EWLP 2014

13TH EUROPEAN WORKSHOP ON LIGNOCELLULOSICS AND PULP

June 24-27, 2014 - Seville, Spain

Proceedings

EWLP 2014

13TH EUROPEAN WORKSHOP ON LIGNOCELLULOSICS AND PULP

PROCEEDINGS

24-27 June 2014
Seville, Spain

Editors: J.C. del Río, A. Gutiérrez, J. Rencoret and Á.T. Martínez
Printed in Spain, 2014
Cover design: E.D. Babot

ISBN: 978-84-616-9842-4

EWLP 2014

13TH EUROPEAN WORKSHOP ON LIGNOCELLULOSICS AND PULP

SPONSORS

novozymes®

Rethink Tomorrow

CELESA

celulosa de levante, s.a.

Special Cellulose Pulps

24-27 June 2014

Seville, Spain

EWLP 2014

13TH EUROPEAN WORKSHOP ON LIGNOCELLULOSICS AND PULP

Local Organizing Committee

José C. del Río, IRNAS-CSIC, Spain, Chair
Ana Gutiérrez, IRNAS-CSIC, Spain
Jorge Rencoret, IRNAS-CSIC, Spain
Angel T. Martínez, CIB-CSIC, Spain

Executive Committee

Monica Ek, Sweden
Dominique Lachenal, France
Carlos Pascoal Neto, Portugal
Thomas Rosenau, Austria

Scientific Committee

Konstantin Bogolitsyn, Russia
Alain Castellan, France
Christine Chirat, France
Claudia Crestini, Italy
José C. del Río, Spain
Dmitry Evtuguin, Portugal
Tommy Iversen, Sweden
Catherine Lapierre, France
Ángel T. Martínez, Spain
Gérard Mortha, France
Antje Potthast, Austria
Bodo Saake, Germany
Herbert Sixta, Finland
Elisabeth Sjöholm, Sweden
Margaretha Söderqvist Lindblad, Sweden
Tarja Tamminen, Finland
Arnis Treimanis, Latvia
Tapani Vuorinen, Finland

Table of Contents

Oral presentations

Poster presentations

ON THE IMPORTANCE OF RAW MATERIAL ASSESSMENT AND SELECTION FOR LOW COST EUCALYPT KRAFT PULP PRODUCTION

Jorge L. Colodette[1] and Fernando J. B. Gomes[1]

[1]*Pulp ad Paper Laboratory, Federal University of Viçosa, Viçosa, MG, Brazil 36.570-000 (colodett@ufv.br)*

ABSTRACT

Wood density and chemical composition (cellulose, hemicelluloses lignin and extractives) are important traits for commodity bleached kraft pulp production cost because they strongly affect specific wood (SWC) consumption and pulping yield. More recently, wood uronic acids content and lignin syringyl/guaiacyl ratio (S/G) have also become relevant and they are focused in this work. The two major costs in the production of bleached eucalyptus Kraft pulp derive from wood and chemicals, which can be minimized by increasing fiber line yield and decreasing bleaching chemical usage. An important alternative for increasing fiber line yield is the optimization of the kappa number at which cooking shall actually terminate before other means of delignification take over. The ideal kappa to terminate cooking is highly dependent on the wood type. It is our belief that cooking shall terminate at the point where pulp achieves maximum HexA/Lignin ratio, regardless of the kappa number. Hence, this study was aimed at determining the exact kappa number at which the HexA/Lignin ratio maximizes for three different eucalyptus woods (*E. globulus, E. urograndis and E. camaldulensis*) and how this affect pulp yield and bleachability. It was observed that maximum HexA/Lignin ratio occurs at kappa 14 for *Eucalyptus globulus* whereas this ratio maximizes at kappa 20 for *E. camaldulensis*. The maximum HexA/Lignin ratio at a given kappa also coincides with maximum pulp yield and bleachability. The kappa number where HexA/Lignin ratio maximizes depends upon wood lignin syringyl/guaiacyl ratio.

I. INTRODUCTION

Industrially, eucalyptus wood quality for kraft pulping is assessed by the following main traits: density and cellulose, hemicelluloses, lignin and extractive contents. These traits are relevant for commodity products because they strongly affect kraft pulp production costs by impacting specific wood consumption (SWC) and pulping yield**.** Wood uronic acids content and lignin syringyl/guaiacyl ratio (S/G) as well as other traits such as fiber morphology (coarseness, fiber population, microfibril angle, etc.), cellulose crystallinity, crystal structure, cellulose and xylan molecular weight distribution, non-process elements (minerals), acetyl group, and others have been recognized as important, but they have not been widely used for wood selection in most forest and pulp and paper companies. Altogether, the traits aforementioned affect not only pulp production costs but also its utilization since they impact pulp refinability, drainability and strength properties, which influence paper machine runnability and productivity [1].

The two major costs in the production of bleached eucalyptus Kraft pulp derive from wood and chemicals, with the first being more significant. Within the industrial domain, the most effective way of decreasing wood costs is by increasing overall fiber line yield and decreasing wastes in the wood preparation room. The decrease of chemical costs is more effectively done through optimization of the pulp bleaching operation where most of the unrecoverable chemicals are used.

Some studies have inferred that is always better to terminate the cook at a higher kappa number, within the limits of equipment runnability, and continue the delignification for example with an oxygen stage [2-4]. Recently, the extended impregnation technology has been developed to minimize the amount of rejects in high kappa pulping [5]. Of course, the ideal kappa to terminate cooking is highly dependent on the wood type [6]. For hardwoods, the approach of terminating the cook at the highest possible kappa number is likely not the right one because the defiberization point for such woods depends upon the syringyl/guaiacyl ratio of their lignins. Some studies have indicated that wood lignin S/G ratio may play a role in wood defiberization point during Kraft cooking [7, 8].

Instead of terminating the cook at the highest possible kappa number, this study proposes that the cook shall terminate at the point where the pulp achieves maximum HexA/Lignin ratio, regardless of the kappa number. Maximization of pulp HexA/Lignin ratio signifies maximization of hemicelluloses retention and as consequence maximization of yield. In spite of some controversies, it is mostly accepted that pulps containing maximum HexA/Lignin ratios at a given kappa number will present highest bleachabilities in ECF bleaching processes as well [9-12]. Therefore, this study aimed at determining the exact kappa number at which the HexA/Lignin ratio

maximizes for three different eucalyptus woods (*E. globulus, E. urograndis and E. camaldulensis*) and how this affect pulp yield and bleachability.

II. EXPERIMENTAL

Eucalyptus wood chips were prepared from 12 yr. old *E. globulus* and *7 yr. old E. urograndis and E. camaldulensis.* The chips were cooked in an M&K digester to kappa number varying in the range from 10-26. Pulps of variable kappa number at fixed residual effective alkali of 6-7 g/L NaOH were prepared by varying process conditions, including three temperatures (160, 165 and 170°C), eight active alkali charges (12, 14, 16, 18, 20, 22, 24 and 26% as NaOH) and 8 times at temperature (30, 60, 90, 120, 150, 180, 210 and 240 min). The time to maximum temperature, liquor to wood ratio and sulphidity were kept constant and equal to 90 min, 4L/1kg and 25%, respectively. Six pulp samples of each one of the three eucalypt species were bleached to ISO brightness 90% with the O-D_{HT}-(EPO)-D-P sequence. These samples were selected of the pool of different pulps on the basis of their kappa numbers (10-24 range) and residual effective alkali (6-7 g/L range). The alkali charge in the O-stage (10% consistency, 100 ^{o}C, 500 kPa, 75 min and 2.2% O_2) were varied in order to achieve 11-11.5 end pH. The charges of chlorine dioxide applied to the D_{HT} (10% consistency, pH 3, 90 ^{o}C, and 120 min) and D-stages (10% consistency, pH 5-5.5, 80 ^{o}C, and 120 min) were varied in order to achieve the target brightness for each one of the selected pulp samples. The ClO_2 charge in the D_{HT} stage was a function of incoming kappa number and established based on a fixed kappa factor of 0.14. Three different charges of ClO_2 were tested in the D_1 stage and the brightness values achieved with the three charges at the end of the bleaching (after the P-stage) were interpolated to 90% ISO brightness. The alkali charge in the (EPO)-stage (10% consistency, pH 10.5-11, 85^{o}C, 120 min, 0.3% H_2O_2) and P-stage (10% consistency, pH 10.5-11, 80^{o}C, 120 min, 0.3% H_2O_2) were varied to reach the end pH of 10-10.5. Wood and pulp analyses were performed as described elsewhere [11].

III. RESULTS AND DISCUSSION

Wood Chemical Characterization

Eucalyptus globulus and *Eucalyptus urograndis* presented much higher uronic acids content than *Eucalyptus camaldulensis* **(Table 1).** The total extractives and mineral contents were significantly higher for *E. camaldulensis* in relation to the other two species. A striking difference among the various eucalypts relates to the syringyl/guaiacyl ratio of their lignins, with *E. globulus* showing a much higher value than the other two eucalypt woods.

Table 1. Chemical composition of the three eucalypt wood species

Chemical Trait	***E. globulus***	***E. urograndis***	***E. camaldulensis***
Acid insoluble lignin, %	20.6	25.3	26.7
Acid soluble lignin, %	4.5	3.4	3.1
Lignin S/G ratio	**5.2**	**2.8**	**1.7**
Glucans, %	46.9	46.5	46.8
Xylans, %	14.5	12.2	11.3
Mannans, %	1.6	1.1	0.9
Arabinans, %	0.3	0.2	0.3
Galactans, %	1.2	1.6	1.1
Total uronic acids, %	4.0	3.9	3.1
Acetyl groups, %	3.2	2.7	2.2
Total extractives, %	2.2	2.7	3.5
Ash, %	0.37	0.42	0.58

Maximizing the HexA/Lignin Ratio

Figure 1 shows that the maximum pulp HexA/Lignin is achieved at kappa numbers of approximately 14, 18 and 20 for *E. globulus*, *E. urograndis* and *E. camaldulensis*, respectively. It is apparent that the maximum HexA/Lignin ratio achievable in a given pulp is affected by the pulp degree of delignification. However, the exact kappa number at which the pulp HexA/Lignin ratio maximizes depends on the wood type. The reason for such behavior stems from differences in the cooking easiness of the various woods evaluated.

Maximizing Pulp Yield

The composition of the kappa number was proven very important to compare yield results. By splitting the kappa number into two fractions, hexenuronic acids and lignin, the important relationship HexA/Lignin was developed; this relationship allows for the comparison of yield and other pulping parameters at different kappa numbers as long as the residual effective alkali of the cooks are similar and only screened yield is taken into account. **Figure 2** show that maximum screened yield tend to occur at the maximum pulp HexA/Lignin ratios, regardless of wood species. The kappa numbers where maximum screened yields were attained for *E. globulus*, *E. urograndis and E. camaldulensis* were about 14, 18 and 20, respectively, and they coincided with the maximum HexA/Lignin ratios for these species. Increasing kappa number over these ranges resulted in increased rejects and decreased pulp xylan contents, which in turn penalized the screened yields. On the other hand, decreasing kappa number under this range resulted in decreased pulp xylan contents with negative consequences on yield. In principle, the kappa number where the ratio pulp HexA/Lignin maximizes for a given wood species should coincide with maximum pulping yield because of maximum xylan retention **(Figure 3).** The wood defiberization point is influenced by the wood density and chemical composition but the lignin syringyl/guaiacyl ratio (S/G) is likely the most important factor affecting this parameter. The higher the S/G ratio the lower is the kappa number at which wood will defiberize. Among the three wood species under investigation, the *E. globulus* showed the highest S/G (**Table 1**) and it defiberized at lower kappa numbers than the other three species.

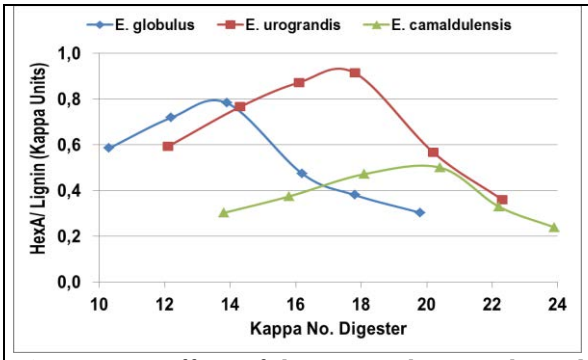

Figure 1 - Effect of kappa number on the pulp maximum HexA/Lignin ratio for *E. globulus*, E. *urograndis* and E. *camaldulensis*, for cooks terminated at constant RES (6-7 g/L).

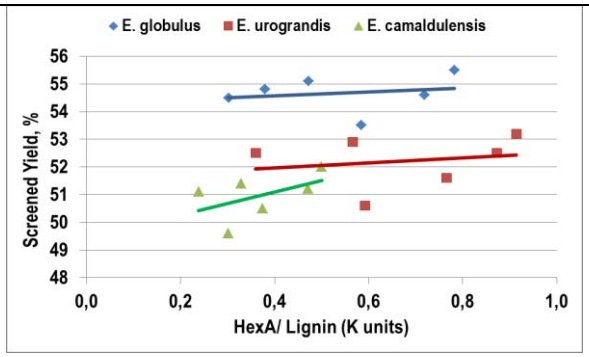

Figure 2 – Effect of pulp HexA/Lignin ratio on pulp screened yield for *E. globulus*, *E. urograndis* and *E. camaldulensis*, for cooks terminated at constant RES (6-7 g/L).

Maximizing Pulp Bleachability

In this study bleachability was defined as the amount of kappa units removed per unit % of chlorine dioxide consumed across bleaching. **Figure 4** shows that pulp bleachability increases with increasing HexA/Lignin ratio. Hence, for minimum chlorine dioxide consumption the cook shall terminate at the kappa number where HexA/Lignin ratio maximizes. Of course, the value of this kappa number cannot be established as a set rule since different eucalypt woods produce maximum HexA/Lignin ratio at different kappa numbers. Thus, technically speaking there is no ideal kappa number for terminating the cook for eucalypt wood aiming at best pulp bleachability since it is species dependent.

IV. CONCLUSIONS

Maximization of pulp yield and bleachability is achieved at the pulp kappa number where pulp HexA/Lignin ratio maximizes. The HexA/Lignin ratio maximizes at different kappa numbers depending upon the eucalypt wood species. The kappa number where HexA/Lignin ratio maximizes is affected by the wood lignin syringyl/guaiacyl ratio (S/G).

V. ACKNOWLEDGEMENT

Funding from the European Community's Seventh Framework Program FP7/2007-2013 under grant agreement no KBBE-2009-3-244362 LignoDeco (EU/Brazil co-operation), and from the Minas Gerais State Research Foundation are greatly appreciated.

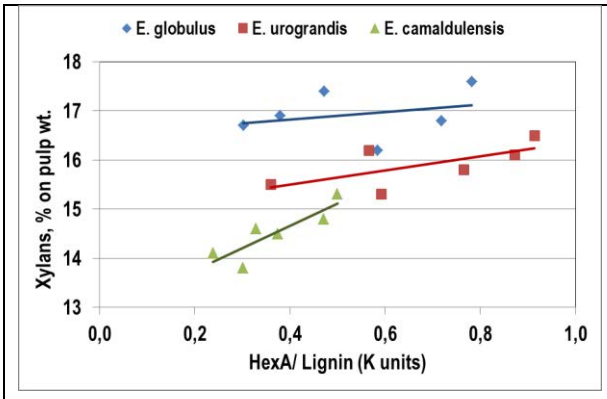

Figure 3. Effect of pulp HexA/Lignin ratio on pulp xylan content for *E. globulus*, *E. urograndis* and *E. camaldulensis*, for cooks terminated at constant RES (6-7 g/L).

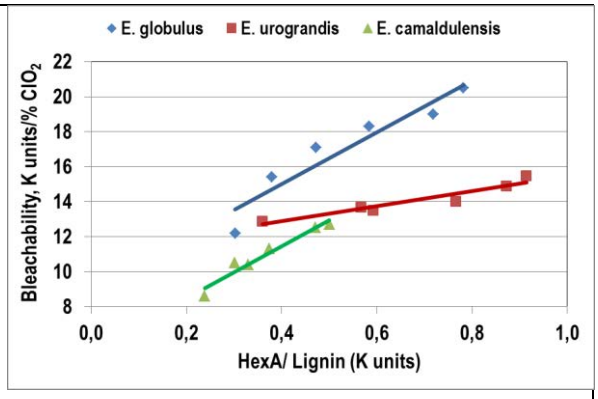

Figure 4. Effect of pulp HexA/Lignin ratio on the bleachability of *E. globulus*, *E. urograndis* and *E. camaldulensis* pulps to 90% ISO brightness (interpolated) with the O-D_{HT}-(EPO)-D-P sequence.

VI. REFERENCES

[1] Magaton, A., Colodette, J.L., Gouvêa, A.F.G., Gomide, J.L., Muguet, M.C.S., Pedrazzi, C., Eucalyptus wood quality and its impact on kraft pulp production and use. Tappi Journal**,** 8(8):32-39 **(2009).**

[2] Parsad, B., Gratzl, J., Kirkman, A., Jameel, H., Rost, T. and Magnotta, V., Extended Delignification by Kraft Pulping Followed by Oxygen-Alkali Treatment: Technical and Economic Evaluation. In: Pulping Conference Atlanta, Atlanta, GA, USA, Book 1, p. 297 **(1993).**

[3] Colodette, J.L., Gomide, J.L., Salles, D.V., Brito, A.C.H. and Oliveira, A.C., "Effect of the Brownstock Kappa Number on Fiber Line Bleached Yield", Proceedings, Tappi Pulping Conference, Chicago, USA, 405-413 **(1995).**

[4] Colodette, J. Gomide, J.L., Longue Júnior, D. and Pedrazzi, C., "Effect of Pulp Delignification Degree on Fiber Line Performance and Bleaching Effluent Load", Bioresources**,** 2(2): 223-234 **(2007).**

[5] Wedin, H., Lindstrom, M. and Ragnar, M., "Extended Impregnation in the Kraft Cook – an Approach to Improve the Overall Yield in Eucalypt Kraft Pulping", Nordic Pulp and Paper Research Journal, 25(1): 7-14 **(2010).**

[6] Colodette, J.L., Mounteer, A.H. and Gomes, F.J.B., "Advanced Technologies for Eucalypt Pulp Bleaching". Proceedings, ANQUE – International Congress of Chemical Engineering. Seville, Spain **(2012).**

[7] Lindstrom, M., "From Simple Theory to Industrial Application – Extended Impregnation Kraft Cooking". Proceedings, 5th International Colloquium on Eucalyptus Kraft Pulp, Porto Seguro, Brazil, CD-ROM **(2011).**

[8] Hart, P.W., Colson, G.W., Antonsson, S. and Hjort, A., "Impact of Impregnation on High Kappa Number Hardwood Pulps", Bioresources 6(4): 5139-5150 **(2011).**

[9] Colodette, J.L, Gomes, C.M., Rabelo, M.S., Eiras, K.M.M., Gomes, A.F. and Oliveira, K.D., "Eucalyptus Kraft Pulp Bleaching: State-of-the-art and new Developments", Tappi Journal Online. 7(2): 18A-18M **(2008).**

[10] Colodette, J.L. and Henricson, K., The hot acid Stage for Hexenuronic Acid Removal. In: Pulp Bleaching and Practices. Tappi Press. Ch. 5, 103-140 **(2012).**

[11] Colodette, J.L., Carvalho, D. M., Souza, C. B., Gomes, F. J. B., Gomide, J.L., A novel approach for maximizing kraft pulp yield and bleachability. 17th International Symposium on Wood, Fibre and Pulping Chemistry (13th ISWFPC), Vancouver, Canada, June 12-14 ***(2013)***.

[12] Martino, D.C., Colodette, J.L., Silva, T.C.F., Longue Junior, D., Paula, D.M.L., Azevedo, M.A.B., 2013. "Factors Affecting Bleachability of Eucalypt Pulp", Proceedings, PAPTAC 99th Conference, Montreal, Canada **(2013).**

PREDICTION OF REAL TIME KRAFT PULP YIELD: FROM SCIENCE TO PULP MILL TRIALS

Denilson da Silva Perez[1*], Adriaan van Heiningen[2], Tiina Liitiä[3], Olli Timonen[4], Kari Kovasin[5], Alexandre Bassa[6], Michel Petit-Conil[1,7].

[1]FCBA, New Materials Division, Domaine Universitaire, CS 90251, 38044 - Grenoble, France; [2]University of Maine, Department of Chemical and Biological Engineering, 5737 Jenness Hall, 04469 - Orono, ME, USA; [3]VTT Technical Research Centre of Finland, P.O. Box 1000, FI02044 VTT, Finland; [4] Stora Enso Oy, Pulp Competence Centre / Tutkimuskeskus, FIN-55800 Imatra, Finland; [5]Metsa Fibre Oy, PO Box 165, FI-26101 Rauma, Finland; [6]Fibria S.A., Centro de Technologia, Jacareí, Brazil; [7]CTP, UST 5, Domaine Universitaire, CS 90251, 38044 - Grenoble, France (denilson.dasilvaperez@fcba.fr)*

ABSTRACT

A new method was developed for the prediction of alkaline pulp yield. The full version of the equation allows predicting pulp yield from the cellulose content and the degree of polymerization of wood raw material used and the corresponding pulps. From the slope and intercept of this linear equation, the lignin-free pulp yield, Y_T', of a pulp sample can be calculated when the cellulose content (G') and its degree of polymerization are determined by sugar analysis and viscosimetry, respectively. This equation was extensively tested and validated at laboratory/pilot scales for the effect of wood variability and process conditions on pulp yield. Then, industrial trials were successfully applied in two mills operating with different wood species (birch and softwoods) and process conditions (modified continuous and batch kraft cooking).

I. INTRODUCTION

As wood is the dominant cost factor for a pulp mill production, an increase in pulp yield has a major impact on its competitiveness. In order to optimize pulp yield, a pulp mill must be able to monitor the pulp yield accurately. Traditionally, the pulp yield is estimated based on wood usage and pulp sales data covering a period of 3-6 months. However, it is inconceivable to perform mill trials over long periods to compare pulp yield gains due to wood or process changes [1]. To overcome this difficulty, several indirect or direct methods for the prediction of the pulp yield have been proposed, but they are often based on empirical considerations and have to be adapted to different situations in a case-by-case approach [1,2,3,4].

Cellulose is a homopolymer subject to wellknown degradation kinetics during alkaline pulping. Therefore, the development of the cellulose mass fraction based on wood may be predicted theoretically. In an earlier work, a theoretical relationship between pulp yield and the cellulose mass fraction based on wood and the cellulose mass fraction of pulp was derived, validated for cotton, then tested for some wood species and process conditions [5,6]. The original form of the equation is the following [6]:

$$\frac{1}{Y_C} = \frac{1}{K_1} + \frac{1}{K_1}\frac{(\Delta DP)_S}{DP} \qquad (1) \qquad \text{where} \qquad K_1 = \frac{\left[DP_0 + (\Delta DP)_s - (\Delta DP)_P\right]}{DP_0} Y_{C,W} \qquad (2)$$

DP_0 = average degree of polymerization of cellulose chains in wood; DP = average degree of polymerization of cellulose chains in pulp; $(\Delta DP)_P$ = loss of degree of polymerization due to primary peeling; $(\Delta DP)s$ = loss of degree of polymerization due to secondary peeling; $Y_{c,w}$, = cellulose mass fraction of the original wood and Y_c = cellulose mass fraction of pulp based on wood.

As DP_0 is more than one order of magnitude larger than $(\Delta DP)_S$ or $(\Delta DP)_P$, and because $(\Delta DP)_S$ and $(\Delta DP)_P$ are of the same order of magnitude and have an opposite sign in equation 1, one may simplify the equation by replacing K_1 in equation 1 by $Y_{C,W}$, resulting in a simplified pulp yield prediction equation which is obtained in the following form:

$$\frac{1}{Y_T'G'} = \frac{1}{Y_{C,W}} + \frac{(\Delta DP)_S}{Y_{C,W}} \cdot \frac{1}{DP} \qquad (3)$$

This simplified equation, called henceforth PulpYield project equation, can be used to calculate the lignin-free pulp yield, Y_T', of a pulp sample when G' (lignin-free cellulose content of the pulp) and the cellulose DP of the pulp [7] are determined by sugar analysis and viscosimetry respectively, and the values of $Y_{c,w}$ and $(\Delta DP)s$ are determined by laboratory cooks or are known for the considered furnish.

II. EXPERIMENTAL

Laboratory cooking

Wood chips were received from pulp mills or produced from manually debarked logs then chipped with a pilot wood chipper. In most cases, the wood chips were air-dried, classified for fines and oversized chips removal and stored. Before cooking, the moisture content of the wood chips was carefully determined using a representative sample. A known weight of chips (usually 500 g o.d.) was cooked in a 3.5-liter rocking, oil-heated, multi batch digesters at a liquid to wood ratio of 4.0 l/kg. Alkali and sulfidity charges, cooking temperature plateau and H-factor values were dependent on the different cases. After cooking, the wood chips were disintegrated, washed and then screened. The total and screened yields were calculated based on the average dryness of the pulp, the total wet pulp weight, the dry weight of the rejects and the dry weight of the chips added to the cook.

Wood and pulp analyses

The intrinsic viscosity was measured according to ISO SCAN C15:62 standard using a RPV-1 automatic viscometer (Rheotek, England). The degree of polymerization of cellulose in the pulp was calculated according to the equation by da Silva Perez and van Heiningen [7]:

$$DP = \left(\frac{(1.65[\eta] - 116H)}{G} \right)^{1.111} \qquad (4)$$

Chemical composition of wood and pulps were determined according to the standards and methods described in an earlier publication [6].

III. RESULTS AND DISCUSSION

Different pure wood species, both softwoods and hardwoods were cooked at different conditions, pure and in mixture. Some examples of the results applied to equation (3) are presented in **Table 1** commented in the sub-sections here below. R^2, (ΔDPs), and Yc,w were obtained from the data plotted according to the equation (3), while Yc,w was measured from sugars analysis of the wood furnish.

Table 1 – Application of PulpYield project equation to different wood supply and process conditions

Wood species	Process conditions	R^2	(ΔDPs)	Yc,w (estimated)	Yc,w (measured)
Beech	Conventional Kraft	0.9203	1107	0.5119	0.5197
Birch	Conventional Kraft	0.9632	1039	0.5042	0.5111
Chestnut	Conventional Kraft	0.8375	229	0.4329	0.4107
Eucalyptus	Conventional Kraft	0.9262	471	0.4852	0.5124
Poplar	Conventional Kraft	0.9554	526	0.5057	0.5211
Chesnut/beech	Conventional Kraft	0.9588	614	0.4477	0.4652
Chestnut/beech	Conventional Kraft	0.9401	1000	0.4610	0.5161
Poplar/beech	Conventional Kraft	0.8919	748	0.5102	0.5204
Chestnut/beech/poplar	Conventional Kraft	0.9046	458	0.4525	0.4838
Eucalyptus clone A	Conventional Kraft	0.9541	782	0.5534	0.5452
Eucalyptus clones B/C	Conventional Kraft	0.9170	959	0.5860	0.6032
Birch	Kraft / AQ (0.1 %)	0.8970	1091	0.4807	0.5111
Eucalyptus	Kraft / AQ (0.1 %)	0.9926	455	0.4879	0.5124
Birch	Multi-stades	0.9702	1400	0.5013	0.5111
Eucalyptus	Multi-stades	0.9253	456	0.4940	0.5124

Effect of inter- and intra- wood species variability

Different pure wood species, both softwoods and hardwoods were cooked at different conditions. The graphical results of the results applied to equation (3) are presented in **Figure 1a** for different hardwoods to illustrate the inter-wood species variability. Results were also obtained for different softwoods, pure and in mixture (not shown here). Very good linearity was observed for all the wood species. Among hardwoods, a slightly weaker performance was observed for chestnut (R^2 around 0.84). The explanation for this particular behavior is the high content of extractives present in chestnut (sometimes up to 15 %) which disturbs the kraft cooking through an important consumption of alkali. Cooking of mixture of wood species both softwood or hardwoods was also performed. Although the results are not shown here due to lack of space, it was observed that mixtures of softwoods can be modeled as an average of the behavior of the individual wood species. For hardwoods, especially the mixtures containing chestnut, interactions occur during pulping of different wood species which

lead to overcooking or undercooking of one of the wood species and therefore affects the overall pulp yield. Therefore, the benefits of pulp yield gains due to one species (poplar for example) are lost due to overcooking. It is also clear that in these cases, chestnut is the wood species governing the behavior of the pulp yield. The intra-wood species effect was tested for eucalyptus clones (**Figure 1b)** and poplar clones (not shown). Three different clones were used for each wood species. For eucalyptus clones, it is clearly seen that clone A differs significantly from clones referred as B and C, which can be treated in a single straight line. These two clones presented similar cellulose content, much higher compared to clone A, which explains the behavior observed.

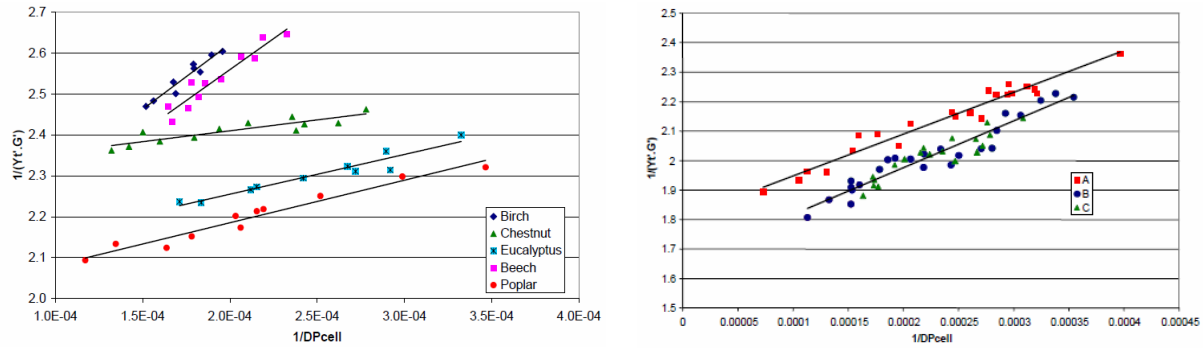

Figure 1 - Application of PulpYield project equation to: **a)** hardwoods (left) and **b)** eucalyptus clones (right).

Effect of process conditions

Different process conditions impacting the pulp yield such as the use of additives (anthraquinone, polysulfide and surfactants), the effect of scale-up (laboratory or pilot), conventional (1 stage) x modified (multi-stages) kraft cooking and the effect of uncooked chips were also studied.

The efforts were concentrated on AQ (0.1 %) as this was the only additive giving consistent and measurable pulp yield gains. Tests were carried out for 4 wood species: birch, eucalyptus, spruce, and pine. Only results obtained for hardwoods are presented here (**Figure 2**). For all wood species, the increase in pulp yield due to the action of AQ is detected by the equation in the form of a reduction in the ΔDPs. This is expected from the mechanism of anthraquinone protection and is observed for all the wood species. A significant impact is observed for birch as the slope is considerably reduced as well as the ΔDPs. However, the estimated Yc,w for AQ-containing cooks is always lower than those obtained for non-AQ and of the measured Yc,w values. AQ and high sulfidity black liquor prevent the primary peeling by stabilizing the original reducing groups in wood cellulose. This occurs at relatively low temperatures during the heat up phase. When secondary reducing groups are formed by alkaline hydrolysis at higher temperatures then the peeling reaction rate is so fast that AQ cannot stop it.

Modified multi-stage kraft cooking is claimed by the equipment suppliers to have a positive impact on pulp yield. In this part of the project, the pulp yield of conventional single stage kraft and a 3-stage kraft cooking (basis for EMCC or Lo-Solids cooking) was carried out for 4 wood species: birch, eucalyptus, spruce and pine. Results obtained for hardwoods are shown in **Figure 2b**. In the conventional cooking, the whole alkaline charge was applied at the beginning with a liquor/wood ratio equal to 4. The modified 3-stage cooking was performed with the same total alkaline/sulfidity charges, but in 3 stages. Black liquor was removed and replaced by fresh liquor at 1/3 and 2/3 of the targeted H-factor. Pulp yield increase was detected by equation (3) due to lower alkaline in modified cooking conditions as evidenced by higher DP and lower values of (ΔDPs).

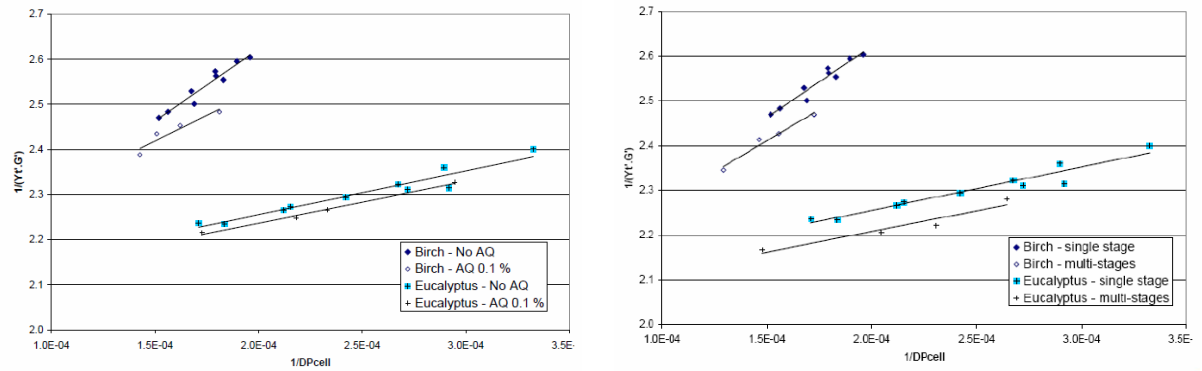

Figure 2 - Application of PulpYield project equation to: **a)** effect of AQ (left) and **b)** multi-stage cooking (right).

Industrial trials

After the work carried out in laboratory, the method for predicting pulp yield presented here was applied in two pulp mills (A = pulp mill operating a continuous modified Kraft cooking of birch and B = operating with softwoods, mainly pine, spruce and sawmill chips and batch cooking). Wood and pulps were sampled during a campaign of production and sent to FCBA laboratories, where they were analyzed individually. Wood samples were grouped into a single lot for birch and two for softwoods (SW1 = rich in spruce and SW2 = rich in pine), characterized and used for laboratory cooking in order to establish the PulpYield project equation parameters (**Figure 3a** for the mill A and **Figure 3b** for the mill B). Then, the acquired parameters were used to predict the yield of the industrial pulp samples based on their properties.

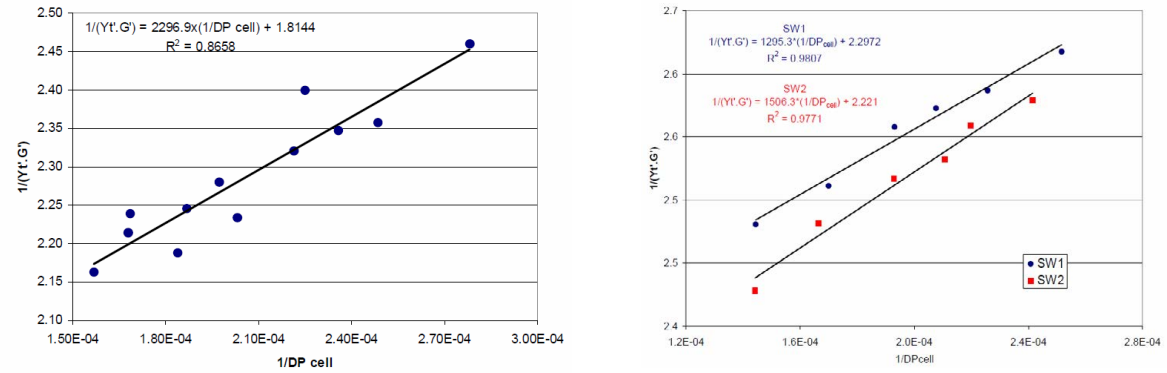

Figure 3 – Application of PulpYield project equation to mill A (birch) and mill B (softwoods).

Then, using the analytical data of the wood and pulps sampled in both mills and the parameters obtained from the equation 3 applied to the different situation, it was possible to predict their pulp yield of the industrial pulps. For the mill A operating with birch and continuous cooking, the average of pulp yield was 52.83 % with a standard deviation of 0.41 % for 8 samples taken along the 8-hour campaign trial. For the mill B, the average of pulp yield was 44.76 % for the spruce-rich wood supply with a standard deviation of 0.35 % for 3 samples obtained in the beginning, the middle and in the end of the batch digester. For the pine-rich pulps, the average value was 45.48 % with a standard deviation of 0.18 %.

IV. CONCLUSIONS

PulpYield project equation was successfully validated at both laboratory/pilot and industrial scales. The results of the project demonstrated that wood variability (both from inter- and intra-wood species) is a very important factor for pulp yield control. Most of the variability sources can be detected by PulpYield project equation but specific calibrations are needed. Process conditions are also important for pulp yield monitoring. Industrial trials were successfully applied in two mills operating with different wood species (birch and softwoods) and process conditions (modified continuous and batch kraft cooking). PulpYield project equation is nowadays ready for routine purposes and will be hopefully tested in other pulp mills in a near future.

V. ACKNOWLEDGEMENT

Financial support from industrial partners is grateful acknowledged. The authors also thank Stora Enso, Metsa Fiber, and Fibria for supplying wood and pulp samples.

VI. REFERENCES

[1] Easty, D.B.; Malcolm E.W. Estimation of pulping yield in continuous digesters from carbohydrate and lignin determinations, *Tappi J.*, **1982**, *65(12)*, 78-80.
[2] MacLeod, J.M.; Pelletier, L.J. Basket cases: kraft pulps inside digesters, *Tappi J.*, **1987**, *70(11)*, 47-53.
[3] Luthe, C.; Berry, R.; Radiotis, T.; Nadeau, T. Measuring Softwood Yield Gain at Kraft Pulp Mils, **2002**, *PRP 1582*.
[4] Marcoccia, B.S.; Stromberg, B.; Prough, J.R. A novel method for real-time measurement of alkaline pulping yield, **1998**, *PAPTAC Pulping Conference*, *Montreal*, *Canada*, Proceedings, pp1485-1499.
[5] van Heiningen, A.R.P.; Gao, Y.; da Silva Perez, D., Prediction of Alkaline Pulp Yield from the Mass Fraction and Degree of Polymerization of Cellulose, *7th EWLP*, **2002**, Turku, Finland, pp63-68.
[6] van Heiningen, A.R.P.; Tunc, M.; Gao, Y.; da Silva Perez, D. Relationship between alkaline pulp yield, the mass fraction and degree of polymerization of cellulose in pulp, *J. Pulp Paper Sci.* **2004**, *30(8)*, 211-217.
[7] da Silva Perez, D.; van Heiningen, A.R.P. Determination of cellulose degree of polymerization in chemical pulps by viscometry, *7th EWLP*, **2002**, Turku, Finland, Proceedings, pp 393-396.

EFFECT OF RAW MATERIAL AND PULPING CONDITIONS ON THE PROPERTIES OF DISSOLVED KRAFT LIGNIN

Olena Sevastyanova[1], Galina Dobele[2], Vilhemina Jurkjane[2], Antonia Svärd[1], and Elisabet Brännvall[1]*

[1]Royal Institute of Technology, KTH, Fiber and Polymer Technology, Stockholm, Sweden,
[2]Latvian State Institute of Wood Chemistry, Riga, Latvia
*(*bettan@kth.se)*

ABSTRACT

Composition, molecular weight and chemical structure of lignin affects its properties, reactivity and performance in various applications. It is thus of great importance to know how processes, in which lignin is dissolved from wood and other plants, affect the characteristics.
In the present study, we investigated the impact of raw material and cooking time on the structure of dissolved lignin. Kraft pulping was performed on wood chips of eucalyptus, pine and spruce. The black liquor was recovered after three different cooking times and the dissolved lignin was thoroughly characterized.
The results indicate that increased cooking time resulted in increased phenolic content and higher glass transition temperature of the dissolved lignin. The sulfur content was higher in the eucalyptus lignin compared to the softwood lignins.

I. INTRODUCTION

Lignin is a main chemical component of lignocellulosic materials, abundantly accessible and easily available. Various technical lignins are currently available in large quantities and viewed as low value by-products from the pulp and paper industry. However, structurally lignin possesses properties which make it a promising starting material for chemical modifications, leading to the preparation of valuable polymeric materials. Detailed characteristic of lignin samples coupled with information on the pulping conditions will help to adjust the pulping process not only with regards to pulp properties but also with respect to obtain lignin with desired characteristics.
Since the main object of the processes in which lignin is recovered is to obtain cellulosic fibres, few efforts have been made to alter process conditions in order to obtain lignin with more suitable characteristics. A number of studies have analyzed the structure of kraft lignin with regard to amount, functional groups, organically bound sulfur and molecular weight [1-3]. The objective of these studies was to get information of the delignification process. Other studies, more aimed at understanding the heating value of black liquor, mainly influenced by the lignin content, have also characterized kraft lignin to some extent [4-5]. As the interest in using lignin as a raw material for value added products has increased, many studies have been conducted to characterize different types of technical lignin [6-7]. These studies have looked into kraft lignin obtained after kraft cooks of different wood raw materials or in spent liquors after different pulping processes. However, there is still a lack of knowledge how pulping conditions influence the kraft lignin characteristics.
The aim of this study was to investigate the effect of raw material (eucalyptus, pine and spruce) and cooking time on the characteristics of dissolved lignin.

II. EXPERIMENTAL

Materials

Industrial wood chips of pine, spruce and eucalyptus wood chips were used in the study. They were dried to a dry solids content of 91-95%. The chips were sorted manually and a fraction of 2-8 mm thickness, without knots and bark, was used.

Kraft cooking

The kraft cooks were performed in steel autoclaves according to cooking parameters presented in **Table 1**. After terminating the cooks, the black liquor was separated from the chips. The black liquors were stored in a fridge until precipitation.

The dissolved lignin in the black liquors was precipitated by acidification according to [8]. The pH of the original black liquors was around 12 and before addition of sulphuric acid, the black liquors after the softwoods cooks were heated to 70°C and the eucalyptus black liquor to 60°C. Sulphuric acid was added during stirring

until a pH of 9 was reached. The beaker with precipitated lignin was cooled in an ice bath and then put into the fridge for 10-12 h. The lignin colloids deposited in the bottom of the beaker and the supernatant was filtered off. The lignin filter cake was then re-dispersed in distilled water and the pH lowered with sulphuric acid to pH 2 under rapid stirring. The lignin was filtered again and collected on a glass dish to dry in a ventilated oven at 65°C.

Table 1 - Pulping conditions

	NaSH [M]	NaOH [M]	Liquor-to-wood ratio, l/kg	Cooking temperature, °C	Cooking time, min
Pine	0,26	1,2	4	157°C	100, 200, 260
Spruce	0,26	1,2	4	157°C	100, 200, 260
Eucalyptus	0,26	1,0	4	157°C	30, 60, 100

Analysis

The phenolic content in lignin using an UV-vis method was determined according to a modified method proposed in [9] using a SHIMADZU UV – 2550 UV-vis spectrophotometer and fused quartz cuvettes.

Total solid content in black liquor was determined by placing 10 ml of each black liquor sample into an oven with a temperature of 105°C for 10-12 h. After gravimetrically determining the dry solids content, the ash content in the black liquor samples was subsequently determined by placing the samples for 6 h in an oven holding a temperature of 500°C. The ash content in precipitated samples was determined by drying 0,3 g of each precipitated lignin sample in the ash oven at 500°C for 6 h.

The chemical composition was determined using both acid hydrolysis in combination with Klason lignin, according to SCAN-CM 71:09, as well as by analytical pyrolysis, Py-GC/MS. The monosugars after acid hydrolysis were analyzed in a high-performance anion exchange chromatograph quipped with a pulsed amperiometric detection (HPAEC-PAD) and CarboPac PA1 column (Dionex, Ca, USA). Analytical pyrolysis was performed on precipitated lignin samples at the Latvian State Institute of Wood Chemistry, Lignin Laboratory using a Frontier Lab (Japan) Micro Double-shot Pyrolyser Py-2020iD , with pyrolysis temperature of 500°C and a heating rate of 600°C/s. Directly coupled with the Shimadzu GC/MS-QP 2010 apparatus (Japan) with capillary column RTX-1701 (Restec, USA), 60 m × 0,25 mm × 0,25 µm film, with injection temperature of 250°C with El of 70 eV, and MS scan range m/z 15-350 with gas helium at the flow rate of 1 ml/min and split ratio of 1:30. The sample size loaded was between 1,0-2,0 mg. The oven temperature program was 1 min isothermal at 60°C, then heating for 6°C/min to 270°C, and finally held at 270°C for 10 min. The identification of the peaks was performed on the basis of GC/MS chromatogram using Library MS NIST 147.LI13. The relative area of the peaks was calculated using the Shimadzu software and for some corrected or integrated manually where it was needed on the basis of the GC/MS data. The relevant peaks were averaged between the double samples.

Differential scanning chromatography (DSC) was performed in a Mettler Toledo DSC 1 STARe System. The samples wer put into 40 µl aluminium standard cups and the sample weight noted. The samples were heated form 25°C to 150 °C at a rate of 10°C/min in nitrogen gas with a flow rate of 50 ml/min. The temperature stayed at 150°C for 3 min and then dynamically cooled to 25°C and reheated to 300°C. The glass transition temperature was recorded at the midpoint temperature of the heat capacity transition of the second heating run using the Mettler software. The results for each samples were reported as the average of two samples.

Elemental analysis was performed on all precipitated lignin samples at the Latvian State Institute of Wood Chemistry, Lignin Laboratory. About 30 mg homogenized sample is packed in tin foil, weighed and placed into carousel of the automatic sample feeder and analyzed with Elementar Analysen system GmbH, (Germany) Vario MACRO CHNS. Oxygen was calculated by subtracting the weight of N, C, H, and s from the total sample weight.

III. RESULTS AND DISCUSSION

The dissolved lignin in black liquors after kraft cooking of eucalyptus, pine and spruce was precipitated by acidification, filtered and dried before analysis, with the exception of phenolic content, which was determined spectrophotometrically. Filtration of precipitated lignin is quite troublesome, as the precipitate easily clogs the filter. An interesting observation is thus that lignin obtained after longer cooking was significantly easier to filter. For the kraft cooking of softwood, the amount of lignin dissolved into the pulping liquor increased up to 200 min of cooking time, **Figure 1A**, after which a decrease was observed. In the case of eucalyptus, although almost half of the lignin in the eucalyptus chips had been dissolved after 30 min of cooking time, **Figure 1B**, the

lignin particles apparently were too small and could not be recovered by filtration, **Figure 1A**. Surprisingly the eucalyptus lignin precipitate was much darker and distinctively green, whereas softwood lignin was light brown to yellowish in color.

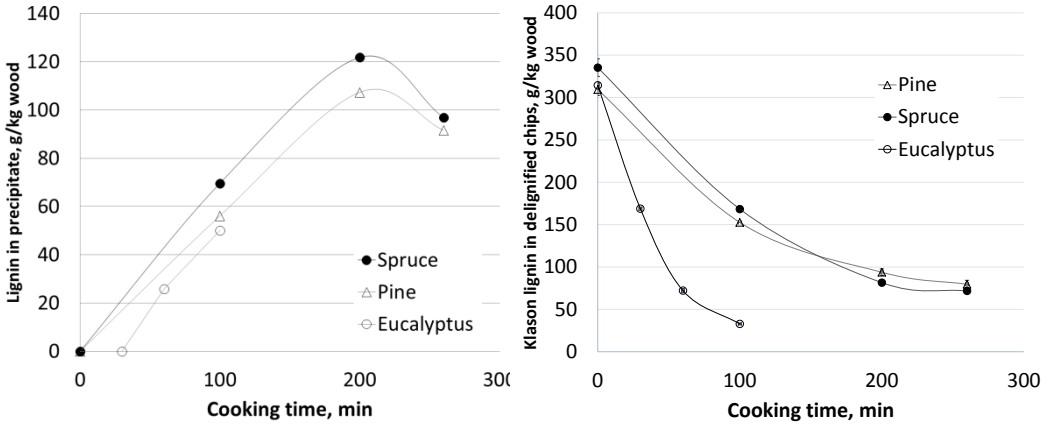

A B

Figure 1. Amount of lignin in black liquor, A; and amount of lignin in chips, B, after different cooking times.

The chemical composition of the precipitates was determined both by acid hydrolysis, **Figure 2A**, and by analytical pyrolysis, Py-GC/MS, **Figure 2B**. There was a discrepancy between the results of the two methods. According to the acid hydrolysis, the precipitate from black liquor after cooking eucalyptus contained higher amount of lignin, whereas according to Py-GC/MS the lignin content was higher in the softwood precipitates.

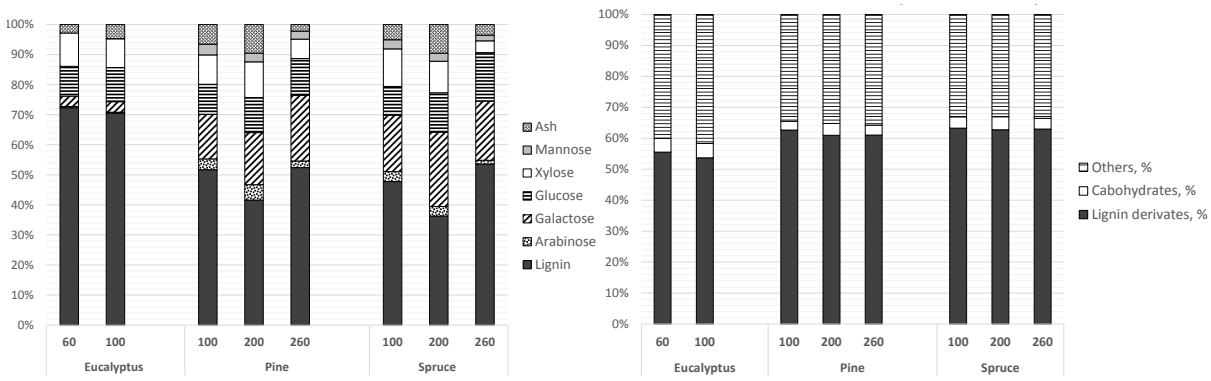

A B

Figure 2. Chemical composition of samples precipitated from black liquor after kraft cooking of eucalyptus, pine and spruce determined by acid hydrolysis, A and by Py-GC/MS, B.

However, in the case of pyrolysis, the sulfur content of the precipitate ends up in the "Others" fraction, whereas in acid hydrolysis, the sulfur will precipitate with the lignin, as it to a large extent is bonded to lignin. As can be seen in **Figure 3**, the sulfur content was higher in the eucalyptus lignin compared to the softwood lignins, especially according to the Py-GC/MS results.

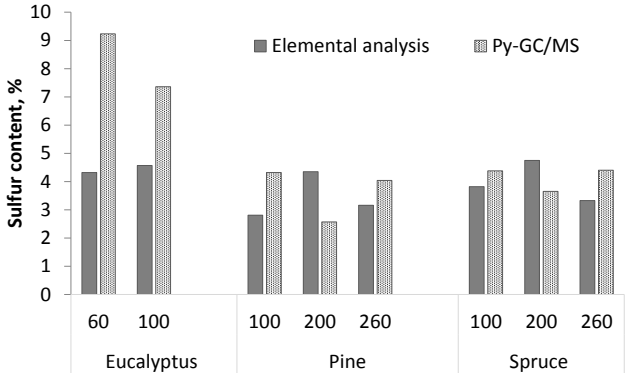

Figure 3. Sulphur content determined by elemental analysis and Py-GC/MS.

As can be expected, the lignin dissolved from eucalyptus was mainly composed of syringyl units, around 60%, whereas the softwood lignins almost entirely consisted of guaiacyl units. Cooking time didn't affect the ratio

between the different lignin units. The phenolic content in the lignin, however, increased with increased cooking time for all wood species as seen in **Figure 4a**. The glass transition temperature was highest for the softwood lignins obtained after the longest cooking time, **Figure 4b**.

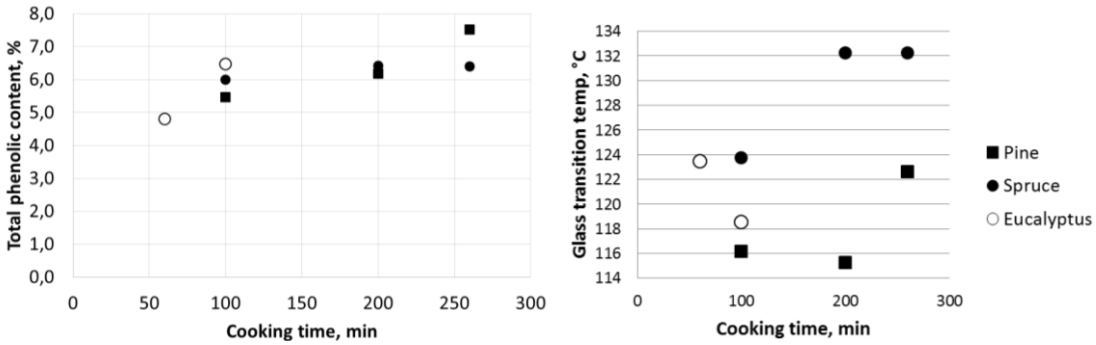

Figure 4. a) Total phenolic content and b) glass transition temperature of lignin.

IV. CONCLUSIONS

Increased cooking time during kraft pulping resulted in a more easily filterable lignin precipitate. The phenolic content of the dissolved lignin increased with cooking time. Eucalyptus lignin contained higher amount of sulfur compared to softwood lignin. The highest glass transition temperature, 132°C, was obtained for spruce lignin obtained after the longest cooking time.

V. ACKNOWLEDGEMENT

COST Action FP1105 (WoodCellNet) is gratefully acknowledged for the financial support of Antonia Svärd during her short-term scientific mission to the Latvian State Institute of Wood Chemistry (IWC). This research was supported by LV PP 5, 2;2,4 program.

VI. REFERENCES

[1] Gellerstedt, G.; Lindfors, E. Structural changes in lignin during kraft pulping. *Holzforschung* **1984**, *38*, 151.

[2] Sjöholm, E.; Nilvebrandt, N.; Colmsjö, A. Characterisation of dissolved kraft lignin by capillary electrophoresis. *J. Wood Chem. Technol.* **1993**, *13*, 529.

[3] Jacobs, A.; Dahlman, O. Characterization of the molar masses of hemicelluloses from wood and pulps employing size exclusion chromatography and matrix-assisted laser desorption ionization time-of-flight mass spectrometry. *Biomacromolecules* **2001**, 23, 894.

[4] Cardoso, M.; de Oliveira, E.; Passos, M. Chemical composition and physical properties of black liquors and their effects on liquor recovery operations in Brazilian pulp mills. *Fuel* **2009**, *88*, 756.

[5] Vakkilainen, E. Estimation of elemental composition from proximate analysis of black liquor. *Paperi Puu* **2000**, *82*, 7, 450.

[6] Prinsen, P.; Rencoret, J.; Gutierrez, A.; Liitiä, T.; Tamminen, T.; Colodette, J.; Berbis, A.; Jimenez-Barbero, J.; Martinez, A.; del Rio, J. Modifcations of the lignin structure during alkaline delignification of eucalyptus wood by kraft, soda-AQ, and soda-O_a cooking. *Ind. Eng. Chem. Res.* **2013**, *52*, 15702.

[7] Mansouri, N.; Salvado, J. Structural characterization of technical lignins for the production of adhesives: Application to lignosulfonate, kraft, soda-anthraquinone, organosolv and ethanol process lignins. *Ind. Crops Products* **2006**, *24*, 8.

[8] Lin, S. Y.; Dence, C. W., Methods in lignin chemistry. **1992**, Springer-Verlag berlin Heidelberg.

[9] Gärtner, A.; Gellerstedt, G.; Tamminen, T. Determination of phenolic hydroxyl groups in residual lignin using a modified UV-method. *Nord Pulp Paper Res. J.* **1999**, *14*, 163.

EFFECT OF PREHYDROLYSIS OF SOFTWOOD CHIPS ON OXYGEN DELIGNIFICATION AND BLEACHING

Christine Chirat, SatyaJit Das, Dominique Lachenal

LGP2 - Grenoble INP - Pagora - 461 rue de la Papeterie, CS 10065, 38402 Saint-Martin d'Hères - France. christine.chirat@pagora.grenoble-inp.fr

ABSTRACT

Prehydrolysed softwood kraft pulps of high (70-78) and classical kappa numbers (20-25) were compared to kraft pulps with corresponding kappa numbers. Depending on the kappa numbers, single or multi-stage oxygen delignification stages were applied on the different pulps. It was shown that PHK pulps could be delignified much more extensively than the control kraft pulps, whatever the starting kappa number. The final viscosities of PHK of high kappa number delignified by oxygen were better than those of the PHK pulps cooked to low kappa numbers. Hydrogen peroxide (P) and ozone (Z) stages were also applied directly on PHK and kraft pulps, and it was shown that the easiest delignification ability was also verified with other oxidants than oxygen. Final bleaching was carried out with a ZEQPP sequence to high brightness levels. The sugar content of the fully bleached PHK pulps was rather low (1.5% xylose, 0.9% mannose and 0.5% arabinose) compared to the control bleached pulp (6.2% xylose, 7.8% mannose, 0.7% arabinose and 0.1% galactose). Lignin carbohydrate bonds were quantified in some of the unbleached pulps and it was shown that their amount was significantly reduced thanks to the prehydrolysis treatment.

I. INTRODUCTION

Pre-hydrolysed kraft (PHK) cooking is one way to produce cellulose for viscose or textile applications. Several mills are converting, or have in project to convert, their kraft process into PHK.
Several studies have been done on the extraction of hemicelluloses from wood, under acidic conditions, prior to chemical pulping [1–16]. Very few articles deal with the bleaching ability of PHK pulps and particularly pre-hydrolyzed softwood pulps [4,14]. The PHK pulps tend to be easier to delignify with oxygen (17). The aim of this work was to investigate further the bleaching ability of pre-hydrolyzed softwood pulps.

II. EXPERIMENTAL

Raw material : Mixed softwood chips, kindly provided by Fibre Excellence Tarascon, were used in this study. The composition is 35% Sylvestre Pine, 24% Black Pine, 18% Alep Pine, 16% Spruce, 7% Douglas fir.

Autohydrolysis : the autohydrolysis step was performed in stainless steel autoclaves placed in a rotating oil bath to adjust the desired temperature. The operating conditions were: liquor to wood ratio of 4, the temperature was 170°C, the time at temperature was 60 minutes and 120 minutes. Wood chips were thoroughly washed after that.

Kraft cooking : cooking was performed in the same autoclaves as for the prehydrolysis. The operating conditions were: liquor to wood ratio of 4, the temperature was 160°C or 170°C, the time at temperature was 110 minutes. The amounts of NaOH and Na_2S are indicated in the tables. The kappa number and viscosity were determined according to Tappi Test Methods T 236 cm-85 and T230 om-99 respectively.

Bleaching : oxygen bleaching (O) was carried out in the same autoclaves as for cooking. The conditions were the following : pulp consistency of 10%, temperature of 100°C, 5 bars of O_2 pressure, and 0.3% $MgSO_4$, $7H_2O$. The NaOH charges are given in the text. Ozone bleaching (Z) was carried out at pH 2.5, high consistency (40°C), in a rotating spherical glass reactor, at room temperature. The ozone charge is given in the text. Hydrogen peroxide bleaching was done according to the following procedure : first a chelation stage (Q) was applied to the pulp (10% pulp consistency, 0.2% EDTA, 80°C, 1 hour), then the pulp was washed and the hydrogen peroxide stage (P) was applied according to the following conditions : 2% NaOH, 1 or 2% H_2O_2, 10% pulp consistency, 80°C, 2 or 3 hours. Duration and hydrogen peroxide charge are given in the tables. Q and P stages were done in polyethylene bags placed in a thermostated water bath.

Isolation of lignin - carbohydrates complexes (LCC) from pulps - The method that was used for the isolation of LCC is described in (18).

Sugar analysis of pulps : the pulps were subjected to acid hydrolysis consisting of a two step treatment : 72% H_2SO_4 followed by dilute acid hydrolysis in an autoclave for 1 h at 120°C (according to TAPPI T 249 cm-00) to hydrolyse all the polysaccharides into sugar monomers. After hydrolysis, the suspensions were filtered. Monosaccharide composition was determined by high-performance anion exchange chromatography with pulse amperometric detection (HPAEC PAD) in a Dionex ICS 5000 apparatus. Sugar separation was done by a CarboPac PA column 10 (250 mm * 4 mm, Dionex).

III. RESULTS AND DISCUSSION

Kraft cooking of control and pre-hydrolysed (PH) wood chips

The wood chips were submitted to autohydrolysis treatments at 170°C for 1 and 2 hours (PH-1hour and PH-2hours). They were then submitted to kraft cooking under different conditions, and the results compared to the control wood chips. The results in Table 1 show that the kraft cooking using conventional conditions from the mill (170°C, 18.9% NaOH and 6.9% Na_2S)(references A and B) gave a pulp with a slightly lower kappa number than the control, and with a significantly reduced DPv. This cellulose degradation is the result of the rather harsh conditions used in the prehydrolysis. A kraft pulp with a reduced cooking temperature (160°C/170°C) and reduced chemicals (16.9% NaOH and 6.9% Na_2S instead of 18.9 and 8.1 respectively) led, logically, to improved viscosity and yield (references C and D, table 1). The kappa numbers were also significantly increased. As the end of a cook is known to be less selective than an oxygen delignification, the idea was to submit these high kappa pulps to an extensive oxygen delignification process.

The use of a milder prehydrolysis treatment (PH-1hour)(reference E) led to a much higher DPv. The sugar content in the resulting unbleached pulps showed that there was not much difference in sugar content whether the prehydrolysis was conducted during one or two hours. In both cases the purity in cellulose was quite high, indicating that the prehydrolysis and the subsequent kraft cooking have eliminated most of the hemicelluloses.

Table 1. Kraft cooking of control and prehydrolysed wood chips

Reference	A	B	C	D	E
Chips	Control	PH-2 hours	Control	PH-2hours	PH-1 hour
Cooking conditions T°C, NaOH%, Na_2S%	170-18.9-8.1	170-18.9-8.1	160-16.1-6.9	160-16.1-6.9	160-16.1-6.9
Kappa number	24.1	21.3	70.3	78.1	73.0
DPv	1360	900	1800	1235	1540
Cooking yield, %	42.9	39.3	53.1	44.6	45.1
Rejects	0.11	0.04	1.00	1.15	0.85
Sugar content, %					
Arabinose, %	1.3	0.5	3.8	0.3	0.4
Galactose, %	0.4	nd	0.7	nd	nd
Glucose, %	83.8	93.6	79.2	95.1	95.0
Xylose, %	7.8	1.6	7.6	3.2	3.4
Mannose, %	7.6	1.0	7.8	0.9	0.9

nd : not detected

Oxygen delignification

The three high kappa pulps (control and PH 1 and 2 hours) were submitted to multistage oxygen delignification (Figure 1). The two prehydrolysed pulps responded extremely well to oxygen delignification compared to the control pulp, which confirms previous results (17). In this previous study, the lignins of the kraft and PHK unbleached pulps were analysed, and it was found that neither the molecular weight distribution of lignin, nor the number of free phenolic groups were significantly modified, which could have explained this result. A modification in the lignin-carbohydrates (LCC) linkages could be an explanation for the easiest oxygen delignification of the PHK pulps compared to the kraft ones.

The fact that the pulp produced from PH1 hour gave even better results than the pulp produced from PH-2hours could be due to some condensation reactions that might have occurred in lignin under the harsher conditions of PH-2hours.

Figure 2 gives the selectivity curves for the oxygen treatment of these three pulps. The kraft pulps that gave low kappa pulps for the control wood chips and PH-2hour wood chips (ref A and B, able 1) were also added to this figure. It can be seen that it is indeed more selective to stop the cook at a high kappa and then apply an oxygen stage, rather than cooking directly to a low kappa pulp.

Single oxygen stage was also applied to the low kappa pulps, referenced A and B, and in this case also the PHkraft pulp gave a higher delignification rate than the kraft pulp from the control chips (64% compared to 52%) when using 2% NaOH in the O stage (Table 2).

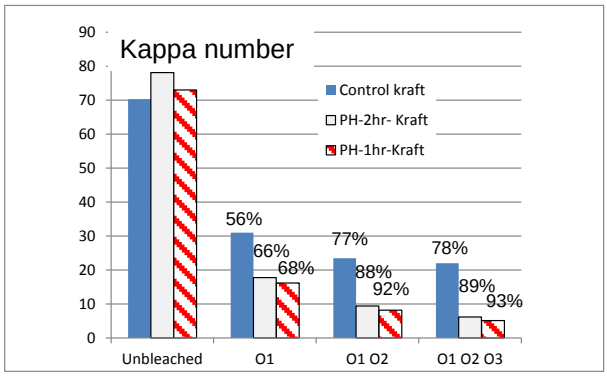

Figure 1. Kappa numbers after multi-stage oxygen delignification of pulps from control and prehydrolysed wood chips. The numbers above the columns indicate the kappa number reduction percentages (NaOH charges: 4% in O1, 1.5% in O2, 1.5 in O3)

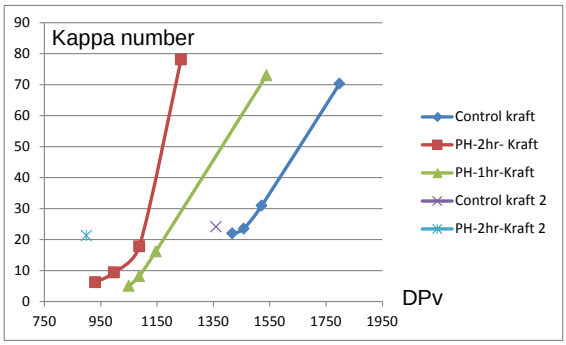

Figure 2. Selectivity curves of oxygen delignification

Effect of other bleaching agents

Hydrogen peroxide (P) and ozone (Z) stages were applied directly on the unbleached pulps to verify if the easiest delignification observed with oxygen also applied to other bleaching agents. The peroxide stage was preceded by a chelation stage. The results, presented in Table 2, show that the delignification was also significantly enhanced with hydrogen peroxide or with ozone due to the prehydrolysis. These results would be in favor of a reduced amount of LCC, thus facilitating the lignin removal from the unbleached pulp during oxidation.

Table 2. Effect of prehydrolysis on P and Z stages. Comparison with an O stage

Starting pulps	Q P stage	Z stage **	O stage***
Control kraft* pulp- kappa number 24.1			
Kappa number after bleaching	14.0	16,1	11.5
% reduction in kappa number	42%	33%	52%
PH-2hrs- kraft* pulp - kappa number 21.3			
Kappa number after bleaching	8.1	11.0	7.8
% reduction in kappa number	62%	48%	64%

*Cooking conditions : 170°C-18.9% NaOH-8.1% Na_2S. **Z stage : 0.5% ozone charge.*** O stage: 2% NaOH

Full bleaching using a OZEQPP sequence

The 78.1 PHK pulp treated by a double oxygen stage to reach a kappa number of 9.4 was compared to the control kappa number 24.1 kraft pulp treated by a single O stage to reach a kappa number of 11.5, as per their bleaching ability using a chlorine free sequence (Table 3). Both pulps could be bleached to high brightness levels. The final sugar content of the PHK pulp showed a high cellulose purity. The molecular weight distribution of the carbohydrates confirmed that almost no hemicelluloses were left. A reduced polydispersity was also obtained.

Table 3. Full chlorine free bleaching of PHK and control pulps

Starting pulps Kappa number - DPv	Control kraft 24.1 - 1360	PH-2hrs- kraft 78.1 - 1235
Oxygen delignification (% NaOH) Kappa number - DPv	Single stage (2%) 11.5 - 1220	Double stage (4% - 1.5%) 9.4 - 880
Z E Q P P % ozone charge Kappa number after Z Final brightness - Final DPv	0,5 3.8 89.7 - 800	0,4 2.9 89.1 - 590
Sugar content in bleached pulps Arabinose, % Galactose, % Glucose, % Xylose, % Mannose, %	 0.7 0.1 85.5 6.2 7.8	 0.5 nd 96.5 1.5 0.9

E: 70°C, 0,5% NaOH, 1 hour, consistency 10%. P : 1% H_2O_2, 90°C, 3 hrs, 0.3% $MgSO_4,7H_2O$

Quantification of LCC bonds

LCC fractions were isolated from the control A pulp and the pulp produced from prehydrolysed wood chips (pulp B) using a method described in (18). The yields obtained for each type of LCC are given in Table 4. LCC1, LCC2 and LCC3 fractions should contain respectively mainly LCC from glucan - lignin, glucomannan - lignin and xylan – lignin. It can be seen that the LCC2 and LCC3 fractions were significantly reduced. A thourough analysis of each LCC fractions is now needed to get a better understanding of the residual LCC's.

Table 4. LCC fractions for control and PH kraft pulps.

Ref -Chips	A -Control			B - PH-2 hours		
Kappa number	24.1			21.3		
	LCC1	LCC2	LCC3	LCC1	LCC2	LCC3
Yield, %	67.2	9.4	17.3	81.5	2.9	5.8

IV. CONCLUSIONS

This study showed that prehydrolysed softwood kraft pulps have a better delignification ability with any oxidant applied directly after cooking than control pulps. Thus, applying a prehydrolysis process and then a kraft cook to high kappa number, followed by an extensive oxygen delignification could be a way to improve the final quality of the pulp (pulp viscosity), compared to a prehydrolysis-kraft pulp to regular kappa numbers. The pulps were fully bleached with a non chlorine containing sequence to high brightness, and a high cellulose purity pulp could be obtained. First trials on LCC fractions isolation were done and showed a reduced amount of LCC related to lignin-hemicellulose fractions. A thorough analysis of these fractions is now needed to investigate this point further.

V. ACKNOWLEDGEMENT

The authors would like to thank the French- Ministère de l'Agriculture, de l'Agroalimentaire et de la Forêt -for the funding of this work in the frame of the EU project WOBAMA (ERANET-WOODWISDOM programme).

VI. REFERENCES

1. Frederick, W. J.; Lien, S. J.; Courchene, C. E.,; DeMartini, N. A.; Ragauskas, A. J.; Iisa, K. Co-production of ethanol and cellulosic fiber from Southern Pine: a technical and economic assessment. *Biomass and Bioenergy*, 2008, *32*: 1293.
2. Hytönen, E. and Stuart P. R. Integrating bioethanol production into a kraft pulp mill – Technology assessment, *95th CPPA Annual Meeting*, 2009: 283.
3. Marinova, M.; Mateos-Espejel, E.; Paris, J. Successful conversion of a kraft pulp mill into a forest biorefinery: energy analysis issues, *23rd International Conference on Efficiency, Cost, Optimization, Simulation and Environmental Impact of Energy Systems*, Lausanne, 2101, June 14-17
4. Chirat, C.; Pipon, G.; Viardin, M. T.; Lachenal, D.; Lloyd, J.; Suckling, I. Hemicelluloses extraction from eucalyptus and softwood chips: pulp properties and ethanol production, *Electronic proceeding, ISWFPC, Oslo*, 2009, June, 15-18: paper no. O038.
5. C. Chirat; D. Lachenal; A. Dufresne. Biorefinery in a kraft pulp mill: from bioethanol to cellulose nanocrystals, *Cellulose Chemistry and Technology*, 2010, *44 (1-3)*: 59.
6. Kämppi, R.; Leponiemi, A.; Hörhammer, H.; van Heiningen, A. Pre-extraction and PSAQ pulping of Siberian larch, *95th CPPA Annual meeting*, 2009: 255.
7. Al-Dajani, W.; Tschirner, U. W.; Jensen, T. Pre-extraction of hemicelluloses and subsequent kraft pulping. Part II: acid and autohydrolysis, *Tappi Journal*, 2009: 30.
8. Leschinsky, M.; Sixta, H.; Patt, R. Detailed mass balance of the autohydrolysis of Eucalyptus globules at 170°C. *Bioresources*. 2009, *4 (2)*: 687.
9. Garrote, G.; DDominguez, H.; Parajo, J. C. Mild autohydrolysis: an environmentally friendly technology for xylooligosaccharide production from wood. *Journal of chemical technology and biotechnology*. 1999, *74*: 1101.
10. Bose, S. K.; Barber, V. A.; Alves, E. F.; Kiemle, D. J.; Stipanovic, A. J.; Francis, R. C. An improved method for the hydrolysis of hardwood carbohydrates to monomers. *Carbohydrate Polymers*, 2009, doi: 10.1016/jcarbpol..04015.
11. Garrote, G.; Parajo, J. C. Non isothermal autohydrolysis of eucalyptus wood. *Wood Science and Technology*. 2002, *36*: 111.
12. Lloyd, J. Suckling I.D.; Allison, R. W.; Manley-Harris, M.; McDonald-Wharry, J. S. Lachenal, D.; and Chirat, C. Hot water prehydrolysis of radiate pine – hemicellulose extraction, *ISWFPC, Oslo*, 2009, June 15-18: P049.
13. Chirat, C., Boiron, L., Pouyet, F., Lachenal, D., Lloyd, J. and Suckling, I., Simultaneous production of ethanol and softwood kraft pulps : adapted operating conditions. 16th ISWFPC, Tianjin, 2011, June 8-10, pp 778-783
14. Kautto, J., Saukkonen, E., Henricson, K. Digestability and paper-making properties of prehydrolysed softwood chips. Bioresources 5(4). 2010, pp 2502-2519.
15. Leschinsky, M., Zuckerstätter, G., Webber, H.K., Patt, R. and Sixta, H. Effect of autohydrolysis of Eucalyptus globules wood on lignin structure. Part 1 : Comparison of different lignin fractions formed during water prehydrolysis.. Holzforschung vol. 62, 2008, pp 645-652.
16. Leschinsky, M., Zuckerstätter, G., Webber, H.K., Patt, R. and Sixta, H. Effect of autohydrolysis of Eucalyptus globules wood on lignin structure. Part 2 : Influence of autohydrolysis intensity. Holzforschung vol. 62, 2008, pp 653-658.
17. Chirat, C.; Boiron, L.; Lachenal, D. Bleaching ability of pre - hydrolysed pulps in the context of a biorefinery mill. *Tappi Proceedings International Pulp Bleaching Conference, Portland, USA*, October 5-7, **2011**, 12–18.
18. Du, X.; Gellerstedt, G.; Li, J. Universal fractionation of lignin - carbohydrate complexes (LCCs) from lignocellulosic biomass: an example using spruce wood. *The Plant Journal*, **2013**, *74*, 328–338.

FORMATION OF HYDROXYL RADICALS DURING OZONE OXIDATION OF UNSATURATED COMPOUNDS: CONSEQUENCES FOR PULP BLEACHING.

Frédéric Pouyet[1], Christine Chirat[1] and Dominique Lachenal[1]*.
[a]*Grenoble INP-Pagora, International School of Paper Print Media and Biomaterials, 461 rue de la papeterie – CS 10065, 38402 St Martin d'Hères Cedex, France,*
**Corresponding Author, Email: dominique.lachenal@grenoble-inp.fr*

ABSTRACT
Several model compounds were added to ozonated water (0.02g/L) at pH 2.5 and room temperature in the presence of 5,5-dimethyl-pyrrolidine-1-oxyl (DMPO). The formation of hydroxyl radical, seen as DMPO-OH radical, was followed by ESR spectroscopy. Acetovanillone was chosen as model for the free phenolic groups present in lignin after oxygen delignification. Maleic acid which presents key similarities with HexA (carboxyl groups on carbon-carbon double bonds) was retained as model for the hexA and 2,5-dimethyl 2,4-hexadienedioic acid was used as model for muconic acid derivatives. In all cases OH formation occurred. It was shown that these radicals would result from the direct reaction of ozone with the carbon-carbon double bond in the models. This finding makes it possible to design TCF bleaching sequences with a much lower impact on pulp viscosity.

I. INTRODUCTION

Unbleached hardwood kraft pulps can be fully bleached with sequences containing oxygen (O), ozone (Z) and hydrogen peroxide (P) stages (TCF bleaching). Among the anticipated advantages are the easier recycling of the bleaching effluents back to the recovery furnace, the absence of AOX formation and a competitive bleaching cost. However pulp viscosity is negatively affected. Minimizing the loss in viscosity would certainly improve the acceptance of TCF bleaching .
Part of the viscosity loss is due to the ozone stage. This problem has been widely investigated and several reasons have been proposed. Ozone may directly oxidize cellulose at its C1 position, cleaving the cellulose chain [1]. Cellulose may be also degraded by OH radicals. OH radicals may be formed by ozone decomposition in the reaction medium [2]. OH radicals may be also generated from the liberated H_2O_2 during the ozonolysis of cabon-carbon double bonds [3]. Finally, OH radicals are produced when ozone reacts with the phenolic units in lignin. This latter reaction has been well documented [4, 5] and is actually considered as the most probable way by which cellulose is oxidized and depolymerised during a Z stage.
However, during a Z stage ozone reacts with other substances than lignin. Hardwood pulp contains hexenuronic acids (HexA) which are prone to react with ozone [6]. When lignin is oxidized by ozone, muconic acid derivatives are formed. These acids could be even more reactive towards ozone than the original lignin since they contain non-aromatic carbon-carbon double bonds [7]. Whether or not these reactions have an impact on the occurrence of cellulose degradation during a Z stage has never been investigated.
The purpose of this work is to better understand the origin of cellulose depolymerization during a Z stage applied to an oxygen delignified eucalyptus kraft pulp. ESR spectroscopy and model compounds will be used to investigate the formation of OH radicals. Knowing the origin of cellulose degradation makes it possible to minimize its occurrence during an ozone stage and thereby to design more efficient TCF bleaching sequences.

II. EXPERIMENTAL

ESR Spectroscopy experiments
Ozonation of three model compounds was followed by ESR spectroscopy. Acetovanillone (Aldrich-Europe) was used as a model for residual lignin after oxygen delignification, (*cis*) maleic acid (Aldrich, 99%) as a model for HexA groups and 2,5-dimethyl 2,4-hexadienedioic (Alfa Aesar, 98%) as a model for muconic acid derivatives. H_2O_2 (Sigma-Aldrich, 35%) was added in some experiments
X-band ESR spectra were recorded at room temperature with a Bruker EMX Plus spectrometer equipped with the ER-4102ST Bruker cavity. It was operating at 9.8 GHz. Samples were analyzed in a water flat cell at room temperature. Hydroxyl radical generated in the medium was trapped with 5,5-dimethyl-pyrrolidine-1-oxyl (DMPO, Sigma-aldrich, 99%) as a stable radical (DMPO-OH), which can be detected with an ESR

spectrometer. In a practice, ozonated water was prepared by bubbling ozone gas in water at pH 2.5 (H_2SO_4) during 90 min. An average concentration of 0.02g/L was reached. A 2-mL water solution of DMPO (and model) was prepared separately. The necessary volume of the ozonated water was added to the latter solution.

Pulp bleaching
An oxygen-delignified Eucalyptus (hybrid between *Eucalyptus grandis x Eucalyptus urophylla*) kraft pulps was provided by a Brazilian pulp mill. Cellulose DP was 1630 and hexA content was 71.7 µeq/g
The ozone was produced from oxygen in an Ozonia (Switzerland) LN 103 laboratory ozone generator.
Prior to the ozone treatment, the pulp was acidified to pH 2.5 with sulfuric acid at a consistency of 1% and then filtered. The filtered pulp was centrifuged to reach a consistency of 40%, and then fluffed. Ozonation was then performed in a rotating spherical glass reactor. The quantity of ozone is expressed as a percentage of ozone charge on pulp (on an oven-dried basis).
For the other stages, the temperature was controlled using a water bath, with the reactions taking place in polyethylene bags. The following procedures were used for pulp characterization: viscosity (ISO 5351/ 1-1981), translated here in DP values [8]; Brightness (ISO 3688 – 1977). The hexenuronic acid (HexA) content was measured according to the procedure described by Chai and Zhu [9].

III. RESULTS AND DISCUSSION

Detection of OH radicals during ozonation of model compounds
Several methods have been proposed in the literature to measure the formation of OH radicals during ozonation. Electron Spin Resonance Spectroscopy (ESR spectroscopy), which is a conventional method for hydroxyl radical analysis in biochemical processes, was used in this work because of its very high sensitivity. 5, 5-dimethyl-pyrrolidine-1-oxyl (DMPO) was added as a spin trapping substance. DMPO forms a stable radical (DMPO-OH) that can be easily detected [10]. Moreover both DMPO and DMPO-OH are resistant to ozone[3]. Several model compounds were added to ozonated water (0.02g/L at pH 2.5 at room temperature in the presence of DMPO. Acetovanillone was chosen as a model for the free phenolic groups present in lignin after oxygen delignification. Maleic acid which presents key similarities with HexA (carboxyl groups on carbon-carbon double bonds) was also retained as model compound. Finally, 2,5-dimethyl 2,4-hexadienedioic acid was used as model for muconic acid derivatives (**Figure 1**)

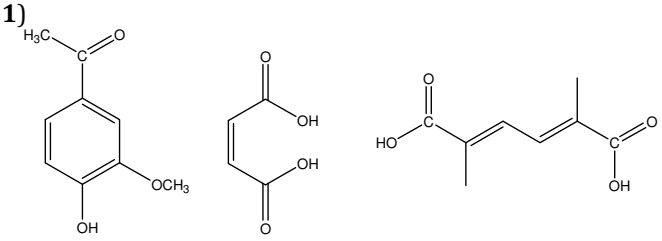

Acetovanillone Maleic acid 2,5-dimethyl 2,4-hexadienedioic acid.

Figure 1. Models used in the ESR study.

As a control test, ozone (as ozonated water) was added to a solution containing only DMPO (2.10^{-7} moles of ozone, and 10^{-4} moles of DMPO). No radical signal was detected straight after the introduction of ozone. However, a small signal was registered after several minutes. This would indicate that ozone would slowly decompose into radicals. It is anticipated that when the models are present ozone will react with the phenolic structures or double bounds before starting to be degraded heavily. Besides, in most of the experiments, the amount of ozone was lower than the amount of model compound. As a consequence, those compounds will rapidly consume most of the ozone. If a signal is registered, it is then safe to say that it comes from the reaction of ozone with the compound rather than from the ozone decomposition.
Ozone was added to a solution containing acetovanillone and DMPO (2.10^{-7} moles of ozone, 2.10^{-6} moles of acetovanillone, and 1.10^{-4} moles of DMPO). In this case, as expected, the DMPO-OH signal was registered. This confirms that ozone produces OH radicals when it reacts with a phenolic compound, as already well known [5, 11].

Figure 2 refers to the ozonation of maleic acid (2.10^{-7} moles of ozone, 3.10^{-6} moles of maleic acid, and 1.10^{-4} moles of DMPO). The corresponding spectrum without maleic acid is given for comparison. It appears clearly that OH radicals are formed when ozone reacts with maleic acid under the conditions of the test. One more experiment was carried out, with a lower amount of maleic acid (2.10^{-7} moles of ozone, 1.10^{-7} moles of maleic acid, and 1.10^{-4} moles of DMPO). The signal observed with this last experiment showed a production of radicals, higher than that of ozone alone with DMPO, but lower than with a higher maleic acid content. As a consequence, the amount of radicals generated when ozone reacts with maleic acid seems to be linked to the concentration of maleic acid. The same behavior was observed with 2,5-dimethyl 2,4-hexadienedioic acid.

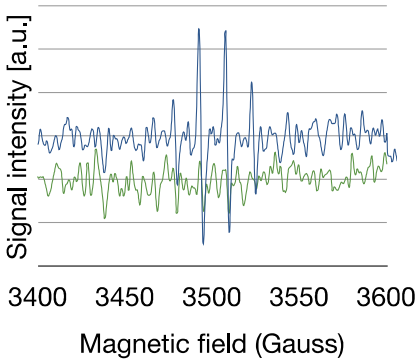

Figure 2. ESR signals obtained for ozone and DMPO (lower spectrum), and for ozone and DMPO + maleic acid (upper spectrum). DMPO-OH radical appears as a 4 peak-signal, g-factor=2.003.

These results were not expected since the ozonolysis of carbon-carbon double bonds described by Criegee [12] is not supposed to generate OH radicals. Several hypotheses can explain this generation.The possibility of OH radical formation by decomposition of the in situ generated H_2O_2 or by reaction of the ozone with peroxide were investigated by performing some tests with addition of H_2O_2. To do so, the maximum theoretical amount of peroxide generated during ozonation (2.10^{-7} moles), considering that one mole of ozone might give a maximum of one mole of H_2O_2 was added to the DMPO solution at pH 2.5 (2.10^{-7} moles of H_2O_2, and 1.10^{-4} moles of DMPO), and the same amount was added to a similar medium just before addition of the ozonated water (2.10^{-7} moles of H_2O_2, 1.10^{-4} moles of DMPO, and then 2.10^{-7} moles of ozone). In those two cases, only very low intensity signals, if any, were registered.
Although the H_2O_2 origin for the formation of OH radicals cannot be totally ruled out by these last trials, other ways are more probable. One is including the formation of the ozonide radical $O_3^{\cdot-}$ by charge transfer with the double bond, which would give a hydroxyl radical after protonation as described in the case of phenolic compounds [5]. Formation of OH radicals, which is well known in the case of gas-phase alkene ozonolysis [13] was also recently seen in water treatment when ozone reacted with unsaturated compounds [14].

Practical relevance
Since OH radicals are produced when ozone reacts with compounds containing carbon-carbon double bonds, it is very likely that this reaction is responsible for the degradation of cellulose, at least to a certain extent. The key for improvement would be to minimize the reaction of ozone with such structures. Apart from lignin which is the target of the bleaching chemicals, the hexenuronic acids present in hardwood kraft pulp and the muconic acid derivatives which are the primary products of lignin oxidation contain such groups in large quantities.
HexA can be partly removed by mild acidolysis with sulfuric acid. Minimizing the quantity of muconic acid can be performed by multi-stage ozonation where the ozone charge is split between 2 or more Z stages each of them being followed by an alkaline extraction (E) (ZEZEZE…). In those cases, most of the muconic acids formed during one Z step would be eliminated in the effluent of the subsequent E step. No washing is really needed after Z. Moreover, considering the low charges of ozone in the Z steps, very short reaction times would be required in Z. Therefore for example (ZE)(ZE)(ZE) is not so different from a 3-stage bleaching process. **Table 1** summarizes some of the improvements which could be brought about to ozone containing TCF sequences.

Table 1. TCF bleaching of oxygen treated eucalyptus kraft pulp including ozone stages.

Treatment	Ozone charge on pulp (%)	Brightness (%)	DP
No	-	51.0	1630
A	-	54.7	1510
ZE	0.8	67.5	1050
AZE	0.8	82.1	1170
AZEZE	0.3 + 0.3	83.5	1250
AZEZEP	0.3 + 0.3	90.0	1220

A: pH3, 90°C, 3h. (hexA after A 26.7 (µeq/g); Z pH 2.5, 25°C, 40% consistency, E:70°C, pH 11; P: 0.5% H_2O_2, 0.5% $MgSO_4$ 7H2O, 1.5% NaOH on pulp. All stages except Z at 10% consistency

IV. CONCLUSION

Hydroxyl radicals are formed when ozone reacts with unsaturated compounds containing carbon-carbon double bonds. Consequently the reaction of ozone with lignin, hexenuronic acids and muconic acid derivatives must be responsible for cellulose degradation during an ozone bleaching stage. This finding is confirmed by the positive effect of acidolysis pretreatment prior to the ozone stage and the split of ozone application, on cellulose DP. It paves the way for the design of new TCF bleaching sequences with a lower impact on cellulose. Tomorrow's bleaching sequences for hardwood kraft pulp might include an extensive HexA removal stage coupled to successive (ZE) phases.

V. ACKNOWLEDGEMENTS

The authors want to acknowledge the assistance of Florian Molton and Carole Duboc (Molecular Chemistry Department, Université Joseph Fourier, Grenoble) in the ESR spectroscopy analysis.

VI. REFERENCES

[1] Katai, A., Schuerch, C., "Mechanism of ozone attack on α-methyl glucoside and cellulosic materials", *J. Polym. Sci*. **1996**, Part A-1, 4, 2683-2703.

[2] Hoigné, J., "The chemistry of ozone in water" in Process Technologies for Water Treatment, Samuel Stucki (ed.), Plenum Publishing Corporation **1988**.

[3] Chirat, C., Lachenal, D., "Effect of Hydroxyl Radicals on Cellulose and Pulp and their Occurrence During Ozone Bleaching", *Holzforschung* **1997**, *51*, 2, 147–154.

[4] Kang, G., Zhang, Y., Ni, Y., Van Heiningen, A. R. P., "Influence of lignins on the degradation of cellulose during ozone treatment", *J. Wood Chem. Technol.* **1995**, *15*, 4, 413-430.

[5] Ragnar, M., Eriksson, T., Reitberger, T. "Radical formation in ozone reactions with lignin and carbohydrate model compounds", *Holzforschung* **1999**, *53*, 3, 292-298.

[6] Ventorim, G., Colodette, J. L., Gomes, A., da Silva, L., "Reaction rates of lignin and hexenuronic acid with chlorine dioxide, ozone and sulfuric acid", *Wood Fiber Sci.* **2008**, *40*, 2, 190-201.

[7] Eriksson, T., Gierer, J., "Relative rates of ozonation of lignin model compounds", Proceedings **1985** International Symposium on Wood and Pulping Chemistry, Vancouver, Canada, Poster book, 29-30 .

[8] Sihtola, H., Kyrklund, B., Laamanen, L., Palenius, I.,"Comparison and conversion of viscosity and DP-values determined by different methods", *Paperi Ja Puu* **1963**, *45*, 4a, 225-232.

[9] Chai, X. S., Zhu, J. Y., "Rapid and direct pulp kappa number determination using Spectrophotometry", *J. Pulp Paper Sci.* **1999***, 25*, 11, 387-392.

[10] Finkelstein, E., Rosen, G., Rauckman, E., "Spin trapping of superoxide and hydroxyl radicals: practical aspects", *Archives of Biochemistry and Biophysics* **1980**, *200*, 1, 1-16.

[11] Han, S.-K., Ichikawa, K., Utsumi, H., "Quantitative analysis for the enhancement of hydroxyl radical generation by phenols during ozonation of water", *Water Research* **1998**, *32*, 11, 3261-3266.

[12] Criegee, R., "The course of ozonization of unsaturated compounds", *Record of Chemical Progress* **1957***, 18*, 2, 111-120.

[13] Anglada, J. M., Aplincourt, P., Bofill, J. M., Cremer, D., "Atmospheric formation of OH radicals and H2O2 from alkene ozonolysis under humid conditions", *Chemphyschem* **2002**, *3*, 2, 215-221.

[14] Audenaert, W. T. M., Vandierendonck, D., Van Hulle, S. W. H., Nopens, I.,"Comparison of ozone and HO• induced conversion of effluent organic matter (EfOM) using ozonation and UV/H2O2 treatment", *Water Research* **2013**, *47*, 7, 2387-2398.

ADVANCES IN CATALYTIC BLEACHING

Naveen Chenna[1]*, Anna-Stiina Jääskeläinen[2], Christian Järnefelt[1,3], Susanna Kuitunen[4], Tapani Vuorinen[1]

[1]*Department of Forest Products Technology, School of Chemical Technology. Aalto University P.O. Box 16300, 00076 Espoo, Finland*

[2]*VTT Technical Research Centre of Finland P.O.Box 1000, 02044 Espoo, Finland*

[3]*Andritz Oy, P.O.Box 500, 48601, Kotka, Finland*

[4]*Department of Biotechnology and Chemical Technology, School of Chemical Technology, Aalto University, P.O. Box 16100, 00076 Espoo, Finland*

**naveen.chenna@aalto.fi*

ABSTRACT

Stoichiometric amount of hypochlorous acid (HOCl) is formed in chlorine dioxide (ClO_2) bleaching during oxidation of phenolic lignin. HOCl further oxidizes residual lignin and hexenuronic acid (HexA) which leads to their degradation. However, a significant part of HOCl is consumed in chlorination of lignin, overoxidation of HexA and formation of chlorate in a reaction with chlorite. The present study focusses on increasing the catalytic selectivity of HOCl towards the lignin and HexA oxidation. In this paper we report on oxidation of residual lignin and HexA in pulp by a quaternary ammonium chloride cation (R_3N^+-Cl) which is a much stronger electrophile than HOCl but lacks the nucleophilic nature. The full catalytic effect was achieved with only 0.1 % charge of catalyst and 1-1.5 % charge of active chlorine equivalent of HOCl. All bleaching reactions were completed at the shortest measurable bleaching time (less than a minute). In these conditions the reduction in kappa number was up to 7-8 units. In addition to bleaching experiments model experiments were carried out to determine the kinetics of the formation and self-decomposition of R_3N^+-Cl of catalyst. Formation of R_3N^+-Cl took place within 0.4ms and whereas degradation took place within 2-10 s. Halftime of the reaction between HexA and R_3N^+-Cl was about 100 ms. We believe that the oxidation of HexA occurs within a second in the pulp suspension. AOX content of the catalytic bleaching liquor was at the same or lower level than in normal chlorine dioxide bleaching. The viscosity of the pulp remained practically unchanged that demonstrated high selectivity towards HexA and lignin oxidation. These findings may open possibilities for more efficient pulp bleaching process of chemical pulp for reduced lignin and/or HexA content. In addition, the number of bleaching stages could possibly be reduced compared with the existing bleaching sequences

.I. INTRODUCTION

Numerous activators have been reported to improve the efficiency of pulp bleaching. For example Prenox process[1], using NO_2 prior to oxygen delignification created more phenolic hydroxyl groups and increased its reactivity towards oxygen. Similarly hydrogen peroxide reinforced with peroxyacids[2] led to increased bleaching efficiency. Until now developments in pulp bleaching has mainly focused on the 'reactivity of pulp with oxidants' approach. However the 'reactivity of oxidants with pulp' approach has not been exploited in detail and discussed well. The present work is an example of how to increase the reactivity and selectivity of hypochlorous acid, formed in situ in today's ECF pulp bleaching, with a catalyst.

Chlorine dioxide (ClO_2) is the main oxidant in elemental chlorine free bleaching sequences. ClO_2 reacts very fast with phenolic lignin producing mainly hypochlorous acid (HOCl) and chlorite (ClO_2^-) in stoichiometric ratio[1]. These intermediates react either with each other forming ClO_2, chlorate (ClO_3^-) and chloride (Cl^-) or with organic substances like lignin, HexA and to smaller extent, other carbohydrates generating oxidized and chlorinated organic compounds[2]. In principle one equivalent of HOCl is sufficient to oxidize one equivalent of HexA, instead several equivalents are consumed during chlorine dioxide bleaching. The present study focuses on increasing the selectivity of HOCl with a tertiary amine as a catalyst to react with HexA and lignin. The effect of reaction conditions (pH, temperature and reaction time, chemical dosage was

studied[3]. The results suggest a way to increase the selectivity and to decrease the overall chemical consumption and reaction time drastically compared with today's bleaching technology.

II. EXPERIMENTAL

Aqueous solution of NaOCl (3.5% available Cl_2, Aldrich) was purchased from VWR. The concentration of NaOCl expressed as active chlorine, was measured before every experiment by iodometric titration as described in the standard method SCAN-C 29:72. 1,4-diazabicyclo [2,2,2]octane (DABCO) 98% was purchased from Sigma-Aldrich. Oxygen delignified eucalyptus pulp was obtained from a Brazilian kraft pulp mill. Kappa number (SCAN-C 1:00) of the pulp was 11.4, HexA content[4] 66 mmol/kg and viscosity (SCAN-CM 15:99) 1130 ml/g. O-methyl-hexenuronic acid was synthesized in laboratory [5].

Oxidations of the pulp were performed at 1% consistency in a stirred batch reactor (1.5l) made of borosilicate glass (Büchi). Desired pH of the pulp suspension (1l) was adjusted with 1M H_2SO_4 or NaOH after the addition of DABCO in catalytic amount. The reactor vessel was thermostated (temperature range of 25-60 °C) and 0.5-2% of NaOCl was added to pulp solution. The bleaching experiment time was set to 10 minutes. Kappa number and viscosity of the pulps were determined according to standard SCAN-C 1:00 and SCAN-CM 15:99, respectively. The content of HexA was quantified through its selective mild acid hydrolysis[4]. Aromatic lignin and HexA contents were determined with UV resonance Raman (UVRR) spectroscopy[6].

The HexA model reactions were followed with a double mixing SFM-3000 Bio-logic stopped flow mixer coupled with diode array spectrophotometer, thermostatted with water flow within 0.1K. The increase in the absorbance maxima of chloroammonium cation was followed at 260 nm and decrease in absorbance maxima of HexA was measured at 230 nm.

III. RESULTS AND DISCUSSION

Oxygen delignified pulp were treated with NaOCl at room temperature for 10 min. Most of the oxidant was not reacted (Figure 1)[3] and change in kappa number was not observed in comparision with original pulp. It was reported earlier that NaOCl does not react much with pulp at room temperature in short times, whereas it reacts faster at higher temperature[7]. It was also reported that NaOCl reacts slow with HexA[8] at room temperature. When catalytic amount of DABCO was added, most of NaOCl was consumed immediately and a large drop in kappa was observed. After the fast initial reaction the oxidation proceeded at a lower rate and significant amounts of the oxidant, lignin and HexA remained unreacted. Clearly the catalysis was inhibited by dynamic changes in the system or the catalyst was partially destroyed as described by Rosenblatt et al [9].

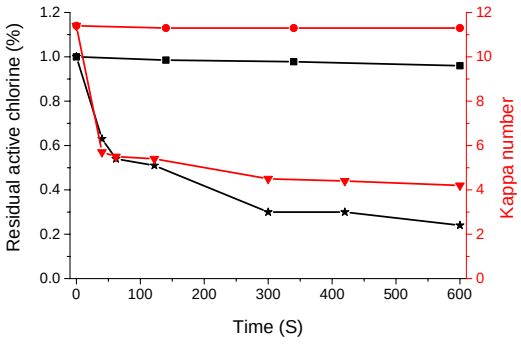

Figure 1: The residual amount of active chlorine (1 % on dry pulp) with (-★-) and without (-■-) DABCO (0.1 % on dry pulp) addition during the 10 minutes of treatment time at pH 8 and 25^{0}C. Development in kappa number was also observed with respect to time and residual active chlorine in presence (-▼-) and absence (-●-) of DABCO[3].

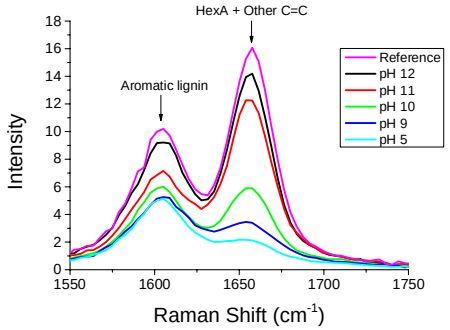

Figure 2. UV-Raman spectra[3] of oxygen delignified eucalyptus kraft pulp before and after 10 min treatment with 1 % active chlorine and 0.1 % DABCO at varying initial pH at 25 ^{o}C. The spectra were normalized relative to the height of the cellulose band at 1094 cm^{-1}.

With the addition of DABCO, the contents of lignin and HexA were reduced by ~45 and 60 %, respectively. Figure 2 shows the UVRR spectra[3] which illustrate the changes in the catalytically bleached pulps treated at varying initial pH. The oxidation was monitored by following the heights of peak at 1605 and 1655 cm^{-1} corresponding to aromatic lignin and HexA respectively [6]. Figure 2 clearly explain that the catalytic oxidation can happen in wide range of pH. The biggest drop in kappa number was observed in a treatment at initial pH 5. UVRR spectra of the treated pulp confirmed this observation. The residual contents of lignin and HexA were lowest at or close to this initial pH.

Additional experiments were carried out with pure chemical compounds to evaluate the reactivity of the components in the catalytic system. The reaction between the tertiary amine and HOCl was studied with a stopped flow mixer coupled with diode array UV-Vis spectrophotometer. When equimolar amounts of NaOCl and DABCO were mixed together, the absorbance at 260 nm (Figure 3) quickly rose due to formation of $DABCO^{+}$-Cl. The full increase in the absorbance was reached within 0.4 ms after which the absorbance declined at a lower rate indicating the degradation of $DABCO^{+}$-Cl that was completed in a few seconds

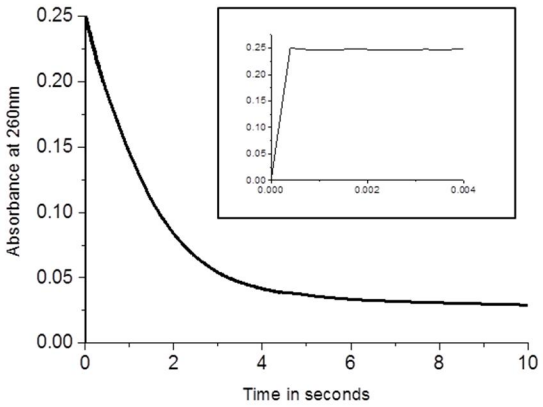

Figure 3. UV absorbance of $DABCO^{+}$Cl at 25 °C and [NaOCl] : [DABCO] = 2:2. The inset shows the change in the absorbance during the first 0.4 ms.

HexA model compound was added to the NaOCl-DABCO system where the decrease in absorbance of HexA was followed at 232nm. As can see from Figure 4 $DABCO^{+}$Cl reacted rapidly with HexA in comparison with uncatalyzed NaOCl. The oxidation of HexA was completeded in 400ms at room temperature. Thus, $DABCO^{+}$-Cl reacted with HexA at a rate about 10 times higher than the self-decomposition rate of $DABCO^{+}$-Cl. Therefore the catalytic oxidation of HexA is very effective. Our preliminary studies demonstrate similar catalysis in removal of lignin. All the above comprised results show that HOCl can be catalyzed with DABCO to react with bleachable components in pulp fibers efficiently with low amount of oxidant and in a very short time.

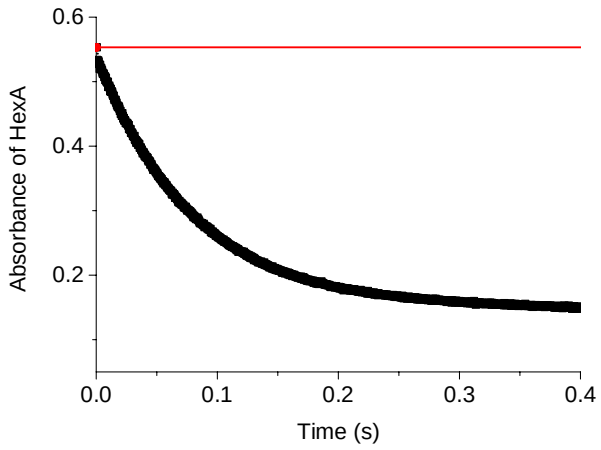

Figure 4. (i) Oxidation of HexA with HOCl followed at 232 nm with (black line) and without DABCO (red line) [10].

IV. CONCLUSIONS

The present work demonstrates an efficient use of tertiary amine catalysis in pulp bleaching. HOCl reacts with DABCO forming $DABCO^{+}$-Cl which is strong electrophile and reacts immediately with unsaturated residual components like HexA and lignin. In ideal conditions the oxidation takes place within seconds and most of HexA and majority of lignin can be removed. The catalysis works over the wide range of conditions like pH, temperature and consistency. These findings may open possibilities for more efficient processing of cellulosic fibers for reduced lignin and/or HexA content. Catalytic oxidation HexA takes place in < 1 s which suggests that in future the bleaching reaction systems could be very quick and efficient.

V. ACKNOWLEDGEMENT

This study was financed by a consortium of Andritz, Kemira, Metsä Fibre, Stora Enso and UPM.

VI. REFERENCES

1. Samuelson, O. and Ötjeg, U.; J. Pulp Paper Sci. 1987, J153.

2. Suchy, M. and Argyropoulos, D. S. Catalysis and activation of oxygen and peroxide delignification of chemical pulps: A review. In ACS Symposium series; ACS Publications: 2001; Vol. 785, pp 2-43.

3. Chenna, N. K., Jääskeläinen, A.-S. and Vuorinen, T., Ind. Eng. Chem. Res. 2013, 17744.

4. Vuorinen, T., Fagerström, P., Buchert, J., Tenkanen, M. and Teleman, A., J. Pulp Paper Sci. 1999, 5, 155-162.

5. Adorjan, I., Jääskeläinen, A.-S. and Vuorinen, T., Carbohydr. Res. 2006, 14, 2439-2443.

6. Jääskeläinen, A.-S., Saariaho, A.-M. and Vuorinen, T. J. Wood Chem. Technol. 2005, 1-2, 51-65.

7. Sandel, J. A. H. L. F. Pulp bleaching: principles and practice, chapter 4, 1996, 395.

8. Chenna, N.K., Jääskeläinen, A.-S, Lehtimaa, T., Kuitunen, S.and Vuorinen, T. Modeling and kinetics of the reaction between hypochlorous and hexenuronic acids, 2012, 12th EWLP proceedings, pp 212.

9. Rosenblatt, D., Demek, M. and Davis, G., J. Org. Chem. 1972, 25, 4148-4151.

10. Chenna, N.K., Jääskeläinen, A.-S, Lehtimaa, T., Järnefelt. C and Vuorinen, T. Catalytic oxidation of residual lignin and hexenuronic acid in pulp, 2013, 6th ICEP proceedings, Colonia, Uruguay.

RECOMBINANT SOYBEAN PEROXIDASE FOR BIOBLEACHING OF EUCALYPTUS PULP

Lisbeth Kalum[1]*, Lars Oestergaard[1] and Henrik Lund[1]

[1]*Novozymes A/S, Krogshoejvej 36, 2880 Bagsvaerd, Denmark*

ABSTRACT

Soybean peroxidase was expressed recombinantly (rSBP) and pH and temperature optimum and stability were determined. The stability of rSBP was observed to be significantly better when subjected to stresses, such as temperature, pH and peroxide when compared to a fungal counterpart from *Coprinus*. Temperature optimum was found to be in the range of 65-70°C. pH optimum depended on the selected mediator, with optimum at pH 4 for N-hydroxy mediators, pH 6 for phenothiazine-3-propionic acid and pH 8 for methyl syringate. Biobleaching of eucalyptus pulp showed superior performance of rSBP with violuric acid as mediator. The very high stability of rSBP makes this enzyme ideal for additional optimization and engineering in order to make biobleaching a realistic solution for the pulp and paper industry.

I. INTRODUCTION

Lignin modifying oxidoreductases have been explored for biobleaching of wood pulp for more than a decade and the technical feasibility has been proven in a vast amount of literature [1]. The most promising biobased solutions constitute a laccase-mediator treatment followed by alkaline peroxide extraction. In order to compete with the chlorine dioxide bleaching technologies currently used for production of bleached kraft pulp, then the cost-performance of an enzyme-mediator system are under strict economical constraints. The enzyme must be commercial available and sufficiently robust to withstand the harsh conditions often applied in the pulp and paper industry. The applied mediator should be effective at low dose, possess low toxicity, produce stabile radicals and have low tendency polymerize. In particular two mediator families have been documented to hold significant biobleaching potential: Low redox potential phenolic mediators (e.g. methyl syringate [2]) and high redox potential N-hydroxy mediators (e.g. 1-hydroxybenzotriazole or violuric acid [3]). Suitable commercial oxidizing enzymes available in the quantities needed for pulp and paper industry currently includes laccases with low redox potential and fungal peroxidases with low temperature stability, while little attention have been given to the plant peroxidases.

Plant peroxidases are famous for their high stability and widely used in medicine as diagnostic tools. Traditionally, they have been obtained from a natural source, which can be a laborious process and affected by the quality of the source material. Recently, Novozymes succeeded in producing a plant peroxidase in a fungal host. The properties and applications of the recombinant soybean peroxidase will be described.

The peroxidases are oxidoreductases and catalyse a range of reactions, such as the oxidation of phenolic compounds in the presence of peroxide. They are heme proteins and contain iron protoporphyrin IX as the prosthetic group. The heme peroxidases are divided into two superfamilies [4]:

1) The superfamily of (archae) bacterial, fungal, and plant heme peroxidases represented by catalase–peroxidases, ascorbate peroxidases, cytochrome c peroxidases, manganese and lignin peroxidases, and plant secretoric peroxidases.

2) The second superfamily is the animal peroxidases (also called the peroxidase– cyclooxygenase superfamily).

II. EXPERIMENTAL

Enzymes

Soybean peroxidase SBP (Sigma P1432), Horseradish peroxidase HRP (type VI-A Sigma P6782), Lignin peroxidase LiP (Sigma 42603), *Coprinus cinereus* peroxidase CiP (Novozym 51004, Novozymes), Versatile peroxidase VP (*Bjerkandera adusta*, Jena Bioscience), recombinant Soybean peroxidase rSBP (Novozymes), *Myceliophthora thermophila* laccase MtL (Novozym 51003, Novozymes), *Polyporus pinsitus* laccase PpL (NS-51002, Novozymes).

pH optimum

The pH optimum of the peroxidase on different mediators was determined by decolourisation of indigo carmine at room temperature. The following ingredients were mixed in a total volume of 200 µl: 50 mM Britton-Robinson buffer (pH 3-10), 0.1 mM indigo carmine, 0.2 mM mediator, and 0.88 mM hydrogen peroxide.

The reaction was started by adding peroxidase and the change in absorption at 610 nm was monitored for 5 min. The rate of the reaction was determined as the change in absorbance per minute.

Temperature optimum
The temperature optimum of the peroxidase was determined using violuric acid in 50 mM Britton-Robinson buffer pH 4. The progress of the reaction was monitored by the change in absorbance at 310 nm in a temperature controlled quartz cuvette. All solutions, apart from enzyme and substrate, were pre-incubated at the desired temperature. The enzyme solution was kept at on ice until start of the assay by addition of enzyme: 50 mM Britton-Robinson buffer (pH 4), 0.2 mM violurc acid and 0.88 mM hydrogen peroxide.

Stability
The stability of the peroxidase was determined by subjecting the enzyme to a given condition for one hour. The pH stability was studied using 25 mM Britton-Robinson buffer pH 3-10 for the incubation, while the thermo- and peroxide stability was studied using 25 mM Britton-Robinson buffer pH 7 only. The residual activity was subsequently determined by decolourisation of indigo carmine at pH 4 using violuric acid as mediator as described above.

Bleaching of pulp

Mini pulp assay: 60 mg dry unbleached pulp was weighed into glass tubes and soaked at room temperature for 30 min in 2 ml buffer. Deionized water, mediator, enzyme solution and hydrogen peroxide were added to reach a final volume of 4 ml (1,3% consistency). The pulp was incubated for 1 hours using stirring block thermostat. The pulp was collected by centrifugation and washed twice with 6 ml of deionized water. Extraction was conducted by addition of 2 mL alkaline solution (0.5 g/L EDTA, 2.0 g/L NaOH and 1 g/L H_2O_2) at 80°C for 30 min. The pulp was collected by centrifugation and resuspended in 8 mL deionized water, filtered under suction. The formed paper pads were pressed using a Labtech automatic sheet press. The pads were dried over night at room temperature. Brightness was determined using a Macbeth Color-Eye 7000 Remissions spectrophotometer, measuring two times on each pad at 460 nm. All experiments were made in duplicates.

10% consistency pulp assay: 5 g dry pulp was weighed into plastic bags and soaked in 22,5 ml buffer for 30 min. at the specified temperature. The pulp was transferred to Labomat beakers and enzyme, mediators and deionized water was added to a total liquid volume of 45 ml. The reaction was started by addition of hydrogen peroxide or 4 bar of oxygen and incubated for 3 hours in water bath. Pulp suspension was filtered and washed twice with 100 ml deionized water. The drained pulp was extracted at 10% consistency using 10 g NaOH/kg dry pulp; 8 g H_2O_2/kg at 85°C for 90 min. The pulp was washed twice and pressed. The pressed pulp was resuspended in 2 L of water and disintegration was carried out at 300 revolutions. Additional 0.5L deionized water was added and 1L of the pulp suspension was used for preparing a sheet in a semiautomatic sheet former. Brightness was measured as described above.

III. RESULTS AND DISCUSSION

Characterization rSBP

The recombinant soybean peroxidase (rSBP) was purified by chromatography and its biochemical properties were compared to those obtained for the commercial fungal peroxidase (CiP). The comparison revealed that soybean peroxidase had much higher thermostability and it retained up to 60% activity even after exposure to 70°C for an hour. Its fungal counterpart did not tolerate temperatures higher than 40°C, **Figure 1A**. The soybean peroxidase was also able to operate at very high temperatures and its activity was observed to increase up to 70°C, **Figure 1B.**The identified temperature optimum was in good agreement with reported thermostability for wild type soybean peroxidase [5].

The pH stability of the enzyme was determined as the residual activity after 1 hour incubation in Britton Robinson buffers ranging from pH 3 to pH 10. Determination of the residual activity revealed that rSBP was slightly more stable than CiP in the acidic pH range. rSBP was thus fairly stable in the range 5-10, while CiP is most stable in the range 7-10. The activity profile was also determined for a selection of mediators of interest and the results show that the activity on different mediators was highly pH dependent. The broadest pH span of 3-8 was observed when using phenothiazine-3-propionic acid (PPT), while it exhibits a narrower pH span for other mediators. Violuric acid and HOBT worked best at acidic pH, whereas methyl syringate (MS) worked best at alkaline pH, **Figure 2**. The right choice of mediator can thus control and secure activity of the peroxidase.

The stability towards hydrogen peroxidase was determined as the residual activity after 1 hour incubation in presence of H_2O_2. The result indicates that rSBP had a better stability towards H_2O_2 than CiP. The rSBPs retained full activity after incubation for an hour in presence of up to 2.5 mM H_2O_2, while the residual activity of CiP dropped to zero in a linear fashion from 0 mM to 5 mM H_2O_2.

rSBP offers a number of advantages over its fungal counterpart. Its stability was observed to be significantly better when subjected to stresses, such as temperature, pH and peroxide. Furthermore, its reactivity and ability to operate at a given pH can be controlled by the right choice of mediator.

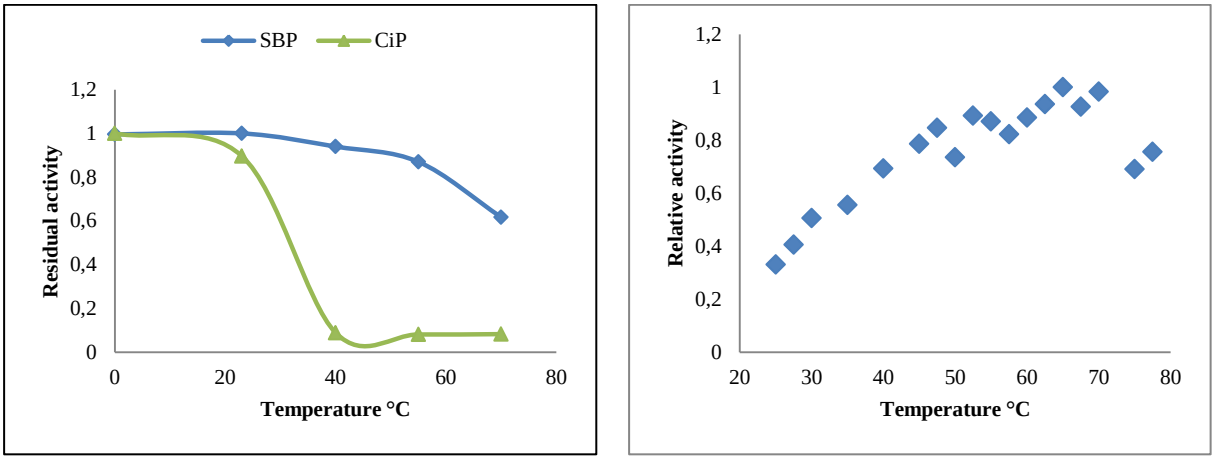

A **B**

Figure 1. A: Comparison of the temperature stability of rSBP and CiP.B: The temperature activity profile of rSBP

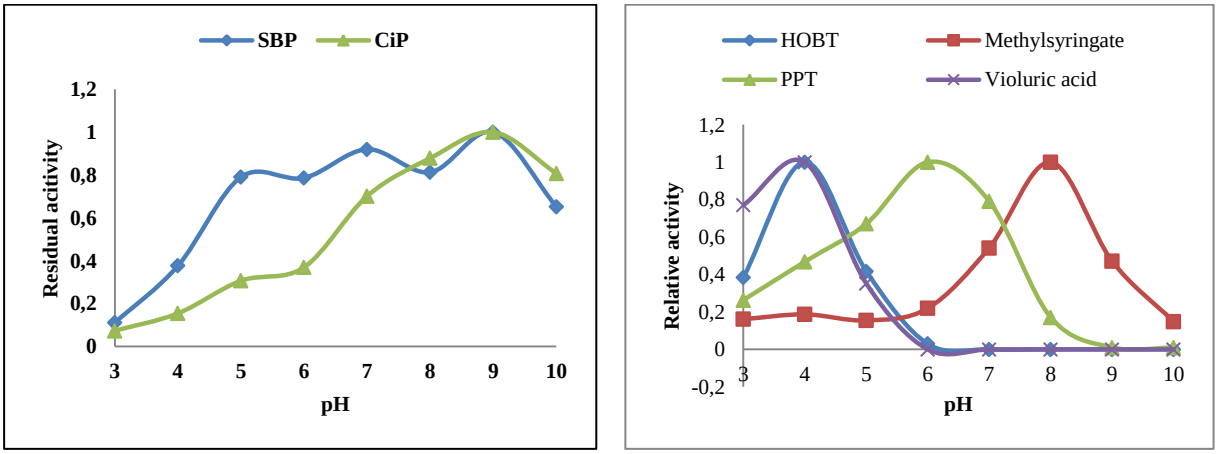

A **B**

Figure 2. A: Comparison of the pH stability of rSBP and CiP. B: The pH activity profile of SBP on selected mediators

Application of rSBP for biobleaching of pulp

A standard bleaching sequence of hardwood kraft pulp is composed of oxygen delignification followed by an acid hydrolysis step possibly combined with chlorine dioxide, alkaline peroxide extraction and a final peroxide stage: OA/DEopDP. Trend is going to even shorter processes balancing cooking yield, fiber integrity, cost and effluent load [4]. In order for an enzymatic biobleaching process to be a viable option for the industry, then it must completely replace or be compatible with one of the mentioned steps. A-stage is performed to eliminate hexenuronic acid which otherwise can cause brightness reversion and consume chlorine dioxide. A-stage is typically performed at pH above 3, temperatures from 85-95°C at 1.5-2 hours [6]. The thermostability and acidic pH optimum of rSBP makes this enzyme a very interesting base for developing a biobased bleaching alternative.

The biobleaching effect of several different peroxidases using VLA as mediator was evaluated in the mini pulp assay using unbleached eucalyptus pulp. VLA is an N-OH mediator which has been reported as ideal for biobleaching with a long lifetime of the iminoxy radical and no observable dimmer formation [3]. The tested peroxidases were evaluated at equal protein level at pH 4.5 and 40°C. SBP and the fungal analog CiP resulted in the highest improvement in brightness. Relatively poor performance was observed with the classical lignolytic peroxidases, LiP and VP when used in combination with violuric acid, **Figure 3**.

rSBP was evaluated at different dose levels in the mini pulp assay using both unbleached and oxygenated eucalyptus pulp. rSBP exhibited excellent bleaching performance at pH 4 and 70°C and worked equally well on unbleached and oxygenated pulp with optimum at 6 POXU(S)/ml. At optimum an increase in brightness of approx. 8 units was observed, irrespectively of pulp type. In order to be compatible with an A-stage temperature and pH must be at least pH 3.5 and 85°C.

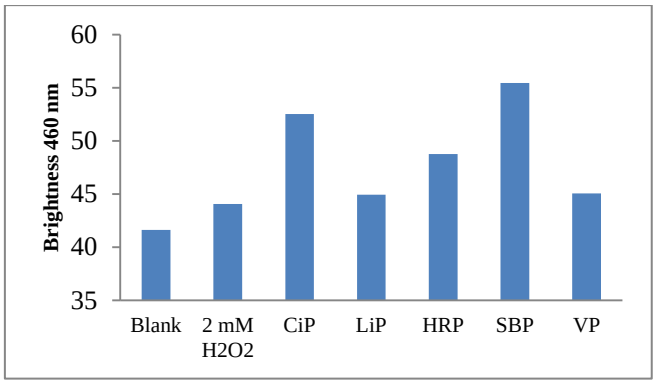

Figure 3. Biobleaching of unbleached eucalyptus pulp in mini pulp assay using various peroxidases with 1 mM VLA and 2 mM H_2O_2 at 50 mM acetate buffer pH 4.5 and 40°C.

The mini pulp assay is excellent for screening purposes, but the low consistency (1.3%) is not representable for industrial processing conditions. rSBP was evaluated at 10% consistency in combination with VLA and compared to MtL-MS or PpL-VLA. Bleaching performance of rSBP-VLA was very good at higher consistency and superior to MtL-MS and PpL-VLA, **Figure 4**.

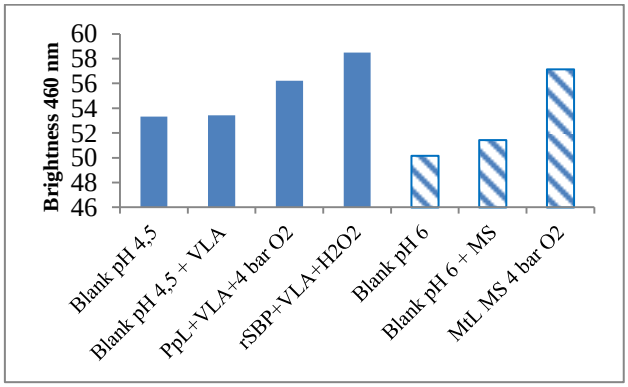

Figure 4. Biobleaching of unbleached eucalyptus pulp in 10% consistency pulp assay using rSBP with 0,5 mM mediator 2 mM H_2O_2 or 4 bar oxygen. pH 4,5: 50 mM acetate, 50°C; pH 6,0: 50 mM phosphate buffer, 55°C.

IV. CONCLUSIONS

Soybean peroxidase was expressed recombinantly and basic characterization indicates temperature optimum at 65-70°C. The stability of rSBP was observed to be significantly better when subjected to stresses, such as temperature, pH and peroxide when compared to a fungal counterpart from *Coprinus*. pH optimum depended on the selected mediator, with optimum at pH 4 for N-hydroxy mediators, pH 6 for phenothiazine-3-propionic acid and pH 8 for methyl syringate. Biobleaching of eucalyptus pulp showed superior performance of rSBP with violuric acid both when compared to other peroxidases and classical fungal laccases. The very high stability of rSBP makes this enzyme ideal for additional optimization and engineering in order to make biobleaching a realistic solution for the pulp and paper industry.

VI. REFERENCES

[1] Martinez, A.T.; Ruiz-Dueñas, F.J.; Martinez, M.J.; del Rio, J.C. and Gutiérrez, A. Enzymatic delignification of plant cell wall: from nature to mill. *Curr. Opin. Biotech.* **2009**, 20, 348–357.

[2] Babot, E.D.; Rico, A.; Rencoret, J.; Kalum, L; Lund, H.; Romero, J.; del Río J.C.; Martínez, A.T. and Gutiérrez, A. Towards industrially-feasible delignification and pitch removal by treating paper pulp with *Myceliophthora thermophila* laccase and a phenolic mediator. *Bioresour Technol*. **2011**, 102, 6717-6722.

[3] Li, K.; Xu, F. and Eriksson, K.E. Comparison of fungal laccases and redox mediators in oxidation of a nonphenolic lignin model compound. *App.l Environ. Microbiol*. **1999,** 65, 2654-60.

[4] Fawal, N.; Li, Q.; Savelli, S.; Brette, M.; Passaia, G.; Fabre, M.; Mathé, C. and Dunand, C. PeroxiBase: a database for large-scale evolutionary analysis of peroxidases. *Nucleic Acids Res*. **2013**, 41 (D1): D441-D444

[5] Kamal, K.J.K. and Behere, D.V. Thermal and Conformational Stability of Seed Coat Soybean Peroxidase. *Biochemistry*. **2002**, 41, 9034-9042

[6] Suess, H.U. Bleaching of chemical pulp (In Pulp bleaching today, Suess, H.U. ed), **2010**, chap. 4, 45-189.

TOWARDS AN OPTIMIZED DECONSTRUCTION OF LIGNOCELLULOSIC BIOMASS: FROM CELL WALL CHARACTERIZATION TO PROCESS MODELING

Baumberger, S.[1*], Berrin, J.-G.[2], Aceves-Lara C.A.[3], Athès, V.[4], Beaugrand, J.[5], Chabbert, B.[5], Guillon, F.[6], Méchin, V.[1], Montanier, C.[3], Paës, G.[5], Tréléa, C.[4]

[1]AgroParisTech, INRA, UMR 1318 Institut Jean-Pierre Bourgin, F-78026 Versailles cedex, France (stephanie.baumberger@agroparistech.fr); [2]INRA, UMR 1163 Biotechnologie des champignons filamenteux, F-13009 Marseille, France ; [3]INRA, CNRS, UMR5504, UMR792 Ingénierie des Systèmes Biologiques et des Procédés, F-31077 Toulouse, France ; [4]AgroParisTech, INRA, UMR 782 Génie et Microbiologie des Procédés Alimentaires, F-78850 Thiverval-Grignon, France ; [5]INRA, URCA, UMR 614 Fractionnement des AgroRessources et Environnement, F-51100 Reims, France ; [6]INRA, UMR 1268 Biopolymères, Interactions, Assemblages, F-44316 Nantes, France

ABSTRACT

In order to improve the understanding of lignocellulose fractionation mechanisms in a biorefinery context, an integrated approach combining exploration of plant variability, design of bioinspired lignocellulosic assemblies and tuning of enzymatic tools has been implemented within the "Lignocellulose biorefinery" INRA-CEPIA priority programme. The results bring insights into the parameters governing grass cell walls enzymatic hydrolysis at different structural levels, from macro- to nano-scales. Focus is made on three major highlights: the influence of lignin-hemicellulose interactions on endoxylanase activity, the influence of lignin structure on cell wall degradability by cellulolytic cocktails, and the influence of the chemical and structural features of cell wall on enzyme mobility. Mathematical models, mechanistic and statistical analysis, were implemented to rank structural parameters controlling lignocellulose enzymatic degradation. The results pave the way for proposing new approaches for optimizing biomass deconstruction to obtain bio-based products for next-generation biorefineries.

I. INTRODUCTION

As non-food renewable feedstock source of polymers, sugars and phenolic compounds for bio-based products, lignocellulose represents a key biomass for the development of future biorefineries [1]. Lignocellulose is composed of a complex cross-linked assembly of plant-cell wall polymers consisting of cellulose microfibrils embedded in a hemicellulose-lignin matrix impeding its degradability. Particular efforts have been paid these last decades to overcome lignocellulose recalcitrance and increase the enzymatic conversion yield of lignocellulose into fermentable sugars during the saccharification step, so as to ensure the competitiveness of second generation biorefineries [2]. Despite considerable advances in understanding the physical and chemical determinants of recalcitrance [3][4] some questions remains, such as the influence of lignin structure, the scale of interaction between lignin and hemicellulose, and the parameters governing enzyme mobility. These questions have been addressed within the "Lignocellulose biorefinery" INRA programme through an integrated approach combining exploitation of plant variability, implementation of bioinspired systems and tuning of enzymatic tools (**Figure 1**). The originality of the programme is to integrate different approaches and observation scales aiming at modeling grass cell wall enzymatic deconstruction. Maize was selected as a model plant allowing the recovery of samples with similar lignin content but contrasted degradability so as to identify the role of lignin structure in cell wall enzymatic recalcitrance. Isolation and synthesis of lignin-hemicellulose assemblies were performed to elucidate the relationships between lignin-hemicellulose interactions and hemicellulose degradability. Finally, bioinspired solid matrixes mimicking plant cell wall were designed in order to investigate parameters governing enzyme mobility and enzyme-substrate interactions.

II. EXPERIMENTAL

Investigation of the biochemical variability of maize lines

Eight maize recombinant inbred lines RILs were selected within the F286 x F7012 RIL population developed at INRA Lusignan to present similar lignin content and contrasted cell wall degradability as predicted by near-infrared reflectance spectrophotometer. The RILs and their two parental lines were cropped at the silage stage for

two successive years (2008 and 2009). After oven-drying (70°C) and grounding (hammer mill, 1 mm screen) the samples were analyzed for *in vitro* degradability (sequential incubation with pepsin then cellulase/amyloglucosidase solutions, protocol adapted from Libramont Limagrain [5]), cell wall residue content (three-stage extraction by toluene/ethanol (1:1, v/v), ethanol, and water, [6]), esterified and etherified *p*-hydroxycinnamic acid content (alkaline hydrolyses combined with LC-MS, [7]), lignin content (Klason method [8]) and lignin structure (thioacidolysis combined with GC-MS, [9]). To compare the relative influence of genetic, year, and plot effects, variance analysis was carried out using the GLM procedure in SAS. Data for RILs were combined over year, field, and analysis replicates before determination of correlation coefficients and multiple regression analysis using R.

Synthesis, isolation and characterization of lignin-carbohydrate fractions

Lignin-carbohydrate fractions were isolated from the stem of maize F2 (INRA) line grown on experimental field condition as described above and harvested at silage stage. Sequential fractionation of the extractive-free maize stems was carried out using two mild alkaline extractions (0.5 and 2 M NaOH, 20°C, 24h) before and after endoglucanase (Novozym 476) treatment according to [10], allowing the recovery of two lignin carbohydrate fractions LC1 and LC2. Lignin glucuronoarabinoxylan complexes (GAX-DHP) were synthesized by oxidative polymerization of coniferyl alcohol using horseradish peroxidase (Sigma) and hydrogen peroxide in the presence of glucuronoarabinoxylan (GAX; 1 g/L). All reactants were either added simultaneously (bulk polymerization) or gradually (end-wise polymerization) thereby allowing to modulate the relative contribution of non-covalent and covalent LCC in the complexes [11]. The resulting stable colloidal suspensions were treated with a purified endoxylanase (GH11 Tx-Xyl from *Thermobacillus xylanilyticus*). Hydrolysis rate was assessed by determining the reducing sugars released by enzymes; LCC were analyzed by size exclusion chromatography and electron microscopy [11].

Implementation of cell wall model to investigate enzyme mobility

Bioinspired model assemblies of grass secondary cell wall were prepared by dispersing ramie fibers cellulose nanocrystals (CNC) into a maize bran feruloylated arabinoxylan (FAX) matrix cross-linked by laccase oxidative treatment [12]. Gels and films with various water contents were obtained by setting the FAX and CNC concentrations of the solution before laccase-induced gelation. Films were obtained by drying gels in a rotating horizontal tube overnight. Fluorescent commercial probes (fluorescein isothioacyanate grafted onto dextran chains) of various sizes were used as well as fluorescently labeled FAX (reaction with 5-(4,6-dichlorotriazinyl)-aminofluorescein) and directly embedded into the assemblies before gelation. The samples were observed by confocal laser scanning microscopy (Leica SP2) using an excitation wavelength of 488 nm. Fluorescence recovery after photobleaching (FRAP) analysis was performed in order to assess the mobility (diffusion and mobile fraction) of probes and FAX polymers into the assemblies. The four principal factors modulated (water content, probe size, FAX and CNC concentrations) were introduced into a full factorial experiment model to compute principal and interaction coefficients. Following a Fischer test and an ANOVA analysis, the different coefficients were ranked according to their influence on diffusion.

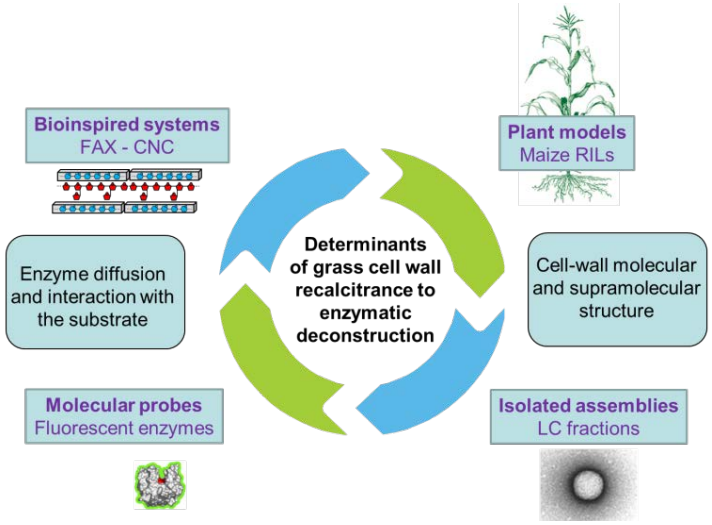

Figure 1. Integrated approach combining exploration of plant models (maize recombinant inbred lines RILs and isolated lignin carbohydrate LC fractions) and bioinspired models (FAX-CNC: feruloylated arabinoxylan – cellulose nanocrystals using molecular probes) for the investigation of grass cell wall enzymatic deconstruction

III. RESULTS AND DISCUSSION

1. Influence of lignin structure and p-coumaroylation on cell wall degradability

Lignin is one of the first factor responsible for the resistance of plant secondary cell-walls to enzymatic degradation. Its negative impact results both from its action as physical hydrophobic barrier restricting the access of cellulose to cellulose and from the irreversible adsorption of cellulases preventing the formation of specific interactions with cellulose [3]. Though both phenomena are likely to be influenced by lignin structure, the establishment of clear-cut relationships between lignin structure and cell wall recalcitrance is often hampered by variations in terms of lignin content. The use of maize recombinant inbred lines displaying similar lignin content permitted to eliminate this factor and show that cell wall enzymatic degradability is significantly linked to the degree of *p*-coumaroylation of lignin syringyl units and to the proportion of lignin β-*O*-4 inter-unit bonds [5]. The detrimental impact of *p*-coumaroylation possibly results from the inhibitory effect of *p*-coumaric esters as shown with model compounds [13], whereas β-*O*-4 bonds are expected to increase the barrier effect of lignin, due to the linearity and extended conformation they confer to the polymer [14]. Analysis of the cabohydrate-lignin fractions LC1 and LC2 isolated by mild alkali extractions of F2 maize imbred line stem suggested that lignin with high β-*O*-4 bonds are specifically associated to hemicellulose fractions [10]. Thus, in addition to lignin conformation, lignin interactions with hemicelluloses might explain the role of β-*O*-4 bonds.

2. Influence of lignin-hemicelluloses interactions on endoxylanases activity

Lignin-carbohydrate complex are known to be involved in the refractory nature of plant cell wall. It is thus necessary to identify the type and organization level of recalcitrant structures, so as to develop more specifically targeted pre-treatments. The association of glucuronoarabinoxylan and *in vitro* polymerized monolignols provided a model to investigate the influence of cabohydrate – lignin supramolecular organization on enzyme action [11]. Electron microscopy indicated that the action of the endoxylanase from *Thermobacillus xylanilyticus* was limited to the peripherical zone where the carbohydrate components was relatively exposed, confirming that enzyme accessibility to the substrate is a key factor. The formation of covalent bonds within the supramolecular assemblies contributed to additional resilience, as indicated by the kinetics of released reducing sugar and change in LCC molecular weight. Covalent bonds are likely to reduce enzyme-subtrat specific interactions. In addition, the question of their possible influence on enzyme mobility within the polymer matrix was raised.

3. Influence of the chemical and structural features of cell wall on enzyme mobility

Bioinspired model assemblies of secondary cell walls with water content ranging from 99.5 to 98% and CNC/FAX ratios of 1:2, 1:1 and 2:1 were recovered [15]. Used as templates to assess progression of fluorescent dextran probes of various sizes, a statistical analysis of the results allowed presenting a quantitative ranking of the parameters influencing the most diffusion. Water content, probe hydrodynamic radius and polysaccharide concentration were found to have decreasing influence levels in this order, with ratios of 75/45/3/1, which means that water content has a 75-fold more important weight than cellulose concentration when measuring diffusion. Moreover, diffusion is directly correlated to FAX cross-linking, as demonstrated by scanning electronic microscopy analysis (honey-comb organized architecture of gels) and FAX mobility (becoming largely decreased after gelation). A mathematical model for predicting diffusion of probes depending on water content, polymer concentration and probe size could therefore be set up. It was applied to a common industrial cellulase Cel7a from *Trichoderma reesei* to demonstrate that when water content increases, diffusion increases more rapidly than substrate accessibility. Several constructs from the fungal multimodular endoglucanase from the glycoside hydrolase family 45 [16] were used as probes in order to study the impact of family 1 carbohydrate binding modules (CBM1) on enzyme mobility into bioinspired models.

IV. CONCLUSIONS

Cell wall recalcitrance to enzymatic degradation is a complex phenomenon involving physical and chemical factors, most of them linked to the presence of lignin. Combining exploitation of maize genetic variability with implementation of bioinspired model systems and tuned enzymatic tools offers a promising approach to understand mechanisms of cell wall enzymatic deconstruction and optimize technological processes. Reducing lignin β-*O*-4 content in lignocellulose, either by lignin engineering or by a mild alkali treatment, appears as one possible strategy to improve conversion yields. The role of lignin β-O-4 bonds in cell wall recalcitrance can be assigned both to lignin conformation and interactions with hemicelluloses. Their influence on enzyme mobility and accessibility to substrate will be further investigated using the cell wall models and enzymatic tools presented in this paper. In these studies, *in silico* models help identifying limiting phenomena and most influent parameters, extensively test virtual scenarios and optimize process designs and control strategies. Furthermore, the use of sugars coming from lignocelluloses deconstruction is under study to produce building blocks using

integrated bioprocesses. The results pave the way for proposing new approaches for optimizing biomass deconstruction up to obtaining bio-based products for next-generation biorefineries.

V. ACKNOWLEDGEMENT

This work was supported by the Regional Council of Champagne-Ardennes, by the French Research National Agency ANR (MAGIC project ANR-08-BLAN-0307-01) and by INRA "Lignocellulose biorefinery" BILI programme (AIC Enzydam and Mobiprot, and Y. Zhang thesis grant from CEPIA and BV divisions).

VI. REFERENCES

[1] FitzPatrick, M., Champagne, P., Cunningham, M.F., Whitney, R.A. A biorefinery processing perspective: treatment of lignocellulosic materials for the production of value-added products **2010**, *101*, 8915-8922.

[2] Limayem, A.; Ricke S.C. Lignocellulosic biomass for bioethanol production: current perpectives, potential issues and future prospects. *Prog. Energy Combust. Sci.* **2012**, *38*, 449-467.

[3] Zhao, X.; Zhang L., Liu, D. Biomass recalcitrance. Part I: the chemical compositions and physical structures affecting the enzymatic hydrolysis of lignocellulose. *Biofuels, Bioprod. Bioref.* **2012**, *6*, 465-482.

[4] Foston, M.; Ragauskas, A.J. Biomass characterization: recent progress in understanding biomass recalcitrance. *Ind. Biotech.* **2012**, *8*, 191-208.

[5] Zhang, Y., Culhaoglu, T., Pollet, B., Melin, C., Denoue, D., Barriere, Y., Baumberger, S., Mechin, V. Impact of Lignin Structure and Cell Wall Reticulation on Maize Cell Wall Degradability. *J. Agric. Food Chem*. **2011**, 59, 10129-10135.

[6] Effland, M. J. Modified procedure to determine acid-insoluble lignin in wood and pulp. Tappi 1977, 60, 143–144.

[7] Mechin, V., Argillier, O., Menanteau, V., Barriere, Y., Mila, I., Pollet, B., Lapierre, C. Relationship of cell wall composition to in vitro cell wall digestibility of maize inbred line stems. *J. Sci. Food Agric.* **2000**, *80*, 574–580.

[8] Dence, C.; Lin, S. Y. The Determination of Lignin. In Methods in Lignin Chemistry; Lin, S. Y., Dence, C. W., Eds.; Springer: Berlin, 1992; pp 33-61.

[9] Lapierre, C., Monties, B., Rolando, C. Preparative thioacidolysis of spruce lignin: Isolation and identification of main monomeric products. *Holzforschung* **1986**, *40*, 47–50.

[10] Sipponen, M., Lapierre, C., Méchin, V., Baumberger, S. isolation of structurally distinct lignin-carbohydrate fractions from maize stem by sequential alkaline extractions and endoglucanase treatment. *Biores. Technol.* **2013**, *133*, 522-528.

[11] Boukari, I., Putaux, J.-L., Cathala, B., Barakat, A., Saake, B., Rémond, C., O'Donohue, M., Chabbert, B. *In vitro* model assemblies to study the impact of lignin carbohydrate interactions on the enzymatic conversion of xylan. *Biomacromolecules* **2009**, *10*, 2489–2498

[12] Paës, G., Chabbert, B. Characterization of arabinoxylan / cellulose nanocrystals gels to investigate fluorescent probes mobility in bio-inspired models of plant secondary cell wall. *Biomacromolecules* **2012**, *13*, 206-214.

[13] Boukari, I., Rémond, C., O'Donohue, M., Chabbert, B. Probing a family GH11 endo-β-1,4-xylanase inhibition mechanism by phenolic compounds: Role of functional phenolic groups *J. Mol. Catal. B: Enz.* **2011**, *72*, 130-138.

[14] Besombes, S., Mazeau, K. The cellulose/lignin assembly assessed by molecular modeling. Part 2: seeking for evidence of organization of lignin molecules at the interface with cellulose. *Plant Physiol. Biochem*. **2005**, *43*, 277–286.

[15] Paës, G., Burr, S., Saab, M., Molinari, M., Aguié-Beghin, V., Chabbert, B. Modeling progression of fluorescent probes in bioinspired lignocellulosic assemblies. *Biomacromolecules* **2013**, *14*, 2196-2205

[16] Couturier, M., Feliu, J., Haon, M., Navarro, D., Lesage-Meessen, L., Coutinho, P.M., Berrin, J-G. A thermostable GH45 endoglucanase from yeast: impact of its atypical multimodularity on activity. *Microb. Cell Fact.* **2011**, 10:103.

HYDROTHERMOLYSIS OF PINE: DISSOLUTION OF WOOD COMPONENTS AT ELEVATED TEMPERATURES

Marina Alekhina[1]*, Kaarlo Nieminen[1], Andreas Ebert[2], Sami Heikkinen[3], Herbert Sixta[1]

*[1]Department of Forest Product Technology, Aalto University School of Science and Technology, Espoo, Finland; [2]Research Division of Biopolymers, Fraunhofer IAP, Potsdam, Germany; [3]Department of Chemistry, University of Helsinki, Helsinki, Finland (*marina.alekhina@aalto.fi)*

ABSTRACT

The objective of this research was to obtain a better fundamental understanding of the extraction of lignin and carbohydrates from pine wood during hydrothermolysis at elevated temperatures. The treatment was performed in a batch reactor at three different temperatures (200, 220 and 240 °C) and a liquid-to-wood ratio of 40:1. The samples were collected at preselected time intervals, covering the treatment up to 120 min. It was found that up to 35% of native pine lignin solubilized at 240 °C within a few minutes of reaction time. A kinetic model fitting the experimental data was proposed to explain the delignification of pine wood during hydrothermolysis. Complete removal of pine wood hemicellulose was accomplished at a concomitant cellulose yield loss of about 12.5%. Overall, this study provided initial fundamental knowledge required for potentially efficient utilization of softwoods using wood biorefinery concept.

I. INTRODUCTION

The concept of wood biorefinery is envisioned as the selective separation of the three main wood components, cellulose, hemicellulose and lignin, and the subsequent utilization of each fraction for production of fuels, high value-added chemicals and other related products. Up to now, it has been a great challenge to design an efficient pretreatment and fractionation process of lignocellulosic materials which would be both technologically feasible and economically viable. Hydrothermolysis, i.e. treatment of wood with water at high temperatures, is a promising method to extract and recover lignin and hemicellulose from wood. It has gained much attention in recent years, because it is considered as a clean and environmentally friendly process where fractionation is achieved by using water and heat only. The majority of the studies deal with the degradation and dissolution of hemicelluloses and lignin during hydrothermal treatment of hardwood species. Softwoods represent the principal lignocellulosics in the Northern hemisphere and therefore their utilization is of interest. Softwoods differ from hardwoods in terms of carbohydrate content, composition and structure as well as in amount and structure of the lignin. So far, very little is known about the behavior of softwood during hydrothermolysis at elevated temperature. In this work, the effect of hydrothermolysis on the reactions of pine wood at different conditions was investigated and a kinetic model for the delignification of pine wood was developed. Further, the effect of hydrothermolysis on the content of the residual carbohydrates in pine wood was presented.

II. EXPERIMENTAL

Pine wood chips were supplied by Metsä Fiber, Finland and stored refrigerated before use. Pine chips were air-dried at ambient temperature and then grinded in a Wiley mill to a particle size between 0.6 and 0.25 mm. The chemical composition of initial pine wood is shown in **Table 1**. The dry matter content was determined by oven drying at 105 °C overnight.

Table 1. Chemical composition of pine wood

Component	Klason lignin	ASL	GGM	AX	CELL	Extractives
Amount, % o.d. sample	27.08	0.56	15.79	9.08	40.85	3.00

**ASL – acid soluble lignin; GGM – galactoglucomannan; AX – arabinoxylan; CELL - cellulose*

Hydrothermolysis experiments were conducted in a 10 L batch reactor, equipped with a mechanical stirrer, a temperature controller, a pressure gauge and a valve for the removal of hot extraction liquors. Liquid-to-wood ratio (L:W) of 40 g/g was used. Such a high L:W was selected in order to minimize the solubility limitations of wood components triggered by mass transfer of wood matrix. The degradation of wood components during preheating was taken into account by conversion of heating up phase into isothermal reaction time using a previously published method [1]. After reaching the set reaction time, the hydrolysate was discharged from the autoclave. The wood residue was recovered from the reactor, washed with hot water and air-dried before the yield was determined on a dry weight basis. Insoluble lignin fractions were recovered by centrifugation of obtained hydrolysates at 5000 rpm for 15 min. The soluble lignin was measured by a Shimadzu UV-2550

spectrometer at a wavelength of 205 nm. For further analysis, the supernatant was mixed with ethyl acetate with a ratio of solvent-to-hydrolysate of 3:1 [2] for extraction of soluble lignin degradation products.

Acid insoluble lignin or Klason lignin, acid soluble lignin (ASL) and carbohydrate contents of solid and liquid samples were determined after acid hydrolysis according to NREL/TP-510-42618 and NREL/TP-510-42623, respectively. Subsequent analysis of the recovered neutral sugar monomers was performed by using a Dionex ICS 3000 high-performance anion exchange chromatograph with pulsed amperometric detection (HPAEC-PAD) equipped with a CarboPacPA20 column (Dionex, Sunnyvale, CA, USA). Water was used as the eluent at a flow rate of 0.4 mL/min at 30º C. The carbohydrate compositionin solid samples was calculated according to previously published method [3]. The molecular mass distribution (MMD) of selected lignin samples was determined by gel permeation chromatography (GPC) equipped with UV detection (UV-Vis Detector 2487). The column was eluted with DMSO with 0.1 LiBr at a flow rate of 1 ml/min. The GPC system consisted of two analytical columns (Suprema 1000 and Suprema 100, 20 µm, 8 mm I.D.*300 mm) and one pre-column (Suprema 20 µm). The columns, injector and UV detector were maintained at 80°C during the analysis.

III. RESULTS AND DISCUSSION

The results showed that up to 35% of the original lignin in wood could be dissolved during hydrothermolysis within a selected range of conditions (**Figure 1**). At the same time the amount of ASL in wood decreased dramatically from 0.6% to 0.1% even at mild treatment conditions. The rate of lignin removal markedly increased at higher temperatures. Interestingly, for each temperature, the lignin removal went through a maximum, after which it decreased mainly triggered by lignin condensation and re-precipitation. This is due to the complex lignin behavior under hydrothermolysis conditions. Homolytic cleavage of α-O-4 and β-O-4 linkages results in formation of phenolic hydroxyl groups, fragmentation and dissolution of lignin. Formation of reactive lignin structures is followed by re-condensation reaction and decreasing lignin reactivity. Therefore, the amount of the residual lignin in the solid phase is decreased as a function of hydrothermolysis intensity until the point where lignin re-condensation occurs. As shown in **Figure 1,** the rate of lignin condensation increased with rising temperatures. A similar observation was reported for birch [1] and eucalyptus [4] wood.

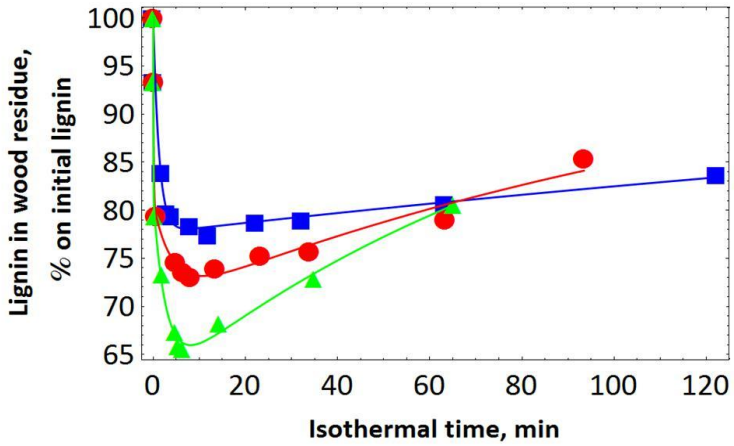

Figure 1. Lignin in wood residue as a function of treatment intensity. Square - temperature 200 °C, circles – 220 °C, triangles – 240 °C. Data points correspond to experimental data. Lines correspond to the proposed kinetic model.

In order to get a better understanding of the delignification during pine hydrothermolysis a kinetic model fitting the experimental data was developed. Native lignin in pine wood was modeled as the sum of three distinct fractions with different degradation rates. Delignification kinetics of pine wood during hydrothermolysis at elevated temperatures was assumed to proceed as,

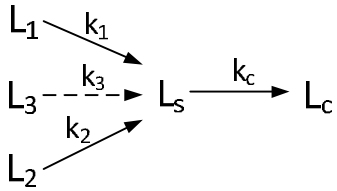

where L_1 and L_2 are fast and slow removable lignin fractions, L_3 is resistant lignin in initial pine wood. L_s and L_c are solubilized and condensed lignin respectively. At t=0, $L_1+L_2+L_3=1$, and $L_s+L_c=0$. k_1 and k_2 are degradation rates of easy and hard removable lignin, and k_3 degradation rates for resistant lignin, k_c is the condensation rate for the lignin solubilized in the extraction liquor.

As shown in **Figure 1**, the proposed kinetic model fitted very well to the experimental data.

The release of lignin into the liquid phase during hydrothermolysis is shown in in **Figure 2**. Two different fractions of lignin appeared in the hydrolysate, one as soluble the other one as insoluble lignin. The latter was recovered by centrifugation as it is readily precipitated during cooling. It was assumed that the insoluble fraction originates entirely from lignin. This assumption was based on a previous study which reported that the insoluble products contain mostly condensed structure from solubilized lignin fragments, especially those of higher Mw [4]. As shown in **Figure 2A**, the amount of insoluble lignin increased rapidly in the beginning of the treatment, reached a certain value, which is characteristic for each temperature. After that the concentration of insoluble lignin levelled-off. Therefore, it can be concluded that the temperature has a major effect on the insoluble lignin content. The second fraction consists of lignin of lower molar mass or lignin degradation products and is completely dissolved in the hydrolysate (**Figure 2B**). It remains soluble after the extraction process and its amount increased from 3.8% to 21.8% of total lignin content or from 1.1% to 6.0% based on original dry wood, with increasing extraction temperature from 200 °C to 240 °C. The release of soluble lignin increased rapidly within a short period of time, followed by a phase where the amount of soluble lignin increases only moderately

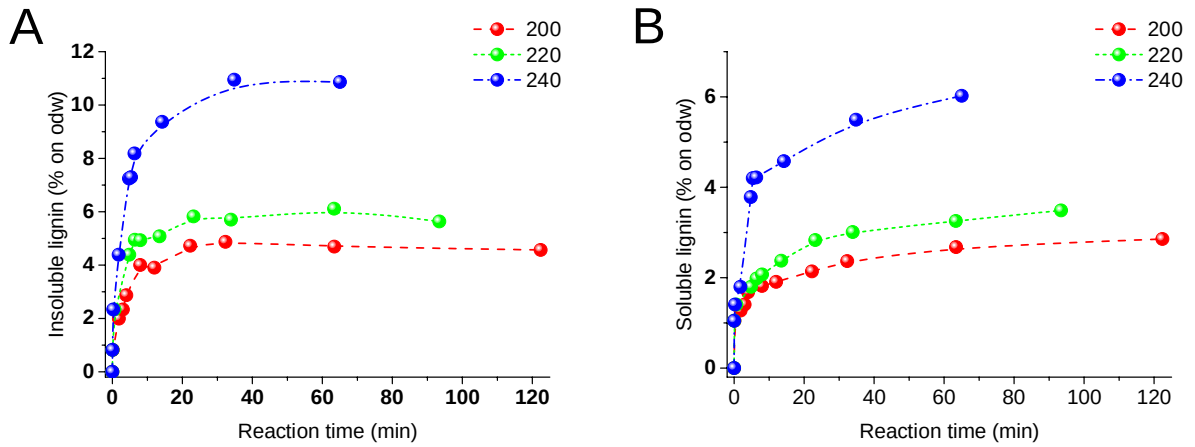

Figure 2. Insoluble (A) and soluble (B) lignin in the hydrolysates

Owing to the formation of insoluble products, most probably through the reaction of carbohydrate and resin derived degradation products with structurally modified lignin, the overall amount of lignin determined as Klason lignin increases with increasing temperature and treatment time.

As a reference, dissolved wood lignin (DWL) was isolated from non-treated pine wood and compared with two lignin fractions formed during hydrothermolysis: lignin precipitated in hydrolysates during cooling separated by centrifugation and lignin degradation products soluble in in the hydrolysates extracted with ethyl acetate. Additionally, kraft lignin is shown for comparison. All lignin fractions were subjected to SEC analysis (**Table 2**). The data indicated that extensive lignin degradation occurs during hydrothermolysis of pine wood due to homolytic cleavage of the aryl-ether bonds which results in a substantial decrease in the Mw of the lignin isolated from hydrolysates. As expected, M_w of soluble lignin was significantly lower than that of insoluble lignin. Additionally, an increase in hydrothermolysis intensity resulted to an increase in polydispersity (PD) of both soluble and insoluble fraction.

Table 2. Molar mass of selected lignin fractions.

Treatment temp., °C	Treatment time, min		M_w	M_n	PD
200	10	Insoluble	1345	107	12.5
200	120		785	60	13.0
200	10	Soluble	488	38	12.8
200	120		427	17	25.7
Pine DWL			6098	2106	2.9
Pine kraft lignin			5542	1347	4.1

Depending on the conditions of hydrothermolysis, up to 35% of the total lignin in pine or 96.8 kg per ton of o.d. wood could be recovered. This is a significant amount of high potential material for the preparation of value added products. Insoluble lignin fraction can be used for the manufacturing of activated carbon, adhesives or lignin polymer blends. The soluble fraction consists mostly of lignin oligomers and monomers, as well as lignin degradation products such as phenols, which can be utilized in the production of polymers or biofuels. Furthermore, the properties of the hydrothermolysis lignin differ significantly from lignin recovered by

conventional pulping technologies. In contrast to kraft lignin the hydrothermolysis lignin is sulfur free which should be advantageous in many applications.

The removal of carbohydrates during the hydrothermolysis of pine wood is shown in **Figure 3**. At 200 ºC, cellulose remained quite stable during the first three minutes, however, gradually decreased from initial 40.9% to 31.7% after 122 min of treatment time. The content of cellulose dramatically decreased to only 16.2% on odw after one hour at 240 °C. As expected, hemicellulose can be more easily removed during hydrothermolysis. Basically, complete degradation of hemicellulose in wood during hydrothermolysis was achieved under conditions with a concomitant cellulose loss of about 12.5% on odw. In addition to carbohydrates in solid residue both monomeric and polymeric sugars in hydrolysates were determined (not shown). At low and medium temperatures, the released carbohydrates consisted mainly of poly- and oligosaccharides. At higher temperature (240 °C), significant amounts of monomeric sugars and their degradation products were formed. In addition to hemicellulose mono- and oligomers, significant amounts of furfural and HMF may be recovered from the hydrolysates.

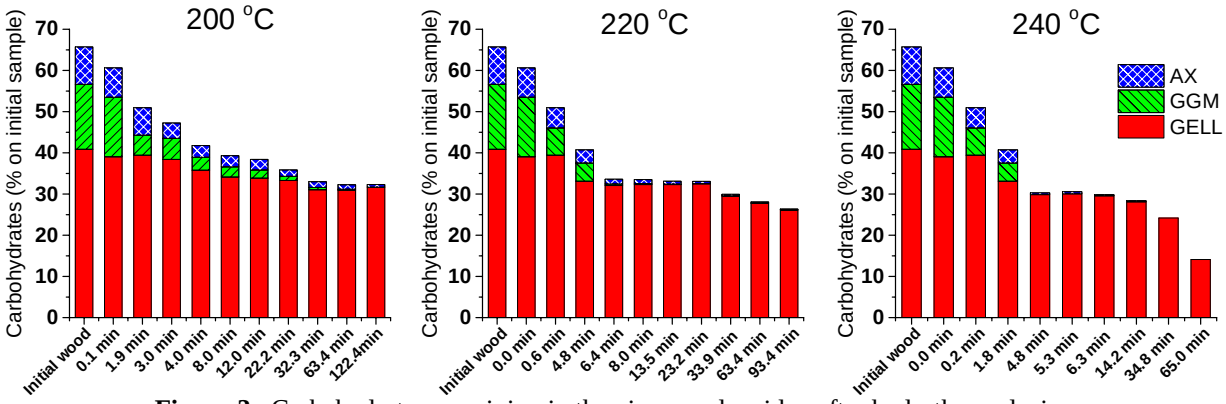

Figure 3. Carbohydrates remaining in the pine wood residue after hydrothermolysis

IV. CONCLUSIONS

Approximately 35% of the native pine lignin was solubilized during hydrothermolysis at 240 °C after less than 10 minutes. Extended reaction time led to excessive condensation of the lignin and therefore increased the amount of lignin in the wood residue. Delignification kinetics of wood during hydrothermolysis was successfully modeled by the assumption of simultaneous dissolution (depolymerization) and condensations reactions of lignin. Native lignin was modeled as the sum of three fractions with different degradation rates (easily removable lignin, resistant lignin and condensed lignin). Lignin in pine wood undergoes extensive structural alteration and degradation during hydrothermolysis. It was proven that soluble lignin in hydrolysates has slightly lower M_w than that of lignin which precipitates during cooling of the hydrolysates. SEC analysis revealed that fragmentation reaction dominated over condensation reactions. Properties and structure of hydrothermolysis lignin differs significantly from lignin recovered by conventional pulping technologies, therefore it is considered to be potential material for the preparation of value added products.

V. ACKNOWLEDGEMENTS

The financial support of this work by TEKES and Forest Cluster as part of Wood Wisdom project is gratefully appreciated. The authors acknowledge Kari Kovasin and Metsä Fiber for their kind offer of wood chips sample. We also thank Dr. Hendrik Wetzel (Fraunhofer IAP) for providing assistance with GPC analysis.

VI. REFERENCES

[1] Borrega, M., Nieminen, K., Sixta, H. Effect of hot water extraction in a batch reactor on the delignification of birch wood. *Bioresources* **2011**, *6(2)*, 1890-1903.

[2] Cruz, J.M., Domingues, J.M., Domingues, H., Parajo, J.C. Solvent extraction of hemicellulosic wood hydrolysates: a procedure useful for obtaining both detoxified fermentation media and polyphenols with antioxidant activity. *Food Chem*. **1999**, *67*, 147–153.

[3] Janson, J., Calculation of the polysaccharide composition of wood and pulp. *Paperi ja puu* **1970**, *5*, 323-329.

[4] Leschinsky, M., Zuckerstätter, G, Weber, H.K., Patt R. and Sixta H. Effect of autohydrolysis of *Eucalyptus globulus* wood on lignin structure. Part 1: Comparison of different lignin fractions formed during during water prehydrolysis. *Holzforschung* **2008**, *62(6)*, 645-652.

CELLULASE SUBSTRATE BINDING AND THE ROLE OF CARBOHYDRATE-BINDING MODULES IN HYDROLYSIS IN AQUEOUS IONIC LIQUID SOLUTIONS

Ronny Wahlström[1]*, Jenni Rahikainen, Kristiina Kruus, Anna Suurnäkki

[1]*VTT – Technical Research Centre of Finland, Tietotie 2, Espoo, Finland;*ronny.wahlstrom@vtt.fi*

ABSTRACT

The enzymatic hydrolysis of the polysaccharide fractions in lignocellulosic biomass requires efficient pretreatment to overcome the natural recalcitrance of lignocellulose. Certain ionic liquids (ILs) dissolve lignocellulose and are thus interesting as pretreatment technology prior to total enzymatic hydrolysis. ILs have, however, been shown to be poorly compatible with enzymes. Enzyme binding to cellulose is a prerequisite for the enzymatic hydrolysis process, but so far binding has not been studied in detail in IL solutions. In this study, we have elucidated the effect of two cellulose-dissolving ILs on the cellulose hydrolysis and cellulose binding using a *Trichoderma reesei* cellobiohydrolase and endoglucanase and their respective catalytic core domains. The results indicate that the carbohydrate-binding module (CBM) in these modular cellulases is sensitive to the presence of IL. In general, the presence of IL had a negative impact on both the hydrolysis yields and the cellulose binding of the studied cellulases. Depending on cellulase type, large differences were observed in how the enzyme binding was affected by ILs.

I. INTRODUCTION

The polysaccharides present in lignocellulosic plant biomass, cellulose and hemicelluloses, can be utilised as starting components in the production of biofuels, most notably ethanol, and a large and growing variety of different chemical products, such as butanol, lactic acid or glycolic acids. To utilise the polysaccharides, they need to be hydrolysed to their constituent monosaccharides prior to fermentation. The hydrolysis step can be carried out either enzymatically or with acid catalysis. Enzymatic hydrolysis has several advantages over acid hydrolysis, such as low formation of harmful side-products, no generation of acid waste, no need for corrosion-resistant processing equipment and a potential for very high yields. Lignocellulosic plant biomass is, however, very recalcitrant towards enzymatic hydrolysis. Therefore, a pretreatment is needed to open the structure of the lignocellulose. Certain ionic liquids (ILs, salts with melting points < 100 °C) have been found to dissolve cellulose and also complete lignocellulose, even wood. It has also been shown that pretreatment with IL greatly facilitates subsequent enzymatic hydrolysis of the lignocellulosic feedstock [1]. The ILs have, however, been found to inactivate the cellulases used for cellulose hydrolysis even in low concentrations [2]. Thus, pretreatment with ILs needs an excessive and expensive washing of the pretreated substrate, or conditions and enzymes need to be found which allow the enzymes to work in the presence of considerable amounts of IL.

The enzymes used for hydrolysing cellulose are termed cellulases, which is a collective term for several different activities. Endoglucanases cleave the cellulose randomly along the chains, whereas cellobiohydrolases work from the chain ends liberating cellobiose in a processive mode and β-glucosidases cleave the small soluble saccharide fragments formed by the endoglucanases and cellobiohydrolases to glucose. Due to their different functions, the structures of the cellulases are different. Endoglucanases generally have their active site in a cleft on the protein surface, whereas the cellobiohydrolases have an active-site tunnel. Cellulases often have a modular structure in which the catalytic core domain (CD) is linked to a carbohydrate-binding module (CBM). The function of a CBM it is to increase the cellulase concentration at the cellulose surface, thus promoting the hydrolysis. Up to date, several factors have been shown to influence the performance of cellulases in the presence of ILs, such as high viscosity, pH, and ionic strength [3]. In addition, other IL-specific factors, *e.g.* conformational changes or protein unfolding, are likely to play a role. In this work, we report a systematic study of how the presence of cellulose-dissolving ILs affect the substrate binding and hydrolytic action of one endoglucanase, *Trichoderma reesei* Cel5A, and the major cellobiohydrolase *T. reesei* Cel7A, in comparison to their isolated core domains [4].

II. EXPERIMENTAL

T. reesei Cel5A, Cel5A core domain (CD), and Cel7A CD were produced, isolated, and purified as described by Suurnäkki *et al.* [5] and *T. reesei* Cel7A according to Rahikainen *et al.* [6]. Enzymatic hydrolysis was carried out with a 1% (w/w) dispersion of microcrystalline cellulose (MCC, Serva research grade, 0.020 mm particle size) as substrate in 0.050 M citrate buffer (nominal pH 5.0) containing 0 – 50 % (w/w) of the ILs 1,3-dimethylimidazolium dimethylphosphate ([DMIM]DMP) or 1-ethyl-3-methylimidazolium acetate ([EMIM]AcO) under constant magnetic agitation. The enzyme concentration in the hydrolysis solution was 400 nM, the hydrolysis temperature was 45 °C and the time 72 h. The hydrolysis was ended by boiling the hydrolysis

tubes for 10 min and separating the solid and liquid fraction after centrifugation. The hydrolysis yields were determined by assaying reducing sugars with the DNS assay using glucose as standard.

The cellulases were labeled with tritium through reductive amination with formaldehyde and tritium-enriched [^{3}H]$NaBH_4$ based on a method by Means and Feeney [7]. After the reaction, the reaction mixture was eluted twice through gel columns. The collected fractions were pooled, concentrated and the buffer was changed to 0.050M citrate buffer (pH 5.0). Binding experiments were carried out in 1% (w/w) MCC suspension in 0.050 M citrate buffer (pH 5.0) containing 0, 20, and 40% w/w [DMIM]DMP or [EMIM]AcO with cellulase concentrations of 0.1–10 mM. The binding experiments were done at 4 °C with an equilibration time of 4h. Enzyme binding was measured after separating the supernatant from the MCC using centrifugation. The binding levels were calculated based on liquid scintillation counting results from the supernatants, by comparing the counts of supernatants incubated with MCC against supernatants incubated without MCC. Both the hydrolysis and the binding experiments were carried out in triplicate.

III. RESULTS AND DISCUSSION

We set out for studying the role of the carbohydrate-binding module (CBM) in hydrolysis and substrate binding in IL matrices because in some earlier studies CBMs have been suggested to be particularly sensitive to the presence of ILs [8,9]. Initially, the impact of the CBM on hydrolysis yield was assessed by comparing the hydrolysis yields of intact Cel5A and Cel7A to their core domains (CDs) in different IL matrices (**Figure 1**). As expected, increasing concentrations of IL led to decreasing hydrolysis yields and [EMIM]AcO was more harmful to hydrolysis than [DMIM]DMP, especially at higher IL concentrations.

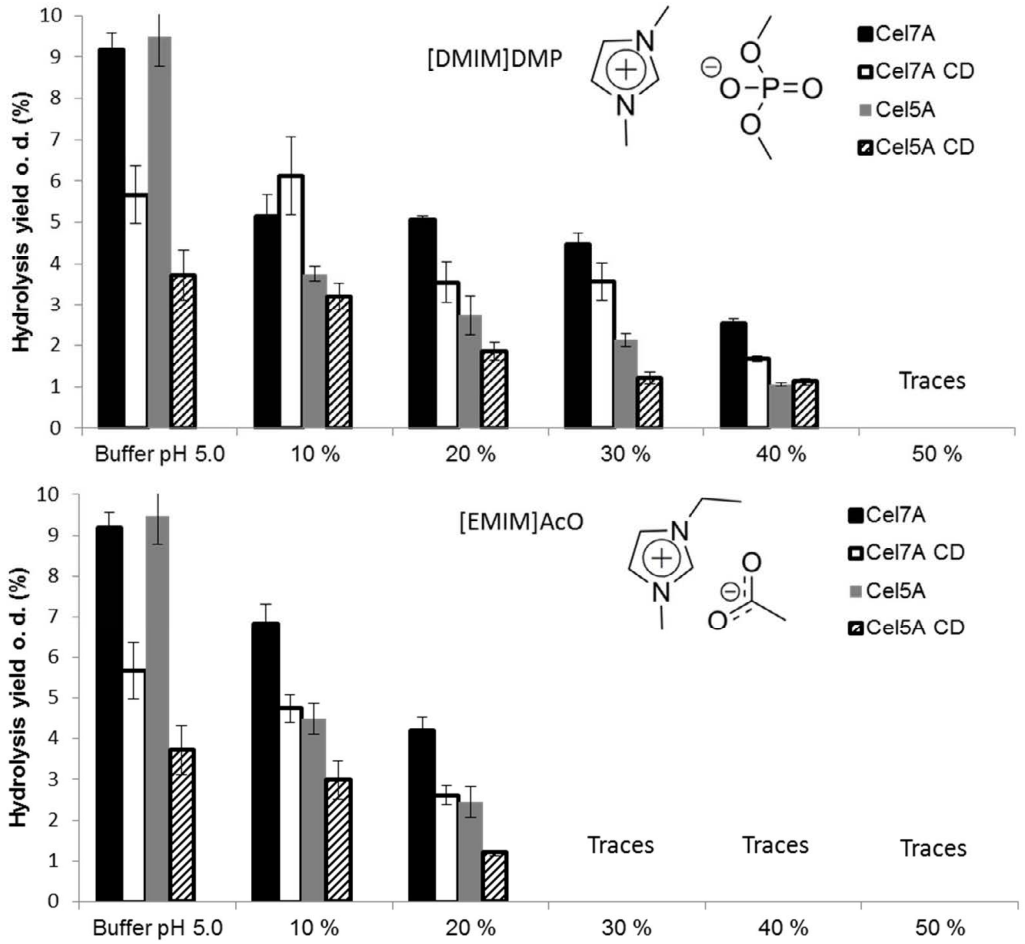

Figure 1. Yields of 72 h hydrolysis of MCC at 45 °C with *T. reesei* Cel5A, Cel5A CD, Cel7A and Cel7A CD, in citrate buffer (pH 5.0) matrices containing 0–50% IL. Hydrolysis yields were measured by a DNS assay with a limit of quantification of 1% yield.

In buffer, the hydrolysis yields of the intact cellulases were clearly higher than those of the CDs, but it was however interesting to notice that introducing IL to the solution had very different impacts on the yields of the intact cellulases and the CDs. The CDs had only slightly reduced yields for every increment of added IL,

whereas the yields of the intact cellulases were reduced to very close to those of the CDs in the presence of ILs. It appears plausible to interpret these hydrolysis results as a strong sensitivity of the function of the CBM in these cellulases to the presence of even low amounts of IL. Cel7A formed the only exception to this pattern in the [EMIM]AcO matrices.

Radiolabeling of cellulases is a very sensitive technique for studying the binding behavior of these proteins. In this work, the free amine groups (lysines and the N terminus) in the cellulases were labeled by reductive amination. In this reaction, formaldehyde initially reacts with a free amine to form an imine, which is reduced by tritium-enriched sodium borohydride, thus introducing the radioactive element to the protein. The protein is only modified by the addition of one methyl group to the formerly free amine. The mild reaction conditions and the minimal chemical modifications introduced to the cellulases during the labeling led to no loss of cellulolytic activity or fragmentation of protein structure. The radiolabeled cellulases were quantified from liquid samples by liquid scintillation counting. ILs have often been noticed to interfere with various analytical methods, but the high specificity and sensitivity of liquid scintillation counting led to high quality result sets where the ILs did not have any impact on the measurement background and the standard deviations within the triplicates were minimal.

The results from the binding experiments supported the conclusions from the hydrolysis experiments of the IL sensitivity of the cellulases' CBM. The four studied cellulases (*T. reesei* Cel7A, Cel7A CD, Cel5A and Cel5A CD) clearly showed different binding behavior to MCC in buffer solution (**Figure 2**). The intact Cel5A and Cel7A both had very similar binding isotherms to MCC and also the binding of Cel7A CD, lacking CBM, was comparatively high. Cel5A CD displayed a clearly different binding behavior, with only very low binding to MCC in buffer (not shown). Thus, the CBM appeared to have a very crucial role for the binding of Cel5A to cellulose, whereas Cel7A does not depend so much on its CBM for substrate binding. The difference in the binding site architecture of the different cellulases (open cleft in the endoglucanase Cel5A, tunnel in the cellobiohydrolase Cel7A) would provide a plausible explanation for the observed difference in the binding of the two studied CDs.

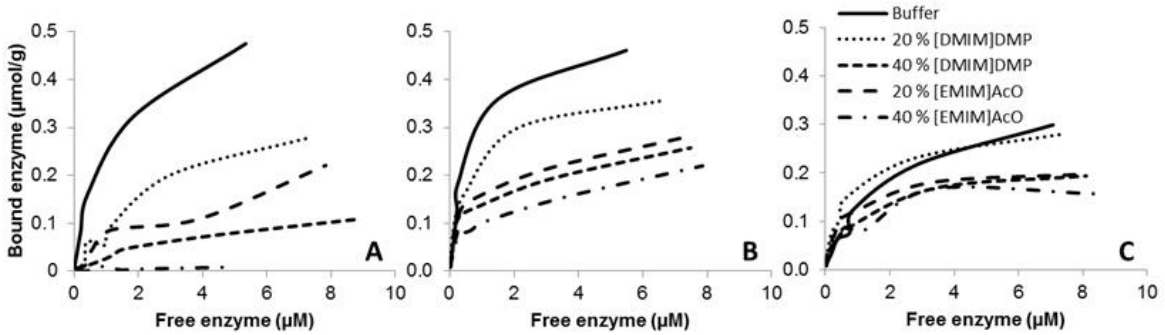

Figure 2. Binding isotherms for *Trichoderma reesei* Cel5A (A), Cel7A (B) and Cel7A CD (C) in five different IL solutions at 4 °C.

The cellulose binding of the studied cellulases responded differently to the presence of IL (**Figure 2**). In all cases, the addition of IL led to reduced binding, [EMIM]AcO having a stronger negative effect on the binding than [DMIM]DMP, similarly as was observed in the hydrolysis results. The binding of Cel7A was reduced by the presence of IL to some extent, whereas the binding isotherms of Cel7A CD were affected to a lower extent in the studied matrices. In fact, the binding isotherms of Cel7A and Cel7A CD appeared to be much alike in 40 % (w/w) [EMIM]AcO, representing the harshest conditions studied, which suggest that the CBM did not in these conditions improve the binding, but that the observed binding was mainly caused by binding of the Cel7A core domain and possibly the active site binding tunnel. The binding of the endoglucanase Cel5A was clearly more sensitive to IL than that of Cel7A and in 40 % (w/w) [EMIM]AcO no binding of Cel5A could be observed, even if the binding of both Cel5A and Cel7A was approximately on the same level in buffer. The interference of IL with the binding and function of CBM can be due to several reasons, which should be the topic of further studies; *e.g.* interference with the hydrophobic actions governing the binding interactions between the CBM and the cellulose ("solvent effect") or partial or complete unfolding of the CBM or other conformational changes.

IV. CONCLUSIONS

Cellulase binding onto cellulose is an essential step in enzymatic cellulose hydrolysis. This study showed that the presence of ILs in the hydrolysis matrix clearly has a negative impact on the cellulases' ability to bind to their substrate. The function of the carbohydrate-binding module (CBM) appeared to be especially sensitive to

the presence of IL. Interesting differences were noticed in how the enzymes with different catalytic site architecture behaved in the presence of IL; cellobiohydrolases with a tunnel-shaped core domain (CD) were able to bind to cellulose even in high IL concentration in which the CBM did not appear to be able to function. The studied endoglucanase with an open catalytic site in a cleft on the surface completely lost its ability to bind onto cellulose in the presence of IL. When developing IL-compatible cellulases both the catalytic activity and the binding properties should be considered. These results show that the presence of a CBM does not necessarily bring any benefits to cellulase action in IL conditions.

V. ACKNOWLEDGEMENT

The Finnish Bioeconomy Cluster's (FIBIC) Future Biorefinery (FuBio) programme and VTT Graduate School are thanked for their financial support. Jenni Lehtonen and Riitta Alander are thanked for skilful technical assistance.

VI. REFERENCES

[1] Dadi, A.P.; Varanasi, S.; Schall, C.A. Enhancement of cellulose saccharification kinetics using an ionic liquid pretreatment step. *Biotechnol. Bioeng.* **2006,** *95,* 904-910.

[2] Turner, M.B.; Spear, S.K.; Huddleston, J.G.; Holbrey, J.D.; Rogers, R.D. Ionic liquid salt-induced inactivation and unfolding of cellulase from *Trichoderma reesei*. *Green. Chem.* **2003,** *5,* 443-447.

[3] Engel, P.; Mladenov, R.; Wulfhorst, H.; Jäger, G.; Spiess, A.C. Point by point analysis: how ionic liquid affects the enzymatic hydrolysis of native and modified cellulose. *Green. Chem.* **2010,** *12,* 1959-1966.

[4] Wahlström, R.; Rahikainen, J.; Kruus, K.; Suurnäkki, A. Cellulose hydrolysis and binding with *Trichoderma reesei* Cel5A and Cel7A and their core domains in ionic liquid solutions. *Biotech. Bioeng.* **2014,** *111,* 726-733.

[5] Suurnäkki, A.; Tenkanen, M.; Siika-aho, M.; Niku-paavola, M.-L.; Viikari, L.; Buchert, J. *Trichoderma reesei* cellulases and their core domains in the hydrolysis and modification of chemical pulp. *Cellulose* **2000,** *7,* 189-209.

[6] Rahikainen, J.L.; Martin-Sampedro, R.; Heikkinen, H.; Rovio, S.; Marjamaa, K.; Tamminen, T.; Rojas, O.J.; Kruus, K. Inhibitory effect of lignin during cellulose bioconversion: The effect of lignin chemistry on non-productive enzyme adsorption. *Bioresour. Technol.* **2013,** *133,* 270-278.

[7] Means, G.E.; Feeney, R.E. Reductive alkylation of amino groups in proteins. *Biochemistry* **1968,** *7,* 2192–2201.

[8] Wahlström R, Rovio S, Suurnäkki A. Partial enzymatic hydrolysis of microcrystalline cellulose in ionic liquids by *Trichoderma reesei* endoglucanases. *RSC Adv.* **2012,** *2,* 4472–4480.

[9] Pottkämper, J.; Barthen, P.; Ilmberger, N.; Schwaneberg, U.; Schenk, A.; Schulte, M.; Ignatiev, N.; Streit, W.R. Applying metagenomics for the identification of bacterial cellulases that are stable in ionic liquids. *Green. Chem.* **2009,** *11,* 957-965.

LACCASE-MEDIATOR PRETREATMENT DELIGNIFIES WOODY AND NONWOODY PLANT FEEDSTOCKS AND IMPROVES ENZYMATIC SACCHARIFICATION

Ana Gutiérrez[1]*, Jorge Rencoret[1], Alejandro Rico[1], Antonio Pereira[1], José C. del Río[1], Angel T. Martínez[2]

*[1]Instituto de Recursos Naturales y Agrobiología de Sevilla, CSIC, Reina Mercedes 10, E-41012 Seville, Spain; [2]Centro de Investigaciones Biológicas, CSIC, Ramiro de Maeztu 9, E-28040 Madrid, Spain (*anagu@irnase.csic.es)*

ABSTRACT

This study shows the ability of laccases to remove lignin when applied on the (milled) whole lignocellulosic biomass in combination with 1-hydroxybenzotriazole or methyl syringate, in a multi-step sequence where the enzymatic stages alternate with alkaline extractions. Eucalypt (*Eucalyptus globulus*) and Elephant grass (*Pennisetum purpureum*) were selected as representative for rapid growth woody and nonwoody plant feedstocks, respectively. Paralleling lignin removal from *E. globulus* and *P. purpureum* (~50% and ~30% of the initial content, respectively) a positive effect on sugar yield was also observed. The modification of lignin was analyzed by 2D NMR of the whole samples at the gel state. Different removal of *p*-hydroxyphenyl, guaiacyl and syringyl lignin units, and a moderate removal of *p*-coumaric acid (present in *P. purpureum*) was observed without a substantial change in polysaccharide signals. However, the most noticeable change was the strong increase of C_α-oxidized syringyl units after the enzymatic sequence.

I. INTRODUCTION

Lignocellulosic biomass serves as feedstock for the lumber and paper pulp industries, and has also attracted increased interest for the production of biofuels and other chemicals and materials. Biomass recalcitrance towards enzymatic hydrolysis is correlated to the content and composition of lignin. Different pretreatments are being studied for deconstructing biomass and removing lignin. Laccases are multicopper oxidases whose direct action on lignin is restricted to the minor phenolic moiety. However, the interest on laccases as industrial biocatalysts steadily increased after discovering that some mediators expand the range of oxidized substrates, 1-hydroxybenzotriazole (HBT) being among the most efficient ones. The present study shows the ability of *Trametes villosa* and *Myceliophthora thermophila* laccases to remove lignin when applied on the (milled) whole lignocellulosic biomass in combination with HBT and methyl syringate (MeS), respectively, in a multi-step sequence where the enzymatic stages alternate with alkaline extractions. *Eucalyptus globulus* and *Pennisetum purpureum* were treated as representative for rapid growth woody and nonwoody plant feedstocks, respectively. The modification of lignin was analyzed by 2D NMR of the whole samples at the gel state [1,2], a promising methodology for the *in situ* analysis of lignin in delignification studies.

II. EXPERIMENTAL

Laccase-mediator treatments

Milled Elephant grass and eucalypt samples were treated with 50 $U \cdot g^{-1}$ (estimated by 2,2'-azino-bis(3-ethylbenzothiazoline-6-sulphonic acid) oxidation at pH 5) of *T. villosa* laccase (from Novozymes) in the presence (or absence) of 2.5% HBT at 6% consistency in 50 mM tartrate (pH 4) under O_2 atmosphere (2 bars) and 170 $rev \cdot min^{-1}$ shaking for 24 h at 50ºC. After washing, samples (6% consistency) were submitted to a peroxide-reinforced alkaline extraction using 1% NaOH and 3% H_2O_2 at 80ºC for 90 min. Cycles of four successive enzyme-extraction treatments were applied. Additionally, eucalypt samples were treated with *M. thermophila* laccase (50 $U \cdot g^{-1}$) (from Novozymes) in the presence (and absence) of 3% MeS under the same conditions described above, but using sodium dihydrogen phosphate (pH 6.5) as a buffer. Treatments with laccase alone and controls without laccase and mediator, were also performed (followed by the corresponding alkaline extractions). Klason lignin content was estimated according to T222 om-88 [3].

Saccharification of pretreated material

The saccharification of samples treated with *T. villosa* laccase (25 $U \cdot g^{-1}$) and 2.5% HBT was performed with a cocktail of commercial enzymes (from Novozymes) with cellulase (Celluclast 1.5 L; 10 $FPU \cdot g^{-1}$) and β-

glucosidase (Novozym 188; 500 nkat·g^{-1}) [4]. The saccharification of eucalypt samples treated with *M. thermophila* laccase (50 U·g^{-1}) and 3% MeS was also carried out with the above enzymatic cocktail [5].

2D NMR spectroscopy

For gel-state NMR experiments, ~100 mg of ball-milled lignocellulose samples after the several steps of the whole multistage sequence were directly transferred into 5-mm NMR tubes, and swelled in 1 mL of dimethylsulfoxide-d_6, forming a gel inside the NMR tube [1,2]. Heteronuclear single-quantum correlation (HSQC) 2D-NMR spectra were acquired as previously described [4,5].

III. RESULTS AND DISCUSSION

Lignin modification by the T. villosa*-HBT pretreatment*

The lignin content in both lignocellulosic materials decreased considerably after the enzymatic sequence applied. For Elephant grass, the decrease was about 32% of the initial lignin content. The reduction in eucalypt wood was even more pronounced, attaining 48% with the same laccase doses. The treatments with laccase alone (without mediator) slightly decreased the lignin content (<5%) in both materials.

The NMR spectra of the whole treated samples at the gel state confirmed the partial removal of lignin *p*-hydroxyphenyl (H), guaiacyl (G) and syringyl (S) units and a more limited removal of *p*-coumaric acid present in Elephant grass, as shown in the aromatic regions of the HSQC spectra of the Elephant grass (**Figure 1B**) and eucalypt wood (**Figure 1D**) treated with laccase and HBT, compared with the corresponding controls (**Figure 1A** and **C**, respectively). A decrease in the intensity of the main (β-*O*-4'-linked) lignin side-chains (**Figure 2,** A) was observed in the aliphatic region of the spectra (not shown), while the amorphous polysaccharide cross-signals remained basically unaffected (crystalline cellulose was silent under the present conditions).

Semi-quantitative evaluation of the relative abundances of the different lignin and cinnamic acid structures (**Figure 2**, PCA, FA, H, G, S and S') after the enzymatic sequence revealed a preferential removal of G (and minor H) units, and the higher recalcitrance of cinnamic acids towards laccase treatment (compared with lignin) resulting in their accumulation. However, the most noticeable modification observed was the massive formation of C_α-oxidized S lignin units during the enzymatic treatment, as revealed by the intensity increase of the characteristic ^{13}C-^{1}H correlation around 106/7.3 ppm ($S'_{2,6}$ in **Figure 1**). This was especially significant in the enzymatically-treated eucalypt wood, and resulted in a very unusual lignin consisting of up to 60% oxidized S units.

Such extensive oxidation is congruent with the concept of lignin degradation as an enzymatic combustion [6], and the C_α modification observed confirms the attack mechanism (H atom abstraction from the C_α position) suggested by degradation studies using model compounds [7].

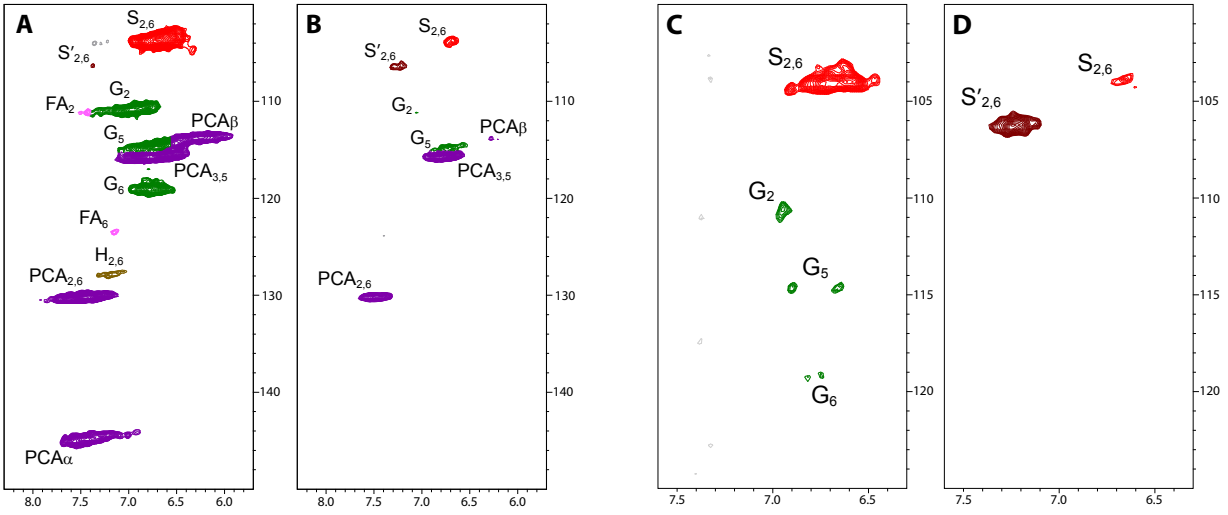

Figure. 1. Aromatic region of the HSQC spectra of Elephant grass (**A**-**B**) and eucalypt (**C**-**D**) treated with *T. villosa* laccase and HBT (swollen in dimethylsulfoxide-d_6): **A** and **C**, Controls without enzyme; **B** and **E**, 50 U·g^{-1} enzyme and 2.5% mediator. See Figure 2 for the main lignin structures identified.

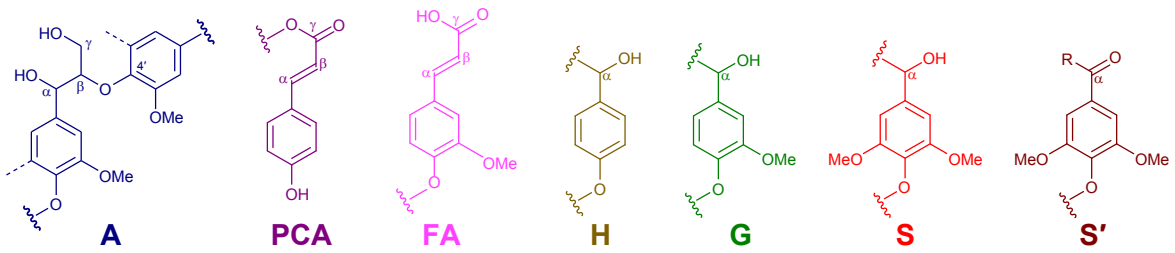

Figure 2. Main lignin and cinnamic acid structures identified: A, β-*O*-4' lignin structure (aliphatic region of the spectra); PCA, *p*-coumaric acid; FA, ferulic acid; H, *p*-hydroxyphenyl unit; G, guaiacyl unit; S, syringyl unit; and S', C_α-oxidized S unit (R can be a hydroxyl in carboxylic acids or a lignin side-chain in ketones).

Lignin modification by the M. thermophila *laccase-MeS pretreatment*

The lignin content of eucalypt sample decreased considerably after the enzymatic sequence reaching a decrease of 47% of the initial lignin content. The treatments with laccase alone (without mediator) decreased the lignin content about 20%.

The HSQC spectrum of the eucalypt sample treated with laccase-mediator at the end of the whole sequence (**Figure 3B**) showed important differences compared to the control (**Figure 3A**). The signals of side-chains in β-*O*-4' lignin substructures (A_α and $A_{\beta(S)}$) decreased considerably with respect to the carbohydrate and S-lignin signals. On the other hand, the G lignin signals completely disappeared with the laccase-mediator treatment, while the S units were C_α-oxidized (and in a significant extent remained as such) as revealed by the increase in the $S'_{2,6}$ signal (after deducting the MeS contribution estimated from the aliphatic signal at δ_C/δ_H 52/3.8 ppm). The results obtained showed a C_α-oxidation mechanism for lignin removal by laccase in the presence of MeS, and revealed that about half of the residual lignin in the laccase-mediator treated wood corresponds to the C_α-oxidized S units. Finally, the low intensity of the aromatic and aliphatic-oxygenated lignin signals in the HSQC spectrum of the laccase-mediator treated sample, compared to the carbohydrate signals, was in agreement with the reduced Klason lignin content.

Interestingly, lignin modification and removal was also shown by the NMR spectra of the eucalypt feedstock treated with laccase alone (not shown), with a relative decrease of the lignin signals compared to the carbohydrate signals, although not as evident as that observed after the laccase-mediator treatment. Among them, the signals of side-chains in β-*O*-4' lignin substructures (A_α and $A_{\beta(S)}$) and especially, the G lignin signals, decreased considerably with respect to the control sample although the changes were less intense than those found in the sample treated with laccase and MeS. Likewise, the C_α-oxidation of S units was much less pronounced than found in the presence of MeS.

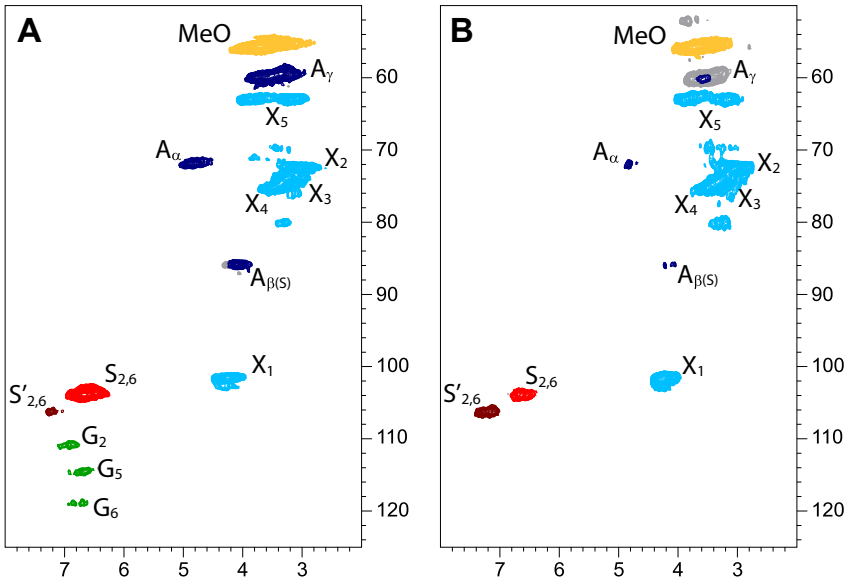

Figure 3. HSQC NMR spectra of whole eucalypt samples treated with *M. thermophila* laccase and MeS (swollen in dimethylsulfoxide-d_6): **A,** Control without enzyme; **B,** Sample treated with laccase-MeS. See Figure 2 for the main lignin structures identified. Correlation signals from xylan (X_1-X_5) are also indicated.

Saccharification of enzyme pretreated materials

The Elephant grass and eucalypt wood samples treated with *T. villosa* laccase and HBT were hydrolyzed using a cellulase and β-glucosidase cocktail, and the main monosaccharides released were analyzed [4]. The effect of hydrolysis time was investigated and 72 h hydrolysis was chosen since monosaccharide release already stabilized after this time period, attaining increases up to 61% and 12% for eucalypt and Elephant grass feedstocks, respectively. In the case of eucalypt wood, the effect of the laccase-HBT treatment increased with cellulase hydrolysis times, the highest increases in glucose and xylose releases were obtained after 72 h. However, for Elephant grass the highest increases in sugar releases by the laccase-mediator treatment were observed after only a 4-h hydrolysis [4]. Interestingly, the treatment with laccase alone (without mediator) also slightly increased the hydrolysis yields for eucalypt and Elephant grass, with respect to that of the controls. The laccase-mediator pretreatment significantly increased ethanol production after 17 h of saccharification-fermentation [4]. Interestingly, the enzymatic treatment was considerably more efficient improving ethanol production from eucalypt (over 4 $g \cdot L^{-1}$ in 17 h) than from Elephant grass (~2 $g \cdot L^{-1}$ in 17 h).

In eucalypt samples pretreated with *M. thermophila* laccase-MeS, an increases in glucose yield up to 41% (with respect to the initial eucalypt wood sample) was attained when low cellulase (2 filter-paper units $[FPU] \cdot g^{-1}$) and β-glucosidase (100 $nkat \cdot g^{-1}$) doses were used. In the samples pretreated with laccase alone (without mediator), an increase in glucose release of 21% was produced. The effect of oxygen and alkaline extraction steps in the control sample were responsible for the increase of 11% in glucose yield with respect to the initial eucalypt sample. On the other hand, an improvement on xylose release of about 37% was obtained after the laccase-MeS treatment of eucalypt wood (with respect to the initial eucalypt wood sample). In the pretreatment with laccase alone an increase in xylose yield of 21% was obtained. The effect of oxygen and alkaline extraction on xylose yield (control sample with respect to the initial one) represented an increase of 12%.

IV. CONCLUSIONS

This work shows the modification of lignin structure and content produced by two laccase-mediator pretreatments, directly on ground lignocellulosic material and its relationship with enzymatic saccharification yields. A better understanding of the action mechanisms of lignin-degrading enzymes, when acting on lignocellulosic substrates, should contribute to the development of knowledge-based transformations in future lignocellulose biorefineries based on fast-growing woody and nonwoody plant species.

V. ACKNOWLEDGEMENT

This study was funded by INDOX (KBBE-2013-7-613549) EU- and LIGNOCELL (AGL2011-25379) Spanish-MICINN (co-financed by FEDER funds) projects. J. Rencoret acknowledges the CSIC JAE-Doc contract of the program JAE co-financed by the ESF. H Lund (Novozymes) is acknowledged for the cellulases and the *M. thermophila* laccase, J Romero (ENCE) and JL Colodette (Univ. of Viçosa) for the eucalypt and Elephant grass, respectively, and M Angulo (CITIUS, Univ. of Seville) for providing technical assistance in the NMR analyses. EM Cadena (Univ. of Colombia) and D. Barth (VTT) are acknowledged for their valuable contribution to first enzymatic pretreatments and saccharification assays, respectively.

VI. REFERENCES

[1] Kim H; Ralph J; Akiyama T. Solution-state 2D NMR of ball-milled plant cell wall gels in DMSO-d_6. *Bioenerg. Res.* **2008**, *1*, 56-66.

[2] Rencoret J; Marques G; Gutiérrez A; Nieto L; Santos I; Jiménez-Barbero J; Martínez AT; del Río JC. HSQC-NMR analysis of lignin in woody (*Eucalyptus globulus* and *Picea abies*) and non-woody (*Agave sisalana)* ball-milled plant materials at the gel state. *Holzforschung* **2009**, *63*, 691-698.

[3] Tappi: *2006-2007 TAPPI Test Methods.* Norcoss, GA 30092, USA: TAPPI Press; **2006**.

[4] Gutiérrez A; Rencoret J; Cadena EM; Rico A; Barth D; del Río JC; Martínez AT. Demonstration of laccase-mediator removal of lignin from wood and non-wood plant feedstocks. *Bioresource Technol*. **2012**, *119*, 114-122.

[5] Rico A; Rencoret J; del Río JC; Martínez AT; Gutiérrez A. Pretreatment with laccase and a phenolic mediator degrades lignin and enhances saccharification of *Eucalyptus* feedstock. *Biotechnol. Biofuels* **2014**, *7*, 6.

[6] Kirk TK; Farrell RL. Enzymatic "Combustion": the Microbial Degradation of Lignin. *Annual Reviews in Microbiology* **1987**, *41*, 465-505.

[7] Fabbrini M; Galli C; Gentili P. Comparing the catalytic efficiency of some mediators of laccase. *J. Mol. Catalysis. B-Enzyme* **2002,** *16*: 231-240.

IMPACT OF STEAM EXPLOSION ON SPRUCE AND WHEAT STRAW LIGNIN STRUCTURES STUDIED BY NMR AND DENSITY FUNCTIONAL CALCULATIONS

Harri Heikkinen[1], Tom Elder[2], Hannu Maaheimo[1], Stella Rovio[1], Jenni Rahikainen[1], Kristiina Kruus[1] and Tarja Tamminen[1*]

[1]*VTT Technical Research Centre of Finland, Biologinkuja 7, Espoo, FI-02044 VTT, Finland*
[2]*USDA-Forest Service, USA*
**tarja.tamminen@vtt.fi*

ABSTRACT

Chemical changes of lignin induced by the steam explosion (SE) process were elucidated. Wheat straw and Spruce were studied as raw materials, and lignins were isolated by the EMAL procedure before and after SE treatment for analyses mainly by HSQC NMR. The β-O4 structures were found to be homolytically cleaved, followed by recoupling to β-5 linkages. The homolytic cleavage / recoupling reactions were also studied by computational methods, which verified their thermodynamic feasibility. The presence of tricin bound to wheat straw lignin was confirmed and it was shown to participate in lignin reactions during the SE treatment.

I. INTRODUCTION

Various pre-treatment methods are crucial steps in the bioferinery concepts, utilising biomass components as raw material for value-added biomaterials and chemicals. Steam explosion (SE) is the most traditional and established of them. It enhances the reactivity of lignocellulosic biomass towards enzymatic hydrolysis for the production of fermentable sugars [1]. Cellulases, used in the enzymatic hydrolysis of biomass, tend to adsorb also on the lignin surfaces, thus making the lignin act as an inhibitory agent and retarding the hydrolysis process. A recent study by Rahikainen *et al.* [2] showed that SE-treated lignins from spruce and wheat straw are actually more active towards binding the hydrolytic enzymes (*Trichoderma reesei* Cel7A and Cel7A-core) compared to the non-pretreated analogues. The same lignin materials as studied by Rahikainen have been used in the present study.

The major lignin reactions in SE have been reported to be the decrease in the content of β-O4 units and increase in the content of C-C condensed structures and other inter-unit linkages (β-1, β-5) formed *via* radical coupling reactions [3,4,5]. Depending on the SE conditions, formation of higher molecular weight lignins has been observed, explained by competing depolymerisation and repolymerisation reactions [6]. The aim of the present study is to elucidate in depth the chemical reactions of lignin during the SE process. The main focus is in wheat straw lignin, but also Spruce lignins have been analysed for comparison, as Spruce lignin is known to be more detrimental in respect to enzyme adsorption. HSQC NMR techniques and theoretical calculations were the main tools.

II. EXPERIMENTAL

Enzymatic mild acidolysis lignins (EMAL) were isolated from ball milled wheat straw and Spruce, and from both raw materials after SE treatment and ball milling. The procedures are explained in detail in [2].

^{31}P NMR analyses were performed after phosphitylation with 2-chloro-4,4,5,5-tetramethyl-1,3,2-dioxaphopholane according to [7].

For the HSQC and HMBC NMR experiments, 50 mg of sample was dissolved in 1 mL of d6-DMSO and the experiments were carried out at 30°C on a 600 MHz Bruker Avance III NMR spectrometer equipped with a CPQCI cryoprobe The quantitative HSQC spectra were acquired using echo/antiecho-TPPI selection and matched sweep adiabatic pulses optimised for ^{13}C sweep width of 200 – 50 ppm were used for all 180° ^{13}C pulses in order to compensate the differences in the $^{1}J_{CH}$ coupling constants [8]. The HMBC experiments were optimised for 8 Hz long range couplings. Matrices of 2048 x 256 (HSQC) or 2048 x 512 (HMBC) data points were collected, zero filled once in F1 and a π/2 shifted squared sine bell weighting function was applied in both dimensions prior to the Fourier transformation.

All calculations using the Density Functional Method were performed with Gaussian 09, C.01 with the facilities of the Alabama Supercomputer Center in Huntsville, Alabama. All structures were optimized at the M06-2X level of theory, using the 6-311++G(d,p) basis set and the fine grid consisting of 75 radial shells and 302 angular points per shell. Frequency calculations were performed on the stationary points identified. Bond dissociation enthalpies were determined as the difference between the enthalpy of the reactant and products.

III. RESULTS AND DISCUSSION

The amounts of the lignin units and the detected inter-unit linkages in spruce and wheat straw EMALs before and after steam explosion are shown in **Table 1**. The amounts are based on the integrals seen in the ^{1}H-^{13}C HSQC NMR spectra where the C9 unit (G2+S2,6/2) is used as an internal standard. The C2 in G units or the C2 and C6 positions in the S units are expected not to be substituted. The inter-unit linkages were determined by integration of the Hα-Cα correlation signals in the HSQC NMR spectra (exception: Hβ-Cβ in α-oxidized β-O4 structure) and comparing to the total C9 unit integral. As example, the HSQC NMR spectrum of wheat straw EMAL and the determined structures are shown in **Figure 1**.

Table 1. Amount of main inter-unit linkages and structural characteristics detected in wheat straw and Spruce lignins before and after the SE treatment from the integration of ^{13}C-^{1}H correlation signals in HSQC spectra.

Interunit linkages [a]	WHEAT STRAW		SPRUCE[c]	
	EMAL	SE	EMAL	SE
β-O4 (G+S)	66	51	50	39
β-O4 (S)	41	26	-	-
β-O4 (G)	25	25	50	39
β-5	10	16	15	16
β-β	5	3	4	4
5-5-O4	8	2	6	2
β-1 (incl. SD)	trace	trace	1	1
α-oxidized β-O-4[b] (S/G)	6	2	0.9	0.1
α,β-diaryl ethers	3	1	-	-
cinnamyl alcohol	0.7	0.6	0.8	0.4
cinnamyl aldehyde	1.4	1.5	5.5	3.6
Aromatic units [a]				
S/G ratio	0.6	0.4	-	-
PCA	11	5	-	-
FA	2.7	1.9	-	-
PCA/FA ratio	4.0	2.6	-	-
Tricin	13	2	c	c

[a] Expressed as No. per 100 C_9 units (0.5 $S_{2,6}$+G_2).
[b] H_β-C_β correlation signal integral.
[c] Some contaminants from the wheat straw lignin detected.

Cleavage of β-O4 structures was found to be the predominant reaction. The level of their reduction was found to be similar (22%) in wheat straw and Spruce, suggesting that the difference in their response to the SE treatment is not due to differences in the main lignin reaction mechanisms. Besides the decrease in the content of β-O4, increase in the level of phenylcoumaran (β-5) linkages after the SE treatment is striking. After the SE treatment, the molar mass values, analysed by SEC, were increased in both raw materials (results not shown). This was contradictory with the observed high degree of cleavage of the aryl ethers, and indicates that competing repolymerisation reactions take place.

Substantial decrease in the amount of p-coumarates (pCA) and tricin (T) was also observed. Recently, incorporation of tricin into the lignin network via β-O4 type linkage from the tricin carbon C4 has been reported [9]. ^{31}P NMR spectroscopy was applied to follow the reactions of tricin in SE treatment using commercially available tricin (SelectLab Chemicals GmbH, Bönen) as model compound. Three distinct chemical shifts 136.4, 137.7 and 142.0 ppm were assigned to correspond to the three hydroxyl groups in the tricin structure. They were also found in the wheat straw EMAL lignin 31P NMR spectrum, confirming the presence of tricin and its decrease in SE treatment. The ^{31}P NMR chemical shifts at 136.4 ppm and 141.67 ppm were well separated, whereas the third signal at 137.7 ppm overlaps partly with lignin-derived p-OH signals. Since the ^{31}P NMR method is quantitative, it provides a means to quantify tricin in the lignin samples (**Table 1**).

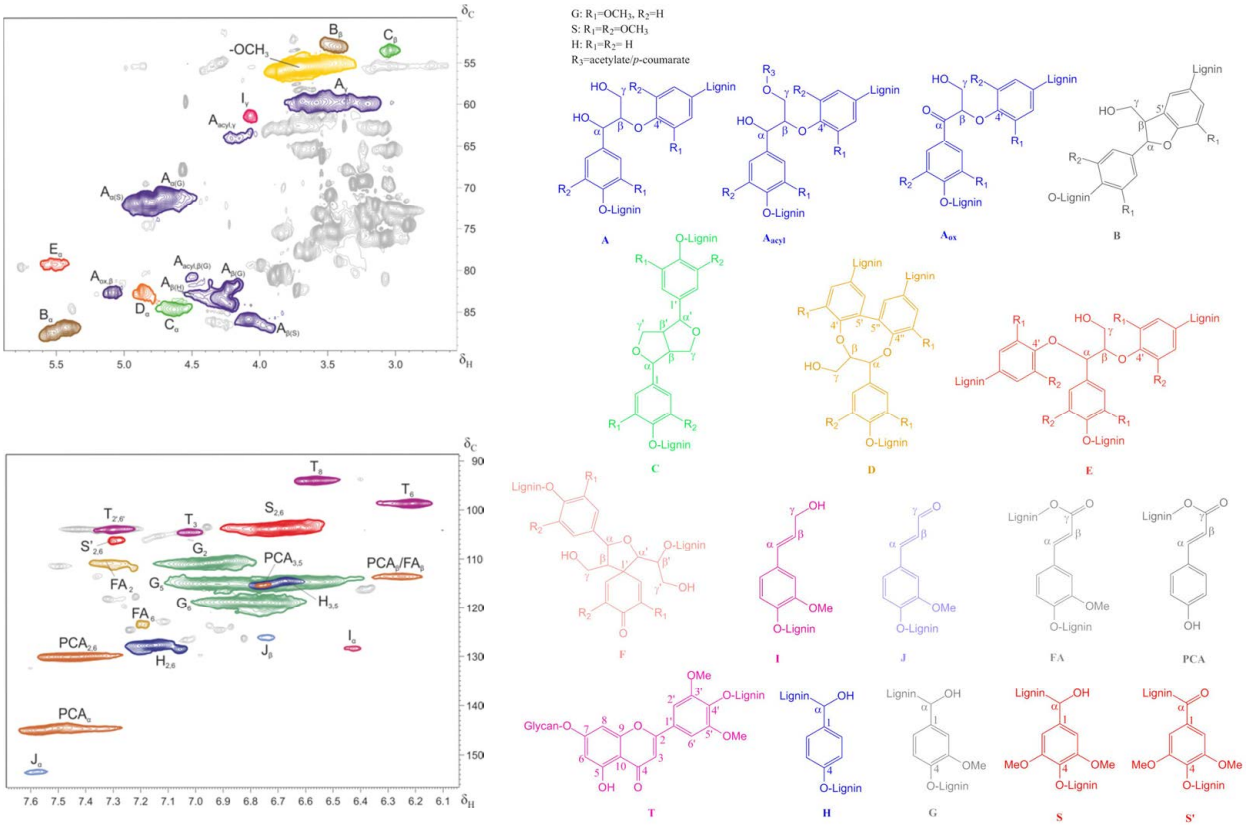

Figure 1. ^{1}H-^{13}C HSQC NMR spectra: side-chain (δC/δH 50-90/2.5-5.8) and aromatic/unsaturated (δC/δH 88-160/6.05-7.65) region of wheat straw EMAL. Signals were assigned according to literature [9]. The structures detected: (A) β-O4; (A_{acyl}) β-O4 alkyl-aryl ethers with acylated γ-OH; (Aox) Cα-oxidized β-O4 structure; (B) phenylcoumaran (β-5); (C) resinol β-β; (D) dibenzodioxocin (5-5-O4); (E) α,β-diarylether; (F) spirodienone (β-1); (I) cinnamyl alcohol; (J) cinnamyl aldehyde; (pCA) p-coumarate; (FA) ferulate; (H) p-hydroxyphenyl unit; (G) guaiacyl unit; (S) syringyl unit; (S) Cα-oxidized S unit.

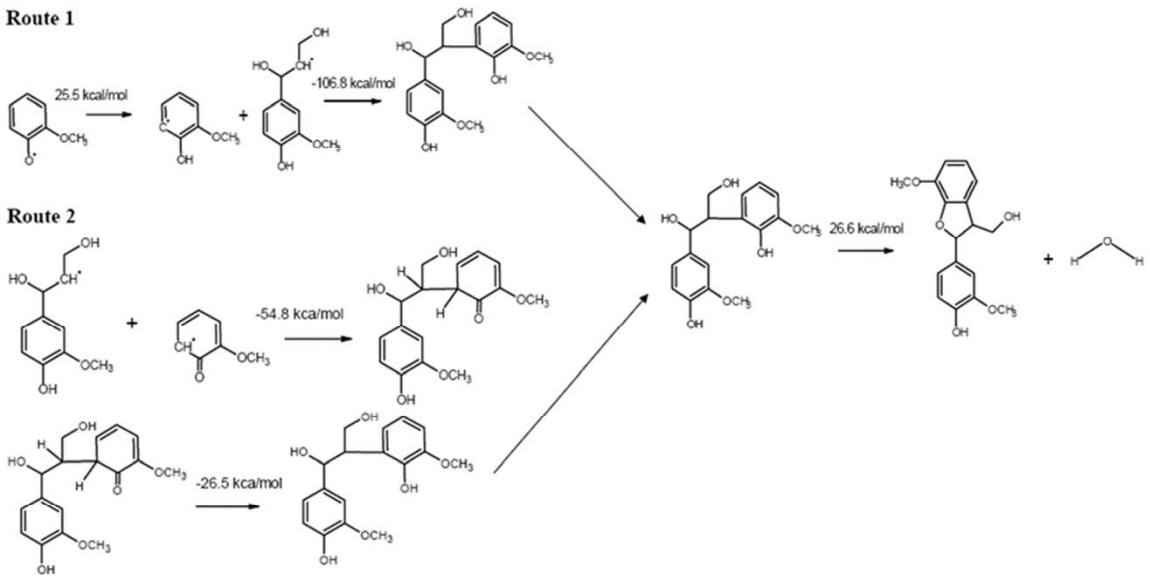

Figure 2. Schematic view of two different routes for the β-O4 to β-5 transformation.

Density Functional Method calculations were performed to analyse the rearrangement from β-O4 to phenylcoumaran (β-5) linkages. From the bond dissociation energy point of view, there are two different routes how the transformation can occur (**Figure 2**). The first route requires the formation of a tautomer from the phenoxy radical, which is a highly endothermic reaction. The second route couples the phenoxy radical and β-O4 radical so that the tautomerization energy is not needed. Altogether, transformation from β-O4 to β-5 (+water) requires energy around 15 kcal/mol, which is available under the SE process conditions. It is also worth pointing out that the β-5 dilignol is actually more stable than the original β-O4 dimer by 11.6 kcal/mol. Thus, the rearrangements concluded to take place by chemical analyses are also thermodynamically justified.

IV. CONCLUSIONS

Homolytic cleavage of the β-O4 linkages and recoupling to β-5 linkages were identified as the main reaction types of lignin in SE treatment, even if the results do not exclude the presence of acidolysis type cleavage and condensation reactions. Tricin was found to have an important role in the reactions of lignin in SE treatment in the case of wheat straw. It is cleaved from lignin probably via homolytic cleavage analogously to syringyl type lignin units. The lignin-bound tricin may exist natively as a glyco-conjugate, possibly linked to the cell wall matrix. In that case, the cleavage of tricin from lignin would simultaneously release lignin from the cell wall matrix and thus enhance saccharification. This would at least partly explain the observed good response of wheat straw to SE treatment as compared to Spruce that does contain tricin.

VI. REFERENCES

[1] L.P. Ramos, C. Breuil, D.J. Kuschner, J.N. Saddler, Steam pre-treatment conditions for effective enzymatic hydrolysis and recovery yields of *Eucalyptus viminalis* wood chips. Holzforschung, 46 (1992) 149-154.

[2] J. L. Rahikainen, R. Martin-Sampedro, H. Heikkinen, S. Rovio, K. Marjamaa, T. Tamminen, O.J. Rojas, K. Kruus, Inhibitory effect of lignin during cellulose bioconversion: the effect of lignin chemistry on non-productive enzyme adsorption. Bioresource Technol., 133 (2013) 270–278.

[3] S. Li, K. Lundquist, Cleavage of arylglycerol β-aryl ethers under neutral and acid conditions, Nordic Pulp Paper Res. J. 15 (2000) 292-299.

[4] J. Li, G. Henriksson, G. Gellerstedt Lignin depolymerization/repolymerization and its critical role for delignification of aspen wood by steam explosion. Bioresource Technology 98 (2007) 3061-3068.

[5] H. Nimz, A new type of rearrangement in the lignin field, Angew. Chem. 5 (1966) 843.

[6] J. Li, G. Gellerstedt, K. Toven, Steam explosion lignins; their extraction, structure and potential as feedstock for biodiesel and chemicals, Bioresource Technology 100 (2009) 2556-2561.

[7] A. Granata, D.S. Argyropoulos, 2-Chloro-4,4,5,5-tetramethyl-1,3,2-dioxaphospholane, a reagent for the accurate determination of the uncondensed and condensed phenolic moieties in lignins. J. Agric. Food Chem. 43 (1995) 1538-1544.

[8] C. Zwahlen, P. Legault, S. J. F. Vincent, J. Greenblatt, R. Konrat, L. E. Kay. Methods for Measurement of Intermolecular NOEs by Multinuclear NMR Spectroscopy: Application to a Bacteriophage λ N-Peptide/boxB RNA Complex J. Am. Chem. Soc. 119 (1997) 6711-6721.

[9] J. C. del Río, J. Rencoret, P. Prinsen, A. T. Martínez, J. Ralph, A. Gutiérrez , Structural characterization of wheat straw lignin as revealed by analytical pyrolysis, 2D-NMR and reductive cleavage methods. Journal of Agricultural and Food Chemistry 60 (2012) 5922-5935.

EFFECT OF LIGNIN CHEMISTRY ON NON-PRODUCTIVE ENZYME ADSORPTION IN THE ENZYMATIC HYDROLYSIS OF LIGNOCELLULOSE

Jenni Rahikainen[1], Raquel Martin-Sampedro[2], Harri Heikkinen[1], Stella Rovio[1], Kaisa Marjamaa[1], Tarja Tamminen[1], Orlando J. Rojas[2,3] and Kristiina Kruus[1]*

*[1]VTT Technical Research Centre of Finland, Espoo, Finland; [2]Aalto University, Department of Forest Products Technology, Espoo, Finland; [3]North Carolina State University, Department of Forest Biomaterials and Department of Chemical and Biomolecular Engineering, Raleigh, USA;*corresponding author: kristiina.kruus@vtt.fi*

ABSTRACT

Lignin is an inhibitory compound in the enzymatic hydrolysis of lignocellulosic feedstocks. Non-productive enzyme adsorption onto lignin and subsequent enzyme inactivation is a major inhibitory mechanism that increases the enzyme dosage and thus the costs, it also restricts enzyme recycling especially with softwood feedstocks. The underlying mechanisms causing non-productive enzyme adsorption have remained mostly unsolved. This paper describes interactions of the major *Trichoderma reesei* cellobiohydrolase Cel7A and its catalytic core domain with well-characterized isolated lignins from different botanical origin, namely from spruce and wheat straw. Both non-treated and steam explosion (SE) pretreated lignocellulosic materials were used for lignin isolation and subsequent preparation of ultrathin lignin films for enzyme adsorption studies. We applied quartz crystal microbalance (QCM) technique for real-time monitoring of enzyme adsorption onto the different lignin films. Interestingly, more enzyme was bound onto the lignin films prepared of steam pretreated materials, whereas botanical origin of lignin had only a minor effect on enzyme binding.

I. INTRODUCTION

Enzymatic hydrolysis of lignocellulosic polysaccharides to monomeric sugars is an attractive process for the production of fermentable sugars for fuel and chemical industry. Biomass pretreatment, which increases enzyme accessibility to the plant polysaccharides, is needed to reach feasible sugar yields in the process. Today, steam pretreatment technologies that preserve lignin insoluble together with the cellulosic fraction are widely employed in demonstration and industrial scale plants. Lignin is an inhibitory compound for the hydrolytic enzymes and non-productive enzyme adsorption onto lignin has been identified as a major inhibitory mechanism, especially with softwood substrates [1]. Interestingly, non-productive adsorption is less pronounced with agricultural residues [2]. The differences in lignin chemistry that result in differences in non-productive enzyme adsorption are poorly understood; for instance, it has remained unclear whether the differences in non-productive binding are due to botanical differences in lignin structure or due to differences in pretreatment conditions. Therefore, in this study, lignins were isolated from steam explosion (SE) pretreated and non-treated spruce and wheat straw and used for preparing ultrathin lignin films for quartz crystal microbalance (QCM) adsorption experiments. QCM is a surface-sensitive technique that can be used to quantify adsorption and desorption phenomena on a solid-liquid interface in real-time.

II. EXPERIMENTAL

Enzymes, lignocellulosic materials and isolation of enzymatic mild acidolysis lignin (EMAL)

Wheat straw (*Triticum aestivum*) and spruce chips (*Picea abies*) were obtained from MTT Agrifood Research (Jokioinen, Finland) and UPM Research Centre (Lappeenranta, Finland), respectively. Both materials were milled through a 1 cm screen and subjected to a non-catalysed steam pretreatment (15.5 bar, 200℃, 10 min). Lignin was isolated from non-treated and steam pretreated spruce and wheat straw using the enzymatic mild acidolysis procedure (EMAL) [3] with optimized enzyme treatments [4,5].
Trichoderma reesei Cel7A (*Tr*Cel7A, CBHI) and the corresponding enzyme without a carbohydrate binding module (*Tr*Cel7A core) were purified as described in [5] and [6], respectively.

Preparation of ultrathin lignin films

The four EMAL lignin preparations were dissolved (5 g/L) in 25% (w/w) aqueous ammonia for at least 48 h until a clear solution was obtained. The lignin solutions were filtered through a 0.2 µm cellulose-acetate filter prior to film preparation. The lignin films were prepared by spin-coating directly onto purified silica QCM sensors (QSX 303; Q-Sense, Sweden). Ca. 200 µl of lignin solution was applied onto a QCM sensor, after which the following spinning program was started: 1 min, 2000 rpm, acceleration 2000 rpm/s. The coating procedure was repeated for

three times after which the coated sensors were incubated at 40°C for 1 h. The coated sensors were stored at room temperature prior to the enzyme binding experiments.

Characterisation of the lignin films

The spin-coated lignin films were visualized by AFM using a Nanoscope IIIa Multimode scanning probe microscope (Digital Instruments Inc., CA, USA) and silicon cantilevers (NSC15/AIBS, Micromasch, Tallinn, Estonia). The microscope was operated in tapping-mode in air. Film thickness was determined by scratching the lignin film with a sharp needle and by height profiling the formed groove with AFM. Water contact angles of the films were analysed with CAM-200 contact angle goniometer (KSV instruments Ltd., Finland) after immersing the films into ultrapure water for 4 hours and drying. Chemical composition of the film surfaces were studied with XPS spectrophotometer AXIS 165 (Kratos Analytical, UK) wih a monochromated Al Kα X-ray source.

Quartz crystal microbalance (QCM) technique to study enzyme adsorption onto lignin films

The binding experiments were run in duplicats at 40°C using a quartz crystal microbalance (model E4, Q-Sense, Sweden). In each measurement, 3.9 µM enzyme was fed to the system with a constant flow of 0.1 ml/min. Each experiment was finalized by rinsing the system with 50 mM Na-acetate pH 5 buffer only. All measurements were recorded at 5 MHz fundamental resonance frequency and its overtones corresponding to 15, 25, 35, 55 and 75 MHz. The third overtone values (15 MHz) were used for data processing.

III. RESULTS AND DISCUSSION

Ultrathin lignin films were prepared onto QCM sensors using isolated EMAL lignins from steam explosion (SE) pretreated and non-treated spruce and wheat straw. AFM height images of the spin-coated lignin films showed that in all cases lignin was evenly distributed on the sensor surface (Figure 1 A-D). Roughness values (Rq) of the films ranged from 4.16 nm to 5.29 nm. In general, these values are higher than some previously reported values for lignin films (0.93-1.38 nm in [7]). With higher magnification (Figure 1 E-F) it can be seen that the film surface is composed of small 10-60 nm globular aggregates that are clustered together. Similar surface morphologies have been previously reported for lignin films [7].

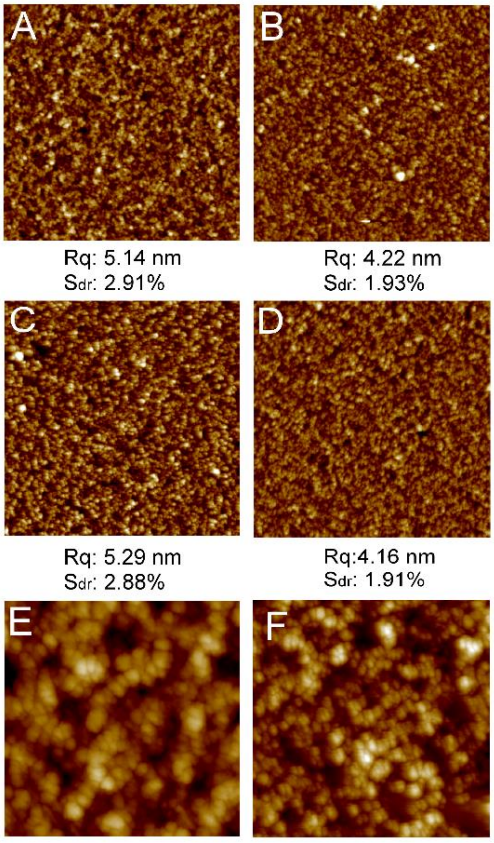

Figure 1. AFM height images of spin coated lignin films: A) Spruce EMAL (5x5 µm), B) Steam explosion pretreated spruce EMAL (5x5 µm), C) Wheat straw EMAL (5x5 µm), D) Steam explosion pretreated wheat straw EMAL (5x5 µm), E) Spruce EMAL (1x1 µm) and F) Wheat straw EMAL (1x1 µm). Surface roughness values (R_q, nm) and ratios of effective surface area and projected surface area (S_{dr}, %) are shown for A–D below each image. Z-scale for all images is 37 nm.

Film thicknesses indicated that the silica sensors were fully covered with lignin polymer in the coating procedure (Table 1), however, in the XPS analysis Si was found to account for 1-5 % of the atomic concentrations of the film surfaces (Table 2) which typically suggests that the underlying silica layer is not fully covered. In further analysis

with Py-GC/MS it was found that the EMAL lignins were contaminated with silica (data not shown). This silica originates likely from industrial grade balls used in the ball milling step of lignin isolation. Nitrogen, which accounts for 2-4 % of the atomic concentration on film surface, is originating from the enzymes used in lignin isolation as well as from the ammonia used in dissolving the lignin samples before film coating. The XPS results show that the SE-treatment decreases the proportion of oxygen and increases the proportion of carbon at the film surface (Table 2). This is likely due to degradation of ether-bonds and formation of condensed structures in the SE treatment [5]. Unexpectedly the water contact angle (WCA) values were lower for SE pretreated films compared to the non-treated films suggesting that the hydrophobicity of lignin is not increasing in SE treatment, which has been proposed in earlier studies [2]. On the other hand, the SE pretreated films were slightly smoother in structure compared to the non-treated films (Figure 1), which may affect the WCA measurement. Water contact angles (WCA) of the lignin films varied between 45.7° and 58.2°. Previously a WCA value 52.5° has been reported for a lignin film prepared from softwood milled wood lignin [7], which is similar to the value obtained for spruce EMAL (51.9°).

Table 1. Properties of ultrathin lignin films. SE=steam explosion, EMAL=enzymatic mild acidolysis lignin

Lignin film	Thickness [nm]	Water contact angle
Spruce EMAL	17.0 ± 2.8	51.9 ° ± 0.1
SE pretreated spruce EMAL	17.0 ± 6.6	45.7° ± 0.8
Wheat straw EMAL	13.7 ± 4.1	58.2° ± 0.4
SE pretreated wheat straw EMAL	9.6 ± 2.9	53.0° ± 0.3

Table 2. Surface chemistry of ultrathin lignin films studied by X-ray photoelectron spectroscopy

	Atomic concentrations (%)			
	O (1s)	C (1s)	N (1s)	Si (2p)
Spruce EMAL	25±1.1	72±1.1	2±0.3	2±0.2
SE pretreated spruce EMAL	22±1.3	74±1.6	2±0.2	1±0.3
Wheat straw EMAL	24±0.2	69±0.5	2±0.6	5±0.1
SE pretreated wheat straw EMAL	22±0.4	73±0.4	4±0.5	2±0.1

Two pure monocomponent cellulase enzymes, *Trichoderma reesei* Cel7A (CBHI, *Tr*Cel7A) and the corresponding enzyme without a carbohydrate binding module (*Tr*Cel7A core) were employed in the QCM adsorption studies. TrCel7A is the major enzyme component in the *T. reesei* enzyme mixture accounting typically ca. 60% of total protein.

The four lignin films were found to adsorb the enzymes to a different extent and most prominently, the SE pretreated lignin films were found to adsorb both *Tr*Cel7A (Figure 2A) and *Tr*Cel7A core (Figure 2B) substantially more than the non-treated lignin films. Among the SE pretreated films, the film prepared from SE pretreated spruce EMAL was found to adsorb slightly more of *Tr*Cel7A than the film prepared from SE pretreated wheat straw EMAL (Figure 2A). Similarly, the film prepared from non-treated spruce EMAL was found to adsorb TeCel7A slightly more than the film prepared from non-treated wheat straw EMAL (Figure 2A). It may be concluded that the botanical differences in lignin chemistry had minor effect on enzyme binding, whereas the effect of pretreatment was more profound.

Carbohydrate binding module (CBM) of *Tr*Cel7A was shown to significantly increase enzyme adsorption onto lignin films (Figure 2) which has also been shown in a previous study [8]. The aromatic amino acids responsible for CBM-cellulose interactions are also shown to have a major contribution in CBM-lignin interactions [9]. Therefore, hydrophobic interactions are likely responsible for the higher binding of *Tr*Cel7A compared to the *Tr*Cel7A core. Hydrophobic, electrostatic and H-bonding interactions are all suggested to contribute to non-productive enzyme binding and therefore underlying mechanism(s) that cause increased enzyme binding onto SE pretreated lignins may thus be complex and difficult to reveal.

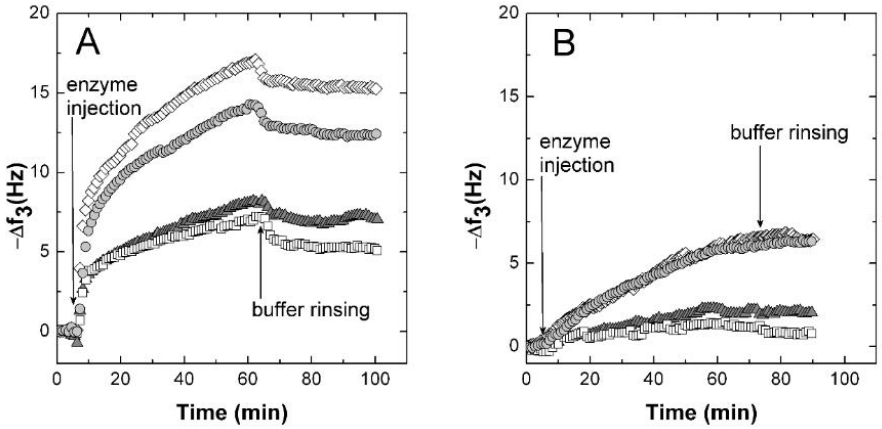

Figure 2. Enzyme binding onto the ultrathin lignin films: ▲ Spruce EMAL lignin, ◊ SE-pretreated spruce EMAL lignin, □ Wheat straw EMAL lignin and ● SE-pretreated wheat straw EMAL lignin. Continuous injection of A) *Trichoderma reesei* Cel7A (CBHI) and B) *T. reesei* Cel7A-core domain at 40˚C. Negative shift in QCM frequency, corresponding to mass addition on the lignin film, is shown as a function of time. Image reproduced with permission from the publisher [5]

IV. CONCLUSIONS

Homogeneous and ultrathin lignin films were successfully generated by spin-coating isolated EMAL lignins from steam pretreated and non-treated spruce and wheat straw. The films were employed to study non-productive cellulase adsorption using quartz crystal microbalance (QCM) technique. Steam pretreatment was found to alter lignin structure in such way that it increased non-productive enzyme adsorption, whereas botanical differences in lignin structure had only minor effect on non-productive binding. Better control over the chemical reactions of lignin in steam pretreatments could alleviate the problems arising from non-productive enzyme adsorption.

V. ACKNOWLEDGEMENT

This work was enabled by funding from Graduate School for Biomass Refining (Academy of Finland), EU-projects DISCO (Grant Agreement No. 211863) and HYPE (Grant Agreement No. 213139) and FiDiPro LignoCell-project (Finnish Funding Agency for Technology and Innovation (TEKES) and Academy of Finland. Taina Ohra-aho and Leena-Sisko Johansson are acknowledged for performing the Py-GC/MS and XPS analysis, respectively.

VI. REFERENCES

[1] Kumar, L.; Arantes, V.; Chandra, R.; Saddler, J. The lignin present in steam pretreated softwood binds enzymes and limits cellulose accessibility. Bioresour. Technol. 2012, 103, 201-208.
[2] Nakagame, S.; Chandra, R.P.; Saddler, J.N. The Effect of Isolated Lignins, Obtained From a Range of Pretreated Lignocellulosic Substrates, on Enzymatic Hydrolysis. Biotechnol. Bioeng. 2010, 105, 871-879.
[3] Wu, S.; Argyropoulos, D.S. An improved method for isolating lignin in high yield and purity. J. Pulp Pap. Sci. 2003, 29, 235-240.
[4] Rahikainen, J.; Heikkinen, H.; Rovio, S.; Tamminen, T.; Marjamaa, K.; Kruus, K. Lignin isolation and characterisation for cellulase adsorption and inhibition studies. 12th European Workshop on Lignocellulosics and Pulp, 27-30 of August 2012, Espoo, Finland.
[5] Rahikainen, J.L.; Martin-Sampedro, R.; Heikkinen, H.; Rovio, S.; Marjamaa, K.; Tamminen, T.; Rojas, O.J.; Kruus, K. Inhibitory effect of lignin during cellulose bioconversion: the effect of lignin chemistry on non-productive enzyme adsorption. Bioresour. Technol. 2013, 133, 270–278.
[6] Suurnäkki, A.; Tenkanen, M.; Siika-aho, M.; Niku-Paavola, M.-L.; Viikari, L.; Buchert, J. Trichoderma reesei cellulases and their core domains in the hydrolysis and modification of chemical pulp. Cellulose 2000, 7, 189-209.
[7] Notley, S.M.; Norgren, M. Surface energy and wettability of spin-coated thin films of lignin isolated from wood. Langmuir 2010, 26, 5484-5490.
[8] Palonen, H.; Tjerneld, F.; Zacchi, G.; Tenkanen, M. Adsorption of Trichoderma reesei CBH I and EG II and their catalytic domains on steam pretreated softwood and isolated lignin. J. Biotechnol. 2004, 107, 65-72.
[9] Rahikainen, J.L.; Evans, J.D.; Mikander, S.; Kalliola, A.; Puranen, T; Tamminen, T.; Marjamaa, K.; Kruus, K. Cellulase-lignin interactions – the role carbohydrate-binding module and pH in non-productive binding. Enzyme Microb. Technol. 2013, 35, 315-321.

REDESIGNING LIGNIN FOR IMPROVED PLANT CELL WALL DECONSTRUCTION – RECENT DEVELOPMENTS

John Ralph,[1,2] Fachuang Lu,[1,2] Hoon Kim,[1,2] Yuki Tobimatsu,[1,2] Yimin Zhu,[1] Jorge Rencoret,[1] Steven Karlen,[2] Dharshana Padmakshan,[2] Sarah Liu,[2] Matt Regner,[1,2] Sally A. Ralph,[3] John Grabber,[4] Ron Hatfield,[4] Jane Marita,[4] Wout Boerjan,[5] Rick Dixon,[6] John Sedbrook,[2,7] Curtis Wilkerson,[8] Nick Santoro,[8] Shawn Mansfield,[9] and Many More Wonderful Collaborators!

[1]Dept. Biochemistry, U. Wisconsin, Madison, WI, USA; [2]Great Lakes Bioenergy Research Center, Wisconsin Energy Institute, U. Wisconsin, Madison, WI, USA; [3]U.S. Forest Products Laboratory, USDA-Forest Service, Madison, WI, USA; [4]U.S. Dairy Forage Research Center, USDA-ARS, Madison, WI, USA; [5]Dept. Plant Systems Biology, VIB, and Dept. Molecular Genetics, Ghent University, Gent, Belgium; [6]Dept. Biological Sciences, U. North Texas, Denton, TX, USA; [7]Dept. Biological Sciences, Illinois State U., Normal, IL, USA; [8]Dept. Plant Biology, and the Great Lakes Bioenergy Research Center, Michigan State U., East Lansing, MI, USA; [9]Dept. Wood Science, U. British Columbia, Vancouver, BC, Canada

ABSTRACT

Redesigning lignin, the aromatic polymer fortifying plant cell walls, to be more amenable to chemical depolymerization can lower the energy required for industrial processing. We have engineered Poplar trees to introduce ester linkages into the lignin polymer backbone by augmenting the monomer pool with monolignol ferulate conjugates. Herein, we describe the isolation of a transferase gene capable of forming these conjugates, and its xylem-specific introduction into Poplar. Enzyme kinetics, *in planta* expression, lignin structural analysis, and improved cell wall digestibility after mild alkaline pretreatment, demonstrate that these trees produce the monolignol ferulate conjugates, export them to the wall, and utilize them during lignification. Tailoring plants to employ such conjugates during cell wall biosynthesis is a promising way to produce plants that are "designed for deconstruction."

I. INTRODUCTION

Lignin is a complex phenolic polymer that is essential for plant growth and development, but concurrently acts as a major impediment to industrial processing. Research efforts globally have therefore focused on altering the natural lignification processes to produce plants with cell walls that process more readily to, for example, liberate carbohydrates with minimal inputs [1-5]. The biosynthetic steps to produce the monomers employed in the synthesis of lignin have been elucidated [1, 4, 5], although new genes continue to be discovered [6, 7], and several transcription factors integral to controlling the lignin biosynthetic network have been identified [8]. It was also empirically discovered that some perturbations led to the synthesis of lignins that incorporated alternative monomers, usually derived from products of incomplete monolignol biosynthesis, spawning the idea that lignins could be designed to encompass significant structural alterations that would engender unique properties [4, 9, 10].

Studies of natural plant tissues, along with those from mutants and transgenics with misregulated monolignol biosynthetic genes, have led to some remarkable discoveries, including plants that produce homopolymers from a range of 'traditional' (*e.g.*, *p*-coumaryl and sinapyl alcohols [11, 12]) as well as 'non-traditional' monomers (*e.g.*, caffeyl and 5-hydroxyconiferyl alcohols, and the hydroxycinnamaldehydes [13-16]). These observations clearly illustrate the inherent pliability of the lignification process [4, 10, 17]. The formal 'design' of an improved polymer using unconventional monomers therefore seems to be a feasible path to tailor plants with superior processing properties for both paper and biofuels production [9, 10]. To that end, the introduction of monolignol ferulate conjugates **2** (**Figure 1**), into the lignin monomer pool appears to be one of the most promising. These exotic conjugates have been shown, but to date only in *in vitro* model systems, to be capable of introducing readily cleavable ester bonds in the lignin backbone, permitting easier depolymerization [10, 18]. Three lines of independent research precipitated the idea that it would be possible to engineer plants to produce such conjugates for lignification. First, although plants have not been shown to use monolignol ferulate conjugates for lignification, all grasses use analogous monolignol *p*-coumarate conjugates (**Figure 1**, *p*-coumarate analogs of **2** without the F-ring methoxyl) [10, 19]. However, due to their preference for radical transfer over radical coupling [10], *p*-coumarates do not polymerize into growing lignin chains and consequently remain almost entirely as free-phenolic pendent entities. Second, unlike the *p*-coumarate moiety, the ferulate, with an additional methoxyl group, is compatible with normal

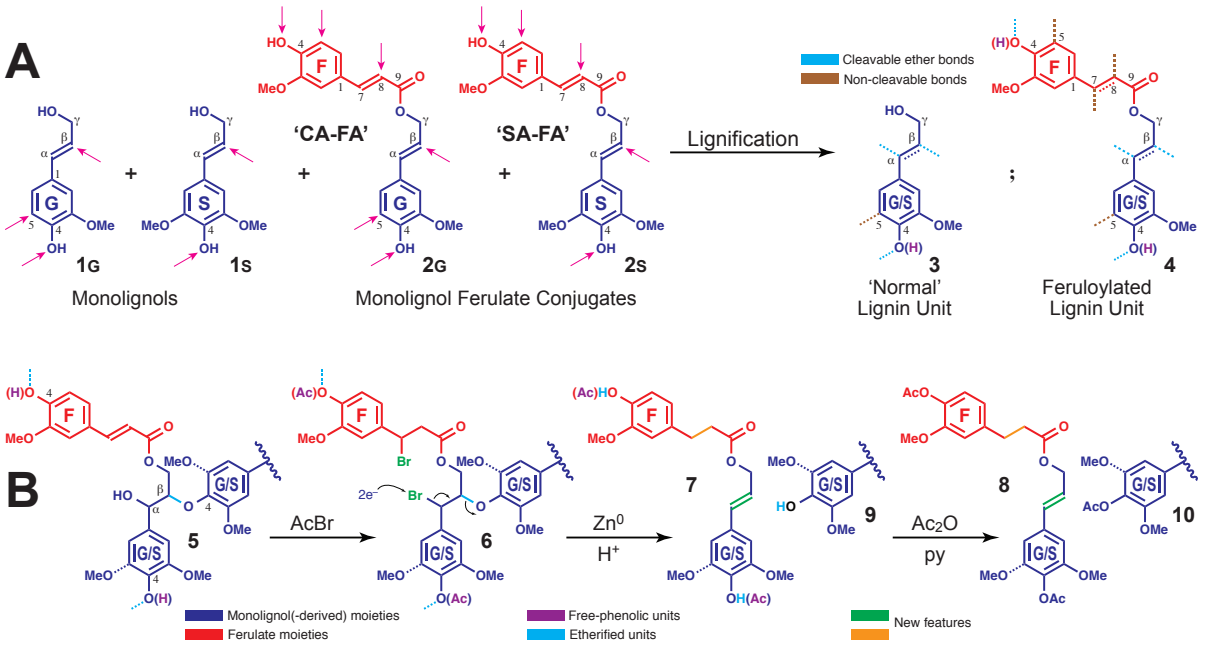

Figure 1. General schemes for lignification and a method to provide evidence for monolignol ferulate conjugate incorporation into lignins. A) Lignification of monolignols **1**, by combinatorial radical cross-coupling reactions, produces a lignin in which the units can be represented by generic structure **3**. Analogous lignification of monolignol ferulate conjugates **2** produces structural units **4** in which lignin moieties are γ-acylated by ferulate. Sites of radical coupling for the monolignols **1** and the conjugates **2** are indicated by magenta arrows. In the final lignin units **3** and **4**, cleavable ether bonds are indicated by dotted bonds in cyan, non-cleavable bonds in brown. B) The DFRC method releases conjugates **8** that diagnostically result from structures **5** within the lignin; the crucial double bond (colored green in **8**) arises only upon cleavage of the signature lignin β-ether bonds, and the ferulate moiety remains attached to its parent unit. Thus, the DFRC method releases an acetylated dihydroferulate analog **8** of the monolignol ferulate conjugate **2** that was incorporated into the lignin, via reactions that specifically cleave lignin β-ethers but leave the γ-esters intact. As the initially free-phenolic *vs*. etherified units are acetate-tagged differentially at the stage of intermediate **7**, acetylation with perdeuteroacetic anhydride in the final step can fully reveal the etherification profile of the released units, as they were in the cell wall.

lignification reactions and can integrally incorporate into the polymer [10]. Polysaccharide-lignin cross-linking results in grasses where the arabinoxylan-bound ferulates (or the diferulates that derive from them by radical dehydrodimerization) radically cross-couple with lignin monomers and higher oligomers during lignification [10]. The full compatibility of ferulate with lignification leads to complex homo- and cross-coupling that renders its products difficult to detect in the lignin polymer, and makes it currently impossible to accurately quantify the extent of its incorporation [10]. As the monolignol ferulate conjugate has two phenolic moieties, it incorporates in a manner that produces ester bonds in the lignin backbone (as schematically shown in **Figure 1**). Third, the substantial research characterizing natural plant lignins and a range of monolignol biosynthetic pathway mutants and transgenic plants with misexpressed biosynthetic genes, revealed that the process of lignification is metabolically plastic; various non-monolignol phenolic monomers have been shown to actively participate in lignification [3-5, 9, 10, 17]. In fact, due to the combinatorial chemical nature of lignification, and the established theory that the polymerization process is not protein- or enzyme-mediated [17], it is logical that a phenolic compound proximal to lignifying tissue may incorporate into lignin subject to its chemical compatibility – its ability to form radicals and to couple and cross-couple with the available phenolics. If a plant could therefore synthesize the monolignol ferulate conjugates **2** with the appropriate temporal and spatial control, and had the ability to transport them to the developing wall, the conjugates would ultimately incorporate into the growing lignin polymer [10]. Recent studies using a corn cell wall synthetic model system clearly demonstrated the feasibility of incorporating such conjugates into lignin and supported the need to implement such a strategy *in planta* [18].

II. EXPERIMENTAL

Experimental details can be now found in the Supplementary Material of Reference [20].

III. RESULTS AND DISCUSSION

The first requirement was to obtain the gene coding for a protein/enzyme capable of catalyzing the formation of the conjugate, a feruloyl-CoA monolignol transferase (FMT). Evidence for the existence of such a gene was found in the Chinese medicinal 'Dong quai' or Chinese Angelica (*Angelica sinensis*) in which the root tissue inherently contained ~2 wt% coniferyl ferulate [21]. Deep EST sequencing led to discovery of many BAHD transferases. The second most abundant transcript had only moderate similarity to any putative Arabidopsis gene (Arabidopsis is not known to make such ferulate conjugates), and ultimately produced a recombinant protein in *E. coli* with the desired transferase activities, namely high activity with feruloyl-CoA and low activity with *p*-coumaroyl-CoA. Such selectivity ensures that the enzyme would not use *p*-coumarate to produce monolignol *p*-coumarate conjugates that, as we know from grasses, do not introduce ester bonds into the lignin backbone. Additionally, the enzyme could employ any of the three monolignols as a target substrate.

A key additional step consisted of expressing the gene spatially and temporally in the tissues that form lignin. This was successfully achieved in hybrid Poplar (*Populus alba* × *grandidentata*) using both a universal *35S* promoter and the Poplar *CesA8* xylem-specific promoter involved in secondary cell wall cellulose biosynthesis. Fusion with a YFP reporter gene demonstrated that the protein was indeed being produced, and facilitated localization for each promoter employed. Examination of leaf extracts showed that, unlike in the control plants, FMT protein was being produced *in planta* in many tissues in the case of the ubiquitous promoter, and only in the leaf vasculature (xylem) when the *CesA8* promoter was employed (**Figure 2**). We subsequently isolated the FMT protein from these plants and demonstrated *in vitro* that it was able to produce the target conjugates from its substrates, feruloyl-CoA and a monolignol. In all cases, the plants showed no phenotypic growth abnormalities in the greenhouse (**Figure 2**). The total lignin levels generally remain the same as in wild-type (WT) controls, and displayed only a very slight consistent increase in the syringyl to guaiacyl (S/G) ratio.

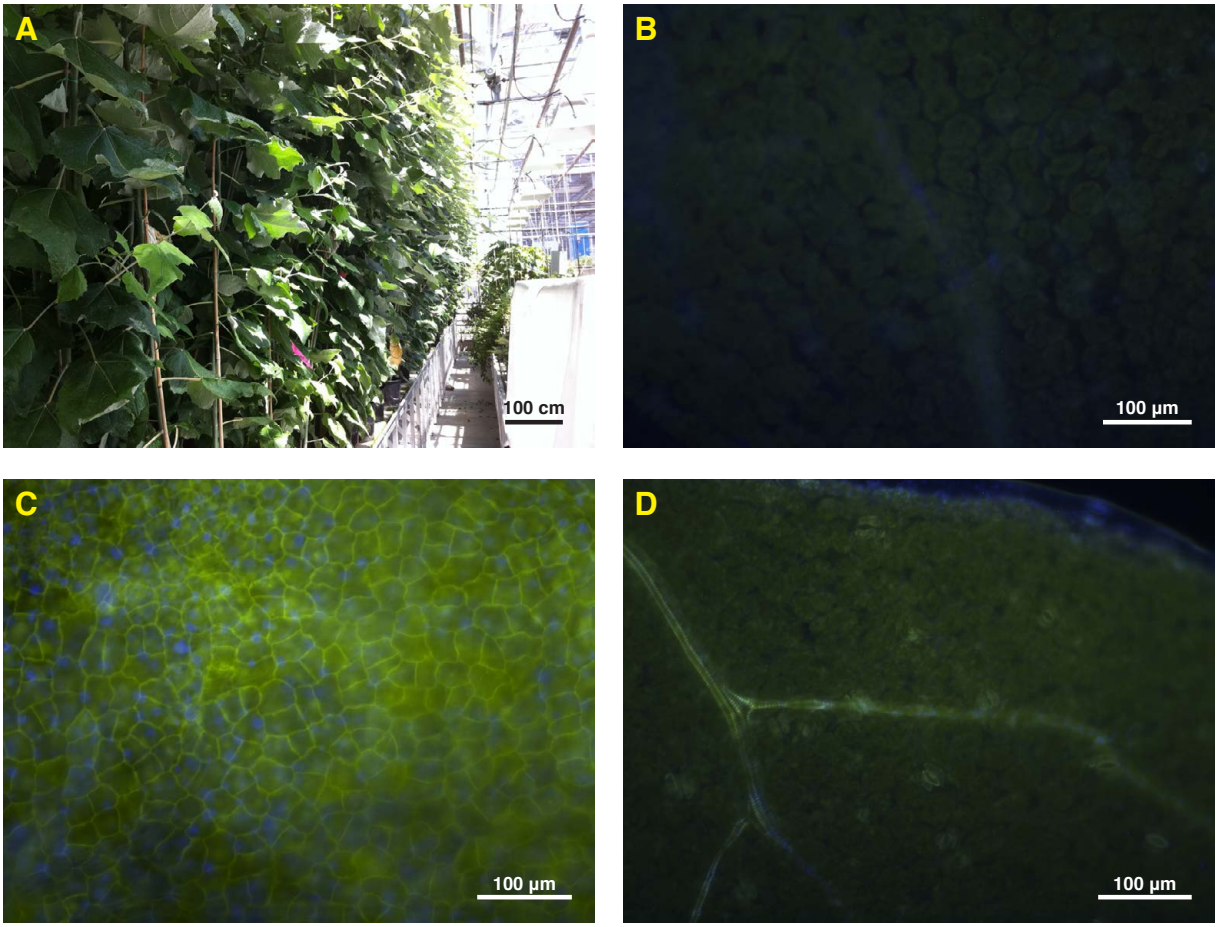

Figure 2. Images showing YFP-tagged FMT protein in Poplar leaves from transgenics in which the *Angelica sinensis FMT* gene was driven by the universal *35S* or the Poplar xylem-specific *CesA8* promoter. A) Poplar FMT transgenics growing in the greenhouse do not display any visible phenotypic differences from WT. B) Non-transgenic control line, C) *35S::FMT*, showing universal FMT expression. D) *CesA8::FMT* line showing vascular-tissue-specific FMT expression.

Unequivocally determining that these plants are capable of incorporating monolignol ferulates into the lignin polymer is particularly challenging because ferulate is naturally integrally incorporated into lignins by combinatorial radical coupling. However, Derivatization Followed by Reductive Cleavage (DFRC) is capable of cleaving the lignin-signature β-ether bonds but leaves γ-esters intact, and has previously been used to analyze *p*-coumaroylated lignins [22]. Using modifications to this method, we were able to show that the novel monolignol ferulates, coniferyl ferulate **2G** and sinapyl ferulate **2S** (**Figure 1**), are indeed incorporated into the lignin of the transgenic trees. Thus, a small fraction of the expected structures **5** in the polymer that would result from incorporating monolignol ferulate conjugates into lignins (**Figure 1**) can be cleaved, releasing monolignol (dihydro)ferulate conjugates **8** that are quantifiable by GC-MS (**Figure 1B**). Importantly, the double bond in the monolignol moiety of **8**, as in the normal DFRC monomers, arises *only* from reductively cleaving the β-ether bond. Compounds **8** are therefore diagnostic markers indicating that the monolignol ferulate conjugate **2** has incorporated into the polymer by radical coupling. However, structures **5** shown in **Figure 1B** are only a small fraction of the many structures (represented by the generic structure **4**) that can result when the combinatorial radical coupling reactions incorporate monolignol ferulates into lignin, but they are the only components that can generate the diagnostic product **8** (**Figure 3**). The methodology does, however, permit confirmation that the trees have incorporated monolignol ferulates, at levels markedly above those of wild type, into the lignin polymer by the radical coupling reactions that typify lignification (**Figure 1A**). Importantly, it indicates that, like the natural monolignol *p*-coumarate analogs in grasses, these non-native monolignol ferulate conjugates are transported intact to the lignifying zone. The GC-MS evidence (**Figure 3**) that our transgenic Poplars, particularly lines with the *FMT* gene driven by the xylem-specific *CesA8* promoter, are performing all of the biochemistry and chemistry desired, is therefore rather compelling.

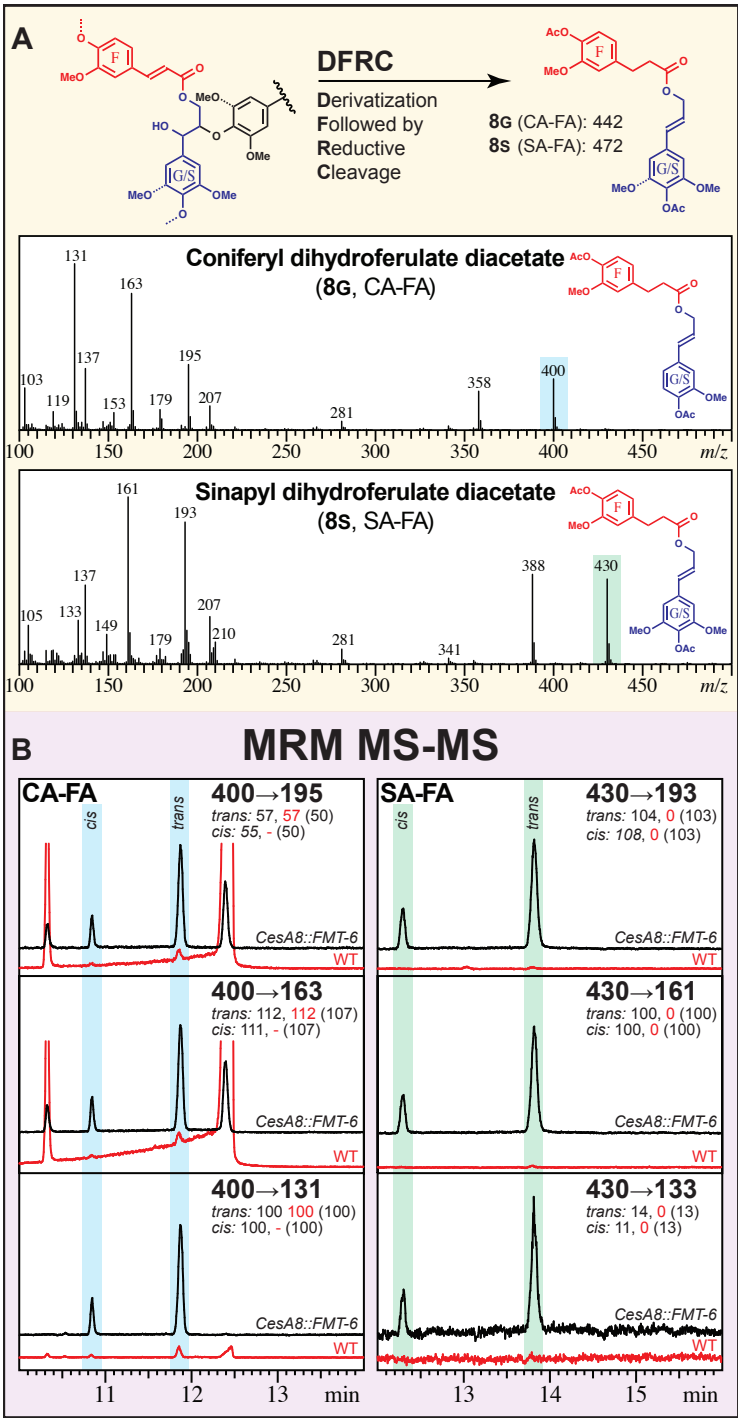

Figure 3. Mass spectrometric evidence for the incorporation of monolignol ferulate conjugates into transgenic Poplar lignins. A) DFRC releasable conjugate **8**; Mass spectra for synthetic compounds **8G** and **8S** are from Q3 scans on a GC-triple-quad MS: molecular ions (*m/z* 442, 472) lose ketene (*m/z* 42) to yield the base peak (*m/z* 400, 430). B) Triple-quad MRM chromatograms of the Poplar-derived *m/z* 400 parent ion to the diagnostic 195, 163, and 131 product ions and *m/z* 430 parent ion to the 193, 161, and 133 product ions; the numbers for the *cis*- and *trans*-isomers are the MRM intensities for transgenic *CesA8::FMT-6* in black and wild-type in red (with the corresponding measured intensities from the synthetic standards in parentheses) relative to the 400→131 (CA-FA) and 430→161 (SA-FA) peak for each. All of the data for the Poplar-released conjugates match (by retention times, mass spectra, collision-induced fragmentation, and MRM relative intensities of daughter ions), providing evidence for the release of the diagnostic conjugates from the lignin in transgenic Poplars.

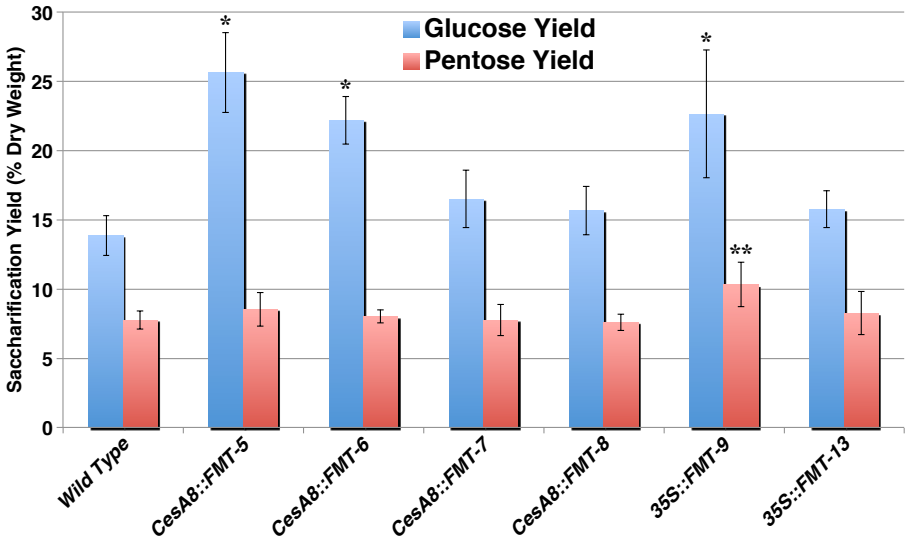

Figure 4. Digestibility data on various mild-alkaline-pretreated transgenic Poplar lines compared to wild type.

A key feature that allows the ensuing modified lignin to be depolymerized under mild conditions is the incorporation of the ferulate unit into the lignin backbone rather than simply existing as a pendant unit. Further insight into how well the conjugates are incorporated is revealed following an isotopically-labeled-reagent modification to the DFRC method [23]. We determined that 53% of the ferulate and 53% of the coniferyl alcohol moieties in the releasable conjugates were from phenol-etherified units, and 36% resulted from units that have both ends of the conjugate etherified. As only a small fraction of units can release the conjugate, and because the double bond in the coniferyl alcohol moiety implies that it is derived from a β-etherified unit, an etherified phenolic level comparable to that of guaiacyl monomers released by DFRC, determined in the same runs here at ~50%, confirms that the conjugate is incorporated into the lignin polymer approximately as well as a conventional monolignol.

Quantifying the level of conjugate incorporation is also a challenge. Currently, no method exists for the analogous quantification of the arabinoxylan-bound ferulates that are incorporated into grass lignins, and it has remained extremely difficult to even detect them, *e.g.*, by NMR, decades after their discovery due in part to the huge range of combinatorial products. An estimate can be made using a model system in which isolated cell walls were ectopically lignified with coniferyl alcohol and 0, 20, 40, and 60% coniferyl ferulate [18]. By plotting the release of the DFRC conjugate in the model system and those released from the current transgenic lines, we estimate that the *CesA8::FMT* Poplar trees are incorporating ~7-23% of the ferulate conjugates **2** into their lignins.

The utility of lignins altered in such a fashion is ultimately determined by how well the ensuing cell walls containing these specialized conjugates can be processed industrially. Significant improvements in saccharification following mild alkaline (6.25 mM NaOH, 90 °C, 3 h) pretreatment [24] are evident in the lines determined to contain high levels of transcripts, proteins, and lignified ferulate conjugates (**Figure 4**).

IV. CONCLUSIONS

The initial concept of inducing plants to use monolignol ferulate conjugates during lignification is clearly realized here; our approach appears to be capable of producing plant materials that are "designed for deconstruction." In a fundamental sense, it supports the idea that we can exploit the inherent metabolic plasticity of lignification [4] to alter lignins for societal benefit by inducing plants to synthesize novel phenolic monomers that are compatible with inherent plant biochemistry and development. The strategic introduction of ester bonds into the backbone of the lignin polymer is an advance that portends the production of crop plants in which cell wall deconstruction can be realized with reduced energy and/or chemical inputs.

V. ACKNOWLEDGEMENT

This work was funded by the DOE Great Lakes Bioenergy Research Center (DOE BER Office of Science DE-FC02-07ER64494). The redesigned polymer presented herein has become known as Zip-lignin™; the method for plant modification and the use of the gene for altering plants have been patented [25]. *Angelica sinensis* plants were obtained with the help of Joe Hollis at Mountain Garden Herbs in Burnsville, NC. The DNA sequence for the *AsFMT* gene (see Supplementary Info) has been deposited in GenBank (http://www.ncbi.nlm.nih.gov/nuccore/JA758320.1) under the accession number JA758320.1.

VI. REFERENCES

[1] Li, X.; Weng, J.K.; Chapple, C. Improvement of biomass through lignin modification. *Plant Journal* **2008,** *54*, 569-581.

[2] Chen, F.; Dixon, R.A. Lignin modification improves fermentable sugar yields for biofuel production. *Nature Biotechnology* **2007,** *25*, 759-761.

[3] Vanholme, R.; Morreel, K.; Ralph, J.; Boerjan, W. Lignin engineering. *Current Opinion in Plant Biology* **2008,** *11*, 278-285.

[4] Ralph, J., Lundquist, K., Brunow, G. Lu, F., Kim, H., Schatz, P. F., Marita, J. M., Hatfield, R. D., Ralph, S. A. Christensen, J. H., Boerjan, W. Lignins: natural polymers from oxidative coupling of 4-hydroxyphenylpropanoids. *Phytochemistry Reviews* **2004,** *3*, 29-60.

[5] Boerjan, W.; Ralph, J.; Baucher, M. Lignin biosynthesis. *Annual Reviews in Plant Biology* **2003,** *54*, 519-549.

[6] Vanholme, R.; Cesarino, I.; Rataj, K.; Xiao, Y.; Sundin, L.; Goeminne, G.; Kim, H.; Cross, J.; Morreel, K.; Araujo, P.; Welsh, L.; Haustraete, J.; McClellan, C.; Vanholme, B.; Ralph, J.; Simpson, G.; Halpin, C.; Boerjan, W. Caffeoyl shikimate esterase (CSE), a newly discovered gene in the lignin biosynthetic pathway. *Science* **2013,** *341*, 1103-1106.

[7] Withers, S.; Lu, F.; Kim, H.; Zhu, Y.; Ralph, J.; Wilkerson, C.G. Identification of a grass-specific enzyme that acylates monolignols with *p*-coumarate. *Journal of Biological Chemistry* **2012,** *287*, 8347-8355.

[8] Li, E.Y.; Bhargava, A.; Qiang, W.Y.; Friedmann, M.C.; Forneris, N.; Savidge, R.A.; Johnson, L.A.; Mansfield, S.D.; Ellis, B.E.; Douglas, C.J. The Class II *KNOX* gene *KNAT7* negatively regulates secondary wall formation in *Arabidopsis* and is functionally conserved in *Populus*. *New Phytologist* **2012,** *194*, 102-115.

[9] Vanholme, R.; Morreel, K.; Darrah, C.; Oyarce, P.; Grabber, J.H.; Ralph, J.; Boerjan, W. Metabolic engineering of novel lignin in biomass crops. *New Phytologist* **2012,** *196*, 978-1000.

[10] Ralph, J. Hydroxycinnamates in Lignification. *Phytochemistry Reviews* **2010,** *9*, 65-83.

[11] Stewart, J.J.; Akiyama, T.; Chapple, C.C.S.; Ralph, J.; Mansfield, S.D. The effects on lignin structure of overexpression of ferulate 5-hydroxylase in hybrid Poplar. *Plant Physiology* **2009,** *150*, 621-635.

[12] Bonawitz, N.D.; Kim, J.I.; Tobimatsu, Y.; Ciesielski, P.N.; Anderson, N.A.; Ximenes, E.; Maeda, J.; Ralph, J.; Donohoe, B.S.; Ladisch, M.; Chapple, C. Disruption of the Mediator rescues the stunted growth of a lignin-deficient *Arabidopsis* mutant. *Nature* **2014**, in press.

[13] Chen, F.; Tobimatsu, Y.; Havkin-Frenkel, D.; Dixon, R.A.; Ralph, J. A polymer of caffeyl alcohol in plant seeds. *Proceedings of the National Academy of Sciences of the United States of America* **2012,** *109*, 1772-1777 and COVER ARTICLE; Editors' choice highlight in *Science*, **335**, 382 (2012).

[14] Vanholme, R.; Ralph, J.; Akiyama, T.; Lu, F.; Rencoret Pazo, J.; Christensen, J.; Rohde, A.; Morreel, K.; DeRycke, R.; Kim, H.; Van Reusel, B.; Boerjan, W. Engineering traditional monolignols out of lignins by concomitant up-regulation *F5H1* and down-regulation of *COMT* in Arabidopsis *The Plant Journal* **2010,** *64*, 885-897.

[15] Weng, J.-K.; Mo, H.; Chapple, C. Over-expression of F5H in COMT-deficient Arabidopsis leads to enrichment of an unusual lignin and disruption of pollen wall formation. *The Plant Journal* **2010,** *64*, 898-911.

[16] Zhao, Q.; Tobimatsu, Y.; Zhou, R.; Pattathil, S.; Gallego-Giraldo, L.; Fu, C.; Shadle, G.L.; Jackson, L.A.; Hahn, M.G.; Kim, H.; Ralph, J.; Chen, F.; Dixon, R.A. Loss of function of *Cinnamyl Alcohol Dehydrogenase 1* causes accumulation of an unconventional lignin and a temperature-sensitive growth defect in *Medicago truncatula*. *Proceedings of the National Academy of Sciences of the United States of America* **2013,** *110*, 13660-13665.

[17] Ralph, J.; Brunow, G.; Harris, P.J.; Dixon, R.A.; Schatz, P.F.; Boerjan, W., Lignification: Are lignins biosynthesized via simple combinatorial chemistry or via proteinaceous control and template replication? In *Recent Advances in Polyphenol Research, Vol 1*, Daayf, F.; El Hadrami, A.; Adam, L.; Ballance, G.M., Eds. Wiley-Blackwell Publishing: Oxford, UK, 2008; Vol. 1, pp 36-66.

[18] Grabber, J.H.; Hatfield, R.D.; Lu, F.; Ralph, J. Coniferyl ferulate incorporation into lignin enhances the alkaline delignification and enzymatic degradation of maize cell walls. *Biomacromolecules* **2008,** *9*, 2510-2516.

[19] Petrik, D.; Karlen, S.D.; Cass, C.; Padmakshan, D.; Lu, F.; Liu, S.; Le Bris, P.; Antelme, S.; Santoro, N.; Wilkerson, C.G.; Sibout, R.; Lapierre, C.; Ralph, J.; Sedbrook, J.C. *p*-Coumaroyl-CoA:Monolignol Transferase (PMT) acts specifically in the lignin biosynthetic pathway in *Brachypodium distachyon*. *The Plant Journal* **2014,** *77*, 713-726.

[20] Wilkerson, C.G.; Mansfield, S.D.; Lu, F.; Withers, S.; Park, J.; Karlen, S.D.; Gonzales-Vigil, E.; Padmakshan, D.; Unda, F.; Rencoret, J.; Ralph, J. Monolignol ferulate transferase introduces chemically labile linkages into the lignin backbone. *Science* **2014,** *344*, 90-93.

[21] Xie, J.J.; Lu, J.; Qian, Z.M.; Yu, Y.; Duan, J.A.; Li, S.P. Optimization and comparison of five methods for extraction of coniferyl ferulate from *Angelica sinensis*. *Molecules* **2009,** *14*, 555-565.

[22] Lu, F.; Ralph, J. Detection and determination of *p*-coumaroylated units in lignins. *Journal of Agricultural and Food Chemistry* **1999,** *47*, 1988-1992.

[23] Martone, P.T.; Estevez, J.M.; Lu, F.; Ruel, K.; Denny, M.W.; Somerville, C.; Ralph, J. Discovery of lignin in seaweed reveals convergent evolution of cell-wall architecture. *Current Biology* **2009,** *19*, 169-175.

[24] Santoro, N.; Cantu, S.L.; Tornqvist, C.E.; Falbel, T.G.; Bolivar, J.L.; Patterson, S.E.; Pauly, M.; Walton, J.D. A high-throughput platform for screening milligram quantities of plant biomass for lignocellulose digestibility. *Bioenergy Research* **2010,** *3*, 93-102.

[25] Ralph, J.; Grabber, J.H.; Hatfield, R.D.; Lu, F. Method of modifying lignin structure using monolignol ferulate conjugates. US 8,569,465 B2, Oct. 29, 2013, 2013; Wilkerson, C.G.; Ralph, J.; Withers, S.; Mansfield, S.D. Feruloyl-CoA:Monolignol Transferase. US2013/0203973, Oct. 29, 2013, 2013.

LIGNIN STRUCTURE: A REVISITATION OF CURRENT PARADIGMS THROUGH NMR ANALYSIS

Claudia Crestini

Dipartimento di Scienze e Tecnologie Chimiche, Tor Vergata University, Rome, Italy
crestini@uniroma2.it

ABSTRACT

Recently, the development of quantitative 2D NMR pulse sequences such as QQ-HSQC allowed for the quantitative determination of lignin interunit bondings by the use of a specific d C2-H signal of the guaiacyl units. This approach permits the characterization of lignin samples in the presence of impurities and contaminants. On the basis of this experimental approach the lignin paradigms about degree of polymerization and branching have been critically revised. By coupling QQ-HSQC with ^{31}P-NMR and DFRC analysis, it was possible to unambigously demonstrate that MWL is an oligomeric system with a high propension to π stacking. The quantitative approach allowed to exclude the significative presence of non-phenolic diphenyl and 4-O-5' substructures. This implies that MWL is a linear oligomeric species.

I. INTRODUCTION

Lignin is a random network polymer lacking of repetitive units and repetitive interunit bondings. Despite the huge amount of studies performed its structure and polymerization degrees are to date not fully understood. This is largely due to lack of suitable analytical tools to reliably and extensively characterise such a complex system. From this viewpoint the determination of lignin molecular weight distribution is an illuminating example. Several analytical techniques have been employed in order to characterise lignin average molecular weight, ranging from vapour osmometry to GPC and light scattering; however different analytical techniques give rise to discordant results.

More specifically vapour osmometry can give informations related to the number average molecular weight, while light scattering provides data about weight average molecular weight of lignins. These techniques suffer from the disadvantage of being affected by supramolecular aggregation processes. Lignin in fact shows a high tendency to aggregate and the results of such analyses are strongly dependent upon the freshness of the lignin preparation studied.

To date the most diffuse analysis method for lignin MW determination is GPC. Data obtained from this technique are however scarcely reproducible. One reason is the lack of MW standards with a hydrodinamic volume comparable to lignin. The second reason that accounts for the variability of the results obtained by GPC analysis of lignins is the variety of eluant systems and derivatization processes employed.

During the last years the development of advanced NMR techniques both homo- and hetero- correlated has provided a new tool for the elucidation of lignin structure. More specifically, ^{31}P-NMR allows an accurate and reliable quantification of the phenolic OH groups. (2D) ^{13}C-^{1}H-correlated (HSQC, HMQC) spectroscopy, which combines the sensitivity of ^{1}H NMR with the higher resolution of ^{13}C NMR, continues to be the best method to reveal the frequencies of the different lignin units and the interunit bonding patterns and has allowed their use as a valid analytical technique in the analysis of complex samples.

More recently the development of quantitative HSQC sequences allowed to quantify different interunit bondings present in lignins[1]. The QQ-HSQC NMR pulse sequence can be successfully applied to lignin structural elucidation. It provides good resolution and signal to noise ratio in a reasonable analysis time. The standard deviations of the results were found ranging from 0,01 to 2 bondings per 100 C_9 units. The choice of the G_2 or $(S_{2,6})/2+G_2$ signal as an internal standard for softwood and hardwood lignins respectively allowed to reduce experimental errors connected to the addition of a low MW compound that could have affected the quantitative analysis due to T_2 effects. Furthermore, the direct evaluation of the C_9 units allowed to use 2D NMR as the sole analytical technique.

NMR spectroscopy is a technique that allows to determine the average degree of polymerization (and thus its number average molecular weight) of a polymer avoiding interferences due to supramolecular aggregation, provided the knowledge of monomer formula weight and the possibility to quantitatively integrate the amount of end groups and monomers of the polymer studied.

Due to its complex structure, the determination of the DP of lignin cannot be directly accomplished by routine NMR experiments. However the joint use of ^{31}P-NMR analysis and QQ-HSQC allowed to develop an analytical tool for the determination of the average degree of polymerization of lignin that does not suffer from interferences due to polymer branching or supramolecular aggregations.

Quantitative 2D-NMR was performed by a recently reported adiabatic quantitative pulse sequence, the quick quantitative HSQC (QQ-HSQC) that allows the direct and accurate determination of the lignin subunits in a few hour time, without suffering from the lack of accuracy typical of wet chemistry methods.

II. EXPERIMENTAL

HSQC and QQ-HSQC NMR spectra were carried as previously reported.[1, 2]

^{31}P-NMR analysis were performed as previously reported. [1, 2]

III. RESULTS AND DISCUSSION

Lignin branching revisited

Lignin branching may originate by the presence of non-phenolic 5-5' and 4-O-5' lignin subunits as shown in figure 1A.

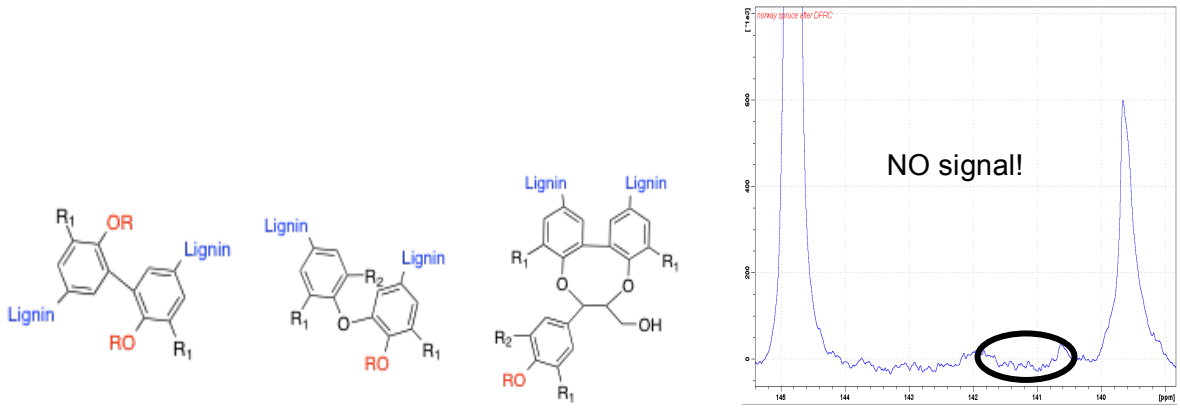

Figure 1. A: Possible branching structures in lignins; B: Quantitative ^{31}P-NMR after DFRC.

In order to evaluate the occurrence of branching in lignin, samples of softwood MWL were submitted to quantitative 31P-NMR after DFRC treatment. The DFRC procedure consists in an acetobromination step that causes the selective functionalization of *β*-aryl ether bondings and simultaneous acetylation of free phenolic groups.[3] The ensuing reduction step causes the cleavage of the *β*-aryl ether bond with release of the phenolic OH groups involved. We applied this technique for the identification of etherified condensed lignin subunits. More specifically, softwood and hardwood MWL samples were submitted to DFRC treatment, and the resulting fragments from the selective *β*-aryl ethers cleavage were submitted to ^{31}P NMR analysis according to the analytical protocol previously reported by Argyropoulos.[4]

Upon DFRC treatment the units reported in Figure 1 are supposed to release free phenolic groups, while the corresponding phenolic subunits result acetylated. As such ^{31}P-NMR after DFRC would show only the occurrence of these branching units in lignin. Our experiments showed that, within the instrumental detection limits, these phenolic units are not present. The results (Figure 1B) indicate that branching is not significantly present in softwood and hardwood MWL.

Toward the Determination of Lignin Degree of Polymerization

In a specific polymer, the average degree of polymerization is defined as the ratio between the monomeric units that constitute the polymer and its end units. The end-group titration method allows, once the monomer average weight is known, to know the average degree of polymerization of a specific polymer. This methodology is completely unsensitive to supramolecular interactions.

The amount of monomeric units in lignin can be easily determined by elemental analysis and methoxy groups determination according to the Zeisel method. In this way it is possible to develop a C9 formula to calculate the average amount of monomeric units.

Nature and Determination of Lignin End Units and Lignin Interunit Bondings

The amount of end units in lignin is more complex to be determined. The terminal phenolic end units can be easily quantitatively evaluated by ^{31}P-NMR. In principle phenolic 5-5'. 4-O-5' and dibenzodioxocines could introduce additional NON end of chain phenolics. However, the terminal biphenyl and 4-O-5' units show well resolved signals in the ^{31}P-NMR spectrum of lignin (Figure 1). Phenolic dibenzodioxocines instead are overlapped with guaiacyl phenolic OH groups. As such the total amount of the terminal phenolic units in lignin can be easily evaluated by subtracting the DBDO amount, as evaluated by QQ-HSQC, from the guaiacyl phenolics quantified by ^{31}P-NMR.

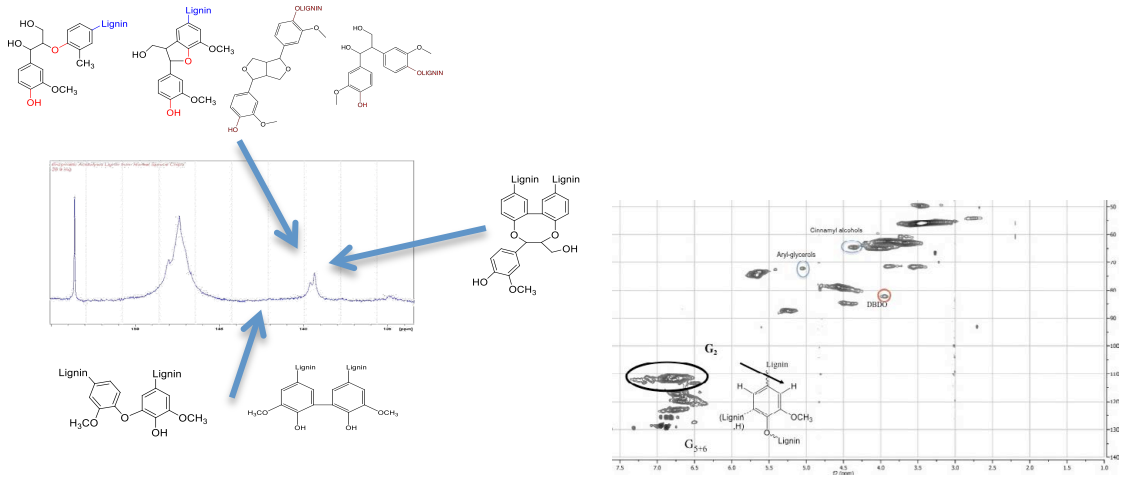

Figure 1. A: Lignin terminal phenolic units and quantitative ^{31}P-NMR of lignin; B: QQ-HSQC of MWL

The terminal aliphatic end groups in lignin consist in cinnamyl and benzoic acids, cinnamyl aldehydes, benzaldehydes, cinnamyl alcohols and arylglycerols. They can be easily quantified by QQ-HSQC and 31P-NMR. However, their occurrence in lignin could be also evaluated by classical wet chemistry methods.

The average degree of polymerization in lignin can thus be calculated as follows:

DP= C9 units/0,5 END GROUPS.

Table 1 shows the average degree of polymerization and the maximim experimental error associated, obtained for three different softwood and hardwood MWL.

Table 1

Lignin sample	DP	DP max error
Black spruce-MWL	5,7	0,7
Norway spruce-MWL	9,4	2,2
Norway spruce-EMAL	7,2	2,0
Beech-MWL	12,1	5,9

IV. CONCLUSIONS

Advances in analytical and spectroscopic chemistry have dramatically refined our knowledge of lignin chemistry over the past two decades. The knowledge gained in these studies, has defined the structure of milled wood lignin, reported in Figure 3, as drastically different polymer from what accepted before. More specifically MWL is composed of supramolecular aggregates of linear oligomers, as was in fact postulated in 1974.[5]

These features now reveal characteristics of lignin structure that will pave the way to addressing key limitations and present us with application opportunities.

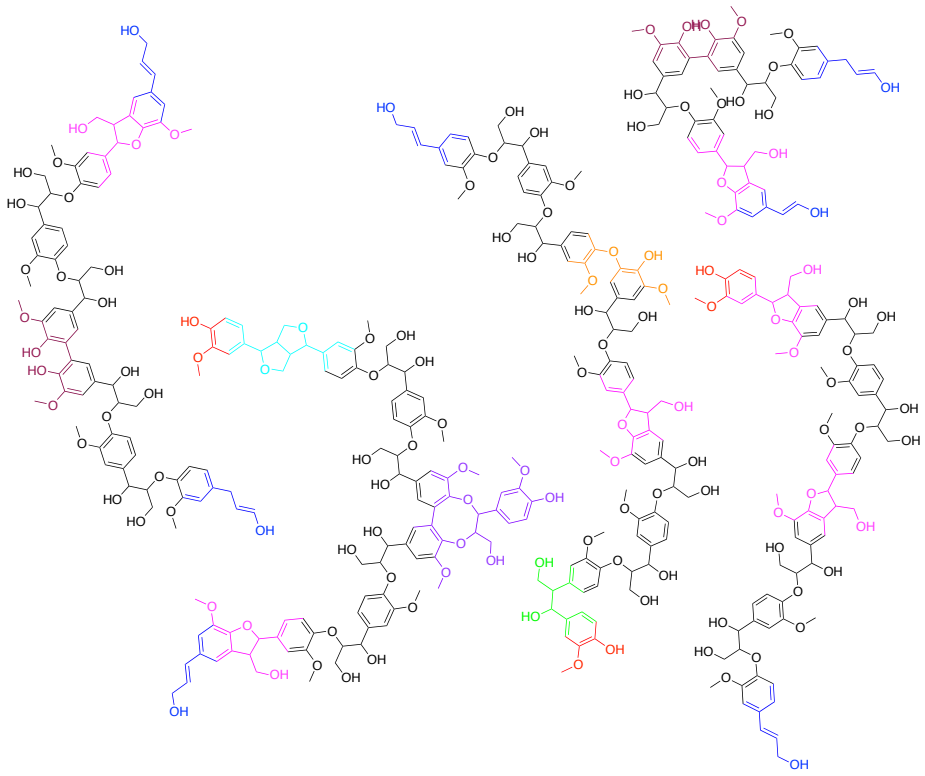

Figure 3. Schematic representation of softwood milled wood lignin. The structures reported are indicative of the occurrence of each interunit bonding and do not strictly reflect the statistical frequency.

V. ACKNOWLEDGEMENT

The EU NMR facility in Utrecht is kindly acknowledged.

VI. REFERENCES

[1] Sette, M., Wechselberger, R., Crestini, C. Elucidation of lignin structure by quantitative 2D NMR **2011** Chemistry - A European Journal, 17 (34), pp. 9529-9535.

[2] *Crestini, C., Melone, F., Sette, M., Saladino, R. Milled wood lignin: A linear oligomer* **2011** Biomacromolecules, 12 (11) 3928-3935

[3] Lu, F.; Ralph, J. **1998**, *J. Agric. Food Chem. 46*, 547−552.

[4] Tohmura, S.; Argyropoulos, D. S. **2001**, *J. Agric. Food Chem. 49*, 536−542.

[5] Wayman, M.; Obiaga, T. **1974**, I. *Can. J. Chem. 52*, 2102−2110.

TOWARDS OPTIMAL METHODOLOGY TO ASSESS MOLECULAR STRUCTURE OF NATIVE AND TECHNICAL LIGNINS

Mikhail Balakshin*, Ewellyn Capanema

*Renmatix Inc., 660 Allendale Rd., King of Prussia, PA 19406 (*mikhail.balakshin@renmatix.com)*

ABSTRACT

The advantages and limitations of different analytical protocols for isolation of lignin preparations and various methods in the analysis of native and technical lignins, such as routine (^{31}P NMR), advanced (^{13}C NMR), and cutting edge NMR techniques (quantitative 2D NMR) are discussed. Our vision on the best analytical strategy for different classes of lignin substrates is proposed.

I. INTRODUCTION

Detailed information on the molecular structure of lignin is a key factor in understanding lignin reactivity in various biorefining processes and for industrial utilization of technical lignins. Therefore, reliable, comprehensive and productive analytical methodology is of primary importance in lignin engineering and commercialization.

A review of the prior art [1] shows a very high variability in the data reported on the structure of the same (or similar) technical lignins (see **Table 1** as an example). This can be caused by variations in different analytical methods used, within method deviations as well as data interpretation. Therefore, important analytical issues have not been sufficiently addressed in the previous studies and more efforts are required towards the standardization and validation. Meanwhile, it is more accurate to compare the structural data obtained with the same analytical method in the same lab. The use of "reference" lignin samples (well-investigated lignins, such as Alcell and Indulin AT) would be also very beneficial to insure at least relative comparison.

As the most common analytical methods for structural lignin analysis nowadays are quantitative ^{31}P NMR, ^{13}C and 2D HSQC techniques, we focus our efforts on their critical evaluation.

Table 1. Summary of the prior art on the analysis of reference Indulin and Alcell lignins (mmol/g).

Lignin	Total OH	PhOH	AliphOH	COOH	Mn, KDa	Mw, KDa
Indulin AT	5.2-9.4	3.2-5.3	2.1-4.1	0.36-1.35	1.3-2.2	3.7-19.8
Alcell	3.7-7.9	2.4-5.7	1.1-3.0	0.23-1.22	0.44-1.5	1.44-21.8

II. RESULTS AND DISCUSSION

Lignin Isolation from Wood (Biomass)

Most of the methods for analysis of lignin in wood/biomass require lignin isolation. Various isolation protocols [2,3] are shown in **Figure 1**. Advantages and limitations of different lignin/LCC preparations are summarized in **Table 2**. The choice of a preparation depends on the research objectives and analytical methods to be used. In general, hardwood (HW) CEL and softwood (SW) CEL or/and MWLp are the most appropriate preparations for detailed structural analysis of HW and SW lignins, correspondingly. However, preparations of other types can be useful in certain specific cases (**Table 2**).

Lignin Analysis

Comparison of quantitative ^{31}P and ^{13}C NMR methods for analysis of lignin OH groups

Factors affecting the accuracy of the analysis of lignin hydroxyl and carboxyl groups with ^{31}P NMR have been further elucidated. Two modifications of ^{31}P NMR analysis of lignin, namely the protocols using 1,3,2-dioxaphospholane (^{31}P NMR-I) and 2-chloro-4,4,5,5-tetramethyl-1,3,2-dioxaphospholane (^{31}P NMR-II) as phosphorylation reagents, with different internal standards were studied. The previous ^{31}P NMR-II standard protocol underestimates OH groups by about 30% whereas ^{31}P NMR-I standard protocol tends to produce overestimated data (**Figure 2**). It has been shown that cholesterol is not an appropriate internal standard resulting in underestimated values for OH groups due to incomplete baseline resolution. The best internal standard has been found to be endo-N-hydroxy-5-norbornene-2,3-dicarboximide. Strong care should be taken related to the stability of the internal standards to avoid inflated results due to IS degradation. Under modified optimized conditions, both methods show a good correlation with the ^{13}C NMR protocol in the quantification of hydroxyl groups as average for a set of 17 HW and SW native and technical lignins with the variability between the

methods in the range of 5-15% (**Figure 2**). However, the ^{31}P NMR protocols reports about twice lower COOH content as compared to the ^{13}C NMR data.
It is important to note that G-condensed and S units cannot be separated in ^{31}P NMR spectra and 5-substituted PhOH should be reported instead. This also implies that the S/G ratio and the degree of condensation (DC) cannot be determined by ^{31}P NMR [4].

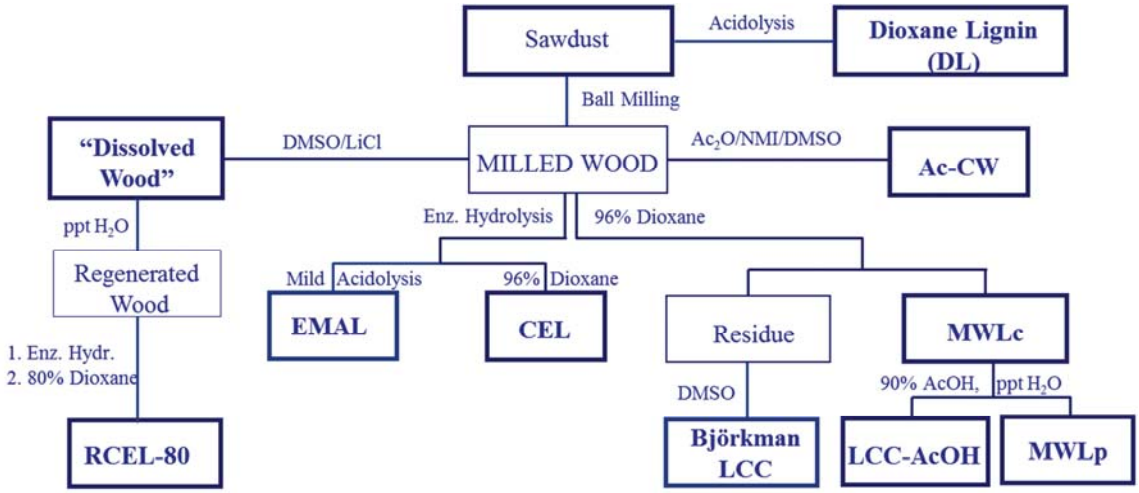

Figure 1. Summary on isolation of lignin/LCC preparation.

Table 2. Comparison of different isolation methods.

Type	Pros	Cons	Recommendations
Dissolved Cell Walls	Whole CW can be analyzed with high-resolution 2D NMR	Not suitable for ^{13}C NMR Limited for LCC analysis	Analysis of the whole CW; Biomass fingerprinting
RCEL-80	Very high yield Very low degradation	Low solubility Enz. esters and PhGly cleavage	Reference for the whole lignin (by 2D NMR)
CEL	Very representative; yield-independent structure; high purity (HW); good solubility	Enzymatic esters and PhGly cleavage	**Best for major lignin structures** and benzyl ether LCC (by ^{13}C/2D NMR)
MWLc and MWLp	No enzymatic degradation; High purity (SW MWLp)	Less representative (HW) Yield-dependent structure (HW) Mechanical degradation	**Good for SW (MWLp)** Analysis of esters and PhGly structures (MWLc)
DL	High yield and purity	Acidic modification	Fast and simple isolation protocol
EMAL	High yield and purity	Some chemical modification	?

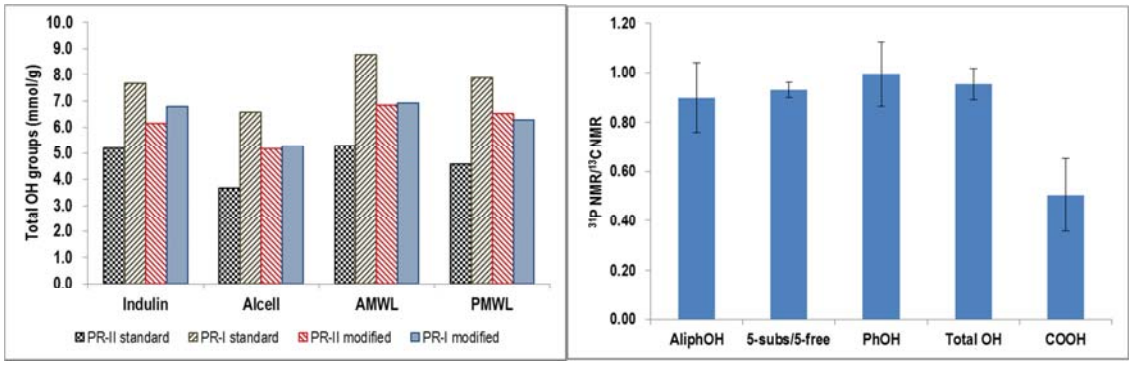

Figure 2. Correlation between the standard and the modified ^{31}P NMR protocols using PR-I and PR-II (left) and between the data obtained by the modified ^{31}P NMR-II and the ^{13}C NMR with IS methods (right).

Comprehensive ^{13}C NMR analysis of technical lignins

The ^{13}C NMR analysis of lignin can provide with a large amount of valuable structural information (20-30 numbers per analyzed lignin sample) in a reasonable experimental time which permits considering the ^{13}C NMR method as one of the most productive in lignin analysis. The analysis of native and technical lignins [1,2] (see **Table 3** as an example) clearly showed dramatic changes in lignin structure during various biomass processing. In addition to between-process variations certain within-process lignin structural changes could be documented. Appreciable differences in the structure of technical lignins from different tree species were obvious and they were significantly larger than the differences in the structure observed for native lignins in these tree species. In fact, species-originated variations are similar or even larger than the variations in major lignin functionalities caused by different delignification and biorefinery technologies. In addition, ^{13}C NMR with IS [4,5] is likely the best analytical approach to obtain lignin structural information expressed both in mol% (units/Ar) and in mmol/g and to establish a correlation between these important modes of data reporting [1,4]. The former is very useful in understanding of the fundamentals of lignin structures and different reaction mechanisms of lignin transformation. The latter is more practical for industrial lignin applications.

Table 3. ^{13}C NMR analysis of main structural moieties of different native and technical lignins (per 100 Ar).

Moieties	Birch MWL	Spruce MWL	Birch Kraft	*E. glob*. kraft	*E. grandis* kraft	Pine kraft	Indulin AT	Alcell	Douglas Fir OS
Total CO	12	21	9	14	12	11	12	35	20
Non-conjug. CO	3	5	4	5	4	4	5	16	7
Conjugated CO	9	14	5	9	8	7	7	19	13
Total COOR	4	5	20	18	16	21	16	19	6
Aliph COOR	3	4	18	16	13	20	15	15	5
Conjug. COOR	1	1	2	2	3	1	1	4	1
Total OH	150	138	107	128	119	108	123	104	118
Aliphatic OH	129	107	27	51	39	34	51	32	37
Primary OH	73	68	23	29	24	23	32	18	27
Secondary OH	56	39	3	22	15	11	19	14	10
Phenolic OH	20	31	80	77	80	74	67	72	81
S/G ratio	3.02	n.a.	1.7	2.5	1.4	n.a.	n.a.	1.3	n.a.
ArH	209	260	172	191	186	218	235	209	
DC	16	38	65	37	55	82	65	33	73
β-O-4	66	45	2	12	5	3	7	8	<5
β-β	11	4	3	2	3	5	4	3	1
β-5	2	9	2	1	2	3	4	3	3
OCH_3	177	95	141	141	125	81	80	117	85
Oxyg. aliphatic	260	215	86	110	79	72	94	94	86
Sat. aliphatic	15	30	64	46	55	85	68	96	62
-OEt	n.a.	n.a.	n.a.	n.a.	n.a.	n.a.	n.a.	13	10

Table 4. Analysis of technical lignins (per 100 Ar) by a combination of ^{13}C and HSQC NMR techniques [7]

Units	Pine Soda Dissolved	Pine Kraft Residual	*E. globulus* Kraft Residual	*E. grandis* Kraft Dissolved
β-O-4-G	0.7	5.2	5.8	1.7
β-O-4-S	na	na	21.8	2.2
Benzyl ether LCC	1.1	2.8	2.3	0.8
β-5	1.3	1.8	0.8	0.7
β-β	2.7	4.0	7.5	4.6
Ar-CH=CH-CH_2OH		1.5	6.4	1.2
Ar-CH_2-CH_2-CH_2OH	2.9	4.2		1.3
Ar-$(CH_2)_n$-COOH	6.9	3.8	7.2	1.5
Ar-CHOH-CHOH-CH_2OH	3.5	0.6		tr
Ar-CH=CH-Ar'	4.1	25.2	3.4	13.1
Ar-CH=CH-O-Ar'	2.0	nd	nd	tr
Alk-Ar'	4.7	2.1	nd	2.4

Advanced 2D NMR approach

2D NMR methods, specifically an HSQC technique, allow to distinguish specific structural characteristics of various lignins and LCC preparations [3,6,7], in contrast to traditional analytical methods including comprehensive ^{13}C NMR. As an example, **Table 4** presents important quantitative information on various structural lignin units, such as condensed lignin moieties, products of β-O-4 bond cleavage, vinyl and alkyl-aryl structures and others, which were not possible to quantify with ^{13}C NMR [7]. The HSQC method can be used alone[6], but it is more powerful in a combination with quantitative ^{13}C NMR [3,7,8]. A good general correlation between the ^{13}C/HSQC approach the prior art in the analysis of spruce MWL has been reported [8]. However, further detailed validation of the method for different lignin/LCC preparations would be desirable.

Table 5. Pros and cons of the different NMR methods for lignin analysis

	^{31}P NMR	^{13}C NMR	2D (HSQC) NMR
Numbers reported	4-5	>20	large
Fingerprinting	no	good	excellent
Molecular structure	no	some	excellent[1]
Functional groups	OH, COOH (?)	various	no
Quaternary C moieties		yes	no
Lignin purity requied	high	high-medium	any
NMR time	1-4 h of prime time	overnight/<1h[2]	overnight/<1h[2]
Qualification required	beginner/intermediate	expert	expert

[1]For the side chain structures; [2]For CryoProbe™ experiment

III. CONCLUSIONS

Among a wide viriety of procedures for lignin isolation from wood, the CEL method appears to be the most suited for detailed characterization of wood lignins. The modified ^{31}P NMR protocols allow for a simple and accurate quantification of major OH lignin functionalities (provided that unjustified conclusions are avoided). A combination of quantitative 2D and ^{13}C NMR methods is the most powerful approach in lignin analysis. At the same time, significant efforts still should be made to address the between-lab deviation and to standardize the analytical methodology. The use of reference lignins is very helpful for methods validation and data comparizon.

IV. REFERENCES

[1] Berlin, A.; Balakshin M. Industrial lignins: Analysis, properties and applications. In: *Bioenergy Research: Advances and Applications*; Gupta V.K.et al. Eds.; Elsevier; **2014**; 315 - 336.

[2] Balakshin, M.Yu.; Capanema, E.A.; Chang, H-m. Recent advances in isolation and analysis of lignins and lignin-carbohydrate complexes. In: *Characterization of Lignocellulosics*; Hu, T., Ed.; Blackwell; **2008**; 148-166.

[3] Balakshin, M. Yu., Capanema, E.A., Berlin, A. Isolation and Analysis of Lignin-Carbohydrate Complexes (LCC) Preparations with Traditional and Advanced Methods. A Review. In: *Studies in Natural Products Chemistry*, v. 42. Elsevier, Amsterdam, **2014**, 83-115.

[4] Balakshin, M. Yu.; Capanema, E.A. On the quantification of lignin hydroxyl groups with ^{31}P and ^{13}C NMR spectroscopy. Submitted for *J. Wood Chem. Techn.*

[5] Xia, P.; Akim, L.; Argyropoulos, D.S. Quantitative ^{13}C NMR of lignins with internal standards. *J. Agric. Food Chem.* **2001**, *49*, 3573-3578.

[6] Del Río, J.C.; Rencoret, J.; Prinsen, P.; Martinez, A.T.; Ralph, J.; Gutiérrez, A. Structural Characterization of Wheat Straw Lignin as revealed by analytical pyrolysis, 2D-NMR and reductive cleavage methods. *J. Agric. Food Chem.* **2012**, *60*, 5922-5935.

[7] Capanema, E.A.; Balakshin, M.Yu.; Chang, H-m.; Jameel, H. Quantitative analysis of technical lignins by a combination of ^{1}H-^{13}C HMQC and ^{13}C NMR methods. *Proc. Int. Conf. Pulping, Papermaking and Biotechn. 2008. Nanjing, China.* 647-651.

[8] Zhang, L.; Gellerstedt G. Quantitative 2D HSQC NMR determination of polymer structures by selecting suitable internal standard reference. *Magn. Res. Chem.* **2007**, *45*, 37-45.

STRUCTURAL ELUCIDATION OF PLANT CELL WALL POLYSACCHARIDES AND THEIR DERIVATIVES USING CHROMATOGRAPHIC AND MASS SPECTROMETRIC TECHNIQUES

Jun Liu[1*], Francisco Vilaplana [2,3], Chunlin Xu [1,2], Stefan Willför [1]

[1] *Process Chemistry Centre, c/o Laboratory of Wood and Paper Chemistry, Åbo Akademi University, Porthansgatan 3-5, FI-20500, Turku/Åbo, Finland;* [2] *Wallenberg Wood Science Centre (WWSC), KTH Royal Institute of Technology Teknikringen 56-58, SE-100 44, Stockholm, Sweden;* [3] *Division of Glycoscience, KTH Royal Institute of Technology, AlbaNova University Centre, SE-106 91, Stockholm, Sweden. (* jun.liu@abo.fi)*

ABSTRACT

The macromolecular structures of plant cell wall polysaccharides, especially heteropolysaccharides or hemicelluloses, are extremely complex due to the presence of different monosaccharides used as building blocks (that usually are isobaric stereoisomers) and the variations in sequence (e.g. linkage, branching, and distribution of side chains). This structure gets even more complicated in their chemical derivatives, when lack of regioselectivity of such chemical modification procedures is typical. Structural elucidation of polysaccharides involves obtaining data from numerous analytical approaches, each of which gives some structural information, and the assimilation/integration of this data into a chemical structure that rigorously and uniquely fits all the available structural information. The present work focused on developing a methodology for the analysis of plant polysaccharides (xyloglucans and galactoglucomannans) and their derivatives by integrating enzymatic approaches with chromatographic (hydrophilic interaction chromatography, HILIC) and mass spectrometric techniques (matrix-assisted laser desorption/ionization-time-of-flight MS, MALDI-TOF-MS, electrospray ionization MS, ESI-MS, and tandem MS). This methodology will be exploited towards the understanding the structural diversity of plant polysaccharides and the chemo-enzymatic modification mechanisms of their derivatives. Semi-quantitative information about the substitution pattern of these derivatives can also be obtained from this powerful approach.

I. INTRODUCTION

Of all the natural plant cell wall polysaccharides, hemicelluloses are the second most abundant biorenewable compounds after cellulose, representing an immense renewable resource of biopolymers. Structural and composition complexities of hemicelluloses, e.g. variety of monosaccharides constituents, glycosidic linkage position, and conformation, result in their previously unperceived application. However, recently they are increasingly attractive as biopolymers, which can be utilized in their native and modified forms in various application areas.

Xyloglucan (XG) is a natural polysaccharide with a common structure of β-(1→4)-linked D-glucan, where three out of four glucose residues are substituted with α-D-(1→6) xylose [1]. Galactoglucomannans (GGMs) from wood, e.g. spruce, consist of both β-(1→4)-linked D-mannose and glucose residues in the backbone and α-D-(1→6) galactose residues attached as single-unit side-chains [2]. Both XG and GGM have been developed for various applications in their native or modified forms. However, detailed structural information of XG and GGM derivatives still need to be elucidated.

Accurately profiling the structural details of plant polysaccharides and their derivatives is fundamental for their application. In addition to the inherent complexity of native polysaccharides, their chemical modification for material applications introduces an additional level of complexity for structural analysis. MALDI-TOF-MS and ESI-MS have become key techniques for identification and molecular mass profiling of polysaccharides that are present in complex mixtures. Coupling of various chromatographic isolation methods with mass analyzers have been developed to reduce the complexity of analyte mixtures.

The present work focused on developing a methodology for the analysis of plant polysaccharides and their derivatives by using chromatographic and mass spectrometric techniques, towards understanding the structural diversity of plant polysaccharides and the chemo-enzymatic modification mechanisms of their derivatives.

II. EXPERIMENTAL

Material and chemicals

XG was obtained from tamarind seed and GGM was prepared from Norway spruce. Preparations of XG and GGM derivatives have been reported previously [3-6]. The 2,5-dihydroxybenzoic acid (DHB) matrix was purchased from Sigma-Aldrich (Sweden AB). Endo-1,4 β-mannanase and xyloglucan-specific endo-β-1,4-glucanase were obtained from Megazyme International (Bray, County Wicklow, Ireland).

Hydrolytic approaches

Incubations of native or derivatives of XG and GGM solution (1 g/L), enzyme and ammonium formate buffer (pH 4.5) were performed for 16 h at 37 ℃ for end point release of oligosaccharides. After incubations, the enzymes were denatured by boiling for 10 min and separated by ultrafiltration (Millipore®, Germany).

Chromatographic isolation and mass spectrometric detection

MALDI-TOF-MS analysis of oligosaccharides was performed by using a MALDI-TOF mass spectrometer (SAI Ltd., UK) equipped with a nitrogen laser of 337 nm, operated in positive ion mode and with accelerating voltage of 20 kV. Positive-ion ESI-MS and collision induced dissociation (CID) MS/MS experiments were carried out on a Q-TOF^2 ESI mass spectrometer (Micromass, UK). Analyte solutions (10-100 ng/μL) were infused into the mass spectrometer by a syringe pump (0.5 μL/min). Chromatographic separations of oligosaccharides were carried out on an Amide column (3.5 μm, 1.0 ×50 mm, Water Corporation, USA) which was coupled to the ESI-MS/MS detector. Mobile phase: (A) 5% ACN and 0.1% formic acid; (B) 95% ACN and 0.1% formic acid.

III. RESULTS AND DISCUSSION

Characterization of XG and its derivatives by MALDI-TOF-MS and ESI-MS

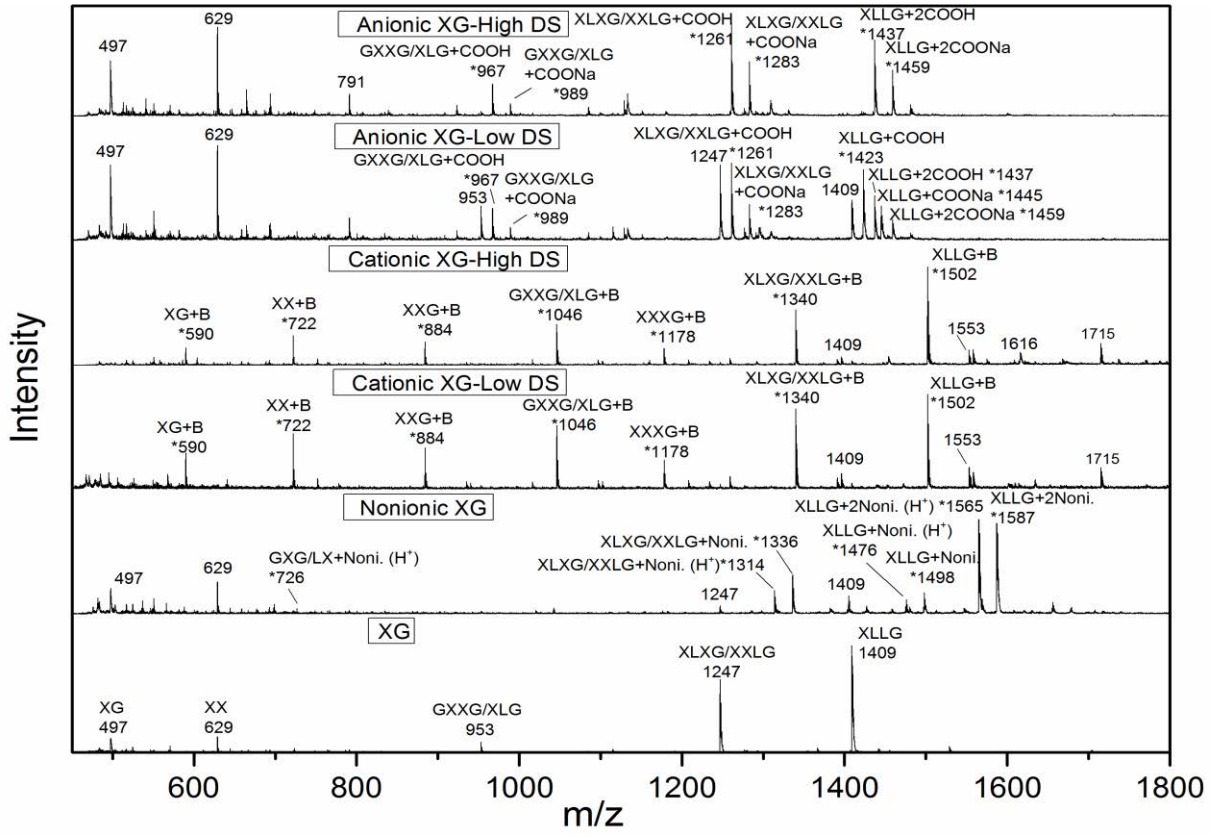

Figure 1. Mass spectrum from MALDI-TOF-MS analysis of XG oligosaccharides and their derivatives. Note: Noni., and B, refer to the nonionic and cationic moieties of the XG derivatives, respectively.

As shown in **Figure 1** and **Figure 2,** the peaks from functionalized XG (spectrum of GGM samples are not shown) oligomers were marked with a star. Most of the glycan oligomers were preferentially in the form of Na^+ adducts and a few of protonated molecular adducts (not including the cationic derivatives). The mass spectrum in **Figure 1** identified the oligomers of XG and its derivatives that were released by enzymatic hydrolysis. The MALDI technique gives qualitative information at most of the time, however, comparison of the spectra between high and low DS of the XG derivatives may give some general semi-quantification information. For example,

the intact XG oligomers ions (m/z 953, 1247, 1409) co-exist with these anionic XG ions (marked with star) and shown high relative intensity in the low DS anionic XG sample, while these anionic molecular ions dominated the spectrum in the high DS anionic XG sample.

The ESI-MS spectra (**Figure 2**) of XG oligosaccharides and its derivatives are basically in agreement with the results from MALDI analysis (**Figure 1**) about the composition of the oligosaccharides and their derivative mixture. However, the relative intensity of some peaks detected by this two techniques were significantly different, especially these of derivatives. For example, the MALDI results of cationic XG shown that the high molecular mass ions have higher relative intensity (e.g. m/z 1502 and 1340), while the ESI method giving an opposite result, i.e. lower molecular weight ions (e.g. m/z 722, 590) tends to have higher relative intensity. The in-source collision induced dissociation (CID) of ESI-MS and the mass discrimination effect of MALDI analysis can explain such differences [7].

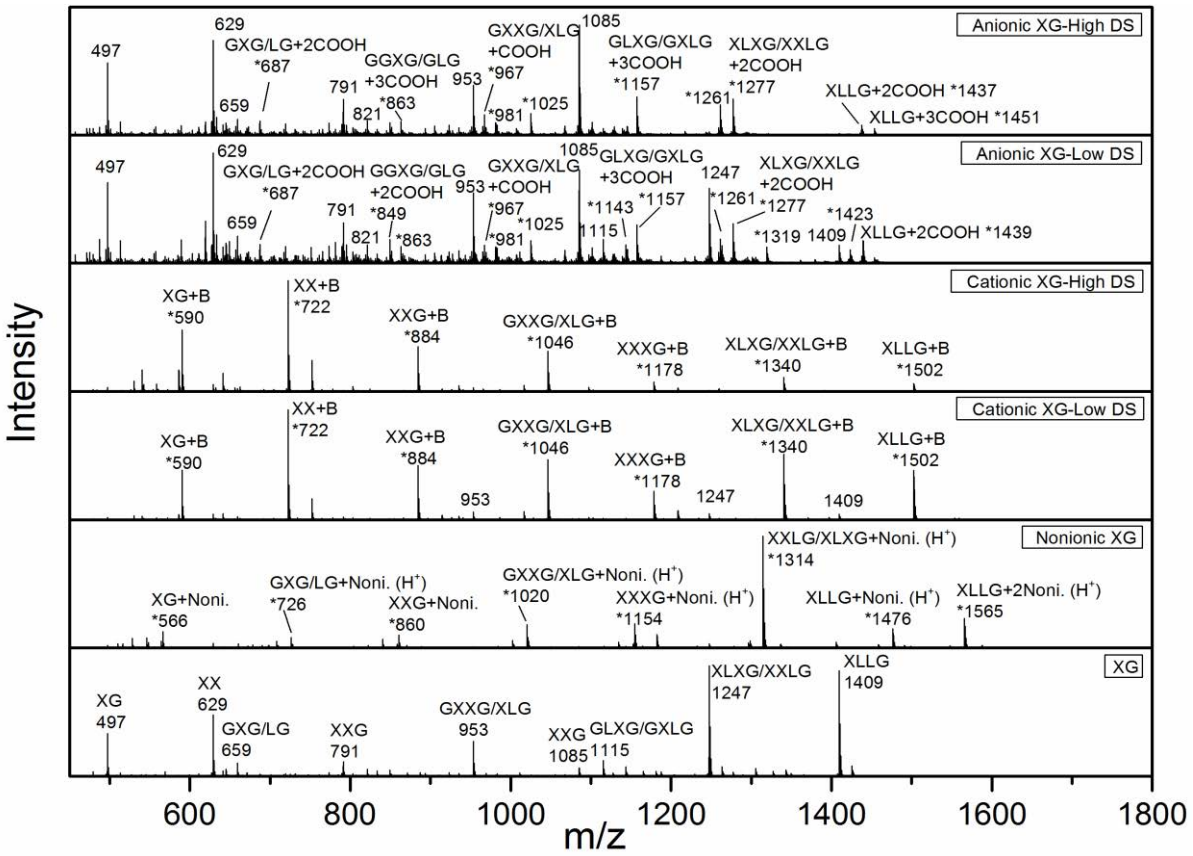

Figure 2. Mass spectrum from ESI-MS analysis of XG/GGM oligosaccharides and their derivatives

Characterization of XG and their derivatives by LC-MS/MS

MALDI-TOF-MS and ESI-MS enable the fast identification of oligosaccharides in the mixture as shown in **Figure 1** and **Figure 2**. However, the presence of isomeric components makes the structural elucidation difficult. Coupling of chromatographic separation and mass spectrometric analysis provides additional analytical approach to profile the analytes and their structures. The chromatograms from HILIC separation in **Figure 3** illustratethat both XG and its derivatives oligomers can be separated sufficiently. However, sometimes there are more than one peak are assigned with a same structure as shown in **Figure 3** and tandem MS analysis (not shown here). For example, as analyzed in **Figure 3**, the "*XG*" oligomers in the cationic XG derivatives showed two peaks at 5.5-6.2 min which is the dehydration product ion (m/z 479) of normal "*XG*" ion (m/z 497), and at 7.0-7.7 min which belongs the normal "*XG*" oligomer respectively. Similarly, the two peaks (**Figure 3**) of cationic XG at 11.6-12.2 min and 12.2-12.9 min sharing the same molecular mass of 590 Da (MS analysis), however, by analyzing their fragmentation pattern (tandem MS, not shown here) we found they have different structures.

IV. CONCLUSIONS

This work presents a comprehensive study of the structures of XG, GGM, and their derivatives (cationic, nonionic and anionic derivatives) via chemo-enzymatic, mass spectrometric, and chromatographic approaches. Semi-quantification information can be obtained from MALDI-TOF-MS and ESI-MS techniques to quickly

distinguish the high or low substitution of the polysaccharides derivatives with prudent evaluation. Combining of the separation by HILIC and fragmentation analysis by ESI-MS/MS enables efficient structure identification and semi-quantification of oligosaccharides and their derivatives in complex mixtures.

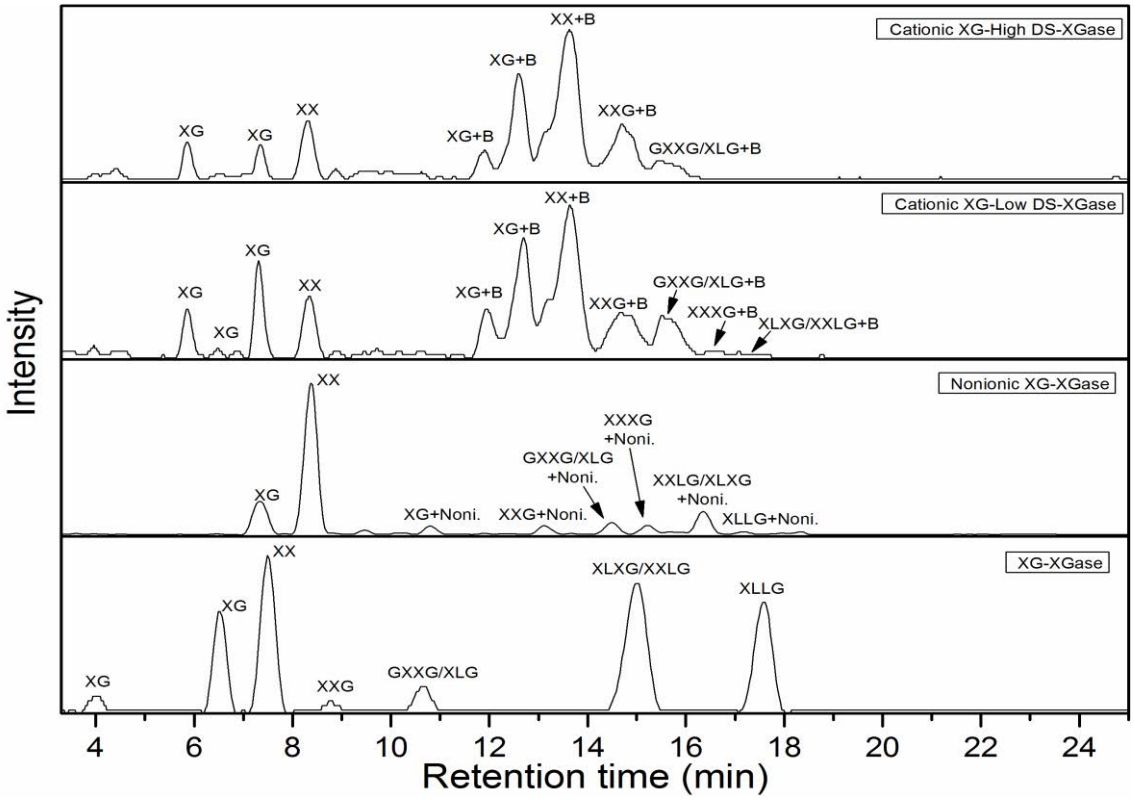

Figure 3. HILIC separation of XG and their derivatives oligomers

V. ACKNOWLEDGEMENT

The authors would like to acknowledge the financial support of the China Scholarship Council, the Wallenberg Wood Science Center, PolyRefNorth network, and Graduate School of Chemical Engineering. This work was also part of the activities at Åbo Akademi University Process Chemistry Centre.

VI. REFERENCES

[1] Gidley, M.J.; Lillford, P.J.; Rowlands, D.W.; Lang, P.; Dentini, M.; Crescenzi, V.; Edwards, M.; Fanutti, C. Structure and solution properties of tamarind-seed polysaccharide. *Carbohydr. Res.* **1991**, *214*, 299-314.

[2] Willför, S.; Sjöholm, R.; Laine, C.; Roslund, M.; Hemming, J.; Holmbom, B. Characterisation of water-soluble galactoglucomannans from Norway spruce wood and thermomechanical pulp. *Carbohydr. Polym.* **2003**, *52*, 175-187.

[3] Kisonen, V.; Eklund, P.; Auer, M.; Sjöholm, R.; Pranovich, A.; Hemming, J.; Sundberg, A.; Aseyev, V.; Willför, S. Hydrophobication and characterisation of O-acetyl-galactoglucomannan for papermaking and barrier applications. *Carbohydr. Res.* **2012**, *352*, 151-158.

[4] Kisonen, V.; Xu, C.; Eklund, P.; Lindqvist, H.; Sundberg, A.; Pranovich, A.; Sinkkonen, J.; Vilaplana, F.; Willför, S. Cationised O-acetyl galactoglucomannans: Synthesis and characterisation. *Carbohydr. Polym.* **2014**, *99*, 755-764.

[5] Leppänen, A.-S.; Xu, C.; Eklund, P.; Lucenius, J.; Österberg, M.; Willför, S. Targeted functionalization of spruce O-acetyl galactoglucomannans—2,2,6,6-tetramethylpiperidin-1-oxyl-oxidation and carbodiimide-mediated amidation. *J. Appl. Polym. Sci.* **2013**, *130*, 3122-3129.

[6] Xu, C.; Spadiut, O.; Araújo, A.C.; Nakhai, A.; Brumer, H. Chemo-enzymatic Assembly of Clickable Cellulose Surfaces via Multivalent Polysaccharides. *ChemSusChem.* **2012,** *5*, 661-665.

[7] Momcilovic, D.; Wittgren, B.; Wahlund, K.G.; Karlsson, J.; Brinkmalm, G. Sample preparation effects in matrix-assisted laser desorption/ionisation time-of-flight mass spectrometry of partially depolymerised carboxymethyl cellulose. *Rapid Commun. Mass Spectrom.* **2003**, *17*, 1107-15.

TOWARDS THERMOPLASTIC LIGNIN POLYMERS; PROGRESS IN THE UTILIZATION OF KRAFT LIGNIN FOR THE SYNTHESIS OF HEAT STABLE POLYMER MELTS

Dimitris S. Argyropoulos [1,2,3], H. Sadeghfifar[2], S. Sen, [2] C. Cui, [2] R. Sun[2]

[1]Department of Forest Biomaterials, & [2]Department of Chemistry

North Carolina State University, Raleigh , North Ccarolina , 27695-800, 5USA

[3]King Abdulaziz University, Center of Excellence for Advanced Materials Research (CEAMR) P.O. Box 80203, Jeddah 21589, Saudi Arabia

ABSTRACT

The work of our group has focused at creating new opportunities for softwood kraft lignin in markets that include value added polymers. During this presentation we will describe our systematic efforts in the following four areas aimed at actualizing our objectives: (i) Providing a detailed molecular understanding of the way the polymeric properties of kraft lignin and its derivatives are affected by thermal treatments. The accumulated data is aimed at providing the foundations for a rational design of single or multi-component lignin-based thermoplastic materials with reproducible polymeric properties when thermally processed in a number of manufacturing cycles. (ii) Creating new thermoplastic lignin polymers and precursors to carbon fibers by applying propargylation derivatization chemistry followed by thermal treatments, offering a versatile novel route for the eventual chain extension & utilization of technical lignins with a significant amount of molecular control. (iii) Refining technical kraft lignin so as to expose its potential as a source for reactive polyphenols of well-defined molecular weight polymers and oligomers. More specifically, we have demonstrated that a continuum of narrow fractions can be isolated from softwood kraft lignin, common to a variety of such sources irrespective of the manufacturing details of the pulping process. Such consistently homogeneous lignin streams from Lignoboost[R] lignins offer significant commercial ramifications. (iv) Creating heat stable kraft lignin copolymers with heat stabilities approaching 300 ^{0}C [8].

I. INTRODUCTION

Most efforts to utilize lignin have been limited by various factors that impart in it characteristics that define it as an unreliable precursor to polymer production. This is because lignin (and more specifically technical lignin) offers relatively unpredictable polymerization characteristics, is of low molecular weight offering materials of no mechanical integrity , is highly functional & reactive causing gel formation and is highly heterogeneous and of variable nature depending on the details of the pulping process.
Consequently, if one is to create new opportunities for softwood kraft lignin in markets of value added polymer products one needs to thoroughly address these limitations.

Thermal and Polymer Characteristics of Kraft Lignin & Derivatives.

Overall, our review of the literature has revealed that the molecular events that occur within technical lignin at low temperatures prevent it from being processed as a thermoplastic polymer. Such molecular events undoubtedly define vital polymeric properties of the material, including its T_g, molecular weight distribution, and thermal stability. Consequently, this work focused on a molecular understanding of the way the thermal properties of kraft lignin are affected by different chemical derivatizations. The conclusions from the accumulated data may provide the foundations for a novel rational design of single-component, kraft lignin-based, thermoplastic materials with consistent thermal properties when thermally processed in a number of heating and cooling manufacturing cycles[1]

Since the primary objective in this effort is the accumulation of data aimed at a rational design of lignin-based thermoplastics, the thermal instability of softwood kraft lignin at temperatures even below its T_g (153 °C) represents a major obstacle that needs to be overcome[2]. For lignin thermoplastic creation, stable melt characteristics are required when thermally processed above its T_g over a number of manufacturing cycles. Furthermore, a variety of radical mechanisms point to the need of derivatization chemistries for kraft lignin to inhibit the onset of radical coupling reactions. The following experiments were, therefore, performed to offer a

molecular understanding of the way the polymer properties of kraft lignin and its derivatives are affected as a function of their thermal treatment.

Since thermoplastic materials are always processed above their T_g, an underivatized softwood kraft lignin and two fully derivatized (oxypropylated and methylated) samples were subjected to heating 20 °C above their T_g as a function of time. The treated samples were then subjected to molecular weight characterization using GPC. It should be noted here that the derivatization protocols applied were specific to the phenolic OH groups of the softwood kraft lignin[3], allowing for meaningful correlations to be made as to their role in defining thermal stability of kraft lignin and its derivatives.

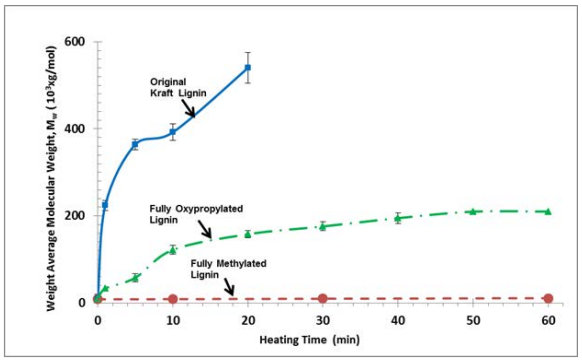

Figure 1. *Effect of heating on the molecular weight of the original underivatized and fully derivatized lignins. Dramatic increase in M_w is obvious in the original underivatized lignin while derivatized lignins show a smaller effect (oxypropylated) or no effect (methylated).*

Figure 1 shows that when the original underivatized softwood kraft lignin was heated under nitrogen at 173 °C (T_g = 153 °C) for only 20 minutes, its M_w increased and eventually exceeded 543,000 g/mol from 7,800 g/mol, a 70-fold increase. This increase is much more than those recorded when it was subjected to temperatures below its T_g, *i.e.*, 130 °C and 140 °C for 30 minutes (Fig. 1B). The same material eventually became highly cross-linked when heated for 30 minutes at 173 °C and could no longer be solubilized in THF, even after acetobromination. This can be explained on the basis of more radicals being activated at a temperature above T_g and the radical coupling reaction rates being significantly increased due to the reduced viscosity of kraft lignin.

For comparison, a fully (≈ 99%) oxypropylated lignin[3] was heated to 148 °C, which is 20 °C above its T_g (T_g = 128 °C) (Fig. 2). There was a gradual increase observed in its M_w, which increased to 212,000 g/mol from 9,100 g/mol (23-fold increase) after 60 minutes of heating at 148 °C (20 °C above its T_g). Such thermal instability issues, therefore, represent a major limitation in processing this derivative as a thermoplastic.

The thermal degeneration observed in the oxypropylated kraft lignin is possibly due to the dehydration of the secondary hydroxyl group of the oxypropyl substituent. For mono-oxypropylated phenolic OH components, their dehydration can be a facile reaction caused by an α-hydride transfer, eventually forming a phenoxonium intermediate so that a new phenolic OH group can be generated by hydrolysis of the cationic intermediate. The newly formed phenolic OH groups will be further thermally activated and, to some extent, trigger radical coupling reactions resulting in further molecular weight increases in a manner similar to the original kraft lignin. The molecular weight increase of this derivative eventually leveled off after being heated for 50 minutes at 20 °C above its T_g (Figure 1)

When the phenolic OH groups of softwood kraft lignin were fully methylated (> 99%) with dimethyl sulfate[3], a remarkable thermal stability of this derivative was apparent upon heating it at 148 °C (20 °C above its T_g) as a function of time (Figure 1). There was practically no observed molecular weight (M_w) increase within the fully methylated lignin when heated for 60 minutes at this temperature. The methylation of the phenolic OH groups of lignin is therefore a feasible derivatization method that enables kraft lignin to be used as thermoplastics. Apparently, the phenoxy radical formation, caused by H abstraction of the phenolic OH groups in kraft lignin, has been avoided by methylation-preventing, thermally induced, radical coupling reactions.

Having understood significant issues related to the way one needs to modulate the structure of kraft lignin in order to induce thermal stabilization within its melt we then turned our attention to modulating its molecular weight [5,6].

Kraft Lignin Chain Extension Chemistry via Propargylation, Oxidative Coupling & Claisen Rearrangement

Despite its aromatic and polymeric nature, the heterogeneous, stochastic and reactive characteristics of softwood kraft lignin seriously limit its potential for thermoplastic applications. Our continuing efforts toward creating thermoplastic lignin polymers have also been focused at exploring propargylation derivatization chemistry and its potential as a versatile novel route for the eventual chain extension & utilization of technical lignins with a

significant amount of molecular control [6]. The installation of propargyl groups in kraft lignin was found to be a seamless and facile reaction operating under basic conditions and highly selective towards the phenolic OH groups of lignin [6]. Furthermore, the cupper mediated oxidative coupling shown in Scheme 1a was also a facile reaction whose significance, details and potential have been enumerated in our patent and full paper in this area [1,6]. In our view the Claisen rearrangement reaction shown in Scheme 1b followed by polymerization is of extreme significance in the context of creating novel materials from kraft lignin , including precursor to carbon fibers. For this reason, more details of it will be discussed below.

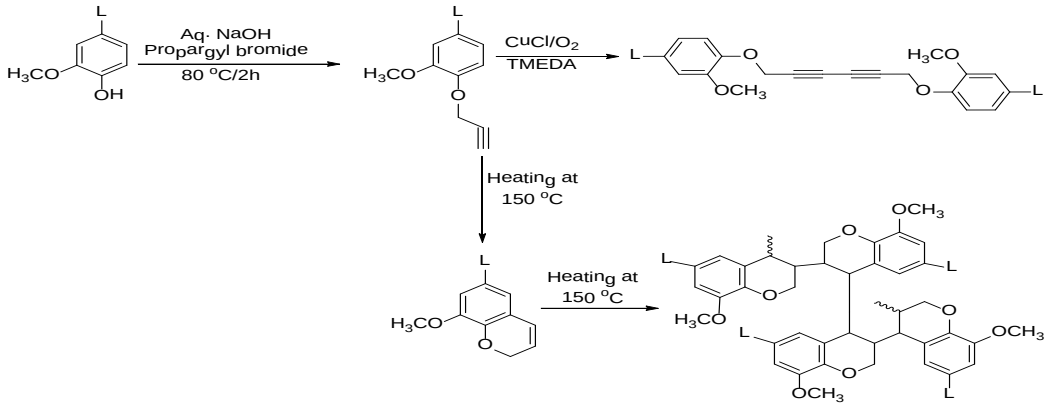

Scheme 1. *Propargylation of Kraft Lignin followed by either (a, top right) oxidative coupling or (b bottom pathway) Claisen rearrangement and subsequent thermal polymerizations .*

Arylpropargyl ether terminated monomers when heated around 220 °C (in a nitrogen atmosphere in the absence of solvent and catalyst) they generally first undergo a thermal sigmatropic Claisen rearrangement to form *2H*-chromenes or *2H*-1-benzopyrans. These intermediates that possess reactive double bonds can subsequently undergo thermal polymerization (Scheme 1). Moreover, the aryl propargyl ether moieties can also undergo polymerization through ethynyl triple bond radical polymerization or ethynyl cyclotrimerization through double bond radical polymerization, generating low molecular weight polymer. As such in our work we have shown that the aryl propargyl ether moieties of the propargylated kraft lignin samples also undergo similar rearrangement and polymerization chemistries when heated at moderate temperatures under a nitrogen atmosphere. Since the propargylated kraft lignins are multifunctional, they initially form chain extended, higher molecular weight polymers, which eventually lead to cross-linked structures at higher temperatures. This major limitation was addressed by appropriately reducing the degree of propargylation (75%) and masking the remaining (25%) phenolic –OHs by alkaline methylation with dimethyl sulfate. Our approach of modulating lignin reactivity via methylation was based on the principles we developed in earlier parts of our work [1, 2, 3, 5].

Fractional Precipitation of Softwood Kraft Lignin; Isolation of Narrow Fractions Common to a Variety of Lignins

In a manner similar to crude oil, technical lignins need refining if their potential as reactive polyphenols of well-defined molecular weight polymers and oligomers is to be actualized. In our work we have also demonstrated that a continuum of narrow fractions can be isolated by the incremental addition of a non polar solvent (hexanes) in a polar (acetone) solution of softwood kraft lignin. Three distinct commercial samples of softwood kraft lignin were used to examine the validity of the developed protocol using detailed chromatographic and quantitative functional group analytical methods. It was shown that all samples contain a common, relatively monodisperse fraction of a polyphenolic material that can be isolated from the different lignins in yields ranging between 10 and 20% w/w.

The versatility of the developed fractional precipitation protocol was further validated by creating artificial physical mixtures of the examined lignins in different proportions and isolating from them precisely calculated fractions of nearly identical molecular weight distributions and composition. Overall, the fractional precipitation approach described in this segment of our work offers the possibility that representative specific narrow fractions, common to a variety of softwood kraft lignins can be isolated irrespective of the manufacturing details of the pulping process. As such, the otherwise known, heterogeneous kraft lignin material, whose composition is relatively unpredictable due to manufacturing variations in making pulp, may now offer consistently homogeneous lignin streams with significant commercial ramifications.

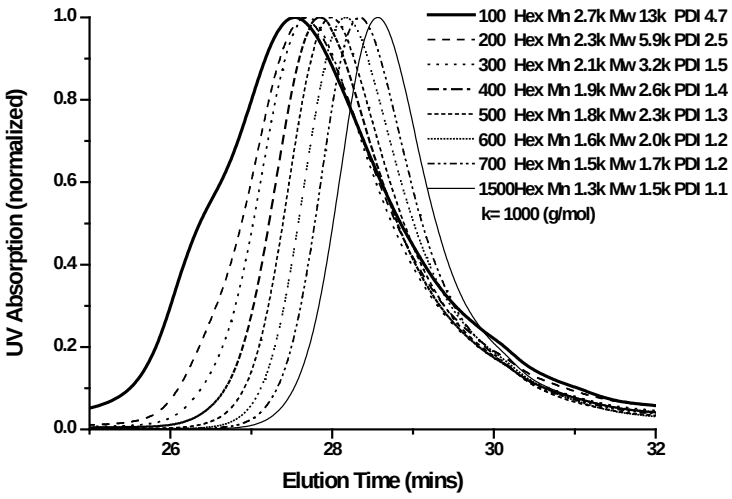

Figure 2. *Normalized and superimposed GPC chromatograms of lignin fractions from a fine fractional precipitation procedure of a softwood kraft lignin obtained via LignoBoost® from a fiber line producing fully bleached kraft pulp.*

II. CONCLUSIONS & OVERALL OUTLOOK

This effort offers novel avenues at creating reactive lignin materials that are stabilized and rendered better suited for industrial applications. It provides methods for creating lignins of controlled and modulated characteristics exhibiting thermal and polymerization stabilities. Such thermal properties and stable narrow molecular weight distributions of lignins and copolymers produced from commercial lignins provides a means for beneficially modulating the properties of an otherwise intractable bio-polymer.

III. REFERENCES

1. Dimitris S. Argyropoulos,. "High Value Lignin Derivatives, Polymers, & Copolymers & Use Thereof in Thermoplastic, Thermoset, Composite and Carbon Fiber Applications. " US Pub. No. : US 2013/0255216A1, Pub Date : Oct.3rd 2013, US Patent Application No,61/601,181, Filed Feb 21 2012.

2. Cui, C., Sadeghifar, H., Sen, S., and Argyropoulos, D. S.. "Toward Thermoplastic Lignin Polymers; Part II: Thermal and Polymer Characteristics of Kraft Lignin and Derivatives," BioResources 8(1), 864-886, (2013).
3. Hasan Sadeghifar, Chengzhong Cui, and Dimitris S. Argyropoulos, "Toward Thermoplastic Lignin Polymers. Part I. Selective Masking of Phenolic Hydroxyl Groups in Kraft Lignins via Methylation and Oxypropylation Chemistries; Ind. Eng. Chem. Res., 2012, 51 (51), pp 16713–16720 Publication Date (Web): December 4, 2012 (Article) DOI: 10.1021/ie301848j
4. George, A. O., and Prakash, G. K. S. (2004). "Carbocation Chemistry," John Wiley & Sons, Inc. New Jersey
5. Dimitris S. Argyropoulos; Journal of Biotechnology & Biomaterials;; "Towards Thermoplastic Lignin Polymers; Progress in the Utilization of Kraft Lignin for the Synthesis of Heat Stable Polymer Melts" ; 2013, 3, 3 ; doi: 10.4172/2155-952X.1000e123
6. Sanghamitra Sen , Hasan Sadeghifar, and D. S. Argyropoulos, "Kraft Lignin Chain Extension Chemistry via Propargylation, Oxidative Coupling & Claisen Rearrangement, Biomacromolecules .doi.org/10.1021/bm4010172 (2013)
7. Chengzhong Cui, Runkun Sun, Dimitris S. Argyropoulos;" Fractional Precipitation of Softwood Kraft Lignin; Isolation of Narrow Fractions Common to a Variety of Lignins" ACS Sustainable Chemistry & Engineering, March 2014.
8. Argyropoulos, D. S., H. Sadeghifar, Cui, C, S. Sen, "Synthesis & Characterization of Poly(arylene ether sulfone) Kraft Lignin Heat Stable Copolymers', ACS Sustainable Chemistry & Engineering, October 2013, DOI http://dx.doi.org/10.1021/sc400085a

NOVEL CHEMICAL MODIFICATIONS OF TECHNICAL LIGNINS FOR COMPOSITE AND RESIN APPLICATIONS

Harri Setälä, Kari Kammiovirta, Riku Talja, Stella Rovio, Tiina Liitiä

VTT Technical Research Centre of Finland, Biologinkuja 7, Espoo, P.O. Box 1000, FI-02044 VTT, Finland

Abstract

In this study, hydroxypropylation and allylation were used for modification of lignin to adjust their properties towards resin, coating and composite applications. The aim of this work was to convert selectively the phenolic hydroxyl groups of lignin to hydroxyalkyl ether substituents still containing the less reactive aliphatic hydroxyl groups. The aim was also at the same time to adjust the final properties of modified lignins, for example, solubility behavior, thermomechanical properties, compatibility with other polymers such as polyesters or polyolefins, and reactivity by adding allylic double bonds into lignin.

Introduction

Lignin and its derivatives are promising materials for resins, coating and composite applications. An efficient method to modify lignin for these purposes is hydroxyalkylation, for example, using propylene oxide or allyl glycidyl ether. This way it is possible to etherify selectively only the phenolic hydroxyl groups in dilute alkaline conditions.[1,2] Derivatization of aliphatic hydroxyl groups of lignin needs more alkaline conditions, higher temperatures and pressures.[3] Allylic double bonds can be utilized, for example, for further modification of lignin by grafting with monomers such as vinyl acetate or acrylic acid,[4,5] crosslinking with other polymeric materials,[6] or they can be converted to other functionalities such as thiosulphates and thioethers,[7] or epoxides.[8]

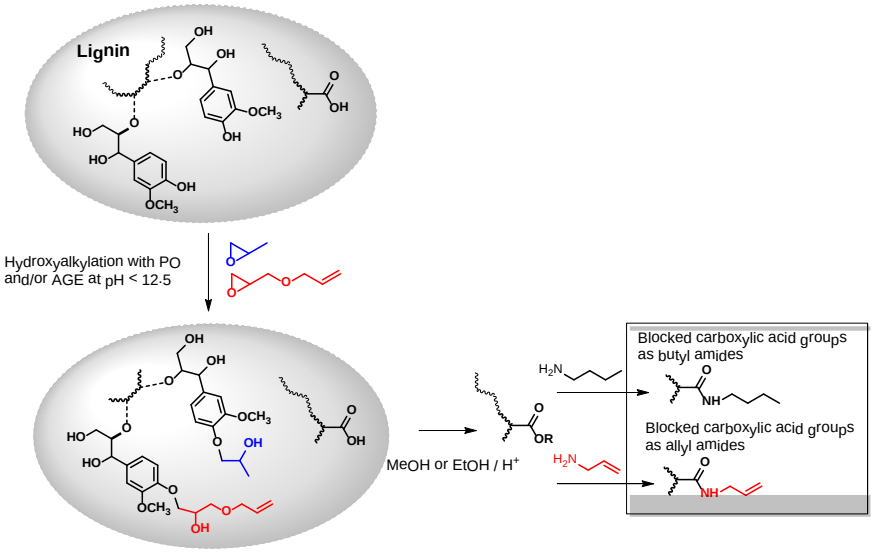

Figure 1. Modification of lignins using methods such as 1) hydroxypropylation with propylene oxide (PO), 2) allylation with allylglycidyl ether (AGE), or 3) esterification with MeOH or EtOH as an activation step followed by formation amides with butylamine or allylamine.

Materials and Methods

Industrial softwood kraft lignin (SW L) provided by Stora Enso and VTT's Lignofibre organosolv (VTT L) lignins[9] were used as starting materials. Methylethylketone (MEK), methanol (MeOH), ethanol (EtOH), butylamine, allylamine, propylene oxide (PO), and allyl glycidyl ether (AGE) were purchased by Sigma-Aldrich.

Procedure for the preparation of butyl or allyl amides of lignins: 10 g of SW L lignin was weighed into a 250 flask. 100 ml of MeOH was added. 0.4 ml of concentrated sulphuric acid was added. The reaction mixture was stirred overnight at +30 ^{o}C. 20 ml of butylamine or allylamine was added and stirred overnight at +30 ^{o}C. The reaction mixture was evaporated to a brown and oily product. This crude product was suspended in water and dialysed. The products butylamide (SWL BAm) or allylamide derivatives (SWL AAm) were then freeze-dried to brown powders.
Procedure for the hydroxypropylation in 0.5 M NaOH (method 1):[2] 1 g of lignin or its amide derivative was weighed into a 100 flask. 10 ml of 0.5 M NaOH, and then 0.53 ml or 1.33 ml of propylene oxide was added. The reaction mixture was stirred overnight at +40 ^{o}C. The reaction mixture was neutralized with HCl, and then dialysed and freeze-dried.
Procedure for the hydroxypropylated in aqueous 90 % MEK (method 2): 1 g of lignin or its amide derivative was weighed into a 100 flask. 20 ml of MEK and 2 ml of 1 M NaOH were added. Then 0.27 ml, 0.53 ml or 1.33 ml of propylene oxide was added. Molar ratios of PO/L were 1:1, 2:1, and 5:1. The reaction mixture was stirred overnight at +30 ^{o}C. The reaction mixture was neutralized with HCl. MEK was first evaporated. The reaction mixture was then dialysed and freeze-dried.
Procedure for the allylated lignins in 30 % aqueous MEK (method 3): 10 g of SWL BAm lignin containing phenolic hydroxyl groups 3.8 mmol/g of was weighed into a 250 ml flask. 70 ml of 0.5 M NaOH and 30 ml of MEK yielding a solution of 30 % aqueous alkaline MEK. The mixture was stirred two hours. 13.5 ml (114 mmol) of allyl glycidyl ether (AGE) was added in ½ hr. Molar ratio of AGE/L was 3:1. The reaction mixture was stirred overnight at +40 ^{o}C. The reaction mixture was neutralized with HCl, then dialysed and freeze-dried. Yield was 14.0 g (yield 98 % based on the phenolic hydroxyl group content of starting material). Unmodified SW kraft and organosolv VTT lignins were also used as starting materials using a similar procedure as described above and molar ratio of AGE/L was also 3:1.
The reaction efficiency and selectivity were investigated. The products and starting materials were characterized using ^{31}P NMR spectroscopy, size exclusion chromatography (SEC) and elementary analysis, as described elsewhere.[9]

Results and discussion

Results on preparation of amide derivatives

The carboxylic acid groups of technical lignins can react with the epoxy group of propylene oxide or with other epoxy groups containing reagents forming ester bonds between lignin and these reagents, and thereby reducing reaction efficiency. However, especially in alkaline conditions where hydroxypropylated and allylated lignin derivatives have been prepared, those ester bonds will be hydrolysed very easily forming free carboxylic acid groups which again can react with epoxy groups. This side-reaction may consume epoxy reagents chancing them to unwanted by-products. Another possible side-reaction is the reaction of epoxy groups with water (OH^-) forming a diol which can further react with epoxy groups forming, for example, oligomers of PO. The blocking of free carboxylic acid groups of lignins have been assumed also to have a positive effect on solubility into organic solvents, on thermomechanical properties lowering the glass transition temperature, and on compatibility with other technical polymers.

The side-reactions such as hydroxylation of epoxy group of propylene oxide can be prevented by blocking carboxylic groups, for example, as amide derivatives. Carboxylic acid groups of lignins have been changed first to methyl or ethyl ester derivatives as an activation step of carboxylic acid group, after which amines react easily with methyl or ethyl derivatives forming amides.[6]

The results of amide derivative syntheses are presented in Table 1. The total content of carboxylic acid groups in the original lignin sample was calculated from the amounts of reacted –COOH with butyl amine and non-reacted residual –COOH. Methyl esters of lignin seemed to be slightly more reactive than ethyl ester derivatives. Based on nitrogen determination, the amount of carboxylic acid groups was observed to be approximately 2.5 times higher than the results from ^{31}P measurements. However, the total carboxylic acid content of 1.0 mmol/g measured this way was very similar to the results obtained by the potentiometric titration studies.

Table 1 Preparation of butyl (BAm) and allyl (AAm) amide derivatives prepared from methyl (Me) or ethyl (Et) esters of lignin. Nitrogen content was determinated using elementary analysis. R = allyl or butyl group.

	N-content in -CONHR	-COOH reacted	-COOH residual	Reacted+residual -COOH
	(wt-%)	(mmol/g)	(mmol/g)	(mmol/g)
	by elementary analysis (N)		by ^{31}P NMR	Total
From ethyl ester to butyl amide (SWL-Et-BAm)	1.2	0.86	0.15	1.01
From methyl ester to butyl amide (SWL-Me-BAm)	1.0	0.71	0.19	0.90
From ethyl ester allyl amide (SWL-Et-AAm)	1.2	0.86	0.12	0.98
From methyl ester to allyl amide (SWL-Me-AAm)	0.9	0.64	0.20	0.84
SW kraft lignin (SWL)			0.41	

Results on preparation of hydroxypropylated and allylated lignins

The performance of hydroxypropylation and allylation reactions with and without blocking of carboxylic groups was investigated using ^{31}P NMR spectroscopy for determination of free aliphatic and phenolic hydroxyl groups before and after the modifications. The phenolic hydroxyl groups should be the most reactive with the epoxy groups of propylene oxide and allyl glycidyl ether, and their amount thus should be decreased when reacted. The effects of reaction conditions and amidation were first studied using hydroxypropylation as a model reaction before using allylation. Three different reaction media were used. Three different molar ratios of PO/L were used: 1:1, 2:1, and 5:1. For example, the code SWL-Et-BAm-HP(1:1) means that SWL lignin was first esterified to ethyl ester (Et), then converted to butyl amide (BAm), then hydroxypropylated (HP) using PO/L ratio 1:1.

Table 2. Hydroxypropylation of SWL, VTT L, and butyl amide derivatives of SWL.

Sample code	Molar ratio	Aliphatic OH	Carboxylic acid	Phenolic OH	Total OH	
	PO:L	(mmol/g L)	(mmol/g L)	(mmol/g L)	(mmol/g L)	Reaction medium
SWL-Me-B-HP (1:1)	1:1	1.67	0.2	1.99	3.86	in aqueous 90 % MEK
SWL-Me-B-HP (2:1)	2:1	2.17	0.22	1.66	4.05	in aqueous 90 % MEK
SWL-Me-B-HP (2:1)	2:1	3.33	0.23	0.68	4.24	in 0.5 M NaOH
SWL-Me-B-HP (5:1)	5:1	3,6	0.23	0.32	4.14	in 0.5 M NaOH
SWL-HP (1:1)	1:1	1.64	0.36	2.17	4.17	in aqueous 90 % MEK
SWL-HP (2:1)	2:1	2.13	0.35	2.07	4.56	in aqueous 90 % MEK
SWL-HP (2:1)	2:1	3.83	0.44	0.29	4.56	in 0.5 M NaOH
SWL-HP (5:1)	5:1	4.48	0.37	0.08	4.93	in 0.5 M NaOH
Organosolv-HP	2:1	3.59	0.16	0.09	3.84	in 0.5 M NaOH
Organosolv-HP	5:1	3.76	0.23	0	3.99	in 0.5 M NaOH
SWL		1.78	0.41	3.64	5.83	

Based on results given in Table 2, the aqueous alkaline 90 % MEK was not a very good reaction system, probably due to too high MEK content and too low alkalinity. Butyl amide derivatives were a bit more reactive than SWL in this reaction system. However, 0.5 M NaOH was a much better reaction medium. Reactivity order of lignins was: organosolv > SWL > SWL-Me-B. In this case, the blocking of carboxylic acids was not necessary in respect of reaction efficiency. The amount of aliphatic hydroxyl groups was increased in every case, but not as much as expected. Total amount of hydroxyl groups was in every case decreased compared to the starting materials. Any good explanation for this rather contradictory behaviour was not found.

The same starting materials were also used and compared in allylation studies without any hydroxypropylation or blocking of free carboxylic acid groups. At this time, aqueous alkaline 30 % MEK was used as reaction medium. Even though the alkaline aqueous conditions were better for the

hydroxypropylation, 30% MEK was used to ensure the solubility of allylation regent (AGE). Molar ratio of AGE/L was now 3:1. Alkalinity of this system seemed to be enough for an effective reaction of phenolic hydroxyl groups with epoxy group of allyl glycidyl ether. Also here, the blocking of carboxylic acids was not necessary, as shown in Table 3.

Table 3 Allylation of SWL, VTT L, and butyl amide derivative of SWL.

Sample code	Molar ratio	Aliphatic OH	-COOH	Phenolic OH	Total OH	
	PO:L	(mmol/g L)	(mmol/g L)	(mmol/g L)	(mmol/g L)	Reaction medium
SWL-A	3:1	3.74	0.30	0	4.04	in aqueous 30 % MEK
VTT L-A	3:1	3.29	0.14	0	3.42	in aqueous 30 % MEK
SWL-Me-BAm-A	3:1	3.06	0.12	0.16	3.35	in aqueous 30 % MEK

CONCLUSIONS

Several modification routes were used to prepare new type of derivatives of lignins such as allyl and butyl amides and/or 3-allyloxy-2-hydroxypropyl ether derivatives of lignins. The most effective etherification routes were either 0.5 M NaOH or 0.5 M NaOH with 30 % of a co-solvent. The blocking of free hydroxyl groups of lignins might be a useful way to adjust the properties of lignins such as solubility, thermoplasticity and/or compatibility with other polymeric materials

V. ACKNOWLEDGEMENT

WoodWisdom-EraNet and Tekes are acknowledged for the funding of ProLignin project. Stora Enso is also acknowledged for providing the industrial kraft lignin.

References

1. R. K. Jain; W. G. Glasser. Lignin derivatives II. Functional ethers. *Holzforschung* **1993**, *47*, 325.
2. H. Sadeghifar; C. Cui; D. S. Argyropoulos. Toward thermoplastic lignin polymers. Part 1. Selective masking of phenolic hydroxyl groups in kraft lignins via methylation and oxypropylation chemistries. *Ind. Eng. Chem. Res*. **2012** , *51*, 16713.
3. Y. Li; A. J. Ragauskas. Kraft lignin-based rigid polyurethane foam. *J. Wood Chem. Technol*. **2012**, *32*, 210.
4. S. S. Panesar; S. Jacob; M. Misra; A. K. Mohanty. Functionalization of lignin: Fundamental studies on aqueous graft copolymerization with vinyl acetate. *Ind. Crops Prod*. **2013**, *46*,191– 196.
5. Z. Zhu, M. Li, E. Jin. Effect of an allyl pretreatment of starch on the grafting efficiency and properties of allyl starch-*g*-poly(acrylic acid). *J. Appl. Polym. Sci*. **2009**, *112*, 2822–2829.
6. H. Pohjanlehto, H. Setälä, K. Kammiovirta, A. Harlin. The use of *N*,*N*'-diallylaldardiamides as cross-linkers in xylan derivatives-based hydrogels. *Carbohydr. Res*. **2011**, *346*, 2736–2745.
7. G. Wenz; P. Liepold; N. Bordeanu; Synthesis and SAM formation of water soluble functional carboxymethylcelluloses: thiosulfates and thioethers. *Cellulose* **2005**, *12*, 85–96.
8. A. M. L. Huijbrechts; R. ter Haar; H. A. Schols; M. C. R. Franssen; C. G. Boeriu; E. J. R. Sudhölter. Synthesis and application of epoxy starch derivatives. *Carbohydr. Polym*. **2010**, *79*, 858–866.
9. Liitiä, T., Rovio, S., Talja, R., Tamminen, T., Rencoret, J., Gutiérrez, A., del Río, J.C., Saake, B., Schwarz, K.U. Vila Babarro, C., Gravitis, J., Orlandi, M. Structural characteristics of industrial lignins in respect to their valorisation, tob e presented in 13th European Worshop on Lignocellulosics and pulp, 24.-27.6.2014, Seville, Spain.

STRUCTURAL CHARACTERISTICS OF INDUSTRIAL LIGNINS IN RESPECT TO THEIR VALORIZATION

Liitiä, T.[1]*, Rovio, S.[1], Talja, R.[1], Tamminen, T.[1], Rencoret, J.[2], Gutiérrez, A.[2], del Río, J.C.[2], Saake, B.[3], Schwarz, K.U.[3] Vila Babarro, C.[4], Gravitis, J.[5], Marco Orlandi[6]

*[1] VTT Technical Research Centre of Finland, P.O. Box 1000, FI-02044 VTT, Finland; [2] IRNAS-CSIC, P.O.Box 1052, 41080-Seville, Spain; [3] University of Hamburg, Department of Wood Science, Germany, Leuschnerstrs. 91, D-21031 Hamburg, Germany; [4] Thünen Institute for Wood Research, Leuschnerstr. 91, D-21031 Hamburg, Germany; [5] Latvian State institute of Wood Chemistry, 27 Dzerbenes Str., LV-1006-Riga, Latvia; [6]University of Milan-Bicocca, Department of Earth and Environmental Science, Piazza della Scienza 1, 20126 Milan, Italy (*Email of corresponding author: Tiina.Liitia@vtt.fi)*

ABSTRACT

The effect of raw material and pretreatment procedure on the structure and properties of industrial lignins was evaluated by detailed chemical and physical characterization. The application potential of studied lignins was considered based on those. Hydrolysis lignin and steam exploded lignins had clearly distinct characteristics compared to the spent liquor lignins; higher molar mass, significantly higher amount of native aryl ether linkages and thereby low phenol content. The hydrolysis lignin also contained significant amount of carbohydrate and protein residues, which may affect the applicability. For resin applications, the kraft lignins seem most reactive in respect of high phenol content. The high molar mass of hydrolysis lignin and steam exploded lignins could be beneficial for dispersants and composites.

I. INTRODUCTION

In future bioeconomy, there is need to generate new biobased fuels, chemicals and materials utilising lignocellulosic feedstocks in order to provide more sustainable renewable alternatives for present oil based products. For transportation, bioethanol is a potential substitute, but its high production costs inhibit rapid commercialisation. Also traditional pulping industry is looking for new added value products. As a phenolic biopolymer, lignin is a potential raw material for the production of biobased aromatic chemicals, as well as building blocks for materials and fuels. The competitiveness of traditional pulp and bioethanol production processes could thus be increased by conversion of the side-stream lignins into new biobased high-value products instead of incineration. Depending on the used feedstock and biomass processing technology, lignin by-products with distinct structural features and variable application potential are produced. Compared to the traditional industrial lignins, the sulphur-free lignin residues produced by lignocellulosic bioethanol plants are not so extensively studied. Especially the utilisation potential of the lignin rich hydrolysis residue recovered after steam explosion pretreatment followed by saccharification and fermentation stages should be better explored.

In this paper, the effect of raw material (softwood, hardwood, wheat straw, bagasse) and pretreatment procedure (kraft, soda, soda-AQ, ethanol organosolv, steam explosion) on the structure and properties of lignin was evaluated by detailed chemical and physical characterization. The application potential of studied lignins was considered based on those. In addition to the purity and composition, the lignin structure (S/G/H ratio, inter-unit linkages) was analyzed using both the degradative (Py-CG/MS) and spectroscopic techniques (2D ^{1}H-^{13}C NMR). Lignin functionalities were analysed by ^{31}P NMR spectroscopy, and molar mass was determined by size exclusion chromatography. Thermal properties were evaluated by DSC. Lignins from industrial or pilot scale processes were mainly used.

II. EXPERIMENTAL

Raw materials. Industrial softwood and hardwood (eucalypt) kraft lignins (**Kraft-SW, Kraft-HW**) were obtained from Stora Enso and Suzano, respectively. Commercially available soda wheat straw lignin (**Soda-WS**) was purchased from Green Value. Wheat straw hydrolysis lignin (**HL-WS**) was obtained from the pilot plant of a bioethanol producer. Steam exploded wheat straw, birch and grey alder lignins (**SE-WS, SE-birch, SE-GA**) were also prepared at lab scale. Steam explosion (SE) was performed at 235°C with 3.2MPa pressure for 1min, after which the lignins were extracted by 0.4% NaOH. Organosolv lignin (**OS-HW**) of *E. globulus* was produced at pilot scale using the lignofibre (LGF) process [1] with ethanol/water (85/15) solvent and 3.5% phosphinic acid [2]. The OS lignin was precipitated by dilution with water (1:4) after some concentration by

evaporation of ethanol. Bagasse (**SAQ-B**) lignin was produced at lab scale by soda-AQ cooking (kappa 9.5) using 16.5% effective alkali in presence of 0.1% anthraquinone (AQ), followed by LignoBoost type lignin separation with two stage pH drop at 35% dry solids with CO_2 and H_2SO_4.

Analytical methods. For composition analyses, the lignin was hydrolysed [3], and the acid insoluble Klason lignin was quantified gravimetrically. Acid soluble lignin was determined spectroscopically at 205 nm (TAPPI UM250 um-83, 1991). The carbohydrate content of hydrolysate was analysed by borate anion-exchange chromatography with post-column derivatisation and detection at 560 nm [4]. The ash content was gravimetrically determined after incineration at 800 °C. The complete oxidation method was used for elemental analysis on a CE Instruments CHNS Flash 1112 Analyzer system. Methoxyl groups were determined according to [5].

The molar mass distributions of lignins were determined by size exclusion chromatography in 0.1M NaOH using MCX 1000 and 100 000 columns with UV detection (280 nm) and polystyrene suphonate (Na-PSS) calibration.

Lignin functionalities were determined by ^{31}P NMR according to Granata and Argyropoulos [6]. Accurately weighted samples (40 mg) were dissolved in 150 µL of *N,N*-dimethylformamide. After dissolution, 100 µL pyridine, 200 µL internal standard solution of 0.05 M *endo*-N-Hydroxy-5-norbornene-2,3-dicarboximide in pyridine/$CDCl_3$ (1.6/1, v/v) and 50 µL $Cr(acac)_3$ solution (11.4 mg/1 mL) in pyridine/$CDCl_3$ (1.6/1, v/v) were added. Then, 100 µL 2-chloro-4,4,5,5-tetramethyl-1,3,2-dioxaphopholane was added drop-wise, followed by 300 µL of $CDCl_3$. The ^{31}P NMR measurements were performed immediately after sample preparation at room temperature with Bruker Avance 500 MHz NMR spectrometer using 90° pulse and 5s pulse delay for 512 scans.

2D HSQC (heteronuclear single quantum coherence) NMR spectra were recorded at 25ºC by a Bruker AVANCE III 500 MHz, equipped with a cryogenically-cooled 5 mm TCI gradient probe with inverse geometry using 'hsqcetgpsisp2.2' pulse sequence (adiabatic-pulsed version). Lignin samples were dissolved (40mg/0.75 mL) in DMSO-d_6. Spectral widths of 5000 Hz (10-0 ppm) and 20,843 Hz (165-0 ppm) for the ^{1}H- and ^{13}C-dimensions were used. The number of transients was 64 for 256 time increments, with $^{1}J_{CH}$ of 145 Hz. The semiquantitative analysis of the correlation peaks was performed using Brukers Topspin 3.1 software. The lignin inter-unit linkages based on C_α–H_α correlations were calculated as described previously [7].

Pyrolysis was performed with a 2020 micro-furnace pyrolyzer (Frontier Laboratories Ltd.) connected to an Agilent 6890 GC/MS system equipped with a DB-1701 fused-silica capillary column and an Agilent 5973 mass selective detector. The pyrolysis was performed at 500 ºC. The GC oven temperature was programmed from 50 ºC (1 min) to 100 ºC at 30 ºC/min and then to 290 ºC (10 min) at 6 ºC/min. Helium was the carrier gas. Peak areas were calculated for the lignin-degradation products, the summed areas were normalized, and the data for two repetitive analyses were averaged and expressed as percentages to determine the proportion of syringyl (S), guaiacyl (G) and p-hydroxy phenyl (H) type lignin units.

The lignin glass transition (Tg) temperatures were determined by Mettler Toledo Differential Scanning Calorimeter model DSC820 system STARe SW 9.20. Temperature profile with following steps was used: 1) heating from 25 ^{o}C to 105 ^{o}C with 20 min isothermic phase for drying, 2) cooling phase to -60 ^{o}C, 3) first actual heating phase from -60 ^{o}C to 200 ^{o}C, 4) cooling phase to -60 ^{o}C, and 5) second heating phase from -60 ^{o}C to 250 ^{o}C. Heating and cooling rate of 10°C/min was used in all cases.

III. RESULTS AND DISCUSSION

Lignins from different raw materials and pretreatment processes were characterized in detail, and their application potential was evaluated based on chemical characteristics. According to the chemical compositions given in Table 1, the actual lignin content varied between 82-96% in most lignins. In hydrolysis residue the lignin content was clearly lower, being only 55%, which is mainly due to the carbohydrate residues of unhydrolysed cellulose. Somewhat higher nitrogen content of hydrolysis lignin also indicates protein residues (Table 2). The impurities may have significant effect on hydrolysis lignin applicability, and based on requirements of the target applications some lignin purification procedure may be needed. Also in Soda-AQ bagasse lignin, the carbohydrate content originating from xylan was slightly higher compared to the others. The high ash contents of HL, SAQ-B and Kraft-HW lignins are probably raw material related, or indications of insufficient washing. The sulphur content of kraft lignins was below 4% (Table 2). Surprisingly, also the wheat straw lignins (Soda-WS, HL-WS) showed some traces of sulphur. The composition in terms of the H:G:S ratios, also widely varied among the lignin samples of different raw materials, the S/G ratio being higher for the hardwood lignins compared to the wheat straw and bagasse lignins (Table 2).

Molar mass is an essential structural feature affecting lignin applicability. Compared to the other lignins, the hydrolysis lignin had significantly higher molar mass, although it was only partly soluble in alkali used as an eluent (Table 2). The high molar mass could be an advantage in lignin based dispersants, providing better

adsorption properties. High molecular weight lignin could also be beneficial in respect of mechanical properties of lignin based composites. For these applications, the hydrolysis lignin solubility and thermoplasticity, respectively, should however be improved by chemical modification. The molar mass of all the other lignins was clearly lower, although the SE lignins and the SW kraft lignin had somewhat higher molar mass compared to the others. The lower molar mass level of the other spent liquor lignins could be beneficial in polyurethane (PU) resin applications to prevent the excess increase of viscosity, or to improve the lignin solubility.

Table 1. Lignin compositions.

Sample	Ash content, %	Klason lignin, %	Acid soluble, %	Total lignin, %	Total carbohydrates, %	Xyl, %	Glc, %	Man, %	Gal, %	Ara, %
Kraft-SW	0.6	90.2	5.1	95.3	2.2	0.8	0.2	0.1	0.8	0.3
Kraft-HW	10.5	82.6	0.0	82.6	1.2	0.5	0.2	0.0	0.3	0.2
Soda-WS	2.7	85.0	7.8	92.8	2.9	1.6	0.5	0.1	0.2	0.5
SAQ-B	6.6	82.8	4.5	87.3	7.1	5.7	0.2	0.1	0.2	0.9
OS-HW	0.6	91.1	2.6	93.7	0.8	0.4	0.1	0.1	0.1	0.1
SE-Birch	0.8	92.4	2.9	95.3	1.2	0.8	0.1	0.1	0.1	0.1
SE-GA	0.7	89.1	2.2	91.3	2.3	1.5	0.3	0.2	0.2	0.1
SE-WS	1.6	91.8	2.0	93.8	1.4	0.6	0.5	0.1	0.1	0.1
HL-WS	12.1	52.9	2.2	55.1	35.3	5.2	29.2	0.4	0.3	0.2

Table 2. Elemental compositions and methoxyl contents together with the average molar masses (Mn, Mw, PD), as well as the proportions of S, G and H type units (by Py-GC/MS) and the glass transitions of first and second heating (Tg_{1st}, Tg_{2nd}).

Sample	Elemental composition*					MeO %*	Type of aromatic units				Molar mass			Glass transition	
	C, %	H, %	O, %	N, %	S, %		S, %	G, %	H, %	S/G	Mn, g/mol	Mw, g/mol	PD	Tg 1st	Tg 2nd
Kraft-SW	65.2	5.9	25.6	0.2	3.1	12.7	-	94	6	-	2400	4700	2.0	140.4	146.7
Kraft-HW	65.0	5.9	26.2	0.2	2.7	16.2	67	32	1	2.1	1800	2800	1.6	177.3	182.0
Soda-WS	65.0	6.0	27.0	0.8	1.1	11.2	40	34	26	1.2	2000	3300	1.7	137.7	140.6
SAQ-B	64.6	6.0	28.9	0.5	0.0	n.d.	33	29	38	1.1	2300	4000	1.7	150.1	151.8
OS-HW	63.8	6.4	29.4	0.4	0.0	23.7	68	31	1	2.2	2000	3100	1.6	121.0	130.6
SE-Birch	63.0	6.1	30.7	0.2	0.0	18.0	75	24	1	3.1	2200	5200	2.4	153.5	162.6
SE-GA	63.1	5.8	30.6	0.5	0.0	n.d.	63	31	6	2.1	2300	5200	2.3	150.3	165.4
SE-WS	n.d.	n.d	n.d.	n.d	n.d	n.d.	27	54	19	0.5	2800	7000	2.5	160.6	186.4
HL-WS	54.8	6.4	37.2	1.3	0.2	nd	nd	nd	nd	nd	.2200	15800#	7.2	-	182.6

* Elemental composition and methoxyl contents have been corrected by ash content. # HL only partly soluble in 0.1M NaOH used as an eluent. n.d. = not determined.

Table 3. Content of most typical lignin inter-unit linkges per 100 C9 unit determined by 2D NMR, and the lignin functionalities determined by ^{31}P NMR (mmol/g lignin, calculated according to the lignin content of the samples, the effect of carbohydrates on aliphatic hydroxyls not taken into account).

Sample	β-O-4	β–β	β-5	β-1	Aliph OH, mmol/g	C + S, mmol/g	G, mmol/g	Catechol, mmol/g	p-OH, mmol/g	Phenolic OH, mmol/g	Total OH, mmol/g	COOH mmol/g
Kraft-SW	2.5	0.8	0.8	-	2,1	1,8	2,2	0,0	0,1	4,1	6,2	0,5
Kraft-HW	2.4	1.5	0.1	-	1,6	3,3	0,9	0,0	0,0	4,2	5,8	0,6
Soda-WS	3.9	0.9	0.4	-	1,4	2,0	0,9	0,0	0,5	3,4	4,8	0,9
SAQ-B	3.0	0.2	0.6	-	1,1	1,6	0,6	0,0	0,9	3,2	4,3	0,5
OS-HW	4.7	3.0	1.6	-	1,7	2,5	0,4	0,2	0,0	3,1	4,9	0,0
SE-Birch	22.3	4.7	1.6	-	2,4	1,9	0,5	0,0	0,0	2,4	4,7	0,3
SE-GA	24.5	2.4	3.9	0.3	3,1	1,7	0,6	0,3	0,2	2,7	5,8	0,2
SE-WS	7.9	3.3	0.8	-	1,4	1,0	0,9	0,0	0,2	2,1	3,5	0,5
HL-WS	20.1	1.9	8.1	-	8,5	0,3	0,3	0,0	0,1	0,7	9,2	0,4

The lignin inter-unit linkages were detected by 2D-NMR measurements, and ^{31}P NMR spectroscopy was used to quantify the different types of lignin functionalities (Table 3). Both methods well describe the depolymerisation occurring during biomass pretreatment. Among the aliphatic hydroxyl and carboxylic acid groups, the phenolic units formed as a result of cleavage of aryl ether linkages are the key functional groups in respect of lignin solubility and reactivity towards crosslinking and further modifications to adjust the lignin properties.

The main inter-unit linkages detected in all the technical lignins were the alkyl-aryl ethers (β–*O*–4´), followed by resinols (β–β´) and phenylcoumarans (β–5´) in different proportions. The abundance of native aryl ether linkages was high in the industrial hydrolysis lignin, which was accompanied with very low phenol content, indicating rather mild biomass pretreatment process. The lignins extracted from steam exploded hardwoods also had high content of alkyl-aryl ether linkages and rather low proportion of phenolic units, whereas the steam explosion clearly had more drastic effect on wheat straw in the same conditions. If the hydrolysis lignin with extremely high content of carbohydrates and thus poor solubility is excluded, the highest total hydroxyl content was detected for kraft lignins and SE-GA, providing highest amount of reactive sites e.g. for crosslinking with isocyanates for polyurethane resins. The proportion of phenolic hydroxyl groups was higher in all spent liquor lignins, but especially in kraft lignins, compared to the HL and SE lignins. The amount of C5 unsubstituted phenols, which is a prerequisite for the reactivity in phenol formaldehyde (PF) resins, was highest in SW kraft lignin. Due to the non-methoxylated *p*-hydroxyphenyl groups detected, also the SAQ bagasse and soda wheat straw lignin could provide sufficient reactivity for PF resin applications. In bagasse the proportion of non-methoxylated *p*-hydroxyphenol groups was higher than in wheat straw.

Thermal properties of lignins were evaluated according to the Tg values (Table 2), which varied between 121 and 177 °C in the first heating. Both the Kraft-HW and the steam exploded lignin of wheat straw had the highest Tg indicating more rigid/condensed structure compared to the other lignins. The lowest Tg was detected for the OS-HW. Some condensation took place during the first heating, which slightly increased the Tg values of all lignins in the 2nd heating. Similarly, some condensation may occur also in process temperatures typically used for processing of thermoplastic composites, unless this could be prevented by chemical modification.

IV. CONCLUSIONS

The hydrolysis lignin and the steam exploded lignins had clearly distinct characteristics (high molar mass, low phenolic content) compared to the spent liquor lignins. For the reactivity required in PU resins, also aliphatic hydroxyl groups are essential. If the hydrolysis lignin with carbohydrate residues and limited solubility is excluded, the highest total hydroxyl content was detected for Kraft lignins and SE-GA. The Kraft-SW had most C5 unsubstituted phenols, which is a prerequisite for the reactivity in phenol formaldehyde (PF) resins. Soda-AQ bagasse and soda wheat straw lignins contain non-methoxylated *p*-hydroxyphenyl groups either as part of the lignin macromolecule or in p-coumaryl esters. These structures may also improve reactivity for PF resin applications. The hydrolysis and SE lignins had the highest molar mass, assumedly providing better adsorption properties for dispersants. Higher molar mass lignin could be beneficial also for the mechanical properties of lignin based composites. However, the effect of carbohydrate and protein impurities may also significantly affect the applicability of hydrolysis lignin. The LGF organosolv lignin had clearly lowest Tg, being in that sense most thermoplastic, although chemical modification is still needed to obtain mouldable thermoplastic lignin for thermal processing. Obviously, only hypothesis on applicability can be made based on chemical characteristics, and these need to be verified with the actual testing in the target applications.

V. ACKNOWLEDGEMENT

WoodWisdom-EraNet and the national funding agencies (Tekes, MIPAFF, INIA-Spain, FNR, Latvian Ministry of Agriculture) are acknowledged for the funding of ProLignin project. Stora Enso, Suzano and Valmet are also acknowledged for providing the industrial and pilot scale lignins.

VI. REFERENCES

[1] Mikkonen, H., Peltonen, S., Kallioinen, A., Suurnäkki, A., Kunnari, V., Malm, T. Process for defibering a fibrous material. **2009**, Patent WO2007/066007.

[2] Liitiä, T.; Barth, D.; Tamminen, T.; Colodette, J.L. Organosolv pulping as a pretreatment for bioethanol production from Eucalyptus and Elephant grass. *17th International symposium on wood, fibre and pulping chemistry.* June 12-14, **2013**, Vancouver, Canada.

[3] Puls, J. Substrate analysis of forest and agricultural wastes. In: *Biotechnology in agriculture; bioconversion of forest and agricultural plant residues*. Ed. Saddler, J.N. CAB International, **1993**, 13-32.

[4] Willför, S.; Pranovich, A.; Tamminen, T.; Puls, J.; Laine, C.; Suurnäkki, A.; Saake, B.; Uotila, K.; Simolin, H.; Henning, J.; Holmbom, B. Carbohydrate analysis of plant materials with uronic acid-containing polysaccharides – A comparison between different hydrolysis and subsequent chromatographic analytical techniques. *Industrial crops and products* **2009**, *29*, 571-580.

[5] Vieböck, F., Schwappach, A. Eine neue Methode zur maßanalytischen Bestimmung der Methoxyl- und Äthoxylgruppe. I. Makro-analyse. *Berichte der deutschen chemischen Gesellschaft (A and B Series)*, **1930**, *63*, 2818–2823.

[6] Granata, A., Argyropoulos, D.S. 2-Chloro-4,4,5,5-tetramethyl-1,3,2-dioxaphospholane, a reagent for the accurate determination of the uncondensed and condensed phenolic moieties in lignins. *J. Agric. Food Chem.***1995**, *43*, 1538-1544.

[7] del Rio, J.C.; Princen, P.; Martinez, A.T.; Ralph, J.; Gutiérrez, A. Structural characterization of wheat straw lignin as revealed by analytical pyrolysis, 2D-NMR, and reductive cleavage methods. *J. Agric. Food. Chem.* **2012**, *60*, 5922-5935.

ON THE UTILIZATION OF FATTY ACID ESTERS OF TECHNICAL LIGNINS IN BIOREFINERY APPLICATIONS

Klaus Koivu*, Hasan Sadeghifar**, Paula Nousiainen*, Dimitris S. Argyropoulos** # , and Jussi Sipilä*

**University of Helsinki, Department of Chemistry. P.O.Box 55, 00014-University of Helsinki, Finland*
***Departments of Forest Biomaterials & Chemistry, North Carolina State University, 2820 Faucette Drive, Rm 3104, Raleigh, NC, 27695-8005, USA*
 # Center of Excellence for Advanced Materials Research Center of Excellence, King Abdulaziz University, PO BOX 80203, Jeddah, 21589, Saudi Arabia.

ABSTRACT

Softwood LignoBoost kraft lignin was esterified with ethanoyl (C2), octanoyl (C8), dodecanoyl (C12) and hexadecanoyl (C16) chloride with various molar ratios with respect to the total OH of lignin. The progress of the reaction and its specific reactivity was studied with quantitative ^{31}P-NMR spectroscopy, FTIR- ATR, molecular weight distribution and DSC. C8-C16 acyl chlorides showed distinct enhanced reactivity toward the aliphatic hydroxyl groups, whereas C2 was found to attach evenly to all groups. Furthermore, partially methylated and acylated, fully substituted lignins, were studied via solution viscosity, melt extrusion, and Differential Scanning Calorimetry (DSC) to understand the effect of the long chain fatty acids on the material properties.

I. INTRODUCTION

The utilization of the second most abundant plant biopolymer lignin as a source for thermoplastics additives in polymeric materials has challenged material chemists over several decades. Only limited success have been achieved despite broad variety of formulations studied so far. This is at least partly due to great variances of lignins obtained from technical processes in terms of structure, chemical reactivity and molecular size.

In the present study we have examined the structure and polymer properties (molecular weight, glass transition temperature, rheological properties) of a variety of conventional Kraft lignins and new non-sulfur technical lignins with comparison to their fatty acid derivatives. The esterified lignins, in particular, have shown interesting properties as fiberboard barrier materials [3] and possess promising properties for thermoplastic additives, in general. We have also successfully applied oligomeric lignin model compounds to increase our knowledge on the behavior of the so called “reactive groups” of lignins in the derivatization procedures to assist the selection of the particular type of technical lignins for special application.

II. EXPERIMENTAL

Chemicals Softwood LignoBoost kraft lignin was obtained from Stora Enso Oyj, Finland. Acetyl chloride (C2), octanoyl chloride (C8), lauroyl chloride (C12), and palmitoyl chloride (C16) were obtained from Sigma-Aldrich and were used as received. Pyridine, tetrahydrofuran (THF), dimethylformamide (DMF) and dimethyl sulfate were obtained from Sigma-Aldrich. Solvents were used from freshly opened bottles.

Synthesis of esters Typically, lignin was dissolved for 30 minutes in a mixture of THF, DMF, and pyridine at 60 °C under argon. Acyl chloride was injected with a syringe. The reaction was kept for 48 hours at 65 °C with efficient stirring (Figure 1 II). Purification of the reaction mixtures was performed by washing with water and ethanol.

Methylation synthesis of lignin Methylation of lignin was performed according to Sadeghifar et al. 2012 [4] (Figure 1 I).

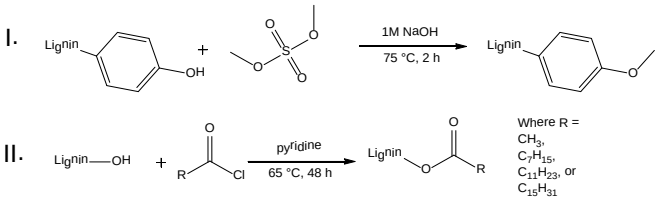

Figure 1. I. The methylation equation of lignin phenolic hydroxyls with dimethyl sulfate in basic aqueous solution. II. The esterification equation of lignin hydroxyls with C_2-C_{16} fatty acid chlorides using pyridine as the catalyst.

Quantitative ^{31}P-NMR spectroscopy Samples were phosphitylated according to method of Granata and Argyropoulos [2]. The internal standard was N-hydroxy-5-norbornene-2,3-dicarbocylic acid imide and the relaxation agent used was chromium(III) acetylacetonate. The ^{31}P-NMR spectra were recorded by inverse gated proton decoupling sequences on a Bruker 300 spectrometer with 5 mm direct detection broadband probe-head.

FTIR-ATR FTIR-ATR were measured with Perkin Elmer Frontier with ATR accessory.

Gel permeation chromatography GPC was performed on Waters setup using a set of Styragel HR5-E and HR-1 columns in series and samples were acetobrominated and filtered before measurement [1].

Differential scanning calorimetry Glass transition temperatures (T_g) and melting temperatures (T_m) of samples were determined using a TA Instruments DSC Q200 with temperature ramp of 10 °C/min.

Viscometry was performed on Ubbelohde viscometer 25, **Extrusion** on DSM Xplore Micro Compounder Extruder 15 ml and **Thermogravimetry** on TA instruments Q500.

III. RESULTS AND DISCUSSION

Synthesis

During the work new convenient methods for the preparation of long chain fatty acid derivatives of lignins have been developed. In the first set, several technical lignins have been fully acylated using acetyl chloride (or acetic anhydride) (C2), octanoyl chloride (C8), lauroyl chloride (C12) and palmitoyl chloride (C16) using pyridine as catalyst. Generally, a 30 mol-% excess has been used in these procedures to provide full derivatization [3]. All samples were fully characterized with ^{1}H, ^{13}C, HSQC, ^{31}P-NMR, GPC and DSC. Also several model compounds have been used to study the behavior of different types of hydroxyl groups in acylation reactions.

In our new approach, we have examined methods for partial acylations of softwood kraft lignin with C2, C8, C12 and C16 fatty acid chlorides. For the preparation of lignin derivatives, the lignin was measured to have 6.67 mmol/g hydroxyls based on quantitative ^{31}P-NMR. Esterifications were performed with 10, 30, 50, 70, and 130 mol-% of these fatty acid chlorides. Altogether 20 samples were measured with quantitative ^{31}P-NMR, FTIR-ATR and GPC. Finally, solution viscosity measurements were performed on the 50 mol-% acylated samples, as a function of concentration, to determine their intrinsic viscosity.

Finally, methylation was incorporated on the phenolic OH groups of the lignin prior to acylation, using dimethyl sulfate [4] to create more stable (thermoplastic) partially acylated lignins. 20g batches were created of 50% methylated fully acylated (C2,C8,C12,C16) lignins and were used for extrusion and DSC.

Characterization of the lignin esters

In order to analyze the structure of esterified lignins, the derivatized materials were first subjected to the IR analysis. From the spectra in Figure 2 a, the acylation can be detected by decline of the OH band at 3440 cm^{-1}, and increase ester bands at 1760 and 1737 cm^{-1} with degree of added C_{12}COCl. Molecular weights were determined by GPC and show an expected increase with added amount of octanoyl chloride (C8) taken as an example (see Figure 2 b).

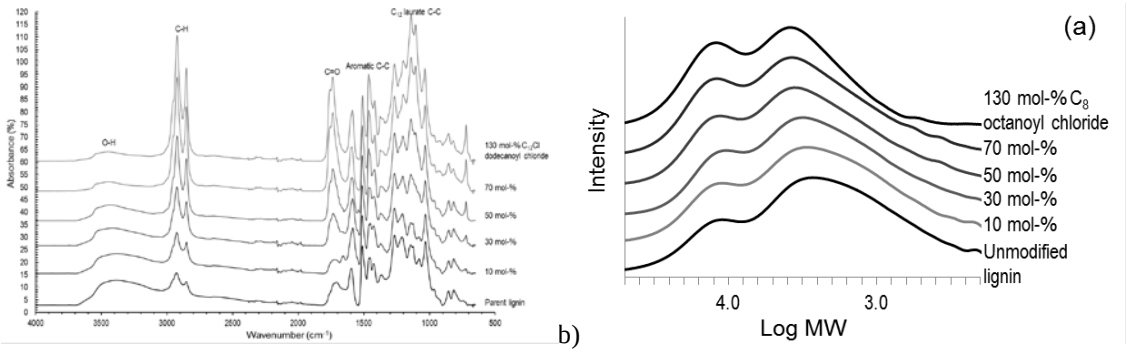

Figure 2. a) FTIR-ATR spectra of $C_{12}C$=OCl acylated lignins and the unmodified lignin with signal assignments (normalized by 1510 cm^{-1} aromatic C-C stretch). b) Molecular weight distributions of unmodified lignin and C_8 esters.

Hydroxyl group reactivity

The amounts of residual free hydroxyl groups were found to decrease with increasing acyl chloride ratio according to quantitative ^{31}P-NMR (see Figure 3 a). At 130 mol-% (99.5% esterification) the free hydroxyls disappeared completely. According to Figure 3 b, the hydroxyl groups were found to react in the order of aliphatic, condensed phenolic and noncondensed phenolic hydroxyls (each about 2.2 mmol/g). Long chain (C8-C16) fatty acids also showed stronger tendency for aliphatic OHs than acetyl chloride (C2).

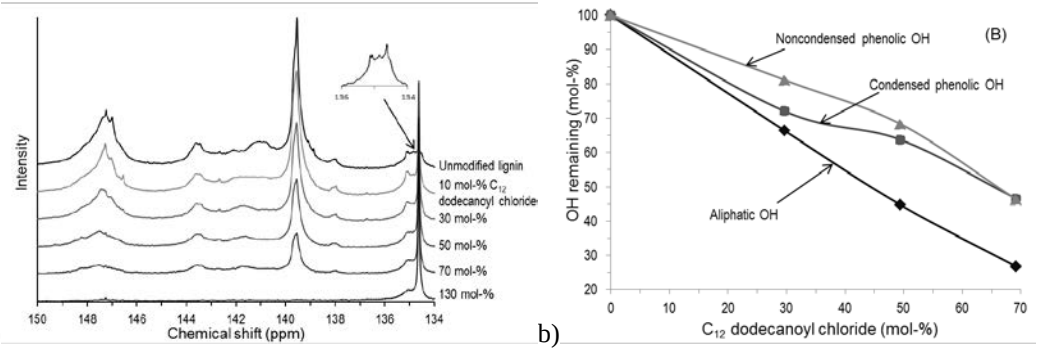

Figure 3. a) Quantitative ^{31}P-NMR spectra of unmodified lignin and C_{12} esters at various loadings. b) Hydroxyl group reactivity as percentages of three main hydroxyl groups with $C_{12}C$=O-Cl.

Thermal behavior

The glass transition temperature T_g of the unmodified lignin was around 145 °C. The C2 and C8 modified lignin esters showed a clear decrease of T_g temperature with increasing degree of esterification (see Figure 4 a). For esterified samples C12 and C16 the T_g was masked or unresolvable, but at lower degrees of acylation showed crystalline melting point T_m values (see Figure 4 b).

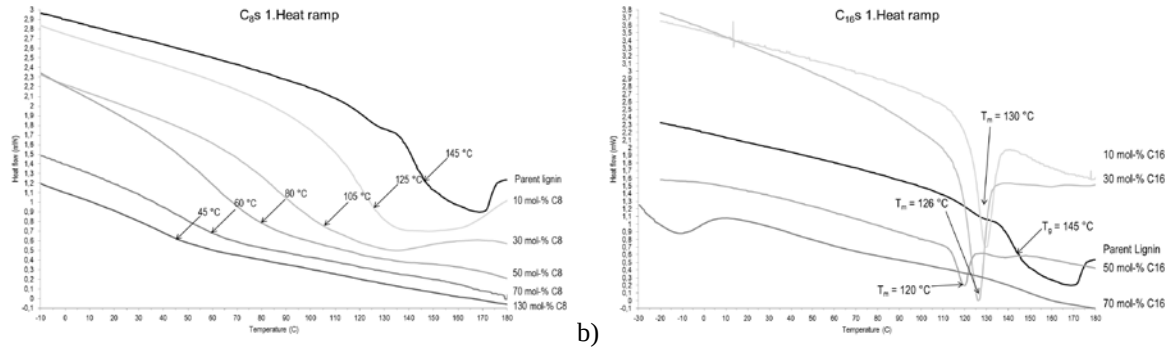

Figure 4. DSC thermograms for a) C8 b) C16 modified lignin esters.

Solution viscosity

Intrinsic viscosity for 50 mol-% modified lignin esters in THF solution is presented in Figure 5. The intrinsic viscosity was found to increase with increasing fatty acid chain length from 0.031 to 0.043 dl/g for C2 to C16.

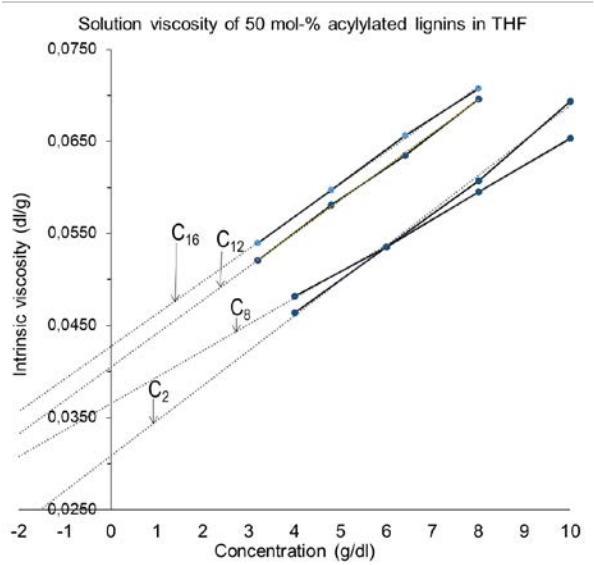

Figure 5. Intrinsic viscosities for 50 mol-% C2, C8, C12 and C16 acylated lignins.

IV. CONCLUSIONS

Softwood kraft lignin esterification can be performed quantitatively as verified by ^{31}P-NMR. A molar ratio of 130 mol-% fatty acid chloride is needed to reach full esterification of the lignin. The aliphatic OHs were determined to be the most reactive amongst the hydroxyl groups. With increasing degree of esterification the T_g of lignin drops considerably.

V. ACKNOWLEDGEMENT

The study is part of a multinational EU-EraNet project titled "High-value products from lignin side-streams of modern biorefineries (ProLignin)". Funding from the Academy of Finland is acknowledged. Our gratitude to Stora Enso Oyj, Finland for providing us with the softwood LignoBoost kraft lignin.

VI. REFERENCES

[1] Asikkala, J.; Tamminen, T.; Argyropoulos D.S. Accurate and reproducible determination of lignin molar mass by acetobromination. *J. Agric. Food Chem.* **2012** *60*, 8968-8973.

[2] Granata, A.; Argyropoulos, D.S. 2-Chloro-4,4,5,5-tetramethyl-1,3,2-dioxaphospholane, a reagent for the accurate determination of the uncondensed and condensed phenolic moieties in lignins. *J. Agric. Food Chem.* **1995** *43*: 1538-1544.

[3] Hult, E.-L.; Koivu, K.; Asikkala, J.; Ropponen, J.; Wrigstedt, P.; Sipilä, J.; Poppius-Levlin, K. Esterified lignin coating as water vapor and oxygen barrier for fiber-based packaging. *Holzforschung* **2013**, *67*, 8, 899-905.

[4] Sadeghifar, H.; Cui, C.; Argyropoulos, D. Toward Thermoplastic Lignin Polymers. Part 1. Selective Masking of Phenolic Hydroxyl Groups in Kraft Lignins via Methylation and Oxypropylation Chemistries. *Ind. Eng. Chem. Res.* **2012** dx.doi.org/10.1021/ie301848j.

HYDROTHERMAL HYDROGEN-FREE CONVERSION OF LIGNIN IN KEY AROMATICS

Richard J. A. Gosselink, Frits van der Klis, Jacco van Haveren and Daan S. van Es

Wageningen UR Food & Biobased Research, Bornse Weilanden 9, NL-6708WG, Wageningen, The Netherlands (richard.gosselink@wur.nl)

ABSTRACT

Lignin depolymerisation into monomeric aromatics is of high interest for the chemical industry to substitute fossil based aromatics, which are becoming more expensive. However, most processes so far show low to moderate yields and selectivity. In this work, a novel hydrothermal catalytic process has been developed to depolymerize technical lignin into a limited number of phenolics. By using heterogeneous catalysis under hydrothermal conditions (250°C) high selectivity can be achieved without the use of external hydrogen. The process combines depolymerisation and in-situ demethoxylation, which by subsequent aqueous phase reforming, leads to in-situ hydrogen formation. Isolated yields of 20% of identified aromatic products can currently be obtained by extraction with organic solvents, with guaiacol being the most abundant phenolic compound (50%).

This novel hydrothermal process allows for the selective conversion of lignin into industrially relevant bulk chemicals with in-situ hydrogen generation.

I. INTRODUCTION

Given the global challenges that humanity is facing with respect to excessive CO_2 emissions, pollution, global warming and diminishing fossil feedstock reserves, new biobased production routes need to be realized in the years to come. In particular the development of second generation lignocellulosic biorefineries aiming at the co-production of biofuels and bio-based chemicals will be expanded. These biorefineries, together with the pulp and paper industry, generate increasing side-streams of technical lignins [1]. Valorization of this lignin by the production of high value aromatic chemicals, beyond the use of lignin for combined heat and power, is a prerequisite for making the lignocellulosic biorefineries economically attractive. As lignin is the largest biobased aromatic resource it is of particular importance to study the conversion of lignin into its aromatic monomers.

So far, most conversion processes show low to moderate isolated yields and selectivity [2]. Currently, many different strategies for converting lignin into phenols and aromatics are being explored. The process conditions vary substantially, ranging from high temperature regimes such as pyrolysis, thermochemical methods, chemocatalytic conversions, reductive or oxidative cleavage, to very mild conditions such as enzymatic degradation. In our study we selected the use of a heterogeneous catalyst in combination with water at relatively mild temperature ranges to selectively depolymerize technical lignins. Earlier work of Matsubara et. al. [3] have shown that aromatic and aliphatic aldehydes and carboxylic acids are efficiently decarbonylated, or decarboxylated, using palladium on carbon under hydrothermal conditions. Here removal of oxygen is accomplished without the need for external hydrogen. This type of catalyst and process conditions were selected for our work in which we firstly showed that a lignin model compound guaiacol (2-methoxyphenol) can selectively be converted with palladium on carbon under hydrothermal conditions in valuable products ranging from phenol to ring-hydrogenated compounds like cyclo-hexanone/cyclohexanol (KA-oil) [4]. In the present work a commercially produced technical soda lignin from non-woods was used to validate the use of a palladium on carbon catalyst for the production of aromatic monomers from a real lignin feedstock.

II. EXPERIMENTAL

Commercially available mixed wheat straw / Sarkanda grass soda lignin (brand name P1000) was supplied by Greenvalue SA, Switzerland.

5.0 g air dried lignin and demineralized water (50 mL) were placed in a 100 mL Parr hastelloy reactor. If used, 1.0 g catalyst was added (10% Pd on activated wood carbon, reduced, 50% wet paste, uniform precious metal distribution, BASF Escat 1931). The desired pH was adjusted by adding aqueous sodium hydroxide. After the reactor was closed, stirring (500 rpm) was started and the reactor was heated to the desired temperature of 250 - 300°C. After reaction, the reactor was rapidly cooled to room temperature by using a water bath. This procedure is described by van der Klis et al. [5]. Gases were collected in gasbags and analysed by GC(-MS).

After opening the reactor, the resulting pH was measured. In order to re-dissolve any residual lignin, the pH was re-adjusted to the starting pH by adding aqueous sodium hydroxide. The reaction mixture was filtered to remove, if present, the catalyst and/or lignin char. Residues were dried in a vacuum oven at 40°C for 18 h. Samples from the aqueous phase were taken to perform SEC analysis as previously described [6].

To precipitate the residual lignin, the pH was adjusted to pH 3 by adding 10% hydrochloric acid in water. The precipitated lignin was removed by centrifugation and subsequently dried in a vacuum oven at 40°C for 18 h. Alkaline SEC analysis, ^{31}P-NMR and FT-IR were measured according to Gosselink et al. 2010 [6].

The acidic water layer was extracted with chloroform (3 x 50 mL) to remove the low molecular weight compounds. The combined organic layers were dried over magnesium sulphate and filtered. The solvent was removed by a rotary evaporator at 40°C under reduced pressure. The compounds in this fraction were further characterized by GC-MS, ^{1}H/^{13}C-NMR, and alkaline SEC.

III. RESULTS AND DISCUSSION

Table 1 displays selected results from the catalytic hydrothermal lignin depolymerization process. Using no catalyst or only the carbon support (entry 1, Table 1) some production of monomeric aromatic compounds was found. However, a relatively large amount of residual char of 39% was obtained. De chloroform solubles showed a yield of 15% with guaiacol (product **2**) and syringol (product **3**) as the main components. Using Pd/C the residual char fraction is decreased. The effect of pH is shown by entries 2-3. An alkaline pH leads to a higher yield of chloroform solubles, while the residual lignin still represents a relative large fraction. These results show that the conversion of lignin seems to be not completed. A clear pH-drop was only observed under basic conditions. At low pH less residual lignin was found, but a low mass balance was obtained. Furthermore, at alkaline pH about 80% of the total detected monomers area was dominated by the five main aromatics (Figures 1 and 2).

Although the mass balances found for the reactions under basic conditions are reasonable (62 – 87%), it might be expected that the dissolved CO_2 accounts for part of the losses. The presence of the catalyst increased the relative amounts of CO_2 in the gas phase as found by the gas analysis. Furthermore, we found that the in situ formation of hydrogen is favored at higher pH and in the presence of the Pd/C catalyst.

Table 1. Isolated fractions after catalytic hydrothermal reaction and monomeric products identified by GC-MS

Entry	Cat.[a]	Time (h)	Temp (°C)	pH (start)	pH (after)	$CHCl_3$ solubles (wt%)	Residual Lignin (wt%)	Char (wt%)	Mass balance (wt%)	**1** (%)[b]	**2** (%)[b]	**3** (%)[b]	**4** (%)[b]	**5** (%)[b]	**1-5** (%)[b]
1	C	4	250	10.0	6.9	15	30	39	84	9	43	23	3	6	84
2	Pd/C	4	250	3.7	4.4	14	14	21	49	3	19	15	-	22	59
3	Pd/C	4	250	10.1	6.7	18	37	18	73	8	53	8	7	4	80
4	Pd/C	4	200	10.0	7.8	5	83	6	94	4	28	17	0	22	71
5	Pd/C	4	300	10.0	6.9	5	39	15	59	17	16	3	3	0	39

[a] Pd/C = 10% Pd on activated wood carbon C = activated wood carbon. [b] % of the total amount of detected monomers.

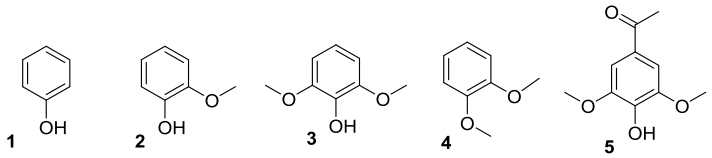

1 = phenol; **2** = guaiacol; **3** = syringol; **4** = dimethoxybenzene; **5** = dimethoxybenzaldehyde

Figure 1. Main aromatic monomers derived from lignin identified by GC-MS

Hydrothermal depolymerisation of lignin at 200, 250 and 300°C (Table 1, entries 3-5) showed that at the lowest temperature 200°C and the highest temperature 300°C a limited fraction of chloroform solubles (5%) was found. Form entry 4 we conclude that the conversion is low as the residual lignin fraction is 83%, while for the highest temperature the mass balance is less complete and more unidentified products were formed. Interestingly at higher temperature more phenol (**1**) was produced next to guaiacol (**2**).,

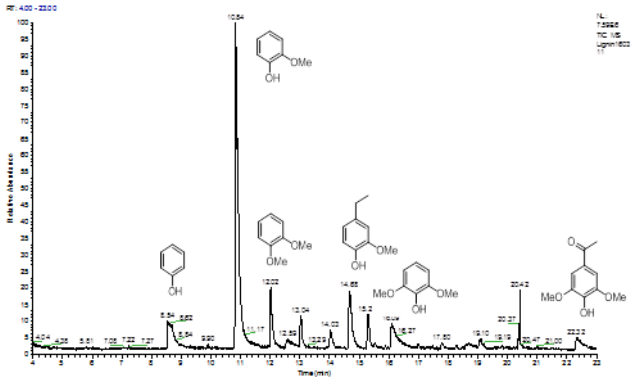

Figure 2. GC-MS chromatogram of the chloroform soluble lignin fraction with identified major compounds

SEC analysis of the extractable monomeric fraction (Figure 3) shows next to the monomeric compounds (rt = 11.5 min) an oligomeric fraction with 2-3 aromatic rings (rt = 9.5 min). At pH 10 the catalyst shifts the ratio of monomers to oligomers in favour of the monomeric species.

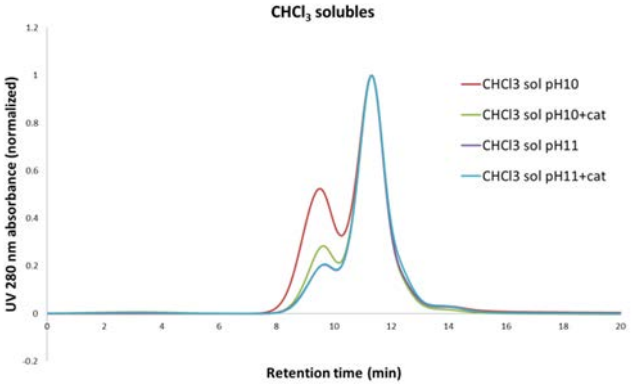

Figure 3. Alkaline SEC analysis of the chloroform soluble lignin fraction under different reaction conditions at 250°C during 4 hours (normalized)

IV. CONCLUSIONS

In this work, we have shown that hydrothermal lignin depolymerisation using a palladium on carbon catalyst leads to increased amounts of monomeric aromatic compounds up to 20 wt% based on dry starting material. Furthermore, under the hydrothermal conditions applied a limited group of aromatic products is obtained, which to our knowledge, has not been reported previously in the absence of external hydrogen. The major compound guaiacol was found in about 50% abundance in the extracted product mixture. In this catalytic depolymerisation process the selectivity towards the main aromatic monomers can be manipulated by changing the process conditions.

V. ACKNOWLEDGEMENT

This research has been performed within the framework of the CatchBio program. The authors gratefully acknowledge the support of the Smart Mix Program of the Netherlands Ministry of Economic Affairs and the Netherlands Ministry of Education, Culture and Science. The authors would like to thank Dr. Guus Frissen, Linda Gootjes BSc, Wouter Teunissen, and Jacinta van der Putten for their contribution to this work.

VI. REFERENCES

[1] Bozell, J.J.; Holladay, J.E.; Johnson, D.; White, J.F. Top value added chemicals from biomass, volume II – Results of Screening for Potential Candidates from Biorefinery Lignin, Pacific Northwest National Laboratory, Richland, WA, **2007**.

[2] Zakzeski, J.; Bruijnincx, P.C.A.; Jongerius, A.L; Weckhuysen, B.M. *Chem. Rev.* **2010**, *110*, 3552.

[3] Matsubara, S.; Yokota, Y.; Oshima, K. *Org. Lett.* **2004**, *6*, 2071.

[4] van der Klis, F., Gosselink, R.J.A., van Haveren, J., van Es, D.S. Lignin valorization, patent filed (**2013**)

[5] van der Klis, F., Gosselink, R.J.A., van Haveren, J., van Es, D.S. Highly selective hydrothermal lignin depolymerization by palladium catalyzed defunctionalisation (*submitted*)

[6] Gosselink, R.J.A.; van Dam, J.E.G.; de Jong, E.; Scott, E.L.; Sanders, J.P.M.; Li, J.; Gellerstedt, G. Fractionation, analysis, and PCA modeling of properties of four technical lignins for prediction of their application potential in binders, *Holzforschung* **2010**, *64(1)*, 193-200.

POTENTIOMETRIC CHEMICAL SENSORS FROM LIGNIN-DERIVED NANOCOMPOSITES

Rudnitskaya, A., Evtuguin D.V. *
*CICECO/ CESAM, Department of Chemistry, University of Aveiro, 3810-193 Aveiro, Portugal (*e-mail:Dmitrye@ua.pt)*

ABSTRACT

Hardwood and softwood lignins obtained from industrial sulphite and kraft and laboratory oxygen-organosolv pulping processes were employed in co-polymerization with tolylene 2,4-diisocyanate terminated poly(propylene glycol). Obtained lignin-based polyurethanes were doped with 0.72 w/w% of multiwall carbon nanotubes (MWCNTs) with the aim to increase their electrical conductivity to the levels suitable for sensor applications. Effect of the polymer doping with MWCNTs were additionally assessed using electrical impedance (EIS) and UV-Resonance Raman (UV-RR) spectroscopy. Potentiometric sensors were prepared by drop casting of liquid polymer on the surface of carbon glass or platinum electrodes. Conducting composite lignin-based polyurethanes doped with MWCNTs were suggested to be promising materials for Cr(VI)-sensitive potentiometric sensors.

I. INTRODUCTION

Lignin, one of the most abundant natural aromatic polymers, is constituted of phenylpropane units linked by carbon-carbon or ether bonds and contains a variety of functional groups such as hydroxyl, carbonyl and carboxyl. These functional groups impart to lignin a capability to complex various compounds, from transition metals to pesticides and humic substances, which made lignin a popular sorbent material for bioremediation needs [1]. Both ion-exchange and redox properties of lignin can be exploited in the chemical sensing. Impedimetric and amperometric electrodes modified by Langmuir–Blodgett lignin films were used for the detection of copper, lead, cadmium and humic substances as discrete sensors and also included in the sensor arrays for the recognition of taste substances and wines and detection of triazine pesticides [2].

All sensors discussed above are based on the lignin thin films, which may have some drawbacks such as for example decreased lifetime and poor reproducibility. An attractive approach to the preparation of bulk sensing material based on lignin is it covalent binding to the polymer matrix which would decrease the leaching of low weight lignin fraction into the solution and, consequently, increase the stability and the lifetime of the final material. Sensing properties of the lignin-based materials have been shown to depend on the delignification or pulping process used for the lignin extraction. This is not surprising, because the reactions taking place during delignification define resulting lignin structure, molecular weight and the functional groups.

The purpose of this work was to elucidate and compare the sensor properties of conductive lignin-poly(propylene oxide) co-polymer membranes doped by carbon nanotubes using three different lignins: eucalyptus kraft lignin, eucalyptus lignosulphonate and spruce organosolv lignin. Furthermore, study on eventual interactions between carbon nanotubes and lignin-based co-polymers in membrane materials for potentiometric chemical sensors have been carried out.

II. EXPERIMENTAL

Reagents and materialsKraft lignin (KL) was isolated from the industrial black liquor from kraft pulping of eucalyptus wood (E. globulus) and catalytically oxidized prior to the polymer synthesis with the aim to increase the amount of carboxyl and carbonyl functional groups (6.4 and 14.8 per 1 phenyl propane unit (PPU), respectively). The amount of hydroxyl groups (aliphatic and phenolic) was 1.24/PPU [1]. Lignosulphonate (LS) was obtained by dialysis from thin spent liquor of the industrial magnesium-based acidic sulphite pulping of eucalyptus wood (E. globulus) and contained 11.2% of HSO_3 groups and 1.10/PPU of hydroxyl groups [3]. Organosolv lignin (OS) was isolated from spent liquor after oxidative delignification of spruce wood (P. abies) by oxygen in aqueous / acetone medium and contained 1.23/PPU of hydroxyl groups, 9.3/PPU of carboxyl and 8.5/PPU of carbonyl groups [4]. The molecular weights of KL, LS and OS were 1580, 2400 and 2800 Da, respectively. Poly(propylene glycol), tolylene 2,4-diisocyanate terminated (PPGDI) with average Mn ~2,300 Da and dibutyltin dilaurate were from Sigma-Aldrich. Multi-wall carbon nanotubes Nanocyl-3150 were from Nancyl, S.A. and had following characteristics: purity >95%, lenght 1–5 μm and diameter 5-19 nm.

Lignin-based sensors

Polycondensation reaction of lignins with isocyanate was carried out using the procedure described in details elsewhere [5]. Films (about 1 mm thickness) used for the polymer characterization were prepared by pouring still liquid polymer into the flat mould. Sensors were prepared by placing a drop of liquid polymer on the tip of the glass carbon or platinum electrode. Polymeric films and sensors were cured during 4 hours at 60 ºC. Direct electrical conductivity (DC) was measured using a 617 Keithley electrometer. Dielectric measurements in an alternative current mode (AC) for frequencies between 40 Hz and 100 MHz were carried out using an Agilent 4294A Precision Impedance Analyzer at the temperatures between -110 and 100 ºC, in a neutral atmosphere. Micro-Raman spectra were recorded using a Jobin Yvon (Horiba) LabRam HR 800 micro-Raman spectrometer @ 325 nm (He-Cd UV laser, Kimmon IK Series) equipped with an air cooled (-70 °C) CCD detector under backscattering configuration using a 40X NUV objective. Neutral density filter (ND 1.0) was used to diminish sample degradation by laser irradiation. Spectra acquisition time was 30 s.

Potentiometric measurements

Electrochemical measurements were carried out in the following galvanic cell: Ag|AgCl, 3M KCl|sample|polymer membrane|Pt or GC. Emf values were measured vs. Ag/AgCl reference electrode with precision of 0.1 mV using custom made multichannel voltmeter with high input impedance connected to the PC for data acquisition and processing. Besides lignin based sensors, pH glass, Pt and Cr(VI)-selective chalcogenide glass electrodes were used. Other specific conditions are described elsewhere [6].

III. RESULTS AND DISCUSSION

DC and AC conductivity

All three synthesized lignin-based polyurethanes were found to be insulating with electrical conductivity of about 10^{-8}–10^{-7} Sm^{-1} at T=350 K (Table 1) and are unsuitable for sensor applications. The doping of lignin-polyurethane co-polymers with MWCNTs increases their electrical conductivity showing percolation threshold at ca 0.18% of MWCNT concentration [5]. Conductivity range of the doped polymers with 0.72% (w/w) of MWCNT increases from 3 to 5 orders of magnitude at 350 K, depending on the lignin type (Table 1). Effect of the doping was smallest for the kraft lignin-based and largest for the lignosulphonate based co-polymers. Non-doped co-polymer based on lignosulphonate also had higher conductivity compared to the others, which can be explained by the presence of ionogenic sulphonic groups.

Table 1. DC conductivity of the polyurethanes based on kraft lignin (KLPU), lignosulphonate (LSPU) and organosolv lignin (OSPU) with and without addition of carbon nanotubes, at T=350 K

Polymer	MWCNT concentration, w/w %	Conductivity, S m^{-1}
KLPU	0	$1.5*10^{-8}$
	0.72	$4.0*10^{-5}$
OSPU	0	$2.6*10^{-8}$
	0.72	$5.2*10^{-4}$
LSPU	0	$1.2*10^{-7}$
	0.72	$2.4*10^{-2}$

A DC conductivity of lignin-based polyurethanes increased exponentially with temperature, which is characteristic for polymer composites. This behaviour indicates that the conductivity σ_{DC} is a thermally activated process, which can be expressed by the well-known Arrhenius relation as follows: $\sigma_{DC} \sim \exp[-E_a/(kT)]$. Values of E_a for the pure polymers were 0.41, 0.69 and 0.71 eV, for lignosulphonate, organosolv and kraft lignin based polyurethanes, respectively. Introduction of MWCNTs decreased activation energy to 0.13, 0.15 and 0.17 eV, respectively. The effect of MWCNTs addition on both DC conductivity and activation energy differs for co-polymers based on different types of lignin suggesting the presence of interaction between MWCNTs and lignin clusters inside polymer composite.

The dielectric analysis was carried out using the modulus formalism and the dielectric relaxation behaviour was modelled using known Cole–Cole expression [6]. Unlike to non-doped lignin polyurethane, which showed the ideal Debye relaxation, the lignin polyurethane doped with MWCNT demonstrated show clearly non-Debye behaviour with deviation from ideal case increasing concurrently with increase of MWCNTs' content. This result indicates the existence of strong interaction of MWCNTs and lignin segments of the polymer composite,

which affects dielectric properties of the polymer itself. The analysis of AC conductivity (σ_{AC}) and real (ε´) and imaginary (ε´´) parts of the complex permittivity (ε*) as a function of frequency for pure and MWCNT-doped lignin polyurethanes allowed the comparison of their fractional exponents *n* and *p* and a cross-over frequency f_c [7]. Dramatic decrease of the *n* low frequency exponent and increase of f_c was observed in all polymers doped with MWCNTs which indicates that the screening increases, and the system is freer with the changes in the electric field followed by the charges. That is the dielectric response results from the prevalence of polarization by the deformation of the electronic cloud wherein the movements of the electrons are uncorrelated. Effect of carbon nanotubes presence on the dielectric response depended on the type of the lignin and was larger in the case of lignosulphonate-based polymer [7]. This indicates that nanotubes do not behave as inert conducting phase dispersed in the polymer matrix but that they interact with lignin segments in the co-polymer composite affecting its properties.

Analysis by UV-RR spectroscopy.

UV-Resonance Raman (UV-RR) spectroscopy was applied to probing the interaction of lignin with MWCNT in the polyurethane. AS an example, UV-RR spectra of OSPU and OSPU+CNT polymers are shown in Fig. 4. Spectra normalization was done using band at 1179 cm^{-1}, which was assigned to C-O stretch in alkyl-substituted ether moieties (C-O-C) in PPGDI. New bands at 1580 and 1351 cm^{-1} in spectrum of OSPU+CNT were assigned to G and D-bands of MWCNTs, respectively, and the band of the aromatic ring stretch shifted to the lower frequency (to 1613 cm^{-1}) and its relative intensity increased. Another two new bands appeared at 1295 and 1446 cm^{-1} assigned to aryl-O stretch in aryl-OH and aryl-OCH_3, and CH_3 bending in OCH_3, respectively. Observed shifts of the bands related to substituted aromatic rings, together with the increase of relative intensity in the doped polymer, result from the interaction between aromatic moieties of lignin segments and carbon nanotubes. This interaction may be a π-π stacking interaction between aromatic ring and carbon nanotubes side wall. Strong interaction between MWCNTs and lignin lead to the increase of the electron delocalization and possibly change of lignin chain conformation allowing better π - overlap along the chain of lignin giving rise to the increased electric conductivity.

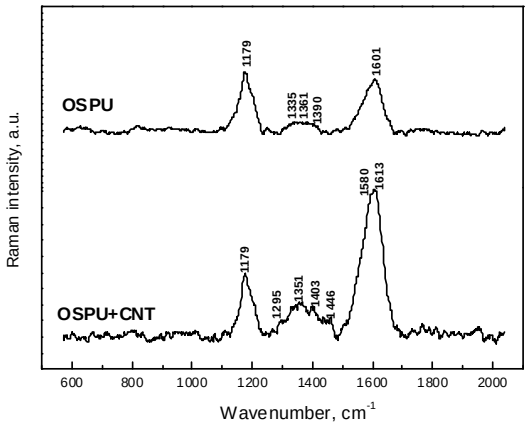

Figure 4. UV-Resonance Raman spectra of the organosolv lignin-poly(propylene oxide) co-polymer: non-doped (OSPU) and doped with MWCNTs (OSPU+CNT).

Sensor properties

Sensors produced from all lignins displayed no response to nitrate, chloride, phosphate, sodium, calcium, zinc(II), cadmium, mercury(II), chromium (III) and iron (III) and low response of about 12 mV/pM to copper(II) and lead(II) ions. pH sensitivity was also relatively low but linear in practically all studied ranges: 11 mV/pH for KL- based sensors in the pH range from 2 to 9 and 14 mV/pH for LS- and OS-based sensors in the pH range from 3 to 9. Significant sensitivity of the studied sensors was observed only towards dichromate at pH 2. Slopes of the electrode function of lignin based sensors and chromate-selective electrode with chalcogenide glass membrane in the chromate solutions at different pH are shown in Fig. 5. Highest sensitivity of 53mV/pCr was observed for LS sensor, which was close to the response of Cr(VI)-selective electrode. Sensor KL displayed lowest response to chromate of 39 mV/pCr. With increase of pH response of lignin sensors diminished and became anionic before disappearing completely at pH 6. Lignin-based sensors displayed higher detection limits but wider linear working range compared to the Cr-selective chalcogenide glass electrode. A mixed ion-exchange – redox mechanism of sensor potential formation for lignin-based electrodes have been proposed. A sorption of Cr(VI) by lignin that requires reduction of Cr(VI) to Cr(III) and concomitant oxidation of lignin moieties followed by the complexation of Cr(III)

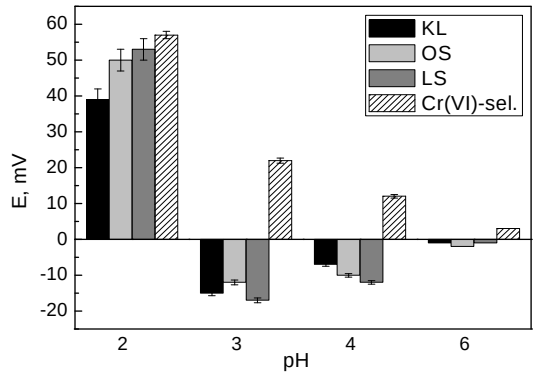

Figure 1. Sensitivity (slopes of the electrode function) together with standard deviations of lignin based polymeric sensors and chalcogenide glass Cr(VI)–selective electrode in the solutions of Cr(VI) at different pH.

ions was proposed. A functioning mechanism may include the formation of reversible hydroquinone/quinone couples in the oxidized lignin.

IV. CONCLUSIONS

Conducting composite polymers based on three types of lignins (kraft, organosolv and lignosulphonate) co-polymerized with poly(propylene oxide) and doped with MWCNT were suggested as promising materials for sensing applications. High conductivity of these materials allows easy preparation of the all-solid-state chemical sensors while maintaining a high chemical stability and low leaching of the membrane components contributed to reproducibility of sensor characteristics. In particular, high sensitivity of the sensors based on organosolv lignin and lignosulphonate towards Cr(VI) in the acid media was observed.

V. ACKNOWLEDGEMENT

Authors acknowledge CESAM, CICECO and I3N (University of Aveiro, Portugal), and the Portuguese Science and Technology Foundation, through the European Social Fund (ESF) and “Programa Operacional Potencial Humano – POPH” for financial support.

VI. REFERENCES

[1] Simoes dos Santos, D.A.; Rudnitskaya, A.; Evtuguin, D.V. Modified kraft lignin for bioremediation applications, *J. Environ. Sci. Health. Part A*, **2012**, *47*, 298-307.

[2] Rudnitskaya A.; Evtuguin D.V. Lignin applications in chemical sensing. In: "Multisensor systems for chemical analysis: materials and sensors", by L. Lvova, D. Kirsanov, A. Legin, C. Di Natale (Eds.), Pan Stanford Publishing, Inc. pp. 181-210 (2014).

[3] Marques, A.P.; Evtuguin, D.V.; Magina, S.; Amado, F.M.L.; Prates, A. Structure of lignosulphonates from acidic magnesium-based sulphite pulping of *Eucalyptus globulus*, *J. Wood Chem. Technol*., **2009**, *29* 337-357.

[4] Evtuguin, D.V.; Andreolety, J.P.; Gandini, A. Polyurethanes based on oxygen-organosolv lignin, *Eur. Polym. J.*, **1998**, *34*, 1163-1169.

[5] Faria, F.A.C.; Evtuguin, D. V.; Rudnitskaya, A.; Gomes, M.T.S.R.; Oliveira, J.A.B.P.; Graça, M.P.F.; Costa, L.C. Lignin-based polyurethane doped with carbon nanotubes for sensorial applications, *Polym. Int.*, **2012**, *61*, 788- 794.

[6] Graça, M.P.F.; Rudnitskaya, A.; Faria, F.A.C.; Evtuguin, D.V.; Gomes, M.T.S.R.; Oliveira, J.A.B.P.; Costa, L.C. Electrochemical impedance study of the lignin-derived conducting polymer, *Electrochim. Acta*, **2012**, *76*, 69- 76.

[7] Rudnitskaya, A.; Evtuguin, D. V.; Costa, L.C.; Graça, L.M.P.F; Fernandes, A.J.S.; Correia, M.R.P.; Gomes M.T.S.R.; Oliveiraa J.A.B.P. Potentiometric chemical sensors using conductive lignin-based polyurethanes. *Analyst*, **2013**, *138*, 501-508.

PREPARATION AND ANALYSIS OF CELLO- OLIGOSACCHARIDES - CLOSING AN ANALYTICAL GAP BETWEEN MONOMER/DIMER AND THE POLYMER

J. T. Oberlerchner[1], P. Vejdovszky[1], T. Zweckmair[1], G. Schild[2], A. Borgards[2], T. Rosenau[1], A. Potthast[1*]

[1]*University of Natural Resources and Life Sciences, Department of Chemistry, Christian Doppler Laboratory "Advanced Cellulose Chemistry and Analytics", Muthgasse 18, A-1190 Vienna, Austria;*
[2] *Lenzing AG, A-4860 Lenzing, Austria*
*(*antje.potthast@boku.ac.at)*

ABSTRACT

Mixtures of cellooligosaccharides were obtained by acetolysis of cellulose. Isolation of fractions which were homogenous with regard to the DP (or did at least have a very narrow molecular weight distribution) was conducted on a semi-preparative scale by normal-phase HPLC on silica with evaporative light scattering (ELS) detection. The obtained monodisperse oligosaccharide fractions in the DP range between 1 and roughly 30 were subsequently subject to different characterization methods, including MALDI-TOF-MS for molecular weight assessment. Oligosaccharide standards are needed for size exclusion chromatography to analyze cellulose fractions below ~10 kDa, even if it is coupled to light scattering detection (SEC-MALLS). The insensitivity of the MALLS detection system in the low molar mass region can often not be compensated by other means, such as higher sample concentration.
Besides providing the cellooligosaccharides as standard compound in SEC, we also focused on analytical methods which are able to quantify cellooligomers. This is important when it comes to biorefinery streams containing degraded polysaccharides, as the spectrum of suitable methods is rather scarce. Here, we present a liquid chromatography method to quantify cellooligomers in their acetylated form, and in parallel we show first results with planar chromatography (HPTLC), addressing this particular analytical problem.

I. INTRODUCTION

The carbohydrate fraction of plant cell walls is the most abundant source for renewable organic raw materials. In that context a complete and comprehensive knowledge of the physical and chemical properties is of great importance in order be able to exploit the full potential of these compounds in the future. Many of the unique properties of these carbohydrates can be related to the degree of polymerization (DP). Oligosaccharides derived as degradation products from the corresponding polysaccharides are useful as model compounds and thus as a tool for basic structural studies on cellulose and hemicellulose. Homologous series of cello- and xylooligomers provide the possibility to investigate MW-related trends of macromolecular characteristics, physical properties and chemical behavior, and thus their application potential as a function of the molecular weight. In addition, such oligosaccharides are valuable standards and calibration compounds for several analytical techniques. Procedures to prepare and isolate oligosaccharides with defined DPs allow to expand the determination window of analytical techniques to cover also the "difficult-to-see" oligomeric range between the well-studied monomeric and dimeric region on one side and the well-covered polymeric compounds on the other side, and makes these compounds amenable to further investigation.

The term cellooligomer refers to the low-molecular mass range of cellulose, normally well below 10.000 $g*mol^{-1}$. The borderline between polymer and oligomers is not very well defined. A common classification in the

case of cellulose is just derived by water solubility, with soluble compounds in the molecular mass range of DP≤8 being referred to as cellooligomers. In nature, such oligomers are produced for instance by enzymatic cleavage of cellulose through microorganisms. In paper and fiber production these cellulose fractions play a minor role since most fiber properties are influenced by the higher molar masses, including all strengths properties and the ability of a polymer to form films or fibers, which is closely related to the molecular weight distribution.

Some pulping methods yield rather polydisperse pulps with a wide range of molar masses present. This is for instance true for sulfite pulps produced according to an acidic process. Those pulps and the associated pulping streams contain considerable amounts of low molecular-weight carbohydrates. Also during viscose (rayon) production, low molecular weight carbohydrates are lost and removed in β- and γ-cellulose fractions. These streams could be an attractive source for cellooligomers to be used in novel applications. However, the utilization of cellooligomers is still poorly conceived. In the future these cellulose fractions could play an important role in crude oil substitution, in particular for the production of block-based chemicals. Methods for appropriate analytical characterization are still rare, and approaches which cover the whole range of a cellulosic sample, from the monomeric to the polymeric level, including the oligomers, are even completely missing.

Our effort is to extend a common SEC-MALLS method for cellulose analysis towards the low molecular range by using monodisperse standards. Therefore, we established a preparative HPLC method to neatly separate such standards after acetolysis of cellulose. In parallel, we used these compounds (masses were verified by MALDI-TOF) to calibrate a HPLC-ELSD system for acetylated cellooligomers up to a DP of 20. Especially wood saccharification requires methods for the analysis of oligomeric carbohydrates which are rapid, robust, and capable of higher throughput - and the developed approach appears to be able to meet such requirements.

II. EXPERIMENTAL

Acetolysis

The acetolysis of cellulose was carried out according to the procedure of Hess and Dziengel with slight modifications [1]. To get batches with different molar mass distributions reaction times were varied. The reaction was controlled by TLC, with cellobiose octaacetate and glucose pentaacetate as references.

Analytical and preparative HPLC

Analytical scale separations of the product mixture were performed by NP-HPLC on a silica column (7 µm, 4.6 x 250 mm) with ethyl acetate and toluene as the eluants. In preparative HPLC fractions were collected with a fraction collector Foxy R1 (Teledyne Isco) according to the ELSD signal used as trigger. A typical chromatogram can be seen in Figure 1b. The product amount in each fraction was between roughly 5 to 20 mg. The individual fractions were further analyzed by means of MALDI-TOF-MS.

HPTLC

Samples were applied using the Automatic TLC Sampler 4 (ATS 4, CAMAG, Muttenz, Switzerland).

For post-chromatographic derivatisation the plate was manually immersed into the derivatisation reagent (anisaldehyde / sulfuric acid) and heated (120°C, 5 min). Plate images were documented using the TLC visualizer (CAMAG). All instruments were controlled by the VisionCats 1.4. program (CAMAG), densitometric evaluation was performed by VideoScan 1.02 (CAMAG).

III. RESULTS AND DISCUSSION

For the generation of cellooligosaccharides by degradation of cellulose a variety of methods has been developed during the last century [2]. Acetolysis was chosen because it is a cheap and simple procedure resulting in sufficient amounts for the subsequent separation step. Avicel cellulose was used as starting material. Analytical HPLC and HPTLC were performed to optimize the preparative HPLC separation system. Particle size is a crucial parameter in chromatography, and a decrease in size leads to a higher resolution for the separation of the cellooligomers which differ only by one acetylated AGU unit per oligomer molecule to be separated. Also anomers can be separated to some extent but as this separation was not required, all fractions finally will contain both isomers). The higher the DP, the more difficult the fractionation eventually becomes. To determine the molar mass of each HPLC fraction, MALDI TOF-MS was performed (cf. Fig.1A). With the above described preparative HPLC system we are able to get monodisperse cellooligomers up to a DP of 18. For the higher DP values we can obtain mixtures of standards with very narrow distribution, which should be sufficient for a SEC-MALLS calibration after removal of acetyl groups.

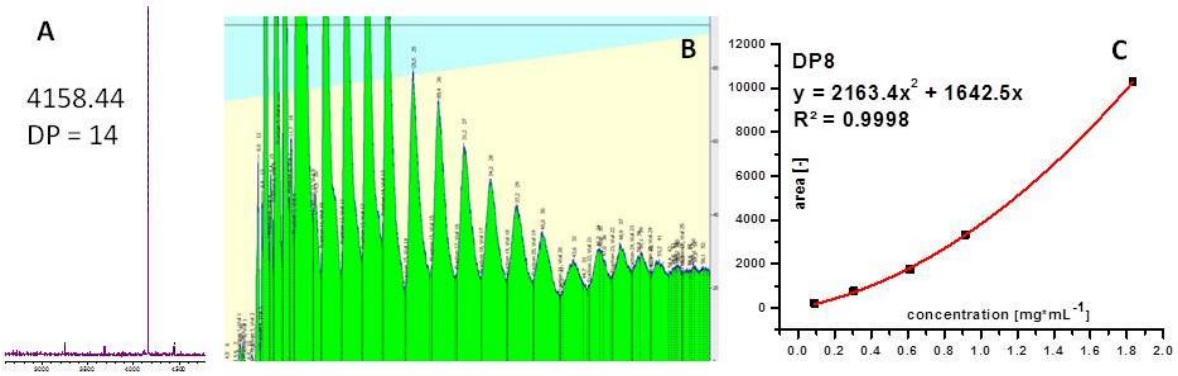

Figure 1. A: Example MALDI-TOF MS spectrum of a pure acetylated cellooligomer (cellotetradecaose, DP=14). **B**: preparative HPLC-ELSD chromatogram of cellooligomers.
C: analytical HPLC-ELSD, calibration curve for cellooctaose (DP=8).

HPLC and HPTLC are by far superior in the region below DP18 when compared to SEC-MALLS. Therefore, we established a HPLC (and consequently HPTLC) methods for per-acetylated cellooligmers. Fig 1C gives an example of a calibration curve obtained by HPLC-ELSD. Real-world samples containing cellooligosaccharides have to be acetylated in advance, which was done in acetic anhydride / pyridine. However, as pyridine has to be removed before injection into the HPLC system, alternative methods for the derivatisation are still in evaluation. Replacing HPLC with HPTLC could have some benefits: increased speed (up to 16 samples/hour), lower running costs, direct sample application after derivatisation and removal of any disturbing matrix directly on the plate. Therefore, we started evaluation of a planar method for cellooligomer analysis. As preliminary tests showed (Fig. 2), this method is capable of separating acetylated cellooligmers up to DP15 within one plate development.

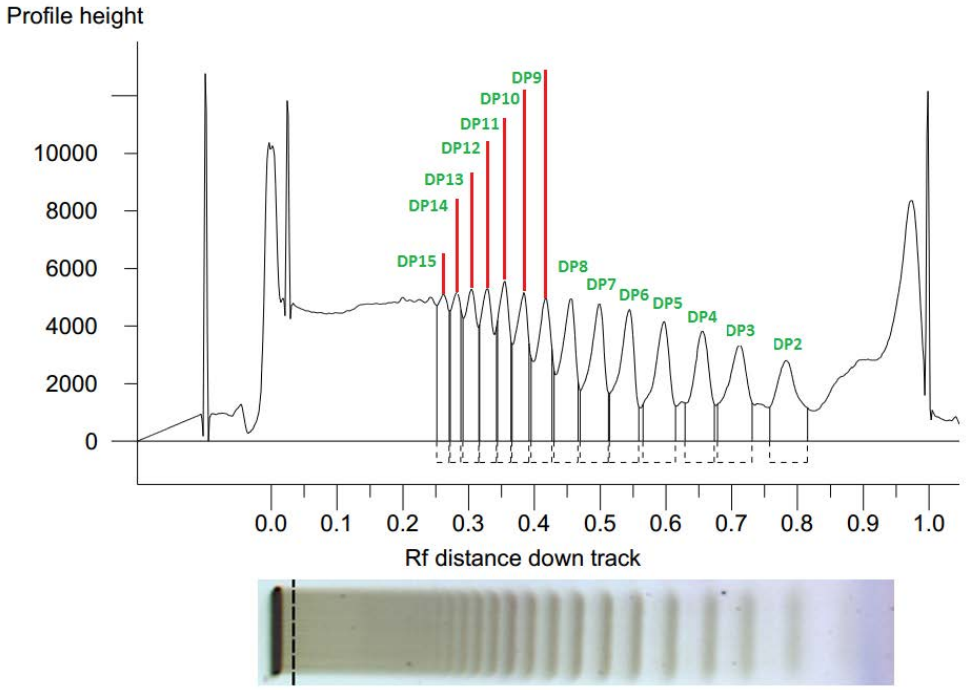

Figure 2. HPTLC chromatogram of acetylated cellooligomers

IV. CONCLUSIONS

To analytically cover the oligomeric range of cellulose and its degradation products in detail, it is important to have cellooligomer standards with defined molar mass available, which were provided in the present project. The preparation of such standards with preparative HPLC using acetylated cellooligomers is an efficient method and can be scaled up to produce largely sufficient amounts. With these standards a HPLC method for quantifying acetylated cellooligomers was established. In parallel, the capability of HPTLC for oligomer analysis in biorefinery product streams was investigated and proved to be very promising. Benefits of planar chromatography are higher throughput, lower costs and exclusion of matrix effects. HPTLC also brings the advantage to separate ubiquitous matrix directly on the plate with a pre-development.

V. ACKNOWLEDGEMENT

Financial supports of the Austrian Christian Doppler Research Society through the Christian Doppler Lab "Advanced cellulose chemistry and analytics" and Lenzing AG are gratefully acknowledged

VI. REFERENCES

[1] Hess, K.; Dziengel, K., Über Cellotriose und ihre Derivate. *Ber. dtsch. chem. Ges. (A and B Series)* **1935**, *68 (8)*, 1594-1605.

[2] Oberlerchner J. T., Characterization of oligomeric cellulose derivatives. Master thesis, University of Natural Resources and Life Sciences Vienna, **2013**.

[3] Vejdovszky, P. Preparation and Analysis of Cello- and Xylooligosaccharides – A Review, *Adv. Polym. Sci.* **2014**, in press.

ENZYMATIC OXIDATION TECHNOLOGY ENABLES MANUFACTURING OF NOVEL LIGHTWEIGHT AND STIFF POLYSACCHARIDE-BASED AEROGELS

Kirsi S. Mikkonen, Kirsti Parikka, Abdul Ghafar and Maija Tenkanen*

Department of Food and Environmental Sciences, P.O. Box 27,
University of Helsinki, FI-00014 Finland
**maija.tenkanen@helsinki.fi*

ABSTRACT

Enzymatic oxidation of galactopyranosyl branches in guar galactomannan (GM) was used as a novel technique to obtain hydro- and further aerogels from polysaccharides. Lyophilization of oxidized GM (GM-OX) hydrogels resulted in stiff, lightweight, and porous materials, i.e., aerogels. The freezing method of the hydrogels was varied to affect the ice crystal formation and orientation of the porous structure. Alternatively, nanofibrillated cellulose (NFC) was added prior to gelation to make composite aerogels. The compressive modulus measurements revealed that the mechanical stiffness of the aerogels increased due to the orientation in the freezing and drying direction, or with the addition of NFC. Microscopy illustrated the orientation of the pores, which were tens to hundreds of micrometers in size. Enzymatic oxidation is an environmentally compatible method to prepare bio-based aerogels for modern pharmaceutical, food, or packaging applications.

I. INTRODUCTION

Aerogels are advanced porous materials that have low weight and density, a large surface area, and high mechanical strength. Due to their high porosity, aerogels are capable of active sorption, and through smart porosity optimizations, they enable a controlled release of desired compounds. They are also thermal super-insulators. Aerogels are obtained in various shapes and sizes by the removal of liquid from a corresponding gel [1,2].

Here, we present a new technique for aerogel preparation applying enzymatic crosslinking of galactose-containing polysaccharides [3]. Galactose oxidase (GaO, EC 1.1.3.9) is a single copper metalloenzyme which catalyzes the oxidation of primary alcohols to the corresponding aldehydes with the high selectivity for C6 in the terminal D-galactopyranosyl (Gal*p*) residues in polysaccharides. Molecular oxygen is used as an electron acceptor and is reduced to hydrogen peroxide during the reaction. The degree of oxidation can be controlled to different levels. Oxidation of aqueous solutions of galactomannan by GaO results in hydrogels with high elasticity already at 0.2–0.4% w/v concentrations. The key mechanism in the hydrogel formation are the inter- and/or intramolecular hemiacetal crosslinks between the polysaccharide chains brought about the carbonyl groups resulting from the enzymatic oxidation [4].

Guar galactomannan (guar gum, GM) is a polysaccharide used as a thickener and stabilizer in various food products due to its water-binding and thickening ability; it is also used in pharmaceutical and cosmetic applications and in the textile, paper, mining, and oil industries [5]. GM is obtained from guar bean seeds (*Cyamopsis tetragonoloba*). It consists of a linear β(1→4)-D-mannopyranosyl (Man*p*) backbone with α-Gal*p* side units attached to the backbone via (1→6)-bonds at Man*p*:Gal*p* ratio of 1.5:1.

Controlled hydrogel formation from water-soluble polysaccharides is advantageous in comparison to widely studied nanofibrillated cellulose (NFC), because the latter forms a gel directly after mechanical fibrillation, which complicates homogenous mixing of active components and other additives in the NFC matrix prior to drying of the aerogel. The aim of the present study was to prepare aerogels from GM using GaO technology and to evaluate the effect of the freezing method and added NFC reinforcement on the morphology and stiffness of the aerogels.

II. EXPERIMENTAL

Materials

Galactose oxidase (GaO) used was from *Fusarium spp*, which was produced recombinantly in *Picihia pastoris*, and donated by Dr. Sybe Hartmans (specific activity of 770 U/mg). Nanofibrillated cellulose (NFC) from birch kraft pulp was obtained from Aalto University, Finland. Guar gum galactomannan (GM), horseradish peroxidase (HRP, P8250, Type II, 181 U/mg) and catalase (C30, from bovine liver, 22000 U/mg) were purchased from Sigma Aldrich (St. Louis, MO, USA).

Preparation of aerogels

GM was dissolved in deionized water (10 mg/ml) at room temperature (RT) and stirred overnight for complete hydration. NFC was added at 25% of polysaccharides by mixing with an Ultra Turrax homogenizer for 5 min at 9500 rpm. Samples were also prepared without the addition of NFC. The enzymes (GaO, catalase, HRP) were added at dosages based on previous studies (0.052 U of GaO/1 mg of galactose) [4]. After stirring at 4°C for 48 h, the enzymes were inactivated by keeping the hydrogels in a boiling water bath for 5 min. Air bubbles were removed by vacuum. The hydrogels were allowed to cool down, samples (ca. 1 ml; 10 mg of polysaccharide) were taken aside, and a previously developed GC-MS method was used to determine the degree of oxidation [4]. The rest of the hydrogels were molded into cubical Petri dishes and frozen at −70 °C. To prepare unidirectionally frozen samples using an ice crystal template, the Petri dishes were placed on top of a CO_2 ice plate in an EtOH bath. After 0.5–1 h the hydrogel was frozen, and the samples were placed in a freezer at −70° C. Water was removed by lyophilization.

Compression testing

The compressive moduli of the aerogels was determined at 23 °C and 50% RH (climate room) using an Instron 33R4465 universal testing machine with a load cell of 100 N. The specimens were compressed for 6 mm at the rate of 1.3 mm min^{-1}. Ten replicate cubic specimens with a width, length, and thickness of approximately 17 mm were tested in either horizontal or vertical direction.

Microscopy

Aerogel specimens were coated with an Au/Pd film, using a Cressington sputter coater, to increase surface conductivity and to improve surface mechanical stability during electron beam imaging. The surfaces of the specimens were viewed using focused ion beam scanning electron microscopy (Quanta 3D 200i FIB-SEM). Optical imaging of aerogels' cross-sections were taken with a Zeiss Axio-Scope A1 polarizing optical microscope (OM) (Carl Zeiss Inc., Oberkochen, Germany) using transmitted light, and the images were collected with AxioCam ICc3 camera.

III. RESULTS AND DISCUSSION

Hydro- and aerogel formation

The hydrogel formation from oxidized GM-OX was similar to that reported previously [4]. The presence of 25% NFC did not hinder the enzyme action and visually similar gel was obtained. The success of the enzymatic treatment was further confirmed by analyzing the degree of oxidation with GC-MS [4], which was 45–63% of the Gal*p* and 18–25% of the total carbohydrates in GM.

Aerogels were successfully prepared from the obtained hydrogels, as freezing and lyophilizing did not affect the outer dimensions of the cubic gel specimens. The ice crystal template, created by unidirectional freezing, induced the formation of an aligned porous structure, which was clearly visible on the aerogel side surface with a naked eye. In comparison, the conventionally frozen samples did not show uniform orientation.

Mechanical properties

The aerogels from GM-OX were lightweight (0.01–0.02 g cm^{-3}) and stiff. To accurately characterize their mechanical properties, the samples were subjected to compression testing at 50% relative humidity, in which the compressive modulus was determined from the initial slope of the stress-strain curve. The oxidized, conventionally frozen GM-OX aerogels showed an average compressive modulus of 73 kPa (**Figure 1**). That value is of the same magnitude, even though on the lower range of the compressive moduli of previously studied polysaccharide aerogels [1].

The effect of ice crystal template freezing was highlighted in the compression testing (**Figure 1**). The specimens were tested on both horizontal and vertical direction. On the horizontal direction, the GM-OX aerogels showed a compressive modulus of 53 kPa. The specimens were much stiffer in the vertical direction, i.e., in the freezing and drying direction, as demonstrated by high compressive modulus of 227 kPa. This large difference was most likely caused by the structure and orientation of the pores and pore walls of the aerogels. We suggest that also the polysaccharide chains could be oriented on the vertical direction during unidirectional freezing, causing higher stiffness on this direction.

The addition of NFC was studied by mixing it with the GM solution prior to oxidation. The hydrogels containing NFC were frozen conventionally in a freezer and thus they did not show orientation. However, the relatively high compressive modulus of the GM-OX aerogels with 25% NFC (167 kPa) showed that NFC indeed acted as a reinforcement and increased the stiffness of the aerogels (**Figure 1**).

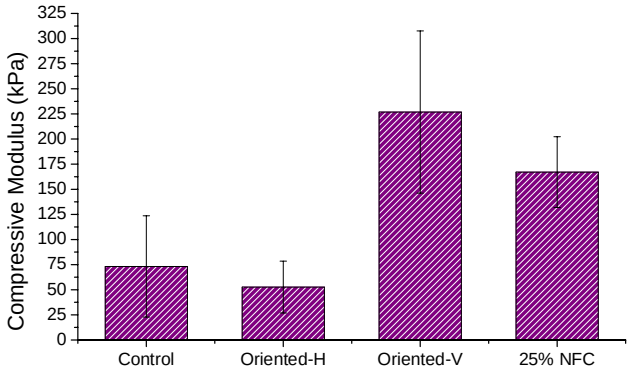

Figure 1. Compressive modulus of conventionally frozen aerogels from enzymatically oxidized guar galactomannan (GM-OX) (Control, determined in vertical, i.e., casting and drying direction), ice-crystal templated GM-OX in horizontal (Oriented-H) and vertical (Oriented-V) direction, as well as conventionally frozen GM-OX aerogels with 25% NFC added (vertical direction). The error bars indicate standard deviations from ten replicate measurements.

Microscopy

To visualize the porous structure of the aerogels, they were viewed with FIB-SEM and optical microscopy. The FIB-SEM images (**Figure 2**) show the morphology of the aerogel specimens on the side surface of the cubic aerogels. **Figure 2A** presents the conventionally frozen GM-OX aerogel, which did not show orientation of the pores. The surface of this sample was also milled open with 30 kV Ga^+ ions, revealing the pores beneath the surface as a rectangular-shaped opening in the middle of the image. The ice crystal templated GM-OX aerogel, on the other hand, showed a honeycomb structure with thick walls in the vertical direction, connected with thinner horizontal walls (**Figure 2B**).

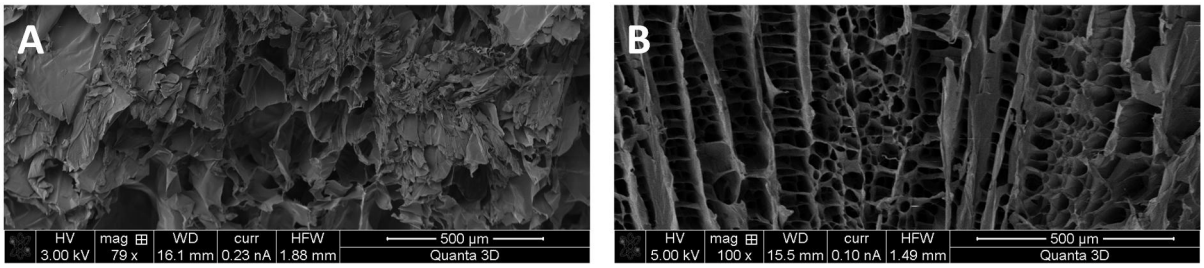

Figure 2. Focused ion beam scanning electron microscopic images of oxidized GM-OX aerogels prepared by (A) conventional freezing or (B) ice-crystal template. The scale bar in both images is 500 µm.

Cross-sections of the aerogels were carefully cut with a sharp knife and the inner structure was viewed with optical microscopy. The optical microscopy of the conventionally frozen GM-OX specimen showed that pores of a diameter from tens to hundreds of micrometers were divided by clearly visible walls (**Figure 3A**). This sample did not show polarizing structures. In contrast, viewing the GM-OX aerogel containing 25% NFC with polarized

light showed bright pore walls, most probably due to the capability of the highly crystalline NFC to orientate polarized light (**Figure 3B**). When viewed with transmitted light without the polarizing filter, the latter sample (not shown) looked similar to the one without NFC.

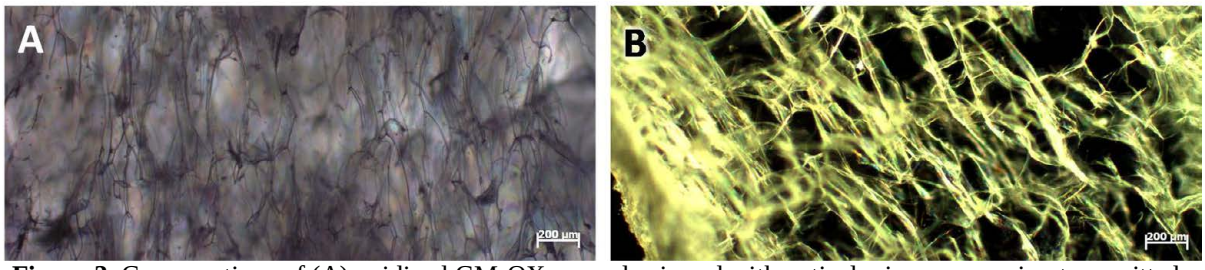

Figure 3. Cross-sections of (A) oxidized GM-OX aerogels viewed with optical microscopy using transmitted light and (B) GM-OX aerogels with 25% NFC, viewed with polarizing optical microscopy. The scale bar in both images is 200 µm.

IV. CONCLUSIONS

The novel, rather stiff aerogels were successfully prepared from oxidized GM-OX hydrogels by freeze-drying. Aerogels were further reinforced by mixing nanofibrillated cellulose prior to oxidation. The aerogel characteristics indicate potential in various applications, such as, active packaging, encapsulation, or absorbents. Their use in food technology is especially interesting due to bio-based origin, biodegradability, and the non-toxic crosslinking technique.

V. ACKNOWLEDGEMENT

We thank Sybe Hartmans for the GO, Monika Österberg (Aalto University, Finland) for the NFC, and Marko Vehkamäki (University of Helsinki) for the FIB-SEM imaging. The Academy of Finland (KSM and KP) and Magnus Ehrnrooth Foundation (AG) are acknowledged for funding.

VI. REFERENCES

[1] Mikkonen, K.S.; Parikka, K.; Ghafar, A.; Tenkanen, M., Prospects of polysaccharide aerogels as modern advanced food materials. *Trends Food Sci. Technol.* **2013**, *34*, 124–136.

[2] García-González, C.A.; Alnaief, M.; Smirnova, I., Polysaccharide-based aerogels – promising biodegradable carriers for drug delivery systems. *Carbohydr. Polym.* **2011**, *86*, 1425–1438.

[2] Mikkonen, K.S.; Parikka, K.; Suuronen, J.-P.; Ghafar, A.; Serimaa, R.; Tenkanen, M., Enzymatic oxidation as a potential new route to produce polysaccharide aerogels. *RSC Adv.* **2014**, *4*, 11884–11892.

[3] Parikka, K.; Leppänen, A.-S.; Pitkänen, L.; Reunanen, M.; Willför S.; Tenkanen M., Oxidation of polysaccharides by galactose oxidase. *J. Agric. Food Chem.*, **2010**, *58*, 262–271.

[4] Wielinga, W.C. Galactomannans. In: Handbook of Hydrocolloids, G.O. Phillips and P.A. Williams, Eds. Woodhead Publishing, Cambridge, UK, 2nd edition, **2009**, pp. 228–251.

THERMOPLASTIC WOOD HEMICELLULOSE-LACTIDE GRAFT-POLYMERS AND FILMS

Olof Dahlman* and Karolina Larsson

Innventia AB, BOX 5604, SE-114 86, Stockholm, Sweden.
*(*olof.dahlman@innventia.com)*

ABSTRACT

Wood-derived hemicelluloses were subjected to grafting with lactide in order to synthesize thermoplastic hemicellulose-based materials and thin self-supporting films intended for packaging applications. Three different kraft pulps from birch, eucalyptus and spruce/pine wood, respectively, were extracted with alkali in order to isolate the hemicelluloses. The extracted hemicelluloses were composed mainly of xylans and exhibited average molar masses in the range 10-13 kDa. The hemicelluloses were modified by grafting L-lactide residues onto the hydroxyl groups via stannous octanoate catalyzed ring opening reaction yielding water insoluble thermoplastic materials. Self-supporting films were produced from the synthesized lactide-grafted hemicellulose materials and characterized with respect to thermal and gas barrier properties. The study showed that the thermal and mechanical properties of the lactide grafted hemicellulose materials varied substantially with the lactide content. The oxygen gas and water vapour barrier properties of the lactide grafted hemicellulose films were good and compared favorably with those for some PLA bioplastics. Moreover, the lactide grafted hemicellulose films exhibited low oxygen gas permeability, OP = 1.4 – 8.3 cm^3mm/m^2 24h atm, at 23 ^oC, 50 % relative humidity.

I. INTRODUCTION

Hemicellulose based films and coatings generally exhibit good gas barrier properties. However, wood hemicelluloses are water soluble polysaccharides exhibiting film properties that are quite sensitive to the humidity of environment. Moreover, hemicelluloses isolated from kraft pulps do not demonstrate thermoplastic properties and, hence, are difficult to process thermally by e.g., extrusion or compression molding to films, fibres and other products.

Chemical modification of the hemicelluloses may reduce the water solubility and introduce thermoplastic properties. For example, Vincendon synthesized xylan phenyl carbamates and benzyl ethers demonstrating thermoplasticity at high temperatures (>200 ^oC) [1,2]. Acetylation was reported to increase the thermal stability of hemicelluloses [3] and nanofibers were produce by electrospinning of acetylated hardwood kraft xylan [4]. Moreover, Jain, et al. [5] demonstrated that acetoxypropylation of xylan produces water insoluble materials exhibiting glass transition temperatures (T_g) in the range 70 – 160 ^oC depending on the degree of acetoxypropyl substitution. However, acetoxypropylation of xylan involves several sequential chemical reactions. It would be desirable to find an efficient one-step procedure to chemically modify kraft pulp derived hemicelluloses in a manner such that the advantageous gas barrier properties are maintained while achieving water insoluble thermoplastic materials suitable for thermal processing into films and other products.

We have previously reported procedures for synthesizing thermoplastic birch xylan materials by grafting lactide onto the hydroxyl groups located on xylan back bone employing a one-step lactide ring-opening reaction [6]. The lactide-g-xylan polymers synthesized were strong water-insoluble materials demonstrating thermoplastic properties e.g., glass transition temperatures ranging from 40 ^oC up to 80 ^oC [6-8]. In the present study we explored the possibility of making thermoplastic lactide grafted hemicelluloses employing three different hemicellulose preparations isolated from bleached hardwood and softwood kraft pulps. The hemicellulose materials synthesized were processed into flexible self-supporting barrier films exhibiting good oxygen gas and water vapor barrier properties.

II. EXPERIMENTAL

Isolation of kraft pulp hemicelluloses

Three different pulps originating from kraft pulping of birch, eucalyptus and spruce/pine wood, respectively were employed for the isolation of the hemicelluloses. The pulp samples were delivered as dry pulp sheets which were stored cold at our laboratory prior to extraction. The pulp sheets were first subjected to disintegration followed by soaking and suspending in aqueous sodium hydroxide solution (10 % NaOH) to a fibre consistency around 10 %. The suspended pulp fibers were subsequently extracted at room temperature for an extraction time

of 60 minutes. Following the extraction the pulp suspension was filtered and the alkaline extraction liquor thus obtained was adjusted to pH~8 resulting in the precipitation of the hemicellulose. The precipitated hemicellulose material was isolated by centrifugation followed by washing and finally freeze-drying to yield a white voluminous solid material.

Synthesis of lactide grafted hemicelluloses

The dried hemicellulose was added to a dry reaction flask and the flask was sealed with a septum. DMSO (dried) was added through the septum. After treated sequentially with vacuum and nitrogen to remove any water residues the mixture was heated to 90 °C to dissolve the xylan under magnetic stirring. L-lactide was then added to the mixture. After another treatment cycle with vacuum and nitrogen of the catalyst stannous octanoate ($Snoct_2$) was added (~5 %-wt. with respect to the amount of hemicellulose). After 24 h reaction time at 90 °C under inert atmosphere, the reaction mixture was allowed to cool to room temperature and subsequently quenched by pouring into deionized water. The water insoluble lactide-g-hemi polymer precipitated from the water/DMSO phase and was subsequently washed three cycles with water and then dried under vacuum.

Film preparation

Thin flexible self-supporting films were made by either solution casting or compression moulding. Solution casted films: about 1 g of the lactide-g-hemi was dissolved in 15 mL THF and transferred to a Teflon coated glass petri dish. The solvent was evaporated in a fume hood for 2-4 days after which the film was removed from the dish. Compression moulded films: the lactide-g-hemi material was put on top of a PET-sheet and compression moulded at 150°C and 50 bar for 10 minutes.

Analysis methods

The carbohydrate composition of the extracted hemicelluloses was determined by enzymatic hydrolysis followed by capillary electrophoresis employing a method described by us previously [9]. The molecular mass for the hemicelluloses were determined by employing aqueous size exclusion chromatography according to the procedure previously described by us [10]. The SEC column system consisted of three columns containing Ultrahydrogel 120, 250 and 500 (Waters Assoc. USA) linked in series to each other and to a refractometer (Waters Assoc. USA). The eluent system utilized was 100 mM sodium acetate and 200 mM sodium hydroxide, pH 13. The lactide graft hemicelluloses were analysed by SEC employing tetrahydrofuran as the eluent. The SEC column system consisted of three Styragel columns (Styragel HR2 and HR1, Ultrastyragel 10^4 Å; Waters Assoc. USA) connected to a reflective index detector (RI). The signal from the refractometer was processed on a standard PC using the Cirrus GPC/SEC software, version 3.1 (Polymer Laboratories Ltd., UK).

Thermal measurements

Differential scanning calorimetry (DSC) was employed to measure the glass transition temperature (T_g). About 2-5 mg of the lactide-g-hemicellulose sample was weighted in a pan for measurements. A Waters DSC Q1000 V9.4 Build 287 instrument was used. The heating rate during measurements was 10°C/min. The thermal degradation temperature (T_d) was measured by TGA. A Perkin Elmer TGA7 instrument with a flow rate of the purge gas (He) at 20–35 ml/min and the balance purge gas (N_2) of 40–60 ml/min was employed. Approximately 4 mg of sample was dried at 105 °C for 20 min prior to heating with a heating rate of 15 °C/min to 300 °C. All reported data are averages of duplicates.

Oxygen gas and water vapour permeability

The oxygen gas permeability (OP) was determined on films by employing Mocon Ox-Tran 2/21 equipment using a temperature of 23 ± 0.5˚C and a relative humidity (RH) of 50 ± 3 % following the standard procedure described in ASTM F 1927-07. The water vapour permeability (WVP) was determined by employing Mocon Permatran-W 3/33 equipment using a temperature of 23°C ± 0.5°C and a relative humidity (RH) of 50 ± 3 % following the standard test method for water vapour transmission rate through plastic film and sheeting using a modulated infrared sensor, ASTM F 1249-05.

III. RESULTS AND DISCUSSION

In this study, three different kraft pulp derived hemicelluloses were subjected to grafting with lactide in order to synthesize thermoplastic hemicellulose-based polymers and thin self-supporting films.

Hemicelluloses

Three different kraft mill pulps from birch, eucalyptus and spruce/pine wood, respectively, were employed for the isolation of the hemicelluloses. The carbohydrate composition and molecular mass properties of the isolated

hemicelluloses are depicted in **Table 1**. According to the carbohydrate analyses the hemicelluloses from the hardwood pulps were pure glucuronoxylans carrying a few 4-*O*-methylglucuronic and hexenuronic acid side-groups. In contrast, the hemicellulose obtained by extraction of the softwood pulp was composed of a mixture of arabinoglucuronoxylan (~90%) and galactoglucomannan. The molecular mass of the spruce/pine and the birch pulp hemicelluloses were rather similar whereas the corresponding eucalyptus xylan exhibited a somewhat higher molecular mass, see **Table 1**.

Table 1. The carbohydrate composition and the average molecular mass of the hemicelluloses.

Hemicellulose origin	**Birch**	**Eucalyptus**	**Spruce/pine**
Carbohydrate composition (weight-%)			
Xylose	96.7	96.4	79.5
4-*O*-Methylglucuronic acid	0.7	1.4	0.0
Hexenuronic acid	2.6	0.7	3.6
Mannose	0.0	0.0	4.3
Galactose	0.0	0.7	0.6
Glucose	0.0	0.9	5.3
Arabinose	0.0	0.0	6.8
Average molecular mass (kDa)			
Number average mass, M_n.	9.2	10.0	9.2
Weight average mass, M_w.	10.9	13.2	10.8

Lactide grafted hemicelluloses

Lactide grafted polymers (lactide-g-hemi) were synthesized from the spruce/pine, eucalyptus and birch pulp hemicelluloses by grafting employing a lactide-to-hemicellulose molar ratio 2:1. **Table 2** depicts the glass transition temperature (T_g) and the decomposition temperature (T_d) for the lactide-g-hemi polymers synthesized. The birch lactide grafted xylan polymer exhibited the highest T_g according to the data in the table. The glass transition temperatures obtained here for the kraft pulp derived lactide-g-hemi polymers were slightly higher than those measured by us previously for some birch black liquor xylan derived lactide-g-hemi polymers [8]

Table 2. The thermal properties of the three different lactide-g-hemicelluloses synthesised from the spruce/pine, birch and eucalyptus hemicelluloses extracted from the bleached kraft pulps.

Polymer and origin	Glass transition temperature T_g (^oC)	Decomposition temperature T_d (^oC)
La-g-hemi, Spruce/pine pulp	88	248
La-g-hemi, Birch pulp	108	250
La-g-hemi, Eucalyptus pulp	98	253

Lactide grafted hemicellulose films

Self-supporting barrier films were manufactured by solvent casting or thermal processing (compression moulding) from the three lactide grafted hemicellulose polymers synthesized. **Table 3** depicts the oxygen gas permeability (OP) and the water vapour permeability (WVP) for the lactide-g-hemi films produced. As can be seen, all films demonstrate good oxygen barrier properties according to the data in **Table 3.** Moreover, the OP values measured here for lactide-g-hemi films compared favourably with the OP values previously reported for PLA and PLA-blends with wood-derived hemicellulose [11]. The oxygen gas permeability for the compression moulded film from the eucalyptus derived lactide-g-hemi was somewhat lower than that for the birch and spruce/pine derived films produced by solvent casting, see **Table 3**. The WVP measured here indicates that the lactide-g-hemi film also can provide some protection against moisture.

Table 3. The oxygen gas permeability (OP) and water vapour permeability (WVP) for films from lactide-g-hemicelluloses from spruce/pine, birch and eucalyptus. The measurements were done at 23°C and 50% RH.

Polymer and origin	Oxygen gas permeability (OP) *cm^3 mm/ m^2 24h atm*	Water vapour permeability (WVP) *g mm/ m^2 24h atm*
La-g-hemi, Spruce/pine pulp	7.1*	n.a
La-g-hemi, Birch pulp	8.3*	n.a
La-g-hemi, Eucalyptus pulp	1.4**	2.7**

* = Solvent casted, ** = Compression moulded, and n.a = not analysed

IV. CONCLUSIONS

The present investigation demonstrates that thermoplastic barrier materials can be synthesized by grafting lactide to birch, eucalyptus and spruce/pine pulp hemicelluloses. The self-supporting films produced from the lactide grafted hemicelluloses exhibited good barrier properties. Thus, the thermoplastic lactide grafted hemicellulose polymers synthesized here may find applications as novel "green" packaging materials derived from renewable raw material resources.

V. ACKNOWLEDGEMENT

This study was performed within the Innventia Cluster Biorefinery Processes and Products.

VI. REFERENCES

[1] Vincendon, M. Xylan derivatives: Aromatic carbamates. *Makromol. Chem.* 1**993**, *194*, 321-328.
[2] Vincendon, M. Xylan derivatives: Benzyl ethers, synthesis, and characterization. *J. Appl. Polymer Sci.* **1998**, *67*, 455-460.
[3] Fang, J. M.; Sun, R. C.; Tomkinson, J.; Fowler, P. Acetylation of wheat straw hemicellulose B in a new non-aqueous swelling system. *Carbohydr. Polym.* **2000**, *41*, 379-387.
[4] Fundador, N. G. V.; Enomoto-Rogers, Y.; Takemura, A.; Iwata, T. Acetylation and characterization of xylan from hardwood kraft pulp. *Carbohydr. Polym.* **2012**, *87*, 170-176.
[5] Jain, R.; Sjöstedt, M.; Glasser, W. Thermoplastic Xylan Derivatives with Propylene Oxide. *Cellulose* **2000**, *7*, 319-336.
[6] Östlund, J.; Dahlman, O. Hemicellulose based polylactide copolymers. In *Proc 2nd Nordic wood biorefinery conference (NWBC).* **2009**, 244-245.
[7] Persson, J.; Dahlman, O. ; Albertsson, A.-C. Birch xylan grafted with PLA branches of predictable length. *BioRes.* **2012**, *7*, 3640-3655.
[8] Persson, J.; Dahlman, O.; Albertsson, A.-C.; Edlund, U. Modification of birch xylan by lactide-grafting *Nord. Pulp Pap. Res. J.* **2012**, *27*, 518-524.
[9] Dahlman, O.; Jacobs, A.; Liljenberg, A.; Ismail Olsson, A. Analysis of carbohydrates in wood and pulps employing enzymatic hydrolysis and subsequent capillary zone electrophoresis. *J. Chromatogr. A* **2000,** *891*, 157-174.
[10] Jacobs, A.; Dahlman, O. Characterization of the molar masses of hemicelluloses from wood and pulps employing size exclusion chromatography and matrix-assisted laser desorption ionization time-of-flight mass spectrometry. *Biomacromolecules.* **2001**, *2*, 894-905.
[11] Saadatmand, S.; Edlund, U.; Albertsson, A.-C. Compatibilizers of a purposely designed graft copolymer for hydrolysate/PLLA blends. *Polymer.* **2011**, *52*, 4648-4655.

CURRENT AND FUTURE APPLICATIONS OF ENZYMES IN THE PULP AND PAPER INDUSTRY

Henrik Lund[1]*, Lisbeth Kalum[1], Pedro E. G. Loureiro[1], Hanne H. Pedersen[1], Pierre Cassland[1] , Kasper T. Klausen[1], Hui Xu[2],and Gregory C. Delozier[3]
[1]*Novozymes A/S, Bagsvaerd, Denmark;*[2]*Novozymes North America, Franklinton, NC, USA;*
[3]*Novozymes, Inc., Davis, CA, USA (*Email of corresponding author: HLU@novozymes.com)*

ABSTRACT

Although the Pulp and Paper industry has been relatively slow to adopt enzyme technologies, tremendous progress has been made in the past 30 years. Xylanase aided bleach boosting, enzymatic deinking, pitch control by lipases, cellulases for drainage improvement and stickies control by esterases have all been implemented in the pulp and paper making processes.
In recent years substantial focus has been on the area of fiber modification, where enzymes are used to fundamentally alter the performance of specific fibers in paper, tissue and board manufacture – and today such applications find widespread use in industry.
The major efforts put into developing commercially viable routes to make ethanol from lignocellulosic biomass has furthermore resulted in a very large diversity of enzymes – both within the known classes of cellulases and hemicellulases, but also within completely new enzyme classes, such as the LPMO's or GH61-type enzymes.
It is likely that more and more enzymatic solutions will find their way into the pulp and paper mills in the years to come.

I. TRENDS IN CURRENT ENZYME APPLICATIONS

As shown in table 1 below around 8-9 enzyme classes are currently used commercially in the pulp and paper industry.

The first application of enzymes in the paper industry was somehow a spill-over from the starch industry – use of amylases for modifying the viscosity of starch so that it becomes applicable for paper coating applications. Then in the mid-80'ties came the discovery that xylanase pre-treatment of pulp could significantly improve the subsequent bleaching process [1]. Today xylanases have been engineered to be used at high temperatures and significant alkalinity in order to ease their implementation at mill scale. Furthermore a new application of xylanases is for post-bleaching application [2], where the enzymatic treatment is done after the final bleaching tower. The benefit of xylanase post-bleaching applications may be a brightness gain in the range of 1.0-1.5% ISO brightness combined with a reduced brightness reversion.

Segment	Application	Enzyme Class
Pulp (i.e. for tissue, towel paper and board manufacture)	Bleach boosting	Xylanase
	Deinking	Amylase, cellulase, lipase
	Strengthening & refining	Cellulase, laccase, hemicellulase
	Drainage/dewatering	Cellulase and hemicellulase
	Vessel element mitigation	Cellulase and hemicellulase
Process & equipment	Starch modification	Amylase
	Pitch control	Lipase
	Stickies control	Lipase
	Cleaning	Protease, lipase, amylase
Process & wastewater	Cationic demand reduction	Pectinase
	Color/odor removal	Laccase, peroxidase
	Residual management	Multiple enzymes

Table 1

Enzymatic solutions for pitch and stickies control have developed into significant industrial applications. Lipase products for pitch control offer an effective tool to reduce productivity losses and quality problems in mills using mechanical pulp fiber [3]. In some respects, pitch control is a business area that shows a relatively high cyclic nature with a significant use in the cold months (where the natural extractives degradation in chip piles is low) and reduced consumption during the summer months. Increasingly, younger trees and/or species with unique extractive profiles comprise a significant fraction regional wood baskets and are availing new, year-round, lipase application opportunities.

Enzymatic stickies control [4] where a special type of lipases is used to prevent agglomeration of adhesive contaminants in recycled pulp furnishes is today well established in industry – in particular in the production of tissue- and towel-grade products from recovered fibers. The mechanism behind enzymatic stickies control is believed to be related to deacetylation of adhesive contaminants such as polyvinylacetate to the less adhesive polyol which in turn increase the colloidal stability of micro-stickies and reduces their agglomeration into macro-stickies.

In recent years a lot of focus in industry has been on the use of enzymes – mostly cellulases - for fiber modification. While many of the multi-component cellulolytic systems found in nature have the potential to dramatically reduce pulp viscosity and reduce most strength measures, it is found that treatment of pulps with selected endoglucanases can do quite the opposite, namely significantly increase strength [5]. Papermakers can take advantage of this strengthening effect in several ways, i.e. by producing a higher quality end-product, by reducing refining energy, by using a less costly furnish and/or by saving on other strengthening agents. The front-runners in the large scale implementation of enzymatic fiber modification have been the tissue- and towel-sectors, where the improvements can be clearly perceived by consumers. Currently, the practices are also transferring to the production of packaging/board grades as well as printing and writing papers.

A related area that has grown in importance is that of enzymatic vessel element mitigation [6]. The problems with vessel elements – i.e. vessel picking – are not new, but the strong growth in export of eucalyptus market pulp from Latin America has resulted in this becoming a global issue. Enzymatic means to control vessel picking take advantage of the distinctive wall structure and the higher content of hemicellulose in the vessel elements compared to the regular fibers, so that combined enzymatic and mechanical treatment of pulps can "selectively" weaken and disrupt the vessels, so that these can be incorporated in the product without causing problems for down-stream users.

While all of the above technologies are still far from full market acceptance and penetration, it is clear that the industry is starting to consider enzymatic solutions as standard tools. No doubt both enzyme producers and solution providers to the paper industry will continue to refine and optimize product and process performances for an even greater use in the future.

II. NOVEL AND FUTURE APPLICATIONS

The enzymes currently used in the pulp and paper industry are almost exclusively representatives of the hydrolase class – and only a very small fraction of enzymes from the remaining classes. Within the coming years this will likely change as more and more applications involving novel enzyme classes are matured to the point of commercialization.

Oxidoreductases for pulp and paper applications have been a major research topic for many years, and we now see mills starting to employ these at commercial scale [7] - mainly for strengthening of packaging grades based on OCC and/or UBSK, as well as in wood composite materials production.

In these applications laccases are believed to induce a redistribution and cross-linking of lignin and other aromatic compounds which impart greater strength (i.e. burst and ring crush strength) and impart new physical properties (e.g. hydrophobicity) to the resulting board. Mills can capitalize on this by optimizing their furnish (i.e. greater use of recovered fiber) and by reducing other functional additives.

Tremendous progress has also been seen in the use of oxidoreductases for bleaching/delignification processes [8] – as will be discussed in another session during this conference. Although there is no doubt that enzymatic bleaching reactions have merit from a technical point of view, enzymatic bleaching technology needs to be further improved to compete with existing bleaching processes.

In the fiber modification area enzymes are being evaluated for more specialized grades and processes. Endoglucanases have emerged as key candidates for cost-effective production of nano-cellulose or MFC by reducing the refining energy needed in the manufacturing process [9].

Another new use of cellulases is in the production of dissolving pulps. Dissolving pulp is one of the high growth sectors of the P&P industry driven by the textile industry seeking alternatives to cotton. Cellulases can be used for a precise adjustment of the intrinsic viscosity of the pulp with the additional benefit of increased pulp reactivity for viscose manufacture (decrease consumption of CS_2) as presented in Figure 1.

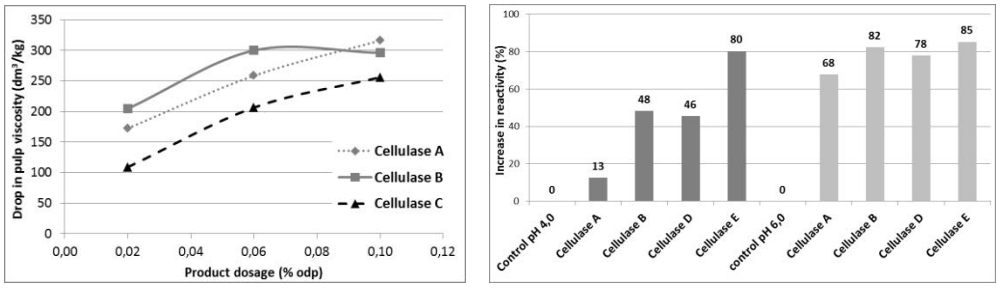

Figure1. Performance of different cellulase products on i) the decrease of the intrinsic viscosity and ii) on the increase in dissolving pulp reactivity for viscose manufacture.

A new class of enzymes that has been found capable of providing fiber modification benefits are the so-called GH61-enzymes [10]- now mostly referred to as lytic polysaccharide monooxygenases (LPMO's). These mono-oxygenases were found to be one of the key enzymes for enabling cost-effective degradation of lignocellulosic biomass to fermentable sugars. In concert with other cellulytic enzymes these enzymes significantly boost the degradation of biomass. However, ithas recently been found that selected LPMO's can provide significant strength benefits to both bleached and unbleached pulp fibers in the absence of other activities. As illustrated in figure 2 it is possible to see substantial increases in both tensile and tear strength of handsheets prepared from unbleached eucalyptus Kraft pulp pre-treated with LPMO. An interesting aspect of the LPMO activity is that the strengthening benefits are noticeable also on highly lignified fibers – a difficult substrate for many endoglucanases.

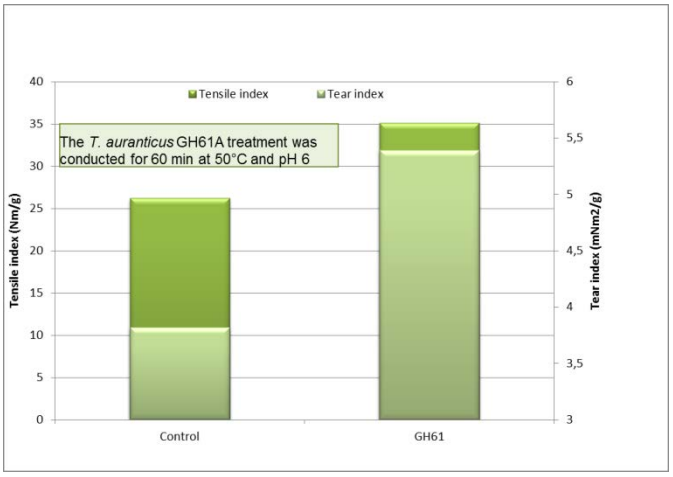

Figure 2. Fiber modification with Ta GH61 on unbleached eucalyptus kraft pulp.

In the pitch control area work has been done to expand enzymatic extractives management from triglycerides to also cover other classes of lipophilic extractives – in particular fatty acids. Several approaches have been found to be effective - treatment of pulps with laccases and selected mediators as well as treatment of extractive rich pulps with lipoxygenases [11]. The lipoxygenases can oxidize unsaturated fatty acids, such as linoleic acid, into fatty acid hydroperoxides. While these enzymes would be expected to be able to act on fatty acid extractives in pulps it has been shown that they may aid in the removal of a far wider range of extractives including sterols, sterol glycosides, fatty alcohols and even alkanes. Additional interest in the lipoxygenases arises from the finding that the formed fatty acid hydroperoxides seem to be able to provide additional delignification/bleaching benefits.

Several grafting technologies are being developed for functionalizing fibers. Various oxidoreductases can be employed to either form or add new functional groups on fiber-surfaces thereby altering their performance on the machine and within the final product. Also transferase enzymes, like xyloglucan endotransferase (XET), can be used to provide new fiber functionalities or to link functional additives onto fiber-surfaces.

III. CONCLUSIONS

The use of enzymes in the pulp and paper industry has been steadily growing over the past 25 years, yet there is still significant room for further growth and implementation of more sustainable ways to manufacture pulp and paper products. Most of this growth has been based on enzymes providing incremental improvements within the existing manufacturing processes. This will for sure also continue in the foreseeable future.With the increasing focus on biorefineries – and in particular integrated forest biorefineries (IFBR's) – it can be envisioned that

enzymes and other biotechnological solutions may become truly enabling technologies for the evolving pulp and paper industry. On one hand, the IFBP-approach may allow the pulp and paper industry to broaden their revenue base by entering and/or creating new markets. On the other, IFBR investigative efforts may boost the progress of self-sufficient manufacturing i.e. via in-situ or on-site production of key-chemicals (solvents, surfactants, strengthening agents etc).

IV. REFERENCES

[1] Viikari, L. et al. Third International Conference in Biotechnology in Pulp and Paper Industry, Stockholm, Sweden, **1986**, 66-69.

[2] Tolan, J. et al., US-patent 7,368,036

[3] Fujita, Y., Awaji, H., Taneda, H., Hata, K., Shimoto, H., Sharyo, M., Sakaguchi, H., and Gibson, K., *Tappi J.* **1992**, 75(4):117.

[4] Jones, D.R. and Fitzhenry, J.W., Pulp Paper **2003,** 2:28

[5] Lumme, M.S., Mansfield, S.D., Saddler, J.N., Proceedings of 7th International conference on Biotechnology in the Pulp and Paper Industry, Vancouver, BC. CPPA **1998,** 3:163.

[6] Bajpai, P.,Biotechnology Progress **1999**, 15(2):147 – 157

[7] Denowski, D.; Hoekstra, O. Tappsa J., **2013**, 1, 11-12

[8] Burnet, A., Meyer, V., Martinez, A., Gutierrez, A., Kalum, L., Lund, H., Romero, J., Petit-Conil, M., "Upscaling TCF bleaching of Eucalyptus globulus pulp using an enzyme catalyzed oxygen delignification stage", **2011,** 5th International Colloquium on Eucalyptus Pulp, Oral presentation, 9-12 May, Porto Seguro, Brazil.

[9] Henriksson, M.; Henriksson, G.; Berglund, L.A.; Lindström, T. European Polymer Journal, **2007,** 43,8, 3434-3441

[10] Quinlan, R.J. et al., Proc Natl Acad Sci U S A., **2011**; 108(37): 15079–15084

[11] Marques, G.; Molina, S.; Babot, E.D.; Lund, H.; del Río, J.C.; Gutiérrez, A., Bioresource Technology, **2011**, 102, 2, 1338-1343

WHAT BASIDIOMYCETE GENOMES TEACH US ABOUT WOOD BIODEGRADATION MECHANISMS

Francisco J. Ruiz-Dueñas[1], Elena Fernández-Fueyo[1], José M. Barrasa[2], Kenneth E. Hammel[3], and Angel T. Martínez[1]*

*[1]CIB, CSIC, Ramiro de Maeztu 9, E-28040 Madrid, Spain; [2]Universidad de Alcalá, Alcalá de Henares, E-28805 Madrid, Spain; [3]US Forest Products Laboratory, One Gifford Pinchot Drive, Madison, WI 53726, USA (*ATMartinez@cib.csic.es)*

ABSTRACT

Considerable confusion existed for years about the mechanisms ultimately responsible for wood biodegradation by basidiomycetes. Interest in wood decay, as a biotechnological model for the sustainable production of fuels and chemicals, led to sequencing of the first basidiomycete genomes. Massive sequencing tools extended the number of white-rot and brown-rot fungal genomes available, enabling us to establish general conclusions on the biodegradation mechanisms involved in each of them. Lignin degradation by white-rot fungi appears always associated with the presence of high redox-potential peroxidase genes in their genomes. Such genes are absent from all the brown-rot fungal genomes. Moreover, polysaccharide degradation by the latter fungi is not associated with an expansion of genes encoding carbohydrate-acting enzymes. This fact, together with the presence of genes encoding peroxide-generating and Fe^{3+}- and quinone-reducing enzymes, supports the chemical depolymerization of wood polysaccharides via Fenton chemistry in the case of brown rot. The genomic analyses also outlined the evolutionary history of the different peroxidase families in wood-rotting basidiomycetes, in particular fixing the origin of lignin-degrading peroxidases at the end of the Carboniferous period, which coincides with the end of coal formation via accumulation of undecayed plant biomass in the soil.

I. FIRST BASIDIOMYCETE GENOMES

The increasing availability of basidiomycete genomes (transcriptomes and secretomes) provides answers to several questions concerning the biodegradation mechanisms of wood-rotting fungi. Most of these genomes were sequenced at the Joint Genome Institute of the US Department of Energy with the purpose of understanding fungal decay of wood, for the biotechnological production of fuels and other chemicals from renewable plant feedstocks. Basidiomycetes have developed two main degradation strategies resulting in so-called white-rot and brown-rot decay of wood (because of the color of the transformed material) [1]. Chemical analysis showed that white-rot fungi remove wood lignin, simultaneously or preferentially with respect to polysaccharides, while brown-rot fungi remove polysaccharides preferentially to leave a modified lignin-rich residue [2]. Simultaneously, using simple and polymeric model compounds, it was shown that white-rot fungi are able to mineralize lignin, which in nature protects wood polysaccharides against hydrolysis by most cellulolytic organisms (brown-rot excluded).

In addition to the so-called ligninolytic peroxidases discovered in the 80's, a variety of other oxidative enzymes (including laccases, different peroxidases, oxidases and other oxidoreductases), as well as redox mediators (such as phenolic and nonphenolic aromatic compounds from fungal metabolism or lignin degradation, lipid and oxygen radicals, metal cations, etc) have been associated with fungal degradation of lignin in a process that was defined as an "enzymatic combustion" [3], in contrast to polysaccharide degradation, which is seen as a generally well understood, largely hydrolytic process. This puzzling situation, already emphasized in some early reviews [4], persisted for more than 20 years until the development of the first genome sequencing platforms.

Phanerochaete chrysosporium, the model white-rot fungus for many years, was the first basidiomycete whose genome was sequenced in 2004 [5]. A few years later, the first brown-rot fungal genome, transcriptome and secretome of *Postia placenta* was available [6] and their comparison with the corresponding *P. chrysosporium* genome [5], transcriptome and secretome [7] provided interesting information on the wood biodegradation mechanisms by these two model white-rot and brown-rot basidiomycetes. This early period of sequencing of individual wood-rotting fungal genomes was completed with the genomes of *Ceriporiopsis subvermispora* [8], a selective lignin degrader, and also those of *Pleurotus ostreatus* [9] and *Agaricus bisporus* [10], which are two representative lignin-degrading agarics that grow on wood and soil, respectively (note that all the above typical lignin-

degrading fungi are polypores). More recently, larger sequencing projects were developed, where the initial conclusions obtained from the genomes of the first fungi sequenced were extended and completed using the genomes of a variety of white-rot and brown-rot basidiomycetes, as reported by Floudas et al. [11], who analyzed 31 ascomycete and basidiomycete genomes.

II. DIVERGENT WHITE-ROT AND BROWN-ROT DEGRADATION MECHANISMS

To obtain general conclusions on the mechanisms of wood degradation, we comparatively analyzed thirteen white-rot and seven brown rot fungal genomes [9,11-13]. Among the different oxidative enzymes mentioned above, genes for ligninolytic peroxidases - the so-called lignin peroxidase (LiP), manganese peroxidase (MnP) and versatile peroxidase (VP) enzymes - appear in all the white-rot fungal genomes but are absent from all the brown-rot fungal genomes, whereas laccases, oxidases and other oxidoreductase families are present in both white-rot and brown-rot fungal genomes.

Among the above peroxidases, MnPs are present in all white rot fungi, being accompanied by LiPs, VPs or both, depending on the type of fungus. LiP is able to degrade nonphenolic lignin model dimers and nonphenolic synthetic lignin (the latter in the presence of the fungal metabolite veratryl alcohol) [14,15] and the same capabilities have been recently shown for VP [16]. On the other hand, MnP, and also VP, oxidize Mn^{2+} to Mn^{3+}, which can: i) initiate lipid peroxidation reactions resulting in lignin degradation by reactive lipid radicals; or ii) oxidize minor phenolic units in lignin or lignin-derived phenols [17]. None of the above peroxidases are found in brown-rot fungi, whose genomes include only a few genes encoding so-called generic peroxidases (GPs), which are characterized by a low redox-potential that limits them to oxidation of phenolic substrates (and some dyes). The specific presence of genes encoding LiP, VP and MnP in white-rot fungal genomes, and their frequent duplication giving rise to numerous isoenzymes, strongly support their involvement in the attack on lignin characteristic of wood-rotting basidiomycetes.

However, the brown-rot fungal genomes not only lack the genes for ligninolytic peroxidases, in agreement with the lifestyle described above that only includes limited modification of lignin [2], but also contain a much smaller number of genes for carbohydrate-acting enzymes (CAZYs) as compared with white-rot fungi. In particular, cellulolytic enzymes that contain cellulose-binding domains are unexpectedly rare. This fact, together with the presence and expression of genes for H_2O_2-generating oxidases and Fe^{3+}- and quinone-reducing enzymes, indicates that polysaccharide attack by brown-rot fungi is largely non-enzymatic, proceeding via Fenton chemistry ($Fe^{2+} + H_2O_2 \rightarrow Fe^{3+} + OH^- + OH\cdot$) [6]. That is, not only lignin depolymerization by white-rot fungi but also polysaccharide depolymerization by brown-rot fungi depend heavily on oxidative processes.

Although a few white-rot fungal species degrade lignin preferentially with respect to polysaccharides (selective decay pattern), most white-rot fungal species degrade polysaccharides simultaneously with lignin [18]. This fact, together with the Fenton-based mechanism for brown-rot decay described above, justifies the apparent paradox raised by the presence of more, and more diverse, genes for carbohydrate-degrading enzymes in the genomes of white-rot fungi (known for their ability to attack lignin) than in those of brown-rot fungi (known for their ability to degrade polysaccharides). The above applies not only to genes encoding carbohydrate hydrolases but also to the recently discovered lytic polysaccharide monooxygenase genes, involved in the initial oxidative attack on recalcitrant carbohydrates [19], which are more abundant in white-rot than in brown-rot fungal genomes [11,20].

A common characteristic of white-rot and brown-rot fungal genomes, and the corresponding transcriptomes and secretomes, is the presence, duplication and expression of oxidase genes responsible for H_2O_2 generation. Interestingly, brown-rot fungi produce methanol oxidase that uses methanol from lignin demethylation for reducing O_2 to H_2O_2, while white-rot fungal oxidases use both carbohydrate-derived (such as glyoxal oxidase and pyranose oxidase) and lignin-derived (such as aryl-alcohol oxidase) reducing substrates. Therefore, considering the main (limiting) reactions as shown by genomic analyses, white-rot and brown-rot decay of wood by basidiomycetes can be seen as an H_2O_2-dependent oxidation (of lignin and polysaccharides, respectively) catalyzed by two different iron species, Fe^{3+} in peroxidase heme cofactors and free Fe^{2+}, respectively.

Concerning laccases, the presence of the corresponding genes is not the determinant factor for white-rot or brown-rot fungal lifestyles since they are widespread in basidiomycete, and also ascomycete, genomes. Therefore, their contribution to lignocellulose biodegradation would differ according to the wood decay pattern and fungal species. In white-rot decay they would oxidize the minor phenolic units in lignin, and the lignin-derived phenols (contributing to similar reactions catalyzed by the MnPs characteristic of white-rot fungi) and it has been suggested that some of the (stable) phenoxy radicals formed could also be involved in lignin degradation as natural redox mediators [21]. In brown-rot species they could contribute

to an alternative mechanism for both Fe^{3+} reduction and H_2O_2 generation via quinone redox-cycling [22]. A similar process was first reported in white-rot fungi [23], although the analysis of fungal genomes does not provide evidence for the involvement of Fenton chemistry in the attack on lignin by these species.

III. WHITE-ROT FUNGI: ORIGIN AND EVOLUTION OF LIGNINOLYTIC PEROXIDASES

The comparative analyses of fungal genomes reveals that not only the number but also the diversity of lignin-degrading peroxidases expanded in the lineage leading to the ancestor of wood-rotting basidiomycetes, which is reconstructed as a white-rot species, and then contracted in parallel lineages leading to brown-rot and mycorrhizal species [11]. The appearance of white-rot decay, made possible by peroxidase evolution leading to the first lignin-degrading enzymes, might have coincided with the sharp decrease in the rate of organic carbon burial around the end of the Carboniferous period, as shown by molecular clock analyses.

Moreover, ancestral state reconstructions [11,12] have shown that an ancestral non-ligninolytic GP (related to those found in ascomycetes and plants) gave rise to the first MnP, by incorporating a Mn^{2+}-oxidation site formed by three acidic residues located near one of the heme propionates. In the subsequent evolutionary history of basidiomycete peroxidases, the ancestral MnPs apparently gave rise at least twice to the first VPs, by incorporating a lignin degradation site that consists of a radical-forming exposed tryptophan that can abstract electrons from the bulky lignin polymer and transfer them to the activated heme cofactor. The last step in ligninolytic peroxidase evolution was the loss of the Mn-oxidation site, conserved in all VPs, thus giving rise to the first LiPs, which represent the most efficient lignin-degrading peroxidases. Interestingly, the last transition occurred only in the evolution of basidiomycetes from the order Polyporales, while VP remained as the only lignin-degrading enzyme in the order Agaricales.

The above evolution of basidiomycete peroxidases followed the evolution of lignin and precursor polymers in land plants, whose functions include protection of polysaccharides from biodegradation. Accordingly, the absence, from the middle Devonian to late Carboniferous periods, of white-rot fungi that can efficiently mineralize these recalcitrant aromatic polymers resulted in the massive accumulation of dead woody and nonwoody plant biomass (from Paleozoic seed ferns, lycophytes, equisetophytes, progymnosperms, and early gymnosperms mainly represented by Cordaitales species). This accumulation generated large coal deposits and also a simultaneous reduction of the very high carbon dioxide content in the primitive atmosphere. This largely irreversible carbon dioxide fixation process by primitive land plants stopped at the end of the Carboniferous period with the evolution of white-rot fungi equipped with lignin-degrading peroxidases, thus enabling the balanced recycling of carbon currently known on earth.

IV. ACKNOWLEDGEMENT

This work was supported by INDOX (KBBE-2013-613549) and PEROXICATS (KBBE-2010-265397) EU projects (to ATM), by Spanish HIPOP project (BIO2011-26694; to FJR-D) and by US DOE grant DE-AI02-07ER64480 (to KEH). The work conducted by the US DOE JGI is supported by the Office of Science of the US DOE under contract DE-AC02-05CH11231. The authors thank D. Cullen (USDA, Madison, USA), D.S. Hibbett (Clark University, Worcester, USA) and A.G. Pisabarro (Universidad de Navarra, Pamplona, Spain), among others, for coordination of basidiomycete genome sequencing projects. EF-F acknowledges a JAE fellowship, and FJR-D acknowledges a Ramón y Cajal contract.

V. REFERENCES

[1] Martínez A.T.; Speranza M.; Ruiz-Dueñas F.J.; Ferreira P.; Camarero S.; Guillén F.; Martínez M.J.; Gutiérrez A.; del Río J.C. Biodegradation of lignocellulosics: Microbiological, chemical and enzymatic aspects of fungal attack to lignin**.** *Int. Microbiol.* **2005**, *8,* 195-204.

[2] Martínez A.T.; Rencoret J.; Nieto L.; Jiménez-Barbero J.; Gutiérrez A.; del Río J.C. Selective lignin and polysaccharide removal in natural fungal decay of wood as evidenced by *in situ* structural analyses**.** *Environ. Microbiol.* **2011**, *13,* 96-107.

[3] Kirk T.K.; Farrell R.L. Enzymatic "combustion": The microbial degradation of lignin**.** *Annu. Rev. Microbiol.* **1987**, *41,* 465-505.

[4] Eggeling L. Lignin-an exceptional biopolymer...and a rich resource? *Trends Biotechnol.* **1983**, *1,* 123-127.

[5] Martinez D.; Larrondo L.F.; Putnam N.; Gelpke M.D.; Huang K.; Chapman J.; Helfenbein K.G.; Ramaiya P.; Detter J.C.; Larimer F. et al. Genome sequence of the lignocellulose degrading fungus *Phanerochaete chrysosporium* strain RP78**.** *Nat. Biotechnol.* **2004**, *22,* 695-700.

[6] Martinez D.; Challacombe J.; Morgenstern I.; Hibbett D.S.; Schmoll M.; Kubicek C.P.; Ferreira P.; Ruiz-Dueñas F.J.; Martínez A.T.; Kersten P. et al. Genome, transcriptome, and secretome analysis of wood decay fungus *Postia placenta* supports unique mechanisms of lignocellulose conversion**.** *Proc. Natl. Acad. Sci. USA* **2009**, *106*, 1954-1959.

[7] Vanden Wymelenberg A.; Gaskell J.; Mozuch M.; Kersten P.; Sabat G.; Martinez D.; Cullen D. Transcriptome and Secretome Analyses of Phanerochaete chrysosporium Reveal Complex Patterns of Gene Expression**.** *Appl. Environ. Microbiol.* **2009**, *75*, 4058-4068.

[8] Fernández-Fueyo E.; Ruiz-Dueñas F.J.; Ferreira P.; Floudas D.; Hibbett D.S.; Canessa P.; Larrondo L.; James T.Y.; Seelenfreund D.; Lobos S. et al. Comparative genomics of *Ceriporiopisis subvermispora* and *Phanerochaete chrysosporium* provide insight into selective ligninolysis**.** *Proc. Natl. Acad. Sci. USA* **2012**, *109*, 5458-5463.

[9] Ruiz-Dueñas F.J.; Fernández E.; Martínez M.J.; Martínez A.T. *Pleurotus ostreatus* heme peroxidases: An *in silico* analysis from the genome sequence to the enzyme molecular structure**.** *C. R. Biol.* **2011**, *334*, 795-805.

[10] Morin E.; Kohler A.; Baker A.R.; Foulongne-Oriol M.; Lombard V.; Nagy L.G.; Ohm R.A.; Patyshakuliyeva A.; Brun A.; Aerts A.L. et al. Genome sequence of the button mushroom *Agaricus bisporus* reveals mechanisms governing adaptation to a humic-rich ecological niche**.** *Proc. Natl. Acad. Sci. USA* **2012**, *109*, 17501-17506.

[11] Floudas D.; Binder M.; Riley R.; Barry K.; Blanchette R.A.; Henrissat B.; Martínez A.T.; Otillar R.; Spatafora J.W.; Yadav J.S. et al. The Paleozoic origin of enzymatic lignin decomposition reconstructed from 31 fungal genomes**.** *Science* **2012**, *336*, 1715-1719.

[12] Ruiz-Dueñas F.J.; Lundell T.; Floudas D.; Nagy L.G.; Barrasa J.M.; Hibbett D.S.; Martínez A.T. Lignin-degrading peroxidases in Polyporales: An evolutionary survey based on ten sequenced genomes**.** *Mycologia* **2013**, *105*, 1428-1444.

[13] Eastwood D.C.; Floudas D.; Binder M.; Majcherczyk A.; Schneider P.; Aerts A.; Asiegbu F.O.; Baker S.E.; Barry K.; Bendiksby M. et al. The Plant Cell Wall-Decomposing Machinery Underlies the Functional Diversity of Forest Fungi**.** *Science* **2011**, *333*, 762-765.

[14] Hammel K.E.; Jensen K.A.; Mozuch M.D.; Landucci L.L.; Tien M.; Pease E.A. Ligninolysis by a purified lignin peroxidase**.** *J. Biol. Chem.* **1993**, *268*, 12274-12281.

[15] Tien M.; Kirk T.K. Lignin-degrading enzyme from the hymenomycete *Phanerochaete chrysosporium* Burds**.** *Science* **1983**, *221*, 661-663.

[16] Fernández-Fueyo E.; Ruiz-Dueñas F.J.; Martínez M.J.; Romero A.; Hammel K.E.; Medrano F.J.; Martínez A.T. Ligninolytic peroxidase genes in the oyster mushroom genome: Heterologous expression, molecular structure, catalytic and stability properties and lignin-degrading ability**.** *Biotechnol. Biofuels* **2014**, *7:2*.

[17] Bao W.L.; Fukushima Y.; Jensen K.A.; Moen M.A.; Hammel K.E. Oxidative degradation of non-phenolic lignin during lipid peroxidation by fungal manganese peroxidase**.** *FEBS Lett.* **1994**, *354*, 297-300.

[18] Blanchette R.A. Delignification by wood-decay fungi**.** *Annu. Rev. Phytopathol.* **1991**, *29*, 381-398.

[19] Quinlan R.J.; Sweeney M.D.; Lo Leggio L.; Otten H.; Poulsen J.C.N.; Johansen K.S.; Krogh K.B.R.M.; Jorgensen C.I.; Tovborg M.; Anthonsen A. et al. Insights into the oxidative degradation of cellulose by a copper metalloenzyme that exploits biomass components**.** *Proc. Natl. Acad. Sci. USA* **2011**, *108*, 15079-15084.

[20] Hori C.; Gaskell J.; Igarashi K.; Samejima M.; Hibbett D.S.; Henrissat B.; Cullen D. Genomewide analysis of polysaccharides degrading enzymes in 11 white- and brown-rot Polyporales provides insight into mechanisms of wood decay**.** *Mycologia* **2013**, *105*, 1412-1427.

[21] Cañas A.I.; Camarero S. Laccases and their natural mediators: Biotechnological tools for sustainable eco-friendly processes**.** *Biotechnol. Adv.* **2010**, *28*, 694-705.

[22] Wei D.S.; Houtman C.J.; Kapich A.N.; Hunt C.G.; Cullen D.; Hammel K.E. Laccase and its role in production of extracellular reactive oxygen species during wood decay by the brown rot basidiomycete *Postia placenta***.** *Appl. Environ. Microbiol.* **2010**, *76*, 2091-2097.

[23] Guillén F.; Gómez-Toribio V.; Martínez M.J.; Martínez A.T. Production of hydroxyl radical by the synergistic action of fungal laccase and aryl alcohol oxidase**.** *Arch. Biochem. Biophys.* **2000**, *383*, 142-147.

EXPLOITING FUNGAL DIVERSITY FOR OPTIMIZED BREAKDOWN AND SACCHARIFICATION OF LIGNOCELLULOSIC BIOMASS

Craig B. Faulds[1,2]*, Jean-Guy Berrin, Anne Favel, Isabelle Gimbert, Laurence Lesage-Meessen, Anthony Levasseur, Anne Lomascolo, Sana Raouche, Yonathon Arfi, Chloé Bennati-Granier, Mathieu Bey, Christophe Boyer, Charlotte Champion, Marie Couturier, Marianne Daou, Annick Doan, Elodie Drula, Marie-Pierre Forquin-Gomez, Soňa Garajová, Sacha Grisel, Mireille Haon, Nadège Liaud, Yann Mathieu, David Navarro, Elise Odinot, Chantal Parodi, Sylvie Piumi, François Piumi, Laetitia Poidevin, Sabine Taussac, Simeng Zhou, Marie-Noëlle Rosso, Eric Record and Jean-Claude Sigoillot

[1]INRA UMR 1163 Biotechnologie des Champignons Filamenteux, 163 avenue de Luminy, 13288 Marseille, France ; [2]Aix-Marseille Université UMR A 1163 BCF, POLYTECH Marseille, 163 avenue de Luminy, 13288 Marseille, France.

ABSTRACT

Efficient biological deconstruction of plant cell walls requires the addition of a great array of enzyme activities. In order to understand how fungi attack lignocellulose and hence apply this knowledge for biotechnological applications, we need to explore the available resources at the genomic, transcriptomic and secretomic level. In this extended abstract, we describe some of the background to the integrated approach we are taking in Marseille utilizing the French National filamentous fungal collection, and the identification of supplementary enzyme cocktails and novel enzymes.

I. INTRODUCTION

Filamentous fungi are an invaluable source of enzymes able to deconstruct and/or modify the complex matrix that comprises the plant cell walls. The wealth of genomic data obtained recently from filamentous fungi has revealed the diversity of lignocellulolytic enzymes they produce. The CIRM-CF collection hosted in Marseille (https://www6.inra.fr/cirm/Champignons-Filamenteux) is dedicated to filamentous fungi involved in lignocellulosic degradation originating from specific temperate and tropical biotopes and from polluted agri-food sites. This collection is a unique tool to explore fungal functional biodiversity with applications in various fields of biotechnology, including the improved pretreatments and saccharification. In this extended abstract, we give examples of how we are exploiting our knowledge of this diverse fungal collection to understand the machinery of lignocellulosic deconstruction.

II. GENOMIC APPROACHES

The expanding numbers of sequenced fungal genomes provide an unprecedented framework for identifying their potential in the deconstruction of lignocellulosic biomass. Comparative genomic studies enable us to decipher the different strategies used by fungi to breakdown the recalcitrant barrier of plant cell wall. This breakdown is carried out by diverse panel of Carbohydrate-Active enzymes (called "CAZymes") [1]. Unravelling the fungal lignocellulolysis requires reliable identification of the main actors involved in and these actors have been integrated and meticulously updated in the CAZy database (http://www.cazy.org). Recently, we added a new category termed Auxiliary Activities (AA) [2]. This novel category groups together the families of redox enzymes and the families of lytic polysaccharide monooxygenases involved in lignin breakdown. Thus, AA category provides a complementary insight into enzymatic lignocellulolysis by focusing on oxidative enzyme families.

In our genomic approaches developed in the laboratory, the purposes consist in focusing on the differences in the fungal lignocellulolytic repertoires to look for convergence and divergence among the families. Each fungal group has its own enzymatic specificity and consequently, specific taxa could be targeted for biotechnological applications. For example, the genome sequence of two white-rot fungi, *P. cinnabarinus* and *P. sanguineus* have been determined (Levasseur et al, in press). Expert annotation of CAZymes and AAs active on lignin revealed that *P. cinnabarinus* possesses a complete genetic portfolio for lignin breakdown, including a total of 6 laccases, 1 ferroxidase, 11 class II ligninolytic peroxidases, 1 cellobiose dehydrogenase, 3 aryl-alcohol oxidases, 1 glucose oxidase, 2 alcohol oxidases, 2 pyranose oxidases, 7 copper radical oxidases, and 1 benzoquinone reductase. This suggests that *P. cinnabarinus* may exploit different strategies for ligninolysis including oxidation mediated by class-II peroxidases via H_2O_2, or by laccases in the presence of redox mediators, or via the Fenton reaction. When grown on birchwood, the fungus secretes laccases, copper radical oxidases, a cellobiose dehydrogenase,

and several aryl-alcohol oxidases, suggesting that these enzymes contribute to lignocellulose deconstruction by the fungus (Levasseur, in press). Under the auspices of a Joint Genome Initiative-sponsored project from the US Department of Energy, we are currently comparing the repertoire of genes encoding enzymes active on carbohydrates or lignin in the genome of 40 Polyporales strains (**Figure 1**). The suite of Polyporales strains has been selected based on their abilities to degrade/deconstruct plant biomass, their phylogenetic position in the taxon or their geo-climatic origin with emphasis on tropical regions where biodiversity is higher and underexplored. In order to facilitate genome assembly, monokaryotic strains have been obtained from dikaryotic strains by in vitro fructification or protoplastization. A consortium of 12 laboratories will analyze and compare the gene repertoires in these Polyporales with other sequenced genomes and explore the diversity of lignocellulose-acting enzymes fungi use to retrieve carbon from plant biomass.

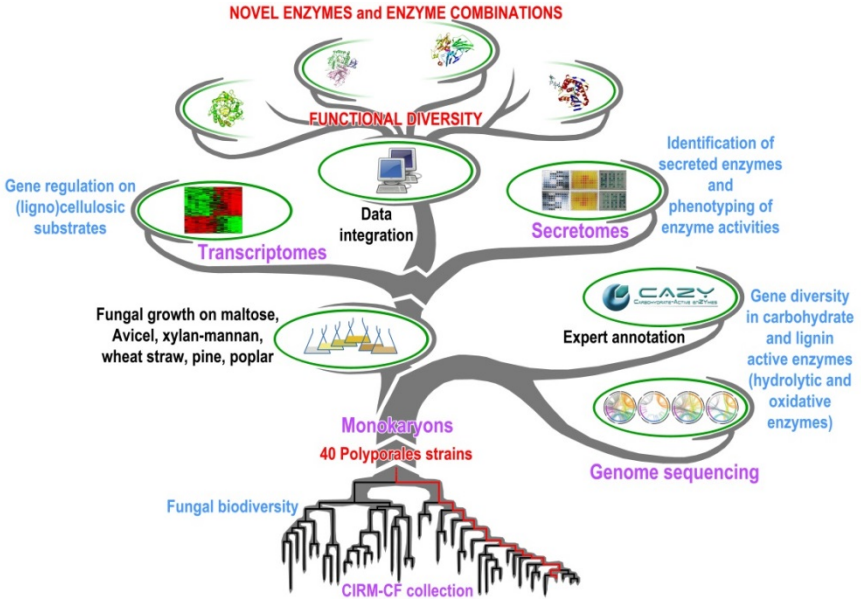

Figure 1. An Integrated Approach to compare genomics, transcriptomics and secretomics data from filamentous fungi within the CIRM-CF collection.

III. TRANSCRIPTOMIC APPROACHES

Beyond the comparison of genome portfolios, the analysis of transcriptome profiles *in vivo* allows identification of the sets of genes encoding the enzyme machineries expressed according to the organisms' strategy for plant cell wall degradation/modification. These analyses reveal which enzymes are produced during the different stages of plant cell wall deconstruction, whether it will be drastic disruption or more subtle modification of wood decay, and under challenging environmental conditions. For instance, the characterization of salt-adapted secreted lignocellulolytic enzymes from the mangrove fungus *Pestalotiopsis* sp. was performed to discover new enzymes of biotechnological interest. Fungi are important for biomass degradation processes in mangrove forests. Given the presence of sea water in these ecosystems, mangrove fungi are adapted to high salinity. *Pestalotiopsis* sp. NCi6, a halotolerant and lignocellulolytic mangrove fungus of the order Xylariales were isolated from the trees of the mangrove swamp. *De novo* transcriptome sequencing and assembly indicate that this fungus possesses of over 400 putative lignocellulolytic enzymes, including a large fraction involved in lignin degradation. We also studied its lignocellulolytic enzymes and analyzed the effects of salinity on its secretomes. Proteomic analyses of the secretomes suggest that the presence of salt modifies lignocellulolytic enzyme composition, with an increase in the secretion of xylanases and cellulases and a decrease in the production of oxidases. As a result, cellulose and hemicellulose hydrolysis is enhanced but lignin breakdown is reduced. This study highlights the adaptation to salt of mangrove fungi and their potential for biotechnological applications.

IV. SECRETOMIC AND ENZYMATIC APPROACHES

A large number of secretomes of fungal isolates originating from temperate and tropical forest environments were explored through an automatic platform developed in our laboratory [3]. The strains displaying potential for the saccharification of lignocellulosic biomass were further investigated through secretomic analyses. For instance the lignocellulose-acting enzymes content of 20 filamentous fungi was investigated by means of activity profiling (**Figure 2**; [4]). Proteomic analyses were also performed on the secretomes of *Fusarium verticillioides* [5], *Trametes gibbosa* [6], *Ustilago maydis* [4], *Pestalotiopsis* sp. [7]. It allowed the identification of hundreds of promising candidates (glycoside hydrolases and oxidative enzymes) to improve the degradation of biomass.

Novel cellobiose dehydrogenases [8,9], lytic polysaccharide monooxygenases [10], hemicellulases (including mannanases) [11] and endoglucanases [12-13] have been identified from genome mining and characterized, demonstrating their potential to enhance the industrial lignocellulose bioconversion process. Overall, analyses of fungal secretomes allowed the identification of the repertoires of enzymes active during *in vivo* plant cell wall degradation, to get insights into the mechanisms involved in lignocellulose degradation and to define the most efficient mixtures of enzymes.

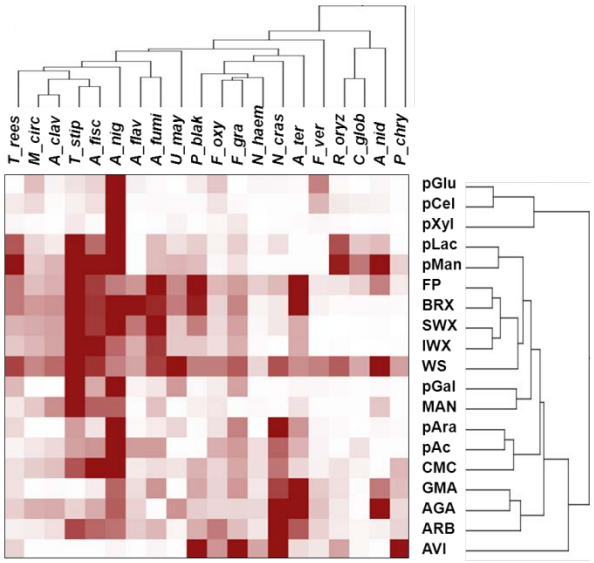

Figure 2. Double clustering of the main carbohydrate-cleaving activities from representative fungi. Enzymatic activities of fungal secretomes (except CL847) on a range of polysaccharides were used to build distance trees. The degree of activity of secretomes on the respective substrate is represented by a colour scale with different strengths of red. Top tree: : *T.rees, Trichoderma reesei (Hypocrea jecorina); M.circ, Mucor circinelloides f lusitanicus; A.clav, Aspergillus clavatus; T. stip, Talaromyces stipitatus (Penicillium emmonsii); A.fisc, Aspergillus fischeri (Neosartorya fischeri); A.nig, Aspergillus niger; A.flav, Aspergillus flavus; A.fumi, Aspergillus fumigatus; U. may, Ustilago maydis; P.blak, Phycomyces blakesleeanus; F.oxy, Fusarium oxysporum f lycopersici; F.gra, Fusarium graminearum (Gibberella zeae); N.haem, Nectria haematococca (Fusarium solani); N.cras, Neurospora crassa*; *A.ter, Aspergillus terreus; F.ver, Fusarium verticillioides (Gibberella moniliformis); R.oryz, Rhizopus oryzae (R. arrhizus); C.glob, Chaetomium globosum*; *A.nid, Aspergillus nidulans (Emericella nidulans); P.chry, Phanerochaete chrysosporium.* Right tree: Enzymatic activities of fungal secretomes were determined on: AVI, Avicel; ARB, arabinan; AGA, arabinogalactan; GMA, galactomannan; CMC, carboxy-methyl cellulose; pAc, *p*NP-acetate; pAra, *p*NP-α–L–arabinofuranoside; MAN, ivory nut mannan; pGal, *p*NP-α–D–galactopyranoside; WS, wheat straw; IWX, insoluble arabinoxylan; SWX, soluble wheat arabinoxylan; BRX, birchwood xylan; FP, filter paper; pMan, *p*NP-β-D–mannopyranoside; pLac, *p*NP-β–D–lactobioside; pXyl, *p*NP-β–D–xylopyranoside; pCel : *p*NP-β–D–cellobioside; pGlu, *p*NP-β-D–glucopyranoside;

V. WHOLE FUNGAL APPROACHES

The diversity and specificity of the enzymes secreted by lignocellulolytic filamentous fungi make these organisms a primary source of powerful enzymes of the microbial world for the breakdown of lignocellulosic plant cell walls. A large number of studies demonstrated their high potential for biotechnological processes, especially those ligninolytic fungi belonging to the group of Basidiomycetes. The CIRM-CF collection offers us a wide wood decaying fungal biodiversity to select the best adapted fungi for a given biorefinery application. The first studies for industrial application of filamentous fungi were performed in the pulp and paper field. In particular, we demonstrated their effectiveness in the pretreatment of wood or other lignocellulosic materials (biopulping) for selective removal of lignin while preserving cellulose [14-16]. Furthermore, the selective delignifying ability of basidiomycetes could also been exploited for renewable bioenergy production processes to improve enzymatic hydrolysis yields improving the accessibility of enzymes to cellulose. At present, we are conducting studies devoted to their implementation for the pretreatment of several lignocellulosic biomasses for energy recovery (bioethanol or biogas). In this frame, more than a hundred strains were screened at the lab scale through a one-pot method (unpublished data) and pilot plant scaling up is underway with the most efficient strains.

VI. CONCLUSIONS

With the growing numbers of fungal genomes, their transcriptomes and the actively secreted enzymes produced, there is no doubt that such an integrated approach as outlined in this extended abstract will provide new insights into the adaptation of fungi to their substrates and thus provide novel enzymatic tools to be targeted and overexpressed for functional validation and eventually incorporated into tailored enzyme preparation for the exploitation of lignocellulosic biomass.

VII. ACKNOWLEDGEMENT

We would like to thank INRA, AIX Marseille Université for general funding of the Unit, l'Agence Nationale de la Recherche (France) for funding through the E-Tricel and Funlock projects, and the DOE Joint Genome Institute (USA) for funding the Polyporales Community Sequencing project.

VIII. REFERENCES

[1] Lombard, V.; Ramulu, H.G.; Drula, E.; Coutinho, P.M.; Henrissat, B. The carbohydrate-active enyme database (CAZy) in 2013. *Nucleic Acid Res* **2014**, *42*, D490-D495.
[2] Levasseur, A.; Drula, E.; Lombard, V.; Coutinho, P.M.; Henrissat, B. Expansion of the enzymatic repertoire of the CAZy database to integrate auxiliary redox enzymes. *Biotechnol Biofuels*. **2013**, *6*:41.
[3] Navarro, D.; Couturier, M.: Ghizzi Damasceno da Silva, G.; Berrin, J-G.; Rouau, X.; Asther, M.; Bignon, C. Automated assay for screening the enzymatic release of reducing sugars from micronized biomass. *Microbial Cell Fact.* **2010**, *9*, 58.
[4] Couturier, M.; Navarro, D.; Olivé, C.; Chevret, D.; Haon, M.; Favel, A.; Lesage-Meessen, L.; Henrissat, B.; Coutinho, P.M.; Berrin, J-G. Post-genomic analysis of fungal lignocellulosic biomass degradation reveal the unexpected potential of the plant pathogen *Ustilago maydis*. *BMC Genomics* **2012**, *13*, 57.
[5] Ravalason, H.; Grisel, S.; Chevret, D.; Favel, A.; Berrin, J-G.; Sigoillot, J-C.; Herpoël-Gimbert, I. *Fusarium verticillioides* secretome as a source of auxilliary enzymes to enhance saccharification of wheat straw. *Biores. Technol.* **2012**, 114, 589-596.
[6] Berrin, J-G.; Navarro, D.; Couturier, M.; Olivé, C.; Grisel, S.; Haon, M.; Taussac, S.; Lechat, C.; Courtecuisse, R.; Favel, A.; Coutinho, P.M.; Lesage-Meessen, L. Exploring the natural fungal diversity of tropical and temperate forests toward improvement of biomass conversion. *Appl. Environ. Microbiol.* **2012**, *78*, 6483-6490.
[7] Arfi, Y.; Chevret, D.; Henrissat, B.; Berrin, J-G.; Levasseur, A.; Record, E. Characterization of salt-adapted secreted lignocellulolytic enzymes from the mangrove fungus *Pestalotiopsis* sp. *Nature Comms.* **2013**, *4*, 1810.
[8] Bey, M.; Berrin, J-G.; Poidevin, L.; Sigoilot, J-C. Heterologous expression of *Pycnoporus cinnabarinus* cellobiose dehydrogenase in *Pichia pastoris* and involvement in saccharification process. *Microbial Cell Fact.* **2011**, *10*, 113.
[9] Turbe-Doan, A.; Arfi, Y.; Record, E.; Estrada-Alvarado, I.; Levasseur, A. Heterologous production of cellobiose dehydrogenases from the basidiomycete *Coprinopsis cinerea* and the ascomycete *Podospora anserina* and their effect on saccharification of wheat straw. *Appl. Microbiol. Biotechnol.* **2013**, *97*, 4873-4885.
[10] Bey, M.; Zhou, S. ; Poidevin, L. ; Henrissat, B. ; Coutinho, P.M. ; Berrin, J-G. ; Sigoillot, J-C. Cello-oligosaccharide oxidation reveals differences between two lytic polysaccharide monooxygenases (Family GH61) from *Podospora anserina*. *Appl. Environ. Microbiol.* **2013**, *79*, 488-496.
[11] Couturier, M. ; Roussel, A. ; Rosengren, A. ; Leone, P. ; Stalbrand, H. ; Berrin, J-G. Structural and biochemical analysis of glycoside hydrolase families 5 and 26 β-(1,4)-mannanases from *Podospora anserine* reveal differences upon manno-oligosaccharide catalysis. *J. Biol. Chem.* **2011**, *288*, 14624-14635.
[12] Couturier, M.; Feliu, J. ; Haon, M. ; Navarro, D.; Lesage-Meessen, L. ; Coutinho, P.M.; Berrin, J-G. A thermostable GH45 endoglucanase from yeast: impact of its atypical multimodularity on activity. *Microbial Cell Fact.* **2011**, *10*, 103.
[13] Poidevin, L.; Feliu, J.; Doan, A.; Berrin, J-G.; Bey, M.; Coutinho, P.M.; Henrissat, B.; Record, E.; Heiss-Blanquet, S. Insights into exo- and endoglucanase activities of family 6 glycoside hydrolases from *Podoposra anserine*. *Appl. Environ. Microbiol.* **2013**, 79, 4220-4229.
[14] Meza, J-C.; Sigoillot, J-C.; Lomascolo, A.; Navarro, D.; Auria, R. New process for fungal delignification of sugar-cane bagasse and simultaneous production of laccase in a vapor phase bioreactor. *J. Agric. Food Chem.* **2006**, *54*, 3852-3858.
[15] Meza, J-C.; Auria, R. ; Lomascolo, A. ; Sigoillot, J-C.; Casalot, L. Role of ethanol on growth, laccase production and protease activity in *Pycnoporus cinnabarinus* ss3. *Enzyme Microb Technol.* **2007**, *41*, 162-168.
[16] Ravalason, H. ; Jan, G. ; Molle, D. ; Pasco, M. ; Coutinho, P.M. ; Lapierre, C. ; Pollet, B. ; Bertaud, F. ; Petit-Conil, M. ; Grisel, S. ; Sigoillot, J-C. ; Asther, M. ; Herpoël-Gimbert, I. Secretome analysis of *Phanerochaete chrysosporium* strain CIRM-BRFM41 grown on softwood. *Appl. Microbiol. Biotechnol.* **2008**, *80*, 719-733.

FUNCTIONALIZATION OF CELLULOSIC MODEL SUBSTRATES VIA LACCASE-MEDIATED COUPLING OF NON-POLAR PARTICLES

Cusola, Oriol[1,2]; Valls, Cristina[1]; Vidal, Teresa[1]; Roncero, M. Blanca[1]*; Rojas, Orlando[2,3]

*[1]CELBIOTECH_Paper Engineering Research Group. Universitat Politècnica de Catalunya-BarcelonaTech. Colom 11, E-08222 Terrassa, Spain; [2]Department of Forest Products Technology. School of Science and Technology. Aalto University 00076 Aalto, Finland; [3]Departments of Forest Biomaterials and Chemical and Biomolecular Engineering. North Carolina State University. Raleigh, North Carolina. (*roncero@etp.upc.edu)*

ABSTRACT

In the present work we investigate the physicochemical interactions between silica and nanofibrillar cellulose (CNF) with a multi component system (MCS) obtained from an enzymatic reaction of a laccase enzyme and a short-chain organic molecule, dodecyl 3,4,5-trihydroxybenzoate (commonly known as lauryl gallate, LG) as well as sulphonated lignin (SL). Hydrophobic chains of enzyme-modified LG were coupled onto CNF and silica surfaces by direct adsorption of the MCS. Quartz crystal microgravimetry (QCM-D), Atomic Force Microscopy (AFM) and water contact angle (WCA) were used to monitor in situ and characterize the hydrophobization process. Efficient adsorption of the MCS onto CNF and silica surfaces increased their WCA by 88° and 78°, respectively. Dynamic Light Scattering (DLS) measurements revealed an effect of the enzyme on LG: reducing particle size from several microns down to 300 nm. The laccase (Lacc) treatment in the presence of SL reduced even more the LG particle size to 80 nm through a dispersive effect of SL.

I. INTRODUCTION

The use of renewable and biodegradable materials has grown enormously in recent years [1]. Nanosized cellulose (cellulose nanofibrils, CNF) has attracted attention as a renewable resource for conversion into high added value products and advanced functional materials. However, expanding the uses of CNF requires its hydrophobization. Waterproof coatings and films, packaging materials and hydrophobic composites are but a few examples of hydrophobized CNF. Hydrophobization of CNF facilitates industrial processing operations such as size pressing, printing or conversion [2]. To be useful for packaging purposes, CNF must be treated with environmentally friendly hydrophobizing agents to facilitate recycling, which is not the case with the currently used conventional waxes and fluoropolymers. The hydrophobization method of choice depends on the particular substrate in each case. For example, "wet chemical reaction" and "electrochemical deposition" methods are commonly applied to metals, whereas "self-assembly" and "layer-by-layer" deposition methods are preferred for glass substrates, and textiles. These and other cellulose hydrophobization methods are the subject of a comprehensive review by Song and Rojas, (2013) [3].

Green chemistry approaches based on enzyme reactions have aroused increasing interest with a view to developing sustainable CNF-based products. Enzymatic functionalization of cellulose fibres by using phenolic moieties to introduce antimicrobial or antioxidant effects, among others, was recently accomplished [4,5]. The use of enzyme systems for surface hydrophobization is still in its infancy, however. A method using laccase enzymes in combination with hydrophobic phenolic compounds has proved effective to confer suspended cellulose fibres and CNF hydrophobic properties [6].

In this work, we devised a novel route to further exploit laccase enzymes with a view to hydrophobizing films or mats of cellulose and CNF (e.g. paper, non-wovens) by direct surface application of the enzyme together with a co-adjuvant to strengthen physico–chemical interactions in aqueous systems. Specifically, we examined physico–chemical interactions of silica and CNF with a multi component system (MCS) obtained by enzymatic reaction of laccase with a short-chain organic molecule (LG), and sulphonated lignin (SL) [7]. MCS proved effective in hydrophobizing CNF by simple immersion, spraying or size-pressing.

II. EXPERIMENTAL

Enzyme, chemicals and substrate preparation

The enzyme used in this work was laccase from *Trametes Villosa* supplied with an activity of 588 U/mL by Novozymes®. Dodecyl 3,4,5-trihydroxybenzoate (LG) was purchased from Sigma Aldrich®. Soluble sulphonated lignin of 5.9 kDa MW and 5% total sulphur content was obtained from Borreegard® (Sarpsborg, Norway) and

used as received. Nanofibrillar cellulose (CNF) was obtained from bleached hardwood (birch) pulp. Model surfaces for adsorption tests consisted of bare silica wafers and QCM-D silica sensors purchased from Q-Sense (Västra Frölunda, Sweden). For adsorption experiments using cellulose the silica sensors were pretreated with polyethyleneimine (PEI) polymer, followed by spin coating with a dispersion of nanofibrillar cellulose (CNF).

Multi component system (MCS) and surface treatment

The multi-component system (MCS) was the product of the enzymatic reaction between *Trametes Villosa* laccase and the low-surface energy phenolic species (LG) in the presence of lignosulphonate (SL). MCS was prepared in a stirred bath, using 250 mL beakers. The preparation conditions were based on previous reports [8]. The role of each MCS component was elucidated by using control treatments.

Quartz Crystal Microbalance with Dissipation Monitoring (QCM-D)

In situ QCM-D tests were performed on a Q-Sense E4 instrument (Västra Frölunda, Sweden) operated in the continuous mode. Molecular interactions between MCS (or the controls) with the substrate caused a shift in resonance frequency (f) which was monitored in order to quantify any gain in mass (e.g. by adsorption). The third overtone (n = 3) was used to interpret QCM data. QCM-D measurements were made at a continuous flow rate of 100 µL/min at 25°C.

Atomic force microscopy

A Nanoscope IIIa Multimode scanning probe microscope from Digital Instruments, Inc. (Santa Barbara, CA, USA) was used to characterize the surface topography of the QCM-D silica sensors and CNF films before and after surface treatment. At least two different areas in each sample were examined, using a scan size of 10x10, 5x5 or 1x1 μm^2. AFM images where flattened following first-order conversion.

Particle size analysis and Water Contact Angle measurement

The hydrodynamic diameter and size distribution of the colloid particles present in MCS and the controls were determined by using a Zetasizer Nano ZS dynamic light scattering (DLS) instrument fromMalvern, UK.

Water contact angles (WCA) were measured with a CAM-200 contact angle goniometer from KSV Instruments, Ltd. (Helsinki, Finland) by depositing a 4 µL water drop onto the substrate from above and using a high-resolution digital camera to capture the drop profile. Measurements were made upon contact, once the water drop had stabilized —the time required for the initial transient fluctuations to cease was 2 s.

III. RESULTS AND DISCUSSION

Particle size analysis with DLS

The particle size of MCS and the controls was determined by dynamic light scattering (DLS); the results are shown in **Table 1**. The LG control, exhibited a highly polydisperse size distribution with a major concentration of particles about 5 µm in size. However, the control LG+Lacc presented a monodisperse particle size around 300 nm; this result is very interesting since it shows the clear effect of the LG after reaction with enzyme. Additionally, the size of the Laccase as far as DLS measurements had to be due to enzyme aggregates, because the typical Laccase individual molecule dimensions are around 5 nm as reported elsewhere. The particle size of the SL was also reduced by means of the reaction with the enzyme as can be seen in **Table 1** comparing the SL and SL+Lacc controls which presented a particle size about 400 and 200 nm respectively. In the control consisting in the mixture LG+SL the particle size was around the 5 µm (the same size as the LG alone before filtration).

Control	Non-filtered (nm)	Filtered (nm)
LG	4900	0
SL	400	60
Lacc	500	45
LG+Lacc	310	200
SL+Lacc	200	230
LG+SL	4800	60
MCS	800	90

Table 1. Particle size of MCS and component systems as measured by DLS before and after passage through syringe filters of 0.45 µm pore size**.**

The particle size of MCS after reaction with the enzyme was about 800 nm. Although there was a marked reduction in size of LG particles, MCS remained highly polydisperse. The particle size of unfiltered MCS was greater than that of the unfiltered LG+Lac control, possibly because of the presence of residual large unoxidized LG particles. However, the fact that filtered MCS particles were approximately 80 nm in size and non-polydisperse suggests that the LG particles passing through the filter were smaller than those of the LG+Lac control. Therefore, MCS was the solution containing the smallest LG particles after filtration. DLS measurements exposed the effect of the enzyme in reducing LG particle size. The whole suspension containing the three main components (MCS) was that leading to the smallest LG sizes after filtration as a result of the favourable effect of SL —the LG+Lac control contained larger particle sizes after filtration.

Adsorption of MCS and MCS components on silica and CNF films

Silica was used as a model for cellulose by virtue of its containing free silanols and geminal silanol groups — which mimic hydroxyl groups in cellulose. Several QCM isotherms were obtained in the form of the variation of the negative value of the frequency shift in terms of mass uptake by the silica surface as a function of time. After the buffer solution (0.1 M sodium acetate) was delivered for 3 min or until no change in Δf was observed, introducing filtered MCS dramatically reduced the frequency by effect of adsorption or deposition of MCS onto the silica surface. In order to determine whether the frequency decrease was due to aggregate deposition or molecular adsorption, the sensor was rinsed with buffer after 70 min. Although rinsing MCS off the silicate surface caused a slight increase in Δf, the initial frequency value was never restored, which was taken as evidence of net adsorption. The difference between the frequency at the beginning (initial signal in the buffer solution) and that after the final rinsing can be assigned to a firmly adsorbed layer of MCS on the silica surface, equivalent to $\Delta f \approx -28$ Hz after 70 min adsorption. This result indicates physic–chemical affinity between silica and MCS.

Similarly to silica surfaces, adsorption of MCS and the control systems onto nanofibrillar cellulose (CNF) substrates was investigated. The adsorption of MCS onto CNF-coated sensors was about –40 Hz after 85 min of adsorption and rinsing with background buffer; this is suggestive of a high affinity between MCS and CNF. A comparison with the results for silica reveals that MCS was adsorbed to a similar extent on both types of surface.

All MCS components (Laccase, LG and SL) also accumulated on the surface of silica and CNF to a different extent with the SL, Lacc, SL+Lacc and LG+Lacc treatments. Based on the results, LG+Lacc was adsorbed to a greater extent than the other controls on both silica and CNF.

Water contact angle and surface hydrophobicity

Water contact angle (WCA) measurements of silica surfaces treated with MCS and the controls were used to relate adsorption to hydrophobization. To this end, bare silica was subjected to the QCM sequences described previously. As shown in **Figure 1**, treating silica with MCS increased WCA to about 50°.

The increased hydrophobicity observed was seemingly directly related to the amounts of material being adsorbed onto the surfaces. Thus, treatment with the SL+Lacc and Lacc controls increased the contact angle to about 35° and 55°, respectively. The most effective treatment as regards increasing WCA or surface hydrophobicity was the LG+Lacc control, which led to a contact angle of 88°.

A relationship between the amount of LG adsorbed and the hydrophobicity introduced by the treatments was also found. The greater adsorption was, the higher the WCA; however, WCA values tended to a plateau and levelled off above a Δf value of ca. –300 Hz.

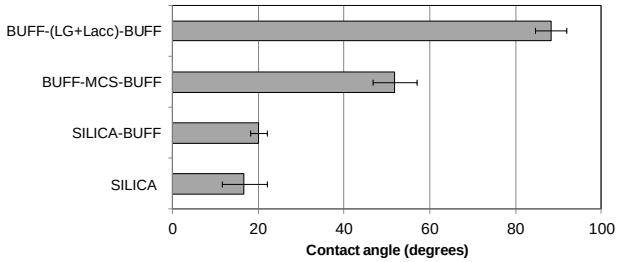

Figure 1. Water contact angle for silica surfaces treated with MCS and respective components and rinsing sequences. (BUFF= buffer rinsing).

Analysis of silica surfaces by AFM

The surfaces of the QCM-D silica sensors treated with MCS and the controls were imaged by AFM. The surface topography of the bare silica surface, was featureless and smooth (rms roughness less than 1 nm). The surface topography of the silica sensor that was treated with the LG+Lacc control, exhibited uniformly distributed large adsorbed particles about 200–300 nm in diameter and 20–40 nm in height. Such particles can only be enzyme-treated LG, which was not observed with the previous controls. The particle diameters were similar to those calculated from the DLS measurements with the LG+Lacc. The silica surface treated with MCS contained uniformly distributed LG particles about 100 nm in diameter and 10–20 nm in height. The particle size of adsorbed MCS as determined by AFM was also similar to that obtained from DLS measurements. Note that SL in MCS boosted the action of the enzyme by reducing the size of LG particles relative to the LG+Lacc control.

IV. CONCLUSIONS

The present investigation offers a novel route to further utilize laccase enzymes to hydrophobize films or mats of cellulose and CNF (as in paper or nonwovens) by direct surface application of the enzyme together with co-adjuvants. It also represents a sustainable substitute to the traditional cellulose-hydrophobing techniques, and a step forward in the implementation of green systems using enzymes.

V. ACKNOWLEDGEMENT

The authors are grateful to the BIOSURFACEL-CTQ2012-34109 and BIOFIBRECELL projects (CTQ2010-20238-CO3-01) within the framework of the Spanish's MICINN. Special thanks are also due to the consolidated research group AGAUR 2009SGR 00327 at Universitat de Barcelona (UB).

VI. REFERENCES

[1] Johansson, C.; Bras, J.; Mondragon, I.; Nechita, P.; Plackett, D.; Simon, P.; Svetec, D. G.; Virtanen, S.; Baschetti, M. G.; Breen, C.; Clegg, F.; Aucejo, S. Renewable fibers and bio-based materials for packaging applications - A review of recent developments. *BioResources.* **2012**, *7* (2), 2506-2552.

[2] Li, S.; Zhang, S.; Wang, X. Fabrication of Superhydrophobic Cellulose-Based Materials through a Solution-Immersion Process. *Langmuir* **2008**, *24*, 5585-5590.

[3] Song, J.; Rojas, O. J. Approaching Superhydrophobicity Based on cellulosic materials: A Review. *Nordic P&P Research Journal* **2013**, *28*, 216-238.

[4] Fillat, A.; Gallardo, O.; Vidal, T.; Pastor, F. I. J.; Díaz, P.; Roncero, M. B. Enzymatic grafting of natural phenols to flax fibres: Development of antimicrobial properties. *Carbohydr. Polym*. **2012**, *87*, 146-152.

[5] Aracri, E.; Fillat, A.; Colom, J. F.; Gutierrez, A.; del Rio, J. C.; Martinez, A. T.; Vidal, T. Enzymatic grafting of simple phenols on flax and sisal pulp fibres using laccases. *Bioresour. Technol*. **2010**, *101*, 8211-8216.

[6] Garcia-Ubasart, J.; Colom, J. F.; Vila, C.; Hernández, N. G.; Blanca Roncero, M.; Vidal, T. A new procedure for the hydrophobization of cellulose fibre using laccase and a hydrophobic phenolic compound. *Bioresour. Technol*. **2012**, *112*, 341-344.

[7] Cusola, O.; Valls, C.; Vidal, T.; Roncero, M,B. Rapid functionalisation of cellulose-based materials using a mixture containing laccase activated lauryl gallate and sulfonated lignin. *Holzforschung*. **2014,** *1–9*, ISSN (Online) 1437-434X, ISSN (Print) 0018-3830, DOI: 10.1515/hf-2013-0128.

[8] Cusola O, Valls C, Vidal T, Blanca Roncero M. Application of surface enzyme treatments using laccase and a hydrophobic compound to paper-based media. *Bioresour Technol.* **2013**, 131,521-526.

HIGH PERFORMANCE THIN LAYER CHROMATOGRAPHY IN ADDRESSING ANALYTICAL PROBLEMS IN THE CHEMISTRY OF RENEWABLES – A METHOD GIFTED WITH GREAT VERSATILITY

Stefan Böhmdorfer[1]*, Josua Oberlerchner[1], Christine Betty Nagawa[1], Markus Gorfer[2], Antje Potthast[1], Thomas Rosenau[1]

*[1]Department of Chemistry, University of Natural Resources and Life Sciences (BOKU University), Konrad-Lorenz-Str. 24, 3430 Tulln, Austria; [2]Institute of Applied Genetics and Cell Biology, University of Natural Resources and Life Sciences (BOKU University), Konrad-Lorenz-Str. 24, 3430 Tulln, Austria (*stefan.boehmdorfer@boku.ac.at)*

ABSTRACT

Similar to other chromatographic method, thin layer chromatography has evolved into a powerful analytical technique during the last decades, although it has suffered from some neglect compared to the more "technical" chromatographic methods. Due to its characteristics, thin layer chromatography can be used for experiments that are impractical or inaccessible by other chromatographic methods. We present the advantages of modern HPTLC (High Performance Thin Layer Chromatography) by means of three illustrative examples from our research.
The simplicity of TLC (Thin Layer Chromatography) allows quick development of normal phase-liquid chromatography methods; this is demonstrated by the development of a preparative method to isolate alkyl resorcinols from wheat bran.
The robustness of HPTLC permits the quantitative analysis of samples with high matrix content. Since the stationary phase is used just once for a single separation, damage inferred to it by sample components has no influence on future analyses. This high matrix resistance is shown by a quantitative analysis of monosaccharide in plant hydrolysates.
The direct accessibility of the plate after separation allows selective detections that are impossible to achieve with other chromatographic methods. This is illustrated by the direct detection of bioactive compounds of whole plant extracts on the TLC plate after separation by microorganisms.

I. INTRODUCTION

The two pillars of chemical analysis are spectroscopy and chromatography. The most common analytical systems consist of a chromatographic unit that separates the sample mixtures and a spectroscopic unit that identifies the isolated compounds. Over the decades, a wide range of different methods have been developed, all with their advantages and drawbacks. Although used less than for example HPLC (High Performance Liquid Chromatography) or GC (Gas Chromatography), HPTLC has developed into a technologically mature and reliable technique as well. Just like other chromatographic systems it has special properties, which easily permit procedures that are very hard to achieve with other chromatographic techniques – parallelization, matrix resistance, chemically selective detection, post separation derivatization and direct detection of bioactive compounds (direct bioautography, DB). This presentation wishes to guide through the first steps into expanding research capabilities by planar chromatography, be it HPTLC or regular TLC.

II. EXPERIMENTAL

Separation Development

A more detailed description of this procedure can be found in Reich et al. [1]. The silica of the TLC plate and of the preparative column must be the same to ensure identical selectivity on both systems. TLC development in sandwich configuration is recommended. Development distances of more than 7 cm usually do not improve the separation, as diffusion becomes more pronounced in the decreased solvent flow. The final solvent mixture must be homogeneous (one phase) and should not contain a too volatile solvent.

In the first step, a solvent system that offers the required selectivity is determined. The sample solution is separated with pure polar solvents of different selectivity groups according to Synder (for example 2-propanol, tetrahydrofuran, dichloromethane, ethyl acetate, toluene and chloroform) [2]. If no separation is observed after development, the solvent is dismissed immediately.

Solvent polarity is adjusted in the second step. Solvent that were able to separate the analytes, but result in too high R_f values are mixed with heptane. This reduces the solvent polarity without altering the separation. If the analytes do not migrate a sufficient distance, the solvent is replaced by a more polar one from the same selectivity group (for example, propanol against ethanol) or mixed with a less polar solvent that also showed good separation.

The third step generates the data necessary for the modeling of the analytes retention behavior. The solvent strength is varied by mixing with heptane or by varying the ratio of the solvents that comprise the mixture. If a preparative isocratic separation is desired, final R_f values of the analytes should be between 0.35 and 0.1, corresponding to *k* values of 2 to 10 (cf. to **Equation 2**). To develop a gradient HPLC method, which requires software assistance, R_f values should cover a wide range to obtain a sound basis for simulation.

Quantitative Analysis of Monosaccharides in Plant Hydrolysates

A detailed description of the method is given in "Revival of thin layer chromatography – separation and quantification of carbohydrates by high performance thin layer chromatography (HP-TLC)" by Oberlerchner, et al. in this book of abstracts.

TLC-Direct Bioautography

TLC separation was performed on 10x20 cm silica gel 60 F254 aluminium sheet TLC plates (Merck, Germany). Plant extracts were applied to the plate and separated with hexane:ethyl acetate 9:1. The separation was conducted twice: one plate was used in the bioassay and the second was used for visualisation of the separated constituents with anisaldehyde staining. Plates were photographed before and after spraying with reagent.

The developed plates were dipped in an overnight nutrient culture of *Escherichia coli* in tripticase soy broth with methyl thiazolyldiphenyl-tetrazolium bromide and then placed in a sterile tray, sealed and incubated at 37°C for 6-24 hours depending on the growth of the bacteria. The formation white clear bands showed the presence of compounds which can inhibit the growth of tested organisms.

III. RESULTS AND DISCUSSION

Development of Preparative Separations by HPTLC

Preparative separations in an organic chemistry laboratory are commonly done by normal phase liquid chromatography. The separation mechanism for normal phase chromatography with silica as stationary phase is based on adsorption of the analytes on the silica surface. The theories describing the separation process are well established, and software to simulate and optimize normal phase separations is available. Still, the behavior of a specific analyte in a specific system cannot be predicted without experimental data.

The goal of chromatography is usually the isolation of a molecule of interest. To achieve this, it has to be retained by the chromatographic system differently from all other molecules in the sample. This selectivity can be achieved by variation of the stationary phase, the mobile phase, the temperature or by additives in the mobile phase. For preparative separation, the stationary phase is usually predefined by the availability of bulk silica or flash columns. The HPTLC layer used for method development must be composed of the same silica, otherwise selectivity will uncontrollably change during the transfer from HPTLC to liquid chromatography. Temperature is usually not controlled in preparative systems, therefore only variation of the mobile phase is available to easily alter selectivity. For this reason, the first step in method development comprises screening of solvents of different selectivities. Solvents that do not show the desired selectivity are dismissed immediately. If no solvent system offers the required selectivity, TLC plates and bulks silica can be impregnated to modify the interaction with the stationary phase. In our case, toluene showed the most promising initial separation of the crude bran extract. The final eluent contained 2-propanol to elute strongly retained molecules.

In the second step of method development, solvent strength is altered to achieve favourable retention values. The retention behavior of a molecule can be described by the modified Soczewinski equation [3]:

$$\log k = \log k_B - n \log \phi \quad (1)$$

k is the retention factor, which describes the molecules retention behavior. It is equals to the solvent volume that is required to elute the compound, expressed in column volumes exceeding the column dead-time t_0. k_B is the retention factor with pure (more polar) solvent B as eluent, *n* is the number of solvent molecules that are replaced by the analyte during adsorption at the stationary phase and ϕ is the volume-fraction of polar solvent B. The dependence of the retention factor on the solvent composition can be predicted by this formula, if *k* has been determined at at least two different concentrations of B. This can be achieved by isocratic HPLC or more simply by TLC. The migration of a compound after development of the TLC plate is measured by the ratio of the analytes migration distance to the migration of the solvent front. This factor is called R_f. The result of each TLC

can be thought to be equivalent to that of an isocratic HPLC run, and R_f values are converted to *k* values according to

(2) $k = (1 - R_f) / R_f$ [4]

The *k* values obtained by TLC screening can then be used to decide on the most useful separation system or fed into software to simulate the behavior of the analytes during isocratic or gradient HPLC.

In the final step, the developed method has to be adapted to the actual system, considering the volume of the tubing, the delay between detector and fraction collector and the column´s volume and diameter.

Quantification of Monosaccharides in Samples with High Matrix Content

Samples of natural origin are usually mixtures of molecules covering a wide range of polarity. Chromatographic techniques usually accept only analytes of a certain polarity; too polar and too apolar molecules interfere with the analysis, deposit on the column or the instrumentation and need to be removed or converted during sample pretreatment. Planar chromatography does not rely on complete elution of the analytes. Instead of monitoring the molecules as they leave the column, the whole stationary phase is inspected after incomplete elution of the analytes. If some analytes are not picked up by the mobile phase and remain and the application spot instead, they will not spoil the stationary phase for future analyses, which would unnoticeably be the case in HPLC. The plate is used just one time, complete sample elution is therefore not required. Thus, planar chromatography deals very well with high amounts of matrix, or unregarded analytes. Still, if the portion of matrix in the sample is very high, the concentration of interesting molecules is very low, rising the detection limit. The application of larger amounts of sample would eventually distort the separation system.

In this project, we quantified monosaccharides in plant hydrolysate samples. Monosaccharide analysis is already challenging, since monosaccharides are very polar molecules, which need to be separated according to small differences in configuration. GC offers the necessary selectivity, but requires time-consuming sample derivatization to lower the analytes polarity. Additionally, each single monosaccharide results in up to five peaks after separation (pyranose, furanose, open chain and two anomers each) [5]. Affinity chromatography with metal ion columns can give useful results, yet when it fails to do so, there are no parameters to effectively affect the selectivity. Also, high matrix load usually lead to distorted results and necessitated more frequent regeneration steps. Furthermore, the application of the very selective lead charged affinity column results in heavy metal contaminated solvent waste, which is expensive to dispose of.

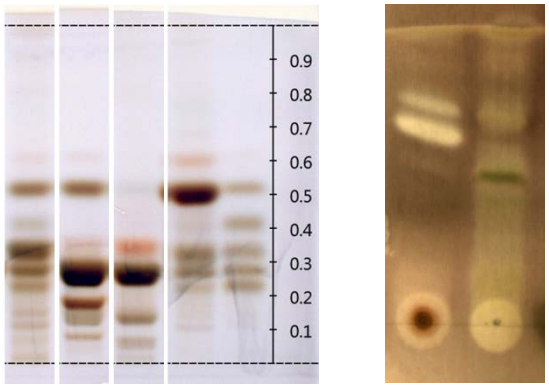

Figure 1. Left: Exemplary quantitative HPTLC analyses of plant hydrolysates. Standard were applied in the rightmost lane; form top to bottom: xylose, arabinose, mannose, glucose, galactose. Right: TLC-DB with *Escherichia coli* of the extracts of *Warburgia ugandensis* bark (left) and leaves (right). Antimicrobial activity can be observed in both samples. Two compounds in the bark extract at R_f 0.7 are apparently very active.

The HPTLC method we developed not only quantitatively separates five monosaccharides, but also tolerates the sample matrix very well (**Figure 1**). The sample preparation consists of simple dilution and filtration. The matrix remains at the application spot and – once separated – does not interfere with the monosaccharide separation. An inherent drawback of the method is it´s large number of manual operations. HPTLC plates need to be transferred manually into the impregnation bath, to the sampling application device, into the developing chamber, into the derivatization solution, onto the heating plate and into the imaging device. Some of the steps (impregnation, derivatization, heating) can influence the result of the measurement (note the streak through sample 4 and the standards in **Figure 1**). It is therefore imperative to record the procedure unambiguously, train the operator very well in both observing the procedure and the changes to the results that can be inferred by alternate procedures.

Direct Bioautography

Additionally to chemical and physical detection methods [6], biological ways can be employed for selective detection on TLC plates. For chemical derivatization, TLC plates are usually dipped into a solution of the derivatization reagent, heated to promote the reaction and the change of color is evaluated. Detection of bioactive compounds by microorganisms works according to the same principle. First, the TLC plate is covered by microorganisms by dipping it into culture medium. For anaerobic bacteria, the plate can also be covered by a solid culture medium. Then the plate is kept in a warm and humid environment that promotes the microorganisms´ growth. Finally, the plate is inspected for areas with increased or reduced growth. A simple way to detect microbial growth is the addition of a tetrazolium salt to the culture medium. For example, colourless 2,3,5-triphenyltetrazolium chloride (TTC) is converted to the pink formazan by microbial organisms. If the colour is absent, the organisms were inactive.

This way, whole plant extracts can be screened very quickly for bioactive compounds. The plant extract is separated by TLC, if necessary several times with solvents that cover a wide range of polarity. The plates are treated with culture medium and incubated. Substances that are active against the used microorganism will not turn pink (see **Figure 1**).

Also, the employed TLC separation can be used in the development of a preparative chromatographic method as described above.

The method has advantages over the classic approach of iterative testing of activity and fractionation, but it also has some pitfalls [7]. Not all TLC plates support the growth of the microorganisms. In our hands, aluminum backed plates worked best. Very apolar compounds give false positives; they do not inhibit growth, but prevent the microorganisms to attach to the TLC plate in the first place. Also, substances with a very dark colour prohibit the observation of the indicator colour. Finally, achieving stable growth conditions takes some experience.

IV. CONCLUSIONS

HPTLC is a mature method with its characteristic advantages and disadvantages. Since the stationary phase (the plate) is only used once, it is very resistant to samples with high matrix load. This is very valuable in the analysis of biological material and biorefinery process samples. Due to the simultaneous analysis of several samples, it is a useful tool for method development, for example for column chromatography methods. A wide range of selective detection methods is available, including the detection of bioactive compounds by microorganisms.

All in all, HPTLCs most pronounced drawback is its dependence on manual operations, which can introduce hard to detect aberrations in the analysis. Yet, it offers methodological properties unavailable to other chromatographic techniques, which can be a valuable addition to an analytical laboratory.

V. ACKNOWLEDGEMENT

The financial support of Christine Nagawa by an ÖAD appear scholarship is gratefully acknowledged.

VI. REFERENCES

[1] Reich, E.; Schibli, A. High-Performance *Thin-Layer Chromatography for the Analysis of Medicinal Plants*. Thieme: New York, Stuttgart, 2006.

[2] Snyder, L. R. Classification of the Solvent Properties of Common Liquids. *J. Chrom Sci.* **1978**, *16* (6), 223-234.

[3] Soczewiński, E. Solvent composition effects in thin-layer chromatography systems of the type silica gel-electron donor solvent. *Anal. Chem.* **1969**, *41*, 179-182.

[4] Snyder, L. R.; Kirkland, J. K.; Dolan, J. W. *Introduction to Modern Liquid Chromatography*. 2nd Ed; John Wiley & Sons: Hoboken, 2010.

[5] Becker, M.; Zweckmair, T.; Forneck, A.; Rosenau, T.; Potthast, A.; Liebner, F. Evaluation of different derivatisation approaches for gas chromatographic-mass spectrometric analysis of carbohydrates in complex matrices of biological and synthetic origin. *J Chrom A* **2013**, *1281*, 115-126.

[6] Jork, H.; Funk, W.; Fischer, W.; Wimmer, H. *Thin-Layer Chromaotography Reagents and Dectection Methods*. VCH Verlagsgesellschaft: Weinheim, 1990.

[7] Choma, I. M.; Grzelak, E. M. Bioautography detection in thin-layer chromatography *J. Chrom. A* **2011**, *1218* (19), 2684-2691.

PINOSYLVINS AS NOVEL BIOACTIVE COMPOUNDS IN FOOD APPLICATIONS

Atte von Wright[1]*, Juan Carlos Parajó[2], Galina Telysheva[3], Oven Primož[4], Stefan Willför[5],
*[1]University of Eastern Finland, Faculty of Health Sciences, P.O. Box 1627, Fi-70211 Kuopio, Finland; (*atte.vonwright@uef.fi) [2]University of Vigo, Chemical Engineering, Edificio Politécnico, University Campus, Es-32004 Ourense, Spain; [3]Latvian State Institute of Wood Chemistry, 27 Dzerbenes str Lv-1006, Riga, Latvia; [3] University of Lubljana, Biotechnical Faculty, Jamnikarjeva ul. 101, Sl-1000, Ljubljana, Slovenia; [4]Stefan Willför, Åbo Akademi, Process Chemistry Centre, Porthansgatan 3, Fi-20500, Åbo, Finland*

ABSTRACT

Pinosylvin and its derivatives are chemically very similar to resveratrol, a stilbene found in grapes and berries. Resveratrol has been associated with many beneficial human health effects. In this study the extraction of pinosylvin and pinosylvin monomethylether from *Pinus* trees was optimized and their biological activities were screened using different in vitro techniques. While the age and growth conditions of the trees affected the pinosylvin contents, the recovery was generally high after relatively straightforward organic extractions. Both pinosylvin and pinosylvin monomethylether proved to be efficient antibacterial and antifungal compounds, and the effects of pinosylvin on the energy metabolism of cultured human cells closely resembled that of resveratrol. Provided that the safety aspects of pinosylvin and pinosylvin monomethylether can be satisfactorily addressed, these compounds could be used as novel biocides and even as nutraceuticals.

I. INTRODUCTION

The three year (2011 – 2014) WoodWisdom-Net 2 project "Pinosylvins as Novel Bioactive Compounds in Food Applications" (PINOBIO) focuses on the novel applications of wood associated polyphenols. Plant-derived stilbenes, especially resveratrol, pterostilbene and piceatannol (**Figure 1)** have interesting bioactivities. Particularly resveratrol, occurring in grapes and berries has been indicated in the prevention of several steps leading to the coronary vascular disease and also several other human ailments such as cancer. These effects and their potential implications to human health have recently been reviewed by Tomé-Carneiro et al. [1]

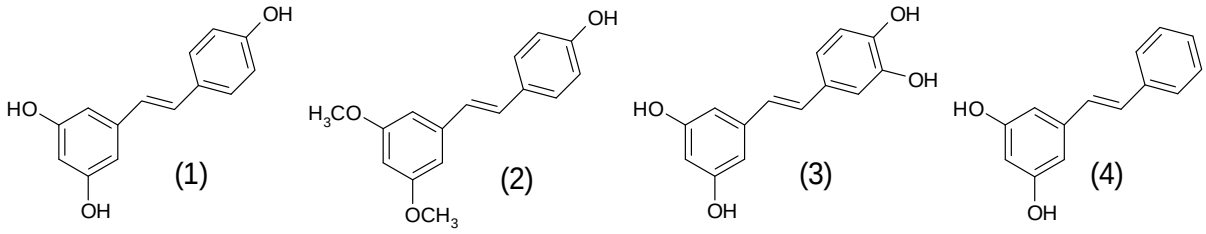

Figure 1. Structures of the stilbenes resveratrol (1), pterostilbene (2), piceatannol (3), and pinosylvin (4).

One of the reported activities of resveratrol has been the increase of energy expenditure, insulin sensitivity, and decrease of glucose levels. These effects are obtained via stimulation of SIRT1. SIRT1 is a nicotinamide adenine dinucleotide dependent deacetylase which is activated in response to nutritional stimulus and maintains energy homeostasis by interacting with the master cellular energy sensor, AMP-activated protein kinase (AMPK) [2].

Wood, especially knotwood of *Pinus* species (at present a side stream of wood industry) is an abundant source of stilbenes, such as pinosylvin and its derivatives [3]. These compounds have demonstrated considerable antimicrobial activities and cytotoxicity against a murine hepatic carcinoma cell line [4]. In further studies pinosylvin was shown to stimulate the SIRT1 expression as efficiently as resveratrol (unpublished results, manuscript in preparation).

The aim of the PINOBIO project has been to upscale the extraction of pinosylvin and its derivatives from wood and further characterize their biological activites with a clear focus on potential applications (antimicrobials in foods and industrial processes, functional ingredients). In this report the main findings are briefly reviewed.

II. EXPERIMENTAL

Optimization of the pinosylvin extraction from Pinus species

Samples of Scots pine (*Pinus silvestris*) from Finland, Latvia and Slovenia, *Pinus nigra* from Slovenia and *Pinus pinaster* from Spain were used in the experiments. Trees of different ages from dry and wet forest lands and from different altitudes were selected for screening. Both sapwood, heartwood and dead and living knots as well as industrial sidestreams (wood chips, discarded knotwood) were sampled. The test materials were subjected to sequential Soxhlet extractions by cyclohexane to remove lipophilic compounds followed by either ethanol water (95:5) or acetone water (95:5) extractions. An alternative was to use Accelerated Solvent Extraction (ASE) with solvents of different polarity. Also pressurized batch extraction with 130-140 °C water, supercritical fluid extraction with CO_2 and CO_2 –ethanol mixtures were applied to certain samples.

Analytical and preparative procedures

The analytical methods applied included HPLC-DAD, GC-FID, GC-MS and HPSEC. Flash chromatography was used to separate and purify the desired compounds.

Derivatization of pinosylvin

In order to study the bioactivity of pinosylvis, including the structure-activity-relationship of modified hydroxyl groups, a selection of different pinosylvin derivatives were prepared. In total 6 esters (1-6), 3 ethers (7-9) one epoxide (10) and a dihydroderivative (11) were semisynthetically obtained (**Figure2**).

Compound 1-6 Pinosylvin was mixed with the corresponding anhydride or acyl chloride (2-3 eqv) in pyridine. The mixture was stirred (1-40h) in room temperature and then the product was precipitated with cold water, filtrated and washed with water and diluted HCl. The residue was purified by column chromatography to give the final products.

Compound 7-9 Pinosylvin was dissolved in acetone and the corresponding alkyl iodide (2-6 eqv) was added followed by K_2CO_3 (8 eqv). The mixture was stirred for 24h and then extracted wit dihloromethane/water. The residue was purified with column chromatography.

Compound 10 Compound 1 was dissolved in dichloromethane and *m*CPBA (3eqv) was added. The mixture was stirred for 72h and the solvent was removed and the residue purified by column chromatography.

Compound 11 Pinosylvin was dissolved in ethanol and 5% Pd/C was added. The mixture was hydrogenated for 72h under 5 atm of H_2. The mixture was filtered and the solvent removed to give the final product.

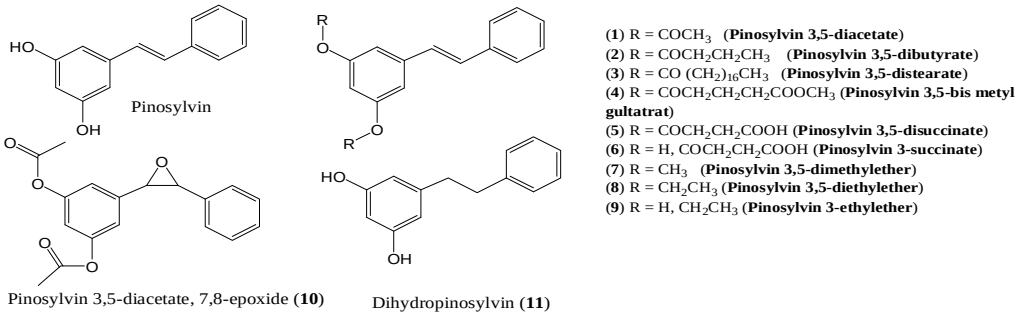

Figure 2. Pinosylvin, dihydropinosylvin and semisynthetic pinosylvin derivatives

Antimicrobial properties

The antimicrobial effects of the pinosylvins and pinosylvin derivatives were turbidometrically determined using a Thermo Bioscreen C automatic turbidometer (Labsystems Oy, Helsinki, Finland) using a Gram positive bacterium *Listeria monocytogenes*, Gram negative *Salmonella* Infantis, and an eukaryotic microorganism *Candida albicans* as representative micro-organisms. The preparation of the test cultures and the practical performance of the assays have been described in [4].

Induction of enzymes involved in xenobiotic metabolism

Three cell lines used in this study are Caco-2 human colorectal adenoma cell line, JEG-3 human choriocarcinoma cell line and HepG2 human hepatoma cell line. After an 8 h exposure to resveratrol, pinosylvin or pinosylvin monomethylether the RNA was extracted , complementary DNA synthesized and the expression of CYP1A1 gene (one of the key enzymes of xenobiotic metabolism) was monitored by quantitative PCR.

SIRT1 and AMPK induction and AMPK phosphorylation

The hypothesis that pinosylvin could regulate energy metabolism through the interaction of AMPK and SIRT1 was tested in 3T3L1 preadipocytes, and in HepG2 and L6 cell lines. The changes in protein expression levels of SIRT1 and AMPK, and the AMPK phosphorylation status were detected by western blotting. Both SIRT1 and AMPK protein concentration was normalized to a loading control. Quantitation of immunoblots was done by Quantity One software.

II. RESULTS AND DISCUSSION

Organic extraction was efficient in recovering pinosylvin and pinosylvin monomethylether from wood samples, while pressurized high temperature water mainly extracted lignans []. While significant amounts of pinosylvin monomethylether could be obtained with cyclohexane, ethanol-water or acetone-water were required for efficient pinosylvin extraction (**Figure 3).** Knotwood and heartwood were consistently superior sources for these compounds compared to sapwood. Certain variation in pinosylvin contents were observed in trees from fifferent environmental conditions. For example, trees grown in wet forests in Latvia contained three times more pinosylvin compared to trees in dry forests. Since pinosylvins apparently are protective compounds, this might reflect a higher exposure to fungal infestations and pathogens in moist conditions.

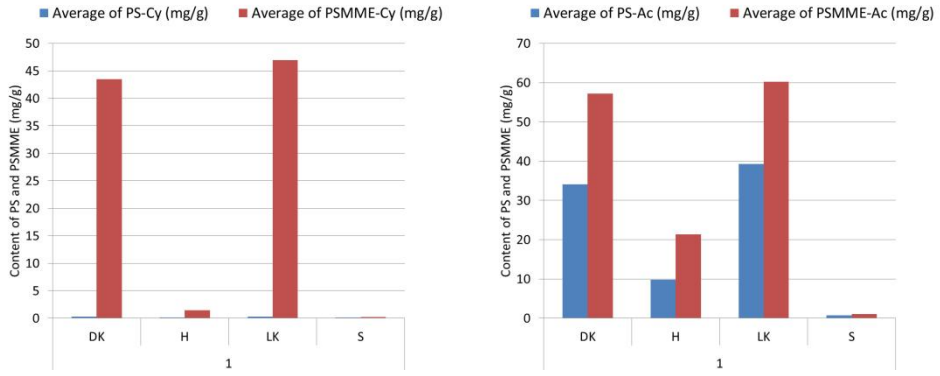

Figure 3. The pinosylvin (PS) and Pinosylvin Momomenthylether (PSMME) contents in cyclohexane (left) and Aceto-water extracts extrasts of *P. silvestris* (right). DK = dry knotwood, H = heartwood, LK = live knotwood, S = sapwood

The antimicrobial potency of pinosylvin and pinosylvin monomethylether was confirmed in this study. While pinosylvin monomethylether was almost as potent as pinosylvin the dimethyl- and monoethyl derivatives as well as dihydropinosylvin had only marginal, if any antimicrobial properties. No clear conclusions could be made regarding the structure-function relationships in antimicrobial activities.

The effects of pinosylvin and pinosylvin monomethylether on the induction of enzymes involved in xenobiotic metabolism varied between the cell lines. While no significant induction of CYP1A1 could be observed with Caco2 (a cell line with intestinal origin), and an actual downregulation was seen in the placental JEG-3 cells, pinosylvin monomethylether (but neither pinosylvin nor resveratrol) caused a strong CYP1A1 induction in the haepatic HepG2 cells.

Treatment with pinosylvin enhanced the phosphorylation of AMPK in 3T3L1 , HepG2 and L6 cells, but SIRT1 protein expression was enhanced only in 3T3L1 (preadipocytes) (**Figure 4)**. These results indicate the tissue-specific role of pinosylvin and also its role in the regulation of adipogenesis as SIRT1 activation is known to trigger lipolysis and improve metabolic efficiency. Our results indicate that pinosylvin is a more potent activator of SIRT1 than resveratrol in 3T3L1 and L6 cells. Therefore, pinosylvin could be used to modulate energy sensing pathways to improve insulin sensitivity in patients with diabetes and prevent the development of metabolic syndrome.

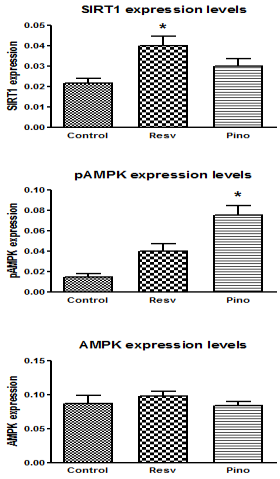

Figure4. SIRT1, pAMPK and AMPK expression levels in 3T3L1 cells exposed to 50 mM of either resveratrol or pinosylvin

IV. CONCLUSIONS

Pinosylvin and pinosylvin monomethylether are potent antibacterial and antifungal compounds, and they both be efficiently extracted from pinewood. Pinosylvin monomethylether efficiently induced the xenobiotic metabolism in exposed haepatic cells, while the influence of pinosylvin on the cellular energy metabolism pathways resembeled that of resveratrol. Provided that the safety aspects of pinosylvin and pinosylvin monomethylether can be satisfactorily addressed, these compounds could be used as novel biocides and even as nutraceuticals.

V. ACKNOWLEDGEMENT

This study was financed by the ERA-program WoodWisdom-Net 2

VI. REFERENCES

[1] Tomé-Carneiro, J.; Larrosa, M.; González-Sarrias, A.; Tomás-Barberán, F.A.; Garcia-Conesa, M.T.; Espin, J.C. Resveratrol and clinical trials: The crossroad from *in vitro* studies to human evidence. *Curr. Pharm. Design.***2013,** *19:*6064-6093.

[2] Lagouge, M. ; Argmann, C.; Gerhart-Hines, Z.; Meziane H.; Lerin, C.; Daussin F.; Messadeq, N.; Milne, J.; Lambert, P; Elliott, P.; Geny, B.; Laakso, M.; Puigserver, P.; Auwerx. J. Resveratrol improves mitochondrial function and protects against metabolic disease by activating SIRT1 and PGC-1α. Cell **2006,** *127*: 1 – 14.

[3] Willför, S.; Hemming, J.; Reunanen, M.; Holmbom, B. Phenolic and lipophilic extractives in Scots pine knots and stemwood. *Holzforschung*, **2003,** *57*: 359-372.

[4] Välimaa, A.-L.; Honkalampi-Hämäläinen, U.; Pietarinen, S.; Willför, S.; Holmbom, B., von Wright, A. Antimicrobial and cytotoxic knotwood extracts and related pure compounds and their effects on food-associated micro-organisms. *Int. J. Food. Microbiol,* **2007,***115*: 235-243.

[5] Conde, E.; Fang, W., Hemming, J.; Willför, S.; Moure, A.; Domíguez, H.; Parajó, J.C. Water-soluble components of *Pinus pinaster* wood. *BioResources* **2013**. *2*: 2047-2063

HIGH VALUE TRITERPENIC ACIDS FROM *EUCALYPTUS* BARK: FROM CHEMICAL CHARACTERIZATION TO ENVIRONMENTALLY FRIENDLY EXTRACTION AND SCALE-UP STUDIES

Carlos P. Neto, Rui M. A. Domingues, Marcelo M.R. de Melo, Carmen S.R. Freire, Armando J.D. Silvestre and Carlos M. Silva*

CICECO, Department of Chemistry, University of Aveiro, Aveiro, 3810-193, Portugal

ABSTRACT

The residues of *E. globulus* contain significant amounts of triterpenic acids, and particularly the outer bark, with a content of 9.2 g $kg^{-1}_{biomass}$. The potential of supercritical fluid extraction has been evaluated for *E. globulus* outer bark, with experiments at lab scale (0.5 L) using CO_2, modified or not with ethanol. The SFE pressure, temperature, ethanol content and CO_2 flow rate were optimized in 200 bar, 40ºC, 2.5 wt.% ethanol, 12 g_{CO2} min^{-1}, respectively, for which the triterpenic acids content in the extract is 38.8 wt.%. Extraction curves were then measured at lab scale and modelled in order to establish an appropriate scale-up criterion. The ratio between mass flow rate and biomass weight was fixed in 10 kg^{-1}_{CO2} $kg^{-1}_{biomass}$ h^{-1}. Upscaling runs were performed in 5 L and 80 L equipment, being confirmed the adequacy of the selected scale-up criterion. In the whole, SFE has been confirmed as a proficient technology for an industrial valorization of *E. globulus* bark.

I. INTRODUCTION

Pulp and paper industry is one of the major industries of the agro-forestry sector. On arrival to the mill, the wood is debarked and the bark is mainly burned for power generation. *Eucalyptus* species are the most important fiber sources for pulp and paper production in southwest Europe (Portugal and Spain) and south America (Brazil and Chile), being observed a fast growing in the last years [1]. In a medium size pulp mill using E. *globulus* wood as feedstock about 1×10^5 tons of bark are generated annually [2], being this a major opportunity for valorization attempts.

Given the importance of this sector and the pertinence of upgrading some of its by-products and wastes, our research group has been engaged on providing knowledge and solutions to the challenge of adding value to *Eucalyptus spp*. bark [2-12], which is among the main low value / high volume by-products streams of this industry. In this respect, we recall the works of Freire et al. [13] and Domingues et al. [2], who studied the composition of *E. globulus* bark. Within the many compounds quantified by gas chromatography–mass spectrometry (GC–MS), several high-value triterpenic acids (TTAs) such as betulinic, betulonic, oleanolic and ursolic acids, as well as the acetylated forms of the latter two, were identified. These TTAs show promising anti-oxidant,anti-inflammatory and anticancer activities [14], making them rather valuable.

The research on the TTAs from *E. globulus* bark evolved then towards the employment of a green separation technology, namely the extraction of with supercritical CO_2, whether used as single solvent [3] or modified with ethanol [12]. From the works on supercritical fluid extraction (SFE) it was concluded that pressure and ethanol content are chief variables for an optimized separation [15-17]. In addition, supercritical extraction curves were measured in order to investigate the kinetic performance of the process, for which modeling was employed. In As a result, improved SC-CO_2 flow rate values were found for the process [4].

In this regard, we now present further developments on the aforementioned research path that has been followed by our group with emphasis on the final approach to exploitation through the upscaling of the SFE process, and through the reference to a patented technique to extract and purify the TTAs in the extracts by conventional technologies, which is communicated for the first time in the academic literature.

II. EXPERIMENTAL

Soxhlet extraction– An amount of ~27 g of deciduous bark was placed inside the Soxhlet apparatus and treated with 300 mL of analytical grade dichloromethane for 7 h. **Supercritical CO_2 extraction** – SFE experiments were accomplished with pure CO_2 and also with ethanol in amounts up to 5% (wt.). Three SFE units were used, being their scales 0.5 L, 5.0 L and 80 L. The laboratorial extractor is described elsewhere [3, 12], and the higher units are available at Natex [18]. The studied range of pressures, temperatures, ethanol content and flow rate comprise 100-200 bar, 40-60ºC, 0-5 wt.%, and 6-14 g min^{-1}. **Characterization –** Extracts were analyzed by GC-

MS. About 20 mg of each dried extract were trimethylsilylated according to the literature [2, 13]. Further details on the method and equipment can be found elsewhere [12, 15].

III. RESULTS AND DISCUSSION

Previous work: Soxhlet extraction & samples characterization – Aiming to evaluate the *E. globulus* bark potential, lipophilic extracts of juvenile and adult leaves, fruits, and barks were characterized. It was found the triterpenoids content of these fractions ranged from 1.2 to 9.2 g $kg^{-1}_{biomass}$. Given the major content of the outer bark (peeling), the results presented below are focused on this fraction.

Patent based on standard technologies – A first approach comprised the purification (up to 98 wt.%) of a mixture of TTAs, mainly ursolic, oleanolic and their acetylated forms. Standard technologies of the chemical industry were selected, consisting of steps such as SLE, LLE, acid-base reactions and decantation/filtration/centrifugation. This process is currently protected by a patent [19].

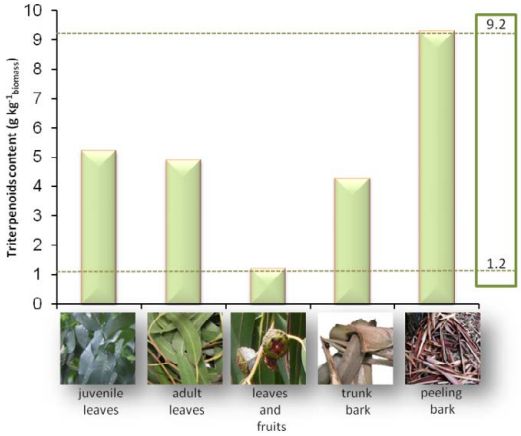

Figure 1 – Triterpenoids in different *E. globulus* parts, obtained by wax collection (leaves, and fruits) and by dichloromethane Soxhlet extraction (barks).

Supercritical Fluid Extraction - Preliminary studies on the SFE of *E. globulus* bark confirmed that this green technology is able to obtain extraction yields equivalent to those achieved by Soxhlet extraction with dichloromethane (ca. 1.3 wt.%), and TTAs concentrations in crude extracts between 5.7% and 43.1% (wt.). Another conclusion was the importance to optimize the SFE operating conditions, particularly pressure (*P*) and ethanol (EtOH) content. This task was performed according to Design of Experiments (DoE) and Response Surface Methodologies (RSM). In Figure 2.a results from this optimization work are presented. In the whole, lab scale experiments showed the optimum condition for the SFE of *E. globulus* bark to be 200 bar, 40ºC, 2.5 wt.% ethanol.

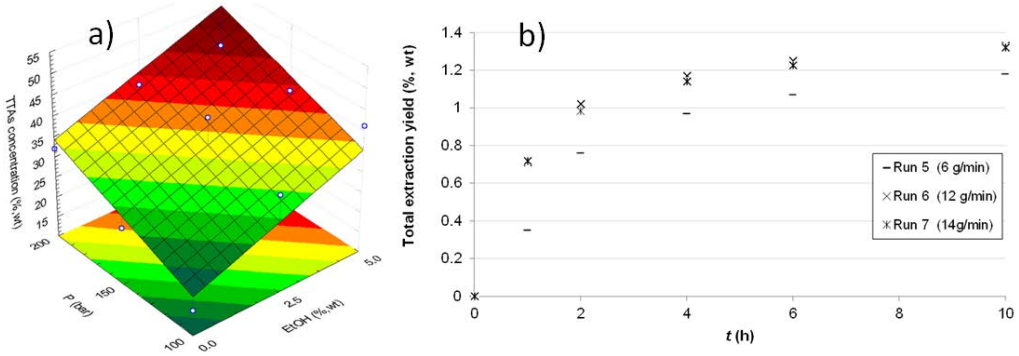

Figure 2 – Supercritical CO_2 extraction of *E. globulus* peeling bark: a) optimization of TTAs extraction at 40ºC; b) total extraction yield *vs.* time at 200 bar, 40ºC and 5 wt.% ethanol, for different CO_2 flow rates.

Subsequently, the kinetic study of the SFE of TTAs from *E. globulus* bark was also carried out aiming to: i) determine the adequate flow rate of supercritical solvent, ii) disclose the existence of external and/or intraparticle mass transfer limitations, and finally iii) establish an appropriate scale-up criterion to guide the experiments at pilot scales. In Figure 2.b, the extraction curves measured at 200 bar, 40ºC and 5 wt.% ethanol are plotted, being possible to observe how important the film resistance to mass transfer can be in the SFE. Under the experimental conditions studied, flow rates in the range 12-14 g_{CO2} min^{-1} are sufficient to eliminate the film – reason why, in further studies, it was fixed in 12 g_{CO2} min^{-1}.

In Figure 3 three extraction curves, measured at different *P*, Q_{CO2} and ethanol content are plotted. Superimposed on the graph are the theoretical curves achieved with four simple expressions taken from the literature (see Table 1) [4, 20], namely, Logistic Model, Desorption Model, Simple Single Plate (SSPM) Model and Diffusion (DFM) Model. The best results were reached by DFM and SSPM models, with average errors ranging 2.6-11.3%, which disclose relevant intraparticle diffusion limitations in the process, since these models were specifically derived for this case.

In view of the abovementioned results, the proper scale-up criterion for the SFE of *E. globulus* bark establishes that the ratio between mass flow rate and biomass weight should be held constant, i.e. $Q_{CO_2}\, w_b^{-1} = \text{const}$ [17, 20]. In our case, it is 10 kg^{-1}_{CO2} $kg^{-1}_{biomass}$ h^{-1}.

Table 1- Simplified SFE models used to disclose the dominant mass transfer mechanisms [12, 17].

Name	Expression	Eq.	Name	Expression	Eq.
Logistic model	$\psi = \frac{x_0}{\exp(b t_m)}\left(\frac{1+\exp(b t_m)}{1+\exp[b(t_m - t)]} - 1\right)$	(1)	Simple Single Plate model	$\psi = x_0\left[1 - \sum_{n=0}^{\infty}\frac{0.8}{(2n+1)^2}\exp\left(-\frac{D_{eff}(2n+1)^2\pi^2 t}{l^2}\right)\right]$	(4)
Desorption model	$\psi = \frac{A}{k_d}[1-\exp(k_d B)]\times[\exp(-k_d t)-1]$	(2)	Diffusion model	$\psi = x_0\left[1 - \frac{6}{\pi^2}\sum_{n=1}^{\infty}\frac{1}{n^2}\exp\left(-\frac{D_m n^2\pi^2 t}{R_p^{\,2}}\right)\right]$	(5)

ψ is the extraction yield, t is time, x_0 is the concentration of the target species in the raw material, and b and t_m are model parameters; A and B are model factors dependent on CO_2 mass flow rate, bed porosity, extractor cross-sectional area, mass of raw material in the extractor, biomass density and solvent density; D_{eff} is the effective diffusivity, l the plate thickness; R_p is the particle radius.

Scale-up of the process - With regard to the upscaling of the SFE process, it was tested based on three different scales, with jumps of at least a factor of 10. Accordingly, experiments at 5 L and 80 L were performed based on the insights and results from lab scale, namely 200 bar, 40ºC, 2.5 wt.% ethanol, and $Q_{CO_2}\, w_b^{-1} = 10$ kg^{-1}_{CO2} $kg^{-1}_{biomass}$ h^{-1}. The results for both total extraction yield and TTAs concentration are essentially concordant.

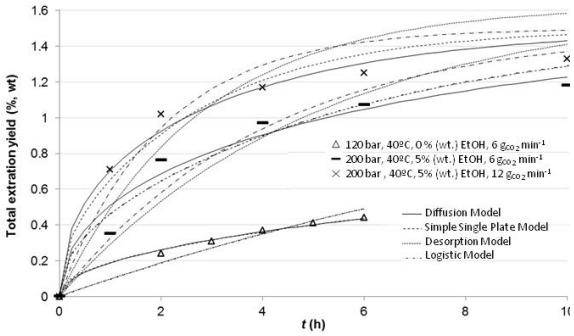

Figure 3 – Modeling of SFE curves of *E. globulus* peeling bark

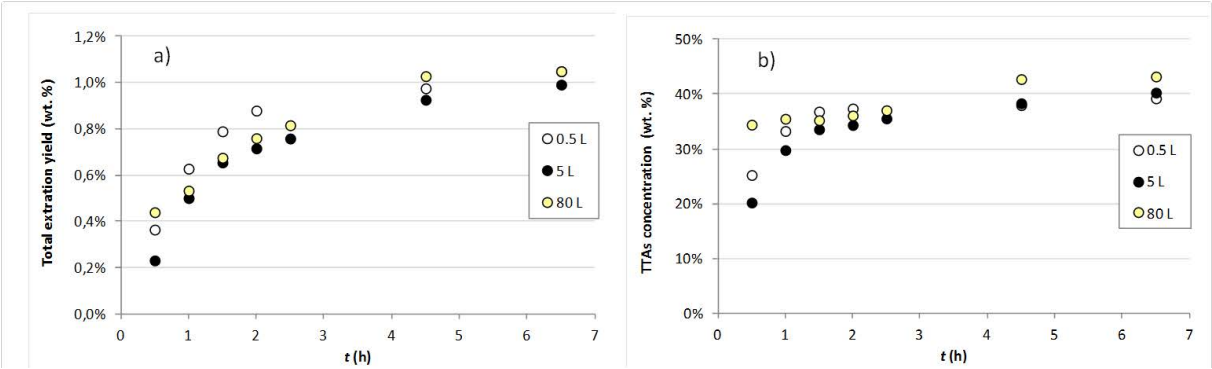

Figure 3 – Total extraction yield (a) and TTAs concentration (b) at 200 bar, 40ºC, 2.5 wt.% ethanol, $Q_{CO_2}\, w_b^{-1} =$ 10 kg^{-1}_{CO2} $kg^{-1}_{biomass}$ h^{-1}, for three different scales: 0.5 L, 5 L and 80 L.

IV. CONCLUSIONS

E. globulus bark is a very promising raw material for future commercial exploitation of extracts rich in triterpenoids, particularly triterpenic acids.

The SFE provide extracts with yields comparable to those obtained by conventional solid-liquid extraction. The variables that mostly govern the process are pressure, ethanol (cosolvent) content, and mass flow rate. Optimization of operating conditions at lab scale (0.5 L extractor) achieved 200 bar, 40ºC, 2.5 wt.% ethanol. From the experimental and modelling results, an appropriate scale-up criterion was established ($Q_{CO_2}\, w_b^{-1} = 10$ kg^{-1}_{CO2} $kg^{-1}_{biomass}$ h^{-1}) and validated at higher scales, namely at 5 L and 80 L. The global yields and the TTAs concentration in the collected extracts measured at 0.5, 5.0 and 80 L are essentially concordant.

SFE technology proficiently meets the technical challenge of adding value to this low-value / high volume residue of pulp and paper industry, giving rise to interesting extracts for pharmaceutical or cosmetic applications.

V. ACKNOWLEDGEMENT

We acknowledge the 7th Framework Programme FP7/2007-2013 for funding project AFORE: Forest Biorefineries: Added-value from chemicals and polymers by new integrated separation, fractionation and upgrading technologies (CP-IP 228589-2). Authors acknowledge Associate Laboratory CICECO (Pest-C/CTM/LA0011/2013).

VI. REFERENCES

[1] CELPA, Statistical bulletin 2007,http://www.celpa.pt/images/pdf/art209_pt_be_2007.pdf, Accessed in: February 2009
[2] R.M.A. Domingues, G.D.A. Sousa, C.S.R. Freire, A.J.D. Silvestre, C.P. Neto, *Eucalyptus globulus* biomass residues from pulping industry as a source of high value triterpenic compounds, Ind.Crop.Prod., 31(**2010**) 65-70.
[3] M.M.R. de Melo, E.L.G. Oliveira, A.J.D. Silvestre, C.M. Silva, Supercritical fluid extraction of triterpenic acids from *Eucalyptus globulus* bark, J. Supercrit. Fluids, 70 (**2012**) 137-145.
[4] R.M.A. Domingues, M.M.R. de Melo, C.P. Neto, A.J.D. Silvestre, C.M. Silva, Measurement and modeling of supercritical fluid extraction curves of *Eucalyptus globulus* bark: influence of the operating conditions upon yields and extract composition, The Journal of Supercritical Fluids, 72 (**2012**) 176-185.
[5] R.M.A. Domingues, E.L.G. Oliveira, C.S.R. Freire, R.M. Couto, P.C. Simões, C.P. Neto, A.J.D. Silvestre, C.M. Silva, Supercritical fluid extraction of *Eucalyptus globulus* bark – a promising approach for triterpenoids production, International Journal of Molecular Sciences, 13(6) (**2012**), 7648-7662.
[6] R.M.A. Domingues, D.J.S. Patinha, G.D.A. Sousa, J.J. Villaverde, C.M. Silva, C.S.R. Freire, A.J.D. Silvestre, C.P. Neto, *Eucalyptus* biomass residues from agro-forest and pulping industries as sources of high-value triterpenic compounds, Cellulose Chemistry and Technology, 45 (**2011**) 475-481.
[7] R.M.A. Domingues, G.D.A. Sousa, C.M. Silva, C.S.R. Freire, A.J.D. Silvestre, C.P. Neto, High value triterpenic compounds from the outer barks of several *Eucalyptus* species cultivated in Brazil and in Portugal, Industrial Crops and Products, 33 (**2011**) 158-164.
[8] C.S.R. Freire, A.J.D. Silvestre, A.M.S. Silva, C.P. Neto, P. Domingues, New glucosides from *Eucalyptus globulus* wood, bark and kraft pulps, Holzforschung, 58 (**2004**) 501-503.
[9] D.J.S. Patinha, R.M.A. Domingues, J.J. Villaverde, A.M.S. Silva, C.M. Silva, C.S.R. Freire, C.P. Neto, A.J.D. Silvestre, Lipophilic extractives from the bark of *Eucalyptus grandis* x *globulus*, a rich source of methyl morolate: selective extraction with supercritical CO_2, Ind. Crop. Prod., 43 (**2013**) 340-348.
[10] S.A.O. Santos, J.J. Villaverde, C.S.R. Freire, M.R.M. Domingues, C.P. Neto, A.J.D. Silvestre, Phenolic composition and antioxidant activity of *Eucalyptus grandis*, *E. urograndis* (*E. grandis x E. urophylla*) and *E. maidenii* bark extracts, Ind. Crop. Prod., 39 (**2012**) 120-127.
[11] S.A.O. Santos, C.S.R. Freire, R.M.A. Domingues, A.J.D. Silvestre, C.P. Neto, Characterization of phenolic components in polar extracts of *Eucalyptus globulus* labill bark by high-performance liquid chromatography–mass spectrometry, Journal of Agricultural and Food Chemistry, 59 (**2011**) 9386-9393.
[12] R.M.A. Domingues, M.M.R. de Melo, E.L.G. Oliveira, C.P. Neto, A.J.D. Silvestre, C.M. Silva, Optimization of the supercritical fluid extraction of triterpenic acids from *Eucalyptus globulus* bark using experimental design, J. Supercrit. Fluids, 74 (**2013**) 105-114.
[13] C.S.R. Freire, A.J.D. Silvestre, C.P. Neto, J.A.S. Cavaleiro, Lipophilic extractives of the inner and outer barks of *Eucalyptus globulus*, Holzforschung, 56 (**2002**) 372-379.
[14] R.M.A. Domingues, A.R. Guerra, M. Duarte, C.S.R. Freire, C.P. Neto, C.M. Silva, A.J.D. Silvestre, Bioactive triterpenic acids: from agroforestry biomass residues, to promising therapeutic tools, Mini-Reviews in Organic Chemistry, (**2014**) DOI: 10.2174/1570193X113106660001.
[15] M.M.R. de Melo, R.M.A. Domingues, A.J.D. Silvestre, C.M. Silva, Extraction and purification of triterpenoids using supercritical fluids: from lab to exploitation, Mini-Reviews in Organic Chemistry, (**2014**) DOI: 10.2174/1570193X113106660002.
[16] M.M.R. de Melo, A.J.D. Silvestre, C.M. Silva, Enhanced technologies for the valorization of waste and side vegetable products using supercritical fluids, in: S. Pandalai (Ed.) Recent Research Developments in Chemical Engineering, Transworld Research Network.
[17] M.M.R. de Melo, A.J.D. Silvestre, C.M. Silva, Supercritical fluid extraction of vegetable matrices: applications, trends and future perspectives of a convincing green technology, The Journal of Supercritical Fluids, (**2014**) (in press).
[18] M.M.R. de Melo, R.M.A. Domingues, M. Sova, E. Lack, H. Seidlitz, F. Lang Jr., A.J.D. Silvestre, C.M. Silva, Scale-up of the supercritical fluid extraction of triterpenic acids from *Eucalyptus globulus* bark, J. Supercrit. Fluids (**2014**) (submitted).
[19] R.M.A. Domingues, C.S.R. Freire, A.J.D. Silvestre, C.P. Neto, C.M. Silva, Method for obtaining an extract rich in triterpenic acids from *Eucalyptus* barks, **2012**, PAT 106278,
[20] M. Perrut, Supercritical Fluid Applications: Industrial Developments and Economic Issues, Industrial & Engineering Chemistry Research, 39 (**2000**) 4531-4535.

THE BARK BIOREFINERY: A SIDE-STREAM OF THE FOREST INDUSTRY CONVERTED INTO RENEWABLE BARRIER NANOCOMPOSITES

Myriam Le Normand, Rosana Moriana Torró and Monica Ek*

*KTH – Royal Institute of Technology, Department of Fiber and Polymer Technology, Division of Wood Chemistry and Pulp Technology, Teknikringen 56-58, 100 44 Stockholm, Sweden (*monicaek@kth.se)*

ABSTRACT

The bark of Norway spruce (Picea abies) is an important side-stream for the forest industry in Nordic countries. The aim of this study was to upgrade the polysaccharides present in the bark to bio-based nanocomposite materials with high oxygen barrier properties. The present study shows for the first time (1) the recovery of cellulose fibers and the isolation of cellulose nanocrystals (CNCs) from the inner bark of Norway spruce and (2) the preparation and characterization of nanocomposites based on non-cellulosic polysaccharides (NCP) reinforced with CNCs, both extracted from the same bark.

I. INTRODUCTION

Norway spruce (*Picea abies*) is the most abundant coniferous tree growing in Northern Europe and is extensively used in the Scandinavian pulp and paper industry. Due to its resistance to pulping and its high content of extractives, bark is considered as an undesirable material and is used as a fuel to process heat and electrical energy in the mill. According to the Swedish Forest Agency, the annual bark yield in Sweden is estimated to be more than 1.5 million tons (dry weight). Part of this considerable amount of bioresidue might be upgraded in a so-called bark biorefinery where high-value components from the bark could be fractionated and upgraded [1].

The major constituents of the bark of Norway spruce are polysaccharides. Altogether, hemicelluloses, pectins and cellulose constitute about 50% of the inner bark, 33% of the outer bark and 40% of the whole bark collected just after the debarking process in a pulp mill [1,2]. Recently, we showed that the recovery of the non-cellulosic polysaccharides (NCP) from the bark of Norway spruce was possible through a series of hot-water extractions and filtration steps [1,3]. The crude NCP extract contained mainly pectin and starch as well as a minor amount of Klason lignin. The purpose of the latest studies was to find direct applications for this crude bark polysaccharide mixture, hence avoiding time-consuming and costly refining steps. One example of such application was described in a previous work and presented the potential utilization of bark hot-water extracts as immunostimulating agents [3]. Another straightforward way of adding value to a polysaccharide mixture, without any further refining process, is the production of functional biomaterials. However, hemicellulose-based films often suffer from poor mechanical properties which restrict their uses in a wide range of applications. In recent years, incorporation of biodegradable nanofillers such as cellulose nanocrystals (CNCs) into polymer matrix was proved to be an important strategy for the obtention of nanocomposites with high mechanical performances. As compared to inorganic reinforcing fillers, CNCs have advantages like positive ecological footprint, low density, ease of recycling.

In this work, we propose a novel way to upgrade spruce bark through the preparation of all-bark nanocomposites base on the NCP fraction obtained in a previous study [3] and reinforced with cellulose nanocrystals (CNCs) isolated from the same bark.

II. EXPERIMENTAL

Materials

Bark of Norway spruce was sampled from a fresh 30-year-old tree cut in Gävleborg County (Sweden) in July 2009. It was stored in the dark at -20°C. The inner and outer bark were separated manually using a scalpel. The inner bark was ground with a hand blender to a particle size of approximately 5×2 mm. The ground inner bark was extracted with an Accelerated Solvent Extractor (ASE) (Dionex, California) following the method described by Le Normand et al. [3]. The non-cellulosic polysaccharides (NCP) fraction, obtained after hot-water extraction

at 140°C, contained around 80% of oligo- and polysaccharides and 4% lignin. The molecular weight averages were Mn=15 kDa and Mw=55 kDa.

Isolation of CNCs

The residue after extraction of NCP at 140°C was freeze-dried and used for isolation of cellulose nanocrystals (CNCs). The isolation process and CNC characterization have been newly reported [4]. Briefly, the residue was bleached with sodium chlorite and hydrolyzed in sulfuric acid solution (60% w/w) at 50°C for 60 min. The CNCs had rod-like aspects with a diameter and length in the range of 2.8 nm and 175 nm, respectively, giving an aspect ratio greater than 60.

Preparation of NCP/CNC formulations

The freeze-dried NCP powder, CNC suspension, and distilled water were mixed together to obtain a solution with a homogeneous dispersion. The CNC contents in the films were 10, 20, 30, 40, 50 wt%. These samples were coded as CNC10, CNC20, CNC30, CNC40 and CNC50. When sorbitol was added, its content was fixed at 30 wt % on the basis of the dry NCP weight. The samples were then coded CNC30S, CNC40S and CNC50S. The films were obtained by casting in polystyrene petri dishes and dried in an oven at 40 °C during 65 hours. Sample thicknesses were determined by a Mitutoyo micrometer by taking the average of five discontinuous spots. The thickness of the films varied between 17 and 22 µm.

III. RESULTS AND DISCUSSION

Isolation of CNCs

CNCs were recovered from the inner bark of Norway spruce after sequential treatment, namely hot-water extraction of the NCP, bleaching of the extraction residue, hydrolysis with sulfuric acid and sonication. The overall yield of CNCs, with respect to the initial amount of inner bark, was close to 11%. Morphological investigation of the CNCs was performed using AFM (**Figure 1**) and showed the presence of nanocrystals with an average length of 175 nm and a diameter of 2.8 nm, giving a high aspect ratio of around 63. X-ray diffraction (XRD) analyses showed that the crystallinity index increased with successive treatments to finally reach a value superior to 80% for CNCs. The thermal degradation of the CNCs started at 190°C. These characteristics make bark CNCs of potential interest for reinforcement in polymer materials.

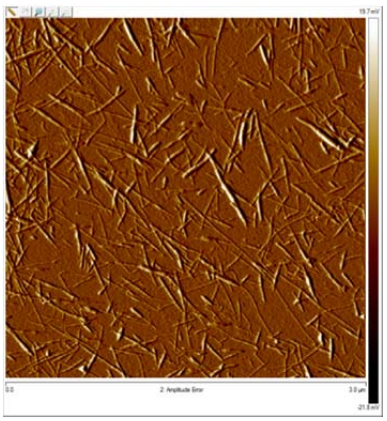

Figure 1. AFM image of bark CNCs.

Preparation and characterization of all-bark polysaccharides

Films prepared from the bark non-cellulosic polysaccharides (NCP) fraction alone were very brittle and fragmented upon drying. In order to improve the film performances, CNCs were introduced to the NCP matrix. Homogeneous transparent films, with a glossy appearance, were obtained by incorporation of more than 30 wt% CNC (**Figure 2**). CNCs obviously prevented crack formation and growth, which resulted in composites with good cohesion. FTIR and XRD analyses showed the presence of strong molecular interaction in the matrix and suggested that CNCs were probably acting as a nucleating agent.

The formulations which allowed the best film formations (CNC content of 30 to 50%) were chosen for the preparation of three new films containing sorbitol. Sorbitol was added as plasticizer to further improve the handling of the films.

Figure 2. Film formation with a CNC content of 10%, 20%, 30%, 40% and 50%, from the left to the right.

Mechanical properties

The mechanical properties of the films were evaluated using tensile testing at 50% RH. The films were strong, with a strength at break between 25 and 60 MPa, and particularly stiff, with a Young's modulus of 6 to 8 GPa. In general, the addition of CNCs improved the mechanical properties of NCP/CNC films. In fact, the tensile strength of the film was improved by more than 3-folds by increasing the CNC content from 30% to 50%. This observation confirmed the presence of strong intermolecular interactions between NCP and CNC, increasing as a function of the CNC content. The strong interactions could be due to the presence of highly branched pectins in the extract and the natural capability of this polysaccharide to bind to cellulose. The strength of the films was comparable or even better than several reported films based on hemicelluloses and CNCs. In addition, the tensile strength and Young's modulus of the NCP/CNC films were in the range of those obtained for synthetic polymer materials such as low-density polyethylene, polypropylene, polystyrene and polyvinylchloride.However, the NCP/CNC films showed very poor flexibility, with an elongation inferior to 1%. Addition of sorbitol as plasticizer increased the elongation of the films, which could reach up to 3.5%.

Thermal properties

The thermal degradation of the NCP/CNC formulations was assessed. **Figure 3** shows the derivative thermogravimetric (DTG) curves of CNC, NCP and the NCP/CNC formulations prepared without sorbitol.

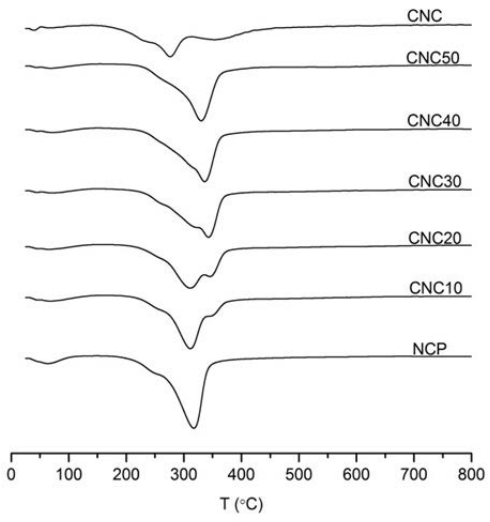

Figure 3. DTG curves of CNC, NCP and NCP/CNC prepared without sorbitol.

In all formulations, it was clear that the blend showed better thermal stability than the individual components. The onset temperature for the thermal degradation of CNCs and NCP was around 190°C, while the NCP/CNC formulations started to degrade above 200°C. Based on this observation, it was possible to conclude that nanocomposite materials with enhanced thermal stability were formed by mixing together NCP and CNC. The improvement of thermal stability could be due to the good intercomponent compatibility and to the nucleating behavior of CNC. In general, increasing the CNC content of the film resulted in better thermal stability.

Oxygen barrier properties

Addition of CNCs to the NCP matrix allowed the formation of resistant films towards oxygen at 50% and 80% RH. The permeability of the films increased with the CNC content. The oxygen permeability (OP) of the films

reached values close to 0.25 µm cm3 m-2 kPa-1 day-1 at 50% RH and 6.5 µm cm3 m-2 kPa-1 day-1 at 80% RH. The addition of sorbitol improved further the barrier properties of the NCP/CNC films at 50% RH (**Figure 3a**), but decreased significantly the barrier performance at 80% (**Figure 3b**). This trend was attributed to the softener behavior of sorbitol at high RH.

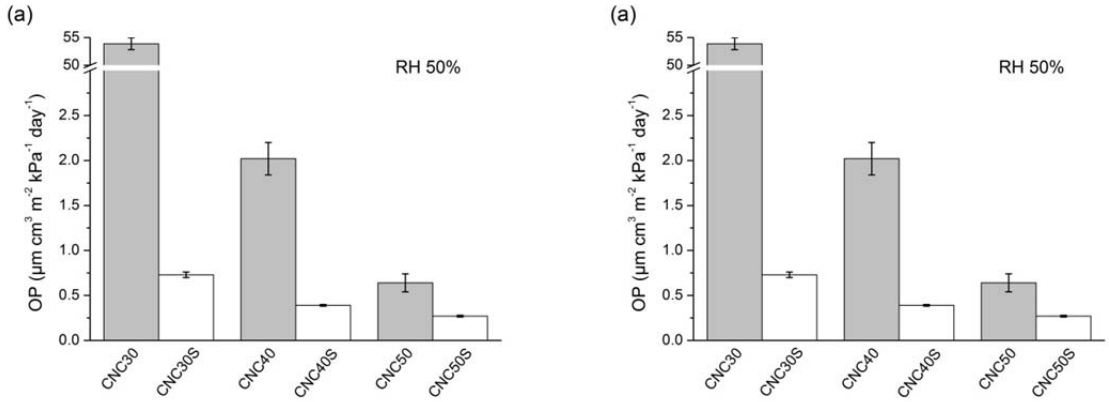

Figure 1. Effect of the addition of CNC and sorbitol on the oxygen permeability (OP) of the NCP/CNC films at (a) 50% RH and (b) 80% RH.

The oxygen permeability of NCP/CNC films was comparable to or lower than the values reported for films obtained from xylan, starch, glucomannan and mixtures of various polysaccharides. Compared with some commercial materials, the OPs of NCP/CNC films were much lower than the values reported for e.g. polylactic acid, polyvinyl chloride and polyethylene-terephtalate which are extensively used for packaging applications.

IV. CONCLUSIONS

The non-cellulosic polysaccharides (NCP) fraction obtained by hot-water extraction of spruce bark was found to be an excellent candidate for making renewable materials. Addition of CNCs was necessary in order to improve the mechanical, thermal and oxygen barrier properties of the films. These properties were tailored by varying the percentage of CNC and sorbitol added into the NCP matrix. The dense structure formed by the mixture of NCP and CNC and their ability to form strong hydrogen bond interactions were believed to contribute to the good properties of the films. Since all the raw materials used for the composite preparation could be obtained from the bark, this work strongly support the bark biorefinery concept.

V. ACKNOWLEDGEMENT

This work was supported by the Wood Wisdom ERA-NET Program (WOBAMA project) as well as the VINNOVA and Ångpanneföreningens Forskningsstiftelse funding agencies (Myriam Le Normand). The authors would like to acknowledge the Wallenberg and Lars-Erik Thunholm Foundation for the research post-doctoral position granted to Rosana Moriana.

VI. REFERENCES

[1] Le Normand, M., Edlund, U., Holmbom, B., Ek, M. Hot-water extraction and characterization of spruce bark non-cellulosic polysaccharides. *Nord. Pulp Pap. Res. J.* **2012**, *27*, 18-23.

[2] Krogell, J., Holmbom, B., Pranovich, A., Hemming, J., Willför, S. Extraction and chemical characterization of Norway spruce inner and outer bark. *Nord. Pulp Pap. Res. J.* **2012,** *27*, 6-17.

[3] Le Normand, M., Mélida, H., Holmbom, B., Michaelsen, T.E., Inngjerdingen, M., Bulone, V., Paulsen, B.S., Ek, M. Hot-water extracts from the inner bark of Norway spruce with immunomodulating activities. *Carbohydr. Polym*. **2014**, *101*, 699-704.

[4] Le Normand, M., Moriana, R., Ek, M. Isolation and characterization of cellulose nanocrystals from spruce bark in a biorefinery perspective. *Carbohydr. Polym.* **2014**, In Press.

CORK SUBERIN ISOLATION USING BIOCOMPATIBLE IONIC LIQUIDS: FROM THE EXTRACTION MECHANISM TO NEW PRODUCTS

Armando J. D. Silvestre,[a] Rui Ferreira,[b] Helga Garcia,[b] Celso Martins,[b] Andreia F. Sousa,[a] Carmen Freire,[a] Luís Paulo N. Rebelo[b] and Cristina Silva Pereira[b]

armsil@ua.pt

[a] *CICECO and Department of Chemistry, University of Aveiro, Campus de Santiago, 3810-193 Aveiro, Portugal*

[b] *Instituto de Tecnologia Química e Biológica, Universidade Nova de Lisboa, Apartado 127, 2781-901, Oeiras, Portugal*

ABSTRACT

The present communication reports a novel method for the extraction of suberin from cork using the cholinium hexanoate. This process yields a material where most suberin components, are in the form of oligoesters resulting mainly from the cleavage of acylglycerol bonds. This selective bond cleavage is promoted by cholinium hexanoate that plays a dual role of solvent and of catalyst in the process. The oligomeric nature of the isolated material allows to foresee new applications as for example in the preparation of bioactive thin films.

I. INTRODUCTION

Biomass feedstocks constitute a source of numerous value-added compounds, such as biopolymers, biofuels, and building-block chemicals [1]. Cork, the outer bark of *Quercus suber L.*, is a remarkable plant composite material displaying a very specific combination of properties, such as elasticity, compressibility, low density, low permeability, and significant chemical and microbial resistance [2]. Historically, cork utility goes back to the ancient Romans, and since then has been used essentially to manufacture stoppers and thermal/sound insulation materials. Globally, ≥ 300,000 ton of cork are processed per annum by industry, generating large amounts of residues (ca. 22 wt %), especially cork of small grains size, which despite its interesting chemical composition, is generally burned to produce energy [3].

Cork is composed of suberin, lignin, polysaccharides, and extractives (approximately 50, 20, 20 and 10 wt %, respectively) [4,5]. Suberin is an aromatic-aliphatic cross-linked bio-polyester with a three-dimensional complex network, occurring in the secondary plant cell wall. The aliphatic domain is composed mostly of even numbered units (C16-C26) of aliphatic alcohols, alkanoic acids, hydroxyalkanoic acids and alkanedioic acids, cross-linked via ester bonds involving glycerol units or aliphatic hydroxyls and carboxylic moieties; whereas the aromatic domain shows some similarities to lignin, being predominantly composed of hydroxycinnamic acid units, with residual amounts of monolignols (p-coumaryl, coniferyl, and sinapyl alcohols) [4, 5].

Depolymerization of suberin involves most frequently ester bond cleavage, normally through harsh alkaline methanolysis or hydrolysis [4,5]. The ensuing depolymerized suberin or its pure components have been considered as promising starting materials for polymer synthesis [4-8] and other additives [4]. The development of innovative and environmentally friendly approaches for suberin depolymerization would certainly contribute to the development of new and more valuable applications for this material. In this context, although it has been shown that some imidazolium-based ionic liquids solubilize suberin isolated enzymatically from potato [9], a landmark was the demonstration, that some nontoxic and biodegradable cholinium alkanoates (Figure 1) can efficiently extract suberin from cork [10].

The present communication is aimed at presenting the global procedure and mechanism of suberin extraction using cholinium alkanoates [11, 12], the detailed characterization of the extracted material, and to point out some of its potential applications, for example in the preparation of bioactive thin films [13].

II. EXPERIMENTAL

Suberin isolation from Quercus suber cork

The extraction procedure and analytical methodologies used to extract suberin from cork using several cholinium alkanoates and methyl imidazolium hexanoate are outlined in Figure 1**.** Their detailed description is reported elsewhere [11].

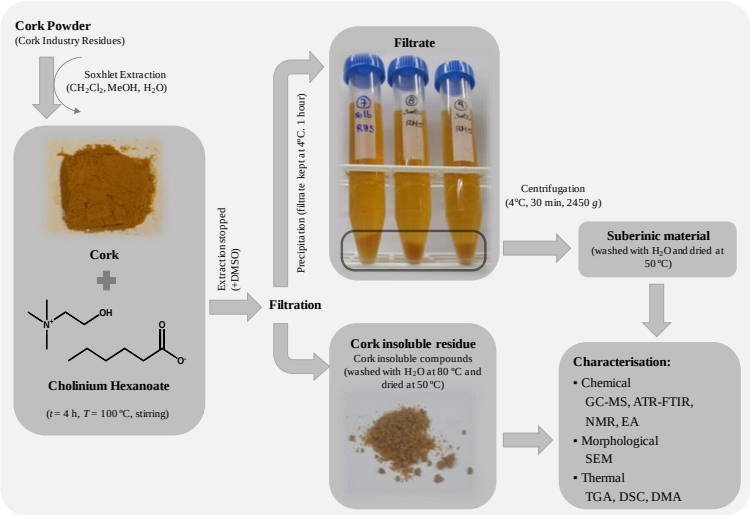

Figure 1. Schematic representation of the methodologies used on the extraction and characterization of cork suberin using cholinium alkanoates.

Suberin depolymerization mechanism

The mechanism of suberin extraction/depolymerization was investigated both by: following the time course of suberin degradation; and testing the lability of the different ester bond types using, e.g., poly(12-hydroxydodecanoic acid), octyl octanoate or glyceryl trioctanoate which were submitted to the same conditions used for cork extraction and following the time course of the products formed as reported in detail elsewhere [12].

Preparation of suberin films

Suberin films have been prepared by solvent casting and characterized in detail as reported elsewhere [13].

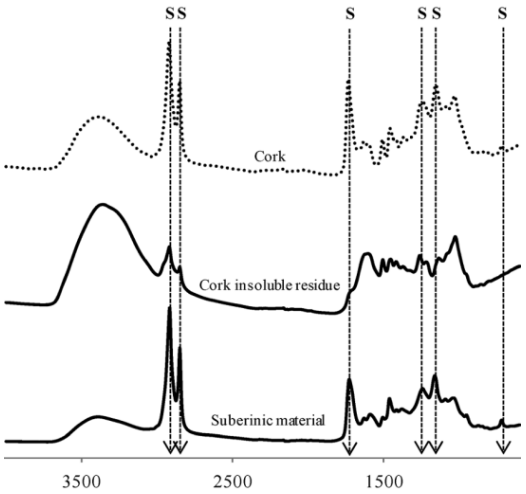

Figure 2. FTIR-ATR spectra of cork, suberinic material extracted with cholinium hexanoate and the cork insoluble residue

III. RESULTS AND DISCUSSION

Composition of extracted suberinic material

Suberin was extracted from cork following the procedure outlined in Figure 1. The best extraction yields (~67 %) were obtained with cholinium hexanoate, even though other alkanoates (C8 and C10) produced good extraction yields (~64 and 58%); on the contrary, methyl imidazolium hexanoate produced fairly low extraction yields (~30%). In this way, it is demonstrated that both the anion and the cation of ILs play an important role in the mechanism of suberin extraction.

The FTIR-ATR analysis of cork, extracted suberinic materil and cork residue (Figure 2) clearly demonstrates that characteristic suberin peaks (2921, 2852, 1737, 1242, 1158, and 724 cm^{-1}) are present both in cork and in suberinic material and drastically reduced in the cork residue as particularly evidenced from the absence of the carbonyl ester peak at 1737 cm^{-1}. Hence, demonstrating that cholinium hexanoate has effectively removed suberin from the starting material; furthermore, the prevalence of the carbonyl ester band in the suberinic material suggests that the obtained material is still in the

Table 1. Main suberin monomers identified by GC-MS: before BH_S and after AH_S alkaline hydrolysis, (detailed composition can be found elsewhere [11]).

Identification	BH_{Sub}	AH_{sub}
Alkan-1-ols	**1,04**	**7,44**
Alkanoic acids	**5,70**	**10,76**
ω-Hydroxyacids	**1,75**	**191,28**
18-Hydroxyoctadec-9-enoic acid	0,04	33,83
22-Hydroxydocosanoic acid	1,43	68,27
9,10,18-Trihydroxyoctadecanoic acid	---	53,00
Alkanedioic acids	**0,43**	**49,71**
Octadec-9-enedioic acid	---	6,32
9,10-Dihydroxyoctadecanedioic acid*	---	26,52
Docosanedioic acid	0,21	8,81
Aromatics	**0,35**	**30,48**
trans-ferulic acid	0,06	27,68
Extractives	**20,50**	**44,29**
Friedelin	9,76	10,14
Betulin	6,95	27,24
Monoacylglycerols derivatives	**8,57**	**0,00**
Glycerol	**1,92**	**0,43**
Others	**3,18**	**24,90**
Total Identified Sample (wt %)	**3,87**	**35,79**

esterified form. These conclusions were further confirmed by ^{13}C solid state NMR analysis of the same fractions [11].

In order to access the monomeric composition of the extracted suberinic material, this was analyzed by GC-MS before and after alkaline hydrolysis (Table 1) Before hydrolysis the major components identified were extractives and accounting only for ~3.9% (Table 1) of the mass of suberinic material extracted. After hydrolysis the typical suberin components, namely ω-hydroxyfatty acids (mainly 22-hydroxydocosanenoic and 9,10,18-tryhydroxyoctadecanoic acids) and α,ω-dicarboxylic acids (mainly docosanendioic and 9,10-dyhydroxyoctadecandioic acids), followed by minor amounts of aromatics, were detected in considerable amounts (~36 % wt.), demonstrating that most components where still present in esterified forms in the extracted material.

The GC-MS results confirm the suggestion made above based on FTIR-ATR that the suberinic material extracted under these conditions is mainly in esterified form, i.e., the process is not fully depolymerizing suberin but rather removing a partially polymerized material of esterified nature.

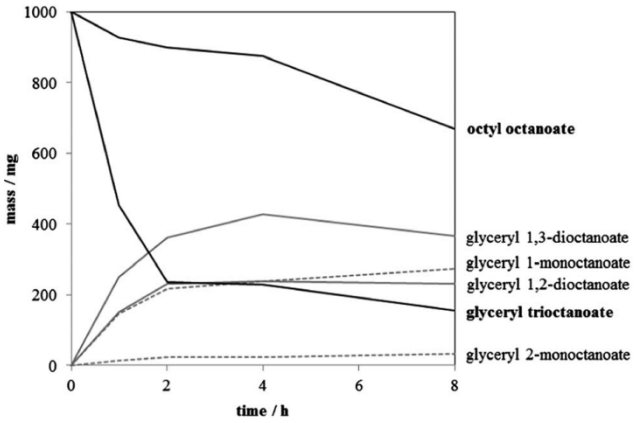

Figure 3. Compounds detected upon treatment of glyceryl trioctanoate and octyl octanoate with cholinium hexanoate for 8h

Suberin extraction/depolymerization mechanism

Given the cross-linked nature of suberin its extraction implies obviously that at least part of the ester bonds are cleaved to remove the partially depolymerized material. To understand this process the time course of suberin depolymerization was followed, as well as the degradation of some ester bonding model compounds, namely octyl octanoate and glyceryl trioctanoate.

The time course of suberin degradation reveals a substantial release of glycerol during cholinium hexanoate extraction, whereas the amount of remaining esterified glycerol in the suberinic materials decreased drastically. This point strongly suggests that glyceride cleavage is the main mechanism of suberin extraction under the studied conditions. Furthermore, the study with model compounds clearly revealed the higher tendency of glyceride bonds to cleave compared to linear ester bonds under these conditions as shown for the course of degradation of glyceryl trioctanoate and octyl octanoate in (Figure 3).

In conclusion this study strongly suggests that the depolymerized material obtained using cholinium hexanoate sould be mainly composed of oligomeric structures mainly linked through ester bonds involving mid-chain or end-chain OH groups of hydroxylated long chain fatty acids rather that glycerol

In this process cholinium hexanoate plays the dual role of solvent and also of catalyst promoting ester bonds hydrolysis by increasing the electrophilic character of the carbonyl ester and at the same time increasing the nucleophilic character of water, and facilitating the leave of the acid-alcohol cleavage (Figure 4)

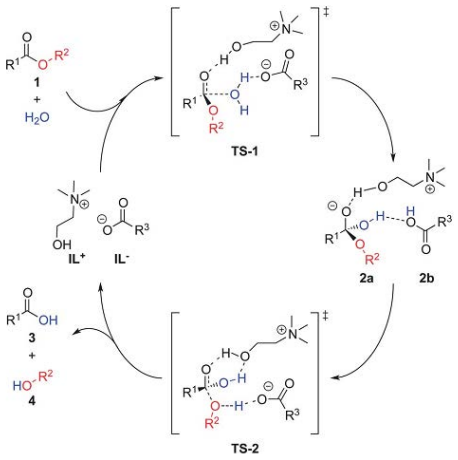

Figure 4. Proposed mechanism for ester cleavage in the presence of Schematic view of cholinium hexanoate (reproduced from [12]

Bioactive thin films from extracted suberin

The suberinic material has been submitted to film casting from an aqueous suspension, yielding very homogeneous and moderately hydrophobic films (Figure 5) which demonstrated to be very active against *S. aureus* and *E. coli.*

IV. CONCLUSIONS

The present study demonstrated the efficiency of cholinium hexanoate to extract an oligomeric suberized material from cork, and the potential of the latter in the preparation of bioactive thin films. This study should inspire the development of other biopolyester-based materials for a broad range of applications. One of the first applications we believe will be implemented is clinical usage, also due to the biocompatibility of suberin films.

Figure 4. Image of a depolymerized suberin film obtained by casting

V. ACKNOWLEDGEMENT

FCT is acknowledged for the grants SFRH/BD/48286/2008 (RF) and SFRH/BPD/73383/2010 (AFS) and for the projects PEst-OE/EQB/LA0004/2013 (ITQB), Pest-C/CTM/LA0011/2013 (CICECO) and PTDC/QUI-QUI/120982/2010. Carmen S.R. Freire also acknowledges FCT/MCTES (Portugal) for a contract under *Investigador FCT 2012*

Fundação Gulbenkian is acknowledged for the grant 21-95587-B (HG).

VI. REFERENCES

[1] Mosier, N.; Wyman, C.; Dale, B.; Elander, R.; Lee, Y.Y.; Holtzapple, M.; Ladisch, M. Features of promising technologies for pretreatment of lignocellulosic biomass. *Bioresour. Technol.*, **2005**, 96, 673.

[2] Silva, S.P.; Sabino, M.A.; Fernandes, E.M.; Correlo, V.M.; Boesel L.F.; Reis, R.L. Cork: properties, capabilities and applications. *Int. Mater. Rev.*, **2005**, 50, 345.

[3] Gil, L., Cortiça: Produção, Tecnologia e Aplicação, INETI, Lisboa, Portugal, 1998.

[4] Gandini, A.; Neto, C.P.; Silvestre A.J.D. Suberin: A promising renewable resource for novel macromolecular materials. Prog. Polym. Sci., **2006**, 31, 878.

[5] Pinto, P.C.R.O; Sousa, A.F.; Silvestre, A.J.D.; Neto C.P.; Gandini, A.; Eckerman, C.; Holmbom, B. *Quercus suber* and *Betula pendula* outer barks as renewable sources of oleochemicals: A comparative study. *Ind. Crops Prod.* **2009**, 29, 126.

[6] Sousa, A.F.; Gandini, A.; Silvestre, A.J.D.; Neto C.P. Synthesis and characterization of novel biopolyesters from suberin and model comonomers. *ChemSusChem* **2008**, 1, 1020.

[7] Sousa A.F.; Silvestre, A.J.D.; Gandini, A.; Neto, C.P. Synthesis of aliphatic suberin-like polyesters by ecofriendly catalytic systems. *High Perform. Polym.* **2012**, 24, 4.

[8] Olsson, A.; Lindström, M.; Iversen, T. Lipase-Catalyzed Synthesis of an epoxy-functionalized polyester from the suberin monomer cis-9,10-epoxy-18-hydroxyoctadecanoic acid. *Biomacromolecules*, **2007**, 8, 757.

[9] Mattinen, M.-L.; Filpponen, I.; Järvinen, R.; Li, B.; Kallio, H.; Lehtinen, P.; Argyropoulos, D. Structure of the polyphenolic component of suberin isolated from potato (Solanum tuberosum var. Nikola), *J. Agr. Food Chem.*, **2009**, 57, 9747.

[10] Garcia, H.; Ferreira, R.; Petkovic, M.; Ferguson, J. L.; Leitão, M. C.; Gunaratne, H. Q.; Seddon, K.; Rebelo, L.; Silva Pereiraa, C., Dissolution of cork biopolymers in biocompatible ionic liquids. *Green Chem.* **2010**, 12, 367 - 369.

[11] Ferreira, R.; Garcia, H.; Sousa, A.F.; Petkovic, M.; Lamosa, P.; Freire C.S.R.; Silvestre, A.J.D.; Rebelo, L.P.N.; Pereira, C.S. Suberin isolation from cork using ionic liquids: characterisation of ensuing products. *New J. Chem.* **2012**, 36, 2014.

[12] Ferreira, R.; Garcia, H.; Sousa, A.F.; Guerreiro, M.; Duarte, F.J.S.; Freire C.S.R.; Calhorda, M.J.; Silvestre, A.J.D.; Kunz, W.; Rebelo, L.P.N.; Pereira, C.S. Unveiling the dual role of the cholinium hexanoate ionic liquid as solvent and catalyst in suberin depolymerisation. *RSC Adv.*, **2014**,4, 2993.

[13] Garcia, H.; Ferreira, R.; Martins, C.; Sousa, A.F.; Freire C.S.R.; Silvestre, Kunz, W.; A.J.D.; Rebelo, L.P.N.; Pereira, C.S. Ex-situ reconstitution of the plant biopolyester suberin as a film. *Biomacromolecules* in press.

POLYESTERS AND COMPOSITES BASED ON BIRCH SUBERIN

Dongfang Li[1]*, Tommy Iversen[2,3], Monica Ek[1]

*[1]Department of Fiber and Polymer Technology, KTH Royal Institute of Technology, Teknikringen 56-58, SE-100 44 Stockholm, Sweden; [2]Innventia AB, Drottning Kristinas väg 61, SE-114 86 Stockholm, Sweden; [3]Wallenberg Wood Science Center, Teknikringen 56, SE-100 44 Stockholm, Sweden (*dongfan@kth.se)*

ABSTRACT

A suberin monomer, *cis*-9,10-epoxy-18-hydroxyoctadecanoic acid (epoxy acid), was isolated from birch outer bark, and polymerized via lipase (immobilized *Candida antarctica* lipase B) catalysis. The epoxy-activated polyesters were characterized by NMR, MALDI-TOF MS, and SEC. The polyester-cellulose composites were prepared through compression molding of polyester and dicarboxylic acids impregnated cellulose. FTIR, CP/MAS ^{13}C NMR, and FE-SEM were used for analyses. All composites were hydrophobic as shown by the contact angle measurement.

I. INTRODUCTION

The hydrophilicity of cellulose is a crucial obstacle for some applications of cellulose-based materials. Natural products that are hydrophobic and biodegradable, such as suberin found in birch outer bark, could be attractive candidates for modifying cellulose surfaces to improve water repellency. Suberin as a natural polymer consists of many monomers, and epoxy acid (**Figure 1**) is the most abundant among the others, amounting to approximately 100 g per kg of dried birch outer bark [1-3]. The epoxy, hydroxyl, and carboxyl functional groups of epoxy acid make it an interesting structure for polymerization and crosslinking.

Figure 1. The structure of *cis*-9,10-epoxy-18-hydroxyoctadecanoic acid (epoxy acid).

In the present report, epoxy acid was isolated from birch outer bark and then polymerized through lipase catalysis [3, 4]. The epoxy-activated polyester was characterized by NMR, MALDI-TOF MS, and SEC. The polyester-cellulose composites were prepared by curing the polyester with dicarboxylic acids on the cellulose surface through compression molding. The composites were analyzed by FTIR, CP/MAS ^{13}C NMR, and FE-SEM. The hydrophobicity was determined by water contact angle measurements.

II. EXPERIMENTAL

Crude epoxy acid was isolated from the birch bark [4], and purified though recrystallization from toluene. The epoxy acid was molten at 85 °C and polymerized for 5 h with lipase (*Candida Antarctic* lipase B) as the catalyst [3]. Cellulose was impregnated in the dry THF solution of polyester and dicarboxylic acids (either oxalic acid or tartaric acid) according to the molar ratios (cellulose/polyester/dicarboxylic acid) of 1/0.2/0.02, 1/0.2/0.06, and 1/0.2/0.1, respectively. The dried mixtures were compression molded at 150 °C for 5 min to prepare the polyester-cellulose composites. All composites were Soxhlet extracted afterwards with THF as the solvent for 24 h to remove the excess chemicals.

NMR, MALDI-TOF MS, SEC, FTIR, DSC, FE-SEM, and contact angle measurement were used to characterize either the intermediate chemicals or products.

III. RESULTS AND DISCUSSION

Isolation of epoxy acid and preparation of polyesters
The final purity of epoxy acid was approximately 95%, as determined by solution NMR, and the isolation yield was 8 wt% (theoretically 10 wt% [3]), calculated on dry birch outer bark.

Size exclusion chromatography revealed that the polyester was successfully prepared through lipase catalysis. MALDI-TOF MS showed poly-linear and cyclic structures, with the former dominating the composition. Solution NMR showed that the epoxy groups were intact, in agreement with the previous study [3].

Preparation of polyester-cellulose composites
The epoxy-activated polyester could be cured by dicarboxylic acids under heating, which was confirmed by FTIR and DSC. By compression molding of the polyester and dicarboxylic acids impregnated cellulose at a high temperature, the curing reaction was introduced on the cellulose surface. Finally, the polyester-cellulose composites with solvent-inert coatings were obtained. All composites were hydrophobic, indicated by contact angle measurements (**Figure 2**), where the polyester-cellulose composite prepared by compression molding of the mixture of cellulose/polyester/oxalic acid according to the molar ratio of 1/0.2/0.02 (composite 4) exhibited the highest hydrophobicity (**Figure 3**) with the average contact angle of 105.5°.

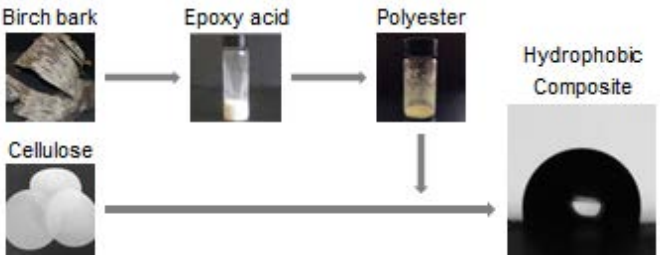

Figure 2. The workflow of preparation of hydrophobic polyester-cellulose composites.

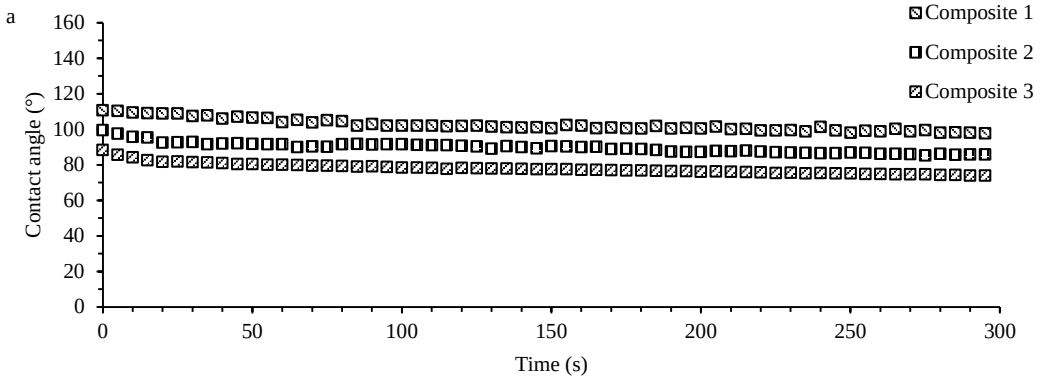

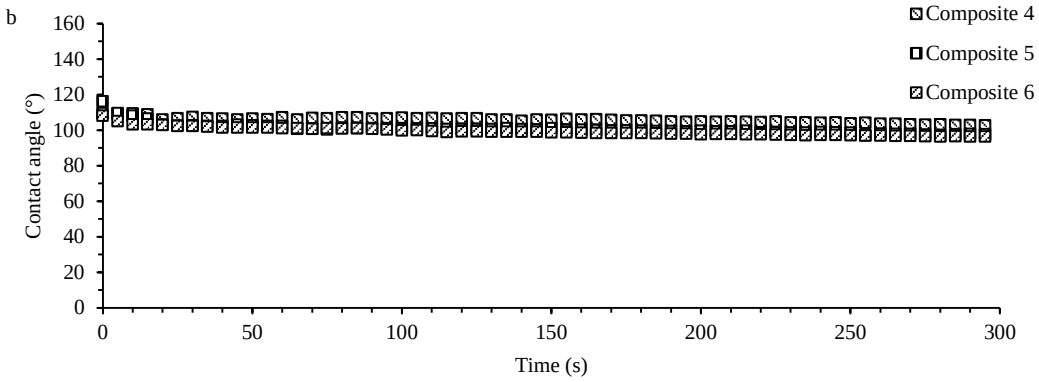

Figure 3. The results of contact angle measurements of all polyester-cellulose composites. Composites 1-3 were prepared by compression molding of mixtures of cellulose, polyester, and tartaric acid according to the molar ratios of 1/0.2/0.02, 1/0.2/0.06, and 1/0.2/0.1, respectively. Composites 4-6 were prepared by compression molding of mixtures of cellulose, polyester, and oxalic acid according to the molar ratios of 1/0.2/0.02, 1/0.2/0.06, and 1/0.2/0.1, respectively.

Based on the results of CP/MAS ^{13}C NMR and FE-SEM, no significant evidence about the chemical reaction between cellulose and the polyester was found, though the coating of cellulose was chemically stable against many organic solvents. In other words, through the current way of surface modification, cellulose preserved its structure, which might be important for the mechanical properties of the prepared composites. Further study about these aspects will be carried out in the near future.

IV. CONCLUSIONS

Here, *cis*-9,10-epoxy-18-hydroxyoctadecanoic acid with high purity and good yield was isolated from birch outer bark, and the corresponding polyester was prepared without affecting the epoxides. The epoxy-activated polyesters were successfully crosslinked by the dicarboxylic acids on the cellulose surface. The polyester-cellulose composites were hydrophobic and stable against many solvents. We demonstrated that the side-stream products from forest industries could be used for value-added applications such as producing functionalized materials, which is in line with the biorefinery concept [5].

V. ACKNOWLEDGEMENT

We would like to express great thanks to WoodWisdom-Net Research Programme and Formas (The Swedish Research Council for Environment, Agricultural Sciences and Spatial Planning) for their financial support.

VI. REFERENCES

[1] Pinto, P.C.R.O.; Sousa, A.F.; Silvestre, A.J.D.; Neto, C.P.; Gandini, A.; Eckerman, C.; Holmbom, B. Quercus suber and Betula pendula outer barks as renewable sources of oleochemicals: a comparative study. *Ind. Crops Prod.* **2009**, *29*, 126-132.

[2] Ekman, R. The suberin monomers and triterpenoids from the outer bark of Betula verrucosa Ehrh. *Holzforschung* **1983**, *37*, 205-211.

[3] Olsson, A.; Lindström, M.; Iversen, T. Lipase-catalyzed synthesis of an epoxy-functionalized polyester from the suberin monomer cis-9, 10-epoxy-18-hydroxyoctadecanoic acid. *Biomacromolecules* **2007**, *8*, 757-760.

[4] Iversen, T.; Nilsson, H.; Olsson, A. A method for separating from suberin and/or cutin containing plants, a solid and/or oil fraction enriched in *cis*-9,10-epoxy-18-hydroxyoctadecanoic acid. WIPO Patent WO/2010/093320.

[5] Cherubini, F. (2010): The biorefinery concept: using biomass instead of oil for producing energy and chemicals. *Energy Convers. Manage.* **2010**, *51*, 1412-1421.

BIOMASS-BASED POLYOLS THROUGH OXYALKYLATION OF ORGANOSOLV LIGNIN BY PROPYLENE CARBONATE

Ralph Lehnen[1*], Isabell Kühnel[2], Jacob Podschun[2], Bodo Saake[2]

[1]*Thünen Institute of Wood Research, Leuschnerstraße 91b, 21031 Hamburg, Germany;*
[2]*University of Hamburg, Wood Technology, Leuschnerstraße 91b, 21031 Hamburg, Germany*
**ralph.lehnen@ti.bund.de*

ABSTRACT

The suitability of lignin as polyol in polyurethane synthesis was usually adjusted by modification with alkylene oxides, especially propylene oxide (PO). Since PO has considerable risks due to high flammability, toxicity and carcinogenicity we investigated an efficient, non-toxic and solvent-free procedure to prepare organosolv lignin based polyols using propylene carbonate (PC). Two modification routes were studied: a direct oxyalkylation of lignin with PC and a two step reaction of lignin with maleic anhydride followed by oxyalkylation with PC. Structural analysis of modified lignins was performed by ^{1}H and ^{31}P NMR spectroscopy and size exclusion chromatography revealing that propylene carbonate was able to almost completely oxypropylate aliphatic and phenolic OH groups, as well as carboxylic groups.

I. INTRODUCTION

During the past, chain-extended hydroxyalkyl lignins were evaluated as substitutes in polyurethane applications because technical lignins lead to low-valued products [1]. Usually chemical modification of lignin was achieved by oxyalkylation with different alkylene oxides, especially propylene oxide (PO) [2-4]. Since propylene oxide is a hazardous material in terms of flammability, carcinogenicity and toxicity, in this study the cyclic organic carbonate propylene carbonate (PC) was investigated as harmless alternative reactant for the oxypropylation of beech wood organosolv lignin from ethanol water pulping. This cyclic organic carbonate is characterized by low toxicity, high boiling and flash point, low vapor pressure, biodegradability and high solubility [5,6].
A synthesis route was developed including the reaction of lignin with propylene carbonate (Figure 1a) and a two-step reaction of lignin with maleic anhydride (MA) [7] followed by oxyalkylation (Figure 1b). Both modified lignins have been characterized in terms of their suitability as polyol component in polyurethane synthesis.

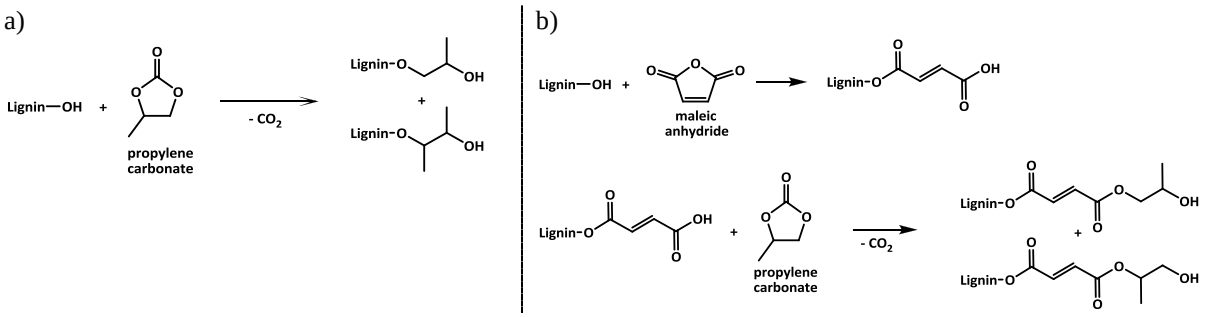

Figure 1. Chemical modification of organosolv lignin via the direct reaction with propylene carbonate (a) and the two-step reaction with maleic anhydride followed by oxyalkylation with propylene carbonate (b).

II. EXPERIMENTAL

Organosolv pulping. Organosolv lignin was produced at the Thünen Institute of Wood Research (Hamburg, Germany) using ethanol water pulping of beech wood as described elsewhere [8].
Direct oxyalkylation of lignin. Beech wood organosolv lignin (1.0 g; 6.52 mmol OH/g) was dissolved in 5.2 ml propylene carbonate and 91.9 mg K_2CO_3 (0.66 mmol) was added. The mixture was allowed to react at 170°C for 3 h under stirring and nitrogen atmosphere. After completion of the reaction the mixture was cooled to room temperature and added to the 10-fold amount of deionized acidified water. The precipitated product was membrane filtered (polyethersulfone, pore size: 0.22 µm) and washed with 5 x 50 ml of water. The isolated product was dried in a vacuum oven at 30°C over phosphorus pentoxide.

Two-step oxyalkylation of lignin. Beech wood organosolv lignin (1.0 g; 6.52 mmol OH/g) was first esterified with maleic anhydride (10.0 g; 0.102 mol) in 20 ml of 1,4-dioxane. A total of 1 ml (0.57 mmol) of the catalyst solution (0.5 g of 1-methylimidazole in 10 ml of 1,4-dioxane) was added to the reaction. The reaction mixture was stirred at 50°C under nitrogen atmosphere overnight. The mixture was cooled to room temperature and added to the 10-fold amount of deionized acidified water. The precipitated maleated lignin was membrane-filtered followed by washing with water until the pH of the filtrate was neutral. The isolated product was dried in a vacuum oven at 30°C over phosphorus pentoxide. The maleated lignin was then oxypropylated as described above for the organosolv lignin.
^{1}H and ^{31}P NMR spectroscopy was performed on a Varian Mercury 400 MHz spectrometer. Acquisition parameters for ^{31}P NMR included: 25°C, 11990 Hz spectral window, 256 scans and a 20 s delay between pulses. Acquisition parameters for ^{1}H NMR spectroscopy included: 40°C, 6006 Hz spectral window, 128 scans and a 2.0 s delay between pulses.
Size exclusion chromatography (SEC). DMSO with 1% LiBr was used as eluent with a polymer standard service (PSS) column set PolarGel-M® (7.5 x 300 mm) and a guard column (8 x 50 mm). The flow rate was 0.5 ml/min at 60°C. About 10 mg of sample material were dissolved (c = 1 mg/ml) and shaken in the eluent for 24 h at room temperature. Detection was performed using an RI detector (RI-71, Showa Denko).

III. RESULTS AND DISCUSSION

The direct oxyalkylation of organosolv lignin (OL) with propylene carbonate was examined using ^{31}P NMR spectroscopy. The analysis of ^{31}P NMR spectra (**Figure 2**) of starting material (OL) and hydroxypropylated organosolv lignin (hOL) shows that both condensed and uncondensed phenolic units were completely hydroxypropylated. Furthermore two distinct broad signals appear in the aliphatic region between 146.5 and 149.5 ppm and between 145.5 and 146.5 ppm. The signal recorded between 146.5 and 149.5 ppm appears in the same region as the primary and secondary aliphatic hydroxy groups originally present in lignin. However, the other signal recorded between 145.5 and 146.5 ppm can be attributed to the new aliphatic hydroxy groups formed by ring-opening attachment of propylene carbonate. As a result of direct oxyalkylation with PC lignin polyols with exclusively aliphatic OH groups were generated. This OH profile of modified organosolv lignin is similar to that of lignin polyols synthesized by oxyalkylation with PO [10].

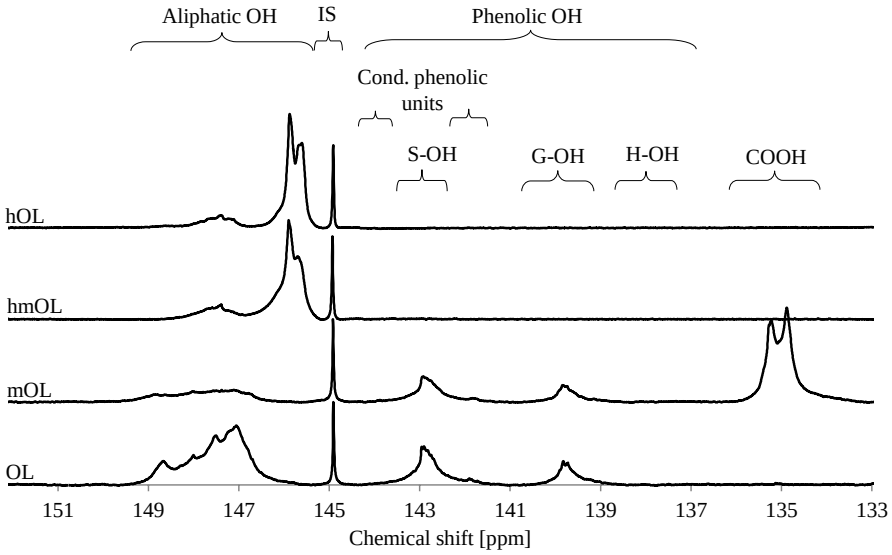

Figure 2. ^{31}P NMR spectra of organosolv lignin (OL), maleated lignin (mOL), hydroxypropylated mOL (hmOL) and hydroxypropylated lignin (hOL).

The comparison of the ^{31}P NMR spectra (**Figure 2**) of OL and maleated organosolv lignin (mOL) suggests that the majority of the OH groups were esterified with maleic anhydride, in which carboxylic acids are formed. Moreover, it can be observed that the aliphatic OH groups react preferably with MA, while the phenolic OH groups have a lower reactivity to MA. ^{31}P NMR spectral analysis of mOL and oxypropylated mOL (hmOL) shows that in addition to the lignin-derived hydroxy groups also the carboxyl groups of the maleic acid spacer reacted with PC. As similar to the spectrum of hydroxypropylated lignin, two distinct broad signals were recorded in the aliphatic region. The signals can be assigned to the remaining lignin-derived (146.5-149.5 ppm) and hydroxypropyl OH groups (145.5-146.5 ppm). By this two-step modification a lignin polyol with an extended carbon skeleton and exclusively aliphatic OH groups can be synthesized.

The ^{1}H NMR data (**Figure 3**) allowed the calculation of hydroxypropyl units appended to each OH function of lignin. While the methine and methylene signals overlap with the methoxyl group signal, the methyl signal was used to determine the degree of oxypropylation. Based on the quantitative ^{1}H NMR analysis 4.67 mmol/g methyl groups were formed. In combination with quantitative ^{31}P NMR analysis 3.64 mmol/g aliphatic hydroxy groups were present in the hydroxypropylated lignin, thus 1.28 hydroxypropyl units per lignin-derived OH group were calculated. Compared to the reactions with propylene oxide multi-oxypropylation is minor for PC [11].

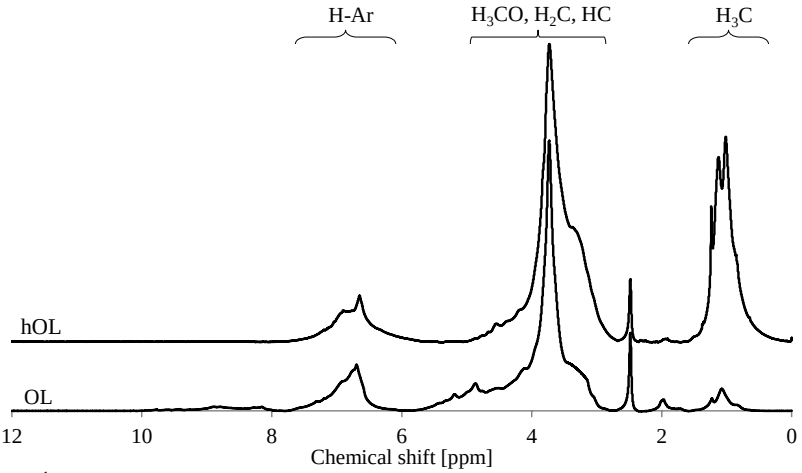

Figure 3. ^{1}H NMR spectra of organosolv lignin (OL) and hydroxypropylated lignin (hOL).

The results of molar mass distributions of the modified lignin samples indicated a shift to higher molar masses (**Figure 4** and **Table 1**). For mOL M_w of 7400 g/mol and polydispersity of 3.6 were determined. This result in combination with spectroscopic analysis showed that esterification with maleic anhydride generated a chain extended polymer of more uniform structure. In contrast hOL has a higher molar mass value (Mw=9900 g/mol) and polydispersity (D=4.7). The molar masses of oxypropylated lignins increased due to the addition of hydroxyalkyl chains and maybe due to thermal induced coupling reactions [12]. In case of hmOL produced by oxypropylation of mOL the molar mass reached up to 86000 g/mol, which is an 11-fold increase in the M_w compared to the starting material mOL. The synthesized hmOL was distributed over a broad molar mass range with significant increase in polydispersity (D=25.5) and modality. Therefore it is doubtful whether such high molecular polyols are compatible with standard polyurethane synthesis.

Table 1. Molar mass and polydispersity of beech wood organosolv lignin (OL), hydroxypropylated OL (hOL), maleated OL (mOL) and hydroxypropylated mOL (hmOL).

	OL	**hOL**	**mOL**	**hmOL**
M_w [g/mol]	4100	9900	7400	86000
M_n [g/mol]	1278	2106	2056	3373
M_w/ M_n	4.1	4.7	3.6	25.5

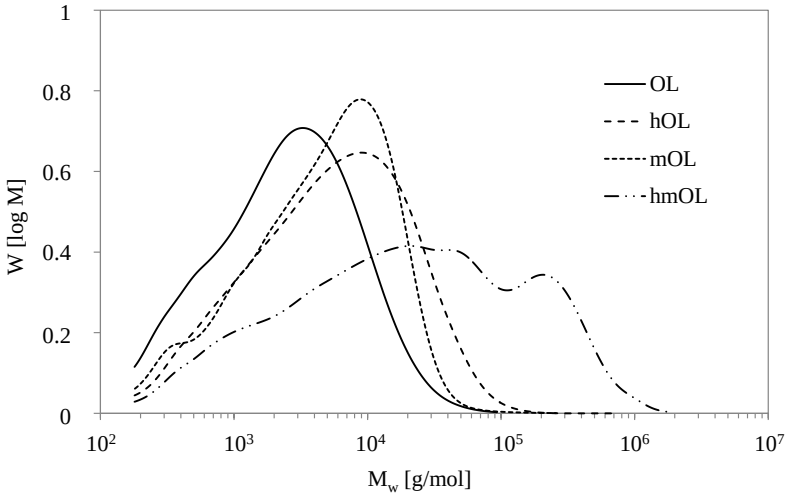

Figure 4. Molar mass distribution curves of organosolv lignin (OL), hydroxypropylated lignin (hOL), maleated lignin (mOL) and hydroxypropylated mOL (hmOL).

The first results in preparing polyurethane foams and films showed that the commercial polyol could be gradually replaced by 10-100% lignin and lignin polyol, respectively. The PU foams synthesized with 10-30% lignin and lignin polyol have properties which correspond to that of commercially available rigid PU foams. The analysis showed that with increasing lignin content PU films with increasing rigidity could be generated. Thus depending on the application the properties of lignin-based polyurethanes can be selectively adjusted by varying the polyol type and composition. These results will soon be published elsewhere.

IV. CONCLUSIONS

Lignin polyols were successfully synthesized using propylene carbonate as oxyalkylating reagent for technical and maleated beech wood organosolv lignin. Based on spectroscopic analysis (^{1}H and ^{31}P) the direct oxypropylation of lignin showed that both condensed and uncondensed phenolic units were completely oxypropylated as well as almost all aliphatic hydroxy groups. Additionally, by the two-step oxyalkylation of lignin the phenolic OH groups and the carboxylic acid groups were completely oxypropylated. These two approaches generated lignin polyols with extended carbon skeleton and exclusively aliphatic hydroxy groups. The molar masses of oxypropylated lignins increased due to the addition of hydroxyalkyl chains and maybe due to coupling reactions. In case of maleated lignin a significant increase of molar mass has been detected.
Compared to oxyalkylation by propylene oxide multioxyalkylation is minor for propylene carbonate. Due to its easy handling, low toxicity, volatility and flammability PC provides a convenient alternative to propylene oxide.
This oxyalkylation procedure shows good potential for the preparation of lignin polyols and will be further investigated with special emphasis on derivatives of cyclic organic carbonates.

V. ACKNOWLEDGEMENT

This research was funded by the Federal Ministry of Food and Agriculture (BMEL), and supported by the Fachagentur Nachwachsende Rohstoffe e.V. (FNR project: Lignocellulose-Bioraffinerie II, FKZ: 22019009).
The authors gratefully acknowledge Andreas Schreiber, Bernhard Ziegler, Sascha Lebioda, Martina Heitmann and Alexander Stücker.

VI. REFERENCES

[1] Wu, L.C.-F., Glasser, W.G. Engineering plastics from lignin. I. Synthesis of hydroxypropyl lignin. *J. Appl. Polym. Sci.* **1984**, *29*, 1111-1123.
[2] Glasser, W.G., Hsu, O.H.H. Polyurethane intermediates and products and methods of producing same from lignin, US Patent 4,017,474, **1977**.
[3] Nadji, H., Bruzzèse, C., Belgacem, M.N., Benaboura, A., Gandini, A. Oxypropylation of lignin and preparation of rigid polyurethane foams from ensuing polyols. *Macromol. Mater. Eng.* **2005**, *290*,1009-1016.
[4] Cateto, C.A., Barreiro, M.F., Rodrigues, A.E., Belgacem, M.N. Optimization study of lignin oxypropylation in view of the preparation of polyurethane rigid foams. Ind. Eng. Chem. Res. **2009**, *48*, 2583-2589.
[5] Liebert, M.A. Final report on the safety assessment of propylene carbonate. *J. Am. Coll. Toxicol.* **1987**, *6*, 23-51.
[6] Clements, J.H. Reactive applications of cyclic alkylene carbonates. *Ind. Eng. Chem. Res.* **2003**, *42*, 663-674.
[7] Thielemans W., Wool, R.P. Lignin esters for use in unsaturated thermosets: Lignin modification and solubility modeling. *Biomacromolecules* **2005**, *6*, 1895-1905.
[8] Puls, J., Schreiber, A., Saake, B. Conversion of beech wood into platform chemicals after organosolv treatment. In: Proceedings of the 15th ISWFPC, Oslo, Norway, **2009**.
[9] Granata A., Argyropoulos, D.S. 2-Chloro-4,4,5,5-tetramethyl-1,3,2-dioxaphospholane, a reagent for the accurate determination of uncondensed and condensed phenolic moieties in lignins. *J. Agric. Food Chem.* **1995**, *43*, 1538-1544.
[10] Ahvazi, B., Wojciechowicz, O., Ton-That T.-M., Hawari, J. Preparation of lignopolyols from wheat straw soda lignin. *J. Agric. Food Chem.* **2011**, *59*, 10505-10516.
[11] Sadeghifar, H., Cui, C.; Argyropoulos, D.S. Toward thermoplastic lignin polymers. Part 1. Selective masking of phenolic hydroxyl groups in kraft lignin via methylation and oxypropylation chemistries. *Ind. Chem. Res.* **2012**, *51*, 16713-16720.
[12] Cui, C., Sadeghifar, H., Sen, S., Argyropoulos, D. S. Toward thermoplastic lignin polymers; Part II: Thermal & polymer characteristics of Kraft lignin & derivatives. *BioRes.* **2013**, *8*, 864-886.

HIGH TENACITY CELLULOSIC FIBRES FROM NOVEL IONIC LIQUID-CELLULOSE SOLUTION BY DRY-JET WET SPINNING

Shirin Asaadi[1*], Anne Michud[1], Michael Hummel[1], Herbert Sixta[1]

[1]*Aalto University, Department of Forest Product Technology PL 16300, FI-00076 Espoo, Finland (*shirin.asaadi@aalto.fi)*

ABSTRACT

Cellulose-dissolving ionic liquids promise a new, safe and environmentally friendly alternative for the Viscose and NMMO-based Lyocell processes for the production of man-made cellulosic fibers (MMCF). Multifilaments were successfully spun from solutions of pulps from four different proveniences in a novel; super base derived ionic liquid using the dry-jet wet spinning technology. The spinning parameters have been optimized by extensive rheological studies. The resulting fibers are characterized by outstandingly high tenacity values. Mechanical properties, i.e. tenacity, elongation at break and elastic modulus are determined and compared to commercial Lyocell fibres. Thus, an understanding of the novel process is developed and the advantages are demonstrated for producing textile and also composite fibres of high added-value.

I. INTRODUCTION

The global demand for textile fibers is expected to increase at a growth rate of 3% pa in 2011-2030. Cotton production cannot meet the growing demand for cellulosic fibers any longer [1]. Currently, man-made cellulosic fibers (MMCFs) are mainly produced by the viscose and Lyocell technique. Since both suffer from certain drawbacks, the need for new, environmentally friendly fiber technologies is strong [2].

Recently, studies on the application of ionic liquids (ILs) in cellulose chemistry have attracted much attention, including the production of regenerated cellulose fibers [3, 4, and 5].

We have studied a dry-jet wet spinning process utilizing a novel IL, [DBNH]OAc. Various cellulosic sources are considered for the production of fibers. This process gives equal or better strength properties than any commercial MMCF.

II. EXPERIMENTAL

The investigations were carried out using four different cellulosic solutes including
Pulp 1: Eucalyptus pre-hydrolysis kraft pulp from Bahia pulp, Brazil (420 ml/g, M_w: 196.4 M_n: 62.9, PDI: 3.1)
Pulp 2: Birch pre-hydrolysis kraft pulp from Enocell, Finland (476 ml/g M_w: 274.3 M_n: 68.2, PDI: 4.0)
Pulp 3: Spruce sulfite pulp from Domsjö, Sweden (540 ml/g, M_w: 406.6 M_n: 54, 4 PDI: 7.5)
Pulp4: Pine sulfite pulp from MetsäFibre, Finland (490 ml/g, M_w: 298.79 M_n: 61, 9 PDI: 4.8)

[DBNH]OAc was kindly supplied by Helsinki University.

The pulp sheets were cut into small particles in a Wiley mill with 1 mm sieve, then oven-dried at 105 °C to constant weight. The pulps were dissolved in the ionic liquid under vacuum and heating in a vertical kneader rotating at 10 rpm, at 80 ºC, for 90 min, then kept under vacuum for an additional hour to remove air bubbles. The solution was press filtered through a layered filter mesh (GKD Ymax2, 5 µm nominal, Gebr. Kufferath AG, Germany) under 2 MPa, and finally stored in a cold room protected from moisture.

The rheological characteristics of the cellulose-IL solutions under shear stresses were measured. The visco-elastic behavior was studied by means of a Anton Paar MCR 300 rheometer by performing dynamic frequency sweep measurements over a range of 0.1-100 s^{-1} and at temperatures from 70 to 85 °C.

Filament spinning (Figure 1) was done with a laboratory spinning system (Fourné Polymertechnik, Germany) with a multifilament spinneret. The dope (200 g) was spun via an air gap into a water bath, where the formed filament was led over a teflon guide roller (at 20 cm depth) and via another guide onto a godet couple. The rate of extrusion (Ve) was kept constant and the properties of fibres obtained after a draw ratio (DR) of 10.60 were measured. The filaments were collected on the godet, carefully cut out with a razor blade, washed first in cold (5

ºC) and then with hot water (50 ºC), dried and stored under controlled conditions (23 ºC, 50% RH) for tenacity measurements.

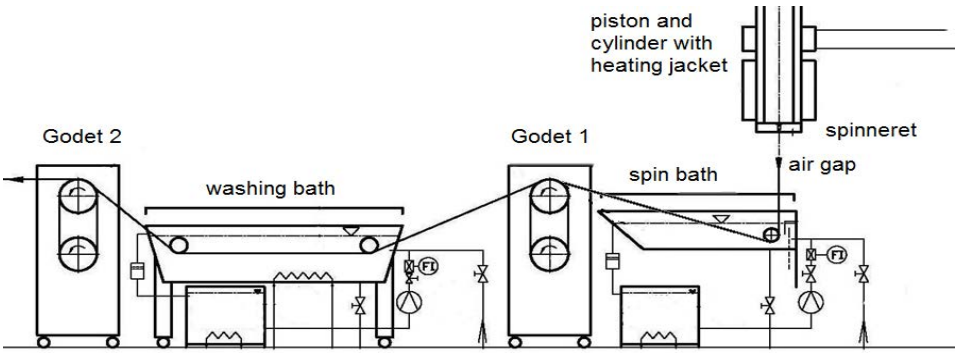

Figure 1. Schematic of dry jet wet spinning.

Filament testing was done with 10 samples of each spinning trial at 23 ºC and 50% RH. Linear density (titer) was determined with a vibroscope (Vibroskop 400, Lenzing Instruments GmbH & Co KG, Austria) with at least 50 mg.dtex^{-1} pretension. Determination of tenacity and elongation was done using a Vibrodyn 400 in both dry and wet mode.

III. RESULTS AND DISCUSSION

Shear rheology of IL/cellulose solutions

The visco-elastic properties of cellulose-IL solutions were assessed by measuring the complex viscosity and the dynamic moduli at different temperatures. Assuming that the Cox-Merz rule is valid for cellulose-IL solutions, the Carreau model has been used to determine the zero shear viscosity.

For the four solutions, Figure 2 shows the changes of complex viscosity |η*| as a function of angular frequency, ω. The measurements were carried out in a temperature range which was anticipated for the spinnabilty of the cellulose-IL solutions (13 wt-%). All samples show shear thinning behavior at high frequencies, typical for polymer melts and solutions.

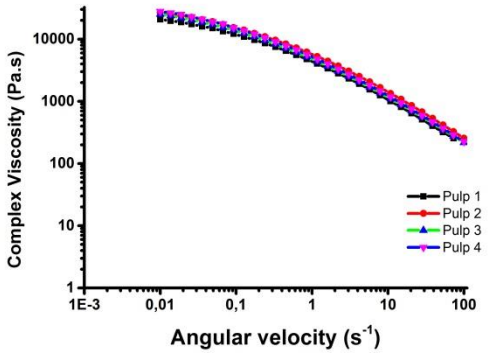

Figure2. Complex viscosity vs. angular frequency of four pulps in ionic liquid solution (13 wt-%) at the respective spinning temperature.

In Figure 3, the master curve from the oscillation test is presented. Spinning temperature could be chosen according to the zero shear viscosity and the cross over point of the dynamic moduli. We found that the dope from novel cellulose solvent, [DBNH]OAc, results in stable spinning conditions at much lower temperature than dope from NMMO.

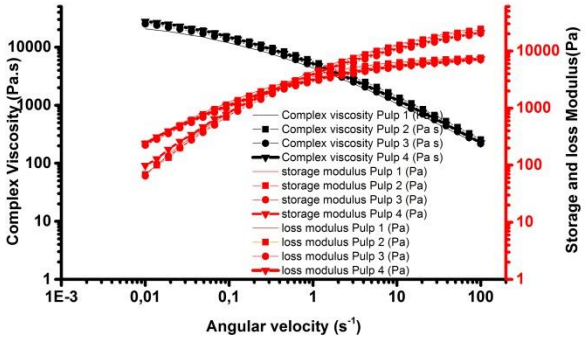

Figure 3. Master curve of four pulps in ionic liquid solution (13 wt-%) at spinning temperature.

Mechanical properties

Figures 4 and 5 reveal a comparison of typical stress-strain curves of the fibers from four different pulps and lyocell fibre in the conditioned and wet state spun with a draw ratio of 10.60. All pulps show similar values with Pulp 1 resulting in slightly higher tenacity values and Pulp 4 slightly larger elongation.

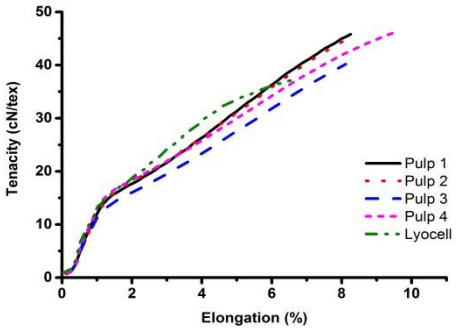

Figure 4. Tenacity (conditioned) vs. elongation of four pulps.

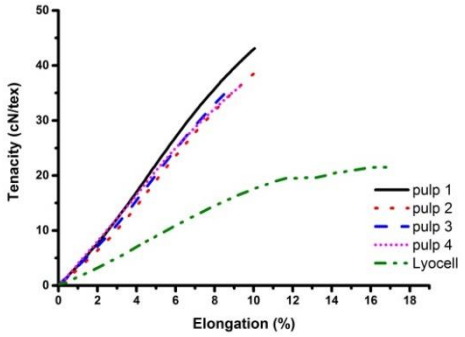

Figure 5. Tenacity (wet) vs. elongation of four pulps.

Figure 6 depicts the tenacity of the fibres at a draw ratio of 10.60 in comparison to the commercial NMMO-spun fibre (Lyocell). The titers of the produced fibres range from 1.75 to 1.95 dtex. Tenacities of 45-52 cN/tex and 40.9 - 51.1 cN/tex have been measured in the conditioned and wet state, respectively.

Figure 7 demonstrates that the IL-spun fibres have slightly lower elongation values than the reference fibres. Measurements revealed elongations of 10.1-10.7% in the conditioned and 10.6 - 12.8% in the wet state, respectively

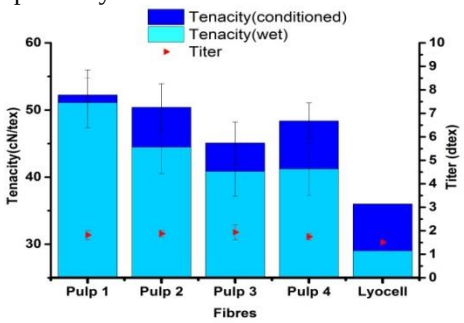

Figure 6. Tenacity and titer of spun fibres compared to Lyocell.

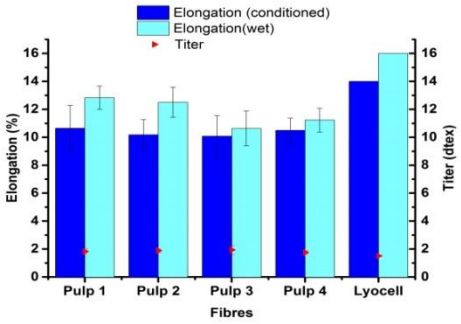

Figure 7. Elongation and titer of spun fibres compared to Lyocell.

The fiber properties in Figure 6 are consistent with the results in Figure 7. These curves confirm that higher stretch leads to higher orientation, higher tenacities and lower elongation for IL-spun fibres.
The elastic modulus of the fibres at draw ratio of 10.60 and the commercial NMMO-spun fibre (Lyocell) are shown in Figure 8. The titers of the produced fibres range from 1.75 to 1.95 dtex. The elastic moduli are 20-25 GPa which is close to the modulus of Lyocell fibres.

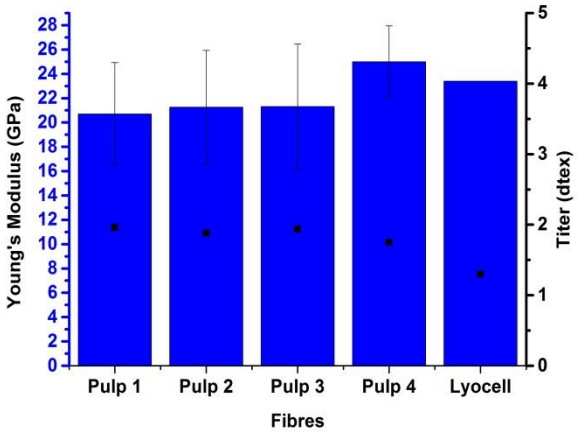

Figure 8. Young Modulus and titer of spun fibres compared to Lyocell.

IV. CONCLUSIONS

Various pulps were spun successfully by means of a dry-jet wet spinning process using a hitherto novel ionic liquid [DBNH]OAc. Drawing the filaments induced high cellulose orientation which resulted in excellent strength properties and elastic moduli similar or surpassing commercial NMMO-spun Lyocell fibers. Additionally, the present procedure requires no stabilizers in the dope and substantially lower process temperatures than in the NMMO-based Lyocell process.

V. ACKNOWLEDGEMENT

This study is part of the Future Biorefinery project financed by the Finnish Bioeconomy Cluster (FIBIC) and the Finnish funding agency for technology and innovation (TEKES).

VI. REFERENCES

[1] Hämmerle F.M.The cellulose gap (the future of cellulose fibres). *Lenzinger Ber* **2011**, 89:12-21.

[2] Hassi H.; Future outlook for man-made cellulosic fibres Towards Bio-Society. *Forest Cluster Ltd's annual seminar* **2011**.

[3] Zhu S.;Wu Y.; Chen Q.; et al. Dissolution of cellulose with ionic liquids and its application: a mini-review. *Green Chemistry* **2006**, 8:325-327.

[4] Zavrel M.; Bross D.; Funke M.; Büchs J.; Spiess AC.; High-throughput screening for ionic liquids dissolving (ligno-) cellulose. *Bioresource Technology* **2009**, 100:2580–2587.

[5] Jiang G.; Yuan Y.; Wang B.; Analysis of regenerated cellulose fibers with ionic liquids as a solvent as spinning speed is increased. *Cellulose* **2012**, 19:1075–1083.

PREPARATION OF LIGNIN-BASED ACTIVATED CARBON FIBER AND ITS ELECTRICAL APPLICATION

Xiangyu You[1], Keiichi Koda[2], Tatsuhiko Yamada[3], and Yasumitsu Uraki[2]*

*[1]Graduate School of Agriculture, Hokkaido University, Sapporo, Japan; [2]Research Faculty of Agriculture, Hokkaido University, Sapporo, Japan; [3]Division of Biomass Chemistry, Forestry and Forest Products Research Institute, Tsukuba, Japan. (*uraki@for.agr.hokudai.ac.jp)*

ABSTRACT

An electric double layer capacitor (EDLC) was successfully prepared from electrospun lignin fibers. The EDLC was prepared by the following process. The electrospun fibers were converted to activated carbon fibers (ACFs) by thermostabilization followed by carbonization and steam activation. The ACFs were suspended together with conductive carbon black (5%) in aqueous carboxymethyl-cellulose solution, and then this suspension was spread on a thin Al foil. The lignin ACFs-coated foil and a paper as a separator were immersed in triethylmethylammonium tetrafluoroborate ($TEAMBF_4$)/propylene carbonate (PC) solution as an organic electrolyte. Finally, these materials were assembled in a measurement cell. This EDLC showed electrostatic capacitance of 133 F/g and impedance of 12 Ω.

I. INTRODUCTION

Lignin is one of the most abundant biopolymer after cellulose on earth, which accounts for 20–30% of wood and possesses high carbon content (about 60 %) among wood components. However, lignin utilizations are limited to energy recovery for pulp mill and inexpensive materials, such as dispersants, emulsion stabilizers, surfactants, and binders [1,2].

Recently, lignin-based carbon fibers (CFs) has been focused on as one of value-added functional materials. So far CFs have been prepared by melt-spinning or dry-spinning followed by thermostabilization and carbonization. The CFs are further converted to activated carbon fibers (ACFs) which have a large surface area. Therefore, ACFs is an excellent adsorbent for environmental purification. Uraki et al. [3] prepared ACFs from softwood acetic acid lignin. The ACFs possessed a large specific surface area of 1930 m^2/g, and had adsorbability comparable to that of high-performance commercial ACFs. The tensile strength was also comparable to that of pitch-derived ACFs. In this study, such lignin-based ACFs were used as a material for electrode of EDLC.

EDLC is a kind of energy storage devices as well as conventional capacitor and secondary battery, such as lithium ion battery. EDLC has several advantages, such as (1) high power density (discharge at high current density), (2) short charging time , (3) long cycle life due to no chemical reactions, (4) high coulombic efficiency (high reversibility), and (5) environmental friendliness (no heavy metals used) over second batteries, even though its energy density is lower than secondary batteries [4]. Therefore, EDLC has been considered to be a next-generation energy storage device to meet the increasing demands of electric power [5]. EDLC consists of three parts, electrode, electrolyte and separator. Carbonaceous materials are considered as prospective electrode materials for industrialization. The advantages of carbon materials over other candidates are abundance, lower price, easy processing, non-toxicity, higher specific surface area, good electronic conductivity, high chemical stability, and wide operating temperature range [6]. Since the electrostatic charge is accumulated at the electrode/electrolyte interface of EDLC, the electrostatic capacitance of EDLC is strongly dependent on the surface area of the electrode [7]. Accordingly, ACFs with a large surface area is suitable material for electrode of EDLC. The objectives of this study are to prepare ACFs with a large surface area from isolated lignin and to assemble an EDLC with the resultant ACFs.

II. EXPERIMENTAL

Preparation of lignin-based ACFs

A preparation process for lignin-based ACFs is shown in **Figure 1**. Hardwood acetic acid lignin (HAL) [8] was dissolved in acetic acid (AcOH) or AcOH/CCl_4 (weight ratio, 8:2), and then hexamethylenetetramine (hexamine) with different amounts was added to the solution. The mixture solution was subjected to electrospinning of lignin fibers by using a homemade electrospinning machine, and it was carried out under the following conditions: applied voltage, 38 kV; solution flow rate, 5 ml/min; tip-collector distance, 13 cm.

Subsequently, the lignin fibers were thermostabilized under air atmosphere by heating up to 250 ^oC at different heating rates. Then, the thermostabilized fibers were, in turn, carbonized under a nitrogen stream at

1000 ℃ to yield lignin based CFs. Finally, the resultant CFs were activated with steam at 900 ^{o}C to yield lignin-based ACFs.

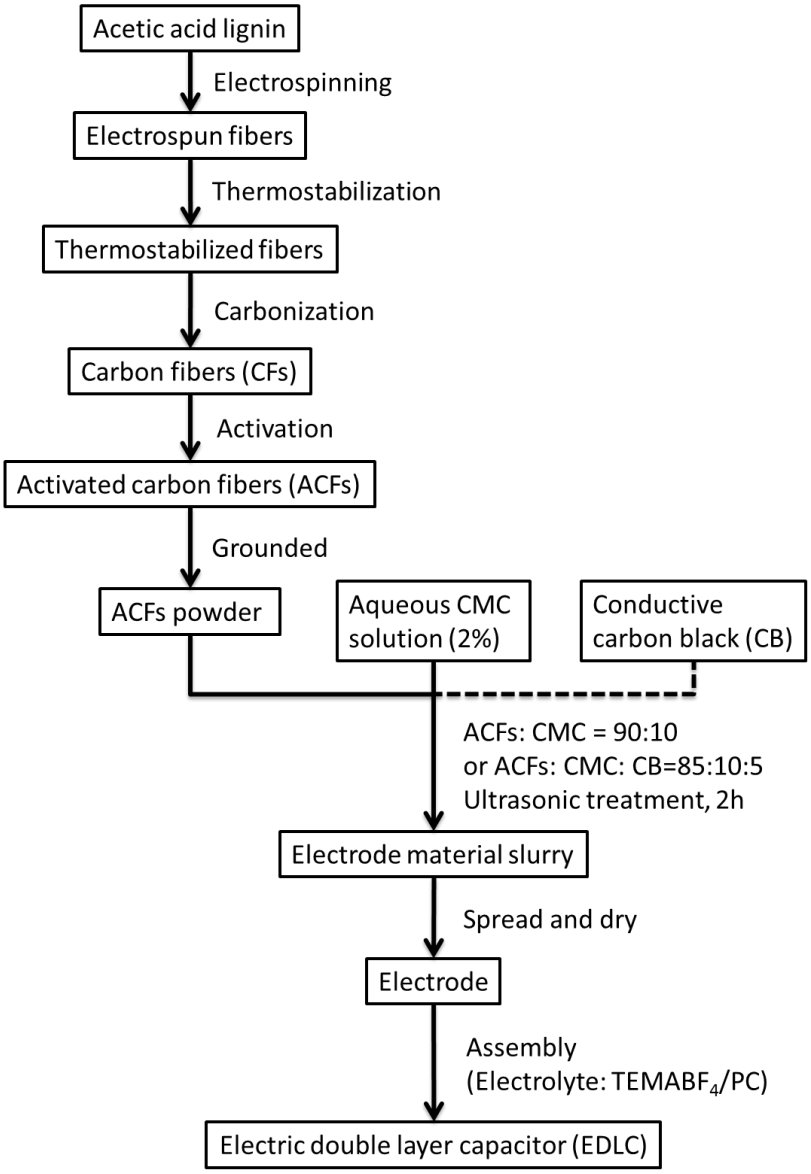

Figure 1. A scheme for lignin-based ACF preparation and EDLC assembly

EDLC assembly and characterization

The resultant ACFs were grounded to powder with a mortor and a pastle, and suspended in aqueous carboxymethyl-cellulose (CMC) solution. These suspensions were ultrasonicated to give homogeneous slurry. Then, 5% of conductive carbon black (CB, Alfa Aesar, Heysham, UK) was added to the carbonaceous sample/CMC suspensions, and the mixtures were spread on an Al foil to yield electrode. The electrodes and a piece of paper sheet (Mitsubishi paper Mills Ltd. Tokyo, Japan) as a separator were immersed in triethylmethylammonium tetrafluoroborate/propylene carbonate solution. The coated Al foil was placed at the bottom of flat cell for assembly of electrode, and the cellulosic separator was put on the foil. Afterwards, the other coated Al foil was placed on the separator to give an EDLC.

The performance of our EDLC was evaluated by cyclic voltammetry (CV), galvanostatic charge/discharge (GCD) method and electrochemical impedance spectroscopy (EIS) using an electrochemical workstation (Autolab PGSTAT302N FRA32M, Metrohm Autolab B.V., Japan).

III. RESULTS AND DISCUSSION

Preparation of lignin-based ACFs

HAL electrospun fibers was obtained by electrospinning from 35 wt% of HAL/AcOH solution. An average fiber diameter was 1.30 μm. However, it took a very long time (2 days) to achieve the complete thermostabilization of electrospun fibers as a second process under air atmosphere. An aim of this process is that the lignin fibers are transformed into infusible fibers by introducing oxygen molecules as a crosslinker into lignin molecules in order to prevent fiber from melting in the following carbonization process. Thus, the thermostabilization process is very important for CFs production. To shorten the thermostabilization time, we tried to add hexamine to the lignin solution, which was expected to act as a crosslinker to suppress thermal mobility of lignin. When hexamine was added to HAL/AcOH solution, no electrospun fiber was obtained because of rapid curing before spinning. When the solvent was changed to a mixture solvent of AcOH and CCl_4, the electrospinning of HAL mixture was carried out. The electrospun fibers (**Figure. 2-A**) with 10% hexamine (on solution) were completely thermostabilized under air atmosphere for 3 h (heated to 250 ^oC for 2 h, and kept at 250 ^oC for 1 h) to give the infusible fibers (**Figure. 2-B**) By carbonization of the thermostabilized one, HAL-based CFs (**Figure. 2-C**) with a large BET specific surface area of 1287 m^2/g were obtained even without activation. The CFs were easily converted into ACFs (**Figure. 2-D**) with a surface area of 2185 m^2/g by steam activation.

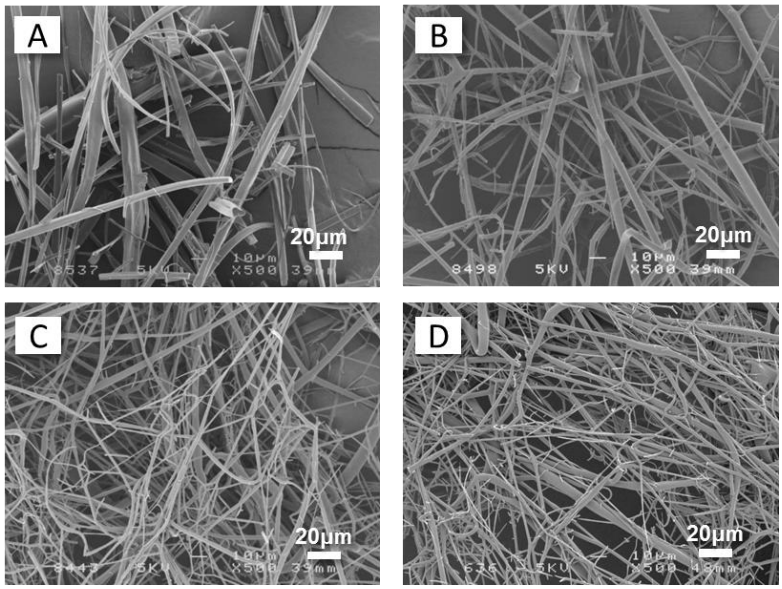

Figure 2. Images of A) electrospun fibers and B) thermostabilized fibers, C) CFs and D) ACFs derived from HAL

EDLC assembly and electrochemical characterization

EDLC was assembled with the HAL-based CFs or ACFs as electrode materials and cellulosic paper as a separator, which contained $TEAMBF_4$/PC as an organic electrolyte, where a commercial activated charcoal (AC) powder was also used as a reference.

As shown in **Table 1**, the specific electrostatic capacitance measure by GCD and charge transfer impedance (R_{ct}) of ACF based EDLC were 25.1 F/g and 37.2 Ω, respectively. These electrochemical properties were remarkably superior to those of EDLC assembled with AC powder. The excellent performance would probably be attributed to the large specific surface area of ACFs. However, these values were quite low, compared to those of EDLC previously reported [7]. By the addition of CB, EDLC performance was drastically improved; R_{ct} of ACF-CB based EDLC was decreased to 12 Ω and the capacitance was remarkably increased to 133.3 F/g, which was comparable to those reported in the previous work[6].

Table 1. The electrochemical properties of EDLC assembled from different electrode materials.

Sample	Specific capacitance[1)] (F/g)	Specific capacitance[2)] (F/g)	Charge transfer resistance (Ω)
AC powder	-	0.1	>4000
AC powder-CB	74.8	90.9	2.4
HAL-ACF	27.9	25.1	37.2
HAL-ACF-CB	142.0	133.3	12.0

1) Specific capacitance was obtained by cyclic voltammetry
2) Specific capacitance was obtained by galvanostatic charge and discharge method.

IV. CONCLUSIONS

Fine lignin fibers were successfully prepared by electrospinng. The thermostabilization time of the fibers was remarkably shortened from 38 h to 3 h by the addition of hexamine to spinning dope. The thermostabilized fibers was easily converted to CFs with a high specific surface area (1287 m^2/g), which was comparable to that of commercial AC powder, by the simple carbonization. Furthermore, the CFs were, in turn, converted into ACFs with a thin diameter of 1.42 μm and a significant specific surface area (2185 m^2/g) by steam activation. The EDLC assembled with HAL-based ACFs, CB and organic electrolyte demostrated superior electrochemical properties, in terms of its large specific capacitance and low inpedance, to that with commercial AC powder. Therefore, lignin-based ACFs can be a promising electrode material for preparing EDLC.

V. ACKNOWLEDGEMENT

This work was supported by a grant from the Ministry of Agriculture, Forestry and Fisheries of Japan, "Development of Technologies for Biofuel Production Systems in Rural Areas (2012-2015)".

VI. REFERENCES

[1] Mathiasson, A.; Kubat, D. G. Lignin as Binder in Particle Boards Using High-Frequency Heating - Properties and Modulus Calculations. *Holz Als Roh-Und Werkstoff*, **1994**, *52*, 9-18.

[2] Calvo-Flores, F. G.; Dobado, J. A. Lignin as renewable raw material. *ChemSusChem*, **2010**, *3*, 1227-35.

[3] Uraki, Y.; Nakatani, A.; Kubo, S.; Sano, Y. Preparation of activated carbon fibers with large specific surface area from softwood acetic acid lignin. *J Wood Sci*, **2001**, *47*, 465-469.

[4] Inagaki, M.; Konno, H.; Tanaike, O. Carbon materials for electrochemical capacitors. *Journal of Power Sources*, **2010**, *195*, 7880-7903.

[5] Simon, P.; Gogotsi, Y. Materials for electrochemical capacitors. *Nat Mater*, **2008**, *7*, 845-854.

[6] Wang, G.; Zhang, L.; Zhang, J. A review of electrode materials for electrochemical supercapacitors. *Chemical Society Reviews*, **2012**, *41*, 797-828.

[7] Zhang, L. L.; Zhao, X. S. Carbon-based materials as supercapacitor electrodes. *Chem Soc Rev*, **2009**, *38*, 2520-2531.

[8] Uraki, Y.; Kubo, S.; Nigo, N.; Sano, Y.; Sasaya, T. Preparation of Carbon Fibers from Organosolv Lignin Obtained by Aqueous Acetic Acid Pulping. *Holzforschung*, **1995**, *49*, 343-350.

POTENTIAL OF RAPESEED STEMS AS AN ALTERNATIVE RAW MATERIAL FOR PAPERMAKING PURPOSES

Roberto Aguado[1]*, Ana Moral[2], Ana Pérez[2], Mª Concepción Monte[1], Antonio Tijero[1]

*[1]Grupo de Celulosa y Papel, Chemical Engineering Dpt., Faculty of Chemistry, Complutense University of Madrid, 28040 Madrid, Spain (*e-mail: rjagarcia@ucm.es);*
[2]Chemical Engineering Dpt., Experimental Sciences Faculty, Pablo de Olavide University of Seville, 41013 Seville, Spain.

ABSTRACT

While wood is still the conventional raw material to manufacture any pulp for papermaking purposes, the use of non-wood fibres is a great source of interest for papermakers and researchers. This can be explained by the demand of certain countries where wood is a scarce resource, the search of new properties, and the decrease of environmental impact.
Cereal straw, bamboo and bagasse are the most used non-wood raw materials, but work is being done towards the characterization of other interesting sources of fibres. Agricultural wastes from rapeseed crops fit that requirement. Rapeseed oil production for energetic purposes is increasing, and so are wastes.
Non-wood materials allow for an effective use of sulphur-free methods that usually result in weaker pulps when applied to wood -e.g., the soda-anthraquinone cooking process is being industrially used to cook straw. Organosolv pulping is another alternative method that removes lignin and achieves higher yield values than other chemical processes.
In this work, pulps from *Brassica napus* (rapeseed) stems were obtained by soda-anthraquinone and Organosolv (using ethanolamine) pulping. Both pulps were refined in a PFI mill. Handsheets made from those pulps were tested. The aim of this work is to evaluate the capabilities of rapeseed stems for papermaking purposes and the influence of refining on mechanical properties.

I. INTRODUCTION

Non-woody wastes from agriculture work in three ways to reduce environmental impact. First, by re-using as raw materials residues which otherwise would be open-burnt –a hazardous activity which causes air pollution. Regarding the pulping process, non-wood materials allow for a satisfying use of sulphur-free methods, such as the SAICA's semichemical process cooking [1]. Finally, this may result in energy savings, as many nonwood species need less energy consumption in the refining process, or do not even require refining al all [2].

European Union is the largest rapeseed (*Brassica napus*) producer in the world. 21.1 million tonnes are produced annually by the Union members, out of a worldwide production of 60 million tonnes. Still, the EU is also the greatest consumer, as 2.2 million tonnes are imported annually and only 0.1 million tonnes are exported [3]. Rapeseed main products are oil, used as a lubricant in industrial applications and for human consumption, and meal for animal feeding. Rapeseed oil is being studied as an interesting source for biodiesel production [4], and as a source of polyacids to manufacture biocomposites. As rapeseed crops for energetic purposes are expected to keep increasing their presence in Europe, greater amounts of waste will be likely generated [5].

Potential of rapeseed wastes for papermaking has already been studied by Mousavi et al. [6], as they analysed rapeseed straw and its papermaking potential. Soda-anthraquinone pulping showed better results than soda alone. Tofanica et al. [7] characterised rapeseed stalk fibres, and found them to be very slender, with length ranging from 0.71 to 1.99 mm, and width from 9.10 to 19.60 μm.

The ancient soda pulping method was relegated in benefit of the kraft process, but the addition of anthraquinone as a homogenous catalyst has made it a competitive technique, as Holton [8] showed, and it seems to be especially competitive for annual plants [9]. If the cooking reagent is an organic solvent, such as methanol or ethanolamine, pulping is called Organosolv. Despite its higher energy consumption, it allows for higher yield values and lignin recovery [10].

In this work, chemical pulps from *Brassica napus* stems were obtained through minimal environmental impact techniques (soda-anthraquinone cooking, ethanolamine cooking), in order to investigate the papermaking

characteristics of rapeseed stems waste. This work aims to evaluate the potential application of rapeseed stems for papermaking purposes, and to discuss the influence of cooking conditions and refining.

II. EXPERIMENTAL

Pulping

Specimens of rapeseed (*Brassica napus*) were grown in Castilla y León, Spain, and stems of all diameters were harvested as raw materials for pulping. Stems were isolated, crushed, and introduced into a stainless steel batch digester. Cooking took place by using two different solvents: monoethanolamine (Organosolv pulping) and sodium hydroxide. In the latter's case, anthraquinone was added to increase selectivity towards lignin. Liquor-to-solid ratio was held at 6. Pulps were crushed, washed, screened and stored at 4 ºC. Remaining lignin was analysed following TAPPI standard UM 246 (Microkappa number).

Refining

Prior to refining, pulps were disintegrated by means of a lab disintegrator ENJO model 692 according to ISO 5263. Pulp refining was carried out by a Maskin's Mark VI PFI mill at 10% consistency according to ISO 5264/2.

The degree of refining was measured using a Canadian Standard Freeness (CSF) tester, following TAPPI standard T227 om-94.

Handsheets

Seven handsheets were obtained from each of the pulps according to ISO 5269-1:1998. The experimental equipment consisted of a pulp dispersing-disintegrator, handsheet former, pressing (130 kPa), and heating system to remove moisture. Brightness was determined according to ISO 2470-1:2009. Stretch and tensile index of handsheets were measured by means of a mechanical tester from HT Hounsfield following UNE 57054 and UNE-EN ISO 1924-2:2009 standards, respectively. Tear index was determined by a MESSMER tester according to UNE-EN 21974:1996. Burst strength was measured by a METROTEC tester according to UNE-EN ISO 2758:2004.

III. RESULTS AND DISCUSSION

Table 1 shows the different conditions in which rapeseed stems were cooked. Reagent specifications refer to the cooking liquor in Organosolv pulping, and to the pure reagent weight for soda-anthraquinone pulping. Yield is expressed as the weight of oven dried pulp obtained per weight of oven dried stems. Kappa number (Microkappa) and ISO brightness are shown too.

Table 2 shows the mechanical properties of the sheets for different numbers of revolutions. Relative standard deviation was never higher than 10%.

Influence of cooking conditions

Mild treatments, at 140 ºC and after 40 minutes of cooking, resulted in higher yields, especially for Organosolv pulp. However, only severe cooking provides enough removal of lignin to make feasibly-bleachable pulps, as it achieves Kappa numbers around 30.

Table 1. Pulping conditions and properties. T: cooking temperature. t: cooking time. AQ: anthraquinone.

Pulp code	Reagent	T (ºC)	t (min)	Yield (%)	Kappa no.	Brightness (%ISO)
ETN40	40% ethanolamine, 60% water	140	40	77.6	46.4	59,1
ETN60	60% ethanolamine, 40% water	180	60	58.7	30.9	62,2
SAQ10	10% NaOH, 0.1% AQ on o.d. pulp*	140	40	69	48.1	59,5
SAQ20	20% NaOH, 0.1% AQ on o.d. pulp*	180	60	54.5	29	62,0

*On the basis of oven dried pulp weight.

Table 2. Influence of refining on mechanical properties.

Pulp	PFI revolutions	Tear index (mN m^2/g)	Stretch (%)	Burst index (kN/g)	Tensile index (N m/g)
ETN40	0	11.1	0.59	0.84	7.5
	250	13.3	0.70	0.97	14.2
	500	15.0	0.45	1.45	16.2
	1000	17.6	0.83	1.87	18.1
ETN60	0	11.5	0.40	0.84	10.2
	250	13.9	0.92	1.53	22.9
	500	14.2	1.73	4.87	45.8
	1000	15.2	1.29	5.14	47.5
SAQ10	0	4.6	0.35	0.73	8.2
	250	12.6	0.59	1.25	12.9
	500	17.8	1.08	1.52	17.2
	1000	19.9	1.19	2.18	26.6
SAQ20	0	14.0	0.39	0.72	9.5
	250	20.1	0.59	1.62	17.1
	500	21.8	1.43	2.12	19.8
	1000	19.5	1.26	3.70	38.5

Unbleached pulps from rapeseed stems showed high values of brightness (around 60%), even under mild conditions. ISO brightness of rapeseed straw pulps lies around 16-18% [6]. Unbleached rice straw kraft pulps, Alfa soda pulps and *Eucalyptus citridiora* kraft pulps show brightness values of 45-50% [11], 47% [12] and 15-20% [13], respectively.

Severe cooking (i.e., high values of temperature, reagent concentration and cooking time) gave out higher burst index and tensile index. These values were particularly high for Organosolv pulp.

Influence of refining

Figure 1 presents the degree of refining, expressed as Canadian Standard Freeness, for the different pulps. For all pulps, 1,000 PFI revolutions were enough to achieve freeness values below 350 mL. Hardwood kraft pulps need around 3,000 PFI revolutions to get to such degree of refining, and softwood kraft pulps need more than 5,000 PFI revolutions [14]. Therefore, the use of rapeseed stems implies great energetic savings at this stage. Pulp ETN60 was found to be the most influenced by refining.

Tear index was slightly improved by refining. Tensile index and burst index were greatly increased from non-refined pulps to 1,000 PFI revolutions. Overall, stretch is in the low range. Burst index was found to be similar to that of rice straw pulps [11]. Tear index is in the high range (Table 2), similar to that of soda pulps from abaca [15].

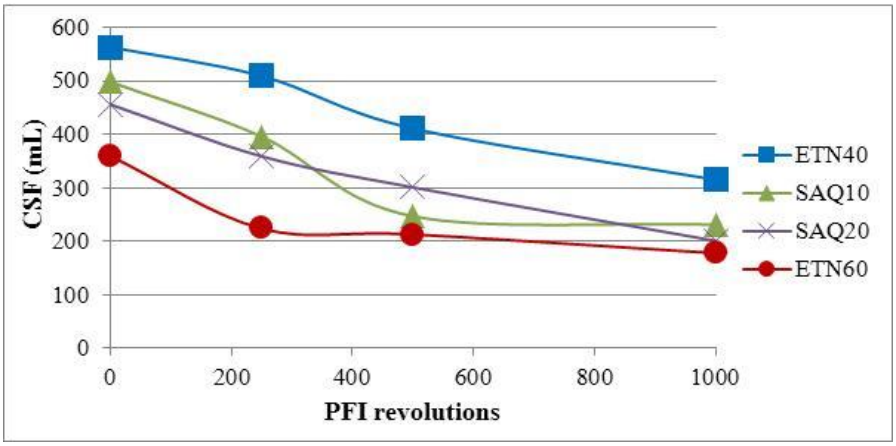

Figure 1. Variation of Canadian Standard Freeness with the number of PFI revolutions.

IV. CONCLUSIONS

Comparing brightness and mechanical properties of pulps from rapeseed stems with pulps of rapeseed straw, rice straw and common hardwoods, it comes out that rapeseed stems are an effective source of fibres to produce market pulp and/or paper. Sheets from the pulps studied showed high brightness values and high tear index. Mechanical properties were notoriously improved by refining.

Organosolv pulping under severe conditions is recommended, as it is the way to achieve low freeness values with little energetic consumption during refining. Moreover, it results in the highest tear index and burst index.

V. ACKNOWLEDGEMENT

The authors wish to acknowledge the Ministry of Science and Innovation of Spain for the financial support of the Project CTQ2010-21660-C03-01 in which the present study is framed**.**

VI. REFERENCES

[1] Delgado, M.; Escudero, E. Chapter 18: The SAICA process. In: Becker, J., editor, *Small Pulp and Paper Mills in Developed Countries*. *Concept Publishing Company*. India **1991**, 214–222.

[2] Stoica, D.E.; Tofanica, B.M.; Gavrilescu, D. Considerations on refining of nonwood pulps. *Celul. Hirtie*. **2010**, *59*, 10–15.

[3] FEDIOL. <http://www.fediol.eu/web/rapeseed/1011306087/list1187970106/f1.html> (Last time consulted on March 25, 2014.)

[4] Abo El-Enin, S.A.; Attia, N.K.; El-Ibiari, N.N.; El-Diwani, G.I.; El-Khatib, K.M. In-situ transesterification of rapeseed and cost indicators for biodiesel production. *Renew. Sust. Energ. Rev.* **2013**, *18*, 471–477.

[5] Bueno-Ferrer, C.; Hablot, E.; Garrigós, M.C.; Bocchini, S.; Averous, L.; Jiménez, A. Relationship between morphology, properties and degradation parameters of novative biobased thermoplastic polyurethantes obtained from dimer fatty acids. *Polym. Degrad. Stabil*. **2012**, *97*, 1964–1969.

[6] Mousavi, S.M.M.; Hosseini, S.Z.; Resalati, H.; Mahdavi, S.; Garmaroody, E.R. Papermaking potential of rapeseed straw, a new agricultural-based fiber source. *J. Clean. Prod*. **2013**, *52*, 420–424.

[7] Tofanica, B.M.; Cappelletto, E.; Gavrilescu, D.; Mueller, K. Properties of Rapeseed (Brassica napus) Stalks Fibers. *J. Nat. Fibers*. **2011**, *8(4)*, 241–262.

[8] Holton, H. Soda additive softwood pulping: A major new process. *Pulp Paper Can*. **1977**, *78(10)*, 1–4.

[9] Rodríguez, A.; Serrano, L.; Moral, A.; Jiménez, L. Pulping of rice straw with high-boiling point organosolv solvents. *Biochem. Eng. J*. **2008**, *42(3)*, 243–247.

[10] Torre, M.J.; Moral, A.; Hernández, M.D.; Cabeza, E.; Tijero, A. Organosolv lignin for biofuel. *Ind. Crop. Prod*. **2013**, *45*, 58–63.

[11] Rodríguez, A.; Moral, A.; Serrano, L.; Labidi, J.; Jiménez, L. Rice straw pulp obtained by using various methods. *Biores. Technol*. **2008**, *99*, 2881–2886.

[12] Marrakchi, Z.; Khiari, R.; Oueslati, H.; Mauret, E.; Mhenni, F. Pulping and papermaking properties of Tunisian Alfa stems (Stipa tenacissima) – Effects of refining process, *Ind. Crop. Prod*. **2011**, 34 (3), 1572-1582.

[13] Khristova, P.; Kordsachia, O.; Patt, R.; Dafaalla, S. Alkaline pulping of some eucalypts from Sudan. *Biores. Technol*. **2006**, *97*, 535–544.

[14] Banavath, H.N.; Bhardwaj, N.K.; Ray, A.K. A comparative study of the effect of refining on charge of various pulps. *Biores. Technol*. **2008**, *102*, 4544-4551.

[15] Jiménez, L.; Ramos, E.; Rodríguez, A.; De la Torre, M.J.; Ferrer, J.L. Optimization of pulping conditions of abaca. An alternative raw material for producing cellulose pulp. *Biores. Technol*. **2005**, *96*, 977–983.

THE INFLUENCE OF VARIOUS PULP PROPERTIES ON THE ENZYMATIC HYDROLYZABILITY

Fredrik Aldaeus[1]*, Karolina Larsson[1], Jasna Stevanic Srndovic[1], Mikaela Kubat[1], Katarina Karlström[1], Ausra Peciulyte[2], Lisbeth Olsson[2], Per Tomas Larsson[1]

*[1]Innventia AB, Box 5604, SE-114 86 Stockholm, Sweden; [2]Chalmers University of Technology, Kemivägen 10, SE-412 58 Göteborg, Sweden (*fredrik.aldaeus@innventia.com)*

ABSTRACT

The enzymatic hydrolyzability of three industrial pulps, five pulps produced by Innventia AB (Stockholm, Sweden), and one microcrystalline cellulose powder was assessed using commercially available enzymes. In addition, the chemical, macromolecular and supramolecular properties of the samples were also determined. Multivariate evaluation revealed that the initial rate for conversion of cellulose to glucose was mainly dependent on specific surface area, glucose content, and fiber saturation point, whereas the conversion at 24 h and 72 h depended on fiber saturation point, specific surface area, and average pore size. Neither the crystallinity nor the lignin content had significant effects on the conversion for the selected pulps (kappa number <19).

I. INTRODUCTION

Conversion of biomass to biofuels is currently an area that attracts large interest, and lignocellulosic biomass offers the abundance and environmental sustainability attributes that can potentially support large-scale biofuel production as an alternative to petroleum-based transportation fuel.

In a recent project, Innventia has developed wood based pulps optimized for conversion to biofuels. These pulps were produced to target a high level of enzymatic hydrolyzability. To assess the hydrolyzability of these pulps, a laboratory protocol has been established using an enzyme mixture containing Celluclast 1.5L® and Novozyme 188® with an activity of 2,5 FPU/g pulp [1]. The results obtained using the recently developed protocol are assumed to be representative for industrial conditions. In addition to assessment of the pulps produced at Innventia AB, the results have been compared to commercial cellulose substrates and pulps of both paper and dissolving grade.

In the present study, the influence of chemical, macromolecular and supramolecular properties of pulp on the enzymatic hydrolyzability is discussed.

II. EXPERIMENTAL

Three industrial pulps and five laboratory pulps produced by Innventia AB (Stockholm, Sweden) were evaluated in the present study. The set of pulps included softwood (spruce/pine) and hardwood (birch and eucalyptus) pulps, sulphite, kraft and soda pulps, as well as dried and never-dried pulps. In addition, microcrystalline cellulose powder Avicel® sample was of the type PH 101 (FMC BioPolymer, USA) was added for comparison of the hydrolyzability. The samples are outlined in **Table 1**.

The kappa numbers were determined according to ISO 302. Limiting viscosities (limiting viscosity number in cupri-ethylenediamine (CED) solution) were determined according to ISO 5351. Carbohydrate compositions were determined according to SCAN-CM 71:09 using high performance anion exchange chromatograph Dionex ISC-5000 system coupled to a CarboPac PA1 (250 mm × 4 mm i.d.) column (Dionex, Sweden) and a pulsed amperometric detector (HPAEC-PAD).

The molecular mass distributions (expressed as peak molecular mass, M_p, number-average molecular mass, M_n, weight-average molecular mass, M_w, and polydispersity PD) were determined by size exclusion chromatography of cellulose tricarbanilates with tetrahydrofuran mobile phase [2, 3].

The supramolecular properties specific surface area and crystallinity were determined in the water-swollen state by an in-house method utilizing solid-state cross polarization magic angle spinning carbon-13 nuclear magnetic resonance (CP/MAS ^{13}C-NMR) [4]. Average pore size was determined from the NMR results combined with fiber saturation point (FSP) measurements. FSP measurement is not applicable to Avicel due to the lack of a

pore system, and hence an equivalent FSP was approximated from water retention value by division with a factor 2, which corresponds to an average correction factor [4]. ,

Table 1. Wood source, pulping and bleaching conditions, drying and source of the samples used in this study.

Designation	Wood source	Pulping and bleaching	Drying	Source
Avicel	unknown	Hydrolysis (microcrystalline cellulose)	Dried	Commercial
HKD	Hardwood (birch)	Kraft (TCF-bleached)	Dried	Commercial
HSi	Hardwood (eucalyptus)	Sulphite (dissolving grade)	Never-dried	Commercial
HSiD	Hardwood (eucalyptus)	Sulphite (dissolving grade)	Dried	Commercial
SKOD	Softwood (spruce)	Kraft (pre-hydrolysis, O-delignified)	Dried	Innventia
SSiD	Softwood (spruce)	Sulphite (dissolving grade)	Dried	Commercial
SSoCOD	Softwood (spruce)	Soda (pre-hydrolysis, circ. dig., O-delig.)	Dried	Innventia
SSoD	Softwood (spruce)	Soda (pre-hydrolysis)	Dried	Innventia
SSoO	Softwood (spruce)	Soda (pre-hydrolysis, O-delignified)	Never-dried	Innventia
SSoOD	Softwood (spruce)	Soda (pre-hydrolysis, O-delignified)	Dried	Innventia

The enzymatic hydrolyzability of the pulps was assessed using the commercially available enzyme mixtures Celluclast1.5L (Sigma-Aldrich, Sweden) and Novozyme 188 (Novozymes, Denmark) in proportions 3:1 (vol:vol). After dilution, the activity in FPU was determined according to NREL/TP-510-42628 “Measurement of Cellulase Activities”. 10 mg of sample (dry basis) was allowed to swell in 0.5 ml acetate buffer (100 mM, pH 4.8) at 50 °C for 1 h. 0.5 ml of diluted enzyme mixture was added. The dilution of the enzyme mixture was done to obtain an activity of 2.5 FPU/g cellulose (corresponds approximately to 0.16 ml undiluted enzyme mixture per g cellulose). The sample was hydrolyzed for 72 h at 50 °C. The enzymes were deactivated by addition of 200 µl 1 M NaOH, and the sample suspensions were filtered through a 0.2 µm cellulose acetate filter. The glucose content in the filtrates was determined using high performance anion exchange coupled to a pulsed amperometric detector (HPAEC-PAD). The conversion (mg g^{-1}) is defined as amount of glucose in hydrolysate (as mg anhydroglucose) per total amount of glucose in sample subjected to hydrolysis (in g, corrected for dry substance). Conversion rate (mg g^{-1} min^{-1}) is defined as conversion per time unit. In the present study, the initial conversion rate was determined at 10 minutes, since it was observed that the rate during the first minutes of the hydrolysis was lower than at 10 minutes.

A multivariate evaluation of the pulp properties [5] – using the initial conversion rate, the conversion at 24, and the conversion 72 h as responses – was performed using the software SIMCA-P+ 12.0.1 (Umetrics AB, Umeå, Sweden).

III. RESULTS AND DISCUSSION

The measured pulp properties are described in **Table 2**. The never-dried samples (HSi and SSoO) had the highest initial conversion rates. It could however be observed that there was not a very pronounced correlation between initial conversion rate and final conversion.

In order to elucidate the relationships between the properties of the pulps, a multivariate model was constructed using principal component analysis (PCA) with two components. A loadings bi-plot (with samples and properties in the same plot) is presented in **Figure 1**. Certain parameters clustered together. As expected, there was a correlation between limiting viscosity and molar mass distribution, as well as between kappa number and total lignin content. No correlation between crystallinity and the other properties was seen. The carbohydrate content parameters were found in the same quadrant as the supramolecular properties. The initial conversion rate and the conversions at 24 h and 72 h were in the PCA plot nearest the fiber saturation point specific surface area.

To further evaluate which properties that had the greatest impact on the conversion, partial least-squares (PLS) models using two principal components were constructed with the response variables Conversion rate at 10 minutes (R^2y_{cum} = 0.81), Conversion at 24 h (R^2y_{cum} = 0.75), and Conversion at 72 h (R^2y_{cum} = 0.75). In these models, the properties limiting viscosity, Mp, Mn and PD were omitted due to the similarities with Mw, and kappa number was omitted due to the similarity with total lignin content.

Table 2. Supramolecular, macromolecular and chemical properties of the samples and results from enzymatic hydrolysis of the samples (initial conversion rate, and conversion at 24 h and 72 h of hydrolysis). n.d. = not determined

Property	**Desig.**	**Avicel**	**Hardwood pulps**			**Softwood pulps**					
			HKD	**HSi**	**HSiD**	**SKOD**	**SSiD**	**SSoCOD**	**SSoD**	**SSoO**	**SSoOD**
Fiber saturation point (g g^{-1})	FSP	0.86	0.72	1.05	0.68	0.69	0.59	0.63	0.60	1.33	0.57
Specific surface area (m^2 g^{-1})	SSA	109	77	152	114	120	98	115	127	130	121
Crystallinity (%)	Cry	58	51	52	53	58	56	57	57	57	57
Average pore size (nm)	Por	16	19	14	12	12	12	11	10	21	10
Kappa number	Kap	n.d.	n.d.	n.d.	n.d.	9.8	n.d.	1.2	18.4	1.5	1.5
Limiting viscosity (ml g^{-1})	Vis	120	540	610	610	1020	760	190	320	260	260
Peak molecular mass (kg mol^{-1})	Mp	36	232	150	150	242	212	55	93	73	71
Number-average molecular mass (kg mol^{-1})	Mn	15	31	23	23	32	25	22	24	25	26
Weight-average molecular mass (kg mol^{-1})	Mw	56	531	339	339	922	448	80	153	116	118
Polydispersity	PD	4	17	15	15	29	18	4	7	5	5
Glucose content (mg g^{-1})	Glc	877	670	943	943	824	923	899	852	898	934
Total carboh. content (mg g^{-1})	CH	927	885	962	962	887	955	921	873	919	954
Total lignin content (mg g^{-1})	Lig	n.d.	n.d.	n.d.	n.d.	19	n.d.	7	36	7	5
Initial conversion rate, 10 min (mg g^{-1} min^{-1})	r10	0.36	0.25	0.75	0.52	0.51	0.50	0.58	0.53	0.84	0.59
Conversion, 24 h (mg g^{-1})	Y24	154	114	279	88	126	136	237	129	441	234
Conversion, 72h (mg g^{-1})	Y72	252	215	585	157	186	192	423	150	697	387

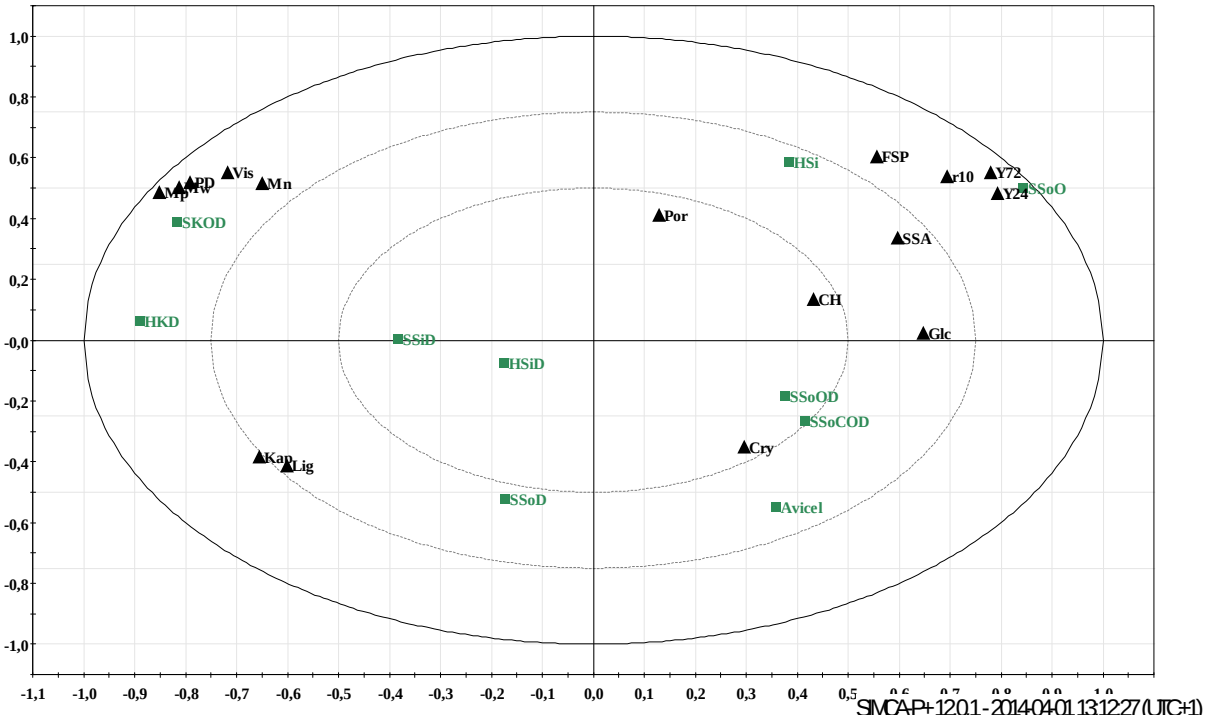

Figure 1. Loadings bi-plot of principal component analysis. Designations as in **Table 1–2**.

For the initial conversion rate, ranking of the parameters in order of importance – with decreasing importance to the right – according to the PLS analysis was:

> Specific surface area > Glucose content > Fiber saturation point > Total carbohydrate content > Weight-average molecular mass (higher conversion rate for lower molecular mass) > Total lignin content > Crystallinity > Average pore size

The effect on initial conversion rate by the specific surface area, glucose content, fiber saturation point, and total carbohydrate content parameters were significant.

A similar ranking for the conversion at 24 h and 72 h was:

> Fiber saturation point > Specific surface area > Average pore size > Weight-average molecular mass (higher conversion rate for lower molecular mass) > Glucose content > Total carbohydrate content > Total lignin content > Crystallinity

The effect by the fiber saturation point, specific surface area, and average pore size parameters were significant on conversion at both 24 h and 72 h. In addition, the effect of weight-average molecular mass was significant on conversion at 24 h, and the effect of glucose content was significant on conversion at 72 h.

The glucose content had a significant effect on the hydrolyzability, despite the conversion numbers were corrected for cellulose content. A reason for this might be that high glucose content corresponds to low hemicellulose contents, and that high abundance of hemicelluloses decrease the conversion rate when using the protocol suggested in this study. The lignin content at the levels of the pulps included in this study (kappa number < 19) was not inhibiting the hydrolysis.

The crystallinity did not have a significant effect on the conversion. The samples included in this study had similar crystallinity, but nevertheless very different hydrolyzability.

From the above results, it can be observed that the supramolecular properties – fiber saturation point, specific surface area, and average pore size – seem to have the greatest influence on the hydrolyzability.

IV. CONCLUSIONS

In conclusion, it seems that the most important factor influencing the hydrolyzability is the supramolecular structure. If producing pulps intended for enzymatic degradation to sugar, the most important consideration should be maintain a high specific surface area and fiber saturation point, i.e. to avoid hornification.

V. ACKNOWLEDGEMENT

Chalmers Energy Initiative is gratefully acknowledged for financial support.

VI. REFERENCES

[1] Andersen, N. *Enzymatic hydrolysis of cellulose – Experimental and modeling studies* **2007**. Doctoral thesis, Biocetrum-DTU, Technical University of Denmark, Denmark.

[2] Kihlman, M.; Aldaeus, F.; Chedid, F.; Germgård, U. Effect of various pulp properties on the solubility of cellulose in sodium hydroxide solutions, *Holzforschung* **2012**, *66*, 601–606.

[3] Drechsler, U.; Radosta, S.; Waltraud Vorwerg, W. Characterization of cellulose in solvent mixtures with N-methylmorpholine-N-oxide by static light scattering, *Macromol. Chem. Phys.* **2000**, *201*, 2023–2030.

[4] Larsson, P.T.; Svensson, A.; Wågberg, L. A new, robust method for measuring average fibre wall pore sizes in cellulose I rich plant fibre walls, *Cellulose* **2013**, *20*, 623–631.

[5] Strunk, P., Eliasson, B., Hägglund, C. and Agnemo, R. The influence of properties in cellulose pulps on the reactivity in viscose manufacturing. *Nord. Pulp Pap. Res. J.* **2011**, *26*, 81–89.

OBTAINMENT OF HEMICELLULOSE DERIVATIVES AND CELLULOSE PULP FROM WHEAT STRAW FOLLOWING COLD ALKALINE EXTRACTION

Alfaro, A.[1]*, García, M.T.[2], García, J.C.[1], Díaz, M.J.[1], Loaiza, J.M. 1, López, F.[1]

*[1]PRO2TEC-Chemical Engineering Department.Campus "El Carmen".University of Huelva, Av. 3 de marzo s/n, 2107, Huelva, Spain; [2]Agrifood Campus of International Excellence (CeiA3).Parque Huelva Empresarial. 21007, Huelva. (*ascension.alfaro@uhu.es)*

ABSTRACT

Wheat straw is an important agricultural residue. It can be used for pulp, paper and chemicals obtention in a framework of biorefinery.
In this work, we addressed the integral exploitation of wheat straw by fractionation of its lignocellulosic components following extraction of hemicelluloses by cold alkaline extraction. The treatment provided a liquid fraction that was used to obtain hemicelluloses by alcoholic precipitation and a solid fraction employed to obtain cellulose pulp by soda–anthraquinone delignification.
The proposed processing scheme is environmentally friendly because it uses cold alkaline extraction to valorize the hemicellulose fraction of wheat straw while facilitating its delignification, which can thus be accomplished under milder conditions. This saves raw material and energy, and provides paper sheets similarly strong to those obtained from untreated cellulose.

I. INTRODUCTION

The amount of wheat produced in Europe each year, which is estimated to exceed 170 million tons, is more than enough for use as a renewable raw material to obtain lignocelluloses chemical derivatives with biorefining technology [1]. Also, the use of crop residues in a biorefinery saves GHG emissions and reduces fossil energy demand [2].

One of the prerequisites of an effective utilization of biomass such as cereal straws and grasses is the fractionation of the main components, polysaccharides and lignin, by a relatively mild procedure, ensuring their minimum physical and chemical changes as well as an acceptable extraction efficiency [3]. Different treatments have been applied to hemicellulose extraction with addition of chemicals such as alkali, acid or hydrogen peroxide, liquid hot water extraction, steam explosion, dilute acid-steam explosion inter alia [4]. Alkaline extraction proved an appropriate pretreatment towards the obtainment of cellulose pulp [5]. The integration of hemicelluloses pre-extraction by alkaline methods into a soda-AQ-based pulping with bagasse as feedstock, was preferred over other pretreatments (dilute acid, hot water treatment) previous kraf pulping processing [6]. Main advantage of these processes is the use of low temperature and pressure [7].
The hemicelluloses obtained can be used to convert them to higher value-added products such as prebiotic xylooligosaccharides or polymers and molecules for chemical and pharmaceutical applications, as natural barriers for packaging films and also in the production of bioethanol, plastics, cellulose pulp and additives [4].

The solid fraction provided by the pretreatment can be used to obtain cellulose pulp by alkaline delignification with a soda–anthraquinone mixture. Soda semichemical process has important environmental and economic advantages in comparation with kraft process. Soda process is a sulfur free process, it is suitable for byproducts obtention, it is a more easy process than conventional schemes and the recovery of chemicals is possible. Then, the mills could have a more little production capacity [8-9].

II. EXPERIMENTAL

Raw material analysis

Wheat straw biomass was obtained on a plantation in Huelva (southwestern Spain). The raw material was analyzed for the following parameters: hot water solubles (TAPPI T 207 cm-93), 1% NaOH solubles (TAPPI T 212 om-07), extractable ethanol-acetone (TAPPI T 204 cm-97), holocellulose [10], α-cellulose (TAPPI T 203 cm-09) and ashes (TAPPI T 211 om-07). Aliquots from the homogenized wheat straw were subjected to quantitative acid hydrolysis with 5 mL of 72% sulfuric acid for an hour (TAPPI T 248 sp-08), the solid residue was recovered by filtration and considered as klason lignin.

Cold alkaline extraction of hemicellulose

Based on previous studies optimum operation conditions were selected [3]. In this study, a 2^n central composite experimental design for extraction process was carried out. This process develops optimally at a temperature of 40ºC, and operation time of 90 min and an alkali concentration of 100 g L^{-1}.

Uniform lignocellulosic material chips were immersed in a thermostated bath and stirred at 5 min intervals. The resulting suspension was filtered and the solid washed of water and neutralizes with 2N acetic acid and drying at room temperature. In this solid were determined the hemicellulosic compounds (glucan, xylan and araban) by HPLC techniques, and in the liquid phase also were determined lignin, glucose and hemicellulose content.

The liquid phase from the extraction was adjusted to pH 4.5–5.5 with 37% HCl, supplied with 4 volumes of 95% ethanol and centrifuged at 4500 rpm for 3 min. Then, the hemicellulose precipitate formed was washed with 95% ethanol and freeze-dried.

Experimental design for soda-anthraquinone pulping

To optimize the process of soda-anthraquinone pulping experimental design was applied. The number of test required was 16. Pulping prior cold alkaline extraction was carried out with the following operation conditions, alkali concentration: 2-5-8%, temperature: 110-125-140ºC and cooking time: 60-90-120 min. The anthraquinone concentration was 0.10% by weight and initial liquor/solid ratio of 8/1 (dry wt. basis). Pulps were obtained using a 8-L bath cylindrical reactor. After completation of the treatment, the reactor was cooled, and the pulp was separated from the liquor and washed in a bag of 0.1 mm mesh.

Pulp characterization experiments involved the following parameters: pulp yield (TAPPI T-257), kappa number (TAPPI T-236), holocellulose [10], α-cellulose (TAPPI T 203 cm-09) and klason lignin. Paper sheets were obtained using an ENJO-F-39.71 sheet former according to TAPPI T 205 sp-06. The resulting paper sheets were analyzed for tensile index (TAPPI T-494 om-96), burst index (TAPPI T-403 om-97) and tear index (TAPPI T-414 om-98).

III. RESULTS AND DISCUSSION

Chemical properties of the raw material

Wheat straw, which contains more than 34% hemicellulose and less than 19% lignin, can provide an effective raw material for the selective separation of the hemicelluloses fraction. Hemicelluloses content is similar to others residues like *Arundo donax* "reed" (29.7%) and *Helianthus annus* "sunflower stalks" (40.4%) and higher than hemicelluloses content in trees like *Eucalyptus globulus* "eucalyptus" (20.1%). α-cellulose in wheat straw (31.05%) is lower than eucalyptus (46.8%). Eucalyptus is a tree very used in Spain for pulp and paper making [9].

Cold alkaline extraction of hemicellulose

The total amount of hemicellulose extracted in the liquid phase was 56.1% of that initially present in the raw material, which contained 3.7% glucan. Therefore, the proposed cold alkaline extraction method affords selective extraction of the hemicellulose fraction, in addition to also highly efficient delignification, 59.1% of all lignin present in the raw material was extracted.

Optimization of pulping procedure

With the solid resulting from cold alkaline extraction carried out in optimal conditions, pulping tests have been made listed in **Table 1**. As shown there in, between 31.8 to 42.2% of the initial feedstock can be transformed into cellulose pulp. These yields are similar to those obtained in non-tree pulps feed stocks such as organosolv pulp with tagasaste without pretreatment with which performances of 42.6% have been achieved [11]. On the other hand, the α-cellulose content is too high in pulps (69.6-98.8%), indicating that there has been low degradation of this component during the alkaline extraction and low Klason lignin content (2-10%). Ethanol-anthraquinone leucaena pulp with hydrothermal pretreatment reached Klason lignin content between 22.6-25.1% [12]. This high delignification will facilitate subsequent bleaching of pulp.

The experimental results were fitted to the following second-order polynomial, where n: number of variables, Y: dependent variables (pulping yield, total yield, kappa number, hollocellulose, α-cellulose, klason lignin, tensile index, tear index, burst index) and X: independent variables (alkali concentration, temperature, operation time).

According to the mathematical models obtained for each of the dependent variables analyzed, the most influential dependent variable (Z axis) has been determined and figures have been represented as shown (**Figure 1**).

$$Y = a_o + \sum_{i=1}^{n} b_i X_{ni} + \sum_{i=1}^{n} c_i X_{ni}^2 + \sum_{i=1;\, j=1}^{n} d_i X_{ni} X_{nj} \quad (i < j)$$

Normalized values of alkali concentration (X_C) temperature (X_t) and operation time (X_T)			Pulping Yield (%)	Total Yield (%)	Kappa Number	Holocellulose (%)	α-Cellulose (%)	Klason Lignin (%)
0	0	0	57,0	38,2	13.91	93,6	91,9	2,1
0	0	0	58,2	39,0	13,5	94,0	92,1	2,0
1	1	1	51,6	34,6	6,9	94,2	69,6	2,5
1	1	-1	52,1	34,9	22,5	93,7	86,4	5,5
1	-1	1	48,9	32,8	9,8	97,1	73,7	10,0
1	-1	-1	55,6	37,3	30,6	94,6	88,3	6,4
-1	1	1	54,2	36,3	8,8	91,3	82,6	2,1
-1	1	-1	57,3	38,4	21,8	93,2	88,9	4,0
-1	-1	1	47,4	31,8	10,4	91,5	87,2	8,6
-1	-1	-1	63,0	42,2	27,3	95,7	91,7	6,7
1	0	0	56,1	37,6	14,3	95,5	79,7	5,7
-1	0	0	59,2	39,7	15,2	93,2	86,0	2,7
0	1	0	54,6	36,6	12,4	97,7	97,1	2,1
0	-1	0	55,9	37,5	14,8	99,2	98,8	5,0
0	0	1	54,6	36,6	8,4	89,8	83,3	2,0
0	0	-1	60,5	40,6	23,6	90,4	91,7	3,5

Table 1. Normalized operational conditions and characterization of solid phase pulp after cold alkaline extraction of hemicellulose. The percentages are referred to initial raw material.

Figure 1.A shows that the highest values of tensile index are obtained at low temperatures, high concentrations of alkali and maximum operating times (+1) or minimum (1).With longer operating time, a greater delignification is achieved, higher α-cellulose content and therefore greater resistance. With low operating times, higher resistances are due to cellulose during treatment suffers less degradation. **Figure 1.B** shows that the higher α-cellulose contents are obtained performed the pulping at low temperatures, with intermediate alkali concentrations and times at the ends, though time variation has low influence on the final content of α cellulose.

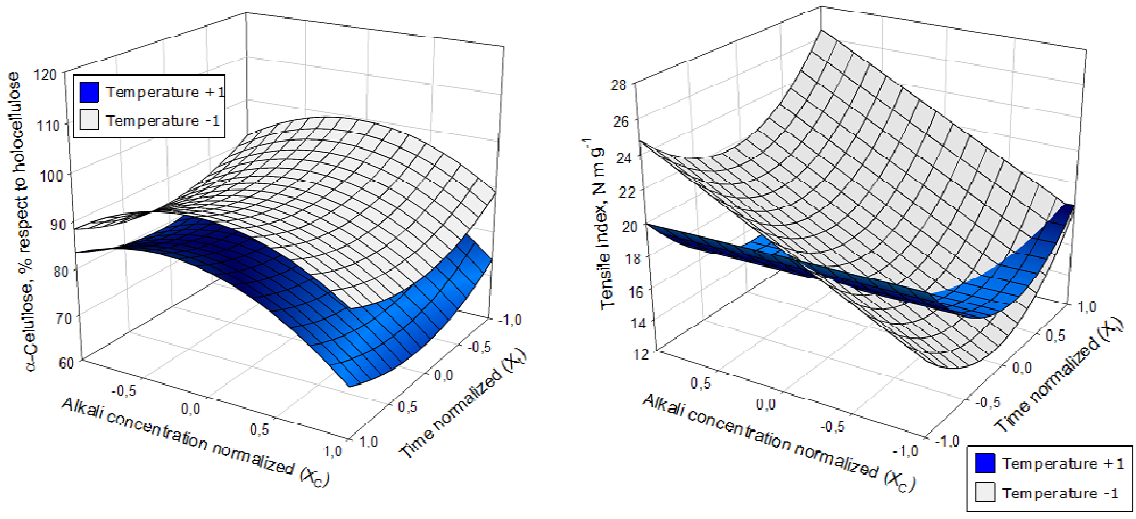

Figure 1.A) α-cellulose of the soda-AQ pulps as function of temperature, alkali concentration and time operation. **B)** Tensile index of the soda-AQ pulps as function of temperature, alkali concentration and time.

Analyzing all the graphics performed (not shown), it concludes that the optimum conditions for the pulping are XT(-0,5) = 117,5ºC , XC(0,5) = 6,5% and Xt(-1) = 60 min, with which it could reach a total cellulose pulp yield of 37.25% of the initial feed stock, with α-cellulose content of 96.99% and leaves with tensile index = 25.64 Nm/g, burst index = 1.68 kPa m^2/g and tear index = 2.63 mN m^2/g. The resistances are lower than those obtained with other agricultural residues such as sunflower stalks without pretreatment [13] and higher than those obtained for tagasaste without pretreatment [14].

IV. CONCLUSIONS

The optimum operating conditions for the cold alkaline extraction of hemicelluloses were applied (temperature: 40ºC, operation time: 90 min and alkali concentration: 100 g/L). These conditions allowed 56.1% of all hemicellulose and 59.1% of all lignin initially present in the raw material to be extracted in the liquid phase.

The solid fraction provided by the pretreatment was used to obtain cellulose pulp by alkaline delignification with a soda–anthraquinone mixture. The process was optimized by using a central composition factor experimental design with alkali concentrations of 2–8%, temperatures of 110–140 ºC and operation times of 60–120 min. The optimum pulping conditions were temperature: 117.5ºC; operation time: 60 min and alkali concentration: 6.5%. The total yield pulp that can be achieved under these conditions was 37.25% with a α-cellulose content of 96.99%. This indicates very little degradation of this component in the previous stage. This method provides paper sheets similarly strong to those obtained from untreated cellulose.

The proposed processing scheme is environmentally friendly because it uses cold alkaline extraction to valorize the hemicellulose fraction of wheat straw while facilitating its delignification, which can thus be accomplished under milder conditions. It can reduce the amount of soda more than 50% with respect to the more usual conditions applied in the soda pulping, working with the minimum operating time.

V. ACKNOWLEDGEMENT

The authors are grateful to Spanish Ministry of Science and Innovation by the “Ramón y Cajal” contract, PhD student grant from Agrifood Campus of International Excellence (CeiA3) and the business group ENCE, S.A. (factory of Huelva). Also they thank to Ministry of Economy, Innovation, Science and Employement of the Junta de Andalucía (Government of Spain), Project number RNM 2323.

VI. REFERENCES

[1] Ruzene, D.S.; Siva, D.P.; Vicente, A.A.; Gonçalves, A.R.; Texeira, J.A. An alternative application to the Portuguese agro-industrial residue: wheat straw. *App. Biochem. Biotechnol.* **2008**, *147*, 85–96.

[2] Cherubini, F.; Ulgiati, S. Crop residues as raw materials for biorefinery systems-A LCA case study. *Appl. Energy.* **2010**, *87*, 47–57.

[3] García, J.C.; Díaz, M.J.; García, M.T.; Feria, M.J.; Gómez, D.M.; López, F. Search for optimum conditions of wheat straw hemicelluloses cold alkaline extraction process. *Biochem. Eng. J.* **2013**, *71*, 127–133.

[4] Brienzo, M.; Siqueira, A.F..; Mialgres, A.M.F. Search for optimum conditions of sugarcane bagasse hemicelluloses extraction. *Biochem. Eng. J.* **2009**, *46*, 199–204.

[5] Huang, H.J.; Ramaswamy, S.; Tschirner, U.W.; Ramarco, B.V. A review of separation technologies in current and future biorefineries. *Sep. Purif. Tecnhol.* **2008**, *62*, 1–21.

[6] Vena, P.F.; García-Aparicio, M.P.,Brienzo, M.; Görgens, J.F.; Rystra, T. Impact of hemicelluloses pre-extraction on pulp properties of sugarcane bagasse. *Cell. Chem. Technol.* **2013**, *47*, 425–441.

[7] Carvalheiro, F.; Duarte, L.C., Gírio, F.M. Hemicellulose biorefineries: a review on biomass pretreatments. *J. Sci. Ind. Res.* **2008**, *67*, 849–864.

[8] Raymond, A.Y., Masood, A. Environmentally Friendly Technologies for the Pulp and Paper Industry. **1997**. Ed. University de Wisconsin. Madison, Wisconsin.

[9] Alfaro, A., F.; Pérez, A., García, J.C.; López, F.; Zamudio, M.A.M.; Rodríguez, A. Ethanol and soda pulp of tagasaste wood: neural fuzzy modeling. *Cell. Chem. Technol*. **2009**, 43, 293–304.

[10] Wise, L.E.; Marphy, M.; D’Adieco, A. Chlorite holocellulose, its fractionation and bearing on summative wood analysis and on studies on the hemicelluloses. *Paper Trade J*. **1946**, 122, 35–43.

[11] Alfaro, A.; Rivera, A.; Pérez, A.; Yánez, R.; García, J.C.; lópez, F. Integral valorization of two legumes by autohydrolysis and organosolv delignification. *Bioresour. Technol*. **2009**, 100, 440–445.

[12] Feria, M.J.; Alfaro, A.; López, F.; Pérez, A.; García, J.C.;Rivera, A. Integral valorization of Leucaena diversifolia by hydrothermal and pulp processing. *Bioresour. Technol.* **2012**, 103, 381–388.

[13] Khristova, P.; Bentcheva, S.; Dafalla, S.; Gabir, S. Soda-anthraquinone pulping of sunflower stalks. *Ind. Crop. Prod.* **1998**, 9, 9–17.

[14] López, F., Alfaro, A., S.; García, M.M.; Díaz, M.J.; Calero, A.M.; Ariza, J. Pulp and paper from Tagasaste (*Chamaecytisus Proliferus* L.F. SSP. Palmensis). *Chem. Eng. Res. Des.* **2004**, 82, 1029–1036.

MONITORING OXIDATION-REDUCTION POTENTIAL OF LACCASE - MEDIATOR SYSTEM: CAN THE EFFICIENCY OF A REDOX MEDIATOR FOR DESLIGNIFYING KENAF PULP BE PREDICTED?

Glòria Andreu[1]*, Teresa Vidal[2]
[1]*Chemical Engineering Department;* [2] *Textile and Paper Engineering Department.*
CELBIOTECH Paper Engineering Research Group.
*Universitat Politècnica de Catalunya-BarcelonaTech. (*gloria.andreu@upc.edu)*

ABSTRACT

The oxidative ability of five phenolic compounds (acetosyringone, syringaldehyde, p-coumaric acid, vanillin and actovanillone) and the laccase–mediator systems was determined by monitoring the oxidation–reduction potential (ORP) during solution oxidation and kenaf lignin oxidation process. The results confirmed the production of phenoxy radicals of variable reactivity and stressed the significant role of lignin structure in the enzymatic process. Although changes in ORP were correlated with the oxidative ability of the mediators, pulp properties determined after the bleaching stage were also influenced by condensation and grafting reactions.

I. INTRODUCTION

The global demand for natural fibers is steadily increasing as well as the demand for cleaner and greener industrial products. Kenaf (Hibiscus cannabinus) is a hard non-wood plant with a fibrous stalk which is resistant to insect damage, adaptable to various types of soil and requiring minimal chemical treatment (typically fertilizer and herbicide applications) to grow effectively. A recent study revealed that the kenaf plant adsorbs approximately 1.5 times its weight in carbon dioxide, which represents the highest level of adsorption among the non-wood plants. This makes it an ideal source of natural fibers for various uses including composite wood, insulation and reinforced materials and paper pulp production.

The use of laccases assisted by redox mediators has aroused much interest for bleaching and fiber functionalization in recent years. One prospective trend in laccase research is screening and identification of low-cost and eco-friendly redox mediators. Natural phenolic compounds (particularly those present in lignin degradation products) have aroused great interest in this respect in recent years [1].

The enzymatic treatment (L stage) described in experimental section was monitored in order to assess changes in the oxidation–reduction potential (ORP) of the system during the oxidation of lignin. This is a key parameter for assessing oxidative power [2] and its monitoring has been deemed a good choice for determining the efficiency of oxidative stress in various processes [3]. This technique may therefore provide an effective predictive tool for selecting enzyme mediators.

II. EXPERIMENTAL

Laccase from *P. cinnabarinus* was supplied by Institut National de la Recherche Agronomique (INRA), Marseille. Unbleached pulp from Chinese kenaf (*H. cannabinus*) obtained by soda–anthraquinone cooking with a kappa number of 12.9 and 35.0% ISO brightness was supplied by CELESA (Tortosa, Spain). The pulp was washed with H_2SO_4 at 3% consistency at pH 2 for 30 min.

Natural phenols

The phenolic compounds used as mediators were acetosyringone, syringaldehyde, p-coumaric acid, vanillin (V) and acetovanillone. They have different functional groups in the aromatic ring as shown in Table 1. These compounds and HBT were all purchased from Sigma–Aldrich (St. Louis, MO, USA).

		Ortho-	Para-
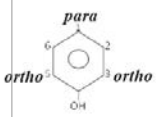	Acetosiyringone (AS)	methoxy (3,5)	ketone
	Syringaldehyde (SA)	methoxy (3,5)	aldehyde
	Acetovanillone (AV)	methoxy (3)	ketone
	Vanillin (V)	methoxy (3)	aldehyde
	p-coumaric Acid (PC)		acid

Table 1. Groups in the ***ortho-*** and para-positions of phenolic compounds assayed as laccase mediators in the delignifying kenaf pulp.

Determination of oxidation–reduction potential (ORP) and ORP ratio

A silver-silver chloride (Ag/AgCl) electrode (Metrohm, Schiedam,The Netherlands) was used as reference electrode. The oxidation-reduction potential was recorded at the enzymatic stage (L), which involved treating 2 g of kenaf pulp at 1% consistency with 20 U/g laccase from *P. cinnabarinus* and a 3% (w/w) concentration of the different phenolic compounds and HBT (all relative to pulp dry weight) in 50 mM tartrate buffer at pH 4.0 in an open reactor at 30 ºC under oxygen saturation. The mediators were added after 500 s and the overall treatment time was 2 h; previously, an identical procedure with 3000 s as processing time was performed in the absence of pulp and the oxidation-reduction potential for laccase, laccase with each phenolic compound and laccase–HBT solutions (20 mmol L^{-1}) recorded. The time sequence of the experiment was as follows: O_2 (under saturation conditions)/laccase (PcL)/mediator, which were added at 500, 1000 and 1200 s, respectively. The ORP ratio was calculated as: ORP ratio = $[(ORP)_t - (ORP)_{t'}]/(ORP)_{t'}$ where $(ORP)_t$ and $(ORP)_{t'}$ are the ORP values measured at time t and that of mediator addition (t´) [4].

After the enzyme treatment, the pulp was filtered and washed with deionized water. Finally, the treated pulp was extracted with 1.5% (w/w) NaOH at 5% consistency at 90 ºC for 2 h (E stage). The brightness and kappa number of the pulp after the bleaching sequence (LE) were assessed according to ISO 2470-1: 2009 and ISO 302: 2004, respectively.

III. RESULTS AND DISCUSSION

Oxidation-reduction potential values for the laccase-phenolic compound solution

a) Without kenaf pulp

Fig. 1a shows the oxidation–reduction potential values measured during the course of the different processes. As can be seen, there was an immediate increase in ORP upon addition of the natural mediators that can be ascribed to the production of the corresponding phenoxy radicals. The increase resulting from the addition of the mediator (between 1200 and 1500 s) is consistent with the ease of radical formation when some electron-releasing group-methoxy-is present in ortho position (C_3 and C_5) with respect to $C_{phenolic}$. The HBT solution also increased ORP (Fig. 1a) by effect of laccase catalyzing the oxidation of N–OH compounds [5]; the presence of NO radical in solution increases its oxidative power.

b) *With kenaf pulp*

The above-described experimental procedure was also used with the five laccase–phenolic compound and laccase–HBT systems in the presence of kenaf pulp. Fig. 1b shows the variation of ORP for the different kenaf–laccase–mediator systems as well as the kenaf–laccase system in the absence of mediator. As can be seen, the oxidative ability at the end of the enzyme treatment (6000–7200 s) decreased in the following sequence: HBT > AS > AV> laccase ≈ V ≈ SA > PC.

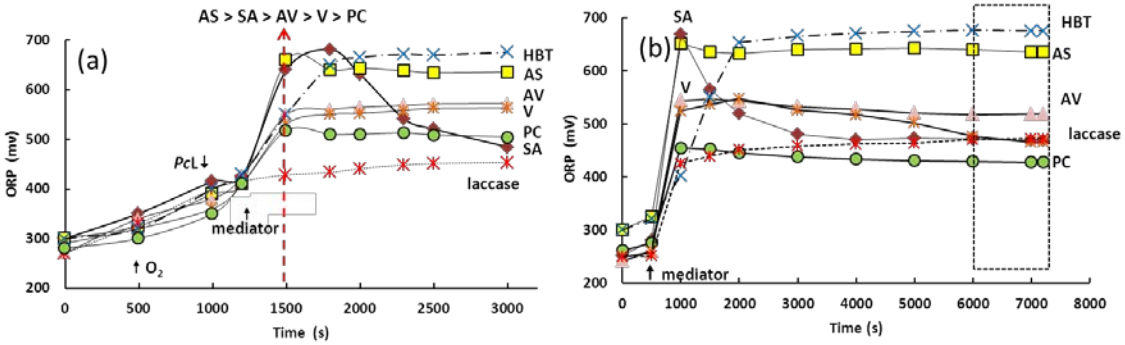

Figure 1. (a) Temporal variation of ORP during the oxidative process with the laccase, laccase–phenolic compounds and laccase–HBT solutions; **(b)** temporal variation of ORP during oxidation of kenaf pulp.

Variation of the ORP ratio during the process

a) Without kenaf pulp

The variation of the ORP ratio during the oxidative process helps to understand the behavior of the different mediators. Fig. 2a shows the calculated ORP ratio for each mediator after time (scored in figure) in the oxidation process (the temporal variation is shown vertically). This variability in the ORP ratio values may have been a result of the concentration of phenoxy radicals in the reaction mixture decreasing through mutual coupling during the oxidative process. With AV and V, the condensation of their respective radicals involves the formation of C_5–C'_5 and C_5–C'_2 (C'_6) intermolecular links [6],[7], [8], and this may also have been the case with the PC phenoxy radical. The intermolecular bonds formed by the phenoxy radicals of AS and SA must be of the $C_{phenolic}$–O–$C'_{phenolic}$ type because both compounds have the *ortho* positions of their aromatic rings occupied by methoxy groups [9]. These authors believe that the SA radical can also be linked via $C_{phenolic}$–O–C'_1 bonds

following oxidation of the aldehyde group (C_1) to a carboxyl group, this special behavior probably being the origin of the large variability in ORP during the oxidative process. The formation of these condensed compounds may account for the differences in oxidative ability between the mediators. Also, differences in stability between phenoxy radicals have been confirmed by several electrochemical studies [10].The NO radical is less active but more stable than phenoxy radicals [11]. The sustained exponential increase in ORP (Fig. 1a), and the fact that it peaked at the end of the process, are consistent with this description.

b) With kenaf pulp

The variation of the ORP ratio during the process illustrates the effect of the presence of the pulp on the oxidative power of the enzyme system (Fig. 2b). The most relevant result was the substantially increased ORP ratios for all mediators and the laccase relative to the absence of pulp (Fig. 2a); this indicates that its presence improves the oxidative ability of the reaction mixture. These results suggest that the chemical structure of lignin in the raw material plays a significant role during the enzyme treatment (Chinese kenaf pulp has a syringyl units/guaiacyl units mole ratio of 3.3 [12]). The increased ORP ratio with all systems may have resulted from an increase in syringyl units coming from the degradation of lignin in the mixed solution [13]. Incorporation of these units (acting as mediators) into the solution may have been the origin of the substantial increase in oxidative ability of laccase in the presence of pulp. It should be noted that this is a specific feature of kenaf in the enzyme treatment. Based on the ORP ratios obtained, the kenaf–*Pc*L–p-coumaric acid system was that with the lowest oxidative power, possibly as a result of the ability of PC radicals to bind to lignin in various lignocellulosic materials with the aid of laccase in ‘‘grafting’’ reactions [14] [15]. The systems with SA and V (two phenolic compounds with an aldehyde group at C_1 on the aromatic ring) exhibited a wider range of ORP values, possibly by effect of oxidation of the aldehyde group during the enzymatic oxidative process [16]. Finally, the kenaf–laccase–HBT system departed from all others in the variation of its oxidative ability; again, its ORP peaked at the end of the enzyme process.

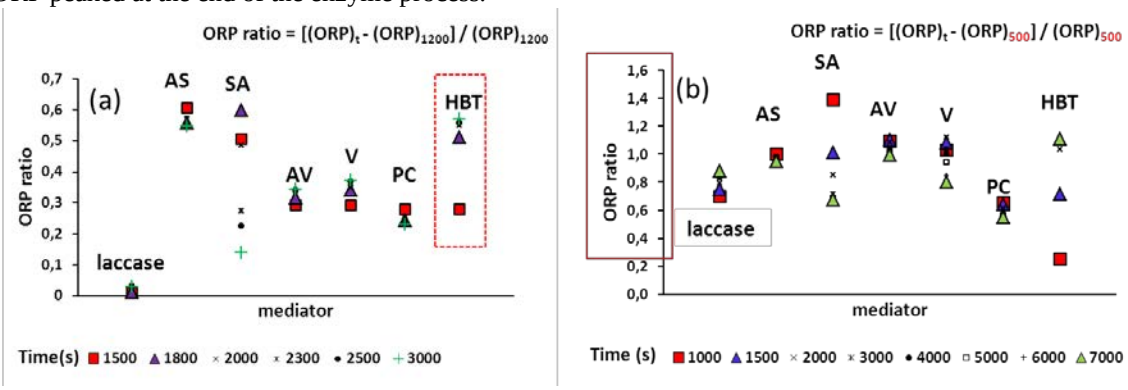

Figure 2. (a) Temporal variation of ORP ratio in the oxidative process with the laccase, laccase–phenolic compounds and laccase–HBT solutions; **(b)** temporal variation of ORP during oxidation of kenaf pulp.

Oxidation lignin and biobleaching process: kappa number and brightness

The ability of the phenolic compounds to bleach kenaf pulp, measured in terms of kappa number and brightness was assessed and used to predict the efficiency of the mediator. The enzyme bleaching treatment was followed by alkaline extraction (an E stage); and a reduction in kappa number and increased brightness were observed respect to unbleached kenaf pulp (kappa number = 12.9 and % ISO brightness= 35.0). Fig. 3 shows the kappa number and brightness obtained after the LE sequence in relation to the average ORP values measured during the treatment. As can be seen, the phenolic compounds reduced kappa number and increased brightness to a variable extent with respect to unbleached pulp. The above-mentioned different tendency of the phenoxy radicals to undergo condensation and grafting reactions on lignin, competing with oxidative degradation, is consistent with the experimental results. Based on the foregoing, HBT is seemingly better balanced as a mediator.

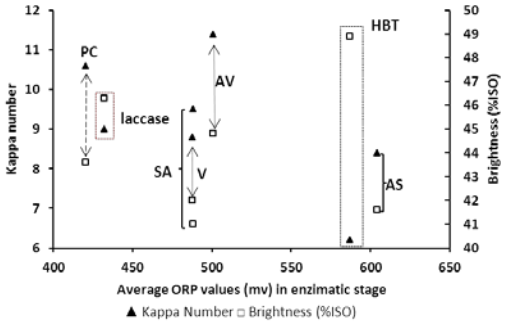

Figure 3. Kappa number and ISO brightness of kenaf pulp after biobleaching with the LE sequence in relation to the average ORP.

IV. CONCLUSIONS

Monitoring ORP **(i)** revealed the formation of phenoxy radicals and their different reactivity depending on the chemical nature of the mediator, **(ii)** permitted to point out the influence of the chemical structure of kenaf lignin on the enzymatic process and **(iii)** realized the increased oxidative ability of laccase in presence of kenaf pulp. The condensation reactions observed in the absence of pulp, and the grafting reactions between the mediator and lignin, compete with oxidative degradation and influence the outcome. The use of ORP measurements as a predictive tool for selecting an enzyme mediator is limited by this competitive reactions. Finally, the most efficient mediator was HBT, which undergoes none of the adverse reactions involving the natural mediators.

V. ACKNOWLEDGEMENT

The authors are especially grateful to Spain's MICINN for funding this research in the framework of Projects AGAUR2009SGR00327, BIOFIBRECELL (CTQ2010-20238-CO3-01) and BIOSURFACEL (CTQ2012-34109). The authors are also grateful to CELESA, S.A. for supplying the starting kenaf pulp.

VI. REFERENCES

[1]-[13] Cañas, A.I.; Camarero, S. Laccases and their natural mediators: Biotechnological tools for sustainable eco-friendly processes. *Biotechnol. Adv.* **2010**, 28, 694-705

[2] Wareham, D.G.; Hall, K.J.; Mavinic, D.S. Real-time control of aerobic-anoxic sludge digestion using ORP. *J. Environ. Eng-ASCE.* **1993,** 119(1), 120-136.

[3] Lin. J-G.; Ma, Y-S. Oxidation of 2-chlorophenol in water by ultrasound/Fenton method. *J. Envionr. Eng.* **2000,** 130-137.

[4] Andreu, G.; Vidal T. Laccase from *Pycnoporus cinnabarinus* and phenolic compounds: Can the efficiency of an enzyme mediator for delignifying knead pulp be predicted? *Bioresour. Tecnol.* **2013,** 131, 536-540.

[5] Astolfi, P.; Brandi, P.; Galli, C.; Gentili, P.; Gerini, M.F.; Greci, L., Lanzalunga, O. New mediators for the enzyme laccase: mechanistic features and selectivity in the oxidation of non-phenolic substrates. *New J. Chem.* **2005,** 29, 1308–1317

[6]Tanaka, T.; Takahashia, M.; Haginoa, H.; Nudejimaa, S.; Usuia, H.; Fujiib, T., Taniguchia, M. Enzymatic oxidative polymerization of methoxyphenols. *Chem. Eng. Scie.* **2010,** 65, 569-573.

[7] Mikolasch, A.; Schauer, F. Fungal laccases as tools for the synthesis of new hybrid molecules and biomaterials. *Appl. Microbiol. Biot.* **2009,** 82, 605-624.

[8] Kudanga, T.; Nyanhongo, G.S.; Guebitz, G.M.;Burton, S. Potential applications of laccase–mediated coupling and grafting reactions: a review. *Enzyme Microb. Tech.* **2011,** 48, 195–208.

[9]-[16] Bollag, J.M.; Myers, C.J.; Minard, R.D. Biological and chemical interactions of pesticides with soil organic matter. *Scie. Total Environ*. **1992,** 123/124, 205-217.

[10] Diaz, M.; Vidal, T.; Tzanova, T. Electrochemical study of phenolic compounds as enhancers in laccase-catalyzed oxidative reactions. *Electroanal.* **2009,** 21(20), 2249-2257.

[11] Xu, F.; Kulys, J.J.; Duke, K.; Li, K.C.; Krikstopaitis, K.; Deussen, H-J.W.; Abbate, E.; Galinyte, V.;, Schneider, P. Redox chemistry in laccase-catalyzed oxidation of N-hydroxy compounds. *Appl. Environ. Microb.* **2000,** 66, 2052-2056.

[12] Andreu, G.; Vidal T. Effects of laccase-natural mediator systems on kenaf pulp. *Bioresour. Tecnol.* **2011,** 102, 5932-5937.

[14] Widsten, P.; Kandelbauer, A. Laccase applications in the forest products industry: A review. *Enzyme Microb. Tech.* **2008,** 42, 293-307.

[15] Fillat, A. Flax fibre modification using enzymatic systems to obtain high-value cellulose products. PhD Thesis, UPC, Department of Textile and Paper Engineering, **2011,** http://www.tdx.cat/handle/10803/38251

.

XYLANASE TREATMENT OF EUCALYPTUS PULPS IN DIFFERENT CHEMICAL BLEACHING STAGES

Ariza, M.[1], Barneto, A.G.[1]., Vidal, T.[2], Ariza, J.[1]

[1]University of Huelva, Department of Chemical Engineering, Physical Chemistry and Organic Chemistry (Campus de Excelencia Internacional Agroalimentario, ceiA3), Campus El Carmen, 21071 Huelva, Spain.
[2]Universitat Politècnica de Catalunya, Textile and Paper Engineering Department, Colom 11, E-08222 Terrassa, Spain.
agustin.garcia@uhu.diq.es

ABSTRACT

Xylanase significantly reduces the kappa number but almost not modifies brightness and viscosity in studied pulps. On average, xylanase decreases the kappa number of chemical pulps 25 %. This intense effect on the kappa number can be explained by enzymatic hydrolysis of hemicellulose. We proved that xylanase treatment on P0 pulp (first chlorine dioxide step) yield a kappa number reduction higher than obtained by chemical PO and D1 steps together.

On the other hand, thermogravimetric analysis shows that xylanase treatment has influence on the thermal degradation path of pulps. As general rule, control treatment (with TrisHCl buffer but without enzyme) leads broads cellulose degradation peak, shown that chlorhydrate of tris(hydroxymethyl) aminoethane adsorb on cellulose surface increasing paracrystalline cellulose content, that is, not-ordered surface crystalline cellulose. When TrisHCl and xylanase are used together, adsorption is less important. In any case, in xylanase-treated pulps cellulose thermally degrades in broader temperature interval than in initial pulps

I. INTRODUCTION

Enzymatic treatments are being studied for a long time. Among the most used enzymes are laccase and xylanase. Laccase directly oxidizes lignin, however, xylanase hydrolyzes hemicellulose leading its removal from cellulosic matrix and dragging lignin [1].

Several studies proves that xylanase pretreatment boosts chemical bleaching, contributing to reduce chemical saving and pollutants emissions [2][3][4]. It seems that xylanase shows two effects: on the one hand hydrolyzes xylans from fibre surface, making more accessible lignin to bleaching chemicals [5], and, on the other hand, removes hexenuronic acids which decrease pulp brightness [6].

Present study carries out a systematic examination of xylanase treatment applied on pulps in different steps of a chemical bleaching which consist of: oxygen delignification (O step), chlorine dioxide (D0 step), hydrogen peroxide (PO step), and chlorine dioxide (D1 step). Usually, this bleaching sequence significantly reduces Klason lignin and hexenuronic acids in O and D0 steps, and substantially increases brightness in the three first steps. The last step (D1) only increases brightness two ISO units. About viscosity, we observed that the initial oxygen delignification in alkaline medium damages cellulosic fiber more than the other steps together.

On the other hand, thermogravimetric analysis has been used to monitor changes in cellulose microfibril [7]. Thermal degradation of pulp is sensitive to changes in cellulose surface. As general rule, cellulose degradation shows two steps: close 300 ºC degrades amorphous cellulose and close 350 ºC crystalline cellulose. However, surface crystalline cellulose degrades as amorphous cellulose (paracrystalline) when chemicals or enzymes adsorb on it. In this case, the amount of cellulose that degrades at low temperature (amorphous plus paracrystalline cellulose) increases and the amount of cellulose that degrades at high temperature (crystalline cellulose from microfibril core) decreases [8]. Complementarily, effects of UV light on chemical and xylanase-treated pulps were compared.

II. EXPERIMENTAL

Eucalyptus kraft pulps were supplied by ENCE mill (Huelva, Spain). P1: Alkaline watched pulp, P2: Alkaline oxygen delignified pulp (O step), P3: chlorine dioxide pulp (P0 step), P4: hydrogen peroxide pulp (PO step) and P5: chlorine dioxide pulp (P1 step).

UV Photobleaching was carried out on Technidyne Color Touch using intensity 765 W/m^2. Eucalyptus kraft pulp sheet (2 cm x 2 cm) was irradiated with light source at room temperature during 96 h, perpendicular to the surface of the sheet, washed with water, and dried.

Thermogravimetric analyses were carried out on a Mettler Toledo TGA/SDTA851e/LF1600 thermobalance, using about 5 mg of sample in each run. Pyrolysis and combustion runs were performed in nitrogen and synthetic air (4:1 N2/O2), respectively. The temperature was raised from 25 to 900 ºC at three different heating rates: 5, 10 and 20 ºC/min.

Brightness, , Kappa index, Viscosity and lignin Klason were measured according ISO 3688, ISO 302, ISO 535-1, and Tappi T-222, respectively. Hexenuronic acids (HexA) content was determined according to Chai el al (2001) [9].

III. RESULTS AND DISCUSSION

	Brightness (% ISO)	Viscosity (cSt)	Kappa Index	HexA (μmol/g)	Klason Lignin (g/100g)
P1	34.2	1021	14.41	44.4	2.6
P2	52.9	918	8.90	27.2	0.9
P3	75.5	842	2.43	10.8	0.6
P4	86.7	843	2.00	10.3	0.6
P5	88.5	826	1,65	6.4	0.6

Table1. Chemical pulps characterization

As can be seen in **table** 1, initial pulp P1 (alkaline washed pulp) was subjected to chemical bleaching according to: Alkaline oxygen delignification (P2), first chlorine dioxide (P3), Hydrogen peroxide (P4), second chlorine dioxide (P5). Two first steps have the greatest importance in chemical bleaching, but damage fibers as shows viscosity reduction. Alkaline oxygen delignification increases brightness 18.7 % and reduces Kappa index, HexA, and Klason lignin 5.51 units (38.2 %), 17.2 μmol/g (38.7 %) and 1.7 % (65 %), respectively. For his part, first chlorine dioxide treatment increases brightness 22.6 % and reduces Kappa index, HexA and Klason lignin 6.47 units (72.7 %), 16.4 μmol/g (60.3 %), and 0.3 % (33.3 %), respectively. Hydrogen peroxide and second chlorine dioxide treatments mainly increase brightness.

Figure 1 depicts that xylanase almost not increases pulp brightness but significantly reduces kappa index without effect on viscosity. Kappa index decreases are 3.0, 2.4, 0.9, 0.5 and 0.3 units for P1 to P5, respectively. These changes represent an average decline of 25 %. Considering only kappa index evolution, xylanase treatment on P3 pulp (after first chlorine dioxide treatment) has similar effect than hydrogen peroxide and second chlorine dioxide jointly.

UV light removes chromophores in both chemical and xylanase-treated pulps. In both cases brightness evolution shows that chromophores removal has first-order kinetics. Representing Ln (brightness change) versus time, a straight line is obtained (see **figure** 2). Slope of this line (kinetic constant) shows the specific rate of photobleaching. Typical values are close 0.012 h^{-1}. On the other hand, intercept values allows obtaining initial amount of chromophores. In all cases, xylanase treatment reduces chromophores content.

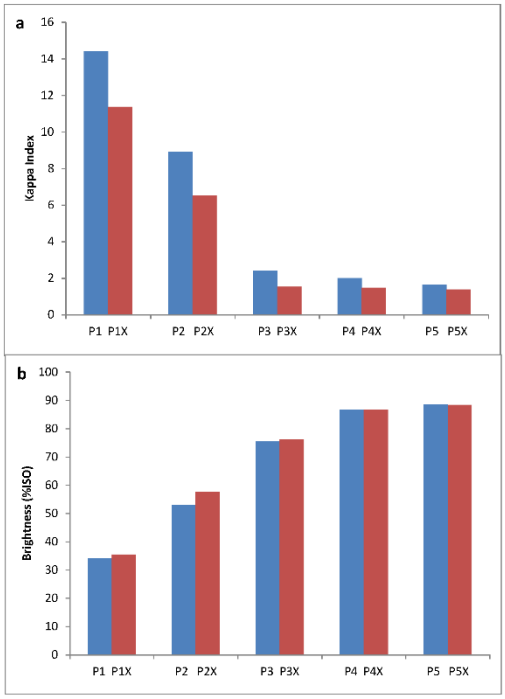

Fig1. Effect of xylanase en kappa index and brightness of several chemical kraft pulps

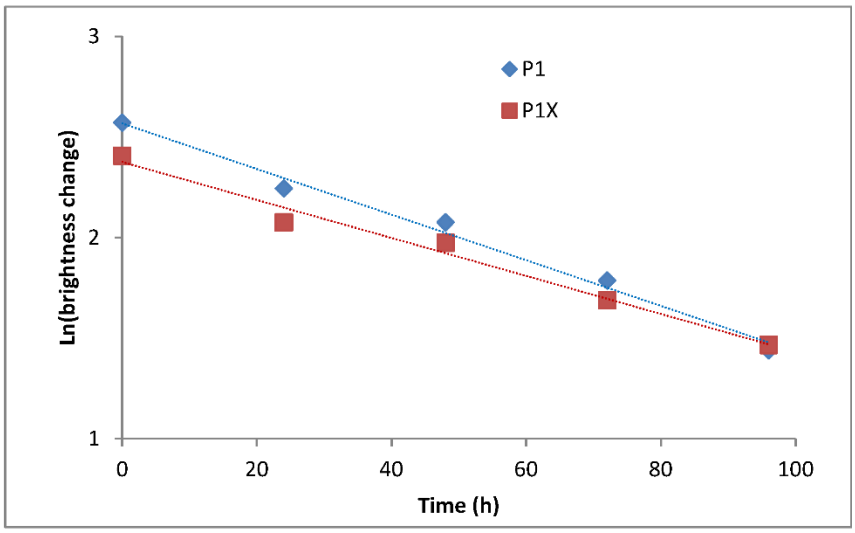

Fig 2. UV photobleaching increases brightness in bot chemical and xylanase-treated pulps.

Figure 3a compares thermal degradation for three pulps: P3, chemical pulp obtained after first chlorine dioxide treatment, P3X, pulp obtained after xylanase treatment, and P3C, pulp obtained after xylanase treatment but without enzyme, that is, after Tris-HCl application. As can be seen, Tris-HCl significantly modify thermal degradation path of P3 pulp, increasing cellulose amount that degrades at low temperature and reducing cellulose amount that degrades at high temperature. This fact is the consequence of Tris-HCl adsorption on cellulose surface. As their molecules has three hydroxyl groups besides one amine group, they can form hydrogen bridges with hydroxyl group of glucose molecules. As consequence crystalline surface modifies their thermal degradation path, behaves like amorphous cellulose. When Tris-HCl is used jointly xylanase (P3X) this phenomenon is less intense. Xylanase bleached pulp has cellulose surface more crystalline. As general rule, Tris-HCl adsorption increases as chemical bleaching progress. As can be seen in **figure** 3b, thermal degradation paths are more similar for P1 and P1X than for P5 and P5X. As chemical bleaching removes lignin on fiber surface, Tris-HCl can remain hydrogen bonded easier.

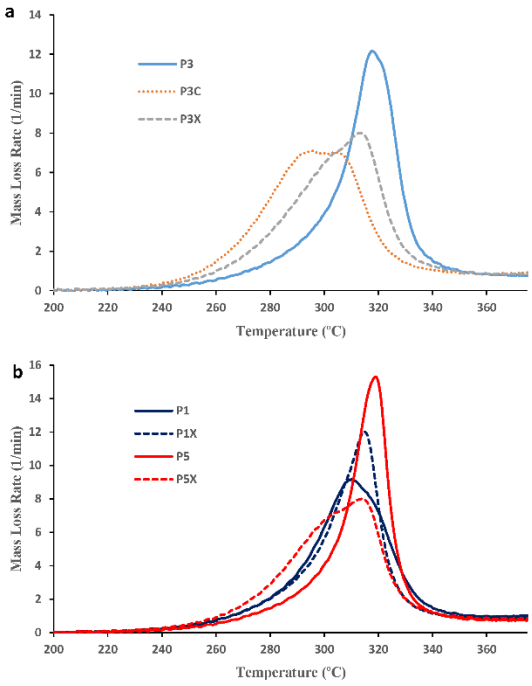

Fig 3. Thermal degradation path for chemical and xylanase-treated pulps.

IV. CONCLUSIONS

Xylanase treatment significantly reduces Kappa index of chemically bleached pulps. For a ECF kraft bleaching sequence based on O,P0,PO,P1 steps, a xylanase treatment on P0 pulp reduces Kappa index more than PO and P1 steps jointly. On the other hand, thermogravimetric analysis proves that Tris-HCl, used as buffer during xylanase treatment, adsorbs on fiber surface, modifying their thermal degradation path.

V. ACKNOWLEDGEMENT

ENCE mill at Huelva (Spain) is gratefully acknowledged for supplying the pulps.

VI. REFERENCES

[1] Barneto, A.G.; Valls. C.; Ariza, J.; Roncero. B. Thermogravimetry study of xylanase- and laccase/mediator-treated eucalyptus pulp fibres. *Bioresource Technology* **2011**, *102*, 9033–9039
[2] Vidal. T.; Torres, A.L.; Colom, J.F.; Siles, J. Xylanase bleaching of eucalyptus kraft pulp—an economical ECF process. *Appita J*, **1997**, *50*, 144–148
[3] Torres, A.L.; Roncero, M.B.; Colom, J.F.; Pastor, F.I.J.; Blanco, A.; Vidal, T. Effect of a novel enzyme on fibre morphology during ECF bleaching of oxygen delignified eucalyptus kraft pulps. *Bioresour Technol*, **2000**, *74*, 135–140
[4] Amin, H.M. Extended usage of xylanase enzyme to enhance the bleaching of softwood kraft pulp. *Tappi J*., **2006**, *5*, 23–26
[5] Roncero M.B.; Torres, A.L.; Colom, J.F.; Vidal, T. The effect of xylanase on lignocellulosic components during the bleaching of wood pulps. *Bioresour Technol*, **2005**, *96*, 21–30
[6] Sevastyanova, O.; Li, J.; Gellerstedt, G. Influence of various oxidizable structures on the brightness stability of fully bleached chemical pulps. *Nord Pulp Pap Res J*, **2006**, *21*, 49–53
[7] Barneto, A.G.; Vila, C.; Ariza, J. Eucalyptus kraft pulp production: Thermogravimetry monitoring. *Thermochimica Acta*, **2011**, *520*, 110–120
[8] Barneto, A.G.; Valls. C.; Ariza, J.; Roncer,. B. Influence of enzyme and chemical adsorption on the thermal degradation path for eucalyptus pulp. *Thermochimica Acta*, **2013**, *551*, 62– 69
[9] Chai, X.S.; Zhu, J.Y.; Li. J.. A simple and rapid method to determine hexeneuronic acid groups in chemical pulps. *Journal Pulp and Paper Science* **2001**, *27*, 165-170

REMOVAL OF HEMICELLULOSES FROM KRAFT PAPER PULP BY CHEMICAL WAYS: SEARCH FOR OPTIMAL CONDITIONS

Benoît Arnoul-Jarriault[1]*, Christine Chirat, Dominique Lachenal

[1] *Laboratoire de Génie des Procédés Papetiers(LGP2), Grenoble-INP Pagora, CS10065, 38402 Saint-Martin-d'Hères Cedex, France (benoit.arnoul-jarriault@pagora.grenoble-inp.fr)*

ABSTRACT

Two chemical processes for hemicellulose extraction have been applied on a fully bleached softwood kraft pulp in an attempt to convert paper pulp into dissolving grade pulp. The cold caustic extraction process (CCE) was performed under conventional and unconventional conditions. Alkali concentration ranged from 3% to 12% and temperature from 25 to 110°C. As expected, the results showed that NaOH concentration had a predominant effect on xylan and glucomannan removal. The effect of temperature was more complex since the best removal was observed below 40°C or above 80°C. Under the best conditions, 80 % of the xylan and 60 % of the glucomannan were removed. A second process consisting in an acid stage at high temperature (up to 150°C) followed by a hot caustic extraction (A-HCE) was also tested. Promising results in terms of hemicellulose removal were obtained when temperature in A was above 140°C. This might be due to a combination of acidolysis during A and peeling reactions during HCE. However, cellulose was partly depolymerized because of the severity of the A step. The two processes were compared in the context of getting to a viscose grade dissolving pulp.

I. INTRODUCTION

Dissolving wood pulps have seen a market growth over the past ten years, mainly driven by the demand for regenerated fibres for textile application [1]. Thus, several kraft paper pulp producers consider the production of dissolving pulp as a new opportunity to improve the economy of their operation. However, the conversion to prehydrolysis kraft process involves important and costly change to remove hemicelluloses. One attractive approach would be the direct purification of kraft paper pulp by adding some appropriate treatments.
In this study, two purification techniques have been investigated. The first one is a cold caustic extraction (CCE) performed under conventional and unconventional conditions and the second one is a sequential treatment consisting in an acid stage at high temperature (up to 150°C) followed by a hot caustic extraction (A-HCE).

II. EXPERIMENTAL

Cold caustic extraction (CCE)

Cold caustic extractions of the pulp were carried out in polyethylene bags at a consistency of 5% for 30 minutes. The concentration of the NaOH solution and the temperature of the reaction for the experiments are given in Table 1. After introduction of the reagents, the bag was placed in a thermostated water bath.

Hot caustic extraction

Hot caustic extractions were carried out in an autoclave placed in an ERTAM rotating reactor. HCE were conducted at 10% consistency during 2 hours. The temperature was set at 110°C and sodium hydroxide charge at 120 kg per dry ton of pulp.

Hot Acid stage (A)

The A stage was performed with sulphuric acid at pH=3, 10% consistency, 150 °C and two reaction times of 60 and 120 min. Reaction was done in an autoclave placed in a ERTAM rotating reactor.

Degree of polymerisation

Degree of polymerization (DPv) were characterized according Tappi Test Method T230 om-99 standard.

Chemical composition of the pulp

The pulps were subjected to acid hydrolysis consisting of a pre-hydrolysis with 72% H2SO4 followed by dilute acid hydrolysis in an autoclave for 1 h at 120°C (according to TAPPI T 249 cm-00) in order to determine their chemical composition. After hydrolysis, the suspensions were filtered. Monosaccharide composition was determined by high-performance anion exchange chromatography with pulse amperometric detection (HPAEC

PAD) in a Dionex ICS 5000 apparatus. Sugar separation was done by a CarboPac PA column 10 (250 mm * 4 mm, Dionex).

III. RESULTS AND DISCUSSION

Effect of cold caustic extraction on hemicelluloses extraction of softwood kraft pulp

Previous studies on cold caustic extraction (CCE) carried out on kraft pulp at low temperature (20-40°C) and high alkalinity (1 to 3 mol.l^{-1} solutions) showed promising results in terms of xylan extraction but only a limited glucomannan removal was observed [3-6]. In the present study, the conditions of the CCE were varied according to an experimental design where alkali concentration ranged from 3% to 12% and temperature from 25 to 95°C. The efficiency of the cold caustic extraction in terms of hemicellulose removal was evaluated on a fully bleached softwood kraft pulp. Table 1 shows the carbohydrate composition of the extracted pulp under the conditions applied in the experimental design. The extraction rate defined by equation (1) was used in the discussion.

Table 1. Carbohydrates composition of the samples after CCE carried out on the fully bleached softwood kraft pulp.

Temperature (°C)	NaOH solution concentration (w/w %)	Cellulose content (%)	Glucomannan content (%)	Xylan content (%)	Hemicellulose content (%)
35	5	90.9	6.3	2.8	9.1
85	5	91.2	6.1	2.7	8.8
35	11	93.7	4.7	1.6	6.3
85	11	94.6	4.1	1.3	5.4
25	8	93.3	5.0	1.7	6.7
95	8	93.2	5.2	1.6	6.8
60	3.8	89.5	7.0	3.5	10.5
60	12.2	94.5	4.1	1.4	5.5
60	8	92.5	5.6	1.9	7.5

$$\text{Extraction rates (\%)} = \left(1 - \frac{X_f}{X_i}\right) \times 100 \quad (1)$$

where X_f is the xylan or glucomannan content of the pulp after extraction
X_i is the initial xylan or glucomannan content of the pulp

In order to observe the influence of the temperature and the NaOH concentration during CCE on hemicellulose removal, the evolution of the extraction rate of xylan and glucomannan was modelled by multi-linear regression (Figure 1 and 2).

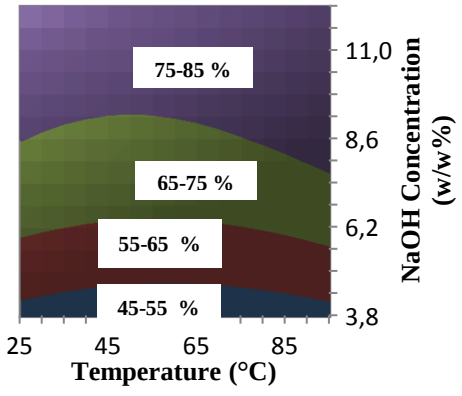

Figure 1. Xylan extraction rates

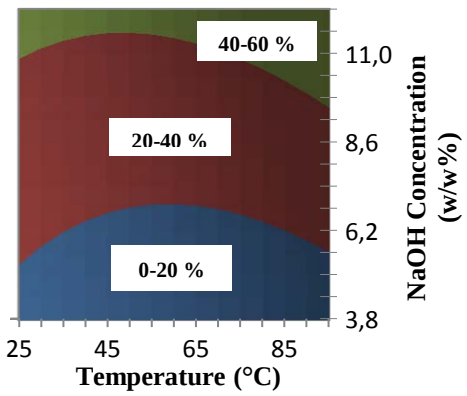

Figure 2. Glucomannan extraction rates

As expected, the results showed that NaOH concentration had a predominant effect on xylan and glucomannan removal. The effect of temperature was more complex since the best removal was observed under 40°C or above 80°C. Under the best conditions, a removal of 80 % of the xylan content and 60 % glucomannan content was reached. The results also indicated that hemicellulose removal could be performed at higher temperature than usual. It is known that under the high alkaline conditions prevailing in CCE cellulose (II) polymorph is formed

[7] and could be detrimental to pulp reactivity [8]. The influence of temperature on cellulose II formation is under investigation.

Impact of A-HCE on hemicellulose content

The extraction of hemicellulose by acid treatment of wood chips has been extensively covered during the past 10 years [9,10,11] but few studies dealt with acid extraction directly applied on kraft pulps. One recent patent described a method for the extraction of xylan by direct application of acid on pulp [12] . Also recently, a study focused on hot water extraction (temperature treatment comprise between 200 and 240 °C) of a hardwood kraft pulp [13]. The residual xylan was around 5-7% which might be suitable for viscose application.
In this study, acid stage (A) at temperature 150 °C was tested on an oxygen bleached pulp to measure the influence of this treatment on hemicellulose removal. The addition of a hot alkaline extraction (HCE) after A stage to enhance hemicellulose removal was studied.

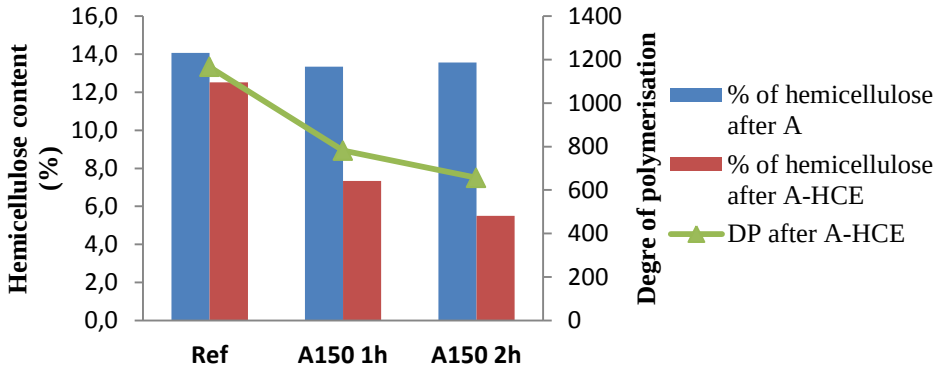

Figure 3. Hemicellulose content after A and A-HCE and degree of polymerization after A-HCE (pulp of initial DP 1600)

The A-HCE process, where the A stage was performed at a temperature higher than 140°C led to promising results in terms of hemicellulose removal (figure 3). In the best conditions the treated pulp contained 5.5% of hemicellulose. This result suggests that some peeling took place during the HCE step. On the other hand cellulose was partly depolymerized because of the severity of the A step.
Although the A-HCE process led to hemicellulose contents which were rather in the upper range for some of the applications sought (higher grade dissolving pulp) this approach deserves consideration since no cellulose II must be formed. This process (A-HCE) could represent an alternative to CCE for pulp purification.

IV. CONCLUSIONS

Two chemical ways of hemicellulose extraction were tested on a softwood kraft pulp. Cold caustic extraction performed under conventional and non-conventional conditions showed that although NaOH concentration was the most important parameter influencing the hemicellulose extraction an increase in temperature might have a beneficial effect. In fact it was shown that when CCE was performed at much higher temperature than usual the hemicellulose removal was improved but cellulose II was formed. An alternative approach was investigated in an attempt to avoid the formation of cellulose II totally. It consisted in an acid stage at high temperature (up to 150°C) followed by a hot caustic extraction at 110°C (A-HCE). Directly applied on the oxygen treated softwood pulp an efficient hemicellulose removal (>60%) was achieved, slightly below the CCE performance. This effect must be the result of some acid hydrolysis of the hemicellulose chains combined with the peeling of the fragments. No cellulose II must be formed during this process, which should favor the pulp reactivity. However the cellulose DP suffered from the A treatment, but could be kept at an acceptable level for viscose grades.

V. ACKNOWLEDGEMENT

This work was conducted in the framework of the "Polywood project" financed by French R&D National Agencies.

VI. REFERENCES

[1] Hämmerle, F.M. 2011: The cellulose gap (the future of cellulose fibres). *Lenzinger Berichte* **2011**, 89, 12–21.

[2] Dinand, E; Vignon, M ; Chanzy, H; Heux, L. Mercerization of primary wall cellulose and its implication for the conversion of cellulose I→cellulose II. *Cellulose* **2002**, 9, 7–18.

[3] Gehmayr, V; Schild, G; Sixta, H. A precise study on the feasibility of enzyme treatments of a kraft pulp for viscose application. *Cellulose* **2010**, 18, 479–491

[4] Ibarra, D; Köpcken V; Larsson, P.T; Jääskeläinen,A.-S; Ek M.Combination of alkaline and enzymatic treatments as a process for upgrading sisal paper-grade pulp to dissolving-grade pulp. *Bioresour. Technol.* **2010**, 101, 7416–7423.

[5] Puls, J; Janzon, R; Saake, B. Comparative removal of hemicelluloses from paper pulps using nitren, cuen, NaOH, and KOH. *Lenzing. Berichte* **2006**, 86, 63–70.

[6] Schild, G; Sixta, H; Testova, L; Multifunctional alkaline pulping, delignification and hemicellulose extraction. *Cellul. Chem. Technol* **2010**, 44, 35–45.

[7] Sixta, H. Handbook of pulp, vol 2. *Wiley-VCH* **2006**, 933–965.

[8] Krässig, H.A. Polymer Monographs **1993**,Vol.11.

[9] Sixta, H. Comparative evaluation of TCF bleached hardwood dissolving pulps. *Lenzing. Berichte* **2000**, 79, 119–128.

[10] Yoon, S.-H.; Macewan, K.; Van, H., Adriaan.. Hot-water pre-extraction from loblolly pine (Pinus taeda) in an integrated forest products biorefinery. *Tappi J.* **2000**, 87, 27–32.

[11] Li, H; Saeed, A; Jahan, M.S; Ni, Y; Van Heiningen, A. Hemicellulose Removal from Hardwood Chips in the Pre-Hydrolysis Step of the Kraft-Based Dissolving Pulp Production Process. *J. Wood Chem. Techn.* **2010**, 30, 48–60.

[12] Heikkil, H; Lindroos, M; Sundquist, J; Kauliomki, S; Rasimus, R. Preparation of chemical pulp and xylose, utilizing a direct acid hydrolysis on the pulp. **2004** US patent 6,752,902

[13] Borrega, M; Sixta, H. Purification of cellulosic pulp by hot water extraction. *Cellulose* **2013**, 20, 2803–2812.

FUNCTIONALITY AND PHYSICAL-CHEMICAL CHARACTERISTICS OF WHEAT STRAW LIGNIN DERIVATIVES FORMED IN THE OXYPROPYLATION PROCESS

A.Arshanitsa[1], L. Vevere[1], G. Telysheva[1*], R.J.A. Gosselink[2], O. Bikovens[1], A. Jablonski[1]

[1]*Latvian State Institute of Wood Chemistry, Riga, Latvia (ligno@edi.lv);* [2]*Wageningen University, Food and Biobased Research, Wageningen, The Netherlands*

ABSTRACT

The new organosolv wheat straw lignin (Biolignin™) was converted into liquid lignopolyols via oxypropylation in the presence of potassium hydroxide. Six batches of lignopolyols differed by the content of Biolignin™ (L) in initial mixture with propylene oxide (PO) varying in the range from 15 up 40% were synthesized in batch Parr reactor. The effect of L/(L+PO)% (w/w) values on oxypropylation process, properties of lignopolyols (hydroxyl value, viscosity, copolymers content) and characteristics of separated Biolignin™ - PO copolymers (structure, functionality, molecular weight distribution) were studied. The lignopolyols obtained at 15 – 30% (w/w) of Biolignin™ correspond to the requirements of commercial polyolpolyethers for rigid polyurethane (PUR) foams production. The further increase of lignin content in reaction mixture leads to the appearance of non-liquefied solid fractions up to ~7% and to the undesirable growth of viscosity of liquefied part (>100 Pa·s).

I. INTRODUCTION

The application of renewable resources instead of petrochemicals is used in the sustainable development of bio-based plastics and composites including polyurethanes (PU) [1-2]. Obtaining of polyolpolyethers using oxypropylation is commonly applied for the production of commercial polyolpolyethers is considered as prospective way to functionalize plant biomass [3-4]. Lignin, the natural phenolic polymer, is separated from the plant biomass processing as multitonnage by-products that is mainly burned to generate energy [4-5]. Its aromatic nature, the presence of free hydroxyl groups allow to use lignin as aromatic macromolecule for PU synthesis. However, the low solubility of technical lignins, their functional and molecular heterogeneity, low steric availability and electronic constraints of hydroxyl groups restrict this application. The oxypropylation of lignin has been recognized as an approach to overcome these disadvantages and to produce liquid lignopolyols suitable for PUR foam production. The oxypropylation of commercial technical lignins from soft wood, hard wood and grasses were studied in some prior works [3-9]. The structure and functionality of technical lignins depends strongly on the method of their isolation [10]. Therefore the effect of lignopolyols application in PUR foam compositions will differ for different lignins. In the present work the aim was to use the novel technical lignin – BIOLIGNIN™ extracted from wheat straw by the CIMV organosolv process [11]. The process of BIOLIGNIN™ oxypropylation, its transformation in the result of copolymerization with PO is described in the present paper.

II. EXPERIMENTAL

Materials

BIOLIGNIN™ was washed with water to pH~4.4 and then air dried up to 5% of water content and finally ground in laboratory scale disintegrator DESI-11.

Oxypropylation of lignin

Six batches of lignopolyols differing by L/(L+PO) values in initial reaction mixture from 15 till 40% (w/w) (on DM of L) were synthesized in one liter Parr reactor. In all cases 140.00 g of PO (Sigma-Aldrich), air dried lignin and KOH (Lachner) (5% on DM of L) were loaded into reactor. Reactor was sealed and heated with stirring to 160-165°C when drastic exothermic reaction was started. The pressure inside reactor increased to maximum (up 30 bars) and then dropped dramatically to value close to atmospheric. After cooling the KOH was neutralized by acetic acid, product was dissolved in dichloromethane and filtered. Dichloromethane was distilled off in vacuum evaporator. The liquid products (lignopolyols) were used for investigation.

Lignopolyols fractionation

The lignopolyols were dissolved in methanol and then five times extracted with hexane to remove homopolymers. The hexane layers were collected and hexane was distilled of vacuum. The methanol layer was separated and the copolymer fractions were precipitated in cool water (t~6°C, pH=4.0), filtered, washed with water and oven dried in vacuum [6]. The yields of hexane soluble fractions and precipitated copolymer fractions were determined gravimetrically. For each lignopolyols three parallel experiments have been carried out.

FTIR analysis

A Spectrum One (Perkin Elmer) spectrometer was used for measurements in the spectral range 4000–500 cm^{-1}; (resolution: 4 cm^{-1}; number of scans 64). The KBr pellet technique was employed.

^{31}P NMR

Prior analysis all samples were dissolved in the solvent mixture (dimethylformamide: pyridine: $CDCl_3$: 2-chloro-4,4,5,5-tetramethyl-1,3,2,-dioxaphopholane=1:1:4:1) as described in [10]. Analyzes were realized by duplicate using NMR spectrometer (Bruker 300 MHz), with 30° pulse angle, inverse gated proton decoupling, a delay time of 5 s and 256 scan.

SEC analysis

The samples dissolved in hexafluorisopropylalcohol + KTFA were injected into 2 columns PSS PFG linear M, 7 µm, 8mm (ID) x 300mm (L) and a PSS PFG guard column, 8mm (ID) x 50mm (L) and eluted with the same solvent. Conditions: flow 0.7 ml/min, temperature 40 °C., RI detection. Polymethylmethaacrylate standards were used for calibration.

Differential scanning calorimetry (DSC)

The glass transition temperatures (Tg) of parent and oxypropylated lignin samples were measured using a Metler Toledo Star DSC 823 e device. Two scans with heating rate 10°C/min in the range -20°C - +180°C has been done. The second scan was used for Tg calculation.

Chemical analysis

Determination of methoxyl groups content in native BIOLIGNIN™, methoxyl and oxypropyl groups in copolymers was carried out using 57% hydroiodic acid (HI) for spliting of ethers bonds in accordance with [8]. Lignins samples were treated with HI during 20 min in a vial at 130°C. The alkyl iodides formed and internal standard (ethyl iodide) were extracted with carbon tetrachloride and determined quantitatively by gas chromatography (GC), using Agilent 6850 Series GC System with FID detector and capillary column CP7946 (25 m x 320 µm x 0.45 µm film). The quantitative determination of methoxyl groups was carried out using calibration by vanillin. The yield of isopropyl iodide was expressed in arbitrary units (AU), defined as ratio of its peak area to that of internal standard in chromatograms.

The hydroxyl values (OHV) of lignopolyols were determined by the acetylation of samples using acetic anhydride, followed by the potentiometric titration of free acid using 0.1 M NaOH solutions in water.

The potasium acetate (KAc) content was determined by potentiometric titration of lignopolyols dissiolved in ethanol with 0.1 M HCL solutions in water.

Viscosity of lignopolyols measurements

The viscosity was determined using a rotation viscometer (HAAKE Viscotester 6L/R plus) at 20 °C.

III. RESULTS AND DISCUSSION

It was shown that increasing the lignin content in reaction mixture from 15 up to 40% (w/w) led to steadily decreasing of PO maximal pressure inside reactor from 30 to 21.7 bars when the close value of temperature in reactor. This can be explained by the partial consumption of PO in low rate copolymerisation reaction with acid groups of lignin. The high rate homopolymerization reaction take place after transformation of acidic lignin groups into an aliphatic one, when the part of PO was converted at copolymerization [6]. It was concluded that at 15 - 30% (w/w) of BIOLIGNIN™ content in the initial reaction mixture the resulting lignopolyols fulfil the requirements of commercial polyolpolyethers for PUR foams production [8]. The further increase of lignin content in reaction mixture leads to the appearance of non-liquefied solid fractions up to ~7wt% and to the undesirable growth of viscosity of liquefied part (Table 1).

Table 1.Effect of L/(L+PO) ratio values on properties and compositions of lignopolyols obtained

L/(L+PO), %(w/w)	Viscosity, at 20°C, Pa·s	OHV, mg KOH/g	KAc content, %	Composition , %		
				Copolymer	PPG	Total
15	1.7	280.8	1.3	20.7±0.6	64.1±1.3	85.3
20	4.9	397.7	1.8	27.5±2.0	60.2±1.8	88.3
25	16.8	414.8	2.2	31.2±1.7	46.0±2.5	77.5
30	73.7	450.1	2.6	43.5±3.2	37.9±2.3	81.3
35	138.5	462.3	2.9	44.9±2.0	38.6±2.1	83.3
40	>200.0	474.9	3.3	46.5±1.0	32.2±0.9	78.3

With increasing L/(L+PO) values the lignopolyols obtained were steadily enriched with copolymer fractions. The content of polypropylene glycols (PPG) soluble in hexane decreased (Table 1). The sum of copolymer and PPG fractions determined is less than 100%. These indicate the presence of soluble in water but insoluble in hexane propylenglycol and its oligomeric derivatives in lignopolyols.

The FTIR data confirms that the process of lignin oxypropylation was realized: content of aliphatic groups CH, CH_2, CH_3 (2975-2909 cm^1, $^-1465$ cm^{-1}) in copolymers increased in comparison with native BIOLIGNIN^{TM}.

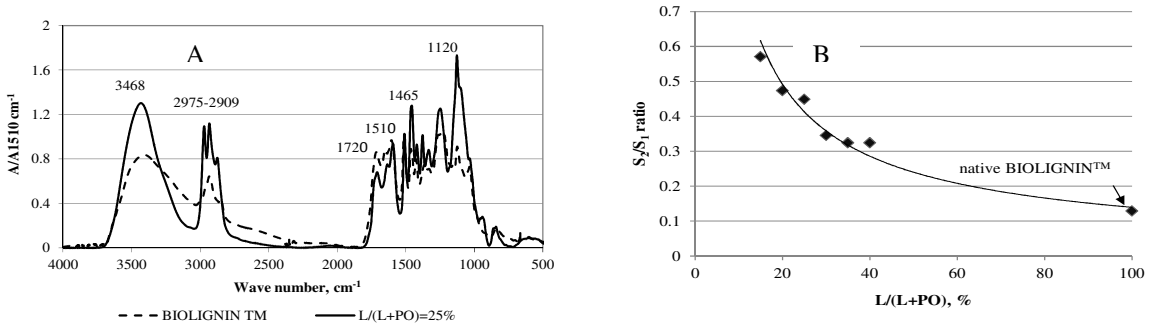

Figure 1. Normalized FTIR spectra of native BIOLIGNIN^{TM} and its oxypropylated derivative (**A**); The ratios of area enclosed by FTIR spectra in the range 3035-2695 cm^{-1}(S_2) to that enclosed in the range3705-3035 cm^{-1}(S_1) for oxypropylated derivatives vs L/(L+PO) values (**B**).

The absorbance of ethers bonds (1100 cm^{-1}) also increased (Fig. 1A). Relative content of aliphatic groups in copolymers, estimated by the FTIR S_2/S_1 ratios, increased with increasing of PO content in initial reaction mixture, confirming the growth of PO grafting onto OH functionalities of BIOLIGNIN^{TM} (Fig. 1B).
The aliphatic OH groups in copolymers are presented mainly by secondary alcohol groups that were confirmed by GC analysis of products obtained at copolymers treatments with HI. The growth of content of isopropyl groups in copolymers is accompanied by decreasing of -OCH_3 groups from 3.7 till 1.4 mmol/g due to reduction of phenylpropane units concentration in copolymers as the result of PO grafting.
The oxypropylation of BIOLIGNIN^{TM} leads to the almost complete transformation of phenolic and carboxylic groups into aliphatic ones. In the result the share of aliphatic OH groups in copolymers increased (Table 2).

Table 2. The functional composition and molecular weights of BIOLIGNIN^{TM} and its copolymers with PO.

L/(L+PO), % (w/w)	Content of OH groups, mmol/g				Ratio OH_{aliph}/OH_{tot}	SEC data		
	Aliphatic	Total phenolic	COOH	Total		M_n, g/mol	M_W, g/mol	M_W/Mn
BIOLIGNIN^{TM}	1.39	1.62	0.50	3.51	0.40	2200	54000	24.5
15	2.26	0.10	0.03	2.39	0.95	8200	30000	3.7
20	2.53	0.10	0.04	2.67	0.95	4900	16300	3.3
25	2.56	0.12	0.05	2.73	0.94	4100	16900	4.1
30	2.59	0.14	0.05	2.78	0.93	4200	21500	5.1
35	2.59	0.14	0.07	2.78	0.93	3600	19700	5.5
40	2.65	0.17	0.06	2.88	0.92	3800	25700	6.8

In the result of oxypropylation the polidispersity of copolymers decreased significantly, reflecting the both processes: the deconstruction of large molecules and PO grafting on to OH groups of lignins [5]. The different relationships between molecular hydrodynamic volumes and molecular weights for various oxypropylated BIOLIGNIN^{TM} derivatives could influence on molecular weight distribution [10].

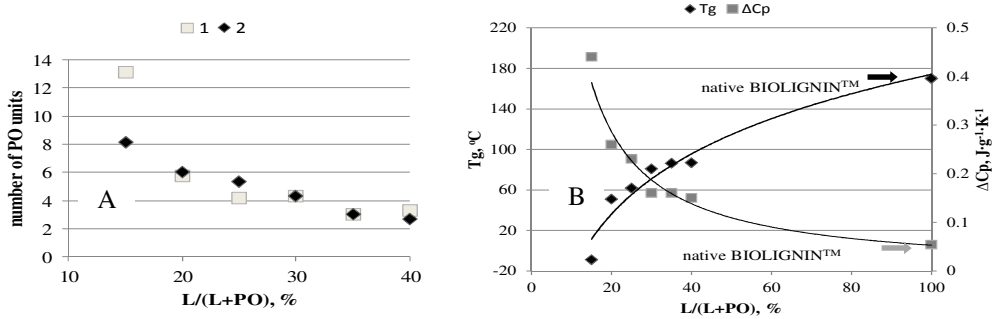

Figure 2. The number of PO units grafted on to each OH function of BIOLIGNIN^{TM} calculated on the basis of Mn values (1) and–OCH_3 content (2) in copolymers (**A**); The DSC data for BIOLIGNIN^{TM} and its oxypropylated derivatives (**B**).

The calculation of average number of PO units grafted onto each OH functional group of BIOLIGNIN^{TM}, made on the basis of two independent experimental data (Mn values and metoxy groups content) have shown the good coinciding for samples with L/(L+PO) values in the range 20-40% (Fig. 2A). In these conditions the similar shape of copolymer macromolecules could be proposed, but in the case of highest amount of PO used (L/(L+PO)=15%)) the significant difference was observed. It can be proposed that in these conditions the longest but no uniform grafted chains are constructed resulting in highest hydrodynamic values of copolymer macromolecule and overestimation of the molecular weight. If the content of lignin in reaction mixture was higher, the grafted oxypropyl chains became shorter, and more uniform. This explanation is in agreement with the results concerning of Alcell lignin oxypropylation [4].
The DSC analysis also confirmed that oxypropyl chains are chemically bonded with macromolecules of lignin and free heat molecular motion in copolymers enhanced with increasing of flexible oxypropyl chains content. The Tg values are decreased but the heat capacity gap at glass transition was steadily increased with enhancing of PO grafting (Fig. 2A; B). The data obtained demonstrate that OH groups in oxypropylated BIOLIGNIN^{TM} derivatives will be highly available for reaction with isocyanates.

IV. CONCLUSIONS

The new type of organosolv wheat straw lignin (BIOLIGNIN^{TM}) was converted into liquid lignopolyol polyethers via bulk oxypropylation. At 15 - 30% (w/w) of BIOLIGNIN^{TM} content in initial reaction mixture the lignopolyols obtained correspond to the requirements of commercial polyolpolyethers for PUR foams production. Further increase of lignin content in reaction mixture leads to the appearance of non-liquefied solid fractions and to the undesirable growth of viscosity. The grafting of oxypropyl chains on to hydroxyl functions of BIOLIGNIN^{TM} was proven by independent chemical and physicochemical methods. In difference with native BIOLIGNIN^{TM} its oxypropylated derivatives had the lower polydispersity, higher molecular segmental mobility and their OH functionalities is near completely presented by secondary aliphatic groups. These feasibilities allowed to characterize the oxypropylated BIOLIGNIN^{TM} derivatives as a high reactive aromatic cross linking constituents of lignopolyols suitable for PUR foams production.

V. ACKNOWLEDGEMENT

The financial support from 7th FP Collaborative project BIOCORE Contract 241566 is gratefully acknowledged. W. Teunissen from WUR-FBR is kindly acknowledged for the SEC analysis.

VI. REFERENCES

[1] Storz, H.; Vorlop, K.D. Bio-based plastics: status, challenges and trends. *APPL Agric Forestry Res.***2013**, *63*, 321-332.
[2]. Ionescu, M. *Chemistry and Technology for Polyurethane*, Rapra Technology limited, UK, **2005**.
[3] Belgacem, M.N.; Gandini, A. Monomers, Polymers and Composites from Renewable Resources, Ed. Oxford UK, **2008**, 273-278.
[4] Cateto, C.A.; Barreiro, M.F.; Rodrigues, A.E.; Belgacem, M.N. Optimization Study of Lignin Oxypropylation in View of the Preparation of Polyurethane Rigid Foams. *Industrial & Engineering Chemistry Research.* **2009**, *48*, p.2583 – 2589.
[5] Li, Y.; Ragauskas A.J. Kraft .Lignin-Based Rigid Polyurethane Foam. *Journal of Wood Chemistry and Technology*. **2012**, *32:3*, 210-224.
[6] Wu, LC.-F.; Glasser, W.G. Engineering plastics from lignin. I. Synthesis of hydroxypropyl lignin. – J. *of Applied Polymer Science*. **1989**, *37*, pp. 3119 – 3135.
[7] Oliveira, W.; Glasser, W. G. Engineering plastics from lignin.XVI.Starlike macromers with propylene oxide. – J. of Applied Polymer Science. **1984**, *29,* pp. 1815 – 1830.
[8] Nadji, H.; Bruzzese, C.; Belgacem, M.N.; Benaboura, A.; Gandini, A. Oxypropylation of Lignins and Preparation of Rigid Polyurethane Foams from the Ensuing Polyols. *Maccromol. Mater. Eng*. **2005**, *290*, 1009-1016.
[9] Gromova, M.; Arshanica, A.; Telysheva, G.; Sevastjanova, A. Ligols - novel hydroxyl-containing multipurpose materials. *In book: "Cellulosic Chemical, Biochemical and Materials Aspects*". Editors: J.F. Kennedy, G.O Phillips., P.A. Williams. Publ: Ellis Horwood, New York, **1993**, 549-553
[10] Gosselink, R.J.A.; van Dam, J.E.G.; De Jong, E.; Scott, E.L.; Sanders, J.P.M.; Li, J. and Gellerstedt, G. Fractionation, analysis, and PCA modeling of properties of four technical lignin for prediction of their application potential in binders. *Holzforschung*, **2010,** *64,* 193-200.
[11] Delmas, G.H; Benjelloun-Mlayah, B.; Bigot, Y.L.; Delmas, M. Functionality of Wheat Straw Lignin Extracted in organic Acid media. *J. of Appl. Pol. Sci.* **2011**, *121*, 491-501.

SOLUBILITY STUDIES OF ALCELL AND INDULIN AT LIGNINS IN PURE SOLVENTS

Mariana M. Barbosa[1], Cláudia F. Lemons[1,2], Maria F. Barreiro[1*], Simão P. Pinho[1]

[1]Laboratory of Separation and Reaction Engineering - Associate Laboratory LSRE/LCM, Polytechnic Institute of Bragança, Campus de Santa Apolónia, 5301-857 Bragança, Portugal (barreiro@ipb.pt)
[2]Engenharia de Biossistemas, Universidade Federal de Pelotas, Rua Gomes Carneiro 1, CEP 96001-970 Pelotas, Rio Grande do Sul, Brasil [#]Presently at UNIFACS-Universidade de Salvador, Rua José Peroba 251, CEP 41770-235 Salvador, Bahia, Brasil

ABSTRACT

In this work the solubility of Alcell and Indulin-AT lignins in a series of pure solvents with different hydrophobicity and hydrogen bonding ability have been measured at 25 ºC, using the shake flask method followed by gravimetric analysis. Infrared spectra and DSC thermograms were acquired for both soluble and insoluble lignin fractions in order to get some knowledge about the involved solubility phenomena. Moreover, the weight percentage of dissolved lignin was related to the solvent molar volume and the Hansen solubility parameter distance (Ra), using a methodology suggested by Hansen. The effect of initial concentration charge in the equilibrium cell, on the lignin solubility, was primarily investigated. For Alcell lignin with acetonitrile, ethyl acetate and methanol, and Indulin-AT with acetonitrile, changing the initial concentration, the maximum difference on the measured solubility was 2.1%, showing the consistency of the experimental procedure. Excepting water, Alcell is more soluble than Indulin-AT, showing big differences in solvents like ethyl acetate or acetonitrile. While for Alcell lignin up to Ra values near 20 $(MPa)^{1/2}$ the solubilities are closer, presenting a weak tendency to decrease for larger molar volumes, for Indulin-AT the change is not yet simple to rationalize. In fact, and based on the preliminary results of this study, the observed difference between the Alcell and Indulin-AT solubilities in acetonitrile, ethyl acetate and water can be related to structural and chemical properties of both solids, as inspected by FTIR and DSC. To the best of our knowledge, no solubility data was found to compare with the values measured in this work.

I. INTRODUCTION

The XXI century brought the concept of bio-refineries as an emerging and intense area of research. In fact, the vision of a modern biorefinery is hotly debated but a broad vision includes a mill that will produce paper, energy, and a variety of chemical feedstocks [1]. However, processing biomacromolecules (BM) presents an inherent difficulty that is related to their solubility. A key problem to be solved is to find a suitable solvent that can effectively destroy the interchain interactions in those materials, turning their dissolution and characterization possible [2]. In that respect, a great lack of information, mainly on solubility data, still remains in terms of studied systems, being difficult to find the solubility values for BM in different solvents. It is then evident the absolute need to establish a systematic procedure that enables to measure solubility values of different BM in several solvents, and therefore to build a reliable database for theoretical and experimental analysis.

Presently, bio-refineries are seen as the big opportunity for lignin since its economic feasibility is intimately related to the valorisation of all generated products. In this context, recent projections indicate that the use of ethanol as fuel in the U.S. is going to increase by about 9.6 billion litres per year, which means that if 25% of the alcohol comes from biomass, at least 1.1 million of tonnes of lignin could be potentially available per year in a near future. The same trend is expected to Europe and other parts of the world, which reveals the need to properly exploit lignin [3]. Studying lignin solubility in different solvents could contribute not only to improve the extraction processes, but also to open new avenues towards its exploitation in more noble applications.

In this work the solubility of Alcell and Indulin AT lignins in acetone, acetonitrile, ethyl acetate, ethanol, methanol, hexane and water have been measured at 25 ºC, using the shake flask method followed by gravimetric analysis. Infrared spectra and DSC thermograms have been acquired for the soluble and insoluble fractions of the lignins in order to rationalize the solubility phenomena and the molecular interactions.

II. EXPERIMENTAL

Lignin samples. The technical lignins chosen in this work proceeded from different pulp processes and vegetal species. Indulin AT is a softwood lignin obtained by the Kraft pulping process of MeadWestvaco (Glen Allen,

VA) and Alcell lignin of Repap Enterprises Inc. (Stamford, CT) was extracted from a mixture of hardwoods (maple, birch and poplar) by an organosolv process using aqueous ethanol. Comparatively to Indulin AT, Alcell lignin has lower molecular weight (760 *versus* 1079), lower total hydroxyl content (5.26 *versus* 6.99 mmol OH/g), lower aliphatic hydroxyl content (1.10 *versus* 2.34 mmol OH/g), and lower OH functionality (4 *versus* 7.5) [4]. The two lignins were used as received. All the used solvents were of analytical grade.

Solubility assays. The solubility experiments were carried out using the analytical isothermal shake-flask method. Initially, mixtures containing 25 g of lignin in 1 kg of solvent were prepared by weighting (±0.1 mg) the appropriate amounts of solid and solvent, into the equilibrium cell of about 80 cm3. To reach equilibrium, the solution is continuously stirred for 24 h and later, the solution is allowed to settle at least 12 h before sampling. Samples (5 cm^3) of the saturated liquid phase were collected using plastic syringes coupled with polypropylene filters (0.45 µm). The gravimetric method was chosen for the quantitative analysis. Therefore, the samples were placed into pre-weighted glass vessels, and immediately weighted. The next step is to evaporate all the solvent, and dry the materials completely in a vacuum stove. Finally, the glass vessels are cooled in a dehydrator with silica gel for one day and weighted. The process is regularly repeated until a constant mass value is achieved. The fraction not dissolved in the equilibrium cell was removed by filtering the saturated solution, using membranes (MFV1, Filter-Lab) with 1.6 µm of pore size, and allowed to dry in the vacuum stove.

Soluble and insoluble fractions characterization. Infrared spectra for both the filtered solid (insoluble fraction) and soluble fraction have been acquired in a FTIR Bomen spectrophotometer (Quebec, Canada), using the KBr pellets technique. The spectra were recorded between 650 and 4000 cm^{-1} at a resolution of 4 cm^{-1} and co-adding 32 scans. DSC thermograms were acquired in the temperature range of -50 to 200 ºC using at a heating rate of 10 ºC/min.

III. RESULTS AND DISCUSSION

The effect of initial concentration on the lignin solubility was primarily investigated using Alcell as the model lignin. The results obtained with the tested solvents (acetonitrile, ethyl acetate and methanol), when changing the initial concentration, pointed out a maximum difference on the measured solubility of 2.1%, showing the consistency of the experimental procedure. The consistency with Indulin AT was thereafter tested using acetonitrile being the tendency corroborated. The final used experimental lignin concentration was fixed in 25 g/1000 g solvent. Each measurement was done in triplicate being the calculated coefficient of variation ($CV = \frac{s}{\bar{x}} * 100$) most often inferior to 5%.

In Figure 1, the percentage of dissolved lignin (given by the circles dimension) is related to the molar volume of the solvent and the Hansen solubility parameter distance (Ra), using a methodology suggested by Hansen [5]. As can be seen, while for Alcell lignin up to Ra values near 20 the solubilities are closer, for Indulin AT the change is not simple to describe. Excepting water, Alcell is generally more soluble than Indulin AT, showing big differences in solvents like ethyl acetate or acetonitrile.

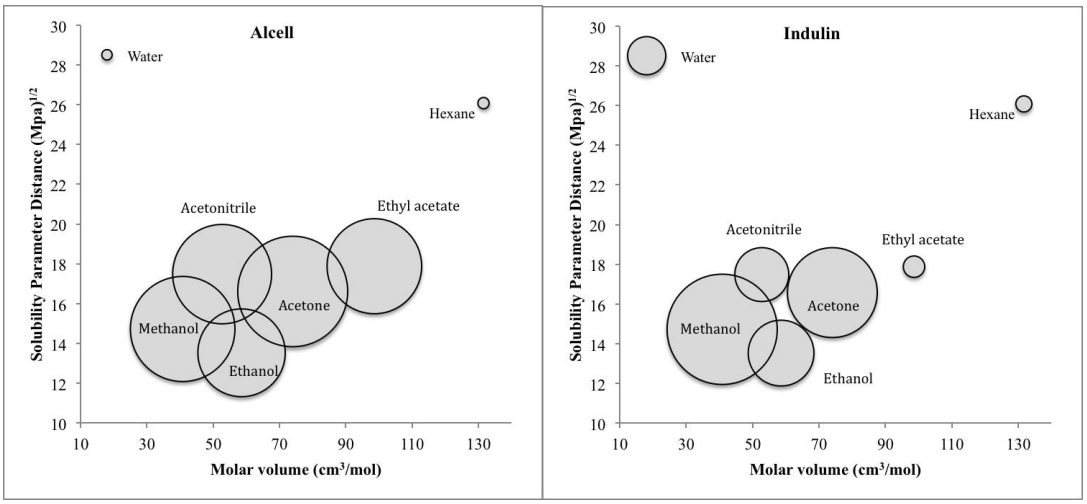

Figure 1. Solubility of Alcell and Indulin AT lignins in different solvents characterized by their molar volume Hansen solubility parameter distance.

In order to get some insights concerning the chemical nature of the soluble and insoluble fractions a FTIR study was conducted considering the analysis of the two fractions together with the original lignin. The comparison between Alcell and Indulin AT is shown in Figures 2 and 3 for ethyl acetate and water solvents, respectively.

All original lignin spectra presented a broad band attributed to OH stretching (3412-3460 cm^{-1}), and peaks corresponding to C-H stretching of methyl and methylene group (2842-3000 cm^{-1}) and methyl group of methoxyl (2689-2880 cm^{-1}). The characteristic vibrations of lignin aromatic rings can be assigned approximately at 1600 cm^{-1}, 1513 cm^{-1} and 1420 cm^{-1}. In Alcell, a band, at approximately 1708 cm^{-1}, attributed to C=O stretching can be identified by a well-defined peak. For Indulin AT only a shoulder was observed.

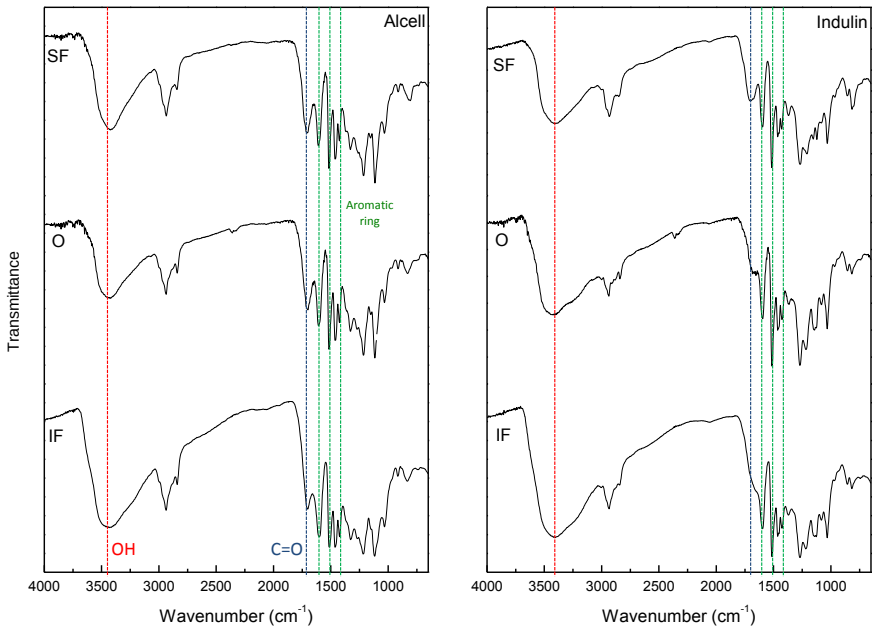

Figure 2. FTIR spectra of Alcell and Indulin AT: Original lignins (O), Soluble (SF) and Insoluble (IF) fractions in ethyl acetate.

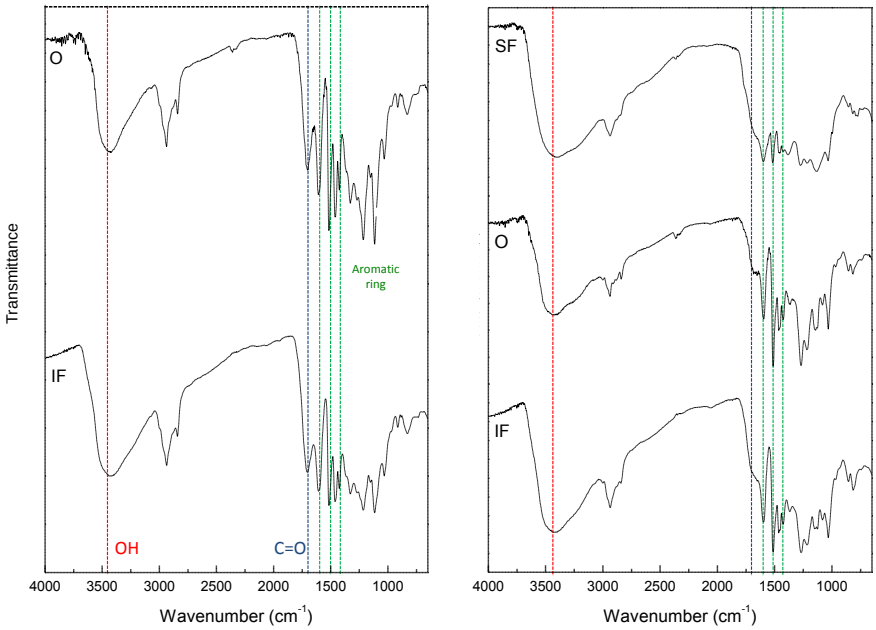

Figure 3. FTIR spectra of Alcell and Indulin AT: Original lignins (O), Soluble (SF) and Insoluble (IF) fractions in water. The spectrum of Alcell SF fraction is not shown due to difficulties related to the scarcity of the sample.

In the case of ethyl acetate, a non-polar solvent (Figure 2), it can be observed that soluble fractions are richer in carbonyl groups as can be depicted by the more prominent peak assigned around 1708 cm^{-1} (see blue line). Moreover, for Alcell lignin, DCS analysis pointed out for the preferable solubility of the low molecular weight fraction (fraction characterized by a Tg of 82.6 ºC, very close the one of the original lignin (99.4 ºC)). The insoluble fraction was characterized by a high Tg (around 182.6 ºC). For the case of Indulin AT, a high molecular weight lignin (Tg of 154.4 ºC), the insoluble fraction was very high (97.9%) and characterized by a high Tg (154.1 ºC).

In the case of water, a polar solvent (Figure 3) the soluble fraction has a low aromatic content, as can be seen by the less prominent bands assigned to the aromatic ring (see bands assigned at 1600, 1513 and 1420 cm^{-1} identified by the green lines). An intensification of the hydroxyl band is also noticed indicating that these fractions are rich in hydroxyl functionalities. The Tgs of the insoluble fractions were 100.4 ºC and 158.1 ºC, respectively for Alcell and Indulin AT lignins.

IV. CONCLUSIONS

To the best of our knowledge, no solubility data was found to compare with the values measured in this work. Based on the preliminary studies performed with FTIR and DCS, the big difference between the Alcell and Indulin AT solubilities in acetonitrile, ethyl acetate and water can be related to structural and chemical properties of both solids, as well as with molecular weight. To get a deeper understanding of the involved phenomena, complementary analysis such as NMR and elementary analysis, are needed. This work is under progress or being planned.

V. ACKNOWLEDGEMENT

To COMPETE, QREN and EU (project QREN-ADI-33969-BIOBLOKS) and LSRE (strategic project PEst-C/EQB/LA0020/2011).

VI. REFERENCES

[1] Chakar, F.S.; Ragauskas, A.J. Review of current and future softwood kraft lignin process chemistry. *Industrial Crops and Products.* **2004**, *20*, 131-141.

[2] Xie, H; Li, S.; Zhang, S. Ionic liquids as novel solvents for the dissolution and blending of wool keratin fibers. Green Chem., **2005**, *7*, 606-608.

[3] Lora, J., Industrial commercial lignins: Sources, properties and applications. In: Monomers, polymers and composites from renewable resources. Belgacem, M.N., Gandini, A. (Eds). Elsevier, **2008**, 225-241.

[4] Cateto, C.A., Barreiro, M.F., Rodrigues, A.E., Brochier-Salon, M.C., Thielemans, W., Belgacem, M.N. Lignins as macromonomers for polyurethane synthesis: A comparative study on hydroxyl group determination. J. Appl. Polym. Sci., **2008**, 109 (5), 3008–3017.

[5] Hansen, C.M., Hansen Solubility Parameters A User's Handbook, Second Edition, CRC Press **2007**, 1-25, 279-283.

A RAPID METHOD FOR THE SIMULTANEOUS TITRATION OF PHENOLIC HYDROXYL AND CARBOXYL GROUPS IN INDUSTRIAL LIGNINS

Fanny BARDOT[1]*, Mathilde FEYDEAU[1], Gérard MORTHA[1]

[1]Laboratory of Pulp and Paper Science and Graphic Arts (LGP2) – UMR 5518 461 rue de la papeterie BP 65 – 38402 Saint Martin d'Hères Cedex France
*(*Fanny.Bardot@lgp2.grenoble-inp.fr)*

ABSTRACT

A rapid method based on simultaneous conductometric and acidic titration with pH measurement was evaluated in aqueous media. It provided good and fast results on a variety of industrial lignin samples. The main advantage of the method is that it provides a simple way for accurate testing of industrial lignins, often available in larger amounts than 1 g. Conversely, this may not be as well suited to the generally smaller amounts of lignins from extracted pulps at lab. scale (like HCl-dioxane extraction). The article presents the results of the analysis of a panel of industrial lignin samples, and as a comparison, the results obtained by the spectroscopic differential-UV method operated at two wavelengths.

I. INTRODUCTION

Lignin is the second most abundant polymer in earth and the main aromatic renewable resource. For a long while confined to energy generation by combustion, recent articles highlight a renewed interest in lignin studies and its applications [1]. Indeed, Laurichesse and Avérous reviewed a large amount of possible modifications on lignin thanks to their functional groups. Those ones are largely represented in this three dimensional polymer since there are methoxyl groups, hydroxyl groups (phenolic and aliphatic), carbonyl groups (ketone, quinone and aldehyde), carboxyl groups and even sulphonic groups as regards lignosulfonates. Thus, functional analysis is a key issue to follow and understand the modifications undergone during a reaction and elucidate the chemical structure of the lignin polymer. Several studies have established and analysed numerous methods to analyse the different functional groups of the lignin, like aminolysis, ultraviolet-spectroscopy method, non-aqueous titration, ^{1}H and ^{13}C NMR for phenolic hydroxyl groups, "acid number" determination, aqueous and non-aqueous titration for carboxyl groups [2, 3, 4, 5].

II. EXPERIMENTAL

Raw materials

The industrial lignins used in this study come from different pulping processes (Kraft, Soda and Organosolv). Kraft Innventia is a kraft lignin derived from wood and Soda EU Innventia, a soda lignin, both purchased from Innventia. Protobind 1000, Protobind 2400 and Protobind 3000 are industrial soda lignin derived from annual plants. They were purchased from GreenValue Enterprises LLC commercializing lignin products from ALM India. Organosolv CIMV (*Avidel* process) is extracted from straw and was purchased from CIMV.

Conductometric titration

1 g of lignin sample was introduced into 500 ml of deionized water, free of carbonates. 8 ml of sodium hydroxide 1M was then added to the mixture leading to a large excess of sodium hydroxide. After stirring until total dissolution (around 15 mn for most of the studied lignin), the solution was conductometrically titrated back with a 1M hydrochloric acid. Two titration end-point volumes were successively detected, in the following order:

- V1, detected by the change of the conductometric curve slope from negative to slightly positive at pH around 11.5-12,
- V3, detected by a sharper increase of the conductometric curve slope at a pH lower than 3.

Results are evaluated in mmol/g and in mol/ C9. Molecular weight of C9 lignin unit is assumed to be 200 g/mol.

Conductometric and pH-metric titration

This method is identical to the previous one except that both pH and conductometry are simultaneously followed all along the titration. The impact of the presence of the pH electrode on the measurement of conductivity was found negligible allowing the simultaneous titration. Another titration end point is also detected:

- V2, detected on the potentiometric curve at pH 7.

Spectrophotometric determination of phenolic hydroxyl groups (Δε method).

The amount of phenolic hydroxyl groups was determined by UV spectroscopy using the method described by Zakis [3]. This method is based on the difference in absorption at 300 and 360 nm between phenolic compounds in alkaline (ionized compounds) and neutral solutions (unionized compounds). The absorbance difference-spectrum is recorded and it is possible to quantify the abundance of the phenolic structure (condensed or uncondensed and bearing or not a carbonyl group) using the equation given by Gartner [6].

III. RESULTS AND DISCUSSION

Part 1: Conductometric titration

Aqueous conductometric titration was conducted on a large amount of industrial lignin. This method allows measuring the total amount of phenolic hydroxyl and carboxyl groups. Indeed, since V1 corresponded to the end-point titration volume of the free hydroxyl ions added in excess and V3 marking the start of an excess introduction of hydronium ions in the medium, the titration of total phenolic hydroxyl and carboxyl groups was obtained by the difference volume between V3 and V1. Results are presented on Table 1. Obviously, kraft and soda lignins exhibit higher amount of those functional groups than Organosolv CIMV since Kraft and Soda pulping lead to higher degradation and oxidation compared to organosolv processes.

Table 1. Phenolic hydroxyl and carboxyl groups by aqueous conductometric titration

	Total (phenolic hydroxyl & carboxyl groups) (mmol/g)	Total (phenolic hydroxyl & carboxyl groups) (mol/C9)
Kraft Innventia	3,24	0,65
Soda EU Innventia	2,97	0,59
Protobind 1000	2,96	0,59
Protobind 2400	2,76	0,55
Organosolv CIMV	2,27	0,45

Protobind 2400 was more fully explored in applying at different time a thermal treatment at 180°C and analysing the effect of this treatment on phenolic hydroxyl and carboxyl groups. The amount of these groups, presented on Table 2, seems to decrease with increasing time of treatment up to 30 mn. Cui [7] have ventured the hypothesis that thermal treatment lead to radical coupling reactions. They supposed that radicals, derived from the phenolic OH groups, seem to create condensed phenolic OH moieties such as 5-5'. Consequently, amount of phenolic hydroxyl groups decreased because of the thermal treatment and therefore, the total amount of functional groups.

Table 2. Effect on total acidic groups of thermal treatment**s** on Protobind 2400

	Total (phenolic hydroxyl & carboxyl groups) (mmol/g)	Total (phenolic hydroxyl & carboxyl groups) (mol/C9)
Protobind 2400	2,76	0,55
5 mn 180°C	1,65	0,33
15 mn 180°C	1,62	0,32
30 mn 180°C	1,51	0,30
60 mn 180°C	2,17	0,43

Part 2: Conductometric & pH-metric titration

Part 1 exhibits only the total of phenolic hydroxyl and carboxyl amount. By using both conductometry and pH-metry, it becomes possible to distinguish the amount of each functional group. Indeed, the titration of free phenols with pKa's in a range of 8-11.5 was obtained by the difference volume between V_2, corresponding to pH

7, and V_1. The remaining acidic groups, *i.e.* carboxylic groups, correspond thus to the difference volume between V_3 and V_2. It should be noticed that the conductivity curve presents no rupture between V3 and V1 (see **Figure 1)**. Equal conductivities of lignin moieties bearing either carboxylic or phenolic functions make it necessary to use pH detection to discriminate them, because of their different pKa.

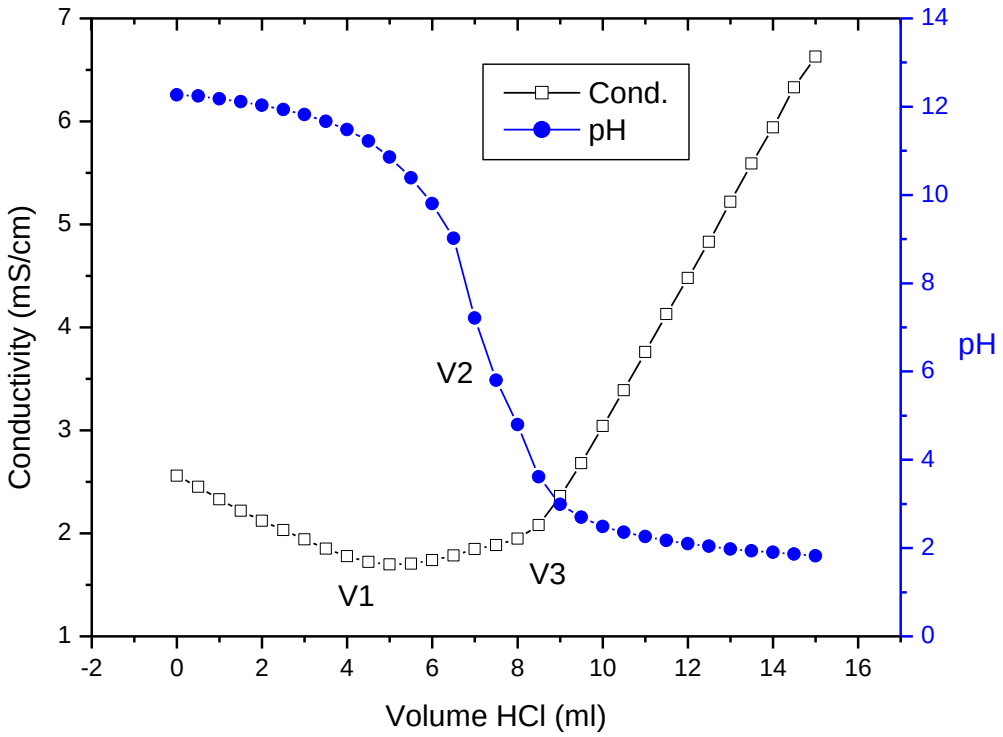

Figure 1. Conductometric and pH-metric curve for Protobind 3000

Results from this method are presented for two industrial soda lignins. The values from **Table 3** are in accordance with values from El Mansouri and Salvado [6] measured by non-aqueous titration on kraft and soda/anthraquinone lignin. Those results were compared to those from the dual-wavelength UV spectroscopy method presented on **Table 4**. This method is known to slightly underestimate the number of phenolic hydroxyl groups [3]. Results from aqueous titration and UV spectroscopy show a poor correspondence regarding Protobind 2400. Indeed, the difference is equal to 0.15 between the two methods, which is quite high. However, functional groups measurements of Protobind 2400 were realised on two completely different batches, which could explain these differences since reproducibility at industrial scale is hardly ever obtained.

Table 3. Phenolic hydroxyl and carboxyl groups by aqueous conductometric & pH-metric titration

	Phenolic hydroxyl groups (mmol/g)	Phenolic hydroxyl groups (mol/C9)	Carboxyl groups (mmol/g)	Carboxyl groups (mol/C9)	Total (phenolic & carboxyl) (mmol/g)	Total (phenolic & carboxyl) (mol/C9)
Protobind 2400	1,69	0,34	1,22	0,24	2,91	0,58
Protobind 3000	2,46	0,49	1,61	0,32	4,06	0,81

Table 4. UV spectroscopy method on industrial lignins from Part 1

UV spectroscopy	Phenolic hydroxyl groups (mmol/g)	Phenolic hydroxyl groups (mol/C9)
Kraft Innventia	2,3	0,46
Soda Innventia	2,7	0,54
Protobind 1000	2,46	0,49
Protobind 2400	2,44	0,49
Organosolv CIMV	1,6	0,32

IV. CONCLUSIONS

A rapid and complete analytical method for the simultaneous measurement of phenolic hydroxyl and carboxyl groups was conducted on industrial lignins. Aqueous titration for measurement of carboxyl groups is already well-known and reliable [4, 5] but results of this study proved that measurement of phenolic hydroxyl groups can dependably be realised at the same time. Furthermore, results tend to show that time of dissolution before titration (usually of 2 h) can be reduced to shorter time (15 mn) for easily dissolving lignin. Functional groups of several industrial lignins were studied showing that kraft lignin and soda lignin had highest amount of both phenolic hydroxyl and carboxyl groups, followed by organosolv lignin. That knowledge is determinant in the choice of an industrial lignin for subsequent application.

V. ACKNOWLEDGEMENT

The authors would like to thank the consortium of industrial companies that supported this study.

VI. REFERENCES

[1] Laurichesse, S., Avérous, L. Chemical modification of lignins: Towards biobased polymers. *Prog. Polym. Sci*. **2013.**
[2] Lin, S.Y., Dence, C.W., Editors. Methods in Lignin Chemistry. *Springer*. **1992.**
[3] Zakis, G.F. Functional Analysis of Lignins and Their Derivatives. *TAPPI Press*. **1994.**
[4] Gosselink, R.J.A., Abächerli, A., Semke, H., Malherbe, R., Käuper, P., Nadif, A., van Dam, J.E.G. Analytical protocols for characterisation of sulphur-free lignin. *Ind. Crops Prod*. **2004**, *19*, 271–281.
[5] El Mansouri, N.-E., Salvadó, J. Analytical methods for determining functional groups in various technical lignins. *Ind. Crops Prod*. **2007**, *26*, 116–124.
[6] Gartner, A., Gellerstedt G., Tamminen T. Determination of phenolic hydroxyl groups in residual lignin using a modified UV-method. *Nord. Pulp Pap. Res*. J. **1999**, *14*, 163–170.
[7] Cui, C., Sadeghifar, H., Sen, S., Argyropoulos, D.S. Toward Thermoplastic Lignin Polymers; Part II: Thermal & Polymer Characteristics of Kraft Lignin & Derivatives. *BioResources*. **2013**, *8*, 864–886.

PHOTOBLEACHING OF EUCALYPTUS KRAFT PULPS. THERMOGRAVIMETRIC MONITORING

Barneto, A.G.[1]., Ariza, M[1]., Vidal, T[2], Ariza, J[1].

[1]*University of Huelva, Department of Chemical Engineering, Physical Chemistry and Organic Chemistry (Campus de Excelencia Internacional Agroalimentario, ceiA3), Campus El Carmen, 21071 Huelva, Spain.*
[2]*Universitat Politècnica de Catalunya, Textile and Paper Engineering Department, Colom 11, E-08222 Terrassa, Spain.*
agustin.garcia@uhu.diq.es

ABSTRACT

This study assesses the potential of UV light as method to bleach eucalyptus pulps in different steps of their chemical bleaching process in a pulp mill. Higher brightness increasing were obtained on dirtier pulps, that is, alkaline washed and oxygen delignified pulps. In any case, photobleaching shows first-order kinetics. Rate of chromophores removal is proportional to the chromophores content in fiber surface. Complementarily, thermogravimetric analysis proved that UV light (400 nm wavelength) do not damages fiber integrity.

I. INTRODUCTION

In a global context which promotes the use of environmentally friendly technologies to bleach pulp, it gain particular relevance studies which illustrate the possibility to replace chemical bleaching by other treatments with low environmental impact based, for example, in the use of enzymes or ultraviolet light (photobleaching).

For long enough, it has been well known that light influences pulp in diverse way according their wavelength: yellowing occurs at wavelengths shorter than 385 nm, but bleaching dominates by wavelengths longer than 385 nm [1]. To improve UV-photobleaching, usually UV irradiation is applied in conjunction with chemical treatment that reduces significantly the bleaching time. For this purpose oxidant reagents like alkaline hydrogen peroxide [2][3] or reducing reagents like $NaBH_4$ or $NaHSO_3$ [2] have been found useful. Photochemical bleaching could be adopted as a part of TCF bleaching sequence. Efficiency of photochemical treatment increases when previously some metallic ions were removed by acid pretreatment. Simultaneous UV and ozone application yield pulp with highly brightness [3].

Present study attempt to assess photobleaching effect in pulps with different bleaching levels. To that, UV light 400 nm (without chemicals) was applied on several eucalyptus mill pulps in different steps of their chemical bleaching, that is, with different lignin or hexenuronics acids contents. Besides, measuring changes of brightness with time, the photobleaching kinetic was obtained.

Complementarily, in order to control UV-light damages on pulp, thermogravimetric analysis was used. As thermal degradation of pulp is sensitive to microfibril surface changes, it is possible to monitor cellulose integrity during bleaching by means thermogravimetry [5].

II. EXPERIMENTAL

Eucalyptus kraft pulps were supplied by ENCE mill (Huelva, Spain). P1: Alkaline watched pulp, P2: Alkaline oxygen delignified pulp (O step), P3: chlorine dioxide pulp (P0 step), P4: hydrogen peroxide pulp (PO step) and P5: chlorine dioxide pulp (P1 step).

UV Photobleaching was carried out on Technidyne Color Touch using intensity 765 W/m^2. Eucalyptus kraft pulp sheet (2 cm x 2 cm) was irradiated with light source at room temperature during 96 h, perpendicular to the surface of the sheet, washed with water, and dried.

Thermogravimetric analyses were carried out on a Mettler Toledo TGA/SDTA851e/LF1600 thermobalance, using about 5 mg of sample in each run. Pyrolysis and combustion runs were performed in nitrogen and synthetic air (4:1 N2/O2), respectively. The temperature was raised from 25 to 900 ºC at three different heating rates: 5, 10 and 20 ºC/min.

Brightness, , Kappa index, Viscosity and lignin Klason were measured according ISO 3688, ISO 302, ISO 535-1, and Tappi T-222, respectively. Hexenuronic acids (HexA) content was determined according to Chai el al (2001) [6].

III. RESULTS AND DISCUSSION

	Brightness (% ISO)	Viscosity (cSt)	Kappa	HexA (µmol/g)	Klason Lignin (g/100g)
P1	34.2	1021	14.41	44.4	2.6
P2	52.9	918	8.90	27.2	0.9
P3	75.5	842	2.43	10.8	0.6
P4	86.7	843	2.00	10.3	0.6
P5	88.5	826	1,65	6.4	0.6

Table1. Pulps characterization

Table 1 depicts main characteristics of studied pulps. As expected, alkaline washed pulp (P1) shows high values for viscosity, kappa index, Klason lignin and hexenuronic acids. Besides, brightness has lower value. Along bleaching process, viscosity, kappa index, HexA and Klason lignin decrease, but, not linearly. Oxygen delignification (P2) and first chlorine dioxide treatment (P3) show more impact than hydrogen peroxide (P4) and second chorine dioxide treatment (P5) on their reduction.
Same behaviour, but in opposite direction, is oberved in brightness evolution. Brightness is a measure of reflectance of blue light at 457 nm and relates with chromophores content. Chromophores are structures that absorb light within the visible range of spectrum. In pulps, main chromophoric structures are based in lignin (aromatic) and HexA (double bond close carboxylic group) produced during wood cooking. As kappa index is a measure of permanganate oxidisable compounds (mainly lignin and HexA) it is expected that an increase in kappa index is accompanied with a reduction (nonlinear) in brightness.

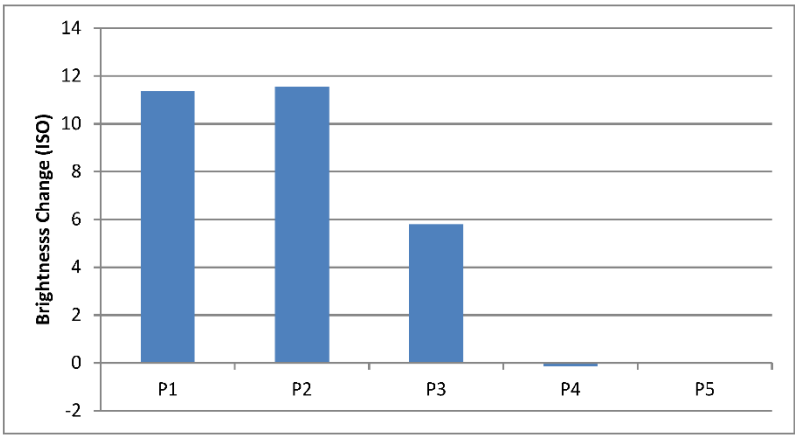

Fig 1. Brightness changes brought about by the UV irradiation in several pulps (Irradiation time 92 h).

As can be seen in **figure** 1, photobleaching is particularly effective when is applied on washed pulp (P1) and oxygen delignified pulp (P2), that is, when UV light acts on dirty pulps. On the contrary, UV light almost has no effect when is applied on pulps in the final steps of chemical bleaching: hydrogen peroxide (P4) or chlorine dioxide (second treatment) (P5). It seems that UV light removes chromophores presents in

the first steps of chemical bleaching. In these pulps (P1 and P2) effectiveness of photobleaching is lower but comparable to effectiveness of chemical treatment. For example, oxygen delignification increases brightness of P1 pulp 18.2 % ISO, and photobleaching (after 96 h) increases brightness 8.8 % ISO.

Monitoring evolution of pulp brightness during UV irradiation, allows obtain photobleaching kinetics. For that, chromophores concentration has been indirectly measured by means pulp brightness. Changes in pulp brightness is a measure of changes in chromophores content during certain time. **Figure** 2 shows that evolution of chromophores content in pulp P1 during UV-photobleaching agrees with a first-order kinetics, that is, the removal rate of chromophores is proportional to the chromophores content. **Figure** 2 allows calculating kinetic constant (k) and initial chromophores content in fiber surface. For both P1 and P2 pulps, kinetic constants (specific rate) are similar: 0.0113 h^{-1} and 0.0124 h^{-1}, respectively. As regards initial chromophores contents (measured by means brightness change that produce), the calculated values are: 13.0; 13.8; 6.6; 2.0 and 2.4 for P1, P2, P3, P4 and P5 respectively. Remarkably, similar values for initial chromophores content in both P1 and P2 shows that, although P2 is cleaner than P1, in both cases the UV-sensitive chromophores (surface chromophores) contents are the same. That is, although oxygen delignification removes chromophores, after this treatment, the surface of fiber even is completely covered by UV-sensitive chromophores. For P3 (after first chlorine dioxide treatment) initial concentration of chromophores is significantly minor, that is, in this case the fiber surface is not completely covered by UV-sensitive chromophores.

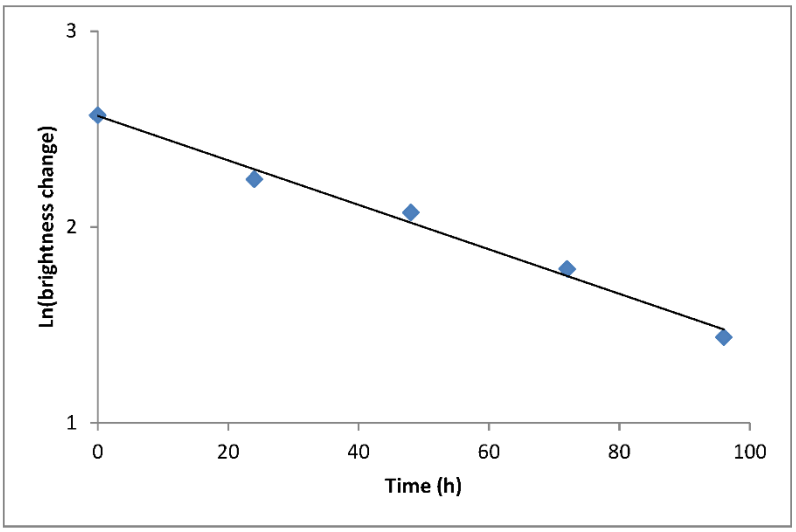

Figure 2. Natural logarithm of brightness change versus time.

.

Thermogravimetric analysis allows comparing thermal degradation path for pulp and UV-bleached pulp. If UV irradiation damages cellulose microfibril, thermal degradation should occur at lower temperature and their maximum mass loss rate should achieve lower value. As can be seen in **figure** 3, neither of those facts occurs in P1 pulp. In this case, DTG (mass loss rate) curve of photobleached pulp (P1B) is shifted toward higher temperature achieving higher degradation rate. This fact shows that UV light do not damages cellulose but, on the contrary, cleans fiber surface. More crystalline surface causes that thermal degradation takes place at higher temperature and occurs in narrower temperature interval. Complementarily, TG curve (mass loss) shows that thermal degradation of P1 pulp yields more residue than P1B. This fact agrees with previous reasoning, because thermal degradation of lignin produces more residues than thermal degradation of carbohydrates (cellulose and hemicellulose). As expected, clean P1B pulp (with lower lignin content), yield lower carbonaceous residues when is heated under nitrogen environment.

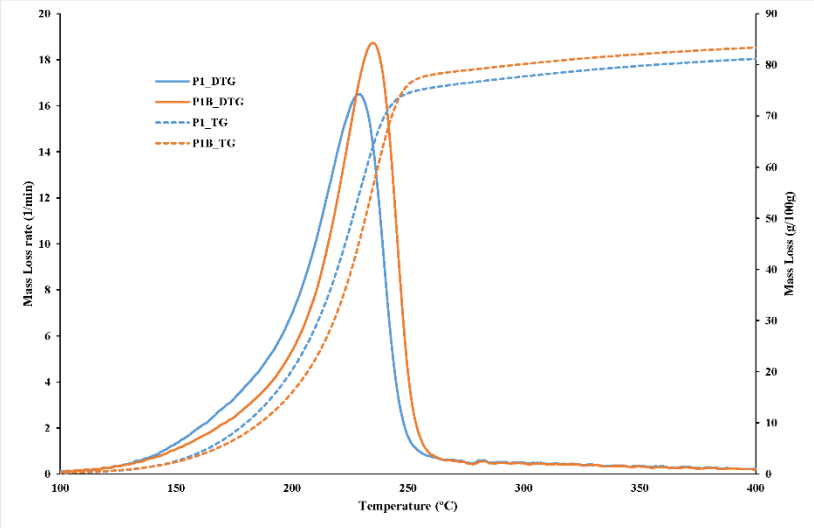

Figure 3. Thermal degradation profiles for P1 and P1B (UV-bleached) pulps. Nitrogen environment, heating rate 10 ºC/min. Mass loss rate was normalised to the initial mass.

IV. CONCLUSIONS

UV light (400 nm wavelength) based photobleaching is useful to remove chromophores from eucalyptus kraft pulps in the first steps of their chemical bleaching. Alkaline washed and oxygen delignified pulps significantly increase brightness because of UV action.

Photobleaching shows first-order kinetics, that is, the rate of chromophores degradation is proportional to the chromophores content which are accessible in fiber surface.

Although washed and oxygen delignified pulps have different chromophores contents (show different brightness), they show similar rate of chromophores degradation because photobleaching is surface phenomenon and in both cases fiber surface is completely surrounded by UV-light sensitive chromophores.

Thermogravimetric analysis proves that photobleaching with UV 400 nm wavelength do not damages cellulose. On the contrary, leads more clean surface that thermally degrades at higher temperature.

V. ACKNOWLEDGEMENT

ENCE mill at Huelva (Spain) is gratefully acknowledged for supplying the pulps.

VI. REFERENCES

[1] Nolan, P.; van de Akker, J.A.; Wink, W.A. The fading of groundwood by light. II. The physical mechanism of fading. *Paper Trade J*. **1945**, *121(11*), 33-37
[2] Ouchi, A. Efficient total halogen-free photochemical bleaching of kraft pulps using alkaline hydrogen peroxide. *Journal of Photochemistry and Photobiology A: Chemistry* **2008**, *200*, 388–395
[3] Kurosu, K.; Miyawaki, S.; Ochi, T. Photochemical Bleaching of Kraft Pulp by UV Radiation. *Japan Tappi Journa*l, **2009**, *63*, 317-324
[4] Ouchi, A.; Saruwatari, A.; Suzuki, T. An efficient photochemical bleaching of kraft pulps using total halogen-free reducing reagents. *Journal of Photochemistry and Photobiology A: Chemistry* **2008**, *193*, 122–128
[5] Barneto, A.G.; Vila, C.; Ariza, J. Eucalyptus kraft pulp production: Thermogravimetry monitoring. *Thermochimica Acta* **2011**, *520*, 110–120
[6] Chai, X.S.; Zhu, J.Y.; Li. J. A simple and rapid method to determine hexeneuronic acid groups in chemical pulps. *Journal Pulp and Paper Science* , **2001**, *27*, 165-170

SECRETION PATTERNS OF LIGNINOLYTIC ENZYMES BY WHITE-ROT WOOD AND HUMUS BASIDIOMYCETES REVEALED BY DYE DECOLORIZATION ON AGAR PLATES

José M. Barrasa[1], Angel T. Martínez[2] and Francisco J. Ruiz-Dueñas[2*]

[1]*Departamento de Ciencias de la Vida, Universidad de Alcalá, E-28805 Alcalá de Henares, Spain*
[b]*Centro de Investigaciones Biológicas, CSIC, Ramiro de Maeztu 9, E-28040 Madrid, Spain*

ABSTRACT

A total of 15 white-rot wood and 19 white-rot humus basidiomycetes were tested for decolorization of two recalcitrant aromatic dyes (Reactive Blue 38 and Reactive Black 5) incorporated to malt extract agar medium. Two dye decolorization patterns were observed that correlated with the wood and humus white-rot lifestyles of basidiomycetes. The former basidiomycetes caused a decolorization ring inside of the fungal colony, whilst the latter caused a decolorization ring outside of the fungal colony, suggesting two different degradation strategies. These two strategies were related to the ability to secrete peroxidases and laccases restricted to the colony area or extending to the surrounding medium, as revealed by enzymatic tests performed directly on the agar plates in four white-rot wood Polyporales (*Abortiporus biennis, Trametes pubescens, Phlebia rufa* and *Polyporus arcularius*), three white-rot wood Agaricales (*Gymnopilus junonius, Cyathus striatus* and *Xerula radicata*) and three white-rot humus Agaricales (*Agrocybe pediades, Mycena polygramma* and *Rhodocollybia butyracea*). Similar oxidoreductases production patterns were observed when these fungi were grown in absence of dyes, although the set of enzymes released was different. These results are consistent with the existence of two colonization strategies developed by white-rot basidiomycetes to degrade the most important types of lignocellulosic materials accumulated on forest soils, such as wood and leaves.

I. INTRODUCTION

Cellulose, hemicelluloses and lignin are the main components of plant cell walls produced by the photosynthetic activity of land plants. Lignin protects cellulose and hemicelluloses and is highly recalcitrant to degradation due to its aromatic nature and structural heterogeneity. A specialized group of basidiomycetes, the so called white-rot fungi, are the most efficient organisms degrading lignin, and constitute one of the most important ecophysiological groups of the mycobiota of soil in forest ecosystems. Lignocellulosic materials accumulated on forest soil are mainly represented by dead wood and leaves. According to the type of lignocellulosic material to be degraded, two types of ligninolytic basidiomycetes can be distinguished: wood and humus white-rot basidiomycetes. The former degrade wood lignin leaving a bleached substrate [1] and the latter degrade lignin and polyphenols of leaves causing the so-called white-rot humus [2]. Whilst white-rot wood basidiomycetes are broadly represented by members of the orders Polyporales and some others of the order Agaricales, white-rot humus basidiomycetes are mainly found among members of Agaricales.

To degrade the complex molecule of lignin, white-rot basidiomycetes have developed an extracellular ligninolytic system, whose composition often differs between species. In general, it is made up of low molar-mass metabolites, oxidases and ligninolytic enzymes such as laccases and especially high redox-potential peroxidases. The latter include manganese peroxidase (MnP), lignin peroxidase (LiP) and versatile peroxidase (VP) being activated by the hydrogen peroxide produced by oxidases [3]. The ligninolytic peroxidase genes are characteristic of white-rot fungal genomes. Ligninolytic peroxidases and laccases have a broad substrate specificity acting directly or through mediators [4] and can also degrade recalcitrant aromatic compounds [5] including synthetic aromatic dyes, such as the phthalocyanine dye Reactive Blue 38 (RB38) and the azo dye Reactive Black 5 (RB5), used in textile industries [6], some of which have been used to detect ligninolytic activity in culture [7].

In the present work, two decolorization patterns, inside or outside of the fungal colony, are described in dye agar cultures of white-rot wood and leaf litter, respectively. Furthermore, assays to detect high and low redox potential oxidoreductase activities on agar plates, with and without dyes, were carried out on representative white-rot wood and humus basidiomycetes. The decolorization patterns and enzymes produced were finally correlated with two possible strategies followed by white-rot fungi to colonize wood and humus respectively.

II. EXPERIMENTAL

II.1. Fungal sampling and culture

Fungal species fruiting on dead wood and leaf litter were isolated from different Spanish native forests. The collected samples consisted of fresh fruit bodies, which were conserved at 4ºC before grown as pure cultures. Fungal isolations were made from mycelium (5x5 mm pieces of context) aseptically removed from fruit bodies that was inoculated in Petri dishes with malt extract (2% wt/vol) agar (MEA) containing ampicillin (1.5 mg/L). Fungal dry material is deposited in AH (Herbario de la Universidad de Alcalá) and pure cultures are conserved in the fungal culture collection of Departamento de Ciencias de la Vida (Universidad de Alcalá).

II.2. Dye decolorization assays in agar plates

Decolorization assays were carried out on Petri dishes (9 cm diameter) with 20 mL of Malt Extract Agar (MEA) containing RB38 and RB5 at two concentrations (75 and 150 mg/L). Plugs of 0.5 cm diameter from MEA cultures were inoculated on plates with the synthetic dyes, which were incubated at 25ºC and examined each two days for decolorization. The radial mycelial growth and decolourized area were measured, and only those species producing a decolorization circle of at least 2 cm diameter, within 15 days of incubation, were selected.

II.3. Enzymatic assays in plates

Enzymatic activities were tested directly on ten fungal colonies grown (at 25ºC) on: i) MEA plates; and ii) RB5 and RB38 containing MEA, where the fungi had previously decolorized these dyes. Ten µl of catechol, guaiacol, syringol and ABTS in 96% (vol/vol) ethanol were dropped on MEA plate cultures in front of, behind or on the edge of the fungal colony. These substrates are oxidized by laccase (EC 1.10.3.2) and by generic peroxidase (GP; EC 1.11.1.7), short MnP (EC 1.11.1.13), VP (EC 1.11.1.16) and dye-decolorizing peroxidase (DyP; EC 1.11.1.19) in the presence of hydrogen peroxide.

Ten µl of 0.1 M RB5 or 25 mM RB38 in 96% (vol/vol) ethanol, which are oxidized by VP and DyP in the presence of hydrogen peroxide were assayed both on MEA plates, as previously described for phenols and ABTS, and on decolorized MEA plates. ABTS, RB5 and RB38 were not completely soluble under the above conditions and they were added as a suspension on the plate. Enzymatic oxidation of dyes mediated by 3,4-dimethoxybenzyl (veratryl) alcohol (VA) radical resulting from VA oxidation by LiP (EC 1.11.1.14) and VP, was also examined. With this purpose, ten µl of 20 mM VA (in H_2O) were added together with ten µl of 0.1 M RB5 or 25 mM RB38 in 96% (vol/vol) ethanol. Five µl of a concentrated catalase solution was also supplied prior to the addition of the above substrates to remove any peroxide traces and avoid peroxidase activity. alternatively, one µl of 10 mm hydrogen peroxide was simultaneously added together with dyes, ABTS or phenols to confirm the presence of peroxidases. Substrate oxidation was easily followed by changes in color.

III. RESULTS

A total of 34 species were selected because of the ability to produce a decolorization circle on plate dyes of at least 2 cm diameter within 15 days of incubation. These species could be divided in two ecophysiological groups. The first group colonized and degraded dead wood causing a white-rot decay pattern due to lignin removal. The second group colonized and degrade dead leaves contributing to soil humus formation causing a white-rot humus decay pattern, which results in bleaching of brown dead leaves due to polyphenol and lignin degradation. The majority of the wood decomposing species studied belongs to the order Polyporales (11) but a few of them belong to the orders Agaricales (4). Otherwise, all the humus basidiomycetes investigated (19 species) belong to the order Agaricales. Two different decolorization patterns were observed when fungal species were grown on MEA plates containing the two dyes assayed. White-rot wood fungi cause a decolorized circle inside the colony and white-rot humus fungi cause a decolorized circle outside the colony.

Enzymatic assays were performed directly on MEA plates where ten species representative of white-rot wood Polyporales (4) and white-rot wood (3) and humus (3) Agaricales under study had been previously grown. The four wood Polyporales and the three wood Agaricales were able to oxidize all the low redox potential substrates (i.e. catechol, guaiacol, syringol and 2,2´-azino-bis:ABTS) added within and on the inner edge of the fungal colony but not the two recalcitrant dyes (RB5 and RB38) even after addition of exogenous hydrogen peroxide and veratryl alcohol (VA). Peroxidase involvement was definitively ruled out, since the addition of catalase did not produce any significant effect on the oxidation of phenols and ABTS, and the reaction could be associated to laccase type activity. The same activity was observed in the three humus Agaricales, but the oxidative activity was mainly detected on the outer edge and in front of the limits of the fungal colony. Oxidation of ABTS and syringol was slowed down, but not completely removed, in the presence of catalase, and conversely it was accelerated when peroxide was added. According to these results, laccases would be responsible for the low activity levels observed in the presence of catalase. We could also confirm both that peroxide is generated by these fungi, and that peroxidases are produced.

Enzymatic assays were also performed by adding RB5 and RB38 on dye plates where the dyes had been previously decolorized by the fungi. *C. striatus*, tested as representative of white-rot wood Agaricales, was unable to decolorize any of the dyes when added on previously decolorized RB38 plates. This confirm the absence of any enzymatic activity able to oxidize these dyes, such as ligninolytic peroxidases and DyPs.

On the other hand, *T. pubescens*, as representative of wood Polyporales, was able to decolorize RB5 but not RB38 when added on the previously decolorized dye plates. In the RB5 plates, high decolorization activity was observed 16 h after RB5 addition within the colony. This ability was enhanced by hydrogen peroxide and dramatically impaired, although not completely removed, by catalase. These results confirm the involvement of both laccase (maybe acting through natural mediators) and peroxidase activities in the oxidation of this dye, as well as the fungal production of the hydrogen peroxide necessary for peroxidase activity. In the RB38 plates, no decolorization of RB5 was observed up to 2 days after its addition. A 6 day period was necessary when catalase was simultaneously added. Again, these results suggest the production of both hydrogen peroxide and peroxidase activity. The long time (days) necessary to decolorize RB5 suggests *de novo* synthesis of the enzymes involved.

Finally, *R. butyracea* was tested as a representative for the white-rot humus Agaricales. This species was unable to decolorize any of the recalcitrant dyes when added alone or together with peroxide or catalase in the inner part of the colony grown on dye-containing MEA. However, both RB5 and RB38 were completely decolorized at the edge and in front of the limits of the colony when incubation was extended to 20 h, except in the presence of catalase. These results suggest *de novo* enzyme synthesis, as mentioned above, and confirm the importance of hydrogen peroxide in the decolorization process by this fungus.

IV DISCUSSION

This is the first time that a correlation between ecophysiological groups of lignin degrading basidiomycetes and dye decolorization patterns is observed. Dye decolorization is a simple assay for the identification of fungal ability to transform lignin. Both lignin and the recalcitrant dyes assayed are aromatic compounds that can be oxidized by ligninolytic peroxidases in the presence of hydrogen peroxide [8]. The enzymatic assays performed in three regions of the fungal plates - within, on the edge, and outside the limits of the fungal colony - revealed that indeed laccases and peroxidases are released in those regions where dyes are decolorized in cultures of white-rot wood Agaricales and Polyporales (within and on the inner edge of the colony) and white-rot humus Agaricales (on the outer edge and outside the limits of the colony). On the other hand, the enzymatic analysis on MEA plates without dyes revealed basically the same wood and humus basidiomycete secretion patterns identified on the dye plates, although the set of secreted enzymes was not competent for dye decolorization. The latter is easily understandable considering that genes encoding the wide range of peroxidases and laccases secreted by white-rot fungi are differentially regulated in response to a variety of environmental signals, including nitrogen and carbon sources, xenobiotics and oxidative stress, among others [9].

All the above results together suggest two different strategies used by wood and humus white-rot basidiomycetes to colonize and degrade their respective substrates. These strategies would be related to the ability of different regions of the fungal colony to release oxidative enzymes acting on aromatic compounds, including the recalcitrant dyes used in the present study and the lignin polymer in nature [2,3]. It is observed that white-rot wood basidiomycetes release their oxidative enzymes in the area initially colonized by the fungal mycelium. We suggest that the decolorization pattern produced by white-rot wood basidiomycetes on agar plates would be related to their strategy for substrate colonization and degradation in nature. Wood constitutes a hardly-colonized substrate where fungal colonies have physical and nutritional limitations to growth and extend their action. In this context, the production of ligninolytic enzymes seems to be more active in secondary hyphae located at the center of the colony, with a limited diffusion to the outer region and the surrounding medium.

On the contrary, white-rot humus basidiomycetes efficiently secrete peroxidases and laccases from young hyphae located at the periphery of the colony. It has been observed that the secreted oxidoreductases subsequently diffuse in the medium acting on the synthetic dyes in the same way as they would act on leaf litter lignin in nature, allowing the fungi to colonize the soil. Thus, the decolorization pattern observed in white-rot humus basidiomycetes - i.e. outside of the limit of colony - would be related to the nature of the decayed substrate. At the contrary of wood, in this case the substrate is constituted by a whole of unrestricted elements (intermixed dead leaves), and all of this entire system provides a habitat for fungal colonization. Under these conditions, the ligninolytic system would be more active in environment exploring by young hyphae, and could involve the secretion and diffusion of ligninolytic enzymes for degradation of lignin and other aromatic compounds in dead leaves.

V. CONCLUSIONS

The differential dye decolorization and enzyme expression/secretion patterns observed suggest that differences in lignocellulose composition and structure could play an important role in wood and humus white-rot (ligninolytic) basidiomycetes diversity. This would include divergent strategies to colonize and degrade wood

and leaf-litter under natural conditions. Such strategies would be related to the metabolic state of the active mycelium, the production of ligninolytic oxidoreductases and their eventual diffusion in the environment, as suggested by the different dye decolorization and enzyme secretion patterns observed in plate cultures of wood and humus fungi. This hypothesis should be corroborated by laboratory studies using more natural (sawdust and leaf litter) growth media. In addition, further investigations aimed to determine the factors regulating oxidoreductase expression and diffusion (or immobilization) are required to explain the differences observed between the two ecophysiological groups of fungi here studied.

VI. ACKNOWLEDGEMENT

This work was supported by the CGL2009-07316 (to JMB) and BIO2011-26694 (to FJR-D) projects of the Spanish Ministry of Economy and Competitiveness (MINECO), and by the PEROXICATS (KBBE-2010-4-265397) and INDOX (KBBE-2013.3.3-04-613549 of the European Union (to ATM). FJR-D thanks a "Ramón y Cajal" contract of the Spanish MINECO.

VII. REFERENCES

[1] Blanchette R.A. Degradation of the lignocellulose complex in wood**.** *Can. J. Bot.* **1995**, *73,* S999-S1010.

[2] Osono T. Ecology of ligninolytic fungi associated with leaf litter decomposition**.** *Ecological Research* **2007**, *22,* 955-974.

[3] Martínez A.T.; Speranza M.; Ruiz-Dueñas F.J.; Ferreira P.; Camarero S.; Guillén F.; Martínez M.J.; Gutiérrez A.; del Río J.C. Biodegradation of lignocellulosics: Microbiological, chemical and enzymatic aspects of fungal attack to lignin**.** *Int. Microbiol.* **2005**, *8,* 195-204.

[4] Ruiz-Dueñas F.J.; Morales M.; García E.; Miki Y.; Martínez M.J.; Martínez A.T. Substrate oxidation sites in versatile peroxidase and other basidiomycete peroxidases**.** *J. Exp. Bot.* **2009**, *60,* 441-452.

[5] Pointing S.B. Feasibility of bioremediation by white-rot fungi**.** *Appl. Microbiol. Biotechnol.* **2001**, *57,* 20-33.

[6] Barrasa J.M.; Martínez A.T.; Martínez M.J. Isolation and selection of novel basidiomycetes for decolorization of recalcitrant dyes**.** *Folia Microbiol. Prague* **2009**, *54,* 59-66.

[7] Gold M.H.; Glenn J.K.; Alic M. Use of polymeric dyes in lignin biodegradation assays**.** *Methods Enzymol.* **1988**, *161,* 74-78.

[8] Tinoco R.; Verdín J.; Vázquez-Duhalt R. Role of oxidizing mediators and tryptophan 172 in the decoloration of industrial dyes by the versatile peroxidase from *Bjerkandera adusta***.** *J. Mol. Catal. B-Enzym.* **2007**, *46,* 1-7.

[9] Janusz G.; Kucharzyk K.H.; Pawlik A.; Staszczak M.; Paszczynski A.J. Fungal laccase, manganese peroxidase and lignin peroxidase: Gene expression and regulation**.** *Enzyme Microb. Technol.* **2013**, *52,* 1-12.

THE EFFICIENCY OF PHYSICOCHEMICAL PRETREATMENT OF SORGHUM AND MISCANTHUS BIOMASS IN THE PRODUCTION OF 2ND GENERATION OF BIOETHANOL

Batog J.*, Wawro A., Pieprzyk-Kokocha D., Skibniewski Z.

Institute of Natural Fibres & Medicinal Plants, Wojska Polskiego 71b, Poznan, Poland
** jolanta.batog@iwnirz.pl*

ABSTRACT

The paper presents the studies on the efficiency of physicochemical pretreatment of lignocellulosic materials i.e. sorghum and miscanthus for the production of 2nd generation of biofuels. Lignocellulosic material must be disintegrated and then subjected to physicochemical pretreatment i.e. saturation with diluted acids and pressure steam explosion. We determined the effect of sulfuric and lactic acid (concentration and incubation time) as well as autoclaving process (time and temperature) on the content of reducing sugar, which parameter was determined with Miller's method in an enzymatic test.
The method of physicochemical pretreatment of sorghum and miscanthus biomass is an important factor affecting efficiency of biofuel production obtained from these raw materials.

I. INTRODUCTION

Bioethanol produced from organic raw materials is a renewable and clean resource for energy production, which is used as fuel and also in chemical, cosmetic and pharmaceutical industries. The main material for bioethanol production is cereal and maize grain, potatoes and also sugar beet. Bioenergetic use of these plants is controversial as it implies reduction of the arable area for production of food and feed. Alternative plants that can be used for bioenergy are for example sorghum and miscanthus and their high calorific value of combustion and high yield of dry biomass make them a suitable material for the production of biofuels (Figure 1).

Figure 1. Plantations of sorghum (left) and miscanthus (right)

Sorghum is an annual plant reaching the height of 4 m, tolerant to drought, and providing high yields of dry mass (28 t/ha) at the so called milk-wax phase of seed [1]. Sorghum biomass contains high amounts of monosaccharides, mainly of fructose (9.75%), what indicates its high usability for obtaining bioethanol [2]. Miscanthus is a perennial tuft grass with low water-mineral needs, resistant to diseases and pests, which can be grown on poor grade soils. It is characterized with high growth of biomass (18-30 t of dry mass/ha), what leads to possible improvement of the cost-efficiency of the production of 2nd generation biofuels [3]. The actual species of *Miscanthus giganteus* is a hybrid bred from two other species i.e. *Miscanthus sinensis* and *Miscanthus sacchariflorus* and it can grow to the height of 3.5 m in one vegetation season. Additionally, both plants have high energetic value of combustion - sorghum of 15 MJ/kg and miscanthus of 14-17 MJ/kg.
Using lignocellulosic biomass as an alternative renewable source of energy can improve energetic security and enhance reduction in greenhouse gases and stability of fuel prices.
Lignocellulosic biomass is characterized with complexity of its chemical composition, as it contains in its structure a polymeric complex called lignocellulose, which is relatively difficult for biodegradation.
The lignocellulosic complex found in cell walls of plants is composed of the cellulose, hemicelluloses and lignin. Cellulose – a glucose polymer and hemicelluloses that mainly consist of galactose, mannose, xylose and arabinose molecules are a potential substrate for efficient use in fermentation processes. Lignin, consisting from

phenolic alcohol derivates such as *p*-coumaryl, coniferyl and sinapyl alcohol, structurally crosslinked by ester and carbon bonds, is an effective obstacle in bioethanol production from plant biomass.
This forces subjecting the biomass to pretreatment, which affects significantly the course of the further stages of bioethanol production i.e. enzymatic hydrolysis and fermentation process, and determines the final efficiency of the process [4-5]. Lignocellulosic material must be subjected to pretreatment i.e. disintegration, saturation with diluted acids and pressure steam explosion. Such processing steps allow for efficient hydrolysis of hemicelluloses and lignin, and prepare cellulose for enzymatic treatment, what ensures effective enzymatic hydrolysis of the cellulose fraction [4].

II. EXPERIMENTAL

The aim of the study is determination of the efficiency of physicochemical processing of sorghum and miscanthus biomass during preparation of the materials for production of bioethanol.
The materials used in the study were:
- Sucrosorghum 506 – from Experimental Farm of INF&MP in Sielec Stary (Poland),
- Miscantus Giganteus – from Institute of Plant Genetics of Polish Academy of Sciences in Poznan.

Chemical components of sorghum and miscanthus biomass were evaluated i.e. cellulose (acc. to PN-P-50092:1992P), hemicelluloses – as the difference holocellulose (acc. to PN-P-050092:1992P) and cellulose, and lignin (acc. to BN-86/7501-11), and also moisture was determined (acc. to PN-Z-04002-13/1997P).
The raw material was subjected to crushing on the crusher for branches, and then dried in the temperature 50°C for the period of 24 hours.
In the first stage of preliminary processing, the material prepared in that way was disintegrated on percussive mill with mesh size 1.8 mm. Sieve analysis of the sorghum and miscanthus biomass was made with the use of rotary laboratory shaker with the use of the sieve set of mesh diameters at: 5, 4, 3, 2, 1, 0.5 and 0.1 mm [6].
The second stage of the study comprised tests for optimization of physicochemical treatment of disintegrated sorghum and miscanthus biomass namely of saturation with diluted acids and pressure steam explosion.
Firstly, the effect of acid type and concentration on sorghum and miscanthus biomass was determined where we tested lactic and sulfuric acids at concentration between 0.1 and 2%, and we studied the effect of incubation time of the materials in the acid within 10-300 minutes. Then the effect of autoclaving process was evaluated. The tests were carried out for temperatures at 100, 121 and 134^{o}C for 15-60 minutes.
A determinant of the efficiency these processes is the content of reducing sugar determined according to Miller's method with DNS (3, 5-dinitrosalicylic acid) in the enzymatic test [7]. This test was performed with the use of the enzymatic preparation Celluclast 1.5L (Novozymes). The vegetable raw material was incubated at 40°C in 0.05 M the citrate buffer of pH 4.8 for 2 hours. Then, absorbance measurement was made against reference sample at the wavelength 530 nm. The reading of the values of the reducing sugar concentration was done from the reference absorbance curve for glucose (Figure 2).

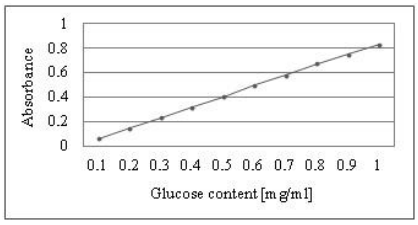

Figure 2. Reference absorbance curve for glucose

The selection of the suitable method of the physicochemical treatment of the sorghum and miscanthus biomass will have a bearing on the efficiency of the entire process of the energy production from these raw materials.

III. RESULTS AND DISCUSSION

As result of the first stage of the study the chemical composition of the sorghum and miscanthus biomass were measured (Table 1).

Table 1. Chemical constitution the sorghum and miscanthus biomass

Raw material	Moisture [%]	Cellulose [%]	Hemicelluloses [%]	Lignin [%]
Sorghum	11.5	26.2	25.9	16.1
Miscanthus	5.0	42.1	36.7	22.4

On the basis of the results it can be observed that:

- the miscanthus biomass has higher cellulose and hemicellulose content in comparison with the sorghum biomass, which components are potential substrates for enzymatic hydrolysis and fermentation process,
- the sorghum biomass has lower lignin content than the miscanthus biomass, what undoubtedly is an advantage of the sorghum in terms of the biofuel production,
- the miscanthus biomass is characterized with the lower moisture than the sorghum biomass, what undoubtedly results from later harvesting of miscanthus from the field than of the sorghum.

The raw materials were subjected to the disintegration on a percussive mill with mesh size 1.8 mm and the sieve analysis was made of the sorghum and miscanthus biomass (Figure 3). The results allow for observing that the distribution of specific fractions of sorghum and miscanthus is similar, where the highest amount were found for fractions at 0.1-0.5 mm and 0.5-1 mm [6]. In terms of further processing the best particles are as small as possible with homogenous size. Disintegration of the raw materials enables to destroy partially the crystalline cellulose structure and improves susceptibility of the lignocellulosic complex polymers to the action of chemical agents.

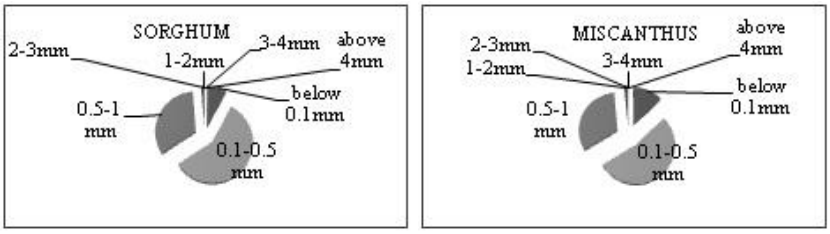

Figure 3. Sieve analysis of the sorghum and miscanthus biomass after the percussive mill disintegration (mesh - 1.8 mm)

In order to determine the efficiency of the physicochemical processing of the sorghum and miscanthus biomass, the content of reducing sugar was measured by Miller's method in the enzymatic test. Figure 4 presents obtained quantities of reducing sugar from the sorghum and miscanthus biomass depending on the concentration of sulfuric and lactic acids.

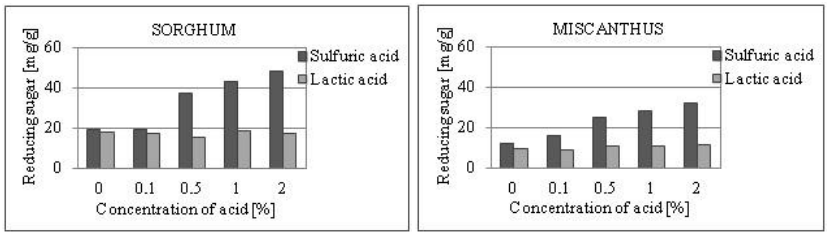

Figure 4. Content of reducing sugar from sorghum and miscanthus biomass after pretreatment with acids

The values of the reducing sugar in the enzymatic test from the sorghum and miscanthus biomass after pretreatment with acids allowed for selection of the optimum type and concentration of the acid, that is sulfuric acid at the concentration from 0.5% and above. This suggests that the raw material, in particular the sorghum biomass, obtained in this way is more susceptible to the enzymatic hydrolysis. Moreover, no significant effect of the incubation time with sulfuric acid (0.5%) was observed on the content of reducing sugar.

Next, we determined the effect of the autoclaving process parameters - temperature and time, on the content of reducing sugar from the sorghum and miscanthus biomass, after 10 minute pretreatment with sulfuric acid (0.5%) - Figure 5.

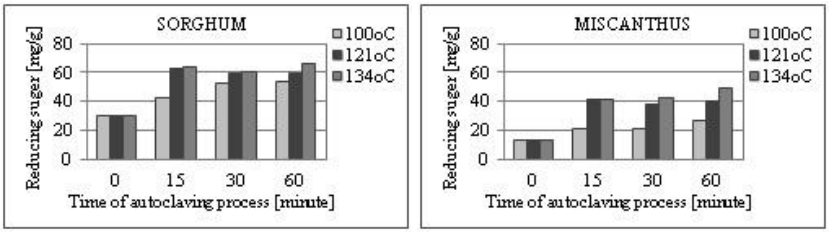

Figure 5. Content of reducing sugar from sorghum and miscanthus biomass after autoclaving process

The content of reducing sugar determined with Miller's method from sorghum and miscanthus biomass after autoclaving process showed that this process increased susceptibility of the raw materials to the enzymatic hydrolysis. The efficiency of the autoclaving process depends mostly on the temperature and to a lesser extent on

the time of the process. It was found that higher values of the reducing sugar from the raw materials were achieved after the autoclaving process run at 121°C, slight increase was also observed for 134°C, in time from 15 to 60 minutes, in particular in case of the sorghum biomass.
The results indicate the necessity of pretreatment in processing of lignocellulosic raw materials and confirm usefulness of saturation with diluted acids and pressure steam explosion for preliminary degradation of lignocellulosic substrate prepared for further stages of bioethanol production i.e. enzymatic hydrolysis and fermentation process.

IV. CONCLUSIONS

- Raw material i.e. sorghum and miscanthus biomass is as much important for bioethanol production as selection of optimal bioprocessing technology, namely, saturation with diluted acids and pressure steam explosion.
- The content of reducing sugar determined with Miller's method from sorghum and miscanthus biomass showed that pretreatment of the raw materials with sulfuric acid (0.5-2%, 2% was regarded as optimal) for 10 minutes, followed by the autoclaving process at temperature 121-134°C for 15-60 minutes (134°C and 60 minutes were regarded as optimal) is an effective method of the pretreatment.
- Sorghum biomass shows higher content of reducing sugar after physicochemical pretreatment in comparison to miscanthus biomass, what might be linked with the presence of high amounts of monosaccharides in the material along with polysaccharides.
- The pretreatment of the lignocellulosic biomass is critical for the production of cellulose ethanol, having significant effect on the consecutive processes.

V. ACKNOWLEDGEMENT

The authors acknowledge the funding by the National Centre for Research and Development, Poland, under the project PBS1/A8/9/2012.

VI. REFERENCES

[1] Burczyk H.; Kołodziej J.; Kowalska M. Plony i wartości energetyczne kukurydzy, sorgo i konopi włóknistych w porównaniu z roślinami egzotycznymi. (Yields and energy value of maize, sorghum and fibrous hemp as compared with exotic plants.) *Materiały XIII Konferencji Naukowej IUNG-PIB* **2009**.

[2] Śliwiński B.; Brzózka F. Historia uprawy sorgo i wartość pokarmowa tej rośliny w uprawie na kiszonkę. (History of cultivation of sorghum and its nutritional value in cultivation for silage.) *Post. Nauk Rol.* **2006**, *1*, 25-37.

[3] Jeżowski S.; Głowacka K.; Kaczmarek Z. Variation on biomass yield and morphological traits of energy grasses from the genus Miscanhus during the first years of crop establishment. *Biomass Bioenergy*, **2011**, *35*, 814-821.

[4] Hendriks A.T.W.M.; Zeeman G. Pretreatments to enhance the digestibility of lignocellulosic biomass. *Bioresour. Technol.* **2009**, *100*, 10-18.

[5] Sims R.E.H.; Mabee W.; Saddler J.N.; Taylor M. An overview of second generation biofuel technologies. *Bioresour. Technol.* **2010**, *101*, 1570-1580.

[6] Wawro A.; Batog J.; Pieprzyk-Kokocha D.; Skibniewski Z. Efektywność obróbki mechanicznej biomasy sorgo i miskanta w produkcji bioetanolu II generacji. (The efficiency of mechanical processing of sorghum and miscanthus biomass in the production of 2nd generation bioethanol.) *Chemik*, **2013**, *67*, 927-934.

[7] Miller G.L. Use of dinitrosalicylic acid reagent for determination of reducing sugar. *Anal Chem.* **1959**, *31*, 426-428.

BATCH ACETONE-BUTANOL-ETHANOL (ABE) FERMENTATION USING *Clostridium beijerinckii* FROM PRETREATED WHEAT STRAW

Carolina Bellido*, Gerardo González-Benito, Marina Loureiro Pinto, Mónica Coca Sanz, María Teresa García-Cubero

*Department of Chemical Engineering and Environmental Technology, University of Valladolid, Dr.Mergelina s/n, 47011, Valladolid, Spain (*Email:cbellido@iq.uva.es)*

ABSTRACT

ABE fermentation of steam-exploded and ozonated wheat straw by *Clostridium beijerinckii* DSM 6422 was studied applying two different operational strategies, separate hydrolysis and fermentation (SHF) and simultaneous hydrolysis and fermentation (SSF). In SHF assays, 11.4 g/L ABE (7.2 g/L butanol) were obtained in steam-exploded hydrolysates from 37.3 g/L total sugars using the whole slurry from pretreatment, while 7.1 g/L ABE (4.9 g/L butanol) were achieved in washed ozonated hydrolysates from 30.8 g/L total sugars after enzymatic hydrolysis. SSF experiments did not result in successful findings probably due to the presence of the solid phase in hydrolysates. Model ABE fermentation of 20 g/L glucose and 10 g/L xylose was also studied in order to observe the diauxic behavior of *C.beijerinckii*.

I. INTRODUCTION

The diminishing crude oil reserves worldwide, the rising demand of fossil fuels, its unstable price in addition to increasing concerns over CO_2 emissions and global warming have reemerged the interest in the production of biobutanol as a chemical and alternative liquid biofuel. Butanol has similar energy value to gasoline and better properties compared to ethanol. Butanol application as a replacement for gasoline will outpace other renewable fuels such ethanol, biodiesel and hydrogen because of its safety and simplicity [1].

Biobutanol from lignocellulosic biomass such low cost sugar crops, grasses and agricultural waste products could be a good alternative to fossil fuels reducing both consumption of crude oil and environmental pollution. Among agricultural products, straw from cereal crops is the major by-product in Europe. In Spain, the annual production of wheat straw exceeds $4x10^6$ tonnes [2], thus this lignocellulosic material represents an abundant, cheap and readily available source for the bioproduction of butanol.

In this study, the use of wheat straw as raw material is analyzed for butanol production. The pretreatment is a crucial step in biofuels production from lignocellulosic biomass via enzymatic pathway. Two different pretreatments have been applied to wheat straw in order to compare its effects, steam explosion and ozonolysis. After this step, the enzymatic hydrolysis of pretreated wheat straw has been carried out and the hydrolysates have been used as a substrate for ABE fermentation by *C.beijerinckii* using both hexoses and pentoses. Simultaneous hydrolysis and fermentation has been also studied.

II. EXPERIMENTAL

II.1. Raw material

Wheat straw was acquired from an agricultural area close to Valladolid, Castilla y León, Spain. Particles sizes about 1-1.5 cm. were obtained using a laboratory scale mill and raw material was kept in an oven at 37 ºC until use.

II.2. Wheat straw pretreatments and enzymatic hydrolysis

Operating conditions of steam explosion and ozonolysis pretreatments of wheat straw have been reported in our previous studies [3],[4]. Stirred tank reactors were used to perform enzymatic hydrolysis of pretreated wheat straw containing 10% (w/w) of dry solid. The assays were carried out applying 175 rpm mechanical agitation, 50ºC, pH 5 and 72 hours of reaction time. Enzymes were kindly donates by Novozymes (Denmark) and a mixture of Celluclast 1.5L and Novozym 188, 0.11 g/g cellulose and 0.05 g/g cellulose, respectively, was added. After hydrolysis, samples were withdrawn, centrifuged, filtered (0.22 mm) and stored for analyses.

II.3. ABE fermentation

II.3.1. Microorganism

Clostridium beijerinckii DSM 6422 was used as a fermentative microorganism in this study and it was obtained from the German Collection of Microorganisms (DSMZ, Leibniz, Germany). Reinforced Clostridial Medium, RCM, (Fluka, Sigma-Aldrich, Spain) in Hungate tubes (18 x 150 mm) in spore form and conserved at -20 ºC under anaerobic conditions.

II.3.2. Fermentation assays

Model fermentation experiments were carried out in a stirred tank bioreactor (Biostat Bplus-2L Sartorius). Temperature was regulated at 35 ºC, pH was measured but not controlled, agitation was set at 175 rpm and total fermentation time was 120h. The growth medium was composed of (I) sugar solution: 20 g/L glucose, 10 g/L xylose and 1g/L yeast extract; (II) vitamins solution: 0.001g/L PABA, 0.001g/L thiamine and 0.00001g/L biotin; (III) salts solution: 0.2g/L $MgSO_47H_2O$, 0.01 g/L $MnSO4H_2O$, 0.01 $FeSO_47H_2O$ and 0.01 NaCl and a (IV) acetate buffer solution composed of: 0.5 g/L KH_2PO_4, 0.5 g/L K_2HPO_4 and 2.2 g/L ammonium acetate. The sugar solution was autoclaved with the reactor while the solutions II, III and IV were sterile filtered thereafter (0.22 μm).

Precultures were grown in serum bottles with rubber septum under anaerobic conditions flushing free O_2 nitrogen. Before inoculating the preculture with the first post-sporal Hungate-tube culture, a heat shock was performed at 80ºC for 3.5 min to stimulate the germination of spores. The preculture was then inoculated (10% v/v) and incubated at 35ºC without agitation for 24 h. Initial pH of fermentation broth was set at 6.2 by addition of NaOH 3M.

Fermentation of wheat straw hydrolysates was carried out at the same conditions as above. The solid fraction of hydrolysates was separated by vacuum filtration. After sterilization, II, III and IV solutions were sterile added to the medium. The preculture was then inoculated (10% v/v) and initial pH was set at 6.2. All the experiments were carried out in duplicate.

II.3.3. Simultaneous Saccharification and Fermentation (SSF)

Steam exploded and ozonated wheat straw was also simultaneously hydrolyzed and fermented in screw cap 250mL flasks with a dry matter content of 10% (w/v). After sterilization, II, III and IV solutions and the enzyme cocktail were sterile added to the medium. All SSF tests were preceded by a prehydrolysis step for 24 hours at the same conditions reported in II.2 paragraph. The preculture was inoculated (10% v/v), initial pH was set at 6.2 and temperature was maintained at 37 ºC.

II.4. Analytical methods

Sugars, acids and solvents concentration were determined by HPLC. The detector was based on the refractive index measurement. An Aminex HPX-87H column was used enabling quantification of glucose, xylose, acetic acid, oxalic acid, butyric acid, ethanol, acetone and butanol. Operational conditions were 0.01 N H_2SO_4 as mobile phase, at a flow rate of 0.6 mL/min and 30 ºC. All the samples were centrifuged at 5000 rpm for 5 minutes and filtered before being analyzed. Biomass concentration was determined by the correlation between the absorbance at 600 nm and dry weight of biomass.

III. RESULTS AND DISCUSSION

III.1. Effect of pretreatments on wheat straw

Wheat straw was subjected separately to different pretreatments: steam explosion (hereinafter denoted as SE), a physical-chemical pretreatment and ozonolysis (hereinafter denoted as OZ), a chemical pretreatment, which improved sugar release in the subsequent enzymatic hydrolysis. The pretreatment conditions were optimized in previous studies [5], [6]. In short, steam explosion caused 56.2% of hemicellulose removal in pretreated biomass compared to raw material, contrary to ozonolysis, which resulted in 33.4% of acid insoluble lignin (AIL) solubilization increasing the percentage of acid soluble lignin (ASL) compared to untreated wheat straw.

III.2. ABE fermentation of model solutions

Model fermentation assays were carried out in order to study the performance of *C.beijerinckii* on a mixed substrate composed of approximately 20 g/L glucose and 10 g/L xylose. **Figure 1** depicts glucose and xylose consumption, solvents production and cell concentration. As regards sugars uptake, a diauxic behavior was observed since *C. beijerinckii* consumed preferably glucose than xylose. These results are in accordance to other

researchers [7] Ezeji *et al.* (2007) who observed glucose preference over xylose, arabinose and mannose in this order on model ABE fermentation by *C.beijerinckii* BA101.

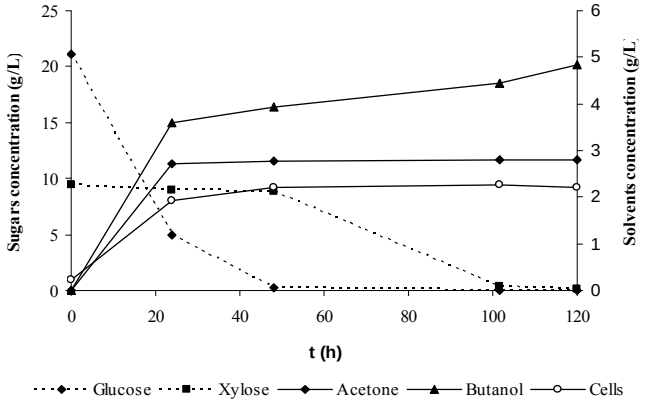

Figure 1. Glucose and xylose consumption, cell growth and solvents production during the fermentation process of mixed substrate by *C. beijerinckii* DSM 6422.

Glucose was exhausted after 48h and xylose was completely consumed in 96h. In regard to solvents production, total ABE concentration reached values of 7.7 g/L, 2.8 g/L acetone and 4.9 g/L butanol, although ethanol did not appear in detectable concentration. The biomass concentration reached a maximum value of 2.3 g/L. The ABE yield, calculated as the ratio between total solvents produced and sugars consumed, reached a value of 0.25 g/g. These results are in the range of those obtained by other researchers [7] who reached 0.32 g ABE/g sugars consumed from 55.0 g/L mixed substrate.

III.3. Comparison between separate hydrolysis and fermentation (SHF) and simultaneous hydrolysis and fermentation (SSF) using pretreated wheat straw.

Two operational strategies, SHF and SSF, were studied for ABE fermentation of steam-exploded and ozonated wheat straw hydrolysates by *C.beijerinckii*.

In SHF assays, the enzymatic hydrolysis was performed separately at optimal temperature of 50 ºC obtaining 37.3 g/L of total sugars (24.7 g/L glucose and 12.6 g/L xylose) in steam-exploded wheat straw hydrolysates using the whole slurry from pretreatment and 30.8 g/L of total sugars (23.7 g/L glucose and 7.1 g/L xylose) in ozonated hydrolysates washing the solid fraction (0.1 L water/g dry matter) after pretreatment. After pretreatments and enzymatic hydrolysis, 65.7% and 63.2% of glucose was released and 61.0% and 34.5% of xylose was recovered in steam-exploded and ozonated hydrolysates, respectively.

Figure 2a-b shows final sugars, acids and solvents concentration after SHF and SSF experiments of pretreated wheat straw hydrolysates.

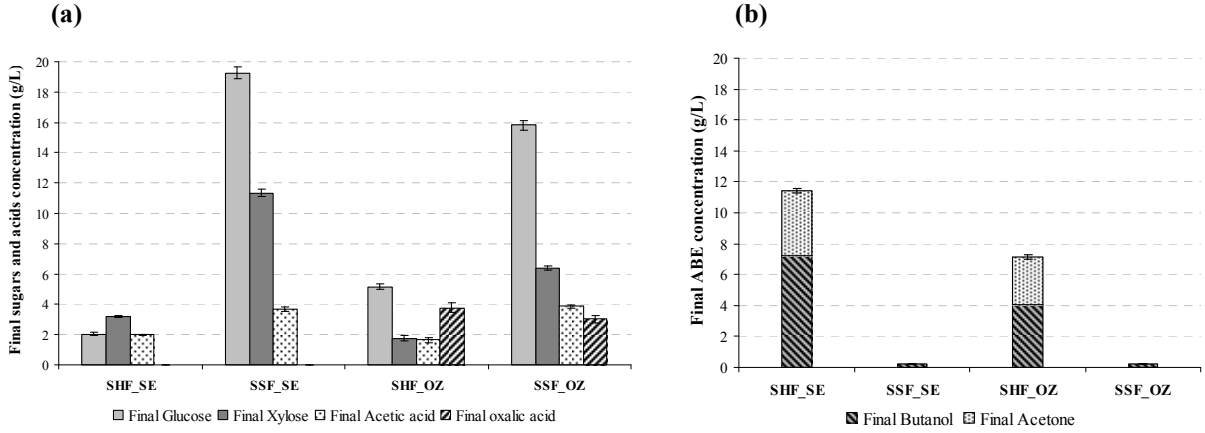

Figure 2a-b. Final sugars, acids and solvents concentration in SHF and SSF experiments.

As shown in the figure, *C.beijerinckii* was not able to ferment sugars in SSF assays and consequently negligible amounts of solvents were detected in samples. In contrast, when performing SHF assays, sugars consumption and solvents production were observed. It can be concluded that the solid phase affected negatively the performance of *C.beijerinckii*.

In steam exploded hydrolysates, 90.8% and 73.1% of glucose and xylose were used respectively after 120h of process. Solvents production resulted in 11.4 g/L ABE, consisting of 4.2 g/L acetone and 7.2 g/L butanol. ABE and butanol yields obtained were 0.40 g/g and 0.25 g/g, respectively. In ozonated wheat straw hydrolysates 75.6% glucose and 77.4 % xylose were consumed by *C.beijerinckii*. In this case, lower solvents production were achieved compared to steam-exploded hydrolysates (7.1 g/L ABE) and 0.32 g/g ABE yield and 0.18 g/g butanol yield were obtained.

IV. CONCLUSIONS

ABE fermentation of steam-exploded and ozonated wheat straw hydrolysates can be performed efficiently by *Clostridium beijerinckii* DSM 6422 performing hydrolysis and fermentation separately. In SHF assays, 0.40 g/g ABE yield was obtained in steam-exploded hydrolysates and 0.32 g/g in ozonated hydrolysates. In SSF experiments, the solid phase could probably affect negatively the performance of *C.beijerinckii*. ABE yield was lower in model fermentations (0.25 g/g), which indicates the presence of some compounds in hydrolysates that affected positively the process.

V. REFERENCES

[1] Huang, W.C., Ramey, D.E., Yang, S.T., 2003. Continuous production of butanol by Clostridium acetobutylicum immobilized in a fibrous bed bioreactor. Applied Biochemistry and Biotechnology 113, 887-898.
[2] MAGRAMA. Ministerio de Agricultura, Alimentación y Medio Ambiente, 2013. Avance Anuario de Estadística 2012. Subdirección General de Estadística, Madrid.
[3] Bellido, C., Bolado, S., Coca, M., Lucas, S., González-Benito, G., García-Cubero, M.T., 2011. Effect of inhibitors formed during wheat straw pretreatment on ethanol fermentation by Pichia stipitis. Bioresource technology, 102, 10868-10874.
[4] Bellido C., González-Benito, G., Coca, M., Lucas, S., García-Cubero, M.T., 2013. Influence of aeration on bioethanol production from ozonized wheat straw hydrolysates using *Pichia stipitis.* Bioresource Technology 133, 51-58.
[5] García-Cubero, M.T., Bolado, S., González-Benito, G., Catalina, I., 2008. "Comparison of ozonolysis and steam explosion of wheat straw to obtain bioethanol." CHEMPOR, BRAGA, Septiembre 2008.
[6] García-Cubero, M.T., González-Benito, G., Indacoechea, I., Coca, M., Bolado, S., 2009. Effect of ozonolysis pre-treatment on enzymatic digestibility of wheat and rye straw. Bioresource Technology 100, 1608–1613.
[7] Ezeji, T., Qureshi, N., Blaschek, H.P., 2007. Butanol production from agricultural residues: Impact of degradation products on *Clostridium beijerinckii* growth and butanol fermentation. Biotechnology and Bioengineering 97, 1460-1469.

USING GLYCOSIDASES TO MODIFY TCF BLEACHED SPECIALTY SISAL FIBERS

Beltramino, Facundo; Valls, Cristina; Vidal, Teresa; Roncero, M. Blanca*

*CELBIOTECH_Paper engineering research group. Universitat Politècnica de Catalunya (UPC. BarcelonaTech). Colom 11, E-08222, Terrassa, Spain. Email: *roncero@etp.upc.edu*
telephone: +34 937398190

ABSTRACT

Modifying fibers in order to upgrade them to dissolving grade involves several changes. Paper grade pulps can be used to yield this kind of raw materials, if the necessary modifications are carried out. Classic processes are capable of producing these changes. However, these classic processes present many drawbacks. In this direction biotechnology, and particularly enzymes, are attracting an increasing interest due to the special features they present.

Enzymes (glycosidases) are applied in this work on an alkaline TCF bleached sisal pulp. A xylanase and a cellulase preparation, both commercial, are applied on this pulp in order to evaluate their potential as catalysts for carrying out the previously stated upgrade. The main objective is to remove hemicelluloses present in starting pulp, which are an undesirable impurity in final product. Other modifications are as well profitable, such as increases in cellulose reactivity, a key parameter in dissolving pulps quality. After application, it is observed that final pulps present a lower content in hemicelluloses, a higher reactivity as well as other positive modifications.

I.INTRODUCTION

A growing interest in society is nowadays observed to move towards a bio-based economy where a bigger part of our daily products can be provided by agriculture. In this direction, making agriculture not just a food provider, but a producer of other raw materials, maybe taking advantage of non-food residues generated by food cropping or cultivating other fiber-providing species, can be a good way to move towards this new economic model. Despite wood pulps are by far the main source for pulp and paper production and non-wood fibers only occupy small niches [1] (e.g. specialty papers), the use of non-wood fibers is attracting a growing attention in the last years.

Dissolving pulps are a raw material used in the manufacture of many products, textile materials such as viscose, or other derivatives from cellulose such as carboxy-methil cellulose (CMC) [2]. Traditionally, dissolving pulps have been produced in industry by two processes: pre-hydrolysis Kraft and sulphite process. Manufacturing of this kind of pulps implies higher costs than the ones for obtaining paper-grade cellulose. Furthermore, pulps obtained through this processes present some problems such as a broad molecular weight distribution or a low viscosity for a specific purity grade. For this reason, there is a growing interest in studying methods for upgrading paper-grade pulps to dissolving-grade pulps. Many possibilities of processes have been studied to carry out this modification, among them enzymatic hydrolysis of different components of lignocellulose has attracted special attention because of its potential as a “green” process. Taking advantage of its selectivity, enzymatic treatments can be held using endoglucanases or xylanases to modify pulps in a desired way. Desired characteristics in final pulp are: Low content of hemicelluloses (below 5%), high proportion of α-cellulose (normally ≥ 94%), a high reactivity and only traces of lignin, extractives or minerals [2–5]. Regarding enzymes, cellulases are mainly used in bibliography to increase reactivity by cleaving cellulose chains. Xylanases, by their side, are used to hydrolyze xylans and therefore reducing their content on pulp. These enzymes have been traditionally used in pulp and paper industry for pulp bleaching [6–8]. However, in this work they are applied on bleached pulps with a different purpose, which is to eliminate hemicelluloses and take their concentration to desired levels. Hemicelluloses are undesirable impurities in dissolving pulps, they affect cellulose processability (filterability and xanthanation in the viscose process), and properties on the final product, such as fiber strength [9].

This study focuses on the possibility of using a bleached - paper grade - non-wood pulp, from sisal (*Agave sisalana*), to obtain a *dissolving quality pulp* by means of enzymatic treatments. A TCF bleached sisal pulp is used. Treatments with cellulase and xylanase are applied to study the possibility of carrying out this

upgrade. The main objective of this work is to remove as much hemicelluloses as possible from initial pulp, whereas treatments with cellulases are intended for other modifications such as increasing pulp reactivity [10].

II.EXPERIMENTAL

Pulp and Enzyme

A TCF bleached pulp from sisal (*Agave Sisalana*) is used. Pulp was provided by Celesa (Spain), and was obtained by an alkaline NaOH-AQ process. A xylanase (X) and a combination of cellulase and xylanase (Cx), both commercial, are used for treatments. They are provided by Fungal Bioproducts (Spain). Activities as U/g extract, measured in our laboratory [11] were: 11000 U/g for the xylanase (X); and 1700 U/g and 680 U/g for the cellulase and xylanase activity on the combination (Cx), respectively. Cellulase activity is expressed as CMCase units.

Enzymatic Treatments

Treatments with Cx enzyme were performed in plastic bags on a thermostatic water bath at 55ºC, 10% consistency and pH 5, adjusted with 50mM sodium acetate buffer. Applied dose was 10U/g odp (always indicated as CMCase units) and reaction was carried out for 2 hours with manual agitation every 10 minutes. Treatments with X enzyme were applied in plastic bags on a thermostatic bath at 50ºC, 10% consistency and pH7, adjusted with 50mM Tris-HCl buffer. Applied dose was 10U/g odp and reaction was carried out for 2 or 5 h, with manual agitation every 10 minutes. Pulps are treated with Cx and X alone and sequentially with Cx and then X for two different time lapses.

Controls (reference pulp) are pulps treated the same way as enzyme-treated pulps but with no enzyme addition.

Pulp properties

Kappa number and viscosity of initial and treated pulps are determined according to ISO 302:2004 and ISO 5351:2010 respectively. HexA content is determined according to Tappi T 282 pm-07 method. Carbohydrate composition of initial and treated pulps is determined using high performance liquid chromatography (HPLC). Samples are studied on a duplicate basis using a modified version of TAPPI 249 cm-09 test method [6,7,9]. Pulp reactivity is determined using a slightly modified version of Fock's method [2]. Carbohydrate presence on effluents is also analyzed by HPLC. Neutralized (pH 7) and filtrated samples are analyzed using a Bio-Rad Aminex HPX-42A column for oligosaccharides resolution.

Samples treated with cellulase mixture are referred as Cx, xylanase treatments are refered as X2 or X5 (2h or 5h). Reference pulps are named the same way with a letter "K" before the sample name (e.g. "KCx").

III.RESULTS AND DISCUSSION

In this work, treatments with xylanase and cellulase were applied with the intention of evaluating their capacity to remove xylans from a pulp with high hemicelluloses content, as well as other modifications. As it has already been said, hemicelluloses represent an undesirable impurity on dissolving pulps.

As seen on **Table 1**, TCF bleached sisal pulp has a high content in hemicelluloses (over 16%). Most of these hemicelluloses need to be eliminated in order to achieve the desired purity of cellulose. Furthermore, this pulp presents a relatively high kappa number (KN) for a bleached pulp, probably because of its high content on hexenuronic acids (HexA), which may affect its value [12]. In order to improve final characteristics of this pulp, it is important to reduce the presence of these compounds as well, and as a consequence, probably reduce KN value to obtain a better quality in final product.

Table 2 indicates pulp characteristics after treatments with X and Cx. Xylanase treatments (X2 and X5) are effective reducing kappa number in pulps on both reaction times. Taking into consideration that lignin content in starting pulp is very low (close to 1%), this reduction is mainly attributable to HexA removal, which values are also indicated and are in fact diminished with treatments. Viscosity is not affected with this hemicellulase, and values actually increase slightly, probably due to the elimination of shorter chains of hemicelluloses [7]. Cellulase combination (Cx), as stated in experimental section, contains also a xylanase activity, in a lower proportion than cellulase but also present. This xylanase activity can be noticed in KN and HexA values, both reduced after treatments with this enzyme. As expected, viscosity is also reduced after all treatments with cellulase. Cleavage of cellulose chains reduces cellulose degree of polymerization and thereafter,

pulp viscosity. Combination of both enzymes provoked a greater reduction in HexA content and KN, even though no synergic effect seems to be observed.

ISO Brightness (%)	82.1 ± 0.3
Kappa Number	4.3 ± 0.2
Viscosity (mL/g)	616 ± 41
HexA (µmol/g odp)	48.1 ± 0.1
Hemicelluloses (%)	16.1 ± 0.2

Table 1 – Starting values of TCF bleached Sisal Pulp

	Sugars (mg/mL)	
Time (h)	**2**	**5**
Xylotriose	0.821	0.936
Xylobiose	0.517	0.788
Xylose	0.096	0.145

Table 3 – Xylooligosaccharides concentration in reaction effluents after treatments with xylanase.

	KN	**Viscosity (cm^3/g)**	**HexA (µmol/g odp)**
X2	3.4 ± 0.02	657 ± 11	36.5 ± 0.9
KX2	4.8 ± 0.1	617 ± 20	40.3 ± 0.7
X5	2.9 ± 0.1	692 ± 22	35.9 ± 5.4
KX5	4.7 ± 0.03	641 ± 8	40.2 ± 0.2
Cx	4.01 ± 0.27	431 ± 6	33.5 ± 2.5
KCx	4.74 ± 0.1	628 ± 1	41.4 ± 2.8
Cx + X2	3.7 ± 0.33	486 ± 3	33.1 ± 1.1
Cx + X5	3.27 ± 0.08	475 ± 16	32.8 ± 2.5
KCx + X2	3.91 ± 0.1	647 ± 23	35.5 ± 2.1
KCx + X5	4.02 ± 0.26	665 ± 6	35.5 ± 0.8

Table 2 – KN, viscosity and HexA content of pulps after treatments with xylanase (X) and cellulase combination (Cx). Reference treatments are also indicated.

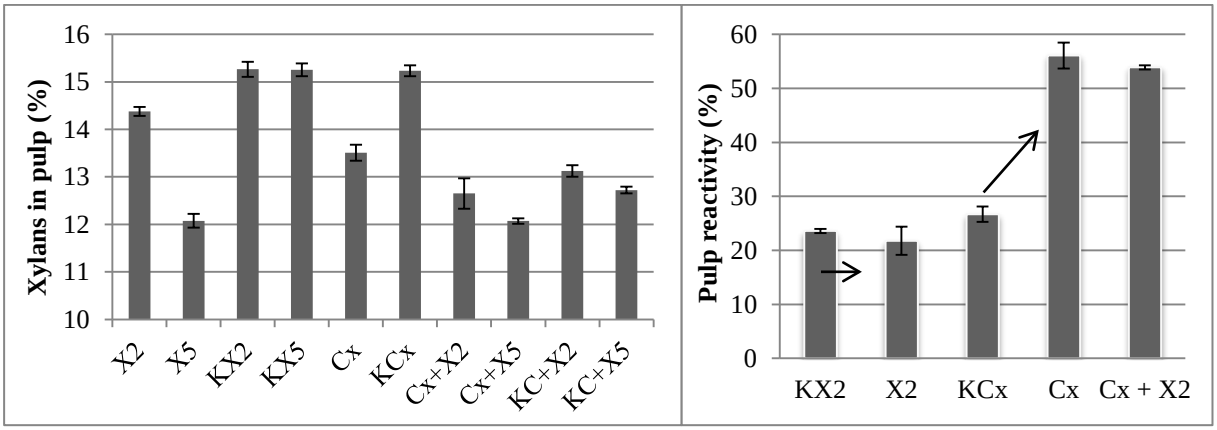

Figure 1a – Hemicelluloses (as % xylans) content of samples after treatments**. Figure 1b –** Pulp reactivity values, as % of reacted cellulose, after treatments with X, Cx and both combined.

As known from literature, HexA are contained in fibers as part of hemicelluloses [13]. So, as it is expected, a good correlation can be observed between contents of both components on **Figure 1a**. Cellulase combination itself reduced hemicelluloses content in fibers with its xylanase activity, as already commented for HexA. The greater reduction in content of hemicelluloses is obtained with the xylanase after 5h of treatment, which does not seem to be enhanced by the pretreatment with cellulase, as similar values are reached for X5 and Cx+X5 samples. Their combination resulted useful for shorter reaction times with xylanase (Cx+X2). However

it does not seem to provide an evident additional benefit in removing hemicelluloses, Cx enzyme shows to be capable of producing another crucial modification in pulps: increasing their reactivity. Pulp reactivity as measured by Fock's method is a key-parameter in *dissolving* quality pulps, especially if their final application is viscose manufacture [10]. **Figure 1b** shows that xylanase does not modify this property, as reference and treated pulps show similar values. Cellulase treatments, by their side, increase reactivity over a 200%. This occurrence has already been reported and explained in literature [10,14] and in this particular case shows the importance of treatments with both enzymes for a proper upgrade of initial pulp to the desired quality

In order to better understand enzyme's action over pulp, sugar presence in reaction effluents is studied. **Table 3** indicates xylose oligosaccharides concentration after treatments. As expected higher concentrations are found after longer treatments (5h compared to 2h), and among oligosaccharides their concentration decreases with their polymerization degree. Xylotriose concentration is almost 10 times higher than xylose, and this proportion remains the same at both times (X2 and X5). It is important to remark that reference treatments show only traces of the mentioned sugars in reaction liquors.

IV.CONCLUSIONS

Treatments with both glycosidases show to be very effective modifying sisal fibers in order to upgrade them to a *dissolving* grade pulp. Xylanase is capable of removing effectively hemicelluloses from fibers, and cellulase utility for this conversion is related to its capacity of increasing pulp reactivity. Both modifications together with other secondary benefits obtained, make these treatments a promising alternative to traditional processes.

V.ACKNOWLEDGEMENTS

This work was funded by the Spanish MICINN BIOSURFACEL- CTQ2012-34109 and BIOFIBRECELL- CTQ2010-20238-CO3-01 projects. Authors are grateful to the consolidated group with the Universitat de Barcelona (UB) AGAUR 2009SGR 00327.

VI.REFERENCES

[1] Moore G. Nonwood Fiber Applications in Papermaking. Pira Int Leatherhead, Surrey, UK. **1996**
[2] Ibarra D, Kopcke V, Ek M. Exploring enzymatic treatments for the production of dissolving grade pulp from different wood and non-wood paper grade pulps. Holzforschung **2009**,63(6),721–730.
[3] Hakala TK, Liitiä T, Suurnäkki A. Enzyme-aided alkaline extraction of oligosaccharides and polymeric xylan from hardwood kraft pulp. Carbohydr Polym. **2013**, 93(1), 102–108.
[4] Ibarra D, Kopcke V, Larsson PT, Jaaskelainen A-S, Ek M. Combination of alkaline and enzymatic treatments as a process for upgrading sisal paper-grade pulp to dissolving-grade pulp. Bioresour Technol **2010**,101(19), 7416–7423.
[5] Quintana E, Valls C, Vidal T, Blanca Roncero M. An enzyme-catalysed bleaching treatment to meet dissolving pulp characteristics for cellulose derivatives applications. Bioresour Technol. **2013**,148,1–8.
[6] Aracri E, Vidal T. Xylanase- and laccase-aided hexenuronic acids and lignin removal from specialty sisal fibres. Carbohydr Polym. **2011,** 83(3),1355–1362.
[7] Fillat A, Roncero MB, Vidal T. Assessing the use of xylanase and laccases in biobleaching stages of a TCF sequence for flax pulp. J Chem Technol Biotechnol; **2011,** 86(12),1501–1507.
[8] Roncero, M B; Colom, J M; Vidal T. Influence ot the xylanase enzymatic treatments on the carbohydrate composition of pulp for paper manufacture. Afinidad. **2003**, 60(503),8–15.
[9] Christov LP. Xylan removal from dissolving pulp using enzymes of Aureobasidium pullulans. Biotechnol Lett. **1993**,15(12),1269–1274.
[10] Kopcke V, Ibarra D, Ek M. Increasing accessibility and reactivity of paper grade pulp by enzymatic treatment for use as dissolving pulp. Nord Pulp Pap Res J. **2008**, 23(4),363–368.
[11] Spiro RG. [1] Analysis of sugars found in glycoproteins. Methods Enzymol. Academic Press; **1966**, 8(C), 3–26.
[12] Valls C, Vidal T, Gallardo O, Diaz P, Javier Pastor FI, Blanca Roncero M. Obtaining low-HexA-content cellulose from eucalypt fibres: Which glycosil hydrolase family is more efficient? Carbohydr Polym **2010,** 80(1),154–160.
[13] Valls C, Gallardo O, Vidal T, Pastor FIJ, Díaz P, Roncero MB. New xylanases to obtain modified eucalypt fibres with high-cellulose content. Bioresour Technol. **2010**, 101(19), 7439–7445
[14] Henriksson G, Christiernin M, Agnemo R. Monocomponent endoglucanase treatment increases the reactivity of softwood sulphite dissolving pulp. J Ind Microbiol Biotechnol. **2005**, 32(5), 211–214.

SOFTWOOD KRAFT LIGNIN ISOLATION FORM BLACK LIQUOR: FROM LABORATORY TO PILOT-SCALE PRODUCTION

Frédérique BERTAUD[1*], Audrey GUILLEMAIN[2], Sandra TAPIN-LINGUA[2], Sonia MOLINA-BOISSEAU[3], Michel PETIT-CONIL[1,2]

*[1]CTP-Centre Technique du Papier, Grenoble, France; [2]FCBA- New materials division, Grenoble, France, [3]CERMAV, Grenoble France (*Frederique.Bertaud@webctp.com)*

ABSTRACT

With the development of sustainable processes and the need for bio-carbon and bio-energy in different industrial sectors, lignin from black liquor gains more and more interest. Kraft black liquor contains approximately 30% of lignin, which are easily isolated by acidification. Softwood kraft lignin from industrial black liquor was precipitated by CO_2 neutralization. Trials were scaled-up from laboratory scale to pilot scale, which allows producing from 100 g to 10 kg o.d. of lignin. Several isolation/washing procedures were tested and compared: sedimentation, centrifugation, and filtration. The production yield, lignin purity, sulfur and minerals contents, as well as elemental composition of prepared lignin showed a relatively good repeatability of the laboratory-scale isolation procedure for five replicates. Nevertheless, the particle size was slightly affected by the separation technique used. The larger-scale production of 1 kg - 10 kg led to a similar quality of Kraft lignin with production yields maintained at 62% (g. of dry lignin/ 100g of initial lignin amount in liquor). Centrifuge and spin dryer filtration appeared as a suitable technology for laboratory and large scale production.

I. INTRODUCTION

50-70 million ton/year of lignins are potentially available from pulp processes in the world. Only 1% is available on the market mainly recovered from cooking liquors of the chemical pulping industry, and marketed as thiolignin and lignosulfonates [1][2][3]. Indeed, most of the lignins solubilized in black liquor are used to feed the recovery boiler, contributing to the production of steam for energy self-sufficiency of the mill. However, recovery boiler capacity is usually the bottle-neck of the pulp productivity. Therefore, lignin extraction from black liquor appears as an interesting solution to increase the pulp mill productivity, together as a promising way to turn the pulp mill into a biorefinery [4][5][6]. .Indeed, lignin with its aromatic chemical structure represents a potential new source of aromatic chemicals and other products for the substitution of petroleum-based products, in addition of its fuel value [1][2][3]. Recent industrial investments in the patented LignoBoost™ technology, show increasing interest of pulp companies for lignin exploitation [7][8].

Kraft pulping process is the dominant chemical pulping process for making pulp from wood. It uses a combination of sodium hydroxide and sodium sulfide to delignify the wood by causing cleavage of α and β-aryl ether linkages of phenylpropane units of the lignin polymer. Phenolic hydroxyl groups (L-OH) are formed as well as few thio-lignins (L-SH). In alkali, lignin degradation products are dissolved under phenolates ($L\text{-}O^-$) and ligno-sulfides ($L\text{-}S^-$) form as it is in the cooking liquors. Thus, black liquor contains between 27% to 37% of lignin, in addition of ~30% of organic acids and 8-12% of extractives and hemicelluloses [9][10].

Kraft lignin is usually extracted by acidification of the black liquor, using sulfuric ac and/or carbon dioxide. After precipitation, lignin is recovered by filtration or centrifugation. Lignin phenolates neutralization occurs at pH 9-11, leading to the lignin precipitation. An additional pH decrease neutralizes carboxylic groups and allows better precipitation yields. Extraction yields of 35%, 70%, 80% and 90% were obtained after acidification of black liquor until pH 9.5; 9; 8 and 2, respectively [11][12] [13]. The quality of the lignin is however highly dependent on the final pH. At pH<4, the lignin was found as a fine powder forming a tacky gel difficult to filtrate [11][16]. Neutralization is usually performed in warm diluted black liquor at 30-35% dry content [14][15]. The precipitation temperature was found to be critical when producing a filterable lignin. The optimum temperature varied between 60°C and 90°C. Tacky lignin, leading to filtration plugging has been formed for temperature higher than 85°C [11][16]. Purifying lignin fractions by washing proved to be difficult due to the problem of lignin re-dissolving in the wash water [17]. Washing with diluted sulfuric acid (pH 1-2) allowed producing a good quality of lignin (Na<0.065% and S<1.2%) [17][18].

In the framework of the forest-based biorefinery deployment in France, and especially in order to develop the use of lignin as new green-chemicals and green products, CTP and FCBA have implemented the extraction of industrial kraft lignin. The reproducibility of standard lab-scale procedure based on carbon dioxide precipitation, and diluted sulfuric acid washing was evaluated on an industrial black liquor of a softwood pulp mill. The

separation of the lignin suspension was worked out in a spin-dryer apparatus for the up-scaling of lignin extraction (10kg batches).

II. EXPERIMENTAL

Industrial black liquor (BL) from a French mixed-softwood kraft pulp mill was collected in the evaporation stage of the chemical recovery circuit, at a concentration about 50% in solids and a pH of 10.3. The lignin content of the liquor was about 35.7% (i.e. 29% KL (Klason lignin) [19] and 6.7% ASL (acidic soluble lignin) [20]).

The laboratory-scale procedure, developed according to Alèn et al.[14][15] and Öhman et al. [21], as already described [22], was performed at 70°C. Carbon dioxide was introduced at 60 L/h in 1 L of diluted black liquor solution (40% dm) under continuous stirring until a final pH 8. The lignin suspension was centrifuged at 8000g/10 min, and washed three times by an acidic solution of diluted sulfuric acid at 2%.

A large-scale procedure was developed according to the laboratory-scale method, in a 50 L thermostatic tank reactor equipped with special turbine, with a CO_2 flow of 120 L/h under stirring until a final pH 9. The lignin suspension was separated in 60L ROBATEL spin-dryers. The lignin was washed by re-dispersing the lignin cake in a diluted sulfuric acid solution at 2%, before spin-drying. Washing sequence was repeated 3 times. The dry matter of the lignin was of 70%, and 90% after 3-5 days air drying at 25°C.

The dry matter, ash, and lignin contents of the prepared lignin samples were determined according to NF EN ISO 638 [23], Tappi T222om-02 [19] and Tappi UM 250 [20] respectively. Elemental analysis (C,H,O,N) was performed with a Vario Micro Cube Elementar. The total sulfur content was determined by ICP-OES according to ISO 11885 [24]. The size distribution of the particles was measured by means of a laser diffraction granulometer Malvern Mastersizer 2000. The powders were coated with Au/Pd and observed in secondary electron mode with a JEOL JSM-6100 scanning electron microscope operated at 8 kV.

III. RESULTS AND DISCUSSION

Five laboratory-scale experiments were performed as described above. Depending mostly on the stirring efficiency, the CO_2 introducing time was between 1 hour to 2,5 hours to reach the final pH of 8 (**Figure 1**). Approximately 100g of lignin samples were isolated. The final dry matter content was of 85-88% after 5-7 days of air-drying. The five laboratory-scale experiments were highly repeatable with extraction yields between 23% and 26% (g o.d. matter/100g of initial o.d. matter in the BL). Considering the initial lignin content of the black liquor (BL), the production yields were between 63% and 70% of the initial lignin (**Figure 2**). The washed lignin presented a high purity of 90-96% of lignin contents, with less than 1.5% of ash, and 63–65.5% of carbon (**Table 1**). Its sulfur content was between 2% and 2.5%, very similar to the lignin LignoBoost-Bächammar samples [7][25].

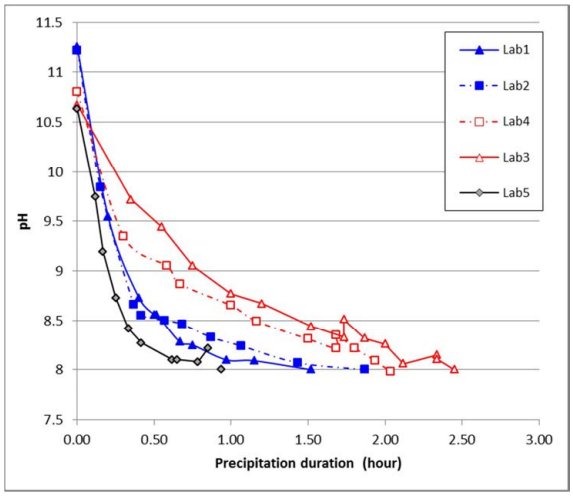

Figure 1: The pH lowering rate of the five laboraty-scale experiments for lignin precipitation

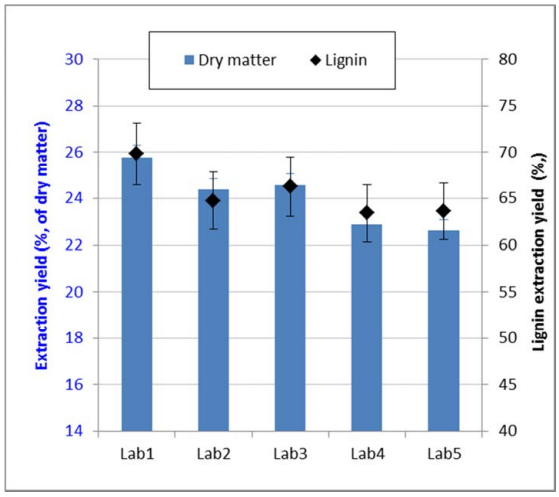

Figure 2: Extraction yields of the five lignin samples prepared at the laboratory-scale, according tot he initial dry matter content and initial lignin content

The up-scaling was firstly performed at medium-scale with 5L of BL. Approx. 500g of lignin (SemiP6) were isolated using a 4L ROBATEL spin-dryer. The washing sequences were optimized and it was found that two re-

dispersing stages of the lignin filter-cake in acidic solution at a ratio of 10 (L/S) were efficient to get pure lignin (> 90%) with low minerals contents (**Table 1)**. This washing methodology was applied for the production of 10 kg of lignin (P7) according to the large-scale procedure, using 60L ROBATEL spin-dryer. The large scale procedure led to highly similar results as laboratory-scale and medium-scale experiments with a high pure lignin (95%), containing only 0.14% of minerals (**Table 1**).

The lignin particles were made up of small agglomerates of grains. The particle size of the different lignin samples was also very similar with a mean diameter around 15 µm, with a slight difference of the particle size distribution (**Figure 3**).

Table 1: Chemical composition of the prepared lignin samples (in % of dry sample)

Experiment	Lignin	Ash	C	H	O	N	S
Lab1	92	1.4	63.9	5.2	26.7	0.1	2.36
Lab2	90	1.5	63.2	5.2	26.9	0.1	2.51
Lab3	92	0.7	64.7	5.2	26.3	<0.1	2.44
Lab4	94	1.0	64.8	5.2	26.6	0.1	2.11
Lab5	96	0.7	64.2	5.2	27.3	<0.1	2.52
SemiP6	96	0.9	65.5	5.2	25.9	<0.1	2.05
P7	95	0.14	-	-	-	-	-

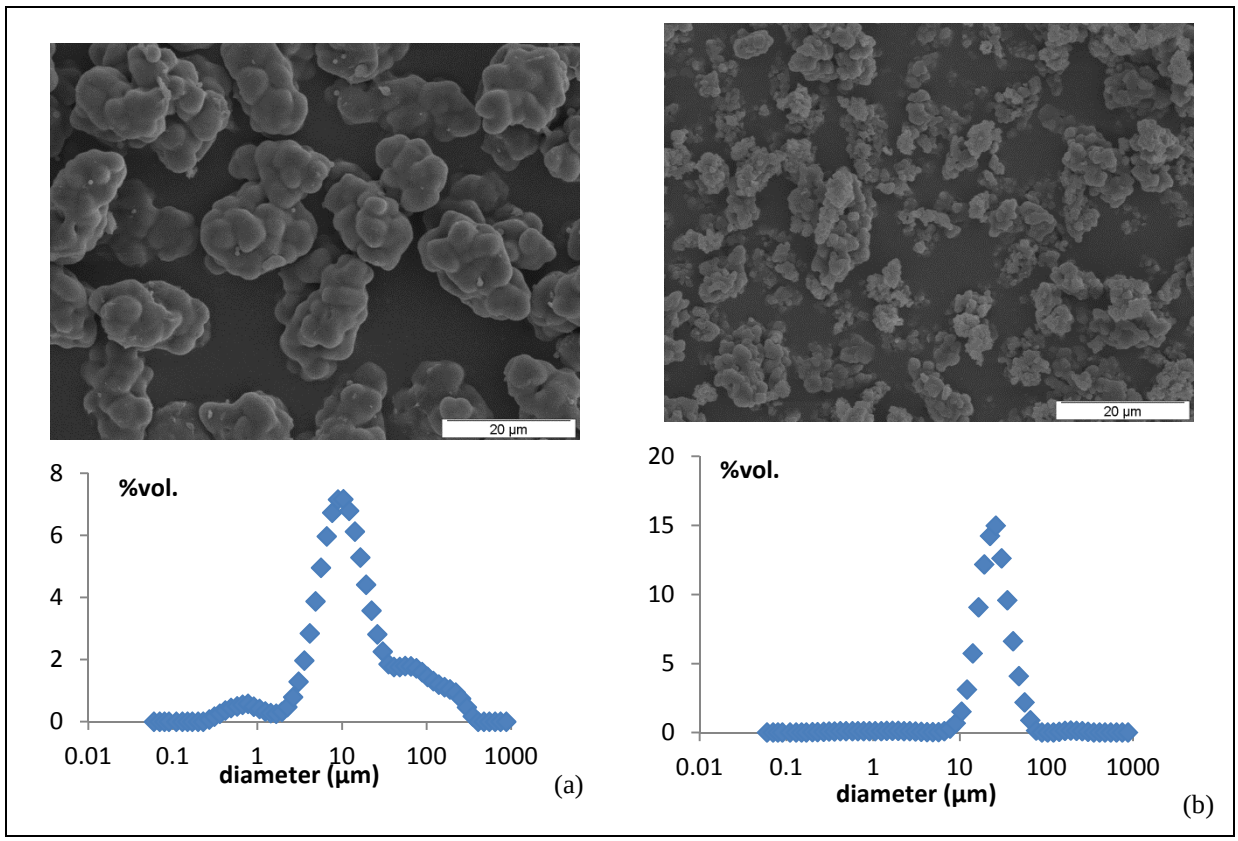

Figure 3: SEM micrographs and particle size distribution of prepared lignin samples Lab 1-5 (a) et SemiP6 (b)

IV. CONCLUSIONS

The preparation of Kraft lignin from industrial black liquor was studied according to a neutralization stage using carbon dioxide and washing stages with a diluted sulfuric acid solution. Laboratory-scale experiments with separation by centrifugation showed high reproducibility. Lignin yields were of 65% ± 5% with 93% ± 3% of purity for the five prepared samples. Spin-dryer technology showed good efficiency in the separation of lignin suspension at large-scale, with similar yield and purity than those laboratory preparations.

V. ACKNOWLEDGEMENT

Fibre Excellence-Tarascon mill is acknowledged for supplying the black liquor.

VI. REFERENCES

[1] Holladay J.E.; Bozell J.J.; White J.F.; Johnson D. Top value-added chemicals from Biomass, Volume II- Results of screening for potential candidates from biorefinery lignin, Pacific Northwest National Laboratory, US Dpt of Energy, **2007**; PNNL-16983
[2] Kendall Pye E. Industrial lignin production and applications, in *Biorefineries – Industrial Processes and Products : Status Quo and Future Directions*, Birgit KAMM, Patrick G. GRUBER and Michael KAMM Eds, Wiley-VCH, Weinheim, **2010**
[3] Grosselink R.J.A. Lignin as a renewable aromatic resource fort he chemical industry, Thesis, Wageningen Unniveristy, **2011**
[4] Lora J.H.; Abächerli A.; Doppenberg F. Debottlenecking the recovery system of soda pulp mills by lignin recovery and wet oxidation – Application to non-wood fibers black liquors, Tappi Pulping Conference Proceedings, Tappi Press, Atlanta, USA, **2000**
[5] Savage D. LignoBoost: lignin from pulp mill black liquor, Products and Solutions, 3, 22-23, **2009**
[6] Larrsson A. LignoBoost – extract lignin from the Kraft pulping process, *Ecochem*, Bâle**,** November 19-21 **2013**
[7] Tomani P.; Berglin N.; Axegard P. The lignoboost process & use of lignin as new bio-fuel, *Tappi Engineering, pulping & environmental Conference*, October 11-14, **2009**, Memphis, Tennessee
[8] Tomani P. LignoBoost makes its world première, *Beyong*, Innventia, 2013
[9] Gullichsen J. Fiber line operations, in *Book 6A: Chemical Pulping, Papermaking Science and Technology*, Johan Gullichsen and Hannu Paulapuro Eds, Tappi Press, **1999**
[10] Vakkilainen E. Chemical recovery, in *Book 6B: Chemical Pulping, Papermaking Science and Technology*, Johan Gullichsen and Hannu Paulapuro Eds, Tappi Press, **1999**
[11] Loufti H.; Blackwell B; Uloth V. Lignin recovery from Kraft black liquor: preliminary process design, *Tappi Journal* January **1991**, 203-210
[12] Sixta H.; Potthasta A;Krotschek W. Chemical pulping processes, in *Handbook of pulp*, Herbert Sixta Ed, Wiley-VCH, Weinheim, **2006**
[13] Axelsson E.; Olsson M.R.; Berntsson T. Increased capacity in kraft pulp mills: Lignin separation and reduced steam demand compared with recovery boiler upgrade, Nordic Pulp and Paper Research Journal, **2006**, 21 (4), 485-492
[14] Alèn R.; Patja P.; Sjöström E. Carbon dioxide precipitation of lignin from pine kraft black liquor, *Tappi*, **1979**, 62(11), 108-110
[15] Alen R.; Len R.; Sjöström E.; Vaskikari P. Carbon dioxide precipitation of lignin from alkaline pulping liquors, *Cellulose Chemistry and Technology*, **1985**, 19, 537-541
[16] Uloth V.C.; Wearing J.T. Kraft lignin recovery: Acid precipitation versus ultrafiltration – Part I: Laboratory test results, *Pulp and Paper Canada*, **1989,** 90(9), 67-71
[17] Öhman F.; Theliander H. Washing lignin precipitated from kraft black liquor, *Paperi ja Puu*, **2006**, 88(5), 287-292
[18] Öhmann F.; Wallmo H.; Theliander H. An improved method for washing lignin precipitated from kraft black liquor – The key to a new biofuel, *Filtration*, **2007**, 7(4), 309-315
[19] Tappi T222om-02, Acid insoluble lignin
[20] Tappi UM250, Acid-soluble lignin in wood in pulp
[21] Öhman F. ; Wallmo H. ; Theliander H. Precipitation and filtration of lignin black liquor of different origin; *Nordic Pulp and Paper Research Journal*, **2007**, 22(2), 188-193
[22] Bertaud F., Tapin-Lingua S., Pizzi A., Navarette P. Petit-Conil Development of green adhesives for fibreboards manufacturing, using tannins and lignin from pulp mill residues, *ATIP*, **2011**; 65(3), 6-12
[23] NF EN ISO 638 (December **2008**), Papiers, cartons et pâtes : Détermination de ma teneur en matières sèches
[24] ISO 11885 (**2007**), Water quality -- Determination of selected elements by inductively coupled plasma optical emission spectrometry (ICP-OES)
[25] Axegard P. The Kraft pulp mill as a biorefinery, *Nordic Wood Biorefinery Conferences***, 2008**, March 11-14, Stockholm, Swedeen, Innventia Conference

INFLUENCE OF WOOD EXTRACTIVES ON CALCIUM BALANCE DURING KRAFT COOKING

Marta Bialik[1]*, Marianne Björklund Jansson[1], Per Törngren[1]

[1]*Innventia AB, Box 5604, SE-114 86 Stockholm; (*marta.bialik@innventia.com)*

ABSTRACT

During the cook, the main part of the fatty and resin acids forms soluble sodium soaps; however, some very insoluble metal soaps with divalent cations, especially calcium and manganese, are also formed, which will affect the balance of the cations. The precipitated divalent metal soaps may form troublesome deposits on the process equipment (e.g. wash presses) and on the pulp product. In this work, a process simulation program, extended with a tool that handles chemical equilibrium calculations, has been used to study the influence of some parameters on the precipitation of calcium soaps of fatty acids in black liquor. The results show that the precipitation is affected by e.g. calcium and fatty acid concentrations, carbonate concentrations, the type and concentration of organic compounds forming soluble complexes with Ca and pH. The simulations may be used to illustrate how changes in mill conditions will affect the formation of calcium soaps and thus to evaluate the risk of their precipitation.

I. INTRODUCTION

Lipophilic extractives, mainly fatty and in softwood also resin acids, are dissolved in the black liquor as sodium soaps during kraft cooking process. The solubility of the soaps decreases with increasing ionic strength during evaporation of softwood liquors, leading to separation of the soap phase which can subsequently be acidified and converted to tall oil. Certain non-process elements, e.g. (Ca, Mg, Mn, Cu and Fe), will also form soaps with fatty acids; their solubility is however extremely low, which may lead to various process problems in the fiber line and the recovery area. The sparingly soluble metal soaps may precipitate in the black liquor evaporators, possibly enhancing the formation of other scales. These soaps are also enriched in the separated soap and thereafter released at the acidulation stage; if the spent brine is returned directly to black liquor evaporation, a dangerous buildup of metal cations in the black liquor may result. If carried to the fiber line, the soaps, especially these of Ca, may form troublesome deposits on pulp thus greatly reducing the quality of the final product.

The solubility of a specific metal soap depends on the length of, and the number of double bonds in, the fatty acid chain. Long, saturated fatty acids form the most insoluble calcium soaps [1] and have earlier been shown to follow the pulp to the fiber line in a higher degree than unsaturated or shorter fatty acids [2]. However, since the unsaturated fatty acids (e.g. oleic and linoleic), dominate in wood resin, their soaps may still constitute a substantial part of the precipitate. The resin acids, which do not form calcium soaps during pulp washing, are washed out very efficiently in the fiber line.

The main source of non-process cations in the kraft process is wood raw material. While this is certainly true for Mn, some Ca can also be introduced to the cooking stage with white liquor, while Mg can deliberately be added as a bleaching aid, in form of $MgSO_4$, to oxygen delignification or as washing aid (talc) to the fiber line. Since there is a great molar abundance of fatty acids compared to metal ions in the digester, the formation of metal soaps will to some extent affect the balance of the cations. Further, depending on the pH and liquor composition, other precipitates can be formed, especially $CaCO_3$, known to form troublesome deposits in both kraft cooking and evaporation, as well as MnS. Understanding the chemistry of metal cations in black liquor solutions is therefore vital for assuring the uniform operation of the kraft process.

When considering the chemical reactions of metal cations in kraft cooking, their interactions with black liquor organic material have to be taken into account. The presence of organics is known to significantly increase the apparent solubility of inorganics, especially $CaCO_3$, the constants for the binding/complexation of Ca to other organic substances, such as lignin or other black liquor organics are not well known, even though a number of different structures have been suggested to bind metal ions [3,4,5].

II. EXPERIMENTAL

Input data for simulations

In order to establish and/or verify some of the formation constants used in the simulations a series of experiments was conducted in model black liquor solutions [6]. The simulations have been based on analytical

data from four different mills: Mill A (pine/spruce, 90/10 %), Mill B (pine/spruce, 20/80 %), Mill C (birch/aspen, 80/20 %; 18 kg of tall oil per ton of pulp added to cook) and Mill D (eucalyptus, 100 %). The calculations corresponded to two positions: the pulp leaving the digester (simulating 1 kg of wet pulp including carry-over) and also for the black liquor withdrawn to the evaporation (1 kg of liquor). The input data is summarized in **Table 1**.

Table 1. Concentrations of basic system components in samples from four mills used in simulations.

Mill/ Parameter	Pulp DS	Fiber cons.	Ca^{2+}	Mg^{2+}	Mn^{2+}	CO_3^{2-}	FA-0	FA-1	FA-2	RA	Pulp-COOH	Lig-COOH	Lig-PhOH	Org-COOH
	%		mmol/kg											
Mill A	24	12.5	4.5	3.5	0.2	165	1	8.6	14.4	8	15.6	14	192	350
Mill B	22,6	12.5	6.5	3.5	0.5	130	0.5	1.7	1.3	1.4	15.6	12	161	350
Mill C	18,3	12.5	4.5	3.5	0.2	200	1.5	1.7	8.3	1.4	15.6	18	236	350
Mill D	22	12.5	8.6	4.4	0.2	165	0.1	0.3	0.6	0	15.6	16	213	350

Equilibrium simulation software

WinGEMS pulp mill simulator (Metso Automation) was used as a base for the soap solubility equilibrium calculations. The program was extended with MeteQ subroutine, a tool for calculation of chemical equilibria based on SOLGASWATER concept [7]. In MeteQ calculation, the user defines a chemical system by specifying a number of elementary components (metal ions, functional groups, hypothetical compounds etc.) and reactions between them, proceeding according to user-defined formation constants. The formation constants are adjusted for temperature and ionic strength according to the Van't-Hoff and Davies equations, respectively. The equilibrium calculation produces concentrations of the final compounds formed for a given set of input concentrations of the elementary components, temperature, ionic strength and pH.

In this work, the following elementary components were used: H^+ (i.e. pH), Ca^{2+}, Mg^{2+}, Mn^{2+}, CO_3^{2-}, carboxyl groups in the pulp fibers (pulp-COOH), kraft lignin phenolic (Lig-PhOH) and carboxyl (Lig-COOH) groups, and carboxyl groups in dissolved organic material, mainly low molecular acids (Org-COOH). The wood extractives were represented by saturated fatty acids (FA-0), monounsaturated fatty acids (FA-1), polyunsaturated fatty acids (FA-2) and resin acids (RA). The formation constants were taken from previous studies: from Ulmgren [8] for water, carbonic acid, and hydroxides and carbonates of Ca, Mg and Mn, and numbers of literature data [1,9] for solubility of undissociated fatty and resin acids as well as their soaps. The pKa value (dissociation constant of the acid) was set to 5.0 for all the fatty acids.

III. RESULTS AND DISCUSSION

The results of the simulations are shown in the form of distribution diagrams, where the concentrations of a certain elementary component, in this case Ca, are presented as fractions (0-1) of the total amount of Ca present in the system. As can be seen in **Figures 1** and **2**, precipitation of calcium soaps of resin acids did not take place in any of the analyzed systems within the simulated pH interval, which is consistent with the expected high solubility of these soaps. In all systems a dominating fraction of saturated fatty acids (98-99%) precipitated as Ca soaps, although in Mill D the amount of saturated fatty acids was so low compared to Ca (see **Table 1**) that the precipitation of soaps did not significantly affect the calcium balance.

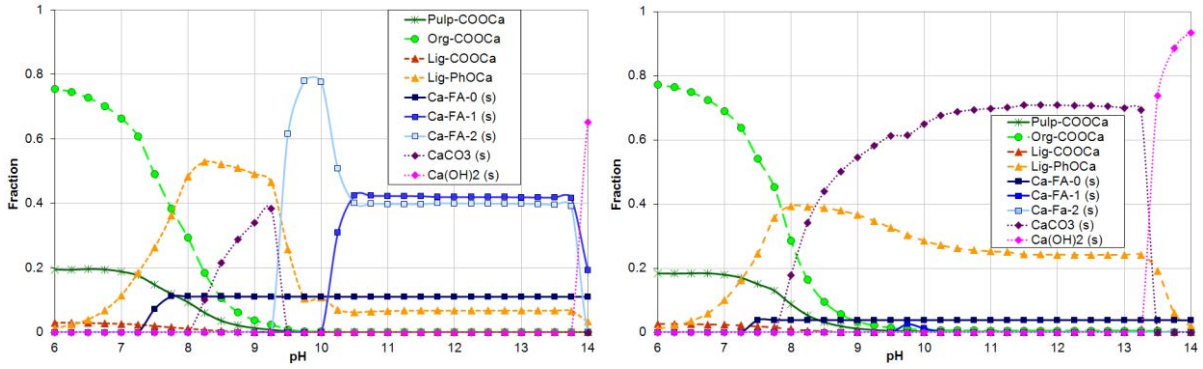

Figure 1. Simulated distribution of Ca in two mill samples: Mill A (left) and Mill B (right); see **Table 1**.

The sample from the softwood Mill A was the only one that contained noticeable amounts of monounsaturated fatty acids (FA-1) compared to Ca and only there could a formation of Ca soaps clearly be seen above pH 10. In Mills A and C, relatively large amounts of polyunsaturated fatty acids (FA-2) were reported: they are present

naturally in wood extractives from pine and birch raw material, and were moreover added deliberately in a form of tall oil as a chemical aid for removal of extractives in Mill C. The simulation results for these two mills also showed a noticeable formation of calcium soaps of polyunsaturated fatty acids. The simulation results confirm a general hypothesis presented above, namely that even though the solubility of unsaturated fatty acid soaps is noticeably higher than the saturated ones, they can still constitute a large part of the formed precipitate if their initial concentration is very high.

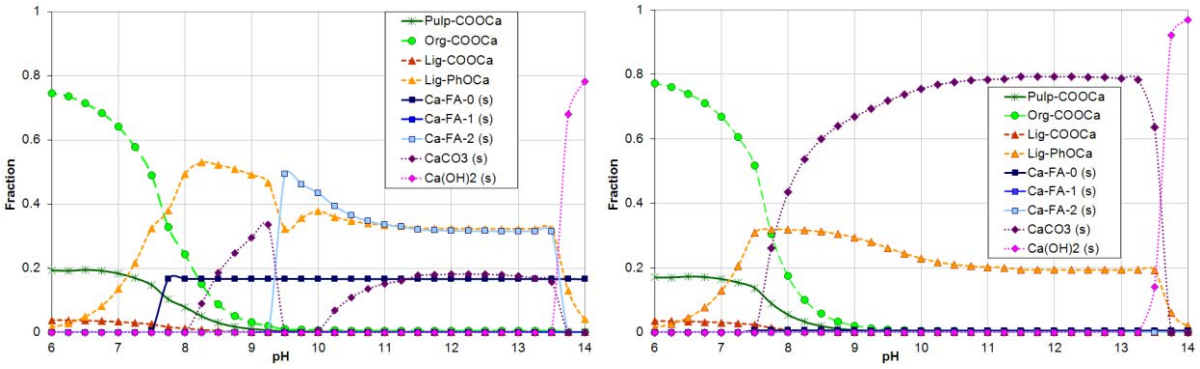

Figure 2. Simulated distribution of Ca in two mill samples: Mill C (left) and Mill D (right); see **Table 1**.

As fatty acids have a valence of one, two moles of a fatty acid are needed in order to precipitate one mole of Ca as a soap. It should be noted that only in cases of Mills A and C is the total amount of fatty acids sufficient to precipitate all Ca; however, in none of the simulated cases was the entire Ca bound to fatty acids. Within the interesting pH interval (9-13) a noticeable fraction of calcium was present as a soluble complex with phenolic functional groups of lignin. This result is consistent with the industrial experience saying that precipitation of sparingly soluble metal salts in solutions containing wood organics is significantly hindered, and that concentrations of metals much above the theoretical solubility limits for purely inorganic solutions can be reached in such systems. The exact molecular mechanisms behind the observed inhibition of solid phase formation are not clear; two, mutually compatible, hypotheses are normally assumed. First, it is believed that certain organic structures, e.g. lignin molecules containing phenolic functional groups in suitable positions, may bind Ca and other metals in stable complexes making them effectively unavailable for precipitate formation. Second, the surface active organic molecules may disturb the crystal growth, acting effectively as crystal-modifying scale inhibitors [10]. In actual industrial systems, these mechanisms may act together; in this work, however, the interactions between Ca and wood organics were for simplicity modelled as complex formation only, and the stability constants were derived from the results of solubility experiments in model solutions [6].

In three of the four simulations: Mills B, C and D, significant amounts of $CaCO_3$ were also formed in the interesting pH interval. This supports the assumption that the high amount of calcium in the pulp leaving the digester is to a large degree present in the form of calcium carbonate. $CaCO_3$ crystals, as well as Ca soaps, may have a tendency to attach to pulp fibers and/or become effectively filtered off by the pulp phase, following it to the fiberline. This also explains the industrial experience saying that Ca is not effectively removed from the pulp either in the digester or in the brownstock wash and tends to follow the pulp to the bleach plant.

Comparison of the analytical and simulation results

Comparison of the simulation results with the analysis data of the four mill samples is slightly difficult to interpret. Resin acids were not expected to form metal soaps and none were found in mill samples either. The fatty acids were expected to form calcium soaps to different degrees in all the mills, which is in agreement with the mill sample analysis, but the results are not possible to use for predicting the situation in the individual mills. For instance the independently taken sample of separated soap from Mill A contained much less calcium compared to the soap samples from Mill B and especially Mill C. In contrast, the pulp sample from Mill A had the highest concentration of calcium soaps from these fatty acids. The soap sample from mill B contained a considerable amount of calcium soaps whereas the simulations of the pulp sample showed only a minor soap formation. It is not clear whether these discrepancies depend on the inefficiency of the simulation tool itself, or rather on difficulties with obtaining representative mill samples, especially with regard to warm pulp from the digester where soap precipitation may happen quickly upon cooling and result in uneven soap distribution.

It can therefore be argued that the simulation results may be used in order to see how changes in mill conditions will affect the formation of calcium soaps. However, the exact equilibrium constants for the components studied, especially metal complexing of organic substances in black liquor are still very uncertain and the area needs more work in order to be fully verified.

IV. CONCLUSIONS

A chemical simulation tool can be very useful in describing the chemical processes in an industrial system. In this work, we have used WinGEMS pulp mill simulator extended with MeteQ subroutine for modelling of chemical equilibria in order to predict the formation of sparingly soluble calcium soaps in pulp samples leaving the digester of the kraft pulping process. The simulations worked well within the defined system boundaries; for certain components (e.g. resin acids) the predictions were very good and in full agreement with the analytical results. For other components, e.g. fatty acids, the results are difficult to interpret, as some differences between the simulated and measured values can be seen. It is however not clear whether the differences depend entirely on inadequate simulation or also on difficulties with obtaining representative mill samples.

It is assessed that the weakest point in defining the chemical system for the simulations is probably a question of interactions between the metal ions and dissolved wood organics. It has been observed that precipitation of sparingly soluble metal salts in solutions containing wood organics is significantly hindered, which may be due to the complex formation but also other means of precipitation inhibition. In this work, the influence of organics was chosen to be modeled as complex formation between the metal ions and, mainly, phenolic functional groups of lignin, based on experiments conducted in model systems. It has been, however, observed that the simulated system is very sensitive to the assumptions regarding the amount of complexing groups as well as the stability constants of the complexes formed. It was therefore concluded that a correct description of these interactions is crucial for a successful prediction of the system behavior.

The new knowledge acquired in this study during the development of simulation tools is useful for better understanding of the mechanisms behind the formation of soap and $CaCO_3$ deposits in the digester and the recovery area. The simulations show clearly that when constructing a balance of metallic non-process elements in cooking and kraft recovery, the reactions of the soap components need to be correctly accounted for.

V. ACKNOWLEDGEMENT

This work has been performed as a project within Innventia Cluster Research Program, clusters Chemical Pulp and Chemical and Energy Recovery in the Kraft Pulp Mill, during the period 2009-2011. The research was supported by Alabama River Pulp, Altri Celbi, Korsnäs, Mercer, Metsä-Botnia, Mondi Kraft Paper, Stora Enso and Södra Cell.

VI. REFERENCES

[1] Irani, R. R.; Callis, C. F. Metal complexing by phosphorus compounds. II. Solubilities of calcium soaps and linear carboxylic acids. *J. Physical Chem.* **1960**, *64*, 1741.

[2] Pettersson, K.; Rutqvist, A.; Björklund Jansson, M. Optimerad hartsuttvättning ur björksulfatmassa. (In Swedish), STFI Report July **1989**.

[3] Westervelt III, H. H. A study of the calcium complex of the potassium salt of cathecol-4-sulfonate in aqueous, alkaline media. Doctoral dissertation, Institute of Paper Chemistry, Appleton, Wisconsin, **1981**.

[4] Lidén. J.; Lindgren, P.; Lukkari, I.; Söderberg, C. The relationship between wood species, $CaCO_3$ scaling and calcium balance in the kraft cook. Proceedings, 5th International conference on new available techniques, June 4-7 **1996**, Stockholm, Sweden. p. 498.

[5] Werner, J.; Ragauskas, A. Evaluation of the intrinsic metal binding capacity of kraft black liquor lignins. Proceedings, Tappi Pulping Conf **1998**, Montreal, Vol III, p.1145.

[6] Björklund Jansson, M.; Bialik, M.; Törngren, P. New insights into soap solubility and separation during kraft cooking. Proceedings of the 13th European Workshop on Lignocellulosics and Pulp, June 24-27 **2014**, Seville, Spain.

[7] Eriksson, G. An algorithm for the computation of aqueous multicomponent, multiphase equilibria. *Anal. Chim. Acta* **1979**, *112*, 375.

[8] Ulmgren, P. Solubility of slightly soluble compounds in bleach plant filtrates - a summary. STFI Report CHEM 88 **2003.**

[9] Al Attar, A.; Beck, W. H. Thermodynamic solubility products of long-chain normal fatty acids and their alkaline earth and lanthanum salts in water. *J Electroanal. Chem* **1970**, *27*, 59.

[10] Flynn, D. J. The Nalco water handbook, 3rd edition, McGraw Hill, New York **2007**.

NEW INSIGHTS INTO SOAP SOLUBILITY AND SEPARATION DURING KRAFT COOKING

Marianne Björklund Jansson*, Marta Bialik and Per Törngren

Innventia AB, Box 5604, SE-114 86 Stockholm, Sweden
**marianne.jansson@innventia.com*

ABSTRACT

The effect of black liquor composition on the solubility and salting out of soap components has been studied. A model black liquor (BL) containing inorganic ions and lignin in relevant concentrations was used. The effect of some kraft process parameters, such as residual alkali and sulphidity was found to have a rather complex influence on the soap solubility. At constant ionic strength the soap solubility was significantly increased in the model BL when the concentration of divalent ions (e.g. carbonate, sulphate and thiosulphate) was increased. Further, a small increase in soap solubility with increased alkali was seen when acetate ions were replaced by hydroxide ions. However, when sulphuric acid was added the effect of the divalent sulphate ion was shown to have a bigger impact and the soap solubility increased in this case even though the alkali decreased. This big impact of small changes in the BL concentrations of different sodium salts on the soap solubility is important when attempts to optimize the soap separation are made.

I. INTRODUCTION

During kraft cooking a high solubility of the wood extractives (=soap) in the black liquor is wanted in the digester in order for the soap to follow the withdrawn liquor and not the pulp. However, in the recovery area where the black liquor is evaporated to a higher concentration before burning, a low soap solubility is preferred instead, in order to maximize the soap separation from the concentrated black liquor. Separation (salting out) of the soaps is mainly achieved by an increased ionic strength during the evaporation. In softwood kraft mills, the separated soap phase is generally recovered from the black liquor before the recovery boiler and acidified to give crude tall oil. Tall oil is a valuable by-product and it is important to optimize the separation from the black liquor.

The solubility of soap is high at the conditions prevailing in weak black liquor at temperatures of 80- 95°C. When the liquor is concentrated the soap solubility will decrease up to a liquor concentration of about 25-30 % DS and then slightly increase [1]. The minimum soap solubility will vary for different mills. In most mills the soap is separated in one or more stages from tanks at a liquor concentration of about 20-30 % DS, but variations are seen between different mills. The black liquor concentration chosen for the soap separation stage is normally a compromise between a lower soap solubility at higher concentrations and a higher viscosity of the black liquor that will make the rising of the soap particles very slow. Since the temperature affects both the solubility and the viscosity the optimal conditions will also vary with temperature. Further, the surface area and the effective residual time for the liquor in the tank will be important.

The major part of the lipophilic extractives in softwoods consists of fatty acids (FA) and resin acids (RA). During a kraft cook these acids will dissolve as sodium soaps in the black liquor. The solubility behaviour of these soaps is quite complex [2, 3]. At lower ionic strengths, sodium soaps of fatty and resin acids are dissolved as micelles. When the ionic strength is increased the solubility of the micelles will decrease, finally resulting in the separation of a liquid crystalline soap phase, i.e. the sodium soaps are salted out.

In a previous study [4] we reported the effect of ionic strength, temperature and lignin addition on the solubility of soap in a model black liquor. Further, the composition of the soap, especially the FA/RA ratio, has a big impact on soap solubility in black liquors [5, 6]. The effect of residual alkali has been investigated by e. g. Ryan [7] and Uloth et al. [6], but the effect has not been fully explained. In this study the effects of variations in composition of the model black liquor, especially alkali concentration, on the soap solubility have been investigated.

II. EXPERIMENTAL

Concentrated model black liquors were prepared from inorganic salts and lignin according to **Table 1**. Sodium acetate was included as a model for organic substances and in order to increase the sodium content. The concentrated model black liquors were diluted to different defined ionic strengths to simulate different levels of

evaporation in the pulping process. Fatty acids (FA) or fatty and resin acids (RA) in the ratio FA/RA = 2.3 were added to the model black liquors after dilution, giving a total concentration of 2 % extractives. The solutions were agitated in a heated water bath at least 24 h to ensure a complete dissolution of the added extractives and then left without agitation for another 18 h to equilibrate. Samples for test were subsequently withdrawn from the bottom of the test tube and dissolved soap was determined according to Saltsman and Kuiken [8], but without the addition of hydrogen peroxide and sodium sulphite. The extracts were subsequently evaporated to dryness under nitrogen, silylated and analysed by GC/MS. Isopalmitic acid was added before the evaporation step and used as an internal standard for quantification of extractives.

Table 1. Starting concentrations in model black liquor BL1 used in figures 1 and 2 and BL2 used after dilution in figure 3. In figure 4 BL2 was used but the acetate was replaced by the different ions tested. The ionic strength was kept constant.

	Na^+	SH^-	OH^-	CO_3^{2-}	$acetate^-$	Lignin	I
	mol/L	***mol/L***	***mol/L***	***mol/L***	***mol/L***	***g/l***	***mol/L***
BL1	*1.57*	*0.18*	*0.19*	*0.16*	*0.6*	*56*	*1.7*
BL2	*3.33*	*0.38*	*0.4*	*0.34*	*1.8*	*0*	*3.6*

The composition of the added soap was: 70 % fatty acids (mainly oleic acid, C18:1, linoleic acid, C18:2 and pinolenic acid C18:3) and 30 % resin acids (mainly abietic acid, dehydroabietic acid and palustrinic acid).

The lignin used was a LignoBoost lignin derived from acidification of a softwood black liquor [9]. Other chemicals used were of p.a. quality.

III. RESULTS AND DISCUSSION

Variation in residual alkali.

A complex influence of residual alkali on soap solubility has been reported by Uloth et.al [6] showing that both at decreased and increased alkali the solubility of soap increases. In their experiment the residual alkali was altered by an addition of sulphuric acid or sodium hydroxide to a mill black liquor.

In this study two different approaches were tested in order to verify the influence of residual alkali on the solubility of fatty and resin acid soaps in black liquor. The experiments were performed at two temperatures, 80 and 95°C.

In the first method (A) the residual alkali was altered by adding sulphuric acid or sodium hydroxide in a controlled way to a model black liquor (BL1 in table 1). This is the most straightforward way and is equivalent to the method used by Uloth et al. The drawback is that the ionic strength is changed by the addition of sodium hydroxide (Na^+, OH^-) or sulphuric acid (SO_4^{2-}). Changing the ionic strength will influence the soap solubility and thus complicate the interpretation of the results. Withdrawn liquor samples were analysed with regard to the amount of dissolved fatty/resin acids at different residual alkali, **Figure 1**. With this method the soap solubility seemed to decrease with increased alkali.

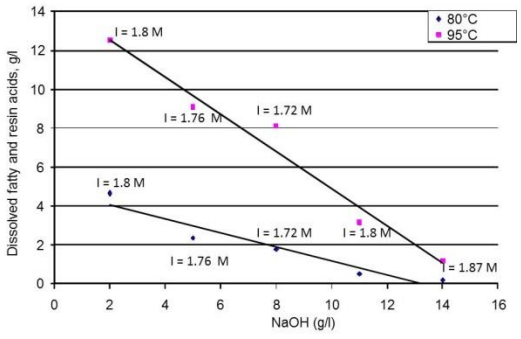

Figure 1. Method A Solubility of FRA in model black liquor as a function of alkali at two different temperatures. Ionic strength shifting within the interval 1.72 – 1.87 M.

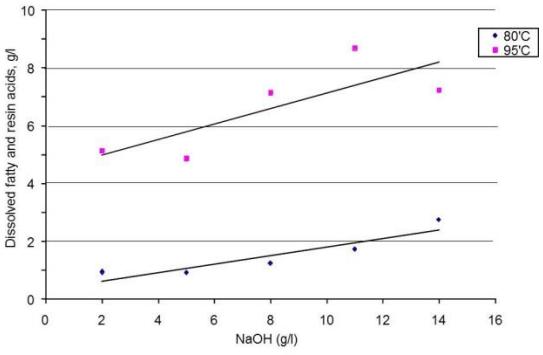

Figure 2. Method B. Solubility of FRA in model black liquor as a function of alkali at two different temperatures. Ionic strength = 1.7 M.

In the second method (B), concentrated model black liquor with reduced amounts of sodium hydroxide and sodium acetate was used. By adding sodium hydroxide to the model black liquor and balance this with sodium acetate, a series of samples with increasing alkali and constant ionic strength could be achieved. Withdrawn liquor samples were analysed similarly as for method A. When the ionic strength was kept constant, **Figure 2**, the solubility increased with higher alkali. Figure 1 and 2 also illustrate the effect of temperature on the soap solubility.

When comparing the results of Figure 1 and 2 a contradicting influence of alkali on the soap solubility is seen. In figure 1 the low solubility at high alkali could be explained by the salting out effect, as the ionic strength increased by the addition of sodium hydroxide. On the other hand, the observed increase in solubility at low alkali is more difficult to explain, since the ionic strength is increased also with the addition of sulphuric acid and thus also should result in a salting out effect similar to the result when sodium hydroxide is added. However, the result at low residual alkali is in agreement with the observations made by Uloth et al [6], when adding sulphuric acid. In some additional experiments acetic acid or formic acid was used instead of sulphuric acid to decrease the alkali according to method (A). Surprisingly no significant increase in soap solubility was observed at low alkali in this case. Obviously there are factors in addition to ionic strength and alkali that seem to affect the soap solubility in these mixtures. Our interpretation was that the addition of sulphate ions was affecting the solubility in a different way than the acetate or formiate ions.

Comparison of various sodium salts.

In one experiment model black liquor (BL2 in table 1) was diluted to ionic strengths in the range 0.5 to 2.0 M and the amount of dissolved fatty/resin acids was determined and plotted against the corresponding ion strength, acetate curve in **Figure 3**. Further, similar series of model black liquors were prepared where different sodium salts were substituted for the sodium acetate in BL2. These curves are included in figure 3.

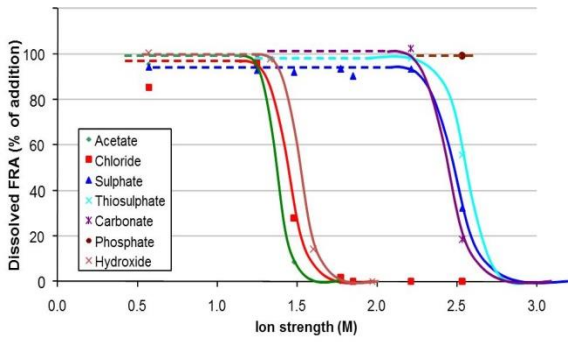

Figure 3. Solubility of sodium soaps of a mixture of fatty acids and resin acids (FRA) as a function of ionic strength, at 80°C. Sodium acetate in BL1 is replaced by different sodium salts. At lower ionic strengths all added soap (14 g/l) is dissolved.

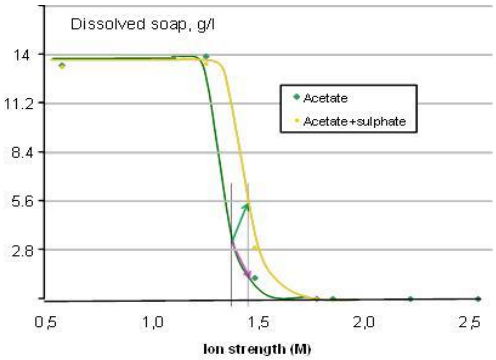

Figure 4. Solubility of sodium soaps of a mixture of fatty acids and resin acids as a function of ionic strength. The effect of changing the ionic strength by addition of acetate and sulphate respectively is illustrated by the arrows. Green arrow = addition of sulphate, red arrow addition acetate. T =80°.

At a low ionic strength, all added FA/RA were dissolved. When the ionic strength is increased the solubility of the micelles is reduced resulting in the separation of a liquid crystalline phase, i.e. the sodium soaps are salted out. In black liquor with acetate (BL2), this occurred in a short interval at an ionic strength of about 1.5 M. As seen, the curves for univalent and divalent ions are arranged in two distinct groups in respect to how they influence the salting out of soaps. Similar results have been reported for solutions of NaCl and Na_2SO_4 by Ström et al. [3]. From these experiments the different anions can be arranged in a tentative sequence from left to right according to how they increase the solubility of sodium soaps.

$$CH_3COO^- < Cl^- < OH^- << CO_3^{2-} < SO_4^{2-} < S_2O_3^{2-} << PO_4^{3-}$$

To verify the effect seen in figure 1 one additional experiment was performed using a low addition of sulphate similar to the addition used in figure 1. The result is shown in **Figure 4**. As seen, the soap solubility increased to 5.5 g/l instead of decreasing to 1.5 g/l when the ionic strength was changed by addition of sulphate instead of acetate. This means that the addition of sulphate can explain the observed increase in solubility when sulphuric acid was added to adjust the residual alkali. Hence, the increase in solubility is an effect of the addition of

sulphate ions and not of the decrease in the residual alkali. On the other hand, the increased solubility when the acetate ions were replaced by hydroxide ions, Figure 2, could be said to be an effect of increased alkali. However, the results show that the soap solubility is sensitive to all changes in the ion composition in the liquor, and the same hydroxide concentrations may thus give different soap solubility if also some other changes e.g. the concentrations of low molecular acids, such as acetate ions, or divalent ions such as e.g. carbonate or sulphate are changed.

IV. CONCLUSIONS

The soap solubility behaviour has been seen to be rather complex even at such basic levels as in this model study. In mill black liquors further complications caused by the divalent cations, especially calcium must be considered.

The following main conclusions were drawn:

- Small changes in ionic composition of BL may have a big impact on soap solubility. At constant ionic strength the soap solubility was significantly increased when the concentration of divalent ions (e.g. carbonate, sulphate and thiosulphate) was increased.
- A small increase in soap solubility with increased alkali was seen at constant ionic strength, i.e. when acetate ions used to adjust ionic strength were replaced by hydroxide ions. However, when sulphuric acid was added the effect of the divalent sulphate ion was shown to have a bigger impact and the soap solubility increased in this case even though the alkali decreased.

It has been shown that a small increase in the concentration of divalent ions, such as sulphate and carbonate, strongly increases the soap solubility in the model liquors used. The importance of this is not fully clear. The concentration of the inorganic ions in the black liquor will be affected by several process variables in the mill recovery cycle. The alkalinity and sulphidity of the liquor as well as the carbonate concentrations will all affect the soap solubility. This new insight may be used in order to explain differences in soap solubility seen when operational parameters in the mill are changed or when comparing the situations in different mills.

V. ACKNOWLEDGEMENT

This work has been performed as a joint project within the Innventia Cluster research program of Chemical pulp - fibre line and the Innventia Cluster research program of Chemical and energy recovery, in the period 2009-2011. The research was supported by Alabama River Pulp, Altri Celbi, Korsnäs, Mercer, Metsä-Botnia, Mondi Kraft Paper, Stora Enso and Södra Cell.

VI. REFERENCES

1. Drew J, Propst M, Tall oil, *Pulp Cemicals Association*, New York **1981**

2. Lindman B and Wennerström H, Micelles. Amphiphilic aggregation in aqueous solution, *Topics in current chemistry*, **1980**, Vol 87, p.3-83, Springer-Verlag, Berlin Heidelberg. Ed. F.L. Boschke

3. Ström G, Stenius P, Lindström M and Ödberg L, Surface chemical aspects of the behaviour of soaps in pulp washing, *Nordic Pulp Paper Res. J*, **1990**, 5:1, 44-51

4. Törngren P and Björklund Jansson M, Proceedings from *11th European Workshop on Lignocellulosics and Pulp*, Hamburg/Germany, August 16 - 19, **2010**

5. Palonen, P Stenius P and Ström G, Surfactant behaviour of wood resin components, *Svensk Papperstidning* **1982**, 85:12, R93-R99

6. Uloth VC, Wong A, Wearing JT, Factors affecting tall oil soap solubility in kraft black liquor *Pulp and Paper reports* PPR 581, **1986**, Pulp and Paper Research Institute of Canada

7. Ryan T, Increased alkali residual improves recovery operations at Calcasieu, *Pulp and Paper*, June **1980**, p 191

8. Saltsman W. and.Kuiken KA, Estimation of tall oil in sulphate black liquor, *Tappi* **1959**, 42:11, 873-874

9. Öhman F, Precipitation and separation of lignin from kraft black liquor, Ph.D. thesis, Department of Chemical Engineering and Environmental Science, Chalmers University of Technology, Gothenburg, Sweden, **2006**

DETERMINATION OF THE FULL ELEMENTAL COMPOSITION OF PULP AND WOOD SAMPLES

K. G. Bogolitsin[1,2], A. V. Malkov[1], E. M. Kashina[1*], A.S. Pochtovalova[1]

[1]Northern (Arctic) Federal University named after M. V. Lomonosov
Severnaya Dvina Emb. 17, Arkhangelsk, Russia; 163002
[2]Institute of Ecological Problems of the North, Ural branch of Russian Academy of Science
Severnaya Dvina Emb. 23, Arkhangelsk, Russia; 163002
*(*e-kashina@mail.ru)*

ABSTRACT

Technique of determination of elemental composition of pulp by x-ray fluorescence is developed. For determination Na and S calibration curves are performed. Light elements C, H, N are determined by elemental analyzer.

I. INTRODUCTION

The content of metals in the pulp has particular importance in the peroxide or ozone bleaching method and in the production of viscose pulp and electrical insulating paper [1]. Sodium assess to the quality of washing. Iron, manganese and copper reduce whiteness of the fibers. Transition metals such as iron, cobalt and manganese are the catalysts for the oxidative degradation of pulp. Aluminum, lead and copper inhibit oxidative processes. Calcium make difficult filtration of viscose solution, silicates impair filtration viscose [2]. Thus the determination of content of elements, presenting in various amounts is interested.

Typically, for the determination of metals in the wood, the pulp and paper a method of atomic absorption spectroscopy is used[3,4]. In recent years, increasingly ICP MS and X-ray fluorescence analysis are used [5,6]. Atomic absorption and ICP MS methods require a lot of time and use of aggressive reagents for sample preparation. X-ray fluorescence analysis is one of the modern spectroscopic methods, allowing the simultaneous determination of the content of elements of the sample from beryllium to uranium without destroying the sample. X-ray spectroscopy is an advanced method for multielemental analysis, but for the determination of light elements (C, N, H) it is not applicable. But the content of these elements is need to know for the correct calculations by method of the fundamental parameters. Therefore it is interest to combinate XRF spectroscopy and elemental analysis on CHN-analyzers.

The aim of this work is the development of method for determination of the elemental composition of the pulp by X-ray fluorescence spectroscopy.

II. EXPERIMENTAL

The objects of investigation are bleached hardwood and softwood pulp, washed and unwashed pulp and wood in chips. Preparation of the samples was performed as follows: before elemental analysis samples were ground in the planetary ball mill Retsch MM 100 to a powder, additionally for XRF – analysis they were pressed into tablets.

For the determination of sodium and sulfur, calibration curves were constructed. For this purpose, initially samples of known content of Na and S were prepared. In a sample of microcrystalline cellulose sodium sulphate weighed was added so that the weight of the resulting tablet made 1g. Then the powder and 2 ml of deionized water were mixed in a mortar for 3.5 minutes, and were dried at 105 ° C for 1h. The powder was pressed into tablets of 20 mm diameter under a pressure of 300 MPa. Thus five tablets to concentrations of 0, 0.2234, 0.5665, 2.1041 and 5.1080% Na and 0, 0.1557, 0.3950, 1.4671 and 3.5615% S were produced. the content of carbon, hydrogen and nitrogen was identified by elemental analyzer EuroEA-3000 by EuroVector company, Italy. The experiment was performed using wavelength dispersive spectrometer Lab Center XRF-1800 by Shimadzu corporation, Japan. Measurements to construct the calibration were performed at the following conditions: atmosphere - a vacuum; x-ray tube parameters: voltage 25 kV, current 130 mA. The spectral crystal for determination Na - TAP, S – Ge were used. The spectra were registered, using K_α-line.

III. RESULTS AND DISCUSSION

At the first stage X-ray fluorescence spectra were recorded. All the spectra were similar character. As a result elements Al, Mg, Zn, Fe, Cr, Mn, Ca, K, Cl, P, Si, Na, S, C and O were found, that is typical for wood and pulp (figure 1).

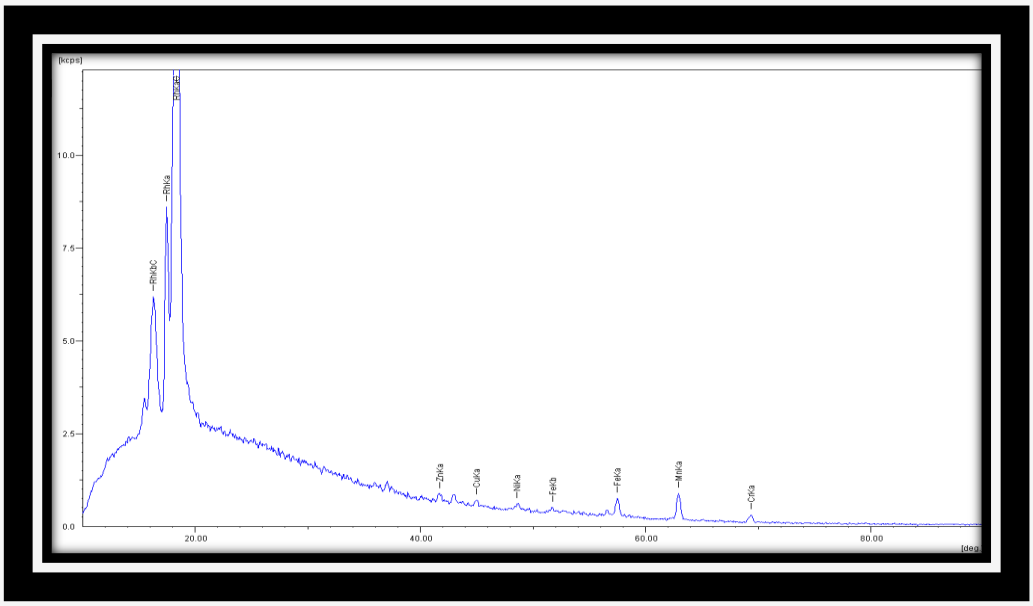

Figure 1. The spectrum of the sample pulp (unbleached washed).

For the determination of the light elements with a relatively high content, such as sodium, calibrations were performed. The results of measurements of intensities against the element content in the sample were plotted on the figure 2.

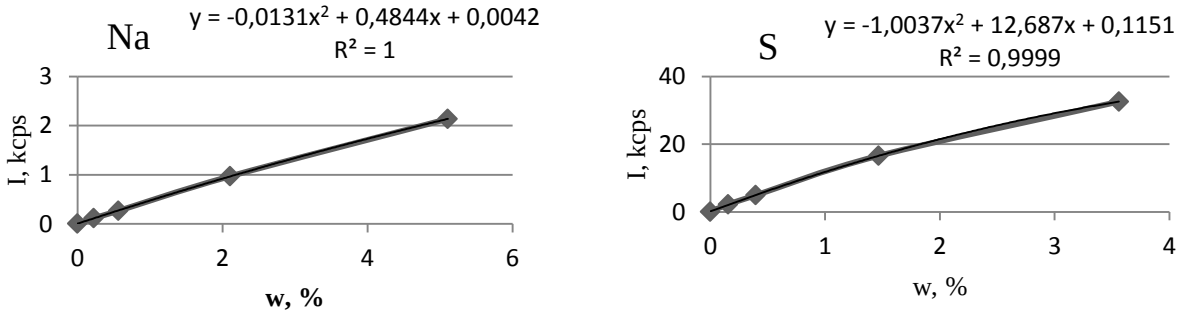

Figure 2. The calibration curve for Na and S.

And finally the content of the remaining elements was identified by quantitative XRF-method. For the determination sodium and sulfur calibration were performed, oxygen was determined by the balance, trace elements - by the fundamental parameters method. The results are presented in the table.

Table. The elemental composition of pulp samples.

Element	Concentration						
	1-C	2-C	3-C	4-C	5-C	2-C-05	3-C-30
S, ppm	*127±2*	*160±2*	*155±2*	*261±4*	*329±6*	*3766±81*	*n/a*
Na, ppm	*59±1*	*11401±492*	*979±49*	*508±9*	*620±22*	*16820±451*	*n/a*
Zn, ppm	*16±1*	*34±1*	*29±1*	-	-	*n/a*	*70±1*
Cu, ppm	*15±1*	*54±1*	*25±1*	*61±3*	*59±2*	*n/a*	*115±3*
Ni, ppm	*17±1*	*65±1*	*22±1*	*65±3*	*78±3*	*n/a*	*106±4*
Fe, ppm	*69±1*	*150±2*	*61±1*	*61±1*	*45±1*	*n/a*	*189±1*
Mn, ppm	*174±1*	*308±2*	*212±1*	-	-	*n/a*	*228±5*
Cr, ppm	*67±1*	*91±1*	*66±1*	*63±1*	*62±1*	*n/a*	*125±1*
Ca, ppm	*1035±10*	*2811±54*	*3871±72*	*673±20*	*637±21*	*n/a*	*n/a*
K, ppm	*565±9*	*284±5*	*73±1*	*32±2*	*22±3*	*n/a*	*n/a*
Cl, ppm	-	-	-	*429±21*	*518±22*	*n/a*	*n/a*
P, ppm	*81±3*	*80±1*	*41±2*	*4±1*	*3±1*	*n/a*	*n/a*
Si, ppm	*833±2*	*1503±8*	*479±1*	*133±4*	*113±6*	*n/a*	*n/a*
Al, ppm	*340±7*	*363±4*	*185±6*	*43±1*	*35±1*	*n/a*	*n/a*
Mg, ppm	*484±3*	*818±2*	*989±18*	*141±3*	*156±15*	*n/a*	*n/a*
O, %	*47.4±1.7*	*43.5±1.4*	*46.2±1.6*	*48.6±0.01*	*48.6±0.01*	*n/a*	*n/a*
N, %	-	-	-	-	-	-	-
C, %	*45.7±1.3*	*48.2±1.9*	*47.1±1.3*	*44.3±1.3*	*44.3±1.3*	*48.2±1.9*	*47.1±1.3*
H, %	*6.48±0.31*	*6.15±0.26*	*5.93±0.21*	*6.89±0.35*	*6.93±0.35*	*6.15±0.26*	*5.93±0.21*

1-C - wood
2-C - unwashed softwood pulp
3-C - washed softwood pulp
4-C - bleached softwood pulp
5-C - bleached hardwood pulp

2-C-05 – 2-C + 0.5% Na, 0.3% S
3-C-30 - 3-C + 30 ppm Zn, Cu, Ni, Fe, Mn, Cr

The data are shown, during the production of pulp from wood chips content of heavy metal increases, such as Zn, Cu, Ni, Fe, Mn, Cr. After washing content of Na and K decreases significantly. In bleached pulp Mn and Zn are absent.
To check the calibration tablet from pulp with the addition of sodium sulfate was made (sample 2-C-05 in the table). Results are shown, that method by calibration curve can be applied for determination light elements. Also the tablet from pulp with the addition 30 ppm Zn, Fe, Cu, Mn, Ni and Cr was made (sample 3-C-30 in the table). Analysis was shown, that acceptable results are obtained for Zn and Mn only. This may be associated with to the low content of elements in the sample and limitations of the fundamental parameters method.

IV. CONCLUSIONS

Research was shown, that materials such as wood and pulp expediently at first to expose to elemental analysis for determination of the content of carbon, hydrogen and nitrogen. In order to obtain more accurate results for light elements need to build calibration curves. Using fundamental parameters method acceptable results are obtained only for heavy metals.

V. ACKNOWLEDGEMENT

Research was done in Center for Collective Use of Equipment “Arktika” by Northern (Arctic) Federal University named after M. V. Lomonosov.

VI. REFERENCES

[1] Milovidova L.A. Bleaching of pulp. *Publisher ASTU, Arkhangelsk* **2005.**

[2] Obolenskaya A.V. Laboratory works on the chemistry of wood and pulp. *Ecology, Moscow*, **1991.**

[3] Carrion N; Zully A.; Elias J. Determination of manganese, calcium, magnesium and potassium in Pine (Pinus Caribaea) Needle samples by flame atomic absorption spectrometry with slurry sample-introduction. *Journal of analytical atomic spectrometry.* **1987**, *2*, 813-817.

[4] Persson J.-A.; Frech W.; Pohl G.; Lundgren K. Determination of aluminium in wood pulp liquors using graphite furnace atomic-absorption spectrometry. *Analyst*, **1980**, *105*, 1163-1170.

[5] Lindsay D.; Anthony T.; John P. Characterization of document paper using elemental compositions determined by inductively coupled plasma mass spectrometry. *J. Anal. At. Spectrom*., **2000**, *15*, 813-819.

[6] Manso M. Carvalho M. L. Elemental identification of document paper by X-ray fluorescence spectrometry. *J. Anal. At. Spectrom*., **2007**, *22*, 164–170.

STUDY OF THE WOOD SUBSTANCE'S MORPHOLOGICAL STRUCTURE CHARACTERISTICS USING THE METHODS OF STEAM EXPLOSION AND SUPERCRITICAL FLUID EXTRACTION TREATMENT

Konstantin Bogolitsyn[1,2], Janis Gravitis[3], Maria Gusakova[1] , Dmitry Chukhchin[2], Anna Krasikova[1]*, Ivan Zubov[1], Artyom Ivakhnov[2], Sergey Khviuzov[1]

[1] *Institute of Ecological Problems of the North, Ural Division, Russian Academy of Sciences, Northern Dvina Embankment 23, Arkhangelsk, 163000,Russia*
[2] *Northern (Arctic) Federal University named after Lomonosov, Northern Dvina Embankment 17, Arkhangelsk, 163000, Russia*
[3]*Latvian State Institute of Wood Chemistry, Dzerbenes str. 27, Riga, LV-1006, Latvia*
**ann.krasikova@gmail.com*

ABSTRACT

Investigation of impact of lignocellulose matrix thermochemical activation by methods of steam explosion and supercritical fluid extraction was carried out in this study. Changes of the chemical composition, morphological structure characteristics at different levels of the wood substance's organization during these treatments were recorded by the methods of scanning electron microscopy (SEM), X-Ray analysis, FTIR- and UV-spectroscopy. Data about changes taking place in the cell wall at micro- and ultramicrolevels during these treatments were obtained. Availability of these methods application for deeper and more detailed study of morphological characteristics of the wood substance's structure and also for labile sites and bonds stability detection during different types of thermochemical activation was shown.

I.INTRODUCTION

According to modern concepts, the structure of wood cell walls has the complicated hierarchical organization. Consideration of submolecular level of wood matrix on the one hand opens a subject of cells' wall synthesis and self-assembly processes, which rule the formation of chaotic objects of biological origin. On the other hand there are questions of thermodynamic compatibility of plant tissue's components [1]. From this point of view, wood is considered as a nanobiocomposite, and its lignin-carbohydrate matrix is a superposition of interpenetrating networks formed by H-bonds, C-C-bonds, ether bonds and lignin-carbohydrate bonds. Thermodynamically incompatible cellulose and lignin form microheterogeneous regions surrounded by hemicellulose gel [2]. The concept of thermodynamic incompatibility of lignin-carbohydrate matrix allows considering of supercritical fluid technologies and steam explosion as a methods aimed at changes of structure and properties of biocomposite on the molecular level. Also they can be used as methods for deeper study and understanding of morphological structure of the wood substance.

Thus, the aim of this work is the investigation of wood substance's structure characteristics by the means of thermochemical activation of lignin-carbohydrate matrix during steam explosion (SE) treatment and CO_2-supercritical extraction (CO_2-SCE), detection of labile sites in the cell wall and search for opportunities of different thermochemical actions application for the system's heterogeneity increase.

II.EXPERIMENTAL

Air-dry grinded (fraction of 1-2 mm) juniper wood (*Juniperus Communis* L.) aged from 80 to 90 years was used as the representative experimental sample.

SE-treatment was carried out at the Laboratory of Biomass Eco-Efficient Conversion (Latvian State Institute of Wood Chemistry) in batch reactor with a capacity of 0,5 l, at pressure of 32 bar, temperature of 235°C for 3 minutes, with subsequent stages of water extraction, alkali extraction by 0,4% NaOH solution and precipitation by HCl.

CO_2-SCE was carried out in autoclave with a capacity of 5 ml (SFE-5000, Thar Process, USA) at temperature of 35°C, pressure of 250 bar for 20 minutes. CO_2 flow rate was 2,4 ml/min, cosolvent flow rate was 0,6 ml/min, washing solvent was acetone. After this treatment the samples were freeze-dried for the next investigations.

Analysis of wood before and after treatment

The composition of investigated samples (content of cellulose, lignin, ash, extractives by water and ethanol) was determined according to standard procedures [3].

FTIR-spectra of wood were registered by Fourier transform infrared spectrophotometer IRAFFINITY-1 ("Shimadzu", Japan) within the range of 4000-400 cm^{-1} with resolution of 4 cm^{-1} in KBr tablets. Values of their relative optical density were calculated as $K = D_{lig} / D_{carb}$ for characterization of lignin and carbohydrate component abundance in wood samples. The band at 1510 cm^{-1} was chosen for lignin abundance because of

absorption of aromatic rings of guatil type, for carbohydrate component abundance - 1060 cm^{-1} because of valency asymmetric fluctuations of ester bonds.
X-Ray analysis and samples' crystallinity degree determination were carried out by X-Ray diffractometer XRD-7000, Shimadzu, Japan.
Investigation of wood sample's ultra-micro and submolecular structure was performed by SEM method. Images were obtained by scanning electron microscope SEM Sigma VP ZEISS (accelerating voltage – 20 kV, In Lens detector). The samples for investigation were in form of transverse and longitudinal splits of juniper wood after freeze-drying. The coating of gold and palladium with 5 nm thickness was applied in order to increase samples' image contrast (with the device for samples preparation Q150TES by QUORUM).
Analysis of extracts after treatment
UV-spectra of extracts were recorded within the range of 190 - 400 nm by UV-spectrophotometer UV-1800 Shimadzu, Japan.

III.RESULTS AND DISCUSSION

According to modern concepts, mechanism of the steam explosion action upon wood matrix includes deacetylation of hemicelluloses at high temperature with acetic acid formation and polysaccharides destruction with formic acid formation. These organic acids act as catalysts of weak bonds hydrolysis in lignin-carbohydrate complex of wood. First, acid catalysis leads to hemicelluloses destruction. Hemicelluloses act as they unite cellulose elementary fibrils and lignin because of the transition layer formation on the cellulose fibrils surface.

Also hemicelluloses have limited thermodynamic compatibility with lignin. Their destruction leads to the phase change, cell wall components stratification and thermodynamic incompatibility increase as a result of destruction of the network between lignin and carbohydrates. Besides, steam explosion has an influence on diffuse regions in cellulose microfibrils. So these regions destruction, decrease of degree of polymerization and increase of cellulose crystallinity (from 30% to 39%) take place. These changes were registered by X-Ray analysis (**Figure 1**) proving the hypotheses from the study [4].

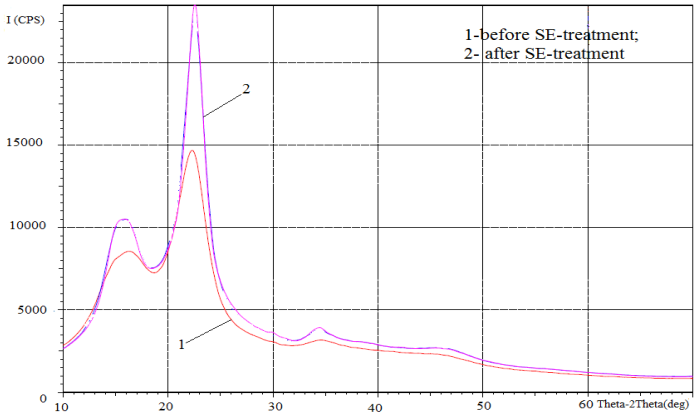

Figure 1. Diffractograms of samples before (1) and after (2) SE-treatment.

The analysis of the chemical composition (**Tables 1, 2**) confirms the destruction of carbohydrates during SE.

Table 1. The fractions ratio during SE process

Sample	Evaporable fractions (%)	Extraction with H_2O		Extraction with 0,4 wt.% NaOH			
		Residue (%)	Water soluble (%)	Residue (%)	Alk. solub. (%)	Precipitation (%)	Residue (%)
Before SE-treatment	-	100	2,7	97,3	4,6	0,4	92,8
After SE-treatment	17,3	87,2	10,3	72,5	18,4	9,7	54,1

Table 2. The chemical composition of juniper wood before and after SE, g/100 g of untreated wood

Sample	Klason lignin	Cellulose	Extractives (water)	Extractives (ethanol)	Ash
Before SE-treatment	30,20	43,10	10,90	4,50	0,20
After SE-treatment	17,08	23,84	12,83	15,92	0,23

Besides, the solid solution of hemicelluloses in lignin of middle lamellae is the most labile. The lignin domains are bonded with carbohydrate matrix by H-bonds [2], which can be easily destructed by acids influence. So, the lignin in such a solution is more mobile during the external impacts on wood, which leads to lignin extraction, coalescence and partial depolymerization of lignin with the formation of compounds with low molecular weight (6-8 phenylpropane units). The decrease of lignin content confirms the hypotheses from the study [4] about the predominance of lignin destruction processes during SE.
Thus, the influence of SE process on lignin-carbohydrate matrix consists of two components. The first of them is mechanical component leading to destruction of linkages between segments of lignin, cellulose and hemicelluloses macromolecules because of local increase of pressure. The second component is chemical one due to interaction of cell wall components. Therefore, thermodynamic incompatibility of a system increases and its internal energy decreases as a result of steam explosion.

The listed processes probably take place during supercritical CO_2 treatment with the same main parameters (high pressure and temperature, chemical additives). Chemical activation by SCE-method provided SC-CO_2 treatment of untreated and SE-treated wood samples. The absence of pure SC-CO_2 delignification impact [5] caused the necessity of modifiers addition. Ethanol and acetic acid were chosen as modifiers. Ethanol is traditionally used in wood chemistry as solvent of lignin. Acetic acid is known for its significant impact on SE process, so it was chosen for further intensification of chemical impact. The chemistry of processes taking place during SCE is similar to SE-chemistry; it is also aimed to weak bond destruction.

The assumptions about system's heterogeneity increase, chemical and mechanical bond destruction during these treatments are confirmed by IR-spectra of wood samples after SE, SCE with modifiers and step-by-step SE and SCE-treatment (**Figure 2**). So, significant differences were found when comparing untreated and SE-treated wood due to decrease of relative content of lignin (K value is 0.498 for sample №2 and 0.649 for sample №1). This trend is also shown for samples treated by SCE after SE (0.469 and 0.492 for samples №5 and 6 respectively). IR-spectra of SCE-treated wood are not so different in comparison with untreated wood (K = 0.603 and 0.615 for samples №3 and 4).

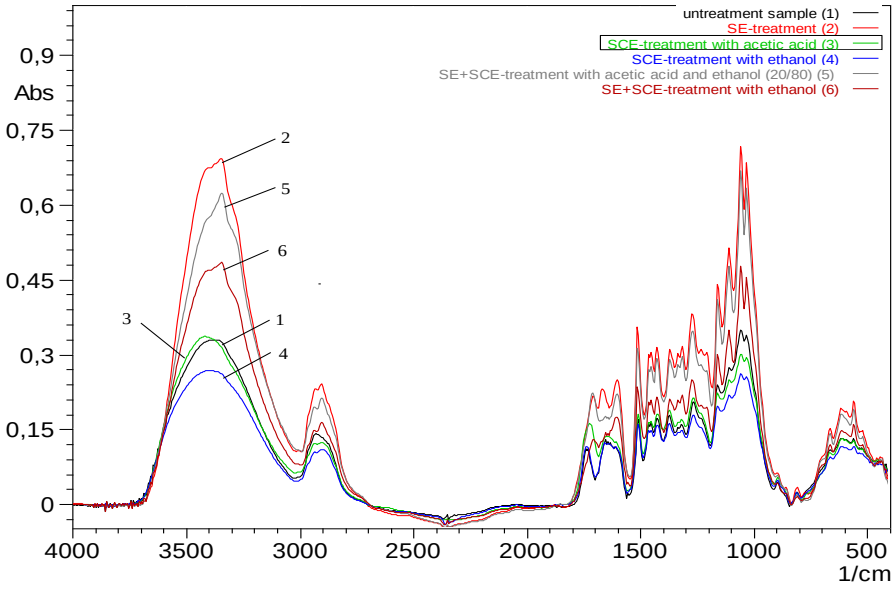

Figure 2. IR-spectra of wood samples

The performed morphological investigations can be the confirmation of stated changes. Figure 3 shows images of late tracheids on the longitudinal slices before and after SE.

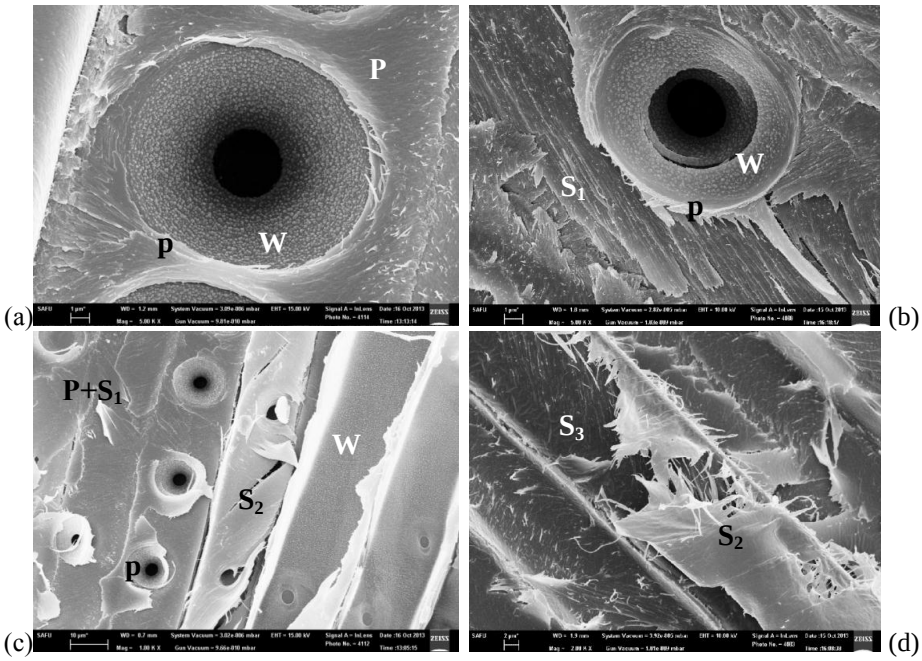

Figure 3. Cell wall changes after SE. (a, c– before SE; b, d – after SE); S_1,S_2, S_3, – second cell wall layers; W – verrucuos layer; P–primary cell wall; p – external pore surface.

As a result of such an impact the primary cell wall (P) was dissolved and separate fibrils of S_1 layer were removed. After SE-treatment the cell wall structure is little changed but there are significant mechanical and chemical impacts due to pressure gradient. The rupture of pores edging (**Figure 3a, b**) and cell wall layers can be seen on these spots, leading to stratification of nanobiocomposite internal structure. It should be noticed that the most voluminous S_2 layer saves its helical structure (**Figure 3c, d**), which is the evidence of such structures stability during SE-process.

SCE-treatment with acetic acid showed the absence of significant changes in cell wall morphological structure. Helical structure stability and little changes of other structural elements prove the stability of low-energetic bonds. The mechanical component of SCE-treatment is less than the same one of SE-treatment, so the access of chemicals to internal bonds and components is rather difficult and the effect of SCE is less expressed.

Acetic acid addition at the SCE-stage after SE did not lead to significant destruction of cell wall components. But ethanol presence in step-by-step treatment resulted in such effects as gradual extraction of lignin from S_2 layer and verrucous layer wash-out (**Figure 4**). The extraction of cell wall components in ethanol medium is confirmed by peak in the region of 280 nm on UV-spectrum corresponding to lignin of conifer species.

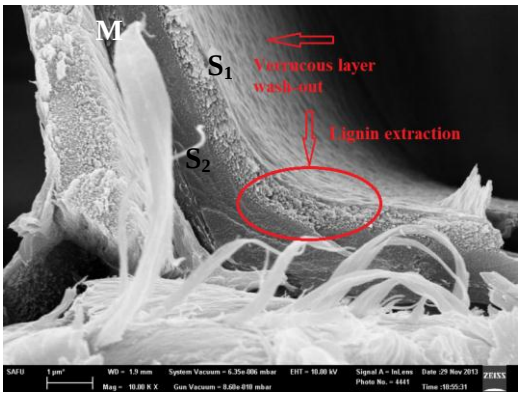

Figure 4. SE+SCE treatment impact on cell wall. S_1,S_2, S_3, – second cell wall layers; M–middle lamellae.

IV.CONCLUSIONS

As a result of performed investigations the new experimental data were obtained. These date confirm the statements about possibility of consideration of wood lignin-carbohydrate matrix as nanobiocomposite having high structure heterogeneity. It appears as a presence of labile and stable regions of lignin-carbohydrate formations distributed in cell wall and middle lamellae. Critical impacts on wood matrix lead to the increase of thermodynamic incompatibility of a system and a diffusion of lignin fragments and carbohydrate components away from wood substance.

V. ACKNOWLEDGEMENT

The researches were performed with the financial support of interdicsiplinary project of Ural Division of Russian Academy of Sciences (№ 12-M-45-2012), and also with the financial support of RFBR, research project №14-03-31551мол_а by the means of the equipment of CCU SE «Critical technologies of RF in the sphere of environmental safety of Arctic» (IEPN,Ural Division of Russian Academy of Sciences) and CCU SE «Arctic» (Northern (Arctic) Federal University named after Lomonosov) with the financial support of the Ministry of Education and Science of Russian Federation.

VI.REFERENCES

[1] Bogolitsyn K.G. Russian chemical journal, 2004. Vol. XLVIII. №6, p.105

[2] Bogolitsyn K.G., Lunin V.V., Kosyakov D.S. Physical chemistry of lignin, – M., Akademkniga, 2010, 492 pp.

[3] Obolenskaya A.V., Yelnitskaya Z.P., Leonovich A.A. Laboratory works on wood and cellulose chemistry. – M., Ecology, 1991. – 320 pp.

[4] Gravitis J. A. Theoretical and applied aspects of steam explosion of plant biomass. – Wood chemistry, 1987, №5, pp.3-21.

[5] Ivakhnov A.D., Bogolitsyn K.G., Skrebets T.E. Chemistry and technology of plant substances: abstracts for V All-Russia scientific conference, Syktyvkar – Ufa, 2008, p.35.

PHYSICO-CHEMICAL PROPERTIES OF LIGNIN-HUMIC COMPOUNDS

Konstantin Bogolitsyn, Larisa Parfenova*, Svetlana Selyanina, Marina Trufanova, Aleksander Orlov

Institute of Environmental Problems of the North, Ural Branch of Russian Academy of Sciences, Severnoy Dviny Emb., 23, Arkhangelsk, 163061
** solombalka@yandex.ru*

ABSTRACT

The fundamental properties of lignin and humic biopolymers include: amphiphility, polydispersity, the heterogeneity of the structural elements. On the one hand humification can be regarded as an important natural process, on the other hand as a method of lignin modification, which allows obtaining new products. As a result of a study, the characteristic of the structural organization of natural and technogenic origin polymeric matrixes containing lignin-humic compounds (hydrolyzed lignin, peat) was obtained. Hydrodynamic and surface-active properties of lignin-humic polymers were investigated and the possibility of their usage as a surfactant has been established.

I. INTRODUCTION

On the one hand, humification can be regarded as an important natural process, on the other hand as a method of lignin modification, which allows obtaining of the new products. Information on lignin-humic or *humic like* compounds properties is less systematized than the one of properties of humic substances obtained from natural raw materials (peat, coal)) as a result of a technological process. Diagram illustrating the possible sources of lignin-humic compounds extraction is presented on **Figure 1**. Comparative analysis of properties of *humic like* substances derived from model compounds and lignin-humic substances isolated from hydrolyzed lignin is described in [1]. Possibilities of transformation of soluble hydrolyzed lignins using water and alcohol solutions of NaOH for obtaining low-molecular destruction products and their application to the synthesis of phenol resins are described in [2]. Physical-chemical properties of humic like compounds extracted from composted biomass and industrial wastes are described in [3].

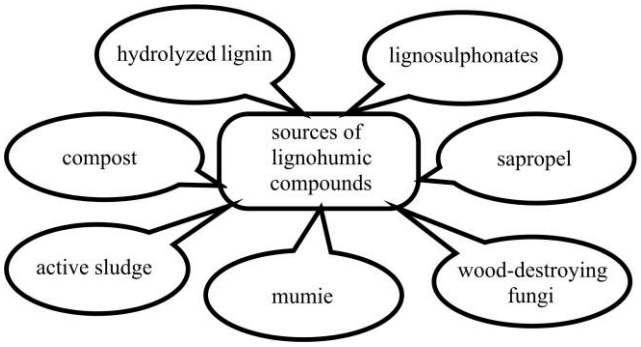

Figure 1. Sources of lignin-humic or *humic like* compounds

Taking into account a similar chemical nature of lignin, humic and lignin-humic biopolymers, their important role in the natural processes and application possibilities it seems reasonable to obtain comparative characteristics of their physical-chemical properties.

II. EXPERIMENTAL

Being sampled at the industrial dumps as well as within the territory of Arkhangelsk region correspondingly humified hydrolyzed lignin and peat have been used for extraction of lignin-humic compounds. Peat and hydrolyzed lignin microstructures were studied by the transmitted light microscopy (AxioScope A1 (Zeiss) laboratory microscope). Thermochemical study of the processes of interaction of hydrolytic lignin and peat with solvents was carried out by using differential microcalorimetric insulated shell at 298,15K. Size distribution of particles in solutions of lignin-humic compounds was studied by the method of dynamic light scattering (HORIBA LB-550 particles size analyzer).

The behavior in solutions and at liquid-gas phase boundary was characterized by the change of surface tension σ of the solutions measured by Wilhelmi method.

III. RESULTS AND DISCUSSION

Figure 2 shows the microstructure of polymeric matrixes of natural and technogenic origin used for extraction of lignin-humic compounds.

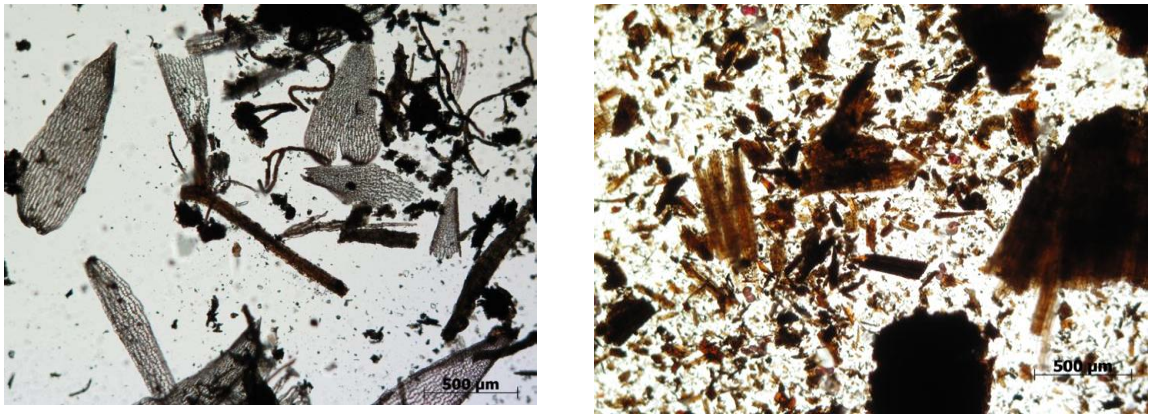

а б

Figure 2. Microphotography of polymeric matrixes of peat (a) and hydrolyzed lignin (b)

The content of lignin-humic substances in hydrolyzed lignin results in 6,8%, while 42% in peat. Lignohumic compounds are usually extracted by alkaline and acidic solutions; it is possible to use alcohols. **Figure 3** describes processes of interaction of hydrolyzed lignin and solvents.

Normally extraction of humic like substances in static mode should be performed within 24 hours. Obtained thermochemical data show that the basic process is completed within 25 minutes (calorimetric curve approaches to the zero line) under dynamic extraction.

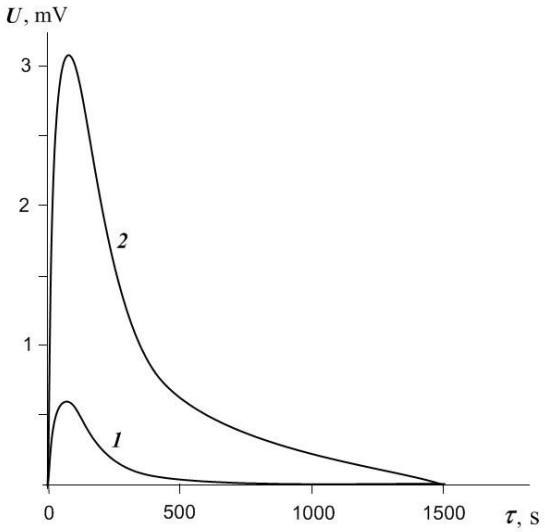

Figure 3. Thermochemical curves describing interaction of hydrolyzed lignin and solvents (water (1) and 0.1 m NaOH (2)) at 298 K.

Extraction at 85-90^{o}C allows to increase the yield of humic like substances, extracted from hydrolyzed lignin 2 times (from 6.8% to 14%). According to [2] a further increase of temperature up to 180^{o}C allows reaching 90% degree of hydrolyzed lignin destruction, however in this case low-molecular extractive substances are formed.

Viscometry shows that the characteristic viscosity of humic like substances extracted from hydrolyzed lignin is $5.1 \cdot 10^{-3}$ l/g. it was compared to the characteristic viscosity of peat humates (sodium salts of humic acids) ($2.3 \cdot 10^{-3}$ l/g), biopolymers of lignin nature - lignosulfonate ($3.5\text{-}4.5 \cdot 10^{-3}$ l/g)). Humic like substances turn to be heavier compared to other polymers of lignin-humic nature (**Table 1**).

Table 1. Hydrodynamic and the molecular-mass characteristics of lignin-humic substances (LGS)

The sample	[η], 10–3 l/g	Mw, Da
LGS	5,1	79000
peat humates	2,3	19000

Dynamic light scattering reveals that polydisperse supramolecular particles of micellar nature are in dynamic equilibrium with individual macromolecules in aqueous solutions of lignin-humic substances (**Figure 4**).

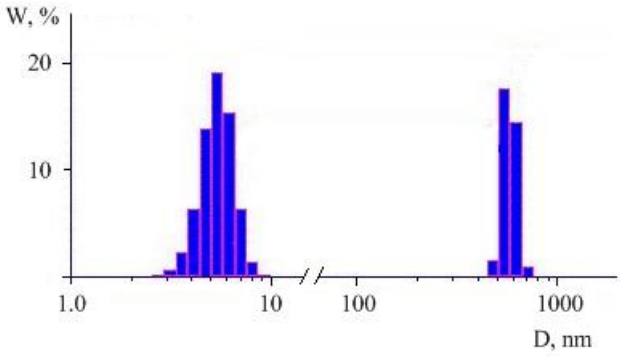

(a)

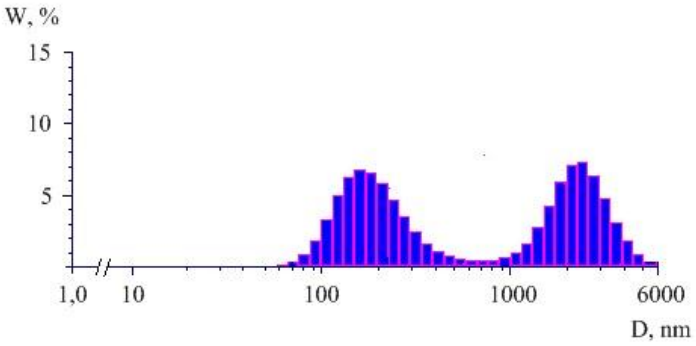

(b)

Figure 4. Size Distribution of particles in diluted (a) and concentrated (b) solutions of lignin-humic biopolymers.

The presence of supramolecular particles of micellar nature in solutions of lignohumic substances define the structure of their molecules and predetermine the surface-active properties. The use of lignin, humus biopolymers and humic like compounds as natural surfactants leads to the reduction of surface tension of water on 37-40 mN/m (**Figure 5)**.

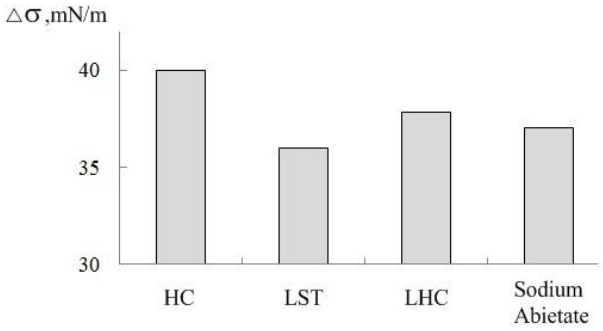

Figure 5. Depression surface tension of water in surfactant solutions: HC – Humic compounds; LST - sodium lignosulfonates; LGS - lignohumic compounds, Sodium abietate

IV. CONCLUSIONS

1. The comparative characteristic of hydrodynamic, molecular mass and surface-active properties of lignin-humic biopolymers, isolated from natural and technogenic matrices is provided.
2. It is shown that the extraction of hydrolyzed lignin at the temperature from 25 to 80^{o}C leads to obtaining of macromolecular lignin-humic compounds, bearing surface-active properties comparable to the other natural surfactants of aromatic nature.

V. ACKNOWLEDGEMENT

The studies were supported by the Program of Interregional and Interdepartmental Fundamental Researches of the Ural Branch of Russian Academy of Sciences (12-C-5-1017) and the Russian Fund of Fundamental Research (project No. 12-03-90018-Bel_a), the equipment of Core Facility “Critical Technologies of the Russian Federation in the Field of Environmental Safety of Arctic” (Institute of Environmental Problems of the North, the Institute of Physiology of Natural Adaptations of the Ural Branch of Russian Academy of Sciences).

The authors are grateful to PhD Chuhchin D.G. and Surso M.V. for the help in obtaining of experimental data.

IV. REFERENCES

[1] Sumarski I.V. Avtoref. dis. ... Cand. chem. Sciences. St. Peterburg, 2010. 18 p.

[2] Gribkov I. V. Avtoref. dis. ... Cand. chem. Sciences. Saint-Petersburg, 2008. 20 p.

[3] Adani F., Tambone F., Davoli E. Surfactant properties and solubilisation ability of humic acid-like substances extracted from maize plant and from organic wastes // Chemosphere – 2003, V.8., P.1017-1022.

FORMATION OF LIGNIN-CARBOHYDRATE MATRIX OF DECIDUOUS WOOD BY THE EXAMPLE OF ASPEN (*POPULUS TREMULA*) UNDER BIOTIC STRESS

Bogolitsyn[1,2]K., Gusakova[1] M., Pustinnaja[1] M., Sloboda[1] A.

[1] Institute of Ecological Problems of the North, Ural Division, Russian Academy of Sciences, nab. Severnoi Dviny23, Arkhangelsk, 163000 (Russia); [2] Northern (Arctic) Federal University named after Lomonosov, nab. Severnoi Dviny 17, Arkhangelsk, 163000 (Russia).

E-mail: lobanova2806@gmail.com

ABSTRACT

The new data, reflecting the impact of biotic stress, expressed by the influence of aspen polypore (*Phellinus tremulae*) on aspen wood (*Populus tremula*) lignin-carbohydrate complex in natural growing conditions were obtained. As the results of the fungus enzymatic system effect change occurs in the functional nature of lignin, which leads to its redox and acid-base properties changing, as well as changing of the chemical nature of the extractive substances, which were expressed in decrease of the content of unsaturated (C18:2, C18:3) and increase of saturated (C16:0, C18:0) fatty acids, and activation of the processes of synthesis of phenolic compounds - lignin precursors.

I. INTRODUCTION

In order to evaluate the wood stability under pathogen a chosen bioobject should correspond to the following criteria: large geographical range and low resistance to the pathogen action. At the same time it is important to note that recently there is an intensive study of tissues of non-woody and woody plants (which include alfalfa, flax, and various types of poplar and eucalyptus) from a position of biochemistry to identify the internal laws of the changes with the implementation of the pathogen.

One of the few biological objects that meets the specified conditions and availability on the north-west of Russia, is aspen (*Populus tremula*). Considering the biological and technical features of aspen, it is important to note the speed of growth, productivity, undemanding to the soil, as well as an extensive range of growth. At the same time, this breed has a low resistance to aspen polypore (*Phellinus tremulae*). Many trees of the age of 15 - 30 years are infected with heart rot, and at maturity age (60 - 70 years) defeat of aspen by mushroom reaches 70 - 90% and above in the European part of Russia.

Interaction of plants and pathogens is a complex dynamic process, which resulted in changes of physiological state of both macro- and micro-organism simultaneously. When implementation of pathogens defense plant mechanisms are activated at the biochemical level, involving special enzymes - oxidoreductases, particularly peroxidases. Activation may be the result of the phenolic structures formation (e.g., lignin) or resinous compounds secretion that the host plant is trying to prevent pathogen colonization.

Thus, the purpose of this paper is to identify changes in the functional nature, structural features and reactivity of lignins, as well as group composition and quantitative ratios of lipophilic substances in response to the action of pathogen in vivo growth. It allows deeper understanding of the process lignin-carbohydrate matrix formation of wood under biotic stress.

II. EXPERIMENTAL

The representative samples of the juniper wood aged from 10 to 70 years were selected on the territory of the Arkhangelsk region, outside the area of anthropogenic and technogenic effects. The wood age is determined by the number of annual rings on the transversal sections at the root neck of the juniper trunks. Wood (age of 20 and 70 years) has damaged parts by action of aspen polypore (degree of damage to wood is more than 50%).

The preparations of dioxan lignin (DL) were extracted from the wood by the Pepper method in amount of 28% of its content in the original wood.

The functional composition of DL is determined by standard methods. The number of phenolic hydroxyl groups is determined by spectrophotometric Δε-method and by the difference between the content of total acid and carboxyl groups, carbonyl groups – by the method of oximation, carboxyl groups – by the chemisorptive method.

The samples of wood and extracted lignins are characterized by infrared technique. IR-spectra are recorded in the tablet of potassium bromide with Fourier transform infrared spectrophotometer IRAffinity-1 („Shimadzu“, Japan) within the range from 4000 to 400 cm^{-1}.
pKa values were determined by method of direct spectrophotometric titration by tetraethylammonium hydroxide (“purum”, Fluka) in the thermostated cell at 25ºC in argon atmosphere. pH was measured with ion meter „Expert-001“with an electrode system made of glass (ЭСЛ-63-07) and silver chloride comparison electrode (ЭВЛ-1-М3). After adding each portion of titrant, solution pH was measured and absorption spectrum relative to the solvent with spectrophotometer Specord-200 PC (Analytic Jena AG, Germanu) in quartz one centimeter cuvettes within the range of 240-400 nm with an interval 0.5 nm was recorded.
Effective potential was determined in the thermostated cell at 25ºC in argon atmosphere and alkaline medium of 0.02M KOH in the reduction-oxidation system of potassium ferrocyanide-ferrocyanide. The electrode system consisted of platinum electrode ЭПВ-1 and saturated silver chloride electrode ЭВЛ-1М3 used as a comparison electrode.
Analysis of quantitative and qualitative composition of extractives was performed as follows: sound and decayed areas of the wood were selected. Then they were grounded in a rotary mill with water-cooling into fractions (to 2 mm), and then extracted in a Soxhlet apparatus to complete extraction of extractive substances. Petroleum, ether, acetone, and ethanol were used as solvents. The organic extracts were dried over anhydrous sodium sulfate, the solvent was distilled off on a water bath and the residue was dried to constant weight at a temperature of 40 ºC. The extracts were dissolved in anhydrous dimethylformamide with addition of deratizational reagent - N, O-bis(trimethylsilyl)trifluoroacetamide (BSTFA) and incubated for one hour at room temperature. GC-MS analysis was performed with Shimadzu QP2010S gas chromatograph equipment. The chromatographic analysis was carried out using capillary column HP-1MS, 100% dimethylpolysiloxane (30 m × 0.25 mm i.d. and 0.25 µm film thickness). Helium was used as carrier gas at a constant flow rate of 1 mL min^{-1}. The oven was programmed to start at 50 °C (held for 3 min) and reach 250 °C at 10 °C min^{-1} where it was maintained 10 min. Identification of compounds was carried out by comparing the mass spectra of compounds with library (MSO8) mass spectra.

III. RESULTS AND DISCUSSION

Lignin is one of the most stable natural compounds with high molecular weight. It plays an important role in the physical block invading pathogens. Newly synthesized lignin takes part in healing up during tissue damage as a protection against the penetration of pathogens [1]. The protective function is manifested in changes of the functional composition due to the action of the enzyme system of the fungus, which in turn affects the reactivity of the polymer.
The functional composition of the extracted preparations of DL of the aspen and acidity constant of the main phenolic structures, **Figure1,** are given in **Table 1**. In general, the functional composition of DLA corresponds to the lignin of deciduous. The ratio of guaiacyl and syringyl structures in samples of aspen DL is 55 - 60% and 40 - 45% respectively by the processing IR spectrum methods of higher derivatives and Fourier self-deconvolution.

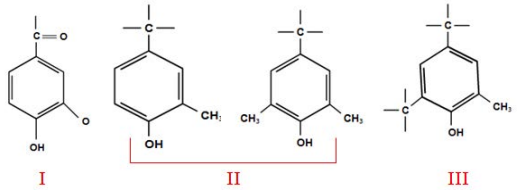

Figure 1. Main Phenolic Structures of Lignin

Table 1. Functional Composition and Values of Acidity Constants of the Extracted Preparations of Dioxane Lignin

Sample of DL	Age, years	Functional Composition, %				Acidity Constants			ORP, mV
		OH com.	OH strong acid	OH phen	CO	pK_{a1}	pK_{a2}	pK_{a3}	
1	10	4,8	0,2	4,6	2,7	7,2	9,2	11,2	856
2	15	3,7	0,2	3,6	4,3	7,5	9,4	11,1	853
3	20	4,9	0,4	4,5	4,3	7,4	10,3	11,3	841
4	20	4,7	0,2	4,2	2,7	7,5	9,4	11,6	831
5*	20	5,2	0,4	4,7	4,7	7,8	10,2	11,5	862
6	30	3,8	0,2	3,6	2,1	7,8	10,3	11,2	846
7	70	4,3	0,2	4,1	2,9	7,6	9,5	11,7	834
8*	70	5,3	0,6	4,7	4,7	7,8	10,3	11,6	860

* Sample with *Phellinus tremulae*

The analyses of the data of functional composition of the extracted preparations of DL allow saying that the content of phenolic hydroxyl groups is growing for an average 12-15% (compared with sound wood). That was because phenyl coumarone structure is broken as a result of demethoxylation. The number of total hydroxyl groups increases because of changes of the amount of carboxyl groups (an average 2 times) in decayed aspen wood.

According to table 1, the highest number of carbonyl groups had DL extracted from decayed aspen wood (4,7%) as a result of biodestruction.

There is change of lignin functional nature, which in turn leads to change in its redox and acid-base properties as a result of enzymatic system of fungi.

In recent years the data array of acidity constants values of monomeric guaiacyl and syringyl structures as lignin modeling phenylpropane units as well as of investigation of directly preparations of DL coniferous species were accumulateed [2, 3].

The analyses of the data obtained allow doing follows classification: the structures of I type have pKa in aqueous medium 7-8. The availability of a carbonyl group conjugated with the benzene ring, due to, mainly, negative mesomeric, as well as negative inductive effect results in reduction of electron density (charge delocalization) in the oxygen atom of the phenolic hydroxyl group and increase of acidic properties. The structures of II type have pKa in aqueous medium about 9-10. The structures of III type having the largest pKa value in aqueous medium 11-12 include the structures with nonconjugated α- carbonyl group and carbon – carbon bond in the fifth position typical for the condensed structures of lignin.

According to the data given in **Table 1**, pKa value of II type in DLA sample is significant change. It is happen because during process of wood biosynthesis and biodegradation the change of functional nature of lignin takes place. And pKa value of I and III type are not changed. Thus, the main contribution in change of DLA acidity constants was made by II type structures. These structures play the main role in lignin formation and its reactionary properties.

All studied lignin preparation has high oxidation-reduction potential (ORP) by experiment. The values of ORP for lignin from sound wood are 834…846 mV, for lignin from decayed is 860…862 mV.

According to indirect oxredmetry theory [2], ORP depends on the logarithm of concentration ratio lg(Cox/Cred), in case we can notice comparative content of phenol (Cred) and quinone (Cox) forms of lignin. Thus, the high values of ORP can be explained by intensive oxidative processes in which quinone structures concentration rises, this fact confirms lignin functional composition data.

According to the data given in Table 1, the main differences in lignin parameters are in sound and decayed wood (70 years).

In this paper the interrelation between analyses and change in group composition and quantitative ratios of main wood cell components were obtained, considering an integrated manner of biosynthesis process and biodestruction.

The characteristic feature of oxidative process during pathogen enzymatic action is formation of low-molecular water-soluble fragments. They forms in process fragmentation and/or oxidation of single and double C-C links in high-molecular fatty acids and dibasic acids (azelaic, suberic and oxalic acid) and oxo(hydroxy) acids (lactic acid). The high contents of water-soluble (more polar) in decayed wood was confirmed by extraction of some solvents with different polar: ethanol, acetone, diethyl ether and petroleum ether. For example, the most polarity ethanol, **Table 2**, extracts 2.6 and 4.3 weight% from the sound and decayed wood respectively. And petroleum ether extracts in 6.5 and 14 times less.

Table 2. The Content of Aspen Wood Extractive Substances According to Solvent Polarity

Solvent	Solvent polarity, E_T^N [4]	Content of extractive substances, % to a.m.u.	
		Sound wood	Decayed wood
Ethanol	0,654	2,6	4,3
Acetone	0,355	2,1	1,8
Diethyl ether	0,117	1,6	1,9
Petroleum ether	–	0,4	0,3

According to the **Table 3**, data reflecting the composition content of the extractives group depends on the solvent polarity and the type of wood. The greatest numbers of identified compounds were represented ether extracts isolated and the smallest one was presented extracts isolated with petroleum ether. The main compound of these extracts were represented by free acids and sterols. Intermediate position is occupied by ethanol and acetone extracts, they are based on one-and dicarboxylic acids and carbohydrates.

Table 3. Group Chemical Composition Aspen Wood Extracts by Chromatographic Analysis

Type of wood, extractant	Total number of compounds	Number of compounds		
		Fatty acid (s/m/p)[1]	Carbohydrates	Steroid, esters
Sound, Ethanol	20	7 (5/1/1)	2	–
Decayed, Ethanol	26	7 (5/1/1)	2	–
Sound, Acetone	24	9 (6/1/2)	1	–
Decayed, Acetone	23	7 (5/1/1)	2	–
Sound, Petroleum ether	21	13 (7/4/2)	–	4
Decayed, Petroleum ether	18	9 (4/3/2)	–	1
Sound, Diethyl ether	39	19 (13/5/1)	–	6
Decayed, Diethyl ether	27	15 (12/2/1)	–	1

1 - s/m/p means saturated/monounsaturated/polyunsaturated fatty acids

Thus it follows that the impact of the parasitic fungus leads to the destruction of plant cell walls, and as a result of enhanced release or secretion of these extractives, having a protective immune response of its biochemical reactions inside the plant cell, mainly oxidative nature. There is a relatively low content of low molecular weight fatty acids (caprylic and caproic acid) and elevated higher fatty acids (palmitic and stearic acids) and polyhydric alcohols (glycerin, glycol). It may indicate the hydrolysis enzyme complexes effects on lipid wood complex or the polymerization oxidative process of low molecular fatty acids. An example of this was the high content of dicarboxylic acids (oxalic acid, suberic acid, azelaic acid, suberic acid) and hydroxy acids (lactic and glycolic acid). Higher content of ethylene glycol of decayed wood can be associated with inactivation of ethylene - the main plant hormone involved in the response of wood to various damaging factors. The presence of xylose and mannose in ethanol and acetone extracts of wood due to the destruction of the wood carbohydrate. In all extracts were indicated the presence of lignin decomposition products (p-hydroxybenzoic, and syringyl tsinnamik acid), which was associated with the availability of lignin in lignin-carbohydrate complex activation processes and enzymatic degradation of chemical bonds.

IV. CONCLUSIONS

Wood as a united matrix composed of lignin-carbohydrate composite and extractives shows the cumulative effect of the enzymatic oxidative degradation of its components. It's noted that in the process of biosynthesis run parallel with structure formation phenolic (lignin) and the isolation of compounds resinous character (terpenes). With the introduction of the pathogen defense mechanisms was activated by plants at the biochemical level. Decrease in the lignins reactivity of decayed wood , reflected in the availability of lignin for enzymatic degradation processes of chemical bonds, as well as the intensification of the extractives formation were observed.

ACKNOWLEDGEMENT

The researches were performed with the financial support of the young research's project Ural Division of Russian Academy of Sciences (№ 14-5-НП-156) and the RAS Presidium Program (the project № 12-П-5-1021) by the means of equipment of CCU KT of Russian Federation - Arctic, (IEPN, IFNA Ural Division of Russian Academy of Sciences) and CCU NO «Arctic» (Northern (Arctic) Federal University named after Lomonosov) with the financial support of the Ministry of Education and Science of Russian Federation.

VI. REFERENCES

[1] Gorshkov, T.A. Plant cell wall as a dynamic system. - Moscow: Nauka, **2007,** 429.

[2] Bogolitsyn, K.G., Lunin, V.V., Kosyakov, D.S.,etc. Physical Chemistry of Lignins: Monography. M.: Akademkniga, **2010,** 492.

[3] Ragnar, M., Lindgren, C.T., Nilvebrant, N-O. pKa-values of Guaiacyl and Syringyl Phenols Related to Lignin. *J. Wood Chem Technol* 20:277–305, **2000**, 180.

[4] Reichardt, C., Harbusch-Görnert, E., Liebigs *Ann. Chem*., **1983**, 721

EXTRACTIVE SUBSTANCES OF COMMON JUNIPER OF SUBARCTIC REGION OF RUSSIA

Konstantin Bogolitsyn, Natalia Selivanova*, Maria Gusakova

Institute of Ecological Problems of the North, Ural Branch of Russian Academy of Sciences
Northern Dvina Embankment 23, Arkhangelsk, 163000 (Russia)
* snatalia-arh@yandex.ru

ABSTRACT

The component composition of bioactive substances (BAS) within the needles of common juniper (*Juniperus Communis L.*) grown in Arkhangelsk region, the Nenets Autonomous Area, Karelia and Kamchatka. It was established that formation of component composition of bioactive substances (BAS) within the needles of common juniper was influenced by climate factors and growing conditions. The data about essential oil output is given for the needles of common juniper grown in the northern part of Russia. The composition of essential oil of common juniper was determined by GC-MS method.

I. INTRODUCTION

Juniper is the unique relict specie and now it's of interest for production of valuable bioactive substances. It is widely used in medicine because of high content of essential oils and bioactive substances in its needles. These substances have wide pharmacological application. The juniper has health impact on forest environment due to its higher secretion of phytoncides in comparison with other coniferous species; also juniper forms microclimate in the surface layer of the atmosphere [1]. The juniper is widely spread at the European North. Considering the fact that content of bioactive substances depends on the growth conditions and the plant species, it's interesting to investigate the content of some kinds of organic substances in wild plants grown in certain conditions. From this point of view the common juniper of northern part of Russia is poorly studied. Archangelsk region, the Nenets Autonomus Area, Karelia and the Kamchatka peninsula are characterized by diversity of natural landscapes with different geological structure and climate characteristics. The juniper underbrush is widely spread in these regions.
The aim of the work is to find out the effect of climate factors and growth conditions on formation of component composition of bioactive substances (BAS) within the needles of common juniper (*Juniperus Communis L.*), which is grown in subarctic region.

II. EXPERIMENTAL

The test platforms for the sampling of juniper from different climate zones were chosen on the base of [1]. The first sampling region is situated in the Northern Taiga (temperate climate zone, Archangelsk region). The second is in the zone of Northern and Middle Taiga (continental zone, Karelia). These regions have almost similar climate conditions. The platforms with similar climate conditions and additional influence of hydrothermal springs were chosen for comparison of abiotic factors impact on component compositions in the needles of common juniper. They are: the Nenets Autonomus Area (NAA, Pym-Va-Shor) situated in tundra (subarctic zone) and the Kamchatka peninsula (natural park "Volcanos of Kamchatka") situated in tundra (temperate zone). The influence of hydrothermal springs is expressed by anomalous temperature gradient in comparison with the environment and also by specific ionic composition of water for nutrition processes. These factors make an impact on characteristics of biosynthesis and component chemical composition of bioactive substances (**Table 1**).

Table 1. The characteristic of regions for juniper sampling

	Archangelsk region	Karelia	NAA	Kamchatka
Average temperature of January, ^{0}C	-12,9	-8-14	-19,6	–7 (February)
Average temperature of July, ^{0}C	15,6	13-14	12,6	12 (August)
Annual precipitation	400-540 mm	450-600 mm	436 mm	1200 mm
Climate	Moderate-continental	Continental	Subarctic	Moderate
Zone	Northern taiga	Northern and middle taiga	Tundra	Tundra

The sampling of representative samples of juniper was made at the specified sites. The feedstock was prepared in the August of 2013 (Archangelsk region, Karelia) and in June of 2013 (Kamchatka, NAA). The selection and averaging of samples (branches of common juniper) were performed according to GOST for the wood greenery [2]. The feedstock was analyzed according to standard methods [3, 4]. Ethanol was used as a solvent for the extractives determination. Ethanol is environmentally safe and transfers water-soluble and liposoluble substances into soluble

state. The determination of extractives was carried out by the infusion method with 96% ethanol solution (duty of water is 1:20; temperature is 50 ^{0}C because of the destruction of vitamins, chlorophyll and carotenoids at a higher temperature). The needles after extraction were dried up to constant weight, the amount of extractives were calculated as a weight loss.
The essential oil of the needles of common juniper was extracted by steam distillation with following calculation of volume and mass fraction of sediment essential oil. The composition of essential oils was determined by spectrometer GC-MS QP-2010 Ultra (Shimadzu).
The identification of separate types of chemical compounds in the extracts was made by the methods of UV-spectroscopy and chromatography-mass spectrometry. UV-spectra were registered by the spectrophotometer «Shimadzu-1800» within the range of 190-900 nm. The composition of volatile extractives was determined by spectrometer GC-MS QP-2010 Ultra (Shimadzu). The analysis was performed by means of two columns with the different polarity. One of them was low-polarity Rtx-5MS and another was average polarity DB-17 MS (the column length is 30 m, the internal diameter is 0.25 mm). The chromatography conditions: isothermal regime at 40 °C during 5 minutes, with programmed increase of temperature at the rate of 10 °C/min up to 250 °C, with exposure at this temperature for 20 min. The evaporator temperature is 230 °C, the ionization chamber temperature is 230 °C, the ionization energy 70 eV.

III. RESULTS AND DISCUSSION

The juniper needles are specific type of wood greenery having a lot of bioactive substances such as essential oils, chlorophyll, carotene, different amino acids, vitamins, phytohormones and ets. The juniper essential oil is valuable bioactive feedstock. The essential oil output can give an information about its participation in plant's growth, plant biological value, possibility for the given plant usage for essential oil production. According to data of other researchers, the essential oil content in the juniper needles depends on its specie, place of growth and season [5, 6].
The object of this investigation is wood greenery of common juniper (*Juniperus Communis L.*). The extractives composition is presented in **Table 2**. The content of water-soluble substances is 23,8% ÷ 28,1%, extractives 33,2% ÷ 41,0 %, essential oil 2,0% ÷ 3,8% depending on the place of growth.

Table 2. The characteristic of wood greenery of juniper

Content, % a.d.	Sampling points			
	Archangelsk region	Karelia	NAA	Kamchatka
Ash	3,3	2,5	3,2	3,7
Extractives, i.e.:	38,1	33,2	41,0	39,3
water soluble	25,9	25,7	23,8	28,1
essential oils	2,5	2,0	3,6	3,8
liposoluble	9,5	5,5	13,6	7,4
Ethanol extracted	34,2	28,2	32,9	30,6
Wax	2,8	2,6	2,4	2,1

According to the obtained data, the juniper grown in Karelia is less valuable (the essential oil output 2,0%); the essential oil output from wood greenery of the juniper grown in Archangelsk region is 2,5%. The sampling points in Archangelsk region and Karelia are situated in mild-continental climate zone with long cold winter and short cool summer. Besides, karstic deposits significantly influence on all physical and geographical conditions of the territory. They sharply change the relief, character and regime of underground water. Fast absorption of atmospheric water leads to dry surface which impact a lot on the processes of soil formation and type of plants.
It should be noticed that higher content of extractives and essential oil in wood greenery is in juniper sampled in NAA (3,6%) and in Kamchatka peninsula (3,8%). Probably it is explained by abiotic stress. On the one hand, Pym-Va-Shor and natural park "Volcanos of Kamchatka" are hydrothermal ecosystems. They present extra-zonal landscapes elements with maximum heat contrasts in comparison with zone background. On the other hand they have harsh climate conditions. Under the stress conditions the plants get the strength to the permanent factor which is illustrated by the data for the essential oil output. The essential oil is obviously acts as a protection from the cold.
The identification of separate compounds in the essential oil was made by the chromatography-mass spectrometry method. The chromatogram is presented at the **Figure 1**.

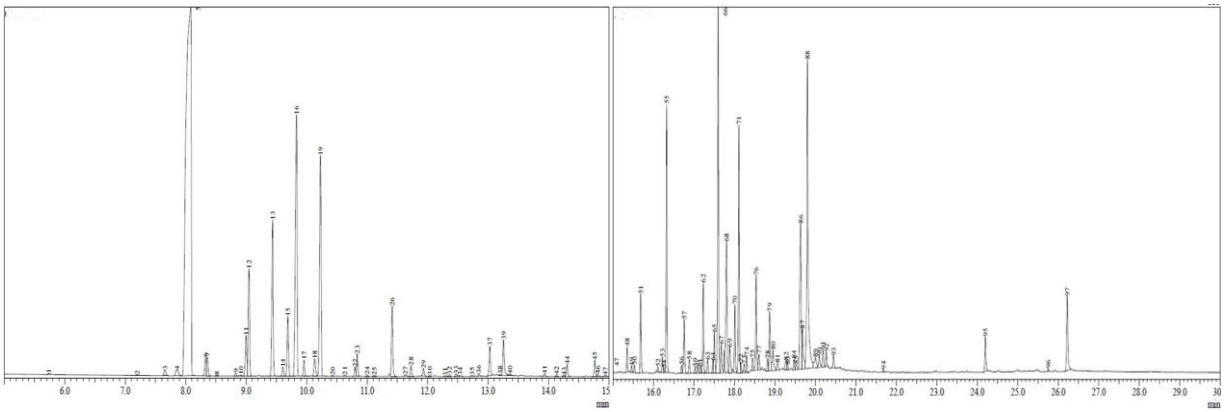

Figure 1 – GC-MS – chromatogram of the essential oil of the juniper wood greenery

Table 3 presents the component composition of the essential oil of the juniper wood greenery sampled in Archangelsk region. The essential oil of *Juniperus Communis L.* wood greenery contains 97 components, 22 of them have the concentration higher than 0,5%.

Table 3. The main component composition of the essential oil of the juniper wood greenery sampled in Archangelsk region

Component	% of total component sum
α-thujene	0,35
Bicyclo[2.2.1]heptane, 2,2-dimethyl-3-methylene	0,60
α-pinene	0,16
Camphene	0,55
β- phellandrene	1,28
Bicyclo[3.1.1] heptane, 6,6- dimethyl -2- methylene	3,31
β-myrcene	4,55
1-phellandrene	1,83
1,3,6-octatriene, 3,7- dimethyl	9,82
Sabinene	7,68
γ-terpinene	0,65
α-terpinolene	2,06
Butanoic acid,3-methyl-,3-methylbutyl ester	0,52
Δ^3-carene	0,04
Terpinen-4-ol	0,87
α-terpineol	1,13
Bornyl acetate	0,48
d-limonene	0,51
Cyclohexane, 1-ethenyl-1-methyl-2,4-bis(1-methylethenyl)-,[1S-(1.alpha.,2.beta.,4.beta.)]	1,67
Caryophyllene	0,40
Humulene	0,60
Germakrene –D	1,14
α-amorphene	0,47
Δ-cadinene	1,63
Farnesol 1	0,68
1-naphthalenol,1,2,3,4,4a,7,8,8a-octahydro-1,6-dimethyl-4-(1-methylethyl)-,[1R-(1.alpha.,4.beta)]	4,38
Epiglobulol	0,64

As a result of this investigation it was found that compounds of terpenes group are prevailing in the essential oil of juniper wood greenery. They are sabinene (7,68%), β-myrcene (4,55%), α-terpinolene (2,06%), β-fellandrene (1,28%), Δ-cadinene (1,63%), α-terpineol (1,13%), terpinene-4-ol (0,87%), camphene (0,55%). Also there are fatty acids ethers, derivatives of azulene and naphthalene in in the essential oil. It should be noticed that the essential oil of the juniper grown in Archangelsk region differs from the essential oil of Siberian juniper by very low content of α-pinene, Δ^3-carene.

The composition of volatile extractives was determined by the chromatography-mass spectrometry method on the spectrometer GC-MS QP-2010 Ultra (Shimadzu). **Table 4** presents the main component composition of the ethanol extract of the juniper wood greenery. As it follows from these data, the ethanol extract of the juniper needles contains more than 100 components with prevalence of terpenes group compounds. They are: mainly α-pinene (16,34%) in contrast to the essential oil with very low content of α-pinene (0,16%), cembrene (4,50%), Δ^3-carene (2,86%), β- fellandrene (2,04%), mannose and glucose derivatives and trace amounts of camphene (0,22%).

Table 4.The main component composition of the ethanol extract of the juniper wood greenery sampled in Archangelsk region

Component	% of total component sum
α-pinene	16,34
Δ^3-carene	2,86
Camphen	0,22
Bicyclo[3.1.1]heptane, 6,6-dimethyl-2-methylene-,(1S)-	0.56
β-myrcene	0,69
Limonene	0,19
β- phellandrene	2,04
Trans- caryophyllene	0,61
α- humulene	0,40
Germakrene –D	2,22
Δ-cadinene	0,13
β-elemene	1,86
α-cadinol	0,27
α-selinene	0,21
1-Naphthalenepropanol,.alpha.-ethyldecahydro-.alpha.,5,5,8a-tetramethyl-2methylene-,[1S-]	1.83
Cembrene	4,50
Thunbergol	6.64
β-D-Glucopyranose	0,57

For the determination of the nature of substances extracted from the juniper wood greenery by ethanol, we investigated the electron absorption spectra of obtained extracts in the UV- and visible regions.
There are significantly expressed absorption bands with maximums at 272-275, 331-335, 536, 611, 664 nm in the absorption spectra of ethanol extracts. It should be noticed that the absorption bands in the region of 270-290 nm can belong to such classes of natural compounds as amino acids, phenolic compounds, flavonoids (250-280 and 330-370 nm) and coumarins (310-350 nm), at the wave lenght of 536 nm – to anthocyanins, at the wavelength of 611 and 664 nm – to chlorophylles “a” (664 nm), chlorophylles “b” (641,611).

IV. CONCLUSIONS

Thus, as a result of the investigation it was found that the formation of component composition of bioactive substances (BAS) within the needles of common juniper (*Juniperus Communis L.*) is influenced by climate factors and growing conditions. The GC-MS method showed that the essential oil of the juniper wood greenery contains 97 components with prevalence of terpenes group compounds, mainly sabinene, β-myrcene, α-terpinolene. Also the ethers of fatty acids, derivatives of azulene and naphthalene were found. The content of such bioactive substances as chlorophylles “a” and“b”, flavonoids, aurones, tannins was determined for the ethanol extracts.

V. ACKNOWLEDGEMENT

The researches were performed with the financial support of interdicsiplinary project of Ural Division of Russian Academy of Sciences (№ 12-M-45-2012) by the means of the equipment of CCU SE «Critical technologies of RF in the sphere of environmental safety of Arctic» (IEPN, Ural Division of Russian Academy of Sciences) and CCU SE «Arctic» (Northern (Arctic) Federal University named after Lomonosov) with the financial support of the Ministry of Education and Science of Russian Federation.

VI. REFERENCES (СПИСОК ИСПОЛЬЗОВАННЫХ ИСТОЧНИКОВ)

[1] Barzut O.S. Ecological and geographical variability of common juniper (*Juniperus Communis L.*) in the forests of Archangelsk region [Text] // abstract for the competition for PhD degree in chemistry – Archanelsk, ASTU, 2007. – 18 p.
[2] GOST 21769-84. Wood greenery. M., 1984. 5p.
[3] Obolenskaya A.V., Yelnitskaya Z.P., Leonovich A.A. Laboratory works on wood and cellulose chemistry. – M., Ecology, 1991. – 320 pp.
[4] Kutakova N.A. BAS and wood greenery analysis. ASTU. 2002.33 p.
[5] Kustova S.D. Reference book for the essential oils. M., 1978. 175 p.
[6] Uvarovskaya D.K. The essential oils of the Far-East kinds of *Juniperus L.:* composition, content, application: dissertation of PhD in biology. Khabarovsk, 2008. 155 p.

SUBMOLECULAR STRUCTURE OF THE SOFTWOOD CELL'S WALL

Konstantin Bogolitsyn[1,2], Dmitry Chukhchin[2], Maria Gusakova[1], Ivan Zubov[1*], Anna Krasikova

[1] *Institute of Ecological Problems of the North, Ural Division, Russian Academy of Sciences, Northern Dvina Embankment 23, Arkhangelsk, 163000 (Russia), e-mail: zubov.ivan@bk.ru*
[2] *Northern (Arctic) Federal University named after Lomonosov, Northern Dvina Embankment 17, Arkhangelsk, 163000 (Russia)*

ABSTRACT

The ultra-micro structure and submolecular structure of coniferous wood matrix were investigated by methods of scanning electron (SEM) and atomic-force microscopy (AFM). New improved method of wood investigation by SEM including the step of cryomechanical sample preparation was suggested. New data on specific features of the composition and cell wall structure of Juniper wood (*Juniperus communis* L) were obtained. Performed investigations experimentally confirm the physic-chemical model of structure and self-assembly of wood substance and prove its application for certain objects.

I. INTRODUCTION

According to modern concepts, wood substance is considered as bionanocomposite. It is formed by polysaccharides (cellulose, hemicelluloses, pectins) and polyphenol with irregular structure (lignin). The biosynthesis process of cell wall components occurs simultaneously, but lignification process can be late, this leads to the formation of complex submolecular structure.

According to the fundamentals of physic-chemical model of structure and self-assembly of wood substance, lignin-carbohydrate matrix is a superposition of interpenetrating networks formed by H-bonds, C-C-bonds, ether bonds and lignin-carbohydrate bonds. Thermodynamically incompatible cellulose and lignin form microheterogeneous regions surrounded by hemicellulose gel. Hemicelluloses act as they unite cellulose elementary fibrils and lignin because of the transition layer formation on the cellulose fibrils surface. Also hemicelluloses have limited thermodynamic compatibility with lignin. Extra strength of this composition is given by mechanical bonds between macromolecules of lignin, hemicelluloses and cellulose [1, 2].

The aim of this work is application of physic-chemical model of structure and self-assembly of wood substance for studying of specific features of ultra-micro and submolecular structure of coniferous wood matrix with assistance of modern methodical approaches and by means of analytical instruments.

Juniper wood (*Juniperus*) is chosen as a bio-object for investigations, because it is one of the most representative, ancient (relic), specific and scantily known coniferous species [3, 4].

Juniper (*Juniperus Communis* L.) is the most wide-spread specie of the genus, it can be found in different environmental conditions between 70 and 30^0N. In Russia its area covers European part, the Urals and Siberia.

II. EXPERIMENTAL

For this investigation the representative samples of the juniper wood (*Juniperus Communis* L.) aged from 60 to 90 years old were selected. Sections and fractures (tangential, radial and cross) of juniper wood samples were used as a material for microscopic studies

For the investigation of ultra-micro structure of wood matrix by SEM the improved method including the step of cryomechanical sample preparation was suggested. This method consists of liquid nitrogen treatment of wood bars (20×5×5 mm) incised at perimeter. After freezing at 77 K a cross section was prepared at the incision. Water and alkali washes of radial and tangential fractures of juniper wood were performed with distilled water and potassium hydroxide at concentrations 0.02 ÷ 0.1V. The samples were freeze-dried after washing. Spectra of the washings were recorded by a UV-spectrophotometer (Shimadzu UV-1800) within the range of 200 – 400 nm.

The images were obtained by scanning electron microscope SEM Sigma VP ZEISS (accelerating voltage – 20 kV, In Lens detector) and by atomic-force microscope ACM Multimod 8 Bruker. In order to increase samples' image contrast (while working on scanning electron microscope) the coating of gold and palladium with the thickness of 5 nanometers were applied (by means of device for samples' preparation Q150TES manufactured by QUORUM).

III. RESULTS AND DISCUSSION

Application of modern methodical approaches and analytical instruments in performed investigations allowed obtaining new scientific results for characterization of ultra- and nanostructure of lignin-carbohydrate wood matrix. It is known that the basis of the juniper wood is formed by tracheids (Tr) put into dense vertical packs, contained between horizontal (radial) medullar rays (Mr). It was experimentally established that tracheids' length exceeds significantly their width and varies from hundred μm up to 1500μm both within a separate annual ring and a whole tree (Figure 1 a-d). Tracheids diameter is 15-25 μm for early wood (SW) and less than 10 μm for latewood (AW). It is 1.5 times less than the same parameters for spruce and 2-2.5 times less – for larch. The number of cells and their diameter within the annual ring grow with the increase of the age of a tree. It can be explained by the increase of

energetic and element flows in the wood associated with the development of roots and crown. Early tracheids of juniper contain a lot of pores (P) and lumen of big diameter. These specific features make tracheids the main conductive element of juniper wood – the vessels' analogue. So, more dense package and small diameter of tracheids explain the high density of juniper wood (~630 kg/m). It is 1.5 times higher than the density of cedar.

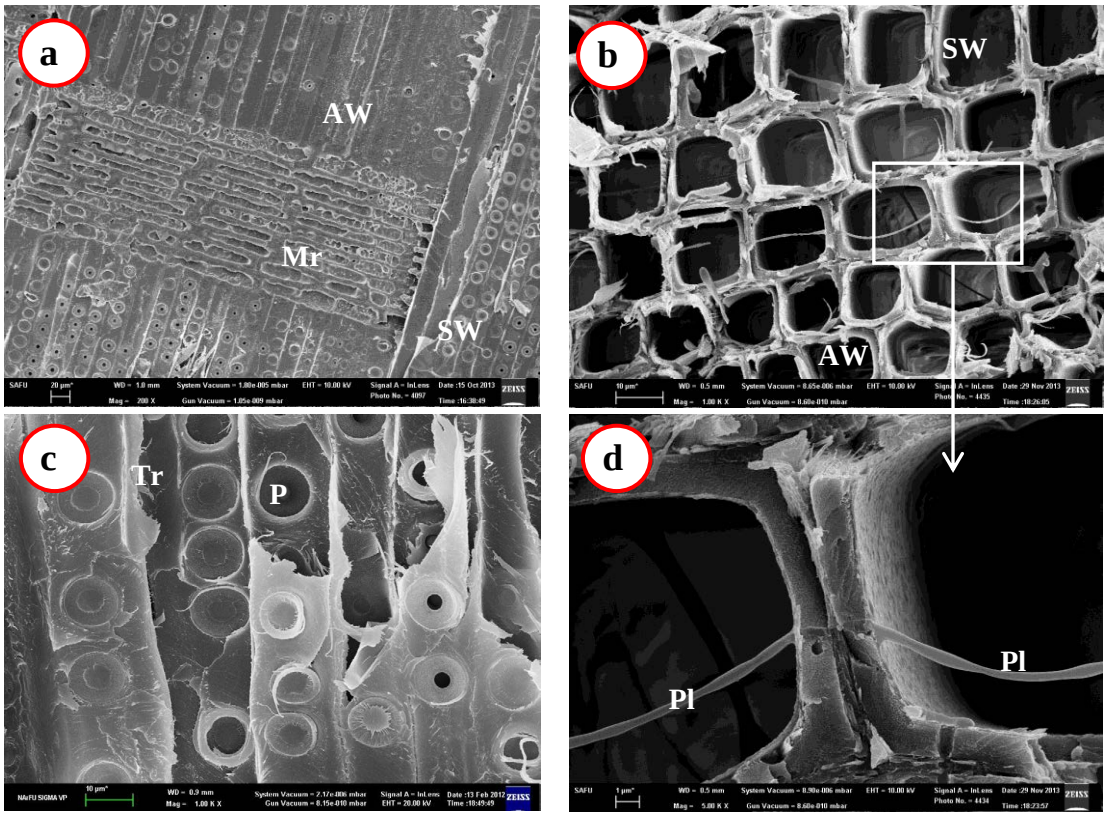

Figure 1. Radial (a,c) and cross (b,d) fractions of juniper wood.
The images with the magnification of 200×(a), 1000×(b) 1000×(c), 5000×(d) were obtained by SEM.
SW – early wood; AW – late wood; Tr – tracheids; Mr - medullar ray; P – pore; Pl – plasmodesmata.

Horizontal medullar rays (Mr) are deposits of parenchymal cells (2÷9 in height and 1÷3 in width), containing double pores. Rays go radially through all the thickness of the trunk (Figure 1a). Their content in juniper wood is 3÷6%.
The distinguishing characteristic of juniper wood is the absence of resin ducts typical for majority of conifer species. Probably the secretory tissue of juniper wood is situated in cambium (near the bark), but there's no references proving that.
During the investigation we found one more characteristic property of juniper wood - plasmodesmata presence (Pl). It is very thin tension bar crossing the cells' cavities (Figure 1b, d). These channels link the protoplast of adjacent cells. They are lined by plasmatic membrane inside. There is hollow desmotubule inside plasmodesmata, which acts for communication between cells and transport of some substances [5]. In most cases this cell wall element goes through pores and ruins together with remains of cytoplasmic membrane during the process of cells' lignification, that's why it can be hardly identified.
According to modern concepts the tracheids' cell wall consists of two components: thin primary (P) and secondary (S) layers, which are different both in composition and in structure [2,6,7]. Secondary layer in its turn consists of three layers S_1, S_2 and S_3, gradually deposited during the growth process. Primary layers of adjacent cells are bonded by intercellular substance and formed complex middle lamellae (P+M+P).
These statements are confirmed by the following results. The arrangements of the cell wall layers of juniper wood and microfibrils orientation can be seen on Figure 2a-b.
The base of cell wall of juniper wood is S_2 layer mainly consisting of unidirectional cellulose microfibrils and providing the necessary stiffness and strength of tracheid and tree. However, the unidirectionality and slight slope of microfibrills with the respect to the cell axis (20-40 degrees) make the layer the most fragile and unstable under conditions of longitudinal mechanical strains. The thinner layers S1 and S3 surround S2 from outer and inner sides of cell wall, respectively. While cellulose microfibrils of S1 are mainly unidirectional, the S3 layer contains intercrossing cellulose plates, lamellae, although only a few (Figure 2b). Besides the primary and secondary layers, the cell wall of juniper wood contains a verrucous layer lining the inner cavities of cells as well as surfaces of pores (Figure 2a, b).
Most of researchers consider that cellulose microfibrils in secondary layer are helically arranged, taking various angles, which provides the necessary stability of cell wall against different impacts. But there were not experimental data proving the presence of helical structure in cell wall. Application of cryomechanical pretreatment allowed

confirming of such a microfibrils arrangement in the cell wall (Figure 2c, d). Such an impact led to splitting and partial destruction of secondary cell wall layers, and helical structure became more visible. The analysis of slope angle and thickness of convolutions allows making a conclusion that the helix base consists of S_2 layer. Microfibrils of S_2 layer are mainly unidirectional and helixes of all cells have the same direction (Figure 2c).

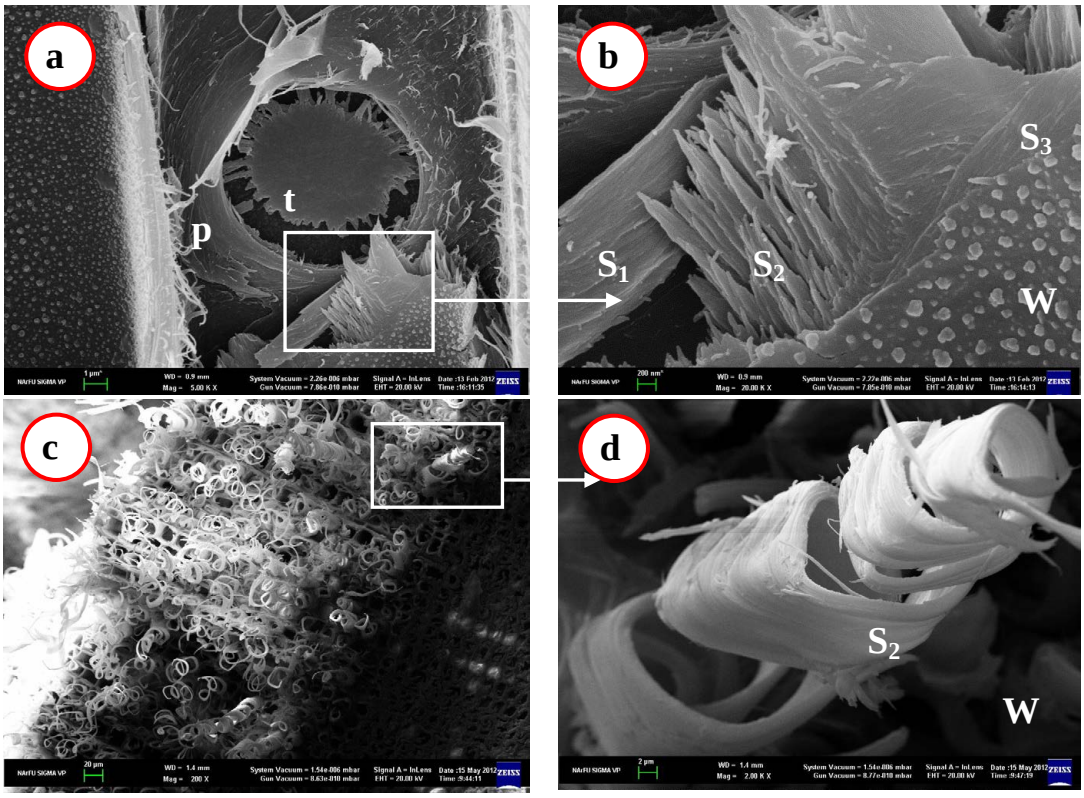

Figure 2. a, b – the rupture of cell wall of juniper wood; c – radial split of juniper wood sample after cryomechanical treatment; d – helical structure of tracheid's cell wall.
Images with the magnification of 5000×(a), 20000×(b), 20000×(c), 20000×(d) were obtained by SEM.
S_1,S_2, S_3, – second cell wall layers; W – verrucuos layer; M – middle lamellae; p – external pore surface; t–torus.

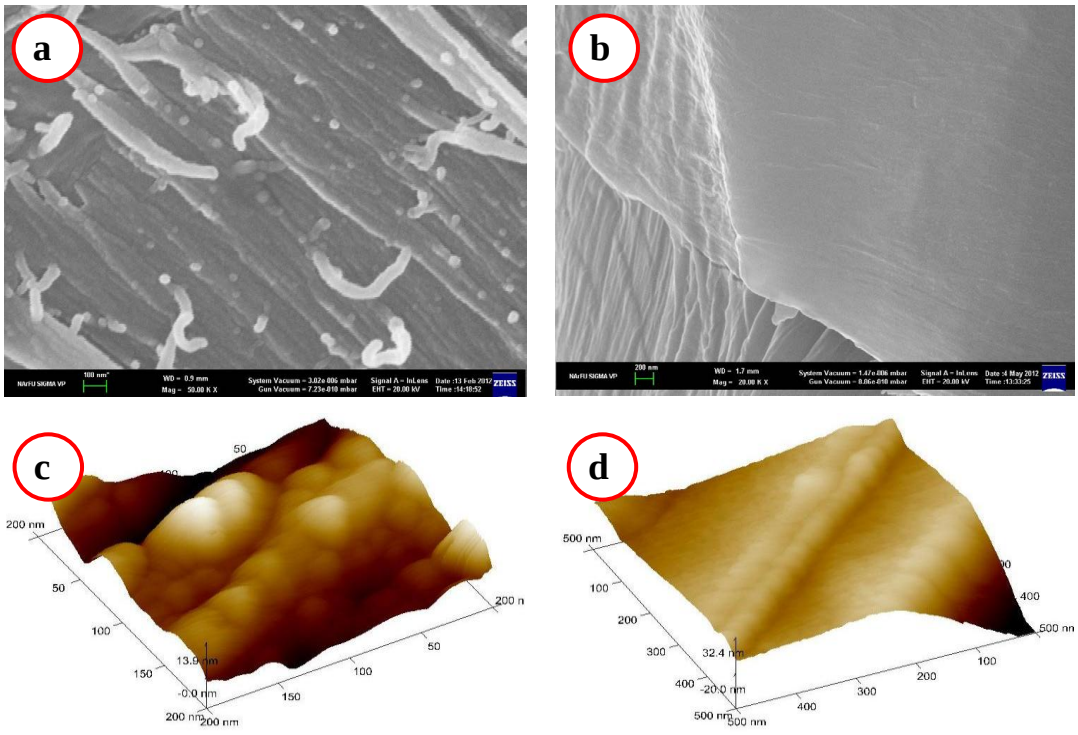

Figure 3. Surface of S_1 layer on radial fracture of juniper wood sample before (a,c) and after (b,d) water treatment. Images with the magnification of 50000× (a), 20000× (b) were obtained by SEM. Images (c,d) were obtained by AFM.

To study the primary cell wall and distribution of lignin in its composition, we prepared radial fractures of juniper wood samples. Radial fracture mainly occurs in the region of early wood in the intercellular substance, thus opening the surface of the primary cell wall P and partly uncovering the S1 layer (Figure 3a-d).
As it can be seen on the images, the remains of layer P on the surface of the secondary cell wall are individual cellulose fibers (up to 50 nm thickness) lacking any directionality, presumably put into solid solution of hemicelluloses in lignin. The last consists of spherical particles (diameter of 5-60 nm) soluble in alkali solutions, dioxan and other solvents. After treatment of the surface with water or alkali solutions, spherical particles on the surface of layer P were not observed (Figure 3b,d), which proves their high mobility with respect to carbohydrate matrix
The evidence of their lignin nature can be confirmed by spectrum investigations. The peak in the region of 280 nm corresponds to lignin of conifer species. According to the analysis of these particles' size, the values are in the range of 10-20 nm. Solubility of the particles in weak aqueous solutions of alkali evidences the presence of carbohydrates.
Thus, such spherical particles discovered in the intercellular substance and primary layer present solid solution of hemicelluloses in lignin [1]. The lignin domains are bonded with carbohydrate matrix by H-bonds. So, the lignin in such solid solution differs from interfibrillar lignin (considering functional composition and polymolecular properties). It is more mobile with respect to carbohydrate matrix during the external impacts on wood.
The presence of such spherical lignin-carbohydrate complexes in the interfibrillar space and their size evidences their inability to cross the cytoplasmic membrane and therefore their inability to be formed inside cells. Thus, similar to exoenzymes, they should be formed on the surface of cytoplasmic membrane. Consequently, microfibrils grow in the space between middle plate and cytoplasmic membrane, which is crossed by monosaccharides and phenylpropane monomers. The enzymes synthesizing cellulose, hemicelluloses and lignin are exoenzymes (they are synthesized in the membrane and diffuse to extracellular space).

IV. CONCLUSIONS

By using the SEM and AFM methods new experimental data about the ultra-micro structure and submolecular structure of coniferous wood matrix were obtained. These data confirm the possibility of consideration of wood substance as nanocomposite, based on cellulose nanofibrils (20-50 nm) and globular lignin-carbohydrate formations (dia. 5 – 60 nm).

V. ACKNOWLEDGEMENT

The researches were performed with the financial support of interdicsiplinary project of Ural Division of Russian Academy of Sciences (№ 12-M-45-2012) by the means of the equipment of CCU SE «Critical Technologies of RF in the Field of Environmental Safety of Arctic» (IEPN, Ural Division of Russian Academy of Sciences) and CCU SE «Arctic» (Northern (Arctic) Federal University named after Lomonosov) with the financial support of the Ministry of Education and Science of the Russian Federation

VI. REFERENCES

[1] Bogolitsyn K.G., Lunin V.V., Kosiakov D.S. etc. Physical chemistry of lignin: Monograph. - Moscow, 2010, 492 p.

[2] Bogolitsyn K., Chuhchin D., Zubov I., Gusakova M. Ultramicroscopic composition and supra-molecular structure of wood matrix // Russian Journal of Bioorganic Chemistry. – 2013. – Vol. – 39. – №7. – P. 671–676.

[3] Adams R. P. Juniperus of the world: The genus Juniperus (2nd ed.) / Vancouver: Trafford Publishing Co. – 2008. – 430 p.

[4] Sokolov S. Ya., Shyshkin B. K. Trees and bushes of USSR. Wild, cultivated and promising for the introduction. – M.-L.: Academy of Sciences of USSR Publishing house. – 1949. – V. I. – 464 p.

[5] Lotova L. I., Nilova M.V., Rudko A.I. Vocabulary of phytoanatomy: tutorial. — M.: LKI Publishing house, 2007. — 112 p. — ISBN 978-5-382-00179-1

[6] Jesper Fahlen. J. The cell wall ultrastructure of wood fibers-effects of the chemical pulp fiber line. Stochholm, 2005. 80 p.

[7] Francis W. M. R. SCHWARZE. Wood decay under the microscope // fungal biology reviews. 2007. №21. P. 133–170

[8] Gorshkova T. A. Plant cell wall as a dynamic system. – M.: Science. – 2007. – 425 p.

EVALUATION OF ALKALINE DECONSTRUCTION PROCESSES FOR BRAZILIAN NEW GENERATION OF EUCALYPT CLONES

Fernando José Borges Gomes [1*], Jorge Luiz Colodette[1], Augusto Milanez[2], Juliana Andreotti[2], Auphelia Burnet[3], Michel Petit Conil[3], José Carlos Del Río[4], Ana Gutierrez[4], Marta Perez Boada[5], Angel T. Martinez[5], Fernando Almeida Santos[1]

*[1]Pulp and Paper Laboratory, DEF-UFV, Viçosa, MG Brazil, 36.570-000; [2]Suzano Paper and Pulp Co., São Paulo, SP, Brazil; [3]CTP, Grenoble, France; [4]CSIC-IRNAS, Seville, Spain; [5]CSIC-CIB, Madrid, Spain (*Corresponding author: fernando.gomes@ufv.br)*

Abstract

Eucalypt wood has become one of the main raw materials for pulp production, mainly in South America. Through this study, 19 eucalypt clones were analyzed regarding their forestry production, and chemical characteristics. After this analysis, among the 19 clones, 5 were chosen to be analyzed concerning their potential for pulp production, including one commercial clone which was used as a reference clone of high quality and performance for pulp production. Two pulping processes were used to convert eucalypt clones into pulps, namely, Soda-AQ and kraft processes. The main findings of this paper were: (1) high technological quality of Eucalyptus clones evaluated, and that they can be used for pulp production since most of the clones had performance similar to clone IP; and (2) the Soda-AQ process seems to be a potentially replace the kraft for a high degree of wood delignification.

I. INTRODUCTION

Eucalyptus is now one of the main raw materials for pulp production, mainly in South America. The wood quality is a factor of extreme importance when the goal is the production of pulp with high industrial yield, low cost and high quality. Regarding the process of pulping, the vast majority of variables have been well studied and they are known and altered depending on the raw material. Thus, in order to achieve the production target pulp of high quality, the biggest challenge industries is the selection of suitable raw materials for their supply. Many studies have been done in order to increase wood productivity and improve its quality aiming at the pulp production through the selection of clones with better performance and crossings between them. Good results have been observed, for example, the average productivity of the Brazilian eucalypt forests increased from 24 m^3/ha/yr in 1980 to 41m^3/ha/yr in 2010, representing a 71% increase in productivity of planted forests in Brazil [1].

A recent study aiming a better characterization of clones of *Eucalyptus* grown in Brazil [2] involved the major pulp Brazilian industries and showed that these plantations in Brazil have the highest global levels of average annual increment (MAI). The eucalypt clones analyzed in his study demonstrate a high productivity, with 20% of clones with MAI higher than 50 m^3/ha/yr, and 70% of the clones showed increments higher than 40m^3/ha/yr. For the scientific community and industries, it is very important to know which are the new opportunities and which are the chances of gain in quality with the available raw materials for pulp production. Therefore, this study aimed to evaluate the wood quality of 19 eucalypt clones with the most recent interbreeding aiming bleached pulp production and testing the best 5.

II. MATERIAL AND METHODS

For this study, 18 wood samples of Eucalyptus in commercial cutting age were used, provided by *GENOLYTPUS* project, located in Minas Gerais State – Brazil and it was also studied one sample of Eucalyptus globulus pure from Europe called IG. The complete list of the eucalypt clones used in this study is presented in the Table 1. The eucalypt clones were investigated regarding their biomass productivity, moisture, basic density, and chemical characteristics according methodology proposed by Gomes [3]. But although this study had 19 eucalypt clones available, only 5 were studied regarding the potential for pulp production due to the high cost of such a study.

Table 1. Description of the eucalypt clones.

	Sample Code	BiomassType
1	U1xU2	*E. urophylla (Flores IP) x E. urophylla (Timor)*
2	U2xC1	*E. urophylla (Timor) x E. camaldulensis (VM1)*
3	G1xUGL	*E. grandis (Coffs Harbour) x [E. urophylla (R) x E. globulus (R)]*
4	U1xUGL	*E. urophylla (Flores IP) X [E. urophylla (R) x E. globulus (R)]*
5	U1xC2	*E. urophylla (Flores IP) x E. camaldulensis(VM2)*
6	C1xC2	*E. camaldulensis (VM1) x E. camaldulensis (VM1)*
7	DGxUGL1	*[E. dunnii* (R) x *E. grandis (R)] x [E. urophylla (R) x E. globulus (R)]*
8	DGxU2	*[E. dunnii* (R) x *E. grandis (R)] x E. urophylla (Timor)*
9	C1xUGL	*E. camaldulensis (VM1) x [E. urophylla (R) x E. globulus (R)]*
10	G1xGL2	*E. grandis (Coffs Harbour)x E. globulus (R)*
11	DGxC1	*[E. dunnii* (R) x *E. grandis (R)] x E. camaldulensis (VM1)*
12	U2xGL1	*E. urophylla (Timor) x E. globulus (R)*
13	DGxGL2	*[E. dunnii* (R) x *E. grandis (R)] x E. globulus (R)*
14	U1xD2	*E. urophylla (Flores IP) x E. dunnii (R)*
15	U1xG2	*E. urophylla (Flores IP) x E. grandis*
16	IP	*E. urophylla (IP) x E. grandis (IP)* commercial clone
17	VC	*E. urophylla x E. grandis* commercial clone
18	CC	*E. urophylla x E. grandis* commercial clone
19	IB	*Iberian Eucalyptus globulus*

In this study were chosen two processes for producing pulp, Soda AQ and kraft processes. The cooking trials of the 5 selected eucalypt clones were done in a CRS digester (CPS 5010 Recycle Digester System), with 2 individual reactors of 10 liters each, equipped with a forced liquor circulation system and electrically heated with temperature and pressure control. The digester is coupled with a cooling system (Coil System with residual liquor, involved with water at room temperature), to ensure the cooling of the liquor after the cooking simulation. With the exception of the alkaline charge, the other cooking conditions were kept (1 kg of wood; 25 % on o.d. chips of Sulfidity as NaOH; liquor to chips ratio of 4/1; 170˚C maximum temperature, being the time to maximum temperature of 90 minutes and time at maximum temperature 50 minute). For the Soda-AQ processes were used a dosage of 0.05 on o.d. chips of anthraquinone. After determination of the delignification curve, two samples of pulp for each clone were prepared at kappa number 20.

III. DISCUSSION AND RESULTS

Selection of clones based on forestry, morphological and chemical characteristics

Forestry characteristics: Two very important factors regarding biomass use for pulp production are moisture content and density since they affect harvesting, transportation and utilization costs. The wood eucalypt analyzed in this studied show average moisture and density of 55% and 500 kg/m^3. These values are considered satisfactory for pulp production [2]. The MAI varied in the range of 16-101.6 m^3/ha/yr. The lowest MAI extreme occurred for the C1xC2 woody raw material. This may be explained due to the fact that eucalypt hybrid is poorly adapted to Minas Gerais State climate conditions and did not develop satisfactorily. Among the woody raw materials, the highest growth (101.6 m^3/ha/yr) was obtained with sample DGxU2. This productivity is much above the average MAI obtained in commercial plantations in the Brazilian Territory (~40-60 m^3/ha/yr) [1].

Chemical characteristics: Table 2 shows the complete chemical characterization of the eucalypt clones. The woody material showed acceptable total extractive contents (1.9-4.9%) for all clones. Regarding the mineral contents the amounts of inorganics present in the eucalyptus woods were very low and quite acceptable for most applications [4] [5]. The total inorganics measured by complete biomass combustion (ash content) varied in the range of 950-2.510 mg/kg biomass. Among the woody biomass, there were significant variations among the total lignin contents, in the range of 27.1-31.3%. The maximum value was obtained for the double crossing U1xC2 hybrid and the minimum for the G1xGL2 one. However, these values are considered acceptable for eucalypt clones, but for pulp production a lower lignin content and high S / G ratio are desired

due to the increase of the pulpability of the wood [6]. About the carbohydrate content, the woody biomass presented values considered satisfactory for eucalypts for pulp production [2].

Table 2. Chemical composition of the eucalypt clones evaluated.

Sample	Sample Code	Total Extractives, %	Total Ash, %	Sugar Composition, %					Acid Soluble Lignin %	Total lignin, %	Lignin S/G ratio	Acetyl Group, %	Uronic Acid Group %	TOTAL
				Glucan	Xylans	Galactans	Mannans	Arabinans						
1	U1xU2	3.6	0.1	46.1	11.8	0.8	0.8	0.2	4.3	30.3	2.8	2.1	3.7	99.5
2	U2xC1	3.4	0.19	45.5	10.7	1.2	1	0.2	4.6	30.8	2.7	1.9	4	98.8
3	G1xUGL	4.9	0.2	43.9	13	0.8	0.9	0.2	4.7	28.9	2.9	2.7	3.8	99.2
4	U1xUGL	3.6	0.12	44.9	11.7	1.1	0.8	0.2	5	29.7	3.1	2.4	4	98.5
5	U1xC2	2.8	0.13	45.6	10	1.4	1.1	0.2	4.5	31.3	3	1.8	3.8	98.3
6	C1xC2	3	0.25	45.6	9.7	1.6	0.9	0.3	5.1	31.1	3	1.6	4.1	98
7	DGxUGL1	2.8	0.2	45.5	13	0.9	0.8	0.3	5.3	29.2	3.2	2.6	4	99.4
8	DGxU2	2.7	0.23	45.3	12.6	0.9	1	0.3	4.4	29.8	2.6	2.5	4	99.2
9	C1xUGL	2.1	0.22	46	11.9	1.1	0.9	0.3	5	30.7	3.2	2.2	4	99.3
10	G1xGL2	2.8	0.18	46.4	14.1	1	0.8	0.3	5	27.1	3.5	3	3.9	99.6
11	DGxC1	1.9	0.14	47.2	10.8	1.2	0.9	0.3	4.7	31	2.8	1.8	4	99.1
12	U2xGL1	2.5	0.18	45.5	13.4	1.2	0.8	0.3	5.6	29.3	3.8	2.6	4	99.7
13	DGxGL2	1.9	0.18	45.8	12.9	1.1	1	0.3	4.4	28.2	2.9	2.5	3.8	97.8
14	U1xD2	3	0.14	48.1	11.4	1	0.9	0.3	4.4	28.6	2.6	2	3.9	99.3
15	U1xG2	2.8	0.19	46.8	11.8	1	0.8	0.3	4.4	30.2	2.6	2	4	99.7
16	IP	2.3	0.16	49.4	12	1.2	0.9	0.3	4.2	27.2	2.7	1.9	4	99.3
17	VC	3.7	0.18	46.9	11.4	0.8	1.1	0.2	4.6	28.4	2.9	2.1	3.8	98.5
18	CC	3.5	0.17	47.4	11.2	1	1.1	0.2	4.1	28.4	2.4	1.9	3.9	98.7
19	IB	2.5	0.32	46.6	13.6	1.5	1.4	0.2	4.8	28.6	4	2.6	3	100.3
Max	-	4.9	0.3	49.4	14.1	1.6	1.4	0.3	5.6	31.3	4.0	3.0	4.1	-
Avg	-	2.9	0.2	46.2	11.9	1.1	0.9	0.3	4.7	29.4	3.0	2.2	3.9	-
Min	-	1.9	0.1	43.9	9.7	0.8	0.8	0.2	4.1	27.1	2.4	1.6	3.0	-
SD	-	0.7	0.1	1.2	1.2	0.2	0.2	0.1	0.4	1.3	0.4	0.4	0.2	-

Based on all the analyses, the five clones selected for the production of pulp were: (1) U1 x U2 that was selected on the basis of its very high annual growth (83 m3/ha/yr), high wood density, excellent morphological traits, very high forest yield (43 ton/ha/yr) and low xylan and uronic acid contents; (2) G1 x UGL which presented a high xylan content and possessed Eucalyptus globulus in its genotype, which is of interest for high S/G ratio, although it is quite challenging for its high content of extractives (4.9%); (3) DG x U2 that was selected due to its highest annual growth (101 m3/ha/yr) among all eucalypts evaluated, good density, outstanding morphological traits, and the highest forest yield (~50 ton/ha/yr); (4) a commercial elite clone (IP) was obtained from a large Brazilian forest company for its excellent forest productivity (38.5 ton/ha/yr), good density, the highest cellulose content and lowest lignin content among all; also for being a very good reference since it is commercially planted by a large pulp company in Brazil. (5) A pure European *Eucalyptus globulus* that was selected in order to compare with the Brazilian wood and a European wood.

***Pulpability of the selected clones*:** Table 3 shows the pulping results. The best performance observed was for the clone IB among all the eucalypt clones in regard to alkali demand, in the whole kappa number range studied. This can be attributed to its high S/G ratio of 4/1. The other eucalypt clone showed similar results, with the exception of IP with a somewhat lower alkali charge for high delignification values. This was attributed to the slightly lower lignin content in relation to the others. Another observed characteristic was that the rejected-pulp fraction decreased with delignification intensity as expected and well described in the literature [2] and [7].The brightness and viscosity obtained for all eucalypt clones in both processes may be considered satisfactory for the most pulp production [2]

Table 3. Cooking results of the eucalypt clones evaluated by kraft process.

	kraft process at kappa number 20				
	U1 x U2	G1 x UGL	DG x U2	IP	IB
Alkaline Charge, %	22	21	22	20	17
Yield Screened, %	51.2	50.4	52,0	52,0	55,5
Reject Content, %	0.3	0.5	0.4	0.4	0.6
Viscosity, dm^3/kg	1073	1193	1054	1100	1064
Brightness, % ISO	31.93	30.57	31.79	31.1	31.6
HexA, mmol/kg	48.8	48.6	48.9	46.4	37.3
	Soda-AQ process at kappa number 20				
	U1 x U2	G1 x UGL	DG x U2	IP	IB
Alkaline Charge, %	24	23	22	22	22
Yield Screened, %	50	51	51,1	51,6	55,2
Reject Content, %	1.1	0.2	0,4	0.6	0,4
Viscosity, dm^3/kg	919	917	1020	1028	1064
Brightness, % ISO	30.82	32.05	30.82	29.59	32.18
HexA, mmol/kg	40.3	48.2	43.4	45.7	41.6

IV. CONCLUSIONS

The results of this study indicate the high technological quality of Eucalyptus clones evaluated, and that they can be used for pulp production since most of the clones had performance similar to clone IP. For the kraft process it was observed a higher cooking yield, highest than 50%. Additionally, Soda-AQ process seems to be a potential process for replacing the kraft for a high degree of wood delignification. These results also indicate that there is still opportunity for more gains in productivity, e.g., if genetic characteristics of the IB clone are passed to the clones of greater forest productivity, as DGXU2 (101.6 MAI).

V. ACKNOWLEDGMENT

Funding provided by the European Community's Seventh Framework Programme FP7/2007-2013 under grant agreement no KBBE-2009-3-244362 LignoDeco, from the Minas Gerais State Research Foundation (FAPEMIG) and from the Brazilian National Council for Science and Technology Development (CNPq) is greatly appreciated.

VI. REFERENCES

[1] ASSOCIAÇÃO DOS FABRICANTES DE CELULOSE E PAPEL – BRACELPA. Disponível em: <http://www.bracelpa.com.br>. Access on: 22 April, 2013.

[2] GOMIDE, J. L.; COLODETTE, J. L.; OLIVEIRA, R. C.; SILVA, C. M. Caracterização tecnológica, para produção de celulose, da nova geração de clones de eucalyptus do Brasil. Revista Árvore, Viçosa-MG, v.29, n.1, p.129-137, 2005.

[3] GOMES, F. J. B. ; COLODETTE, J. L. ; BURNET, A. ; BATALHA, L. A. R. ; BARBOSA, B. M. . Potential of elephant grass for pulp production. Bioresources (Raleigh, N.C), v. 8, p. 4359-4379, 2013.

[4] MOREIRA, E. Efeito da lixiviação ácida de cavacos de eucalipto no processo Kraft. Dissertação apresentada à Universidade federal de Viçosa, fevereiro de 2006.

[5] FOELKEL, C. E. B. Qualidade da madeira de eucalipto para atendimento das exigências do mercado de celulose e papel. In: Conferência IUFRO sobre silvicultura e melhoramento de eucalipto, 1997, Salvador. Anais... Salvador: IUFRO, 1977, v.1, p.1.

[6] GOMES, F. J. B.; GOMES, A. F.; COLODETTE, J.L.; GOMES, C. M.; SOUZA, E.; MACEDO, A. M. L. Influência do teor e da relação S/G da lignina da madeira no desempenho da polpação Kraft. O Papel (São Paulo), v. 12, p. 95-105, 2008.

[7] GOMIDE, J. L.; FANTUZZI, N. H.; REGAZZI, A. J. Análise de critérios de qualidade da madeira de eucalipto para produção de celulose kraft. Rev. Árvore, Viçosa, v.34, n.2, Apr. 2010.

ACCLIMATIZATION OF MICROORGANISMS FOR DIRECT FERMENTATION OF CONCENTRATED HYDROLYSATES

Jérémy Boucher[1], Christine Chirat[1]*, Javier Carvajal[2], Bernardo Bastidas[2], Dominique Lachenal[1]

[1]LGP$_2$-Grenoble INP Pagora, 461 rue de la Papeterie CS10065 - 38402 Saint Martin d'Hères Cedex, France ; [2]Pontificia Universidad Católica del Ecuador, Av. 12 de Octubre 1076 y Roca Quito, Ecuador (christine.chirat@pagora.grenoble-inp.fr)*

ABSTRACT

The objective of this project is to develop a process for the parallel production of hemicellulosic ethanol and cellulose in the same pulp mill. This paper deals more precisely with the fermentation of hemicelluloses extracted without detoxification. A hydrolysate was obtained by autohydrolysis and evaporated to reach a concentration of 86 g/L of hexoses. Four strains of *Saccharomyces cerevisiae* and two strains of *Zygosaccharomyces bailii* were acclimatized to this hydrolysate. The most efficient strain of *S. cerevisiae* was able to ferment a medium composed of 75% of hydrolysate and reached an ethanol yield of 0.42 g/g after 72 hours. *Z. Bailii* showed less important volumetric productivities than *S. cerevisiae* but finally enabled the fermentation of the concentrated hydrolysate, even if the productivity reached was 0.16 g/(L.h), which means that more than ten days would be required to achieve the fermentation.

I. INTRODUCTION

Decreasing the consumption of oil derivatives has become one of the main world issues nowadays. As the major part of oil is turned into transport fuels, the development of biofuels is encouraged [1]. The only green substitute for gasoline potentially available in large quantities today is ethanol, given that it is the second bioproduct consumed in the world after paper pulp [2]. Unfortunately, first generation ethanol is produced from crops, which can have harmful repercussions on the prices of food resources. It is therefore important to develop the production of second generation ethanol, which consists in using lignocellulosic biomass as raw material, such as bagasse, straw or wood. Among all the possibilities existing to produce it, this paper deals with the co-production of hemicellullosic ethanol and cellulose in a kraft pulp mill using softwood as raw material.

In a kraft mill, hemicelluloses, and more particularly galactoglucomannans (GGM) in the case of softwood species, are lost during the process and burnt in a boiler, which is not profitable regarding their low calorific value [4]. The developed process would consist in the hydrolysis and extraction of the GGM prior to the kraft process. GGM are made up of hexoses which could be fermented into ethanol in a second phase.

Several treatments can be used to extract hemicelluloses such as hot water (autohydrolysis), acid hydrolysis, alkaline extraction, near neutral extraction or enzymatic hydrolysis [3,4]. Autohydrolysis and acid hydrolysis allow higher rates of sugar extraction. During the autohydrolysis, acetic acid, coming from the deacetylation of hemicelluloses, catalyzes the hydrolysis of GGM. The efficiency of the treatment can be improved by the addition of a mineral acid to perform an acid hydrolysis. Nevertheless, the severity of the treatment has to be limited to avoid damaging the cellulose, which could then reduce the properties of the pulp [5]. In acidic medium, hexoses and pentoses can be subjected to dehydratation reactions, leading to the formation of 5-hydroxymethylfurfural (HMF) and furfural respectively. HMF can further be degraded into levulinic acid and formic acid, and furfural into formic acid. Furthermore, some phenolic compounds coming from lignin and extractives are also present in the hydrolysates [6]. Unfortunately, HMF, furfural, acetic acid, levulinic acid, formic acid and phenolic compounds are known to be potential inhibitors of the fermentation [7]. The limitation of the concentrations of such inhibitors is necessary to obtain a profitable process. Alternatively, a post-treatment of detoxification can be added, such as overliming treatment, ions exchange resins, evaporation, activated charcoals or enzymatic detoxification [8].

A secondary hydrolysis or a step of concentration can also be implemented before the fermentation. A secondary hydrolysis can be applied to increase the rate in monomers, given that only monosaccharides can be fermented. It could be performed with an acid or with enzymes. A step of sugar concentration might also be necessary to have a profitable distillation after fermentation. The higher the concentration in ethanol, the lower the demand in energy for the distillation. A concentration of 3—5% (w/w) is the minimum admitted, meaning that at least 6—10% (w/w) of fermentable sugars are required prior to the fermentation [9,10].

The fermentation of extracted sugars can be performed by a large variety of wild or genetically modified microorganisms. Among them *Saccharomyces cerevisiae* and *Zygosaccharomyces bailii* were selected for this

study. These yeasts can only ferment hexoses, which are the main saccharides present in the softwood hemicelluloses. *S. cerevisiae* is known to have good fermentation yields, to be robust and to be quite tolerant to inhibitors [11]. *Z. bailii* is less efficient than *S. cerevisiae* [12] but is known to be very tolerant to organic acids [13].
In this study, the possibility of the extraction, the concentration and the fermentation of the hemicelluloses without detoxification step was evaluated. To overcome this issue, four wild strains of *S. cerevisiae* and two wild strains of *Z. bailii* were acclimatized to the hydrolysate.

II. EXPERIMENTAL

Extraction of the hemicelluloses

Wood chips used for this study were a mixture of different softwood species containing sylvester pine (35%), black pine (24%), alep pine (18%), douglas fir (16%) and spruce (7%). The average composition is given in **Table 1**.
The hemicellulose extraction was performed by an autohydrolysis and a secondary hydrolysis. This extraction was optimized in previous works to limit the degradation of sugars and therefore the apparition of inhibitors [14]. The autohydrolysis was performed in an autoclave immersed in an oil bath. The liquor was composed of distilled water and the liquor to wood ratio was 4. The temperature was raised during 30 min to reach 170°C and maintained for 65 min. The hydrolysate was then cooled, separate from wood chips by filtration and concentrated by evaporation, using a rotary evaporator: a round-bottom flask containing the hydrolysate was immersed in a bath at 70°C. The extraction was performed at a pressure of 35 kPa. The hydrolysate was concentrated until it contained about 85 g/L of hexoses. Part of acetic acid and furfural was lost in the vapors during the evaporation. As the objective was to test the fermentations in the most unfavorable case, acetic acid and furfural were added back to the hydrolysate to offset the losses. In order to depolymerize the oligomers, an acid hydrolysis was finally performed on the liquor during 60 min at 120 °C, with the addition of sulfuric acid to reach a concentration of 41 g/L.

Chemical component	Amount (% by wt.)	Chemical component	Amount (% by wt.)
Arabinan	2.0 ± 0.2	Acetyl groups	1.3 ± 0.01
Galactan	2.1 ± 0.0	Klason lignin	27.9 ± 0.5
Glucan	40.0 ± 0.5	Acid soluble lignin	0.35 ± 0.02
Xylan	4.90 ± 0.6	Acetone extractives	2.5 ± 0.5
Mannan	10.1 ± 0.2	Others	8.9

Table 1 : Composition of the wood chips used in the study

Fermentation

Five strains of *S. cerevisiae* (referenced at the *Colección de levaduras quito católica* as INT-005, INT-041, 19-001 and 10-386) and two strains of *Z. bailii* (referenced as INT-044 and INT-045) furnished by the *Pontificia Universidad Católica del Ecuador* (PUCE, Ecuador) were acclimatized to the hydrolysate. The acclimatization of the strains of *S. cerevisiae* was performed at the LGP_2 (Grenoble INP Pagora, France) whereas the acclimatization of *Z. bailii* was performed at the PUCE. The strains were put to 50 mL sterile liquid medium and incubated 24h at 35 °C. The sterile liquid medium was composed of Yeast Nitrogen Base (Sigma-Aldrich) at 134 g/L and glucose at 100 g/L. Yeast Nitrogen Base was also added to the hydrolysate as nitrogen source, to reach a concentration of 134 g/L. The pH of the hydrolysate was then adjusted (5.5 for *S cerevisiae* and 4.5 for *Z. Bailii*) and the hydrolysate was sterilized by filtration (0.45µm). Acclimatization was then performed in centrifuged tubes of 15 mL under agitation. The strains were transfer in 4 mL of media containing successively 25%, 50%, 75% and 100% (v/v) of this hydrolysate. The other part of the media was composed of the sterile medium used previously for incubation. The times of fermentation for each step are summarized in the **Table 2.** The temperatures of fermentations were 35°C for *S. cerevisiae* and 25°C for *Z. Bailii*.

Proportion of hydrolysate	25%	50%	75%	100%
S. cerevisiae	24h	24h	72h	-
Z. bailii	72h	72h	96h	120h

Table 2: Times of fermentations for each step of the acclimatization

Between each step, the medium was centrifuged (3000 rpm for 5 min), removed from the yeasts, filtered (0.45 µm) and frozen before analysis. The yeasts were then washed three times with sterile distilled water. The water was removed after each washing by centrifugation. Then, the next fermentation medium was added to the yeasts to start a new step of the acclimatization.

Analytical methods

At the LGP_2, the concentrations in monosaccharides in the hydrolysates and in the media of fermentations were measured by High Pulsed Anion Exchange Chromatography with Pulsed Amperometric Detection (HPAEC-PAD). The column used was a CarboPac PA 10 (250*4 mm, Dionex) after a guard column (50*4 mm, Dionex). The column and the detector were in a compartment regulated at 25°C. The eluent was composed of KOH 2 mM at a flow rate of 1 mL/min. The injection volume was 20 µL. The concentrations in HMF, furfural, acetic acid, formic acid, levulinic acid and ethanol were measured by HPLC. A ligand exchange column Pl Hi-Plex H (300*7.7 mm, Varian) was used and placed after a guard column (5*3 mm, Varian). The columns were placed in a compartment regulated at 65°C. A refractive index detector was used at 35°C. The eluent was composed of sulfuric acid at 5 mM with a flow rate of 0.6 mL/min. The injection volume was 10 µL.
At the PUCE, the concentrations in ethanol, glucose and mannose were measured by HPLC. The column used was a Rezex ROA-Organic Acid H+ (300*7.8 mm, Phenomenex) placed in a compartment regulated at 79°C. A refractive index detector was used. The eluent was composed of sulfuric acid at 0.25 mM with a flow rate of 0.6 mL/min. The injection volume was 10 µL.

III. RESULTS AND DISCUSSION

A hydrolysate was produced after an autohydrolysis, evaporated and depolymerized. Acetic acid and furfural were added to offset the losses during the evaporation. The final composition of the hydrolysate is given in **Table 3**. The total concentration in hexoses was 86.0 g/L. Except acetic acid, the concentrations in inhibiting species were quite low. Previous works showed that the amount of HMF and furfural obtained here are not harmful alone for *S. cerevisiae*, whereas acetic acid at 11.5 g/L can be really inhibiting if no acclimatization is performed. Formic acid can also decrease the productivity [14]. This explains why *Z. Bailii*, known to be very tolerant to organic acids, was chosen to be compared to *S. cerevisiae*.

Composition of the hydrolysate (g/L)			
Arabinose	11,2 ± 0.6	Acetic acid	11.5 ± 0.6
Galactose	15.7 ± 0.8	Levulinic acid	3.2 ± 0.2
Glucose	17.4 ± 0.9	Formic acid	3.0 ± 0.2
Xylose	19.5 ± 1.2	HMF	2.0 ± 0.1
Mannose	52.9 ± 2.7	Furfural	3.7 ± 0.2

Table 3 : Composition of the hydrolysate used for the fermentations

This hydrolysate was used for the acclimatization of fours strains of *S. cerevisiae* and two strains of *Z. Bailii*. The results of the fermentations are given by the ethanol yield and the volumetric productivity (**Figure 1**).

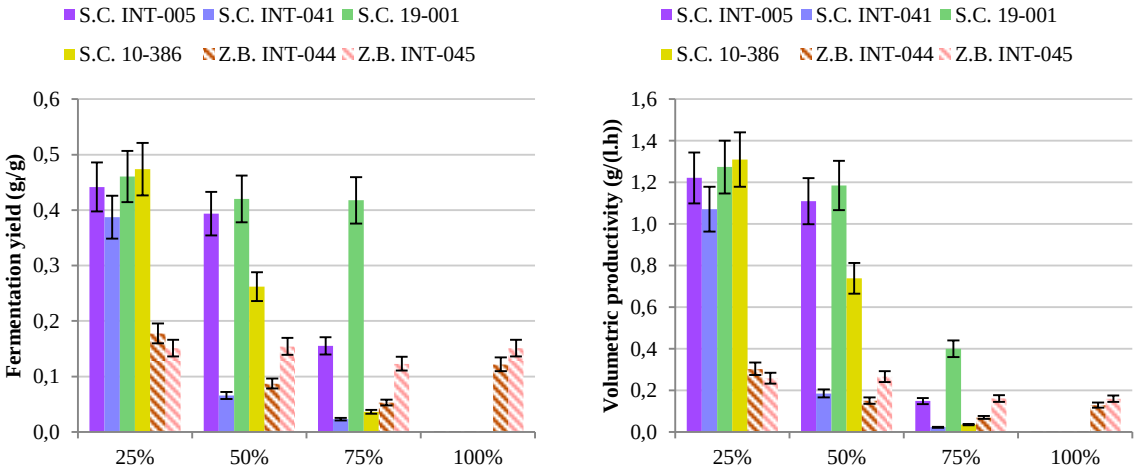

Figure 1: Ethanol yields (left) and volumetric productivities (right) calculated at the end of the fermentation for the acclimatization for the six strains

As galactose was not consumed by the yeasts, only glucose and mannose were taken into account as fermentable sugars for the calculation of yields and productivities. Indeed, galactose is used by *S. cerevisiae* only when no other fermentable hexose is available for the yeast [15]. The ethanol yield is then defined as the final amount of ethanol formed per gram of initial mannose and glucose. Theoretically, the maximum ethanol yield is 0.511 g/g. The volumetric productivity is defined as the amount of ethanol produced per liter of medium and per hour.
Only fermentations led with the strains of *S. cerevisiae* INT-005, 19-001 and 10-386 with 25% of hydrolysate led to the total consumption of mannose and glucose. All the other fermentations were not complete, even if the

times of fermentations were increased. The strains INT-005 and 19-001 reached also good yields with 50% of hydrolysate after 24 hours. However, only the strain 19-001 was able to ferment efficiently a medium containing 75% of hydrolysate, with a final yield of 0.42 g/g. However, the decrease in the productivity of this strain from 1.18 to 0.40 g/(L.h) showed that it was inhibiting, and 72 hours were necessary to reach such a yield. Moreover, no strain of *S. cerevisiae* acclimatized was able to ferment a medium containing 100% hydrolysate.
The productivities obtained with the two strains of *Z. Bailii* were very low compared to those obtained with *S. cerevisiae*, even with a low level of inhibitions. Thus, with a medium composed of 25% of hydrolysate, the productivities of *Z. Bailii* were 4 times lower than the productivities reached with *S. cerevisiae*. Nevertheless, the repercussions of the inhibition were less important with *Z. Bailii* and both of the strains were able to ferment a complete hydrolysate. By increasing the proportion of hydrolysate from 25 to 100%, the productivities decreased from 0.30 to 0.13 g/(L.h) for INT-044 and from 0.26 to 0.16 g/(L.h) for INT-045. The productivities were too low to achieve good yields in the times of fermentation chosen. Thus, with the productivities measured, 5 to 6 days would be necessary for the strains of *Z. Bailii* to ferment the medium containing 25% of hydrolysate, and 10 to 13 days for a medium composed of 100% of hydrolysate.

IV. CONCLUSIONS

The acclimatization of yeasts was efficient to ferment a concentrated hydrolysate. The most interesting strain of *S. cerevisiae*, INT-041, was nearly able to reach a complete fermentation of a medium containing 75% of hydrolysate, even if its productivity was divided by 3. The two strains of *Z. Bailii* were less efficient for media containing up to 75% of hydrolysate. But, unlike *S. cerevisiae*, they enabled the direct fermentation of a concentrated hydrolysate even if their productivities were very low. The fermentation of a concentrated hydrolysate without any detoxification step is then possible with *S. cerevisiae* or *Z. Bailii*. The choice of the microorganism depends on the final ethanol concentration required. These results can allow to develop a profitable process to produce ethanol in a kraft pulp mill.

V. ACKNOWLEDGEMENT

The authors thank the Enerbio fund of the Tuck foundation and the KIC InnoEnergy (SYNCON project) for their financial support. Part of the equipment used in this study was funded by la Région Rhône-Alpes.

VI. REFERENCES

[1] Ragauskas AJ, Nagy M, Kim DH, Eckert CA, Hallett JP, Liotta CL. From wood to fuels: Integrating biofuels and pulp production. *Ind Biotechnol*.**2006**, *2*, 55–65.
[2] Hytönen E, Stuart P. Integrating Bioethanol Production into an Integrated Kraft Pulp and Paper Mill: Techno-Economic Assessment. *PULP Pap Can.* **2009,** 25-32.
[3] Mosier N. Features of promising technologies for pretreatment of lignocellulosic biomass. *Bioresour Technol.* **2005**, *96* ,673–686.
[4] Jørgensen H, Kristensen JB, Felby C. Enzymatic conversion of lignocellulose into fermentable sugars: challenges and opportunities. *Biofuels Bioprod Biorefining.* **2007**, *1*, 119–134.
[5] Yoon S-H, Van Heiningen A. Kraft pulping and papermaking properties of hot-water pre-extracted loblolly pine in an integrated forest products biorefinery. *Tappi J.* **2008**, *7*, 22–27.
[6] Larsson S, Quintana-Sáinz A, Reimann A, Nilvebrant NO, Jönsson LJ. Influence of lignocellulose-derived aromatic compounds on oxygen-limited growth and ethanolic fermentation by Saccharomyces cerevisiae. *Appl Biochem Biotechnol.* **2000**, *84*, 617–632.
[7] Palmqvist E, Hahn-Hägerdal B. Fermentation of lignocellulosic hydrolysates. II: inhibitors and mechanisms of inhibition. *Bioresour Technol.* **2000**, *74*, 25–33.
[8] Palmqvist E, Hahn-Hägerdal. Fermentation of lignocellulosic hydrolysates. I: inhibition and detoxification. *Bioresour Technol.* **2000**,*74*, 17–24.
[9] Al-Dajani WW, Tschirner UW. Pre-extraction of hemicelluloses and subsequent ASA and ASAM pulping: Comparison of autohydrolysis and alkaline extraction. *Holzforschung,* **2010**, *64*, 411–416.
[10] Vane LM. Separation technologies for the recovery and dehydration of alcohols from fermentation broths. Biofuels *Bioprod Biorefining.* **2008**, *2*, 553–588.
[11] Maris A, Abbott D, Bellissimi E, Brink J, Kuyper M, Luttik M, et al. Alcoholic fermentation of carbon sources in biomass hydrolysates by Saccharomyces cerevisiae: current status. *Antonie Van Leeuwenhoek.* **2006**, *90*, 391–418.
[12] Martín C, Jönsson LJ. Comparison of the resistance of industrial and laboratory strains of Saccharomyces and Zygosaccharomyces to lignocellulose-derived fermentation inhibitors. *Enzyme Microb Technol.* **2003**, *32*, 386–395.
[13] Thomas DS, Davenport RR. Zygosaccharomyces bailii — a profile of characteristics and spoilage activities. *Food Microbiol.* **1985**, *2*, 157–169.
[14] Simultaneous production of ethanol and softwood kraft pulp: extraction, concentration, secondary hydrolysis and fermentation step, *Proceedings of 17th ISWFPC, Vancouver.* **2013**, 2556–2563.
[15] Johnston M, Flick JS, Pexton T. Multiple mechanisms provide rapid and stringent glucose repression of GAL gene expression in Saccharomyces cerevisiae. *Mol Cell Biol.* **1994**, *14*, 3834–3841.

EFFECT OF THE COMPOSITION AND MOLECULAR WEIGHTS OF LIGNOSULFONATE AND CHITOSAN ON STRENGTH AND DEFORMATION PROPERTIES OF POLYMER FILMS ON THEIR BASIS

[1]O. Brovko, [2]Y. Kazakov, [1,2]K. Bogolitsyn, [1]T. Boitsova, [1]I. Palamarchuk, [1]N. Rusanova

[1] Institute of Environmental Problems of the North, Ural Branch of Russian Academy of Sciences, 23 Severnoy Dvinu Emb., Arkhangelsk, 163000,Russia (Email: brovko-olga@rambler.ru)
[2] Northern (Arctic) Federal University named after Lomonosov, 17, Severnoy Dvinu Emb., Arkhangelsk, 163000, Russia

ABSTRACT
The influence of composite compound and molecular weight distribution of lignosulfonate and chitosan on the strength properties of the films derived from them was studied. To improve the mechanical characteristics of the films in the composition, unbleached softwood pulp (15 or 25 %) was added. It has been shown that the strength properties of the films increased with increasing lignosulfonate molecular weight, whereas for chitosan molecular weight this dependence is extreme. Increasing the molecular weight of chitosan up to 1000 kDa reduces the tensile stiffness of the films and lead to increasing their elongation to failure. Thus the use of chitosan having a molecular mass greater than 500 kDa in the composition does not improve the mechanical properties of the films. Mechanical behavior of composite materials is determined by the presence of the main film-forming polymer – chitosan. The highest strength and deformation properties has the film composed of interpolyelectrolyte complex based on the lignosulfonate and chitosan with a molecular weight of 500 and 90 kDa, respectively, and the addition of softwood unbleached kraft pulp in an amount of 25 %.

I. INTRODUCTION

Polyelectrolyte complexes (PEC) are a special class of polymers used for the production of separation membranes used for dialysis and pervaporation processes [1-3]. Such polymer materials have different composition, whose main element is a PEC, can also be incorporated plasticizer and fibrous filler [4]. Promising materials for such membranes are natural polymers having biocompatibility and biodegradability in the absence of toxicity, which opens the possibility of their use in medicine and pharmacy. Macromolecules of polymers used to prepare the membranes must be sufficiently stiff to form rigid supramolecular structures. An important characteristic of the membranes is their mechanical strength, that is depend on the composition of the film and the molecular weights of the polymers included in its composition. Knowledge of the conditions under which the membrane can exist as a body and not to lose its integrity, is important to choose conditions under which it is possible to carry out research of membranes and their use for practical purposes.

II. EXPERIMENTAL

To obtain polymer films based on biopolymers used:
- Lignosulfonates (LS) – according technical specifications TU 13-0281036-029-94, fractionated and purified by ultrafiltration using a polysulfone membrane. We used lignosulfonate samples with an average molecular weight (M_W) 24, 45, 63, 67, 90 kDa, which was determined by gel permeation chromatography [5].
- Chitosan (Ch) – according technical specifications TU 9289-002-11418234-99 derived from the shells of king crab, fractionated on JSC "Bioprogress", Moscow region. We used Chitosan samples with molecular weight 30, 87, 150, 330, 500, 1000 kDa, and a deacetylation degree of 85-87 %.
- As crosslinking agent in the composition was added unbleached softwood kraft pulp (15 or 25 % by mass) whose fibers have a large length, flexibility and increased durability. Refining of the samples was carried in a laboratory Jokro mill up to 30° SR.

The films were prepared by mixing solutions of components in volume ratio LS:Ch = 10:7. We used water solution of LS and an acetic acid solution (concentration of 2 % acid) of Ch (concentration of 2,5 g/l). Pulp was introduced into the composition as an aqueous suspension with concentration of 10 g/l. Films were prepared by the method of irrigation on an inert substrate (glass covered with polyethylene film), followed by drying at constant room temperature and humidity. The resulting membrane in the air-dry state have a smooth surface, they are transparent and flexible, and are swellable in water. To assess the strength and deformation properties, the samples of the films were tested on vertical tensile tester Testsystem–101 (made in Ivanovo, Russia). The test results of each sample were transferred to the PC, for the receipt and mathematical processing of stress – strain ("σ – ε") curve, obtained by treatment of the load – elongation ("F – Δl") dependence. For testing the films we used cut samples of 80×25 mm. The distance between the clamps was 50 mm, tensile speed – 10 mm/min, sample width – 25 mm. When performing mathematical processing of experimental stress-strain curves obtained in parallel tests, builds the middle curve, consisting of 21 points, and calculated characteristics: maximal force (F_{max}), N; elongation at maximal force (Δl), mm; failure stress (σ_f), MPa, the failure deformation (ε_f), %, elastic modulus (E_1), MPa; work to extension (A_f) , mJ, tensile energy absorbed (TEA), J/m^2.

III. RESULTS AND DISCUSSION

The influence of cellulose content on the mechanical properties of the films is shown in **Table 1**. The composition of the films includes LC and Ch with molecular weight 67 and 87 kDa respectively, and cellulose (Cell) in amount 15 or 25 %. All tested samples have low strength and increased fragility. They differ in thickness (δ, μm) and basic weight, which should be considered when analyzing the results.

Table 1 – The results of tensile tests of the films

The material	δ, μm	F_{max}, N	Δl, mm	ε_f, %	σ_f, MPa	E_1, MPa	A_f, mJ	*TEA*, J/m^2
Ch87LS67	31	1,91	1,068	2,14	2,50	239	0,853	683
Ch87LS67-15Cell	41	1,60	0,864	1,73	2,61	331	0,436	580
Ch87LS67-25Cell	53	20,37	0,573	1,15	25,72	3820	6,076	8100

Ch87LS67 sample not containing cellulose fibers in the composition has a minimum thickness, and its amorphous structure can't provide sufficient strength and extensibility. Introduction of cellulose fibers in the composition increased the thickness of the films through the introduction of thick fibers and spreading the mixture in a confined space between the fibers. If we introduce a small amount of cellulose fibers (sample Ch87LS67-15Cell), the fibers don't form ab own grid structure in the film, and it leads to a slight increase in the film thickness and a corresponding increase in strength. Sample Ch87LS67-25Cell with high cellulose content in the composition, shows the mechanical behavior fundamentally different from the other samples, which is reflected in the load-elongation and stress-strain curves. It has the highest strength and deformation properties. This may be due to the formation of an independent grid of cellulose fibers, which has the primary mechanical load (**Figure 1**).

a *b*

Figure 1 – The microphotographs of films obtained by a digital microscope.
The cellulose fibers introduced into the composition: *a* – 15 %; *b* – 25 %

For tests evaluating the effect of molecular weights Ch and LS on the properties of the films, were sampled Ch with molecular weight 30, 150, 330, 500, 1000 and LS samples M_W: 24, 45, 63, 90 kDa, the addition cellulose is 25 %. The results are shown in **Table 2**.

Table 2 – Results of tensile tests of samples of films from LS and Ch with cellulose additive 25 %

The material	δ, μm	F_{max}, N	Δl, mm	ε_f, %	σ_f, MPa	E_1, MPa	A_f, mJ	*TEA*, J/m^2
M_W LS 24 kDa								
LS24Ch150	50	2,41	0,756	1,51	1,93	277	1,215	972
LS24Ch330	48	3,21	0,622	1,24	2,68	335	1,134	907
LS24Ch500	62	2,92	0,815	1,63	1,88	198	1,240	992
LS24Ch1000	40	1,46	1,044	2,09	1,46	143	0,931	745
M_W LS 45 kDa								
LS45Ch30	95	8,16	0,799	1,60	3,44	510	3,483	2786
LS45Ch150	74	4,06	0,522	1,04	2,21	445	1,098	878
LS45Ch330	58	3,49	0,614	1,23	2,43	326	1,260	1008
LS45Ch500	65	7,31	0,867	1,73	4,50	461	3,502	2801
LS45Ch1000	40	2,31	0,741	1,48	2,33	230	0,786	629
M_W LS 63 kDa								
LS63Ch330	63	3,39	0,670	1,34	2,15	256	1,395	1116
LS63Ch500	64	4,74	1,071	2,14	2,96	342	3,206	2565
LS63Ch1000	50	1,80	1,269	2,54	1,44	113	1,135	908
M_W LS 90 kDa								
LS90Ch330	72	7,79	0,693	1,38	4,36	560	2,937	2350
LS90Ch500	73	8,72	0,811	1,62	4,81	511	3,860	3088
LS90Ch1000	53	5,43	1,096	2,19	4,13	305	2,513	2010

The films with Ch weight of 1000 kDa have a minimum thickness, low strength, high elongation and toughness, in all cases. Film samples of Ch with molecular weight 500 kDa are the thickest, have most high strength and deformation properties. An increase chitosan molecular weight up to 1000 kDa reduces the tensile stiffness of the films and increases their extensibility. The use of Ch in the composition with molecular weight more than 500 kDa does not improve the mechanical properties of the films. Thus, the dependence of the strength characteristics of the films versus the molecular weight of main film-forming polymer chitosan has an extreme character that is typical for films prepared from chitosan [6]. It suggests that the mechanical behavior of studied composite materials largely determined by the presence of this particular polymer.

An increase of M_W lignosulfonate in the polymer composition increases the thickness of the films due to the higher viscosity of the mixture in the liquid state and at the spreading area, while also increasing the strength and extensibility of the films. Film samples of with LS M_W 90 kDa exhibit mechanical behavior fundamentally different from other specimens and has the highest strength and deformation properties.

Swellable membranes usually possess good dialysis properties; however the resulting polymer composite was tested as a semipermeable membrane for the dialysis process. **Table 3** shows characteristics of sodium lignosulfonate before and after dialysis through synthesized polymer films. The ash content during dialysis decreased by 1.4 times, i.e. main amount of inorganic salts gone into diffusate. Weight average molecular weight of lignosulfonate after dialysis increased by 1.5 times, and the polydispersity index M_w/M_n decreased.

Table 3 – Characteristics of the samples before and after dialysis

LS	Ash content, %	M_w, kDa	M_w/M_n
before dialysis	13,8	24	5,5
after dialysis	10,2	37	4,5

Gel-chromatograms of the initial sample and the product of membrane separation are shown in **Figure 2**. Curve for dialyzed LS (**Figure 2*b***) has peak at high molecular weight fraction of the bimodal molecular weight distribution curve. It is shown more clearly in comparison with curve for not dialyzed LS (**Figure 2*a***).

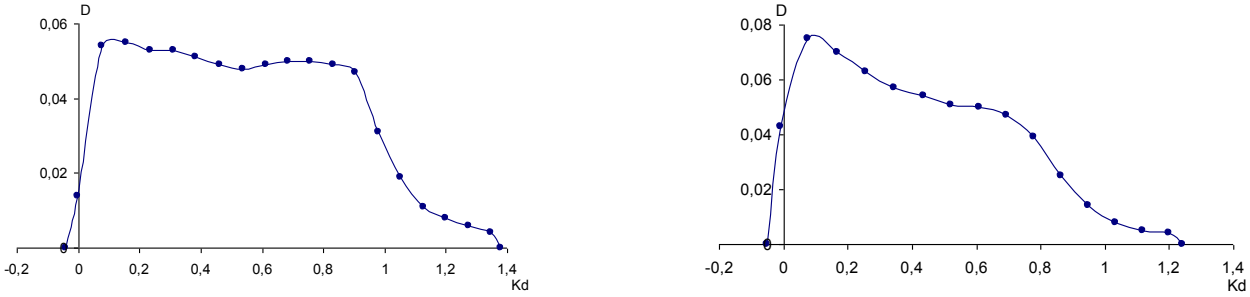

a *b*

Figure 2 – The LS gel-chromatogram before (*a*) and (*b*) after dialysis

IV. CONCLUSIONS

As a result of the research, a method of producing of composite biopolymer films based on different mixture compositions LS and Ch with additives softwood unbleached sulphate pulp was developed and tested. These films are intended for use as a dialysis membrane.

It was found that the films without cellulosic fibers do not have the required level of strength and deformation characteristics, and it requires the introduction of a fibrous material for reinforcing films. The amount of softwood fibers must be at least 25 %. The fibers in the structure of the film should form an independent grid.

It is shown that the strength characteristics of the investigated films increase with lignosulfonate molecular weight, whereas for chitosan this dependence has an extreme character.

The evaluation of the mechanical properties allows propose the process and the best composition for the dialysis membrane. The composition of the optimal films is composed of a lignosulfonate with a molecular weight of 90 kDa, chitosan with a molecular weight of 500 kDa with addition of unbleached softwood kraft pulp 25 %. Films of such compositions exhibit the highest and stable strength and deformation properties.

V. ACKNOWLEDGEMENT

The financial support from Ural Branch of Russian Academy of Sciences (interdisciplinary project № 12-M-45-2012) is gratefully acknowledged.

VI. REFERENCES

[1] Izumrudov, V.; Sibachin, A. Determining influence on the phase lyophilized polyion separation in solutions of polyelectrolyte complexes. *Polymer Science A*. **2006**, *48(10)*, 184-185.

[2] Kabanov, V. Polyelectrolyte complexes in solution and in the condensed phase. *Russian Chemical Reviews*. **2005**, *74(1)*, 5-23.

[3] Palamarchuk, I.; Makarevich, N.; Brovko, O.; Boitsova, T.; Afanasyev, N. Cooperative interactions in the system lignosulphonate – chitosan. *Khimija Rastitel'nogo Syr'ja*. **2008**, *4*, 24-29.

[4] Brovko, O.; Kazakov, Y.; Boitsova, T.; Palamarchuk I. Application of cellulose fibers for increased strength polymer dialysis membranes. Proceedings of the Ist International Scientific and Technical Conference "The Issues in mechanics of the pulp and paper materials", Arkhangelsk, Russia, 13-17 September **2011**, 251-256.

[5] Sokolov, O. Determination of lignin molecular weight on ultracentrifuge and by gel filtration. **1978**. 75.

[6] Fedoseeva, E.; Alekseeva, M.; Nistratov, V.; Smirnov, L. Features mechanical testing chitosan films. *Zavodskaya Laboratoriya. Diagnostika Materialov*. **2009**, *75(7)*, 42-46.

.

APPLICABILITY OF LIGNOCELLULOSIC FIBERS FROM PLANTAIN (*Musa paradisiaca*) AS REINFORCEMENT OF POLYMER COMPOSITES

Edith M. Cadena Ch.[1*], J. Manuel Vélez R.[1], J. Felipe Santa M.[2], Viviana Otálvaro G.[2]

*[1]Universidad Nacional de Colombia, A.A. 1779-Medellín, Colombia; [2]Instituto Tecnológico Metropolitano, A.A. 54959-Medellín, Colombia (*emcadenac@unal.edu.co)*

ABSTRACT

Post-harvest and processing technologies of agricultural crops produce a significant amount of lignocellulosic wastes and they are usually considered worthless (e.g. crop residues such as straws, leaves, stalks, husks, bagasse, among others). Accordingly, in this study, new materials reinforced with vegetal waste from plantain plants (stems) were studied. Natural fibers were extracted through mechanical processing of pseudo stems; lignocellulosic fibers were processed to be used as a reinforcing material in a polymer matrix composite. The samples were prepared by using a polyester resin, methyl ethyl ketone peroxide (MEKP) and a cobalt-based promoter to speed up the curing reaction. Three types of composites (CI, CII, and CIII) were obtained using a 3.8% wt. of lignocellulosic reinforcement with a fiber length from 2 to 5 mm. The CII and CIII composites were prepared after alkaline extraction and acetylation treatment of the fibers in order to enhance the compatibility of organic loads with the polymer matrix. The results showed that the fibers can be used to obtain a polymer composite as a filler material; in this case, the acetylation procedure improved the mechanical properties, but fibers in the alkaline treatment did not have a positive effect as reinforcement. Furthermore, bio-composites can be used for several applications as an alternative to conventional polymers.

I. INTRODUCTION

Clean technologies promote the use of agro-industrial waste in new materials with potential applications in several fields (e.g. food and pharmaceutical sector, industrial packaging). In the recent years, researchers have focused on renewable and biodegradable materials in order to reduce the global production of synthetic polymers manufactured mainly from crude oil. In order to reduce the global production of synthetic polymers, fundamental research and technological development are required to reduce the environmental impacts caused by plastic materials.

On the other hand, the characteristics of residues obtained from the agricultural sector depend on the source and postharvest processes. In most of the cases, the residues are made of lignocellulosic materials composed of cellulose, lignin, hemicellulose, extractives and other compounds. They contain a significant fiber fraction that can be processed in order to produce new materials. Composites reinforced with natural fibers in comparison to synthetic materials reinforced with glass or carbon fibers, offer competitive production because the former are non-abrasive materials, they have a lower production cost, lower density, flexibility during processing because of their biodegradability, high availability of woody and non-woody plant sources (wood, cane fiber, pineapple, banana, cotton, flax, hemp, kenaf, sisal, coconut, etc.) from agricultural and agroindustrial practices.

A critical aspect of producing composites reinforced with natural fiber is the compatibility of the interface between lignocellulosic materials and the polymer matrix. In this area, researchers have tried to generate coupling and grafting by functionalization techniques and morphological modifications of the fibers in order to find improve the interface to obtain high adhesion of the plant material to the polymer matrix [1] and to generate structures with different mechanical properties. Chemical treatments, such as alkaline, silane, acetylation, peroxide treatments, are some examples of techniques used to create reactive groups on the fiber's surface, permitting a positive coupling with the matrix.

Recent developments related to physical-mechanical and chemical properties of plantain fibers extracted from the pseudostem, have allowed the development of medium and long term technologies to produce "green" materials reinforced with plantain fibers that can be applied in industries needing for composite reinforced with natural fibers.

In this work, residues from plantain cultivation of a monocotyledon plant of the Musaceae family and the Musa genus were selected to be studied. In Colombian agriculture, the plantain crops are around 378,884 ha. From those crops, 4 million metric tons of residues are generated every year and 95% of the residues (leaves, buds, stems) are used as compost, with potential applications still unknown. Consequently, the use of plantain stems to

extract lignocellulosic fibers as raw material for the production of composites is an interesting area for researchers and producers.

II. EXPERIMENTAL

Fiber samples

Fibers derived from plantain stems were characterized in terms of extractives (UNE 57-013), ash - mineral compounds, and holocellulose and cellulose (Tappi 203), Klason lignin (Tappi 222) contents and the morphology was studied using Scanning Electron Microscopy (SEM). The physical properties were evaluated by using Differential Scanning Calorimetry (DSC), X-ray Diffraction (XRD) and Fourier Transform Infrared Spectroscopy (FTIR).

Alkaline and acetylation treatments on the fibers were carried out in order to enhance the compatibility of the organic load with the polymer matrix. For the alkaline treatments, the fibers were immersed in 5, 10 and 20 % NaOH solutions at 10 % wt. of concentration at 50 °C for 2 hours. The acetylation method [2] was carried out on fibers previously treated with the 20 % alkaline procedure. After the treatments, the fibers were rinsed with distilled water and dried overnight in an oven at 60 °C.

Composites manufacturing

Three types of composites (C) were obtained. The CII and CIII composites were prepared using fibers after alkaline extraction and acetylation, respectively, CI composite corresponds to control sample with fibers without treatment. The composites were obtained using polyester resin and as accelerator and initiator agents were employed cobalt and methyl ethyl ketone peroxide (MEKP), respectively. The samples were prepared by adding 0.1% wt. of Cobalt at 45g of polyester resin, afterwards 3.8% wt. of lignocellulosic fibers (length from 2 to 5 mm) was added to the resin. The resin with the fibers was stirred to obtain a homogeneous solution. Finally 2 % wt. of MEKP was added to initiate the polymerization reaction. The curing was done at room temperature.

Mechanical tests

The mechanical properties were evaluated using universal testing machine (Shimadzu AG-X 100 kN). Three-point bend tests were performed on the cylinders made of the composite material. A span of 50 mm was used and the rupture load was recorded. After the tests, the surfaces of failed samples were analyzed to observe the adhesion of fibers to the polymeric matrix.

III. RESULTS AND DISCUSSION

Structural compositions of plantain fibers

A transverse section of plantain pseudostem is shown in **Figure 1**. Pores (average diameter: 79,3 µm) and cavities were found in the vascular bundle of monocotyledonous plants from the muse genus (**Figure 1a** and **1c**). Mechanical extraction from the pseudotem generates fibers with a length from 0.2 to 1 m and a high length/diameter relation (**Figure 1b**). The morphology of the plantain fibers after cleaning and is similar to other fibers found in the literature like yute, sisal and fique. From **Figure 1d**, it can be concluded that the fibers are composed of a lignocellulosic network and a interfibrillar matrix creating a microporous structure. The porosity of the fibers can be useful when surface treatments are performed since the chemicals can get directly into the fibers. The surface of the fibers is uniform with a flat wall without external fibrillation.

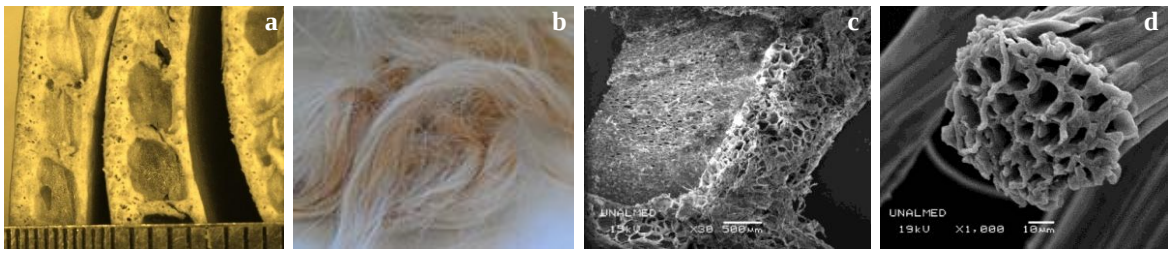

Figure 1. Micrographs (a) plantain stems, (b) Plantain fibers obtained from the stem, (c) SEM micrograph of cross section of stem- 500 µm, (d) SEM micrograph of fiber -10 µm.

The chemical composition of the plantain fibers is shown in **Table 1**. High cellulose contents were found and the plantain fibers have higher cellulose contents compared with other woody fibers. From the Infrared analysis, the FTIR spectra shows a typical lignocellulosic material with stretching vibration of OH groups and intermolecular

hydrogen by single bridge at frequencies around 3500 - 3300 cm^{-1}. Absortion bands related to aromatic ring (around 1500 - 1600 cm^{-1}) were also observed caused by the lignin in the fibers. The cristallinity of the fibers measured by XRD reported 50.2 %. This cristallinity is typical of crystalline I_α and I_β. The intensity is increased when the analysis is performed on cellullose reporting 61.3% of cristallinity. This value is important since mechanical strength of fibers mainly depends on the content of crystalline cellulose [3]. Accordingly, the plantain fibers are a good option to be used in composites.

Table 1. Structural compositions of plantain fibers obtained from stem

Minerals		Component (% dw)	
Calcium, %	0.54	Klason lignin	19.13
Iron, ppm	67	Cellulose	56.83
Magnesium, %	0.26	Holocellulose	68.86
Manganese, ppm	60	Acetone extractives	1.27
Potassium, ppm	110	Water-solubles	10.75
Sodium, ppm	91	Ash	2.37
Zinc, ppm	20		

The results of tensile tests performed on the fibers reported a high tensile strength (620 MPa). The fibers also have high elongation. The results indicate that the fibers can be used to reinforce polymers since their tensile strength is seven times higher than the polymer. On the other hand, the transition temperature (by differential scanning calorimetry), Tg is around 127 ºC meaning that the fiber are very stable at high temperature and indicating that the fibers can be used in thermoforming processes.

Composites: mechanical properties

Alkaline treatment changes the morphology and molecular structure of the plantain fibers. When a higher concentration of NaOH is used, the rupture of celullose and hemicellulose bonds is increased and the lignin and extractives are partially removed. Usually, an Alkaline treatment is performed before other surface treatments in order to improve the efficiency of additional chemical agents. However, in alkalized cellulose "fibre-cell-O-Na", a reduction of the hydrophilic properties can be found leading to higher wet resistance [4, 5]. The use of NaOH also improves the adhesion between the fibers and the polymeric matrix [6].

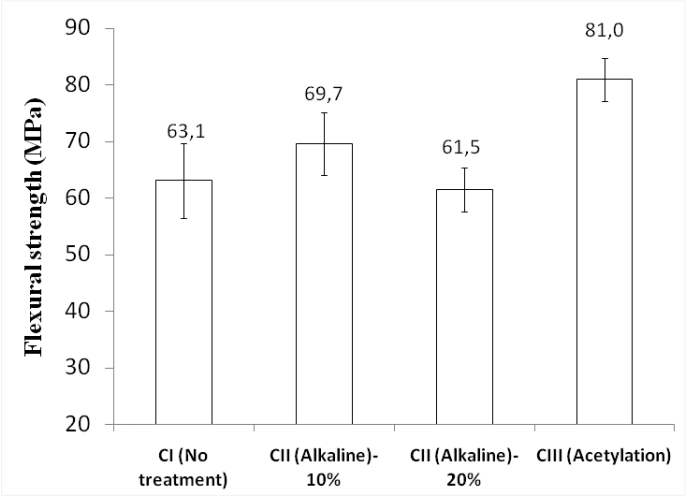

Figure 2. Flexural strength of composites reinforced with plantain fiber. CI: No surface treatment, CII: Alkaline treatment , CIII: Acetylation treatment

The results obtained from the three-point bend tests are shown in **Figure 2**. It shows the average flexural strength and the standard deviation. From the results it can be concluded, that composites reinforced with plantain fiber have high mechanical resistance. The acetylation treatment reported the highest mechanical resistance improving 25% the flexural strength. On the other hand, for the alkali treatments there was no improvement.

In acetylation treatment, the acetyl group CH_3CO reacts with hidroxyl groups and a coupling is created in the celullosic polymer reducing its hydrophilic properties. The coupling is useful to improve the properties of the composites since it enhances dimensional stability [7]. In plantain fibers, acetylation treatment is done after the alkaline procedure in order to improve the functionalization of the fibers. The reaction between the fibers-OH and CH_3COOH, also improves the wet resistance, thermal properties and the adhesion of the fibers to the polymer actinng as the matrix [8, 9] .

IV. CONCLUSIONS

Biodegradable lignocellulosic fibers from non-woody plant, showed the feasibility to obtain composites suitable for several applications, the natural fibers exhibit many advantages and environmental benefits. Plantain fibers are composed mainly of cellulose (56%) and lignin (19%) and their cristallinity is around 50%. Additionally, their high cellulose content indicates that plantain fibers can be used to reinforced composites with a polymeric matrix.

Plantain fibers have an average diameter around 90 µm with pores and their morphology is similar to other fibers found in the literature like yute. The fibers have pores that can be useful when surface treatments are performed since the chemicals can get directly into the fibers.

Mechanical resistance of the composite can be improved by performing an acetylation treatment. The flexural strength of acetylated fibers reported the highest mechanical resistance improving 25% the flexural strength of the composites with no surface treatment.

V. ACKNOWLEDGEMENT

The authors would like to acknowledge to Centro de Investigación of Instituto Tecnológico Metropolitano for the financial support provided project No. P13127. Programa Nacional de Semilleros de Investigación, Creación e Innovación (2013-2015) of Universidad Nacional de Colombia is also acknowledged for their financial support provided. Code: 18311. Mod 1.

VI. REFERENCES

[1] Ragoubi, M.; George, B.; Molina, S.; Bienaimé, D.; Merlin, A.; Hiver, J.-M.; Dahoun A. Effect of corona discharge treatment on mechanical and thermal properties of composites based on *miscanthus* fibres and polylactic acid or polypropylene matrix. *Composites Part A*. **2012**, 43(4),675-685.

[2] Kabir, M.M.; Wang, H.; Lau, K.T.; Cardona, F. Effects of chemical treatments on hemp fibre structure. *Applied Surface Science*. **2013**, 276, 13-23.

[3] Azwa, Z.N.; Yousif, B.F.; Manalo, A.C.; Karunasena, W. A review on the degradability of polymeric composites based on natural fibres. *Mater. Design.* **2013**, 47, 424-442.

[4] John M.J.; Anandjiwala, R.D. Recent developments in chemical modification and characterization of natural fibre-reinforced composites. *Polym Compos*. 2008, 29 (2), 187–207.

[5] Mwaikambo, L.Y.; Tucker, N.; Clark, A.J. Mechanical properties of hemp fibre reinforced euphorbia composites. *Macromol Mater Eng.* **2007**, 292 (9), 993-1000.

[6] Li, X.; Tabil, L.G.; Panigrahi, S. Chemical treatment of natural fibre for use in natural fibre-reinforced composites: A review. *Polym Environ.* **2007**, 15, 25-33.

[7] Sreekala, M.S.; Kumaran, M.G.; Joseph, S; Jacob, M. Oil palm fibers reinforced phenol formaldehyde composites: influence of fibers surface modifications on the mechanical performance. *Appl Compos Mater*. **2000**, 7, 295-329.

[8] Mishra, S.; Mohanty, A.K.; Drzal, L.T.; Misra, M.; Parija, S.; Nayak, S.K.; Tripathyc, S.S. Studies on mechanical performance of biofiber/glass reinforced polyester hybrid composites. *Compos Sci Technol*. **2003**, 63, 1377-1385.

[9] Bledzki, A.K.; Mamun, A.A.; Lucka-Gabor, M., Gutowski, V.S. The effects of acetylation on properties of flax fibre and its polypropylene composites. *Express Polym Lett*. **2008**, 2 (6), 413-422.

PURIFICATION AND CHARACTERIZATION OF A RECOMBINANT XYLOSIDASE FROM ENTEROBACTER SP.

Eleonora Campos[1], Maria Jose Negro[2], Paloma Manzanares[2], Felicia Sáez[2], Paola Talia[1], Angel A. Cataldi[1], Mercedes Ballesteros [2]*

*[1]Inst. de Biotecnología, CICVyA. Instituto Nacional de Tecnología Agropecuaria (INTA), Buenos Aires, Argentina. [2]Unidad Biocarburantes, Centro de Investigaciones Energéticas, Medioambientales y Tecnológicas (CIEMAT), Madrid, Spain. (*m.ballesteros@ciemat.es)*

ABSTRACT

Beta-xylosidases are hemicellulases that hydrolyze beta-1,4 bonds between two units of xylose in xylobiose and short xylo-oligoscharides, activity that is essential for complete breakdown of xylan. The objective of this work was the characterization of enzymatic activity for a GH43 beta-xylosidase from *Enterobacter* sp, identified and cloned from a soil bacteria consortium. Sequence analysis revealed two distinct modules, a GH43 catalytic domain and an uncharacterized module in the C-terminal portion of the protein, common to many GH43 proteins. The enzyme was expressed in *E. coli* as an N-terminal His- tagged fusion and purified under native conditions. The recombinant enzyme had a MW of 64.5 kDa and a pI of 5.8. Biochemical enzymatic assays of purified protein showed an optimal activity pH range from 6 to 7 in citrate/phosphate buffer using pNPX as substrate, with typical Michaelis-Menten kinetics. It also showed activity on xylobiose (X2), but with cooperative binding kinetics. Substrate specificity tests on xyloarabinan and low DP xylooligosaccharides and xylose inhibition have also been tested.

I. INTRODUCTION

In order for cellulosic biomass to become a viable feedstock for meeting the demand for liquid biofuels, efficient and cost effective processes must exist to break down cellulosic materials into their primary components. Biomass recalcitrance and hydrolytic enzymes are the key limiting steps in obtaining cellulosic ethanol. Lignocellulosic biomass is mainly formed by cellulose (35–50%), hemicellullose (20–35%), lignin (10–25%) and other less represented components. The synergistic action of multiple enzymes is required to fully hydrolyze complex biomass feedstocks [1]. At present, commercial enzymes come mainly from fungi (*Trichoderma reesei* and *Aspergillus niger*). However, depending on the biomass and pre-treatment process, it is necessary to supplement enzymatic cocktails with a greater number of enzymatic activities that would allow overcoming the inhibition of the reaction due to insoluble substrate or intermediate toxic compounds [2]. Hemicellulases represent an array of enzymes such as xylanases, mannases, arabinases (both endo and exo) and their corresponding glycosidases [3]. Among them, beta-xylosidases are responsible for the hydrolysis of xylo-oligosacharides into xylose units, therefore completing degradation of hemicelluloses and providing fermentable pentoses. In this context, bacterial GH43 beta-xylosidases (EC 3.2.1.37) are being thoroughly studied [4]. A common structural feature of GH43 enzymes is a 5-bladed beta-propeller domain that contains the catalytic acid and catalytic base. A C-terminal conserved domain of unknown function (DUF) is also present in many GH43 described so far. In *T. fusca* Xyl43A this module is necessary for activity [5]. We have previously identified and cloned a novel *E. cloacae* GH43 beta-xylosidase [6]. In this work we have further characterized its activity and identified crucial residues involved in activity and substrate binding.

II. EXPERIMENTAL

Activity assays

For enzymatic activity characterization of EcXyl43 and mutans, β-xylosidase activity was assayed in a mixture (0.2 mL) containing 0.1% *p*-nitrophenyl β-D-xylopyranoside (pNPX, Sigma-Aldrich ref. N2132), 50 mM citrate/phosphate buffer (I=0.3 M, adjusted with NaCl) pH 6 and appropriately diluted enzyme solution. After 5 min, the reaction was stopped by adding 0.2% Na_2CO_3 (0.5 mL) and the A_{400} was measured. A standard curve was prepared by using *p*-nitrophenol (*p*NP). One unit (IU) of β-xylosidase activity was defined as the amount of enzyme that liberates 1 μmol *p*NP per minute in the reaction mixture under these assay conditions. Specific activity is defined as the number of international units per milligram of protein.

For protein content quantification, BCA protein assay kit (Pierce) was used using bovine serum albumin as standard. For the determination of the optimum pH of His-Xyl43, 50 mM citrate-phosphate buffer (pH 3.5-8) at constant ionic strength (I=0.3 M with NaCl) was used.
Optimum temperature assay was performed at the interval 30-70 ºC. A continuous monitoring method was employed for determining initial-rate reactions for determination of kinetics parameters of the His-Xyl43 acting on *p*NPX substrate. Reactions were monitored at 400 nm for 5 min. For incubation, 10 µl of enzyme (0.97 mg protein/mL) were added to 270 µL of substrate solution (0.5-20 mM of *p*NPX) in citrate/phosphate buffer 50 mM, pH 6 (adjusted with NaCl to I=0.3M). Temperature incubation was 40 ºC. A standard curve was prepared by using p-nitrophenol (*p*NP) at pH 6. K_{cat} is expressed in moles of substrate hydrolyzed per second per mole of enzyme. The kinetic parameters K_{cat} and K_m were calculated by nonlinear regression fitting of the Michaelis-Menten equation using the program OriginPro 7.5 (OriginLab Corporation, Northampton, USA). Kinetic parameters with substrate 1,4-β-D-Xylobiose (X2) were determined in reaction mixtures 0.2 mL containing 50 mM citrate/phosphate (I=0.3 M, adjusted with NaCl) at pH and 40ºC, 10 µL enzyme (1 mg/mL), from duplicated 30 min endpoint assays. X2 concentrations varied from 2.5 to 20 mM. Xylose concentrations were determined using an enzyme coupled spectrophotometric assay (Megazyme Xylose-kit). Data were fit to Hill equation [6].

Site directed mutagenesis and purification of recombinant proteins.

PCR mutagenesis was performed with QuickChange II kit from Agilent Technologies, based on His- EcXyl43 [6]. Primers were designed by Agilent primer design website and the ones selected for mutagenesis were D14A(a5213c) 5'gcttcaacccggccccgtccctgtg3' and W73G (t5389g) 5'ctccggcggtatcggggcgccgt3' and their corresponding antisense versions. Mutation was confirmed by complete sequencing of plasmid insert. Recombinant proteins were expressed in *E. coli* BL21 and purified by IMAC with Ni-NTA resin as previously described [6].

III. RESULTS AND DISCUSSION

Characterizarion of recombinant EcXyl43 activity.

Ecxyl43 was expressed in *E. coli* as an N-terminal His fusion and purified in a soluble way to high homogeneity [6]. The purified enzyme can be lyophilized and stored at room temperature for over a year. Optimal activity was achieved at 40°C and in a range of pH from 6 to 7 (Figure 1).

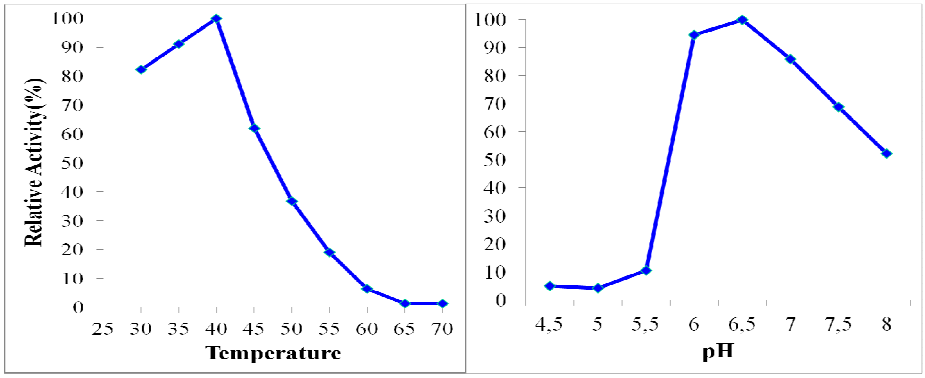

Figure 1: Determination of optimal activity on pNPX.

Kinetic studies of beta-xylosidase activity with pNPX as substrate showed Michaelis–Menten kinetic, with K_m of 2.92 mM and K_{cat} of 1.32 seg^{-1}. Activity on the natural substrate, xylobiose (X2), was also proved, although a different kinetic was observed. Surprisingly on X2, the saturation curve displayed positive cooperativity of binding, with a Hill coefficient of 2.8. The K_{cat} value was 380 s^{-1} and K_m was 17.8 mM (Figure 2).

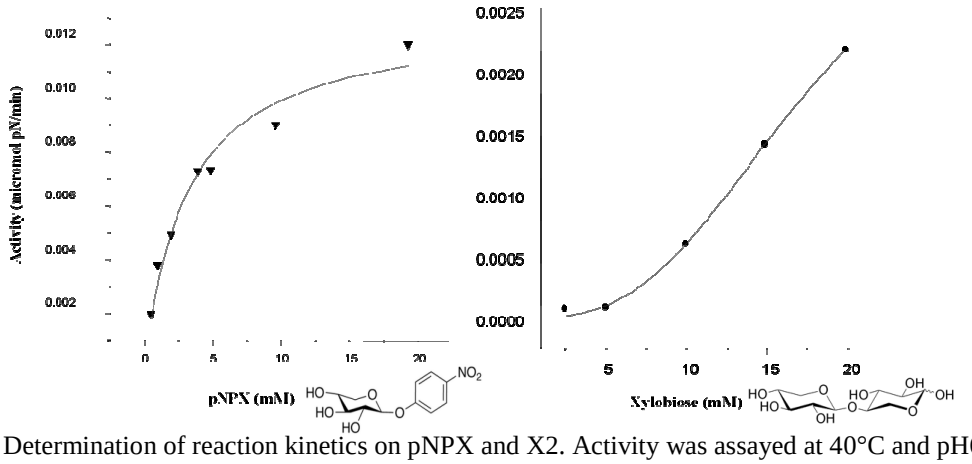

Figure 2: Determination of reaction kinetics on pNPX and X2. Activity was assayed at 40°C and pH6.

Modelling and identification of catalytic and binding residues

EcXyl43 model was obtained based on its aminoacid sequence and multiple similar GH43 solved crystal structures using the HHPRED MODELLER pipeline (http://proteinmodelportal.org/) [7]. Candidate residues for the catalytic site were predicted as well as aromatic residues that could be involved in substrate binding. Predicted model revealed a pocket structure as the active site. Predicted catalytic residues were aminoacids D14 and E186. Among important residues for binding, a tryptophan, W73, located close to the catalytic site was identified (Figure 3).

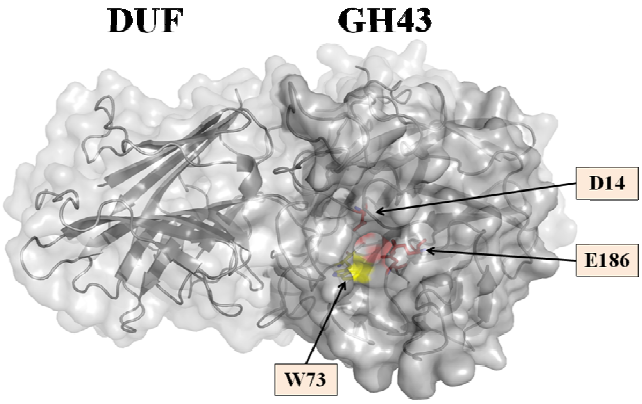

Figure 3. Model of EcXyl43. GH43 and conserved module of unknown function DUF1349, as well as predicted catalytic site, are indicated.

Production of mutated EcXyl43(D14A) and EcXyl43(W73G).

To prove the model prediction, aspartic acid in position 14 was replaced by alanine (D14A) and tryptophan in position 73 was replaced by glycine (W73G). Recombinant mutant proteins were expressed in *E.coli* and purified in a soluble way, retaining their native structure. Activity was assayed on pNPX. Mutant EcXyl43(D14A) presented no activity, demonstrating that mutation D14A completely abolishes activity. On the other hand, mutation W73G, still presented activity, although it was dramatically diminished (Table 1).

	Molecular weight (MW)	Isoelectric point (pI)	Molar extinction coefficient (ε)	Specific Activity (IU/mg)
EcXyl43 (wt)	64,5	5.8	151.19	2,21
D14A	64,5	5.85	150.69	0,03
W73G	64,4	5/8	145.9	0,70

Table 1. Activity and biochemical properties of recombinant EcXyl43 and mutants.

IV. CONCLUSIONS

In this work we have demonstrated that *Enterobacter* sp. Xyl43 has beta-xylosidase activity on pNPX and xylobiose, its natural substrate. The recombinant protein was expressed in a soluble, active form. Activity assays on xylobiose showed a cooperative binding kinetic, suggesting more than one binding site. We have confirmed the catalytic site by site directed mutagenesis and have identified a tryptophan (W730) relevant for activity, possibly by affecting substrate binding. Based on the models presented in this work, we will aim to identify residues involved in secondary biding sites as well as inhibitors binding sites, in order to design enzyme variations with improved activity parameters suitable for different industrial conditions.

V. ACKNOWLEDGEMENTS

This research was supported by INTA National Project PNEG141130 and by Binational MinCYT (Argentina)-MINECO (Spain) project PICT2011-2735. The authors thank Nathan Kruer-Zehusen and Dr. David Wilson, from the Dept. of Molecular Biology and Genetics, Cornell University, Ithaca, NY, USA, for protein models.

VI. REFERENCES

[1] 1: Gao D, Uppugundla N, Chundawat SP, Yu X, Hermanson S, Gowda K, Brumm P, Mead D, Balan V, Dale BE. Hemicellulases and auxiliary enzymes for improved conversion of lignocellulosic biomass to monosaccharides. *Biotechnol Biofuels*. **2011**, 4:5.

[2] Ballesteros M. Enzymatic hydrolisis of lignocellulosic biomass. *In: Waldron K, editor. Bioalcohol Production. Head Publising Series in Energy, number 3. WashingtonDC: CRC Press*. **2010,** 159–77.

[3] Lombard V, Golaconda Ramulu H, Drula E, Coutinho PM, Henrissat B. The Carbohydrate-active enzymes database (CAZy) in 2013. *Nucleic Acids Res*, **2014,** D490–D495

[4] Jordan DB, Wagschal K, Grigorescu AA, Braker JD. Highly active β-xylosidases of glycoside hydrolase family 43 operating on natural and artificial substrates. *Appl Microbiol Biotechnol*. **2013**, 4415-28.

[5] Moraïs, S., Salama-Alber, O., Barak, Y., Hadar, Y., Wilson, DB., Lamed, R., Shoham, Y., Bayer E. Functional association of catalytic and ancillary modules dictates enzymatic activity in glycoside hydrolase family 43 β-xylosidase. *The Journal of biological chemistry*. **2012**, 9213–21.

[6] Campos E, Negro Alvarez MJ, Sabarís di Lorenzo G, Gonzalez S, Rorig M, Talia, P, Grasso DH, Sáez F, Manzanares Secades P, Ballesteros Perdices M, Cataldi AA. Purification and characterization of a GH43 β-xylosidase from Enterobacter sp. identified and cloned from forest soil bacteria. *Microbiol Res.* **2014**, 213-20.

[7] Haas J, Roth S, Arnold K, Kiefer F, Schmidt T, Bordoli L, Schwede T. The Protein Model Portal-a comprehensive resource for protein structure and model information. *Database* (Oxford). **2013**, bat031.

FEASIBILITY OF USE OF BANANA (MUSA ACCUMINATA) RACHIS IN PAPERMAKING

Carbajo J.M.[1*], González, F.[2], Santos, S.M.[1], Revilla, E.[1], Villar, J.C.[1]

[1]*Cellulose and Paper Laboratories. INIA-CIFOR Ctra.de la Coruña km 7. 28040 Madrid, Spain;*
[2]*Canary Paper. c/ 12 de octubre,36. 38300 La Orotava, Sta. Cruz de Tenerife. Spain*
*(*chema@inia.es)*

ABSTRACT

Banana (*Musa accuminata*) rachis is an agricultural residue extensively produced in several areas like Canary Islands. It is produced continuously during the whole year and its elimination it is a problem for the banana producers. The possibility to use cellulosic fibers from other parts of the plants, as the pseudo stem, has been explored, but the use of the rachis has not been developed yet.

In this work, *Musa accuminata* rachis is chemically characterized in terms of extractives, ashes, lignin, pentosans and holocellulose. α-,β- and γ-cellulose has been also determined using hollocelulose as raw material. Biometric characteristics (length and width) of fiber have also been measured. The most significant results are the high amount of extractives (even in cold water) and subsequently, low levels of lignin and hollocelulose.

Due to the low content in hollocelulose and lignin, a mechanical procedure is proposed to produce pulp. Banana rachis has been defibered in a Sprout-Waldron Laboratory refiner and the energy consumption has been determined.

Three different pulps have been produced. The first one with just a defibering stage (Schopper-Riegler drainage index near 50), the second one with a refining stage after the defibering (Schopper-Riegler drainage index near 75) and, finally, the third one mixing the first and second pulps. Handsheets has been formed and characterized in terms of grammage, thickness, porosity, mechanical resistance (tear, burst and tensile strength) and optical properties (brightness and opacity). Results shows moderate mechanical properties so, this pulp can be used for purposes where resistance is not essential, or can be mixed with other pulps in order to use this residue and produce papers with good properties and a reduced cost.

I. INTRODUCTION

In the last years the consumption of paper and board products has increased. In order to preserve the sustainability and protection environment, as well as to satisfy the increasing demand in pulps, new non-wood sources of lignocellulosic fibres are being used as an important alternative fibrous sources for papermaking industries. Some agricultural residues, such as wheat and rice straws, sorghum stalks and some annual plants such as hemp and jute, are used as raw materials for pulp and paper production [1,2] .

Among these non-woody plants available as byproducts in agriculture, the banana (*Musa accuminata*) is still unexplored. Banana is one of the most important crops in agriculture, reaching its global production $83x10^6$ (FAO January 21, 2013). In general, the different species and varieties of bananas are differentiated by their size, layout and size of the leaves, the shape and size of the fruits, but mainly by the conformation of the bunch of bananas.

One of the challenges that the banana producing countries face is the removal of organic waste generated in the production, picking and packing fruit. After harvesting of a single bunch of bananas, a great amount of agricultural residues are produced. Pseudo-stems and foliage are usually left in the plantation soil to be used as organic fertilizer. However, these banana tree counterparts and some other byproducts of banana processing such as rachis could represent an economically interesting renewable source of fiber material.

Recent preliminary studies on the utilization of pseudo-stems and rachis as raw materials for papermaking [3] and composite materials [4] respectively, have shown rather promising results. Further investigations on the potential industrial utilization of banana residues require detailed knowledge of their chemical composition. As part of a research project aiming to use the rachis of *Musa accuminata* in papermaking after the harvesting of fruits, we have studied the morphological and chemical composition of the plant harvested in Canary islands as well as the quality of pulps produced mechanically using this lignocellulosic material.

II. EXPERIMENTAL

Raw material description and characterization

The banana rachis material studied was collected in Canary Islands. It was air dried and cut in pieces of 5 – 10 cm width. After drying was cut in pieces of about 15 cm. length and stored in plastic bags.

For microscopic inspection, a small piece of banana rachis was prepared by heating in Schultz solution (4 g $KClO_3$, 80ml HNO_3, 200 ml distilled water) until fibers separated. Then, the fibers were washed with distilled water and stained with Herzberg stain. Fiber length was measured by projection with a Reichert "Visopan" microscope. Fiber diameter was measured with an Olympus VANOX microscope attached to a digital camera and the software "CellD". At least 100 fibers were measured. Microphotographs were also obtained with this microscope and camera.

Chemical analyses included ash content (TAPPI T-211), extractives in hot and cold water (TAPPI T-207), acetone (SCAN CM49) and 1% NaoH (TAPPI T-212), lignin content (TAPPI T-222), holocellulose content [5] and pentosan content (TAPPI T-223). The hollocelulose fraction was characterized in terms of α-,β- and γ-cellulose (TAPPI T-203). The sample was previously milled in a willey mill and screened. The fraction able to pass to a 0.4mm screen and retained in a 0.3mm one was selected for the chemical analysis.

Mechanichal pulping and handsheet evaluation

Previously to produce mechanical pulp, the raquis material was soaked in tap water for two hours. After that was pulped mechanically in a 12" Sprout Waldron laboratory refiner. For one pulp, two pulping stages were applied (defibering and refining) and the power consumption was measured for both stages. For other one, only defibering stage was applied. The third pulp was obtained mixing equal parts of the other two pulps. Drainability (Schopper Riegler; ISO 5267-1) was determined and handsheet formed in a rapid-kothen sheet former according to ISO 5269-2. Bulk, Gurley porosity and Strength (tensile, tear and burst indexes) and optical properties (brightness, opacity) were also measured for the pulps according to ISO standards

III. RESULTS AND DISCUSSION

Fiber Morphology and chemical characterization

Figure 1A shows individual fibers from *Musa accuminata* rachis. Fibers show morphological characteristics in the same range of other cellulosic fibers (Table1). For example, its length (1.61mm) is higher than hardwoods like eucalyptus or aspen (1.1 mmm and 0.9 mm respectively) but lower than softwood (3.4 mm for *Picea abies* or 3.0 mm for *Pinus radiate*) [6]. Probably, one problem to its papermaking potential is the presence of high number of other types of cells (parenchyma cells) as can be shown in figure 1B.

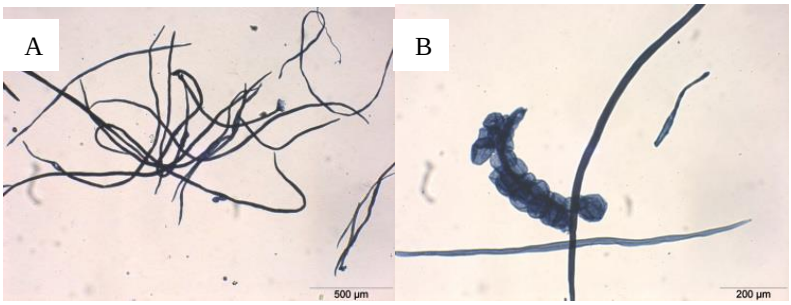

Figure 1. (A) Fibers from *Musa accuminata* rachis. (B) Parenchyma cells

	Length (mm)	Diameter (µm)
Mean	1.61	20.94
Maximum	3.11	33.10
Minimum	0.48	12.40

Table 1. Morphologic data from *Musa accuminata* rachis fibers

Chemical composition (Table 2) shows high levels of extractable material, probably due to the presence of salts (ashes values are also high). Other parts of rachis like pseudostem have also high content of extractable material,

near 30%, but lower than rachis [7]. Due to this characteristic a mechanical pulping process is proposed in order to maintain an acceptable yield.

Ash (%)	525 ºC	31.8
	900 ºC	20.8
Solubility (%)	Cold water	48.4
	Hot water	49.1
	1% NaOH	66.0
Extractives (%)		1.2
Lignin (%)		17.8
Holocellulose (%)		32.9
α-cellulose (%)		73.2
β-cellulose (%)		6.6
γ-cellulose (%)		21.2
Pentosans (%)		17.8

Table 2. Chemical characterization of *Musa accuminata* rachis fibers

Mechanical pulping and handsheet characterization

Mechanical pulping of *Musa accuminata* rachis shows low yield for a mechanical process due to the high level of extractable material but not lower than a conventional chemical process (table 3). On the other hand, energy consumption is notably lower that the figures obtained for pulping woody materials. Typical values for pulping pine in our system are 2000-2500 Wh/Kg for the first stage and 1000-1500 Wh/Kg for the second one. Yield and energy consumption for pulping in one or two stages (Pulp A and B respectively) are slightly different, so, pulping in one or two stages will depend of the quality of the products obtained

	Pulp A	Pulp B
Energy consumption (Wh/kg raw material)	233	306
Yield (%)	44.7	39.5

Table 3. Pulping yield and energy consumption of *Musa accuminata* rachis.

For studying paper properties, three group of handsheets are produced, using pulp A, pulp B and mixing equal amounts of both pulps (pulp C). Properties are shown in figure 2. Gurley air permeance has been also determined and is > 900 s in all cases showing that the paper has a very "closed" structure, probably due to the high amount of parenchyma cells. Except for tear index there are not important differences in the pulps so, producing pulp in one stage looks like the best option. However, producing paper using rachis as sole raw material is difficult, and may be more adequate to assay mixing rachis with other sources of fibers.

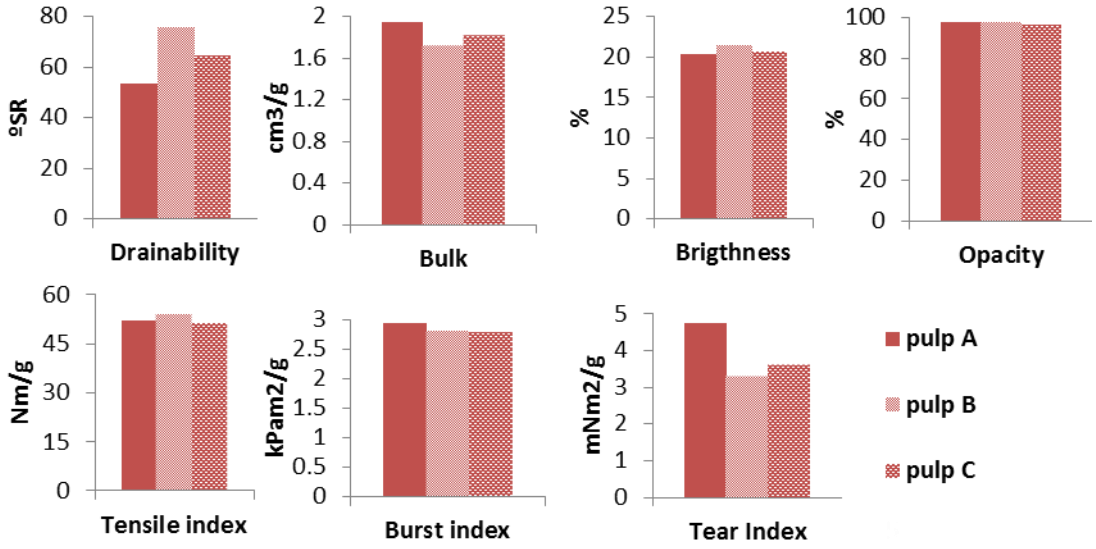

Figure 2. Properties of handsheets elaborated with *Musa accuminata* rachis.

IV. CONCLUSIONS

The possibility of produce paper using fibers from banana rachis has been demonstrated. Mechanical pulping has low energy consumption. Nevertheless, to produce paper with enough quality and runability, raquis fibers might be used in combination with other complementary ones.

V. ACKNOWLEDGEMENT

Samaria Atondo and Fernando Romero are acknowledged for their technical contribution to this project

VI. REFERENCES

[1] Rousu, P.; Rousu, P; Anttila, J. Sustainable pulp production from agricultural waste. *Resour. Conserv. Recy.* **2002**, *35*, 85-103.

[2] Ashori, A. Nonwood fibers – A potential source of raw material in papermaking. Polym. Plast. Techno.l Eng. **2006**, *10*, 1133-1136.

[3] Cordeiro, N.; Belgacem, M.N.; Torres, I.C.; Moura, J.V.C.P. Chemical composition and pulping of banana pseudo-stems. *Ind. Crops Prod.* **2004**, *19*, 147-154.

[4] Faria, H.; Cordeiro, N.; Belgacem, M. N.; Dufresne, A. Dwarf Cavendish as a source of natural fibers in polypropylene-based composites. *Macromol. Mater. Eng.* **2006**, *291*, 16-26.

[5] Wise, L.E.; Murphy, M; d'Addieco, A. A. Chlorite Holocellulose, Its Fractionation and Bearing on Summative Wood Analysis and on Studies on the Hemicelluloses *Paper Trade J.* **1946,** *122*, 35-43.

[6] Ilvessalo-Pfäffli M.S. Fiber Atlas: Identification of papermaking fibers **1995**. Springer

[7] Akpabio, U.D.; Udiong, D.S.; Akpakpan, A.E. The physicochemical characteristics of plantain (musa Paradisiaca) and banana (Musa Sapientum) pseudostem wastes. *Adv. Nat. Appl. Sci*. **2012**, *6*, 167-172.

HYDROXYL AND CARBONYL OXIDATION DURING BIOTRANSFORMATION OF HEXOSE-DERIVED HYDROXYMETHYL FURFURAL BY FUNGAL ARYL-ALCOHOL OXIDASE

Juan Carro[1], Leonor Rodríguez[1], Alicia Prieto[1], Patricia Ferreira[2], Ángel T. Martínez[1]*

[1]*CIB, CSIC, Ramiro de Maeztu 9, 28040 Madrid, Spain*
[2]*Facultad de Ciencias, Universidad de Zaragoza, Pedro Cerbuna s/n, 50009 Zaragoza, Spain*
*(*e-mail:atmartinez@cib.csic.es)*

ABSTRACT

Aryl-alcohol oxidase (AAO) is an extracellular flavooxidase from the glucose-methanol-choline oxidase (GMC) superfamily, involved in degradation of lignin by *Pleurotus* species and other white-rot fungi. AAO continuously supplies the H_2O_2 needed by ligninolytic peroxidases, due to its ability to redox cycling lignin-derived compounds and aromatic fungal metabolites, in collaboration with mycelium dehydrogenases. Taking advantage of the wide range of aromatic molecules likely to be oxidized by AAO, we wanted to test the oxidative ability of the *Pleurotus eryngii* enzyme on new aromatic molecules, such as 5-hydroxymethylfurfural (HMF) and its oxidized derivatives. HMF can be produced by dehydration of fructose and other sugars, which may be obtained from lignocellulosic biomass by a number of procedures. Oxidation of the hydroxyl and carbonyl groups of HMF provides a series of aromatic heterocycles of industrial interest, such as 2,5-diformylfuran, a biofuel, and furancarboxylic acids. The latter have a broad potential as platform chemical building blocks. Among them, 2,5-furandicarboxylic acid (FDCA) can replace terephthalic acid in the production of polyethylene polymers, but the chemical synthesis of this compound is expensive and polluting. The final aim of the work was to test whether AAO from *P. eryngii* was able to carry out the mentioned reactions. Firstly, we performed a series of reactions with AAO and HMF and we analyzed them by gas chromatography coupled to mass spectrometry to find out which compounds were present after different times of incubation. Then, we estimated the kinetic constants of AAO for HMF and the other molecules potentially involved in its biotransformation to FDCA, and proposed a pathway for HMF oxidation to FDCA.

I. INTRODUCTION

Biotransformations have gained interest during the last years because of the importance of sustainable conversion of chemicals, which use renewable materials and are environmentally friendly [1]. As a consequence, biorefineries have come up as the industries being capable of carrying out such processes. Their development focuses on two main goals: the displacement of petroleum in favor of renewable materials (which constitutes an energy goal) and the establishment of a biobased industry (economic goal). Thus, the production of high-valuable biobased chemicals might draw the necessary financial incentive that could eventually permit the expansion of the biorefining industry [2].

Lignocellulose represents a promising raw material for biorefineries because it possesses some properties that make it unique as a renewable resource. First and foremost, lignocellulose is widespread and very abundant, consisting of the two most abundant biopolymers on Earth. Moreover, it is cheap, can be easily converted into energy, biofuels and chemicals, and can be stored. Therefore, it has drawn much attention as a raw material that could substitute for fossil fuels.

Lignocellulose is made up of lignin, cellulose and hemicelluloses and it is the main constituent of the plant cell-wall. It confers protection and rigidity to plants and its biodegradation is important since it allows carbon sequestered inside its chemical structure to cycle back to the atmosphere. Cellulose and hemicelluloses are of high importance as they are formed from monomers of glucose and other hexoses and pentoses; thus, they can be used as a carbon source in multiple processes. There exists a broad range of chemicals considered as building blocks derived from carbohydrates. One of these is 5-hydroxymethylfurfural (HMF), which can be obtained from fructose through dehydration using a great deal of procedures, most of them based on acidic treatments [3]. Subsequent oxidations of the hydroxyl and carbonyl groups of HMF lead to the final formation of 2,5-furandicarboxylic acid (FDCA), a building block of great importance, since it is a potential biorenewable replacement monomer for terephthalic acid in plastics [4]. Besides, the intermediate compounds of the route may play roles as biofuels or surfactants. **Figure 1** depicts the possible oxidative cascade leading from HMF to FDCA. Many different routes have been described to FDCA, but all of them proceed via oxidation of HMF with air over different catalysts.

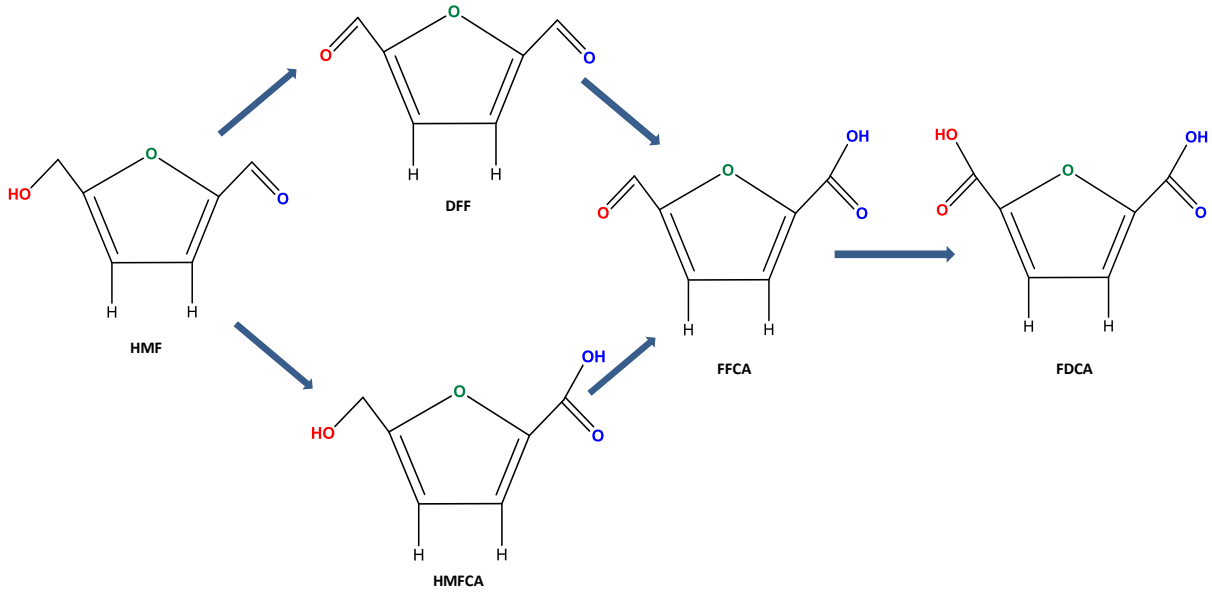

Figure 1. Oxidative pathway from HMF to FDCA showing the intermediates of the route and the carbonyl and hydroxyl groups involved in it (DFF: 2,5-diformylfuran, HMFCA: 5-hydroxymethyl-2-furancarboxylic acid, FFCA: 5-formylfuran-2-carboxylic acid).

Due to the great interest HMF and its oxidation draw and the convenience to find a biological catalyst that could replace the expensive and often polluting chemical processes traditionally used to carry out the mentioned reaction, the discovery of an enzyme capable of oxidizing this compound, and its different oxidized derivatives, would be of great importance.

Aryl-alcohol oxidase (AAO) is an extracellular flavooxidase from the glucose-methanol-choline oxidase (GMC) superfamily of oxidoreductases involved in degradation of lignin by *Pleurotus* species and other white-rot fungi. It oxidizes aromatic and non-aromatic polyunsaturated primary alcohols, as well as their corresponding aldehydes with lower efficiency. In Nature, AAO continuously supplies the H_2O_2 needed by ligninolytic peroxidases, due to its ability to redox cycling lignin-derived compounds an aromatic fungal metabolites, in collaboration with mycelium peroxidases [5].

II. EXPERIMENTAL

Chemicals

HMF, DFF, HMFCA, FDCA and *t*-butyl-methyl ether were purchased from Sigma-Aldrich. FFCA was purchased from TCI America. AmplexRed® and horseradish peroxidase (HRP) were obtained from Invitrogen.

Enzyme production

Recombinant AAO from *Pleurotus eryngii* was obtained by expressing the mature AAO cDNA (GenBank® accession number AF064069) using *Escherichia coli* as heterologous expression host and by *in vitro* activating and purifying the protein as previously described [6].

Kinetic studies

Steady-state kinetic constants for AAO oxidation of the different chemicals were calculated by monitoring AAO production of H_2O_2 upon reacting with the substrates using a HRP-coupled assay with AmplexRed® as HRP substrate, at 25ºC in air-saturated 50 mM sodium phosphate buffer, pH 5.5. The reactions were initiated by adding the enzyme with an adder-mixer. In the presence of the H_2O_2 generated by AAO, HRP (6 U/ml) oxidizes AmplexRed® (60 µM) in a 1:1 stoichiometry forming resorufin (ε_{563} 52000 $M^{-1}\cdot cm^{-1}$). Kinetic constants were obtained by fitting the data to the Michaelis-Menten equation using Sigmaplot software.

Gas chromatography-mass spectrometry (GC-MS) studies

In order to analyze the reaction products, HMF (3 mM) was incubated up to 24 h in the presence of AAO (500 nM) in 50 mM sodium phosphate, pH 5.5. After different incubation times, samples were taken and reactions were stopped by adding 6 M HCl (to pH 2-3) and then liquid-liquid extracted using *t*-butyl-methyl ether. The

extracts were evaporated and dissolved in chloroform. The GC-MS analyses were performed using derivatized and non-derivatized samples. Derivatization was performed by bis(trimethylsilyl)trifluoroacetamide (BSTFA) silylation in the presence of pyridine, at 80ºC for 1 h. A chromatograph equipped with a HP-5MS column (30 m x 0.25 mm internal diameter; 0.25 µM film thickness) coupled to a quadrupole mass detector was used. The oven programme started at 110ºC (2 min) increasing 20 ºC·min-1 until 310 ºC. Helium was the carrier gas at a flow rate of 1.2 ml·min^{-1}. Compounds were identified by comparing their mass spectra with standards, which were also used to obtain response factors.

III. RESULTS AND DISCUSSION

GC-MS studies

After the incubation of HMF with AAO, amounts of FFCA and also FDCA were observed. In contrast, no significant amounts of HMFCA or DFF could be identified after the different incubation times. In two hours, almost all HMF had been converted into FFCA (84%), whose levels decreased as time passed by yielding a small amount of FDCA after 24 hours (14%) **(Figure 2**).

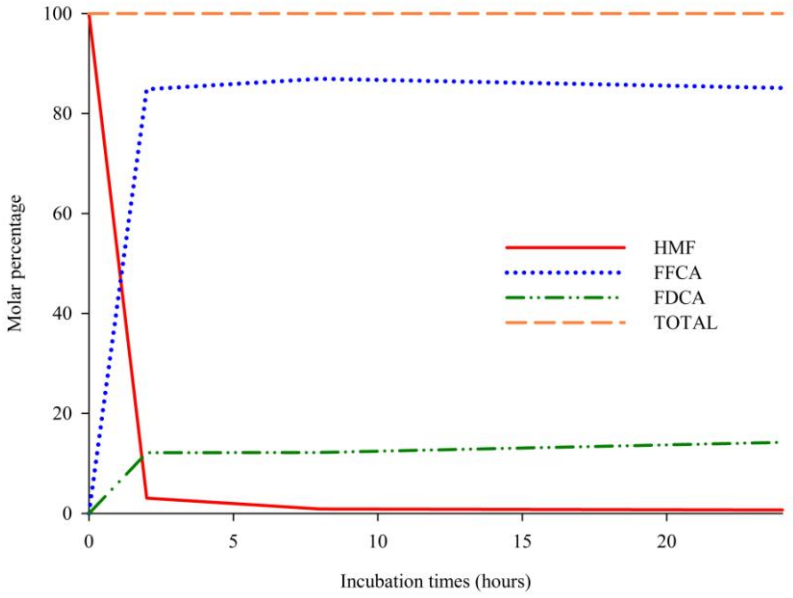

Figure 2. Evolution of HMF incubated with AAO up to 24 h and appearance of its oxidized derivatives. The compounds were separated and identified by GC-MS.

These results suggest that AAO is capable of oxidizing HMF and other derivatives to yield FDCA. However, it seems that the enzyme is not very efficient at reacting with FFCA, since the latter accumulates while the yield of the subsequent oxidized compound (FDCA) is low when compared to the levels of FFCA. In the light of these results it is not possible to reveal if the enzyme reacts preferentially with the carbonyl or the hydroxyl group of HMF, that is, if the reaction proceeds through DFF or HMFCA formation (see **Figure 1**).

Kinetic studies

With the aim of obtaining further information on the above reactions, we estimated the kinetic constants of AAO for HMF and the other molecules (DFF, HMFCA and FFCA) potentially involved in the biotransformation to FDCA, through a coupled reaction where the H_2O_2 released by AAO was used by a peroxidase forming a colored product. The estimated constants are shown in **Table 1.** In the case of HMFCA the enzyme could not be saturated at increasing substrate concentrations, therefore, a k_{obs}/concentration value was only obtained.

The constants show that AAO has no apparent activity on FFCA, in agreement with its presence as the main product of the biotransformation of HMF by AAO analyzed by GC-MS. However, it can oxidize both HMF and DFF, and even HMFCA; although, due to the higher apparent affinity of AAO for HMF, it is more efficient at oxidizing it than DFF. This is in accordance with the fact that, normally, AAO has much higher catalytic efficiency oxidizing aromatic alcohols than aldehydes, with those ring substituents promoting alcohol oxidation decreasing aldehyde oxidation and vice versa [7].

Table 1. Estimated kinetic constants of AAO for HMF, DFF, HMFCA and FFCA.[a]

Substrate	Structure	K_m (mM)	k_{cat} (min^{-1})	k_{cat}/K_m ($min^{-1} \cdot mM^{-1}$)
HMF	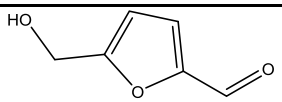	1.6 ± 0.2	40.1 ± 1.2	25.8 ± 2.4
DFF	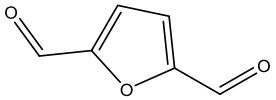	3.3 ± 0.2	31.4 ± 0.7	9.4 ± 0.5
HMFCA	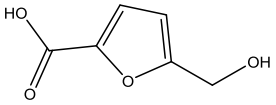	-	-	1.0 ± 0.1[b]
FFCA	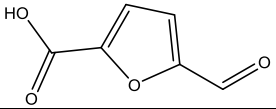	-	0	0

[a]The kinetic constants were estimated from H_2O_2 release measured in a HRP-coupled reaction. [b]AAO was not saturated at increasing HMFCA concentrations and only a k_{obs}/concentration value could be obtained.

IV. CONCLUSIONS

In the present study, the alcohol oxidase and aldehyde oxidase activities of AAO are shown in a double reaction, resulting in the oxidation of the corresponding carbonyl and carboxyl groups in the HMF molecule, at the same time that equimolecular amounts of H_2O_2 are formed in each step, although with catalytic efficiencies lower than for the best aryl-alcohol substrates of the enzyme. The complete enzymatic conversion of HMF into FDCA, if intended, would require the cooperation of a second oxidoreductase oxidizing FFCA, such as a hemethiolate peroxidase [8], at expenses of the H_2O_2 generated by AAO.

V. ACKNOWLEDGEMENT

The present work has been supported by the INDOX EU project (KBBE-2013-7-613549) and the HIPOP Spanish project (BIO2011-26694). J.C thanks an FPU fellowship of the Spanish Ministry of Education.

VI. REFERENCES

[1] Thomas S.M.; DiCosimo R.; Nagarajan A. Biocatalysis: applications and potentials for the chemical industry**.** *Trends Biotechnol.* **2002**, *20,* 238-242.

[2] Bozell J.J.; Petersen G.R. Technology development for the production of biobased products from biorefinery carbohydrates-the US Department of Energy's "Top 10" revisited**.** *Green Chem.* **2010**, *12,* 539-554.

[3] Moreau C.; Belgacem M.N.; Gandini A. Recent catalytic advances in the chemistry of substituted furans from carbohydrates and in the ensuing polymers**.** *Topics in Catalysis* **2004**, *27,* 11-30.

[4] Rosatella A.A.; Simeonov S.P.; Frade R.F.; Afonso C.A. 5-Hydroxymethylfurfural (HMF) as a building block platform: Biological properties, synthesis and synthetic applications**.** *Green Chem.* **2011**, *13,* 754-793.

[5] Ruiz-Dueñas F.J.; Martínez A.T. Microbial degradation of lignin: How a bulky recalcitrant polymer is efficiently recycled in nature and how we can take advantage of this**.** *Microbial Biotechnol.* **2009**, *2,* 164-177.

[6] Ruiz-Dueñas F.J.; Ferreira P.; Martínez M.J.; Martínez A.T. In vitro activation, purification, and characterization of *Escherichia coli* expressed aryl-alcohol oxidase, a unique H2O2-producing enzyme**.** *Protein Express. Purif.* **2006**, *45,* 191-199.

[7] Ferreira P.; Hernández-Ortega A.; Herguedas B.; Rencoret J.; Gutiérrez A.; Martínez M.J.; Jiménez-Barbero J.; Medina M.; Martínez A.T. Kinetic and chemical characterization of aldehyde oxidation by fungal aryl-alcohol oxidase**.** *Biochem. J.* **2010**, *425,* 585-593.

[8] van Deurzen M.P.J.; van Rantwijk F.; Sheldon R.A. Chloroperoxidase-catalyzed oxidation of 5-hydroxymethylfurfural**.** *J. Carbohyd. Chem.* **1997**, *16,* 299-309.

SYNTHESIS OF FUNCTIONALIZED XYLAN DERIVATIVES FOR MACROMOLECULAR ENGINEERING

Maud Chemin[1,2], Alex Rakotovelo[1,2], Frédérique Ham-Pichavant[1,2], Carine Alfos[3], Denilson da Silva Perez[4], Michel Petit-Conil[4], Henri Cramail[1,2], Stéphane Grelier[1,2]*

[1]Univ. Bordeaux, LCPO, UMR 5629, 16 av. Pey Berland, Pessac, F-33600, France
[2]CNRS, LCPO, UMR 5629, 16 av. Pey Berland, Pessac, F-33600, France
[3]ITERG, 11 rue Gaspard Monge, Parc Industriel, Pessac cedex, F-33600, France
[4]FCBA, New Materials Division, Domaine universitaire, CS90251, Grenoble cedex9, F-38044, France
*(*stephane.grelier@enscbp.fr)*

ABSTRACT

The purpose of this study was to target functionalized xylan derivatives for the design of functional materials. On the one hand, periodate oxidation was conducted on xylan from beechwood. A rate of 0.2 $NaIO_4$/xylose leads to 5-7 oxidized units per chain. On the other hand, controlled sulfuric acidic hydrolysis of xylan from beechwood was performed to get well-defined xylooligosaccharides. The reaction took place at 0.7 M H_2SO_4 at 90°C for 45 minutes of hydrolysis with 27 wt.% yield. Finally, reductive amination was used on the aldehyde functions of xylan derivatives to functionalize them, either with a double bond or with an azide function. The whole process involves renewable starting materials whose chemical modification can open the route to the design of new functional biomaterials.

I. INTRODUCTION

Nowadays, the scientific community is working on renewable resources to find an alternative to fossil resources towards sustainable development. Lignocellulosic biomass knows a growing interest as starting materials for biofuels, biochemicals or new highly valued biomaterials. Hemicelluloses represent roughly one-fourth to one-third of the total organic material. The most important ones are O-acetyl-(4-O-methylglucurono)xylans, amounting to about 80-90% of total hardwood hemicelluloses [1]. Xylans have many potential commercial applications in healthcare, cosmetics, food and other industries. Extensive literature data reports on the isolation, characterization, derivatization and applications of xylans [2]–[6]. The chemical modification and/or degradation of hemicelluloses into oligomers could further widen the range of future uses of these materials.

This work aims at studying chemical modifications of xylan from beechwood though periodate oxidation and acidic hydrolysis. More precisely, the oxidation of xylan brings new aldehyde functions in a controlled manner and acidic hydrolysis leads to well-defined oligomers with an aldehyde group at the reductive end. Those aldehyde groups, using reductive amination, allow the functionalization of these xylan derivatives. Click chemistry will then open the route to macromolecular engineering and thus new opportunities to add value to this high potential bioresource as functional materials.

II. EXPERIMENTAL

Ultrafiltration

Beechwood xylan obtained from Sigma Aldrich (X-4252) was solubilized in deionized water at 50 g/L under magnetic stirring over night. Ultrafiltration was performed in a cross flow filtration system (Startoflow Slice 200 Benchtop System) using a Slice 200 cassette holder together with a peristaltic pump. The membrane used was a 0.45 µm molecular weight cut-off hydrosart membrane. Both the retentate and the filtrate were then freeze-dried.

Periodate oxidation

Periodate oxidation was conducted following an adapted method from Gomez et al. [7]. Ultrafiltrated xylan (1 g) was dissolved in 60 mL of deionized water in a dark flask. Then 10 mL of sodium periodate solution was added under magnetic stirring to have 0.2 $NaIO_4$/xylose ratio. Deionized water was then added to reach a final volume of 100 mL. The solution was stirred in the dark for 6 hours in a thermostatic water bath at 25°C. Unreacted $NaIO_4$ was then quenched with 1 mL of ethylene glycol. The oxidized product was purified using precipitation,

first by the addition of NaCl and ethanol twice and then using NaCl and acetone. The precipitate was then washed with ethanol and dried under vacuum. The determination of the aldehyde content was achieved by the hydroxylamine hydrochloride method [8]. In this process, one equivalent of hydrochloride acid is released for one equivalent of aldehyde on the xylan backbone; the hydrochloride acid is then titrated using NaOH.

Synthesis of oligosaccharides

Xylan was solubilized in sulfuric acidic media (0.7M) at 50 g/L. The solution was heated at 90°C for 45 minutes under magnetic stirring. After reaction the solution was cooled down with ice and neutralized using a saturated barium hydroxide solution. Finally, centrifugation was conducted to remove the salt that precipitated and the supernatant was freeze dried. Oligosaccharides were purified by selective ethanol purification (1:9). The purification was done twice before drying the precipitate under vacuum.

Reductive amination

Xylan was dissolved in deionized water at 100 g/L. 5 eq. of amine (2-aminoethylazide or allylamine) was added under magnetic stirring, followed by $NaBH_3CN$ (5 eq.). The mixture was stirred at 50°C for three days. The solution was then precipitated in ethanol three times (1:10) to remove the excess of amine and $NaBH_3CN$. The product was finally dried under vacuum [9].

Size Exclusion Chromatography (SEC)

Molecular masses (M_w) of xylan and derivatives' were determined by SEC, with three TSK gel columns G3000PW G4000PW G3000PW from TOSOH BIOSCIENCE with a refractive index (RI) detector (RID-10A, Shimadzu). The columns were calibrated using pullulan standards. Samples were dissolved in deionized water at a concentration of 6 g/L and the flow rate was 0.7 mL/min (H_2O pH 12 as eluent). Pullulan standards for RI detection SEC were purchased from Polymer Standards Service for lower M_w and from Showa Denko for higher M_w.

Mass spectroscopy

MALDI-TOF analyses were performed on a Voyager mass spectrometer (Applied Biosystems). The instrument is equipped with a pulsed N_2 laser (337 nm) and a time-delayed extracted ion source. Spectra were recorded in the positive-ion mode using the reflectron and with an accelerating voltage of 20 kV. Samples and matrix were dissolved in H_2O. The matrix 2,5-dihydroxybenzoic acid solution was prepared at 10 g/L. The solutions were combined in a 10:1 volume ratio of matrix to sample. One to two microliters of the obtained solution was deposited onto the sample target and vacuum-dried.

III. RESULTS AND DISCUSSION

Periodate oxidation on beechwood xylan

Raw xylan was filtrated and characterized by SEC-RI to obtain a degree of polymerization (DP) around 50. The oxidation reaction was conducted at 0.2 $NaIO_4$/xylose ratio and the periodate concentration was measured throughout the reaction by following the absorption at 225 nm over 6 hours [7], [10]. The reaction was repeated twice, and good repeatability of the results was obtained (**Figure 1**). The periodate concentration reaches a constant value superior to zero after 210 minutes of reaction and 90% of the total periodate was consumed.

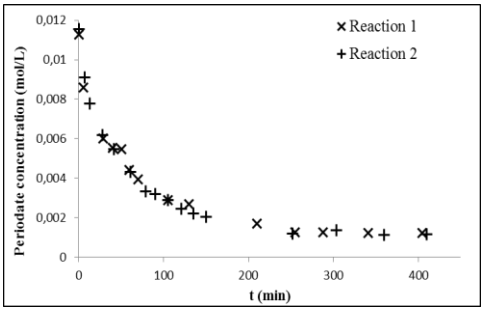

Figure 1. Spectrometric follow-up

Periodate oxidation of hemicelluloses often leads to non-desired depolymerization [11]. SEC-RI analyses were then performed on the oxidized samples after purification in order to study a potential variation of molar mass. A slight diminution - but not significant - of the molar mass was observed. The degree of oxidation was determined by the hydroxylamine hydrochloride method [8] allowing the titration of aldehyde functions and was found to be

0.15, a value close to the theoretical one (0.18 according to the maximal of 90% consumed periodate). Taking into account the DP of filtrated xylan, one can conclude the opening of 5-7 xylose units per chain for 0.2 $NaIO_4$/xylose ratio.

Synthesis of oligomers

The hydrolysis of 500 mg of xylan in 0.7 M sulfuric acid medium at 90°C for 45 minutes was performed several times and the procedure was found reproducible, with a yield close to 85 wt.%. SEC-RI showed a typical chromatogram exhibiting a multimodal feature (dashed curve on **Figure 2**).

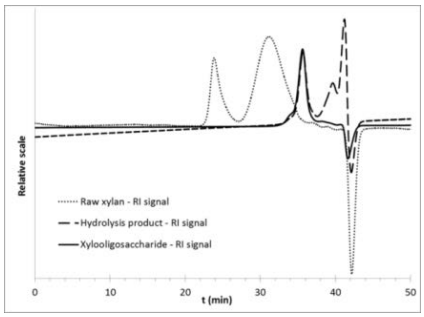

Figure 2. SEC-RI chromatograms of raw xylan, hydrolysis product and oligosaccharide

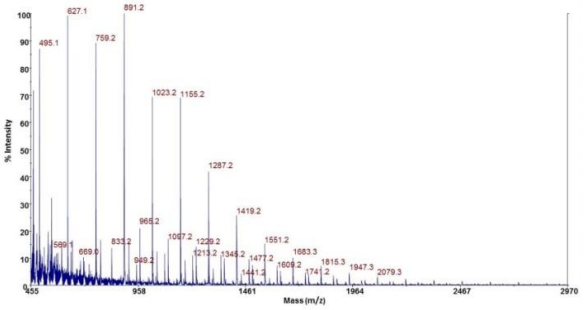

Figure 3. MALDI-TOF spectrum of oligosaccharides showing three overlapping series

A first population eluted at 36 min corresponded to oligomers with an M_w of about 3000 g/mol (pullulan calibration). The peak at 41 min was attributed to free xylose units produced by the acidic hydrolysis, as proved by the elution of commercial xylose under the same conditions. A third peak at 39 min was assumed to correspond to the elution of dimer composed of one xylose unit bonded to one glucuronic acid unit. Indeed, the α-(1→2) link between the xylose and glucuronic acid units is more resistant to acidic hydrolysis than the β-(1→4) link between two xylose units [7]. The so-formed oligosaccharides were isolated by precipitation in ethanol (solid curve on **Figure 2**) and represented 27 wt.% of the total mass. The positive-ion MALDI-TOF spectrum of so-formed oligosaccharides (**Figure 3**) showed three partially overlapping series of oligosaccharides. The difference in the masses of two adjacent peaks in each series corresponded to one anhydroxylose unit, i.e. 132.0 mass units. The peaks in the most important series were identified on the basis of their exact molar mass as corresponding to oligomers with DP values 2-14 and 1 glucuronic acid substituent per chain. In a similar manner, the two remaining series consisted of either neutral xylooligosaccharides with DP values of 4-13 or oligomers with DP values 4-10 with 2 glucuronic acid substituents. For molar masses higher than 2100 g/mol, however it was difficult to distinguish between all series.

Functionalization by reductive amination

The reducing end of the so-formed oligosaccharides was functionalized by the amination (see experimental section) of the reducing end. On one hand, a double bond has been introduced on the oligomer using allylamine, on the other hand an azide function has been introduced using 2-aminoethylazide (**Figure 4**).

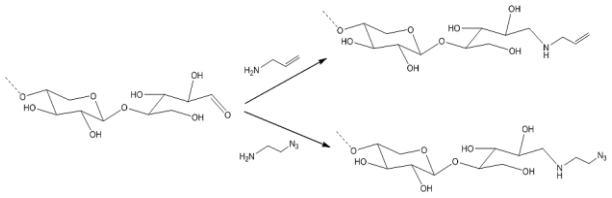

Figure 4. Scheme of reductive amination on the reductive end

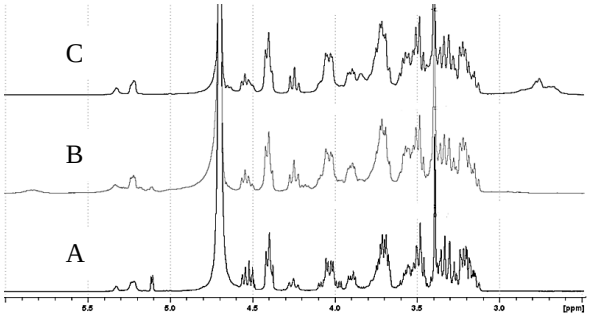

Figure 5. ^{1}H NMR spectra of A-oligosaccharides, B-oligosaccharides with allylamine and C-oligosaccharides with aminoethylazide

^{1}H NMR analyses were performed to check that the reaction worked. Data revealed the appearance of new proton signals. On **Figure 5-B**, signals at 5.10-5.45 (2H, $=CH_2$) and 5.75-5.95 (1H, -CH=) ppm was assigned to allylamine. On **Figure 5-C**, signals at 2.55-3.00 (4H, $-CH_2-CH_2-$) ppm was assigned to 2-aminoethylazide.

IV. CONCLUSIONS

On one hand, beechwood xylan was oxidized using sodium periodate to obtain aldehyde functionalized xylan. Xylan was oxidized at a ratio of 0.2 $NaIO_4$/xylose without any degradation to have 5-7 modified xylose units per chain. On the other hand, well-defined oligosaccharides were obtained by the partial hydrolysis (45 min in 0.7 M sulfuric acid at 90 °C) of xylan. The latter mostly contain two to eight xylose units in their backbone and have only one glucuronic acid unit, i.e. they have a molar mass of 500-1300 g/mol. The reductive end of oligosaccharides was functionalized by reductive amination on the aldehyde group, which allowed bringing a specific functionality on these xylan derivatives, i.e. double bond or azide function. The use of these new functional blocks in the design of original functional biomaterials will broaden the potential of xylan.

V. ACKNOWLEDGEMENT

This work is financially supported by the Aquitaine Council, ITERG, FCBA and ANR-10-EQPX-16 XYLOFOREST. The authors thank C. Absalon (CESAMO, Institut des Sciences Moléculaires, Université de Bordeaux, Talence (33), France) for MALDI-TOF experiments.

VI. REFERENCES

[1] P. Mäki-Arvela, T. Salmi, B. Holmbom, S. Willför, and D. Y. Murzin, "Synthesis of sugars by hydrolysis of hemicelluloses--a review.," *Chem. Rev.*, vol. 111, no. 9, pp. 5638–66, Sep. 2011.

[2] M. S. Izydorczyk and C. G. Biliaderis, "Cereal arabinoxylans: advances in structure and physicochemical properties," *Carbohydr. Polym.*, vol. 28, no. 1, pp. 33–48, 1995.

[3] A. Ebringerová and Z. Hromádková, "Xylans of industrial and biomedical importance," *Biotechnol. Genet. Eng. Rev.*, vol. 16, pp. 325–346, 1999.

[4] A. Ebringerova and T. Heinze, "Naturally occurring xylans structures , isolation procedures and properties," *Macromol. Rapid Commun.*, vol. 21, pp. 542–556, 2000.

[5] F. Peng, P. Peng, F. Xu, and R.-C. C. Sun, "Fractional purification and bioconversion of hemicelluloses," *Biotechnol. Adv.*, vol. 30, no. 4, pp. 879–903, 2012.

[6] R. Deutschmann and R. F. H. Dekker, "From plant biomass to bio-based chemicals: Latest developments in xylan research," *Biotechnol. Adv.*, vol. 30, pp. 1627–1640, 2012.

[7] C. G. Gomez, M. Rinaudo, and M. A. Villar, "Oxidation of sodium alginate and characterization of the oxidized derivatives," *Carbohydr. Polym.*, vol. 67, no. 3, pp. 296–304, 2007.

[8] H. Zhao and N. D. Heindel, "Determination of degree of substitution of formyl groups in polyaldehyde dextran by the hydroxylamine hydrochloride method," *Pharm. Res.*, vol. 8, no. 3, pp. 400–402, 1991.

[9] C. Schatz, S. Louguet, J.-F. Le Meins, and S. Lecommandoux, "Polysaccharide-block-polypeptide Copolymer Vesicles: Towards Synthetic Viral Capsids," *Angew. Chemie Int. Ed.*, vol. 48, no. 14, pp. 2572–2575, 2009.

[10] K. Babor, "Periodate oxidation of saccharides . III .* Comparison of the methods for determining the consumption of sodium periodate and the amount of formic acid formed," vol. 27, no. 5, pp. 0–4, 1973.

[11] I. M. N. Vold, K. A. Kristiansen, and B. E. Christensen, "A study of the chain stiffness and extension of alginates, in vitro epimerized alginates, and periodate-oxidized alginates using size-exclusion chromatography combined with light scattering and viscosity detectors.," *Biomacromolecules*, vol. 7, no. 7, pp. 2136–46, Jul. 2006.

[12] E. L. Springer, "Prehydrolysis of hardwoods with dilute sulfuric acid," *Ind. Eng. Chem. Prod. Res. Dev.*, vol. 24, no. 4, pp. 614–623, 1985.

EFFECT OF AMPHIPATHIC LIGNIN DERIVATIVE ON SIMULTANEOUS SACCHARIFICATION AND FERMENTATION (SSF) OF SOFTWOOD PULP FOR BIOETHANOL PRODUCTION

Ningning Cheng[1], Keiichi Koda[2], Yutaka Tamai[2] and Yasumitsu Uraki[2]*

[1] Graduate School of Agriculture, Hokkaido University, Sapporo 060-8589, Japan. (luna@for.agr.hokudai.ac.jp)
[2] *Research Faculty of Agriculture, Hokkaido University, Sapporo 060-8589, Japan.*
*(*uraki@for.agr.hokudai.ac.jp)*

ABSTRACT

We have already reported that amphipathic lignin derivatives from hardwood acetic acid lignin and soda-lignin of sago significantly improved saccharification efficiency of lignocellulose, and maintained cellulase activity at a high level even after enzymatic saccharification [1, 2]. In this study, a similar amphipathic derivative was prepared from cedar soda-lignin by the reaction with dodecyloxy-polyethylene-glycol-glycidylether (DAEO) under alkaline conditions, and applied to simultaneous saccharification and fermentation (SSF) process.

Prior to an SSF experiment, we confirmed that the amphipathic lignin derivative (A-SL) did not suppress glucose fermentation with Japanese sake yeast. Subsequently, an SSF for unbleached soda-pulp of cedar in the presence or absence of A-SL was conducted with Genencor GC220 (10 FPU/g of substrate) and the Sake yeast. After pre-enzymatic saccharification for 12h and SSF for 6 days, the finally produced ethanol concentration in the presence of A-SL was 49.4 g/L, while that in the absence of A-SL as a reference run was 37.8 g/L. These values corresponded to 64.1% and 49.0%, respectively, based on the theoretical maximum ethanol production. Thus, the amphipathic lignin derivative is a very useful additive to increase bioethanol production on SSF.

I. INTRODUCTION

Japanese cedar (*Cryptomeria japonica*) is a typical and abundant plantation wood in Japan among several Japanese softwoods. Recently, the utilization of cedar timber from forest thinning became an urgent task to promote [3]. A possible approach to this is to convert the cedar components to chemicals, such as bioethanol and other fermented products, through saccharification of polysaccharides in the wood.

SSF processes have been proposed to be a promising method for bioethanol production, because an end-product inhibition for cellulolytic enzyme was very scare [4], resulting in reduction in the processing time, and an increase in the ethanol production. However, a traditional SSF, in which all substrates were added to the SSF media and processed simultaneously, was not necessarily highly efficient, because enzymatic saccharification of a substrate was a limiting step. As a modified process, continuously charge of a substrate was proposed in SSF, which was termed as fed-batch SSF [5].

Lignin is one of the most abundant woody biomass components, and is used only for fuel in pulp and paper manufacturing. To create a sustainable human society based on recycling of natural resources, utilizations of lignin, especially its conversion to added-value biorefinery products, have drawn much attention [6]. As one of functional lignin-based materials, we have already developed amphipathic lignin derivatives, which were prepared by coupling of technical lignin with epoxylated poly (ethylene glycol). These derivatives were found to efficiently improve enzymatic saccharification of lignocellulose, and maintains cellulase activity at a high level for a long period even after repeated runs of enzymatic saccharification [1, 2] in addition to significant surface activity and dispersibility for cement [7]. In the present study, a similar amphipathic lignin derivative was prepared from cedar soda-lignin, and effect of the amphipathic lignin derivative on the fed-batch SSF was investigated.

II. EXPERIMENTAL

Preparation of an amphipathic lignin derivative

Cedar soda-lignin (SL) was obtained from the spent liquor of the soda pulping of cedar by precipitation with HCl solution. The crude lignin was washed with water until pH 4, and then lyophilized. SL (10 g) was reacted with dodecyloxy-polyethylene-glycol-glycidylether (45 g, **Figure 1**) under alkaline conditions, and the reactant was purified by combination of ultrafiltration (cut-off molecular mass, 1000 Da, Advantec) and washing with water. The ultrafiltration residue was lyophilized to yield A-SL.

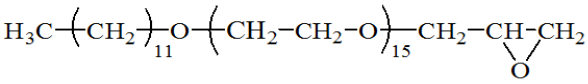

Figure 1. Chemical structure of dodecyloxy-poly (ethylene glycol) glycidylether

PEG content in A-SL was determined by modified Morgan method [8]. Water surface tension in the presence of A-SL was measured by Du Noüy ring method [7].

Glucose fermentation of Japanese sake yeast

Japanese sake yeast, *Saccharomyces cerevisiae*, (2 g of dry powder, Mauri Yeast Australia Pty Ltd., Queensland, Australia) was dispersed in 100 mL of YP medium (0.05 M, citrate buffer pH 4.8 including 10 g/L of yeast extract and 20 g/L of peptone) with 3 g of glucose, and incubated for 2 days at 38 °C. Ten grams of glucose was dissolved in 80 mL of YP medium, and 20 mL of the incubated yeast in YP medium and A-SL (0.25 g) were added to the glucose solution. The mixture was incubated for 4 days at 38 °C with gentle shaking at 100 rpm. An aliquot was taken out every day, and ethanol concentration in the aliquot was measured by GC (Shimadzu-GC2010) with a capillary column (0.25 mmϕ × 30 m; TC-WAX, GL Science, Tokyo, Japan).

Fed-batch SSF with and without A-SL

Anthraquinone-soda unbleached pulp of Japanese cedar with 6.9 % Klason lignin content as a substrate for SSF was kindly supplied from Forestry and Forest Products Research Institute, Tsuka, Japan. An outline of SSF process is illustrated in **Figure 2**. Firstly, 6 g of pulp was pre-hydrolyzed in 70 mL of citrate buffer (0.05 M, pH 4.8) with an addition of 60 filter paper unit (FPU) [9] of cellulase, Genencor GC220 (solution; Genencor International Inc., USA; Lot # 4901121718), for 12 h at 50 °C together with or without 0.25 g of A-SL. Afterwards, the incubated medium of sake Yeast was inoculated into the pre-hydrolyzed pulp suspension, and the mixture was gently shaken at 100 rpm at 38 °C until the produced ethanol concentration became constant. During this fermentation, the pulp and the cellulase were added intermittently, as shown in **Figure 2**. The total charges of the cellulase and the pulp in this SSF were 180 FPU and 18 g, respectively; the charge ratio of cellulase was 10 FPU/g of substrate. An aliquot was taken out every day, and its ethanol concentration was measured by GC. SSF experiment under the same condition was attempted in duplicate, therefore, the ethanol concentration was represented as the average. The ethanol yield based on theoretical maximum ethanol production was calculated according to the following equation:

$$\%\ of\ theoretical\ ethanol\ yield = \frac{[EtOH]_f - [EtOH]_o}{0.51\ (f\ [biomass]1.11)} \times 100\%$$

where $[EtOH]_f$ is ethanol concentration at the end of the fermentation (g/L), $[EtOH]_o$ is ethanol concentration at the beginning of the fermentation (g/L), [Biomass] is biomass consistency at the beginning of the fermentation (g/L), *f* is cellulose fraction of dry biomass (g/g; 0.756 in this study) and 0.51 is conversion factor for glucose to ethanol based on stoichiometrical fermentation of yeast [10]. In this study, the denominator value in the equation was 77.1.

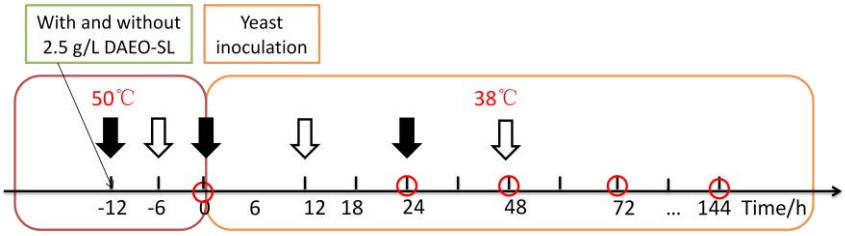

Figure 2. Time schedule for reactant charge and sampling during SSF process

(○, sampling for ethanol determination every day;

⇩, charge of 3 g pulp; ⬇, charge of 3 g pulp and 60 FPU cellulase)

III. RESULTS AND DISCUSSION

Surface tension of A-SL

A-SL comprised of hydrophobic SL and hydrophilic PEG (66.1 wt% on A-SL), the structure of which was essentially similar to those of amphipathic compounds in general. Such compounds, represented as a detergent, generally showed surface activity. To examine the surface activity of A-SL, water surface tension upon

increasing A-SL concentration was monitored by using Du Noüy tensiometer. **Figure 3** shows water surface tension vs. A-SL concentration. The profile consisted of two lines. The crossing point reveals a citrate micelle concentration (CMC). Therefore, the amphipathic lignin derivative from cedar soda-lignin clearly show the CMC at 2.0×10^{-4} g/mL, suggesting that it has high surface activity as well as amphipathic lignin derivatives from different isolated lignins previously reported [1].

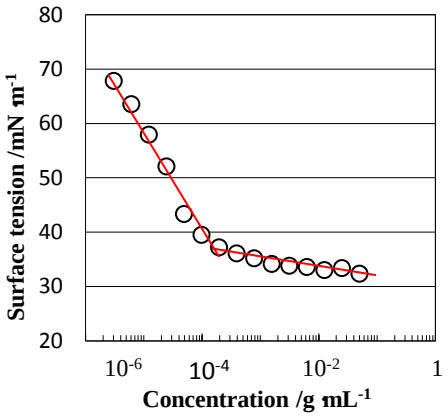

Figure 3. Surface tension-concentration isotherm for A-SL

Influence of A-SL on ethanol fermentation of glucose with Japanese sake yeast

An SSF process includes two kinds of main reactions. One is enzymatic hydrolysis of cellulose to convert it to fermentable sugar (mainly glucose). The other is ethanol fermentation of the produced glucose with yeast. As a preliminary experiment, we confirmed that A-SL also significantly improved enzymatic saccharification efficiency for unbleached cedar pulp, and maintained the cellulase activity at a high level even after saccharification as well as other amphipathic lignin derivatives from different origins [1, 2]. However, the influence of A-SL on yeast fermentation of glucose has not been studied. So we examined influence of A-SL on yeast fermentation prior to SSF experiment. **Figure 4** shows the relationship between fermentation time and ethanol production. The maximum ethanol concentration in the presence and absence of A-SL was identical. However, the fermentation time to reach the maximum ethanol concentration in the presence of A-SL was 2-days shorter than that in the absence of A-SL as a control experiment. This result suggested that A-SL did not suppress the yeast fermentation, rather it accelerated the fermentation.

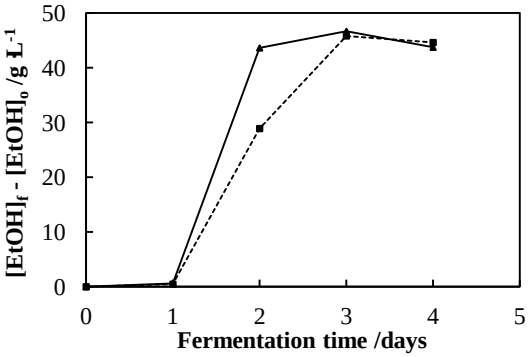

Figure 4. Effect of A-SL on ethanol fermentation of glucose.
-▲-, in the presence of A-SL; -■-,in the absence of A-SL.

Effect of A-SL on fed-batch SSF

Figure 5 shows ethanol production in SSF with and without A-SL. The ethanol production at the first day of SSF was dramatically enhanced by the addition of A-SL, due to the fact that a larger amount of glucose was produced in the pre-hydrolyzed process by the help of A-SL. Furthermore, the produced ethanol concentration in the presence of A-SL almost reached maximum at 4-days SSF, while the concentration gradual increased until 6 days. After SSF for 6 days, the produced ethanol concentration in the presence of A-SL was 49.4 g/L, which was corresponded to 64.1 % based on the theoretical maximum ethanol production. On the other hand, the final ethanol concentration and the yield on the theoretical value in absence of A-SL as a control were 37.8 g/L and 49.0 %, respectively. These results obviously suggest that the amphipathic lignin derivative from cedar soda-lignin is also very useful for SSF.

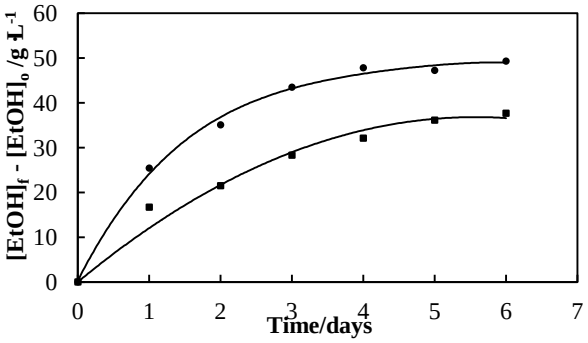

Figure 5. Ethanol production in SSF with cellulase of 10.0 FPU/g cedar pulp in the presence of A-SL (-●-) and absence of A-SL (-■-).

IV. CONCLUSIONS

From the preliminary experiments, A-SL was found to improve enzymatic saccharification efficiency of unbleached pulp and ethanol fermentation of glucose with Japanese sake yeast. On the basis of these functions of A-SL, the fed-batch SSF process of unbleached soda-pulp from Japanese cedar was conducted with pre-incubated yeast and cellulase (total charge, 10 FPU/g of substrate). The ethanol production in SSF was remarkably improved by the addition of A-SL, probably due to a combination of increased saccharification efficiency and improved yeast fermentation. Thus, this amphipathic lignin derivative prepared from cedar soda-lignin is considered to be a promising additive for SSF. Now, we are under the investigation on the ethanol production at high concentration.

V. REFERENCES

[1] Winarni, I.; Oikawa, C.; Yamada, T.; Igarashi, K.; Koda, K.; Uraki, Y. Improvement of Enzymatic Saccharification of Unbleached Cedar Pulp with Amphipathic Lignin Derivatives. *Bioresources* **2013**, 8(2), 2195-2208

[2] Winarni, I.; Koda, K.; Pari, G.; Waluyo, T.K.; Uraki Y. Enzymatic saccharification of sago pulp from starch extraction waste using sago lignin-based amphipathic derivatives. *J. Wood Chem. Technol.* **2014**, 34, 157-168

[3] Amirta, R.; Tanabe, T.; Watanabe, T.; Honda, Y.; Kuwahara, M.; Watanabe, T. Methane fermentation of Japanese cedar wood pretreated with a white rot fungus, Ceriporiopsis subvermispora. *J Biotechnol.* **2006**, 123, 71-77

[4] Olofsson, K.; Bertilsson, M.; Lidén G. A short review on SSF – an interesting process option for ethanol production from lignocellulosic feedstocks. *Biotechnology for Biofuels* **2008**, 1:7

[5] Elliston, A.; Collins, S. R. A.; Wilson, D. R.; Roberts, I. N.; Waldron, K. W. High concentrations of cellulosic ethanol achieved by fed batch semi simultaneous saccharification and fermentation of waste-paper. *Bioresour. Technol.* **2013**, 134, 117–126

[6] Uraki, Y.; Ishikawa, N.; Nishida, M.; Sano, Y. Preparation of amphiphilic lignin derivative as a cellulase stabilizer. *J. Wood Sci.* **2001**, 47, 301-307

[7] Aso, T.; Koda, K.; Kubo, S.; Yamada, T.; Nakajima, I.; Uraki, Y. Preparation of novel lignin-based cement dispersants from isolated lignins. *J. Wood Chem. Technol.* **2013**, 33(4), 286-298

[8] Homma, H.; Kubo, S.; Yamada, T.; Matsushita, Y.; Uraki, Y. Preparation and characterization of amphiphilic lignin derivatives as surfactants. *J. Wood Chem. Technol.* **2008**, 28(4), 270-282

[9] Ghose, A. T. K. Measurement of cellulase activities. *Pure Appl. Chem.* **1987**, 59(2), 257-268

[10] Hayward,T. K.; Combs, N. S.; Schmidt, S. L.; Philippidis, G. P. SSF Experimental Protocols: Lignocellulosic Biomass Hydrolysis and Fermentation. *National Renewable Energy Laboratory, Golden, CO, USA LAP-008* **1995**

CHARACTERIZATION OF *EUCALYPTUS GLOBULUS* LIGNINS PRODUCED BY KRAFT AND ORGANOSOLV PROCESS

C.A. Costa *, P.C.R. Pinto, A.E. Rodrigues

Laboratory of Separation and Reaction Engineering - LSRE, Associate Laboratory LSRE/LCM,
Department of Chemical Engineering, Faculty of Engineering,
University of Porto, Rua Dr. Roberto Frias s/n, 4200-465 Porto. Portugal

ABSTRACT

In this study a comprehensive and comparative analysis of *Eucalyptus globulus* lignins was performed in order to evaluate the impact of the delignification process in the structure of lignin (functional groups, linkages and type of structures), and to find the main structural features related with the lignin potential to produce aldehydes. Another objective was the study of *E. globulus* lignin structure produced by bark mild acidolysis, and the further comparison, presented for the first time, with the lignin from the respective wood. The structural analysis of the different *E. globulus* lignins reveals the influence of the chemical process applied on lignin functionality and reactivity. This conclusion represents an important tool for the selection of lignin types and processes to a valorization route within a lignocellulosic-based biorefinery.

I. INTRODUCTION

Lignin is a three dimensional phenolic polymer composed by three sub-units types, p-hydroxyphenyl (H), guaiacyl (G) and syringyl (S). These units are linked through aryl ether bonds (β-*O*-4, α-*O*-4, 4-*O*-5) and C-C linkages (5-5', β-5, β-1, β–β) [1]. Lignin is the second most abundant biopolymer on the earth next to cellulose, and obtained as industrial waste from pulp and paper industries. Moreover, the emerging biorefining activity is also producing side streams containing lignin that claims for valorization due to environmental and economic issues. The chemistry and structure of lignin makes it an interesting raw material for a wide variety of applications, and a potential source of high-added-value chemicals [2]. However its reactivity toward chemical processes depends of the chemical structure, which is related with biomass species and delignification process [3]. In this work, a full characterization of four *E. globulus* lignins was performed in order to evaluate the influence of the delignification type on its structure. To the best of our knowledge, there is no comparative study for *E. globulus* lignins from different processes with the aim of evaluating their potential as source of added-value compounds, as vanillin and syringaldehyde. The structural analysis of an *E. globulus* lignin produced by bark mild acidolysis was also presented, for the first time, since no information about this lignin is available. The knowledge about this lignin will help to define a new valorization strategy for bark generated in pulp and paper industries.

II. EXPERIMENTAL

In this work four different *Eucalyptus globulus* lignins were characterized in order to evaluate the influence of the industrial process on its structure: L*Eg*Org –lignin produced by organosolv process, L*Eg*Kraft – lignin isolated and further purified from industrial black liquor (obtained by kraft process), and lignins produced by wood (LD*Eg*) and bark (LDEg_{bark}) mild acidolysis. The contaminants content of lignin samples were analyzed with reference to inorganic material (gravimetric quantification of ashes after incineration of lignin samples at 650 °C for 6h) and carbohydrates. For carbohydrate analysis the lignins were submitted to acid methanolysis; about 15 mg of sample was suspended in 3 mL of 2 M HCl methanolic solution, and the reaction was performed at 100 °C for 4 hours, as previously described [4]. The products were identified by GC-MS and quantified GC-FID with the equipment, experimental conditions and calibration as already described in literature [4]. Yields and types of simple phenolic aldehydes were obtained by nitrobenzene oxidation (NO). The NO experiments were performed as already described for reaction and products analysis [4]. About 30 mg of lignin was dissolved in 7.00 mL of 2 M NaOH, and 0.45 mL of nitrobenzene was added, the experiments were run at 170 °C during 4 hours. The content of functional groups and typical structures/linkages were determined by quantitative ^{13}C, ^{1}H and ^{31}P nuclear magnetic resonance (NMR) analysis, using a Bruker AVANCE III 400 spectrometer operating at 400 MHz. Molecular weight of phenylpropane unit (M_{ppu}) was determined with the data obtained from elemental analysis.

III. RESULTS AND DISCUSSION

The analysis of contaminants shows that the ash content of all the lignin samples is lower than 1.0% while carbohydrate percentage is lower than 2.0%. These results allow inferring about the low degree of contamination of the samples. NO is a widely applied method to determine the noncondensed fraction of lignin structure. High total yields of NO are indicative of advantageous structural characteristics of lignin, considering the production of vanillin and syringaldehyde. For the studied *E. globulus* lignins higher values of NO yield were found for mild acidolysis lignins, LD*Eg* (30%) and LDEg_{bark} (32%), confirming that these samples have higher content of uncondensed structures than L*Eg*Org (25%) and L*Eg*Kraft (21%).

^{13}C NMR provides data about the carbons in different structural and chemical environments (linkages, functional groups) in lignin structure (**Figure 1**). L*Eg*Org and L*Eg*Kraft show a higher number of aromatic C-C and a slight decrease in the number of aromatic C-H comparatively to mild acidolysis lignins. This trend is related with the higher content of condensed structures in the industrial processed lignins. However, if only organosolv and kraft lignins are considered, L*Eg*Kraft has higher content of condensed structures than L*Eg*Org, demonstrating that lignin undergoes fewer transformations in the organosolv process. A low content of condensed structures is favorable for the route of valorization through vanillin and syringaldehyde production. The results also indicate that L*Eg*Org and L*Eg*Kraft show a lower content of β-*O*-4 structures and OCH_3 groups than LD*Eg* and LDEg_{bark}. The cleavage of β-*O*-4 and α-*O*-4 linkages as also the formation of condensed structures and the demethoxylation of lignins are a consequence of the reactions that occur during the delignification process that inevitably led to a change on native characteristics of lignin [5, 6].

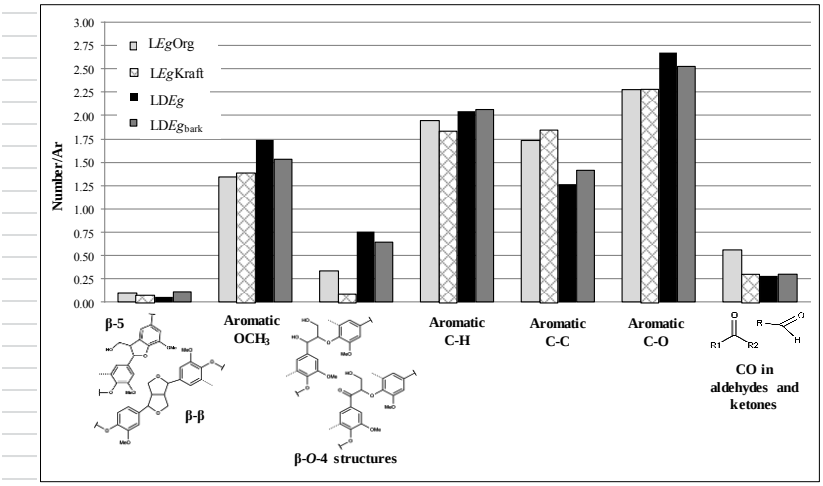

Figure 1. Quantification (number per aromatic ring) of the structures/linkages and functional groups identified by ^{13}C NMR.

With the ^{13}C NMR results it is also possible to obtain the degree of condensation (DC) and the syringyl:guaiacyl:*p*-hydroxyphenyl ratio (S:G:H) of each lignin sample (**Table 1**). Among the studied lignins, L*Eg*Org and L*Eg*Kraft show the highest values of DC, as consequence of the higher content of condensed structures in these samples than in LD*Eg* and LDEg_{bark}. DC is an important parameter for studies about lignin applications, since it represents a negative impact on lignin reactivity. The ratio S:G:H found for all the samples revels a predominance of S units as expected for this type of lignins.

Table 1. S:G:H ratio and DC calculated for the *E. globulus* lignins.

Lignin	DC (%)	S:G:H
L*Eg*Org	35	70:30:00
L*Eg*Kraft	43	74:26:00
LD*Eg*	15	80:20:00
LDEg_{bark}	17	73:23:04

Quantitative ^{31}P NMR was also applied. This method allows quantifying each type of hydroxyl groups present in lignin structure (**Figure 2**). The comparison between ^{31}P NMR results of kraft, organosolv and mild acidolysis lignins shows that de delignification process causes an increase in free phenolic OH units and a decrease in aliphatic OH groups present in lignin structure. As reported before, these structural changes result from aryl-ether cleavage that are a consequence of the delignification process conditions, that are more drastic in kraft and organosolv than in mild acidolysis [7]. Regarding the production of added-value aldehydes it is advantageous that lignin structure presents a higher content of free phenolic OH, since these units promotes lignin solubility.

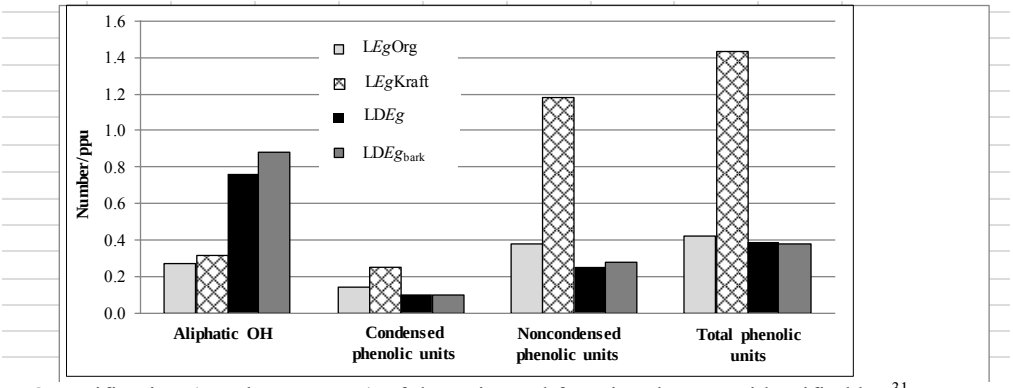

Figure 2. Quantification (number per ppu) of the units and functional groups identified by ^{31}P NMR.

Data obtained from ^{1}H NMR are in accordance with the structural features observed for ^{13}C and ^{31}P NMR; kraft and organosolv lignins present a lower content of aliphatic OH and aryl-ether structures and more phenolic OH groups than mild acidolysis lignins. NMR results also allow observing that LD*Eg*$_{bark}$ has a higher content of condensed structures than LD*Eg*. Another difference between mild acidolysis lignins is the presence of H units only in bark lignin, which leads to a S:G:H (73:23:4) different from wood lignin (80:20:0). However, LD*Eg* and LD*Eg*$_{bark}$ do not show significant differences for the other types and contents of interunit linkages and functional groups, demonstrating that *E. globulus* lignins structure produced by wood and bark mild acidolysis are similar.

Correlations between data obtained from NMR results and aldehydes yields from NO were established. The NO yields were successful correlated with DC values (**Figure 3**), clearly demonstrating that the reactivity of lignin towards NO decreases with the increases of condensed structures content.

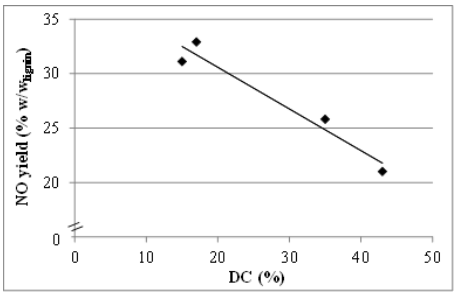

Figure 3. Plot of NO yield versus DC values obtained for *E. globulus* lignins.

A good correlation between NO yields and β-*O*-4 structures content, from ^{13}C NMR, was also obtained (**Figure 4**). This trend ascertains the correlation between the content of uncondensed structures and the content of β-*O*-4 structures obtained for each lignin sample: the higher is the content of β-*O*-4 structures, higher is the total of uncondensed structures. For lignins produced by mild acidolysis, LD*Eg* and LD*Eg*$_{bark}$, high yields of monomeric phenolic aldehydes were obtained by NO and high contents of β-*O*-4 structures were quantified by ^{13}C NMR. The results allow concluding that mild acidolysis lignins preserved a considerable fraction of its original ether structures, comparing with organosolv and kraft lignins.

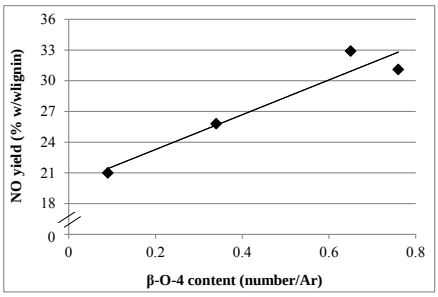

Figure 4. Plot of NO yield versus β-*O*-4 content obtained for *E. globulus* lignins.

Concerning the obtained M_{ppu} values for each lignin sample it is observed that industrial processed lignins (193-196 g/mol) have lower values than mild acidolysis lignins (207-219 g/mol), proving that the molecular mass of phenylpropane units decrease with the delignification process. The structural alterations identified for kraft, organosolv and mild acidolysis lignins have particular impact on its chemical reactivity and it allows predicting the potential of each lignin to produce aldehydes by oxidation, namely vanillin and syringaldehyde.

IV. CONCLUSIONS

The overall results show that L*Eg*Kraft and L*Eg*Org have a low content of β-*O*-4 structures and a high amount of phenolic OH groups, since during the delignification process β-aryl ether bonds are predominantly cleaved. Kraft and organosolv lignins are also more condensed (higher condensed structures content) and have lower NO yield than mild acidolysis (close to native lignins). The extent of these reactions revealed to be higher for kraft lignin than for organosolv lignin. The NO yield of each *E. globulus* lignin proved to have a good correlation with DC value and total β-aryl ether content, from ^{13}C NMR. Lignins produced by wood and bark mild acidolysis have similar structures, though the presence of H units only for LDEg_{bark} and the higher content of condensed structures for this sample than for LD*Eg*. With the obtained results is also possible to conclude that the industrial processing, particularly the kraft one, induced unfavorable changes for a valorization route involving production of functionalized phenolics by depolymerization. For this reason organosolv or a mild delignification process would be a preferable process to obtain lignin from *E. globulus* wood or bark for production of functionalized phenolics.

V. ACKNOWLEDGEMENT

Project No. 33969 Conception of bio-based products from renewable lignocellulosic sources as precursors for bioindustry of chemical synthesis and biomaterials - funded by the European Regional Development Fund (ERDF) through the Operational Programme for Competitiveness Factors (POFC) of the National Strategic Reference Framework (NSRF). This work was co-financed by FCT and FEDER under Programe COMPETE (Project PEst-C/EQB/LA0020/2013). Carina Costa thanks FCT - Fundação para a Ciência e Tecnologia (Portugal) for PhD grant SFRH/BD/89570/2012.

VI. REFERENCES

[1] Lin, S.Y.; Dence, C.W. (Eds.) *Methods in Lignin Chemistry*. 1992, Springer-Verlag: New York.
[2] Calvo-Flores, F.G.; Dobado, J.A. Lignin as renewable raw material. *Chemsuschem* **2010**, *3*, 1227-1235.
[3] Pinto, P.C.; Evtuguin, D.V.; Neto, C.P. Effect of structural features of wood biopolymers on hardwood pulping and bleaching performance. *Ind. Eng. Chem. Res.* **2005**, *44*, 9777-9784.
[4] Pinto, P.C.R.; Costa, C.E.; Rodrigues, A.E. Oxidation of lignin from *Eucalyptus globulus* pulping liquors to produce syringaldehyde and vanillin. *Ind. Eng. Chem. Res.* **2013**, *52*, 4421-4428.
[5] Pinto, P.C.; Evtuguin, D.V.; Neto, C.P.; Silvestre, A.J.D. Behavior of *Eucalyptus globulus* lignin during kraft pulping I. Analysis by chemical degradation methods *J. Wood Chem. Technol.* **2002**, *22*, 93-108.
[6] Wen, J.L.; Sun, S.L.; Yuan, T.Q.; Xu, F.; Sun, R.C. Structural elucidation of lignin polymers of *Eucalyptus* chips during organosolv pretreatment and extended delignification. *J. Agric. Food. Chem.* **2013**, *61*, 11067-11075.
[7] Ibarra, D.; Chávez, M.I.; Rencoret, J.; Del Río, J.C.; Gutiérrez, A.; Romero, J.; Camarero, S.; Martínez, M.J.; Jiménez-Barbero, J.; Martínez, A.T. Lignin modification during *Eucalyptus globulus* kraft pulping followed by totally chlorine-free bleaching: A two-dimensional nuclear magnetic resonance, fourier transform infrared, and pyrolysis−gas chromatography/mass spectrometry study. *J. Agric. Food. Chem.* **2007**, *55*, 3477-3490.

POLYALCOHOL LIQUEFACTION OF AGROFORESTRY RESIDUES

Luísa Cruz Lopes, L. P.[1]*, Sónia Lopes[1], Sónia O. Prozil[1,2], Dmitry V. Evtuguin[2], Idalina Domingos[1], José V. Ferreira[1], Hélder Viana[1] and Bruno Esteves[1]

[1] Polytechnic Institute of Viseu and CI&DETS, Viseu, Portugal; [2] University of Aveiro - Department of Chemistry, 3810-193 Aveiro, Portugal

Email: lvalente@amb.estv.ipv.pt

ABSTRACT

Liquefaction of lignocellulosic materials has been studied over the years but due to the search for new sources to replace oil-derived products the studies have increased in the last decade. Liquefaction of lignocellulosic residues was held on a double shirt reactor with heated oil using ethylene glycol (EG) catalyzed by sulfuric acid (SA) at 3%. The liquefied lignocellulosic materials were dissolved in a solution of dioxane-water in the proportion 4: 1 and filtered, determining the insoluble residue gravimetrically. Liquefaction time and temperature was optimized. To determine the chemical composition influence on liquefaction reaction, the complete chemical characterization was made: cellulose, hemicelluloses, lignin, ashes, tannins and proteins were determined.The results of the chemical analysis showed that all materials are composed mainly of cellulose, hemicelluloses, lignin, tannins and proteins. The results show that the higher the temperature, the higher the percentage of liquefaction. At the same temperature liquefaction percentage increases with the time of treatment according to a logarithmic curve approximately until it reaches a maximum and then decreases, possibly due to condensation reactions of liquefaction products.

I. INTRODUCTION

Liquefaction of lignocellulosic materials has been studied over the years but due to the search for new sources to replace oil-derived products the studies have increased in the last decade. The main liquefaction processes that have been studied in the last years are based on liquefying agents with catalysts that allow the liquefaction to be done at low temperatures and pressure. The most studied liquefied agents are phenol using an acid or base catalyst [1], polyhydric alcohols generally with an acid catalyst and cyclic carbonates [2], ionic liquids and dibasic esters. The main applications for these liquefaction procedures have been the liquefaction of wood to produce different resins in accordance with the liquefaction agent. When phenol is used there are mainly three types of resins that have been tested: Novolac type phenolic resins [3] and Resol type resins [4] from acid catalyzed liquefied wood and phenolic resins [5], from alkaline catalyzed liquefied wood [1]. Tests were also make to study the potential use of pine liquefied wood for the partial substitution of MUF resin [6].

The central region of Portugal is essentially an agroforestry region dominated by the production of residues from wood transformation (sawdust from local sawmills), hazelnut and almond shelling, olive cake from the olive oil production and grape stalks from wine production.

II. EXPERIMENTAL

Sample preparation

Hazelnut and almond shells, grape stalks and Maritime pine (Pinus Pinaster Ait) sawdust were used in the tests. The samples were sieved into three fractions > 40 Mesh, 40-60 Mesh and < 60 Mesh. The 40-60 Mesh fraction was selected for the tests.

Liquefaction reaction

Ethylene glycol (EG) was used as solvent and was used 4 parts of EG for each part of lignocellulosic material (LM) in dry state and 3% of Sulfuric Acid (SA) was added as a catalyzer based on the EG mass. In order to achieve a better liquefaction percentage the mixture was pre-stirred to obtain a more homogenous preparation. After closing the reactor the automatic stirrer was placed at ±70rpm. The liquefaction process was carried out in a Parr cylinder glass 600ml LKT PED reactor with double jacket. The liquefaction temperature was 180ºC (temperature of the oil in the jacket), and the time ranged between 15-120 min. The EG+SA+LM were inserted

inside the reactor when the oil achieved the desired temperature. To filter the residues a mixture of dioxane and water at 4:1 ratio was used to solubilize the liquefied material. A pump and a Buckner Funnel with a paper filter were used to separate the solid residues that resulted from the liquefaction. This allowed us to determine the liquefaction percentage that was calculated using the following formula:

$$\text{Liquefaction percentage (\%)} = \left(1 - \frac{Mass\ of\ residue\ (g)}{Mass\ of\ dry\ wood\ (g)}\right) \times 100$$

The water and dioxane were evaporated using a Rotary evaporator by using reduced pressure, 700mmHg provided by a vacuum pump.

Chemical composition determination

The hazelnut and almond shells, grape stalks and Maritime pine were characterised regarding the ash content, extractives (in acetone, dichloromethane and in hot water), proteins, tannins, cellulose, lignin and hemicelluloses. The ashes content was determined by calcinations of the material at 525 ºC, according to the standard procedure Tappi T 211 om-93.

The extractives content in acetone and dichloromethane were determined by Soxhlet extraction according to the Tappi T 204 om-88. The determination of extractives in hot water was carried out with a solution of ammonium citrate (10 g/L) for 1 hour under reflux (liquid-to-solid ratio 100). The proteins content in extractives-free shells, after extraction with acetone, was determined by treatment with 1% pepsin solution in 0.1 M HCl at 37ºC for 16 hours. The tannins content was assessed in extractives- and proteins-free shells by reflux with 0.3% NaOH solution (liquid-to-solid ratio 100) under nitrogen atmosphere for 1 hour. The extracted material was filtered, washed with hot water until neutral reaction of filtrate and dried at 60ºC to a constant weight. The content of tannins was assessed by the difference in weights of initial and extracted materials. The alkaline extract was precipitated by adding 3M H_2SO_4 until pH 3. After 24 hours, precipitated tannins were centrifuged and washed with water to pH 5. Finally, the tannins fraction was freeze dried. The cellulose was determined by 4 consecutive treatments with HNO_3: EtOH mixture (1:4, v/v) under reflux for 1h each according to the Kürschner and Höffer method (Browning, 1967). The lignin content in hazelnut shells free of extractives, proteins and tannins was determined by Klason method with 72% H_2SO_4 (according to Tappi T 204 om-88).

III. RESULTS AND DISCUSSION

Liquefaction reaction

The highest liquefaction was attained by wood. Even with only 15 minutes it is possible to obtain a liquefaction percentage of over 50% but the maximum liquefaction percentage (80%) is attained for about 60 min. For hazelnut shells the maximum liquefaction (60%) is attained for 30 min. The liquefaction reaction for almond shells and grape stalks is similar, both reaching a maximum liquefaction of about 40%. The only difference was that for almond shells the maximum was attained earlier, at 45 min while for grape stalks was for 60 min.

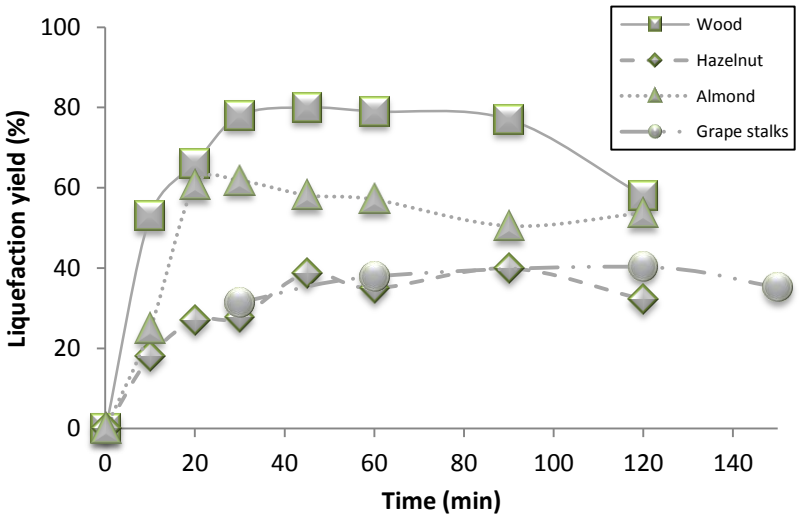

Figure 1. Liquefied material yield (%) for different reaction times.

All the reaction curves presented a similar development. With the increase in treatment time the liquefaction percentage increases, having a higher slope in the beginning of the process with a tendency similar to a

logarithmic curve. At the end there is a clear reduction on the liquefaction percentage for all the samples. The reduction at the end of the liquefaction curve has often been attributed to condensation reactions [6]. Looking at the chemical composition (Figure 2) we can see that almond shells and grape stalks have a higher percentage of tannins in relation to the other residues. It is possible that their presence influences the liquefaction percentage due to condensation reactions with other compounds at an earlier stage.

Chemical analysis

The results of the chemical analysis showed that all materials are composed mainly of cellulose, hemicelluloses, lignin, tannins and proteins as shown in Figure 2.

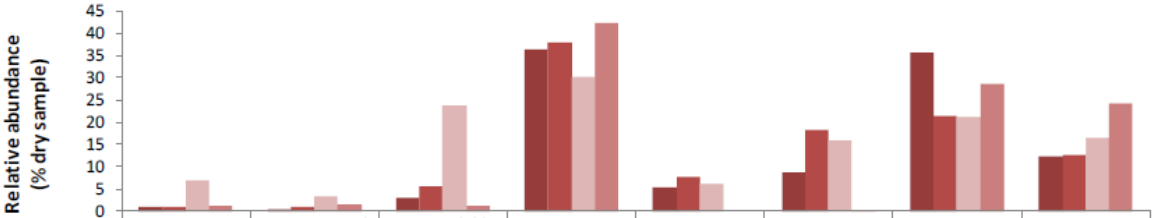

	Ash	Extractives with Acetone	Water-soluble Extractives	Cellulose	Proteins	Tannins	Lignin	Hemicelluloses
Hazelnuts Shells	0,94	0,37	2,96	36,33	5,39	8,8	35,74	12,43
Almond Shells	0,992	0,97	5,65	38,01	7,65	18,32	21,42	12,64
Grape Stalks*	7,00	3,30	23,70	30,30	6,10	15,90	21,00	16,40
Wood Sawdust	1,23	1,50	1,2	42,4	0,00	0,25	28,6	24,12

Figure 2. Chemical analysis of lignocellulosic materials.

Studies on the chemical composition revealed that all materials are lignocellulosic. The major compound in grape stalks is cellulose with about 30.3% followed by lignin (21%) and hemicelluloses (17.4%). Regarding hazelnut shells, they are mainly cellulose (36.3%), lignin (35.7%) and hemicelluloses (12.4%). Almond shells are composed mostly by 38.0% of cellulose, lignin 21.4% and 18.3% tannins. Finally the wood sawdust has 42.4% cellulose, 28.6% lignin and 24.1% hemicelluloses.

IV. CONCLUSIONS

Wood and hazelnut shells presented the highest potential for liquefaction, much higher than almond shells and grape stalks. New test have to be made to determine the best conditions for each residue.

V. ACKNOWLEDGEMENT

The authors would like to thank CI&DETS (Viseu) and the Portuguese Science Foundation for the financial support through (PEst-OE/CED/UI4016/2014).

VI. REFERENCES

[1] Zhang, Q., Zhao, G., Jie, S. 2005. Liquefaction and product identification of main chemical compositions of wood in phenol, Forestry Studies in China, 7(2), 31-37.

[2] Xie, T., Chen, F. 2005. Fast liquefaction of bagasse in ethylene carbonate and preparation of epoxy resin from liquefied product. Journal of Applied Polymer Science, 98, 1961-1968

[3] Pan, H., Shupe, T. F., Hse, C-Y, 2009. Characterization of novolac type liquefied, Eur. J. Wood Prod., 67: 427–437.

[4] Kobayashi, M., Tukamoto, K., Tomita, B. 2000. Application of liquefied wood to a new resin system-synthesis and properties of liquefied wood/epoxy resins, Holzforschung, 54(1), 93-100.

[5] Alma, M. H., Yoshioka, M., Yao, Y., Shiraishi, N., 1998. Preparation of sulfuric acid-catalyzed phenolated wood resin. Wood Sci Technol,32:297–308.

[6] Cruz Lopes, L., Martins, J., Martins, J. M., Esteves, B. 2013 Study of the potential use of pine liquefied wood for the partial substitution of MUF resin. In Proceedings of: ACCMES 2013-Asian Conference on civil, material and environmental science. 15-17 March Tokyo.

COATING OF LACCASE-ACTIVATED PHENOLS FOR THE INDUSTRIALLY-FEASIBLE FUNCTIONALIZATION OF CELLULOSE-BASED SUBSTRATES

Cusola, Oriol[1]; Valls, Cristina[1]; Vidal, Teresa[1]; Roncero, M. Blanca[1]*

*[1]CELBIOTECH_Paper Engineering Research Group. Universitat Politècnica de Catalunya-BarcelonaTech. Colom 11, E-08222 Terrassa, Spain. (*roncero@etp.upc.edu)*

ABSTRACT

The present work describes an innovative method for the hydrophobization of cellulosic material by impregnation with an enzymatically obtained functionalization solution (FS). Application of FS to the surface of previously formed cellulose sheets was found to confer them hydrophobic properties. The absorbance of functionalized sheets was assessed with the water-drop test (WDT), and their hydrophobicity from their contact angle (WCA) and the surface free energy (SFE) as determined with a goniophotometer. The proposed method is an effective choice for the hydrophobization of paper sheets, with absorption times of up to 4000 s and WCA values around 130°. Treating eucalyptus paper sheets dramatically decreased SFE (from 55 to 10 mJ/m^2), and evidences on the grafting of the FS onto the cellulosic sheets were assessed by using ATR-FTIR. The stability of FS and the control solutions was characterized in terms of Z potential and light scattering measurements.

I. INTRODUCTION

One way of hydrophobizing paper substrates is by grafting hydrophobic compounds onto lignocellulosic fibers. This, however, entails chemically altering the paper surface or using a product or reagent to bind functional groups to paper fibers. Enzymes have been shown to catalyze coupling reactions with potential use in various areas, including the field of lignocellulosic materials. This has aroused increasing industrial interest in them in recent years. Enzymes provide substantial advantages over chemical catalysts. Societal interest in green chemistry and advances in biotechnology have brought to the forefront the use of enzymes to address many of the challenges of modern synthetic organic chemistry [1]. Laccase (benzenediol:oxygen oxidoreductase, EC 1.10.3.3) is a blue multi-copper oxidase capable of catalyzing the oxidation of various low-molecular weight compounds while concomitantly reducing molecular oxygen to water. Laccases have been successfully used in biobleaching [2], and also to functionalize cellulose fibers for purposes such as internal sizing of paper [3], or obtaining paper sheets with antimicrobial properties [4], or improved wet strength properties [5]. Also, Garcia-Ubasart et al., (2012) and Sipponen et al., (2010) [6, 7] obtained hydrophobic fibers by applying laccase in combination with hydrophobic phenolic compounds to a fiber suspension. However, all previous enzyme treatments were conducted in aqueous suspensions consisting of cellulose fibers, an enzyme and the functional compound (i.e. before the paper or paper substrate was formed).

Industrially, introducing chemicals or enzymes before paper formation can alter the natural interaction between fibers and lead to paper with impaired strength-related properties and less easily recycled effluents as a result. In a previous work [8], this problem was addressed by applying a laccase treatment for the first time to finished paper in order to improve its hydrophobicity and avoid the shortcomings of the procedure traditionally applied to fiber suspensions. Although an effective method for hydrophobizing finished paper via enzymatic coupling was developed, the processing time was rather long. In fact, paper sheets required soaking in the enzyme solution for 4 h, which is a strong hindrance for industrial application since paper machines can currently operate at rates in the region of 1500 m/min. Therefore, the previously reported method by Cusola et al., (2013) [8], was not feasible to be implemented industrially in the papermaking process.

In this work, we developed a new, fast method for the surface treatment of paper sheets that is compatible with these paper processing rates. The surface treatment has the advantages that it does not affect sheet formation, uses small amounts of chemicals per functionalized area unit, is compatible with the high throughput of paper machines, can be implemented at various points in the industrial process and can be applied to sheet surfaces with existing devices. The proposed method provides an innovative tool for functionalizing paper surfaces by using the enzyme laccase to make them hydrophobic. The functionalization solution is compatible with most papermaking technologies (size pressing, speed sizing, spraying). The method is the basis for a patent filed by Cusola et al., (2012) [9].

II. EXPERIMENTAL

Paper, enzyme and chemicals

Filter paper sheets (PS) were purchased from FILTERLAB. Eucalyptus ECF pulp was supplied by ENCE® (Spain), and unbleached flax and sisal pulps were kindly supplied by CELESA®. The enzyme used was laccase (Lacc) from *Trametes Villosa* supplied by Novozymes® (Bagsvaerd, Denmark). Lauryl gallate (LG) was purchased from Sigma–Aldrich. Soluble sulfonated kraft lignin (SL) was obtained from Borreegard and used as received. The eucalyptus, flax and sisal pulp samples were refined to a variable degree (°SR) according to ISO 5264-1:1979 on a Valley mill.

Preparation of laboratory handsheets and sonication

Refined and unrefined samples from eucalyptus, flax, and sisal pulp were used to prepare handsheets in a Rapid-Köten lab former according to ISO 5269-2:2004. Filter paper sheets were used as received. All sheets were cut into circles 4 cm in diameter for surface treatment. An aqueous solution of lauryl gallate (LG) in 50 mM sodium tartrate buffer at pH 4 was sonicated on a Hielscher® UP100H at 100% amplitude for 30 min.

Laccase treatments to obtain the functionalization solution (FS) and surface application to paper sheets

The enzymatic reaction was performed in the absence of paper sheets (PS) and the resulting functionalization solution (FS), was used to impregnate paper sheets by dipping. Enzymatic treatments were performed according to the method previously reported [10]. The resulting, functionalization solution (FS) was then applied to the surface of paper sheets by dipping, and the sheets were allowed to dry in a normalized athmosphere (23ºC; 50% RH). Various control treatments were also performed by using control functionalization solutions (KFS).

Hydrophobicity assessment

Contact angles were measured with a Dataphysics® OCA15 contact angle goniometer, using a 4 µL water drop for delivery to the sample surface in each measurement. Surface free energy (SFE) was determined by applying 4 µL droplets of deionized water, ethylene glycol and 99% diiodomethane to the surface of paper sheets and determining the corresponding contact angles. Water drop tests (WDT) were performed on each treated paper specimen according to Tappi standard T835 om-08.

Z potential tests and paper properties

The stability of enzymatic products was assessed by measuring the electrophoretic mobility of the solutions with a Malvern Zetamaster device equipped with a laser Doppler velocimeter. The physicomechanical properties of the paper samples after treatment with FS were assessed by using commercial grade laboratory filter paper in accordance with ISO standards. The target properties were Bendtsen permeability (ISO 5636), burst strength (ISO 2758), tear strength (ISO 1974), folding endurance (ISO 5626), tensile strength (ISO 1924), wet tensile strength (ISO 3781), Cobb60 (ISO 535) and zero-span tensile strength (ISO 15361).

III. RESULTS AND DISCUSSION

Hydrophobization of paper sheets

The hydrophobization of paper was achieved by having the enzyme react with lauryl gallate (LG), albeit in the absence of paper sheets, in order to obtain a post-enzymatic solution (FS) containing an enzyme-modified phenol. The resulting FS was applied to paper sheets by impregnation/immersion, after which the sheets were allowed to dry in a normalized atmosphere (23°C, 50% RH). The ensuing method involves the following steps: (1) initial sonication of LG in the reaction buffer (50 mM sodium tartrate); (2) enzymatic reaction under conditions described elsewhere, but in the absence of paper sheets to obtain the FS; (3) impregnation of paper sheets with FS; and (4) drying of impregnated sheets under a normalized atmosphere or with forced drying.

Control functionalization solutions (KFS) were obtained by using various modifications of the original standard procedure to assess the influence of each individual agent, namely: laccase (Lacc), lauryl gallate (LG) and lignosulfonate (SL). Several filter paper sheets were treated using the FS as described above. Then, the sheets were subjected to the WDT. **Table 1** shows the WDT values of the filter paper sheets impregnated using the different control solutions (LG, LG+SL, SL, Lacc, LG+Lacc and SL+Lacc) and the functionalization solution (FS; LG+SL+Lacc). As can be seen, none of the compounds improved hydrophobicity by itself, and only the LG+Laccase control solution increased it significantly. In fact, only the tree compounds in combination (LG+SL+Lacc) resulted in a dramatic increase in paper hydrophobicity. Also, the combined contribution of the LG+Lacc and SL+Lacc solutions to hydrophobicity as measured with the WDT was lower than that of the LG+SL+Lacc solution. This confirms the presence of a synergistic effect between LG and SL. The results were

suggestive of chemical or physicochemical interaction between enzyme-modified LG and paper sheets. The treated sheets were subjected to strong washing with hot water and Soxhlet extraction with acetone to assess the strength of paper–chemical linkages. The measured contact angles (WCA) for the treated sheets were insignificantly decreased by hot washing and Soxhlet extraction (about 4 and 5% respectively); this suggests that LG was strongly bound to the paper sheets even after washing and acetone extraction.

Table 1. WDT of filter paper sheets after impregnation with the control solutions (LG, SL, Lacc, LG+Lacc, SL+Lacc, LG+SL) and the complete functionalization solution FS (LG+SL+Lacc).

Control	WDT (seconds)
LG	5 ± 1
SL	5 ± 1
Lacc	4 ± 1
LG+Lacc	187 ± 16
SL+Lacc	5 ± 1
LG+SL	6 ± 1
FS (LG+SL+Lacc)	3810 ± 200

Hydrophobic characterization of treated paper sheets

The free energy of a surface is a measure of its readiness to interact with other surfaces or liquids. In this work, SFE was used to assess the tendency of treated sheets to interact with water. A high SFE value is indicative of easy wetting by water and leads to a low contact angle. **Figure 1** shows the SFE values of eucalyptus sheets before and after impregnation with FS and the control solutions (KFS). As can be seen, SFE for sheets to which no FS or KFS was applied ranged from 50 to 60 mJ/m^2, which is consistent with previously reported values for this material [11]. Only the LG+Lacc control treatment and the FS treatment reduced SFE to a significant extent. Application of FS was especially effective in this respect; thus, it reduced SFE from an initial value around 55 mJ/m^2 to one in the region of 10 mJ/m^2. The reduction in SFE testifies to the hydrophobizing ability of FS and is consistent with the WDT results.

In order to extend the use of the FS to other types of paper-based substrates and assess the influence of the pulp type and the refining process in the hydrophobization, laboratory sheets were obtained from refined and unrefined flax and sisal pulps. Afterwards, the sheets were treated using the FS, and subjected to similar experiences. The obtained results in terms of hydrophobicity and SFE reduction were similar than the obtained with eucalyptus.

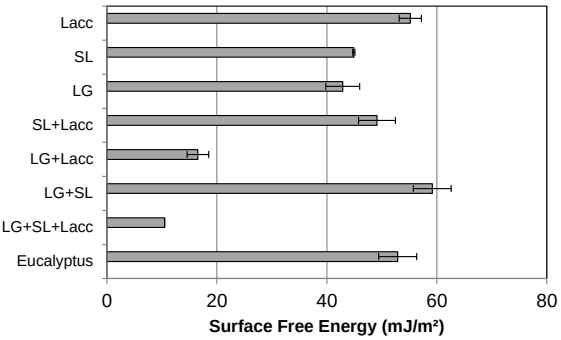

Figure 1. Surface Free Energy (SFE) eucalyptus sheets before (Eucalyptus) and after impregnation with FS (LG+SL+Lacc) and control solutions (LG+SL, LG+Lacc, SL+Lacc, LG, SL and Lacc).

Z potential measurements

The stability of the control solutions was assessed and compared via Z potential, which is illustrative of the behavior of colloid suspensions. The sonicated LG solution had Z potential ≈ –30 mV and was thus scarcely stable. The SL solution had Z potential ≈ –50 mV and was thus highly stable; in fact, SL never precipitated in the aqueous medium. On the other hand, the combination of SL with laccase exhibited a significantly reduced Z potential (ca. –35 mV) compared with to SL alone; however, the solutions exhibited no visual signs of agglomeration, turbidity or large particles. One possible explanation for this result is that the reaction with laccase may have partially dissolved SL and reduced Z potential to a near-zero level closer to the electrokinetic properties of water. Combining LG with laccase increased its Z potential to about –40 mV and improved its LG stability even though the solution still looked turbid to the naked eye. The most interesting result was derived

from the measurements of the solutions containing LG, SL and laccase (FS). One would have expected the synergistic effect of SL in combination with laccase to result in a dramatic increase in Z potential with respect to LG alone; however, Z potential remained at ca. –38 mV and the solutions looked clear and contained no suspended particles. The enzyme may have facilitated dissolution of LG, thereby reducing the Z potential.

IV. CONCLUSIONS

This paper reports an innovative green methodology for preparing a functionalization solution (FS) via an enzymatic reaction between laccase and lauryl gallate. Application of FS to the surface of finished paper substrate makes it hydrophobic as assessed by WDT and WCA measurements. The functionalization solution (FS) is highly stable as confirmed by Z potential measurements. This simple, expeditious method improves on the existing enzymatic alternatives and is amenable to industrial application.

V. ACKNOWLEDGEMENT

The authors are grateful to the BIOSURFACEL-CTQ2012-34109 and BIOFIBRECELL projects (CTQ2010-20238-CO3-01) within the framework of the Spanish's MICINN. Special thanks are also due to the consolidated research group AGAUR 2009SGR 00327 at Universitat de Barcelona (UB).

VI. REFERENCES

[1] Cherry JR, Fidantsef AL. Directed evolution of industrial enzymes: an update. *Curr Opin Biotechnol*. **2003**, *14*, 438-443.

[2] Valls, C., Roncero, M.B. Antioxidant property of TCF pulp with a high hexenuronic acid (HexA) content. *Holzforschung*. **2012,** *67*, 257.

[3] Garcia-Ubasart J, Esteban A, Vila C, Roncero MB, Colom JF, Vidal T. Enzymatic treatments of pulp using laccase and hydrophobic compounds. *Bioresour Technol.* **2011**, *102*, 2799-2803.

[4] Fillat, A.; Gallardo, O.; Vidal, T.; Pastor, F. I. J.; Díaz, P.; Roncero, M. B. Enzymatic grafting of natural phenols to flax fibres: Development of antimicrobial properties. *Carbohydr. Polym*. **2012**, *87*, 146-152.

[5] Aracri E, Roncero MB, Vidal T. Studying the effects of laccase-catalysed grafting of ferulic acid on sisal pulp fibers. *Bioresour Technol*. **2011**, *102*,7555-7560.

[6] Garcia-Ubasart, J.; Colom, J. F.; Vila, C.; Hernández, N. G.; Blanca Roncero, M.; Vidal, T. A new procedure for the hydrophobization of cellulose fibre using laccase and a hydrophobic phenolic compound. *Bioresour. Technol*. **2012**, *112*, 341-344.

[7] Sipponen MH, Pastinen OA, Strengell R, Hyötyläinen JMI, Heiskanen IT, Laakso S. Increased water resistance of CTMP fibers by oat (Avena sativa L.) husk lignin. *Biomacromolecules*, **2010**, *11*, 3511-3518.

[8] Cusola O, Valls C, Vidal T, Blanca Roncero M. Application of surface enzyme treatments using laccase and a hydrophobic compound to paper-based media. *Bioresour Technol.* **2013**, 131,521-526.

[9] Cusola O, Roncero MB, Valls C, Vidal T. Preparación enzimática acuosa aislada y uso para la funcionalización de la superficie del papel o soportes celulósicos. **2012**, ES20120030852 20120604.

[10] Cusola, O.; Valls, C.; Vidal, T.; Roncero, M,B. Rapid functionalisation of cellulose-based materials using a mixture containing laccase activated lauryl gallate and sulfonated lignin. *Holzforschung*. **2014,** *1–9*, ISSN (Online) 1437-434X, ISSN (Print) 0018-3830, DOI: 10.1515/hf-2013-0128.

[11] Persin Z, Stana-Kleinschek K, Sfiligoj-Smole M, Kreze T, Ribitsch V. Determining the Surface Free Energy of Cellulose Materials with the Powder Contact Angle Method. *Text Res J*, **2004**, *74*, 55.

STUDIES ON THE PRETREATMENT OF NATIVE CELLULOSE AND LIGNOCELLULOSIC RESIDUES OF STONE PINE (*PINUS PINEA),* CARNAÚBA (*COPERNICIA PRUNIFERA*) AND MACAÚBA PALM *(ACROCOMIA ACULEATA)* IN IONIC LIQUIDS FOR BIOFUEL PRODUCTION

Viviane da Silva-Lacerda[1], Anderson Barbosa-Evaristo[2], Adriana Correa-Guimaraes[1], Salvador Hernández-Navarro[1], Luis M. Navas-Gracia[1], Pablo Martín Ramos[1], Luis F. Sánchez-Sastre[1], Eduardo Pérez-Lebeña[1] and Jesús Martín-Gil[1]*

*[1] Department of Agricultural and Forestry Engineering, Higher Technical School of Agricultural Engineering, University of Valladolid, Avenida de Madrid 44, Palencia, 34004 Spain; [2]Universidade Federal de Viçosa, Viçosa, MG, 36570-000, Brazil (*jesusmartingil@gmail.com)*

ABSTRACT

In the study presented herein, research has been conducted on the pretreatment in ionic liquids of native cellulose and lignocellulosic wastes (pine nut shells from Stone Pine (*Pinus pinea)*, palm leaves from Carnaúba palm (*Copernicia prunifera*) and residues from Macaúba palm *(Acrocomia aculeata)* (*viz.*, pulp, shell) for the production of bioethanol, bio-hydroxymethylfurfural (bio-HMF) and bio-furfural. The heat treatment has been carried out in a microwave oven at different temperatures and times and the results have been compared with those obtained upon operation in a low-pressure reactor and ultrasound treatments. In order to promote the dissolution of cellulose and lignocellulosic wastes, different ionic liquids (ILs) have been assayed, namely, eutectic mixtures of choline chloride/urea, choline chlorine/oxalic acid, choline chloride/betaine, tetraethyl ammonium chloride (TEAC) and tetraethyl ammonium bromide (TEAB). To facilitate the hydrolysis process of the cellulose and lignocellulosic residues, different types of solvents have been used: water/sulfolane and/or 2-ethylhexanol, along with acid and basic catalysts which promote the process of isomerization of glucose. The characterization and quantification of the produced HMF and furfural has been performed by UV spectrophotometry at 275 nm and 285 nm and by high-performance liquid chromatography (HPLC) at 280 nm. Carbohydrates characterization has been conducted by VIS spectrophotometry and by Ionic Chromatographic (IC). The study confirms that ILs promote the dissolution reaction of cellulose and/or lignocellulose residues leading to the formation of mono-, di- and trisaccharides, HMF and furfural. It has been observed that, when the temperature is increased, the eutectic mixture of choline chloride/oxalic acid has the highest yields of HMF and furfural, while the eutectic mixture of choline chloride/urea leads to the best yields in terms of sugars or carbohydrates formation. Aforementioned studies aim to optimize the processes of production of biofuels, such as bioethanol, bio-HMF or bio-furfural.

I. INTRODUCTION

Lignocellulosic materials have become attractive precursors for energy production, since they are abundant, renewable and do not compete with food crops both for human and animal consumption [1,2]. In general, lignocellulosic materials are composed of cellulose, hemicellulose and lignin, being cellulose the most important component in energy crops, agricultural and forestry residues [3].

The objective of this work is the production of second generation biofuels from cellulose and lignocellulosic wastes for their conversion into bio-alcohols, bio-HMF and/or bio-furfural, using ionic liquids and different proportions of water, organic solvents, catalysts, acids, times, temperatures, etc. either in microwave reactors with ultrasound pretreatment or in a Parr reactor operating at low-medium pressure with stirring. Production yields for sugars and/or bio-HMF/furfural obtaining from cellulose and various palm and pine lignocellulosic wastes have been assessed.

II. EXPERIMENTAL

Native cellulose (Merck™) and different lignocellulosic materials (*viz.*, palm leaves from Carnaúba palm (*Copernicia prunifera*) from Ceará, Brasil; pulp and shell from Macaúba palm (*Acrocomia aculeata*) from Minas Gerais, Brasil; and pine nut shells from Stone Pine (*Pinus pinea*) from Valladolid, Spain) were assayed as substrates. The lignocellulosic materials were dried in oven at 60 °C, milled and sieved prior to their utilization. Anatase titanium oxide (TiO_2, Sigma Aldrich™) was used as a catalyst. Choline chloride (ChCl), urea, oxalic acid, tetraethyl ammonium chloride (TEAC) and tetraethyl ammonium bromide (TEAB) were also supplied by Sigma Aldrich™.

Studies both at lower temperatures (100ºC and 120°C), aimed at sugars production, and at 140°C (aimed at bio-furfural and bio-HMF obtaining) have been conducted for different catalysts and organic solvents (**Table 1** and **Figure 1**), working both in a Milestone™ mod. Ethos One microwave apparatus or in a low-pressure Parr reactor. For the hydrolysis of different substrates to bio-furfural and bio-HMF, 100 mg of substrate were used, together with 20 mg of TiO_2 catalyst, 5 mL of ionic liquid and 5 mL of a (water+organic solvent) mixture (see Table 1). When only sugars obtaining is pursued, the 5 mL of the (water+organic solvent) mixture are replaced by 5 mL of acid (HNO_3, 10% or H_3PO_4, 30%), in order to favor the rupture of the 1,4-β-glycosidic bonds of cellulose. The 10 mL mixture was sealed in a reaction vessel and heated in the microwave apparatus, preceded by an ultrasonic homogenization pretreatment in some cases. The attack was also carried out in a low-pressure Parr reactor with stirring (**Table 1**). Upon completion of the desired reaction time, the reaction mixture was rapidly cooled to room temperature. Bio-HMF/furfural production was quantified for both treatments according to Chi [4] methodology by means of a Hitachi U-series UV spectrophotometer, measuring at 277 nm and at 285 nm for bio-furfural and bio-HMF, respectively; sugars concentration was determined by the 3,5-dinitrosalicylic acid (DNS) method [5].

III. RESULTS AND DISCUSSION

In order to promote the dissolution of cellulose and lignocellulosic residues in ionic liquids, different eutectic mixtures have been assayed: choline chloride (ChCl)/urea, ChCl/oxalic acid, ChCl/betaine, tetraethyl ammonium chloride (TEAC) and tetraethyl ammonium bromide (TEAB) (**Table 1** and **Figure 1**). The best results for bio-HMF/furfural and/or sugars production have been attained for the ChCl/urea and ChCl/oxalic acid mixtures.

Table 1 summarizes the conversion rates of cellulose and lignocellulosic biomass into bio-HMF and bio-furfural for 60 minutes at 140°C in a microwave reactor. When 2-ethylhexanol (2-EH) organic diluent is used, furfural formation is favored vs. that of HMF, and furfural concentrations vary from 349 to 426 mg/L depending on the substrate. The ChCl/oxalic acid mixture proves to be very reactive with lignocellulosic residues when sulfolane is used as a solvent, while the ChCl/urea mixture would be the preferred option for native cellulose. In agreement with Nakaiama and Imai [6], when a 15 min sonication pretreatment is performed, the HMF production is significantly promoted vs. that of furfural, reaching HMF concentrations of 3489 mg/L for Carnauba leaves. When the low-pressure Parr reactor with stirring is used instead of a microwave oven, furfural formation is enhanced for all substrates except for Macauba pulp (in which HMF formation increases). It should be noted that when native cellulose is attacked in the Parr reactor, concentrations of 1551 mg/L and 1663 mg/L are achieved for HMF and furfural, respectively (i.e., 3114 mg/L of biofuel or a 31.14 % yield).

Table 1. Conversion of cellulose and lignocellulosic biomass into bio-HMF and bio-furfural in a microwave (MW) oven (140ºC, 60 min) *vs*. in a low-pressure Parr reactor with stirring (140ºC, 60 min).

Substrate	Ionic liquid	Diluting agent	Procedure	HMF (mg/L)	Furfural (mg/L)
Carnauba leaves	ChCl/oxalic acid	2-EH	MW	0.0	348.8
	ChCl/oxalic acid	Sulfolane	MW	1023.3	0.0
	ChCl/urea	Sulfolane	MW	195.6	203.6
	ChCl/oxalic acid	Sulfolane	15’ sonication + MW	3489.1	0.0
	ChCl/urea	Sulfolane	Parr reactor	1122.1	1152.7
Macauba shell	ChCl/oxalic acid	2-EH	MW	0.0	426.6
	ChCl/oxalic acid	Sulfolane	MW	593.2	0.0
	ChCl/urea	Sulfolane	MW	104.8	64.2
	ChCl/oxalic acid	Sulfolane	15’ sonication + MW	404.0	411.8
	ChCl/urea	Sulfolane	Reactor Parr	645.2	973.1
Macauba pulp	ChCl/oxalic acid	2-EH	MW	0.0	327.0
	ChCl/oxalic acid	Sulfolane	MW	671.7	107.5

	ChCl/urea	Sulfolane	MW	37.1	24.9
	ChCl/oxalic acid	Sulfolane	15' sonication + MW	0	892.0
	ChCl/urea	Sulfolane	Reactor Parr	2255.3	628.0
Pine nut shell	ChCl/oxalic acid	2-EH	MW	0.0	358.2
	ChCl/oxalic acid	Sulfolane	MW	1200.9	0.0
	ChCl/urea	Sulfolane	MW	25.2	11.9
	ChCl/oxalic acid	Sulfolane	15' sonication + MW	869.6	7.0
	ChCl/urea	Sulfolane	Reactor Parr	607.8	762.1
Native cellulose	ChCl/oxalic acid	2-EH	MW	21.4	389.6
	ChCl/oxalic acid	Sulfolane	MW	391.0	459.2
	ChCl/urea	Sulfolane	MW	1682.7	374.5
	ChCl/oxalic acid	Sulfolane	15' sonication + MW	959.8	0.0
	ChCl/urea	Sulfolane	Reactor Parr	1550.8	1562.6

The formation of reducing sugars from cellulose and lignocellulosic residues in ionic liquids (ChCl/Oxalic acid and ChCl/Urea at 100ºC and 120°C) in an acidic medium with either H_3PO_4 or HNO_3 is shown in **Figure 1**.

In **Figure 1** (a), it should be pointed out that the ChCl/oxalic acid, TEAC and TEAB ionic liquids in acidic medium with H_3PO_4 30%, at 100°C and 120ºC, did not lead to the production of reducing sugars. It can also be observed that when oxalic acid was replaced with urea, the native cellulose substrate treated at 100°C in the microwave reactor yielded a 8.6% (95.9 g/L) of reducing sugars, whereas lignocellulosic residues led to disparate sugars production yields: 15.2% (168.5 g/L) for carnauba leaves and 13.2% (146.7 g/L) for macauba pulp, *vs*. 5.5% (60.6 g/L) for pine nut shell and 7.3% (80.6 g/L) for macauba shell. When the tests were conducted at 120°C, native cellulose led to a significant production of reducing sugars 14.8% (164.4 g/L), followed by macauba pulp 14.6% (162.03 g/L), pine nut shell 11.9% (132.5 g/L), carnauba leaves 10.2% (113.02 g/L) and, finally, macauba shell 9.1% (100.7 g/L). Consequently, the increase in temperature from 100ºC to 120ºC favors the sugars production in H_3PO_4 30% medium.

On the other hand, in **Figure 1** (b) is it noticeable that the highest yields for the ChCl/oxalic acid eutectic mixture in HNO_3 10% medium are obtained for carnauba leaves, with values as high as 18,8% (209.2 g/L), followed by macauba shell 17.3% (192.1 g/L), native cellulose 10.5% (117.2 g/L), macauba pulp 7.2% (80.1 g/L) and pine nut shell (0%). No sugar production could be detected when working with the ChCl/urea mixture in nitric acid at 100°C, but formation of sugars can be attained by rising the microwave oven temperature to 120ªC for 30 minutes.

The bio-HMF/furfural concentrations generated by the hydrolysis of cellulose are very low, ranging from 0 to 0.4 g/L for HMF (the highest production was obtained for carnauba leaves in ChCl/Oxalic acid and H_3PO_4) and from 0 to 0.74 g/L for furfural (in this case, the highest concentration corresponds to carnauba leaves in TEAB and H_3PO_4).

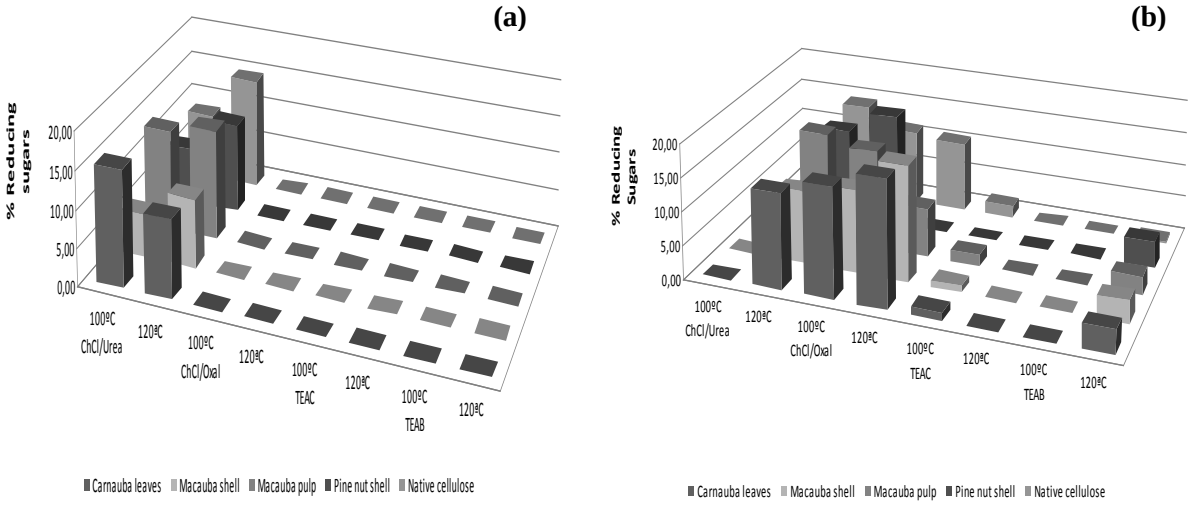

Figure 1. Sugars production in a microwave oven in ionic liquids (ChCl/oxalic acid and ChCl/urea, at 100ºC and 120ºC) for 30 minutes in acidic medium: (*a*) H_3PO_4 30% and (*b*) HNO_3 10%.

IV. CONCLUSIONS

The operative conditions for the production of biofuels derived from furfural and HMF and for the obtaining of reducing sugars from cellulose and lignocellulosic waste have been optimized, working in ionic liquids and utilizing either a microwave oven with ultrasonic pretreatment or a low-pressure Parr reactor with stirring for conducting the treatment.

It can be concluded that for the production of biofuels -derived from furfural and HMF- in a pilot plant, Parr-type reactors and ionic liquids at temperatures of 140°C for 60 min are to be used. ChCl/oxalic acid mixture proves to be the most reactive, amongst those assayed, in order to attack lignocellulosic waste substrates when sulfolane is used as solvent and TiO_2 as a catalyst, while the ChCl/urea mixture would be more advisable for native cellulose. When the MW oven is replaced with a low-pressure Parr reactor, the formation of furfural is favored for all substrates, except for macauba pulp.

In relation to the production of reducing sugars in a pilot plant, ionic liquids and either Parr reactors or microwave apparatus shall be used, but lower temperatures (100ºC or 120°C) are desirable. When nitric acid (HNO_3 10%) is used, the best yields are attained for ChCl/oxalic acid eutectic mixture, while ChCl/urea proves better when H_3PO_4 acid is chosen. The small amounts of furfural and HMF produced in the formation of sugars (lower than 0.8 g/L in all case) can be removed with acetonitrile so as to have pure sugar than can be readily used for the synthesis of bio-alcohols by fermentation.

V. ACKNOWLEDGEMENTS

Viviane da Silva-Lacerda would like to thank Universidad de Valladolid for its financial support under FPI PhD scholarship program. Support by Junta de Castilla y León under project VA036A12-2 is gratefully acknowledged by the UVA group.

VI. REFERENCES

[1] Huber, G.W., Iborra, S., Corma, A. Synthesis of transportation fuels from biomass: chemistry, catalysts, and engineering. *Chem Rev*. **2006**, *106*, 4044–98.

[2] Merino, S.T., Cherry, J. Progress challenges in enzyme development for biomass utilization. *Adv Biochem Eng Biotechnol.* **2007**, *108*, 95–120.

[3] Datta, S., Holmes, B., Park, J.I., Chen, Z., Dibble, D.C., Hadi, M., *et al*. Ionic liquid tolerant hyperthermophilic cellulases for biomass pretreatment and hydrolysis. *Green Chem*. **2010**, *12*, 338–345.

[4] Chi, C., Zhang, Z., Chang, H.M., Jameel, H. Determination of Furfural and Hydroxymethylfurfural Formed from Biomass under Acidic conditions. *J. of Wood Chem. and Techn.* **2009**, 29, 265–276.

[5] Miller, G.L. Use of dinitrosalicylic acid reagent for determination of reducing sugar. *Analytical Chem.* **1959**, 31, 426–428.

[6] Nakayama, R., Imai, M. Promising ultrasonic irradiation pretreatment for enzymatic hydrolysis of Kenaf. *J. of Environ. Chem. Engin.* **2013**, 1, 1131–1136.

TECHNO-ECONOMIC ASSESSMENT OF GASIFICATION SCHEMES FOR ELECTRICITY GENERATION FROM OLIVE TREE PRUNING

Javier A. Dávila[1], Valentina Hernández[1], Juan M. Romero[2], Eulogio Castro [2]*, Carlos A. Cardona [1]

*[1] Grupo de Investigación en Procesos Químicos, Catalíticos y Biotecnológicos, Universidad Nacional de Colombia, Sede Manizales; [2]Dpto. Ingeniería Química, Ambiental y de los Materiales, Universidad de Jaén, España (*Email: ecastro@ujaen.es)*

ABSTRACT

More than nine million hectares of olive trees are cultivated worldwide, especially in the Mediterranean countries. Pruning of olive trees is yearly performed resulting in a huge amount of biomass lacking of applications. As a renewable source of energy, pruning biomass has been proposed as raw material for a number of uses, e.g. biofuels, chemicals, or electricity production. According to the afore-mentioned, this work examines three schemes for electricity generation from olive tree pruning biomass by gasification. The commercial software ASPEN Plus® v.8 was applied to carry out techno-economic analysis of the three proposed schemes, e.g., gasification with cryogenic CO_2 recovery (scheme 1), gasification with combined gas and steam turbines (scheme 2) and gasification with only gas turbine (scheme 3). The first scheme has advantages from an environmental point of view because the CO_2 recovered can decrease the greenhouse gases besides, this CO_2 could be sold as credits in the electricity generation plants. On the other hand, the scheme 2 has not environmental advantages but has lower capital cost due to the use of fewer units. Finally, scheme 3 gives less electricity but at the same time consumes fewer units. Three different volumes of feedstock were used for the three schemes of electricity generation: 1, 20 and 50 tonnes per hour in order to analyze the effect of the amount of raw material over the feasibility. The mass and energy balances generated were used for the economic evaluation using Aspen Process Economic Analyzer software, calculating the production cost per kWh generated. Economic parameters were taken considering the Spanish market. Results show that schemes 2 and 3 present the lower production cost per kWh generated and that these schemes are feasible when the raw material have no cost. According to the results, 334, 302 and 299 kWh/t of olive tree pruning biomass were obtained for schemes 1, 2 and 3 respectively.

I. INTRODUCTION

Olive tree pruning biomass is one of the most important agroindustrial wastes generated in Spain due to its large production and its availability [1]. It has been estimated that more than three million tonnes of biomass from olive tree pruning are yearly available in Spain [2]. This residue should be eliminated because it generates serious environmental problems, such as propagation of vegetal diseases. In this sense, this biomass can be used as a source of alternative energy because it is a renewable biomass, which does not contribute significantly to increase the greenhouse gases, and it is an available biomass, lacking of economic applications. According to the mentioned above approximately 400 t/h could be available in Spain to be used in electricity generation processes. In this order, gasification of olive tree pruning constitutes an excellent alternative to electricity production. This work presents a techno-economic point of view of the electricity generation from olive tree pruning using three schemes of electricity generation. Gasification with cryogenic CO_2 recovery (scheme 1), gasification with combined gas and steam turbines (scheme 2) and gasification with only gas turbine (scheme 3). Three different volumes were used in the feedstock: 1, 20 and 50 tonnes per hour in order to analyze the effect of the amount of raw material over the feasibility.

II. EXPERIMENTAL

The proposed schemes of electricity generation are shown in **Figure 1**. Raw material composition was taken according to previous works and it is showed in **Table 1** [3-5]. Aspen Plus v.8.0 was used to generate the mass and energy balances of each proposed scheme of electricity generation. Then, mass and energy balances were used for the economic evaluation using Aspen Process Economic Analyzer software, calculating the production cost per kWh generated. Economic parameters according to Spain were used and are showed in **Table 2**.

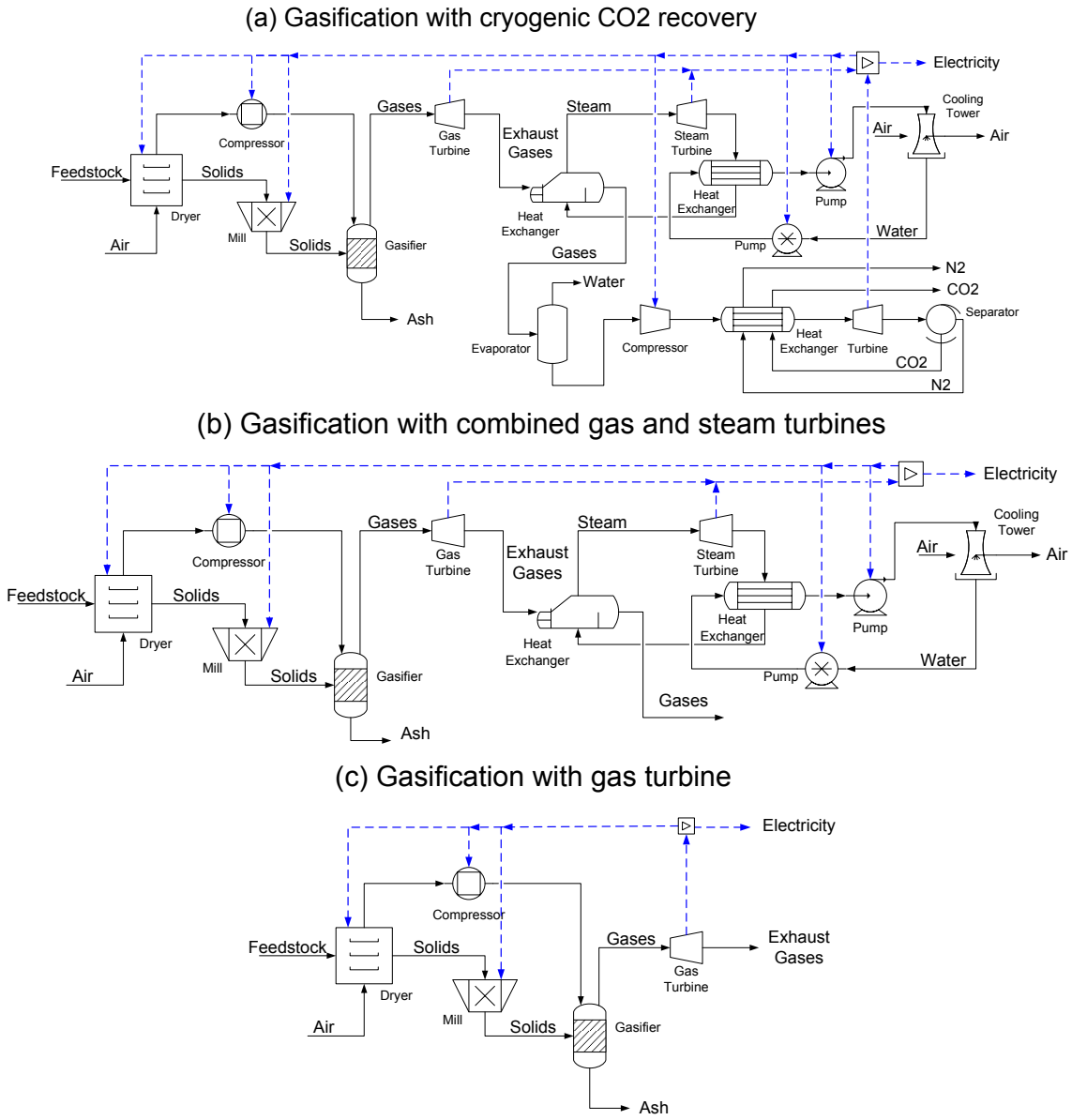

Figure 1. Gasification schemes for electricity generation from olive tree pruning. (a) Gasification with cryogenic recovery of CO_2. (b) Gasification with combined gas and steam turbines. (c) Gasification with gas turbine.

Table 1. Chemical composition of olive tree pruning biomass

Compound	(%)
Cellulose	28.08
Hemicellulose	15.80
Lignin	18.81
Ash	3.40
Water	33.90

Table 2. Economic parameters for techno-economic assessment

Parameter	Price	Unit
Operator	22.36	USD/h
Supervisor	24.55	USD/h
Electricity	0.11	USD/kWh
Potable water	0.22	USD/m^3
Fuel	7.86	USD/MMBTU
Olive tree pruning	28.8	USD/tonne
Tax rate	35	%
Desired rate of return	6	%

III. RESULTS AND DISCUSSION

Figures 2 and **3** show the total production cost with and without raw material cost respectively. When olive tree pruning has a cost (28.8 USD/t) the lowest production cost are obtained for 20 and 50 t/h of feedstock and the total production cost ranges from 0.12 to 0.16 USD/kWh. On the other hand, without raw material cost and with flows of 20 and 50 t/h of olive tree pruning, total production cost from 0.02 to 0.07 USD/kWh are obtained. This indicates that there is a price of olive tree pruning that permits to obtain the same electricity price consumed for the gasification plant (0.11 USD/kWh), this was found as 26.4 USD/t for flows of 20 t/h and scheme 3 which was the best scheme of production.

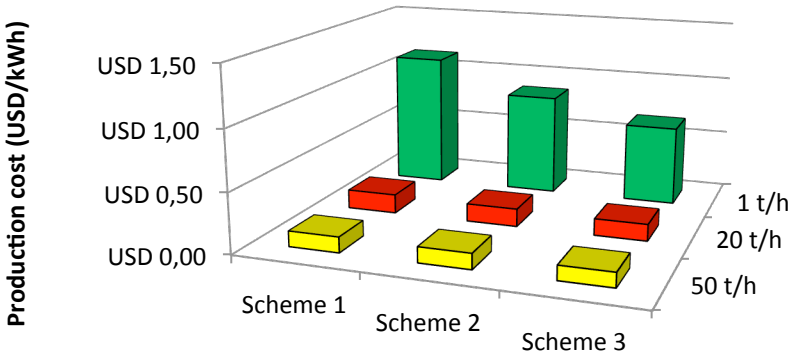

Figure 2. Total production cost with 28.8 USD/t of olive tree pruning.

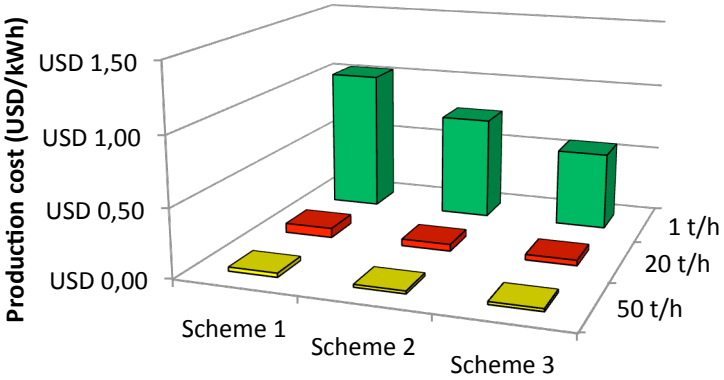

Figure 3. Total production cost without cost of olive tree pruning.

Table 3 shows the distribution of the total production cost to the best scheme (scheme 3) with 50 t/h. It is clear that the raw material cost is the most important item in the economic evaluation because it has a contribution of 82.67% of the total production cost. Despite that the raw material cost has an important contribution over total production cost, low flows of olive tree pruning (1 t/h) resulted in low significant contribution as is shown in **Figure 4**.

Table 3. Distribution of the total production cost.

Economic Parameter	Cost (USD/Year)	Share (%)
Depreciation Expense	384635	2.59
Total Raw Materials Cost	12272400	82.67
Total Utilities Cost	293542	1.98
Operating Labor Cost	411213	2.77
Maintenance Cost	69470.6	0.47
Operating Charges	102803	0.69

Plant Overhead	240342	1.62
G and A Cost	1071180	7.22
TOTAL	**14845585**	**100**

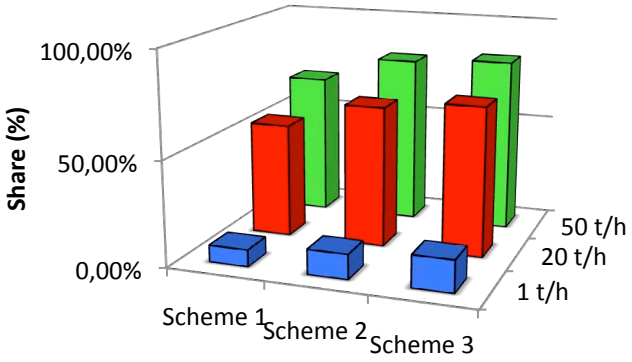

Figure 4. Share of the raw material cost over total production cost.

IV. CONCLUSIONS

Olive tree pruning is an attractive raw material to be employed in gasification processes due to its large quantities and its availability.

When the olive tree pruning has cost (28.8 USD/t), any of the schemes are infeasible using the flows of feedstock evaluated and the final production cost to all schemes is higher than the typical electricity cost (0.11 USD/kWh). On the other hand, when the olive tree pruning has not cost, all schemes are feasible only when flows of feedstock are above of 20 tonnes per hour obtaining productions cost lower than 0.07 USD/kWh. 26.4 USD/t of olive tree pruning was found as the price to obtain a feasible gasification with 20 t/h in scheme 3 which was the most promising scheme of electricity generation.

The raw material cost is the most important economic parameter to take into account in the economic evaluation especially when high flows of feedstock are used because as the flow of feedstock increases, the production cost decreases.

V. ACKNOWLEDGMENTS

Financial support from Junta de Andalucía (Proyecto de Excelencia AGR-6103) is gratefully acknowledged. JMR and VH express also their gratitude for their scholarships received from Junta de Andalucía and Agrifood International Doctorate School (eidA3).

VI. REFERENCES

[1] Castro E, Ruiz E, Moya M, Romero I, Cara C, Díaz M. La poda del olivar: Avances hacia el desarrollo de una biorefinería. Residuos. Revista Técnica 110, 38-44, 2009.

[2] Velázquez-Martí B, Fernández-González E, López-Cortés I. Quantification of the residual biomass obtained from pruning of trees in Mediterranean olive groves. Biomass and Bioenergy 35, 3208-3217, 2011.

[3] Cara C, Ruiz E, Oliva J, Sáez F, Castro E. Conversion of olive tree biomass into fermentable sugars by dilute acid pretreatment and enzymatic saccharification. Bioresource Technology 99, 1869 – 1876, 2008.

[4] Cara C, Ruiz E, Ballesteros I, Negro M, Castro E. Enhanced enzymatic hydrolysis of olive tree wood by steam explosion and alkaline peroxide delignification. Process Biochesmistry 41, 423 – 429, 2006.

[5] Cara C, Romero I, Oliva J, Sáez F, Castro E. Liquid hot water pretreatment of olive tree pruning residues. Applied Biochemistry and Biotechnology, 136, 136 – 140, 2007.

[6] Rincón LE, Hernández V, Cardona CA. Analysis of technological schemes for the efficient production of added-value products from Colombian oleochemical feedstocks. Process Biochemistry 39, 474 – 489, 2014

INFLUENCE OF LIGNIN SOURCE AND MODIFICATION ON THE PROPERTIES OF LIGNIN-POLYETHYLENE BLENDS

Dehne, L.[1], Vila Babarro, C.[2], Schwarz, K.U.[1], Saake, B.[1]*

[1]*University of Hamburg, Department of Wood Science, Chemical Wood Technology, Leuschnerstr. 91, 21031 Hamburg, Germany; Thünen Institute of Wood Research, Leuschnerstr. 91, 21031 Hamburg, Germany (*bodo.saake@uni-hamburg.de)*

ABSTRACT

Esterification of Soda Grass, Hardwood and Softwood Kraft lignins with acetic, propionic and butyric anhydride was performed to improve compatibility of lignin and polyethylene (PE-HD) in blends. Mechanical properties were determined by tensile and flexural tests. In comparison to pure PE-HD the blends are still too rigid, yet, the performed modifications enhance the mechanical properties compared to blends containing unmodified lignin. Best results were observed for propionated lignin-polyblends. Light microscopic images confirmed an improved compatibility of the feedstocks with increasing length of the substituent. Interestingly, no significant differences occurred among the technical lignins concerning the behavior of the modified products in the blends.

I. INTRODUCTION

Modification of lignin has extensively been studied during the last decades, and its use has successfully been promoted for a wide range of applications, comprising e.g. adhesives and foams [1]. Due to its inherent features, lignin is also a suitable component to be used in lignin-polyblends [2]. Here, investigations mainly focused on the incorporation of unmodified lignins into the polymer matrix [3, 4, 5]. However, comparably little research has been conducted so far on suitable modifications to improve lignin applicability in composites with thermoplastic polymers as matrix material [6, 7, 8].

In this paper three technical lignins from different sources were esterified with acetic, propionic, and butyric anhydride before melt mixing with polyethylene (PE-HD) in order to improve compatibility of the two feedstocks. Properties of the resulting blends were determined by means of tensile and flexural tests. Light microscopic images of the blends were taken to analyze changes in the miscibility and adhesion of lignin and PE-HD.

II. EXPERIMENTAL

Raw materials. Industrial Hardwood (eucalypt) and Softwood (pine/spruce) Kraft lignins (**HW-K, SW-K**) were provided by Suzano and Stora Enso, respectively. Commercially available Soda Grass Lignin (**SG**) from wheat straw was purchased from Green Value. High density polyethylene (PE-HD) named Hostalen GC 7260 (LyondellBasell) served as matrix polymer for the lignin-polyblends. Density: 0.96 g/cm³, MFR: 0.8 g/10 min (190 °C/2.16 kg), T_{pm}: 125-135 °C.

Methods. Esterification of each lignin sample was performed according to a revised protocol by [6]. Lignin was suspended in acetic, propionic, and butyric anhydride, respectively, with a 2:1 weight ratio of solvent to lignin, adding 0.01 mL N-methylimidazol (N-MIM) as catalyst per gram of lignin. The reaction was performed at 50 °C in a stirred glass reactor. After 3 h, the mixture was poured into cold deionised water to stop the reaction, and subsequently washed until the filtrate reached pH 5. The esterified lignin was dried in an oven at 50 °C for several days.

Melt mixing of lignin and polymer was accomplished using a Haake Rheomix OS 3000 torque-rheometer (Thermo Fisher Scientific, Germany) with a weight proportion of 1:1. Process parameters: 160 °C, 50 rpm, 60 % filling degree; lignin was added after stabilization of the PE-HD torque curve. The resulting blends were encoded according to the lignin type and the applied modification (acetylation a, propionation p, butyration b).

Test specimens were injection moulded using a Haake MiniJet II (Thermo Fisher Scientific, Germany). Melt temperature was adjusted for each formulation, varying between 160-168 °C. The casting moulds had a constant temperature of 90 °C; first and second pressures were kept at 500 and 300 bar, respectively, for 15 s each. Dumbbell-shaped specimens (type 1BA) were prepared for tensile tests according to [9]. Rod-shaped specimens in accordance with [10] were used for flexural tests.

Investigations of mechanical properties were conducted using a Zwick Roell Z050, testing three specimens for each formulation. Tensile tests were performed at 1 mm/min test speed and 20 mm gauge length [11]. For the flexural test, 2 mm/min test speed and 64 mm supporting width were set [10]. Before testing, all specimens were conditioned at 20 °C/ φ= 65 %.

Light microscopic images were taken using AxioCam MRc5 and ZEN 2012 software (both Zeiss).

III. RESULTS AND DISCUSSION

Unmodified lignin is not compatible with unpolar polyethylene (PE-HD) and therefore needs to be modified prior to the blending process. ^{31}P-NMR and FTIR analysis confirmed complete disappearance of OH group signals in the spectra of the modified lignin samples. The latter one moreover showed the apparition of the peak corresponding to the ester group at 1757 cm^{-1}.

To evaluate the effects of lignin modification on its distribution in the polymer matrix and the adhesion of the two feedstocks, light microscopic images were taken from blends containing unmodified and modified lignin, respectively. As depicted in **Figure 1a**, unmodified lignin accumulates in unevenly distributed grains, well demarcated from the transparent polymer matrix. Compared to this, the images of modified lignin-polyblends display an increasing homogeneity with increasing chain length of the substituent on the lignin (C2 to C4 chain). In the acetylated lignin-polyblend the grainy texture is partly dissolved (**Figure 1b**). The lignin rather seems to be associated in threadlike structures, running through the polymer matrix. This phenomenon may be attributed to the mixing process in the torque-rheometer and is even more pronounced in the images of the propionated lignin-polyblends in **Figure 1c**. The blends containing butyrated lignin are characterized by a smooth brown matrix (**Figure 1d**). Based on this, it can be assumed that the modification positively affects the compatibility of lignin and polyethylene. With increasing chain length of the substituent the adhesion at the interface of the two feedstocks is improved and the lignin is able to distribute homogeneously within the polymer matrix. This, furthermore, goes in line with experiences made during the blending and injection molding processes. With increasing chain length of the substituent, the blended material appears to be more homogeneous and less crumbly. The reduction of the melt temperature from 168 °C for the acetylated lignin-polyblends to 160 °C for those containing butyrated lignin also indicates a better compatibility.

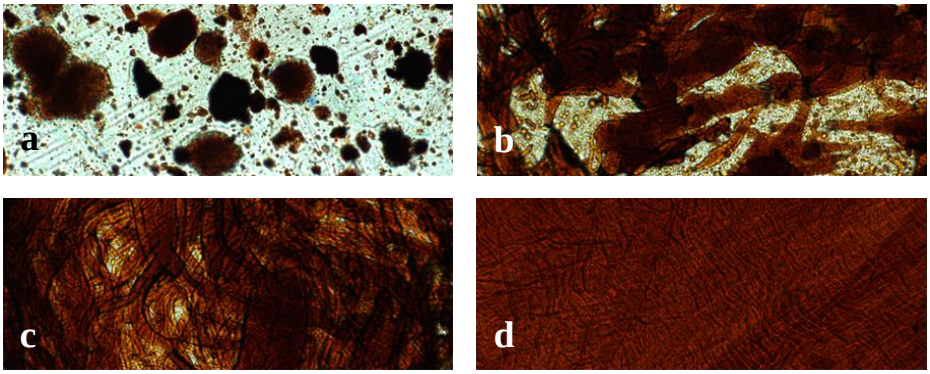

Figure 1. Light microscopic images of PE-HD blended with unmodified (a), acetylated (b), propionated (c), and butyrated (d) lignin, showing an increasing homogeneity of the blends from a to d.

Mechanical properties were determined by tensile and flexural tests in accordance to DIN EN ISO norms, the results being displayed in **Figure 2** and **Figure 3**. In both test series, neat PE-HD specimens served as reference samples.

Regarding the tensile tests (**Figure 2**), all lignin-polyblends are characterized by significantly reduced strength and elongation values compared to neat PE-HD (σ_M= 22,7 N/mm²), Young's modulus being distinctly increased. As depicted in the figure, blends containing unmodified lignin show tensile strengths between 9.4 N/mm² (SG) and 11.2 N/mm² (HW-K) which correspond to only half the value of the reference. The elongation values decrease to less than 1/5. Youngs's Modulus roughly doubles, indicating an increased rigidity of the blends compared to pure PE-HD.

Yet, the tensile tests of the modified blends confirm that the esterification of lignin with acid anhydrides is beneficial for the mechanical characteristics of the resulting blends. Consistent with the light microscopic images, the modified blends are characterized by significantly higher tensile strengths than blends containing unmodified lignin. Furthermore, the modifications differ among each other; with increasing chain length of the

substituent an increase of the tensile strengths can be determined. Interestingly, there exist no significant differences among the three lignins. All of them show the same trend, and, concerning HW-K and SG, even quite similar values for the respective modifications. For HW-K and SG best results for the tensile strenghts were achieved using propionated lignin (σ_M= 17 N/mm²), whereas for SW-K highest values were observed for acetylated blends (σ_M= 17 N/mm²). The butyrated blends all show a distinct decline of the strength values, which contradicts to the assumptions based on their microscopic images. The decline may be attributed to damages on the surfaces of the specimens as they tend to stick on the metal surface of the casting moulds. This phenomenon is predominantly observed for modified SW-K lignin-blends, which explains the significantly reduced strength of the butyrated SW-K lignin blends. All modified blends are characterized by further decreased elongation values to roughly 1/10 of the reference, showing brittle fractures during the tensile tests. However, there is a slight (re)increase of elongation values visible from acetylated to butyrated substituent. In combination with a constantly decreasing Young's Modulus this indicates that the blends become less rigid as the length of the side chain increases.

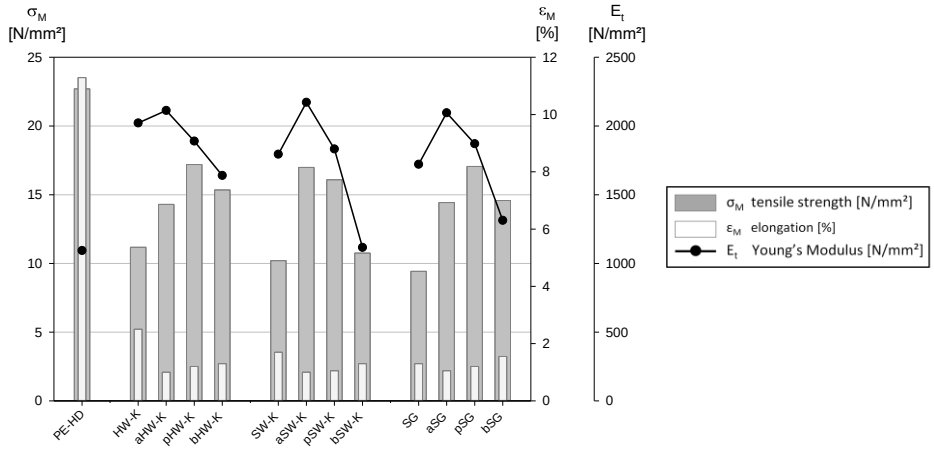

Figure 2. Results of the tensile tests: pure PE-HD is shown in comparison to 1:1 mixtures with unmodified and modified Hardwood Kraft, Softwood Kraft, and Soda Grass lignins

The results of the flexural tests confirm the results of the tensile tests (**Figure 3**). Blends containing unmodified and modified lignins, respectively, show a comparably moderate reduction of the flexural strengths compared to the reference. Blending polyethylene with unmodified lignin results in a higher stiffness as the flexural modulus in distinctly increased and the deflection of the blends is reduced to ca. 1/3 of the reference. With exception of SW-K lignin, an increase of the flexural strength can be observed for the modified blends as the substituent becomes longer. The deflection, too, increases. Highest strengths were again determined using propionated HW-K (σ_{fM}= 25 N/mm²) and SG (σ_{fM}= 24 N/mm²) lignin, respectively, whereas for SW-K the acetylated blends (σ_{fM}= 23 N/mm²) showed the best results. The aforementioned damages on the surface of the specimens may explain the decline of the flexural strengths measured for the butyrated blends, and the propionated SW-K lignin in contradiction to HW-K and SG.

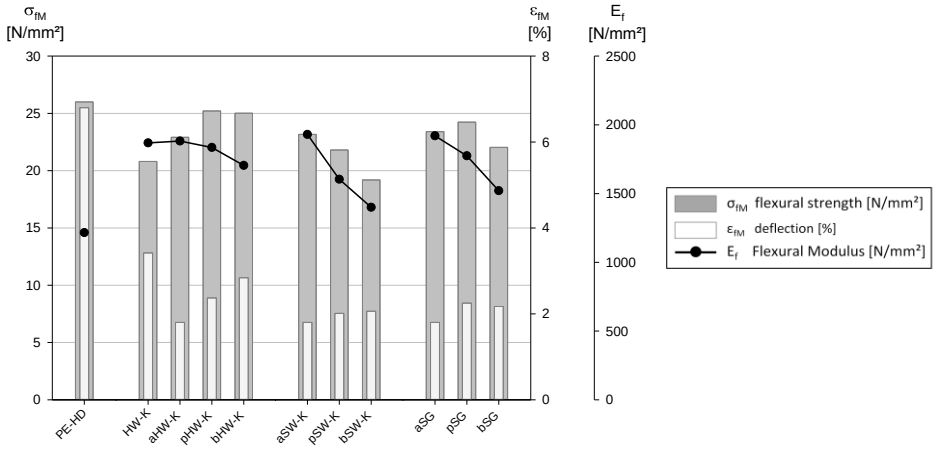

Figure 3. Results of the flexural tests: pure PE-HD is shown in comparison to 1:1 mixtures with unmodified and modified Hardwood Kraft, Softwood Kraft, and Soda Grass lignins

IV. CONCLUSIONS

Three technical lignins (Soda Grass, Hardwood and Softwood Kraft) from different sources were modified with acetic, propionic, and butyric anhydride before melt mixing with high density polyethylene (PE-HD). Test specimens to evaluate the mechanical properties of the resulting blends were produced by injection moulding.

Regarding the results of pure PE-HD, the lignin-polyblends are still more rigid, showing brittle fractures during the tensile tests. Yet, modification with short chain acid anhydrides improves the mechanical properties compared to blends containing unmodified lignin. In this context, the modification reagent is more decisive for the processability and properties than the lignin source.

Compatibility of lignin and polyethylene and the adhesion at their interface are progressively enhanced with increasing chain length of the substituent. The mechanical tests reveal an increase of the strength and elongation/deflection values, as well as a decline of the respective moduli the longer the esterified side chain becomes. Concerning the respective modification reagents, there are no significant differences to be pointed out among the three lignins.

V. ACKNOWLEDGEMENT

WoodWisdom-EraNet and the German funding agency “Fachagentur für nachwachsende Rohstoffe” (ref. no. 22020811) are acknowledged for the funding of ProLignin project.

VI. REFERENCES

[1] Lora, J.H.; Glasser, W.G. Recent Industrial Applications of Lignin: A Sustainable alternative to Nonrenewable Materials. *J. Polym. Environ.* **2002**, 10, 39-48.

[2] Cazacu, G.; Pascu, M.C.; Profire, L.; Kowarski, A.I.; Mihaes, M.; Vasile, C. Lignin Role in a Complex Polyolefin blend. *Ind. Crops Prod.* **2004**, *20*, 262-273.

[3] Ciemniecki, S.L.; Glasser, W.G. Multiphase Materials with Lignin: 1. Blends of Hydroxypropyl Lignin with Poly(methylmethacrylate). *Polymer*. **1988**, *29*, 1021-1029.

[4] Alexy, P.; Košíková, B.; Podstránska, G. The Effect of Blending Lignin with Polyethylene and Polypropylene on Physical Properties. *Polymer*. **2000**, *41*, 4901-4908.

[5] Nitz, H.; Semke, H.; Mülhaupt, R. Influence of Lignin Type in the Mechanical Properties of Lignin Based Compounds. *Macromol. Mater. Eng.* **2001**, *286*, 737-743.

[6] Thielemans, W.; Wool, R.P. Lignin Esters for Use in Unsaturated Thermosets: Lignin Modification and Solubility Modeling. *Biomacromolecules.* **2005**, *6*, 1895–1905.

[7] Olsson, S.; Östmark, E.; Ibach, R.E.; Clemons, C.M.; Segerholm, K.B.; Englund, F. The Use of Esterified Lignin for Synthesis of Durable Composites. *Proceedings of 7th meeting of Nordic-Baltic Network in Wood Material Science & Engineering (WSE)*. **2011**.

[8] Maldhure, A.V.; Ekhe, J.D.; Deenadayalan, E. Mechanical Properties of Polypropylene Blended with Esterified and Alkylated Lignin. *J. Appl. Polym. Sci.* **2012**, 125, 1701-1712.

[9] DIN EN ISO 527-2:2012. Kunststoffe – Bestimmung der Zugeigenschaften – Teil 2: Prüfbedingungen für Form- und Extrusionsmassen (ISO 527-1:2012); Deutsche Fassung EN ISO 527-2:2012.

[10] DIN EN ISO 178:2006: Kunststoffe – Bestimmung der Biegeeigenschaften (ISO 178:2001 + Amd. 1:2004); Deutsche Fassung EN ISO 178:2003 + A1:2005.

[11] DIN EN ISO 527-1:2012. Kunststoffe – Bestimmung der Zugeigenschaften – Teil 1: Allgemeine Grundsätze (ISO 527-1:2012); Deutsche Fassung EN ISO 527-1:2012.

A DETAILED STRUCTURAL CHARACTERIZATION OF THE LIGNIN FROM WHEAT STRAW

José C. del Río[1]*, Jorge Rencoret[1], Pepijn Prinsen[1], Ana Gutiérrez[1], John Ralph[2], and Ángel T. Martínez[3]

[1]IRNAS-CSIC, P.O. Box 1052, 41080-Seville, Spain; [2]The University of Wisconsin, Madison, USA; [3]CIB-CSIC, Ramiro de Maeztu 9, E-28040 Madrid, Spain (delrio@irnase.csic.es)*

ABSTRACT

The structure of the lignin in wheat straw has been investigated by 2D-NMR and DFRC. It is a p-hydroxyphenyl-guaiacyl-syringyl lignin (with a H:G:S ratio of 6:64:30) associated with p-coumarates and ferulates. The main substructures present are β–O–4´-ethers (~75%), followed by phenylcoumarans (~11%), with lower amounts of other units. The lignin is partially acylated (~10%) at the γ-carbon, predominantly with acetates that preferentially acylate guaiacyl (12%) rather than syringyl (1%) units. p-Coumarate esters were barely detectable (<1%) on monomer conjugates released by selectively cleaving β-ethers in DFRC, indicating that they might be preferentially involved in condensed or terminal structures. A major new finding is that the flavone tricin is apparently incorporated into the lignins.

I. INTRODUCTION

Nowadays, increasing attention is being paid to the use of lignocellulosic biomass as a renewable feedstock for the production of second generation bioethanol [1]. Common lignocellulosic feedstocks considered for biofuel production include woods, perennial energy crops, and agricultural wastes (e.g., corn stover or cereal straws). Among them, wheat straw has the greatest potential of all agricultural residues because of its wide availability and low cost [1]. Wheat straw contains 35–45% cellulose, 20–30% hemicelluloses, and around 15% lignin, which makes it an attractive feedstock to be converted to ethanol and other value-added products. The conversion of lignocellulosic biomass to bioethanol involves saccharification of carbohydrates to fermentable reducing sugars via hydrolysis and then fermentation of these free sugars to ethanol. However, the presence of lignin limits the accessibility of enzymes to cellulose, thus reducing the efficiency of the hydrolysis. Pretreatment of lignocellulosic materials to remove or modify the lignin is therefore needed to enhance the hydrolysis of carbohydrates. The knowledge of the structure of the lignin polymer is important to develop appropriate pretreatment methods for lignin modification and/or removal. In this paper, a more in-depth and complete characterization of the lignin of wheat straw has been performed by 2D-NMR and DFRC. The knowledge of the composition and structure of wheat straw lignin will help to maximize the exploitation of this important agricultural waste as a feedstock for biofuels and other biorefinery products.

II. EXPERIMENTAL

Wheat straw (*Triticum durum*) was air-dried and the dried samples were milled using a knife mill and successively extracted with acetone in a Soxhlet apparatus for 8 h and hot water. 'Milled-Wood Lignin' (MWL) was obtained by dioxane extraction according to the classical method, from extractive-free wheat straw [2,3].

For NMR analysis, around 40 mg of MWL were dissolved in 0.75 mL of DMSO-d_6. NMR spectra were recorded at 25 ºC on a Bruker AVANCE III 500 MHz instrument equipped with cryoprobe. HSQC experiments used Bruker's 'hsqcetgpsisp2.2' pulse program with spectral widths of 5000 Hz and 20,843 Hz for the ^{1}H- and ^{13}C-dimensions. The number of collected complex points was 2048 for the ^{1}H-dimension with a recycle delay of 1.5 s. The number of transients was 64, and 256 time increments were always recorded in the ^{13}C-dimension. The $^{1}J_{CH}$ used was 145 Hz. Processing used typical matched Gaussian apodization in the ^{1}H dimension and squared cosine-bell apodization in the ^{13}C dimension. Prior to Fourier transformation, the data matrixes were zero-filled up to 1024 points in the ^{13}C-dimension. The central solvent peak was used as an internal reference (δ_C 39.5; δ_H 2.49). Long range *J*-coupling evolution times of 66 and 80 ms were used in different HMBC acquisition experiments. HSQC correlation peaks were assigned by comparing with the literature [2–6]. A semiquantitative analysis of the volume integrals of the HSQC correlation peaks was performed using Bruker's Topspin 2.1 processing software. In the aliphatic oxygenated region, the relative abundances of side-chains involved in the various inter-unit linkages were estimated from the C_α–H_α correlations, except for substructures A_{ox} and I, for which C_β–H_β and C_γ–H_γ correlations were used. In the aromatic/unsaturated region, C_2–H_2 correlations from H, G and S lignin units and from *p*-coumarate and ferulate were used to estimate their relative abundances.

III. RESULTS AND DISCUSSION

The structural characteristics of the MWL isolated from wheat straw were analyzed in detail by 2D-NMR. The side-chain (δ_C/δ_H 50-90/2.5-5.8) and the aromatic/unsaturated (δ_C/δ_H 90-155/6.0-8.0) regions of the HSQC NMR spectrum are shown in **Figure 1**, together with the main substructures found. The aliphatic-oxygenated region of the spectra gave information about the different inter-unit linkages present in the lignin. In this region, correlation peaks from methoxyls and side-chains in β–*O*–4´ substructures (**A**) were the most prominent. Other substructures were also clearly visible, including signals for phenylcoumarans (**B**), resinols (**C**), dibenzodioxocins (**D**), and spirodienones (**F**). Minor amounts of α,β-diaryl ether substructures (**E**) could also be detected. The main correlation peaks in the aromatic/unsaturated region of the HSQC spectra corresponded to the aromatic rings and unsaturated side-chains of the different lignin units and hydroxycinnamates. Signals from *p*-hydroxyphenyl (**H**), guaiacyl (**G**), and syringyl (**S**) units were observed. In addition, prominent signals corresponding to *p*-coumarate (**PCA**) and ferulate (**FA**) structures were also observed. Other signals in this region of the spectrum are from the unsaturated side-chains of cinnamyl alcohol end-groups (**I**) and cinnamaldehyde end-groups (**J**).

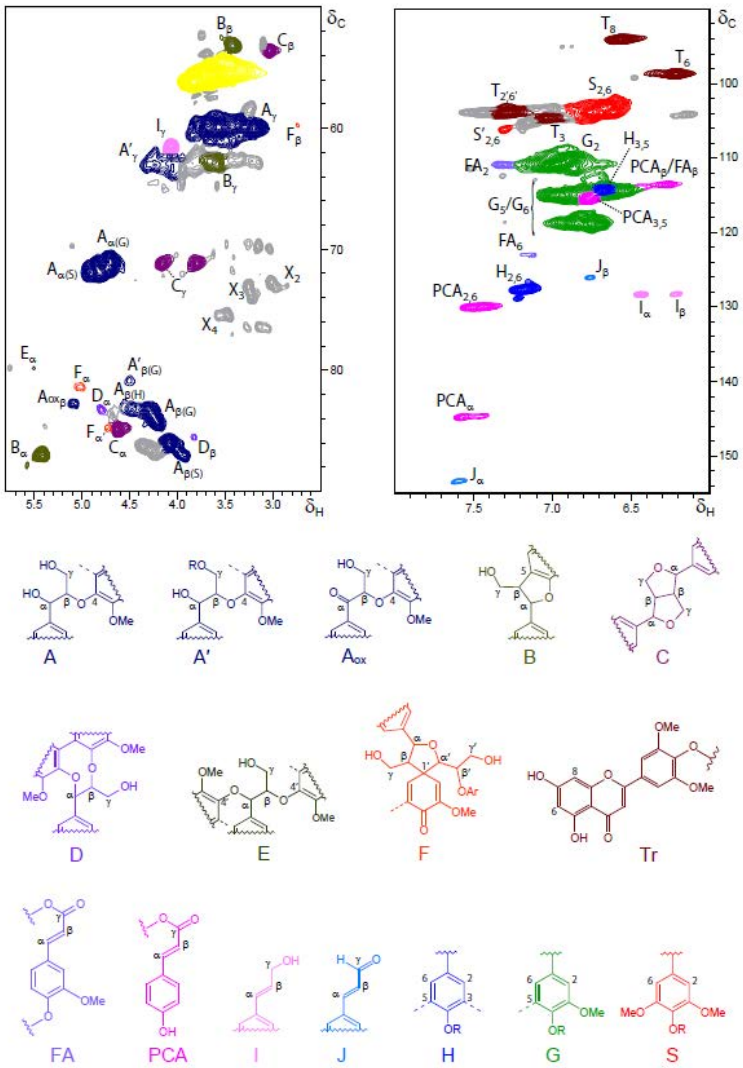

Figure 1. Side-chain (δ_C/δ_H 50-90/2.5-5.8) and aromatic/unsaturated (δ_C/δ_H 90-155/5.5-8.0) regions in the 2D HSQC NMR spectrum of wheat straw MWL. Main structures present: (**A**) β–*O*–4´ alkyl-aryl ethers; (**A'**) β–*O*–4´ alkyl-aryl ethers with acylated γ-OH; (**A_{ox}**) Cα-oxidized β–*O*–4´ structures; (**B**) phenylcoumarans; (**C**) resinols; (**D**) dibenzodioxocins; (**E**) α,β-diaryl ethers; (**F**) spirodienones; (**I**) cinnamyl alcohol end-groups; (**J**) cinnamyl aldehyde end-groups; (**PCA**) p-coumarates; (**FA**) ferulates; (**H**) *p*-hydroxyphenyl units; (**G**) guaiacyl units; (**S**) syringyl units; (**Tr**) tricin.

The main structural characteristics of wheat straw lignin are shown in **Table 1**. The structure of the lignin is mostly made up of β–*O*–4´ linkages (accounting for 75% of all the inter-unit linkages), followed by phenylcoumarans (11%) and lower amounts of resinols, dibenzodioxocins, α,β-diaryl ethers, and spirodienones.

Table 1. Structural Characteristics from Integration of ^{13}C-^{1}H Correlation Peaks in the HSQC of the Wheat Straw MWL

	Wheat straw MWL
Lignin inter-unit linkages (%)	
β–*O*–4´ aryl ethers (**A/A'**)	75
α-oxidized β–*O*–4´ aryl ethers ($\mathbf{A_{ox}}$)	2
Phenylcoumarans (**B**)	11
Resinols (**C**)	4
Dibenzodioxocins (**D**)	3
α,β-diaryl ethers (**E**)	2
Spirodienones (**F**)	3
Lignin end-groups[a]	
Cinnamyl alcohol end-groups (**I**)	4
Cinnamaldehyde end-groups (**J**)	4
Lignin side-chain γ-acylation (%)	**10**
Lignin aromatic units[b]	
H (%)	6
G (%)	64
S (%)	30
S/G ratio	0.5
***p*-Hydroxycinnamates**[c]	
p-Coumarates (%)	4
Ferulates (%)	2
p-Coumarates/ferulates ratio	2.0

[a]Expressed as a fraction of the total lignin inter-unit linkage types **A-F**
[b]Molar percentages (H+G+S=100)
[c]*p*-Coumarate and ferulate molar contents as percentages of lignin content

Additional HMBC experiments indicated that *p*-coumarate is acylating the γ-position of the lignin side-chains in wheat straw, as also occurs in other grasses [2–7]. In addition, the HBMC spectrum also revealed that acetates are also acylating the γ-OH of the lignin side-chain. Acetates have also been previously found acylating the γ–OH in the lignins of many plants, including grasses [2,3,5,8–10]. Further confirmation regarding the lignin acylation in wheat, via *p*-coumarate and acetate, was provided by DFRC, a degradation method that cleaves α- and β-ether linkages in the lignin polymer leaving γ-esters intact [10.11]. *p*-Coumarate esters were barely detectable (<1%) on monomer conjugates released by selectively cleaving β-ethers in DFRC, indicating that they might be preferentially involved in condensed or terminal structures. In addition, DFRC confirmed the occurrence of native acetylation at the γ-carbon of the lignin side-chain of wheat straw. The analyses indicated that up to 12% of the G-lignin units are acetylated, while only 1% of the total S-lignin units are acetylated.

Identification of the flavone tricin in wheat straw lignin

We also report here the structural elucidation of a component giving unusual correlation peaks in the aromatic regions of HSQC spectrum, and provide the first evidence that a flavone is linked to lignin in wheat and other grasses. Two strong and well resolved signals from unknown structures, not previously reported in lignin, were readily observed at δ_C/δ_H 94.1/6.56 and 98.8/6.20 in the HSQC spectrum (**Figure 1**). Further valuable information about the nature of this structure was obtained by performing long-range ^{13}C–^{1}H correlation (HMBC) experiments [3]. From the HMBC data, it was then possible to conclude that the structure of the flavone moiety present in the MWL of wheat straw is tricin (5,7,4´-trihydroxy-3´,5´-dimethoxyflavone).

The signals appearing in the HSQC spectrum at δ_C/δ_H 94.1/6.56 and 98.8/6.20 (**Figure 1**) thus correspond to the C_8-H_8 and C_6-H_6 correlations, respectively. The HSQC also shows the C_3-H_3 correlation at δ_C/δ_H 104.5/7.04, near the $S_{2,6}$ signal. On the other hand, the phenyl moiety linked at C-2 is of syringyl-type, the correlations for $C_{2',6'}$-$H_{2',6'}$ being also observed at δ_C/δ_H 103.9/7.31. Tricin has two phenolic hydroxyls at C-5 and C-7 of the chroman-4-one skeleton, with diagnostic phenolic proton chemical shifts that are readily apparent in the HMBC. In addition, the absence of the signals for the phenolic 4´-OH of tricin in the HMBC proton indicates that it is not free. Therefore, incorporation of tricin into the lignin network through 4–*O*–β ether linkages is indicated. In fact,

a signal for the correlation of the tricin C4′ carbon (at 139.5 ppm) and a proton at the β-position of a G-unit at 4.28 ppm was clearly observed in the HMBC spectrum [3], providing evidence for this incorporation. Interestingly, tricin has also been recently found in the lignin from coconut coir [11]. Coconut, like the grasses, belongs to the monocots. Therefore, it is beginning to appear that tricin may be a feature restricted to monocot lignins although its clade range remains to be determined.

IV. CONCLUSIONS

The lignin from wheat straw is a H:G:S lignin, with a strong predominance of G-lignin units (S/G 0.5), and with associated *p*-coumarates and ferulates. The main lignin inter-unit linkages are β–*O*–4′ alkyl-aryl ethers, followed by phenylcoumarans and minor amounts of resinols, spirodienones, dibenzodioxocins and α,β-diaryl ethers, together with cinnamyl alcohol and cinnamaldehyde end-groups. The lignin is partially acylated (~10% of all side-chains), and exclusively at the γ-carbon of the side-chain, with acetates and *p*-coumarates. Finally, we present the first evidence that the flavone tricin was found in wheat lignin, etherified by a G-type unit. If it is ultimately shown to have incorporated, in the cell wall, into the lignin by the radical coupling reactions that typify lignification (as it appears), the definition of lignin, and what constitutes a lignin monomer, will need further refinement.

V. ACKNOWLEDGEMENT

This study has been funded by the EU-project LIGNODECO (KBBE-244362) and the Spanish project AGL2011-25379 (co-financed by FEDER funds). Jorge Rencoret thanks the CSIC for a JAE-DOC contract of the program “Junta para la Ampliación de Estudios” co-financed by Fondo Social Europeo (FSE). John Ralph was funded by the DOE Great Lakes Bioenergy Research Center (DOE Office of Science BER DE-FC02-807ER64494).

VI. REFERENCES

[1] Sarkar, N.; Ghosh, S.K.; Bannerjee, S.; Aikat, K. Bioethanol production from agricultural wastes: An overview. *Renew. Energy* **2012**, *37*, 19–27.

[2] del Río, J.C.; Prinsen, P.; Rencoret, J.; Nieto, L.; Jiménez-Barbero, J.; Ralph, J.; Martínez, A.T.; Gutiérrez, A. Structural characterization of the lignin in the cortex and pith of elephant grass (*Pennisetum purpureum*) stems. *J. Agric. Food Chem.* **2012**, *60*, 3619–3634.

[3] del Río, J.C.; Rencoret, J.; Prinsen, P.; Martínez, A.T.; Ralph, J.; Gutiérrez A. Structural characterization of wheat straw lignin as revealed by analytical pyrolysis, 2D-NMR, and reductive cleavage methods. *J. Agric. Food Chem.* **2012**, *60*, 5922–5935.

[4] Ralph, J.; Hatfield, R.D.; Quideau, S.; Helm, R.F.; Grabber, J.H.; Jung, H.-J.G. Pathway of *p*-coumaric acid incorporation into maize lignin as revealed by NMR. *J. Am. Chem. Soc.* **1994**, *116*, 9448–9456.

[5] del Río, J.C.; Rencoret, J.; Marques, G.; Gutiérrez, A.; Ibarra, D.; Santos, J.I.; Jiménez-Barbero, J.; Zhang, L.; Martínez, A.T. Highly acylated (acetylated and/or *p*-coumaroylated) native lignins from diverse herbaceous plants. *J. Agric. Food Chem.* **2008**, *56*, 9525–9534.

[6] Ralph, J.; Landucci, L.L. NMR of Lignins. In: *Lignin and Lignans; Advances in Chemistry*, Heitner, C., Dimmel, D.R., Schmidt, J.A., Eds.; CRC Press (Taylor & Francis Group): Boca Raton, FL, pp. 137–234, 2010.

[7] Ralph, J. Hydroxycinnamates in lignification. *Phytochem. Rev.* **2010**, *9*, 65–83.

[8] del Río, J.C.; Marques, G.; Rencoret, J.; Martínez A.T.; Gutiérrez, A. Occurrence of naturally acetylated lignin units. *J. Agric. Food Chem.* **2007**, *55*, 5461–5468.

[9] Ralph, J. An unusual lignin from kenaf. *J. Nat. Prod.* **1996**, *59*, 341–342.

[10] Ralph, J.; Lu, F. The DFRC method for lignin analysis. 6. A simple modification for identifying natural acetates in lignin. *J. Agric. Food Chem.* **1998**, *46*, 4616–4619.

[11] Lu, F.; Ralph, J. Derivatization followed by reductive cleavage (DFRC method), a new method for lignin analysis: protocol for analysis of DFRC monomers. *J. Agric. Food Chem.* **1997**, *45*, 2590–2592.

[12] Rencoret, J.; Ralph, J.; Marques, G.; Gutiérrez, A.; Martínez, A.T.; del Río, J.C. Structural characterization of lignin isolated from coconut (*Cocos nucifera*) coir fibers. *J. Agric. Food Chem.* **2013**, *61*, 2434−2445.

ISOLATION AND STRUCTURAL CHARACTERIZATION OF LIGNIN-CARBOHYDRATE COMPLEXES FROM SISAL AND ABACA FIBERS

José C. del Río[1]*, Jorge Rencoret[1], Pepijn Prinsen[1], Edith M. Cadena[1], Ángel T. Martínez[2] and Ana Gutiérrez[1]

[1]IRNAS-CSIC, P.O. Box 1052, 41080-Seville, Spain; [2]CIB-CSIC, Ramiro de Maeztu 9, E-28040 Madrid, Spain (delrio@irnase.csic.es)*

ABSTRACT

Lignin carbohydrate complexes (LCC) were isolated from sisal and abaca. Two LCC fractions, namely GL and XL, were isolated in a quantitative manner. GL fractions were enriched in glucans and depleted in lignin whereas XL fractions were depleted in glucans but were enriched in xylans and lignin. The lignin moieties in the different LCC fractions of sisal and abaca are structurally different from each other, with a lignin that is enriched in S-units, less condensed, that is preferentially associated to xylans, and a lignin with more G-units, more condensed, that is preferentially associated to glucans. In addition, the analyses indicated that the acetate groups attached to the γ-carbon of the lignin side-chains in abaca and sisal were completely hydrolyzed and removed during the isolation procedure.

I. INTRODUCTION

Lignin, cellulose and hemicelluloses are the three major structural components of plant cell-walls. However, selective separation or fractionation of these components is not an easy task because they are physically entangled with one another in the cell-wall [1]. In addition, chemical linkages can also occur between these components, forming the so-called lignin–carbohydrate complexes (LCCs) [1,2]. The linkage types and numbers are still not well understood, although it is generally accepted that there are three types of lignin-carbohydrate linkages present in wood, namely phenyl glycosides, esters, and benzyl ethers [1].

However, and in order to investigate LCCs structure, a clear and complete fractionation with proper preservation of the bonds between the lignin and carbohydrate must be obtained. Recently, a simple fractionation method was established to isolate LCCs from lignocellulosic biomass based on mild milling and dissolution using a mixture of dimethyl sulfoxide (DMSO) and 50% aqueous tetrabutylammonium hydroxide (TBAH) [3,4]. Two LCC fractions, a glucan-lignin (GL) and a xylan-lignin (XL) fractions can be quantitatively obtained, while a glucomannan-lignin (GML) fraction was additionally obtained from softwoods. It was claimed that this method can isolate all cell-wall components, including lignin, in a chemically unaltered form. In this work, we have applied the LCC isolation method recently developed [3,4] to two plants that are known to have lignins with high extent of acetylation, as sisal (*Agave sisalana*) and abaca (*Musa textilis*). The structure of the lignin as well as the preservation of the acetylated lignin units was monitored by using a modification of the so-called Derivatization Followed by Reductive Cleavage (DFRC) degradation method [5].

II. EXPERIMENTAL

Plant samples

The plant samples selected for this study consist of leaf fibers of sisal (*Agave sisalana*) and abaca (*Musa textilis*). The fibers were finely ground to sawdust using a knife mill before analysis.

Lignin-carbohydrate complex (LCC) fractionation

The LCC fractionation was performed according to the method previously described [3,4]. A ball-milled sample (ca. 3 g) was completely dissolved in a mixture of 30 ml DMSO and 30 ml TBAH (40% w/w in water). Then, the clear solution was dispersed into 500 ml deionized water until a precipitate was formed. The precipitate was washed with deionized water until neutral pH, and was then freeze-dried to obtain the glucan-lignin fraction (GL). The xylan-lignin fraction (XL) was obtained, after separation of the precipitate, by neutralizing the solution with HCl, followed by dialysis and freeze-drying. The barium hydroxide step detailed in [4] was skipped since glucomannan is not a major hemicellulose in these plants.

DFRC (derivatization followed by reductive cleavage) degradation

A modification of the standard DFRC method by using propionyl instead of acetyl reagents (DFRC´) was used [5], and the detailed protocol has been published elsewhere [6].

III. RESULTS AND DISCUSSION

Sisal and abaca were fractionated according to the LCC fractionation approach previously developed [3,4]. Two different LCC fractions, namely a glucan-lignin (GL) and a xylan-lignin (XL) fraction, were efficiently and quantitatively isolated from sisal and abaca. The yields of the GL and XL fractions isolated from sisal and abaca, as well as the Klason lignin content and the composition of the sugars in these fractions, are detailed in **Table 1**. In sisal, GL and XL fractions accounted for 68.5% and 31.5%, respectively, whereas in abaca GL and XL fractions accounted for 78.8% and 21.2%, respectively. Interestingly, the total of both fractions amounted to nearly 100% of the initial material, indicating that the fractionation was quantitative. In both plants, the yields of GL were higher than XL, as also occurred in hardwoods and softwoods [3,4]. In addition, in both plants, the GL fractions were enriched in glucan and depleted in lignin, while the XL fractions were depleted in glucan and enriched in xylan and lignin. Hence, in sisal, GL was enriched in glucan (88.4% of the sugars were glucose) with low Klason lignin content (7.8%), whereas XL was enriched in xylose (89.4% of the sugars) with a high Klason lignin content (24.1%). In abaca, GL was also enriched in glucose (95% of all the sugars) and depleted in lignin (4.4% Klason lignin), whereas XL was enriched in xylose (72.6% of all sugars) and presented a high Klason lignin content (29.4%).

Table 1. Yield of GL and XL fractions isolated from sisal and abaca, and content of klason lignin and carbohydrates.

	Sisal		Abaca	
	GL	XL	GL	XL
Yield (%)	68.5	31.5	78.8	21.2
Klason lignin (%)	7.8	24.1	4.4	29.4
Carbohydrates (relative %)				
Arabinose	1.5	0.6	0.3	3.9
Xylose	9.0	89.4	4.1	72.6
Mannose	0.9	2.6	0.5	15.0
Galactose	0.2	0.3	0.1	0.3
Glucose	88.4	7.1	95.0	8.2

The lignins from sisal and abaca are known to be highly acetylated at the γ-carbon of the lignin side-chain [6-8]. Since it might exist the possibility of some structural modifications of the lignin due to the use of TBAH, a strong basic salt that may alter the structure of the lignin during the fractionation, the occurrence of naturally acetylated lignin in the GL and XL fractions isolated from sisal and abaca was analyzed in detail. For this, we used a modification of the so-called Derivatization Followed by Reductive Cleavage (DFRC) method, that cleaves α-ether and β-ether linkages but leaves γ-esters intact allowing the analysis of native γ-acylated lignin, by using propionyl instead of acetyl reagents (DFRC′) [5]. The chromatograms of the DFRC′ degradation products of the XL and GL fractions isolated from sisal and abaca are shown in **Figure 1**. The chromatograms of the DFRC′ degradation products of the MWL isolated from the same plants are also shown for comparison.

The MWL from sisal and abaca released the *cis* and *trans* isomers of guaiacyl (*c*-G and *t*-G) and syringyl (*c*-S and *t*-S) lignin monomers in different proportions, arising from normal (γ-OH) units in lignin. In addition, the presence of originally γ-acetylated guaiacyl (*c*-Gac and *t*-Gac) and syringyl (*c*-Sac and *t*-Sac) lignin units could be clearly observed in the chromatograms of the DFRC′ of the MWL isolated from sisal and abaca (**Figure 1**). The relative abundances of γ-OH and γ-acetylated lignin units (G, Gac, S and Sac), as well as the percentage of acetylated Gac- and Sac- units and the S/G ratios, in the GL and XL fractions isolated from sisal and abaca, and in their respective MWLs, are shown in **Table 2**. In both MWLs, the acetylation occurred predominantly on syringyl units, as has been observed in most lignins [6-9]. The high extent of γ-acetylation of sisal MWL included both S units (80%) and G units (48%), whereas in the case of abaca MWL γ-acetylation occurred predominantly on S units (84%) and only a minor degree of acetylation was observed on G units (4%), in agreement with previous studies [6-8]. The S/G ratios of the MWL from sisal and abaca, as determined by DFRC′, were 1.4 and 1.3, respectively.

The analyses indicated that the composition of the lignin moiety in the XL and GL fractions isolated from sisal and abaca were completely different from each other and from the respective MWL. Sisal XL fraction presented a lignin enriched in S-units (S/G ratio 2.8), whereas sisal GL fraction presented a lignin with more G-units (S/G ratio 1.0). Likewise, abaca XL fraction presented a lignin enriched in S-units (S/G ratio of 3.3), whereas abaca GL fraction presented a lignin with more G-units (S/G ratio of 1.1). Similar results were also found in the LCC fractions of eucalyptus [3] and spruce [4]. This fact suggests that the lignin moiety in the different LCC fractions

of sisal and abaca are structurally different from each other, and indicates the presence of two types of lignins in each plant, a lignin that is enriched in S-units, less condensed, that is preferentially associated to xylans, and a lignin with more G-units, more condensed, that is preferentially associated to glucans.

Interestingly, XL and GL fractions only released lignin monomers arising from normal (γ-OH) units in lignin. The γ-acetylated guaiacyl (*c*-Gac and *t*-Gac) and syringyl (*c*-Sac and *t*-Sac) lignin units were completely absent in the chromatograms. This indicates that the acetate groups acylating the γ-carbon of the lignin side-chain have been extensively hydrolyzed during LCC fractionation, most probably due to the use of TBAH, a strong basic salt. Therefore, this LCC fractionation seems to affect the structure of lignins, particularly those having a large extent of γ-acylation. Acetylated lignin units are known to occur in all angiosperms, including mono- and eudicotyledons [6-12]. Likewise, it can be envisaged that other groups (*p*-coumarates and *p*-hydroxybenzoates) that are also acylating the γ-carbon of the lignin in other plants [10-12] may behave similarly and suffer from hydrolysis during the LCC fractionation. Moreover, we also observed that acetates attached to carbohydrates (as in xylans) were also be hydrolyzed during LCC fractionation.

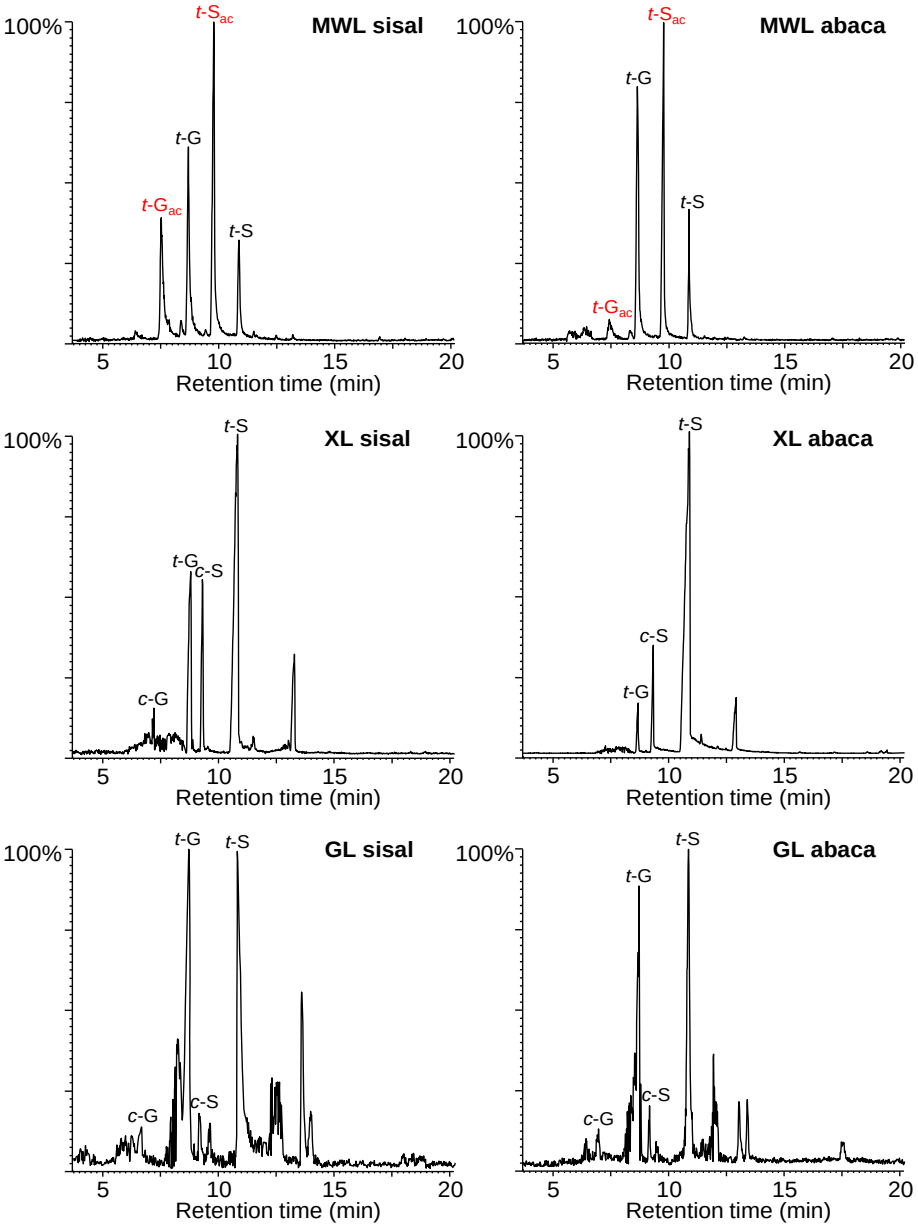

Figure 1. Reconstructed Ion Chromatograms (*m/z* 222+236+252+266) of the DFRC′ degradation products of XL fractions isolated from sisal and abaca. The DFRC′ degradation products of the respective MWL are shown for comparison. *c*-G, *t*-G, *c*-S and *t*-S are the *cis*- and *trans*-guaiacyl and syringyl monomers, respectively. *c*-Gac, *t*-Gac, *c*-Sac and *t*-Sac are the originally γ-acetylated *cis*- and *trans*-guaiacyl and syringyl monomers, respectively.

Table 2. Relative abundance (%) of γ-OH and γ-acetylated lignin units (G, Gac, S and Sac), percentage of acetylated G and S units and S/G ratios, in the GL and XL fractions isolated from sisal and abaca, and in their respective MWLs, as determined upon DFRC′

	Sisal			Abaca		
	MWL	GL	XL	MWL	GL	XL
Gac	20	0	0	2	0	0
G	22	50	26	43	47	23
Sac	46	0	0	46	0	0
S	12	50	74	9	53	77
% acetylated G units	48	0	0	4	0	0
% acetylated S units	80	0	0	84	0	0
S/G ratio	1.4	1.0	2.8	1.3	1.1	3.3

IV. CONCLUSIONS

Sisal and abaca were fractionated into different LCC fractions. Two different LCC fractions, namely a glucan-lignin (GL) and a xylan-lignin (XL) fraction, were quantitatively isolated. The GL fractions were enriched in glucan and depleted in lignin, while the XL fractions were depleted in glucan and enriched in xylan and lignin. The structural characteristics of the lignins in the XL fractions, in particular the extent of acetylation of the γ-carbon of the side-chain, were studied by DFRC that indicated that the acetate groups that are natively present in these lignins were completely hydrolyzed and removed during the LCC fractionation.

V. ACKNOWLEDGEMENT

This study has been funded by the EU-project LIGNODECO (KBBE-244362) and the Spanish project AGL2011-25379 (co-financed by FEDER funds). Jorge Rencoret thanks the CSIC for a JAE-DOC contract of the program “Junta para la Ampliación de Estudios” co-financed by Fondo Social Europeo (FSE).

VI. REFERENCES

[1] Fengel, D.; Wegener, G. *Wood: Chemistry, Ultrastructure,Rreactions*. Berlin: Walter de Gruyter, 1984.

[2] Balakshin, M.; Capanema, E.; Gracz, H.; Chang, H.M.; Jameel, H. Quantification of lignin-carbohydrate linkages with high-resolution NMR spectroscopy. *Planta* **2011**, *233*, 1097–1110.

[3] Li, J.; Martin-Sampedro, R.; Pedrazzi, C.; Gellerstedt, G. Fractionation and characterization of lignin–carbohydrate complexes (LCCs) from eucalyptus fibers. *Holzforschung* **2011**, *65*, 43–50.

[4] Du, X.; Gellerstedt, G.; Li, J. Universal fractionation of lignin-carbohydrate complexes (LCCs) from lignocellulosic biomass: an example using spruce wood. *Plant J.* **2013**, *74*, 328–338.

[5] Ralph, J.; Lu, F. The DFRC method for lignin analysis. 6. A simple modification for identifying natural acetates in lignin. *J. Agric. Food Chem.* **1998**, *46*, 4616–4619.

[6] del Río, J.C.; Marques, G.; Rencoret, J.; Martínez A.T.; Gutiérrez, A. Occurrence of naturally acetylated lignin units. *J. Agric. Food Chem.* **2007**, *55*, 5461–5468.

[7] del Río, J.C.; Rencoret, J.; Marques, G.; Gutiérrez, A.; Ibarra, D.; Santos, J.I.; Jiménez-Barbero, J.; Zhang, L.; Martínez, A.T. Highly acylated (acetylated and/or *p*-coumaroylated) native lignins from diverse herbaceous plants. *J. Agric. Food Chem.* **2008**, *56*, 9525–9534.

[8] Martínez, A.T.; Rencoret, J.; Marques, G.; Gutiérrez, A.; Ibarra, D.; Jiménez-Barbero, J.; del Río, J.C. Monolignol acylation and lignin structure in some nonwoody plants: A 2D-NMR study. *Phytochemistry* **2008**, *69*, 2831–2843.

[9] Ralph, J. An unusual lignin from kenaf. *J. Nat. Prod.* **1996**, *59*, 341−342.

[10] Rencoret, J.; Ralph, J.; Marques, G.; Gutiérrez, A.; Martínez, A.T.; del Río, J.C. Structural characterization of lignin isolated from coconut (*Cocos nucifera*) coir fibers. *J. Agric. Food Chem.* **2013**, *61*, 2434−2445.

[11] del Río, J.C.; Rencoret, J.; Prinsen, P.; Martínez, A.T.; Ralph, J.; Gutiérrez, A. Structural characterization of wheat straw lignin as revealed by analytical pyrolysis, 2D-NMR, and reductive cleavage methods. *J. Agric. Food Chem.* **2012**, *60*, 5922−5935

[12] del Río, J.C.; Prinsen, P.; Rencoret, J.; Nieto, L.; Jiménez-Barbero, J.; Ralph, J.; Martínez, A.T.; Gutiérrez, A. Structural characterization of the lignin in the cortex and pith of elephant grass (*Pennisetum purpureum*) stems. *J. Agric. Food Chem.* **2012**, *60*, 3619–3634.

INDUCED PRODUCTION OF THE HYDROLYTIC ENZYMES BY *ASPERGILLUS ACULEATUS* IN SUBMERGED FERMENTATION ON STEAM-EXPLODED WHEAT-STRAW AS CARBON SOURCE

Marie Demuez*, Cristina González-Fernández, María-José Negro, Mercedes Ballesteros

*IMDEA Energy Institute, Biotechnology Processes for Energy Production Joint Unit IMDEA Energy-CIEMAT, Mostoles, Spain (*marie.demuez@imdea.org)*

ABSTRACT

The present study describes the production of cellulolityc and xylanolytic enzymes from the filamentous fungi *Aspergillus aculeatus* CECT 20387 in submerged fermentation using pretreated lignocellulosic biomass as carbon source. This fungus was grown at 25ºC with agitation during 20 days on steam-exploded pretreated wheat straw (SEWS): washed water insoluble fraction (WIS) and whole slurry. Additionally, sigma-cellulose standard medium (Sigmacell) was used as model cellulosic substrate.
Maximal β-glucosidase, endoxylanase and β-xylosidase activities measured on Sigmacell were 31.8 IU/g $_{DW}$, 76 IU/g $_{DW}$ and 1.35 IU/g $_{DW}$ of substrate, respectively. When slurry, containing soluble and insoluble solids, was used, 47.3 IU of β-glucosidase /g $_{DW}$ of glucan, 6341 IU of endoxylanase /g $_{DW}$ of xylan and 26.6 IU β-xylosidase /g $_{DW}$ of xylan were quantified. In experiments using the WIS fraction, the highest levels of β-glucosidase, endoxylanase and β-xylosidase activities detected were 28.6 IU /g $_{DW}$ of glucan, 2915 IU/g $_{DW}$ of xylan and 53.7 IU /g $_{DW}$ of xylan respectively. WIS fraction induced preferentially β-xylosidase production whereas the whole slurry seems to induce β-glucosidase and endoxylanase production. The differences in xylanolytic enzymes production profiles are a matter of the substrate composition and seems to be due to the presence of soluble compounds (inhibitors and sugars) in liquid fraction of slurry.

I. INTRODUCTION

Hydrolysis step is regarded as the key-limiting step in the production of biofuels and biochemical from lignocellulosic biomass. Since the production cost of hydrolytic enzymes is one of the major problems for industrial application, big efforts have been directed to the characterization and optimization of the enzymes produced by wood-degrading fungi. During this decade, efforts have been focused on the discovery of new xylanases and other accessory enzymes to increase the hydrolysis of all the components present in the lignocellulosic biomass. It has been shown that hydrolytic enzymes production is induced and affected by the nature of the substrate used in fermentation [1-2]. Therefore, the cultivation of fungus on a particular lignocellulosic material could induce different enzyme mixture with a composition and proportion especially suitable for the hydrolysis of this particular material. By finding a tailored enzymatic cocktail for the hydrolysis of the certain material, the enzyme loading would be lowered and the efficiency of the process increased.

This study was aimed at the characterization of enzymes production by the wild-type filamentous fungus *Aspergillus aculeatus* CECT 20387, using pretreated lignocellulosic substrates (SEWS) with different composition (washed water insoluble fraction and whole slurry), and sigma-cellulose standard medium. Hydrolytic enzymes production profiles obtained in the different substrates were compared.

II. EXPERIMENTAL

Microorganisms and growing conditions

The mesophilic *Aspergillus aculeatus* CECT 20387 was maintained at 25ºC on agar composed of 20 g L^{-1} malt extract, 20 g L^{-1} glucose, 1 g L^{-1} peptone, 15 g L^{-1} agar.

Black conidia from 3 days-old agar plates were harvested with sterile saline solution composed of 0.9% NaCl and 0.1% Tween 80. The suspension was adjusted to 1.5- 2.10^8 spores, and was used to inoculate Erlenmeyer flask containing 150 mL sterile Mandel's medium supplemented with 0.1% Tween 80 and 10 g L^{-1} glucose as carbon source [3]. Fungal preculture was incubated at 25ºC at 180 rpm rotary shaker for 4 days. To homogenize the biomass in the culture, *A. aculeatus* mycelium balls were disrupted with IKA T18 disruptor (S18N-10G). 10 % of homogenous mycelium was inoculated into each of the cultures with different cellulosic substrates.

For enzyme production, 2-fold concentrated Mandel's medium supplemented with 12 mM of phosphate buffer without glucose was used. *A. aculeatus* cultures with 4% (w/v) substrate consistency (WIS, slurry and Sigmacell) were incubated at 25ºC, 180 rpm agitation for 20 days.

Raw and pretreated material

Wheat straw was supplied by CEDER-CIEMAT (Soria, Spain). The composition of this material was (% dry weight, w/w): cellulose, 40.5; hemicelluloses, 26.1 (xylan, 22.7; arabinan, 2.1; and galactan, 1.3); lignin, 18.1; ash, 5.1; and extractives, 14.6 [4].

The SEWS was obtained by treating milled wheat straw by steam explosion (200 ºC for 10 min) without acid impregnation, considering a severity factor of 3.94. One part of SEWS was used as whole slurry. This slurry contained both soluble (hemicellulosic-derived sugars, acetic acid, and degradation compounds) and insoluble fraction. Other part was thoroughly washed with water and vacuum-filtered, obtaining a water insoluble solids (WIS) fraction composed mainly by cellulose and lignin. Both substrates (WIS and slurry) were kept at 4 ºC until use.

Analytical methods

Raw material, slurry and WIS were analyzed using the National Renewable Energy Laboratory (NREL) standard methods for determination of structural carbohydrates and lignin [5]. Dry weights were determined by drying a representative sample at 105ºC for 24 h. Total phenolic content of the supernatants from fungi culture was determined according to a slightly modified version of the Folin-Ciocalteau method described by Moreno *et al*., [6].

Enzymatic assays

Enzymatic activity assays were performed in micro-volumes using different substrates. Total cellulase activity (FPase) and endoxylanase activity were determined using Whatman No. 1 filter paper disks (5.5 mm) [7] and xylan birchwood solution [8] as substrates, respectively. Subsequently formed reducing sugars were measured by DNS method [9]. β-Glucosidase and β-xylosidase activities were determined using synthetic ρ-nitrophenyl-β-d-glucopyranoside and ρ-nitrophenyl-β-d-xylopyranoside as substrate, respectively [10]. Proteins from the culture supernatant were precipitated using methanol/chloroform, and further quantified using reducing agent compatible BCA protein assay kit (Pierce Ref. 23250). In this later analysis, bovine serum albumin was used as standard. Enzymatic activities are expressed in International Units (IU), where one unit of enzyme activity is definied as catalyzing the formation of 1 µmol product in 1 min (glucose for filter paper activity, xylose for xylanase and p-nitrophenol for β-glucosidase and β-xylosidase) under the assay conditions.

III. RESULTS AND DISCUSSION

Pretreatment of raw material

After steam explosion pretreatment, the chemical composition of water insoluble fraction of SEWS (WIS and slurry) was compared with the one of the raw material. The pretreatment produces high hemicellulose solubilization from 26.1 to 4.9 % (w/w) while the cellulose and Klason lignin content increased from 40.5% and 18.1% to 58.8% and 33.6% (w/w), respectively. Hemicellulose solubilization is typically observed during steam explosion pretreatment [11].

The soluble fraction of the SEWS was analyzed to evaluate the effect of steam-explosion pretreatment (**Table 1**). This liquid fraction contained soluble sugars in oligomeric and monomeric forms and degradation products.

Table 1. Composition of the soluble fraction of slurry after steam-explosion pretreatment (g L^{-1}).

Total sugars (oligomers)		Degradation products	
Glucose	5.46 (3.48)	Furfural	2.11
Xylose	17.56 (11.78)	HMF	0.33
Arabinose	1.16 (0.4)	Formic acid	10.46
Galactose	1.75 (1.05)	Acetic acid	13.36
Mannose	0.87 (0.87)	Vanillin	0.06
		Ferulic acid	0.04
		Syringaldehyde	0.02

Reducing sugars content

The concentration of reducing sugars was followed during culture **(Figure 1)**. No reducing sugar was observed in *A. aculeatus* culture growing on Sigmacell and WIS, as fungus was growing as much as reducing sugars were consumed. At the initial stage of the culture on slurry, high reducing sugars content was measured, which means that fungus was going through a lag phase due to the presence of toxic compounds (furan derivates, weak acids, and phenolic substances) and has to adapt to this substrate. However, reducing sugars was subsequently consumed after 3 days of culture on slurry, indicating that *A. aculeatus* was starting to grow due to presence of free sugars. After 14 days of culture, (**Figure1**. arrow) nitrogen source was added into the culture media as

ammonium sulfate powder (2.8 g L^{-1}) to re-equilibrate C/N ratio, promoting mycelium growth and extracellular protein synthesis [1, 12].

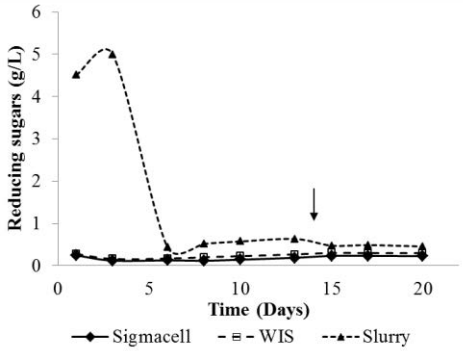

Figure 1. Reducing sugars content profile of *A. aculeatus* (g L^{-1}); Arrow: addition of N-source.

A. aculeatus cellulolytic enzymes production

Aspergillus genus is known to produce high quantity of β-glucosidase [1, 14]. In the present study, β-glucosidase enzyme was secreted steadily on Sigmacell and WIS, while it gets a maximum at the 10th days of culture on Slurry (**Figure 2A)**. Out of the three substrates, the highest induction was achieved on the slurry (47.3 IU/g $_{DW}$ of glucan).

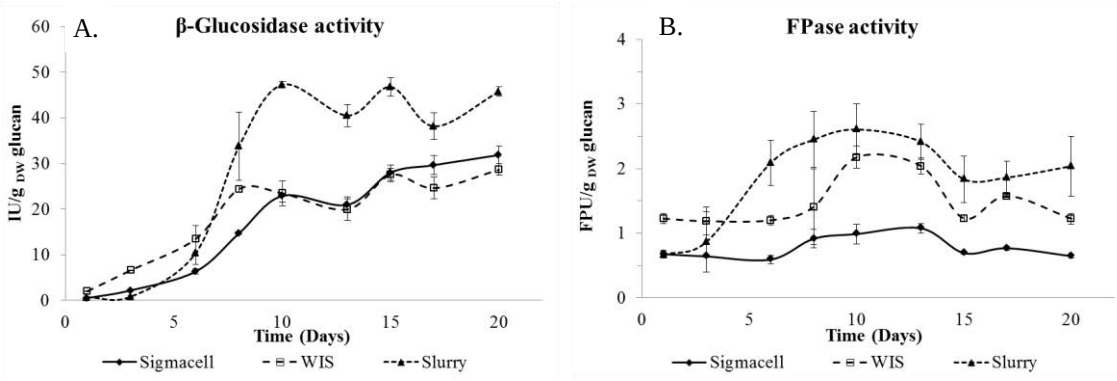

Figure 2. Time course profiles of cellulolytic activity produced by *A. aculeatus* in submerged fermentation on Sigmacell, WIS and whole slurry; A) β-glucosidase activity is expressed in IU/g $_{DW}$ of glucan; B) FPase activity is expressed in FPU/g $_{DW}$ of glucan.

Low levels of FPase activity were observed for the three substrates (**Figure 2B**), attaining a maximum activity of 2.2, 2.6 FPU/g $_{DW}$ and 1.1 FPU/g $_{DW}$ of glucan on WIS, slurry and Sigmacell, respectively, which is comparable with *Aspergillus* FPase production observed in other studies [1, 14].

A. aculeatus xylanolytic enzymes production

Aspergillus genus and *A. aculeatus* strain have been also described as a good xylanase producer and were used for xylanase production on industrial and agro-industrial wastes [13-14].

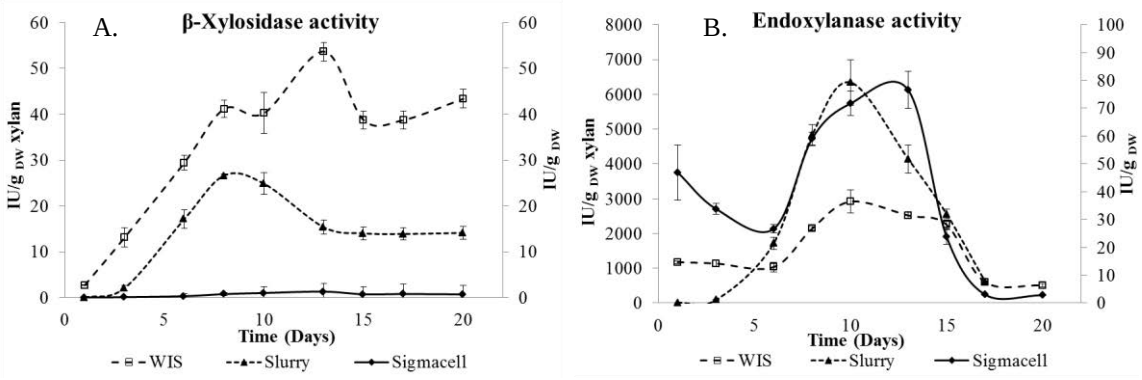

Figure 3. Time course profiles of xylanolytic activity in *A. aculeatus* submerged fermentation WIS, slurry and Sigmacell; A) β-xylosidase; B) Endoxylanase. On the right axe, activities measured on SEWS are expressed in IU/g $_{DW}$ of xylan; on the left axe, in IU/g $_{DW}$ of Sigmacell.

The results in **Figure 3** showed that WIS fraction induced more the production of β-xylosidase than endoxylanase, while the opposite was observed in the slurry. This could be explained by the presence of toxic compounds present in slurry that inhibit the expression and/or activity of β-xylosidase, whereas endoxylanase is induced [2, 14].

Xylanase enzymes are preferentially induced when *Aspergillus* is growing on a xylan-containing substrate, however, xylanase production also takes place at low level when fungus is grown on a cellulosic substrate. On Sigmacell, endoxylanase activity reached 76 IU/g $_{DW}$, which is in the range of previous reports (30-100 IU/g $_{DW}$), whereas β-xylosidase remained very low [13].

IV. CONCLUSIONS

In this study, hydrolytic enzymes production of *Aspergillus aculeatus* CECT 20387 were assessed in submerged fermentation using three different materials as carbon sources: water insoluble fraction (WIS) and whole slurry of SEWS, and Sigmacell as model cellulosic substrate. The use of different substrates led to the induction of distinctive cellulolytic and xylanolytic enzymes. WIS fraction induced preferentially β-xylosidase production whereas the slurry induced β-glucosidase and endoxylanase production due to the presence of free sugars and soluble compounds in the liquid fraction of slurry.

Xylanolytic enzymes production by *A. aculeatus* could be further optimized by better controlling operating conditions (pH) of fungus cultures to promote fungal growth. Moreover, SEWS is probably not the best substrate for xylanase production due to the low hemicellulose content after steam-explosion pretreatment. Using another kind of pretreatment would be a potential alternative to enhance the xylanolytic enzymes production.

V. REFERENCES

[1] Duff, S.J.B.; Cooper, D.G.; Maynard Fuller, O. Effect of media composition and growth conditions on production of cellulase and β-glucosidase by a mixed fungal fermentation. *Enz. Microb. Technol.* **1987**, *9*, 47-52.
[2] Manju, S.; Chadha, B.S. Production of Hemicellulolytic Enzymes for Hydrolysis of Lignocellulosic Biomass, *Chapter 9*, In: Biofuels- Alternative Feedstocks and Conversion Processess; Pandey, A., Larroche, C., Ricke, S.C., Dussap, C-G., Gnansounou, E. (Eds.), Academic Press **2011**, 203-228.
[3] Mandels, M.; Weber, J. Production of cellulases. *Adv Chem Ser*. **1969,** *95*, 391–414.
[4] Alvira, P.; Negro, M.J.; Ballesteros, M. Effect of endoxylanase and α-L-arabinofuranosidase supplementation on the enzymatic hydrolysis of steam exploded wheat straw. *Bioresour. Technol.* **2011**, *102*, 4552-4558.
[5] Sluiter, J.B.; Ruiz, R.O.; Scarlata, C.J.; Sluiter, A.D.; Templeton, D.W. Compositional analysis of lignocellulosic feedstocks. 1. Review and description of methods. *J. Agricultural Food Chem.*, **2010,** *58*, 9043-9053.
[6] Moreno, A.D.; Ibarra, D.; Ballesteros, I.; González, A.; Ballesteros, M. Comparing cell viability and ethanol fermentation of the thermotolerant yeast Kluyveromyces marxianus and Saccharomyces cerevisiae on steam exploded biomass treated with laccase. *Bioreour. Technol*. **2013**, *135*, 239-245.
[7] Xiao, Z.; Storms, R.; Tsang, A. Microplate-based filter paper assay to measure total cellulase activity. *Biotech. Bioeng.* **2004**, *88*, 832-837.
[8] Bailey, M.J.; Biely, P.; Poutanen, K. Interlaboratory testing of methods for assay of xylanase activity. *J. Biotechnol.* **1991**, *23*, 257–270.
[9] Miller, G.L.; Blum, R.; Glennon, W.E.; Burton, A.L. Measurement of carboxymethylcellulase activity. *Anal. Chem.* **1960** *1*, 127–132.
[10] Biely, P. Xylanolytyic enzymes, *Chapter 71*, In: Handbook of Food Enzymology; Marcel Dekker Inc., New York, **2003,** 879-916.
[11] Alvira, P.; Tomas-Pejo E.; Ballesteros, M.; Negro MJ. Pretreatment technologies for an efficient bioethanol production process based on enzymatic hydrolysis: A review. *Bioresour. Technol.* **2010**, *101*, 4851-4861.
[12] Betini, J.H.; Michelin, M.; Peixoto-Nogueira, S.C.; Jorge, J.A.; Terenzi, H.F.; Polizeli, M.L. Xylanases from *Aspegillus niger*, *Aspergillus niveus*, and *Aspergillus ochraceus* under solid state fermentation and their application in cellulose pulp bleaching. *Bioprocess. Biosyst. Eng.* **2009**, *32*, 819-824.
[13] Guimaraes, N.C.A.; Sorgatto, M.; Peixoto-Nogueira S.C.; Betini, J.H.; Zanoelo, F.F.; Marques, M.R.; Polizeli M.L.T.M.; Giannesi, G.C. Xylanase production form *Aspergillus japonicus var. aculeatus*: Production using agroindustrial residues and biobleaching effect on pulp. *J. Biocatal. Biotransformation* **2013**, *2*, 1.
[14] de Vries, R. ; Visser, J. Aspergillus enzymes involved in degradation of plant cell wall polysaccharides. *Microbiol. Mol. Biol. Rev.* **2001,** *65*, 497-522.

SILICA-BASED NANOCOATINGS FOR TAILORED MODIFICATION OF PAPER SURFACES

Vânia M. Dias*, Rui F. Duarte, Inês Portugal, Dmitry V. Evtuguin

*CICECO, Chemistry Department, University of Aveiro, Campus de Santiago, 3810-193 Aveiro, Portugal (*vania.dias@ua.pt)*

ABSTRACT

Targeted modification of cellulosic fibres may be accomplished by *in situ* deposition of silica employing a mild sol–gel procedure. The use of pre-hydrolyzed trialkoxysilanes bearing variable functions (propylamine, allyl, alkyl, etc.) and active substances (e.g. redox or acid/base catalysts) widely expands the application areas of the resultant cellulosic hybrids for example as functionalized materials (barrier coating, active filters, etc.) for packaging and insulation applications. This work presents new cellulose-based materials and the targeted modification of paper surfaces using silica-based formulations.

I. INTRODUCTION

Organic–inorganic hybrids (OIHs) are a relatively new type of composites with advanced mechanical, optical, electrical and thermal properties, which arise from the synergism between the properties of the starting organic and inorganic components and depend on the synthesis mode [1]. A significant part of OIHs is synthesised in a sol–gel process where starting materials, such as natural or synthetic polymers and metal alkoxides, react in the presence of a small amount of an acid or basic catalyst [2]. The advantage of this method is that inorganic particles are generated *in situ* and randomly dispersed on a polymeric host matrix, bounding to the polymer through hydrogen or covalent bonds thus forming an organic–inorganic network. In addition to the primary hydrolysis and polycondensation reactions of the precursors a sol–gel process involves other important steps such as gelation, aging, drying, stabilization and densification [1, 2].

A mild acid catalyzed sol–gel process has been reported for incorporating silica on cellulose derivatives and unmodified cellulosic fibers (pulp) using tetraethyl orthosilicate (TEOS) as silica precursor [3]. The resultant cellulose/silica hybrid materials are remarkable due to enhanced thermal stability, improved lipophilic behavior and affinity towards specific substrates [4,5]. Therefore, although cellulosic pulp is mainly used for papermaking the synthesis of cellulose/silica hybrid materials may be considered a high-added value alternative.

Paper-coating is another promising application of cellulose/silica hybrids, herein presented. TEOS based formulations are synthesized by a sol–gel method and applied on a paper surface that acts as cellulose source. Silica oligomers are formed *in situ* and linked to the paper surface via strong hydrogen bonds involving the free hydroxyl groups of cellulose. The impermeable silica network formed enables the controlled modification of paper surfaces aiming better printability and moisture resistance.

II. EXPERIMENTAL

Synthesis of silica-based nanocoatings

Paper sheets without any surface treatment (73 g/m², A3 size) were supplied by Grupo Portucel-Soporcel, Portugal. Silica precursors (tetraethyl orthosilicate – TEOS, triethoxymethylsilane – TEMS, diethoxydimethylsilane – DEDMS, triethoxypropylsilane – TEPS, 3- aminopropyltriethoxysilane – TEAP) were supplied by Sigma-Aldrich with 96-98% purity. Silica-based formulations were prepared by sol-gel synthesis, using TEOS, or a mixture of TEOS (95%) and a secondary precursor (5%), or a mixture of TEOS (94%) and two secondary precursors (3% each). The formulations were applied (ca. 2-3g/m^2) on uncoated paper sheets using a conventional roll-to-roll technique and subsequently cured by heat using an infrared lamp (ca. 5min).

Characterization methods

Silica coated papers were characterized by scanning electron microscopy with X-ray microanalysis (SEM/EDS), using a FEG-SEM Hitachi SU-70 microscope operating at 15 kV. Contact angle measurements were done in a

Data Physics Instrument OCA 20 using the sessile drop method. The surface energies and relative contribution of dispersive and polar (donor-acceptor) forces were evaluated by the Owens-Wendt theory [6]. Porosity was analyzed by the mercury porosimetry method in a Micromeritics Poresizer 9320. The affinity of modified papers to water was evaluated by penetration dynamic analysis (PDA) using a Surface and Sizing Tester Model EST 12.2 EMTEC. Printing quality was accessed in RAIZ by internal procedures (Gamut area, optical density, width of line, circularity of dot and inter color bleed) using an office ink-jet printer and a set of commercial inks.

III. RESULTS AND DISCUSSION

Aiming better-quality printing silica-based formulations were applied on paper surfaces without any prior surface treatment (uncoated paper). After deposition the silica formulation was cured by heat (ageing process) to form the silica-cellulose composite depicted in **Figure 1(a)**. The silica domains (SD) are attached to cellulosic fibrils (EF) via hydrogen bonds, forming clusters or films surrounding the fibers (**Figure 1(b)**). Due to their relatively low viscosity silica formulations penetrate the paper being located mainly at the outer surface but also in depth (**Figure 1(c)**). The silica-coated papers revealed no significant change in microporosity but, in contrast, the pore average size and surface areas changed significantly, particularly for the TEOS/DEDMS/TEAP formulation (**Figure 2**).

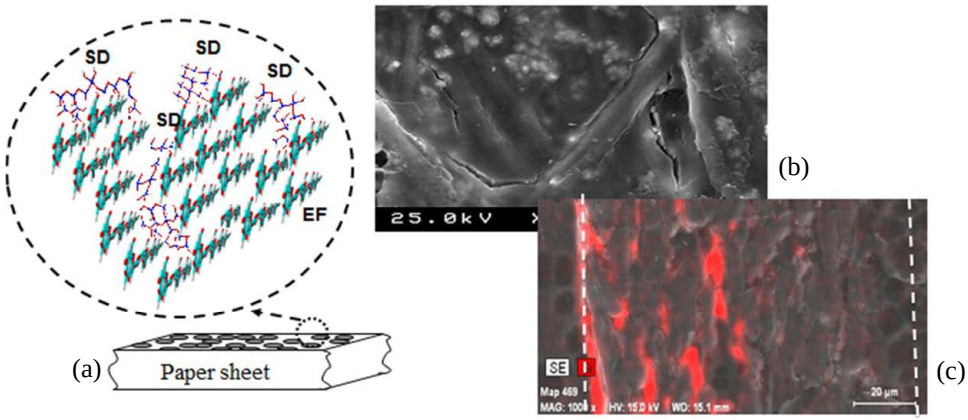

Figure 1. Schematic representation (a) of silica formulations dispersed on a paper surface and the resultant silica domains (SD) attached to cellulosic fibrils (EF). SEM-EDS images show the silica domains surrounding the cellulose fibers (b) and the distribution of silica (red color) along a transversal paper cut paper (c) (paper margins are depicted by dashed lines).

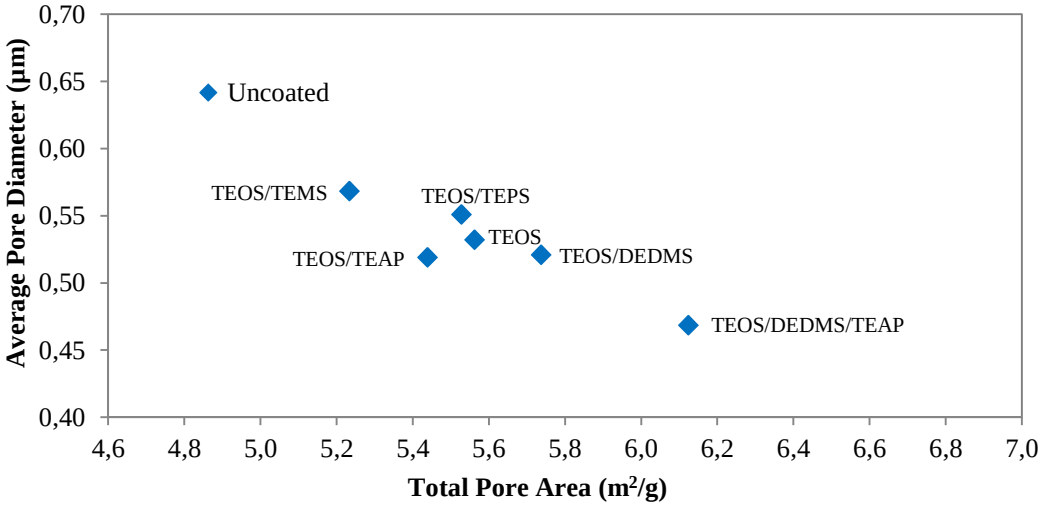

Figure 2. Relationship between average diameter and total area of the pores of uncoated paper and silica-coated (ca. 2 g/m^2) papers.

Overall, silica coating altered the paper surface parameters such as water contact angle (θ_w), total surface energy (γ_s) and the corresponding polar (γ_s^p) and dispersive (γ_s^d) components (**Table 1**). TEOS coating formulations increase γ_s^p and wettability (lower θ_w). However, adding 5% of a secondary precursor bearing alkyl groups (e.g. DEDMS) to the TEOS formulations, or combining alkyl and amino functionalities (i.e. DEDMS and TEAP), lowers the surface energy polar component thus creating a more hydrophobic surface.

Table 1. Water contact angles and surface energies of papers coated by different silica formulations.

Silica formulation (ca. 2 g/m^2)	Water contact angle, θ_w(º)	Surface Energy (mJ/m^2)		
		Dispersive component, γ_s^d	Polar component, γ_s^p	Total (γ_s)
---	100.9	35.9	0.1	36.0
TEOS	66.4	35.8	10.6	46.4
TEMS/TEOS	79.5	41.8	3.8	45.6
TEPS/TEOS	93.2	34.5	1.0	35.5
DEDMS/TEOS	112.7	20.3	0.03	20.3
TEAP/TEOS	75.6	39.7	5.5	45.2
DEDMS/TEAP/TEOS	115.0	19.2	0.01	19.2

Inkjet printing quality is highly dependent on the nature and properties of the inks (dyes for the colours and pigments for black) and the paper surface but also on their interactions. Therefore, surface properties of silica-coated papers may be tailored to improve those interactions so that better colour reproduction (measured as Gamut area) and printing quality (optical density, point and line firmness, inter-color-bleed) are attained. Printing tests with different inks (cyan, magenta, yellow and black) revealed that paper coating with TEOS formulation has a negative effect on printing quality i.e. Gamut area and optical densities are lower (**Figure 3).** However, introducing a secondary silica precursor with methyl or amino groups (e.g. TEMS or TEAP) increases Gamut area, whereas black optical density was increased by incorporating DEDMS (higher hydrophobicity of the surface prevents black ink penetration into the paper). The TEOS/TEAP/DEDMS formulation combines the properties of both precursors (TEAP and DEDMS) making it the most promising to increase the printing quality. The outstanding potential of this formulation is quiet visible from the inkjet printing tests images (**Figure 4**).

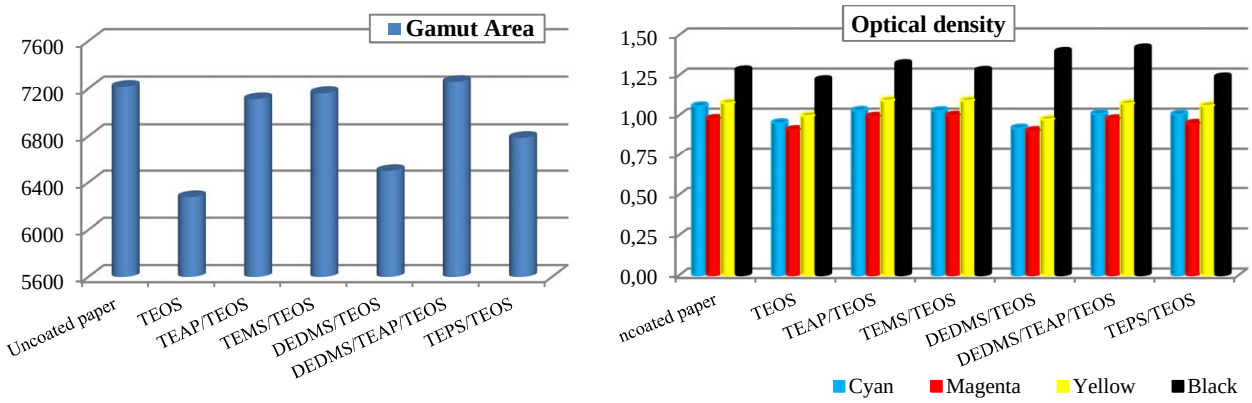

Figure 3. Gamut area (left) and optical density (right) of uncoated and silica-coated (2 g/m^2) papers.

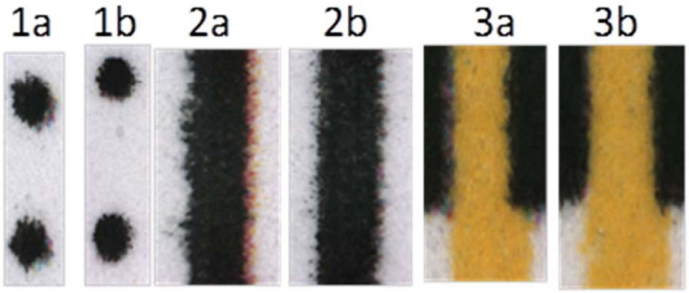

Figure 4. Inkjet printing tests for uncoated paper (series a) and DEDMS/TEAP/TEOS coated paper (2 g/m^2). (1) point firmness, (2) line firmness and (3) inter-color-bleeding.

Since water is the most common ink vehicle (inkjet printers) uncoated and silica-coated papers were scrutinized by water penetration dynamic analysis (PDA). The results, presented in **Figure 5** for uncoated and coated papers, reveal the strong affinity of water and the paper coated with TEOS formulation. The secondary silica precursor DEDMS reduces water affinity of the coated paper due to the increased surface hydrophobicity (**Table 1**).

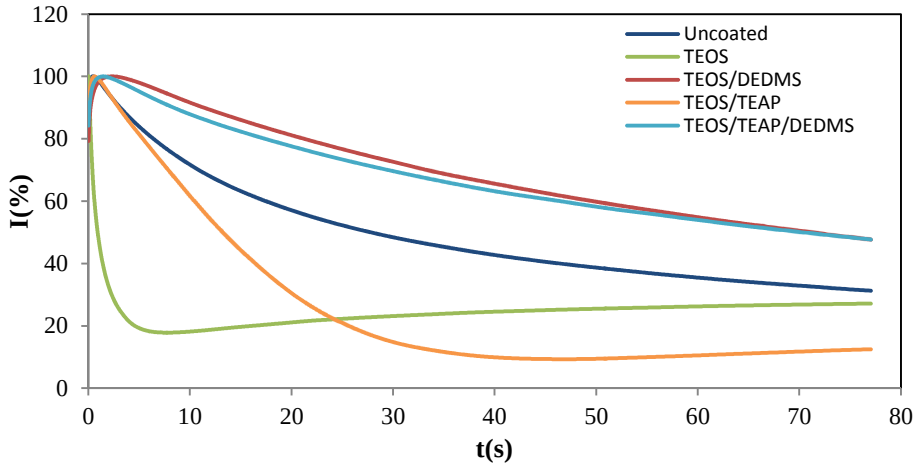

Figure 5. Intensity of water penetration versus time on uncoated (control) and silica-coated papers (2 g/m^2).

IV. CONCLUSIONS

Silica formulations bearing different functional moieties (alkyls, amines, isocyanates, etc) were deposited *in situ* on paper surfaces (2 g/m^2) with a significant impact on water penetration dynamics, surface energy, porosity and other parameters that influence printing quality. Paper surface modification with silica based formulations is suggested as a prospective tool for surface engineering towards tailored printing performance.

V. ACKNOWLEDGEMENT

Authors acknowledge the project NANOBARRIER financed by EU funds of FP7 program (FP7-NMP-2011-LARGE-5), QREN project candidature 5348 (PADIS), FEDER, AdI (Agência de Inovação), Compete (Programa Operacional Factores de Competitividade) and CICECO grant PEst-C/CTM/LA0011/2011. Authors also thank the the Prado Karton SA and Portuguese Research Institute on Forestry and Paper (RAIZ) for the technical support.

VI. REFERENCES

[1] Smith, W.F.; Principles of Materials Science and Engineering, *McGraw-Hill, New York*. **1996**.

[2] Brinker, C.J.; Scherer, G.W.; Sol–Gel Science: The Physics and Chemistry of Sol–Gel Processing. *Academic Press*, San Diego, **1990**.

[3] Sequeira, S.; Evtuguin D.V.; Portugal I.; Esculcas, A.P.; Synthesis and characterisation of cellulose/silica hybrids obtained by heteropoly acid catalysed sol–gel process. *Mat. Sci. Eng. C-Bio S*, **2007**, 27, 172-179.

[4] Sequeira S.; Evtuguin D.V.; Portugal I.; Preparation and properties of cellulose/silica hybrid composites. *Polymer Composites*, **2009,** 30(9), 1275-1282.

[5] Portugal, I.; Dias, V.M.; Duarte, R.F.; Evtuguin, D. V.; Hydration of cellulose/silica hybrids assessed by sorption isotherms. *J. Phys. Chem. B*, **2010**, 114, 4047–4055.

[6] Owens, D.K.; Wendt, R.C.; Estimation of the surface free energy of polymers. *J. Appl. Polym. Sci.* **1969**, 13, 1741–1747.

WOOD BASED ACTIVATED CARBONS FOR SUPERCAPACITORS

Galina Dobele[1], Aleksandrs Volperts[1], Galina Telysheva[1*], Darya Vervikishko[2], Evgeny Shkolnikov[2]

[1]Latvian State Institute of Wood Chemistry, 27 Dzerbenes St., 1006 Riga, Latvia (lingo@edi.lv); [2]Scientific Association for High Temperatures, Russian Academy of Sciences, 13/2 Izhorskaya St., 125412 Moscow, Russia

ABSTRACT

Influence of thermocatalytical synthesis on the porous structure formation and properties of microporous carbon wood-based materials is demonstrated. It has been found that increase of activation temperature and alkali activator addition ratio can be used to control not only total pore volume, but also micro- and mesopores proportion. The results of tests of the synthesized carbon materials as electrodes in supercapacitors are shown, as well as properties of carbon materials porous structure influencing on electrodes working characteristics. It was demonstrated that increase of activation temperature from 600°C to 800°C leads to increase of mesopores proportion in the porous structure which negatively influences on supercapacitor cell capacity. It was found that the most feasible way of activated cabons production for use as electrodes in supercapacitors is low-temperature activation.

I. INTRODUCTION

The traditional way of biomass conversion is production of wood chars and carbon materials with developed porous structure, activated carbons (AC), which are used as sorbents in many areas. Nowadays elucidation of AC structure is of scientific and practical interest since areas of these materials application are constantly widening: membrane technologies of rare earth metals separation, metallurgy, electronics, electrochemistry, aerospace technologies, and nuclear energy. This broad spectrum of AC application is justified by diversity of their structures with completely different physical and chemical properties, which can be achieved by certain physical-chemical treatment of carbonaceous precursors. One of distinctive features of plant biomass based AC is the fact that they can be obtained from extremely wide choice of precursors varying conditions of pyrolysis and activation: wood chips, cellulose and lignin, lignocellulosics, nut shells, straw, peat, husks, etc. As the results properties of AC will be different depending of precursor and synthesis conditions.

Wood based carbonizates have low porosity and their structure consists of elementary crystallites divided by multiple slit-like pores [1]. These pores are filled with pyrolysis products – pyrolytic tar. In the process of activation closed pores open up and porous structure forms. Varying carbon materials and activation conditions (temperature, time, atmosphere) it is possible to control total porosity, pore size distribution and nature of inner space.

Chemical activation is a widely used method for production of AC with developed porosity. The most important advantage of chemical activation is a possibility to synthesize carbonaceous materials with very high specific surface which is close to theoretical limits for carbon materials.

Alkali metals hydroxides are one of the most effective activating agents allowing in certain cases to synthesize microporous carbon sorbents with specific surface more than 3000 m^2/g [2].

There are numerous examples of application of AC as electrodes for the perfection of storage and transmission of electrical energy. The main ways of research are aimed at high specific surface and low electric resistance of carbon matrix with low costs of production. AC, synthesized with the use of alkali metals hydroxides, correspond to the above mentioned demands [3-4].

In the development of new systems for the modern electric-power industry one of important problems is the research devoted to application of electric double layer capacitors or supercapacitors (SC) where porous AC are used the main material for electrodes. Development and research of SC is an important subject worldwide. It is known that energy capacity of carbon electrode is influenced by the following AC properties: raw material, its dispersity end elemental composition, modes of carbonization and activation, porous structure characteristics, etc [5].

This work is devoted to the study of influence of wood based carbon material porous structure characteristics for the use in electric double layer capacitors (supercapacitors) with sulfuric acid as electrolyte.

II. EXPERIMENTAL

Materials and methods

***Raw material*:** birch wood chips, 0.2 – 0.4 mm fraction.

AC synthesis is schematically illustrated in the Fig. 1. It consists of two stages of thermal treatment - at the first one raw material was carbonized in the nitrogen atmosphere at 400°C for 150 minutes.

At the second carbonizate was impregnated with NaOH water solution (50 ww %). Ratio of carbonizate to activator was varied from 1:2 to 1:4. The mixture was activated at the temperatures 600-800°C for 120 minutes. Pyrolysis product was washed with deionized water, demineralized with hydrochloric acid and washed with dionized water again up to filtrate pH 5. The obtained AC was dried overnight at 105°C. Ash content in the AC was found to be 0.1-0.4%. The main variables in the experiment were activation temperature and carbonizate/activator ratio.

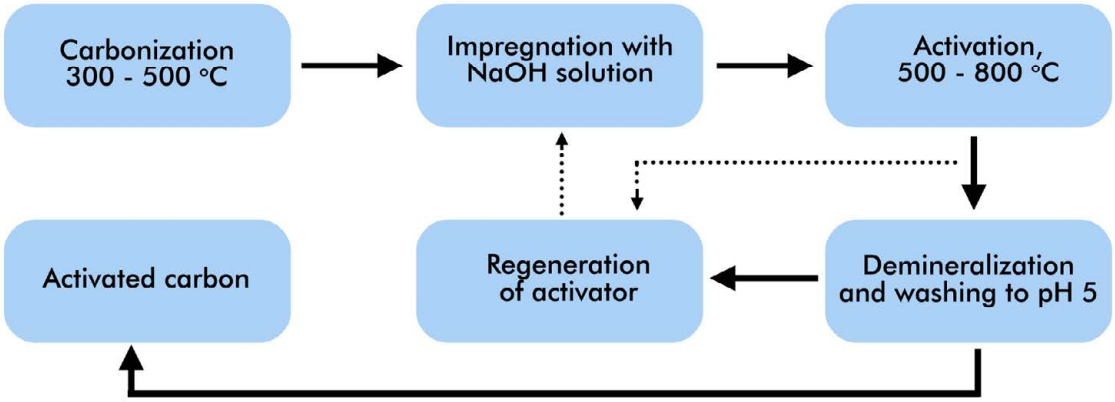

Figure 1. Schematics of microporous carbon materials thermocatalytical synthesis.

Porous structure was evaluated by nitrogen adsorption isotherms at 77 K (Quantachrome Autosorb 6B). Micropores volume was calculated using Dubinin-Radushkevich method [6].

Electrodes were prepared using calandering method, water suspension of PTFE F-4D (5-10% from electrode mass) was used as a binder. Electrodes were dried and impregnated with 4.9 M solution of sulfuric acid under vacuum. Porous PP membrane was used as a separator between electrodes. Thermoexpanded graphite foil was used as substrate-current collector. Energy capacity of supercapacitor was determined at complete discharge with direct current after 10 minute exposure at 1v voltage drop.

II. RESULTS AND DISCUSSION

AC porous structure characteristic for use as electrodes in supercapacitors were evaluated using nitrogen sorption isotherms (Fig. 2).

The samples under study were first carbonized at 400°C and then activated at carbonizate to NaOH ratio 1:2 (Fig. 2, isotherms 2-5) and 1:4 (Fig. 2, isotherm 1) in the isothermal conditions at the temperatures 600, 650, 700 and 800°C. Judging by the shape of isotherms samples obtained at temperatures 600, 650 and 700°C (Fig. 2, isotherms 2-4) are microporous. With increase of activation temperature volume of adsorbed nitrogen increases as well. At activation temperature 800°C (Fig.2, isotherm 5) the shape of isotherm changes. The appearance of hysteresis is indication of capillary condensation of sorbate, which also indicates increase of mesopores number. With the increase of carbonizate/activator ratio to 1:4 (activation temperature 700°C) volume of adsorbed nitrogen, as well as number of mesopores in AC structure, increase (Fig. 2, isotherm 1).

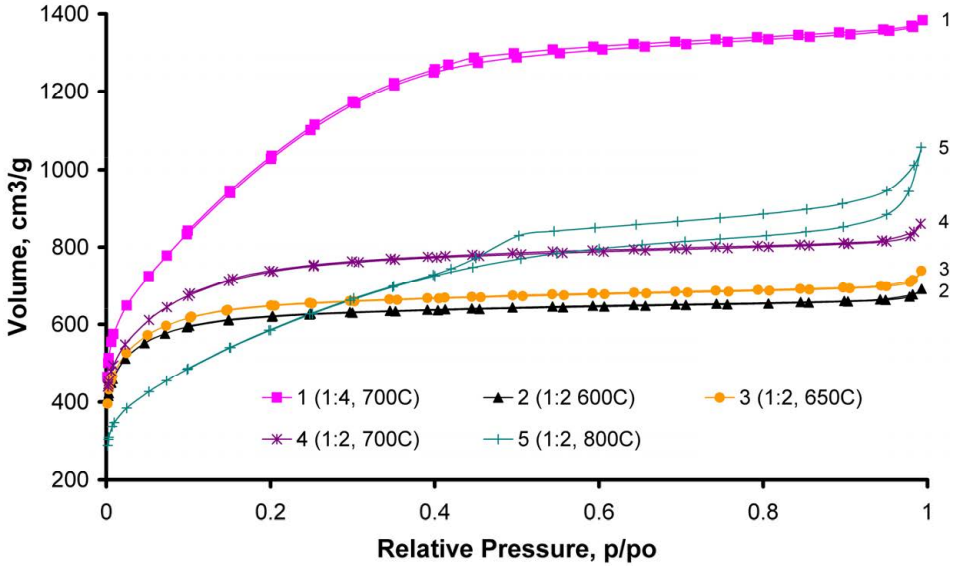

Figure 2. AC nitrogen adsorption isotherms at 77K with alteration of activation temperature and carbonizate/activator ratio.

Volume of micropores increases with the increase of activator ratio and activation temperature in the range 600 – 700°C (Fig. 3). Activation at the temperature 800°C leads to decrease in micropores proportion in the structure of AC, which obviously is explained by elimination of pore walls and combination of smaller pores into the larger ones. Alongside with this proportion of microporosity in the total pore volume decreases with increase of activation temperature and with increase of activator ratio, both (Fig. 3).

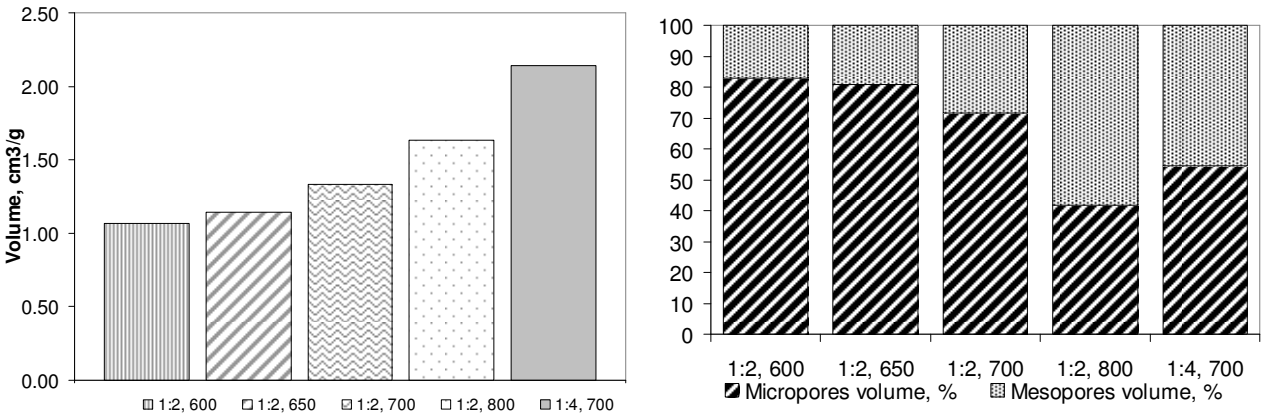

Figure 3. Micropores volume (left) and micropores/mesopores ratio (%) (right) with alteration of activation temperature and carbonizate/activator ratio.

Characteristics of supercapacitor cells made with electrodes from AC prepared at different activation temperatures and carbonizate/activator ratio 1:2 are illustrated in the Figure 4. At the low carbonization temperatures – 600 and 700°C capacitance is 330 and 320 F/g, correspondingly. Increase of carbonization temperature negatively influences on electrochemical properties - at the activation temperature 800°C capacitance decreases to 220 F/g.

As it is shown in the Figure 4 total volume of electrolyte retained by electrode considerably increases with the increase of activation temperature. This parameter is important when evaluating efficiency of the device under development, namely for the calculation of specific characteristics to the mass of elementary capacitor cell.

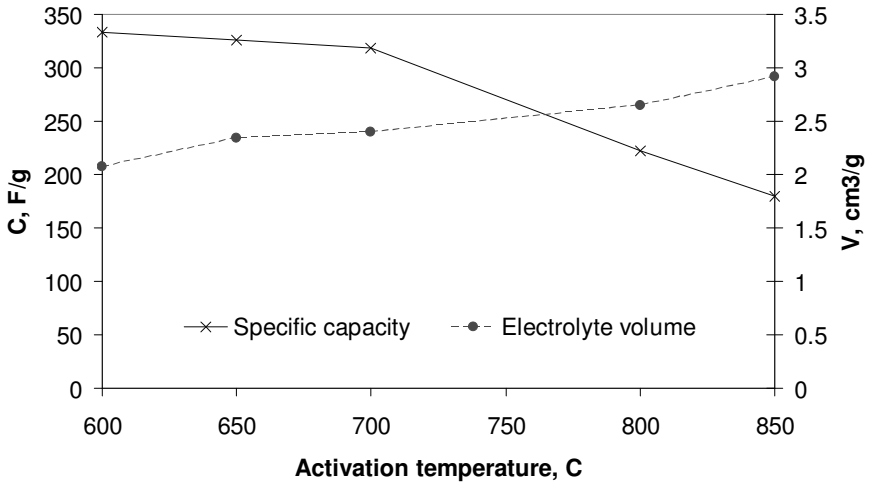

Figure 4. Dependence of supercapacitor cell capacitance and volume of electrolyte retained by AC from the activation temperature (carbonizate/activator ratio 1:2).

Thus the choice of lower activation temperatures positively influences not only on microporous structure of AC, but on electrode quality as well. This makes the described activation process more feasible from the commercial standpoint.

IV. CONCLUSIONS

Microporous wood based carbon materials were obtained using thermocatalytical synthesis, which includes carbonization and consequent alkali activation. The synthesized carbon materials have good electrode characteristics for the capacitors with double electric layer with sulfuric acid as electrolyte. Maximal capacity of supercapacitor – 330 F/g - is achieved at the activation temperature 600^{o}C and carbonizate/activator ratio 1:2. Capacity decreases with temperature increase, which corresponds to decrease of micropores proportion in activated carbons porous structure.

V. ACKNOWLEDGEMENT

This research was supported by LV PP 5,2;2,4 program and cooperation project 666/2014.2.

VI. REFERENCES

[1] Tsyganova, S.; Korolkova, I.; Bondarenko, G.; Chesnokov, N.; Kuznetsov, B. Synthesis of Active Carbons from Birch Wood modified by phosphoric Acid and Potassium Hydroxide. *J. Siberian Fed University Chemistry* **2009**, *.2*. 3, 275-281.

[2] Torne-Fernandez, V.; Mateo-Sanz, J.M.; Montane, D.; Fierro, V. Statistical Optimization of the Synthesis of Highly Microporus Carbons by Chemical Activation of Kraft Lignin with NaOH. *J. Chem. Eng. Data.* **2009,** *54*, 2216–2221.

[3] Marsh, H.; Rodri´Guez-Reinoso, F**.** *Activated Carbon***. 2006,** 243-265.

[4] Dobele, G.; Dizhbite, T.; Gil, M.,V.; Volperts,,A..;Centeno,T.,A. Production of Nanoporous Carbons from Wood Processing Wastes and their use in Supercapacitors and CO_2 Capture. *Biomass and Bioenergy.* **2012,** *46,* 145-154.

[5] Inagaki, M.; Konno, H.; Tanaike, O. Carbon Materials for Electrochemical Capacitors. *J. Power Sources.* **2010,** *195,* 7880-7903.

[6] Dubinin, M.; Radushkevich, L. Regarding activated carbons characteristic curve equation (in Russian). *Academy of Science Reports*. **1947,** *55,* 4, 331–334.

WOBAMA – WOOD BASED MATERIALS

Monica Ek[1], *Christine Chirat*[2], *Dongfang Li*[1], *Tommy Iversen*[3], *Eva Malmström*[1], *Emelie Norström*[1], *Herbert Sixta*[4], *Lidia Testova*[4], *Dariouz Wawro*[5]

[1]*KTH Royal Institute of Technology, Department of Fibre and Polymer Technology, Teknikringen 56-58, SE 100 44, Stockholm, Sweden*

[2] *Grenoble INP Pagora, 461 rue de la Papeteri BP 65, F-38402 St-Maritn-d´Hères Cedex France*

[3] *Innventia, Box 5604, SE 11486 Stockholm, Sweden*

[4] *Aalto University, Dept of Forestry Products Technology, P.O. Box 16300, FI-00076 Aalto, Finland*

[5] *IBWCh Institute of Biopolymers and Chemical Fibers, Lodz, Poland*

ABSTRACT

WOBAMA – Wood Based Materials and Fuels is a biorefinery oriented scientific research project, financed by Wood Wisdom-Net Research Program and ERA-NET Bioenergy. This project includes participants from academics and industries in European Union member states. The aim of WOBAMA is to converse wood based raw materials to a range of value added products, both materials and fuels, using different conversion technologies, within the biorefinery concept:

Wood Based Material → Conversion Technologies → Bioproducts
The project is supposed to result in a series of demonstrators, e.g. bioethanol, adhesive, composite, film and cellulose acetate.

I. INTRODUCTION

The project is performed in the following work packages:

- Pre-extraction of hemicelluloses and impact on the subsequent cooking and bleaching
- Post extraction of hemicelluloses and impact on the subsequent bleaching
- Cellulose functionalization for high-tenacity films and biocomposites
- Hemicellulose for adhesives

The project is also organizing a series of Summer Schools connecting Young Scientists with Senior Professionals from both academia and industry on European basis.

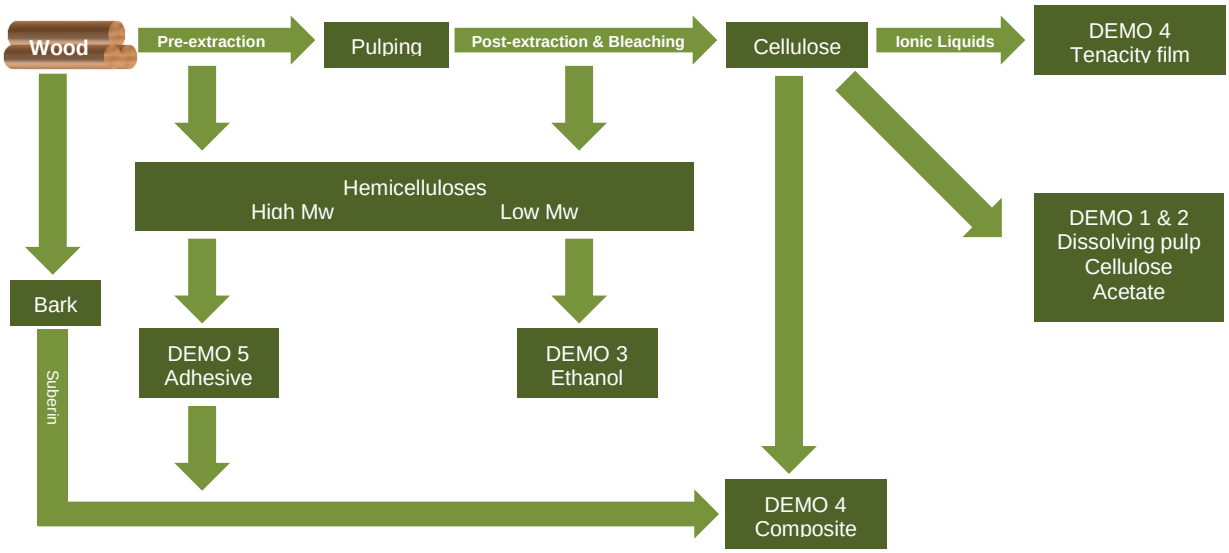

III. Results and Discussion

Pre-extraction of hemicelluloses and impact on the subsequent cooking and bleaching
High-purity cellulose pulp manufactured by hydrothermolysis followed by alkaline delignification
Approximately half of the dissolving wood pulp is currently manufactured by the prehydrolysis-kraft (PHK) process. However, conventional application of aqueous-phase prehydrolysis, as opposed to its steam equivalent, has been limited due to the formation of sticky lignin precipitates. On the other hand, steam prehydrolysis does not allow the recovery of the hemicellulose-rich dissolved organic fraction. Here, a prehydrolysis by consecutive recirculation and percolation modes is seen as a process combining the advantages of the both modes. The aim is

to develop a novel method that would remove most of the pine wood hemicelluloses during the prehydrolysis in order to produce high purity dissolving pulp.
First, a prehydrolysis in recirculation (batch) mode is performed at elevated temperature until the side reactions start to take place. Second, subsequent percolation mode with a continuous fresh water feed is applied in order to maximize the removal of hemicelluloses while avoiding carbohydrate degradation and lignin recondensation. The reference prehydrolysis is performed by water recirculation only. Remaining hemicelluloses and lignin are removed during the following pulp production steps. The effects of the prehydrolysis on wood composition were evaluated. The treatment with circulation mode only and the treatment with consecutive circulation and percolation of water have been studied at 170 and 200°C. The results show that a batch prehydrolysis of 10 minutes at 200°C and 90 minutes at 170°C result in similar removal of hemicelluloses; 52.0 and 50.5% of initial hemicelluloses, respectively, while cellulose is not notably affected.
Experiments with prehydrolysis treatment followed by a kraft cook were then carried out. The aim is to adjust the process conditions so that pulp with Kappa number around 20 and a high purity in cellulose would be produced. Prehydrolysis with consecutive circulation and percolation of water has been performed under 170 and 200°C with different treatment times and liquid-to-wood ratios. The chosen prehydrolysis conditions for reference experiments (batch mode) are 90 minutes at 170°C, with liquid-to-wood ratio of 7.2:1. Kraft cooks have been performed at 160°C with effective alkali of 22%, sulfidity of 40% and liquor-to-wood ratio of 4:1.

Table 1: Circulation or circulation/percolation prehydrolysis followed by a kraft cook.

Sample	Reference	1	2	3
Prehydrolysis	*Circulation*	*Consecutive circulation and percolation*		
Temperature, °C	170	170	200	200
Time, min	90	60 and 30	10 and 5	15 and 15
Liquid:Wood	7.2:1	7.2:1 and 45:1	7.2:1 and 8:1	7.2:1 and 22:1
Prehydrolysis yield, %	81.7	77.9	74.1	69.3
Kraft cook	*160°C, EA 22%, sulfidity 40%, Liquor:wood 4:1*			
H-factor	1600	1800	1600	1550
Kraft yield, %	42.4	44.6	42.1	43.2
Total yield, % on wood	34.6	34.7	31.2	30.0
Kappa number	16	13	25	46
Viscosity, ml/g	790	730	620	450
Cellulose, % of sample	93.8	93.7	95.3	92.0
Glucomannan, % of sample	1.0	1.6	0.0	0.3
Xylan, % of sample	2.5	2.8	1.4	1.0
Lignin, % of sample	2.7	1.8	3.3	6.7

High-purity cellulose pulps by post-extraction in caustic-borate solution
Sodium borate ($Na_2B_4O_7$) has a potential of improving glucomannan (GGM) extraction from softwood pulps (1). In the present study, the pulps with the hemicellulose content of 1% of xylan and under 2% of GGM were obtained after post-extraction (CCE+B) of bleached commercial pine kraft pulp in optimised conditions. However, under the highly alkaline extraction conditions the major concern for the acetate grade pulp production is the formation of cellulose II. At present conditions 70% of cellulose I in the pulp was converted to cellulose II. Xylanase treatment (X) before CCE+B enhanced extraction efficiency and the caustic concentration could be reduced to 10 wt.% (Table 2). However, the further reduction of caustic concentration to 8 wt.% resulted in a pulp with the residual content of xylan and GGM of 1.2 and 3.3%, respectively, which cannot comply with the typical acetate grade specification. The pulp obtained after xylanase and CCE/B extraction at the caustic concentration of 10 wt.% demonstrated promising performance in laboratory acetylation trials but the content of cellulose II remained high (Table 2).

Table 2. Properties of the acetate-grade pulp produced from commercial paper-grade bleached pine kraft pulp in comparison with two commercial sulphite acetate grade pulps (pine and spruce).

	Pulp				Acetate dope	
	Xylan	GGM	Cellulose II	Molar mass	Yellowness	Transmittance
	%			kg/mol		%
Pine	0.8	0.7	0	595	0.11	85
Spruce	1.8	1	0	475	0.14	81
X-CCE/B	***0.6***	***1.9***	***63***	***540***	***0.27***	***65***

Extraction of hemicelluloses and impact on the subsequent bleaching

Prehydrolysed softwood kraft pulps of high (50-55 and 70-78) and classical kappa numbers (20-25) were prepared. Producing PHK of high kappa could be a way to improve the viscosity of the pulp, which can be interesting for high grades cellulose usages. Single oxygen stages were applied and PHK pulps were delignified much more extensively than the corresponding control kraft pulps: The 55.5 kappa number PHK pulp could be delignified down to 9.2 in a single O stage (83.4% delignification) compared to 25.3 (50.3%) for the control kraft pulp (starting kappa number 50.9). The 78.1 kappa number PHK pulp could be delignified down to 9.4 in two oxygen stages, to be compared to 23.5 for the control kraft pulp. With three oxygen stages the kappa number was 6.0 for the PHK OOO pulp. This very good reactivity of PHK pulps to oxygen delignification, would thus enable to stop the cooking at higher kappa numbers, to save yield and viscosity.

Table 3. Two stage oxygen delignification of 70-78 kappa number kraft and PHK pulps.

Pulping	Kraft	PHK
T, °C	160	
$NaOH/Na_2S/AQ$	16.1/6.9	
Kappa number	70.3	78.1
Viscosity, ml/g	1176	837
Oxygen bleaching (100 °C, 1 hr, 5 bars O_2, 0.3% $MgSO_4$, $7H_2O$)		
1^{st} stage oxygen delignification		
4% NaOH, kappa	31.0	17.8
4% NaOH, viscosity, ml/g	908	673
2^{nd} stage oxygen delignification		
1.5% NaOH, kappa	23.5	9.4
1.5% NaOH, viscosity, ml/g	894	616

In a previous study by Chirat et al [2], the lignins of the kraft and PHK unbleached pulps were analysed, and it was found that neither the molecular weight distribution of lignin, nor the number of free phenolic groups were significantly modified. A modification in the lignin-carbohydrates (LCC) linkages could be an explanation for the easiest oxygen delignification of the PHK pulps compared to the kraft ones. Direct P and Z stages were also applied after PHK and kraft pulps to verify if this easiest delignification ability was also verified with other oxidants, and it was confirmed that it was also the case. Hemicellulose content is rather low and would be suitable at least for viscose applications.

Cellulose Functionalization to High-Tensile Strength Films

ILs as cellulose solvents aroused interest presenting the chance of spinning cellulosic fibres and casting film. The ILs offer the chance to elaborate an environment-friendly, save-to-humans and low energy-consuming route to prepare cellulosic film. Good transparency and high tensile strength is expected from the film. The hydrothermal treatment enables a controlled reduction of the polymerization degree and improves cellulose properties: increases solubility, decreases polydispersity, and removes traces of lignin [3-5].

Films were prepared by casting from solutions of cellulose in ionic liquids (ILs), [EMIM]OAc and [BMIM]OAc, both producing stabile spinning solutions of cellulose at 90 °C. Prior to the dissolution, cellulose pulp was hydrothermally treated (HT cellulose). Samples of transparent cellulose film were prepared with a low polydispersity index (PDI) of 2.2, and satisfactory mechanical properties: strength up to 126 MPa and elongation of 60%. PHK dissolving pulp after hydrothermal treatment was used to prepare the solution, characterized by DP 290 - 440 and a low polydispersity. The HT cellulose concentration in the IL solutions was in the range of 10 - 16 wt%. All films showed strength of about 100 MPa which is close to commercial cellophane. Films made of the HT cellulose with DP of 325 were comparable in tensile strength with films made from higher DP cellulose. Films made both from ([EMIM]OAc) and ([BMIM]OAc) are similar in structure and quality. Both films are highly transparent. The films prepared in laboratory scale showed tensile strength in the range of 90 - 126 MPa and elongation of 25 - 60% and good transparency.

Table 4. Mechanical properties of cellulose films made from HT cellulose/IL solution.

Type of solvent	DP of HT cellulose	Cellulose concentration in solutions	Thickness	Tensile strength	Elongation at maximum stress
		wt%	mm	MPa	%
([EMIM]OAc) ([BMIM]OAc)	255 - 440	10 - 16	0.024 - 0.060	90 - 126	25 - 60

Preparation of polyester-cellulose composites
The hydrophilicity of cellulose is a crucial obstacle for some applications of cellulose-based materials. Natural products that are hydrophobic and biodegradable, such as suberin found in birch outer bark, could be attractive candidates for modifying cellulose surfaces to improve water repellency. Suberin consists of many sub-units, and epoxy acid is the most abundant among the others, amounting to approximately 100 g per kg of dried birch outer bark [6-8]. The epoxy, hydroxyl, and carboxyl functional groups of epoxy acid make it an interesting monomer for polymerization and crosslinking. A suberin monomer, *cis*-9,10-epoxy-18-hydroxyoctadecanoic acid (epoxy acid), was isolated from birch outer bark, and polymerized via lipase (immobilized *Candida antarctica* lipase B) catalysis. The epoxy-activated polyesters were characterized by NMR, MALDI-TOF MS, and SEC. The polyester-cellulose composites were prepared through compression molding of polyester impregnated cellulose. The polyesters were successfully crosslinked by the dicarboxylic acids. FTIR, CP/MAS ^{13}C NMR, and FE-SEM were used for analyses. All composites were hydrophobic. The polyester-cellulose composites were hydrophobic, shown by the contact angle measurement, and stable against many solvents. We demonstrated that the side-stream products from forest industries could be used for value-added applications such as producing functionalized materials, which is in line with the biorefinery concept.

Hemicellulose for adhesives
Wood adhesives of today perform very well in terms of bonding performance such as bond strength, water resistance and heat resistance. From an economic view they are also inexpensive. However, most wood adhesives are derived from petroleum-based chemicals. This is a limited and non-renewable resource. Furthermore, some of these chemicals also have a negative impact on the environment and human health for example the formaldehyde. Therefore, there is an urge to find bio-based alternatives. It has proved difficult to find a bio-based alternative that fulfill all requirements, such as price and poor water resistance. Polysaccharides have shown interesting properties that can be useful for wood adhesives. Gums are relatively high molecular weight polysaccharides that can be obtained from different plants and bacteria and are for example used as thickeners in the food industry. Several gums were evaluated as binders in wood adhesives and were compared with a commercial polyvinyl acetate-based wood adhesive used for indoor applications. The gum locust bean gum showed remarkable results in this study with properties comparable to the commercial wood adhesive. The bonding performance was remarkably good regarding the bond strength, water resistance, as well as the heat resistance. Surprisingly, it was possible to use the adhesive both at room temperature and at elevated temperatures. In the present project the potential of using chemicals from a wood biorefinery as binders in wood adhesives is investigated, such as different hemicelluloses. Some recent results will be presented.

IV. CONCLUSIONS

The alkali/borate extraction of softwood pulp hemicelluloses demonstrated a great potential towards the production of high purity cellulosic pulps suitable for cellulose acetate production
Oxygen delignification of PHK vs kraft pulps have been evaluated
Cellulose solutions have been prepared using selected solvents of ionic liquids, and production of cellulose films has been evaluated. Morphology and mechanical properties of selected films have been tested.

The polyesters based on epoxy fatty acid were successfully prepared via lipase-catalysis. Efforts were made to prepare fatty acid-cellulose biocomposites through environmentally friendly ways
polysaccharides can work as binders in wood adhesives

V. ACKNOWLEDGEMENT

We would like to express great thanks to WoodWisdom-Net Research Programme and ERA-NET Bioenergy, Formas, Akzo Nobel, Andritz, Metsä fibre, OrganoClick, Processum and StoraEnso, for the financial support.

VI. REFERENCES

1 Wells, F.L.; W.C. Schattner, L.E. Ekwell. Tappi J., 54(4), 1971, p.525-529.
2 Chirat, C. Boiron, L, Lachenal D., Int Pulp Bleaching Conf, Tappi Proceedings, October 5-7, 2011, Portland, USA
3 Wawro D, Steplewski W, Bodek A., FIBRES TEXT EAST EUR 17 (3): 18-22 JUL-SEP 2009.
4 Wendler F, et al., FIBRES TEXT EAST EUR 18 (2): 21-30 APR-JUN 2010.
5 Kuzmina O, Sashina E, Troshenkowa S, Wawro D., FIBRES TEXT EAST EUR 18 (3): 32-37 JUL-SEP 2010.
6 Pinto P C R O, Sousa A F, Silvestre A J D, Neto C P, Gandini A, Eckerman C, Holmbom B (2009). Ind. Crops Prod., 29, p. 126-132.
7 Ekman R (1983), Holzforschung, 37, p. 205-211.
8 Olsson A, Lindström M, Iversen T (2007): Biomacromolecules, 8, p. 757-760.

EFFECT OF ANATOMICAL FEATURES OF *EUCALYPTUS GLOBULUS* AND *E. NITENS* WOOD QUALITY

Juan Pedro Elissetche[1,]*, Isabel Carrillo[1], Regis Teixeira Mendonça[1,2] and Sofía Valenzuela[1,2]

[1]Biotechnology Center, Universidad de Concepción, Concepción; [2]Forest Sciences Faculty, Universidad de Concepción, Concepción
*(*jelisset@udec.cl)*

ABSTRACT

Eucalyptus globulus and *E. nitens* are two species widely used at the Chilean forestry industry. The importance of *E. globulus* is due of its high quality of fiber for pulp and paper production and high pulp yield; however, it does not present frost tolerance. On the other hand, *E. nitens* has cold tolerance and fast growth, but a lower fiber quality. Current efforts of the main forestry companies are focused on developing *E. globulus* x *E. nitens* hybrids presenting additive traits of both species. Basic wood density is a parameter that indicates wood quality and can be used as fast selection criteria of genotypes. In this work, basic wood density of 30 *E. globulus* and 30 *E. nitens* trees was evaluated for further anatomical characterization. *E. globulus* trees presented a basic wood density average of 477.6 kg/m^3, while *E. nitens* was 490.3 kg/m^3. Both micro-drillings tools showed significant correlation indexes with basic wood density. Correlation coefficient between basic wood density and Pilodyn values showed negative indexes, being -0.53 (p=0.01) and -0.68 (p<0.001) for *E. globulus* and *E. nitens*, respectively. For both species a positive correlation was observed between basic density and Resistograph mean amplitude. *E. globulus* correlation index was 0.84 (p<0.001), and for *E. nitens* was 0.85 (p<0.001). *E. nitens* genotypes presented higher density and amplitude average, and less Pilodyn values than *E. globulus* genotypes, while *E. globulus* trees had higher coarseness, fiber length and DBH than *E. nitens* trees.

I. INTRODUCTION

In Chile, *E. globulus* is the mainly commercial hardwood for pulp and paper production because of its fast growth, high basic wood density, high pulp yield and good fiber and handsheet properties, but it has a poor frost tolerance [1, 2]. *E. nitens* have been introduce to the country for forest plantation and pulp production because of its frost tolerance, but its wood has a poor quality and low basic density [3, 4]. For this reason, current efforts of the main Chilean forestry companies are focused on developing *E. globulus* x *E. nitens* hybrids presenting additive traits of both species, combining frost tolerance and high wood quality. For this reason, trees of 6 year-old *E. globulus* and *E. nitens* were anatomically analyzed, determining basic wood density and fiber quality of both *Eucalyptus* species using fiber analyzer equipment and micro-drilling tools in order to generate information for further selection of trees in genetic improvement programs.

II. EXPERIMENTAL

Wood material. The Chilean forest company CMPC provided 6 year-old *E. globulus* and *E. nitens* trees growing in field plantation established in forest sites of the Bio-Bio Region (Chile). A pre-screening of 100 *E. globulus* trees and 100 *E. nitens* trees at breast height (BH) was made using Pilodyn micro-drilling tool as an indicator of wood density. Using this information, 30 *E. globulus* trees and 30 *E. nitens* trees with high and low density were selected. Incremental cores were sampled at breast height for further anatomical analysis.

Basic density determination. Incremental cores were sampled and basic density of each tree was measured according to the Tappi Standard Method T258 om-94.

Fiber quality analysis. Matchsticks obtained from longitudinal cuts of sub-samples taken along the incremental core were macerated and treated using Franklin solution (30% H_2O_2 and CH_3COOH, 1:1 v/v) for 8 hours at 70°C. The solution was decanted and the remaining fibrous material was washed with water until a neutral pH was achieved. Fiber length and fiber width average and coarseness were determined in a Fiber Tester equipment (Lorentzen &Wettre, Sweden) where 200 mg of sample were previously disaggregated in 200 mL of distiller water for 10 minutes. During the analysis of this suspension, the equipment was setting to measure approximately 35.000 fibers of each sample.

Resistograph measurements. Trees were drilled bark-to-bark at DBH (diameter at breast height) using IML Resistograph PD400 (Instrumenta Mechanik Labor GmbH, Germany). The drilling speed was set to 100 cm/min during all measurements. Resistance profiles stored in the electronic unit were downloaded using PD-Tools Pro software that was provided with the Resistograph. Using a SAS macro script with the EXPAND and MEANS procedures (SAS Institute Inc. 2008) centered moving averages and centered moving minimum averages functions were applied to the exported amplitude profiles in order to reduce profiles irregularities, as suggest [5].

III. RESULTS AND DISCUSSION

Wood density. *E. globulus* showed a basic density range of 408.6 to 540.8 kg/m^3, with an average of 477.6 kg/m^3, while *E. nitens* ranged 432.8 – 558.1 kg/m^3, with an average of 490.3 kg/m^3. Some reports shows that *E. globulus* has much higher basic density than *E. nitens*. Whole-tree averages densities reported for 8 year-old *E. globulus* was 476 kg/m^3 and *E. nitens* was 440 kg/m^3 [4]. Similar species difference was found for basic density by [3] and [6], which are not agree with the results found in this work. Correlation coefficient between basic wood density and Pilodyn values showed negative indexes, being -0.53 (p=0.01) and -0.68 (p<0.001) for *E. globulus* and *E. nitens*, respectively (**Table 1 and 2**).

Fiber biometry characterization. Fiber length and fiber width of *E. globulus* ranged 0.51 – 0.88 mm and 17.8 – 20.1 µm, respectively, while coarseness ranged between 49.4 and 82.4 µg/m. Fiber length and fiber width of *E. nitens* ranged 0.55 – 0.73 mm and 17.1 and 20.7 µm, respectively, while coarseness ranged 47.9 and 77.3 µg/m. Correlation analysis showed positive and significant relations between fiber length and fiber width with coarseness of *E. globulus* and *E. nitens*, which is expected due that coarseness is a parameter that involve both variables. DBH also showed higher correlations indexes with fiber length and coarseness in both *Eucalyptus* species (**Table 1 and 2**).

Wood characterization by Resistograph measurements. Mean amplitude of *E. globulus* genotypes was 27.1%, while for *E. nitens* was 31.9%, being *E. nitens* amplitude average significantly superior to *E. globulus* amplitude average. In order to test data variation, standard deviation of amplitude profiles was determined for each species, which allows determining transversal wood homogeneity. *E. globulus* standard deviation was of 4.3, while for *E. nitens* was of 5.5, showing that *E. globulus* wood has more homogeneity than *E. nitens* wood (**Figure 1, A)**. *E. globulus* resistograms shows less amplitude variation between averages of peaks and valleys than *E. nitens* resistograms. This indicates a higher difference between features of spring and summer *E. nitens* wood in a growth ring. Regression analysis was made between basic density and mean amplitude of drilling made by Resistograph for *E. globulus* and *E. nitens* (**Figure 1, B**). For both species a positive correlation was observed between basic density and mean amplitude. *E. globulus* correlation index was 0.84 (p<0.001), and for *E. nitens* was 0.85 (p<0.001).

Finally, to integrate all variables evaluated, a principal component analysis was made (PCA). Variables included were DBH, fiber length, coarseness, basic density, and micro-drilling methods by Pilodyn and Resistograph. PCA allows to obtain two principal components, which explains a 75.39% of the total variation of data. Loading graph (**Figure 2, A**) shows that the first component explains Resistograph amplitude, basic density and Pilodyn values variation, while the second component explains coarseness, fiber length and DBH variation. At **Figure 2, B** both components are presented, which enables to group *E. globulus* and *E. nitens* genotypes. *E. nitens* genotypes presented higher density and amplitude average, and less Pilodyn values than *E. globulus* genotypes, while *E. globulus* trees had higher coarseness, fiber length and DBH than *E. nitens* trees. However, is also possible to determine trees of *E. nitens* and *E. globulus* with similar characteristics respect to variables under analysis.

Table 1. Pearson correlation indexes between variables evaluated of *E. globulus*.

	Basic density	Pilodyn	DBH	Coarseness	Fiber length	Fiber width
Basic density	1					
Pilodyn	-0.53**	1				
DBH	NS	NS	1			
Coarseness	0.31*	NS	0.55**	1		
Fiber length	0.33*	NS	0.65**	0.46**	1	
Fiber width	-0.39**	0.57**	0.36**	0.43**	NS	1

NS: No significant. * Significant at p=0.1. ** Significant at p=0.05.

Table 2. Pearson correlation indexes between variables evaluated of *E. nitens*.

	Basic density	Pilodyn	DBH	Coarseness	Fiber length	Fiber width
Basic density	1					
Pilodyn	-0.68**	1				
DBH	NS	NS	1			
Coarseness	NS	NS	0.56**	1		
Fiber length	NS	NS	0.64**	0.31*	1	
Fiber width	-0.3*	0.42**	NS	0.45**	NS	1

NS: No significant. * Significant at p=0.1. ** Significant at p=0.05.

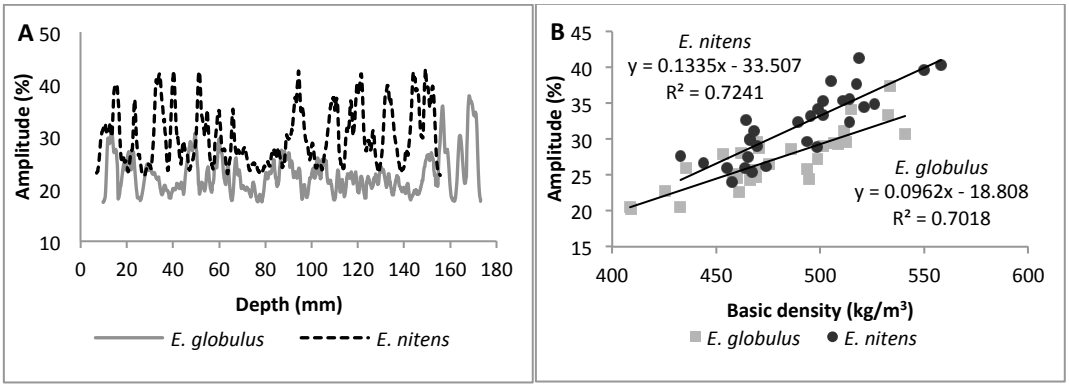

Figure 1. **A.** Resistogram profile of *E. globulus* versus *E. nitens*. **B.** Linear regression between basic density and mean amplitude of *E. globulus* and *E. nitens* trees.

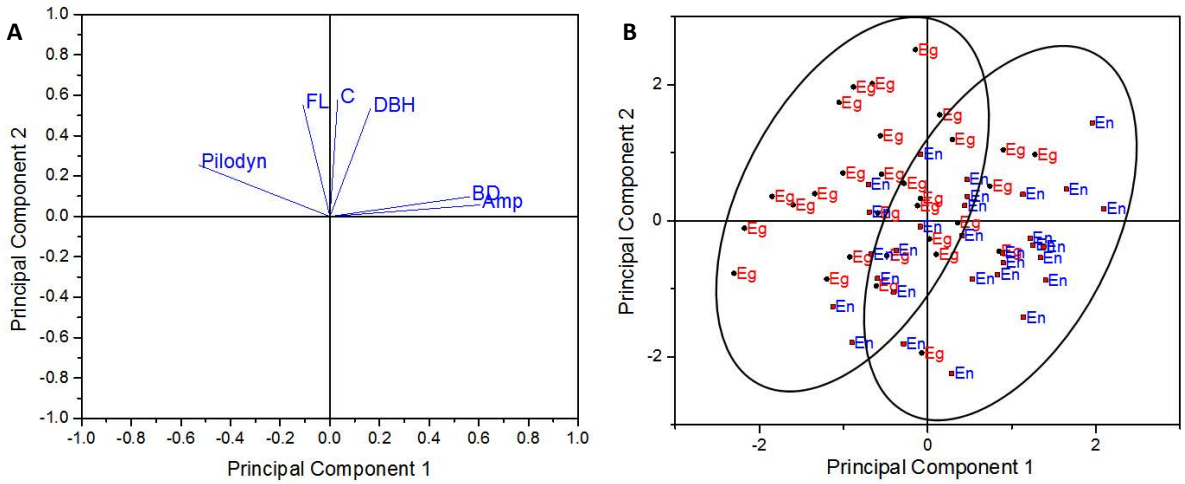

Figure 2. Principal component analysis. **A**: loadings graph, **B**: score graph. **FL**: Fiber length, **C**: coarseness, **DBH**: diameter at breast heigth, **BD**: basic density, **Amp**: amplitude, **Eg**: *E. globulus*, **En**: *E. nitens*.

IV. CONCLUSIONS

E. nitens genotypes had higher basic wood density and Resistograph amplitude averages than *E. globulus* genotypes. However, *E. globulus* wood presented more homogeneity than *E. nitens* wood, which showed a higher difference between features of spring (earlywood) and summer wood (latewood) in a growth ring. *E. globulus* trees also had higher coarseness, fiber length and DBH than *E. nitens* trees.

V. ACKNOWLEDGEMENT

FONDECYT Project 1130472 and Genómica Forestal S.A.

VI. REFERENCES

[1] Doughty, R.W. The *Eucalyptus*: a natural and commercial history of the gum tree. John Hopkins University. **2000**, Press, Baltimore, MD.

[2] Patt, R.; Kordsachia, O.; Fehr, J. European hardwoods versus *Eucalyptus globulus* as a raw material for pulping. *Wood Sci. Technol*. **2006**, *40*:39–48.

[3] Kibblewhite, R.P.; Johnson, B.I.; Shelbourne, C.J.A. Kraft pulp qualities of *Eucalyptus nitens*, *E. globulus*, and *E. maidenni*, at ages 8 and 11 years. *N.Z.J. Forestry Sci.* **2000**, *30*:447–457.

[4] McKinley, R.B.; Shelbourne, C.J.A.; Low, C.B.; Penellum, B. and Kimberley, M.O. Wood properties of young *Eucalyptus nitens*, *E. globulus* and *E. maidenii* in Northland, New Zealand. *N.Z.J. Forestry Sci.* **2002**, *32*:334–356.

[5] Isik, F. and Li, B. Rapid assessment of wood density of live trees using Resistograph for selection in tree improvement programs. *Can. J. For. Res.* **2003,** *33*:2426–2435

[6] Jensen, G.R. Wood density and biomass evaluation of *Eucalyptus nitens, E. globulus* and *E. maidenii* on two sites. B.Sc (Technology) Industry report. **1998**, University of Waikato, Hamilton, New Zealand.

KINETICS STUDY OF FURFURAL FORMATION FROM XYLOSE IN NON-CATALYZED MICROWAVE-ASSISTED REACTIONS

Olga Ershova[1*], Jaana Kanervo[2], Juha Lehtonen[2], Herbert Sixta[1]

[1] *Aalto University, Department of Forest Products Technology,* [2] *Aalto University, Department of Biotechnology and Chemical Technology (*olga.ershova@aalto.fi)*

ABSTRACT

The work addresses the determination of furfural formation kinetics in a non-catalyzed, microwave-assisted conversion of xylose in the temperature range from 180 to 220°C. The abundance of xylose as a monomer unit of xylans in hardwoods suggests significance of this study also for the wood industry. Xylose is used as a model compound for our in-depth kinetic evaluation studies. The effects of initial xylose concentration and the formation of the important intermediate compound, xylulose, were investigated in a comprehensive mechanistic modeling study including thermodynamic considerations.

I. INTRODUCTION

Furfural is a platform chemical produced from plant pentosans. It is utilized in chemical industry for synthesizing solvents, adhesives, medicines, and plastics. The main sources of these hemicelluloses are corn cob, bagasse, wheat and rice straw. Hardwoods can be used as alternative source for furfural production as they are rich in pentosans and prehydrolysis of birch allows separation of xylan up to almost 9 % of the wood [1].

Different reaction mechanisms of furfural formation from xylose were proposed by different researchers [2]. Some authors believed the reaction proceeds via xylose acyclic form (route C in **Figure 1**) [2] but most recent studies showed the reaction starts from the pyranose form of xylose (route B in **Figure 1**) [3]. This intermediate compound (luxose [2] or xylulose [4]) is subsequently dehydrated into furfural. Antal *et al.* [2] proposed the formation of both acyclic and cyclic forms of xylose at high temperatures (250 °C). Still, most of the authors calculated the kinetic parameters for xylose dehydration using a simplified mechanism with direct conversion of D-xylose to furfural (route A in **Figure 1**) [5, 6, 7].

As well as for any other chemical reaction, the rate of furfural formation depends on the temperature, reaction time, concentration of the initial reactant (xylose) and the presence of substances accelerating the process. At the moment, many studies have investigated the kinetics of furfural formation under different conditions in order to increase the production efficiency.

$$-\frac{d[Xyl]}{dt} = (k_{xyl-xylul} + k_{xyl-dp})[Xyl]$$

$$\frac{d[Xylul]}{dt} = k_{xylul-xyl}[Xyl] - k_{xylul-furf}[Xylul]$$

$$\frac{d[Furf]}{dt} = k_{xylul-furf}[Xylul] - k_{furf-dp}[Furf]$$

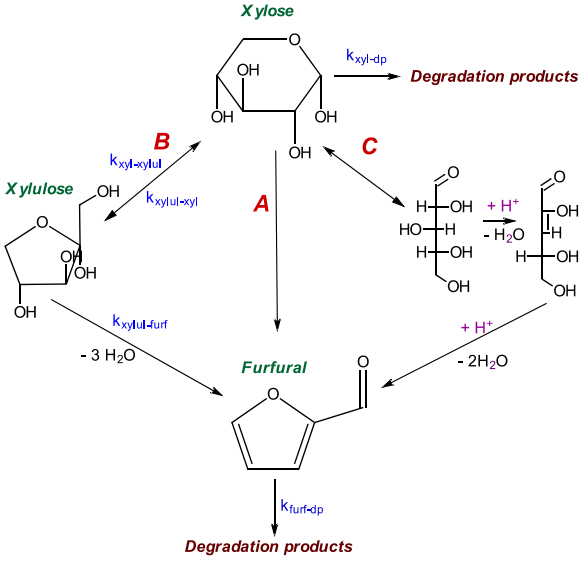

Figure 1. Different routes suggested for furfural formation from xylose and the rate equations for xylose consumption and furfural formation according to route B. (*xyl* - xylose, *xylul* – xylulose, *furf* – furfural, *dp* – degradation products)

Jing and Lu [8] studied the effect of temperature in non-catalyzed decomposition of 72 mM aqueous xylose solution. The result indicated that furfural yield can be changed by temperature manipulation and its maximum yield was 50%.

The effect of xylose concentration on the xylose dehydration was studied by Weingarten *et.al.[*5] at 160 °C. The authors demonstrated that the furfural yield was independent on the xylose concentration. In contrast, Gairola and Smirnova [9] illustrated that while there is no significant difference in yield in the initial xylose concentration range of 2-4 wt.%, an almost linear decline in furfural yield was observed (from 68% to 37%), when the effect of initial xylose concentration was examined in a broader concentration range, from 4 wt.% up to 20 wt.%.

Microwave irradiation is an alternative rapid and efficient heating method. It has been shown to accelerate reaction rates and to give a slightly higher furfural yield, which is nonetheless comparable to the conventional heating method [5].

This study focused on the evaluation of kinetic parameters of the non-catalyzed dehydration of D-xylose to furfural under microwave irradiation at temperature range 180-220 °C taking into account the formation of the intermediate compound, xylulose.

II. EXPERIMENTAL

Solutions of high purity D-xylose powder (E. Merck AG) in water with different concentrations (0.05, 0.2, 0.5 M) were freshly prepared.

3 ml of D-xylose-water mixture were treated in a Monowave 300 single-mode microwave reactor (Anton Paar GmbH, Graz, Austria) using borosilicate glass vial of 10 ml capacity. During the reaction the solution was mixed by a magnetic stirrer at 600 rpm. Time-to-maximum temperature was set as 1.5 min with 850 W maximum output power employed. The temperature inside the vessel was controlled by a fiber optic sensor. The prepared solutions were tested for furfural yield at treatment temperatures 220, 200 and 180 °C with the reaction time 1-240 min. The reaction vial was rapidly cooled after the treatment by compressed air inside the reactor.

The samples were analyzed by High Performance Liquid Chromatography (HPLC) in a Dionex UltiMate 3000 HPLC (Dionex, Sunnyvale, CA, USA) equipment outfitted with refractive index (RI) and ultraviolet (UV) diode array detectors and HyperREZ XP Carbohydrate Ca^{+} column (Thermo Scientific). Solution of HPLC grade sulfuric acid (Sigma-Aldrich) in Millipore water (0.0025M H_2SO_4) was used as eluent at a flow rate of 0.8 ml/min, and the temperature was set to 70 ºC.

Computations of kinetic model were implemented in MATLAB 2013b. The ordinary differential equations were solved by ode15s and optimization was done by Nelder-Mead algorithm. Equal weighing was applied in calculating the SSQR (sum of squared residuals).

III. RESULTS AND DISCUSSION

The effect of treatment temperature, residence time and reactant xylose concentrations on furfural yield during non-catalyzed microwave assist reactions are displayed in **Figure 2**. The yield is strongly influenced by treatment temperature. After the first 25-35 min of the treatment the furfural yield increases up to 4.5-5 times with the temperature increasing from 180 to 200 °C and up to 2-2.5 times from 200 to 220 °C, respectively. At the highest studied temperature (220°C) the furfural yield started to decrease after reaching its maximum (45-48 mol%) due to the furfural decomposition reactions and formation of solid residues – humins. The same trend could be estimated at other temperatures during prolonged treatment times.

The furfural yield was somewhat influenced by the initial reactant concentration. During the first 20-25 min this dependence is very minor, but with the extended reaction time the dependence becomes more obvious. The lowest furfural yield was obtained from the solution with the lowest xylose concentration. At the same time, the solution with xylose concentration 0.5M showed similar or even slightly lower furfural yield compare to 0.2M xylose solution. From **Figure 2** it can be seen that the decreasing of furfural yield at 220 °C started earlier and with increased rate for the solution with the highest xylose concentration. Probably, it can be explained by side reaction between furfural and xylose (or it's intermediate).

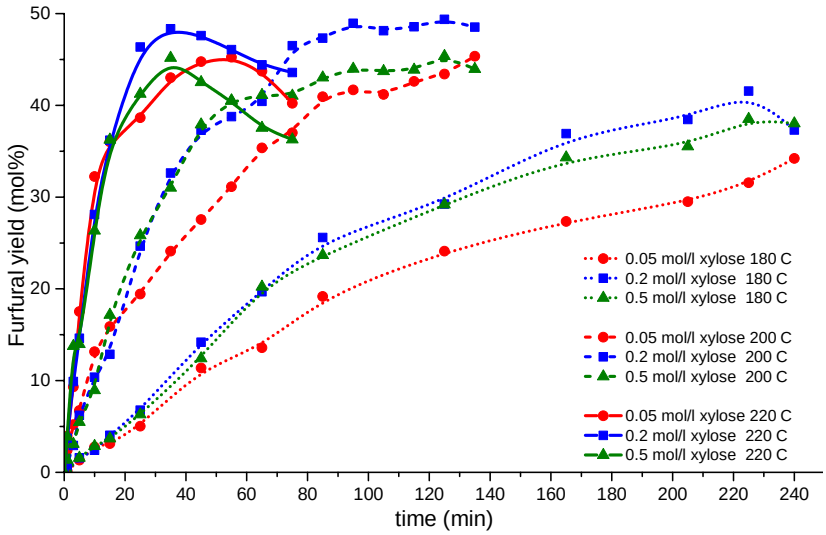

Figure 2. The temperature dependence and xylose concentration dependence on furfural yield during non-catalyzed furfural formation under microwave irradiation.

As it can be seen from **Figure 3a** the xylose conversion is strongly influenced by reaction temperature. The dependence of xylose conversion *vs.* initial xylose concentration becomes less significant with the temperature increasing. At 220°C the xylose conversion reached 100% already after 45 min of treatment. During the initial stage of this non-catalyzed xylose dehydration (25-45 min) the selectivity (**Figure 3b**) was also dependent on the reaction temperature. The selectivity to furfural formation has the maximum around 48-52% for all the temperatures.

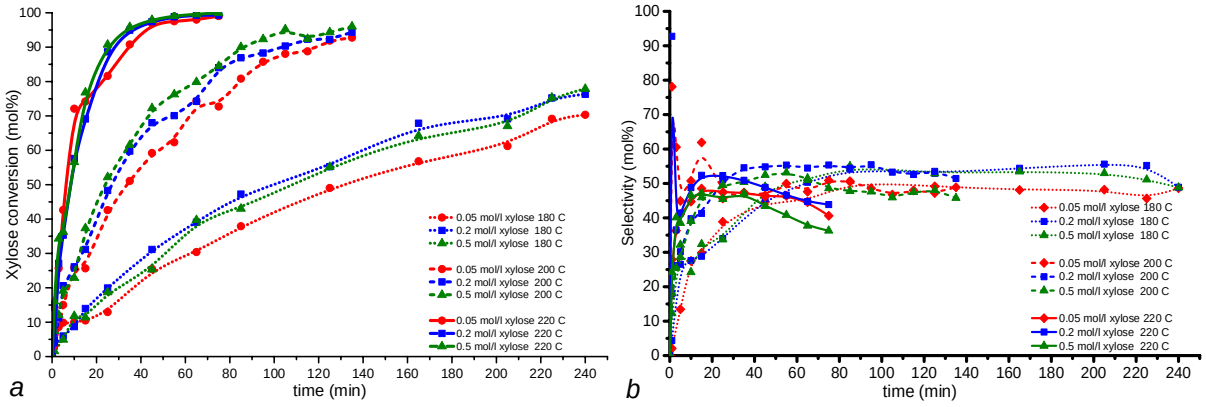

Figure 3. Xylose (a) conversion and (b) selectivity during non-catalyzed furfural formation under microwave irradiation.

The reaction scheme according to route B on **Figure 1** was applied for kinetics modeling of non-catalyzed xylose dehydration. All the reactions are reported to be in first order. The concentration of intermediate compound, xylulose, has been determined by HPLC method for each sample and utilized for kinetic model calculation. The side reaction between xylose and furfural was not taken into account. The rate equations of xylose consumption, xylulose and furfural formations are shown in **Figure 1**. The obtained values for rate constants and corresponding activation energies are listed in **Table 1**.

All the reaction rates were increased with the temperature increasing. The ratio of reaction rate constants $k_{xyl\text{-}xylu}/k_{xyl\text{-}dp}$ was raised along with the temperature increasing from 0.83 to 1.03. From these results it can be concluded that at temperatures above 200 °C the formation of degradation products from xylose monomer is more preferable than furfural formation. Each temperature increase on 20 °C resulted in an almost three times higher furfural decomposition rate compare to the respective previous step (**Table 1**, *F→dp*). The direct comparison of evaluated kinetic parameters for non-catalytic xylose dehydration with the previously published

results seems to be not possible, because of either utilization of simplified reaction mechanism [6, 7, 8] or implementation of subcritical and supercritical reaction conditions [4].

Table 1. Evaluated kinetic parameters for xylose dehydration in non-catalyzed aqueous system

Reaction	***A (scaled) 1/min***	***Ea kJ/mol***	***Rate constants at experimental temperatures, L/(mol*s)***		
			180	**200**	**220**
xyl→xylul	0,0148	126	0,216	0,888	3,258
xylul→xyl	0,00206	110	0,036	0,124	0,384
xylul→F	0,000109	0 (fixed)	0,007	0,007	0,007
F→dp	0,00832	100(fixed)	0,162	0,499	1,400
xyl→dp	0,0138	136	0,180	0,828	3,367

IV. CONCLUSIONS

The kinetic model for the non-catalyzed dehydration of xylose under microwave irradiation at temperature range of 180-220 °C has been developed in this study taking into account the formation of the intermediate compound, xylulose. The reaction rate constants for decomposition of furfural and xylose were also determined in the studied temperature range.

The effect of reaction temperature and initial xylose concentration on furfural yield has been investigated.The results of the kinetics modeling have shown that at the temperature above 200 °C the formation of degradation products from xylose is more preferable than furfural formation. The effect of initial xylose concentration was more obvious at extended reaction times, where the lowest initial xylose concentration resulted in the lowest furfural yield and xylose conversion.

In non-catalytic process the maximum obtained furfural yield of 48 mol% has been corresponded to the following conditions: 35 min reaction time at 220 °C or 90 min at 200 °C.

V. ACKNOWLEDGEMENT

The authors would like to acknowledge financial support from The International Doctoral Programme in Bioproducts Technology (PaPSaT) and Walter Ahlström Foundation. We also sincerely thank Rita Hatakka for her contribution in HPLC method development.

VI. REFERENCES

[1] Testova, L., Vilonen, K., Pynnönen, H., Tenkanen, M., Sixta, H., Isolation of hemicelluloses from birch wood: distribution of wood components and preliminary trials in dehydration of hemicelluloses, *Lenzinger Berichte* **2009**, 87, 58.

[2] Antal, M.J., Leesomboon, T., Mok, W.S., Richards, G.N., Mechanism of formation of 2-furaldehyde from D-xylose, *Carbohydrate research* **1991**, 217, 71-85.

[3] Danon, B., Marcotullio, G., de Jong, W., Mechanistic and kinetic aspects of pentose dehydration towards furfural in aqueous media employing homogeneous catalysis, *Green Chemistry* **2014**, 16,39-54.

[4] Aida, T.M., Shiraishi, N., Kubo, M., Watanabe, M., Smith, Jr. R.L., Reaction kinetics of D-xylose in sub- and supercritical water, *The Journal of Supercritical Fluids* **2010**, 55, 208-216.

[5] Weingarten, R.; Cho, J.; Conner, W.C.,Jr.; Huber, G. W., Kinetics of furfural production by dehydration of xylose in a biphasic reactor with microwave heating, *Green Chemistr*, **2010**, 12(8), 1423-1429.

[6] Borrega, M., Nieminen, K., Sixta, H., Degradation kinetics of the main carbohydrates in birch wood during hot water extraction in a batch reactor at elevated temperatures, *Bioresourse Technology* **2011**, 102, 10724-10732.

[7] Kim, S.B., Lee, M.R., Park, E.D., Lee, S.M., Lee, H.K., Park, K.H., Park, M.J., Kinetic studies of the dehydration of D-xylose in high temperature water, *Reac. Kinet. Mech. Cat.* **2011**, 103, 267-277.

[8] Jing, Q.; Lu, X., Kinetics of non-catalyzed decomposition of D-xylose in high temperature liquid water, Chinese *Journal of Chemical Engineering* **2007**, 15(5), 666-669.

[9] Gairola, K.; Smirnova, I., Hydrothermal pentose to furfural conversion and simultaneous extraction with SC-CO2 - Kinetics and application to biomass hydrolysates, *Bioresource Technology* **2012**, 123, 592-598.

PAPERMAKING POTENTIAL OF WOOD AND PRE- HYDROLYZED BARKS OF *Eucalyptus globulus*

Luís Fernandes[1], Duarte Neiva[2], Maria Emília Amaral[1], Jorge Gominho[2], Helena Pereira[2], Ana Paula Duarte[3*], Rogério Simões[1]

[1]*Unidade de Materiais Têxteis e Papeleiros, Universidade da Beira Interior, 6200 Covilhã, Portugal;* [2]*Centro de Estudos Florestais, Instituto Superior de Agronomia, Universidade Lisboa, Tapada da Ajuda, 1349-017 Lisboa, Portugal; 3Centro de Investigação em Ciências da Saúde, Universidade da Beira Interior, 6200 Covilhã, Portugal (**apcd@ubi.pt*)*

ABSTRACT

The pulping and papermaking potential of *Eucalyptus globulus* bark and wood was evaluated. The chemical composition of the bark sample studied did not differ significantly from that of wood, which suggests a good potential for pulping. After auto-hydrolysis, the delignification extent and the pulp yield of the bark was only slightly lower than those for wood. As a consequence of the higher kappa number of the pulps from bark, the chlorine dioxide consumption in the bleaching process was higher. The morphological characteristics of the bark pulp fibers are very similar to those from wood and the corresponding papermaking potential does not differ significantly. One drawback observed was the higher drainage resistance of the pulp from bark in respect to the corresponding pulps from wood.

I. INTRODUCTION

The cost of raw-material has an important impact on the total production costs of the pulp, particularly in the Europe. The increasing demand of wood for pulping and other applications, including biomass for energy, rises concern in the pulp and paper industry regarding raw-material supply at a competitive cost. The shortage of raw-material for pulping has a negative impacts on the costs of raw-material and consequently in the industry competitiveness. Therefore, research on alternative species and residual materials has been intensified. Bark from eucalypt has been traditionally used as biomass for energy production. Several studies have focused on eucalypt bark, namely in their chemical composition, their potential as source of chemicals or biofuels or as adsorbent, and more recently their pulping potential was studied [1-4]. The high ash and extractives contents, as well as the high amount of parenchyma cell and vessels are the main disadvantages of the bark as raw-material for pulping; some advantages, like fast impregnation were also referred [4]. A recent study has shown the potential of *E. globulus* bark and tops for pulping [4]. The present study aims to further explore the pulping and papermaking potential of eucalypt bark.

II. EXPERIMENTAL

Heartwood and sapwood from a 40 year-old *Eucalyptus globulus* tree, and industrial *E.globulus* bark was used in this study. These materials were chipped in a knife mill (Retsch SM 2000) with an output sieve of 6 mm x 6 mm and screened using a vibratory apparatus (Retsch AS 200 basic) with a 10 mesh (2.0 mm) sieve in order to separate the fines. The chips were approximately 8 mm x 3 mm x 2 mm. Industrial *E. globulus* chips were also used in the study. To determine the chemical composition of the materials , representative milled samples were extracted successively with dichloromethane, ethanol, and water, according to TAPPI T204 cm-07. Klason and acid-soluble lignin contents were determined in the extracted material according to TAPPI T222 om-11. Klason lignin was determined as the mass of the solid residue after drying at 103 ± 2 ºC. The acid-soluble lignin was determined on the filtrate by measuring the absorbance at 205 nm. Total lignin content was calculated as the sum of Klason lignin and acid-soluble lignin. The monosaccharide composition was determined in the hydrolysate, after their derivatization to alditol acetates and separation by gas chromatography, according to a method adapted from TAPPI standard 249 cm-00.

The wood and bark chips were pulped in a forced circulation reactor with 6 litters of capacity with a West N4400 Single Loop Temperature Controller. The wood chip charge was 1000 g oven dry wood, and the general kraft cooking conditions were as follows: active alkali 22% (Na_2O), sulfidity 30%, liquor/wood ratio 4:1, time to temperature 100 min, and time at maximum temperature (160ºC) 60 min. The bark was submitted to kraft cooking after pre-hydrolysis. The pulped material was washed and screened. The screened pulp yield and rejects, kappa number (ISO 302), and pulp viscosity (ISO 5351/1) were determined according to standard methods.

Hexenuronic acids (Hex Ac) were determined acording to Tenkanen et al. **[5].** The unbleached pulps were submited to an elemental chlorine free sequence $D_0ED_1D_2$.

The morphological properties of unbleached and bleached pulp fibers were determined by image analysis of a diluted suspension in a flow chamber in Morfi® (TECHPAP). The bleached pulps were beaten in a PFI mill at 500, 2500 and 4500 revolutions under an refining intensity of 1.66 N/mm. Paper sheets were prepared according to the Scan standard, and tested regarding structural, mechanical and optical properties, according to the TAPPI standards.

III. RESULTS AND DISCUSSION

Table 1 presents the chemical composition of the different samples tested. The industrial chips exhibit higher holocellulose and glucose content than the other wood samples. The industrial bark presents slightly higher ash content, but the content of the remaining components is similar, including the polar extract content. Miranda et al. [4] have reported higher values for these compounds which may be due to the different source of the barks.

Table 1. Chemical characterization of the wood and bark.

Sample		Industrial chips (%)	Heartwood (%)	Sapwood (%)	Industrial Bark (%)
ash		0.4	0.3	1.1	2.0
Extractives	CH_2Cl_2	0.3	0.3	0.3	0.3
	Ethanol	1.8	2.5	3.3	1.4
	Water	1.8	1.8	2.1	2.6
	Total	3.8	4.6	5.7	4.3
Klason		17.0	19.7	16.3	15.0
Soluble lignin		4.3	3.7	3.5	3.6
Total lignin		21.4	23.3	19.9	18.5
Holocellulose		74.5	69.5	71.6	74.2
Sugars	Arabinose	0.5	0.5	0.5	0.6
	Xylose	10.9	11.8	11.9	9.3
	Mannose	1.0	1.6	1.6	0.9
	Galactose	1.1	0.6	0.6	1.2
	Glucose	41.0	35.3	35.4	41.4

Table 2 presents the results of the cooking process. The industrial chips presents a pulp yield slightly higher than the corresponding wood samples from the 40 year-old tree. The lower pulp yield of the older material may be related with the lower holocellulose and glucose content of the raw-material (**Table 1**). The pulp yield of the industrial eucalypt bark is of the same magnitude of the industrial wood chips, which confirms the pulping potential of the bark. It should be emphasized that the bark was submitted to an auto-hydrolysis stage (140ºC, 45 min) before kraft cooking. The bark delignification extent is lower than that observed for the wood, particularly for the same cooking conditions (Bark (9)), which cannot be ascribed to the lignin or extractives content (**Table 1**) and probably are other factors playing a role. Miranda et al. [4], working with wood and bark from *E. globulus*, have reported a higher solubility of the bark components in 1% NaOH solution, respecting to wood. The same authors also reported lower bark pulp yield and higher kappa number. Regarding to the pulp bleaching response, no significant differences were observed between bark and wood, but the different unbleached kappa number were taken in account in the chlorine dioxide charge in D_0, using a kappa factor of 0.2. The pulps were bleached according a $D_0ED_1D_2$ bleaching sequence, using a chlorine dioxide charge of 1.2% and 0.5% in D_1 e D_2 stages respectively and a final brightness of 80% ISO was obtained. This topic deserves further research.

Table 2. Pulping conditions and results (*Auto-hydrolysis, L: W=15:1;** Auto-hydrolysis, L: W=4:1)

Chips	Alkali (%)	T max (ºC)	Time at Tmax (min)	Yield (%)	Kappa	Hex Ac (mmol/Kg)	Kappa (corrected)	Viscosity (cm^3/g)
Industrial	22	160	60	48.4	13.3	39.0	9.9	780
Heartwood	22	160	60	44.6	14.9	43.2	11.2	841
Sapwood	22	160	60	44.6	13.5	46.3	9.5	871
Lab. chips	22	160	60	47.7	9.3	35.4	6.2	853
Bark* (8)	15	165	114	43.9	18.4	31.8	15.7	969
Bark** (9)	22	160	60	44.3	25.1	47.6	21.0	810

Table 3 presents the morphological properties of the unbleached and bleached pulp fibers obtained from the wood and the bark. As expected, there are differences between the pulp fibers from heartwood and sapwood, but the bark pulp fibers compare favorably with the corresponding wood pulp fibers. In addition, these results are in very good agreement with the expected results for *E. globulus* wood pulps, suggesting the high potential of *E. globulus* bark for papermaking.

Table 3. Fiber characteristics of wood and bark pulp samples from E. globulus.

Pulp	bleaching	beating (PFI)	Fibers(millions/g)	Lenght (µm), arithmetic	Lenght (µm), weighted in length	Width (µm)	Coarseness (mg/m)
Heartwwod	Before bleaching	0	17.3	657.3	784.3	19.50	0.07
	After bleaching	0	21.4	651.7	780.7	19.50	0.07
		500	20.8	649.7	782.0	19.43	0.07
		2500	22.6	650.7	780.3	19.57	0.07
		4500	22.1	639.3	771.7	19.77	0.07
Sapwood	Before bleaching	0	12.7	713.7	859.7	20.67	0.10
	After bleaching	0	14.3	707.6	855.6	20.82	0.10
		500	14.6	705.6	858.0	21.06	0.10
		4500	15.6	690.9	842.8	21.94	0.09
Pre-hydrolized Bark (9)	Before bleaching	0	14.1	662.7	807.0	19.90	0.10
	After bleaching	0	17.7	662.8	805.0	19.23	0.08
		500	18.3	668.7	812.7	18.83	0.08
		2500	17.9	655.0	797.7	19.03	0.08
Pre-hydrolized Bark (8)	Before bleaching	0	13.1	662.3	813.3	20.30	0.10
	After bleaching	500	16.4	664.0	810.3	19.47	0.09
		2500	16.6	653.4	795.6	19.98	0.09
		4500	17.1	634.7	779.0	20.43	0.09

Figures 1 and **2** present the behavior of the bleached pulps in beating. The densification of the paper structure with beating is similar for sapwood and bark pulps; heartwood pulp develops faster densification due to lower diameter, length and coarseness of the pulp fibers. In consequence, the tensile index of the heartwood pulp is higher than that of the other pulp samples at a given beating level. However at a given paper density no significant differences were observed. Regarding tear index, the heartwood pulp exhibit lower values than the corresponding sapwood pulp, which is an expected result considering the lower fiber length; bark pulps exhibit lower values than the wood samples. These results may not be ascribed to differences in fiber length; the large proportion of parenchyma cell and vessels [4] certainly play a role in the behavior of the bark pulps. In general,

however, the mechanical properties of the bark pulps compare well with the wood pulp. On the contrary, a clear drawback of the bark pulps is the higher drainage resistance of the pulp suspensions (**Figure 2-b**).

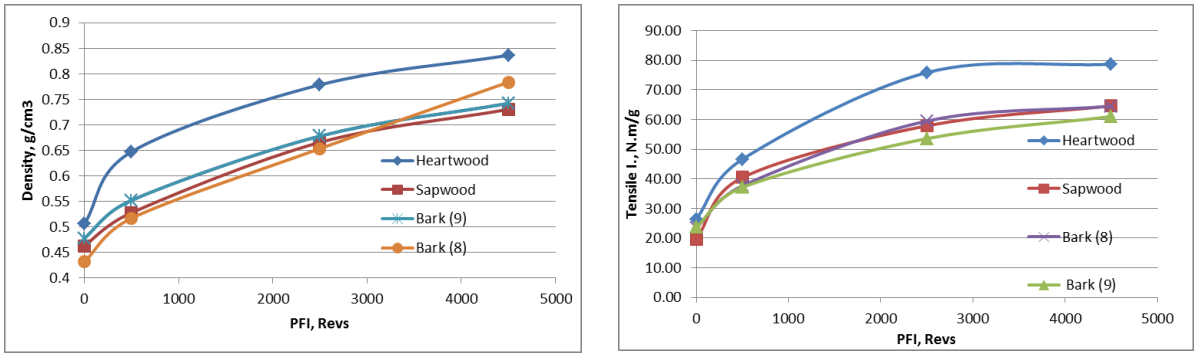

Figure 1. Paper density (a-left) and tensile index (b-right) vs. beating extent.

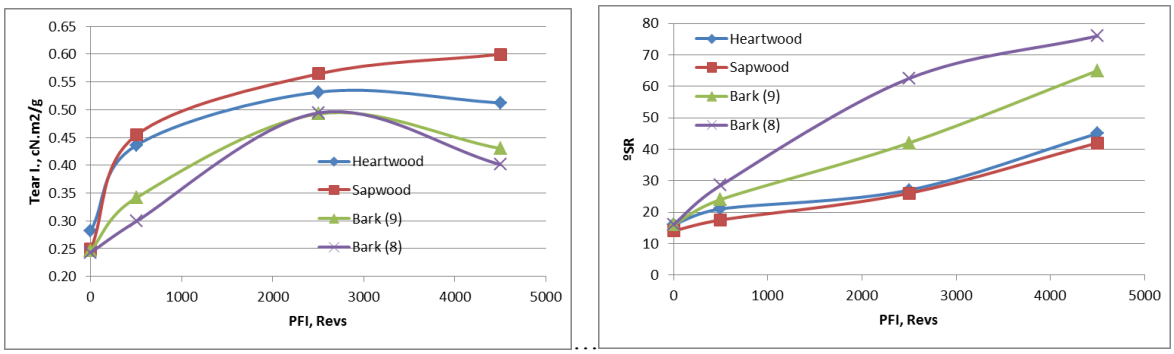

Figure 2. Tear index (a-left) and drainage resistance (b-right) vs. beating extent.

IV. CONCLUSIONS

The *Eucalyptus globulus* bark tested exhibited good performance in the kraft cooking process and the papermaking properties displayed were also promising. The pulping yield was only 4 % lower than the corresponding for wood and the delignification extent in cooking was also lower, which obliges an increasing of the chlorine dioxide consumption in the bleaching process. Regarding the papermaking potential, the strength properties are comparable with the wood pulps, but the drainage resistance of the bark stocks is higher, which implies a lower paper production rate on industrial scale.

V. ACKNOWLEDGEMENT

This work was carried out in the scope of the PTDC/AGR-CFL/110419/2009 project supported by the national funding of FCT - Fundação para a Ciência e Tecnologia.

VI. REFERENCES

[1] Miranda, I.; Gominho, J.; Mirra, I.; Pereira, H. Fractioning and chemical characterization of barks of Betula pendula and Eucalyptus globulus. Industrial Crops and Products **2013**, *41*, 299-305.

[2] Lima, M.; Lavorente, G.; da Silva, H.; et al. Effects of pretreatment on morphology, chemical composition and enzymatic digestibility of eucalyptus bark: potentially valuable source of fermentable sugars for biofuel production – part 1, Biotechnology for Biofuels **2013**, *6*, 75-92.

[3] Khosla, E.; Kaur, S.; Dave, P. Adsorption mechanism of basic red-12 over Eucalyptus bark and its surface derivatives, J. Chemical and Eng. Data, **2012**, *57*(7): 2004-2011.

[4] Miranda, I.; Gominho, J.; Pereira, H. Incorporation of bark and tops in Eucalyptus globulus wood pulping. BioResources **2012**, *7(3)* 2012, 4350-4361.

[5] Tenkanen, M.; Gellerstedt, G.; Vourinen, T.; Teleman, A.; Perttula, M.; Li, J.; Buchert, J. Determination of hexeneuronic acid in softwood kraft pulps by three different methods. Journal of Pulp and Paper Science **1999**,. *25(9)*, 306-311.

2D-NMR DEMONSTRATION OF LIGNIN REMOVAL FROM WOOD AND NON-WOOD PLANT FEEDSTOCKS BY FUNGAL VERSATILE PEROXIDASE

Elena Fernández-Fueyo[1], Jorge Rencoret[2], M. Alvaro Berbis[1], Francisco J. Ruiz-Dueñas[1], Ana Gutiérrez[2], José C. del Río[2], Jesús Jiménez-Barbero[1], Kenneth E. Hammel[3], Angel T. Martínez[1]*

*[1]CIB, CSIC, Ramiro de Maeztu 9, E-28040 Madrid, Spain; [2]IRNAS, CSIC, PO Box 1052, E-41080 Seville, Spain; [3]FPL, USDA, 1 Gifford Pinchot Dr, Madison, WI 53726, USA (*atmartinez@cib.csic.es)*

ABSTRACT

The ability of versatile peroxidase to modify/degrade lignin (in conjunction with veratryl alcohol as a mediator) in both wood (*Eucalyptus globulus*) and non-wood (*Pennisetum purpureum*) lignocellulosic feedstocks was demonstrated using the *Pleurotus ostreatus* enzyme heterologously expressed in *Escherichia coli* and "in vitro" folded. Two-dimensional nuclear magnetic resonance (NMR) of the treated materials, swollen in dimethylsulfoxide-d_6, revealed a reduction in the number of lignin side-chain linkages after both treatments. However, a significant removal of lignin by the enzymatic treatment was only observed in the case of eucalypt wood, as shown by the decrease of lignin aromatic signals referred to carbohydrate anomeric signals.

I. INTRODUCTION

Lignin removal is a key step for recycling the carbon fixed by land photosynthesis and a limiting issue for the use of lignocellulosic biomass by the pulp and paper industry and in the sustainable production of fuels and other chemicals. Only a group of basidiomycetes, the so-called white-rot fungi, are efficient lignin degraders in nature [1]. According to the genomic data, ligninolytic peroxidases - the so-called lignin peroxidase (LiP, EC1.11.1.14), manganese peroxidase (MnP, EC1.11.1.13) and versatile peroxidase (VP, EC 1.11.1.16) - are exclusive of lignin-degrading white-rot basidiomycetes and play a central role in lignin degradation [2]. The presence of LiP has been associated with the ability to degrade lignin in white-rot fungi and *in vitro* depolymerization of lignin by LiP was demonstrated [3]. On the other hand, a recent study show the presence in the model agaric *Pleurotus ostreatus* of a peroxidase repertoire in which VPs play the role that LiPs do in white-rot polypores, being able to depolymerize lignin in the presence of VA [4].

In the present study, eucalypt (*Eucalyptus globulus*) and Elephant grass (*Pennisetum purpureum*), two fast growing plant species, were treated with VP from *P. ostreatus* in the presence of VA to investigate its ability to modify natural lignin in lignocellulosic feedstocks, as it has been previously demonstrated for the laccase-mediator system [5,6]. The eventual modification of the cell-wall polymers during the enzyme treatment of the whole plant material was analyzed by hetereonuclear single quantum correlation (HSQC) solution NMR of gels prepared by lignocelluloses swelling in dimethylsulfoxide-d_6 [7,8].

II. EXPERIMENTAL

Recombinant VP

VP (isoenzyme VP1) from the basidiomycete *P. ostreatus* was produced heterologously in *Escherichia coli*. The mature protein-coding sequence of gene model 137757 from the PC9 monokaryon genome, after manual curation, was synthesized by ATG:biosynthetics (Merzhausen, Germany) after verifying that all the codons had been previously used for expressing other genes in the same *E. coli* strain (and substituting them when required). Mature protein-codifying sequence was cloned in the expression vector pET23a (+) (Novagen). The resulting plasmid pET23a-137757, was directly used for expression. The peroxidase was produced in *E. coli* BL21(DE3)pLysS. Cells were grown for 3 h in Terrific Broth, induced with 1 mM isopropyl-β-D-thiogalactopyranoside, and grown further for 4 h. The apoenzyme accumulated in inclusion bodies, as observed by sodium dodecyl sulfate-polyacrylamide gel electrophoresis, was solubilized using 8 M urea. Subsequent *in vitro* folding was performed using 0.16 M urea, 5 mM Ca^{2+}, 20 µM hemin, 0.5 mM oxidized glutathione, 0.1 mM dithiothreitol, and 0.1 mg/ml protein, at pH 9.5. Active enzyme was purified by Resource-Q chromatography using a 0-300 mM NaCl gradient (2 ml·min^{-1}, 20 min) in 10 mM sodium tartrate, pH 5.5.

Wood and grass treatments with VP

Milled Elephant grass and eucalypt wood samples (100 mg) were treated with 5 mg of VP from *P. ostreatus* in 10 mM Na acetate (pH 4.5) containing 10 mM VA and 60 mM H_2O_2 at 25 ºC for 24 h. Treatments without

enzyme were also performed. For NMR analysis, the whole samples recovered after washing (70-85 mg) were swollen in dimethylsulfoxide-d_6 and HSQC spectra were acquired at the gel state [7,8]. A Bruker Biospin (Billerica, MA) AVANCE 500 MHz spectrometer fitted with a cryogenically cooled 5-mm TCI gradient probe with inverse geometry (proton coils closet to the sample) was used. The ^{13}C-^{1}H correlation experiment was an adiabatic HSQC experiment (Bruker standar pulse sequence ´hsqcetgpsisp.2´; phase-sensitive gradient-edited-2D HSQC using adiabatic pulses for inversion and refocusin). Spectra were acquired from 10 to 0 ppm in F2 (^{1}H) with 1000 data points for an acquisition time (AQ) of 100 ms, an interscan delay (D1) of 500 ms, 200 to 0 ppm in F1 (^{13}C) with 400 increments (F1 acquisition time 8 ms) of 40 scans. The $^{1}J_{CH}$ used was 145 Hz. Processing used typical matched Gaussian apodization in 1H and a squared cosine bell in ^{13}C. Prior to Fourier transformation, the data matrices were zero filled up to 1,024 points in the ^{13}C dimension. The central solvent peak was used as an internal reference (δ_C/δ_H 39.5/2.49). The aromatic ^{13}C-^{1}H correlation signals of the different lignin units were used for estimation of its composition in guaicyl (G) and syringyl (S) lignin units. The *p*-coumaric and ferulic acid contents and the percentages of main lignin substructures (including β-O-4' and β-β' side-chain linkages) were referred to total lignin. Signal assignement was based on previous studies on *E. globulus* and *P. purpureum* lignins [9,10].

III. RESULTS AND DISCUSSION

The detailed assignments of aliphatic-oxygenated (top) and aromatic-unsaturated (bottom) signals in the control and VP-VA treated eucalypt wood and Elephant grass samples are shown in the spectra expansions included in **Fig. 1**. The main lignin and cinnamic structures identified are shown in **Fig. 2**.

The aliphatic oxygenated region of the spectrum of control (**Fig. 1a** and **c**) showed signals of both lignin and carbohydrates, the latter mainly corresponding to xylan units (X). In addition to methoxyl signals, signals of lignin side-chains were observed, the latter corresponding to C_α–H_α correlations (A_α) in β-O-4´ alkyl–aryl ether substructures, and C_β–H_β correlations in β-O-4 alkyl–aryl ether substructures including a second S-unit (A_β(S)). The main signals in the aromatic-unsaturated region of the HSQC spectrum of control eucalypt wood (**Fig. 1a**) corresponded to the lignin benzene rings, including the G and S whereas in the case of the Elephant grass **(Fig. 1c)** *p*-coumaric acid signals are also present together with lignin signals.

The oxidation of VA, used as mediator, results in the production of veratraldehyde which remains attached to the sample, despite the exhaustive washing, overlapping some signals. This can be due to the coupling of VA radical on the lignin units.

Enzymatic modification of eucalypt lignin as shown by 2D NMR

As shown by the NMR spectra of the whole treated sample at the gel state, a single step VP-VA treatment (without a subsequent alkaline extraction) led to a significant reduction in the molar frequency of both β-β' (B_α signal) and β-O-4' (A_β signal) inter-unit linkages (per 100 lignin units) in the treated sample (40% and 1%, respectively, in **Fig. 1b**) with respect to the control (44% and 4%, respectively, in **Fig. 1a**). Moreover, a reduction of the lignin content was produced, as shown by the lignin-to-carbohydrate molar ratios (L/CH) estimated from the intensity of the lignin aromatic signals referred to the carbohydrate anomeric signals (X_1 and X'_1), passing from a L/CH ratio of 2.3 in the control to a L/CH ratio of 1.6 in the treated sample (**Fig 1**). Finally, a slightly preferential removal of G units was observed, resulting in higher S/G molar ratio in the treated sample (1.5) compared with the control (1.4), in agreement with related studies [5,6].

Enzymatic modification of Elephant grass lignin as shown by 2D NMR

The single step VP-VA treatment (without subsequent alkaline extraction) resulted in a reduction (>10%) of β-O-4' linkages per 100 lignin units in the treated sample (**Fig. 1d**) with respect to the control (**Fig. 1c**) (β-β linkages were not detected in the Elephant grass samples). However, in contrast with that observed for eucalypt wood, no significant reduction of lignin content was produced, as shown by the unchanged lignin-to-carbohydrate molar ratios (1.0 in both samples), and the *p*-coumaric acid (PCA signals) signals remained basically unchanged.

IV. CONCLUSIONS

In the present study, the ability of a high-redox ligninolytic peroxidase from *P. ostreatus* (VP) to remove lignin from two lignocellulosic samples is demonstrated by NMR analysis, in agreement with its central role in lignin degradation in Agaricales and with our previous results in which VP was able to degrade both a non phenolic lignin-model dimer and synthetic polymeric lignin (DHP). The results obtained showed that VP was more effective against eucalypt wood lignin than against Elephant grass lignin, leading to both a significant reduction in the frequency of main inter-unit linkages and a moderate reduction of the lignin content, while the carbohydrate signals remain basically unchanged.

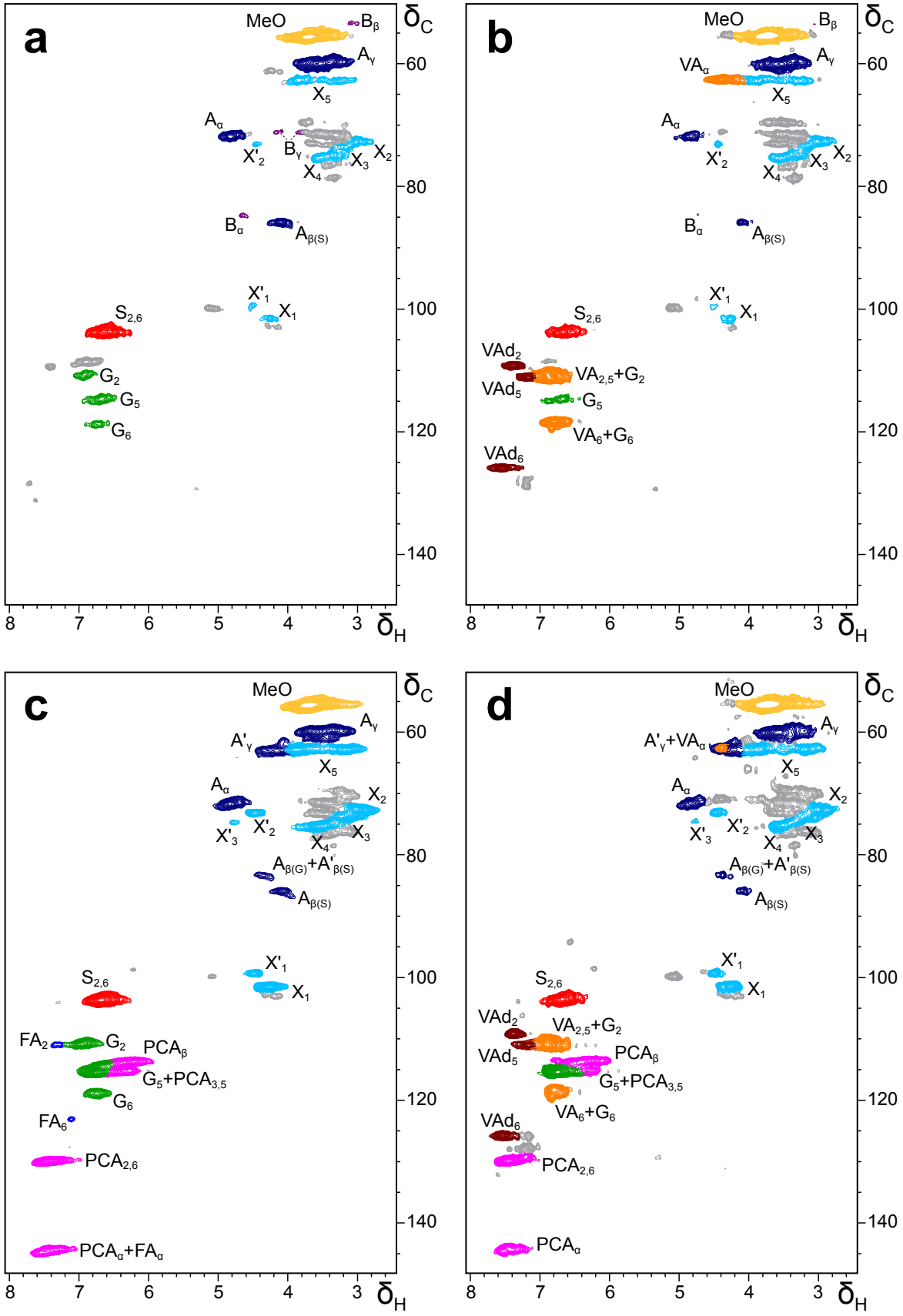

Figure 1. Aromatic region of the HSQC spectra of eucalypt wood (top) and Elephant grass (bottom) treated with *P. ostreatus* VP and VA (as mediator). **A** and **C** controls without enzyme; **B** and **D** treatments with enzyme. See **Fig. 2** for identification of the lignin, cinnamic acid and mediator-derived structures assigned (MeO correspond to methoxyl groups). X and X' signals correspond to normal and acetylated carbohydrates, respectively.

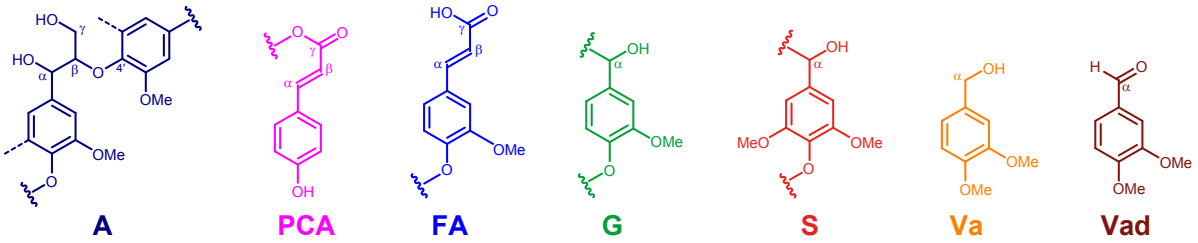

Fig. 2. Main lignin, cinnamic acid and mediator-derived structures identified in the Elephant grass and eucalypt samples analyzed by HSQC NMR (Fig. 1): **A**, β-O-4´ lignin structure (aliphatic region of the spectra); **PCA**, p-coumaric acid; **FA**, ferulic acid; **G**, guaiacyl units; **S**, syringyl units; **Va**, veratryl alcohol (mediator); and **Vad**, veratraldehyde (Va oxidation product).

V. ACKNOWLEDGEMENT

E.F.-F. and J.R. thank Junta de Ampliación de Estudios of CSIC for a JAE PhD fellowship and a JAE-DOC contract (co-funded by the European Social Fund). M.A.B. acknowledges an FPI fellowship from the Spanish Ministry of Economy and Competitiveness. This work was supported by the Spanish HIPOP (BIO2011-26694) and LIGNOCELL (AGL2011-25379) projects (co-financed by FEDER funds) and the European projects PEROXICATS (KBBE-2010-4-265397) and INDOX (KBBE-2013-7-613549).

VI. REFERENCES

[1] Martínez A.T.; Speranza M.; Ruiz-Dueñas F.J.; Ferreira P.; Camarero S.; Guillén F.; Martínez M.J.; Gutiérrez A.; del Río J.C. Biodegradation of lignocellulosics: Microbiological, chemical and enzymatic aspects of fungal attack to lignin**.** *Int. Microbiol.* **2005**, *8,* 195-204.

[2] Floudas D.; Binder M.; Riley R.; Barry K.; Blanchette R.A.; Henrissat B.; Martínez A.T.; Otillar R.; Spatafora J.W.; Yadav J.S. et al. The Paleozoic origin of enzymatic lignin decomposition reconstructed from 31 fungal genomes**.** *Science* **2012**, *336,* 1715-1719.

[3] Hammel K.E.; Jensen K.A.; Mozuch M.D.; Landucci L.L.; Tien M.; Pease E.A. Ligninolysis by a purified lignin peroxidase**.** *J. Biol. Chem.* **1993**, *268,* 12274-12281.

[4] Fernández-Fueyo E.; Ruiz-Dueñas F.J.; Martínez M.J.; Romero A.; Hammel K.E.; Medrano F.J.; Martínez A.T. Ligninolytic peroxidase genes in the oyster mushroom genome: Heterologous expression, molecular structure, catalytic and stability properties and lignin-degrading ability**.** *Biotechnol. Biofuels* **2014**, *7:2*.

[5] Gutiérrez A.; Rencoret J.; Cadena E.M.; Rico A.; Barth D.; del Río J.C.; Martínez A.T. Demonstration of laccase-mediator removal of lignin from wood and non-wood plant feedstocks**.** *Bioresource Technol.* **2012**, *119,* 114-122.

[6] Rico A.; Rencoret J.; del Río J.C.; Martínez A.T.; Gutiérrez A. Pretreatment with laccase and a phenolic mediator degrades lignin and enhances saccharification of *Eucalyptus* feedstock**.** *Biotechnol. Biofuels* **2014**, *7:6*.

[7] Kim H.; Ralph J.; Akiyama T. Solution-state 2D NMR of ball-milled plant cell wall gels in DMSO-*d6***.** *Bioenerg. Res.* **2008**, *1,* 56-66.

[8] Rencoret J.; Marques G.; Gutiérrez A.; Nieto L.; Santos I.; Jiménez-Barbero J.; Martínez A.T.; del Río J.C. HSQC-NMR analysis of lignin in woody (*Eucalyptus globulus* and *Picea abies*) and non-woody (*Agave sisalana)* ball-milled plant materials at the gel state**.** *Holzforschung* **2009**, *63,* 691-698.

[9] Rencoret J.; Gutiérrez A.; Nieto L.; Jiménez-Barbero J.; Faulds C.B.; Kim H.; Ralph J.; Martínez A.T.; del Río J.C. Lignin composition and structure in young versus adult *Eucalyptus globulus* plants**.** *Plant Physiol.* **2011**, *155,* 667-682.

[10] del Río J.C.; Prinsen P.; Rencoret J.; Nieto L.; Jiménez-Barbero J.; Ralph J.; Martínez A.T.; Gutiérrez A. Structural characterization of the lignin in the cortex and pith of Elephant grass (*Pennisetum purpureum*) stems**.** *J. Agric. Food Chem.* **2012**, *60,* 3619-3634.

ACETOSOLV PULPING: A STAGE IN THE FRACTIONATION OF EFB (EMPTY FRUIT BUNCHES) FROM OIL PALM INDUSTRY

Ana Ferrer[1], Alberto Vega[2], Pablo Ligero[2], Luis Jiménez[1], Alejandro Rodríguez[1*]

*[1]Chemical Engineering Department, Campus of Rabanales, Building C3, University of Córdoba, 14071 Córdoba, Spain [2]Department of Physical Chemistry and Chemical Engineering. University of A Coruña, Spain, 15071 A Coruña, Spain, *corresponding author: a.rodriguez@uco.es*

ABSTRACT

Empty fruit bunch is a residue generated by the oil palm industry after a sterilization process and the separation of the fruits for oil extraction. This residue, which in many countries, especially in Malaysia and Indonesia, is produced in very high levels, is simply used as mulch, burnt for energy production or even burnt in the plantations without any benefits.

Acetosolv pulping could be seen as a stage in the fractionation of empty fruit bunches for pulp production used in various applications as; pulps for specialty papers or other applications such as obtaining microcrystaline cellulose, microfibrilled cellulose or bioethanol by simultaneous saccharification and fermentation.

The aim of this work was to study the influence of operational variables in the empty fruit bunches acetosolv pulping process [acetic acid (60-95%), hydrochloric acid (0.10-0.25%) and time process (60-180 min)], on the solid yield, Schopper Riegler index, Kappa number, lignin content and viscosity of pulps. By using an experimental factorial design, polynomial equations were obtained that reproduced the experimental results for the dependent variables with errors less than 9-18%. These equations could be used to find the suitable conditions, so that operating with not too high values of operating variables (with minor costs of operation and capital) pulps with acceptable properties could be obtained: operating with 86.25% acetic acid, 0.25% hydrochloric acid and 120 min time, produced pulps with 46.56% solid yield, 15.9 ºSR drainability, 36.3 Kappa number, 10.3% lignin content and 303 mL/g viscosity, values all of them close to the optimal predicted.

I. INTRODUCTION

Plant biomass has been for centuries a resource used by humanity worldwide, for energy and cellulosic pulp production. The production of paper pulp has traditionally been a highly polluting process.

Organosolv methods use organic compounds of relatively low molecular weight as delignification agents, and are a good alternative to Kraft because of the possibility of eliminate the sulphur compounds in cooking. Although lignin removal can be achieved with high efficiency, in some cases, the physical properties of the paper sheets from these pulps was lower to those of Kraft pulps. Therefore, these pulps may be applied to the manufacture of special papers or obtaining high purity cellulose, with a possible final destination as dissolving pulps [1-5].

However, the fact of being able to use compounds with very different characteristics makes organosolv cooking processes very different versus Kraft. Some of them may be performed at atmospheric pressure and therefore at a much lower temperature, which results in a decreased severity of treatment and, consequently, a reduced formation of degradation compounds from sugars and lignin. This is of particular interest in the concept of the lignocelluloses biorefinery [6], which could be designed to get the most interesting products from all compound families found in lignocellulosic materials. Due to the very different susceptibility of these families against chemical reagents, a mill of this type should integrate, or a sequence of treatments of increasing severity, or some processes capable of separating fractions mildly. The set of procedures able to perform this separation is known as fractionation.

The Acetosolv process uses acetic acid enriched (70-90% by weight) aqueous mixtures with the addition of small amounts of hydrochloric acid (typically 0.1-0.2% by weight) which contributes to enhance the delignification through partial hydrolysis and solubilisation of hemicelluloses and lignin.

Oil palm empty fruit bunch (EFB) is a waste generated by the oil palm industry after a sterilization process and the separation of the fruits for oil extraction. This residue, which in many countries, especially in Malaysia and Indonesia, is produced in very high levels, is simply used as mulch, burnt for energy production or even burnt in the plantations without any profit. Due to its high production and uniformity resulting from the use of specific plant species EFB may not only be a waste but an important resource for obtaining various high-value products through chemical processing [7].

The aim of this work was to study the Acetosolv treatment of EFB by means of an experimental design factor, considering the influence of the operational variables on the composition of the resulting pulp, with the aim of finding the optimum conditions of operation to obtain a pulp for specialty papers or other applications such as obtaining microcrystaline cellulose, microfibrilled cellulose or bioethanol by simultaneous saccharification and fermentation.

II. EXPERIMENTAL

Raw material

African palm from Western Africa supplied by Straw Engineering S.L (Zaragoza) were used. Each hectare of oil palm produces an average of 10 tons of fruits per year which give about 3000 kg of palm oil (the main product) [8,9].

Pulping and pulps characterization

Mixtures of EFB, water and acetic acid (proportions ranging from 60 to 95% by weight of liquor) were heated to the boiling point in glass Pyrex flasks. Hydrochloric acid was added (0.10-0.25% by weight of liquor) when boiling started (zero time), and mixtures were maintained at total reflux with stirring for different times (60-180 min) at atmospheric pressure. After the reaction, the pulps were separated by filtration and the solids washed with concentrated acetic acid solutions (80%w) in order to avoid the deposition of the dissolved lignin on pulp. Finally the pulps were treated with water until neutrality and let to dry at room temperature before measuring the following parameters; pulp yield (oven drying to constant weight), Kappa number (T236), lignin content (T222), beating grade (Shopper-Riegler index, UNE 57-025), and intrinsic viscosity (T230).

Experimental design

A second order factorial design of experiment was used [10] consisted in a central experiment (in the centre of a cube) and several additional points (additional experiments lying at the cube vertices and side centers).

Experimental data were fitted to the following second-order polynomial:

$$\mathbf{Y_e = a_0 + a_1X_A + a_2X_H + a_3X_T + a_{11}X_A^2 + a_{12}X_AX_H + a_{13}X_AX_T + a_{22}X_H^2 + a_{23}X_HX_T + a_{33}X_T^2} \quad (1)$$

where Y_e denotes the response variables [viz. yield (YI), beating grade or Shopper Riegler index (SR), Kappa number (KN), lignin (LI) or viscosity (VI)]; X_A, X_H and X_T are the normalized values of the operational variables (acetic acid concentration –A-, hydrochloric acid concentration –H- and processing time –T-, respectively); and a_0 to a_{33} are constants.

The values of the operational variables were normalized to values from -1 to +1 by using the following expression:

$$\mathbf{X_n = 2\frac{X - X_m}{X_{max} - X_{min}}} \quad (2)$$

where X_n is the normalized value of A, H or T; X is the actual experimental value of the variable concerned; X_m is the mean of X_{max} and X_{min}; and X_{max} and X_{min} are the maximum and minimum value, respectively, of such a variable.

The operational values for the independent variables in the 15 experiments conducted are given in **Table 1**.

A(%)	H(%)	T(min)	Yield (%)	Beating grade (°SR)	Kappa number	Lignin (%)	Viscosity (mL/g)
77.5	0.175	120	58.6	17	55.5	13.5	283
95.0	0.25	180	41.3	14	41.1	11.1	306
60.0	0.25	180	52.3	19	58.0	11.6	384
95.0	0.25	60	46.4	12	32.2	8.9	226
60.0	0.25	60	67.3	13	71.0	15.4	291
95.0	0.10	180	75.4	13	77.7	16.6	185
60.0	0.10	180	74.4	18	75.8	16.3	302
95.0	0.10	60	83.2	12	73.6	15.9	183
60.0	0.10	60	84.3	14	69.3	16.3	213
77.5	0.25	120	47.4	18	39.7	9.8	345
77.5	0.10	120	74.8	13	70.0	15.9	262
77.5	0.175	180	54.9	18	51.3	13.1	297
77.5	0.175	60	63.2	13	55.8	15.3	312
95.0	0.175	120	51.8	13	47.6	10.8	251
60.0	0.175	120	67.6	17	76.8	16.1	318
A: acetic acid concentration; H: hydrochloric acid concentration; T: time process							

Table 1. Values of operational variables of the properties of pulp obtained by Acetosolv pulping of EFB

III. RESULTS AND DISCUSSION

Pulping of EFB

First a series of previous experiments was carried out, based on the results of other researchers on different raw materials, in order to define the ranges of operating variables. In this way the following ranges were chosen: acetic acid concentration from 60 to 95% by weight, hydrochloric acid concentration, which acts as a catalyst, from 0.10 to 0.25% by weight, and processing time from 60 to 180 minutes. Always operating at the boiling point and with the same liquid/solid ratio (10:1 by weight).

Table 1 shows the experimental values of the pulp properties, which differed by less than 5-10% from their means as obtained in triplicate measures. The experimental results were fitted to polynomial model by multiple regression using the software BMDP©. The terms possessing a Snedecor F-value greater than 6 and a Student t-

value greater than 2.5 were deemed statistically significant. Equations found, as well as the lowest Snedecor-F value, the highest p value and lowest Student t- value for the terms, are the following:

$\mathbf{YI = 59.22 + 5.46X_H^2 - 3.97X_AX_H - 4.61X_T - 4.76X_A - 13.76X_H}$ (F>10.56; p<0.010; t>3.25) (3)

$\mathbf{SR = 14.9 - 1.7X_A + 1.8X_T}$ (F>11.70; p<0.005; t>3.42) (4)

$\mathbf{KN = 54.5 + 7.9X_A^2 - 7.7X_AX_H - 7.9X_A - 12.4X_H}$ (F>6.88; p<0.025; t>2.62) (5)

$\mathbf{LI = 13.8 - 1.2X_A - 2.42X_H}$ (F>6.83; p<0.023; t>2.61) (6)

$\mathbf{VI = 300 - 34X_A^2 + 25X_T - 36X_A + 41X_H}$ (F>10.56; p<0.01; t>3.25) (7)

where YI is the pulp yield, SR the Shopper Riegler index or beating grade number, KN the Kappa number, LI the lignin content, VI the viscosity, and X_A, X_H and X_T the normalized values of acetic acid concentration, hydrochloric acid concentration and time process, respectively.

The predictions of the previous equations reproduced the experimental results for the dependent variables with errors lower than 9% for yield, 17% for SRº, 17% for Kappa number, 18% for lignin content and 16% for viscosity of pulps**.**

The values of the operational variables providing the best pulp properties (yield, beating grade, Kappa number, lignin content and viscosity) were identified by using equations (3) to (7) and **figure 1a and 1b** and other similar. **Table 2** shows the optimum values of the dependent variables and those of the operational variables required to obtain them**.**

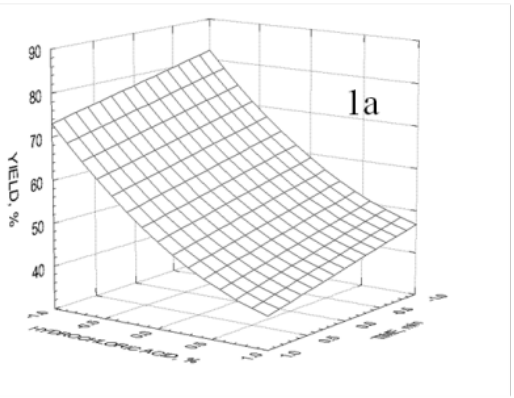

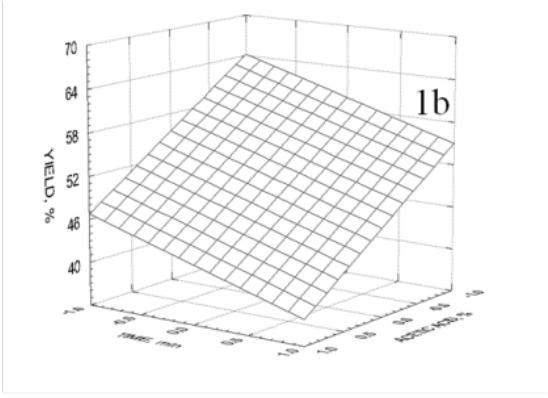

Figure 1a. Yield pulp vs hydrochloric acid concentration and time, at low acetic acid concentration
Figure 1b. Yield pulp vs acetic acid concentration and time, al low hydrochloric acid concentration

The polynomial equations allowed the identification of the more influencing operational variables on the pulp properties. The maximum variations in the dependent variables with changes in the operational variables over the studied range were obtained by altering one independent variable at a time while keeping all others constant. The results are shown in **Table 2** together with the maximum percent differences in the dependent variables from their optimum values over the studied variation ranges. The maximum yield (83.84 %) corresponded to low values of operating variables. The hydrochloric acid concentration influences on pulp yield more significantly than the process time (**Figure 1a**), while the latter variable affects more than the concentration of acetic acid (**Figure 1b**). The maximum Shopper Riegler index (18.4 ºSR) occurs when the concentration of acetic acid is low and the processing time long, being the most influential variable this last one. The Kappa number increased more sharply with the hydrochloric acid concentration that with acetic acid concentration. The minimum Kappa number (34.4) was obtained when hydrochloric acid concentration and acetic acid concentration were high. The lignin content has a parallel behaviour, with a minimum value of 10.2% for when the concentrations of the two acids are high, being the most influential variable the hydrochloric acid concentration. The viscosity was maximum (376 mL/g) when operating with medium-low level of acetic acid concentration and high values of processing time and hydrochloric acid concentration. Process time has minor influence on the viscosity that the acetic acid concentration, while hydrochloric acid concentration is the most influential variable.

Dependent variable	Optimum value of dependent variable	Values of the operational variables required to obtain the optimum values of dependent variables			Maximum variation of dependent variable with operational variable		
		X_A	X_H	X_T	Acetic acid	HCl acid	Time
Yield, %	83.87	-1	-1	-1	1.58(1.88%)	19.64(23.43%)	9.22(11.00%)
ºSR	18.4	-1	-	+1	3.4(18.48%)	-	7.0(38.04%)
Kappa N	34.4	+1	+1	-	31.2(90.70%)	40.2(116.86%)	-
Lignin, %	10.2	+1	+1	-	2.4(23.5%)	4.8(47.1%)	-
Viscosity, mL/g	376	-0.52	+1	+1	80(21.28%)	82(21.81%)	50(13.30%)

Optimum operating conditions

Considering the "Yield/Kappa" ratio (which is desirable to have a maximum value), adjusting the experimental data to a polynomial model gives the equation:

$$\text{"Yield}/\text{Kappa"} = 1.07 + 0.07X_A + 0.09X_AX_H - 0.10X_T \text{ (F>6.34; p<0.029; t>2.52)} \quad (8)$$

The values of the operational variables providing the maximum "Yield/Kappa" were identified by using Eq. (8): the maximum value, 1.33, is for high acetic acid concentration (95%), hydrochloric acid concentration (0.25%) and short processing time (60 minutes).

The Eq. 3 to 7 and data of **Table 2** can be used to select values of the operational variables providing near-optimal pulp properties while saving chemicals, energy and immobilized capital by using lower values of some of the operational variables. One combination leading to near-optimal properties with reduced costs with properties is using a processing time of 120 min, an acetic acid concentration of 86.25% and a hydrochloric acid concentration of 0.25%. Operating under these conditions the following values for the dependent variables were obtained: yield 46.56%, Shopper Riegler index 15.9 ºSR, Kappa number 36.3, lignin 10.3% and viscosity 303 mL/g; these values deviate by 44.5%, 13.6%, 5.5%, 5.9% and 18.6%, respectively of the maximum values of yield, Shopper Riegler index, Kappa number, lignin content and viscosity. Operating under these conditions the values obtained for the ratios "Yield/Kappa" (1.15) is very near from the optima predicted by the corresponding regression equation

IV.CONCLUSSIONS

Acetosolv pulping can be a stage in the EFB fractionation. The pulp obtained has low viscosity, but can be used for specialty papers, microcrystalline-cellulose, microfibrilled-cellulose, or bioethanol by simultaneous saccharification-fermentation.

Polynomial equations obtained by multiple regression can be used to find the suitable conditions that, operating with not too high values of operational variables (minor operation and capital costs), procedure pulps with acceptable properties. Specifically, operating at 86.25% acetic acid, 0.25% hydrochloric acid 120 min time, brings pulps with 46.56% yield, 15.9ºSR drainability, 36.3 Kappa, 10.3% lignin and 303 mL/g viscosity; all these values are close to the optimal.

V. ACKNOWLEDGEMENTS

The authors are grateful to Ecopapel, S.L. (Écija, Sevilla, Spain) for their support, and to Spain's DGICyT and Junta of Andalucía for funding this research within the framework of the Projects CTQ-2010-19844-C02-01 and TEP-6261.

VI. REFERENCES

[1] Sixta, H.; Harms, H.; Dapia, S.; Parajo, J.C.; Puls, J.; Saake, B.; Fink, H.-P.; Roeder, T. Evaluation of new organosolv dissolving pulps. Part I: Preparation, analytical characterization and viscose processability. *Cellulose* **2004** *11*, 73-83

[2] Vila, C.; Santos, V.; Parajo, J.C. Dissolving pulp from TCF bleached acetosolv beech pulp. *J Chem Technol Biotechnol* **2004** *79*, 1098-1104

[3] Shansan, L.; Fang, G.; Deng, Y.; Wang, W. Preparation of microcrystalline cellulose from cotton linter ethanol pulp. *Advanced Materials Research* **2011** *295-297*, pp. 653-658

[4] Serrano, L.; Urruzola, I.; Nemeth, D.; Belafi-Bakob, K.; Labidi, J. Modified cellulose microfibrils as benzene adsorbent. *Desalination* **2011** *270*, 1-3

[5] Requejo, A.; Peleteiro, S.; Rodríguez, A.; Garrote, G.; Parajó, J.C. Second-generation bioethanol from residual woody biomass. *Energ Fuel*,**2011** *25*, 4803-4810

[6] Kamm, B.; Kamm, M. Principles of biorefineries *Appl Microbiol Biotechnol* **2004** *64*, 137-145

[7] Noor, M.; Azemi M.; Sarip, H. Oil palm (*Elaeis guineensis*) wastes as a potential source of cellulose. Cellulosic Pulps, Fibres and Materials, [International Cellucon Conference. In: Pulp for Papermaking: Fibre and Surface Properties and Other Aspects of Cellulose Technology], 10th, Turku/Abo, Finland, Dec. 14-17, 1998 **2000**, 13-17. Edited by: Kennedy, John F

[8] Ferrer, A.; Vega, A.; Rodríguez, A.; Ligero, P.; Jiménez, L. Milox fractionation of empty fruit bunches from *Elaeis guineensis*. *Bioresource Technol* **2011** *102*, 9755-9762

[9] Ferrer, A.; Vega, A.; Ligero, P.; Rodríguez, A. Pulping of empty fruit bunches (EFB) from the palm oil industry by formic acid. *Bioresources* **2011** *6*, 4282-4301

[10] Montgomery D.C. Design and analysis of experiments. Grupo Editorial Iberoamericana, Mexico, p. 303. México. **1991**

BIOETHANOL PRODUCTION FROM *Cistus ladanifer* PRETREATED BY STEAM EXPLOSION

M. Ferro[1], A.F.C Paulino[1], J.Gravitis[2], D.V. Evtuguin[3], A.M.R.B.Xavier[3] and M.C. Fernandes[1]

[1]*Centro de Biotecnologia Agrícola e Agro-Alimentar do Alentejo (CEBAL)/Instituto Politécnico de Beja (IPBeja), 7801-908 Beja, Portugal.*

[2] *Laboratory of Eco-Effective Conversion, Latvian State Institute of Wood Chemistry, Riga, Latvia*

[3]*Centre for Research in Ceramics & Composite Materials (CICECO), University of Aveiro, 3810-193 Aveiro, Portugal*

** Corresponding author. E-mail: dmitrye@ua.pt*

ABSTRACT

Thermochemical pretreatment, saccharification and fermentation of *Cistus ladanifer* (rockrose) wildly grown in Alentejo (Portugal) were studied. Rockrose was subjected to steam explosion treatment (SE) and a subsequent alkali treatment (SE-OH). Enzymatic hydrolysis of untreated, SE and SE-OH materials was compared. The biomass resulting from the best pretreatment was used for a comparative study in Separate Hydrolysis and Fermentation (SHF), and Simultaneous Saccharification and Fermentation (SSF) assays.

Steam explosion treatment was rather selective for hemicelluloses solubilization, producing a residue with higher glucan content (mainly cellulose). Alkali post-treatment with 2% of NaOH increased the proportion of hexosans in rockrose residue due to the elimination of a part of degraded lignin and hemicelluloses. Enzymatic hydrolysis of untreated biomass (R) and pretreated with SE and SE-OH, was carried out using commercial cellulase and cellobiase. Rockrose was very recalcitrant to enzymes providing 1% of saccharification yield, whereas steam explosion pretreatment and subsequent alkali treatment improved digestibility up to 40 and 70 % of saccharification yield, respectively.

Fermentation assays carried out in SHF and SSF modes with 8% of biomass, 43 FPU and 50 β-glucosidase UI of commercial cellulase and cellobiase, respectively showed that SSF process is more efficient than SHF process with an overall efficiency of 66% allowing the production of 14.8 g/L of bioethanol with a productivity of 0.62 g/(Lh) after 24h of saccharification/.fermentation.

I. INTRODUCTION

Cistus ladanifer L. (known as gum cistus or rockrose) is a well adapted species to the edaphoclimatic conditions of Alentejo, south region of Portugal, that grows widely and that can be exploited as feedstock for second generation bioethanol production. This plant is an important part of the semiarid-Mediterranean ecosystem and forms dense stands on siliceous soils [1]. The accumulation of rockrose is a permanent danger to the Portuguese forest, making it more vulnerable to the outbreak emergence and spread of fire [2]. As a consequence it is necessary to manage the ground by buffing the rockrose periodically, to prevent forest fires. The use of these wood residues that grow in marginal areas could be a good alternative for biomass feedstock of biofuel production.

Due to the recalcitrance of the woody biomass like rockrose, usually it is necessary to subject the lignocellulosic material to a previous pretreatment process in which the cellulose is made accessible for further conversion. The most used pretreatments are steam explosion, liquid hot water, concentrated acid hydrolysis and dilute acid pretreatment [3]. Dilute acid pretreatment was already applied to rockrose, producing lower enzimatic saccharification when compared to other shrub like broom [4].

The central objective of this investigation is to assess the potential of biomass from rockrose, directly (R) and after SE or SE-OH pretreatments, in the production of fermentable sugars, through enzymatic hydrolysis for the production of ethanol by separate hydrolysis and fermentation (SHF), and simultaneous saccharification and fermentation (SSF).

II. EXPERIMENTAL

Raw material: Rockrose (R) with more than 10 years old was collected from Monte do Vento in the county of Mértola in 2011. After collection, rockrose was size reduced with a knife mill and sieved in order to obtain particles between 40 and 60 mesh. For steam explosion treatment samples were reduced to 18 mesh.

Steam Explosion: SE treatment of rockrose was carried out in a laboratory pilot unit designed by Latvian company "FIL & KO" for the Latvian State Institute of Wood Chemistry. The sample was treated with saturated steam for 1 min. at 235 ºC, 32 bar, in a 0.5 L reactor and a receiving chamber of 30L. The reactor was equipped with a quick-opening ball valve and an electronic device programmed for accurate control of steam time and temperature. The severity factor was calculated using the reaction ordinate R_0, which can be expressed as: R_0 = t x exp [(T-100)/14.75]; where: duration of treatment (t, minutes) and temperature (T, ºC) express the severity against the base temperature, T base or reference =100 ºC. Log R_0= 3.97 in the tested conditions. Resultant water insoluble solid fraction from rockrose (R-SE) was air dried.

Alkali delignification: R-SE was rehydrated for 24h in distilled water and then treated with sodium hydroxide [5]. 50 ml of 2% (w/w) aqueous sodium hydroxide solution was used for 10 g of dry weight of R-SE, during 15 min, to remove the depolymerized lignin from the cellulose residue. The obtained residues were thoroughly washed with hot deionized water, till alkali removal (pH reached 4.8), and then dried at 40 ºC or frozen for analysis and enzymatic hydrolysis, respectively.

Enzymatic Hydrolysis: The pre-treated samples used for the enzymatic assays were hydrated during 24h with deionized water and then thoroughly washed, to remove inhibitors that could be impregnated in the material. Saccharification was applied to R, R-SE and R-SE-OH samples with 5% solid loading in 50 mM sodium citrate buffer (pH 4.8), sodium azide (0.1%) using 15 FPU Celluclast 1.5L and 15 β-glucosidase (CBU) Novozyme 188 per gram of dry biomass, respectively. Assays were performed at 50ºC, 130 rpm for 72 h and stopped by boiling the reaction mixtures for 5 minutes. After centrifugation supernatants were filtered and analyzed by HPLC. All assays were performed in duplicate with the respective substrates and enzyme controls. Saccharification yield was calculated by dividing the obtained glucose by the potential glucose multiplied by 100.

SHF studies were done with 8% of solids, 43 FPU of Celluclast 1.5L and 50 CBU Novozyme 188 per g of dry biomass. All assays were done with total volume of 50 mL in closed 250 mL Erlenmeyer flasks. R-SE-OH was mixed with citrate buffer, pH was adjusted to 4.8 and the mixture was sterilized in autoclave for 15 min at 121°C, as sodium azide cannot be used. Enzymes after sterile filtration were added aseptically, and saccharification conditions were the same as stated above.

Fermentations: Two *Saccharomyces cerevisiae* strains were used. The NCYC-1119 for SHF assays and the thermotolerant strain PYCC-2613 in SSF assays. Inocula were obtained by growing the yeasts in YPD medium containing: 10 g/L of yeast extract (YE), 20 g/L of peptone (Pept), and 50 g/L of glucose, for 15 h with 130 rpm at 30°C or 42°C for NCYC-1119 and PYCC2613, respectively. After saccharification step of SHF assay and for SSF process after sterilization, sterile Pept and YE were added to each flask, to obtain a final concentration similar to that of YPD medium. For SHF and SSF experiments a 5.0 mL inoculum was added to the respective flasks. Ethanol production was carried out under the same conditions as for inocula preparation. Samples were taken over time, and analyzed by HPLC after centrifugation. Overall efficiency was calculated dividing the obtained ethanol concentration by the theoretical ethanol concentration, assuming that all the glucose in the starting material, known after cellulose quantification, is available for fermentation and that theoretical fermentation yield is 0.51 g of ethanol/g of glucose. All assays were performed in duplicate.

Biomass characterization: R, R-SE and R-OH were characterized according to NREL protocols[6]. No extraction was made before quantitative acid hydrolysis as indicated in NREL protocols of the pre-treated solids.

High Performance Liquid Chromatography analysis: Glucose, xylose, arabinose and ethanol were analyzed by HPLC (Merck Hitachi LaChrome equipment). The D-7000 HSM software was used associated to a L7000 interface module, a L7200 auto sampler, a L7490 RI detector, a L7350 column oven and a L7100 pump. An Aminex HPX-87H cation exchange column and a Micro-Guard Cation H Cartridges both from Bio-Rad (USA), were used at 50°C. with 5 mM H_2SO_4 solution used as the mobile phase. Concentrations were determined with external standard, through standard curves for each component analyzed.

III. RESULTS AND DISCUSSION

Characterization of R, R-SE and R-SE-OH is shown in **Table 1**. Steam explosion treatment was rather selective for hemicelluloses solubilization, producing a residue with higher glucan content (mainly cellulose). Alkali post-treatment with 2% of NaOH increased the proportion of hexosans in rockrose residue due to the elimination of a

part of degraded lignin and hemicelluloses. A similar effect was also observed by Fernández-Bolaños *et al* [7], with steam exploded olive stones.

Table1. Composition of rockrose (R) and respective solid residues obtained after steam explosion (R-SE) and alkali treatment (R-SE-OH), according NREL procedures in g per 100g of dry biomass.

Component	Rockrose (R)	R-SE	R-SE-OH
*Glucan**	22.9 ± 0.1	26.8 ± 0.1	54.1 ± 0.3
Hemicelluloses	22.0 ± 0.1	10.6 ± 0.1	15.5 ± 0.3
Xylan	14.7 ± 0.1	8.9 ± 0.1	6.3 ± 0.0
Arabinan	0.0 ± 0.0	1.7 ± 0.0	0.0 ± 0.0
Acetyl group	7.3 ± 0.0	0.0 ± 0.0	9.2 ± 0.3
*Klason lignin**	26.7 ± 0.7	41.6 ± 0.2	28.6 ±0.2
Ashes	2.7 ± 0.1	3.5 ± 0.0	6.6 ± 0.0

*- Glucan is assumed as cellulose content.

Saccharification yields and glucose concentrations obtained after the enzymatic hydrolysis of R, R-SE and R-SE-OH are presented in **Table 2**. Untreated rockrose presented practically no saccharification. Glucose concentration increased after pretreatments, corresponding to a saccharification yield increase of 40 and 72 times after steam explosion and alkali post-treatment, respectively, due to the reduction of the hemicellulosic fraction. R-SE and R-SE-OH presented 94 and 381 mg of glucose per g of dry substrate, respectively. The release of glucose from R-SE-OH is higher than the 242 mg/g of rockrose pretreated with diluted acid hydrolysis found by Ferreira et al. [4].

Table2. Enzymatic hydrolysis yields of rockrose without pretreatment and after treatment with steam explosion (R-SE) and alkali treatment (R-SE-OH).

Sample	Glucose concentration (g/L)	Saccharification yield (%)
Rockrose	0.2 ± 0.0	0.9 ± 0.0
R-SE	5.8 ± 0.0	39.1 ± 0.3
R-SE-OH	21.0 ± 0.1	69.6 ± 0.2

So, it was notorious that the best pretreatment for glucose solubilization was the R-SE-OH, being this the one chosen for the comparative study in Separate Hydrolysis and Fermentation (SHF), and Simultaneous Saccharification and Fermentation (SSF).

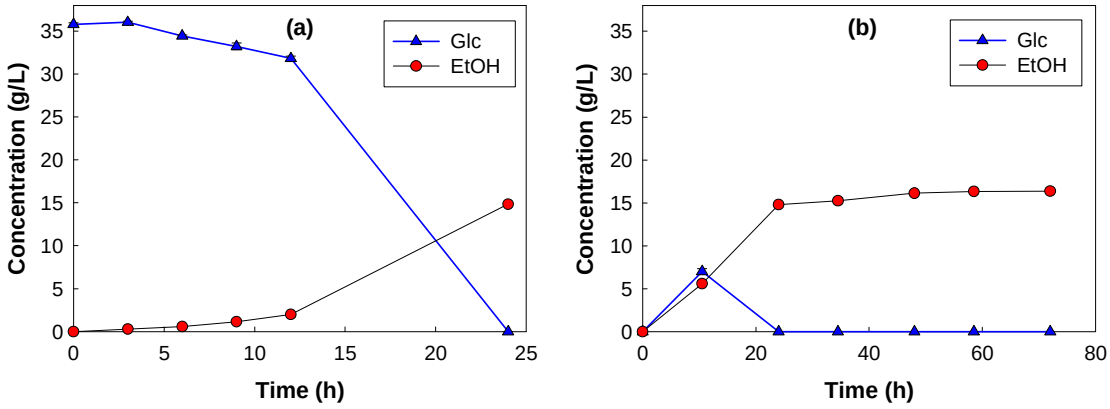

Figure 1. Glucose (Glc), and ethanol (EtOH) concentration during SHF (a) and SSF (b) of R-SE-OH, with 8% solid loading with 43 FPU and 50 CBU per g of dry biomass.

Figure 1 shows the results for the SHF and SSF processes. In SHF process, saccharification with higher enzyme loading per gram of biomass during 72h, resulted in higher conversion of the cellulose, 73.6%, which represents a 4% gain. This result shows that the increment on enzyme loading besides enhancing the cellulose conversion may also improve cellulose conversion rate that is an important asset for the SSF process. The initial glucose concentration was almost 36 g/L and it remained practically constant until 12 h of fermentation. After that it abruptly decreased, with a reverse increase in ethanol concentration, that reached the maximum of 14.9 g/L after 24 h, corresponding to an overall efficiency of 62% and a volumetric ethanol productivity of 0.62 g/(Lh).

For the SSF experiment a glucose peak was observed at 10h, dropping again to 0 and maintained constant at this value until the end of the assay. As it was expected, the produced glucose was quickly consumed for the growth of yeasts and for their bioethanol fermentation. At 24 h the ethanol concentration reached 14.8 g/L with a productivity of 0.61 g/(Lh) and an overall efficiency of 66%. A higher overall efficiency of 73% was reached with an ethanol concentration of 16.4 g/L and a productivity of 0.23 g/(Lh). These results indicate that most of the cellulose fraction from R-SE-OH was solubilized and converted in ethanol during the first 24h showing a clear advantage of the SSF bioprocess over the SHF that took a total time of 96 h.

IV. CONCLUSIONS

Untreated rockrose is a very recalcitrant material to the enzymatic hydrolysis. Pretreatments increased the polysaccharides accessibility to cellulolytic enzymes, especially after alkali treatment, allowing saccharification yields of 70-74%. Study of SHF and SSF process with R-SE-OH showed that SSF process was more efficient than SHF process with an overall efficiency of 66% allowing the production of 14.8 g/L of bioethanol with a productivity of 0.61 g/(Lh) after 24h of fermentation. A higher overall efficiency of 73% can be attained if the bioprocess is extended.

V. ACKNOWLEDGEMENT

This research was co-financed by INALENTEJO 2007.2013/QREN, within the project BioEcos— Valorização Integrada de Biomassa. CICECO is Associated Laboratory of the Portuguese Ministry of Science, Technology and Higher Education, being partially supported by FCT, the Portuguese Foundation for Science and Technology by Pest-C/CTM/LA0011/2011 contract. The authors would like to thank Associação de Defesa do Património de Mértola (ADPM), for kindly supplying the *Cistus ladanifer*.

VI. REFERENCES

[1] Fernández-Arroyo S, Barrajón-Catalán E, Micol V, Segura-Carretero A, Fernández-Gutiérrez A. High-performance liquid chromatography with diode array detection coupled to electrospray time-of-flight and ion-trap tandem mass spectrometry to identify phenolic compounds from a *Cistus ladanifer* aqueous extract. *Phytochem Anal* **2010**;21:307–13.

[2] Nunes MCS, Vasconcelos MJ, Pereira JMC, Dasgupta N, Alldredge RJ, Rego FC. Land Cover Type and Fire in Portugal: Do Fires Burn Land Cover Selectively? *Landsc Ecol* **2005**;20:661–73.

[3] Harmsen P, Huijgen W, Bermudez L, Bakker R. Literature review of physical and chemical pretreatment processes for Lignocellulosic biomass. *Wageningen UR, Food & Biobased Research*; **2010**.

[4] Ferreira S, Duarte A, Ribeiro M, Queiroz J, Domingues F. Response surface optimization of enzymatic hydrolysis of *Cistus ladanifer* and *Cytisus striatus* for bioethanol production. *Biochem Eng J* **2009**;45:192–200.

[5] Fernández-Bolaños J, Felizón B, Heredia A, Rodríguez R, Guillén R, Jiménez A. Steam-explosion of olive stones: hemicellulose solubilization and enhancement of enzymatic hydrolysis of cellulose. *Bioresour Technol* **200**1;79:53–61.

[6] Sluiter JB, Ruiz RO, Scarlata CJ, Sluiter AD, Templeton DW. Compositional Analysis of Lignocellulosic Feedstocks. 1. Review and Description of Methods. *J Agric Food Chem* **2010**;58:9043–53.

[7] Fernández-Bolaños J, Felizón B, Heredia A, Guillén R, Jiménez A. Characterization of the lignin obtained by alkaline delignification and of the cellulose residue from steam-exploded olive stones. *Bioresour Technol* **1999**;68:121–32.

ACID PRETREATMENT OF *JATROPHA CURCAS* SHELLS FOR ENZYMATIC HYDROLYSIS OF CELLULOSE

Ariel García[1,2], Cristóbal Cara[2], Manuel Moya[2], Jorge Rapado[1], J. Carlos Linares[2], Eulogio Castro[2], Carlos Martín[1,3]

[1]Departamento de Química e Ingeniería Química, Universidad de Matanzas, 44740 Matanzas, Cuba; [2]Departamento de Química Ambiental e Ingeniería de los Materiales, Universidad de Jaén, 23071 Jaén, España; [3]Department of Chemistry, Umeå University, SE-901 87, Umeå, Sweden

ABSTRACT

Since *Jatropha curcas* shells, a subproduct from biodiesel production, are rich en hexosans, they can be considered for ethanol production using *Saccharomyces cerevisiae* as fermentable microorganism. In this work, acid pretreatment conditions were applied to *J. curcas* shells, and the effect of temperature (110-150°C), H_2SO_4 concentration (0.5-2.5%) and pretreatment time (15-45 min) on the formation of sugars during pretreatment and on the enzymatic hydrolysis of cellulose was evaluated. Cellulose conversion during enzymatic hydrolysis, which was evaluated by both separate hydrolysis and simultaneous saccharification and fermentation, was positively affected by pretreatment, and in some experimental runs it reached values above 80%. Based on the experimental results, analytical models describing the effect of the operational conditions on the response factors were built. The models predicted maximal cellulose-to-ethanol conversion (82.0%) for the material pretreated at 136°C, 1.5% H_2SO_4 and for 30 min. That value is higher than the optimal glucan yield previously reported for the pretreatment performed at 178°C, 0.9% H_2SO_4.

I. INTRODUCTION

Jatropha curcas L. is a drought-resistant plant belonging to the *Euphorbiaceae* family. Its seeds are rich in a non-edible oil [1], which can be used for biodiesel production [2]. In Cuba, *J. curcas* grows in the whole island as a wild plant, and now it is been specially cultivated in some provinces for biodiesel production. Because of its oil yield and its fatty acid composition, *J. curcas* was identified as the most promising non-edible-oil plant for biodiesel in Cuba [3]. Besides to oil, *J. curcas*, produces considerable amount of biomass. The net biomass production, including fruits, branches, and leaves can reach around 11.8 t/ha/year [4]. A high percent of this biomass is discarded or burned in the fields.

In the biodiesel process solid residues, such as press cake and shells, are generated. The fruit shells are rich in cellulose and hemicelluloses, and can, therefore, be considered potential feedstocks for ethanol production. For that aim, the shells should be pretreated to break the lignocellulose matrix and improving cellulose reactivity. Afterwards, the pretreated cellulose can be hydrolysed, preferably by enzymes leading to a glucose-rich hydrolysate [5]. Among the investigated pretreatment methods [6], sulfuric acid pretreatment is one of the most promising, and it has recently been used for *J. curcas* shells [7, 8].

This work is aimed to investigate the sulfuric acid pretreatment and the enzymatic hydrolysis of cellulose of *J. curcas* fruit shells in order to obtain sugars that can be converted in ethanol and other added products.

II. EXPERIMENTAL

Material

The *J. curcas* fruit shells were air dried at 50°C during 24 h. Afterwards, they were knife-milled, screened through a 2 mm-sieve and stored in a plastic bag at room temperature until further use. A small part was screened under 1 mm-sieve a used for raw material analysis.

Acid pretreatment

50 g (dry matter) of shells were suspended in 500 g of sulfuric acid solution and pretreated in a 1 L-reactor (Parr Instrument Company, Moline, IL) following a Box–Behnken response surface experimental design (Table 1). By the end of the pretreatment, the reactor was cooled by immersion in an ice-water bath to approximately 30-35°C.

Enzymatic hydrolysis

1.25 g of dried pretreated solids were supended in 25 mL of 0.1 M citrate buffer (pH 4.8). A commercial preparation of *Trichoderma reesei* cellulases (Celluclast 1.5 L) and a β-glycosidase preparation (Novozym 188), were used. The cellulases were added at a loading of 15 FPU/g DM, and the β-glycosidase as 15 IU/mL. The reaction mixture was incubated at 50°C and 150 rpm for 48 h. At the end of the hydrolysis, glucose was quantified by HPLC, and the results were used for calculating the enzymatic convertibility of cellulose. All of the experiments were performed in duplicates.

Simultaneous saccharification and fermentation

Suspensions of 1.25 g of the pretreated solids in 24 mL of citrate buffer (pH 4.8) were prepared in Erlenmeyer flasks. The suspensions were supplemented with yeast extract (5 g/L), NH_4Cl (2 g/L), KH_2PO_4 (1 g/L) and $MgSO_4 \cdot 7H_2O$ (0.3 g/L). Enzymes were added in the same amounts as for the enzymatic hydrolysis. A *Saccharomyces cerevisiae* culture (1

mL) was inoculated, and the reaction mixture was incubated at 35°C and 150 rpm for 72 h. All of the experiments were performed in duplicates.

III. RESULTS AND DISCUSSION

Dilute acid pre-treatment

Initially, the chemical composition of the raw shells was determined. The cellulose content (32.8%) was comparable to that of other lignocellulosic materials [9]. It also contained 5.0% of other hexosans (mannan and galactan). That rather high content of hexosans makes *J. curcas* shells a raw material of interest for ethanol production. In order to release fermentable sugars (glucose, mannose and galactose), the hexosans have to be hydrolysed, and the material should be pretreated if enzymatic hydrolysis is the choice. Dilute acid prehydrolysis was used as pretreatment method, and a Box-Behnken experimental design was applied. The pretreatment resulted in the solubilization of 25-50% of the initial material (see the yields of solids Table 1). The analysis of significance of the independent factors showed that the yield of solids significantly decreased with the temperature, the sulphuric acid concentration and their interaction, whereas it significantly increased with the quadratic effect of the pretreatment time (Data no shown).

Table 1. Pretreatment conditions and yield of solids achieved under each experimental run

No.	Temperature, °C	H_2SO_4 conc., % (w/w)	Time, min	Yield of solids, %
1	110	0.5	30	73.4
2	110	1.5	15	75.3
3	110	1.5	45	75.3
4	110	2.5	30	70.7
5	130	0.5	15	73.3
6	130	0.5	45	69.6
7	130	1.5	30	65.0
8	130	1.5	30	64.0
9	130	1.5	30	63.4
10	130	2.5	15	64.2
11	130	2.5	45	59.0
12	150	0.5	30	65.5
13	150	1.5	15	62.4
14	150	1.5	45	58.8
15	150	2.5	30	51.1

Enzymatic hydrolysis

The pretreated material was submitted to enzymatic hydrolysis by both separated hydrolysis (SH) and simultaneous saccharification and fermentation (SSF). Both hydrolysis schemes led to high hydrolytic conversions, and the responses for both of them were strongly affected ($P < 0.01$) by the temperature and the quadratic effect of acid concentration. The best conversions (above 80%) were achieved for the pretreatments performed at intermediate severity (Fig. 1). The materials pretreated at either low or high values of the independent factors gave rise to values below 70% of the theoretical yield.

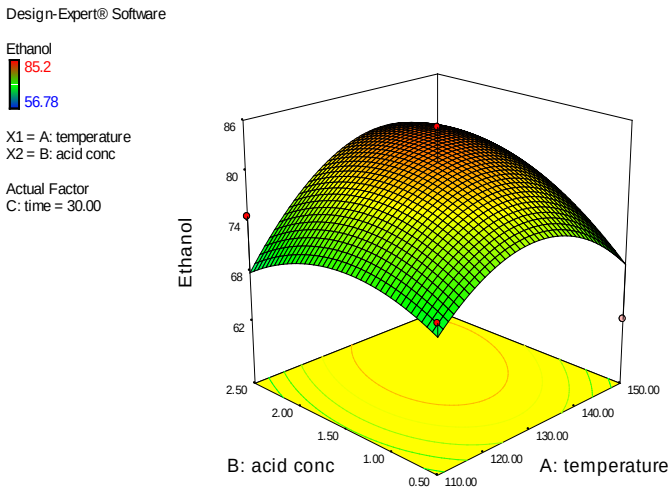

Figure 1. Response surface graph for the cellulose-to-ethanol conversion in the SSF

The experimental results were used for building up analytical models predicting the cellulose-to-glucose conversion (CGC) in the separate hydrolysis (Eq. 1) and the cellulose-to-ethanol conversion (CEC) in the SSF (Eq. 2) under

different temperature (T), acid concentrations (AC) and pretreatment time (PT).

$$\mathbf{CGC} = 85.3 - 9.1*T + 14*AC - 8.0*AC^2 \qquad \text{(Eq. 1)}$$

$$\mathbf{CEC} = 81.3 + 8.0*T - 11.3*T^2 + 5.0*AC - 8.3*AC^2 - 18.3*PT^2 \qquad \text{(Eq. 2)}$$

The developed models predicted optimal conversions for both schemes. The optimal cellulose-to-glucose conversion in the separate hydrolysis was 87.1%, and maximal cellulose-to-ethanol conversion predicted for the SSF experiments was 82.0%, and they are expected for rather low temperatures (135°C) and moderate acid concentrations (1.5%). The predicted optima are higher than the optimal glucan yield reported previously for pretreatment performed at 178°C and 0.9% H_2SO_4 [7]. That indicates that low temperature pretreatments combined with moderate acid concentrations are more favorable for activating the cellulose contained in *J. curcas* shells than high temperature pretreatments at lower acid concentration.

IV. CONCLUSION

The suitability of dilute-acid prehydrolysis as pretreatment method for preparing J. curcas shells for enzymatic hydrolysis was demonstrated. It was found that pretreatments at with moderate acid concentrations (1 – 1.5%) at relatively low temperature (130 – 140°C) are effective for achieving high hydrolytic conversion of cellulose.

V. ACKNOWLEDGMENT

The financial support of Estancias de Excelencia, Junta de Andalucía (Spain), the Alexander von Humboldt Foundation and the Swiss Agency for Development and Cooperation are gratefully acknowledged.

VI. REFERENCES

[1] Openshaw, K. A review of *Jatropha curcas*: an oil plant of unfulfilled promise. *Biomass Bioenerg.* **2000**, *19*, 1 – 15.
[2] Berchmans, H.J.; Hirata, S. Biodiesel production from crude *Jatropha curcas* L. seed oil with a high content of free fatty acids. *Bioresource Technology*. **2008**, *99*, 1716 – 1721.
[3] Martín, C.; Moure, A.; Martín, G.; Carrillo, E.; Domínguez, H. ; Parajó, J.C. Fractional characterisation of jatropha, neem, moringa, trisperma, castor and candlenut seeds as potential feedstocks for biodiesel production in Cuba. *Biomass Bioenerg.* **2010**, *34*, 533 – 538.
[4] Sotolongo, J.A.; Beatón, P.; García, A.; Montes de Oca, S.; del Valle, Y.; García, S. Potencialidades energéticas y medioambientales del árbol *J. curcas* L. en las condiciones edafoclimáticas de la región semiárida de la provincia de Guantánamo. *Tecnología Química.* **2007**, *27*, 76 – 82.
[5] Taherzadeh, M.; Karimi, K. Enzyme-based hydrolysis processes for ethanol from lignocellulosic materials: review**.** *BioResources*. **2007**, *4*, 707 – 738**.**
[6] Mosier, N.; Wyman, C.; Dale, B.; Elander, R.; Lee, Y.; Holtzapple, M.; Ladisch, M. Features of promising technologies for pretreatment of lignocellulosic biomass. *Bioresour. Technol.* **2005,** *96*, 673 – 686.
[7] Marasabessy, A., Maarten, A., Kootstra, J., Sanders, J.P.M., Weusthuis, R.A. Dilute H_2SO_4-catalyzed hydrothermal pretreatment to enhance enzymatic digestibility of *J. curcas* fruit hull for ethanol fermentation. *Int. J. Energy Environ. Eng.* **2012**, *3*, 1 – 15.
[8] Visser, E.M., Filho, D.O., Tótola, M.R., Martins, M.A., Guimarães, V.M. Simultaneous saccharification and fermentation of *J. curcas* shells: utilization of co-products from the biodiesel production process. *Bioprocess Biosyst. Eng.* **2012**, *35*, 801 – 807.
[9] Martín, C., López, Y., Plasencia, Y., Hernández, E. Characterisation of agricultural and agro-industrial residues as raw materials for ethanol production. *Chem. Biochem. Eng. Q.* **2006**, *20*, 443 – 446.

EUCALYPTUS GLOBULUS BIOPULPING: OPTIMIZATION ENZYMATIC - MEDIATOR TREATMENT

Mª Trinidad García[1, 2], Juan C. García[2], M. Jesús Díaz[2], Francisco López[2]

[1]Agrifood Campus of International Excellence (CeiA3). University of Huelva Business Park. 21007 Huelva. [2]PRO[2]TEC- Chemical Engineering Department. Campus "El Carmen". University of Huelva. 21071 Huelva. Spain. Corresponding author. Tel.: +34959219940. E-mail: mtrinidad.garcia@diq.uhu.es

ABSTRACT

The aim of this study was the influence and optimization of operating variables in the enzymatic treatment (laccase-mediator, (LMS)) in Eucalyptus globulus wood with a hydrolytic pretreatment. This treatment was performed with laccase and HBT as mediator of eucalyptus wood with hydrolytic pretreatment in a concentration range of 15 to 35 U/g in o.d.b. (over dry basis) of laccase, concentration range of 1.5 to 4.5 % in o.d.b. of HBT and time between 60 and 180 minutes. The ratio liquid/solid was 8/1 for all experiments. The operating temperature and pH were 45 and 4.5, respectively. For this study design was performed centrally composed of experiments in order to investigate the influence of independent variables, concentration of laccase, concentration of HBT and time on the dependent variables: yield, percentage de cellulose and percentage of residual lignin in the solid. The results showed that the best operating conditions in the treatment of Eucalyptus globulus with laccase mediator system were 21.6 U/g in o.d.b of laccase, 2.25% in o.d.b. of HBT and a time of 60 minutes.

I. INTRODUCTION

Biopulping could be defined as the operation of paste obtained by procedures that include biological treatments. Its justification is the substitution from the chemical reagents or of the mechanical energy by the action of microorganisms (fungi) or enzymes with capacity to degrade the lignin and to obtain as a result the environmental improvement of the pulping procedure, due to reduced energy expenditure and reagents in the pulping process [1-2].

The enzymes that play a key role in the degradation of the lignin are peroxidases (lignin peroxidase (LiP), manganese peroxidase (MnP)) and laccases (Lac). These enzymes come from lignolitic fungi, like for example the fungi of white rot. Laccases, enzymes of type phenol oxidase, use molecular oxygen as substrate and reduces it until water. Laccases are enzymes that catalyze the oxidation of a large amount of phenolic substrates, much of the lignin is made by no laccase phenolic compounds alone cannot modify. With the laccase-mediator system (LMS), the enzyme can extend its work, including non-phenolic compounds. Mediators are molecular organic compounds of low molecular weight that can be easily oxidized by the enzyme, which in turn oxidize other substances with higher redox potential before returning to its original state [3].

One disadvantage of enzymes for biopulping is their low effectiveness due to difficulties in penetrating the chips [4]. In the this study, hydrolytic treatment is being explored as a means to facilitate enzymes penetration. This process consists in the treatment of lignocellulosic materials with water high temperature. During this process, the water high temperature causes the release of acids from the acetylated wood components which catalyze hydrolytic reactions in the wood polymers. These autohydrolysis reactions result in a loss of hemicellulose [5-6].

In the current study, the influence and optimization of operating variables in the LMS treatment in Eucalyptus globulus wood following hydrolytic pretreatment.

II. EXPERIMENTAL

2.1. Raw material and analysis of raw material.

Eucaliptus globulus samples from local plantations (Huelva, Spain). The raw materials were chemically characterized. Thus, ash, ethanol-toluene extractives, hot water and 1% NaOH solubles, lignin, cellulose and hemicelluloses content were determined according to the methodology described by Lopez et al. (2014) [7]

2.2. Hydrothermal pretreatment

Raw material and water were mixed in the desired proportions and treated in a 600 cm^3 stainless steel reactor (Parr Instruments Company, Moline, Illinois, USA) using a liquid/solid ratio (LSR) of 6 kg water/kg raw material, on dry basis (the moisture content of material was considered as water). The operating conditions the hydrothermal treatment were 181 ºC temperature and 37.5 minutes time. After treatment, solid residues were recovered by filtration, washed with water, air-dried, weighted for yield determination. Aliquots of the solid were assayed for yield and composition (duplicate) using the same methods as for raw material analysis.

2.3. Laccase - Mediator treatments

The solid fraction obtained from the hydrothermal pre-treatment was subjected to the laccase treatment. The enzyme used was laccase from Trametes versicolor of Sigma-Adrich. Assays were performed in 500 mL flasks placed in a thermostatic shaker at 100 revolutions per minute. Based on the enzyme product sheetsprovided by themanufacturer, 45 ºC and pH 4.5 were the fixed conditions selected for the laccase treatments. For the laccase treatments, flasks were equipped with an air bubbling system, and 1-hydroxybenzotriazole (HBT) was used as mediator. Other conditions, were: citrate buffer concentration, 1mol L^{-1} and liquid/solid ratio of 8 kg water/kg raw material, on dry basis. After the enzymatic treatments, the solid fractions were isolated and aliquots of the solid were assayed for yield and composition using the same methods as for raw material analysis.

2.4. Experimental design for Laccase - Mediator treatments

A 2n central composite experimental design that enabled the construction of second-order polynomial in the independent variables and the identification of statistical significance in the variables was used. This allowed relating the dependent (yield, glucan, hemicellulose and Klason lignin) and independent (laccase concentration (Xl), HBT concentration (X_m) and operation time (Xt)) variables of the Laccase - Mediator treatments with a minimum number of experiments.

Independent variables were normalized by using the following equation:

$$X_n = \frac{X - \overline{X}}{(X_{\max} - X_{\min})/2}$$

Where X is the absolute value of the independent variable concern $\overline{X}$ is the average value of the variable, and Xmax and Xmin are its maximum and minimum values, respectively. The laccase concentration, HBT concentration and operation time used in the different experiments of the design were 15, 25 and 35 U/g o.d.b., 1.5, 3 and 4.5 % o.d.b. and 60,120 and 180 min, respectively.

The number of tests required was calculated as $N = 2^n + 2*n + nc$, 2^n being the number of points constituting the factor design, 2*n that of axial points and nc that of central points. Under our conditions, N = 15.

The experimental results were fitted to the following second-order polynomial:

$$Y = a_o + \sum_{i=1}^{n} b_i X_{ni} + \sum_{i=1}^{n} c_i X_{ni}^2 + \sum_{i=1;\, j=1}^{n} d_i X_{ni} X_{nj} \quad (i < j)$$

For the multiple regression analysis was used statistical programs STATISTICA 9.0 and JMP 8.0.

III. RESULTS AND DISCUSSION

Eucalyptus globulus chemical characterization gave the following values: Glucan 42.78 %, hemicellulose 21.05 and Klason lignin 21.17 %, over dry raw material.

Table 1 shows results for yield, glucan, hemicelluloses and klason lignin contents in solid phase after the treatment with laccase. Also, the normalized values of laccase concentration, mediator concentration and operation time where showed.

Results of yield were similar for all experiments. After laccase treatment this variable is between 94.1 % and 95.0% to respect the solid phase after autohydrolysis treatment of raw material. Taking into account that the process yield of autohydrolysis was 73.4%, the yield of the global process in two stages was between 69.1 % and 69.7 %.

The glucan content varied between 48.7 % and 53.3 % in solid phase after laccase treatment and values shows from table 1 when this result was expressed respect to the original raw material. In the same manner, the hemicelluloses and Klason lignin contents varied between 2.3 % - 2.7 % and 24.6 % - 34.5 % respectively.

Table 1: Normalized operational conditions and composition of solid after LMS treatment. The concentrations are referred to initial raw material.

Normalized values of laccase concentration (Xl) , HBT concentration (Xm) and operation time (Xt)			Yield , %	Glucan*, %	Hemicelluloses*, %	Klason Lignin*, %
0	0	0	94.43	35.45	1.88	18.04
1	1	1	94.56	35.11	1.74	23.78
1	1	-1	94.75	34.83	1.81	23.99
1	-1	1	94.73	36.61	1.81	22.40
1	-1	-1	94.14	36.38	1.69	22.14
-1	1	1	94.48	35.93	1.59	23.02
-1	1	-1	94.78	35.77	1.64	23.02
-1	-1	1	94.49	36.22	1.68	17.55
-1	-1	-1	94.66	37.01	1.62	17.59
1	0	0	94.39	36.45	1.83	21.27
-1	0	0	94.39	36.70	1.69	19.28
0	1	0	94.34	33.70	1.86	20.92
0	-1	0	94.10	34.31	1.83	17.89
0	0	1	94.92	35.50	1.88	17.11
0	0	-1	94.96	35.25	1.92	17.11

*over dry raw material

According results of characterizacion of raw material, the relative proportion of glucan in the solid phase after laccase treatment was increased and hemicelluloses fraction decreased. More of 87.2 % of hemicellulose fraction en raw material was extracted in liquid phases.

Table 2: Equations yielded for each dependent variable for solid after LMS treatment of eucaliptus.

Equation	Adjusted R^2	F- Snedecor
$Y_{yld} = 94.44 - 0.02\ X_l + 0.07\ X_m X_m + 0.44\ X_t\ X_t + 0.11\ X_l\ X_t - 0.11\ X_m X_t$	0.81	11.64
$Y_{Glu} = 35.32 - 0.23\ X_l - 0.58\ X_m + 1.45 X_l\ X_l - 0.82\ X_m\ X_m - 0.19\ X_l\ X_m$	0.941	31.77
$Y_{Hem} = 1.89 - 0.06\ X_l - 0.15\ X_l\ X_l - 0.05\ X_m\ X_m + 0.02\ X_l\ X_m - 0.04\ X_m\ X_t$	0.976	81.95
$Y_{lk} = 17.77 + 1.31\ X_l + 1.71\ X_m + 2.64\ X_l\ X_l + 1.77\ X_m\ X_m - 0.52\ X_t\ X_t - 0.95\ X_l\ X_m$	0.985	173.00

Table 2 and figures 1-2 shown the models and surface response to represent the variation of dependent variables (glucan, hemicelluloses and Klason lignin contents) respect to independent variables: operation time and laccase concentration at two levels of mediator (HBT) concentration. All the models in table 3 show a good fit to the experimental values, with values higher than 0.9 of r^2 for the characteristics of the solid phase.

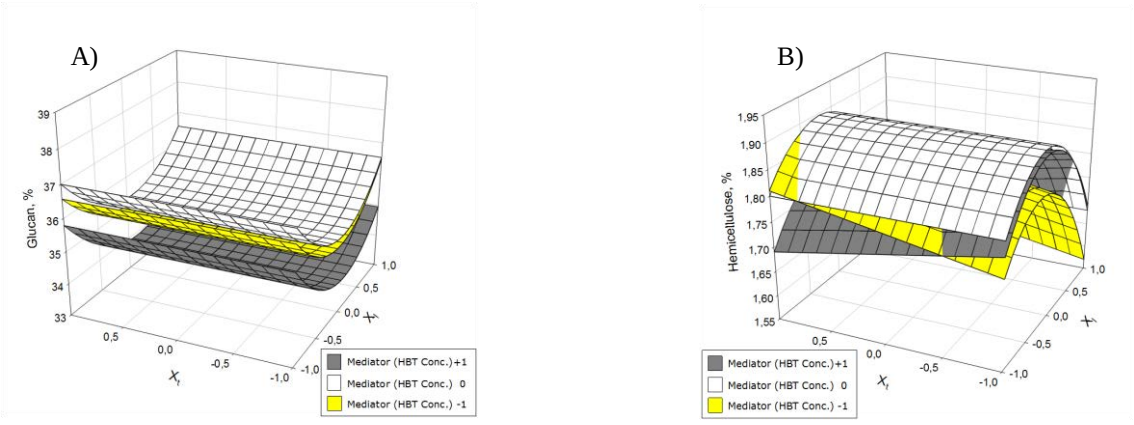

Figure 1: Variation dependent variables as a function of independent variables of LMS process. A) Glucan B) Hemicelluloses

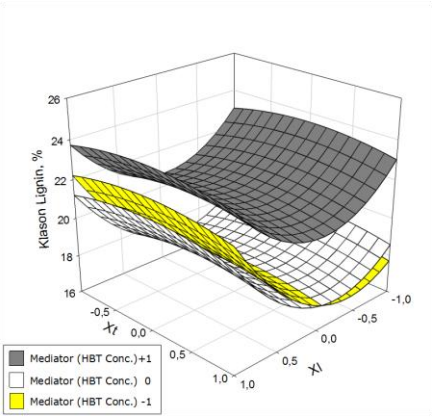

Figure 2: Klason lignin variation as a function of independent variables of LMS process

The best results in delignification (figure 1) can be obtained by operating at low or intermediate mediator and laccase concentrations. The operation time is a variable with low influence. Then, a suitable delignification can be achieved in these conditions (operation time in the low range of variation interval). On the other hand, the best result for glucan content (figure 1.A) can be obtained at intermediate mediator concentration and low laccase concentration. Again, the time of operation is a little influential in the considered range variable. Differences in hemicelluloses concentration are little because most of them have been extracted in the autohydrolysis stage.

The optimum operating conditions (determined with JMP 8.0 statistical software) were 21.6 U/g (-0.35 normalized) in o.d.b of laccase, 2.25 % in o.d.b. of HBT (-0.5 normalized) and a treatment time of 60 minutes (-1 normalized). Process optimization is made considering the lowest percentage of Klason lignin and the higher percentage of glucan (cellulose) existing in the final solid with respect to the initial raw material.

IV. CONCLUSIONS

The variables that most influence the LMS treatment were HBT concentration, followed by laccase concentration. The least influential variable was the time treatment. Optimum operating conditions were -0.35, -0.5 and -1 for normalized values of laccase concentration, HBT concentration and operation time, respectively. Hydrolytic treatment followed by LMS treatment the *Eucaliptus globulus* seems to be a promising pretreatment for increasing the delignification rate in a biopulping process.

V. ACKNOWLEDGEMENT

The authors are grateful to Spanish Ministry of Science and Innovation by the “Ramón y Cajal” contract and PhD student grant from Agrifood Campus of International Excellence (CeiA3). Also they thank to Ministry of Economy, Innovation, Science and Employement of the Junta de Andalucía (Government of Spain), Project number RNM 2323.

VI. REFERENCES

[1] Martín-Sampedro, R., Eugenio, M.E., Carbajo, J.M., Villar, J.C. Combination of steam explosion and laccase-mediator treatments prior to Eucalyptus globulus kraft pulping. Bioresour. Technol. **2011,** 102 ,7183–7189.
[2] Widsten, P., Kanderbauer, A. Laccase applications in the forest products industry. A review. Enzyme Microb. Technol. **2008**, 42, 293-307.
[3] Grethlein, H.E.. The effect of pore size distribution on the rate of enzymatic hydrolysis of cellulosic substrates. Nat. Biotechnol. **1985**, 3, 155–160.
[4] Martín-Sampedro, R., Eugenio, M.E., García, J.C., Lopez, F., Villar, J.C., Diaz, M.J. Steam explosion and enzymatic pre-treatments as an approach to improve the enzymatic hydrolysis of Eucalyptus globulus. Biomass Bioenerg. **2012**, 42, 97-106.
[5] Li H, Saeed A, Jahan MS, Ni Y, Van Heiningen A., Hemicellulose removal from hardwood chips in the prehydrolysis step of the kraft-based dissolving pulp production process. J Wood Chem Technol. **2010,**3 0, 48-60.
[6] López, F., García, M.T., Feria, M.J., García, J.C., Diego, C.M., Zamudio, M.A.M., Díaz, M. J. Optimization of furfural production by acid hydrolysis of Eucalyptus globulus in two stages. Chem. Eng. J. **2014**, 240, 195–201.

RADIAL AND AXIAL VARIATION OF NON-POLAR EXTRACTIVES IN *EUCALYPTUS GLOBULUS*

Jorge Gominho[1*], Ana Lourenço[1], Isabel Miranda[1], António Velez Marques[1,2] and Helena Pereira[1]

*[1] Centro de Estudos Florestais, Instituto Superior de Agronomia, Universidade de Lisboa, Tapada da Ajuda, 1349-017 Lisboa, Portugal; [2] Superior Institute of Engineering of Lisbon, Polytechnic Institute of Lisbon, Rua Conselheiro Emídio Navarro 1, 1959-007 Lisboa, Portugal (*Jgominho@isa.ulisboa.pt)*

ABSTRACT

In order to evaluate the radial and axial variations of the extractives in *E. globulus*, one mature tree with 32 m was harvested and six discs were taken at different height levels: 0%, 5%, 10%, 35%, 50%, and 60%, of height. The heartwood was present at all levels and contained more extractives than sapwood. The bole section from stump to 60% height level represented 81.8 kg (o.d.) with 36.9 kg sapwood and 44.9 kg heartwood. Extractives amounted to 2.94 kg of which 1.83 kg in heartwood. The extractives content decreased with height and with radial position. The main contribution for the total content was done by ethanol extracts (1.3 – 8.9 %). Non-polar compounds represented respectively in sapwood, outer heartwood and inner heartwood 0.30 %, 0.50 % and 0.43 % at base level and 0.25 %, 0.30 % and 0.32% at 60 % of total height. In non-polar extractives the major compounds identified were fatty acids and sterols.

I. INTRODUCTION

Extractives are important non-structural components of wood that show a high chemical diversity e.g. hydrophilic and lipophilic compounds, and have a large impact on wood properties and processing. They are responsible for wood colour, odour and they protect the tree from microbial and insect attacks, [2]. Their occurrence, composition and distribution depend of species, growing site, position within the tree and genetic factors, [1]. The extractives content varies axially and radially within the tree: they decrease to the tree top and from the inner to the outer part [3]. The heartwood is the preferential region where the tree accumulates extractives, [4]. In pulping, the effect of both non-polar and polar extractives is highly negative as regards yield and product quality as well as process and equipment, [5]. Therefore wood extractives are one of the main concerns for pulping engineers. This problem is significant even in pulp industries using *E. globulus* wood which is a raw-material known to have a low content of total extractives (2.9-5.7 %), [6]. The lipophilic fraction of wood extractives plays an important role in pulp and paper production, since it induces formation of pitch and stickies, even if present in the wood in only small amounts as in *e.g. E. globulus* where the dichloromethane extractives range between 0.4-0.8 %, [7]. The objective of this work is to study the radial and axial variations of non-polar compounds in *E. globulus* trees using as a case study mature trees for which a higher content in extractives is expected.

II. EXPERIMENTAL

One mature tree with 40 years of age was chosen and stem disks with 20 cm thickness were taken at different height levels: 0%, 5%, 10%, 15%, 20%, 25%, 35%, 45%, 50%, 60%, 75% of total tree height and top (< 6 cm of diameter). The wood samples were air-dried, and the regions of sapwood and heartwood were marked and the respective area measured using an image analysis system, [8]. The tree volume, and the sapwood and heartwood volumes were calculated by sections corresponding to the different height levels of sampling according to Gominho and Pereira [8]. For basic density and chemical analysis the heartwood was divided in outer heartwood and inner heartwood (at 1/2 of the heartwood radius). In this study, only six height levels were analyzed: at 0%, 5%, 10%, 35%, 50% and 60% (Figure 1). The basic density was calculated using the oven-dry weight and the green volume determined by water immersion. For extractives analysis the samples were grinded and sieved. The 40-60 mesh fractions (5 g) were Sohxlet-extracted successively with dichloromethane, ethanol and water until the completed extraction (16 h with each solvent) and the extractives content was determined gravimetrically. All the analyses were done in duplicate. The dichloromethane extracts were dried under N_2, derivatized with BSTFA and

analyzed by GC-MS (Agilent 7890 A - 5975 C inert MSD) with a high-temperature capillary column ZB-5HT Inferno (30 m × 0,25 mm x 0,10 μm). The compounds were identified by comparing their electron-impact mass spectra (EIMS) with spectra libraries (Wiley and NIST), published spectra, standard spectra and/or interpretation of the mass spectra.

III. RESULTS AND DISCUSSION

Tree characterization

Figure 1 represents the sapwood and heartwood variation along the height of the harvested tree. The tree had a total height of 32 m, a merchantable bole of 29.1 m and a below-crown height (to the first live branch) of 22.9 m.

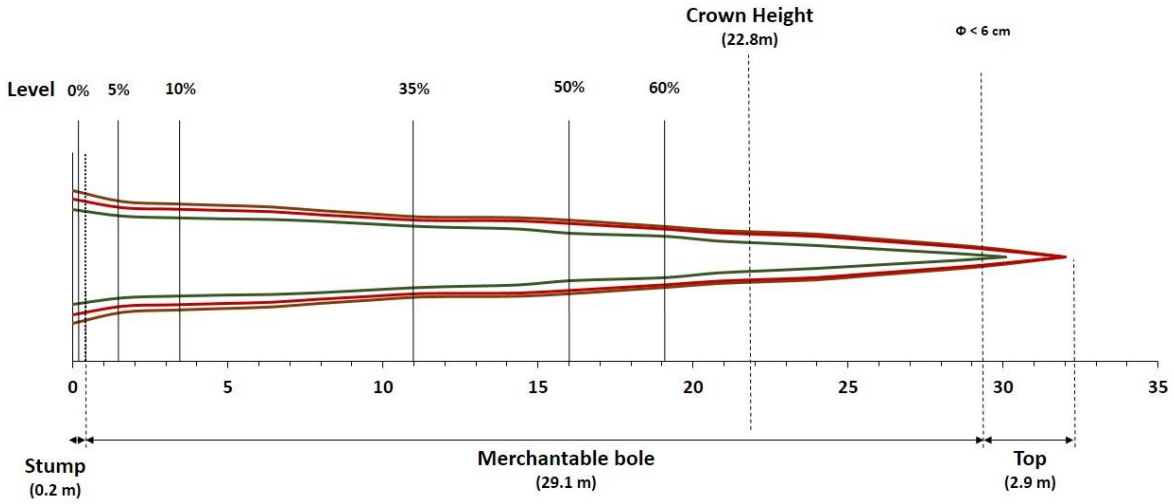

Figure 1. Heartwood and sapwood variation along the harvested *E. globulus* tree.

Heartwood content decreased from bottom to the top (13.6 cm of radius at 0% to 5.9 cm at 60% of height). The sapwood thickness was fairly constant along the tree *e.g.*, ranging between 3.1 cm and 2.1 cm (Table 1). This behavior was described by Gominho and Pereira [8] for *E. globulus* and Gominho *et al.* [9] for the eucalypt hybrid urograndis. Regarding basic density, outer heartwood showed higher values when compared with inner heartwood due to the thick fiber walls of such mature wood and the accumulation of more extractives [1].

Table 1. Biometric data and basic density at different height levels of the *E. globulus* tree.

Level	**0 %**	**5 %**	**10 %**	**35 %**	**50%**	**60 %**
Height level (m)	0.2	1.6	3.2	11.2	16.0	19.2
Total radius (cm)	19.1	15.9	15.2	11.5	10.6	8.7
Bark thickness(cm)	2.4	1.7	1.4	0.9	0.9	0.7
Sapwood thickness (cm)	3.1	2.5	2.6	1.8	2.9	2.1
Heartwood radius (cm)	13.6	11.7	11.2	8.7	6.8	5.9
Heartwood area (% of total area)	50.8	54.2	54.2	57.8	41.4	45.5
Basic density (g/cm^3)						
Sapwood	0.578	0.666	0.669	0.666	0.680	0.663
Outer Heartwood	0.760	0.721	0.732	0.702	0.776	0.724
Inner Heartwood	0.613	0.592	0.615	0.633	0.737	0.726

The total volume for the bole section between the stump and 60% of height was 121.2 dm^3 with a partition in sapwood and heartwood of 59.85 dm^3 and 61.33 dm^3 respectively.

Extractives variation

The results show that the content in extractives (dichloromethane, ethanol and water) decreased in the stem with height and with radial position (Figure 2). For the total extractives content, the main contribution was done by ethanol extracts (1.3 – 8.9 %) followed by the water extracts (0.7 - 1.7 %) and to a small extent by dichloromethane extract (0.19 - 0.49 %). Non-polar extracts soluble in dichloromethane represented respectively in sapwood, outer

heartwood and inner heartwood 0.30 %, 0.50 % and 0.43 % at base level and 0.25 %, 0.30 % and 0.32% at 60 % of total height. The variation of the total content of extractives showed that the values for inner heartwood remained constant at different height levels, the values for the outer heartwood decreased and increased for the sapwood. The increase in sapwood extractives in the upper part of the tree could be explained by the proximity to the crown with more translocation of organic compounds.

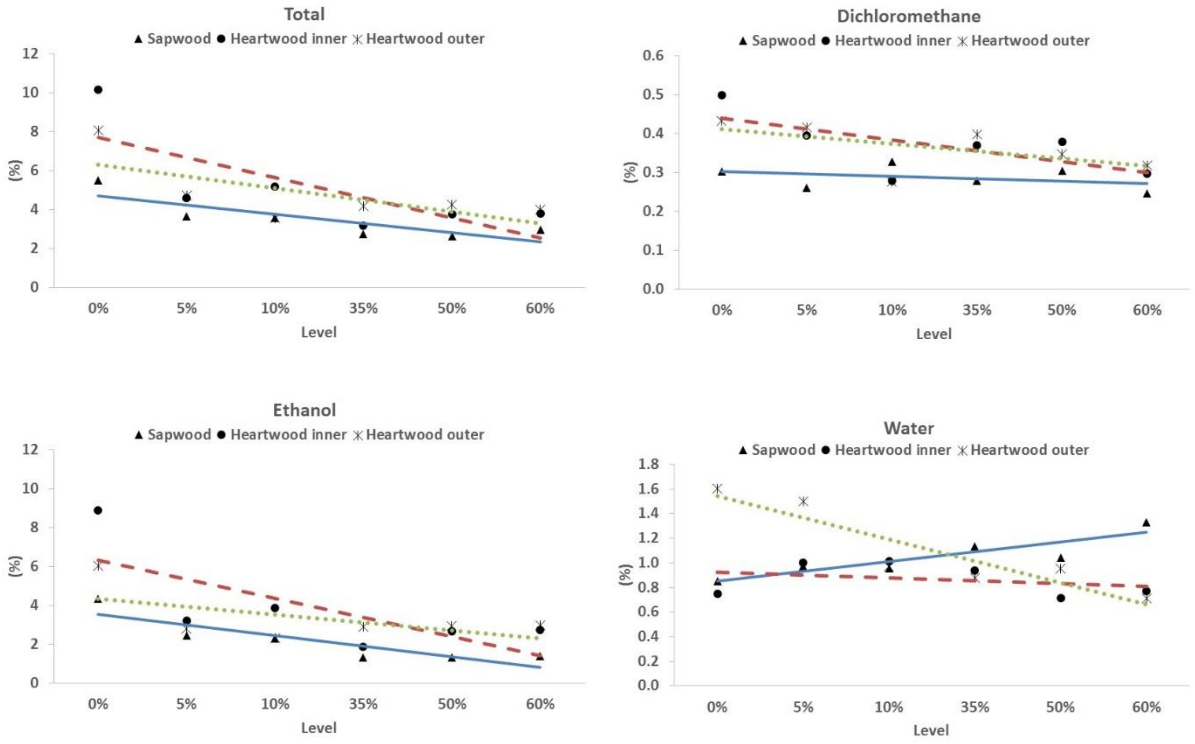

Figure 2. Extractives variation (total, dichloromethane, ethanol and water) at different height levels.

Based on volume and basic density, the portion of the stem analyzed corresponded to 81.8 kg with 36.9 kg sapwood and 44.9 kg heartwood (Table 2). Taking in account the extractives content, the mass of extractives was 2.94 kg of which 1.83 kg in heartwood. The inner heartwood was responsible for 54 % of the total extractives accumulated in this wood region. Concerning the solvents, dichloromethane extracted 0.28 kg, ethanol 1.84 kg and water 0.82 kg.

Table 2. Partitioning of extractives in sapwood and heartwood of the *E. globulus* tree (base to 60% of height).

Dry weight	Wood (kg)	Extractives (kg)			
		Dichloromethane	Ethanol	Water	Total
Sapwood	36.9	0.11	0.60	0.40	1.11
Heartwood	44.9	0.17	1.25	0.42	1.83
Inner heartwood	24.6	0.09	0.66	0.22	0.97
Outer heartwood	20.3	0.08	0.59	0.20	0.86
Total	81.8	0.28	1.84	0.82	2.94

Composition of non-polar extractives

Figure 3 represents the chromatograms of the non-polar extractives for the sapwood at 0% and 60 % of height. The major compounds identified in the non-polar extractives were fatty acids and sterols and their relative distribution could be charted within the stem.

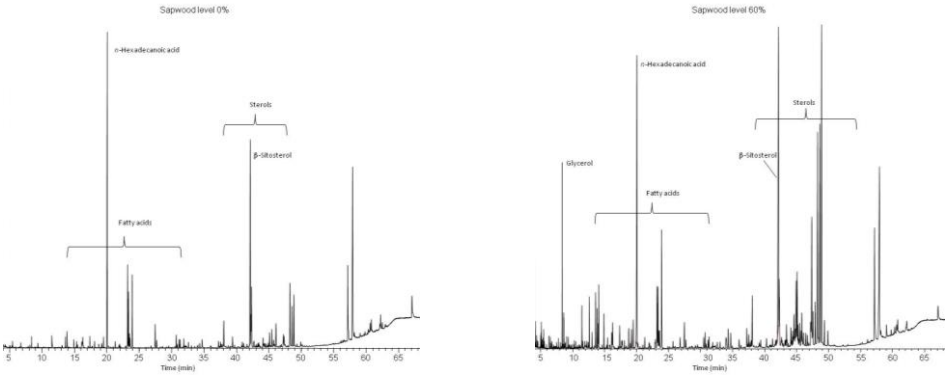

Figure 3. Gas chromatography-mass spectrometry (GC-MS) of dichloromethane extracts from sapwood at 0% and 60 % of height.

IV. CONCLUSIONS

The bole section of the *E. globulus* tree analyzed in this study presented a heartwood proportion of 50.8 – 45.5 % in the cross-sectional area that decreased from bottom to the top. The extractives content decreased in the stem with height and with radial position. The ethanol extracts are the main compounds (1.3 – 8.9 %) in the extractives. The dichloromethane extract represented 0.28 kg of the bole and the major compounds identified are fatty acids and sterols.

V. ACKNOWLEDGEMENT

The authors thank the ALTRI and Clara Araújo for the field sampling. Financial support was given by research funding of FCT (Fundação para a Ciência e a Tecnologia) to CEF (Centro de Estudos Florestais) under its Strategic Project (PEst-OE/AGR/UI0239/2014), and two projects (PTDC/AGRCFL/110419/2009 and PTDC/AGR-FOR/3872/2012).

VI. REFERENCES

[1] Hillis, W. E. Heartwood and tree exudates. Springer-Verlag. Berlin. **1987**.

[2] KAI, Y. Chemistry of extractives. In, D. N.-S. Hon e N. Shiraishi (Eds.). Wood and cellulosisc chemistry. Marcel Dekker, INC. New York. **1991.**

[3]. SJÖSTRÖM, E. Wood chemistry - Fundamentals and applications. Academic press. New York. **1981.**

[4]. Rowell, R. M. Wood Chemistry and Wood Composites, ed., Taylor and Francis, New York, USA. **2005.**

[5]. Rydholm, S. A. *Pulping Processes*, ed., John Wiley and Sons, New York, USA. **1965.**

[6]. Pereira, H., Miranda, I., Gominho, J., Tavares, F., Quilhó, T., Graça, J., Rodrigues, J., Shatalov, A., Knapic, S. *Qualidade tecnológica do eucalipto (Eucalyptus globulus)*, Centro de Estudos Florestais ed., Instituto Superior de Agronomia, Universidade Técnica de Lisboa, Lisboa. **2010**.

[7]. Gutiérrez, A., Rencoret, J., Ibarra, D., Molina, S., Camarero, S., Romero, J., del Río, J.C., Martínez, A.T. Lipophilic extractives forming pitch deposits can be removed from paper pulp using laccase and lignin-derived phenols as natural mediators. *Environmental Science & Technology* **2007**, 41, 4124-4129.

[8]. Gominho, J., and H., Pereira. Variability of heartwood content in plantation grown *Eucalyptus globulus* Labill.. *Wood Fiber Sci*, **2000**, 32(2): 189-195.

[9]. Gominho, J., Figueira, J., Within-tree variation of heartwood, extractives and wood density in the eucalypt hybrid urograndis (Eucalyptus grandis× E. urophylla). *Wood and Fiber Sci*, **2001**. 33, 3–8.

ORANGE TREE PRUNINGS AS RAW MATERIAL FOR CELLULOSE PRODUCTION BY ETHANOL PROCESS

Zoilo González, Fátima Vargas, Eduardo Espinosa, Luis Jiménez, Alejandro Rodríguez*

*Chemical Engineering Department, University of Córdoba, Spain, *corresponding author: Alejandro Rodríguez. Chemical Engineering Department. Campus of Rabanales, C-3. University of Córdoba. Córdoba. Spain. Phone: +34 957 212274 Fax+34 957 218625 E-mail: a.rodriguez@uco.es*

ABSTRACT

The rational use of natural resources should be a priority in the policies aimed to make what is known as sustainable development. The epitome of rational use is the comprehensive utilization of these resources. Thus, when it comes to food crops, interest should focus not only on obtaining actual food (fruit, vegetables, cereals, etc), but in turn into product or by-product which can initially be considered as waste.

Orange tree pruning consists of lignocellulosic material from the felling operation. The Spanish production of oranges is about 6,500,000 t/year, Andalusia contribute with more than 20%. Considering that the relationship "prune/fruit" can be 0.8, the production of pruning can be more than 5,000,000 tons/year.

Within the wide range of organic solvents used in organosolv process, ethanol is the most used and the most ancient delignified agents. This is due to its low price, ease of recovery and low toxicity (regarding other organic solvents). The ethanol pulps have highest α-cellulose content and lower hemicellulose, in relation to the Kraft pulp, providing the benefits of increased yield and a minor loss of hemicelluloses in the refining.

The aim of this work was to study the influence of operational variables in the orange tree pruning ethanol pulping [temperature (170-200ºC), time process (60-120 min) and ethanol concentration (60-80%) at constant values of liquid solid ratio of 8:1, on the pulp yield and viscosity of pulps and tensile index, burst index and tear index of papersheets. The experimental data obtained were used to estimate the parameters or constants in the equation for the neural fuzzy model. The predictions for the yield, viscosity, tensile index, burst index and tear index differ by less than 5, 8, 13, 8 and 20% of their experimental values.

I.INTRODUCTION

Since the 1970s, pulp production from non-woody plants using non-conventional raw materials has increased from approximately 7% to almost 12% of the total pulp produced, growing at a rate of 2 to 3 times greater than wood pulps [1-4].

The use of agricultural and agro-industry residues and alternatives to food crops seems to be a good alternative to raw wood material, which can lead to excellent paper products with special properties and can serve as the sole source of raw materials in some geographical areas [5].

Orange tree prunings could provide a new source of non-wood raw material. Spanish production of orange tree prunings from felling operations is more than 5 million tons per year [6]. Orange tree prunings and crop residues in general must be removed to control pollution, fire, pests, interference with soil cultivation, and occupation of large areas. It is advantageous to try to exploit the different fractions of waste as a method to reduce disposal costs.

The aim of this work was to study the influence of operational variables in the orange tree pruning ethanol pulping [temperature (170-200ºC), time process (60-120 min) and ethanol concentration (60-80%) at constant values of liquid solid ratio of 8:1, on the pulp yield and viscosity of pulps and tensile index, burst index and tear index of papersheets. The experimental data obtained were used to estimate the parameters or constants in the equation for the neural fuzzy model. The predictions for the yield, viscosity, tensile index, burst index and tear index differ by less than 5, 8, 13, 8 and 20% of their experimental values

II. EXPERIMENTAL

Raw material

This work uses the main fraction of the orange tree prunings (*Citrus sinensis*), constituted by the wood from the branches and stems with diameters larger than 1 cm

Pulping

Pulp was obtained by using a cylindrical reactor of 1.9 L capacity, operating in discontinuous. The reactor vessel is enveloped by electrical resistances for heating. The vessel is designed to achieve pressures higher than 30 kg/cm^2.
The main fraction of the orange tree pruning was pulped in the reactor under certain conditions of ethanol concentration, temperature, time and liquid/solid ratio (**Table1**). Next, the cooked material was fiberized in a wet desintegrator at 1200 rpm for 30 min and the screenings were separated by sieving through a screen of 1 mm mesh size.
Paper sheets were prepared on an ENJO-F-39.71 sheet machine according to the TAPPI 220 standard method.

Experiment	T, ºC	t, min	E, %	YI, %	VI, mL/g	TI, Nm/g	BI, kN/g	TeI, mNm^2/g
1	185	90	70	44.9	362	15.1	0.66	1.45
2	200	120	80	39.7	667	11.5	0.54	1.25
3	170	120	80	58.0	162	6.3	-	0.98
4	200	120	60	34.7	638	12.9	0.51	1.18
5	170	120	60	48.7	244	14.5	0.61	1.43
6	200	60	80	44.9	496	15.5	0.60	1.33
7	170	60	80	61.5	112	-	-	0.74
8	200	60	60	36.6	689	13.4	0.52	1.25
9	170	60	60	55.6	157	7.0	-	0.89
10	185	120	70	47.1	538	18.9	0.73	1.52
11	185	60	70	47.4	337	16.5	0.73	1.52
12	185	90	80	47.0	309	16.3	0.70	1.53
13	185	90	60	41.5	523	17.3	0.74	1.52
14	200	90	70	36.9	699	12.9	0.54	1.41
15	170	90	70	57.6	169	8.0	0.33	1.02
T, t, and E = Temperature, time and ethanol concentration, respectively YI: yield; VI: viscosity; TI: tensile index; BI: burst index; TeI: tear index								

Table1. Values of the operational variables and of the properties of the pulps obtained pulping orange tree pruning with ethanol

Characterization of the pulp and paper sheets
The products (pulp and paper) obtained from raw material were characterized according to the following standard methods: Yield (gravimetrically), viscosity (Tappi T230-om-94), tensile index (Tappi T494om-96), burst index (Tappi T403om-97) and tear index (Tappi T414om-98).
Experimental design
The relationships between the dependent variables (viz. yield, viscosity, tensile index, burst index and tear index) and the independent (operational) variables were established by using a fuzzy neural model. This type of model combines the advantages of fuzzy logic systems [7] and neural networks [8], and provides a powerful prediction tool based on the following equation [9] with three independent variables, the use of a singleton defuzzifier (a constant parameter) and a linear membership function for the independent variables:

$$Y_e = \frac{\sum_{l=1}^{8} c_l \left[\prod_{i=1}^{4} \prod_{j=1}^{2} x_{ij} \right]}{\sum_{l=1}^{8} \left[\prod_{i=1}^{4} \prod_{j=1}^{2} x_{ij} \right]} \qquad (1)$$

where Ye is the estimated value of the property to be modelled and c_l the defuzzifier of a fuzzy rule, x_i denoting the values of temperature (T), time (t) and ethanol concentration (E), and j being 1 or 2 in the equations:

$$x_{i1} = 1 - \frac{1}{(x_{high} - x_{low})}(x - x_{low}) \qquad x_{i2} = \frac{1}{(x_{high} - x_{low})}(x - x_{low}) \qquad (2)$$

with x_{high} and x_{low} the extreme values of each variable.

With three independent variables, one can establish the following 8 fuzzy rules (R_i) based on the extreme (high and low) values of such variables:
R1: low T, low t and low E
R2: low T, low t and high E
.....
R7: high T, high t and low E
R8: high T, high t and high E
With a Gaussian membership function with three levels (low, medium and high) for one of the variables and a linear membership function with two levels (low and high) for the other two, Eq. 1 would contain 12 terms in the numerator and another 12 in the denominator. The Gaussian membership function would be of the form:

$$x_i = \exp\left(-0.5\left(\frac{x - x_c}{L}\right)^2\right) \quad (3)$$

where x is the absolute value of the variable concerned; x_c its minimum, central or maximum value; and L the width of its Gaussian distribution.
The parameters and constants in the previous equation were estimated by using the ANFIS© (Adaptive Neural Fuzzy Inference System) Edit tool in the Matlab v. 6.5 software suite.

III. RESULTS AND DISCUSSION

Experimental data from **Table 1** were adjust to the equation of neurofuzzy model to estimate the parameters or constants (a_i) of this equation, with functions of linear belonging to two different levels (low and high) for two variables of operation, and a function of membership Gaussian at three levels (high, medium and low) for another operation variable (**table 2**)

Rules	T, ºC	t, min	E, %	Value of a_i for				
				YI, %	VI, mL/g	TI, Nm/g	BI, kN/g	TeI, mNm^2/g
1	170	60	60	57.1	290	6.53	0.198	0.708
2	170	60	80	63.1	247	5.82	0.245	0.542
3	170	120	60	49.6	226	12.6	0.595	1.278
4	170	120	80	58.8	165	5.73	0.202	0.795
5	185	60	60	41.7	417	16.8	0.764	1.395
6	185	60	80	47.5	228	16.22	0.742	1.431
7	185	120	60	42.3	632	19.69	0.764	1.389
8	185	120	80	48.1	439	18.5	0.711	1.405
9	200	60	60	36.1	701	13.19	0.500	1.112
10	200	60	80	44.2	508	15.49	0.590	1.206
11	200	120	60	33.9	1001	12.49	0.490	1.048
12	200	120	80	38.9	763	11.06	0.530	1.116
9	170	90	60	-	-	-	-	-
10	170	90	80	-	-	-	-	-
11	200	90	60	-	-	-	-	-
12	200	90	80	-	-	-	-	-
R^2				0.98	1.00	0.98	0.99	0.97
T, t, and E = Temperature, time and ethanol concentration, respectively YI: yield; VI: viscosity; TI: tensile index; BI: burst index; TeI: tear index								

Table 2. Values of the constant a_i of the neurofuzzy model, and values of R^2

Table 3 show the estimated values of the dependent variables provided by the neurofuzzy models and the corresponding errors with respect to the experimental values (**table 1**). As shown, the predictions for yield, viscosity, tensile index, burst index and tear index differ in less than the 5, 8, 13, 8 and 20%, respectively, of their respective experimental values.

Experiment	T, ºC	t, min	E, %	YI, %	VI, mL/g	TI, Nm/g	BI, kN/g	TeI, mNm^2/g
1	185	90	70	45,2 (0,8)	436 (0,4)	17,0 (12,1)	0,710 (7,89)	1,358 (6,14)
2	200	120	80	39,4 (0,9)	744 (0,7)	11,5 (0,4)	0,541 (0,34)	1,133 (9,23)
3	170	120	80	58,2 (0,3)	181 (3,5)	6,5 (2,6)	0,232 (1,27)	0,831 (14,90)

4	200	120	60	34,4 (1,0)	979 (1,3)	12,9 (0,3)	0,507 (0,49)	1,068 (9,75)
5	170	120	60	49,2 (0,9)	249 (2,4)	13,0 (1,1)	0,605 (0,44)	1,285 (10,21)
6	200	60	80	44,4 (1,0)	492 (0,8)	15,5 (0,3)	0,599 (0,41)	1,219 (8,64)
7	170	60	80	62,1 (1,1)	246 (2,4)	6,4 (2,6)	0,275 (1,12)	0,595 (19,62)
8	200	60	60	36,4 (0,4)	684 (0,7)	13,4 (0,3)	0,515 (0,42)	1,129 (9,85)
9	170	60	60	56,2 (1,1)	298 (1,9)	7,1 (2,3)	0,232 (1,44)	0,749 (16,26)
10	185	120	70	45,2 (3,9)	536 (0,4)	18,1 (3,8)	0,707 (2,74)	1,360 (10,60)
11	185	60	70	45,2 (4,6)	335 (0,4)	15,8 (4,3)	0,713 (2,50)	1,356 (10,60)
12	185	90	80	48,2 (2,5)	343 (1,9)	16,5 (1,0)	0,690 (1,56)	1,363 (11,12)
13	185	90	60	42,2 (2,5)	528 (1,1)	17,5 (0,9)	0,729 (1,25)	1,353 (11,24)
14	200	90	70	38,7 (4,8)	725 (3,6)	13,3 (3,4)	0,540 (0,33)	1,137 (19,59)
15	170	90	70	56,4 (2,1)	244 (7,4)	8,3 (3,0)	0,336 (1,40)	0,865 (15,01)
T, t, and E = Temperature, time and ethanol concentration, respectively YI: yield; VI: viscosity; TI: tensile index; BI: burst index; TeI: tear index								

IV. CONCLUSIONS

The neurofuzzy models are effective for a typical experimental design of three operational variables, with a total of 15 experiments. A neurofuzzy model offers physical interpretation of the constants (parameters) in so far as they represent averages of the destination properties values (dependent variables) under the conditions defined by the specific used fuzzy rule.

V. ACKNOWLEDGEMENTS

The authors are grateful to Ecopapel, S.L. (Écija, Sevilla, Spain) for their support, and to Spain's DGICyT and Junta of Andalucía for funding this research within the framework of the Projects CTQ-2010-19844-C02-01 and TEP-6261.

VI. REFERENCES

[1]Atchinson, J. E. Twenty-five years of global progress in non-wood plant fiber repumping, *Tappi J.* **1996** *79(10)*, 87-97

[2] Simula, M. Fibre supply: The achilles heel of the global pulp and paper industry, *Paperi Ja Puu-Paper and Timber*, **2002** *84(1)*, 16-19.

[3] Alaejos, J.; López, F.; and Eugenio, M. E. Using of non-wood raw materials for cellulose pulp. Review *Afinidad* **2004** *61(513)*, 400-410

[4] González, Z.; Rosal, A.; Requejo, A.; and Rodríguez, A. Production of pulp and energy using orange tree pruning, *Bioresour. Technol.* **2011** *102 (19)*, 9330-9334

[5] Jiménez, L. Pastas Celulósicas de Materias Primas Alternativas a las Convencionales. **2005** Editorial Gráficas Sol, Sevilla.

[6] Rodríguez, A.; Rosal, A.; and Jiménez, L. Biorefinery of agricultural residues by fractionation of their components through hydrothermal and organosolv processes, *Afinidad* **2010** *67(545)*, 14-19

[7] Zadeh, L.A. Fuzzy sets. *Information and Control,***1965** *8*, 338-353

[8] Works, G.A. Neural network basics. Proceeding AUTOFACT'89, **1989**, 29, 1-9

[9] Jang, J.S.R. ANFIS: adaptive-network-based fuzzy inference system. *IEEE Transactions on Systems, Man and Cybernetics,* **1993** *23 (3)*, 665-685

SCREENING MUTANT LIBRARIES OF VERSATILE PEROXIDASE FROM *Pleurotus eryngii* TO ENHANCE OXIDATIVE STABILITY

David González-Pérez[1], Alina Roman[1], Eva García-Ruiz[1], Francisco Javier Ruiz-Dueñas[2], Angel T. Martínez[2] and Miguel Alcalde[1]*

*[1]Institute of Catalysis, CSIC, Cantoblanco, 28049 Madrid, Spain; [2]Centro de Investigaciones Biológicas, CSIC, Ramiro de Maeztu 9, 28040 Madrid, Spain (*malcalde@icp.csic.es)*

ABSTRACT

Versatile peroxidases (VPs) are promiscuous high-redox potential biocatalysts with broad substrate specificity. VPs are strongly inhibited by modest concentrations of hydrogen peroxide which hampers their application in different industrial settings. In the current work, a VP mutant evolved in our laboratory for functional expression was used as departure point to tailor oxidative stability. A high-throughput assay based on the analysis of the apparent half-life using different H_2O_2:enzyme molar ratios was designed and employed to explore mutant libraries. After only one round of directed evolution two variants were selected showing apparent half-life of 10-23 min with a 3,000-fold H_2O_2:enzyme molar excess.

I. INTRODUCTION

Broadly distributed in nature, peroxidases (EC 1.11.1) are an important group of oxidoreductases that are capable to oxidize a wide variety of substrates in the presence of hydroperoxides [1, 2]. Peroxidases find tens of potential applications ranging from bioremediation to organic synthesis but their low oxidative stability preclude many biotechnological use. Typically, peroxidases undergo a mechanism-based inhibition process mediated by catalytic concentrations of H_2O_2 (referred to as suicide inactivation). Several studies have been carried out to regulate the oxidative stability of peroxidases, either by process engineering (in an attempt to control the H_2O_2 dosage during reaction) or by protein engineering. Site-directed mutagenesis experiments for oxidative stability focus on the substitution of the most oxidizable residues of the protein (Met, Cys, Trp, His, Tyr) by less-oxidizable amino acids [3, 4]. On the other hand, the use of directed evolution provides the opportunity to unmask residues involved in the oxidative stability of the peroxidase that otherwise could hardly be anticipated by rational approaches. High-throughput screening (HTS) assays reported to date for evolving towards oxidative stability are based on the rough incubation of mutant supernatants in the presence and in the absence of H_2O_2 [5-7]. All these protocols do not take into account the H_2O_2:enzyme molar ratio, which is an important parameter to avoid the selection of false positives during the directed evolution experiment: the same molar excess of H_2O_2 applied in the screening led to different responses depending on the activity and secretion levels of each mutant. Recently, the high-redox potential versatile peroxidase (VP) from *Pleurotus eryngii*, was evolved for secretion, activity and thermostability in *Saccharomyces cerevisiae* [8]. In the current work, we have used the VP secretion mutant (R4 variant) to tailor oxidative stability. A robust HTS-assay based on the determination of apparent half-life ($\Delta t_{1/2}$) at several H_2O_2:enzyme molar ratio was adapted to the specific conditions of the yeast expression system and used to screen mutant libraries towards oxidative stability.

II. EXPERIMENTAL

VP from *P. eryngii* (R4 mutant of the allelic variant *vpl2*, GenBank AF007222) was used as parent type for library construction. R4 was engineered after 4 rounds of directed evolution for secretion achieving expression levels of 22 mg/L [8]. ABTS (2,2´-azino-bis(3-ethylbenzothiazoline-6-sulfonic acid), bovine hemoglobin, *Taq* polymerase and the Yeast transformation kit were purchased from Sigma-Aldrich (Madrid, Spain). The *E.coli* XL2-blue competent cells were from Stratagene (La Jolla, CA, US). *S. cerevisiae* BJ5465 was from LGCPromochem (Barcelona, Spain). Zymoprep yeast plasmid miniprep kit I and Zymoclean gel DNA recovery kit were from Zymo Research (Orange, CA). NucleoSpin plasmid kit was from Macherey-Nagel (Germany) and restriction enzymes *BamH*I and *Xho*I were from New England Biolabs (Hertfordshire, UK).

Library construction and cloning

PCR products were cleaned, concentrated and loaded onto a low melting point preparative agarose gel and purified using the Zymoclean gel DNA recovery kit I (Zymo research). PCR products were cloned by replacing the corresponding parental gene in pJRoC30 vector. To remove the parental gene, the plasmid was linearized

(with *Xho*I and *BamH*I). The parent R4 mutant was subjected to error-prone PCR (a mutagenic library of 1044 clones was constructed). The primers used for amplification were: RMLN sense (5'-CCTCTATACTTTAACGTCAAGG-3', which binds to bp 420-441 of pJRoC30-R4) and RMLC antisense (5'-GGGAGGGCGTGAATGTAAGC-3', which binds to bp 1792-1811 of pJRoC30-R4). To promote *in vivo* ligation, overhangs of 40 and 66 bp homologous to the linear vector were designed. Reaction mixture was prepared in a final volume of 50 µL containing 90 nM RMLN, 90 nM RMLC, 0.1 ng/µL pJRoC30-R4, 0.3 mM dNTPs (0.075 mM each), 3% dimethylsulfoxide (DMSO), 1.5 mM $MgCl_2$, 0.05 U/µL *Taq* polymerase and 0.01 mM $MnCl_2$. Error prone-PCR was carried out on a gradient thermocycler (Mycycler, BioRad, US) using the following parameters: 95ºC for 2 min (1 cycle); 94ºC for 45 s, 53ºC for 45 s, 74ºC for 1.30 min (28 cycles); and 74ºC for 10 min (1 cycle). The PCR product (400 ng) was mixed with the linearized vector (100 ng) and transformed into competent cells using the Yeast transformation kit (Sigma). Transformed cells were plated in SC drop-out plates and incubated for 3 days at 30ºC.

High-throughput oxidative stability assay

Individual clones were picked and cultured in 96-well plates (Greiner Bio-One) containing 50 µL of minimal medium lacking uridine per well. In each plate, column number 6 was inoculated with parental R4 as internal standard, and well-H1 (containing minimal medium supplemented with uridine) was inoculated with untransformed *S. cerevisiae* as negative control. Plates were sealed and incubated at 30°C, 225 rpm in a humidity (80%) shaker (Minitron-INFORS, Biogen, Spain). After 48 h, 160 µL of expression medium were added to each well, and the plates were incubated for 24 h. The plates (master plates) were centrifuged (Eppendorf 5810R centrifuge, Germany) for 15min at 3,000 rpm at 4°C. The master plate was duplicated with the help of a robot (Liquid Handler Quadra 96-320, Tomtec, Hamden, CT, USA) by transferring 20 µL of supernatant onto two replica plates: the initial activity plate (IA plates) and the residual activity plate (RA plates). Subsequently, 180 µL of stability buffer (20 mM sodium tartrate buffer pH 5.0, Buffer A) was added to the IA plates and 180 µL of incubation solution (0.3 mM H_2O_2 in 20 mM sodium tartrate buffer pH 5.0, Buffer B) was added to the RA plates with the help of a Multidrop robot (Multidrop Combi, ThermoFischer Scientific, Vantaa, Finland). Both plates were briefly stirred and the incubation took place at room temperature for 60 min (so that the assessed activity in RA plates was reduced 2/3 of the initial activity). 20 µL of supernatants were transferred from both RA and IA plates to new plates to measure the residual and initial activity values by adding ABTS containing specific buffers: 180 µL of 100 mM sodium tartrate buffer pH 3.5 containing 2 mM ABTS and 0.1 mM H_2O_2 for the estimation of residual activity and 180 µL of 100 mM sodium tartrate buffer pH 3.5 containing 2 mM ABTS and 0.13 mM H_2O_2 for the estimation of initial activity. Plates were stirred briefly and the absorption at 418 nm ($\varepsilon_{ABTS}^{\bullet+}$ = 36,000 M^{-1} cm^{-1}) was recorded (end-point mode) in the plate reader (SPECTRAMax Plus 384, Molecular Devices, Sunnyvale, CA). The plates were incubated at room temperature until a green color was developed, and the absorption was measured again. Relative activities were calculated from the difference between the absorption after incubation and that of the initial measurement normalized against the parental type in the corresponding plate. Oxidative stability values came from the ratio between residual activity and initial activity values. To rule out false positives, two consecutive re-screenings were carried out. A third rescreening was incorporated to determine the increment (expressed in minutes) in the apparent half-lives ($t_{1/2}$ H_2O_2) for each selected variant over parent R4 in different H_2O_2:enzyme molar ratios.

Protein modeling

The structure of wild-type VPL2 (purified from *P. eryngii* culture) at a resolution of 2.8 Å (1 Å=0.1 nm) (PDB code 3FJW) was used as a template to generate a molecular model where the new found mutations were mapped. The resulting model was analyzed with PyMOL Molecular Visualization System (http:// pymol.org).

III. RESULTS AND DISCUSSION

Validation of the screening assay

Typically, an appropriate selection pressure for screening towards stability in directed evolution experiments is chosen so that the residual activity is about 30 % of the initial activity. At 0.3 mM H_2O_2, R4 kept 1/3 of its initial activity value, for an incubation time of 60 min and this concentration and incubation time were selected for the HTS-assay. ABTS was chosen as reporter substrate since it shows high sensitivity and hardly interferes with the *S. cerevisiae* culture broth. Activities from 96-well plates supernatants preparations were evaluated (coefficient of variation=13 %). The final value of oxidative stability in the HTS-assay come from the ratio of residual activity to initial activity (RA/IA) normalized with the parent type.

Library construction and analysis

An error-prone PCR mutant library of ~1,000 clones was constructed and explored, **Fig. 1**. After 2 consecutive re-screenings, two clones were selected (3B10 and 6H5 mutants with improvements of 2.1- and 1.4-fold over

parental R4). The selected clones were subjected to a third re-screening in which total activities and apparent $t_{1/2}$ H_2O_2 were evaluated at several H_2O_2:enzyme molar ratios.

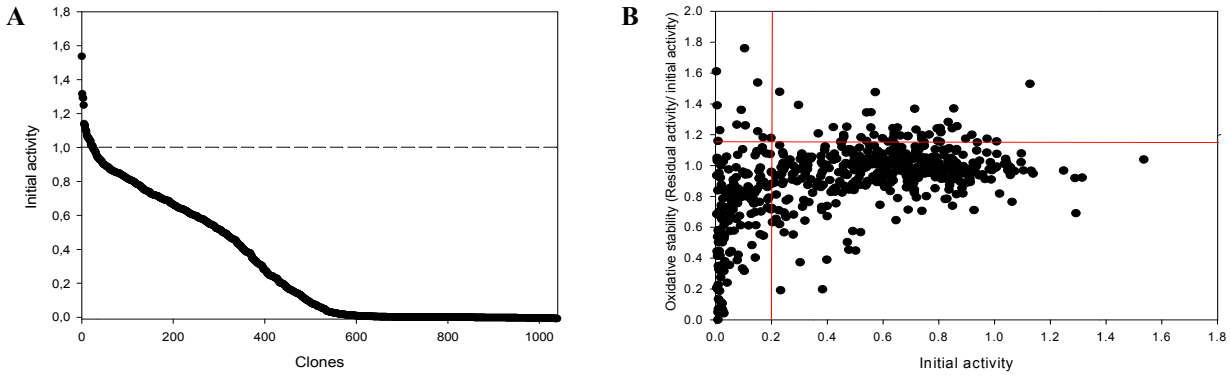

Figure 1. Directed evolution landscapes. A) Activities of clones from the library prepared by mutagenic PCR (*Taq*/$MnCl_2$), plotted in descending order. Dashed black line represents activity of the parental R4. B) Initial activities *vs* oxidative stability. Red lines highlight the improvements in stability (1.15-fold retaining over 0.2 - fold of the parental activity).

The apparent H_2O_2 $t_{1/2}$ was defined as the time at which the enzyme (from supernatants) retains 50 % of its initial activity at a given concentration of H_2O_2 under a defined molar ratio H_2O_2:enzyme. Regardless of the molar ratio used, both 3B10 and 6H5 showed higher oxidative stability than the parental type. With a molar ratio of 3,000-fold, the H_2O_2 apparent $\Delta t_{1/2}$ over R4 parental type were 23 min and 10 min for 3B10 and 6H5, respectively, **Fig. 2**. Parental R4 showed 2,230±52 ABTS-Units/L whereas the mutant´s total activities decreased to 915±4 and 970±7 ABTS-Units/L for 3B10 and 6H5, respectively. The trade-off between activity and oxidative stability was not unexpected since there are several studies in which improvements in oxidative stability are associated with a reduction of total activity [3, 5, 6]. 6H5 mutant showed the mutations that conferred high secretion levels in the parental R4 (E37K-V160A-T184M-Q202L) plus one new mutation, I171V (**A**TT_{511}**G**TT). Interestingly, 3B10 conserved only three of the four mutations of R4 reverting mutation T184M to M184T (A**T**G_{551}A**C**G). The mutations were mapped in a model based on *P. eryngii* VP crystal structure. It has been shown that the substitution of Met by non-oxidizable residues can improve the H_2O_2 resistance [3, 4]. The drop in total activity upon mutation may be attributed to the fact that the original mutation T184M conferred to R4 mutant a considerable enhancement in secretion levels by promoting a more proper folding in yeast [8]. Mutation I171V is placed in a loop near the proximal His169, the latter acting as the fifth coordinating ligand of Fe^{3+} of the heme prosthetic group. The change from Ile to Val represents a substitution by a less bulky residue, which could modify the topology of the VP inner structure due to its proximity (4.5 and 5.6 Å) to the disulfide bridge Cys114-Cys34 and to the proximal structural Ca^{2+}, respectively.

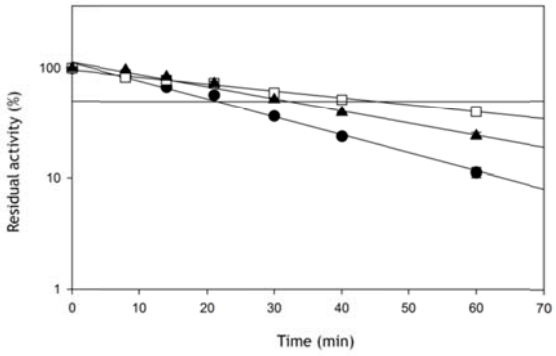

Figure 2. Inactivation of parental and VP mutants in the presence of H_2O_2. R4-parent type (black circles), 6H5 (black triangles) and 3B10 (white squares) variants. H_2O_2:enzyme molar ratio = 3,000 fold. Black line indicates 50 % of residual activity. Each point is represented as the average of three independent measurements including standard deviation.

IV. CONCLUSIONS

The oxidative stability HTS-protocol described here is a valuable tool to study suicide inactivation in VP. The use of specific H_2O_2:enzyme molar ratio during the screening assay and the estimation of H_2O_2 apparent $\Delta t_{1/2}$

have been successfully employed to discriminate between clones when screening libraries. We have recently applied this protocol to perform focused directed evolution to improve further the VP oxidative stability [9].

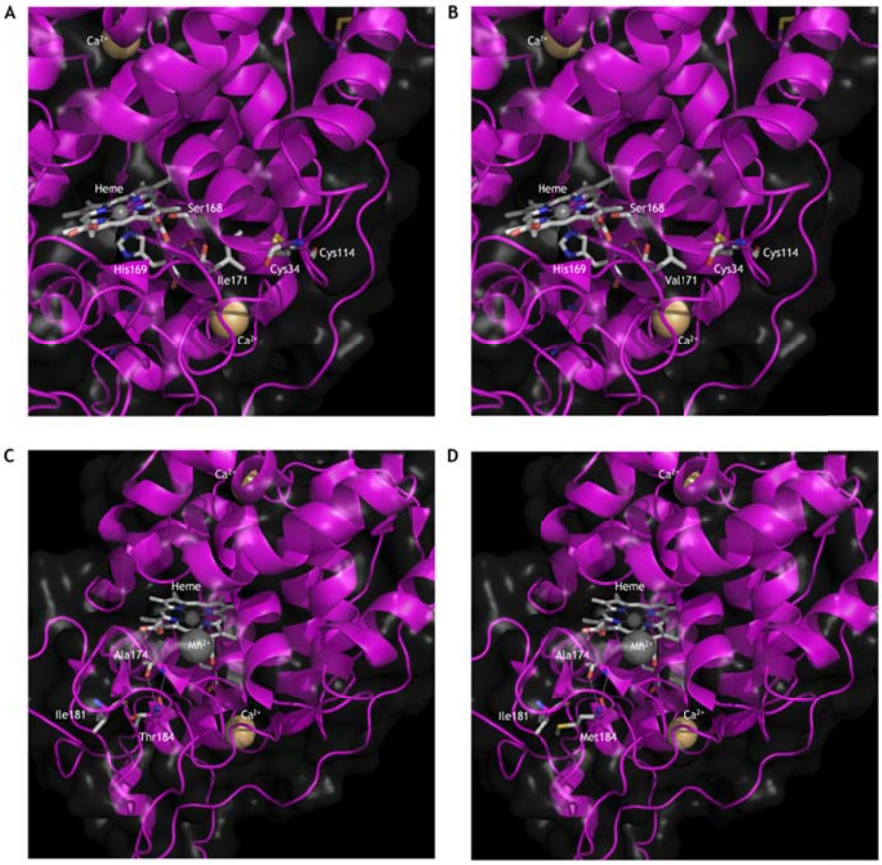

Figure 3. Location and surroundings of stabilizing mutations in 6H5 (A,B) and 3B10 (C,D).

V. ACKNOWLEDGEMENTS

This work was supported by European Commission Projects (Peroxicats-FP7-KBBE-2010-4-26537; Indox-FP7-KBBE-2013-7-613549; COST-Action CM1303: Systems Biocatalysis) and the National Project (Evofacel) [BIO2010-19697].

VI. REFERENCES

[1] Fawal, N.; Li, Q.; Savelli, B.; et al. PeroxiBase: a database for large-scale evolutionary analysis of peroxidases. *Nucleic Acids Res.* **2010**, *41*, 441–444.

[2] Martinez, AT. High redox potential peroxidases.*J. Polaina and A.P. MacCabe (eds.), Industrial Enzymes*. Springer, the Netherlands. **2007**, 475–486.

[3] Ogola, H.J.; Hashimoto, N.; Miyabe, S.; Ashida, H.; Ishikawa, T.; Shibata, H.; Sawa, Y. Enhancement of hydrogen peroxide stability of a novel Anabaena sp. DyP-type peroxidase by site-directed mutagenesis of methionine residues. *Appl. Microbiol. Biot*. **2010**, *87*,1727-1736.

[4] Miyazaki, C.; Takahashi, H. Engineering of the H_2O_2 -binding pocket region of a recombinant manganese peroxidase to be resistant to H_2O_2. *FEBS Lett*. **2001**, *509*, 111-114.

[5] Morawski, B.; Quan, S.; Arnold, F.H. Functional expression and stabilization of horseradish peroxidase by directed evolution in *Saccharomyces cerevisiae*. *Biotechnol Bioeng.* **2001**, *76*, 99-107.

[6] Cherry, J.R.; Lamsa, M.H.; Schneider, P.; Vind, J.; Svendsen, A.; Jones, A.; Pedersen, A.H. Directed evolution of a fungal peroxidase. *Nat Biotechnol*. **1999**, *17*, 379-84.

[7] Miyazaki-Imamura, C.; Oohira, K.; Kitagawa, R.; Nakano, H.; Yamane, T.; Takahashi, H. Improvement of H_2O_2 stability of manganese peroxidase by combinatorial mutagenesis and high-throughput screening using in vitro expression with protein disulfide isomerase. *Protein Eng*. **2003**, *16*, 423-428.

[8] Garcia-Ruiz, E.; Gonzalez-Perez, D.; Ruiz-Dueñas, F.J.; Martinez, A.T.; Alcalde, M. Directed evolution of a temperature-peroxide- and alkaline pH-tolerant versatile peroxidase. *Biochem. J.* **2012**, *441*, 487–498.

[9] Gonzalez-Perez, D.; Molina-Espeja, P.; Garcia-Ruiz, E.; Alcalde, M. Mutagenic organized recombination process by homologous in vivo grouping (MORPHING) for directed enzyme evolution. *PlOS ONE*. **2014**, 9(3): e90919.

PHYSICOCHEMICAL PROPERTIES OF PLA LIGNIN BLENDS

Oihana Gordobil, Itziar Egüés, Rodrigo Llano-Ponte, Jalel Labidi

Chemical and Environmental Engineering Department, University of the Basque Country, Plaza Europa, 1, 20018, Donostia-San Sebastián, Spain
**E-mail: jalel.labidi@ehu.es, tel.:+34-943017178; fax: +34-943017140*

ABSTRACT

Commercial alkali lignin (CL) and lignin extracted from almond shells by organosolv process (OL) were used for the preparation of blends with poly(lactic acid) (PLA) with different percentages (0.5,1,5,10 and 20%) by extrusion method. Both lignins were acetylated to improve their compatibility with PLA. PLA/acetylated lignin blends exhibited greater compatibility than non-acetylated PLA/lignin. Characterization of lignins has been performed using HPLC, FT-IR, GPC, DSC and TGA. All lignins showed high purity. Acetylated lignins had lower T_g and higher thermal stability than original lignins. Thermal and mechanical properties of different blends were investigated. Lignin content increased the thermal stability of PLA but does not favour the crystallization of PLA. Maximum strength decreased with high percentages of originals lignins. However, PLA/acetylated lignin blends remains fairly constant, even at high percentages. In all cases, the elongation at break was increased.

I. INTRODUCTION

Lignin is the second most abundant biopolymer on earth. It confers mechanical support of the plant and also provides rigidity, internal transport of water, nutrients and protection against attack by microorganisms [1]. The chemical structure of lignin is difficult to define because its structure and properties are largely related to isolation process and the types of sources used for its extraction. Generally, is an amorphous polyphenolic macromolecule which is composed of a large number of polar functional groups [2]. Commercially, lignin is a by-product mainly obtained from the pulp and paper industry. Most of the raw material is burnt as an energy source, although it can offer many other added value uses. Some papers described the efficiency of lignin as flame retardant additive [3]. Also, lignin is utilized as a stabilizer (antioxidant) for plastics [4]. Other authors have found that lignin has an important influence on the thermal behaviour in different composites [5]. Furthermore, lignin has been investigated as compatibilizer between natural fibers and polymer matrix [6, 7]. The effective use of lignin in blends with various synthetic polymers such as poly(propylene) [8], poly(ethylene terephthalate) [3], poly(vinyl alcohol), poly(ethylene oxide) [4], polystyrene [9], low-density polyethylene and linear low density polyethylene [10] has been also reported in literature. However, the environmental concerns and a shortage of petroleum resources have driven efforts on the preparation of bioplastics made from renewable materials. Several works have been reported about biopolymer/lignin blends. Some authors showed that the addition of lignin into thermoplastic starch matrix (TPS), improved mechanical properties, increasing the tensile strength. Thermal stability also increased and a reduction of moisture absorption was achieved [11]. Biocomposites of (3-hydroxybutyrate) (PHB) and acetylated lignin were prepared by other authors, in this case the decrease of PHB crystallization rate and the increase of thermal stability were observed [5]. This study was focused on the obtaining of composites formed by PLA and lignin as filler. In this research, blends with different percentages of lignin were prepared by extrusion method. Two kinds of lignin were used, commercial alkaline lignin and the lignin extracted from natural resources such as almond shells. Both lignins were acetylated to increase lignin affinity with PLA. The object of this study was to evaluate the effect of lignin addition in PLA thermal and mechanical properties.

II. EXPERIMENTAL

Lignin extraction and acetylation

Two different lignins were used. One was Commercial alkaline lignin and was supplied by Sigma ALDRICH®. The other was extracted from almond shells (Klason lignin 52.6±3.7, Celluloses 41.3±2.2 and hemicelluloses 8.6±0.8). Milled almond shells were treated with a mixture of ethanol-water (70 wt%). The treatment was carried out at 180 ºC for 90 min and the solid to liquid ratio was 1:6 (w/w).

Dissolved lignin was isolated by precipitation. Then was filtered and was dried at 50ºC. Each lignin was chemically modified by the esterification of its hydroxyl groups in order to enhance the interaction with PLA in the composite. Dry lignin samples (1.00 g) were dispersed in formamide (25 mL) about 3 h, until complete solubilization. Pyridine (40 mL) was added, followed by acetic acid anhydride (6.6 mL). After stirring at room temperature for 3 h, another portion of acetic anhydride (6.6 mL) was added, followed by the same amount after another 3 h. After 30 h, the viscous dark solution was poured into 1.3 L of 2% ice-cold hydrochloric acid. The precipitate was filtered on a buchner funnel with filter paper and washed with excess (0.5 L) deionized water and 0.5 L diethyl-ether. The samples were then dried at 50ºC.

Preparation of blends by extrusion

An extruder THERMO HAAKE Minilab Rheomex CTW5 model with double screw (109.5mm) was used for the preparation of mixtures. PLA (NatureWorks®PLA Polymer 3051D) was from NatureWorks LCC. Process conditions were the same for all blends, 165 ºC, at rate 25 min^{-1} and recirculation time was 30 min, optimum conditions previously determined for successful mixing of the materials. The blends are made using PLA as matrix with different percentages of nonacetylated and acetylated lignin (0.5, 1, 5, 10, 20%).

III. RESULTS AND DISCUSSION

Results of acidic insoluble lignin and sugars content and the values of weight average (M_w), number average (M_n) and polydispersity index (M_w/M_n) of unmodified and acetylated lignins are presented in Table 1. All the used lignins for blends elaboration, both modified and non-acetylated, showed high purity (>80%) with low quantities of sugars (0.3-3.8%). In both cases, acetylated lignins reflected increased purity and a reduction of sugar content. Unmodified lignins presented a little more high weight average than acetylated lignins. This may be affected by the loss of hemicellulose sugars in the acetylation process. Thermal properties of different lignins were analyzed by DSC and TGA in order to kwon the change in glass transition temperature and thermal stability. The obtained results are shown in Table 1. In both cases, a decrease in the glass transition temperature of the acetylated lignins with respect to unmodified lignins can be appreciated. After acetylation process, hydroxyl groups were replaced by ester substituent. Thus, reduce the number of hydrogen bonding and lead an increased free volume in the molecule and thus the mobility of the chains [12]. The results of TGA showed that both unmodified lignins had a small weight loss (1-4 %) below 100 ºC due to gradual evaporation of moisture, however, acetylated samples did not show any weight loss due to moisture. The initial degradation temperature corresponding to 5% weight loss ($T_{5\%}$) of both acetylated lignins is marked higher than unmodified lignins. The main degradation step occurs in the temperature range between 300-500ºC, and it is associated with the fragmentation of inter-units linkage [5]. Also, it can be observed an improvement in the thermal stability of acetylated lignins with respect unmodified lignins, appreciating further improvement in the case of acetylated organosolv lignin.

Table 1. Lignin purity analysis and weight average (M_w), number average (M_n) and polydispersity index (M_w/M_n) of different lignins and thermal properties.

	CL	**ACL**	**OL**	**AOL**
Klason Lignin %	82.6	88	81.4	90.2
Total Sugars %	1.2	0.3	3.8	0.7
Xylose	1	0.3	3.6	0.7
Arabinose	0.2	-	-	-
Glucose	-	-	0.1	-
M_n	1129	1598	1953	2409
M_w	10324	9295	16167	14974
M_w/M_n	9.1	5.8	8.3	6.2
T_g	158	127	144	132
$T_{5\%}$	259	266	182	297
T_{max}	365	182	380	395
Char Residue %	52	297	36	42

In the case of thermal properties of blends, TGA was used to know how affected lignin addition on thermal stability of PLA and DSC was also used to study the effect of lignin on the crystallization and melting behaviour of blends. The results are presented in Table 1. Addition of different lignins increases the thermal stability of the PLA, all the blends, showed higher degradation onset and maximum decomposition temperature than PLA. The pure PLA exhibited a T_g at 59.2 ºC and a melting temperature (T_m) around 146 ºC. Crystallinity of PLA was 35.9%, and crystallization temperature (T_c) was around 106 ºC. Similar results were obtained by other authors [13]. No significant change in glass transition temperature (T_g) of the samples was found. As it can be observed, PLA/lignin blends presented an increase in cold crystallization and melting temperatures. The normalized heat of fusion decreases with lignin addition in the blends. This behaviour may point to a lower nucleation density, then to the formation of poorer and fewer crystals. The introduction of lignin (amorphous in nature) affected the interactions among the PLA chains. Tensile tests have been performed to study the different lignins effect on mechanical properties of PLA. Mechanical properties of blends with different percentages are showed in Figure 1. The maximum strain was not severely affected by the low percentages (0.5-1%) of unmodified lignin, mainly in the case of organosolv lignin. However, at percentages greater than 5%, the maximum strain decreased with increasing lignin content, especially in blends formed by PLA and commercial lignin. Other study in which was elaborated a blend of PLA / unmodified commercial lignin by similar methods were also observed a decrease in the stress at percentages of 5% and 10% [11]. In the case of blends with acetylated lignin, both showed an improvement respect to composites with unmodified lignin, particularly, at high percentages. Moreover, the elongation at break decreased upon the addition of high percentages of unmodified lignin, but blends with low content of unmodified lignin presented an improvement compared to PLA. Furthermore, have seen an increase in the deformation in all blends blended with acetylated lignin. The improvement in ductility on compatibilization can be attributed to both esterification as esters act like internal plasticizers [14]. Other author [13] also demonstrated a slight increase in the deformation of films formed with starch and lignin. The Young's modulus shows a slight decrease in all cases although the addition of acetylated lignin at high percentages (20%) enhanced these properties.

Table 2. Thermal properties of blends containing 5% of unmodified and acetylated lignins.

	$T_{5\%}$	T_{max}	Char Residue %	T_g (ºC)	T_c (ºC)	T_m (ºC)	ΔH_m (J/g)	ΔH_c (J/g)	*Xc*
PLA	264	314	7.5	59.2	106.4	146.5	33.4	32.0	35.9
CL5	337	367	8.6	59.3	120.2	149.5	31.4	30.5	35.6
ACL5	325	360	9.5	59.8	124.5	150.5	25.3	24.0	28.7
OL5	335	365	9.7	59.8	123.2	150.5	26.4	26.5	29.9
AOL5	318	365	7.3	59.5	123.0	150.1	27.0	26.8	30.6

Figure 1. Mechanical properties of PLA and blends.

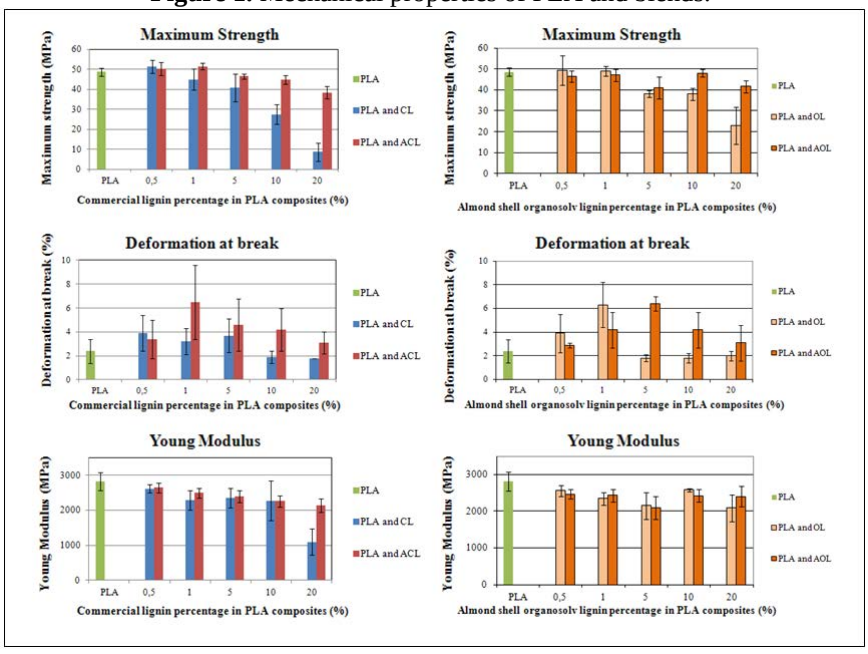

IV. CONCLUSIONS

In this work two different lignins were used, commercial alkaline lignin and lignin extracted from almond shells. Original and acetylated lignins were used as PLA filler. Acetylation process of lignins resulted successful with high yield and besides improvement in the compatibility between the two components of the mixture was achieved. All lignins presented high purity with very low content of polysaccharides. Acetylated lignins have lower Tg and higher thermal stability than original lignins. The addition of lignin greatly improved the thermal stability of PLA but PLA crystallization behaviour is not favoured. Mechanical properties of PLA worsen with the addition of high percentages of lignin; however, PLA/acetylated lignin blends properties remain similar to those of pure PLA. In all cases, the elongation at break was increased.

V. ACKNOWLEDGEMENT

The authors are grateful for the financial support received from the Department of Education, Universities and Investigation of the Basque Government (Grant of I.E., ref BFI09.164), Diputacíon de Gipuzkoa and Saiotek program.

VI. REFERENCES

[1] Jia-Long, W.; Bai-Liang, X.: Feng, X.; Run-Cang, S.; André, P. Unmasking the structural features and property of lignin from bamboo. *Ind Crop Prod*. **2013**, *42*, 332–343.

[2] Saswata, S.; Manjusri, M.; Amar, K.M. Enhanced properties of lignin-based biodegradable polymer composites using injection moulding process. *Composites: Part A*. **2011**, *42*, 1710–1718.

[3] Maurizio, C.; Fabio, B. Supermolecular structure and thermal properties of poly(ethylene terephthalate)/lignin composites. *Compos Sci Technol*. **2007**, *67*, 3151– 3157.

[4] John, F.K.; Satoshi, K. Lignin-based polymer blends: analysis of intermolecular interactions in lignin–synthetic polymer blends. *Composites: Part A*. **2004**, *35*, 395–400.

[5] Fabio, B.; Maurizio, C.; Adriana, C.; Graziano, E.; Marco, O.; Luca, Z. Effect of lignoderivatives on thermal properties and degradation behaviour of poly(3-hydroxybutyrate)-based biocomposites. *Polym Degrad Stab.* **2012**, *97*, 1979-1987.

[6] Nina, G. Application of lignin as natural adhesion promoter in cotton fibrereinforced poly(lactic acid) (PLA) composites. *J Mater Sc.i* **2008**, *43*, 5222–5229.

[7] Andréia, A.M.; José Augusto, M.A.; Bruno, Z.L.; Rodrigo, M.; Suzan, A.C.; Sílvia H.P.B. Lignin as additive in polypropylene/coir composites: Thermal, mechanical and morphological properties. *Carbohyd Polym*. **2012**, *87*, 2563– 2568.

[8] Charlyse, P.; Patrice, D.; Bernard, C.; Luc, A.; N, B. Antioxidant properties of lignin in polypropylene. *Polym Degrad Stab*. **2003**, *81*, 9–18.

[9] Charlyse, P.; Stéphanie, B.; Bernard, C.; Patrice, D. Lignin–polymer blends: evaluation of compatibility by image analysis. *C. R. Biologies*. **2004**, *327*, 935–943.

[10] Alexy, P.; Kosiková, B.; Podstránska, G. The effect of blending lignin with polyethylene and polypropylene on physical properties. *Polym*. **2000**, *41*, 4901–4908.

[11] Kaewta, K.; Jariya, T. Effect of kraft lignin and esterified lignin on the properties of thermoplastic starch. *Mater Design*. **2013**, *49*, 701–704.

[12] J, L.; P, P.; S, U. Structure and thermal properties of lignins: characterization by infrared spectroscopy and differential scanning calorimetry. *J Chil Chem Soc*. **2009**, *54*, 460-463.

[13] S, B., C, L.; B, M. Use of kraft lignin as filler for starch films. *Polym Degrad Stab*. **1998**, *59*, 213-211.

[14] K, W.; S, B.; R, S. Structural Transformation of Miscanthus × giganteus Lignin Fractionated under Mild Formosolv, Basic Organosolv, and Cellulolytic Enzyme Conditions. *J Agric food chem*. **2012,** *60*, 144–152.

HIGH YIELD COOKING OF WOOD CHIPS WITH SULPHITE IN NEUTRAL MEDIA

Saara Hanhikoski[1]*, Antero Varhimo[1], Klaus Niemelä[1], Elina Warsta[2], Tapani Vuorinen [2]

[1] VTT Technical Research Centre of Finland, P.O. Box 1000, 02044 VTT, Finland; [2] Aalto University, School of Chemical Technology, Department of Forest Products Technology, P.O. Box 16300, 00076 Aalto, Finland
*(*saara.hanhikoski@vtt.fi)*

ABSTRACT

The cost of wood raw material is one of the key factors affecting the competitiveness of pulp and paper industry. The efficient use of wood raw material and dissolved wood components is thus essential. The existing chemical pulping technologies, kraft and sulphite, are operating in severe conditions, which leads to the loss of at least part of the valuable wood components, cellulose, hemicelluloses, and lignin. The sulphite cooking carried out in neutral conditions offers technology, which preserves cellulose and hemicelluloses in high yield. Lignin is dissolved as lignosulphonate, a commercial by-product.

In this paper we present results from cooking of wood chips with sodium sulphite solution under neutral conditions. Sulphite (SO_3^{2-}) and bisulphite (HSO_3^-) are strong nucleophiles, which are able to depolymerize, demethylate and sulphonate lignin. The neutral conditions result in high carbohydrate yield, as the acid and base catalysed carbohydrate degradation reactions are slow.

Pine wood chips were exposed to neutral sodium sulphite liquor (pH 6-9) boosted by anthraquinone (AQ) at high temperature of 180 °C. This treatment resulted in high polysaccharide yield and complete defibration of wood raw material at high residual lignin content of 5-11%. The brightness of the pulp was high, over 60% ISO, which may be an advantage in pulp bleaching.

The carbohydrate yield of pulps produced at neutral conditions was high, at kappa number 60 over 7% point higher compared to the kraft pulp at the same kappa number. Especially, the retention of glucomannan seemed to be responsible for the high yield. High contents of sulphonic and carboxylic acid groups were shown by conductometric titration. It seemed to be possible to affect the degree of sulphonation of the pulp by varying the process conditions. Resulting from a high temperature and a long cooking time the viscosity of the pulp was found poor.

It is possible to affect the delignification degree, gained yield and thus the fibre and polymer properties of pulp obtained, by modifying neutral sulphite cooking conditions. Carbohydrates consisting mainly of cellulose and glucomannan isolated from wood in high yield offers a potential platform for the development of many types of fibres, chemicals and polymers. However, the form and properties of dissolved lignosulphonate and sugars will need further research. So far these results give an encouraging base for future research to explore the potential of the neutral sulphite biorefinery concept.

I. INTRODUCTION

Sulphonation is the most important reaction of lignin in neutral sulphite pulping. Demethylation occurs also to some extent introducing new phenolic hydroxyl groups, and thus new reactive sites of the lignin are formed [1]. Anthraquinone is added to improve rate and selectivity of delignification in neutral sulphite pulps. Sulphite is capable to act as a reducing agent for AQ, and thus it can act as a catalyst at pH at least as low as 7 [2].

Softwood sulphite pulps produced in neutral or slightly alkaline conditions are noticed to improve the carbohydrate yield. This yield gain is thought to result from stabilization of softwood glucomannan. It is suggested that the cleavage of acetyl units allows the adsorption of glucomannan on the cellulose protecting glucomannan against the acid and base catalysed carbohydrate degradation reactions [3]. The advantage to gain high yield has been used in two-stage sulphite pulping processes such as Stora process [4]. However, single stage neutral sulphite cooking has not existed as its own process, since cooking at neutral conditions is slow and requires high cooking temperature and long cooking time.

The results presented in this paper concentrate to describe the effect of Na_2SO_3 charge and AQ on the total pulp yield and the content of sulphonic and carboxylic acid groups. In addition, the effect of initial pH on the total yield and chemical composition of pulps are presented.

II. EXPERIMENTAL

Cooking trials were executed in 1-litre air heated autoclaves at 180 °C for 240 min. In addition, a larger scale experiment was performed in a 15-litre digester at the same conditions. Screened pine wood chips were used as a raw material. The cooking liquor consisted of solid Na_2SO_3 dissolved in deionized water and the initial pH of the liquor was adjusted with H_2SO_4. Liquor-to-wood ratio varied from 3.5 to 3.75. The autoclaves were pressurized with N_2 gas into 5 bar before the temperature rise. After the cooking the spent liquor pH was measured and the recovered chips were defibrated with a British disintegrator, and screened in a TAP03 laboratory screen with 0.15 mm slots.

The total pulp yield was determined using the gravimetric method. Kappa number according to ISO 302:2004, brightness according to ISO 2470 and viscosity according to ISO 5351:2004 were analysed from the laboratory sheets. The amounts of sulphonic and carboxylic acid groups in pulps were estimated by analysing the total acidic groups using the conductometric titration method (SCAN-CM 65:02). In addition, the lignin content and carbohydrate composition of the pulps produced at different initial pH were analysed by HPAEC (Dionex ICS-5000) after acid hydrolysis using the laboratory procedure of VTT.

III. RESULTS AND DISCUSSION

Neutral sulphite cooking produced pulps with the total yield of 52-65% at a residual lignin content of 5-11%. Regardless of the high yield, the screenings remained under 3%. The brightness of the pulps was relatively high, between 59-66% ISO. Viscosities were between 570-840 ml/g. The effect of chemical charge and AQ on the pulp yield and the content of acid groups and the effect of initial pH on the chemical compositions of pulps are discussed below.

The effect of Na_2SO_3 charge and AQ

The effect of Na_2SO_3 charge and AQ on total yield of pulps as a function of kappa number is compared with the conventional kraft cooks in **Figure 1**. The yield advantage of neutral sulphite pulps is 5-10% point at the same kappa number level compared to the conventional kraft pulps. The higher Na_2SO_3 charge clearly promoted delignification, which is seen as linearly decreasing kappa number when the higher amount of Na_2SO_3 is added. AQ is participating in both delignification and preservation of the carbohydrates in the neutral sulphite cooks. The cooks carried out in the absence of AQ remain in higher kappa number level and the total yield is at the same level with the cooks where AQ is used.

The larger scale experiment produced pulp with the highest total yield of 64.6% at kappa number 59. Chip steaming was possible to execute only during the large scale experiment, which apparently improved impregnation of cooking chemicals and thus led to a higher pulp yield.

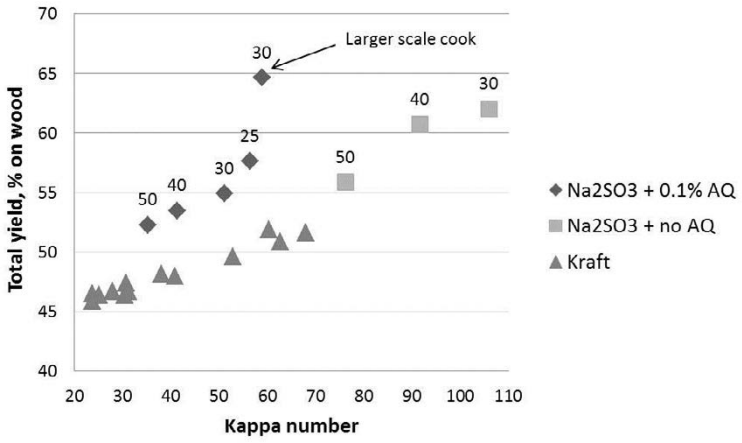

Figure 1. Total yield (% on wood) as a function of kappa number of neutral sulphite pulps compared with the conventional kraft pulps produced from the same pine raw material. Neutral sulphite cooks were carried out at 180 °C for 240 min at initial pH 8 with varying Na_2SO_3 and AQ charges.

The content of sulphonic and carboxylic acid groups in neutral sulphite pulps produced with varying Na_2SO_3 and AQ charges is shown in **Figure 2**. It is notable that the content of sulphonic acid groups is at the same level in pulps produced with and without AQ though the differences in kappa numbers are considerable.

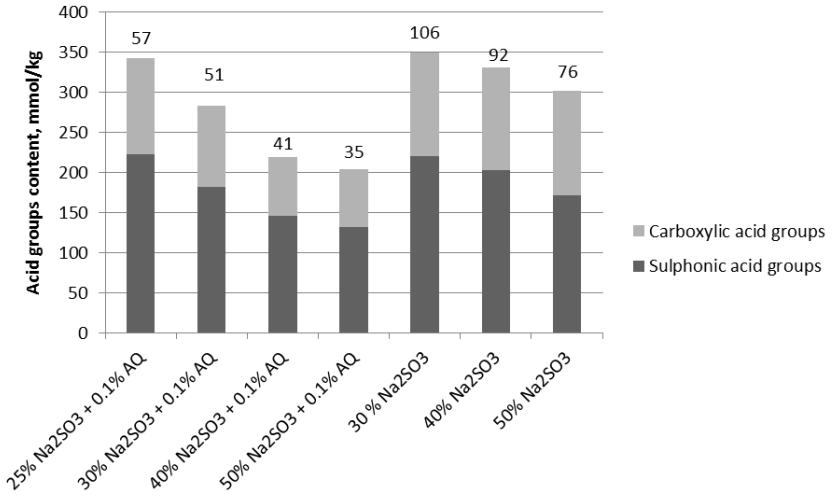

Figure 2. The sulphonic and carboxylic acid group contents of neutral sulphite pulps cooked at 180 °C for 240 min at initial pH 8 with varying Na_2SO_3 and AQ charges. The kappa numbers of pulps are marked above the columns.

The effect of initial pH

The initial pH had a significant effect on the cooking selectivity as shown in **Figure 3**. Kappa number decreased from 63 to 48 while the initial pH was increased from 7.5 to 9 while the total yield remained at the same level between 55-60%.

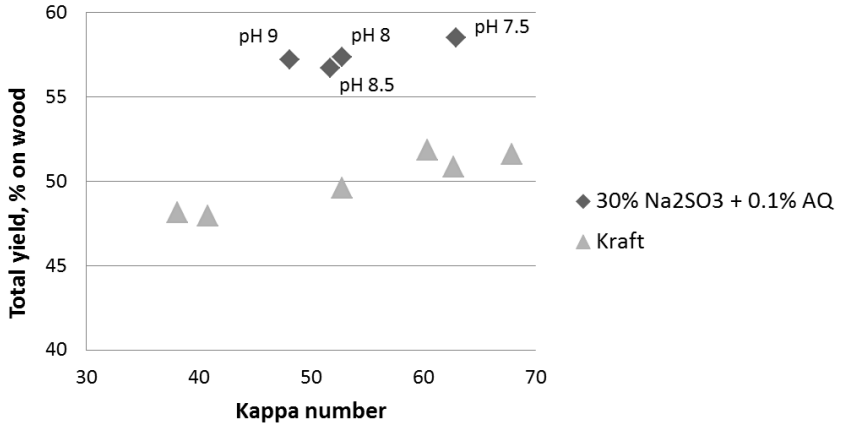

Figure 3. Total yield (% on wood) as a function of kappa number of neutral sulphite pulps compared with the conventional kraft pulps produced from the same pine raw material. Neutral sulphite cooks were carried out at 180 °C for 240 min with 30% Na_2SO_3 and 0.1% AQ charges.

The chemical composition of neutral sulphite pulps produced by varying the initial pH is shown in **Figure 4**. Approximately 7% of the total pulp yield consisted of glucomannan. Around 4% point unaccountable material was excluded from the results in **Figure 4**. However, this material probably consists of polysaccharides.

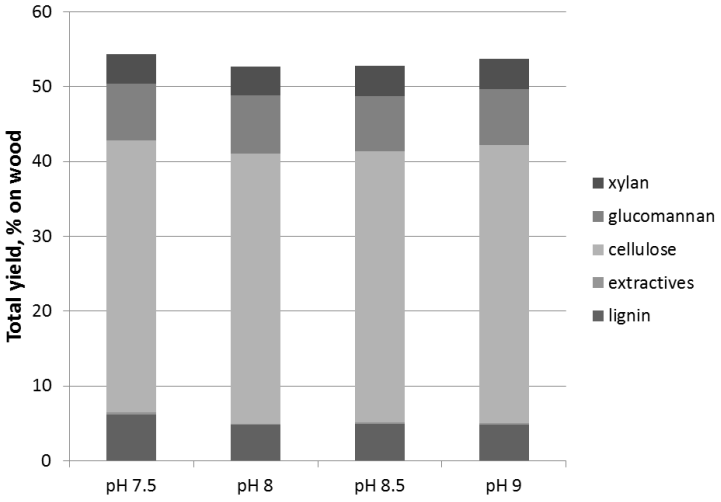

Figure 4. The chemical composition of neutral sulphite pulps cooked at 180 °C for 240 min, with 30% Na_2SO_3 and 0.1% AQ charge using different initial pH.

IV. CONCLUSIONS

Neutral sulphite cooks executed at 180 °C for 240 min produced high yield pulps at high residual lignin content of 5-11%. Compared to the conventional kraft pulps at the same kappa number level the yield advantage of neutral sulphite pulps was 5-10% point higher. Delignification was improved using higher chemical charge and AQ, which was seen as decreasing kappa number from 57 to 35 when Na_2SO_3 charge was increased from 25% to 50%. The content of sulphonic and carboxylic acid groups in neutral sulphite pulps showed that AQ may also improve the sulphonation reactions. The initial pH seemed to have the major contribution to cooking selectivity and carbohydrate retention. The total yield remained at the same level while kappa number decreased from 63 to 48.

V. ACKNOWLEDGEMENT

This work has been partly funded by TEKES and FIBIC in EffFibre program of FIBIC.

VI. REFERENCES

[1] Gellerstedt, G. The reactions of lignin during sulfite pulping. *Svensk Papperstidn.* **1976**, *79*, 537-543.

[2] Suckling, I.D. Enhanced cleavage of β-aryl ether bonds in lignin model compounds during sulphite-anthraquinone pulping. *J. Wood Chem. Technol.* **1988**, *8*, 43-71.

[3] Annergren, G.E; Rydholm, S.V. On the stabilization of glucomannan in the pulping processes. *Svensk Papperstidn.* **1960**, *63*, 591-600.

[4] Lagergren, S. The Stora pulping process and its implications for European paper makers. *Svensk Papperstidn.* **1964**, *67*, 238-243.

IMMUNOLOCALIZATION OF ARABINOXYLAN IN WHEAT BRAN TO MONITOR THE EFFECT OF DIFFERENT TREATMENTS

Hell J.[1,2,3], Donaldson L.[4], Michlmayr H.[2,3], Kneifel W.[2,3], Rosenau T.[1], Potthast A.[1], Böhmdorfer S.[1]*

*[1]Department of Chemistry, University of Natural Resources and Life Sciences, Konrad Lorenz Straße 24, 3430 Tulln, Austria; [2]Department of Food Science and Technology, University of Natural Resources and Life Sciences, Muthgasse 18, Vienna, Austria;[3]Christian Doppler Laboratory for Innovative Bran Biorefinery; [4]Scion, Rotorua, New Zealand; *stefan.boehmdorfer@boku.ac.at*

ABSTRACT

There is a multitude of techniques available for the selective extraction of arabinoxylan from wheat bran, but comparisons between these methods are scarce. We evaluated a broad range of treatments, such as lye treatment, ball-milling, fermentation, treatment with xylanase and a combination of esterase and xylanase. Chemical analysis was corroborated by immunolocalization of arabinoxylan by confocal microscopy, which has proven valuable in the assessment of cell-structural changes.

Extensive ball-milling showed the best selectivity. Lye treatment gave the highest yields, but did so at the cost of specificity. Fermentative and enzymatic treatments were hampered by coextraction.

I. INTRODUCTION

Wheat bran, the outer layer of the wheat kernel, is an abundant by-product of white flour production. Given the bran´s high content of nutritionally valuable and technologically desirable compounds, it is gaining interest as a raw material for biorefineries [1]. However, these valuable constituents cannot be accessed directly, which makes pretreatment imperative to down-stream processing. The pretreatment has to be chosen and adjusted according to the objective of fractionation [2].

With about 32% of total dry matter, arabinoxylan represents the most abundant valuable in wheat bran [3]. It is a dietary fiber that exhibits both nutritional and rheological benefits [4]. Approaches to extract arabinoxylan range from chemical treatments, such as lye-based or oxidizer-assisted, [5-7] over enzymatic treatments [8] to mechanical treatments, such as ball-milling [9]. However, few studies have been undertaken to relate the effectiveness of different treatments. Whether the aim is to isolate arabinoxylan or to remove it in the purification of other target compounds, tracking its course is mandatory.

Arabinoxylan can be quantified indirectly as monosaccharides after acidic cleavage of the polysaccharide. The favored method is methanolysis, routinely combined with GC-MS or GC-FID analysis [10, 11]. The information gained, however, is limited in the way that it does not assess the spatial distribution among cell wall layers and is impartial to cell integrity.

Adopted from antibody-markers of polysaccharides in wood, fluorescent-labeled monoclonal antibodies against arabinoxylan epitopes have been applied to wheat bran in order to get a comparative visual reading of the effects of various treatments and processes on the arabinoxylan distribution on a cellular level [12, 13]. Samples were analyzed for residual arabinoxylan and subjected to an enzymatic peeling in order to obtain a cross-sectional profile of polysaccharide distribution. Thereby, the liberation of arabinoxylan and changes in its extractability were evaluated. Treatments were lye treatment, ball-milling, fermentation with *Lactobacillus plantarum* and treatment with xylanase and a combination of esterase and xylanase.

II. EXPERIMENTAL

Methanolysis

In order to remove mobilized arabinoxylan prior to methanolysis, 200 mg of bran sample were stirred in 10 mL water for 1 h, filtrated and washed twice with 10 mL of water before drying *in vacuo* at room temperature.

Methanolysis was performed according to Sundberg et al. [10]. For silylation, dried samples after methanolysis were left to equilibrate in 400 µL of pyridine for 1 h. 200 µL of BSTFA (N,O-bis(trimethylsilyl)-trifluoroacetamide) containing 10% TMCS (trimethylchlorosilane) were added and the samples kept at 70 °C for 2 h. Samples were diluted with 600 µL of ethyl acetate, filtered through a 0.45 µm PTFE syringe filter and analyzed by GC-MS.

GC-MS: 0.2 µL of silylated sample was injected (260 °C, splitless) on a 30 m/0.25 mm HP-5 capillary (film thickness 0.25 µm) in an Agilent 6890N Series GC system with an Agilent 5973 Series mass-selective detector. The temperature program was 140 °C (1 min); 4 °C min^{-1} to 210 °C (0 min); 30 °C min^{-1} to 260 °C (5 min). The carrier gas was helium (0.9 ml min^{-1}, constant flow). Detector conditions were 70 eV with a scan range from 45

to 950 Da. Data was acquired and processed with MSD Chemstation E.2.01.1177 software from Agilent Technologies.

Enzymatic peeling
The procedure for enzymatic peeling was adopted from Sjöberg et al. [14] with modifications to suit wheat bran polysaccharides. 20 mg of washed sample were stirred in a sodium acetate buffer adjusted to pH 4 at 40 °C for 1 h prior to addition of 100 µL of the internal standard sorbitol (20 mg/mL) and 700 µL of enzyme mix. The suspension was kept at 40 °C and 0.2 mL aliquots were taken after 5, 10, 30, 60 and 120 minutes. Aliquots were filtered through a 0.45 µM PTFE filter and incubated for 48 h at 40 °C for complete enzymatic hydrolysis. Samples were used for HPLC in a dilution of 1:10. A blank was recorded to correct for residual sugars in the enzyme mix.
Sugars were quantified on a DionexUltiMate 3000 HPLC system (Dionex, Sunnyvale, CA, USA) equipped with a Phenomenex 300x7.8 mm Rezex™ ROA-Organic Acid H+ (8%) column kept at 80 °C (Phenomenex, Aschaffenburg, Germany) and a HP 1100 Series G1362A RID refractive index detector (Hewlett-Packard, Palo Alto, CA, USA). The mobile phase was 5 mM sulfuric acid at a flow of 0.4 mL/min. Data was recorded with DionexChromeleon 6.8.

Immunolocalization
Samples were prepared for immunolocalization by pouring the wheat bran flakes/powder into molten paraffin wax and letting it harden. The wax was trimmed to blocks and chafed with a microtome so that cross sections of wheat bran were located at the surface.
Immunolocalization of arabinoxylan was performed by placing a droplet of a 1:20 dilution of primary rat monoclonal antibody hybridoma cell culture supernatant LM11 (PlantProbes, Leeds, UK) in 0.1 M phosphate-buffered saline (PBS, pH 7, containing 1% w/v acetylated bovine serum albumin as a blocking agent and 5 mM sodium azide) on a wax block so that it covered its surface over night at 4 °C. Wax blocks were rinsed five times with PBS and dried before being covered with a droplet of fluorescently labeled secondary antibody Alexa647 (goat anti-rat; Invitrogen, Paisley, UK) at a 1:100 dilution in PBS (20 µg/mL) for 2 h under light exclusion at room temperature. Blocks were washed five times with PBS, mounted in SlowFade at pH 9 (Molecular Probes Inc., Eugene, Oregon, USA) and measured on the same day.
Confocal laser scanning microscopy was performed on a Leica SP5 MA II. For autofluorescence, excitation was 488 nm and 561 nm and emission was recorded at 500-535 nm and 570-620 nm. The fluorescent antibody was excited at 633 nm and recorded at 650-750 nm.

III. RESULTS AND DISCUSSION

Figure 1 shows results for enzymatic peeling, f**igure 2** for immunolocalization of arabinoxylan.
Percent values are given relative to untreated wheat bran and refer to residual samples after washing, i.e. negative values indicate an increase in solubilization.

Lye treatment
Despite an increase of 88% in total solubles compared to untreated wheat bran, average amounts of xylose-based polysaccharides (-30%) and high amounts of glucose (-61%) were solubilized. The seeming increase in arabinose (+25%) is due to the removal of other components, but points to a preferred extraction of non- or lowly-substituted xylan over highly branched xylan. The residual bran was only incompletely depleted of xylan-based polysaccharides. Immunolocalization revealed a thorough elimination of the aleurone layer as well as a swelling of the nucellar epidermis layer. The thick cell walls of the remaining outer layers of wheat bran are very resilient to enzymatic hydrolysis.

Ball-milling
Extensive ball-milling is known to cause fragmentation of arabinoxylan into oligosaccharides and thus to increase solubility [9]. 60 min of ball-milling increased overall solubility by 16% with a strong preference for xylan-based polysaccharides (-66%) over glucose (+28%). Consequently, we found very reduced concentrations of xylan upon the enzymatic profiling. The findings were substantiated by immunolocalization, which showed a complete disintegration of cell structures and a loose association of arabinoxylan to particles, implying ready extractability.

Fermentation with Lactobacillus plantarum
In addition to carbohydrates, *Lactobacillus plantarum* can also ferment protein [15]. Despite an increase in overall solubility of 40%, we also observed an increase of insoluble polysaccharides (arabinose +13%, xylose -2.5% and glucose +52%), which indicates that mainly protein and only small amounts of arabinoxylan have been solubilized to concentrate the remaining compounds. *Lactobacillus plantarum* showed high amounts of

accessible arabinoxylan throughout the layers, with the largest total amount of xylose among all samples being released. Immunolocalization exposed arabinoxylan thinly concentrated in the aleurone layer comparable to untreated bran, making it highly accessible to enzymatic attack.

Xylanase and esterase/xylanase treatment

Xylanase treatment increased total solubility by 30%. Arabinose moieties were increased by 3%, xylose reduced by 8% and glucose increased by 42% in residual material. The addition of esterase brought overall solubility to 40%. The synergistic effect is presumed to be due to esterase being able to cleave ester bonds between arabinoxylan and phenolics as well as between two arabinoxylan chains, which can be ester-linked through ferulic acid at arabinose side chains. This gives xylanase access to more substrate for depolymerization [16]. However, the fact that residual polysaccharides showed the same trend (arabinose -2%, xylose -13% and glucose +26%) implied a concomitant increase in extraction of other compounds. Both treatments showed a severely reduced concentration of xylose moieties throughout all layers accessible to enzymatic peeling. As revealed by immunolocalization, xylanase treatment effected a pronounced swelling of aleurone cell walls as well as damage to inward-facing cell walls so that the distribution of arabinoxylan was concentrated towards the nucellar epidermis. This change can be expected to render arabinoxylan less accessible to further enzymatic attack. As for the combination of esterase and xylanase, cell walls were swollen, perforated or even partially disintegrated. Arabinoxylan was distributed in broader strokes and smaller intensity across the aleurone layer lending reason to the reduced concentration observed in enzymatic peeling.

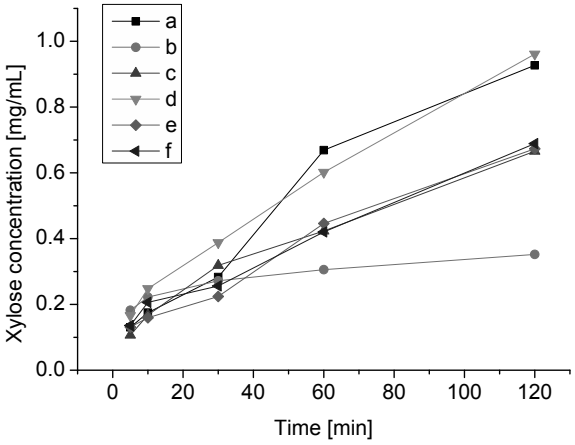

Figure 1. Enzymatic peeling. Concentration of released xylose over time for: (a) untreated wheat bran, (b) lye treatment, (c) ball-milling, (d) *Lactobacillus plantarum* fermentation, (e) xylanase treatment, (f) esterase + xylanase treatment

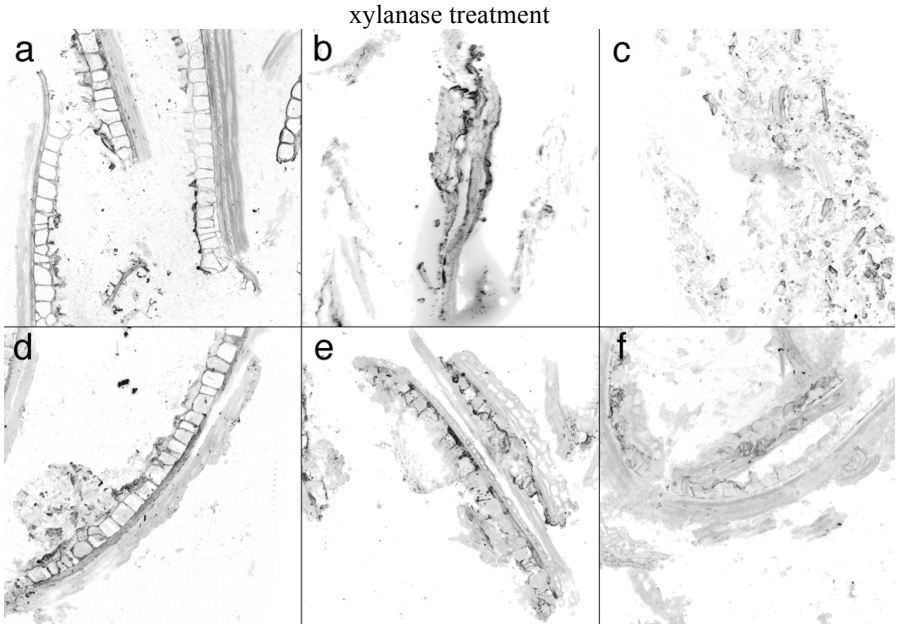

Figure 2. Confocal fluorescent images of arabinoxylan localization shown in black on white. (a) Untreated wheat bran, (b) lye treatment, (c) ball-milling, (d) *Lactobacillus plantarum* fermentation, (e) xylanase treatment, (f) esterase + xylanase treatment

IV. CONCLUSIONS

The application of immunolocalization augments the chemical analysis of the effects of pretreatments on arabinoxylan. As a complementary method it is very helpful at assessing pretreatment strategies.
Lye treatment solubilized by far the highest percentage of wheat bran, but did so at the cost of substantial coextraction of other compounds and, given its severe conditions, probably caused degradation of other valuables as well as formation of inhibitory and hazardous substances.
Enzymatic extraction, fermentation or both showed little selectivity for arabinoxylan and mostly influenced degrees of overall solubilization. Enzymatic removal of arabinoxylan is ostensibly always concomitant with extraction of other cell compounds. Treatment with *Lactobacillus plantarum* even showed a strong preference for non-carbohydrate material.
Extensive ball-milling exhibited the most promising results with a strong specificity for xylan-based polysaccharides. Since it applies mere mechanical force, the results point towards a less rigid implementation of arabinoxylan into the cell wall or a greater disposition for depolymerization as compared to cellulose.

V. ACKNOWLEDGEMENT

This work was supported by Bühler AG, Switzerland, GoodMills Group GmbH, Austria, and the Christian Doppler Forschungsgesellschaft, Austria (CD lab "Innovative wheat bran biorefinery").

VI. REFERENCES

[1] Apprich, S.; Tirpanalan, T.; Hell, J.; Reisinger, M.; Böhmdorfer, S.; Siebenhandl-Ehn, S.; Novalin, S.; Kneifel, W. Wheat bran-based biorefinery 2: Valorization of products. *LWT - Food Science and Technology*. **2014**, *56*, 222-231.
[2] Prückler, M.; Siebenhandl-Ehn, S.; Apprich, S.; Höltinger, S.; Haas, C.; Schmid, E.; Kneifel, W. Wheat bran-based biorefinery 1: Composition of wheat bran and strategies of functionalization. *LWT - Food Science and Technology*. **2014**, *56*, 211-221.
[3] Maes, C.; Delcour, J.A. Structural characterisation of water-extractable and water-unextractable arabinoxylans in wheat bran. *Journal of Cereal Science*. **2002**, *35*, 315-326.
[4] Bauer, J.L.; Harbaum-Piayda, B.; Stockmann, H.; Schwarz, K. Antioxidant activities of corn fiber and wheat bran and derived extracts. *Lwt-Food Science and Technology*. **2013**, *50*, 132-138.
[5] Sun, Y.L.; Cui, S.W.; Gu, X.H.; Zhang, J.M. Isolation and structural characterization of water unextractable arabinoxylans from Chinese black-grained wheat bran. *Carbohydrate Polymers*. **2011**, *85*, 615-621.
[6] Maes, C.; Delcour, J.A. Alkaline hydrogen peroxide extraction of wheat bran non-starch polysaccharides. *Journal of Cereal Science*. **2001**, *34*, 29-35.
[7] Bataillon, M.; Mathaly, P.; Cardinali, A.P.N.; Duchiron, F. Extraction and purification of arabinoxylan from destarched wheat bran in a pilot scale. *Industrial Crops and Products*. **1998**, *8*, 37-43.
[8] Swennen, K.; Courtin, C.M.; Lindemans, G.C.J.E.; Delcour, J.A. Large-scale production and characterisation of wheat bran arabinoxylooligosaccharides. *Journal of the Science of Food and Agriculture*. **2006**, *86*, 1722-1731.
[9] Van Craeyveld, V.; Holopainen, U.; Selinheimo, E.; Poutanen, K.; Delcour, J.A.; Courtin, C.M. Extensive dry ball milling of wheat and rye bran leads to in situ production of arabinoxylan oligosaccharides through nanoscale fragmentation. *J Agric Food Chem*. **2009**, *57*, 8467-73.
[10] Sundberg, A.; Sundberg, K.; Lillandt, C.; Holmbom, B. Determination of hemicelluloses and pectins in wood and pulp fibres by acid methanolysis and gas chromatography. *Nordic Pulp and Paper Research Journal*. **1996**, *11*, 216-219+226.
[11] Willför, S.; Pranovich, A.; Tamminen, T.; Puls, J.; Laine, C.; Suurnakki, A.; Saake, B.; Uotila, K.; Simolin, H.; Hemming, J.; Holmbom, B. Carbohydrate analysis of plant materials with uronic acid-containing polysaccharides-A comparison between different hydrolysis and subsequent chromatographic analytical techniques. *Industrial Crops and Products*. **2009**, *29*, 571-580.
[12] McCartney, L.; Marcus, S.E.; Knox, J.P. Monoclonal antibodies to plant cell wall xylans and arabinoxylans. *Journal of Histochemistry & Cytochemistry*. **2005**, *53*, 543-546.
[13] Donaldson, L.A. Immunocytochemistry of xylem cell wall. *New Zealand Journal of Forestry Science*. **2009**, *39*, 161-168.
[14] Sjöberg, J.; Potthast, A.; Rosenau, T.; Kosma, P.; Sixta, H. Cross-sectional analysis of the polysaccharide composition in Cellulosic fiber materials by enzymatic peeling/high-performance capillary zone electrophoresis. *Biomacromolecules*. **2005**, *6*, 3146-3151.
[15] Fadda, S.; Vildoza, M.J.; Vignolo, G. The Acidogenic Metabolism of Lactobacillus Plantarum Crl 681 Improves Sarcoplasmic Protein Hydrolysis during Meat Fermentation. *Journal of Muscle Foods*. **2010**, *21*, 545-556.
[16] Lewis, N.G.; Yamamoto, E. Lignin - Occurrence, Biogenesis and Biodegradation. *Annual Review of Plant Physiology and Plant Molecular Biology*. **1990**, *41*, 455-496.

REDUCTIVE TREATMENTS OF CELLULOSIC PULP AND PAPER FOR BETTER COLOR AND ALKALI STABLITY

Ute Henniges*, Thomas Rosenau, Antje Potthast

*Department of Chemistry, Division of Chemistry of Renewable Resources, Konrad Lorenz Straße 24, 3430 Tulln, BOKU – University of Natural Resources and Life Sciences, Vienna, Austria (*ute.henniges@boku.ac.at)*

ABSTRACT

An increased amount of oxidized cellulose functionalities, especially carbonyl groups, increases the susceptibility of cellulose towards chain scission and decreases brightness stability. Reductive treatment thus might be a suitable means to reduce the carbonyl content in cellulosics, and different protocols are available to chemically reduce carbonyls. Sodium borohydride ($NaBH_4$) was found to be very suitable for this purpose with regard to efficiency. However, aqueous borohydride solutions themselves generate an alkaline environment that is potentially harmful for oxidized cellulose. A treatment with this reagent would thus be only meaningful if the reduction proceeds faster than the competitive process of alkali-induced beta-elimination which causes cellulose chain degradation.
In the present work, the impact of reductive treatments was investigated on pure cellulose. The parameters molar mass and carbonyl group content as key parameters for the efficient reduction were evaluated. We were able to demonstrate that the reduction treatment is fast enough to avoid negative impact on the molar mass of cellulose, and to determine the extent of carbonyl group removal by $NaBH_4$.

I. INTRODUCTION

While the native and "ideal" cellulose molecule contains only one reducing end group, many oxidized functionalities are introduced by industrial processing into the cellulose molecule. Especially carbonyl groups are discussed in the context of stability of pulp towards natural aging and degradation reactions. Carbonyl groups increase the tendency of paper to turn yellow with age [1]. Depending on their type, carbonyl groups have a detrimental influence on brightness stability of the pulp. It was found that a combination of ketone and aldehyde groups in pulps impair brightness stability [2]. Next to their influence on brightness stability, carbonyl groups introduce reactive sites into the cellulose molecule where degradation processes, such as β-elimination, can attack and split the molecule, thus leading to significantly decreased molar mass, and, in the long run, to lower mechanical stability [3]. The increased sensitivity towards alkalinity has been linked to misleading results when determining the viscosity of cellulose as cellulose solvents such as cupriethylene diamine are strongly alkaline and will cause β-elimination in the pulps to investigate. This leads to an underestimation of the viscosity of the pulp [4].
There are various reduction treatments available to decrease the amount of carbonyl groups, the most frequently used one is sodium borohydride ($NaBH_4$). In the context of industrial pulp bleaching the interactions of reduction treatments and bleachability have been studied. The addition of $NaBH_4$ in small quantities during the alkali treatment of O_3-prebleached pulps resulted in higher bleaching degree and a better preservation of the degree of polymerisation of cellulose, compared with bleaching tests conducted in the absence of $NaBH_4$. The results are explained by a reduction of carbonyl groups present in the pulp by $NaBH_4$ resulting in stabilization of the polysaccharides against oxidative degradation [5,6]. The $NaBH_4$ assisted peroxide bleaching process of mechanical pulps (the so-called PR process) improves its bleaching efficiency and increases the brightness of pulps. The improvement of the PR process was assigned to the stabilization of transition metal ions, and to the reduction of carbonyl groups of lignin [7,8].
However, in oxygen-delignified eucalyptus Kraft pulps, the reduction of pulp with $NaBH_4$ under conditions for removing carbonyl groups had no impact on bleachability [9]. The same observation was made on stone groundwood pulp from spruce (*picea abies*), when the reduction treatment had no dramatic effect on the light-induced brightness reversion [10]. It was also assumed that carbonyl groups in sulfite pulps promote cellulose degradation during oxygen delignification. The addition of a catalytic quantity of $NaBH_4$ improved the process in terms of better pulp yield, viscosity, and strength properties [11]. Nevertheless, $NaBH_4$ is quite alkaline, and might damage oxidized cellulose.
In this study, different types of carbonyl groups introduced into pure cellulosic pulp, generally highly oxidized by purpose to study their efficiency, were submitted to $NaBH_4$ treatment at different conditions, such as varying reaction time, different pH levels, and concentrations of the reducing agent.

II. EXPERIMENTAL

Cellulose analysis
General molar mass determination by GPC-MALLS-RI combined with fluorescence labelling by **C**arbazole-9-**C**arbonyl-**O**xy-**A**mine (CCOA) of carbonyl groups was performed as described earlier [12].

Pulp
All experiments were performed using cotton linters pulp from Buckeye. According to the following descriptions this pulp was first oxidized to increase the amount of carbonyl groups. As different oxidation treatments have specific preference on the type of carbonyl groups formed, three variations were chosen to provide a broad variety. All three oxidation treatments were performed with 2 g of dry pulp in total, except for the sodium periodate oxidation when 10 g of wet pulp were used. To improve accessibility, the pulp was suspended in water and shortly disintegrated. The excess water was removed, and the wet pulp was transferred into a 2 L beaker, re-suspended and stirred on with the aid of a magnetic stirrer throughout the oxidation procedure that takes place as described below.

Sodium periodate-Oxidation
The wet pulp was re-suspended in 2 L of sodium periodate solution (0.1 M at pH 5). The oxidation was stopped after 60 minutes by addition of ethanol and followed by thorough washing with water. The pulp was freeze-dried.

Hypochlorite-Oxidation
The wet pulp was re-suspended in a sodium acetate buffer (1 M, adjustment with glacial acetic acid to pH 5). To start the oxidation, 50 mL of HOCl (active chlorine 10-13 %, Sigma Aldrich) were added. Soon, the pH increased to 6.5 where it remained over the whole reaction period. The oxidation was stopped after 45 minutes by addition of ethanol and followed by thorough washing with water.

TEMPO-Oxidation
The pH was adjusted to 10.8 by slowly adding NaOH (0.4 M). 20 mg of 2,2´,6,6´-tetramethylpiperidine-1-oxyl (*TEMPO*) were dissolved in 500 µL of absolute ethanol before adding it with 1.9 g of sodium bromide and 20 mL of sodium hypochlorite (active chlorine 10-13 %, Sigma Aldrich) to the pulp suspension. The pH was continuously controlled and stabilized at pH 11.2. The reaction was stopped 25 minutes after a faint yellow colour developed in the reaction mixtures by addition of ethanol and followed by thorough washing with water.

Sodium borohydride reduction
The $NaBH_4$ reduction treatment of all three oxidized pulp modifications ($NaIO_4$, HOCl, and *TEMPO*) was performed at three different concentrations (0.05 M, 0.25 M, and 1 M), at three different pH (non-buffered solution with a pH of 10, buffered at pH 8, and buffered at pH 12), and at five different time intervals (5', 10', 30', 120', and 24 h). $NaBH_4$ (Sigma Aldrich) was dissolved in demineralised water at the chosen concentrations. The pH was adjusted by NaOH (0.4 M for treatment at pH 12), respectively by borate buffer at pH 8. The reaction was performed in closed glass vials containing 40 mg of wet oxidized pulp and 4 mL of $NaBH_4$ solution. The reaction time was stopped after the designated time intervals by addition of ethanol and followed by thorough washing in water. The wet pulp was stored in dark at 4°C no longer than 24 h before the labelling procedure started.

III. RESULTS AND DISCUSSION

Influence of time
It is known that $NaIO_4$ introduces dialdehyde structures at C2 and C3, accompanied by ring opening. These structures are obviously more difficult to reduce than the carbonyl structures introduced by *TEMPO* at C6 and random oxidation by HOCl. The relative rate of dialdehyde reduction is slowest for $NaIO_4$ oxidized pulp, followed by *TEMPO* and HOCl oxidized pulps (figure 1 left). However, after 120 minutes the remaining amount of carbonyl groups is roughly the same.
Neither *TEMPO*-oxidized nor HOCl-oxidized pulps show any severe decrease of molar mass during the reduction treatment with $NaBH_4$, but $NaIO_4$-oxidized pulps do (figure 1 right). After only five minutes of reduction treatment the molar mass is decreased from 160 kg/mol to less than 80 kg/mol. However, the starting molar mass of 160 kg/mol is surprisingly high compared to the two other starting Mws, even though the amount of carbonyl groups is equally high in all three modified pulps that originate from the same starting material. The reason is the higher tendency of dialdehyde cellulose to engage in hemiacetal cross-linking, which are often not broken during cellulose dissolution. Hence the observed molar mass is slightly higher.

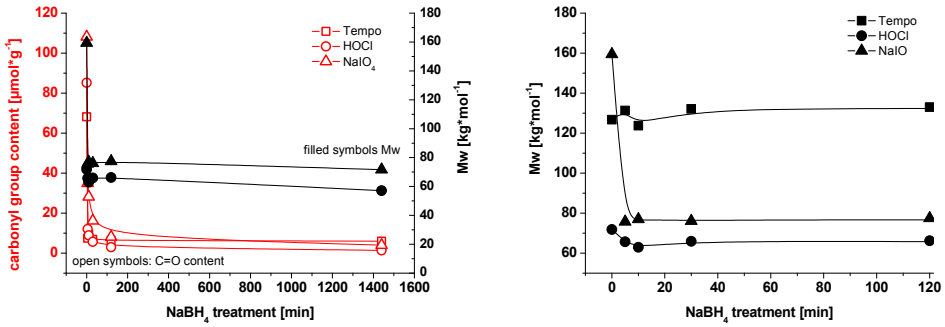

Figure 1: Reduction of differently oxidized pulps by $NaBH_4$. Left: Absolute values for carbonyl group content and molar mass. Right: Detail of the molar mass development within the initial phase of the reduction treatment.

Influence of concentration

The concentration of $NaBH_4$ pulps influences the rate of reduction of $NaIO_4$-oxidized (figure 2). For the experiments 0.05 M, 0.25 M, and 1 M were chosen. The increase of the concentration does not significantly improve the results, while a decrease negatively influences the carbonyl group reduction capacity (figure 2 left). The impact on the average molar mass is only slightly influenced by the concentration. The lowest concentration tested (0.05 M) does not prevent the decrease of molar mass it only slows the reaction down (figure 2 right). Note the considerably lower Mw right in the beginning of the reduction experiments in HOCl pre-treated Cotton Linters.

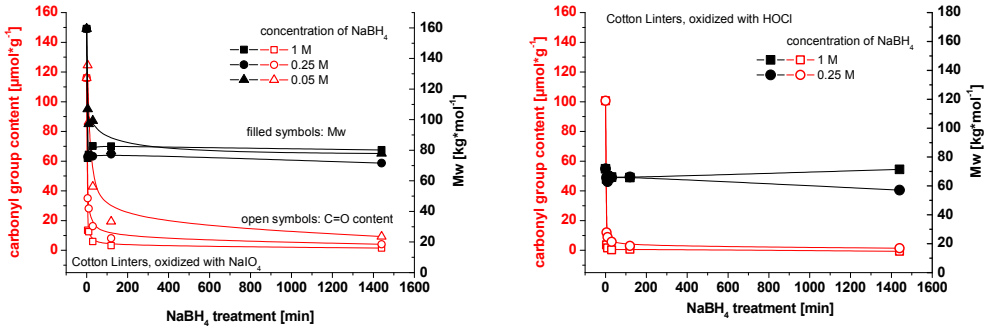

Figure 2: Impact of $NaBH_4$ concentration on oxidized Cotton Linters. Left: Carbonyl group content and molar mass in $NaIO_4$-oxidized pulp. Right: Carbonyl group content and molar mass in HOCl-oxidized pulp.

Influence of pH

The influence on the average molar mass is controlled by the pH and by the reduction treatment (figure 3).

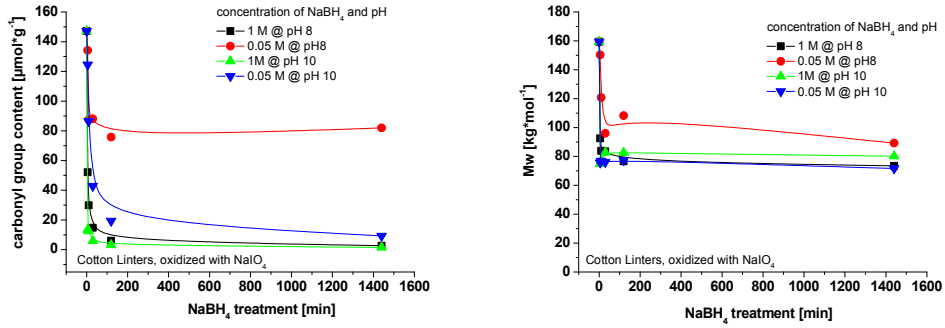

Figure 3: $NaBH_4$ reduction treatment on $NaIO_4$-oxidized Cotton Linters. Left: Impact of pH and concentration on carbonyl group content. Right: Impact of pH and concentration on molar mass.

The $NaIO_4$-oxidized pulp contains a high amount of carbonyl groups that render this type of pulp vulnerable to *β*-elimination. Generally there is no difference in the efficiency to reduce carbonyl groups between $NaBH_4$ treatments performed at pH 8 or 10 in $NaIO_4$-oxidized pulps (figure 3 left). However, when additionally lowering the concentration from 0.25 M to 0.05 M and adjusting the pH to 8 the efficiency of the reduction treatment is considerably lowered (figure 3 right). This correlates to a higher Mw caused by cross links that still survived the reduction treatment and seemingly increase the Mw.

IV. CONCLUSIONS

The influence of time, pH, concentration, and type of carbonyl groups introduced into Cotton Linters pulp was studied. The efficiency to reduce carbonyl groups and the impact on molar mass were the parameters to evaluate the different modifications.
The carbonyl groups of $NaIO_4$-oxidized pulp, dialdehyde functions at C2 and C3, are rather difficult to reduce and the impact on the decrease on Mw is very pronounced. As dialdehyde functions are known to encourage cross linking rendering cellulose dissolution more difficult, the decrease in Mw after only five minutes of reduction treatment may be attributed mainly to a process of breaking the cross links, thus lowering a Mw the has been determined to high beforehand. This observation was discussed in detail in [13].
This thesis is supported by the observation that in HOCl and TEMPO-oxidized pulps with comparable high amounts of carbonyl groups a lower Mw has been determined in the starting material. In HOCl-oxidized pulp only a minor decrease in Mw is observed during the initial phase of the reduction treatment.
The impact of time was mainly studied in $NaIO_4$-oxidized pulp, however, the other two modifications, HOCl and *TEMPO*-oxidized pulps, underline the results found in $NaIO_4$-oxidized pulp. $NaBH_4$ treatment generally takes two hours to efficiently reduce most carbonyl groups. $NaBH_4$ treatment at slightly alkaline conditions (pH 8) still allow reduction of carbonyl groups, however, the process is more efficient at pH 10.
In conclusion, $NaBH_4$ treatment is recommended for an efficient reduction of carbonyl groups within a reasonable short time of treatment. After only two hours virtually no carbonyl groups are left and even after shorter treatment periods around 30 minutes considerable amounts of oxidized cellulose functions have been removed. Depending on the type of carbonyl groups present in the pulp, some decrease of Mw has to be expected. The treatment should be performed in alkaline conditions (pH 10) without further pH adjustments at a concentration of 0.25 M.

V. ACKNOWLEDGEMENT

The authors would like to thank Dr. Sonja Schiehser for her assistance with the analysis of the cellulosic pulps.

VI. REFERENCES

[1] Rapson, W. H.; Anderson, C. B.; Magued, A. Brightness of naturally aged laboratory-bleached pulps. *Tappi J.* **1989**, *72*, 147-151.
[2] Chirat, C.; De la Chapelle, V. Heat- and Light-Induced Brightness Reversion of Bleached Chemical Pulps. *J. Pulp Pap. Sci.* **1999**, *25*, 201-205.
[3] Knill, C. j.; Kennedy, J. F. Degradation of cellulose under alkaline conditions. *Carbohyd. Polym.* **2003**, *51*, 281-300.
[4] Malesic, J.; Kolar, J.; Strlic, M. Effect of pH and Carbonyls on the Degradation of Alkaline Paper. *Restaurator* **2002**, *23*, 145-153.
[5] Chirat, C.; Viardin, M. T.; Lachenad, D. Use of a reducing stage to avoid degradation of softwood kraft pulp after ozone bleaching. *Pap, Puu/ Pap Tim.* **1994**, *76*, 417-422.
[6] Kordsachia, O.; Reipschläger, B.; Patt, R., ASAM pulping of birch wood and chlorine free pulp bleaching *Pap, Puu/ Pap Tim.* **1990**, *72*, 44-50.
[7] Bouchard, J.; Polverari, M.; Morelli, E.; Gagnon, P.; Picotte, R. Brightness reversion and brightness loss in fully-bleached kraft pulp: a case study. *Pulp Pap.-Canada* **2000**, *101,* 46-50.
[8] He, Z.; Ni, Y.; Qian, X. The strength properties of the bleached mechanical pulps from the $MG(OH)_2$-based peroxide bleaching process. In: *Annual Meeting of the Pulp and Paper Technical Association of Canada (PAPTAC)*, **2005**, 721-731.
[9] Costa, M. M.; Colodette, J. L. The impact of kappa number composition on eucalyptus kraft pulp bleachability. *Braz. J. Chem. Eng.* **2007**, *24*, 61-71.
[10] Ek, M.; Lennholm, H.; Iversen, T. A comment on the effect of carbonyl groups on the light-induced reversion of groundwood pulp. *Nord. Pulp Pap. Res. J.* **1990**, *5*, 159-160.
[11] Ni, Y.; Ghosh, A.; Li, Z.; Heitner, C.; McGarry, P. Photostabilization of bleached mechanical pulps with DTPA treatment. *J. Pulp Pap. Sci.* **1998**, *24*, 259-263.
[12] Potthast, A.; Röhrling, A.; Rosenau, T.; Borgards, A.; Sixta, H.; Kosma, P. A novel method for the determination of carbonyl groups in cellulosics by fluorescence labeling. 3. Monitoring oxidative processes. *Biomacromolecules* **2003**, *4*, 743-749.
[13] Potthast, A.; Kostic, M.; Schiehser, S.; Kosma, P.; Rosenau, T., Studies on oxidative modifications of cellulose in the periodate system: Molecular weight distribution and carbonyl group profiles. *Holzforschung* **2007**, *61*, 662-667.

TECHNO ECONOMIC AND ENVIRONMENTAL ASSESSMENT OF THE ETHANOL PRODUCTION FROM OLIVE STONE

Valentina Hernández[1]*, Juan M. Romero-García[2], Eulogio Castro[2], Carlos A. Cardona[1]*

*[1]Instituto de Biotecnología y Agroindustria, Departamento de Ingeniería Química. Universidad Nacional de Colombia Sede Manizales. Cra. 27 No. 64-60, Manizales, Colombia; [2]Department of Chemical, Environmental and Materials Engineering, Agrifood Campus of International Excellence (ceiA3), University of Jaén, 23071 Jaén, Spain (*ccardonaal@unal.edu.co)*

ABSTRACT

Olive tree cultivation is spreading worldwide as a consequence of beneficial effects of olive oil consumption. Olive stones constitute an important byproduct generated in the olive oil extraction and pitted table olive industries. In the 2009/2010 season, the world olive oil and table production were 2.97 and 2.37 million tons, respectively. In the same season, approximately $1.7 \cdot 10^5$ tons and 2.1 million tons of stones from table olives and olive oil industries, respectively, were produced. Currently, the main use of this byproduct is the direct combustion to produce energy as electricity or heat. Although, crushed olive stones have a potential application as biofuel for heat and power production, they have also been considered as raw material for other kind of value-added products. For instance, the reducing sugar and lignin content in this residue are 50 and 40% approximately. In this work, the techno-economic and environmental assessment of the ethanol production from olive stones is presented based on three scenarios: The base case, where neither energy integration nor cogeneration is considering. The second scenario presents the case when integration is considered. In the last case, besides energy integration, cogeneration of the solid residues is evaluated.

I. INTRODUCTION

Currently, there are several environmental, economic and social concerns related to the use of the energy and chemicals based on fossil raw materials, which have increased the interest on renewable feedstocks. Many countries, including Spain, have as an objective to replace either fully or partially the fossil raw materials. Since the fossil supply in Spain is almost entirely of foreign origin, it is interesting to use local biomass such as agricultural, forest, agro-industrial and industrial wastes, due to its low cost and large availability.

Beneficial effects of olive oil consumption have made that olive tree cultivation is spreading worldwide (United States, Argentina or Australia) being Spain the largest producer of olive oil and pitted table olives in the world. Olive oil and pitted table olive production are the most important agrifood industries in the Mediterranean countries. Olive stone is an important by-product generated in the olive oil extraction and pitted table olive production. It represents 10-30 % wt [1] of the fruit, implying an annual production of three million tonnes, approximately. Currently, the main use of this by-product is the direct combustion to produce energy as electricity or heat [2]. In this context, the olive stone valorization would be an economic improvement in farms, since it has lower handling and transport costs due to its small size, high density and concentration in the same manufacturing plants.

The aim of this work is to perform the economic and environmental assessment of the ethanol production from olive stone. Three scenarios have been considered. The first one presents the base case where ethanol is producing neither considering energy integration nor cogeneration. The second scenario, describes the bioethanol production with energy integration. Finally, the third scenario shows the process considering energy integration as well as cogeneration of the solid residue.

II. PROCESS DESCRIPTION

Raw material

Table 1 shows the olive stone composition used for the simulation procedure. Sugar polymers sum up to fifty percent of dry weight.

Table 1. Olive stone composition

Compound	Cellulose	Hemicellulose	Lignin	Extractives	Ash
%	20.10	29.92	38.87	10.54	0.57

Moisture content: 7.71%

Sugar extraction

In order to achieve the sugar extraction, the olive stone is submitted to a process consisting in two hydrolysis steps [3, 4]. The first stage is carried out at 100 °C with sulfuric acid (1.2% by weight) to hydrorolyze the hemicellulose fraction. As a result, a non-converted solid fraction and a rich-pentose liquor are obtained and separated by filtration. In the second stage, the solid undergoes to a hydrolysis with sulfuric acid (4% by weight) at 2.68 atm and 150°C to obtain a rich-hexoses liquor and a solid residue rich in lignin. A detoxification process based on overliming [5-7] is required in order to remove the furfural and hydroxymethyl furfural (HMF) obtained as by-product in the two hydrolysis steps, as a result of the decomposition reactions of the sugars. This procedure is carried out to avoid poisoning and inhibition by the acids, furfural and HMF in the fermentation stage.

Ethanol production
Liquors obtained from both stilirization steps together with the last solid obtained are sent to sent to a sterilization process at 121 °C to neutralize the biologic activity. Later the simultaneous saccarifitation fermentation process is carried out at based on the kinetic expressions reported by Morales-Rodríguez et al. [8], at 37°C using Spezyme CP and Novozym 188 for the enzymatic hydrolysis step and *Escherichia coli* as microorganism for the fermentation step. Afterwards, cell biomass is separated from the culture broth. After the fermentation stage, the culture broth is taken to the separation zone, which consists of two distillation columns. In the first column, ethanol is concentrated nearly to 50-55% by weight. In the second column, the liquor is concentrated until the azeotropic point (96% wt) to be led to the dehydration zone with molecular sieves for obtaining an ethanol concentration of 99.7% by weight [9].

Cogeneration process
The biomass integrated gasification combined cycle (BIGCC) [10-12] is used as technology for energy cogeneration. Gasification is a thermo-chemical conversion technology of carbonaceous materials (coal, petroleum coke and biomass), to produce syngas added to small amounts of char and ash. The Gas properties and composition of syngas changes according to the gasifying agent used (air, steam, steam-oxygen, oxygen-enriched air), gasification process and biomass properties [13]. Gasification temperatures range between 875-1275 K [13]. The BIGCC system include biomass dryer, gasification chamber, gas turbine and heat steam recovery generator (HRSG). A gas turbine is a rotator engine that extracts energy from a flow combustion gas. It is able to produce power with an acceptable electrical efficiency, low emission and high reliability. The gas turbine is composed by three main sections: compression (air pressure is increased, aimed to improve combustion efficiency), combustion (adiabatic reaction of air and fuel to convert chemical energy to heat) and expansion (obtained pressurized hot gas at high speed passing through a turbine generating mechanical work) [14]. The HRSG is a high efficiency steam boiler that uses hot gases from a gas turbine o reciprocating engine to generate steam, in a thermodynamic Rankine Cycle. This system is able to generate steam at different pressure levels.

III.SIMULATION PROCEDURE

For all the scenarios, flowsheet synthesis is carried out using process simulation tools in order to generate the mass and energy balances for calculating the raw materials, consumables, utilities and energy requirements. The main simulation tool used is the commercial package Aspen Plus v8.0 (Aspen Technology, Inc., USA). Specialized package for performing mathematical calculations especially for kinetic analysis such as Matlab is also used. The Non-Random Two-Liquid (NRTL) thermodynamic model was applied to calculate the activity coefficients of the liquid phase and the Hayden-O'Conell equation of state was used for the description of the vapor phase. Also the UNIFAC-DORTMUND and Soave Redlick Kwong models for liquid and vapor phases were needed when the NRTL model do not predict properties (e.g. distillation columns).

Energy consumption
The estimation of the energy consumption was performed based on the results of the mass and energy balances obtained from the simulation. Then, the required thermal energy in the heat exchangers and re-boilers was calculated, as well as the electric energy needs for the pumps, compressors, mills and other equipment.

Economic assessment
The capital and operating costs were calculated using the software Aspen Economic Analyzer V8.0 (Aspen Technologies, Inc., USA). On the other hand specific parameters regarding to some Spain conditions such as the raw material costs, income tax (35%), annual interest rate (6%) and labor salaries, among others, were incorporated in order to calculate the production costs per unit for the different obtained products. This analysis was estimated in US dollars for a 10-year period. The Capital depreciation was calculated using the straight-line method.

Environmental assessment
The Waste Reduction Algorithm WAR, developed by the National Risk Management Research Laboratory from the U.S. Environmental Protection Agency (EPA) is used as the method for the calculation of the Potential Environmental Impact (PEI). The PEI for a given mass or energy quantity could be defined as the effect that those (energy and mass) will have on the environment if they are arbitrary discharged. The environmental impact is a quantity that cannot be directly measure; however, it can be calculated from different measurable indicators. The WAR GUI software incorporates eight categories: Human toxicity by ingestion (HTPI), human toxicity by dermal exposition or inhalation (HTPE), aquatic toxicity potential (ATP), Global warming (GWP), Ozone depletion potential (ODP), Photochemical oxidation potential (PCOP) and acidification Potential (AP). This tool considers the impact by mass effluents and the impact by energy requirements of a chemical process, based on the energy and mass balances generated in Aspen Plus. Then the weighted sum of all impacts ends into the final impact per kg of products.

IV.RESULTS AND DISCUSSION

Process Simulation
For simulation purposes a raw material flow of 10 tonne/h is considered and a yield of 0.129 litters of ethanol per kg of olive stone. Simulations of the three studied scenarios were used to generate their respective mass and energy balance, which are the basic input for the techno-economic and environmental assessment.

Economic Evaluation
The annualized costs are presented in **Table 2** for each scenario as well as the unit cost of ethanol and the profit margin. As can be seen the feature that contributes with a higher proportion on the total costs are the operating costs followed by utilities, raw materials and depreciation. However, scenario 3 shows higher values due to the addition of the cogeneration scheme. The third scenario presents a lower ethanol cost because of the electricity obtained through the cogeneration system, which is sold to the electric grid.

Table 2. Annualized costs for ethanol production

	Scenario 1	**Scenario 2**	**Scenario 3**
Depreciation	1.667.278,93 USD	1.667.278,93 USD	1.732.164,93 USD
Raw materials	9.268.144,00 USD	9.268.144,00 USD	9.268.144,00 USD
Utilities	1.024.681,39 USD	696.783,35 USD	650.415,79 USD
Operating	4.055.131,63 USD	4.055.131,63 USD	4.582.298,74 USD
Total	**16.015.235,95 USD**	**15.687.337,90 USD**	**16.233.023,46 USD**
Unit cost of ethanol	1,20 USD	1,17 USD	0,96 USD
Profit margin	3%	6%	23%

Environmental Assessment
The environmental assessment is based on the criteria of the potential environmental impacts, described above. The results of the potential environmental impact per kg of product are presented in **Figure 1**. This Figure shown that the scenario 3 is the less environmental friendly. According to **Figure 1** that human toxicity by ingestion (HTPI) and terrestrial toxicity (TTP) potentials affect the most to the environmental impacts. The HTPI and TTP potentials are high due to organic waste present in liquid streams leaving the process.

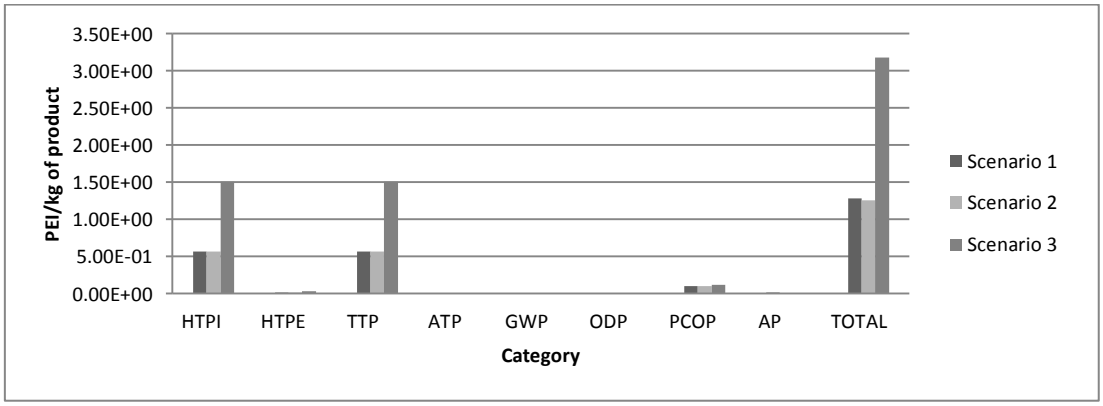

Figure 1. Potential Environmental Impact per kg of Product

V. CONCLUSIONS

According to the results, the olive stone is an interesting material to be used as feedstock to obtain ethanol. Showing good profit margin when cogeneration of the solid residues is used. Although, the environmental results show that the less environmental friendly scenario is the third one.

Acknowledgements

The authors express their gratitude to the Universidad Nacional de Colombia at Manizales, to the Investigation and extension direction, from the Engineering and Architecture Faculty from Universidad de Colombia Sede Manizales, to the Design of Sustainable Biorefineries (code 157) and Chemical, catalytic and biotechnological Processes (code 16081) projects from the Investigation Direction at Manizales (DIMA), to the Agrifood Excellence Campus (ceiA3) in University of Jaén and to the Agrifood International Doctorate School (eidA3) for funding this work. Financial support from Junta de Andalucía (Proyecto de Excelencia AGR-6103) is gratefully acknowledged.

VI. REFERENCES

1. Garrido-Fernández, A., M.J. Fernández-Diez, and M.R. Adamos, *Physical and Chemical Characteristics of the Olive Fruit*, in *Table Olives*, C. Hall, Editor 1997.
2. Romero-García, J.M., et al., *Biorefinery based on olive biomass. State of the art and future trends.* Bioresource Technology. **In press**.
3. Quintero, J.A., J. Moncada, and C.A. Cardona, *Techno-economic analysis of bioethanol production from lignocellulosic residues in Colombia: A process simulation approach.* Bioresource Technology, 2013. **139**(0): p. 300-307.
4. Moncada, J., M.M. El-Halwagi, and C.A. Cardona, *Techno-economic analysis for a sugarcane biorefinery: Colombian case.* Bioresource Technology, 2013. **135**(0): p. 533-543.
5. Martinez, A., et al., *Detoxification of dilute acid hydrolysates of lignocellulose with lime.* Biotechnology Progress, 2001. **17**(2): p. 287-293.
6. Millati, R., C. Niklasson, and M.J. Taherzadeh, *Effect of pH, time and temperature of overliming on detoxification of dilute-acid hydrolyzates for fermentation by Saccharomyces cerevisiae.* Process Biochemistry, 2002. **38**(4): p. 515-522.
7. Purwadi, R., C. Niklasson, and M.J. Taherzadeh, *Kinetic study of detoxification of dilute-acid hydrolyzates by Ca (OH) 2.* Journal of Biotechnology, 2004. **114**(1-2): p. 187-198.
8. Morales-Rodriguez, R., et al., *A Mathematical Model for Simultaneous Saccharification and Co-fermentation (SSCF) of C6 and C5 Sugars.* Chinese Journal of Chemical Engineering, 2011. **19**(2): p. 185-191.
9. Pitt Jr, W., G. Haag, and D. Lee, *Recovery of ethanol from fermentation broths using selective sorption–desorption.* Biotechnology and Bioengineering, 1983. **25**(1): p. 123-131.
10. Balat, M., et al., *Main routes for the thermo-conversion of biomass into fuels and chemicals. Part 2: Gasification systems.* Energy Conversion and Management, 2009. **50**(12): p. 3158-3168.
11. Herron, J.S., J.D. King, and D.C. White, *Recovery of poly-β-hydroxybutyrate from estuarine microflora.* Applied and environmental microbiology, 1978. **35**(2): p. 251-257.
12. Rincón, L.E., et al., *Techno-Economic Analysis of the Use of Fired Cogeneration Systems Based on Sugar Cane Bagasse in South Eastern and Mid-Western Regions of Mexico.* Waste and Biomass Valorization, 2013.
13. Ahmed, I.I. and A.K. Gupta, *Sugarcane bagasse gasification: Global reaction mechanism of syngas evolution.* Applied Energy, 2012. **91**(1): p. 75-81.
14. Najjar, Y.S.H., *Gas turbine cogeneration systems: a review of some novel cycles.* Applied Thermal Engineering, 2000. **20**(2): p. 179-197.

HETEROGENEOUS SURFACE MODIFICATION OF CELLULOSE: SYNTHESIS OF PHOTOACTIVE MATERIALS VIA CLICK CHEMISTRY

Hubert Hettegger[1], Wolfgang Harreither[2], Katharina Merz[2], Christian Rohrer[2], Antje Potthast[1], Thomas Rosenau[1]*

[1]*University of Natural Resources and Life Sciences Vienna (BOKU), Department of Chemistry, Christian-Doppler Laboratory "Advanced Cellulose Chemistry and Analytics", Konrad-Lorenz-Straße 24, A-3430 Tulln, Austria; thomas.rosenau@boku.ac.at*
[2]*Lohmann & Rauscher GmbH & Co. KG, Heilsberger Straße 16, D-56566 Neuwied, Germany*

ABSTRACT

The objective of the current project is the development of photoactive materials based on cellulose as a backbone material for the destruction of low molecular weight molecules, which are responsible for the unpleasant odor of chronic wounds. The destruction process is triggered by release of radicals or singlet oxygen ($^1O_2$) as the actual active agents. Various xanthene dyes, including well-established photosensitizers (PS) such as Fluorescein, Eosin Y, Rhodamine B and Rose Bengal, were derivatized in order to make them accessible to Cu(I)-catalyzed Huisgen-Meldal-Sharpless 1,3-dipolar cycloaddition, in a so-called *click chemistry* approach. The synthesized photosensitizers were characterized by means of spectroscopic methods including NMR, FTIR, UV/Vis absorption and fluorescence techniques. The photo-oxidative impact of the sensitizers regarding the production of singlet oxygen in solution was investigated using an indirect spectrometric approach: the decomposition of 1,3-diphenylisobenzofurane (DPBF), a molecule possessing a highly specific reactivity towards singlet oxygen, was recorded after illumination with white light. The xanthene derivatives, equipped with an alkyne moiety as immobilization anchor, were appended onto 6-azido-6-deoxycellulose under mild reaction conditions in a heterogeneous reaction. The resulting photoactive cellulosic materials were characterized *inter alia* by solid-state NMR spectroscopy.

I. INTRODUCTION

Photoactive materials, once a domain of technical and material disciplines, nowadays find also wide applications in biosciences and medicine, such as wastewater treatment, cancer therapy, photodynamic treatments, antimicrobial surfaces, or blood sterilization. Another potential application is the destruction of odorous molecules, which are generated in putrid wounds by the action of bacteria (e.g. *Pseudomonas* and *Klebsiella* species), necrosis or tissue degradation. Malodor of cancerous wounds and ulcers is mainly based on low molecular weight molecules, including short chain fatty acids, such as butyric and valeric acid, amines including putrescine and cadaverine as well as sulfides, such as dimethyl trisulfide.

Current methods for wound odor treatment are based on antibacterial cleansing and debriding of the concerned wound, adsorption of odorous molecules onto activated charcoal or cyclodextrins, or inactivation of bacteria by antibacterial substances, such as silver particles, PHMB or metronidazole [1, 2]. However, because of the different nature of wounds it is not possible to use each method in every single case, and performance might decrease due to saturation phenomena. Until today no dressing with an active material that actually destroys molecules and bacteria responsible for malodor is available.

The actual destruction process in our approach toward this issue is based on singlet oxygen, which is produced by photoactive substances attached to cellulosic matrices. Upon illumination, photosensitizers get activated by the absorption of energy. By transferring part of the energy to ordinary (triplet) oxygen they are producing highly reactive singlet oxygen from ambient air [3]. This reactive intermediate causes a variety of reactions based on oxidative processes, including the potential destruction of odorous molecules as well as the inactivation of bacteria by cell wall destruction.

The fixation of above mentioned photosensitizers onto cellulosic matrices allows application in wound coverage materials. The Cu(I)-catalyzed Huisgen alkyne-azide cycloaddition serves as a facile and efficient route for the heterogeneous modification of pre-activated cellulose under mild conditions, even at room temperature. The advantages of a covalent attachment of active molecules onto cellulose include longer durability, the prevention of aggregation and minimization of leaching [4].

II. EXPERIMENTAL

Materials and Methods

Solution NMR experiments were recorded on a Bruker Avance II 400 instrument (Rheinstetten, Germany) with a resonance frequency of ^{1}H at 400.13 MHz and ^{13}C at 100.61 MHz, respectively. Dry samples were dissolved either in DMSO-d_6 (Euriso-top, 99.9 %D) or $CDCl_3$ (Euriso-top, 99.8 %D) at room temperature with standard Bruker pulse programs. The raw data were processed with ACD/NMR Processor academic edition. Assignment of the signals was accomplished by means of 2D NMR techniques (COSY, HSQC, HMBC). Solid state ^{13}C CP-TOSS NMR spectra were recorded on a Bruker Avance III HD instrument with a resonance frequency of ^{13}C at 100.68 MHz. A PerkinElmer Frontier IR Single-Range spectrometer (Waltham, Massachusetts, US) was used in ATR mode for FTIR measurements. UV/Vis absorption and fluorescence spectroscopy experiments were carried out on a PerkinElmer Lambda 35 UV/Vis and PerkinElmer LS 45 fluorescence spectrometer. Elemental analyses were operated on a EURO EA 3000 CHNS-O instrument from HEKAtech (Wegberg, Germany). Illumination for the light-triggered destruction of DPBF was carried out with both a TRIO 20W/12V halogen bulb desk lamp (Arnsberg, Germany) and an OSRAM FQ 54W/840 halogen fluorescent tube (Munich, Germany). Flash column chromatography was performed on Silica Gel 60 from Merck (Darmstadt, Germany). Solvents were purchased from ROTH, Sigma-Aldrich and VWR and used as received. Reagents for synthesis were obtained from Sigma-Aldrich, Fluka and TCI. As a cellulose backbone material microcrystalline cellulose (Avicel® PH-101 50 µm) was used.

Preparation of alkyne derivatives of xanthene dyes

Ethyl 2-[3-oxo-6-(prop-2-yn-1-yloxy)-3*H*-xanthen-9-yl]benzoate **1**: Fluorescein ethyl ester as an intermediate was prepared as reported by Adamczyk et al. [5] using EtOH instead of MeOH and fluorescein free acid as reagents. To a suspension of the corresponding ethyl ester (3.20 g, 8.88 mmol) in acetone (50 mL) was added DMF until complete dissolution of the reagent. Finely grounded K_2CO_3 (1.85 g, 13.4 mmol) was added followed by the addition of propargyl bromide solution in toluene (1.50 mL, 13.4 mmol). The suspension was allowed to stir at 60°C overnight. The reaction mixture was poured into water (300 mL) and the orange voluminous precipitate was filtered off. The product was washed with water until the filtrate became colorless and then lyophilized. The already pure product was allowed to crystallize from acetone in order to remove traces of remaining reagents. The crystals were washed with cold acetone and dried under high vacuum overnight. Yield: 3.05 g of an orange solid **1** (7.64 mmol, 86%).

Prop-2-yn-1-yl 2-[3-oxo-6-(prop-2-yn-1-yloxy)-3*H*-xanthen-9-yl]benzoate **2** and prop-2-yn-1-yl 2-(6-hydroxy-3-oxo-3*H*-xanthen-9-yl)benzoate **3**: The reaction conditions for the synthesis of both substances in one pot follow the protocol described above using DMF instead of acetone as a solvent and fluorescein as a reagent. After evaporation of the solvent the mixture of products was extracted with EtOAc, the combined organic phases were washed with water and brine and finally dried over anhydrous $MgSO_4$. After filtration and evaporation of the solvent the products were separated by flash column chromatography using gradient elution from EtOAc to EtoAc/EtOH 2:1. Fractions containing pure products were combined, filtered and the solvent was evaporated. Drying overnight under high vacuum yielded **2** as an orange solid (51%, R_f = 0.30 in EtOAc) and **3** as a red solid (7%, R_f = 0.07 in EtOAc).

3,6-Bis(diethylamino)-9-[2-[(2-propyn-1-yloxy)carbonyl]phenyl]-xanthylium chloride **4** was prepared with modification as reported by Birnbaum and Kuckling [6] starting from Rhodamine B as reagent. After completion of the reaction the mixture was evaporated to dryness, the residue dissolved in CH_2Cl_2 and filtered. The filtrate was evaporated and the product purified via flash column chromatography using stepwise gradient elution from CH_2Cl_2/MeOH 10:1 to 5:1, yielding **4** as a dark purple solid (78%, R_f = 0.31 in CH_2Cl_2/MeOH 10:1).

Sodium 2,4,5,7-tetraiodo-3-oxo-9-{2,3,4,5-tetrachloro-6-[(prop-2-yn-1-yloxy)carbonyl]phenyl}-3*H*-xanthen-6-olate **5** (Rose Bengal disodium salt as a reagent) and sodium 2,4,5,7-tetrabromo-3-oxo-9-{2-[(prop-2-yn-1-yloxy)carbonyl]phenyl}-3H-xanthen-6-olate **6** (Eosine Y disodium salt as a reagent) were synthesized following a protocol published by Fall et al. [7] with modification regarding the purification. Raw compound **5** was purified by flash column chromatography using elution from CH_2Cl_2/MeOH 10:1 to 5:1 yielding a dark purple solid (94%, R_f = 0.10 in CH_2Cl_2/MeOH 10:1). Compound **6** was purified by crystallization in Et_2O followed by filtration and washing with Et_2O and water. Lyophilization followed by further drying under high vacuum at room temperature yielded pure **6** as a dark red-to-brown solid (65%).

Surface modification of cellulose

Microcrystalline cellulose was modified according to a protocol derived from Feese et al. [4] yielding solid white cellulose material (elemental analysis [w-%]: C: 42.96, H: 6.29, N: 1.16, S: 0.08, O: 49.09). Reaction conditions for the Cu(I)-catalyzed immobilization of photosensitizers **1**-**6** were set in accordance with [4] as well.

UV/Vis and fluorescence spectroscopy

All spectroscopic experiments were carried out in DMF as a solvent. For the comparative $^1O_2$ production experiments a similar setup as described by Garcia et al. [8] was used. A solution of DPBF (10 µM) and respective photosensitizer (5 µM) was prepared in the dark and air-saturated with an aquarium air pump for 10 min. The solution (20 mL) was irradiated with white light at room temperature for 16 min at constant flushing with air. Aliquots (2 mL) were taken at 2 min intervals and the UV/Vis spectra were recorded. The same setup without additional photosensitizer was used as for blank value determination.

III. RESULTS AND DISCUSSION

Synthesis aspects

A total of six xanthene derived photosensitizers comprising different substitution patterns at the aromatic ring structure were synthesized and obtained in pure form, which was evaluated by NMR and FTIR methods. The structures of compounds **1-6** are given in **Figure 1** including respective spectroscopic properties. Fluorescein, Rhodamine B, Rose Bengal disodium salt and Eosin Y disodium salt were used as precursor molecules. With the exception of Rhodamine B, all educts were esterified with propargyl bromide. In case of Rhodamine B-derived compound **4**, Steglich esterification using propargyl alcohol, DCC and DMAP afforded the corresponding propargyl ester after purification via flash column chromatography.

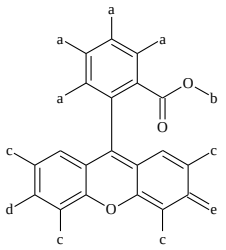

1: a = H; b = Et; c = H; d = OCH_2CCH; e = O
2: a = H; b = OCH_2CCH; c = H; d = OCH_2CCH; e = O
3: a = H; b = OCH_2CCH; c = H; d = OH; e = O
4: a = H; b = OCH_2CCH; c = H; d = $N(Et)_2$; e = $N^+(Et)_2Cl^-$
5: a = Cl; b = OCH_2CCH; c = I; d = O^-Na^+; e = O
6: a = H; b = OCH_2CCH; c = Br; d = O^-Na^+; e = O

Compound	$\lambda_{max\ abs}$ [nm]	$\lambda_{max\ em}$[nm]	log ε
1	455	526	4.34 ± 0.01
2	459	529	4.30 ± 0.01
3	456	556	4.41 ± 0.03
4	563	588	4.65 ± 0.02
5	572	-	4.72 ± 0.04
6	544	552	4.96 ± 0.05

Figure 1. Structure of the synthesized xanthene dyes **1-6** including corresponding UV/Vis and fluorescence properties. Compounds **1-3** are based on Fluorescein, whereas **4-6** represent derivatives of Rhodamine B, Rose Bengal and Eosin Y, respectively.

It is important to mention that regioselective propargylation is challenging in the case of reagents containing both a carboxylate and phenoxide functional group, which is especially true for fluorescein (free acid) as an educt. Because of resonance stabilization of the carboxylate, the alkoxide possesses higher nucleophilicity and therefore the Williamson ether products are favored. However, in case of disodium salts as precursors the respective alkyne esters were obtained as major compounds and were separated from minor byproducts by means of flash column chromatography and crystallization. Esterification instead of etherification was confirmed both by FTIR and long-range heteronuclear coupling in 2D NMR (HMBC) experiments. Cellulose as a backbone material for immobilization of previously synthesized xanthene derivatives was pre-modified by surface tosylation and nucleophilic tosyl-azide exchange yielding 6-azido-6-deoxycellulose in two steps with a DS = 0.06 calculated by the amount of nitrogen present in the sample (1.16 w-%).

Comparative $^1O_2$ production study

The results of the singlet oxygen production of compounds **1-6** are shown in **Figure 2a**. DMF was chosen as a solvent for the present study because no significant photolysis of DPBF without photosensitizer occurs in this solvent (as it e.g. happens in the case of $CHCl_3$) [9]. The singlet oxygen production rate of compounds **1-3** and **6** are almost identical. These four substances are based on fluorescein (**1-3**) and tetrabromofluorescein (**6**). The Rhodamine B-based sensitizer **4** shows lower production rates compared to the four mentioned above; on the other hand, the Rose Bengal-derived sensitizer **5** is the most efficient one and complete destruction of DPBF resulting in *o*-dibenzoylbenzene was observed after already 6 min. The decrease of typical DPBF absorption in case of **6** is shown as a detail in **Figure 2b**. As a reference also the non-derivatized educts were used, indicating that derivatization did not affect the overall singlet oxygen production (data not shown).

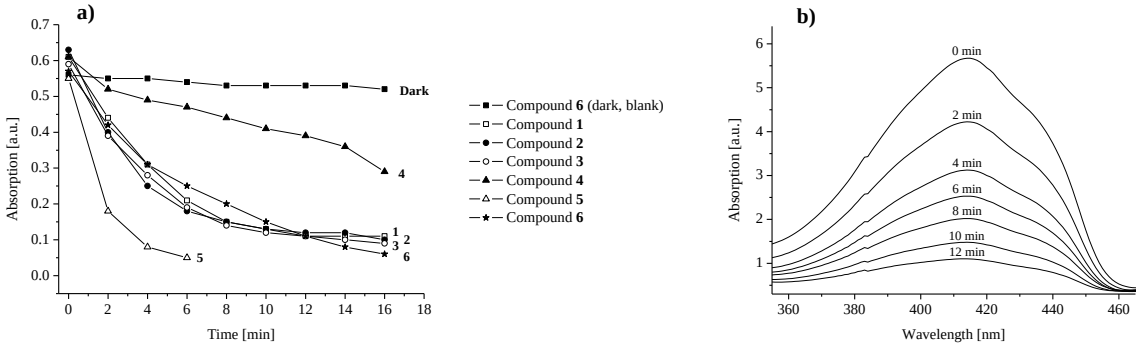

Figure 2. Comparative $^1O_2$ production study. a) Decrease of DPBF-absorption at 414.5 nm over time. Conditions: DPBF (10 µM) and PS **1-6** (5 µM) in DMF, air-saturated solution, illumination with white light. Reference (dark, blank) = DPBF (10 µM) and PS **6** (5 µM) in DMF, air-saturated solution, without illumination; b) Decrease of DPBF-absorption in case of PS **6** over time.

IV. CONCLUSIONS

A total of six xanthene derived dyes with alkyne moieties have been synthesized successfully and characterized by means of spectroscopic methods including a comparative study of the $^1O_2$ production rate, in which Rose Bengal derived compound **5** has shown to be the most powerful sensitizer. The compounds were attached onto pre-modified cellulose according to Cu(I)-catalyzed *click chemistry* resulting in photoactive cellulosic materials. Their potential oxidative action and applicability in modern wound treatment approaches will be studied in further experiments by means of GC/MS and UV/Vis spectroscopy, which have been developed for this special analytic scenario.

V. ACKNOWLEDGEMENT

The financial support by the Christian Doppler Research Society through the CD-laboratory for "Advanced Cellulose Chemistry and Analytics" is gratefully acknowledged.

VI. REFERENCES

[1] Fleck, C.A. Palliative Dilemmas: Wound Odour. *Wound Care Canada* **2006**, 4(3), 10-13.
[2] Shirasu, M.; Nagai, S.; Hayashi, R.; Ochiai, A.; Touhara, K. Dimethyl trisulfide as a characteristic odor associated with fungating cancer wounds. *Biosci., Biotechnol., Biochem.* **2009**, 73, 2117-2120.
[3] DeRosa, M.C.; Crutchley, R.J. Photosensitized singlet oxygen and its applications. *Coord. Chem. Rev.*, **2002**, 233-234, 351-371.
[4] Feese, E.; Sadeghifar, H.; Gracz, H.S.; Argyropoulos, D.S.; Ghiladi, R.A. Photobactericidal Porphyrin-Cellulose Nanocrystals: Synthesis, Characterization, and Antimicrobial Properties. *Biomacromolecules* **2011**, 12, 3528-3539.
[5] Adamczyk, M.; Grote, J.; Moore, J.A. Chemoenzymatic synthesis of 3'-*O*-(carboxyalkyl)fluorescein labels. *Bioconjug Chem* **1999**, 10, 544-547.
[6] Birnbaum, W.; Kuckling, D. Synthesis of *α*-biotinyl poly(ethylene glycol-*b*-*N*-isopropylacrylamide) block copolymers with different fluorescent dyes at the *ω*-side. *Polymer Chemistry* **2012**, 3(8), 2039-2049.
[7] Fall, A.; Sene, M.; Diouf, O.; Gaye, M.; Gomez, G.; Fall, Y. Synthesis and use of imidazolium-bound Rose Bengal derivatives for singlet oxygen generation. *Open Org. Chem. J.* **2012**, 6, 21-26.
[8] Garcia, G.; Naud-Martin, D.; Carrez, D.; Croisy, A.; Maillard, P. Microwave-mediated click-chemistry' synthesis of glyco-porphyrin derivatives and in vitro photo-cytotoxicity for application in photodynamic therapy. *Tetrahedron* **2011**, 67, 4924-4932.
[9] Zhang, X.-F.; Li, X. The photostability and fluorescence properties of diphenylisobenzofuran. *J. Lumin.* **2011**, 131, 2263-2266.

PHASE SEPARABLE IONIC LIQUIDS FOR LIGNOCELLULOSE PROCESSING

Ashley J. Holding,[1] Héctor Rodríguez,[2] Ilkka Kilpeläinen,[1*] Alistair W. T. King[1*]

*[1] Department of Chemistry, University of Helsinki, Helsinki, Finland; [2] Department of Chemical Engineering, University of Santiago de Compostela, Galicia, Spain (*alistair.king@helsinki.fi, ilkka.kilpelainen@helsinki.fi)*

ABSTRACT

We have demonstrated a new series of phase-separable ionic liquids (PSILs), based on the hydrophobic tetraalkylphosphonium cation ($[P_{RRRR}]^+$), that can dissolve lignin in the neat state but also hemicellulose and high purity cellulose in the form of their electrolyte solutions with dipolar aprotic solvents. For example, the IL trioctylmethylphosphonium acetate ($[P_{8881}][OAc]$) was demonstrated to dissolve up to 19 wt% of microcrystalline cellulose (MCC) at 60°C with the addition of 40 wt% of DMSO. It was found that the MCC saturation point is dependent on the molar ratio of DMSO and IL in solution. At the optimum saturation, a ~1:1 molar ratio of $[P_{8881}][OAc]$ to anhydroglucose units is observed, which demonstrates highly efficient solvation. This is attributed to the positive contribution that these more amphiphilic cation-anion pairs provide, in the context of the Lindman hypothesis. This effective dissolution is further illustrated by solution-state HSQC NMR spectroscopy on MCC. Finally, it is also demonstrated that these electrolytes are phase separable by the addition of aqueous solutions enabling the ionic liquid to be recovered and separated from DMSO.

I. INTRODUCTION

A major limiting factor for the commercialisation of ionic liquids (ILs) for cellulose dissolution and wood fractionation is the ability of the IL to be effectively recycled and purified by a suitable method. Distillation of the biopolymer-precipitating anti-solvent can be cost-prohibitve on a large scale, requiring high temperatures and low pressures [1]. Contaminants including oligomeric, monomeric and inorganic materials may also build up after several process cycles which need to be removed from the IL before further use. Recent generational advances have been made; including the advent of distillable ILs [2] wherby the IL may be ‚distilled' at lower temperatures and pressures than previous generations of cellulose dissolving ILs. The next generation of ILs for cellulose dissolution are predicted by us to be phase-separable ILs[1], circumventing the need for distillation of ILs. We aimed to test the cellulose, lignin, and hemicellulose dissolution capabilities and recycling strategies of a range of phosphonium based ILs. Their high polarity and strong hydrogen bond basicity would suggest them to be good candidates for cellulose dissolution solvents, along with their attractive potential for recycling *via* phase-separation due to the hydrophobicity of the cation. In addition, phosphonium based ILs have a number of other advantages, such as increased thermal and chemical stabilities [3]

II. EXPERIMENTAL

Ionic Liquid Synthesis

Methyltrioctylphosphonium chloride ($[P_{8881}]Cl$) was prepared by quaternization of trioctylphosphine, with methyl chloride in an autoclave at 100 °C for 12 h. Tetraoctylphosphonium chloride ($[P_{8888}]Cl$) and (tetradecyl)trioctylphosphonium chloride $[P_{14888}]Cl$ were prepared by quaternization of trioctylphosphine, with 1-octylchloride in an autoclave at 145°C for 24 h. The acetate salts tetrabutylphosphonium acetate ($[P_{4444}][OAc]$,), tetraoctylphosphonium acetate ($[P_{8888}][OAc]$). (tetradecyl)trihexylphosphonium acetate ($[P_{14666}][OAc]$) and (tetradecyl)trioctylphosphonium acetate $[P_{14888}][OAc]$ and (Tetradecyl)tributylphosphonium chloride $[P_{14444}][OAc]$) were prepared by anion metathesis from potassium acetate or silver acetate in isopropanol from the commercial or synthesized chloride salt. Methyltrioctylphosphonium acetate ($[P_{8881}][OAc]$) was prepared by quaternization of trioctylphosphine with dimethylcarbonate in an autoclave at 140 °C for 24 h. A metathesis reaction was then carried out by addition of acetic acid to give the acetate salt.

Biopolymer Dissolution

The IL was added to a pre-weighed sample vial and a co-solvent was added (if used). Each addition was weighed to give accurate compositions. The biopolymer was weighed separately on a filter paper and added to the solvent in one addition. After mixing briefly with a mechanical vortex mixer, a stirrer bar was added and the biopolymer solution was mixed at a steady rate with magnetic stirring at 100°C. The dissolution state was confirmed by

visual inspection of a clear solution and by observation by optical microscopy, which confirmed the absence of undissolved fragments.

Cellulose Dissolution Saturation Limit in Electrolyte Solutions

With constant stirring of the solution, under an argon atmosphere, mass portions, relative to the mass of solution (typically 0.25 wt%), of cellulosic pulp were added to the solutions and allowed to homogenise at 60°C. This low temperature was chosen to avoid error due to de-polymerisation or evaporation of co-solvent over the extended dissolution times required for the incremental addition of pulp. In the case of [emim][OAc], lower co-solvent (more viscous) concentrations were heated to 100°C briefly to aid in dispersion of the pulp. The solution is stirred between each addition until it becomes optically clear (confirmed by optical microscopy, ESI) and the next portion added. The end-point is taken when the solution no longer becomes clear after stirring for 24 h.

Ternary Phase Diagrams

Two methods of constructing phase diagrams are used: first, an NMR method[5], whereby ^{1}H NMR spectrum integrals are used to calculate mass fractions, and second, a GC method [6], whereby GC chromatogram peak areas are used to calculate mass fractions, in combination with an internal standard. Prior to data collection, a calibration is established using samples of known concentrations, with an average standard error of ~0.005 mass fractions. Phases are sampled from the ternary mixtures with a needle and syringe without disturbing the interface, after mixing and sufficient phase-equilibration time at 298.15K.

III. RESULTS AND DISCUSSION

Qualitative polysaccharide and lignin dissolution experiments (Table 1) were performed on some of the purified and dried acetate ILs in addition to chloride ILs, with 5 wt% microcrystalline ecellulose (MCC), 5 wt% Norway spruce dioxane-acidolysis lignin (Lignin). In addition, alkaline-extracted birch xylan (Xylan) and Norway spruce hot water-extracted galactoglucomannan (GGM) were dissolved in the representative ILs [P_{8881}][OAc], [P_{14666}]Cl, and [P_{14666}][OAc]. For these initial tests we assessed biopolymer solubility "qualitatively". Lignin was found to dissolve rapidly at 100°C in all the ILs and electrolyte solutions studied (Table 2). However, in all of the neat ILs, the dissolution of MCC did not proceed even after heating at 100°C for up to 48 h. In fact, none of the polysaccharides (MCC, Xylan, or GGM) dissolved in any of the pure ILs tested. This demonstrates some motivation for the extraction of lignin from lignocellulosic materials.

Under the same conditions, the use of DMSO as a co-solvent afforded rapid cellulose dissolution in under 1 h. GGM and xylan were also soluble and partially soluble, respectively, in 40 wt% DMSO solutions of the acetate ILs that were tested ([P_{8881}][OAc] and [P_{14666}][OAc]). The dissolution of cellulose in the phosphonium acetate ILs was confirmed by optical microscopy. Following dissolution, it was possible to precipitate cellulose with water, ethanol, and brine solutions. The attenuated total reflectance (ATR) IR spectra of the cellulose regenerated from ethanol confirmed the absence of acetate peaks and XRD confirmed a loss of crystallinity and a partial conversion to the cellulose II polymorph.

Table 1. Biopolymer Solubility in PSILs and their DMSO electrolytes.

Ionic Liquid	Lignin (5 wt%)	MCC (5 wt%)	Xylan (5 wt%)	GGM (5 wt%)	MCC + DMSO (5 + 38 wt%)	Xylan + DMSO (5 + 38 wt%)	GGM + DMSO (5 + 38 wt%)	Water Miscibility
[P_{4444}][OAc]	S	I	-	-	S	-	-	M
[P_{14444}][OAc]	S	I	-	-	S	-	-	M
[P_{8881}][OAc]	S	I	I	I	S	P	S	I
[P_{8888}][OAc]	S	I	-	-	S	-	-	I
[P_{14666}][OAc]	S	I	I	I	S	P	S	I
[P_{4444}]Cl	S	I	-	-	I	-	-	M
[P_{14444}]Cl	S	I	-	-	I	-	-	M
[P_{8881}]Cl	S	I	-	-	I	-	-	I
[P_{8888}]Cl	S	I	-	-	I	-	-	I
[P_{14666}]Cl	S	I	I	I	I	I	I	I

Lignin = Norway spruce dioxane-acidolysis lignin, MCC = microcrystalline cellulose, Xylan = alkaline-extracted birch xylan, MCC = hot water-extracted Norway spruce galactoglucomannan, S = soluble, I = insoluble/immiscible, P = partially soluble, M = miscible

To test the full effect of the variation of the amount of co-solvent on cellulose dissolution, DMSO was chosen as the best solvent for this purpose. A range of solutions, with various mass compositions of the co-solvent DMSO and IL were prepared. Two ILs were chosen for comparison: [P_{8881}][OAc] and [emim][OAc], the second of

which is the most common and successful structure quoted in the literature for cellulose dissolution. A new method was developed to determine quantitatively the wt% dissolution capacities and molar dissolution capacities for the different mixtures, the wt% of cellulose in electrolyte solution and the anhydroglucose unit (AGU)/IL molar ratio. The most effective cellulose dissolution in terms of weight capacity in [P_{8881}][OAc]/DMSO electrolyte solutions occurs at around 40 wt% DMSO/[P_{8881}][OAc], with a decreased capacity above and below this composition (Figure 1). The optimum cellulose dissolution composition of [P_{8881}][OAc]/DMSO corresponds with the formation of a relatively defined cellulose/IL complex of approximately a 1:1 molar ratio of AGU/IL between 30 and 60 wt% DMSO compositions (maximum of 1.12:1 mol equiv. at 50:50 wt%). More IL per AGU is required to go above and below these compositions at the maximum dissolution capacities. As a comparison, the maximum molar dissolution capacity of 1.12 AGU/IL (50 wt% DMSO) is significantly higher than that of the [emim][OAc]/DMSO electrolytes. It seems that, for the maximum dissolution capacity, less acetate anions are needed per mole of AGU for the more bulky phosphonium structure than for the less bulky imidazolium structure. One possible explanation for the enhanced molar dissolution effect is the amphilicity of the ILs, creating a positive interaction via the hydrophobic effect as speculated by the Lindman hypothesis.[4]

Figure 1. Cellulose (MCC) saturation in [P_{8881}][OAc] and [emim][OAc]-DMSO electrolyte solutions.

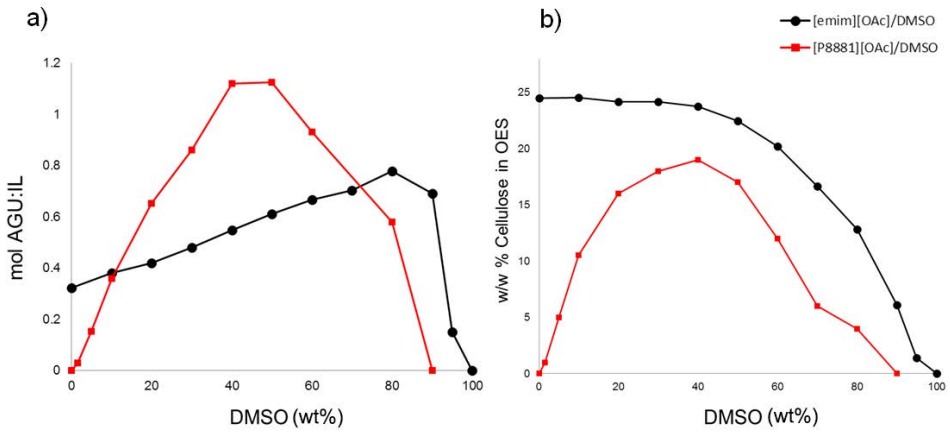

As a more definitive demonstration of the dissolution capabilities of these electrolytes, IL [P_{8881}][OAc] (60 wt%) and d6-DMSO (40 wt%) were used to prepare a 7.7 wt% solution of MCC. A high-resolution solution-state HSQC NMR spectrum was collected and processed for the optimum viewing of cellulose correlations (Figure 2). All of the cellulose backbone peaks can be differentiated clearly and correlated in both the $_1$H and $_{13}$C dimensions without overlapped solvent resonances. These ILs are unique in that they do not have any major resonances that interrupt the biopolymer C_1^H region in the $_1$H dimension, which enables high-resolution solution-state HSQC, ^{1}H and ^{13}C NMR on cellulose with a high degree of polymerization (DP) (MCC DP~100), to be obtained without deuteration of the IL or solvent suppression techniques.

Figure 2. HSCQ & 1D NMR assignments for MCC in [P_{8881}][OAc]/DMSO.

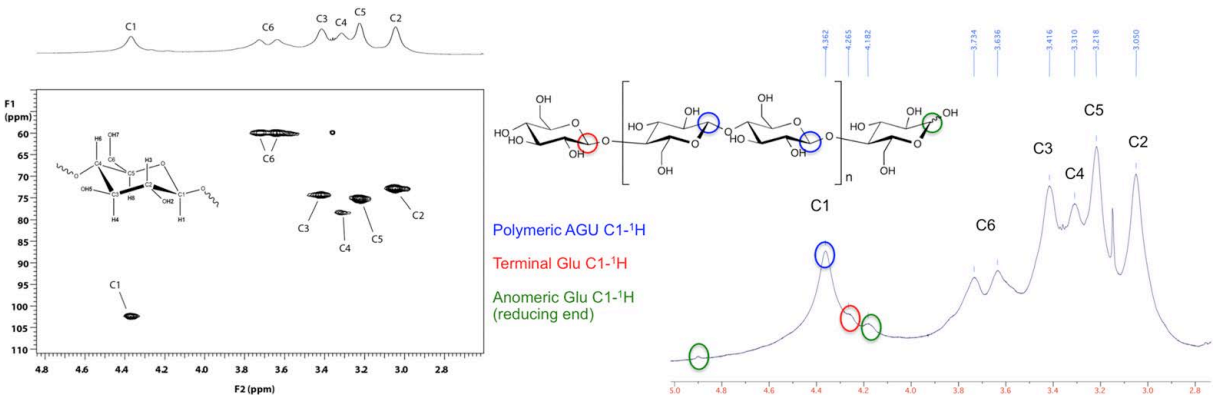

Figure 3 a) Phase diagram of [P_{8881}][OAc]/DMSO/water, b) recovery of [P_{8881}][OAc] after separation.

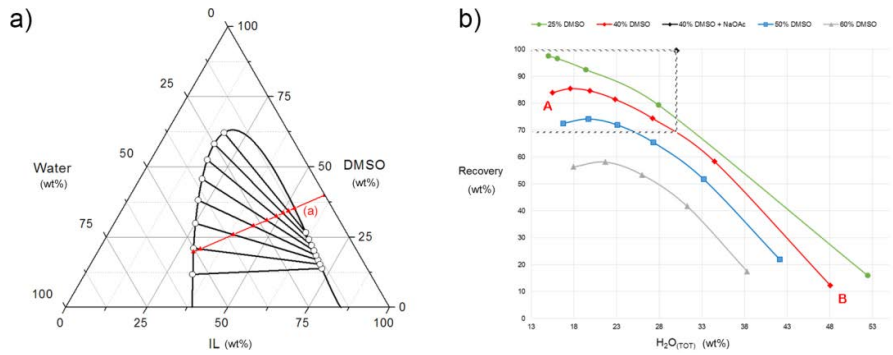

Gibbs diagrams of the ILs, DMSO and water were constructed according to previously used methods.[5][6] Three ILs were studied, $[P_{8881}][OAc]$, an IL with a small bi-phasic region, and $[P_{14,888}]$ and $[P_{8888}][OAc]$, with larger biphasic regions. Although they are described as water immiscible, these hydrophobic ILs are slightly hygroscopic, and a small amount of water is soluble in the IL phase and vice versa (15 wt% for $[P_{8881}][OAc]$ and <0.5 wt% for $[P_{14888}][OAc]$ and $[P_{8888}][OAc]$). Thus, the maximum % recovery of the IL is effectively limited by the solubility of the IL in pure water and the slope of the tie-lines. If we take a defined concentration (e.g., 40 wt%) of a DMSO solution of $[P_{8881}][OAc]$, the addition of more water to the mixture (e.g., Figure 3a, line (a)), increases the size of the water-rich phase and decreases the size of the IL-rich phase (intersections of AB with tie lines). From the tie-line data, in all ILs studied, the DMSO distribution constants ($\beta_{DMSO} > 1.0$) and selectivities ($S > 1$) indicated that the IL may be recovered in the upper phase, and the DMSO may be extracted into the aqueous phase for most ILs. The recovery in $[P_{8881}][OAc]$ drops drastically as a function of water content and has a reduced biphasic region when compared to $[P_{14888}][OAc]$ and $[P_{8888}][OAc]$ and thus is not able to be easily recovered from a simple phase-separation at useful water concentrations. However, kosmotropic salt solutions utilizing salts of the same anion (ie. NaOAc) boost the recovery of IL by lowering the solubility of the IL in water (Figure 3 b) and additionally reverse the distribution of DMSO by favoring solubility in the IL phase. For example, an aqueous solution of NaOAc (10 wt% in water) was added to a solution 40% DMSO and 60% $[P_{8881}][OAc]$ and the recovery of the IL in the IL-rich layer after one phase separation increased from approximately 68 to >95 wt%.

IV. CONCLUSIONS

Phosphonium ILs in combination with polar aprotic co-solvents are powerful non-derivatizing solvents for cellulose and with or with co-solvents are promising media for the fractionation of wood. Cellulose can be dissolved rapidly to a high concentration in the mixed solutions, with the cellulose saturation limit in different ILs being determined mostly by the length of the cation alkyl chains and their spatial arrangement. When compared to [emim][OAc], phosphonium ILs $[P_{8881}][OAc]$ and $[P_{14444}][OAc]$ have an increased ratio of AGU units per mol of IL at lower DMSO concentrations indicating the possibility of a positive contribution from the increased amphiphilicity of the solvent, as hypothesized by Lindman. The water-immiscible ILs may be recovered from water, the cellulose anti-solvent, by phase separation and separated from the DMSO co-solvent by washing with water. Alternatively, kosmotropic salt solutions can be added to the aqueous phase to shift the DMSO partitioning to the IL phase. Recovery of the IL is limited by the solubility of IL in the aqueous phase and the slope of the tie-lines.

V. ACKNOWLEDGEMENT

Funding provided by FIBIC (Finnish Bioeconomy Cluster) as part of the FUBIO (Future Biorefinery) program, Joint Research 2, Work Package 2. COST (European Co-operation on Science and Technology) are acknowledged for providing funding towards the short term scientific mission (STSM) with the University of Santiago de Compostela.

VI. REFERENCES

[1] Holding, A. J.; Heikkilä, M.; Kilpeläinen, I.; King, A. W. T. *ChemSusChem* **2014**, DOI: 10.1002/cssc.201301261
[2] King, A. W. T.; Asikkala, J.; Mutikainen, I.; Järvi, P.; Kilpeläinen, I. *Angew. Chem. Int. Ed.* **2011**, *50*, 6301–5.
[3] Bradaric, C. J.; Downard, A.; Kennedy, C.; Robertson, A. J.; Zhou, Y. *Green Chem.* **2003**, *5*, 143–152.
[4] Medronho, B.; Romano, A.; Miguel, M. G.; Stigsson, L.; Lindman, B. *Cellulose* **2012**, *19*, 581–587.
[5] Anderson, K.; Rodríguez, H.; Seddon, K. R. *Green Chem.* **2009**, *11*, 780.
[6] Rodríguez-Cabo, B.; Francisco, M.; Soto, A.; Arce, A. *Fluid Phase Equilib.* **2012**, *314*, 107–112.

2,5-DIHYDROXY-[1,4]-BENZOQUINONE AS A KEY CHROMOPHORE IN AGED CELLULOSICS - MOLECULAR MECHANISMS OF ITS REMOVAL IN A PEROXIDE STAGE

Takashi Hosoya[1], Ute Henniges[1], Antje Potthast[1], Thomas Rosenau[1]*

[1] *University of Natural Resources and Life Sciences, Department of Chemistry, Muthgasse 18, A - 1190 Vienna, Austria (takashi.hosoya@boku.ac.at; thomas.rosenau@boku.ac.at)*

ABSTRACT

2,5-Dihydroxy-[1,4]-benzoquinone (DHBQ) is one of the key chromophores occurring in all types of aged cellulosics. In the present work, we have addressed the molecular mechanisms of DHBQ degradation by hydrogen peroxide by a combination of synthesis, kinetic and computational approaches, attempting to provide a solid knowledge base for optimization of bleaching sequences aiming at DHBQ removal. Experimental investigation under neutral conditions (3.0 % H_2O_2, to choose a system as simple as possible) showed that DHBQ degraded into malonic acid, acetic acid, and carbon dioxide with the activation energy (E_a) being 20.4 kcal/mol. DFT(B3LYP) computation presented a plausible mechanism for the degradation of DHBQ involving an intermediate $\mathbf{I_{OH}}$ having an intramolecular O-O bridge between C-2 and C-5 of the 1,4-cyclohexadione structure. $\mathbf{I_{OH}}$ then undergoes the homolysis of the O-O bond followed by β-fragmentation of the resulting biradical, giving ketene and oxaloacetic acid. While ketene yields acetic acid, oxaloacetic acid eventually gives malonic acid and carbon dioxide. Under conditions more relevant to pulp bleaching (3.0% H_2O_2, NaOH, pH 10 and above), DHBQ is degraded quantitatively into malonic acid with an E_a of 16.1 kcal/mol. The DFT computation indicated that this degradation formed a dianionic intermediate $\mathbf{I_O^-}$, which is the doubly deprotonated form of $\mathbf{I_{OH}}$. The intermediate $\mathbf{I_O^-}$ undergoes O-O homolysis to form a biradical, which is fragmented into malonate anions. The O-O bond homolysis of the dianionic intermediate $\mathbf{I_O^-}$, under alkaline conditions is favored over that of the neutral counterpart $\mathbf{I_{OH}}$, with the unpaired electrons being stabilized by the geminal anionic oxygens. This difference in the stability of the intermediates translates into significant variations in the reaction rate and the product distribution between pH 10 and neutral conditions. It was also clarified that coordination of Na^+ to $\mathbf{I_O^-}$ during this reaction decreases the energies and enhances the O-O homolysis rate. This finding led us to the idea of investigating the effects of other metal cations on the degradation reaction.

I. INTRODUCTION

On one hand, 2,5-dihydroxy-[1,4]-benzoquinone (DHBQ) is one of the key chromophores formed upon aging ("brightness reversion") in cellulosic materials [1]. On the other hand, due to its extensive resonance stabilization, which results in highly delocalized double bonds, it also "survives" conventional bleaching treatments much longer than other chromophores. Degradation of DHBQ is thus a crucial issue in pulp bleaching, and hence clarification of the degradation mechanism of DHBQ by bleaching agents is indispensable for fine-tuning bleaching stages.

Previous accounts have addressed the general chemistry of DHBQ which mainly undergoes electrophilic substitution, nucleophilic substitution, and condensation with amines [2]. However, these works have employed DHBQ as a starting material in organic synthesis. With the revival of the compound which is connected to its pivotal role in cellulose yellowing, the degradation and "discoloration" of DHBQ became a matter of much interest. It is thus important to investigate the detailed behavior of DHBQ towards bleaching agents and elucidate the compound´s degradation mechanisms. In this study, we would like to communicate our attempts to clarify the detailed mechanism of the reaction between DHBQ and hydrogen peroxide as one of the most common bleaching agents, trying to combine experimental investigation with computational studies (DFT calculations).

II. MATERIALS AND METHODS

The degradation reaction was started by adding a 30% aqueous solution of hydrogen peroxide (2.2 mL, 19.6 mmol of hydrogen peroxide) to 20 mL of an pH 10 NaOH buffer solution or deionized water solution of DHBQ (10.7 mg, 0.0763mmol) in a 50 mL round bottom flask. The buffer solution of DHBQ contained 4.0 mg of 1,3,5-tricarboxylbenzene as internal standard. The solution was preheated at temperatures between 278.15 and 353.15 K before addition of the hydrogen peroxide solution. After the reaction started, sampling of the reaction mixture was done by adding 2.0 mL of the reaction solution separately into 10.0 mL of deionized water. After freeze drying of the sample at this temperature, the sample was analyzed by ^{1}H NMR in DMSO-d_6 to quantify the amount of non-reacted DHBQ. In the experiment in the pH 10 buffer, the degradation was also carried out in the presence of 1.63 g (11.4 mmol) of sodium sulfate. In this case, sodium sulfate was added into the buffer solution of DHBQ in advance and the degradation was started in the same manner as described above. Sampling was

carried out according to the procedure described above. The freeze-dried mixture was extracted with dimethyl ether and the soluble part was subject to ^{1}H NMR analysis in DMSO-d_6 after removal of the solvent *in vacuo*.
In quantum chemical computation, geometry optimization was carried out by the DFT method with the B3LYP functional. The 6-31G(d) basis sets were employed for H, C, O, Na where a diffuse function was added to each of C and O and a p-polarization function was added to H. For single point calculations, we employed MP2 or DFT(UB3LYP) method, the latter was used only for the calculations of radical species. In the single point calculations, cc-pVDZ basis stets were employed for H and Na and aug-cc-pVDZ basis sets were employed for C and O. In all calculations, the solvation energy in water was evaluated with the PCM method. It was ascertained that each equilibrium geometry exhibited no imaginary frequency and each transition state exhibited one imaginary frequency. Enthalpy, entropy, and Gibbs energy changes were evaluated at 298.15 K. Zero-point energy, thermal energy, and entropy change were evaluated with the DFT(B3LYP) method.

III. RESULTS AND DISCUSSION

Degradation under neutral conditions

Kinetic analysis of the degradation reaction under neutral conditions with an excess amount of H_2O_2 gave a linear relationship between the reaction time and the ln of the concentration of DHBQ, indicating the reaction to follow a pseudo-first-order kinetic rate law. Further investigation of temperature dependency of the pseudo-first-order rate constant (k) gave an Arrhenius plot, from which we determined an experimental activation energy (E_a) of 20.4 kcal/mol and activation entropy ($\Delta S^{0‡}$) of -27.7 cal/mol·K at 313.15 K, as summarized in **Table 1**. Product characterization with ^{1}H NMR and GC/MS analyses indicated that DHBQ degraded into malonic acid in around 50 % yield with the other 50 % of the products being acetic acid and carbon dioxide.
The DFT(B3LYP) computation to clarify the detailed mechanism showed an initial nucleophilic attack of H_2O_2 to DHBQ, forming an intermediate with an intramolecular O-O bridge between C2 and C5 of the 2,5-dihydoxy-1,4-cyclohexadione structure (**I_{OH}**) (**Figure 1**). This intermediate **I_{OH}** then undergoes homolysis of the O-O bond followed by β-fragmentation of the resulting biradical **BR_{OH}** to give ketene and oxaloacetic acid. While ketene is converted into acetic acid through reaction with water, oxaloacetic acid further degrades into malonic acid and carbon dioxide. The rate determining step of the degradation is the homolysis of the O-O bridged intermediate, and the E_a value was calculated to be 23.3 kcal/mol, which agrees well with the experimental value above [3].

Table 1. Experimental pseudo-first-order rate constants (k) and activation parameters in the degradation of DHBQ by H_2O_2 at 313.15 K.

	Without sodium sulfate				With sodium sulfate [b]
		Activation parameters [a]			
	k (s^{-1})	$\Delta H^{0‡}$ (kcal/mol)	$\Delta S^{0‡}$ (cal/mol·K)	$\Delta G^{0‡}$ (kcal/mol)	k (s^{-1})
Neutral conditions	4.66×10^{-4}	19.9	-16.7	24.9	–
Alkaline (pH 10) conditions	1.44×10^{-3}	15.5	-27.7	24.1	2.13×10^{-2}

[a] The activation energies (E_a) were determined to be 20.4 kcal/mol under neutral conditions and 16.1 kcal/mol under alkaline conditions. [b] The amount of sodium sulfate was 150 eq. (mole) against DHBQ.

Degradation under alkaline (pH 10) conditions

We next investigated the degradation under conditions more relevant to pulp bleaching (3.0% H_2O_2, NaOH, pH 10). Kinetic analysis indicated that the degradation followed a pseudo-first-order rate law also under these alkaline conditions. Interestingly, the degradation occurred with smaller E_a (16.1 kcal/mol) and $\Delta S^{0‡}$ (-27.7cal/mol·K) than under neutral conditions (**Table 1**), indicating that the degradation under pH 10 conditions is favorable from the viewpoint of enthalpy but unfavorable regarding entropy. Considering both factors, the effect of enthalpy is stronger than that of entropy, leading to a smaller activation Gibbs energy ($\Delta G^{0‡}$) under alkaline conditions. This means that the degradation becomes faster by increasing the pH to 10. The product characterization showed that DHBQ gave quantitatively malonic acid, whereas malonic acid was produced only in 50 % yield under neutral conditions (see previous section). These results suggest the degradation under pH 10 conditions to involve some mechanisms different from those under neutral conditions, as shown in **Figure 1A**.
The reaction pathway shown in **Figure 1B** was proposed for the degradation under pH 10 conditions from the DFT(B3LYP) computations [4]. In the first step of the degradation, deprotonated DHBQ reacts with H_2O_2 to form an intermediate **I_O^-**, which is the doubly deprotonated form of the intermediate **I_{OH}**. The O-O bond homolysis of **I_O^-** then occurs to give a biradical **BR_O^-**, which fragments into two molecules of radical **R1**. The radical **R1** further reacts with H_2O_2 resulting in the formation of two molecules of malonate anion. The rate

determining step of the degradation is the O-O bond homolysis, the same as that under the neutral conditions, with an E_a calculated to be 17.8 kcal/mol. This E_a value very well agrees with the experimental one (16.1 kcal/mol, see **Table 1**), indicating the correctness of the proposed mechanism. It is also noted that coordination of Na^+ to $\mathbf{I_O^-}$ and $\mathbf{BR_O^-}$ significantly decreased the energies and enhanced the O-O bond homolysis of $\mathbf{I_O^-}$. This computational result is well supported by the experimental fact that addition of Na_2SO_4 to the reaction solution considerably increased the degradation rate, and by the considerably negative $\Delta S^{0\ddagger}$ values calculated under alkaline conditions, as already mentioned above (see **Table 1**).

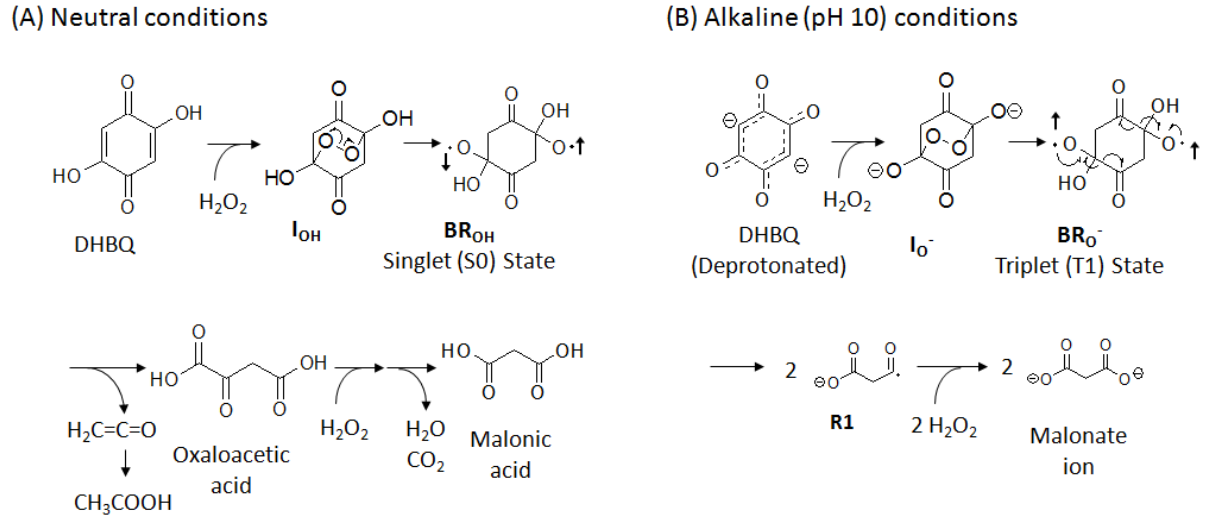

Figure 1. Degradation mechanisms under neutral conditions (A) and alkaline (pH 10) conditions (B), as proposed based on DFT computation, kinetics and product analyses [3,4]. In the mechanism for alkaline media, sodium cations coordinating to $\mathbf{I_O^-}$ and $\mathbf{BR_O^-}$ are not shown.

Degradation of DHBQ under alkaline and neutral conditions - a comparison

The mechanism for the degradation of DHBQ under alkaline conditions is considerably different from that under neutral conditions. One important difference is the stability of the biradicals formed by the O-O bridge homolysis, $\mathbf{BR_{OH}}$ (neutral) and $\mathbf{BR_O^-}$ (alkaline): $\mathbf{BR_O^-}$ is more stable than $\mathbf{BR_{OH}}$. In other words, deprotonation of the two hydroxyl groups of $\mathbf{I_{OH}}$ stabilizes the biracial. In fact, the E_a value calculated for the degradation under alkaline conditions (17.8 kcal/mol, see above) is much lower than that calculated for the degradation in neutral medium (23.3 kcal/mol), and so are the experimental E_a values (16.1 kcal/mol vs. 20.4 kcal/mol, see **Table 1**). Orbital analysis based on the DFT computation suggested that this difference in energy between $\mathbf{BR_O^-}$ and $\mathbf{BR_{OH}}$ was explained by the orbital interactions shown in **Figure 2**. In $\mathbf{BR_O^-}$, the unpaired electrons interact with the lone pairs of the geminal anionic oxygens. This interaction stabilizes the biradical with two electrons stabilized and one electron destabilized: $E_{SO} = 2\Delta E_{1O} - \Delta E_{2O} > 0$, see **Figure 2A**. In $\mathbf{BR_{OH}}$, by constrast, this stabilizing effect becomes much weaker as the orbital energy of the lone pair orbital is significantly decreased by the protonatin of the geminal oxgens, which renders the interaction between the lone pair electrons and the unpaired electron much weaker ($E_{SO} >> E_{SOH}$, see **Figure 2**). The activation energy required for the O-O bond homolysis therefore becomes much lower in the formation of $\mathbf{BR_O^-}$ from $\mathbf{I_O^-}$ (alkaline conditions) than that of $\mathbf{BR_{OH}}$ from $\mathbf{I_{OH}}$ (neutral conditions).

Another important difference between the degradation under alkaline vs. neutral conditions is the product distribution: DHBQ produces malonic acid in quantitative yield in alkaline medium, while a maximum of 50 % yields was obtained under neutral conditions (see previous sections). This difference in the products is well explained from the difference in the spine state from which the β-fragmentation of the biradicals starts, as shown in **Figure 1**. The DFT computation indicated that $\mathbf{BR_O^-}$ (alkaline conditions) underwent the β-fragmentation in a triplet (T1) state, where the two unpaired electrons have the same spin so that they cannot form a covalent bond (**Figure 1B**). Thus, β-fragmentation does not proceed further to form non-radical species, and two molecules of the radical **R1** are formed. Under the neutral conditions, on the other hand, the β-fragmentation occurs predominantly in the singlet (S0) state, in which the unpaired electrons can readily form a covalent bond afterwards (**Figure 1A**). Hence, ketene and oxaloacetic acid are produced as non-radical products. Since only oxaloacetic acid is a precursor of malonic acid, the yield of the latter comes down to 50% yield under neutral conditions.

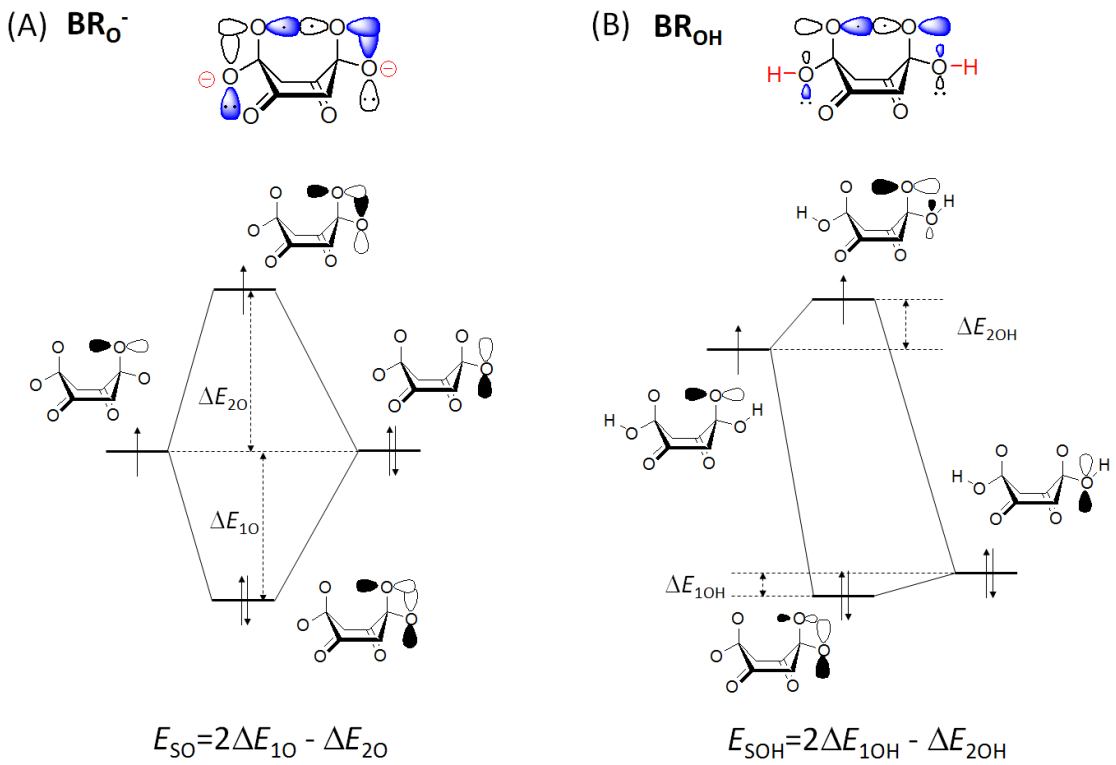

Figure 2. Orbital interaction between the unpaired electron and the lone pair electron at the germinal oxygen in the biradical **BR$_O^-$** (A) and **BR$_{OH}$** (B).

IV. CONCLUSIONS

The mechanisms of the degradation of DHBQ by hydrogen peroxide were significantly different between neutral and alkaline conditions. This clearly disqualifies the conventional assumption in pulp bleaching with H_2O_2 ("P-stage) that a change in pH influences only the reaction rate for chromophore removal, but not the actual mechanism. DHBQ is degraded more easily under alkaline conditions. In a P-stage, alkaline media are used anyway in order to minimize damage to the carbohydrates. The use of an alkaline pH would now get additional support as it is needed not only from the viewpoint of carbohydrate preservation, but also with regard to a faster degradation of DHBQ-based chromophores. The beneficial effect of Na^+ was also revealed. The addition of salts during the P-stage, such as sodium sulfate that is a byproduct in many pulp production units, would be an interesting conclusion to be tested in real-world bleaching of cellulosic pulps. In further work, effects of various metal cations, such as Li^+, K^+, Mg^{2+}, Ca^{2+}, and Al^{3+}, on the degradation mechanism will be examined in more detail.

V. ACKNOWLEDGEMENT

We performed quantum chemical calculations at the workstation in the Sakaki group, Fukui institute for fundamental chemistry at Kyoto University, Japan. The financial support of the Austrian Christian Doppler Research Society (CDG) through the CD-lab "Advanced cellulose chemistry and analytics" and of the Austrian Research Promotion Agency (FFG, project 829443) is gratefully acknowledged.

VI. REFERENCES

[1] Rosenau, T.; Potthast, A.; Krainz, K.; Yoneda, Y.; Dietz, T.; Shields, Z. P.; French, A. D. Chromophores in cellulosics, VI. First isolation and identification of residual chromophores from aged cotton linters. *Cellulose* **2011**, *18*, 1623-1633.

[2] Hosoya, T.; French, A. D.; Rosenau, T. Chemistry of 2,5-dihydroxy-[1,4]-benzoquinone, a key chromophore in aged cellulosics. *Mini Rev. Org. Chem.* **2013**, *10*, 309–315.

[3] Hosoya, T.; Rosenau, T. Degradation of 2,5-dihydroxy-[1,4]-benzoquinone by hydrogen peroxide: a combined kinetic and theoretical study. *J. Org. Chem.* **2013**, *78*, 3176-3182.

[4] Hosoya, T.; Rosenau, T. Degradation of 2,5-dihydroxy-[1,4]-benzoquinone by hydrogen peroxide under alkaline conditions resembling pulp bleaching: a combined kinetic and computational study. *J. Org. Chem.* **2013**, *78*, 11194-11203.

EFFECTS OF MAIN GROUP METAL SALTS ON H_2O_2 DEGRADATION OF 2,5-DIHYDROXY-[1,4]-BENZOQUINONE AS A KEY CHROMOPHORE IN AGED CELLULOSICS

Takashi Hosoya[1], Ute Henniges[1], Antje Potthast[1], Thomas Rosenau[1]*

[1] *University of Natural Resources and Life Sciences, Department of Chemistry, Muthgasse 18, A - 1190 Vienna, Austria (takashi.hosoya@boku.ac.at; thomas.rosenau@boku.ac.at)*

ABSTRACT

2,5-Dihydroxy-[1,4]-benzoquinone (DHBQ) is one of the key chromophores, both surviving conventional bleaching longer than other chromophores due to extensive resonance stabilization and re-formed upon aging ("brightness reversion") in cellulosic materials. Degradation of DHBQ is thus one of the key reactions in pulp bleaching, and hence clarification of the degradation mechanism of DHBQ by bleaching agents is indispensable for improvising pulp bleaching processes. Our work on the degradation of DHBQ under model conditions for pulp bleaching (3.0 % hydrogen peroxide/ pH 10) showed that the degradation was strongly enhanced by the presence of sodium cations, which stabilized anionic reaction intermediates by electrostatic interaction. This result led us to investigate the effects of other metal cations on the degradation reaction. This study addresses the effects of alkaline metal salts (Li_2SO_4, Na_2SO_4, and K_2SO_4), alkaline earth metal salts ($MgSO_4$ and $CaCl_2$), and $Al_2(SO_4)_3$ on the degradation of DHBQ under the same conditions. Kinetic analysis of the degradation showed that the degradation followed a pseudo first-order rate law in the presence of the alkaline metal and the alkaline earth metal salts, when excess of hydrogen peroxide was used. While the alkaline metal salts significantly enhanced the degradation, the alkaline earth metal salts slowed down the degradation. Visible spectra, ^{1}H NMR analyses and MP4(SDQ)//DFT(M06-2X) computation provide mechanical insights on the effects of these salts: Li^+, Na^+, and K^+ stabilize several reaction intermediates by forming complexes, leading to the enhancement of the degradation. On the other hand, Mg^{2+} and Ca^{2+} coordinate and stabilize the reactant (dianionic conjugate base of DHBQ) as well as the intermediates, resulting in a decreased degradation rate. $Al_2(SO_4)_3$ exhibited a strong enhancing effect. In this case, however, the degradation did not follow pseudo-first order, but second order kinetics regarding the concentration of DHBQ. This result strongly suggests that $Al_2(SO_4)_3$ completely changes the degradation mechanism, enabling reaction pathways different from the ones of the degradation in the presence of alkaline and alkaline earth metal salts.

I. INTRODUCTION

2,5-Dihydroxy-[1,4]-benzoquinone (DHBQ) is one of the key chromophores formed upon aging ("brightness reversion") in cellulosic materials [1]. Due to its extensive resonance stabilization, which results in highly delocalized double bonds, it "survives" conventional bleaching treatments much longer than other chromophores. Degradation of DHBQ is thus a crucial issue in pulp bleaching, and hence clarification of the degradation mechanism of DHBQ by bleaching agents is indispensable for fine-tuning bleaching stages. With the revival of studies of the compound, which is connected to its pivotal role in cellulose yellowing, the degradation and "discoloration" of DHBQ became a matter of much interest [2]. It is thus important to investigate the detailed behavior of DHBQ towards bleaching agents and elucidate the compound´s degradation mechanisms.

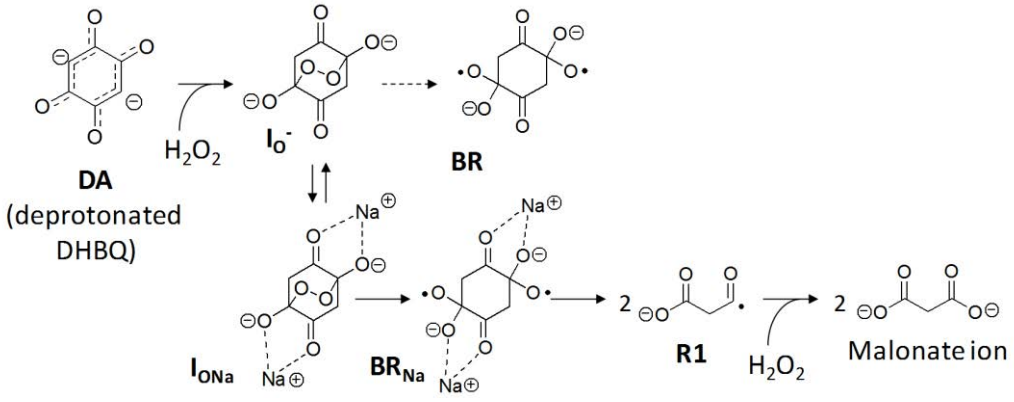

Figure 1. Degradation mechanism of DHBQ by H_2O_2 under alkaline pH 10 conditions, proposed in our previous study [3].

Our previous investigation demonstrated that H_2O_2 degradation of DHBQ under pulp bleaching conditions (3.0% H_2O_2/ pH 10 NaOH buffer solution) occurred according to the mechanism shown in **Figure 1** [3]. The degradation is initiated by an attack of H_2O_2 to deprotonated dianionic DHBQ **DA**, resulting in the formation of an intermediate $\mathbf{I_O^-}$. $\mathbf{I_O^-}$ is then coordinated by two sodium cations to form $\mathbf{I_{ONa}}$ and undergoes O-O bond homolysis to form a biradical $\mathbf{BR_{Na}}$, which is finally converted to the final product, malonic acid, via several intermediates. One of the key processes of this degradation is the coordination of Na^+ to $\mathbf{I_O^-}$, as the coordination significantly stabilizes $\mathbf{I_O^-}$ and enhances the homolysis of its intramoleculer O-O bridge. Based on this observation, we set out to investigate the effects of other metal cations on the H_2O_2 degradation of DHBQ under similar conditions. The effects of various metal cations on the degradation behavior of DHBQ are not only scientifically interesting, but also of industrial importance, since different metal cations are expected to prevail in actual bleaching stages. In this study, we investigate the effects of several main group metal cations, such as alkaline and alkaline earth metal cations and the aluminum cation, on the H_2O_2 degradation of DHBQ in pH 10 NaOH buffer solution, combining experimental and computational approaches.

II. MATERIALS AND METHODS

DHBQ (14.0 mg, 0.100 mM) was dissolved in 20.0 mL of the pH 10 NaOH buffer. The DHBQ solution (0.5 mL, corresponding to 2.5×10^{-3} mM of DHBQ) was taken to a quarts cell and diluted by adding another 3.0 mL of the buffer solution containing 4.5 mM of the metal cation: Na_2SO_4, Li_2SO_4, K_2SO_4, and $Al_2(SO_4)_3$: 2.25 mM, and $MgSO_4$ and $CaCl_2$: 4.5 mM. After inserting the cell in the UV-Vis spectrometer, the degradation was started at 295.15 K by adding 0.33 mL of a 30% aqueous solution of hydrogen peroxide (2.9 mM of H_2O_2) to the solution. The reaction was traced on the basis of the light absorbance at the λ_{max} of the reaction solution.

In quantum chemical calculations, the geometry optimization was carried out by the DFT method with the M06-2X functional. The 6-311G(d) basis sets were employed for H, C, O and metal atoms, where a diffuse function was added to each of C and O and a p-polarization function was added to H. It was ascertained that each equilibrium geometry exhibited no imaginary frequency. Zero-point energy was evaluated with the DFT(M06-2X) method. In the energy evaluation, we employed MP4(SDQ) and DFT(M06-2X) methods. The aug-cc-pVTZ basis set was employed for O atoms and cc-pVTZ basis sets were used for H, C, and metal atoms. In all calculations, the solvation energy was evaluated with the PCM method.

III. RESULTS AND DISCUSSION

Kinetic analysis

Kinetic innvestigation on the degradation of DHBQ with an excess of H_2O_2 in the presence of Li_2SO_4, Na_2SO_4, K_2SO_4, $MgSO_4$, $CaCl_2$ indicated that the degradation reactions followed pseudo-first-order: there relationships between the reaction time and the logarithm of the DHBQ concentration was linear, as shown in **Figure 2A**. In addition to the enhancing effect of Na_2SO_4 reported in our previous study, similar enhancing effects were also observed for the degradation in the presence of Li_2SO_4 and K_2SO_4. On the other hand, it was evident that the reaction was slowed down by $MgSO_4$ and $CaCl_2$.

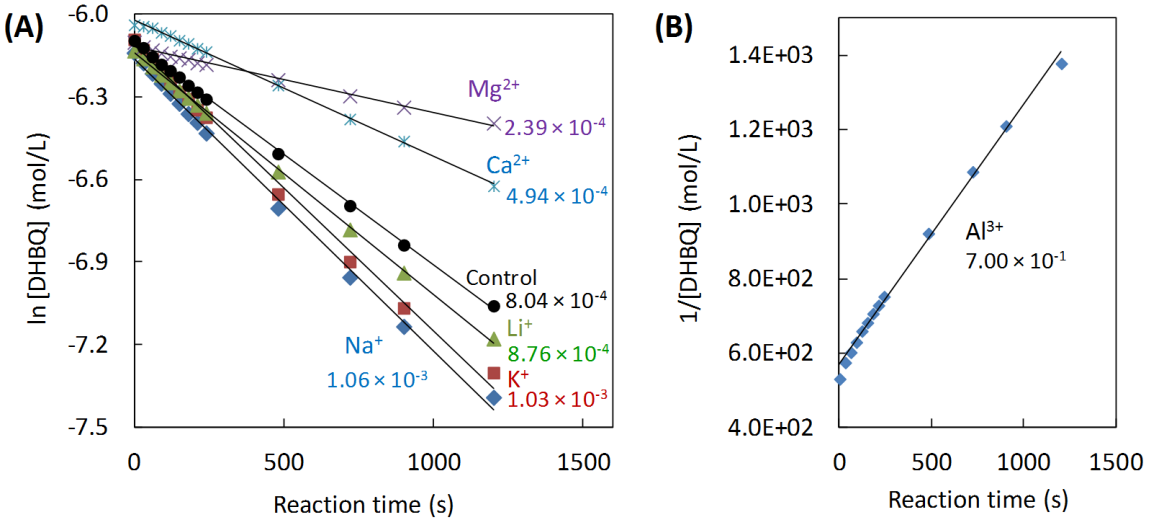

Figure 2. Kinetic analyses of the DHBQ degradation under alkaline pH 10 conditions, upon addition of different monovalent, divalent and trivalent cations: alkaline and alkaline earth metal salts (A) and $Al_2(SO_4)_3$ (B).

Besides the good correlation according to pseudo first-order approximation for the reactions with the mono- and divalent cations, the reaction in the presence of $Al_2(SO_4)_3$ did not follow pseudo-first order, but pseudo-second order: a linear relationship was found for the plot of the reciprocal of DHBQ concentration against reaction time (see **Figure 2B**). This result strongly suggests that $Al_2(SO_4)_3$ completely altered the degradation mechanism, and that the mechanism in **Figure 1** was no longer valid when $Al_2(SO_4)_3$ was present in the reaction system.

Complex formation between deprotonated DHBQ and metal cations

To clarify in what form the deprotonated dianionic DHBQ **DA** exists in the reaction solution, we investigated the dependency of the visible spectrum of DHBQ on the presence of the metal cations. $MgSO_4$, $CaCl_2$, and $Al_2(SO_4)_3$ caused considerable changes in the visible spectrum compared to the spectrum of DHBQ alone: the absorbance between 370-550 nm was considerably decreased by the addition of these salts. By contrast, addition of the alkaline metal salts produced no significant variation in the spectrum. ^{1}H NMR analysis also showed that the chemical shift of the C-H protons of **DA** shifted toward lower magnetic fields by 0.19 ppm by the presence of $MgSO_4$ whereas the alkaline metal salts caused almost no change in chemical shift. A plausible explanation for these experimental observations is that **DA** has a strong affinity for Mg^{2+}, Ca^{2+}, and Al^{3+} and formed complexes with these cations, but did not form such complexes with Li^+, Na^+, and K^+.

To support the above hypothesis of the complex formation, we carried out quantum chemical calculations to calculate binding energies between **DA** and the metal cations (two cations due to the symmetry properties of the molecule). As listed in **Table 1**, the Mg^{2+}, Ca^{2+}, and Al^{3+} complexes (**DA_{Mg}**, **DA_{Ca}**, and **DA_{Al}**, respectively) clearly exhibited much higher biding energy than the Li^+, Na^+, K^+ complexes (**DA_{Li}**, **DA_{Na}**, and **DA_K**, respectively). These computational results well support the complex formation hypothesis. The high binding energy in the case of $Mg^{2+}$is particularly noteworthy.

Table 1. Binding energy between metal cations and **DA**, calculated at the MP4(SDQ) level.

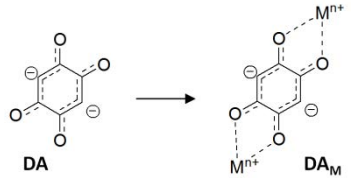

DA_M	Binding energy (kcal/mol)
DA_{Li}	25.1
DA_{Na}	17.6
DA_K	13.2
DA_{Mg}	83.1
DA_{Ca}	46.6
DA_{Al}[a)]	41.0

[a)] The binding energy was calculated at the DFT(M06-2X) level. MP4(SDQ) computation was impossible due to the large size of the complex.

Mechanistic insights

The degradation of DHBQ without the additional salts proceeds according to the mechanism in **Figure 1**. In the presence of the salt other than $Al_2(SO_4)_3$, the degradation mechanisms of DHBQ is similar to that in **Figure 1**, since the degradation reactions in the presence of the salt follow pseudo first-order rate laws (**Figure 2**) as does the degradation without any addition of salt. Metal salt addition (apart from Al^{3+}) just has an effect on the reaction rate, but not on the mechanism. We thus evaluated the potential energies of the reactant **DA**, the intermediate **I_O^-**, the biradical **BR**, and their cation complexes.

While the biradical **BR** without the coordination of the metal cations was calculated to be 41.1 kcal/mol less stable than the reactant **DA**, coordination of Na^+ to **BR** significantly stabilized the biradical: **BR_{Na}** is only 22.9 kcal/mol less stable than **DA** (see **Figure 3**). The ΔE values of **BR_{Li}** and **BR_K** relative to **DA** exhibited similar values to that of **BR_{Na}**. This result is consistent with the experimental observation that Li_2SO_4 and K_2SO_4 had an enhancing effect similar to that of Na_2SO_4.

As mentioned in the previous section, **DA** formed complexes with Mg^{2+} and Ca^{2+} as well. The ΔE values of the biradicals **BR_{Mg}** and **BR_{Ca}** was thus eveluated relative to the **DA**-Metal complexes, **DA_{Mg}** and **DA_{Ca}**. **BR_{Mg}** and **BR_{Ca}** were extremely unstable compared to the biradicals with alkali metal cations, **BR_{Li}**, **BR_{Na}** and **BR_K**: the ΔE values of **BR_{Mg}** and **BR_{Ca}** are 52.2 and 44.5 kcal/mol higher than **DA_{Mg}** and **DA_{Ca}**, respectively. This is

essentially because the coordination stabilizes the reactant **DA** as well as the biradical **BR**. These computational results are consistent with the experimental observation that the addition of $MgSO_4$ and $CaCl_2$ slowed down the reaction (see **Figure 2A**). We also calculated the biradical $\mathbf{BR_{Al}}$, the Al^{3+}-coordinated **BR**. The ΔE value of $\mathbf{BR_{Al}}$ was calculated to be 70.0 kcal/mol relative to the complex $\mathbf{DA_{Al}}$, indicating that the formation of $\mathbf{BR_{Al}}$ is unlikely to occur. This computational result corresponds to the result from the kinetic analysis that the reaction mechanism is altered from that in **Figure 1** to different one in the presence of Al^{3+}. Since the reaction follows second-order regarding to DHBQ concentration, the altered mechanism would involve two moleucles of **DA**, but further investigation is necessary to clarify more detailed mechanisms involved there. It should be noted as well that aluminum cations at alkaline pH are present as $[Al(OH)_4]^-$ rather than trivalent Al^{3+} which certainly affects the mechanism.

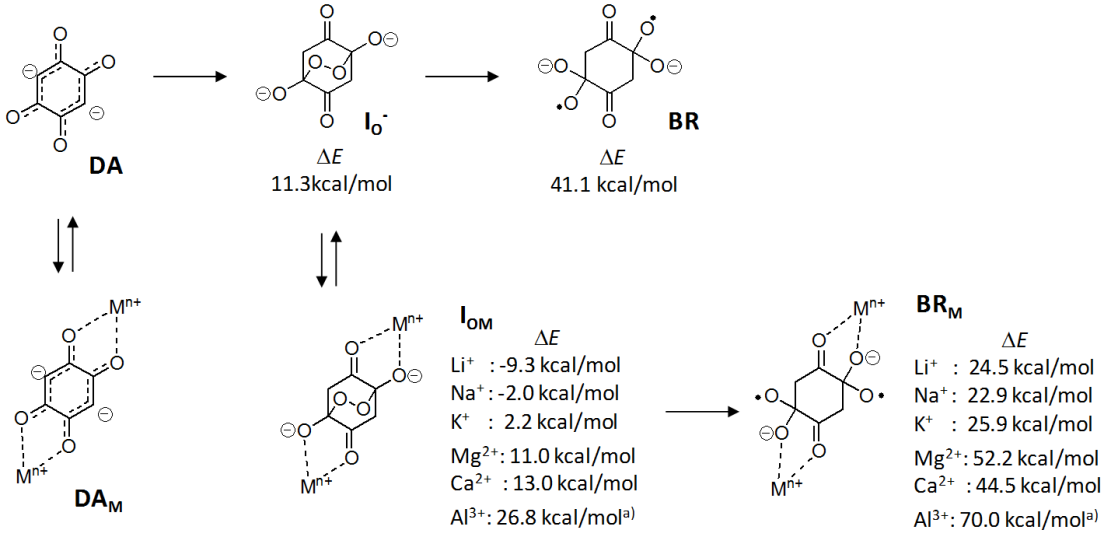

Figure 3. Potential energies (ΔE) of $\mathbf{I_O^-}$, **BR**, and their complexes with the cations, $\mathbf{I_OM}$ and $\mathbf{BR_M}$, calculated at the MP4(SDQ) level. The energy of **R** was taken to be energy zero in the reaction without any cation and those in the presence of Li^+, Na^+, and K^+, while the energies of $\mathbf{R_M}$ were taken as energy zero in the reactions with Mg^{2+}, Ca^{2+}, and Al^{3+}. [A)] DFT(M06-2X) was employed in the energy evaluation of $\mathbf{DA_{Al}}$, $\mathbf{I_OAl}$, and $\mathbf{BA_{Al}}$.

IV. CONCLUSIONS

We made quantitative evaluation of the effects of alkaline metal salts (Li_2SO_4, Na_2SO_4, and K_2SO_4), alkaline earth metal salts ($MgSO_4$ and $CaCl_2$), and $Al_2(SO_4)_3$ on the degradation of DHBQ by hydrogen peroxide at pH 10. The alkaline metal salts significantly enhanced the degradation, which was attributed to the stabilization of the intermediate $\mathbf{I_O^-}$ and the biradical **BR** through complex formation with the alkaline metal cations. The alkaline earth metal salts, on the other hand, slowed down the degradation, as these salts stabilizes the reactant **DA** through complexes formation. For the degradation in the presence of $Al_2(SO_4)_3$, the kinetic analysis strongly suggested an altered degradation mechanism. The results are important also from the viewpoint of metal cation management in the bleaching stages. While alkali metals promote the removal of DHBQ by H_2O_2, magnesium - which has a desired protective effect on carbohydrates - has an unwanted protective effect also on DHBQ.

V. ACKNOWLEDGEMENT

We performed quantum chemical calculations with the workstation in the Sakaki group, Fukui institute for fundamental chemistry at Kyoto University, Japan. The financial support of the Austrian Christian Doppler Research Society (CDG) through the CD-lab "Advanced cellulose chemistry and analytics) and of the Austrian Research Promotion Agency (FFG, project 829443) is gratefully acknowledged.

VI. REFERENCES

[1] Rosenau, T.; Potthast, A.; Krainz, K.; Yoneda, Y.; Dietz, T.; Shields, Z. P.; French, A. D. Chromophores in cellulosics, VI. First isolation and identification of residual chromophores from aged cotton linters. *Cellulose* **2011**, *18*, 1623-1633.

[2] Hosoya, T.; French, A. D.; Rosenau, T. Chemistry of 2,5-dihydroxy-[1,4]-benzoquinone, a key chromophore in aged cellulosics. *Mini Rev. Org. Chem.* **2013**, *10*, 309–315.

[3] (a) Hosoya, T.; Rosenau, T. Degradation of 2,5-dihydroxy-[1,4]-benzoquinone by hydrogen peroxide under moderately alkaline conditions resembling pulp bleaching: a combined kinetic and computational study. *J. Org. Chem.* **2013**, *78*, 11194–11203. (b) Hosoya, T.; Rosenau, T. Degradation of 2,5-dihydroxy-[1,4]-benzoquinone by hydrogen peroxide: a combined kinetic and theoretical study. *J. Org. Chem.* **2013**, *78*, 3176-3182.

ONE-STEP PRODUCTION OF CELLULOSE NANOFIBERS DISPERSED IN BOTH HYDROPHOBIC AND HYDROPHILIC SOLVENTS

Pei Huang, Min Wu, Shigenori Kuga and Yong Huang*

*National Engineering Research Center for Engineering Plastics, Technical Institute of Physics & Chemistry, Chinese Academy of Sciences, Beijing100190 China (*yhuang@mail.ipc.ac.cn)*

ABSTRACT

A facile and quick one-step method was developed for producing cellulose nanofibers dispersible in organic liquids. Planetary ball milling of native cellulose in an aprotic polar solvent doped with an esterifying agent resulted in highly dispersed nanofibers with esterified surfaces. Successful combinations include hexanoyl chloride/DMF and succinic anhydride/DMSO. Ball milling for 16 h was sufficient to give complete dispersion showing flow birefringence. The dispersion medium could be exchanged from DMF to other solvents such as THF and butyl alcohol via centrifugation-redispersion cycles. The hexanoylated nanofibers could be dried up to form dense film, which could be readily redispersed in THF by sonication. The succinated nanofibers were hydrophilic due to introduction of unesterified carboxyls and could be dispersed in water as anionic nanofibers. The bulk degree of substitution of the fully esterified products ranged from 0.4~ 0.6. These values correspond to nanofiber width of 3~5 nm by assuming complete esterification of surface hydroxyls. These results demonstrate remarkable efficacy of simultaneous application of mechanical and chemical actions for dispersing cellulose into the thinnest fiber units.

I. INTRODUCTION

Disintegration of native cellulose into its intrinsic fibrillar unit, i.e. cellulose nanofiber (CNF), is pursued intensively. Unlike several exotic cellulose sources such as vinegar bacteria and tunicate (lower sea animal), higher plant cellulose is difficult to disintegrate into nanofibers due to its intricate mutual bundling. Several physical[1-3] and chemical[4,5] techniques have been developed to cause effective disintegration of wood pulp, which is the most important practical raw material.

One of the promising use of cellulose nanofiber is fabrication of nanocomposites with thermoplastic polymers, which can replace glass fiber-based automotive components. One drawback of CNF, however, is its hydrophilic nature due to abundant hydroxyl groups, which cause poor adhesion with synthetic resins and water sensitivity of the composite. For overcoming these problems, hydrophobic modification of CNF surface is also sought after.

In the pursuit of effective methods of CNF preparation and surface modification, we found that simultaneous application of physical and chemical actions, i.e. a mechanochemical approach, can be the answer of said challenges. It consists of planetary ball milling of the cellulose material in an organic solvent together with an esterifying agent[6,7]. This method can give hydrophobically modified CNF in one step, possible useful in practical manufacturing of high-performance composites.

II. EXPERIMENTAL

Materials

Microcrystalline cellulose (Whatman CF11) or a commercial bleached kraft pulp was used as starting materials. All chemicals were used as received. Water means deionized or distilled water.

Procedure

a) Hydrophobic esterification[6]: A 40 ml zirconia pot with 17 zirconia balls (1.0 cm diameter) was loaded with 1.7 g of CF11, 23 mL of N,N-dimethylformamide (DMF), and 4.3mL of hexanoyl chloride (HC). The pot was operated by a Fritsch Pulverisette 7 at 300 rpm for desired time. A 10 min pause was set after every 20 min run for preventing heating up. Starting from room temperature, temperature of the pot during operation stayed at 30-40^{o}C. The solid product was washed with DMF by repeated centrifugation to remove unreacted HC.

b) Hydrophilic esterification: Performed as in a), but DMF and HC were replaced by DMSO, and succinic anhydride, respectively. Unlike HC's case, this reaction needs catalyst, as which dimethylaminopyridine or calcium carbonate was found effective. Catalyst 0.2-1.0 g per pot was examined.

c) Swelling pretreatment of pulp

The starting cellulose material was immersed in a large amount of water or 2 % NaOH at room temperature for 3 days[7]. The latter was then thoroughly washed with water. Wet cellulose was solvent-exchanged to DMF by 12,000-rpm centrifuge-redispersion repeated twice.

Characterization

Products were analyzed by X-ray diffraction (XRD), FTIR, and thermogravimetry (TGA).

III. RESULTS AND DISCUSSION

The solid material recovered from ball milling with HC could be readily dispersed in DMF, alcohols, chloroform, or toluene. Light sonication in these solvents gave non-sedimenting suspensions, which showed flow birefringence observed between crossed polarizers (Fig. 1). This behavior indicates successful disintegration of cellulose into nanofibers. TEM and SEM images also show nearly homogeneous individualization of nanofibers.

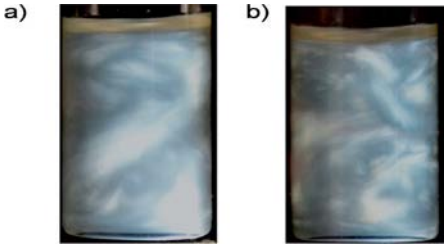

Figure 1. Flow birefringence of esterified cellulose nanofiber suspension. a) Nanofiber/DMF suspension after 16 h of ball milling in HC/DMF, and b) same sample once dried and redispersed in THF.

In spite of extensive ball milling, the cellulose nanofibers have not been subjected to visible damage, as confirmed by Fig. 2. Also, XRD (Fig. 4) showed nearly no change in crystallinity. This is remarkable because the disintegrated nanofibers are actually smallest fiber unit that existed in the starting material. That unit in higher plant cellulose is believed to be approx. 3.5 nm wide, so-called "elementary fibrils". Assuming that all hydroxyls on the surface of nanofibers were esterified, one can calculate the width of cellulose core as 5.5 nm. This value agrees well with estimation from XRD peak (Fig. 4) by the Scherrer formula, 5.7 nm.

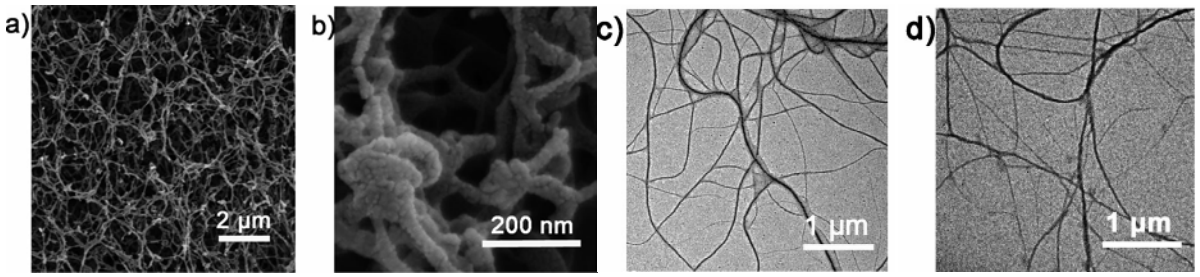

Figure 2. SEM (a, b) and TEM (c, d) images of HC-esterified cellulose.

Fig. 3 shows the change in FTIR spectra of HC-esterified cellulose for varied milling time. It shows a gradual increase in the relative intensity of the ester C=O (1740 cm^{-1}) and C-H stretching (2900 cm^{-1}) peaks. The growth of ester peak indicates near saturation by 16 h-milling. The ratio of the height of the 1740 cm^{-1} peak and the 1059 cm^{-1} peak (C-O stretching of glucopyranoside) allowed to estimate the a degree of substitution (DS) as 0.60 after 24 h of ball milling. This value agreed well with the level of weight gain of the product.

Esterification of kraft pulp was harder than CF11, but swelling pretreatment with water or 2% NaOH was very effective, giving similar levels of nanofiber dispersion and DS.

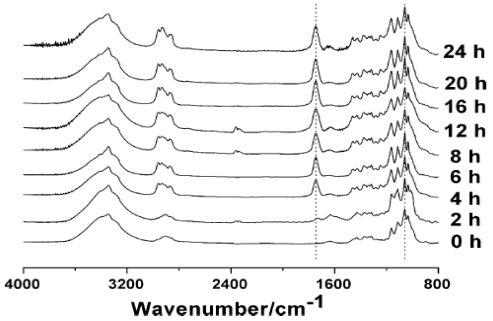

Figure 3. FTIR spectra of HC-esterified cellulose.

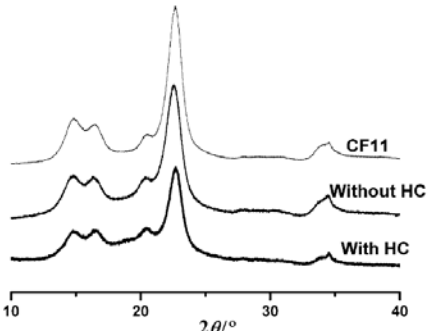

Figure 4. XRD of HC-esterified cellulose.

Ball mill treatment with succinic anhydride in DMSO also resulted in nanofiber dispersion. This reaction forms half ester of succinic acid attached to cellulose, and the nanofiber surface becomes anionic. Therefore the product can be dispersed in water as well as in DMSO. Results of characterization were similar to those for HC esterification. Milling time to reach maximum DS was approx. 20 h. By the use of DMAP catalyst (0.6 g/pot), the bulk DS reached 0.36, much lower than HC's case (0.60). A possible cause this difference is steric hindrance. Calcium carbonate, an inexpensive and safe substance, could be used instead of DMAP. The reaction efficiency was somewhat lower, but it opens possibility of using this process for food or cosmetic applications. Because succinic acid is also a very safe material permitted as food ingredient. This situation would be favorable in practical utilization.

Figure 5. Flow birefringenc of succinylated cellulose nanofiber suspension in DMSO (left) and water (rght).

IV. CONCLUSIONS

While various combinations of mechanical and chemical treatments as pre- or post-treatments, our study revealed remarkable effectiveness of the simultaneous application of them, i.e. mechanochemical method. This technique may be applied to devices other than planetary ball mill, such as high-energy vibration mill, ultrasonicator, high-pressure homogenizer, and disc mill. Also, chemical treatments would not be limited to esterification only; possible reactions include etherification, oxidation etc. Mechanochemistry of cellulose is just starting.

V. ACKNOWLEDGEMENT

This work was supported by the National Natural Science Foundation of China (51043003, 51172247, 50821062), the National Program on Key Basic Research Project (973 Program, 2011CB933700), and the Chinese Academy of Sciences Visiting Professorships.

VI. REFERENCES

[1] Abe, K.; Iwamoto, S.; Yano, H. Obtaining Cellulose Nanofibers with a Uniform Width of 15 nm from Wood. *Biomacromolecules* **2007**, *8*, 3276 –3278.

[2] a) Chakraborty, A.; Sain, M.; Kortschot, M. Cellulose microfibrils: A novel method of preparation using high shear refining and cryocrushing. *Holzforschung* **2005**, *59*, 102–107; b) Sundari, M. T.; Ramesh, A. Isolation and characterization of cellulose nanofibers from the aquatic weed water hyacinth—Eichhornia crassipes. *Carbohydr. Polym.* **2012**, *87*, 1701 –1705.

[3] Zhao, H. P.; Feng, X. Q.; Gao, H. Ultrasonic technique for extracting nanofibers from nature materials. *Appl. Phys. Lett.* **2007**, *90*, 073112.

[4] Dong, X. M.; Revol, J. F.; Gray, D. G. Effect of microcrystallite preparation conditions on the formation of colloid crystals of cellulose. *Cellulose* **1998**, *5*, 19– 32.

[5] Saito, T.; Isogai, A. TEMPO-Mediated Oxidation of Native Cellulose. The Effect of Oxidation Conditions on Chemical and Crystal Structures of the Water-Insoluble Fractions. *Biomacromolecules* **2004**, *5*, 1983 –1989.

[6] Huang, P.; Wu, M.; Kuga, S.; Wang, D.; Wu, D.; Huang, Y. One-Step Dispersion of Cellulose Nanofibers by Mechanochemical Esterification in an Organic Solvent. *ChemSusChem* **2012**, *5*, 2319 – 2322.

[7] Huang, P.; Wu, M.; Kuga, S.; Huang, Y. Aqueous pretreatment for reactive ball milling of cellulose. *Cellulose* **2013**, *20*, 2175-2178.

PREDICTION OF SCALING RISK IN CHEMICAL PULP BLEACH PLANTS

Patrick HUBER*, Auphélia BURNET, Michel PETIT-CONIL

Centre Technique du Papier, CS 90251, 38044 Grenoble Cedex 9, France
*(*Patrick.Huber@webctp.com)*

ABSTRACT

The general tendency in the pulp industry towards reduced fresh water consumption and minimum effluent causes major deposit problems in mills. Chemical pulp bleach plants are affected by several types of mineral deposits, the most frequent being calcite, calcium oxalate and barite.
We present a chemical speciation model, which predicts local scaling risk in chemical pulp bleach plants. The interest for magnesium salts to reduce calcium oxalate scaling risks is discussed and simulated.

I. INTRODUCTION

The pulp industry has made great efforts to reduce its specific water consumption over the last few decades. With the increasing closure of bleach plants in chemical pulp mills, many dissolved species accumulate in process loops, which may lead to scale deposits. Various methods may be used to prevent deposits, such as metal removal (by acid washing and/or chelation). In severe cases, the bleach plant has to be shut down, as only hydro-blasting techniques and/or acid cleaning procedures can remove the most encrusted deposits. The most frequent types of scale in bleaching lines are composed of calcium carbonate, calcium oxalate and barium sulphate [1].

Calcite: $$CaCO_{3(s)} = Ca^{+2} + CO_3^{-2}$$

Calcite deposits form in supersaturated solutions containing both calcium and inorganic carbon. The main source of calcium is the wood material itself (0.5-1.0 kg/T, see [1]). Calcium is released during the cooking stage. Carbonate ions mostly come from the white liquor (as carry-over from the re-caustification cycle). In bleach plant filtrates, various dissolved organic species can complex with calcium, thus reducing free calcium available for precipitation.

Calcium oxalate: $$CaOxalate:H_2O_{(s)} = Ca^{+2} + Oxalate^{-2} + H_2O$$

Calcium oxalate deposits form in supersaturated solutions containing both calcium and oxalate. Oxalic acid ($C_2O_4H_2$) is a dicarboxylic acid naturally present in wood (0.1-0.4 kg/T, and up to 10-15 kg/T in bark) [2]. It is also formed from reactions with wood during bleaching as an oxidation product of lignin (mainly) and hemicelluloses (xylan/uronic acids) (to a lesser extent). Oxalic acid formation is proportional to Kappa number reduction [3]. Typically, the largest oxalic acid release occurs during oxygen delignification and ozone bleaching stages. Like other dissolved wood organics, oxalate plays the role of a weak chelating agent with respect to most metal cations.

Barite: $$BaSO_4 = Ba^{+2} + SO_4^{-2}$$

Barite deposits form in supersaturated solutions containing both barium and sulphate ions. The main source of barium in the bleaching line is the wood itself. There are large differences among wood species, but typically there is more barium in hardwood chips (20-60 ppm) than in softwood chips (10 ppm) [4]. As in the case of the other metal cations, the barium content of the bark is much higher than that of the stem wood. The main source of sulphate in the bleaching line is pH regulation with sulphuric acid.

In order to reduce scaling, it is crucial to understand the physicochemical parameters that govern the phenomenon, in the conditions of a closed bleach plant (i.e. at high ionic strength, and in the presence of dissolved wood organics and fibres). Chemical speciation methods are an invaluable way of predicting scaling risks [5].

In this work, we present a method to calculate the saturation index of pulps or bleaching effluents, with respect to the main mineral deposits. The model can simulate several basic bleaching operations that affect scaling, such as pulp washing, pH regulation, etc. Curative solutions to scale deposits are discussed and simulated.

II. EXPERIMENTAL

Scaling is a complex phenomenon, involving many dissolved species, together with solid and gas phases. The scaling potential of a solution is defined by its supersaturation [6]. Supersaturation quantifies how far the solution is from equilibrium.

In an aqueous solution, a chemical element may be involved in several chemical reactions, so that it is distributed as various soluble species. Thus, only a fraction of the element participates in the scaling process. For instance, in the case of calcium carbonate scaling, only a fraction of the total inorganic carbon is actually in carbonate form, and this depends on carbonic acid equilibria, thus mainly on pH.

In order to estimate scaling, the saturation index with respect to the precipitating phase has to be calculated. This involves estimating the ionic activity product (IAP), i.e. the activities of the precipitating species in the solution (for instance with calcite: IAP = $a(Ca^{+2}).a(CO_3^{-2})$, where a() denotes activity). This is achieved through the simultaneous resolution of all chemicals equilibria in the system. The ionic activity product can then be compared with the solubility product Ks, and the ratio is the supersaturation (S=IAP/Ks). The saturation index (SI) is defined as log(S). If a solution has SI<0, there is no scaling risk, as it could dissolve more solids before reaching equilibrium. If a solution has SI>0, there is a scaling risk, as it would tend to precipitate some solid in order to reach equilibrium (which corresponds to SI=0).

In this work, all speciation calculations were performed with PHREEQC [7]. Ion-exchange phenomena with fibres are resolved with the EXCHANGE feature in PHREEQC. The ion exchange reactions with fibres and constants are taken from [8]. Reference solution composition and conditions are given by (Temp.=50°C, all [ ] given in mM: $[Ba]=10^{-3}$, [S(6)]=20, [Oxalate]=1, [Ca]=1, [C]=5, [Na]=20, [Mg]= 1, [Cl]=10, [Acetate]=3), unless otherwise specified. More details concerning the simulation methods can be found in [9]. In this case, dozens of chemical equilibria must be resolved simultaneously, involving up to 46 soluble species.

III. RESULTS AND DISCUSSION

The modelling can predict the conditions which favour mineral deposits in the bleaching line (**Figure 1**).

Barite is a very insoluble mineral. It is less soluble at cold temperatures (like calcium oxalate, but unlike calcite), so that it is important to avoid temperature drops anywhere in the bleaching line, especially on washers. The precipitation tendency of barite is pH-dependent; this is because the availability of sulphate anions is governed by the second dissociation of sulphuric acid ($HSO_4^- \rightleftarrows SO_4^{-2} + H^+$). Barite precipitation may start at any pH>2 (however this situation is changed when sulphuric acid is used for pH regulation).

Calcite precipitates in alkaline conditions only (8<pH<13). The precipitation tendency also depends on temperature. Calcite is less soluble at high temperature. In the bleaching line, calcite deposits may be expected during the oxygen delignification, extraction and peroxide bleaching stages. Note that, when the pulp or the effluent comes into contact with air, inorganic carbon may have a tendency to escape to the atmosphere as gaseous CO_2, thereby enhancing calcite deposition [10]. This may occur on washers after alkaline extraction.

The availability of the $Oxalate^{-2}$ species involved in scaling problems is determined by the two dissociations of oxalic acid. Thus calcium oxalate is likely to be deposited as soon as pH>3. Calcium oxalate deposits are also less likely to happen in highly alkaline conditions (pH>12.5) as calcium is mobilised in other soluble complexes and no longer available for precipitation. Calcium oxalate deposits prevail at low temperatures (T<40-50°C). This explains why calcium oxalate is deposited preferentially on washing filters.

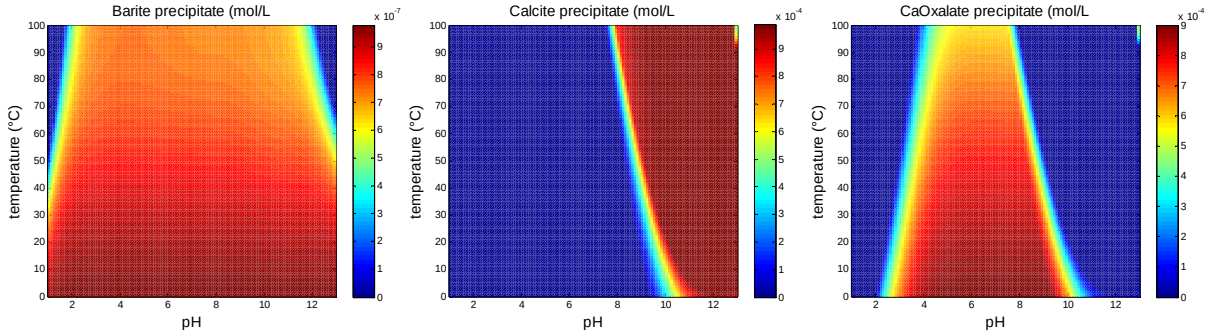

Figure 1. *Combined effect of temperature and pH on simultaneous precipitation of barite, calcite and calcium oxalate, for the reference bleaching effluent*

If we take typical pH and temperature profiles throughout a bleaching line, the following scaling risks can be anticipated at each bleaching stage (see **Figure 2**):

ECF sequences potential deposits:

- O: calcite and calcium oxalate
- D0: barite
- E: calcite and calcium oxalate
- D1: barite and calcium oxalate
- D2: calcium oxalate

TCF sequences potential deposits:

- O: calcite and calcium oxalate
- Q: calcium oxalate
- Z: barite
- P: calcite and calcium oxalate

The calculation presented takes into account the main physicochemical phenomena occurring in the pulp suspension during bleaching (pH, temperature, ionic strength, complexations, ion exchange with fibres, additives such as EDTA, etc.).

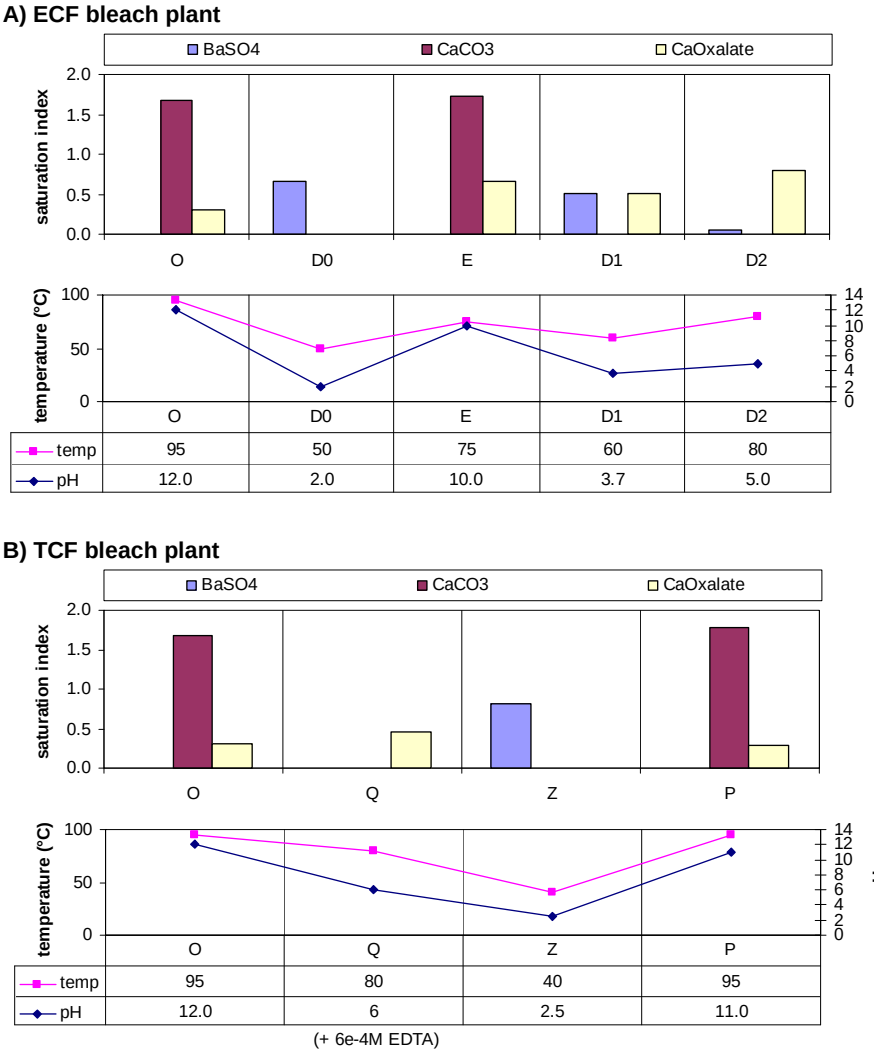

Figure 2. *Evaluation of scaling risk throughout bleach plant A) ECF, B) TCF (same effluent composition in each stage, ion exchange with fibres taken into account).*

From the scaling point of view, introducing magnesium into the system has great potential advantages. The introduction of magnesium salts is a large source of Mg^{+2} that competes with Ca^{+2} in the formation of calcium oxalate. Magnesium forms soluble magnesium oxalate complex (log(K)=3.56). Therefore less oxalate is available to precipitate with calcium. Our calculations show that this effect is anticipated to reduce problems related to calcium oxalate deposits considerably (**Figure 3**). Interestingly, magnesium salts have the greatest beneficial effect in conditions where calcium oxalate deposits are most severe (4<pH<11 and temperature<50°C) (**Figure 4**). This offers opportunities for reducing calcium oxalate deposits during peroxide bleaching by using alternative alkali sources such as $Mg(OH)_2$, or magnesium salts such as $MgCl_2$.

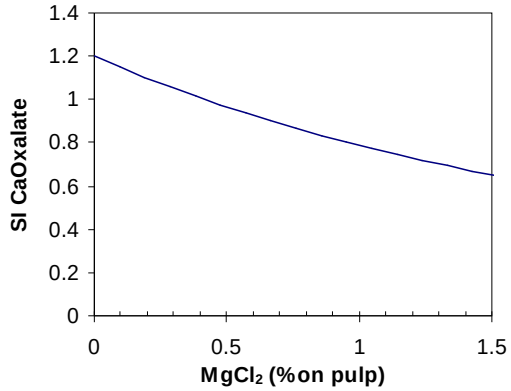

Figure 3. *Effect of magnesium chloride addition on saturation index of calcium oxalate (T=50°C, pH=7)*

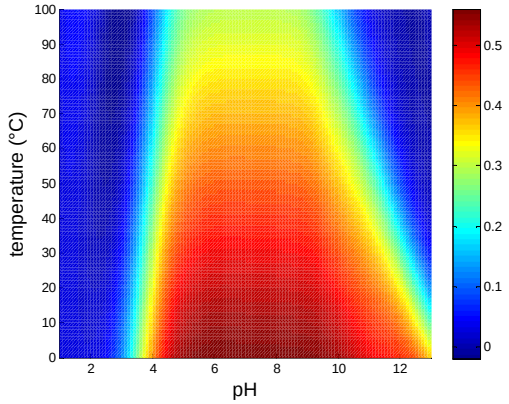

Figure 4. *Reduction of saturation index of calcium oxalate vs. temperature and pH, for 1% $MgCl_2$ added on pulp*

IV. CONCLUSIONS

The saturation index of precipitating phases can be calculated with the chemical speciation model. This allows calculating the potential scaling risks throughout a chemical pulp bleaching line. The modelling demonstrates the interest for using magnesium salts to limit calcium oxalate deposits.

Perspectives to this work are to integrate the scaling chemistry model into our process simulation tool. This will make it possible to evaluate potential scaling problems throughout the fibre line and study the interest of curative strategies to be implemented in the bleach line to combat and solve scaling problems.

V. ACKNOWLEDGEMENT

The authors would like to express their acknowledgements to the CTPi members, who supported this project.

VI. REFERENCES

[1] Ulmgren, P. Non-Process Elements in a Bleached Kraft Pulp Mill with a High Degree of System Closure-State of the Art. *Nord. Pulp Pap. Res. J.*, **1997**, *12*, 32–41.

[2] Häärä, M.; Sundberg, A.; Willför, S. Calcium Oxalate-a Source of “Hickey” Problems-A Literature Review on Oxalate Formation, Analysis and Scale Control. *Nord. Pulp Pap. Res. J.*, **2011**, *26*, 263–282.

[3] Elsander, A.; Ek, M.; Gellerstedt, G. Oxalic Acid Formation during ECF and TCF Bleaching of Kraft Pulp. *Tappi J.*, **2000**, *83*, 73–77.

[4] Bryant, P.S.; Samuelsson, A.; Basta, J. Minimizing BaSO4 Scale Formation in ECF Bleach Plants. *Tappi J.*, **2003**, *2*, 3–7.

[5] Ferguson, R.J. Predicting Calcium Oxalate Scale. In *CORROSION 2002*; NACE International: Denver, CO, USA, **2002**.

[6] Mersmann, A. *Crystallization Technology Handbook. Second Edition Revised and Expanded*; Marcel Dekker, **2001**.

[7] Parkhurst, D.L.; Appelo, C.A.J. User’s Guide to PHREEQC (version 2)- A Computer Program for Speciation, Batch-Reaction, One-Dimensional Transport, and Inverse Geochemical Calculations, **1999**.

[8] Yantasee, W. Kinetic and Equilibrium Analysis of Metal Ion Adsorption onto Bleached and Unbleached Kraft Pulps, Ph.D. Thesis, Oregon State University, Ph.D. thesis, Oregon State University, **2001**.

[9] Huber, P.; Burnet, A.; Petit-Conil, M. Scale Deposits in Kraft Pulp Bleach Plants with Reduced Water Consumption: A Review. *J. Environ. Manage.*, **2014**.

[10] Huber, P. Kinetics of CO2 Stripping and Its Effect on the Saturation State of CaCO3 upon Aeration of a CaCO3-CO2-H2O System: Application to Scaling in the Papermaking Process. *Ind. Eng. Chem. Res.*, **2011**, *50*, 13655–13661.

BLACK LIQUOR SUPERCRITICAL WATER GASIFICATION IN THE CASE OF A SULFUR-FREE COOKING PROCESS.

Marion HUET[1*], Anne ROUBAUD[1,] and Dominique LACHENAL[2]

*[1] CEA /LITEN/ Biomass Technologies Laboratory, Grenoble, France ; [2] LGP2 - Grenoble INP - Pagora, Saint-Martin-d'Hères, France. (*marion.huet@cea.fr)*

ABSTRACT

Supercritical water gasification (SCWG) is one of the most promising technologies to convert biomass into a combustible gas rich in methane and hydrogen. Through this process, it is possible to convert biomass with water content higher than 80% without prior drying.

An energetic valorization of black liquor avoiding the evaporation step, directly from the high water content stream, could improve the thermal and economic efficiencies of the whole pulping process. The objective of this work is to establish whether SCWG of black liquor is more efficient than the conventional recovery process, with real data obtained from gasification of a black liquor from NaOH / Anthraquinone cooking of softwood.

Semi-batch reactor experiments of black liquor supercritical water gasification were performed. Devices allowing injection and sampling were set up. Temperatures between 430 and 470°C, pressure between 24 and 26 MPa, and reaction times between 2 and 60 minutes have been tested. The results showed that the gas produced was a mixture of mainly hydrogen (26%), methane (24%) and carbon dioxide (44%) in 30 minutes reaction time. About 46% of the LHV (Low Heating Value) and 34 % of the carbon initially present in black liquor were converted into gases. It appeared that under those conditions the thermodynamic equilibrium was not reached. Energetic assessment through thermodynamic calculations indicates that further work at higher temperature is needed in order to optimize the gasification and energetic efficiencies.

I. INTRODUCTION

A softwood kraft pulp mill is already working as a biorefinery producing material (cellulosic fibers), chemicals (tall oil and turpentine) and energy needed for running the mill. During this process the main part of the lignin and a significant amount of hemicelluloses are dissolved during the cooking step, ending up in the black liquor (BL). This liquor is then concentrated by evaporation and burned in the recovery boiler of the mill, with a boiler energetic efficiency of 64% when BL dry solid is at 80 % when entering in the boiler [1]. Taking into account the energy needed to evaporate black liquor before the boiler, the energetic yield is lower than 39 % (39 % when BL dry solid is at 20 % after washing, 30 % when BL dry solid is at 11.5 %). The cooking chemicals are also recovered making this process 99% autonomous in chemicals.

Supercritical water gasification (SCWG) is particularly relevant for biomasses with high content of water like black liquor. This process is using the specific properties of supercritical water. Above its critical point (221 bar, 374°C), water behaves like a non-polar solvent, with a low dielectric constant (from 80 at 20 °C to 5 at 450 °C), a high diffusivity, and a low dissociation constant. Organic matters are solubilized but salts are precipitated.

Biomass components are rapidly decomposed by hydrolysis into smaller species and fragmented up to the production of a gas mixture. This gas is mainly composed of CH_4, H_2 and CO_2. Under those conditions, if formed, CO is rapidly converted into CO_2 and H_2 through the water gas shift reaction, catalyzed by alkali like Na [2].

In the literature, it was demonstrated that supercritical water gasification of black liquor could be advantageously integrated in a pulping process, in terms of energetic valorization of lignin and of recovery of the cooking reagents [3]. However data and assumptions used presented in this earlier work did not come from tests on black liquor directly but on wood. Previous studies also showed that an increase of temperature enhanced the gasification but variation of pressure did not have any significant effect [4].

The aim of this study is to examine the supercritical water gasification of black liquor and to compare it to the usual recovery process. The black liquor used is this study is from a soda/AQ cooking process applied to prehydrolyzed softwood chips.

II. EXPERIMENTAL

Gasification experiments were performed in a batch autoclave (500 mL) made of stainless steel 1.4571 designed to work up to 300 bars and 500°C. The experimental pressure is related to the selected heat up temperature, the weight of water introduced and the initial N2 pressure (about 10 bars). An injection device was added, allowing to inject at pressure up to 300 bar. The BL is injected when the reactor is at the desired temperature. BL takes less than 1 minute to reach the supercritical conditions. A sampling system at the top of the reactor was also added to take about 10% of the reactive medium at the desired time. This sample is thereafter quenched and analyzed. As the reactor is heated with a small quantity of water, the black liquor is found slightly diluted to 11.5%$_{WT}$ after the injection, with a total carbon content of 51 g/L.

Black liquor is supplied by our project partner at PAGORA. This black liquor is sulfur free. Its initial carbon content is 61 g/L and Na concentration is 16 g/l. Black liquor is a high alkaline solution of pH≈13.

After each experiment three different phases are recovered: an aqueous phase, a gas phase and a solid phase. Gas composition is determined with a µGC Varian CP-4900. Initial and final organic carbon in the aqueous phase is measured with a Shimadzu TOC-L CSH. Total carbon content for solids and liquids is measured via the TOC SSM. Sodium concentration in the liquid phase is measured by Ion Chromatography (Dionex ICS-3000). GC-MS (Perkin Elmer Clarus 500/Clarus 600S) was performed on the ethyl acetate extract of the liquid phase. **Gas yield** is characterized by the percentage of the C or H initially present in black liquor, found in the gas. Energetic efficiency is calculated via the Low Heating Value (LHV) of the gases and called **Cold Gas Efficiency** (CGE) which is calculated via this formula: $\mathbf{CGE = \sum LHV_{gases} / LHV_{BL}}$.

III. RESULTS AND DISCUSSION

Gasification of the black liquor was done at three different temperatures (430, 450 and 470 °C), different reaction times (between 2 and 64 min) and at a resulting pressure between 24 and 27 MPa.

Main trends

A longer time increases the degradation of the organic compounds and the production of gases although they both finally reach a plateau. Moreover, the higher the temperature, the faster is the degradation.

The Total Organic Carbon in the aqueous phase decreases dramatically in the first minutes of gasification and reaches a plateau at about 20% of its initial concentration. This non-converted organic matter essentially contains aromatic compounds originating from the lignin. At 450°C-12min, GC-MS analysis reveals the presence of phenol (peak area multiplied by 6 compared to original BL), 2-methoxy phenol (peak area multiplied by 4), methoxy benzene, methyl, dimethyl and trimethyl phenols These compounds are reported to be difficult to gasify at a temperature inferior to 600 °C due to the formation of resonance-stabilized phenoxy radicals [5].

The gas phase is mainly composed of carbon dioxide, hydrogen and methane, with a small amount of C_2 and C_3 hydrocarbons (C_2H_4, C_2H_6 and C_3H_8). No CO is measured; we considered that the high concentration of sodium in black liquor promoted the water gas shift reaction, which consumed CO and generated H_2 and CO_2. The results show that gas yield increases with temperature and time. However a plateau is reached, the level of which increases with temperature. At 430 °C and 60 min., 21 % of the carbon and 28 % of the hydrogen initially in the black liquor are found in the gas. At 470°C and 60 min the values are 34 % and 53 %, respectively. The gas is composed of 48 % CO_2, 32 % H_2, 15 % CH_4, 3% C_2 and 1 % C_3 at 430 °C (36 % of CO_2, 39 % of H_2, 21 % CH_4, 3% C_2 and 1 % C_3 at 470 °C).

Furthermore, H_2 and CO_2 are closer to equilibrium (minimum of Gibbs Energy) than CH_4: at 470 °C and 60 minutes, only 16.1 % of the CH_4 that could be formed at equilibrium is measured whereas 68 % of H_2 is found. This confirms the effect of water gas shift which catalyzes the formation of CO_2 and H_2.

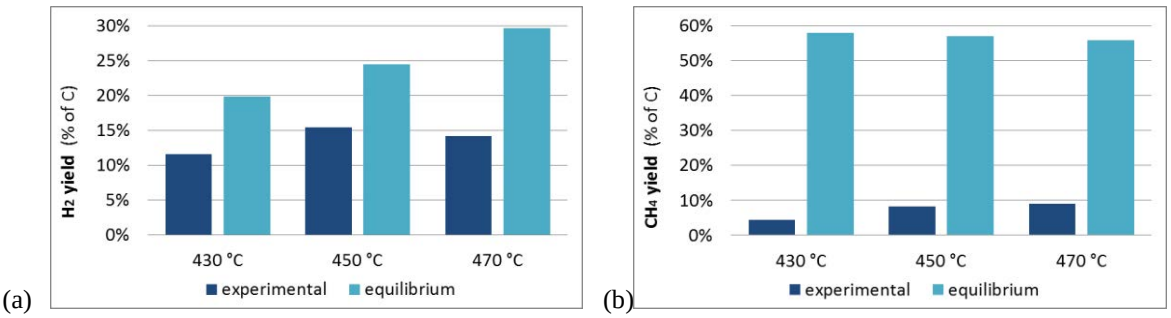

Figure 1: experimental and at thermodynamic equilibrium gas yields for H_2 (a) and CH_4 (b) (60 min).

Finally, increasing the temperature allows the gas yield to be closer to the thermodynamic equilibrium. Figure 1 shows that at 430 °C for 60 min, yield of CH4 is at 7.7 % of its equilibrium value whereas it is at 16.1 % at 470 °C. We can guess that at 700 °C, gas yield should be close to equilibrium.

Evolution of the Cold Gas Efficiency (CGE) and total yield

The **CGE** is a way to evaluate the gasification efficiency and represents the ratio of energy in the gases to that initially present in the black liquor. Evolution of CGE is parallel to that of the gas yield: increasing with time and temperature and reaching a plateau with time. The level of the plateau increases with temperature and reaches 46 % at 470 ° and 60 min (see figure 2).

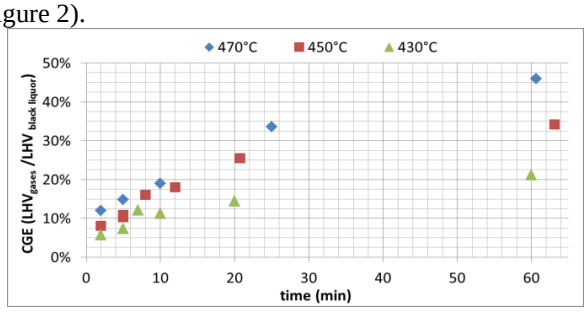

Figure 2 : effect of time and temperature on CGE

In order to take into account the energy needed to bring black liquor to the SCWG conditions and the energy recovered, we simulated a continuous process via the software Prosim+. The behavior of inorganics is not considered in this balance. The process scheme is given in figure 3 for a flow of a black liquor of 1kg/h (at a dry solid content of 11.5 $\%_{WT}$).

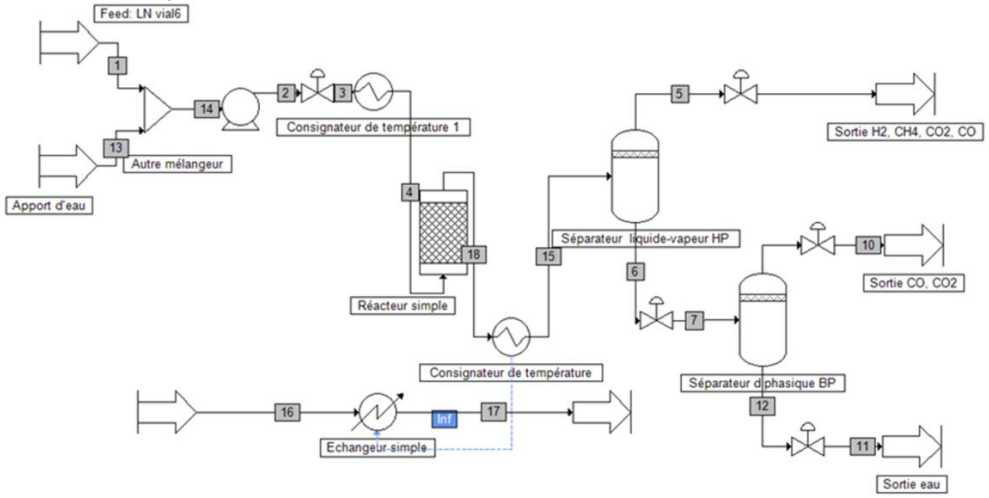

Figure 3: process scheme of SCWG of black liquor

In this scheme dry black liquor is mixed with water (in *autre mélangeur)*. This weak black liquor is then pressurized and heated at 350 °C (in *consignateur de temperature 1*). In the reactor (*réacteur simple*) black liquor reacts according to a set series of reaction at a set temperature (430, 470, 700 °C). The products are then cooled to 20 °C in *consignateur de temperature* and are separated at high pressure in a liquid-vapor separator. The liquid phase is then depressurized to 5 bars and gases and water are separated.

Hypotheses are the following:

- Composition at equilibrium is calculated by Gibbs energy minimum;
- The formula of the dry black liquor molecule $C_{600}H_{939}O_{156}$ is calculated from its CHON composition. As we know its High Heating Value (HHV), enthalpy of formation is calculated. Some thermodynamic properties of guaiacol are used to simulate BL behavior.
- Cooling enthalpy is recovered at 70 % and is used to heat the black liquor ;
- The supply of energy is brought about by a bark boiler with a yield of 80 %
- Energy is recovered from gas by cogeneration with a yield of 80 % [6];
- To simplify the system, the organic compounds present in the liquid phase are represented by xylene C_8H_{10} (one of major components identified by GC-MS) and the char is represented by biphenyl, $C_{12}H_{10}$, which is considered as a char precursor.

Total energetic yield is defined by: $\frac{\sum energy\ recovered}{\sum brought\ energy} = \frac{0.8 * \sum_{gases} LHV}{(LHV_{BL} + \Delta H_{14\to4} + \Delta H_{4\to18} - 0.7 * |\Delta H_{15\to15}|)/0.8}$ (given in table 1).

Evaporation + Thomlinson	yield at 430 °C	yield at equilibrium at 430 °C	yield at 470 °C	yield at equilibrium at 470 °C	yield at equilibrium at 700 °C
30 %	12 %	68 %	20 %	67 %	64 %

Table 1: total yield under different conditions

Total energetic yield is 20 % at 470 °C (12 % at 430 °C) whereas the yield of the kraft recovery system is 30 % with a BL dry content of 11.5% (evaporation + Thomlinson recovery). At thermodynamic equilibrium total energetic yield of SCWG of this black liquor is of 67 % at 470 °C and 68 % at 430 °C. At 700°C, the calculated total energetic yield at equilibrium will be 64 %. According to these calculations, increasing temperature to 700 °C will permit to increase the gas yield to be closer to its thermodynamic equilibrium value and to reach a larger total energetic yield than that for a conventional recovery cycle in a pulp mill.

Sodium behavior

When the temperature is above the critical point, the water dielectric constant is inferior to 5 and thus the inorganic compounds are insoluble. We assume that the sodium is precipitated in the reactor during gasification. As the sampling is at the top of the reactor, alkalis are not taken with the liquid during sampling. The inorganics which precipitate in supercritical water should solubilize in the liquid remaining in the reactor during the cooling.

To confirm this assumption, we compared the concentration of sodium in the liquid phase taken during the sampling to that in the liquid phase remaining in the reactor: the concentration of sodium was approximately of 0.5 g/L in the sampling phase against 15.8 g/L in the remaining phase. Therefore, the quantity of sodium in the liquid remaining in the reactor is above 90% of the quantity introduced in the reactor, which will facilitate the caustic soda recovery (by causticizing of the sodium carbonate)

IV. CONCLUSIONS AND PERSPECTIVES

Gasification of sulfur free black liquor was performed in a semi batch reactor at temperatures between 430°C and 470 °C for 2 to 64 minutes. The sodium initially present in black liquor catalyzes the water gas shift reaction and enhances the formation of H_2. At a temperature inferior to 470 °C, black liquor is not completely converted by supercritical water gasification (SCWG) and a substantial part of aromatic compounds remains stable. At 470 °C, the total energetic yield of SCWG for a black liquor with a dry solid content of 11.5% is about 20 % whereas it is around 30 % with a similar black liquor in the standard kraft recovery process.

Increasing the temperature will accelerate the reaction and permit to obtain a higher gas yield. Moreover, product composition will be closer to the one corresponding to the thermodynamic equilibrium. The total energetic yield is expected to reach 64 % at 700 °C..

Additional experiments will be done at temperatures up to 700 °C to validate this conclusion and to study sodium recovery in continuous process.

V. ACKNOWLEDGEMENT

The authors would like to thank Institut Carnot Energie du Futur for the funding of this study.

VI. REFERENCES

[1] Adams, T.N. Kraft recovery boilers. *Tappi press, AF&PA*. 1997.

[2] Kruse, A. Hydrothermal biomass gasification. *The Journal of Supercritical Fluids*. **2009**, 49, 391–399.

[3] Naqvi, M.; Yan, J.; Froling, M. Bio-refinery system of DME or CH4 production from black liquor gasification in pulp mills. *Bioresource Technology*. **2010**, 101, 937–944.

[4] Roubaud, A., Chirat, C., Huet, M., Monot, C., Lachenal, D. Development of a new pulp production process and black liquor gasification. *Récents progress en genie des procédés*. 2013, 104.

[5] Huelsman, C.M., Savage, P.E. Intermediates and kinetics for phenol gasification in supercritical water. *Physical Chemistry Chemical Physics*, 2012, 2090–2910.

[6] Comodi, G., Cioccolanti, L., Pelagalli, L., Renzi, M., Vagni, S., Caresana, F. A survey of cogeneration in the Italian pulp and paper sector. *Applied Thermal Engineering*, 2013, 54, p 336–344.

INFLUENCE OF HARDWOOD SPECIES ON ALTERNATIVE DISSOLVING PULP PRODUCTION

Christian Hutterer[1], Gabriele Schild[2*], Antje Potthast[3]

[1]*Kompetenzzentrum Holz GmbH, Altenberger Str. 69, A-4040 Linz, Austria*
[2]*Lenzing AG, Werkstraße 1, A-4860 Lenzing, Austria (* g.schild@lenzing.com)*
[3] *Universität für Bodenkultur Wien, Department für Chemie, A-1190 Wien, Austria*

ABSTRACT

The upgrading of paper pulps to dissolving pulps is of high economical interest. Therefore, a new process strategy was developed to modify existing kraft mills to facilitate the production of high quality dissolving pulps [1]. The process adaptation includes steam activation with subsequent alkaline cooking. After oxygen bleaching, the hemicelluloses are removed in a cold caustic extraction stage (CCE). The final TCF bleaching includes an ozone stage, an enzymatic treatment or an acid hydrolysis for the adjustment of the degree of polymerisation of the cellulose.
In this study, focus was placed on the applicability of economically interesting hardwood species, namely beech (*Fagus sylvatica*), birch (*Betula papyrifera*) and eucalyptus (*Eucalyptus globulus*). Due to differences in both, morphology and chemical composition between the different hardwood species, their behavior during each process step is not yet fully understood and requires characterization by more advanced analytical methods. Initial investigations revealed strong effects of process conditions in the CCE stage on fiber and hemicellulose accessibility and reactivity, especially temperature and alkalinity. The knowledge of these supramolecular interactions allows further process optimization.
For investigating these interactions, process conditions were varied in the cold caustic hemicellulose extraction step for a birch kraft paper pulp. Focus was placed on the investigation of the extracted hemicelluloses via SEC and β/γ-cellulose determination.

I. INTRODUCTION

For the extraction of hemicelluloses from paper pulps, alkaline post extraction at low temperatures from 25 to 45°C, called cold caustic extraction, represents an effective method [2] [3]. During this treatment, only physical phenomena are dominating the extraction and no peeling reactions occur in any significant extent that could lead to cellulose losses [4]. The physical phenomena include intermicellar and intramicellar swelling permitting short-chain celluloses and especially xylan to dissolve [5]. In this study, the impact of process conditions, namely effective alkali and temperature, on xylan extraction efficiency is studied using an industrial birch paper grade pulp after oxygen bleaching.

II. EXPERIMENTAL

CCE bleaching

All CCE-treatments were performed in a lab high-shear mixer for 30 min at 10% consistency. To simulate industrial conditions, synthetic white liquor was used as an alkali source. This lye is generated out of cooking liquors through the conversion of sodium carbonate (Na_2CO_3) in the smelt to sodium hydroxide (NaOH) in a recausticizing plant. Thereby, a certain amount of inert salts and non-process elements are accumulated in the white liquor according to equilibrium conditions [6]. Hence, white liquor with a sulfidity of 30% and a causticizing degree of 90% was used for CCE bleaching experiments reflecting a typical white liquor composition. The term effective alkali (EA) of the lye describes the measured alkalinity out of fully dissociated hydroxide and hydrogen sulfide ions in the liquor.

Beta / Gamma ratio determination

The quantification of β- and γ- cellulose in alkaline process lyes was achieved through the precipitation of the β-fraction by sulfuric acid and the subsequent determination of the dissolved carbon containing molecules by DOC (dissolved organic carbon) measurement. The method was performed according to TAPPI T 203 om-93.

Size exclusion chromatography

The molar mass distribution of alkali soluble carbohydrate fractions, in this case dissolved hemicelluloses, was achieved by size exclusion chromatography (SEC) coupled with RI and UV detection according to [7][8].

III. RESULTS AND DISCUSSION

The extraction of hemicelluloses in a CCE bleaching step can be monitored via the determination of the β/γ-ratio. **Figure 1** demonstrates the content of β-cellulose of the extraction lyes. The figure reveals a slightly rising β-cellulose content with increasing effective alkali at 20°C and 40°C respectively due to an increasing hemicellulose extraction efficiency. β/γ-ratio determinations of lyes treated at 60°C show a reverse behavior due to peeling reactions of hemicelluloses at this temperature.

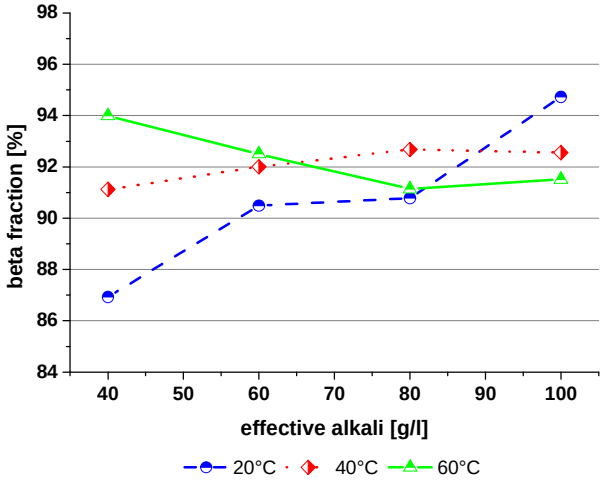

Figure 1. β- and γ-cellulose composition of the CCE process lyes at different effective alkali and treatment temperature.

As the high molecular weight xylans in process lyes after CCE extraction possess a high potential as valuable co-products, their behavior in terms of possible changing molar masses as a consequence of variable process conditions should be monitored. The determination of the molar mass distribution will indicate degradation reactions triggered by improper process conditions. **Figure 2** shows the molar mass distribution of the β-cellulose fraction at different effective alkali concentrations at treatment temperatures of 20°C and 60°C. The figure indicates a molar mass average of about 9.0 kDa for all fractions at 20°C. Higher effective alkali concentrations slightly increase the polydispersity due to xylans with higher molar mass dissolved at these conditions. This is a clear indication for the xylans being physically dissolved. The situation is different at 60°C. Here, high effective alkali concentrations cause a significant degradation. This is caused by degradation reactions of the extracted xylans including peeling reactions and alkali induced cleavages of glycosidic bonds. The polydispersity index increases. The peakshape does not change to any significant extent. The traces of the UV signal show the presence of residual lignin bound to extracted xylans, which dominates in the low molecular mass region. The signals reveal similar trends independent from the treatment conditions.

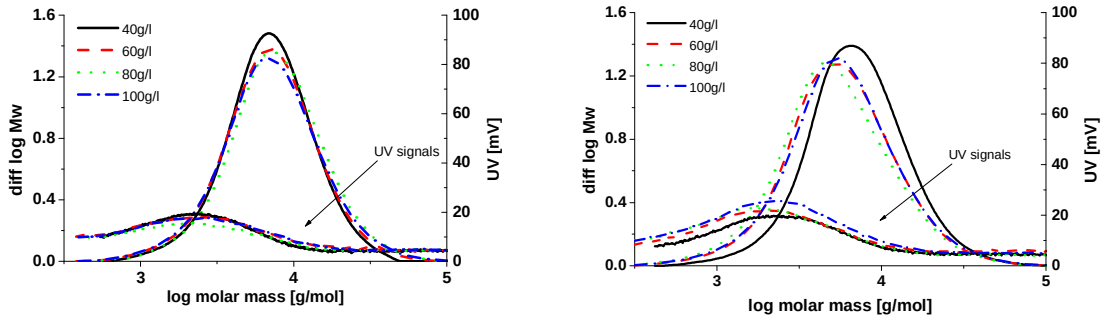

Figure 2. Molar mass distribution of CCE extracted birch hemicelluloses in process lyes depending on effective alkali at 20°C (a) and 60°C (b).

IV. CONCLUSIONS

Experiments studying the influence of process conditions during CCE treatment were conducted varying temperature and effective alkali of the white liquor used. The temperature ranged from 20°C to 60°C and the effective alkali from 40g/l to 100g/l. Data about the hemicellulose extraction efficiency using a birch paper pulp revealed a rising behavior with increasing effective alkali and temperature when looking at the β/γ-ratio. The high ratio also revealed practically no cellulose loss. Treatment temperature and effective alkali respectively are slightly affecting the molar mass distributions of extracted hemicelluloses due to peeling reactions and alkaline hydrolyses.

V. ACKNOWLEDGEMENT

Financial support was provided by the Austrian government, the provinces of lower Austria, upper Austria, and Carinthia as well as by Lenzing AG. We also express our gratitude to the Johannes Kepler University, Linz, the University of Natural Resources and Life Sciences, Vienna, and Lenzing AG for their in-kind contributions.

VI. REFERENCES

[1] Sixta, H., et al., Method for producing a type of pulp. *WO 2007/128024 A1*, **2007**: p. 1-50.
[2] Jayme, G. and E. Roffael, Einfluss von Natriumhyroxidlösungen verschiedener Konzentration auf die Feinstruktur und die Reaktivität der Cellulose. *Das Papier*, **1969**. *23*(7): p. 405-412.
[3] Wallis, A.F.A. and R.H. Wearne, Does borate inhibit cellulose mercerization during cold alkali extraction of wood pulps? *Tappi Journal*, **1990**: p. 226-228.
[4] Glaus, M.A. and L.R. Van Loon, Degradation of Cellulose under Alkaline Conditions: New Insights from a 12 Years Degradation Study. *Environ. Sci. Technol.*, **2008**. *42*: p. 2906-2911.
[5] Sixta, H., *Handbook of Pulp* , **2006**. *2*: p. 609-1348.
[6] Sixta, H., *Handbook of Pulp*, **2006**. *1*: p. 3-1352.
[7] Eremeeva, T.E. and T.O. Bykova, High-performance size-exclusion chromatography of wood hemicelluloses on a poly(2-hydroxyethylmethacrylate-co-ethylene dimethylacrylate) column with sodium hydroxide solution as eluent. *Journal of Chromatography*, **1993**. *639*: p. 159-164.
[8] Wong, K.K.Y. and E. De Jong, Size-exclusion chromatography of lignin- and carbohydrate- containing samples using alkaline eluents. *Journal of Chromatography A*, **1996**. *737*: p. 193-203.

MODIFICATION OF HYDROLYSIS LIGNIN FOR VALUABLE APPLICATIONS

Elena V. Ipatova,[1] Dmitry V. Evtuguin,[2] Stepan M. Krutov,[1]

Sonia A.O. Santos,[2] Uriy N. Sazanov [3]

[1] *Department of Organic Chemistry, St. Petersburg Forest Technical University, Institutsky per. 5, 194021 St. Petersburg, Russian Federation*

[2]*CICECO, Chemistry Department, University of Aveiro, Campus de Santiago, P-3810-193 Aveiro, Portugal*

[3]*Institute of Macromolecular Compounds Russian Academy of Sciences, V.O. Bolshoy pr. 31, 19900, St. Petersburg, Russian Federation*

ABSTRACT

Particles (ca 0.25 mm) of technical hydrolysis lignin (THL) were grinded by a rotary-jet mill to obtain a fraction of THL ca 5 μm. Both initial and milled THL were liquefied by thermal alkaline treatment at 220 ºC for 2h. Upgraded THL from non-milled (L1) and milled (L2) were desalted by treatment with cation-exchanged resin and dried. The molecular weights (M_w) of L1 and L2 were 1100 and 1000 Da, respectively, as determined by SEC. Structural characterization carried out employing ESI-MS^n and 1D and 2D NMR spectroscopy revealed that small amounts of β-O-4 (ca 6 mol.%), β-5 and β-β structures still remained in L1 and L2. Overall, upgraded lignins are oligomers (trimers-pentamers) with highly degraded propane chains and possessing polyconjugated aromatic structures. L2 produced from milled THL didn´t contain concomitant polysaccharides and showed lower polydispersity than L1 and was suggested as a promising raw material for polymeric formulations.

I. INTRODUCTION

The use of biomass instead of fossil resources for the production of fuels and materials is a perspective trend involved in the biorefinary concept. One of the industrial areas of biomass use is the method of acid hydrolysis, focused on the production of ethanol, feed yeast, furfural or levulinic acid derivatives and sugar alcohols. Acid hydrolysis with diluted sulphuric acid was widely used in XX century in the former Soviet Union where was built about 50 plants. Technical hydrolysis lignin (THL) is a large-scale underutilized by-product of hydrolysis industry, which end-disposal may cause serious environmental problems. Only in Russia, dumps plants accumulated tens of millions of tons THL. The difficulties in THL utilization are related to it complex structure and relatively poor reactivity. In fact, THL is a cellolignin containing ca 20-30% of polysaccharides (mainly cellulose) and highly condensed lignin [1]. Lignin is of particular interest as a promising feedstock for the production of aromatic compounds for further organic synthesis. One of the lignin depolymerisation methods is it degradation with bases under appropriate conditions [1-3]. This work deals with alkali-catalyzed thermal upgrading of THL aiming to transform it into series soluble products suitable for polymeric formulations. The obtained lignins were characterised for their molecular weights and general structural features.

II. EXPERIMENTAL

Upgrading of hydrolysis lignin

Air-dried THL from Kirovski hydrolysis plant was sieved and particles of ca 0.25 mm were grinded by a rotary-jet mill to obtain a fraction of ca 5 μm (weighted length as analyzed by Laser Particle Sizer ANALYSETTE 22 MicroTec plus). The thermal treatments under alkaline conditions (NaOH, 5%) were carried out in autoclave at 220 ºC for 2h. The conversion of THL reached up to 99%. The dissolved alkaline lignin was filtered off on a glass filter and treated by cation-exchange resin to remove cations giving raise the water-soluble lignin, which was further isolated by vacuum drying.

Analyses

The lignins **L1**, obtained from 0.25 mm particles, and **L2**, obtained from 5 μm particles THL, were analyzed for molecular weight by SEC and ESI-MS and structurally characterized by 1D/2D ^{13}C NMR and ESI-MS^n. SEC analysis was carried out as described previously [4]. ESI-MS and ESI-MS^n analyses were performed using a LXQ linear ion-trap mass spectrometer (Finningan). The lignin sample (ca 1 mg) was firstly dissolved in 100 μL of 0.1% ammonia hydroxide solution followed by addition of 900 μL of acetonitrile. The final sample was

diluted ca 30-50 times by methanol before the direct injection in the electrospray source. The spectra were acquired on a LCQ Fleet ion trap mass spectrometer (ThermoFinnigan, San Jose, CA, USA), equipped with an electrospray ionization source and operating in negative mode. The nitrogen sheath gas was 10 (arbitrary units). The spray voltage was 5 kV and the capillary temperature was 275 ºC. The capillary and tune lens voltages were set at -28 V and -115 V, respectively. CID-MS^n experiments were performed on mass-selected precursor ions in the range of m/z 150–2000. The isolation width of precursor ions was 1.0 mass units. The scan time was equal to 100 ms and the collision energy was optimized between 20 and 35 (arbitrary units), using helium as collision gas. The data acquisition was carried out by using Xcalibur® data system. The quantitative ^{13}C NMR spectra of lignins (L1 and L2) were recorded on a Bruker AVANCE 300 spectrometer operating at 75.47 MHz (323 K) with TMS as internal reference. Lignins were dissolved in DMSO-d_6 (ca. 25% concentration) and placed into 5-mm-diameter tubes. The acquisition parameters were as follows: 4.1 ms pulse width (90°pulse angle), 12 s relaxation delay, 16 K data points and 18000 scans. The same lignin samples in DMSO-d_6 were placed into 5-mm-diameter tube and 2D NMR spectra were recorded on a Bruker AVANCE 300 spectrometer. The phase sensitive 1H-detected Heteronuclear Single Quantum Coherence (HSQC) spectrum was acquired over a F1 spectral weight of 12000 Hz and a F2 width of 2000 Hz with a 2048 x 1024 matrix and 128 transients per increment. The delay between scans was 2 s and the delay for polarization transfer was optimized for $^1J_{C-H}$ =149Hz.

III. RESULTS AND DISCUSSION

Molecular weights of upgraded hydrolysis lignins

Two lignins obtained from THL of different granulometric composition (L1 and L2) showed similar molecular weight distributions in SEC analysis (figure is not shown) though the molecular weight (Mw) of L1 was slightly higher than of L2 (1100 against 1000 Da) with higher polydispersity (1.25 against 1.17). More detailed information on the abundance of lignin oligomers was obtained from ESI-MS spectra (**Figure 1**).

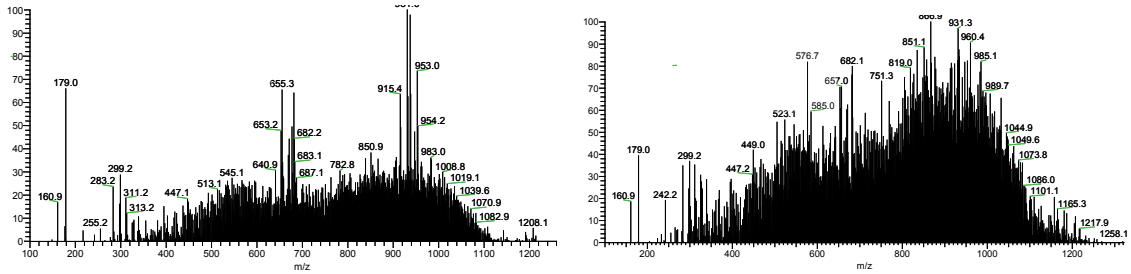

Figure 1. ESI-MS spectra of L1 (left) and L2 (right) acquired in a negative mode.

The analysis of both lignins by ESI-MS revealed wide distribution of molecular masses of oligomers (from ca 200 to 1500 Da) with predominant presence of trimers (ca 550 Da) and pentamers (ca 900 Da). The efforts on the structural elucidation of lignin oligomers by tandem ESI-MS spectrometry were only partially successful due to the prevalence of alkyl-aryl and alkyl-alkyl linkages between structural units. Intensive signal at *m/z* 179 was assigned to coniferyl alcohol, which was presented both in L1and L2. Two dimmers at *m/z* 299 and 319 were assigned, according to the analysis of MS/MS spectra, to dimers linked by β-O-4 bonds.

A series of rather abundant oligomers at *m/z* 653 and 655 in ESI-MS spectra of L1 showed the characteristic loss of MeGlcA (-206 Da) and were assigned, based on ESI-MS^n spectra (not shown), to partially degraded acidic xylo-oligosaccharides (XOS) of general composition $Xyl_{3\text{-}4}MeGlcA$. These XOS were not found in ESI-MS spectrum of L2.

Structural studies

The structural studies were carried out using proton-carbon correlation spectroscopy (HSQC) and the quantitative ^{13}C NMR spectroscopy. The analysis of HSQC spectrum of (**Figure 2**) revealed that despite drastic conditions of industrial percolation acid hydrolysis of wood and posterior alkaline treatment certain amounts of β-*O*-4, β-β and β-5 lignin structures still maintained in upgraded THL. HSQC spectrum of L1 also showed the presence of associated to lignin carbohydrates and extractives (proton/carbon resonances at 1.0-2.5/10-35 ppm).

The comparison of quantitative ^{13}C NMR spectra allowed the conclusion about similarity of two upgraded THLs though some structural differences could be highlighted. Thus, unlike to L2, L1 contained noticeable amounts of concomitant polysaccharides (**Figure 3**). Strong signals at 173-178 ppm in L1, assigned to carboxylic moieties

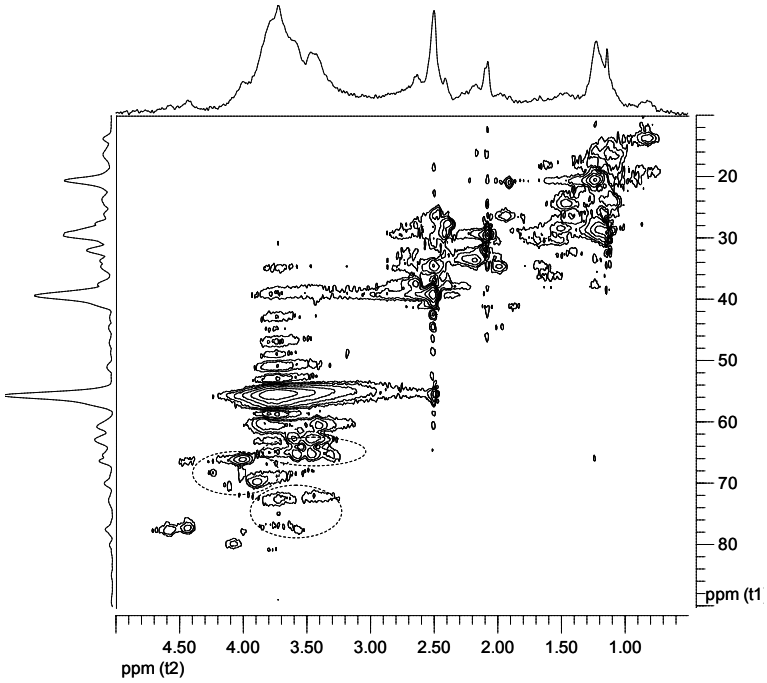

Figure 2. Aliphatic region of HSQC spectrum (DMSO-d_6, 40ºC) of sample L1. The signals from polysaccharides are depicted by dashed circles.

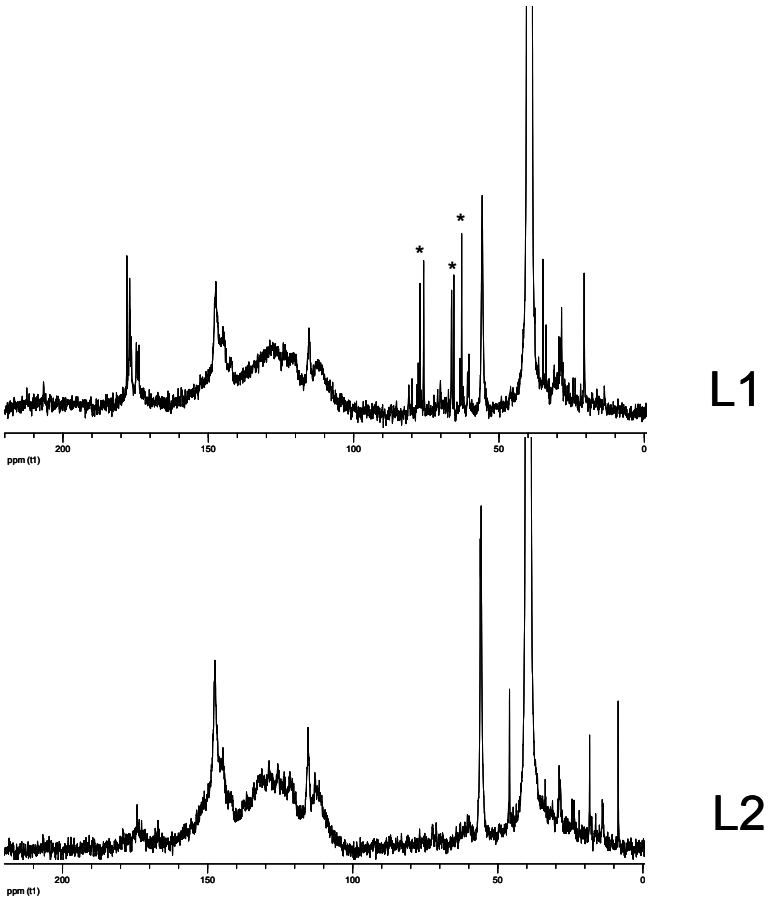

Figure 3. Quantitative ^{13}C NMR spectra of upgraded hydrolysis lignins L1 and L2 (DMSO-d_6; 50 ºC). Signals from polysaccharides are marked by asterisks.

Table 1. Quantitative estimation of structural elements in upgraded THL as revealed by ^{13}C NMR.

Structural element	Integrated region, ppm	Amount, per C6	
		L1	L2
β-O-4	59.3-60.6 (Cγ in β-O-4)	0.06	0.06
OCH_3	54.5-56.7 (methoxy C)	0.45	0.52
Ar-H	100.0-126.0 (tert. C)	2.07	1.94
Ar-C	126.0-140.0 (quat. C)	1.86	1.96
Ar-O	140.0-158.0 (ox. quat. C)	2.07	2.09

in extractives, were much less abundant in L2. The same may be noticed for the ketones showing resonances at 200-215 ppm.

The quantitative evaluation of structural features in L1 and L2 is summarized in **Table 1**. Both upgraded lignins contained few amounts of β-*O*-4 structures and were partially (almost 50%) demethoxylated. Also, both lignins were strongly condensed as follows from unusually high abundance of quaternary aromatic carbons in structural units (about twice additional Ar-C bonds that in spruce dioxane lignin [5]). It is worth noting the higher condensation degree of L2 when compared to L1. The propane chain is much degraded in both lignins, which is follows from the fairy low abundance of carbons intensity at 60-90ppm (Figure 3). The results obtained allow a proposition about formation of polyconjugated aromatic structures. Regarding the results of structural analyses of L1 and L2, the second may be considered as the most promising for using in polymer formulations since possess the lower M_w and PD that L1 and is not contaminated with polysaccharides.

IV. CONCLUSIONS

The results of this study demonstrated thermal alkaline treatment as a promising way for the liquefaction of THL into water-soluble products. The grinding of THL by a rotary-jet mill allowed a fraction of ca 5 μm free of polysaccharides, which could be completely transformed into water-soluble product of relatively low molecular weight (ca 1000 Da) and polydispersity (ca 1.17). Upgraded THL represent a strongly condensed lignin with highly degraded propane chain. Water-soluble lignin from THL may find interesting applications being involved in different polymeric formulations, which work is currently in course.

V. ACKNOWLEDGEMENT

Authors are grateful to Prof. A.V. Pranovich (Åbo Akademi University, Laboratory of Wood and Paper Chemistry) and I.V. Sumerskiy (University of Natural Resources and Life Sciences, Vienna) for the participation in this work. This work was carried out with the support of STC «Otkrytye innovacii».

VI. REFERENCES

[1] Chudakov, M.I., Industrial Utilization of Lignin (in Russian), Moscow: Lesnaya Promyshlennost.,1972.

[2] Vishtal, A; Kraslawski, A. Challengers in industrial application of technical lignins. *BioResources* 2011, 6(3), 3547- 3568.

[3] Sazanov, Yu. N. et al. Thermochemical Transformations of Hydrolysis Lignin. *Russ. J. Appl. Chem*., **2010**, 83(9), 1607-1614.

[4] Evtuguin, D.V.; Pascoal Neto C., Silva, A.M.; Domingues, P. M.; Amado, F. M. L.; Robert D.; Faix O. Comprehensive study on the chemical structure of dioxane lignin from plantation *Eucalyptus globulus* Labill wood. *J. Agric. Food Chem.* **2001**, 49, 4252-4261.

[5] Evtyugin, D.V.; Robert, D.; Zarubin, M.Ya. Structural study of oxygen-acetone lignins by quantitative ^{13}C NMR spectroscopy. *Russ. J. Appl. Chem. (Engl.transl.)* **1994**, 67(10), 1486-1491.

ALLOCATION OF KRAFT LIGNIN BY SUPERCRITICAL CARBON DIOXIDE

A.Ivahnov[1], T.Skrebets[1], O.Brovko[2]

[1]*Northern (Arctic) Federal University named after M.V.Lomonosov*
Russia, Arkhangelsk, Northern Dvina Emb., 17
[2]*Institute of Ecological Problems of the North, Ural Department of Russian Academy of Sciences*
Russia, Arkhangelsk, Northern Dvina Emb., 23

ABSTRACT

In this work possibility of use of supercritical carbon dioxide to isolate kraft lignin from technological solutions is shown. The influence of carbon dioxide pressure on completeness of kraft lignin allocation and its functional structure is established. Comparison of received preparations with kraft lignin allocated by acidulation of pulping liquors with sulfuric acid is carried out. Advantages of use of carbon dioxide in an offered way in comparison with a classical method of lignin allocation are shown. The lignin isolated by means of supercritical processing is characterized as less oxidated and more reactive at yield comparable with classical method.

I. INTRODUCTION

The directed modification of a kraft lignin for the purpose of receiving new perspective products on its basis assumes not only quantitative allocation of a lignin from spent pulping liquors, but also preservation of high reactionary ability of the allocated lignin [1]. Several techniques are available for the isolation of lignin from commercial spent pulping liquors. They may be based on the differences between lignin and contaminents in solubility (extraction by various solvents or acidification) or on the difference in molecular weight (gel permeation or ultrafiltration).

Traditional precipitation of lignin by lowering the pH of spent pulping liquors is based on solubility fractionation. But acidification by sulfuric acid may cause the loss of considerable fraction of an acidsoluble lignin. Also acid makes hard effect on lignin and changes it structure considerably. We made an attempt of sedimentation of a kraft lignin with use of supercritical dioxide of carbon as strong acidifying agent and at the same time lignin anti-solvent.

II. EXPERIMENTAL

For allocation of kraft lignin commercial spent pulping liquors after coniferous wood cooking of cellulose production of Arkhangelsk Pulp and Paper Mill were used. Experiments were executed on a supercritical fluid extractor SFE 400 (production of Institute of Analytical Instrument Making of Russian Academy of Sciences, State Petersburg, Russia). Black liquor (15 ml) placed in the 25 ml autoclave and the last filled with carbon dioxide with a demanded excessive pressure and temperature of 60 ^{O}C. Liquor processing by carbon dioxide continued within an hour. When dumping pressure the rest of cooking liquor deleted from the autoclave at the same time. During experiences temperature was constant and pressure was varied (100 – 400 atm, a step of 50 atm).

The main lignin functional groups (methoxyl, carbornyl, hydroxyl) were determined by modified Zeisel-Viebock-Schwappach method, by oxidation with hydroxylammonium chloride in a dimethysulfoxide-triethanolamine buffer and by chemisorption method, correspondingly. The sedimentation extent of lignin were established by spectrophotometry in UV-range.

III. RESULTS AND DISCUSSION

The influence of carbon dioxide pressure on extent of sedimentation of lignin and its chemical composition is presented on schedules (to zero pressure there corresponds structure and an yield of the lignin besieged by sulfuric acid), figures 1-3.

From figure 1 it is visible that extent of sedimentation of a lignin from liquor in supercritical carbon dioxide with a pressure over 250 atm corresponds to this indicator for a classical method. So supercritical carbon dioxide allowes allocate lignin from spent pulping liquors completely .

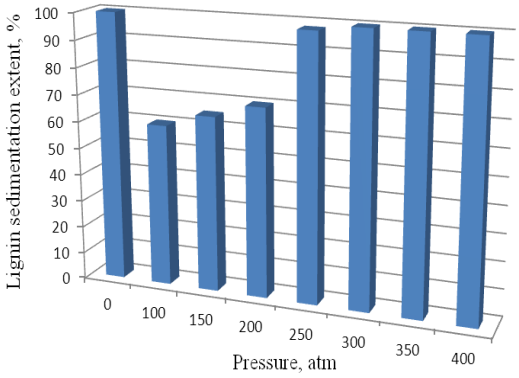

Figure 1. The influence of CO_2 pressure on the lignin sedimentation extent

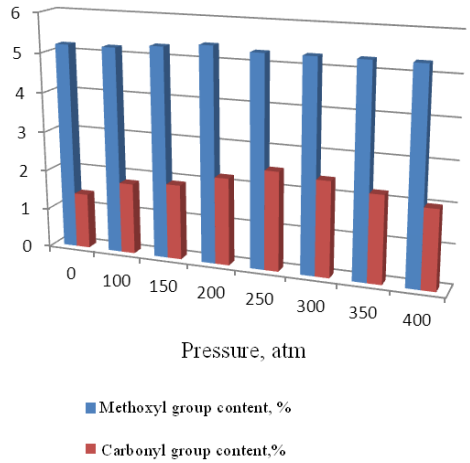

Figure 2. The influence of CO_2 pressure on the methoxyl and carbonyl groups content

Methoxyl group content stays practically constant and has not been influenced by allocation method. Carbonyl group content increases with pressure till 250 atm, then slightly decreases, but remains more then for acid presipitated lignin.

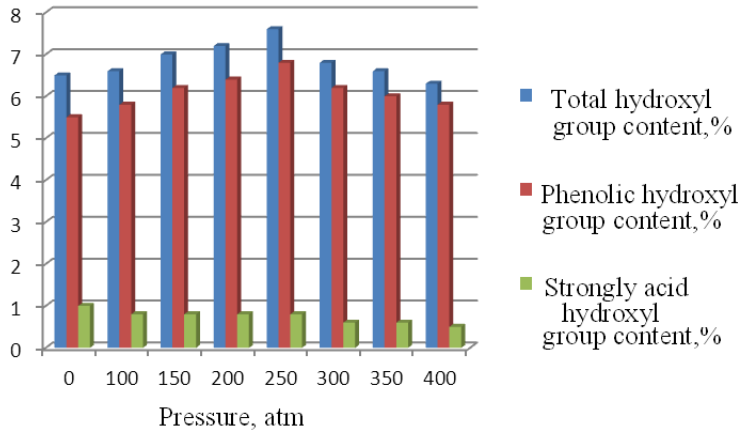

Figure 3. The influence of CO_2 pressure on the hydroxyl groups content

Figure 3 shows that lignin allocated with pH lowering is more oxidized – strongly acid hydroxyl (carboxyl) group content is approximately twice more for it then for lignin allocated by supercritical CO_2. Total hydroxyl group content increases with increasing of CO_2 pressure till 250 atm. Phenolic hydroxyl group content depends on CO_2 pressure such as total hydroxyl groups. So lignin allocated with supercritical carbon dioxide from black cooking liquors looks more reactive then acid isolated one.

IV. CONCLUSIONS

On the basis of the work that has been carried out, we can conclude that practically complete allocation of lignin from spent cooking liquors is possible. The isolated lignin is less oxidized and more reactive then lignin isolated by pH lowering with mineral acids.

V. ACKNOWLEDGEMENT

The study was supported the Ministry of Education and Science of the Russian Federation and by the Russian Foundation of Basic Research (grant no. 13-03-12238-ofi-m-2013).

VI. REFERENCES

[1] Physical chemisty of lignin/ K.Bogoltsyn, V.Lunin, etc. Akademkniga, **2010**, 492 p.

[2] S.Y.Lin, C.W.Dence. Methods in lignin chemistry. Springer Verlag. **1992**. 578 p.

MOLECULAR MASS DISTRIBUTION OF LIGNIN FROM BLACK LIQUOR – METHODS COMPARISON

Anna Jacobs*[1], Fredrik Aldaeus[1], Fadia Chedid[2]

[1]Innventia AB, Box 5605, SE 114 86 Stockholm, Sweden; [2]BillerudKorsnäs Karlsborg AB, SE 952 83 Karlsborgsverken, Sweden,
*(*Email:anna.jacobs@innventia.com)*

ABSTRACT

The aim of the present work was to evaluate different SEC calibration parameters for analysis of kraft black liquor lignin. Off-line matrix-assisted laser desorption/ionization time-of-flight mass spectrometry (MALDI-TOF-MS) was compared to calibration using the commonly utilized polystyrene standards. The results from this comparison showed that calibration using polystyrene standards gave calibration lines with different slopes compared to calibration using MALDI-TOF-MS. As a consequence, calibration with polystyrene gives an overestimation of weight-average molecular mass (Mw) and underestimation of number-average molecular mass (Mn), and an overestimation of the polydispersity index by up to 50%. The effect was most pronounced for low- and high molecular mass lignins.

I. INTRODUCTION

The basis of the wood biorefinery concept is to utilize the wood components released during for example pulping for value-added products. Utilization of lignin for different applications however requires certain chemical and molecular properties, e.g. purity, chemical composition, molecular mass distribution, thermal properties etc. This in turn puts demands on relevant analytical methods for these parameters. In the case of determination of molecular mass distribution, size-exclusion chromatography (SEC) is by far the most commonly used technique for lignin. However, SEC of lignin can be carried out using different mobile phase systems, different columns, different pretreatments such as derivatization, and using different calibrants. Several attempts have been made to harmonize methods, one example being the work carried out by the Eurolignin network [1], but still no standard method is available. One widely used method for SEC analysis of lignins is using tetrahydrofuran (THF) as mobile phase [1]. When THF is used, linear polystyrene standards are often used for calibration. However, polystyrene and lignin have different three-dimensional structures, which causes different hydrodynamic volumes and, consequently, elution behavior during SEC. In order to obtain absolute molecular mass values, the use of narrow-polydisperse lignin fractions have been reported [2], as well as the use of light scattering detectors [3, 4]. We have previously employed off-line matrix-assisted laser desorption/ionization time-of-flight mass spectrometry for SEC calibration [5]. Due to the development of the recently commercialized LignoBoost process [6], our interest has lately been focused on analysis of lignins from black liquor. The aim of the present work was therefore to compare SEC calibration using MALDI-TOF-MS or polystyrene for analysis of kraft black liquor lignin [7].

II. EXPERIMENTAL

Samples and reagents

Two lignin samples were used, from Swedish hardwood mix (HW) and Swedish softwood mix (SW), isolated using the LignoBoost process [6]. The samples were kind gifts from Lars-Erik Åkerlund at Innventia AB. The samples were dissolved in THF and filtered prior to analysis using Millex-HV13 syringe filters with 0.45 μm pore size (Millipore, Milliford, USA).

Polystyrene standards with nominal M_p values of 580, 3100, 10200, 34500 were obtained from Polymer Laboratories (Salop, UK).

All reagents were of p.a. grade.

Acetylation

The softwood lignin sample was subjected to acetylation. 50 mg lignin was dissolved in 2 ml pyridine and 2 ml acetic anhydride was added. This mixture was left to react over night at 25 °C, before it was put on ice and mixed with 2 ml methanol. Two hours later the process of evaporation was started. The evaporation was performed at 60 °C and consisted of 6 rounds. At each round, 5 ml toluene was added. When the sample was completely dried, acetone was added and the sample was transferred to a vial where it was dried under nitrogen gas flow.

Size-exclusion chromatography

Size-exclusion chromatography was used to separate the lignins into low-polydisperse fractions. A Waters SEC system with a Waters 410 RI detector, a Waters 625 HPLC pump and three columns (Styragel HR1, HR2 and Ultrastyragel 104 Å, Waters assoc. USA) were used in series. Calculations were made with the software Cirrus version 3.1 from Polymer Laboratories. The mobile phase was THF with a flow of 0.8 ml/min and the temperature of about 25 °C. The lignin was dissolved in THF to a final concentration of 10 mg/ml. DMSO was added to the sample as a flow marker for the SEC system. The sample solutions were filtrated in order to remove all insoluble material using hydrophobic PTFE syringe filters from Advantec with a pore size of 0.20 µm. Thereafter, a sample amount of 100 µl was injected into the SEC column system. The lignins were collected from the outlet of the RI detector in 0.15 ml fractions, during a period of 10 minutes and 2 fractions/minute.

MALDI-TOF-MS

MALDI-TOF-MS analysis were performed using a Micro-flex LT system (Bruker Daltonik, Bremen, Germany) with a nitrogen (337 nm) laser beam. Around 600-800 single pulse raw spectra were averaged and transformed into a spectrum. Evaluation of the analysis was made using the Bruker Daltonik Flex series software package, 2008. The matrix consisted of 10 mg DHB dissolved in 1 ml THF. It was required to prepare the matrix on a daily basis since DHB is easily oxidized. The sample and matrix solutions were mixed in different ratios to find the optimal amounts. About 0.5 µl of the sample/matrix solution was pipetted onto the sample probe and dried by evaporation to form a sample/matrix co-crystal.

Before analyzing the SEC fractions by MALDI-TOF-MS, the fractions were evaporated to dryness and re-dissolved in 50 µl THF obtaining a concentration of 0.1-0.2 mg/ml.

III. RESULTS AND DISCUSSION

The MALDI-TOF-MS spectra obtained upon analysis of the softwood lignin fractions are presented in **Figure 1**. Due to the heterogeneity of the kraft lignin (no repeating unit) the spectra of these fractions contain broad and rather noisy signals. Nonetheless, it was possible to determine the peak-average molecular mass (M_p) of the lignin fractions from their MALDI-TOF-MS spectra.

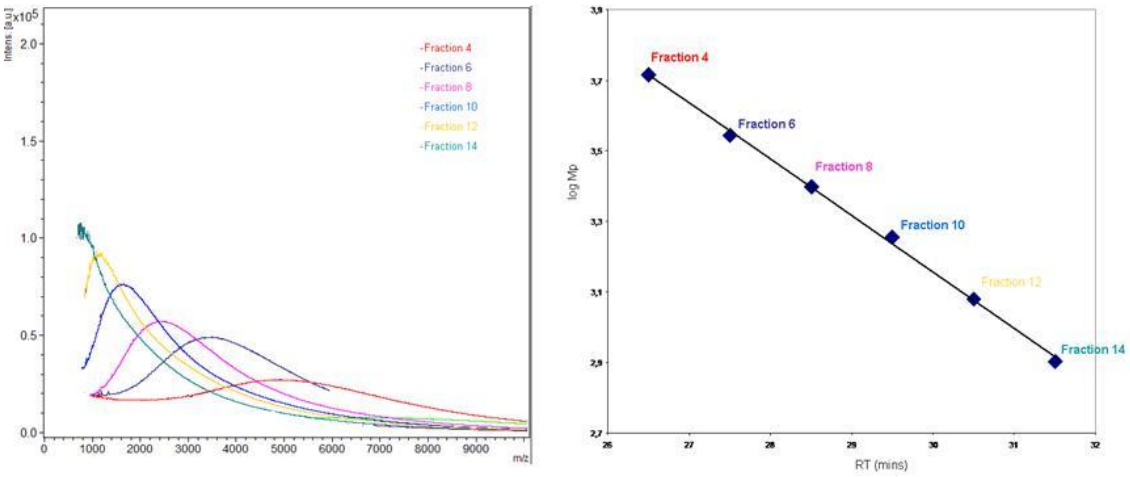

Figure 1. MALDI-TOF-MS spectra for softwood kraft lignin fractions and SEC calibration line constructed from the peak-average molecular mass values obtained from the MALDI-TOF-MS spectra.

The M_p values were then used to create a SEC calibration lines (Figure 1). For comparison, a conventional calibration line was constructed by SEC analysis of polystyrene standards. The three calibration lines obtained are compared in **Figure 2**. The calibration lines are overlapping but the line originating from polystyrene standards has a steeper slope compared to the calibration lines constructed from MALDI-TOF analysis of the lignin fractions. Also, the calibration line for hardwood lignin seemed to differ somewhat from that for softwood lignin. However, conclusions about any differences between hardwood and softwood lignin needs further investigation. The calibrations were used for calculation of the average molecular masses and molecular mass distributions of the lignin samples from the SEC chromatograms (**Table 1**).

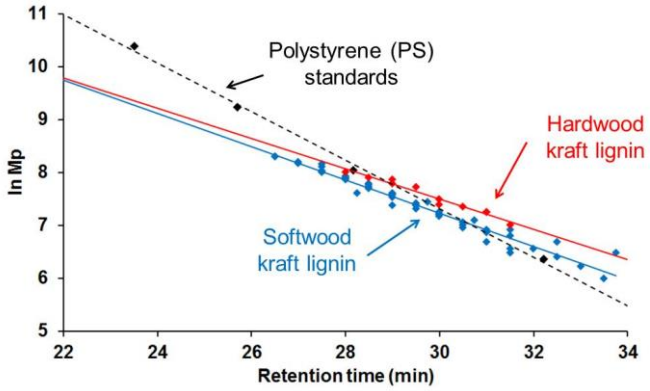

Figure 2. Calibration lines obtained by polystyrene standards and by MALDI-TOF-MS analysis of hardwood and softwood lignin fractions.

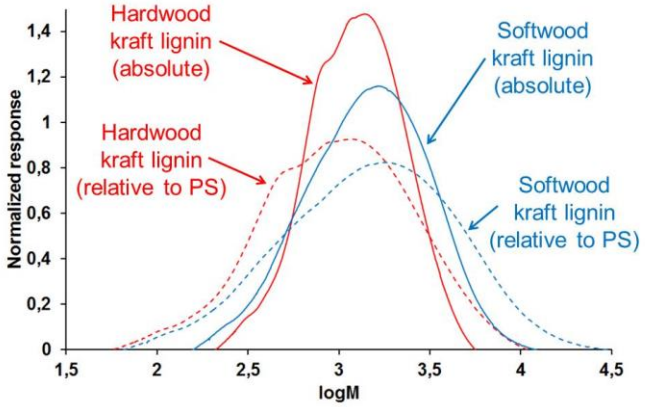

Figure 3. SEC chromatograms for hardwood and softwood kraft lignins while employing polystyrene (dashed) or the more absolute MALDI-TOF-MS (solid) calibration.

In Figure 3, the MALDI-TOF-MS and polystyrene calibrations have been employed to calibrate the x-axis of the SEC chromatograms from retention time to log M scale. This illustrates clearly the effect of the different calibrations on the resulting molecular mass calculations. Due to the steeper slope of the polystyrene calibration line, this calibration gives an overestimation of weight-average molecular mass (Mw) and underestimation of number-average molecular mass (Mn), and consequently also overestimation of the polydispersity index (PDI) by up to 50%.

The hardwood kraft lignin used in this study was completely soluble in THF, but the softwood lignin sample was not. Therefore the softwood kraft lignin was acetylated, which made this sample completely soluble in THF as well. The SEC fractionation/MALDI-TOF-MS calibration was performed also for the acetylated softwood kraft lignin.

Table 1. Average molecular mass, mass distribution and polydispersity index (PDI) for hardwood (HW) and softwood kraft lignin (SW).

Sample	Polystyrene calibration			MALDI-TOF-MS calibration		
	M_w	M_n	PDI	M_w	M_n	PDI
HW	1400	700	2.1	1400	1100	1.4
SW	2700	1000	2.7	2000	1200	1.7
SW (acetylated)	-	-	-	3500	1300	2.6

As expected, the average molecular mass of the acetylated softwood kraft lignin is higher than that for the underivatized sample. The molecular mass increase is higher than the theoretical increase due to the addition of acetyl groups, and is most likely due to increased solubility of the high molecular mass portion of the sample (**Table 1**).

IV. CONCLUSIONS

Calibration with polystyrene gives an overestimation of weight-average molecular mass (Mw) and underestimation of number-average molecular mass (Mn).

Calibration with polystyrene overestimates the polydispersity index by up to 50%.

The effect is most pronounced for low- and high molecular mass lignins.

V. ACKNOWLEDGEMENTS

We wish to acknowledge Johanna Persson for skillful technical assistance, and Lars-Erik Åkerlund and Dr Fredrik Öhman for supplying the lignin samples. Research Institutes of Sweden (RISE) is gratefully acknowledged for financial support.

VI. REFERENCES

[1] Baumberger, S.; Abaecherli, A.; Fasching, M.; Gellerstedt, G.; Gosselink, R.; Hortling, B.; Li, J.; Saake, B.; de Jong, E. Molar mass determination of lignins by size-exclusion chromatography: towards a standarization of the method. *Holzforschung* **2007**, *61*, 459-468.

[2] Botaro, V R.; da Silva Curvelo, A A. Monodisperse lignin fractions as standards in size-exclusion analysis – Comparison with polystyrene standards, *J. Chromatogr. A* **2009**, *1216*, 3802-3806.

[3] Faix, O.; Beinhoff, O. Improved calibration of high-performance size-exclusion chromatography of lignins using ligninlike model compounds. *Holzforschung* **1992**, *46*, 355-356.

[4] Gidh, A.; Decker, S-R.;Vinzant, T-B.; Himmel, M-E.; Williford, C. Determination of lignin by size-exclusion chromatography using multi angle light scattering. *J. Chromatogr. A* **2006**, *1114*, 102-110.

[5] Jacobs, A.; Dahlman, O. Absolute molar mass of lignins by size exclusion chromatography and MALDI-TOF mass spectrometry. *Nordic Pulp Paper Res J*. **2000**, *15(2)*, 120-127.

[6] Öhman, F. *Precipitation and separation of lignin from kraft black liquor* **2007**. Doctoral thesis, Chalmers University of Technology, Sweden.

[7] Chedid, F. *Determination of absolute molecular mass distribution and other structural properties of kraft lignin samples: Investigation using SEC in combination with MALDI-TOF-MS and Py-GC/MS* **2010**. Master of Science thesis, Linköping University, Sweden, LITH-IFM-A-EX-10/2271-SE.

EVALUATION OF GREY ALDER BARK TANNIN AS PHENOL SUBSTITUTE IN THE SYNTHESIS OF PHENOL-FORMALDEHYDE RESINS SUITABLE FOR PLYWOOD

Sarmite Janceva[1], Electra Papadopoulou[2], Laimonis Kulinsh[3], Maris Lauberts[1], Tatiana Dizhbite[1], Galina Telysheva[1]*

*[1]Latvian State Institute of Wood Chemistry, 27 Dzerbenes st., LV-1006 Riga, Latvia; [2]Chimar Hellas S.A., 88 Them. Sofouli, 55131 Thessaloniki, Greece; [3]Latvia University of Agriculture, 41 Dobeles st., LV-3001 Jelgava, Latvia; (*ligno@edi.lv)*

ABSTRACT

With the aim to develop green adhesives for wood, an adhesive system formed by condensed tannins (CT), isolated from grey alder bark, polyethyleneimine (PEI) and phenol-formaldehyde resins (PF) including this one containing micro/nanoparticles of extracted bark as a filler, and a PF resin, where CT were used as phenol substitute on the synthesis stage were studied for plywood manufacture. The results of the gluing quality tests have shown that the modulus of elasticity of plywood glued using the (CT-PEI):PF based adhesives with 40-60% substitution of PF was very close to that for plywood obtained with the traditional 100% PF glue and meet the European norms EN 312 (2004) in terms of share strength for plywood used both in indoor or outdoor conditions. Introduction of extracted bark residue micro/nanoparticles into composition of adhesives investigated led to increasing of physical-mechanical properties and strength of gluing. The experimental PF resin was prepared by substitution of 20% phenol following processes proprietary of CHIMAR. The produced resin had properties close to that of a typical PF resin. Plywood panels produced with this CT:PF resin (PFT) may be used for exterior application. The resins obtained using both (CT:PEI) gel and CT extract are suitable for the fabrication of plywood panels for interior application because their formaldehyde emission is very low.

I. INTRODUCTION

Phenol-formaldehyde (PF) based wood adhesives still today dominate in markets. However, toxic formaldehyde emission [1] and necessity to diminish petrochemicals consumption stimulate the search of alternative environmentally safe adhesives. Tannins, natural polyphenolic compounds, are present in large concentrations in wood barks. They are natural hydrophilic complexing agents. Wood adhesives from condensed tannins have been developed, especially on the basis of acacia (Mimosa – *Acacia mearnsii* De Wild) and quebracho (*Schinopsis lorentzii*) tannins [2]. It has been established earlier [3] that the bark of grey alder (*Alnus incana*), the tree widely spread in the European countries including Latvia, contains condensed tannins (CT) in rather large quantity (about 12% on o.d. bark) Using ^{13}C NMR spectroscopy, it has been shown that the grey alder CT contain mostly epicatechin units connected by C4-C8 and C4-C6 interflavonoid bonds to B-type procyanidins double bond flavanyl units in the molecule (2C-O-7C), which is typical for A-type procyanidins. The TOF-MS analysis has shown that oligomeric CT of grey alder bark ranged from the dimer to the heptamer (Figure 1). The preliminary experiments have shown suitability of alder bark tannins for obtaining of eco-friendly wood adhesives [3,4].

The present study continues our works aimed on the developing of green adhesives and is focused on investigation of the alder bark oligomeric tannins as substitutes of petrol-based adhesives used in plywood panels manufacturing. With this aim, a polymeric gel obtained on the basis of CT by its modification with polyethylenimine (PEI) was tested as an additive in a typical PF resin for plywood manufacturing. Besides, the grey alder CT were tested as a phenol substitute during the synthesis of PF wood adhesive (PFT).

II. EXPERIMENTAL

Formulation of CT-based polymeric gel and (CT-PEI):PF adhesives

Grey alder bark (*Alnus incana*) was collected from the forest in East-South part of Latvia. Tannin fraction of bark extractives was sequentially extracted as described in [3] using solvents with increasing polarity: hexane, ethyl acetate and finally aqueous ethanol (1:1, v/v). The ethanol was removed under vacuum and the remaining aqueous solution was frozen and freeze-dried. CT content in the tannin extract was measured by buthanol–HCl method [5] using procyanidin dimer B2 from Extrasynthese as a reference compound.

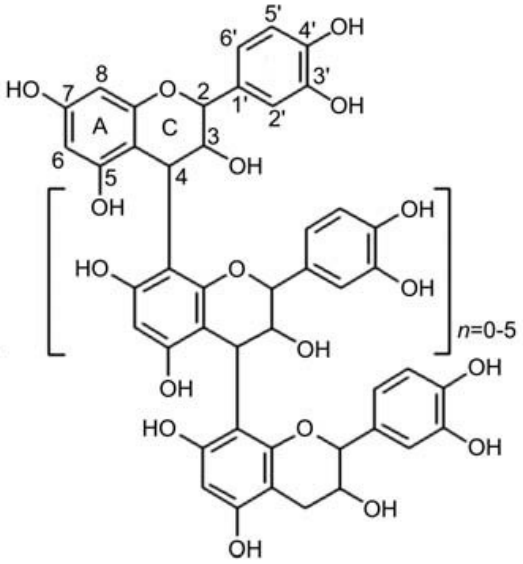

Figure 1. B-type oligomeric structure of grey alder condensed tannins.

The CT–based gel was obtained by mixing of aqueous tannins solution (pH 7) with 50% (w/v) aqueous polyethylenimine (PEI) solution (mass ratio 2:1,w/w) was purchased from Sigma-Aldrich. The tannin adhesive were characterized by differential scanning calorimetry (DSC) on a Metter Toledo DSC 828. and the results obtained from the DSC scans show a large heat absorption peak at about 120°C, which indicated that the reaction CT with PEI proceeds in the temperature range 100-140°C.

Adhesives for plywood manufacture were made by mixing of (CT-PEI) gels with PF resin at the mass ratios (CT-PEI):PF = 20:80, 40:60, 50:50, 60:40, 80:20. The resulting adhesives were tested for obtaining of plywood panels.

Synthesis of a PFT resin with phenol substitution by CT

For the synthesis of the phenolic resins, phenol 90% and formaldehyde water solution 37.4% were used. A PFT resin with 20% phenol replacement by CT was produced smoothly following the CHIMAR proprietary process for the synthesis of a PFT type resin.

Plywood panels production and characteristics

The (CT-PEI) based adhesives were applied for obtaining of birch plywood panels. The plywood panel samples were made using tree layers of birch (thickness of 2 mm each), and 170 g/m2 of adhesive. The panels were pressed for 10 minutes at 140°C and pressure of 2 MPa. The samples obtained were conditioned in a climate room (25˚C and 65% humidity) for 24 h. Then the quality of plywood panel gluing was evaluated by the statistic bending (modulus of elasticity) and bonding shear tests, carried out according to EN 314 -1 [6].

The bonding ability of PFT resin with 20% phenol substitution by CT under study was tested in the production of laboratory plywood panels of 3 layers: the face veneers were from okoume and the core veneer was from poplar. The plywood panels were produced with a process simulating industrial practices, while panel testing and evaluation was conducted according to the European standards EN 314.1 and EN 314.2. Formaldehyde emissions were determined according to the Desiccator (JIS A 1460) method.

III. RESULTS AND DISCUSSION

(CT-PEI)-based PF adhesive

It was found that the major components (0.36 g/g of extract or 12 % on bark dry mass) of the tannins extract isolated from grey alder bark are condensed tannins (proanthocyanidins). The new (CT-PEI):PF adhesive compositions were prepared on the basis of this extract.

The results of the gluing quality tests of the birch plywood panels glued using the all (CT-PEI):PF based adhesives showed (Table 1) that the values of elasticity modulus for plywood panels obtained with PF substitution by 20-60% were close to those for control panels glued by the typical PF only.

It was found that the values of share strength for these panels after treatment by immersion in water at 20°C for 24 h (bonding class for dry interior) and cyclic treatment in boiling water (bonding classes for exterior application) passes the threshold values requested by the EN standard 314.2 (Table 1). However, the adequacy of the plywood panels to the standard requirements has to be confirmed further by evaluation of the gluing quality using the apparent cohesive wood failure criteria.

Table 1. Influence of composition of adhesives prepared on (CT-PEI) basis on the modulus of elasticity of plywood panels glued

Adhesive composition	Plywood panel elasticity modulus, N/mm^2		Shear strength, N/mm^2	
	Transverse modulus	Longitudinal modulus	After immersion in water at 20°C	After cyclic treatment in boiling water
Control: traditional PF	1190±160	16270±1800	2.28±0.38	1.68±0.30
(CT-PEI):PF = 20:80	1000±150	14610±660	1.79±0.38	1.56±0.28
(CT-PEI):PF = 40:60	1070±140	14480±880	1.84±0.34	1.36±0.27
(CT-PEI):PF = 50:50	1030±110	14085±1300	2.04±0.29	1.30±0.32
(CT-PEI):PF = 60:40	1030±120	13980±1730	1.45±0.30	1.3±0.29
(CT-PEI):PF = 80:20	1060±200	11720±1380	0	0

Introduction of extracted bark residue micro/nanoparticles into composition of (CT-PEI):PF adhesives led to increasing of physical-mechanical properties and strength of gluing.

Phenol substitution by CT during PF synthesis

An experimental resin was prepared by substitution of 20% phenol during the synthesis of the PFT resin following processes proprietary of CHIMAR. The produced PFT resin had properties close to that of a typical phenol-formaldehyde PF resin.

The results of evaluation of quality of gluing for plywood panels produced with a process simulating industrial practices, have shown (Figure 2, Table 2) that the experimental PFT resin passes the threshold values requested by the EN standard 314.2, for all classes: for Class 1 - dry interior and Class 3 – non covered exterior (the conditions of corresponding tests are shown in the Table 2).

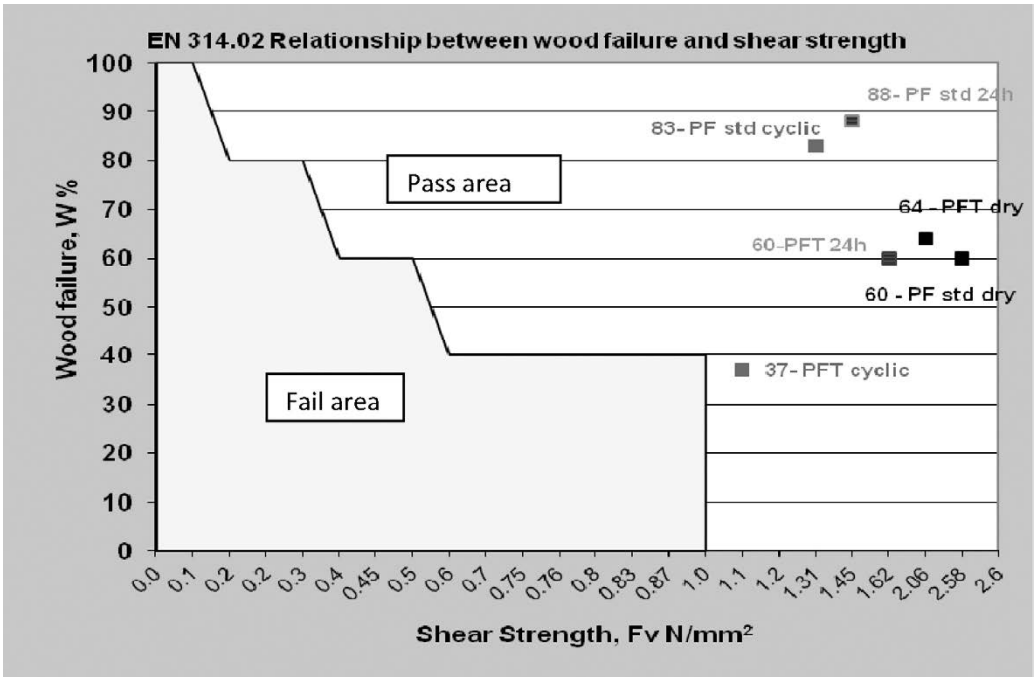

Figure 2. The relationship between wood failure and share strength of plywood panels and the experimental results. std dry – panels without pretreatment; std 24 h – panels after pretreatment required by Class 1; std cyclic – panels after pretreatment required by Class 3.

For all three bonding classes (EN 314. 2), each glue line has to satisfy two criteria, namely, the mean share strength and the mean apparent cohesive wood failure as combined in the Figure 2.

Table 2. The results of evaluation of plywood panels produced with PFT

Index	Resin	
	Standard PF	PF with 20% phenol substitution by CT
No treatment		
Shear strength, N/mm^2	2.58±0.23	2.06±0.31
Wood failure, %	60±2	64±1
Pretreatment required by Class 1: immersion in water of 20°C for 24 h		
Shear strength, N/mm^2	1.45±0.22	1.62±0.35
Wood failure, %	88±2	60±1
Pretreatment required by Class 3: 4 h in boiling water–16 h drying at 60°C–4 h in boiling water–1 h in cool water		
Shear strength, N/mm^2	1.31±0.19	1,14±0.11
Wood failure, %	83±2	37±1
Formaldehyde emission: desiccator values, mg/L	0.090±0.008	0.047±0.009

Comparison of the desiccator values showed (Table 2) that the plywood panels fabricated with the experimental PFT resin (20% substitution of phenol by CT) showed much lower formaldehyde emission than that released by the panel produced using a typical PF resin. The reducing formaldehyde emission provide the advantage of the CT-based adhesive interior application in comparison with typical PF resins.

IV. CONCLUSIONS

The synthesised wood adhesives containing oligomeric tannins that are available in large quantities from grey alder bark, could be used for production of plywood for exterior applications, although the further investigations needed for improvement their wood failure performance.

Due to very low level of formaldehyde emission, the synthesised CT-containing adhesives are suitable for the fabrication of plywood panels for interior needs.

V. ACKNOWLEDGEMENT

Financial support from Collaborative European project BIOCORE, Contract FP7-241566, LSC Research Grant 564/2012 and Latvian Government Research Program 2010.10-4/VPP-5 is gratefully acknowledged.

VI. REFERENCES

[1] International Agency for Research on Cancer (IARC) and World Health Organisation (WHO), June 14, **2004**.
[2] Bertaud, F.; Tapin-Lingua, S.; Pizzi, A.; Navarrete, P.; Petit-Conil, M. Development of green adhesives for fibreboard manufacturing, using tannins and lignins. *Cellulose Chem. Technol*., **2012**, *46*, 449-455.
[3] Telysheva, G.; Dizhbite, T.; Bikovens, O.; Ponomarenko, J.; Janceva, S., Krasilnikova, J. Structure and antioxidant activity of diarylheptanoids extracted from bark of grey alder (*Alnus incana*) and potential of biorefinery-based bark processing of European trees. *Holzforschung,* **2011**, *65*, 623 – 629.
[4] Janceva, S.; Dizhbite, T.; Telysheva, G.; Arshanitsa, A.; Spulle, U.; Kulinsh, L.; Dzenis, M. Isolation and testing of condensed tannins from alder bark for obtained environment friendly adhesives and biofuel granules. Proceedings of NWBC 2011, Stockholm, March 22-24, **2011**, 351 – 352.
[5] Waterman, P.G.; Mole, S. Analysis of phenolic plant metabolites.Blackwell Scientific Publications, Oxford, 1994.
[6] Zanuttini, R.; Cremonini, C. Optimization of the test method for determining the bonding quality of core plywood (blackboard). Mater. Struct., **2002,** *35*, 126-132.

IMPORTANCE OF H_2SO_4 OR NAOH CONCENTRATION ON REMOVAL OF XYLAN AND LIGNIN FOR ENZYMATIC CELLULOSE HYDROLYSIS

Mirjam A. Kabel[1]*, Patricia Murciano Martínez[1], Arjen Punt[1], Harry Gruppen[1]

[1]*Laboratory of Food Chemistry, Bornse Weilanden 9, 6708 WG, Wageningen, The Netherlands (*mirjam.kabel@wur.nl)*

ABSTRACT

Future biobased chemicals and materials are preferably based upon agricultural side streams. An example of such side streams are bagasse (Bag) and palm empty fruit bunches (EFB), which are both rich in lignin, hemicellulose (xylan) and cellulose. Although the composition of Bag and EFB was rather similar, different structural features for lignin and for xylan were observed prior to pretreatment. EFB contained a highly acetylated 4-O-methylglucuronoxylan, while Bag-xylan was much less substituted.
In this study, the effect of hemicellulose and lignin solubilization by H_2SO_4 and NaOH catalyzed pretreatments, was correlated to the extent of subsequent enzymatic cellulose hydrolysis. For both EFB and Bag, alkali pretreatment resulted into extensive lignin removal. This removal resulted in up to 90% (w/w) conversion of glucan into glucose by enzymes. But, the alkaline conditions also provoked unwanted xylan losses up to 50% (w/w). Acid pretreatment resulted into solubilization (60-80% (w/w)) of xylan, with almost no losses, while lignin remained. Although xylan solubilization increased enzymatic cellulose hydrolysis of residual glucan, extensive removal of xylan decreased glucan hydrolysis. In this study, under the applied treatment conditions, the alkali treatments were the most efficient in terms of enzymatic release of xylose and glucose from the insoluble residues.

I. INTRODUCTION

The use of renewable resources is the key in the transition to a sustainable society that will allow future generations to have a standard of living similar to ours. Hence, future biobased chemicals and materials are preferably based upon agricultural side streams. An example of such side streams are bagasse (Bag) and palm empty fruit bunches (EFB). Bag is the remaining stream from the extraction of sucrose from sugarcane, while EFB are the empty bunches remaining after removal of the oil containing berries as present in the oil palm. Both belong to the monocots or true grasses and are typical lignocellulosic materials composed of around 25% (w/w) hemicellulose, 35% (w/w) cellulose and 25% (w/w) lignin [1, 7, 8]. Cellulose is a homoglucan of which the backbone consists of β-D-(1-4)-linked glucosyl units, forming a crystalline polymer. Lignin is a highly heterogeneous, complex aromatic polymer synthesized from phenylpropanoid precursors.

The conversion of the (hemi-) celluloses of such agricultural side streams into fermentable monosaccharides, mainly glucose and xylose, comprises various steps. These are harvest, storage of lignocellulosic biomass, pretreatment, enzymatic saccharification and fermentation/modification of the resulting monosaccharides [2]. Pretreatment is a critical prerequisite to achieve high monosaccharide-yields together with the enzyme hydrolysis. Leading chemical pretreatments, resulting in increased enzymatic hydrolysis of the (hemi) celluloses, usually comprise acid or alkaline based processes. While acid provokes GAX solubilization, alkali promotes swelling of the biomass and the cleavage of ester-bonds in GAX and in GAX-lignin complexes. The fate of lignin and its distribution over solid and liquid phases during pretreatment is not well understood, although alkali is known to promote the solubilization of lignin [3], supporting enzymatic cellulose hydrolysis. Also, recently it was shown that by dilute acid treatment lignin-droplets deposited on the cellulose surface, which retarded enzymatic hydrolysis [4]. So, for both acid and alkali treatments, there is a remarkable effect on the composition and structure of the insoluble material. Clearly, the concentration of the acid or alkali is an important factor. At present, there are no studies that compare the effects of different concentrations of alkali or acid on enzymatic hydrolysis of the insoluble residues obtained. Usually, only a limited number of conditions are applied. Or in case of many conditions applied, no detailed quantitative information is given with respect to carbohydrates present in the different fractions obtained.

The present study evaluates for Bag and EFB the effects of acid and alkali treatments at elevated temperatures on their enzymatic hydrolysis, the research described is based on Murciano Martínez *et al.* [5]. Various concentrations of acid (0-6 %w/w) and alkali (0-12 %w/w) are applied. Carbohydrate and lignin mass distributions over insoluble residues and soluble hydrolysates after catalysis are determined, and enzymatic hydrolysis of the residues is correlated to the ratio of hemicellulose/lignin/cellulose.

II. EXPERIMENTAL

Bag and EFB were supplied by Purac Thailand (Banchang, Thailand) and Sime Darby (Kuala Lumpur, Malaysia), respectively. Enzyme cocktails CellicCTec2 (CCT) and CellicHTec (CHT) were kindly provided by Novozymes (Bagsvaerd, Denmark) and stored at 4°C.

Stainless steel, non-stirred reactors (0.1 L) were loaded with a fixed solid:liquid ratio of 1:10 (w/w). Residence time for acid (0, 2, 4 or 6 % H_2SO_4 (%w/w dry matter (DM) was 30 minutes at 140°C, and for alkali treatment (0, 4, 8 or 12% NaOH (%w/w DM)) 60 minutes at 120°C. The reactors were equipped with a controlled thermocouple (Pico Technology, Saint Neots, UK). The reactors were introduced into silicon oil preheated at the desired pretreatment temperature. Reactors removed from the oil after pretreatment were directly submerged in ice-water. The maximum heating and cooling times were 22 and 15 min, respectively. After cooling down to ambient temperature the pretreated mixture was transferred to 0.25 L polypropylene tubes and centrifuged (10000 *g*, 15 min, ambient temperature). The supernatant was decanted and the residue was recovered and washed 3 times with water. For each raw material, the first supernatant and 3 wash supernatants were combined and freeze dried (denoted as "soluble fraction"). The remaining washed residues were denoted as "residues".

Enzyme incubations were performed as described by Murciano Martínez *et al.* [5]. In short, CCT and a combination of CCT+CHT (ratio 10:1 (protein (Nx6.25) basis) was used. Residues (milled; <1 mm) were incubated in 50mM sodium acetate buffer pH 5.5. The milled substrate load was 1% (w/w) based on dry matter. The enzyme incubations were performed in duplicate at 55°C, and rotated head-over-tail for 72h. Enzyme dosage was in total 3% (w/w) of protein based on dry matter of the amount of residue/sample loaded. The protein contents (N%*6.25) of CCT and CHT were 127 mg/ml and 120 mg/ml, respectively. Sodium azide 0.01% (w/v) was used to prevent bacterial growth. After incubation, the digests were heated at 100°C for 5 min, centrifuged, and analyzed for their total carbohydrate content and constituent monosaccharide composition.

Neutral carbohydrate content and composition, as well as uronic acid content, Klason lignin content (corrected for ash), and ash content, was determined as described previously [6]. High-performance anion exchange chromatography (HPAEC) was used to quantify release of the various monosaccharides [6].

III. RESULTS AND DISCUSSION

Composition of the feedstocks

EFB and Bag were composed of mainly cellulose (Bag 37%; EFB 26 %w/w), glucoronoarabinoxylans (GAX) (both 27 %w/w), and lignin (Bag 28%; EFB 24 %w/w), which corresponded to literature values [7,8]. The degree of substitution (DS) of the xylan backbone was calculated as mol% of arabinosyl, acetyl and glucuronic acid residues on xylosyl residues. It must be considered that double substitution and chains longer than 1 substituent are not taken into account. The DS of EFB-xylan was 60%, while for Bag-xylan a much lower DS (38%) was found.

Carbohydrate distribution over hydrolysates and residues after pretreatment

Acid treated samples showed xylan solubilization reaching a maximum (80 w/w% of original amount of xylan present in Bag) in 6% (w/w) H_2SO_4 for Bag, mainly as xylose monosaccharides. For EFB, similar conditions resulted in a much lower xylan solibilization (60%), of which only 20% as monosaccharides and 40% as oligosaccharides.

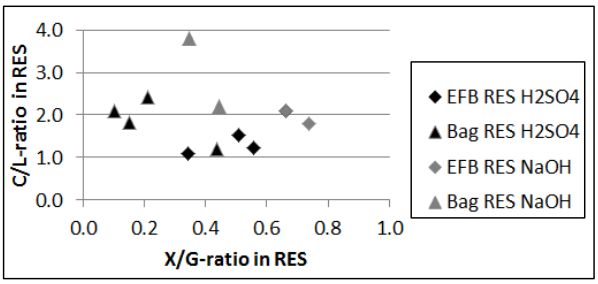

Figure 1. Xylan/glucan (X/G-) ratio versus carbohydrate/ lignin (C/L-) ratio in residues remaining after pretreatment catalyzed with H_2SO_4 or NaOH, modified from [5].

Corresponding glucan solubilization was low (<15 %w/w). The amount of lignin solubilized is for all acid samples around 20% (w/w) based on the original amount of lignin present. Alkaline pretreatment showed visible swelling of the material, but it resulted in less than 20 %w/w solubilization of carbohydrates, while up to 50% w/w of lignin was solubilized (**Figure 1**). The amount of calculated losses of GAX (up to 40% (w/w)) was

remarkable. The amount of losses was much higher for Bag compared to EFB. The lost fraction was calculated taking the total amount of xylan in the feedstock prior to pretreatment, minus the amount of xylan analyzed in residue and corresponding hydrolysate. It was hypothesized, that part of the xylan present was converted into non-carbohydrate degradation products during alkaline pretreatment, for example, caused by peeling.

GAX and lignin removal by the pretreatments used, resulted in residues with different contents of xylan and lignin next to cellulose. This was expressed as the ratio of xylan versus glucan (X/G-ratio), and as the ratio of carbohydrates versus lignin (C/L-ratio) in the residues (**Figure 1**). No clear correlation between the two ratios was observed.

Enzymatic degradability of residues resulting from the various pretreatments

To study the enzymatic degradability of the residues described above, they were incubated by using 2 different enzyme cocktails: CCT and a combination of CCT+CHT. CCT is, principally, a cellulose degrading enzyme cocktail, while CHT is enriched in xylan degrading enzymes.

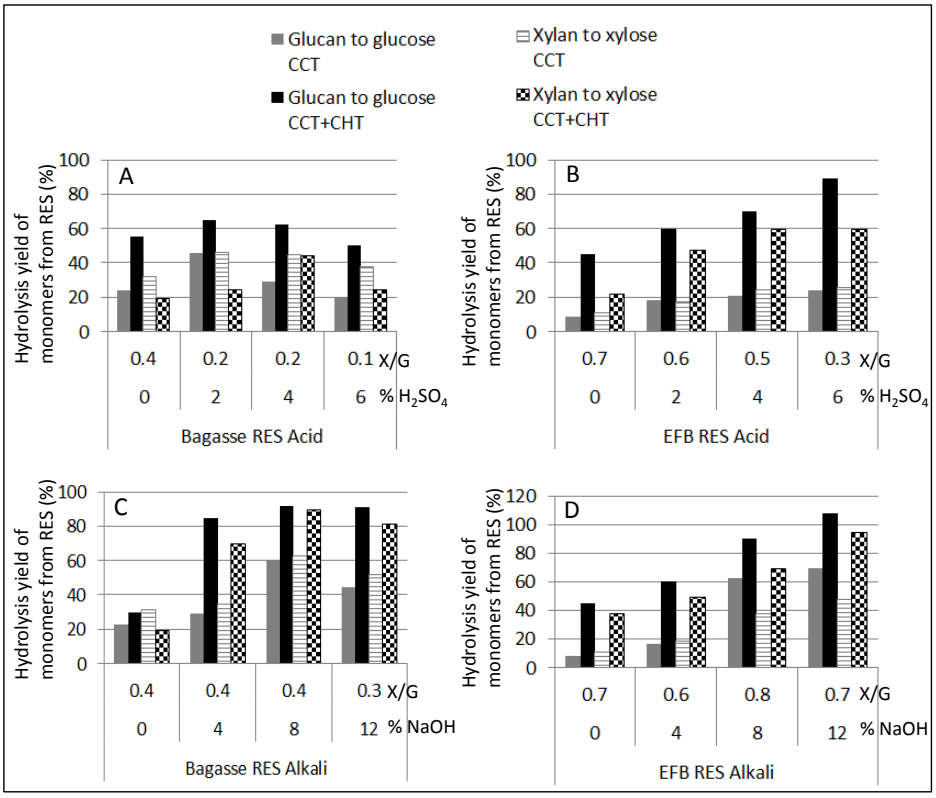

Figure 2. Hydrolysis yield of monosaccharides, glucan to glucose or xylan to xylose, by the enzyme cocktails CCT and by CCT+CHT, from residues remaining after H_2SO_4-pretreatment (Bag (A) and EFB (B)) or NaOH-pretreatment (Bag (C) and EFB (D)), modified from [5].

Degradation of glucan and xylan into corresponding glucose and xylose is shown in **Figure 2**. It should be remarked that enzyme studies were performed with freeze dried material to allow good comparison between samples and to minimize inhomogeneity issues, although drying may negatively affect enzyme hydrolysis. Nonetheless, the results are expected to reflect the comparisons made.

Acid pretreatments of Bag resulted in residues with lower X/G-ratios compared to the EFB residues obtained under similar conditions. Nevertheless, residues obtained after acid treatment with lower X/G-ratios were better hydrolysed by CCT. Also in literature, xylan removal was shown to enhance enzymatic cellulose hydrolysis [9]. Interestingly, at very low X/G-ratios, the enzyme degradability decreased. For EFB, this point was reached at X/G-ratios lower than 0.4, while for Bag this was lower than 0.2. This trend of decreased cellulose hydrolysis was more pronounced for Bag than for EFB. Hydrolysis by CCT+CHT showed for acid pretreated Bag residues again that the yield of monosaccharides decreased at lowest X/G-ratios (**Figure 2**). On the contrary, for the EFB acid residues the hydrolysis yield by CCT+CHT increased at low X/G-ratios (**Figure 2**).

To understand these phenomena, the remaining composition of the residues should be considered. The residues of the acid pretreatment were high in both glucan content and lignin content. Both were hardly solubilized during pretreatment, while xylan was progressively removed upon higher acid concentrations (lower X/G-ratio). The remaining lignin may have formed droplets on the cellulose surface hindering the enzymatic hydrolysis, which

was shown to occur in dilute acid pretreatments [4]. As this was less observed for the EFB acid treated residues, it may implicate that the relatively high amounts of residual xylan present prevented re-condensation of lignin present on cellulose fibers. The physical hindrance by xylan was partly overcome by addition of endoxylanase activity to the cellulase cocktails, especially for the more xylan-rich EFB residues. So, excessive removal of xylan from glucan fibers before addition of cellulases and xylanases, in the presence of lignin, negatively influenced glucan conversion into glucose. From microscopic studies [9], the same conclusion was drawn. During alkaline pretreatment mainly lignin was removed for Bag and EFB. The corresponding residues were hydrolyzed by CCT and CCT+CHT and the results are shown in **Figure 2**. The various concentrations of NaOH resulted in residues with rather similar X/G-ratios for EFB and Bag, but the enzymatic cellulose to glucose hydrolysis yields differed. For the alkaline pretreated residues of EFB, an increase in hydrolysis by CCT of glucan was observed with decreasing lignin contents. The same trend was observed for Bag, but less pronounced. Apparently, lignin solubilization together with the swelling of the material during treatment facilitated the hydrolysis of the residual glucan, while X/G-ratios remained the same.

IV. CONCLUSIONS

Acid pretreatment solubilized large amounts of xylan and increased subsequent enzymatic cellulose hydrolysis. But, at extensive removal of xylan while lignin remained, glucan hydrolysis became less efficient. On the contrary, solubilization of lignin in alkaline pretreatements resulted in a rather high residual cellulose hydrolysis. This showed that, in this study, alkali pretreatment resulted in the highest glucose from cellulose yield.

V. ACKNOWLEDGEMENT

This project is jointly financed by BE-Basic (The Netherlands), and Wageningen University (The Netherlands).

VI. REFERENCES

[1] Escarnot, E., Aguedo, M., Paquot, M. Characterization of hemicellulosic fractions from spelt hull extracted by different methods. *Carb. Polymers*, **2011**, *85*, 419-428.

[2] Himmel, M.E., Ding, S.Y., Johnson, D.K., Adney, W.S., Nimlos, M.R., Brady, J.W., Foust, T.D. Biomass recalcitrance: Engineering plants and enzymes for biofuels production. *Science*, **2007**, *315*, 804-807.

[3] Park, Y.C., Kim, J.S. Comparison of various alkaline pretreatment methods of lignocellulosic biomass. *Energy*, **2012**, *47*, 31-35.

[4] Li, H., Pu, Y, Kumar, R., Ragauskas, A.J., Wyman, C.E. Investigation of lignin deposition on cellulose during hydrothermal pretreatment, its effect on cellulose hydrolysis, and underlying mechanisms. *Biotechnol. Bioeng*., **2013**, *111*, 485-492.

[5] Murciano Martínez, P., Bakker, R., Harmsen, P., Gruppen, H., Kabel, M.A. Importance of acid or alkali concentration on the removal of xylan and lignin for enzymatic cellulose hydrolysis. *Submitted* **2014**.

[6] Jurak, E., Kabel, M.A., Gruppen H. Carbohydrate composition of compost during composting and mycelium growth of *Agaricus bisporus*. *Carb. Polymers*, **2014**, *101*, 281-288.

[7] Canilha, L., Santos, V.T.O., Rocha, G.J.M., Almeida E Silva, J.B., Giulietti, M., Silva, S.S., Felipe, M.G.A., Ferraz, A., Milagres, A.M.F., Carvalho, W. A study on the pretreatment of a sugarcane bagasse sample with dilute sulfuric acid. *J. Ind. Microbiol. Biotechnol*., **2011**, *38*, 1467-1475.

[8] Hamzah, F., Idris, A., Shuan, T.K. Preliminary study on enzymatic hydrolysis of treated oil palm (*Elaeis*) empty fruit bunches fibre (EFB) by using combination of cellulase and β 1-4 glucosidase. *Biomass and Bioenergy*, **2011**, 35, 1055-1059.

[9] Ding, S.Y., Liu, Y.S., Zeng, Y., Himmel, M.E., Baker, J.O., Bayer, E.A. How does plant cell wall nanoscale architecture correlate with enzymatic digestibility? *Science*, **2012**, *338* 1055-1060.

CHEMICAL AND THERAPEUTIC PROPERTIES OF THE ROOT BARK EXTRACTS OF *MYRIANTHUS ARBOREUS*

Pierre Betu Kasangana[1,2,3], Pierre Haddad[2,3] and Tatjana Stevanovic[1,3,*]

[1]*Département des sciences du bois et de la forêt, Faculté de foresterie, de géographie et de géomantique, Université Laval, Québec ;* [2]*Département de pharmacologie, Faculté de médecine, Université de Montréal, Montréal ;* [3] *Institut de la nutrition et des aliments fonctionnels (INAF), Québec, Canada*

*E-mail address: tatjana.stevanovic@sbf.ulaval.ca (T. Stevanovic)

ABSTRACT

We report the results on phytochemical analyses and antidiabetic effects of six extracts obtained from *M. arboreus* root bark: water, dichloromethane, methanol (MeOH), ethanol (EtOH) and two sub-fractions from EtOH extract, ethyl acetate (ACE) and hexane (Hex) sub-fractions. Various classes of polyphenols were determined quantitatively in EtOH extract by UV-visible spectrophotometry. This extract was found to have high levels of total phenols, hydroxycinnamic acids and proanthocyanidins, while flavonoids were less concentrated. On the other hand, the chemical screening of the same extract by GC-MS revealed the presence of triterpenes which still remain to be identified. Alkaloids (Alk) were revealed from the MeOH extract by HPLC method and confirmed by TLC using Dragendorff reagent. *In vitro* assays were used to evaluate the antidiabetic activity of the plant extracts. Cytotoxicity was determined by using lactate dehydrogenase (LDH) assay for all studied extracts and fractions in order to determine the maximal nontoxic concentrations. Glucose-6-phosphatase (G6Pase) and Glucose uptake activities were assessed respectively in cultured hepatocytes (H4IIIE cells) and myocytes (C2C12 cells) treated with all extracts. Results showed that EtOH, two sub-fractions and Alk extract significantly decreased G6Pase activity, with insulin used as the positive control. Extracts and fractions of *M. arboreus* did not stimulate glucose transport into muscle cells compared with control DMSO. Metformin (400µM) and insulin (100nM) were used as positive control. The results of our study confirm the potential of using forest resources for the development of new natural health products.

I. INTRODUCTION

Myrianthus arboreus originates from the secondary forests of Africa. This small tree is widely used in folk medicine for its therapeutic effects. In Democratic Republic of Congo, the root barks of *M. arboreus* are used to treat diabetes. Several studies on *M. arboreus* reported the isolation of peptide alkaloids from the leaves as well as pentacyclic triterpene acids from the root wood and from the trunk bark [3]. However, no research has yet been done so far on root bark extracts namely on their phytochemical composition and antidiabetic effects. Diabetes is a metabolic disease characterized by hyperglycemia resulting from defects in insulin secretion, insulin action or both [2]. Type 1 diabetes is caused by a deficiency of insulin secretion from β-pancreatic cells. On the other hand, Type 2 diabetes is characterized by decreased insulin sensitivity in major target organs such as liver, muscle, and adipose tissues, in addition to a decreased insulin secretion by beta pancreatic cells [1, 2]. The aim of this study was to first identify different phytochemical classes of polyphenols, terpenes and alkaloids in the studied root bark extracts and fractions and then to determine their antidiabetic potential through the cell-based bioassays using the glucose-6-phosphatase activity (H4IIE cells) and the activity of glucose transport in muscle cells (C2C12).

II. METHODOLOGY

II.1.Sampling and phytochemical analyses

The root bark of *M. arboreus* was collected in the city of Bas-Congo, from Jardin botanique de Kisantu, in December 2012. The plant was identified at the Departement des sciences, of Kinshasa. The root barks were dried for a week and ground into powder. This crude powder was used to prepare six extracts in order to study their polyphenols, terpenoids and alkaloids contents. Thus, water extract was obtained after 2 hours of decoction using reflux system. Dichloromethane extract, methanol extract and ethanol (95%) extract were obtained by using Soxhlet apparatrus. The ethanol extract was divided into two sub-fractions, namely hexane and ethyl acetate fractions. The various types of polyphenols and triterpens compounds were determined in ethanol solution [4].

1. Determination of polyphenols content

Total phenols content: The total phenol content was measured spectrophotometrically according to the Folin–Ciocalteu method [4]. Gallic acid was used for the calibration curve and the results are expressed in gallic acid equivalents (mg GAE/g dry extract)
Flavonoids content: The flavonoids content was determined spectrophotometrically according by the $AlCl_3$ method developed by Brighente et al. [4]. Quercetin was used for the calibration curve and the results are expressed as quercetin equivalent (mg QE/g dry extract).
Hydroxycinnamic acids content: The hydroxycinnamic acids content was determined according to the method developed by Arnow (1937) [4]. Chlorogenic acid was used for the calibration curve and results are expressed as chlorogenic acid equivalents (mg CGE/g dry extract).
Proanthocyanidins content: The content of proanthocyanidins was measured following the method developed by Porter et al. (1986) [4].Cyanidin chloride was used for the calibration curve and the results are expressed as cyanidin chloride equivalents (mg CCE/g dry extract).

2. *Triterpenes characterization*
The identification of triterpènes compounds were performed by the use of gaseous chromatography coupled to mass spectroscopy (GC-MS). The method developed by Saint-Pierre et al. (2013) [4] was applied with a slight modification. The MS signal acquired was the total ion count for all the m/z included between 50 and 500. The identification of molecules was made by comparing the mass spectrum to those from the existing databases.

3. HPLC analysis of alkaloid extract

Alkaloid extract was obtained according to the method developed by Choudhary et al. (2011) [5]. The presence of alkaloids was confirmed by TLC ($CHCl_3$: MeOH, 50:50) using Dragendorff reagent. The extract was then studied by HPLC with UV detection at 320 nm. Analytical separations were performed on a 4.6 x 250 mm Zorbax SB-C18, 5µm reversed-phase column using CH_3CN-H_20 system for elution. The mobile phase was programmed on a gradient from 90% to 50% over 40 min, followed by 50% to 0% H_20 over the next 25 min at a flow rate of 0.5 mL/min.

II.2. Biological activity

1. *LDH Test:* Hepatic cells (H4IIE) and differentiated C2C12 cells were treated overnight (16-18h) with extracts and sub-fraction of M. *arboreus* at different concentrations. LDH release was measured spectrophotometrically at 492 nm. The determined maximal non-toxic concentrations were subsequently used for the antidiabetic effects experiments (G6P and GT).

2. Glucose-6-phosphatase (G6P) activity: Cells H4IIE (90% confluent in 12 well plates) were treated for 18 h with negative control (0.1%DMSO vehicle), positive control (Insulin, 100 nM), and extracts and sub-fractions of *M. arboreus* at their respective optimal nontoxic concentrations. After 18 h, cells were washed then lysed in 15mM phosphate buffer. Cell lysates were incubated in glucose-6-phosphate-containing buffer (200 mM) for 40 min at 37 C where the G6P serves as a substrate for endogenous G6Pase to yield glucose. Quantification of the glucose generated in this reaction was measured using Wake Autokit Glucose colorimetric assay. Results are presented relative to Insulin equivalent [1].

3. Glucose transport (GT) assay: The deoxy-D-glucose uptake assay was performed as described by (Spoor et al., 2006) [7], with a few modifications [7].Confluent and differentiated C2C12 myotubes (in 12- well plates) were incubated for 18 h in differentiation medium (DMEM with 2% HS) containing different concentrations of extracts and fractions of *M. arboreus* at their selected concentration obtained by LDH assay. DMSO (0.1%) and metformin (400 μM) were taken as negative and positive controls, respectively.

III. RESULTS AND DISCUSSION

1. *Determination of polyphenols content*

Table 1. Total phenol and different classes polyphenols contents in ethanol extracts

Parameter	**Average contents**		
	M. *arboreus*	**Y.birch**	**S. maple**
Phénols totaux (mg GAE/g)	278 ± 1.4^{ab}	223 ± 30^{b}	296 ± 27^{a}
Flavonoides (mg QE/g)	2.7 ± 0.6^{b}	3.7 ± 0.6^{b}	22 ± 8^{a}
Hydroxycinnamic acids (mgCAE/g)	173 ± 1.5^{a}	91 ± 60^{a}	117 ± 10^{a}
Proanthocynanidines (mg GAE/g)	123.9 ± 0.2^{a}	65 ± 48^{ab}	52 ± 10^{b}

Different letters indicate significantly different results according to Tukey's tests at 95% confidence level.

Results from **Table 1.** show variability in the content of phenolic compounds in EtOH extract. Flavonoids (FL) content is considerably lower than that of other classes of polyphenols. The concentration of proanthocyanidines (PAs) and hydroxycinnamic acids (HA) are determined to be very high in this extract. Comparing these results with those obtained by St-Pierre et al. on EtOH extract of bark trunk from Yellow birch (Y.B) and Sugar maple (S.M), it appears that the content of HA is not statistically difference in all three plants. The content of PAs is higher in *M. arboreus* (173±1.5 mg GAE/g) than in S.M (52±10 mg GAE/g), while it remains the same statistically in Y. B (65±48 mg GAE/g). Futhermore, the content of total phenols and FL are the same in Y. B and in *M. arboreus* [4]. The presence of PAs and HA in *M. arboreus* extract could contribute to its therapeutic proprieties. Interestingly, recent studies report that HA and its derivatives namely ferulic acid, m-hydroxycinnamic and p-methoxy cinnamic acides were potential agents of many antidiabetic activities determined namely from aqueous extract of *Syzygium alternifolium* seeds [6].

2. GC-MS triterpens compounds characterization

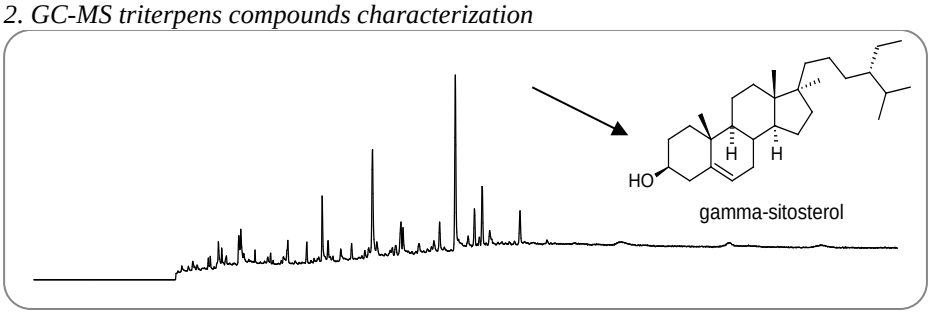

Figure 1. GC-MS chromatogram of ethanol extract

GC-MS chromatogram was developed in order to identify triterpens and sterols contained in the EtOH extract. The major peak indicating the main compound in this extract appeared at 14.6 min. Comparing it with the mass profiles of the compounds present in the database of the chromatogram (GC-MS), this peak corresponds to the gama-sitosterol (**Figure 1.**). However, we were unable to identify the others peaks with the database available in our instrument. The rest of the peaks will be identified in the future study using the GC-MS analysis on authentic triterpenes and/or after isolation and identification of triterpenes from this extract.

3.HPLC analysis of alkaloid fraction

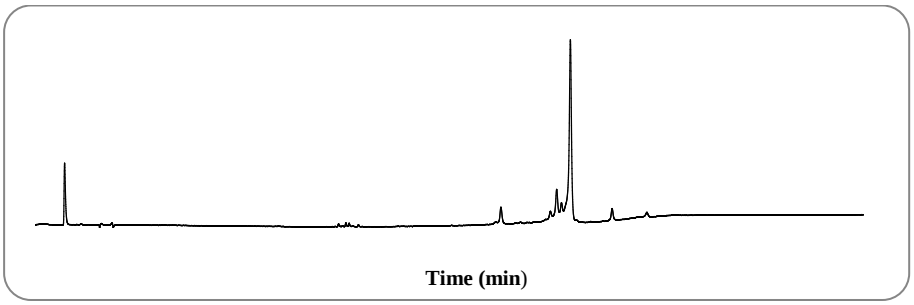

Figure 2. HPLC chromatogram of *M. arboreus* root bark ether extract

The presence of Alk in the ether extract was confirmed by TLC, using Dragendorff reagent. This extract was then analyzed by HPLC with UV detection at 320 nm. The **Figure 2.** shows the presence of three peaks corresponding, probably, to Alk compounds in this extract. As the recent work reported that the cyclopeptide type alkaloids were isolated from other part of *M. arboreus* [3, 5] these will be further studied. Other studies on cyclopeptidic Alk showed that these compounds seem to have an interesting potential to control the postprandial hyperglycemia, and associated diabetes complications [5].

4. Cell-bassed bioassays for antidiabetic activity

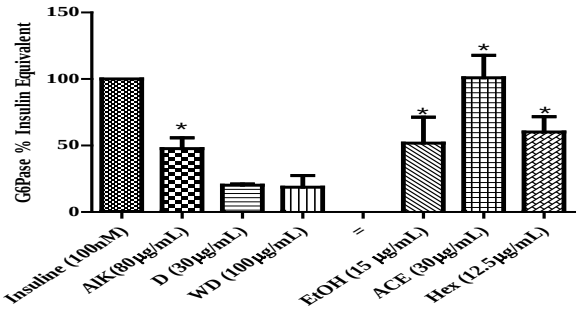

Figure 3. Effect of extracts/ fractions of *M. arboreus* on G6Pase activity. Results are expressed as Insulin Equivalent. Mean±SEM for n=4 to 5. *P < 0.05 significantly different after one-way ANOVA analysis followed by Dunnett's t test vs the positive control (Insulin 100nM)

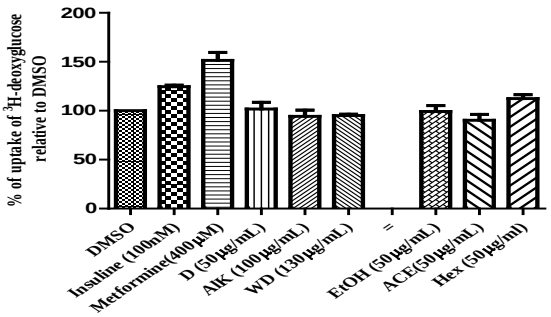

Figure 4. Effect of extracts/fractions of *M. arboreus* tested on glucose uptake assay in C2C12 cells. Each value is the mean±SEM (n= 4) in each group. *P < 0.05 significantly different after one-way ANOVA analysis followed by Dunnett's t test vs the negative control (DMSO 0.1%)

The antidiabetic potential of the root bark extracts of *M. arboreus* was first studied to determine glucose -6-phosphatase activity. G6Pase is a key enzyme involved in hepatic gluconeogenesis. The results are expressed in insulin equivalent. **Figure 3.** shows that the inhibitory effect of EtOH extract, sub- fractions (Hex and ACE) and Alk extract is not statistically difference with insulin used as a positive control. Interestingly, the ACE sub-fraction had antidiabetic potential comparable to insulin, while the EtOH extract and Hex fraction inhibited about 50 %. In addition, the effects of Alk extract should attract special attention because of the HPLC profile described in **Figure 2**. A thorough study of this extract should be performed in order to determine the bioactive molecule. The dichloromethane and water extracts, did not inhibit the enzymatic reaction. As for the activity of glucose transport in muscle cells, **Figure 4.** reports that none of the extracts of *M. arboreus* was determined to stimulate glucose transport. Metformin (400 µM) and insulin (100nM) were used as positive control.

IV. CONCLUSIONS

The results of phytochemical analyses of various extracts from root bark of *M. arboreus* have demonstrated a high concentration of proanthocyannidins and hydroxycinamic acids in EtOH extract, the polyphenols recognised for antidiabetic effect. The presence of triterpenes and phytosterols has also been recognised, the gamma-sitosterol being the only constituent identified by GC-MS of EtOH extract so far. Alkaloid rich extract is particularly interesting due to its simple HPLC profile revealing the presence of a few peaks. The tests on G6Pase activity and the glucose transport in muscle cells have produced the best results for the ACE fraction of EtOH extract which inhibited the G6Pase to the extent comparable to that of insulin. The EtOH extract, its Hex sub-fraction, as well as AlK fraction have been determined to reach the 50% of insulin efficiency. These results indicate that root bark extracts of *M. arboreus* have the potential to reduce hepatic glucose.

V. ACKNOWLEDGEMENT

The authors wish to thank Institue of Nutrition and functional food (INAF) for the financial support.

VI. REFERENCES

[1] Nachar, A.; Vallerand, D.; Musallam, L.; et al. *Evidence-Based Complementary and Alternative Medicine*, **2013**, ID 189819, 1-9.
[2] Haddad, P. S.; et al. *Evidence-Based Complementary and Alternative Medicine*, **2012**, ID 893426, 1-9.
[3] Ojinnaka, C.M.; et al. Myrianthic acid; A triterpene acid from the rootwood of *Myrianthus arboreus*. *Phytochemistry*, **1984**, 23, 1125-1127.
[4] St-Pierre, F.; Achim A.; Stevanovic, T. *Industrial Crops and Products*, **2013**, 41, 179-187.
[5] Choudhary, I. et al. *Phytochemistry*, **2011**, 4, 404-406.
[6] Kasetti, R.; Nabi, S.; Swapna, S.; Apparao, C. Cinnamic acid as one of the antidiabetic active principe(s) from the seeds of *Syzygium alternifolium*, *Food and chemical toxicology*, **2012**, 50, 1425-1431.
[7] Motaal, A.; Ezzat, S.M.; Haddad, P.S. *Phytomedicine*, **2011**, 38-41.
[8] Royer, M.; Diouf, P.N.; Stevanovic, T. *Food and Chemical Toxicology*, **2011**, 49, 2180-2188.

PHOTOMETRIC DETERMINATION OF LIGNIN IN LIGNOCELLULOSIC MATERIALS

Khabarov Yu. G., Babkin I.M., Komarova G.V., Rekun A.A., Kuzyakov N.Yu.

Russia, Arkhangelsk, Northern (Arctic) Federal University named after M.V. Lomonosov
e-mail: khabarov.yu@mail.ru

ABSTRACT

Rapid photometric method of lignin determination was developed on the basis of reaction of lignocellulosic materials (LCM) with nitric acid in water-dioxane solution. Complete delignification of lignocellulosic materials with the formation of colored products occurs in reaction with nitric acid within 5-10 minutes.

I.INTRODUCTION

Natural lignins undergo significant changes in the structure and properties during the chemical processing of plant materials. Quantitative determination of lignin is of crucial practical importance for estimation of the amount of lignin compounds in wastewater [1], for process control of chemical and biochemical processing LCM [2], for proper assessment of reagents consumption at different stages of processing LCM [3]. A large number of direct and indirect methods of determining lignin were proposed [4].
In direct methods the carbohydrate part of plant material is dissolved and undissolved lignin is determined gravimetrically. Klason method is the most common direct method for determining lignin by two-step hydrolysis of lignocellulosic material. In the first step the hydrolysis is carried out with 72% sulfuric acid and the second step after dilution - 3% sulfuric acid. After separation of the precipitate lignin, acid-soluble lignin in the filtrate is determined by UV spectroscopy. In Russia, this method is applied in Komarov modification [5]. Popov method provides for a two-step hydrolysis of carbohydrates, the first - 37% HCl with the addition of ZnCl2, the second - the final hydrolysis under boiling for 1 h after dilution with water [6]. In the autoclave method for determining lignin [7] hydrolytic dissolution of polysaccharides is carried out in one step for 6-7 hours using a 1% solution of HCl at 5 ... 6 atm. In Clark one-step method carbohydrate hydrolysis occurs under anhydrous or 80% hydrofluoric acid, it takes 30 minutes at 20-30 ° C [8].
In indirect methods, the lignin is quantified by measuring a property which is associated with lignin. When implementing the indirect methods of determining the physico-chemical devices are widely used [9]. Nitric acid is also one of the reactants which have a delignifying effect. The advantage of nitric acid is that the reaction products are colored compounds that are easily detected using photometry. Hendrickson method consists in treating the lignocellulosic material by 14 % nitric acid under heating for 20 min. As a result of this treatment, lignin is nitrated and partially dissolved. The absorbance of the filtrate is determined at 425 nm after separation of cellulosic residues [10].

II. EXPERIMENTAL

For the experiments, nitric acid (64.7%), dioxane, 1 M solution of NaOH were used.
In experiments the lignocellulosic materials obtained in laboratory pulping and in mill pulping of various types of pulping processes have been used. Content of Klason lignin in LCM samples ranged from 1 to 18%. LCM samples were previously crushed by a laboratory analytical mill. Further air-dry LCM sample (approximately 100 mg) was placed in a test tube and 1 ml of nitric acid solution prepared from the concentrated acid and dioxane in the ratio of 1:4 by volume was added. The test-tube with the reaction mixture was heated in a water bath for a predetermined time. The test-tube was then cooled and the reaction mixture was alkalized with 1M sodium hydroxide. Reaction volume was adjusted to 25 ml after alkalization. Electronic spectra or absorbance of the filtrates were recorded after preliminary filtration cellulosic residue. Lignin modified by nitric acid went into solution, where it is determined by photometry at an interval 200 ... 500 nm.
The methodology was tested on samples of different lignins extracted from the spent cooking liquor of laboratory and mill pulping. A certain amount of lignin was treated with the reagent in test-tube, under boiling

on a water bath for 5 min. The reaction mixture was alkalized with 1M NaOH. Then the reaction volume was adjusted to 25 ml with water and electronic spectra were recorded in region 200 ... 500 nm.

III. RESULTS AND DISCUSSION

Delignification efficiency of nitric acid on the LCM depends largely on the nature of the solution. It has been found that the use of water-dioxane solution of nitric acid allows rapid (within 5 ... 10 min) and almost complete delignification of LCM with nitric acid**.**

The reaction product of LCM with nitric acid in aqueous dioxane is white fibrous material. An IR spectrum of the reaction product indicates the high degree of delignification. The IR spectra of the semicellulose (curve 1) and of the cellulose residue (curve 2) after the reaction with nitric acid in aqueous dioxane for 5 minutes are shown in figure 1 . Compared with the IR spectrum of the original semicellulose in the spectrum of the reaction product are practically no absorption bands in the interval 1500 and 1600 cm^{-1}, which are attributed to the stretching vibrations of the benzene ring [11].

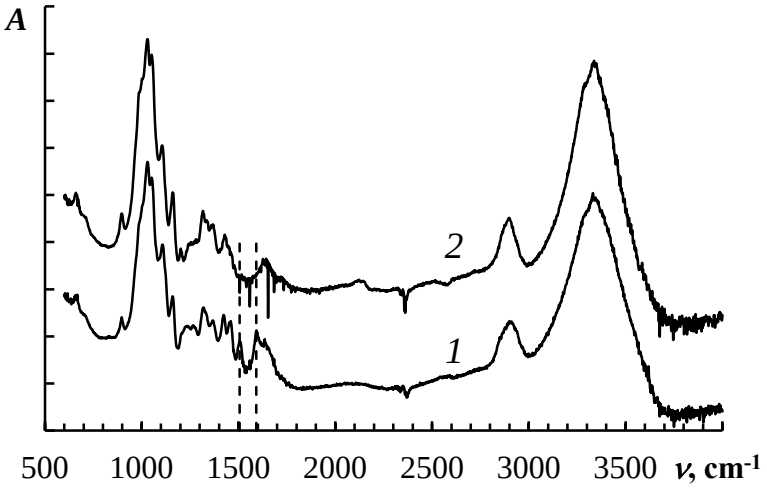

Figure 1. IR spectra original semicellulose (1) and the product of the reaction (2)

The resulting soluble lignin derivatives are intensely colored. In figure 2 the electronic spectra of initial reagent and electronic spectra of solutions resulting from the reaction of nitric acid with LCM in water-dioxane medium are shown. As compared with the spectrum of the initial reagent (curve 1) the intense overlapping absorption bands with maxima at 340 and 400 nm have appeared for spectra of solution.

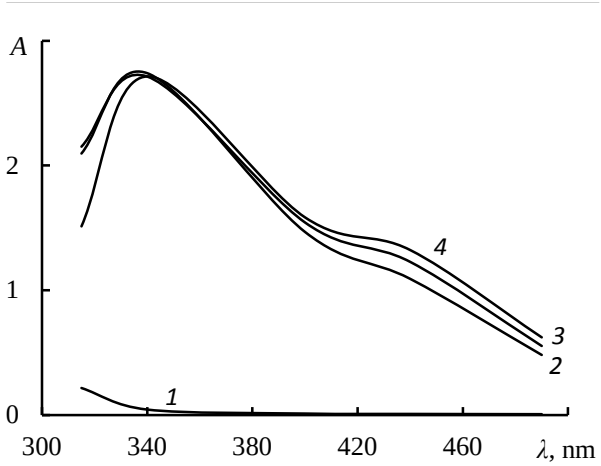

Figure 2. Electronic spectra of initial reagent (1) and filtrates after reaction of neutral sulphite semichemical pulp with nitric acid in water-dioxane medium within 15 (2), 10 (3), 5 (4) minutes.

Duration of the treatment, the charge of alkali and of nitric acid in a water-dioxan medium influence on the photometric reaction. As the result of studies optimum conditions were chosen.

High rate of photometric reaction is confirmed by the results shown in Fig. 3. The reaction is completed in 5-10 min and then the optical density is constant. It was established experimentally that the photometric result of the reaction is practically independent from the fluid module in the range from 5 to 25. Therefore further experiments were carried out in the fluid module 10. Application of alkalizing allowed increasing significantly the optical density, i.e. sensitivity of the reaction. To achieve maximum optical density the alkali consumption is to be not less than 5 ml of 1 M solution of NaOH.

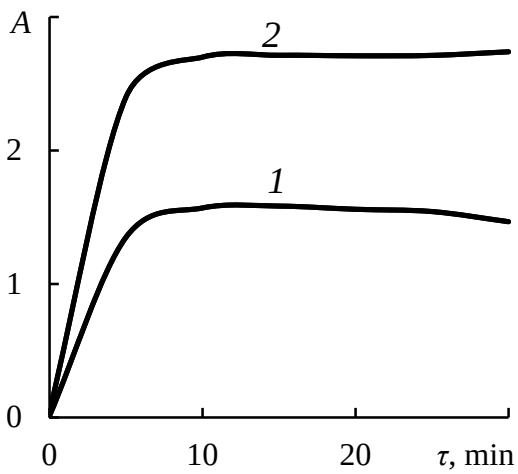

Figure 3. Dependence of optical density at 400 (1) and 340 (2) nm on duration of reaction

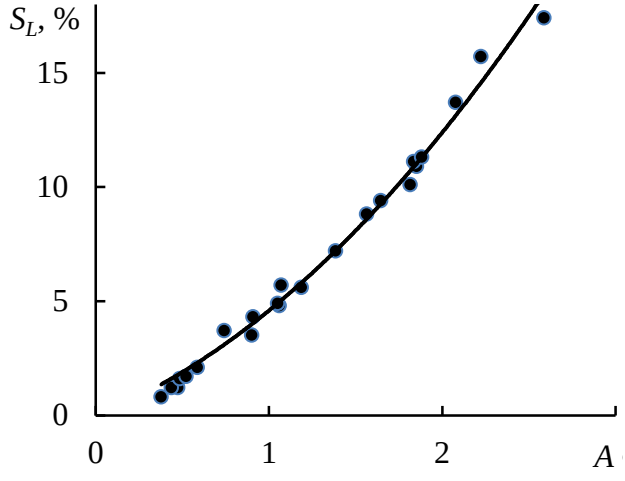

Figure 4. Calibration graph. *A* - Optical density at 340 nm. S_L - Klason lignin content in LCM,%

Each result given in the article is the average of 3-5 replicates. Reproducibility of experiments is estimated on the value of variation coefficient, which does not exceed 3-5%.

Photometric method of analysis involves the use of standard substances for the construction of calibration curve. We have constructed calibration curves for different types of lignins (Table 1).

Table 1. Coefficients *a* and *b* of the calibration equations of dependence for different lignins

Type of lignin	Coefficients *a* and *b* of the calibration equations $S_L=aA+b$		The coefficient of pair correlation R^2
	a	*b*	
Klasone spruce lignin	19.0	0.02	0.9691
Klasone birch lignin	25.8	0.06	0.9773
Sodium lignosulphonate	18.8	0.01	0.9893
Kraft lignin industrial	27.0	0.05	0.9898
Kraft lignin industrial	26.1	0.34	0.9848
Kraft lignin pine (laboratory)	21.4	0.46	0.9928
The dioxane birch lignin	28.6	0.41	0.9977
The dioxane pine lignin	25.1	0.45	0.9744

It turned out that they are linear, but with different angular coefficients. Therefore it is difficult to choose a specific lignin as standard. For this reason, all the experimental results were summarized on one graph (Fig. 4). The obtained dependence is well approximated by a polynomial of the second degree.

$$S_L = 1.6025\,A^2 + 2.9898\,A\ (R^2 = 0.9906)$$

IV. CONCLUSION

Thus, it was found that the reaction of lignocellulosic material with nitric acid in an aqueous-dioxane medium relates to photometric and it can be used for determining lignin content.

V. REFERENCES

[1] Lozovik, P.A.; Kaflyuk, A.E. Application of differential UV spectroscopy to the determination of lignin substances in polluted water. *Journal of Analytical Chemistry*. **2005**, *60*, 833-837.

[2] Karin Öhgrena, Renata Burab, Jack Saddlerb, Guido Zacchia. Effect of hemicellulose and lignin removal on enzymatic hydrolysis of steam pretreated corn stover. *Bioresource Technology*. **2007,** *98*, 2503–2510.

[3] Shin, S.-J.; Lai, Y.-Z. Impact of lignin determination method on oxygen delignification chemistry // Palpu Chongi Gisul/*Journal of Korea Technical Association of the Pulp and Paper Industry*. **2005**, *37*, 50-55.

[4] Khabarov, Yu.G.; Pesyakova L.A. Analytical chemistry of lignin. Archangelsk. **2008**. 172 P.

[5] Obolenskaya A.V. at al. Laboratory work on the chemistry of wood and cellulose. M.: «Ekologiya», 1991.-320 p.

[6] Popov, I.D. A new method for the quantitative determination of lignin. *Izv. In-ta Biol. Bulg. AS.* **1957**, *7*, 149–154.

[7] Fuchs, W. Die Chemie des Lignins. Verlag von Springer. Berlin. **1926**.

[8] Clark, I.T. Determination of lignin by hydrofluoric acid. *Tappi J*. **1962**, *45*, 310–314.

[9] Schwanninger, M.; Rodrigues, J.C.; Gierlinger, N.; Hinterstoisser, B. Determination of lignin content in Norway spruce wood by Fourier transformed near infrared spectroscopy and partial least squares regression. Part 1: Wavenumber selection and evaluation of the selected range. *Journal of Near Infrared Spectroscopy*. **2011**, *19*, 319-329.

[10] Henriksen, A.; Kesler, R.B. The Nu-number, a measure of lignin in pulp. *Tappi J*. **1970**, 53, 1131–1140.

[11] Lignins: Occurrence, formation, structure and reactions, K.V. Sarkanen and C.H. Ludwig, Eds., John Wiley & Sons, Inc., New York, 1971. 916 pp.

DEPOLYMERIZATION OF CONDENSED LIGNINS UNDER THE INFLUENCE OF NITRIC ACID

Khabarov Yu.G., Lakhmanov D.E.

Russia, Arkhangelsk, Northern (Arctic) Federal University named after M.V. Lomonosov (e-mail: khabarov.yu@mail.ru)

ABSTRACT

We have found that the depolymerization of condensed lignins with nitric acid in aqueous-organic media can significantly increase the efficiency of the process. Ethanol, 1.4-dioxane and dimethylsulphoxide (DMSO) were used as organic solvent. The depolymerization of condensed lignins is accompanied by not only splitting the connection between phenylpropane units but nitration as well. In aqueous-alcoholic medium depolymerization runs a little better than in aqueous environment. The best results were achieved when using dioxane and DMSO. Complete depolymerization takes place for about 20...30 minutes at the boiling temperature of the reaction mixture. The share of the undissolved residue of condensed lignins is approximately 20%, which corresponds to the experimentally determined content of carbohydrates in the hydrolytic lignin.

I. INTRODUCTION

Hydrolytic lignin (HL) refers to the most altered lignins [1, 2, 3], its macromolecules contain fused aromatic naphthalene, anthracene, phenanthrene, benzofuran structural fragments. In general the structure of hydrolytic lignin mesh and three-dimensional.

Modification leads to new properties of lignins and enhances market attractiveness. Depolymerization is an important direction of technical lignin modifications, which can be used to obtain low molecular weight products of different nature.

Nitric acid is the reagent which promotes the formation of lignin derivatives with nitrogen containing groups, the molecular weight of modified lignin decreases and solubility increases. Now it is known a large number of lignin processing methods by nitric acid. One known method for depolymerization HL - its treatment with an aqueous solution of nitric acid [4]. The ecological load of lignin nitration process can be reduced [5].

The aim of this study was to investigate the depolymerizing effect of nitric acid on lignin in an aqueous-organic solvent medium.

II. EXPERIMENTAL

During the experiments were used nitric acid (65 %); ethanol (96 %), sulphuric acid (94 %); dioxane; dimethylsulfoxide (DMSO).

The experiments were held on the laboratory obtained samples of Klason spruce (LKS), birch (LKB) lignins and on the air-dry factions of industrial hydrolytic lignin. Fraction size of hydrolytic lignin was 0.2-1 mm.

Determination of sugars in HL was held after hydrolysis of polysaccharides by Klason method [6].

Klason lignin was isolated from spruce and birch wood sawdust (size of sawdust 0.2 ... 1 mm) according to [7].

The reaction was carried out with nitric acid in flask with a reflux condenser on a water bath for a predetermined time. To perform the experiment 2.5 g of lignin and a predetermined amount of reagent was placed in a flask. The reagent was prepared by mixing nitric acid with the solvent in a ratio of 1:4 by volume. After the reaction, the insoluble part of lignin was separated from the solution. The precipitate was washed with water until neutral pH, and then it was dried to constant weight in a vacuum. Effectiveness of lignin depolymerization was assessed by the degree of lignin dissolving.

III. RESULTS AND DISCUSSION

To compare the effect of nitric acid on HL experiments were carried out in aqueous and aqueous-organic solvent medium. Reaction time was 2 hours. The reaction was held in flask with a reflux condenser on a water bath. Liquid module ranges from 13 to 25, Table 1.

Table 1 shows that in an aqueous-alcoholic medium depolymerizing action of nitric acid appears slightly stronger than in an aqueous medium. And liquid module from 19 to 21 is the most optimal for depolymerization. Overall, these results show that the insoluble fraction of HL is rather high even after 2 hours of reaction.

Polysaccharides as a part of the HL may participate in chemical processes occurring in the interaction with nitric acid, making it difficult to interpret the results. The content of carbohydrate in HL sample in our experiment reaches 21,2 ± 0,2 %. Therefore, to assess the effects of nitric acid on polysaccharides in similar conditions, experiments were held with cotton cellulose and bleached sulphate pulp of hardwood and softwood. It was found that hydrolysis effect of nitric acid in an aqueous medium is stronger, dissolved 9.1 % cotton, 17.8 % bleached kraft hardwood pulp and 7.9 % bleached softwood kraft pulp. In aqueous-alcoholic these figures were 3.6, 9.4 and 8.0 %, respectively.

Table 1. Effect of liquid module on HL depolymerization.

Solvent	Liquid module	Part of undissolved lignin, %
Ethanol	13	30,4
Ethanol	17	44,4
Ethanol	19	56,0
Ethanol	21	59,2
Ethanol	25	38,8
Water	25	29,6

To exclude the influence of polysaccharides on the interaction of lignin with nitric acid, experiments were carried out with condensed Klason lignins (spruce and birch), which were obtained in the laboratory. The results of these experiments are shown in Table 2.

Table 2. Klason lignin depolymerization by nitric acid in different conditions.

Solvent	The reaction time, min	Part of dissolved lignin, %	
		Spruce	Birch
Ethanol	15	3,7	26,0
	120	43,6	84,5
Water	15	5,4	23,1
	120	32,1	74,2
Dioxane	15	100	100
DMSO	15	100	100

The data in table 2 indicate that the reaction time has a significant effect on the dissolving process not only HL but also Klason lignins. Therefore, further experiments were carried out on the kinetics of the HL depolymerization. The results of these experiments are shown in Figure 1.

As shown in Figure 1 depolymerizing action of nitric acid in an aqueous and aqueous-alcoholic medium is approximately the same. Only after long-term treatment percentage of undissolved lignin in aqueous-alcoholic medium becomes larger than in the reaction in an aqueous medium. The dissolution rate of HL in water-alcohol medium depends little on the reaction time and in an aqueous medium there is a tendency of constant velocity reduction process. Even after 2 h only half of the HL dissolves. To solve the problem of complete HL depolymerization in an aqueous or aqueous-alcoholic medium, unfortunately, is not possible.

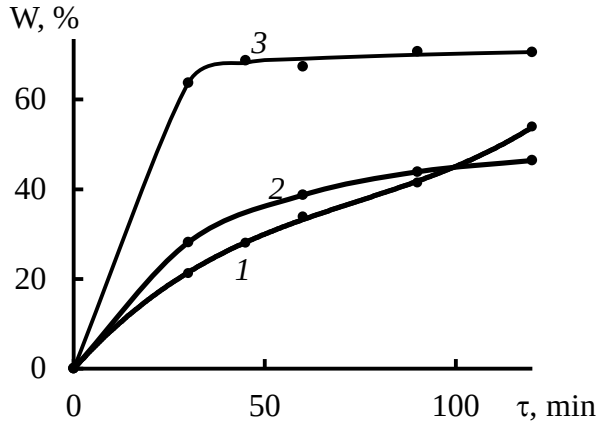

Figure 1. Kinetics of technical HL depolymerization by nitric acid in an aqueous alcohol (1), water (2) and the aqueous-dioxane (3) medium. W - percentage of undissolved lignin. τ - the reaction time, min

As shown in Figure 1 depolymerizing action of nitric acid in an aqueous and aqueous-alcoholic medium is approximately the same. Only after long-term treatment percentage of undissolved lignin in aqueous-alcoholic medium becomes larger than in the reaction in an aqueous medium. The dissolution rate of HL in water-alcohol medium depends little on the reaction time and in an aqueous medium there is a tendency of constant velocity reduction process. Even after 2 h only half of the HL dissolves. To solve the problem of complete HL depolymerization in an aqueous or aqueous-alcoholic medium, unfortunately, is not possible.

It is known that solvation has a great influence on the reaction. If you change the type of solvent chemical reaction rate can change in 10^9 times. Solvation determines the relative stability of the tautomers, conformers, isomers, effects on the reaction mechanism [6]. Aprotic solvents such as dioxane, dimethylsulfoxide have strong solvating properties. Our assumption that their use will have a positive effect completely justified. Experiments with Klason lignins also met expectations, after 15 minutes, spruce and birch Klason lignins completely dissolved. Complete HL depolymerization by nitric acid in water-dioxane medium runs 20 ... 30 min (Figure 1, curve 3).

The insoluble residue is a light gray mass. In experiments with aqueous and aqueous-alcoholic medium insoluble HL residue has red and brown tones. Large differences are observed in the IR spectra (Figure 2). Comparing the IR spectrum of the original HL and spectra of undissolved HL products after the reaction the spectra of undissolved HL products have greatly reduced absorption at 1506 and 1593 cm^{-1} due to the skeletal vibrations of aromatic rings and increases the absorption at 1720 cm^{-1}, which is usually referred to the stretching vibrations of the carbonyl and carboxyl groups.

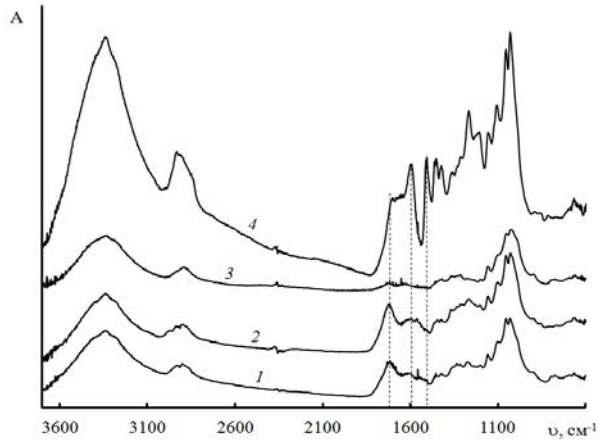

Figure 2. IR spectra of undissolved HL residues after the reaction with nitric acid in water (1), aqueous-alcohol (2) and aqueous-dioxane (3) and original hydrolytic lignin (4)

Significant changes have occurred with lignin which passed into the solution, as evidenced by the ionization spectra. Three absorption bands are detected in the ionization spectra of most soluble lignins. The bands at 250 nm and 300 nm are caused by ionization of the phenolic hydroxyl groups.

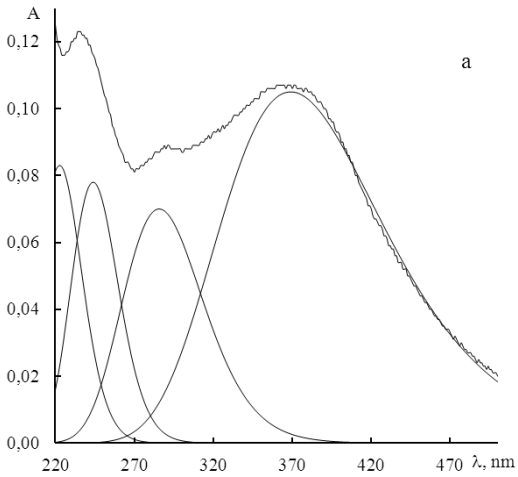

Figure 3. Ionization Spectra of HL depolymerization product (a) and lignosulfonates (b) and modeling them by Gaussian curves

Absorption at 350 nm caused by carbonyl groups, which are conjugated with aromatic rings, Figure 3(b). Ionization spectrum of the soluble products of the HL is very different from the ionization spectrum of lignosulfonates (a). Modelling ionization spectra by Gauss curves confirms differences in the electronic structure. Selected models describe ionization spectra with good accuracy. The average error of the Gauss curve fitting is 6.4 % for lignosulfonates and 1.4 % for HL depolymerization product respectively. Absorption bands at 250 and 300 nm are very weak, but at 370 nm we can observe intense absorption

IV. CONCLUSIONS

Thus, for the first time was found that in aqueous-dioxane, dimethylsulfoxide medium nitric acid completely dissolves condensed lignins.

V. REFERENCES

[1] Reznikov, V.M. Reactivity of lignin and its transformation in wood delignification processes. *Wood chemistry*. **1977**, 3, 3-23.

[2] Kholkin, Yu. I. Hydrolysis technology industries. *Lesnaya promishlennost*, Moscow. **1989**.

[3] Spirina, T.N.; Saprikina, N.N.; Andreeva, O.A. et. al. Morphology of modified hydrolytic lignin. *Journal of Applied Chemistry*. **2012**, 85, 794-798.

[4] Kebich, M.S.; Zilbergleit, M.A.; Gorbatenko, I.V. et. al. Conversion of technical lignin by nitric acid solutions. *Materiali. Tehnologii. Instrumenti.* **1999**, 3, 87-89

[5] Gogotov, A.F.; Panasenkov,Yu.V.; Panchukov, I.L. et. al. Improving the eco-safety technology of lignin nitration. *Khimiya v interesakh ustoychivogo razvitiya*. **1996**, 4, 245-257

[6] Veshnyakov, V.A.; Khabarov, Yu.G.; Kamakina, N.D. Comparison of methods for the determination of reducing substances: Bertrand method, ebulliostatical and photometric methods. *Khimiya rastitelnogo syrya*. **2008**, 4, 47-50.

[7] Obolenskaya, A.V.; Yelnitskaya, Z.P.; Leonovich, A.A. Laboratory work on the chemistry of wood and cellulose. *Moscow: Ekologiya*. **1991**.

[8] Burger, K. Solvation, ionic and complex formation reactions in non-aqueous solvents: Experimental methods for their investigation. *Amsterdam: Elsevier Scientific Pub. Co.* **1983**.

2D NMR (HSQC) PROFILING OF TRANSGENIC *POPULUS TRICHOCARPA* LIGNINS

Hoon Kim,[1,*] Quanzi Li,[2] Jie Liu,[2] Chenmin Yang,[2] Rui Shi,[2] Jack Wang,[2] Hsi-Chuan Chen,[2] Chien-Yuan Lin,[2] Ying-Chung Lin,[2] Ying-Hsuan Sun,[2,3] Ting-Feng Yeh,[2,4] Sermsawat Tunlaya-Anukit,[2] Ron Sederoff,[2] Vincent L. Chiang,[2,*] and John Ralph.[1,*]

1) DOE Great Lakes Bioenergy Research Center, and Department of Biochemistry, Wisconsin Energy Institute, University of Wisconsin, Madison, WI, USA (jralph@wisc.edu; hoonkim@wisc.edu)
2) Forest Biotechnology Group, Department of Forestry and Environmental Resources, North Carolina State University, Raleigh, NC, USA (vchiang@ncsu.edu)
3) Department of Forestry, National Chung Hsing University, Taichung 40227, Taiwan.
4) School of Forestry and Resource Conservation, National Taiwan University, Taipei 10617, Taiwan

ABSTRACT

Lignin, one of the major polymers in the plant cell wall, remains a significant problem in lignocellulosic biomass processing for liquid fuel production. Understanding the monolignol biosynthetic pathway in plants provides a foundation for solving such problems. Altering lignin composition and structure via plant biotechnology is an approach towards understanding the pathway, and towards finding methods to enhance biomass quality to obtain biofuels and various bio-based products. The Chiang group at NCSU has identified, in *Populus trichocarpa*, all known pathway (22 monolignol and 4 *peroxidase*) genes and transcription factors and their corresponding proteins, affecting lignin biosynthesis in differentiating xylem. They generated transgenics using artificial microRNA (amiRNA) and RNAi suppression. To support the study, isolated lignins from the WT and transgenic lines were examined using high-field (700 MHz) and high-sensitivity (cryoprobe) NMR. Lignin composition and inter-unit linkage profiles were elucidated and comparatively quantified by 2D HSQC NMR to identify pathway components and for modeling the formation of lignin structures. The cellulolytic enzyme lignins (CELs), i.e., the entire lignin fractions, were used directly in the DMSO-d_6:pyridine-d_5 (4:1) NMR solvent system that was originally developed for whole cell wall materials.

I. INTRODUCTION

Recent studies of transgenic and mutant plants have allowed researchers to misregulate the monolignol biosynthetic pathway [*1*]. This has opened new windows to explore cell wall structure. Consequently, an increasing number of research plant samples requires us to use more rapid, but still detailed, structural analysis methods.

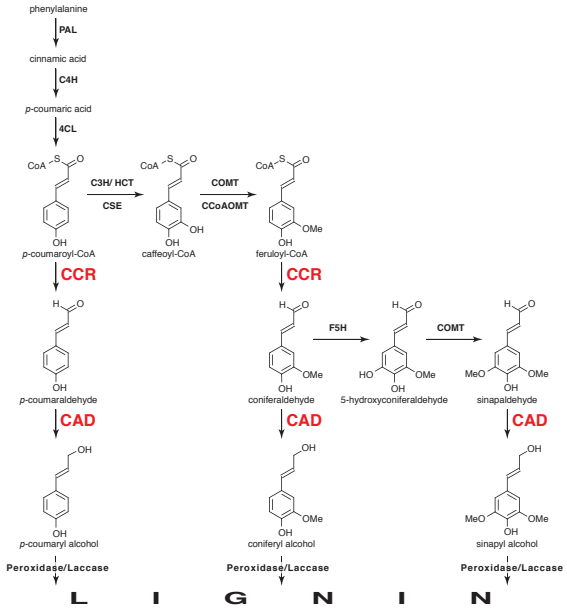

Figure 1. Monolignol biosynthetic pathway

The gel-state 2D NMR method was developed as an independent research tool for ball-milled plant cell wall material [*2*]. DMSO-d_6 was chosen for the original gel-state NMR method because it is not only an excellent swelling reagent for cellulose and other wall components but is also a commercially available NMR solvent**.** The method has been improved via a mixed solvent [*3*]. The mixture of DMSO-d_6 and pyridine-d_5 provides better quality 2D NMR spectra, and allows much easier sample handling. This mixed solvent system is currently being used not only for whole plant cell wall samples but also for isolated lignins; a substantial assignment database is developing.

Vincent Chiang's group at North Carolina State University produced various transgenic plants of *Populus trichocarpa* (genotype Nisqually-1) as part of their NSF-funded 'Regulation and Modeling of Lignin Biosynthesis' Project. Here we report recent NMR data on the transgenics in two final enzymes in the monolignol biosynthetic pathway, CAD (cinnamyl alcohol dehydrogenase) and CCR (cinnamoyl-CoA reductase).

CAD is the last enzyme on the monolignol biosynthetic pathway (**Figure 1**). When CAD is downregulated, the hydroxycinnamaldehyde precursors to the monolignols, *p*-coumaraldehyde, coniferaldehyde and sinapaldehyde, build up and may be incorporated into the polymer by radical coupling [*4, 5*].
CCR is the enzyme that reduces the CoA-activated hydroxycinnamic acid to the cinnamaldehyde in the pathway (**Figure 1**) [*6*]. Downregulation of CCR in angiosperms resulted in lignin reductions up to 50% [*7*], and the S/G ratio was increased in tobacco [*8*]. In an earlier study, downregulation of CCR in tobacco also caused the accumulation of ferulic acid [*5*], and we reported the identification of a thioacidolysis marker compound, 1,2,2-trithioethyl ethylguaiacol [1-(4-hydroxy-3-methoxyphenyl)-1,2,2-tris(ethyl-thio)ethane][*6*]. The origin of the marker compound, a bis-8-O-4-ether structure, was also produced in a synthetic lignin (DHP, dehydrogenation polymer) and identified using NMR.

II. EXPERIMENTAL

Transgenic Plant Materials.

Samples were collected from 6-month-old *Populus trichocarpa* (Nisqually-1) WT and transgenic trees maintained in a greenhouse as described [*9*].

CEL and NMR Sample Preparation, and NMR Experiments.

Two grams of 40- to 60-mesh wood meal samples were ball-milled using a Planetary micromill Pulverisette 7 (Fritsch, Germany) in a 50-mL ZrO_2 bowl with 18 ZrO_2 ball bearings (1 cm diameter) at 600 rpm, with 15 min of rest after every 30 min of milling. The total milling time for each sample was 3 h. Cellulolytic enzyme lignin (CEL) was isolated according to Chang et al. [*10*]. One gram of the ball-milled material was suspended in 20 mL 20 mM NaOAc buffer (pH 4.5). Crude cellulase (50 mg) was added, and the reaction was incubated at 48 °C for 48 h. The solution was centrifuged, and the residues were washed with 20 mL distilled water three times and freeze-dried.
The NMR experiments were performed as described earlier [*11*]. The CELs were collected directly into NMR tubes (40 mg for each sample) and dissolved using DMSO-d_6/pyridine-d_5 (4:1) [*2, 3*]. NMR spectra were acquired on a Bruker Biospin Avance 700 MHz spectrometer equipped with a cryogenically cooled 5-mm TXI $^{1}H/^{13}C/^{15}N$ gradient probe with inverse geometry (proton coils closest to the sample). The central DMSO solvent peak was used as an internal reference (^{13}C, 39.5; ^{1}H, 2.49 ppm). The $^{13}C–^{1}H$ correlation experiment was an adiabatic heteronuclear single-quantum correlation (HSQC) experiment (Bruker standard pulse sequence "hsqcetgpsisp.2"; phase-sensitive gradient-edited-2D HSQC using adiabatic pulses for inversion and refocusing) [*12*]. HSQC experiments were carried out using the following parameters: acquired from 11.5 to −0.5 ppm in F2 (^{1}H) with 3,366 data points (acquisition time, 200 ms) and 215 to −5 ppm in F1 (^{13}C) with 560 increments (F1 acquisition time, 7.2 ms) of 32 scans with a 1-s interscan delay; the d_{24} delay was set to 0.86 ms (1/8J, J = 145 Hz). The total acquisition time for a sample was 6 h. Processing used typical matched Gaussian apodization (GB = 0.001, LB = −0.5) in F2 and squared cosine-bell and one level of linear prediction (32 coefficients) in F1. Volume integration of contours in HSQC plots used Bruker's TopSpin 3 (Mac version) software and used spectra reprocessed without linear prediction.

III. RESULTS AND DISCUSSION

CAD Transgenics.

Aldehyde structures had been elucidated and the cross-coupling propensities were previously studied using NMR methods (**Figure 2**) [*13-15*]. The aldehyde monomers were shown to have been incorporated into the growing lignin polymers by forming mainly 8–O–4-linked radical coupling structures (**Figure 2**).

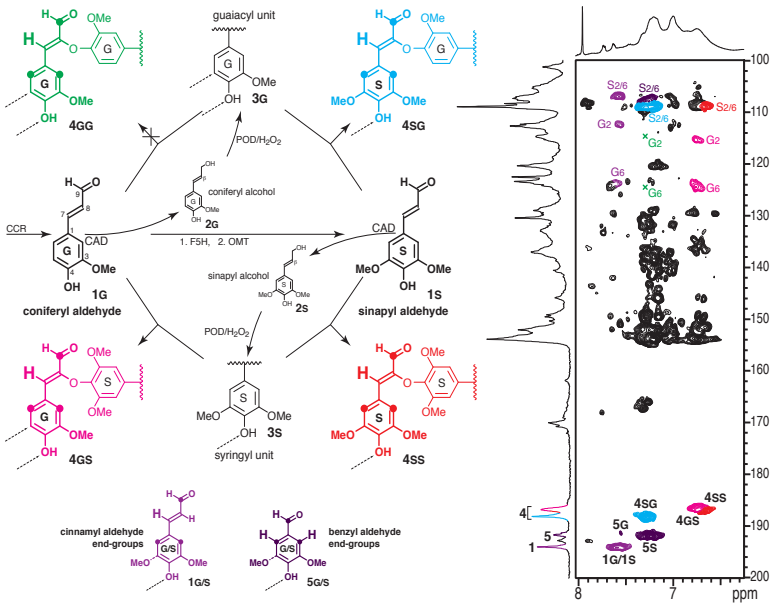

Figure 2. Cross-coupling of hydroxycinnamaldehydes **1G** and **1S** with guaiacyl and syringyl lignin units **3G** and **3S**

Correlation of the aldehyde carbonyl carbons in cross-products **4** to the H7-protons three-bonds away identifies the type of lignin units involved. Of the four possible aldehyde 8–O–4-linked incorporation products **4**, **Figure 2**, only three can be detected in the antisense-CAD tobacco lignin by NMR methods. Product **4gg** is notably absent in HMBC spectra.

In this study, lignin structural components and linkages were determined using NMR spectroscopy on lignins remaining after cellulolytic enzyme digestion [*16*]. Three transgenic lines, i33-2, i33-5, and i33-10, covering the range of the observed lignin reduction levels were analyzed and compared with WT. The *PtrCAD1* transcript levels were reduced by 77%, 92%, and 34%, in the three lines. As the result, the i33-5 line had the highest aldehyde abundance among the transgenic lines (**Figure 3**). The 2D HSQC NMR spectra of the i33-5 also showed 8–O–4-cross-coupled structures in the aromatic region as newly appearing peaks (to form cross-coupled structures **SG** and **SS**), but that coniferaldehyde cross-couples 8–O–4 only with syringyl units and not with guaiacyl units as described earlier (see **Figure 2**). Thus, cross-coupling product **GS** was readily detected, whereas **GG** cannot be detected even when spectra are viewed at close to the base-plane noise level (**Figure 4**).

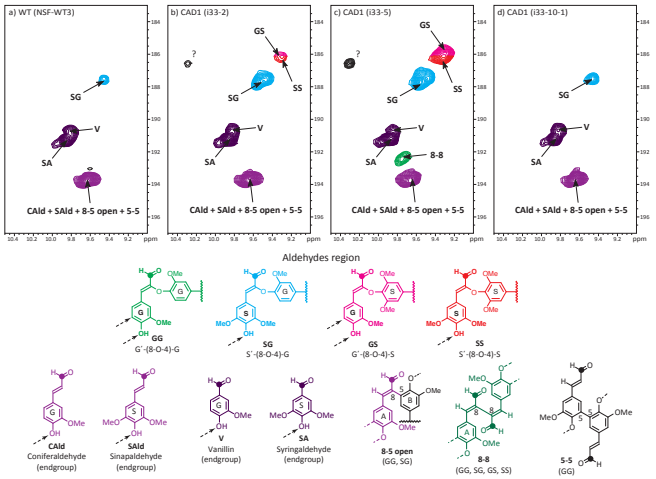

Figure 3. Aldehyde regions of *Populus trichocarpa PtrCAD1* transgenics

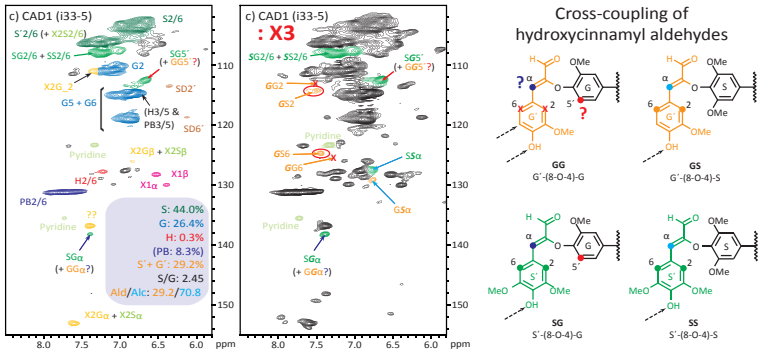

Figure 4. Aromatic regions of *Populus trichocarpa PtrCAD1* transgenics

CCR Transgenics.

A ^{13}C–^{1}H correlation diagnostic for structure "FA Marker" can also be detected in a difference NMR spectrum of CCR-downregulated poplar (not shown) [*6*]. The ferulic acid content is similar to that from other CCR-deficient angiosperms previously reported [*6*], and can be detected by NMR. This provides evidence for the involvement of free ferulic acid in lignification in CCR-deficient plants. Two *PtrCCR2* transgenic lines, i26-4 and i26-9 were analyzed using NMR and compared with WT. The i26-4 line showed a low level (0.9%) of linked ferulic acid (144/7.6 ppm and 117/6.5 ppm, the 7 and 8-C/H correlation) (**Figure 5**).

IV. CONCLUSIONS

This study shows that downregulating genes in monolignol-biosynthetic-pathway can alter lignin structures in plants. The lignin structures in mutant and transgenic plants are often just simple compositional changes, but in some lines (such as those here), significant structural changes can be observed.

In CAD transgenics, coniferaldehyde cross-couples only with syringyl units in 8–O–4-(cross-)coupling reactions, whereas sinapaldehyde cross-couples with both guaiacyl and syringyl units, as noted in a previous study on CAD transgenic tobacco [*13, 15*]. These results support the prevailing theory of the radical coupling of phenols into growing lignin polymers based on the phenolic's simple chemical coupling propensities.

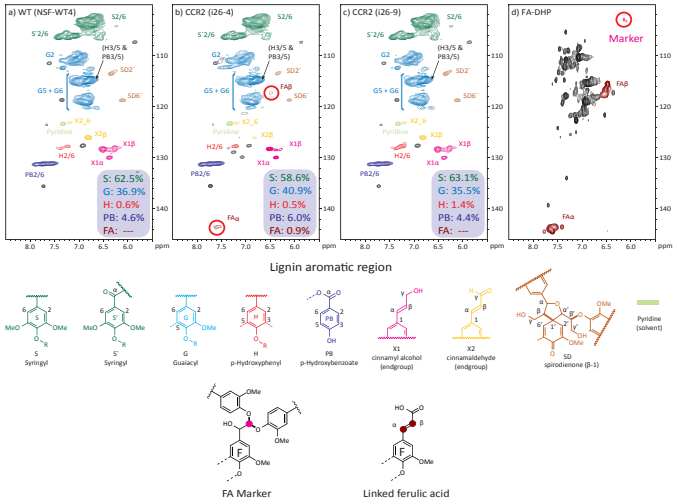

Figure 5. Aromatic regions of *Populus trichocarpa PtrCCR2* transgenics

The transgenic *Populus trichocarpa* trees here are therefore displaying several of the characteristics of CAD and CCR gene downregulation seen previously in model systems. This is not always the case and it is crucial to determine the response in the species of interest. However, these results, along with a growing compendium of results from other species, suggest that hydroxycinnamaldehyde incorporation in CAD-deficient plants, and trace levels of ferulic acid incorporation into CCR-deficient lines, are general phenomena in angiosperms. Importantly, but not explicitly shown here, the alterations in these and other structures in the lignins help delineate the impact of the various gene misregulations on this important tree species. It also adds to the growing evidence that various other phenolics are used in lignification in transgenic as well as 'normal' plants and supports the notion that lignification is quite malleable.

V. ACKNOWLEDGEMENT

This work was supported by grants from National Science Foundation Plant Genome Research Program Grant (DBI-0922391) to V.L.C. and the DOE Great Lakes Bioenergy Research Center (DOE Office of Science BER DE-FC02-07ER64494) to J.R. and H.K.

VI. REFERENCES

[1] Vanholme, R.; Morreel, K.; Ralph, J.; Boerjan, W., Lignin engineering. *Current Opinion in Plant Biology* **2008**, *11*, (3), 278-285.
[2] Kim, H.; Ralph, J.; Akiyama, T., Solution-state 2D NMR of Ball-milled Plant Cell Wall Gels in DMSO-d_6. *BioEnergy Research* **2008**, *1*, (1), 56-66.
[3] Kim, H.; Ralph, J., Solution-state 2D NMR of ball-milled plant cell wall gels in DMSO-d_6/pyridine-d_5. *Organic & Biomolecular Chemistry* **2010**, *8*, (3), 576-591.
[4] Ralph, J.; MacKay, J. J.; Hatfield, R. D.; O'Malley, D. M.; Whetten, R. W.; Sederoff, R. R., Abnormal lignin in a loblolly pine mutant. *Science* **1997**, *277*, 235-239.
[5] Ralph, J.; Hatfield, R. D.; Piquemal, J.; Yahiaoui, N.; Pean, M.; Lapierre, C.; Boudet, A.-M., NMR characterization of altered lignins extracted from tobacco plants down-regulated for lignification enzymes cinnamyl-alcohol dehydrogenase and cinnamoyl-CoA reductase. *Proc. Nat. Acad. Sci.* **1998**, *95*, (22), 12803-12808.
[6] Ralph, J.; Kim, H.; Lu, F.; Grabber, J. H.; Leplé, J.-C.; Berrio-Sierra, J.; Mir Derikvand, M.; Jouanin, L.; Boerjan, W.; Lapierre, C., Identification of the structure and origin of a thioacidolysis marker compound for ferulic acid incorporation into angiosperm lignins (and an indicator for cinnamoyl-CoA reductase deficiency). *The Plant Journal* **2008**, *53*, (2), 368-379.
[7] Leplé, J.-C.; Dauwe, R.; Morreel, K.; Storme, V.; Lapierre, C.; Pollet, B.; Naumann, A., Gilles; Kang, K.-Y.; Kim, H.; Ruel, K.; Lefèbvre, A.; Josseleau, J.-P.; Grima-Pettenati, J.; De Rycke, R.; Andersson-Gunnerås, S.; Erban, A.; Fehrle, I.; Petit-Conil, M.; Kopka, J.; Polle, A.; Messens, E.; Sundberg, B.; Mansfield, S. D.; Ralph, J.; Pilate, G.; Boerjan, W., Downregulation of cinnamoyl coenzyme A reductase in poplar; multiple-level phenotyping reveals effects on cell wall polymer metabolism and structure. *Plant Cell* **2007**, *19*, 3669-3691.
[8] Piquemal, J.; Lapierre, C.; Myton, K.; O'Connell, A.; Schuch, W.; Grima-Pettenati, J.; Boudet, A.-M., Down-regulation of cinnamoyl-CoA reductase induces significant changes of lignin profiles in transgenic tobacco plants. *Plant J.* **1998**, *13*, (1), 71-83.
[9] Li, Q. Z.; Min, D. Y.; Wang, J. P. Y.; Peszlen, I.; Horvath, L.; Horvath, B.; Nishimura, Y.; Jameel, H.; Chang, H. M.; Chiang, V. L., Down-regulation of glycosyltransferase 8D genes in Populus trichocarpa caused reduced mechanical strength and xylan content in wood. *Tree Physiology* **2011**, *31*, (2), 226-236.
[10] Chang, H.-M.; Cowling, E. B.; Brown, W.; Adler, E.; Miksche, G., Comparative studies on cellulolytic enzyme lignin and milled wood lignin of sweetgum and spruce. *Holzforschung* **1975**, *29*, (5), 153-159.
[11] Lu, S.; Li, Q.; Wei, H.; Chang, M.-J.; Tunlaya-Anukit, S.; Kim, H.; Liu, J.; Song, J.; Sun, Y.-H.; Yuan, L.; Yeh, T.-F.; Peszlen, I.; Ralph, J.; Sederoff, R. R.; Chiang, V. L., Ptr-miR397a is a negative regulator of laccase genes affecting lignin content in *Populus trichocarpa*. *Proceedings of the National Academy of Sciences of the United States of America* **2013**, *110*, (26), 10848-53.
[12] Kupče, E.; Freeman, R., Compensated adiabatic inversion pulses: Broadband INEPT and HSQC. *J. Magn. Reson.* **2007**, *187*, 258-265.
[13] Kim, H.; Ralph, J.; Yahiaoui, N.; Pean, M.; Boudet, A.-M., Cross-coupling of hydroxycinnamyl aldehydes into lignins. *Org. Lett.* **2000**, *2*, (15), 2197-2200.
[14] Kim, H.; Ralph, J.; Lu, F.; Pilate, G.; Leplé, J. C.; Pollet, B.; Lapierre, C., Identification of the structure and origin of thioacidolysis marker compounds for cinnamyl alcohol dehydrogenase deficiency in angiosperms. *J. Biol. Chem.* **2002**, *277*, (49), 47412-47419.
[15] Kim, H.; Ralph, J.; Lu, F.; Ralph, S. A.; Boudet, A.-M.; MacKay, J. J.; Sederoff, R. R.; Ito, T.; Kawai, S.; Ohashi, H.; Higuchi, T., NMR Analysis of Lignins in CAD-deficient Plants. Part 1. Incorporation of hydroxycinnamaldehydes and hydroxybenzaldehydes into lignins. *Org. Biomol. Chem.* **2003**, *1*, 158-281.
[16] Balakshin, M.; Capanema, E.; Gracz, H.; Chang, H. M.; Jameel, H., Quantification of lignin-carbohydrate linkages with high-resolution NMR spectroscopy. *Planta* **2011**, *233*, (6), 1097-1110.

CHARACTERISATION OF TECHNICAL LIGNINS BY NMR SPECTROSCOPY

Philipp Korntner, Markus Bacher, Ivan Sumerskii, Thomas Rosenau,* Antje Potthast*

University of Natural Resources and Life Sciences, Department of Chemistry, Division of Chemistry of Renewable Resources, Konrad-Lorenz-Str. 24, A-3430 Tulln, Austria
*(*thomas.rosenau@boku.ac.at; *antje.potthast@boku.ac.at)*

ABSTRACT

Phosphorous NMR, based on the derivatization reagent 2-chloro-4,4,5,5-tetramethyl-1,3,2-dioxaphospholane, has been widely used in lignin analytics for hydroxyl group determination, but sometimes suffers from poor reproducibility compared to other methods. In the present work, in particular solubility problems and deviations of the ^{31}P method from other established techniques to characterize technical lignins, such as kraft lignins and lignosulfonates, were addressed. As the choice of relaxation times is essential to achieve quanitative data, also the relaxation delays of the internal standards used in the experiments were revisited. Finally, a set of four different technical lignins from different raw materials, pulping and isolation processes are compared with the studied methods.

I. INTRODUCTION

Advancing depletion of fossil raw materials, increasing concerns about climate change and the subsequent demand of renewable resources promote the utilization of biomass for value-added chemicals and products. As a by-product in pulp and paper industry, technical lignin in the form of black liquors is produced in vast amounts; 50 million tons in 2004, of which only two per cent have been commercially used [1]. Even if a majority of the spent liquors was directly used and burnt in the mills for chemical recovery and energy production, [2] an estimated amount of 6-7 percent of those spent liquors are available for discharge from the process without affecting the energy balance of the mill. Combined with potentially available lignin from other biorefinery processes, a serious amount of petrochemical products could be replaced in the future [3], as well as the feasibility of certain biorefinery processes increased. Current applications already include a wide area of high and lower value products, such as concrete additives, adhesives, oil well drilling muds, phenol-formaldehyde resins and UV stabilizers in polyolefins, or specialty products, such as pesticides and food flavouring [4-7].
One of the main obstacles in the utilization of lignin has been, and still is, its irregular, non-uniform structure. It is basically built by phenylpropanoid monomers, which are crosslinked in a combinatorial-like radical coupling reaction. This results in a structurally highly variable polymer, with a huge number of possible isomers, rendering nearly each molecule of lignin unique [8]. The three main monomeric units differ in abundance by the origin of the lignin. Thus softwood lignin predominantly consists of coniferyl alcohol units (G), while hardwood additionally incorporates sinapyl alcohol (S) in the lignin polymer. Lignin of annual plants have a *p*-coumaryl (H) alcohol as major building block [9]. These units are linked by a combination of several typical links, such as β-O-4; β-5, β-β and other carbon-carbon or carbon-oxygen bonds [10]. Furthermore, the pulping processes increase the heterogeneity of the lignins, now termed "technical lignins" to a large extent, as ether bonds are cleaved and functional groups are introduced, altered or eliminated from the polymer, highly dependent on the pulping process and process conditions. Regarding technical lignins derived from pulp and paper industry, the main process today is Kraft pulping, cleaving the beta-ether bonds of the lignin under strong alkaline conditions, resulting in a highly condensed lignin with small amounts of organically bound sulfur [11, 12]. Nevertheless, the majority of the commercially available lignin is lignosulfonate, mainly produced by acidic sulfite pulping. The main reaction step is the sulfonylation in benzylic position of the lignin monomer unit, which extensively improves the water solubility[13]. Additionally, also degradation of α- and partially β-ether bonds occurs by acid-catalyzed hydrolysis, resulting in highly polydisperse lignin with molar weight distributions from 10-40 kDa [3] or smaller. On the other hand, lignin provides an exceptional number of accessible aromatic and aliphatic hydroxyl and carboxylic acid groups paired with an aromatic backbone which is unique for a biopolymer [14].
The key to make these features accessible for utilization, while being able to handle the disadvantages, requires reliable techniques for analyses and a constant-quality lignin, with low batch-to-batch variations for industry and researchers. Nuclear magnetic resonance spectroscopy has proven to be a valuable tool to gain qualitative and quantitative information. NMR spectroscopy is in fact rather insensitive compared to most other spectroscopic techniques, but has the advantage of offering highly resolved spectra and advanced multidimensional experiments for maximum information on the sample [15]. For quantitative data, mostly one dimensional experiments of ^{13}C, ^{1}H and ^{31}P are acquired. While ^{13}C suffers from the low sensitivity and the low natural abundance of the NMR-active carbon isotope, there is on the other hand no need for derivatization of the sample, and the broad spectral dispersion of about 200 ppm gives reasonable resolution. Furthermore, optimized experimental parameters and

improved instruments, such as spectrometers equipped with cryo-probes, nowadays afford acceptable experimental times.[16, 17]. Proton and phosphorous NMR can both benefit from a highly sensitive nucleus with nearly 100 % natural isotopic abundance, but ^{1}H suffers from low resolution, due to its low spectral width of about 10 ppm. In case of quantification of hydroxyl groups [18], also tedious and time consuming sample preparation has to be taken into account. For ^{31}P experiments, the nucleus needs to be introduced into the sample by derivatization as well, however, the derivatization procedure is fast and thus also suitable for high throughput analysis. Moreover, phosphorous gives adequate resolution for several distinct moieties, which for example proton NMR cannot resolve, and additionally has an advantage over carbon-13 experiments in terms of experiment time. [19]

In this study, we compare ^{31}P-NMR spectroscopy of technical lignins to other derivatization methods, as well as present an inter-lab comparison along with relevant current literature [3, 19-21]. As lately questions have been raised about the reproducibility of ^{31}P-NMR techniques in lignin analysis [3] we also reconsider basic parameters of the experiment, such as the choice of internal standard and relaxation times.

II. EXPERIMENTAL

Materials and sample preparation

Kraft Lignin samples, hardwood, softwood and Indulin AT, as well as milled wood lignin, were provided by project partners. The samples were already purified and freeze dried. The ammonium lignosulfonate sample was purchased from Lignotech SA, converted into the sulfonic acid with a strong ion exchange resin DOWEX 50WX8 and additionally purified by ultrafiltration (MWCO 1000 Da) and Amberlite XAD-7 resin [22]. For storage it was freeze dried. As the lignosulfonate does not readily dissolve in $CDCl_3$/pyridine, used for ^{31}P-NMR, it turned out to be beneficial to dissolve, respectively swell it in very small amounts of DMSO and again freeze dry, in order to promote complete dissolution. Prior to further analyses all samples have been routinely checked for purity by FTIR and for their carbohydrate content by methanolysis and subsequent GC/MS.

Determination of methoxyl groups and acetylation of lignins has been done according to Zakis, 1994. [23]

For ^{31}P-NMR, 25 mg of lignin was completely dissolved in 700 µl of a 1:1.6 mixture of deuterated chloroform ($CDCl_3$) and pyridine (non-deuterated). Dissolution was achieved only by shaking, no ultrasonic bath or similar means was applied. Furthermore 200 µl of a stock solution containing the internal standard (0.02 mmol/ml) and relaxation agent, chromium acetylacetonate ($Cr(acac)_3$; 5 mg/ml) were added. After thoroughly mixing 100 µl of phosphitylation reagent, 2-chloro-4,4,5,5-tetramethyl-1,3,2-dioxaphospholane, were injected through a closed septum into the vial, to avoid contact of the reagent with moisture. The sample was shaken for two hours at room temperature, and then transferred into an NMR tube. The internal standard used was cyclohexanol resulting in one rather sharp ^{31}P signal for its hydroxyl group, separating the aliphatic and aromatic region in the spectrum at 145.15 ppm or *N*-hydroxy-5-norbornene-2,3-dicarboxylic acid imide (e-HNDI) at 153.8 ppm. Both spectra were calibrated to the anhydride of the derivatization reagent (2-chloro-4,4,5,5-tetramethyl-1,3,2-dioxaphospholane) at 132.2 ppm. [24].

Hydroxyl group determination by ^{1}H and ^{31}P-NMR spectroscopy

For quantitative ^{1}H-NMR analysis a Bruker Avance II 400 instrument (^{1}H resonance at 400.13 MHz, ^{13}C resonance at 100.61 MHz and ^{31}P at 162 MHz, respectively) with a 5 mm broadband observe probe head (BBFO) equipped with z-gradient in $CDCl_3$ (euriso-top, 99.9% D) at room temperature with standard Bruker pulse programs was used. ^{1}H-NMR data were collected with 32k data points and apodized with an exponential window function (lb = 0.3) prior to Fourier transformation. A 2.5 s acquisition time and a 30 s relaxation delay were used. A total 64 scans were collected. Proton signals of aromatic-bound acetoxy groups (2.4-2.2 ppm) and aliphatic-bound acetoxy groups (2.2-1.7) were integrated and referred to the integrated signal of the methoxyl protons (4-3.5 ppm), which were taken as an internal standard, for further quantification of aliphatic and phenolic hydroxyl groups content. ^{31}P data was collected with 64k data points and apodized with an exponential window function (lb = 5) prior to FT. A 2.5 s acquisition time and delays from 1 to 30 s were used (30 s is actually suggested to ensure complete relaxation of IS, instead of 5 s used in many studies). 16 to 512 scans were acquired for different experiment (16 scans actually already giving very reasonable results). Integration was done after automatic baseline correction (Bruker TopSpin) according to Granata et al.[19]

III. RESULTS AND DISCUSSION

From the comparisons in **Figure 1 (A)** and **(B)** it was evident that for milled wood lignin both methods, ^{1}H-NMR and ^{31}P-NMR, agreed precisely with each other, and also with the inter-laboratory measurement, thus proving that the set of parameters chosen for the NMR and derivatization work well with all functional groups commonly evaluated by those methods. However, looking at the Kraft lignins, the ^{1}H-NMR for the acetylated lignins showed a drastically higher value for the aliphatic hydroxyls and a slightly lower value for the aromatic OH groups. This

could be an indication that the acetylation procedure also acetylates impurities of the Kraft lignin which stay underivatized upon phosphitylation or are just better resolved in the ^{31}P spectrum. On the other hand, the phosphitylation reagent might not react completely with some aliphatic moieties in the sample, and so underestimate the aliphatic value in the technical lignin. For the aromatics, also the two ^{31}P experiments differ slightly from each other, but as shown in **(C)** there are also differences to literature averages [3, 19-21] of ^{31}P experiments with Indulin (the only Kraft lignin available in literature for comparison). However, this could just be a matter of reaction time, as for the parallel measured samples in lab 2 no reaction time for the derivatization is given. **Figure 1 (D)** finally shows a comparison of a selection of technical lignins and one milled wood lignin measured in house. Particularly worth mentioning is the result for lignosulfonate, which perfectly dissolved in the phosphitylation mixture only after pre-swelling in DMSO and a subsequent drying step in between, thus rendering it now possible to measure all kinds of lignins according to the original ^{31}P method. Since the raw material for the lignosulfonate was hardwood, the hydroxyl group value for the syringyl & condensed value is rather low in contrast to hardwood Kraft pulp investigated, indicating a very low degree of condensation.

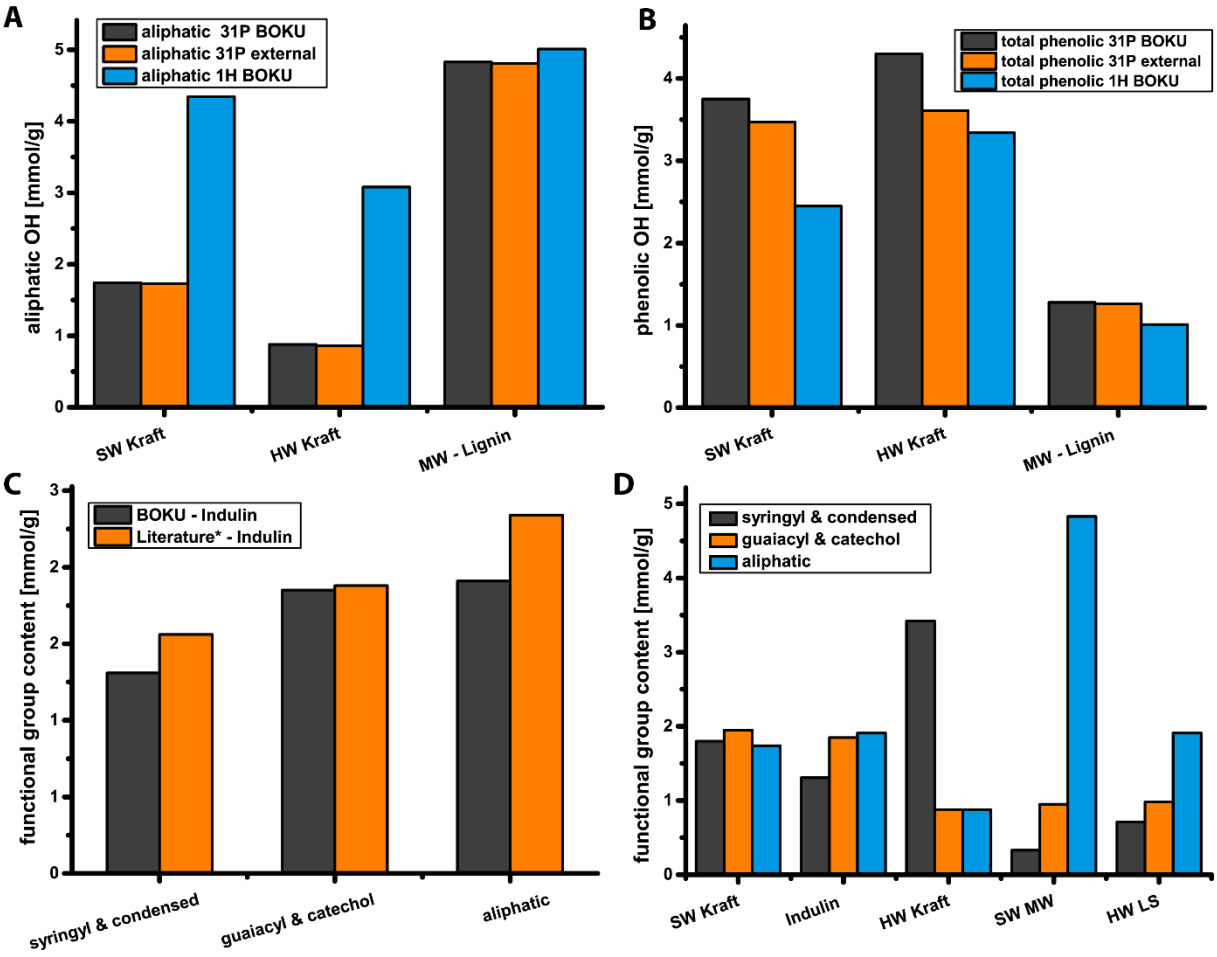

Figure 1: Comparison of different technical lignins with a milled wood lignin (MWL), measured with two different methods on two different spectrometers. (A) and (B) show measurements of MWLwith ^{31}P-NMR at BOKU Vienna and another lab, compared to ^{1}H-NMR of acetylated lignin measured at BOKU. (C) compares the averages of the ^{31}P-NMR experiments on Indulin at BOKU with literature values given in Bioenergy Research: Advances & Applications [3]. (D) shows a selection of measured technical lignin samples at BOKU.

IV. CONCLUSIONS

When the right parameters are chosen, ^{31}P-NMR gives very consistent results for conventional lignins, such as milled wood lignin. When it comes to technical lignins, the reactivity of the phosphitylation reagent has to be evaluated further, and the outcome must be compared to other methods, such as ^{13}C-NMR spectroscopy, which are independent of derivatization influences. However, for relative comparison of lignins, ^{31}P-NMR is a fast and reproducible method within one laboratory, which is able to deal with all kinds of lignins, only depending on the pretreatment of the sample before measurement. For evaluation of lignosulfonates, more data is needed and measurements have to be repeated successfully in other laboratories. Furthermore, side reactions of the phosphitylation and acetylation reagent in the respective solvents need to be evaluated.

V. ACKNOWLEDGEMENT

We thank VTT, Finland, for custom ^{31}P-NMR analysis of technical lignins used for comparison. The authors acknowledge the company partners of the FLIPPR° project for their generous financial support.

VI. REFERENCES

[1.] Gosselink, R.J.A., et al., Co-ordination network for lignin—standardisation, production and applications adapted to market requirements (EUROLIGNIN). Industrial Crops and Products, 2004. 20(2): p. 121-129.
[2.] Lora, J.H. and W.G. Glasser, Recent industrial applications of lignin: A sustainable alternative to nonrenewable materials. Journal of Polymers and the Environment, 2002. 10(1-2): p. 39-48.
[3.] Berlin, A. and M. Balakshin, Chapter 18 - Industrial Lignins: Analysis, Properties, and Applications, in Bioenergy Research: Advances and Applications, V.K. Gupta, et al., Editors. 2014, Elsevier: Amsterdam. p. 315-336.
[4.] Doherty, W.O.S., P. Mousavioun, and C.M. Fellows, Value-adding to cellulosic ethanol: Lignin polymers. Industrial Crops and Products, 2011. 33(2): p. 259-276.
[5.] Gosselink, R.J.A., et al., Characterisation and application of NovaFiber lignin. Industrial Crops and Products, 2004. 20(2): p. 191-203.
[6.] Stewart, D., Lignin as a base material for materials applications: Chemistry, application and economics. Industrial Crops and Products, 2008. 27(2): p. 202-207.
[7.] Mansouri, N.-E.E. and J. Salvadó, Structural characterization of technical lignins for the production of adhesives: Application to lignosulfonate, kraft, soda-anthraquinone, organosolv and ethanol process lignins. Industrial Crops and Products, 2006. 24(1): p. 8-16.
[8.] Ralph, J., et al., Lignins: Natural polymers from oxidative coupling of 4-hydroxyphenyl- propanoids. Phytochemistry Reviews, 2004. 3(1-2): p. 29-60.
[9.] Sarkanen, K.V.L.C.H., Lignins: occurrence, formation, structure and reactions. 1971, New York: Wiley-Interscience.
[10.] Brunow, G., K. Lundquist, and G. Gellerstedt, Lignin, in Analytical Methods in Wood Chemistry, Pulping, and Papermaking, E. Sjöström and R. Alén, Editors. 1999, Springer Berlin Heidelberg. p. 77-124.
[11.] Balakshin, M.Y., et al., Elucidation of the Structures of Residual and Dissolved Pine Kraft Lignins Using an HMQC NMR Technique. Journal of Agricultural and Food Chemistry, 2003. 51(21): p. 6116-6127.
[12.] Smook, G.A., Handbook for Pulp and Paper Technologists. 2002: Angus Wilde Publications Incorporated.
[13.] Gratzl Josef, S. and C.-L. Chen, Chemistry of Pulping: Lignin Reactions, in Lignin: Historical, Biological, and Materials Perspectives. 1999, American Chemical Society. p. 392-421.
[14.] Gösta, B. and L. Knut, Functional Groups and Bonding Patterns in Lignin (Including the Lignin-Carbohydrate Complexes), in Lignin and Lignans. 2010, CRC Press. p. 267-299.
[15.] Keeler, J., Understanding NMR Spectroscopy. 2006, John Wiley & Sons, Ltd. p. 526.
[16.] Capanema, E.A., M.Y. Balakshin, and J.F. Kadla, A Comprehensive Approach for Quantitative Lignin Characterization by NMR Spectroscopy. Journal of Agricultural and Food Chemistry, 2004. 52(7): p. 1850-1860.
[17.] Capanema, E.A., M.Y. Balakshin, and J.F. Kadla, Quantitative characterization of a hardwood milled wood lignin by nuclear magnetic resonance spectroscopy. Journal of Agricultural and Food Chemistry, 2005. 53(25): p. 9639-9649.
[18.] Lundquist, K., NMR studies of lignins. 4. Investigation of spruce lignin by 1H NMR spectroscopy. Acta Chem. Scand., 1980. 34(1): p. 21-26.
[19.] Granata, A. and D.S. Argyropoulos, 2-Chloro-4,4,5,5-tetramethyl-1,3,2-dioxaphospholane, a reagent for the accurate determination of the uncondensed and condensed phenolic moieties in lignins. Journal of Agricultural and Food Chemistry, 1995. 43(6): p. 1538-1544.
[20.] Cateto, C.A., et al., Lignins as macromonomers for polyurethane synthesis: A comparative study on hydroxyl group determination. Journal of Applied Polymer Science, 2008. 109(5): p. 3008-3017.
[21.] Gosselink, R.J.A., et al., Fractionation, analysis, and PCA modeling of properties of four technical lignins for prediction of their application potential in binders. Holzforschung, 2010. 64(2): p. 193-200.
[22.] Sjöström, J.D.S.i.P.a.P.P.P.T., Åbo Akademi University, Turku/Åbo, Detrimental Substances in Pulp and Paper Production. 1990, Åbo Akademi University: Turku/Åbo.
[23.] Zakis, G.F., Functional analysis of lignins and their derivatives. 1994: TAPPI Press (Atlanta, Ga.).
[24.] King, A.W.T., et al., A new method for rapid degree of substitution and purity determination of chloroform-soluble cellulose esters, using 31P NMR. Analytical Methods, 2010. 2(10): p. 1499-1505.

MILD ALKALINE HOT-WATER EXTRACTION OF LIGNIN FROM SPRUCE WOOD

Ekaterina Korotkova*, Andrey Pranovich, Stefan Willför

Åbo Akademi University, Process Chemistry Centre, c/o Laboratory of Wood and Paper Chemistry Porthansgatan 3 FI-20500 Åbo/Turku, Finland,

**E-mail: ekaterina.korotkova@abo.fi*

ABSTRACT

The aim of this study was to isolate lignin from spruce wood with an Accelerated Solvent Extractor (ASE) using low concentration of aqueous NaOH and characterise the products in order to understand how the process parameters affects the chemistry involved. Two concentration of alkali were studied – 1% and 2% aqueous NaOH. Extraction was performed for 4 hours total time, but different extraction sequences were studied: 1×240 min, 2×120 min, 4×60 min, 6×40 min, and 12×20 min. It was found that higher alkali concentration allows extracting more lignin from spruce wood. The extraction sequence has great influence on the process – shorter extraction times extracted up to 10 times more lignin compared to longer extraction times. Xylose and galactose were the most abundant carbohydrate impurities in the isolated lignins. The average molar mass of lignin increased with the extraction time and concentration of alkali.

I. INTRODUCTION

Lignin is the second most abundant component in wood after cellulose. It is well known that lignin structure depends on plant origin, isolation technique, and conditions. However biosynthesis of lignin macromolecule in the cell wall stems from polymerisation of three types of phenylpropane units: coniferyl, sinapyl and *p*-coumaryl alcohols. Lignin represents the main potential renewable source of aromatic fine chemicals.

Lignin is a by-product in kraft pulp mills and usually burnt to generate energy and recover chemicals. Only a small part of the kraft lignin is used for different chemical and material applications. Kraft lignin has a condensed structure and therefore low reactivity, as well as high sulphur content. But lignin could also be isolated by more tailor-made processes with respect to the specificity of further transformations within the biorefinery concept [1]. Due to ecological and economical aspects sulphur-free lignin is of increasing interest. Biorefining of natural feedstock is a promising approach to promote broader use of lignin. Advanced technique and methodology for efficient isolation of sulphur-free lignin in less altered form are needed. Scientists are continually challenged to accomplish desired results faster, better, cheaper, and more efficiently. The now used ASE is an elegant, accurate, and reproducible method, which uses a combination of elevated temperature and pressure to increase the efficiency of the extraction process resulting in faster run times and major reduction in solvent use. Later the methods can be scaled-up to large batch extractions. Previously ASE was successfully used for hot-water extraction of hemicelluloses from spruce wood [2].

II. EXPERIMENTAL

Sample preparation

Norway spruce knot-free sapwood was manually separated from bark and heartwood, ground with a Thomas Wiley® Mill (Thomas Scientific, Swedesboro, NJ), and fractionated. The fraction with particle size of 0.5-1 mm was used for further experiments.

In order to remove lipophilic extractives the wood meal was extracted with acetone in a Soxhlet apparatus for 15 h and then conditioned in a hood for 12 h to evaporate the solvent. The extracted wood meal was stored at -19°C in sealed polyethylene bags in the dark.

Lignin extraction

Extraction of lignin was performed in an ASE 350 extractor (Thermo Fisher Scientific, Waltham, USA). Approximately 18 g (dry weight) of wood meal was weighed in zirconium cells. 1% and 2% aqueous NaOH solutions were used as extraction solvents. Extraction was performed at a temperature of 170°C and pressure of

10.34 MPa (1500 psi) for 4 hours total time but different extraction sequences were studied; 1×240 min, 2×120 min, 4×60 min, 6×40 min, and 12×20 min. The volume and weight of all extracts were measured.

Extracts characterization

Residual alkali and pH of all extracts were determined by titration with 0.1M HCl using a 665 Dosimat titrator (Metrohm, Herisau, Switzerland) and further calculations.

Total dissolved solids content of the extracts and the extraction solvents were gravimetrically determined after drying of 2mL of liquid at 105°C to a constant weight.

Lignin isolation from extracts

The pH of all extracts were adjusted to 3 in order to precipitate lignin. After precipitation lignin was filtered and washed from the acid with warm water through a G3 glass filter [3]. After that lignin was freeze-dried and weighted.

Average molar mass determination

Average molar masses (Mw) of isolated lignins were determined by HP-SEC coupled with an RI detector (RID-10A) (Shimadzu, Tokyo, Japan). The system consisted of a Jordi gel GBR Mixed Bed (Glucose) 250×10mm i.d. column + a Jordi gel (Glucose) DVB 500Å 50mm×7.8 mm i.d. guard column. Lignin was dissolved in DMSO (3mg of sample in 1 mL of DMSO) and filtered through a 0.22-mm Teflon syringe filter before injection. Eluent: 0.05 M LiBr in DMSO; flow rate: 0.5 mL min^{-1}; injection volume: 100 µL, the temperature of column oven: 60°C. The calibration was done using the series of pullulan standards.

Residual carbohydrates in lignin

The amount of residual hemicelluloses in extracted lignin was determined by GC after acid methanolysis followed by silylation and gas chromatography [4]. 10 mg of sample were transferred to pressure resistant pear-shaped flasks with a Teflon coated screw caps. Calibration samples were prepared by evaporation of 1 mL 0.1 mg/mL of carbohydrate calibration solution in a steam of nitrogen at ~50°C. The calibration is necessary for the determination of correction coefficients for quantitation of carbohydrates after methanolysis.
About 2 mL of 2 M HCl in water free methanol was added to all samples and separately to the flasks containing dried calibration mixture. Flasks were placed in the oven at 105°C for 3 hours. After that pear-shaped flasks with metahanolysed samples were taken out and cooled down to room temperature to equalize the pressure. Excess HCl was neutralized by adding 150 µL of pyridine.
Exactly 1 mL of internal standard (0.1 mg/mL resorcinol or sorbitol solution in MeOH) was added to the extracts samples and to the calibration samples. The methanol was evaporated in a stream of nitrogen at about 50°C. All samples were further dried in a vacuum desiccator at 40°C for 30 minutes.
After that samples were silylated. 150 µL of pyridine, 150 µL HMDS and 70 µL TMCS were added to each sample. The samples were left overnight at room temperature. Silylated samples were transferred to GC vials using Pasteur pipettes and analysed by GC. GC PerkinElmer AutoSystemXL was used for analysis. Calculations were made with TotalChrom software (PerkinElmer, Inc).

III. RESULTS AND DISCUSSION

pH of extracts

At the beginning of the extraction, the consumption of alkali was observed due to splitting of acetyl groups from galactoglucomannan and formation of acetic acid. After first 3 extraction runs in case of 1% NaOH concentration and after first 2 extraction runs in case of 2% NaOH concentration, the pH of the extracts was stabilised (Figure 1).

Yield of extracted lignin

It was found that consecutive short extraction times were more effective compared to long ones. After 4 hours of total extraction time up to 10 times more lignin was extracted with 12×20 minutes extraction sequence compared to the long 240 minutes extraction, as fresh portions of alkali were added more frequently. Figure 2 shows that it is possible to extract up to 22% of wood as lignin with 2% aqueous NaOH and 12×20 minutes extraction sequence. The amount of extracted lignin after the first extraction run was almost the same for all extraction sequences at given alkali concentration. It can be concluded that the extraction process depends strongly on the consumption of alkali, and once alkali neutralisation happens, extraction run time does not affect the amount of extracted lignin.

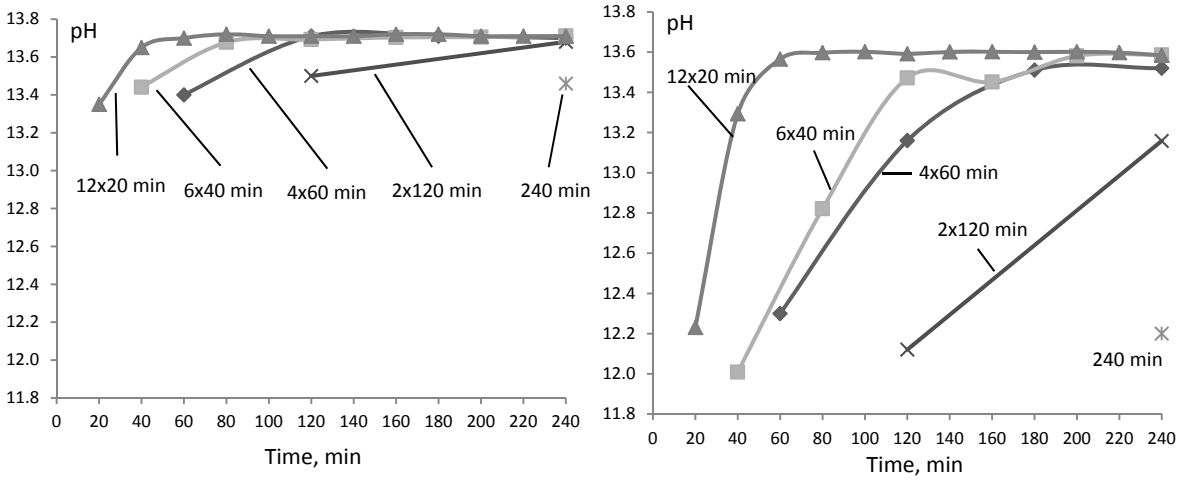

Figure 1. pH of extracts at a) 2% NaOH concentration and b) 1% NaOH concentration

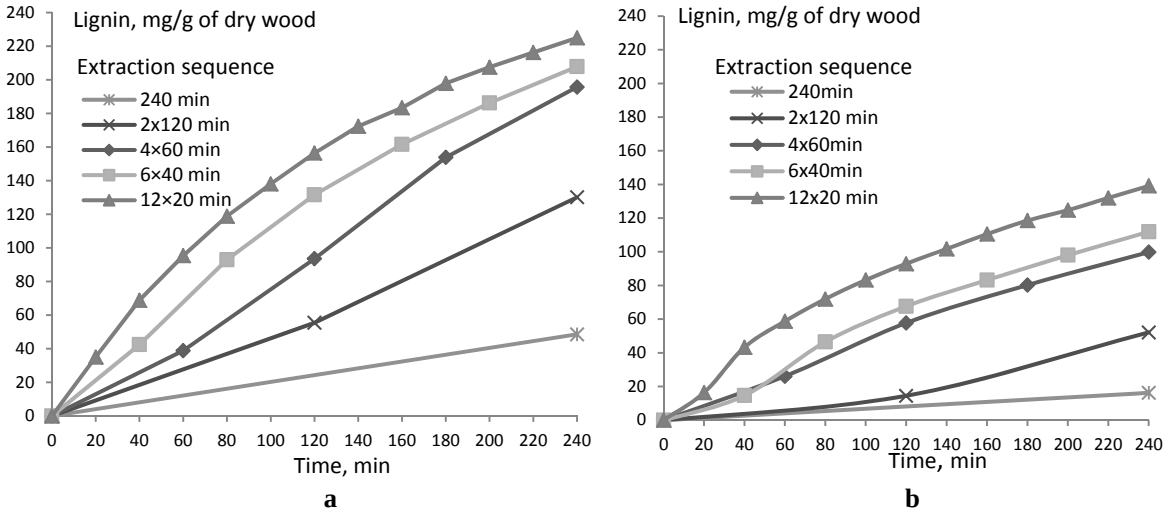

Figure 2. Amount of lignin extracted with a) 2% NaOH concentration and b) 1% NaOH concentration

Average molar mass of extracted lignin

As it can be seen in Figure 3, the average molar mass of extracted lignin depended on the alkali concentration. Higher concentration of NaOH led to higher molar mass of the extracted lignin. At the beginning of the extraction the molar mass of the extracted lignin was significantly lower than at the end of the extraction. More frequent addition of alkali, i.e. shorter extraction run times, leads to increase of molar mass of the extracted lignin.

Residual carbohydrates in extracted lignin

Even though galactoglucomannan is the main hemicellulose in spruce wood, the main carbohydrate impurities found in extracted lignin were xylose and galactose (results not shown). The amount of mannose in extracted lignins was found to be significantly smaller than the amount of xylose. Possibly the complex of lignin with xylan is more stable in alkaline conditions. In addition Du et. al. proposed that in the secondary cell wall xylan is mainly associated with lignin, whereas glucomannan is associated with cellulose [5]. No uronic acids were found in extracted lignin probably due to degradation of pectins in alkaline conditions. The amount of hemicelluloses in lignin at the beginning of extraction was found to be higher than at the end of extraction.

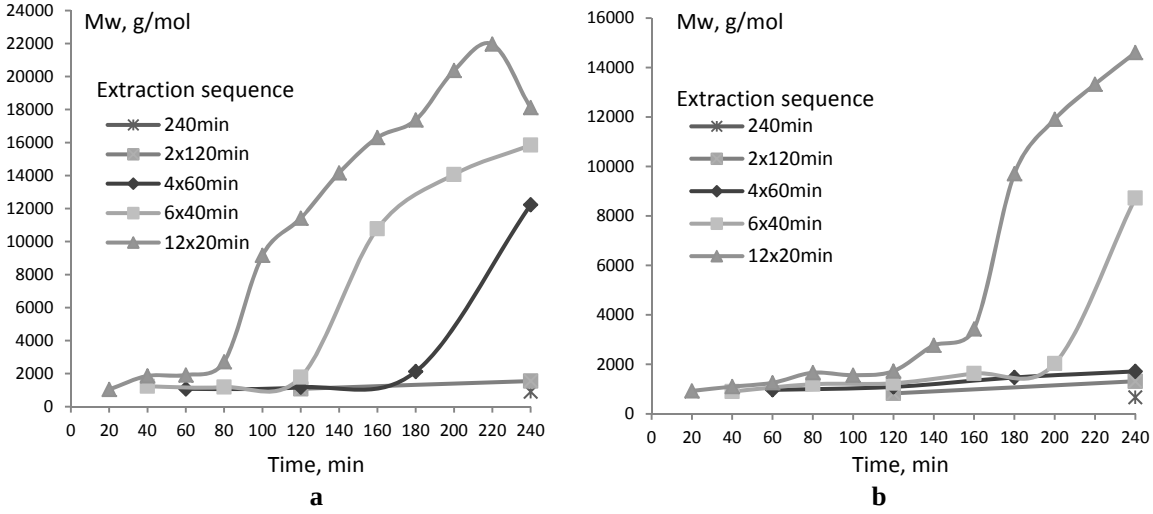

Figure 3. Average molar mass of lignin extracted with a) 2% NaOH concentration and b) 1% NaOH concentration

IV. CONCLUSIONS

Extraction of lignin from spruce wood with low-concentration aqueous alkaline solution (1-2%) was performed. It was possible to extract up to 22% of wood as a lignin. The extraction process is more effective in case of higher alkali concentration and shorter consecutive extraction runs. The average molar mass of lignin increases with the extraction time and concentration of alkali. The amount of carbohydrates in lignin, i.e. impurity, at the beginning of extraction is higher than at the end of extraction. Main carbohydrate impurities in extracted spruce lignin are xylose and galactose.

V. ACKNOWLEDGEMENT

This research was part of activities at Åbo Akademi Process Chemistry Centre. The financial support from The International Doctoral Programme in Bioproducts Technology PaPSaT is gratefully appreciated.

VI. REFERENCES

[1] Lange, H.; Decina, S.; Crestini, C. Oxidative upgrade of lignin – Recent routes reviewed. *Eur. Polym. J.* **2013**, *49*, 1151–1173.

[2] Song, T.; Pranovich, A.; Holmbom, B. Hot-water extraction of ground spruce wood of different particle size. *Bioresources*, **2008**, *7(3)*, 4214-4225.

[3] Gosselink, R.J.; Snijder, M.H.B.; Kranenbarg, A.; Keijsers, E.R.P.; de Jong, E.; Stigsson, L.L. Characterisation and application of NovaFiber lignin. *Ind. Crops Prod.* **2004**, *20*, 191–203.

[4] Willför, S.; Pranovich, A.; Tamminen, T.; Puls, J.; Laine, C.; Suurnäkki, A.; Saake, B.; Uotila, K.; Simolin, H.; Hemming, J.; Holmbom, B. Carbohydrate analysis of plant materials with uronic acid-containing polysaccharides–A comparison between different hydrolysis and subsequent chromatographic analytical techniques. *Ind Crops Prod*. **2009**, *29*, 571–580.

[5] Du, X.; Gellerstedt, G.; Li, J. Universal fractionation of lignin-carbohydrate complexes (LCCs) from lignocellulosic biomass: an example using spruce wood. *Plant J.* **2013**, *74*, 328–338.

NEW INORGANIC-ORGANIC COMPOSITE PIGMENTS IN PAPER

Jonna Kuusisto[1]*, Thaddeus C. Maloney[1]

[1]*Department of Forest Products Technology, School of Chemical Technology, Aalto University, PO Box 16300, FI-00076 AALTO, Finland (*jonna.kuusisto@aalto.fi)*

ABSTRACT

The influence of two polysaccharides, native corn starch and carboxymethyl cellulose (CMC) on the precipitation of calcium carbonate ($CaCO_3$) was studied. Precipitation was performed in two different conditions. In a batch reaction, CO_2 gas was bubbled through a $Ca(OH)_2$ slurry at a pH of 11.5-12.0, until the reaction was complete. In a fed-batch reaction, the CO_2 was dissolved in water in the reactor, while $Ca(OH)_2$ was pumped into the water, keeping a constant pH of 6.0±0.5. The structures of precipitated calcium carbonate (PCC) architectures were characterized by scanning electron microscopy (SEM), particle size analyzer (Malvern Mastersizer 2000), and specific surface area analyzer (Micromeritics Tristar II 3020). In application testing, the effect of pigment modification on paper properties was examined. The results showed that polysaccharides greatly affect the crystallization of $CaCO_3$, but their influence is dependent on the precipitation process. Polysaccharide-modified PCC can be applied in papermaking to produce paper with engineered properties like enhanced strength and stiffness.

I. INTRODUCTION

Traditional fillers or pigments are used in papermaking because they are inexpensive and have positive effect on many properties, such as the dimensional stability and optical performance of paper. Paper characteristics can be controlled by varying the pigment properties, for instance, the particle size, size distribution, specific surface area, and morphology. The disadvantage of traditional pigments is that they are incapable of forming bonds with fibers and they also prevent fiber-fiber bonding thus impairing mechanical paper properties, e.g., stiffness and tensile strength. In addition, pigments increase the chemical consumption and two-sidedness of paper. At the same time, the need for reducing production costs is putting pressure on manufacturers to increase pigment content. Since one of the main limiting factors for pigment content is paper strength, interest in designing pigments with diminished interference on fiber-fiber bonding has increased. [1]

Calcium carbonate ($CaCO_3$) is an inorganic mineral, which is abundant in nature and widely used in many industrial applications, such as paper, paints, and plastics. It occurs in three crystalline polymorphs: calcite, aragonite and vaterite. Calcite is the most thermodynamically stable and can exhibit e.g. scalenohedral or rhombohedral morphology. In the industrially conventional method, precipitated calcium carbonate (PCC) is crystallized by reacting carbon dioxide (CO_2) gas with the aqueous slurry of calcium hydroxide ($Ca(OH)_2$) i.e. slaked lime.

The crystallization of $CaCO_3$ is a complicated phenomenon and the properties of precipitated particles are determined by the process variables, such as the temperature, pH, and ionic strength of solution. Crystallization can also be influenced by different organic additives, e.g. polysaccharides, to modify the properties of precipitated particles. Controlled nucleation and growth of inorganic crystals is believed to result from the specific molecular interactions at inorganic-organic interfaces [2]. Interfacial molecular recognition between calcium carbonate and polysaccharides includes geometric matching (epitaxis), as well as electrostatic and stereochemical complementarity.

In this study, the crystallization of $CaCO_3$ was influenced by two polysaccharides, starch and carboxymethyl cellulose (CMC), typically used as strength additives in papermaking. The influence of polysaccharide concentration and precipitation process on the pigment properties and the effect of pigment modification on the paper properties were studied. Polysaccharides were found to have a substantial effect on PCC and consequently the properties of paper were modified depending on the type of polysaccharide and precipitation process.

II. EXPERIMENTAL

Materials

La Mède lime was provided by Lhoist Ltd. Native corn starch was obtained from Roquette Ltd and CP Kelco Oy supplied technical grade CMC (Calexis L-H1). Stora Enso Oyj, Varkaus mill (Finland) provided bleached

softwood and hardwood kraft pulps. Two-component retention aid system consisting of cationic and anionic polyacrylamides (Kemira Ltd.) was applied in a sheet making. Deionized water was used in all experiments.

Crystallization and characterization of $CaCO_3$

$CaCO_3$ was produced by a precipitation process in a cylindrical laboratory-scale reactor (5 dm^3). The reactor was equipped with a high-shear impeller mixer, a CO_2 gas feed system with a rotameter, thermoelement casings, and a pH, conductivity, and temperature sensors. In a lime slaking process, calcium oxide (i.e. burnt lime) and water were mixed with a high-shear mixer for 10 minutes to form $Ca(OH)_2$. Lime to water ratio was 1:5 and initial water temperature 50 °C. Starch was cooked into soluble form by heating at 95 °C for 30 minutes. CMC was dissolved in water at room temperature.

In a batch precipitation process, the aqueous slurry of $Ca(OH)_2$ was first adequately mixed with a polysaccharide solution in the reactor before starting to feed CO_2 through the slurry. As a reference experiment, $CaCO_3$ was precipitated in the absence of a polysaccharide. The initial temperature was 50 °C, $Ca(OH)_2$ concentration 7.4%, and batch volume 2.5 dm^3. Initial pH of the slurry was 11.5-12.0. CO_2 was fed to the reactor at constant flow rate (2.5 dm^3/min) and mixing rate was 800 rpm. Conductivity and pH were continuously monitored and the reaction was completed when pH dropped to 7.

A fed-batch process was started by bubbling water (1 dm^3) with CO_2 to form carbonic acid (H_2CO_3), which caused pH in the reactor to decrease to 5.0-6.0. The polysaccharide solution was then added into the reactor and mixed well. $Ca(OH)_2$ was slowly fed into the reactor at the flow rate adjusted to maintain the pH of solution at 6.0±0.5. Same initial temperature, total $Ca(OH)_2$ concentration, batch volume, CO_2 flow rate, and mixing rate were applied as in the batch precipitation.

The size of precipitated particles was measured with Malvern Mastersizer 2000 and the specific surface area was determined by the multi-point BET method (Micromeritics Tristar II 3020) by using nitrogen gas as an adsorbate. The morphology of $CaCO_3$ precipitates was analyzed with Field Emission Scanning Electron Microscopes (FE-SEM; JEOL JSM-7500FA and Zeiss Sigma VP, acceleration voltage 3 kV).

Preparation and testing of paper

Paper sheets with a basis weight of 80 g/m^2 were prepared in a laboratory sheet mold according to a standard ISO 5269-1. A mixture of softwood and hardwood pulp (30/70) and a two-component retention aid system with C-PAM (300 g/t) and A-PAM (400 g/t) were used. Reference paper sheets, which contained unmodified PCC, were prepared at two different PCC contents, 20% and 30%, and the results were normalized to 25% of PCC. The sheets containing composite pigments were made to 25% of PCC. The physical properties of prepared paper sheets were tested according to the standards shown in **Table 1.**

Table 1. Measurement standards used in paper testing.

Paper property	Bulk	ISO Brightness	PPS roughness	Tensile strength	Tear strength	Bending stiffness
Standard	ISO 534	ISO 2470	ISO 8791-4	ISO 1924-2	ISO 1974	ISO 5629

III. RESULTS AND DISCUSSION

Effect of polysaccharide concentration on pigment properties

Figure 1 shows the effect of different concentrations of starch on the morphology of PCC particles prepared by the batch precipitation. At low starch concentration (**Figure 1 b**) the particles still showed scalenohedral structure, which is characteristic of calcite, but further addition of starch (**Figure 1 c** and **1 d**) changed the morphology of particles. The detected transition may be attributed to the adsorption of starch on the crystal surfaces of calcite when high enough concentrations of starch is used [3]. Consequently the crystal growth of calcite can be inhibited and the formation and growth of vaterite enhanced. The underlying mechanism has been proposed by Yang et al. [4]. The secondary structure of starch and crystal lattice of calcium carbonate have an excellent geometric match. The spatial arrangement of hydroxyl groups is ordered in the secondary structure of starch and Ca^{2+} ions combine with these hydroxyl groups. Crystal nucleus is formed when CO_3^{2-} ion aggregates around the Ca^{2+} ion.

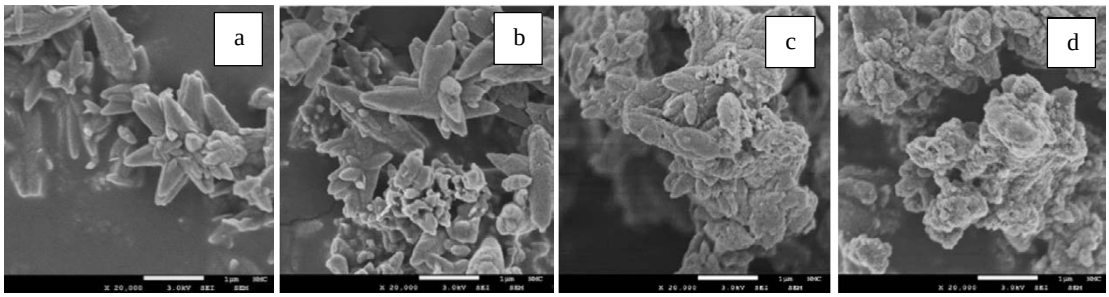

Figure 1. SEM micrographs of the batch precipitated PCC with 0 (a), 1.0 (b), 2.5 (c), and 5.0 wt% starch of $Ca(OH)_2$ (d).

The addition of starch increased the average particle size and decreased the specific surface area of particles, as shown in **Figure 2**. Increased particle size can be ascribed mainly to the particle aggregation caused by starch. Changes were rather small at the lowest starch concentration, but the increase of the concentration to 2.5 wt% of $Ca(OH)_2$ emphasized the effect of polysaccharide. Further increase of the starch concentration had no influence on the size and surface area of particles.

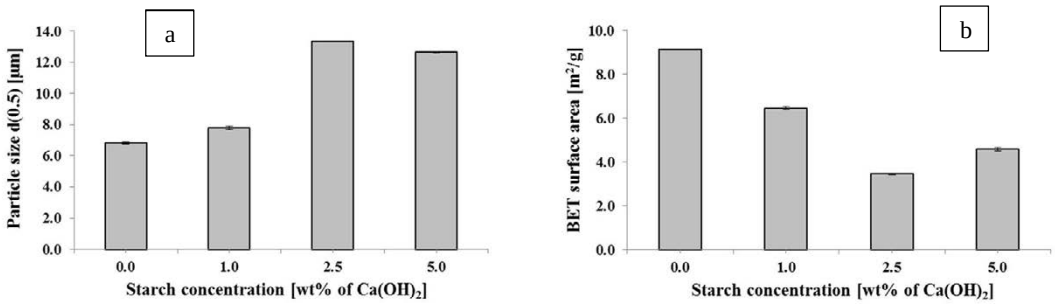

Figure 2. Average particle size (a) and BET surface area (b) of the batch precipitated reference system and PCC modified with different mass percentages of starch.

Effect of polysaccharide type and precipitation process on pigment and paper properties

The effect of starch and CMC on the batch and fed-batch precipitation of $CaCO_3$ at the polysaccharide content 2 wt% of $Ca(OH)_2$ was examined. Starch and CMC were found to behave differently depending on the precipitation process. As already illustrated in **Figure 1**, the scalenohedral morphology of PCC produced by the batch process was lost in the presence of higher concentrations of starch, whereas in the presence of CMC, bundled particles were precipitated. This is shown in **Figure 3 a - c**. Both polysaccharides induced an abrupt decrease in the surface area of particles and increased their average size (**Table 2**).

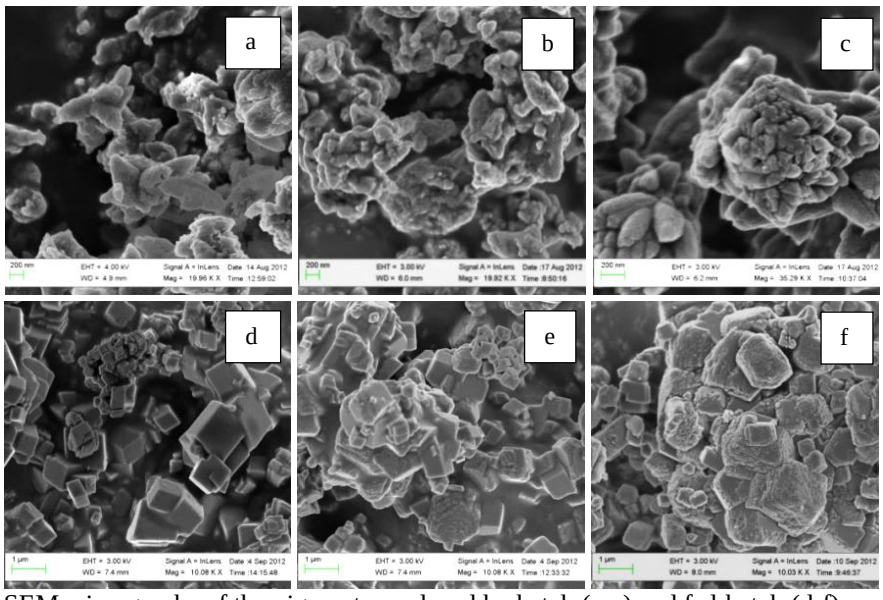

Figure 3. SEM micrographs of the pigments produced by batch (a-c) and fed-batch (d-f) precipitation: reference (a, d), starch-modified (b, e), and CMC-modified PCC (c, f).

Fed-batch precipitation (acidic pH) produced cubic particles, which is illustrated in **Figure 3 d – f**. Unlike in the batch precipitation (alkaline pH), neither the morphology nor the surface area of particles was affected by starch, but it highly aggregated the particles (**Table 2**). On the contrary, CMC had an impact on morphology. Possibly due to the electrostatic interaction between Ca^{2+} ions and carboxyl groups, the edges and acute corners were dissipated and smooth surfaces became rough, which is consistent with the findings by Liang et al. [5]. As shown in **Table 2**, CMC increased the surface area of particles, but they were marginally smaller than pure PCC.

Table 2. The properties of the batch and fed-batch precipitated reference and polysaccharide-modified pigments and corresponding properties of paper sheets (80 g/m^2, PCC content 25%).

Pigment type		Pigment properties		Paper properties					
Poly-saccharide addition	Precipitation process	Particle size d(0.5) [µm]	BET surface area [m^2/g]	Bulk [cm³/g]	ISO Brightness R457 C	PPS roughness [µm]	Tensile index [Nm/g]	Tear index [mN*m²/g]	Bending stiffness index [10^6 Nm^7/kg^3]
None	Batch	5.44	11.5	1.68	90.1	8.80	18.6	6.90	0.47
Starch	Batch	7.54	4.13	1.75	89.7	8.99	17.6	7.27	0.42
CMC	Batch	7.69	5.22	1.75	91.0	8.02	15.7	6.10	0.40
None	Fed-batch	4.93	3.25	1.53	90.6	8.79	23.4	6.57	0.44
Starch	Fed-batch	14.0	2.25	1.57	89.1	9.13	26.7	7.80	0.47
CMC	Fed-batch	3.79	4.61	1.64	90.5	8.54	20.7	6.24	0.48

The effect of pigment modification on the paper properties is illustrated in **Table 2**. Polysaccharide-modified pigments gave higher bulk to the paper. CMC-modified PCC improved the brightness and smoothness of the paper, especially the pigments produced by the batch precipitation, but the strength properties were impaired. The influence of starch was highly dependent on the precipitation process. Aggregated particles produced by the fed-batch precipitation increased the strength and stiffness of paper, but optics and smoothness were negatively affected. However, the loss of brightness could be overcome by the increase of pigment content enabled by the improved mechanical properties.

IV. CONCLUSIONS

Polysaccharides have an effect on the crystallization of $CaCO_3$ and they can be utilized to produce pigments with engineered characteristics. The morphology, particle size and surface area of the modified particles depend on the type of polysaccharide and its concentration, as well as the process conditions during the precipitation. Composite pigments can be exploited in different applications, e.g. to produce paper with high performance. Pigments with CMC were found to improve the smoothness, bulk, and brightness of the paper but the strength was impaired. On the contrary, starch-modified PCC had negative effect on the paper brightness and smoothness, but enhanced strength, stiffness, and bulk were achieved when the fed-batch precipitation was employed. Enhanced stiffness and strength properties concede raise in the paper pigment content, which restores the optical performance diminished by starch and reduces the manufacturing costs.

V. ACKNOWLEDGEMENT

This study was conducted as a part of the EffNet program (Finnish Bioeconomy Cluster Ltd.).

VI. REFERENCES

[1] Krogerus, B. Papermaking additives. Papermaking chemistry. 2nd edition. Ed. Alén, R. Publ. Finnish Paper Engineers' Association/Paperi ja Puu Oy. Helsinki **2007**, pp. 54-121.

[2] Mann, S.; Archibald, DD. Crystallization at inorganic-organic interfaces: Biominerals and biomimetic synthesis. *Science*. **1993**, *261*, 1286-1292.

[3] Kontrec, J.; Kralj, D.; Brečević, L.; Falini, G. Influence of some polysaccharides on the production of calcium carbonate filler particles. *J Cryst Growth*. **2008**, *310*, 4554-4560.

[4] Yang, L.; Zhang, X.; Liao, Z.; Guo, Y.; Hu, Z.; Cao, Y. Interfacial molecular recognition between polysaccharides and calcium carbonate during crystallization. *J Inorg Biochem.* **2003**, *97*, 377-383.

[5] Liang, P.; Zhao, Y.; Shen, Q.; Wang, D.; Xu, D. The effect of carboxymethyl chitosan on the precipitation of calcium carbonate. *J Cryst Growth*. **2004**, *261*, 571-576.

FRACTIONATION OF WOOD USING 1-BUTYL-3-METHYLIMIDAZOLIUM BASED IONIC LIQUIDS

A.V. Ladesov[1], D.S. Kosyakov[1], K.G. Bogolitsyn[1], A.S. Amosov[1], D.I. Falev[1], S.A. Pokryshkin[1]*

[1]*Northern (Arctic) Federal University named after M.V.Lomonosov, Arkhangelsk, Russia*

[*] lokoal13@gmail.com

ABSTRACT

The imidazolium based room temperature ionic liquids are known as promising green solvents for wood dissolution and fractionation leading to obtaining of lignin and polysaccharide parts.

Earlier we proposed two such ionic liquids, 1-butyl-3-methylimidazolium acetate and methylsulfate, as the media with extremely high dissolution power towards lignin and perspective cooking agents for plant biomass chemical treatment.

In present work the treatments of softwood with ionic liquids acetate 1-butyl-3-methylimidazolium and methylsulfate 1-butyl-3-methylimidazolium and their binary mixtures with DMSO at different temperatures were done. It was found that wood is completely dissolved in both ionic liquids and IL-DMSO systems at 150°C. The method of sequential sedimentation of lignin and polysaccharide fractions from solution was proposed. The obtained products were characterized using the IR and NMR spectrometry as well as the pyrolytic gas chromatography mass spectrometry methods. The molecular weight distributions of lignins were determined by size exclusion chromatography. Gaseous products evolved during the treatments were identified by gas chromatography-mass spectrometry technique.

I. INTRODUCTION

To date, it is still impossible to study naturally occurring lignin in its unaltered form, because all known isolation procedures result in chemical modification of its three dimensional network [4,6]. After the first report in 2002 that some ILs can dissolve cellulose, wood scientists were gradually becoming aware of the immense potential of ILs for their research [7]. In 2007, Kilpelainen *et al.* reported the complete dissolution of wood in ILs [6]. The possibility to dissolve lignin in ILs triggered investigations on both the nature and the chemical behaviour of IL-derived lignin [8-11] including studies on the depolymerisation of the IL-dissolved biopolymer [5, 12-15].

Pu *et al.* [16] investigated a range of imidazolium ILs for their ability to dissolve Kraft lignin. In their study, up to 0.2 mass fraction of lignin could be dissolved in ILs containing triflate or methylsulfate anions, and it was suggested that the IL anion dominates the dissolution behaviour. Imidazolium chlorides and bromides were less potent to dissolve Kraft lignin, compared to sulfur containing anions, and both tetrafluoroborates and hexafluorophosphates did not dissolve the polymer. However, the chemical nature of Kraft lignin containing sulfur residues from the pulping process cannot be compared with that of native wood lignin, and caution is required when interpreting these observations [3].

Most ILs with cellulose-dissolving ability also dissolve lignin to a certain degree. This behaviour is exploited to reduce of lignocellulosic biomass towards enzymatic hydrolysis. Especially the IL 1-ethyl-3-methylimidazolium acetate ([EMIM]Ac) has been used to reduce both the lignin content and the crystallinity of biomass prior to its hydrolysis [17, 18].

Only a few reports are available that describe efforts to selectively extract lignin with ILs. Sun *et al.* [1] completely dissolved wood in [EMIM]Ac, isolating up to 0.3 mass fraction of the initial wood lignin by selective precipitation in a mixture of acetone and water. Major drawbacks were long dissolution times (48 h) and a considerable loss of carbohydrates (0.4 mass fraction). In subsequent studies, these authors used polyoxymetalate (POM) catalysts to both reduce the long dissolution times and increase the pulping efficiency. Unfortunately, a number of problems arose, including the loss or degradation of both lignins and carbohydrates, and the instability of the POM catalyst during recycling [19].

Inspired by the effectiveness of sodium xylenesulfonate as a pulping agent in a process known as *hydrotropic* pulping, Tan *et al.* studied the use of 1-ethyl-3-methylimidazolium alkylbenzsulfonates ([EMIM]ABS) to selectively dissolve lignin from sugarcane bagasse. Remarkable lignin extraction yields of up to 0.93 mass fraction were achieved, but at the expense of considerable carbohydrate losses (0.55 mass fraction). More drawbacks include comparatively high extraction temperatures (463 K), the necessity to pretreat the biomass with steam, and difficulties in the recovery of the IL [2].

II. EXPERIMENTAL

2.1 Materials and Instruments

2.1.1 Materials. 1-Butyl-3-methylimidazolium acetate ([BMIM]Ac), 1-butyl-3-methylimidazolium methylsulfate ([BMIM]$MeSO_4$), dimethylsulfoxide (DMSO) were purchased from Fluka. Unless otherwise stated, all reagents were used without further purification. All ILs were dried prior to their use in cellulose dissolution experiments. Water was deionised with a Millipore MilliQ to a final resistivity of 15 MΩcm. Lignin, alkali with a low sulfonate content, was purchased from Sigma Aldrich. Wood samples (*Pinus sylvestris*) were collected from pulp and paper mill in Arkhangelsk.

2.1.2 Instruments. Fourier transform infrared (FT-IR) spectra were recorded on a Bruker Vertex 70 FT-IR spectrometer over a range of (4000 to 400) cm^{-1}. A total of 128 scans at a resolution of 4 cm^{-1} was taken for each sample. Liquid and solid samples were recorded with ATR accessory GladiATR. Nuclear magnetic resonance (NMR) spectra were recorded on a Bruker AVANCE III spectrometer (600 MHz and 150 MHz for ^{1}H and ^{13}C, respectively), using the signals of the residual solvent protons and the solvent carbons as internal references (δ_H 2.6 ppm and δ_C 39.6 ppm for DMSO-d_6). The pyrolytic gas chromatography mass spectrometry was used (Shimadzu GCMS-2010Plus GC-MS system) for determination products of pyrolise of lignin and cellulose, extracting with ionic liquids. Size exclusion chromatography was used (Shimadzu LC-20 Prominence system with SPD-20 UV/Vis detector) for determination of molecular mass distribution.

2.2 Extraction of wood lignin.

All experiments were conducted in N_2 atmosphere. Fifty grams of dried IL was transferred to a 100 mL flask, equipped with a magnetic stirring bar. The IL was heated to 373-423 K, and 0.05 mass fraction of wood was added and stirred at constant temperature for 6 h. A graphical overview of the extraction procedure is provided in Figure 1.

The extraction of wood lignin with a mixture of IL+DMSO was performed in the same manner as the lignin extraction with the pure IL. The only difference was the extraction solvent, now a mixture of 0.8 mass fraction of [BMIM]Ac or [BMIM]$MeSO_4$ and 0.2 mass fraction of dried DMSO.

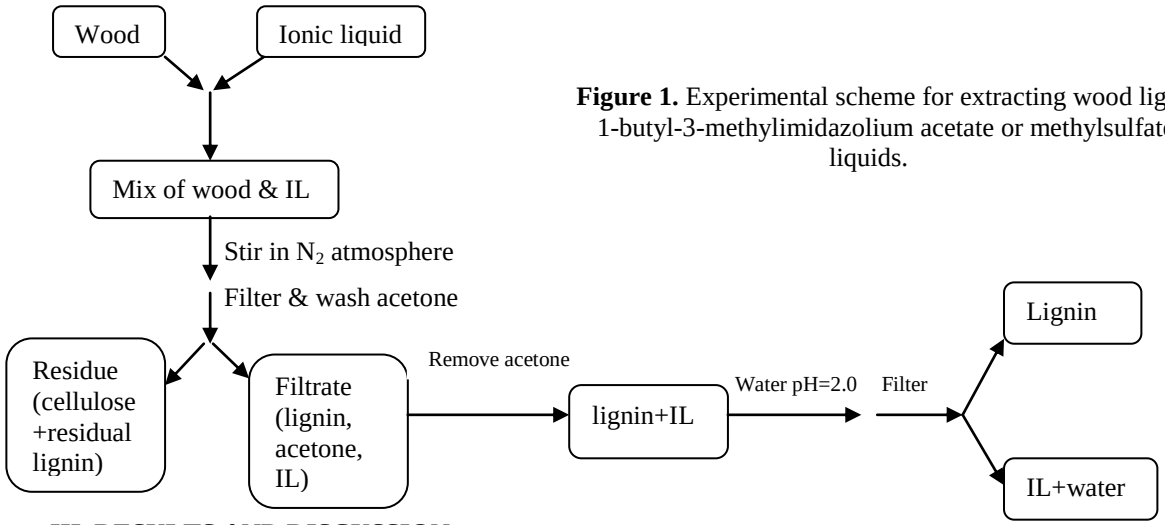

Figure 1. Experimental scheme for extracting wood lignin with 1-butyl-3-methylimidazolium acetate or methylsulfate ionic liquids.

III. RESULTS AND DISCUSSION

Lignin extraction efficiencies, obtained in our experiments, are shown in Table 1.

Table 1. Efficiencies of extraction of wood

Product	Efficiencies of extraction, w, %		
	373 K	393 K	423 K
Lignin	12	15	20
Cellulose	86	80	78

Similarly, the presence of small amounts of a cosolvent with the ability to swell cellulose without dissolving it, such as DMSO can prove beneficial for the overall extraction efficiency. The results show that the addition of DMSO is indeed beneficial for the extraction of wood lignin, increasing the extraction efficiency from e = 0.15 to 0.25, while still maintaining a gentle extraction temperature (393 K) and a short extraction time (6 h). This significantly improved extraction yield, in the presence of DMSO, is potentially due to two factors: loosening the tight H–bond network of wood cellulosics, and decreasing the overall viscosity of the mixture.

Analysis of the IR spectra confirms both extracts as lignin, agreeing with other published data,3 but the results also suggest that there are structural differences between lignin samples, which is attributed to both the different lignin sources and the different extraction methods (Figure 2).

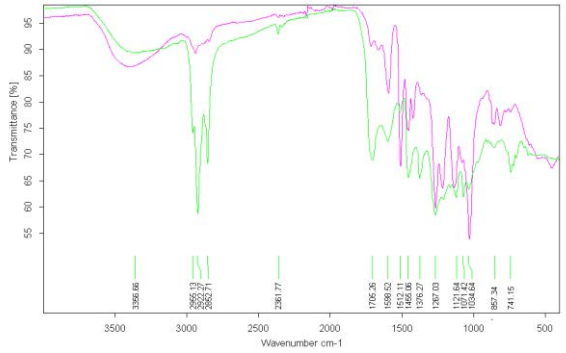

Dioxane lignin (red) and IL-lignin (green)

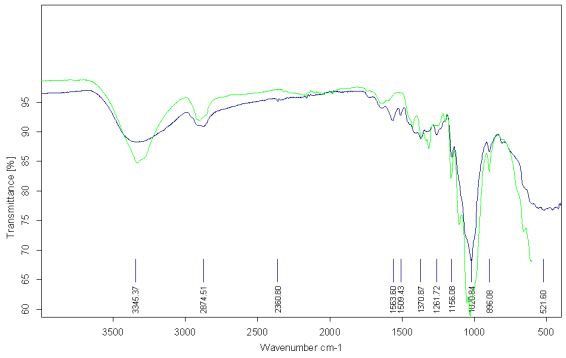

Cellulose (blue) and cotton cellulose (green)

Figure 2. IR spectra of products of extraction

The separated cellulose-rich residues still show bands in the region from (1740 to 1590) cm^{-1}, characteristic for the presence of C=O and C=C bonds and indicating the presence of residual lignin.

Increasing treatment temperatures result in a reduced intensity for a number of bands that are associated with aromatic and ether-containing structures: phenolic OH–groups (3500 to 3200, and 2890) cm^{-1}, aromatic C=C and C–H stretching (1510) cm^{-1}, C–H deformation of $–O–CH_3$, aryl–O–alkyl stretching (1260) cm^{-1}, and C–O stretching of cyclic diaryl ethers (1060) cm^{-1}. All those peaks are also present in the lignin extracts, indicating an increasing degree of wood delignification with increasing extraction temperatures (Figure 2).

Size exclusion chromatography (SEC) is a common method to determine the molar mass of polymers. In our experiments we obtained next average molecular mass: $\bar{M}_w$=5.2x10^3 g·mol^{-1}, $\bar{M}_n$=2.75x10^3 g·mol^{-1}, PDI=2.2

Main functional group of lignin was determinated by NMR. NMR spectra was shown in Figure 3.

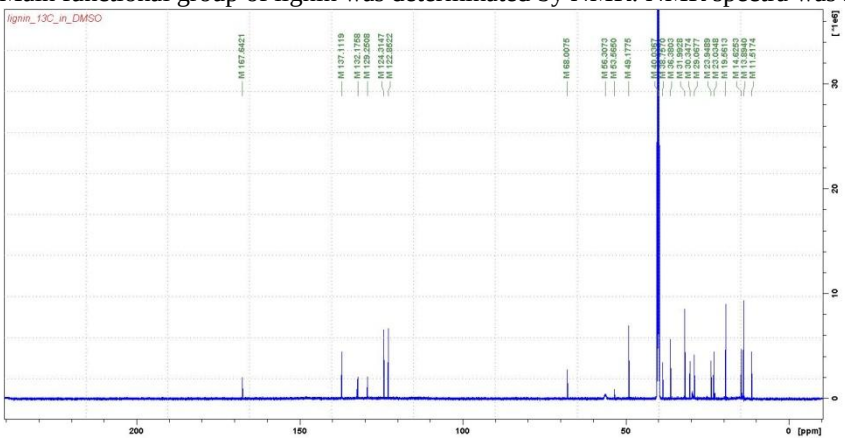

Figure 3. NMR spectra of lignin

The pyrolytic gas chromatography mass spectrometry method is shown (Figure 4), that our products have model lignin compaunds (on figure: 24-eugenol, 30-guaiacol and etc.)

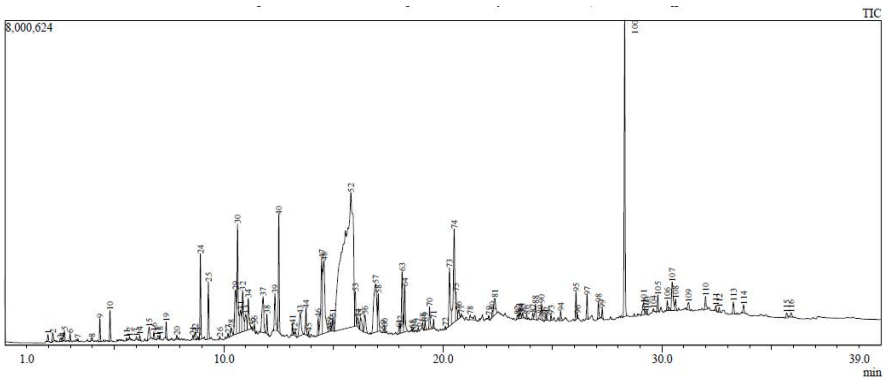

Figure 4 – Gas chromatogramm of lignin

IV. CONCLUSIONS

Imidazolium ILs have the ability to dissolve wood lignin without dissolving cellulose. In particular, 1-butyl-3-methylimidazolium acetate and 1-butyl-3-methylimidazolium methylsulfate exhibits physical properties that are desirable in industrial processing. The extracted lignins possess both a larger average molar mass and a more uniform molar mass distribution compared to lignin obtained from the Kraft process, which is the dominant process for the extraction of lignin in the pulp and paper industry. Viewed from a different perspective, it allows to transform native wood into a lignin-deficient material with an increased cellulose content, but without compromising its crystallinity. IL lignin removal has numerous advantages, compared to prevailing methods, representing an opportunity for future biorefineries—producing renewable feedstock material for aromatic biochemicals and cellulosic biocomposites— with the potential to transform current industries such as the pulp and paper industry. In conclusion, IL extraction of wood lignin holds promising potential for being a low-cost and environmental benign method to obtain both uniform lignins and cellulosic-rich wood residues with a high degree of crystallinity, which can be used for the manufacturing of biocomposites with superior mechanical properties. Although the incorporation of the IL anion into the extracted lignin was only observed at elevated extraction temperatures, this does not imply a nonreactive IL anion in general. IR spectroscopy, NMR spectroscopy are shown that residual lignin have small different from other lignins. In cellulose-rich material was found small quantities of lignin.

V. ACKNOWLEDGEMENT

The authors are greatful to Ministry of Science and Education of Russian Federation for finance support. Research was done using instruments of Core Facility Center of Scientific Equipment “The Arctic” of Northern (Arctic) Federal University named after M.V.Lomonosov

VI. REFERENCES

[1] N.Sun, M.Rahman, Y.Qin, M.L.Maxim, H.Rodriguez and R.D.Rogers, *Green Chem.*, 2009, **11**, 646–655.

[2] S.S.Y.Tan, D.R.MacFarlane, J.Upfal, L.A.Edye, W.O.S.Doherty, A.F.Patti, J.M.Pringle and J.L.Scott, *Green Chem.*, 2009, **11**, 339–345.

[3] J.Gierer, *Wood Sci. Technol.*, 1980, **14**, 241–266.

[4] S.M.Notley and M.Norgren, *The Nanoscience and Technology of Renewable Biomaterials*, ed. L.A.Lucia and O.J.Rojas, John Wiley & Sons, Ltd, Chichester, 2009, ch. 7, pp. 173–205.

[5] K.Stark, N.Taccardi, A.Bosmann and P.Wasserscheid, *Chem-SusChem*, 2010, **3**, 719–723.

[6] I.Kilpelainen, H.Xie, A.King, M.Granstrom, S.Heikkinen and D.S.Argyropoulos, *J. Agric. Food Chem.*, 2007, **55**, 9142–9148.

[7] R.P.Swatloski, S.K.Spear, J.D.Holbrey and R.D.Rogers, *J. Am. Chem. Soc.*, 2002, **124**, 4974–4975.

[8] L.Zoia, A.W.T.King and D.S.Argyropoulos, *J. Agric. Food Chem.*, 2011, **59**, 829–838.

[9] A.W.T.King, L.Zoia, I.Filpponen, A.Olszewska, H.Xie, I.Kilpelainen and D.S.Argyropoulos, *J. Agric. Food Chem.*, 2009, **57**, 8236–8243.

[10] H.Xie, A.King, I.Kilpelainen, M.Granstrom and D.S.Argyropoulos, *Biomacromolecules*, 2007, **8**, 3740–3748.

[11] J.Zakzeski, A.L.Jongerius and B.M.Weckhuysen, *Green Chem.*, 2010, **12**, 1225–1236.

[12] J.B.Binder, M.J.Gray, J.F.White, Z.C.Zhang and J.E.Holladay, *Biomass Bioenergy*, 2009, **33**, 1122–1130.

[13] S.Jia, B.J.Cox, X.Guo, Z.C.Zhang and J.G.Ekerdt, *Chem-SusChem*, 2010, **3**, 1078–1084.

[14] J.Songyan, B.J.Cox, G.Xinwen, Z.C.Zhang and J.G.Ekerdt, *Holzforschung*, 2010, **64**, 577–580.

[15] B.J.Cox, S.Jia, Z.C.Zhang and J.G.Ekerdt, *Polym. Degrad. Stab.*, 2011, **96**, 426–431.

[16] Y.Pu, N.Jiang and A.J.Ragauskas, *J. Wood Chem. Technol.*, 2007, **27**, 23–33.

[17] S.H.Lee, T.V.Doherty, R.J.Linhardt and J.S.Dordick, *Biotechnol. Bioeng.*, 2009, **102**, 1368–1376.

[18] D.Fu, G.Mazza and Y.Tamaki, *J. Agric. Food Chem.*, 2010, **58**, 2915–2922.

[19] N.Sun, X.Jiang, M.L.Maxim, A.Metlen and R.D.Rogers, *ChemSusChem*, 2011, **4**, 65–73.

NANOPARTICLE FILLERS OBTAINED FROM BARK FOR THEIR USE IN PAPER COATINGS

Marianna Laka*, Arnis Treimanis, Svetlana Chernyavskaya, Marite Skute, Linda Rozenberga

*Latvian State Institute of Wood Chemistry, 27 Dzerbenes Str., LV-1006 Riga, Latvia (*lamar@edi.lv)*

ABSTRACT

The effect of coatings, obtained from unextracted and extracted bark nanoparticle gels as well as their mixtures with chitosan solution in 1% acetic acid, on barrier and mechanical properties of paper sheets was investigated. For obtaining the nanoparticle gels, the bark was destructed by the thermocataytic method and then dispersed in water medium in a ball mill. The obtained gels contained nanoparticles with dimensions ~300 nm. Coatings were made on both sides of paper sheets produced by the Ligatne Paper Mill (Latvia). It has been established that Gurley air resistance increases with increasing thickness of the coatings obtained from pure bark nanoparticle gel and with increasing gel concentration. At the gel concentration 10% and coating thickness 34.5 μm, the air resistance in the case of unextracted and extracted black alder bark increases by 57 and 72%, respectively, in comparison with the case of uncoated paper sheets. The coatings from mixtures of bark nanoparticle gels and chitosan solutions essentially increase the air resistance. At a coating thickness of 20μm and a nanoparticle content of 30% in the coatings, the air resistance increases 425 times. Investigating the effect of coatings on mechanical properties, it has been found that coatings from bark nanoparticle gel improve the burst and tensile strength in a dry state (in the latter case, till the gel concentration 6%). The coatings from mixtures with chitosan improve all investigated mechanical properties. The coatings increase the water vapour sorption of paper sheets.

I. INTRODUCTION

The residues that remain after the mechanical processing of wood are commonly used as a fuel. However, it would be more attractive to process them so that they could be used in composites with other materials, for example, with papers to improve their properties. There are a lot of publications in which it has been established that coatings improve the barrier properties of papers. Thus, chitosan-caseinate bilayer coatings lead to a decrease in the water vapour permeability (WVP) of paper sheets [1]. Chitosan coatings improve also the gloss, oxygen barrier properties and water absorption capacity [2,3]. In the same manner, the use of microfibrillated cellulose (MFC) as a surface coating on various papers considerably reduces the air permeability and improves the oil barrier properties of papers [4]. It is because the coating agent fills the pores between the cellulose fibres in paper sheets and makes their structure denser. In the present work, nanoparticle gels obtained from black alder bark were used in coatings for paper to improve its barrier properties.

II. EXPERIMENTAL

Unextracted bark and that extracted in biorefinery were used as a raw material for production of nanoparticle gels. The bark was destructed by a thermocatalytic method developed at our Institute [5]. According to this method, the bark was impregnated with a weak hydrochloric acid and thermally treated at 120^{o}C until a dry state. Then the partially destructed bark was dispersed in water medium in a ball mill. Gel-like dispersions were obtained, which contained nanoparticles with dimensions of around 300 nm. Coatings were made on both sides of the paper sheets produced by the Ligatne Paper Mill (Latvia). Those were made by pure bark nanoparticle gels at concentrations of 4–10 % as well as by mixtures of the nanoparticle gels with chitosan solution in acetic acid. The chitosan solution and nanoparticle gel concentration in mixtures was 2%. In the suspension form, the coatings' thickness was 24, 40, 60 and 100 μm. Owing to the partial diffusion of the gel into the paper pores and water evaporation, the coatings' thickness after drying decreased approximately by 30%. Air resistance according to Gurley (SCAN-P 19) was determined using a L&W Air Permeance Tester. Besides, the mechanical properties such as tensile strength (ISO 1924-1:1992 (E)) and burst strength (ISO 2758-1983 (E)), as well as water vapour sorption of paper sheets with coatings were investigated. Water vapour sorption was investigated at a relative air humidity of 95%. The samples of paper sheets were weighed, held in an exicator till the equilibrium state and weighed again.

III. RESULTS AND DISCUSSION

Figure 1 demonstrates the Gurley air resistance versus thickness of coatings made from a 6% extracted black alder bark nanoparticle gel. It can be seen that the air resistance increases with increasing thickness of coatings from the bark nanoparticle gel. In the case of the 34.5 µm thickness of the coatings obtained using a 6% black alder nanoparticle gel, the air resistance increases by 35% in comparison with the case of uncoated paper sheets. It is because the bark nanoparticles cover the micro and submicrovoids between the fibres and fibrils, and increase the barrier properties. With increasing coating thickness, the tensile strength and burst strength of paper sheets also increase (**Figure 2**, curves 1 and 2). At the coating thickness 34.5µm, the tensile strength and burst strength increase by 12.6 and 27.7%, respectively. However, the tensile strength in a wet state, with increasing coating thickness, decreases (**Figure 2**, curve 3). At the coating thickness 34.5 µm, the tensile strength in a wet state decreases by 11%. It can be explained by the fact that the nanoparticle gel films are more hydrophylic than the cellulose fibres.

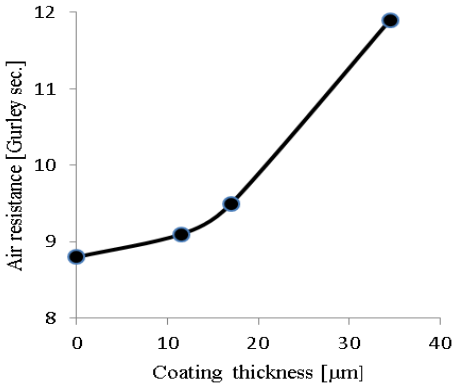

Figure 1. Gurley air resistance versus thickness of coatings made from 6% extracted black alder nanoparticle gel.

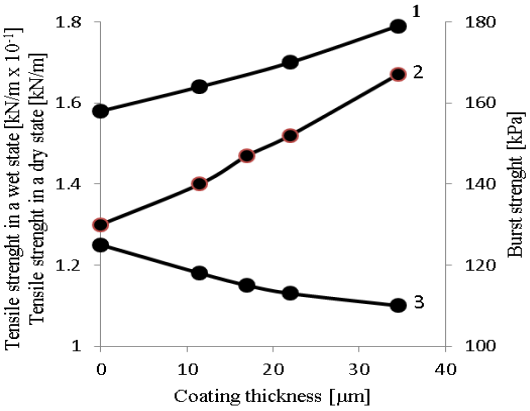

Figure 2. Tensile strength in a dry state (1), burst strength (2) and tensile strength in a wet state (3) of paper sheets versus thickness of coatings made from 6% extracted black alder nanoparticle gel.

Gurley air resistance increases with increasing concentration of the bark nanoparticle gel (**Figure 3**, curves 1 and 1a). At the gel concentration 10% and coating thickness 34.5 µm, the air resistance in the case of unextracted and extracted bark increases by 57 and 72%, respectively, in comparison with the case of uncoated paper sheets. The higher air resistance for extracted bark can be explained by the fact that the extractives hinder the binding formation between the bark nanoparticles and cellulose fibres. The sorption of paper sheets increases with increasing bark nanoparticle gel concentrations due to the greater hydrophylity of nanoparticle films (**Figure 3**, curves 2 and 2a). The tensile strength in a dry state and a wet state decreases with increasing nanoparticle gel concentration (**Figure 4**, curves 1, 1a, 3), while the burst strength changes little (**Figure 4** curves 2, 2a). Tensile strength and burst strength are greater when the coatings are made from extracted bark gels.

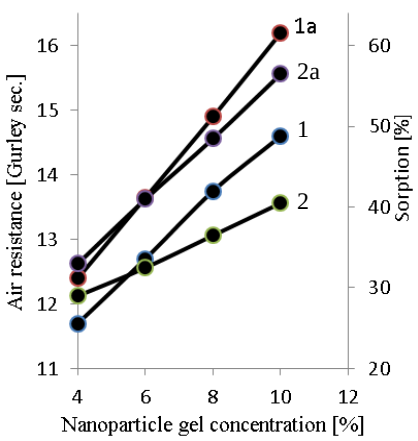

Figure 3. Gurley air resistance (1, 1a) and water vapour sorption (2, 2a) of paper sheets with 34.5 µm thick coatings versus alder bark nanoparticle gel concentration. a – extracted bark.

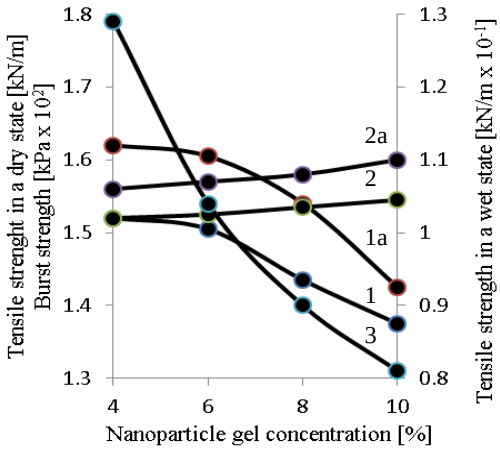

Figure 4. Tensile strength in a dry state (1, 1a), burst strength (2, 2a) and tensile strength in a wet state (3) of paper sheets with 34.5 µm thick coatings versus alder bark nanoparticle gel concentration. a – extracted bark.

The coatings made from mixtures of black alder bark nanogels with chitosan solutions essentially improve the barrier properties. It is because chitosan ensures more homogenous coatings and higher degree of adhesion. **Figure 5** shows the dependences of Gurley air resistance and mechanical indices on the coating thickness in the case of mixtures, which contain 70% of chitosan and 30% of unextracted black alder bark nanoparticles. It can be seen that air resistance and mechanical indices increase with increasing coating thickness. Thus at a coating thickness of 20 μm, air resistance increases 425 times. Tensile strength in a dry state and a wet state, and burst strength increase 1.5, 3.4 and 2 times, respectively.

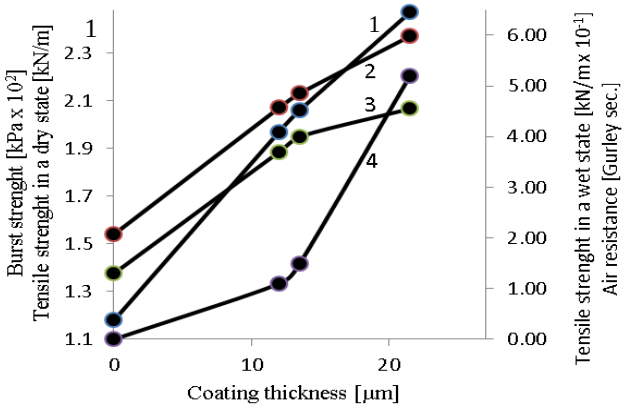

Figure 5. Burst strength (1), tensile strength in a dry state (2), tensile strength in a wet state (3) and Gurley air resistance(4) versus thickness of coatings made from mixtures of unextracted black alder nanoparticle gel and chitosan solution. Coatings contain 70% of chitosan and 30% of bark nanoparticles.

With increasing nanoparticle content in the mixture, air resistance decreases (**Figure 6**, curve 1), and at a nanoparticle content of 70% (air resistance is 50 Gurley sec), is only 5 times higher than that in the case without coatings. The sorption properties, with increasing nanoparticle content in the mixtures, decrease (**Figure 6**, curves 2 and 2a). The mechanical indices, with increasing nanoparticle content till 30%, change little, then fall dramatically **(Figure 7)**, although remaining higher than those for uncoated paper sheets.

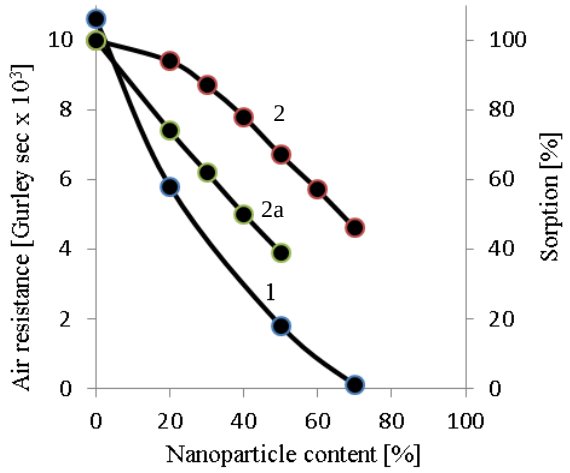

Figure 6. Gurley air resistence (1) and water vapour sorption (2, 2a) of paper sheets with 20 μm thick coatings versus the black alder bark nanoparticle content in the coatings.
a – extracted bark

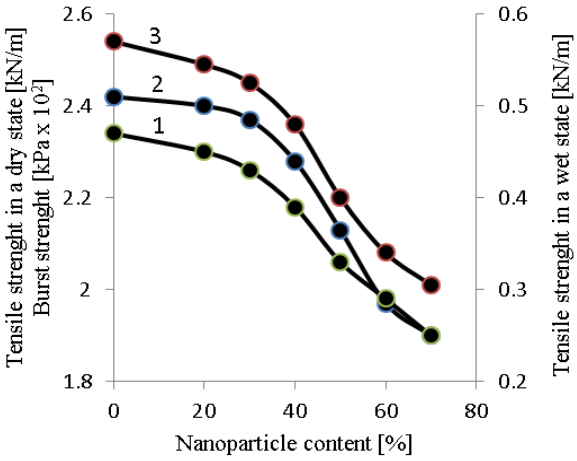

Figure 7. Tensile strength in a wet state (1), tensile strength in a dry state (2) and burst strength (3) of paper sheets with 20 μm thick coatings versus the unextracted black alder nanoparticle content in the coatings.

IV. CONCLUSIONS

The coatings made from black alder bark nanoparticle gels improve the paper barrier properties in respect to Gurley air resistance.

The barrier properties increase with increasing coating thickness and nanoparticle gel concentration.

The coatings made from mixtures of bark nanoparticle gels and chitosan acetic solution improve the barrier properties to an essentially greater extent, which is connected with a greater coating homogeneity and a higher degree of adhesion.

V. ACKNOWLEDGEMENT

The research leading to these results has received funding from the National Research Programme 2010-2013 „Sustainable Use of Local Resources (Entrails of the Soil, Forest, Food and Transport) – New Products and Technologies" (Nat Res).

VI. REFERENCES

[1] Khwaldia, K.; Basta, A. H.; Aloui, H.; El-Saied, H. Chitosan-caseinate bilayer coatings for paper packaging materials. *Carbohyd. Polym.* **2014**, *99*, 508–516.

[2] Vartiaine, J.; Motion, R.; Kulonen, H.; Ratto, M.; Skytta, R.; Ahvenainen, R. Chitosan-coated paper: Effects of nisin and different acids on the antimicrobial activity. *J. Appl. Polym. Sci.* **2004**, *94*, 986–993.

[3] Reis, A. B; Yoshida, C. M. P; Reis, A. P. C.; Franco, T. T. Application of chitosan emulsion as a coating on Kraft paper. *Polym. Int.: Special Issue: Advances in Chitin and Chitosan Research* **2011**, *6*, 963–969.

[4] Aulin, C.; Gaelstedt, M. Oxygen and oil barrier properties of microfibrillated cellulose films and coatings. *Cellulose* **2010**, *17*, 559–574.

[5] Laka, M.; Chernyavskaya, S. Method of obtaining microcrystalline cellulose, Latvian Republic Patent No. 11184. *Patents and Trademarks* **1996**, *4*, 878.

CHEMICAL ANALYSIS AND FRACTIONAL SEPARATION OF SPENT LIQUORS FROM PULP AND PAPER INDUSTRY

Sabrina Laun[1], Ilka Lehmann[1], Helga Mölleken[1], Hans-Willi Kling[1]*

[1]*University of Wuppertal, Communication and Management of Chemical Processes in Industry, 42119 Wuppertal, Germany (*kling@uni-wuppertal.de)*

ABSTRACT

In this research different spent liquors were examined; a kraft liquor, a sulfite liquor and an organosolv liquor. The three liquors were characterised and compared by different analytical parameters, e.g. ash-, lignin- and sulfur content.
For fractionation of kraft liquor a pH shift was used. To generate a precipitate enriched with lignin, hydrochloric acid (6 M) was added to decrease the pH to different values (pH 10, pH 6, pH 4, pH 2). These precipitates were analysed in terms of fractional yield, behavior on incineration and structural changes of the separated lignin. The results show that separated fractions were almost free of inorganics. Some structural changes are shown in ^{1}H-NMR. Due to the increase of the number of aromatic hydrogen in relation to methoxy-groups, the aliphatic signals in ratio to methoxy-signals decrease with stronger acidification.

I. INTRODUCTION

Chemical pulping is one of the most important processes in paper industry. Wood delignification takes place under alkaline, neutral or acidic conditions. The resulting liquors consist of different ingredients for example lignin, carbohydrates and inorganic [1]. Currently, the most common procedures are sulfite and kraft pulping, however, the use of organosolv pulping has increased considerably in recent years. During the pulping procedure, only up to 50 % of the utilised wood yields pulp, while the remainder accrues as spent liquor [1]. After a thickening process, most of the spent liquors are burned in order to recycle inorganic agents and to generate energy [2,3]. From an economical and ecological point of view the use of spent liquors as a renewable resource is desirable, due to the phenolic structures of lignin degradation products.
For industrial applications of lignin as a renewable resource a comparable composition and similar physico-chemical properties among various batches are necessary.
Although a large number of methods are available to determine functional groups [4,5], these methods often vary in scope and are not the most suitable for the analysis of such complex samples.
In this work three liquors of different processes (kraft-, organosolv- and sulfite process) have been characterised and compared by different analytical techniques in order to identify the composition of such complex mixtures. Due to the differences in several batches, a fractionation of spent liquors is required to get comparable "products" for use as renewable resources. Therefore kraft liquor was fractionated by pH reduction and the fractions were characterised.

II. EXPERIMENTAL

For magnesium-based acidic sulfite pulping (sulfite liquor) 50 % spruce and 50 % beech wood were used. Kraft liquor originates from pulping of 70 % spruce and 30 % pine wood. Organosolv liquor was also characterised.
Fine chemicals were purchased from Sigma-Aldrich and Merck KGaA.

Analysis of spent liquors and fractions

Dry matter content of spent liquors was determined by oven drying at 105 °C for 48 h [6]. For thermogravimetric analysis the samples were incinerated by a muffle furnace in steps of 50 °C for 1 h to a maximum temperature of 600 °C.

The quantification of optical active lignin degradation products was carried out on a Thermo Heλios Gamma UV/VIS spectrometer at 278 nm [7]. Therefore, dry solids were dissolved in 10 mM NaOH (kraft liquor) or in 100 mM HCl (sulfite liquor). The calibration was carried out by isolated lignins.
For the isolation of lignin degradation products from liquors established methods have been used [8,9].
A Varian ICP-OES 720-ES was used for elemental analysis of heavy metals and sulfur. The samples (300 mg/L in diluted nitric acid) were filtered. The calibration of the system was performed with a multi-element standard (solution 4, Merck KGaA).
The NMR spectra were obtained on a Bruker Avance III 600 instrument. Approximately 50 mg of each fraction was dissolved in 3 M NaOD in D_2O.

Fractionation of kraft liquor

For the fractionation of kraft liquor established methods have been used [9].
Kraft lignin was isolated from industrial kraft black liquor by precipitation with hydrochloric acid (6 M) to pH 10, pH 6, pH 4 and pH 2. The filtrate was dried and washed with MeOH. The precipitates were filtered and washed with a corresponding pH-dilution (expection: pH 10) and finally dried at 105 °C.

III. RESULTS AND DISCUSSION

Characterisation of spent liquors

Table 1 shows the characteristic features of the examined spent liquors. The varieties between the spent liquors could be explained by the different pulping processes and may result out of the biodiversity of wood.

Table 1. Main characteristics of examined spent liquors

Properties		**Kraft liquor**	**Organosolv liquor**	**Sulfite liquor**
colour		dark brown to black	brown	brown to dark brown
odor		pungent	intense aroma of almonds	intensive
pH-value		12,9	2,4	4,6
dry solid (105 °C)		17 %	7 %	16 %
lignin content (278 nm) (related to dry matter)		32 %	not measured	51 %
ash content (450 °C) (related to dry matter)		73 %	2 %	45 %
S - content (related to dry matter)		4,2 %	0,2 %	7,2 %
metal content (related to dry matter)	K	1,5 %	0,1 %	0,2 %
	Ca	0,4 %	1,4 %	0,3 %
	Mg	0,1 %	0,3 %	4,5 %

The results show that there is a correlation between ash and lignin content. During the incineration at 450 °C the major amount of lignin has been decomposed.

The sulfur and metal content corresponds to the used pulping chemicals of the pulping processes. According to literature, in sulfite liquor sulfur is available as lignin sulfonates, while in kraft liquor sulfur is probably not bonded to lignin degradation products [10,11].

Fractionation of kraft liquor

For the use of spent liquors as source of renewable resources, a comparable composition and similar physico-chemical performance is very important. Due to the significant changes between different batches of a spent liquor, a fractionation of this liquor is inevitable.
Therefore, kraft liquor was precipitated up to different pH values (pH 10, pH 6, pH 4, pH 2). The effects of various pH values on the yield of the lignin fractions are presented in table 2.

Table 2. Yields of the kraft liquor fractions

pH value	**yield [%]** (related to dry matter of kraft liquor)
10	13
6	35
4	37
2	38
2 (without washing the precipitate)	54

The precipitation up to pH 2 with and without washing shows that it is necessary to wash the precipitates with the corresponding pH-solution to remove impurities. Results indicate that the majority of lignin was separated at pH > 6, afterwards only a small amount was precipitated. So it can be assumed that a precipitation of kraft liquor to pH 6 is sufficient.
A comparison of the thermogravimetric analysis, shown in figure 1, reveals comparable properties of the fractions of pH 6 and pH 4, however the ash content of pH 2 decreases more than the others.
The changes in composition of the fractions are also noticed at the rate of methoxy-, aliphatic and phenolic hydrogen, which were analysed by ^{1}H-NMR (600 MHz). The signals around 2.7-3.8 ppm can be assigned to the number of hydrogen in methoxy-groups, the aromatic signals have been found at 6.0-7.5 ppm and the aliphatic ones are localised at 0.0-2.3 ppm (Fig.2).

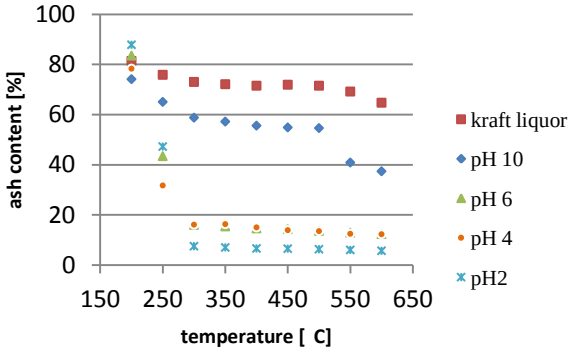

Figure 1. Thermogravimetric analysis – steps of 50 °C for 1h

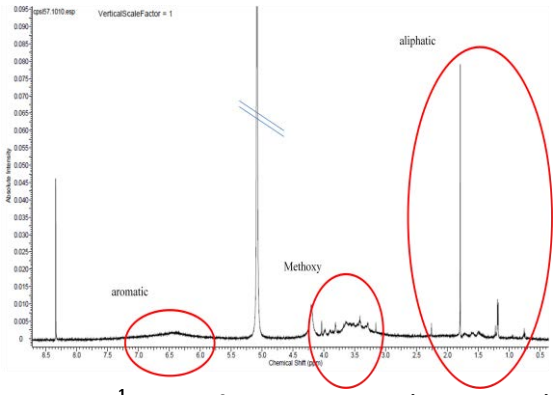

Figure 2. ^{1}H-NMR of pH 10 precipitate (NaOD in D_2O)

Based on different precipitation pH values, the corresponding ^{1}H-NMR spectra shows different signal intensities in the characteristic regions of molecular functions. In comparison of the integration areas of methoxy- with aromatic signals a ratio of 3:1.01 (kraft lignin), 3:1.42 (pH 10) and 3:1.85 (pH 2) and a methoxy- with aliphatic signal ratio of 3:2.67 (kraft lignin) 3:1.67 (pH 10) and 3:0.97 (pH 2) were determined.

IV. CONCLUSIONS

Industrial spent liquors of the important processes in paper industry like kraft pulping and acidic magnesium-based sulfite pulping as well as the innovative organosolv pulping have been characterised and compared by different analytical techniques, in order to identify their chemical composition.

Depending on the process, spent liquors contain high amounts of lignin, which correlates with the ash content. Due to the use of sulfur compounds in the kraft and sulfite pulping, the sulfur contents of about 4 % and 7 % are explainable.

The ash content in fractions of kraft liquor decrease proportional with the pH reduction, assuming that the precipitate is relatively free from impurities. This is confirmed by the results of ^{1}H-NMR. It is shown that aromatic hydrogen increase in relation to the methoxy-groups, while aliphatic protons decrease with stronger acidification.

V. ACKNOWLEDGEMENT

Industrial thick spent liquors from magnesium-based acidic sulfite pulping were provided by Sappi Alfeld mill (Alfeld, Germany). The kraft liquor was supplied by Zellstoff- und Papierfabrik Rosenthal GmbH (Blankenstein, Germany). The organosolv liquor is courtesy of Fraunhofer Zentrum für Chemisch-Biotechnologische Prozesse CBP (Leuna,Germany).

VI. REFERENCES

[1] Sixta,H. Handbook of Pulp. Wiley-VCH, Weinheim **2006**

[2] Gosselink,R.J.A.; de Jong,E.; Guran,B.; Abächerli,A. Coordination network for lignin – standardisation, production and applications adapted to market requirements (EUROLIGNIN). *Ind. Crop. Prod.* **2004**, *20*, p.121-129

[3] Lora,J.H.; Glasser,W.G. Recent Industrial Applications of Lignin: A Sustainable Alternative to Nonrenewable Materials. *J. Polym.Environ.* **2002**, *10*, p.39-48

[4] Lin,S.Y.; Dence,C.W. Methods in lignin chemistry. Springer-Verlag, Berlin, Heidelberg **1992**

[5] Sjöström,E.; Alen,R. Analytical Methods in Wood Chemistry, Pulping and Papermaking. Springer-Verlag Berlin, Heidelberg **1999**

[6] TAPPI. TAPPI Test Methods 1998-1999. TAPPI Press, Atlanta **1998**

[7] Marques, A.P.; Evtuguin,D.V.; Magina,S.; Amado,F.M.L.; Prates,A. Chemical Composition of Spent Liquors from Acidic Magnesium-Based Sulphite Pulping of Eucalyptus globulus. *J Wood Chem Technol* **2009**, *29*, p.322–336.

[8] Ringena,O. Isolation and fractionation of lignosulfonates by amine extraction and ultrafiltration: A comparative study. *Holzforschung* **2005,** *59(4)*, p.405-412

[9] Pastusiak,R. Charakterisierung von Zellstoffkomponenten - Analytik, Spektroskopie, Reaktionskinetik, Modellierung. Dissertation Technische Universität München **2003**

[10] Gierer,J. The Chemistry of Delignification. *Holzforschung* **1982,** 36 (1), p.43-51

[11] Björsvik, H.-R.; Liguori,L. Organic processes to pharmaceutical chemicals based on fine chemicals from lignosulfonates. *Organic Process Research & Development* **2002**, 6, p.279-290

EFFECT OF WET TORREFACTION PRETREATMENT ON THE COMPOSITION OF BIO-OIL FROM FOREST BIOMASS

Étienne Le Roux[1]*, Papa Niokhor Diouf[2], Tatjana Stevanovic[1]

*[1] Centre de Recherche sur les Matériaux Renouvelables, Departement of Wood and Forest Science, Faculty of Forestry, Geography and Geomatic, Laval University, Quebec City, Quebec; [2] Service de recherche et d'expertise en transformation des produits forestiers (SEREX), Amqui, Quebec (*etienne.le-roux.1@ulaval.ca)*

ABSTRACT

Fast pyrolysis is a promising technology to promote wood biomass utilisation. This thermochemical process produces mainly a liquid product, called bio-oil which could serve as a feedstock for chemicals and fuels.
The wet torrefaction was performed as a pretreatment on trembling aspen (hardwood) and white spruce (softwood) with an aim to improve the quality of the pyrolysis oil. Bio-oil composition, product distribution and relative amount of the pretreated biomass and of the original raw material were investigated by analytical pyrolysis coupled with gas chromatography/mass spectrometry (Py-GC/MS). The identified products issued from pyrolysis could be classified in eight chemical groups: phenolics, anhydrosugars, furans, pyrans, acids, fatty acids, ketones, and aldehydes.
Wet torrefaction pretreatment increased the yield of bio-oil, indicating that this pretreatment enhances the woody biomass conversion through fast pyrolysis. The analysis of the pyrolysis products composition revealed that the phenolics were the predominant products in bio-oil produced from both original and pretreated wood. The wet torrefied wood pyrolysis yielded higher anhydrosugars. Moreover, the anhydrosugars production seemed to increase significantly with increase of pretreatment severity.

I. INTRODUCTION

Ever growing number of studies has been reported on biomass fast pyrolysis [1]. The major product of this process is a liquid called pyrolysis oil or bio-oil. It has been proven that bio-oil could replace fossil resources as chemical feedstock or energy carrier. However, due to the complex nature of lignocellulosic biomass, some of the physical and chemicals properties of the pyrolytic oil impede its direct application. Some improvements could be brought about the reactor design or directly on bio-oil in order to correct this situation. The pretreatment of the biomass represents an interesting alternative. A number of studies have shown that a wet torrefaction treatment removed hemicelluloses and ash from lignocellulosic biomass [2,3]. The acidity and the instability of the bio-oil are mainly related to the ash content and hemicelluloses transformation products. Therefore, the wet torrefaction process could represent a path to improvement of pyrolysis oil quality through modification of biomass chemical composition by pretreatment. The effect of wet torrefaction of wood on the composition of bio-oil has been studied by analytical pyrolysis coupled with gas chromatography/mass spectrometry (Py-GC/MS). Py-GC/MS has usually been performed to investigate the structure of wood components, in particular lignins [4]. However, there are few GC/MS studies on the impact of pretreatment on both wood composition and bio-oil composition.

The analytical pyrolysis was designed as to simulate the fast pyrolysis applied in bio-oil production. It was performed on two wood species, trembling aspen *(Populus tremuloides)* and white spruce (*Picea glauca*), which had previously undergone wet torrefaction at different severity levels. Since the Py-GC/MS was carried out in order to simulate a fast pyrolysis process, its results could be useful for predicting the bio-oil yield and its chemical composition.

II. EXPERIMENTAL

Wood biomass

The forest biomasses used for this study were trembling aspen and white spruce in form of chips. They were received oven dried to 8% moisture content. It is noteworthy that wood chips contained also some bark.

Wet torrefaction

Each severity factor, S, corresponds to a specific wet torrefaction temperature. Thus S=0 corresponds to the original non-treated raw wood, S=3.9 stands for wood pretreated by wet torrefaction at 175°C, S=4.6 for wood pretreated at 195°C, and S=5.2 for wood pretreated at 215°C [5].

Py-GC/MS

The analytical pyrolysis was performed using a CDS Pyroprobe 2000 heated coil pyrolyzer. The fast pyrolysis was achieved at 350°C–400°C–450°C–500°C for trembling aspen and at 400°C–450°C–500°C–550°C for white spruce. This study was focused on pyrolysis performed with a heating rate of 1000°C/min. The previous analysis was carried out at heating rate of 100°C/min but it appeared that an increase of heating rate enhanced the effect of the pretreatment. About 0.15 mg of biomass sample was pyrolyzed during 3 min. The pyrolysis products were separated in capillary column VF-5 ms. Helium was the carrier gas with a flow rate of 1 mL/min. The column oven program was the following: isothermal for 4 min at 45°C, then the temperature increased to 250°C (5°C/min) and then held during 10 min. Afterwards the gas was set into a mass spectrometer operating in Electron Ionization mode at 70 eV. The mass spectra were obtained from m/z 40 to 400 with a scan rate of 1 scan/s. All samples were pyrolyzed twice.

The identification of the chromatographic peaks was based on the NIST library and on the data available in the literature [6]. For each significant peak, an average peak area and average relative intensity were calculated. The peak area values were divided by the weight of the corresponding sample to remove its influence.

III. RESULTS AND DISCUSSION

Effect of wet torrefaction on bio-oil yield

The evolution of the bio-oil yield could be evaluated on the basis of the total peak area value, e.g. the production of pyrolysis vapors. The results according to the severity and the pyrolysis temperatures are displayed in **Figure 1**.

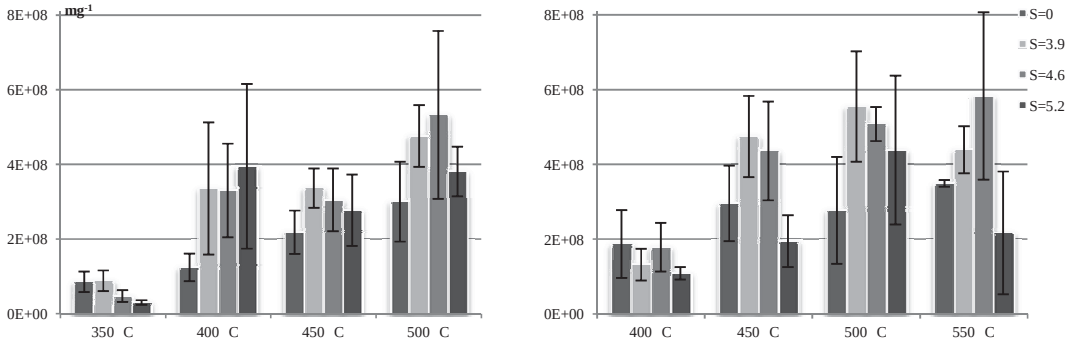

Figure 1. Total peak area values from fast pyrolysis of trembling aspen (left) and white spruce samples (right)

The increase due to the wet torrefaction was shifted to higher pyrolysis temperatures for spruce when compared to aspen. There was no noticeable difference between the severities for hardwood while for softwood the higher severity yielded a lower production of vapors.

Effect of wet torrefaction on bio-oil composition

The relative amount of identified peaks could be taken to predict the bio-oil chemical composition. The pyrolysis products are regrouped in eight chemical families: phenolics, anhydrosugars, furans, pyrans, acids, fatty acids, ketones, and aldehydes.

Phenolics were the main chemical group identified from both spruce and aspen pyrolysis. For hardwood, the relative amount of phenolics peaks decreased with the increase of pyrolysis temperatures: from 66% at 350°C to 46% at 500°C. The wet torrefaction pretreatment seems to amplify this effect: at 500°C the phenolics content decreased from 46% for S=0 to 34% for S=5.2. The relative amount of phenolics peaks from spruce pyrolysis has not been determined to vary with pyrolysis temperature.

The second largest chemical group among the identified peaks is represented by anhydrosugars. For both woods, the pretreated samples yielded higher anhydrosugars content upon pyrolysis than the raw samples. The highest severity seemed to have the greatest impact in that relation. Thus, for spruce at 500°C, the anhydrosugars content

increased from 15% for S=0 to 23% for S=5.2. Anhydrosugars content was generally higher for pyrolysis of softwood than for hardwood.

Concerning furans, it seemed that pretreatment had little effect on their generation through pyrolysis. As for fatty acids, although the standard deviations were large, these were important constituents released by pyrolysis from raw wood. However, the pretreatment seemed to reduce their contents. Wet torrefaction appeared to affect acids content more in aspen pyrolysis vapors than in spruce. More severe pretreatments seem to contribute to the lower acid content in the pyrolysis products.

Effect of wet torrefaction on production of pyrolysis products

To understand better the impact of pretreatment on pyrolysis vapors production, an assessment of the total peak area values for each chemical group had been done.

As shown in **Figures 2 and 3**, the pretreatment seems to promote the production of phenolics. However, the lower phenolics content obtained from harshly pretreated aspen and pyrolyzed at high temperatures could be partially explained by the decrease of production of both syringol derivatives and guaiacol derivatives. The lower production of guaiacol derivatives was also observed from spruce pyrolysis for the harsh pretreatment.

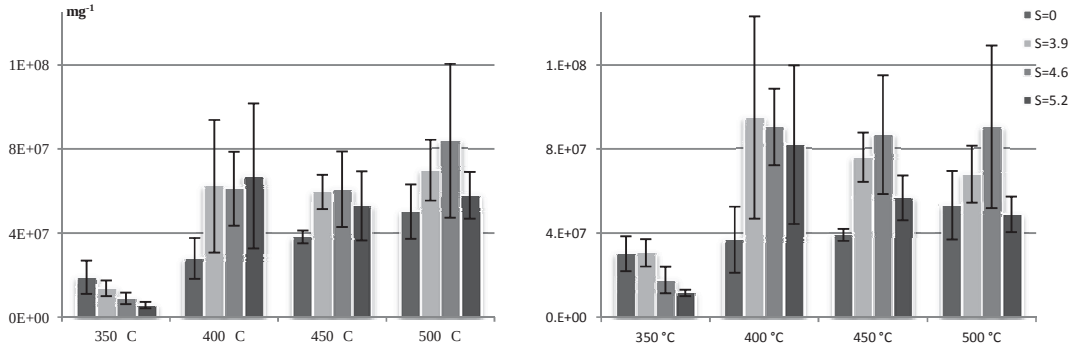

Figure 2. Total peak area values of guaiacol (left) and syringol derivatives (right) from fast pyrolysis of trembling aspen

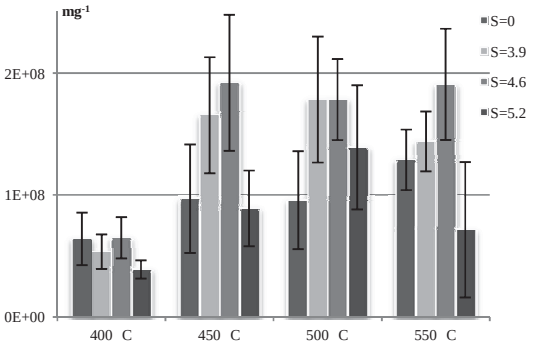

Figure 3. Total peak area values of guaiacol derivatives from fast pyrolysis of white spruce

The main anhydrosugar identified was levoglucosan. As shown in **Figure 4**, pretreatment affected the production of levoglucosan, but in different ways for hardwood and softwood.

For aspen, the yield of low temperature pyrolysis products increased greatly when applied to the biomass pretreated at high severity factor. The yield increased significantly at higher temperatures, even for the moderate wet torrefaction pretreatment.

For spruce, except for the pyrolysis performed at 500°C, the wet torrefied samples under harsh conditions seemed to give the lowest bio-oils yields.

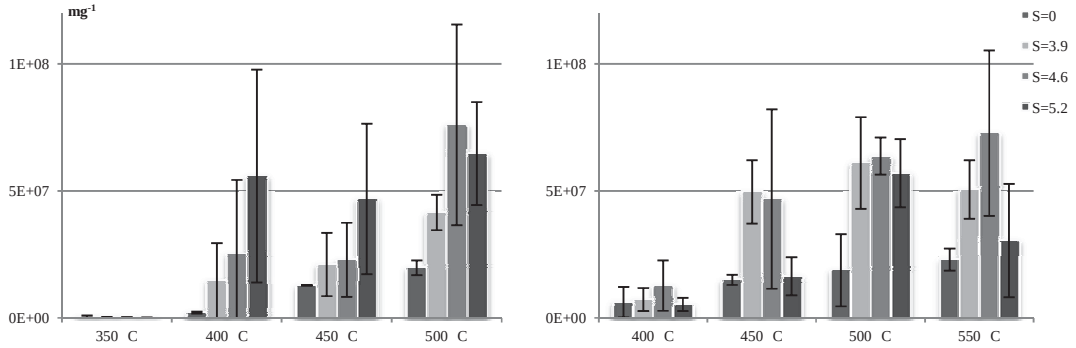

Figure 4. Total peak area values of levoglucosan from fast pyrolysis of trembling aspen (left) and white spruce samples (right)

IV. CONCLUSIONS

To improve the bio-oil quality, actions could take place before, during or after the fast pyrolysis. In this study, pretreatment of the biomass had been chosen to modify the composition of the biomass and consequently the composition of the bio-oil.

The analytical pyrolysis was performed to reproduce the thermal degradation occurring in a fast pyrolysis process. It allowed studying the influence of wet torrefaction on the chemical distribution and composition of the bio-oil. First, it has been shown that pretreatment could improve the production of pyrolysis vapors and consequently the yield of pyrolitic bio-oil. Eight chemical groups have been identified among pyrolysis products: phenolics, anhydrosugars, furans, pyrans, fatty acids, acids, ketones and aldehydes.

The major impact of pretreatment seems to be on the formation of anhydrosugars. As a result the content of anhydrosugars was determined to be substantial among pyrolysis products. It has also been found that acids content seemed to decrease with the increase of severity pretreatment. This seems to be particularly the case for the hardwood studied in this research. These two phenomena have already been observed in studies performed on straw [7].

A better comprehension of the influence of wet torrefaction on bio-oil composition may lead to the improvement of bio-oil quality but may also lead to new research directions such as the production of levoglucosan, for example.

V. ACKNOWLEDGEMENT

This research was supported by funding from the Consortium de Recherche et Innovations en Bioprocédés Industriels au Québec (CRIBIQ). The authors would like to thank Groupe BSL for supplying the forest biomasses. Special thanks are due to Yves Bédard for technical assistance.

VI. REFERENCES

[1] Meier, D.; van de Beld, B.; Bridgwater, A.V.; Elliott, D.C.;Oasmaa, A.; Preto, F. State-of-the-art of fast pyrolysis in IEA bioenergy member countries. *Renew. Sustain. Energy Rev*. **2013**, *20*, 619–641.

[2] Ando, H.; Sakaki, T.; Kokusho, T.; Shibata, M.; Uemura, Y.; Hatate, Y. Decomposition behavior of plant biomass in hot-compressed water. *Ind. Eng. Chem. Res.* **2000**, *39*, 3688–3693.

[3] Yan, W.; Acharjee, T.C.; Coronella, C.J.; Vasquez, V.R. Thermal Pretreatment of Lignocellulosic Biomass, *Environ. Prog. Sustain. Energy*. **2009**,*28*, 435–440.

[4] Shafidazeh, F. Introduction to pyrolysis of biomass. *J. Anal. Appl. Pyrolysis.* **1982**, *3*, 283–305.

[5] Le Roux, E.; Diouf, P.N.; Stevanovic, T. Characterization of the properties of thermally pre-treated forest biomass. *J--J. Sci. Technol. For. Prod. Process.* **2012**, *2*, 33–37.

[6] Nonier, M.F.; Vivas, N.; de Gaulejac, N.V.; Absalon, C.; Soulié, P.; Fouquet, E. Pyrolysis–gas chromatography/mass spectrometry of Quercus sp. wood: Application to structural elucidation of macromolecules and aromatic profiles of different species. *J. Anal. Appl. Pyrolysis.* **2006**, *75*, 181 – 193.

[7] Johnson, R.L.; Liaw, S.-S.; Garcia-Perez, M.; Ha, S.;. Lin, S.S.-Y; McDonald, A.G; Chen, S; Pyrolysis Gas Chromatography Mass Spectrometry studies to evaluate high-temperature aqueous pretreatment as a way to modify the composition of bio-oil from fast pyrolysis of wheat straw. *Energy Fuels*. **2009**, *23*, 6242-6252.

ANALYSIS OF LIGNIN DEGRADATION PRODUCTS IN SPENT LIQUORS BY APCI-MS/MS

Ilka Lehmann[1], Sabrina Laun[1], Helga Mölleken[1], Hans-Willi Kling[1]*

[1]*University of Wuppertal, Communication and Management of chemical processes in Industry, 42119 Wuppertal, Germany*
*(*kling@uni-wuppertal.de)*

ABSTRACT

Based on this research the degradation products could be a potential source of raw materials for the chemical industry. Consequently, this approach could allow an application of spent liquors as a source of renewable resources.
Industrial spent liquors of alkaline kraft and acidic magnesium-based sulfite pulping have been characterised by a mass spectrometric technique in order to identify some of the structures of lignin degradation products.
To determine the structure of the complex ingredients a mass spectrometric method was developed using model compounds. Compared to ESI the best results were accomplished by APCI in negative and positive ionisation mode. The lignin degradation products were isolated from spent liquor, followed by detection with the developed APCI-MS method. The possible structures of these substances were identified by MS/MS measurements.

I. INTRODUCTION

Wood consists of approximately 30 % lignin [1]. Lignin, which is one of the most abundant biological polymers found in nature, is classified as an aromatic heteropolymer that is responsible for the necessary strength of the plant. It consists of phenylpropanoid units linked by ether and carbon-carbon bonds. The main precursors are three cinnamyl alcohols: coumaryl alcohol, coniferyl alcohol and sinapyl alcohol [2-4]. Soft wood is composed mainly of coniferyl units, whereas hard wood mainly consists of coniferyl and sinapyl units [5-6].
Wood is one of the major raw materials for paper and cellulose production. The by-product spent liquor contains the water soluble degradation products of lignin with about 30-50 % (dry matter). Here two major chemical pulping processes, the sulfite and kraft pulping, are fundamental. The kraft pulping process is a soft procedure that results in a strength pulp and a spent liquor with a high percentage of lignin degradation products. The liquor of the sulfite process consists additionally of sulfonated lignin units. The spent liquors are mostly incinerated in order to recycle the inorganic reagents and to generate the required process heat for the pulping process [7].
It seems evident, that more efficient applications of liquors are of technological, ecological and economical interest. From a long-term perspective it is certainly necessary to gain extensive knowledge of the structure of lignin degradation products. A single substance analysis enables a statement about the applicability of these compounds. One example of such an application represents the utilisation of vanillin from the spent liquors.

Due to the complex mixture of lignin degradation products a powerful analytical method is required, like atmospheric pressure chemical ionisation mass spectrometry (APCI-MS). In literature, a limited set of methods for the identification of lignins by MS and the fragmentation of existing bonding-types are published and were used for the interpretation of mass spectra [8-10].

II. EXPERIMENTAL

For magnesium-based acidic sulfite pulping (sulfite liquor) 50 % spruce and 50 % beech wood were used. Kraft liquor originates from pulping of 70 % spruce and 30 % pine wood. 3,3‘-Dimethoxy-5,5‘-dimethyl-biphenyl-2,2‘-diol, 1-(3,4-Dimethoxy-phenyl)-2-(2-methoxy-phenoxy)ethanone, 6,6‘-Dihydroxy-5,5‘-dimethoxy-biphenyl-3,3‘-dicarbaldehyde, sodium (4-hydroxy-3-methoxyphenyl)-methansulfonate), vanillin, (3,4-Dimethoxy-phenyl)-methanol and sodium 4-(vinylbenzene)sulfonate were used as model compounds.

Isolation of lignin degradation products:

For the isolation of the lignin degradation products from liquors already established methods were used. During the isolation from sulfite liquor lignin components were transferred to an organic phase as a lignin-dicyclohexylamine-complex [11,12]. The lignin degradation products from kraft liquor were precipitated by a reduction of pH from pH 12 to pH 2 [13].

Mass analysis with APCI:

All mass spectra were obtained using an Agilent Infinity 1290 System coupled with an Agilent 6530/6538 Ultra High Definition Accurate-Mass QTOF-System (Agilent Technologies, Santa Clara, USA) equipped with an APCI source. The MS spectra were analysed with Masshunter software (B05.01).
Model compounds were dissolved in MeOH/NH_3(10mM) (1:1, v/v) with a concentration of 10 µg/mL. The concentration of lignin samples were 100 µg/mL.
Analytes were ionised using the following parameters:
injection volume 10 µL; LC flow 0.5 mL/min; eluent 50 % MeOH/50 % H_2O
negative mode: drying gas temperature 300 °C; vaporiser temperature 350 °C; drying gas (nitrogen) flow rate 4 L/min; nebuliser pressure 20 psig; capillary voltage 3500 V; corona current 20 µA; fragmentation voltage 125 V; skimmer voltage 65 V; octopol voltage 750 V; scan rate 1 spectra/sec; scan mode 50 – 3000 Da.
positive mode: drying gas temperature 300 °C; vaporiser temperature 325 °C; drying gas (nitrogen) flow rate 6 L/min; nebuliser pressure 20 psig; capillary voltage 3500 V; corona current 4 µA; fragmentation voltage 125 V; skimmer voltage 65 V; octopol voltage 750 V; scan rate 1 spectra/sec; scan mode 50 – 3000 Da.
MS/MS spectra were generated using nitrogen as collision gas and a collision energy between 5 and 30 V.

III. RESULTS AND DISCUSSION

Figure 1 shows mass spectra of model compounds using the optimised method (see above).

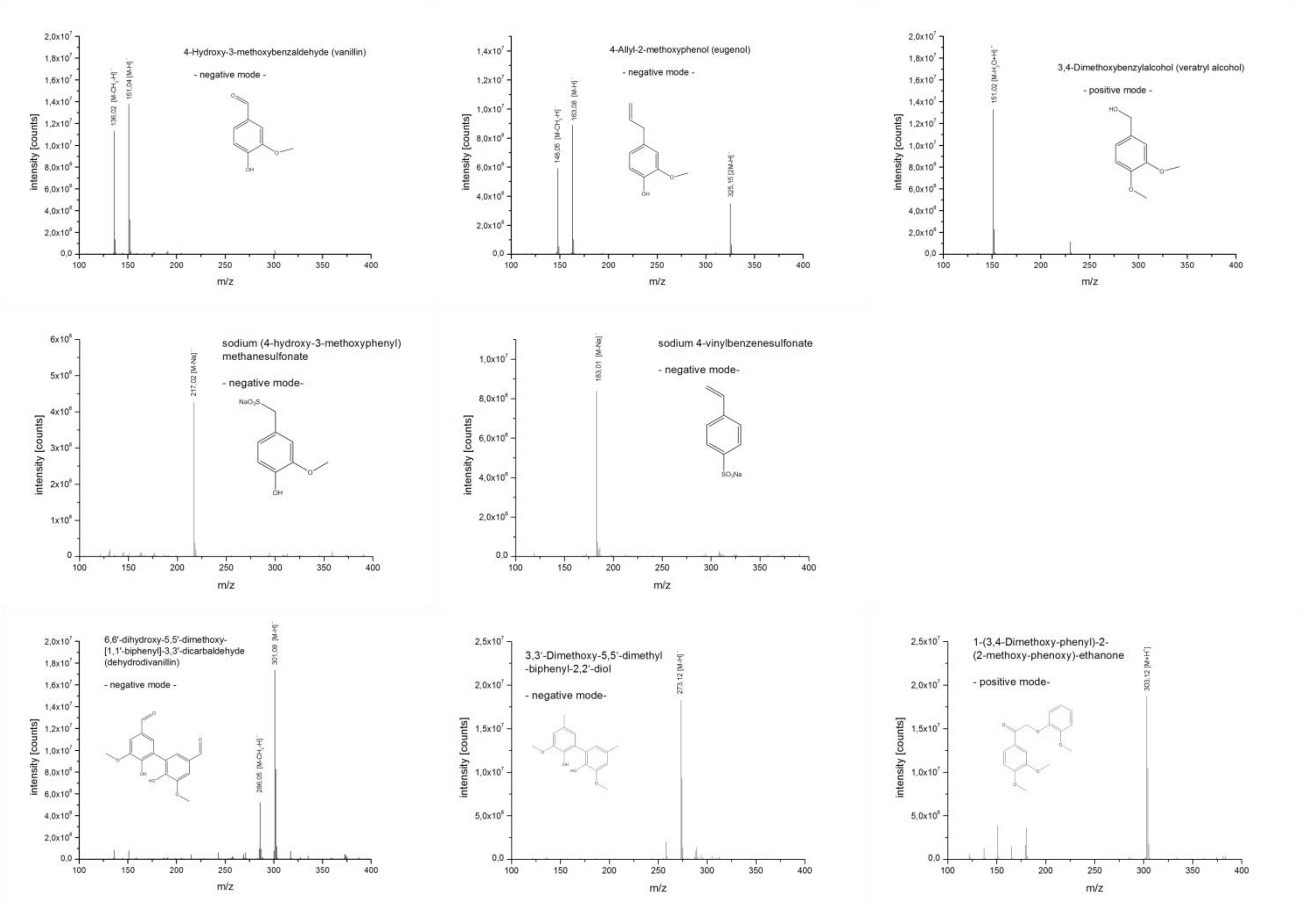

Figure 1. Optimised APCI mass spectra of model compounds

The optimised method for mass analysis of model compounds also allows a determination of the isolated kraft lignin and the isolated lignosulfonate. Figure 2 shows the obtained spectra of these complex mixtures.

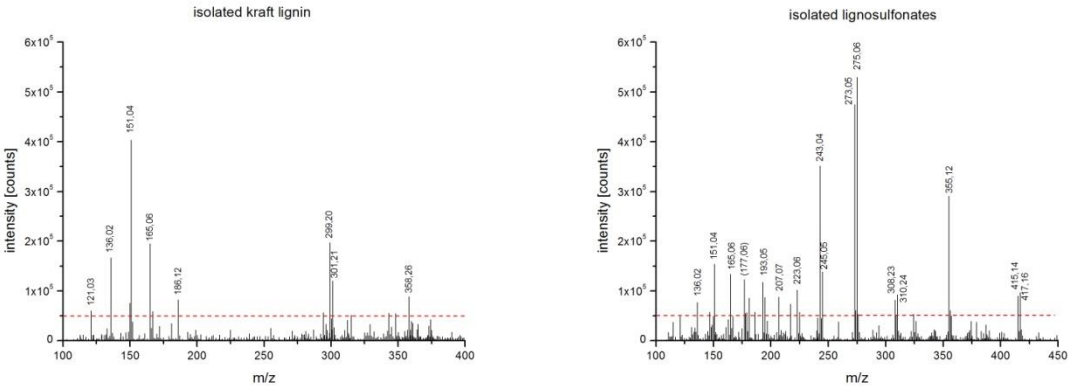

Figure 2. (-)APCI mass spectra of isolated kraft lignin and isolated lignosulfonates

By means of MS/MS experiments of the obtained signals it is possible to determine potential structures of the detected substances. It must be noted that the structures were based only on assumptions. Table 1 summarises the results obtained for the isolated lignin degradation products (structures or formulas).

Table 1. Potential structures of the isolated lignin degradation products

kraft lignin		lignosulfonates	
m/z	potential structure	m/z	potential structure
136,02 (40 %) $[M\text{-}CH_3\text{-}H]^-$ 151,04 (100 %) $[M\text{-}H]^-$	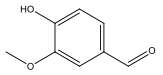 vanillin	136,02 (40 %) $[M\text{-}CH_3\text{-}H]^-$ 151,04 (100 %) $[M\text{-}H]^-$	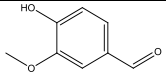 vanillin
165,06 $[M\text{-}H]^-$	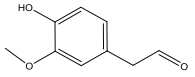 2-(4-hydroxy-3-methoxyphenyl)acetaldehyde	165,06 $[M\text{-}H]^-$	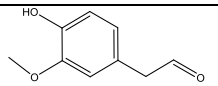 2-(4-hydroxy-3-methoxyphenyl)acetaldehyde
186,12	$C_{10}H_{19}OS$	243,04 (100%) 245,05 (40 %) $[M\text{-}Na]^-$	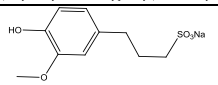 sodium 3-(4-hydroxy-3-methoxyphenyl)propane-1-sulfonate
299,20 (100 %) 301,21 (60 %) $[M\text{-}H]^-$	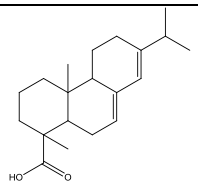 abietic acid	273,05 (90 %) 275,06 (100 %) $[M\text{-}Na]^-$	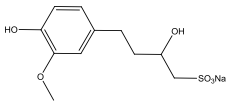 sodium 2-hydroxy-4-(4-hydroxy-3-methoxyphenyl)butane-1-sulfonate
358,26 (100 %) 360,15 (40%) $[M\text{-}H]^-$	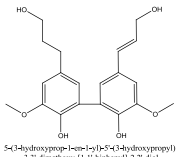 5-(3-hydroxyprop-1-en-1-yl)-5'-(3-hydroxypropyl)-3,3'-dimethoxy-[1,1'-biphenyl]-2,2'-diol	308,23 (90 %) 310,24 (100 %)	$C_{22}H_{31}O$ $C_{19}H_{35}OS$
		355,12 $[M\text{-}H]^-$	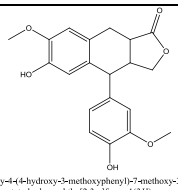 6-hydroxy-4-(4-hydroxy-3-methoxyphenyl)-7-methoxy-3a,4,9,9a-tetrahydronaphtho[2,3-c]furan-1(3*H*)-one
		415,14 (90 %) 417,16 (100 %)	$C_{23}H_{30}O_3S_2$ $C_{26}H_{26}O_5$

Table 1 shows the compliance of several potential structures with detected masses. Under these circumstances the main substances in kraft lignin are vanillin, 2-(4-hydroxy-3-methoxyphenyl)acetaldehyde and abietic acid. The difference of *m/z* = 2 could be explained by a quinone-methide-conversion.

Isolated lignosulfonates contain mainly sulfonated substances like sodium 3-(4-hydroxy-3-methoxyphenyl)propane-1-sulfonate and sodium 2-hydroxy-4-(4-hydroxy-3-methoxyphenyl)butane-1-sulfonate. However, identification of sulfonated degradation products is difficult due to the fragmentation of $[M\text{-}Na]^-$ results exclusively in the $[SO_3]^-$ and the $[M\text{-}CH_3\text{-}Na]^-$ fragment.

IV. CONCLUSIONS

In this work an optimised APCI-method was developed, which allows a determination of several low molecular lignin degradation products in spent liquors. Potential structures were identified by MS/MS experiments.
In both spent liquors from the pulping processes, the lignin polymers were partly degraded to low molecular aromatic substances. These substances could be used as raw materials for biobased chemical industry.
Finally, at this point of research the first identification of structures shows, that the spent liquors from the pulp industry have a great potential for substantial use. Further research needs to examine fractions (e.g. soxhlet- and HPLC-fractions) of lignin degradation products to enable a comprehensive identification of the major structures.

V. ACKNOWLEDGEMENT

Industrial thick spent liquors from magnesium-based acidic sulfite pulping were provided by Sappi Alfeld mill, Germany. The kraft liquor was supplied by Zellstoff- und Papierfabrik Rosenthal GmbH, Germany.
Some model compounds (3,3‘-Dimethoxy-5,5‘-dimethyl-biphenyl-2,2‘-diol and 1-(3,4-Dimethoxy-phenyl)-2-(2-methoxy-phenoxy)ethanone) were synthesised by the working group of inorganic chemistry (Prof. Mohr).

VI. REFERENCES

[1] Fengel, D., Wegener, G.; *Lignin in Wood – Chemistry, Ultrastructure, Reactions*, **2003**, Chapter 6, 132-182, Kessel Verlag, Remagen

[2] Boerjan, W.; Lignin Biosynthesis. *Annual review of plant biology*. **2003**, 54, 519-546

[3] Forss, K.G.; The Nature and Reactions of Lignin - a New Paradigm. **2003**, Oy Nord Print Ab, Helsinki

[4] Sjöström, E.; Analytical Methods in Wood Chemistry, Pulping and Papermaking. **1999**, Springer Verlag, Berlin

[5] Ek, M.; Wood Chemistry and Wood Biotechnology. **2009**, Chapter 6, 121-124, Walter de Gruyter

[6] Sakakibara, A.; A Structural Model of Softwood Lignin. *Wood Science and Technology*. **1980**, 14, 89-100

[7] Sixta, H.; Chemical Pulping Processes in Handbook of Pulp. **2006**, Volume 1; Wiley-VCH, Weinheim

[8] Morreel, K.; Mass Spectrometry-Based Fragmentation as an Identification Tool in Lignomics. *Analytical Chemistry*. **2010**, 82, 8095-8105

[9] Morreel, K.; Mass Spectrometry-Based Sequencing of Lignin Oligomers. *Plant Physiology*. **2010**, 153, 1464-1478

[10] Peterson, J.R.; Method for Tiered Production of Biobased Chemicals and Biofuels from Lignin. **2013**, Pub.No. US2013/0232852 A1

[11] Bottger, J.; Isolation of Pure Lignin-Sulfonates on Sulfite Waste Liquor. *Papier*. **1975**, 29 (7), 305-308

[12] Ringena, O.; Isolation and Fractionation of Lignosulfonates by Amine Extraction and Ultrafiltration: A Comparative Study. *Holzforschung*. **2005**, 59 (4), 405 - 412

[13] Lappan, R.E.; Kraft Lignin-poly(DADMAC) Precipitate Formation. *Industrial & Engineering Chemistry Research*. **1997**, 36 (4), 1171 - 1175

FROM LIGNIN-AEROGELS TO CARBOGELS

Sebastian P Leitner[1,*], Christian Paulik[2], Hedda K. Weber[1]

[1]*Kompetenzzentrum Holz GmbH, Wood and Cellulose chemistry, Altenbergerstraße 69, 4040 - Linz, Austria; (*s.leitner@kplus-wood.at)*

[2]*Institute for chemical technology of organic materials, Johannes Kepler University Linz, Altenbergerstraße 69, 4040-Linz, Austria*

ABSTRACT

Carbon aerogels can be used in a variety of applications. Here we present a way to produce them from lignin precursors. Aerogels and carbogels were prepared from a pure lignin formaldehyde solution without further addition of phenols. Different formaldehyde to lignin ratios were tested with a constant reaction concentration at nearly 10 percent. These conditions led to reproducible hydrogels and subsequent the water was exchanged by ethanol to prepare them for a supercritical carbon dioxide extraction step. Results from thermo gravimetrical analysis yielded the desired conditions for pyrolysis of the aerogels to carbogels. The material was quite brittle, but the sample form was unchanged though the expected shrinkage occurred during the carbonization procedure. All sample materials were measured by nitrogen BET adsorption to obtain the specific surface area and the surface was further investigated by scanning electron microscopy. Higher formaldehyde to lignin ratio gave a higher specific surface area in the resulting aerogels and carbogels.

I. INTRODUCTION

Aerogels are not well defined. The best way to describe them is being materials that are prepared from a wet, highly porous gel system by supercritical extraction as the drying process. In this step the liquid pore content of the gel material is replaced by gas. In addition to the term aerogel there also exist xerogels (by conventional drying) and cryogels (by freeze drying)[1].

Since the first publication on organic aerogels from Pekala [2] there has been quite a big effort to obtain new and better organic aerogels and also a trend to produce them of renewable resources. Their characteristic properties are interesting for several applications, for example insulating material due to their very low thermal conductivity because of the porous structure [3]. Moreover the pyrolized carbon aerogels (or carbogels) are reported to show electrical conductivity so that there are ideas to use it as anode material in batteries or as storage material for hydrogen [4], [5].

The high abundance of lignin and its derivatives makes it an ideal renewable "bio-ingredient" for aerogel synthesis, replacing the well-established petrochemical based phenol and resorcinol in the resin synthesis. And although the reactivity of lignin is lower than that of phenol or resorcinol it is a considerable alternative in the synthesis of bio-organic-aerogels.

II. EXPERIMENTAL

Used materials and methods

"Indulin AT" (a Kraft lignin) was bought from Sigma-Aldrich. Indulin was dissolved in water for better adjustment of the synthesis conditions. Formaldehyde was taken from a 37% aqueous solution bought from Sigma-Aldrich.

Scanning electron microscopy (SEM) analysis was performed on a Zeiss 1540XB CrossBeam equipped with an Oxford Instruments EDX system. BET surface measurements were done on a Quantachrome Nova 3000e analyzer. For High pressure extraction a self-assembled super critical extractor with a 250 mL steel extraction thimble was used. Carbonization was done on a high temperature oven GERO HTK8 under N_2 atmosphere.

Preparation of Lignin hydrogels

The lignin solution and the formaldehyde solution were mixed within an Erlenmeyer flask. Subsequently NaOH solution (20%w/w) was added to raise the pH value over 11 and then the lignin-formaldehyde concentration (LF concentration) was adjusted to a value of nearly 10% by adding the desired amount of distilled water. Afterwards the reaction solution was divided into several sealable tubes and placed into a drying oven at a temperature of 90 °C. The solution reacted for about 48 h until gelation was visible. In total the material was being kept at temperature for five days for better solidification of the material. The samples showed a brownish color and rubber-like behavior on slight deformation.

Table 1 Aerogel synthesis

Sample Name	L/F mass-ratio	LF-content
A	1.00	0.10
B	0.51	0.10
C	0.33	0.09
D	1.014	0.134

Preparation of Lignin aerogels

The reaction tubes were opened after polycondensation time and then cut at the closed end. With a spatula the hydrogels were very carefully loosened from the tube walls. They could be pushed out of the vessel with a slight overpressure by compressed air. Each sample could be placed in a small screw mountable polypropylene container, which was large enough to cover the sample with ethanol (p.A.). This was necessary because of the following supercritical extraction step. The solvent exchange took about four to five days. The sample material was daily filtered and then covered with fresh ethanol (p.A.). After the solvent exchange step the samples shrank slightly. The brownish color remained unchanged. Afterwards the supercritical extraction was performed with CO_2 (critical point: 31 °C, 73.8 bar). The extraction step took 2 h at 40 °C and 100 bar. After the drying the samples were lighter colored than before. After the SCE samples were degassed in a desiccator under reduced pressure and silica gel as drying agent.

Carbonization of aerogels

The samples were placed in ceramic containers covered with a perforated carbon plate and the put into a high temperature oven. The oven was purged with N_2 and then the temperature program started (temperature program: 20°C to 500°C: 1°C min^{-1}; hold 1 hour; 500°C to 900°C: 2°C min^{-1}; hold 2 hours; cooling as fast as possible.; N_2 flow: 150 L h^{-1}). The choice of the temperature program was based on the thermo gravimetrical analysis, which showed the highest decrease in mass at a range of 400°C to 500°C. T

III. RESULTS AND DISCUSSION

Pure lignin formaldehyde aerogels could be synthesized by the method described. Gelation in the hydrogel preparation step occurred after about 24 h. However, it was necessary to cure the samples for about 5 days at 90°C to obtain the desired stability. In case of shorter reaction times the samples remained highly viscous fluids that could not be removed from the reaction tubes without significant deformation of the material. Sample C could not be further investigated because it was not possible to detach it from the tube and obtain a dimensionally stable sample that keeps it shape.

The solvent exchange step takes with a duration of several days, as mentioned in literature [1], a very long time but is necessary for the supercritical fluid extraction with CO_2.

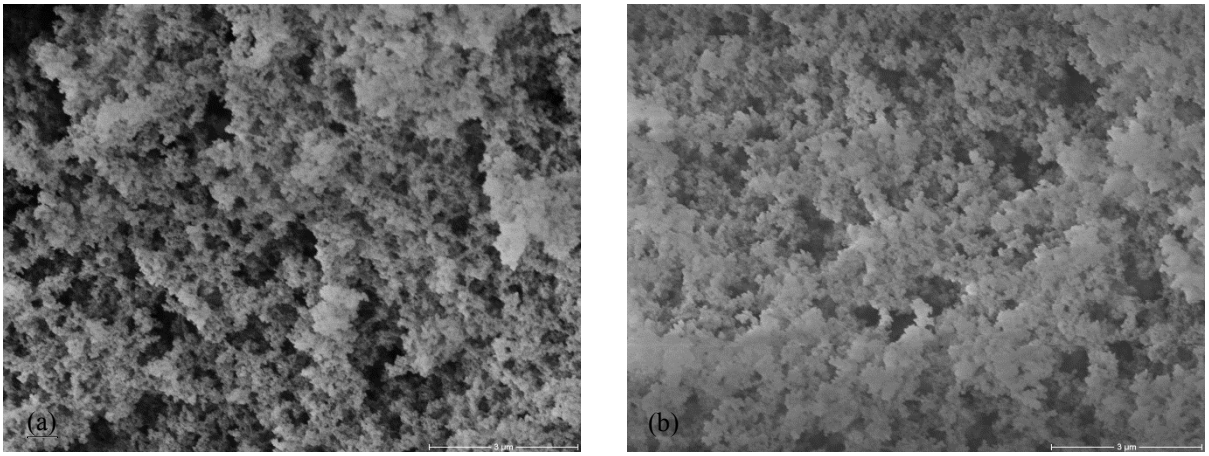

Figure 1. Comparison of two different lignin formaldehyde aerogels by SEM. (Sample A (a) and D (b), (magnification 10.000, 10.00kV)

In Figure 1 the difference of an aerogel with a LF-content of nearly 10% compared to an LF-content of around 14% is visible. Sample B (Figure 1 (b)) shows a slightly tighter arranged solid and Sample A (Figure 1 (a)) looks like the more porous material. Carbonization of the aerogels under described conditions yields the carbon aerogels shown in Figure 2. Due to their electric conductivity of the surface of the carbon samples can be investigated without prior gold sputtering of the samples. Figure 2.depicts no obvious difference to see via electron-microscopy between the carbonized samples A and B, and a more suitable method to compare them is described in Table 2 with the N_2 adsorption measurements.

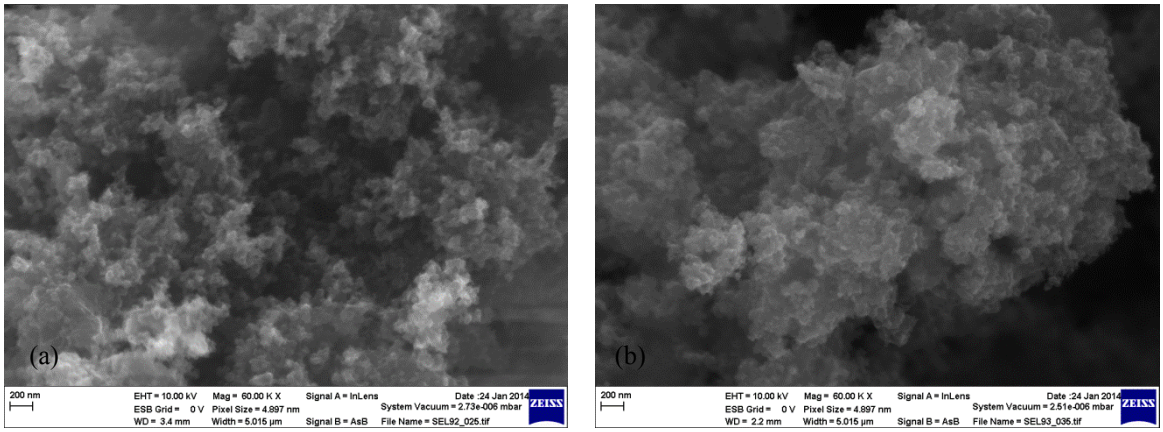

Figure 2. Comparison of carbon aerogels with different lignin formaldehyde-ratio by SEM (carbonized Sample A (a) and carbonized sample B (b), magnification 60.000; 10.00kV).

The surface BET areas of the lignin aerogel samples A and B are around 180 m²/g to 230 m²/g. With increasing formaldehyde ratio higher BET surface areas are obtained and the pore size is with nearly 40 nm in the mesoporous region. One can conclude that higher formaldehyde content leads to an increase in specific surface area probably because of the reduced pore size.

Furthermore the carbonization under described conditions leads to an increase in the surface area of samples A and B. Carbonized sample A has an increased specific surface area from 330 m²/g and carbonized Sample B from 356 m²/g. The ratio from the surface area, which origins from the micro pores, has also increased compared to the lignin aerogel structures because in these cases the carbonization increases the micro pores in the system. The shape of the material samples remained unchanged during the pyrolization but showed shrinkage of about 30%. The carbon residue of the samples after carbonization is between 45 to 54 %. In Table 2 the comparison of the surface areas is shown.

Table 2 surface areas of different samples

Sample	**Specific surface area [m²/g]**	**Specific surface area [m²/g]**
	Non carbonized	carbonized
Sample A	180	230
Sample B	330	356

IV. CONCLUSIONS

In this work it was possible to synthesize aerogels and also carbon aerogels based on a pure Kraft-lignin source without the addition of phenol or resorcinol. The surface area of the samples with around 200 m²/g was in accordance with the literature. It could also be shown that a higher formaldehyde content during condensation reaction leads to a higher surface area. This could be explained by an enhanced possibility of reaction of formaldehyde with the reactive sites of the aromatic system of the lignin increases. This leads to smaller pores that do have higher effect on the specific surface area.

With the carbonization step it was possible to increase the surface area of the material to a value of nearly 350 m²/g and also the microporous ratio of the total pores in the system.

V. ACKNOWLEDGEMENT

The work was performed within the XpremES project, which is funded by the European Regional Development Fund (EFRE) and the province of Upper Austria

The authors gratefully thank Jürgen Schoiber and Prof. Nicola Hüsing from the University of Salzburg for SEM and BET measurements of the samples.

VI. REFERENCES

[1] N. Hüsing, U. Schubert, Aerogels—Airy Materials: Chemistry, Structure, and Properties, Angewandte Chemie International Edition 37 (1998) 22–45.

[2] R.W. Pekala, Organic aerogels from the polycondensation of resorcinol with formaldehyde, Journal of Materials Science 24 (1989) 3221–3227.

[3] L.W. Hrubesh, R.W. Pekala, Thermal Properties of organic and inorganic aerogels, Journal of Materials Research 9 (1994) 731–738.

[4] H. Kabbour, T.F. Baumann, J.H. Satcher, A. Saulnier, C.C. Ahn, Toward New Candidates for Hydrogen Storage: High-Surface-Area Carbon Aerogels, Chem. Mater. 18 (2006) 6085–6087.

[5] R.W. Pekala, J.C. Farmer, C.T. Alviso, T.D. Tran, S.T. Mayer, J.M. Miller, B. Dunn, Carbon aerogels for electrochemical applications, Journal of Non-Crystalline Solids 225 (1998) 74–80.

ORGANOSOLV FRACTIONATION OF BEECH WOOD – THE FIRST YEAR OF OPERATION AT PILOT SCALE

Moritz Leschinsky[1]*, Marlen Verges[1], Gerd Unkelbach[1]

[1]*Fraunhofer Center for Chemical-Biotechnological Processes (CBP), Am Haupttor, 06237 Leuna, Germany (*moritz.leschinsky@igb.fraunhofer.de)*

ABSTRACT

A new pilot plant for organosolv fractionation of wood chips started its operation in May 2013 within the new Fraunhofer-Center for Chemical-Biotechnological Processes in Leuna, Germany. The plant is designed to fractionate beech wood using ethanol-water pulping with the aim to further develop and optimize the process and to provide all major fractions (lignin and sugars) in sufficient amounts for the development of new value chains. After successful scale-up from the laboratory main results of the first year of operation are presented.

I. INTRODUCTION

The fractionation of lignocellulosic biomass into lignin, cellulose and hemicellulose can pave the way for new sustainable materials. Especially the separation of lignin in high purity is interesting for the substitution of phenolic resources. In conventional pulping processes however lignin is mostly combusted or destroyed but not used as a material. The ethanol organosolv pulping process enables a gentle extraction of lignin and hemicellulose and thus a clear fractionation of lignocellulose. It was first patented in 1932 by Kleinert and Tayenthal [1].

To establish a pilot scale plant of an organosolv pulping process was an aim of the "German Lignocellulose Feedstock Biorefinery Project" [2]. It was intended to develop and scale-up a process for maximum material usage of the components of national wood resources. Beech wood was identified as the most available and suitable species for the conversion into platform components for the chemical industry. Pulping with ethanol-water was selected as the most appropriate process for the fractionation of beech wood forest residues with the aim to achieve the highest material usage. In the second phase of the project the pilot plant was built within the new Fraunhofer-Center for Chemical-Biotechnological Processes in Leuna [3]. Main results of the first year of operation are presented in this paper. The process can be regarded as the basis of a lignocellulose biorefinery.

II. EXPERIMENTAL

Description of the pilot plant

The "lignocellulose biorefinery" pilot plant is designed to fractionate wood chips by ethanol-water-pulping using batch processes. The plant is divided into the following process units, which are shortly described and shown in a process scheme (**Figure 1.**):

- Pulping: The pulping section consists of a batch digester with forced circulation containing 400 L of industrial wood chips. Two additional temperature controlled pressure vessels and one atmospheric tank allow the preparation, preheating and storage of the cooking and washing liquors. The whole pulping section is built in Duplex steel and can be operated at maximum 200 °C and 36 bars. Wood chips can be pre-steamed prior to cooking and pulping liquors can be displaced from bottom to top through the digester for washing with ethanol and water.
- Washing and dewatering: The pulped wood chips are discharged into a blow tank where the pulp is diluted to ~5 % solids content and the fibers are disintegrated by an in-line disperser. The pulp is then dewatered by a screw press.
- Enzymatic hydrolysis: Two temperature controlled stirred tanks with a volume of 1000 L are used for the enzymatic saccharification of pulp. A chamber filter press is used to separate the hydrolysis residue from the liquid. Optionally a fall film evaporator can be used to concentrate the glucose solution for stabilization.

- Lignin precipitation: Lignin is precipitated in a 1200 L stirred tank by the addition to water and filtered using a chamber filter press. Optionally lignin can be precipitated by evaporating ethanol. The obtained organosolv-lignin can be washed on a membrane filter press and dried in a vacuum drier.
- Solvent recovery: Ethanol is recovered from the filtrates of lignin precipitation and from the washing liquors in a batch rectification column.

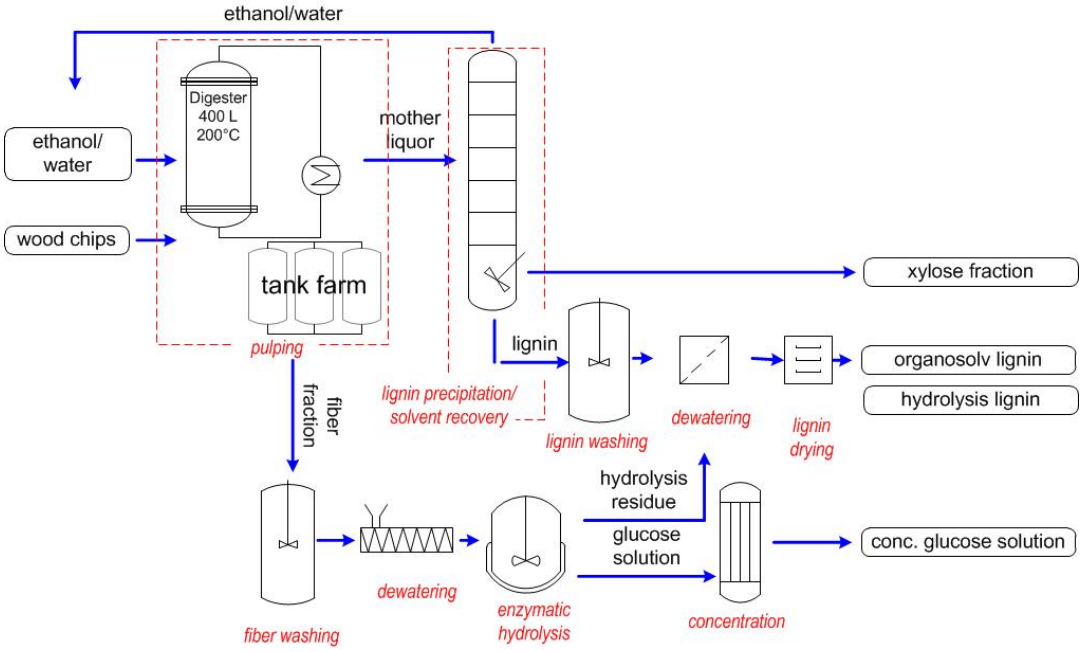

Figure 1. Process scheme of the organosolv pilot plant in Leuna.

Operation of the pilot plant

Ethanol-water pulping is carried out discontinuously with batches of 70 kg o.d. debarked beech wood chips. Starting conditions from the scale-up are described as follows. After presteaming at 100 °C, the pulping process is running for 100 minutes at a temperature of 170 °C and 20 bar in a cooking liquor consisting of a 50 % (w./w.) ethanol-water solution. The liquor-to-wood ratio is 3.2:1. As a catalyst, sulphuric acid is added in a concentration of 0.5 % based on o.d. wood. After pulping the cooking liquor is displaced by a 50 % (w./w.) ethanol-water solution of 100 °C. Washing and cooling is done two times by displacement with water in order to remove ethanol from the fibers.

During cooking lignin and hemicelluloses are dissolved in the cooking liquor. The hemicellulose present in solution after the filtration of the precipitated lignin is purified and concentrated at the solvent rectification. The cellulose fraction is disintegrated and washed. After dewatering the enzymatic hydrolysis of cellulose is carried out at a solids concentration of 10 % (w./w. o.d. pulp) in a stirred tank reactor for 48 hours. Temperature is set to 50 °C and a pH value of 5 is realized. Enzymes are provided by Novozymes. 6 % of Cellic® CTec3 and 0.25 % Cellic® HTec3 (based on o.d. pulp) are used. The glucose solution obtained is finally concentrated for preservation by means of evaporation.

The design of the pilot plant is modular in order to allow optimization of pulping and downstream processing. To evaluate the process, the composition of the products and intermediates are analyzed according to adopted NREL procedures. Mass balances of the process are established on this basis.

III. RESULTS AND DISCUSSION

The organosolv pilot plant started operation in May 2013 and is running in day-shift operation since. The selection of the scalable unit operations could be confirmed and no major modifications of the plant have been deemed necessary so far. The scale-up of the processes from the laboratory experiments was successful and similar yields and product compositions as at the laboratory-scale were obtained. Ethanol-water fractionation of 70 kg of debarked beech (Fagus sylvatica) wood chips at 170 °C for 100 minutes using 0.5% of sulphuric acid (based on o.d. wood) at a liquor-to-wood ratio of 3.2:1 resulted in the pulp, lignin and glucose syrup compositions described in **Table 1**.

Table 1. Compositions of pulp and organosolv-lignin obtained from ethanol-water fractionation of beech wood and sugar syrup from enzymatic hydrolysis of pulp.

Fraction / Components	Pulp	Sugar Syrup	Organosolv-Lignin
Glucose [% dry mass]	72.1	74.8	0.0
Xylose [% dry mass]	16.9	18.2	3.6
Lignin [% dry mass]	14.9	n.d.	88.5

During further operation first parameters like temperature, heating time and concentration of sulphuric acid were varied leading to different product amounts and compositions. **Figure 2** shows the composition of the pulp obtained using 70 kg of debarked beech wood chips at different sulphuric acid concentrations.

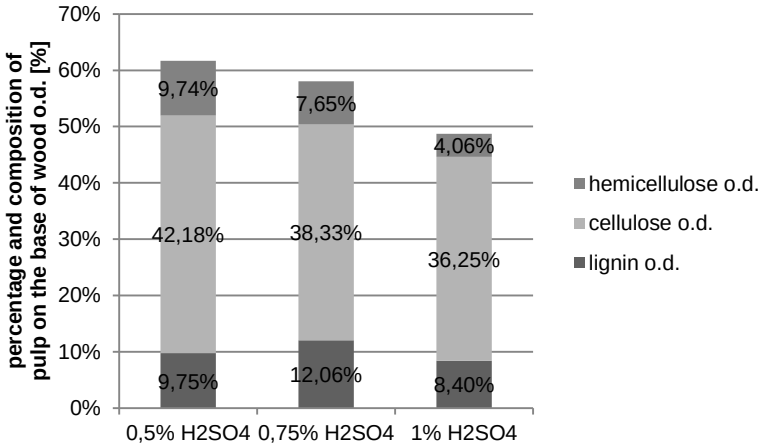

Figure 2. Percentage and composition of o.d. pulp obtained from the ethanol-water fractionation of 70 kg o.d. debarked beech wood chips at 170 °C and 20 bar and addition of sulphuric acid in different concentrations (% w./w. o.d. wood).

A higher amount of sulphuric acid led to lower pulp yield containing less hemicellulose. But also the yield of cellulose in the pulp was lowered. The single-stage enzymatic hydrolysis at 50 °C and a solid concentration of 10 % (w./w. o.d. pulp) resulted in the sugar concentrations shown in **Figure 3**. The concentration of glucose is higher if more sulfuric acid is used during cooking, while the amount of hemicellulose is lower. The results show a clear influence of pulping conditions on the enzymatic hydrolysis. To improve the glucose concentration and yield the influence of pulping conditions will be more closely investigated. Therefore an increasing severity of the pulping process is planned. Also investigations of a second hydrolysis step of the residue material will follow. Utilization pathways for the hydrolysis residue have to be analyzed.

At the moment around 50 % of the lignin contained in beech wood is extracted and obtained as organosolv-lignin. To improve yield an optimization of the pulping process is necessary. Additionally a washing of the disintegrated pulp will be investigated in order to increase the yield of lignin and glucose.

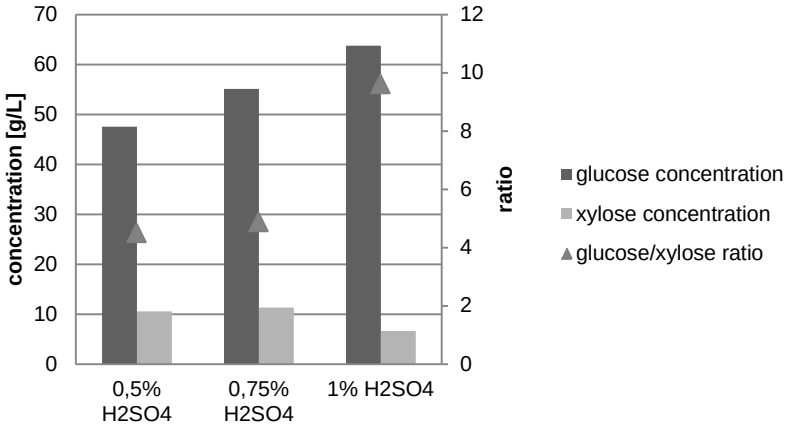

Figure 3. Sugar concentrations in filtrate after the single-stage enzymatic hydrolysis at 50 °C of the pulp obtained with different concentrations of sulphuric acid (% w./w. o.d. wood).

Within the project, products of the pilot plant were sent to project partners for the development of utilization pathways. The lignin fraction was used for the development of duro-and thermoplastic applications . Glucose was used for various fermentations. Promising results for all applications were obtained. The aim of further operation is to optimize the process as far as possible to improve yield, process stability and purity of the products. In addition, the fractionation products are used in various national and European projects for the development of new products and value chains.

IV. CONCLUSIONS

A lignocellulose fractionation pilot plant was successfully established at the Farunhofer CBP in Leuna confirming the expected results from laboratory scale. The main fractionation products are glucose, lignin and xylose. Process optimization is continuing. The pilot plant is used as basis for a concept of a demonstration plant in future. Products are used for the development of new applications by project partners leading to promising results.

V. ACKNOWLEDGEMENT

This work is partly funded by the German Ministry of Education and Research (BMBF) within the Leading-Edge Cluster “Bioeconomy”. It is also part of the research project “Lignocellulose Bioraffinerie – Aufschluss lignocellulosehaltiger Rohstoffe und vollständige stoffliche Nutzung der Komponenten (Phase 2)”, funded by the German Federal Ministry of Food and Agriculture (BMEL) via the Agency for Renewable Resources (FNR). The authors are responsible for the content. The authors are grateful for funding and for the support of all project partners.

VI. REFERENCES

[1] Tayenthal, K.; Kleinert, T. Process of decomposing vegetable fibrous matter for the purpose of the simultaneous recovery both of the cellulose and of the incrusting ingredients. *patent US 1, 856,567*, **1932**.

[2] DECHEMA - BMELV-Verbundvorhaben: „Pilotprojekt Lignocellulose Bioraffinerie“. Gemeinsamer Schlussbericht zu den wissenschaftlich-technischen Ergebnissen aller Teilvorhaben. URL: www.fnr-server.de/ftp/pdf/berichte/22014406.pdf. **2009.**

[3] DECHEMA: working title: BMELV-Verbundvorhaben „Lignocellulose Bioraffinerie – Aufschluss lignocellulosehaltiger Rohstoffe und vollständige stoffliche Nutzung der Komponenten (Phase 2)“. Gemeinsamer Schlussbericht zu den wissenschaftlich-technischen Ergebnissen aller Teilvorhaben. In preparation, **2014.**

DEHYDROGENATIVE POLYMERIZATION OF CONIFERYL ALCOHOL ON THE XYLAN-DEPOSITED HONEYCOMB-PATTERNED CELLULOSE FILMS

Qiang Li[1)], Yuka Tasaki[1)], Keiichi Koda[2)], Yasumitsu Uraki[2)*]

[1]*Graduate School of Agriculture, Hokkaido University, Sapporo, Hokkaido 060-8589, Japan*
[2]*Research Faculty of Agriculture, Hokkaido University, Sapporo, Hokkaido 060-8589, Japan*
*(*Email of corresponding author: uraki@for.agr.hokudai.ac.jp)*

ABSTRACT

To elucidate functions of wood cell wall components on the formation and mechanical properties of the cell wall, a bio-mimetic model, termed "artificial cell wall," was created in this research. Honeycomb-patterned bacterial cellulose film (HPBC) was fabricated as a skeleton of the artificial cell wall. As a second process, xylan adsorption onto the skeleton was attempted. The adsorption amount of xylan onto HPBC was much higher than that onto the normal BC pellicle as a flat BC film (FBC), indicating HPBC had a larger accessible area of xylan than FBC did. The mechanical properties, tensile strength and modulus of elasticity (MOE) were significantly strengthened by the xylan adsorption. Thus, it was evident that xylan reinforced the cell wall.

Finally, coniferyl alcohol was polymerized by alternative dropping coniferyl alcohol and hydrogen peroxide together with peroxidase onto the xylan-deposited HPBC. The content of the generated dehydrogenative polymer (DHP) in xylan-deposited HPBC was slightly larger than HPBC without xylan. However, the nitrobenzene oxidation yield as a measure of *β*-O-4 linkage frequency was much larger than that without xylan. Therefore, it was confirmed that xylan affected the formation of *β*-O-4 linkage. In addition, mechanical strength was remarkably enhanced by DHP generation.

I. INTRODUCTION

Wood is one of the most abundant natural resource on earth, and one of its unique characteristic lies in high mechanical strength for its low specific gravity. This characteristic is assumed to be highly dependent not only on the nature and deposition process of wood cell wall components, cellulose, hemicellulose and lignin, but also on the cell wall arrangement.[1] However, these assumptions were not necessarily proved empirically. To clarify this point, we have developed "artificial cell wall," which mimics cell wall arrangement and deposition process of the cell wall components.

We have already demonstrated the fabrication process of honeycomb-patterned cellulose with cellulose I structure, whose morphology resembled cell wall array.[2-4] This fabrication was carried out by culture of cellulose-producing bacterium, *Gluconacetobacter xylinus*, on the agarose medium with concave honeycomb-like grooves. In this study, xylan as a hemicellulose component was deposited on the HPBC, and then the polymerization of coniferyl alcohol was attempted in order to fabricate artificial cell wall and to elucidate the functions of cell wall componets in cell wall formation. In addition, we monitored mechanical strength of the artificial cell wall at each deposition process of cell wall components.

II. EXPERIMENTAL

Fabrication of artificial cell wall

HPBC was fabricated accroding to the previous report.[2] Briefly, a convex honeycomb-patterned film as a first template was prepared from a mixture of polycaprolactone and acrylate copolymer, named (CAP) (weight ratio, 9:1) by blowing humid air onto the mixture/chloroform solution. Poly(dimethyl siloxane) (PDMS) was poured to the first template together with curing agents to give a second template with concave honeycomb-patterned surface. By repeating transcription of second template with PDMS, a third template with convex honeycomb morphology was obtained. Hot agarose aqueous solution with HS medium [5] was poured onto the third template, and then cooled to yield agarose gel with concave honeycomb-like grooves. Finally, *G. Xylinus* (ATCC53582) was inoculated and cultured on this agarose film at 28 ^{o}C for 48 h under a 90 % CO_2 atmosphere. As a reference, normal BC pelicle was prepared by static culture of the bacterium. Both BC films were soaked in 1 M sodium hydroxide solution at 65 ^{o}C for 1 h, and then washed with pure water and air-dried.

The prepared BC films were immersed in aqueous beech xylan solution, which was purchased from Wako Pure Chemicals Co. Ltd. (Osaka, Japan) for 24 h at ambient temperature. The xylan concentration in a supernatant was measured by HPLC (Shimadzu VP series, Kyoto, Japan) with a Corona detector (ESA Bioscience Inc., Chelmsford, MA, USA) and a column of Ashipak GF 7M HQ at 40 ^{o}C at a flow rate of 0.5 mL/min. Pure water was used as an eluent. The adsorption amount of xylan was calculated by the difference in

the concentration between before and after immersion.

Both types of films with and without xylan were immersed in horse radish peroxidase (HRP)/phosphate buffer saline (PBS) solution (pH 6.1, 0.01 M). The buffer solution of coniferyl alcohol and hydrogen peroxide were added to the film suspension by using two pumps at a constant volume rate of 5 mL/h for 10 h. After complete addition, the mixture was allowed to stand for 16 h. The resultant films were washed two times with pure water and air-dried. The films were further washed with 1,4-dioxane.

Chemical analysis of DHP

DHP content in BC films was determined by acetyl bromide method.[6] Two point five millilitter of freshly prepared acetyl bromide (25 % in acetic acid, v/v) was added into 5 mg of sample, and then the sample was heated at 50 ^{o}C for 4 h. The DHP content was calculated from the absorbance at 280 nm on an UV spectrophotometer (Shimadzu UV-1800, Tokyo, Japan).

Alkaline nitrobenzene oxidation for DHP samples was carried out as follows.[7] Four millilitter of aqueous NaOH (2 M) and 0.24 mL of nitrobenzene were added to 10-15 mg of sample in a 10-mL stainless autoclave. The reaction was performed at 160 ^{o}C for 2 h. Afterwards, 0.2 mg of acetovanillone as an internal standard was added to the reactant. The reaction products were determined by GC analysis (Shimadzu GC-2010, Kyoto, Japan) under the following conditions: detector, FID; column, Intercap 1701; split ratio, 5.0; carrier gas, He (110 mL/min); injector temperature: 250 ^{o}C; detector temperature: 280 ^{o}C; the oven temperature program was 150 ^{o}C (5 min), 5 ^{o}C/min to 230 ^{o}C (1 min), 10 ^{o}C/min to 250 ^{o}C (10 min).

All the experiments described above were run in duplicates, and the average was shown as a result.

Mechanical test

Tensile strength, MOE and elongation were measured on a special designed testing apparatus reported previously by Uraki *et al*.[3] Films were gently pressed with 300 g load for 10 min, and then cut into 1-2 mm in width and 5 mm in length. The measurement was conducted at 22 ^{o}C with 50 % relative humidity.

III. RESULTS AND DISCUSSION

Xylan adsorption on HPBC and FBC

HPBC has been confirmed to consist of highly ordered cellulose microfibrils with cellulose I structure as well as FBC as BC pelicle.[2] Surface molphologies of HPBC and FBC were shown in **Figure 1**. HPBC was constructed with narrow cellulose wall and big pores with the pore size of 20 μm, having a very similar array to cross section of wood cell wall. On the other hand, the surface of FBC was apparently very flat and no pore was observed in this magnification image.

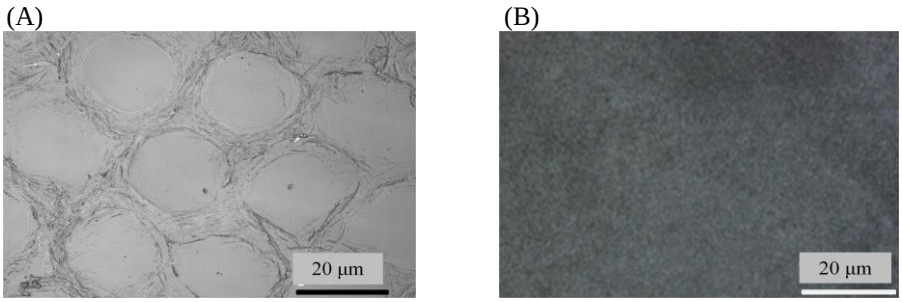

Figure 1. Morphology of bacterial cellulose film: (A) HPBC; (B) FBC

The adsorption isotherms of xylan on both HPBC and FBC were shown in **Figure 2**. The adsorption amount of xylan on HPBC at 1.0 mg/mL was 0.77 g/g of cellulose, while that on FBC was 0.27 g/g of cellulose. Likewise, the adsorbance of xylan on HPBC was much higher than that on FBC at any concentration. This result indicates that HPBC had a larger accessible area of xylan than FBC did. These reasons might be explained by the following facts. Most cellulose microfibrils in HPBC were exposed outwards, such as air and solvent, and easily accessible with adsorbate, whereas only microfibrils at the surface of FBC could contact with adsorbate. Therefore, HPBC is considered to a suitable test specimen for the evaluation of interaction between cellulose microfibrils and guest molecules.

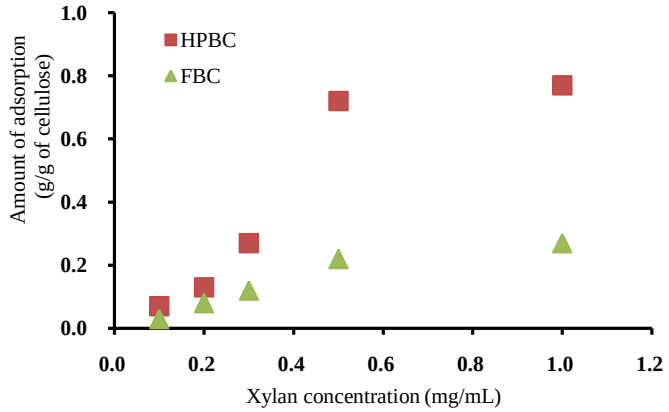

Figure 2. Amount of xylan adsorption on HPBC and FBC films

Polymerization of coniferyl alcohol on xylan-deposited HPBC

Polymerization of coniferyl alcohol as one of monolignols was attempted in the presence of xylan-deposited HPBC by the same manner as the endwise polymerization (Zutropfverfahren) for DHP preparation.[8] DHP content determined by acetyl bromide method and alkaline nitrobenzene oxidation yield are listed in **Table 1**. DHP content was slightly increased by the xylan adsorption by 2.1%. When the DHP-deposited HPBC was rinsed with 1,4-dioxane, DHP content was markedly decreased. We considered that washable DHP was free, while unwashable DHP was tightly associated with cellulose, i. e. that was lignin-carbohydrate complex (LCC). The difference in washable DHP content between in the presence and absence of xylan was negligible. Therefore, these results indicate that the xylan affected DHP formation very slightly as well as pectin reported by Touzel *et al*.[9]

Table 1. Chemical analysis of DHP

	DHP content (%)		Nitrobenzene oxidation yield (μmol/g)
	Before rinsing with dioxane	After rinsing with dioxane	
DHP-HPBC	26.2[a]	7.1[b]	45.5[c] (641)[d]
DHP-Xyl-HPBC	28.3[a]	8.9[b]	67.0[c] (752)[d]

a, DHP content of artificial cell wall; b, DHP content of artificial cell wall after rinsing with 1,4-dioxane; c, based on the weight of artificial cell wall; d, based on the weight of DHP.

Subsequently, 1,4-dioxane-rinsed HPBC with and without xylan were subjected to nitrobenzene oxidation, the yield of which was one of the measures for estimation of *β*-O-4 linkage that was a major interunitary linkage in lignin. The nitrobenzene oxidation yield of DHP-Xyl-HPBC was 67.0 μmol/g of cell wall (752 μmol/g of DHP), which was higher than that of DHP-HPBC (45.5 μmol/g of cell wall, 641 μmol/g of DHP). Thus, *β*-O-4 linkages remarkably increased when the xylan was present. This finding is in agreement with Barakat *et al*,[10] who reported that higher concentration of arabinoxylan induces higher thioacidolysis yied of DHP. The increase in *β*-O-4 linkage in the presence of hemicellulose suggests that regulate lignin structure during polymerization process.

Mechanical properties of artificial cell wall

Table 2 shows the effect of the cell wall components deposited onto HPBC on mechanical properties of resultant materials. Xylan deposition increased tensile strength and MOE by 1.2 times. Interestingly, both mechanical parameters were dramatically enhanced by DHP deposition by 1.6-1.7 times even without xylan. By deposition of both xylan and DHP onto HPBC, MOE was further enhanced; 1.7 times as compared with DHP-HPBC and 3 times as compared with HPBC. However, in terms of tensile strength, that of DHP-Xyl-HPBC was only 1.9 times as large as that of intact HPBC. From the mechanical test, we conclude that both of xylan and lignin reinforce cellulose as a framework of artificial cell wall. Especially, lignin seems to give the cell wall rigidity.

Table 2. Mechanical properties of HPBC

	Tensile strength (MPa)	MOE (MPa)	Elongation (%)	Film thickness (μm)
HPBC	19.4±6.9	278±100	6.3±1.4	0.77±0.03
Xyl-HPBC	23.6±5.7	352±110	6.9±3.2	0.79±0.05
DHP-HPBC	31.9±9.2	486±128	7.1±3.1	0.76±0.06
DHP-Xyl-HPBC	36.6±14.3	833±256	6.4±3.8	0.77±0.05

IV. CONCLUSIONS

We fabricated "artificial cell wall" upon successive depositions of xylan and DHP as a result of coniferyl alcohol polymerization onto HPBC. From the lignin analyses and mechanical test, we have come to the following conclusions: (i) xylan induced *β*-O-4 linkage with high frequency, although it scarcely contributed to DHP generation; (ii) both of xylan and DHP contributed to the mechanical strength of a cellulose framework, especially DHP contributed to the formation of rigid cell wall.

VI. REFERENCES

[1] Terashima, N.; Kitano, K.; Kojima, M.; Yoshida, M.; Yamamoto, H.; Westermark, U. Nanostructural assembly of cellulose, hemicellulose, and lignin in the middle layer of secondary wall of ginkgo tracheid. *J. Wood Sci.* **2009**, *55*, 409-416.

[2] Uraki, Y.; Nemoto, J.; Otsuka, H.; Tamai, Y.; Sugiyama, J.; Kishimoto, T.; Ubukata, M.; Yabu, H.; Tanaka, M.; Shimomura, M. Honeycomb-like architecture produced by living bacteria, *Gluconacetobacter xylinus*. *Carbohydr. Polym.* **2007**, *69*: 1-6.

[3] Uraki, Y.; Matsumoto, C.; Hirai, T.; Tamai, Y.; Enoki, M.; Hiroshi, Y.; Tanaka, M.; Shimomura, M. Mechanical effect of acetic acid lignin adsorption on honeycomb-patterned cellulosic films. *J. Wood Chem. Technol.* **2010**, *30*, 348-359.

[4] Uraki, Y.; Tamai, Y.; Hirai, T.; Koda, K.; Yabu, H.; Shimomura, M. Fabrication of honeycomb-patterned cellulose material that mimics wood cell wall formation processes. *Mater. Sci. Eng. C* **2011**, *31*, 1201-1208.

[5] Hestrin, S.; Schramm, M. Synthesis of cellulose by *Acetobacter xylinum*. II. Preparation of freeze-dried cells capable of polymerizing glucose to cellulose. *Biochem. J.* **1954**, *58*, 345-352.

[6] Hatfield, R. D.; Grabber, J.; Ralph, J.; Brei, K. Using acetyl bromide assay to determine lignin concentrations in herbaceous plants: Some cautionary notes. *J. Agric. Food Chem.* **1999**, *47*, 628-632.

[7] Chen, C.-L. Nitrobenzene and cupric oxide oxidations. In: Methods in lignin chemistry. Eds. Lin, S. Y.; Dence, C. W. Springer-Verlag, New York, USA. **1992**, pp. 301-321.

[8] Cathala, B.; Saake, B.; Faixb, O.; Monties B. Evaluation of the reproducibility of the synthesis of dehydrogenation polymer models of lignin. *Polym. Degrad. Stab.* **1998**, *59*, 65-69.

[9] Touzel, J.P.; Chabbert, B.; Monties, B.; Debeire, P.; Cathala, B. Synthesis and characterization of dehydrogenation polymers in *Gluconacetobacter xylinus* cellulose and cellulose/pectin composite. *J. Agric. Food Chem.* **2003**, *51*, 981-986.

[10] Barakat, A.; Chabbert, B.; Cathala, B. Effect of reaction media concentration on the solubility and the chemical structure of lignin model compounds. *Phytochemistry* **2007**, *68*, 2118-2125.

ELUCIDATION OF DEGRADATION PRODUCTS IN RAYON SPINNING BATHS

Eva Liftinger[1], Thomas Zweckmair[3]*, Gabriele Schild[2], Gottfried Eilenberger[3], Stefan Böhmdorfer[3], Thomas Rosenau[3], Antje Potthast[3]*

[1]*Kompetenzzentrum Holz GmbH, Altenberger Straße 69, A-4040 Linz, Austria*

[2]*Lenzing AG, Werkstraße 2, A-4860 Lenzing, Austria*

[3]*University of Natural Resources and Life Sciences, Division of Chemistry of Renewable Resources, Konrad-Lorenz-Strasse 24, A-3430 Tulln, Austria*

**Corresponding author: antje.potthast@boku.ac.at, thomas.zweckmair@boku.ac.at*

ABSTRACT

The manufacturing of viscose fibers has been optimized for many decades. Nevertheless, various improvements are desirable for environmental and economic reasons. This cherishes the need for more appropriate analytical methods, which are able to cope with the rather extreme conditions.

In the course of fiber production, the cellulose xanthate is introduced into a highly complex acidic spinning bath for regeneration of cellulose. Only the characterization of the inorganic compounds was established so far. An entire characterization of the spinning bath including organic degradation products was not feasible yet due to the extremely high content of inorganics.

In this study, a method was successfully implemented which enables the determination and quantification of the main organic degradation products in the viscose spinning bath. The organic fraction was extracted from the spinning bath by different techniques, which allowed separation of the organic from the vast inorganic fraction. Extensive removal of salts was a prerequisite for the analysis of the contained organic compounds. The samples were subsequently silylated and analyzed by GC-MS. The intricacy was the quantification of the degradation products, because standard compounds are often not commercially available.

Analyte recovery was optimized with regard to pH and lyophilization conditions. Since the spinning bath analytes show a very broad range of volatility, internal standardization by ^{13}C-labeled compounds should ideally be carried out of each single analyte. The degradation product spectrum of uniformly ^{13}C-labeled glucose converted in acidic media was used to approximate this target.

The developed method for the characterization of the viscose spinning bath opens new perspectives to keep track of the formation and origin of organic degradation products. It is a prerequisite for all further efforts to avoid undesired degradation of polysaccharides and contamination of the spinning bath for a higher product quality and a better closure of process cycles. Furthermore, it can be transferred to other highly complex acidic or alkaline industrial process streams.

I. INTRODUCTION

The analysis of a viscose spinning bath is not straightforward due to the huge variety of substances in a complex inorganic matrix with extremely high salt content. Today, the standard method to evaluate viscose spinning baths is an estimation of total organic carbon level (TOC), without a more detailed analysis of its chemical composition. The analysis of this extremely complex mixture is markedly difficult. The main part of the organic amount constitutes of hydroxy-monocarboxylic acids from carbohydrate degradation [1].

The increasing pressure to lower TOC levels in all process streams, based on environmental concerns and economic reasons, led to the attempt to better understand the composition of the degradation products in the viscose spinning bath. Furthermore, detailed information about its constituents would allow better handling of dirt fractions in the spinning bath and the following process.

Novotny et al. investigated the formation of carboxylic acids during degradation of monosaccharides. They succeeded in identification and quantification of three low molecular carboxylic acids, 2,4-hydroxy-carboxylic acids and 12 corresponding lactones by GC-MS. Hydroxy-carboxylic acids and their lactones were monitored as their trimethylsilylated derivates [2]. They are formed during degradation of reducing sugars. In general, the acids produced during sugar transformation can be divided into those which include the entire carbon skeleton of the sugar, and the acids with shorter carbon chains [3]. Typical products of degradation of sugars in strong alkaline media are saccharinic acids, although their formation was also observed in acidic media [4]. Acids with

shorter carbon chains than the parent sugars can be formed as direct cleavage products of sugar intermediates or by subsequent reactions with carbonyl fragments [1].

In the current study, the organic components of the viscose spinning bath were the point of interest. A new advanced methodology for identification and quantification of hydroxy-carboxylic acids was developed. In the past years researchers at Lenzing AG had already worked on identification of some components. These investigations served as a base of the current scientific method. Lactic acid, glycolic acid, 2-deoxytetronic acid, 2,3-deoxypentonic acid, 3-deoxy-2-(hydroxymethyl)-tetronic acid, 3-deoxypentonic acid, 3-deoxy-2-(hydroxymethyl)-pentonic acid and 2-(2,3-dihydroxypropyl)-tartronic acid were identified as possible spinning bath components. They also found that the organic acids originate to some extent in the viscose production process. In alkaline media, the acids are present as sodium salts. The major part of dicarboxylic acids probably originates from 4-*O*-methylglucuronic acids from xylan.

For separation of the organic fraction from the vast inorganic residue different extraction techniques were performed. An accelerated solvent extraction with pyridine compared to a batch extraction was examined. Real spinning bath samples were used for evaluation of analyte signal recovery with respect to pH and lyophilization conditions. Since the spinning bath analytes show a very broad range of volatility, internal standardization by ^{13}C-labeled compounds should be carried out for each single analyte in an ideal case. Hence, we degraded perlabeled ^{13}C-glucose in alkaline media for this purpose.

II. EXPERIMENTAL

As a first step, an industrial spinning bath sample, which was adjusted to pH 3 with sodium hydroxide solution (18.87 %), was submitted to headspace analysis. A closed loop sampler and a VF-WaxMS-column were used. The resulting gas chromatograms were compared with databases (see figure 1).

^{13}C-labeled glucose conversion products obtained after alkali degradation were used as internal reference. They were produced by degradation of ^{13}C perlabeled glucose in 18.87 % sodium hydroxide solution at 60 °C for 40 minutes. 3 g of glucose per 100 mL sodium hydroxide solution was used.

For further analysis, spinning bath samples were adjusted to different pH between pH 3 and pH 8 at integer pH-steps using 18.87 % sodium hydroxide solution. Lyophilization of individual sample sets was carried out at -34°C for 24h or at -105°C for 48 hours.

Two methods for sample preparation were compared. On the one hand the lyophilized samples were subjected to an accelerated solvent extraction (ASE) with pyridine. On the other hand, they were extracted with pyridine in a vial directly used for derivatization. In case of ASE an aliquot of the pyridine phase was transferred into a new vial. In both cases derivatization was carried out by mixing with pyridine, which contains ethoxyamine·HCl and methyl-*α*-*D*-galactopyranoside as an internal standard. Then the aliquot was heated to 70 °C for one hour in an oven. Pyridine containing 4-(dimethylamino)-pyridine (DMAP), bis(trimethylsilyl)trifluoro-acetamide (BSTFA) and trimethylchlorosilane (TMS) were added. The mixture was heated again to 70 °C for two hours and after cooling was diluted with ethyl acetate and filtered through a PTFE membrane. An aliquot was injected into the GC-MS for analysis [5].

III. RESULTS AND DISCUSSION

The headspace sample, which was adjusted to pH 3, was analyzed in order to determine the volatile sample compounds in the gas phase at 50 °C. **Figure 1** shows the resulting chromatogram including a number of analytes which were identified by a database search. The highest peaks that were recognized were 1-pentanol, 2-ethyl-1-hexanol, isobutyric acid, benzothiazole and 4-ethyl-guaiacol. These substances could be used for calibration in GC-MS in order to increase the ratio of TOC described by GC-MS analysis.

Two ways of pyridine extraction were investigated. The extraction was conducted as batch reaction or as accelerated extraction by ASE. Interestingly, the batch reaction revealed higher analyte yields as it is not necessarily accompanied by sample dilution. Signal yields for the ten most abundant spinning bath peaks were evaluated at defined pH-levels. A strong dependence on pH was obvious. At pH=8 the highest number of analytes showing a maximum in signal recovery was observed. Thus, this parameter is considered to be useful for the all subsequent investigations.

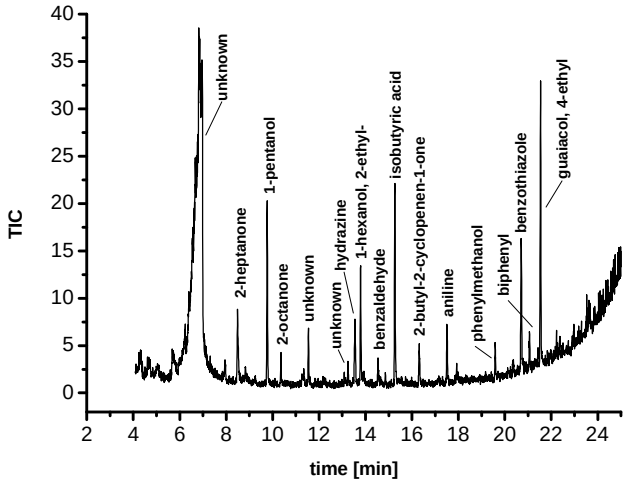

Figure 1. Results of headspace GC (pH 3)

Also different conditions of lyophilization were examined. Samples which were lyophilized at -34 °C for 24 h were compared with samples which were lyophilized at -105 °C for 48 h. It was ascertained that lower temperatures for a longer time range had a positive impact on analyte recovery.

Spinning bath samples present a huge variety of components, each with a different volatility. A simple internal standard would not accommodate the different volatilities of all the analytes. In an ideal case every analyte should be internally standardized by uniformly ^{13}C-labeled compounds to ensure unambiguous differentiation in MS-detection.

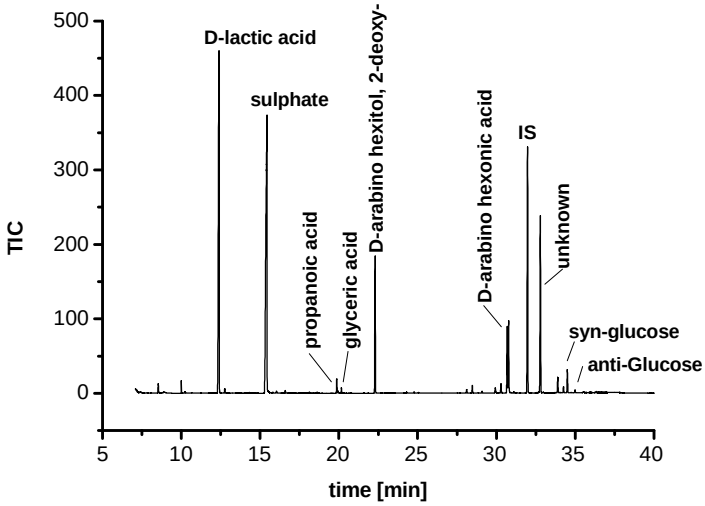

Figure 2. Chromatogram of the glucose conversion product

The glucose conversion product obtained in alkaline media ideally corresponds to the components in the spinning bath and as a consequence also to their volatilities. In reality, the product spectrum differs to a certain extend which forces the analyst to divide the spinning bath chromatogram into sections and to introduce one internal standard with a representative volatility for each group (**Figure 2, Figure 3**).

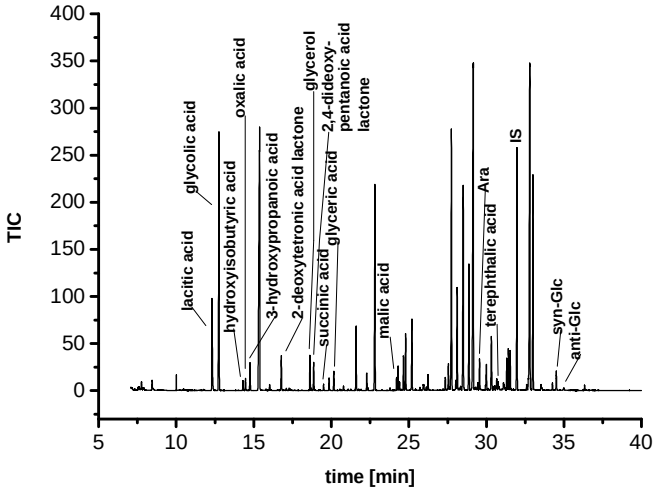

Figure 3. Chromatogram from spinning bath at pH 8

IV. CONCLUSIONS

- Headspace analysis shows several volatile compounds to be quantified. Their quantitative information would help to describe a bigger TOC-ratio by GC-MS.
- For analysis of spinning bath components it is inevitable to compare samples at different pH as the signal intensities vary over a larger pH range.
- Lyophilization turned out as a crucial point. Lower temperatures obviously had better impact on the analyte yield.
- Batch extraction with pyridine was more expedient for analyte signal recovery.
- The usage of the ^{13}C-glucose conversion product as internal reference was confirmed as a suitable approach because the degradation products cover all compound classes present.
- Further investigations have to be performed to optimize the method developed.

V. ACKNOWLEDGEMENT

Financial support was provided by the Austrian government, the provinces of Lower Austria, Upper Austria and Carinthia as well as by the Lenzing AG. We also express our gratitude to the Johannes Kepler University, Linz, the University of Natural Resources and Life Sciences (Boku), Vienna, and the Lenzing AG for their in kind contributions.

VI. REFERENCES

[1] Niemelä K., (1988) Gas-Liquid Chromatography-Mass Spectrometry
Studies on Pine Kraft Black Liquors. 3. The Liberation of
Carboxylic-Acids in the Initial Phase of Pulping, *Journal of Chromatography*, 446:247 – 252.

[2] Novotný O., Cejpek K., Velišek J. (2008) Formation of carboxylic acids during degradation of monosaccharides, *Czech Journal of Food Science*, 26: 117-131.

[3] Yaylayan V.A., Huyghues-Despiontes A. (1996) Identification of per-O-(trimethylsilyl) derivtes of aldoses generated from thermal composition of N-(1-deoxy-D-fructopyranos-1-yl)proline: reversibility of the Amadori rearrangement, *Carbohydrate Research* 280: 27-45.

[4] Mizuno T., Weiss A.H. (1974) Synthesis and utilization of formose sugars, *Advances in Carbohydrate Chemistry and Biochemistry* 29: 173-227.

[5] Bogolitsyna A., Becker M., Borgards A., Liebner F., Rosenau T., Potthast A. (2012) Degradation products of lignocellulosics in pulp mill effluents – comparison and evaluation of different gas chromatographic techniques for a comprehensive analysis, *Holzforschung* 60: 917-925.

EFFECT OF STEAM EXPLOSION ON FIBRE LIGNIN STRUCTURE FOR SELF-BINDING FIBER BOARDS

Liitiä, T.[1*], Rovio, S.[1], Talja, R.[1], Tamminen, T.[1], Rencoret, J.[2], Gutiérrez, A.[2], del Río, J.C.[2], Sutka, A[3]., Tupciauskas, R.[3], Andzs, M.[3], Gravitis, J.[3]

*[1] VTT Technical Research Centre of Finland, P.O. Box 1000, FI-02044 VTT, Finland; [2] IRNAS-CSIC, P.O.Box 1052, 41080-Seville, Spain; [3] Latvian State Institute of Wood Chemistry, 27 Dzerbenes Str., LV-1006-Riga, Latvia; (*Tiina.Liitia@vtt.fi)*

ABSTRACT

The structural changes induced in fiber lignin by steam explosion was studied to better understand the effect of steam explosion conditions on bonding mechanisms of lignin containing fibers in self-binding fiber boards. In all the steam exploded lignin samples, the main lignin inter-unit linkage after 1 min treatment was the β–*O*–4´ alkyl aryl ether that accounts for up to nearly 80% of all inter-unit linkages. With increased steam explosion times a drastic decrease in the content of β-O-4 linkages was detected, which was accompanied with the formation of new phenolic units and decrease in molar mass. However, at the same time, some condensation of lignin occurred as well. After steam explosion, the lignin was more prone to thermally induced condensation reactions. The formation of the new phenolic groups during steam explosion, and the enhanced tendency to condensate during thermal processing, most likely contribute to the higher bonding ability of steam exploded fibers when manufacturing self-binding fiber boards.

I. INTRODUCTION

Steam explosion (SE) is a potential pretreatment method to produce self-binding fiber boards, utilizing the fiber lignin as such or together with added lignin as a binder without any synthetic resins [1-3]. This way the negative effects of synthetic phenol-formaldehyde resins, e.g. emissions of volatile formaldehyde, could be avoided. It has also been shown that the properties of produced boards in many cases are comparable with the conventional commercial boards, especially for dry-use in interior grades [1]. To better understand the effect of steam explosion conditions on bonding mechanisms of lignin containing fibers, it is essential to better understand the structural changes induced in fiber lignin.

In this study, steam explosion was performed in different conditions at laboratory scale for grey alder, birch, and wheat straw, and fiber lignin was isolated by alkaline extraction for chemical characterization. The lignin samples were analyzed in detail by 2D ^{1}H-^{13}C correlation NMR spectroscopy that provided information of the structure of the whole lignin macromolecule and is a powerful tool for lignin structural characterization revealing both the aromatic units and the different inter-unit linkages present in the lignin polymer [4]. The functional groups of lignin, *i.e.* aliphatic and phenolic hydroxyls and carboxylic acids, were detected by ^{31}P NMR spectroscopy, and the lignin molar mass distributions were detected by size exclusion chromatography (SEC). Thermal properties were evaluated by differential scanning calorimetry (DSC).

II. EXPERIMENTAL

Steam explosion. Steam explosion (SE) was performed for wheat straw (WS), birch and grey alder (GA) at 235°C with 3.2MPa pressure for 1min. For gray alder also longer SE times of 2 and 3 min were performed. The steam exploded fibers were used for production of fiber boards. For the analytical purposes, lignin was extracted from steam exploded fibers by 0.4% NaOH and precipitated by acid.

Analytical methods. The molar mass distributions of lignins were determined by size exclusion chromatography (SEC) in 0.1M NaOH eluent using MCX 1000 and 100 000 columns with UV detection (280 nm). The molar mass distributions and the average molar mass values (Mn, Mw) were calculated relative to the polystyrene suphonate (Na-PSS) calibration using Waters Empower 3 software.

Lignin functionalities were determined by ^{31}P NMR according to Granata and Argyropoulos [5]. Accurately weighted samples (40 mg) were dissolved in 150 µL of *N,N*-dimethylformamide. After dissolution, 100 µL pyridine, 200 µL internal standard solution of 0.05 M *endo*-N-Hydroxy-5-norbornene-2,3-dicarboximide in pyridine/$CDCl_3$ (1.6/1, v/v) and 50 µL $Cr(acac)_3$ solution (11.4 mg/1 mL) in pyridine/$CDCl_3$ (1.6/1, v/v) were

added. Then, 100 µL 2-chloro-4,4,5,5-tetramethyl-1,3,2-dioxaphopholane was added drop-wise, followed by 300 µL of $CDCl_3$. The ^{31}P NMR measurements were performed immediately after sample preparation at room temperature with Bruker Avance 500 MHz NMR spectrometer using 90° pulse and 5s pulse delay for 512 scans.

2D ^{1}H-^{13}C HSQC (heteronuclear single quantum coherence) NMR spectra were recorded at 25ºC by a Bruker AVANCE III 500 MHz, equipped with a cryogenically-cooled 5 mm TCI gradient probe with inverse geometry using 'hsqcetgpsisp2.2' pulse sequence (adiabatic-pulsed version). Lignin samples were dissolved (40mg/0.75 mL) in DMSO-d_6. Spectral widths of 5000 Hz (10-0 ppm) and 20,843 Hz (165-0 ppm) for the ^{1}H- and ^{13}C-dimensions were used. The number of transients was 64 for 256 time increments, with $^{1}J_{CH}$ of 145 Hz. The semiquantitative analysis of the correlation peaks was performed using Brukers Topspin 3.1 software. The lignin inter-unit linkages based on C_α–H_α correlations were calculated as described previously [2].

The lignin glass transition (Tg) temperatures were determined by Mettler Toledo Differential Scanning Calorimeter model DSC820 system STARe SW 9.20. Temperature profile with following steps was used: 1) heating from 25 ^{o}C to 105 ^{o}C with 20 min isothermic phase for drying, 2) cooling phase to -60 ^{o}C, 3) first actual heating phase from -60 ^{o}C to 200 ^{o}C, 4) cooling phase to -60 ^{o}C, and 5) second heating phase from -60 ^{o}C to 250 ^{o}C. Heating and cooling rate of 10°C/min was used in all cases.

III. RESULTS AND DISCUSSION

The structural changes induced in fiber lignin by steam explosion was studied to better understand the effect of steam explosion conditions on bonding mechanisms of lignin containing fibers. Based on 2D ^{1}H-^{13}C HSQC NMR results given in Table 1, the main lignin substructure present in all the steam exploded lignin samples was the β–*O*–4´ alkyl aryl ether. It accounts for up to nearly 80% of all inter-unit linkages in 1 min steam exploded wood lignin, while condensed linkages (β–β´ resinols, β–5´ phenylcoumarans and β–1´ spirodienones) were present in lower amounts. Interestingly, the 2D-NMR data also indicated that the steam exploded grey alder lignins showed a drastic decrease in the content of lignin substructures, particularly β-O-4 linkages, with increasing steam explosion time. Compared to the hardwoods, the steam explosion had more drastic effect on wheat straw in the same conditions.

The cleavage of β-O-4 linkages during steam explosion pretreatment was accompanied with the formation of new phenolic units (Table 2) and decrease of molar mass (Mw) (Table 3). However, at the same time, some condensation of lignin occurred as well. As shown in the molar mass distributions (Figure 1), the decrease of molar mass was mainly due to the degradation of high molecular weight lignin or lignin-carbohydrate complexes (LCCs), whereas the molar mass of the main lignin fraction increased at the same time. Also the proportion of condensed phenolic units (C+S) was increased (Table 2). It is thus evident that both lignin degradation and condensation takes place during steam explosion.

Table 1. Content of most typical lignin inter-unit linkges per 100 C9 unit determined by 2D NMR.

Sample	β-O-4	β–β	β-5	β-1
SE-WS	7.9	3.3	0.8	-
SE-Birch	22.3	4.7	1.6	-
SE-GA-1	24.5	2.4	3.9	0.3
SE-GA-2	12.5	2.4	3.4	0.3
SE-GA-3	4.6	1.4	1.9	0.1

Table 2. The lignin functionalities determined by ^{31}P NMR (mmol/g lignin, calculated according to the lignin content of the samples).

Sample	Aliph OH, mmol/g	C + S, mmol/g	G, mmol/g	Catechol, mmol/g	p-OH, mmol/g	Phenolic OH, mmol/g	Total OH, mmol/g	COOH mmol/g
SE-WS	1,4	1,0	0,9	0,0	0,2	2,1	3,5	0,5
SE-Birch	2,4	1,9	0,5	0,0	0,0	2,4	4,7	0,3
SE-GA-1	3,1	1,7	0,6	0,3	0,2	2,7	5,8	0,2
SE-GA-2	2,1	1,9	0,6	0,2	0,2	2,9	5,0	0,3
SE-GA-3	1,4	2,3	0,7	0,3	0,2	3,5	4,9	0,3

The glass transition temperatures detected after second heating cycle (Table 3) were higher than after the first heating, which indicates that some condensation reactions most likely takes place during thermal processing of steam exploded lignins. Also here, the prolonged steam explosion slightly increased the tendency for thermally induced condensation. Formation of the new phenolic units during steam explosion, and the enhanced tendency to condensate during thermal processing most likely contribute to the higher bonding ability of steam exploded fibers in self-binding fiber boards.

Table 3. The average molar masses (Mn, Mw, PD) and the glass transitions of first and second heating (Tg_{1st}, Tg_{2nd}).

Sample	Molar mass			Glass transition	
	Mn, g/mol	Mw, g/mol	PD	Tg 1st	Tg 2nd
SE-WS	2800	7000	2.5	160.6	186.4
SE-Birch	2200	5200	2.4	153.5	162.6
SE-GA-1	2300	5200	2.3	150.3	165.4
SE-GA-2	2400	5000	2.1	154.2	166.4
SE-GA-3	2500	4800	1.9	150.5	168.5

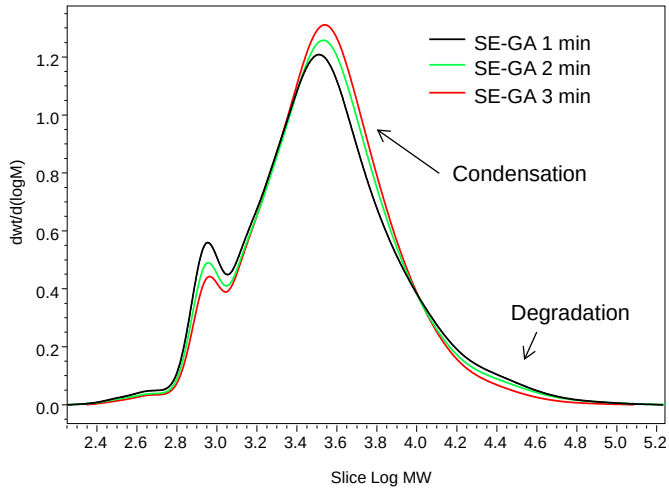

Figure 1. The molar mass distributions of the SE-GA lignins after variable steam explosion times of 1-3 min.

IV. CONCLUSIONS

In all the steam exploded lignin samples, the main lignin substructure present was the β–*O*–4´ alkyl aryl ether that accounts for up to nearly 80% of all inter-unit linkages in 1 min steam exploded wood lignin. Interestingly, the steam exploded grey alder lignins showed a drastic decrease in the content of β-O-4 linkages with increasing steam explosion time, which was accompanied with the formation of new phenolic units and decrease of molar mass. However, at the same time, some condensation of lignin occurred as well. After steam explosion, the lignin was also more prone to thermally induced condensation reactions. Both the formation of the new phenolic groups during steam explosion, and the enhanced tendency to condensate during thermal processing most likely contribute to the higher bonding ability of steam exploded fibers when manufacturing self-binding fiber boards.

V. ACKNOWLEDGEMENT

WoodWisdom-EraNet and the national funding agencies (Tekes, INIA-Spain, Latvian Ministry of Agriculture) are acknowledged for the funding of ProLignin project.

VI. REFERENCES

[1] Gravitis, J., Abolins, J., Tupciauskas, R., Veveris, A., Alksnis, B. Substitution of phenolic components by steam-exploded lignin in plywood and self-binding boards with account of energy vecessary for steam explosion

treatment, *Scientific Journal of Riga Technical University – Material Science and Applied Chemistry*, **2010**, *21*, 7-11.
[2] Tupciauskas, R., Gravitis, J., Belkova, L., Tuherm, H., Grey alder fiber board processed by modified steam explosion unit, *16th International Scientific Conference on Research for Rural Development 2010*, Jelgava, Latvia, May 19-21, **2010**, 248-254.
[3] Tupciauskas, R., Gravitis, J., Veveris, A., Tuherm, H., *Forest & Landscape Working Papers*, **2009**, 43, 141.
[4] del Rio, J.C.; Prinsen, P.; Martinez, A.T.; Ralph, J.; Gutiérrez, A. Structural characterization of wheat straw lignin as revealed by analytical pyrolysis, 2D-NMR, and reductive cleavage methods. *J. Agric. Food. Chem.* **2012**, *60*, 5922-5935.
[5] Granata, A., Argyropoulos, D.S. 2-Chloro-4,4,5,5-tetramethyl-1,3,2-dioxaphospholane, a reagent for the accurate determination of the uncondensed and condensed phenolic moieties in lignins. *J. Agric. Food Chem.***1995**, *43*, 1538-1544.

STRUCTURAL CHARACTERIZATION OF THE LIGNINS FROM SUGARCANE BAGASSE AND STRAW

Alessandro G. Lino[1,2], Jorge Rencoret[1], Ana Gutiérrez[1], Jorge L. Colodette[2], Claudio F. Lima[3], Ángel T. Martínez[4] and José C. del Río[1]*

[1]IRNAS-CSIC, P.O. Box 1052, 41080-Seville, Spain; [2]Department of Forestry Engineering, Federal University of Viçosa, Viçosa, MG 36570-000, Brazil; [3]Department of Chemistry, Federal University of Viçosa, Viçosa, MG 36570-000, Brazil; [4]CIB-CSIC, Ramiro de Maeztu 9, E-28040 Madrid, Spain (delrio@irnase.csic.es)*

ABSTRACT

The structure of the lignins of sugarcane bagasse and straw was investigated. The lignins were characterized both *in situ* and in isolated preparations (Milled-Wood Lignin, MWL, and Cellulolytic Lignin, CEL) by Py-GC/MS and 2D-NMR. It was concluded that they are *p*-hydroxyphenyl-guaiacyl-syringyl lignins with associated *p*-coumarates and ferulates. 2D-NMR indicated that the main substructures present are β–*O*–4´-ethers, followed by β–5´ phenylcoumarans and with lower amounts of β–β´ resinols and β–1´ spirodienones.

I. INTRODUCTION

Sugarcane bagasse and straw are wastes from the process of sugar extraction, and are abundant and low-cost materials of the alcohol and sugar industries. Sugarcane bagasse and straw are composed of cellulose (ca. 41%), hemicelluloses (ca. 39%) and lignin (19-21%), with high amounts of extractives (2.4-4.8%) and ash (ca. 5%), and are attractive feedstocks to produce second–generation bioethanol and other value-added products in the context of the lignocellulosic biorefinery. The conversion of lignocellulosic biomass to bioethanol involves saccharification of carbohydrates to fermentable reducing sugars and then fermentation of these free sugars to ethanol. However, the presence of lignin limits the accessibility of enzymes to cellulose, thus reducing the efficiency of the hydrolysis. Pretreatment of lignocellulosic materials to remove or modify the lignin is therefore needed to enhance the hydrolysis of carbohydrates. The efficiency of pretreatment methods is highly dependent on the lignin structure, and hence the knowledge of the structure of the lignin polymer in sugarcane bagasse and straw is important to develop appropriate pretreatment methods for lignin modification and/or removal.

In this paper, we report the structural characteristics of the lignins in sugarcane bagasse and straw by analytical pyrolysis (Py-GC/MS) and 2D-NMR. The knowledge of the composition and structure of the lignin of sugarcane will help to maximize the exploitation of these important agroindustrial as a feedstocks for biofuels and other biorefinery products.

II. EXPERIMENTAL

Samples

Sugarcane bagasse and straw were supplied by the University of Viçosa (MG, Brazil). Klason lignin content was estimated as the residue after sulphuric acid hydrolysis according to the TAPPI method T222 om-8. The acid-soluble lignin was determined, after the insoluble lignin was filtered off, by UV-spectroscopic determination at 205 nm wavelength using 110 L cm^{-1} g^{-1} as the extinction coefficient (TAPPI method UM 250).

Isolation of 'Milled-Wood' Lignin (MWL) and Cellulolytic lignin (CEL)

'Milled-wood' lignin (MWL) was extracted from finely ball-milled (50 h) plant material, free of extractives and hot water soluble material, using dioxane-water (9:1, v/v), followed by evaporation of the solvent, and purified as described [1]. The final yields ranged from 5-15%. Cellulolytic lignin (CEL) preparations were isolated by enzymatically saccharifying polysaccharides as described [2]. Cellulysin cellulase (Calbiochem), from *Trichoderma viride* was used. The final yields were higher than 90%.

Analytical pyrolysis

Pyrolysis (ca. 100 µg) was performed with a 3030 micro-furnace pyrolyzer (Frontier Labs) connected to an Agilent 7820A GC using a DB-1701 capillary column (60 m x 0.25 mm i.d., 0.25 µm film thickness) and an Agilent 5975 mass selective detector. The pyrolysis was performed at 500 ºC. The oven was programmed from 45 ºC (4 min) to 280 ºC (10 min) at 4 ºC min^{-1}. Helium was the carrier gas (1 mL min^{-1}).

III. RESULTS AND DISCUSSION

The abundance of the main constituents (water solubles, acetone extractives, Klason lignin, acid-soluble lignin, holocellulose, α-cellulose, and ash) of sugarcane bagasse and straw are shown in **Table 1**.

Table 1. Abundance of the main constituents (% dry-weight) of sugarcane bagasse and straw.

	Sugarcane bagasse	Sugarcane straw
Water soluble extractives	1.4 ± 0.2	2.2 ± 0.2
Acetone extractives lipids	0.8 ± 0.1	1.3 ± 0.1
Klason lignin	17.8 ± 0.6	17.0 ± 0.2
Acid-soluble lignin	2.2 ± 0.2	1.9 ± 0.2
Holocellulose (α-cellulose)	75.8 ± 0.5 (40.1 ± 0.2)	72.9 ± 0.7 (37.9 ± 0.3)
Ash	2.0 ± 0.1	4.7 ± 0.5

MWL and CEL preparations were isolated from sugarcane bagasse and straw according to traditional lignin isolation procedures [1,2], and were subsequently analyzed by Py-GC/MS and 2D-NMR. The pyrograms of sugarcane basse and straw, and of their corresponding MWL and CEL preparations are shown in **Figure 1**. The identities and relative molar abundances of the released compounds are listed in **Table 2**.

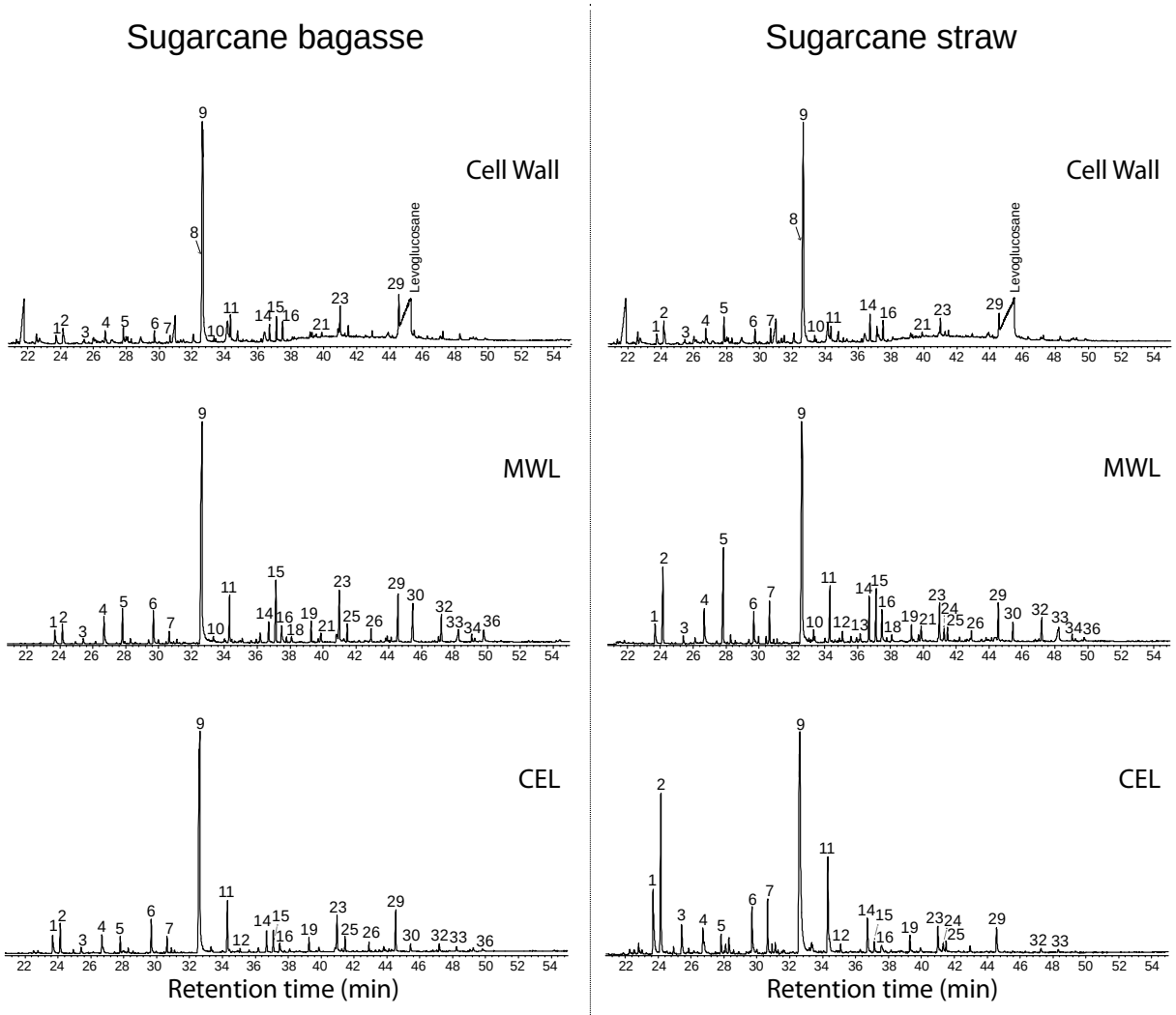

Figure 1. Py-GC/MS of sugarcane bagasse and straw (whole cell-walls), and their isolated MWL and CEL lignin preparations. The identities and relative abundances of the released compounds are listed in **Table 2**.

Table 2. Identities and relative molar abundances of the compounds released after Py-GC/MS of sugarcane bagasse and straw (whole cell walls) and their isolated MWL and CEL preparations.

		Sugarcane bagasse			Sugarcane straw		
	Compounds	CW	MWL	CEL	CW	MWL	CEL
1	phenol	2.46	2.67	4.12	3.06	3.05	10.17
2	guaiacol	2.54	2.18	3.55	3.87	8.03	13.59
3	3-methylphenol	1.05	0.66	0.97	1.06	0.83	3.32
4	4-methylphenol	2.49	4.21	2.84	3.10	4.38	2.91
5	4-methylguaiacol	2.33	2.98	1.70	4.00	8.87	1.36
6	4-ethylphenol	1.48	3.67	3.97	2.14	2.87	4.38
7	4-ethylguaiacol	0.83	0.99	1.44	1.75	2.80	3.44
8	4-vinylguaiacol	10.99	3.30	7.09	16.97	8.72	9.09
9	4-vinylphenol	53.27	41.72	47.40	43.85	29.98	31.30
10	eugenol	0.42	0.35	0.49	0.78	0.77	0.59
11	syringol	3.13	4.17	5.47	2.08	4.26	7.74
12	*cis*-isoeugenol	0.27	0.35	0.37	0.46	0.73	0.55
13	*trans* 4-propenylphenol	0.46	1.02	0.65	0.48	0.81	0.29
14	*trans*-isoeugenol	1.75	1.55	2.12	3.13	3.03	2.61
15	4-methylsyringol	2.39	5.10	1.93	1.70	3.49	0.72
16	vanillin	2.36	1.88	1.34	2.58	2.52	0.91
17	propynylguaiacol	0.17	0.36	0.13	0.21	0.26	0.09
18	propynylguaiacol	0.27	0.51	0.15	0.29	0.55	0.08
19	4-ethylsyringol	0.48	1.24	1.08	0.31	0.91	1.05
20	vanillic acid methyl ester	0.00	0.25	0.09	0.00	0.44	0.00
21	acetovanillone	0.48	0.89	0.54	0.76	1.28	0.42
22	4-hydroxybenzaldehyde	0.00	1.35	0.67	0.00	0.30	0.00
23	4-vinylsyringol	2.97	3.97	3.08	1.92	2.52	1.65
24	guaiacylacetone	0.24	0.21	0.22	0.55	0.83	0.49
25	4-allylsyringol	0.87	1.06	1.06	0.57	0.67	0.48
26	*cis*-4-propenylsyringol	0.51	0.81	0.66	0.30	0.58	0.27
27	propinylsyringol	0.00	0.29	0.44	0.45	0.05	0.07
28	propinylsyringol	0.00	0.30	0.18	0.15	0.03	0.06
29	*trans*-4-propenylsyringol	3.19	3.22	3.28	2.00	2.08	1.56
30	syringaldehyde	0.62	3.20	0.78	0.00	1.26	0.14
31	syringic acid methyl ester	0.12	0.27	0.11	0.08	0.11	0.00
32	acetosyringone	0.65	1.82	0.72	0.36	1.37	0.30
33	syringylacetone	0.62	1.21	0.39	0.40	0.93	0.22
34	propiosyringone	0.19	0.45	0.17	0.10	0.34	0.06
35	syringyl vinyl ketone	0.19	0.28	0.35	0.25	0.15	0.09
36	*trans*-coniferaldehyde	0.21	1.26	0.43	0.28	0.22	0.00
37	*trans*-sinapaldehyde	0.00	0.27	0.00	0.00	0.00	0.00
	S/G[a]	1.1	1.7	1.3	0.5	0.5	0.5

[a]All G- and S-derived peaks were used for the estimation of the S/G ratio, except 4-vinylguaiacol (which also arises from ferulates), and the analogous 4-vinylsyringol.

Pyrolysis of the whole cell-walls of sugarcane bagasse and straw released compounds from carbohydrate and lignin moieties, as well as from *p*-hydroxycinnamates. Among the lignin derived phenols, the pyrograms showed compounds derived from *p*-hydroxyphenyl (H), guaiacyl (G) and syringyl (S) lignin units as well as from the cinnamic acid esters in the wall. The most prominent cinnamate or lignin-derived compounds released were 4-vinylguaiacol (8) and 4-vinylphenol (9) with important amounts of other lignin-derived compounds such as phenol (1), guaiacol (2), 4-methylguaiacol (5), syringol (11), 4-methylsyringol (15) and 4-vinylsyringol (23). However, the high amounts of 4-vinylphenol released upon pyrolysis is mostly due to the presence of *p*-coumarates which decarboxylates efficiently under pyrolytic conditions [3–6]. Similarly, 4-vinylguaiacol, which is present in high abundance among the pyrolysis products of the whole cell-walls, also arises from ferulates after decarboxylation upon pyrolysis.

Pyrolysis of the MWL and CEL preparations released a similar distribution of cinnamate- and lignin-derived compounds as from their respective whole cell-walls, except for the much lower relative abundance of 4-vinylguaiacol (8). The most prominent compound in the pyrograms of the MWL and CEL preparations was still

4-vinylphenol (9), derived largely from the *p*-coumarate esters acylating lignin sidechains, and as also occurred in the pyrolysis of their whole cell-walls. The presence of *p*-hydroxycinnamates in the whole cell walls, as well as in the isolated lignins, however, could be addressed by pyrolysis in the presence of a methylating agent, tetramethylammonium hydroxide (data not shown). The relative abundances of *p*-hydroxycinnamates (*p*-coumarate/ferulate ratio) present in the whole cell-walls and in their isolated lignins revealed that ferulate is mostly attached to the carbohydrates while *p*-coumarate is primarily attached to the lignin polymer, as occur in other grasses [5,6].

It is obvious then that these vinyl compounds cannot be used for the estimation of the lignin H:G:S composition upon Py-GC/MS, as the major part of them do not arise from the core lignin structural units but from *p*-hydroxycinnamates. A rough estimation of the S/G ratio of the lignins in sugarcane bagasse and straw and their isolated MWL and CEL lignins was, however, performed by ignoring 4-vinylguaiacol (and the analogous 4-vinylsyringol), and revealed that sugarcane bagasse lignin is enriched in S-lignin units (S/G of 1.1–1.7) whereas the lignin from sugarcane straw is enriched in G-lignin units (S/G of 0.5) (**Table 2**).

Additonal analysis by 2D-NMR revealed that the main lignin substructures present were β–*O*–4′ aryl ethers followed by smaller amounts of phenylcoumarans, resinols and spirodienones. The S/G ratios obtained by 2D-NMR closely matched those determined by Py-GC/MS, indicating a predominance of S-lignin units in sugarcane bagasse lignin and a predominance of G-lignin units in sugarcane straw lignin. The spectra indicated that *p*-coumarates are acylating the γ-position of the lignin side-chains, as also occurs in other grasses [5–7]. The spectra also revealed that the flavone tricin was incorporated into the structure of these lignins, as also occurred in other grasses [5,6].

IV. CONCLUSIONS

Analysis of sugarcane bagasse and straw and their isolated MWL and CEL lignin preparations indicated that they are H-G-S lignins with some amounts of associated *p*-coumarates (acylating the γ-position of the lignin moiety) and ferulates (associated to the carbohydrates). Whereas the lignin in sugarcane bagasse is more enriched in S-lignin units, the lignin from sugarcane straw is enriched in G-lignin units. The main lignin inter-unit linkages present were the β–*O*–4′ aryl ethers, followed by phenylcoumarans, resinols and spirodienones. The flavone tricin was also found to be incorporated into these lignins, as also occurs in other grasses.

V. ACKNOWLEDGEMENT

This study has been funded by the Spanish project AGL2011-25379 (co-financed by FEDER funds). Jorge Rencoret thanks the CSIC for a JAE-DOC contract of the program “Junta para la Ampliación de Estudios” co-financed by Fondo Social Europeo (FSE). AGL thanks CAPES (Coordenação de Aperfeiçoamento de Pessoal de Nível Superior) for financial support.

VI. REFERENCES

[1] Björkman, A. Studies on finely divided wood. Part I. Extraction of lignin with neutral solvents. *Sven. Papperstidn.* **1956**, *59*, 477–485.

[2] Chang, H.; Cowling, E.B.; Brown, W.; Adler, E.; Miksche, G. Comparative studies on cellulolytic enzyme lignin and milled wood lignin of sweetgum and spruce. *Holzforschung* **1975**, 29, 153–159.

[3] del Río, J.C.; Martín, F.; González-Vila, F.J. Thermally assisted hydrolysis and alkylation as a novel pyrolytic approach for the structural characterization of natural biopolymers and geomacromolecules. *Trends Anal. Chem.* **1996**, 15, 70–79.

[4] del Río, J.C.; Gutiérrez, A.; Rodríguez, I.M.; Ibarra, D.; Martínez A.T. Composition of non-woody plant lignins and cinnamic acids by Py-GC/MS, Py/TMAH and FT-IR. *J. Anal. Appl. Pyrol.* **2007**, 79, 39–46.

[5] del Río, J.C.; Prinsen, P.; Rencoret, J.; Nieto, L.; Jiménez-Barbero, J.; Ralph, J.; Martínez, A.T.; Gutiérrez, A. Structural characterization of the lignin in the cortex and pith of elephant grass (*Pennisetum purpureum*) stems. *J. Agric. Food Chem.* **2012**, *60*, 3619–3634.

[6] del Río, J.C.; Rencoret, J.; Prinsen, P.; Martínez, A.T.; Ralph, J.; Gutiérrez A. Structural characterization of wheat straw lignin as revealed by analytical pyrolysis, 2D-NMR, and reductive cleavage methods. *J. Agric. Food Chem.* **2012**, *60*, 5922–5935.

[7] Ralph, J. Hydroxycinnamates in lignification. *Phytochem. Rev.* **2010**, *9*, 65–83.

PREPARATION AND STABILIZATION OF GOLD NANOPARTICLES USING CELLULOSE DERIVATIVES AS THE REDUCING AND STABILIZING AGENT

Weiwei Li, Junjun Tan, Ruigang Liu*, Huang Yong

*Sate Key Laboratory of Polymer Physics and Chemistry, Beijing National Laboratory of Molecular Sciences, Institute of Chemistry, Chinese Academy of Sciences, Beijing 100190, China (*rgliu@iccas.ac.cn)*

ABSTRACT

In present work, cellulose derivatives were used as the green reducing and stabilizing agent for preparation of gold nanoparticles (AuNPs). First, a pH-sensitive gold nanoparticles cysteamine/carboxymethyl cellulose (AuNPs-CA/CMC) dispersion system was prepared by a simple approach. Gold nanoparticles (AuNPs) were firstly synthesized by directly reducing chloroauric acid ($HAuCl_4$) with sodium carboxymethyl cellulose (CMC). Then the AuNPs were decorated by an electrostatic compound of cysteamine hydrochloride (CA) and sodium carboxymethyl cellulose (CMC) through ligand exchange to get the assembly of AuNPs-CA/CMC. The AuNPs-CA/CMC dispersion system exhibits strongly reversible pH-responsive behavior with the aggregation of the AuNPs caused by the combined action of the chain conformation change of CMC and electrostatic interactions between CA and CMC at different pH value. In order to avoid using CA for stabilizing AuNPs, amidoxime functionalized cellulose (AOFC) was synthesized and used for the preparation of AuNPs. It was found that AOFC can be used as both reducing agent and stabilizer for preparing gold nanoparticles (AuNPs). The AOFC stabilized AuNPs have the excellent stability in whole pH range, which may have the promising applications in the fields of catalyst, biotechnology and medicine.

I. INTRODUCTION

Cellulose is one of the oldest natural polymers and is the most abundant biomass in nature. It is renewable, biodegradable, biocompatible, and can be converted into various derivatives for versatile applications.[1] Gold nanoparticles (AuNPs) have attracted increasing interesting in the last decades due to their unique physicochemical properties and have the potential applications in optoelectronics, sensors, catalysis biotechnology, and medicine.[2-3]. The popular methods for preparation of AuNPs are generally based on the reduction of Au(III) derivatives using citrate or toxic compounds such as sodium borohydride (NaBH4) and hydroxylamine hydrochloride.[4-6] Moreover, further stabilization or functionalization using ligands is generally needed for the stabilization of AuNPs prepared via the above mentioned methods.[5-7] In this work, cellulose derivatives were used as both the reducer and stabilizer for preparing AuNPs in aqueous media. The present work provides a "green" approach for preparing AuNPs with good stability.

II. EXPERIMENTAL

Materials

Hydrogen tetrachloroaurate tetrahydrate ($HAuCl_4 \cdot 4H_2O$) (Shenyang Jinke Reagent Plant, China), sodium carboxymethylcellulose (CMC, DS = 1.2, $M_w = 2.5 \times 10^5$ g/mol) (Acros Organics) and cysteamine hydrochloride (CA, Alfa Aesar) were used as received. Aidoxime functionalized cellulose (AOFC) was synthesized in the lab and the details are shown in elsewhere.[3]

Preparation and Fabrication of Au-CA/CMC

Typically, 600 μL of 0.05 M $HAuCl_4$ aqueous solution was added to 200 mL 0.2 wt.% CMC aqueous solution in a reaction vessel followed by constant stirring. The mixture was kept at 110 °C for 12 h to obtain colloidal AuNPs stabilized by CMC (Au/CMC). The obtained colloidal solution was used for characterization without further treatment. To the above obtained Au/CMC solutions, 5 mg/mL CA aqueous solution was added. The final concentration of CA in the mixture was kept at about 8.6×10^{-3} mg/mL. The mixture solution was further stirred at room temperature for 2 days at room temperature to get the dispersion of Au-CA/CMC assembly.

Preparation of AOFC-stabilized gold nanoparticles

$HAuCl_4$ aqueous solution (0.05M, 100 μL) was added to 50 mL of AOFC aqueous solution (0.5 wt.%) in a reaction vessel, followed by constant stirring. The mixture was kept at desired temperature for 30 min to obtain colloidal gold nanoparticles stabilized by AOFC (AuNPs/AOFC). The obtained colloidal solution was used for characterization without further treatment.

Characterization

The pH value of the samples was adjusted by HCl and NaOH aqueous solutions and measured by a Shanghai Leici digital pHS-2F acidic meter. The UV-vis spectroscopy measurements were performed on a Shimadzu UV-1601PC spectrophotometer. The morphology of AuNPs and their hybrids were observed by a Hitachi H-800 transmission electron microscope (TEM) operated at 100KeV and a JEOL FS-2200 high-resolution transmission electron microscope (HRTEM) operated at 200 KeV. The samples for TEM and HRTEM observation were prepared by dropping the colloidal solution to the carbon coated copper grid and drying in air.

III. RESULTS AND DISCUSSION

When CMC reacted with $HAuCl_4$ at 110 °C for 12 h, the nearly colorless original solution turns into pink and finally bright ruby red. Figure 1a shows HRTEM images of the obtained AuNPs. Dispersed spherical AuNPs with fairly uniform size, about 20 nm in diameter, were obtained and the wavelength of surface plasmon resonance (SPR) absorbance appears at 521 nm on the UV-vis spectra (Figure 1b, solid line). This phenomenon demonstrates that the CMC served as both reducing agent for gold ions and stabilizer for AuNPs. When suitable amount of CA, e.g. 8.6×10^{-3} mg/mL, was added to Au/CMC solution the mercapto group (-SH) would anchor on the surface of AuNPs instead of carboxylic groups by the ligand exchange. Meanwhile, the ammonium ions ($–NH_3^+$) on CA molecules have electrostatic interactions with carboxylic ions ($–COO^–$) of CMC. The wavelength of surface plasmon resonance (SPR) absorbance of the AuNPs shifts slightly from 521 nm to 522nm (Figure 1b). The red shift maybe attributes to the changes of the AuNPs surface surrounding by the bounding of -SH group.

The initial pH value of Au-CA/CMC solution is 6.4 and the solution shows a bright ruby red color. When pH of Au-CA/CMC solution was adjusted, the color of the solution changes accordingly. The original ruby red color turns into violet in a narrow pH range of 2.6 – 2.1 and blue at pH < 2.1 (Figure 2, insert). The color change of the AuNPs dispersion is reversible. When the pH value of the AuNPs dispersion was adjusted from 1.5 back to 6.4, the color recovered to red. The SPR peak position changes from 520 nm at pH 6.4 to 598 nm at pH 1.5 to exhibit a critical point at about pH 2.6. When the pH value of the system decreased from 6.4 to 2.6, the SPR band of AuNPs shifted slightly from 520 nm to 526 nm. When the pH value is below 2.6, the SPR band is broadened and red shifted sharply from 527 nm to 598 nm. This process is reversible and the SPR band of the AuNPs gradually recovered to its initial position by adjusting pH value from 1.5 to 6.4 (Figure 2). This phenomenon of the system can be used for the colorimetric detection of amino acid.[8]

CMC can be used as both the reducing and stabilization agent for the preparation AuNPs. However, stabilizer such as CA is still needed for further stabilizing the AuNPs at different pH. Figure 3 shows the UV-vis spectra and the changes of the color of the reaction mixture during the preparation of the AuNPs using AOFC with DS_{AO} of 2.39. DS_{AO} is defined as the substitution degree of amidoxime groups per glucose ring of AOFC. The results show that the peak position of the UV-vis spectra remains unchanged during the procedure of the reaction (Figure 3a). However, the absorbance intensity of the peak increases with reaction time (Figure 3b) and the color of the reaction mixture was also changed from clear colorlessness to pink and then to ruby. The absorbance intensity of the peak reaches it maximum at about 210 min in the reaction conditions indicated, which suggest the finish of the reaction.

The stability of the Figure 3c shows the UV-vis spectra and the color of the AOFC stabilized AuNPs colloid solutions. The results indicate that the UV-vis spectra, as well as the color, of the AOFC stabilized AuNPs colloid solution remain unchanged at pH values in the range of 0.38-13.42, which confirm that the AOFC stabilized AuNPs colloid solutions have super stability in both acid and basic conditions. It has been reported that the adsorption of metal ions of amidoxime groups is generally carried out at low pH range (2-6.5), in which the amidoxime group has strong affinity with metal ions and prevent the precipitation of the metal ions.30 The adsorbed metal ions is generally regenerated by eluting with acid solution such as 1-4 M HCl. At a pH above 7, the de-protonated amidoxime groups have an even stronger interaction with AuNPs. Moreover, AOFC could remain its hydrophilicity due to the abundant remaining hydroxyl groups of the cellulose chains. The AOFC stabilized AuNPs the promising applications in the field of catalyst, biotechnology and medicine that can work in a wide pH range.

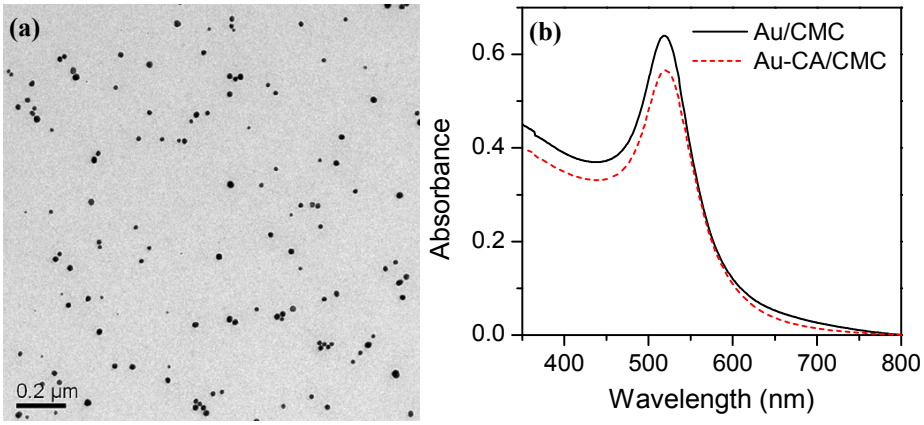

Figure 1. (a) HRTEM of AuNPs dispersed in CMC solution (AuNPs/CMC) and (b) UV-vis spectra of AuNPs/CMC and AuNPs-CA/CMC.

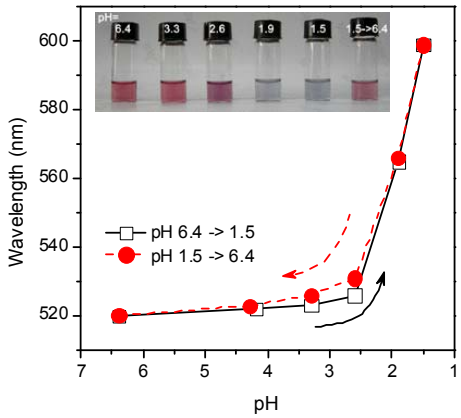

Figure 2. The effect of pH to the surface plasma absorbance wavelength and the AuNPs-CA/CMC dispersion solution at different pH values

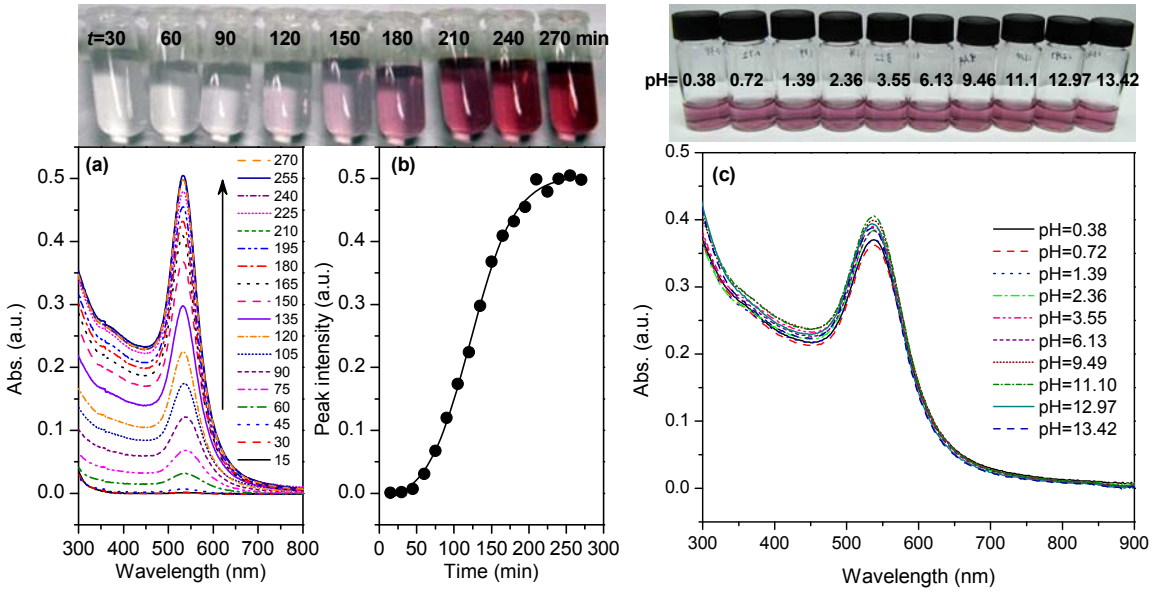

Figure 3. UV-vis spectra (a) and the peak intensity (b) of the aqueous reaction solution with $HAuCl_4$ (10^{-4} M) and AOFC (0.2 wt.%) as a function of reaction time at 80°C. The photos show the changes of the color of the reaction solution at the reaction time indicated. (c) Photos and UV-vis spectra of AuNPs/ AOFC (DS_{AO}=2.39) colloid solution at pH that indicated.

IV. CONCLUSIONS

Cellulose derivatives, CMC and AOFC, have been successfully used as the green reducing and stabilizing agent for preparation of AuNPs. In case of using CMC, AuNPs were prepared by directly reducing $HAuCl_4$ with CMC and stabilized in aqueous media. The AuNPs were further stabilized by assembling with CA to result pH-sensitive AuNPs-CA/CMC. The AuNPs-CA/CMC dispersion system exhibits strongly reversible pH-responsive behavior with the aggregation of the AuNPs caused by the combined action of the chain conformation change of CMC and electrostatic interactions between CA and CMC at different pH value. In order to avoid using CA for stabilizing AuNPs, amidoxime functionalized cellulose (AOFC) was synthesized and used for the preparation of AuNPs. It was found that AOFC can be used as both reducing agent and stabilizer for preparing AuNPs. The AOFC stabilized AuNPs have the excellent stability in whole pH range, which may have the promising applications in the fields of catalyst, biotechnology and medicine.

V. ACKNOWLEDGEMENT

The financial support of the National Natural Science Foundation of China (Grant No. 20974114, 21174156 and 21174150), China Ministry of Science and Technology (Grant No. 2011IM030400, 2011CB606100, and 2011CB605600) and the Knowledge Innovation Program of the Chinese Academy of Sciences (Grant No. KJCX2-YW-H19) is greatly appreciated.

VI. REFERENCES

[1] Klemm, D.; Heublein, B.; Fink, H. P.; Bohn, A., Cellulose: Fascinating biopolymer and sustainable raw material. *Angew. Chem. Int. Ed.* **2005,** *44*, 3358-3393.

[2] Tan, J. J.; Liu, R. G.; Wang, W.; Liu, W. Y.; Tian, Y.; Wu, M.; Huang, Y., Controllable aggregation and reversible pH sensitivity of aunps regulated by carboxymethyl cellulose. *Langmuir* **2010,** *26*, 2093-2098.

[3] Li, W. W.; Liu, R. G.; Kang, H. L.; Sun, Y. M.; Dong, F. Y.; Huang, Y., Synthesis of amidoxime functionalized cellulose derivatives as a reducing agent and stabilizer for preparing gold nanoparticles. *Polym. Chem.* **2013,** *4*, 2556-2563.

[4] Frens, G., Controlled nucleation for regulation of particle-size in monodisperse gold suspensions. *Nature-Phys. Sci.* **1973,** *241*, 20-22.

[5] Daniel, M. C.; Astruc, D., Gold nanoparticles: Assembly, supramolecular chemistry, quantum-size-related properties, and applications toward biology, catalysis, and nanotechnology. *Chem Rev* **2004,** *104*, 293-346.

[6] Rosi, N. L.; Mirkin, C. A., Nanostructures in biodiagnostics. *Chem Rev* **2005,** *105*, 1547-62.

[7] Wang, Z.; Ma, L., Gold nanoparticle probes. *Coord. Chem. Rev.* **2009,** *253*, 1607-1618.

[8] Wei, X. Y.; Qi, L.; Tan, J. J.; Liu, R. G.; Wang, F. Y., A Colorimetric sensor for determination of cysteine by carboxymethyl cellulose-functionalized gold nanoparticles. *Anal. Chim. Acta* **2010,** *671*, 80-84.

EVALUATION OF BLOOM ALGAE AS RAW MATERIAL FOR PAPERMAKING

María M. López[1], Ana Moral[1*], Roberto Aguado[2], Mª Lourdes Campaña[1] and Antonio Tijero[2]

*[1]Chemical Engineering Dpt. Experimental Sciences Faculty, Pablo de Olavide University. 41013 Seville, Spain *e-mail: amoram@upo.es*
[2]Chemical Engineering Dpt. Faculty of Chemistry, Complutense University of Madrid, 28040 Madrid, Spain

ABSTRACT

The main source of cellulose has always been wood from trees and other vascular plants. The cellulose obtained from these sources is associated with other natural polymers, mainly lignin. Algae can be considered as an alternative source of cellulose to traditional raw materials. One of the principal problems regarding the conventional extraction of cellulose is the removal of lignin. The lignin content in the algae cell wall is so low that there are not problems associated with lignin removal. This study aims to evaluate the potential of two of the most important bloom forming kinds of algae, *Ulva sp.* and *Cladophora sp.*, as a raw material for papermaking.
The amount of solvent-substances, lignin and holocellulose in dried algae pulp is estimated. The results show that the studied algae have low lignin-like compounds and solvent-soluble substances content, which supposes an enormous advantage over the current cellulose extraction methods as it eliminates the need of pre-treatment, cooking and bleaching stages. Therefore, the application of extremely toxics reagents used nowadays is not necessary. The holocellulose content obtained in this study ranged from 47 to 54%, lower than that of wood or herbaceous species.
The algae genus presented in this work stand as a proper source of reinforcing fibers for papermaking purposes. Also, represent an excellent opportunity to valorize tidal wastes obtained from bloom episodes.

I. INTRODUCTION

Eutrophication is a natural process which causes an excessive algal growth [1]. The current problem is that, due to the increase of pollution, temperature and organic effluents, eutrophication is reaching disproportionate rates [2]. This massive growth affects the dynamics of nutrients and resources, compromising the ecosystem balance [3]. Furthermore, enormous amounts of these algae get accumulated in the beach, increasing bacterial and insect's growth [4] and causing problems to the beach users [5]. The withdrawal and storage of these tidal residues are raising the volume of wastes and the costs of waste management. During the last summers, the amount of algal wastes collected was up to 3.000 tonnes, only in one province of Spain [6] Algae used in this paper belong to the genus *Ulva* and *Cladophora*, two of the most bloom forming genus worldwide [7-8].

To solve this problem, many works using algae from blooms have been published over the last years. They have been used as a fertilizer in composting process [9], in wastewater treatment [10], anaerobic digestion [11], ethanol fermentation [12] construction materials [13] or filter membranes [14], among others.

The great availability of a feedstock with a photosynthetic efficiency around six times higher than terrestrial biomass [15], made seaweed a raw material with three times more energetic potential than the whole terrestrial biomass [16]. Among the algae structural characteristics, their most striking quality for papermaking is their almost lack of lignin [17], as the removal of lignin generates most of the polluting effluents, and a huge energetic cost in pulp production. Also it is always necessary further steps of bleaching to eliminate lignin rest [18].

There are few references of paper from algae [19-22], and all of them show the benefits arising from the lack of pulping and bleaching stages. Nevertheless, technologic uses of algae are still in their early stages and needs preliminary studies in order to determinate the useful characteristics of algae for their potential applications.

In this work, we evaluate the characteristics of dried pasta of *Ulva sp* and *Cladophora sp* as a pulp for papermaking, in a way to convert tidal wastes into high-added value products and, at the same time, to minimize the environmental impact and the tree felling generated by the current papermaking processes.

II. EXPERIMENTAL

Algae collection

All the specimens used in this study were collected from tidal wastes after episodes of natural blooms in "La Cachucha" beach, Puerto Real (Spain), during the month of March 2013. Seaweeds were identified according to Cabioc´h et al [23] as *Ulva sp.* and *Cladophora sp*. The seaweeds were freed from attached impurities, washed thoroughly with water and dried at 40°C for three days.

In order to characterise the algae potential as paper pulp, the chemical pulp characterization essays and the holocellulose content were carried out.

Soluble extractives

To determinate the amount of non-volatile substances. TAPPI T204 [24] was followed.

Lignin content

The method used to determinate the percentage of lignin in the samples was TAPPI T222 [24].

Holocellulose content

Holocellulose content was measured by Wise´s method [25], which includes the alpha- and hemi-cellulose content in the algal dried pulp.

III. RESULTS AND DISCUSSION

Soluble extractives

Algae have a considerable amount of oils and pigments, substances all included on the non-volatile material measured by this essay. **Table 1** shows a comparative between the results obtained from the studied algae and other materials used for pulp production.

Table 1. Percentages of solvent –extractives, lignin and hollocelulose in several materials used for paper making

Species	% EEB	% E1	% LIG	% HOLOCEL
Ulva sp	2.00	98.00	3.27	46,89
Cladophora sp	0.90	99.12	4.17	53,81
Agricultural remains	10.40-0.60[26]			
Alternative vegetables	7.30-2.20[26]		13-24[30]	60[32]
Conifers and hardwoods	2.60- 1.20[26]		25-33[29]	70[31]

Both of the studied algae present a low content of non-volatiles; 2% for *Ulva* and 0, 9% for *Cladophora sp.* The percentages found in other materials range from 2 %, in woody plants, to 10%, in olive pruning [26].The best candidate for paper-pulp production seems to be *Cladophora sp*, as it contains less extractives. However, *Ulva sp* presents a percentage of extractives that is accepted for hardwoods and even lower than those of alternative materials. The great amount of chlorophyll in these algae, 21.21mg/g DW in *Ulva* species [27] and 15-10mg/g DW in *Cladophora* species [28] suggests that the most abundant extractive is chlorophyll and a mild pre-treatment with ethanol or another polar-solvent can be used to avoid a possible colour on the final product.

Lignin-like compounds content

The lignin-like compounds measured were around 3% in *Ulva sp* and 4% in *Cladophora sp.*, considerably lower than lignin content obtained for wood species [29], and herbaceous plants [30]. **Table 1** shows the percentage of lignin in *Cladophora sp*, *Ulva sp* and other materials.

Holocellulose content

The analysed species have an average holocellulose content of 50.35%. **Table 1** shows a comparison of the obtained results.

The holocellulose content of the studied macroalgae is lower than the percentage found in hardwoods and other plant species used in papermaking. However, in traditional species a large part of the cellulose is tightly linked to lignin, as hemicellulose. In the case of woody species, the α-cellulose percentage is 56 to 55% [31], and for herbaceous species it changes from 35 to 47%,[32] the rest is hemicellulose. The used method usually shows high values because a high proportion of hemicellulose remains attached to lignin, thus the calculated residue contains lignin remainders. As algae have remarkably less lignin than terrestrial plants, it is expected to measure a lower value in the first ones.

IV. CONCLUSIONS

Algae analysed in this study represent a raw material that could be used for papermaking. Although holocellulose content is lower than that of vascular plants, it is high enough to be interesting for the manufacturing of fibre-based products. The amount of soluble extractives was found to be similar than traditional feedstock.

Based on the low amount of lignin-like components, we conclude that it can be made algal pulp for paper production without any pre-treatment or aggressive reagent to remove lignin.

As the cellulose content could be insufficient, we suggests that this pulp could be better used as reinforcing fibres in paper-making, supporting the traditional or recycled pulp.

On the other hand, the possibility to create a market based on this kind of resources, symbolize an excellent outputting to tidal wastes, as the algal species treated in this document have been reported as two of the most problematic genus in bloom-forming.

V. ACKNOWLEDGEMENT

The authors wish to acknowledge the Ministry of Science and Innovation of Spain for the financial support of the Project CTQ2010-21660-C03-01 to which the present study is related.

VI. REFERENCES

[1] de Jonge; V.N.; Elliott, M.; Orive, E. Causes, historical development, effects and future challenges of a common environmental problem: eutrophication. *Hydrobiologia*. **2002**, 475, 1–19.

[2] Sweeny, A. Eutrophication in the world's oceans. Future United Nations environmental programme topic a backgrounder. *Connect model united nations.* **2013.**

[3] Corzo A. Respuestas ecológicas del microbentos intermareal a la eutrofización: metabolismo neto, estructura de la comunidad y flujo de nutrientes. Repercusiones sobre la fauna bentónica*. Proyecto Microbentos*. **2004** (REN2002-01281/MAR).

[4] Schramm, W.; Nienhuis, P.H. Marine benthic vegetation: recent changes and the effects of eutrophication. **1996,** 400 p.

[5] Byappanahalli, M. N.; Sawdey, R.; Ishii, S.; Shively, D. A.; Ferguson, J. A.; Whitman, R. L.; Sadowsky, M. J. Seasonal stability of Cladophora-associated Salmonella in Lake Michigan watersheds. *Water Res***. 2009,** 43, 806-14.

[6**]**http://www.huelvainformacion.es/article/provincia/1343353/las/algas/vuelven/ocupar/otra/vez/la/arena/las/playas.html: *Andalucía información*, Septiembre. **2012.**

[7] Higgins, S.N.; Malkin, S. Y.; Howell, E. T.; Guildford, S.J.; Campbell, L.; Hiriart-Baer, V.; Hecky, R.E. An ecological review of Cladophora glomerata (Chlorophyta) in the Laurentian Great Lakes. *J. Phycol***. 2008**, 44, 839-854

[8] Berezina, N.A.; Golubkov, S.M. Effect of drifting macroalgae Cladophora glomerata on benthic community dynamics in the easternmost Baltic Sea. *Journal of Marine Systems*. **2008**, 74, 80-85.

[9] Han, W.; Clarke, W.; Pratt, S. Composting of waste algae: A review. *Waste Management*. Available online 3 March **2014**.

[10] Sode, S.; Bruhn, A.; Balsby, T.J.S.; Larsen M.M.; Gotfredsen A.; Rasmussen M.B. Bioremediation of reject water from anaerobically digested waste water sludge with macroalgae (Ulva lactuca, Chlorophyta). *Bioresource Technology*. **2013**, 146, 426-435.

[11] Vergara-Fernandez, A.; Vargas, G.; Alarcon, N.; Velasco, A. Evaluation of marine algae as a source of biogas in a two-stage anaerobic reactor system. *Biomass Bioenergy*. **2008,** 32, 338–344.

[12] Borines, M.G.; de Leon, R.L.; McHenry, M.P. Bioethanol production from farming non-food macroalgae in Pacific island nations: chemical constituents, bioethanol yields, and prospective species in the Philippines. *Renew. Sustain. Energy Rev.* **2011**, 15, 4432–4435.

[13] Johnson, M.; Shivkumar, S. Filamentous green algae additions to isocyanate based foams. *J. Appl. Polym. Sci*. **2004**, 93, 2469–2477.

[14] López-Simeon, R.; Beltrán-Conde, H.; Campos-Terán, J.; Hernández-Guerrero, M. Extracción y caracterización interfacial de celulosas extraídas de desechos residuales de la industria del agar, para su posible uso en la formación de membranas mesoporosas con ordenamiento hexagonal. *XIV Congreso Nacional de Biotecnología y Bioingeniería*. Junio, **2011**.

[15] Aresta M.; Dibenedetto A.; Barberio G. Utilization of macro-algae for enhanced CO2 fixation and biofuels production: Development of a computing software for an LCA study. *Fuel Processing Technology*. 2005, 86, 14–15, 1679-1693.

[16] Chynoweth, D. P.; Owens J.M.; Legrand, R .Renewable methane from anaerobic digestion of biomass. *Renewable Energy*. **2001**, 22(1-3): 1-8.

[17] Roesijadi, G.; Jones, S.B.; Snowden-Swan, L.J.; Zhu, Y. Macroalgae as a Biomass Feedstock: A Preliminary Analysis. Technical Report. **2010,** US DOE, PNNL-19944.

[18] Jiménez, L.; Ramos, E.; de la Torre, M.J.; Ferrer, J.L. ECF and TCF Bleaching Methods as Applied to Abaca Pulp. *Afinidad.* **2005**, 62 (515), 14-21.

[19] Sakai, M.; Seto, T.; Kanaeko, M.; Hada, M.; Kinomoto, K. Method for producing pulp from green algae. Patent number: 5500086. Filing date: 30 Apr. Issue date: 19 Mar **1996.**

[20] You, H.C.; Park, J.H. Pulp and paper made from Rhodophyta and manufacturing method thereof. Patent number: 7622019. Filing date: Nov 12, 2004. Issue date: Nov 24, **2009**.

[21] Kiran, E.; Teksoy, I.; Guven, K.C.; Guler, E.; Guner, H. Studies on seaweeds for paper production. *Bot. Mar.* **1980,** 23, 205–207.

[22] Chao, K. P.; Y. C. Su. Feasibility of utilizing Rhizoclonium in pulping and papermaking. *Journal of Applied Phycology*. **2000**, 12(1): 53-62.

[23] Cabioc'h, J. Guía de las algas de los mares de Europa: Atlántico y Mediterráneo. Ed. Omega. **1995.**

[24] TAPPI Standards. TAPPI Test Methods. Atlanta. **1997.**

[25] Wise, L.E.; Murphy, M.; D'Addieco, A. Chlorite Holocellulose, its fractionation and bearing attach the flask to a vacuum source and evacuate the flask to on summative wood analysis and on studies on the hemicelluloses. *Paper Trade J*. **1946**, 122, (2): 35-43.

[26] Gonzalez-Granados, Z. Idoneidad de las podas de naranjo como materia prima para la producción de pasta celulósica para diversos usos. Tesis doctoral. *Universidad de Córdoba, Servicio de Publicaciones*. **2013.**

[27] Abd El-Baky H.H; El Baz F.K; El-Baroty G.S. Evaluation of Marine Alga Ulva lactuca as a Source of Natural Preservative Ingredient. *American-Eurasian J. Agric. & Environ. Sci*. **2008,** 3 (3), 434-444.

[28] Ensminger, I.; Xyländer, M.; Hagen, C.; Braune, W. Strategies providing success in a variable habitat: III. Dynamic control of photosynthesis in Cladophora glomerata. *Plant, Cell & Environment*. **2001**, 24, 769–779.

[29] Aitken, I. ; Cadel, F. ; Voillot, C. Constituants fibreux des pates papiers et cartons pratique de l'analyse, 1st edition. **1988.**

[30] Sixta, H. Handbook of pulp.Weinheim: Wiley-Vch Verlag Gmbh & Co. **2006.**

[31] Alonso, L. Análisis químico de diferentes especies forestales. INIA, Ministerio de Agricultura. Madrid. **1976.**

[32] Jiménez, L.; Sánchez, I; López, F. Characterization of Spanish agricultural residues with a view to obtaining cellulose pulp. *Tappi Journal*. **1990**, 73 (8), 173-176.

LIGNIN CHARACTERIZATION OF TEAK WOOD FROM MATURE TREES FROM EAST TIMOR BY PY-GC/MS(FID)

Ana Lourenço[1]*, Duarte Neiva[1], Jorge Gominho[1], António Velez Marques[1,2] and Helena Pereira[1]

[1]*Centro de Estudos Florestais, Instituto Superior de Agronomia, Universidade de Lisboa, Tapada da Ajuda, 1349-017 Lisboa, Portugal*
[2]*Instituto Superior de Engenharia de Lisboa, Instituto Politécnico de Lisboa, Rua Conselheiro Emídio Navarro 1, 1959-007 Lisboa, Portugal*
*(*analourenco@isa.ulisboa.pt)*

ABSTRACT

Tectona grandis trees with 70-years of age were collected in East Timor. The heartwood and sapwood were characterized by analytical pyrolysis (Py-GC-MS/FID). Heartwood and sapwood presented similar lignin content (37.3% vs. 35.4%). Regarding lignin composition both presented a high values for guaiacyl-units (in average 20.3%), while syringyl-units represented 16.4% in heartwood and 14.4% of total area in sapwood. The *p*-hydroxyphenyl-units only amounted to 0.7%. Teakwood is characterized by a GS type of lignin, with a S/G ratio of 0.8. The major lignin derivative compounds found in the pyrograms were: 4-vinylsyringol, *trans*-coniferyl alcohol, coniferaldehyde, 4-vinylguaiacol, 4-methylguaiacol, vanillin, and sinapinaldehyde, with respectively, 6.6%, 4.5%, 2.0%, 1.6%, 1.6%, 1.5% and 1.2%. The high content of lignin and its composition, with a predominance of guaiacyl-units, leading to a lignin with a more condensed structure, may explain the wood stiffness and resistance to biological attack.

I. INTRODUCTION

Lignin, the second major compound in lignocellulosic materials, gives stiffness and mechanical resistance to the cellular matrix, as discussed by Koehler and Telewski [1], and is though to contribute to biological resistance. The lignin in hardwoods represents 18% to 30% of the wood [2]. In *Tectona grandis*, a species with particularly durable wood, the lignin content is comparatively high, representing 32.5% [3], and 33.6% [4] of oven dry wood. The lignin content and composition could explain the high durability of the teak wood. However few studies are focused on the identification of lignin in teak wood [5,6]. In teakwood, besides the lignin, extractives are also present in high amounts (from 8.5% to 10.0%) [4,3], particularly in heartwood.

Teak is highly appreciated for a wide range of noble end uses (carpentry, boat construction or outdoor equipment) [7]. In particular heartwood is very appreciated due to its esthetic characteristics and durability, as discussed by Moya et al. [8]. Besides, the noble wood uses, an additional added-value could be achieved from the teakwood processing residues by using their chemical value. In fact, extractives are used for a wide range of bioproducts, from antioxidants and compounds with antitumor activity; while lignin is used for the production of polymers, resins, adhesives [9]. In this perspective, an increased knowledge of the structural components of teak is important as a background to this potential added-value as raw material.

In this paper, heartwood and sapwood of *Tectona grandis* were characterized by PY-GC/MS(FID) and the lignin composition was studied.

II. EXPERIMENTAL

Samples

Three teak trees (*Tectona grandis*) were harvested with approximately 70 years of age from a pure teak stand in East Timor, as described elsewhere [4]. A disc was cut at 1.3 m of the tree height, and heartwood and sapwood were manually separated. Each was milled and sieved, and the 40-60 mesh fraction kept for analysis. The samples were extracted, using a sequence of dichloromethane, ethanol and water during 24h each, previously to the pyrolysis analysis.

Pyrolysis

Analytical pyrolysis was performed using a CDS platinum coil Pyroprobe 2000 apparatus with a CDS 1500 valved interface. The sample (80 µm) was placed in a quartz boat and pyrolysed at 625 ºC for 10s with a temperature rise time of ca. 20 ºC/ms (ramp-off) with the interface kept at 270 ºC. The pyrolysates were purged from the pyrolysis interface into the gas chromatograph injector with a constant helium gas flow of 1.0 mL/min. The pyrolyser was connected to a Thermo Finnigan GC equipped with a fused-silica capillary column DB-17HT (30 m x 0.25 mm x 0.15 µm) from Agilent, and coupled with a Thermo Trace Ultra Polaris Ion Trap mass spectrometer. The conditions for GC-MS/FID where: injector temperature: 240 ºC; FID detector: 250 ºC; column temperature program: 50 ºC (2 min), 50-80 ºC (heating rate: 6 ºC/min), 80-150 ºC (heating rate: 4 ºC/min), 150-220 ºC (heating rate: 5 ºC/min), 220-300 ºC (7 ºC/min), 300 ºC during 10 min. For mass spectra analysis, electronic ionization at 70 eV, 220 ºC for ion source temperature and 0.3 mL of damping helium gas were used. The lignin compounds were classified in S-, G- and H-lignin monomeric units and their proportions calculated as well as the S/G ratio.

III. RESULTS AND DISCUSSION

The sapwood and heartwood chromatograms are presented in Figure 1. The peak assignment of the main lignin derived compounds is shown in Table 1. Sapwood and heartwood presented no differences regarding peak assignment, and minor differences were noticed at a quantitative level. In average, 72% of the total area was identified; in the initial part of the chromatogram, the compounds are mainly carbohydrates derivatives, while the lignin derivatives appear in the middle and the end of the chromatogram.

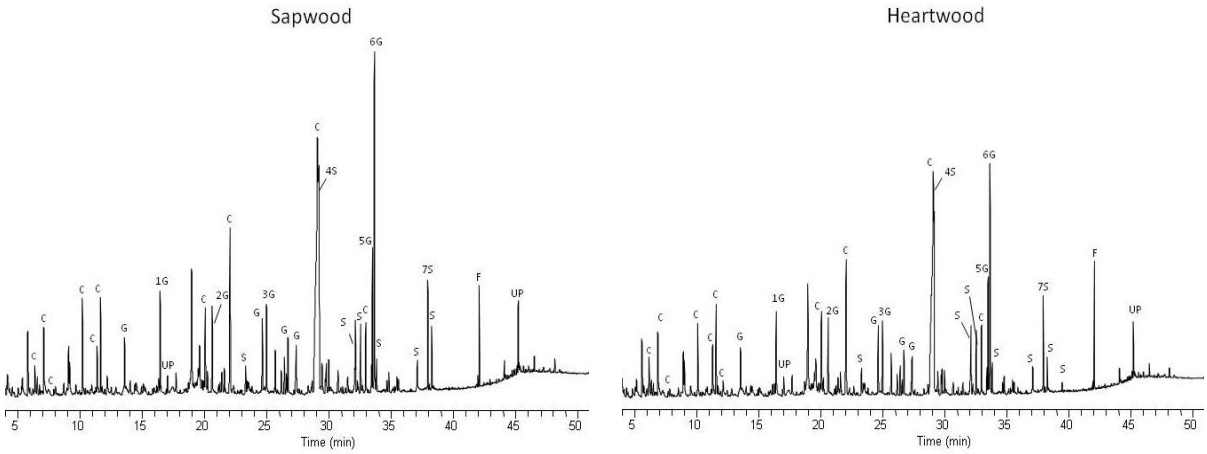

Figure 1. Py-GC/FID of sapwood and heartwood from teak; C – carbohydrates derivatives; Lignin derivatives: S - syringyl units; G - guaiacyl units; UP – undetermined phenolic source.

Table 1. Main lignin derivatives compounds (% of total area) and their peak assignment.

Peak/Origin*	Name	Sapwood	Heartwood
4S	4-vinylsyringol	6.3%	6.9%
6G	*trans*-coniferyl alcohol	4.5%	4.4%
5G	coniferaldehyde	2.0%	2.0%
1G	4-methylguaiacol	1.6%	1.6%
2G	4-vinylguaiacol	1.6%	1.6%
3G	vanillin	1.5%	1.5%
7S	sinapinaldehyde	1.1%	1.3%

*S, syringyl-units; G, guaiacyl-units.

The main lignin-derived compounds obtained were 4-vinylsyringol (6.6% of the total pyrolysis compounds), *trans*-coniferyl alcohol (4.5%), followed by coniferaldehyde (2.0%), 4-vinylguaiacol (1.6%), 4-methylguaiacol (1.6%), vanillin (1.5%) and sinapinaldehyde (1.2%), as described in Table 1. Compounds derived from H-units, for example phenol, represented less than 0.1% of the total area. A group of compounds with a phenolic base (designed by UP: e.g. methoxy-1,2-benzenediol, or 3,4-dimethoxystyrene) were also identified, and represented almost 4% of the total area.

The lignin content (in % of total area) and its monomeric composition are presented at Figure 2. Sapwood had a total lignin content of 35.4%, and heartwood 37.3%. On average teakwood presented 36% of lignin, which is a high value compared to other hardwoods, e.g. 24.0% in *Quercus faginea* [10]. The lignin content is an important component for wood durability, since lignin protects wood against microbial degradation while the lignin monomeric composition has a role in the wood mechanical resistance, as discussed by Koehler and Telewski [1]. In teak, the guaiacyl-units represented 20.4% of the total area, while the syringyl-units represented 14.4%, and the *p*-hydroxyphenyl-units only 0.6%. These results show that teakwood has a GS type of lignin, with a S/G ratio of 0.8. No differences were found between sapwood and heartwood. The high content in the guaiacyl-units is indicative of a more condensed lignin (with more C-C inter-units linkages), thereby inducing an increase of wood strength. This relation between lignin content and composition with the mechanical resistance has not been referred in relation to teakwood.

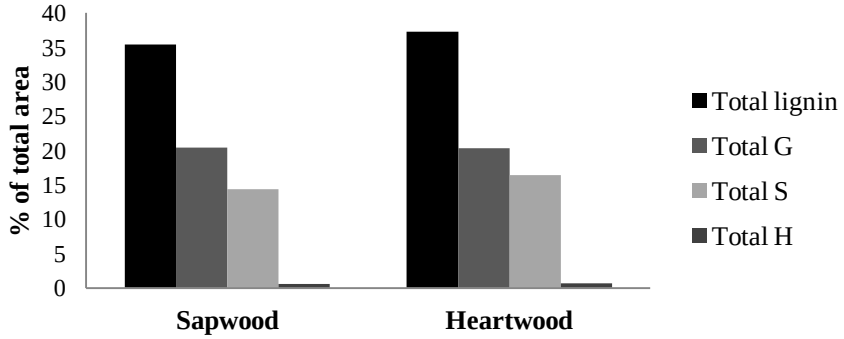

Figure 2. Lignin values from sapwood and heartwood of *Tectona grandis* (% of total area of the chromatogram), and its monomeric units (G, S and H).

IV. CONCLUSIONS

Sapwood and heartwood from teak had a high content of lignin that was characterized by a monomeric composition of a GS type, where the G-unit predominates comparatively to S-units (S/G ratio of 0.8). Both the lignin content and the predominance of guaiacyl-units compared to syringyl-units may explain the durability and mechanical strength of teak wood.

V. ACKNOWLEDGEMENT

The authors are grateful for all the help of the staff of the Rural Development in East Timor (PADRTL) in particular Nuno Moreira, Paulo Maio and Filipe Suspiro, for the sampling and wood transportation from East Timor to Portugal. The financial support for the laboratorial analysis was given by research funding of FCT (Fundação para a Ciência e a Tecnologia) to CEF (Centro de Estudos Florestais) under Strategic Project (PEst-OE/AGR/UI0239/2014), and the research projects PTDC/AGR-CFL/110419/2009, PTDC/AGR-FOR/3872/2012.

VI. REFERENCES

[1] Koehler, L.; Telewski, F.W. Biomechanical and transgenic wood. *Am. J. Bot.* **2006**, *93(10),* 1433-1438.

[2] Pereira, H.; Graça, J.; Rodrigues, J.C. Wood chemistry in relation to quality. Cap. 3. In: Barnett, J.R.; Jeronimidis, G. (Eds) Wood quality and its biological basis. CRC Press, Blackwell Publishing, Oxford, **2003**, pp 53.

[3] Miranda, I.; Sousa, V.; Pereira, H. Wood properties of teak (*Tectona grandis*) from a mature unmanaged stand in East Timor. *J. Wood Sci.* **2011**, *57*, 171-178.

[4] Windeisen, E.; Klassen, A.; Wegener, G. On the chemical characterization of plantation teakwood from Panama. *Holz als Roh-und Werkstoff* **2003**, *61*, 416-418.

[5] Meier, D.; Faix, O. Pyrolysis-gas-chromatography-mass spectroscopy. In: Lin, S.Y.; Dence, C.W. (Eds.) Methods in lignin chemistry. Springer Series in Wood Science, New York, **1992**, pp 177.

[6] Faix, O.; Meier, D. Pyrolytic and hydrogenolytic degradation studies on lignocellulosics, pulps and lignins. *Holz als Roh-und Werkstoff* **1989**, *47*, 67-72.

[7] Keogh, R.M. La teca y su importancia económica a nivel mundial. In: Camino, R.; Morales, J.P. (Eds) Las plantaciones de teca en América Latina: mitos y realidades. Centro Agronómico Tropical de Investigación y Enseñanza (CATIE) Turrialba, Costa Rica, **2013**, pp 8.

[8] Moya, R.; Bond, B.; Quesada, H. A review of heartwood properties of *Tectona grandis* trees from fast-growth plantations. *Wood Sci. Technol.* **2014**, *48*, 411-433.

[9] Stewart, D. Lignin as a base material for materials applications: chemistry, applications and economics. *Ind. Crop. Prod.* **2008**, *27*, 202-207.

[10] Sousa, V.B.; Cardoso, S.; Miranda, I.; Pereira, H. Overview of *Quercus faginea* characteristics and growth tendency. IUFRO conference Division 5 Forest Products, Estoril, Lisbon, Portugal, 8-13 July **2012**, pp 244.

CHARACTERIZATION OF *CYNARA CARDUNCULUS* L. LIGNIN BY PY-GC/MS(FID)

Ana Lourenço*[1], Duarte Neiva[1], Jorge Gominho[1], Maria Dolores Curt[2], Jesús Fernández[2], António Velez Marques[1,3] and Helena Pereira[1]

*[1]Centro de Estudos Florestais, Instituto Superior de Agronomia, Universidade de Lisboa, Tapada da Ajuda, 1349-017 Lisboa, Portugal; [2]Departamento de Producción Vegetal: Botánica y Protección Vegetal, Universidad Politécnica de Madrid, Av. Complutense s/n, 28040 Madrid, Spain; [3]Instituto Superior de Engenharia de Lisboa, Instituto Politécnico de Lisboa, Rua Conselheiro Emídio Navarro 1, 1959-007 Lisboa, Portugal (*analourenco@isa.ulisboa.pt)*

ABSTRACT

Four outstanding *Cynara cardunculus* L. plants were selected from two field experiments located in Sesimbra (Portugal) and Alcalá de Henares (Spain), and used for vegetative propagation, producing four clones. In this work, two plants from each clone were collected. The plant stalks were separated in depithed stalks (Stalks $_{DP}$) and pith (P) samples, for lignin characterization by Py-GC/MS(FID). The lignin derivative compounds with more expression were: 4-vinylsyringol (with values from 1.8% to 5.7%), 4-propenylsyringol (1.7% to 2.5%), syringol (0.63% to 1.9%), 4-methylguaiacol (0.56% to 1.7%), 4-vinylguaiacol (0.21% to 1.1%). The total lignin represented in average 23.9% in depithed stalks, slightly higher than in the pith samples (21.8%). The syringyl-units were predominating in both depithed stalks and pith, with average values of respectively, 12.6% and 13.9%. The depithed stalks samples presented more guaiacyl-units (11.1%), while in pith samples only 7.9% was attained. The *p*-hydroxyphenyl units represented less than 2.0% in both. Overall, *Cynara* was characterized by an SG type of lignin, where in average the S/G ratio was 1.3 and 2.1, respectively for depithed stalks and pith.

I. INTRODUCTION

Cardoon *(Cynara cardunculus* L.) is a Mediterranean herbaceous plant with high biomass production in dry and hot environments. At the end of cycle, the biomass production varies from 14 to 20 t.ha^{-1} [1,2,3], thus it have been considered a promising plant for industrial uses in Southern Europe.

Cynara cardunculus produces about 40% stalks, 25% leaves and 35% capitula [4], where the main advantage of this crop is that at time of harvesting the plant is almost dry (10-15%), avoiding problems of conservation. The stalks of cardoon presents a high content in ashes (5-11%), a total extractives of 13-21%, mainly ethanol (7.2%) and water extracts (5.7%), a total lignin varying from 17.0 % to 20.3%, and 53 % of polysaccharides [5,6].

Cardoon has diverse traditional applications, as discussed by Fernández et al. [7]: in food chain (for cheese making, soups and salads [8]), for pharmaceutical purposes [9], for energy production: by gasification, combustion or pyrolysis [10,11]. Moreover, from the seeds can be produced oil, and subsequently, biodiesel [12,13]. Other studies referred the ability of the aerial biomass to for the production of pulp and paper [14,15]. Besides, the crop has been studied regarding its phenotypic variability, mainly for either biomass production or seed production [16].

The efficient conversion of the biomass to value-added materials and chemicals relies on the ability to manipulate the chemistry of the raw materials. Thus, their chemical characterization, and the efficient fractionation are fundamental steps to maximize their exploitation. For instance, the lignin is one of the main compounds of the lignocellulosic material, but its isolation for posterior production of added-value materials has been studied for other materials, except cardoon. In fact, the lignin content in *Cynara* could influence its diverse uses, although as far as we known, this subject has never been explored. In order to overcome this, the lignin composition in four clones of *Cynara* was characterized by Py-GC-MS/FID.

II. EXPERIMENTAL

Samples

Cynara cardunculus plants grown in the period 2006/07 in two different environments of Peninsula Iberia, were selected for micropropagation. Four outstanding plants were selected from a field experiment in Sesimbra (Portugal) and Alcalá de Henares (Spain) (2 plants per location). The selected plants were harvested, and the stumps carefully removed from the soil and transported to a tissue culture laboratory in Madrid (Spain). The vegetative propagation was performed in three phases: 1) plant multiplication from division of plant stumps; 2) in-vitro culture of the meristematic tissues and 3) transfer of the offsprings to the soil. The field trial was established in June 2008, and only during that summer was provided irrigation, maintained in dry conditions, afterwards. At the end of the 4th growth cycle, the stalks of two plants per clone were separatedly collected for this study. Plants 1 to 4 are from clones of Spanish plants, while the plants 5 to 8 from Portuguese plants. The stalks of each plant were fractionated by hand in depithed stalks (Stalks $_{DP}$) and pith (P). The samples were milled and extracted before pyrolysis analysis.

Pyrolysis

Analytical pyrolysis was performed using a CDS platinum coil Pyroprobe 2000 apparatus with a CDS 1500 valved interface. The samples were weighed (80 µg) and placed in a quartz boat and pyrolysed at 625 ºC for 10s with a temperature rise time of ca. 20 ºC/ms (ramp-off) with the interface kept at 270 ºC. The pyrolysates were purged from the pyrolysis interface into the gas chromatograph injector with a constant helium gas flow of 1.0 mL/min. The pyrolyser was connected to a Thermo Finnigan GC equipped with a fused-silica capillary column DB-17HT (30 m x 0.25 mm x 0.15 µm) from Agilent, and coupled with a Thermo Trace Ultra Polaris Ion Trap mass spectrometer. The conditions for the GC-MS/FID analysis where: injector temperature (240 ºC); FID detector (250 ºC). The column temperature program was: 50 ºC (2 min), 50-80 ºC (heating rate: 6 ºC/min), 80-150 ºC (heating rate: 4 ºC/min), 150-220 ºC (heating rate: 5 ºC/min), 220-300 ºC (7 ºC/min), 300 ºC during 10 min. For mass spectra analysis the conditions used were: electronic ionization at 70 eV, 220 ºC for ion source temperature and 0.3 mL of damping helium gas. The lignin derived compounds were classified in S-, G- and H-lignin monomeric units and their proportions calculated as well as the S/G ratio.

III. RESULTS AND DISCUSSION

Figure 1 represents the Py-GC-FID chromatograms of the clone 1, respectively depithed stalk (1Stalks $_{DP}$) and pith (1P), as an example of the chromatograms obtained. A total of 110 compounds were identified, corresponding in average to 57% of the area identified. The lignin derived compounds represented from 18.2% to 26.7% of the total area, while the carbohydrates varied from 25.4% to 35.4%.

The main lignin derivative compounds were 4-vinylsyringol (varying from 1.8% to 5.7%), 4-propenylsyringol (1.7% to 2.5%), syringol (0.63% to 1.9%), 4-methylguaiacol (0.56% to 1.7%), 4-vinylguaiacol (0.21% to 1.1%).

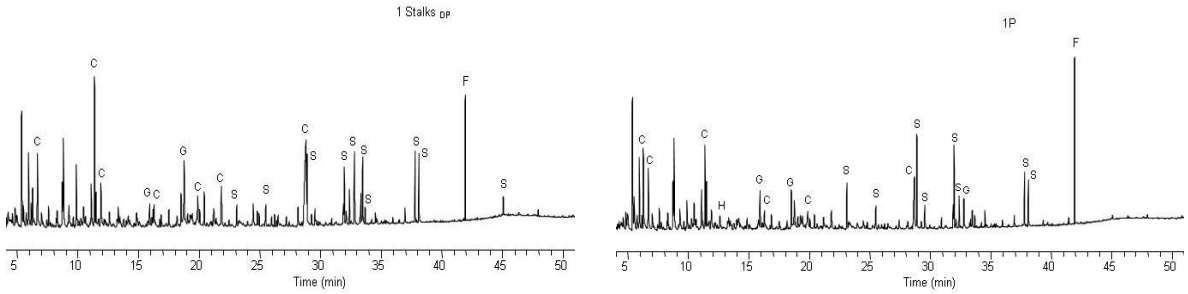

Figure 1. Py-GC/FID of depithed stalks (Stalks $_{DP}$) and pith (P) from *Cynara* plant 1.

The characterization of the depithed stalks (Stalks $_{DP}$) and the pith (P) of the four *Cynara* clones by Py-GC-FID are presented in Table 1. The depithed stalks (Stalks $_{DP}$) presented in average 23.9% of lignin content, varying from 22.2% to 26.7%, slightly higher than in the pith samples, which average was 21.8% (18.2% to 25.4%).

The pith samples presented slightly higher values of syringyl-units (S), varying from 11.3% (plant 7) to 15.7% (plant 2). Although, in averaged the difference between P and Stalks $_{DP}$ is small, respectively 13.9% and 12.6%. On the contrary, the Stalks $_{DP}$ presented more guaiacyl-units (G), reaching 11.1% (plant 3) while the P samples reached only 7.9% (plant 2). The *p*-hydroxyphenyl units (H) represented less than 2.0% of the total area, meaning that, either, Stalks $_{DP}$ and P samples are characterized by a lignin of SG type. Overall, cardoon lignin can be considered as a SG type, the same as in hardwoods, but different from *Arundo donax*, where the lignin is HGS-type [17]. Since the P samples presented more S-units, the S/G ratio was slightly higher (from 1.9 to 2.8), where the maximum and minimum values were attained in plant 8 and 7, respectively. The Stalks $_{DP}$ only attained S/G ratios in between 1.2 to 1.5.

The difference of the lignin composition in the depithed stalks and pith samples is a result of their anatomical features. The pith is mainly characterized by parenchyma cells, while the depithed stalks by vessels and fibers [18], each presenting diverse lignin composition: the vessels are characterized by guaiacyl-units while fibres present more syringyl-units [19].

Table 1. Characterization of the depithed stalks (Stalks $_{DP}$) and the pith (P) of the *Cynara* plants by Py-GC-FID (% of total area).

	Stalks $_{DP}$								
Plant number	1	2	3	4	5	6	7	8	Av ±STDEV
Total lignin	23.2	22.2	26.7	24.4	23.0	22.4	24.7	25.0	23.9±1.5
S	11.7	10.9	14.1	12.3	12.5	11.8	13.6	13.6	12.6±1.1
G	9.6	9.4	11.1	10.4	8.6	9.0	9.3	9.9	9.7±0.8
H	1.9	1.9	1.5	1.6	1.9	1.6	1.8	1.5	1.7±0.2
S/G	1.2	1.2	1.3	1.2	1.5	1.3	1.5	1.4	1.3±0.1
Total others*	36.3	36.8	32.3	34.5	35.3	34.1	35.6	34.4	34.9±1.4
	Pith								
Total lignin	23.7	25.4	20.7	22.7	23.0	21.3	18.2	19.4	21.8±2.3
S	14.7	15.7	13.6	14.5	14.8	13.1	11.3	13.4	13.9±1.4
G	7.4	7.9	5.6	6.3	6.2	6.3	5.8	4.8	6.3±1.0
H	1.6	1.9	1.4	1.8	2.0	1.9	1.1	1.2	1.6±0.3
S/G	2.0	2.0	2.4	2.3	2.4	2.1	1.9	2.8	2.1±0.3
Total others*	29.7	28.2	35.4	36.3	29.8	34.6	37.7	35.1	33.7±4.0

* Sum of total undetermined phenolic compounds and total carbohydrates; S, syringyl; G, guiaicyl; H, hydroxyphenyl-units; Av, average; STDEV, standard deviation.

IV. CONCLUSIONS

The *Cynara* plants were characterized by total lignin of 23.9% in the depithed stalks, and with 21.8% in the pith. Both samples presented more syringyl-units comparatively to the guaiacyl-units, although the S-units predominated in the pith. Cardoon was characterized by a SG type of lignin, differing from other herbaceous which are usually characterized by a HGS-type of lignin.

V. ACKNOWLEDGEMENT

The financial support for the laboratorial analysis was given by research funding of FCT (Fundação para a Ciência e a Tecnologia) to CEF (Centro de Estudos Florestais) under Strategic Project (PEst-OE/AGR/UI0239/2014), and the research projects: PTDC/AGR-CFL/110419/2009, PTDC/AGR-FOR/3872/2012.

VI. REFERENCES

[1] Fernández, J.; Curt, M.D. State-of-the-art of *Cynara cardunculus* as an energy crop. In: Sujunnesson L., Carrasco J.E., Helm P., Grassi A. (Eds.), Proc. 14th European Biomass Conference, Biomass for Energy,

Industry and Climate Protection. 17-21 October, Paris, France. ETA-Renewable Energies & WIP Renewable Energies (Pub.), **2005**, 22-27.

[2] Gominho, J.; Lourenço, A.; Palma, P.; Lourenço, M.E.; Curt, M.D.; Férnandez, J.; Pereira, H. Large scale cultivation of *Cynara cardunculus* L. for biomass production – A case study. *Ind. Crop. Prod*. **2011**, 33, 1-6.

[3] Ciancolini, A.; Alignan, M.; Pagnotta, M.A.; Vilarem, G.; Crinò, P. Selection of Italian cardoon genotypes as industrial crop for biomass and polyphenol production. *Ind. Crop. Prod*. **2013**, 51, 145–151.

[4] Fernández, J. Production and utilization of *Cynara cardunculus* L. biomass for energy, paper-pulp and food industry. In: Grassi, G., Collina, A. & Zibetta, H. (Eds), Biomass for Energy, Industry and Environment. 6th E.C. Conference, Athens, Greece, 22-26 April **1991**, 312-316.

[5] Pereira, H.; Miranda, I.; Paes, M.S.; Gominho, J. The chemical composition and raw-material quality of *Cynara cardunculus* biomass as pulp fibre source. In: D.O.Grassi, H.Scheer (Eds.), *Biomass for Energy and Industry*. Ponte Press, Bochum, **1992**, 1133-1137.

[6] Gominho, J.; Fernández, J.; Pereira, H. *Cynara cardunculus* L. – a new crop for pulp and paper production. *Ind. Crop. Prod*. **2001**, *13*, 1-10.

[7] Fernández, J.; Curt, M.D.; Aguado, P.L. Industrial applications of *Cynara cardunculus* for energy and other uses. *Ind. Crop. Prod*. **2006**, *24*, 222-229.

[8] Sousa, M.J.; Malcata, F.X. Comparison of plant and animal rennets in terms of microbiological, chemical and proteolysis characteristics of ovine cheese. *J. Agric. Food Chem*. **1996**, *45*, 74–81.

[9] Kukić, J.; Popović, V.; Petrović, S.; Mucaji, P.; Ćirić, A.; Stojković, D.; Soković, M. Antioxidant and antimicrobial activity of *Cynara cardunculus* extracts. *Food Chem.* **2008**, *107*, 861-868.

[10] Abelha, P.; Franco, C.; Pinto, F.; Lopes, H.; Gulyurtlu, I.; Gominho, J.; Lourenço, A.; Pereira, H. Thermal conversion of *Cynara cardunculus* L. and mixtures with *Eucalyptus globulus* by fluidized-bed combustion and gasification. *Energ. Fuel.* **2013**, *27*, 6725-6737.

[11] Grammelis, P.; Malliopoulo, A.; Basinas, P.; Danalatos, N.G. Cultivation and characterization of *Cynara cardunculus* for solid biofuels production in the Mediterranean region. *Int. J. Mol. Sci*. **2008**, 9, 1241-1258.

[12] Encinar, J.M.; González, J.F.; Rodríguez, J.J., Tejedor, A. Biodiesel fuels from vegetable oils: transesterification of *Cynara cardunculus* L. oils with ethanol. *Energ. Fuel*. **2002**, *16*, 443-450.

[13] Sengo, I.; Gominho, J.; D'Orey, L.; Martins, M.; D'Almeida-Duarte, E.; Pereira, H.; Ferreira-Dias, S. Response surface modeling and optimization of biodiesel production from *Cynara cardunculus* oil. *Eur. J Lipid. Sci. Technol.* **2010**, *112*, 310-320.

[14] Gominho, J.; Fernández, J.; Pereira, H. *Cynara cardunculus* L. – a new crop for pulp and paper production. *Ind. Crop. Prod*. **2001**, *13*, 1-10.

[15] Abrantes, S.; Amaral, M.E.; Costa, A.P.; Duarte, A.P. *Cynara cardunculus* L. alkaline pulps: alternatives fibres for paper and paperboard production. *Biores. Technol*. **2007**, *98*, 2873-2878.

[16] Ierna, A.; Mauromicale, G. *Cynara cardunculus* L. Genotypes as a crop for energy purposes in a Mediterranean environment. *Biomass Bioenergy* **2010**, *34*, 754-760.

[17] Seca, A.M.; Cavaleiro, J.A.S.; Domingues, F.M.J.; Silvestre, A.J.D.; Evtuguin, D.; Neto, C.P. Structural characterization of the lignin from the nodes and internodes of *Arundo donax* reed. *J Agric. Food Chem.* **2000**, *48*, 817-824.

[18] Quilhó, T.; Gominho, J.; Pereira, H. Anatomical characterization and variability of the thristle *Cynara cardunculus* in view of pulping potential. *IAWA J*, **2004**, *25(2)*, 217-230.

[19] Takabe, K.; Miyauchi, S.; Tsunoda, R.; Fukazawa, K. Distribution of guaiacyl and syringyl lignins in Japanese beech (*Fagus crenata*): variation within annual ring. *IAWA Bull* **1992**, *13*, 105–112

HAKEA SERICEA SCHRADER: A SOURCE OF BIOACTIVE COMPOUNDS

Ângelo Luís, Carla Cruz, Fernanda Domingues, Ana Paula Duarte*

*CICS-UBI Health Sciences Research Centre, University of Beira Interior, Covilhã, Portugal (*apcd@fcsaude.ubi.pt)*

ABSTRACT

Bioconversion of lignocellulosic biomass into value-added products offers numerous geopolitical, environmental, and strategic benefits. Lignocellulosic biomass is the most abundant renewable organic resources (~200 billion tons annually) on earth that are readily available for conversion to value-added products (industrial enzymes, organic acids, pharmaceuticals, commodity chemicals, and food/feed). *Hakea sericea* Schrader is an invasive shrub in Portuguese forests. In a previous report of our team, it was made an exhaustive study of several methanolic shrubs extracts, including the aerial parts of *H. sericea*. These extracts have demonstrated great antioxidant, antimicrobial and antibiofilm properties. Moreover, the methanolic extract of *H. sericea* fruits presented no toxicity towards NHDF cells, but for MCF-7 cells, this extract was able to decrease mitochondrial dehydrogenases activity in about 60% as MTT test results had demonstrated, indicating a relevant cytotoxicity towards these cancer cells and potential anti-carcinogenic properties. Based in these results, it was decided to make a bioassay-guided fractionation of this extract in order to identify the compound or compounds responsible for such bioactivity. It was used the direct bioautography technique to visualize the activity of different extract components separated by TLC against microorganisms, in order to screen the antimicrobial activity. Finally the resazurin microtiter assay was employed to determine the MIC values of fractions. The fractions of methanolic extract of *H. sericea* fruits have demonstrated great MIC values (ranging from 0.02 to 1.25 mg/mL) against *S. aureus* strains including some clinical-isolates of MRSA. The fractions presenting the best antimicrobial activities and, in addition, the highest purity, were submitted to analytical characterization by NMR and IR spectroscopy, and HRMS to elucidate the structure of the main compound responsible for the biological activity. It was possible to conclude that one major compound was present in all bioactive fractions, an alkenylresorcinol derivative, the 9-(3,5-dihydroxy-4-methylphenyl)nona-3(*Z*)-enoic acid.

I. INTRODUCTION

Hakea is a genus of shrubs and small trees native to South Australia. Some taxa are disseminating very fast and have become invasive species through both non-protected and protected areas of New Zealand, South Africa and the Mediterranean basin. In Portugal, *H. sericea* Schrader (family Proteaceae) has been introduced for ornamental purposes and the formation of hedgerows, especially near the coastline [1]. A key characteristic of *H. sericea* is its extreme serotinous habit; all of its seeds are retained in pairs in tough woody follicles, which accumulate along the branches throughout the life of the plant [2]. In a previous report *H. sericea* methanolic extracts were studied [3]. These demonstrated very good antioxidant properties, namely radical scavenging activity of DPPH free radicals and the inhibition of linoleic acid oxidation, which is an indicator of inhibition of lipid peroxidation [3]. These antioxidant properties could be associated with the presence of phenolics, tannins and flavonoids. It was also found that *H. sericea* possesses high concentrations of some secondary metabolites, namely alkaloids [3]. Other researchers have studied *Hakea* spp. extracts and their promising antimicrobial properties against *Staphylococcus aureus* strains [1]. In a previous study focused on characterizing this shrub, the crude methanolic extract of *H. sericea* fruits exhibited pronounced antimicrobial activity, namely against *S. aureus*, including some methicillin resistant strains, together with inhibition of biofilm formation [4]. Moreover, it was also found that the fruit extract presented no toxicity towards NHDF cells, whereas for MCF-7 cells, this extract was able to decrease mitochondrial dehydrogenases activity by about 60% in the MTT test, indicating a relevant cytotoxicity towards these cancer cells and potential anti-carcinogenic properties [4].
In the present study, the methanolic extract of *H. sericea* fruits exhibited pronounced antimicrobial activity against *S. aureus*, including some methicillin resistant strains. Based on such results it was decided to fractionate the extract to identify the compounds responsible for such biological activity.

II. EXPERIMENTAL

Plant material: Fruits of *H. sericea* were collected in Serra da Estrela (GPS coordinates: N 40º20.296'; W 07º27.491'; Altitude: 730 m). Plant materials were dried at 35ºC in a ventilated oven for 48 h and reduced to a coarse powder (< 2 mm) using a laboratory cutting mill. Harvesting, transport and storage of this plant species

were authorized by the Portuguese Institute for Nature Conservation and Biodiversity (ICNB). The species was identified by a botanist and a voucher specimen (No. LISI 13/2011) has been deposited in the Herbarium of the Instituto Superior de Agronomia (Jardim Botânico d'Ajuda, Lisboa).

Extraction procedure: The methanolic extract of *H. sericea* fruits was obtained with a Soxhlet apparatus until the solvent became colorless, using approximately 100 g of raw material and 1000 mL of solvent. The extract solutions were filtered under vacuum using a crucible of porosity #2 and then distilled under reduced pressure until a final volume of 100 mL. Prior to use, the extracts were dried using a rotary evaporator under reduced pressure, and then dissolved in dimethyl sulfoxide (DMSO).

Bioassay-guided fractionation and isolation: Based on the results of exploratory TLC, the methanolic crude extract of *H. sericea* fruits was fractionated by CC using silica-gel 60 (0.06-0.2 mm; 70-230 mesh) packed in light petroleum/diethyl ether (7:3). Elution was performed stepwise with solvents of increasing polarity, starting with light petroleum containing increasing amounts of diethyl ether and then eluted sequentially with chloroform, ethyl acetate, methanol and water. Fractions of 10 mL were recovered and the course of elution was monitored by TLC. Solvents were removed using a rotary evaporator at 45ºC. The fractionation process was repeated 4 times to achieve greater amounts of each fraction. At the end, 25 fractions were obtained. The fractions were analyzed by TLC using precoated TLC plates (silica-gel 60 F_{254} aluminum sheets) eluted with two different polarity mixtures of solvents, as mobile phase: chloroform/ethyl acetate (1:1) and ethyl acetate/methanol (1:1). Fractions were dissolved in methanol and aliquots were applied to TLC plates. After elution, plates were visualized under visible and ultra-violet light (254 and 365 nm). Folin-Ciocalteu's reagent (0.2 N) was also used to identify phenolics; aluminum chloride (10%) for flavonoids; and methanolic solution of DPPH (40 µg/mL) for antioxidant activity. The fractions with the same R_f value for the major spot were pooled together and thus the number of fractions was reduced from 25 to 5. These were sub-fractionated under the same conditions in order to obtain the purest fractions possible. Finally, 9 sub-fractions (A: 278.0 mg; B: 173.8 mg; C: 135.2 mg; D: 80.0 mg: E: 48.5 mg; F: 52.4 mg; G: 32.3 mg; H: 3.5 g; I: 499.4 mg) of the initial methanolic crude extract of *H. sericea* fruits were obtained and used to evaluate potential antimicrobial activity.

Bioautography: After elution, the TLC plates were subjected to direct bioautography [5]. The TLC plates spotted with sub-fractions were manually immersed (for about 10 s) in the bacterial suspensions. The inoculum was prepared by diluting 1:10 in Müller-Hinton broth (MHB) the direct bacterial suspension in saline solution of 0.5 McFarland (about $1\text{-}2\times10^8$ CFU/mL to non-fastidious bacteria). Then, TLC plates were placed in a moistened plastic box lined with wetted paper and incubated at 37ºC for 18 h. After incubation, they were sprayed with 0.2% MTT aqueous solution and incubated again at 37ºC for 30 min. One drop of TritonX-100/10 mL aqueous MTT was found to enhance the intensity of the color. In places with antimicrobial compounds, cream-white inhibition zones were observed [6].

Resazurin microtiter assay: The antimicrobial activity of crude extract, sub-fractions and new compound was assessed using resazurin microtiter assay. Plates were prepared under aseptic conditions. A sterile 96 well plate was labeled. A volume of 100 µL of sub-fractions in 10%, v/v, DMSO (stock concentration of 20 mg/mL in MHB) was pipetted into the first row of the plate. To all other wells 50 µL of MHB was added. To each well, 10 µL of resazurin indicator solution (0.1 % diluted in MHB) was added. Using a pipette, 30 µL of fresh MHB was added to each well. Finally, 10 µL of bacterial suspension (0.5 McFarland) was added to the wells. The plates were prepared in triplicate, and placed in an incubator set at 37ºC for 18 h. The color change was then assessed visually. Any color changes from purple to pink or colorless were recorded as positive. The lowest concentration at which change occurred was taken as the Minimum Inhibitory Concentration (MIC) value [7].

III. RESULTS AND DISCUSSION

The crude methanolic extract was successively eluted with solvents of increasing polarity using silica gel column chromatography. The fractions were analyzed by TLC, which revealed the presence of phenolics (Folin-Ciocalteu's reagent), flavonoids (aluminum chloride), and antioxidant substances (DPPH). Direct bioautography was used to evaluate the potential antimicrobial activity of the fractions. The developed chromatoplates were dipped into a cell suspension, and after incubation, it was possible to visualize the inhibition zones by using a vital dye. The evaluation of the activity was performed directly on the adsorbent layer [8]. Some fractions demonstrated good antimicrobial properties, especially for *S. aureus* strains, where cream-white inhibition zones were observed indicating the inhibition of growth. It was then possible to decide which fractions could be pooled and which ones had some biological activity; nine sub-fractions were obtained. The minimum inhibitory concentration (MIC) of each one of them against three strains of *S. aureus* was determined using the resazurin microtiter assay (**Table 1**). Resazurin, a blue colored redox dye, allows the detection of microbial growth in extremely small volumes of solution in microtiter plates without the use of a spectrophotometer [7]. This assay is based on the ability of viable and metabolically active cells to reduce resazurin to resorufin and finally colorless dihydroresorufin [9]. The MIC value for some sub-fractions was slightly lower than that of the crude extract.

Specifically, sub-fractions C, D, F and I had the lowest MICs for *S. aureus* strains, indicating a potential antimicrobial activity.

Table 1 - MIC values (mg/mL) of methanolic crude extract of *H. sericea* fruits and its sub-fractions (modal values).

Strain	Crude extract	Sub-fractions								
		A	B	C	D	E	F	G	H	I
S.aureus ATCC 25923	0.31	0.31	0.02	0.02	0.005	5	0.005	5	>10	0.005
MRSA 10/08	0.31	0.31	0.08	0.02	0.08	10	0.02	5	>10	0.02
MRSA 12/08	0.31	1.25	0.08	0.02	0.08	10	0.02	5	>10	0.02

From **Table 1**, fractions D, F and I showed the best antibacterial activity and, in addition, were the purest ones (only one spot on TLC with some residual impurities). For that reason, these fractions were then analyzed by NMR and IR spectroscopy, and HRMS to elucidate the structure of the main compound responsible for the biological activity. It was possible to conclude that one major compound was present in all bioactive sub-fractions.

The compound was obtained as colorless oil. The IR spectrum displayed absorptions at 3550 - 3200 (broad, s) and at 1710 cm^{-1}, indicating the presence of hydroxyl and carbonyl groups, respectively. The HRMS of the compound exhibited a molecular ion at *m/z* 278.151, which corresponded to the molecular formula $C_{16}H_{22}O_4$. Analysis of the NMR spectra indicated that 9-(3,5-dihydroxy-4-methylphenyl)nona-3(*Z*)-enoic acid (**Figure 1**) is the main compound of all the sub-fractions collected from column chromatography, giving a single spot on TLC.

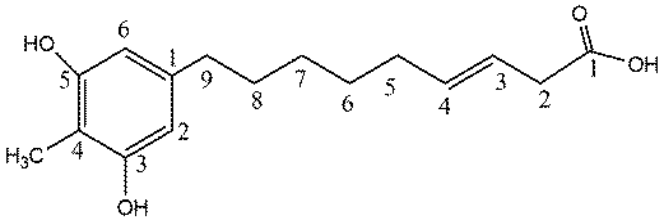

Figure 1 - Structure of 9-(3,5-dihydroxy-4-methylphenyl)nona-3(*Z*)-enoic acid.

The antimicrobial activity of the new resorcinol was tested against several strains of Gram-negative and Gram-positive bacteria, using the resazurin microtiter assay (**Table 2**). Very good antibacterial properties were demonstrated against the Gram-positive strains, with inhibition of the growth of *E. faecalis*, *L. monocytogenes* and *B. cereus* with MIC values of 0.31, 0.02 and 0.16 mg/mL, respectively. Good MIC values (0.005 – 0.16 mg/mL) were obtained for *S. aureus*, including the clinical isolates SA 01/10, SA 02/10 and SA 03/10, and MRSA strains. This is consistent with the phenolic nature of the compound.

By comparing the MIC results for the new compound against *S. aureus* strains with those obtained for the sub-fractions D, F and I of *H. sericea* fruits, it is possible to verify that the values are very similar (**Table 1** and **Table 2**), indicating that the antimicrobial activity of the extracts is probably due to the new alkenylresorcinol derivative.

Table 2 - MIC values (mg/mL) of 9-(3,5-dihydroxy-4-methylphenyl)nona-3(*Z*)-enoic acid) (modal values).

Strain	MIC (mg/mL)
Salmonella typhimurium ATCC 13311	> 5
Pseudomonas aeruginosa ATCC 27853	> 5
Escherichia coli ATCC 25922	> 5
Klebsiella pneumoniae ATCC 13883	> 5
Enterococcus faecalis ATCC 29212	0.31
Bacillus cereus ATCC 11778	0.02
Listeria monocytogenes LMG 16779	0.16
Staphylococcus aureus ATCC 25923	0.005
MRSA 10/08	0.02
MRSA 12/08	0.02
S. aureus SA 01/10	0.16
S. aureus SA 02/10	0.16
S. aureus SA 03/10	> 5

IV. CONCLUSIONS

In conclusion, in this work a new alkenylresorcinol derivative, 9-(3,5-dihydroxy-4-methylphenyl)nona-3(*Z*)-enoic acid, was isolated and characterized from the methanolic extract of *H. sericea* fruits. This compound demonstrated very good activity against Gram-positive bacteria. It was possible to conclude that the antimicrobial activity of this shrub is probably due to the new alkenylresorcinol derivative.

V. ACKNOWLEDGEMENT

Ângelo Luís acknowledges a PhD fellowship from Fundação para a Ciência e a Tecnologia (Reference: SFRH/BD/65238/2009), co-funded by Fundo Social Europeu (POPH–QREN) and by national funds of Ministério da Educação e Ciência. Carla Cruz acknowledges the post-doctoral grant from FCT (SFRH/BPD/46934/2008). Authors wish to thank Prof.ª Dr.ª Dalila Espírito-Santo and Dr.ª Paula Paes, from the Herbarium of the Instituto Superior de Agronomia (Jardim Botânico d'Ajuda, Lisboa), for the identification and deposit of the voucher specimens of the plant species used in this work.

VI. REFERENCES

[1] Madureira, A. M.; Duarte A.; Teixeira, G. Antimicrobial activity of selected extracts from Hakea salicifolia and *H. sericeae* (*Proteaceae*) against *Staphylococcus aureus* multiresistant strains. *South African J. Bot.* **2012**, *81*, 40–43.

[2] Le Maitre, D. C.; Krug, R. M.; Hoffmann, J. H.; Gordon, A. J.; Mgidi, T. N. *Hakea sericea*: Development of a model of the impacts of biological control on population dynamics and rates of spread of an invasive species. *Ecol. Modell.* **2008**, *212*, 342–358.

[3] Luís, Â.; Duarte, A. P.; Domingues, F. Bioactive Compounds, RP-HPLC Analysis of Phenolics, and Antioxidant Activity of Some Portuguese Shrub Species Extracts. *Nat. Prod. Commun.* **2011**, *6*, 1863–1872.

[4] Luís, Â.; Breitenfeld, L.; Ferreira, S.; Duarte, A. P.; Domingues, F. Antimicrobial, antibiofilm and cytotoxic activities of *Hakea sericea* Schrader extracts. *Pharmacognozy Mag.* **2013**, In Press.

[5] Choma, I. M.; Grzelak, E. M. Bioautography detection in thin-layer chromatography. *J. Chromatogr. A.* **2011**, *1218*, 2684–2691.

[6] Grzelak, E. M.; Majer-Dziedzic, B.; Choma, I. M. Development of a Novel Direct Bioautography–Thin-Layer Chromatography Test: Optimization of Growth Conditions for Gram-Negative Bacteria, *Escherichia coli. J. AOAC Int.*, **2011**, *94*, 1567–1572.

[7] Sarker, S. D.; Nahar, L.; Kumarasamy, Y. Microtitre plate-based antibacterial assay incorporating resazurin as an indicator of cell growth, and its application in the in vitro antibacterial screening of phytochemicals. *Methods*, **2007**, *42*, 321–324.

[8] Móricz, A. M.; Szarka, S.; Ott, P. G.; Héthelyi, E. B.; Szoke, E.; Tyihák, E. Separation and identification of antibacterial chamomile components using OPLC, bioautography and GC-MS. *Med. Chem.* **2012**, *8*, 85–94.

[9] Karuppusamy, S.; Rajasekaran, K. M. High Throughput Antibacterial Screening of Plant Extracts by Resazurin Redox with Special Reference to Medicinal Plants of Western Ghats. *Glob. J. Pharmacol.* **2009**, *3*, 63–68.

[10] Smith-Palmer, A.; Stewart, J.; Fyfe, L. Antimicrobial properties of plant essential oils and essences against five important food-borne pathogens. *Lett. Appl. Microbiol.* **1998**, *26*, 118–122.

COMPOSITE FIBRE SPINNING OF CELLULOSE AND LIGNIN FROM IONIC LIQUID

Yibo Ma[1], Shirin Asaadi[1], Michael Hummel[1], Herbert Sixta[1].

[1] *Department of Forest Products Technology, School of Chemical Technology, Aalto University, P.O. Box 16300, FI-00076 Aalto, Finland.*

**Corresponding author: Yibo.ma@aalto.fi*

ABSTRACT

Ionic liquids (ILs) have been identified as effective solvent media for lignocellulosic biomass. The solution produced by dissolution of lignocellulosic biomass in ionic liquid can potentially be applied for regenerating cellulose-based fibres using air-gap spinning. In this study, we present the production of wood-like fibres. As a model solute, different blends of Eucalyptus dissolving pulp and Organosolv lignin were dissolved in a novel ionic liquid. Kraft lignin was also used in order to compare the effect of the lignin source on the properties of fibres. A highly viscous wood-IL solution was prepared using a vertical kneader, followed by pressure filtration in order to remove insoluble residues. After degassing, the resulting solution was utilized as a spinning dope for dry-jet wet fibre spinning according to a Lyocell process. Composite fibres containing cellulose and lignin in different ratios were successfully spun. The draw ratio was varied systematically by regulating the extrusion and the take-up velocities at a given polymer concentration and geometry of the holes of the spinneret. The spun fibre has a unique brown and shiny appearance. The composite fibres revealed high strength properties with slightly decreasing values for fibers with an increasing share of lignin. The fibres were further analysed in terms of chemical composition and molar mass distribution.

I. INTRODUCTION

Cellulose is one of the most important raw materials for textile fibres. Due to diminishing fossil resources, cellulose is considered as a good alternative to a petroleum-based synthetic polymer since it is a renewable, widely abundant raw material and ensures a superior moisture absorption and excellent mechanical properties. Cotton plays a major role in the global textile market. However, there is an increasing demand for regenerated cellulose fibres due to a limited growth of cotton. Due to the crystalline structure and the strong hydrogen bonding, cellulose is difficult to dissolve in a conventional solvent. Therefore, efficient solvents or processes are needed for the production of regenerated cellulose fibres. [1]

The viscose fiber process is still by far the dominating process for the production of man-made cellulosic fibers (MMCF). This process requires the derivatization of cellulose by carbon disulphide forming cellulose xanthate, which is soluble in diluted aqueous sodium hydroxide. Despite the high production volume, this process causes severe environmental impacts due to the demand of toxic chemicals, the discharge of hazardous waste material and the consumption of large volumes of fresh water. As the only commercial alternative to Viscose, the Lyocell technology came on stream in the beginning of the 1990s after more than 20 years of research. Lyocell is the generic name for a regenerated cellulosic fiber obtained by spinning of a chemical pulp in a direct solvent. The only commercial direct solvent so far is N-methylmorpholine-N-oxide (NMMO). Fibers manufactured from this process exhibit higher mechanical strength properties than viscose fibres, especially in the wet state. NMMO is a solid at room temperature and the dissolution of cellulose and the spinning of the dope are carried out at relatively high temperature. However, NMMO is thermally not very stable and undergoes exothermic runaway reactions at high temperature and in the presence of traces of transition metal ions. Therefore stabilizers have to be added to avoid both solvent and cellulose degradation. [2]

Ionic liquids are salts with a melting point lower than 100 °C and are entirely composed of ions. They are characterized by very low vapour pressure and high thermal stability. Ionic liquids (ILs) have been identified as effective solvents for cellulose or even lignocellulosic substrates. The dissolved matters can be easily regenerated by immersing the resulting solution with water. [3] This opens up a new pathway for the production of regenerated cellulosic fibers. Roger's group was the first who reported about the use of an ionic liquid for the manufacture of MMCFs. [4] Quite recently, researchers at Aalto and Helsinki Universities have successfully developed a novel ionic liquid, an excellent direct cellulose solvent, which revealed high spinning stability of the formed dope. The regenerated cellulose fibers revealed outstanding fiber properties. This new dry-jet wet spinning technology, referred to as IONCELL-F, belongs to the category of Lyocell fiber technology. The strength properties of IONCELL fibres are comparable to those obtained from the NMMO-based Lyocell process, *e.g.* the Tencel® process. The IONCELL-F process is operated at moderate temperatures, far below those applied in the NMMO-based Lyocell process. This results in a highly stable process with basically no degradation of both the solvent and the cellulose.

In this study, composite fibres were spun from an ionic liquid solution of different cellulose-lignin blends. The effect of the cellulose-to-lignin ratio on the fibre properties was thoroughly investigated. With the spun lignin-containing fibres

two potential applications are pursued. The first approach is to utilize the composite fibre as a precursor for carbon fibre production. The second approach aims at producing naturally dyed textile fibres. The color and color depth can be tuned by the lignin source and the lignin content in the fiber.

II. EXPERIMENTAL

Lignin, originated from either beech Organosolv (Organosolv lignin; courtesy to Fraunhofer CBP) pulping or from Pine Kraft pulping (Kraft lignin) was blended with *Eucalyptus* Prehydrolysis-Kraft dissolving pulp (Bahia pulp) in fractions of 10 wt%, 15wt%, 20 wt%, 30 wt% (Organosolv only). 13 wt% solutions of cellulose blends with lignin in different ratios were prepared using the novel ionic liquid as the solvent. To produce a reference fibre, a dope with neat Bahia pulp at the same concentration was made. The dissolution was carried out in a vertical kneader followed by press filtration equipped with a metal filter fleece of 5-6 µm absolute fineness to remove the insolubles. Subsequently, the dope was spun in a dry-jet wet air gap spinning system. The spinneret with 18 holes (Ø = 0.1 mm) was used to generate a multi-filament. The extrusion temperature was set according to the zero shear viscosity of the dope. The draw ratio of fibres was expressed as $V_{take\text{-}up}/V_{extrution}$. The coagulation medium was water and the temperature was kept at temperatures below room temperature. Linear density (titer), conditioned and wet tenacity were measured at 23 °C and 50% relative humidity using the Lenzing Instrument devices Vibroskop 400 and Vibrodyn 400, respectively. The compositions of the raw material and the resulting fibre were analysed according to the NERL method. The molar mass distributions of the pulp and fibre samples were analysed by size exclusion chromatography from a solution in LiCl/DMAc. The lignin in the fibres was removed prior to dissolution.

III. RESULTS AND DISCUSSION

Figure 1. Comparison of regenerated cellulose fibre and composite fibre.

Figure 1 illustrates the different colors of the fibres regenerated from pure Bahia pulp and a Bahia pulp/lignin blend. Due to the presence of lignin, the composite fibres exhibit a unique shiny brown appearance. The brightness of the fibre has a strong correlation with the lignin content. The color of the composite fibres tends to turn darker as the lignin concentration increases. While the filaments went through the coagulation bath, lignin is partially dissolved in water. Table 1 presents the composition of the pulp/lignin blends and the corresponding composite fibres.

Table 1. The maximum draw ratio and compositions of initial blend polymer and fibres.

		Blend %			Composite fibres %		
Sample	**Max. draw ratio**	Cellulose	Hemicellulose	Lignin	Cellulose	Hemicellulose	Lignin
10 wt% Kraft lignin	15.02	86.56	2.66	10.68	91.13	2.17	6.7
15 wt% Kraft lignin	12.37	81.52	2.7	15.78%	83.86	2.74	13.58
20 wt% Kraft lignin	9.72	76.1	2.74	21.16	78.74	2.74	18.79
10 wt% organosolv. lignin	15.02	86.55	3.28	10.18	89.51	2.39	8.46
15 wt% organosolv. lignin	14.14	81.32	3.67	15.01	85.38	2.31	12.31
20 wt% organosolv. lignin	10.06	75.88	4.07	20.06	82.17	2.03	15.8
30 wt% organosolv. lignin	12.37	65.22	4.85	29.94	72.32	2.25	25.43

In general, the fiber titer decreases with increasing draw ratio. As shown in Table 1, the maximum draw ratio decreases with increasing lignin concentration. Meanwhile, a similar trend between the draw ratio and the titer of the fibres are expected (Figure 2). The lignin content in the fibres showed a considerable effect on the tensile properties. Figure 2 provides a comparison between the tensile strengths and the elongations of the fibers in the dry and wet stages. As expected, the tenacities decrease with rising lignin content. The tenacities of fibres in the dry state containing 10% Kraft and Organosolv lignin were 45.6 and 42.7 cN/tex, respectively, while their tensile strengths decreased to 42.7 and 36.0 cN/tex in the wet state. Due to their higher stretchability, the composite fibers containing Organosolv lignin have a lower linear density and show slightly higher tensile strength as compared to those containing Kraft lignin.

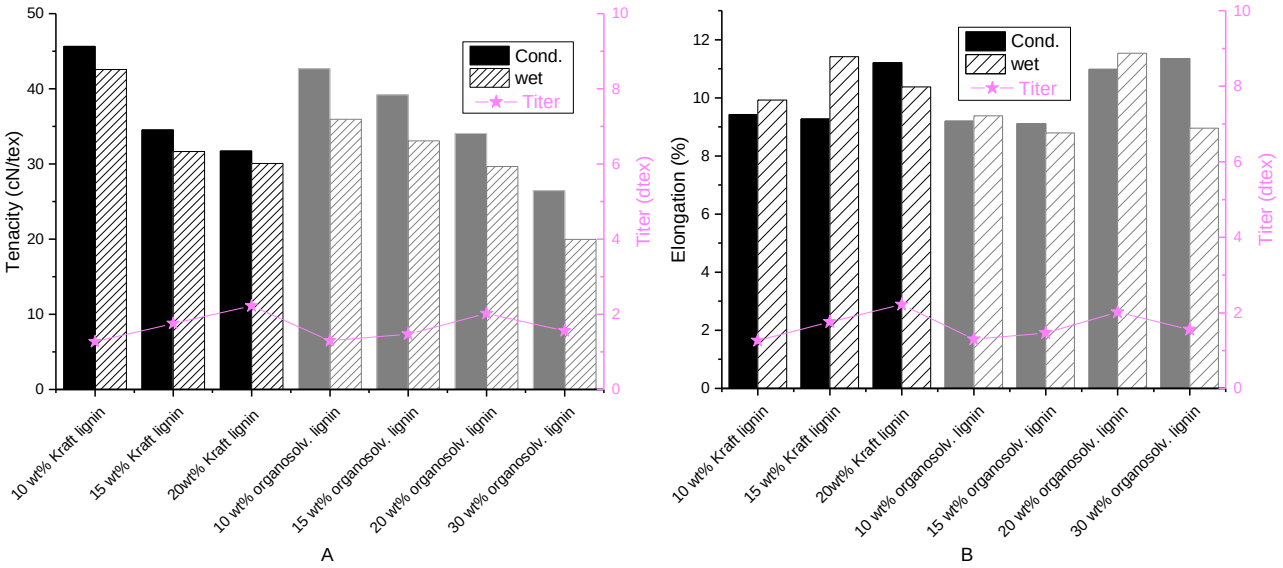

Figure 2. Tensile properties of the composite fibres at highest draw ratio. A: Tenacity. B: Elongation.

Figure 2b shows that lignin acts as a softener. In the dry state, the elongation at break increases with increasing lignin content. No effect on elongation, however, is observed in the wet state.

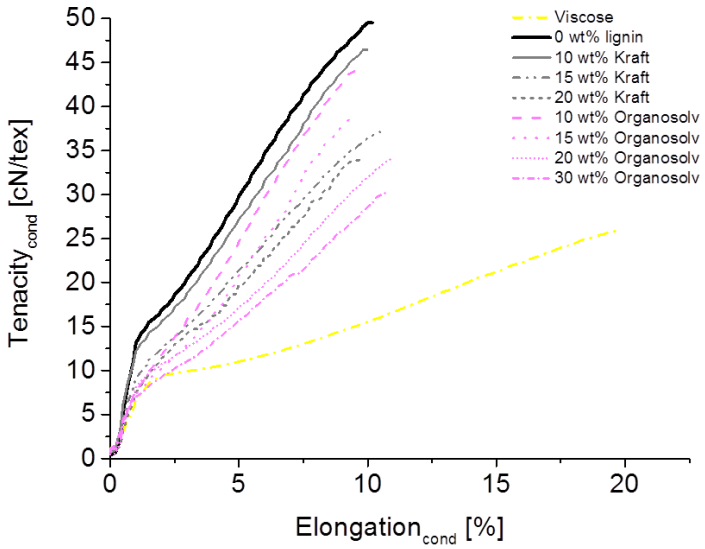

Figure 3. Stress and strain curves of the composite fibres (titer at highest DR), reference fibre (1.2 dtex) and the viscose fibre (1.4 dtex).

To study the mechanical properties of the composite fibres, stress-strain curves were recorded and compared with those of viscose and reference fibres. As shown in Figure 3, the IONCELL-F fibers show significantly higher tensile strengths even with the highest lignin content as compared to the reference Viscose fiber, albeit exhibiting lower elongation.

Molar mass (MM) and molar mass distribution (MMD) are key parameters, determining the raw material and fibres properties. At a given polymer concentration, the dope rheology is largely determined by the MM and the MMD of the dissolved polymer(s). The spinnability is very sensitive to the complex viscosity and the dynamic moduli of the spinning dope. Furthermore, the dissolution conditions shall be controlled in order to prevent the cellulose degradation which may reduce the dope viscosity. Table 3 reveals the MM and MMD distribution of the Bahia pulp and the regenerated fibres after delignification. It has been observed that the MMDs of the fibres are comparable to that of the Bahia pulp, the starting material. This observation confirms the high stability of the novel IONCELL-F spinning process.

Table 3. Molecular weight distribution of composite fibres

Sample	Mn	Mw	PDI	DP 50	DP 100	DP 2000
10 wt% Kraft lignin	71959	201285	2.8	1.02%	3.41%	17.51%
15 wt% Kraft lignin	73233	202297	2.76	1.02%	3.32%	17.61%
20wt% Kraft lignin	75393	207802	2.76	0.93%	3.16%	18.34%
10 wt% organosolv. lignin	69089	202800	2.94	1.41%	3.83%	17.94%
15 wt% organosolv. lignin	67384	201907	3.00	1.53%	3.98%	17.50%
20 wt% organosolv. lignin	72559	206050	2.84	1.19%	3.48%	18.07%
Bahia pulp	72337	202878	2.8	1.17%	3.38%	17.57%

IV. CONCLUSIONS

Composite fibres of cellulose and lignin were produced by means of the IONCELL-F process, a novel IL-based Lyocell spinning process. Although the tensile strength of the composite fiber decreases with increasing lignin content, it remains significantly higher as compared to that of a commercial viscose fiber even at the highest lignin content of 30 wt%. It was shown that blends with Organosolv lignin allowed higher draw ratios than those with Kraft lignin, which resulted in slightly stronger fibers at lower linear density (titer). In the dry state, the presence of lignin acts as a softener, resulting in a higher elongation of the fibers. The MMDs of the fibers confirmed the high chemical stability of the IONCELL-F process.

V. ACKNOWLEDGEMENT

The research project of Design Driven Value Chains in the World of Cellulose is grateful acknowledged for financial support.

VI. REFERENCES

[1] Olsson, C.; Westman, G. Wet Spinning of Cellulose from Ionic Liquid Solution-Viscometry and Mechanical Performance. *J. APPL. POLYM. SCI.* 2013, 127, 4542-4548.

[2] Hermanutz, F.; Meister, F.; Uerdingen, E. New Developments in the Manufacture of Cellulose Fibers with Ionic Liquid. *Chemical Fibers International*. 2006, 56, 342-343.

[3] Jiang, W.; Sun, L. F.; Hao, A.; Chen, J. Y. Regenration Cellulose Fibers from Waste Bagasse Using Ionic Liquid. Textile Research Journal. 2011, 0, 1-10.

[4] Hong, J. H.; Ku, M, K.; Ahn. Y. J.; Kim, H. J.; Kim, H. S. Air-gap Spinning of Cellulose/Ionic Liquid Solution and Its Characterization. *Fibers and Polymer*s. 2013, 14, 2015-2019.

INTEGRATION OF A DISSOLVING PULP MILL AND A CELLULOSE BASED TEXTILE FIBER PLANT

Hans Magnusson, Niklas Kvarnlöf and Ulf Germgård

Department of Engineering and Chemical Sciences, Karlstad University,
SE 65188 Karlstad, Sweden
Email: hans.magnusson@kau.se

ABSTRACT

Textile fibers based on cellulose can soon become a very important product for the pulp and paper industry and it is believed that it would be beneficial to locate such a textile fiber production unit at the same site as the pulp mill. By an integration of pulp production and textile fiber preparation, products from the pulp mill could then easily be transported to the textile fiber plant and some of the by-products from the textile fiber plant could be recycled to the pulp mill. The integrated two processes could also share for example the fresh water supply and the effluent treatment plant. The paper discusses different alternatives and their pros and cons.

I. BACKGROUND

It is today well-known that environmental protection activities will become very critical for the survival of mankind: the greenhouse effect, emissions of harmful chemicals and the shortage of land and water for food production are examples of the problem areas. However, only one activity cannot solve all problems but each step that is taken in the right direction is beneficial. Research into the development of new technologies can give us environmental benign textile fibers that can replace oil based fibers like polyester and nylon but also cotton due to its problems when growing in the fields. The future textile fibers will be based on cellulose from trees, the target is to produce a similar textile fiber quality as today and at a competitive prize. Preliminary studies have indicated that this goal is not too far away.

Textile production

The global textile fiber consumption will increase dramatically in the future and some experts have predicted that the demand in 2050 will be three times the current level [1]. Thus, new types of textile fibers based on cellulose are needed and preferentially should the fiber production be integrated with a dissolving pulp mill. It is also important to know how the chemicals added to the combined production will react and how the chemicals can be regenerated and effluent streams can be taken care of.

During the last decades an increasing interest has been concentrated towards the development of new environmental acceptable cellulose solvents which could be used in an economical feasible production process for textile fibers. Different solvent systems for the dissolution of cellulose have been listed and investigated by several researchers [2, 3, 4] but the main problem is that the chemicals used are often toxic, harmful to the environment, expensive, requiring complicated process conditions or a combination of these factors.

It has been shown that cellulose is soluble in aqueous sodium hydroxide in a small window in the ternary cellulose-sodium hydroxide –water phase diagram [5]. This area is somewhat enlarged with for instance urea, thiourea [6] and some other compounds, like zinc oxide or combinations of these. [7]. No systematic studies of the impact on the solubility window in the face diagram cellulose – sodium hydroxide - water seems to have been done.

A process for production of cellulose carbamate was patented by Hill & Jacobson in 1938 [8]. The process is based on impregnation of the cellulose with an urea – alkali solution and treatment at elevated temperature (above 130 °C) and afterwards dissolution in sodium hydroxide.

An alternative way to produce cellulose carbamate [6], includes impregnation of the dissolving pulp (or other suitable cellulose material) with sodium hydroxide/urea at a low temperature (around – 8 °C) and then heating it to a slightly higher temperature. The produced cellulose carbamate solution can be used to produce both films and fibers of cellulose. The chemicals involved in the production of cellulose carbamate are water, urea and sodium hydroxide. Depending on which process is used, also thiourea and/or zinc compounds can be used. For the spinning of fibers a conventional coagulation bath of sulfuric acid and sodium sulfate is used [9].

II. METHODS

A simplified flowsheet for the integrated pulp/fiber plants was used as basis for an EXCEL model that calculates the relevant mass balances for different elements and for water. Data for the model was mainly taken from the literature [10, 11].

III. RESULTS AND DISCUSSION

The size of a production line for conventional viscose fibers is today of the magnitude 50000 t/year and larger plants consists of more than one line [12]. Therefore 50000 t/year was chosen as the capacity of a theoretical textile plant in our calculation.

One obvious result is the importance of high cellulose content in the spinning dope. In the viscose process a typical amount is 10 % cellulose [11]. For NaOH/ZnO it is reported a cellulose content of the magnitude 3 – 6 % [10], the content is limited by the formation of gel particles if higher cellulose content is used. An increase from 6 % to for example 12 % cellulose corresponds to a decrease of the water volume of 15 to 7 m^3/ton fiber which would be very interesting from en economical point of view.

NaOH for pretreatment and mercerization can be supplied from a kraft pulp mill and it can be evaporated to get the specified strength. A better alternative is to use this input as the input to the combined pulp and textile plant system and to use the overflow/effluent from the textile plant as sodium make-up for the pulp mill.

A greenfield mill can be built according to the principles outlined here, but it is important to design the systems in such a way that the two plants also can operate independent of each other. To add a textile fiber plant to an existing pulp mill and convert it to production of dissolving pulp is a challenge, and detailed knowledge of both the pulping and the textile fiber processes are necessary.

The most common spinning bath composition includes sulfuric acid and sodium sulfate as well as additives like $ZnSO_4$ improving the coagulation and increasing the strength of the fibers [13]. It is important to remember that the strength of the fibers, wet or dry is not the same as the strength of the spin yarn or the finished textile.

Zinc compounds are used both in the dissolution of cellulose and in the coagulation baths. For protection of the environment it is important to minimize the zinc content in the effluents from the combined pulp and textile fiber plant. In this case is the chemistry favorable, as zinc sulfide has a very low solubility under alkaline conditions. Green liquor from the pulp mill can be used to selectively precipitate zinc sulfide and thus to make it possible to remove this precipitate and send concentrated zinc slurry to recycling and reuse elsewhere.

Such a combined pulp mill/textile plant could be very interesting for many pulp mills in Sweden which today need to change their pulp/paper processes to other products with better future potential.

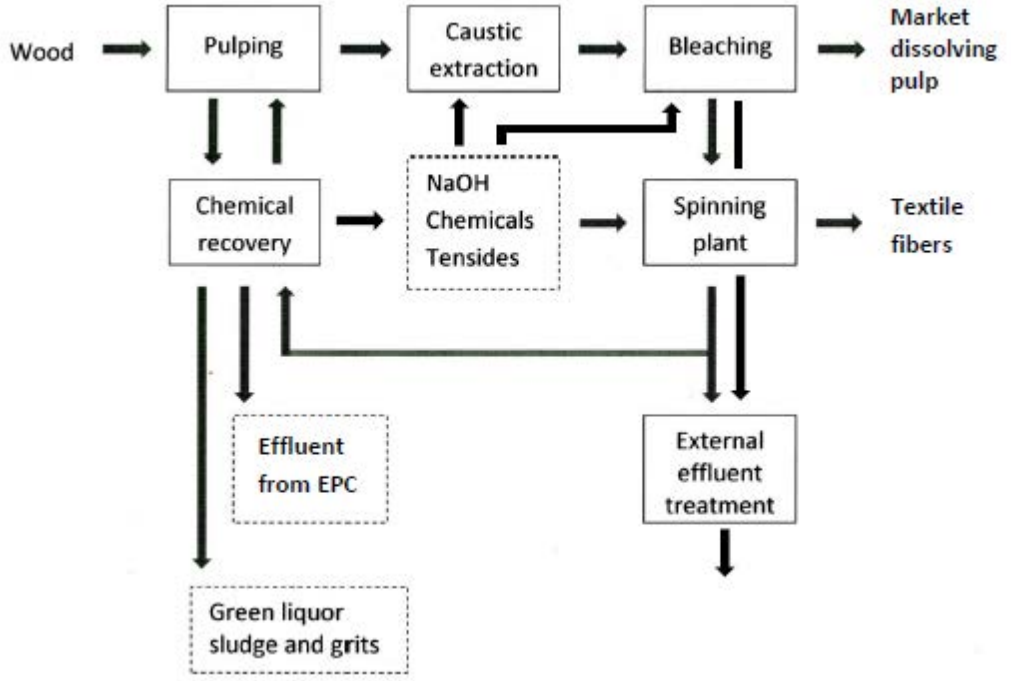

Figure 1. A pulp mill integrated with a textile fiber plant.
EPC, Electrostatic Precipitator Catch, a process to remove potassium and chloride from the recycled electrostatic precipitator dust.

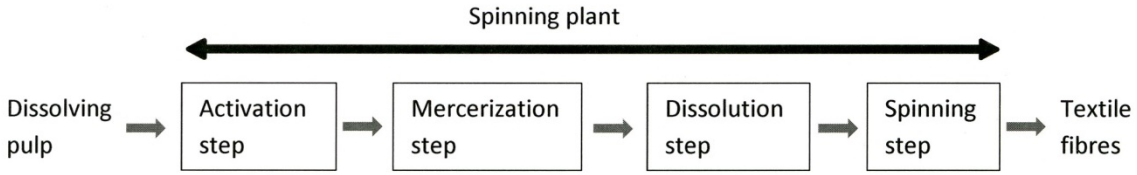

Figur 2 The principal stages in a spinning plant

IV. CONCLUSIONS

There are substantial benefits from an integration of a pulp mill and a textile fiber plant which is studied in an on-going project at Karlstad University. The intention is to present an environmental benign combined process with a favorable economy. Detailed mass and energy balances will show the necessary data for dimensioning of the production lines. Research in the areas improved dissolution processes and spinning conditions may change today's limitations and give new opportunities for the production of textile fibers of sufficient strength at a viable cost.

V. ACKNOWLEDGEMENTS

Thanks are due to the Bo Rydin Foundation for the economical support of Hans Magnusson´s travel cost to EWLP 2014, Seville, Spain.

VI. REFERENCES

[1] Johnson, Tim F.N. Current and future market trends, p 273 – 289
In *Woodings, C. Regenerated Cellulose Fibres, The Textile Institute, 2001.*
[2] Turbak, A. Other Processes. p 174 – 198
In *Woodings, C. Regenerated Cellulose Fibres, The Textile Institute, 2001.*
[3] Wang, Y. Cellulose fiber dissolution in sodium hydroxide solution at low temperature: Dissolution kinetics and solubility improvement, *Diss. Georgia Inst of Technology, 2008.*
[4] Heinze, T.; Koschella, A. Solvents applied in the field of cellulose chemistry – A mini review. *Polimeros* **2005,** *15*, 84-90
[5] Sobue, H.; Kiessing, H.; Hess, K. The cellulose-sodium hydroxide –water system as a function of the temperature. *Physik Chem B* **1939**, *43*, 309–328.
[6] Cai, J, et al. Novel fibers prepared from cellulose in NaOH/urea aqueous solution. *Macromolecular Rapid Communications* **2004,** *25*, 1558 – 1562.
[7] Zhang, S. et al. Dissolution behavior and solubility of cellulose in NaOH complex solution.
Carbohydrate Polymers **2010**, *81*, 668-674.
[8] Hill, J.W.; Jacobson, R.A. Chemical process. U.S.Patent 2 134 825, **1938.**
[9] Mao, Y. et al. Effects of coagulation conditions on properties of multifilament fibers based on dissolution of cellulose in NaOH/urea aqueous solution. *Ind. Eng.Chem.Res.* **2008**, *47*, 8676-8683.
[10] Kihlman, M., et al. Effect of various pulp properties on the solubility of cellulose in sodium hydroxide solutions. *Holzforschung*, **2012**, *5*, 601-606.
[11] Söderlund, C-A. Personal communication. **2013.**
[12] Wright, T. Sateri starts up viscose staple fiber plant in China. *Nonwovens Industry Magazine* **2014-01-06.** www.nonwovens-industry.com/contents/view_breaking-news.
[13] Wilkes, A.G. The viscose process, p 37-61.
In *Woodings, C. Regenerated Cellulose Fibres, The Textile Institute, 2001.*

WATER EXTRACTION, DILUTE-SULFURIC PRETREATMENT AND ENZYMATIC HYDROLYSIS OF *Jatropha curcas* SHELLS

Carlos Martín[1,2*], Ariel García[3], Andreas Schreiber[4], Jürgen Puls[1], Bodo Saake[4]

*[1]TI-Institute for Wood Research, 21031 Hamburg, Germany; [2]Department of Chemistry, Umeå University, SE-901 87 Umeå, Sweden; [3] Department of Chemistry and Chemical Engineering, Universidad de Matanzas, 44740 Matanzas, Cuba; [4]Hamburg University, Wood Science Centre, Chemical Wood Technology, 21031 Hamburg, Germany; *carlos.martin@chem.umu.se*

ABSTRACT

Jatropha curcas is an oil-bearing tree, whose fruits are a raw material of high interest for biodiesel production. The shells, which represent up to one third of the weight of the fruits, are discharged prior to the extraction of *J. curcas* oil, and because of their relatively high carbohydrate content, they can be considered a potential feedstock for bioethanol production. In this work, dilute-acid pretreatment was applied to *J. curcas* shells, which were previously extracted with water at 100ºC and 60 min in a pilot-scale reactor. The water extraction yielded 64.7% of solids containing 35.1% of glucans, which is 53% higher than the glucan content in the raw material. The water-extracted shells were submitted to dilute acid pretreatment at 110-180°C, 0.1-1.5% H_2SO_4 concentration and for 20-60 min following a Box-Behnken experimental design. The yield of pretreated solids ranged between 75 and 95%, and the recovery of glucan was above 87% in all the experimental runs. Xylan solubilisation was relatively low (13-20%) in the less severe pretreatments and up to 45% in the most severe runs. The enzymatic conversion of cellulose upon hydrolysis with commercial cellulases was above 70% for the material pretreated at 145 and 180°C. The analysis of significance showed that the temperature was the factor exerting the most important effect on the enzymatic convertibility, which reached values above 75% in pretreatments performed at 180ºC. The analysis of the contour diagrams revealed that a region with maximal overall conversion can be reached at around 190ºC, short pretreatment time and low H_2SO_4 concentration. These results show the potential of the combination of water extraction and dilute-acid hydrolysis for enhancing the enzymatic hydrolysis of *J. curcas* shells.

Keywords: *Jatropha curcas* shells, dilute-acid pretreatment, enzymatic hydrolysis, lignocellulosic materials

I. INTRODUCTION

Biodiesel is an environmentally friendly fuel that can be used as transportation fuel [1], but the use of edible oils as raw materials is a restriction for the further development of biodiesel industry. Therefore, alternative feedstocks, such as non-edible oils should be considered [2]. The potential of different non-edible oilseeds is being investigated in Cuba [3, 4], and *J. curcas* is one of the most attractive options.

Prior to extraction of the oil, *J. curcas* seeds should be separated from the fruits, and huge amounts of residual shells are generated in that operation. Among the uses that could be applied to that voluminous residue should be considered the production of ethanol [5]. The *in situ* produced ethanol could be directed, together with the oil, to biodiesel production in an integrated configuration. The integration of ethanol and biodiesel production processes using a single source of biomass would allow considerable reduction of the energy costs compared with the autonomous production of each of them, and would lead to decrease of the generation of solid wastes.

Enzymatic hydrolysis is a way for obtaining fermentable sugars from of lignocellulosic materials [6], and a pretreatment is required for making cellulose accessible to the enzymes. The reports on pretreatment and hydrolysis of *J. curcas* shells are rather scarce, but the potential of acid pretreatment has recently been stressed [7, 8, 9]. In the current work, we water extraction was applied prior to the pretreatment in order to remove potential inhibitors of the enzymatic hydrolysis contained in the water-soluble extracts.

II. EXPERIMENTAL

Water extraction of the raw material

Milled *J. curcas* shells corresponding to 2.3 kg dry matter (DM) were suspended in 24 L of water in a 100-L rotating reactor (Herbst Machinenfabrik GmbH, Buxtehude, Germany). The mixture was heated to 100ºC and hold for 1 h. After that, the solid material was separated from the extract by filtration, washed with abundant water, and dried for 5 days at room temperature.

Pretreatment

Sixty grams of extractive-free *J. curcas* shells was mixed with diluted H_2SO_4 (LSR 10) in 1-L stainless steel reactors mounted on a rotary autoclave. A Box-Behnken response surface experimental design was applied (Table 1). By the end of the pretreatment, the reactors were cooled in a cold water bath. After that, the slurry was vacuum-filtered, and the pretreated solids were washed with warm water. The liquors were stored in plastic containers at 4ºC. A portion of the pretreated solids was stored frozen in sealed plastic bags until enzymatic hydrolysis tests, and the rest was dried at room temperature in a climatization chamber and then used for compositional analysis.

Table 1. Experimental design used for investigating the acid pretreatment of pre-extracted *J. curcas* shells

Experiment	Temperature, ºC	Time, h	H_2SO_4 concentration, %
1	110	20	0.8
2	110	40	0.1
3	110	40	1.5
4	110	60	0.8
5	145	20	0.1
6	145	20	1.5
7	145	60	0.1
8	145	60	1.5
9	145	40	0.8
10	145	40	0.8
11	145	40	0.8
12	180	20	0.8
13	180	40	0.1
14	180	40	1.5
15	180	60	0.8

Enzymatic hydrolysis

One gram, on DM basis, of the washed pretreated material was suspended in 25 mL of citrate buffer (pH 5.0). A commercial preparation of *T. reesei* cellulases (Celluclast 1.5L) and a β-glycosidase preparation (Novozym 188) (Novozymes, Denmark) were added at loadings of 25 FPU g^{-1} and 0.46 CBU mL^{-1}, respectively. The reaction mixture was incubated at 45ºC and 150 rpm for 72 h. At the end of hydrolysis, glucose was quantified by HPLC, and the enzymatic convertibility of cellulose was calculated. All experiments were performed in triplicate.

Analytical methods

The chemical composition of both raw and pretreated bagasse was determined by analytical acid hydrolysis of the extractive-free material, followed by quantification of the sugars by borate complex ion exchange chromatography [10]. The sugars were separated on a MCI Gel CA08F (Mitsubishi) column at 60ºC, using a linear gradient of 0.3 to 0.9 M potassium borate buffer (pH 9.2) at a flow rate of 0.7 mL min^{-1} within 35 min. For spectrophotometric detection of sugars at 560 nm, derivatisation with cuprum bicinchoninate was performed. The content of cellulose and xylan was calculated based on the concentrations of glucose and xylose, respectively. Acid-insoluble lignin was determined gravimetrically. Furfural and 5-hydroxy methylfurfural were analyzed by reverse-phase high-performance liquid chromatography (RP-HPLC) using an Aquasil C18 column (Thermo Scientific, Waltham, MA, USA) and UV detection at 210 nm. The sugar content in the pretreatment liquors was determined by posthydrolysis with 0.2 M H_2SO_4, followed by chromatographic analysis. The extractive compounds were determined by accelerated solvent extraction (ASE 200, Dionex, Sunnyvale, USA) with four different solvents in the following sequence: petrol ether, acetone/water mixture, ethanol/water mixture, and water. In parallel, a sample was processed only water extraction. The mineral components were determined as ash, after incineration of an aliquot of the material at 550ºC, in a muffle oven (Heraeus Instruments GmbH, Hanau, Germany). All analyses were performed in triplicate. The experimental results were processed with the software STATGRAPHICS Plus 5.0 for Windows.

III. RESULTS AND DISCUSSION

Water extraction

The yield of solids achieved after water extraction indicate that 35.3% of the initial dry matter was solubilised (Table 2). The removal of the extractive fraction lead to increases of the content of structural components. Cellulose and the other polysaccharides were completely recovered in the extractive-free material.

Pretreatment

The extractive-free solids resulting from the extraction step were submitted to dilute-acid pretreatment. A Box-Behnken response surface experimental design was applied for investigating the effect of the temperature, H_2SO_4 concentration and pretreatment time on the response factors. The Box-Behnken design offers a number of advantages over other experimental designs. It allows keeping the sample size at a value that is relatively low, but that is sufficient to fit a quadratic model [11]. The selection of the factors and their ranges was based on preliminary results [7].

Table 2. Yield of solids and recovery of carbohydrates and lignin in the extraction and pretreatment, %

Experiment	Yield of solids[1]	Cellulose	Xylan	Arabinan	Mannan	Galactan	Lignin
Extraction	64.7	100	100	100	100	100	100
1	95.4	93.4	87.5	97.0	95.4	95.4	100
2	96.0	92.8	87.1	96.1	96.0	96.0	99.1
3	93.3	91.9	83.8	93.3	97.4	93.3	96.8
4	93.8	91.8	84.5	93.1	97.1	98.3	96.4
5	93.0	92.7	86.1	84.5	97.0	93.0	93.6
6	92.5	92.0	84.8	67.3	92.5	82.2	95.3
7	91.1	91.8	83.5	66.2	91.1	80.9	93.0
8	86.9	90.0	78.9	47.4	86.9	77.2	90.9
9	88.0	91.3	79.9	72.0	91.8	83.1	92.3
10	87.6	91.6	79.5	71.7	92.4	82.8	92.0
11	88.4	91.7	81.1	72.4	92.3	83.5	91.5
12	79.2	90.7	82.1	28.8	79.2	57.2	86.9
13	75.1	91.1	66.8	27.3	78.4	58.4	85.8
14	73.4	86.6	56.4	20.0	79.8	53.0	86.6
15	73.5	87.9	54.2	20.0	73.2	52.9	87.2

A clear decrease of the yield of solids was observed with increasing the temperature (Table 2). In the pretreatments at 110ºC the yield was above 93%, which corresponds to more than 61% of the raw material, considering that the yield of the extraction step was 65.6%. The yield, based on the pre-extracted material, was 87 – 93% for the experiments at 145ºC, and 73-79% for those at 180ºC.

Figure 1. Pareto chart (A) and three-dimensional response surfaces under constant time (B) and constant sulfuric acid concentration (C) for cellulose recovery after pretreatment

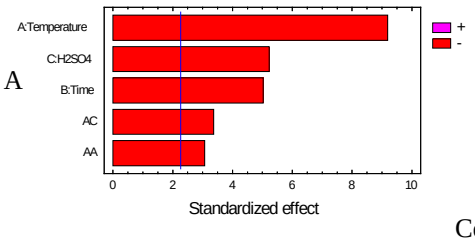

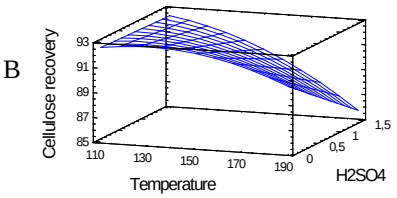

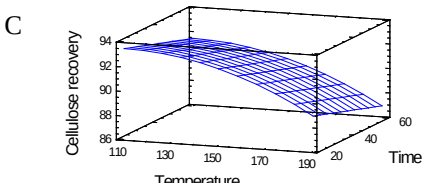

Cellulose recovery in the pretreated solids ranged between 86.6 and 93.4% (Table 2). The temperature exerted the most important effect on cellulose recovery (Fig. 1-A). Acid concentration and time, as well as the interaction between the temperature and concentration, and the quadratic of the temperature also exerted significant effects. The negative signs indicate that the increases of each factor lead to decrease of cellulose recovery. This is confirmed by the response surface diagrams (Fig. 1-B and 1-C).

The recovery of xylan was lower than that of cellulose (Table 2), indicating a relatively high degree of solubilisation. Even at the mildest conditions (experimental runs 1 and 2), around 13% of xylan was solubilised. The solubilisation degree of xylan increased with the severity, and it reached 44-46% in some of the pretreatments performed at 180ºC (experiments 14 and 15). Lignin was only marginally affected by the pretreatment. Its recovery was around 100% in the least severe pretreatments, remained high for most of the experimental runs, and it was below 90% only in the pretreatments performed at 180ºC (Table 2).

The recovery of carbohydrates in the liquid fraction was consistent with the above discussed trend of polysaccharides recovery in the pretreated solids. The glucose in the prehydrolysates was almost negligible, which indicates that little cellulose was hydrolysed during the pretreatment. Anyway, not all the solubilised carbohydrates were recovered as simple sugars in the prehydrolysates, which was due to their partial degradation to furan aldehydes.

Enzymatic hydrolysis

The effect of the pretreatment on enhancing the enzymatic hydrolysis of *J. curcas* shells is shown by the increased enzymatic convertibility of cellulose in all the pretreated solids as compared to the raw material and to the extracted but not acid-pretreated shells (Fig. 2). At 110ºC, the convertibility (55.6 – 59.2% of the cellulose contained in the pretreated material) was only slightly higher than in the extracted material not submitted to acid pretreatment (53.8%), but it was clearly higher than in the raw material (45%). As the temperature increased, the enzymatic convertibility also increased reaching values above 75% in some of the pretreatments performed at 180ºC.

Figure 2. Enzymatic conversion of cellulose in the pretreated shells (white bars), raw material (black bar) and extracted material (gray bar).

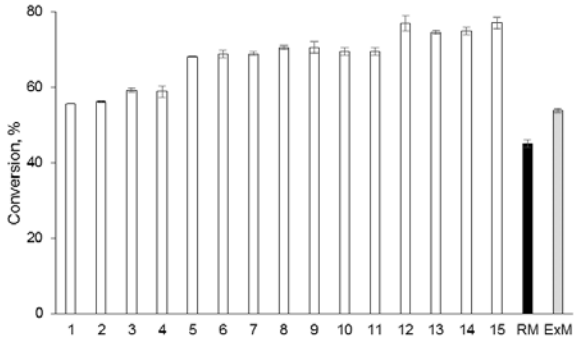

Figure 3. Three-dimensional response surface for the overall conversion of cellulose. Obtained for 0.8% sulfuric acid.

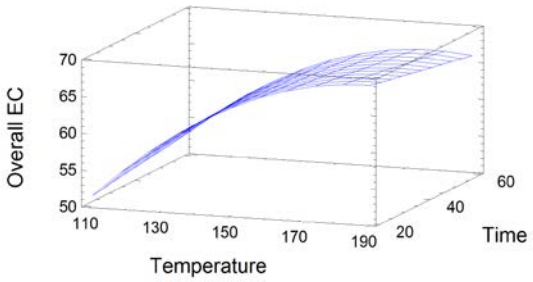

The analysis of significance showed that the estimated effect of the temperature is the most important one affecting the overall enzymatic conversion, and that it has a positive sign, indicating that its increase leads to an increase of the overall conversion of cellulose. On the other hand, the interactions of the temperature with both the pretreatment time and the sulfuric acid concentration, as well as the quadratic term of the temperature also exert significant standardized effects, but with negative signs.

The estimated effect of the temperature is better described by the three-dimensional response surface graph (Fig. 3). It is evident that the overall conversion increased sharply when the temperature was raised from 110ºC to around 170ºC, while the effect of further temperature increases was more moderate. The contour diagrams revealed that a region with maximal overall conversion can be reached at around 190ºC, short pretreatment time and low H_2SO_4 concentration.

IV. CONCLUSIONS

The potential of a water extraction step prior to acid pretreatment of *J. curcas* shells was confirmed. A region of pretreatment conditions leading to a maximal overall conversion of cellulose was identified.

V. ACKNOWLEDGEMENT

The financial support given by the Alexander von Humboldt foundation is gratefully acknowledged.

VI. REFERENCES

[1] Agarwal, A.K. Biofuels (alcohols and biodiesel) applications as fuels for internal combustion engines. *Progr. Energy Comb. Sc.* **2007**, *33*, 233 – 271.

[2] Azam, M.M.; Waris, A.; Nahar, N.M. Prospects and potential of fatty acid methyl esters of some non-traditional seed oils for use as biodiesel in India. *Biomass Bioenerg.* **2005**, *29*, 293 – 302.

[3] Martín. C.; Moure. A.; Martín. G.; Carrillo. E.; Domínguez. H.; Parajó. J.C. Fractional characterization of jatropha, neem, moringa, trisperma, castor and candlenut seeds as potential feedstocks for biodiesel production in Cuba. *Biomass Bioenerg.* **2010**, *34*, 533 – 538.

[4] Hernández, E.; García, A.; López, M.; Parajó, J.C.; Puls, J.; Martín, C. Dilute sulfuric acid pretreatment of Moringa oleifera pods for enzymatic hydrolysis. *Ind. Crop. Prod.* **2013**, *44*, 227 – 231.

[5] Visser, E.M.; Filho, D.O.; Martins, M.A.; Steward, B.L. Bioethanol production potential from Brazilian biodiesel co-products. *Biomass Bioenerg.* **2011**, *35*, 489 – 494.

[6] Taherzadeh, M.J.; Karimi, K. Enzyme-based hydrolysis processes for ethanol from lignocelulosic materials: A review. *BioResources* **2007**, *2*, 707 – 738.

[7] García, A.; Cara, C.; Moya, M.; Rapado, J.; Puls, J.; Castro, E.; Martín, C. Dilute sulphuric acid pretreatment and enzymatic hydrolysis of *J. curcas* fruit shells for ethanol production. *Ind. Crops Prod.* **2014**, *53*, 148 – 153.

[8] Marasabessy, A.; Maarten, A.; Kootstra, J.; Sanders, J.P.M.; Weusthuis, R.A. Dilute H_2SO_4-catalyzed hydrothermal pretreatment to enhance enzymatic digestibility of *Jatropha curcas* fruit hull for ethanol fermentation. *International J. Energy Environm. Eng.* **2012**, *3*, 1 – 15.

[9] Visser, E.M.; Filho, D.O.; Tótola, M.R.; Martins, M.A.; Guimarães, V.M. Simultaneous saccharification and fermentation (SSF) of Jatropha curcas shells: utilization of co-products from the biodiesel production process. *Bioprocess Biosyst. Eng.* **2012**, *35*, 801 – 807.

[10] Puls J. Substrate analysis of forest and agricultural wastes. In: *Bioconversion of forest and agricultural residues*. Ed. Saddler J.N. CAB International, Wallingford. **1993**. pp. 13 – 32.

[11] Box, G.E.P.; Behnken, D.W. Some new three level designs for the study of quantitative variables. *Technometrics* **1960**, *2*, 455 – 75.

CHEMICAL COMPOSITION AND TOPOCHEMISTRY OF DELIGNIFICATION IN *EUCALYPTUS GLOBULUS* GENOTYPES WITH DIFFERENT PULPWOOD CHARACTERISTICS

Regis Teixeira Mendonça[1]*, María Graciela Aguayo[1], Paulina Martínez[1], André Ferraz[2]

[1]Universidad de Concepción, Facultad de CienciasForestales y Centro de Biotecnología, Concepción, Chile; [2]Universidade de Sao Paulo, Escola de Engenharia de Lorena, Lorena-SP, Brazil.
**rteixeira@udec.cl*

ABSTRACT

Six different genotypes of *Eucalyptus globulus* were selected on the basis of their differences in wood density and pulp yield. The trees were separated in 2 groups, one with high density and high pulp yield (573 kg/m^3 and 54.5%, respectively) and other with low density and low pulp yield (471 kg/m^3 and 57,8%, respectively). Averaged chemical composition showed that samples of group I presented high glucans and low lignin content as compared with samples from group II. Xylans content was lower in samples of group I than in group II. During kraft delignification, samples of group I retained more xylans (54-59%) than samples from group II, which was associated with the degree of substitution with methylglucuronic acids. Characterization of the wood and pulp samples by thioacidolysis indicated that the content of syringyl units in β-O-4 linkages (S-β-O-4) was higher in samples of group I than group II. Topochemistry studies by UV microspectrophotometric (UMSP) revealed that the samples with the lowest lignin levels and high S-β-O-4 have the lowest UV absorbances at 278 nm (A_{278} nm) in the secondary walls (S2). Results showed that glucans content, xylans structure, lignin structure and topochemistry are important parameters that affected the pulpwood performance of different genotypes of *E. globulus*.

I. INTRODUCTION

Eucalyptus globulus is an important raw material for the pulp and paper industry. Large breeding programs with this species are performed worldwide to select the best genotypes. Usually, trees were selected based on phenotypic and pulpwood traits, such as tree form, height, volume, wood density and pulp yield. These breeding programs usually select plants based on growth rates and tree quality parameters. Previous works showed that the kraft pulpability of this species correlates positively with the glucan content and negatively with the lignin content[1,2]. More recently, anatomical features of *E. globulus* clones were also assessed as a breeding selection parameter[3]. Aside from lignin content, lignin structure also plays a key role in pulping processes[4]. The syringyl/guaiacyl ratios (S/G), and especially the frequency of beta-aryl-ether (ß-O-4) linkages, have important effects on delignification rate, alkali consumption and pulp yield. Moreover, the composition and structure of the xylans in hardwoods could also play a role in explaining the variation in pulp yield observed and can also be a characteristic to include in clonal breeding programs. In the present work, the chemical characteristics and the kraft delignification of different *E. globulus* genotypes were evaluated in terms of pulpwood quality. Xylans retention, lignin composition and distribution in the cell wall layers were associated with the different pulpability of the species during kraft pulping.

II. EXPERIMENTAL

Samples and chemical characterizacion: Six trees of 15-years old *E. globulus* were provided by a Chilean forest company located in the Bio Bio Province. The trees were selected based on a previous study and showed significant variation in wood density (from 471 to 573 kg/m^3) and pulp yield (from 54.5% to 57.8%). Wood chips from each genotype was milled in a knife mill and sieved to 45/60 mesh. Extractives were determined after extraction with 90% acetone for 16 h in a Soxhlet apparatus. Extractive-free samples were characterized for carbohydrates and lignin content by the acid hydrolysis with 72% H_2SO_4 following the procedure detailed by Ferraz et al.[4] Thioacidolysis was performed on 20 mg of extracted milled wood in 10 mL of reagent according to the method published by Rolando et al.[4] Detailed composition of hemicelluloses from wood and pulps were determined by acid methanolysis/GC-FID according to the procedure described by Sundberg et al.[6] Xylans were isolated from wood holocellulose and pulp according to Shatalov et al.[7] Xylans were characterized by HPLC/SEC and 1H-RMN.

Kraft pulping: Wood chips were submitted to kraft pulping in a rotary digester equipped with 4 independent 1.5-L vessels (Regmed, Brazil). Each vessel was loaded with 50 g of wood chips (dry basis) and 200 mL of cooking

liquor with 18% active alkali (AA) and 30% sulfidity, liquor:wood ratio 4:1, (both calculated on dry wood basis and expressed as NaOH equivalents). Reactor heating ramp was from 40°C to 80°C in 40 min, then 80°C to 165°C in 120 min, and then the temperature was maintained for 30 min at 165°C. Samples were immerse in water for 24 h for residual liquor removal and were not fiberized or screened previous the UMSP analysis.

UV microspectrophotometry: Small wood blocks (approximately 1 x 1 x 0.5 mm) were cut from the samples and dehydrated in a graded series of acetone and embedded in Spurr's epoxy resin. Sections of 1 µm thick were prepared from these samples with a diamond knife and transferred to quartz microscope slides. The topochemical analysis was carried out using a microspectrophotometer (UMSP Zeiss MSP800) equipped with a scanning stage enabling the determination of image profiles at defined wavelengths using the scan program MSP Tidas 800 (Zeiss). Wavelengths at 278 - 280 nm were selected for the distribution of hardwood lignin[8-10].

III. RESULTS AND DISCUSSION

Chemical characterization: Chemical composition of the 6 genotypes showed that the samples from GI contain the highest amounts of glucans and the lowest amounts of lignin, where as the samples from GII have low glucan and high lignin contents (Table 1). The data concerning the pulp yield and chemical composition of these samples are consistent with previously published data from another *E. globulus* sample sets. Xylans content was slightly lower in genotypes of GI (11.2-11.6%) than in GII (12.6- 14.3%), and no significant differences were found for the amount of MeGlcA and acetyl groups attached to the xylan chains. The amount of galactose found was due to the residues of α-D-galactopyranose attached to MeGlcA, as previously reported for *Eucalyptus* species[7,11].

Table 1. Wood characteristics of *E. globulus* genotypes.*

	Group I			Group II		
	E1	E2	E3	E4	E5	E6
Density (kg/m3)	573	563	547	485	484	471
Glucans (%)	53.3	53.8	52.1	49.2	48.7	48.5
Xylose (%)	11.6	11.6	11.2	12.6	14.3	13.8
Arabinose (%)	0.1	0.1	0.2	0.1	0.2	0.2
Galactose (%)	0.5	0.4	0.6	0.4	0.7	0.4
MeGlcA (%)	1.2	1.6	1.2	1.0	1.2	1.2
Acetyl (%)	3.1	3.0	3.1	3.1	3.5	3.3
Lignin (%)	24.1	24.2	24.9	26.9	25.8	26.9
G-units (µmol/g lig)	547	618	511	561	642	941
S-units (µmol/g lig)	2304	2073	2258	1790	1787	1500
β-O-4 linkages (%)	60	57	58	52	51	52
Extractives (%)	1.3	1.1	0.8	1.3	1.7	2.4

* Standard deviations for wood density and chemical characteristics were lower than 3% of the average value.

Kraft pulping: Kraft pulps produced with kappa numbers of 16±1 presented significant differences in the retention of xylans (in relation with the original amount in wood), which was in the range of 54-59% for pulps of GI and, 43-51% for pulps of GII. These results indicated that, despite their lower initial amount, the xylans from genotypes of GI were less degraded than xylans of genotypes from GII, during kraft pulping process. The formation of HexA from MeGlcA during kraft pulping also stabilizes the reducing ends of xylan chains and contributes to their retention in pulps. Good correlations were found for the amount of xylans retained in pulp and the amount of MeGlcA and HexA (determined by 1H-RMN) in wood and pulp (figure 1).

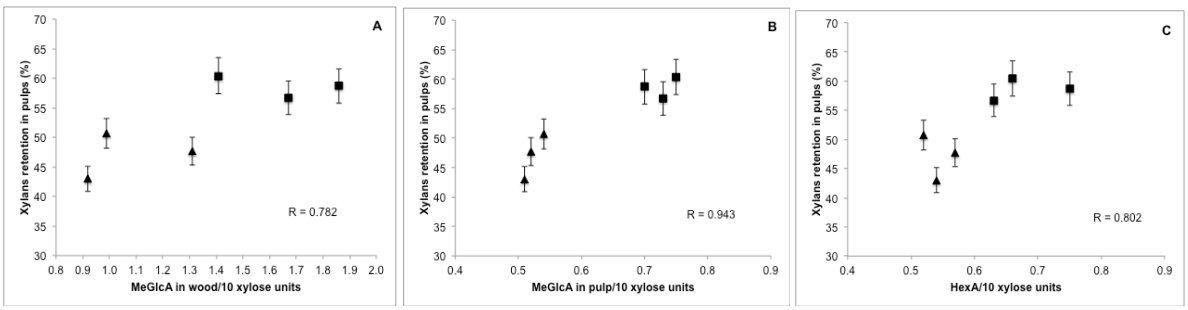

Figure 1. Effect of the MeGlcA/10 xylose units in A) wood and B) pulps, and C) HexA/10 xylose units with the retention of xylans in kraft pulps of *E. globulus*. Samples of group I (black filled squares) and group II (black filled triangles).

The total yield of thioacidolysis monomers recovered from the uncooked wood chips indicated that the samples with the lowest lignin levels (GI) led to slightly higher yields of thioacidolysis monomers, suggesting that their lignin contains more β-O-4 linkages and less-condensed structures (Figure 2A). Syringyl (S) units predominated in the β-O-4 structures of the lignin of all wood samples as the yields of S-thioacidolysis monomers were 2-3 times higher than those of the yields of G-thioacidolysis monomers (Figure 2B and 2C). S units in β-O-4 linkages were also a contrasting characteristic of the studied genotypes because the GI samples give rise to higher yields of S-thioacidolysis monomers compared with data from the GII samples (Figure 2B). The total yield of thioacidolysis monomers detected in the residual lignins from P1 and P2 pulps decreased with pulping, confirming that β-O-4 cleavage is one of the main reactions in kraft cooking, while more condensed structures are left in the residual lignin of the produced pulps.[12]

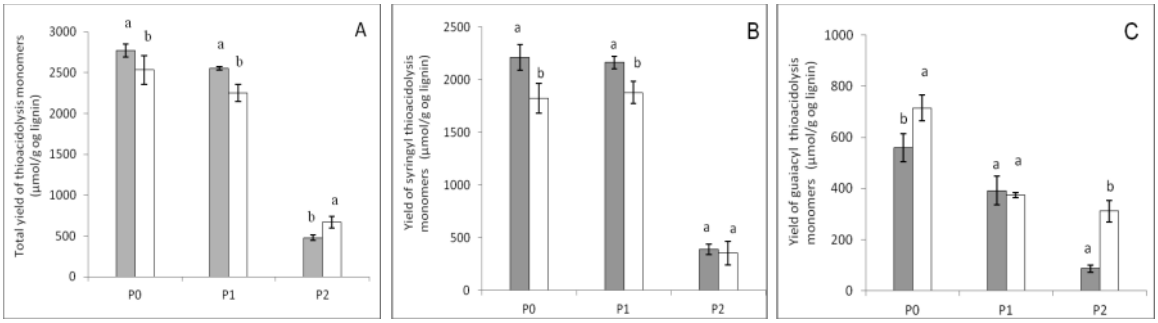

Figure 2. (A) Yield of thioacidolysis monomers, (B) yield of syringyl thioacidolysis monomers and (C) yield of guaiacyl thioacidolysis monomers recovered from selected *E. globulus* genotypes with varied pulp wood quality, before and after kraft pulping. P0, P1 and P2 denote uncooked wood and pulps sampled at the initial and intermediary steps of the bulk delignification phase, respectively. Grey bars represent average samples of group I genotypes and white bars represent samples average of group II. The letters above the bars indicate significant differences between the groups determined by Tukey test at $p<0.05$.

Results of UMSP studies: UV spectra recorded from l-µm^2 spots localized in the secondary walls of the wood chips of the studied genotypes are shown in Figure 3. Intense UV absorptions were observed in the range from 274 to 281 nm, which is consistent with UV spectra of guaiacyl-syringyl lignin from angiosperms[13]. The absorption intensity at 278 nm of the secondary walls of the wood samples were in accordance with the values previously published for S2 layers of angiosperms that are lower than the values often observed in the guaiacyl lignins from gymnosperms[14]. UV-microspectrophotometric data of each genotype followed the same trend as observed for total lignin contents in the samples (Table 1). The GI, with the lowest lignin contents, also presented the lowest UV absorbance values for the secondary walls at 278 nm. The lower absorbance values at 278 nm obtained for the GI wood samples also corroborate with the higher syringyl contents of these samples (Figure 2B), since for angiosperms lignins, the absorptivity at the 278 nm region decreases at increasing OCH_3/C_9 ratios[15].

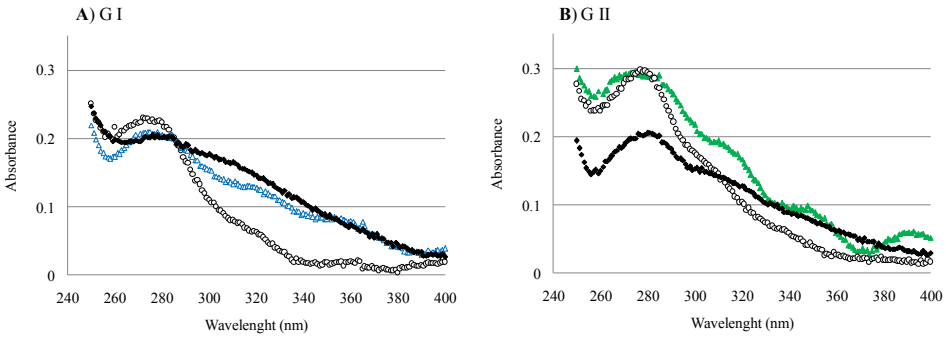

Figure 3. UV spectra from the S2 of fibres from different *E. globulus* genotypes. At least 15 spectra were recorded from the S2 layers of each genotype. A) and B) show spectra of uncooked wood samples of group I and II, respectively.

IV. CONCLUSIONS

Eucalyptus globulus genotypes with high pulp yields were those with high glucan, low lignin contents, high abundance of syringyl units in β-O-4 linkages. In superior genotypes, lignin distribution in secondary cell wall showed lower absorbance at 278 nm in comparison with inferior genotypes. Genotypes with high pulp yield also

presented higher retention of xylans. Retention was associated with high molar mass of xylans and high degree of substitution with presented a high degree of substitution of xylose residues with methylglucuronic acid in both wood and pulps, and also a high degree of substitution with methylglucuronic and hexenuronic acids. All these characteristics provided useful information for the selection and management of the species in clonal plantations for the pulp and paper industry.

V. ACKNOWLEDGEMENT

Financial support from FONDECYT (grant 1110828) and INNOVA-CHILE (grant 05CTE04-01) in Chile, and FAPESP (grant 2011/50535-2) in Brazil is acknowledged. M.G. Aguayo thanks a PhD grant from MECESUP (UCO 0702).

VI. REFERENCES

[1] Wallis, A.F.A.; Wearne, R.H.; Wright, P.J. Analytical characteristics of plantation eucalypt woods relating to kraft pulp yields. *Appita J*. **1996**, *49(6)*, 427–432.

[2] Miranda, I.; Pereira, H. (2002) Variation in pulpwood quality with provenances and site in *Eucalyptus globulus*. *Ann. Forest Sci*. **2002**, *59*, 283–291.

[3] Ramirez, M.; Rodríguez, J.; Balocchi, C.; Peredo, M.; Elissetche, J.P.; Mendonça, R.; Valenzuela, S. Chemical composition and wood anatomy of *Eucalyptus globulus* clones: variations and relationships with pulpability and handsheet properties. *J. Wood Chem. Technol*. **2009**, 29, 43-58.

[4] Ferraz, A.; Mendonca, R.; Guerra, A.; Ruiz, J.; Rodríguez, J.; Baeza, J.; Freer, J. Near Infrared Spectra and chemical characteristics of *Pinustaeda* (Loblolly Pine) wood chips biotreated by the white rot fungus *Ceriporiopsissubvermispora*. *J. Wood Chem. Techn*. **2005**, *24(2)*, 99-113.

[5] Rolando, C.; Monties, B.; Lapierre, C. Thioacidolysis. In: Methods in Lignin Chemistry, Lin S.Y., Dence C.W. Eds: Springer, Berlin. **1992**, pp.334-350.

[6] Sundberg, A.; Sundber, K.; Lillandi, C.; Holmbom, B. Determination of hemicelluloses and pectins in wood and pulp fibres by acid methanolysis and gas chromatography. *Nordic Pulp Pap Res. J*. **1996**, *4*, 216–220.

[7] Shatalov, A.A.; Evtuguin, D.V.; Neto, C.P. (2-O-α-D-Galactopyranosyl-4-Omethyl-α-D glucurono)-D-xylan from *Eucalyptus globulus*Labill.*Carbohydrate Res*. **1999**, *320*, 93–99.

[8] Koch, G.; Grünwald, C. Application of UV microspectrophotometry for the topochemical detection of lignin and phenolic extractives in wood fibre cell walls. In: Wood Fibre Cell Walls: Methods to Study their Formation, Structure and Properties. Schmitt U. Uppsala: Swedish University of Agricultural Sciences. **2004**. pp.119-130.

[9] Koch, G., Kleist, G. (2001) Application of scanning UV microspectrophotometry to localiselignins and phenolic extractives in plant cell walls. *Holzforschung*. **2001**, *55*, 563-567.

[10] Lehringer, C.; Gierlinger, N.; Koch, G. Topochemical investigation on tension wood fibres of Acer spp., Fagussylvatica L. andQuercusrobur L. *Holzforschung.* **2008**, *62*, 255-263.

[11] Magaton, A.S.; Silva, T.; Colodette, J.; Pilo-Veloso, D.; Reis Milagres, F. Behavior of xylans from *Eucalyptus* species. Part 1. The influence of structural features of eucalyptus xylans on their retention in kraft pulp. *Holzforschung*. **2013**, *67*, 115–122.

[12] Guerra, A.; Elissetche, J.;Norambuena, M.; Freer, J.; Valenzuela, J.; Rodríguez, J.; Balocchi, C. Influence of lignin structural on *Eucalyptus globulus* kraft pulping. *J. Agric. Food Chem*. **2008**, *47*, 8542-8549.

[13] Fergus, B.J.; Goring D.A.I. The location of guaiacyl and syringyl lignins in birch xylem tissue. *Holzforschung*. **1970**, *24*, 113–117.

[14] Prislan, P.; Koch, G.; Cufar, K.;Gricar, J.; Schmitt, U. Topochemical investigations of cell walls in developing xylem of beech (*Fagus sylvatica* L.). *Holzforschung*. **2009**,*63*, 482-490.

[15] Musha, Y.; Goring, D.A.I. Distribution of syringyl and guaiacyl moieties in hardwoods as indicated by ultraviolet microscopy.*Wood Sci. Technol*. **1975**, *9*, 45–58.

INFLUENCE OF MOLAR MASS DISTRIBUTION ON THE FINAL PROPERTIES OF REGENERATED FIBERS FROM CELLULOSE DISSOLVED IN IONIC LIQUID BY DRY-JET WET SPINNING

Anne Michud, Michael Hummel and Herbert Sixta*

Department of Forest Products Technology, Aalto University, P.O. Box 16300, 00076 Aalto, Finland
**herbert.sixta@aalto.fi*

ABSTRACT

Regenerated cellulose fibers were produced by dry-jet wet spinning from cellulose blends dissolved in ionic liquid with different molar mass distribution (MMD) but fixed intrinsic viscosity in order to investigate the influence of MMD on the spinnability and on the mechanical properties of the final fibers. Polymer solutions were prepared by dissolution of blends, constituted of cotton linters and spruce sulfite pulp, in 1,5-diazabicyclo[4.3.0]non-5-ene acetate ([DBNH]OAc) in a vertical kneader. Dynamic shear measurements of the different polymer solutions were conducted to define their visco-elastic properties and thus the appropriate spinning temperature needed to establish stable spinning. Blends with a certain share of high molecular weight cellulose and wider polydispersity index (PDI) showed enhanced spinnability. Higher draw ratios were accessible and, consequently, stronger fibers were produced.

I. INTRODUCTION

Spinning of cellulose-ionic liquid solutions in the so called IONCELL-F process is presented as an alternative to the currently used viscose and Lyocell processes for the production of man-made cellulosic fibers. Ionics liquids are a novel class of solvents which have been proven to be efficient non-derivatizing solvents for lignocellulosic materials [1]. In a dry-jet wet spinning process a polymer solution is extruded at elevated temperature through a spinneret via an air gap into a coagulation bath. In the air gap, the fluid filament is drawn which provokes the orientation of the polymer chains and, thus, affects the properties of the resulting fibers. The final properties of the fibers are strongly influenced by the chosen spinning parameters (extrusion velocity, draw ratio, air gap) as well as the properties of the raw material (cellulose and hemicellulose contents, intrinsic viscosity, molar mass distribution) [2].
The molar mass distribution and the polydispersity index of cellulose dissolved in ionic liquid has a great influence on the rheological behavior of spinning solutions which is important to consider in order to anticipate the processability [3]. Further, the strength properties of the produced fibers are highly connected to the intrinsic characteristics of the original cellulose and to the way the regenerated cellulose chains are oriented during the regeneration process.
In this study, the influence of the MMD of cellulose on the spinnability of cellulose-[DBNH]OAc and on the mechanical properties of the regenerated cellulose fibers was investigated.

II. EXPERIMENTAL

Preparation of blends

Five blends of different molar mass distribution but fixed intrinsic viscosity (420 ml/g) were prepared by combining two pulps presenting different distribution properties. Cotton linters (CL729, CL420, CL415, CL318) and spruce sulfite pulp (S1521, S577, S218, S174) of different starting intrinsic viscosity were used as raw materials in this study. The different pulps have been selected in order to form blends with a wide range of PDI. The blends were prepared by combining the two different pulps in water and by stirring the suspension for 15 min by means of an ultra-turrax disperser. The intrinsic viscosity of the blends was determined according to the standard method SCAN-CM 15:99 and the molar mass distribution characterized by gel permeation chromatography (GPC).

Dissolution in [DBNH]OAc

The different blends (15 wt% concentration except Blend 4 that has also been prepared at 13 wt%) were dissolved in [DBNH]OAc by means of a vertical kneader at 80 ºC. The cellulose-IL mixture was first homogenized manually before being transferred in the pre-heated vertical kneader. Temperature, torque moment, vacuum and revolution per min (rpm) were recorded on-line and plotted as a function of time. A dissolution time of 45 min at 10 rpm, 80ºC and vacuum of 100 mbar was sufficient for complete cellulose dissolution. The dissolution state of the cellulose in the IL was checked with an optical microscope. Subsequently, the solutions were filtered via a hydraulic pressure filtration unit to remove any impurities or un-dissolved particles.

Characterization of cellulose-IL solutions

The rheological behavior of the cellulose-IL solutions was investigated under shear stresses. The visco-elastic behavior was studied by means of a MCR 300 rheometer from Anton Paar by performing dynamic frequency sweep measurements at a strain of 0.5% over a range of 0.01-100 s^{-1} and at temperatures from 70 to 90 °C.

Dry-jet wet spinning of cellulose-IL solutions

Fibers were spun using a dry-jet wet piston spinning unit. The spinning temperature was chosen according to the rheological behavior of each polymer solutions. The chosen temperature was thus different for each blend but in the same range from 70 to 85 °C. The extrusion and take-up velocities were the only parameters varied during the spinning process in order to determine the maximum draw ratio applicable on the fibers. The spinneret (36 holes, diameter of 100 µm, and capillary length of 20 µm), air gap distance (1cm), coagulation bath temperature (10-15 °C) and immersion depth in the coagulation bath were kept constant.

Testing of regenerated fibers

The quality of the resulting fibers was assessed by using Lenzing Instrument devices (Vibroskop and Vibrodyn 400). They were characterized in terms of linear density (dtex), tenacity (cN/tex) and elongation at break (%).

III. RESULTS AND DISCUSSION

Blend composition and molar mass determination

The composition and the molar mass distribution of each blend are summarized in Table 1. The intrinsic viscosity of the different blends is very close to the target value 420 ml/g, except for Blend 1 which is slightly higher. The weight average molar masses (M_w) are comparable. The PDI ranges between 2.0 and 5.9 and indicates the broadness of the MMD in the blends. The MMD of the different blends, obtained by GPC, are depicted in Figure 1.

Table 1: Composition and molar mass distribution of each blend.

	Composition	**Intrinsic viscosity ml/g**	**Mn kDa**	**Mw kDa**	**Mz kDa**	**PDI**	**w (DP<50) %**	**w (DP<100) %**	**w (DP>2000) %**
Blend 1	S1521/S157	477	44.6	236.9	1779.4	**5.3**	2.4	7.0	12.1
Blend 2	S577/S174	413	46.6	276.5	1101.8	**5.9**	3.1	7.1	22.9
Blend 3	CL729/CL415	410	101.3	210.7	372.9	**2.1**	2.3	1.0	18.1
Blend 4	CL420	424	104.6	209.9	368.2	**2.0**	0.1	0.8	17.9
Blend 5	S1521/CL318	410	72.2	231.0	1239.5	**3.2**	0.9	2.5	13.3

Shear rheology of cellulose-IL solution

The understanding of visco-elastic properties of a polymer solution is an essential point for its good processability. In order to determine the adequate conditions for a successful spinning, visco-elastic properties of cellulose-IL solutions were assessed by measuring the complex viscosity and the dynamic moduli at different angular frequency between 70 and 90ºC. Assuming that the Cox-Merz rule is valid for cellulose-IL solution rheology, the Carreau model has been used to determine the zero shear viscosity. Figure 2 illustrates the zero-shear viscosity and the dynamic moduli as a function of the angular frequency value of the cross-over point (COP) of the different blends. Despite having similar intrinsic viscosities, the blends show significantly different visco-elastic behavior. The influence of the MMD on the rheology of cellulose-IL solution is herein demonstrated. The spinning temperature for each blend-IL solution was determined according to the zero-shear viscosity, a value of 30000 Pa.s was chosen as reference.

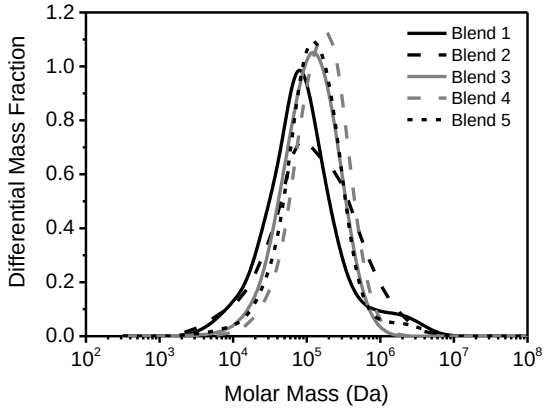

Figure 1. Molar mass distribution of the blends.

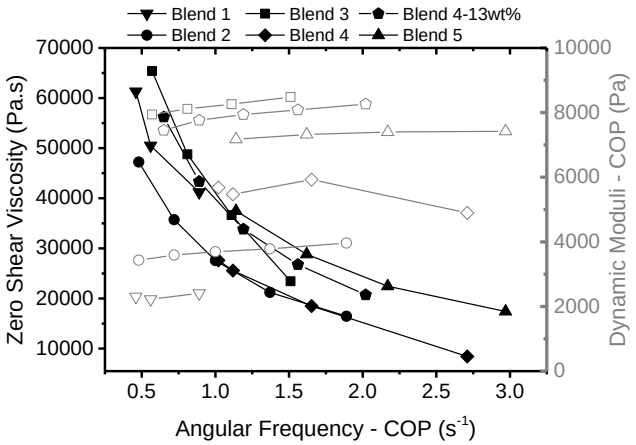

Figure 2. Zero-shear viscosity (full symbols) and cross-over moduli (open symbols) as a function of COP-angular frequency.

Dry-jet wet spinning and mechanical properties of regenerated fibers

Table 2 summarizes the spinning temperatures and velocities at which the polymer solutions were extruded, as well as the maximum draw ratio applied to the fibers at each extrusion velocity. Clear and stable extrusions were obtained for all cellulose-IL solutions. However, the spinnability, or the ability of the fluid filaments to be stretched, significantly differed from one to another. An extrusion velocity of 1.6 cm^3/min was used as starting point; in the case of successful spinning, the extrusion velocity was then gradually reduced in order to study the behavior of the solutions under higher draw ratio (the maximum take-up velocity was 100 m/min). Only Blend 2 showed good spinning ability and could be stretched at very low extrusion velocities (Table 2). Therefore, high draws could be applied and fiber samples collected. Blends 1, 3, 4 and 5, despite stable extrusions, could be stretched and taken-up only at low draw ratios; frequent filament breaks in the air gap were observed and became greater with the increase of the draw ratio preventing the take-up of the filaments. The different responses of the solutions under similar spinning conditions emphasize the importance of visco-elastic properties of cellulose-IL solutions and therefore the influence of cellulose molar mass distribution in dry-jet wet spinning. According to our experiments, the zero-shear viscosity and the angular frequency and dynamic modulus of the COP of a cellulose-IL solution need to be within specific ranges to obtain successful spinning. A zero-shear viscosity between 27000 and 30000 Pa.s and a cross-over point located between 0.8 and 1.2 s^{-1} and 3000 and 5500 Pa, respectively, seem to be required. The importance of this matrix can be observed with Blend 4. Fibers could be collected at very low draws at a concentration of 13 wt% while no draw at all could be applied at a concentration of 15 wt%. This slight improvement has been achieved by lowering the dynamic moduli through the decrease of the concentration while the zero-shear viscosity and angular frequency were kept constant by reducing the spinning temperature. In terms of MMD, it seems that the spinnability of a cellulose-IL solution is very sensitive to high molecular weight fraction of the cellulosic solute and to the polydispersity index. A share of high molecular weight greater than 20% and a PDI higher than 3 appeared to be favorable for successful spinning.

Table 2. Dry-jet wet spinning conditions for the blends-IL solutions

	$T_{spinning}$ °C	$V_{extrusion}$ cm^3/min	Maximum draw ratio
Blend 1 – 15 wt%	80	1.6	3.0
Blend 2 – 15 wt%	77	1.6	18.0
		1.0	23.0
		0.8	28.3
		0.6	5.0
Blend 3 – 15 wt%	80 – 82	1.6	-
Blend 4 – 13 wt%	70	1.6	1.5
Blend 4 – 15 wt%	80 – 84	1.6	-
Blend 5 – 15 wt%	75	1.6	3.0

Figure 3 and 4 represent the mechanical properties of the fibers collected at different draw ratios during the spinning of the blends. Figure 3 shows the superiority of Blend 2 in terms of spinnability. High quality fibers (1.4 dtex, 38.1 cN/tex) could be produced at an extrusion velocity of 1.6 cm^3/min and draw of 18 while the other blends could not be highly drawn. Acceptable tenacities were obtained with blend 4 and 5 despite the low draws applied. However, due to the low draws, the resulting fibers show too high linear densities. During the regeneration process, in the air gap, the drawing of the fluid filaments provokes the orientation of the cellulose chains and thus directly influences the final properties of the fibers. Draw increase leads to thinner and higher tenacity fibers. Figure 4 illustrates the properties of the fibers collected from blend 2 at different extrusion velocities. The strongest fibers were collected at a velocity of 1 cm^3/min and draw ratio of 23.5; fibers with a titer of 1 dtex and a tenacity of 43.8 cN/tex were produced.

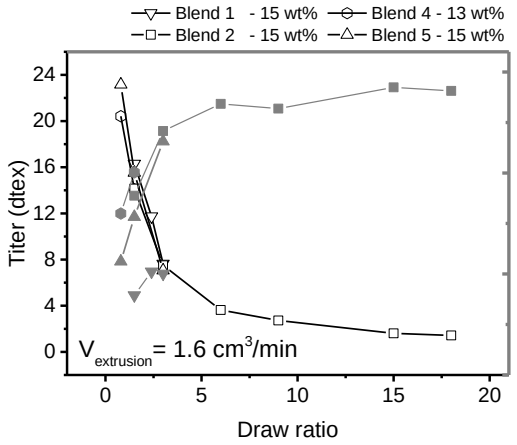

Figure 3. Titer and tenacity as a function of draw ratio

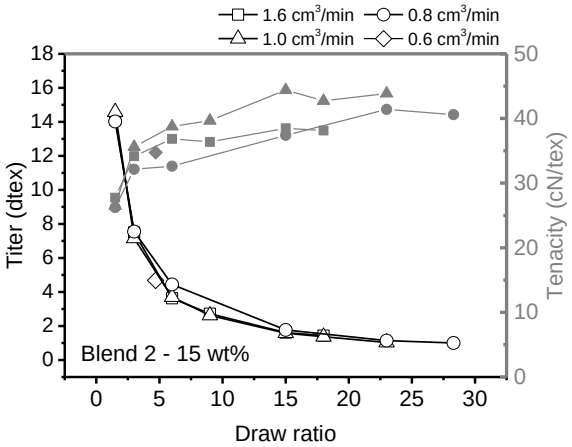

Figure 4. Titer and tenacity of fibers collected from Blend 2 as a function of draw ratio

IV. CONCLUSIONS

The influence of the molar mass distribution on the spinnability of cellulose-[DBNH]OAc solutions and on the mechanical properties of the resulting fibers has been investigated by conducting dry-jet wet spinning experiments. The importance of the molar mass distribution of cellulose chains in the visco-elastic behavior of cellulose-IL solutions and thus on the spinnablity have been elaborated. A specific matrix of zero-shear viscosity and dynamic modulus and angular frequency of the cross-over point in dynamic frequency sweep measurement appear to be an important requirement for the spinnability of cellulose-IL solutions. A certain high molecular weight fraction and high PDI of the cellulosic solute seem to favor a good processability and therefore the production of high quality fibers.

V. ACKNOWLEDGEMENT

This study is part of the Future Biorefinery program financed by the Finnish Bio-economy Cluster (FIBIC) and the Finnish Funding Agency for Technology and In-novation (TEKES).

VI. REFERENCES

[1] Maeki-Arvela P., Anugwom I., Virtanen P., Sjoeholm R., Mikkola J.P. Dissolution of lignocellulosic materials and its constituents using ionic liquids-A review. *Ind. Crops Prod.* **2010**, 32, 175-201.

[2] Mortimer, S.A.; Péguy, A.A.; Ball, R.C. Influence of the physical process parameters on the structure formation of lyocell fibres. *Cellulose Chem. Technol.* **1996**, 30, 251-266.

[3] Plog, J.P.; Kulicke, W.-M.; Clasen, C. Influence of the molar mass distribution on the elongational behaviour of polymer solutions in capillary breakup. *Appl. Rheol.* **2005**, 15, 28-37.

EXPLORING MONO-OXYGENASE ACTIVITY IN MUTANT LIBRARIES OF UNSPECIFIC PEROXYGENASE FROM *Agrocybe aegerita*

Patricia Molina-Espeja[1], David Gonzalez-Perez[1], Javier Martín-Díaz[1], Eva García-Ruiz[1] and Miguel Alcalde[1]*.

[1]*Institute of Catalysis, CSIC, Cantoblanco, 28049 Madrid, Spain; (*malcalde@icp.csic.es)*

ABSTRACT

The unspecific peroxygenase (UPO) from *Agrocybe aegerita* is a highly efficient biocatalyst for oxygen transfer reactions but its use in synthetic applications is hindered by an unspecific oxidative (peroxidative) activity. To uncouple the unwanted peroxidative activity from the mono-oxygenase (peroxygenase) activity, a sensitive colorimetric dual HTS-protocol based on the oxidation of 2,2'-azino-bis(3-ethylbenzothiazoline-6-sulphonic acid (ABTS) and the hydroxylation of 5-nitro-1,3-benzodioxole (NBD) was developed. Four mutant libraries with different mutational rates were constructed from several UPO variants, which were previously evolved for secretion in *Saccharomyces cerevisiae*, and screened for improved peroxygenation/reduced peroxidation. After one round of random mutagenesis and *in vivo* DNA-shuffling, a mutant with a 5-fold drop in peroxidative activity and an improvement of 1.7-fold in peroxygenase activity was identified. The evolved variant harbors T120P mutation, which is close to the heme entrance channel, addressing this region as suitable departure point for further engineering.

I. INTRODUCTION

The unspecific peroxygenase (UPO) -also referred to as aromatic peroxygenase; EC 1.11.2.1- secreted by the mushroom *Agrocybe aegerita* is arousing a big expectation due to its potential uses for many synthetic applications [1]. Since its discovery almost 10 years ago, UPO has been exhaustively studied but its role in nature is still unclear (detoxification and conversion of lignin-derived compounds are among the possible enzymatic targets). The versatile peroxide-dependent monoxygenase activity of UPO based on a two-electron oxygenation mechanism (in short peroxygenase activity) is extremely attractive as selective oxyfunctionalizations are among the most important transformations in organic synthesis. Indeed, regio- and enantio-oxyfunctionalizations has been a forbidden territory for most biocatalysts excluding P450 monooxigenases, but unlike the latter, UPO is soluble and neither require expensive cofactors (NAD[P]H) nor auxiliary flavoproteins [2]. However, there are two big obstacles for the real exploitation of this versatile biocatalyst: i) the lack of a suitable heterologous host that guarantees the functional expression of the enzyme and its further engineering, and ii) the presence of a natural and spontaneous oxidative activity (so called peroxidative or phenol oxidizing activity), which somehow limits its practical use as many of the aromatic substrates and oxyfunctionalized compounds converted by UPO are further oxidized by the enzyme giving rise to a pool of products of different complexity. The heterologous functional expression bottleneck was recently solved by our laboratory using a strategy that combined several cycles of directed evolution and rational design to achieve high secretion levels of UPO in *Saccharomyces cerevisiae* [3, 4]. Yet, enhancing the UPO peroxygenase activity while reducing (or even removing) its peroxidative activity is a crucial issue. In the current work, we have constructed and explored several mutant libraries using as departure points different UPO-secretion variants. The error-prone PCR libraries were *in vivo* shuffled by yeast and screened with the help of a dual HTS-assay, which has allowed us to identify improved peroxygenation UPO variants.

II. EXPERIMENTAL

UPO mutants (I13D3, M4D8 and M5D2 from the third generation of directed evolution and 2A12 from the fourth generation) were used as parent types for library construction. These variants are from previous engineering work carried out on the *upo1* gene clone C1A-2 from *A. aegerita* for functional expression in *S. cerevisiae* by directed evolution [3]. NBD (5-nitro-1,3-benzodioxole) was purchased by TCI America (USA). ABTS (2,2'-azino-bis(3-ethylbenzothiazoline-6-sulfonic acid)), Taq polymerase and the *S. cerevisiae* transformation kit were from Sigma-Aldrich (Madrid, Spain). The zymoprep yeast plasmid miniprep kit and zymoclean gel DNA recovery kit were purchased from Zymo Research (Orange, CA, USA). The *Escherichia coli* XL2-blue competent cells were from Stratagene (La Jolla, CA, USA). The uracil independent and ampicillin resistance shuttle vector pJRoC30 was from the California Institute of Technology (CALTECH, USA). The protease deficient *S. cerevisiae* strain BJ5465 was obtained from LGCPromochem (Barcelona, Spain).

NucleoSpin Plasmid kit was purchased from Macherey-Nagel (Germany) and the restriction enzymes BamHI and XhoI were from New England Biolabs (Hertfordshire, UK). All chemicals were of reagent-grade purity.

Library construction for laboratory evolution

PCR products were cloned under the control of the GAL1 promoter of the expression shuttle vector pJRoC30. BamHI and XhoI were used in order to linearize the plasmid and remove the parental gene. Linearized vector was loaded onto a low melting point preparative agarose gel and purified with Zymoclean gel DNA recovery kit. For library 1 (L1, 2,000 clones), I13D3, M4D8 and M5D2 mutants were used as parental types. Error-prone PCR (epPCR, with Taq DNA polymerase/$MnCl_2$) and *in vivo* DNA shuffling were used as genetic diversity generation tools. The primers used for this purpose were: RMLN-sense (5'-CCTCTAATACTTTAACGTCAAGG-3') and RMLC-antisense (5'-GGGAGGGCGTGAATGTAAGC-3'). PCR reactions were performed in a final volume of 50 µL containing 90 nM RMLN, 90 nM RMLC, 0.3 mM dNTPs, 3% dimethylsulfoxide (DMSO), 0.05 U/µL of Taq DNA polymerase, 1.5 mM $MgCl_2$, 0.01 mM $MnCl_2$ and 0.1 ng/µL of plasmids containing I13D3, M4D8, M5D2 and 2A12 (individual PCR reactions for each parent type). For libraries 2, 3 and 4 (L2, 522 clones; L3, 427 clones; L4, 522 clones), the 2A12 mutant from fourth round of evolution was used as parental type. Reaction mixture was prepared in a final volume of 50 µL containing 0.1 ng/µL pJRoC30-UPO1 (mutant 2A12), 3% dimethylsulfoxide (DMSO), 1.5 mM $MgCl_2$, and 0.05 U/µL Taq polymerase (Sigma) and variable concentrations of primers, dNTPs and $MnCl_2$ depending on the mutagenic library: 250 nM each RMLN and RMLC, 1 mM dNTPs (0.25 mM each) and 0.01 mM $MnCl_2$ for L2; 90 nM each RMLN and RMLC, 0.3 mM dNTPs (0.075 mM each) and 0.01 mM $MnCl_2$ for L3; 90 nM each RMLN and RMLC, 0.2 mM dATP, 0.2 mM dGTP, 1 mM dTTP, 1 mM dCTP and 0.25 mM $MnCl_2$ for L4. All PCRs were carried out using a gradient thermocycler (Mycycler, Bio-Rad, USA). The thermal cycling parameters fixed for the PCRs were: 95°C for 2 min (1 cycle), 94ºC for 45 s, 53ºC for 45 s, 74ºC for 3 min (28 cycles) and 74ºC for 10 min (1 cycle). Purified PCR products were then recombined by *in vivo* DNA shuffling. PCR mutated products were mixed equimolarly (200 ng of each product) and transformed together with the linearized vector (ratio PCR product:vector, 6:1) into *S. cerevisiae* competent cells using the yeast transformation kit.

High-throughput dual-screening assay

Individual clones were picked and inoculated in sterile 96-well plates (Greiner Bio-One GmbH, Germany) containing 50 µL of minimal medium per well. In each plate, column number 6 was inoculated with the corresponding parental type, and one well (H1-control) was inoculated with untransformed *S. cerevisiae* cells. Plates were sealed to prevent evaporation and incubated at 30°C, 220 rpm and 80% relative humidity in a humidity shaker (Minitron-INFORS, Biogen, Spain). After 48 h, 160 µL of expression medium were added to each well, and the plates were incubated for 48 h. The plates (master plates) were centrifuged (Eppendorf 5810R centrifuge, Germany) for 10 min at 3,500 × rpm at 4°C. 20 µL of supernatant were transferred from the master plate to two replica plates by a robot (Liquid Handler Quadra 96-320, Tomtec, Hamden, CT, USA). 180 µL of reaction mixture with ABTS or NBD were added to each replica plate. Reaction mixture with ABTS contained 100 mM sodium citrate/phosphate buffer pH 4.4, 0.3 mM ABTS and 2 mM H_2O_2. Reaction mixture with NBD contained 100 mM potassium phosphate buffer pH 7.0, 1 mM NBD, 15% acetonitrile and 1 mM H_2O_2. Plates were stirred briefly and the initial absorptions at 418 nm ($\varepsilon_{ABTS}^{\bullet+}$ = 36,000 M^{-1} cm^{-1}) and 425 (ε_{NBD} = 9,700 M^{-1} cm^{-1}) were recorded in the plate reader (SPECTRAMax Plus 384, Molecular Devices, Sunnyvale, CA). The plates were incubated at room temperature until a green (ABTS) or yellow (NBD) color developed, and the absorption was measured again. The values were normalized against the parent type in the corresponding plate. To rule out false positives, two re-screenings were carried out. Finally a third re-screening was performed in order to preliminarily characterize the best mutants obtained, **Figure 1**.

Protein modeling

A structural model of the UPO1 from *A. aegerita* crystal structure at a resolution of 2.1 Å (Protein Data Bank Europe [PDB] accession number 2YOR, [5]) was used as scaffold to build protein models, obtained by PyMol v1.3r1 (DeLano Scientific LLC).

III. RESULTS AND DISCUSSION

Design of a dual HTS-assay for peroxygenation

The improvement of UPO mono-oxygenase activity whilst reducing the peroxidative activity requires a dual HTS-assay, in which positive selection (for peroxygenation) and negative selection (for peroxidation) can be simultaneously applied during directed evolution. To design this assay, two colorimetric substrates were chosen: 2,2'-azino-bis(3-ethylbenzothiazoline-6-sulphonic acid (ABTS) for peroxidative activity and the 5-nitro-1,3-benzodioxole (NBD) for peroxygenase activity. ABTS has been extensively employed by our laboratory to screen mutant libraries of different ligninolytic oxidoreductases secreted by *S. cerevisiae* (medium and high-redox potential laccases and versatile peroxidases). With a high affinity to the UPO active site (K_m = 27 µM; [3]), high sensitivity, and low interference with supernatant of culture broth, ABTS was in all likelihood the best compound to accurately measure peroxidative activity. The oxidation of ABTS to $ABTS^{\bullet+}$ by UPO produces a

strong and stable colorimetric response ($\varepsilon_{ABTS}^{\bullet+}$ = 36,000 M^{-1} cm^{-1}) which is suitable to screen mutant libraries in *S. cerevisiae*. Recently, a peroxygenase-specific colorimetric assay based on NBD was reported [6]. This compound is hydroxylated by UPO into 4-nitrocatechol (ε_{425} = 9,700 M^{-1} cm^{-1}), which can be further converted at basic pH to strong red (ε_{514} = 11,400 M^{-1} cm^{-1}) since the color of 4-nitochatechol is pH-dependent. Further analysis of the UPO tolerance towards acetonitrile (ACN) concentration was necessary since the low concentration of ACN in the reaction mixture makes NBD insoluble whereas high amounts of organic solvent inhibits the UPO activity. A compromise between substrate availability and UPO stability was established with 1 mM NBD and 15 % (v/v) ACN. Under the aforementioned conditions, we were capable to perform reproducible measurements in both kinetic and end-point mode for ABTS- and NBD-assays without significant interferences with the culture broth. The HTS-dual assay was validated by assessing the responses of UPO concentrations from yeast supernatants *vs* the two colorimetric assays. Fresh transformants containing I13D3 mutant were inoculated, induced for expression and different volumes of supernatant (0.5 to 20 µL) were tested. A linear relationship between the amount of UPO and the responses of both colorimetric assays was found. To calculate the coefficient of variation (CV) of both assays, test plates containing the same parental type in different wells were prepared. *S. cerevisiae* cells harboring the I13D3-pJRoC30 construct were placed on SC selection plates. Individual clones were transferred to test plates and after inducing expression, the activities were evaluated from fresh supernatants preparations. The CV for the ABTS and NBD HTS-assays were 13.5 % and 22 %, respectively.

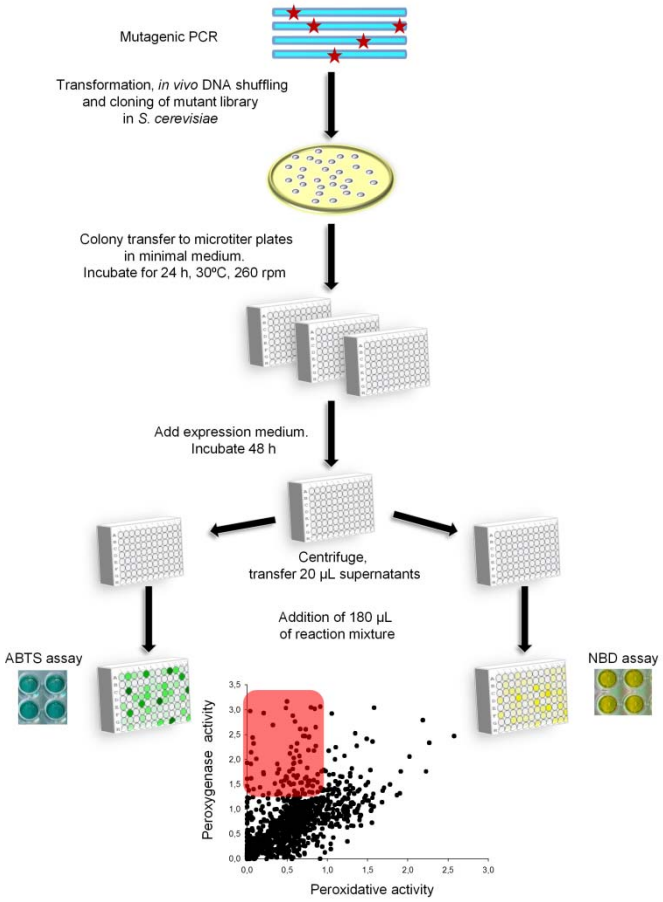

Figure 1. Dual high-throughput screening (HTS) assay for Directed evolution towards peroxygenation.

Library construction and analysis

Four different mutant libraries were constructed and explored using several parental types from different generations of directed evolution for secretion (*i.e.* with broad differences in their levels of detected activity). Mutational rates were adjusted by varying the $MnCl_2$ and DNA template concentrations as well as the dNTPs composition during the error prone PCR. The mutagenized DNA inserts were not *in vitro* cloned with the linearized plasmid but *in vivo* shuffled by yeast, which promoted the appearance of new crossover events and the reparation of the whole autonomously replicating plasmid in one single step. Library 1 (L1, ~2,000 clones) was constructed from parental types I13D3, M4D8 and M5D2, which were subjected to error-prone PCR (with mutational rate of 1 amino acid per whole protein sequence) and *in vivo* DNA shuffling. Libraries 2, 3 and 4 (L2, L3 and L4, ~500 clones each) were prepared from 2A12 mutant testing different mutational rates, **Figure 2**. Three consecutives re-screens were used to rule out the presence of false positives. Even though some clones with important improvements for both substrates were located, the screening was directed to those with reduced peroxidase activity and increased peroxygenase activity. Systematically, the best 50 clones were picked and subjected to the first re-screening. Thereafter, the best 10 mutants were selected for a second re-screening, in which all the mutants were produced at the same metabolic stage. Finally, best variants from each library were isolated, produced in larger scale and preliminary characterized in terms of thermostabilities (T_{50}), pH profiles and initial activities. Using this protocol, several variants with improved peroxygenase abilities were identified. Among then, IAP4 mutant (from L1) showed 5-fold lower peroxidative activity and 1.7-fold higher peroxygenative activity than the parent type. IAP4 harbors only one mutation in mature protein (T120P). According to our homology model, this residue is located at the entrance of the heme group becoming even more

hydrophobic the access to the substrate binding pocket. Although this change did not substantially affect the pH activity profile, it does exert a negative effect on the thermostability (with a drop in the T_{50} of 7ºC), which addresses the significance of this region for the protein stability.

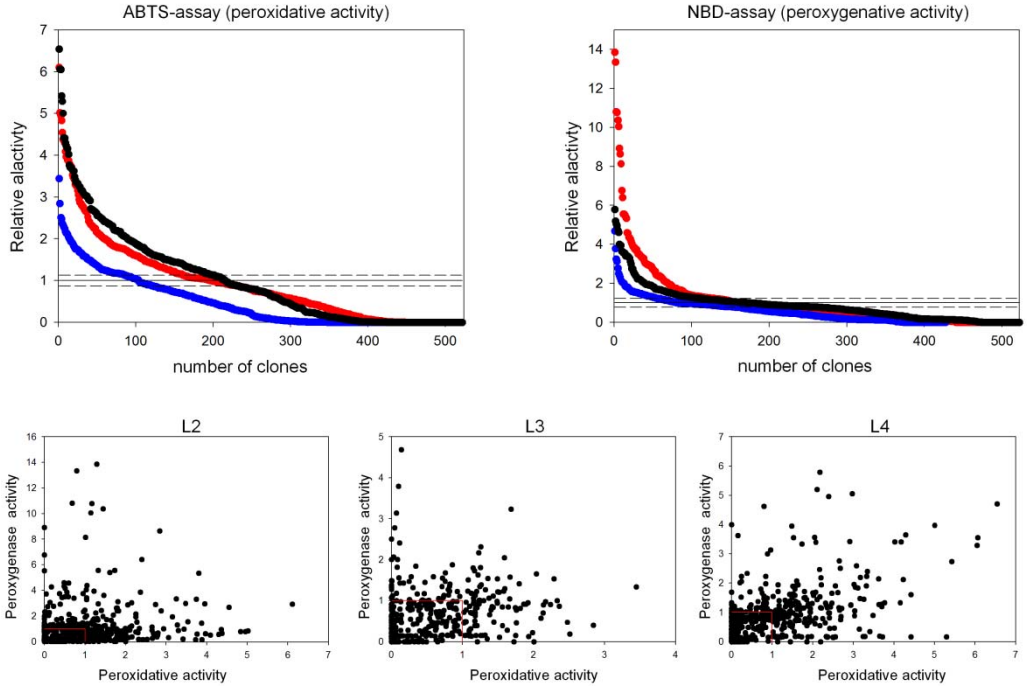

Figure 2. Mutant libraries landscapes. Red, L2; Blue L3; Black, L4. The dashed lines represent the CV in the corresponding assays and the solid line the parental type activity.

IV. CONCLUSIONS

The synthesis of hydroxylated aromatic compounds for industrial or pharmaceutical purposes has been traditionally achieved by chemical methods, which show low selectivity generating undesirable by-products. In the last couple of decades, we are witnessing a growing interest in the use of enzymes for such remarkable transformations. UPO represents a very promising starting point to engineer aromatic hydroxylations in a high selective and efficient way as long as its peroxidative activity can be quenched. The HTS assays shown here for the directed evolution of UPO together with its yeast heterologous expression system are promising biomolecular tools to convert this enzyme into a true self-sufficient monooxygenase.

V. ACKNOWLEDGEMENTS

This work was supported by European Commission Projects PEROXICATS (FP7-KBBE-2010-4-26537), INDOX (FP7-KBBE-2013-7-613549), COST-Action CM1303-Systems Biocatalysis; and the National Project EVOFACEL (BIO2010-19697).

VI. REFERENCES

[1]Hofrichter, M.; Ullrich, R.; Pecyna, M.J.; Liers, C.; Lundell, T. New and classic families of secreted fungal heme peroxidases. *Appl. Microbiol. Biot.* **2010**, *87*, 871-897.

[2]Hofrichter, M.; Kellner, H.; Pecyna, M.; Ullrich, R Fungal unspecific peroxygenases: heme-thiolate proteins that combine peroxidase and cytochrome P450 properties. *In*: E. G. Hrycay ed., Monooxygenase, peroxidase and peroxygenase properties and mechanisms of cytochrome P450. Springer, Heidelberg, **2014**, in press.

[3]Molina-Espeja, P.; Garcia-Ruiz, E.; Gonzalez-Perez, D.; Ullrich, R.; Hofrichter, M.; Alcalde, M. Directed evolution of unspecific peroxygenase from agrocybe aegerita. *Appl. Environ. Microb.* **2014**, In press.

[4]Gonzalez-Perez, D.; Molina-Espeja, P.; Garcia-Ruiz, E.; Alcalde, M. Mutagenic organized recombination process by homologous in vivo grouping (MORPHING) for directed enzyme evolution. *PlOS ONE*. **2014**, 9, 3: e90919.

[5]Piontek, K.; Strittmatter, E.; Ullrich, R.; Gröbe, G.; Pecyna, M.J.; Kluge, M.; Scheibner, K.; Hofrichter, M.; Plattner, D.A. Structural basis of substrate conversion in a new aromatic peroxygenase: P450 functionality with benefits. *J. Biol. Chem*. **2013**, *288*, 34767-3476.

[6]Poraj-Kobielska, M.; Kinne, M.; Ullrich, R.; Scheibner, K.; Hofrichter, M. A spectrophotometric assay for the detection of fungal peroxygenases. *Anal. Biochem*. **2012**, *421*, 327-329.

STUDY OF THE ACTION OF AUTO-HYDROLYSIS OF SOFTWOOD CHIPS ON LIGNIN AND LIGNIN - CARBOHYDRATES COMPLEXES (LCC)

Claire Monot[1]*, Christine Chirat[1], Xueyu Du[2], Jiebing Li[2]

*[1] LGP2 - Grenoble INP - Pagora - 461 rue de la Papeterie, CS 10065, 38402 Saint-Martin d'Hères - France; [2] KTH - Department of Fibre and Polymer Technology, Teknikringen 56-58, SE-10044, Stockholm - Sweden (*claire.monot@lgp2.grenoble-inp.fr)*

ABSTRACT

Several pulp and paper biorefinery projects are under development. In particular, the extraction of hemicelluloses using an autohydrolysis step before the production of cellulose fibers is studied. The extracted hemicelluloses could constitute a major source of sugars, oligomers and polymers for the production of bio-products, bio-fuels or biomaterials. It has been shown that this hemicelluloses extraction could improve the manufacturing process of cellulosic fibers, by facilitating the cooking, as well as oxygen delignification and bleaching. The first part of our study compares different types of cooking (kraft, soda, soda/AQ) on prehydrolysed and control softwood chips. The prehydrolysis would enable to apply a sulfur free cooking on softwood wood chips, which is hardly possible on control wood chips.

To understand the reasons for this better cooking ability of softwood chips, some lignin analyses were carried out. The molecular mass distribution obtained for prehydrolysed and control softwood lignins indicated that only a slight depolymerisation of the lignin occurred during the autohydrolysis treatment. ^{13}C NMR analysis of the isolated lignins indicated that after autohydrolysis the lignin contained slightly more aromatic carbons and free phenolic groups and less secondary hydroxyl groups and aliphatic carbons than the control lignin. Lignin - carbohydrate complexes (LCC) were also isolated using a method described in [1].

I. INTRODUCTION

A biorefinery consists in the production of materials and energy. A pulp biorefinery produces fibers, chemicals (tall oil and turpentine), ethanol, and energy needs for the process. In modern kraft mills, extra energy is produced and sold to the market. The common process in kraft mills uses Na_2S and NaOH as reagents, at a temperature between 160 and 170°C during a couple of hours. During this process, the main part of lignin and hemicelluloses of wood are dissolved, which form the effluent of the process called black liquor. This effluent is concentrated and burned in a recovery boiler to produce the energy. During this stage, chemicals are recovered to be used again in the process. However the calorific potential of the hemicelluloses is much lower than that of lignin and a better valorization of the hemicelluloses should be looked for. Autohydrolysis was chosen to extract part of the hemicelluloses prior to alkaline cooking, and valorize them either by fermentation into ethanol or to produce chemicals such as surface active agents [2, 3]. It has been shown that prehydrolysis improves cooking and bleaching [4, 5, 6]. Therefore, sulfur free cooking (like soda cooking) could be considered.

The first objective of this study is to develop a sulfur free cooking of prehydrolysed softwood chips. The advantage of this type of cooking is that the black liquor will then not contain sulfur and could be used for another valorization such as gasification [7]. The second objective is to understand the easier ability of the wood to be delignified after a prehydrolysis. Lignins of control and prehydrolysed chips were extracted and compared for their chemical composition and molecular weight distribution. The quantification of the linkages between lignin and carbohydrates (LCC) was also carried out, using a method developed by [1].

II. EXPERIMENTAL

Sulfur free production process - Mixed softwood chips, kindly provide by Fibre Excellence Tarascon, were used in this study. The composition is 35% Sylvestre Pine, 24% Black Pine, 18% Alep Pine, 16% Spruce, 7% Douglas fir. The autohydrolysis step was performed in autoclaves placed in a rotating oil bath to adjust the desired temperature. Autohydrolysis consists in an acidic hydrolysis without addition of any external acid. Acetic acid released from the wood when it is heated in water is the acid source. The operating conditions were: liquor to wood ratio of 4, the temperature was 170°C, the time at temperature was 60 minutes. Cooking was performed in the same rotating oil bath as the prehydrolysis. Two types of cooking were carried out: kraft cooking, according to the common industrial process, and soda - anthraquinone cooking. The operating conditions were the same for both types of cooking: liquor to wood ratio of 4, the temperature was 170°C, the time at temperature was 110 minutes. The amounts of NaOH and Na_2S are indicated in the text. The percentage

of anthraquinone (AQ) varied between 0.1 and 0.2% of the dry mass of wood. After cooking, the pulp obtained was characterized by its yield and its kappa number, which is proportional to the lignin content, to evaluate the performance of cooking. The kappa number is determined according to the T 236 cm-85 standard.

Isolation and analysis of lignin and lignin - carbohydrates complexes (LCC) - Extractives were first eliminated from the wood chips prior to isolation and analysis by acetone extraction. The isolation of lignin was performed according to Björkman [8]. The method that was used for the isolation of LCC is described in [1]. To perform ^{13}C NMR, 300 mg of lignin were dissolved in 4 mL of DMSO-d_6. An acetylation was performed on both types of lignin to better determine the different types of hydroxyl groups using the method described in [9] replacing hydrochloric acid by ethanol and the ice - water mixture by diethyl ether. The molecular mass distribution was realized on a size exclusion chromatography thanks to the dissolution of lignin in DMAc/LiCl (0.5%). The standard used is polystyrene.

Analysis of wood - The analyses of different components of wood were performed, especially to know their proportion in the wood. The determination of the percentage of lignin was carried out as described in the Tappi Standard T 222 om-02. The saccharides percentages were determined according to T 249 cm-09 and using a high - performance anion exchange chromatography with pulse amperometric detection (HPAEC PAD) in a Dionex ICS 5000 apparatus.

III. RESULTS AND DISCUSSION

Sulfur free production process

First of all, an autohydrolysis was performed on the softwood chips and gave a yield of 80.1%. The results presented in **Table 1** show that the percentages of lignin and cellulose in the prehydrolysed wood were higher than the ones in control wood, which is due to the solubilization of a part of the hemicelluloses during this step.

Table 1. Relative proportions of lignin and carbohydrate content in the control and prehydrolysed chips

	Lignin	Cellulose	Hemicelluloses*	
			GGM	Xylans
Control chips	31.4	39.6	17.7	11.2
Prehydrolysed chips	36.7	50.2	9.0	4.1
Variation in composition due to the autohydrolysis, %	+ 16.8%	+ 26.7%	- 49.9%	- 63.4%

*: acetyl and methylglucuronic acid groups are not included

Two types of cooking, kraft and soda - AQ, were carried out on both types of wood chips. The yields and the kappa number are given in **Table 2**.

Table 2. Kappa numbers and yields obtained after kraft and soda - AQ cooking of control and prehydrolysed wood chips

	Kraft (Na_2S 8.1%, NaOH 18.9%)		Soda - AQ (NaOH 27%, AQ 0.1%)	
	Yield*	Kappa number	Yield*	Kappa number
Control softwood	44.0	24.4	46.0	46.6
Prehydrolysed softwood	34.5	27.9	37.1	31.7

*: yield = yield after prehydrolysis x yield after cooking

The yields of prehydrolysed (PH) chips are lower than the ones of control chips because the yield of the prehydrolysis is taken into account. It can be seen that even if there is a higher lignin content in the prehydrolysed chips, the final lignin content is quite the same after a kraft cooking, which implies that a higher delignification rate was obtained.

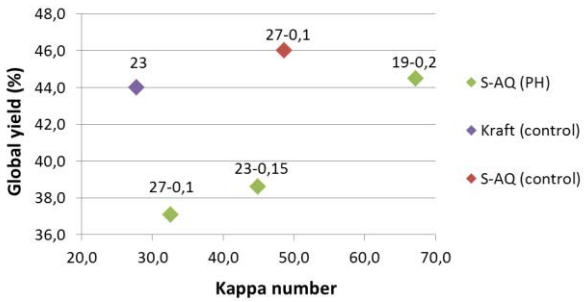

Figure 1. Yield versus kappa number for the soda AQ cooking of the softwood prehydrolysed and control chips (the first number above the point indicates the NaOH %, and the second the AQ %) and kraft control (the number indicates the NaOH %).

After a soda - AQ cooking, the prehydrolysed wood chips showed a much higher delignification ability than the control chips: the kappa number after PH soda cooking was in the same range as the one obtained after PH kraft treatment, whereas the control wood chips exhibited a much higher kappa number of 46.6. Additional experiments were made by varying the NaOH and AQ charges, **Figure 1**. As expected, a reduction in the alkali charge led to increased kappa number, and increased yield. A previous study showed that pulps from PH wood chips were also very easy to delignify in a subsequent oxygen bleaching stage and that it could be advantageous, from a yield point of view, to stop the cooking at a higher kappa, as the oxygen delignifiation is more selective than the end of a cooking [4]. One could then imagine a process using PH - soda with a high kappa number (65 in this case), followed by oxygen delignification to obtain low kappa numbers.

Analyses of lignin and lignin - carbohydrates complexes

Reasons for the better delignification ability of the prehydrolysed softwood chips to soda AQ cooking could be either that the lignin has been modified [10], or that some lignin carbohydrate complexes have been hydrolysed during the acidic treatment. Lignin isolation was performed using a mixture of water - dioxane and hydrochloric acid. The yield of this isolation was between 70 and 75% for both types of wood. Molecular mass distribution and ^{13}C NMR analysis were carried out on the two lignins. The molecular weight distribution of prehydrolysed wood lignin was slightly shifted to the small masses which indicate that only a slight depolymerisation of the lignin occurred during the prehydrolysis, **Figure 2**.

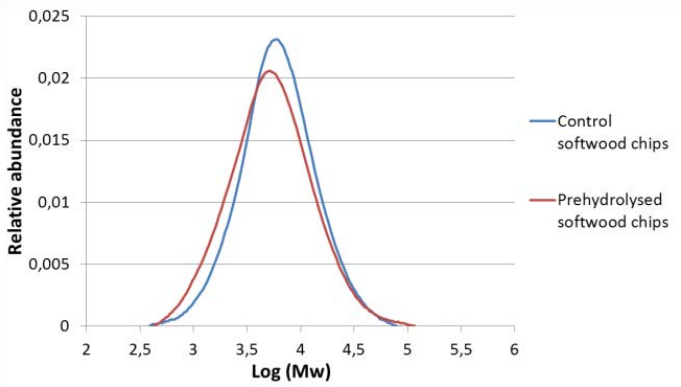

Figure 2. Molecular mass distributions of control and prehydrolysed softwood chips

The results of ^{13}C NMR showed that lignin of autohydrolysed wood contained more aromatic carbons and free phenolic groups and less secondary hydroxyl groups and aliphatic carbons (between 15 and 20% less) than the lignin of control wood, **Table 3**. Whether these differences would be enough to explain the efficiency of the cooking of prehydrolysed wood chips is not sure. For the other functional groups the differences were not significant.

Table 3. Contents of functional groups of acetylated lignin (for an aromatic unit)

Group/aromatic unit	Control softwood chips lignin	Prehydrolysed softwood chips lignin
Aromatic OCH3	0.86 (± 0.043)	0.89
Primary OH	0.63 (± 0.032)	0.61
Secondary OH	0.32 (± 0.016)	0.27
Phenolic OH	0.29 (± 0.015)	0.36
Aliphatic C=O of RCOOR'	0	0.003
Cβ of β-β and β-5	0.03 (± 0.0015)	0
Cβ of β-O-4	0.15 (± 0.008)	0.22
Overall OH	1.24 (± 0.062)	1.24
Condensed aromatic C	1.88 (± 0.094)	1.95
Protonated aromatic C	2.32 (± 0.116)	2.44
Aliphatic C	1.78 (± 0.089)	1.39

LCC were isolated from control and prehydrolysed wood chips, and the yields of each type of LCC are given in **Table 4**. LCC1, LCC2 and LCC3 fractions contain respectively mainly LCC from glucan - lignin, glucomannan - lignin and xylan - lignin. The results obtained for the control wood used in this study were compared to that of spruce wood obtained at KTH. Higher yields could be obtained with spruce, but the general tendencies were about the same at least for LCC1 and LCC2: about 53 - 54% of the LCC can be attributed to glucan - lignin LCC and 33 - 36% to the glucomannans - lignin LCC. For the xylan - lignin LCC fraction (LCC3) there were more differences between the wood species: 9% for the mixed softwood and almost 14% for the spruce. One reason for that could be that the spruce wood contained more xylans than our mixed softwood species.

The proportions of LCC2 and LCC3 decreased after a prehydrolysis, whereas LCC1 increased, which is normal given the fact that the prehydrolysis eliminated mainly hemicelluloses. The proportion of lignin in LCC1 was

about the same for the control and prehydrolysed wood chips, and the relative change in carbohydrate in LCC1 was the same as the increase in cellulose content in wood chips, which implies that the cellulose lignin bonds do not seem to have been significantly affected by the prehydrolysis. The relative change in carbohydrate content in LCC2 was 45%, which is of the same order than the reduction in GGM in wood chips due to the autohydrolysis. The lignin content in LCC2 was however higher than for the LCC2 in control wood. The reduction in LCC3 (lignin - xylan) was particularly high. A thorough analysis of the carbohydrate composition of the LCC fractions is now needed to investigate the effect of prehydrolysis further.

Table 4. LCC yields for control and prehydrolysed softwood chips (the number between brackets indicates the relative contribution of a given type of LCC: yield LCCi/Yields (LCC1 + LCC2 + LCC3))

	LCC1	LCC2	LCC3	Total
Control wood	42.4 (54.4%)	28.3 (36.3%)	7.3 (9.3%)	78.0
Lignin content in LCC, %	19.7	41.1	52.0	
Data from spruce wood (KTH study, [1])	49.5 (53.1%)	30.9 (33.2%)	12.8 (13.7%)	93.2
Lignin content in LCC, %	19.3	29.2	42.7	
Prehydrolysed wood	55.9 (69.1%)	23.0 (28.4%)	2.0 (2.5%)	80,9
Lignin content in LCC, %	20.9	58.7	Non determined	
Relative change of carbohydrate content in LCC% due to autohydrolysis, %	+ 25.1%	- 45%	-	
Relative change of lignin in LCC due to autohydrolysis	+ 26%	+ 9.4%		

V. CONCLUSIONS

The implementation of a prehydrolysis before the cooking on softwood allowed a better delignification of the wood. Thus, it could be possible to replace the traditional kraft cooking by a sulfur free cooking, a soda - anthraquinone cooking for instance. To understand the influence of prehydrolysis on cooking, a study of lignin and lignin - carbohydrates complexes (LCC) was performed. The size exclusion chromatography and ^{13}C NMR did not show big differences between the lignins of control wood and of prehydrolysed wood. Yields of LCC indicated a loss of lignin - hemicelluloses complexes, particularly for the xylan - lignin complexes. Lignin - cellulose complexes did not seem to be degraded by the prehydrolysis. The next steps will be to continue the analyses on LCC and to show that cellulose of suitable properties, either for paper application or for textile application, can be obtained from these pulps.

V. ACKNOWLEDGEMENT

The authors would like to thank Institut Carnot Energie du Futur for the funding of this study.

VI. REFERENCES

[1] Du, X.; Gellerstedt, G.; Li, J. Universal fractionation of lignin - carbohydrate complexes (LCCs) from lignocellulosic biomass: an example using spruce wood. *The Plant Journal*, **2013**, *74*, 328–338.
[2] Sanglard, M.; Chirat, C.; Jarman, B.; Lachenal, D. Biorefinery in a pulp mill: simultaneous production of cellulosic fibres from Eucalyptus globulus by soda/anthraquinone cooking and surface-active agents. *Holzforschung*, **2013**, *67*, 481–488.
[3] Boucher, J.; Chirat, C.; Lachenal D. Simultaneous production of ethanol and softwood kraft pulp: extraction, concentration, secondary hydrolysis and fermentation step. *Paptac Electronic Proceedings 17th ISWFPC, Vancouver*, **2013**, 2556–2563.
[4] Chirat, C.; Boiron, L.; Lachenal, D. Bleaching ability of pre - hydrolysed pulps in the context of a biorefinery mill. *Tappi Proceedings International Pulp Bleaching Conference, Portland, USA*, October 5-7, **2011**, 12–18.
[5] Ragauskas, A.J.; Nagy, M.; Kim, D.H.; Eckert, C.A.; Hallett, J.P.; Liotta, C.L. From wood to fuels-Integrating biofuels and pulp production. *Industrial Biotechnology*, **2006**, *1*, 55–65.
[6] Chirat, C.; Lachenal, D.; Sanglard, M. Biorefinery in a kraft pulp mill: extraction of xylans from hardwood chips prior to the production of cellulosic paper pulp. *Process Biochemistry*, **2012**, *47*, 381–385.
[7] Roubaud, A.; Chirat, C.; Huet, M.; Monot, C.; Lachenal, D. Development of a new pulp production process and black liquor gasification. *Récents Progrès en Génie des Procédés*, **2013**, *104*, [sfgp2013120618].
[8] Björkman, A. Studies on finely divided wood. Part I. Extraction of lignin with neutral solvents. *Sven. Papperstidn.* **1956**, *59*, 477–485.
[9] Thring, R.W.; Chornet, E.; Bouchard, J.; Vidal, P.F. Evidence for the heterogeneity of glycol lignin. *Ind. Eng. Chem. Res.* **1991**, *30*, 232–240.
[10] Leschinsky, M.; Zuckerstätter, G.; Weber, H.K.; Patt, R.; Sixta, H. Effect of autohydrolysis of Eucalyptus globulus wood on lignin structure. Part 1: Comparison of different lignin fractions formed during water prehydrolysis. *Holzforschung*, **2008**, *62*, 645–652.

SYNERGISTIC EFFECT OF CELLULOSE NANOCRYSTALS AND GRAPHENE ON THE PROPERTIES OF POLYMERIC BIOCOMPOSITES.

Sarah Montes[1]*, Pedro Mª Carrasco[1], Ibon Odriozola[1], Germán Cabañero[1], Hans Grande[1], Jalel Labidi[2], Virginia Ruiz[1]

[1]*Materials Division, IK4-CIDETEC, Paseo Miramón 196, 20009 San Sebastián, Spain (smontes@cidetec.es)*

[2] *Chemical and Environmental Engineering Department, University of the Basque Country. Plaza Europa 1, 20018 San Sebastian, Spain.*

ABSTRACT

As renewable and biodegradable nanofillers, cellulose nanocrystals (CNC) are currently attracting and will continue drawing attention both from academic and industrial sectors. In the last decade, there has been growing interest in incorporating polysaccharide-based nanocrystals into biopolymers as efficient reinforcing materials, affording higher toughness, thermal stability and barrier properties[1,2]. On the other hand, graphene has emerged as a material of enormous scientific interest due to its exceptionally high surface area and mechanical, thermal and electron transport properties, among many others. In the field of nanocomposites, these atomically thin carbon sheets have proven to be very promising additives that can significantly improve several physical properties of host polymers at extremely small loadings[3]. Here, we present an innovative route to prepare CNC and graphene based biocomposites where the nanofillers are produced by a method recently reported[4]. Specifically, CNC-modified graphene were produced by CNC-assisted liquid phase exfoliation of graphite, a method that allows stabilization of resulting graphene flakes in aqueous dispersions at high concentrations. Incorporation of these CNC-modified graphene fillers in a polymeric matrix produced significant enhancement of the resulting biocomposite properties.

I. INTRODUCTION

In the last few decades, the use of naturally occurring polymers derived from renewable resources has gained increasing attention due to their availability and renewability besides economical reasons. Cellulose stands out among biomaterials as it is considered the most abundant renewable polymer on Earth[5] and can be biosynthesized by a number of living organisms ranging from higher to lower plants, some amoebae, sea animals, bacteria and fungi[6]. Due to the hierarchical structure and semicrystalline nature of cellulose, nanoparticles such as microfibrillated cellulose (MFC) can be extracted from this naturally occurring polymer. MFC are commonly obtained by mechanical treatment of native cellulose fibers consisting of alternating crystalline and non-crystalline domains and cellulose nanocrystals or nanowhiskers are the result of submitting microfibrils to a strong acid hydrolisis treatment, allowing dissolution of amorphous domains[7]. Cellulose nanocrystals have been extensively investigated in the preparation of polymer nanocomposites[8]. Impressive mechanical properties and reinforcing capability, abundance, low weight, and biodegradability of cellulose nanocrystals make them ideal candidates for processing polymer bionanocomposites, above all those based on biodegradable polymers.

As well as reinforcing nanomaterial, cellulose nanocrystals have been recently reported[4] to effectively stabilize graphene aqueous dispersions prepared by liquid phase exfoliation of graphite. Graphene, a single layer of carbon atoms arranged in a hexagonal lattice, has been widely used in the preparation on conductive polymer nanocomposites. However, preparation of graphene polymer nanocomposites require the application of chemical or physical methods for a good dispersability of graphene in hydrophilic polymeric matrix[9]. CNC-assisted liquid phase exfoliation of graphite has been suggested as a simple, economic and non-toxic method to prepare highly stable aqueous dispersions of graphene.

On the other hand, poly(vinyl alcohol) (PVA), a highly polar, water-soluble polymer, has been widely utilized in polymer blends with natural polymeric materials. In addition to being compatible with many biopolymers, such as cellulose or chitosan, PVA is also biodegradable[10]. The preparation of graphene oxide or graphene nanoplatelets/PVA composites has been reported, in all cases resulting in nanocomposites with improved mechanical, thermal or electrical properties.

Here we show a simple and environmentally friendly method to prepare graphene-cellulose nanocrystals/PVA biocomposites by direct incorporation of previously exfoliated graphene with cellulose nanocrystals into PVA. To the best of our knowledge, there are no previous reports on PVA nanocomposites with the two nanomaterials. Interestingly, the combination of graphene and cellulose in PVA had a pronounced synergistic effect on the properties of the nanocomposite material. The investigation of the thermal properties of the novel nanocomposites was carried out.

II. EXPERIMENTAL

Materials

Triton X-100 was purchased from Panreac and high purity graphite powder (SP-1) was obtained from Bay Carbon Inc. Microcrystalline cellulose and Mowiol 4-88 (M_w ~31,000) PVA, were purchased from Sigma-Aldrich.

Preparation of nanofillers

Prior to the preparation of biocomposites, cellulose nanocrystals (CNCs) and cellulose-nanocrystals-stabilized-graphene (GR-CNC) were prepared. CNCs were extracted from microcrystalline cellulose (MCC) by acidic hydrolysis with sulfuric acid, according to a protocol reported elsewhere[12]. GR-CNC nanofillers were prepared by CNC-assisted liquid phase exfoliation of graphite, following a protocol recently reported[4]. Briefly, graphite (4 mg mL^{-1}) and CNCs (16 mg mL^{-1}) were co-dispersed in Millipore water and sonicated (tip sonicator Hielscher UP400S, 0.5 s pulse, 70% amplitude) for 4 h in an ice bath to avoid overheating. Unexfoliated graphite was removed by centrifugation at 4500 rpm for 1.5 h. The resulting dark black dispersions were very stable, with negligible levels of sedimentation over periods of months. For comparative purposes, CNCs previously dispersed in water and sonicated for four hours and graphene produced using the organic surfactant Triton X100 (GR-T) and the same conditions as for CNC-GR, were also prepared.

Preparation of GR-CNC/PVA nanocomposites

For the fabrication of GR-CNC/PVA biocomposite, 5 g of PVA were dissolved in 150 mL of distilled water at 100 ºC and the solution was subsequently cooled to room temperature. Then, 1 wt% of GR-CNC was added to the polymer solution while stirring. For film formation the blend was poured into a Petri dish and allowed to dry at room temperature until reaching a constant weight.

A series of PVA biocomposite films with different nanofillers at the same loading level (1 wt%) were similarly prepared for comparison, namely CNC/PVA and GR-T/PVA. As a reference sample, a neat PVA film was prepared following the same procedure.

The resulting films were of excellent quality, transparent (although those containing Graphene were slightly greyish) and apparently uniform to the naked eye.

Characterization

Melting temperatures (Tm) of the biocomposites were determined with a Pyris Diamond DSC (Perkin Elmer) at a scan rate of 10 °C min^{-1} over the temperature range 25-220 °C. The measurements were carried out using 5.00 $\pm$ 0.50 mg samples under a nitrogen atmosphere (50 mL min^{-1}). The glass-transition temperature (Tg) and the melting temperature (Tm) were recorded as the onset and the peak maximum temperature on the second heating process, respectively. Relative crystallinity of PVA in blends was calculated from the area of the melting peak on the basis of the heat of fusion of 100% crystalline PVA (138.6 J g^{-1}) [11]. Thermogravimetric analysis (TGA) was performed on a TGA Q500 (TA instruments) at a heating rate of 10 °C min^{-1} in a nitrogen atmosphere until 600 ºC and then in air until 800 ºC.

III. RESULTS AND DISCUSSION

Exfoliation of graphene

The exfoliation of graphite was supported by several techniques. UV–Vis absorption spectra for Triton X-100 and CNC-stabilized graphene dispersions obtained under identical exfoliation conditions were comparable, both featuring a band centred at λ_{max} = 269 nm (that can be attributed to $\pi \rightarrow \pi^*$ transitions of aromatic C–C bonds), in agreement with λ_{max} reported for reduced graphene oxide dispersions[13]. Raman spectroscopy was additionally used to further corroborate graphite exfoliation. **Figure 1** shows representative FE-SEM images of GR-CNC samples obtained with different CNC concentrations.

Depending on the initial CNC:graphite ratio, the relative percentage of CNC in produced GR-CNC flakes varies. This concentration was estimated from the weight loss in the temperature range 130–575 °C measured by TGA,

which for the case of GR-CNC used as nanofillers here was 95:5 (CNC:GR). The same dispersant:graphene ratio was used for Triton-stabilized graphene (TR-GR).

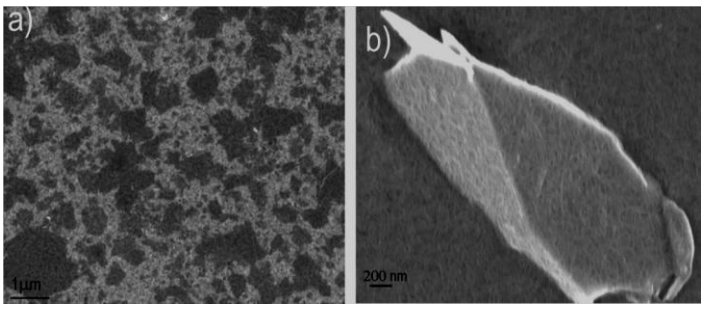

Figure 1. FESEM (a, b) images of graphene flakes produced at 10:1 graphite:CNC concentration ratio.

Properties of PVA nanocomposites

The thermal stability of the nanocomposites was assessed by thermogravimetric analysis (TGA). Thermograms showed several weight losses for the degradation of neat PVA and the biocomposites. Both pure PVA and its biocomposite decomposed in a two-step process, and the TGA curve of the bionanocomposite was shifted towards a higher temperature when compared to that of pure PVA.

On the other hand, DSC was performed for the different PVA biocomposites films. **Table 1** shows themelting temperature (Tm) and degree of crystallinity for the prepared biocomposites. It was observed that the melting temperature and the degree of crystallinity of CNC/PVA nanocomposites decreased compared to GR-T/PVA, GR-CNC and neat PVA. Disorder and decrease of PVA nucleation in the presence of CNC has already been reported in the case of CNC-filled PVA produced by casting evaporation technique[14]. Such effect is ascribed to stronger interactions between the cellulosic surface and polymeric matrix for the latter. These interactions most probably restrict the capability of the matrix chains to form large crystalline domains. However, the presence of a small loading (0.05 wt%) of graphene, both in GR-CNC/PVA and GR-T/PVA seems to counteract this effect as the degree of crystallinity is slightly increased.

Table 1. Melting temperatures (Tm) and degree of crystallinity $(\chi^c)^a$ for PVA bionanocomposites.

Nanocomposite composition	Tm (ºC)	**ΔH** (J g^{-1})	χ^c
PVA	191.6	21.57	0.16
GR-T/PVA	191.6	19.25	0.14
CNC/PVA	188.8	16.3	0.12
GR-CNC/PVA	188.7	18.8	0.14

$^a\chi^c = (\Delta H_m)/ (\Delta H^0_m \times \omega)$, with ΔH^0_m, is the heat of fusion for the 100% crystalline polymer, ω, is the weight fraction of polymeric material in the bionanocomposite (1%).

IV. CONCLUSIONS

CNC-assisted liquid phase exfoliation of graphite has been used to prepare highly stable aqueous dispersions of graphene. We have successfully prepared PVA biocomposites by direct incorporation of these aqueous dispersions of graphene in a water solution of PVA and subsequent casting evaporation process. This method has proven to be simple, clean and environmentally friendly for the production of PVA biocomposites films.

Assessment of the thermal properties showed that GR-CNC nanofiller had a synergistic effect in the thermal stability of PVA. DSC analysis revealed that the incorporation of GR-CNC nanofiller can improve the crystallinity of the biocomposite compared with the addition of plain CNC nanofillers that avoid the formation of large crystalline domains. The presence of graphene can partially counteract this effect favouring the nucleation.

V. ACKNOWLEDGEMENTS

Financial support from the Basque Government (Etortek Program, nano-IKER project IE11-304 and ACTIMAT IE13-380) and the European Commission (FP7 Program, ECLIPSE project FP7-NMP-280786) is gratefully acknowledged.

VI. REFERENCES

[1] Tingaut, P; Zimmermanna, T.; Sebe, G. Cellulose nanocrystals and microfibrillated cellulose as building blocks for the design of hierarchical functional materials. *J. Mater. Chem.*, **2012**, *22*, 20105.

[2] Siqueira, G.; Bras, J.; Dufresne, A. Cellulosic Bionanocomposites: A Review of Preparation, Properties and Applications. *Polymer*, **2010**, *2*, 728-765.

[3] Kim, H.; Abdala, A.; Macosko, C. Graphene polymer nanocomposites. *Macromolecules,* **2010**, *43* (16), 6515–6530.

[4] Carrasco, P.; Montes, S.; García, I.; Borghei, M.; Jiang, H.; Odriozola, I.; Cabañero, G.; Ruiz, V. High-concentration aqueous dispersions of graphene produced by exfoliation of graphite using cellulose nanocrystals. *Carbon*, **2014**, *70*, 157-163.

[5] Dufresne, A. Polymer nanocomposites from Biological Sources. In *Encyclopedia of Nanoscience and Nanotechnology*, 2nd ed.; Nalwa, H.S., Ed.; American Scientific Publisher: Valencia, CA, USA;

[6] Heux, L.; Dinand, E.; Vignon, M.R. Structural aspects in ultrathin cellulose microfibrils followed by 13C CP-MAS NMR. *Carbohydr. Polym.*, **1999**, *40*, 115-124.

[7] Siqueira G.; Bras, J.; Dufresne, A. Cellulosic Bionanocomposites: A Review of Preparation, Properties and Applications. *Polymer*, **2010**, *2*, 728-765.

[8] Kalia, S.; Dufresne, A.; Cherian, M.; Kaith, B. S.; Avérous, L.; Njuguna, J.; Nassiopoulos, E. Cellulose based bio and nanocomposites–a review. *International Journal of Polymer Science*, **2011**, 2011, 1-35.

[9] Tantis,I.; Psarras,G.C.; Tasis,D. Functionalized graphene – poly(vinyl alcohol) nanocomposites: Physical and dielectric properties. *eXPRESS Polym. Lett.*, **2012**, *6*, 283–292.

[10] Kubo, S.; Kadla, J. F. The Formation of Strong Intermolecular Interactions in Immiscible Blends of Poly(vinyl alcohol) (PVA) and Lignin. . *Biomacromolecules*, **2003**, *4*, 561-567.

[11] Liang, J.; Huang,Y.; Zhang, L.; Wang, Y.; Ma, Y.; Guo, T.; Chen, Y. Molecular-Level Dispersion of Graphene into Poly(vinyl alcohol) and Effective Reinforcement of their Nanocomposites. *Adv. Funct. Mater*., **2009**, 19, 1–6.

[12] Cranston E.D.; Gray D.G. Morphological and optical characterization of polyelectrolyte multilayers incorporating nanocrystalline cellulose. *Biomacromolecules*, **2006**, *7*, 2522–30.

[13] Khan, U.; O'Neill, A.; Lotya, M.; De S, Coleman JN. High concentration solvent exfoliation of graphene. *Small*, **2010**, *6*, 864–71.

[14] Roohani, M.; Habibi, Y.; Belgacem , N. M.; Ebrahim, G.; Karimi A., Dufresne, A. Cellulose whiskers reinforced polyvinyl alcohol copolymers Nanocomposites. *Eur. Polym. J.*, **2008**, *44*, 2489–2498

TCF BLEACHING OF ORGANOSOLV PULP FROM ORANGE TREE TRIMMINGS

Ana Moral[1], Roberto Aguado[2]*, Elena Cabeza[1], M. Menta Ballesteros[1], Antonio Tijero[2]

[1]*Chemical Engineering Dpt., Experimental Sciences Faculty, Pablo de Olavide University of Seville, 41013 Seville, Spain;*
[2]*Grupo de Celulosa y Papel, Chemical Engineering Dpt., Faculty of Chemistry, Complutense University of Madrid, 28040 Madrid, Spain (*e-mail: rjagarcia@ucm.es).*

ABSTRACT

The revalorization of agricultural wastes is attracting the attention of researchers and manufacturers. One of the many ways to carry out this revalorization is the pulping and bleaching of those residues for papermaking.
Spain annually produces more than 300 thousand tonnes of *Citrus sinensis* (orange tree) trimmings. If they are not re-used, they end up being open-burnt. Chemical composition of these residuals is similar to that of common hardwoods.
The kraft process is the most used method to obtain pulp for papermaking purposes, but the use of sodium sulphide and the burning of the black liquor are related to some environmental problems. A lot of research has been carried out to evaluate alternative methods to remove lignin, such as soda-anthraquinone and Organosolv processes.
Nowadays, most of the bleaching plants work on ECF (elemental chlorine-free) bleaching methods. Although chlorine dioxide is less harmful than elemental chlorine, it also creates halogenated pollutants. This can be avoided by the development of total chlorine-free methods, such as hydrogen peroxide bleaching.
The work aims to obtain bleached pulp that is environmentally friendly in three ways: first, by using agricultural wastes (orange tree trimmings) as the raw material; second, by using Organosolv pulping, and third, by bleaching the pulp with hydrogen peroxide. A design of experiments was used to discuss the influence of peroxide concentration, time and temperature on the yield, brightness, viscosity and Kappa number of pulps.

I. INTRODUCTION

The manufacturing of fibre-based products from agricultural wastes has been a field of interest for the past decades. The reasons for this trending research are the expectation of the reduction of the availability of wood in the future, the demand of certain countries where wood is a scarce resource, the care for environmental impact, and the convenience to discover different new properties, be it mechanical or optical [1].

European production of pulp from wastes such as bagasse and cereal straw accounted only for 211,000 tonnes in 2012, making it the 0.6% of total pulp production, 18.2% less than the previous year, according to CEPI's report [2]. However, China's non-wood pulp production was as high as 12.4 million tonnes in 2011, according to FAO's survey [3]. Finland is the greatest alternative pulp producer in Europe, Spain being the second. Cereal straw, bamboo and bagasse are the most usual alternative raw materials. Many other plants or parts of plants are being studied for papermaking purposes, namely esparto grass [4], hemp core [5], cotton stalk [6].

In Spain, the total production of trimmings implies a large wood potential, over 6.5 million tonnes. This includes trimmings from sweet orange tree (*Citrus sinensis*) with a potential from 300 to 400 thousand tonnes, mainly located in Eastern and Southern Spain. Orange tree pruning has been recently used by González et al. [7] to make paper and evaluate the influence of cooking conditions. This material consists mainly of 73% of holocellulose and 20% of lignin [8].

As it is known, the kraft process is the main method to obtain cellulosic pulp for papermaking purposes, but the use of sulphur salts is related to contamination problems and bad odours. Organosolv pulping, using various organic solvents that selectively dissolve lignin, stands as one of the most popular alternative ways. It allows for higher yield values, since it is less-damaging to cellulose and hemicellulose, and lignin recovery. As a major drawback, in the current market it cannot be obtained enough profit from pure lignin yet [9].

To achieve the brightness usually required by printing paper or market pulp, a bleaching process is needed. Generally speaking, bleaching is more selective towards lignin removal than cooking, but also more expensive per unit of lignin removed, and it requires an already-cooked pulp. Traditional bleaching processes used to be based on elemental chlorine, related to various pollution problems. This reagent was progressively displaced by chlorine dioxide, less hazardous, since its first use in 1946 [10]. Stages involving ClO_2 are present in the majority of

bleaching plants today [11], but a next step is being taken by trying new bleaching processes only with oxygen, ozone and/or hydrogen peroxide [12] These reagents do not form chlorinated organic derivatives needing to be removed [13].

The aim of this work is to study the influence of three variables (temperature, time, reagent concentration) in a one-stage bleaching process with hydrogen peroxide. The convenience of this bleaching process to remove lignin and increase brightness of cellulosic pulp obtained from orange tree trimmings through Organosolv pulping, using ethanolamine as the solvent, is discussed.

II. EXPERIMENTAL

Harvesting and pulping

Trimmings were harvested from orange trees grown in the East of Spain. An ethanolamine commercial solution was purchased from Panreac.

First, the wood fraction of orange tree trimmings, i.e., stems whose diameter was greater than 5 mm, was separated from the rest, washed, crushed, and then cooked to obtain the pulp. Cooking was performed in a stainless steel batch reactor. Liquor to solid ratio was held at 6. Cooking liquor consisted of ethanolamine (60%) and water (40%). Temperature was held at 180 ºC thorough the process. After 60 minutes of cooking, the resulting pulp was washed, pressed, crumbled and stored at temperatures below 10 ºC. Prior to bleaching, the pulp was disintegrated in a lab disintegrator ENJO model 692.

Bleaching

Peroxide bleaching of Organosolv pulp was performed following a fractional experimental design: 3 factors, 3 levels, and 15 different runs. The factors selected were: peroxide concentration, temperature, and bleaching time. In each essay, a pulp sample was mixed with deionized water, hydrogen peroxide, sodium hydroxide, magnesium sulphate and diethylentriaminepentaacetic acid (DTPA). The pulp sample and the bleach liquor were placed in a polyethylene bag, which was sealed and kept at the desired temperature by means of a water bath. Consistency was held at 10% for all the experiments. Amounts of NaOH, $MgSO_4$ and DTPA added per gram of oven-dry pulp were held constant (1.8%, 0.2% and 0.5%, respectively).

The hydrogen peroxide concentration was 2%, 6% and 10%, on the basis of oven-dried pulp weight. Bleaching temperature was 55, 70 and 85 ºC. Duration of peroxide bleaching was 30, 90 and 150 minutes. Once bleaching was complete, the sample was quenched to room temperature, washed, filtered, air-dried and weighted.

Analytic method

Up to six handsheets were made from unbleached pulp and from the bleached pulp obtained through each of the experiments. Standard ISO 5269-1:1998 was followed. Handsheets were pressed at 130 kPa and dried at 140 ºC for 10 minutes. The grammage of the handsheets was 60 g/m^2 approximately. Brightness was determined according to ISO 2470-2 standard.

Microkappa number was measured according to TAPPI standard UM 246, for both the unbleached pulp and the one-stage bleached samples. Intrinsic viscosity was determined following UNE 57-039.

III. RESULTS AND DISCUSSION

Table 1 shows the normalized values of independent variables and the four dependent variables, according to the proposed experimental design. The codes for the normalized factors are X_P (peroxide concentration), X_T (temperature) and X_t (time). Yield is expressed as the weight of oven-dried bleached pulp per weight of oven-dried pulp prior to bleaching. Each experiment was replicated enough times that relative standard deviation was less than 6% for intrinsic viscosity and Kappa number, and less than 2% for ISO brightness.

Table 1. Properties of unbleached pulp and properties of bleached pulp for different conditions. BR: ISO brightness. KN: Kappa number. IV: intrinsic viscosity. YI: Yield.

Code	X_P	X_T	X_t	BR (%)	KN	IV (mL/g)	YI (%)
Unbleached	--	--	--	34,5	49,8	286	--
1	1	1	1	72,9	38,5	192	90
2	1	1	-1	70,0	40,6	184	90,1
3	1	-1	1	68,3	43,2	211	93,8
4	1	-1	-1	68,2	42,3	215	89,6
5	-1	1	1	67,5	44,2	246	94,2
6	-1	1	-1	67,4	44,8	234	94,3
7	-1	-1	1	67,6	44,1	246	95,7
8	-1	-1	-1	67,3	44,5	250	95,5
9	0	0	0	68,3	42,6	200	92,4
10	1	0	0	68,8	41,9	184	93,5
11	-1	0	0	67,6	43,7	219	94
12	0	1	0	68,1	41,8	188	94,4
13	0	-1	0	67,9	42,1	234	94,3
14	0	0	1	68,4	41,5	211	93,7
15	0	0	-1	67,0	44,6	223	92,8

Kappa number and yield were found to decrease mainly with peroxide concentration, although time and temperature also showed significant negative influences. A low Kappa number is associated with low values of intrinsic viscosity, because of the degradation of carbohydrates. Nonetheless, viscosity of the most severe-treated sample is not the lowest. This is probably due to the removal of hemicelluloses [14].

Comparing with unbleached pulp, even a mild bleaching process raises brightness greatly. Such a high increment in brightness corresponds to a low decrement in Kappa number. This is due to the mechanism of peroxide hydrogen bleaching: brightness gain is mainly caused by the oxidation of lignin's chromophoric groups, rather than the removal of lignin itself [15]. However, very severe conditions cannot achieve brightness values higher than 71.1%. Brightness was found to increase with time, temperature and, especially, peroxide concentration.

That could only be achieved by additional bleaching stages. A regression for ISO brightness was performed, considering individual and binary influences that were statistically significant:

$$BR = 67.8 + 1.073X_P + 0.652X_T + 0.487X_t + 0.455X_P^2 + 0.805X_PX_T + 0.308X_PX_t + 0.287X_T^2 + 0.321X_t^2$$

The correlation coefficient R^2 was 0.84. Figure 1 shows response surfaces relating brightness to normalized values of temperature and peroxide concentration (A), and to normalized values of peroxide concentration and time (B).

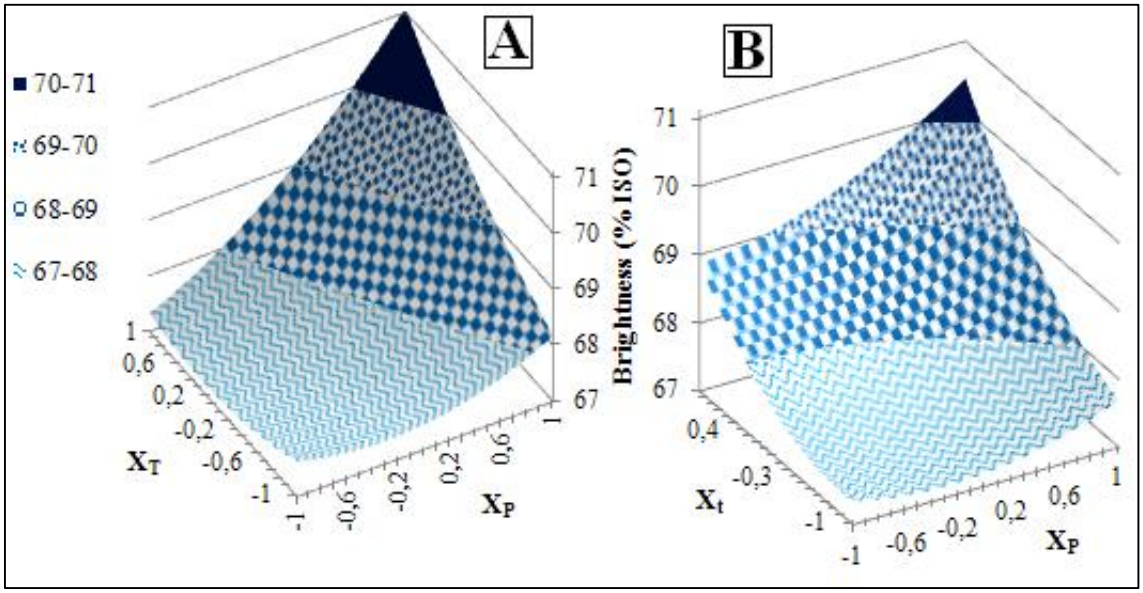

Figure 1. Response surfaces for ISO brightness. A) Bleaching time is 90 minutes. B) Temperature is 70 ºC.

IV. CONCLUSIONS

One-step alkaline bleaching with hydrogen peroxide, using DTPA as activator, achieved a high brightness gain in Organosolv pulp from orange tree trimmings, although delignification was poor. For brightness values above 71%, a multi-stage bleaching process is necessary. Temperature, peroxide concentration and duration of the process affected brightness positively. Temperature and concentration showed negative influences over Kappa number and yield. Viscosity usually decreased with those factors, due to the partial degradation of carbohydrates, but it was found to increase in certain cases, due to the removal of hemicelluloses.

V. ACKNOWLEDGEMENT

The authors wish to acknowledge the Ministry of Science and Innovation of Spain for the financial support of the Project CTQ2010-21660-C03-01 in which the present study is framed**.**

VI. REFERENCES

[1] Jiménez, L.; Rodríguez, A. Fabricación de papel a partir de materias primas alternativas a las convencionales. *Curr. Opin. Ecopapel S.L.* **2010**, Écija (Spain).

[2] CEPI's Key Statistics, **2013**. Downloaded on March 10, 2014, from: <http://www.cobelpa.be/pdf/cepi%20Key%20Statistics%20Report%202012.pdf>

[3] FAO. Survey of World Pulp and Paper Capacities, 2011-2016. Food and Agriculture Organization of the United Nations. **2012**, Rome (Italy).

[4] Marrakchi, Z.; Khiari, R.; Oueslati, H.; Mauret, E.; Mhenni, F. Pulping and papermaking properties of Tunisian Alfa stems (Stipa tenacissima) – Effects of refining process. *Ind. Crop. Prod*. **2011**, *34(3)*, 1572-1582.

[5] Barberà, L.; Pélach, M.A.; Pérez, I.; Puig, J.; Mutjé, P. Upgrading of hemp core for papermaking purposes by means of organosolv process. *Ind. Crop. Prod*. **2011**, *34(1)*, 865-872.

[6] Reddy, N.; Yang, Y. Properties and potential applications of natural cellulose fibers from the bark of cotton stalks. *Biores. Technol.* **2009**, *100*, 3563-3569.

[7] González, Z. Idoneidad de las podas de naranjo como materia prima para la producción de pasta celulósica para diversos usos. Ph.D. Thesis. **2013**, Cordoba University (Spain).

[8] González, Z.; Rosal, A.; Requejo, A.; Rodríguez, A. Production of pulp and energy using orange tree prunings, *Biores. Technol*. **2011**, 102 (19), 9330-9334.

[9] Jiménez, L.; Rodríguez, A.; Serrano, L.; Moral, A. Organosolv ethanolamine pulping of olive wood: Influence of the process variables on the strength properties, *Biochem. Eng. J*. **2008**; 39 (2), 230-235.

[10] Rapson, W.H. Bleaching – Chlorine Dioxide. In: Britt, K.W. (Editor). *Handbook of pulp and paper technology*, 2nd edition. *Van Nostrand Reinhold Company*. **1970**, Nueva York (U.S.A.), 275-286.

[11] Reinstaller, A. The technological transition to chlorine free pulp bleaching technologies: lessons for transition policies, *J. Clean. Prod*. **2008**, *16S1*, S133-S147.

[12] Fennell, F.L. Peroxide Bleaching. In: Britt, K.W. (Editor). *Handbook of pulp and paper technology*, 2nd edition. *Van Nostrand Reinhold Company*. **1970**, Nueva York (U.S.A.), 315-321.

[13] Shatalov, A.A.; Pereira, H. Arundo donax L. reed: new perspectives for pulping and bleaching. Part 4. Peroxide bleaching of organosolv pulps. *Biores. Technol*. **2005**, *96*, 865-872.

[14] López, F.; Díaz, M.J.; Eugenio, M.E.; Ariza, J.; Rodríguez, A.; Jiménez, L. Optimization of hydrogen peroxide in totally chlorine free bleaching of cellulose pulp from olive tree residues. *Biores. Technol*. **2003**, *87*, 255-261.

[15] Qin, W.; Cui, G.; Liang, W.; Yu, H. Study on DMD pretreatment and totally chlorine free bleaching. *Chemistry and Industry of Forest Products*. **1999**, *19(3)*, 1-15.

CELLULOSE FROM ULVA SP. AS A REINFORCING FIBRE FOR THE PULP AND PAPER INDUSTRY

Ana Moral[1]*, María M. López, Roberto Aguado, José S. Torrecilla, Antonio Tijero

[1]*Chemical Engineering Dpt. Experimental Sciences Faculty, Pablo de Olavide University. 41013 Seville, Spain (*e-mail: amoram@upo.es)*
[2]*Chemical Engineering Dpt. Faculty of Chemistry, Complutense University of Madrid, 28040 Madrid, Spain*

ABSTRACT

Due to the current energetic and environmental crisis, and to the increase of value and use limitations of wood fibres, a lot of attention is being led to the search of new and cleaner extraction methods. The objective of the research is the recovery or production of cellulose from new sources, such as: agro-industrial wastes, annual plants, bagasse and even mud and bacteria. However, few works consider the use of algae for that goal.
Algae, besides being a new, cheaper and more sustainable raw material, lack lignin or show scarce amounts of it. This low or non-existent lignin content grants improved economic and environmental performance.
It has been proved that cellulose from algae has the required properties for its use in papermaking, and there are patented methods and works regarding the manufacturing of paper and paper-related products from algal fibres. Besides the profits implied by the suppression of the pulping and bleaching stages, cellulose from macroalgae shows an exceptionally low degree of hornification, which delays its degradation upon use, improving its utilization as reinforcing fibres in the manufacturing of both virgin and recycled paper.
The aim of this work is to optimize the process of extraction of cellulose from *Ulva sp*. A design of experiments with three factors (hydrogen peroxide concentration, temperature, and time) was carried out. The influence of these variables in the capabilities of algal cellulose as reinforcing fibre in the paper industry is studied.

I. INTRODUCTION

While wood is still the main source of cellulose, a great amount of research has been conducted lately into new ways to obtain this polymeric material from alternative sources and by alternative methods [1-5]. Most of the attention is paid to annual plants and agricultural wastes, but other raw materials should be taken into consideration. Among them, algae stand as simple and feasible sources of cellulose fibres. Unlike wood, algae do not need expensive (and usually polluting) cooking and screening processes to obtain a cellulose-concentrated product. Lignin content is a major limitation when obtaining cellulosic pulp from higher plants, thus the lack of lignin in seaweed eases the extraction and use of cellulose. Some lignin-like compounds at low concentrations have been found [6], and even a very low content of true lignin [7].

Seaweed in the division *Chlorophyta*, or green algae, has cell walls constituted by up to 70% of cellulose. Species in the genus *Ulva*, also known as sea lettuce, are particularly interesting for papermaking, to be used as reinforcing fibres, due to ease of extraction and availability. Algae belonging to the genus *Ulva* are very common worldwide, fast colonizers of coastal sites and tolerant to severe conditions [8]. *Ulva sp*. have been studied for different applications: manufacturing of composites [8]; removal of copper from aqueous streams [9]; oil extraction [10]; bioindication of metal contamination in water [11]. However, to the best of our knowledge, little research has been done to evaluate their potential applications for papermaking since Monegato and Nicolucci [12] invented a method to manufacture paper from seaweed, mainly *Ulva rigida*, along with bleached wood-pulp. Later, You and Park [13] invented a method to manufacture paper from *Rodophyta algae.*

Obtention of cellulose from seaweed can be performed by means of acids, alkalis, enzymes, selective solvents and/or several oxidants, such as ozone, hydrogen peroxide and hypochlorite. Extraction with hydrogen peroxide is a minimal environmental impact method. This reagent is widely used in bleaching processes, since it is an efficient oxidizer of colouring compounds [14], namely lignin in vascular plants, chlorophyll in seaweed.

In this work, algal samples from genus *Ulva* were analysed chemically to determine their content of holocellulose, lignin and extractives. Algae underwent an extraction process with hydrogen peroxide with no

prior treatment, following an experimental design with three factors and three levels. Brightness and mechanical properties (breaking length, elongation, tear index, burst index) were measured. The influence of temperature, hydrogen peroxide concentration and time through the extraction process was evaluated. Also, results are compared to those obtained for conventional pine kraft pulp and pine sulphite pulp.

II. EXPERIMENTAL

Materials

For this work, seaweed was harvested by hand at the beach "La Cachucha" (Puerto Real, Cadiz, Spain) in March of 2013. Samples were exhaustively washed with freshwater and screened in order to isolate *Ulva sp.* from other algae, sand and impurities of any kind, and dried at 40 ºC for three days.

Commercial benzene and ethanol (95%) were purchased from Sigma-Aldrich. A solution consisting of 2 volumes of benzene by 1 volume of ethanol was prepared. Sulphuric acid (72%), glacial acetic acid (99.7% at least) and sodium chlorite (0.1 N) solutions were obtained from Panreac. Solid $MgSO_4$ and solid NaOH were supplied by Panreac too, while solid diethyltriamminpentacetic acid (DTPA) was purchased from Fluka.

Chemical characterization of the samples

Extraction ethanol-benzene was performed according to TAPPI standard method T264 cm-97. Standard method T222om-06 for the determination of the content of acid-insoluble lignin was followed. Holocellulose content was determined according to Wise and Murphy (1946), using sodium chlorite and acetic acid as reagents [15].

Cellulose extraction

The reagent used was prepared by dissolving NaOH, $MgSO_4$ and DTPA in a solution of hydrogen peroxide. Per gram of o.d. sample, 0.018 g of NaOH, 0.005 g of DTPA and 0.002 g of $MgSO_4$ were added to enhance the process and preserve the cellulose chains.

Experiments were planned following a design with three factors: temperature, time, and percentage (in weight) of hydrogen peroxide in relation to o.d. sample. **Table 1** shows the codes adopted for the independent variables and the normalized values. The criteria used to discern statistically-significant data from non-significant values were: having a Snedecor F-value greater than 4 and having a Student t-value greater than 2. Only significant data were fitted.

Each *Ulva sp.* sample were put in a polyethylene bag, along with the required addition of reagents, and distilled water was poured into the bag until the consistency of the mixture was 10%. Each sample was held at constant temperature for the desired time, then quenched, washed, and screened.

Table 1. Experimental planning for the cellulose extraction process.

Independent variable	Code	Normalized values		
		-1	0	1
Peroxide hydrogen (%)	X_p	1	2	3
Temperature (ºC)	X_T	50	60	70
Time (min)	X_t	15	30	45

Formation and characterization of handsheets

Samples that had undergone extraction were mixed at a 50:50 ratio with pine kraft pulp. Handsheets were obtained from each of the mixed samples according to ISO 5269-1:1998. Brightness was determined according to the standard method ISO 2470-2:2008. Elongation and breaking length were measured by means of equipment from HT Hounsfield according to UNE 57054 and UNE-EN ISO 1924-2:2009 standards. Tear index was determined by a MESSMER tester according to UNE-EN 21974:1996 standard. Burst index was measured by a METROTEC tester according to UNE-EN ISO 2758:2004 standard.

III. RESULTS AND DISCUSSION

Chemical analysis of the raw material

Results of the determination of the amount of extractives in ethanol-benzene, lignin and holocellulose are shown in **Table 2**. Compared to wood or, generally speaking, higher plants, algae show a very low content of undesired

components, such as lignin-like compounds and extractives. This makes unnecessary a treatment prior to the cellulose extraction process, unless very pure cellulose is to be obtained. Holocellulose content is around 10-30% lower than that of conventional wood and most of annual plants. This is made up by those materials usually needing to undergo delignification processes that also remove a large amount of cellulose and hemicellulose.

Table 2. Chemical characterisation of *Ulva spinulasa.*

Holocellulose (%)	46,89
Extractives in ethanol-benzene (%)	2,00
Acid-insoluble lignin-like compounds (%)	2,47

Characterization of handsheets

The ISO brightness and mechanical properties of the handsheets for each of the experiments planned are shown in **Table 3**. The addition of treated seaweed samples to pine kraft pulp resulted in an increase of tear index, and a decrease of the rest of the properties measured.

Table 3. Average value and standard deviation for the physical properties of paper sheets.

Essay	BR		TI		EL (%)		BL (m)		BI (kN/g)	
	AV	SD	AV	SD	AV	SD	AV	SD	AV	SD
PKP	25.03	0.22	14.04	1.03	0.32	0.09	7723	46	5.1	0.07
PSP	16.90	0.16	15.50	0.94	0.24	0.04	3756	28	4.3	0.1
1	12.43	0.65	30.36	1.82	0.5	0	1846	184	1.66	0.05
2	12.75	0.96	25.97	0.15	0.36	0.02	1321	82	1.22	0.02
3	13.27	0.23	26.52	0.07	0.7	0.03	2273	20	1.87	0.12
4	11.36	0.42	25.88	1.05	0.97	0	3004	21	2.16	0.07
5	12.89	1.3	24.8	1.68	0.53	0.04	1301	2	1.17	0
6	14.4	1	25.36	2.35	0.39	0.01	1630	25	1.65	0.01
7	13.3	0.62	26.14	0.24	0.5	0	1971	139	1.69	0.05
8	12.8	0.29	23.29	1.29	0.62	0.01	1934	11	2.06	0.02
9	14.48	0.41	27.55	0.67	0.55	0.04	2143	31	1.39	0.01
10	11.5	0.39	34.62	0.45	0.41	0.04	1620	142	1.42	0.11
11	12.55	0.11	21.92	1.34	0.49	0.05	2090	149	2.23	0.03
12	13.09	0.39	25.62	0.04	0.6	0.01	1728	24	1.29	0.02
13	12.31	0.34	20.52	0.06	0.71	0.01	2208	80	1.91	0.08
14	14.3	0.29	27.14	0.25	0.48	0.05	1730	26	1.17	0.09
15	13.81	0.21	27.71	0.31	0.64	0.11	2716	35	1.93	0.02

Abbreviations: PKP: pine kraft pulp; PSP; pine sulphite pulp; AV: average value; SD: standard deviation; BR: brightness; TI: tear index; EL: elongation; BL: breaking length; BI: burst index.

Fitting and modelling

Average values found for each of the dependant variables selected in the design of experiments were adjusted to a polynomial model. Non-significant influences were neglected, which includes ternary and cubic influences. The results of multiple regressions upon brightness, tear index, elongation, breaking length and burst index and are shown in the next equations, along with the correlation coefficient in each case.

$$BR = 13.02 + 0.002X_P^2 + 0.024X_T^2 + 0.02X_PX_T + 0.025X_T + 0.079X_t \qquad r^2=0.917$$

$$TI = 25.497 + 1.04X_t^2 + 0.769X_tX_T + 0.822X_PX_T + 2.45X_T - 0.754X_t \qquad r^2=0.923$$

$$EL = 0.56 + 0.121X_t^2 - 0.08X_T^2 + 0.02X_tX_T + 0.017X_PX_T + 0.042X_T - 0.082X_t - 0.011X_P \qquad r^2=0.875$$

$$BL = 1967 - 58.8X_t^2 - 172X_T^2 - 196X_P^2 - 29.2X_tX_T + 162X_PX_T - 78.5X_P \qquad r^2=0.738$$

$$BI = 1.675 - 0.294X_PX_t \qquad r^2=0.911$$

As expected, higher brightness values are obtained for larger additions of hydrogen peroxide. Medium temperature and long-time extraction are also advised. To optimize tear index, we recommend high temperature, 2% hydrogen peroxide to o.d. sample, and a time of 30 minutes. The best performance in tensile properties is achieved at low concentrations of hydrogen peroxide, 15 to 30 minutes of extraction and medium-to-high temperature. For burst index, low peroxide concentration (1%) and short extraction processed are advised.

IV. CONCLUSIONS

Ulva sp.'s cellulose content is lower than that of vascular plants, but, given the low content of undesired compounds to remove prior to extraction, it can be concluded that its chemical composition provides ease to the manufacturing of cellulosic products.

Comparing sheets from pine kraft pulps to sheets consisting of both pine kraft pulp and algal cellulose, it can be seen that the incorporation of algal fibres greatly enhances tear resistance and elongation, but worsens the performance in tensile and burst essays. Although these properties were decreased, it should be noted that they are still acceptable for many applications, and this method implies notorious savings in terms of costs of raw materials, energy, reagents, and equipment. Brightness values were found to be low, as the remaining chlorophyll has a large colouring power.

V. ACKNOWLEDGEMENT

The authors wish to acknowledge the Ministry of Science and Innovation of Spain for the financial support of the Project CTQ2010-21660-C03-01 to which the present study is related.

VI. REFERENCES

[1] Jiménez, L., Rodríguez, A., Serrano, L., Moral, A.; Organosolv ethanolamine pulping of olive wood: Influence of the process variables on the strength properties. *Biochem. Eng. J.* **2008,** *39*, 230-235.

[2] Jonoobi, M., Mathew, A.P., Oksman, K.; Producing low-cost cellulose nanofiber from sludge as new source of raw materials. *Ind. Crop. Prod.* **2012**, *40*, 232-238.

[3] Khristova, P., Kordsachia, O., Patt, R., Karar, I., Khider, T.; Environmentally friendly pulping and bleaching of bagasse. *Ind. Crops. Prod.* **2006**, *23*, 131-139.

[4] Rodríguez, A., Moral, A., Sánchez, R., Requejo, A., Jiménez, L.; Influence of variables in the hydrothermal treatment of rice straw on the composition of the resulting fractions. *Biores. Technol*. **2009**,*100*, 4863-4866

[5] Yang, L., Zhang, H.-Y., Yang, Q., Lu, D.-N.; Bacterial cellulose-poly (vinyl alcohol) nanocomposite hydrogels prepared by chemical crosslinking. *J. App. Polym. Sci.* **2012,** *126* (SUPPL. 1), E244-E250.

[6] Dewilche, C.F., Graham, L.E., Thomson, N.; Lignin-like compounds and sporopollenin in Coleochaete, an algal model for land plant ancestry. *Scienc.* **1989,** *245*, 399–401.

[7] Martone, P.T., Estevez, J.M., Lu, F., Ruel, K., Denny, M.W., Somerville, C., Ralph, J.; Discovery of Lignin in Seaweed Reveals Convergent Evolution of Cell-Wall Architecture. *Current Biol.* **2009**, *19*, 169-175.

[8] Smith, G.M.; On the reproduction of some Pacific coast species of Ulva. *Am. J. Bot.* **1947**, *34*, 80-87.

[9] Karthikeyan, S., Balasubramanian, R., Iyer, C.S.P.; Evaluation of the marine algae Ulva fasciata and Sargassum sp. for the biosorption of Cu(II) from aqueous solutions, *Biores. Technol*. **2007**, *98*, 452–455.

[10] Suganya, T., Renganathan, S.; Optimization and kinetic studies on algal oil extraction from marine macroalgae Ulva lactuca. *Biores. Technol.* **2012**, *107*, 319-326.

[11] Pereira, P., De Pablo, H., Guilherme, S., Carvalho, S., Santos, M.A., Vale, C., Pacheco, M.; Metal accumulation and oxidative stress responses in Ulva spp. in the presence of nocturnal pulses of metals from sediment: A field transplantation experiment under eutrophic conditions. *Marine Env. Res.* **2014**, *94*, 56-64.

[12] Monegato, A., Nicolucci, C.; Paper comprising cellulose fiber and seaweed particles in integral form. Patent number: US5472569. Filling date: Oct. 24, 1994. Issue date: Dec. 5, **1995.**

[13] You, H.C., Park, J.H.; Pulp and paper made from Rhodophyta and manufacturing method thereof. Patent number: 7622019. Filling date: Nov 12, 2004. Issue date: Nov 24, **2009.**

[14] Cort, C.J., Bohn, W.L.; Alkaline, peroxide and mechanical pulping of hardwoods. *Tappi J.* **1991**, *74*, 79-84.

[15] Wise, L.E., Murphy, M., D'Addieco, A.; *Paper Trade J.* **1946,***122*, 35.

DEPOLYMERISATION OF CELLULOSE DURING COLD ACIDIC CHLORITE TREATMENT

Gérard Mortha[1]*, Jennifer Marcon[1], David Dallérac[1], Christophe Vallée[2], Nadège Charon[2], Agnès Le Masle[2]

*[1]LGP2, UMR 5518, Institut Polytechnique de Grenoble, 461 rue de la papeterie, CS 10065, F-38402 Saint Martin d'Hères, France; [2] IFP Energies nouvelles, Rond-Point de l'échangeur de Solaize, BP 3, F-69360 Solaize, France (*gerard.mortha@grenoble-inp.fr)*

ABSTRACT

A cold holocellulose treatment (CH) was studied on a bleached Eucalyptus kraft pulp to see whether the chlorite reaction on pulp at room temperature, slightly acidic pH and high reactant charge (313 % active chlorine) could degrade cellulose. Indeed Ragauskas and col. (2010) reported some cellulose depolymerization by chlorite treatments at 70°C and reinforced conditions compared to the classical so-called holocellulose treatment, although lignin was found to protect cellulose. In our study, cellulose depolymerization was followed by measuring the TAPPI viscosity and by multidetection size-exclusion chromatography. It could not be clearly concluded that the CH treatment induced some cellulose degradation. This study opens the way to the set-up of inert delignification procedures to be applied on raw or processed lignocellulosic samples from biorefinery studies.

I. INTRODUCTION

During wood biorefinery studies, one main parameter to be monitored is the degree of polymerization (DP) of cellulose in the raw material and during the applied processes. Size-exclusion chromatography (SEC) coupled to multidetectors – differential refractometry (DRI) and light-scattering (LS) – is the preferred characterization method used in several laboratories. Prior to SEC, samples are either directly dissolved in LiCl-DMAC or derivatized to form cellulose tricarbanilates (CTC's) which are soluble in THF or LiCl-DMAC. This method is well reported on pure cellulose like cotton or low-viscosity chemical pulps that contain few amounts of hemicelluloses and no trace of lignin. It is less applicable on samples that contain significant amounts of lignin and hemicelluloses, like partially bleached wood chemical pulps. Its application remains virtually impossible on raw vegetal or much lignified pulps like mechanical pulps. The quality of dissolution may also depend of the cellulose DP, small chains being more easily dissolved or derivatized than long chains. However, even for well-dissolved pulps, artefacts can be observed on the chromatograms, like irregular elution caused by the formation of molecular aggregates between cellulose chains or interactions with the SEC columns. Aggregates are detected by peaks in the high molar mass region of the chromatograms with very high light-scattering signals. They may also cause poor column resolution with tailing chromatograms, exhibiting rather constant molar masses in the tailing part, as measured by the detectors. Aggregates may result from polar interactions or cross-linking between cellulose chains in which the residual hemicelluloses and lignin bonded to hemicelluloses play a role. Therefore a rigorously correct analysis of the cellulose degree of polymerization should require a complete elimination of lignin and few or no hemicelluloses remained in the sample prior to direct dissolution or derivatization into CTC's.

Lignin extraction and purification from raw or processed lignocellulosic samples that contain important amounts of lignin and hemicelluloses, without affecting the DP of cellulose, is not straightforward. Highly lignified samples can originate from plants or wood samples, untreated or treated during biorefinery studies, or from papers containing mechanical pulps or semi-chemical pulps, such as old patrimonial papers manufactured during the XIXth century. Even in the more recent studies that deal with the effect on cellulose of purification methods for lignocellulosic samples [1-3], only CUED viscosities or SEC with simple DRI detection that relies on standard calibration, but not highly precise measurements such as SEC-multidetection, has been reported.

Chlorite delignification of kraft pulps at slightly acidic pH, 70°C, reaction time 2h, is the so-called "holocellulose test". Delignification in one step is not fully achieved on plants and wood samples, and several studies have reported the use of reinforced conditions: repeated stages at 70°C, prolonged time, high reactant charge introduced in several steps [1, 2] [4, 5]. However, by testing some reinforced procedures on poplar milled wood (unpublished results), we found that serious degradation of the TAPPI viscosity occurred. This was also confirmed by molar mass distribution (MMD) measurements by SEC-multidetection on the fully-delignified

samples, which revealed abnormally small DP's of cellulose (lower than that of kraft pulps). This at least confirmed the observation of Hubbell and Ragauskas [1] who treated pure cellulose samples by reinforced holocellulose at 70°C and found some protection effect of added dissolved lignin.

In this paper, we investigated a cold holocellulose (CH) procedure reported in 1997 by Lapierre and Bouchard [6]. We measured the TAPPI viscosity and the MMD of cellulose tricarbanilates by SEC-multidetection during successive CH treatments with or without insertion of an alkaline extraction (E) treatment between the chlorite stages. We used a SEC-multidetection system that includes differential refractometry, UV, dual-angle light-scattering (LALS/RALS) and viscometry, allowing the quantification of the MMD, intrinsic viscosity, hydrodynamic radius and gyration radius of the CTC's.

II. EXPERIMENTAL

An industrial south-American Eucalyptus kraft pulp (ECF bleached) was used as cellulosic substrate containing hemicelluloses (mostly xylans) and no lignin, with no further treatment (except washing with deionized water and air drying). CUED viscosity was measured by the TAPPI standard procedure. Viscosity-average degree of polymerization in CUED (DP_v) was calculated from TAPPI viscosity using a conventional formula.

Cold holocellulose (CH) treatment was made according to the method described in [6]: 1 g (on dry basis) of wet pulp sample is placed in a glass flask. 50 mL of a solution containing 0.442 mol/L of sodium chlorite and 0.167 mol/L of pure acetic acid (pH of about 3.6) is added. The flask is tightly closed and left for reaction in a dark box at room temperature during 16 h. After reaction, the pulp is washed with a large volume of deionized water. A part of the pulp is dried at room temperature for viscosity measurement; the remaining is kept undried for solvent exchange with pure DMAC and phenylisocyanate derivatization followed by SEC measurement.

Alkaline extraction (E) was made in polyethylene bags immersed in a water bath in the following conditions: 2% NaOH/pulp, 10% solids consistency, 70°C, and 2 h.

Cellulose derivatization to form CTC's followed a procedure modified from Berggren *et.al.* [7]. Solvent exchange with pure/dry DMAC is applied on the wet pulp sample (100 mg o.d. basis). DMAC-LiCl (6% LiCl) and phenylisocyanate are added and the reaction is carried out in closed stirred flasks at 40°C. It is stopped after 5 days with an excess of MeOH. Dilution in DMAC and final dilution in THF allow reaching a CTC concentration of about 1 mg/mL for SEC injection. The SEC system includes a Malvern GPCmax system equipped with DRI, UV, LALS, RALS and viscometer detectors, 3 PLGEL mixed-B columns and a precolumn, all kept at 35°C. The system was eluted with THF at a flow rate of 1 mL/min. Data were treated with OMNISEC 4.5^{TM} from Malvern Corporation.

III. RESULTS AND DISCUSSION

The measured CUED viscosities and mean chromatographic data are reported in **Table 1**. It is shown that a single or two successive CH treatments did not affect the TAPPI viscosity of the pulp, while three treatments induced a slight decrease of the viscosity. With an E treatment after CH, a more significant viscosity decrease was induced, but viscosity kept rather stable after an end CH treatment. Tendencies shown by the chromatographic analysis appear slightly different, since it might be concluded that either very little or no degradation would be induced by the repeated cold holocellulose and E treatments. The peak degree of polymerization data exhibit a slight decreasing tendency, slightly more pronounced when E is applied. Weight-average DP data (DP_w) tend to correlate the latter. Since the DP_w is mostly affected by the high molar mass population, the biggest molecules might suffer little damages. However, variations of the weight-average intrinsic viscosity $<[\eta]>$ or weight-average hydrodynamic radius $<R_h>$ appear at the limit of significance. Variations of the weight-average gyration radius $<R_g>$ appear to be slightly more pronounced than for $<R_h>$. However the calculation of R_g with a dual-angle light-scattering detector may not be very accurate. It is interesting to note the rather constant values obtained for the identified MHS-law parameters K and a, very close to previously calculated values on cotton pulps. The DP_v of the CTC's was recalculated from K, a and $[\eta]$. As for the DP_{peak} and DP_w values, it exhibits a slightly decreasing tendency with the multiplication of the applied treatments. The polydispersity (DP_w/DP_n) appears to be rather constant, except for (CH + E). Here again, variations can be assumed at the limit of significance since the precision depends on column resolution, partly affected by the presence of a small population of molecular aggregates. Data treatment of the chromatograms has been made using linear interpolation of the Log M *vs.* retention volume curves, which usually provides only an approximate evaluation of the DP_n. Moreover, the low molar mass region is affected by the presence of hemicelluloses which lowers the value of DP_n and increase the polydispersity.

	Untreated pulp	CH	CH+CH	CH+CH+CH	CH + E	CH+E+CH
TAPPI viscosity (mPa.s)	10.8	11.0	10.8	10.4	10.2	10.2
DP_v in CUED calculated from TAPPI viscosity*	949	960	951	925	912	915
Peak DP	1541	1690	n.d.	1640	1550	1430
DP_w	2416	2601	n.d.	2564	2516	2453
DP_n	391	427	n.d.	419	452	402
Polydispersity (DP_w/DP_n)	6.2	6 .1	n.d.	6.1	5.6	6.1
$<[\eta]>$ (dL/g)	4.58	4.32	n.d.	4.26	4.32	4.06
$<R_h>$ (nm)	40.6	41.4	n.d.	40.9	40.9	39.1
$<R_g>$ (nm)	80.2	74.7	n.d.	70.4	69.3	65.8
MHS-law parameters (Log K; a)**	(-3.559; 0.703)	(-3.683; 0.714)	n.d.	(-3,503; 0.685)	(-3.662; 0.713)	(-3.690; 0.716)
Recalculated DP_v from MHS-law parameters	1940	2150	n.d.	2080	2050	1920

*Calculated by the formula: $DP_V = 10^{\frac{\log\left[0.75\times(954\times\log T-325)\right]}{0.905}}$ (T = TAPPI viscosity)

** Mark-Houwink-Sakurada law: $DP_V = \frac{1}{M_{monomer}}\left(\frac{[\eta]}{K}\right)^{1/a}$ (a; K: MHS-law parameters)

Table 1. CUED viscosities and size-exclusion chromatographic data of the different samples.

Results for molar mass distribution and R_h *vs.* Log M curves are presented in **Figures 1 and 2**. The MMD curves appear to be quite well reproducible and superimposed. DP values can be calculated from M by dividing by 519, the molar mass of the CTC repeating unit. The main peak at $10^{5.9}$ Da (DP of about 1500) represents the main cellulose population. A second peak that appears as a shoulder at $10^{6.7}$ – $10^{6.8}$ Da corresponds to high molar mass molecules (DP of about 10^4), likely to be molecular aggregates. This peak exhibits a rather similar intensity on the different curves and seems not to be affected by the CH or E treatments. At $10^{4.8}$ Da (DP of about 80), the peak corresponds to the small chains of hemicelluloses, which appear to be rather stable and therefore not eliminated during the treatments.

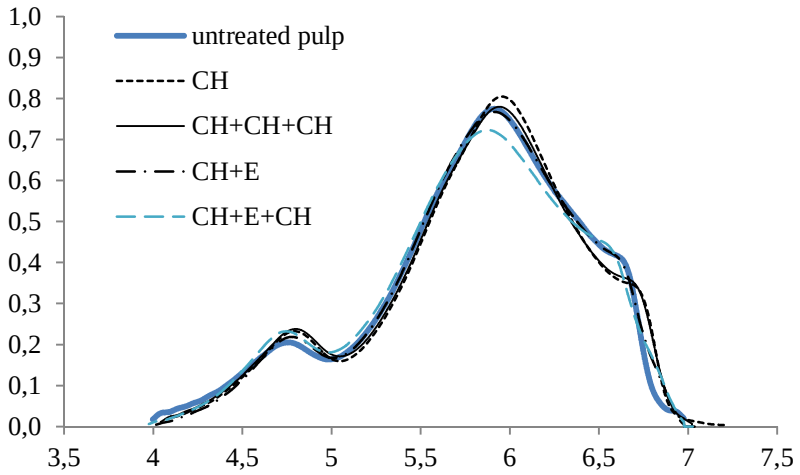

Figure 1. Molar mass distribution curves (dW/d Log M *vs.* Log M) of the different samples.

The evolution of the hydrodynamic radius *vs.* Log M curve (**Figure 2**) also exhibits quasi-perfect superimposition of the curves, which shows no change in the molecular conformation of cellulose during the different treatments. Similar superimposition of the curves was observed for the $[\eta]$ *vs.* Log M curves (not represented), from which R_h was calculated by the Einstein law: $R_h = \left(\frac{3[\eta]M}{10\pi N_{av}}\right)^{1/3}$.

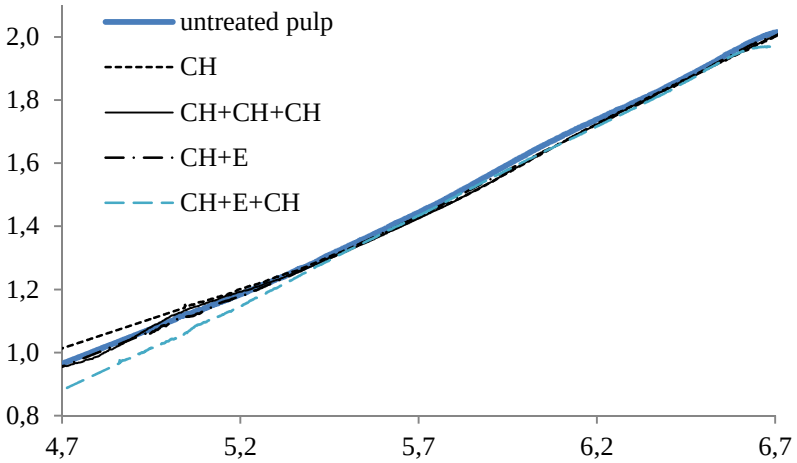

Figure 2. Log R_h *vs.* Log M curves of the different samples.

IV. CONCLUSIONS

Repeated holocellulose treatments, applied on a bleached Eucalyptus kraft pulp at room temperature, high chlorite charge (313% active chlorine), with or without alkaline extraction, appear to be quite innocuous for the cellulose degree of polymerization and preservative for hemicelluloses. CUED viscosity and SEC-multidetection measurements exhibited slightly different results and tendencies, from which no evidence for significant degradation of the pulp was found, but possibly, a slight tendency for very few depolymerization of cellulose. This work is a preliminary step for further studies on inert delignification treatments to be applied on lignified samples from biorefinery studies. The cold holocellulose procedure appears to induce very little or no cellulose degradation, contrary to reinforced hot holocellulose procedures described in the literature.

V. ACKNOWLEDGEMENT

The authors acknowledge Mrs. K. Janel for assistance in the preparation of the treated samples.

VI. REFERENCES

[1] Hubbell, C.A.; Ragauskas, A.J. Effect of acid-chlorite delignification on cellulose degree of polymerization. *Bioresource Technology*. **2010**, *101*, 7410–7415.

[2] Kumar, R.; Hu, F.; Hubbell, C.A.; Ragauskas, A.J.; Wyman, C.E. Comparison of laboratory delignification methods, their selectivity, and impacts on physiochemical characteristics of cellulosic biomass. *Bioresource Technology*. **2013**, *130*, 372–381.

[3] Hussain, A.; Germgard, U. Using chlorite delignification to simplify characterisation of chemical pulps. *Appita*. **2011**, *64*, 257–261.

[4] Ahlgren, P.A.; Goring, D.A.I. Removal of wood components during chlorite delignification of black spruce. *Can. J. Chem.* **1971**, *49*, 1271–1275.

[5] Kerr, A.J.; Goring, D.A.I. The role of hemicellulose in the delignification of wood. *Can. J. Chem.* **1975**, *53*, 952–959.

[6] Lapierre, L., Bouchard, J. Molecular weight determination of softwood kraft cellulose. *9th ISWPC*, Montreal, Canada, **1997**, *Proceedings vol. 1*, L6-1–L6-6.

[7] Berggren, R., Berthold, F., Sjöholm, E., Lindström, M. Fibre strength in relation to molecular mass distribution of hardwood kraft pulp. Degradation by ozone and acid hydrolysis" *NPPRJ*. **2001**, *16*, 333–338.

CARBOHYDRATE LOSS REACTIONS DURING VISCOSE MANUFACTURE

Danuta J. Mozdyniewicz[1], Kaarlo Nieminen[2], Gabriele Schild[3], Herbert Sixta[2]*

[1]Kompetenzzentrum Holz GmbH, Altenberger Str. 69, 4040 Linz, Austria ; [2]Department of Forest Products Technology, Aalto University School of Chemical Technology, Vuorimiehentie 1, P.O. Box 16300, Espoo; [3]Lenzing AG, Werkstrasse.1, 4860 Lenzing, Austria;

*(*herbert.sixta@aalto.fi)*

ABSTRACT

Although the production of viscose fibres has been known for more than a century now, improvements are still of high economical interest, such as increasing the fibre yield or the isolation of by-products of high added value. The pulp components are exposed to varying conditions during the manufacturing process. Strong alkaline conditions are applied during steeping to dissolve most of the hemicellulose and to activate the cellulose for subsequent xanthation. Additionally, the carbohydrate fractions are subjected to alkaline degradation reactions of varying extent.

A comprehensive kinetic model was developed for process simulation of alkaline cellulose degradation comprising primary and secondary peeling, stopping and alkaline hydrolysis.

For this purpose a TCF bleached beech sulfite dissolving pulp was treated with sodium hydroxide at 40, 50 and 60 °C for time periods up to 80 hours. Oxygen was excluded to inhibit undesired oxidation of the substrate. An attempt of detailed characterisation of all obtained fractions was made using both, established and novel analytical methods. Molar mass distribution, carboxyl and carbonyl group content of the alkali insoluble fraction were determined and confirmed the assumptions of the model. Further, a variety of alkali soluble degradation products was identified.

In the last step of the viscose process, cellulose fibres are regenerated in an acidic spinning bath. Viscose samples of different composition were prepared and spun in a lab scale spinning machine under standardized conditions. Further, the never dried viscose fibres with different hemicellulose contents were subjected to long term degradation in a standard spinning bath at 50 °C. The changes in fibre properties and the gain of the TOC in the solution were monitored.

I. INTRODUCTION

During the viscose process, carbohydrates are exposed to extreme conditions concerning the pH. Especially cellulose is subjected to a broad range of different types of reactions, mostly leading to undesired yield loss. In the first step the pulp is mixed with alkali to dissolve the remaining hemicellulose and to convert cellulose I into cellulose II in order to enhance the reactivity. Under alkaline conditions an enolate group is formed at the reactive reducing end group of a cellulose molecule, leading to endwise degradation due to chemical peeling (β-elimination). As a result a shortening of the molecule and the elimination of the soluble isosaccharinic acids occurs. Stopping is a competing reaction to peeling and leads to an alkali stable metasaccharinic acid (3-deoxy-D-gluconic acid) end group [1]. At higher temperatures and pH values alkaline hydrolysis may occur as a third possible reaction [2]. It results in random chain scission and forming of new reducing end groups that undergo secondary peeling. So far, secondary peeling has not been considered in the models present in the literature.

The strong acidic conditions during spinning lead to cellulose bond cleavage due to hydrolysis. Under strong acidic conditions, the amorphous parts of the cellulose are degraded in the first place. After prolonged treatment times, the reaction proceeds, until the Level-off-DP is reached [3]. The residual crystalline fraction is degraded with a markedly lower reaction rate. Hemicellulose is assumed to degrade by a similar mechanism with a much higher reaction rate due to its amorphous character [4].

II. EXPERIMENTAL

Alkaline treatment

A TCF bleached beech sulfite pulp was treated with sodium hydroxide at 40, 50 and 60 °C for time periods up to 40 hours to derive the time dependence of the cellulose degradation. An initial ten minutes steeping by vigorous stirring was applied to remove residual hemicelluloses and ensure a homogenous cellulose suspension in the aqueous lye. Oxygen was excluded to inhibit undesired oxidation of the substrate. The insoluble cellulose was separated, washed neutral and air dried. The resulting filtrate contained acid precipitable hemicelluloses (β-fraction) as well as soluble cellulose degradation products (γ-fraction). The formation and properties of the solid residue as well as the degradation products in the lye were monitored.

Acidic treatment

Viscose dope was prepared from the same pulp as used for the steeping experiments. The fibers were spun into a standard spinning bath, collected, washed neutral and stored cooled. Additionally to common fiber composition, xylan enriched fibers were prepared by using hemicellulose rich lye as dissolving lye. The never dried fibers were, again, treated with standard spinning bath at 50 °C for time periods up to 260 hours in Erlenmayer flasks. After a certain time period, the fibers were separated from the solution, washed neutral and their mass and intrinsic viscosity was determined after air drying. The TOC of the remaining solutions was measured.

III. RESULTS AND DISCUSSION

Alkaline reaction kinetics

As already mentioned, no appropriate model describing the cellulose reactions, including secondary peeling was present in the literature. Therefore a suitable solution for the problem had to be found. In our approach, the fraction of degraded cellulose units P may be calculated with following equations

$$P = 1 - \left(\frac{1}{2} + \gamma\right) e^{-(\alpha+\beta)t} - \left(\frac{1}{2} - \gamma\right) e^{(\alpha-\beta)t}$$

$$\alpha = \frac{1}{2}\sqrt{(k_s - k_h)^2 - 4k_h k_p}\,, \quad \beta = \frac{1}{2}(k_h + k_s) \text{ and } \quad \gamma = \frac{k_h + 2R_0 k_p - k_s}{2\sqrt{(k_h - k_s)^2 - 4k_h k_p}}$$

where k_p is the first-order rate constant for the peeling reaction, k_s is the first-order rate constant for the stopping reaction and k_h represents the rate constant of alkaline hydrolysis [5, 6].

Based on the model, further calculations enable to determine the contribution of the particular reaction type [7]. The results for our data are visible in **Figure 1**. The relevance of secondary peeling for the cellulose yield loss is increasing with treatment time, whereas primary peeling does not longer proceed after the formation of metasaccharinic acid at the reducing end.

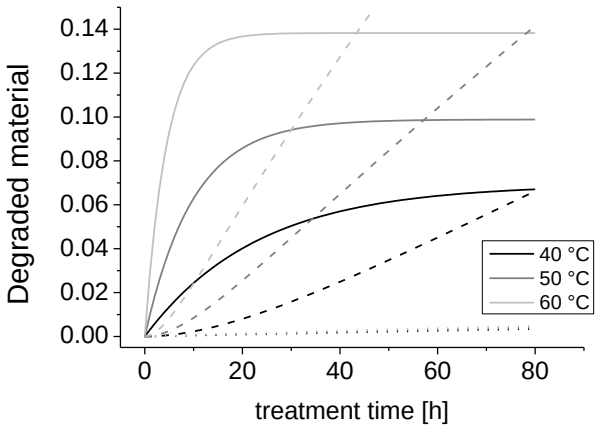

Figure 1. Partition of degraded cellulose respectively the reaction type; solid lines – primary peeling, dashed lines – secondary peeling, dotted lines – alkaline hydrolysis

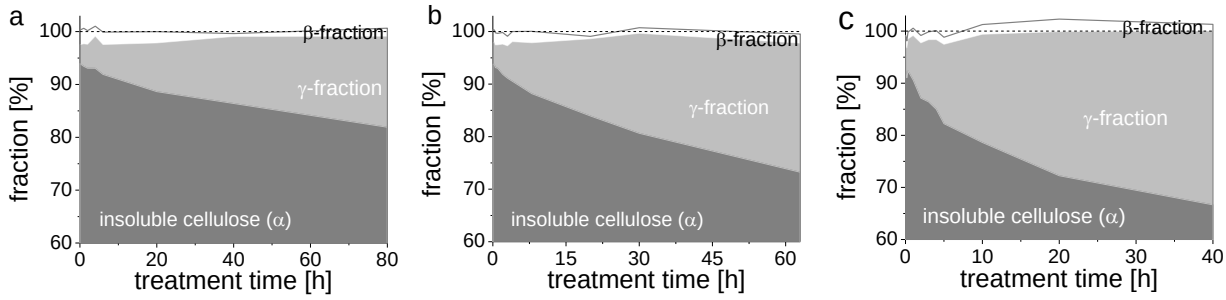

Figure 2. Fractional distribution of the solid residue and degradation products dependent on the treatment temperature; a: 40 °C; b: 50 °C and c: 60 °C in wt%.

Besides the investigation of insoluble cellulose, the influence of the treatment conditions on the lye soluble residues was examined. A fractionation of the dissolved matter was accomplished by changes in the pH to lower values. The amount of the fractions was indirectly determined by TOC-analysis of the lye and the acidic solution. The mass balance of the entire system was obtained by calculation of the yields of all of the fractions and their sum for each experiment. The following assumptions were made for the mass calculation: the β-fraction was considered to be consisting of anhydroxylan units with a conversion factor of TOC/xylan = 0.4545 and the γ-fraction was treated as anhydrocellulose with a factor of TOC/cellulose = 0.4440. The addition of the insoluble cellulose yield and the soluble components resulted in a recovery rate of 100 % with a deviation of ± 2 %. The distribution of all fractions for the different temperatures is illustrated in **Figure 2**.

Acidic reaction kinetics

Viscose Fibers with comparable DP and different hemicellulose content were subjected to degradation in a standard spinning bath. The reaction rates were calculated with the equation introduced by Calvini [3]

$$\left(\frac{1}{DP_t}\right) - \left(\frac{1}{DP_0}\right) = \left(\frac{1}{LODP} - \frac{1}{DP_0}\right)(1 - e^{-kt})$$

where DP_0 is the initial degree of polymerization, DP_t is the degree of polymerization at the time t and $LODP$ is the Level-off degree of polymerization.

A LODP of 90 was determined for the fibers. The same model was used for both, standard and xylan enriched fibers, as hemicellulose was assumed to follow a similar degradation mechanism [4]. Slightly higher reaction rate constant was determined for the hemi-rich fibers ($k = 9.3*10^{-3}$ h^{-1}) in comparison with the standard ($k = 6.6*10^{-3}$ h^{-1}). The progression of the chain scissions is illustrated in **Figure 3**. Hemicellulose is known to degrade with a higher rate compared to cellulose. Yet, in this case, the higher reaction rate could not be ascribed to xylan degradation, since its DP was significantly lower and the amount present was small.

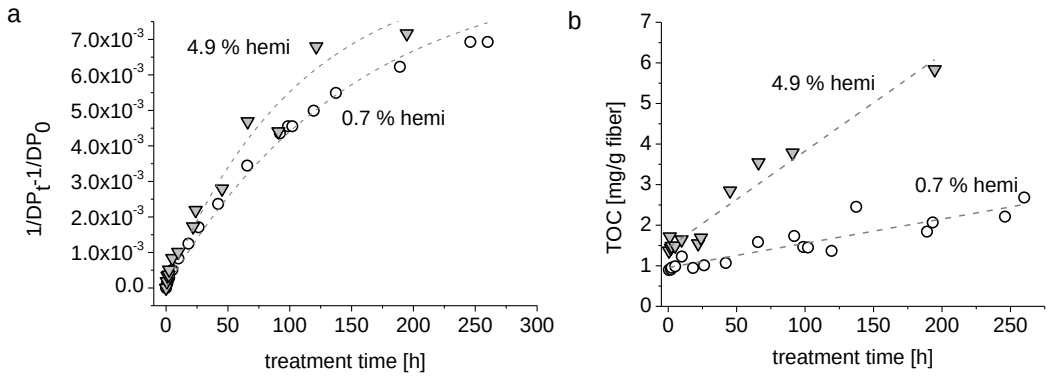

Figure 3. Kinetics of fiber degradation after acidic treatment (a) and the corresponding TOC formation in the solution (b)

Therefore, higher cellulose accessibility was assumed, as a consequence of xylan dissolution and the resulting gaps [8]. A negligible increase in degradation products concentration was determined in the solutions after standard fiber treatment. This seems reasonable, since no significant yield loss was observed, even after long treatment times. Degradation of xylan enriched fibers resulted in higher TOC increase in the liquid phase, due to a higher hemicellulose loss reaction rate.

IV. CONCLUSIONS

A novel model was developed, describing cellulose degradation in alkaline media, including secondary peeling:

- it enables a detailed description of cellulose reactions
- contribution of the particular reaction type may be calculated
- improved steeping process control

Standard viscose fibers and xylan enriched fibers were subjected to acidic degradation in spinning bath:

- good agreement for description of the reaction kinetics with an existing model
- higher degradation rate of xylan enriched fibers due to higher cellulose accessibility
- increased reaction rate leads to enhanced formation of degradation products

V. ACKNOWLEDGEMENT

Financial support was provided by the Austrian government, the provinces of lower Austria, upper Austria, and Carinthia as well as by Lenzing AG. We also express our gratitude to the Johannes Kepler University, Linz, the University of Natural Resources and Applied Life Sciences, Vienna, and Lenzing AG for their in-kind contributions.

VI. REFERENCES

[1] Van Loon, L.R., et al.; Degradation of cellulosic materials under the alkaline conditions of a cementitious repository for low- and intermediate-level radioactive waste. II. Degradation kinetics. *J Environ Polym Degrad*, **1999**. *7*(1), 41-51.

[2] Lai, Y.-Z. and Sarkanen, K.V.; Kinetics of alkaline hydrolysis of glycosidic bonds in cotton cellulose. *Cellul Chem Technol*, **1967**. *1*, 517-527.

[3] Calvini, P.; The influence of levelling-off degree of polymerisation on the kinetics of cellulose degradation. *cellulose*, **2005**. *12*, 445 - 447.

[4] Jacobsen, S.E. and Wyman, C.E.; Celllulose and hemicellulose hydrolysis models for application to current and novel pretreatment processes. *Appl Biochem Technol*, **2000**. *84 - 86*, 81 - 96.

[5] Mozdyniewicz, D.J., Nieminen, K., and Sixta, H.; Alkaline steeping of dissolving pulp. Part I: Cellulose degradation kinetics. *Cellulose*, **2013**. *20*(3), 1437 - 1451.

[6] Testova, L., et al.; Cellulose degradation in alkaline media upon acidic pretreatment and stabilisation. *Carbohyd Polym*, **2014**. *100*, 185 - 194.

[7] Nieminen, K., Paananen, M., and Sixta, H.; A kinetic model for carbohydrate degradation and dissolution during kraft pulping. *submitted to Ind Eng Chem Res*, **2014**.

[8] Gehmayr, V., Schild, G., and Sixta, H.; A precise study on the feasibility of enzyme treatments of a kraft pulp for viscose application. *Cellulose*, **2011**. *18*(2), 479-491.

EFFECTIVENESS OF THE RAPID RELEASE OF PRESSURE DURING THE STEAM EXPLOSION PRETREATMENT

Muhammad Muzamal, Anders Rasmuson*
Chemical and Biological Engineering
Chalmers University of Technology, Gothenburg, Sweden
rasmuson@chalmers.se;

ABSTRACT

Wood material is difficult to digest by enzymes during enzymatic hydrolysis to obtain fermentable sugar and ethanol because of its complex chemical composition and physical structure. Steam explosion (SE) is a promising pretreatment that increases the enzymatic accessibility by chemical and physical effects. In this process wood is treated with high pressure steam for a certain time. After this treatment step, the pressure is reduced rapidly which causes the vapour inside the wood to expand and exert pressure on the cell walls. This pressure causes alteration in cell structure which increases enzyme penetration. Existing literature on the steam explosion process provides limited information about the parameters that should be considered for SE equipment design. In this study, we have performed experiments on single wood pieces to study the effectiveness of the explosion step. Mercury porosimetry analysis is performed to characterize the structural changes in steam exploded wood. It has been found that the ratio of area of steam discharge valve to volume of steam treatment vessel (A/V) is an important parameter that can affect the explosion step. A large increase in average pore diameter of steam exploded wood is observed with increase in A/V ratio. Efficient explosion depends on pressure decrease rate inside wood chip and in the vessel. Net pressure experienced by cells in the wood is the difference between pressure inside the wood cells and the pressure in the vessel at any instant. A/V ratio is an important parameter that should be considered during the steam explosion equipment design.

I. INTRODUCTION

Fermentable sugar obtained by enzymatic hydrolysis of untreated wood is almost negligible because of complex chemical composition and physical structure of wood [1]. A pretreatment process which increases the accessibility of enzymes to hemicelluloses and cellulose is thus necessary. The steam explosion (SE) pretreatment is the most widely employed pretreatment for lignocellulosic biomass [2]. Grous et al. [1] found remarkable increase in glucose yield in steam exploded wood as compared to unexploded wood.

The SE process is a combination of both chemical and physical effects. First wood chips are treated with steam at high pressure and temperature for certain time (2 - 20 min) which causes the chemical linkages between lignin and polysaccharides to cleave. Then the pressure is rapidly decompressed inducing physical effects where the vapours inside the wood expand and exert stresses on the cell walls [3]. These physical effects cause an increase in pore size of the wood [4] and cracks in the cells and rupture in pits which increase the effectiveness of the SE process [5].

The SE process is optimized if both chemical and physical effects are optimized. Several studies have been conducted to find the conditions (time and temperature) to optimize chemical effects for obtaining high yield for different biomass [6], [7]. Maximum efficiency of steam explosion process is obtained if the physical effects are also optimized [8], [9]. The stresses experienced by the cells during rapid decompression depend on the net pressure difference ΔP exerted on the cell walls. The ΔP can be calculated by the difference in pressure inside and outside the wood.

$$\Delta P = P_{inside\ wood} - P_{vessel}$$

The pressure inside the wood is the saturated steam pressure at the corresponding temperature [10]. The temperature inside wood chips is controlled by heat and mass transport mechanisms and depends on the

permeability of the wood material and surrounding pressure. There is no study available to calculate the change in pressure inside the wood during rapid decrease of vessel pressure.

The outside pressure is the vessel pressure. The ΔP is high if the pressure in the vessel decreases at high rate. The present study focuses on the parameter that influences the pressure decrease rate in the vessel. This parameter is the ratio of the area of steam discharge valve to volume of steam treatment vessel (A/V).

II. EXPERIMENTAL:

Two steam explosion vessels, with A/V = 0.13 m^{-1} and A/V = 0.28 m^{-1}, were built. In these vessels, experiments with single wood chips could be performed. During the SE experiments the wood pieces were contained inside a wire frame in which they were free to move and expand due to vapour expansion but not escape from the frame and collide with the walls of the equipment.

Wood pieces with dimensions of 60 mm x 20 mm x 4 mm of Norway spruce (sapwood) were used as samples. These were divided into two parts (small pieces with dimension 30 mm x 20 mm x 4 mm). These small wood pieces were taken from the same annual rings which make the samples comparable. The wood pieces were impregnated in water under 5 bar pressure at room temperature for 24 hr before SE. Experiments were performed with saturated steam at 10 bar (180 ^{O}C) with treatment time of 10 min. After the experiments mercury porosity analysis was performed to analyze the effects of steam explosion on available pore size.

Mercury porosimetry analysis of wood

Mercury porosimetry is a useful technique for structural characterization of wood [11]. This technique can be used to find sample's total pore volume, porosity and pore size distribution. The pore diameter is calculated by the Washburn equation [12]:

$$D = -\frac{4\gamma cos\theta}{P}$$

where D is the pore diameter, γ is the surface tension = 0.485 N/m, θ is contact angle = 130^{O} and P is pressure. An average pore diameter is calculated as

$$D_{avg} = 4V/A$$

where V is total intrusion volume and A is total pore area.

III. RESULTS AND DISCUSSION

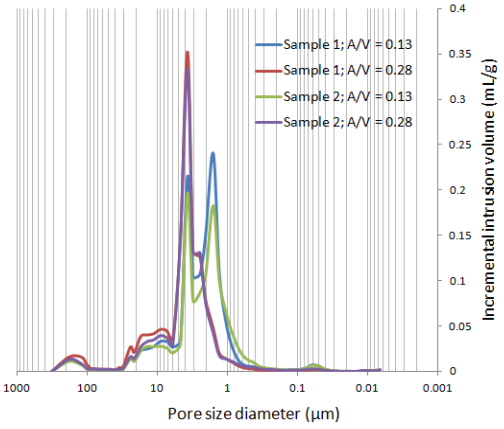

Figure 1. Incremental intrusion volume for different pore size in wood

Figure 1 illustrates pore size distribution for steam exploded wood in two different steam treatment vessels. There are significant differences in intrusion volume for different A/V ratio. Also an increase in average pore diameter is observed with increase in A/V ratio. Average pore diameter of two samples increased from 770 and 940 µm at A/V = 0.13 m^{-1} to 1420 and 1140 µm at A/V = 0.28 m^{-1}. Thus A/V ratio is an important parameter in steam explosion equipment design. The increase in A/V ratio causes the pressure in the vessel to decrease faster. Below we have calculated the effect of A/V ratio on pressure decrease in the vessel.

Pressure in vessel

As the explosion starts the pressure in the vessel decreases rapidly and the flow can be shown to enter the choked (sonic) flow regime. This occurs when the ratio of source pressure to the downstream pressure is equal to or greater than $[(k+1)/2]^{k/(k-1)}$, where k is specific heat ratio. For steam, k = 1.3 and the term becomes 1.83. Thus if the vessel pressure is higher than 1.83 atm (usually the case), and the decompression pressure is atmospheric pressure, the condition for choked flow is fulfilled. At this condition the pressure in the vessel can be calculated using expression [13]:

$$P_{vessel}^{(1-k)/2k} = P_0^{(1-k)/2k} + (t - t_0).\frac{CA}{V}.\frac{(k-1)}{2k}\sqrt{\frac{g_c R k^3}{M}.\left(\frac{T_0}{P_0^{(k-1)/k}}\right)\left[\frac{2}{k+1}\right]^{(k+1)/(k-1)}}$$

For vessels with A/V = 0.13 or 0.28 m^{-1}, discharge coefficient = 0.59 [14], with initial pressure of 10 bar at t = 0; the vessel pressure decrease with time as shown in Figure 2.

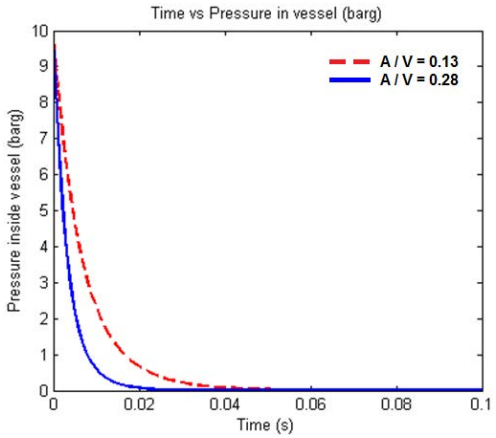

Figure 2. Pressure decrease in steam explosion vessel with time

It can be seen that the pressure decrease is faster for large A/V ratio. If the pressure decrease from the vessel is faster, then the ΔP will be higher. In order to obtain maximum effect from the explosion step, the pressure release rate in the vessel must be high. For batch steam explosion equipment this can be achieved by increasing the A/V ratio.

IV. CONCLUSIONS

Steam explosion increases digestibility of the wood material by chemical and physical effects. The process is optimized if both effects are optimized. The rapid decrease of pressure during the explosion step causes the increase in pore size of the wood. In order to obtain maximum effects from the explosion step, pressure release rate in the vessel must be high. For the batch steam explosion process, the pressure release rate increases with increase in the ratio of area of steam discharge valve to volume of steam treatment vessel. Badly designed steam explosion equipment may cause less pressure difference on cell walls resulting in no effect of explosion and no opening of structure.

V. ACKNOWLEDGMENT

Chalmers Energy Initiative is gratefully acknowledged for financial support.

VI. REFERENCE

[1] Grous, W. R.; Converse, A. O.; Grethlein, H. E. Effect of steam explosion pretreatment on pore size and enzymatic hydrolysis of poplar. *Enzyme Microb Technol.* **1986**, 8, 274-280.

[2] Alvira, P.; Tomás-Pejó, E.; Ballesteros, M.; Negro, M. J. Pretreatment technologies for an efficient bioethanol production process based on enzymatic hydrolysis: A review. *Bioresource Technol*. **2010**, 101, 4851-4861.

[3] Muzamal, M.; Gamstedt, E. K.; Rasmuson, A. Modeling Wood Fiber Deformation Caused by Vapor Expansion during Steam Explosion of Wood. *Wood Sci Technol*. **2014**, 48, 353-372.

[4] Muzamal, M. Steam Explosion of Wood. Licentiate Thesis, *Chalmers University of Technology, Gothenburg*. **2014**, ISSN1652-943X.

[5] Zhang, Y.; Cai, L. Effect of steam explosion on wood appearance and structure of sub-alpine fir. *Wood Sci Technol.* **2006**, 40, 427-436.

[6] Toussaint, B.; Excoffier, G.; Vignon, M. R. Effect of steam explosion treatment on the physico-chemical characteristics and enzymic hydrolysis of poplar cell wall components. *Animal Feed Sci Technol.* **1991,** 32, 235-242.

[7] Vivekanand, V.; Olsen, E. F.; Eijsink, V. G. H.; Horn, S. J. Effect of different steam explosion conditions on methane potential and enzymatic saccharification of birch. *Bioresource Technol.* **2013**, 127, 343-349.

[8] Zhang, Y.; Chen, H. Multiscale modeling of biomass pretreatment for optimization of steam explosion conditions. *Chem Eng Sci*. **2012,** 75, 177-182.

[9] Zhengdao, Y.; Bailiang, Z.; Fuqiang, Y.; Guizhuan, X.; Andong, S. A real explosion: The requirement of steam explosion pretreatment. *Bioresource Technol.* **2012,** 121(0), 335-341.

[10] Li, X.; Zhou, Y.; Yan, Y.; Cai, Z.; Feng, F. A single cell model for pretreatment of wood by microwave explosion. *Holzforschung*. **2010**, 64, 633-637.

[11] Moura, M. J.; Ferreira, P. J.; Figueiredo, M. M. The use of mercury intrusion porosimetry to the characterization of eucalyptus wood, pulp and paper. *Iberoamerican Congress Pulp Pap Res.* **2002**.

[12] Washburn, E. W. Note on a Method of Determining the Distribution of Pore Sizes in a Porous Material. *Proc Natl Acad Sci USA*. **1921,** 7(4), 115-116.

[13] Rasouli, F.; Williams, T.A. Application of dispersion modelling to indoor gas release scenarios. *J Air Waste Manag Assoc.* **1995**, 45(3), 191-195.

[14] Grose, R. D. Orifice Contraction Coefficient for Inviscid Irrotational Flow. *J Fluid Eng*. **1985**, 107 (1), 36-43.

TWIN-SCREW EXTRUSION PRETREATMENT OF OLIVE-TREE PRUNING FOR FERMENTABLE SUGARS PRODUCTION

*Negro María José, Duque Aleta, Manzanares Paloma, Sáez Felicia, Oliva José Miguel, Ignacio Ballesteros, Mercedes Ballesteros

Biofuels Unit. Energy Department. CIEMAT . Avda Complutense 40, 28040 Madrid –Spain (mariajose.negro@ciemat.es)

ABSTRACT

The present study focuses on the extrusion of olive tree pruning biomass in a one-step alkaline-extrusion process, in order to fractionate biomass and improve sugar production. In this work, a range of pretreatment conditions (temperature, catalyst concentration and screw speed) were evaluated according to different parameters: composition of pretreated substrates, glucose and xylose recovery, degradation products generation, enzymatic hydrolysis yield and overall sugars yield. Results show that enzymatic digestibility is remarkably improved by extrusion although not significant variations are found on the chemical compositions of material extruded at different conditions. The maximum glucose sugar production value, after pretreatment and enzymatic hydrolysis, was close to 210 g/Kg raw material, which corresponds to about 69 % of the theoretical production yield.

I. INTRODUCTION

Olive tree pruning (OTP) biomass is a large available renewable agricultural residue in the Mediterranean countries with no industrial applications. In Mediterranean areas, the residual biomass from olive pruning reaches an average 1.31 t ha-1 in annual and 3.02 t ha-1 in biennial pruning [1]. A typical OTP lot includes leaves (around 25% by weight), thin branches (around 50% by weight), and thick branches or wood (25% by weight), although the proportions may vary depending on culture conditions, tree age, production and local pruning practice. This biomass constitutes an important energy and chemicals source that, till date, is not being used. This residue contains variable amounts of carbohydrate as well as phenolic and terpenic compounds, etc., which makes it an interesting source for bio-refinery products [2]. The composition of OTP biomass permits to develop a multiproduct industry that takes advantage of the various components in biomass and their intermediates therefore maximizing the value derived from the biomass feedstock.

As an alternative, olive tree pruning residues may be used as raw material for ethanol production or other added value products from sugars. Due to the recalcitrant nature of the lignocellulose, a pretreatment step is required for increasing fermentable sugars in the hydrolysis step. It is necessary to choose pretreatment conditions that produce highly digestible solid material resulting in high sugar yields from enzymatic hydrolysis and at the same time preventing the degradation of soluble sugars, so maximizing overall sugar yield. Many pretreatment methods have been evaluated for ethanol production [3]. . Extrusion process is a novel and promising physical pretreatment method for biomass fractionation that offers several attractive features when compared to other pretreatment technologies. In extrusion pretreatment, the materials are subjected to heating, mixing and shearing, resulting in physical and chemical modifications during the passage through the extruder [4]. Screw speed and barrel temperature are believed to disrupt the lignocellulose structure causing defibrillation and shortening of the fibers, and, in the end, increasing accessibility of carbohydrates to enzymatic attack [4]. The different extrusion parameters must be taken into account to achieve the highest efficiency in the process. Recent studies showed a significant improvement on sugar recovery from switchgrass [4], corn stover [5], Miscanthus *(M. sacchariflorus*) [6], pine wood [7] and barley straw [8] through enzymatic hydrolysis.

II. EXPERIMENTAL

OTP was collected after fruit-harvesting, air-dried at room temperature to equilibrium moisture content of about 10%, and milled using a hammer mill to a particle size smaller than 4 mm. fraction 1-4 mm was utilized.

Extrusion was performed in a twin-screw extruder (Clextral Processing Platform Evolum® 25 A110, Clextral, France), composed of 6 modules of 100 mm length each. The screw profile has been previously described [8]. Operating conditions were set to achieve moderate values of NaOH/DM ratio, 5 and 10 % (w/w), barrel temperature (70, 90 and 110 ºC) and screw speed of 70 and 150 rpm. Run pretreatments were performed in triplicate. After extrusion, solid extruded material was recovered and washed thoroughly with distillate water until neutral pH. The filtrate was also collected and their content in total soluble solids and sugars were analyzed. A portion of washed solid extrudate was dried and analyzed for carbohydrates and lignin composition.

The washed water-insoluble residue of pretreated OTP was enzymatically hydrolyzed by the novel enzyme preparations Cellic CTec2 and Cellic HTec2, both from Novozymes. The assays were run in 50 mM sodium citrate buffer (pH 5) at 50 ºC, 150 rpm, for 72 h and 5% (w/w) substrate consistence. Samples were withdrawn, centrifuged at 9300 g for 10 min and the supernatants were analysed for sugars concentration measured by HPLC as described elsewhere [8]. Additionally, blanks of the enzyme mixtures were analyzed by HPLC to subtract the sugar content present in the enzyme preparations used. Enzymatic hydrolysis yields (EH) were calculated as the glucose/xylose release during enzymatic hydrolysis divided by the potential glucose/xylose (calculated based on the glucan/xylan content in the insoluble solid), and expressed as percentage. Average values of the three replicates were presented.

Raw material and solid fraction obtained after pretreatment (WES) composition were determined according to National Renewable Energy Laboratory (NREL) analytical methods for biomass [7].

III. RESULTS AND DISCUSSION

OTP biomass has 22.3% of cellulose and 17.4% hemicellulose (o.d.w.). Acid insoluble lignin content (AIL) accounts for 14.6%. Considering acid-soluble lignin content (fraction of lignin that is solubilized during the hydrolysis process used to determine AIL), the total lignin value increases up to 17.8%. Acetyl groups represent about 2.3% of raw material and 4.1 % total ash. It is worth noticing that this lignocellulosic residue has an extractive content of 24.5%, which includes 6.2% of glucose (mostly as oligosaccharides, mainly starchyose and raffinose). Other sugars were present in the water extract in trace amounts. The proportion of the extractive fraction was greater than that reported for other agricultural residues like barley straw. The high proportion of extractives could be related to a higher content of leaves in the raw material.

In order to evaluate the efficiency of extrusion as a method to fractionate olive tree punning and so affect the enzymatic digestibility of the carbohydrates, changes in the composition of washed extruded solid (WES) obtained at different pretreatment conditions with respect to the raw material were measured. In addition, filtrate fraction was analyzed for sugar composition.

The sugar compositions in the filtrate fraction are depicted in **Figure 1**. The sugar content ranged from 6.9 to 11.8 g/100 g OTP. It is worth noting that glucose is the most abundant sugar in the liquid fraction at any condition. Considering that non-structural derived glucose was present at high proportion in the aqueous extract fraction of raw material, it is likely that the most part of this component was transferred to liquid fraction after one-step alkaline-extrusion process. The second major sugar found in filtrates was mannitol, sugar concentration of this sugars ranged from 1.65 to 3.5 g/100 g OTP. This component, with interesting applications in the food and pharmaceutical industries, is also present in olive tree leaves [10].

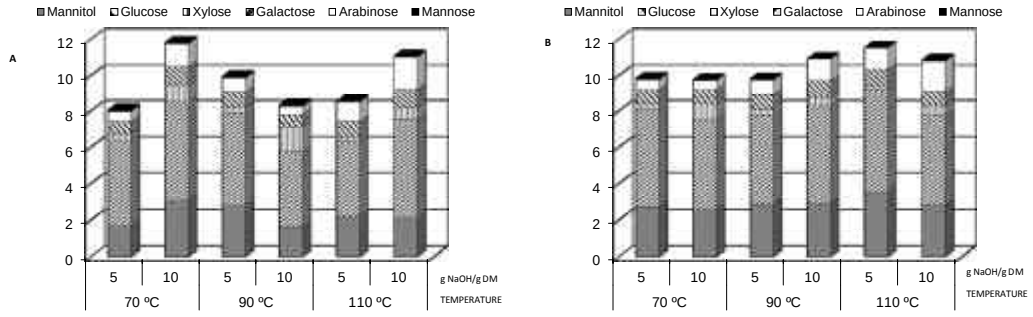

Figure 1. Sugars composition in filtrate (g/100 g OTP). Screw speed: A) 70 rpm and B) 150 rpm

The alkali-extrusion pretreatment resulted in cellulose and hemicellulose enriched-solid (results in **Table 1**). Glucan (values ranging from 31.4 to 38.8 %), is the main component of WES. Hemicellulose content in WES ranges from 21.2 to 26.5 %, while AIL was 24.4-27.3%. The recovery of glucan is in the range 92-100 % in the solid fraction. Xylan recovery in both liquid and the solid fraction varies from 95 to 100%. High values of hemicellulose-sugars recovery in the pretreated solid would be interesting to increase the total fermentable sugars production by enzymatic hydrolysis.

The main objective of pretreatment is to alter the structure of the fibers in order to increase the accessibility of enzymes to cellulose. So, the effect of temperature, alkali concentration and screw speed on the enzymatic digestibility of the solid fraction obtained after extrusion pretreatment was evaluated and results are shown in **Table 1**. EH_G yield depends on the barrel temperature and in general, EH_G yield increases as the temperature rises. The untreated raw material displayed maximum EH_G yield about 8 % after 72 h enzymatic hydrolysis in tests performed in parallel to pretreated substrates and 13-15% EH_G yield when extrusion pretreatment was undertaken with water instead of alkali (data not shown). The alkali extruded samples exhibited a higher digestibility, yielding up to 65%. The EH yield increased with NaOH loading and barrel temperature, but screw speed effect was not significant.

Table 1. Composition of washed extruded solid (WES), glucan enzymatic hydrolysis yield ($EH_{G,}$ %), xylan enzymatic hydrolysis yield ($EH_{X,}$ %), overall glucose yield ($g.Kg^{-1}$ OTP) and overall xylose yield ($g.Kg^{-1}$ OTP)

Screw speed (rpm)	Temperature (ºC)	Composition content (%)				Enzymatic hydrolysis yield ($EH_{G,}$ %)	Enzymatic hydrolysis yield ($EH_{x,}$ %)	Overall glucose yield $g.Kg^{-1}$ OTP	Overall xylose yield $g.Kg^{-1}$ OTP
		NaOH g/100g biomass	Glucan	Hemi-cellulose	Lignin				
70	70	5	31.7	21.4	24.4	27.0	24.3	126.3	32.8
		10	31.4	22.3	24.5	46.0	42.3	161.4	61.3
	90	5	35.3	21.2	25.5	28.7	31.1	128.3	41.0
		10	32.7	22.2	25.1	35.1	34.2	144.4	48.1
	110	5	38.3	24.5	25.8	33.1	35.7	154.6	49.7
		10	37.0	26.0	25.2	46.7	49.5	194.7	83.9
150	70	5	33.8	23.6	25.2	29.2	22.1	121.8	28.5
		10	34.9	23.3	24.8	51.7	57.0	163.4	74.7
	90	5	34.5	22.9	24.6	22.7	40.9	107.3	50.6
		10	37.2	22.9	24.7	58.3	63.2	190.7	86.5
	110	5	38.8	26.5	24.5	32.4	33.9	137.7	48.7
		10	36.4	23.7	27.3	65.8	69.4	210.1	95.4

On the other hand, xylan conversion yield increases also in all temperatures tested as alkaline concentration raises, attaining values 70% of theoretical in WES at 110ºC and 10 NaOH/g DM and 150 rpm. In untreated material yield was 3%. It means that the digestibility of xylan is greatly improved by one-step alkaline extrusion pretreatment by deconstructing lignocellulose matrix and facilitating the xylanases enzymes. Similar results in xylan hydrolysis were reported on barley straw using the same equipment, where the hydrolysis yield for xylan resulted in 71% of theoretical [8].

In order to optimize the overall process, attention must be paid to several partial objectives, e.g. both cellulose and hemicellulose recovery in the solid residue in the pre-treatment step, and hydrolysis yield in the enzymatic step, some of which may interact with each other. Overall sugar yield, calculated in relation to the raw material for the two phases: pretreatment and enzymatic hydrolysis, is the major indicator of the potential amount of sugars that could be used for ethanol production. Overall sugar yields were evaluated and results are shown in **Table 1.** At the best conditions (150 rpm, 110ºC, 10 g NaOH /100 g DM) an overall yield of glucose of 210.1 g/Kg OTP and 95.4 g xylose/Kg OTP was obtained. A 68.7% of total glucose is available after one-step extrusion pretreatment and enzymatic hydrolysis yield. The maximum sugars recovery recorded in this study was comparable to those obtained in this study was similar to those obtained in pine were a maximum of 66.1% of sugars was obtained (150 rpm 180ºC, 25% moisture) [7].

IV. CONCLUSIONS

- ✓ Extrusion pretreatment has been proved as a method to improve fermentable sugars production by enzymatic hydrolysis of olive tree pruning biomass.

- ✓ Alkali concentration and temperature have significant effect in enzymatic digestibility.
- ✓ One-step alkaline –extrusion process followed by enzymatic saccharification leads to a glucose yield equivalent to 68% of potential glucose present in raw material.

V. ACKNOWLEDGEMENT

This research was supported by funding from Ministerio de Economía y Competitividad (Spain) ref. ENE2011-29112-C02.

VI. REFERENCES

[1] Velázquez-Martín, B.; Fernández-González, E.; López-Cortés, I.; Salazar-Hernández, D.M. Quantification of the residual biomass obtained from pruning of trees in Mediterranean olive groves. Biomass Bioenerg. **2011**, *35*: 3208-3217.

[2] Romero-García, J.M; Niño, L.; Martínez-Patiño, C.; Álvarez, C.; Castro, E.; Negro, M.J. Biorefinery based on olive biomass. State of arte and future trends. http://dx.doi.org/10.1016/j.biortech. 2014.03.062. **2014**

[3] Alvira, P.; E. Tomás-Pejó; M.J. Negro. Pretreatment technologies for an efficient bioethanol production process based on enzymatic hydrolysis: A review. *Biores. Technol.* **2010**, *101*: 4851-4861.

[4] Karunanity C.; Muthukumarappan K. Effect of extruder parameters and moisture content of switchgrass, prairie cord grass on sugar recovery from enzymatic hydrolysis. Appl. Biochem. Biotechnol. **2010**, *162*: 1785-1803.

[5] Liu, C., van der Heide, E., Wang H., Li B., Yu, G., Mu, X. 2013. Alkaline twin-screw extrusion pretreatment for fermentable sugar production. Biotechnology for Biofuels 6: 97.

[6] Kang, K.E.; Han M.; Moon S.K.; Kang H.W.; Kim Y.; Cha Y.L.; Choi G.W. Optimization of alkali-extrusion pretreatment with twin-screw for bioethanol production from Miscanthus. *Fuel* **2013**, *109*: 520-526.

[7] Karunanithy, C.; Muthukumarappan, K. ; Gibbons W.R. Extrusion pretreatment of pine wood chips. *Appl. Biochem. Biotechnol*. **2012**, *167*: 81-99.

[8] Duque, A.; Manzanares, P.; Ballesteros, I.; Negro, M.J.; Oliva, J.M.; Sáez, F.; Ballesteros, M. Optimization of integrated alkaline-extrusion pretreatment of barley straw for sugar production by enzymatic hydrolysis. Process Biochem. **2013**, *48*: 775-781.

[9] Sluiter, J.B.; Ruiz, R.O.; Scarlata, C.J; Sluiter, A.D.; Templeton, D.W. Compositional analysis of lignocellulosic feedstocks. 1. Review and description of methods. *J. Agri. Food Chem*. **2010**, *58*: 9043-9053.

[10] Ghoreishi, S.M.; Shahrestania, R.G. Subcritical water extraction of mannitol from olive leaves. *J. Food Eng.* **2009**, *93*: 474–481.

KRAFT PULPING AND WOOD CHEMICAL COMPOSITION FOR 12 EUCALYPTUS SPECIES

Duarte M. Neiva[1]*, Solange Araújo[1], Ana Lourenço[1], Jorge Gominho[1] and Helena Pereira[1]

[1] *Centro de Estudos Florestais, Instituto Superior de Agronomia, Universidade de Lisboa, Tapada da Ajuda, 1349-017, Lisboa, Portugal; (*duarteneiva@isa.utl.pt)*

ABSTRACT

There are more than 700 species of eucalypts worldwide although only a few are suited and used as pulpwood. In this work we compared the delignification yield and Kappa number of pulps obtained from 12 eucalypt species. We also conducted and compared the chemical analysis regarding ash, extractives, lignin and holocellulose contents, as well as carbohydrate composition. Samples of *E. globulus*, *E. botryoides*, *E. sideroxylon*, *E. viminalis*, *E. grandis*, *E. rudis*, *E. maculata*, *E. camaldulensis*, *E. saligna*, *E. resinifera*, *E. propinqua* and *E. ovata*, with six years of age, were collected from an eucalypt arboretum in Portugal. In terms of yield and kappa number the highest and lowest results were obtained for *E. globulus* (η=49%, K=12) and *E. camaldulensis* (η=38%, K=23), respectively. The chemical analysis showed significant variation among species, which in some cases reached differences in the order of magnitude of six to seven times. The overall results suggest that *E. globulus* is the best species among the 12 in terms of the pulping characteristics studied. *E. ovata*, *E. sideroxylon*, *E. viminalis*, *E. grandis* and *E. saligna* also showed good results.

I. INTRODUCTION

There are more than 700 species within the Eucalyptus genus, most with origin in Australia, and a few species from Indonesia and Papua New Guinea. Worldwide, Eucalypts are among the most important hardwoods, accounting for 18 million ha over 90 countries, spanning from temperate to subtropical and tropical regions. Eucalypt plantations managed as short-rotation constitute the major source of wood for the pulp and paper industry, and despite the genus variability only four species and their hybrids (*E. grandis*, *E. urophylla*, *E. camaldulensis* and *E. globulus*) comprise 80% of the world plantations [1], with a few others also used for pulping purposes (*E. saligna*, *E. nitens*, *E.viminalis*).

In the extensive literature about Eucalypts, the less used species have received comparatively less attention. Most of the existent studies compare species with potential for pulping or biomass, by focusing on the morphological and anatomical characteristics [2,3,4], chemical composition or delignification process [5,6]. Chemical composition affects wood potential for pulp and paper [7] and thus provides an indication of the chemical likeness between different species. Pulp yield and degree of delignification (kappa number) are two key-parameters that describe the potential of wood in papermaking industry based on kraft cooking [6].

The objective of this study is to compare the chemical composition, pulp yield and kappa number of six year's *E. globulus*, *E. botryoides*, *E. sideroxylon*, *E. viminalis*, *E. grandis*, *E. rudis*, *E. maculata*, *E. camaldulensis*, *E. saligna*, *E. resinifera*, *E. propinqua* and *E. ovata*. These results will provide a baseline for comparison between kraft pulping potential of the species.

II. EXPERIMENTAL

Sampling

Wood samples from 12 eucalypt species (*E. botryoides*, *E. camaldulensis*, *E. grandis*, *E. globulus*, *E. maculata*, *E. ovata*, *E. propinqua*, *E. resinifera*, *E. rudis*, *E. saligna*, *E. sideroxylon*, *E. viminalis)* with six years of age, were collected from an arboretum located in the campus fields of the School of Agriculture, University of Lisbon (ULisbon), at Tapada da Ajuda, Lisboa, Portugal (38°42´N; 09°10´W). The stem was debarked, the wood from the base height was chipped, fractionated using a knife mill, screened to a size ranging between 2 and 10 mm and homogenized in single lots.

Chemical Analysis

The samples from homogenized lots were milled, sieved and the 40-60 mesh fraction used for the summative chemical analysis.

Ash content was determined by TAPPI standard method T15 os-58. Extractive content (successively in dichloromethane, ethanol and water) was obtained using extraction thimbles in a Soxhlet apparatus for no less than 16h for each solvent. The thimbles were oven-dried and weighted after each extraction determining the extractive content by weight variation. Holocellulose was determined by using the modified chlorite method [8] and the insoluble and soluble lignin content was determined according to TAPPI standard methods T222 om-88 and UM 250 om-83, respectively. Holocellulose and lignin were determined in extractive-free wood samples. All summative chemical analysis results were reported as percentage of initial mass.

Determination of the neutral monosaccharides and acetate content in wood was based on the monomers present in the hydrolysate from the lignin analysis, through a Dionex ICS-3000 High Pressure Ion Chromatographer, using an Aminotrap plus Carbopac SA10 column. The results were reported as percentage of total sugars.

Kraft Pulping

Kraft pulping was conducted in stainless steel microdigestors (*ca.* 100ml) under rotation in an oil bath. The conditions used for the pulping of five grams of oven-dried wood were: liquid to wood ratio of 4:1, active alkalinity and sulfidity as Na_2O of 22% and 30%, respectively, 165ºC maximum temperature, five minutes to achieve maximum temperature and 60 minutes of reaction time under isothermal conditions. The solid residue was defibrated and thoroughly washed with hot and cold water till neutral pH. All the species were pulped in triplicate. Yield was determined after weighing the oven-dried pulp and kappa number was achieved using TAPPI Useful Test Method UM.

III. RESULTS AND DISCUSSION

Chemical Analysis

The summative chemical analysis of the 12 species of eucalypts is shown in **Table 1**. The ash content varied from 0.4% for *E. grandis*, *E. propinqua* and *E. sideroxylon* to 2.2% for *E. maculata* with the remaining varying between 0.6% and 0.8%. Regarding extractives content *E.camaldulensis* showed the highest amount (18.9%), over three times the lowest value found for *E. globulus* and *E. viminalis* (6.1%). Apolar extractives (soluble in CH_2Cl_2) were the least predominant (0.4-1.2%), as opposing to ethanol extractives (2.3-14.8%), with exception for *E. globulus* with water extractives exceeding the ethanol's. Lignin content varied among the species of almost 10% with *E. maculata* showing the lowest value (21.6%) and *E. resinifera* the highest (30.8%). Holocellulose content showed also a high variation with *E. camaldulensis* and *E. globulus* with the lowest (55.4%) and highest (70.1%), respectively.

Table 1. Summative chemical analysis of the 12 species of eucalypts.

	E. globulus	*E. botryoides*	*E.sideroxylon*	*E. viminalis*	*E. grandis*	*E. rudis*	*E. maculata*	*E. camaldulensis*	*E. saligna*	*E. resinifera*	*E. propinqua*	*E. ovata*
Ash	0.6	0.6	0.4	0.6	0.4	0.7	2.2	0.8	0.8	0.6	0.4	0.6
Extractives	6.1	9.7	13.5	6.1	6.7	14.5	10.0	18.9	10.1	8.2	8.8	6.4
CH_2Cl_2	0.4	0.4	0.7	0.8	0.7	1.2	1.1	1.1	0.9	0.9	0.6	0.9
EtOH	2.3	5.8	10.8	2.9	4.2	10.7	6.5	14.8	7.2	5.2	6.7	2.8
H2O	3.4	3.5	2.0	2.3	1.8	2.7	2.4	3.0	2.0	2.1	1.5	2.7
Lignin	24.8	27.1	26.6	26.8	27.8	26.8	21.6	24.0	26.6	30.8	29.9	26.0
Klason lignin	21.1	24.3	23.3	23.2	25.1	23.4	18.5	21.8	23.7	28.1	27.7	22.2
Soluble lignin	3.7	2.8	3.2	3.6	2.7	3.5	3.1	2.3	2.9	2.8	2.2	3.8
Holocellulose	70.1	64.7	61.1	68.1	66.8	59.0	64.8	55.4	64.2	61.0	62.7	68. 3

Table 2 presents the results for the carbohydrate composition in relation to the proportion of neutral monosaccharides and acetates. The acetate derives from the depolymerization of the hemicelluloses and the hydrolysis of the acetyl groups [9]. The percentage of glucose varied between 61.0-68.6% and xylose from 21.6% to 28.2%. This gives an approximate idea of the cellulose to hemicellulose ratio within the different species: *E. sideroxylon* and *E. propinqua* showed the lowest and highest ratio of glucose/(xylose+acetate) of 1.7 and 2.4, respectively.

Table 2. Monosaccharides and acetates percentage in relation to total sugars in the 12 eucalypt species studied.

	E. globulus	*E. botryoides*	*E.sideroxylon*	*E. viminalis*	*E. grandis*	*E. rudis*	*E. maculata*	*E. camaldulensis*	*E. saligna*	*E. resinifera*	*E. propinqua*	*E. ovata*
Arabinose	1.1	1.1	1.1	1.1	1.1	1.1	1.1	1.2	1.1	1.2	1.1	1.0
Galactose	1.1	1.1	2.2	1.1	1.1	2.2	1.1	1.8	2.3	2.4	2.1	1.0
Glucose	64.3	68.2	61.0	63.1	68.0	65.5	63.3	62.3	65.0	63.5	68.6	63.6
Xylose	25.4	22.3	27.7	26.1	22.7	23.5	26.1	26.4	23.8	24.9	21.6	28.2
Acetates	8.1	7.3	7.9	8.5	7.1	7.7	8.5	8.3	7.8	8.0	6.6	6.1

Kraft Pulping

The results for pulp yields and respective kappa number of the pulps are shown in **Figure 1**.

E. globulus pulping resulted in the highest yield (49.3%) and lowest kappa number (12) as opposed to *E. camaldulensis* which only reached 37.8% yield with kappa number of 23. *E. ovata* appears to be the next best species in terms of the pulping characteristics studied, with *E. sideroxylon*, *E. viminalis*, *E. grandis* and *E. saligna* also showing good results. *E. rudis* and *E. camaldulensis* pulps were obtained with low yield and high kappa number, according to the low holocellulose content and large amount of extractives [10]. *E. resinifera* and *E. propinqua* were pulped to a kappa number around 19, probably due to high initial lignin content.

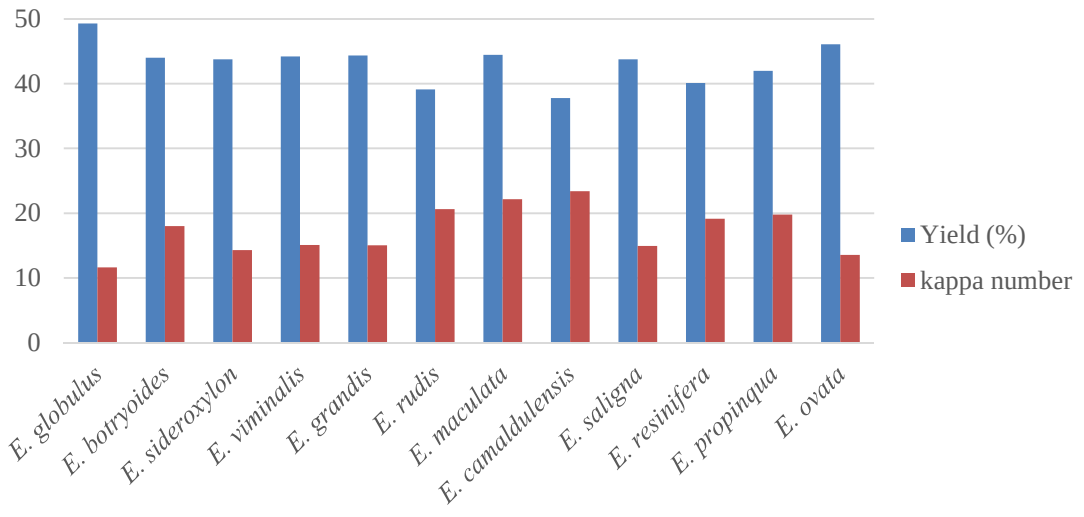

Figure 1. Yield and kappa number for the kraft pulping of 12 species of eucalyptus

IV. CONCLUSIONS

The 12 species of eucalypts showed a large variation regarding the chemical composition, which could in part explain the variation of the results of yield and kappa number. Eucalypts with excessive extractives in their composition will produce pulps with low yield and high kappa number. *Eucalyptus globulus* showed the best results in terms of yield and kappa number under the experimental conditions used but *E. ovata*, *E. syderoxylon*, *E. viminalis*, *E. grandis* and *E. saligna* also showed good pulping potential.

V. ACKNOWLEDGEMENT

We are grateful to Dr. Paula Soares for providing the samples and the information about the trial which was sponsored by CELPA – Associação da Indústria Papeleira (Portuguese Pulp and Paper Industry Association). Financial support for the laboratorial analysis was given by research funding of FCT (Fundação para a Ciência e Tecnologia) to CEF (Centro de Estudos Florestais) under its Strategic Project (Pest-OE/AGR/UI0239/2014), and two projects (PTDC/AGR-CFL/110419/2009 and PTDC/AGR-FOR/3872/2012). The authors also wish to acknowledge the Federal University of Viçosa, Capes (Coordination for the development of Higher Level Personnel) and CNPq (National Council for Scientific and Technological Development) for financial support.

VI. REFERENCES

[1] Rockwood, L.D.; Rudie, W.A.; Ralph, S.A.; Zhu, Y.J.; Winandy, E.J. Energy product options for Eucalyptus species grown as short rotation woody crops. International Journal of Molecular Science 2008, 9 (8), 1361–1378.

[2] Pirralho, M.; Flores, D.; Sousa, V.B.; Quilhó, T.; Knapic, S.; Pereira, H. Evaluation on paper making potential of nine Eucalyptus species based on wood anatomical features. Ind. Crops and Prod. 2014, 24, 327-334.

[3] Dutt, D.; Tyagi, C.H. Comparison of various eucalyptus species for their morphological, chemical, pulp and paper making characteristics. Indian Journal of Chemical Technology 2011, 18, 145-151.

[4] Knapic, S.; Pirralho, M.; Louzada, J.L.; Pereira, H. Early assessment of density features for 19 Eucalyptus species using X-ray microdensitometry in a perspective of potential biomass production Wood Sci. Technol 2014, 48, 37-49.

[5] González-Vila, F.J.; Almendros, G.; del Rio, J.C.; Martín, F.; Gutiérrez, A.; Romero, J. Ease of delignification assessment of wood from different Eucalyptus species by pyrolysis (TMAH)-GC/MS and CP/MAS ^{13}C-NMR spectrometry. Journal of Analytical and Applied Pyrolysis 1999, 49, 295-305.

[6] Khristova, P.; Kordsachia, O.; Patt, R.; Dafaalla, S. Alkaline pulping of some eucalypts from Sudan. Bioresources Technology 2006, 97, 535-544.

[7] Seca, A.M.L.; Domingues, F.M.J. Basic density and pulp yield relationship with some chemical parameters in eucalyptus trees. Pesquisa Agropecuária Brasileira 2006, 41(12), 1687-1691.

[8] Rowell, R.M. Handbook of Wood Chemistry and Wood Composites, CRC Press, Boca Raton, Florida 2005.

[9] Spiridon, I.; Popa, V.I. "Hemicelluloses: Structure and Properties" in: Polysaccharides Structural Diversity and Functional Versatility, S. Dumitriu (ed), CRC Press 2004.

[10] Foelkel, C.E.B.; Barrichelo, L.E.G.; Milanez, A.F. Estudo comparativo das madeiras de Eucalyptus saligna, E. paniculata, E. citriodora, E. maculata e E. tereticornis para produção de celulose sulfato. I.P.E.F. 1975, 10, 17-37

NOVEL INSIGHT IN CARBOHYDRATE DEGRADATION DURING ALKALINE TREATMENT

Kaarlo Nieminen*, Markus Paananen, Lidia Testova, Herbert Sixta

*Aalto University P.O. Box16400, 00076 Aalto, FINLAND (*Kaarlo.Nieminen@aalto.fi)*

ABSTRACT

We present a mathematical model for the yield loss and decline in polymerization of carbohydrates. The model is applicable to the treatment of cellulose and hemicellulose in alkaline media and it features the actions of peeling, stopping and alkaline hydrolysis on the polymer chains. The reaction rates are estimated by fitting the model to experimental data. Experiments conducted at several temperatures enable the evaluation of activation energies for the reactions. The peeling reaction is further divided into primary and secondary peeling, depending on whether it originates from an initial reducing end group or from a reducing end group created by alkaline hydrolysis. We are able to evaluate the impact of the different processes on degradation and the portion of polymer chains possessing reducing end groups.

I. INTRODUCTION

Background

Peeling, stopping and alkaline hydrolysis are central reactions involved in the degradation of chain molecules such as cellulose, (galacto)glucomannan (GGM) and xylan. There are several studies on the interplay between those reactions in the context of disposal of nuclear waste, where the focus has been on the degradation of cellulosic material under moderate ambient conditions over the course of thousands or millions of years. However, it seems that modeling of the same reactions under conditions relevant to biorefineries has received far less attention. In the present study a mathematical model incorporating peeling, stopping and alkaline hydrolysis is employed to describe the degradation of carbohydrates in biorefineries during alkaline treatment. Cellulose and hemicelluloses consist of long chains of monosaccharide units. If a chain has a reducing endgroup (REG), the end monosaccharide unit can be eliminated from the chain by the peeling reaction. The subsequent element in the chain then forms a new reducing end group admitting further peeling. The peeling reaction plays a central role in the degradation of the polysaccharide chains and the resulting loss of yield in the kraft pulping process. The stopping reaction terminates the endwise peeling by transforming a reducing end group to a nonreducing one. These two reactions alone would after some time lead to a situation where all the reducing endgroups have been eliminated and degradation has terminated. However, the reaction of alkaline hydrolysis alters the scene by eliminating a non-end element, thus cleaving the chain in two. One of the new chain end units then becomes a reducing end group susceptible to the peeling reaction. Peeling descending from initially existing reducing end groups is classified as primary peeling whereas peeling with first origin in a reducing endgroup created by alkaline hydrolysis as secondary peeling. Similarly the REGs are called primary or secondary depending on their source.

Kinetic model

The joint effect of the different end reactions on a carbohydrate was described with the following system of differential equations [1]:

$$\begin{cases} \dfrac{dR}{dt} = -k_s R + k_h\left(\Gamma_0 - P - H\right) \\ \dfrac{dP}{dt} = k_P R \\ \dfrac{dH}{dt} = k_h\left(\Gamma_0 - P - H\right) \end{cases} \quad (1)$$

Here R is he amount of REGs, P the material degraded by peeling and H the material degraded by alkaline hydrolysis. The amount of initial material is denoted by Γ_0 and the reaction rates for peeling, stopping and alkaline hydrolysis by k_p, k_s and k_h respectively. The system of differential equations was transformed to a second order differential equation, which was solved analytically. From this solution the amount of nondegraded material was calculated by subtracting the expressions for P and H from Γ_0.

Fitting the mathematical model to the experimental data gives estimates for the reaction rates. The presence of several different temperatures in the experimental data enables the calculation of the frequency factors and activation energies for the reactions according to the well-known Arrhenius equation.

The equation system can be modified to describe separately the portions of primary and secondary peeled carbohydrate material.

Model for the degree of polymerization

A peeling reaction reduces the polymer chain length by one element, whereas an alkaline hydrolysis reaction apart from removing one element from the chain also splits the chain in two parts, thus on the average reducing the chain to half of its previous length. Hence, the degree of polymerization (DP) can be expressed as a function of the amount of material degraded by the endwise reactions:

$$DP = \frac{DP_0 - P - AH}{1 + AH} \tag{2}$$

Here DP_0 designates the initial degree of polymerization. In this context P stands for the number of peeled off chain elements and AH for the number of chain elements removed by alkaline hydrolysis. These quantities are calculated from the solution of Equation system (1) with Γ_0 interpreted as the initial DP. Now, fitting the expression for DP to experimental data enhances the evaluation of the kinetic parameters obtained from the yield loss fit.

II. EXPERIMENTAL

Two categories of data were utilized in this study. Firstly, raw material from Scots pine was subjected to kraft treatment [2], producing degradation data on glucomannan, xylan and cellulose. Secondly, soda-anthraquinone treatment of cotton linters [1], in addition to generating cellulose degradation data, as a result of the absence of lignin, also allowed for an evaluation of the degree of polymerization.

Kraft treatment of Scots pine

The wood material was chipped and screened according to SCAN-CM 40:01. Subsequently, the screened chips were milled with a Wiley mill to pass through a 1 mm slot screen. The experiments were conducted in a 10 L batch reactor at a liquor-to-wood-ratio 200:1. The hydroxide ion concentration levels were 0.5 and 1.55 M. For the lower [OH-] level the temperature was 160 °C and for the higher [OH-] level the each cook underwent one of the temperatures 130, 140, 150 or 160 °C. Addition of NaCl fixed the ionic strength at a constant level of 2.00 M [Na+]. For all cooks the sulfidity was kept at 33%. At each hydroxide level – temperature combination a series of approximately ten cooks of increasing duration were made – the shortest lasting under ten minutes the longest a few hours. Both the wood residue and the black liquor were analyzed for carbohydrate content.

Soda-anthraquinone treatment of cotton linters

Cotton linter pulp was grinded in a Wiley mill with mesh size 0.5 mm. Within the soda-anthraquinone treatment three types of experiments, with regard to acid pretreatment and stabilization, were carried out: 1) no pretreatment (CL), 2) pretreatment with oxalic acid (OA) and 3) pretreatment with oxalic combined with borohydride stabilization attempted in-situ in the alkaline degradation stage (OA+BH). The acid pretreatment took place at a 15 ml/g liquid-to-solid ratio and a temperature of 110 °C. The isothermal duration was 80 min. The alkaline degradation trials were conducted at a temperature of 160 °C, a liquid-to-solid ratio of 40 ml/g, an alkali concentration of 20 g/l and the addition of dispersed 0.1 g/l AQ.

III. RESULTS AND DISCUSSION

Apart from the endwise degrading reactions, which remove one element a time from the polymer chains, the carbohydrates in the kraft cooking experiment can also be dissolved into the black liquor in longer fragments. To be able to fit the model expression for the remaining carbohydrate to the data it is assumed that the endwise reactions proceed with the same reaction rates in the black liquor as in the wood residue. The model was then fitted to the joint amount of carbohydrate in the wood residue and the black liquor. **Figure 1** shows the fit for GGM and xylan **Table 1** shows the estimated activation energies and frequency factors related to the various reactions.

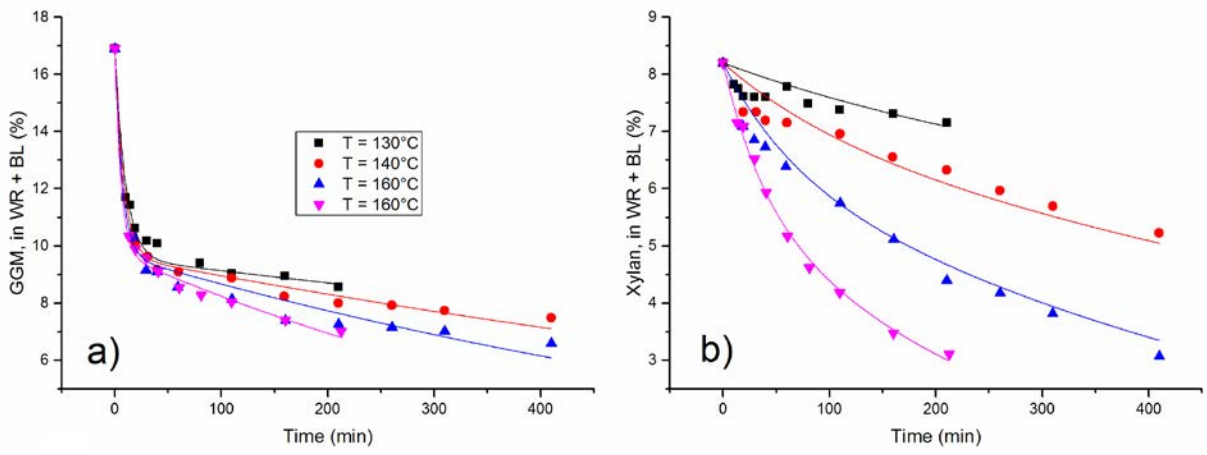

Figure 1. Fit of kinetic model to the amounts of a) GGM and b) xylan remaining in either the wood residue or the black liquor at different temperatures.

To further analyze the dissimilarity between GGM and xylan we divide the degraded material into groups according to the generating reaction, distinguishing between primary and secondary peeled material. **Figure 2** shows the cumulative amounts of primary peeled, secondary peeled and alkaline hydrolysis degraded material. We observe that in the case of the GGM the primary peeling is extensive, but almost all of it takes place during the first half an hour, indicating fast peeling and stopping reactions. After the primary reducing end groups have been consumed by the stopping reaction, degradation is dominated by secondary peeling. For xylan the regimes of primary and secondary peeling are more interlaced and the primary peeling is more temperature dependent than for GGM. This indicates slower peeling and stopping reactions with a longer lasting supply of primary reducing end groups. The amount of material explicitly degraded by alkaline hydrolysis is minor, but alkaline hydrolysis is crucial for the secondary peeling in creating new reducing end groups.

Table 1. Estimated kinetic parameters in the Arrhenius equation related to the endwise reactions

Reaction	Parameter (Unit)	GGM	Xylan	Cellulose
Peeling	A (min^{-1})	11700	2.9×10^{14}	1.69×10^{13}
	E_a (kJ/mol)	25.5	120	98
Stopping	A (min^{-1})	290	1.2×10^{8}	8.54×10^{11}
	E_a (kJ/mol)	26.7	80	106
Alkaline hydrolysis	A (min^{-1})	982	636	6.64×10^{15}
	E_a (kJ/mol)	62.4	57	175

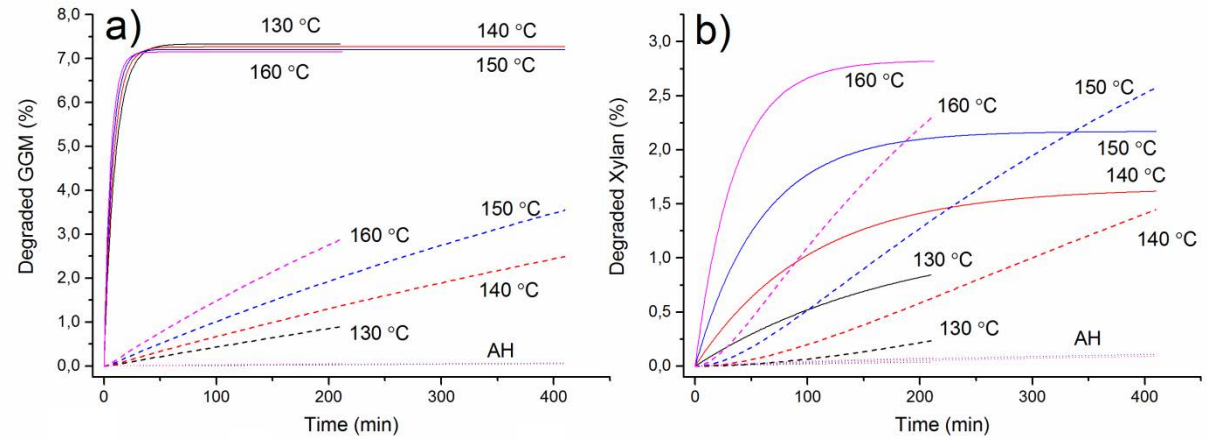

Figure 2. Degradation of a) GGM and b) xylan subdivided into portions contributed by primary peeling (solid lines), secondary peeling (dashed lines) and alkaline hydrolysis (dotted lines close to zero)

For the alkaline treated cotton linters experimental data on the degree of polymerization was available. Further, both the amount of remaining carbohydrate material and the degree of polymerization can in the mathematical model be expressed as functions of time with the reaction rate constants of the various end wise reactions and the

initial amounts of reducing end groups as parameters. Consequently, it is possible to perform a simultaneous fit to the degradation data and the DP data. **Figure 3** shows such fits for differently treated cotton linter pulps and **Table 2** the corresponding estimated parameters. The estimations of the amounts of REGs are in accordance with the fact that acid treatment breaks the chains creating new REGs whereas stabilization turns reducing end groups into nonreducing ones.

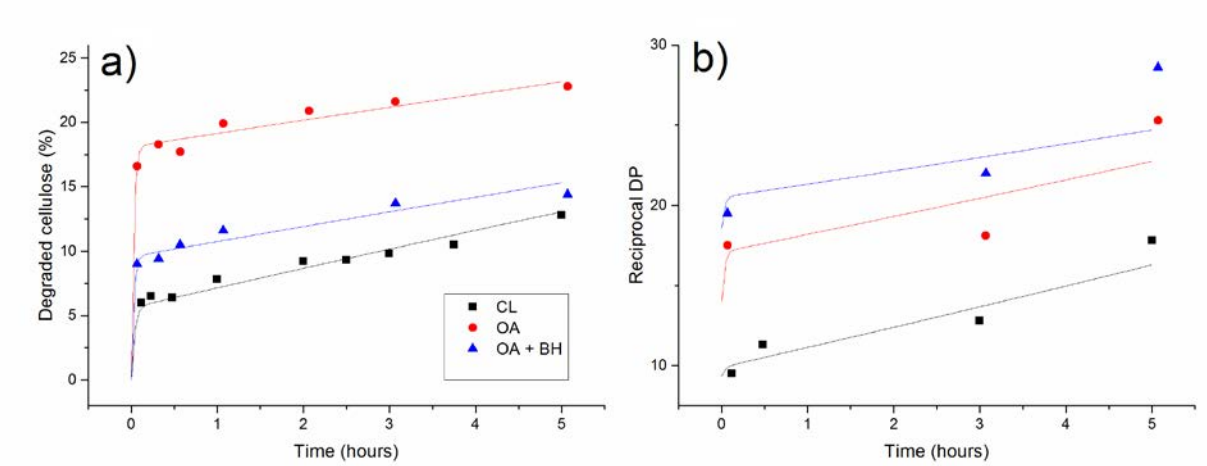

Figure 3. Simultaneous fit to a) degradation and b) DP data for untreated cotton linter pulp (CL), cotton linter pulp pretreated with oxalic acid without stabilization (OA) and cotton linter pulp pretreated with oxalic acid and stabilized with borohydride (OH + BH).

Table 2. Estimated kinetic parameters as well as the initial amount of reducing and nonreducing end groups obtained from simultaneous degradation and DP data fit.

Pretreatment	k_p (h^{-1})	k_s (h^{-1})	k_h (h^{-1})	REG	NREG
Untreated	2474	26.2	1.72E-4	5.99E-4	9.15E-4
Oxalic acid	3189	36.2	1.43E-4	2.06E-3	2.09E-4
Stabilization	5341	36.0	8.79E-5	6.48E-4	2.36E-3

IV. CONCLUSIONS

A mathematical model capable of describing the endwise degradation reactions in alkaline treatment of pulp was introduced. The model distinguishes between primary and secondary peeling and demonstrates the differences in degradation conduct between the carbohydrates. For GGM primary peeling dominates initially, but ceases rapidly, whereas secondary peeling proceeds at a constant rate. Temperature affects secondary peeling but not primary peeling. For xylan the duration of primary peeling is longer and both primary and secondary peelings are affected by temperature. For the yield loss alkaline hydrolysis is relevant through the production of new reducing end groups. The degradation model can further be combined with a model of DP. In the case of the cellulose of the cotton linter pulp the simultaneous fit shows that pretreatment with oxalic acid increases both the peeling and the stopping rate and also the initial number of REGs due to cleavage of the polymer chains. Stabilization further increases the peeling rate coefficient, but this is prevailed by the decreased number of reducing end groups.

V. ACKNOWLEDGEMENT

Funding from the FuBio JR2 research program is gratefully acknowledged.

VI. REFERENCES

[1] Testova, L.; Nieminen, K.; Penttilä, P.; Serimaa R.; Potthast .; Sixta H. Cellulose degradation in alkaline media upon acid pretreatment and stabilization. *Carbohyd Polym.* **2014**, *100*, 185–194.

[2] Paananen, M.; Liitiä, T.; Sixta, H. Further insight into carbohydrate degradation and dissolution behavior during kraft cooking under elevated alkalinity without and in the presence of anthraquinone. *Ind. Eng. Chem Res.* **2013**, *52*, 12777–12784.

ENZYMATIC SACCHARIFICATION OF HARDWOOD SEMICHEMICAL PULPS: LIGNOCELLULOSE BIOREFINERY ASPECTS

Novozhilov E.V.[1]*, Aksyonov A.S. [1], Demidov M.L. [1], Chukhchin D.G. [1], Tyshkunova I.V. [1], Sinitsyn A.P. [2,3], Dotsenko G.S. [2], Osipov D.O. [2]
[1]*Northern (Arctic) Federal University named after M.V. Lomonosov, Arkhangelsk, Russia;*
[2]*A.N. Bach Institute of Biochemistry, Russian Academy of Sciences, Moscow, Russia;*
[3]*Department of Chemistry, M.V. Lomonosov Moscow State University, Moscow, Russia*
**E-mail: biotech@narfu.ru*

ABSTRACT

Lignocellulosic substrates were obtained using two alternative methods of hardwood cooking: neutral sulphite pulping and pulping with green liquor pretreatment in industrial and laboratory conditions. The reactivity was obtained using two *Penicillium verruculosum* enzyme preparations. It was demonstrated, that cooking methods provide differences in morphological structure of fibers. Green liquor pretreated hardwood pulp possesses higher reactivity for enzymatic hydrolysis. Conversion degree of glucanes to glucose is equal to 76-78 % under enzyme dosage 9,4 FPU/g substrate. Pulp beating improves reactivity of lignocellulose matrix and in twain reduces the time for achievement of maximum conversion yield. Saccharification of substrate produced by neutral sulphite pulping is limited by low cellulose availability. It is induced by fiber swelling limitation and composition of residual lignin.

I. INTRODUCTION

The realization of biorefining technologies providing enzymatic hydrolysis of cellulose-containing materials allows to obtain monosaccharides which further might be used as a final products or as a raw-materials for production of ethanol or butanol, organic acids, amino acids and other useful products. New preparations with high content of cellulases and xylanases are produced by genetic engineering for plant material saccharification [1].
Neutral sulphite pulping and green liquor (sodium carbonate and sodium sulfide) pulping are used for industrial production of hardwood semichemical pulp. Neutral sulphite semichemical (NSSC) pulp and green liquor pretreatment (SCGL) semichemical pulp are used for production of paper and cardboard. The advantages of semichemical pulp production using green liquor are cost cut out for cooking liquor preparation and simplification of spent liquor regeneration.
The development of a new process, which utilizes green liquor as a pretreatment for the production of ethanol is described in article Jin et al. [2]. The low pH prevents the random hydrolysis of polysaccharides and secondary peeling reactions during the pretreatment, resulting in higher retention of the polysaccharides in pulp. The yield of pulp produced by the green liquor pretreatment process is about 80% with nearly 100% cellulose and 75% xylan in retention in mixed southern hardwood [2]. Residual lignin content in chemical pulp plays an important role on the efficiency of enzymatic hydrolysis. Noncellulosic compounds of semichemical pulps such as hemicelluloses and lignin may limit access of biocatalysts for cellulosic fibrils. Enzymatic hydrolysis of semichemical pulps is under research.

II. EXPERIMENTAL

Semichemical pulp
SCGL pulp 1 was laboratory obtained. Aspen cooking was carried out using glycerine bath in following conditions: penetration at 110 °C during 15 min, cooking at 170 °C during 35 min, green liquor consumption was 8 % (in terms of Na_2O). After cooking chips were separated by beating on laboratory mill for fibers production, washed with water, dewatered to level of dry solids 20-25 % and kept at 4 °C. Pulp yield was 78,0±0,2 % based on dry weight of wood, number kappa was 110±2. SCGL pulp 2 was obtained after beating of SCGL pulp 1 on Jokro mill to 70 °SR. SCGL pulp 3 was obtained from SCGL pulp 1 after beating on Jokro mill to 30 °SR and handsheets production. Sample mass produced on Rapid Koten sheet-making apparatus was 125 g/m^2.

Number kappa of NSSC pulp 1 was 106, freeness – 14°SR. This sample was pulp produced from aspen and birch mixture using neutral sulphite pulping in industry. NSSC pulp 2 was obtained after beating of NSSC pulp 1 to freeness value 22 °SR on industrial disk mill.
Characteristics of semichemical pulp fibers were studied on Fiber Tester (Lorentzen & Wettre Company). Semichemical pulps samples were freeze-dried on Labconco apparatus (FreeZone 2,5L) and photographed on electron microscope ZEISS «SIGMA VP». Samples were covered with gold and palladium mixture to thickness of 5 nm using Q150TES apparatus (Quorum).

Enzymes and enzymatic hydrolysis
The laboratory fungal preparations, produced by *P. verruculosum* were used. B151#3.147.2 preparation contained cellulase complex and preparation F10#3.201.2 contained *Aspergillus niger* β-glucosidase (80%). Detailed characteristics of the preparations were reported previously [1]. Filter paper activity was measured towards «Whatman» filter paper (England) (FPU/g) using Ghose method [3] and dinitrosalicyl acid method for reducing sugars (RS) analysis.
Enzymatic hydrolysis of substrates with concentration 100 g/l (reduced to dry matter) was carried out at 50 ?C using thermostatic cells at stirring rate 250 rpm. Substrate sample and 0,1 M sodium acetate buffer were placed in the cell (pH 5,0). Dosage of the *P. verruculosum* B151 preparation was 10 mg of protein per 1 g of dry substrate, *P. verruculosum* F10 preparation dosage was 0,88 mg per 1 g of dry substrate. After 48 hours samples were centrifuged (10000 rpm, 3 min) and RS content was measured by Somogyi-Nelson method. Glucose was measured by glucose oxidase and peroxidase test.

III. RESULTS AND DISCUSSION

Semichemical pulp cooking with green liquor was carried out at pH media closed to neutral. Thus the destruction of polysaccharide complex including cellulose and xylan decreased. Hard wood delignification during green liquor pulping corresponds to mechanism, which is equal to kraft pulping mechanism. During aspen and birch mixture pulping with such yield of semichemical pulp about half of the lignin from raw-material was removed. Residual lignin content was about 14,1–15,4 %. In comparison, during mixture of mostly oak and sweet gum pulping with yield of 77–78%, the lignin content was higher, and equal to 17–18% [2].
SCGL pulp 1 fibers preserved form and entirety of external walls and substantially had not fibrils (Figure 1). Production SCGL pulp 2 including beating to 70 °SR provided decreasing of the average length and width of the fibers, increasing of fine fraction yield and breaking value. Influence of beating on semichemical pulp was studied using scanning electron microscopy of freeze-drying sample. Essential destruction of external cell walls, fragments separation and release of internal fiber layers were observed (Figure 1). Appearance of additional defects in structure of SCGL pulp 2 fibers provided new sites for biocatalysis.
Biocatalysts based on recombinant fungi *P. verruculosum* in small dosages allowed to provide high RS yield due to balanced composition of enzyme complex. SCGL pulp 1 sample had high reactivity corresponding to 53%. The result was achieved using enzyme dosage 9,4 FPU/g. Enzymatic hydrolysis of SCGL pulp 2 practically stopped after 24 hours at reactivity 56 % (Figure 2). At the same time SCGL pulp 1 conversion occurred partially and needed time increase up to 48 hours for hydrolysis to be completed. Maximum conversion degree measured respectively RS for SCGL pulp 2 was higher than for SCGL pulp 1 sample by 6 % (Table 1).
Additionally SCGL pulp produced from birch was used as a substrate for reference. SCGL pulp had yield, which was equal to 76,7 % based on wood. After 48 hours enzymatic hydrolysis RS yield to SCGL from birch was smaller on 0,8–1,6 % than SCGL pulp 1 from aspen.
Basic cellulosic part in semichemical pulp was enzymatically hydrolyzed. High content of the residual lignin in semichemical pulps was not a problem for destruction of polysaccharides. Glucose yield reduced to dry matter of raw-material (aspen) was 37–38 % (Table 1).
During enzymatic hydrolysis of SCGL pulp conversion degree of aspen glucans (cellulose and glucomannan [4]) to glucose was 76–78 %. In the article [2] similar saccharification degree for hardwood SCGL pulp was achieved using enzyme dosage 40 FPU/g substrate.

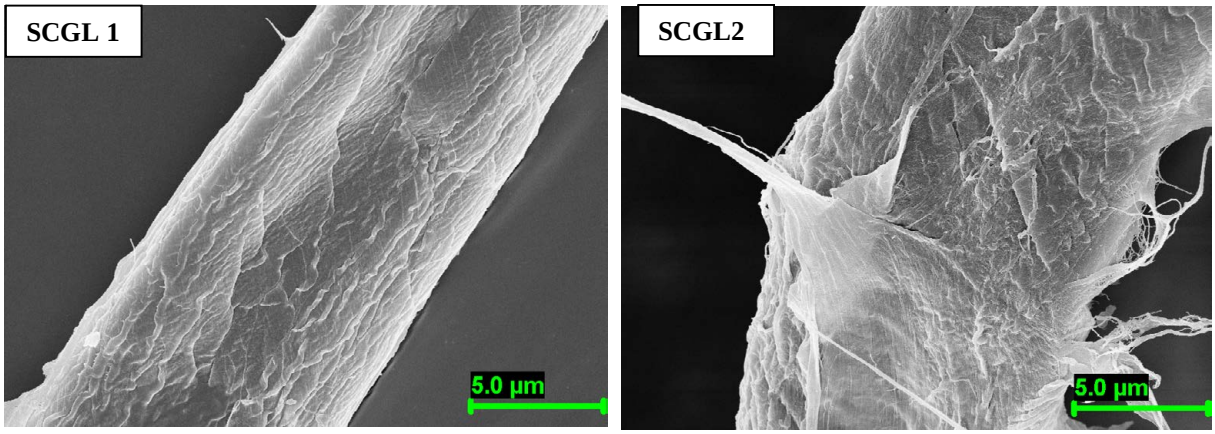

Figure 1. Scanning electron microscopy of SCGL pulp fibers.

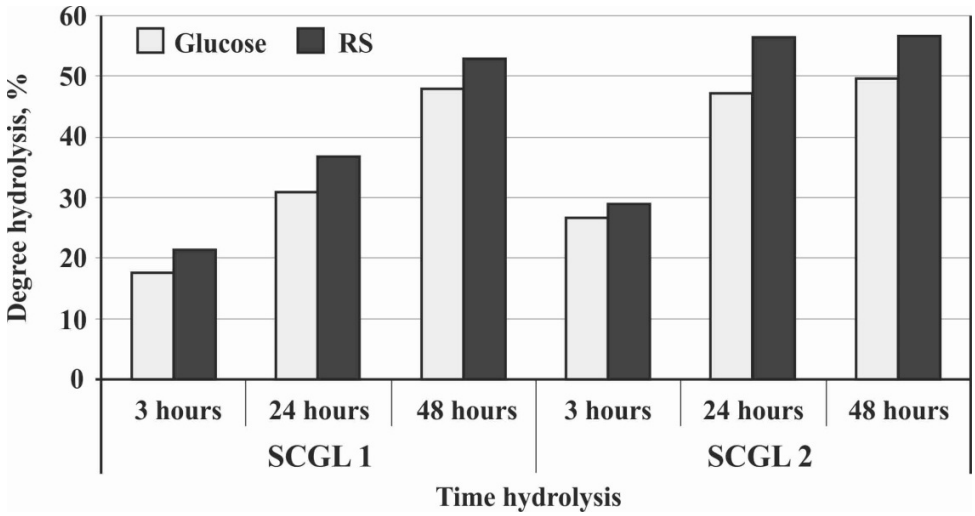

Figure 2. Hydrolysis yield for SCGL pulp (% from initial substrate mass, on dry weight of wood).

Table 1. Reactivity of the semichemical pulps after 48 hours hydrolysis with *P. verruculosum* B151 and *P. verruculosum* F10 preparations.

Semichemical pulp sample	Pulp yield, % based on dry weight of wood	RS yield, % based on dry weight of pulp	Glucose yield, % based on dry weight of pulp	Glucose yield, % on dry weight of wood
SCGL pulp 1	78	53	47	37
SCGL pulp 2	78	56	49	38
SCGL pulp 3	78	31	29	23
NSSC pulp 1	77	31	23	18
NSSC pulp 2	77	35	26	20

SCGL pulp 3 sample was handsheeted. Irreversible changes of the structure happened during fiber drying, which had negative influence on enzymatic hydrolysis of polysaccharides. The reactivity of SCGL pulp 3 decreased to 31 % (Table 1).

Additionally industrial NSSC pulp produced from aspen and birch mixture was used as a substrate for reference. SCGL pulp and NSSC pulp had similar yields, which were equal to 77–78 % based on wood. Other parameters – number kappa, lignin and xylan content in these semichemical pulps hadn't got significant differences.

After chips separation for fibers production the NSSC pulp surface had slight development, fibrillation was absent (Figure 3). Mechanical treatment during beating to 22 °SR provided increasing of microdefects, partial destruction of external fiber cell walls. Reactivity of NSSC pulp 1 was average - 31% (Table 2). After beating NSSC pulp 2 still had average reactivity, which was equal to 35 % (Table 1).

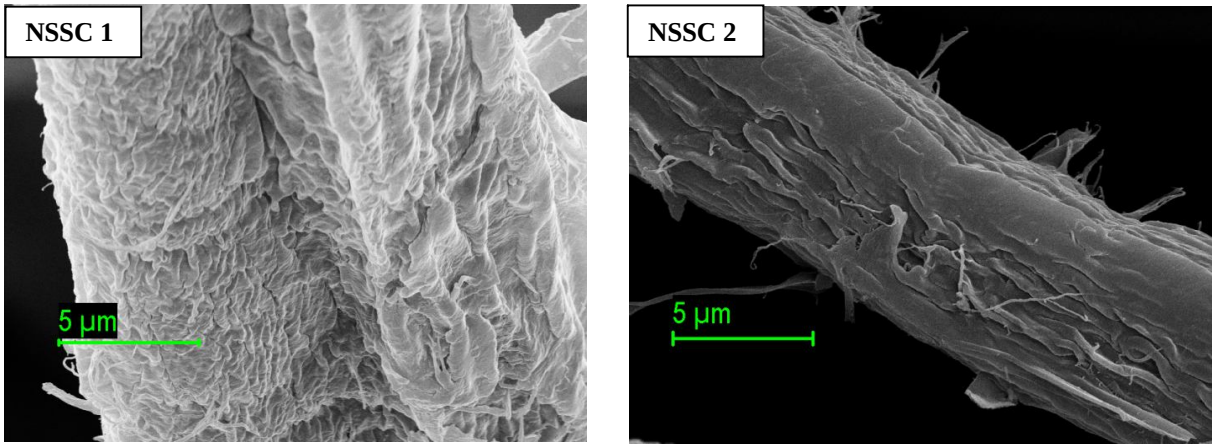

Figure 3. Scanning electron microscopy of NSSC pulp fibers.

Lignin sulphanation with sulfo-groups addition occurs during neutral sulphite pulping. Partially carbohydrates sulphanation leads to carbohydrate-sulfonic acid formation. Sulfo-groups create steric hindrance for biocatalysis limiting enzymes contact with substrate. Green liquor provides more alkaline media than neutral sulphite liquor and leads to higher fiber swelling of semichemical pulp. It is documented by the phenomenon evidence that average fiber width of SCGL pulp was more than by 4–6 % higher in comparison with average fiber width of NSSC pulp. Microcapillary structure development improves enzyme diffusion to substrate inside the fiber cell walls and increases biocatalytic destruction of semichemical pulp polysaccharides.
It is important that SCGL pulp 3 after drying was hydrolyzed with the same degree as a wet NSSC pulp. It demonstrated differences in structure and properties of the fibers of these two semichemical pulp types.

IV. CONCLUSIONS

Green liquor application for semichemical pulp production in combination with following enzymatic hydrolysis for glucose production is a new advanced approach for hardwood biorefining. This technology allows to convert a part of industrial capacities on substrate production for enzymatic saccharification in pulp and paper industry.
Enzymatic preparations based on *Penicillium verruculosum* fungi are effective biocatalysts for hardwood semichemical pulp hydrolysis. The advantages of SCGL pulp as a raw-material for saccharification have been revealed. Significant swelling of fibers in alkaline media, which improves enzyme diffusion to substrate in internal structure of cell walls have been demonstrated. The beating of SCGL pulp additionally increases its ability to biocatalytic influence and in twice decreases process time. Conversion degree of glucans to glucose was 76-78 % at enzyme dosage 9,4 PFU/g substrate.

V. ACKNOWLEDGMENT

The research involved scientific equipment of Shared Use of Equipment Center “Arktika" (Northern (Arctic) Federal University named after M.V. Lomonosov) with financial support from The Russian Foundation for Basic Research (Grant 14-04-98825).

VI. REFERENCES

[1] Chekushina A.V.; Dotsenko G.S.; Sinitsyn A.P. Comparing the efficiency of plant material bioconversion processes using biocatalysts based on Trichoderma and Penicillium verruculosum enzyme preparations. *Catalysis in industry*. **2013**, *5*, 98-104.
[2] Jin Y.; Jameel H.; Chang H.; Phillips R. Pretreatment of mixed hardwood for ethanol production in a repurposed kraft pulp mill. *Journal of wood chemistry and technology*. **2010**, *30*, 86-104.
[3] Ghose T.K. Measurement of Cellulase Activities. *Pure Appl. Chem.* **1987**, *59*. 257-268.
[4] Sharkov V.I.; Kuybina N.I.; SolovievaYu.P. Quantitative analysis of plant raw materials.*M.: Lesnaya promyshlennost.* **1976**, 72 P.

REVIVAL OF THIN LAYER CHROMATOGRAPHY – SEPARATION AND QUANTIFICATION OF CARBOHYDRATES BY HIGH PERFORMANCE THIN LAYER CHROMATOGRAPHY (HP-TLC)

J.T. Oberlerchner[1], S. Böhmdorfer[1], T. Zweckmair[1], S. Koch[2], A. Kindler[2], T. Rosenau[1], A. Potthast[1]*

[1]*University of Natural Resources and Life Sciences, Department of Chemistry, Christian Doppler Laboratory "Advanced Cellulose Chemistry and Analytics", Muthgasse 18, A-1190 Vienna, Austria;*
[2] *BASF Ludwigshafen, D-67056 Ludwigshafen, Germany*
*(*antje.potthast@boku.ac.at)*

ABSTRACT

The separation and quantification of monomeric carbohydrates today is mainly done by means of gas and liquid chromatography, requiring derivatization in several cases. The accurate determination of the sugar composition and content in plant material is of great importance, e.g. in industrial routine analysis.
In this study, it is demonstrated that the modern variant of Thin Layer Chromatography (TLC), mostly denoted as High Performance TLC (HP-TLC), is a highly advantageous method that stands fully emancipated among other separation techniques. We established a method for the quantification of the most common sugars appearing in plant hydrolysates (e.g. glucose, galactose, mannose, xylose and arabinose). To benchmark this method we compared it with GC-MS and HPLC-RI. Plant hydrolysates are often difficult to analyze by GC or HPLC due to a highly complex matrix which may falsify the results. With HPTLC such matrix-associated problems can be easily avoided since the disturbing compounds are directly removed on the plate.

I. INTRODUCTION

The need for fast and accurate analysis methods of plant-derived low-molecular weight carbohydrates is associated with the fact that the development of biorefineries is rapidly progressing: crude oil as a starting material, for a vast number of applications, will be more and more replaced by renewable materials in the future. For this purpose, either the polymeric constituents are used directly (cellulosic products) or they are hydrolyzed (e.g. glucose production for subsequent fermentation). Since plant material can differ strongly in its composition, fast and robust screening methods are of great importance. A disturbing matrix, consisting of dissolved lignin, furfural, formic and acetic acid, sugar acids, various oils and other products can falsify results or even can clog columns or capillaries which lead to increased maintenance needs and costs.

Quantification of the sugar components after hydrolysis is nowadays mainly done by chromatographic methods. Gas chromatography (GC) and liquid chromatography (LC) with all their inherent benefits - and some inherent drawbacks - are by far the most common methods for the quantification of plant-derived sugars. These well established methods are still time consuming and expensive when it comes to analysis of high sample numbers..
The first chromatographic method and actually the one which gave chromatography its name (the separation of colored plant components on paper was called "color writing": chromatography) was TLC, which after the advent of instrumental separation techniques has unfortunately been increasingly neglected, and has only recently been revived. HPTLC is an enhanced TLC method which includes fully automated steps using high performance silica layers for increased sensitivity.
To test the capability of HPTLC for quantifying wood sugars, different layers, impregnation techniques and eluents were tested. For evaluating the feasibility of this method we compared the results obtained with standard HPLC and GC-MS methods for carbohydrate quantification.

II. EXPERIMENTAL

HPTLC

Planar chromatography was performed on impregnated HPTLC plates silica gel 60 (20 x 10 cm, layer thickness 0.2 mm, Merck). For the impregnation of the HPTLC layers the plates were dipped for 15 min in a sodium phosphat buffer (pH 6.2, 0.1 M). After drying in an oven (100 °C, 1 hour) the plates were stored in a desiccator over saturated LiCl solution (RH 11%). Samples and standards were applied by an Automatic TLC Sampler 4 (ATS 4, Camag, Muttenz, Switzerland), using the following settings for 20 tracks per plate: band length 8.0 mm, track distance 10.0 mm, dosage speed 150 nL/s, application position x-axis 10 mm and y-axis 8 mm, needle heating 40°C. The application volumes for the standard solutions were 5, 10, 15 and 20 µL / band and for the sample solutions 2, 3.5 and 10 µl / band. The instrument was controlled by winCATS 1.3.1.2. Chromatography was carried out on in an Automated Developing Chamber (ADC2, CAMAG) using acetonitrile: 1-pentanol: water 4:1:1 (v/v/v) up to a migration distance of 70 mm, drying time was 5 min. For the second development exactly the same conditions were used and mobile phase was renewed before each development step. For post-chromatographic derivatization the following reagent was employed: 70 ml aniline solution and 70 ml diphenylamine solution (both 2% in acetone) were mixed and 10 ml phosphoric acid, 85% was added. The plate was manually immersed in the reagent for 1 second. Then, the plate was heated on a plate heater for 3 min at 120°C. Plate images were documented using the Camag TLC visualizer. Exposure time was 20 ms, gain 1 (white light, transmission mode). Quantitative evaluation of the image was done by Camag VideoScan 1.02.00 via peak height. For evaluating different layers, eluents and impregnation techniques the CAMAG Vario System was used.

HPLC

Sugars were quantified on a Dionex UltiMate 3000 HPLC system (Dionex, Sunnyvale, CA, USA) equipped with a Bio Rad HPLC Carbohydrate Analysis Column Aminex HPX-87P 300mm x 7.8mm column kept at 80 °C and a HP 1100 Series G1362A RID Refractive Index Detector (Hewlett-Packard, Palo Alto, CA, USA). The mobile phase was pure water at a flow of 0.6 mL/min. Calibration was performed externally relative to sorbitol as the internal standard. All standards were purchased from Sigma-Aldrich. Data was recorded with Dionex Chromeleon 6.8.

GC-MS

Sugars were derivatised according to the ethoximation-silylation approach [1]. The derivatized samples were diluted with ethyl acetate and filtered prior to injection. Aliquots of 0.2 ml were introduced into the splitless injector with an Agilent GC Sampler 120GC/MS analysis was performed on an Agilent7890A gas chromatograph coupled with an Agilent 5975C mass selective detector. Column: HP-5 MS (30m 0.25 mm 0.25mm; J&W Scientific, Folsom, CA, USA); carrier gas: helium, injector: 2801C; column flow: 0.9 ml/min; purge flow: 32.4 ml/min, 0.6 min; oven program: 50°C (2 min), 5°C/min, 280°C (20 min); MS: EI mode,70 eV, source pressure:1.13 10–7 Pa, source temperature: 230°C. Scan range was set from 50 to 950 Da.

III. RESULTS AND DISCUSSION

Quantification of plant-derived carbohydrates needs methods which are reliable, especially in routine analysis, as e.g. for control of fermentable sugars in samples. Methods which are simple, rapid and capable of being run in large numbers are of particular interest. Paper chromatography (PC) and TLC have been extensively used in the analysis for sugars [2]. However, quantification of sugars is mainly done by GC oder LC approaches. HPTLC offers a lot of benefits when compared to other methods: low running costs, high sensitivity, high throughput or the ability to simultaneously isolate and identify the sugars,to name but a few.

One drawback of the HPTLC method is that mobility of sugars on silica layers depends mainly on the molecular weight and the number of hydroxyl groups, and diastereomers are thus poorly resolved [3]. Therefore the selectivity of commercially available layers has to be adjusted. Preliminary tests showed that impregnation with phosphate buffer gave the best selectivity for aldohexoses, arabinose and xylose (fig. 1). However, two developments of the chromatogramm after separation are necessary to get appropriate Rf values. Using the ADC device for plate developing, the error of a two-step development remains negligible since all the steps are fully automated, which largely improves reproducibility. The total run time of the whole chromatographic procedure is less than 1.5 h.

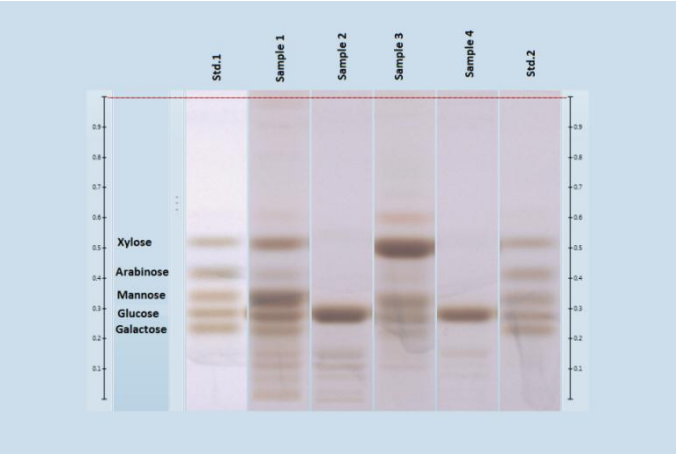

Figure 1. HPTLC chromatogram of wood-hydrolyzate sugars.

Since carbohydrates have no chromophores or fluorophores attached, a postchromatographic derivatisation is necessary for the detection on silica layers. Three different derivatisation approaches were investigated. With p-aminobenzoic acid all sugars showed a blue fluorescence when inspected at 366 nm. The thymol-dye has the benefit to distinguish sugars by color, with aldohexoses giving orange spots, arabinose a blue and xylose a brown spot. However, the signal-to-noise ratio was best in th ecase of the anilin-diphenylamine dye. This dye was used for quantification. The possibility of using different derivatisation methods is also an asset of (HP)TLC since this delivers agood optical impression of a sample as required for automated processing. For a first proof of concept, the whole image was processed by the VideoScan software (CAMAG). The use of a TLC scanner, for densitometric analysis with defined wavelength sensitivity, further improved the overall performance. Although the relative humidity is said to be less critical when using polar eluents [4], we settled that an increased humidity worsens the separation and shape of the spots. Therefore, a well controlled environment is a necessary prerequisite for such a separation.

For comparing results obtained by HPTLC with alternative methods, samples were also analyzed according to common HPLC and GC-MS methods. Focusing on the analysis time, the HPTLC method is by far the fastest method. Table 1 gives an overview of results obtained by these three different methods. The findings of sugars were comparable for all three methods, despite for mannose in sample A, xylose in sample B and glucose in sample C which had standard deviations above 10 %. However, it is more difficult to determine which method delivers the most accurate results. Matrix interference is by far most problematic for the HPLC method. For GC-MS analysis of carbohydrates a derivatisation step is needed, which is time demanding and error-prone. Also the processing and interpreting of partly very complex GC spectra (due to the presence of isomers and anomers) can be tedious.

Table 1. Example of results obtained by HPTLC, HPLC and GC/MS

	Sample A			Sample B			Sample C		
	HPTLC [g*l^{-1}]	**HPLC [g*l^{-1}]**	**GCMS [g*l^{-1}]**	**HPTLC [g*l^{-1}]**	**HPLC [g*l^{-1}]**	**GCMS [g*l^{-1}]**	**HPTLC [g*l^{-1}]**	**HPLC [g*l^{-1}]**	**GCMS [g*l^{-1}]**
Ara	13.9	12.8	-	10.12	28.5	7.6	-	-	-
Gal	23.9	22.0	28.3	28.3	-	8	-	-	-
Glu	29.6	46.2	47.1	20.8	32.5	11.9	38.9	115.9	112.3
Man	44.4	95.1	93.4	27.8	49.3	-	1.2	-	-
Xyl	34.6	54.1	57.3	60.4	231.6	248.6	2.1	0.4	-

As shown in fig. 2 the HPTLC method can be extended to analyze additional compounds, which were also abundant in such hydrolyzate samples for instance cellobiose, sucrose, or sugar acids can be easily covered with this system.

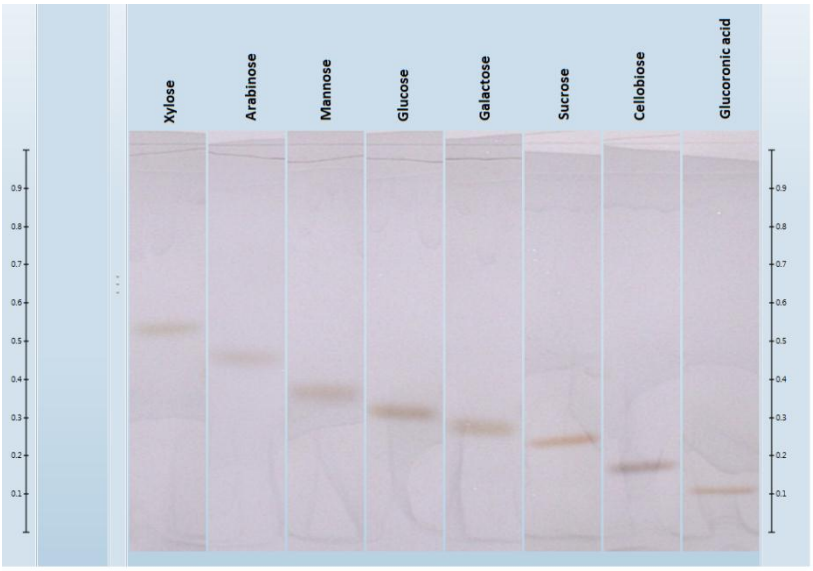

Figure 2. Extension of the HPTLC method to compounds other than monomeric pentoses and hexoses; in this example: sucrose, cellobiose and gluconic acid.

IV. CONCLUSIONS

The performance of HPTLC for quantification of monosaccharides and related compounds in real-world wood hydrolyzate samples was investigated. The aim of this study is to develop a fast quantification method for wood-derived carbohydrates.

We demonstrated the usefulness of planar chromatography in routine quantification of sugars derived from plant hydrolyzates. Especially in industry (e.g. for control of fermentation processes) the accurate quantification of the sugar content is of great importance. As matrix problems are a minor issue in HPTLC, the method is very flexible with regard tosample origins and impurities. Within two hours, 16 samples can be analysed, which is by far superior to HPLC or GC-MS. The comparison with those methods that are conventionally normally used for quantification of wood sugarsshowed HPTLC to stand fully emancipated among alternative separation techniques. A full validation of the HPTLC method is still in progress, but so far the results are quite promising that a quantification of sugars in plant material by HPTLC can compete with other chromatographic techniques.

V. ACKNOWLEDGEMENT

The generous financial support by BASF SE is gratefully acknowledged.

VI. REFERENCES

[1] Becker, M; Zweckmair, T; Forneck, A; Rosenau, T; Potthast, A; Liebner, F. Evaluation of different derivatisation approaches for gas chromatographic-mass spectrometric analysis of carbohydrates in complex matrices of biological and synthetic origin. *J Chromatogr A.* **2013**; 1281(2):115-126

[2] Robards, K.; Whitelaw M. Chromatography of monosaccharides and disaccharides. *J Chromatogr A.* **1986**: 373: 81-110

[3] Stahl E.; Thin-Layer Chromatography – A Laboratory Handbook. *Springer Verlag* **1969**

[4] Morlock G. E.; Sabir G. Comparison of two orthogonal liquid chromatographic methods for quantification of sugars in food. *J. Liq. Chromatogr.* **2011**; 34:10-11, 902-919

COMPARISON OF PINOSYLVIN CONTENT IN PINE SPECIES FROM DIFFERENT LOCATIONS IN EUROPE

Primož Oven[1]*, Ida Poljanšek[1], Viljem Vek[1], Stefan Wilfför[2], Juan Carlos Parajó[3]

[1]*University of Ljubljana, Biotechnical faculty, Department of wood science and technology, Rozna dolina VIII/34, 1000 Ljubljana, SI-Slovenia,*
[2]*Process Chemistry Centre, Åbo Akademi University, Porthansgatan 3, FI-20500, Turku, Finland*
[3]*Department of Chemical Engineering, Polytechnical Building, University of Vigo (Campus Ourense). As Lagoas. 32004 Ourense, Spain. (*primoz.oven@bf.uni-lj.si)*

ABSTRACT

The aim of this research was examination of content of pinosylvins in wood of three pine species (*Pinus nigra, P. sylvestris and P. pinaster*) originating from different locations in Europe. European black pine (*Pinus nigra*) trees were cut-down in SW Slovenia, Scots pine (*Pinus sylvestrias*) in Finland, and *Pinus pinaster* trees were sampled in NW Spain. Samples of sapwood, heartwood, and dead and living knots were sequentially extracted in a Soxhlet apparatus with cyclohexane and then with acetone/water. The content of lipophilic and hydrophilic extractives was determined gravimetrically. The content of pinosylvin (PS) and pinosylvin monomethyl ether (PSMME) were analysed by HPLC. Content of PS and PSMME was highest in dead and linving knots in all investigated species. *P. sylvestris* exhibited higher content of pinosylvin than other two species. On the other hand, heartwood of *P. nigra* contained more PSMME than *P. sylvestris* and *P. pinaster*.

I. INTRODUCTION

Woody biomass represent increasingly important source of products other than wood, including structural polymers of the cell walls, cellulose, lignin and hemicelluloses, and extracellular low molecular weight compounds, which are referred to as extractives. Extractives comprise compounds that are involved in primary metabolism of living cells as well as the compounds that are usually characterized as secondary metabolites or natural products. The later have important ecological functions in the living tree including protection against colonization by microorganism and protection against attack by herbivores and insects.

Composition of wood extractives is species specific and highly variable among species, growth sites and within the tree. It has been demonstrated recently that heartwood and especially knots of softwood and broadleaved species represent rich source of phenolic compounds [1, 2, 3]. Knots of softwood contain mostly lignans, oligolignans and stilbens, whereas flavonoids were found in hardwood tissues. Stilbene pinosylvin and its monomethyl ether are the characteristic compounds of heartwood and knots of the genus *Pinus* (1).

Pinosylvins exhibited antimicrobial activity against a battery of both gram positive and negative bacteria, yeasts, and filamentous fungi [4, 5]. The antimicrobial effects of pinosylvin were even more prominent than those of a related stilbene, resveratrol, well known for its various bioactivities [5]. Extracts obtained from pine knotwood showed also cytotoxicity against a mouse hepatoma cell line [4]. It was concluded that pinosylvin could have potential as a natural disinfectant or biocide in some targeted applications [5]. Optimal extraction procedures [6] as well as pine species, growth sites and tissues containing high concentration of pinosilvins should be identified for eventual industrial recovery of pinosylvin from pinewood. The aim of this research was examination of content of pinosylvins in wood of three pine species (*Pinus nigra, P. sylvestris and P. pinaster*) originating from different geographic and climatic locations in Europe, namely Slovenia, Finland, and Spain.

II. EXPERIMENTAL

European black pine (*Pinus nigra*) trees were cut-down in SW Slovenia, Scots pine (*Pinus sylvestris*) in Finland, and *Pinus pinaster* trees were felled in NW Spain. Discs were removed from the stems at about 1 m above the ground and bolts containing bases of dead and living branches from the upper parts of trees. These tissues will be referred to as dead and living knots. Samples of sapwood, heartwood, and dead and living knots were isolated, air dried, milled, and extracted in a Soxhlet apparatus. Lipophilic compounds were extracted with cyclohexane and hydrophilic compounds with acetone/water (95:5 v/v)

The content of lipophilic and hydrophilic extractives was determined gravimetrically by drying until constant weight. The content of pinosylvin (PS) and pinosylvin monomethyl ether (PSMME) were analysed by Thermo Fischer Scientific Accela HPLC modular system (Waltham, USA), equipped by Accela 600 quarter pump and Accela photo-diode array detector (PDA). Extractives were separated on the Accucore PFP column (Thermo Fischer Scientific) with dimensions of 2.1mm × 150 mm and the particle size of 2.6 µm. The column was thermostatted on 30°C. The mobile phase was consisted of water with 0.1% of formic acid (v/v) as solvent A and methanol containing 0.1% of formic acid as solvent B. The 10 minutes gradient from 5 to 65% of solvent B was applied for elution, where mobile phase flow rate was defined at 400 µL/min. The detection wavelength was adjusted to 275 nm. Quantitative analysis based upon three point calibration curve, consisting of standard solutions. Chromatograms were evaluated by ChromQuest 5.0 software. Peak identification was achieved by comparison of retention times and UV spectra of separated compounds with analytical standards. The content of pinosylvins was expressed in mg of compound per gram of dry wood (mg/g).

III. RESULTS AND DISCUSSION

Gravimetric determination of lipophilic and hydrophilic extractives (**Figure 1**) showed that knots contain essentially more extractives than sapwood and heartwood. Knots contained more lipophilic extractives than heartwood, whereas dead knots contained more lipophilic extractives than living knots in the three investigated pine species. The amount of lipophilic extractives was largest in *P. nigra*, whereas *P. pinaster* revealed the lowest values.

The content of hydrophilic extractives revealed the same distribution pattern among tissues in the investigated trees. *Pinus sylvestris* contained more hydrophilic extractives than *P. nigra* and *P. pinaster*.

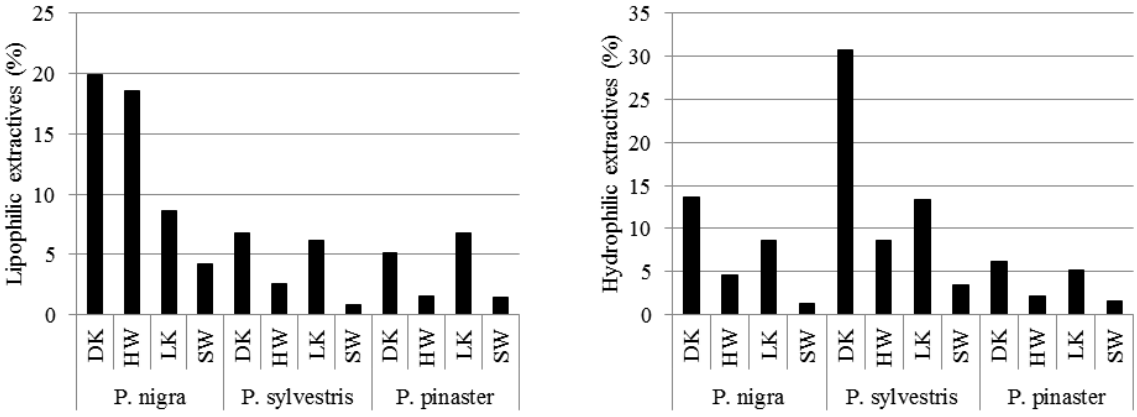

Figure 1. The contents of lipophilic and hydrophilic extractives in different tissues of *Pinus nigra*, *P. sylvestris* and *P. pinaster*. DK = dead knot, HW = heartwood, LK = living knot, SW = sapwood.

Pinosylvin (PS) and pinosylvin monomethyl ether (PSMME) were present in both the cyclohexane and the acetone extract (**Table 1**). Only small amounts of pinosylvin were extracted by cyclohexane from knots (0.30 mg/g dw) comparing to acetone extracts where up to 35.0 (mg/g) of pinosylvin was found in dead knots. *P. sylvestris* from Scandinavia revealed highest values of PS. As well, the amount of PSMME extracted by cyclohexane was largest in *P. sylvestris* and only small amounts were found in *P. pinaster*. In the acetone extracts, the amount of PSMME was slightly larger in *P. nigra* than in *P. sylvestris*.

Table 1 Content of pinosylvin (PS) and pinosylvin monometyl ether (PSMME) in extracts of various tissues of *Pinus nigra*, *P. sylvestris* and *P. pinaster* obtained by sequential extraction, first with cyclohexane and thereafter with acetone/water. DK = dead knot, HW = heartwood, LK = living knot, SW = sapwood.

	Extraction with cyclohexane		**Extraction with acetone/water**	
	PSMME (mg/g)	**PS (mg/g)**	**PSMME (mg/g)**	**PS (mg/g)**
P. nigra				
SW	0,15	n.d.	0,18	0,23
HW	20,18	0,07	44,08	20,44
DK	46,16	0,34	54,02	22,34
LK	34,16	0,39	48,84	15,78
P. ylvestris				
SW	n.d.	n.d.	0,13	0,07
HW	18,76	0,10	15,94	17,60
DK	54,49	0,47	44,85	35,17
LK	40,54	0,16	33,16	23,00
P. pinaster				
SW	0,14	n.d.	n.d.	n.d.
HW	0,30	n.d.	6,06	5,91
DK	0,92	0,54	2,47	1,08
LK	0,89	n.d.	2,61	0,87

IV. CONCLUSIONS

This study confirmed the known variability in content of pinosylvins within the tree, i.e. knots represent the richest source of valuable bioactive phenolic compounds. These preliminary results indicate, that heartwood of P. nigra contain more PSMME than *P. sylvestris* and P. *pinaster*. On the other hand, *P. sylvestris* form Scandinavia revealed highest content of PS than other two species. Our study demonstrated considerable variability in content of pinosylvins among three pine species from different locations in Europe.

V. ACKNOWLEDGEMENT

The transnational research was conducted within the frame of FP7 WoodWisdom-Net Research Programme and was founded by national founding organizations within the framework of the ERA-NET WoodWisdom-Net2.

VI. REFERENCES

[1] Willför, S.; Hemming, J.; Reunanen, M.; Holmbom, B. (2003a). Phenolic and lipophilic extractives in Scots pine knots and stemwood. Holzforschung. **2003a**, *57*, 359-372.

[2] Willför, S.M.; Ahotupa, M.O.; Hemming, J.E.; Reunanen, M.H.T.; Eklund, P.C.; Sjöholm, R.E.; Eckerman, C.S.E.; Pohjamo, S.P.; Holmbom, B.R.. Antioxidant activity of knotwood extractives and phenolic compounds of selected tree species. J Agric Food Chem. **2003b**, *51*, 7600-7606.

[3] Pietarinen, S.P.; Willför, S.; Sjöholm R.E.M.; Holmbom, B.R. Bioactive phenolic substances in important tree species. Part 3: Knots and stemwood of *Acacia crassicarpa* and *A mangium*. Holzforschung. **2005**, *59*, 94-101.

[4] Välimaa, A.-L.; Honkalampi-Hämäläinen, U.; Pietarinen, S.; Willför, S.; Holmbom, B.; von Wright, A. Antimicrobial and cytotoxic knotwood extracts and related pure compounds and their effects on food-associated micro-organisms. Int J Food Microbiol. **2007**, *115*, 235-243.

[5] Plumed-Ferrer, C.; Väkeväinen, K.; Komulainen, H.; Rautiainen M.; Smeds, A.; Raitanen, J.; Eklund, P.; Willför, S.; Alakomi H.; Saarela M.; von Wright, A. The antimicrobial effects of wood-associated polyphenols on food pathogens and spoilage organisms. Int J Food Microbiol. **2013**, *164*, 99–107.

[6], Fang W.; Hemming, J.E.;, Reunanen M.; Eklund P.; Pineiro E. C., Poljanšek I; Oven P.; Willför, S. Evaluation of selective extraction methods for recovery of polyphenols from pine. Holzforschung. **2013**, *67*, 843-851.

A NOVEL TITRATION METHOD OF OXOAMMONIUM SALT CONVERTED FROM RADICAL TEMPO

Timo Pääkkönen[1]*, Gopi Krishna Tummala[1], Raili Pönni[1], Markus Nuopponen[2], Tapani Vuorinen[1]

*[1]Aalto University, School of Chemical Technology, Department of Forest Products Technology, P.O. Box 16300, 00076 Aalto, Finland; [2]UPM, Tekniikantie 2 C, 02150 Espoo, Finland (*timo.paakkonen@aalto.fi)*

ABSTRACT

A separate activation treatment of 2,2,6,6-tetramethyl-1-piperidinyloxy (TEMPO) prior to the TEMPO-mediated oxidation of pulp and a novel titration method for oxidized TEMPO ($TEMPO^+$) is introduced. TEMPO can be activated without NaBr in neutral conditions using high enough concentrations of HOCl. The formation of $TEMPO^+$ was verified with the novel iodometric titration method. The new method provides useful information on the activation of radical TEMPO in the absence of NaBr (bromide interferes with the titration). Oxidation of pulp at slightly alkaline conditions (pH 8) began immediately after adding the activated catalyst and NaOCl. A carboxylate content of 0.7 mmol/g pulp was achieved by using 2.3 mmol NaOCl *per* g pulp with less than 3 hours reaction time.

I. INTRODUCTION

TEMPO-mediated oxidation of alcohols to aldehydes and further to carboxylates was introduced in 1980`s [1-3]. Later the method was applied for the oxidation of cellulose [4]. Preparation of nanofibrillated cellulose (NFC) through TEMPO-mediated oxidation of cellulosic fibers was reported some years later [5, 6] and has been studied widely since then. TEMPO-mediated oxidation can be used for easier disintegration of chemical pulps to form a transparent gel of NFC [7, 8]. The energy consumption in the production of NFC can be reduced from 700-1400 MJ kg^{-1} to less than 7 MJ kg^{-1} by applying the TEMPO-mediated oxidation for wood pulps [9]. The most common oxidation process of pulp is based on the use of NaBr/TEMPO/NaOCl at pH $\geq$ 10 [7, 10]. The reaction rate of bromide-free TEMPO-mediated oxidation (e.g. electro-mediated TEMPO-oxidation or acid-neutral TEMPO/NaOCl/$NaClO_2$ oxidation) is clearly too low for industrial purposes. However, a process without bromide would be more attractive since its presence in the waste water stream is highly undesired [11]. Activation of TEMPO, which is the commercially available stable radical compound, to the more reactive oxoammonium cation ($TEMPO^+$) must take place to oxidize the hydroxymethyl groups in cellulose.

In this study we introduce a separate activation step for TEMPO prior to the oxidation of cellulose. The conversion of TEMPO to $TEMPO^+$ by HOCl, which is the main form of hypochlorite at pH < 7.5, is effective in HOCl concentrations higher that those during the following pulp oxidation.

II. EXPERIMENTAL

Materials

Dried bleached birch pulp from a Finnish pulp mill was used as the raw material in the TEMPO-mediated oxidations. TEMPO (Sigma Aldrich (St Louis)) and 13 % NaOCl solution (Merck (Darmstadt, Germany) were used as the catalyst and stoichiometric oxidant, respectively. Orthoboric acid (22 g, VWR (Leuven, Belgium)) and NaOH pellets (1.8 g, VWR (Leuven, Belgium)) were diluted to 2000 ml of distilled water to prepare a borate buffer (pH 8.3). $NaClO_2$ (Sigma Aldrich (Germany)) was used to convert the residual aldehydes in the oxidized pulp to carboxylates. The pulp oxidations were carried out in a Büchi reactor (volume 1.6 dm^3) equipped with a Metrohm 718 Stat Titrino titrator to control pH during the oxidation. 1 M NaOH (Merck, (Darmstadt, Germany)) and 1 M HCl (Merck (Darmstadt, Germany)) were used to control pH. The carboxylate contents of the oxidized pulp were determinated by conductometric titration with Metrohm 751 GPD Titrino titrator and Tiamo 1.2.1. software.

Activation of TEMPO

A stoichiometric excess of NaOCl was mixed with solid TEMPO in water and the pH was adjusted to neutral. The solution was mixed in a closed vessel until TEMPO was completely dissolved. In reference, TEMPO was activated with NaOCl in the presence of NaBr at pH 10.

Oxidation of bleached pulp

Aqueous pulp suspension and the activated TEMPO solution were mixed well in a closed vessel and added to the Büchi reactor (continuous mixing, temperature 25 °C, volume of pulp solution 1.2 dm^3). NaOCl solution was added to the reactor with a pump and pH was adjusted to 8 by 1 M NaOH added with an automatic titrator. The reaction was monitored by iodometric titration for active chlorine until all HOCl was consumed. The pulp was washed through a wire cloth. The carboxylate content (SCAN-CM 65:02) and the CED viscosity (SCAN-CM 15:99) were analyzed from the washed pulp samples.

Conversion of residual aldehydes to carboxylates

After the washing, the acidity of the pulp suspension (1 % consistency) was adjusted to pH 3 by 1 M HCl. $NaClO_2$ (10 mM concentration) was added to the solution and conversion was executed in the Büchi reactor (2 hours, 50 °C). The washing and the analysis of the pulp were conducted according to the same procedures described in the previous section.

HOCl and $TEMPO^+$ titration

The titration is based on the method of Wartiovaara [12] except for the analysis of $TEMPO^+$. The liberated iodine was titrated with $Na_2S_2O_3$ using starch as an indicator. The iodometric titration is based on the following reaction (Eq. 1):

$$I_2 + 2\ S_2O_3^{2-} \rightarrow S_4O_6^{2-} + 2\ I^- \quad \text{(Eq. 1)}$$

First, borate buffer (pH 8.3) was added to two sample containers. Then, DMSO was added to one of the sample containers. A known amount of the sample solution together with an excess amount of KI was added to both of the containers. Both samples were titrated against $Na_2S_2O_3$ using starch as an indicator. The following reactions occur under the neutral medium:

$$HOCl + H^+ + 2\ I^- \rightarrow Cl^- + I_2 + H_2O \quad \text{(Eq. 2)}$$

$$2\ TEMPO^+ + 2\ I^- \rightarrow 2\ TEMPO^* + I_2 \quad \text{(Eq. 3)}$$

Because DMSO reacts rapidly with HOCl, the consumption of thiosulphate in the presence of DMSO corresponds to the amount of $TEMPO^+$ present (Eq. 1 and Eq. 3). The titration result without DMSO gives the total amount of HOCl and $TEMPO^+$ (Eqs. 1-3).

III. RESULTS AND DISCUSSION

Activation of TEMPO to form $TEMPO^+$ was monitored with iodometric titration with added DMSO as a function of reaction time using stoichiometric amounts of TEMPO and NaOCl at two concentrations (**Figure 1**). The reaction was carried out at pH 8.3 (borate buffer) at room temperature. Most of TEMPO (85 %) was converted into $TEMPO^+$ during 4 hours reaction time at 10 mM added concentration of TEMPO and NaOCl. The halftime of the reaction was < 30 min at this concentration. At 2 mM added concentration of TEMPO and NaOCl the reaction was very slow and the conversion into $TEMPO^+$ was only 40 % after 4 hours reaction time. Clearly, a separate activation treatment of TEMPO in concentrated solution is an effective pretreatment for the bromide-free TEMPO-mediated oxidation.

Consumption of NaOCl during the activation of TEMPO (2 mM) was monitored by iodometric titration at several concentration levels of NaOCl (**Table 1**). Because NaOCl undergoes also self-decomposition, blank solutions of NaOCl without added TEMPO were titrated correspondingly. NaOCl consumption by TEMPO activation was calculated by correcting the values for the self-decomposition of NaOCl under similar conditions, assuming that the self-decomposition and consumption by $TEMPO^+$ formation are additive. The rate of the self-decomposition is proportional to the square of the concentration of HOCl [13]. The thus measured stoichiometry of HOCl consumed relative to $TEMPO^+$ formed was 1:1.5. Because of the non-additivity of the two reactions, the actual ratio must be smaller, most probably 1:2 similar to the stoichiometry proposed in literature [11].

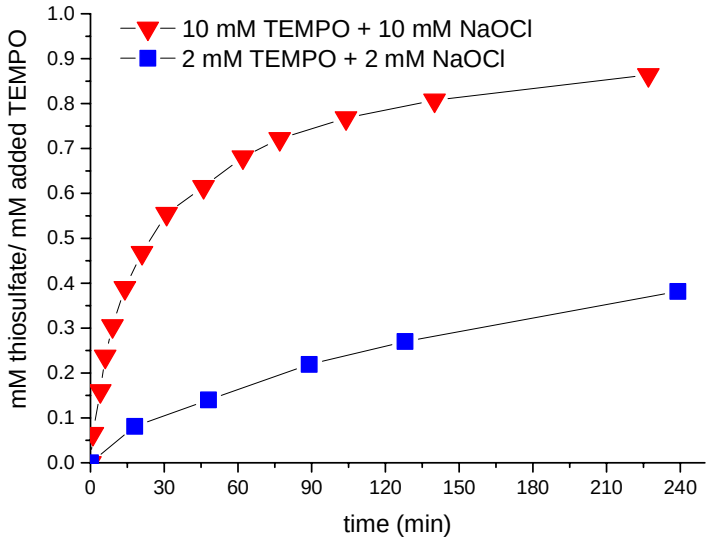

Figure 1. Formation of $TEMPO^+$ in treatment of equimolar amounts of NaOCl and TEMPO at pH 8.3 (borate buffer) at room temperature. The consumption of thiosulphate in iodometric titration in the presence of DMSO (shown) corresponds to the amount of $TEMPO^+$ formed.

Table 1. Formation of $TEMPO^+$ (stoichiometry by Eqs.1 and 3) and consumption of NaOCl (corrected for self-decomposition) in reaction of 2 mM TEMPO with NaOCl at pH 8.3 (borate buffer) for 120 min at room temperature.

[NaOCl]/[TEMPO]	0	0.25	0.5	0.75	1	1.5	2	3	6
$[TEMPO^+]$ (mM)	0	0.124	0.23	0.37	0.52	0.73	1.05	1.41	1.93
$-\Delta$[NaOCl] (mM)	0	0.082	0.15	0.28	0.32	0.47	0.65	0.96	1.37

Bromide-free TEMPO/NaOCl (pH 8) and NaBr/TEMPO/NaOCl treatments (pH 9-10) with and without a separate TEMPO activation step were applied to oxidize birch pulp to high carboxylate content (**Table 2**). Formation of the oxoammonium cation ($TEMPO^+$) in the separate TEMPO activation stage was verified by iodometric titration. Bromine compound formed in the presence of NaBr interfered with $TEMPO^+$ in the iodometric titration and therefore $TEMPO^+$ could not be quantified in the presence of NaBr. When NaBr was not used, the separate activation step reduced the oxidation time from 317 min to 170 min. On the other hand, there was no benefit from the preactivation in the NaBr/TEMPO/NaOCl system, which was much faster than the bromide-free oxidation.

Table 2. Effect of preactivation of TEMPO on oxidation of bleached kraft pulp. The oxidation was carried out at pH 8 (without NaBr) or at pH 9-10 (with NaBr). All oxidations were performed at 4 % pulp consistency at 25 °C.

Preactivation	Yes	No	Yes	No
Radical TEMPO activator	NaBr/NaOCl	NaBr/NaOCl	NaOCl	NaOCl
TEMPO (mM)	2	2	2	2
TEMPO (mmol/g)	0.05	0.05	0.05	0.05
NaOCl (mmol/g)	2.4	2.4	2.3	2.3
Molar ratio (activator/TEMPO)	2.0	-	2.5	-
$TEMPO^+$ formed (mM)	nd	nd	1.75	-
Reaction time (min)	28	28	170	317
COOH (mmol/g)	0.79	0.88	0.70	0.74
after aldehyde conversion	0.99	0.98	0.92	0.92

IV. CONCLUSIONS

$TEMPO^+$ titration seems to be a valuable tool to study the chemistry of the bromide-free TEMPO-mediated oxidation. A separate activation step by NaOCl prior to the TEMPO-mediated oxidation increases the reaction rate of bromide-free oxidation drastically. However, in the case of NaBr/TEMPO/NaOCl oxidation there is no clear benefit to use a separate TEMPO preactivation.

V. ACKNOWLEDGEMENT

This study was supported by UPM Nanocenter and the Finnish Funding Agency for Innovation (TEKES). We thank Mrs Mirja Reinikainen and Mrs Kristel Kosk for excellent laboratory work.

VI. REFERENCES

[1] Anelli, P.L.; Biffi, C.; Montanari, F.; Quici, S. Fast and selective oxidation of primary alcohols to aldehydes or to carboxylic acids and of secondary alcohols to ketones mediated by oxoammonium salts under two-phase conditions. *J Org Chem.* **1987,** 52**,** 2559-2562.

[2] Semmelhack, M.F.; Chou, C.S.; Cortes D.A. Nitroxyl-mediated electro-oxidation of alcohols to aldehydes and ketones. *J Am Chem Soc*. **1983**, 105, 4492-4494.

[3] Semmelhack, M.F.; Schmid, C.R.; Cortes, D.A.; Chou, C.S. Oxidation of alcohols to aldehydes with oxygen and cupric ion, mediated by nitrosonium ion. *J Am Chem Soc.* **1984**, 106, 3374-3376.

[4] Isogai, A.; Kato, Y. Preparation of polyuronic acid from cellulose by TEMPO-mediated oxidation. *Cellulose.* **1998**, 5, 153-164.

[5] Saito, T.; Okita, Y.; Nge, T.; Sugiyama, J.; Isogai, A. TEMPO-mediated oxidation of native cellulose: Microscopic analysis of fibrous fractions in the oxidized products. *Carbohydr Polym*. **2006**, 65, 435-440.

[6] Saito, T.; Nishiyama, Y.; Putaux, J.; Vignon, M.; Isogai, A. Homogeneous suspensions of individualized microfibrils from TEMPO-catalyzed oxidation of native cellulose. *Biomacromolecules*. **2006**, 7, 1687-1691.

[7] Saito, T.; Isogai, A. TEMPO-mediated oxidation of native cellulose. The effect of oxidation conditions on chemical and crystal structures of the water-insoluble fractions. *Biomacromolecules.* **2004**, 5, 1983-1989.

[8] Tanaka, R. Cellulose nanofibrils prepared from softwood cellulose by TEMPO/NaClO/$NaClO_2$ systems in water at pH 4.8 or 6.8. *Int J Biol Macromol*. **2012**, 51, 228-234.

[9] Isogai, A. TEMPO-oxidized cellulose nanofibers. *Nanoscale*. **2011**, 3, 71-85.

[10] Bragd P.L.; van Bekkum, H.; Besemer, A.C. TEMPO-mediated oxidation of polysaccharides: Survey of methods and applications. *Top Catal*. **2004**, 27, 49-66.

[11] Bragd, P.L. Bromide-free TEMPO-mediated oxidation of primary alcohol groups in starch and methyl alpha-D-glucopyranoside. *Carbohydr Res*, **2000**, 328, 355-363.

[12] Wartiovaara, I. The influence of pH on the D_1 stage of a D/CED_1 bleaching sequence. *Paperi ja Puu*. **1982**, 64, 534-545.

[13] Lister, M.W. The decomposition of hypochlorous acid. *Can J Chem*, **1952**, 30, 879-889.

EFFECT OF HYDROXIDE AND SULFITE ION CONCENTRATION ON THE CARBOHYDRATE PRESERVATION DURING ALKALINE SULFITE ANTHRAQUINONE (ASA) PULPING

Markus Paananen[1]*, Tiina Liitiä[2], Stella Rovio[2], Herbert Sixta[1]

[1]Aalto University, School of Chemical Technology, Department of Forest Products Technology, Vuorimiehentie 1, FI-00076 AALTO
[2]VTT Technical Research Centre of Finland, P.O.Box 1000, FI-02044 VTT, Finland

**markus.paananen@aalto.fi*

ABSTRACT

The effect of hydroxide [OH^-] and sulfite [SO_3^{2-}] ion concentration on the polysaccharide degradation and dissolution behavior during alkaline sulfite anthraquinone (ASA) pulping was investigated by a comprehensive characterization of the solid residue and black liquor samples. At a constant temperature of 160˚C, two cooking series were studied at a liquor-to-wood ratio of 200:1 comprising low, L-ASA (0.50 M [OH^-] + 0.375 M [SO_3^{2-}]) and high, H-ASA (1.55 M [OH^-] + 1.163 M [SO_3^{2-}]), concentrations of active cooking chemicals. In both cases, an anthraquinone (AQ) charge of 3 % on wood was applied, which represents an AQ concentration of 0.15 g /L, typical for a commercial cook. Contrary to the expectations, L-ASA cooks revealed rapid delignification, expressed in an H-factor of only 350 to achieve a kappa number-60 pulp. Thus, under H-ASA conditions, the H-factor could only moderately be reduced to 300 to attain the same kappa number. However, H-ASA cooks resulted in a slightly higher yield of 1-2% on wood than the L-ASA cooks but only until a kappa number of about 60 was reached. With progressing delignification the yield advantage was gradually lost. The higher pulp yield at H-ASA conditions was due to an improved galactoglucomannan (GGM) retention, which was approximately 2% on wood above kappa number 60 and approximately 0.5% on wood below kappa number 60. The xylan content, on the other hand, was found to be 1% on wood lower under H-ASA conditions, which may be attributed to an increased solubility of short-chain polysaccharides at high alkali concentration.

I. INTRODUCTION

In chemical pulping, kraft pulping has retained its dominant position as a method of choice owing to fast delignification producing fibers with high strength properties. In addition, the kraft process and its various modifications ensure the utilization of a wide raw material range including softwood and hardwood species. However, as a disadvantage during kraft pulping, substantial yield losses take place owing to unwanted carbohydrate degradation reactions. Today, the industry is struggling with pulp overproduction, thus further savings are pursued through better raw material utilization, or in other words, increasing pulp yield. Parallel to kraft pulping, sulfite pulping has developed many modifications, which are mainly characterized by different bases and pH-ranges. Neutral and alkaline sulfite processes, however, require the use of cations, such as sodium, which form soluble sulfites under these conditions [1, 2]. Increased alkalinity in sulfite processes has ensured the utilization of a wider raw material range, while tolerating even coniferous species containing a notable amount of extractives. Later, it was noticed that the addition of anthraquinone (AQ) substantially accelerated delignification, which was the major disadvantage compared to the kraft process. In the resulting alkaline sulfite anthraquinone process, ASA, the delignification rate was significantly accelerated [3, 4]. However, an additional increase in temperature or longer pulping time compared to kraft pulping was still necessary to obtain a fully bleachable pulp grade. Owing to the presence of AQ, not only the delignification rate was enhanced, but also the retention of hemicelluloses, in particular of galactoglucomannan (GGM), was improved, thus resulting in a higher pulp yield at a target kappa number. The objective of this study was to investigate the effect of the [OH^-] and the [SO_3^{2-}] concentrations on the polysaccharide preservation and the rate of delignification. Following the observations from McDonough et al., it is expected that an increase of both active chemical concentrations will result in an increased rate of delignification [5].

II. EXPERIMENTAL

To diminish the effect of mass transfer and the rapid consumption of cooking chemicals, experiments were conducted with wood meal and liquor-to-wood ratio of 200:1. At a constant temperature of 160˚C, low and high chemical concentration levels were studied during alkaline sulfite anthraquinone (ASA) pulping, namely L-ASA (0.50 M [OH^-] + 0.375 M [SO_3^{2-}]) and H-ASA (1.55 M [OH^-] + 1.163 M [SO_3^{2-}]) in the presence of 0.15 g/L anthraquinone (3% on wood). *Pinus sylvestris L.* raw material from southern Finland was milled to pass through 1mm hole screen and air-dried. Wood meal, together with cooking liquor and AQ was charged into the reactor. The reactor was flushed with nitrogen and pressurized to 0.5 MPa. After 5 minutes, the pressure was released and the reactor was heated to 160˚C temperature in 20 minutes. After the preset time at temperature, the pulp suspension was cooled in the reactor, filtered with a 6 µm pore diameter tissue filter and washed with deionized water. Wood residue was acetone extracted (SCAN 49:03) and analyzed for chemical composition [6, 7]. The dissolution of hemicelluloses was evaluated according to the carbohydrate composition of black liquors.

III. RESULTS AND DISCUSSION

Wood residue

In respect to the delignification rate and the pulp chemical composition, comparison is made to previously published data on kraft and kraft-AQ pulping using exactly the same raw material and otherwise similar pulping conditions [8]. Based on the previous study, the chemical concentration of the active cooking chemicals had a pronounced influence on the rate of pulping. Therefore, the acceleration of the delignification rate through high concentrations of [OH^-] and [SO_3^{2-}] was surprisingly insignificant and not expected, since in a similar comparison of kraft-AQ cooks it was shown that under high alkali (1.55 M [OH^-]) concentration the delignification rate was substantially higher than under moderate alkali (0.50 M [OH^-]) concentration. The low effect of high [OH^-] and [SO_3^{2-}] concentrations on the delignification rate was also reflected in the H-factors to obtain a kappa-60 pulp, which was 300 for H-ASA and 350 for L-ASA, respectively. The delignification, however, slowed down under L-ASA compared to H-ASA conditions when continuing to kappa number 30, which was also apparent in a higher H-factor of 750 compared to only 600 for the latter conditions (Figure 1). Interestingly, at a constant 0.50 M [OH^-] in a comparison between kraft, kraft-AQ and ASA process, L-ASA had the fastest delignification rate, while the opposite behavior was observed at a constant 1.55 M [OH^-], where the delignification in H-ASA proceeded even slower than in an analogous kraft process. In general, the GGM preservation accounts for the major part of the yield increase in alkaline processes of softwoods where AQ has been added. It was shown that a high and constant [OH^-] throughout the cook, e.g. 1.55 M [OH^-], effectively stabilizes the reducing end groups of GGM due to a higher stopping rate, thus resulting in less unwanted degradation reactions [8, 9]. A similar behavior was observed also during the ASA process. In terms of pulp yield, H-ASA was found to be advantageous during the initial delignification, resulting in a notable pulp yield increase owing to better GGM preservation (Figure 2). Interestingly, the GGM stability under H-ASA conditions decreased when cooking proceeded to a lignin content below 10% on pulp (Figure 3). In addition to the enhanced GGM preservation, regardless of the chemical concentration, the ASA process was found to be beneficial in preserving cellulose and xylan in pulp compared to kraft and even kraft-AQ (Table 1).

Black liquor

Under alkaline conditions, degradation and dissolution account for pulp polysaccharide losses in the resulting pulp. The degradation pathway by endwise peeling reactions is by far the most important loss reaction during alkaline treatment of polysaccharides. As a result of the end-group cleavage, various acids are formed, such as glucoisosaccharinic and xyloisosaccarinic acids (Gisa, Xisa), formic, acetic, lactic, 2-hydroxybutanoic and 2,5-dihydroxypentanoic acids in the case of pine wood [10]. The extent of degradation and dissolution is mainly influenced by the pulping liquor composition; however, in order to initiate dissolution of a polymer, the chain length needs to be adjusted to the power of the solvent (sodium hydroxide). Thus, with increasing [OH^-] the solubility of hemicelluloses with increasing chain lengths increases. Similar to pulp polysaccharides, dissolved polysaccharides are unstable at alkaline conditions and thus susceptible towards further degradation. Previously it has been shown that elevated chemical concentration in kraft pulping liquor increase the amount of dissolved polysaccharides [8]. It was also suggested that in the presence of AQ, a further increase of the amount of dissolved polysaccharides could be explained by the enhanced stability of the soluble fraction. The amount of dissolved hemicelluloses is comparable for kraft-AQ and ASA at 0.50 M [OH^-] throughout the cook (Figure 4). However, at 1.55 M [OH^-], the extent of dissolution during H-ASA is significantly lower than in kraft or kraft-AQ as shown in Table 1. This can be explained by a higher hemicellulose retention in the solid residue for the kappa number-60 pulp, however, not for the kappa number-30 pulp.

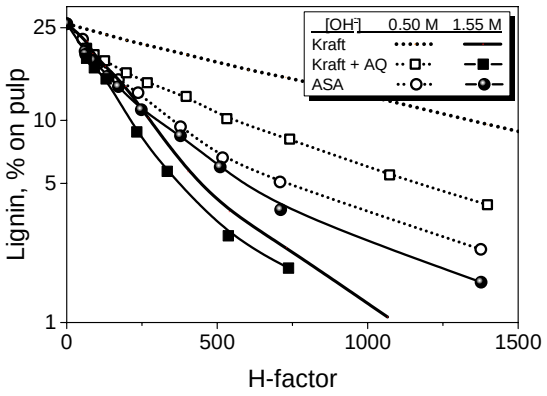

Figure 1. Delignification rate. *Abbreviations:* Kraft (+AQ) performed at 0.50 or 1.55 M [OH^-], 33% sulfidity; 160˚C; (0.15g AQ/L) [8].

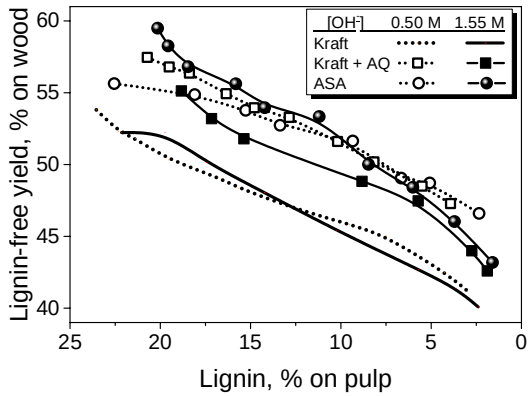

Figure 2. Lignin-free yield as a function of pulp lignin content.

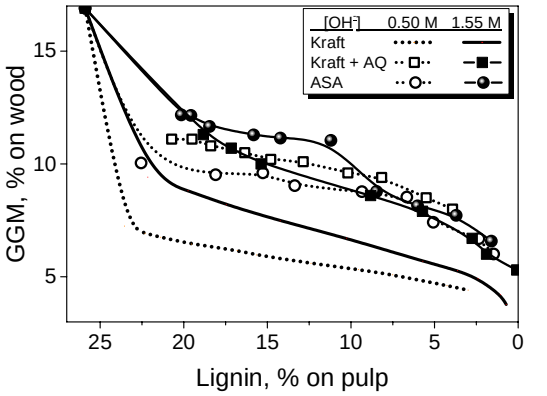

Figure 3. GGM preservation as a function of pulp lignin content.

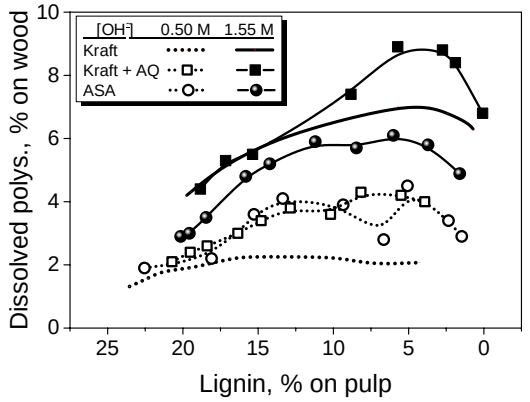

Figure 4. Dissolved polysaccharides in black liquor as a function of pulp lignin content.

Table 1. Wood residue and black liquor composition at kappa number 60 and 30 (corresponding to a pulp Klason lignin content of 9.0% and 4.5%, respectively). *[8]

κ-60 (κ-30)	**0.50 M [OH^-]**			**1.55 M [OH^-]**		
Pulping process	Kraft*	Kraft + AQ*	L-ASA	Kraft*	Kraft + AQ*	H-ASA
AQ charge (g/L)	-	0.15	0.15	-	0.15	0.15
H-factor	1480 (2370)	660 (1270)	410 (870)	300 (480)	230 (390)	350 (650)
Wood residue (% on wood)						
Cellulose	37.0 (35.2)	37.7 (36.8)	38.3 (38.0)	36.4 (35.4)	38.0 (37.3)	38.3 (36.8)
Galactoglucomannan	5.2 (4.6)	9.5 (8.2)	8.7 (7.3)	6.4 (5.5)	8.6 (7.5)	9.3 (7.8)
Xylan	3.4 (2.9)	3.7 (2.8)	4.2 (2.8)	1.9 (1.1)	2.3 (1.4)	3.1 (2.2)
Lignin	4.6 (2.0)	5.1 (2.2)	5.2 (2.3)	4.5 (2.0)	5.0 (2.2)	5.1 (2.2)
Total Polysaccharides	45.6 (42.7)	50.9 (47.8)	51.2 (48.1)	44.7 (42.0)	48.9 (46.2)	50.7 (46.8)
Wood residue yield	50.2 (44.7)	56.0 (50.0)	56.4 (50.4)	49.2 (44.0)	53.9 (48.4)	55.8 (49.0)
Black liquor (% on wood)						
Cellulose	0.1 (0.1)	0.1 (0.1)	0.2 (0.1)	0.2 (0.3)	0.3 (0.3)	0.3 (0.3)
Galactoglucomannan	0.7 (0.9)	1.4 (1.7)	1.3 (1.1)	2.5 (2.9)	3.3 (4.4)	2.2 (2.6)
Xylan	1.4 (1.1)	2.6 (2.3)	2.6 (2.9)	3.9 (3.8)	4.0 (4.5)	3.4 (3.0)
Total dissolved polysaccharides	2.2 (2.1)	4.1 (4.1)	4.1 (4.1)	6.6 (7.0)	7.6 (9.2)	5.9 (5.9)
Polysaccharides in wood residue and in black liquor (% on wood)						
Total polysaccharides	47.8 (44.8)	55.0 (51.9)	55.3 (52.2)	51.3 (49.0)	56.5 (55.4)	56.6 (52.7)

IV. CONCLUSIONS

The increase of the [OH^-] from 0.50 M to 1.55 M at a constant [SO_3^{2-}]/[OH^-] of 0.75 in high liquor-to-wood ASA cooking has a surprisingly low effect on the delignification rate, which is in contrast to kraft-AQ cooking under otherwise comparable conditions. Obviously, the high AQ charge, caused by the high liquor-to-wood ratio, affects the pulping reactions in a more pronounced way in ASA than in kraft cooking. The delignification rates in ASA cooking are higher than in kraft-AQ cooking and almost not affected by the [OH^-] in the high kappa number range. Only at kappa numbers below 60-80, the delignification velocity is progressively increasing at high [OH^-] in reference to the low [OH^-]. Similar to kraft cooking, high [OH^-] promotes the stabilization of GGM. However, the stabilizing effect of high [OH^-] towards GGM diminishes with decreasing kappa number. Overall, the L-ASA pulps reveal a composition and a yield comparable to the kraft analogue at both kappa number levels, however, with a slightly lower GGM-to-xylan ratio. At high [OH^-], ASA cooking results in a higher pulp yield (+1.9%) than kraft-AQ when cooking to kappa number 60. However, the overall carbohydrate yield is almost identical for both processes owing to the higher amount of dissolved polysaccharides in the case of kraft-AQ cooking. However, cooking to kappa number 30 affords a much higher intensity in the case of H-ASA (H-factor 650) than for kraft-AQ cooking (H-factor 390), which might be the reason for the lower total polysaccharide yield of the former due to enhanced degradation reactions.

V. ACKNOWLEDGEMENT

Authors would like to acknowledge the Finnish Funding Agency for Technology and Innovation (Tekes) and FIBIC Ltd. for financial support.

VI. REFERENCES

[1] Ingruber, O. Alkaline sulfite anthraquinone pulping – A brief review of its nature, development and present status. *Proceedings in the TAPPI Pulping conference*, **1985**, 461–469.

[2] Sixta, H. Comparative evaluation of different concepts of sulfite pulping technology. *Lenzinger Berichte*, **1998**, *78*, 18–27.

[3] Kettunen, J., Virkola, N.-E., Yrjälä, I. The effect of anthraquinone on neutral sulphite and alkaline sulphite cooking of pine. *Paperi ja Puu*, **1979**, *61*, 685–700.

[4] Ingruber, O., Stradal, M., Histed, J.A. Alkaline sulphite-anthraquinone pulping of eastern Canadian woods. *Pulp & Paper Canada*, **1982**, *83*, 79–88.

[5] McDonough, T.J., van Drunen, V.J., Paulson, T.W. Sulphite-anthraquinone pulping of southern pine for bleachable grades. *JPPS*, **1985**, *11*, 167–176.

[6] Sluiter, A., Hames, B., Ruiz, R., Scarlata, C., Sluiter, B., Templeton, D., Crocker, D. *Determination of structural carbohydrates and lignin in biomass. Technical Report NREL/TP-510-42618*, **2008**.

[7] Janson, J. Calculation of polysaccharide composition of wood and pulp. *Paperi ja Puu*, **1970**, *52*, 323–329.

[8] Paananen, M., Liitiä, T., Sixta, H. Further insight into carbohydrate degradation and dissolution behavior during kraft cooking under elevated alkalinity wihtout and in the presence of anthraquinone. *Industrial and Engineering Chemistry Research Journal*, **2013**, *52*, 12777–12784.

[9] Paananen, M., Tamminen, T., Nieminen, K., Sixta, H. Galactoglucomannan stabilization during the initial kraft cooking of Scots pine. *Holzforschung*, **2010**, *64*, 683–692.

[10] Sjöström, E. The behavior of wood polysaccharides during alkaline pulping process. *Tappi J.*, **1977**, *60*, 151–157.

LIGNIN FLUORESCENCE IN SOLID STATE

M.V. Panfilova*, D.S. Kosyakov, K.G. Bogolitsyn
Northern (Arctic) Federal University named after M.V. Lomonosov,
Northern Dvina Emb. 17, 163002, Arkhangelsk, Russia
**m.panfilova@narfu.ru*

ABSTRACT

2D excitation-emission fluorescence spectra of wide range of lignin preparations and lignin containing materials in solid state were recorded using the Horiba Fluorolog-3 double monochromator luminescent spectrometer. The presence of long wavelength emission bands in visible region of spectrum is shown for solid lignin samples, which is not usual for polymer solutions. The obvious dissimilarity in excitation-emission spectra and fluorescence intensities for lignins of different origin is demonstrated. These facts are of great significance for the rapid identification of lignins and their determination in lignocellulosic materials. Effect of lignin functional composition on its fluorescent properties and the role of carbonyl groups in fluorescence quenching are studied. The excitation energy transfer in lignin macromolecules is discussed.

I. INTRODUCTION

Natural lignin and related aromatic compounds are characterized by a rather intense fluorescence – the quantum yields for them can reach a few tenths. The excitation source may be the absorption of UV-radiation, and some chemical reactions, which are taking place during the biosynthesis of lignin in plants and manufacturing processes of delignification of wood in pulp production. The study of photoexitation of lignin and properties of natural polymer in exited states is also of great importance of understanding the processes of photoyellowing and photoaging of lignocellulosic materials, and developing the new technologies of pulp bleaching. [1]

The emission intensity and position of bands in the spectrum of lignin and lignin model compounds are depended on the molecular structure comprising a fluorophore and its nearest environment. [2] Removal of the carbonyl groups in macromolecule of natural polymer did not change maximum of excitation and emission band position, but intensity of fluorescence increased dramatically. [3]

Different researchers were studied fluorescent properties of lignin and lignin model compounds in a solvent medium. In general, lignin fluorescence was revealed at excitation range of wavelength from 240 to 350 nm. [4, 5] Also were studied cellulosics and bleached kraft pulps using fluorescence spectroscopy, but lignin fluorescence in solid state did not research. [6, 7]

Given the foregoing, the purpose of this study is estimate role of functional composition of lignin and influence of medium on its fluorescent properties.

II. EXPERIMENTAL

As objects of study, we chose dioxane lignin extracted from spruce wood by the method of Pepper, reduced dioxane lignin ($NaBH_4$-reduction), lignin alkali (Sigma Aldrich) and kraft lignin extracted from black leach from production of sulphate spruce pulp at Arkhangelsk Pulp and Paper Mill (Arkhangelsk, Russia).

Fluorescence spectra were collected using a Fluorolog-3 spectrofluorimeter (Jobin Yvon Horiba, France) equipped with a 450 W xenon lamp, a photomultiplier tube and detection system based on single photon counting. Before measurement the sample was compressed into a tablet and located in sample holder. The spectral slit width in the excitation and emission monochromator was 3 nm. The sample surface was at an angle of 35° with respect to the excitation beam to avoid self-absorbtion.

N,N-dimethylformamide is good solvent of lignin which significantly influence the processes its dissociation. Concentration of solution of lignin in N,N-dimethylformamide was adjusted so that optical density did not exceed 0.1 to avoid inner filter effect. Immediately before measurement solution in 1 cm quartz cuvetts were bubbled with argon to remove dissolve oxygen, which is known as a phenol fluorescence quencher. The spectra of solution are obtained in similar conditions that solid sample.

III. RESULTS AND DISCUSSION

Fluorescence spectra at room temperature of lignin samples in solid state are presented in **Figure 1**.

The fluorescence intensity and wavelength of maximum emission are dependent on the origin of the lignins. Maximum intensity of fluorescence is obtained for dioxane lignin and kraft lignin at wavelength excitation 450 nm. Maximum emission for reduced dioxane lignin is shifted at wavelength excitation 370 nm and observed modification of shape excitation-emission region. For lignin alkali is obtained two maximum intensity of fluorescence at 350 and 450 nm. This is due to different content of carbonyl groups in lignins.

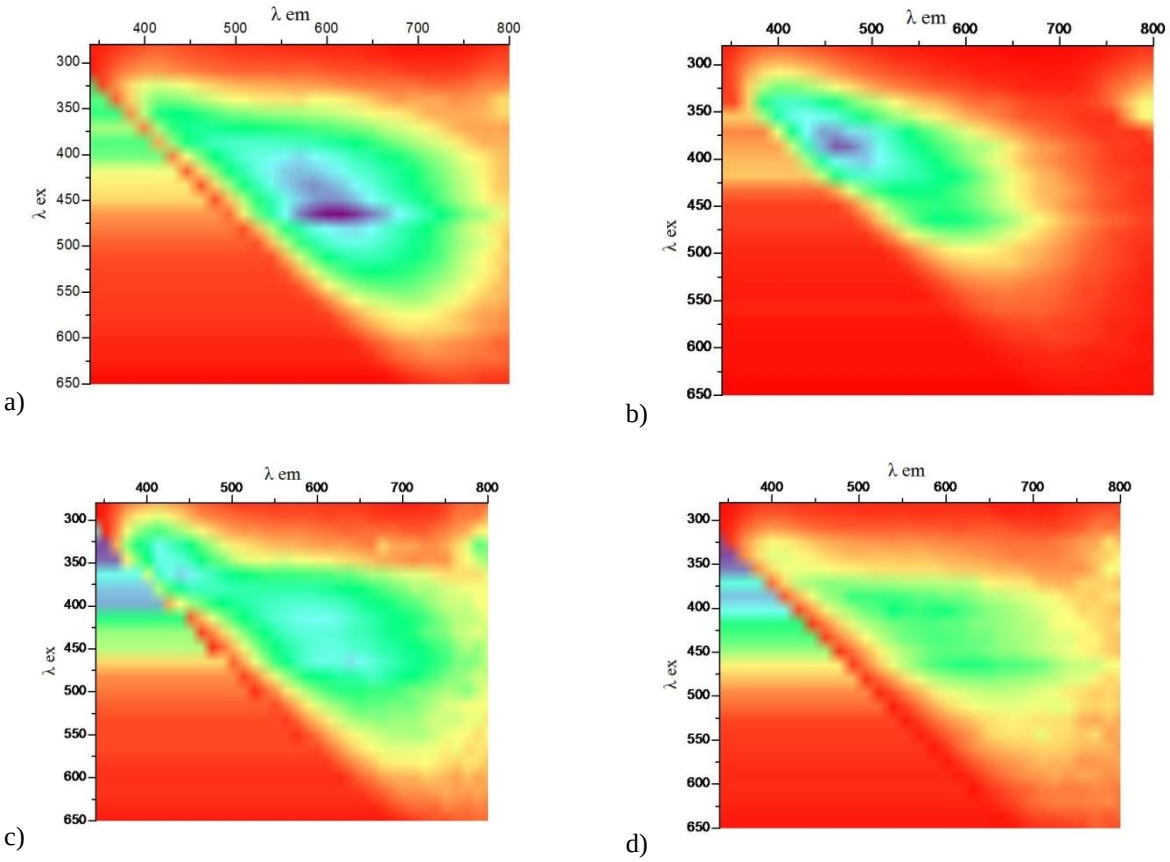

Figure 1. 2D excitation-emission spectra of lignin samples recorded in the solid state in front face mode: a) dioxane lignin; b) reduced dioxane lignin; c) lignin alkali; d) kraft lignin. Color changes from red to violet are showed an increase in fluorescence intensity.

Carbonyl group content was determined by oximation method and shown in Table 1.

Table 1 – Content of carbonyl group in lignin samples

Dioxane lignin, %	Reduced dioxane lignin, %	Lignin alkali, %	Sulphate lignin, %
6.58±0.12	0.83±0.04	1.83±0.14	4.84±0.15

Removal of the carbonyl groups in the lignin by borohydride reduction change the position of emission maximum and intensity of the fluorescence increased dramatically. The mechanism of energy transfer is the following: one fluorophore is absorbed energy at excitation source and emitted it; next fluorophore absorbed emitted energy from first group and fluorescent at more long wave region. Last fluorophore in lignin, emitted energy at 600 nm is carbonyl group conjugated with aromatic ring.

Fluorescence spectra solutions of lignin in N,N-dimethylformamide are shown in **Figure 2**.

Excitation-emission region has a similar shape for four samples. Maximum intensity of fluorescence (400 nm) is obtained at wavelength excitation 370 nm.

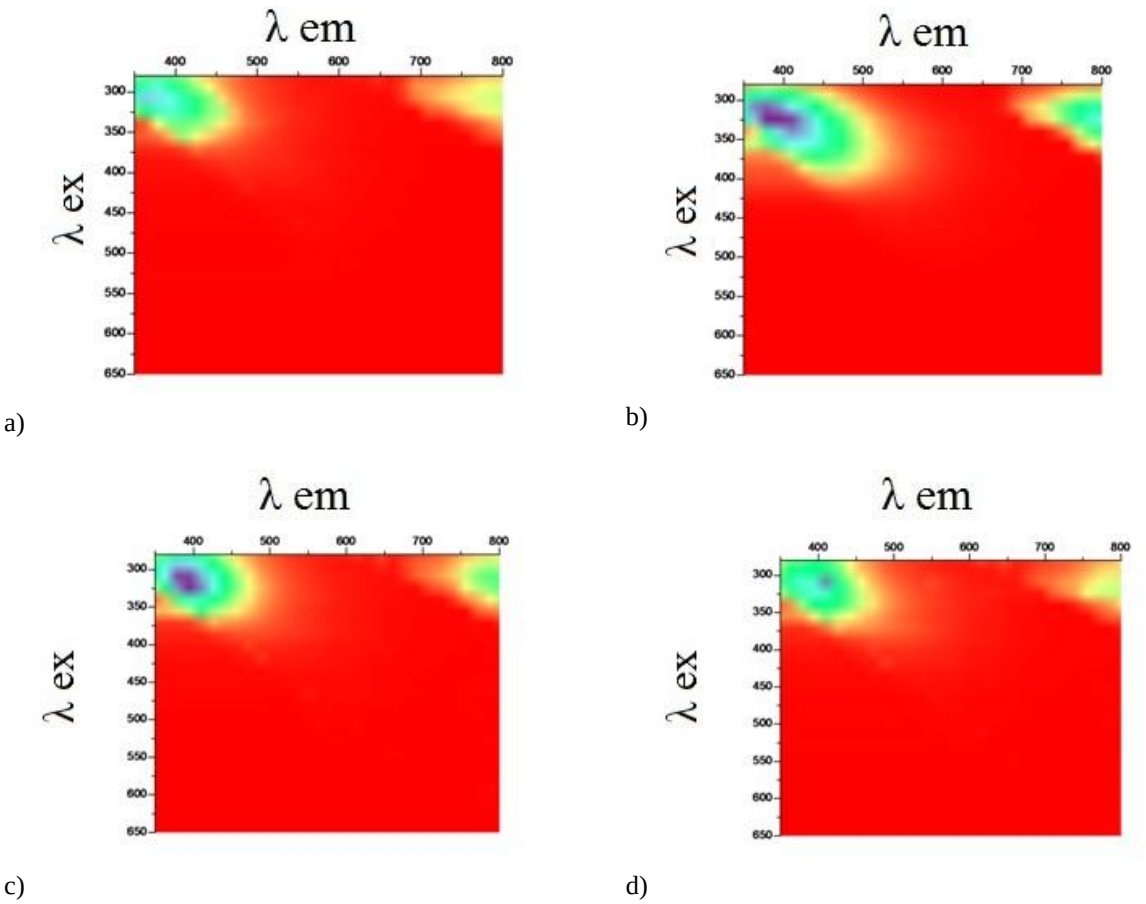

Figure 2. 2D excitation-emission spectra solution of lignin samples:
a) dioxane lignin; b) reduced dioxane lignin; c) lignin alkali; d) kraft lignin.
Color changes from red to violet are showed an increase in fluorescence intensity.

Spectra are shows that in an aprotic solvent the quenching of fluorescence due to solvation effects.

IV. CONCLUSIONS

2D excitation-emission spectra different lignins in solid state are obtained. Carbonyl groups conjugated with aromatic ring in lignin are responsible for long wave fluorescence at 600 nm. Shown that lignin in solid state and solution of lignin had a different band position and intensity of fluorescence due to solvation effects.

V. ACKNOWLEDGEMENT

The authors are grateful to Russian Foundation for Basic Research (project No. 14-03-31593) and Ministry of Science and Education for financial support. Research was done using equipment of Core Facility Center "Arktika" Northern (Arctic) Federal University named after M.V. Lomonosov

VI. REFERENCES

[1] Ragnar, M., Lindgren, C.T., Nilvebrant, N.-O. pKa-value of guaiacyl and syringyl phenols related to lignin. *Journal of Wood Chemistry and Technology*. **2000**, 20 (3), 277 – 305.

[2] Chupka, E. I., Burlakov, V.M., Energetika obmennykh protsessov v lignine. 9 Vozmozhnyye napravleniya vnutrimolekulyarnykh protsessov perenosa zaryada i energii v lignine. (Energy exchange processes in lignin. 9. Possible directions of intermolecular charge transfer processes and energy in lignin) *Khimiya drevesiny*. 1984, 2, 31 – 38.

[3] Albinsson, B., Shiming, L., Lundquist, K., Stomberg, R. The origin of lignin fluorescence. *Journal of Molecular Structure*. **1999**, 508, 19 – 27

[4] Grabner, G., Köhler, G., Marconi, G., Monti, S., Venuti, E. Photophysical Properties of Methylated Phenols in Nonpolar Solvents. *J. Phys. Chem.* **1990**, 94, 3609 – 3613

[5] Radotić, K., Kalauzi, A., Djicanović, D., Jeremić, M., Leblanc, R.M., Cerović, Z.G. Component analysis of the fluorescence spectra of a lignin model compound. *Journal of Photochemistry and Photobiology B: Biology*. **2006**, 83, 1 – 10

[6] Castellan, A., Ruggiero, R., Frollini, E., Ramos, L.A., Chirat, C. Studies on fluorescence of cellulosics. *Holzforschung* . **2007**, 61, 504 – 508

[7] Liukko, S., Teasapuro, V., Liitia, T. Fluorescence spectroscopy for chromophore studies on bleached kraft pulps. *Holzforschung* . **2007**, 61, 509 – 515

DOMAIN SWAPPING BETWEEN TWO HIGH-REDOX POTENTIAL LACCASES: EFFECT ON ENZYME PROPERTIES

Isabel Pardo[1]*, Susana Camarero[1]

[1]*Centro de Investigaciones Biológicas, Ramiro de Maeztu 9, 28040, Madrid, Spain*
*(*iparmen@cib.csic.es)*

ABSTRACT

Laccases from wood-rotting fungi are of great interest as "green" biocatalysts for the development of lignocellulose biorefineries, due to their oxidative versatility and low catalytic requirements. However, for their industrial application, enzymes active and stable under operational conditions are desired. Recombination of related genes can lead to hybrid mutants with improved properties that could not have been predicted beforehand. In this work, we describe the construction and preliminary characterization of "swapped" mutants obtained by exchanging the cupredoxin domains of two different laccases.

I. INTRODUCTION

Laccases are blue multicopper oxidases with huge biotechnological applicability, capable of oxidizing many different aromatic compounds using oxygen as co-substrate and generating water as the only by-product. These enzymes typically present three cupredoxin domains (D1, D2 and D3) and four copper atoms (one T1 Cu, one T2 Cu and two T3 Cu), although two-domain laccases lacking D2 and that form trimers have also been described. The Cu atoms are coordinated by ten histidine and one cysteine residues located in domains D1 and D3. Substrate oxidation takes place at the T1 Cu site and, after the monovalent oxidation of four substrate molecules, the abstracted electrons are transferred to the T2 and T3 Cu sites, where one molecule of O_2 is reduced to two molecules of H_2O. The substrates susceptible to be oxidized by laccase are determined by the redox potential of the T1 Cu and by the size and properties of the substrate binding pocket, which is delimited by residues from domains D2 and D3.

Laccases from white-rot fungi, the only organisms able to completely degrade lignin, are of special interest due to their high-redox potential which, in principle, broadens their substrate range. Directed evolution, which mimics the natural evolution process of mutation, recombination and selection in the laboratory, is a very powerful tool for the design of tailor-made enzymes appropriate for industrial purposes. Recently we have described the engineering of chimeric laccases by random DNA shuffling, using as parent types two high-redox potential laccase variants previously evolved *in vitro*: OB1, evolved from PM1 basidiomycete laccase (PM1L), and 3PO, evolved from *Pycnoporus cinnabarinus* laccase (PcL) [1, 2]. The new chimeric variants, functionally secreted by *S. cerevisiae*, presented novel properties different from those of both parent types, such as varied pH activity profiles, increased stability and/or modified affinities towards phenolic substrates, even though the exchanged sequence blocks were relatively small [3]. All the recombination events in the selected chimeric laccase sequences were found in D1 and D3 domains, where the conserved signatures for Cu binding are located.

In the present work we describe the construction of new hybrid laccases by "domain swapping", this is, by exchanging the second cupredoxin domain (D2) between the evolved laccase variants OB1 and 3PO. This way we obtained two variants: OB1::3PO (OB1 with D2 from 3PO) and 3PO::OB1 (3PO with D2 from OB1), which have been preliminarily characterized.

II. EXPERIMENTAL

Construction of swapped mutants

By studying structure models of 3PO-PcL and OB1-PM1L, cross-over points were selected in loops between domains, taking into account that no polar contacts were broken between surrounding residues (distance < 5 Å). Swapped mutants were obtained by PCR overlap extension. All PCR conditions are described in [3]. Individual domains from each parent were amplified and purified products were mixed and assembled in a primer-less PCR. This reassembly product was amplified by PCR and co-transformed together with the linearized expression vector in competent *S. cerevisiae* cells [1-3].

Laccase production

Culture media and conditions used for yeast growth and laccase production are described previously [1-3]. Briefly, laccase production was carried out by growing cells in 30 mL of expression media in 100 mL flasks with agitation, until maximum activity was reached. Laccase activity was monitored by measuring ABTS oxidation at 418 nm (ε = 36000 M^{-1} cm^{-1}) in acetate buffer pH 5. Cultures were then centrifuged and supernatants containing secreted laccase were filtered and concentrated through 10,000 MWCO membranes.

Characterization of swapped mutants

For the laccase mutants described in this work and parent types 3PO and OB1, T_{50} (10 min), pH activity profiles, and K_M values for ABTS and DMP were studied, following the procedures described previosuly [1-3].

III. RESULTS AND DISCUSSION

Construction and production of swapped laccase mutants

Swapped laccase mutants OB1::3PO and 3PO::OB1 were obtained by PCR overlap extension (**Figure 1**). The effect of temperature on the production of swapped laccases by *S. cerevisiae* was studied by carrying out fermentations at 20 and 30 ºC, which were the optimum temperatures for production of parent laccases 3PO and OB1, respectively. For both swapped mutants, maximum production was achieved at 20 ºC, though laccase activity in the culture was much lower than that obtained with parent types: around 120 U/L for OB1::3PO and 45 U/L for 3PO::OB1 (compared to 350 and 1000 U/L reached with 3PO and OB1). We checked whether domain swapping affected the high redox potential of the new laccases by assessing their ability to oxidize violuric acid [4], and both mutants retained activity over this substrate.

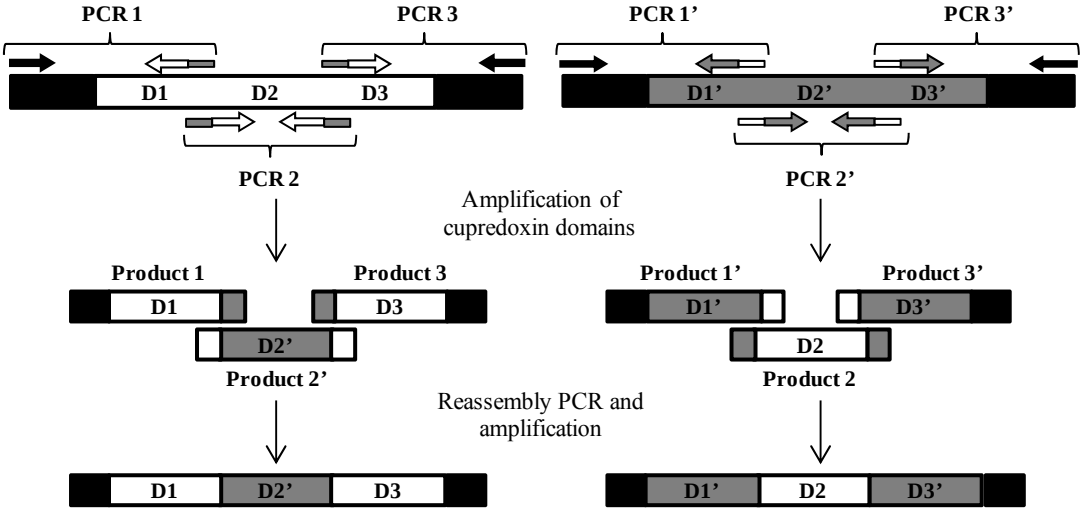

Figure 1. Schematic representation of the construction of swapped mutants. cDNA sequences of both parents are represented in white and gray and the expression vector is represented in black.

Characterization of swapped laccase mutants

Although parent laccases 3PO and OB1 presented similar properties, the swapped mutants obtained in this work were quite different. Regarding the optimum pH for ABTS oxidation, OB1::3PO mutant presented a slightly more acidic activity profile, with maximum activity at pH 2, whereas 3PO::OB1 mutant presented no activity at this pH and retained the same relative activity as parent types at higher pH values. In the case of DMP, OB1::3PO showed the same activity profile as parent OB1, but 3PO::OB1 had a significant loss of activity at pH values below 5 (**Figure 2**). This type of profile was also found in another laccase mutant, 2C4, obtained from the random chimeragenesis of laccases 3PO and OB1 [3]. This chimera was in its most part identical to OB1 and it incorporated two small fragments from 3PO in the third cupredoxin domain. One of these fragments included mutation P394H from 3PO parent, contiguous to the His395 residue that coordinates T1 Cu. During the laboratory evolution of PcL, its pH activity profile shifted from acidic to more neutral values, and this mutation was selected and maintained from the second generation onwards [2]. We believe that mutation P394H is responsible for the shift in optimum pH in 3PO, 2C4 and 3PO::OB1. However, in 3PO laccase, residues from D2

located in the surroundings of residue 394 in the protein's tridimensional structure may modulate the effect of this mutation in such a way that the loss of activity at acidic pH is not so severe.

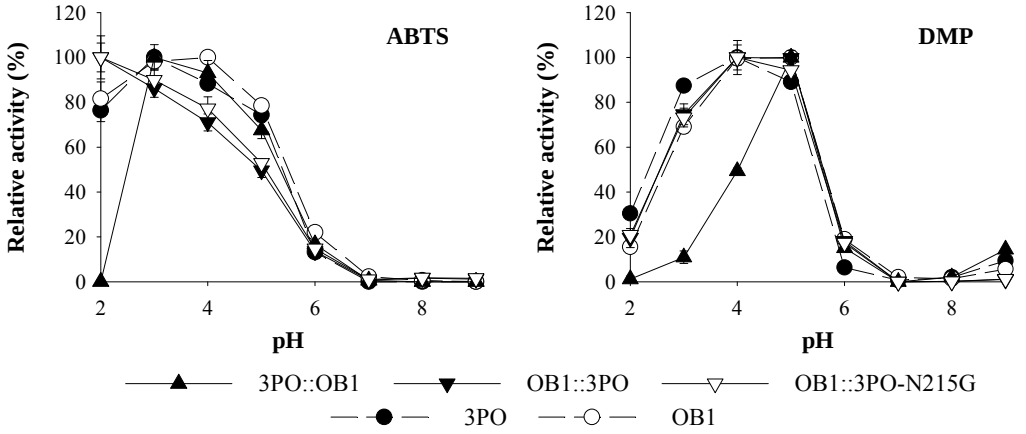

Figure 2. pH activity profiles of swapped laccase variants and parent types for ABTS and DMP.

Concerning thermostability, variant OB1::3PO showed an important increase in its T_{50} (10 min) of 7 ºC, whereas for 3PO::OB1 it decreased in 5 ºC, respecting parent type laccases (**Table 1**). In the case of mutant OB1::3PO, the exchange of D2 for that of 3PO involves the introduction of a new glycosilation site in residue Asn 215. In order to check if the increase in thermostability was due to a higher degree of glycosilation, Asn 215 was substituted for a Gly residue originally found in OB1. Mutant OB1::3PO-N215G however showed the same T_{50} as OB1::3PO, suggesting that the increase in thermostability is in fact due only to new stabilizing interactions introduced by domain swapping. Besides T_{50}, the deglycosilated mutant behaved in the same manner as OB1::3PO for the properties studied in this work.

Table 1. T_{50} values for swapped laccase mutants and parent types. Values represent the temeprature at which laccases retain 50 % of intial activity after a 10 minute incubation.

Clone	3PO	OB1	3PO::OB1	OB1::3PO	OB1::3PO-N215G
T_{50} (10 min) (ºC)	70.8 ± 0.2	71.4 ± 0.3	65.8 ± 0.2	78.1 ± 0.6	78.6 ± 0.2

Finally, K_M values for ABTS and DMP at pH 5 were obtained (**Table 2**). Mutant 3PO::OB1 presented an important loss of affinity towards both substrates, with increases in K_M values of approximately 5-fold for ABTS and 12-fold for DMP. On the other hand, for OB1::3PO mutant K_M values were not so different from those of parent types. In the case of ABTS, it presented a K_M more similar to that of parent 3PO, whereas K_M for DMP was closer to the one of parent OB1.

Table 2. K_M values (μM) for ABTS and DMP for swapped mutants and parent types obtained at pH 5.

Clone	3PO	OB1	3PO::OB1	OB1::3PO	OB1::3PO-N215G
ABTS	42.9 ± 1.3	9.1 ± 0.5	204.7 ± 13.0	53.2 ± 5.2	52.8 ± 4.2
DMP	243.5 ± 6.7	93.1 ± 3.3	3005.3 ± 161.8	133.8 ± 4.6	120.9 ± 5.2

In the swapped mutants, the residues from D2 that delimit the substrate binding pocket are exchanged (**Figure 3**). Thus 3PO::OB1 mutant holds the same binding pocket as OB1, whereas the residues of OB1::3PO binding pocket are the same as in 3PO. D2 from 3PO presents three large hydrophobic phenylalanines while D2 from OB1 presents three small residues that enlarge the substrate binding pocket: one hydrophobic alanine and two polar residues, a threonine and a serine. However, since the mutations introduced by domain swapping are so numerous (69 % amino acid sequence identity in D2 versus 81 % in D1 and 79% in D3), it is not likely that changes in affinity of the mutants are caused by these substitutions alone.

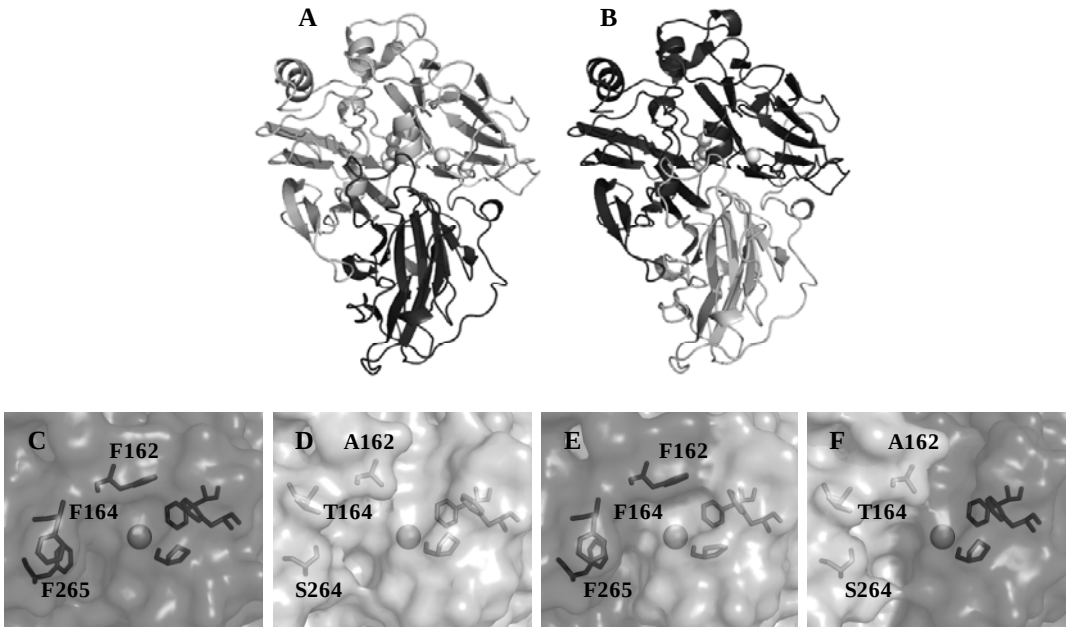

Figure 2. Model structures for mutants OB1::3PO (A) and 3PO::OB1 (B). Close-ups of the substrate binding pockets of 3PO parent (C), OB1 parent (D), OB1::3PO mutant (E) and 3PO::OB1 mutant (F) are shown.

IV. CONCLUSIONS

One of the aims of directed molecular evolution in protein engineering is to enhance the applicability potential of enzymes, making them more stable under operational conditions. Throughout the natural evolution of enzymes, natural selection drives the preservation of advantageous mutations while random genetic drift contributes with neutral mutations to sequence divergence. In this manner, neutrality relates to numerous genotypes accommodating the same phenotype. The results presented here demonstrate that it is possible to "play" with this neutrality in the lab without affecting the function and structure of the protein. So far, the exchange of the second cupredoxin domain between two high-redox potential laccases led to the substitution of amino acids that in principle are not determinants for enzyme activity but changed the protein properties, including an unexpected increase in stability.

V. ACKNOWLEDGEMENTS

This work has been funded by the Spanish Project BIO2010-19697. I. Pardo thanks CSIC for a JAE-Predoc Fellowship.

VI. REFERENCES

[1] Maté, D; García-Burgos, C; García-Ruiz, E; Ballesteros, A.O.; Camarero, S; Alcalde, M. Laboratory evolution of high-redox potential laccases. *Chem Biol.* **2010**, *17*(9):1030-41.

[2] Camarero, S; Pardo, I; Cañas, A.I.; Molina, P; Record, E; Martínez, A.T.; Martínez, M.J.; Alcalde, M. Engineering platforms for directed evolution of laccase from Pycnoporus cinnabarinus. *Appl Environ Microbiol*. **2012**, *78*(5):1370-84

[3] Pardo, I; Vicente, A.I.; Mate, D.M.; Alcalde, M; Camarero, S. Development or chimeric laccases by directed evolution. *Biotechnol Bioeng*. **2012**, *109*(12):2978-86

[4] Pardo, I; Chanagá, X.; Vicente A.I.; Alcalde, M; Camarero, S. New colorimetric screening assays for the directed evolution of fungal laccases to improve the conversion of plant biomass. *BMC Biotechnol.* **2013,** *13*(1):90

ENGINEERING HIGH-REDOX POTENTIAL LACCASES IN THE LAB TO AID BIOMASS CONVERSION INTO CHEMICALS, MATERIALS AND BIOFUELS

Pardo I.[1], Vicente A. I.[1,2], Alcalde M.[2] and Camarero S.[1]*

[1]*Centro de Investigaciones Biológicas, CSIC. Ramiro de Maeztu 9. ES-28040 Madrid. Instituto de Catálisis y Petroleoquímica, CSIC. Marie Curie 2. ES-28049 Madrid. (*susanacam@cib.csic.es)*

ABSTRACT

Laccases are multicopper oxidases able to catalize the oxidation of a variety of aromatic compounds without any other requirement than oxygen from air. In previous studies we have highlighted the biotechnological potential of fungal laccases to improve the utilization of plant biomass in the modern biorefineries. In this context, lignin derived compounds that are released during lignocellulose processing can be used as redox mediators of laccases, promoting degradation reactions catalyzed by the enzyme, or as bioactive precursors for the enzymatic synthesis of natural products. However, the industrial implementation of these enzymes is hampered by the lack of powerful expression systems to produce fungal recombinant laccases and the need for active and stable enzymes under the harsh operational conditions.

Recently, we developed fungal laccases of high-redox potential functionally expressed in *S. cerevisiae* by directed molecular evolution. Using these platforms as the starting points for further engineering studies, in combination with *ad-hoc* high-throughput screening methods, we have developed a more robust laccase with improved catalytic activity towards phenolic compounds under preferred pH conditions.

I. INTRODUCTION

Laccases (EC 1.10.3.2, p-diphenol oxidase) catalyze the oxidation of substituted phenols, polyphenols, aromatic amines and other aromatic compounds without any other requirement than oxygen from air. As a result, these multicopper oxidases are valuable green biocatalysts for several industrial sectors such as textile, food, wood and pulp or organic synthesis. Laccases are widely distributed in nature. Above all, the high-redox potential laccases ($E^0 \approx + 0.8$ V) secreted by white-rot fungi exhibit the highest biotechnological applicability due to the wider range of potential reducing substrates used. Besides, the enzyme applicability potential is notably broadened in the presence of redox mediator compounds which, once oxidized by the enzyme, act as electron shuttles and promote the oxidation of recalcitrant substrates and complex polymers.

In previous studies we have highlighted the biotechnological potential of fungal laccases in the presence of lignin-derived phenolic compounds acting as redox mediators for improving the utilization of plant biomass in the modern lignocellulose biorefineries [1]. Moreover, the synthesis of a variety of new added-value products from cellulose and lignin can be obtained using laccase as biocatalyst and these phenols as precursors. One example is the enzymatic functionalization of cellulosic pulp to confer new properties to paper by grafting of phenolic derivates to fibers surface [2]. It is worth mentioning these phenolic compounds might be easily obtained from the processing of the lignocellulosic materials [3], pulping and thermo-chemical pretreatment for ethanol production [4].

The implementation of these fungal laccases as industrial biocatalysts is still about to happen due to the harsh industrial operational conditions and the lack of efficient expression systems to produce the recombinant enzymes. However, protein engineering by directed evolution can help us overcome these obstacles. In recent studies, we developed high-redox potential laccases functionally expressed in *S. cerevisiae* with improved catalytic efficiencies towards phenolic and non-phenolic compounds [5, 6]. We have engineered a chimeric laccase by *in vitro* and *in vivo* DNA recombination of these two fungal laccases (from *Pycnoporus cinnabarinus* and PM1 basidiomycete). The use of high-throughput screening methods precisely designed for this purpose [7] allowed us to obtain a more robust laccase, with improved catalytic activity towards lignin-derived phenolic compounds under chosen pH conditions.

II. EXPERIMENTAL

Laccase production and purification

Culture media and conditions used for yeast growth and laccase production are described previously [5]. Briefly, *S. cerevisiae* cells were grown in 300 mL of expression media in 1 L flasks with agitation until maximum activity was reached. Then, cultures were centrifuged and supernatants were filtered and concentrated through

10,000 MWCO membranes. Laccase was purified by HPLC using two steps of anionic exchange and a final step of molecular exclusion, using 20 mM Bis-Tris buffer, pH 6, and NaCl for elution (detailed protocols for laccase purification are described in [5]. Throughout production and purification, laccase activity was measured with 3 mM ABTS (ε_{418} = 36,000 M^{-1} cm^{-1}) in acetate buffer pH 5.

Characterization of laccases

Procedures for determining pH activity profiles, T_{50} and kinetic constants are described previously [5]. To determine laccase temperature stability, dilutions of 0.1 U/mL were prepared in 100 mM acetate buffer, pH 5, and incubated at different temperatures. For pH stability, dilutions were prepared in 100 mM Britton and Robinson buffer at different pH values and incubated at room temperature. Aliquots were taken at different time-points and residual activity was measured in the plate reader with ABTS.

III. RESULTS AND DISCUSSION

The combination of random *in vitro* and *in vivo* DNA shuffling of the two parental laccases genes previously evolved in the lab [5,6] rendered a set of laccase mutants whose activities were screened using a multiple colorimetric high-throughput screening assay. Diverse protein block exchanges and different properties were found among the active laccases secreted by *S. cerevisiae* [8]. Some of these new laccases showed improved thermal stabilities respecting the parental types, and they also presented different substrate affinities for the model phenolic compound 2,6-dimethoxyphenol -DMP- (**Table 1**). Laccase 3A4 exhibited significantly higher T_{50} value than both parental types, with increases of up to 3 ºC over that of the most stable parent type. Besides, it showed a significant improvement of substrate affinity for DMP, for which we selected this laccase for further characterization studies.

Table 1. Thermal stabilities ($T_{50,}$ 10 min) and Michaelis constant for DMP oxidation of several laccases engineered by chimeragenesis of two fungal laccases previously evolved in the lab (P1: evolved PM1L; P2: evolved PcL).

Laccase	T_{50} (ºC)	K_M (µM)
P1	73.3	93.1 ± 3.3
P2	70.9	243.5 ± 6.7
7D5	74.9	361.4 ± 12.0
2C4	75.5	777.8 ± 22.2
3A4	76.1	61.8 ± 4.8
4A11	76.6	86.2 ± 2.9

Yeast cells expressing 3A4 mutant were cultured in flasks (in the presence of $CuSO_4$ and ethanol as laccase inducers) and up to 300 U/L of laccase 3A4 were obtained (**Figure 1**).

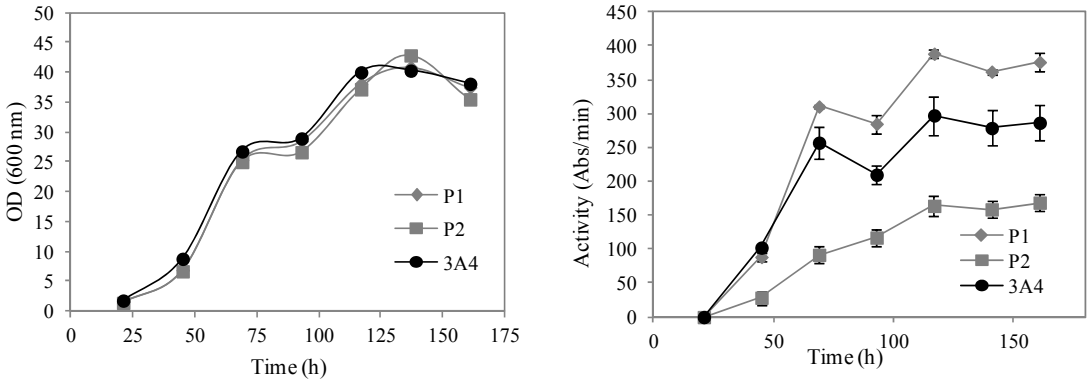

Figure 1. Optical density (**A**) and laccase activities (**B**) from the liquid cultures of *S. cerevisiae* cells expressing the 3A4 laccase or the parent laccases (P1: evolved PM1L; P2: evolved PcL) grown at 20ºC.

The enzyme was purified and characterized. Laccase 3A4 displayed sharper acidic optimal pH than the parent laccases, especially for the oxidation of ABTS. Only 40 % ABTS activity was retained at pH 5 compared to the 70–80 % of the parental types (**Figure 2**).

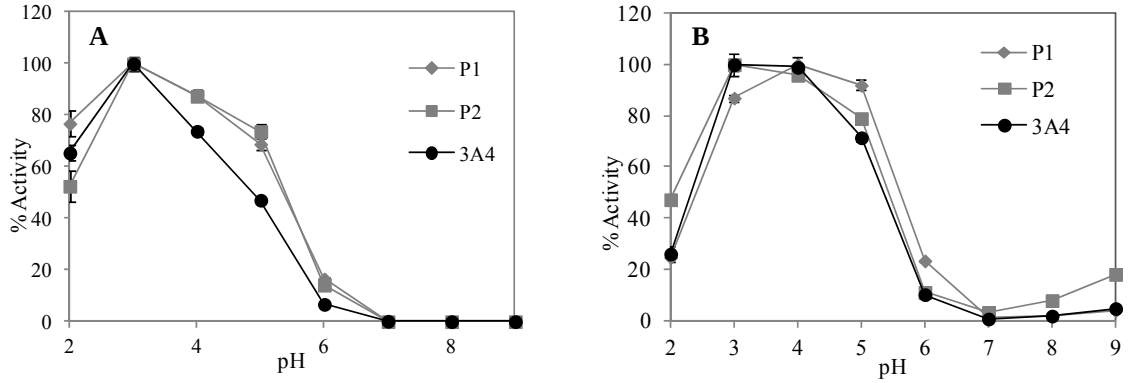

Figure 2. Optimum pH of 3A4 laccase for the oxidation of ABTS (A) and DMP (B) compared with those of the laccases used in this study as parent types (P1: evolved PM1L; P2: evolved PcL).

3A4 laccase showed improved thermal stability at long times (8h) when compared with those of the parent types and in particular its stability at acidic pH was notably improved respecting the parent types (**Figure 3**).

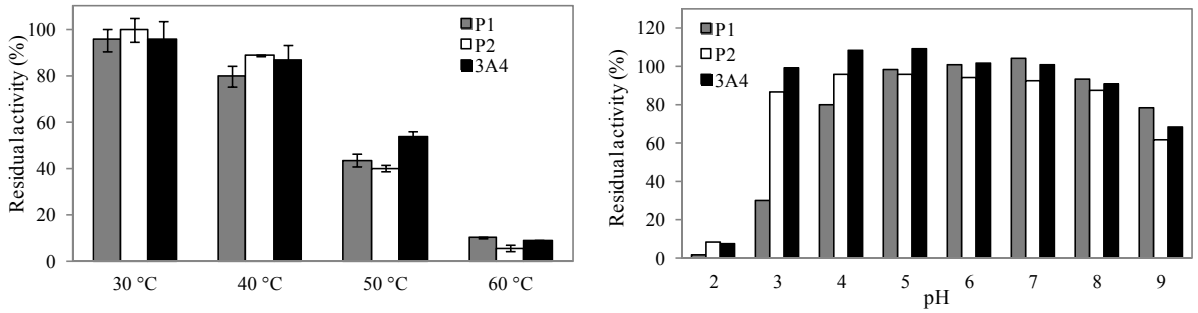

Figure 3. Thermal stability of 3A4 laccase (8h) and pH stability (6h). (P1: evolved PM1L; P2: evolved PcL)

Finally, the catalytic efficiency of 3A4 laccase towards phenolic compounds raised around 3 fold for DMP and up to 7 fold for sinapic acid respecting the parent types (**Table 2**). All these properties may be of much interest for processes such as the enzymatic detoxification of thermo-chemically pretreated lignocellulosic biomass by removing the phenols that inhibit the fermentation stage for second generation bioethanol production [9].

Table 2. Kinetic constants of 3A4 laccase engineered by chimeragenesis of two fungal laccases previously developed in the lab (evolved PM1L and evolved PcL).

	ABTS			**DMP**			**Sinapic acid**		
	k_{cat} (s^{-1})	K_M (mM)	k_{cat}/K_M	k_{cat} (s^{-1})	K_M (mM)	k_{cat}/K_M	k_{cat} (s^{-1})	K_M (mM)	k_{cat}/K_M
P1 (evolved PM1L)	185	0.006	29365	125.0	0.14	893	129.0	0.073	1778
P2 (evolved PcL)	482.6	0.024	19944	196.9	0.213	923	191.1	0.023	8459
Chimeric laccase 3A4	140	0.011	12652	166.2	0.064	2618	141.0	0.011	12605

Further attempts for improving 3A4 laccase efficiency towards phenols, by using random mutagenesis, were not successful. Only minor laccase improvements towards acetosyringone and syringaldehyde were found. On the light of these results a semirational approach is being currently undertaken by mutating specific 3A4 laccase residues, to attain an outstanding biocatalyst to be used for aiding the utilization of lignocellulose biomass in different industrial processes.

IV. CONCLUSIONS

We have engineered a laccase by random DNA shuffling of two high-redox potential fungal laccases from basidiomycetes PM1 and *Pycnoporus cinnabarinus*. The enzyme holds higher thermal stability, increased stability at acidic pH and improved catalytic efficiency towards phenolic compounds. The design of laccases *a la carte*, with improved activities/specificities towards natural phenolic compounds released during lignocellulose processing represents a valuable step forward for the utilization of these enzymes to aid the conversion of plant biomass into chemicals, materials and biofuels.

V. ACKNOWLEDGEMENT

This work has been funded by the Spanish Project BIO2010-19697. I. Pardo thanks CSIC for a JAE Predoc Fellowship.

VI. REFERENCES

[1] Cañas AI, Camarero S: Laccases and their natural mediators: Biotechnological tools for sustainable eco-friendly processes. *Biotechnol Adv* **2010**, *28*:694-705.

[2] Aracri E, Fillat A, Colom JF, Gutiérrez A, del Río JC, Martínez AT, Vidal T: Enzymatic grafting of simple phenols on flax and sisal pulp fibres using laccases. *Bioresource Technol* **2010**, *101*:8211-8216.

[3] Camarero S, Ibarra D, Martínez AT, Romero J, Gutiérrez A, del Río JC: Paper pulp delignification using laccase and natural mediators. *Enzyme Microb Technol* **2007**, *40*:1264-1271.

[4] Parawira W, Tekere M: Biotechnological strategies to overcome inhibitors in lignocellulose hydrolysates for ethanol production: review. *Crit Rev Biotechnol* **2011**, *31*:20-31.

[5] Camarero S, Pardo I, Cañas AI, Molina P, Record E, Martínez AT, Martínez MJ, Alcalde M: Engineering platforms for directed evolution of laccase from *Pycnoporus cinnabarinus*. *Appl Environ Microbiol* **2012**, *78*:1370-1384.

[6] Maté D, García-Burgos C, García-Ruiz E, Ballesteros A, Camarero S, Alcalde M: Laboratory evolution of high redox potential laccases. *Chem Biol* **2010**, *17*:1030-1041.

[7] Pardo I, Chanaga X, Vicente AI, Alcalde M, Camarero S: New colorimetric screening assays for the directed evolution of fungal laccases to improve the conversion of plant biomass. *BMC Biotechnol* **2013**, *13*:90.

[8] Pardo I, Vicente AI, Alcalde M, Camarero S: Development of chimeric laccases by directed evolution. *Biotechnol Bioeng* **2012**, *109*:2978-2986.

[9] Jurado M, Prieto A, Martínez-Alcalá MA, Martínez AT, Martínez MJ: Laccase detoxification of steam-exploded wheat straw for second generation bioethanol. *Bioresource Technol* **2009**, *100*:6378-6384.

DESIGNING ROBUST CATIONS FOR DISTILLABLE AND CELLULOSE DISSOLVING ACID-BASE CONJUGATE IONIC LIQUIDS

Arno Parviainen,[1] K. Juhani Helminen,[1] Uula Hyväkkö,[1] Ilpo Mutikainen,[1] Michael Hummel,[2] Christoph Selg,[1] Lauri K. J. Hauru,[2] Herbert Sixta,[2] Alistair W. T. King,[*1] Ilkka Kilpeläinen[*1]

*[1] Department of Chemistry, University of Helsinki, Helsinki, Finland; [2] Department of Forest Products Technology, Aalto University, Espoo, Finland (*alistair.king@helsinki.fi, ilkka.kilpelainen@helsinki.fi)*

ABSTRACT

A variety of acid-base conjugate ionic liquids were prepared by combining a range of bases and superbases with acetic and propionic acid. Cellulose dissolving capability was obtainable only with conjugates containing superbases. Proton affinities were calculated for all of the bases. A range, within which cellulose dissolution occurred, when combined with acetic or propionic acid, was defined for further use. This was above a proton affinity value of about 240 kcal mol^{-1} at the MP2/6-311+G(d,p)//MP2/ 6-311+G(d,p) *ab initio* level. Rationalising this allowed us to determine that cation acidity contributed considerably to the ability of ionic liquids to dissolve cellulose and not just the basicity of the anion.

I. INTRODUCTION

Cellulose is a prime candidate for the production of renewable materials, chemicals and energy. The inter- and intramolecular H-bonding network in cellulose makes it insoluble to conventional nondestructive molecular solvents. In 1934, Graenacher demonstrated that molten salts, such as the alkylpyridinium chlorides, are capable of dissolving cellulose.[1] This was extended to ILs by Swatlowski in 2002, with the use of dialkylimidazolium chlorides.[2] One disadvantage of this and other imidazolium-based ILs is the solubility of oligomeric lignocellulosic materials in both IL and polymeric lignocellulose non-solvents (regeneration solvents). Distillation has also been proven to be possible for these structures but only under short-path and high-vacuum conditions. Recently, we published the combination of 1,1,3,3-tetramethylguanidine (TMG) and organoacids, such as acetic and propionic acid, in the preparation of distillable ILs (DILs), which were capable of dissolving cellulose.[3] Herein we would like to describe the further development and understanding of these acid-base conjugates, as potential structures for lignocellulose processing.

II. EXPERIMENTAL

A series of acid-base conjugates were prepared from a range of bases and propionic acid, as can seen from **Table 1**: Equimolar equivalents of the acid and base were mixed in screw-cap vials. The materials were characterized using NMR, IR, mp, X-ray crystal structure determination and dissolving pulp (Bahia eucalpytus pre-hydrolysis kraft pulp) solvation capability, where appropriate. Proton affinities (ΔH_{PA}, MP2/6-311+G(d,p)//MP2/6-311+G(d,p)) were calculated, using GAMESS[4] 2009, as a measure of basicity of the unconjugated bases. The capability of each synthesized acid-base conjugate to dissolve cellulose was qualitatively tested by heating and stirring the mixtures in an oil bath at 85°C overnight. The dissolution was evaluated visually and using optical microscopy. The results by Hauru *et al.*[5] on the Kamlet-Taft (KT) parameterization of different potential solvents for cellulose have already suggested that the $\beta-\alpha$ value (net basicity = basicity-acidity) was a better discriptor for the cellulose dissolving capability of a solvent system than the β value alone. To compare this with our computational results, KT parameters for a short series of propionate ILS were evaluated. These parameters, combined with values from the literature, can be seen from **Table 2.**[6]

Table 1. ***Qualitative dissolution capability, viscosities and melting points for different bases and superbases, arranged in order of increasing proton affinity (ΔH_{PA}), combined with propionic acid (1:1). Below a ΔH_{PA} value of -240 kcal mol^{-1}, the ionic liquids no longer dissolve cellulose.***

Base	Acid	*Base ΔH_{PA} (kcal/mol)*	*RT Viscosity (cP)*	*IL m.p. (^oC)*	*Pulp Dissolution*
[emim]:	Propionic	-262.90	111	< RT	Yes
HMPI	Propionic	-253.90	-	51	Yes
MTBD	Propionic	-251.02	458	< RT	Yes
DBU	Propionic	-248.88	9430	45	Yes
DBN	Propionic	-246.44	135	< RT	Yes
DMP	Propionic	-246.14	201	< RT	Yes
TMG	Propionic	-244.88	8360	63	Yes
DMAP	Propionic	-238.01	-	74	No
Hünigs base	Propionic	-235.93	-	< RT	No
DIPA	Propionic	-232.16	-	70	No
EIM	Propionic	-228.88	-	< RT	No
DEA	Propionic	-227.58	-	< RT	No
Pyridine	Propionic	-220.68	-	< RT	No

[emim]: - [emim]-carbene, HMPI - *N,N,N,N,N,N*- hexamethylphosphorimide triamide (phosphazene), MTBD - 7-methyl-1,5,7-triazabicyclo[4.4.0]dec-5-ene, DBU - 1,8-diazabicyclo[5.4.0]undec-7-ene, DBN - 1,5-diazabicyclo[4.3.0]non-5-ene, DMP - 1,2-dimethyl-1,4,5,6-tetrahydropyrimidine, TMG - *N,N,N,N*-tetramethylguanidine, DMAP - 4-(dimethylamino)pyridine, Hünigs Base - *N,N*-diisopropylethylamine, DIPA - *N,N*-diisopropylamine, EIM - 1-ethylimidazole, DEA, *N,N*-diethylamine

Table 2. ***Kamlet-Taft parameters for selected propionate room-temperature ionic liquids (RTILs) or electrolytes at 20^{o}C.***[5]

RTIL	$E_T(30)$[a]	π^*	α	β	β-α	B: $-\Delta H_{PA}$ [kcal mol^{-1}]
[emim][OAc][5]	50.1	1.01	0.50	1.09	0.59	262.90
[emim][CO_2Et]	50.3	0.96	0.54	1.09	0.56	262.90
[DMPH][CO_2Et]	51.3	1.02	0.56	1.08	0.52	246.14
[DBNH][CO_2Et]	52.6	1.04	0.64	1.11	0.47	246.44
[DBNH][CO_2Et][b]	51.3	1.07	0.53	1.03	0.50	246.44
[TMGH][CO_2Et][5]	53.2	1.00	0.71	1.16	0.46	244.88
[DMAPH][CO_2Et][5]	-	0.85[c]	-	0.79[c]	-	238.01
[HünigsH][CO_2Et]	-	0.79	-	1.00	-	235.93
[eimH][CO_2Et][5]	-	0.85[d]	-	0.71[d]	-	230.31
[PyrH][CO_2Et]	-	0.76	-	0.60	-	220.68

[a] Dimroth-Reichardt polarity scale, [b] 60 wt % solution of [DBNH][CO_2Et] in 40 wt % of DMSO, [c] Values were determined at 70 ^{o}C, [d] Values were determined at 25 ^{o}C.

III. RESULTS AND DISCUSSION

When propionic acid was combined with the differing range of bases, it was found that the combination of propionic acid with superbases (ΔH_{PA} < -240 kcal mol^{-1}) afforded ILs that were capable of dissolving cellulose (**Table 1**). Those bases, which were less basic than the superbase series either did not ionise or could not dissolve cellulose. As the basicity of the unconjugated base is also a measure of the acidity of the cation, these indicate that too acidic cations prevent cellulose dissolution by increased H-bond donation to the anion (**Scheme 1**). This stabilization of charge on the anion prevents H-bond breakage between cellulose chains once a certain threshold has been reached (**Figure 1**). This threshold corresponds to the enthalpy gain contribution to the Gibbs free energy of dissolution. Degree of H-bond donation between cation and anion seems to be critical for both cellulose dissolution and distillation of the resulting ILs. Distillability of [DBNH][CO_2Et] was demonstrated using a kugelrohr (170 ^{o}C, 5 mbar). ^{1}H NMR showed high cation purity after distillation. X-ray crystal structures were determined for suitable crystals (**Figure 2**). These showed strong interactions with the carboxylate anions

and the N-H positions on the protonated bases. The TMG-based structure ([TMGH][CO_2Et]) forms a dimer ion-pair in the crystal lattice,[3] as does the HMPI structure ([HMPIH][CO_2Et]). Both form 12-membered cyclic structures holding the dimer ion pairs together, with H-bonding between ions.

Figure 1. Acidic cation-anion interaction reducing the enthalpy gain upon cellulose dissolution (left). Illustrative MP2 surface charge-density for an optimised $[DBNH]^+$---$[OAc]^-$---Glc conjugate (right).

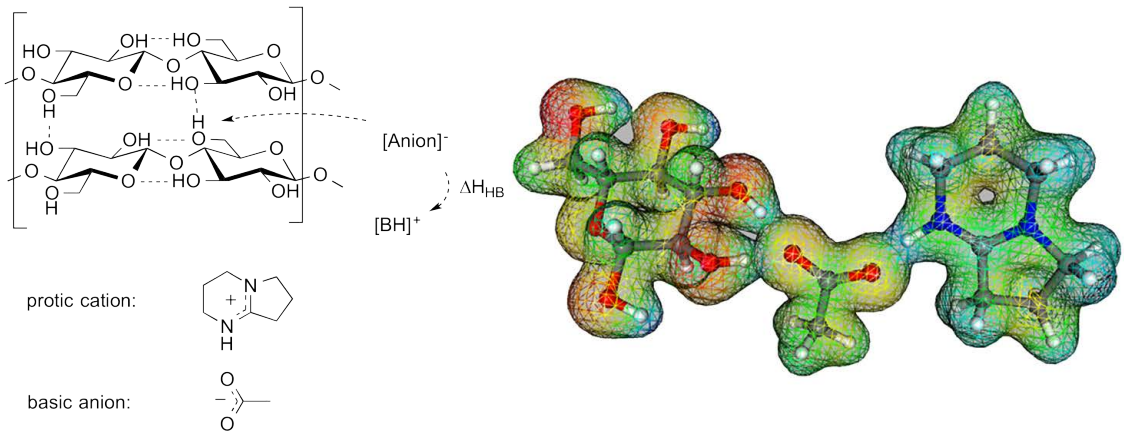

Figure 2. X-ray structures for [TMGH][CO_2Et] (a), [DBUH][CO_2Et] (b), [DBNH][OAc] (c) and [MTBDH][OAc] (d).

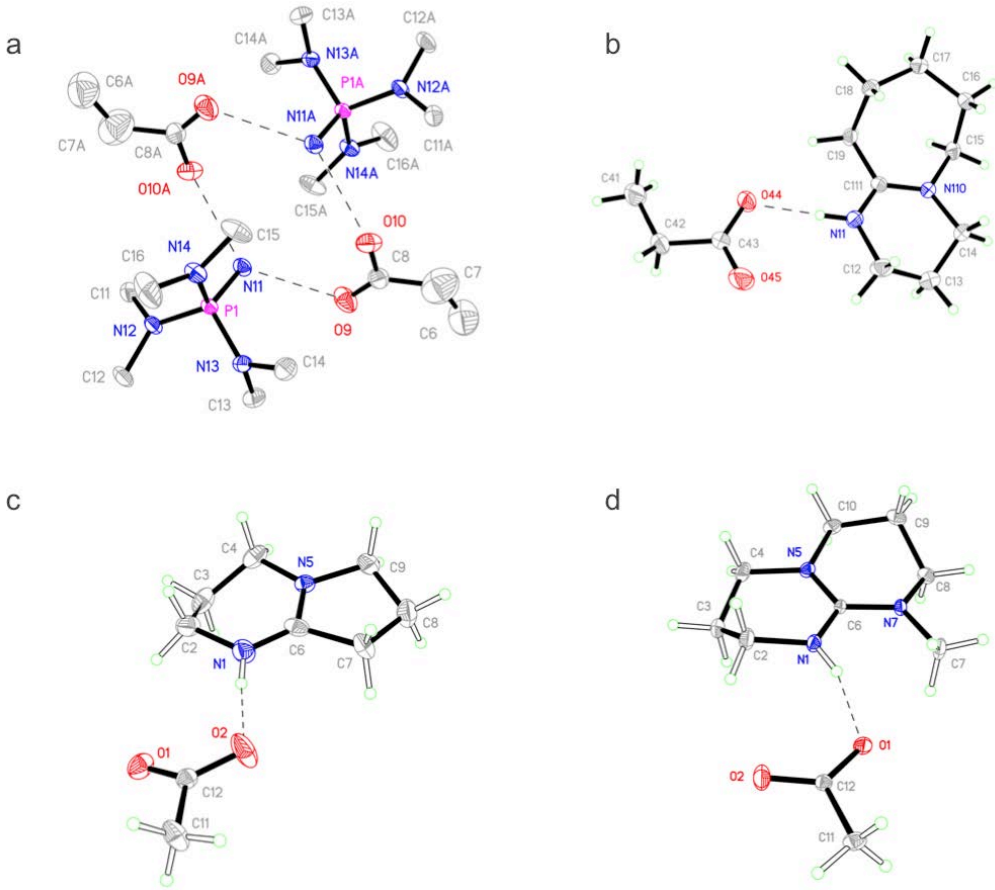

One drawback of the new cations is that superbases are prone to hydrolysis, which could complicate matters when recycling the ionic liquid. However it was found that after hydrolysis of [DBNH][OAc] it was possible to convert the hydrolysis product back to the ionic liquid by adding excess DBN, Amberlyst 15 and heating under vacuum (**Figure 3**).

Figure 3. Hydrolysis of [DBNH][OAc] and dehydration back to the starting ionic liquid.

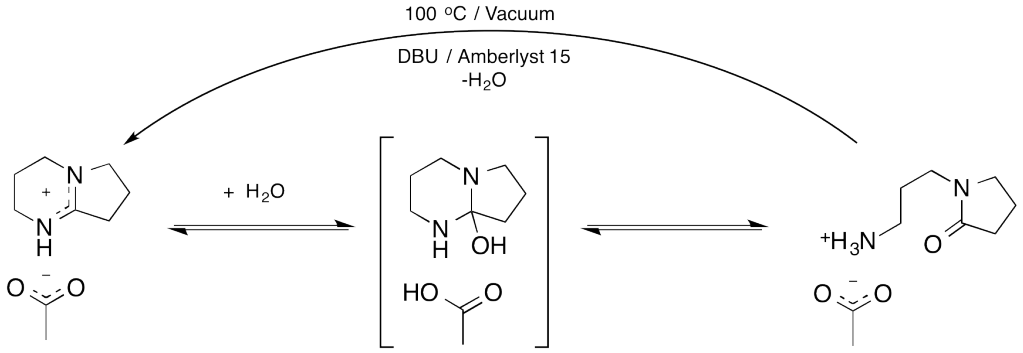

IV. CONCLUSIONS

New low-viscosity ILs, based on the conjugation of DBN with propionic or acetic acid, have been developed that can rapidly dissolve cellulose. These are comparable to [emim][OAc] in their abilities to dissolve cellulose. They are also distillable, allowing for purification at conditions of around 170 °C and > 5 mbar. Hydrolysis of superbase-derived ionic liquids may be problematic for recycling the mixtures but the hydrolysis product can be converted back to the starting ionic liquid under vacuum conditions. It was found that H-bond donation from the IL cation to anion is critical for cellulose dissolution capability of an IL. The more acidic the cation, the less likely the IL will be able to break H-bonds between cellulose chains. This is expected to be the major contribution to enthalpy gain in the Gibbs free energy of dissolution of cellulose.

V. ACKNOWLEDGEMENT

The authors wish to thank Forestcluster Ltd, now called the Finnish Bioeconomy Cluster (FIBIC) Oy, and TEKES for funding, provided under the Future Biorefinery (FuBio) program: FUBIO2 | JOINT RESEARCH 2 | WORK PACKAGE 2

VI. REFERENCES

1. Graenacher, C. Cellulose solutions. *U.S. Patent*, 1934, 1943176.
2. Swatloski, R. P., Spear, S. K., Holbrey, J. D., Rogers, R. D. Dissolution of cellose (sic) with ionic liquids. *J. Am. Chem. Soc.,* 2002, **124**, 4974-4975.
3. King, A. W. T. Asikkala, J. Mutikainen, I. Järvi, P. Kilpeläinen, I. Distillable acid-base conjugate ionic liquids for cellulose dissolution and processing. *Angew. Chem. Int. Ed.,* 2011, **50**, 6301-6305.
4. Schmidt, M. W. Baldridge, K. K. Boatz, J. A. Elbert, S. T. Gordon, M. S. Jensen, J. H. Koseki, S. Matsunaga, N. Nguyen, K. A. Su, S. J. Windus, T. L. Dupuis, M. Mongomery, J. A. General atomic and molecular electronic structure system. *J. Comput. Chem*., 1993, **14**, 1347-1363.
5. L. K. J. Hauru, M. Hummel, A. W. T. King, I. Kilpeläinen, H. Sixta, *Biomacromol*. **2012**, *13*, 2896-2905.
6. Parviainen, A., King, A. W. T., Mutikainen, I., Hummel, M., Selg, C., Hauru, L. K. J., Sixta, H. and Kilpeläinen, I. (2013), Predicting Cellulose Solvating Capabilities of Acid–Base Conjugate Ionic Liquids. *ChemSusChem*, 6: 2161–2169.

MECHANICAL PROCESSING OF SORGHUM AND MISCANTHUS IN THE PRODUCTION OF 2ND GENERATION BIOETHANOL

Dominika Pieprzyk–Kokocha*, Jolanta Batog, Aleksandra Wawro, Zbigniew Skibniewski

Institute of Natural Fibres & Medicinal Plants, Poznan, Poland
**dominika.kokocha@iwnirz.pl*

ABSTRACT

The paper presents the studies on the efficiency of mechanical pretreatment of lignocellulosic materials i.e. sorghum and miscanthus for the production of 2nd generation of biofuels. The energy consumption required for disintegration of sorghum and miscanthus biomass was measured; their fractions were evaluated by sieve analysis. Also enzymatic hydrolysis was tested and the reducing sugar content was determined with the use of Miller's method. The results of the tests allowed for selection of efficient and economically viable method of pretreatment of the sorghum and miscanthus biomass for the production of bioethanol.

I. INTRODUCTION

Bioethanol produced from plant biomass is a renewable and basic alternative source of energy, which is used both as fuel and in chemical, cosmetic and pharmaceutical industries. The main source for the production of 1st generation of bioethanol is grain of cereals and maize, potatoes, sugar beet and others. However the use of these crops for bioenergy is controversial as it causes reductions in the cultivation area for food and feed production. Taking into account domestic climatic conditions, lignocellulosic plants such as sorghum and miscanthus can become an alternative for bioenergy production.
Sorghum, similarly to maize, sugar cane and proso millet is classified in the *Panicoideae* family, *Poaceae*, in genus *Sorghum* [1]. Sorghum biomass contains high amounts of monosaccharides, what indicates its high usability for obtaining bioethanol [2]. Miscanthus is characterized with high growth of biomass, what leads to possible improvement of the cost-efficiency of the production of 2nd generation biofuels [3].
Considering high energetic value of combustion of sorghum and miscanthus and high yield of biomass, both plants can be used as raw material for production of biofuel.
It should be noted that lignocellulosic biomass is characterized with complexity of its chemical composition, as it contains in its structure a polymeric complex called lignocellulose, which is relatively difficult for biodegradation.
For bioethanol production raw material is as much important as optimal bioprocessing technology. Its efficiency can be increased by optimization of technological parameters. Lignocellulosic material must be subjected to pretreatment i.e. disintegration, saturation with diluted acids and pressure steam explosion. Processing of the material will allow for effective hydrolysis of the hemicellulose and will prepare cellulose for enzymatic treatment, what will ensure proper and efficient course of the following stages of bioethanol production i.e. enzymatic hydrolysis and fermentation.
The first stage of the pretreatment is mechanical processing involving disintegration of the plant material, most commonly done by grinding, what allows for improvement of cellulose accessibility to cellulolytic enzymes and thus increases monosaccharides that are further decomposed by distillation yeasts in fermentation process [4-5]. Mechanical pretreatment does not cause separation of specific fragments of the lignocellulosic complex, but leads to decreasing the particle sizes and consequently to lowering the resistance of transported mass and heat, change in macro and microscopic structure of the biomass, what generally has positive effect on the efficiency of the whole process of biofuel production [6-7]. Therefore, mechanical processing of the biomass is significant for the rate and degree of enzymatic hydrolysis of the cellulosic fraction.
Moreover, it is advisable to take into account the economic aspect of mechanical processing, as optimization of physical processes, which are energy consuming in their nature, will contribute to reduction of costs of the production of 2nd generation biofuels.

II. EXPERIMENTAL

The aim of the study was determination of the efficiency of mechanical processing of sorghum and miscanthus biomass during preparation of the materials for bioethanol production.
The materials used in the study were:
- Sucrosorghum 506 – from Experimental Farm of INF&MP in Sielec Stary (Poland),

- Miscantus Giganteus – from Institute of Plant Genetics of Polish Academy of Sciences in Poznan.
The raw material was subjected to crushing on the crusher for branches, and then dried at the temperature of 50°C for the period of 24 hours. The material prepared in that way was transferred for further processing on mills.
Percussive mills with sieves of the mesh size: 1, 1.8, 3 and 4 mm were used.
The measurement of the electrical energy consumption was performed on samples of crushed sorghum and miscanthus biomass of 200 g each, on every sieve, with the use of the analyser of the electric horsepower.
Furthermore, a sieve analysis of the sorghum and miscanthus biomass, for every sieve, was made with the use of a rotary laboratory shaker with the use of the sieve set of mesh diameters at: 5, 4, 3, 2, 1, 0.5 and 0.1 mm.
The determinant of the mechanical processing efficiency of the sorghum and miscanthus biomass is the content of reducing sugar determined according to Miller's method in an enzymatic hydrolysis test [8]. This test was performed with the use of the enzymatic preparation CELLUCLAST 1.5L (Novozymes) which cellulolytic activity is at 700 EGU/g. The vegetable raw material was incubated at 40°C in 0.05 M the citrate buffer of pH 4.8 for 2 hours. Then, absorbance measurement was made against the reference sample at the wavelength of 530 nm. The reading of the values on the reducing sugar content was done from the reference absorbance curve for glucose.
The selection of a suitable method of the disintegration of the sorghum and miscanthus biomass will have a bearing on the efficiency of the entire process of the energy production from these raw materials.

III. RESULTS AND DISCUSSION

In the study, the raw materials were subjected to the disintegration on the percussive mill (mesh size – 1, 1.8, 3 and 4 mm) and then electrical energy consumption was measured.
The average consumption of electrical energy per 100 g of the raw material in the percussive mill amounted to 0.0075 kWh. The mean duration of disintegration of the sample was about 2 minutes. For the sorghum biomass, the demand for energy was linearly decreasing in time, depending on the mesh size and it ranged between 0.023 kWh (the mesh - 1 mm) and 0.014 kWh (the mesh - 4 mm). In case of miscanthus the lowest energy consumption occurred for the biomass ground with the use of the sieve with mesh size at 1 mm and it amounted to 0.008 kWh.
Furthermore, the study included the sieve analysis of the sorghum and miscanthus biomass disintegrated with the percussive mill for every mesh size – 1, 1.8, 3 and 4 mm. The results of the sieve analysis are presented in Table 1.

Table 1. The sieve analysis of the sorghum and miscanthus biomass

		Amount of the material in each fraction [%]						
Raw material	Mesh diameter	below 0.1 [mm]	0.1 - 0.5 [mm]	0.5 - 1 [mm]	1 - 2 [mm]	2 - 3 [mm]	3 - 4 [mm]	above 4 [mm]
Sorghum	1 [mm]	9	79	9	1	0	0	0
	1.8 [mm]	7	57	33	1	0	0	0
	3 [mm]	7	39	46	5	0	0	0
	4 [mm]	3	27	38	27	3	0	0
Miscanthus	1 [mm]	11	72	15	0	0	0	0
	1.8 [mm]	12	53	32	1	0	0	0
	3 [mm]	7	38	44	9	0	0	0
	4 [mm]	3	28	33	30	3	0	0

The sieve analysis of the sorghum and miscanthus permitted the comparison of the decomposition of individual fractions of the biomass, what is an important element in the choice of the method of mechanical pretreatment. In terms of further processing the best particles are as small as possible with homogenous size.
The obtained results allow for observing that:
- the distribution of specific fractions of sorghum and miscanthus is similar,

- the highest amount of fractions at 0.1-0.5 mm and 0.5-1 mm was found for mesh sizes at 1, 1.8 and 3 mm, while for the mesh diameter 4 mm the distribution of specific fractions was similar – at about 30% in fractions: 0.1-0.5 mm, 0.5-1 mm and 1-2 mm.

In order to determine the efficiency of the mechanical processing of the sorghum and miscanthus biomass, the content of reducing sugar was measured by Miller's method in the enzymatic hydrolysis test of the fractions obtained after disintegration of raw materials on the percussive mill for every mesh size – 1, 1.8, 3 and 4 mm.
Table 2 presents differences in the quantity of reducing sugar in tests on the sorghum and miscanthus biomass subjected to action of the enzymatic preparation CELLUCLAST 1.5L and in control tests – without the use of the enzyme.

Table 2. The reducing sugar content in the sorghum and miscanthus, for mesh sizes – 1, 1.8, 3 and 4 mm

Raw material	Mesh size [mm]	Content of reducing sugar [mg/g]		
		Enzyme	Control	Difference
Sorghum	1	58.9	31.6	27.3
	1.8	74.3	32.8	41.5
	3	76.4	45.0	31,4
	4	76.9	53.9	23.0
Miscanthus	1	18.9	2.4	16.5
	1.8	24.4	9.0	15.4
	3	18.3	5.8	12.5
	4	19.0	6.6	12.4

The values of the reducing sugar in tests on the sorghum and miscanthus biomass ground on the percussive mill with sieves – 1, 1.8, 3 and 4 mm, obtained as the difference of the content of sugars determined in tests with the use of the CELLUCLAST 1.5L enzyme and control tests – without the use of the enzyme, allowed for selection of the optimum fractions of the raw materials. For the sorghum biomass, it was the fraction ground on the sieve with mesh size at 1.8 mm (the difference in sugar content of 41.5 mg/g), and for the miscanthus biomass it was the fraction obtained with mesh size of 1 mm (the difference in sugar content of 16.5 mg/g). The differences in the reducing sugar quantity in these fractions suggest that the raw material processed in this way is most susceptible to the enzymatic hydrolysis. This is an important factor as the fraction size of the raw material will influence significantly further stages of the pretreatment i.e. the treatment with acids and the pressure steam explosion, because it will permit more effective loosening of the lignocellulosic structure and thus more effective preparation of the raw material for the enzymatic treatment.
Furthermore, it is notable that the selected fractions are characterized with the lowest energy consumption during their disintegration and this will contribute to lowering the costs of the mechanical pretreatment of the sorghum and miscanthus biomass.

IV. CONCLUSIONS

- The use of the percussive mill, due to time, efficiency and energy consumption is advisable and allows for analysing disintegration with sieves of different mesh sizes – 1, 1.8, 3 and 4 mm, what leads to differentiation in the electrical energy consumption needed for disintegration of both sorghum and miscanthus.
- The content of reducing sugar determined with Miller's method in ground sorghum and miscanthus biomass showed that an effective method of the disintegration of raw materials was grinding on the percussive mill: for sorghum with mesh at 1.8 mm, and for miscanthus with mesh at 1 mm, what is justified also from the economic point, because it requires the lowest energy consumption for the process.

V. ACKNOWLEDGEMENT

The authors acknowledge the funding by the National Centre for Research and Development, Poland, under the project PBS1/A8/9/2012.

VI. REFERENCES

[1]. Dalhberg J.; Berenji J.; Sikora V.; Latkocić D. Assessing sorghum (*Sorghum bicolor (L) Moench*) germplasm for new traits: food, fuels and unique uses. *Maydica* **2011**, *56*, 85-92.

[2]. Burczyk H.; Kołodziej J.; Kowalska M. Plony i wartości energetyczne kukurydzy, sorgo i konopi włóknistych w porównaniu z roślinami egzotycznymi. (Yields and energy value of maize, sorghum and fibrous hemp as compared with exotic plants.) *XIII Konferencja Naukowa IUNG-PIB* **2009**.

[3]. Jeżowski S. Rośliny energetyczne – produktywność oraz aspekt ekonomiczny, środowiskowy i socjalny ich wykorzystania jako ekopaliwa. (Energy plants - efficiency and economic, environmental and social aspects of their use as ecofuel.) *Post. Nauk Rol.* **2003**, *3*, 61-73.

[4]. Taharzadeh M.J.; Karimi K. Pretreatment of lignocellulosic wastes to improve ethanol and biogas production: a review. *Int. J. Mol. Sci.* **2008**, *9*, 1621–1651.

[5]. Chmielewska J.; Sowiński J.; Nowakowski P. Wykorzystanie lignocelulozowej biomasy sorgo do produkcji etanolu. (Using lignocellulosic sorghum biomass for ethanol production.) *Przem. Chem.* **2013**, *92*, 1106-1009.

[6]. Świątek M.; Lewandowska M.; Bednarski W. Znaczenie doboru metody wstępnej obróbki substratów lignocelulozowych z uwzględnieniem wydajności produkcji bioetanolu. (The importance of selection of the pretreatment method for lignocellulosic substrates in terms of bioethanol production efficiency.) *Post. Nauk Rol.* **2011**, *1*, 109–119.

[7]. Biopaliwa. Technologie dla zrównoważonego rozwoju. (Biofuels. Technologies for sustainable development.) Redakcja E. Klimuk, M. Pawłowska, T. Pokój. Wydawnictwo Naukowe PWN, Warszawa **2012**, 109-113.

[8]. Miller G.L. Use of dinitrosalicylic acid reagent for determination of reducing sugar. *Anal. Chem.* **1959**, *31*, 426-428.

MACROPOROUS, MECHANICALLY STABLE CELLULOSE PHOSPHATE AEROGELS FOR TISSUE ENGINEERING APPLICATIONS

Nicole Pircher[1], Thomas Rosenau[1], Falk Liebner[1]*

*Department of Chemistry, Division of Chemistry of Renewables, University of Natural Resources and Life Sciences Vienna, Konrad-Lorenz-Straße 24, A-3430 Tulln, Austria (*falk.liebner@boku.ac.at)*

ABSTRACT

Cellulose phosphate aerogels of low DS have shown promise when tested for hemocompatibility aiming at biomedical applications. However, insufficient macroporosity as well as lacking mechanical strength are the limiting factors that hitherto prevented the respective aerogels from being used as cell scaffolding materials in bone tissue engineering.
The current paper demonstrates that these limitations can be overcome by creation of a secondary void system consisting of interconnected, large macropores (≤ 300 µm) and by reinforcing the obtained macroporous composite aerogel with biocompatible biopolymers, such as PMMA or cellulose acetate. This has been accomplished by a) preparation of a temporary templating scaffold composed of fused spheres of a suitable polymer, b) filling the voids of the templating network with a solution of cellulose in a suitable solvent, c) cellulose coagulation, d) removal of the temporary templating porogens scaffold, e) phosphorylation, and f) reinforcement. The obtained aerogels have been characterized with regard to their material properties (density, morphology, specific surface area, mechanical stability under uniaxial compression) and biocompatibility (viability and distribution of mesenchymal stem cells, biomineralization).

I. INTRODUCTION

Functional scaffolds for bone tissue engineering have to fulfill numerous demands regarding their biocompatibility, resorbability, porosity characteristics and mechanical properties. An interconnected pore network with a micro-structured surface is required for cell migration and diffusion of physiological nutrients and gases to cells, removal of metabolic by-products from cells, in vitro cell adhesion, in-growth and in vivo neovascularization.

Cellulose, either in its native form, e.g. bacterial cellulose (BC), or as the readily shapeable cellulose II polymorph, is considered to be a promising cell scaffolding material, as respective aerogels form hierarchical fibrous networks that contain micro-, meso- and macropores. [1]. However, despite the use of high purity BC in a range of tissue engineering applications, e.g. [2-4], both bacterial cellulose and regenerated cellulose require chemical modification prior to implant applications, due to its potential inflammatory response via the alternative pathway and the insufficient binding and crystallization tendency of hydroxyl apatite, which impedes both quantitative biomineralization and osseointegration of the cellulosic scaffold [5-7]. Cellulose phosphate aerogels of low degree of phosphorylation (DS ≤ 0.20) obtained from NMMO·H_2O solutions showed good hemocompatibility and ability to induce formation of a thin hydroxy apatite layer under simulated physiological conditions. [8]

For bone tissue engineering, interconnected macropores larger than 75 µm are crucial to promote osteogenesis [9-12]. The mesh size of cellulose fibrils in gel networks is much lower (>10 µm). However, spherical pores of these dimensions have previously been introduced into cellulose gels using porogens [13, 14]. Even without the introduction of macropores, the innately low elastic modulus and yield strength of cellulosic aerogels under compressive strain are a major drawback to applications in bone tissue engineering. Our group previously achieved reinforcement of the microfibrillar network structure by precipitation of a second polymeric constituent therein, ideally merging the cellulose fibrils at their contact points. [15]

In the present work, cellulose (phosphate) aerogels are reinforced by introducing a secondary biocompatible polymeric constituent, such as polylactic acid (PLA), cellulose acetate (CA), poly(methyl methacrylate) (PMMA) or sodium polyphosphate (SPP), into the cellulose fibril network, according to liquid or supercritical antisolvent precipitation techniques. To achieve an interconnected hierarchical porosity ranging from single-digit nanometers to several hundred micrometers, porogens were used as a scaffold during cellulose coagulation.

II. EXPERIMENTAL

Preparation of cellulose-based aerogels

Cotton linters (M_w143.2 kg/mol), in their native or phosphorylated form were dissolved either in an ionic liquid (EMIM acetate:DMSO, 30:70, RT, 2h) or a salt hydrate melt ($Ca(SCN)_2 \cdot 4H_2O$, 140°C, 2h). Cellulose was coagulated and washed using water or ethanol.

Cellulose and cellulose phosphate aerogels have been reinforced by introducing a secondary organic polymer constituent. Prior to reinforcement, the cellulose gels were transferred to the solvent used to dissolve the secondary reinforcing polymer. Thereafter, the cellulose lyogels were immersed in the respective reinforcing polymer solutions, which were loaded into the voids of the cellulose fibril network. After a residence time of at least 24 hours, the samples were removed from the loading bath. Precipitation was carried out using either a liquid or a supercritical gas. Reinforcement conditions for selected reinforcing polymers are summarized in Table 1.

Table 1: Selected loading and precipitation conditions.

Reinforcing polymer	Loading solvent	Loading temperatur (°C)	Antisolvent
PLA	THF	50°C	EtOH
CA	Acetone	RT	$scCO_2$
PMMA	Acetone	RT	$scCO_2$
SPP	Water/urea	RT	EtOH

$ScCO_2$ precipitation and drying (Separex, France) were carried out using the following conditions: Constant $scCO_2$ flow (40 g/min) at 10 MPa and 40°C (2-3 hours), slow (<0.1 $MPamin^{-1}$), and isothermal depressurization.

Macroporous cellulosic aerogels have been prepared by filling a template of porogens (paraffin wax or PMMA spheres) with the respective cellulose solution and subsequent regeneration of cellulose. The porogens were extracted with THF (paraffin) or acetone (PMMA).

Characterization

Scanning electron microscopy (SEM) of gold-sputtered samples was performed on a Tecnai Inspect S50 instrument under high vacuum and an acceleration voltage of 5.00 kV. Compressive tests were performed on a Zwick/Roell Materials Testing Machine Z020 in a 500 N load cell. Yield strength (RP0.2) was defined as the stress at 0.2% plastic deformation. Nitrogen adsorption/desorption isotherms at 77 K have been obtained on a Micromeritics ASAP 2020 analyzer. All samples were degassed in vacuum prior to analysis.

III. RESULTS AND DISCUSSION

The internal morphology of the composite aerogels as investigated by SEM revealed that small, isolated PLA particles were precipitated at low polymer concentrations of the loading bath, whereas a continuous, interpenetrating PLA network was obtained at concentrations above 8% (w/v). In contrast, CA and PMMA were deposited as thin films on the cellulose fibrils, affording a reinforcing effect already at low concentrations. At higher concentrations, the microstructure of the composite aerogels was comparable to CA and PMMA-based open porous films obtained by $scCO_2$ processing [16].

The mechanical response profiles towards compression stress showed a higher stiffness (elastic modulus) and strength (yield strength at 0.2% compression stress) for CA and PMMA reinforced aerogels compared to unmodified cellulose aerogels already at low concentrations of the loading bath, and did so increasing with higher contents. The highest increase in specific modulus (density normalized Young's modulus) compared to pure cellulose aerogels was achieved for composites obtained from loading bath containing 8% (w/v) (4.8-fold) and 12% (w/v) PMMA (5.5-fold). PLA had a reinforcing effect only once an interconnected PLA network had been formed. While the incorporation of PLA caused a reduction of specific modulus at lower concentrations (increase in density without a reinforcing effect), it increased once the interpenetrating network was established throughout the cellulose network.

The increase in density due to the introduction of a second polymeric component usually causes a reduction of the specific surface area. However, in most cases a maintenance or even increase in the surface-area-to-volume

ratio (SA:V) was observed, which, in conjunction with the SEM micrographs, confirms the preservation of an open porous morphology throughout the antisolvent precipitation and drying procedures.

Homogeneous percolation of the secondary polymer network inside the cellulosic aerogel has been demonstrated for one of the composite aerogels (cellulose-PMMA) by re-dissolving cellulose with EMIM acetate. The obtained self-standing, largely homogeneous PMMA scaffold confirms that cellulose aerogels can be used as a templating temporary scaffold for the preparation of open-porous materials from other sources as well.

The application of paraffin wax or PMMA microspheres as porogens during cellulose coagulation allows tailoring the hierarchical pore structure that contains interconnected macropores of controllable size (up to 300 µm, Figure 1) next to meso- and micropores found in the walls of the macrovoids.

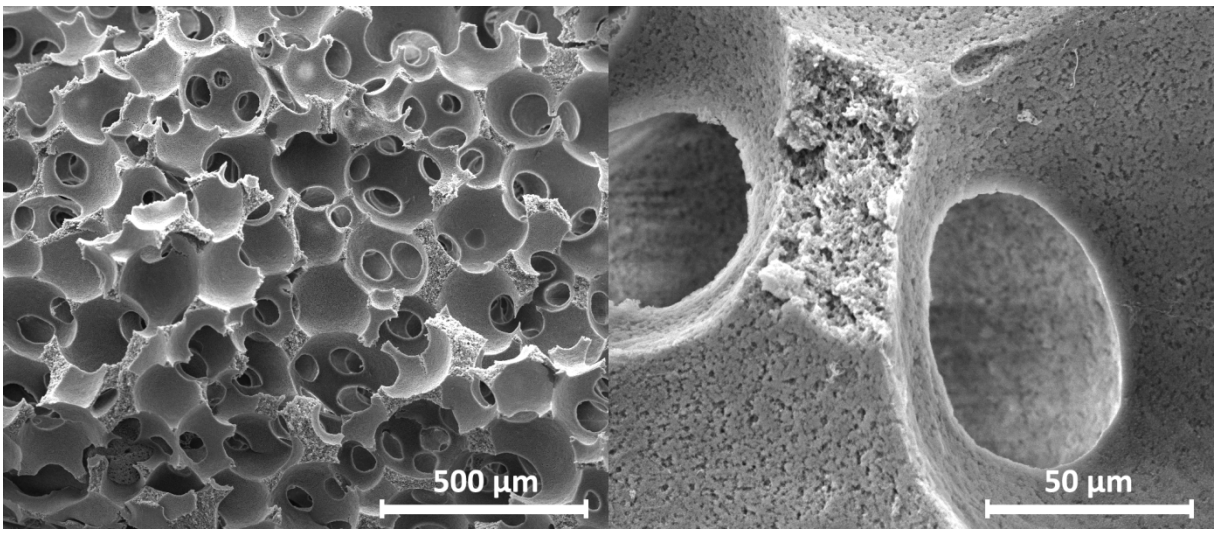

Figure 1: SEM images of a cellulose aerogel with pore sizes ranging from single-digit nanometer to several hundred micrometers. Interconnected macropores were obtained using 200-300µm paraffin wax spheres as porogens (pore templates). Right: Breaking edge illustrating the inner morphology of the hierarchical, open-porous scaffold.

IV. CONCLUSIONS

Biocompatible macroporous and mechanically stable cellulose-based aerogels for bone tissue engineering were prepared by i) introducing phosphate groups to render cellulose hemocompatible in terms of homeostasis and inflammatory response and to promote the formation of hydroxyapatite and thus osteogenesis; ii) porogens to obtain interconnected macropores and to control their size distribution to optimize the scaffold morphology with regard to cell adhesion, ingrowth, and proliferation; and iii) reinforcing the fragile lightweight cellulose (phosphate) based materials with an intercalating secondary, biocompatible polymeric component under preservation of the hierarchical, interconnected pore system.

V. ACKNOWLEDGEMENT

The financial support by the Austrian Science Fund (FWF) and the Agence Nationale de la Recherche (ANR) through the Austrian-French project CAP-Bone (FWF I848-N17) is thankfully acknowledged.

VI. REFERENCES

[1] Helenius, G.; Bäckdahl, H.; Bodin, A.; Nannmark, U.; Gatenholm, P.; Risberg, B. In vivo biocompatibility of bacterial cellulose. *Journal of Biomedical Materials Research Part A*. **2006**, *76A*, 431-438.

[2] Svensson, A.; Nicklasson, E.; Harrah, T.; Panilaitis, B.; Kaplan, D.L.; Brittberg, M.; Gatenholm, P. Bacterial cellulose as a potential scaffold for tissue engineering of cartilage. *Biomaterials*. **2005**, *26*, 419-431.

[3] Bodin, A.; Bäckdahl, H.; Fink, H.; Gustafsson, L.; Risberg, B.; Gatenholm, P. Influence of cultivation conditions on mechanical and morphological properties of bacterial cellulose tubes. *Biotechnology and Bioengineering*. **2007**, *97*, 425-434.

[4] Bodin, A.; Concaro, S.; Brittberg, M.; Gatenholm, P. Bacterial cellulose as a potential meniscus implant. *Journal of Tissue Engineering and Regenerative Medicine*. **2007**, *1*, 406-408.

[5] Granja, P.L.; Pouysegu, L.; De Jeso, B.; Rouais, F.; Baquey, C.; Barbosa, M.A. Cellulose phosphates as biomaterials. mineralisation of chemically modified regenerated cellulose hydrogels. *J. Mater. Sci.***2001**, *36*, 2163-2172.

[6] Fricain, J.C.; Granja, P.L.; Barbosa, M.A.; de Jéso, B.; Barthe, N.; Baquey, C. Cellulose phosphates as biomaterials. In vivo biocompatibility studies. *Biomaterials*. **2002**, *23*, 971-980.

[7] Ishihara, K.; Nakabayashi, N. Hemocompatible Cellulose Dialysis Membranes Modified with Phospholipid Polymers. *Artificial Organs*. **1995**, *19*, 1215-1221.

[8] Liebner, F.; Dunareanu, R.; Opietnik, M.; Haimer, E.; Wendland, M.; Werner, C.; Maitz, M.; Seib, P.; Neouze, M.-A.; Potthast, A.; Rosenau, T. Shaped hemocompatible aerogels from cellulose phosphates: preparation and properties. *Holzforschung*. **2012**, *66*, 317–321.

[9] Lu, J.X.; Flautre, B.; Anselme, K.; Hardouin, P.; Gallur, A.; Descamps, M.; Thierry, B. Role of interconnections in porous bioceramics on bone recolonization in vitro and in vivo. *Journal of Materials Science: Materials in Medicine*. **1999**, *10*, 111-120.

[10] Hutmacher, D.W. Scaffolds in tissue engineering bone and cartilage. *Biomaterials*. **2000**, *21*, 2529-2543.

[11] Karageorgiou, V.; Kaplan, D. Porosity of 3D biomaterial scaffolds and osteogenesis. *Biomaterials*. **2005**, *26*, 5474-5491.

[12] Hulbert, S.F.; Young, F.A.; Mathews, R.S.; Klawitter, J.J.; Talbert, C.D.; Stelling, F.H. Potential of ceramic materials as permanently implantable skeletal prostheses. *Journal of Biomedical Materials Research*. **1970**, *4*, 433-456.

[13] Bäckdahl, H.; Esguerra, M.; Delbro, D.; Risberg, B.; Gatenholm, P. Engineering microporosity in bacterial cellulose scaffolds. *Journal of Tissue Engineering and Regenerative Medicine*. **2008**, *2*, 320-330.

[14] Tsioptsias, C.; Panayiotou, C. Preparation of cellulose-nanohydroxyapatite composite scaffolds from ionic liquid solutions. *Carbohydrate Polymers*. **2008**, *74*, 99-105.

[15] Pircher, N.; Veigel, S.; Aigner, N.; Nedelec, J.-M.; Rosenau, T.; Liebner, F. Reinforcement of bacterial cellulose aerogels with biocompatible polymers. *Carbohydrate Polymers*. **2014**, *submitted*.

[16] Reverchon, E.; Cardea, S.; Rappo, E.S. Production of loaded PMMA structures using the supercritical CO2 phase inversion process. *Journal of Membrane Science*. **2006**, *273*, 97-105.

PINOBIO – PINOSYLVINS AS NOVEL BIOACTIVE AGENTS FOR FOOD APPLICATIONS

Carme Plumed-Ferrer[1]*, Patrik Eklund[2], Markus Storvik[3], Markku Pasanen[3], Stefan Willför[2], Atte von Wright[1]

*[1]University of Eastern Finland, Institute of Public Health and Clinical Nutrition, P.O. box 1627, FI-70211 Kuopio, Finland; [2]Åbo Akademi University, Process Chemistry Centre, Porthansgatan 3, FI-20500 Åbo, Finland; [3]University of Eastern Finland, School of Pharmacy, P.O. box 1627, FI-70211 Kuopio, Finland. *Email of corresponding author: carme.plumed@uef.fi*

ABSTRACT

Pinosylvin and pinosylvin monomethyl ether (PMME) are naturally occurring compounds found in the heart-wood of Scot pine (*Pinus sylvestris*). They are protective stilbenoids, suggested to act against any fungal infection. Pinosylvin is structurally very similar to resveratrol, a stilbene compound commonly known as the miracle molecule in red wine because of its wide range of pharmacological actions (anti-aging, anti-diabetic, anti-inflammatory, anti-oxidation, cardio- and neuro-protector, etc.). The aim of this project was to elucidate whether pinosylvin and some derivatives can have similar properties as resveratrol, and could thus be used as bioactive agents in food applications. The project focused on elucidating the anti-microbial potential of the pinosylvins and some derivatives as natural biocides against a wide range of food-associated pathogens and spoilage organisms. Moreover, their role in the human xenobiotic and cancer metabolism was studied *in situ* using three cell models; enteric-, placental- and hepatic-cell lines. The results showed that pinosylvin was the most effective stilbene against *Listeria* and *Salmonella*, followed by PMME and pinosylvin monoethyl ether (PMEE). However, PMME and PMEE were more effective against *Candida* than pinosylvin. Other derivatives showed very little antimicrobial activity. Their effect in the xenobiotic and cancer metabolism was cell line-, compound- and dose-dependent, pinosylvin and PMME showing surprisingly different effects from those of resveratrol.

I. INTRODUCTION

Pinosylvin (3,5-dihydroxystilbene) and its monomethyl ether (3-hydroxy-5-methoxy-stilbene) are naturally occurring compounds found in the heart-wood of Scot pine (*Pinus sylvestris*). They are protective stilbenoids, suggested to act against any fungal infection (Plumed-Ferrer et al. 2013). Pinosylvin is structurally very similar to resveratrol (3,5,4´-trihydroxystilbene, Fig. 1), a stilbene compound commonly known as the miracle molecule in red wine because of its wide range of pharmacological actions (anti-aging, anti-diabetic, anti-inflammatory, anti-oxidation, cardio- and neuro-protector, etc.). The aim of this project was to elucidate whether pinosylvin and some derivatives can have similar properties as resveratrol, and could thus be used as bioactive agents in food applications. The project focused on elucidating the anti-microbial potential of the pinosylvins and some derivatives as natural biocides against a wide range of food-associated pathogens and spoilage organisms. Moreover, their role in the human xenobiotic and steroid metabolism was studied *in situ* using three cell models; enteric-, placental- and hepatic-cell lines.

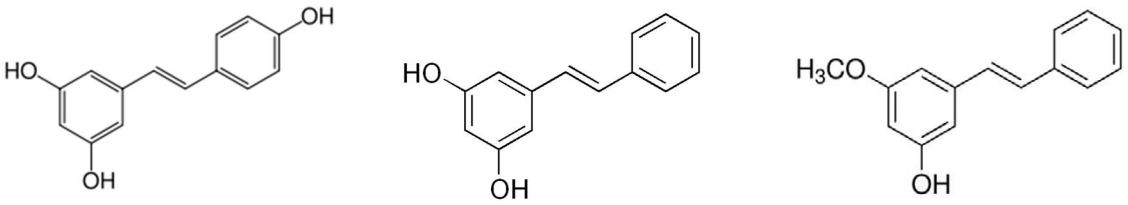

Resveratrol Pinosylvin Pinosylvin monomethyl ether

Figure 1. Chemical structure of resveratrol, pinosylvin and pinosylvin monomethyl ether

II. EXPERIMENTAL

Tested compounds

A total of 13 compounds were tested for the antimicrobial assay: Pinosylvin (PS); 7,8-dihydropinosylvin (DPS); Pinosylvin monomethyl ether (PMME); Pinosylvin 3,5-dimethyl ether (PDME); Pinosylvin 3,5-diethyl ether (PDEE); Pinosylvin monoethyl ether (PMEE); Pinosylvin 3,5-distearate (PDST); Pinosylvin 3,5-diacetate (PDAC); Pinosylvin monosuccinate (PMSC); Pinosylvin 3,5-dibutyrate (PDBT); Pinosylvin 3,5-diglutarate (PDGT); Pinosylvin 3,5-disuccinate (PDSC); Pinosylvin 3,5-diacetate 7,8-oxide (PDACOX).

DPS: Pinosylvin was dissolved in ethanol and 5% Pd/C was added. The mixture was hydrogenated for 72h under 5 atm of H_2. The mixture was filtered and the solvent removed to give the final product.

PDME, PDEE, PMEE: Pinosylvin was dissolved in acetone and the corresponding alkyl iodide (2-6 eqv) was added followed by K_2CO_3 (8 eqv). The mixture was stirred for 24h and then extracted wit dichloromethane/water. The residue was purified with column chromatography.

PDAC, PDBT, PDST, PDGT, PMSC, PDSC: Pinosylvin was mixed with the corresponding anhydride or acyl chloride (2-3 eqv) in pyridine. The mixture was stirred (1-40h) in room temperature and then the product was precipitated with cold water, filtrated and washed with water and diluted HCl. The residue was purified by column chromatography to give the final products.

PDACOX: Compound 1 was dissolved in dichloromethane and *m*CPBA (3eqv) was added. The mixture was stirred for 72h and the solvent was removed and the residue purified by column chromatography.

Three compounds were used for the gene expression assay: PS, PMME and resveratrol. Resveratrol was purchased from Sigma-Aldrich (Steinheim, Germany).

Microbial strains and culture conditions

The microbial strains used included a gram-positive bacteria, *Listeria monocytogenes* L211 (The Finnish Food Safety Authority (EVIRA), Helsinki, Finland), a gram-negative bacteria, *Salmonella infantis* EELA 72 (EVIRA) and a eukaryotic yeast, *Candida tropicalis* 4068 (Valio, Espoo, Finland). *Listeria* was grown in trytone soy agar or broth at 37 °C, *Salmonella* in blood agar and brain heart infusion broth at 37 °C, and *Candida* in OGYE agar or broth at 30 °C. All media were purchased from Lab M Ltd., UK.

Antimicrobial assay

The antimicrobial effects of the pinosylvins and pinosylvin derivatives on the microbial strains were determined using a Thermo Bioscreen C automatic turbidometer (Labsystems Oy, Helsinki, Finland). Four different concentrations of the compounds were assessed: 0.25, 0.5, 0.75 and 1 mM for *Listeria* and *Salmonella*, and 0.1, 0.25, 0.5, and 1 mM for *Candida*. The preparation of the test cultures and the practical performance of the assays have been described in Välimaa et al. 2007. The growth inhibition was calculated by subtracting the percentage of turbidity of the test culture from that of the control.

Cell lines and cell culture

Three cell lines used in this study are Caco-2 human colorectal adenoma cell line (ATCC HTB-37), JEG-3 human choriocarcinoma cell line (ATCC HTB-36) and HepG2 human hepatoma cell line (ATCC HB-8065). All cell lines were grown in 6-well plates, seeded at 1-2 million cells/well (in triplicates) and incubated at 37 °C in 5% CO_2 humidified incubator. Caco-2 cells were additionally differentiated for 14 days before the test started. Caco-2 and JEG-3 cells were grown in DMEM (Dulbecco´s Modified Eagle´s Medium, Biowhittaker) supplemented with 10% (v/v) heat inactivated fetal bovine serum, 1% L-glutamine (x100), 1% (v/v) non-essential amino acids and 1% penicillin/streptomycin (x100). HepG2 cells were grown in MEM (Minimum Essential Medium Eagle, Sigma-Aldrich) supplemented with 10% (v/v) heat inactivated fetal bovine serum, 1% L-glutamine (x100) and 1% (v/v) non-essential amino acids. All reagents were purchased from EuroClone (Siziano, Italy).

Cells were incubated with different concentrations (0.1-100 mM) of PS, PMME and resveratrol for 8 hours. After incubation, cells were washed with PBS and lysed with Trizol for 5-10 min.

RNA isolation and RT-PCR

Total RNA was extracted with Trizol followed with centrifugation in chloroform, isopropanol precipitation and 75% ethanol washing. The RNA pellet was diluted with DEPC-H_2O and treated with DNase (Ambion Turbo DNA-free kit). Complementary DNA (cDNA) was synthesized as described in Storvik et al. 2011. The expression of CYP1A1 gene was monitored and normalized with β-actin as reference gene. Each sample was measured in triplicate.

III. RESULTS AND DISCUSSION

Antimicrobial assay of pinosylvins and some derivatives against food pathogens

Pinosylvin and 12 pinosylvin derivatives were tested for their antimicrobial effect against different model microorganism (*Listeria* as a gram-positive, *Salmonella* as a gram-negative and *Candida* as a eukaryotic yeast), being all common food pathogens. PS has two hydroxyl groups (Figure 1), while the pinosylvin derivatives had one or both hydroxyl groups replaced by a methyl ether, ethyl ether, stearate, acetate, succinate, butyrate, or glutarate group. Concentrations considerably lower than the ones used with commercial disinfectants were chosen.

The results showed that PS was the most effective stilbene against *Listeria* and *Salmonella*, followed by PMME and PMEE (Table 1). However, PMME and PMEE were more effective against *Candida* than PS. This might probably be due to their increased polarity and thus increased capacity to penetrate the bacteria cell wall or membrane. On the other hand, PDME and PDEE had no inhibition effects against the microorganisms tested (Table 1) suggesting that at least one hydroxyl group is needed for their antimicrobial activity. All the other derivatives showed none or very little antimicrobial activity (not shown).

Table 1. Antimicrobial activity of pinosylvin and 5 pinosylvin derivatives (MIC, mM)

Compounds	***Listeria***	***Salmonella***	***Candida***
Pinosylvin (PS)	0.75	0.5	0.25
7,8-dihydropinosylvin (DPS)	>1	>1	1
Pinosylvin monomethyl ether (PMME)	>1	0.5	0.1
Pinosylvin 3,5-dimethyl ether (PDME)	>1	>1	>1
Pinosylvin 3,5-diethyl ether (PDEE)	ND	ND	> 0.5*
Pinosylvin monoethyl ether (PMEE)	1	>1	0.1

Minimum inhibitory concentration (MIC) considered when the % of inhibition was 50 or higher.
ND, not detected because of interfering background.
* Concentrations higher than 0.5 mM were not detected due to interfering background.

Effects of pinosylvin on xenobiotic and carcinogen metabolims

Pinosylvin is chemically very similar to resveratrol (Figure 1), a well-known polyphenol associated with life extension, cancer prevention, cardiovascular and neurodegenerative diseases, diabetes and inflammation. Resveratrol has been shown to modulate the expression of the CYP450 enzyme system. CYPs are key factors for human health, specifically CYP1A1, which has been showing a dual activity. CYP1A1 is involved in the metabolism of xenobiotics (pharmaceuticals, pesticides, food contaminant, etc.), acting as a detoxifying enzyme. However, it is also a carcinogen activator. Resveratrol has been shown to both, activate (acting as xenobiotic) and inhibit (acting as anti-cancer) the expression of CYP1A1 in a dose-dependent manner. The effects of resveratrol, PS, and PMME in the xenobiotic and cancer metabolism have been shown to be cell line-, compound- and dose-dependent, pinosylvin and PMME showing surprisingly different effects from those of resveratrol. Specifically, in colorectal epithelial cells (Caco-2), no significant differences were found between the three compounds or between the different concentrations tested (Figure 2). In the placental cells (JEG-3), a clear down-regulation of all three compounds occurred with the increased in concentration (Figure 3) suggesting that all these compounds might have an effect reducing the cancer activators. In the hepatic cells line (HepG2), resveratrol and PS did not show significant differences between different concentrations. However, an extremely

high over-expression occurred with PMME at high concentrations, suggesting that at those concentrations, this compound could have an important effect on the xenobiotic metabolism.

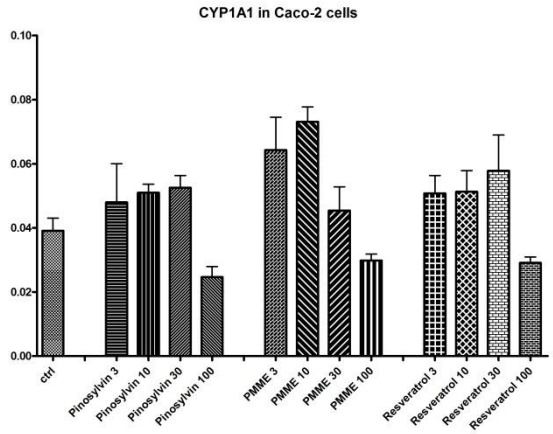

Figure 2. CYP1A1 expression in Caco-2 cells after 8 h of exposure.

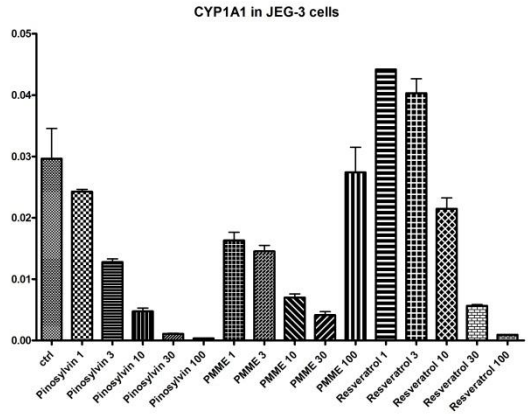

Figure 3. CYP1A1 expression in JEG-3 cells after 8 h of exposure.

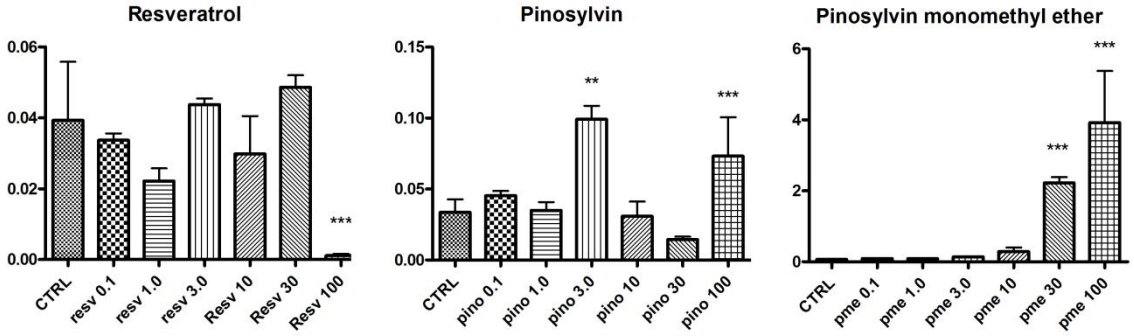

Figure 4. CYP1A1 expression in HepG2 cells after 8 h of exposure.

IV. CONCLUSIONS

1- PS, PMME and PMEE have the potential to be natural biocides against a wide range of food-associated pathogens and spoilage organisms.

2- PS and PMME in the xenobiotic and cancer metabolism have been shown to be cell line-, compound- and dose-dependent, these compounds showing different effects from those of resveratrol in some cells lines. More information is needed in order to conclude whether *in vivo* PS and PMME would act differently than resveratrol.

VI. REFERENCES

[1] Plumed-Ferrer, C.; Väkeväinen, K.; Komulainen, H.; Rautiainen, M.; Smeds, A.; Raitanen, J.; Eklund, P.; Willför, S.; Alakomi, H.; Saarela, M.; von Wright, A. The antimicrobial effects of wood-associated polyphenols on food pathogens and spoilage organisms. *Int. J. Food Microbiol.* **2013,** 164, 99-107.

[2] Storvik, M.; Huuskonen, P.; Kyllonen, T.; Lehtonen, S.; El-Nezami, H.; Auriola, S.; Pasanen, M. Aflatoxin B1-a potential endocrine disruptor - up-regulates CYP19A1 in JEG-3 cells. *Toxicol. Lett.* **2011**, 202, 161-167.

[3] Välimaa, A.; Honkalampi-Hämäläinen, U.; Pietarinen, S.; Willför, S.; Holmbom, B.; von Wright, A. Antimicrobial and cytotoxic knotwood extracts and related pure compounds and their effects on food-associated microorganisms. *Int. J. Food Microbiol.* **2007**, 115, 235-243.

PHENOLATION OF LIGNINS: EFFECT OF STRUCTURE ON REACTIVITY

Jacob Podschun[1]*, Alexander Stücker[2], Bodo Saake[1], Ralph Lehnen[2]*

[1] *University of Hamburg, Chemical Wood Technology, Leuschnerstraße 91b, 21031 Hamburg, Germany*
[2] *Thünen Institute of Wood Research, Leuschnerstraße 91b, 21031 Hamburg, Germany*
(jacob.podschun@uni-hamburg.de; ralph.lehnen@ti.bund.de)*

ABSTRACT

The material utilization of lignin for high value products is one attempt to enhance the efficiency of lignocellulosic biorefineries. Lignin could function as a structural backbone in phenol formaldehyde resin prepolymers. However, the low number of reactive sites with respect to phenol-formaldehyde chemistry hinders effective condensation reactions. Organosolv, Kraft, soda and sulfite lignin were phenolated to increase their cross-linking ability. The products were characterized concerning their functional groups by ^{31}P-NMR spectroscopy as well as sulfur and ash content. The results revealed that the degree of phenolation differs significantly due to structural features of the lignins. Additionally, the cross-linking ability of phenolated lignin was studied by synthesizing a lignin phenol formaldehyde resin and comparing its wood bonding properties with plain PF and LPF with unmodified lignin.

I. INTRODUCTION

Thermosetting resins require numerous reactive sites to achieve a high cross-link density. The approach to partially substitute phenol formaldehyde (PF) resoles with lignins results in a decrease in the number of reactive functionalities. The comparable low reactivity of lignin is already established during shikimate biosynthesis resulting in lower free ortho-positions and no free para-positions in the phenolic ring. To overcome this obstacle, several methods have been reported to increase lignin reactivity [1]. The hydroxymethylation of lignin does not directly increase the number of reactive sites, but sterical hindrances and competing reaction with phenol are lowered. Demethylation of lignin is another promising approach with high potential. However, the reagents applied (halide or sulfur compounds) are undesired for future applications, and catalytic pathways do not yet exist. A demethylated lignin can also be prepared by combining oxidation and reduction of the aromatic ring. This method however still lacks suitable reagents and reaction control. Alternative to the methods above, which focus on the functionalization of the aromatic moiety, the reactivity in the side chain of lignin could be used. The direct reaction of lignin model compound guaiacylglycerol-β-guaiacyl ether with phenol was intensively studied by Lin et al. [2]. They found that the dominant reaction product result from condensation of phenol and guaiacylglycerol-β-guaiacyl in its C_α. Furthermore, they reported the cleavage of β-O-4- and C_β-C_γ-bonds to generate new reactive sites. This pathway to increase lignin reactivity was investigated by Alonso et al. for ammonium lignosulfonate [3]. They revealed that long reaction time, high temperature and low lignosulfonate concentration are optimal (160 min, 110-160°C, 30%). Cetin and Özmen investigated the application of phenolated Alcell® lignin in particleboards and found that a higher fraction of lignin could be added to PF resin upon phenolation compared to plain lignin [4,5]. However, it remains unresolved how lignin source and structural features affect the degree of phenolation. In this study, a comparison of different lignins in the phenolation reaction (see **Figure 1**) is presented towards the improvement of lignin-PF resins. Furthermore, one could deduce the reactivity of the lignins for other nucleophiles than phenol in similar reactions.

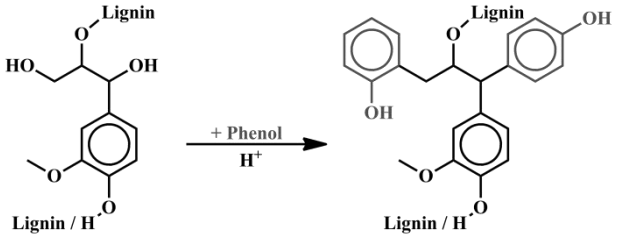

Figure 1. Schematic representation of the phenolation of lignin

II. EXPERIMENTAL

Lignins: Organosolv lignins were produced at Thünen Institute of Wood Research (Hamburg, Germany) by ethanol water pulping of beech wood, pine wood and wheat straw as described in **Table 1** followed by precipitation of the black liquor in water, filtration and vacuum drying over P_2O_5. The other lignins were obtained from Stora Enso (spruce/pine, Kraft), Suzano (eucalyptus, Kraft), Tembec (softwood, sulfite-NH_4) and Green Value (wheat, soda).

Table 1. Pulping conditions of organosolv lignins

	Time [h]	Liquor ratio	Temperature [°C]	H_2SO_4 [% of dry mater]	EtOH : H_2O
Wheat straw	2	1 : 4	180	2	1 : 1
Pine wood	1,5	1 : 4	170	1	1 : 1
Beech wood	1,5	1 : 4	170	0,5	1 : 1

Phenolation of Lignins: Phenolation of lignins was performed by treating 1 g of lignin with 2 g (21 mmol) of phenol and 108 µL (2 mmol) conc. H_2SO_4 at 110°C for 20 minutes. The reaction mixture was quenched with 25 mL acetone-H_2O (9:1) and precipitated into the 4-fold amount of dilute H_2SO_4 (pH 1). The precipitate was collected on a PES membrane (0.45 µm pores), washed with water until neutral and dried over P_2O_5 in vacuum. All lignins had excellent solubility in phenol, except for the sulfite lignin. Here, 0.8 mL of water was required to obtain a homogenous mixture. Further adaptations were necessary in case of sulfite lignin, including T=90°C, quenching with water, precipitation and washing with iso-propanol and RC-membrane filtration.

Ash removal: Kraft lignins were dissolved in the 10-fold amount of acetone-water (8:2) and the solution was precipitated into the 4-fold amount of dilute H_2SO_4 (pH 1). The precipitate was collected on a PES membrane (0.45 µm pores), washed with water until neutral and dried over P_2O_5 in vacuum.

Reduction of sulfur content in Kraft lignin: A quantity of 2 g softwood Kraft lignin was dissolved in 50 mL of 1 M NaOH and treated for 24 h with 200 mg (5.3 mmol) of $NaBH_4$ under nitrogen at RT. The purification was performed like mentioned above.

^{31}P-NMR spectroscopy: The structural features of lignin were characterized by means of ^{31}P-NMR spectroscopy on a Varian Mercury 400 MHz Spectrometer following a published procedure [6]. Acquisition parameters included: 25°C, 11990 Hz spectral window, 256 scans, acquisition time 1.0 s and a 20 s delay between pulses.

Wood bonding: Organosolv and phenolated organosolv lignin were co-condensed in phenol formaldehyde resins (20wt % pure lignin, P : F : NaOH = 1 : 2 : 0.4) and compared to plain PF resin regarding the wet internal bond strength of particleboards (8 wt% of resin, 3 wt% K_2CO_3, core layer particles, 16 mm board thickness, Siempelkamp laboratory press, press temperature 220°C, press time 240 s) following EN 1087-1.

III. RESULTS AND DISCUSSION

The approach to increase the number of reactive sites was studied for three different lignin sources (hardwood, softwood, annual plants). In each category, an organosolv lignin was compared to the typical technical lignins. The results in **Figure 2** show the number of reactive sites of the lignin educts in comparison to the phenolated lignin products based on ^{31}P-NMR measurements of the hydroxyl groups (counting one reactive site for guaiacyl OH and two for p-hydroxyphenyl OH).
Across all organosolv lignins, hardwood showed the highest degree of phenolation with about 7.7 mmol reactive sites per gram. Thus, the number increased by the factor of 10.5 compared to the lignin educt. Furthermore, the achieved number equals half of the reactive sites of 2,4,6-tris(hydroxymethyl)phenol, the most reactive constituent of pure PF resin with 16.3 mmol/g. The other lignins showed a minor increase, which could partially be attributed to acid-catalyzed condensation reactions and to low molecular lignin fractions not precipitated during work up. Sulfite lignin showed the lowest degree of phenolation. This finding can be related to the low solubility of ammonium lignosulfonate in phenol, thus water as co-solvent and a decrease in reaction temperature <100°C were required.

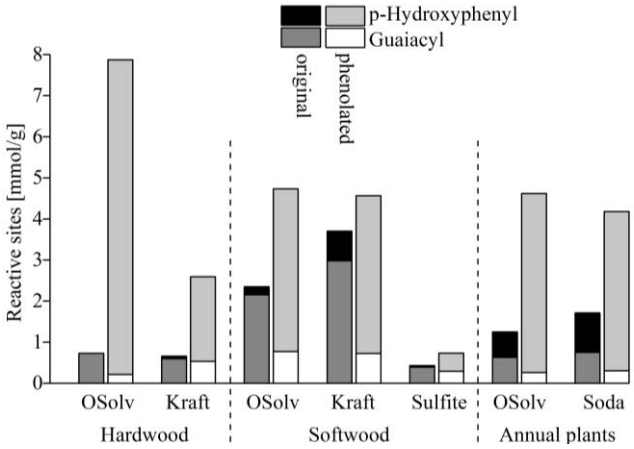

Figure 2. Comparison of number of reactive sites of the lignin educts and the phenolated lignin products based on ^{31}P-NMR measurements

To elucidate other factors affecting the reactivity, the number of aliphatic hydroxyl groups of the lignin educts was compared to the number of aromatic hydroxyl groups introduced upon phenolation (equivalent to p-hydroxyphenyl). The results illustrated in **Figure 3** show that for both functional groups, similar values were measured. The exception of the lignosulfonate might again be related to the unfavorable reaction conditions due to solubility problems. Both Kraft lignins showed lower p-hydroxyphenyl-OH compared to the aliphatic hydroxyl groups. The mismatch in hydroxyl groups found for the lignins from annual plants might be attributed to p-hydroxyphenyl units that were already present in the lignin educt (cf. **Figure 2**). However, it can be assumed that the large differences in the degree of phenolation were mainly related to variations of the amount of aliphatic hydroxyl groups in the lignin educts which in turn depends on the intensity of the pulping (cf. **Table 1**). Thus, the major mechanism of lignin phenolation is in accordance with the results found for the model compounds [2]. However, it should be noted that the ^{31}P-NMR results are given per gram, thus higher values for phenol-OH are realistic, when correlated to a lignin-C_9 unit. This indicates that other reactive sites beyond aliphatic hydroxyl groups are involved as well, e.g. cleavages of β-O-4 and C_β-C_γ-bonds [2].

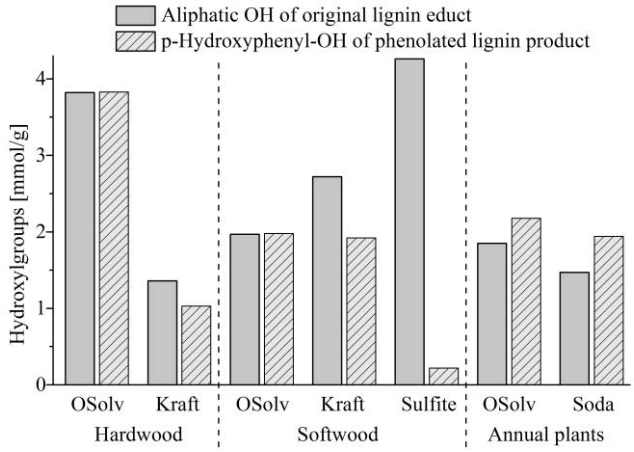

Figure 3. Correlation of phenol-OH (product) with aliphatic OH (educt)

Beside the aliphatic hydroxyl groups, the influence of two major differences between Kraft and organosolv lignin was investigated, namely the ash and sulfur content (**Figure 4**). For hardwood lignin, it was found that a large reduction in the ash content resulted in an increase in the degree of phenolation. Whereas the minor change in the ash content of the softwood lignin did not show this effect. It can be assumed that the ash present in the samples reduced the action of the sulfuric acid catalyst during phenolation. The large reduction of the sulfur content of lignin did not result in a significant change in the degree of phenolation.

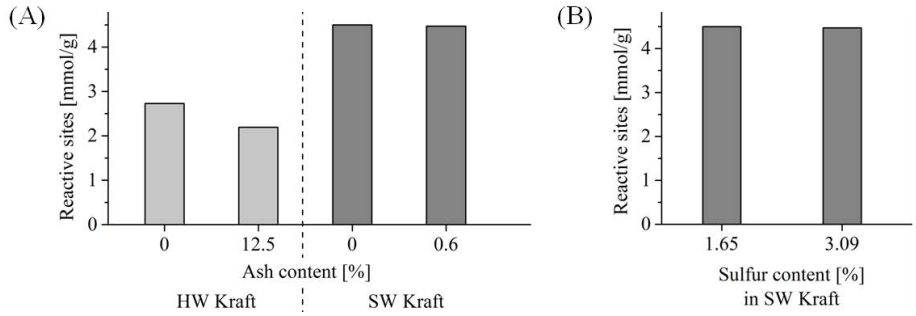

Figure 4. Influence of ash content (A) and sulfur content (B) of lignin educts on the degree of phenolation for hardwood and softwood Kraft lignin.

The wet internal bond of particleboards bonded with the different resins is listed in **Table 2**. It can be seen that the resin with phenolated organosolv lignin (pOSolv PF) resulted in higher bond strength, which might be attributed to the more intense chemical incorporation in the resin network.

Table 2. Wet internal bond strength (IB) of PF resins with/without organosolv and phenolated organosolv lignin including categories of particleboards (EN 312: P5 - load-bearing humid, P7 - heavy load-bearing humid)

	PF	OSolv PF	pOSolv PF	P5	P7
wet IB [N/mm²]	0.31	0.18	0.22	0.14	0.23

IV. CONCLUSIONS

In view of functional substitution of phenol formaldehyde resins by lignin, the chemical activation of lignin to increase the number of reactive sites was investigated. The phenolation of lignins from different sources was studied resulting in remarkable differences between hardwood, softwood and annual plants, as well as between organosolv and technical lignins (Kraft, sulfite, soda). The difference could be mainly attributed to the number of aliphatic hydroxyl groups of the original lignins. Additionally, a reduction of the ash content was beneficial, whereas a reduction of the sulfur content did not result in improvement. In conclusion, it could be shown that hardwood organosolv lignin is extraordinarily suitable for chemical activation by phenolation. Applying this activation, a remarkable improvement of the particleboard's wet IB strength by about 20 % was achieved.

V. ACKNOWLEDGEMENT

The research was funded by the Federal Ministry of Food and Agriculture (BMEL), and supported by the Fachagentur Nachwachsende Rohstoffe e. V. (FNR projects: Lignocellulose-Bioraffinerie II, no.: 22019009 and ProLignin, no.: 22020811). The authors gratefully acknowledge Mr. Andreas Schreiber from the Thünen Institute for the isolation of organosolv lignins, as well as the other lignin producers: Stora Enso, Tembec and Suzano.

VI. REFERENCES

[1] Hu, L., Pan, H., Zhou, Y., and Zhang, M. Methods to improve Lignin's Reactivity as a Phenol Substitute and as Replacement for other Phenolic Compounds: A brief Review. *BioResources* **2011**, 6, 3515–3525.
[2] Lin, L., Yao, Y., and Shiraishi, N. Liquefaction Mechanism of β-O-4 Lignin Model Compound in the Presence of Phenol under Acid Catalysis, Part 1. Identification of the Reaction Products. *Holzforschung* **2001**, 55, 617–624.
[3] Alonso, M. V., Oliet, M., Rodríguez, F., García, J., Gilarranz, M. A., and Rodríguez, J. J. Modification of ammonium lignosulfonate by phenolation for use in phenolic resins. *Bioresource Technology* **2005**, 96, 1013–1018.
[4] Cetin, N. S. and Özmen, N. Use of organosolv lignin in phenol – formaldehyde resins for particleboard production I. Organosolv lignin modified resins. *International Journal of Adhesion & Adhesives* **2002**, 22, 477–480.
[5] Cetin, N. S. and Özmen, N. Use of organosolv lignin in phenol-formaldehyde resins for particleboard production II. Particleboard production and properties. *International Journal of Adhesion & Adhesives* **2002**, 22, 481–486.
[6] Granata, A. and Argyropoulos, D. S. 2-Chloro-4,4,5,5-tetramethyl-1,3,2-dioxaphospholane, a Reagent for the Accurate Determination of the Uncondensed and Condensed Phenolic Moieties in Lignins. *Journal of Agricultural and Food Chemistry* **1995**, 43, 1538–1544.

ENZYMATIC OXIDATION OF LIGNIN IN WATER-DMSO BINARY SOLVENT

S.A. Pokryshkin[1]*, K.G. Bogolytsin[1]

[1] *Northern (Arctic) Federal University named after M.V.Lomonosov, Arkhangelsk, Russia, (*serge.physchem@yandex.ru)*

ABSTRACT

The investigation on the reaction of enzymatic oxidation of different lignin types by hydrogen peroxide in the presence of horseradish peroxidase in water-DMSO binary solvents was done. By UV-VIS spectrophotometry and size-exclusion liquid chromatography it was shown that enzyme exhibit its activity in lignin oxidation in the presents up to 30% DMSO. It was found that oligo- and polymeric fraction of lignin as well as monomeric phenols may undergo the enzymatic oxidation. The calibration curves for initial reaction speed, maximum optical density of the reaction solution and lignin concentration were obtained for dioxane lignin and Kraft-lignin samples. Obtained results are promising for the determination of lignin in aqueous-organic media using enzyme biosensors.

I. INTRODUCTION

Nowadays the objective of monitoring water quality industry is a very relevant. At pulp and paper mills toxic phenolic compounds are found throughout the process technology in water. After removal of easily oxidized monomeric phenols effluents contain large amounts of lignin substances that are accumulated in the aquatic environment. Their destruction by ultraviolet radiation from the sun, microorganisms and air oxidation creates a constant background of toxic components in the reservoir and reduces the level of oxygen in it [1, 2, 3]. Therefore, determination of oligo- and polymeric lignin compounds is relevant for technological process optimization as well as environmental monitoring [4]. The use of enzyme-based biosensors is one of the promising directions of the analysis which can help improve the rapidity of analysis, and increase the sensitivity and selectivity [5].

Horseradish peroxidase as a classical plant peroxidase is a high stability, high-pH optimum peroxidase. It has ability to directional oxidation of phenolic compounds without a mediator or second substrates. This enzyme is widely used in analytical purposes - in ELISA, in the construction of enzyme electrodes [1] and as a biomarker. Native horseradish peroxidase catalyses the oxidations of a wide range of phenolic substrates [2, 3] in presence of hydrogen peroxide. For the oxidation of water-immiscible high molecular weight phenolic compounds the use of aqueous-organic mixed solvents is promising. Dimethylsulfoxide (DMSO) is a well-known solvent for lignin compounds [4]. The possibility of oxidation of phenolic compounds by horseradish peroxidase in aqueous-organic media was shown in [5, 6, 7].

The aim of this work was to study the process of enzymatic oxidation of lignin in water-DMSO binary solvent and to study the possibility of determining lignin substances by enzyme-based methods. Horseradish peroxidase (HRP), EC 1.1.11.7 - heme- containing enzyme belonging to the class of plant peroxidases was chosen as the object of research.

II. EXPERIMENTAL

Commercial type C2 horseradish peroxidase (BBI Enzymes) with a spectral purity index Rz = 2.30 was used as enzyme. Enzyme activity was determined by the rate of oxidation reaction of guaiacol by hydrogen peroxide.

The concentration of hydrogen peroxide was monitored by 230 nm absorption band (molar absorptivity 72.7 $M^{-1}cm^{-1}$) using a UV-VIS spectrophotometer Specord300 (Analytik Jena). Guaiacol (Sigma-Aldrich) was used as a substrate. All reagents qualification was "purris".

In our previous work [7, 8, 9] the optimal parameters of the enzymatic oxidation of lignin model compounds was determined. Reaction of peroxidase oxidation of lignin (5…500 * 10^{-3} g/l), by hydrogen peroxide (0.1 * 10^{-3}M) was performed at 25°C (thermostatted) in 0.1 M pH6.0 phthalate buffer solution and in a presence of 30% DMSO wt. The process was initiated by the adding horseradish peroxidase (0.015 mg/mL) solution in 3 ml of the reaction mixture. Spectra recording and kinetic curves were obtained on double-beam spectrophotometer Specord300 (Analytik Jena). The reaction rate was measured by absorbance at absorption band of the product of the enzymatic oxidation of guaiacol. Initial reaction rate was calculated as the slope of the initial linear part of the kinetic curve.

Analysis of the molecular weight distribution was carried out by size exclusion chromatography using HPLC system LC- 20 (Shimadzu, Japan) equipped with a pump LC- 20 ADsp, autosampler SIL-20A, column oven CTO-20A, spectrophotometric detector SPD-20A. Separation was performed on a Styragel column (300 * 4.6 mm), filled with 5 um styrene-divinylbenzene gel particles (Waters, USA) at 50°C. Dimethylformamide was used as eluent with the addition of lithium bromide (0.05M) for suppressing polyelectrolyte effects. Sample volume was 10 ul with approximate concentration 1 mg/ml. System calibration was carried out using polystyrene standards with monodisperce distribution in a range from 100 Da to 100 kDa. Detection was performed at 280nm band. Data was collected and processed by WinGPC software (PSS, Germany).

Spruce dioxane lignin and sodium wheat straw lignin was isolated in laboratory, spruce Kraft lignin and lignosulfonate was obtained from pulp and paper plant were used as model substrates of the enzyme samples were used. Reaction mixture was prepared using a lignin - DMSO solution with concentration 10 g / liter, which was added to the reaction mixture to obtain the desired concentration of lignin. In the presence of hydrogen peroxide without the enzyme reaction mixture was stable for more than three hours. After adding a horseradish peroxidase to a reaction mixture an increase of absorbance at 400 ... 600 nm was observed. During the enzymatic oxidation reaction a maximum at 490 nm band, which is absent in the original spectra, was clearly seen and then it was used in the future calculation of the reaction rate.

III. RESULTS AND DISCUSSION

According to science resources, the enzymatic oxidation of phenols is followed by polymerisation reactions. In **Figure 1** the diagram of peroxidase-catalyzed oxidation of guaiacol in the presence of horseradish peroxidase is presented.

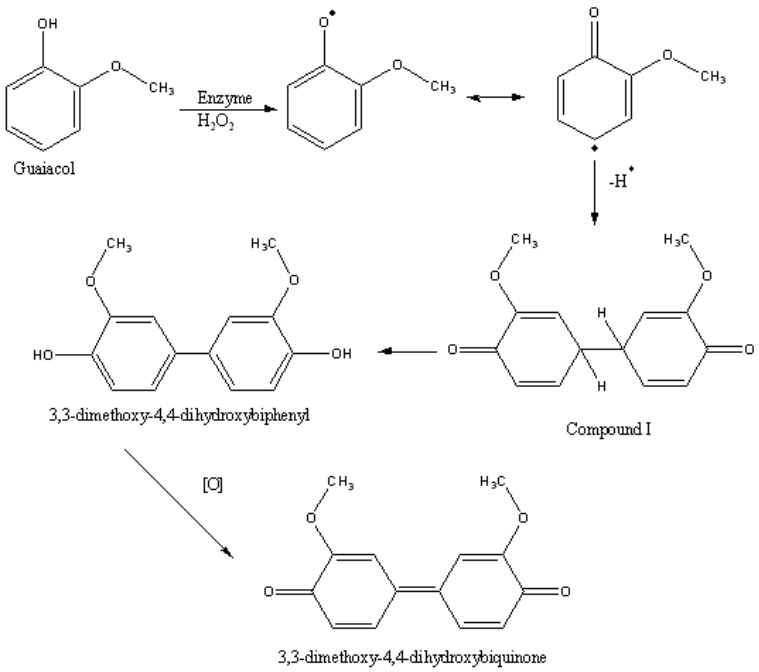

Figure 1. Peroxidase-catalyzed oxidation of guaiacol [10].

In a range of lignin concentrations 5 ... 500 mg/l the initial reaction rate and dependences of initial reaction rate and maximum optical density of the reaction mixture from lignin concentration was determined and plotted (Figure 2).

For dioxane lignin and Kraft lignin samples the increasing of the optical density during reaction was found. With sodium lignin and lignosulfonate no signs of reaction were observed. This can be explained by an ionic form of phenolic OH groups of lignin in the enzyme's pH optimum. In the lignin concentration range from 5 to 100 mg/l linear dependences of the initial speed and the maximum absorbance from the lignin concentration (**Figure 2**) was obtained. These dependences can be described by equations: $V_0 = a \cdot C$ and $D_{max} = b \cdot C$, where V_0 is the initial reaction rate (a.u.·s^{-1}), D_{max} is maximum optical density of the reaction mixture (a.u.), *a* and *b* is angular coefficient and *C* is the lignin concentration (mg/l).

The angular coefficients *a* and *b* are given in **Table 1**. Deviation of the experimental points from the linear dependence at high concentrations of lignin is due to saturation of the substrate-binding site of the enzyme. The

data obtained provide the prerequisites for the development of the method for determining the content of lignin after its transfer into the water- DMSO solution.

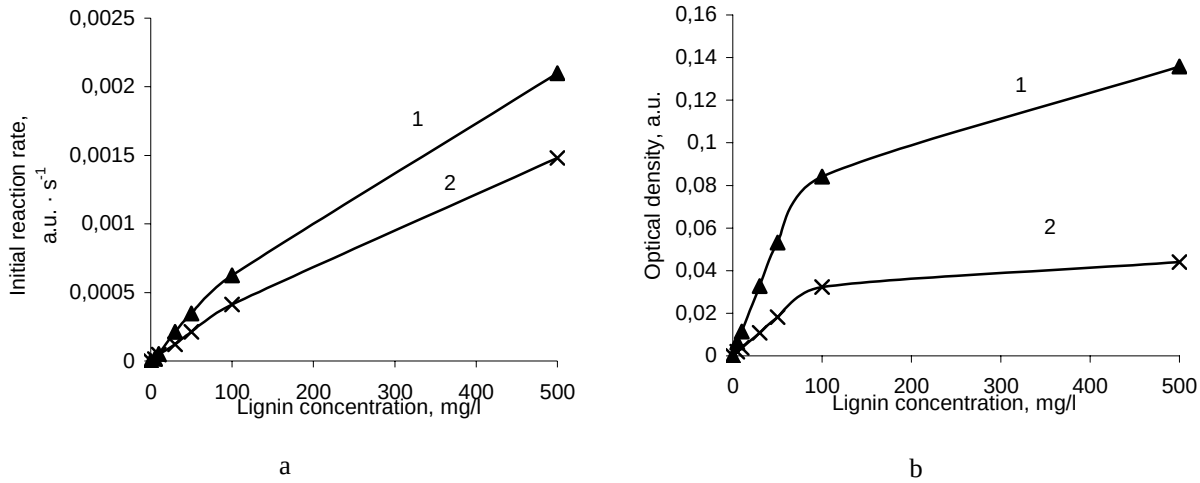

Figure 2. Dependences of initiall reaction rate (a) and maximum optical density (b) from: Kraft lignin concentration (1); dioxanlignin concentration (2)

Table 1. Angular coefficients *a* and *b* for different lignin types

Coefficient	Dioxanlignin	Kraft lignin
a	$4{,}16 \cdot 10^{-6}$	$6{,}42 \cdot 10^{-6}$
b	$3{,}63 \cdot 10^{-4}$	$1{,}06 \cdot 10^{-3}$

In addition for dioksanlignin sample change of the molecular weight distribution during reaction was studied by exclusion chromatography. Results indicate a decrease of low molecular weight fractions amount. Also some increase in the average molecular weight accompanied with reducing of polydispersity index was found (**Table 2**).

Table 2. Characteristics of molecular-mass distribution of dioxanlignin sample

Characteristic	Sample	
	intact	oxidized
Mn	1540	2030
Mw	4660	5480
Mz	9040	10100
Polydispersity index	3,0	2,7

This suggests joint processes of oxidation and polymerization of lignin by peroxidase, as well as reactivity of both low molecular weight and high-molecular lignin fragments.

IV. CONCLUSIONS

It was shown that the enzyme shown activity in the oxidation of lignin substances with a significant content of DMSO in the solution (30%). It was found that both monomeric phenols and oligo-and polymer fraction of

soluted lignin shows possibility of the enzyme-catalytic oxidation. The results show development prospects of enzyme biosensors in aqueous-organic media for the determination of lignin.

V. ACKNOWLEDGEMENT

Work was performed at the Center for collective use of scientific equipment "Arctic" Northern (Arctic) Federal University with the support of Ministry of Education of the Russian Federation.

VI. REFERENCES

[1] Yao, H.; Hu, N. pH-switchable bioelectrocatalysis of hydrogen peroxide on layer-by-layer films assembled by concanavalin A and horseradish peroxidase with electroactive mediator in solution. *J. Phys. Chem. B.* **2010**, *114*, 3380-3386.

[2] Torres, E.; Ayala, M. Biocatalysis Based on Heme Peroxidases. *Springer-Verlag Berlin Heidelberg.* **2010,** *358*.

[3] Shehovtsova, T.N.; Lyalyulin, A.L.; Kondratief, E.I.; Ghazarian I.G.; Dolmanova, I.F. Different origin peroxidases usage for determining phenols. *J. Analytical Chem.* **1994**, *49*, 1317 -1323.

[4] Bogolitsyn, K.G., Lunin, V.V.; Kosyakov, D.S. Physical chemistry of lignin (in rus.) *Akademkniga.* **2010,** *492*.

[5] Azevedo, A.M.; Durate, M.F. Stability of free and immobilized peroxidase in aqueous-organic solvent mixtures. *J. of Mol. Cat. B: Enzymatic.* **2001,** *15*, 147-153.

[6] Veselov, I.A.; Kireyko, A.V.; Shehovtsova, T.N. Increasing catalytic activity and stability of horseradish peroxidase by its inclusion in the polyelectrolyte complex with chitosan (in rus.) *Prikladnaya biochimiya i mikrobiologiya*. **2009,** *45*, 143-148.

[7] Pokryshkin, S.A.; Bogolitsyn, K.G.; Aksenov, A.S. Kinetic regularities of the enzymatic oxidation of guaiacol in the aqueous and aqueous-organic media. (in rus.) *Izvestiya Vuzov – Lesnoy Journal*. **2012**, *3*, 100 - 106.

[8] Aizenstadt, M.A.; Bogolitsyn, K.G.; Pokryshkin, S.A. Catalytic oxidation of lignin model compounds with hydrogen peroxide in the presence of horseradish peroxidase as catalyst (in rus.). *Himiya rastitelnogo syria.* **2009,** *4*, 31-37.

[9] Bogolitsyn, K.G.; Aizenstadt, M.A.; Pokryshkin, S.A.; Pryakhin, A.N.; Lunin, V.V. Kinetics of the catalytic oxidation of model compounds of lignin with hydrogen peroxide in the presence of peroxidase from horse-radish. *Rus. J. of Phys. Chem. A.* **2010,** *84*, 1511-1515.

[10] Doerge, D.R.; Divi, R.L.; Churchwell, M.I. Identification of the colored guaiacol oxidation product produced by peroxidases *Analytical biochem*. **1997,** *250*, 10-17.

NANOCOMPOSITES FROM ACETYLATED FREEZE DRIED NANOFIBRILLATED CELLULOSE (NFC) AND PLA

Ida Poljanšek [1]*, Vesna Žepič [2], Primož Oven [1], Aleš Hančič [2]

[1] *University of Ljubljana, Biotechnical Faculty, Department of Wood Science and Technology, Rožna dolina, Cesta VII/34, SI-1000 Ljubljana, Slovenia;* [2] *TECOS, Slovenian Tool and Die Development Center, Kidričeva 25, SI-3000 Celje, Slovenia (*ida.poljansek@bf.uni-lj.si)*

ABSTRACT

The aim of this study was to disperse nanofiblillated cellulose (NFC) homogeneously within a hydrophobic polymeric matrix. In order to acquire the nano-reinforcement component in dried form with hydrophobic surface characteristics, NFC aqueous suspension was dried by the means of a freeze drying procedure and afterward heterogeneously acetylated using different reaction times and catalyst concentrations with the aim to find optimal reaction conditions. The non-modified and acetylated NFC powders were characterized by attenuated total reflection infrared spectroscopy analysis (ATR-IR) and field emission scanning electron microscopy (FE-SEM). Afterward nanocomposite films containing 2, 5 and 10 wt% of unmodified and acetylated NFC were prepared by solution casting of mixtures of poly(lactic acid) (PLA) solution and cellulose nanofibre suspension in chloroform. The mechanical properties of the composites were evaluated using tensile tests measurements.

I. INTRODUCTION

During the past decades environmental concerns are favourable for eco-friendly innovations, and hence, nanotechnology shows vast potential in finding new uses for cellulosic materials [1]. In biosynthesis, cellulose polymers aggregate to form substructures, nanofibrils, which in turn aggregate to form cellulosic fibres. Using new effective methods these fibrils with a diameter ranging from 20 to even 100 nm and length of several micrometers, can be disintegrated from fibres to form uniform nanosized material ideal for incorporation into other materials as a reinforcing agent. However, as for any nanoparticle, the main challenge is related to their homogeneous dispersion within a hydrophobic polymeric matrix [2-5]. Hydrophilic character of the nanofibrillated cellulose (NFC) represents a major obstacle for its use in combination with hydrophobic polymers. With a chemical modification of the NFC surface, its hydrophilicity and a tendency toward hornification can be drastically reduced [2, 3].

II. EXPERIMENTAL

Materials

Poly(lactic acid) (PLA), trade name Ingeo™ Biopolymer 2003D (D-lactide of 4 to 5%, density of 1.24 g/cm3 and a melting point of 145-160 ºC), from Natureworks™ was used as a matrix material. Nanofibrillated cellulose (NFC) was supplied by the Centre for Biocomposite and Biomaterial Processing, University of Toronto, Canada, as a water suspension of cellulose nanofibrils with diameters in the range of 20 to 60 nm, with a solid content of 1.6 wt%. Acetic anhydride (Ac_2O, ≥99%), N,N-dimethylformamide (DMF, anhydrous, 99.8%), pyridine (anhydrous, 99.8%), toluene (99.5%), chloroform (anhydrous, ≥99%, with 0.5-1.0% ethanol as stabiliser), ethanol (96%) and acetone (99.5%) were all purchased from Sigma-Aldrich (Steinheim, Germany).

Pre-treatment and the acetylation of NFC

Prior to freeze drying, the NFC suspension was frozen using liquid nitrogen and then lyophilised (LyoQuest freeze dryer, Telstar). The pressure within the freeze drying system was set to 0.040 mbar, the temperature of the plates to 22 °C and the temperature of the condenser to -50 °C. The dried forms of NFC were dispersed into DMF at a concentration of 1 wt% using homogenisation (Ultra Turrax T 25 basic, IKA-Werke, Staufen,

Germany) and high intensity ultrasonication (Ultrasonic Vibra cell VC500 (Sonics and Materials, USA), 19 mm needle probe tip, 60% output amplitude). The DMF/NFC suspensions obtained are hereafter referred to as freeze dried (NFC_{FD}) nanofibrillar cellulose.

A 100 mL suspension of DMF/NFC (1% based on the dry weight) was mixed with 35 mL of acetic anhydride. A predetermined amount of pyridine (catalyst) was added into the beaker and mixed thoroughly with the reaction mixture under slow homogenisation. The pre-treated NFC sample was added into a round-bottomed flask equipped with a condenser and a magnetic stirrer. The reaction was performed under a nitrogen flow and kept at the required temperature of 105 ± 5 °C. At specific reaction intervals samples were withdrawn from the reaction mixture. A series of acetylated products $A\_NFC_{FD,}$ with different degrees of substitution (DS) were obtained.

Preparation of PLA/NFC nanocomposites

Films were prepared through solvent casting method. PLA pellets were primarily dissolved in $CHCl_3$ at a constant stirring for 10 h. Separately NFC/$CHCl_3$ dispersions (with unmodified and modified NFC) were prepared using homogenization and high intensity ultrasonication process. NFC dispersions were then added into a PLA solution and homogenized/ultrasonicated. The resulting solutions were casted into Petri dishes and chloroform was allowed to evaporate.

Characterisation of the unmodified and acetylated NFC

The infrared spectra of the unmodified and acetylated NFC_{FD} were recorded using a Spectrum One FTIR spectrometer (Perkin Elmer, USA) in attenuated-total-reflection (ATR) mode on a ZnSe crystal. The spectra were collected at a resolution of 4 cm^{-1}, over the range from 650 to 4000 cm^{-1}. Bands of FT-IR spectra were assigned according to Tingaut et al. (2010)[3], Adebajo and Frost (2004) [6] and Sun et al. (2002) [7]. The acetyl content (Ac %) of the modified NFCs was determined according to Tingaut et al. (2010) [3] using FT-IR calibration curves.
For the FE-SEM analysis (Zeiss ULTRA plus, Germany) a droplet of the 0.5 wt% suspensions of NFC_{FD} and A_NFC_{FD} in $CHCl_3$ was deposited on a glass plate and dried. Samples were coated with a highly conductive film of gold.
The tensile properties were evaluated with Zwick/Roell Z005 testing device according to ASTM D882. The crosshead speed was maintained at 50 $mm \cdot min^{-1}$ during testing. The testing samples were cut from the neat PLA and nanocomposite sheets, containing unmodified and modified NFC into a 15 mm wide and 85 mm long tapes. The results presented in this paper are the average values of six individual specimens.

III. RESULTS AND DISCUSSION

During freeze drying of NFC bulk material did not form [8]. The generated end-product was in the form of coarse powder (**Figure 1a**). Freeze dried NFC was composed of agglomerated fibrillar fragments in the form of convoluted plates with barely identifiable nanofibrils (**Figure 1a**). Examination of freeze dried NFC at higher magnifications revealed that nanofibrils (35 nm) and ribbon like structures (1.2 μm) were connected to form an open porous structure (**Figure 1a**). The structure of freeze dried NFC sample significantly differed from acetylated NFC_{FD} ($A\_ NFC_{FD}$) samples (**Figure 1b**), the acetylated nanofibrillar units became visible already after 60 min of reaction. Longer reaction times did not essentially change the morphology of acetylated NFC_{FD}.

FT-IR spectrum of A_NFC_{FD} exhibited pronounced acetylation peaks. The intensity of three main ester bands increased with increasing reaction time. We did not observe the typical twin bands of acetic anhydride, which indicated that there was no reactant present in acetylated NFCs. The absence of a peak at 1700 cm^{-1} for a carboxylic group in the spectra of the acetylated samples also indicated that the acetylated products were free of the acetic acid by-product, as reported by Sun et al. [7].

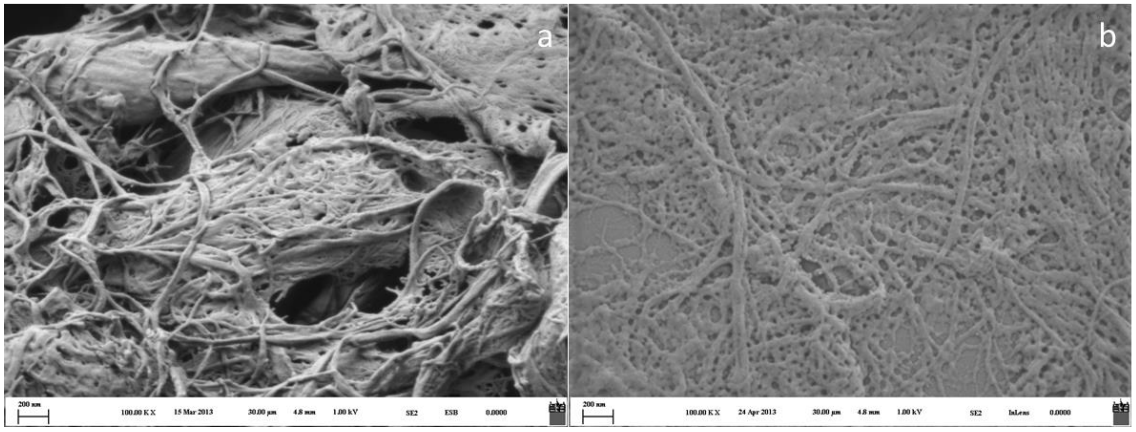

Figure 1. FE-SEM images of unmodified (a) and acetylated NFC_{FD} at 1200 min, pyridine concentration of 3 %.

Degree of substitution for acetylated NFC_{FD} materials increased with reaction time, the DS values increased rapidly during the first hour of acetylation. After 900 min, the DS values started to reach a constant value (equilibrium). The high degree of substitution (DS) of NFC_{FD} can be ascribed to the low quantity of water in the starting material [9]. Additionally, we assumed that the drying pre-treatment significantly increased the swelling ability of the cellulose and the diffusion rate of the acetic anhydride and pyridine. Despite the fact that the pyridine is highly effective catalyst for acetylation reaction [10, 11] higher pyridine concentration has no impact on the DS.

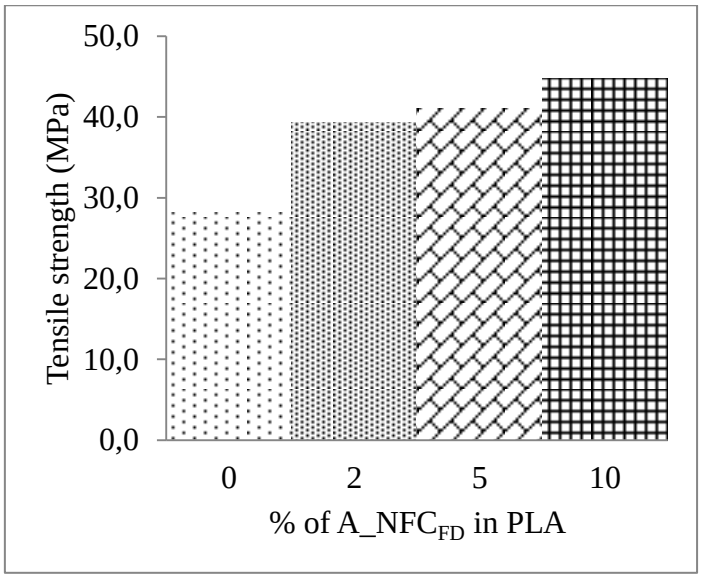

Figure 2. Tensile strength of nanocomposites as a function of concentration of A_NFC_{FD}.

The mechanical properties of the composites were evaluated using tensile tests measurements (**Figure 2**). As compared with neat PLA, a gradual increase in modulus of elasticity (E') and tensile strength (σ) was noted upon the incorporation of acetylated nanofibers (**Figure 2**), while for unmodified NFC_{FD} the reinforcing effect was not that significant.

IV. CONCLUSIONS

It was proved that acetylation reaction is a highly efficient in modifying the surface of NFC with various DS, which exhibit higher thermal stability than unmodified samples. A gradual increase in modulus of elasticity (E') and tensile strength (σ) was noted upon the incorporation of acetylated nanofibers in PLA matrix. The addition of modified NFC_{FD} importantly altered the elongation at break of the resulting nanocomposites, meaning that chemical affinity of the nanofibrils to the matrix is essential in order to achieve a good polymer-matrix interaction.

V. ACKNOWLEDGEMENT

The authors wish to gratefully acknowledge the Ministry of Higher Education, Science and Technology of the Republic of Slovenia, within the Programs P4-0015. This work was also co-supported by the European Union, European Social Fund, whose contribution is fully recognized.

VI. REFERENCES

[1] Miao C, Hamad WY (2013) Cellulose reinforced polymer composites and nanocomposites: a critical review. Cellulose, 20:2221-2262.

[2] Eyholzer C, Bordeanu N, Lopez-Suevos F, Rentsch D, Zimmermann T, Oksman K (2010) Preparation and characterization of water-redispersible nanofibrillated cellulose in powder form. Cellulose, 17(1):19-30.

[3] Tingaut P, Zimmermann T, Lopez-Suevos F (2010) Synthesis *and* characterization of bionanocomposites with tunable properties *from* poly*(*lactic acid*)* and acetylated microfibrillated cellulose. Biomacromolecules, 11: 454–464

[4] Dufresne A (2010). Processing of polymer nanocomposites reinforced with polysaccharide nanocrystals. Molecules, 15(6): 4111–4128.

[5] Eichhorn SJ, Baillie CA, Zafeiropoulos N, Mwaikambo LY, Ansell MP, Dufresne A, Entwistle KM, Herrera-Franco P, Escamilla GC, Groom L, Hughes M, Hill C, Rials TG, Wild PM (2010) Review: Current international research into cellulosic fibres and composites. Journal of Materials Science, 36(9): 2107-2131.

[6]Adebajo MO, Frost RL (2004) Acetylation of raw cotton for oil spill cleanup application: an FTIR and 13C MAS NMR spectroscopic investigation. Spectrochimica Acta, Part A: Molecular and Biomolecular Spectroscopy, 60(10): p. 2315-2321.

[7] Sun XF, Sun R, Sun JX (2002) Acetylation of rice straw with or without catalysts and its characterization as a natural sorbent in oil spill cleanup J Agric Food Chem 50(22):6428-33.

[8] Žepič V, Fabjan EŠ, Kasunič M, Korošec RC, Hančič A, Oven P, Perše L, Poljanšek I (2014) Morphological, thermal, and structural aspects of dried and redispersed nanofibrillated cellulose (NFC). Holzforschung, doi: 10.1515/hf-2013-0132

[9] Lee KY, Bismarck A (2012) Susceptibility of never-dried and freeze-dried bacterial cellulose towards esterification with organic acid, Cellulose, 19:891-900

[10] Hill CAS, Cetin NS, Ozmen Z (2000) Potential catalysts for the acetylation of wood. Holzforschung, 54, 269-272.

[11] Satchell DPN (1963) An outline of acylation. Q. ReV. (London) 1963, 17, 160-203.

ALKALI TREATMENT OF BIRCH KRAFT PULP TO ENHANCE ITS TEMPO CATALYZED OXIDATION WITH HYPOCHLORITE

Raili Pönni[1], Timo Pääkkönen[1], Markus Nuopponen[2], Jaakko Pere[3], Tapani Vuorinen[1]

[1] Aalto University, School of Chemical Technology, Department of Forest Products Technology, P.O. Box 16300, 00076 Aalto, Finland; [2] UPM, Tekniikantie 2 C, 02150 Espoo, Finland; [3] VTT, Tietotie 2, PO Box 1000, 02044 VTT, Finland
*(*raili.ponni@aalto.fi)*

ABSTRACT

Alkali treatment of birch kraft pulp was applied to increase the pulp reactivity during 2,2,6,6-tetramethyl-1-piperidinyloxy (TEMPO) catalyzed oxidation, which is a process commonly applied to prepare nanofibrillated cellulose (NFC). TEMPO was activated with HOCl prior to the oxidation instead of using NaBr as a cocatalyst. Commonly, the lack of bromine increases the oxidation time and decreases the formation of carboxylic groups. By applying the alkali treatment, the reaction time of the TEMPO catalyzed oxidation could be shortened from 2.5 hours to 0.5 hours when the pulp was treated with 1 M NaOH prior to the oxidation. The alkali treatment was effective at room temperature and required only a few minutes incubation time. Furthermore, the alkali treatment enabled production of a pulp with carboxylate content as high as 1.6 mmol/g with NaOCl dosage of 4.4 mmol/g pulp. The changes in the cellulosic raw material during the alkali treatment were evaluated by water retention value (WRV) and carbohydrate analysis.

I. INTRODUCTION

The catalytic conversion of the primary hydroxyl groups to carboxylates via aldehydes has been studied widely during the last two decades. TEMPO catalyzed oxidation of pulp has been shown to be an efficient chemical pretreatment for the production of nanofibrillated cellulose (NFC) [1]. The TEMPO oxidized pulp can be converted to NFC by merely a mild homogenization. The reduction in the energy consumption of the homogenization is determined by the carboxylate content obtained during the oxidation of the pulp. Commonly, radical TEMPO is activated with NaBr that is used as a cocatalyst in stoichiometric oxidation of pulp with NaOCl at pH range from 10 to 11 [1]. However, some procedures without the cocatalysis by NaBr have been introduced, such as an electromediated oxidation [2] and an acid-neutral process applying TEMPO/NaOCl/$NaClO_2$ [3]. Even though these bromine-free oxidations can produce pulps with high carboxylate contents, the reaction is slow in comparison with the bromine assisted TEMPO catalysis.

Strongly alkaline pretreatments of cellulosic raw materials have been studied widely since the mercerization process was developed. To date, such pretreatments are used in many chemical processes, including the production of carboxymethyl cellulose and viscose for textile fibers. Mercerization causes native cellulose or cellulose I to become swollen and after washing to shrink back to another allomorph, cellulose II. The most severe changes in the crystallinity of cellulose occur under the conditions of mercerization, corresponding NaOH concentrations above 8-9% [4]. However, alkaline treatment of pulp alters the pulp properties by increased swelling already at mild conditions [5]. Mild alkaline treatments are used for several purposes, including regaining the bonding properties of recycled pulps and improving the prospects of natural fibers in composites. Swelling is diffusion controlled and occurs in only a few minutes. The maximum extent of swelling is reached at high alkaline concentration, around 10% NaOH, slightly depending on the cellulosic raw material [6]. In addition, temperature has a significant effect on the phenomenon as swelling is favored under low temperature [7]. In novel processes' point of view, swelling improves cellulose accessibility and, thus, makes it more reactive in many heterogeneous chemical and enzymatic treatments.

II. EXPERIMENTAL

Materials

Never-dried and industrially dried bleached birch kraft pulps were obtained from a Finnish pulp mill. The chemicals used for the oxidations were TEMPO (Sigma Aldrich (St. Louis, USA)), 13% NaOCl (VWR (Radnor

(PA), USA)), $NaClO_2$ (Sigma Aldrich (St. Louis, USA)), 1 M NaOH (Merck (Darmstadt, Germany)), 1 M HCl (Merck (Darmstadt, Germany)), and H_2SO_4 (Emsure (Darmstadt, Germany)). An 8 M NaOH solution was prepared from solid NaOH pellets (VWR (Leuven, Belgium)) to adjust the alkalinity in the pretreatments of the pulps. Water was purified in a Milli-Q system (Millipore Corporation, resistivity 18.2 MΩcm) for reagent solution preparations. Deionized water was used for all washings.

Alkali treatment of pulps

The treatments were executed at room temperature (RT). First, an 8 M NaOH solution together with water was added to the pulp to obtain the desired alkalinity and pulp consistency of 5%. The pulp suspension was stirred with a mechanical stirrer throughout the reaction time. After the desired reaction time, the pulp was washed immediately with deionized water to pH 9. The pH of the suspension was measured with a pH meter (Mettler Toledo) at 5% pulp consistency. Finally, the pulp was manually pressed to a dry matter content of approximately 20% and homogenized mechanically.

TEMPO catalyzed oxidation of pulps and conversion of residual aldehydes to carboxylates by chlorous acid

The oxidations were performed in a Büchi reactor (volume 1.6 dm^3), with a Metrohm 718 Stat Titrino titrator for the pH adjustment. TEMPO was mixed with an excess of NaOCl in water and the pH of the TEMPO solution was adjusted to 7.5 with H_2SO_4. First, the pulp (48 g dry matter content) and the activated TEMPO (2.4 mmol) were mixed well in a closed vessel. Then, the pulp suspension and water were added to the Büchi reactor to make a total volume of 1.2 dm^3. The reactor was provided with a continuous mixing and temperature control at 25 °C. NaOCl (58-218 mmol) was added to the reactor with a pump during 5-32 min and the acidity was adjusted to pH 9 with 1 M NaOH. After the addition of NaOCl, pH was kept constant (pH 9) by adding 1 M NaOH with the automatic titrator. The oxidation rate was followed by iodometric titration until all active chlorine was consumed. The standard deviation for the oxidation time was determined from four parallel measurements. After the reaction, the pulp was washed with deionized water. To convert the residual aldehydes to carboxylates, the oxidized pulp suspension at 1 % consistency was adjusted to pH 3 with 1 M HCl. $NaClO_2$ was added to the suspension (1 mM final concentration) which was then mixed in the Büchi reactor for 2 hours at 50 °C. Finally, the pulp was washed with deionized water. The carboxylate content of the pulps was determined by a conductometric titration, which was conducted according to the standard SCAN-CM 65:02. The titration was executed using an automatic titrator (Metrohm 751 GPD Titrino) together with Tiamo 1.2.1. software. The standard deviation is according to the standard.

Pulp characteristics

The pulp characteristics were evaluated by WRV and carbohydrate composition. Prior to the WRV analysis, the pulp samples were converted to their Na^+-form. All of the treatments were done at 1% consistency. First, the samples were converted to their protonated form under 0.01 M HCl for 1 hour. Then, the samples were washed twice with water. Conversion to Na^+-form was done in 0.001 M $NaHCO_3$ for 2 hours with pH adjusted to 9.5-10 with 0.1 M NaOH. Then, the samples were washed with water until the conductivity of the slurry was less than 5 µS/cm. The WRV analysis was done according to the standard SCAN-C 102 XE with a Jouan GR 4.22 centrifuge. The standard deviation was determined from four parallel measurements. The carbohydrate composition of the pulps was determined by quantitative saccharification upon acid hydrolysis according to the standard procedure [8]. The monosaccharides were determined by high performance anion exchange chromatography with pulse amperometric detection (HPAEC-PAD) in a Dionex ICS-3000 system (Sunnyvale (CA), USA). The content of xylan was calculated from the monosaccharide content using a correction factor [8]. The standard deviation was determined from four parallel measurements.

III. RESULTS AND DISCUSSION

NaOH concentration during the alkali treatment

The progress of the catalytic oxidation was monitored by iodometric titration of the residual NaOCl in the reaction mixture. Without any pretreatment of a never-dried birch kraft pulp its oxidation was relatively slow. A short pretreatment of the pulp with 0.25 M NaOH did not change the reactivity. When 0.5 M or higher concentration of NaOH was applied in the pretreatment, a marked increase in the reaction rate was observed. Thus, the total reaction time, corresponding to the time needed to consume all NaOCl, could be reduced from 2.5

to 0.5 h by applying a pretreatment with 0.75 M NaOH at RT (**Figure 1**). A similar 80% reduction of reaction time took place when a dry birch kraft pulp was pretreated with 1 M NaOH prior to the catalytic oxidation at RT.

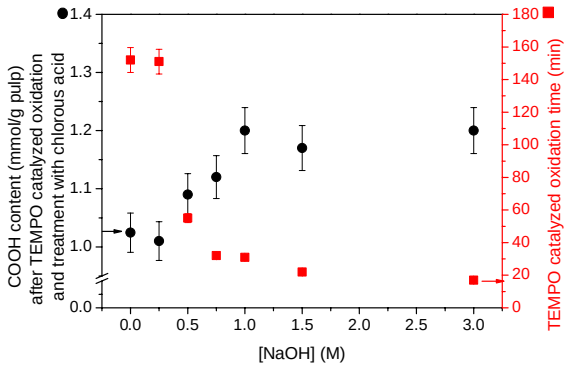

Figure 1. Effect of NaOH concentration in alkali treatment (15 min at RT) of never dried birch pulp (5 % consistency) on its TEMPO (0.05 mmol/g) catalyzed oxidation with NaOCl (2.4 mmol/g). The carboxylate content of the pulp is shown after the oxidation and a post-treatment with chlorous acid that converts aldehydes to carboxylic acids (circle). The total reaction time (square) refers to the time during which NaOCl was fully consumed. Pulp consistency was 4 % and reaction temperature 25 °C during the TEMPO catalyzed oxidation.

When the TEMPO oxidized pulps were post-treated with chlorous acid, almost 20% higher carboxylic acid contents were measured for the pulps treated with 1 M NaOH or higher (**Figure 1**). The observed increase in the total amount of the oxidized hydroxymethyl groups after the treatment with concentration higher than 0.5 M NaOH indicated an increase in the accessibility of cellulose, which levelled off at around 1 M NaOH concentration. Since the changes in the supramolecular structure of cellulose should occur only at concentration above 2 M NaOH, the increased reactivity with the milder treatments could not be related with any interconversion between the allomorphs of cellulose [4].

NaOCl dosage during TEMPO catalyzed oxidation

A never-dried birch kraft pulp pretreated with 1 M NaOH for 15 minutes at RT and then washed to pH 9 was oxidized with varying NaOCl dosage (2.4-4.5 mmol/g) to obtain pulps with varying carboxylate contents. The oxidation rate of the pretreated pulp remained high when NaOCl dosage was increased from 2.4 to 3.1 mmol/g. However, further oxidation of the pulp slowed down when higher NaOCl dosages were applied (3.8-4.5 mmol/g), indicating that the number of available unreacted hydroxymethyl groups was reduced. The alkaline pretreatment of pulps enabled reaching very high carboxylate contents without using bromide in the catalytic oxidation. When NaOCl dosage of 4.5 mmol/g was applied, the final carboxylate content was above 1.6 mmol/g. Previously, the traditional TEMPO catalyzed oxidation with NaBr as cocatalyst and applying NaOCl dosage of 5 mmol/g has produced carboxylate contents ranging from 1.25 to 1.5 mmol/g for bleached hardwood pulp [1]. However, the reaction time (240 min) is still longer compared to the bromine-aided oxidation (125 min) [1]. The reaction time is significantly shorter than the previously reported bromine-free alternatives with reaction times up to 80 hours [3].

Pulp characteristics

WRV of dry birch kraft pulp increased by 12% when it was treated with 1M NaOH for 15 min at RT. However, treating the never-dried birch kraft pulp with NaOH concentrations higher than 1 M (15 min at RT) decreased its WRV by up to 15% (**Figure 2**). The xylan content of both pulps was significantly decreased by alkali. Since the alkali treatment activated both the dry and never-dried pulps towards the TEMPO catalyzed oxidation, it seems obvious that the increase in the accessibility of cellulose was affected more by the dissolution of xylan than fiber wall swelling that correlates with WRV. The changes in WRV could be explained by the dissolution of the highly accessible xylan and reversible aggregation of microfibrils in alkali.

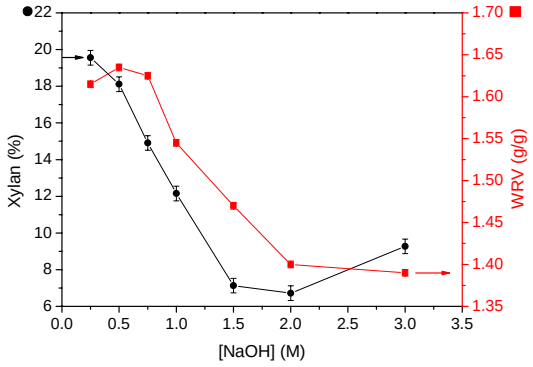

Figure 2. Effect of alkalinity (15 min treatment) on the residual xylan content (circles) and WRV (squares) of never-dried birch kraft pulp in aqueous suspension at RT.

IV. CONCLUSIONS

An alkali treatment was introduced as a means to improve bromine-free TEMPO catalyzed oxidation of cellulosic pulps. A very short pretreatment of a never-dried birch pulp with 0.75 M NaOH at RT was shown to decrease the oxidation time from 2.5 hours to 0.5 hours. In addition, a carboxylate content as high as 1.6 mmol/g was reached when the dosage of hypochlorite was 4.5 mmol/g. Thus, the alkali treatment enabled a bromine-free oxidation with slightly better oxidation outcome compared to the conventional TEMPO catalyzed oxidation. Similar benefits were recorded for both dry and never-dried birch pulps. Hemicellulose content decreased for both dry and never-dried pulps as a function of the alkalinity and the removal of xylan seemed to be partly responsible for the increased reactivity of cellulose. Surprisingly, WRV was shown to increase for the dry pulps but to decrease for the never-dried pulps.

V. ACKNOWLEDGEMENT

This study was funded by UPM and the Finnish Funding Agency for Technology and Innovation (TEKES). We thank Mrs Mirja Reinikainen and Ms Kristel Kosk for excellent laboratory work.

VI. REFERENCES

[1] Saito, T.; Kimura, S.; Nishiyama, Y.; Isogai, A. Cellulose nanofibers prepared by TEMPO-mediated oxidation of native cellulose. *Biomacromolecules* **2007,** 8, 2485-2491.

[2] Isogai, T. Wood cellulose nanofibrils prepared by TEMPO electro-mediated oxidation. *Cellulose* **2011**, 18, 421-431.

[3] Hirota, M.; Tamura, N.; Saito, T.; Isogai, A. Oxidation of regenerated cellulose with NaClO2 catalyzed by TEMPO and NaClO under acid-neutral conditions. *Carbohydr. Polym.* **2009**, 78, 330-335.

[4] Dinand, E.; Vignon, M.; Chanzy, H.; Heux, L. Mercerization of primary wall cellulose and its implication for the conversion of cellulose I → cellulose II. *Cellulose* **2002**, 9, 7-18.

[5] Lindström, T.; Carlsson, G. The effect of carboxyl groups and their ionic form during drying on the hornification of cellulose fibers. *Sven. Papperstidn.* **1982**, 85, R146-R151.

[6] Saito, G. Das Verhalten der Zellulose in Alkalilösungen. *Kolloid-Beih.* **1939**, 49, 365-454.

[7] Porro, F.; Bedue, O.; Chanzy, H.; Heux, L. Solid-state 13C NMR study of na-cellulose complexes. *Biomacromolecules* **2007**, 8, 2586-2593.

[8] Sluiter, A.; Hames, B.; Ruiz, R.; Scarlata, C.; Sluiter, J.; Templeton, D.; Crocker, D. Determination of Structural Carbohydrates and Lignin in Biomass. **2011**, Golden, National Renewable Energy Laboratory

STRUCTURE-ANTIOXIDANT ACTIVITY RELATIONSHIP FOR LOW-MOLECULAR AND HIGH-MOLECULAR PLANT PHENYLPROPANOIDS: ACYCLIC DIARYLHEPTANOIDS AND LIGNINS

Jevgenija Ponomarenko[1], Patrick Trouillas[2], Tatiana Dizhbite[1], Maris Lauberts[1], Liga Roze[1], Vilhelmina Jurkjane[1], Jelena Krasilnikova[3], Galina Telysheva[1]*

*[1]Latvian State Institute of Wood Chemistry, 27 Dzerbenes st., LV-1006, Riga, Latvia; [2]Université de Limoges, 2 rue du Docteur Marcland, Limoges, France; [3]Riga Stradin University, 16 Dzirciema Street, LV-1007, Riga, Latvia (*ligno@edi.lv)*

ABSTRACT

A methodology for the evaluation of the antioxidant activity of plant derived monomeric and polymeric phenylpropanoids was developed. The joined experimental (tests with $DFPH^{\bullet}$, $ABTS^{\bullet+}$, $O_2^{\bullet-}$, $ROO^{\bullet}$ radicals) and theoretical (quantum chemistry calculations) studies allowed establishing the structure-activity relationships and elucidating the mechanisms of diarylheptanoids reactions with different oxidants. The antioxidant properties of 50 lignin samples differed by botanical origin (annual plants, coniferous trees, deciduous trees) and by the isolation technique (delignification by alkali, kraft process, Bjorkman method, solvolysis, fast pyrolysis, hydrolysis, isolation by ionic liquids) were compared. The structure and functionality of these lignins was characterized, using analytical pyrolysis (Py-GC-MS-FID), FTIR, EPR, DSC, TG, UV/VIS spectroscopy, SEC, titrimetric methods. The "structure – (antioxidant) activity" relationships (SAR and QSAR) of lignins were rationalized, using pair correlation, partial correlation and multivariate regression analyses, including CCR – correlated components regression. It was established that the main structure factors and mechanisms governing the radical-scavenging activity are the same for the acyclic diarylheptanoids (DAHs) and the polymeric phenylpropanoids – lignins.

I. INTRODUCTION

Different materials, food products, means for human health care, etc. undergo oxidative degradation. In order to protect their properties and prolong their shelf life, antioxidants have to be added to almost all oxidizable organic substrates. In June 2013, the antioxidant market was 1.5 billion USD [1]. The use of a traditional synthetic antioxidant is not safe from the ecological point of view, and it can threaten humans health. For example, an antioxidant can migrate from the packaging and get into the food. There is an increasing discontent of the society with synthetic antioxidants for food, because their safety is doubtful. Due to their biodegradability and significantly lower toxicity, naturally originated antioxidants, in particular, polyphenols, can be a good alternative to the synthetic ones [2,3].

Despite the huge number of researches devoted to antioxidant activity of plant polyphenols, their results often are not comparable. Besides, the possible correlations between the antioxidant properties of monomeric and polymeric polyphenols are poorly considered. The aim of the present work was characterization the structure – antioxidant activity relationship for lignins and diarylheptanoids for future development of a theoretic basis for effective application of these plant polyphenols as antioxidants for living organisms and variety of materials.

II. EXPERIMENTAL

Materials and methods of analysis

The DAHs under study were isolated from the bark of Latvian hardwood trees and purified as previously described [4]. The 50 technical lignins under study were obtained from different botanical sources and in different processes of phytomass chemical processing. To characterize the composition and chemical structure of the samples, the Py-GC-MS-FID, FTIR and UV/VIS spectroscopy methods were used. The Py-GC-MS-FID method was adjusted for the characterization of lignin structural descriptors. For the determination of the content of the functional groups (hydroxy-, methoxy- groups), titrimetric methods (conductometric titration, the method of Ceizel-Fibek-Schwapahh) were used. For the determination of the size of the π-conjugated systems, the EPR method was used. To characterize the distribution of molecular mass, size exclusion chromatography was used. To characterize the thermal stability and determine the glassing temperature of the lignins, the DSC and TG methods were used.

Characterization of antioxidant activity
For the investigation of the structure and antioxidant activity relationships of low-molecular and high-molecular plant polyphenols, the methods of the deactivation of $DPPH^{\bullet}$ and $ABTS^{\bullet+}$ radicals were adjusted. Radical scavenging activity against $DPPH^{\bullet}$, $ABTS^{\bullet+}$ radicals was measured spectrophotometrically as described in [5,6]. At the same time, for the evaluation of the ability of antioxidants to protect the substrate from oxidation, competitive methods, such as the ORAC (oxygen radicals absorbance capacity) method and the method of the deactivation of $O_2^{\bullet-}$, generated in the fermentative system, were chosen. ORAC assay was performed according to the method described in [7]. For the evaluation of the possibility to use the polyphenols under study as antioxidants in different areas, their action in real chemical and biological systems was investigated. To investigate the influence of the lignins under study on the thermo-oxidative destructions of the polyurethane (PU) films, lignins and their fractions were inducted in the films in the content of 2.5 % (by mass) and thermogravimetric analysis was made in oxidative atmosphere [8]. The compounds under study were tested as inhibitors of rapeseed oil, using OXIPRESS equipment.

Determination of qualitative (SAR) and quantitative (QSAR) structure-antioxidant activity relationships
For the rationalization of the antioxidant activity of diarylheptanoids and obtaining valuable information about the mechanisms of their reactions with radicals, the molecular modelling methods, which allow characterizing the main descriptors, connected with the antioxidant activity of polyphenolic compounds (dissociation enthalpies of O-H bonds, the energies of deprotonation and ionization), were used. For calculation of energies and geometry optimization, the DFT B3P86/6-31+G(d,p) and DFT ωB97XD/6-31+G(d,p)//ωB97XD/6-31G(d) schemes were chosen. All calculations were carried out with the Gaussian09® software from Gauss Inc, USA.
For the rationalization of the structure and antioxidant activity relationships of lignins, the correlation, partial correlation and multivariate regression analyses were used, including CCR – correlated components regression. The calculations were made, using SPSS Statistics 21 and XLSTAT 2013.

III. RESULTS AND DISCUSSION

Structure-antioxidant activity relationships for diarylheptanoids
The structures of the diarylheptanoids, used in the antioxidant activity study, are shown in the Figure 1.

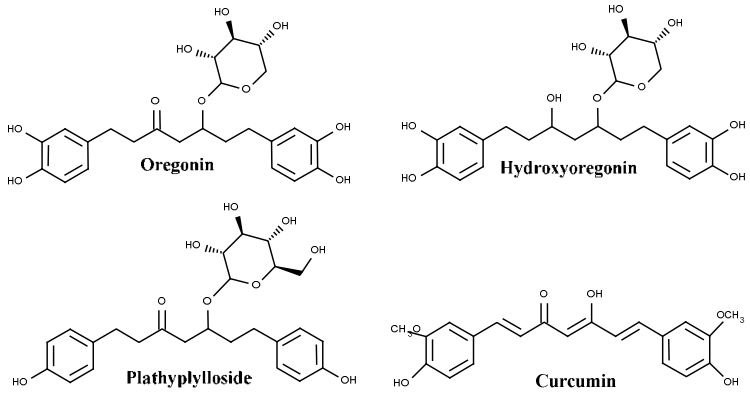

Figure 1. Structures of the diarylheptanoids

The highest antioxidant activity in $ABTS^{\bullet+}$ and $DPPH^{\bullet}$ test was shown by oregonin and hydroxyoregonin. In ORAC test, hydroxyoregonin had the highest antioxidant activity among the studied alder bark DAHs, while the activity of oregonin and plathyphyloside was lower (Table 1). In comparison with IC_{50} - the concentration of the antioxidant, needed to reduce by half the initial concentration of the radical, RDI - the number of deactivated radicals, calculated per number of phenolic hydroxyl groups, gives more trustworthy information about the redox-reactivity of diarylheptanoids under study and enhances the contribution of other structural properties, in addition to phenolic hydroxyl groups. The values of RDI, which are > 1, show that the formed phenoxyl radicals take part in the reactions with radicals as secondary antioxidants. RDI<1 shows that not all oregonin and hydroxyoregonin phenolic hydroxyl groups (Table 1) take part in the reaction with $ABTS^{\bullet+}$ radicals.
The results of the calculations of the thermodynamic descriptors have shown that *PCET* is the main mechanisms of the diarylheptanoids reactions with free radicals. The comparison of the results of the $ABTS^{\bullet+}$ test with the values of the calculated thermodynamic descriptors allowed to evaluate the contribution of the SPLET mechanisms in the antioxidant activity of diarylheptanoids.
The results of the $DPPH^{\bullet}$ test together with the calculated BDE values allowed to establish the structure-antioxidant activity relationships of diarylheptanoids in the reactions by PCET mechanism.

Table 1. Antioxidant activity of diarylheptanoids in $ABTS^{\bullet+}$, $DPPH^{\bullet}$ and ORAC tests.

Compound	**IC_{50}** - the concentration of the antioxidant, needed to reduce by half the initial concentration of the radical, mmol•L^{-1}		**RDI-**the number of deactiveted radicals per one group of DAH		**TEAC**- Trolox equivalent antioxidant capacity, mmol•L^{-1} (concentration of the antioxidant, in which it shows the same activity, as 1 mmol•L^{-1} Trolox
	$ABTS^{\bullet+}$	$DPPH^{\bullet}$	$ABTS^{\bullet+}$	$DPPH^{\bullet}$	ORAC
Oregonin	6.5±0.3	10.7±0.4	0.71±0.04	1.22±0.06	0.18± 0.02
Hydroxyoregonin	5.6±0.2	10.0±0.4	0.82±0.04	1.33±0.06	0.13 ± 0.03
Platyphylloside	5.8±0.3	Non-active	1.52±0.08	Non-active	0.22± 0.02
Curcumin	6.9±0.2	34.5±0.8	1.2±0.06	0.80±0.04	0.28 ± 0.02

The positive influence on the antioxidant activity of o-methoxy groups, as well as the negative influence of the carbonyl groups of the aliphatic chain, was confirmed. The found relationships are useful for further searching of natural polyphenols for healthcare and healing, working out of purposeful methods for their modification, and synthesis of novel preparations for pharmacy and veterinary. The results of the present study were used for development of two new market products containing the diarylheptanoid fraction of *Alnus spp.* bark: a cosmetic after sun cream and a dietary supplement.

Structure-antioxidant activity relationships for lignins

Antioxidant activity of different lignins is close to that of the reference antioxidant Trolox and to that of active low-molecular polyphenols. The TGA data clearly testified the antioxidant effect of polymeric fractions (obtained by the sequential extraction of lignins by organic solvents as propanol and methanol soluble fractions) of LignoBoost kraft lignins and Biolignin^{TM}, which revealed itself in increasing temperatures of starting (Tstart) and maximal development (T_{max}) of PU thermo-oxidative destruction as well as decreasing the process rate on the first stage of PU thermo-oxidative degradation. The data of DTA also confirmed the changes in thermo-oxidative behavior of model PU films: the exothermal maximum connected with oxidizing of PU destruction volatile products shifted to the high temperature region by 25-30 K. The oligomeric fraction (obtained by the sequential extraction of lignins by organic solvents as dichloromethane soluble fraction) of softwood LignoBoost kraft lignin and pyrolysis lignins showed high antioxidant activity in the rapeseed oil oxidation test.

In the studies of the structure-activity relationships, the antioxidant activity was expressed as the number of deactivated radicals per one phenolic hydroxyl group of lignin. To establish SAR, partial correlation analysis was used (Table 2).

Table 2. Partial correlation analysis results

The parameter, which characterizes the structural properties	Pearson's correlation coefficient* (n=50, α=0.05)	
	$DFPH^{\bullet}$	$ABTS^{\bullet+}$
Relative content of G+S phenols, %	**0.52**	-0.20
CH_2-groups in the α-position of the side chain, %	**0.53**	**0.33**
Oxygen-containing groups in the side chain, %	**-0.42**	-0.25
Size of the π–conjugated systems, n C	**-0.40**	**-0.50**
Double bonds in the α-position of the side chains, %	0.15	0.21
Carbohydrates, %	-0.21	**-0.61**
$(ArC_1+ArC_2)/ArC_3$	0.17	**0.77**
$-OCH_3$/FPV	0.14	0.01
M_w, g/mol	0.04	-0.08

***Values, which are marked with bold, significantly differ from 0, α=0.05.**

In the case of lignins, the structural parameters, which influence the antioxidant activity in the $DPPH^{\bullet}$ tests, can easily be explained by means of the SPLET mechanism. The factors, which determine the antioxidant activity in the $ABTS^{\bullet+}$ test, show the contribution of other mechanisms.

For the *QSAR* studies, the multivariate "*Correlated Component Regression*" (*CCR*) analysis was used. The following structure-activity relationship equation was obtained on the basis of the $DPPH^{\bullet}$ test results:

$$\mathbf{Y_1 = -3.08+0.043\times X_1+0.018\times X_2-0.018\times X_3-0.014\times X_7+0.24\times X_8} \quad (1.1.),$$

where Y_1 –number of the deactivated DPPH$^\bullet$ radicals per 1 phenolic hydroxyl group; $\mathbf{X_1}$ – relative content of G+S phenols, %; $\mathbf{X_2}$ **–** relative content of the phenylpropane units with CH_2-groups in the α-position of the side chains, %; $\mathbf{X_3}$ – relative content of the phenylpropane units with oxygen-containing groups in the side chains, %; $\mathbf{X_7}$ – size of the π–conjugated systems (the number of atoms); $\mathbf{X_8}$ – OCH_3/FPU (Figure 2).

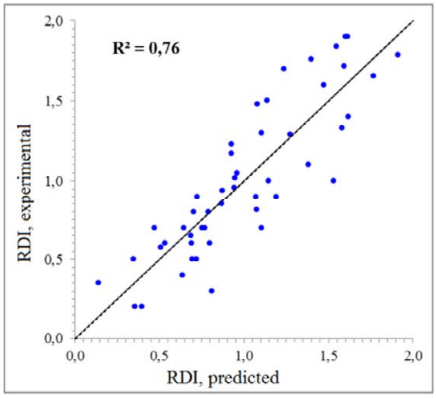

Figure 2. Predicted and experimental RDI values in the DPPH$^\bullet$ test

IV. CONCLUSIONS

The joined theoretical and experimental studies allowed establishing structure-antioxidant activity relationships of the bark diarylheptanoids and obtaining information about the mechanisms of their antioxidant action. Relative low-molecular and high-molecular polyphenols have similar structure-antioxidant activity relationships and mechanisms of action. The most important structural properties, which influence the antioxidant activity of lignins by *PCET* mechanism, are: *o*-methoxy groups, CH_2-groups in the α-position of the aliphatic chain, carbonyl groups in the aliphatic chains, and the size of π-conjugated systems. The most important structural properties, which influence the antioxidant activity of lignins by single electron transfer mechanisms (*SPLET, ET-PT* – electron transfer-proton transfer), are ether bonds in the aliphatic side chains, the content of carbohydrates, the number of the methoxyl groups per phenylpropane unit, and the size of π-conjugated systems.

V. ACKNOWLEDGEMENT

The financial supports from Latvian budget: Government Research Program 2010.10-4/VPP and LSC grant 564/2012 are gratefully acknowledged. Authors thank COST action CM0804 “Chemical Biology with Natural Compounds” and ERA-NET WOODWISDOM-NET project PINOBIO.

VI. REFERENCES

[1] Butti, M.; Vischetti, A. Songwon looks to emerging markets & Middle East for growth; expands portfolio to inlude HALS in tie-up with SABO. Polymer stabilizers. *Chem. Weekly*, **2013**, May 25, 209 – 210.
[2] Malik, J.; Krohnke, C. Polymer stabilization: present status and possible future trends. *Comptes Rendus Chimie* **2006**, *9*, 1330-1337.
[3] Jamshidian, M.; Tehrany, E. A.; Desobry, S. Release of synthetic phenolic antioxidants from extruded poly lactic acid (PLA) film. *Food Control* **2012**, *28*, 445-455.
[4] Telysheva G.; Dizhbite T.; Bikovens O.; Ponomarenko J.; Janceva S.; Krasilnikova J. Structure and antioxidant activity of diarylheptanoids extracted from bark of grey alder (*Alnus incana*) and potential of biorefinery-based bark processing of European trees. *Holzforschung* **2011**, *65*, 623-629.
[5] Baltrusaityte, V.; Venskutonis, P.; Cheksteryte, V. Radical scavenging activity of different floral origin honey and beebread phenolic extracts. *Food Chem*. **2007**, *101*, 502-514.
[6] Dizhbite, T.; Telysheva, G.; Jurkjane, V.; Viesturs, U. Characterization of the radical scavenging activity of lignins—natural antioxidants. *Biores. Technol.* **2004**, *95*, 309-317.
[7] Prior, R. L.; Wu, X.; Schaich, K. Standardized methods for the determination of antioxidant capacity and phenolics in foods and dietary supplements. *J. Agric. Food Chem.* **2003**, *53*, 4290-4302.
[8] Pei, N.; Thring, R. W. Syntheis of polyurethanes from solvolysis lignin using a polymerization catalyst: mechanical and thermal properties, *Int. J. Polym. Mater*. **2003**, *52*, 685 - 707.

EXTRACTION OF POLYMERIC ACETYL-GALACTOGLUCOMANNAN IN HIGH YIELD FROM SPRUCE WOOD WITH HOT WATER

Andrey Pranovich*, Bjarne Holmbom and Stefan Willför

Process Chemistry Centre, Laboratory of Wood and Paper Chemistry,
*Åbo Akademi University, FI-20500 Turku/Åbo, Finland (*Email: apranovi@abo.fi)*

ABSTRACT

Hemicelluloses constitute 25-30% of the wood in conifers and have a large potential value as natural polymers in applications as hydrogels and packaging films, and have also various bioactive properties and might find use as food additives and pharmaceuticals.
Ground spruce sapwood of different particle sizes were subjected to a series of consecutive two-stage extractions with plain water at a liquid/wood ratio of 4, at different temperatures in the range from 150°C to 180°C using an Accelerated Solvent Extraction (ASE) apparatus. The aim was to find optimal conditions for extraction of acetyl-galactoglucomannans (GGM) in native polymeric form in high yield.
The total yields of dissolved material (TDS) after two-stage extraction with a total extraction time of 1 hour amounted, irrespectively of the time ratios between the 1st and the 2nd extraction, to 110 mg/g, 170 mg/g, 220 mg/g and 260 mg/g at 150°C, 160°C, 170°C and 180°C, respectively.
The partial release of acetic acid lowered the pH of extracts and catalyzed not only hydrolytic cleavage of polymeric carbohydrates, but also further deacetylation of GGM, which leads to a lower water solubility and even to re-adsorption of GGM to the cellulosic matrix of wood fibers.
Polymeric GGM was precipitated by adding ethanol to the water extracts. The yield of polymeric GGM was quite similar for the different extraction temperatures. By extraction at 150°C, 52% of TDS consisted of polymeric GGM (ca 6% based on wood) while at 180°C only 27% of TDS was precipitable polymeric GGM (7% of wood).

I. INTRODUCTION

Since the last decade there is a renewed and growing interest in forest biomass utilization mainly because of the anticipated future shortage and high price of oil. The modern biorefinery concept, however, can provide even a broader spectrum of products which may give enough profit to ensure long-term success. Besides biofuels, biomass-derived specialty chemicals and pharmaceuticals, there is a growing interest in natural biopolymers as alternatives to synthetic polymers [1]. To extract such biopolymers from wood in intact form requires a deeper knowledge of the physico-chemical phenomena during the extraction processes.

Accelerated Solvent Extraction (ASE) is a very efficient extraction technique that enables convenient sequential extractions on the same sample with high repeatability at extraction temperatures up to 200°C.

Water as solvent for wood extraction is attractive because it is truly “the green door to natural products”. Much effort have been made to explore hot-water extraction of hemicelluloses, mainly of xylans from hardwood species ([2]. Softwood species, such as Norway spruce, are a promising source for another abundant type of hemicelluloses, the galactoglucomannans (GGM) [3].

Because extraction involves both physical and chemical processes, finding the means to provide the best mass-transfer, i.e. extraction yield, conditions with minimum damage of the native polymer structures in wood is a great challenge. In contrast to common hydrolysis/autohydrolysis processes, it is necessary to prevent chemical reactions of the native hemicelluloses, in particular their acid-catalyzed hydrolytic depolymerisation and deacetylation. Therefore, careful control of pH, temperature and time is needed [4-5].

The proton concentration (pH-value) is the most critical factor determining the initiation/catalysis of these hydrolytic reactions. It is important to keep the end pH of water extracts in a narrow range about 4, also because alkali-induced hydrolysis of acetyl groups occurs already at pH 5 [4]. If the galactoglucomannans are deacetylated they will become less soluble in water and cannot anymore be extracted in polymeric form. In order to keep pH during water extraction at the desired level buffering agents may be added [5].

In case of extraction with plain water (no buffers added, autohydrolytic pH drift occurring) it is necessary to control the extraction process by optimizing the temperature and time, and to have an enough small wood particle size.

The aim of this study was to isolate the principal hemicellulose in spruce wood, i.e., GGM, in high yield and with preserved structure, i.e., with high-molar-mass and high acetyl content.

II. EXPERIMENTAL

A mature, healthy Norway spruce tree was felled in South of Finland, and part of the stem at the height between 0.7 m – 2.2 m above the ground was taken for study. Handmade chips from sapwood were air-dried overnight, ground and screened into fractions of different particle size. The fraction with the particle size 0.25-1.0 mm was used in the study. Some comparative extractions were performed with the particle size fraction 0.05-0.1 mm.

Accelerated Solvent Extraction (ASE-350) (Dionex, Sunnyvale, Calif.) apparatus equipped with 100-ml Zr-type cells was used for hot-water extractions. Approximately 20 g o.d. ground wood was extracted at the pressure 10 MPa at temperatures of 150°C - 180°C with 1 hour total extraction time. After extraction, the water extracts were cooled to room temperature and their end pH-values were measured.

Total Dissolved Solids (TDS) in water extracts were determined gravimetrically by freeze-drying of corresponding aliquots to a constant weight. The amount of acetyl groups spit off from wood during hot-water extraction was determined by analysis of acetic acid in extracts by HPLC using a reversed-phase a Synergi Hydro-RP 80R column (Phenomenex®) and a RI detector [4]. Monosaccharides in the extracts were determined by GC after silylation of freeze-dried aliquots [6]. Total carbohydrates in the water extracts and the isolated products were analysed by GC after freeze-drying, acid methanolysis and silylation [7]. Polymeric non-cellulosic carbohydrates were isolated from water extracts by precipitation in ethanol:water (85:15% v/v) [8]. Molar-mass characteristics of precipitated carbohydrates were determined by SEC-HPLC equipped with MALLS (miniDAWN, Wyatt Technology) and RI detectors as described earlier [4]. Lignin and lignin-like substances in water extracts were measured by UV absorption at 280 nm in acetic acid (AcOH) with acetyl bromide (AcBr) [9]. Aliquots of total water extracts, including some lignin precipitated during cooling, were freeze-dried and then dissolved in AcOH with AcBr.

III. RESULTS AND DISCUSSION

The total yield of dissolved material (TDS, determined gravimetrically) increased along the extraction time and temperature (**Figure 1**). At 180°C about 4% of the wood material was dissolved already during the first minute of extraction, which was four times higher than that at 150°C. TDS amounted to about 21% wood at 180°C and 30 min extraction time. The yield did not increase further, but actually even decreased slightly. The total yield of dissolved material after 60 min extraction at 150°C was about 9% of wood. With fine wood particles (0.05-0.1 mm) the yield at 150°C and 60 min was about 40% higher than of that obtained by extraction of larger wood particles (0.25-1 mm).

End-pH profiles exhibited a corresponding pattern, so that higher temperatures resulted in lower pH values (**Figure 2**). At 180°C the pH level decreased dramatically with extraction time, to the level of 3.3 after 60 min. During extraction at 150°C the pH value decreased much less than at higher temperatures, down to 3.7 after 60 min. The pH profile obtained with fine wood particles was very similar to that for larger wood particles. The amount of polysaccharides precipitated in ethanol from water extracts obtained at 180°C had a maximum yield after 15 min extraction, amounting to ca 6.6% of wood (**Figure 3**). Extended extraction resulted in severe depolymerisation of the non-cellulosic carbohydrates, thus lowering the yield of polymeric precipitates. After 60 min extraction the yield was only 1.2% of wood. In the extracts obtained at 170°C and 160°C the highest yield of polysaccharides (ca 6.0% of wood) was obtained after 30 min and 40 min extraction, respectively. In the extracts obtained at 150°C, a yield of 4.7% was obtained after 60 min extraction. However, by extraction of finer wood particles (0.05-0.1 mm) the yield of precipitated polysaccharides increased up to 6.8% of wood, i.e. more than 40%. This is in agreement with our early findings [10]. In extracts obtained at different temperatures and times, 50-52% of TDS (4.7-6.6% of wood) were polymeric non-cellulosic carbohydrates, mainly GGM. The portion of polymeric carbohydrates in TDS can be increased to about 60% (6.8% of wood) by extraction of fine wood particles. The molar-mass characteristics of the precipitated polysaccharides were strongly influenced by the temperature, extraction time and pH profile (Fig. 4). Decreasing the temperature from 180°C to 150°C will increase the molar mass substantially. During extraction up to 30 min at 180°C the average molar mass (Mw) decreased from 35 kDa to 7.0 kDa (**Figure 4**). After 30 min extraction probably induces secondary reactions resulting in formation of some aggregates, because Mw increased again to 16 kDa for 60 min extraction time.

As expected, due to relatively high pH-values and lower depolymerisation rate the average molar mass of precipitated carbohydrates was relatively high at 150°C; the Mw value decreased along the extraction time from 47 kDa to about 12 kDa. This is also true for the polysaccharides obtained by extraction of the fine wood particles.

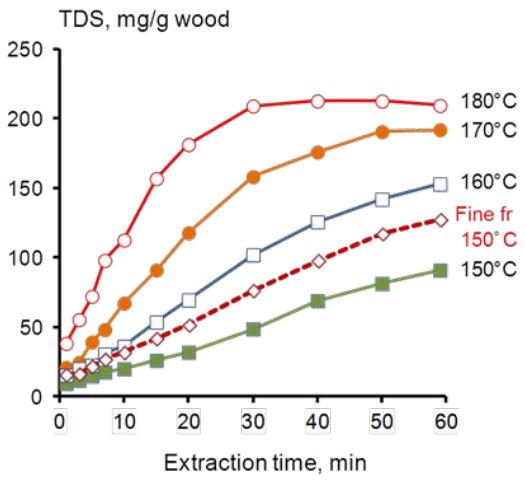

Figure 1. Total Dissolved Solids released from ground spruce wood by hot-water extraction at different temperatures.

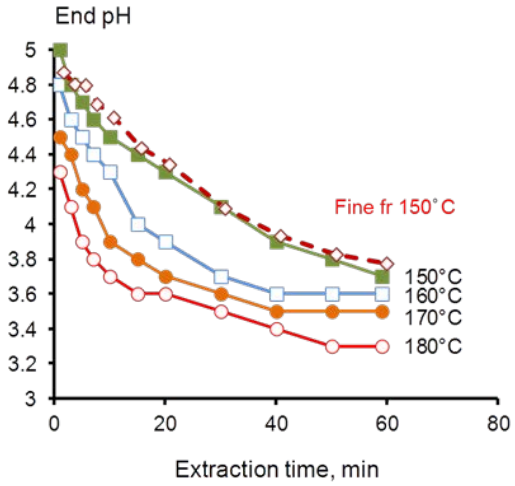

Figure 2. End pH of water extracts obtained from ground spruce wood at different temperatures.

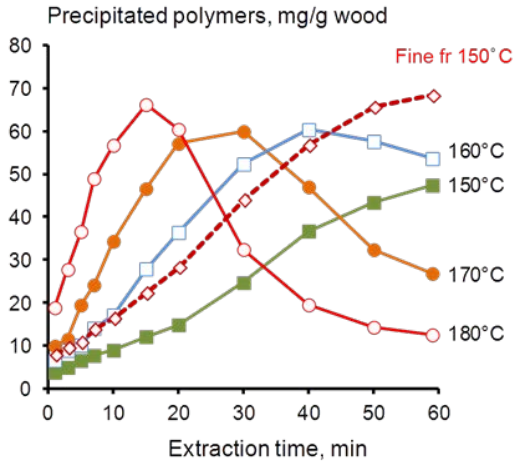

Figure 3. EtOH-precipitated polymeric GGM from extracts obtained from ground spruce wood at different temperatures.

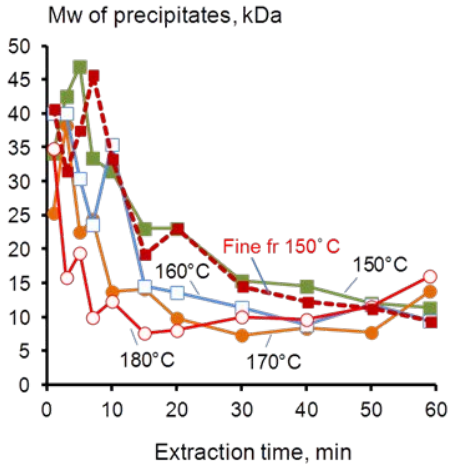

Figure 4. Molar mass Mw of precipitated polymeric GGM from extracts obtained from ground spruce wood at different temperatures.

The pH profile during hot-water extraction is related to the kinetic profile of the autohydrolysis of acetyl groups, as seen in the amounts of free acetic acid released. The acetyl groups in spruce wood are mainly found at C-2 and C-3 in mannose units of the galactoglucomannans.

At 150°C, 160°C and 170°C the release of acetic acid increased steadily, and were after 60 min extraction 1.4 mg/g, 3.0 mg/g and 4.0 mg/g of acetic acid/wood, respectively. However, at the most severe conditions, 180°C and 60 min, about half of the acetyl groups in spruce wood, i.e. 9.9 mg/g acetic acid/wood, were hydrolyzed.

The amount of lignin and lignin-like substances extracted at 180°C increased with time steadily from 1.0% to 5.4% of wood. However, at 150°C, the release of lignin and lignin-like substances after 60 min of extraction was low and amounted only to 1.8% of wood.

The yield of total dissolved carbohydrates also increased at higher temperatures. At 180°C, however, a notable degradation of pentoses and hexoses occurred. About half of the dissolved carbohydrates were hydrolysed at

180°C to monosaccharides. Moreover, also hexosans also were hydrolysed. Almost no hexosan degradation was observed at 150°C.

The content of non-cellulosic carbohydrates, including GGM, in all precipitates obtained from spruce extracts at different temperatures was determined by acid methanolysis and GC in range between 88% and 92% (calculated as anhydro-sugars).

The carbohydrate composition in the EtOH-precipitated polysaccharides was almost similar for all temperatures and times. Hexoses C-6 (mannose, galactose and glucose) from GGM were the main sugar units in the precipitates, comprising 76-78% of polysaccharides. Pentoses (arabinose and xylose) from xylan and, probably also from arabinogalactan, comprised 6.8-8.0% of the polysaccharides. The content of uronic acid units was between 3.7% and 4.0%. The main uronic acid unit was galacturonic acid derived from pectins.

IV. CONCLUSIONS

Extraction of ground spruce sapwood with plain water by Accelerated Solvent Extraction at 150-180°C enabled isolation of galactoglucomannan with a DP about 60 in a yield of 7% of the wood (40% of the GGM in the wood).

By applying lower temperatures, 150-160°C, and fine wood particles (0.05-0.1 mm) it is possible to obtain polymeric GGM with a higher molar mass without substantial loss in yield.

Lower temperatures are also preferred because of less degradation in the residual wood.

V. ACKNOWLEDGEMENT

Financial support from the Finnish Bioeconomy Cluster (FIBIC), the Finnish Funding Agency for Technology and Innovation (Tekes) and several industrial companies is acknowledged. This work was part of the activities at the Åbo Akademi Process Chemistry Centre.

VI. REFERENCES

[1] Willför, S.; Sundberg, K.; Tenkanen, M.; Holmbom, B. Spruce-derived mannans - a potential raw material for hydrocolloids and novel advanced natural materials. *Carbohydr. Polym.* **2008**, 72, 197-210.

[2] van Heiningen, A. Converting a kraft pulp mill into an integrated forest biorefinery. *Pulp Pap. Can.* **2006**, 107, 38-43.

[3] Casebier, R.L.; Hamilton, J.K.; Hergert, H.L. Chemistry and mechanism of water prehydrolysis on Southern pine wood. *Tappi* **1969,** 52, 2369-2377.

[4] Song, T.; Pranovich A.; Holmbom. B. Characterisation of Norway spruce hemicelluloses extracted by pressurised hot-water extraction (ASE) in presence of sodium bicarbonate. *Holzforschung* **2011,** 65, 35-42.

[5] Song, T.; Pranovich A.; Holmbom. B. Effects of pH control with phthalate buffers on hot-water extraction of hemicelluloses from spruce wood. *Biores. Technol.* **2011,** 102, 10518–10523.

[6] Willför, S.; Sundberg, A.; Hemming, J.; Holmbom, B. Polysaccharides in some industrially important softwood species. *Wood Sci. Technol.* **2005,** 39, 245–257.

[7] Sundberg, A.; Sundberg, K.; Lillandt, C.; Holmbom, B. Determination of hemicelluloses and pectins in wood and pulp fibres by acid methanolysis and gas chromatography. *Nord. Pulp Pap. Res. J.* **1996,** 11, 216–219, 226.

[8] Song, T.; Pranovich A.; Holmbom. B. Separation of polymeric galactoglucomannans from hot-water extract of spruce wood. *Biores. Technol.* **2013**, 130, 198-203.

[9] Iiyama, K.; Wallis, A.F.A. An improved acetyl bromide procedure for determining lignin in woods and wood pulps. *Wood Sci. Technol.* **1988,** 22, 271–280.

[10] Song, T.; Pranovich A.; Holmbom. B. Hot-water extraction of ground spruce wood of different particle size and thermomechanical pulp. *BioResources* **2012,** 7, 4214-4225.

CHEMICAL COMPOSITION OF LIPOPHILIC COMPOUNDS FROM WHEAT STRAW

Pepijn Prinsen, Ana Gutiérrez, José C. del Río*

IRNAS-CSIC, P.O. Box 1052, 41080-Seville, Spain (delrio@irnase.csic.es)*

ABSTRACT

The chemical composition of the lipids in wheat straw was studied in detail by gas chromatography and mass spectrometry. The predominant lipids identified were series of long-chain free fatty acids (25% of total extract), followed by series of free fatty alcohols (ca. 20%). High molecular weight esters were also found (11%), together with lower amounts of other aliphatic series such as *n*-alkanes, *n*-aldehydes and glycerides (mono-, di- and triglycerides). Relatively high amounts of β-diketones (10%), particularly 14,16-hentriacontanedione, which is the second most abundant single compound among the lipids in wheat straw, were also identified. Finally, steroid compounds (steroid hydrocarbons, steroid ketones, free sterols, sterol esters and sterol glycosides) were also found, with sterols accounting for nearly 14% of all identified compounds.

I. INTRODUCTION

Plant biomass is the main source of renewable materials in Earth and represents a potential source of renewable energy and biobased products. Biomass is available in high amounts at very low cost (as forest, agricultural or industrial lignocellulosic wastes and cultures) and could be a widely available and inexpensive source for biofuels and bioproducts in the near future. The high abundance, wide availability and very low-cost of some agricultural wastes, as cereal straws, makes them excellent raw materials for future biorefineries. Among them, wheat straw has the greatest potential of all agricultural residues because of its wide availability and low cost [1]. Wheat straw contains 35–45% cellulose, 20–30% hemicelluloses, and around 15% lignin, which makes it an attractive feedstock to be converted to ethanol and other value-added products [2]. Wheat straw also contains significant amounts of lipids (*ca.* 1-2% by weight) that can be extracted to produce high-value waxes [3].

Studies concerning the composition of lipids in wheat straw have been relatively scarce, although some papers have been published in this regard [3,4]. In the present work, a thorough and comprehensive characterization of the lipophilic extractives in wheat straw has been performed by gas chromatography-mass spectrometry (GC-MS) using medium-length high temperature capillary columns with thin films, which enables the elution and analysis of a wide range of compounds from fatty acids to intact high molecular weight lipids such as sterol esters, sterol glycosides or triglycerides [5]. The knowledge of the precise composition of the lipophilic extractives in wheat straw will help to maximize the exploitation of this important agricultural waste.

II. EXPERIMENTAL

Samples

Wheat straw (*Triticum durum* var. Carioca) was harvested from an experimental field in Seville (South Spain) in June 2009. Wheat straw was air-dried and the dried samples were milled using a knife mill, and subsequently extracted with acetone in a Soxhlet apparatus for 8 h. The acetone extracts were evaporated to dryness, and resuspended in chloroform for chromatographic analysis.

GC-MS analyses

The GC-MS analysis were performed on a Varian Star 3400 gas chromatograph coupled with an ion-trap detector (Varian Saturn) equipped with a high-temperature capillary column (DB-5HT, 15 m × 0.25 mm i.d., 0.1 μm film thickness). Helium was used as carrier gas at a rate of 2 mL/min. The samples were injected directly onto the column using a SPI (septum-equipped programmable injector) system. The temperature of the injector during the injection was 60 ºC, and 0.1 min after injection was programmed to 380 ºC at a rate of 200 ºC min-1 and held for 10 min. The oven was heated from 120 ºC (1 min) to 380 ºC (5 min) at 10 ºC min-1. The temperature of the transfer line was set at 300 ºC. Bis(trimethylsilyl)trifluoroacetamide (BSTFA) silylation were used to form the TMS-derivatives. Compounds were identified by comparing their mass spectra with mass spectra in the Wiley and NIST libraries, by mass fragmentography and, when possible, by comparison with authentic standards. Peaks were quantified by area, and a mixture of standards (octadecane, palmitic acid, sitosterol, cholesteryl oleate, and sitosteryl 3β-D-glucopyranoside) with a concentration range between 0.1 and 1 mg/mL, was used to elaborate calibration curves.

III. RESULTS AND DISCUSSION

The total acetone extractives of wheat straw accounts for 2.7% of dry material. However, the lipohilic content, estimated as the chloroform solubles is lower and accounts for 2% while the rest (0.7%) correspond to polar compounds. This content is similar to that reported in other grasses and nonwoody materials [6,7].

The lipophilic extracts from wheat straw were analyzed (as TMS-ether derivatives) by GC-MS using medium-length high-temperature capillary columns with thin films, according to the method previously described [5]. The GC-MS chromatogram of the TMS-ether derivatives of the lipid extracts from wheat straw is shown in **Figure 1**.The identities and abundances of the main lipid compounds identified are detailed in **Table 1**.

The predominant lipids present in wheat straw were series of fatty acids that accounted for 25% of all identified compounds, followed by series of free fatty alcohols (*ca.* 20%). High molecular weight esters of long-chain fatty acids esterified to long-chain fatty alcohols were also found in significant amounts (11%). Additionally, lower amounts of other aliphatic series such as *n*-alkanes, *n*-aldehydes and glycerides (mono-, di- and triglycerides), were also observed. Important amounts of β-diketones (10% of all identified compounds) were also found in the extracts of wheat straw. Steroid compounds (hydrocarbons, ketones, free sterols, sterol esters and sterol glycosides) were also present among the lipophilic extracts of wheat straw in important amounts, with sterols accounting for nearly 14% of all identified compounds.

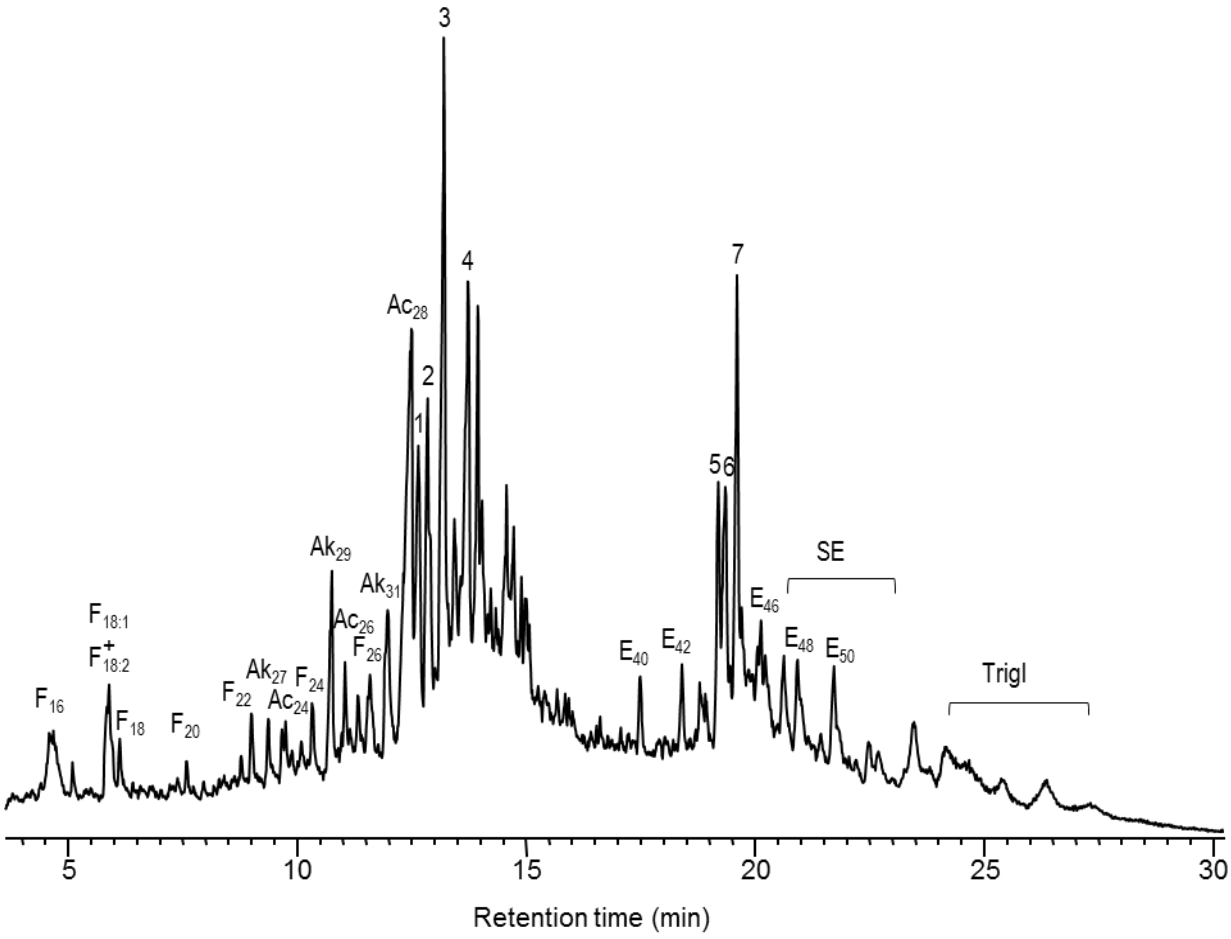

Figure 1. GC-MS chromatograms of the lipid extracts from wheat straw, as TMS-ether derivatives. F(n): *n*-fatty acid series; Ak(n): *n*-alkane series; Ac(n): *n*-fatty alcohol series; Ad(n): *n*-aldehyde series; E(*n*): high molecular weight ester series; n denotes the total carbon atom number. SE: sterol esters; Trigl: triglycerides. Other compounds reflected are: 1: campesterol; 2: stigmasterol; 3: sitosterol; 4: 14,16-hentriacontanedione; 5: campesteryl 3β-D-glucopyranoside; 6: stigmasteryl 3β-D-glucopyranoside; 7: sitosteryl 3β-D-glucopyranoside.

Aliphatic series

Free fatty acids were the most predominant series, accounting for 2080 mg/Kg. The series ranges from tetradecanoic acid (C_{14}) to tetratriacontanoic acid (C_{34}), with a strong even-over-odd carbon atom number predominance, and palmitic acid being the most predominant. The unsaturated oleic and linoleic acids were also found in important amounts. Free fatty alcohols were the second most abundant class of aliphatic series in wheat straw, accounting for 1615 mg/Kg. Free fatty alcohols were found in the range from *n*-docosanol (C_{22}) to *n*-triacontanol (C_{30}), with a strong even-over-odd carbon atom number predominance, and *n*-octacosanol being the most predominant homolog in the series. The series of *n*-alkanes was present in lower amounts (371 mg/Kg) and ranged from *n*-tricosane (C_{23}) to *n*-tritriacontane (C_{33}), with a strong odd-over-even atom carbon number predominance and nonacosane being the predominant homolog, followed by hentriacontane. Finally, minor amounts of *n*-aldehydes (99 mg/Kg) were identified from *n*-eicosanal (C_{20}) to *n*-dotriacosanal (C_{32}), with a strong even-over-odd atom carbon atom predominance and *n*-octacosanal being the major compound. The distribution of aldehydes parallels that of free alcohols, as usually occurs in the plant kingdom and observed in other plants [6], suggesting that aldehydes are intermediates in the biosynthesis of alcohols from fatty acids [8].

The series of high molecular weight esters occurred in important amounts (915 mg/Kg). This series was found in the range from C_{38} to C_{48} with a strong predominance of the even atom carbon number homologues, and the C_{44} and C_{46} analogs being the most abundant ones. A close examination of each chromatographic peak indicated that they consisted of a mixture of esters of different long-chain fatty acids esterified to different long-chain fatty alcohols. The identification and quantitation of the individual long-chain esters in each chromatographic peak was resolved based on the mass spectra of the peaks [6]. Quantitation of individual esters was accomplished by integrating the areas in the chromatographic profiles of the ions characteristic for the acidic moiety. The esterified fatty acids ranged from dodecanoic acid (C_{12}) to octacosanoic acid (C_{28}) and the esterified fatty alcohols from octadecanol (C_{18}) to triacontanol (C_{30}). According to our analyses, the predominant high molecular weight ester in wheat straw was C_{44}, which was mostly constituted by hexadecanoic acid, octacosyl ester.

Finally, glycerides (mono-, di- and triglycerides), were also found among the lipophilic extractives in wheat straw, although in lower amounts. Monoglycerides accounted for 127 mg/Kg, and ranged from 2,3-dihydroxypropyl tetradecanoate to 2,3-dihydroxypropyl triacontanoate, with a strong even-over-odd carbon atom number predominance, and with 1-monopalmitin being the most abundant. The unsaturated monoglycerides 1-monoolein and 1-monolinolein were also present in minor amounts. Diglycerides were also found in low amounts (85 mg/Kg), the most abundant being 1,2-dipalmitin and 1,3-dipalmitin. Finally, triglycerides were also identified and accounted for 198 mg/Kg, dioleoylpalmitin being the most abundant.

β-diketones

The analysis of the lipophilic extractives of wheat straw revealed the presence of important amounts (883 mg/Kg) of a compound with a β-diketone structure. The identification of this compound was achieved based on its mass spectrum. The molecular ion at *m/z* 464 indicates that this is a hentriacontanedienone, and the fragments at *m/z* 250 and *m/z* 278 that arise from the McLafferty rearrangement at both sides of the diketone group followed by loss of water [9] clearly indicate that the structure of this β-diketone is 14,16-hentriacontanedione. 14,16-hentriacontanedione was the second most abundant single compound among the lipophilic extractives in wheat straw. Minor amounts of 12,14-tritriacontanedione were also present among the lipophilic compounds of wheat straw. β-Diketones are relatively common constituents of plant waxes and have been identified in the leafs of different grasses, including wheat straw [7,10].

Steroid compounds

Different classes of steroid compounds were present in the extracts of wheat straw, namely steroid hydrocarbons, steroid ketones, sterols, sterol glycosides and sterol esters. Free sterols were the most abundant steroid compounds, accounting for 1135 mg/Kg. Sitosterol was the most important sterol, together with campesterol and stigmasterol. Minor amounts of sterols were found esterified forming sterol esters (70 mg/Kg), sitosteryl palmitate being the most important one. Sterol glycosides were also identified in important amounts (680 mg/Kg). Sitosteryl 3β-D-glucopyranoside was the most predominant with lower amounts of campesteryl and stigmasteryl β-D-glucopyranosides. The identification of sterol glycosides was accomplished (after BSTFA derivatization of the lipid extract) by comparison with the mass spectra and relative retention times of authentic standards [11]. Steroid ketones were observed in low amounts (88 mg/Kg) and consisted mainly of stigmasta-4,22-dien-3-one, stigmasta-3,5-dien-7-one, ergost-4-ene-3,6-dione, stigmast-4-ene-3,6-dione, ergostane-3,6-dione, stigmastane-3,6-dione, stigmasta-4,22-diene-3,6-dione, and stigmast-22-ene-3,6-dione. Finally, minor amounts of steroid hydrocarbons (16 mg/Kg) were also identified, stigmasta-3,5-diene being the most important one, and with lower amounts of ergosta-3,5-diene, stigmasta-3,5,22-triene, stigmasta-4,22-diene and stigmasta-3,5,7-triene. Most probably, these steroid hydrocarbons might arise from degradation of free and conjugated sterols, either within the plant or during the lipids isolation and/or analysis.

Table 2. Composition and Abundance (mg/Kg fiber, d.a.f.) of Main Lipids Identified in the Extracts of Wheat Straw

Compound	Abundance
n-Fatty acids	2080
n-Fatty alcohols	1615
n-Alkanes	371
n-Aldehydes	99
High molecular weight esters	915
Monoglycerides	127
Diglicerides	85
Triglycerides	198
β-Diketones	883
Steroid hydrocarbons	16
Steroid ketones	88
Sterols	1121
Sterol glycosides	680
Sterol esters	70

IV. CONCLUSIONS

The present paper provides a detailed description of the lipophilic compounds in wheat straw, which is a highly valuable information for a more complete industrial utilization of this lignocellulosic material.

V. ACKNOWLEDGEMENT

This study has been funded by the EU-project LIGNODECO (KBBE-244362) and the Spanish project AGL2011-25379 (co-financed by FEDER funds).

VI. REFERENCES

[1] Sarkar, N.; Ghosh, S.K.; Bannerjee, S.; Aikat, K. Bioethanol production from agricultural wastes: An overview. *Renewable Energy* **2012**, *37*, 19–27.

[2] del Río, J.C.; Rencoret, J.; Prinsen, P.; Martínez, A.T.; Ralph, J.; Gutiérrez, A. Structural characterization of wheat straw lignin as revealed by analytical pyrolysis, 2D-NMR, and reductive cleavage methods. *J. Agric. Food Chem.* **2012**, *60*, 5922–5935.

[3] Deswarte, F.E.I.; Clark, J.H.; Hardy, J.J.E.; Rose, P.M. The fractionation of valuable wax products from wheat straw using CO_2. *Green Chem.* **2006**, *8*, 39–42.

[4] Sun, R.C.; Sun, X. F. Identification and quantitation of lipophilic extractives from wheat straw. *Ind. Crops & Prod.* **2001**, *14*, 51–64.

[5] Gutiérrez, A.; del Río, J.C.; González-Vila, F.J.; Martín, F. Analysis of lipophilic extractives from wood and pitch deposits by solid-phase extraction and gas chromatography. *J. Chromatogr. A* **1998**, *823*, 449–455.

[6] Gutiérrez, A.; del Río, J.C. Lipids from flax fibers and their fate in alkaline pulping. *J. Agric. Food Chem.* **2003**, *51*, 4965–4971.

[7] Prinsen, P.; Gutiérrez, A.; del Río, J.C. Lipophilic extractives from the cortex and pith of elephant grass (*Pennisetum purpureum* Schumach.) stems. *J. Agric. Food Chem.* **2012**, *60*, 6408–6417.

[8] Bianchi, G.; Plant waxes. In *Waxes: Chemistry, Molecular Biology and Functions*; Hamilton, R.J., Ed.; The Oily Press: Dundee, Scotland, 1995; pp 175–222.

[9] Evans, D.; Knights, B.A.; Math, V.B.; Ritchie, A.L. β-Diketones in *Rhododendron* waxes. *Phytochemistry* **1975**, *14*, 2447–2451.

[10] Tulloch, A.P. Carbon-13 NMR spectra of β-diketones from wax of the gramineae. *Phytochemistry* **1985**, *24*, 131–137.

[11] Gutiérrez, A.; del Río, J.C. Gas chromatography/mass spectrometry demonstration of steryl glycosides in eucalypt wood, kraft pulp and process liquids. *Rapid Commun. Mass Spectrom.* **2001**, *15*, 2515–2520.

EVALUATION OF GRAPE STALKS AS A FEEDSTOCK FOR PELLETS PRODUCTION

S. O Prozil[1], D.V. Evtuguin[1*], S. M. Lopes [2], L.P. Cruz Lopes[2], A. S. Arshanitsa[3], V. P. Solodovnik[3], G. M. Telysheva[3]

[1] *CICECO, Department of Chemistry, University of Aveiro, 3810-193 Aveiro, Portugal*

[2] *CI&DETS, Department of Environment, Polytechnic Institute of Viseu, 3504-510 Viseu, Portugal*

[3] *Laboratory of Lignin Chemistry, Dzerbenes st. 27, LV-1006, Latvian State Institute of Wood Chemistry, Riga, Latvia*

**corresponding author: dmitrye@ua.pt*

ABSTRACT

Grape stalks are the massive by-product of winemaking composed essentially of cellulose (ca 30%), hemicelluloses (ca 20%), lignin (ca 18%), tannins (ca 16%) and proteins (ca 6%) and could be an interesting source of solid biomass for energy needs. Among others agriculture residues (e.g. wheat straw or corncobs), grape stalks contain the relatively low ash content (2.90%), which is, however, ten times higher than in softwoods (e.g. spruce or pine). In this work grape stalks were evaluated for the first time as a pelletized solid fuel and compared with those produced from softwood. It was found that the specific energy consumption for pelletizing of grape stalks was approximately 25% lower when compared to that for softwood sawdust. The bulk density of produced grape stalks pellets (670 kg/m^3) was similar to that of pellets produced from softwoods (660 kg/m^3), whereas the particle density was slightly higher for grape stalks than for softwood pellets (1129 against 1098 Kg/m^3). The durability of pellets from grape stalks and softwood was practically the same: 95.8% and 95.6%, respectively. The grape stalks' higher heating value was of 16.7 MJ/kg, which is slightly lower than that obtained for softwood (18.2 MJ/Kg).

I. INTRODUCTION

The present global energy model is mainly based on the use of fossil fuels. However, the growing demand for energy, the high dependence on fossil fuels and the negative impacts on the environment has led the European Union (EU) to review its energy policy strategies. Several reasons have prompted the EU to revise this policy, including: increased use of renewable energy sources in order to reduce carbon dioxide (CO_2) emissions, the need to reduce on imported energy sources and the diversification of energy sources and increased international cooperation [2]. The Energy Policy Strategy for 2020 of the European Commission predicts increased use of renewable resources in the energy system. The projections based on renewable energy in the EU includes biomass, which should represent more than 50% renewable energy supply in the EU-27 in 2020 [3]. The utilization of biomass as an alternative to fossil energy sources has emerged recently for domestic heating and electric energy production. Within classes of biomass, forest biomass and agricultural biomass take prominent roles. Agriculture biomass such as, residual stalks, straw, leaves, roots, husk, nut or seed shells, is widely available, renewable, and virtually free. Despite there is an emerging trend in the use of biomass and conversion technologies (combustion, gasification, pyrolysis, pelletization, etc.), the agriculture biomass is still largely under-utilized (abandoned in fields and in water lines or burned openly in the fields), especially in countries lacking strong regulatory instruments to control polluting practices [4]. These polluting practices are damaging to the environmentally and to human health (propagation of odors and fires, disease transmission, contamination of soils and aquifers, etc) and for this reason it is urgent to valorize this type of biomass.

The potential of biomass from agricultural sector as an energy source, including the by-products of wine making process, is not enough studied. In particular, grape stalks are the massive by-product of winemaking composed by cellulose (ca 30%), hemicelluloses (ca 20%), lignin (ca 18%), tannins (ca 16%) and proteins (ca 6%) [5]. In apriori, this agricultural residue could be an interesting source of solid biomass for energy needs. Hence the main goal of this work was the evaluation of grape stalks as a pelletized solid fuel.

II. EXPERMENTAL

2.1. Raw materials

Grape stalks of the variety *Vitis vinifera L.* (Touriga Nacional) used to produce pellets in this study were supplied by Tavfer Group (Quinta do Serrado in Penalva do Castelo in Dão Region of Portugal). The raw material was collected after mechanical destemming, which separate the grapes from woody fraction (grape stalks), and was dried at room temperature. Softwood (essentially spruce) sawdust with small proportion of pine sawdust of ca 1mm fraction were prepared in the laboratory.

2.2 Chemical analyses

The elemental composition, the ash content, the moisture content and the sulphur content of grape stalks biomass were determined according to EN 15104:2010, EN 14775:2009, EN 14774-1: EN 15289 standards, respectively.

2.3 Pelletizing and pellets analysis

Before pelletizing, grape stalks were grinded in a hammer mill AGICO TSF420C with screening hole diameter of 3.5 mm. The biomass was granulated using a flat die laboratory press KAHL 14-175. The die hole diameter was 6.0 mm and the channel length of 24 mm. The pellets were produced without any additives or adhesives. The durability and bulk density values of pellets obtained were determined according to EN 15210-1:2009 and ~~2011~~ EN 15103:2009, respectively. The higher heating values (HHV) were determined according to ISO 1928:2009 using PARR 1341 Oxygen Bomb calorimeter. TGA and DTA analyses were realized for samples grinded in a ball Mixer mill Retsch MM 200 and dried in an oven using the Mettler Toledo Star System TOA/SDTA 851 at a heating rate of 10 K/min, air flow rate of 50 mL/min and sample weight of ca 8 mg.

III. RESULTS AND DISCUSSION

3.1 Element composition of grape stalks and fuel characteristics

Table 1 shows the results on elementary analysis and heating values of grape stalks and commonly used in the European market softwood sawdust (spruce/pine mixture) taken for the comparative reasons. In addition, the literature data on grape pomaces have been also presented. The contents of C and H detected for grape stalks are quite similar to those observed for softwood. The nitrogen content in grape stalks is slightly higher than for spruce wood, but lower than that reported for grape pomaces by other researchers (**Table 1**). Hence, it could be expected that grape stalks will not cause problems of excessive NO_x emissions. The sulfur content observed for the grape stalks is very low compared to the percentages reported by other authors for grape pomaces. The low sulfur content avoids the generation of toxic/corrosive SO_x emissions derived from sulphur during the combustion process. The ash content in grape stalks was of 2.9%, a much higher value when compared to woods, but a rather low value when compared to typical agriculture residues such as wheat straw [1]. Note worthy that the heating values of grape stalks and softwood sawdust were close each other (**Table 1**).

Table 1. Quality parameters on DM of biomass used for the pelletizing.

Characteristics	Softwood	Grape stalks	Other literature references	
			Grape pomace [6]	Grape pomace [7]
Carbon content, %	49.6	50.1	47.2	42.9
Hydrogen content, %	6.4	6.1	6.33	9.28
Nitrogen content, %	0.2	1.1	2.37	2.05
Sulphur content, %	<0.05	<0.05	0.14	0.17
Ash content, %	0.37	2.90	5.30	7.47
Higher heating value , MJ/kg	19.6	19.1	18.20	19.54
Lower heating value. MJ/kg	18.2	17.8	16.37	-

Thermogravimetric analysis has been employed to study the thermal behaviour of biofuels. The thermal analysis in air atmosphere (**Figure 1**) revealed three major stages of weight loss for grape stalks and softwood sawdust. The first stage takes place at temperatures around 373 K and is attributed to the water evaporation present in the sample, while the second stage (523-632 K) and the third stage (632-725 K) corresponds to the phases of combustion process. The first combustion phase was assigned to gasification stage accompanied by volatile combustion (oxidation) in gaseous phase (523-632 K) and the second to the heterogenic oxidation of charcoal residue (632-725 K). The maximum rates of volatile combustion and charcoal residue oxidation were achieved at ca 583 K and ca 663 K for grape stalks and at ca 593 K and ca 723 K for softwood, respectively. It was suggested that the complete thermodegradation of grape stalk proceeds faster than spruce wood and the char combustion proceeds at lower temperature. According to DTA analysis (curves are not shown) the total amount of heat released by volatile combustion of grape stalks was almost 30% less than that released by combustion of softwood, whereas the total amount of heat released by char oxidation was similar for both types of biomass sources. The incomplete combustion of volatiles at grape stalks combustion was suspected.

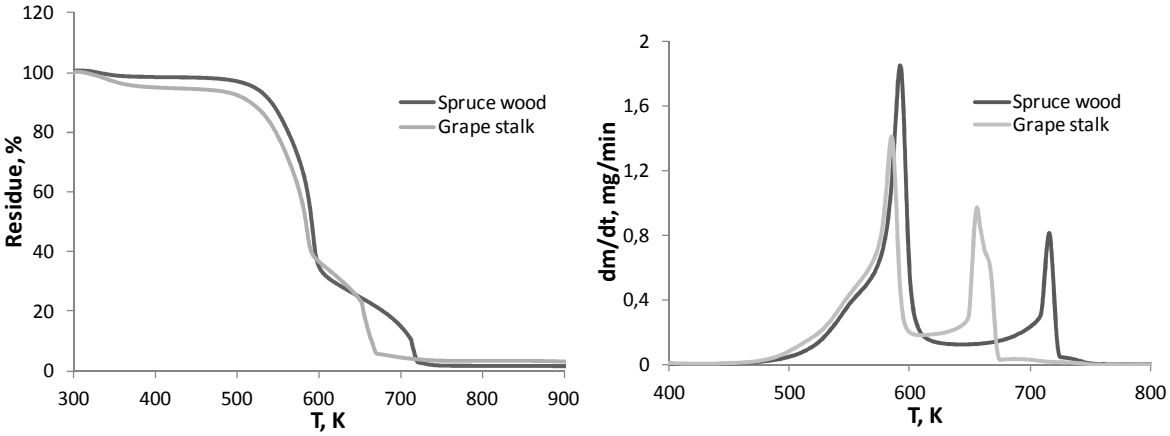

Figure 1. TGA (left) and DTG (right) curves of grape stalks and spruce wood in air.

The results of analyses on densified/pelletized biomass obtained in this study are summarized in **Table 2**. Under optimized conditions of pelletizing, the moisture content in grape stalks pellets was higher than in pellets from softwood though been in the optimal range of moisture content for biomass (between 10 and 20%). The water content is an important parameter because it has an influence on the basic parameters of fuel, such as calorific value, combustion efficiency, temperature of combustion, and also affecting the storage conditions and durability [8].

Table 2. Physical characteristics of grape stalks and spruce pellets.

Parameters	Softwood pellets	Grape stalk pellets
Water content, %	8.10	12.6
Higher heating value, MJ/kg	18.2	16.7
Lower heating value, MJ/kg	16.6	15.3
Length, mm	16.7±2.5	17.4±1.2
Diameter, mm	6.06±0.04	5.89±0.07
Bulk density, kg/m^3	660±10	670±2
Particle density, kg/m^3	1098±47	1129±47
Energy density, MWh/m^3	3.05	2.85
Durability, %	95.6	95.8
Specific energy consumption for pelletizing on DM, kWhe/kg	0.137	0.110

The grape stalks pellets have shown that its particle density, bulk densities and durability values are similar to pellets produced from softwood sawdust. The HHV of grape stalk pellets was 16.7 MJ/kg, a slightly lower value than that one obtained for spruce wood pellets (18.2 MJ/kg). The lower value can be explained by higher content of water (12.6%) and ash (near 3%). Interestingly, the specific energy consumption for pelletizing of grape stalks is approximately 25% lower when compared to that for softwood sawdust. The lower specific energy consumption for pelletizing together with the low cost of the raw material acquisition makes grape stalks one of the promising raw materials for the pelletized fuel from agricultural biomass.

IV. CONCLUSIONS

The physical properties and energetic value of pellets from grape stalks were evaluated and compared with those of pellets prepared from softwood sawdust. For the main physical properties (bulk/particle density and durability) and heating value, pellets from grape stalks were very close to pellets prepared from softwood, but required almost 25% lower energy for pelletizing. Last fact together with low cost of raw material make grape stalks as an attractive raw material for the production of granulated solid fuel However, the increased ashes content could affect the operating comfort for end users in the residential heating sector and the comparative environmental impact (e.g. emission factors) from grape stalks pellets burning need to be evaluated.

V. ACKNOWLEDGEMENT

Authors wish to thank the Portuguese Foundation for Science and Technology (FCT project PTDC/AGR-AAM/104911/2008) and the Operation Program of Competitive Factors (COMPETE, ref. FCOMP-01-0124-FEDER-008734) for the financial support of this work.

VI. REFERENCES

1. Demirbaş, A. Calculation of higher heating values of biomass fuels. *Fuel*, **1997, 76** (5): p. 431-434.
2. Mantzos, L.; P. Capros. European Energy and Transport - Scenarios on energy efficiency and renewables, E. Commission, Editor 2006, European Commission: Luxembourg.
3. Bentsen, N.; Felby, C. Biomass for energy in the European Union - a review of bioenergy resource assessments. *Biotechnology for Biofuels,* **2012**. **5**(1): p. 25.
4. Programme, U.N.E., Converting Waste Agricultural Biomass into a Resource - Compendium of Technologies. **2009**, United Nations Environmental Programme, Division of Technology, Industry and Economics International Environmental Technology Centre: Osaka/Shiga, Japan.
5. Prozil, S.O., D.V. Evtuguin, and L.P.C. Lopes, Chemical composition of grape stalks of Vitis vinifera L. from red grape pomaces. *Industrial Crops and Products*, **2012**, **35**(1): p. 178-184.
6. Celma, A.R., S. Rojasa, and F. Lopez-Rodrıguez, Waste-to-energy possibilities for industrial olive and grape by-products in Extremadura. *Biomass and Bioenergy*, **2007**, *31*, 522-534.
7. Miranda, M.T., et al., Characterization of grape pomace and pyrenean oak pellets. *Fuel Processing Technology*, **2011**. *92*, 278–283.
8. O'Dogherty, M.J. and J.A. Wheeler, Compression of straw to high densities in closed cylindrical dies. *J. Agric. Eng. Res.*, **1984**, *29*, 61-72.

CHEMICAL CHARACTERIZATION OF *Eucalyptus globulus* FROM DIFFERENT PROVENANCES BY ANALYTICAL PYROLYSIS AND CHEMOMETRICAL TOOLS

Carolina Puentes,* Carlos Cofré, KimenaRojo, Sofía Valenzuela, Regis Teixeira Mendonça

Universidad de Concepción, Facultad de CienciasForestales y Centro de Biotecnología, Concepción, Chile.
*capuentes@udec.cl

ABSTRACT

In this work, approximately200 different genotypes of *Eucalyptus globulus* with age between 6 and 8 years old from two different provenances in the Biobio Province (Chile) were sampled for chemical characterization. A set of 50 samples was characterized by acid hydrolysis (Klason method) and the other 150 samples by analytical pyrolysis (Py-GC/MS). Chemometric analyses of the data were performed using Principal Component Analysis (PCA) and Partial Least Squares regression (PLS). By this procedure, it was possible to establish predictive models for the chemical composition based on the combination of the information generated by pyrolysis and PLS. By PCA, it was also possible to segregate the samples by provenance based solely on the analytical pyrolysis data. The application of this methodology allowed the use of the technique as a tool for fast determination of chemical composition and classification of wood for breeding programs and industrial uses.

I. INTRODUCTION

Eucalyptus genus is an important raw material for the pulp and paper industry worldwide and, specifically in the case of Chile,*E. globulus* is the main species. Its main characteristics are fast growth, high quality of fiber and pulp, and easy adaptation to new agricultural land [1]. Actually, genetic improvement programs for *E. globulus* in Chile were based mainly on volumetric growth and form of tree. Remarkable efforts have been dedicated to select and develop genotypes with emphasis on increasing yield and quality of pulp. The selection and use of highly sensitive analytical techniquesto determinechemical composition and structural differences in wood coming from different genotypes is a need in clonal selection programsfor tree improvement. Due to the great number of samples generated in these studies it is necessary to develop rapid prediction methods of the most important features. In this work, analytical pyrolysis [2] was used as a tool for chemical characterization of different genotypes of *E. globulus.* The information generated was analyzed by chemometric tools [3] with the aim todetermine not only the chemical compositionbut also the classification of the samples based on the provenance site.

II. EXPERIMENTAL

Eucalyptus globulus samples (200genotypes) were obtained from commercial plantations (Figure 1) located in (A) coast and (B) middle valley of the Bio-Bio Region (southern of Chile).

Figure 1. Sampling sites of commercial plantations of *Eucalyptus globulus* in the Bio-Bio Region.

Incremental cores of each tree were obtained at diameter breast height (DBH) and were ground to 40/60 mesh and extracted with 90% acetone. For Klason analysis, 150 mg of milled wood and 1.5 mL 72% H_2SO_4 was added to a test tube and hydrolyzed in a water bath at 30°C for 1 h [4]. The acid was diluted to a final concentration of 4% and the mixture was autoclaved at 121°C for 1 h.The residue material was cooled and

filtered on Gooch No. 4. The solids were dried to constant weight at 105°C and the result reported as insoluble lignin. The concentration of the soluble lignin was determined by measuring absorbance at 205 nm and using the value of 110 L / g.cm and the absorptivity of the soluble lignin [5].The concentration of monomeric sugars in the soluble fraction was determined by HPLC using a BioRad HPX-87H column at 45°C, with 0.005 mol / L of sulfuric acid at 0.6 mL/min.Analytical pyrolysis was performed using a CDS AS-2500 autosampler for 36 samples (CDS Analytical). Approximately 100 µg was weighed into a quartz tube of 2 mm x 40 mm. Pyrolysis was carried out at 550°C for 10 s.The pyrolysis chamber was maintained at 250°C and purged with helium gas in order to transfer the products of pyrolysis to the column of the gas chromatographer (Agilent 6890). The column was of fused silica (DB-1701, 60 m x 0.25 mm x 0.25 mm thickness) coupled to an Agilent 5973N mass detector. The chromatograph was programmed from 50°C (4 min) to 280°C at a rate of 4°C/min. The final temperature was maintained for 15 minutes. The injector temperature was 250°C while the GC/MS interface was maintained at 280°C.The generated fragments are separated by gas chromatography and the products identified by mass spectrometry. In the pyrograms obtained from the different samples it was possible to identify compounds associated to the lignin and carbohydrates degradation [6].The Unscrambler 9.7 software (CAMO) was used to perform chemometrics and multivariate analysis of each chemical property measured and to classify the samples by provenance.

III. RESULTS AND DISCUSSION

A typical pyrogram obtained for the eucalyptus samples analyzed is shown in Figure 2. Based on the chemical characterization by the Klason method and with the data of the pyrograms, multivariate regression analysis were performed and allowed the development of prediction models for the amount of glucose, xylose and lignin for the samples of the difference provenances, as shown in Figure 3 for site A and Figure 4 for site B.

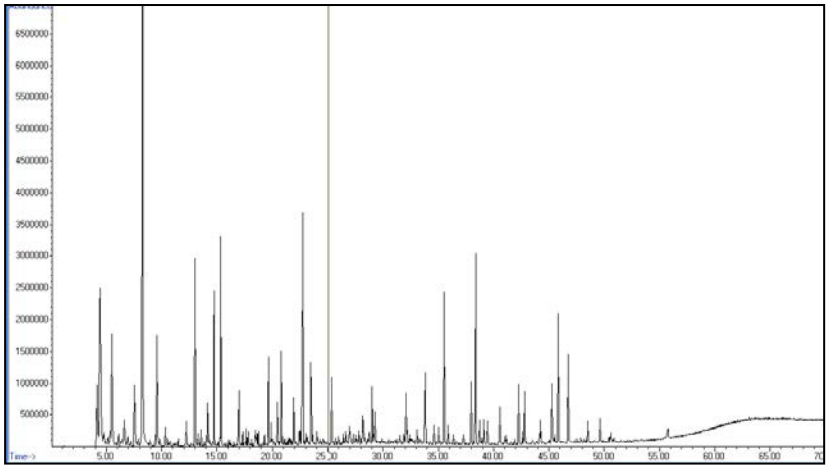

Figure 2. Typical pyrogram obtained for the *Eucalyptus globulus* genotypes.

Prediction models with high correlations for the three chemical properties were obtained by the PLS analysis of the pyrolytic data. For site A, correlations for calibration and validation models were, respectively, 0.92 and 0.76 (glucose),0.89 and 0.56 (xylose),0.96 and 0.62 (lignin). For site B, correlations for calibration and validation models were, respectively, 0.87 and 0.63 (glucose), 0.84 and 0.70 (xylose), 0.82 and 0.72 (lignin).

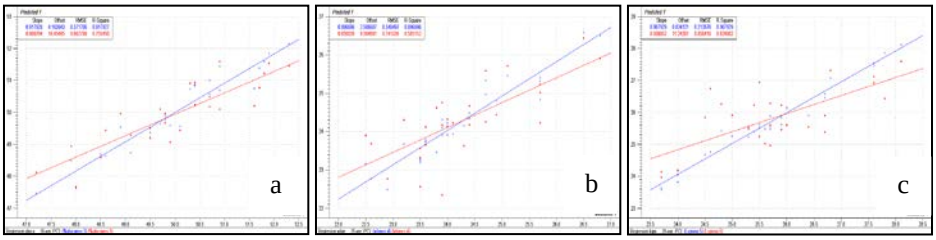

Figure 3. Multivariate calibration (PLS) for (a) glucose, (b) xylose and (c) lignin for samples of site A.

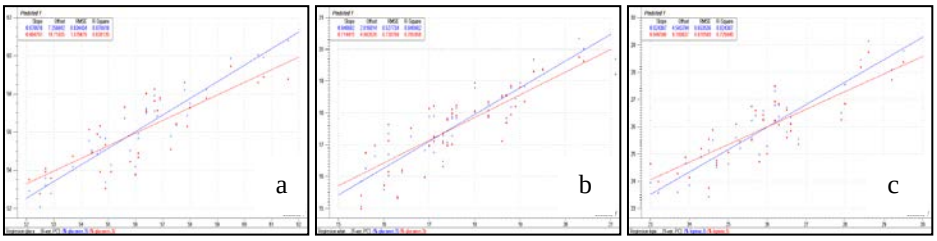

Figure 4. Multivariate calibration (PLS) for (a) glucose, (b) xylose and (c) lignin for samples of site b.

The prediction models based on analytical pyrolysis were applied for all the samples and the range of chemical characteristics determined is shown Table 1. A wide variation in the main chemical traits is observed, showing that is possible to use this information for further genetic improvement of the species.

Table 1. Range of values for the chemical characteristics for *Eucalyptus globulus* samples from sites A and B.

	A	B
Glucose(%)	47- 52	47-60
Xylose (%)	21-27	14-22
Lignin (%)	23-28	21-35

All the chemical data obtained were also analyzed by PCA, and it was possible to obtained a clearly separation of the sample from sites A and B based solely in the chemical information from the analytical pyrolysis and multivariate analysis using 2 principal components that explained more than 90% of the variance (Figure 5).

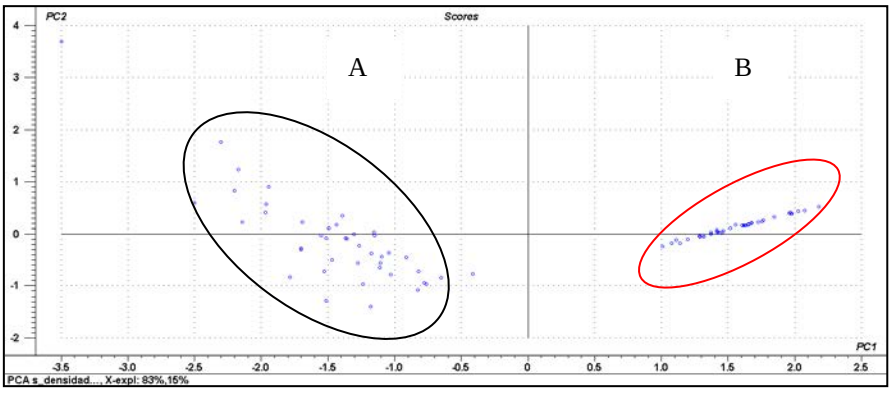

Figure 5. Principal component analysis (PCA) of *Eucalyptus globulus* samples from sites A and B using data obtained by analytical pyrolysis and PLS.

IV. CONCLUSIONS

- Py-GC/MS associated with chemometric tools is a method able to be used for predicting chemical properties of wood.
- High correlationsfor calibration and validation were found for glucose, xylose and lignin content in *Eucalyptus globulus* after multivariate regression of analytical pyrolysis data.
- Py-GC/MS and multivariate methods were useful for classification of wood samples based on site origin and can a tool for ranking and selection genotypes for improvement and industrial use.

V. ACKNOWLEDGEMENTS

FONDEF D10i-1221, CONICYT 21120106.

VI. REFERENCES

[1] Teulieres, C.; Marque, C. *Biotechnology in agriculture and forestry*. Transgenic Crops V.Springer Berlin Heidelberg: Berlin, **2007**, Vol. 60, 387-406.
[2] del Rio, J.; Gutiérrez, A.; Hernando, M.; Landin, P.; Romero, J.; Martinez, A. *J. Anal. Appl. Pyrolysis*. **2005**, 74, 110-115.
[3] Malkavaara, P.; Alén, R.; Kolehmainen, E. *J. Chem. Inf. Comput. Sci.* **2000**, 40, 438-441.
[4] Mendonça RT; Jara J; González V; Elissetche J, Freer J. Microbiology and Biotechnology, **2008**, 35:1323-1330. Evaluation of the white-rot fungi *Ganodermaaustrale* and *Ceriporipsissubvermispora* in biotechnological applications. Journal of Industrial.
[5] Dence, C. The determination of lignin.In *Methods in Lignin Chemistry*. Lin, S., Dence, C.W., Eds.; Springer – Verlag: Berlin, **1992**, 38-39.
[6] Ohra, T; Gomez F; Colodette J; Tamminem T. Structural differences in lignin between Eucalyptus clones determined by analytical pyrolysis-gas chromatography/mass spectrometry. 5thInternational Colloquium on Eucalyptus Pulp, May 9-12, **2011**. Porto Seguro, Bahia, Brazil.

EVALUATING CHANGES ON CELLULOSIC BIOBLEACHED FIBERS BY MEANS OF THERMOGRAVIMETRIC ANALYSIS

Elisabet Quintana[1], Agustín A. Barneto[2], Cristina Valls[1], Teresa Vidal[1], José Ariza[2] and M. Blanca Roncero[1]*

[1]*CELBIOTECH_Paper Engineering Research Group. Universitat Politècnica de Catalunya-BarcelonaTech. Colom 11, E-08222 Terrassa, Spain.*
[2]*Chemical Engineering, Physical Chemistry and Organic Chemistry Department, University of Huelva (ceiA3), Spain*
**E-mail: roncero@etp.upc.edu, Phone n: (+34) 937398210*

ABSTRACT

The effects on fibre surface produced by the laccase-mediator system on softwood sulphite fibres were analysed in terms of surface crystallinity using thermogravimetric analysis. The starting pulp presented low content of lignin and hemicelluloses and these characteristics were clearly reflected on TGA graphs, indicating a clean and crystalline surface. Unbleached sulphite pulps were subjected to a biobleaching process using the well-know laccase-mediator system (LMS). From all studied mediators, violuric acid, VA, was the most efficient biobleaching compound. By contrast, HBT also provided a good delignification but affected negatively the fibre "surface". The natural mediators, SA and PCA were not grafted on sulphite pulp unlike what have been observed with other raw materials. These observations led to the development of an extended biobleaching sequence named L_{VA}QPo, using a laccase from *Trametes villosa* in combination with VA as a mediator. The characterization of treated pulp in terms of dissolving pulp characteristics showed that this enzymatic sequence could satisfy the market-like requirements. In addition, TGA results showed that the introduction of an enzymatic stage let to reduce the adverse effect caused by a hydrogen peroxide treatment in terms of pulp crystallinity.

I. INTRODUCTION

Recently, several studies have shown that enzymatic and chemical bleaching treatments modify the structure and ultrastructure of fibres surfaces. These investigations suggested that laccase-mediator system is able to interact on fibre surface in several ways: can produce deposits on fibre surface as a result of mediator condensation, can promote the grafting of the mediator on lignin surface or can lead to oxidative degradation of lignin. The adsorption of laccase on fibre surface has been proved by Saarinen et al. [1] using a quartz crystal microbalance, and by Barneto et al. [2] using XPS (X-ray photoelectron spectroscopy) and thermogravimetry analysis (TGA). XPS technique shows an increasing of nitrogen in fibre surface after enzyme treatment, and TGA provides information on the thermal degradation behaviour of surface and interior of cellulose, showing an increase of cellulose that degrades at low temperature.

In order to understand the effect of laccase adsorption on the thermal degradation of pulps, it is necessary to take into consideration that fibre contains amorphous and crystalline celluloses. In higher plants, cellulose is present as long bundles of cellulose polymer chains called microfibrils. In each one, there are crystalline and amorphous zones. Within crystalline cellulose region (so-called cellulose crystallite), cellulose chains form planes in which equatorial hydroxyl groups of pyranose rings are hydrogen bonded. The amorphous cellulose, which consists of non-ordered cellulose chains, is mainly located between cellulose crystallites in microfibrils. Studying the thermal degradation of bleached pulp, two phases are clearly observed. First, amorphous cellulose is degraded (close to 300 ºC) and subsequently crystalline cellulose, yielding fast mass loss at higher temperature (close to 350 ºC). Differences or changes of surface and interior cellulose are reflected in the thermal degradation profiles. Therefore, TGA is an interesting technique to monitor changes that cellulose surface fibres underwent during pulping and biobleaching processes [3]. In the present work, thermogravimetric analysis was used to evaluate the alterations of surface fibre during an enzymatic bleaching treatment of sulphite pulps [4].

Initially, the potential of different compounds, namely 1-hydroxybenzotriazole (HBT), violuric acid (VA), syringaldehyde (SA) and *p*-coumaric acid (PCA) in combination with a laccase from *Trametes villosa* were extensively studied. Then, an extended biobleaching sequence, termed L_{VA}QPo, was developed in order to meet dissolving pulp characteristics by means of enzymatic treatments.

II. EXPERIMENTAL

Raw material

Unbleached sulphite cellulose obtained from a mixture of 60% spruce (*Picea abis*) and 40% pine (*Pinus sylvestris*) and cooked at Domsjö mill (Sweden) was used as a raw material. The carbohydrate composition of the initial pulp, determined by high-performance liquid chromatography (HPLC), were as follows: 90.2 ± 0.38% glucan, 4.3 ± 0.1% mannan, 2.1 ± 0.06% xylan, 0.8 ± 0.0% glucuronic acid, 0.04 ± 0.01% acetyl groups and 1.6 ± 0.1% klason lignin.

Biobleaching treatments

Unbleached sulphite pulps were subjected to an enzymatic stage (L) followed by a chemical bleaching stage (P) resulting in a biobleaching sequence named LP.
In the enzymatic stage (L), a commercial laccase from *Trametes villosa* was used in combination with the natural mediators, syringaldehyde (SA) and *p*-coumaric acid (pCA), and the synthetic mediators, 1-hydroxybenzotriazole (HBT) and violuric acid (VA). All treatments, at 5% pulp consistency, were conducted in an pressurized oxygen reactor (0.6 MPa), at stirring rate of 30 rpm, using 50mM sodium tartrate buffer at pH 4, a laccase dose of 20U/g odp (oven dried pulp) and a dose of 1.5% odp of each mediator, at 50ºC for 4h. A few drops of the surfactant Tween 20 (0.05% w/v) were also added. The sequence was completed with a chemical bleaching stage involving alkaline peroxide bleaching procedure. Fibre samples, at 5% consistency, were treated with 2% odp H_2O_2, 1.5% odp NaOH, 1% odp DTPA and 0.2% odp $MgSO_4$ in a Datacolor Easydye AHIBA oscillating individual reactor at 90ºC for 2h [4]. After each stage, residual liquors were collected for subsequent analysis, and pulp samples filtered and extensively washed for further processing. A conventional hydrogen peroxide bleaching treatment, i.e. a P stage applied directly to the starting pulp, was also performed in order to compare the bleaching efficiency of the laccase–mediator system in combination with a hydrogen peroxide bleaching stage. Complementary, a laccase control treatment named KL, with no presence of mediator. Finally, an extended biobleaching sequence, LVAQPo (being Q a chelating stage and P a hydrogen peroxide stage reinforced with pressurized oxygen) was intensely studied.

Characterization: surface and bleaching properties.

The effects of the respective bleaching treatments produced on fibre surface were analysed by thermogravimetric analysis (TGA). Additionally, the crystallinity of the different pulps was determined by X-Ray Diffraction (XRD) measurements. The experimental XRD signal was fitted by means of gaussian distributions, which include amorphous background. Therefore, the crystallinity values were calculated as the ratio between the area of the crystalline cellulose peaks and the total area, which includes the amorphous background contribution.
In terms of bleaching properties, the pulp changes resulted from the bleaching treatments were evaluated via kappa number, cellulose integrity (viscosity), ISO brightness and colour coordinates (CIE *L*a*b**), and alpha cellulose, according to ISO 302:2004, ISO 5351:2004, ISO 2470:2009 and TAPPI method T-203 cm-99.

III. RESULTS AND DISCUSSION

In the present work, natural and synthetic mediators in combination with a *Trametes villosa* laccase were applied to softwood sulphite fibres in order to assess their potential for meeting dissolving pulp characteristics.

In terms of cellulose integrity, the enzymatic treatment caused no significant change in viscosity, which was only 6% lower after the L stage, with respect to initial pulp (**Table 1**). This finding reflects that the incorporation of LMS treatment boosted biodelignification (i.e. diminution of the lignin content) without degrading carbohydrate chains. However, after a hydrogen peroxide (P) stage, the degradation of cellulose was more pronounced, which in turn resulted in a greatest reduction of lignin content and a marked increase of ISO brightness (data not shown). As known from the literature, viscosity is an important parameter for dissolving pulp applications. Importantly, during the viscose process, final quality rayon requires viscosity values in the 200–300 mL/g range [5]. Relevantly, all treated pulps, at the end of the bleaching sequence (i.e. L stage followed by a P stage) presented higher values of viscosity (data not shown). In terms of ISO brightness, a brightness loss was observed after the laccase treatment (L) for all tested compounds. These observations may indicate the coexistence of lignin removal with condensation and oxidation of compounds from the mediator effluents or formation of chromophores groups in the pulp. Nevertheless, this negative effect was overcome due to a hydrogen peroxide stage, but with the important benefit that higher values of brightness than a conventional hydrogen peroxide stage were achieved. Altogether, VA exhibited the best results in all studied properties and was suggested as a potential industrial application.

Table 1. Viscosity and ISO brightness results obtained after an enzymatic stage (L) for each mediator. Initial value is also included.

	Viscosity (mL/g)	**ISO brightness (%)**

Initial	511 ± 19	61.25 ± 1.0
	L stage	
KL	492 ± 6	60.85 ± 0.2
PCA	494 ± 18	51.20 ± 0.5
SA	490 ± 20	52.10 ± 0.2
HBT	480 ± 2	55.60 ± 0.3
VA	509 ± 8	56.70 ± 0.4

The respective characteristics of initial unbleached sulphite pulp were clearly reflected in thermogravimetric curves. As can be seen from **Figure 1**, initial pulp presented a sharp peak around 300-350ºC indicating high content of crystalline cellulose. Furthermore, the absence of a shoulder at low temperatures (~250ºC) pointed out the low content of hemicelluloses, which is consistent with carbohydrate composition of pulp. According to our results, the action of tartrate buffer on softwood sulphite pulps is proposed as a cleaning effect on fibre surface (i.e. peaks are shifted to higher temperatures) rather than being adsorbed on pulp surface, as other authors described elsewhere [3, 6]. On the contrary, the respective enzymatic treatments shifted all the thermogravimetric curves to lower temperatures and as a result the amount of crystalline cellulose was reduced. In particular, the damages on pulp surface provided by laccase-HBT treatment were significantly greater than pulps treated with the other mediators. According to Barneto et al. [2], the laccase-HBT system partially oxidizes the external cellulosic layer, changing hydroxyl groups to carbonyl groups, disordering crystalline surface and increasing the paracrystalline cellulose content (i.e reduction of peak height).

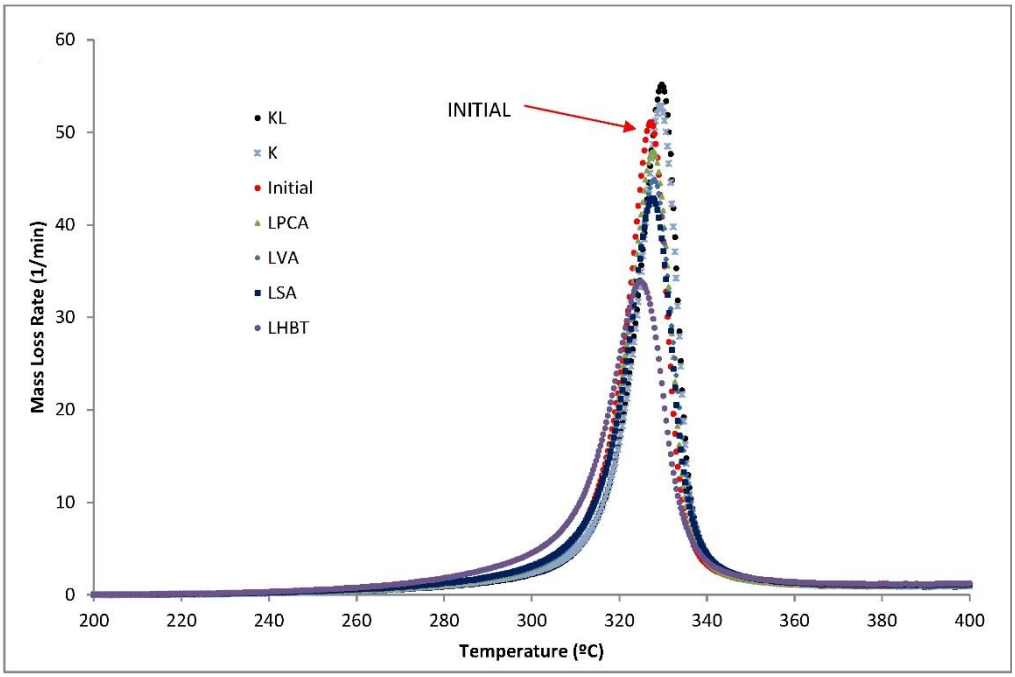

Figure 1. Changes in the thermal degradation pathway for the initial pulp during the biobleaching process at 10ºC/min in an air atmosphere. Mass loss rate was normalised to the initial mass of sample

The effect of a full-biobleaching sequence (L_{VA}QPo) on fibre surface was also studied using thermogravimetric analysis. In the course of biobleaching process, pulp underwent surface changes (**Figure 2**), appearing a drastically reduction of cellulose that degrades at high temperature and an increase of cellulose that degrades at low temperature when a hydrogen peroxide treatment is introduced. Overall, the L_{VA}QPo sequence offered biobleached fibres with dissolving pulp characteristics and with better surface features than commercial dissolving pulps.

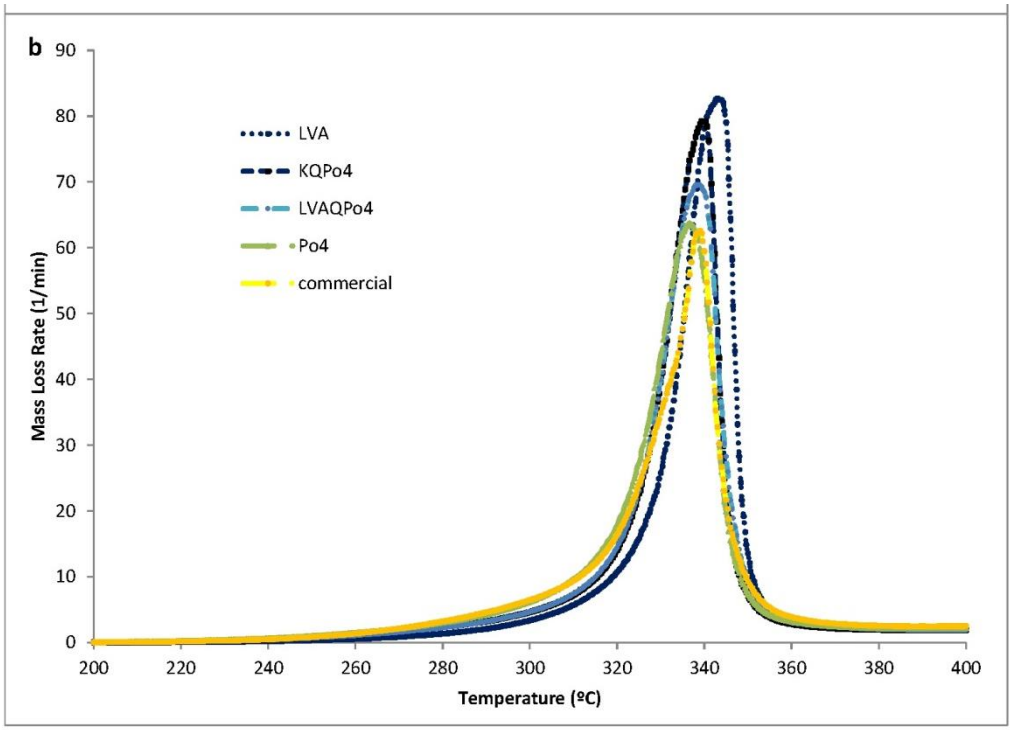

Figure 2. DTG curves for pulps in different steps of biobleaching process. Heating rate 20 ºC/min. Environment: air. L_{VA} (enzymatic treatment), L_{VA}QPo (enzymatic stage and pressurized hydrogen peroxide stage), KQPo (control treatment), Po (conventional treatment) and commercial bleached dissolving pulp.

IV. CONCLUSIONS

Natural and synthetic mediators used in combination with *Trametes villosa* laccase were evaluated in terms of bleaching and fibre surface properties. In contrast to other pulps, the natural mediators were not grafted on the sulphite fibres and did not produce a delignification effect. These observations were also confirmed by TGA analysis since no changes on fibre surface were detected. Synthetic mediators, SA and VA, contributed to delignification being the latter the best. Moreover, according to TGA results, VA exhibited better fibre surface characteristics than HBT. Complementary, a completed biobleaching sequence was conducted and compared with a simple hydrogen-peroxide treatment in terms of dissolving pulp characteristics, showing that this enzymatic sequence could satisfy the market-like requirements.

V. ACKNOWLEDGEMENT

This work was supported by the Spanish MICINN BIOSURFACEL-CTQ2012-34109 and BIOFIBRECELL-CTQ2010-20238-C03-01 projects. The authors are grateful to the consolidated group with the Universitat de Barcelona (UB) AGAUR 2009SGR 00327.

VI. REFERENCES

[1] Saarinen, T.; Orelma, H.; Grönqvist, S.; Andberg, M.; Holappa, S.; Laine, J. Adsorption of different laccases on cellulose and lignin surfaces. BioResources. **2009**, 4, 94–110.

[2] Barneto, A.G.; Valls, C.; Ariza, J.; Roncero, M.B. Influence of enzyme and chemical adsorption on the thermal degradation path for eucalyptus pulp. Thermochim. Acta. **2013**, 551, 62–69.

[3] Barneto, A.G.; Valls, C.; Ariza, J.; Roncero, M.B. Thermogravimetry study of xylanase- and laccase/mediator-treated eucalyptus pulp fibres. Bioresour. Technol. **2011a**, 102, 9033–9.

[4] Quintana, E.; Valls, C.; Vidal, T.; Roncero, M. B. An enzyme-catalysed bleaching treatment to meet dissolving pulp characteristics for cellulose derivatives applications. Bioresour. Technol. **2013**, 148, 1–8.

[5] Kvarnlöf N.; Germgård U.; Jönsson L.J.; Söderlund C. Enzymatic treatment to increase the reactivity of a dissolving pulp for viscose preparation. Appita J. **2006**, 59:242-246.

[6] Andreu, G.; Barneto, A.G.; Vidal, T. A new biobleaching sequence for kenaf pulp: Influence of the chemical nature of the mediator and thermogravimetric analysis of the pulp. Bioresour. Technol. **2013**, 130, 431–438.

EXPLORING BIOBLEACHING POSSIBILITIES OF DISSOLVING PULPS BY MEANS OF ENZYMATIC TREATMENTS

Elisabet Quintana, Cristina Valls, Teresa Vidal and M. Blanca Roncero*

CELBIOTECH_Paper Engineering Research Group. Universitat Politècnica de Catalunya-BarcelonaTech. Colom 11, E-08222 Terrassa, Spain.
**E-mail: roncero@etp.upc.edu, Phone n: (+34) 937398210*

ABSTRACT

Unbleached sulphite cellulose was subjected to an LQPo biobleaching sequence with the intention to elucidate the potential of LMS as an alternative to conventional bleaching processes. The enzymatic stage (L) was performed with the presence of *Trametes villosa* laccase and violuric acid. This enzymatic stage was followed by a chelating stage (Q) and then by a hydrogen peroxide stage reinforced with pressurized oxygen (Po). The outstanding results obtained with laccase-violuric acid system fulfil the characteristics of commercial dissolving-grade pulp (high reactivity, high ISO brightness, preserved cellulose integrity and low content of hemicellulose). Additionally, the enzymatic treatment saved 2h of reaction time and about 70% of hydrogen peroxide consumption, relative to a conventional hydrogen peroxide sequence (Po).

I. INTRODUCTION

According to FAO (2012) [1], demand for dissolving pulp has grown rapidly in latest years and the prospective consumer markets indicate that this trend will continue in the next decades. Importantly, these pulps have traditionally been used in the production of viscose filament and viscose staple fibres. But, the recent interest in this high-purity bleached pulp can be attributed to the new end-uses that have provided, such as cellulose based casings and sponges, thickeners in food and paints, capsules for medicine, among others. In addition, agricultural restrictions on cotton cultivation and the fact that dissolving pulp can be an environmentally friendly alternative to synthetic fibers have also contributed to this market upturn.
Dissolving pulps are characterized by a high content of cellulose, low amount of hemicellulose (<10%) and traces of residual lignin, extractives and minerals. These particular features can be obtained by a sulphite or a pre-hydrolysis kraft cooking process. However, these two long-established procedures present some disadvantages in terms of economic cost, chemical consumption and production rate [2]. Hence, the increasing interest to convert paper-grade pulps into dissolving-grade pulps. There are new alternatives that have been studied in order to carry out this modification, in particular, biotechnological procedures using cellulases and xylanases [3,4,5]

Based on the above observations, the aim of this work was to explore new bleaching possibilities of unbleached sulphite cellulose using the well-known Laccase-Mediator System. This biobleaching sequence was proposed as a potential alternative to traditional bleaching process.

II. EXPERIMENTAL

Raw material

Unbleached sulphite cellulose obtained from a mixture of 60% spruce (*Picea abis*) and 40% pine (*Pinus sylvestris*) and cooked at Domsjö mill (Sweden) was used as a raw material. The main characteristics of the starting pulp were as follows: 5.3 ± 0.12 kappa number, 58.65 ± 0.6% ISO brightness, 552 ± 8mL/g viscosity and no presence of hexenuronic acids (HexA). Carbohydrate contents, as determined by high-performance liquid chromatography (HPLC), were as follows: 90.2 ± 0.38% glucan, 4.3 ± 0.1% mannan, 2.1 ± 0.06% xylan, 0.8 ± 0.0% glucuronic acid, 0.04 ± 0.01% acetyl groups and 1.6 ± 0.1% klason lignin.

Biobleaching sequence: LQPo

A biobleaching sequence named LQPo was performed. In the first stage, a laccase from *Trametes villosa* in combination with violuric acid (synthetic mediator) were used. The enzymatic treatment, at 5% pulp consistency, was conducted in an oxygen pressurized reactor (0.6 MPa), at stirring rate of 30 rpm, using 50mM sodium tartrate buffer at pH 4, a laccase dose of 20U/g odp (oven dried pulp) and 1.5% odp of mediator at 50ºC for 4h. Then, treated pulp was washed with deionized water and was followed by a Q stage involving the use of chelating agents to reduce the contents in metal ions (Fe^{2+}, Cu^{2+}, Mn^{2+}) capable of degrading the bleaching agents and cellulose during the subsequent peroxide bleaching treatment. The biobleaching sequence was

completed with a chemical bleaching stage involving alkaline hydrogen peroxide bleaching procedure (Po). The treatment was carried out at 5% consistency in oxygen pressurized (0.6 MPa) reactor, using a stirring rate of 30 rpm under the following conditions: 1.5% odp NaOH, 0.3% odp DTPA and 0.2% odp $MgSO_4$ at 90ºC for 4h. This stage was performed in three consecutive steps (Po_1 = 1h, Po_2 = 1h, Po_4 = 2h) each involving the addition of 10% odp H_2O_2 and no interstep washing. The mentioned biobleaching sequence was compared with a conventional hydrogen peroxide treatment (Po) where the enzymatic stage was omitted, in order to elucidate the effect of an enzymatic stage (L) for a prospective industrial application. A control sequence with no presence of laccase neither mediator was also performed (KQPo) as a reference[6].

Pulp characterization

On one hand, treated pulps were characterized via bleaching properties: kappa number, viscosity, ISO brightness, brightness stability (aging treatments), hydrogen peroxide consumption and effluent properties (colour, toxicity and residual laccase activity). On the other hand, pulps were evaluated in terms of dissolving pulp characteristics: carbohydrate composition, cellulose reactivity, alpha cellulose and alkali solubility.

III. RESULTS AND DISCUSSION

Table 1 shows the values of kappa number and ISO brightness for the respective bleaching treatments. Concerning brightness results, despite the drop in brightness observed after the enzymatic stage (L), the laccase–VA system was more efficient in raising pulp brightness at the end of the whole sequence than was the control sequence (KQPo) or even the conventional bleaching sequence (Po). In fact, the control and conventional sequence required three additions of H_2O_2 and 4h of reaction while the enzymatic sequence needed only one addition of H_2O_2 and 1h of reaction to reach similar values. In terms of lignin content, the laccase–VA system efficiently reduced kappa number from 5.3 to 2.3 after the enzymatic stage. The kappa number reduction can be directly ascribed to the removal of residual lignin, since the starting pulp contained low amount of xylan (2%), so the presence of no hexenuronic acids did not contribute to these results. The enzymatic sequence (LQPo) caused 56% delignification after the L stage; however, the buffering stage of the control sequence (KQPo) also afforded 13% delignification with respect to the initial pulp. Therefore, the actual delignification contributed by the laccase–mediator stage in the LQPo sequence was about 43%. The delignifying effect of Po_1 step with respect to the previous stage in the LQPo sequence was 79%. The marked decrease obtained after Po_1 step was directly due to the laccase–VA system since the control sequence (KQPo) only provided 56% delignification after $KQPo_1$. The conventional hydrogen peroxide process (Po) caused 61% delignification at Po_1 relative to the initial pulp, but failed to reach the same brightness level as the $LQPo_1$ sequence. This result further confirms the boosting effect of L stage and the alkaline pH used in the Po stage facilitated the dissolution of degraded lignin.

Table 1. Kappa Numbre values (± confidence interval) and ISO Brightness values (± confidence interval) for LQPo (enzymatic sequence), KQPo (control sequence) and Po (conventional bleaching sequence).

Initial	KN : 5.3 ± 0.12		ISO Br (%): 58.75 ± 0.6			
	LQPo		**KQPo**		**Po**	
	KN	ISO Br (%)	KN	ISO Br (%)	KN	ISO Br (%)
L/K	2.3 ± 0.06	55.45 ± 0.4	4.7 ± 0.18	55.0 ± 1.0	-	-
Q	2.5 ± 0.07	56.85 ± 1.0	4.2 ± 0.19	57.85 ± 0.5	-	-
Po_1	0.5 ± 0.33	84.20 ± 0.2	1.9 ± 0.24	77.95 ± 0.1	2.1 ± 0.35	76.10 ± 0.3
Po_2	0.6 ± 0.37	87.50 ± 0.1	1.1 ± 0.00	83.06 ± 0.1	1.9 ± 0.04	81.80 ± 0.3
Po_4	0.2 ± 0.00	89.15 ± 0.1	1.0 ± 0.21	84.40 ± 0.2	1.5 ± 0.00	84.0 ± 0.05

Figure 1 depicts the evolution of ISO Brightness values when treated pulps are subjected to a moist heat aging treatment. The particular characteristics of starting pulp (i.e. no presence of hexenuronic acids and low content of lignin) showed high brightness stability when were thermally aged [7]. Concerning this observation, the control treatment (K) only suffered 0.3% brightness loss but, the L_{VA} treatment underwent a 10.1% brightness loss. These results suggested that the enzymatic treatment generated amounts of chromophores or oxidizable structures, which in turn resulted in increased reversion of optical properties. However, the final brightness loss detected for $L_{VA}QPo_4$ and $KQPo_4$ after an aging treatment, was very similar in both cases (13.0% and 12.2%, respectively), suggesting that the chromophore groups created during the laccase treatment were removed or modified along the hydrogen peroxide stage (Po). Importantly, the enzymatic biobleaching sequence achieved the highest brightness value (89% ISO) and without detriment to brightness stability.

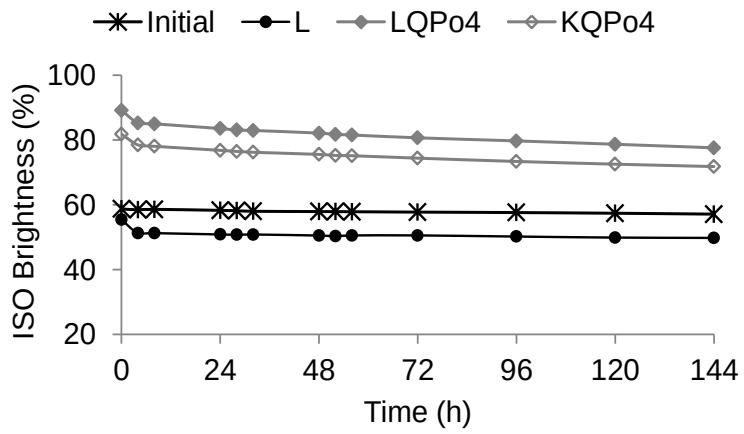

Figure 1. Effect of accelerated ageing by moist heat treatment on ISO brightness for initial pulp, L (enzymatic treatment), $KQPo_4$ (control sequence) and $L_{VA}QPo_4$ (enzymatic sequence).

As can be seen from **Figure 2**, the highest viscosity loss was detected by the enzymatic sequence (LQPo) after the Po stage; however this sequence gained the highest brightness value (~90%). Moldes et al. [8] reported that in the case of laccase treatment in combination with HBT or VA, during the P stage, the hydrogen peroxide is consumed mainly to oxidize chromophoric groups and as a result a brightness improvement is detected. Conventional bleaching sequence used the first addition of hydrogen peroxide to remove lignin and a decrease on viscosity was not produced. Viscosity is an important parameter for dissolving pulp applications. During a viscose process it is necessary to decrease viscosity around 200–300 mL/g with a pre-aging stage because too high viscosity affects the cellulose processability. The enzymatic sequence did not provide excellent levels of viscosity (343 ± 13 mL/g) and limits its applications for certain final applications [9, 10, 11]. In terms of reacted cellulose, no important differences between bleaching treatments were observed. However, the obtained values were similar to reported by other authors elsewhere [3, 4]. According to Gehmayr and Sixta [5], the reactivity measured by Fock test describes the amount of pulp which was dissolved in the viscose-like solution. Consequently, the results are strongly influenced by the pulp viscosity and the amount of alkali soluble hemicellulose.

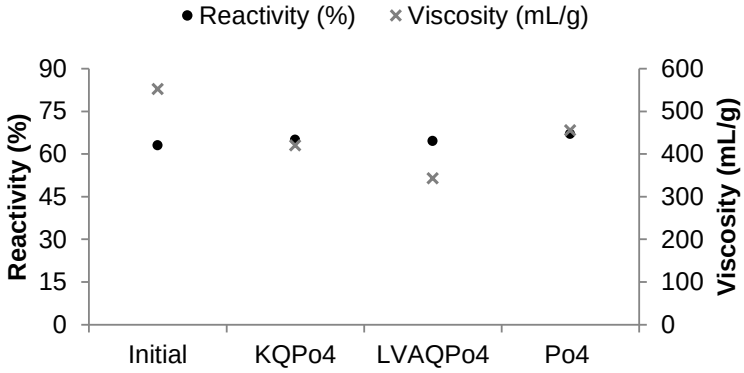

Figure 2. Viscosity and reactivity values for the different bleaching treatments. Initial (unbleached sulphite pulp), $KQPo_4$ (control sequence), $L_{VA}QPo_4$ (enzymatic sequence) and Po_4 (conventional bleaching treatment).

Taking the above results together, it is therefore possible to conclude that the introduction of an enzymatic stage during the bleaching process, led to obtain biobleached dissolving pulps with commercial specifications.

IV. CONCLUSIONS

The main objective of this study was to obtain high-quality cellulose meeting industrial specifications of dissolving grade-pulp by means of an enzymatic treatment during the bleaching process.

The introduction of an enzymatic stage (L) in a bleaching sequence provided important benefits that were reflected during a Po stage. Specifically, L stage reduces 2h of reaction time and let to save about 70% of H_2O_2 dose, for a target brightness value of 84% ISO and with respect to a conventional hydrogen peroxide treatment (Po), where the enzymatic stage (L) was omitted. In addition, under this brightness value, the enzymatic sequence did not cause significant cellulose degradation and reached a final viscosity value (413 ± 0.85 mL/g) similar to conventional and control treatments. The particular characteristics of the starting pulp provided high brightness stability when a moist heat treatment was applied. Relevantly, the incorporation of an enzymatic stage did not negatively affect brightness stability. Although the proposed biobleaching sequence needs to be optimized in terms of H_2O_2 charge, the use of LMS in combination with unbleached sulphite cellulose offered a good alternative for traditional bleaching processes since the properties of the final treated pulps fulfil the requirements for dissolving pulps.

V. ACKNOWLEDGEMENT

This work was supported by the Spanish MICINN BIOFIBRECELL-CTQ2010-20238-C03-01 and BIOSURFACEL CTQ2012-34109. The authors are grateful to the consolidated group with the Universitat de Barcelona (UB) AGAUR 2009SGR 00327. The authors would like to knowledge DÖMSJO (Sweden) for providing the starting pulp and Novozymes (Denmark) for kindly supplying the laccase.

VI. REFERENCES

[1] FAO. Food and Agriculture Organitzation of the United Nations. In: http://faostat.fao.org. Accessed September **2012.**

[2] Hillman, D. Do Dissolving Pulps Really Dissolve?. Paper Asia. **2006**, 12-18

[3] Ibarra, D.; Köpcke, V.; Ek, M. Exploring enzymatic treatments for the production of dissolving grade pulp from different wood and non-wood paper grade pulps. Holzforschung. **2009**, Vol. 63, 721-730.

[4] Köpcke V.; Ibarra D.; Ek M. Increasing accessibility and reactivity of paper grade pulp by enzymatic treatment for use as dissolving pulp. Nordic Pulp Paper Research Journal, **2008**, 23:363-368.

[5] Gehmayr, V.; Sixta, H. Pulp properties and their influence on enzymatic degradability. Biomacromolecules. **2012**, 13, 645–651.

[6] Quintana, E.; Valls, C.; Vidal, T.; Roncero, M.B. An enzyme-catalysed bleaching treatment to meet dissolving pulp characteristics for cellulose derivatives applications. Bioresour. Technol. **2013**, 148, 1–8.

[7] Cadena, E.M.; Vidal, T.; Torres, A.L. Influence of the hexenuronic acid content on refining and ageing in eucalyptus TCF pulp. Bioresour. Technol. **2010**, 101, 3554–3560.

[8] Moldes, D.; Vidal, T. Laccase-HBT bleaching of eucalyptus kraft pulp: Influence of the operating conditions. Bioresour Technol. **2008**, 99:8565-8570.

[9] Henriksson G.; Christiernin M.; Agnemo R. Monocomponent endoglucanase treatment increases the reactivity of softwood sulphite dissolving pulp. Journal Industrial Microbiol Biotechnology. **2005**, 32:211-214.

[10] Kvarnlöf N.; Germgård U.; Jönsson L.J.; Söderlund C. Enzymatic treatment to increase the reactivity of a dissolving pulp for viscose preparation, Appita J. **2006,** 59:242-246.

[11] Batalha L.A.R.; Colodette J.L.; Gomide J.L.; Barbosa L.C.; Maltha C.R.; Gomes F.J.B. Dissolving pulp production from bamboo. BioResources. **2011**, 7:0640-0651.

PHENOLIC COMPOSITION AND ANTIOXIDANT ACTIVITY OF *CYNARA CARDUNCULUS* L. VAR. *ALTILIS* (DC) EXTRACTS

Patrícia A. B. Ramos*[1,2], Sónia A. O. Santos[1], Ângela R. Guerra[2], Olinda Guerreiro[2], Carmen S. R. Freire[1], Maria F. Duarte[2], Armando J. D. Silvestre[1]

*[1]CICECO and Department of Chemistry, University of Aveiro, 3810-193 Aveiro, Portugal; [2]Centro de Biotecnologia Agrícola e Agro-Alimentar do Alentejo (CEBAL) / Instituto Politécnico de Beja (IPBeja), 7801-908 Beja, Portugal (*patriciaaramos@ua.pt)*

ABSTRACT

The phenolic composition of stalks, capitula and leaves of *Cynara cardunculus* L. var. *altilis* (DC) from south of Portugal was determined by analyzing their methanol/water/acetic acid (49.5:49.5:1) extracts, through high temperature-ultra high pressure liquid chromatography coupled to tandem mass spectrometry (HT-UHPLC-MS^n). From the twenty eight phenolic compounds identified, eriodictyol hexoside was referenced for the first time as *C. cardunculus* L. component, and six as cardoon components, namely 1,4-di-*O*-caffeoylquinic acid, naringenin 7-*O*-glucoside, naringenin rutinoside, naringenin, luteolin acetyl-hexoside and apigenin acetyl-hexoside. Stalks outer part and capitula florets extracts showed the highest hydroxycinnamic acids and flavonoids contents, respectively. 1,5-di-*O*-caffeoylquinic acid represented the most abundant hydroxycinnamic acid, while apigenin glucuronide, apigenin 7-*O*-glucoside and apigenin 7-*O*-rutinoside were the main flavonoids. Finally, stalks outer part and capitula receptacle and bracts extracts showed the strongest antioxidant activity, by using the 2,2-diphenyl-1-picrylhydrazyl (DPPH) scavenging effect assay, which was mainly related to phenolic compounds, particularly to hydroxycinnamic acids.

I. INTRODUCTION

Cynara cardunculus L. (Asteraceae) is a Mediterranean species that includes three varieties: the ancestor wild cardoon (var. *sylvestris* (Lamk) Fiori) and their cultivated forms, known as artichoke (var. *scolymus* (L.) Fiori) and cultivated cardoon (var. *altilis* DC). Wild cardoon grows naturally in the Iberian Peninsula, north Africa, west Turkey and Macaronesia, while artichoke production is distributed worldwide, with particular importance in Italy, Spain, France and Turkey, owing to the economic value of the edible immature capitula. Additionally, cultivated cardoon production is located in Spain, Italy, France and south of Portugal, once the blanched fleshy stems and leaf petioles are much enjoyed in regional plates. Since cardoon is rich in cellulose and hemicelluloses, several industrial applications have been studied, namely pulp for paper production, power and biodiesel generation [1]. Traditionally, capitula cardoon is used in Portugal and Spain for the manufacturing of DOP cheeses. Moreover, infusions of cardoon and artichoke leaves are used in folk medicine, due to their hepatoprotective, choleretic and anti-cholestatic benefices [2]. These biological activities have been mostly attributed to the phenolic compounds, especially to caffeoylquinic acids (e.g. 5-*O*-caffeoylquinic and 1,3-di-*O*-caffeoylquinic acids) [3] and flavones (e.g. luteolin and luteolin 7-*O*-glucoside) [2]. Furthermore, artichoke and cardoon extracts, containing phenolic compounds, have also shown antimicrobial [4], antioxidant [4-7], anti-inflammatory [8] and antitumor [9, 10] activities.

Nevertheless, a detailed chemical characterization of phenolic compounds in cardoon extracts is scarce [4, 5, 10-12], especially in what concerns to cultivated cardoon. The detailed knowledge of the chemical composition of cultivated cardoon extracts can contribute to valorize this crop, prompting the economic development of Mediterranean countries. In this way, the present work aims to determine the phenolic composition of methanol/water/acetic acid (49.5:49.5:1) extracts of stalks (outer and inner parts), capitula (receptacle, bracts and florets) and leaves of cultivated cardoon from south of Portugal, by using high temperature-ultra high performance liquid chromatography-diode array detection (HT-UHPLC-DAD) and tandem mass spectrometry (MS^n) analysis. Moreover, the antioxidant activity is evaluated by the DPPH scavenging assay.

II. EXPERIMENTAL

Extraction

C. cardunculus L. var. *altilis* (DC) was collected in June 2010 at the Experimental Center of the Agriculture School from Instituto Politécnico de Beja, south of Portugal. Outer and inner parts of stalks, receptacle, bracts

and florets of capitula, and leaves were milled and submitted to Soxhlet extraction with dichloromethane for 7 h to remove the lipophilic fraction, as reported elsewhere [13]. Then, the extraction of phenolic compounds was carried out according to the procedure of Santos, *et al* (2013) [14]. The extracts were kept at room temperature, protected from the light until analysis.

HT-UHPLC-DAD-MS^n analysis

Cultivated cardoon extracts were previously dissolved in HPLC grade methanol/water mixture at 10 mg/mL, and then filtered through a 0.2 μm PTFE syringe filter. Methanol/water extracts (5 μL) were injected in the HPLC system equipped with an Accela 600 LC pump, an Accela autosampler (16ºC) and an Accela 80 Hz photo DAD. The separation of compounds was carried out on a Hypersil Gold RP C18 column (100 x 2.1 mm; 1.9 μm particle size, Thermo Fisher Scientific, San Jose, CA, USA), maintained at 45ºC. The mobile phase was constituted by (A) water:acetonitrile (99:1, v/v) and (B) acetonitrile, both with 0.1% of formic acid. A gradient elution program was applied from 3% to 100% B at a flow rate of 0.48 mL/min, during a 38 min period. The chromatograms were recorded at 280, 330 and 350 nm and UV/Vis spectra recorded from 210 to 600 nm. Pure standards were used for the quantification of phenolic compounds. The HPLC system was coupled to a LCQ Fleet ion trap mass spectrometer (ThermoFinnigan, San Jose, CA, USA), equipped with an electrospray ionization source and operated at the negative ionization mode. The operational conditions were according to the procedure of Santos, *et al* (2013) [14].

Antioxidant activity

The antioxidant activity of cultivated cardoon extracts was evaluated through the DPPH scavenging assay, following the procedure of Santos, *et al* (2013) [14]. The inhibitory concentration providing 50% DPPH scavenging effect (IC_{50}) was determined. Ascorbic acid and 3,5-di-*tert*-4-butylhydroxytoluene (BHT) were used as antioxidant reference compounds from natural and synthetic origin, respectively.

III. RESULTS AND DISCUSSION

Phenolic composition by HT-UHPLC-DAD-MS^n analysis

The methanol/water/acetic acid (49.5:49.5:1) extracts of cultivated cardoon were analyzed by HT-UHPLC-DAD-MS^n. Twenty eight phenolic compounds were identified, based on their UV spectra and MS^n fragmentation, by comparing with pure standards or, when these were not available, with literature data. Eriodictyol hexoside (**Figure 1**) was reported for the first time as *C. cardunculus* L. component. Additionally, six of these compounds were described for the first time as cardoon components (**Figure 1**), namely: 1,4-di-*O*-caffeoylquinic acid, naringenin 7-*O*-glucoside, naringenin rutinoside, naringenin, luteolin acetyl-hexoside and apigenin acetyl-hexoside.

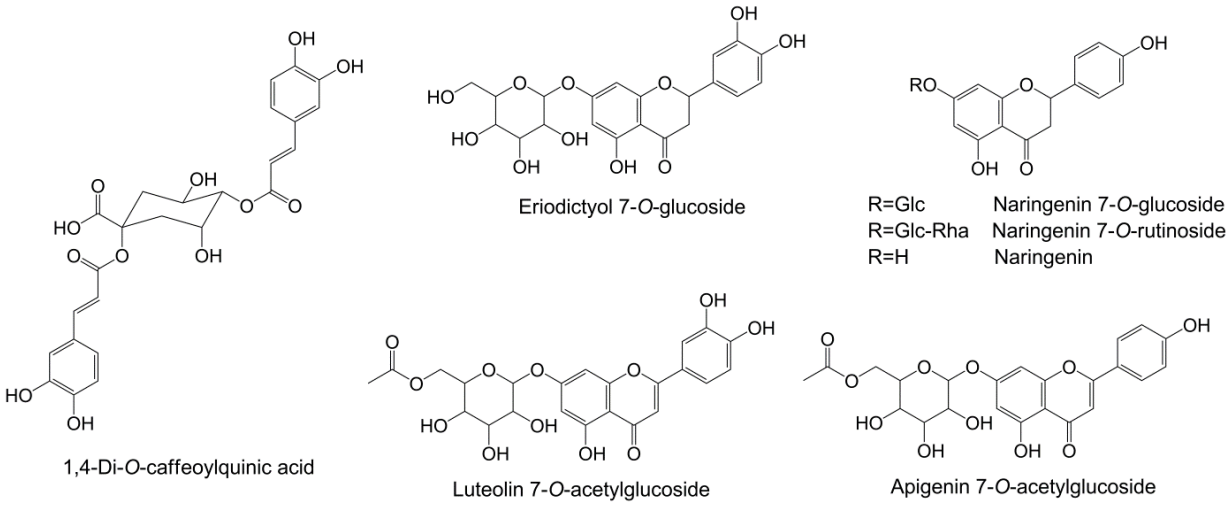

Figure 1: Structures of phenolic compounds identified in *C. cardunculus* L. var. *altilis* (DC) extracts. Abbreviations: Glc, glucosyl; Rha, rhamnosyl.

The total content of phenolic compounds in cultivated cardoon extracts ranged from 10.4 mg/g in leaves to 63.5 mg/g in stalks outer part (**Figure 2**). Stalks outer part extract showed the highest hydroxycinnamic acids content (59.1 mg/g), while capitula florets extract displayed the highest flavonoids content (30.7 mg/g), besides coumarins (1.2 mg/g) (**Figure 2**). Extracts of capitula receptacle and bracts, and stalks inner part also presented considerably high hydroxycinnamic acids contents. Finally, leaves extract was mainly constituted by flavonoids (10.2 mg/g). Dicaffeoylquinic acids (**Figure 2**) were the most abundant hydroxycinnamic acids, particularly in capitula receptacle and bracts (28.8 mg/g), mainly represented by 1,5-*O*-dicaffeoylquinic acid. Dicaffeoylsuccinoylquinic acids (**Figure 2**) were only detected in stalks extracts (16.1-18.5 mg/g). Moreover, apigenin derivatives (**Figure 2**) were the major flavonoids, especially in capitula florets (19.3 mg/g). Apigenin glucuronide, apigenin 7-*O*-glucoside and apigenin 7-*O*-rutinoside represented the major flavonoids. Naringenin derivatives (**Figure 2**) were only detected in capitula florets extract (7.6 mg/g), while luteolin derivatives (**Figure 2**) were the most common flavonoids in leaves extract (5.7 mg/g).

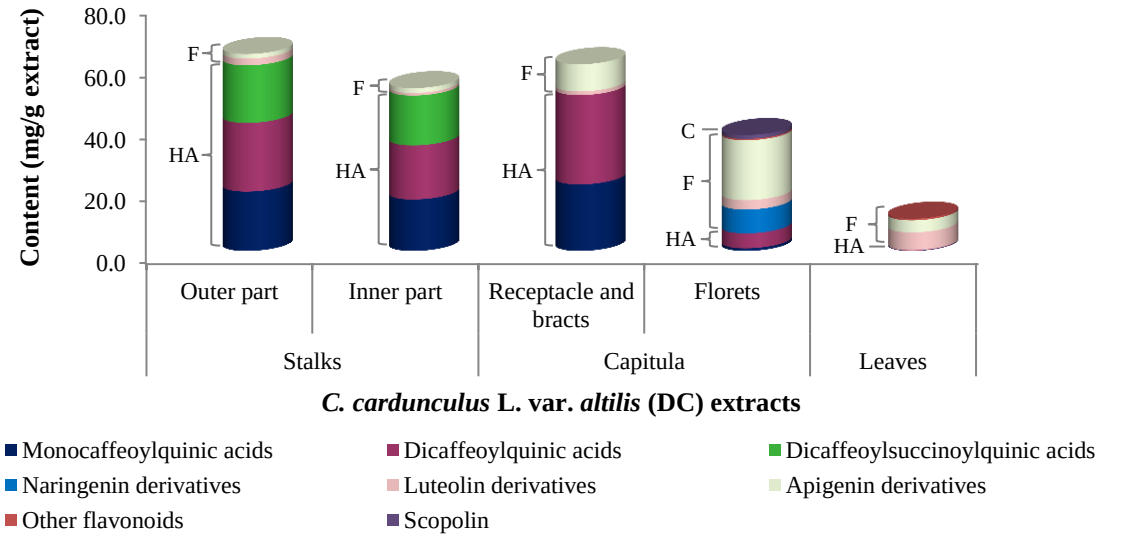

Figure 2: Phenolic composition of *C. cardunculus* L. var. *altilis* (DC) extracts. Abbreviations: C, coumarins; F, flavonoids; HA, hydroxycinnamic acids.

Antioxidant activity

Extracts of stalks outer part and capitula receptacle and bracts were the most effective to scavenge DPPH free radicals (**Figure 3**). Stalks inner part extract was weaker than the previous two (~1.7-fold). Extracts of capitula florets and leaves were the least active. Additionally, these extracts were less active than ascorbic acid (IC_{50}=2.29 µg/mL) and BHT (IC_{50}=16.02 µg/mL). The antioxidant activity of cultivated cardoon extracts was mainly related to their phenolic contents, as shown by the linear correlation between the IC_{50} and the total content of phenolic compounds (r=-0.897). More specifically, it is mainly related to hydroxycinnamic acids content (r=-0.990), as well as to the monocaffeoylquinic acids content (r=-0.996) and the dicaffeoylquinic acids content (r=-0.961). Contrary, IC_{50} values of the DPPH scavenging effect increased with the total contents of flavonoids, luteolin and apigenin derivatives. In fact, previous studies showed that apigenin glycosides were less active to scavenge DPPH free radicals compared to caffeoylquinic acids [6].

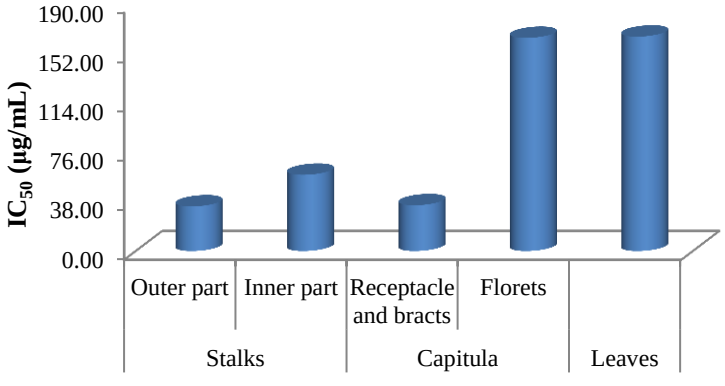

Figure 3: Antioxidant activity of *C. cardunculus* L. var. *altilis* (DC) extracts, determined by the DPPH scavenging assay.

IV. CONCLUSIONS

The present work details the phenolic composition of *C. cardunculus* L. var. *altilis* (DC) extracts from south of Portugal, using HT-UHPLC-DAD-MS^n analysis, as well as the antioxidant activity, using the DPPH scavenging assay. From the twenty eight phenolic compounds identified, eriodictyol hexoside was reported for the first time as *C. cardunculus* L. component, and six as cardoon components, namely 1,4-di-*O*-caffeoylquinic acid, naringenin 7-*O*-glucoside, naringenin rutinoside, naringenin, luteolin acetyl-hexoside and apigenin acetyl-hexoside . Extracts of stalks (outer and inner parts) and capitula receptacle and bracts were mainly constituted by hydroxycinnamic acids, where dicaffeoylquinic acids were the most abundant compounds of this family. Capitula florets extract was rich in flavonoids, mainly represented by apigenin derivatives. Luteolin derivatives were the main phenolic compounds present in leaves extract. Stalks outer part extract was the most active to scavenge DPPH free radicals, mainly due to their phenolic content, particularly to hydroxycinnamic acids content. In this way, the extraction of phenolic compounds from cultivated cardoon can be integrated in an industrial value chain, involving energy, food and pharmaceutics, for the economic development of Mediterranean countries.

V. ACKNOWLEDGEMENT

The authors acknowledge Fundação para a Ciência e a Tecnologia for the award of PhD grants to P.A.B. Ramos (SFRH/BD/70845/2010) and O. Guerreiro (SFRH/BD/84406/2012) and postdoctoral grant to S.A.O. Santos (SFRH/BPD/84226/2012), CICECO (Pest-C/CTM/LA0011/2013), QOPNA (PEst-C/QUI/UI0062/2013) and INALENTEJO 2007.2013 / QREN (ALENT-09-0140-FEDER-000705 (QREN)) for funding. C.S.R. Freire also thanks FCT/MCTES for a research contract ("Investigador FCT 2012"). The authors also thank School of Agriculture from Instituto Politécnico de Beja for kindly supplying the *C. cardunculus* var. *altilis* (DC) samples.

VI. REFERENCES

[1] Fernández, J.; Curt, M.; Aguado, P., Industrial applications of *Cynara cardunculus* L. for energy and other uses, *Ind. Crops Prod.*, **2006**, *24*, 222-229.

[2] Gebhardt, R., Choleretic and anticholestatic activities of flavonoids of artichoke (*Cynara cardunculus* L. subsp. *scolymus* L. Hayek), *Acta Hort. (ISHS)*, **2000**, *684*, 429-436.

[3] Adzet, T.; Camarasa, J.; Laguna, J. C., Hepatoprotective activity of polyphenolic compounds from *Cynara scolymus* against CCl_4 toxicity in isolated rat hepatocytes, *J. Nat. Prod.*, **1987**, *50*, 612-617.

[4] Falleh, H.; Ksouri, R.; Chaieb, K.; Karray-Bouraoui, N.; Trabelsi, N.; Boulaaba, M.; Abdelly, C., Phenolic composition of *Cynara cardunculus* L. organs, and their biological activities, *C. R. Biol.*, **2008**, *331*, 372-379.

[5] Kukic, J.; Popovic, V.; Petrovic, S.; Mucaji, P.; Ciric, A.; Stoikovic, D.; Sokovic, M., Antioxidant and antimicrobial activity of *Cynara cardunculus* L. extracts, *Food Chem.*, **2008**, *107*, 861-868.

[6] Wang, M. F.; Simon, J. E.; Aviles, I. F.; He, K.; Zheng, Q. Y.; Tadmor, Y., Analysis of antioxidative phenolic compounds in artichoke (*Cynara scolymus* L.), *J. Agric. Food Chem.*, **2003**, *51*, 601-608.

[7] Brown, J. E.; Rice-Evans, C. A., Luteolin-rich artichoke extract protects low density lipoprotein from oxidation *in vitro*, *Free Radic. Res.*, **1998**, *29*, 247-255.

[8] Kammoun, M.; Koubaa, I.; Ben Ali, Y.; Jarraya, R.; Gargouri, Y.; Damak, M.; Bezzine, S., Inhibition of pro-inflammatory secreted phospholipase A2 by extracts from *Cynara cardunculus* L., *Appl. Biochem. Biotechnol.*, **2010**, *162*, 662-670.

[9] Mileo, A. M.; Di Venere, D.; Linsalata, V.; Fraioli, R.; Miccadei, S., Artichoke polyphenols induce apoptosis and decrease the invasive potential of the human breast cancer cell line MDA-MB-231, *J. Cell. Physiol.*, **2012**, *227*, 3301-3309.

[10] Velez, Z.; Campinho, M.; Guerra, Â.; García, L.; Ramos, P.; Guerreiro, O.; Felício, L.; Schmitt, F.; Duarte, M., Biological characterization of *Cynara cardunculus* L. methanolic extracts: antioxidant, anti-proliferative, anti-migratory, and anti-angiogenic, *Agriculture*, **2012**, *2*, 472-492.

[11] Pinelli, A. F.; Comino, C.; Lanteri, S.; Portis, E.; Romani, A. P., Simultaneous quantification of caffeoyl esters and flavonoids in wild and cultivated cardoon leaves, *Food Chem.*, **2007**, *105*, 1695-1701.

[12] Pandino Courts, F. L.; Lombardo, S.; Mauromicale, G.; Williamson, G. G., Phenolic acids and flavonoids in leaf and floral stem of cultivated and wild *Cynara cardunculus* L. genotypes, *Food Chem.*, **2011**, *126*, 417-422.

[13] Ramos, P. A. B.; Guerra, A. R.; Guerreiro, O.; Freire, C. S. R.; Silva, A. M. S.; Duarte, M. F.; Silvestre, A. J. D., Lipophilic extracts of *Cynara cardunculus* L. var. *altilis* (DC): a source of valuable bioactive terpenic compounds, *J. Agric. Food Chem.*, **2013**, *61*, 8420-8429.

[14] Santos, S. A. O.; Vilela, C.; Freire, C. S. R.; Neto, C. P.; Silvestre, A. J. D., Phenolic composition and antioxidant activity of industrial cork by-products, *J. Chromatogr. B*, **2013**, *938*, 65-74.

BIOGRAFTING OF FERULIC ACID ONTO LIGNOCELLULOSIC FIBERS BY THE USE OF LACCASES

Jorge Rencoret[1*], Elisabetta Aracri[2], Ana Gutiérrez[1], José C. del Río[1], Antonio L. Torres[2], Teresa Vidal[2] and Angel T. Martínez[3]

*[1]IRNAS-CSIC, PO Box 1052, E-41080 Seville, Spain; [2]UPC, Colom 11, E-08222 Terrassa, Spain; [3]CIB-CSIC, Ramiro de Maeztu 9, E-28040 Madrid, Spain (*jrencoret@irnase.csic.es)*

ABSTRACT

Laccases can functionalize paper pulps with phenolic compounds but little is known about the formed linkages. Treatment of a high-kappa sisal pulp with *Trametes villosa* laccase and ferulic acid resulted in strong increases of kappa-number and acid-group content. This suggested extensive incorporation of ferulic acid, as confirmed by pyrolysis in the presence of tetramethylammonium hydroxide. The coupling linkages were investigated by 2D-NMR of the lignin isolated from pulps. The aromatic region of the spectra showed incorporation of the cinnamic molecule, representing ~4% of the lignin content. Interestingly, the spectra revealed that ferulic acid is C_4-etherified. The aliphatic region of the spectra showed that ferulic acid also incorporates as the corresponding β-β' dilactone (another ~4% of the total lignin) with characteristic $^{13}C_\alpha$-$^1H_\alpha$ and $^{13}C_\beta$-$^1H_\beta$ correlations. The lignin composition and interunit linkages in the treated pulps were only slightly modified revealing that the main effect of the treatment was ferulic acid biografting.

I. INTRODUCTION

Laccases are multi-copper oxidases widely distributed in fungal and plant species, where they play multiple functions. Laccases present broad substrate specificity including substituted phenols, aromatic amines and thiols and many others, which are converted into reactive radicals using oxygen as the electron acceptor. By virtue of these characteristics, laccases are being intensively investigated as eco-friendly biocatalysts for a wide array of biotechnological applications [1]. Within the pulp and paper field, a novel subject of research is the application of laccase-catalyzed radical coupling reactions to modify lignocellulosic fiber chemistry with a view to altering paper properties [2]. Two main approaches are used for laccase-assisted modification of lignocellulosic fibers: i) laccase-mediated cross-linking of lignin molecules in situ; and ii) coupling of low molecular weight (generally phenolic) compounds onto fibers (biografting). The second approach provides a versatile method for functionalizing lignocellulosic fibers and imparting desirable properties to pulps. Although much research has been carried out to explore the potential of biografting for tailoring the properties of lignocellulosic materials, few of them have assessed the mechanistic aspects of this process and the nature of the chemical bonds formed and they mainly involved the use of lignin model compounds due to the complexity of the lignin polymer. In the present study, a high-kappa pulp from sisal was treated with laccase and *trans*-ferulic acid (FA) according to the conditions reported by Aracri et al. [3]. After extensive washing, the treated pulp was directly analyzed by pyrolysis, in the presence of tetramethylammonium hydroxide (TMAH) [4], to confirm the FA incorporation. Then, in order to gain additional information on the amount of FA incorporated with respect to pulp lignin, and identify the lignin-FA linkages formed in the biografting reaction, analysis of the lignin isolated from treated pulp was performed by HSQC (heteronuclear single quantum correlation) 2D-NMR spectroscopy.

II. EXPERIMENTAL

2.1. Enzyme, chemical and pulps

Laccase from *Trametes villosa* was kindly provided by Novozymes (Bagsvaerd, Denmark) and the chemicals for enzyme assay were purchased from Sigma-Aldrich. Pulp was obtained from a laboratory cooking of sisal (*Agave sisalana*) fiber bundles kindly supplied by Celesa mill (Tortosa, Spain). Refined pulp samples were treated in an oxygen-pressurized (0.6 MPa) reactor at 5% consistency [3], using 50 mM sodium tartrate (pH 4), 40 U/g laccase and 3.5% (w/w) FA (all relative to pulp dry weight). Tween 80 (0.05% w/v) was added as surfactant. Treatments were conducted for 4 h at 30 rev/min shaking, and 50 °C. After treatment, the pulp samples were filtered in a fritted glass funnel and washed with de-ionized water until a colorless, neutral filtrate was obtained. Pulp properties were analyzed after Soxhlet extraction with acetone aimed at removing the fraction of FA that failed to covalently bind to fibers [5]. Kappa number was determined according to the standard methods ISO 302 and cellulolytic enzyme lignins were isolated by enzymatically saccharifying polysaccharides as described by Chang et al. [6].

2.2. Analytical pyrolysis and NMR analysis

Pyrolysis-gas chromatography/mass spectrometry (Py-GC/MS) was performed in the presence of TMAH. Approximately 0.1 mg of milled pulp was mixed with 1 μL of TMAH (25%, w/w, methanol solution). The pyrolysis was carried out at 500 ºC, using an EGA/PY-3030D micro-furnace pyrolyzer (Frontier Laboratories Ltd.) connected to an Agilent 7820A gas chromatograph using a DB-1701 fused-silica capillary column (60 m x 0.25 mm i.d., 0.25 μm film thickness) and an Agilent 5975 mass detector (EI at 70 eV). The oven was programmed from 45 ºC (4 min) to 280 ºC (10 min) at 4 ºC min^{-1}. Helium was the carrier gas (2 mL min^{-1}).

For NMR analysis of isolated lignins, around 20 mg of the isolated lignin was dissolved in 0.75 mL of DMSO-d_6. 2D-NMR HSQC spectra were acquired at 25ºC on a Bruker AVANCE III 500 MHz spectrometer fitted with a cryogenically cooled 5 mm TCI gradient probe with inverse geometry. The 2D ^{13}C-^{1}H correlation spectra were carried out using an adiabatic HSQC pulse program. The central solvent peak was used as an internal reference (δ_C/δ_H 39.5/2.49) and 2D-NMR cross-signals were assigned and integrated as in previous publications [7,8].

III. RESULTS AND DISCUSSION

The laccase-FA treatment increased the kappa number of sisal pulp by 11 units relative to control (laccase alone). To confirm the enzymatic incorporation of FA, the acetone extracted pulps were analyzed by pyrolysis in the presence of TMAH. Pyrolysis/TMAH of laccase-FA treated sisal pulp released important amounts of the methyl derivative of FA, which was detected in the m/z 222 ion chromatographic profile (**Fig. 1c**) but which was absent from the pyrograms of both the untreated (control) pulp and the pulp treated with laccase alone (**Fig. 1a** and **b**). This fact confirms that the cinnamic FA molecule was successfully incorporated by the laccase into the sisal pulp. Its relative abundance was ~10% of the total degradation products in the laccase-FA treated pulp.

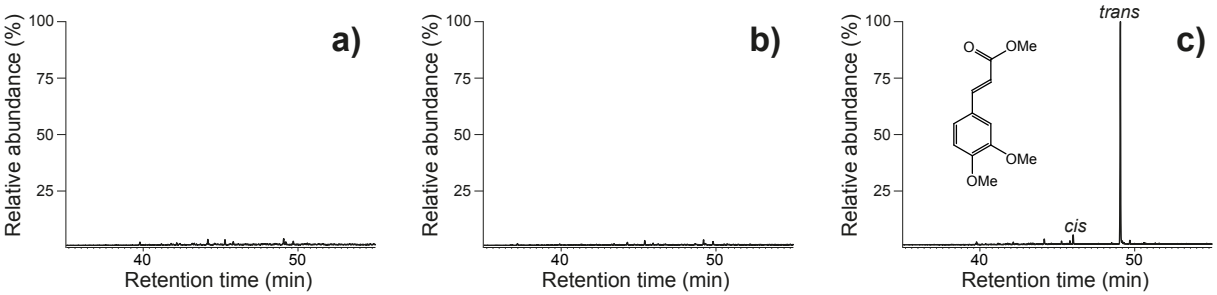

Figure 1. Pyrolysis/TMAH of sisal pulp control (a), laccase alone (b) and treated with laccase-FA (c). Selected-ion (m/z 222) chromatographic profiles.

Since the aim of the study was to get further information of the laccase biografting of phenols onto pulp, the lignins were enzymatically isolated from the laccase-FA treated sisal pulps and subsequently analyzed by 2D-NMR spectroscopy. The HSQC spectra of the lignins isolated from the laccase-FA treatment (and the respective untreated control pulp) are shown in **Fig. 2**. The main cross-signals in the aromatic/unsaturated region (δ_C/δ_H 98−148/5.2−8.7 ppm) of the spectra of the lignins isolated from the laccase-FA treated sisal pulp, and the untreated control (**Fig. 2d** and **b**, respectively) corresponded to the aromatic rings of the G and S lignin units, and the FA attached to the lignin (in the laccase-FA treated pulp). Signals for the C_α–H_α and C_β–H_β correlations in the FA cinnamic structure were observed at δ_C/δ_H 144/7.5 and 117/6.4 ppm, respectively. Interestingly, the latter olefinic signal was displaced with respect to the position found in the spectrum of free FA (116/6.4 ppm) and matched with that reported for 3,4-dimethoxycinnamic acid [9]. The presence of this signal, (and the absence of the above-mentioned C_β–H_β correlation signal characteristic of free FA), clearly indicated that FA is C_4-etherified during its incorporation onto the sisal lignin.

The main cross-signals in the aliphatic-oxygenated region of the spectra (δ_C/δ_H 45-95/2.5-6.0/ppm) of the lignins isolated from the laccase-FA treated sisal pulp, and the untreated control (**Fig. 2c** and **a**, respectively) corresponded to side chains of lignin and FA-derived structures (in the laccase-FA treated pulp) forming different inter-unit linkages and end-units (**Fig. 2,** structures **A** to **I**). Moreover, a comparison of the aliphatic region of the 2D-NMR spectra revealed that FA also incorporates to lignin (in the laccase-FA treated pulp) as the corresponding β-β' dilactone dimer (structure **CL**) with characteristic C_α-H_α and C_β-H_β correlations at δ_C/δ_H 82/5.7 and 48/4.2 ppm, respectively [9]. A semiquantitative estimation of the different (i) lignin (**S, S'** and **G**) and etherified FA units and (ii) lignin (**A** to **I**) and FA dilactone side-chain structures, in the HSQC spectra of control (**Fig. 2a** and **b**) and laccase-FA treated (**Fig. 2c** and **d**) pulps is provided in **Table 1**.

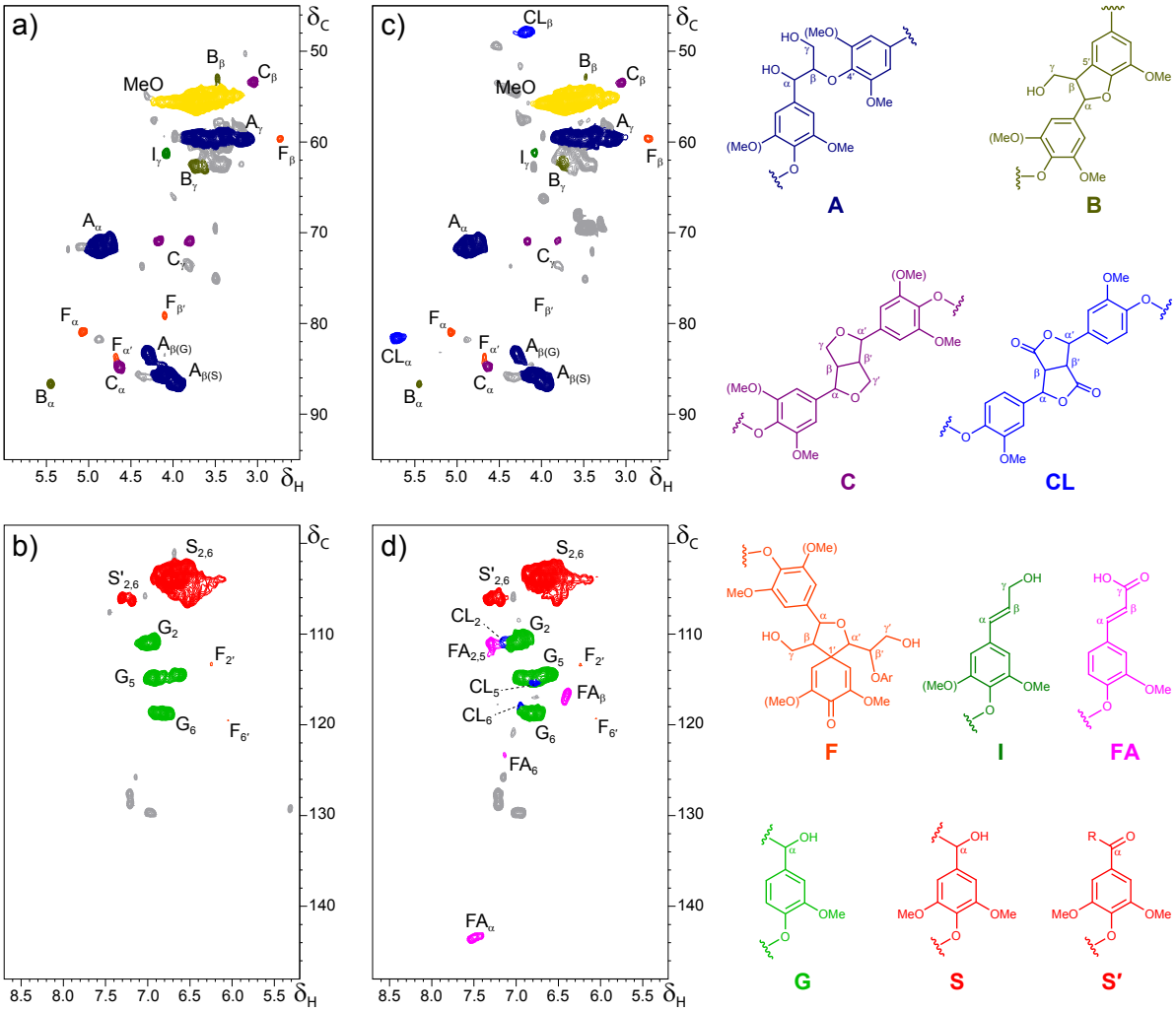

Figure 2. HSQC spectra of the lignins isolated from sisal pulp treated with laccase-FA and the respective control without enzyme. The aliphatic-oxygenated and aromatic regions of the control pulp are shown in **a** and **b**, respectively. The aliphatic-oxygenated and aromatic regions of the laccase-FA treated pulp are shown in **c** and **d**, respectively. Main substructures identified: (**A**) β-O-4' ether structure; (**B**) phenylcoumaran; (**C**) resinol; (**CL**) FA dilactone; (**F**) spirodienone; (**I**) trans cinnamyl end-group; (**FA**) etherified trans ferulic acid; (**G**) guaiacyl unit; (**S**) syringyl unit; (**S'**) Cα-oxidized syringyl unit.

Table 1. Quantification of main lignin structures and units, and FA-derived structures in control and laccase-FA treated sisal pulps, as estimated from HSQC spectra (**Fig. 2**).

	Control pulp	Treated pulp
Lignin substructures (%)[1]		
β-*O*-4' (**A**)	88	90
Phenylcoumaran (**B**)	2	1
Resinol (**C**)	4	3
Spirodienone (**F**)	3	2
Cinnamyl alcohol end-group (**I**)	3	3
Lignin units (%)[2]		
Syringyl units (**S**)	85	77
Oxidized syringyl units (**S'**)	3	6
Guaiacyl units (**G**)	11	17
Ferulic structures/units (%)		
FA dilactone structures (**CL**)[1]	0	7.0 (4.5[2])
Etherified ferulic acid units (**FA**)[2]	0	4.2

[1]Percentage of side-chains (A+B+C+F+I); [2]Percentage of lignin (S+S'+G)

The values obtained showed over 4% etherified FA referred to the lignin content in the lignin isolated from the laccase-FA treated pulp. Moreover, the aliphatic region of the spectrum of the lignin isolated from the laccase-FA treated pulp revealed that a similar percentage of the lignin-linked FA (~4% referred to the lignin content estimated by NMR) is coupled to a second FA molecule forming a dilactone structure (CL in Fig. 2). Slight differences in lignin composition, in terms of S and G units were observed, including higher amounts of S' and G units and lower amounts of S units in the lignin from the laccase-FA treated sisal pulp. Concerning the different interunit linkages in sisal lignin, the percentage of side chains involved in β-O-4' linkages (88-90%), resinols (3-4%), spirodienones (2-3%) and phenylcoumarans (1-2%) were very similar in the treated and the control pulps, and the same happened for the cinnamyl end-groups (3%) (**Table 1**).

IV. CONCLUSIONS

Laccase is highly efficient in incorporating FA on high lignin sisal pulp, as shown by the increases of kappa number (11 points). Such modification confers new properties to pulps, and the aim of the present study was to elucidate the chemical linkages formed during FA biografting. Pyrolysis/TMAH demonstrated that FA in the pulp is linked by covalent bonds. 2D-NMR of the enzymatically isolated lignins confirmed that grafting is produced on the lignin component of the pulp. Moreover, information on the linkage types formed during laccase grafting of phenols onto pulp was provided by both the aromatic/unsaturated and aliphatic-oxygenated regions of the NMR spectra. While the former showed significant amounts of FA etherified (to lignin) at its C_4 position, the latter revealed formation of a similar amount of FA dilactone structures from coupling at the side chain level. Although minor modification of the lignin composition was observed after the laccase-FA treatment, we could conclude that biografting is the predominant modification during sisal pulp treatment with laccase-FA.

V. ACKNOWLEDGEMENT

This study was supported by the EU projects LIGNODECO (KBBE-2009-3-244362) and PEROXICATS (KBBE-2010-4-265397) and the Spanish projects AGL2011-25379, CTQ2010-20238-CO3-01, CTQ2012-34109 and BIO2011-26694 (co-financed by FEDER funds). J.R. thanks the CSIC for a JAE-DOC contract, co-financed by Fondo Social Europeo.

VI. REFERENCES

1. Riva, S. Laccases: blue enzymes for green chemistry. *Trends Biotechnol.* **2006**, *24*, 219-226.
2. Kudanga T.; Nyanhongo, G.S.; Guebitz G.M.; Burton, S. Potential applications of laccase-mediated coupling and grafting reactions: A review. *Enzyme Microb. Technol.* **2011**, *48*, 195-208.
3. Aracri, E.; Roncero, M.B.; Vidal T. Studying the effects of laccase-catalysed grafting of ferulic acid on sisal pulp fibers. *Bioresource Technol.* **2011**, *102*, 7555-7560.
4. del Río, J.C.; Martín, F.; González-Vila, F.J. Thermally assisted hydrolysis and alkylation as a novel pyrolytic approach for the structural characterization of natural biopolymers and geomacromolecules. *Trends Anal. Chem.* **1996**, *15*, 70-79.
5. Aracri, E.; Fillat, A.; Colom, J.F.; Gutiérrez, A.; del Río, J.C.; Martínez, A.T.; Vidal T. Enzymatic grafting of simple phenols on flax and sisal pulp fibres using laccases. *Bioresource Technol.* **2010**, *101*, 8211-8216.
6. Chang, H.; Cowling, E.B.; Brown, W.; Adler, E.; Miksche, G. Comparative studies on cellulolytic enzyme lignin and milled wood lignin of sweetgum and spruce. *Holzforschung*. **1975**, *29*, 153-159.
7. Ralph, J.; Helm, R.F.; Quideau, S.; Hatfield, R.D. Lignin-Feruloyl Ester Cross-Links in Grasses. 1.Incorporation of Feruloyl Esters into Coniferyl Alcohol Dehydrogenation Polymers. *J. Chem. Soc. Perkin Trans*. **1992**, *1*, 2961-2969.
8. Rencoret, J.; Ralph, J.; Marques, G.; Gutiérrez, A.; Martínez, A.T.; del Río, J.C. Structural characterization of lignin Isolated from coconut (*Cocos nucifera*) coir fibers. *J. Agric. Food Chem.* **2013**, *61*, 2434-2445.
9. Ralph, S.; Ralph, J.; Landucci, L. NMR database of lignin and cell wall model compounds, US Forest Prod. Lab., One Gifford Pinchot Dr., Madison, WI 53705. (http://ars.usda.gov/Services/docs.htm?docid=10491) (accessed: July 2009), **2004**.

STRUCTURAL CHARACTERIZATION OF THE MILLED WOOD LIGNIN ISOLATED FROM BREWER´S SPENT GRAIN

Jorge Rencoret,[1] Pepijn Prinsen,[1] Ana Gutiérrez,[1] Ángel T. Martínez[2] and José C. del Río[1]

[1]IRNAS-CSIC, P.O. Box 1052, 41080-Seville, Spain; [2]CIB-CSIC, Ramiro de Maeztu 9, E-28040 Madrid, Spain (delrio@irnase.csic.es)*

ABSTRACT

Brewer´s spent grain (BSG) is the major by-product generated by the brewing industry. BSG is rich in carbohydrates, lignin, proteins and lipids, and has a high potential as source of food, energy and chemicals. In this work, the composition and structural characteristics of the lignin from BSG have been studied in detail by Py-GC/MS and 2D-NMR. The data demonstrated that this lignin is a *p*-hydroxyphenyl-guaiacyl-syringyl (H-G-S) lignin, with a predominance of G units (S/G ratio of 0.4). 2D-NMR indicated that the main substructures present include β–*O*–4´ alkyl-aryl ethers followed by small amounts of phenylcoumarans and resinols.

I. INTRODUCTION

Brewer´s spent grain (BSG) is the solid residue obtained from barley (*Hordeum vulgare* L.) after mashing and filtration from the brewing process. BSG basically consists of the husk–pericarp–seed coat layers that covered the original barley grain [1]. BSG represents up to 30% (w/w) of the starting malted grain, which makes this a readily available, high volume and low cost by-product within the brewing industry, and a potentially valuable resource for industrial exploitation. BSG is a lignocellulosic material containing cellulose (17-25%), non-cellulosic carbohydrates (25-35%), protein (15-24%) and lignin (8-28%), with lower amounts of lipids (10%) [1,2]. For an appropriate valorization of BSG as a source for added-value products, the complete characterization of the different components present is of high interest. Previous studies have mostly dealt with the composition of carbohydrates, proteins, lipids and *p*-hydroxycinnamic acids [2,3]. In comparison, studies concerning the composition and structure of lignin in BSG have been relatively scarce and mostly limited to its interactions with gastrointestinal microbiota [4]. In this paper, an in-depth and complete characterization of the lignin polymer of BSG has been performed. For this, a 'milled-wood' lignin (MWL) preparation was isolated according to traditional lignin isolation procedures, which was subsequently analyzed by Py-GC/MS and 2D-NMR.

II. EXPERIMENTAL

Samples

BSG was obtained from Adnams brewery (Southwold, UK) and was kindly provided by Prof. Craig B. Faulds (INRA, Marseille). Klason lignin content was estimated as the residue after sulphuric acid hydrolysis of the pre-extracted material according to the TAPPI method T222 om-8. The Klason lignin content was then corrected for proteins, determined from the N content and using a 6.25 factor, and ash, estimated as the residue after 6 h of heating at 575 ºC. The acid-soluble lignin was determined, after the insoluble lignin was filtered off, by UV-spectroscopic determination at 205 nm wavelength using 110 L cm^{-1} g^{-1} as the extinction coefficient.

Milled-wood lignin' isolation

The lignins were obtained according to the classical procedure, and the detailed protocol has been explained somewhere else [5,6]. The final yields were 10% of the original Klason lignin content.

Analytical pyrolysis

Pyrolysis of MWL (approximately 100 μg) was performed with a 3030 micro-furnace pyrolyzer (Frontier Laboratories Ltd.) connected to an Agilent 7820A GC using a DB-1701 fused-silica capillary column (60 m x 0.25 mm i.d., 0.25 μm film thickness) and an Agilent 5975 mass selective detector (EI at 70 eV). The pyrolysis was performed at 500 ºC. The oven temperature was programmed from 45 ºC (4 min) to 280 ºC (10 min) at 4 ºC min-1. Helium was the carrier gas (1 mL min-1). Peak molar areas were calculated for the lignin-degradation products, the summed areas were normalized and expressed as percentages.

NMR spectroscopy

2D-NMR spectra were recorded at 25 ºC on a Bruker AVANCE III 500 MHz instrument, equipped with a cryoprobe. MWL (40 mg) was dissolved in 0.75 mL of dimethylsulfoxide (DMSO)-d_6. The central solvent peak

was used as internal reference (DMSO δ_C/δ_H 39.5/2.49). The HSQC (heteronuclear single quantum coherence) experiment used Bruker's "hsqcetgpsisp2.2" pulse program (adiabatic-pulsed version) with spectral widths of 5000 Hz and 20,843 Hz for the ^{1}H- and ^{13}C dimensions. The number of transients was 64, and 256 time increments were always recorded in the ^{13}C dimension. The $^{1}J_{CH}$ used was 145 Hz. Processing used typical matched Gaussian apodization in the ^{1}H dimension and squared cosine-bell apodization in the ^{13}C dimension. Prior to Fourier transformation, the data matrices were zero-filled up to 1024 points in the ^{13}C-dimension. 2D-NMR cross-signals were assigned by literature comparison [5-7]. A semiquantitative analysis of the HSQC correlation peaks was performed using Bruker's Topspin 3.1 processing software. Relative abundances of inter-unit linkages were estimated from C_α–H_α correlations, and the relative abundance of side-chains involved in different substructures and terminal structures were calculated. In the aromatic/unsaturated region, C_2–H_2 from G and $C_{2,6}$–$H_{2,6}$ from S lignin units were used to estimate their abundances.

III. RESULTS AND DISCUSSION

The Klason lignin content of the BSG was relatively low (8.8%) compared to previous published data for the same sample (16-20.1%). The main reason for this discrepancy is that previous works did not consider the high amounts of proteins and ashes when quantifying the Klason lignin content, which was corrected here. In this work, we have thoroughly studied the lignin composition and structure of BSG. For this purpose, a 'milled-wood' lignin (MWL) preparation was isolated and was then analyzed by Py-GC/MS and 2D-NMR.

Py-GC/MS

The pyrogram of the MWL from BSG is shown in **Figure 1**. Pyrolysis released phenolic compounds that are derived from *p*-hydroxyphenyl (H), guaiacyl (G) and syringyl (S) lignin units. The most predominant phenolic compounds were phenol (1), guaiacol (2), 4-methylphenol (4), 4-methylguaiacol (6), 4-vinylphenol (10), 4-vinylguaiacol (11), syringol (15), *trans*-isoeugenol (19), 4-methylsyringol (20), 4-vinylsyringol (26), guaiacylacetone (27) and *trans*-4-propenylsyringol (33). The high levels of phenol, 4-methylphenol and 4-vinylphenol released, together with the presence of indol, indicates a major contribution from proteins. In addition, the high amounts of 4-vinylphenol released upon pyrolysis, as also occurs in other grasses, also point to the presence of *p*-coumarates esters, which decarboxylates under pyrolytic conditions [5-9]. Similarly, 4-vinylguaiacol (11), which is present in high abundance, also arises from ferulates after decarboxylation upon pyrolysis. A rough estimation of the S/G ratio (by using the molar areas of all G- and S-derived compounds, except 4-vinylguaiacol, that also arises from ferulates, and its respective 4-vinylsyringol), indicate a S/G ratio of 0.4. The occurrence of *p*-hydroxycinnamates in BSG was assessed by pyrolysis in the presence of TMAH [5-9]. Previous studies have indicated that *p*-coumarates in grasses are esterified to the lignin side-chains, and more specifically acylates the γ-OH of the lignin side-chain [5,6,10,11].

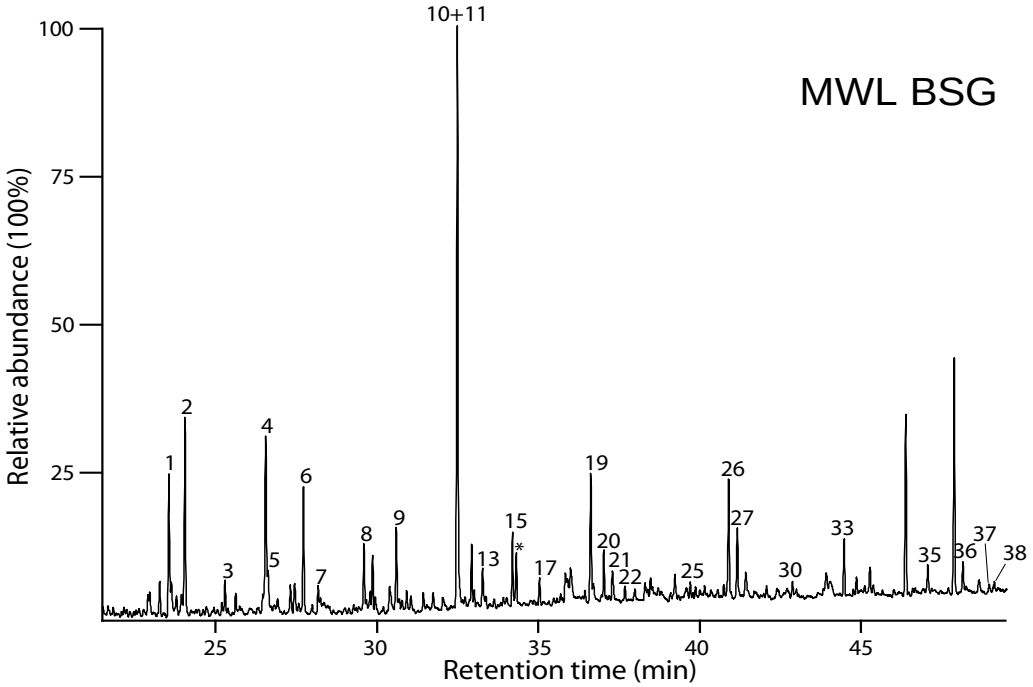

Figure 1. Py-GC/MS of the MWL isolated from BSG.

2D-NMR

The MWL from BSG was also analyzed by 2D-NMR. The side-chain (δ_C/δ_H 69−88/3.8−5.6) and the aromatic (δ_C/δ_H 90−150/5.8−8.0) regions of the spectrum are shown in **Figure 2**. The main substructures present are also depicted in **Figure 2**. The spectrum shows prominent signals corresponding to β–*O*–4′ aryl-ether linkages (**A**), together with smaller signals for phenylcoumarans (**B**), resinols (**C**) and dibenzodioxocins (**D**). The main cross-signals in the aromatic region of the HSQC spectra corresponded to the aromatic rings of the H, G and S lignin units, and the *p*-hydroxycinnamates ferulates and *p*-coumarates. Strong signals corresponding to $C_{3,5}$–$H_{3,5}$ and $C_{2,6}$–$H_{2,6}$ correlations in "H-lignin" units were observed, confirming that the high abundance of 'H-units' observed upon pyrolysis was also due to the presence of proteins. Interestingly, in this region of the HSQC spectra, it was also possible to detect two characteristic signals at δ_C/δ_H 94.1/6.56 and 98.8/6.20 corresponding to the C_8–H_8 and C_6–H_6 correlations of tricin (**T**), a flavone that is apparently incorporated into the lignins in some grasses [6], and that also occur in other monocotyledons, as in the lignin of coconut coir [7].

The relative abundances of the main lignin inter-unit linkages, the molar abundances of the different lignin units (H, G and S), and *p*-coumarates, ferulates and tricin, are shown in **Table 1**. The main substructure present in the lignin of BSG was the β–*O*–4′ aryl ether, that accounts for 91% of all inter-unit linkages, followed by smaller amounts of phenylcoumaran that involved 6.8% of all linkages and resinols with 2.2%. The lignin S/G ratio determined upon NMR (0.4) was similar to that obtained upon Py-GC/MS.

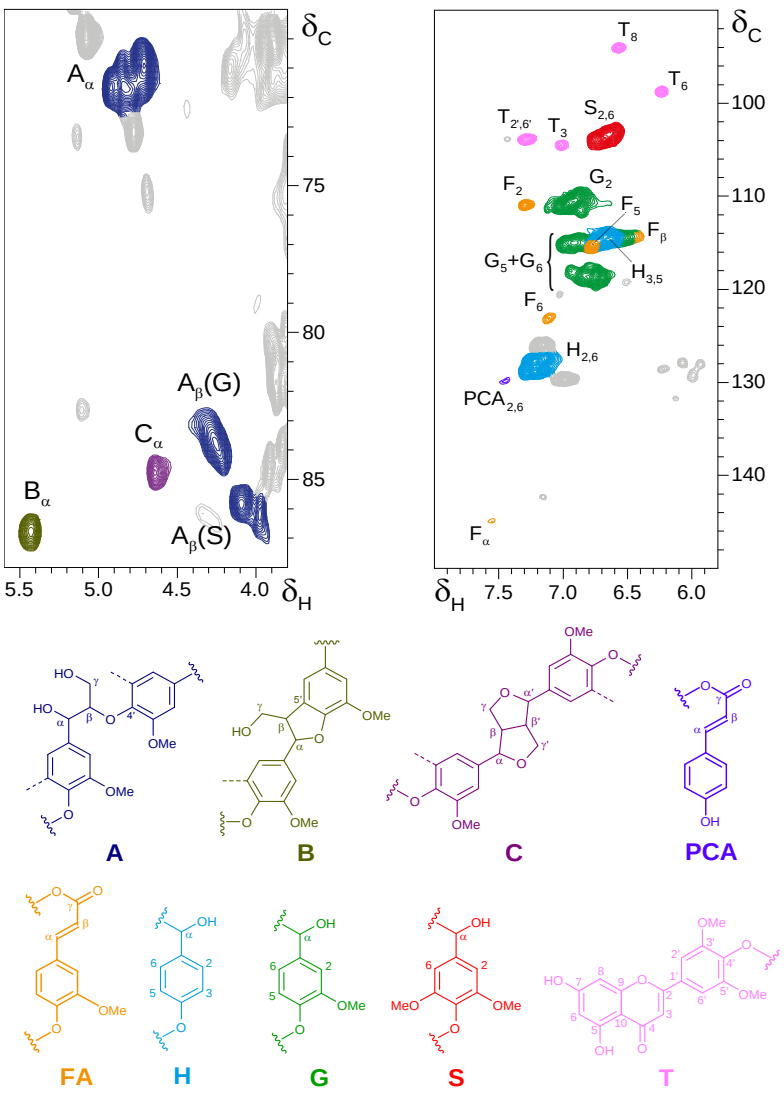

Figure 2. Side-chain and aromatic/unsaturated regions in the HSQC spectrum of the MWL from BSG. Main structures present: (**A**) β–*O*–4´ alkyl-aryl ethers; (**B**) phenylcoumarans; (**C**) resinols; (**PCA**) *p*-coumarates; (**FA**) ferulates; (**H**) *p*-hydroxyphenyl units; (**G**) guaiacyl units; (**S**) syringyl units; (**T**) tricin.

Table 1. Structural Characteristics (Lignin Inter-Unit Linkages, Aromatic Units, *p*-Coumarates and Ferulates Content) of the MWL Isolated from Brewer′s Spent Grain

	Abundance
Lignin inter-unit linkages (%)	
β–*O*–4′ aryl ethers (**A**)	72
Cα-oxidized β–*O*–4′ aryl ethers (**Aox**)	5
Phenylcoumarans (**B**)	12
Resinols (**C**)	6
Dibenzodioxocins (**D**)	5
Lignin aromatic units	
H (%)	31
G (%)	51
S (%)	18
S/G ratio	0.35
p-Hydroxycinnamates	
p-Coumarates (%)	2
Ferulates (%)	7
p-Coumarates/Ferulates ratio	0.28
Tricin	6

IV. CONCLUSIONS

Py-GC/MS and 2D-NMR analysis of the MWL isolated from BSG indicated that it is a H:G:S lignin with a S/G ratio of 0.4, and with some amounts of associated *p*-coumarates and ferulates. The main lignin inter-unit linkages present was the β–*O*–4′ aryl ether, followed by smaller amounts of phenylcoumaran and resinols. The flavone tricin was incorporated into this lignin, as also occurs in other grasses.

V. ACKNOWLEDGEMENT

This study has been funded by the EU-project LIGNODECO (KBBE-244362) and the Spanish project AGL2011-25379 (co-financed by FEDER funds). Jorge Rencoret thanks the CSIC for a JAE-DOC contract of the program “Junta para la Ampliación de Estudios” co-financed by Fondo Social Europeo (FSE).

VI. REFERENCES

[1] Mussatto, S.I.; Dragone, G.; Roberto, I.C. Brewers' spent grain: generation, characteristics and potential applications. *J. Cer. Sci.* **2006**, *43*, 1–14.

[2] Robertson, J.A.; I'Anson, K.J.A.; Treimo, J.; Faulds, C.B.; Brocklehurst, T.F.; Eijsink, V.G.H.; Waldron, K.W. Profiling brewers' spent grain for composition and microbial ecology at the site of production. *LWT-Food Sci. Technol.* **2010**, *43*, 890–896.

[3] del Río, J. C.; Prinsen, P.; Gutiérrez, A. Chemical composition of lipids in brewer´s spent grain: A promising source of valuable phytochemicals. *J. Cereal Sci.* **2013**, *58*, 248–254.

[4] Niemi, P.; Aura, A.-M.; Maukonen, J.; Smeds, A.I.; Mattila, I.; Niemelä, K.; Tamminem, T.; Faulds, C.B.; Buchert, J.; Potanen, K. Interactions of a lignin-rich fraction from brewer´s spent grain with gut microbiota in vitro. *J. Agric. Food Chem.* **2013**, *61*, 6754–6762.

[5] del Río, J.C.; Prinsen, P.; Rencoret, J.; Nieto, L.; Jiménez-Barbero, J.; Ralph, J.; Martínez, A.T.; Gutiérrez, A. Structural characterization of the lignin in the cortex and pith of elephant grass (*Pennisetum purpureum*) stems. *J. Agric. Food Chem.* **2012**, *60*, 3619–3634.

[6] del Río, J.C.; Rencoret, J.; Prinsen, P.; Martínez, A.T.; Ralph, J.; Gutiérrez A. Structural characterization of wheat straw lignin as revealed by analytical pyrolysis, 2D-NMR, and reductive cleavage methods. *J. Agric. Food Chem.* **2012**, *60*, 5922–5935.

[7] Rencoret, J.; Ralph, J.; Marques, G.; Gutiérrez, A.; Martínez, A.T.; del Río, J.C. Structural characterization of lignin isolated from coconut (*Cocos nucifera*) coir fibers. *J. Agric. Food Chem.* **2013**, *61*, 2434−2445.

[8] del Río, J.C.; Gutiérrez, A.; Rodríguez, I.M.; Ibarra, D.; Martínez A.T. Composition of non-woody plant lignins and cinnamic acids by Py-GC/MS, Py/TMAH and FT-IR. *J. Anal. Appl. Pyrol.* **2007**, *79*, 39–46.

[9] del Río, J.C.; Martín, F.; González-Vila, F.J. Thermally assisted hydrolysis and alkylation as a novel pyrolytic approach for the structural characterization of natural biopolymers and geomacromolecules. *Trends Anal. Chem.* **1996**, *15*, 70–79.

[10] Ralph, J.; Hatfield, R.D.; Quideau, S.; Helm, R.F.; Grabber, J.H.; Jung, H.-J.G. Pathway of *p*-coumaric acid incorporation into maize lignin as revealed by NMR. *J. Am. Chem. Soc.* **1994**, *116*, 9448–9456.

[11] Ralph, J. Hydroxycinnamates in lignification. *Phytochem. Rev.* **2010**, *9*, 65–83.

2D NMR STUDY OF LIGNIN MODIFICATION DURING THE PRETREATMENT OF *EUCALYPTUS* WOOD FEEDSTOCK WITH A FUNGAL LACCASE AND A PHENOLIC MEDIATOR

Alejandro Rico[1], Jorge Rencoret[1], José C. del Río[1], Ángel T. Martínez[2], Ana Gutiérrez[1]*

*[1]Instituto de Recursos Naturales y Agrobiología de Sevilla, CSIC, Reina Mercedes 10, E-41012 Seville, Spain; [2]Centro de Investigaciones Biológicas, CSIC, Ramiro de Maeztu 9, E-28040 Madrid, Spain (*anagu@irnase.csic.es)*

ABSTRACT

The delignification of eucalypt feedstock during enzymatic pretreatment with the laccase from *Myceliophthora thermophila*, in conjunction with methyl syringate as mediator, when applied in a multistage sequence consisting of successive enzymatic and alkaline extraction stages, directly on the ground lignocellulosic material was thoroughly studied by two-dimensional nuclear magnetic resonance (2D NMR) of the whole wood (at the gel stage) after each step of the sequence. The 2D NMR analyses of eucalypt feedstock after the enzymatic pretreatment, revealed the removal of guaiacyl and syringyl lignin units (with preferential removal of the former) and aliphatic (mainly β-*O*-4'-linked) side-chains of lignin without a substantial change in polysaccharide cross-signals. However, the most noticeable modification was the formation of C_α-oxidized syringyl lignin units in the enzymatic steps that were partially removed in the alkaline extraction stages. This study revealed that the first cycle of pretreatment of eucalypt with *M. thermophila* laccase and methyl syringate did not produce any delignification effect and consequently did not increase the saccharification yields. However, at the end of the whole sequence (4 cycles), a high delignification (~50%) of eucalypt feedstock and increases (~40%) in glucose yield after enzymatic hydrolysis was attained with this laccase-mediator pretreatment.

I. INTRODUCTION

Biotechnology can contribute to plant biomass deconstruction in lignocellulose biorefineries for the sustainable production of chemicals, materials and fuels, by providing biocatalysts being able to degrade or modify lignin [1]. Physical, chemical and biological pretreatments are being studied for deconstructing lignocellulosic biomass and removing lignin. Most biological pretreatments for delignifying lignocellulosic materials employ lignin-degrading fungi from the group of white-rot basidiomycetes but such pretreatments require long application periods. In the present study, eucalypt (*Eucalyptus globulus*) wood was treated with the so-called laccase-mediator system [2], which has been often investigated for paper pulp delignification [3]. The eventual modification of cell-wall polymers during the enzymatic treatment of the whole plant material was analyzed by heteronuclear single-quantum correlation (HSQC) solution NMR of gels prepared by lignocellulose swelling in dimethylsulfoxide-d_6 [4,5]. In addition to lignin removal, the effect of the enzymatic treatments on sugar yield from the pretreated eucalypt feedstock was assessed.

II. EXPERIMENTAL

Wood, enzyme and mediator

Eucalypt (*E. globulus*) wood chips from ENCE (Pontevedra, Spain), were air-dried and grounded and then finely milled in a planetary mill using an agate jar and agate ball bearings. The total ball-milling time for the samples was 5 h. A commercial (recombinant) fungal laccase from the ascomycete *Myceliophthora thermophila*, provided by Novozymes (Bagsvaerd, Denmark), was used in this study. Its activity was measured as initial velocity during oxidation of 5 mM 2,2'-azino-bis(3-ethylbenzothiazoline-6-sulphonic acid) (ABTS) to its cation radical (ε_{436} 29 300 $M^{-1}\cdot cm^{-1}$) in 0.1 M sodium acetate (pH 5) at 24ºC. The laccase activity of the enzyme preparation was 945 U/ml. One activity unit (U) was defined as the amount of enzyme transforming 1 µmol of ABTS per min. Methyl syringate (MeS) was used as mediator.

Laccase-mediator treatments

The eucalypt samples were treated with the *M. thermophila* laccase in the presence (and absence) of MeS, as mediator. Laccase doses of 50 $U\cdot g^{-1}$ were assayed, together with 3% MeS, both referred to wood dry weight. The treatments were carried out in pressurized bioreactors placed in a thermostatic shaker at 170 $rev\cdot min^{-1}$ and 50 ºC,

using 10 g (dry weight) samples at 6% consistency (w:w) in 50 mM sodium dihydrogen phosphate (pH 6.5) under O_2 atmosphere (2 bars) for 24 h. After the treatment, the samples were filtered through a Büchner funnel and washed with water. In a subsequent stage, samples at 6% consistency (w:w) were submitted to a peroxide-reinforced alkaline extraction using 1% (w:w) NaOH and 3% (w:w) H_2O_2 (with respect to sample dry weight) at 80 ºC for 90 min, followed by water washing. Cycles of four successive enzyme-extraction treatments were applied. Treatments with laccase (50 $U \cdot g^{-1}$) alone (without mediator) and controls without laccase and mediator, were also performed (followed in both cases by the corresponding alkaline extractions). Klason lignin content was estimated according to T222 om-88 [6].

Saccharification of treated wood

The laccase-pretreated samples were hydrolyzed with a cocktail of commercial enzymes (Novozymes, Bagsvaerd) with cellulase (Celluclast 1.5 L; 2 $FPU \cdot g^{-1}$) and β-glucosidase (Novozym 188; 100 $nkat \cdot g^{-1}$) activities, at 1% consistency in 3 mL of 100 mM sodium citrate (pH 5) for 72 h at 45 ºC, in a thermostatic shaker at 170 $rev \cdot min^{-1}$. The different monosaccharides released were determined as alditol acetates [7] by GC. An HP 5890 gas chromatograph equipped with a split−splitless injector and a flame ionization detector was used. The injector and detector temperatures were set at 225 and 250 °C, respectively. Samples were injected in the split mode (split ratio 10:1). Helium was used as the carrier gas. The capillary column used was a DB-225 (30 m × 0.25 mm i.d., 0.15 µm film thickness). The oven was temperature-programmed from 220 °C (held for 5 min) to 230 °C (held for 5 min) at 2 °C min^{-1}. Peaks were quantified by area and glucose, xylose and arabinose were used as standards to elaborate calibration curves.

2D NMR spectroscopy

For gel-state NMR experiments, ~100 mg of ball-milled wood samples after the several steps of the whole multistage sequence were directly transferred into 5-mm NMR tubes, and swelled in 1 mL of dimethylsulfoxide-d_6, forming a gel inside the NMR tube [4,5]. HSQC 2D-NMR spectra were acquired at 25ºC on a Bruker AVANCE III 500 MHz spectrometer fitted with a cryogenically cooled 5 mm TCI gradient probe with inverse geometry (proton coils closest to the sample). The 2D ^{13}C-^{1}H correlation spectra were carried out using an adiabatic HSQC pulse program (Bruker standard pulse sequence 'hsqcetgpsisp2.2') and the following parameters: spectra were acquired from 10 to 0 ppm (5000 Hz) in F2 (^{1}H) using 1000 data points for an acquisition time of 100 ms, an interscan delay (D1) of 1 s, and from 200 to 0 ppm (25,168) in F1 (^{13}C) using 256 increments of 32 scan, for a total acquisition time of 2 h 34 min. The $^{1}J_{CH}$ used was 145 Hz. Processing used typical matched Gaussian apodization in ^{1}H and a squared cosine bell in ^{13}C. The central solvent peak was used as an internal reference (δ_C/δ_H 39.5/2.49). The ^{13}C-^{1}H correlation signals from the aromatic region of the spectrum were used to estimate the lignin composition in terms of G, S and oxidized S (S') units, and those of the aliphatic-oxygenated region were used to estimate the inter-unit linkage and end-unit abundances. The S lignin content in the laccase-mediator treated sample was corrected for the contribution of MeS to the 106/7.3 ppm signal, which was estimated from the integral of its characteristic signal at 52/3.8 ppm.

III. RESULTS AND DISCUSSION

Lignin modification along the M. thermophila *laccase-MeS pretreatment*

The modification of lignin structure during the laccase-mediator treatment of eucalypt wood was studied after each of the 8 stages, including 4 enzymatic treatments under oxygen (stages 1,3,5 and 7) followed each of them by an alkaline peroxide extraction (stages 2, 4, 6 and 8). With this purpose, all the pretreated eucalypt samples (and the corresponding controls) were analyzed by 2D NMR at the gel state. The initial wood sample (without any treatment) was also analyzed (**Figure 1**, left). The main lignin structures identified are shown in **Figure 1** (right). The aliphatic-oxygenated region of the HSQC spectrum of the initial eucalypt wood shows signals of lignin and carbohydrates, the latter mainly corresponding to xylan (X) and acetylated xylan (X') units. In this region, signals of side-chains in β-*O*-4' alkyl-aryl ether lignin substructures (A), including C_γ-H_γ, C_β-H_β and C_α-H_α correlations (A_γ, A_β and A_α, respectively) were observed. The C_β-H_β correlations gave two different signals corresponding to β-*O*-4' substructures where the second unit is an S unit or a G unit ($A_{\beta(S)}$ and $A_{\beta(G)}$). Other less prominent signals for resinol (β–β') substructures (C) were also observed in the spectrum, with their C_α–H_α, C_β–H_β and the double C_γ–H_γ correlations (C_α, C_β and C_γ). The main signals in the aromatic region of the HSQC spectrum corresponded to the benzenic rings of the S and G lignin units. The S-lignin units showed a prominent signal for the $C_{2,6}$-$H_{2,6}$ correlation ($S_{2,6}$), while the G-lignin units showed different correlations for C_2-H_2 (G_2), C_5-H_5 (G_5) and C_6-H_6 (G_6). Signals corresponding to $C_{2,6}$-$H_{2,6}$ correlations in C_α-oxidized S-lignin units ($S'_{2,6}$) were also observed although in low amount. From the integrals of the above signals an S/G ratio around 3.5, and a large predominance of β-*O*-4' ether linkages, together with some resinols, were estimated for lignin in *E. globulus* wood.

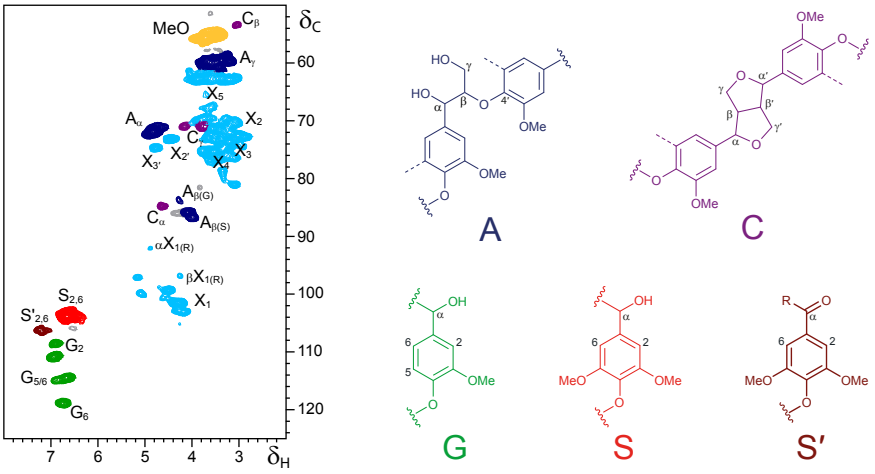

Figure 1. HSQC NMR spectra of whole eucalypt wood (initial sample) swollen in dimethylsulfoxide-d_6 (left) and main lignin structures identified (right): (**A**) β-*O*-4' lignin substructures (including a second S or G unit); (**C**) resinols; (**G**) guaiacyl units; (**S**) syringyl units; and (**S'**) C_α-oxidized S units.

In the pretreatment of eucalypt wood with *M. thermophila* laccase in the presence of MeS (**Figure 2**), an evident modification of lignin structure was produced. This included the complete absence of G units and resinol substructures, together with a high decrease in β-*O*-4' alkyl-aryl ethers, after two cycles of laccase-mediator treatment and alkaline extraction (stage 5), although the most remarkable decreases in these units and substructures were already observed after the first cycle of treatment (stage 3) at the same time that the signals corresponding to β-*O*-4' substructures where the second unit is a G unit ($A_{\beta(G)}$) disappeared. Likewise, the most remarkable increase in C_α-oxidized lignin units (S') was also observed in stage 3. Interestingly, the amount of these oxidized lignin units decreased in all cases with the alkaline extraction (stages 2, 4, 6 and 8).

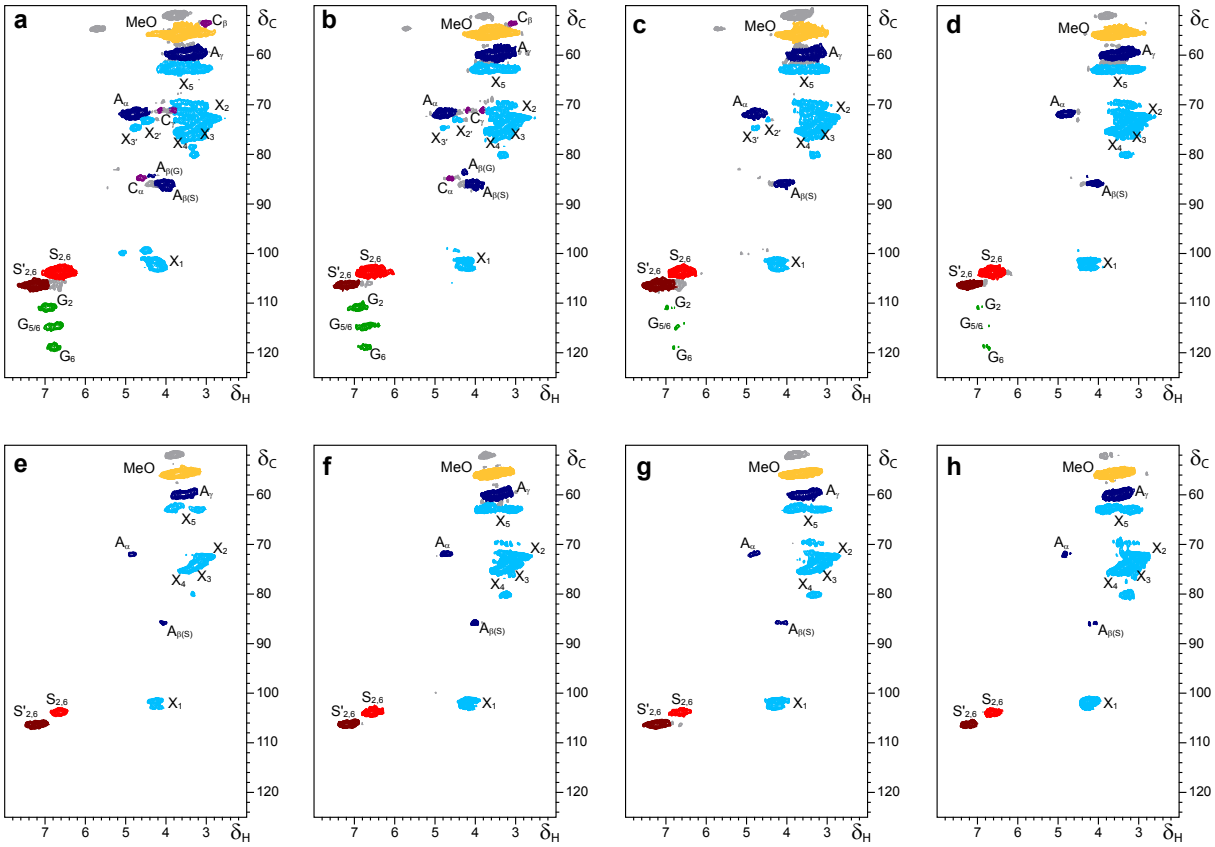

Figure 2. HSQC NMR spectra of whole eucalypt samples from a multistage enzymatic sequence, including four treatments with *M. thermophila* laccase-MeS and four alkaline extractions: **a**), **c**), **e**) and **g**) Samples from first, second, third and fourth enzymatic pretreatment with laccase and MeS (stages 1, 3, 5 and 7, respectively); **b**), **d**), **f**) and **h**) Samples from first, second, third and fourth alkaline peroxide extractions (stages 2, 4, 6 and 8, respectively).

The 2D NMR analyses of eucalypt samples treated with *M. thermophila* laccase alone (followed by alkaline peroxide extractions) (data not shown) revealed a decrease in the β-*O*-4' alkyl-aryl ethers and resinol substructures along the sequence showing the sharpest decrease in the second enzymatic treatment (stage 3). Concerning lignin units an increase in the S/G ratio was observed along the sequence, which was especially significant along the third and fourth cycles of treatment. One effect of the enzymatic treatment with *M. thermophila* laccase (not observed along the control sequence) was the increase in C_α-oxidized lignin units (S') produced in the enzymatic stages 3, 5 and 7. In the aliphatic oxygenated region of the spectra of control samples, acetylated xylan units (X´) decreased considerably after the first alkaline extraction (stage 2) and completely disappeared with the second alkaline extraction (stage 4) while the non-acetylated ones (X) remained. The β-*O*-4' alkyl-aryl ethers and resinol substructures decreased slightly along the sequence and after the last stage the lignin in control were mainly constituted by the former substructures although the latter were still present (data not shown). The most significant effect of the control pretreatment conditions was the increase in the S/G ratio along the sequence that particularly took place in the oxygen stages and was especially evident in the stage 7.

Saccharification of wood pretreated with M. thermophila *laccase-MeS*

The pretreatment of eucalypt wood with *M. thermophila*-MeS produced a decrease in lignin content after the four cycles of about 50%. This decrease in lignin content paralleled the increase in enzymatic saccharification yield of glucose of almost 40%. The pretreatment with the laccase alone produced a decrease of lignin content of about 20% and an increase of glucose release of 9%. On the other hand, the lignin content and saccharification yield with the laccase alone or in the presence of mediator were not modified after the first cycle of pretreatment.

IV. CONCLUSIONS

This work shows the potential of an oxidative enzymatic pretreatment using a recombinant laccase in the presence of a phenolic mediator to delignify and improve cellulase saccharification of a hardwood feedstock (eucalypt wood) when applied directly on the ground lignocellulosic material, and reveals the main chemical changes in the pretreated material, and its recalcitrant lignin moiety, behind the above results.

V. ACKNOWLEDGEMENT

This study was funded by the INDOX (KBBE-2013-7-613549) EU-project and the LIGNOCELL (AGL2011-25379) Spanish MICINN project (co-financed by FEDER funds). J. Rencoret acknowledges the CSIC JAE-Doc contract of the program “Junta para la Ampliación de Estudios” co-financed by the European Social Fund (ESF). H. Lund and L. Kalum from Novozymes (Bagsvaerd, Denmark) are acknowledged for the cellulases and the *M. thermophila* laccase and J. Romero (ENCE, Spain) for the eucalypt wood samples. Manuel Angulo (CITIUS, University of Seville) is acknowledged for providing technical assistance in the NMR analyses.

VI. REFERENCES

[1] Martínez AT; Ruiz-Dueñas FJ; Martínez MJ; del Río JC; Gutiérrez A. Enzymatic delignification of plant cell wall: from nature to mill. *Curr. Opin. Biotechnol.* **2009**, *20*, 348-357.

[2] Bourbonnais R; Paice MG. Oxidation of non-phenolic substrates. An expanded role for laccase in lignin biodegradation. *FEBS Lett* **1990**, *267*, 99-102.

[3] Babot ED; Rico A; Rencoret J; Kalum L; Lund H; Romero J; del Río JC; Martínez AT; Gutiérrez A. Towards industrially feasible delignification and pitch removal by treating paper pulp with *Myceliophthora thermophila l*accase and a phenolic mediator. *Bioresource Technol.* **2011**, *102*, 6717-6722.

[4] Rencoret J; Marques G; Gutiérrez A; Nieto L; Santos I; Jiménez-Barbero J; Martínez AT; del Río JC. HSQC-NMR analysis of lignin in woody (*Eucalyptus globulus* and *Picea abies*) and non-woody (*Agave sisalana)* ball-milled plant materials at the gel state. *Holzforschung* **2009**, *63*, 691-698.

[5] Kim H; Ralph J; Akiyama T. Solution-state 2D NMR of ball-milled plant cell wall gels in DMSO-d_6. *Bioenerg. Res.* **2008**, *1*, 56-66.

[6] Tappi: *2006-2007 TAPPI Test Methods.* Norcoss, GA 30092, USA: TAPPI Press; **2006**.

[7] Selvendran RR; March JF; Ring SG. Determination of Aldoses and Uronic-Acid Content of Vegetable Fiber. *Anal. Biochem.* **1979**, *96*, 282-292.

IONCELL-P: SELECTIVE HEMICELLULOSE EXTRACTION METHOD WITH IONIC LIQUIDS

Annariikka Roselli[1]*, Sari Asikainen[2], Agnes Stepan[1], Alireza Monshizadeh[1], Niklas von Weymarn[3], Kari Kovasin[3], Michael Hummel[1], Herbert Sixta[1]

[1]*Aalto University, School of Chemical Technology, Department of Forest Products Technology, P.O. Box 16300, 00076 Aalto, Finland*
[2]*VTT Technical Research Centre of Finland, P.O.Box 1001, FI-02044 VTT, Finland*
[3]*Metsä Fibre Oy, Revontulenpuisto 2, FI-02100 Espoo, Finland*

ABSTRACT

The IONCELL-P(ulp) process is a method that selectively extracts hemicelluloses from bleached paper grade kraft pulp, using a mixture of ionic liquid and water. The selectivity is achieved by tuning the ionic liquid's solvent properties by the addition of water. The IONCELL-P method refines the paper grade pulp to high purity dissolving pulp and polymeric xylan with no yield losses or polymer degradation. In this study, the IONECELL-P process was applied on both softwood and hardwood pulps and the purified cellulose fractions were evaluated for cellulose triacetate production. Also, the effect of endoglucanase pretreatment was investigated in order to see whether i) the pulp viscosity could be adjusted for the following process steps before the hemicellulose extraction and ii) if decreasing the pulp viscosity would open the fibre structure and thus enhance the extraction.
The hemicelluloses could be efficiently extracted from all the tested kraft pulps (birch, eucalyptus and pine), but the selectivity was better with hardwoods. With the pine pulp, both xylan and glucomannan were decreased down to 0.9 and 2.2 wt %, respectively, but the relatively high residual glucomannan content prevented good quality cellulose acetate production. The endoglucanase pretreatment was damaging the dissolution selectivity, preventing the possibility to open up the fiber structure for the extraction or adjusting the pulp intrinsic viscosity before the IONCELL-P process.

I. INTRODUCTION

The market for cellulose based products is expanding. While the sales figures for paper are declining, the demand for high purity cellulose for various applications is predicted to rise significantly. Thus, the pulp industry needs to shift its production focus from paper grade to dissolving pulp, aiming for new products such as regenerated cellulose fibers and cellulose derivatives.[1]

In our recent studies we have shown that ionic liquids can be used to produce high purity cellulose from birch paper grade pulp, when mixed with a co-solvent.[2] This method, called IONCELL-P(ulp) process, allows the almost quantitative extraction of hemicelluloses without any polymer losses or degradation. Meanwhile, the cellulose retains its cellulose I crystalline form. In addition, the polymeric hemicellulose can be utilized as raw material for new products increasing the value of the overall process. Thus, IONCELL-P represents an attractive alternative to the currently used process steps of dissolving pulp production, e.g. pre-hydrolysis or cold-caustic extraction.

In the present study we compare softwood paper grade pulp in the IONCELL-P process to the previously published results of hardwood paper grade pulps and examine the reactivity of the obtained high purity cellulose fractions.[2,3,4] The reactivity of the IONCELL-P treated hard and softwood pulps is tested by heterogeneous acetylation to produce the acetic acid soluble cellulose triacetate. Finally the quality of the prepared cellulose acetate solutions are compared to ones made from commercial acetate grade pulps by measuring the yellowness and transmittance of the solutions.

II. EXPERIMENTAL

The tested pulps were bleached birch, eucalyptus and pine kraft pulps, containing 25.4 wt %, 16.6 wt % xylan, and 8.1 wt % xylan and 7.1 wt % glucomannan, respectively. The applied ionic liquids were 1-ethyl-3-methylimidazolium dimethylphosphate ([emim][DMP]) purchased from IoLiTec and 1-ethyl-3-methylimidazolium acetate ([emim][OAc]) from BASF.

In the IONCELL-P process the pulp is treated with a mixture of ionic liquid and water at 60°C for 3h. The dissolved hemicelluloses are then removed via filtration and the cellulose fraction is first washed with the mixture of the

ionic liquid and water and then two times with hot water in order to remove all the dissolved hemicelluloses and finally the ionic liquid. The dissolved hemicellulose fraction is first precipitated by adding more water that acts as anti-solvent when it is added excessively. Then the hemicelluloses are collected via centrifugation and washed two times with hot water. The IONCELL-P process is described in more detail by Froschauer *et al*.[2] The water content of the solvent system was optimized for each tested pulp. The gravimetric yield and sugar compositions were determined for both the cellulose and dissolved hemicellulose fractions. The molar mass distributions of the pulps and purified cellulose fractions were determined via gel permeation chromatography (GPC) according to Borrega *et al*.[5] The intrinsic viscosities of the extracted pulps were adjusted by sulfuric acid treatment to values which are suitable for cellulose triacetate production. The acetylation was done via a method described by Testova *et al* with acetic anhydride in acetic acid.[6]

The effect of decreasing pulp intrinsic viscosity before the fractionation process was investigated for the pine pulp. The pulp viscosity was adjusted from 893 ml/g to 660 ml/g and 450 ml/g, with endoglucanase, Ecopulp R treatment (AB Enzymes Oy), and the enzyme dosages were optimized to 0.04 and 0.22 mg protein per g of dry pulp, respectively. The treatment conditions were as follows: temperature 50 °C, retention time 120 minutes and pulp consistency 6 %. Initial pH of the treatment was adjusted to pH 5 with sulfuric acid. After the treatment the pulp was dewatered. Then the enzyme was deactivated by suspending the pulp in hot water (95 °C) for 20 minutes, at 4 % consistency. Then the pulp was dewatered again and (in order to remove the inactivated enzyme) the pulp was washed twice with cold deionized water, each time with ten times the equivalent amount of the absolutely dry pulp's weight.

III. RESULTS AND DISCUSSION

The extraction results under optimum conditions are presented in **Figure 1**. It was remarkable that when the process was optimized for the individual pulps, all the pulps were extracted most efficiently at the same water content (15 wt % for [emim][OAc] and 6.5 wt % for [emim][DMP]) of the solvent system. Another significant finding was that the most potent ionic liquid depended on the used pulp. The solvent system using [emim][DMP] was the most efficient and selective solvent for hardwood pulps, resulting in residual xylan contents of 1.3 and 2.4 wt % for birch and eucalyptus, respectively, while the system using [emim][OAc] was a better for pine. However, the difference between the ionic liquids on pine pulp was mostly seen in the extraction efficiency of the glucomannan**.**

The extraction efficiency did not depend on the amount of the extractable hemicelluloses. The birch pulp that contained 25 wt % of xylan was purified as effectively as the eucalyptus pulp that contained 16.6 wt % of xylan. All the purified pulps presented similar GPC characteristics (**Figure 2**) after the extraction. Based on the molar mass distributions of the purified pulps, the purification is possibly limited by some overlap between the molecular weights of hemicellulose and cellulose. This would support our theory, that the extraction is dependent on the size of the polymers. In that case the residual hemicelluloses are the size of low molar mass cellulose polymers. Still the residual hemicelluloses cannot be removed by decreasing the water amount of the solvent system, as this decreases the selectivity of the process, which leads to the partial dissolution of cellulose and insufficient hemicellulose removal during filtration.[5]

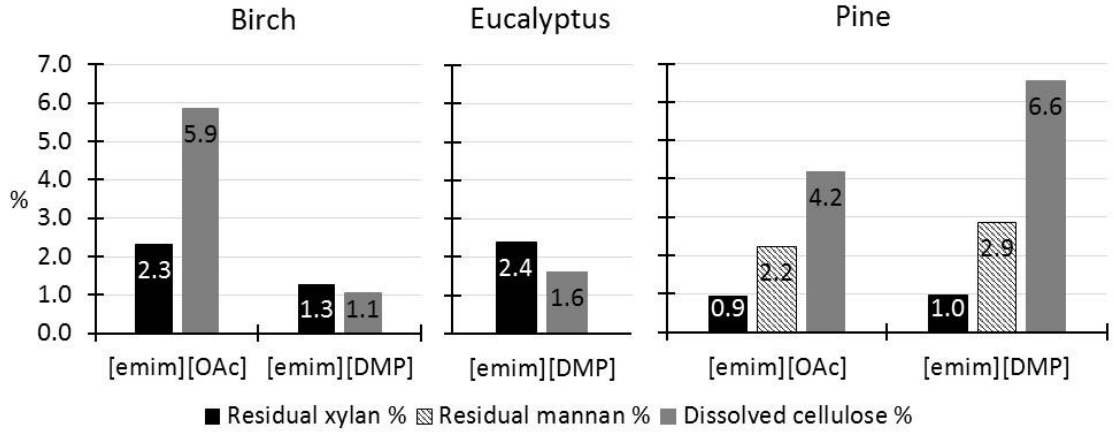

Figure 1. The residual hemicellulose contents and dissolved cellulose fractions of the tested pulps as wt % of the bleached pulp.

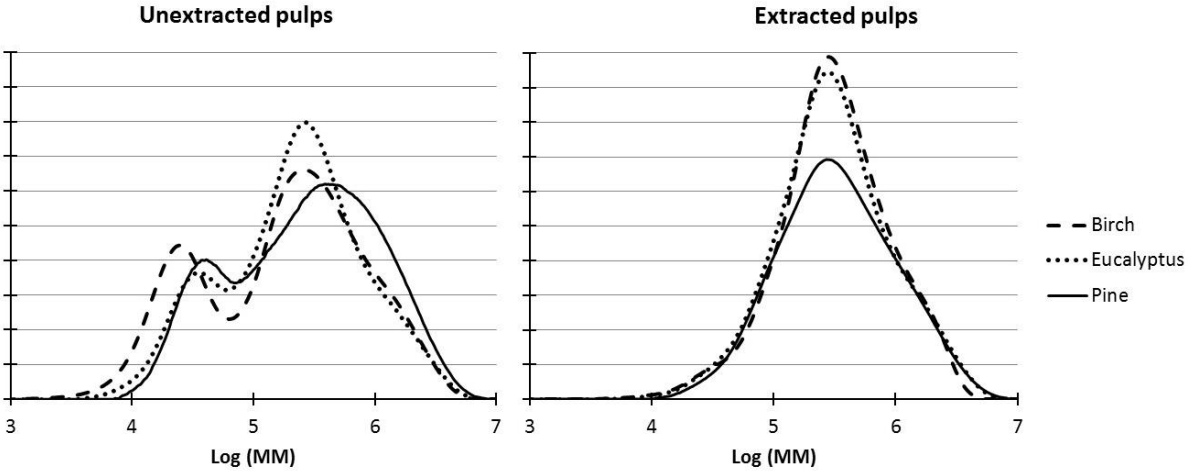

Figure 2. The molar mass distributions of the pulps before and after the IONCELL-P process. Birch and pine pulps are extracted with [emim][OAc] containing 15 wt % of water and the eucalyptus pulp with [emim][DMP] containing 6.5 wt % water.

The pine pulp intrinsic viscosity was decreased via endoglucanase pretreatment, but instead of opening up the pulp structure to enhance the hemicellulose removal, the IONCELL-P process suffered from a loss of extraction selectivity. The decrease in the intrinsic viscosity was directly proportional to the celluloses losses, again supporting the theory that the selectivity is dependent on the polymer size (see **Figure 3**).

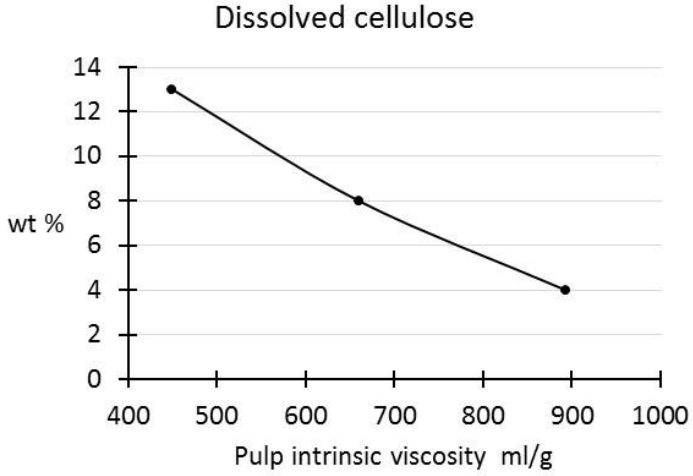

Figure 3. The effect of enzymatic viscosity adjustment of the pulp on the selectivity of the IONCELL-P process.

Cellulose triacetate was prepared from purified eucalyptus and pine pulps and compared to commercial acetate grade pulps. The residual xylan of the eucalyptus remained at 2.2 wt % after viscosity decreasing acid treatment, but its triacetate still had yellowness and transmittance values comparable to the one prepared from commercial eucalyptus pulp that contained 1.8 wt % xylan. The IONCELL-P treated eucalyptus pulp reached the hemicellulose level of the commercial acetate grade eucalyptus pulp when it was first pretreated with endoxylanase and viscosity decreasing acid treatment, resulting in superior yellowness and comparable transmittance values to the commercial pulp.[5] On the other hand, the relatively high glucomannan content of pine wood had an adverse effect on the quality of the produced cellulose triacetate, when compared to the commercial pine pulp that contained only 0.8 wt % of xylan and 0.7 wt % of glucomannan. The yellowness and transmittance results are presented in **Figure 4** as a function of residual hemicelluloses.

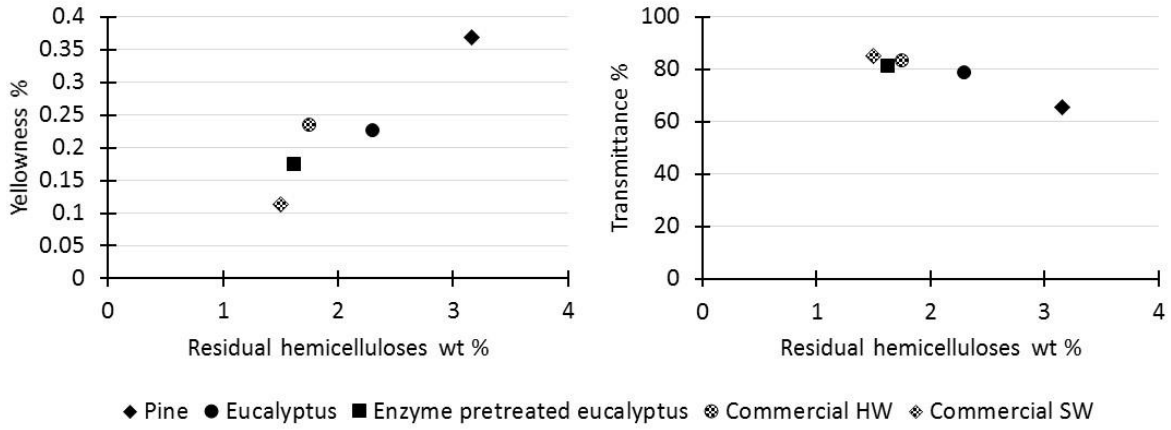

Figure 4. Yellowness and transmittance of the prepared cellulose acetates as function of residual hemicelluloses.

IV. CONCLUSIONS

From our results it can be seen that even though the optimum co-solvent content of a selected ionic liquid may be comparable for hardwood and softwood, other factors, like efficiency of the ionic liquid itself can differ strongly depending on the used pulp. The efficiency was evaluated based on the amount of dissolved cellulose and residual hemicelluloses. The difference in used ionic liquid was highlighted with pine pulp glucomannan.

Comparing the different pulps, it can be seen that it is not the amount of extractable hemicelluloses, but the nature of the pulp polymers that limit the extraction efficiency. The GPC results show that the smaller polymers are readily extracted, while the larger (cellulose) polymers remain undissolved. Moreover, the results indicate that the residual hemicelluloses are probably overlapping with the molecular weight of the cellulose fraction. If this overlapping is increased with endoglucanase pretreatment, the selectivity of the process suffers severely. As glucomannan was more difficult to remove than xylan, an endomannanase pretreatment could be introduced into the process for the pine pulp in order to enhance the glucomannan removal and reach the purity of acetate grade pulp.

V. ACKNOWLEDGEMENT

This research was conducted as part of the Future Biorefinery programs (FuBio) coordinated by the Finnish Bioeconomy Cluster (FIBIC), and as a separate project funded by Metsä Fibre Oy. The funding from companies linked to the FuBio programs and the Finnish Funding Agency for Technology and Innovation (TEKES) enabled long time research to be done. Lidia Testova (Aalto University) is warmly thanked for her assistance in the acetylation experiments.

VI. REFERENCES

[1] Shen, L.; Haufe, J; Patel, M. Product overview and market projection of emerging bio-based plastics. **2009**.

[2] Froschauer, C.; Hummel, M.; Iakovlev, M.; Roselli, A.; Schottenberger, H.; Sixta, H. Separation of Hemicellulose and Cellulose from Wood Pulp by Means of Ionic Liquid/Cosolvent Systems. *Biomacromolecules*, **2013**, 14, 1741-1750.

[3] Roselli, A.; Froschauer, C.; Hummel, M.; Sixta, H. IONCELL: Selective xylan extraction with ionic liquids. **2013**, Proceedings of the 17th International Symposium of Wood, Fibre and Pulping Chemistry, Vancouver, Canada, June 12-14.

[4] Roselli, A.; Hummel, M.; Monshizadeh, A.; Maloney, T.; Sixta, H. Ionic liquid extraction method for upgrading eucalyptus kraft pulp to high purity dissolving pulp. *Cellulose*, submitted **2014**.

[5] Borrega, M.; Tolonen, L.; Bardot, F.; Testova, L.; Sixta, H. Potential of hot water extraction of birch wood to produce high-purity dissolving pulp after alkaline pulping. *Bioresour. Technol*. **2013**, 135, 665-671.

[6] Testova, L.; Borrega, M.; Tolonen, L.; Penttilä, P.; Serimaa, R.; Larsson, P.; Sixta, H. Dissolving-grade birch pulps produced under various prehydrolysis intensities: quality, structure and applications. *Cellulose*, accepted: DOI: 10.1007/s10570-014-0182-x.

SEPARATION AND CHARACTERIZATION OF SULFUR-FREE LIGNIN FROM DIFFERENT AGRICULTURAL RESIDUES

Christine Rossberg[1], Martina Bremer[1], Susanne Machill[2], Steffen Fischer[1]*

[1]Institute of wood and plant chemistry, Technische Universität Dresden, Pienner Straße 19, 01737 Tharandt, Germany; [2]Institute of bioanalytical chemistry, Technische Universität Dresden, Bergstraße 66, 01069 Dresden, Germany
(sfischer@forst.tu-dresden.de)*

ABSTRACT

Wheat straw, as one of the most abundant agricultural residues in Europe, was subjected to alkaline pulping, microwave-assisted alkaline pulping and natural pulping using formic acid and hydrogen peroxide. The obtained lignins were characterized by means of KLASON-lignin, FT-IR spectroscopy, molecular weight determination, elementary analysis and different wet chemical methods. The emphasis here was on their structural differences, especially the content of functional groups like total hydroxyl, phenolic hydroxyl, carboxyl, carbonyl and methoxyl groups.
In addition, numerous agricultural residues, for example barley straw, maize straw, sunflower stalks and horse manure, were characterized and subjected to alkaline pulping, which was carried out based on the optimum parameters found for wheat straw: θ = 160 °C, t = 30 min and c(NaOH) = 3 wt%. As they showed different suitability for carbohydrate and lignin separation using this pretreatment, modification of parameters were necessary for other starting materials. The resulting lignins were characterized with the methods described above. By this, lignin with interesting structural features could be proposed for further studies.

I. INTRODUCTION

Second-generation bioethanol uses agricultural residues, as they are abundant and have no application in food industry. Before hydrolysis and fermentation, the lignocellulosic material needs to be pretreated in order to increase accessibility and to remove potential enzyme inhibitors [1]. Lignin, which is often a byproduct of the pretreatment procedure, could be used for several applications, for example as binder, as additive in asphalt or for the production of basic chemicals.
As lignin structure is strongly dependent on the used biomass, pretreatment procedure and pretreatment parameters, obtained lignins can vary in composition and hence, in their utilization possibilities. Microwave-assisted alkaline pulping has been studied for wheat straw regarding the enhancement of pulp hydrolysis [2,3]. As this is an interesting approach, due to shortening of reaction time and lowering the energy consumption compared to conventional alkaline pulping, further studies on the effect on lignin are necessary.
In order to understand the effect of different raw materials used in a pretreatment process, extensive studies have been conducted with e.g. wheat straw, switchgrass, corn stover and sunflower stalks [4–8]. Unfortunately, these often focus on pulp properties or are not comparable as different pulping procedures or parameters were used.
In this study, different agricultural residues were subjected to alkaline pulping using the same parameters. The aim is, on the one hand, to find lignins of unusual composition and, on the other hand, to find lignins, which seem to be very similar and thus, could be substituted by one another in a future application. Furthermore, three pretreatment procedures were used for wheat straw to show the influence of natural pulping and microwave-assisted alkaline pulping in comparison to conventional alkaline pulping on lignin composition.

II. EXPERIMENTAL

The following agricultural residues served a raw material for the conventional alkaline pulping procedure: pretreated alfalfa (pa), miscanthus (mi), wheat straw (ws), barley straw (bs), oat husk (oh), maize straw (ms), horse manure (hm), coconut shell powder (cp), hemp shives (hs), sunflower stalks (ss), canola straw (cs). Wheat straw was furthermore subjected to microwave-assisted alkaline pulping and natural pulping.
Alkaline pulping was carried out using an autoclave of 2-L capacity. The parameter used were as follows: liquid/solid ratio: 6.1 mL/g, c(NaOH) = 3 wt%, T = 160 °C, t = 30 min. Microwave-assisted alkaline pulping was conducted using a CEM microwave system (MDS 2000) with following parameters: liquid/solid ratio: 6.1 mL/g, c(NaOH) = 3 wt%, power = 609 Watt. After pulp removal, lignin was separated by precipitation at pH 1, followed by washing with hydrochloric acid (0.1 M) and dialysis. Natural pulping was carried out at Saxon Institute for Applied Biotechnology, Leipzig University following a procedure described by Siegle [9]. The pretreatment was performed in a 3 L round bottom flask with reflux condenser at the following parameters:

liquid/solid ratio: 27 mL/g, c(HCOOH): 60 wt%, maximum temperature: 101 °C, time at maximum temperature: 60 min. After separation of pulp, lignin was precipitated in water.
Lignin was determined as the residue after sulfuric acid hydrolysis in two steps according to TAPPI method T222 om-88 [10]. Carboxyl and phenolic hydroxyl groups were determined by nonaqueous potentiometric titration according to [11]. Carbonyl groups were determined after oximation using hydroxylammonium chloride following the procedure suggested by [12]. Methoxyl groups were determined according to [13].
Total amount of hydroxyl groups was determined after acetylation. 0.5 g lignin was weighed into an Erlenmeyer flask and 10 mL of pyridine (distilled) and 10 mL of acetic anhydride (distilled) were added. The flask was closed under a nitrogen stream and left in a shaking device at 40 °C for eight hours. Lignin was precipitated in 100 ml of 0.1 M hydrochloric acid and washed thoroughly to remove residual pyridine and separated over a glass frit (porosity G4). 60 mg of acetylated lignin and 4 ml of sulfuric acid (50 %) are heated under reflux for one hour. After rinsing the condenser the acetic acid is distilled by short-path distillation and finally titrated with sodium hydroxide (0.05 M) and phenolphthalein.
Elementary analysis was carried out on a Hekatech EA 3000 Euro Vector CHNSO. FT-IR spectra were obtained on a Nicolet 210 using KBr pellet technique. Spectra were measured between 400 and 4000 cm^{-1} at a resolution of 4 cm^{-1} with 100 scans.

III. RESULTS AND DISCUSSION

Wheat straw lignin obtained by alkaline pulping, microwave-assisted alkaline pulping and natural pulping

Lignin was separated from wheat straw (composition: 48.9 % cellulose, 27.3 % hemicelluloses and 22.8 % lignin) after alkaline, microwave-assisted alkaline and natural pulping. Yield, expressed as lignin content of the precipitation product in relation to lignin content of wheat straw, and purity of the separated products are shown in Table 1. The highest yield was obtained by alkaline pulping using an autoclave, followed by microwave-assisted alkaline pulping and finally by natural pulping. No significant difference was found for the purity of lignin derived by both alkaline procedures, as the only parameter influencing their purity was found to be the concentration of sodium hydroxide used (data not shown), being the same for both procedures. However, the purity of NP-lignin was found to be considerably higher due to its lower content of carbohydrate impurities.

Table 1 Yield and KLASON-lignin content of precipitation product obtained by alkaline pulping (AP), microwave-assisted alkaline pulping (AM) and natural pulping (NP)

	Yield of precipitation product* [%]	KLASON-lignin content of precipitation product [%]	Yield of lignin** [%]
Alkaline pulping (AP)	22	65.9	64
Microwave-assisted alkaline pulping (AM)	17	66.9	51
Natural Pulping (NP)	11	82.4	39

* in relation to wheat straw ** in relation to KLASON-lignin content in wheat straw

These carbohydrate impurities are also reflected in the content of aliphatic hydroxyl shown in Figure 1, which was found to be lower for NP-lignin compared to both alkaline lignins. Furthermore, alkaline pulping leads to more reactive lignin than natural pulping, since alkaline lignin contains more phenolic hydroxyl groups as the cleavage of α-ether-linkages is particularly promoted by neighbouring group participation in alkaline media [14]. Given that NP-lignin contains less phenolic hydroxyl groups and methoxyl groups as alkaline lignin, it might be more cross-linked due to condensation reactions. This is supported by its comparatively high molecular weight ranging between 7000 and 14500 g/mol (AP-lignin: 3000 – 6500 g/mol), depending on pulping parameters. Furthermore, the content of carbonylic groups differs significantly. Though alkaline treatment promotes the formation of carbonylic groups, this does not seem to be as crucial as oxidation by performic acid generated during natural pulping treatment.

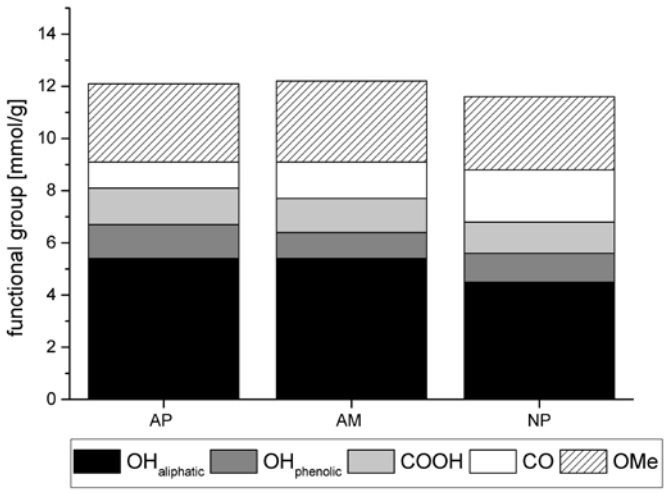

Figure 1 Content of functional groups in lignin obtained by alkaline pulping (AP), microwave-assisted alkaline pulping (AM) and natural pulping (NP)

Lignin of agricultural residues obtained by alkaline pulping

Pretreated alfalfa (pa), miscanthus (mi), wheat straw (ws), barley straw (bs), oat husk (oh), maize straw (ms), horse manure (hm), coconut shell powder (cp), hemp shives (hs), sunflower stalks (ss), canola straw (cs) were submitted to alkaline pulping. The highest lignin yields were attained for pretreated alfalfa, miscanthus, wheat and barley straw, though the maximum amount was separated from coconut shell powder (data not shown). High purities were obtained for lignin from sunflower stalks, hemp shives and coconut shell powder containing KLASON-lignin of 90.4, 89.0 and 86.5 %, respectively.

Figure 2 shows the content of functional groups of the separated lignins in comparison to the commercial Kraft-lignin Indulin AT (IAT). Their composition is strongly dependent on the raw material used. The overall content of functional groups varies between 9.9 mmol/g for pretreated alfalfa and 13.2 mmol/g for hemp shives. Furthermore, lignin from coconut shell powder was found to be remarkable, having a high overall functional group and phenolic hydroxyl content in addition to a low amount of methoxyl groups.

The degree of oxidation and aromatization is shown in Figure 3. With its high degree of aromatization and the described composition of functional groups the lignin from coconut shell powder is of special interest. As expected, lignin from similar botanical origins showed similar H/C and O/C ratios. It is worth noting, that lignin from pretreated alfalfa showed a very low degree of aromatization, despite its low content of aliphatic hydroxyl and carbohydrate impurities.

However, the degree of aromatization as well as the content of carbonyl groups was confirmed by FT-IR spectroscopy (data not shown).

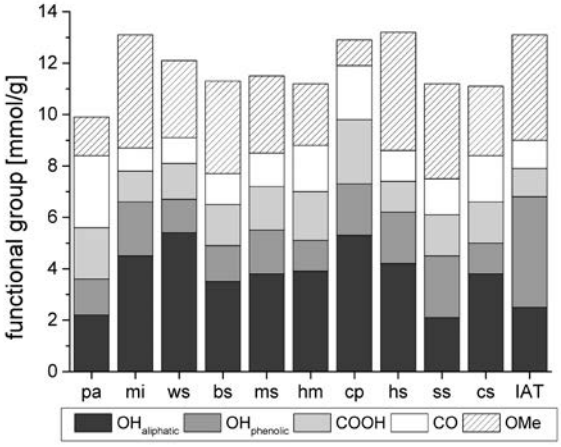

Figure 2 Content of functional groups in lignin from different agricultural residues

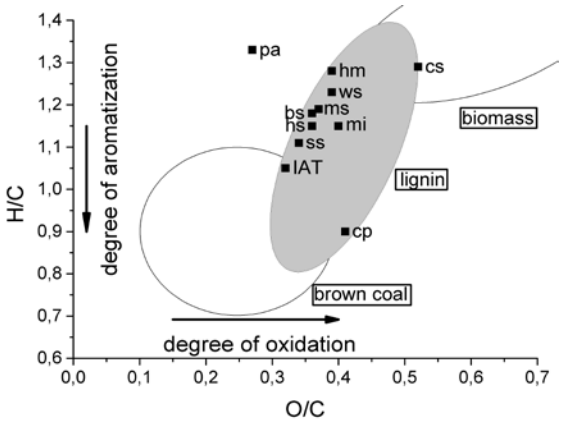

Figure 3 Van-Krevelen diagramm obtained by elementary analysis (assignment adapted from [15])

IV. CONCLUSIONS

1. Reduction of pulping time by using microwave-assisted pulping is possible obtaining lignin with similar purity and composition, but lower yield compared to conventional alkaline pulping.
2. Lignins with purities of > 85 % were separated from sunflower stalks, hemp shives and coconut shell powder by alkaline pulping.
3. Following lignins are suggested for detailed studies: lignin from coconut shell powder, pretreated alfalfa, sunflower stalks

V. ACKNOWLEDGEMENT

The financial support by Staatsministerium für Wissenschaft und Kunst Sachsen (SMWK) is gratefully acknowledged.

The authors thank S. Koenig and M. Hoernicke from Saxon Institute for Applied Biotechnology at Leipzig University for providing wheat straw lignin obtained by natural pulping as well as Dr. Carmen Boeriu (Wageningen UR) for molecular weight determination.

VI. REFERENCES

[1] Talebnia, F.; Karakashev, D.; Angelidaki, I. Production of Bioethanol from Wheat Straw: An Overview on Pretreatment, Hydrolysis and Fermentation. *Bioresour. Technol.*, **2010**, *101*, 4744–4753.
[2] Hu, Z.; Wen, Z. Enhancing Enzymatic Digestibility of Switchgrass by Microwave-Assisted Alkali Pretreatment. *Biochem. Eng. J.*, **2008**, *38*, 369–378.
[3] Zhu, S.; Wu, Y.; Yu, Z.; Chen, Q.; Wu, G.; Yu, F.; Wang, C.; Jin, S. Microwave-Assisted Alkali Pre-Treatment of Wheat Straw and Its Enzymatic Hydrolysis. *Biosyst. Eng.*, **2006**, *94*, 437–442.
[4] Chen, M.; Zhao, J.; Xia, L. Comparison of Four Different Chemical Pretreatments of Corn Stover for Enhancing Enzymatic Digestibility. *Biomass Bioenergy*, **2009**, *33*, 1381–1385.
[5] Cybulska, I.; Brudecki, G.; Rosentrater, K.; Julson, J.L.; Lei, H. Comparative Study of Organosolv Lignin Extracted from Prairie Cordgrass, Switchgrass and Corn Stover. *Bioresour. Technol.*, **2012**, *118*, 30–36.
[6] F. Lopez; M.E. Eugenio; M.J. Diaz; J.A. Nacimiento; M.M. García; L. Jiménez. Soda Pulping of Sunflower Stalks. Influence of Process Variables on the Resulting Pulp. *J Ind Eng Chem*, **2005**, *11*, 387–394.
[7] Ruiz, E.; Cara, C.; Ballesteros, M.; Manzanares, P.; Ballesteros, I.; Castro, E. Ethanol Production from Pretreated Olive Tree Wood and Sunflower Stalks by an SSF Process. *Appl. Biochem. Biotechnol.*, **2006**, *130*, 631–643.
[8] Mousavioun, P.; Doherty, W.O.S. Chemical and Thermal Properties of Fractionated Bagasse Soda Lignin. *Ind. Crops Prod.*, **2010**, *31*, 52–58.
[9] Siegle, S. Method of Producing a Pulp from Cellulosic Material Using Formic Acid and Hydrogen Peroxide. Patent US6183597, 02 **2001**.
[10] Technical Association of the Pulp and Paper Industry. TAPPI Test Methods.
[11] Dence, C.W. Determination of Carboxyl Groups. In *Methods in Lignin Chemistry*; Lin, D.S.Y.; Dence, P.E.D.C.W., Eds.; Springer Series in Wood Science; Springer Berlin Heidelberg, **1992**; pp. 458–464.
[12] Zakis, G.F. *The Functional Analysis of Lignins and Their Derivatives*; Joyce, T.; Brezny, R., Eds.; illustrated edition.; Tappi Pr, **1997**.
[13] Vieböck, F.; Schwappach, A. Eine neue Methode zur maßanalytischen Bestimmung der Methoxyl und Äthoxylgruppe. *Berichte Dtsch. Chem. Ges. B Ser.*, **1930**, *63*, 2818–2823.
[14] Gierer, J. Chemistry of Delignification. *Wood Sci. Technol.*, **1985**, *19*, 289–312.
[15] Schimmelpfennig, S.; Glaser, B. One Step Forward toward Characterization: Some Important Material Properties to Distinguish Biochars. *J. Environ. Qual.*, **2012**, *41*, 1001.

SCOTS PINE GROWING IN LATVIA AS A SOURCE OF PINOSYLVIN STILBENES

Liga Roze[1], Maris Lauberts[1], Tatiana Dizhbite[1], Stefan Willför[2], Galina Telysheva[1]*

*[1]Latvian State Institute of Wood Chemistry, 27 Dzerbenes st., LV-1006, Riga, Latvia; [2] Laboratory of Wood and Paper Chemistry, Åbo Akademi University, Turku, Finland (*ligno@edi.lv)*

ABSTRACT

The content and distribution of pinosylvin stilbenes in Scots pine (*Pinus sylvestris*) wood, sampled in Latvia, have been investigated. Results indicated that heartwood from pines grown in the wet forests have higher pinosylvins content than for trees grown in the dry forests. Our results showed that contents of pinosylvin and pinosylvin monomethyl ether in heartwood varied in the range of 0.1-2.0% (w/w), depending on the height of sampling from the ground. The highest content of pinosylvins was observed for the samples taken at 0.5 m height of tree from ground. Comparison of pinosylvins content in the heartwood of 90 and 60 years old pine trees has shown that for the latter it is higher (0.86 and 2.0 % w/w, respectively). Screening of pinosylvins content in pine trees, using boring technique, (heartwood was taken at the hight 0.5 m from 30 pine trees of 50-60 years old grown in wet forests) showed that pinosylvin and pinosylvin monomethyl ether content can achieve more than 2% on wood dry mass. All heartwood hydrophilic extracts showed antioxidant activity close or higher than the reference sample Trolox (water-soluble analog of vitamin E). The crude ethylacetate and ethanol water extracts of heartwood were purified by preparative liquid chromatography. The results showed that pinosylvin with a higher purity (> 85%) can be obtained from water ethanol extract, but pinosylvin monomethyl ether with higher purity (> 95%) can be obtained from ethyl acetate extract. The analysis of extracts from industrial waste of wooden windows frames (Scots pine taken from Latvian forests) manufacture demonstrated that these waste have good prospects for pinosylvins production due to the pinosylvins yield was of 2% *w/w).*

I. INTRODUCTION

Forests are covering more than 40% of the Latvian territory. Two-thirds of the Latvian forests consist of Scots pine. In the next 50 years pine will remain the leading tree species in Latvia and will be widely available. During recent years pine wood is considered as an abundant source of biologically active compounds, in particular stilbenes. Large amount of bioactive compounds are present in wood knots of several trees species. Pinosylvins possess potent anti-fungal activity against a wide assortment of fungi and is secreted in situations in which the tree is susceptible to infection by fungal agents. Pinosylvins are structurally similar to the anti-cancer stilbene resveratrol. It may be assumed that this structural similarity has also to be accompanied by anticancer activity. The bioactivities of pinosylvins make them exceptionally interesting as active compounds with many potentially beneficial effects [1].

The aim of this work, carrying out in the frame of the ERA-NET Project „PINOBIO", was evaluation of heartwood of pine growing in Latvian forests as a source of pinosylvin stilbenes. Using the methodology developed by scientists of the Abo Academy University (Finland), the heartwood samples of pine trees differing by age, growth location and conditions (wet and dry forests) were analyzed regarding the content of pinosylvin stilbenes. The evaluation of industrial pine wooden waste available as residue after window frames manufacturing from Scots pine taken from Latvian forests was also in focus of the present study.

II. EXPERIMENTAL

The heartwood samples were taken during forest felling from healthy Scots pine trees grown in dry and wet forest. The samples were cut into small discs of 5cm height, then air-dried at room temperature, milled to 50 mesh using Retch equipment and further air-dried to moisture content of about 10 %. Heartwood samples were taken at different heights (0.5 m, 2.5 m and 4 m). Industrial wastes (pine wood chippings with knots) were taken from two different windows producers. The special sorting did not used, all samples under study contained heartwood and knots.

Screening of pinosylvins content in pine trees were performed using boring technique. Samples were taken from 50 – 60 years old 30 Scots pine trees (wet forests) at the height 0.5 m. Pines were sampled in April, 2013. Samples were taken in double. One sample was separated into heartwood and sapwood, second was milled without separation.

Extraction procedure

Extraction was made with ASE apparatus (ASE 350, Dionex Corp.), the lipophilic extractives were first extracted with hexane (solvent temperature 90°C, three 5-min static cycles), then more hydrophilic extractives were extracted with ethylacetate or ethanol water (E/W) mixtures in the same conditions. The yields of extractives were determined gravimetrically after freeze drying.

High performance liquid chromatography analysis (HPLC)

HPLC analysis was performed with an HPLC Agilent Technologies 1100 Series coupled with a UV diode - array detector. The separation of the analytes was done with a column Zorbax Eclipse XDB - C18, 4.6 x 250 mm. Elution was carried out with a flow rate of 1 mL/min using the following solvent systems: solvent A = water/methanol/formic acid (974 : 25 : 1v/v) and solvent B = methanol/formic acid (999 : 1 v/v). The elution conditions were: 0 - 20 min from 60 % B to 80 % B; 20 - 25 min 100% B; 25 - 30 min from 100 % B to 60 % B. The operating conditions were: column temperature 30°C; injection volume 20 μL and detection wavelenght 300 nm. The calibration curves were made by diluting pinosylvin and pinosylvin monomethyl ether standard solutions with methanol water solution to give concentration of the standard in the range 10 - 100 mg/L. The curves were plotted from chromatograms as a peak area vs. concentration of the standard.

Total soluble phenolic compound content

The content of total phenolic compounds in the extracts was determined spectrophotometrically by the Folin-Ciocalteu method with gallic acid as reference. Results are given in gallic acid equivalent (mg GAE g^{-1} of dry extract).

Purification of crude extracts

The crude (ethyl acetate and ethanol water 60 : 40) extracts of heartwood were purified by SP1™ Purification System using Biotage column KP - C18 - HS (12 x 150 mm, 35 - 70 μm)-and after freeze drying analysed with HPLC - DAD as described above.

Assessment of antioxidant activity

Testing radical scavenging activity was performed against stable radicals 2,2-azino-bis(3-ethylbenzthiazoline-6-sulphonic cation radical ($ABTS^{\bullet+}$). $ABTS^{\bullet+}$ was produced by reacting 2,2-azino-bis(3-ethylbenzothiazoline-6-sulphonic acid) (ABTS) with potassium persulfate ($K_2S_2O_8$). The $ABTS^{\bullet+}$ solution was produced reacting 50 mL of stock solution with 200 L of 70 mM $K_2S_2O_8$ water solution. The mixture was left to stand in the dark at room temperature for 15–16 h before use. For the evaluation of the antioxidant capability, the $ABTS^{\bullet+}$ solution was diluted with PBS to obtain the absorbance of 0.800 ± 0.030 at 734 nm. 0.03 mL of the sample solution in DMSO were mixed with 3 mL of the $ABTS^{\bullet+}$ solution in the 1 cm path length microcuvette. The absorbance at 734 nm was read at ambient temperature after 10 min. PBS solution was measured as a blank sample.

III. RESULTS AND DISCUSSION

We have made pinosylvin stilbenes analysis (total was examined 60 wood samples) of different morphological parts of pine wood, highest values of pinosylvins content are showed in Table 1. The pine heartwood was chosen as the object for studies of pinosylvins obtaining, because extracts from heartwood contained less impurities.

Table 1. Content of pinosylvin (PS) and pinosylvin monomethyl ether (PSMME) in Latvian pine; %, w/w o.d.

Sample	**Content of PS and PSMME, % w/w o.d.**			
	Heartwood		**Knots**	
Pine 60 years, dry forest	In extract	In sample	In extract	In sample
Pinosylvin	10.94	0,20	4.78	0.62
Pinosylvin monomethyl ether	28.65	0,53	16.40	2.14
In Total	**39.59**	**0.73**	**21.18**	**2.76**
Pine 60 years, wet forest				
Pinosylvin	17.3	0.60	6.60	1.03
Pinosylvin monomethyl ether	22.0	0.70	21.30	3.34
In Total	**39.3**	**1.30**	**27.90**	**4.37**
Pine 90 years, wet forest				
Pinosylvin	18.7	0.48	-	-
Pinosylvin monomethyl ether	15.1	0.38	-	-
In Total	**33.8**	**0.86**	-	-

Results indicated that heartwood from pines grown in the wet forests have higher pinosylvins content. Comparison of pinosylvins content in the heartwood of 90 and 60 years old pine trees has shown that for the latter it is higher (0.86 and 2.0% w/w, respectively). Compared with knots, the amounts of pinosylvin stilbenes in heartwood were lower, but stilbenes were of higher purity in extracts (40%, w/w). This observation is in compliance with the results obtained in [2].

The screening of pine heartwood samples from wet forest showed that pinosylvin and pinosylvin monomethyl ether content varied depending on the height of sampling and can achieve more than 2 % on heartwood dry mass at the height of 0.5 m (Figure 1).

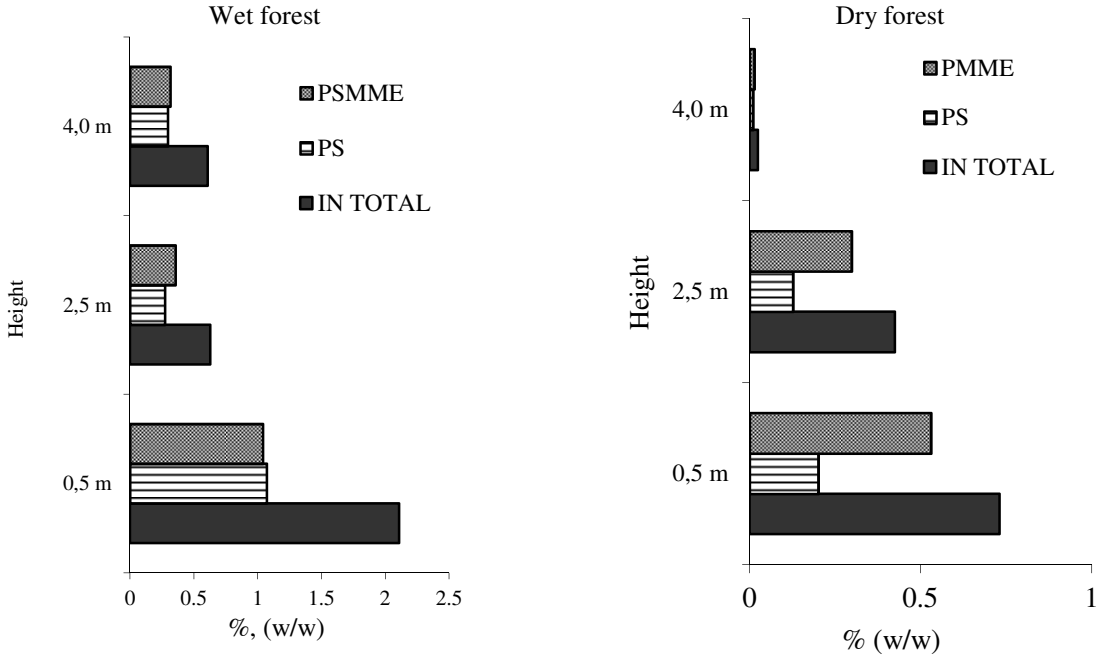

Figure 1. Pinosylvin (PS) and pinosylvin monomethyl ether (PSMME) analysis of Latvian pine heartwood; content %, w/w) and distribution

Our results for the distribution of pinosylvin and pinosylvin monomethyl ether are close to reported data for Norwegian pines [3]. The highest content of pinosylvins was observed for the samples taken at 0.5 m height of tree. Variations of the pinosylvin stilbenes content within tree and between trees were high. We found that the pinosylvin content in pine heartwood ethanol water extracts was on average 14 - 25 % (w/w), pinosylvin monomethyl ether 16 - 30 % (w/w).

The concentration of pinosylvin and pinosylvin monomethyl ether was higher in heartwood than in heartwood + sapwood, the same results was obtained for extracts. Experimental data indicated that for getting of more pinosylvins with lower impurity from pine wood, it is better to take only heartwood. The extract of heartwood of trees grown in wet forest showed the highest radical scavenging activity in the $ABTS^{\bullet+}$ test that was on the level of the reference antioxidant Trolox, it is higher then reported for Pinus pinaster wood extracts obtained by supercritical CO_2 (one third of trolox) [4].

To isolate pure pinosylvin (PS) and pinosylvin monomethyl ether (PMME) we used reverse phase or normal-phase preparative chromatography. The experiment showed that both these chromatography methods can be used for PS and PSMME isolation (HPLC purity $\geqslant$ 85% in each case). The results showed that pinosylvin with a higher purity (> 85%) can be obtained from water ethanol extract, but pinosylvin monomethyl ether with higher purity (> 95%) can be obtained from ethyl acetate extract.

The analysis of extracts from industrial waste of wooden windows frames manufacture demonstrated that these waste have good prospects for pinosylvin stilbenes production because summarized PS and PMME yield was of 1.9 % w/w o.d. (Table 2).

Table 2. Content of phenolic compounds in industrial samples

Industrial sample	Gravimetric yield, % w/w					Total phenols (g Gal.Acid/100g extract)
	Hexane extract	E/W 60:40	PSMME (%' w/w)	PS (%' w/w)	Total (%' w/w)	
1	5.92	2.88	0.910±0.003	0.509±0.002	1.419±0.005	21 ± 2
2	12.24	4.27	1.290± 0.005	0.641±0.002	1.931±0.007	27 ± 2

Differences between industrial samples taken from different producers were extracts yield that could be explained by the differences between heartwood, sapwood and knots content in under study samples.

It was found that the stability of pinosylvins content in wood at room temperature is rather high (Table 3).

Table 3. Pinosylvins content (%, w/w) in milled wood sample during storage at room temperature and in 60% ethanol water solution during storage at 4°C.

Storage	Summary content of PS and PSMME, % of o.d. sample
Wood sample	
1 day	1.38
150 days	1.30
Ethanol water extract	
1 day	0.184
205 days	0.182

The ethanol water extract (containing 34 % w/w pinosylvins) is quite stable in 60 % ethanol water solution stored at 4°C. The chromatography study revealed that there was no apparent degradation of pinosylvin and pinosylvin monomethyl ether. However the storage under low temperature is preferable.

IV. CONCLUSIONS

The data obtained have shown that the tree growing in wet forest characterized with enhanced content of pinosylvins in heartwood in comparison with trees growing in dry forest. According to literature data approximately average content of pinosylvins in the pine wood is about 0.01 - 1 % (w/w). Summarizing the results, the heartwood of Latvian pine trees of approximately 60 years old growing in wet forests is a prospective source for pinosylvin stilbenes obtaining (1.3 – 2%, w/w). Pinosylvin stilbenes could be isolated with good yield from industrial waste from wooden windows frames (pine) manufacture.

V. ACKNOWLEDGEMENT

The research leading to these results has received finding from the WOODWISDOM–NET Research programme, which is transnational R and D programme jointly funded by national funding organization with the framework of the ERA-NET WOODWISDOM-NET and the financial support from the Latvian National Programme is gratefully acknowledged.

VI. REFERENCES

[1] Yeo, S.C., Luo, W., Wu, J., Ho, P.C., Lin, H.S. Quantification of pinosylvin in rat plasma by liquid chromatography-tandem mass spectrometry: application to a pre-clinical pharmacokinetic study. J Chromatogr B Analyt Technol Biomed Life Sci. **2013**, *931*, 68-74

[2] Fang, W., Hemming, J., Reunanen, M., Eklund, P., Pineiro, E.C., Poljanšek, I., Oven, P., Willför, S. Evaluation of selective extraction methods for recovery of polyphenols from pine. Holzforschung, **2013**, *67*, 843–851

[3] Hovelstad, H., Leirset I., Oyaas, K., Fiksdahl, A. Screening analysis of pinosylvin stilbenes, resin acids and lignans in Norwegian conifers. Molecules, **2006**, *11*, 103-114

[4] Conde, E., Fang, W., Hemming, J., Willför, S., Moure, a., Dominguez, H., Parajo, J.C. Water-Soluble Components of Pinus pinaster Wood. BioResources, **2013**, *8*, 2047-2063

COMPARATIVE STUDY OF NANOCELLULOSE PREPARATION METHODS

Inese Sable[1]*, Laura Vikele[1], Arnis Treimanis[1], Liene Anteina[2]

[1]*Latvian State Institute of Wood Chemistry, 27 Dzerbenes Str., Riga, Latvia*
[2]*University of Latvia, 19 Raina Blvd., Riga, Latvia*
**inese.sable@inbox.lv*

ABSTRACT

The aim of the study was to compare three different nanostructurated cellulose (NSC) preparation methods: the thermocatalytic method, regeneration of nanoparticles from ionic liquids and traditional acid hydrolysis. The thermocatalytic method: materials were impregnated with a weak acid (HCl) solution and thermally treated, then dispersed in water medium in a ball mill; thermocatalytically destructed pulp was also oxidized with 2,2,6,6-tetramethyl-piperidinyl-1-oxyl (TEMPO). Acid hydrolysis was carried out in the traditional way with 64% H_2SO_4, followed by dialysis. The regeneration method was performed with BmimCl, Bmim HSO_4 and Bmim PO_4Me_2 ionic liquids (IL). Bmim HSO_4 was found as the most appropriate. Particles obtained were analyzed with Malvern "ZetaNanosizer", atomic force microscopy (AFM) and x-ray diffraction (XRD). NSC cellulose particles obtained by all methods exhibited a rod like shape, in the size range of 100-1000 nm (Nanosizer). AFM studies showed somewhat smaller dimensions. Crystallinity degree of NSC by XRD showed 48% in the case of the thermocatalytic method, 60% after TEMPO modified and 78% in the case of the traditional acid hydrolysis method. Regeneration from ILs yielded NSC with the highest crystallinity degree of 82%.

I. INTRODUCTION

Nanocellulose has gained attention due to its nanoscale dimensions and superior properties. Finding the most appropriate method is an urgent theme in this study of cellulose processing. The aim of the study was to compare three different nanocellulose preparation methods: the thermocatalytic method, regeneration of nanoparticles from ionic liquids and the traditional acid hydrolysis.

The hydrolysis method with following mechanical treatment is applied to obtain cellulose fibrils from different cellulose materials. In sum, these mechanical operations can be accompanied by chemical treatments, to remove the amorphous material. Likewise, an increase of the interfibrillar repulsive forces can be achieved through oxidation (usually employing 2,2,6,6-tetramethyl-piperidinyl-1-oxyl radical (TEMPO) region selective oxidation) [1].

Discovering and applying of ionic liquids (IL) as a new eco-friendly solvent in cellulose dissolution and processing have been initiated in recent age. Good dissolution and regeneration of cellulose in alkyl substituted imidazolium IL's have been reported [2]. In addition, the ability of IL's to modificate cellulose, both physically and chemically [3], even to nanoparticles in case of specific IL and sonification, is shown [4].

Acid hydrolysis is used to obtain crystalline particles from a variety of cellulose sources. The process preferentially removes (hydrolyzes) the amorphous regions within the cellulose nanofibrils. Sulfuric acid is most typically applied as it creates a negative surface charge on the particles, but other acids are also employed. The mechanism of acid hydrolysis is incompletely understood. The acid hydrolysis process is reported in detail elsewhere [5, 6].

II. EXPERIMENTAL

Thermocatalytic method

In compliance with the thermocatalytic method elaborated at the Latvian State Institute of Wood Chemistry [7], polysaccharide-containing materials were impregnated with small quantities of a weak acid (HCl) solution and thermally treated at elevated temperature. Then the partially destructed materials were dispersed in water medium in a ball mill. This process utilizes very small quantities of acid, which is partly evaporated during the heating. The remaining acid can be washed out or left within the fibers. The drawback of the method is a rather intense milling. This method is very efficient when larger volumes of cellulose nano/micro particles have to prepared in laboratory scale.

TEMPO catalyzed oxidation

To oxidize the thermocatalytically destructed pulp sample, it was disintegrated at 4000 RPM during 2 min in 1% water suspension. After draining on a Buehner funnel, cellulose fibers were transferred to stock and filled with distillate water. TEMPO and NaBr were added to the fiber suspension with constant stirring until the solids dissolved. The reaction started with the addition of NaOCl. After 1.5 h, 0.5M NaOH was added for 1.5 h (at pH 11) and then 0.5M HCl for 1h (pH 6). The reaction was performed by stirring constantly at +4^{o}C. To prepare NSC gel after draining and washing with distillate water, the pulp sample was dispersed with water at high shear stress in a ball mill for 3 h [8].

Traditional acid hydrolysis

Traditional acid hydrolysis of birch bleached kraft pulp was carried out with 64% H_2SO_4 at an initial concentration of cellulose of 0.08 g/ml. The mixture was treated at 45°C for 15 min. Hydrolysis was stopped by adding 500 ml of cold water. After hydrolysis, the resulting suspension was centrifuged and dialyzed against water for 14 days.

Regeneration from ionic liquids

Microcrystalline cellulose, obtained by the thermocatalytic method [9] from bleached (using H_2O_2, and NaOH liquid to pulp ratio 16.7 ml/g) kraft pulp of aspen hybrid (*Populus tremuloides* Michx. X *Populus tremula* L.), was mixed (10% w/w) and dissolved in three types of ILs (1-butyl-3-metylimidazolium chloride BmimCl; 1-butyl-3-metylimidazolium hydrogen sulfate Bmim HSO_4 and 1-butyl-3-metylimidazolium dimethyl phosphate Bmim PO_4Me_2). The cellulose solution was stirred continuously in an oil bath in the temperature range of 70°-100°C for 1 to 3 h. The reaction was quenched by adding deionized water to the mixture. Sonification was applied in the cellulose regeneration stage. The suspension was washed with deionized water, and centrifugation was used to isolate cellulose nanoparticles.

The hydrolysis of microcrystalline cellulose by BmimHSO_4 is found to be rather similar to acid hydrolysis. In this reaction, the ionic liquid is expected to react with microcrystalline cellulose in a similar manner as acids in acid hydrolysis. IL causes the hydrolytic cleavage of glycosidic bonds that results in the rearrangement of the interlinking chain ends [6]. The dissolution process of microcrystalline cellulose did not provide any difficulties – the regeneration step (adding of cold water and sonification) caused the formation of an emulsion, and particles appeared in the shape of a white precipitate.

In the case of BmimCl, the regeneration process depended on the temperature of the mix of cellulose and IL, and water applied. If both liquids were hot and pre-filtration took place before regeneration, an emulsion was formed and particles appeared in the form of a white precipitate. In another case, adding water caused the formation of non-crystalline aggregates in the solution. It has been reported [10] that gelation processes start in the solution of cellulose in BmimCl and water, which continue with the preparation of flexible gel materials from these aggregates.

In the case of BmimPO_4Me_2, when water was added, one-piece gel-type material was formed, even sonification did not cause its decomposition in particles.

Methods of NSC characterization

Characterization of the nanostructured cellulose samples was carried out by a Malvern "ZetaNanosizer", atomic force microscopy (AFM) and x-ray diffraction (XRD).

III. RESULTS AND DISCUSSION

Regeneration of cellulose nanoparticles from ionic liquids

The dissolution process of cellulose in ILs was attributed to their ability to break the network of hydrogen bonds existing in cellulose [11].

We conclude that the process strongly depends on the above mentioned parameters and if NSC is the preferred outcome, temperature and other parameters should be precisely provided. In the case of BmimHSO_4, the regeneration process provides NSC.

The aim of using BmimPO_4Me_2 for our experiments was to examine the ability to regenerate cellulose in nanoparticles from the IL solution. In that respect there is limited information about detailed process parameters of dissolution of cellulose in phosphate-based ILs. A material was obtained in accordance with [12], where preparing one-piece (film) product from the BmimPO_4Me_2/cellulose solution is reported.

Deliberating on the primary aim of this study, we conclude that $BmimHSO_4$ is the most appropriate type of the ion liquid for the preparation of cellulose nanoparticles.

Characterization of particles obtained

On the average, the cellulose nanoparticles obtained by acid hydrolysis and regeneration from IL, and TEMPO modified NSC cellulose particles exhibit a rod like shape. The dimensions of the cellulose particles were found to be in the size range of 100-1000 nm. The results of the Zeta-nanosizer measurement of NSC are summarized in **Table 1.**

Table 1 The size and charge of nanostructured cellulose particles

	Thermocatalytic NSC	TEMPO modified NSC	IL method NSC	Acid hydrolysis method NSC
Average size of particles, nm	308	102	439	679
ζ potential, mV	-20.4 ± 0.2	-29.4 ± 0.5	-20.7 ± 0.2	-18.0 ± 0.2

AFM images of NSC showed both nanorods and abundant nanoparticles whereas uniformly shaped nanorods were observed for TEMPO-modified NSC (**Figure 1a**). AFM height profiles and distribution showed abundant nanoparticles of NSC obtained by the thermocatalytic method (**Figure 1b**). It was shown that crystallites were broken by prolonged mechanical treatment. The observation of both nanoparticles and nanorods in TEMPO modified NSC showed more heterogeneous morphology.

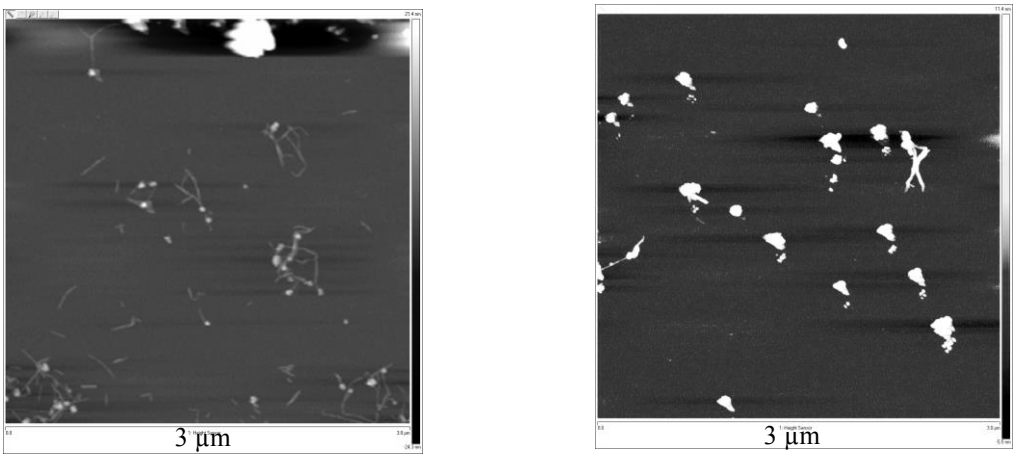

Figure 1. AFM images of TEMPO modified NSC (a) and thermocatalytic NSC (b).

AFM height images exhibited thermocatalytically obtained NSC nanoparticles to be 83 ± 4 nm and TEMPO modified NSC 48 ± 2 nm (**Table 2**). TEMPO modified NSC nanorods appeared to be bimodally distributed to lengths of 167 ± 10 nm and 331 ± 23 nm.

Table 2 Size of NSC as determined by AFM

Sample		Size, nm
TEMPO NSC	Abundant nanoparticles	48 ± 2
	Nanorod length 1	167 ± 10
	Nanorod length 2	331 ± 23
	Nanorod diameter	32 ± 2
Thermocatalytic NSC	Abundant nanoparticles	83 ± 4

The crystallinity degree was calculated, and it is shown in Table 3. It can be seen that cellulose in the nanoparticles obtained by the IL and acid hydrolysis methods had much higher crystallinity than cellulose in raw pulp fibers. The crystallinity degree calculated from XRD patterns of cellulose in the pulp sample was

59%.When applying the thermocatalytic method by weak acid treatment and ball mill grinding, the process produced NSC with a lower crystallinity degree of 48% due to prolonged mechanical treatment. The NSC isolated by traditional sulfuric acid hydrolysis and the IL method yielded the highest crystallinity degree in the range of 78-82%. As a result of the TEMPO oxidation of thermocatalytically obtained NSC, the CrI gave a considerably higher crystallinity degree around 60%. However, TEMPO oxidized cellulose from various sources has been previously reported to show unchanged crystallinity [10].

Table 3 Crystallinity degree of NFC by XRD

	Bleached pulp	Thermocatalytic NSC	TEMPO modified NSC	IL method NSC	Acid hydrolysis method NSC
Crystallinity degree, %	59	48	60	82	78

IV. CONCLUSIONS

The ongoing investigation to find original and efficient methods for preparing cellulose nanoparticles has attracted considerable attention. Nevertheless the matter should be conceived as being still in its infancy and hence the need exists of further research involving both novel strategies and the optimization of those outlined here. The obvious next effort should focus on systems bearing a green character, an economically viable application potential and also ability of process transfer to pilot-scale amounts.

V. ACKNOWLEDGEMENT

The financial support by the Latvian Council of Science (project 564/2013) and Latvian State Project "NatRes" is acknowledged.

VI. REFERENCES

[1] Saito, T.; Nishiyama, Y.; Putaux, J.L.; Vignon, M.; Isagai, A. Homogeneous suspensions of individualized microfibrils from TEMPO-catalyzed oxidation of native cellulose. *Biomacromolecules*. **2006**, *7*, 1687–1691.

[2] Swatloski, R.P.; Spear, S.K.H.; Rogers, R.D. Dissolution of cellulose with ionic liquids. *J. Am. Chem. Soc*. **2002**, *124*, 4974–4975.

[3] Feng, L.; Chen, Z.L. Research progress on dissolution and functional modification of cellulose in ionic liquids. *J. Mol. Liq*. **2008**, *142*, 1–5.

[4] Zakaria, M.; Nawshad, M.; Ariyanti, S.; Mohamad, A.B.; Vignesh, K.; Sikander, R. Preparation of cellulose nanocrystals using an ionic liquid. *J. Polym. Environ*. **2011**, *19*, 726–731.

[5] Elazzouzi-Hafraoui, S.; Nishiyama, Y.; Putaux, J. L.; Heux, L.; Dubreuil, F.; Rochas, C. The shape and size distribution of crystalline nanoparticles prepared by acid hydrolysis of native cellulose. *Biomacromolecules.* **2008**, *9*, 57–65.

[6] Moon, R. J.; Martini, A.; Nairn, J.; Simonsen, J.; Youngblood, J. Effect of microcrystallite preparation conditions on the formation of colloid crystals of cellulose. Cellulose nanomaterials review: structure, properties and nanocomposites. *Chem. Soc. Rev.* **2011**, *40*, 3941–3994.

[7] Laka M.; Chernyvskaya, S.; Maskavs, M. Cellulose-containing fillers from polymer composite. *Mech. Compos. Mater*. **2003**, *39 (2)*, 183–188.

[18] Saito, T.; Isogai, A. TEMPO-mediated oxidation of native cellulose. The effect of oxidation conditions on chemical and crystal structures of the water-insoluble fractions. *Biomacromolecules*. **2004**, *5(5)*, 1983–1989.

[9] Laka, M.; Chernyavskaya, S. Obtaining microcrystalline cellulose from softwood and hardwood pulps, *BioResources*. **2007**, *2(3)*, 583–589.

[10] Kadokawa, J.; Murakami, M.; Kaneko, Y. A facile preparation of gel materials from a solution of cellulose in ionic liquids. *Carbohyd. Res.* **2008**, *343*, 769–772.

[11] Cao, Y.; Wu, J.; Zhang, J.; Li, H.; Zhang, Y.; He, J. Room temperature ionic liquids: A new and versatile platform for cellulose processing and derivatization. *Chem. Eng. J.* **2009**, *147*, 13–21.

[12] Zhao, D.; Li, H.; Zhang, J.; Fu, L.; Liu, M.; Fu, J.; Ren, P. Dissolution of cellulose in phosphate-based ionic liquids. *Carbohyd. Polym*. **2012**, *87*, 1490–1494.

DEMOSTRATION OF LIGNOSULFONATES OXIDATION BY VERSATILE PEROXIDASE FROM *Pleurotus eryngii*

Verónica Sáez-Jiménez[1], Maria Camilla Baratto[2], Rebecca Pogni[2], Angel T. Martínez[1]* and Francisco Javier Ruiz-Dueñas[1]*

[1]*Centro de Investigaciones Biológicas, CSIC, Ramiro de Maeztu 9, E-28040 Madrid, Spain;*
[2]*Department of Chemistry, University of Siena, Via Aldo Moro, I-53100 Siena, Italy*
*(*atmartinez@cib.csic.es, *fjruiz@cib.csic.es)*

ABSTRACT

Versatile peroxidase (VP) is a high redox-potential peroxidase of biotechnological interest due to its ability to oxidize a wide range of substrates including phenolic and non-phenolic aromatics, and dyes. The ability of VP from the white-rot fungus *Pleurotus eryngii* to oxidize water-soluble technical lignins (lignosulfonates) was demonstrated using electron paramagnetic resonance (EPR) and stopped-flow rapid spectrophotometry. In addition, the electron transfer reaction produced between the peroxidase and the lignin macromolecule was for the first time unequivocally related to the presence of a solvent-exposed tryptophan residue (Trp164) using mutated variants. Finally, the tryptophan radical formed after VP activation by H_2O_2 was identified as catalytically active, since it was reduced during lignosulfonate oxidation, as shown by EPR spectroscopy.

I. INTRODUCTION

Around 20% of the total carbon fixed in nature is incorporated into lignin [1]. It is the only biomass component with an aromatic origin, and a valuable raw material [2]. Lignin can be an important source of aromatic chemicals and polymers with numerous applications. The only organisms being able to significantly modify and degrade lignin in nature are the white-rot fungi, acting through a battery of oxidoreductases secreted to the extracellular medium [1]. One of these enzymes is versatile peroxidase (VP), which is able to oxidize lignin and a variety of other recalcitrant substrates.

During the catalytic cycle, VP at resting state (containing a Fe^{3+}-heme) is activated by H_2O_2 yielding Compound I (CI) (with an Fe^{+4}=O - porphyrin radical complex). CI catalyzes a one-electron substrate oxidation and forms Compound II (CII) which contains an Fe^{+4}=O complex. Through another one-electron substrate oxidation the resting state is recovered. Moreover, VP oxidizes high redox-potential compounds through an exposed catalytic tryptophan which forms a radical (both in the CI and CII transient states) on the surface of the protein through an electron transfer from this residue to heme [3].

In this work, the ability of VP to act on lignin was investigated using water soluble lignosulfonates (LS). LS are technical lignins obtained in the paper pulp industry through the sulphite pulping of wood, being commercialized for a wide range of applications. LS representative of two types of wood were used in this study: one from *Picea abies* (softwood) which contains a high proportion of monomethoxylated (guaiacyl, G) lignin units and other from *Eucalyptus globulus* (hardwood) which has both monomethoxylated and dimethoxylated (syringyl, S) lignin units. The main aim of the work was to study the ability of VP to oxidize LS, and investigate the role played by the putative catalytic tryptophan during the oxidation.

II. EXPERIMENTAL

Enzyme production

VP from *P. eryngii* and its W164S and R257A/A260F mutated variants [4,5] were produced in *Escherichia coli* as follows. pFLAG1 expression plasmid containing the mature protein-coding sequence of VPL2 was transformed into *E. coli* W3110. The cells were grown in Terrific Broth medium until OD~ 1.Then protein expression was induced by addition of 1mM IPTG and cells were further grown for 4 hours. The apoprotein accumulated as inclusion bodies and was recovered in a solution containing 8 M urea, 1 mM DTT and 1 mM EDTA in 50 mM Tris-HCl, pH 8. The subsequent *in vitro* reactivation process was carried out overnight in a solution containing 0.16 M urea,15 µM hemin, 5 mM $CaCl_2$, 0.1 mM DTT, 0.5 mM GSSG and 0.1 mg/ml protein concentration in 20 mM Tris-HCl, pH 9.5. Finally, native VP and its variants were purified by anion exchange chromatography (Resource Q column, GE

Healthcare) using a 0-0.3 M NaCl gradient. The R_z (A_{410}/A_{280} ~ 4) of the variants was indicative of the purity of the proteins. The UV-vis spectrum was checked in order to confirm the correct folding of the reactivated enzymes.

Lignosulfonates

Two types of LS were selected for this study, softwood LS from *P. abies* and hardwood LS from *E. globulus*, both kindly provided by Borregaard (Sapsborg, Norway). LS were prepared by a first dialysis in 10 mM EDTA, 50 mM Tris, pH 8, with the aim of removing Mn^{2+} traces, and then a second one in milli-Q water to remove salts and EDTA.

Transient-state kinetics

Reduction of CI and CII of native VP, and its W164S and R257A/A260F directed variants, by LS was measured using a stopped-flow equipment (Bio-Logic) with a three-syringe module (SFM300) synchronized to a diode array detector (J&M) and BioKine software.

CI reduction experiments were carried out mixing the variants (1µM final concentration) with H_2O_2 (1µM final concentration) in 0.1 mM sodium tartrate, pH 3.5. After 0.6 s, CI was formed. Next, LS were added at different concentrations and the reaction was followed at 416 nm (isosbestic point of VP CII and resting state). CII reduction was studied by mixing a solution of enzyme and ferrocyanide (both at 1µM final concentration) with H_2O_2 at equimolar ratio. The solution was aged for 6 s and CII formation was achieved. Then an excess of LS was added (different concentrations) and the reaction was followed at 406 nm (Soret maximum of resting enzyme).

All kinetic traces exhibited single-exponential character from which pseudo first-order rate constants (k_{2obs} and k_{3obs} for CI and CII reduction, respectively) were calculated. Plots of k_{2obs} *vs* LS concentration fitted to a linear or hyperbolic model from which apparent second-order rate constants (k_{2app}) were obtained. On the other hand, plots of k_{3obs} *vs* LS concentration were fitted to a Michaelis-Menten model from which K_{D3} (dissociation constant) and k_3 (first-order rate constant) were obtained. R257A/A260F CII reduction kinetics were fitted to a sigmoid model from which k_3 and $K_{0.5}$ (equivalent to K_{D3}) constants were obtained. The corresponding k_{3app} rate constants were calculated with the equation: $k_{3obs} = (k_3/K_{D3})[S]/(1+[S]/K_{D3})$.

Electron paramagnetic resonance (EPR) spectroscopy

EPR measurements were performed in solutions containing 0.16 mM VP, 1.3 mM H_2O_2 and 0.64 or 1.92 mM softwood LS in 50 mM sodium tartrate, pH 3. The reactions were initiated by addition of H_2O_2 and stopped by immersion in liquid nitrogen after 2 s or 10 s reaction. CW-X-band (9 GHz) EPR measurements were carried out with a Bruker E500 Elexsys Series using the Bruker ER 4122 SHQE cavity and an Oxford helium continuous flow cryostat (ESR900).

III. RESULTS AND DISCUSSION

The kinetic constants for LS oxidation under transient-state conditions were obtained from spectrophotometric measurements (Figure 1, Table 1). Native VP was able to oxidize LS from softwood and hardwood with similar efficiency, although some differences were observed in CII reduction. The dissociation constant (K_{D3}) using hardwood LS was 3.4 lower than for softwood LS, indicating a higher affinity of the enzyme for the hardwood LS. This improvement in affinity was compensated with a similar decrease in the first-order rate constant (k_3) for the oxidation of this LS, this being the reason that finally explain the similar efficiency in the oxidation of both LS.

Besides native VP, two variants were tested for the oxidation of LS. In the W164S variant the exposed catalytic tryptophan [4], was substituted by a serine with the intention to remove this catalytic site. As expected, the variant without catalytic tryptophan showed kinetic constants impaired for the oxidation of both LS, meaning that the electron transfer between VP and LS was reduced. In the case of softwood LS, k_{2app} (CI reduction) was impaired 2.3 times and k_{3app} (CII reduction) 4.3 times. The worsening in the constants was more accentuated in the case of the hardwood LS oxidation, where the k_{2app} and k_{3app} values experienced 12-fold and 150-fold decreases, respectively. These results are in agreement with data obtained for this variant oxidizing simple high redox-potential compounds, which evidenced a 17-50-fold k_{2app} decrease depending on the substrate tested, whereas k_{3app} was 175-fold reduced or the activity was even not observed [5]. Electron transfer between synthetic lignin (DHP) and LiP had been previously shown [6] but this is the first time that electron transfer between peroxidase and lignin is established being this ability related unequivocally to the presence of the catalytic tryptophan since the removal of Trp164 led to an enzyme with impaired lignin oxidation.

EPR spectra of VP reactions with different equivalents of softwood LS (after enzyme activation by H_2O_2) were obtained in order to know which radicals were formed during the reaction (Figure 2). It was found that when a low amount of LS was present in the reaction (4 equivalents, referred to the amount of enzyme), a mixed radical signal centered on both the catalytic tryptophan and LS was detected after 2 s reaction. This signal remained finally located on the Trp164 residue when the reaction time was increased to 10 s. By contrast, when a higher amount of LS was present in the reaction (12 equivalents), the tryptophan radical signal was substituted by the LS radical signal. These data evidenced that the tryptophan radical formed after VP activation by H_2O_2 was the responsible for LS oxidation, and that LS oxidation led to the formation of a substrate radical. This is the first direct proof of the fact that the tryptophan radical formed in VP is catalytically active since its reduction was observed when LS was oxidized, as previously demonstrated for the radical formed in LiP [7].

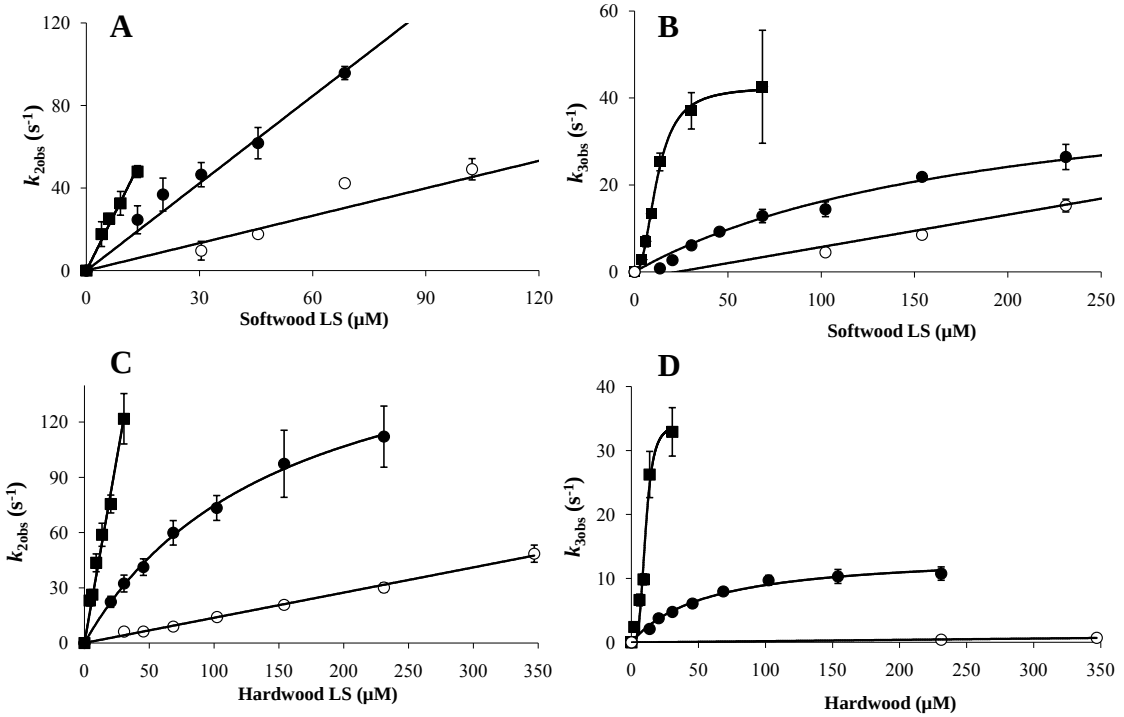

Figure 1. Kinetics of reduction of CI (A, C) and CII (B, D) of native VP (●)and its W164S (○)and 257A/A260F (■)variants by softwood (A, B) and hardwood (C, D) LS. Means and 95% confidence limits.

Table 1. Transient-state kinetic constants for reduction of CI and CII of native VP and its W164S and R257A/A260F variants by softwood and hardwood LS. k_3(s^{-1}), K_{D3} (μM), $k_{2app}$and k_{3app}($s^{-1}mM^{-1}$).

	CI reduction		**CII reduction**					
	Softwood	**Hardwood**	**Softwood**			**Hardwood**		
	k_{2app}	k_{2app}	k_3	K_{D3}	k_{3app}	k_3	K_{D3}	k_{3app}
VP	1410 ± 30	1240 ± 50	48 ± 2	194 ± 21	250 ± 20	14 ± 1	57 ± 7	250 ± 20
W164S	660 ± 90	140 ± 3	-	-	70 ± 10	-	-	2 ± 0.2
R257A/A260F	3680 ± 150	4020 ± 130	40 ± 1	11 ± 1	3540 ± 70	34 ± 3	10 ± 1	3260 ± 240

The second VP variant analyzed was R257A/A260F, which harbors two mutations near the catalytic tryptophan and showed improved kinetic constants for the oxidation of some lignin model compounds under transient state conditions [5]. Interestingly, this variant also showed enhanced catalytic constants for the oxidation of LS. An 11-fold improvement in the apparent second-order rate constant (k_{3app}) was observed using both LS as substrates, indicative of a higher efficiency in the oxidation. CI reduction was similarly improved, although the increases in k_{2app} were not as high (2.6-3.3-fold increment). The improvements achieved were mainly due to changes in the dissociation constant (K_{D3}) which suffered a 17-fold and 6-fold decrease for softwood LS and hardwood LS respectively, indicative of a higher affinity for LS. The results achieved for LS oxidation by this variant show that the efficiency of the electron

transfer from the catalytic tryptophan depends on its surface environment and can be improved by modifying it.

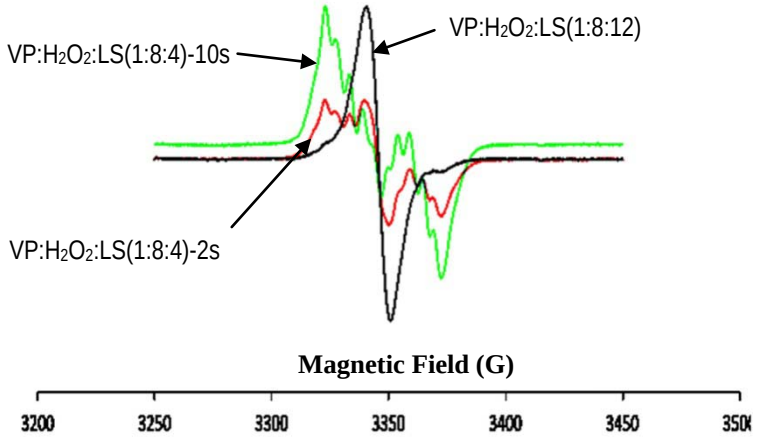

Figure 2. EPR spectra of the reaction of VP, H_2O_2 and softwood LS at different molar ratios and times.

IV. CONCLUSIONS

The ability of VP to oxidize softwood and hardwood lignin was demonstrated by stopped-flow rapid spectrophotometry using water soluble lignosulfonates. In this way, the electron transfer produced between VP and lignin was established, and this ability was for the first time unequivocally related to the presence of Trp164 using site-directed variants. Moreover, the EPR experiments showed Trp164 as catalytically active since its reduction happened concomitant to the oxidation of LS. Finally, improvements in the oxidation of LS after the R257A/A260F double mutation illustrated the relevance of the Trp164 environment in the activity of the enzyme.

V. ACKNOWLEDGEMENT

The study was funded by the PEROXICATS (KBBE-2010-265397) and INDOX (KBBE-2013-613549) EU projects and the HIPOP (BIO2011-26694) Spanish Project. We are grateful to Borregard for providing the LS preparations.

VI. REFERENCES

[1] Ruiz-Dueñas F.J.; Martínez A.T. Microbial degradation of lignin: How a bulky recalcitrant polymer is efficiently recycled in nature and how we can take advantage of this**.** *Microbial Biotechnol.* **2009**, *2,* 164-177.

[2] Lora J.H.; Glasser W.G. Recent industrial applications of lignin: A sustainable alternative to nonrenewable materials**.** *J. Polym. Environ.* **2002**, *10,* 39-48.

[3] Ruiz-Dueñas F.J.; Pogni R.; Morales M.; Giansanti S.; Mate M.J.; Romero A.; Martínez M.J.; Basosi R.; Martínez A.T. Protein radicals in fungal versatile peroxidase: Catalytic tryptophan radical in both Compound I and Compound II and studies on W164Y, W164H and W164S variants**.** *J. Biol. Chem.* **2009**, *284,* 7986-7994.

[4] Pérez-Boada M.; Ruiz-Dueñas F.J.; Pogni R.; Basosi R.; Choinowski T.; Martínez M.J.; Piontek K.; Martínez A.T. Versatile peroxidase oxidation of high redox potential aromatic compounds: Site-directed mutagenesis, spectroscopic and crystallographic investigations of three long-range electron transfer pathways**.** *J. Mol. Biol.* **2005**, *354,* 385-402.

[5] Ruiz-Dueñas F.J.; Morales M.; Mate M.J.; Romero A.; Martínez M.J.; Smith A.T.; Martínez A.T. Site-directed mutagenesis of the catalytic tryptophan environment in *Pleurotus eryngii* versatile peroxidase**.** *Biochemistry* **2008**, *47,* 1685-1695.

[6] Johjima T.; Itoh H.; Kabuto M.; Tokimura F.; Nakagawa T.; Wariishi H.; Tanaka H. Direct interaction of lignin and lignin peroxidase from *Phanerochaete chrysosporium***.** *Proc. Natl. Acad. Sci. USA* **1999**, *96,* 1989-1994.

[7] Smith A.T.; Doyle W.A.; Dorlet P.; Ivancich A. Spectroscopic evidence for an engineered, catalytically active Trp radical that creates the unique reactivity of lignin peroxidase**.** *Proc. Natl. Acad. Sci. USA* **2009**, *106,* 16084-16089.

ALLYLATION AND CLAISEN REARRANGEMENT AS NOVEL CHEMICAL MODIFICATION OF LIGNIN

Anika Salanti[1], Marco Orlandi[1], Frigerio Paola[1], Luca Zoia[1]

Department of Environmental and Earth Sciences, University of Milano-Bicocca, Piazza della Scienza, 1 Milan, I-20126 Italy. (luca.zoia@unimib.it)

ABSTRACT

The conversion of lignin into value-added products is traditionally hampered by its stochastic structure and its complex reactivity. In this work, is for the first time reported the allylation reaction and the aromatic Claisen rearrangement of the allyl group on lignin as potential chemical modification aimed at the development of new lignin-based materials and the improvement of its compatibility and ease of processing. In particular, the Claisen rearrangement of lignin was foreseen as a valuable approach to release phenols in an already chemically modified lignin giving additional reactive sites for further transformation. Finally, a screening of the antioxidant activity of reference, allylated, and Claisen rearranged lignins was carried out. Rearranged lignins exhibited satisfying antioxidant activities if compared to the reference ones.

I. INTRODUCTION

Lignin is the second most abundant polymer in the world after cellulose and it constitutes about 15-25% of the dry weight of woody plants [1]. Between 40 and 50 million tons/year of lignin are produced worldwide as a mostly non commercialized waste product (www.ili-lignin.com). Even if a major part of industrial lignin is still incinerated for the production of process steam and energy, attempts to valorize lignin waste produced by industry go back to the first half of 1900 [2].

The highly and heterogeneous functionalization extent of lignin macromolecules enables a variety of chemical modifications, chain extension, and polymerization to be conducted opening the avenue to the development of new lignin-based materials. Chemically, lignin has a variety of functional groups, namely hydroxyl, methoxyl, and carboxyl groups. Phenolic hydroxyl groups in the aromatic rings are the most reactive functional groups in lignin and can significantly affect the chemical reactivity of the material. To improve upon this limitation, different types of modifications have been proposed with the aim to increase lignin chemical reactivity, reduce the brittleness of derived polymers, increase its solubility in organic solvents, and improve its ease of processing.

Within these research topics, the present work is focused on the study of lignin allylation reaction and subsequent Claisen rearrangement of the allyl group as potential chemical modifications aimed at the development of new lignin-based materials. In particular, the Claisen rearrangement of lignin was foreseen as a valuable approach to release phenols in an already chemically modified lignin giving additional reactive sites for further transformation.

II. EXPERIMENTAL

Lignin allylation: method A. In a round bottom flask, oven-dried lignin (1 g) was solubilized in 40 mL of an acetone/0.5 M aqueous NaOH (1:3) solution. Excess allyl bromide was then added and the mixture was reacted at 40°C. After 5 hs acetone was rotary evaporated and the crude was acidified to pH 2 adding 37% HCl dropwise. Allylated lignin was recovered by Buchner filtration.

Lignin allylation: method B. In a round bottomed flask equipped with a condenser, oven-dried lignin (100 mg) was refluxed in acetone in the presence of excess allyl bromide and potassium carbonate. After 8 hs, the mixture was poured dropwise, under vigorous stirring, into an Erlenmeyer flask containing cool acidic water (pH=1). Allylated lignin was collected by Buchner filtration and air dried.

Claisen rearrangement. In a round bottom flask equipped with a magnetic stirrer and a condenser, 100 mg of allylated lignin was refluxed in 10 mL of dimethylformamide (DMF) for 15 hs. DMF was then removed by freeze-drying.

Radical Scavenging Activity Evaluation. The radical scavenging activity of reference, allylated, and Claisen rearranged Protobind1000® lignin was determined by means of a spectroscopic assay involving the consumption of the stable free radical originated by DPPH (2,2-diphenyl-1-picrylhydrazyl) in a methanolic solution. The colorimetric assay was performed according to a published method [3].

III. RESULTS AND DISCUSSION

Lignin P1000 allylation

Two different strategies for hydroxyls allylation were tested on P1000® lignin. The one designed as Method A involved the reaction of lignin with excess allyl bromide in aqueous NaOH 0.5 M in the presence of about 25% v/v acetone to reduce the precipitation of allylated products during the reaction. According to the procedure designed as Method B, lignin was reacted with excess allyl bromide in the presence of K_2CO_3 as deprotonating agent in acetone.

Table 1. Distribution of labile hydroxyl groups in reference and allylated P1000®, as found by ^{31}P NMR quantitative analysis.

Assignment (mmol/g)	P1000® Ref	P1000® Allylated Met.A	P1000® Allylated Met. B
Aliphatic OH	1.70	1.18	0.89
Cond + S-OH	2.00	n.d.	0.38
G-OH	1.12	n.d.	0.20
P-OH	0.48	n.d.	0.12
COOH	1.07	0.80	0.02

The *Table 1* reports the ^{31}P NMR quantification of different hydroxyl groups present in purified lignin and in allylated lignin. The aliphatic OH groups remain present in high amount after allylation with both methods. The first method has allowed the modification of 80% of the phenolic units while for the second reaction method all the available phenols present have been allylated. The acid moieties are almost totally disappeared in the B method while in the A method they have been modified in a small percentage. ^{31}P NMR is an indirect method for evaluating the occurred allylation because it allows quantifying the residual hydroxyl groups after the functionalization reaction, while the allylated ones have been calculated by difference.

The direct evidence of the allylation reaction has been obtained by ^{13}C NMR spectroscopy. The ^{13}C NMR spectra of acetylated lignin and acetylated allylated P1000 (method A) have been collected and reported in the *Figure 1*.

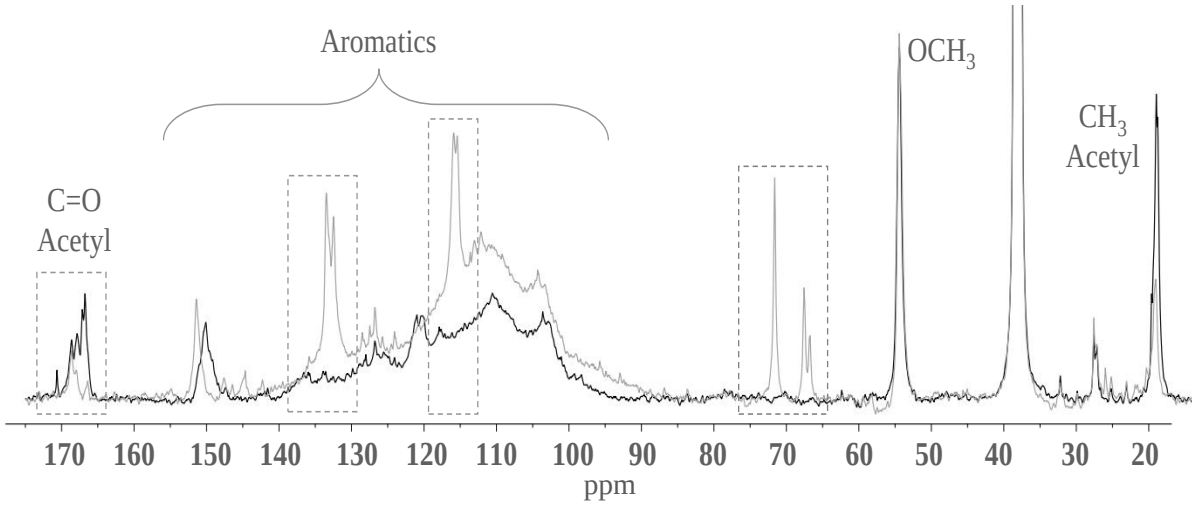

Figure 1. Overlapped ^{13}C NMR spectra of acetylated samples of reference (black) and allylated (grey) P1000® lignin registered in DMSO-d_6.

More specifically, it possible to observe that at the chemical shifts of carbonyl groups region, there is a decrease of carbonyl group bonded to the phenolic units (168 ppm): this is clearly due to the allylation reaction occurred

at these functionalities. The spectrum also shows a decrease of intensity of CH_3 in α-position to carbonyl (19 ppm). All these peaks are presented in the ^{13}C NMR spectra of allylated lignin. Moreover it is possible to observe the peaks related to the allyl chain (γ at around 138 ppm, β around 117 ppm and α with different peaks at 73, 70 and 69 ppm related to the different kind of phenolic units present in the lignin structure).

Claisen rearrangement

The Claisen Rearrangement is a [3,3]-sigmatropic reaction in which an allyl ether is thermally converted to an unsaturated carbonyl compound. In the case of the aromatic Claisen Rearrangement it is accompanied by a rearomatization. The etherification of alcohols or phenols and their subsequent rearrangement makes possible an extension of the carbon chain of the molecule (*Figure 2*).

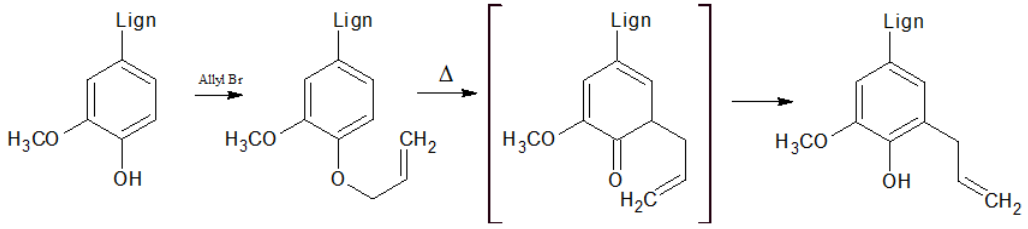

Figure 2. Mechanism of Aromatic Claisen rearrangement of allylated lignin.

In *Figure 3* the ^{31}P-NMR spectra of reference, allylated, and rearranged P1000® lignin are reported. Starting from P1000 reference lignin, it is possible to observe the different derivatized -OH groups (namely aliphatic, syringyl and condensed, guaiacyl, parahydroxycumaryl and carboxylic acids). After allylation as told before it possible to observed the total disappearing of phenol (method A). After thermal rearrangement of allylated lignin in DMF a signal related to condensed or syringyl units appeared in the spectrum.

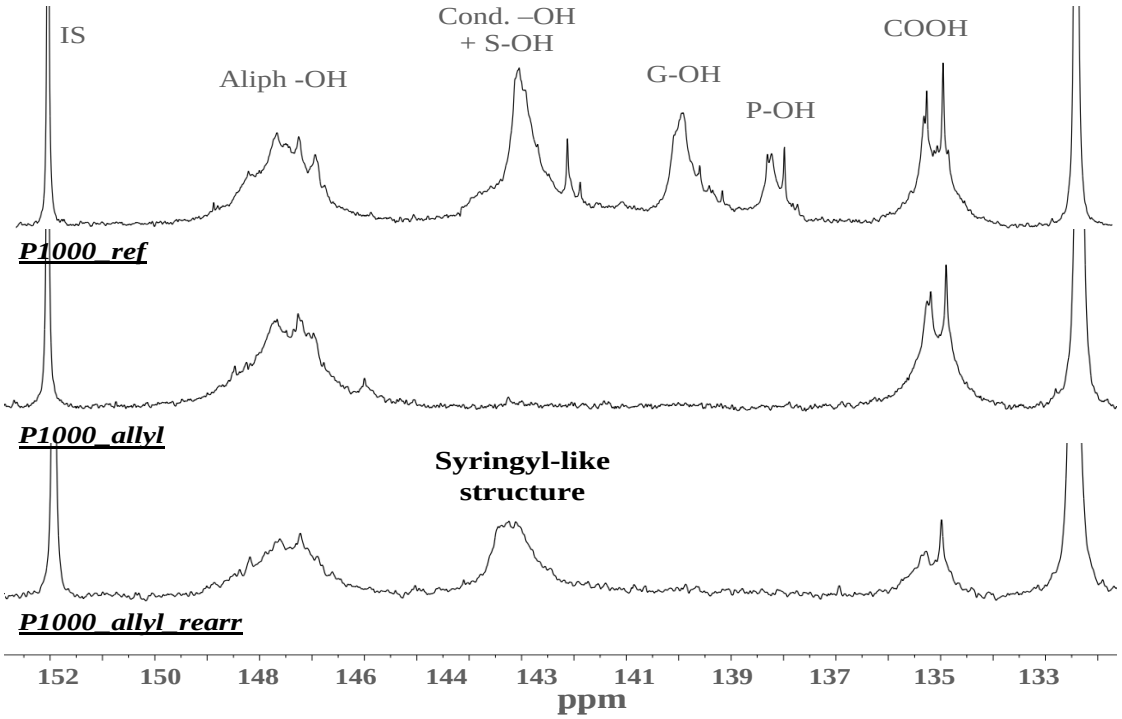

Figure 3. ^{31}P NMR spectra of reference, allylated, and rearranged P1000® lignin showing the interchange of guaiacyl phenols into syringyl-like phenols after Claisen rearrangement.

As experimental screening, the DPPH assay for antioxidant activity has been performed. The radical scavenging activity of pristine, allylated, and Claisen rearranged Protobind1000® lignin was determined by means of a spectroscopic assay involving the consumption of the stable free radical originated by DPPH (2,2-diphenyl-1-picrylhydrazyl) in a methanolic solution. The inhibition percentage (% I) of the free radical DPPH• was calculated according to the following formula:

$$\% I = [(A_0\text{-}A) / A_0] \times 100$$

where A_0 is the absorbance of the DPPH reference solution and A is the absorbance of the DPPH solution in present of different amount of lignins after 15 minutes of reaction. The obtained data were plotted on a log dose-inhibition curve and the resulting linear calibration curves were used to derive the half maximal inhibitory concentration IC_{50} reported in *Table 2*.

Table 2. Radical scavenging activity of reference, allylated, and Claisen rearranged P1000® lignin, expressed as IC_{50} concentration. The total phenols concentration is also reported.

	IC_{50} (ug/mL)	**PhOH (mmol/g)**
P1000® Ref	10.0	3.60
P1000® allyl	398.1	0.00
P1000® rearr	50.1	1.35

As observed from the data, after allylation and Claisen rearrangement the antioxidant properties of lignin preparation has been recovered. In this work, the Claisen rearrangement of lignin was foreseen as a valuable approach to release phenols in an already chemically modified lignin. Available phenols could act both as potential chain extension or cross-linking sites and antioxidants, attaining a tailor-made lignin derivative of controlled properties.

IV. CONCLUSIONS

Allylation is a straightforward reaction and provides a versatile product, prone to several chemical modifications, as typical of double bonds. On the other hand, the Claisen rearrangement can be used as a simple reaction to introduce C–C bonds and release phenolic groups and results, as is the case of the pristine allylated lignin, in a still reactive, chemically modified lignin, but having in addition a certain degree of antioxidant activity.

VI. REFERENCES

[1] W. Boerjan, J. Ralph, M. Baucher, Lignin biosynthesis. *Annu. Rev. Plant Biol*. **2003**, 54, 519.

[2] Harris, E.E. Utilization of waste lignin, current chemical research. *Industrial and Engineering Chemistry*, **1940**, 32(8), 1049-1052

[3] Salanti, A.; Zoia, L.; Orlandi, M.; Zanini, F. Elegir, G. Structural characterization and antioxidant activity evaluation of lignins from rice husk. *J. Agric. Food Chem*. **2010**, 58, 10049-10055.

[4] Claisen, L. *Chem. Ber.* **1912**, *45*, 3157.

STRUCTURAL CHANGES IN RECYCLE PULP INDUCED BY HIGH PRESSURE TREATMENT

Ana M. Salgueiro[1], Dmitry V. Evtuguin[1*], Jorge A. Saraiva[2], Filipe Almeida[3]

[1]*CICECO, Chemistry Department, University of Aveiro, Campus de Santiago, P-3810-193 Aveiro, Portugal;* [2] QOPNA, Chemistry Department, University of Aveiro, Campus Universitario de Santiago, Aveiro, 3810-195 Portugal; [3] Renova FAP S.A., Torres Novas, 2354 Portugal

*(*to whom correspondence should be addressed: dmitrye@ua.pt)*

ABSTRACT

Industrial recycled pulp (RP) was subjected to ultra high pressure (UHP) treatment and cellulose structural changes were assessed by X-Ray Diffraction (XRD), solid state ^{13}C NMR and FTIR spectroscopy. The interactions between water and cellulosic fibers were also evaluated by calorimetric analysis, sorption isotherms, H/D exchange, surface energy evaluation, ζ-potential and capillarity. Cellulose rearrangement upon UHP treatment led to small increase of its crystallinity degree and average crystallite width. Forced fiber hydration by UHP led to the formation of strongly bound water and an increased fibrils hydration thus decreasing substantially the pulp hornification. An increased isosteric heat of sorption, specific area of recycled fibers, integral heat of wetting, and capillary absorption was found. The structural changes observed represent a significant beneficial effect on papermaking properties, on the lifetime and the end life disposal of UHP-processed recycled fibers. The study of the papermaking properties of UHP-treated recycled pulp is in progress.

I. INTRODUCTION

Hydrostatic UHP treatment applied to virgin cellulosic pulp induces structural changes in supramolecular structure of cellulose and hemicelluloses [1]. The rearrangement of cellulose crystallites and forced hydration of cellulose fibrils leads to better accessibility of pulp components towards chemical reagents and enzymes and to radical improvement of papermaking properties. In particular, UHP treatment reduces drastically pulp's hornification culprit to the loss of hydration abilities [1]. This point may be important regarding recycled pulp, which brings economic and environmental benefits, when compared to virgin fibers, but exhibits known drawbacks such as the loss of hydration/swelling capacity (hornification) and mechanical properties [2]. Hornification is responsible for the loss of fiber properties, resulting from consecutive processing/stress to which fibers are submitted during their life cycles, such as wetting, drying, printing, storage, repulping and deinking. Although impurities, such as inks (mostly hydrophobic), calcium salts of fatty acids, non-ionic surfactants, dispersants, stikies, glues, dirt, etc., still remain attached to fibers and affect greatly fibers properties, hornification is essentially responsible for the loss of paper strength suffered by fibers throughout their life cycle. It causes irreversible structural changes, such as porosity loss (surface area), loss on hydration ability, and turning fiber stiffer.
The main goal of this work was to study the structural changes occurring upon UHP treatment of recycled pulps through the prism of eventual diminishing of hornification effect and papermaking benefits.

II. EXPERIMENTAL

Eucalyptus globulus bleached industrial kraft pulp, EP, and Industrial Recycled pulp, RP, were kindly supplied by Renova FAP, S.A. RP and EP were analysed for ash (NP 3192), extractives (TAPPI T204 om-88 norm), intrinsic viscosity (SCAN-CM 15:18 norm), carbonyls [3, 4], carboxyls (T 237 om-1993), neutal sugars [5] and acid methanolysis for hemicelluloses analysis [6]. Residual lignin and hexeuronic acids were also analysed according known procedure [7]. EP and RP dispersions (2% consistency) were sealed in plastic flasks, submitted to hydrostatic high pressure (400MPa, 15min, 20ºC), filtered, dried at room conditions and then stored in sealed plastic bags. Handsheets were prepared according to ISO 5269/2 norm.
Structural changes were monitored by X-ray diffraction scattering analysis at 4-40º (2θ) and scanning steps of 0.02º/scan on pulp pellets. Cross Polarization/Magic Angle Spinning (CP/MAS) ^{13}C RMN spectra were registered on a Bruker Avance 400 spectrometer (magnetic field of 9.4 T). The H/D exchanged pulps were analysed on a FTIR spectrometer Mattson 7000. RP and EP suspensions of D_2O and pulp were submitted to UHP treatment while blank tests remained dispersed in heavy water for an equal amount of time. Samples were then filtered and left over room conditions. All samples were then

dried at 105ºC and stored on a desiccator over P_2O_5. Pellets of KBr and pulp (ca 2mg pulp per 300mg KBr) were prepared and submitted to FTIR analysis.

Capillarity rise was tested following NP 686, 1990 standard. C**ontact angle analysis** was performed on handsheets using the sessile drop method for water, formamide, and diiodomethane standard liquids. The surface energy (γ_s) and its corresponding polar (γ_s^p) and dispersive (γ_s^d) components were determined following the Owens-Wendt-Rable-Kaeble (OWRK) model [8]. **Surface texture parameters** were also acquired by microtopographic analysis (scanning area 4.8x4.8 mm^2, resolution of 2µm). Samples charge was analysed by **zeta potential** measurements with disposable plastic cells. **Gravimetric Water Sorption** was performed to determine moisture sorption isotherms (25, 30 and 35ºC), for different values of relative humidity. Samples were dried, beforehand, over P_2O_5 and then placed on closed flasks containing the saturated salt solutions (controlled HR%), over controlled temperature environment. The samples were weighted periodically until equilibrium.

Calorimetric analysis was carried out on a thermally isolated container with 200g of water and 2g of pulp using a thermometer of ±0.01 ºC accuracy.

III. RESULTS AND DISCUSSION

Composition analysis showed that recycled pulp (RP) had general composition very similar to that of hardwood pulp (EP) though a small contribution of softwood pulp is possible due to the detected presence of mannan (**Table 1**). Hence, RP and EP were considered as analogs. A relatively high content of ash in RP is due to the residual fillers still not eliminated during pulp purification (**Table 2**). Residual lignin and hexeuronic acids content were not possible to determine in RP most likely due to interference from the concomitant impurities. As could be expected, RP polysaccharides revealed to be more degraded than in virgin EP, as follows from data on their intrinsic viscosity and oxidized groups (**Table 2**).

Table. 1 Results on sugars analyses by H_2SO_4 hydrolysis and acid methanolysis.

	Neutral sugars (wt%)					Monosaccharides from acid methanolysis (wt%)						
Sample	Glc	Xyl	Arab	Man	Gal	Glc	Xyl	Arab	GalA	4-*O*-Me-GlcA	Gal	Man
RP	78.8	17.7	0.54	2.8	0.19	43.8	43.5	0.6	0.3	0.8	1.0	9.9
EP	75.4	24.6	Tr.	Tr.	Tr.	34.7	62.6	0.0	0.4	0.8	0.8	0.7

Table. 2 General analysis on RP and EP samples.

Sample	RP	EP
Ash content (%)	1.83	0.14
Extractives (in acetone)	0.15	0.24
Intrinsic viscosity (ml/g)	540	925
Carbonyls (mmol/100g pulp)	1.26	0.76
Carboxyls (mmol/100g pulp)	7.0	6.80
Residual Lignin	-	0.11
Hexeuronic acids	-	5.2

Table. 3 Results of pulp analyses by XRD and solid-state ^{13}C NMR

Sample	XRD					^{13}C NMR
	$2\theta_{002}$(º)	$2\theta_{040}$(º)	D_{002}(nm)	b(nm)	DC(%)	Crystallinity index (%)
R	22.54	34.54	4.485	1.0380	70.9	46,5
R HP	22.54	34.62	5.212	1.0300	71.5	48,2
E	22.54	34.60	5.029	1.0357	71.1	45,4
E HP	22.52	34.60	5.641	1.0362	71.7	46,0.

Structural changes induced by UHP in RP and EP cellulose were assessed by XRD and solid-state ^{13}C NMR (**Table 3**). A very similar increase on average crystallite width (D_{002}) and the degree of crystallinity (DC) was observed in cellulose of both pulps. The rearrangements suffered by cellulosic chains, leading to the convergence of conveniently orientated fibril, yielding larger crystallizes, are the explanation found to explain such results [1]. Forced hydration upon UHP treatment resulted on the formation of strongly bound water, which was confirmed by FTIR spectra of pulp samples subjected to H/D exchange with heavy water (**Figure 1**). The chacteristic OD band at ca 2490 cm^{-1} remained after rehydration of RP with H_2O and oven-drying at 105ºC after the UHP treatment only. A small peak at ca 2940 cm^{-1} remained after

rehydration and drying of non-pressurized EP, which is explained by irreversible changes suffered by pulp during the drying process, which hindered the H/D exchange (resistant OD)[9, 10]. Besides, a OD peak shoulder at ca 2450 cm^{-1} suggests stronger binding interactions in the case of virgin fibers after UHT treatment.

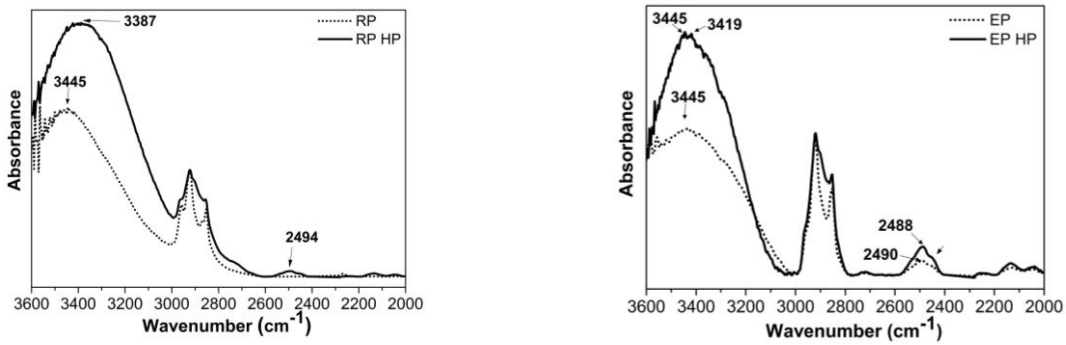

Figure. 1 – FTIR spectra of deuterated samples before (RP and EP) and after UHP (EP HP and RP HP) treatment.

Zeta potential measurements revealed a decrease from -19.5 to -2.5 mV for RP sample and from -15.4 to -9.9 mV for EP. These features may be tentatively explained by the presence of strongly bound water on the fiber surface affecting the increase of Stern layer. Capillarity tests revealed an increase of the capillary for RP upon UHP, from 49.5mm to 55.0mm bringing further confirmation that UHP rearrangements induce fibrils disaggregation. Virgin fibers, however, didn't manifest significant changes in capillarity tests showing 126-130 mm. The paper sheets prepared from UHP treated pulps revealed slightly increased surface roughness and contact angle with water for RP or it small decrease for EP (**Table 4**). The ambiguous enhancement of hydrophobic character of paper surface after UHP pre-treatment of RP may be due to the hydrophobic inorganic/organic impurities still attached to its fiber walls [2].

Table 4. Surface parameters determined by contact angle and surface texture analyses.

Sample	Water contact angle (º)	Roughness (μm)	Surface energy, (γ_s) (mJ/m^2)	Polar, (γ_s^p) (mJ/m^2)	Dispersive, (γ_s^d) (mJ/m^2)
RP	43,9±1,1	4.44	53.6	37.3	16.3
RP HP	47,7±1,3	4.55	50.9	28.0	22.9
EP	54,5±1,5	4.10	49.5	23.4	26.1
EP HP	43,1±1,3	4.53	54.5	32.6	21.9

Sorption isotherms exhibited a huge increase of water sorption after UHP treatment of RP (**Figure 2a**). This might be associated with forced hydration of hornified fibers leading to disaggregation of fibrils and substantial development of available surface area necessary for the formation of monolayer similar of that in virgin fibers. In contrast to RP, EP showed after UHP treatment a sorption isotherm with less monolayer capacity (**Figure 2b**). The last phenomenon may be addressed to highly increased amount of strongly bound water in virgin fibers after UHP treatment that diminished the monolayer capacity. Noteworthy the perfect simulation of sorption isotherms while fitting to Guggenheim-Anderson-de Boer (GAB) model describing multilayer adsorption and condensed film formation in the temperature range of 25-35 ºC.

The isotherm sorption studies were complemented by the determination of integral heat of wetting (ΔH_w). Thus, ΔH_w of RP increased from 43.4 J/g to 50.9 J/g while subjecting pulp to UHP treatment and indicated an increased number of free cellulose hydroxyl groups available for interaction with water. The decrease in ΔH_w found for EP after the pulp processing by UHP (from 53.5 J/g to 42.8 J/g) was in agreement with the diminishing of sorption capacity in monolayer suggested, based on isotherms analysis (**Figure 2b).**

The results on ΔH_w are in tune with calculated total heat of sorption, Q_s, as presented in **Figure 3.** Hence Q_s of RP in monolayer increased substantially when fibers were previously subjected to UHP treatment. This was not a case for the EP, which showed any significant increase of Q_s after UHP treatment of pulp.

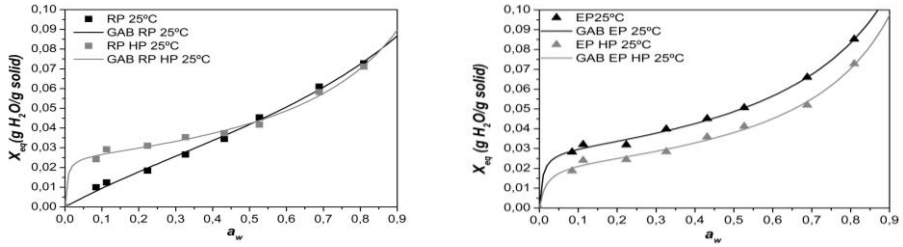

(a) (b)

Figure.2- Moisture sorption isotherm for UHP treated and non-treated pulps at 25ºC.

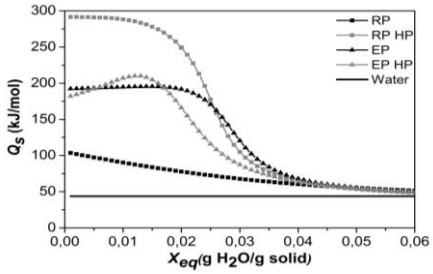

Figure 3. Total heat of sorption as a function of moisture content for UHP treated and non-treated pulps.

IV. Conclusions

The effect of UHP treatment on structural changes and hydration of cellulose in recycle pulp have been demonstrated. UHP pre-treatment induced structural changes in cellulose supramolecular structure and forced hydration of fibrils resulted in their disaggregation and introduction of strongly bound water. This set of phenomena enables the regeneration of recycled fibers enhancing their hydration properties highly degraded before due to hornification. UHP technology appears to be a powerful tool to enhance recycled fibers properties and eventually to prolong their lifetime.

V. ACKNOWLEDGEMENT

The authors acknowledge FCT-Fundação para a Ciência e Tecnologia and Renova FPA, SA for the PhD grant SFRH/BDE/51855/2012. The authors also thank Pest-C/CTM/LA0011/2013 and funding from of Project RENOVA PAPTIS (Ref. 30203)) co-funded by FEDER through POFC-COMPETE from QREN (Quadro Nacional de Referência). Finally, authors thanks RAIZ (Portuguese Research Institute on Forestry and Paper) for surface texture analysis.

VI. REFERENCES

1. Figueiredo, A.; Evtuguin, D.V.; Saraiva J. Effect of high pressure treatment on structure and properties of cellulose in eucalypt pulps, *Cellulose*, **2010**, *17*, 1193–1202.
2. Hubbe, M. A. V., R.A.; Rojas, O. J. What happens to cellulosic fibers during papermaking and recycling? A Review. *BioResources*, **2007**, *2*, 739-788.
3. Rikhter, N. E. A., Akim, G.L.; Nikitin, V.M. Comparing the Sabolks and hydroxyamine methods for the determination of small amounts of carbonyl groups in dissolving pulps. *Russian J. Appl. Chem* **1965,** *38* (8), 1848-1853.
4. Obolenskaya, A. V. E., Z.P. ; Leonovitch, A.A. *Laboratory practicum in wood and cellulose chemistry*: Moscow, 1991.
5. Selvendran, R. R.; March, J. F.; Ring, S. G. Determination of aldoses and uronic acid content of vegetable fiber. *Analytical Biochemistry* **1979,** *96* (2), 282-292.
6. Marques, G.; Gutiérrez, A.; del Río, J. C.; Evtuguin, D. V. Acetylated heteroxylan from Agave sisalana and its behavior in alkaline pulping and TCF/ECF bleaching. *Carbohydrate Polymers* **2010,** *81* (3), 517-523.
7. Evtuguin, D. V.; Daniel, A. I. D.; Pascoal Neto, C. Determination of Hexenuronic Acid and Residual Lignin in Pulps by UV Spectroscopy in Cadoxen Solutions. *Journal of Pulp and Paper Science* **2002,** *28* (6), 189-192.
8. Owens, D. K.; Wendt, R. C. Estimation of the surface free energy of polymers. *Journal of Applied Polymer Science* **1969,** *13* (8), 1741-1747.
9. Mann, J.; Marrinan, H. J. The reaction between cellulose and heavy water. Part 1. A qualitative study by infra-red spectroscopy. *Transactions of the Faraday Society*, **1956**, *52*, 481-487.
10. Mann, J.; Marrinan, H. J. The reaction between cellulose and heavy water. Part 3.-A quantitative study by infra-red spectroscopy. *Transactions of the Faraday Society*,**1956**, *52*, 492-497.

ACID HYDROLYSIS OF *PINUS RADIATA* IN 1-BUTYL-3-METHYLIMIDAZOLIUM CHLORIDE

Tamara M. Santos*, Mercedes Oliet, Juan C. Domínguez, M. Virginia Alonso, and Francisco Rodriguez

Chemical Engineering Department, Complutense University of Madrid.
Avda. Complutense S/N, 28040 Madrid, Spain
**E-mail: tmsantos@quim.ucm.*es

ABSTRACT

Lignocellulosic biomass is a renewable feedstock, which can be converted to fuels or chemicals. The use of ionic liquids (IL) as green solvents for the pretreatment of this biomass is considered a promising alternative. Recent studies show the possibility to isolate the carbohydrates components of biomass dissolved in IL. In this work, a solution of *Pinus radiata* wood in 1-butyl-3-methylimidazolium chloride (BmimCl) ionic liquid with 5 % (wt/wt) was preheated at 120 ºC and 1 h. Then, the 10 % (wt/wt) hydrochloric acid was added to this reaction mixture and the hydrolysis was carried out at different temperatures (80, 100 or 120 ºC) for 7 h. The samples were analyzed by HPLC to determinate the concentration of monosaccharides and degradation products. The best operating conditions to achieve the highest monosaccharides yield are 100 ºC and 3 h.

I. INTRODUCTION

Bioethanol produced from lignocellulosic biomass is referred to as 'second generation' biofuel, which presents advantages over conventional biofuels from the environmental and economic aspects [1]. Biomass is an attractive feedstock due to the fact that it is sustainable and CO_2 neutral [2]. The production of lignocellulosic ethanol is a process divided into four steps: 1) pretreatment, 2) hydrolysis, 3) fermentation, and 4) distillation [3]. Thermal or chemical pretreatment of lignocellulosic biomass to access to sugars from cellulosic and hemicellulosic components is required, overcoming its recalcitrance [4].
The ionic liquids (ILs) have shown great potential for pretreatment of biomass. ILs have been recognized as efficient and green solvent due to their minimal vapour pressure and low volatility at room temperature. The pretreatment reduces the crystallinity of cellulose to improve the enzimatic hydrolysis for obtaining fermentable sugars. In addition, it can deslignify the lignocelullosic biomass and recover the lignin as co-product [5].
A recent approach to sugar production is the use of ILs as medium reaction to obtain sugars and other compounds using acid as catalysts. Thus, the hydrolysis of biomass is carried out 'in situ' with the addition of the mineral acid, after dissolving lignocelullosic materials in imidazolium chloride ILs [6].
The aim of this work has been to study the influence of temperature and time on the acid-catalyzed hydrolysis of softwood specie dissolved in 1-butyl-3-methylimidazolium chloride IL. In addition, the generation and evolution of degradation products has been analyzed.

II. EXPERIMENTAL

Materials

The scheme of the experimental procedure in this work is shown in **Figure 1**. Pine wood employed (*Pinus radiata*) was supplied by CIFOR-INIA ("Instituto Nacional de Investigación y Tecnología Agraria y Alimentación"). The ionic liquid 1-butyl-3-methylimidazolium chloride (BmimCl, 99 %) was purchased from Iolitec. Wood chips were pretreated in order to promote their solubility in the ionic liquid [7]. Firstly, pine wood was extracted with acetone and water to remove the wood extractives. The resulting extractive free wood was milled to particle size 150 µm, and dried in a vacuum oven at 60 ºC for 24 h.

Procedure for Pinus radiata hydrolysis

Pinus radiata wood powder (0.250 g) and 1-butyl-3-methylimidazolium chloride (BmimCl) ionic liquid (5 g) was dissolved in 25 mL flask, and was preheated at 120 ºC for 1 h in an orbital shaker (RS900, Barnstead Stem). At this moment, the hydrochloric acid solution 10 % (wt/wt) was added for beginning the hydrolysis. This process was carried out in the orbital shaker at different temperatures (80, 100 and 120 ºC). Aliquots were taken at 0.25, 0.5, 1.5, 3, 5 and 7 h of reaction.

Analysis method

The concentration of sugars and degradation products in the aliquots were determinated by HPLC (Agilent 1260 liquid chromatography) using a Refractive Index detector and a Phenomenex ROA Organic Acid column. These analyses were carried out using 0.005 M H_2SO_4 as mobile-phase and a flow rate of 0.6 mL/min. The column compartment temperature was 60 ºC.

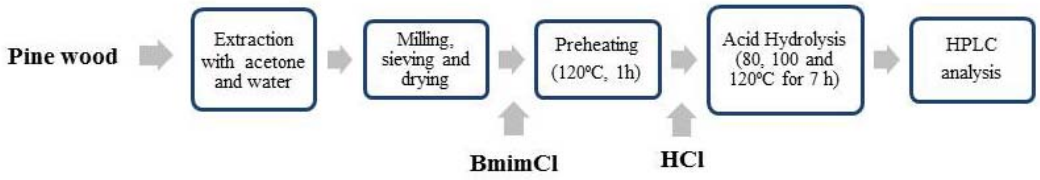

Figure 1. Scheme of the experimental procedure

III. RESULTS AND DISCUSSION

The glucose formation and decomposition in the hydrolysis carried out for 7 h at a temperature range of 80-120 ºC are shown in **Figure 2**. The initial rate of formation of glucose increased with increasing temperature. This behavior can be explained due to the increment of temperature produces the viscosity reduction of the mixture. Then, it facilitates the dissolution of wood and improves the hydrolysis [2,8]. Li et al., 2008 [9] explained that the formation of the solution of biomass and ionic liquid induces that H^+ is more accessible to the β-glucosidic bonds of the lignocelullosic materials, overcoming the physical barriers for hydrolysis. In addition, the dissociation of the anion Cl^- and the electron-rich aromatic system of cation $Bmim^+$ weaken the glycosidic linkage to improve hydrolysis. In the reactions at 100 and 120 ºC, high glucose concentrations of 3.6 and 3.4 g/L were reached at 3 h and 0.5 h, respectively. After these maximum, the concentration decreases due to the decomposition of glucose. However, this decrease is higher for reaction at 120 ºC than at 100 ºC. These maximum concentrations correspond to a glucan yield of 15.7 % and 14.6 %, respectively.

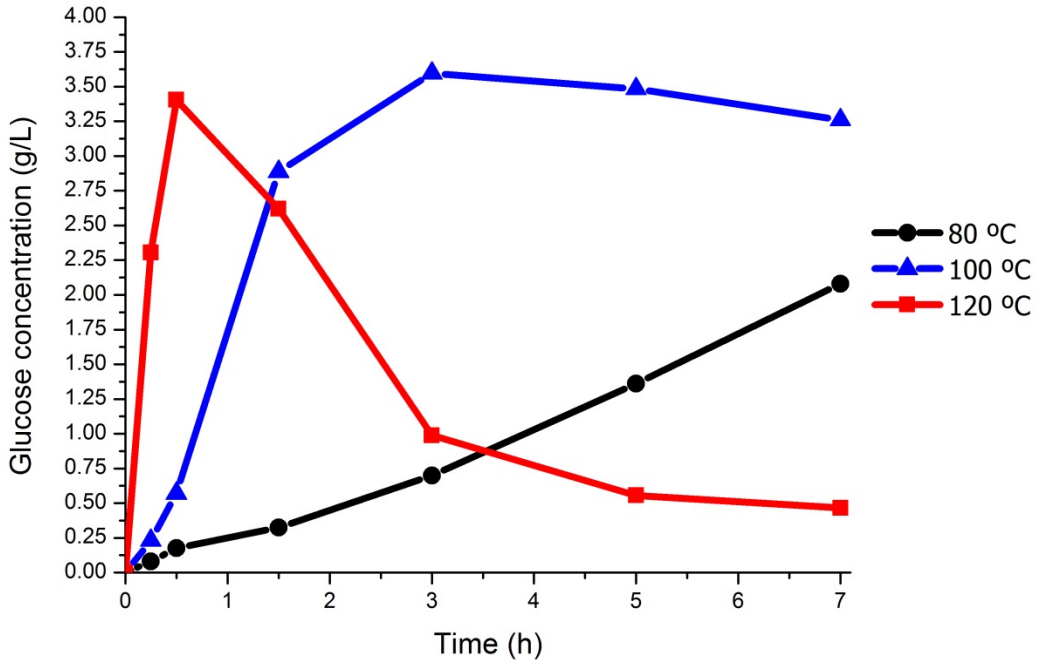

Figure 2. Glucose concentrations in the hydrolysis at 80, 100 and 120 ºC.

Figure 3 presents the concentration of sugar from hemicellulosic components of wood released in acid-catalyzed hydrolysis. These monosaccharides which appeared in the hydrolysate are xylose and arabinose. As can be seen, the trend of these components is the same that glucose and depends on the temperature. For xylose, the maximum concentration of 0.8 g/L (6.7 % of xylan yield) was reached at 100 and 120 ºC, at 3 and 0.5 h, respectively. However, for arabinose, the highest concentration of 0.13 g/L (21 % of arabinan yield) was achieved at 0.5 h and 100 ºC. This can be explained because rate of decomposition is faster than the formation when temperature and time are upper.

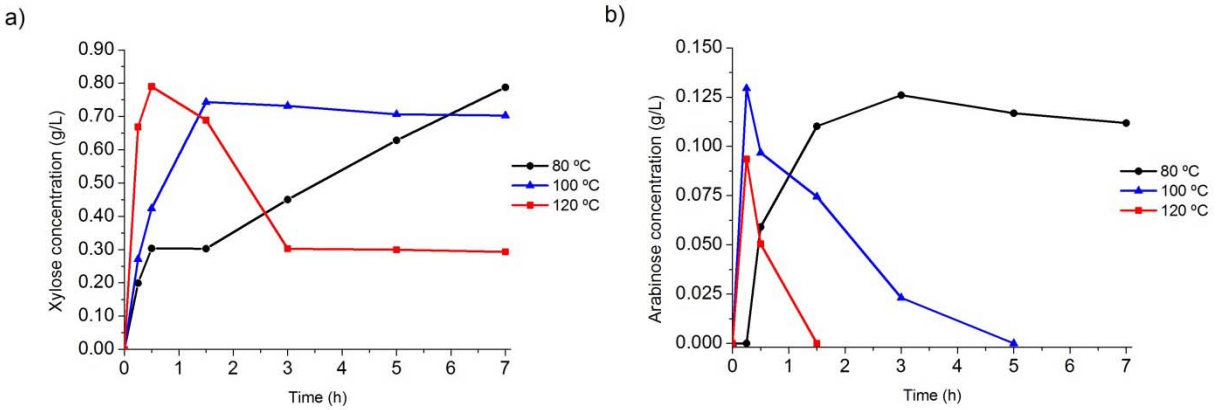

Figure 3. Sugars concentrations in hydrolysis at 80, 100 and 120 ºC: a) Xylose, b) Arabinose.

In the present work, we observed that the degradation products were negligible when the operating conditions used were lower than 100 ºC and 3 h. However, when the experimental conditions were severe, as shown **Figure 4**, then, hydroxymethylfurfural (HMF) and furfural appeared. The maximum sugar concentrations under these hydrolysis conditions were 3.4 g/L of glucose (14.7 % of glucan yield) and 0.8 g/L of xylose (6.7 % of xylan yield) at 0.5 h. The concentrations of these sugars decrease from this point, as a result of the transformation into subproducts. HMF and furfural were generated from hexoses (glucose) and pentoses (xylose) by reactions of dehydration. The trends of these dehydration products are similar and both reached a maximum of concentration at 1.5 h of reaction (1.8 g/L HMF and 0.3 g/L furfural). Moreover, HMF and furfural reduce their concentrations by reactions of rehydration into levulinic and formic acids after these maximums. Therefore, the components produced as dehydration products (HMF and furfural) are subject to decomposition, which occur at the same time that sugar descomposition [10]. Sievers et al., 2009 [2] observed the trend of furfural and HMF were comparable; however, furfural yield was lower than HMF as in the present work.

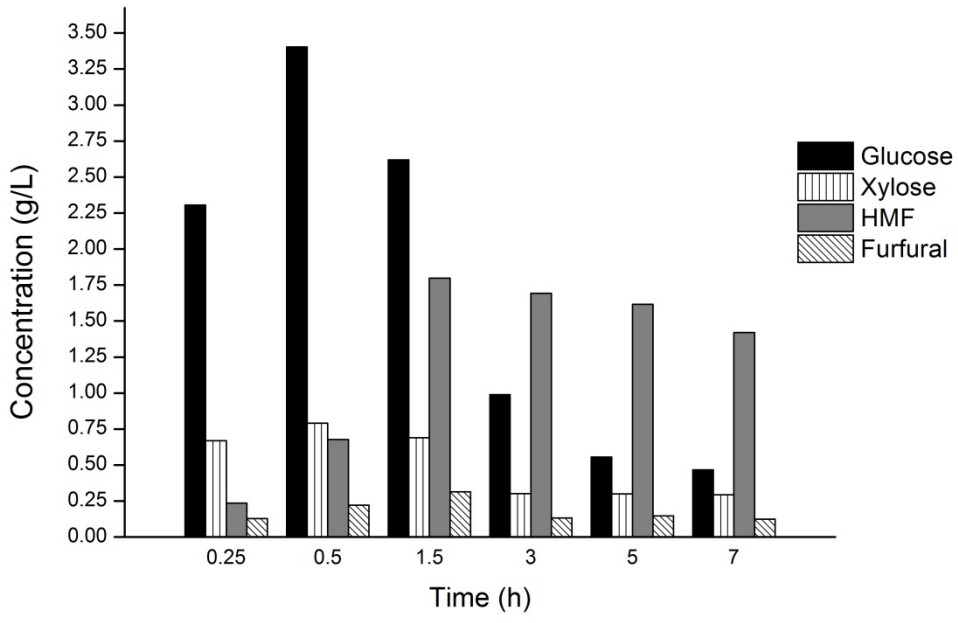

Figure 4. Monosaccharides and decomposition products concentrations at 120 ºC.

IV. CONCLUSIONS

This study shows that the combination of 1-butyl-3-methylimidazolium chloride (BmimCl) ionic liquid and hydrochloric acid as catalyst is effective for hydrolysis of *Pinus radiata* into sugars. Note that under mild conditions, temperature and time lower than 100 ºC and 3 h, the decomposition products are negligible. Thus, the best operating conditions to achieve the highest monosaccharides are 100 ºC and 3 h. Under this reaction conditions, the yields for glucan, xylan and arabinan are 15.7 %, 6.4 % and 4.0 %, respectively.

V. ACKNOWLEDGEMENT

The authors are grateful to the "Ministerio de Economía y Competitividad" and the "Comunidad de Madrid" for the financial support of Projects CTQ2010-15742 and S2009/PPQ-1545, respectively.

VI. REFERENCES

[1] Stephen, J.D.; Mabee, W.E.; Saddler, J.N. Lignocellulosic ethanol production from woody biomass: The impact of facility siting on competitiveness. *Energy Policy.* **2013**, *59*, 329-340.

[2] Sievers, C.; Valenzuela-Olarte, M.B.; Marzialetti, T.; Musin, I.; Agrawal, P.K.; Jones, C.W. Ionic-liquid-phase hydrolysis of pine wood. *Ind. Eng. Chem. Res.* **2009**, *48*, 1277-1286.

[3] Balat, M. Production of bioethanol from lignocellulosic materials via the biochemical pathway: A review. *Energ. Convers. Manage*. **2011,** *52*, 858-875.

[4] Dee, S.; Bell, A. Effects of reaction contidions on the acid-catalyzed hydrolysis of miscanthus dissolved in an ionic liquid. *Green Chem.* **2011**, *13*, 1467-1475.

[5] Sen, S.M.; Binder, J.B.; Raines, R.T.; Maravelias, C.T. Conversion of biomass to sugars via ionic liquid hydrolysis: process synthesis and economic evaluation. *Biofuels, Bioprod. Biorefin.* **2012**, *6*, 444-452.

[6] Sun, N.; Liu, H.; Sathitsuksanoh, N.; Stavila, V.; Sawant, M.; Bonito, A.; Tran, K.; George, A.; Sale, K.L.; Singh, S.; Simmons, B.A.; Holmes, B.M. Production and extraction of sugars from switchgrass hydrolyzed in ionic liquids. *Biotechnol. Biofuels.* **2013**, 6:39.

[7] Casas, A.; Alonso, M.V.; Oliet, M.; Santos, T.M.; Rodriguez, F. Characterization of cellulose regenerated from solutions of pine and eucalyptus woods in 1-allyl-3-methilimidazolium chloride. *Carbohydr. Polym.* **2013**, *92*, 1946-1952.

[8] Hu, X.; Xiao, Y.; Niu, K.; Zhao, Y.; Zhang, B.; Baozhong, H. Functional ionic liquids for hydrolysis of lignocellulose. *Carbohydr. Polym.* **2013**, *97*, 172-176.

[9] Li, C.; Wang, Q.; Zhao, K.Z. Acid in ionic liquid: An efficient system for hydrolysis of lignocellulose. *Green Chem*. **2008**, 10, 177-182.

[10] Jeong, T.S.; Choi, C.H.; Lee, J.Y.; Oh, K.K. Behaviors of glucose decomposition during acid-catalyzed hydrothermal hydrolysis of pretreated Gelidium amansii. *Bioresour. Technol.* **2012**, *116*, 435-440.

PRODUCTION OF METALLIC NANOPARTICLES USING *EUCALYPTUS GLOBULUS* BARK PHENOLIC EXTRACTS: UNVEILING THE MECHANISM OF AN ENVIRONMENTALLY FRIENDLY PROCESS

Sónia. A. O. Santos[1]*, Ricardo J. B. Pinto[1,2]*, Sílvia M. Rocha[3], Paula A. A. P. Marques[2], Carlos Pascoal Neto[1], Armando J. D. Silvestre[1], and Carmen S. R. Freire[1]

*[1] Department of Chemistry-CICECO University of Aveiro, 3810-193 Aveiro, Portugal; [2] TEMA-NRD, Mechanical Engineering Department and Aveiro Institute of Nanotechnology (AIN), University of Aveiro 3810-193 Aveiro, Portugal; [3] Department of Chemistry-QOPNA, University of Aveiro, 3810-193 Aveiro, Portugal (*santos.sonia@ua.pt; r.pinto@ua.pt)*

ABSTRACT

Nanobiotechnology has emerged as a fundamental domain in modern science, with metallic nanoparticles (NPs) being one of the largest classes of NPs studied, due to the wide-spectrum of possible applications in several fields. The use of plant extracts as reducing and stabilizing agents in their synthesis is an interesting and reliable alternative to conventional methodologies. However, the role of the different components of such extracts in the metal ions reduction/stabilization has not yet been clearly understood and addressed. Here we studied the behaviour of the main components of an *E. globulus* bark aqueous extract during metal ions reduction, followed by advanced chromatographic techniques, allowing establishing their specific role in the process. The obtained results showed that phenolic compounds, particularly galloyl derivatives, are the main responsible for the metal ions reduction, while sugars are essentially involved on the stabilisation of the NPs.

I. INTRODUCTION

The recent advances in the field of Nanoscience and Nanotechnology lead to a variety of physical and chemical strategies for the selective preparation of inorganic NPs with precise control over the shape and dimensionality [1]. Among the chemical methodologies, the most commonly used are based on soluble metal salt precursors and different reducing agents, which can act also as stabilizers to avoid coalescence of the NPs. Most of the reducing agents as e.g. hydrazine, sodium borohydride or *N,N*-dimethylformamide, are commonly associated with environmental risks and toxicity [2]. The green synthesis of metal NPs has been studied as a reliable and promising alternative to overcome the use of these harmful substances [3]. Green synthetic processes comprise either microorganisms such as bacteria or fungi, as well as plant biomass and several plant extracts. The use of plant extracts from different plant parts, including leaves, fruits, seeds, and bark, revealed more advantageous than microorganisms, due to the simplicity, easier scale-up, and cost-effectiveness [4]. Despite the remarkable number of reports found in literature regarding the synthesis of metal NPs using distinct plant extracts[5], a precise understanding of their formation mechanism and the clear-cut role of the natural compounds involved in this process is still imprecise. Some works have put forward hypothetical mechanisms proposing that the reduction of the metal ions to metal NPs may be due to the distinct compounds present in the extracts, such as reducing sugars, phenolic compounds and proteins [4]. However, these generic suggestions have been based essentially on qualitative routine-based spectrophotometric analysis, as FTIR, colorimetric assays or UV spectroscopy, which cannot unambiguously differentiate the presence or absence of the different families of compounds in the extracts and resulting NPs.

In this vein, and considering the relevance of such fundamental knowledge, particularly on the optimization and control of the final properties of the NPs and on the up-scaling of these green processes, in the present study we intended to clarify the role of the different components of a plant extract in NPs formation mechanism and kinetics and stabilization. Here, an aqueous extract of *Eucalyptus globulus* bark, a typical residue from the pulp and paper industry, well recognized for its high content on phenolic compounds [6] was chosen as reducing and stabilizing system for silver (Ag) and gold (Au) NPs synthesis. The clear identification of the natural reducing agents, involved on the formation of the metal NPs, was achieved by qualitative and quantitative analysis of sugars and phenolic compounds present in the plant extracts before and after Ag and Au synthesis, by using advanced chromatographic techniques.

II. EXPERIMENTAL

Eucalyptus globulus bark extraction: About 20 g of bark were submitted to water extraction at 100 ºC for 2 minutes under constant stirring. The suspension was then filtered and the extract was used as reducing and stabilizing agent for Ag and Au NPs synthesis.

Preparation of the metal NPs: Typically, 100 mL of the bark extract were added to 300 mL of 1 mM $AgNO_3$ or 1mM $HAuCl_4$ aqueous solutions, under stirring. A brownish yellow colloid was obtained in case of Ag NPs, while for Au NPs a deep-red colloid was achieved. After 1 h, the metal NPs were removed from the initial solution by high speed centrifugation. The bark extract after the reduction was analysed directly after the centrifugation while the NPs were washed several times. The assays with standard compounds were carried out by replacing the bark extract by the same volume of aqueous solutions of: 1) glucose, fructose, gallic acid, ellagic acid and isorhamnetin, individually, 2) the mixtures of the compounds belonging to the same family (phenolic and sugars) and 3) the mixture of all standard compounds. In all cases the concentrations were equivalent to those found in the initial extract.

Analysis of protein content by Nitrogen (N) elemental analysis: The N content of the bark extract (before and after the NPs biosynthesis) was determined on a freeze dried aliquot by elemental analysis, and converted into protein content using the standard 6.25 conversion factor.

Analysis of sugars by HPLC-RI: The monosaccharides content present in *E. globulus* bark extract (before and after Ag and Au NPs synthesis) was determined on HPLC system with a refractive index detector, using a 10 µm ion-exchange column, 300 × 7.5 mm, equipped with a 30 x 8 mm pre-column.

Analysis of phenolic compounds by HPLC-DAD-MS: The separation of the compounds was carried out on a HPLC system equipped with DAD detector, by using a C-18 column (150 x 2.1 mm x 5 µm) as reported elsewhere [6].

III. RESULTS AND DISCUSSION

Synthesis of Au and Ag NPs using E. globulus bark extract

In this study, comparative experiments using *E. globulus* aqueous extracts as reducing and stabilizing agent in the preparation of Ag and Au hydrosols were carried out in order to elucidate the role of the different components of plant extracts in green processes. As expected, the obtained Au colloidal solution showed the typical absorption band at around 530 nm without any significant shift over time, excepting a gradual increasing of intensity, most noticeable in the first minutes of reaction. Similarly, the addition of the *E. globulus* extract to the silver salt solution leads to the formation of Ag NPs, however following a slower kinetic. One hour after the addition of the extract, the UV-Vis spectrum shows two weak and broad absorbance bands at around 375 nm and 445 nm. Figure 1 shows the STEM images of the Au and Ag NPs obtained by reduction with *E. globulus* bark extract, after 1 hour of reaction. The Au NPs exhibit a homogeneous distribution of well-defined nanoparticles predominantly with spherical morphology, with a narrow size distribution (average diameter of 18±3 nm). Contrarily, the Ag NPs showed a spherical and polydisperse distribution with average diameters in the range 15 to 73 nm. The crystalline structure of the obtained Au and Ag NPs was confirmed by XRD of dried samples.

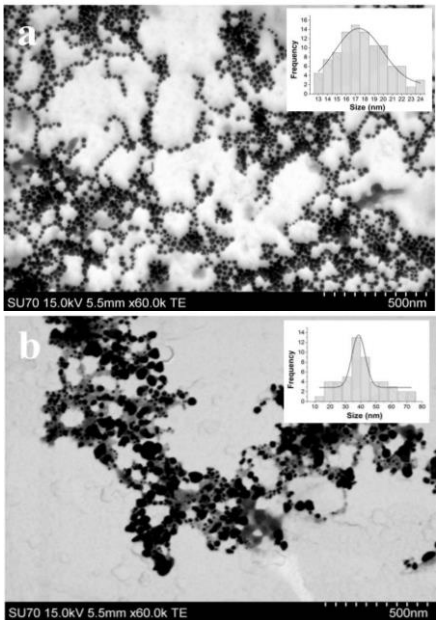

Figure1. STEM images of (a) Au and (b) Ag NPs, with the respective histogram of size distribution, obtained after reduction (1 h) with the E. globulus aqueous extract.

Identification of the biomolecules responsible for Au and Ag NPs synthesis and stabilization using E. globulus bark extract

In order to assess the role of the different extract components in the Au and Ag green synthesis and stabilization, the protein content, the composition of phenolic compounds and sugars of the bark extracts was investigated before and after the NPs formation.

The role of proteins: Several authors have attributed the reducing capacity of plant extracts in NPs synthesis to proteins, despite the fact that most of the extracts used have been obtained employing conditions (e.g. absence of a proper buffer and/or mechanical processes suitable to disrupt the cell walls) that commonly do not allow proteins removal or promote their degradation. Nonetheless, we decided to verify the presence of proteins in the extracts studied here and to access their possible participation in the NPs synthesis. The protein content of the *E. globulus* bark extract, determined by elemental analysis, represented about 0.8 wt.% of the total extract, which corresponds to a concentration of about 19.0 µg mL^{-1} of aqueous extract. This value is extremely low (four and

nineteen-fold lower than the phenolic compounds and sugars content, respectively). Additionally, this value is in a range of concentration that was previously reported not to have a linear relationship with Au NPs synthesis [8]. Moreover, the protein content determined by elemental analysis was probably overestimated because other extract components could also contribute to the nitrogen content. This result clearly suggested that, in the conditions studied, proteins are not involved in metal ions reduction. However, they might play an important role on the stabilization of the NPs.

The role of sugars: Only detected two monosaccharides in the *E. globulus* extract, namely glucose and fructose, representing 127.7 and 233.7 μg mL^{-1} of aqueous extract, respectively. These concentrations are in the same range of those reported for several other plant extracts [9], commonly used in the biogenic synthesis of NPs. After the Ag and Au NPs synthesis a considerable decline in both monosaccharides content in the extracts was observed. Glucose concentration decreased to 52.7 and 71.4 μg mL^{-1} of extract after Ag and Au NPs synthesis, respectively, while fructose content decreased to 114.4 and 119.7 μg mL^{-1} of extract (Figure 2). This first outcome suggested the involvement of these reducing sugars in the reduction process of Ag^{+} and Au^{3+} or on the stabilization of the obtained NPs. Indeed, the participation of reduction sugars, as glucose, in reduction of metal ions in NPs synthesis using plant extracts have been previously suggested and several mechanisms have been proposed [10]; however most of the authors neglects the co-existence of other reducing agents in these type of plant extracts. Thus, in order to verify the specific role of glucose and fructose on the NPs synthesis, standard solutions with the same concentration as observed in the bark extract (130 and 230 μg mL^{-1} of extract for glucose and fructose, respectively) were also tested. After one hour of reaction, no metal ions reduction was perceived with glucose or fructose standard solutions, or even when the two reducing sugars were mixed together. This behaviour could be essentially related with the relatively low concentration of these reducing sugars in the bark extract. These results indicated that sugars are essentially involved on the NPs stabilisation, as will be discussed below.

The role of phenolic compounds: 16 Phenolic compounds were identified in the aqueous extract of *E. globulus* bark. Most of them were previously described as constituents of this Eucalyptus species [6] or even on plant tissues of other *Eucalyptus* species [11]. The phenolic fraction of *E. globulus* bark aqueous extracts is mainly composed of galloyl-glucose, ellagic acid and isorhamnetin derivatives. The total amount of quantified phenolic compounds account for 70.27 μg mL^{-1}, with an isomer of isorhamnetin-pentoside, gallic acid and galloyl-bis-HHDP-glucose as the major components among the 16 compounds identified, with concentrations of 14.27±0.55, 11.13±0.43 and 10.27±0.25 μg mL^{-1} of the aqueous extract, respectively.

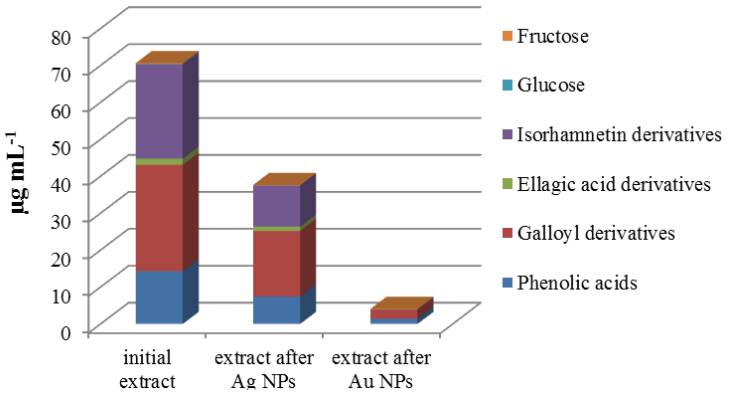

Figure 2. Abundance of compounds identified in *E. globulus* bark extract before and after NPs synthesis

After Ag NPs synthesis the content of phenolic compounds decreased down to 37.97 μg mL^{-1} (Figure 2), being this decline more accentuated for isorhamnetin and phenolic acids derivatives, with decreases of 54 and 48%, respectively. Specifically, an isomer of isorhamnetin-pentoside and gallic acid were the compounds whose concentration diminished most. In contrast, after Au NPs synthesis the majority of the phenolic compounds present initially in the *E. globulus* bark disappeared (accounting only for 4.36 μg mL^{-1}), being detected only quinic acid, HHDP-glucose, galloylglucose, gallocatechin dimer and galloyl-bis-HHDP-glucose. These results indicated that phenolic compounds have a dominant role on this green process of producing NPs.

In this sense, in order to confirm their specific starring role in NPs synthesis, gallic and ellagic acids and isorhamnetin standards were tested individually, using equivalent concentrations to those found in the bark extract. In the Ag NPs synthesis, gallic acid showed the faster redox kinetics. In the Au NPs synthesis, after the addition of gallic acid, the colour of the $HAuCl_4$ solution changed in a few seconds from light yellow to pink, identically to that observed in the case of the *E globulus* extract, indicating the successfully synthesis of Au NPs. However, no metal reduction was even observed when ellagic acid or isorhamnetin were added to gold hydrosol. These observations established undoubtedly that phenolic compounds, and in particular derivatives of gallic acid, are the main responsible for metal ions reduction in both Au and Au NPs synthesis using *E. globulus* bark extracts. It must be noticed that non oxidation products of phenolic compounds have been detected in the *E. globulus* bark extract after NPs synthesis. This may be related with the fact that these components are certainly aggregated at the surface of Ag and Au NPs; but also with the possibility that they cannot be detected by HPLC-MS at the conditions used (e.g. due to their higher polarity).

The combined role of sugars and phenolic compounds: To understand the possible combined effect of the main monossacharides and phenolic compounds identified in *E. globulus* aqueous extract, a mixture of glucose, fructose, gallic and ellagic acids and isorhamnetin were testedin the production of Au and Ag NPs. After the addition of the mixture, a prompt formation of Ag and Au NPs was observed, with the appearance in both cases of the correspondent UV absorption bands.
The NPs obtained using the sugars and phenolic standards mixtures showed to be more stable than those formed after the addition of the standard phenolic compounds mixture alone, with the zeta potential values changing from −36.2 (with phenolic compounds) to −40.4 mV (with phenolic and sugar compounds) in Au NPs and from −24.4 to −30.3 mV for Ag NPs. This trend suggested that, in the studied conditions, reducing sugars have a more significant effect on the NPs stabilization, and particularly in the case of Ag NPs, which is in agreement with the higher decrease of glucose in the extract after the Ag NPs synthesis.

IV. CONCLUSIONS

We established a strategy to identify the natural reducing agents involved on the formation of Ag and Au NPs when plant extracts are applied in their green synthesis. This study relied on the identification of sugars and phenolic compounds present in *E. globulus* aqueous extract before and after Ag and Au NPs synthesis using advanced chromatographic techniques. An evaluation of the proteins content of the extract was also carried out. Evidence of the role of these components in NPs synthesis, as well as in their stabilization, was provided by using different sugars and phenolic compounds standard solutions. We have demonstrated that glucose and fructose, the main sugars present in plant extracts, have a negligible responsibility in both Ag and Au NPs synthesis; however these sugars could be aggregated at the NPs surface turning them more stable. In opposition, gallic acid, and galloyl derivatives, showed to be the main responsible for the Ag and Au hydrosols reduction, allowing a quick formation of NPs. In addition, ellagic acid and isorhamnetin show to have a decisive role on the stabilization of Au NPs. Considering that the composition of plants water extracts is broadly similar in what concerns to the main families of components present, these conclusions are expected to be extrapolated to the vast majority of extracts used in this context. In this perspective, we anticipate that these results can be a driving force to the optimization of green synthesis of metal NPs in order to a better control of their properties.

V. ACKNOWLEDGEMENT

The authors wish to thank to FCT (Fundação para a Ciência e Tecnologia) and POPH/FSE for the postdoctoral grants to S.A.O. Santos (SFRH/BPD/84226/2012) and R.J.B. Pinto (SFRH/BPD/89982/2012) and for funding CICECO (Pest-C/CTM/LA0011/2013) and QOPNA (PEst-C/QUI/UI0062/2013). C.S.R. Freire and P.A.A.P. Marques also acknowledges FCT/MCTES for a research contract under the Program Investigador FCT 2012 and 2013, respectively. Microscopy analysis was supported by Rede Nacional de Microscopia Eletrónica (RNME-Pole UA FCT) project REDE/1509/RME/2005.

VI. REFERENCES

[1] Xia, Y.; Xiong, Y.; Lim, B.; Skrabalak, S.E. Shape-controlled synthesis of metal nanocrystals: Simple chemistry meets complex physics? *Angew. Chem.-Int. Edit.* **2009**, *48*, 60-103.
[2] Raveendran, P.; Fu, J.; Wallen, S.L. Completely "green" synthesis and stabilization of metal nanoparticles. *J. Am. Chem. Soc.* **2003**, *125*, 13940-13941.
[3] Sanchez-Mendieta, V.; Vilchis-Nestor, A.R. Green synthesis of noble metal (Au, Ag, Pt) nanoparticles, assisted by plant extracts in *Nanotechnology and Nanomaterials, Noble Metals* (ed Yen-Hsun Su), InTech, **2012**, *Ch18*, 391-408.
[4] Duran, N.; Marcato, P.D.; Durán, M.; Yadav, A.; Gade, A.; Rai, M. Mechanistic aspects in the biogenic synthesis of extracellular metal nanoparticles by peptides, bacteria, fungi, and plants. *Appl. Microbiol. Biotechnol.* **2011**, *90*, 1609-1624.
[5] Iravani, S. Green synthesis of metal nanoparticles using plants. *Green Chem.* **2011**, *13*, 2638-2650.
[6] Santos, S.A.O.; Freire, C.S.R.; Domingues, M.R.M.; Silvestre, A.J.D.; Neto, C.P. Characterization of phenolic components in polar extracts of *Eucalyptus globulus* Labill. bark by high-performance liquid chromatography-mass spectrometry. *J. Agric. Food Chem.* **2011**, *59*, 9386-9393.
[7] Pinto, R.J.B; Marques, P.A.A.P.; Neto, C.P.; Trindade, T.; Daina, S.; Sadocco, P. Antibacterial activity of nanocomposites of silver and bacterial or vegetable cellulosic fibers. *Acta Biomater.* **2009**, *5*, 2279-2289.
[8] Li, S.; Shen, Y.; Xie, A.; Yu, X.; Qiu, L.; Zhang, L.; Zhang, Q. Green synthesis of silver nanoparticles using *Capsicum annuum* L. extract. *Green Chem.* **2007**, *9*, 852-858.
[9] Ma, C., Sun, Z., Chen, C., Zhang, L. & Zhu, S. Simultaneous separation and determination of fructose, sorbitol, glucose and sucrose in fruits by HPLC–ELSD. *Food Chem.* **2014**, *145*, 784-788.
[10] Lin, Z.; Wu, J.; Xue, R.; Yang, Y. Spectroscopic characterization of Au^{3+} biosorption by waste biomass of Saccharomyces cerevisiae. *Spectrochim. Acta A* **2005**, *61*, 761-765.
[11] Santos, S.A.O.; Vilela, C.; Freire, C.S.R.; Neto, C.P.; Silvestre, A.J.D. Ultra-high performance liquid chromatography coupled to mass spectrometry applied to the identification of valuable phenolic compounds from Eucalyptus wood. *J. Chromatogr. B* **2013**, *938*, 65-74.

EVALUATION OF PHYSICO-MECHANICAL TREATMENTS ON SUGARCANE BAGASSE CELLULOSE HYDROLYSIS

Santucci, B.S. [1,2]; Curvelo, A.A.S.[1,2], Pimenta, M.T.B.[1]*,

[1]*Laboratório Nacional de Ciência e Tecnologia do Bioetanol, Centro Nacional de Pesquisa em Energia e Materiais, Campinas, São Paulo, Brazil.*
[2]*Instituto de Química de São Carlos – Universidade de São Paulo, São Carlos, São Paulo, Brazil.*

**mtborges@bioetanol.org.br*

ABSTRACT

The effect of two different physico-mechanical treatments, refining and cryogenic grinding, in sugarcane bagasse samples was studied in this paper. Three different chemical composition samples were employed: raw fibers, hydrothermally pretreated and organosolv delignified bagasse. Refining process was performed in a laboratory centrifugal Jokro mill, being the refining time the only process variable. Cryogenic grinding was carried out under established conditions to pulverize the wet samples. Glucose yield by enzymatic hydrolysis and porosity results were related. Refining process provided increases until 60% in porosity, resulting in glucose yield increments of until 60%, 100% and 200% (delignified pulp, raw bagasse and hydrothermal bagasse, respectively) regarding unrefined materials. The highest glucose yield was obtained for organosolv pulp after refining at 60 minutes, correspondent to 72%. In contrast, cryogenic grinding doesn't change significantly the porosity of the materials, what results in inexpressive increasing in enzymatic digestibility.

I. INTRODUCTION

The use of sugarcane bagasse as energy feedstock is encouraged by its position as the greatest Brazilian agroindustrial surplus. Its use for cellulosic ethanol production needs previous reduction on recalcitrance of biomass. When bagasse is submitted to chemical treatments, the lignin-carbohydrate matrix becomes more susceptible to enzymatic hydrolysis as a result of changes in the chemical composition and physical structure, such as lignin and hemicelluloses removal and/or decrease in degree of polymerization and increase in surface area and porosity. However, there's a need for a further increase in digestibility yields of biomass, providing higher concentrations of fermentable sugars. In order to improve accessibility to cellulose without using chemical reagents, different physico-mechanical treatments have been studied for the ultrastructure modification of lignocellulosic materials concerning the defibrillation and the increase in active surface area.

Refining is a mechanical treatment that shears and compresses the fibers in aqueous medium and provokes delaminations that modify the cell wall morphology and increases the degree of hydration of biomass substrate, affecting the binding forces between the fibers which change the material porosity. Physical modifications, which occur in fibers structure, increase the chemical fiber components accessibility. Chemical treatments promote the cell wall disintegration by partial removal of major components, creating spaces between cellulose microfibrills, which can be further defibrillated by refining [1,2,3,4].

In this context, this paper proposes the use of two different physico-mechanical treatments, refining and wet grinding, combined with mild chemical pretreatments, in order to increase the fibers active surface area to hydrolytic enzymes using environmentally friendly treatments.

II. EXPERIMENTAL

Raw Material

Raw bagasse was washed in flowing water using a 40 mesh sieve. The retained fibers were used in following experiments, storing the collected pith.

Chemical Pretreatments

Hydrothermal pretreatment was carried out in a 20L laboratory rotate digester AU/E-20 (Regmed), rotating at a speed of 6 rpm. The reaction was performed at 160°C, 30 minutes and solid : liquid ratio 1:10 (g of fibers : mL of water). The cellulignin obtained was washed in flowing water until neutral pH.

Organosolv pulping was carried out in a 7,5L stainless steel reactor (Parr Instruments Company) at 190°C and 120 minutes using a solvent mixture of ethanol : water (1:1 v/v) at solid : liquid ratio 1:10 (g/mL). The pulp was defibrated with 1% NaOH in a laboratory disintegrator, and then washed in flowing water until neutral pH.

Chemical compositions of raw and pretreated materials were determined by National Renewable Energy Laboratory's (NREL) Laboratory Analytical Procedures [5,6].

Physico-Mechanical Treatments

Refining process was performed in a laboratory centrifugal Jokro mill JK-21 (Regmed), acting in planetary movement at 150 rpm and low solid consistency (6%), being the refining time the studied process variable (number of equipment revolutions), ranging between 6.7 and 120 minutes (1000 to 18000 revolutions).

Cryogenic grinding was carried out in a 6970EFM Enclosed Freezer Mill - 6970D (SPEX Sample Prep.), pulverizing the wet samples (about 70% moisture) at cryogenic temperatures by the action of a steel impactor driven by electromagnets. The equipment parameters adjusted for the process was: 10 minutes of precooling, 6 grinding cycles of 2 minutes and grinding rate of 6 cps.

Enzymatic Hydrolysis

Enzymatic hydrolysis were performed using a mixture of commercial enzyme preparations, Celluclast 1.5L (cellulose), with an activity loading of 10 FPU/g substrate, and Novozym 188 (β-glucosidase), with an activity loading of 20 IU/g substrate. Hydrolysis experiments were carried out with solid content of 10% (w/w) substrate in citrate buffer (pH 4.8). All samples were incubated at 50°C in an air incubator shaker of 150 rpm for 72h with aliquots collected each 24h. Hydrolysate analysis was performed by HPLC.

Substrate Characterization

The thermoporometry analysis was performed by differential scanning calorimetry in a TA Q200 instrument with RCS90 cooling unit (TA Instruments). The morphologies of selected substrates were examined using an optical microscope Axio.Imager A2 with the AxioCam MRm camera and magnification of 100x (Carls Zeiss).

III. RESULTS AND DISCUSSION

The chemical composition of raw bagasse (*B*), hydrothermal bagasse (*H*) and organosolv pulp (*O*) are shown in **Table 1**. The mass yield obtained in hydrothermal pretreatment and organosolv deslignification were 79% e 55%, respectively.

Table 1. Chemical composition and total mass balance of the tree studied bagasse samples (*B*, *H* and *O*).

Sample	Extractives (%)	Ashes (%)	Cellulose (%)	Lignin (%)	Hemicelluloses (%)	Total (%)
B	1.2 ± 0.2	0.5 ± 0.0	44.1 ± 0.4	22.3 ± 0.1	31.8 ± 0.7	99.8 ± 0.9
H	n.d.	0.4 ± 0.0	56.2 ± 0.1	24.9 ± 0.1	19.3 ± 0.1	100.7 ± 0.1
O	n.d.	0.6 ± 0.1	82.5 ± 0.2	5.0 ± 0.4	13.4 ± 0.1	101.5 ± 0.0

*n.d. = not determined.

The results of enzymatic digestibility after the physico-mechanical treatment for the three samples (*B*, *H* and *O*) are shown in **Figure 1**, which relates glucose yields with the hydrolysis reaction time.

It could be noted from de obtained curves for the three studied materials an increase in glucose yield according to the increase in refining times in Jokro mill; the obtained values were higher as longer the enzymatic hydrolysis time, reaching the highest values at the 72th hour of reaction. Hydrothermal bagasse (*H*) and organosolv pulp (*O*) refined at a low process time (6.7 minutes) showed increments about 50% on glucose yield regarding unrefined materials. In contrast, cryogenic grinding provided a significant gain of enzymatic digestibility just for hydrothermal bagasse (28% in 72h of hydrolysis), whereas for raw bagasse (*B*) the process was unfavorable (decrease of 45% in glucose yield).

For the raw bagasse samples (*B*) (untreated and mechanically treated), the highest obtained value was 16% (72 h) at 100 minutes of refining, correspondent to 100% increase in glucose yield with respect the hydrolysis of unrefined material (7.8%).

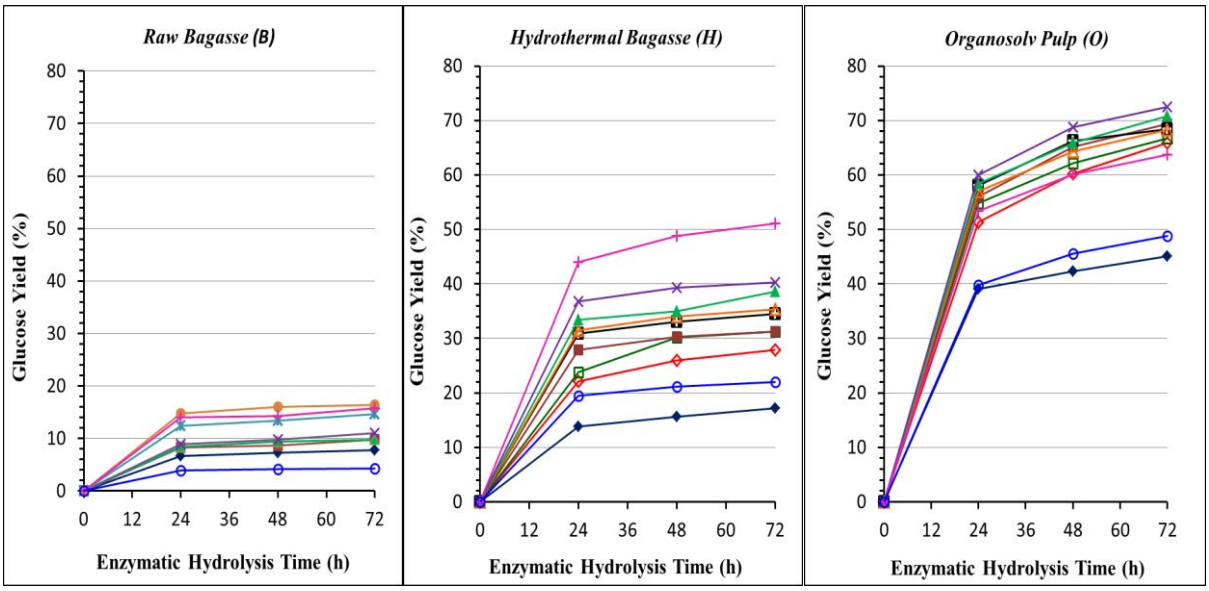

Figure 1. Glucose yield according to enzymatic hydrolysis time, obtained for the three studied samples (***B***, ***H*** and ***O***), either unrefined(—◆—), refined at different times (6.7 min = —◇— ; 13.3 min = —□—; 20.0 min = —■—; 26.7 min = —▪—; 33.3 min = —△—; 40.0 min = —▲—; 60.0 min = —×—; 80.0 min = —✳—; 100.0 min = —●—; 120.0 min = —+—) and cryogenically ground (—○—).

The variation in enzymatic digestibility for hydrothermal bagasse (*H*) was more expressive than for raw bagasse, providing a glucose yield of 51% (72h) when refined at 120 minutes, which corresponds to an increase about 200% concerning the unrefined material. Organosolv pulp (*O*) refined by 20 minutes provided a glucose yield of 69%, an increment about 53% with respect to the unrefined sample and about 604% e 123% with respect to the raw bagasse (*B*) and hydrothermal bagasse (*H*) refined at the same conditions. The higher response of chemically pretreated materials may be justified by the high removal of hemicelluloses (about 52% for (*H)* and 77% for (*O*)) and lignin (about 12% for (*H)* and 88% for (*O*)), what reduces the material recalcitrance and provides an increase in active surface area and porosity, supporting the delamination and hydration process induced by refining.

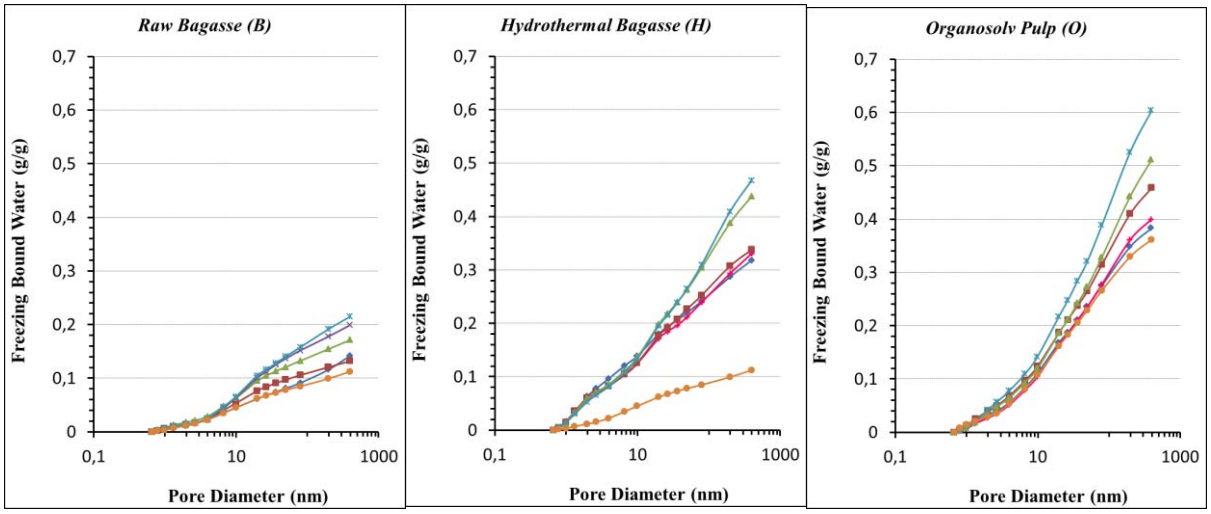

Figure 2. Cumulative pore size distribution determined by thermoporometry obtained for the tree studied samples (***B***, ***H*** and ***O***), either unrefined (—◆—), refined at different times (6.7 min = —+—; 20.0 min = —■—; 60.0 min = —▲—; 80.0 min = —×—; 120.0 min = —✳—) and cryogenically ground (—●—).

Thermoporometry graphs obtained for the three studied samples (*B*, *H* and *O*), showed in **Figure 2,** denote wet porosity increasing, represented by cumulative water increase in larger pore diameters, with refining time. On the other hand, cryogenically ground samples shows porosities close to or lower than unrefined samples, justifying the enzymatic digestibility observations. Both raw bagasse (*B*) and hydrothermal bagasse (*H*), refined

at 120 minutes, showed porosity increments about 50%, related respectively to 100% and 200% glucose yield increments. The higher glucose yield reached in the study was 72% (72h of hydrolysis) from *O - 60 minutes Jokro refined* - whose porosity increment was 33%.

Optical microcopy images obtained from unrefined organosolv pulp (*O*), Jokro refined at 60 minutes and cryogenically ground illustrate the physico-mechanical treatments effects. While **Figure 3-(A)** shows sugarcane bagasse vegetal fibers, the **Figure 3-(B)** shows the disruption and delamination of fibers walls by refining process. Furthermore, it can be observed in **Figure 3-(C)** that cryogenic grinding promotes just the "cut" of fibers to produce smaller particles.

Figure 3. Optical microscopy from **(A)** fibers of organosolv pulp (*O*), **(B)** organosolv pulp refined for 60 minutes and **(C)** organosolv pulp cryogenically ground.

IV. CONCLUSIONS

The improvement in enzymatic digestibility can be reached by physical structure modifications caused by mechanical treatments. The refining in Jokro mill is an efficient treatment, providing increases up to 200% in enzymatic hydrolysis, obtained for hydrothermal bagasse, related to porosity increment about 50%. A Jokro refined organosolv pulp (60 minute) exhibited a high porosity increment (33%) and, consequently, the higher glucose yield (72%). Oh the other hand, cryogenic grinding didn't promote significant increments in porosity, being inefficient in increase of the active surface area. It follows that refining causes an opening in the physical structure of cell walls, facilitating the enzymatic digestibility, which is not observed in conventional grinding process, even if they do not involve the material drying.

V. ACKNOWLEDGEMENTS

This study was supported by FAPESP (process 2010/08691-4) and CNPq (process 152685/2013-8).

VI. REFERENCES

[1] Chen, X.; Kuhn, E.; Wang, W.; Park, S.; Flanegan, K.; Trass, O.; Tenlep, L.; Tao, L.; Tucker, M. Comparison of different mechanical refining technologies on the enzymatic digestibility of low severity acid pretreated corn stover. *Bioresource Technol*. **2013**, 147, 401-408.

[2] Ertas, M.; Han, Q.; Jameel, H.; Chang, H., T. Enzymatic hydrolysis of autohydrolyzed wheat straw followed by refining to produce fermentable sugars. *Bioresource Technol*. **2014**, 152, 259-266.

[3] Miura, T.; Lee, S. H.; Inoue, S.; Endo, T. Improvement of enzymatic saccharification of sugarcane bagasse by dilute-alkali-catalyzed hydrothermal treatment and subsequent disk milling. *Bioresource Technol.* **2012**, 105, 95-99.

[4] Silva, A. S.; Inoue, H.; Endo, T.; Yano, S.; Bon, E. P. S. Milling pretreatment of sugarcane bagasse and straw for enzymatic hydrolysis and ethanol fermentation. *Bioresource Technol*. **2010**, 101, 7402-7409.

[5] Sluiter, A.; Hames, B.; Ruiz, R.; Scarlata, C.; Sluiter, J. and Templeton, D. Determination of Ash in Biomass. Technical Report, NREL/TP-510-42622, National Renewable Energy Laboratory, **2005**.

[6] Sluiter, A.; Hames, B.; Ruiz, R.; Scarlata, C.; Sluiter, J. and Templeton, D. and Crocker, D. Determination of Structural Carbohydrates and Lignin in Biomass. Technical Report, NREL/TP-510-42618, National Renewable Energy Laboratory, **2008**.

KRAFT LIGNIN DEPOLYMERISATION BY BASE CATALYSED DEGRADATION (BCD) - THE EFFECT OF PROCESS PARAMETERS ON CONVERSION DEGREE AND STRUCTURAL FEATURES OF BCD-FRACTIONS

Detlef Schmiedl[1]*, Sarah Böringer[1], Rainer Schweppe[1], Tiina Liitiä[2], Stella Rovio[2], Tarja Tamminen[2], Jorge Rencoret[3], Ana Gutiérrez[3], José C. del Rio[3]

*[1]Fraunhofer Institute for Chemical Technology, Pfinztal, Germany; [2]VTT-The Technical Research Center of Finland, Espoo, Finland; [3]IRNAS-CSIC, Seville, Spain (*detlef.schmiedl@ict.fraunhofer.de)*

ABSTRACT

The objective of the study is the generation of oxy-aromatic compounds (monomer, oligomer) from Eucalyptus-Kraft-lignin via multi-stage processes. These processes (1st base catalysed degradation & 2nd separation of the organic phase from reactor water) have to be feasible in bio refineries & in new Pulp-mill bio refineries as a new technology module. The Eucalyptus-Kraft-lignin (Suzano Pulp & Paper) was used for catalyzed conversion into oxy aromatics. Subsequently, the effect of process parameters: catalyst & catalyst conc., mineral content, p: ≤250bars, τ≤15min), T:≤350°C)) was investigated. Liquid-liquid extraction of reactor water (pH=3) was performed with MIBK for isolation of the monomer rich phase. The BCD fractions (oils) & (tars) were characterized regarding their yields via carbon balance, & their composition. A characterization of the monomer composition was done (GC-MS/FID & EA (CHONS), ^{31}P-NMR, 2D-NMR (HSQC), TGA). Types of monomers were summarized into groups (guaiacols (G), syringols (S), catechols (C)). Oligomer degradation products in the oil were characterized by Infusion MS Ion Trap & the composition of the oligomer phase by ^{Py}GC-MS, SEC, EA, ^{31}P-NMR, 2D-NMR (HSQC) & TGA. On the one hand, depending on the botanical source & the lignin recovery process (Organosolv, Kraft etc.), useful lignins differ in their structure (inter unit linkages) & monomer composition, mineral & sulphur content, M_W, M_N. These substrate factors effecting the degradation process during the catalysed cleavage of aryl-aryl-ether & aryl-methyl-ether bonds. On the other hand, process factors e. g.: p, ϑ, τ, catalyst conc. & type of alkaline elements have a main effect on the cleavage processes, on the yield & composition of the monomer rich phase (oil), on the molecular characteristic (Mw, Mn, OH-number (aliphatic & phenolic -OH)) of the oligomer rich phase (tar) & on the carbon balance. To get an overview about the main & side effects in such complex situation, the study on the Kraft-lignin was done using DoE (Box-Behnken). A detailed evaluation regarding the main & side effects of process factors on the yield of oil & tar, on the concentration of (G), (S) & (C) in the oil phase, on the carbon balance, on M_W & M_N of the tars as well on functional groups (OH-number, differentiated into aliphatic & phenolic), presence of inter unit linkages & methoxy groups will be given.

I. INTRODUCTION

Depletion of crude oil, an increase in the greenhouse gas concentration, economical/ecological challenges of the pulp & paper industry force into the utilization of lignocellulose biomass. Only by economical biomass conversion processes the production of sustainable bio-based materials, chemicals, & semi-finished chemical goods will be reasonable. Lignin (renewable resource) contains aromatic structures, & has sustainable & economical potential in bio based chemicals & materials. Lignin depolymerisation for the generation of phenolic building blocks has been investigated over some decades. The degradation of lignin (Kraft-lignin, Organosolv-lignin) in alkaline, hot compressed solution, so called "base catalysed degradation - BCD" is based on the selective catalytic cleavage of inter unit linkages (α-O-4, β-O-4, 4-O-5) & methyl-aryl-ether bonds in the presence of strong bases (e.g. NaOH, KOH) [**1-5**]. Under defined conditions the generation of a monomer rich phase (BCD-oil) & an oligomer rich phase (BCD-tar) is possible. A detailed study was done regarding the BCD of Eucalyptus-Kraft-lignin (25wt. % of ash), supported by DoE (Box-Behnken). The high mineral content of the lignin was used as additional catalytic active component. The experiments were done in a plug flow reactor at selected T 300, 325 & 350°C, with selected additional NaOH of 1, 2 & 3wt.-% as well as at selected reaction times of 5, 10 & 15min respectively. The pressure was ~ 200-250bars. The BCD-oil & BCD-tar phases were analysed by weight, EA (CHONS), ^{31}P-NMR, 2D-NMR (HSQC) & TGA. Additionally, the BCD-oils were analysed by GC-MS/FID (composition of monomer oxy aromatic compounds (G, S, C)) & by infusion MSD Ion Trap (APCI negative) (oligomer composition). Furthermore, the acetylated BCD-tars were analysed by SEC regarding their molecular weight (M_N, M_W). The 3D assessment of the complex data sets was supported by the software Statgraphics centurion XV. Based on the analysis results the carbon balance was used for the description of the conversion degree into BCD-oil and BCD-tar over the test cube.

II. EXPERIMENTAL

GC-MS/FID: Monomers were determined according a method describe in [5].
Elemental analysis (NCHS & O): EA was performed according a method described in [5].
^{31}P-NMR- Analysis: OH-Number was determined according a method described in [6].
2D-NMR- Analysis (HSQC): 2D-NMR-analysis was done according a method described in [7].
SEC-Analysis: M_N &M_W of acetylated samples were determined according a method described in [8].

III. RESULTS AND DISCUSSION

Depending on the process parameters the Kraft-lignin could be converted into 15-20% of BCD-oil & 30-75% of BCD-tar (by carbon balance, Figure 1. & 2.). The liberation of primary monomer cleavage products (G & S) & the formation of secondary monomer cleavage products (C) depend significantly on T, τ & the concentration of NaOH. The highest amounts of C (approx. 4.5wt. % of lignin) were generated at the process parameter combination: T: 350°C, t: 15min & 3wt.-% of NaOH (Figure 3.).

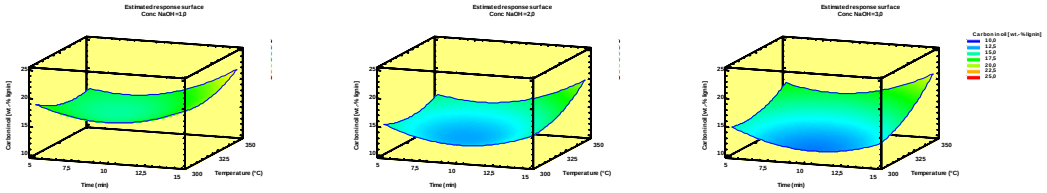

Figure 1. Conversion degree-**Carbon balance of used lignin** over the **BCD-oil** (z-axis: 10 - 25%) depending on process parameters (y-axis: T: 300-350 [°C], τ: 5-15 [min], NaOH- [%]: 1% left, 2% centre, 3% right.

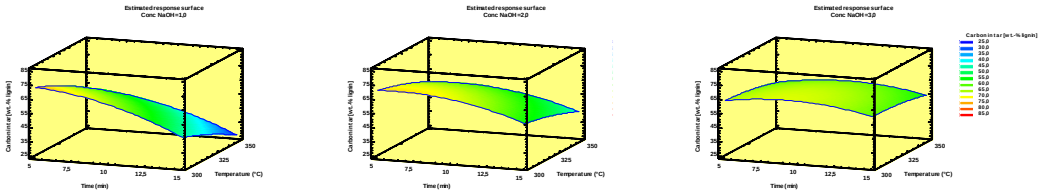

Figure 2. Conversion degree-**Carbon balance of used lignin** over the **BCD-tar** (z-axis: 25 – 85%) depending on the process parameters (y-axis: T: 300-350 [°C], τ: 5-15 [min], NaOH- [%]: 1% left, 2% centre, 3% right.

^{31}P-NMR analyses on selected BCD-oils show an increase in the phenolic OH-number depending on BCD process conditions. ^{31}P-NMR analyses on corresponding BCD-tars illustrate more or less the same trend in the phenolic OH-number. The used Kraft-Lignin showed a lower phenolic OH (Table1.). The stronger the process conditions (**01:** 5min, 300°C → **08:** 5min, 350°C → **03:** 15min, 350°C,const.NaOH:2%) the higher the phenolic OH number, indicating additional de-methylation. An additional de-methoxylation is remarkable. Para-hydroxy phenolic units were also formed (Table 1.). During the BCD aliphatic OH-groups were lost (**Table 1.**).

Table 1. Results of ^{31}P-NMR of Eucalyptus-Kraft-Lignin & of some BCD-oils & tars regarding aliphatic & phenolic OH-number & their distribution into condensed & S, G, C, para-hydroxy-phenyl.

sample	**Aliphatic -OH** **mmoles/g**	Cond. & Syringols -OH mmoles/g	Guaiacols -OH mmoles/g	Catechols -OH mmoles/g	para-OH -OH mmoles/g	**Phenolic -OH** **mmoles**/g	**Total -OH** **mmoles/g**
K-Lignin	**1.58**	2.10	0.69	-	-	**2.79**	**4.37**
BCD oil 01	**0.24**	3.30	2.0	0.29	0.20	**5.78**	**6.02**
BCD oil 08	**0.20**	2.88	3.18	0.63	0.39	**7.08**	**7.28**
BCD oil 03	**0.16**	1.26	6.74	0.58	0.80	**9.39**	**9.55**
BCD tar 01	**0.15**	2.64	0.72	0.61	0.27	**4.24**	**4.39**
BCD tar 08	**0.10**	2.39	1.00	1.19	0.38	**4.96**	**5.06**
BCD tar 03	**0.04**	1.16	1.23	1.70	0.62	**4.71**	**4.75**

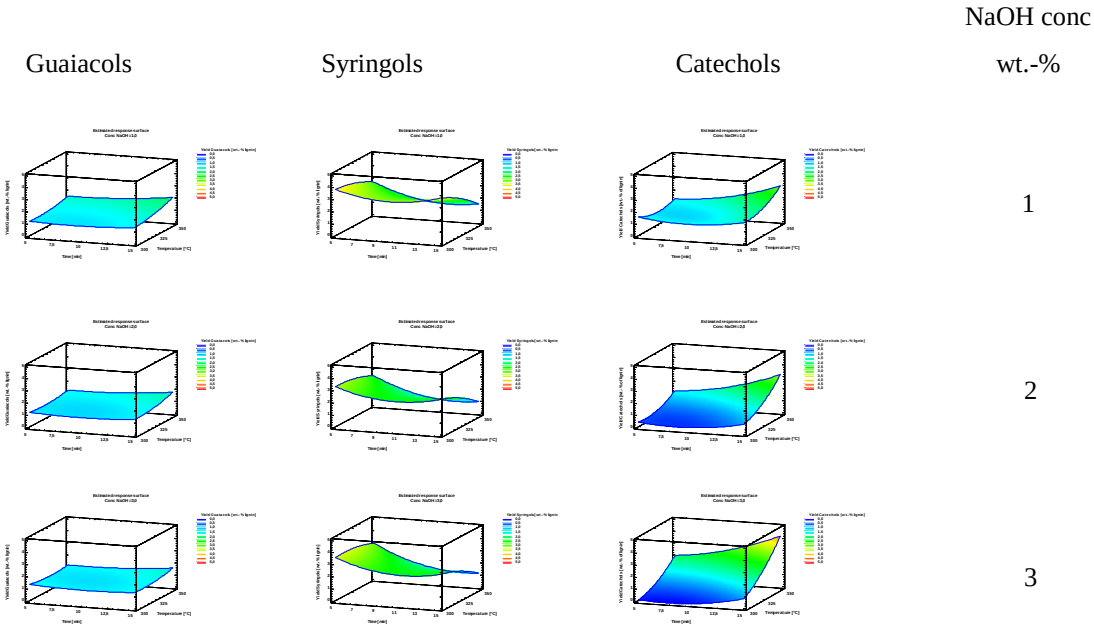

Figure 3. Yield of G (z-axis: 0 - 5wt.-% of lignin), S (z-axis: 0 - 5wt.-% of lignin) & C (z-axis: 0 - 5wt.-% of lignin) depending on the BCD process parameters (T [°C], τ [min], Conc. NaOH.

TG-Analyses on BCD-oils illustrate that ~ 50-65 wt.-% of the samples are volatile up to a temperature of 250°C. The residues represent the non-volatile, oligomer fraction in BCD-oils. Infusion MSD Ion Trap analysis on BCD-oils illustrates a complex picture of single charged & multi charged oligomer molecules in the scanning range from 225 to 500amu.

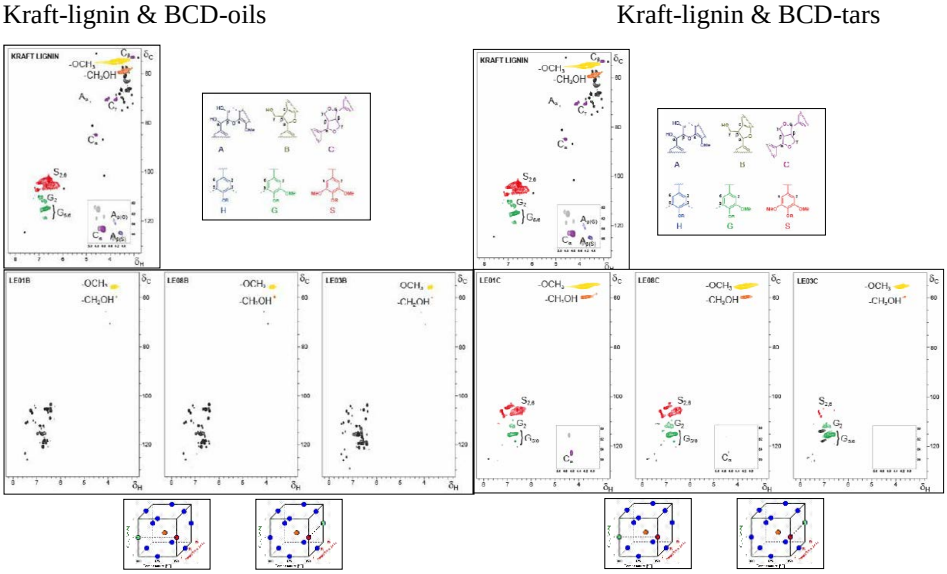

Figure 4. 2D-NMR (HSQC, δ_C/δ_H ppm) Spectra of Eucalyptus-Kraft-Lignin, BCD-Oils 01, 08, 03 (left) & of BCD-Tars 01, 08, 03 (right), **(LE01→ LE08→ LE03:** points in DoE, Box -Behnken**),** generated by BCD.

2D-NMR analyses (HSQC) on some BCD-oils illustrate the absence of inter-unit linkages β-O-4 & β-β` (Figure 4.). 2D-NMR analyses (HSQC) on selected BCD-tars show that the presence/absence of inter unit linkages of the type β-O-4 & β-β` depends on the process conditions (Figure 4.). The results of SEC on Kraft-lignin & on BCD-tars illustrate a significant reduction on M_W: 700-1300g/moles & M_N: 300-360g/moles as well as on M_W/M_N: 2. The Kraft-lignin showed following values for M_W: 8569g/moles, M_N: 1351g/moles, M_W/M_N: 6.3 (Figure 5.).

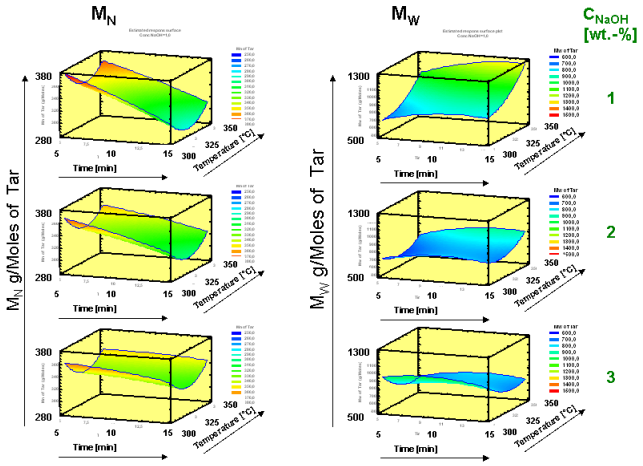

Figure 5. Result of SEC (M_N, M_W) on BCD-tars depending on parameters, τ [min], T [°C] & NaOH [wt.-%].

IV. CONCLUSIONS

BCD of hard wood Kraft-lignin leads to the formation of primary cleavage products (guaiacols, syringols) & secondary cleavage products (catechols, p-OH-phenolics) by additional de-methylation & de-methoxylation. The formation of the monomers depends on the process parameters: T, τ & catalyst conc.. The inter-unit linkages (β-O-4, 4-O-5, β-β`resinol) are not more present in BCD-oils & in the oligomer BCD-fractions depending on the process parameters. The formed oligomer material shows lower M_W, M_N & M_W/M_N than the Kraft-lignin, & contains very high amounts of "phenolic-OH"- functional group. The "aliphatic OH"-group will be lost during BCD of lignin. The oligomer main product (BCD-tar) shows also interesting structures for material applications. The properties are adjustable by process parameters. Further investigations are necessary.

V. ACKNOWLEDGEMENT

The authors would like to thank the company Suzano Pulp & Paper, the national funding organisations (Agency for Renewable Resources, BMELV, Germany; TEKES, Finland; INIA, Spain).

VI. REFERENCES

[1] Miller, J.E.; Evans, L.R.; Mudd, J.E.; Brown, K.A.: Batch Microreactor studies of lignin depolymerisation by bases. 2. Aqueous solvents, SAND2002-1318, *Sandia National Laboratories, Albuquerque, New Mexico, USA* **2002**, 1-51.

[2] Vigneault, A.; Johnson, D.K.; Chornet, E.: Advance in the thermal depolymerisation of lignin via base-catalysis. In: *Science In Thermal And Chemical Biomass Conversion*, **2006**, *2*, 1401-1419. Edited by A.V. Bridgwater and D.G.B. Boocock, CPL Press, Newbury Berks, UK.

[4] Thring, R.W., Chornet, E., Overend, R.P. Fractionation of woodmeal by prehydrolysis and thermal organosolv. Alkaline depolymerisation, chemical functionality, and molecular weight distribution of recovered lignins and their fractions. *Can. J. Chem.* **1993**, 71, 779-789.

[5] Schmiedl, D.; Endisch, S.; Pindel, E.; Rückert, D.; Unkelbach, G.; Schweppe, R. Base Catalysed Degradation of lignin for the generation of oxy-aromatic compounds – Possibilities and challenges. *Erdöl, Erdgas, Kohle*, **2012**, 128, Heft 10, 357 – 363.

[6] Granata, A., Argyropoulos, D.S. 2-Chloro-4,4,5,5-tetramethyl-1,3,2-dioxaphospholane, a reagent for the accurate determination of the uncondensed and condensed phenolic moieties in lignins. *J. Agric. Food Chem.* **1995**, 43, 1538-1544.

[7] Rencoret J., Marques G., Gutiérrez A., Ibarra D., Li J., Gellerstedt G., Santos J.I., Jiménez-Barbero J., Martínez A.T. and del Río J.C. Structural characterization of milled wood lignin from different eucalypt species. *Holzforschung*, **2008**, 62, 514-526.

[8] Baumberger, S.; Abaecherli, A.; Fasching, M.; Gellerstedt, G.; Gosselink, R. Hortling, B.; Li, J.; Saake, B., de Jong, E. (2007): Molar mass determination of lignins by size-exclusion chromatography: towards standardisation of the methods. *Holzforschung*, **2007**, 61, 459-468.

SORBENTS FROM KRAFT LIGNIN: IMPACT OF THE CHEMICAL MODIFICATION ON THE THERMAL STABILITY AND POROUS STRUCTURE

Sevastyanova Olena,[1*] Podkościelna Beata,[2] Gawdzik Barbara,[2] Sobiesiak Magdalena,[2] Bartnicki Andrzej,[2] Poddubnaya Olga,[3] Lindström E. Mikael,[1] Puziy Alexander[3]

*[1]KTH, The Royal Institute of Technology, Department of Fibre and Polymer Technology, Division of Wood Chemistry and Pulp Technology, SE-10044 Stockholm, Sweden(*olena@kth.se);[2]Department of Polymer Chemistry, Faculty of Chemistry, Maria Curie-Skłodowska University, pl. M. Curie-Skłodowskiej 5, 20-031 Lublin, Poland; [3]Institute for Sorption and Problems of Endoecology, National Academy of Sciences of Ukraine, Naumov Street 13, 03164 Kyiv, Ukraine*

ABSTRACT

In this paper the novel method for the synthesis of microspheres from lignin co-polymerised with styrene (St) and divinylbenzene (DVB) is presented. The copolymers were obtained by the emulsion-suspension polymerization at constant mole ratio of tetrafunctional monomer divinylbenzene (DVB) to styrene St (1:1 w/w) and different amounts of lignin. Thermal stabilities and degradation behaviour of the obtained microspheres were studied by means of thermogravimetric (TG/DTG/DSC) analysis. Due to the presence of the specific functional groups and well developed porous structure the obtained Lignin-St-DVB microspheres have potential application as specific sorbents for the removal of phenolic pollutants from water by using e.g. Solid Phase Extraction (SPE) technique.

I. INTRODUCTION

Lignin is one of the main components of the lignocellulosic material. Various technical lignins are currently available in large quantities and considered as a low value by-products from the pulp and paper industry. However, lignin possesses structural features which make it promising starting material for chemical modifications, leading to the preparation of valuable polymeric materials with special properties [1]. Kondo et al. reported the method of preparation and ozonation of allilated lignins to obtain their epoxy derivatives [2]. Epoxy resins from the carboxylic acid system consisting of ester-carboxylic acid derivatives of alcoholysis lignin and ethylene glycol were successfully prepared by Hirose et al. [3]. Another possible way of lignin modification is the reaction with acrylic or methacrylic acid. As the result of the introduction of vinyl groups into lignin structure, new derivatives, capable for further polymerization can be obtained.

In this paper the novel method of the synthesis of microspheres from lignin or lignin vinyl derivatives co-polymerised with styrene (St) and divinylbenzene (DVB) is investigated. Due to the presence of different functional groups e.g. hydroxyl, carbonyl and thiol, the obtained microspheres have a potential application as sorbents for environmental pollutants. For chromatography purposes particles of sorbents should possess uniform spherical form. Such shape improves the efficiency of sorption process, as flow resistance for mobile phase and widening of chromatographic band due to diffusion are minimised. Equally important is also porous structure of polymeric microspheres. Well-developed surface area and presence of micro- and meso- pores provide effectiveness of sorption processes [4]. Thermal properties are crucial feature of polymer-based materials because the heat resistance determines the scope of application the sorbents used in different chromatographic techniques (GC, SPE-HPLC or SPME).

II. EXPERIMENTAL

Scheme of lignin modification is presented in Figure 1. According to a first method, lignin was reacted directly with acrylic acid in the presence benzene, sulphuric acid and hydroquinone at reflux temperature for 5 h. The obtained modified lignin was washed and dried. In the second method, lignin was derivatized with epichlorohydrine and acrylic acid. Lignin reacted first with epichlorohydrine in presence of propan-2-ol, and then an aqueous solution of NaOH was dropping out for 30 min. The lignin with introduced epoxy groups, was filtered off, washed and dried. To the epoxy-lignin (LE), acrylic acid, triethylbenzylammonium chloride and hydroquinone were added and heated at 90-95^{o}C for 5 h. The course of the modification of lignin was controlled by Attenuated Total Reflectance (ATR) spectroscopic method. Copolymerisation of styrene with divinylbenzene and lignin or lignin derivatives was performed in the aqueous medium in suspension-emulsion procedure [5].

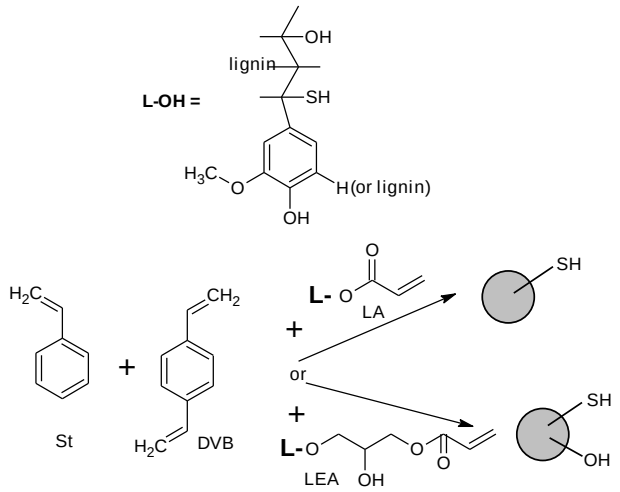

Figure 1. Chemical structure of monomers and copolymerization scheme.

Lignin was added to the monomers before polymerization in three forms: a) unmodified (L-OH) (0, 1, 3 and 6 g), b) modified with acrylic acid (LA), c) modified with epichlorohydrin and then with acrylic acid (LEA). The reaction mixture was stirred at 350 rpm for 18 h at 80^{o}C. Figure 1 presents chemical structure of monomers and lignins used in synthesis. The weight ratios of various types of the lignin derivatives for the syntheses are listed in Table 1.

Tabela 1. Experimental parameters of the synthesis

Copolymer	L-OH	LA	LEA
	[g]		
St-DVB*	0	-	-
St-DVB-L1	1	-	-
St-DVB-L3	3	-	-
St-DVB-L6	6	-	-
St-DVB-LA	-	3	-
St-DVB-LEA	-	-	3

*St and DVB amounts were the same in each case: 8 g St and 10 g DVB

ATR-IR spectra were obtained on a Bruker FTIR spectrophotometer TENSOR 27. The porous structure of copolymers was characterised by nitrogen adsorption at 77K using an adsorption analyser ASAP 2405 (Micrometrics Inc., USA). Thermal stabilities and degradation behaviours of copolymers were studied by means of TG/DTG/DSC analyses (STA 449 F1 Jupiter, Netzsch, Selb, Germany). Analyses were carried out in helium atmosphere in temperature range of 50 to 800°C.

III. RESULTS AND DISCUSSION

Figure 2 shows that the obtained copolymers possess spherical shape. Figure 3 presents the exemplary sample of St-DVB copolymers without lignin (1), and obtained with different amounts of unmodified lignin (2 - 1g, 3 - 3g of 4 - 6g).

By means of ATR spectroscopy the changes in the lignin structure introduced during chemical modification were confirmed. In Figure 4, ATR spectra for unmodified lignin (L) and its derivative obtained in reaction with acrylic acid (LA) are shown. Disappearance of signals of hydroxyl and methoxyl groups (4 peaks in the range of 1000-1300 cm^{-1}) in lignin spectrum and appearance new peaks at 1175 cm^{-1} and 1720 cm-1 which correspond to the ester and carbonyl species vibrations, confirm the correct course of modification.

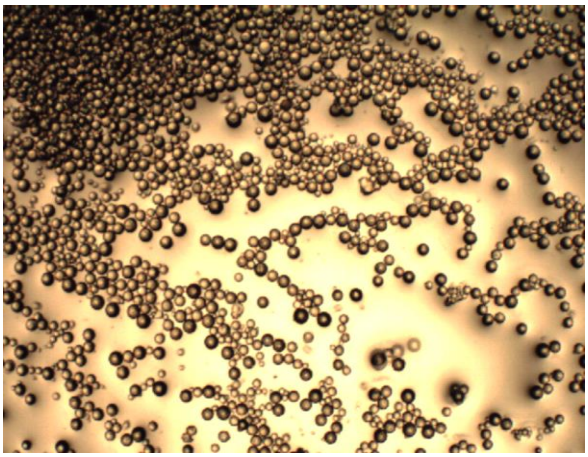

Figure 2. Microspheres St-DVB-L1

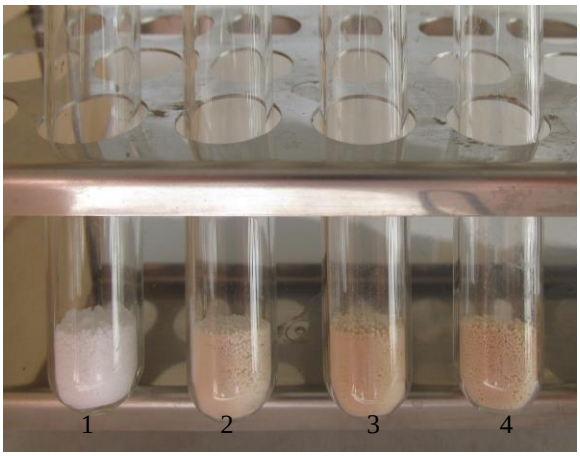

Figure 3. Photos of St-DVB with lignin

In Table 2 characterization of the porous structure of the St-DVB and its lignin copolymers obtained by the nitrogen adsorption-desorption method is presented. The largest specific areas and pore volumes are observed for the copolymers obtained in syntheses No. 1 (St-DVB) without the addition of lignin. Comparing with parent St-DVB copolymer for samples containing modified lignin decrease of specific surface area and total pore volume are observed. Probably, some pores are blocked by lignin derivatives. This assumption seems to confirm the fact, that for St-DVB-lignin copolymers mean pore width is about 11 nm, whereas for St-DVB copolymers 15,6 nm.

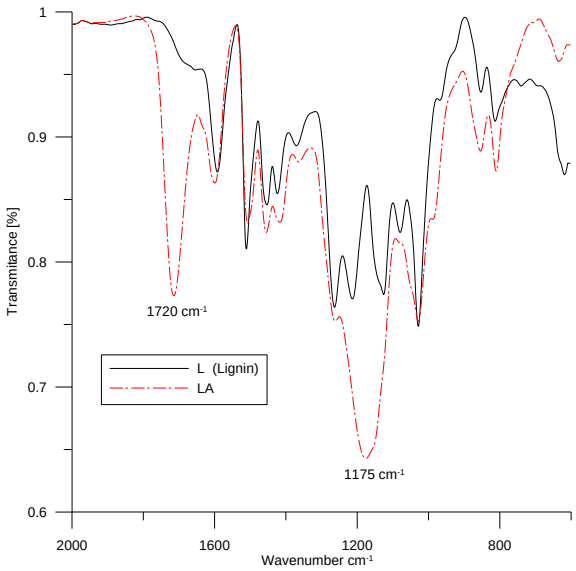

Figure 4. ATR spectra

Table 2. Porous structure parameters of the St-DVB copolymers

Copolymer	S_{BET} [m^2/g]	V_{TOT} [cm^3/g]	W [nm]
St-DVB	235	0.84	15.6
St-DVB-L1	166	0.41	10.9
St-DVB-L3	154	0.36	11.0
St-DVB-L6	149	0.25	8.0
St-DVB-LA	196	0.66	11.9
St-DVB-LEA	105	0.12	10.0

The DSC curves (Figure 5) show similarity in thermal behavior of all the studied copolymers. A slight increase of decomposition temperature is visible by increasing the amount of lignin. The endothermic peaks at 415.0-427.4°C are related to the thermal degradation of copolymers.

Some additional results obtained from TG/DTG analysis are presented in Table 3. According to this data thermal decomposition of lignin starts at 113°C and the most intensive mass changes proceed in two stages at 309 and 390°C with mass loss ca 20 and 10%, respectively. After the reaction with acrylic acid thermal behaviour of lignin has been changed. Decomposition of LA material starts at 159°C. It also proceeds in two stages, but the course of process is different. First stage is in the range of 200-300°C, while the second proceeds in the range of 350-450°C. It means LA is more thermally stable than unmodified lignin.

Thermal decomposition of St-DVB copolymer is quite different. In the range of 125°C to 250°C only 3% of mass is lost by this material. It is connected with evaporation of unreacted monomers. The main thermal changes proceed in the range of 300 to 500°C. Similar thermal behaviour is observed for polymers St-DVB containing lignin component. Nevertheless influence of the lignin additives can be noticed. St-DVB-L3 and St-DVB-LA are more thermally stable than unmodified St-DVB, their initial decomposition temperatures are about 10 °C higher. The temperatures of maximum rate of mass loss (T_{peak2}) also possess higher values. The obtained residue in form of chars after thermal treatment of St-DVB-L3 and St-DVB-LA was about 5%.

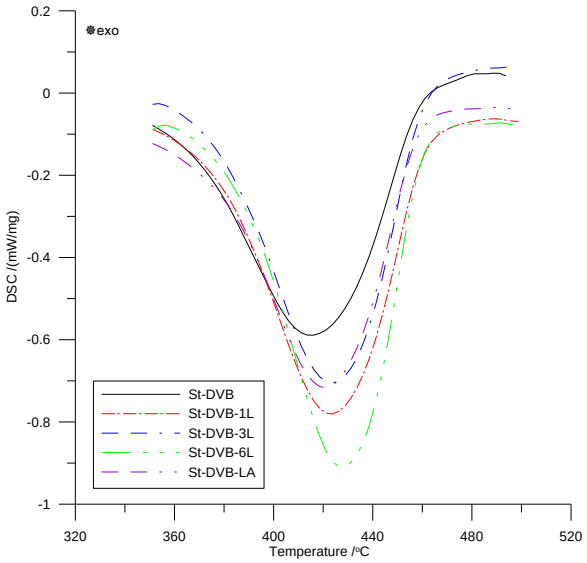

Figure 5. DSC analysis

Table 3. Results from the thermo-gravimetric analysis (TG) for chosen materials.

Material	$T_{initial}$ [°C]	T_{peak1} [°C]	W_{loss1} [%]	T_{peak2} [°C]	W_{loss2} [%]	Residue at 800°C
L	113.1	309.3	21.28	390.3	10.26	29.75
St-DVB	125.4	152.4	2.84	418.6	90.65	4.53
St-DVB-3L	133.9	166.6	0.38	430.5	91.14	5.42
St-DVB-LA	135.7	163.3	1.32	424.9	91.13	4.63
LA	158.9	246.4	14.24	389.2	27.53	41.95

IV. CONCLUSIONS

- Vinyl derivatives of lignin were successfully prepared by reaction with acrylic acid (LA) and in two-step reaction with epichlorohydrin and acrylic acid (LEA) which was confirmed by ATR spectra.
- Polymeric porous materials in form of microspheres were prepared from lignin derivatives copolymerized with styrene and divinylbenzene.
- Surface area and total pore volume for copolymers containing lignin were smaller in comparison to parent St-DVB copolymer.
- Some advantageous influence of lignin and lignin derivatives on thermal properties of the presented lignin-containing St-DVB microspheres was observed.

V. ACKNOWLEDGEMENT

- Knut and Alice Wallenberg foundation in association with the Wallenberg Wood Science Center (WWSC)
- The Swedish Institute (Baltic Sea cooperation program, project 001-3053)

VI. REFERENCES

[1] Dournel, P.; Randrianalimanana, E.; Deffieux, A.; Fontanille, M. Synthesis and polymerization of lignin macromonomers I. *Eur. Polym. J.* **1988**, *24*, 843-847.

[2] Kondo, T.; Meshitsuka G.; Ishizu, A.; Nakando, J. Preparation and ozonation of completely allylated and methallylated lignins. *Mokuzai Gakkaishi* **1987**, *33*, 724-727.

[3] Hirose, S.; Hatakeyama T.; Hatakeyama H.; Glass transition and thermal decomposition of epoxy resins from the carboxylic acid system consisting of ester-carboxylic acid derivatives of alcoholysis lignin and ethylene glycol with various dicarboxylic acids. *Thermochimica Acta* **2005**, *431*, 76–80.

[4] Sobiesiak, M.; Podkościelna B. Preparation and characterization of porous DVB copolymers and their applicability for adsorption (solid-phase extraction) of phenol compounds. *Appl.Surf. Sci.* **2010,** *257*, 1222-1227.

[5] Podkościelna, B.; Bartnicki, A.; Gawdzik, B. New crosslinked hydrogels derivatives of 2-hydroxyethyl methacrylate: Synthesis, modifications and properties. *Express Polym. Lett.* **2012,** *6(9)*, 759-771.

CHANGE IN ENZYMATIC DIGESTIBILITY OF AGRO-CROP LIGNOCELLULOSIC BIOMASS DURING SELECTIVE HYDROLYTIC REMOVAL OF XYLAN

Anatoly A. Shatalov [1]*, Rita C. Morais[1], Luís C. Duarte[2], Florbela Carvalheiro[2]

*[1] Universidade de Lisboa, Instituto Superior de Agronomia, Centro de Estudos Florestais (CEF), Tapada da Ajuda, 1349-017 Lisboa, Portugal; [2] LNEG-Laboratório Nacional de Energia e Geologia I. P., Unidade de Bioenergia, Estrada do Paço do Lumiar 22, 1649-038 Lisboa, Portugal (*anatoly@isa.utl.pt; anatoly@isa.ulisboa.pt)*

ABSTRACT

The low temperature dilute sulfuric acid hydrolysis has been employed for selective single-stage conversion of agro-crop hemicelluloses (consisted mainly of xylan) to monomeric sugars, viewing as entry point to complex biorefining scheme with separate processing/utilization of different carbohydrate streams. The combined severity parameter (CS), applied in the range of 1.07-2.44, was used to assess the effects of hydrolysis conditions on selectivity and efficiency of xylan conversion to xylose as well as on enzymatic digestibility improvement of insoluble solid residue for bioethanol production. Two potential energy crops – giant reed and cardoon, possessing different morphological features, were chosen as model biomass feedstocks. The maximum xylose recovery in solution of 0.94 and 0.86 was achieved at CS 1.90 and 1.97, respectively for giant reed and cardoon, with formation of only 2.4-2.7% glucose, 0.9-1.4% furfural, 0.3-0.7% 5-hydroxymethylfurfural and 2.9-3.7% acetic acid. At these optimal CS levels, the enzymatic cellulose saccharification of 0.51 and 0.64, for giant reed and cardoon respectively, was observed under standard NREL conditions. The digestibility was further linearly increased to 0.73 and 0.98 with increase in hydrolysis severity up to CS 2.44, while substantial loss in xylose (up to 40%) and formation of toxic furan substances (up to 4.8-5.3% furfural) had also place. The essential effect of stem morphology on established correlations was noted.

I. INTRODUCTION

The integrated upgrading of low-cost lignocellulosic biomass feedstocks, such as agro-based crops and residues, into transportation fuel and high-value products within a multi-product biorefining concept is viewed now as a more reliable way to ensure the sustainable bio-based economy [1,2].

Such Mediterranean perennial herbs as giant reed (*Arundo donax* L.) and cardoon (*Cynara cardunculus* L.), possessing remarkable characteristics of biomass yield and quality, are being considered now among the most promising non-food agro species for industrial utilization, and as a particularly attractive feedstocks for biorefinery schemes [3,4].

The main chemical constituents of lignocellulosic biomass (cellulose, hemicellulose and lignin) form complex and rigid cell-wall structure, recalcitrant to chemical and enzymatic degradation. The development of effective and selective methods of biomass fractionation is a challenge of primary importance in biorefining technology. Since the carbohydrate portion reaches up to 80% of lignocellulosic biomass, sustainable separation and conversion of hemicelluloses and cellulose would define the commercial viability of the whole biorefining chain [5]. The agro-based hemicelluloses are basically composed (by 90-95%) of xylan polysaccharide, which can be used as a valuable source of xylose for many (bio)chemical technologies, e.g., for biotechnological production of xylitol. For selective conversion of hemicellulosic xylan to monomeric sugars, the dilute acid hydrolysis was proved to be the most reliable and easily performed low cost method [6]. The yield of xylose is strongly dependent on the type of raw material and operation conditions. The high efficiency and selectivity of process can be provided under controlled hydrolysis conditions. After selective xylan hydrolysis, the remaining solid residue, consisting essentially of cellulose, can be used for bio-ethanol production. Since hemicelluloses removal destroys the lignin-carbohydrate matrix shielding cellulose micro-fibrils [7], the dilute acid pre-hydrolysis can substantially improve enzymatic digestibility (saccharification) of cellulose, being an important pre-treatment step and entry point to complex biorefining scheme.

The effect of selective hydrolytic removal of hemicellulosic xylan on enzymatic digestibility of energy crops giant reed and cardoon for bioethanol production has been studied and is discussed in the present communication.

II. EXPERIMENTAL

The cardoon (*Cynara cardunculus* L.) and giant reed (*Arundo donax* L.) biomass was sampled respectively from the university experimental plantation field (Institute of Agronomy, Lisbon) and the naturally growing crop population (Tapada da Ajuda, Lisbon). The air-dry whole stems of both crops were manually stripped of leaves, milled and screened to uniform particle size of 40-60 mesh and stored in sealed plastic bags at room temperature until using.

Commercial enzymatic preparations Celluclast 1.5L (cellulases from *Trichoderma reesei*) and Novozyme-188 (β-glucosidases from *Aspergillus niger*) were purchased by Sigma Co. Enzymatic activity (FPU/mL and pNPGU/mL, respectively) was determined before enzyme application.

Dilute sulfuric acid hydrolysis was performed in stainless steel digesters rotated in an oil bath, as described elsewhere [8,9]. Insoluble solid residue was separated by vacuum filtration, thoroughly washed by deionized water to neutral pH and kept frozen for subsequent analysis and enzymatic saccharification. Hydrolysate was combined with washing waters and analyzed on degree of monosaccharide recovery and degradation.

The enzymatic digestibility of insoluble residue after acid hydrolysis was performed by NREL standard [10]. The release of soluble sugars was determined by HPLC and corrected by blank tests on substrate and enzymes. The enzymatic digestibility (saccharification) was defined as a ratio of cellulose digested to cellulose loaded (g/g).

Residual lignin in process solids was determined as acid-insoluble (Klason) lignin after two-step acid hydrolysis, according to NREL standard [11].

The concentration of monosaccharides and their degradation products in liquid process steams was quantified by HPLC using Aminex HPX-87H column (Bio-Rad, Hercules, CA, USA) operating at 50ºC, in combination with a cation H^+-guard column (Bio-Rad, Hercules, CA, USA). The mobile phase was 5mM sulfuric acid and the flow rate 0.4 ml min^{-1}.

Xylose recovery after acid hydrolysis was defined as a ratio of xylose content in solution to xylose content in untreated biomass. Acid hydrolysis selectivity was defined as a ratio of xylose to glucose in solution.

III. RESULTS AND DISCUSSION

Following the multi-stage fractionation scheme, the whole stem material of two potential European energy agro-crops giant reed and cardoon was pre-hydrolyzed by acid for hemicellulosic carbohydrates recovery and valorization prior to cellulose conversion to fuel bioethanol The low temperature (below 150ºC) dilute sulfuric acid hydrolysis has been designed to produce a high quality xylose-enriched organic substrate for xylitol production and reactivity (digestibility) improvement of insoluble xylan-free residue in the following enzymatic saccharification by cellulases. The combined severity parameter (CS) was applied to assess the effects of hydrolysis conditions (time, temperature and acid concentration), combined into a single reaction ordinate, on selectivity and efficiency of xylan conversion to xylose as well as on enzymatic digestibility of residual cellulose to glucose:

$$CS = \text{Log } R_O - pH$$

$$R_O = t \cdot \exp[(T - 100)/14.75$$

where R_O is severity factor; t is reaction time (20-70 min); T is reaction temperature (120-150ºC); pH was calculated from the acid concentration (0.2-1.8%).

As can be seen from Fig. 1, under tested range of combined hydrolysis severity of 1.04-2.44, the maximum xylose recovery in solution of 0.94 and 0.86 (94% and 86% of total) was achieved at CS 1.90 and 1.97, respectively for giant reed and cardoon, showing very good correlation of experimental data (R^2=0.93 and R^2=0.90). Under these levels of CS, only limited cellulose hydrolysis (formation of 2.4-2.7% glucose) and monosaccharide decomposition (formation of 0.9-1.4% furfural, 0.3-0.7% 5-hydroxymethylfurfural and 2.9-3.7% acetic acid) was observed, providing high process selectivity.

To examine the effect of single-stage selective xylan-to-xylose hydrolysis on enzymatic digestibility of remaining cellulose for bioethanol production, the insoluble residues with different degree of xylan removal were saccharificated by commercial cellulase preparations under standard NREL conditions. As shown in Fig. 2, under optimum hydrolysis conditions providing maximum monomeric xylose recovery at solution (at CS 1.90 and 1.97), the enzymatic digestibility (or cellulose-to-glucose conversion) of 0.51 and 0.64 (51% and 64% of

total cellulose conversion) can be obtained for giant reed and cardoon, respectively, versus 0.09 and 0.19 for untreated material.

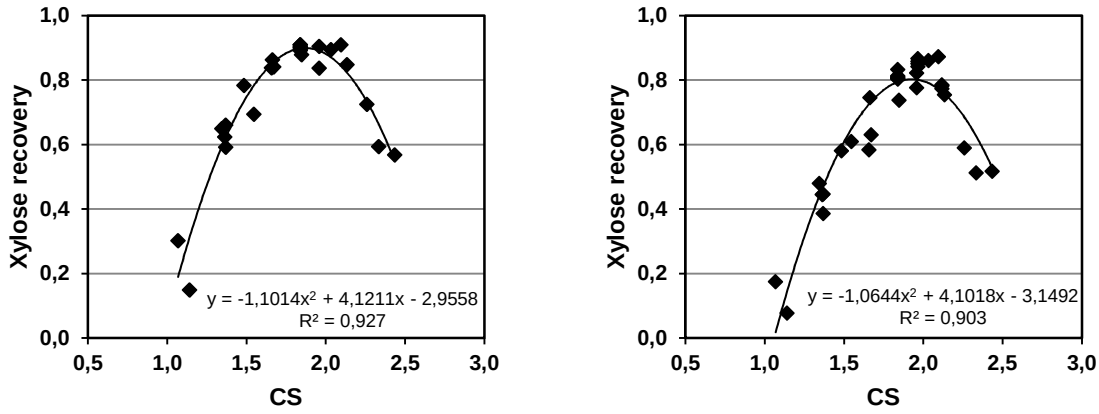

Figure 1. Effect of combined severity of single-stage dilute sulfuric acid hydrolysis of giant reed (left) and cardoon (right) on monomeric xylose recovery in solution.

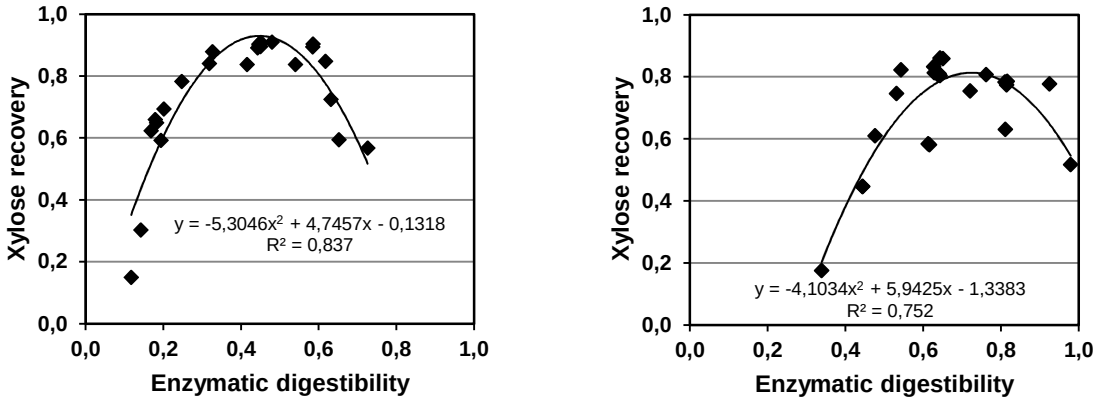

Figure 2. Correlation between monomeric xylose recovery during single-stage dilute sulfuric acid hydrolysis of giant reed (left) and cardoon (right) and enzymatic digestibility of insoluble residue.

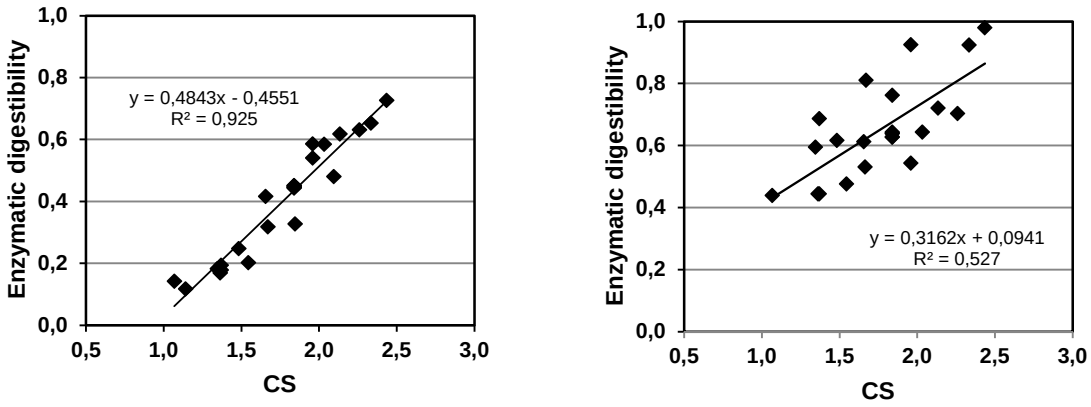

Figure 3. Effect of combined severity of single-stage dilute sulfuric acid hydrolysis of giant reed (left) and cardoon (right) on enzymatic digestibility of insoluble residue.

Generally, the low temperature dilute sulfuric acid hydrolysis performed at the CS range 1.04-2.44 improved linearly the following enzymatic digestibility of pre-hydrolyzed giant reed and cardoon up to 0.73 and 0.98 (73% and 98% of cellulose conversion to glucose), respectively (Fig. 3), being obviously very effective pre-treatment

method for bioethanol production. However, the substantial degradation of xylose (up to 40%) and the formation of toxic substances (up to 5% of furfural) occurred when the hydrolysis was performed at levels CS over 1.90 and 1.97, respectively for giant reed and cardoon, thereby reducing significantly the commercial value of the hemicelluloses. To gain the most benefits of hemicellulose and cellulose portions in biorefining technology, the enzymatic saccharification of insoluble crop residues obtained after acid pre-hydrolysis at CS 1.90 and 1.97, respectively for giant reed and cardoon, must be improved by process optimization.

The comparison between two tested crops revealed substantial effect of crop morphology on biorefining results. The less dense cardoon stalks showed higher readiness and thus effectiveness to enzymatic hydrolysis. At the same time, the anatomic heterogeneity of cardoon whole stalks, consisted of centrally located pith and surrounding fibro-vascular bundles, affected the process uniformity (topochemical effect) leading to significant dispersion of experimental data and difficulties in process modeling, as compared with giant reed.

IV. CONCLUSIONS

The single-stage low temperature dilute sulfuric acid hydrolysis can be very effective entry point for integrated fractionation of agro-crop lignocellulosics, such as energy crops giant reed and cardoon, providing selective conversion of xylan into monomeric xylose and significantly improving the enzymatic digestibility of cellulose.

V. ACKNOWLEDGEMENT

Financial support was provided by FCT (Portugal) within research contract PTDC/AGR-CFL/103840/2008.

VI. REFERENCES

[1] Kamm, B.; Kamm, M. Biorefineries – Multi Product Processes. *Adv. Biochem. Eng. Biotechnol*. **2007**, *105*, 175–204.

[2] FitzPatrick, M.; Champagne, P.; Cunningham, M.F.; Whitney, R.A. A biorefinery processing perspective: Treatment of lignocellulosic materials for the production of value-added products. *Biores. Technol*. **2010**, *101*, 8915-8922.

[3] Lewandowski, I.; Scurlock, J.M.O.; Lindvall, E.; Christou, M. The development and current status of perennial rhizomatous grasses as energy crops in the US and Europe. *Biomass Bioenergy* **2003**, *25*, 335–361.

[4] Fernández, J., Curt, M.D.; Aguado, P.L. Industrial applications of *Cynara cardunculus* L. for energy and other uses. *Ind. Crops Prod.* **2006**, *24*, 222-229.

[5] Zhang, Y.H.P. Reviving the carbohydrate economy via multi-product lignocellulose biorefineries. *J. Ind. Microbiol. Biotechnol.* **2008**, *35*, 367–375.

[6] Martin, C.; Alriksson, B.; Sjode, A.; Nilvebrant, N.-O.; Jonsson, L.J. Dilute sulfuric acid pretreatment of agricultural and agro-industrial residues for ethanol production. *Appl. Biochem. Biotechnol*. **2007**, *136*, 339-352.

[7] Zhang, Y.-H.P. Reviving the carbohydrate economy via multi-product lignocellulose biorefneries. *J. Ind. Microbiol. Biotechnol.* **2008**, *35*, 367-375.

[8] Shatalov, A.A.; Pereira, H. Biorefinery of energy crop cardoon (*Cynara cardunculus* L.) - Hydrolytic xylose production as entry point to complex fractionation scheme. *J. Chem. Eng. Proc. Technol.* **2011**, *2*, 118-125.

[9] Shatalov A.A.; Pereira H. Xylose production from giant reed (*Arundo donax* L.): Modeling and optimization of dilute acid hydrolysis. *Carbohydr. Polym.* **2012**, *87*, 210-17.

[10] Selig, M.; Weiss, N.; Ji, Y. Enzymatic saccharification of lignocellulosic biomass. Laboratory analytical procedure (LAP), NREL/TP-510-42629, **2008**.

[11] Sluiter, A.; Hames, B.; Ruiz, R.; Scarlata, C.; Sluiter, J., Templeton, D.; Crocker, D. Determination of structural carbohydrates and lignin in biomass. Laboratory analytical procedure (LAP), NREL/TP-510-42618, **2008**.

INTEGRATED UPGRADING OF AGRO-CROP LIGNOCELLULOSIC BIOMASS FOR PRODUCTION OF HIGH GRADE CELLULOSE FIBERS

Anatoly A. Shatalov*, Helena Pereira

*Universidade de Lisboa, Instituto Superior de Agronomia, Centro de Estudos Florestais (CEF), Tapada da Ajuda, 1349-017 Lisboa, Portugal (*anatoly@isa.utl.pt; anatoly@isa.ulisboa.pt)*

ABSTRACT

Integrated upgrading of the potential European energy agro-crops giant reed and cardoon has been carried out for valorization of the main chemical constituents of the whole stem biomass. After selective single-stage hydrolytic conversion of hemicellulosic xylan to monomeric xylose for enzymatic xylitol production, the high purity dissolving grade cellulosic fibers were produced by sulfur-free soda-AQ pulping technology. Response surface methodology was employed for statistical pulping modelling and optimization. The effect of principle process variables on such pulping outputs as pulp yield, Kappa number, brightness, viscosity, α-cellulose content and lignin recovery was assessed and modelled using 2^4 central composite rotatable design (CCRD). Cellulosic fibers having 96-98% of α-cellulose and DP 2500-2700 were obtained for both crops under optimized conditions. About 80-85% (as a max) of total crop lignin was recovered from the black pulping liquor, as a high purity precipitated technical lignin.

I. INTRODUCTION

The multi-product biorefining of lignocellulosic biomass with complete fractionation and co-utilization of the principal chemical components has been the focus of much attention for the last few years, as a more potential biorefinery scheme [1,2]. The agro-based lignocellulosics, such as industrial crop residues and perennial herbaceous species (grasses), represent abundant and cheap feedstock for biorefining technologies. Among a group of the more potential perennial herbs evaluated as energy crops in Europe, the particular attention has been given to giant reed (*Arundo donax* L.) [3] and cardoon (*Cynara cardunculus* L.) [4]. The remarkable biomass productivity of giant reed and cardoon combined with high ability to intensive cultivation and appropriate chemical composition made these herbs as the most promising energy crops for industrial utilization and particularly attractive lignocellulosic feedstock for biorefinery.

In biorefinery of fiber agro-crops (such as giant reed and cardoon) the isolated cellulose can be used as a valuable source of fibers, alternatively to ethanol production. After selective hemicellulose (basically xylan) removal and appropriate delignification, the high purity dissolving grade pulps can be produced, substantially enhancing the economy of biorefinery process. Nowadays, the dissolving grade pulps with 92-96% of α-cellulose are commercially produced from woody species using pre-hydrolysis kraft or acid sulfite processes followed by elemental chlorine-free (ECF) bleaching [5]. The application of sulfur-free delignification in combination with totally chlorine-free (TCF) bleaching would be a significant step in meeting environmental and economic concerns related to conventional industrial technologies.

The production of high-grade cellulosic fibers by soda-AQ pulping of pre-hydrolyzed (xylan-free) stem material of giant reed and cardoon has been studied as an integrated stage of complex upgrading scheme. The principal results on pulping modelling and optimization are discussed in the present communication.

II. EXPERIMENTAL

The air dried stems of giant reed and cardoon, sampled respectively from the naturally growing native crop population and the university experimental plantation field, were manually stripped of leaves, milled, screened and stored in sealed plastic bags until using.

The selective hydrolysis (removal) of hemicelluloses (consisted by 90-95% of xylan) was performed before pulping, using previously established optimum reaction conditions, as described elsewhere [6,7].

The soda-AQ pulping of pre-hydrolyzed (xylan-free) crop stems was carried out in stainless steel digesters rotated in an oil bath. The process variables were reaction time (80-160 min), reaction temperature (150-170ºC), alkali (NaOH) concentration (14-26% oven-dry material) and AQ concentration (0.1-0.3% oven-dry material).

Residual lignin was determined as a Kappa number according to TAPPI T 236 cm-85. Pulp intrinsic viscosity was measured in CED solution according to SCAN-cm 15:88. ISO Brightness and DIN yellowness index were measured by CM-3630 spectrophotometer (Minolta). The α-cellulose content was determined according to T 203 om-93 TAPPI standard.

Response surface methodology (RSM) [8] was employed for statistical data treatment and conditions optimization (Statistica 6.0, Statsoft, USA). The statistical significance of regression coefficients and effects was checked by analysis of variance (ANOVA).

III. RESULTS AND DISCUSSION

According to pre-defined fractionation scheme with separate utilization of hemicelluloses and cellulose fractions, the stem material of both giant reed and cardoon was hydrolyzed by diluted sulfuric acid under moderate reaction conditions specifically designed for selective single-stage conversion of polymeric xylan to monomeric sugars [6,7]. Under established optimal reaction conditions, the xylose recovery of 94% and 86%, respectively for giant reed and cardoon, was achieved in solution with only limited cellulose hydrolysis and monosaccharide decomposition to furans. The insoluble residue after selective hydrolysis (removal) of hemicelluloses from both crops hold only 0.2-0.5% of residual xylan, indicating almost total (by 98.5-99.5%) xylan removal during hydrolysis. The content of cellulose accounted for 53% and 65% of the insoluble residue, respectively for giant reed and cardoon. Only 6-8% of total crop cellulose was dissolved during hydrolysis, representing the less ordered amorphous cellulose fraction. Exploring the fiber properties of residual high molecular cellulose portion, the insoluble residue after acid hydrolysis of both crops was used for production of high purity dissolving grade pulps. The sulfur-free soda-AQ pulping process, as the most successfully and frequently used for agro-crop biomass approach, was chosen as a basic technology for dissolving pulp production.

Optimization of soda-AQ pulping was done using response surface methodology (RSM) [8]. The 2^4 central composite rotatable design (CCRD) was applied to optimize the effect of the principal independent process variables such as alkali concentration (X_1), AQ concentration (X_2), reaction temperature (X_3) and reaction time (X_4) on the main reaction responses (outputs) such as residual lignin in pulp (as Kappa number) (Y_1), pulp brightness (Y_2), pulp yield (Y_3), pulp viscosity (Y_4), α-cellulose content (Y_5) and lignin recovery from spent liquor (Y_6).

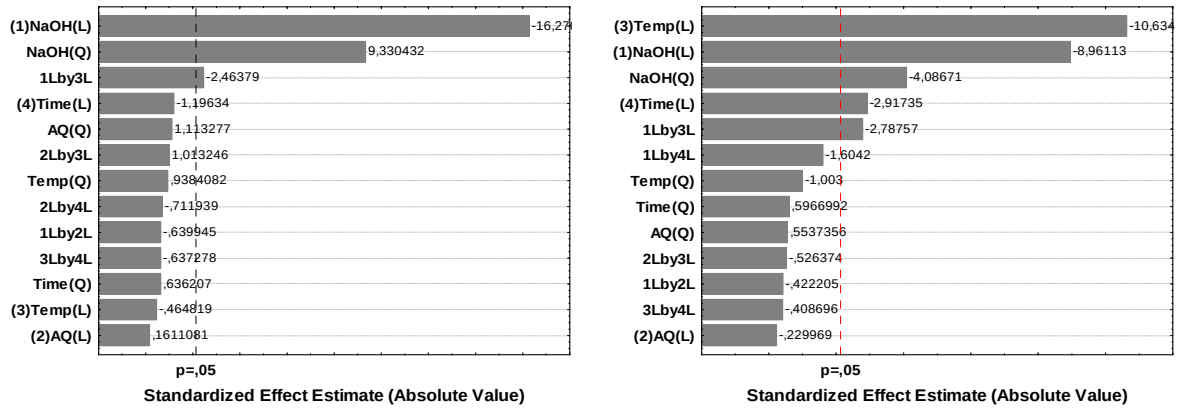

Figure 1. Pareto charts of standardized effects affecting degree of pulp delignification (left) and CED intrinsic viscosity (right) during soda-AQ pulping of pre-hydrolyzed (xylan-free) giant reed stems.

The standardized pulping effects, sorted by their absolute magnitude in relation to the statistical significance (p) level of 0.05, are shown on the Pareto graphs (Fig. 1). As was expected, the alkali concentration in reaction solution had critical importance on degree of pulp delignification (and brightening as well) during soda-AQ

pulping of pre-hydrolyzed crop stems. The ANOVA of estimated linear and quadratic effects of alkali concentration showed absolute confidence interval of 100% (p=0). The interaction effect between alkali concentration and temperature also revealed some importance for delignification results (p=0.026). At the same time, the degree of cellulose degradation, expressed as pulp intrinsic viscosity in CED solution, was mainly affected by process temperature, followed by alkali concentration. The effect of process duration (time) as well as the interaction effect between alkali concentration and temperature also showed some equal significance for cellulose degradation. The effect of AQ concentration was found to have some statistical significance only for pulp brightness (p=0.018).

The second-order polynomial model was fitted to experimental data to define the optimum set of reaction conditions by multiple regression analysis. The model equations for prediction of pulping outputs were obtained using statistically significant regression coefficients. The response surfaces illustrating the modeled effects of pulping conditions on Kappa number and intrinsic viscosity of produced pulps are shown in Fig. 2.

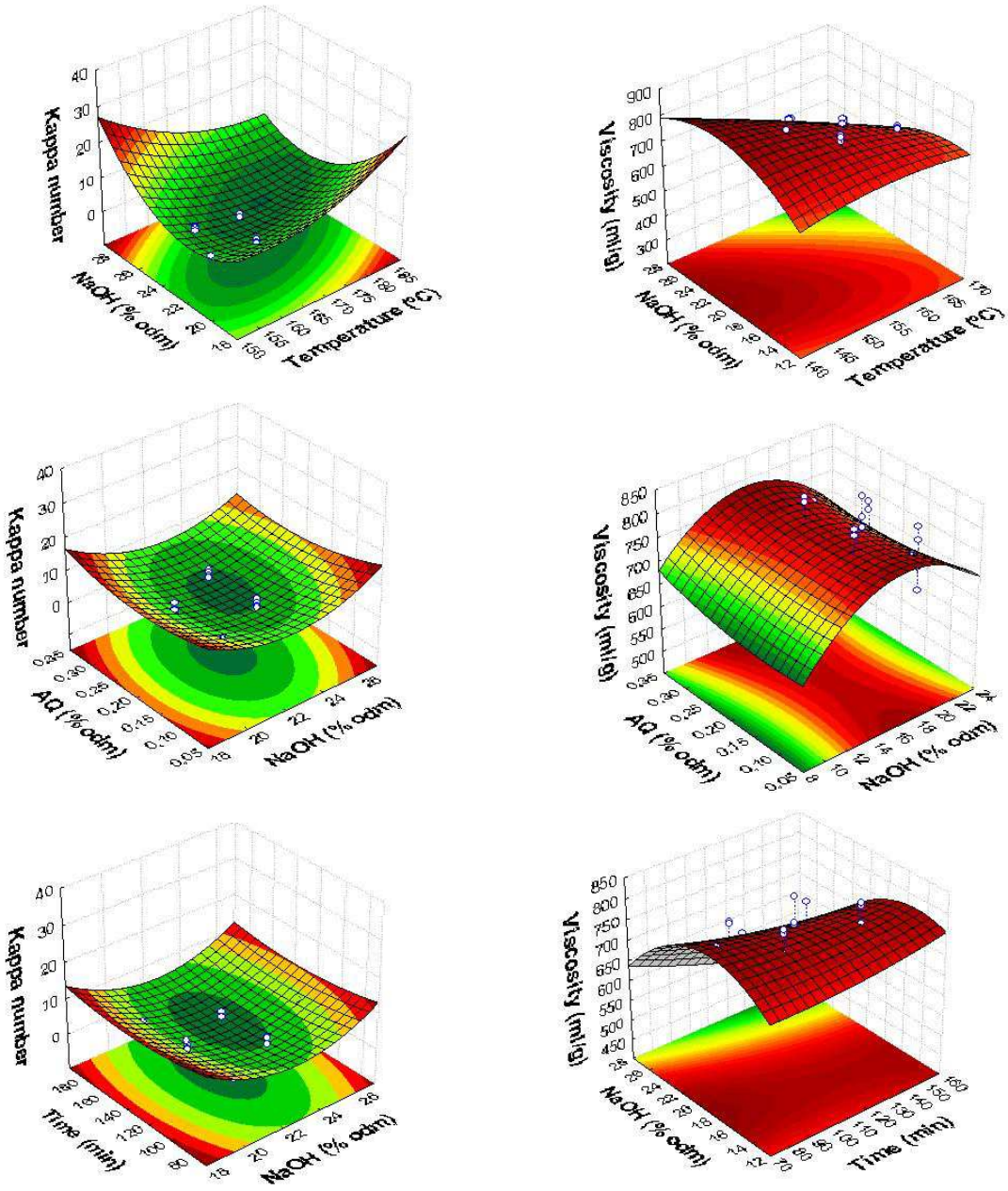

Figure 2. Response surfaces and contour plots of modeled delignification (left) and cellulose degradation (right) under variable conditions of soda-AQ pulping of pre-hydrolyzed (xylan-free) giant reed stems.

As can be seen from Fig. 2, under desirable ranges of independent process variables providing maximum expected degree of pulp delignification (up to 4-5 Kappa number), the CED intrinsic viscosity of 600-750 ml/g (or DP 2075-2700) of produced cellulosic pulps can be expected, what is fairly high for dissolving grade pulps.

The soda-AQ pulping of pre-hydrolyzed cardoon, generally, showed similar to giant reed tendency, despite some deviations in numerical values.

The partial differentiation of the fitted polynomial functions in respect to each process variable gave the set of optimal reaction conditions at extreme points of the surface plots. The control pulping experiments performed under found optimum reaction conditions resulted in pulps with Kappa 4.2-4.8; ISO brightness 50-52%; CED intrinsic viscosity 700-750 ml/g and α-cellulose content 96-98%, exhibiting very good correlation between predicted and experimental data and providing the validity test of the developed statistical model.

Completing the full biomass fractionation, the precipitated technical lignin was recovered from the black liquors after soda-AQ pulping of pre-hydrolyzed giant reed and cardoon. About 80-85% (as a max) of total lignin was recovered for both crops, substantially increasing the commercial viability of the entire biorefining sequence.

IV. CONCLUSIONS

The effective integrated upgrading of agro-crop lignocellulosic biomass, such as energy crops giant reed and cardoon, can be realized by combination of low-temperature dilute sulfuric acid hydrolysis followed by soda-AQ delignification. After statistical modelling and optimization of each separation process, the xylose-enriched organic substrate for biotechnological xylitol production, the dissolving grade cellulosic fibers and the precipitated technical lignin can be produced with high yield and quality.

V. ACKNOWLEDGEMENT

Financial support was provided by FCT (Portugal) within research contract PTDC/AGR-CFL/103840/2008.

VI. REFERENCES

[1] Zhang, Y.-H.P. Reviving the carbohydrate economy via multi-product lignocellulose biorefneries. *J. Ind. Microbiol. Biotechnol.* **2008**, *35*, 367–375.

[2] FitzPatrick, M.; Champagne, P.; Cunningham, M.F.; Whitney, R.A. A biorefinery processing perspective: Treatment of lignocellulosic materials for the production of value-added products. *Bioresour. Technol.* **2010**, *101*, 8915-8922.

[3] Lewandowski, I.; Scurlock, J.M.O.; Lindvall, E.; Christou, M. The development and current status of perennial rhizomatous grasses as energy crops in the US and Europe. *Biomass Bioenergy* **2003**, *25*, 335–361.

[4] Fernández, J.; Curt, M.D.; Aguado, P.L. Industrial applications of *Cynara cardunculus* L. for energy and other uses. *Ind. Crops Prod.* **2006**, *24*, 222-229.

[5] Sixta, H. Dissolving grade pulp, in: Sixta, H. (Ed.), *Handbook of Pulp*. Wiley-VCH Verlag GmbH and Co. KGaA, Weinheim, **2006**, pp.1022–1067.

[6] Shatalov, A.A.; Pereira, H. Biorefinery of energy crop cardoon (*Cynara cardunculus* L.) - Hydrolytic xylose production as entry point to complex fractionation scheme. *J. Chem. Eng. Proc. Technol.* **2011**, *2*, 118-125.

[7] Shatalov A.A.; Pereira H. Xylose production from giant reed (*Arundo donax* L.): Modeling and optimization of dilute acid hydrolysis. *Carbohydr. Polym.* **2012**, *87*, 210-17.

[8] Myers, R.H.; Montgomery, D.C.; Anderson-Cook, C.M. Response surface methodology: Process and product optimization using designed experiment, third ed. John Wiley and Sons, New York, **2009**.

UTILIZATION OF *CLADOPHORA* IN PAPER/PAPERBOARD PRODUCTION

Bo Shi*, Peter Lortscher and Doris Palfery

Corporate Research and Engineering, Kimberly-Clark Corporation
*2100 Winchester Road, Neenah, WI 54956 (*bshi@kcc.com)*

ABSTRACT

Global paper and paperboard consumption is over 450 million metric tons per year and is expected to increase in the future. Currently, wood-based fibers are a primary source of raw material for papermaking. Pulp and paper industries are energy intensive using large volumes of water and releasing many tons of carbon dioxide (CO_2). Fiber represents a very large portion of the cost to manufacture pulp and paperboard. As society becomes more conscious of environmental concerns and responsible resource utilization, pulp and paper manufacturers constantly strive to seek lower cost solutions for natural fibers. This presentation addresses the use of filamentous algae such as Cladophora as an alternative low-cost, renewable and sustainable fiber for papermaking.

Green Cladophora alga, one of the photosynthetic aquatic species having cellulosic or fibrous characteristics, was collected from Lake Winnebago in Neenah, WI. Unlike conventional mechanical or chemical pulping, the algal sample was subjected to a fast biological process for releasing cementing materials embedded in filamentous Cladophora algae using anaerobically digested sludge collected from Appleton Wastewater Treatment Plant, Appleton, WI. This biopulping stage took place at 35^o C and completed within two weeks. The biogas generated in the process could be collected for use as a fuel, which prevents it from causing atmospheric pollution. At the end of the biopulping, the green Cladophora sample was washed with tap water and bleached using 1% sodium hypochlorite. Standard handsheets with a basis weight of 60 g/m^2 were made with algal fiber inclusion up to 30% and the remaining is balanced by Eucalyptus pulp. The results indicate handsheet tensile, tear and burst indexes increased proportionally as the amount of Cladophora in the fiber blend was increased. A plausible explanation to the unexpected strength development may be attributed to the presence of algae micro fibrillation. The SEM data for the samples comprising Eucalyptus and Cladophora supports this observation.

I. INTRODUCTION

Cladophora is well known as one of the nuisance algae present in the aquatic environment globally. Mihranyan [1] offered a comprehensive summary of the beneficial utilizations of Cladophora in animal food, plastics, paper-based battery, etc. One of the attractive characteristics from Cladophora algae is high cellulose content [2], which supports an idea to use it as one of non-woody raw materials in the pulp and paper industry in order to replace or reduce a consumption of tree-based commodity fibers.

Non-woody material pulping methods outlined by Sridach [3] are suitable for Cladophora pulping and the earlier studies [4] focused on using conventional mechanical or chemical pulping method to generate algal pulp for paper and paper product manufacturing. In this paper, we describe a fast biological pulping process for releasing cementing materials embedded in filamentous Cladophora algae using anaerobically digested sludge, which is evolved from basic principles detailed by Manilal [5] and Aykroyd [6].

Cladophora pulp obtained from anaerobic sludge digestion was used for handsheet making and the results indicate handsheet tensile, tear and burst indexes increased proportionally as the amount of Cladophora in the fiber blend was increased. A plausible explanation to the unexpected strength development may be attributed to the presence of algal micro fibrillation.

II. EXPERIMENTAL

Anaerobic Biopulping

A schematic description of anaerobic biopulping apparatus is shown in Figure 1, where Cladophora sample, collected from Kimberly Point Park, Neenah, WI was loaded into the vessel after nitrogen purging (5 minutes) of anaerobically digested sludge, collected from Appleton Wastewater Treatment Plant, Appleton, WI. The whole vessel was housed in a chamber, capable of maintaining 35 ^{o}C through anaerobic sludge digestion of Cladophora

sample. The methane generated during the sample biopulping was released continuously with a gas regulator. At the end of two weeks biopulping, the green Cladophora sample was washed with tap water and bleached using 1% sodium hypochlorite (Clorox bleach).

Figure 1. Anaerobic Biopulping Apparatus

Handsheet Study

Handsheets were prepared according to a modified method, which is approved by Kimberly-Clark in 2007. The major difference, in comparison to TAPPI T205 [7], is that the sheet is pressed one at a time and only once without a plate during K-C sheet making. The sheet is then dried by steam instead of air dried with a plate. All other general procedures are the same unless otherwise noted. A total of twenty five grams of the mixed pulp materials (Cladophora algal and Eucalyptus pulps, respectively) at given ratios was weighed, considering respective moisture in the algal pulp and Eucalyptus pulp (Aracruz, Brazil). The two fibrous materials were soaked in British disintegrator and disintegrated for 5 minutes. The resulted slurry about 2 liters was further diluted to 4000 mL, where 480 mL of the pulp slurry was taken to make a 60 g/m^2 handsheet. For each sample code, five handsheets were made for tensile, tear and burst index measurements.

All testing was done under laboratory conditions of 23.0 ± 1.0 ^{o}C, 50.0 ± 2.0 % relative humidity, and after the sheet had equilibrated to the testing conditions for a period of not less than four hours. The testing was done on a tensile testing machine maintaining a constant rate of elongation, and the width of each specimen tested was 2.54 cm. The specimens were cut into strips having a 2.54 ± 0.04 cm width using a precision cutter. The "jaw span" or the distance between the jaws, sometimes referred to as gauge length, was 12.7 cm. The crosshead speed was 1.27 cm per minute. A load cell or full scale load was chosen so that all peak load results fall between about 20 and about 80 percent of the full scale load. Suitable tensile testing machines include those such as the Sintech QAD IMAP integrated testing system (Rockford, IL), recording at least 20 load and elongation points per second.

Scanning electron microscopy images of the handsheets containing Cladophora fibers were obtained using a JSM-6490LV scanning electron microscope (Peabody, MA). The surface images were generated at 300X magnifications for all samples that were coated with gold of about 15 nanometer thickness prior to taking any observations. The cross-sectional images were generated at 500X magnifications for all samples. The cross-section of the sample was prepared by cleaving the sheet with a fresh and ultra-keen razor blade at liquid nitrogen temperatures. The sample was mounted with double-stick tape and metalized with gold using a vacuum sputter for proper image in the SEM.

III. RESULTS AND DISCUSSION

Algal Fiber Characterization

The cleaned algal sample after anaerobic sludge digestion was tested for fiber length, width and distribution, etc. using MorFi (Fiber Quality Analyzer). Average Cladophora algal fiber arithmetical length is 0.61 mm and weighted Cladophora algal fiber length is 0.94 mm. The Cladophora algal fiber width is 45.5 µm. The fiber coarseness is 0.366 mg/m and fiber curl is 11.8%.

Tensile Index

Three codes of the handsheet sample were made at Eucalyptus/Cladophora algal fiber ratios of 90/10, 80/20 and 70/30, including one control handsheet comprising 100% Aracruz Eucalyptus. Figure 2 is a plot, which represents tensile index values as amount of Cladophora algal fiber is increased from nothing up to 30% inclusion. Normally, inclusion of non-woody fiber such as wheat straw or corn stover [8] would decrease tensile index of the composite handsheet. However, tensile index clearly to increases as more Cladophora algal fiber is added into the handsheets. A plausible explanation to the unexpected strength development may be attributed to the presence of algae micro fibrillation.

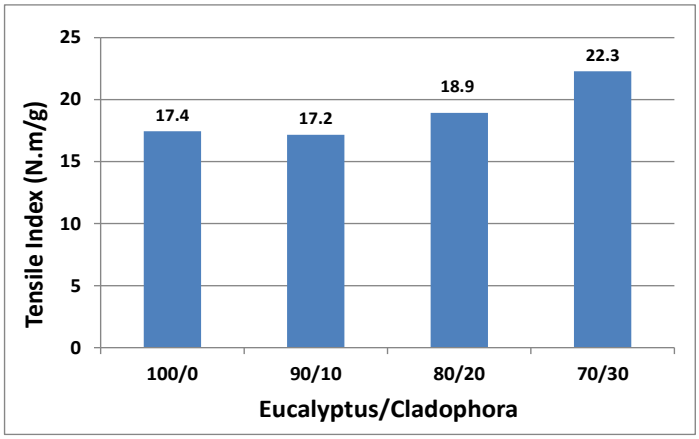

Figure 2. Tensile Index for Handsheets of Eucalyptus and Cladophora algal Fiber

Tear Index

Similar to the plot shown in Figure 2, tear index values are presented in Figure 3A, where the tear index is also increased as an inclusion of Cladophora algal fiber is increased. The tear index value for Eucalyptus/Cladophora (90/10) is 3.5, which is unexpectedly higher than Eucalyptus/Cladophora (80/20).

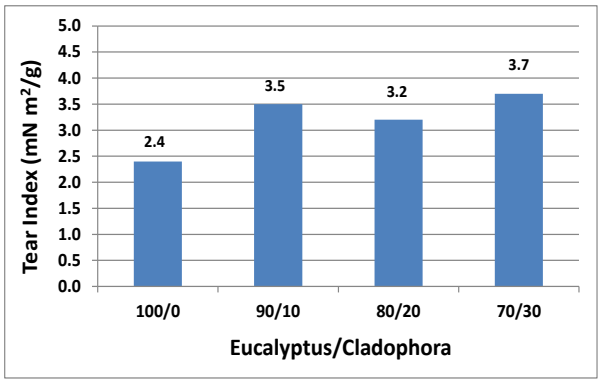

Figure 3A. Tear Index

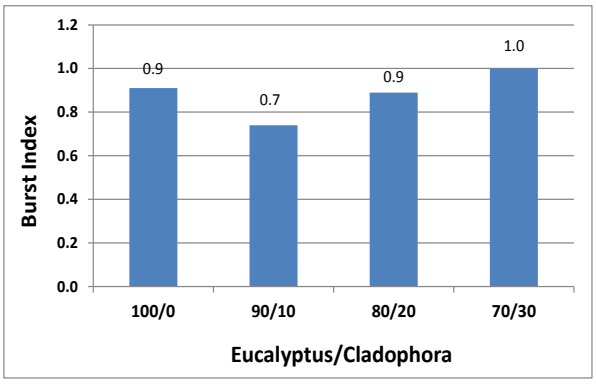

Figure 3B. Burst Index

Burst Index

Figure 3B displays handsheet burst index values as Cladophora algal fiber is increased up to 30%. There is an initial decrease in burst index at 10% Cladophora algal fiber and then this value increased to the same level as the control sample. It is 10% greater than the control sample when Cladophora algal fiber is added at 30% in the handsheets.

SEM Study

Scanning electron microscope (SEM) images of a series of handsheets containing Eucalyptus and Cladophora algal fibers at ratios of 90/10, 80/20 and 70/30 were obtained using JSM-6490LV scanning electron microscope under the following operating conditions: Accelerating voltage was 10 kilovolts, Spot size was 40, and working distance was 20 millimeters. Presented here is for the handsheet, containing 70% Eucalyptus and 30%

Cladophora. It is visible from Figure 4A (handsheet surface SEM) that Cladophora algal fiber is much larger than Eucalyptus. Figure 4B is a cross-sectional view, showing a well-mixed fiber configuration in the handsheet.

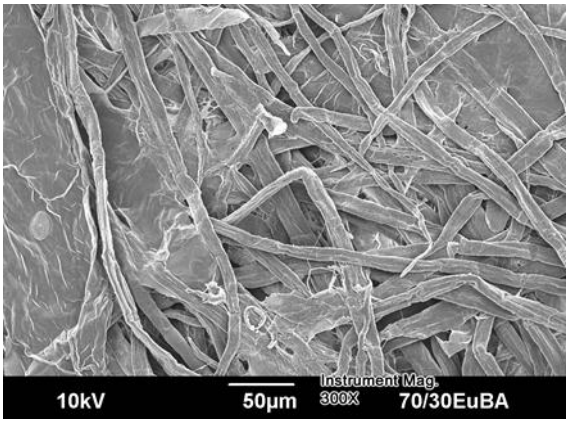

Figure 4A. Surface SEM

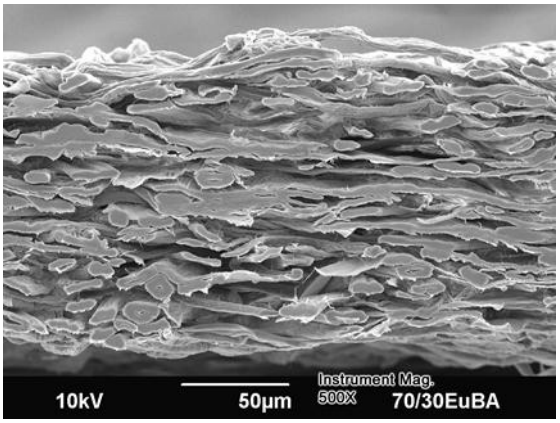

Figure 4B. Cross Sectional SEM

IV. CONCLUSIONS

Algae as a natural and low-cost fiber or wood fiber substitute shows promising results. Anaerobic biopulping of Cladophora can be done without releasing any unwanted chemicals commonly used in other pulping methods. The presence of Cladophora algal fiber increased tensile, tear and burst indexes for Eucalyptus-based handsheets. The higher of Cladophora algal fiber in the handsheet, the more pronounced effect can be observed. This behavior may be attributed to Cladophora algal micro fibrillation. The SEM data indicate Cladophora has larger fiber dimension in comparison to Eucalyptus pulp.

V. ACKNOWLEDGEMENT

Authors sincerely thank Jonathan Thom for testing handsheet samples and Mike Shlepr for SEM data acquisition.

VI. REFERENCES

[1] Mihranyan, A. Cellulose from Cladophora green Algae: from environmental problem to high-tech composite materials. J. Appl Polym Sci. **2010**, *119*, 2449–2460.

[2] Knoshaug, E.P. Shi, B., Shannon, T.G., Mleziva, M.M., Pienkos, P.T. The potential of photosynthetic aquatic species as sources of useful cellulose fibers – a review. *J. Appl Phycol*. **2013**, *25*, 1123–1134.

[3] Sridach, W. The environmentally benign pulping process of non-wood fibers. *Suranaree J. Sci. Technol.* **2010**, *17(2)*, 105-123.

[4] Berlowitz, L., Tarrant, T. Algal pulps and pre-pulps and paper products made from therefrom. WO patent 1994004745 A1

[5] Manilal, V.B. A method for anaerobic process coupled separation and refining of plant materials. WO patent 2009109994 A1

[6] Aykroyd, H. Processing fiber crops. WO patent 200175198 A1

[7] TAPPI T205. Forming handsheets for physical tests of pulp

THERMOCHEMICAL PROPERTIES OF LIGNIN MODEL COMPOUNDS

N. Shkaeva, D. Kosyakov, T.Skrebets, K.Bogolitsyn

Northen (Arctic) Federal University named after M.V. Lomonosov
163002 Russia, Arkhangelsk, Northern Dvina Embankment, 17(email: nshkaeva@mail.ru)

ABSTRACT

A wide range of phenolic compounds simulating structural fragments of lignin is investigated using the differential scanning calorimetry method. The data on the fusion points, specific enthalpy and entropy of fusion were obtained. The dependences of the isobaric heat capacity on temperature were established. A comparison of the experimental values of the isobaric heat capacity at 298 K with the theoretical values calculated by the group additivity method were done. The relationship between the structure of lignin model compounds and their thermochemical properties is discussed.

I. INTRODUCTION

Currently, data on the thermochemical properties of lignin and its model compounds presented not enough. However, parameters such as enthalpy, entropy of fusion, isobaric heat capacity are very important for further investigation of these compounds and understanding the nature of the their interaction with solvents. Differential Scanning Calorimetry (DSC) is one of the most convenient methods for studying these parameters. Results of lignins study by DSC method are shown in some papers [1-5]. However, the complex lignin structure makes it difficult for study and does not allow to distribute conclusions obtained for a particular sample for other types of lignins. In this connection it is interesting to study the lignin model compounds having a different structure as well as various functional groups. Previously, substances of similar structure have been successfully investigated by DSC method [6-8]. The authors of paper [6] successfully used the DSC method for analysis of polycyclic aromatic hydrocarbons. The heat capacities of same organic substances in the liquid state were analyzed in paper [7]. Results of the ferulic acid as pharmaceutical ingredient study contained in [8] are very interesting. Several studies compared the experimental and of calculated values of thermodynamic characteristics of the organic substances [9-11]. Methods of calculations used for a long time and allow to calculate some characteristics of the compounds through their additive components. These studies are very important and interesting. However, most authors did not consider these compounds as lignin models.

II. EXPERIMENTAL

Thirteen lignin model compounds with different chemical structures (aldehydes, ketones, acids, phenols and alcohols) were investigated. Compounds with guaiacilic, syringilic and other structures were taken: 2,6-dimetoxyphenol, acetosyringone, vanilin, veratrumaldehyd, vanillic alcohol, vanillic acid, acetovanillone, syringaldehyde, coniferyl aldehyde, p-coumaric acid, trans-cinnamic acid, ferulic acid, syringic acid. All substances are ALDRICH or SIGMA-ALDRICH production and have high purity (not less than 98%). Research have been performed using differential scanning calorimeter DSC Q2000 (TA Instruments, USA). 5-10 mg of the sample were placed in an aluminum pan. All measurements were performed in the linear mode of heating up to a temperature which is 20 ^{o}C higher than the expected temperature of fusion, heating rate is 10 degrees per minute. The experiment was performed in argon atmosphere. Pre-calibration was carried out, it includes the determination of the resistance and capacitance of the cell. Calibration includes an experiment with an empty cell and calibration sapphire samples. Cell constant calibration was performed with a sample of indium. Control of DSC system, data collection and processing was performed using software «TA Instrument Explorer» and «TA Universal Analysis». Specific enthalpies of fusion were calculated by integrating the peak in the DSC-curve. Specific entropy of fusion values were calculated from the Gibbs equation:

$$\Delta S = \frac{\Delta H}{T}$$

II. RESULTS AND DISCUSSION

Fusion temperatures as well as the specific enthalpy and entropy of fusion were obtained, **Table 1**.

Table 1. Temperature, enthalpies and entropies of fusion for lignin model compounds

Compound	T_{fus}/K	$\Delta_{fus}H_m$/kJ mol^{-1}	$\Delta_{fus}S_m$/J mol^{-1} K^{-1}
2,6-dimetoxyphenol	327.3 ± 0.3	16.2 ± 0.3	48.38
acetosyringone	398.0 ± 0.2	27.2 ± 0.3	66.23
vanilin	355.1 ± 0.9	20.3 ± 0.6	56.56
veratrumaldehyd	316.8 ± 0.3	18.6 ± 0.4	58.73
vanillic alcohol	384.0 ± 0.4	26.5 ± 0.2	68.39
vanillic acid	482.9 ± 0.1	21.2 ± 0.9	48.44
acetovanillone	386.0 ± 0.8	22.6 ± 0.9	58.42
syringaldehyde	384.6 ± 0.8	28.6 ± 0.6	72.67
coniferyl aldehyde *	345.9 ± 0.5 353.0 ± 0.5	20.6 ± 0.5	-
p-coumaric acid	492.0 ± 0.8	41.8 ± 0.8	84.85
trans-cinnamic acid	406.0 ± 0.9	18.3 ± 0.4	44.93
ferulic acid	444.9 ± 0.1	30.5 ± 0.9	70.08
syringic acid	482.0 ± 0.2	20.7 ± 0.5	42.85

** specific enthalpy of coniferyl aldehyde was calculated as the total for the two peaks*

The differences in fusion enthalpies obtained for acids can be explained by the presence of intermolecular hydrogen bonds, the breaking of which requires additional energy. The maximum value was observed for the p-coumaric acid. Its molecule has a phenolic hydroxyl in addition to carboxyl. Fusion enthalpy for ferulic acid is less than p-coumaric because methoxy group increases the formation of intramolecular hydrogen bonds and decreases intermolecular ones. Fusion enthalpy of vanillin and syringic acid are even less. It can be assumed that a carboxyl group connected to the propane chain forms stronger bonds than the one which is connected directly to a benzene ring. The minimum fusion enthalpy value was obtained for trans-cinnamic acid, because of its benzene ring has no other groups capable of forming hydrogen bonds. Very similar fusion enthalpies were obtained for most aldehydes and ketones. Higher values were obtained for acetosyringone and syringaldehyde. Alcohols fusion enthalpies were higher than those aldehydes, ketones and acids. Comparatively small enthalpies of fusion defined for phenols, it must be assumed that phenolic hydroxyls form less strong hydrogen bonds. Two peaks was found for coniferyl aldehyde **(Figure 1)**. Since the sample is a mixture of cis- and trans-isomers, such effect may be related to their different fusion temperatures.

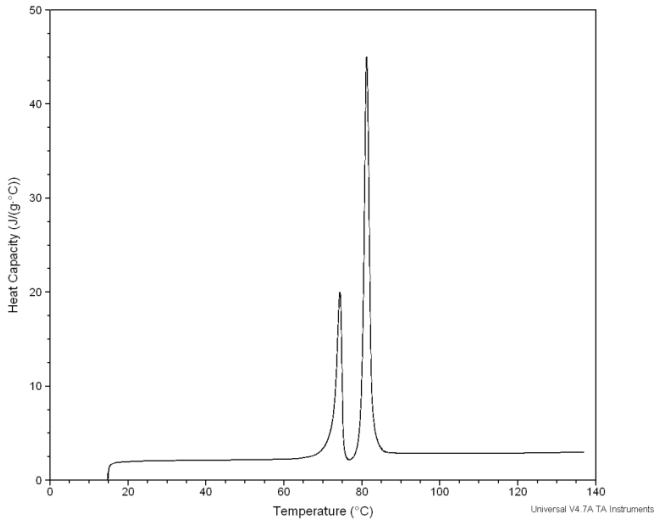

Figure 1. DSC-curve for coniferyl aldehyde

The dependences of the isobaric heat capacity on temperature are established. These dependencies are describes of third-degree polynomial most adequately: $C_p = a + bT + cT^2 + dT^3$ The coefficients of equation Cp = f (T) are shown in **Table 2**.

Table 2
Coefficients of equation $C_p = a + bT + cT^2 + dT^3$

Compound	a	b	c	d	δ	r
2,6-dimetoxyphenol	$-2.33\cdot10^4$	$2.31\cdot10^2$	$-7.56\cdot10^{-1}$	$8.29\cdot10^{-4}$	0.09	0.99
acetosyringone	$-3.67\cdot10^4$	$3.57\cdot10^2$	-1.15	$1.23\cdot10^{-3}$	0.09	0.99
vanilin	$-3.56\cdot10^3$	$3.41\cdot10$	-1.04	$1.08\cdot10^{-4}$	0.31	0.99
veratrumaldehyd	$-1.88\cdot10^5$	$1.87\cdot10^3$	-6.17	$6.80\cdot10^{-3}$	0.11	0.99
vanillic alcohol	$-4.77\cdot10^3$	$4.35\cdot10$	$-1.28\cdot10^{-1}$	$1.27\cdot10^{-4}$	0.66	0.99
vanillic acid	$-1.69\cdot10^3$	$1.48\cdot10$	$-3.72\cdot10^{-2}$	$3.21\cdot10^{-5}$	2.84	0.99
acetovanillone	$-4.41\cdot10^3$	$4.17\cdot10$	$-1.27\cdot10^{-1}$	$1.32\cdot10^{-4}$	0.49	0.99
syringaldehyde	$-1.58\cdot10^3$	$1.54\cdot10$	$-4.47\cdot10^{-2}$	$4.51\cdot10^{-5}$	0.18	0.99
coniferyl aldehyde *	$-6.30\cdot10^4$	$6.07\cdot10^2$	-1.94	$2.07\cdot10^{-3}$	0.60	0.99
p-coumaric acid	$-6.89\cdot10^2$	6.36	$-1.72\cdot10^{-2}$	$1.70\cdot10^{-5}$	2.77	0.99
trans-cinnamic acid	$-1.56\cdot10^3$	$1.58\cdot10$	$-4.53\cdot10^{-2}$	$4.46\cdot10^{-5}$	0.63	0.99
ferulic acid	$-4.49\cdot10^2$	3.80	$-5.49\cdot10^{-3}$	$2.31\cdot10^{-6}$	2.89	0.99
syringic acid	$-5.62\cdot10^2$	5.21	$-1.25\cdot10^{-2}$	$1.10\cdot10^{-5}$	1.71	0.99

*δ - standart error; r – correlation coefficient

The authors of papers [9-11] have calculated some characteristics theoretically using additive methods. They investigate a some solid aldehydes, similar in chemical structure of lignin models. The paper compares the theoretical and experimental values of the heat capacity. We performed a similar comparison for the studied lignin model compounds. Results of the comparison of the experimental values of the isobaric heat capacity at 298 K, obtained by DSC with the theoretical values calculated by the method proposed by the authors of [9], [11] are shown in **Table 3**.

Table 3
Calculated and experimental values of the lignin model compounds isobaric heat capacity

Compound	C_p^{298}, J mol^{-1} K^{-1}	
	experimental	calculated
2,6-dimetoxyphenol	233.95	225.07
acetosyringone	259.61	259.52
vanilin	196.15	196.37
veratrumaldehyd	232.21	234.67
vanillic alcohol	217.24	213.67
vanillic acid	251.01	216.37
acetovanillone	194.00	206.73
syringaldehyde	241.12	249.16
coniferyl aldehyde	363.93	239.17
p-coumaric acid	131.59	206.38
trans-cinnamic acid	317.43	191.89
ferulic acid	258.24	181.20
syringic acid	172.18	269.16

As can be seen from the table, the difference between calculated and experimental values for aldehydes (except coniferyl), ketones, alcohols and phenols are small. Very large differences observed for acids. It is possible that intermolecular hydrogen bonds and the formation of dimers influence significantly to the heat capacity.

IV. CONCLUSIONS

1. Fusion temperatures and specific enthalpies for model lignin compounds were determined. Specific entropies of fusion were calculated .
2. The dependences of the isobaric heat capacity on temperature were established.
3. It was shown that the formation of intermolecular and intramolecular hydrogen bonds influences significantly to the substance formation enthalpy as well as to the heat capacity. This can explain the differences between the calculated and experimental values of the heat capacity. This is typical for acids. Small differences between theoretical and practical values were obtained for other compounds.

V. ACKNOWLEDGEMENT

This study performed using equipment of Joint use center of scientific equipment “Arctica”.

VI. REFERENCES

1. Sho-ichi Tsusioma, J. Wood Sci (**2001**) 47: 495-501
2. Arima T. (**1973**) Differential scanning calorimetry of wood and wood components. I.Thermogravimetry and differential scanning calorimetry of wood. Mokuzai Gakkaishi 19:435-442
3. Arima T. **1973**) Differential scanning calorimetry of wood and wood components. II.Thermogravimetry and differential scanning calorimetry of wood components. Mokuzai Gakkaishi 19:443-450
4. Justo Lispergueer, Patricio Perez, Silvio Urisar, J. Chil. Chem. Soc., v.54, n.4(**2009**) p.460-463
5. Aurelio De Chirico, Guido Audisio, Francesco Provasoli et al., Die Angewandte Macromoleckulare Chemie 228 (**1995)** p.51-58 (Nr 3976)
6. K. Drozdzewska, V.Kestens, A. Held et al. Journal of Thermal Analysis and Calorimetry, vol. 88 (**2007**) 3, p.757-762
7. M. Zabransky, V. Ruzicka, V.Majer, J. Phys. Chem. Ref. Data, vol.19, n.3, **1990**, p.719-762
8. Young Tack and Jin Hee Oh, Arh. Pharm. Res., vol. 26, n.12, p.1002-1003, **2003**
9. J.S. Chikos, D.G.Hesse, J.F. Liebman, Structural Chemistry, vol.4, n.4, **1993**, p.261-269
10. Benson, S.W. Thermochemical kinetics, 2nd ed.; Wiley: New York, **1978**
11. M. Temprado, M.V. Roux, J.S. Chikos, Joural of Thermal Analysis and Calorimetry, vol. 94 (**2008**) 1, p.257-262

MODIFICATION OF ASPEN WOOD MICROPARTICLES BY AMMOXIDATION METHOD AND THEIR USE IN WOOD-POLYMER COMPOSITES

Galia Shulga[1]*, Brigita Neiberte, Anrijs Verovkins, Sandra Livcha, Sanita Vitolina, Jevgenijs Jaunslavietis

Latvian State Institute of Wood Chemistry, 27 Dzerbenes St., Riga LV 1006, Latvia
*(*E-mail: shulga@junik.lv)*

ABSTRACT

The modification of aspen microparticles (<100 mk), obtained by milling aspen sawdust after its low temperature hydrolysis with dilute hydrochloric acid, was performed by the ammoxidation method using ammonium hydroxide and persulphate ammonium as an oxidizing agent at normal pressure and room temperature. The effect of the ammonium hydroxide concentration and the ratio of its volume to the mass of the oxidising agent on the nitrogen fixation and the yield of the modified particles was studied. The formation of salt and amide bonds in the aspen wood as a result of its ammoxidation was found. The ammoxidised microparticles were used as a filler in the composite materials based on recycled polypropylene. The mechanical properties of the obtained composites as well as their contact angles and water sorption were discussed.

I. INTRODUCTION

Nowadays, wood-polymer composites are increasingly applied in different functional areas. The use of lignocellulosic materials as a filler in composite materials is evidently beneficial in terms of their good mechanical properties with a low specific mass, economic and environment aspects [1, 2]. However, to improve the compatibility between the synthetic polymer and the lignocellulosic filler for obtaining wood-polymer composites with high-performance properties, the surface modification of lignocelluloses is necessary. The lignocellulosic modification can be realised by various techniques, the main of which being the treatment with alkali (mercerisation), acetylation, benzylation, graft copolymerisation, treatment with fatty acids, peroxide, anhydride, permanganate, silane and plasma [3]. Each of the offered methods has its own advantages as well as drawbacks represented by the costs, complicated techniques, usage of organic solvents, etc.

Owing to the efficiency and high yield of the end product, and the simplicity of the implementation of the modification process, the low content of by-products and the use of water as a reaction medium, ammoxidation method of wood and its components can be one of the promising ways of its modification [4, 5].

The aim of the work was to apply the ammoxidation method for modification of aspen wood microparticles and to study the mechanical properties and hydrophobicity of recycled polypropylene-based composites filled with the ammoxidated particles.

II. EXPERIMENTAL

The hydrolysed aspen wood microparticles with the size <100 mk obtained by the procedure described in the previous work [6] were used for modification by the ammoxidation method. Ammoxidation was carried out at normal pressure and room temperature by adding the aspen microparticles to a NH_4OH solution at stirring and then, after obtaining a stable suspension, the required amount of persulphate ammonium was applied as an oxidising agent. The studied concentration of the NH_4OH solution was 5% and 20%. The value of the ratio of its volume to the mass of the oxidising agent (ml/g) in the suspension was varied in a wide range. The hydromodulus (mass ratio of sawdust particles to the NH_4OH solution, g/g) was equal to 1:50. The duration of modification was 120 h. After the treatment, the ammoxidated particles were washed to a neutral medium and dried over prolonged periods at 60^{o}C, and then for 3 h at 105^{o}C. The elemental composition of the microparticles was determined by Elementar Analysensysteme GmbH (Germany). Changes in the functional composition were identified by Fourier Transform Infrared (FTIR) using a spectrophotometer (Perkin-Elmer Spectrum One, USA) with KBr tablets. For making composites, recycled polypropylene (RPP) was used as a thermoplastic polymer matrix. It had a density of 0.9 t m^{-3} and a melt flow index of 5.2/10 min (230^{o}C, 2.16 kg). The wood polymer samples were prepared from a blend of powder RPP with the aspen microparticles, using a twin extruder and a moulding machine (HAAKE MiniLab II with MiniJet II, Thermo Scientific "HAKKE") at temperatures of 170-180^{o}C. The microparticles content in the composites was 30 mass %. For the wood particles and the composite samples, contact angles were measured in distillate water by the Washburn sorption method and the Wilhelmy method, respectively, using a Kruss K100 tensiometer. Before measuring, all the samples were conditioned. Water sorption of the composite samples was determined using a desiccator method at a humidity of 98% and a

temperature of 20 ± 2°C. Mechanical tests for the composite samples were carried out according to ASTM D638 and EN ISO 178, using a universal machine "Zwick" (Germany).

III. RESULTS AND DISCUSSION

Figure 1 shows the values of the content of the incorporated N and the yield of the N-modified particles depending on the ratio of the NH_4OH solution volume to the mass of persulphate ammonium in the reaction mixture. It can be seen that, with increasing this ratio, namely, decreasing content of the oxidising agent in the mixture, irrespective of the concentration of the ammonium hydroxide solution, the amount of fixed nitrogen in the lignocellulosic matrix decreases from 2.1% to 1.1% in the 5% NH_4OH solution and from 3.4 to 2.8% in the concentrated solution of ammonium hydroxide. At the same time, with decreasing content of the oxidising agent in the mixture, the yield of the modified particles increases.

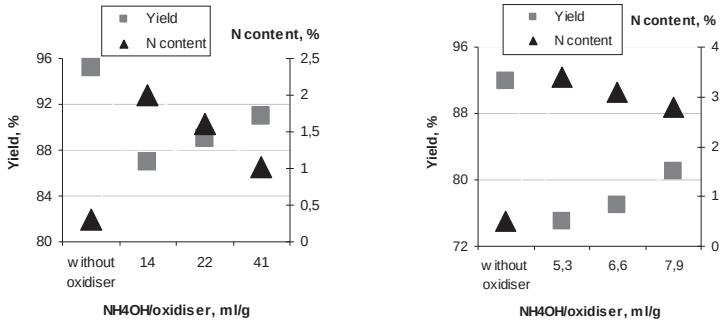

Figure 1. Effect of a ratio of NH_4H/oxidiser on nitrogen content and yield of the modified microparticles depending of NH_4OH solution concentration: 5% (on the left) and 20% (on the right).

It also follows from **Figure 1** that the higher concentration of the NH_4OH solution, the greater amount of nitrogen can be introduced into the wood microparticle. The maximum content of nitrogen in the microparticles, treated with a 20% solution of H_4OH in the presence of the oxidiser, is almost 1.6-1.8-fold higher than that in the particles treated with a 5% ammonium hydroxide solution, and the yield of N-modified particles is lower by 15-18%.

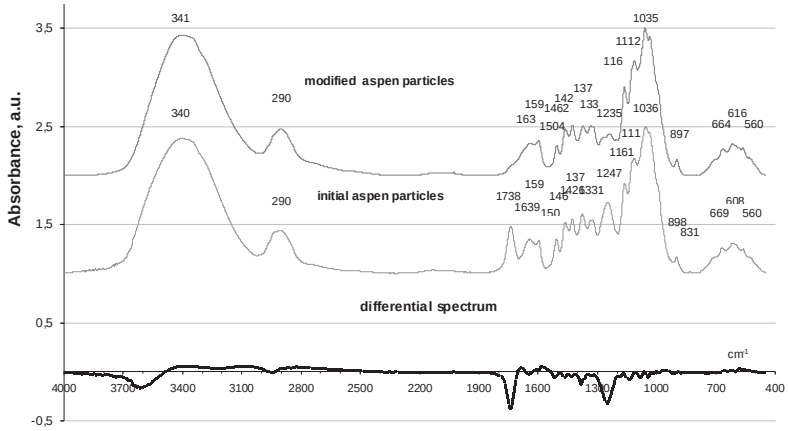

Figure 2. FTIR spectra of initial and modified aspen microparticles and their differential spectrum.

The latter can be caused by the more pronounced destruction of the lignocellulosic matrix in the concentrated solution of NH_4OH, accompanied by a decrease in the content of hemicelluloses and lignin therein. It is known that the ammoxidation process has a complex chemical nature and is accompanied by both couplings and cross-linking and the reactions of destructive nature. As a rule, the most sensitive to such a type of reactions are the hydroxyl groups of the wood components – lignin and hemicelluloses, as well as ether and ester bonds in the lignocellulosic matrix This can be testified by the comparative analysis of FTIR (**Figure 2**) of aspen microparticle spectra before and after the ammoxidation. It can be seen that the ammoxidation of aspen particles

is accompanied by a decrease in absorption in the wavelength ranges 3700-3470 cm^{-1}, 1800-1700 cm^{-1}, 1640-1610 cm^{-1} and 1520-980 cm^{-1} and an increase of adsorption in the wavelength ranges 3470-2940 cm^{-1}, 2900-2500 cm^{-1}, 1690-1640 cm^{-1} and 1610-1520 cm^{-1}. It is known that, in the region 3700-3470 cm^{-1}, free and bound hydroxyl groups of lignocellulose are adsorbed; therefore, the decrease of absorption in this region in the FTIR spectrum of ammoxidated particles can indicate the decrease in the amount of the hydroxyl groups of wood components as a result of chemical transformations. The decrease in absorption in the region 1800-1700 cm^{-1} with a maximum at 1734 cm^{-1} can be connected with the hydrolysis of ester bonds in hemicelluloses (xylan) and the shift of this absorption peak to the region of lower wavelengths (1610-1600 cm^{-1}) as a result of the formation of salt bonds. The region 1500-900 cm^{-1} is characterised by the presence of C-H, C-O, O-H in hemicelluloses and is assigned mainly to the region of the absorption with the glycosidic bond and glucopyranose ring. A comparative decrease of absorption in this region with pronounced minima at 1370 cm^{-1} and 1245 cm^{-1} conforms the destruction of ester bonds in the lignocellulosic matrix as a result the ammoxidation and the formation of carboxylate ions. The observed decrease of absorption in the region 1640-1610 cm can be connected with the consumption of the carbonyl groups of lignin, capable of forming different types of covalent bonds with nitrogen: imine, amide, heterocyclic, etc. The increase in absorption in the region 1690-1640 cm^{-1} with a maximum at 1666 cm^{-1} is determined by the presence of C=O and C-N stretching, and C-N-H bending vibrations in amide I and amide II [4]. A comparative increase in absorption in the region 1600-1520 cm^{-1} with a maximum at 1556 cm^{-1} in the spectrum of ammoxidated particles can be connected with the formation of amide bonds in the lignocellulosic matrix. The increase of absorption at 1640 cm^{-1} can indicate the formation of NH_4^+ salt bonds in the lignin macromolecules due to the formation of carboxylic groups. At the same time, the analysis of the main absorption bands in the spectrum of ammoxidated microparticles did not indicate the destruction of the aromatic rings of lignin.

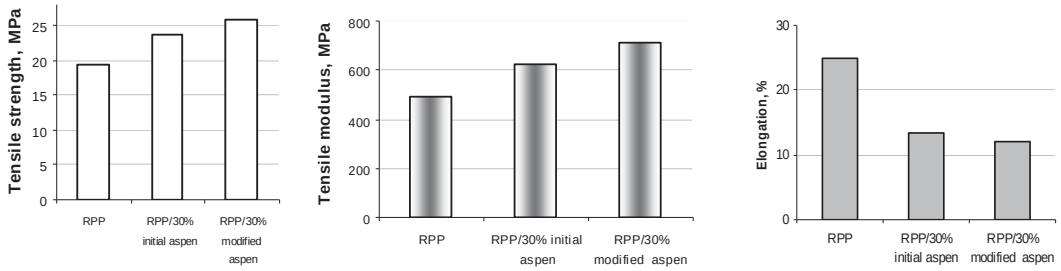

Figure 3. Tensile strength, tensile modulus and deformation of RPP and the obtained composites.

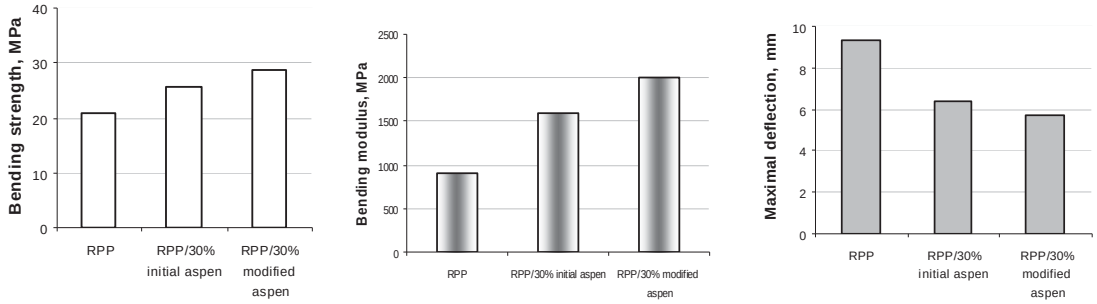

Figure 4. Bending strength, bending modulus and deformation of RPP and the obtained composites.

It is known that the type of the wood filler and its content in a polymer composite material are crucial for its physico-mechanical properties. Ammoxidation of the initial aspen particles, resulting in the introduction of amide bonds in the lignocellulosic structure and a drop in the hydroxyl groups' content, has to favour the improvement of the compatibility between RPP and the aspen microparticles. **Figure 3** shows the values of maximal tensile strength (a), Young's modulus (b) and deformation (c) of the composite materials, containing 70 mass % of recycled PP and 30 mass % of the initial and ammoxidised aspen microparticles with the minimal N content (1.1%). According to the given results (**Figure 3**), the filling of RPP with the ammoxidised micropaticles leads to the increase of its tensile strength by 30% and Young's modulus by 45%, and a twofold decrease of its elongation. Simultaneously, with filling of RPP with the ammoxidised wood particles, bending strength (**Figure 4**) is enhanced by 37%, bending modulus increases twice, but the value of maximal deflection decreases by more than 60%. The improvement of the compatibility of the filler with the polymer matrix, which is reflected in the

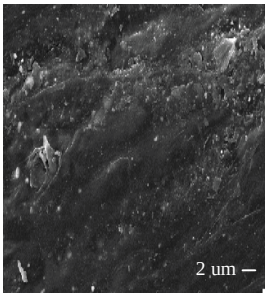

Figure 5. SEM image of composite containing modified aspen particles.

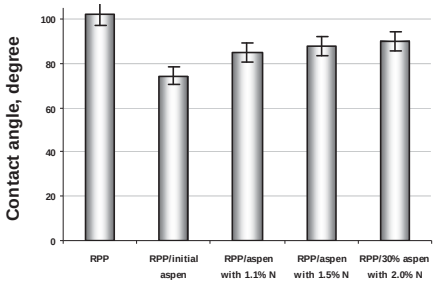

Figure 6. Contact angles of the composites.

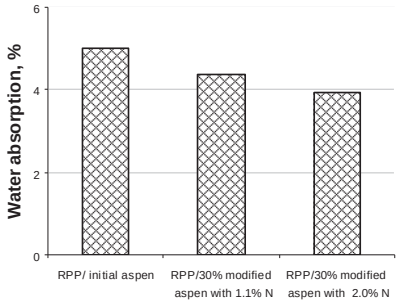

Figure 7. Water sorption of the composites.

growth of the mechanical properties of the obtained composite, is also testified by its morphology study. The SEM image of the composite, containing 30% of the modified microparticles, indicates the homogeneity of the obtained complex structure and its consolidation (**Figure 5**). The results testify that the purposeful modification of the aspen microparticles, obtained by the low temperature acid hydrolysis [6], favours the drop in the ability of the obtained composites to be wetted by water (**Figure 6**) and to adsorb water vapours (**Figure 7**).

IV. CONCLUSIONS

Ammoxidation, resulting in the drop of the hydroxyl groups' content and the formation of amide bonds in aspen lignocelluloses favours the compatibility between RPP and the aspen microparticles. This is testified by the improvement of the mechanical properties, the increase of contact angles and the reduction of water sorption by the obtained composites.

V. ACKNOWLEDGEMENT

The authors have received funding for this study from the Latvian State Research Programme VPP-5 "NatRes" (2010-2014).

VI. REFERENCES

[1] Bledzki, A.K.; Faruk, O. Wood fibre reinforced polypropylene composites: Effect of fibre geometry and coupling agent on physico-mechanical properties. *Appl.Compos. Mater*. **2003**, *10*, 365-379.
[2] Shulga, G.; Neiberte, B.; Verovkins, A.; Laka, M.; Chernyavskaya, S.; Shapovalov, V.; Valenkov, A.; Tavroginskaya, M. The new polymer composites integrating modified wood originated products. **2009**, *Proc. Italic-5*, Varenna, Italy, September 1-4, 2009, 185–188.
[3] La Mantia F.P.; Morreale M. Green composites: A brief review. *Composites: Part A.* **2011,** *42*, 579–588.
[4] Capanema, E.A.; Balakshin, M.Y.; Chen, C-L.; Gratzl, J.S. Oxidative anmmonolysis of technical lignins. *J. Wood Chem Tech*. **2006,** 26, 95-109.
[5] Verovkins, A.; Neiberte, B.; Zakis, G.; Avotins, F.; Shulga G. Lignocellulose nitrogen derivatives. 2. Oxyammonolysis of wood bark. *Latvian Journal of Chemistry*. **2014**, (in print).
[6] Shulga G., Vitolina S., Neiberte B., Verovkins A., Jaunslavietis J., Ozolins J., *Obtaining lignocellulosic microparticles using energy saving pre-treatment method.*13th European Workshop on Lignocellulosics and Pulp (EWLP-2014), Seville, Spain, June 24-27, **2014**.

OBTAINING LIGNOCELLULOSIC MICROPARTICLES USING ENERGY SAVING PRE-TREATMENT METHOD

Galia Shulga[1]*, Sanita Vitolina, Brigita Neiberte, Anrijs Verovkins, Jevgenijs Jaunslavietis, Jurijs Ozolins[2*]

[1]*Latvian State Institute of Wood Chemistry, 27 Dzerbenes St., Riga LV 1006, Latvia*
[2]*Riga Technical University, Azenes 14/24, Riga LV-1048, Latvia*
*(*E-mail: shulga@junik.lv)*

ABSTRACT

In this work, aspen sawdust, a by-product of the mechanical processing of aspen wood, was studied as a feedstock for obtaining microparticles as a filler for polymeric composites. It is known that, due to enhanced energy requirements, milling of untreated wood is not economically beneficial. With the aim to partially destruct and activate the lignocellulosic matrix for the following modification, low temperature acid hydrolysis of aspen sawdust under mild conditions was carried out. The effect of the acid concentration, the hydrolysis duration and the hydromodulus on the components and fractional composition of milled hydrolysed aspen sawdust was investigated.

I. INTRODUCTION

Lignocellulose is the most abundant renewable biomass, consisting of three polymers, namely, cellulose, hemicellulose and lignin, which all provide its perfect mechanical properties. In Latvia, aspen trees, along with pine and birch ones, annually give the highest wood yield. By-products, i.e. sawdust, bark and other wood biomass residues that are formed during forest management and wood mechanical processing are used mainly for energetic needs. At the same time, waste lignocellulosics are a feedstock for obtaining various value-added products. In recent years, intensive studies have been carried out on the application of lignocellulosics as a filler in wood-polymer composites [1-3] due to their renewability, easy availability, low cost, biodegradability, light mass, enhanced filling degree, etc. The obtaining of wood-polymer composites occurs by incorporating lignocellulosics in the form of fibres or particles in a polymer matrix. For the wood polymer composites filled with lignocellulosic fibres, their length and orientation in the polymer matrix are very important. The properties of the composites, containing wood microparticles, depend on the particle size, as well as size distribution, shape and charge. In most cases, smaller sizes of wood particles promote their compatibility with the polymer matrix and decrease the melt viscosity of the wood-polymer blend during the processing. For obtaining microparticles, wood has to be milled. However, due to the enhanced energy requirements, the milling of untreated wood is not economically beneficial, because it requires considerable energy consumption and energy input. With the target to facilitate and decrease the required energy for chemical and enzymatic processing of wood, various pre-treatment technologies are offered [4]. The acid hydrolysis of wood for production of ethanol and other chemicals is well known [5, 6]. The hydrolysis for bioethanol production can be realised using dilute or concentrated acids. As a rule, the dilute acid hydrolysis technology applies high temperatures (> 100^{o}C) and enhanced pressures. The acid pre-treatment of wood at high temperature is used for energy saving in wood thermomechanical pulping [7, 8]. On the other hand, very scarce information is available on the effect of low temperature hydrolysis (< 100^{o}C) with dilute acids on the wood composition and properties. Such information is useful for obtaining wood finest particles for wood-polymer composites, with simultaneous decreasing the energy input at wood milling and grinding. The cleavage of ether linkages at the wood surface is accompanied by changes in its functional groups' composition. The latter enhances the specific surface of the lignocellulosic matrix and facilitate its accessibility for chemical modifiers.

The aim of the study was to investigate the effect of acid hydrolysis parameters (acid concentration, duration, hydromodulus) at a low temperature (< 100^{o}C) on the changes in the aspen wood components and fractional composition after milling, as well as on the time of milling that is equivalent to energy input. The hydrolysis served as the first step for obtaining wood microparticles for their following modification.

II. EXPERIMENTAL

The aspen sawdust represented a by-product of the mechanical processing of aspen wood (*Populus tremula*). The main part of its fractional composition consisted of particles with a size from 1 mm to 0.5 mm (67 mass %). The elemental composition of the sawdust was determined by an Elementar Analysensysteme GmbH

(Germany). The composition of the sawdust was determined according to analytical chemical procedures – Klason and Kürschner ones – for lignin and cellulose, respectively. The content of extractives in the sawdust represented the sum of the content of the wood substances dissolved in acetone, using a Soxlet extractor, and in hot water (100°C) during 3 h. The elemental component composition of aspen wood was the following: 48.77% C, 6.25% H, 44.71% O, 0.11% N and 0.16% S. The content of cellulose, lignin, hemicelluloses, extractives and ash in aspen wood was 50.52%, 18.45%, 26.12%, 4.51% and 0.4%, respectively. Acid pre-hydrolysis was carried out by using a 5-L three-neck flask equipped with a return condenser, a thermometer and a stirrer under the following conditions: 0.05-0.5 g/dl HCl concentration, temperature 60°C and duration 1-7 h at a hydromodulus (sawdust/water mass ratio) of 1/10, 1/20 and 1/50. After the pre-hydrolysis, the treated sawdust was separated from the hydrolysate by filtration and dried, at first, at 60°C, and then at 105°C. The mass losses of the hydrolysed sawdust and the dry matter of the obtained hydrolysates were used for calculating the amounts of the degraded products. The hydrolysed sawdust milling was carried out with a planetary ball mill (Retsch, Germany) at 300 min^{-1} during 15 min. The milled sawdust fractionation was performed by using Pulverizette 0 (Fritsch, Germany) with a set of sieves during 15 min. The size distribution in the particles fraction < 100 mk was investigated with a laser particle granulometer (Annalizetto-22 NanoTec, Fritsch, Germany). The shape of the finest microparticles was fixed by transmission electron microscopy (Leo 912 AB Omega microscope, Carl Zeiss, Germany). The microstructure of the hydrolysed wood particles was examined using a scanning electron microscope (Tesla, Czech Republic). The UV-spectra of the obtained hydrolysates was performed with the help of an UV-VIS Spectrometer Genesys™ 10 (Thermo, USA).

III. RESULTS AND DISCUSSION

A study of the effect of the acid concentration on the yield of the extractives, consisting of water-soluble extractives and lignocellulosic degradation products (low molecular hemicelluloses and lignin fragments), as a result of the low temperature hydrolysis during 1 h at a hydromodulus of 1/20, shows that, with applying 0.05 g/dl HCl, the amount of the water-soluble products in the hydrolysate increases 1.6-1.8 times (**Figure 1**).

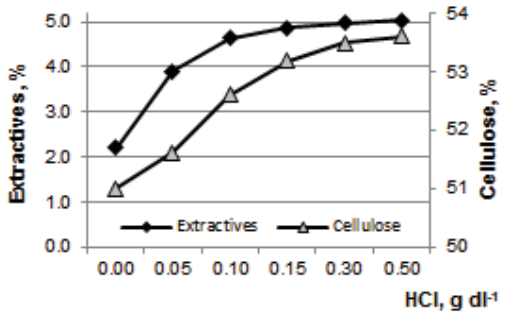

Figure 1. Effect of acid concentration on extractives amount in the hydrolysate and cellulose content in wood.

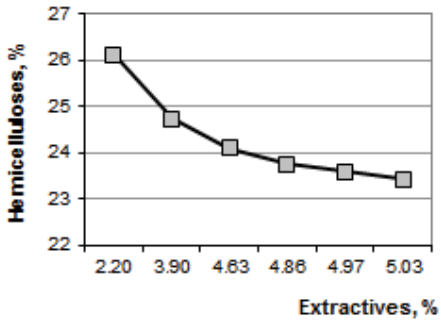

Figure 2. Hemicellulose content in sawdust *versus* extractives concentration in the hydrolysate.

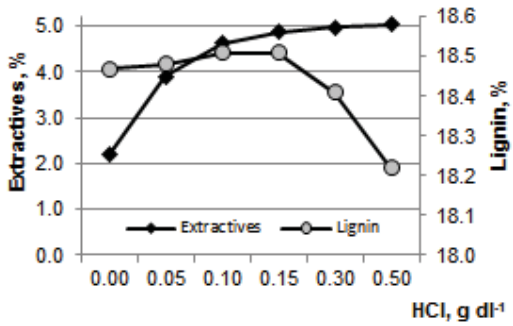

Figure 3. Effect of acid concentration on lignin content in wood.

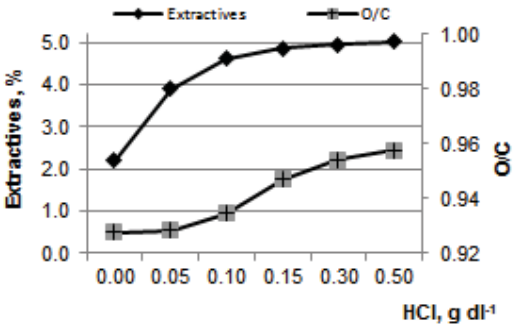

Figure 4. Effect of acid concentration on oxidation degree of wood.

The highest content of the degraded products is in the hydrolysate obtained by the treatment of the sawdust with the highest HCl concentration (0.5 g/dl): the amount of the degraded products in the hydrolysate increases more than twice in comparison with the case of the hydrolysis in water. At the same time, the correlation between the released extractives and acid concentration has a saturation character. According to **Figure 2**, the

main water-soluble degraded products passing to the hydrolysate are hemicelluloses fragments, the amount of which decreases in the lignicellulosic matrix with increasing concentration of the degraded products in the hydrolysate. The relative content of cellulose in the hydrolysed residue is enhanced with increasing HCl concentration (**Figure 1**). At a lower concentration of the acid, the transition of hemicelluloses' fragments to water is dominant, but, at the HCl concentration > 0.15 g/dl, the amount of lignin aromatic fragments in the hydrolysate starts to increase (**Figure 3**). The cleavage of the glucosidic linkages in the lignocellulosic matrix influences the functional groups' composition. This testifies the increase in the values of O/C with growing applied HCl concentration (**Figure 4**).

The UV-spectrum of the hydrolysate obtained with the highest HCl concentration was characterised by pronounced absorbance bands at 238, 288 and 338 nm, indicating the presence of biphenyl derivatives and aromatic fragments, containing non-etherified hydroxyl groups, carbonyl and carboxyl groups.

According to **Figure** 1, the hydrolysis with the HCl concentration more than 0.15 g/dl does not lead to an essential change in the amount of the released water-soluble degraded products. However, the application of higher concentrations of HCl increases the content of low molecular lignin fragments in the hydrolysate that is not rational, taking into account the following modification of the obtained wood microparticles.

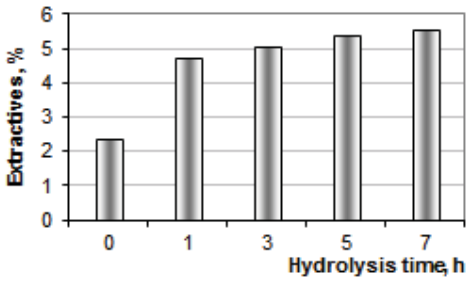

Figure 5. Extractives concentration in the hydrolysate *versus* hydrolysis time.

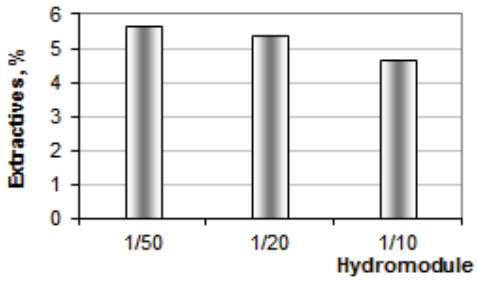

Figure 6. Extractives concentration in the hydrolysate *versus* hydrolysis hydromodulus.

The results shown in **Figure 5** reflect the effect of the hydrolysis duration, using a 0.15 g/dl HCl concentration, on the yield of the degraded products. It is seen that, with increasing hydrolysis time, the concentration of the extractives in the hydrolysate grows. It is found that the relative content of cellulose increases, but the relative lignin content in the sawdust decreases after the hydrolysis time 5 h. The found correlation of the degraded products' concentration with time has the same saturation character as the dependence of the extractives on the acid concentration.

According to **Figure 6**, with decreasing hydrolysis hydromodulus (mass ratio of sawdust to water) from 1/10 to 1/50, the extractives concentration in the hydrolysate, obtained with a 0.15 g/dl HCl concentration at a hydrolysis duration of 5 h, remarkably enhances. The components composition analysis of the hydrolysed residue obtained at a hydromodulus of 1/50 showed that the extractives had mainly the hemicelluloses nature. However, the use of a hydrolysis hydromodulus of 1/50, in spite of the absent of a large amount of the lignin's fragments, is not beneficial, because the hydrolysis requires a considerable consumption of water.

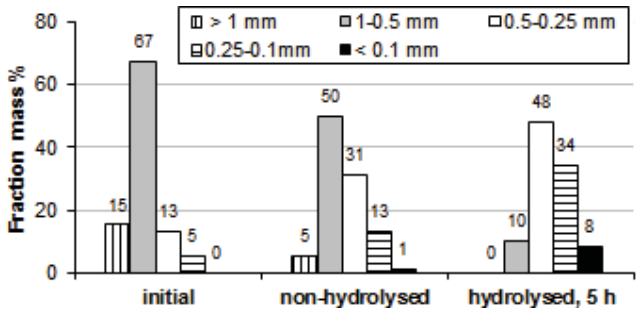

Figure 7. Fractional composition of milled initial, non-hydrolysed and hydrolysed aspen sawdust.

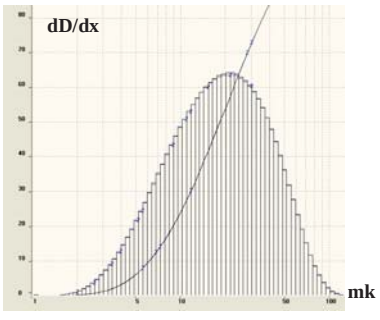

Figure 8. Size distribution histogram of hydrolysed aspen microparticles (< 100 mk).

The components composition changes in the lignocellulosic matrix lead to the reduction of its mechanical strength. This is testified by a pronounced shift in the fractional composition of the milled aspen sawdust, hydrolysed with a 0.15 g/dl HCl concentration for 5 h at a hydromodulus of 1/20, toward the content of the microparticles with the sizes < 250 mk (**Figure 7**) and a 3-fold decrease in the milling time for obtaining the fine

particles (< 250 mk), in comparison with the case of non-hydrolysed sawdust. The analysis of the particle size distribution within the fraction < 100 mk showed that more than 50% of the fraction volume was occupied by the lignocellulosic particles with sizes of 10-30 mk (**Figure 8**).

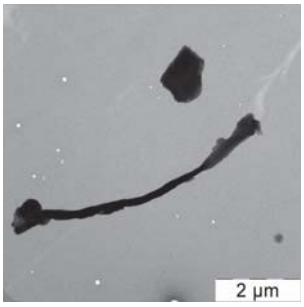

Figure 9. TEM image of the obtained aspen microparticles.

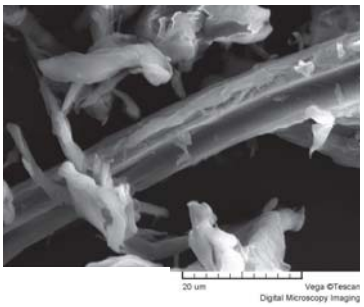

Figure 10. SEM image of the obtained aspen microparticles.

The study of the obtained microparticles by TEM revealed the prevalence of two types of the microparticles' shape, namely, oval and extended ones (**Figure 9**) with average sizes of 1-2 mk and 6-8 mk , respectively.

The performed low temperature pre-treatment of wood with dilute HCl is gentle and thus has a negligible effect on the morphology of aspen wood fine fibres that is testified by their SEM image given in **Figure 10**.

IV. CONCLUSIONS

The optimal parameters of the low temperature hydrolysis of the aspen sawdust with dilute acid for reducing sawdust particle sizes, with the aim of their further chemical modification, are found. These parameters are compromised from the point of view of the lignocellulosic matrix destruction and the lignin content. The pronounced growth of the finest particles in the milled wood and the essential drop of the milling time were achieved mainly by the partial hydrolysis of hemicelluloses. At the same time, the performed hydrolysis is gentle and has a negligible effect on the morphology of aspen wood.

V. ACKNOWLEDGEMENT

The authors have received funding for this study from the Latvian State Research Programme VPP-5 "NatRes" (2010-2014).

VI. REFERENCES

[1] Farsi, M. Effect of surface modification on thermo-mechanical behaviour of wood-polymer composite. *Asian J. Chem*. **2012**, *24(6)*, 2775–2779.
[2] Safdari, V.; Khodadadi, H.; Hosseinhashemi, S.K. The effects of poplar bark and wood content on the mechanical properties of wood/polypropylene composites. *BioResourses*. **2011**, *6(4)*, 5180–5192.
[3] Shulga, G.; Neiberte, B.; Verovkins, A.; Laka, M.; Chernyavskaya, S.; Shapovalov, V.; Valenkov, A.; Tavroginskaya, M. The new polymer composites integrating modified wood originated products. **2009**, *Proc. Italic-5*, Varenna, Italy, September 1-4, 2009, 185–188.
[4] Mosier, N.; Wyman, C.; Dale, B.; Elander, R.; Lee, Y.Y.; Holtzapple, M. Features of promising technologies for pre-treatment of lignocellulosic biomass. *Bioresource Technol*. **2005**, *96(6)*, 673–686.
[5] Taherzadeh, M.J.; Karimi, K. Pretreatment of lignocellulosic wastes to improve ethanol and biogas production: a review. *Int. J. Mol. Sci*. **2008**, *9*, 1621–1651.
[6] Kumar, P.; Barrett, D.M.; Delwiche, M.J.; Stroeve, P. Methods for pre-treatment of lignocellulosic biomass for efficient hydrolysis and biofuel production. *Ind. Eng.Chem. Res.* **2009**, *48(8)*, 3713–3729.
[7] Carvalheiro, F.; Duarte, L.C.; Gírio, F.M. Hemicellulose biorefineries: a review on biomass pretreatments. *J. Sci. Ind. Res*. **2008**, *67*, 849–864.
[8] Maache-Rezzoug, Z.; Pierre, G.; Nouviare, A.; Maugard, T.; Rezzoug, S.A. Optimizing thermomechanical pretreatment conditions to enhance enzymatic hydrolysis of wheat straw by response surface methodology. *Biomass Bioenerg*. **2011**, *35(7)*, 3129–3138.

SYNTHESIS OF NOVEL CATIONIC CELLULOSE DERIVATIVE FOR WASTEWATER TREATMENT

Katja Sievänen[1]*, Jari Kavakka[1], Pirjo Vainio[2], Kaisa Karisalmi[2], Juha Fiskari[1], Ilkka Kilpeläinen[1]

[1]*Laboratory of Organic Chemistry, Department of Chemistry, University of Helsinki, P.O. Box 55, 00014 Helsinki, Finland.*

[2]*Kemira Oyj, Luoteisrinne 2, P.O. Box 44, FIN-02271 Espoo, Finland*

**Email: katja.sievanen@helsinki.fi*

ABSTRACT

A water-soluble cationic cellulose N-chlorobetainate has been synthesized and tested for wastewater treatment applications. Starting materials, cellulose and betaine are both renewable biomaterials and are not part of the human food chain. In the synthesis of cellulose N-chlorobetainate, high molecular-weight dissolving pulp was acylated with betaine in a traditional dimethylacetamide / lithium chloride solvent system with good yield.

Extensive application testing was carried out to examine the performance of cellulose betainate as a flocculant. Commercial synthetic cationic polyacrylamide and polyamine flocculants were used as reference materials in the testing. In the fixing test, the cellulose betainate showed very good results: the performance was equal or even better than that of the reference material. The floc strength of the synthetized material was excellent in flocculation tests. In the capillary suction test, the performance of cellulose betainate was somewhat lower than that of the reference material. In all, the cellulose betainate showed excellent flocculation power, and could be used in wastewater purification applications. These results indicate that conventional synthetic polymers could be replaced with bio-based polymers in many applications, including flocculation.

I. INTRODUCTION

Municipal and industrial wastewaters can be hazardous to environment if disposed untreated to natural water bodies. Therefore the effective treatment of wastewaters is imperative. Substantial quantities of water is typically needed in many operations, such as those associated to pulp and paper manufacturing. Widely-used and important, yet cost-effective treatment methods for wastewaters are chemical coagulation and flocculation, in where a rapid solid-liquid separation takes place for large quantities of wastewater. Chemical coagulation is typically combined with floc formation in a process that involves rapid mixing in a flocculation tank.[1] Small solid particles then form larger flocs, which can be removed by filtration, flotation or sedimentation. Flocculants, which are typically high molecular weight polyelectrolytes, and usually cationic polymers, are added with rapid mixing to enhance flocculation. Flocculants act on a molecular level on the surfaces of the particles to reduce repulsive forces and increase attractive ones.[2] Moreover, effective agitation is necessary for thorough mixing of chemicals. Most importantly, however, the properties of flocculants determine the efficiency of a flocculation process.

The flocculants are either inorganic or organic compounds, latter having an advantage of being effective in very small doses. Organic compounds can be devided into two different categories: 1) synthetic organic flocculants, such as polyacrylamide, cationic derivatives of acrylic acid polymers and diallyldimethylammonium chloride (DADMAC) polymers and 2) natural organic flocculants that are based on naturally occurring biopolymers, such as cellulose, chitin and starch, as well as their derivatives. The latter are typically biodegradable, and thus they are gaining more important role as raw materials for flocculants. Being the most abundant biopolymers in the world, cellulose is a good starting material for products which could replace the existing oil-based synthetically produced materials. In this work high molecular-weight cellulose was esterified with naturally occurring cationic betaine (N,N,N-trimethylglycine), which is non-toxic and can be found in plants, microbes and humans.[3] The goal was to create a novel polyelectrolyte product from dissolving pulp for wastewater treatment applications.

II. EXPERIMENTAL

Materials

Betaine hydrochloride, LiCl, $SOCl_2$, DMAc (dimethylacetamide), toluene and pyridine were purchased from Sigma-Aldrich. Betaine hydrochloride and LiCl were used as such. $SOCl_2$ and toluene were distilled prior to their use. Pyridine was dried with KOH prior to its use. Dissolving pulps produced by Domsjö Fabriker and Borregaard ChemCell were dried in high vacuum overnight prior to their use. For application testing, the commercial reference materials, Fennopol K506, Fennopol K3400R and Fennofix 50 were provided by Kemira Oyj.

Synthesis of cationic cellulose N-chlorobetainate

First, chlorobetainyl chloride was prepared from betaine hydrochloride according to the procedure by Vassel *et al.*[4] In a typical procedure, $SOCl_2$ (72 ml) was added into 21.4 g of betaine hydrochloride. The mixture was stirred at 75 ^{o}C for 3 h under argon atmosphere. Next, 134 ml of dried toluene was added and the mixture was stirred at 75 ^{o}C for 5 to 10 min. Mixture was cooled down during which the product crystallized. The toluene-$SOCl_2$-mixture was decanted, new toluene was added and the procedure was repeated two times. The product was dried in high vacuum, grained under argon atmosphere and used as such. Quantitative yield 24.0 g.

In the synthesis of cellulose N-chlorobetainate both Domsjö and Borregaard dissolving pulps were used as starting material. The procedure was similar to both dissolving pulp samples. Dissolving pulp sheet was cut to small pieces and dried in high vacuum prior to use. Cellulose (7.5 g) was added into 375 ml of dry DMAc and the mixture was heated at 130 ^{o}C for 3 hours under argon atmosphere. After cooling down to 90 ^{o}C 26 g of dry LiCl was added and resulting mixture was stirred at room temperature overnight. Into the resulting viscous homogenous solution 10.5 ml of dry pyridine was added and stirring was continued for 30 min. Powdery chlorobetainyl chloride (22 g) was added in one portion and resulting mixture was stirred for 2 d at 40 ^{o}C using mechanical stirrer. After cooling the brown gel-like mixture was poured into acetone and filtered. Precipitate was washed three times with ethanol and dried in high vacuum for several days. The water soluble products made of Domsjö dissolving pulp (9.22 g, DS ~0.5) and Borregaard dissolving pulp (18.11 g, DS ~1.3) were analyzed with IR and NMR.

Analytical methods

IR spectra (650-4000 cm-1) were recorded with Bruker alpha-P ATR-FT-IR spectrometer. 1H NMR spectra were recorded with a Varian Unity INOVA 500 NMR spectrometer (500 MHz 1H-frequency) equipped with a 5 mm triple-resonance (1H, 13C, 15N) z-gradient probehead at 27 °C. Elemental analyses were performed with a Vario Micro Cube.

Application tests

Capillary Suction Time (CST) is a standardized method to evaluate the time of water draining from the sludge into a standard board. Testing equipment (Triton CST) and standard boards were manufactured by Triton. Time is measured with ring electrodes. CST describes how fast the free water of the sludge is penetrating into a board sheet, with various dosing of the polymer (2–17 mg of dry polymer / g of dry sludge). Tests were carried out using digested sludge from the Suomenoja wastewater plant. The reference material in the CST tests was Fennopol K506, which is a cationic polyacrylamide.

Focused Beam Reflectance Measurement (FBRM) is a laboratory test to describe paper machine first pass retention. FBRM tests were run with Lasentec D600 measuring device, particle/floc size analysed relative to time. The probe of Lasentec immersed into the investigated solution emits a laser beam. When a solid particle transcribes the beam, light reflects back to the probe. Lasentec is a time related measurement for flocculation and floc strength (shear resistance). Neutral pulp was used in the tests and polymer doses were 2–17 mg of dry polymer / g of dry pulp. The neutral pH pulp (solid contents 5.0 g per kg) consisted of 60% bleached mechanical pulp (Stora-Enso Kvarnsveden Mill GWD) and 40 % of filler (PCC Albacar 5970 by Specialty Minerals). Tap water was used in the preparing of the pulp and pH 7.5 was adjusted with acetic acid. In each test point, the pulp amount was 500 grams and mixing speed was 1500 rpm. Polymer was added at 15 seconds and data collection time was 2 minutes. The reference material used in the FBRM tests was Fennopol K3400R, a cationic polyacrylamide.

The fixing procedure is to add the studied chemical into the pulp, to mix using a blender, filtrate or centrifuge, and measure the turbidity of the water phase. The addition of cationic polymer fixes pitch onto a fiber surface decreasing the turbidity of the water phase. The two mechanical pulp samples used in the fixing tests were, as follows: refined thermomechanical pulp (TMP) from the UPM-Kymmene Rauma Mill and pressure groundwood (PGW) from the Rhein Papier Plattling Mill. The reference material used in the fixing tests was Fennofix 50, a cationic polyamine.

III. RESULTS AND DISCUSSION

We investigated the possibility to prepare a cationic cellulose based flocculation chemical where the cationic substituent would fulfill the environmental restrictions. When evaluating a suitable substituent, few things had to be considered, which are conceivable attachment to cellulose, eco-friendliness of the substituent and price of the substituent and the chemistry involved. This evaluation led to betaine (trimethylglycine). Although the synthesis of highly reactive acid chloride form of betaine has been reported already by Vassel *et al*.,[4] only few esters of betaine have been reported, which could be due to a poor solubility of the chlorobetainyl chloride in aprotic solvents. After several solvent trials, our attention turned to a common cellulose solvent system (DMA/LiCl) which allowed smooth esterification at close to ambient temperature (Scheme 1). The resulting cellulose N-chlorobetainate with DS values of ~0.5 and ~1.3 for Domsjö and Borregaard cellulose derivative, respectively, were obtained from the elemental analysis. IR and NMR spectra of the products were measured.

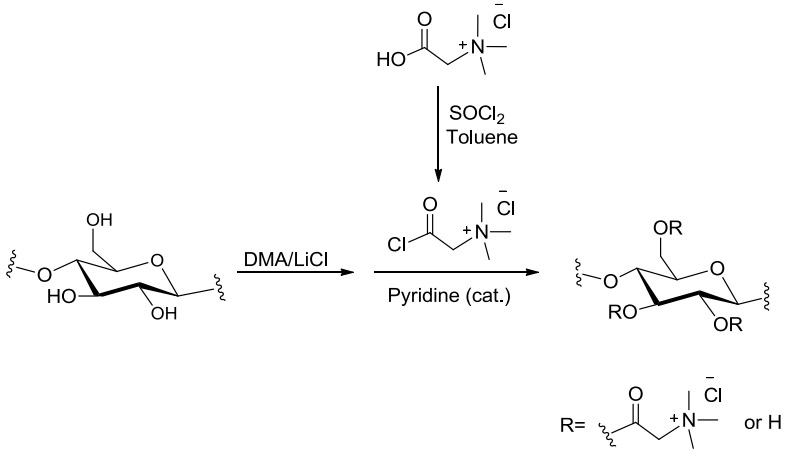

Scheme 1. Synthesis of cationic cellulose N-chlorobetainate.

The products were characterized by measuring viscosities of their water and salt solutions in order to compare their molecular weights. The charge of the products was measured by streaming current titration. Viscosities of the products were relatively high and charges in pH 4 were 1.9 meq/g for Domsjö cellulose derivative and 2.6 meq/g for Borregaard cellulose derivative, which is in agreement with the DS values.

The flocculation performance was tested with three different methods: dewatering of sludge with Capillary Suction Time (CST), flocculation of pulp with Focused Beam Reflectance Measurement (FBRM) and the fixing test with pulp. In CST tests, both cellulose derivatives exhibited a relatively good dewatering effect at dewatering time of < 30 seconds. However, the products did not meet the performance of reference polyacrylamide material, Fennopol 506. However, flocculation tests (FBRM) yielded good results for the cellulose betainate. Maximum floc size was 35 µm with a dose of 12 mg of dry polymer per one gram of dry pulp. The floc strength of the cellulose betainate was also very good. After 120 seconds of shearing, the floc size of the cellulose derivatives kept their floc size much better than the reference polyacrylamide flocculant.

Fixing tests were run with both of the cellulose derivatives with two different mechanical pulp samples: thermomechanical pulp (TMP) from the UPM-Kymmene Rauma Mill and Rhein Papier Plattling pressurized groundwood (PGW). Fennofix 50 was used as the reference material. Results of the fixing tests are shown in Figure 1. Both parallel fixing tests yielded consistent results. The performance of Domsjö cellulose betainate was equal or better than the reference material with both TMP and PGW. Borregaard cellulose betainate showed lesser turbidity decrease with both mechanical pulps than the reference and the other cellulose betainate.

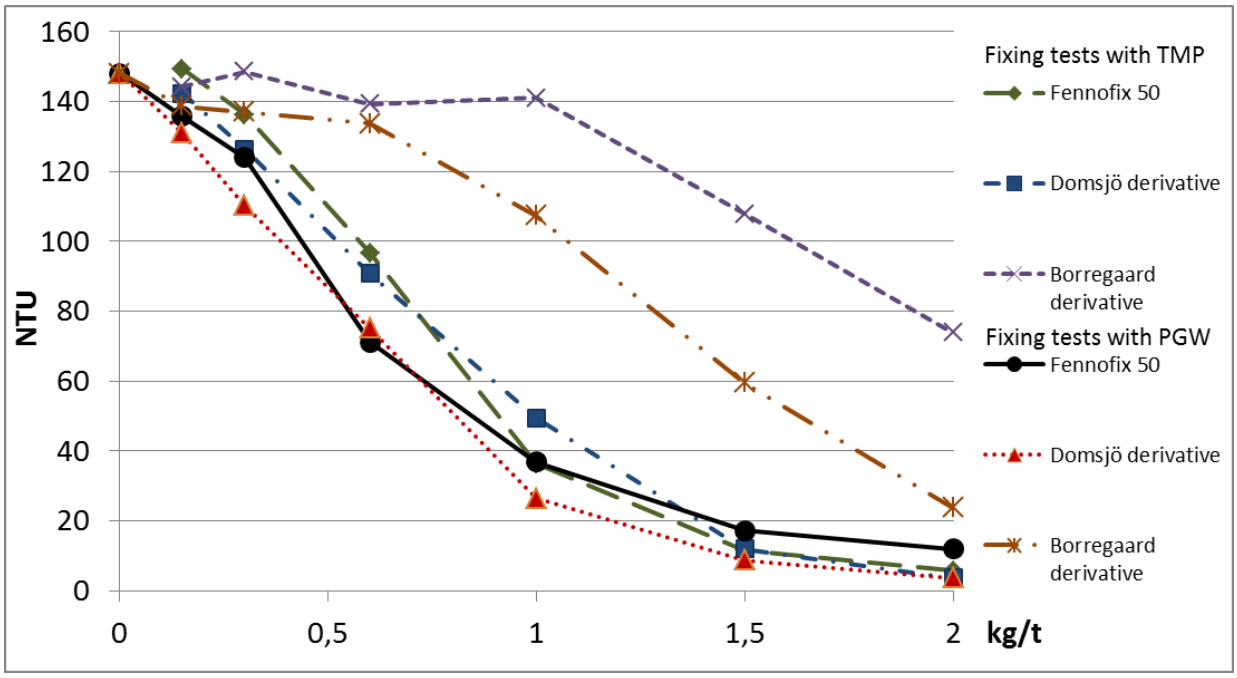

Figure 1. Turbidity decreasing in fixing test with TMP and PGW mechanical pulps

IV. CONCLUSIONS

Successful esterification of cellulose and chlorobetainyl chloride was achieved in a DMA/LiCl. In the application tests good results were obtained, which indicate that the bio-based polymers could replace the conventional synthetic polymers as flocculants. Cationic cellulose betainates are potential candidates for wastewater and paper process applications, such as flocculation, sludge dewatering and fixing.

V. ACKNOWLEDGEMENT

This research has been supported by Kemira Oyj and FIBIC (Finnish Bio-economy Cluster), who are gratefully acknowledged. The authors would like to thank Gustaf Komppa foundation for financial support.

VI. REFERENCES

[1] Hynninen, P. Effluent treatment. In: *Environmental Management and Control*. O. Dahl (Ed.). Finnish Paper Engineers' Association, Helsinki, 2008; pp. 86–116.

[2] Heitner, H.I. Flocculating Agents. In: Kirk-Othmer Concise Encyclopedia of Chemical Technology, 4th ed., John Wiley & Sons, New York, 1999; pp. 869–871.

[3] Mäkelä, P. Agro-industrial uses of glycinebetaine. *Sugar Tech.* **2004**, *6*, 207–212.

[4] Vassel, B.; Skelly, W.G. N-chlorobetainyl chloride. *Org. Synth*. **1955**, *35*, 28–30.

DETERMINATION OF FUNDAMENTAL THERMAL CHARACTERISTICS OF LIGNIN – A COMPARATIVE STUDY

Elisabeth Sjöholm[1]*, Fredrik Aldaeus[1], Anders Reimann[1], Jarmo Ropponen[2], Riku Talja[2]

*[1]Innventia, Box 5604, SE-114 86 Stockholm, Sweden; [2]VTT Technical Research Centre of Finland, P.O. Box 1000, FI-02044 VTT, Finland (*elisabeth.sjoholm@innventia.com)*

ABSTRACT

The applicability of thermal characterization methods for the determination of glass-transition temperature (T_g) and decomposition temperature (T_d) of lignin have been evaluated. Nine laboratories used their respective in-house and/or common methods to analyse five types of lignin samples; kraft lignin from birch/aspen wood and pine/spruce, respectively, organosolv spruce lignin, soda wheat straw lignin and enzymatic treated steam explosion poplar wood lignin. The samples thus represent different raw materials and types of processing of interest in today's research and development.
Good reproducibility between the laboratories was observed for the T_d irrespective of the lignin sample type and purity. The determination of T_g was more difficult for lignin samples containing large amounts of non-lignin components such as ash and/or carbohydrates. Eventual residues from proteins did not appear to obstruct the T_g (or the T_d) analysis. The best agreement between the laboratories for the T_g determination were for the two kraft lignin samples and the lignin sample obtained from enzymatic hydrolysis of steam explosion lignin. A large scatter in the data was obtained for the organosolv and soda lignin samples, respectively. The scatter in the T_g values was considerably less when the common method was used as compared to when all results were included

I. INTRODUCTION

To make a lignocellulose biorefinery concept viable, all raw material constituents of the plant should be recovered and commercialised. Much attention has been paid to the valorisation of lignin since it is the most underutilized component in all woody plants. It is well known that the composition of the lignin sample depends on origin, delignification technique and isolation conditions. The main source of technical lignin is found in the spent liquor of the kraft paper pulp mill. Even if a pure kraft lignin can be obtained by the LignoBoost method some carbohydrates, extractives and inorganics still remain. Other types of lignin studied for potential use in the future is e.g. organosolv wood lignins and soda lignins from annuals. In all cases, non-lignin constituents may be an obstacle for accurate characterisations of the lignin samples at hand.
Thus, the increasing interest in valorising lignin makes the use of properly analytical methods of great concern. For evaluation of suitable potential applications and conversions, e.g. adhesives and carbonised products, thermal properties like the decomposition temperature (T_d) and the glass-transition temperature (T_g) are frequently used. The T_d is measured by following the mass loss during heating, and is commonly defined as the temperature when a specified amount of sample remains. The T_g is the temperature at which an amorphous polymeric material undergoes a reversible transition from a glassy state to a rubbery state. The change between the two is observed in a broad temperature range, and the specific T_g is determined by convention either as the on-set temperature or as the middle point of the temperature range. The most commonly analytical methods used today is thermal gravimetric analysis (TGA) for T_d determination and differential scanning calorimetry (DSC) for T_g determination. The method used may also differ in the conditions such as drying cycles and different heating rates. The reported T_g values depend on the sample properties like molecular mass, degree of crosslinks and extent of polar groups that can take part in hydrogen bonds as well as applied analytical procedure [1]. In addition it can also be expected that non-lignin constituents will influence the results. This presentation reports about a comparative study of the glass-transition temperature (T_g) and the decomposition temperature (T_d) of five types of lignin samples performed at nine laboratories. The samples represent different raw materials and types of processing of interest in today's research and development; kraft lignin from birch/aspen wood and pine/spruce, respectively, organosolv spruce lignin, soda wheat straw lignin and enzymatic treated steam explosion poplar wood lignin.

II. EXPERIMENTAL

The details of the experimental section are described in [2]. Five lignin samples were used; hardwood kraft lignin from birch/aspen (KLHM), softwood kraft lignin from pine/spruce (KLSM), organosolve spruce lignin (Orgsolv), Soda lignin from wheat straw (Soda) and enzymatic treated steam explosion poplar lignin (ESEL).

The lignin content and the carbohydrate content were determined after acid hydrolysis according to Tappi T249-cm 00, using the coefficients 128 l g^{-1} for KLSM and 113 l g^{-1} for KLHM for determination of the acid soluble fraction at 205 nm (Theander and Westerlund, 1986). Carbohydrates were determined by HPAEC-PAD. The ash content was determined after combustion at 525°C essentially according to ISO 1762. The molecular mass characteristics were determined on acetylated samples in a THF-SEC system, using three Styragel columns (HR2, HR1, Ultrstyragel 10^4), and a flow rate of 0.8 ml/min. Polystyrene standards covering the M_p range 1.38 to 115 kDa, were used to determine the relative MMD of the lignins, and evaluations were done with PL Cirrus GPC software v 3.1.

For the determination of glass-transition temperature (T_g) and decomposition temperature (T_d), 1-3mg of lignin sample were used for each measurement [3]. Prior to the T_d determination, the sample was dried at 105°C for 20 min, before quenching to room temperature. The analysis was done by increasing the temperature to 350°C while recording the mass loss. The reported T_d, was defined as the temperature where 95% of the initial dry sample remained. The T_g determination was made by modulated reversed calorimetry where the temperature is increased by oscillation of ±3°C every 60 seconds. The drying cycle was 1°C/min to 105°C, isothermal for 20 min, quenched to 20°C, where it was held for 10 min. The following test cycle was 3°C/min temperature increase to 250°C. T_g was defined as the inflection point of the heat capacity-temperature curve. The described T_g method were modified by some laboratories and is then denoted "In-house" method in the text, along with a description of the main deviation.

III. RESULTS AND DISCUSSION

Sample description

In Table 1 show a summary of the main components of the lignin samples. The total lignin is the combined amount of Klason lignin and acid insoluble lignin. The main part of the lignin sample composition is explained by the content of total lignin, carbohydrates and ash for the kraft lignins (KLHM and KLSM) and the soda lignin. However, the Orgsolv sample and the ESEL sample also contain other components. It can be assumed that the unidentified part of the Orgsolv sample may originate from organically bound and/or inorganic phosphorus, since phosphinic acid is used as catalyst in the delignification process. The ESEL sample may contain protein (residues), and thus nitrogen analysis could reveal such indicative information.

The molecular mass characteristics reveal unusual high values for the KLSM sample. Whereas the corresponding high values for the ESEL sample may be attributed to presence of proteins and the high values for the Soda lignin sample may be due to presence of hemicelluloses, a reason for the high values of the KLSM sample is not clear.

Table 1. Table showing the main composition of the lignin samples used and macromolecular characteristics of the studied lignins. M_w= weight average molecular mass (M), M_n= number average M, PD = polydispersity. For sample designation, see the Experimental section.

Sample	Sum of main components	Total lignin (%)	Carbo-hydrates (%)	Ash (%)	M_w	M_n	PD (M_w/M_n)
KLHM	98.2	96.0	1.5	0.7	3300	900	3.7
KLSM	97.7	95.7	1.2	0.8	7000	1400	4.9
Orgsolv	87.5	80.9	3.0	3.6	2300	600	3.7
Soda	96.4	72.5	13.3	10.6	6200	2100	2.9
ESEL	91.2	87.4	0.9	2.9	7100	1300	5.6

Determination of the decomposition temperature (T_d)

Seven laboratories analysed the kraft lignin samples and the Orgsolv sample, whereas six laboratories analysed the samples Soda and ESEL respectively. Five determinations were made except one lab who made two measurements. In **Table 2** the average, temperature range and span, respectively are given. The accuracy of the determination does not seem to be negatively influenced by the large fraction of non-lignin content of the Soda and ESEL sample.

Table 2 The average, temperature range and span of T_d measurements on five lignin samples, designation, given in the Experimental section.

	KLHM	KLSM	OrgSolv	Soda	ESEL
Average T_d, °C	251	268	238	249	269
T_d range, °C	238-264	251-294	225-250	237-260	260-281
T_d span, °C	26	43	25	23	21

Determination of the glass transition temperature (T_g)

The T_g measurements were more difficult to perform than the T_d determination. One problem that may arise is to distinguish a clear transition, which of course will make the evaluation hard. The number of successful measurement of each sample differed between the labs, and in addition not all were using the same method. Six labs followed the distributed method for T_g determination. The In-house methods differed from the distributed method mainly with respect to heating rate during the test cycle; 10 to 40°C/min were used by three labs, as compared to the suggested 3°C/min. The long drying cycle applied by one lab (105°C for 16 hours) did however not seem to influence the T_g result.

As expected, the T_g determined by the common method scattered less between the laboratories, see **Table 3**, as compared to when the results for the in-house methods were included, see **Table 4**. The T_g of the Orgsolv sample was most difficult to determine irrespective of method applied, likely due to the deviating lignin structure/incorporated phosphorus groups. Also the Soda sample which contained a large fraction of both carbohydrates and ash gave scattered T_g results, indicating the importance of purification prior to T_g determination to get reliable values for the lignin in the samples.

Table 3. Comparison of the average T_g as determined with a common method. Data from six labs.

	KLHM	KLSM	OrgSolv	Soda	ESEL
Average T_g, °C	116	162	122	168	147
T_g range, °C	109-122	155-169	88-172	146-180	144-149
T_g span, °C	13	14	84	35	5

Table 4. Comparison of Tg determined with either a common or an in-house method. Number of participating labs shown within parenthesis for each lignin sample.

	KLHM (9)	KLSM (8)	OrgSolv (9)	Soda (5)	ESEL (7)
Average T_g, °C	115	160	126	155	141
T_g range, °C	92-123	142-169	88-172	128-180	127-149
T_g span, °C	32	28	84	53	22

Two laboratories analysed the samples both with the Innventia method and with their own in-house method. Lab A made one determination per sample and method. The in-house method for Lab A deviated from the Innventia method mainly by using about twice as much sample, and the use of silicon oil as an antioxidant and to ensure good heat transfer. The test cycle included heating at 10 °C/min (cf. 1 °C/min to 105 °C for the Innventia method). The other in house method (Lab B) differed from the Innventia method with regard to the temperature programme; by cycling from 25 to 120 °C to -60 °C to 200 °C to -60 °C to 200 °C using a heating/cooling rate of 10 °C/min. The largest difference between the two methods was obtained for the Orgsolv and Soda sample by Lab B. No systematic difference between the two pair of methods could however be observed.

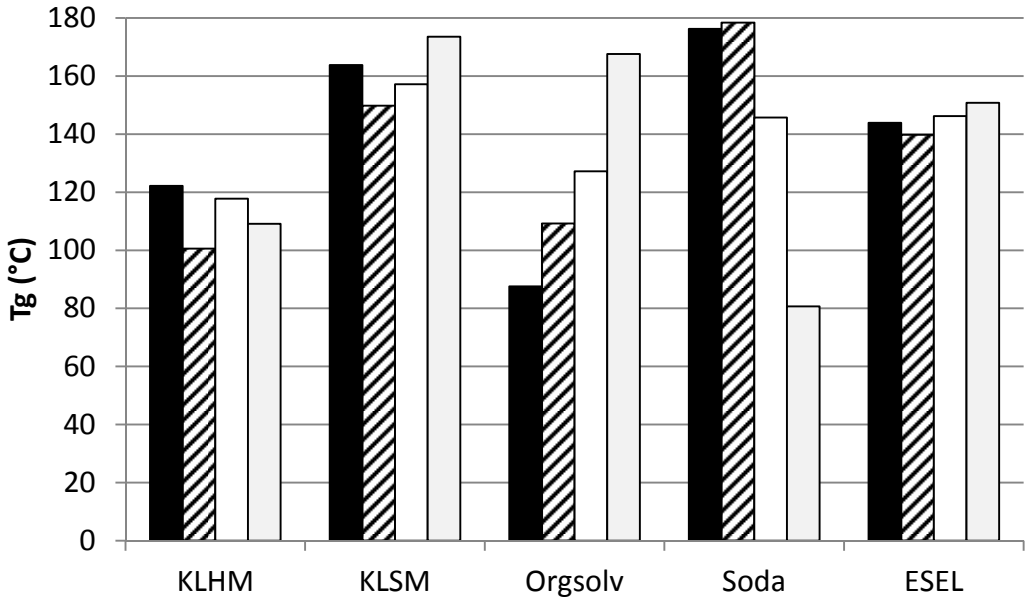

Figure 1. T_g obtained by the Innventia method (black and white) versus In-house method (striped and grey) at two laboratories. The values from Lab A (black/striped) is based on one measurement and the values from Lab B (white/grey) is based on five measurements except for Soda and ESEL (n=4).

IV. CONCLUSIONS

- Irrespective of lignin sample type and purity, good reproducibility between laboratories seems to be possible when using the same method for determination of the degradation temperature (T_d) of lignin samples.
- The determination of the glass transition temperature (T_g), is more difficult for samples containing large amounts of non-lignin components such as ash and/or carbohydrates.
- No systematic difference could be observed between In-house methods and the Innventia method, according to data from two labs. Since one of the labs made single measurements, the importance of a certain method on the obtained T_g value remains to be settled

V. ACKNOWLEDGEMENT

The study has been carried out within the frame of COST Action FP0901 “Analytical techniques for biorefineries”. Tarja Tamminen VTT Technical Research Centre of Finland (VTT), Richard Gosselink, Wageningen UR Food & Biobased Research (WUR), the Netherlands and Bodo Saake Johann Heinrich von Thünen-Institut (vTI), Germany are acknowledged for supplying the non-kraft lignin samples. Laboratories contributing to the analysis were (contact persons within parenthesis): VTT (Jarmo Ropponen), Latvian State Institute of Wood Chemistry (Tatiana Dizhbite), North Carolina State University NCSU (Dimitris Argyropoulos), Nab Labs Oy (Ritva Savolainen), Vienna University of Technology (Simone Knaus), WUR (Richard Gosselink), vTI (Ralph Lehnen), Romanian Academy “P Poni” – ICMPP (Cornelia Vasile) and Innventia (Elisabeth Sjöholm).

VI. REFERENCES

[1] Hatakeyama, H., Thermal analysis, In Methods in lignin chemistry, Eds. Lin, S.Y. and Dence, C.W., Springer Verlag, Berlin **1992**, pp. 200-214.

[2] Sjöholm, E., Aldaeus, F., Nordström, Y. and Reimann, A.. Cost Action FP0901, Round Robins of lignin samples. Part 2: Thermal properties, **2013**, Innventia Report No. 388.

[3] Nordström, Y., Norberg, I., Sjöholm, E., Drougge, R.. A New Softening Agent for Melt Spinning of Softwood Kraft Lignin. *J. Appl. Polym. Sci.*, **2013**, 129, 1274–1279.

MECHANOCHEMICAL TREATMENT OF COTTON LINTERS IN THE PRESENCE OF STYRENE

Iina Solala[1]*, Ute Henniges[2], Katharina F. Pirker[3], Bojan Stefanovic[2], Thomas Rosenau[2], Antje Potthast[2], Tapani Vuorinen[1]

*[1]Department of Forest Products Technology, Aalto University, Vuorimiehentie 1, Espoo, Finland; [2]Christian-Doppler-Laboratory, Department of Chemistry, University of Natural Resources and Life Sciences, Vienna, Konrad Lorenz Strasse 24, 3430 Tulln a.d.Donau, Austria; [3]Department of Chemistry, Division of Biochemistry, University of Natural Resources and Life Sciences, Vienna, Muthgasse 18, 1190 Vienna, Austria (*iina.solala@aalto.fi)*

ABSTRACT

Mechanochemical treatment of cotton in the presence and absence of styrene was studied with electron paramagnetic resonance (EPR) spectroscopy, gel permeation chromatography (GPC), ultraviolet resonance Raman (UVRR) spectroscopy and gas chromatography-mass spectrometry (GC-MS). The well-known phenomenon of mechanoradical formation in ball milling of cellulose was detected, but the radical content was significantly lower when styrene was added in the system. Further tests showed that there was no covalent attachment of styrene to cellulose despite the lower radical content in the presence of styrene. Instead, the styrene most likely formed homopolymers or homo-oligomers initiated by the cellulosic mechanoradicals.

I. INTRODUCTION

Cellulose, the most common biopolymer in the world, has become increasingly important in the development of sustainable materials and biofuels, in addition to its traditional uses in pulp and papermaking. Mechanochemical activation by ball milling may provide useful alternatives for traditional polymer chemistry because it requires no hazardous solvents and has higher energy efficiency than for example ultrasound or microwave treatments [1, 2]. In this study we have investigated the formation of mechanoradicals in cotton cellulose in the presence and absence of styrene. Previously a similar approach has been used for bacterial cellulose and methyl methacrylate, producing block copolymers of the two [3, 4]. The main objective of our work was to see if the well-known occurrence of cellulosic mechanoradicals in ball milling will cause copolymerization between cotton and styrene.

II. EXPERIMENTAL

Air-dry cotton linters were torn into small pieces (approx. 0.5 cm x 0.5 cm) by hand and 1.0 g of sample was placed in a 50-mL ball milling chamber with two stainless steel balls (Ø 9 mm) and 1.0 mL of styrene. The >99% styrene was purified by running it through an aluminum oxide column before use (both purchased from Sigma-Aldrich). The milling was done at 25 Hz in a Retsch CryoMill (Retsch, Haan, Germany) equipped with continuous liquid nitrogen cooling for periods of 20, 30, 40, 50 and 60 min. Pure cotton milled in the same conditions was used as a control for all subsequent analyses.

Electron paramagnetic resonance (EPR) spectroscopy

Two parallel room temperature samples were prepared for each data point. The EPR spectra were recorded as first derivatives of the microwave absorption with a Bruker EMX cw EPR spectrometer, operating at X-band frequencies (9 GHz), equipped with a high-sensitivity (HS) cavity, using 0.318 mW microwave power and 2.5 mT modulation amplitude, and 50-77 scans per sample. Non-saturating conditions were chosen based on a saturation curve. All signal intensities were obtained by double integration of the (cubically) baseline-corrected signal with Bruker WinEPR software. The results were then normalized to account for the differences in sample mass and number of scans.

Gel permeation chromatography (GPC)

GPC analysis was done according to the method used by Borrega *et al.* [5] through a water – acetone – N,N-dimethylacetamide (DMAc) activation sequence followed by dissolution in 9 % DMAc/LiCl.

Ultraviolet resonance Raman (UVRR) spectroscopy

The spectra were recorded out of acetone-extracted (5h in a Soxhlet apparatus), air-dried (overnight in room temperature) powder-like samples that were pressed into a smooth, even layer between two microscope slides prior to measuring with a Renishaw 1000 UV Raman spectrometer operated by Grams32 (Galactic Industries Corporation) computer program. The measurement parameters were 244 nm, 10 mW, focusing depth ~30 µm from the sample surface, measuring time 30 s. The sample was rotated continuously to avoid damage from the laser. An average of two parallel spectra was calculated after normalizing with respect to the cellulose band at ~1093 cm-1.

Gas chromatography-mass spectrometry (GC-MS)

Acid hydrolysis was done as described by Willför *et al.* [6] by measuring approx. 0.1 g of sample, adding 1 mL of 72% H_2SO_4, heating at 30 °C for 1 h, adding 28 mL of ultrapure water, heating in an autoclave to 121 °C for 1 h and filtering through a 0.45 µm GHP filter. 500 µL of hydrolysate was neutralized with 200 µL of pyridine and left overnight in a fume hood to evaporate. The next day the hydrolysates were dried in a vacuum oven at 40 °C for a total of 6 h until completely dry.

Trimethylsilylation was done by adding 80 µL of pyridine and 250 µL of freshly prepared derivatization agent (*N*,*O*-bis(trimethyl silyl)-trifluoroacetamide with 5 % of trimethylchlorosilane) to the completely dry samples. Samples were then sonicated for 30 min and left in room temperature overnight. Parameters for GC-MS analysis were taken from Laine *et al.* [7] except for split ratio, which was 1:100 in our case. Data was collected with ISQ GC-MS (Thermo Fisher Scientific Inc.) and handled with Xcalibur software.

In order to look for styrene moieties attached to cellulose, we looked for fragments of possible monomers or oligomers of styrene on glucose (**Figure 3**). The assumption was that the glycosidic bond would be the site of the breaking, and that styrene would attach either to a carbon or an oxygen atom after the homolysis. Thus we looked if there were fragments at m/z 77, 91 and 105 present in GC peaks that also yielded typical fragments of trimethylsilylated pyranoses (m/z 217, 204 and 191 being the most characteristic).

III. RESULTS AND DISCUSSION

Based on the intensity of EPR spectra, the radical contents were significantly higher when there was no styrene in the system (**Figure 1**). Both sample types demonstrated a notable increase in radical content over the milling time, followed by a decrease after reaching a maximum at ~40 min.

The most apparent change in the Raman spectra of cryomilled cotton and styrene was a small but systematic increase at the aromatic band at ~1605 cm^{-1} (**Figure 2**), which may suggest covalent bonding between cellulose and styrene. However, this hypothesis was further tested with GPC and GC-MS.

At milling levels of 0, 20 and 40 min (both pure cotton and cotton + styrene) there were no significant differences in Mw distributions or average values (around 200 kg/mol in all tested samples), despite the fact that the radical contents were highest at ~40 min milling time. Also the polydispersity index remained unchanged, at 1.95 ± 0.11.

Comparison of mass spectra of GC peaks with elution time of about 8.3 min to data available at Mass Bank indicated that they originated mainly from 1,2,3,4,6-*O*-pentatrimethylsilyl glucopyranose. No styrene-derived structures were detected at the cellulose-derived fractions, which leads us to the conclusion that no covalent bond formation took place between styrene and cellulose. Instead, something other than a copolymerization reaction must cause the decrease in radical content when styrene is present in the system, possibly homopolymerization of styrene initiated by the formed mechanoradicals. Mechanochemically initiated homopolymerization of styrene has been reported also in the case of ball milling of quartz [8].

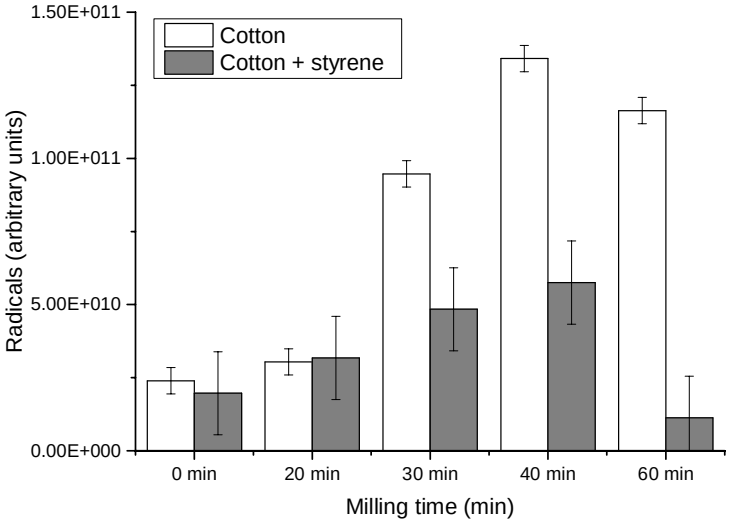

Figure 1. Intensities of free radical EPR spectra measured at room temperature after cryomilling cotton with and without styrene.

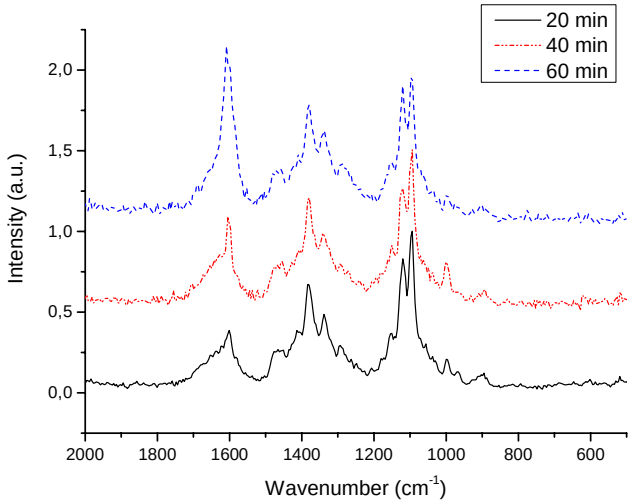

Figure 2. Comparison of UVRR spectra of samples milled for 20, 40 and 60 min in the presence of styrene.

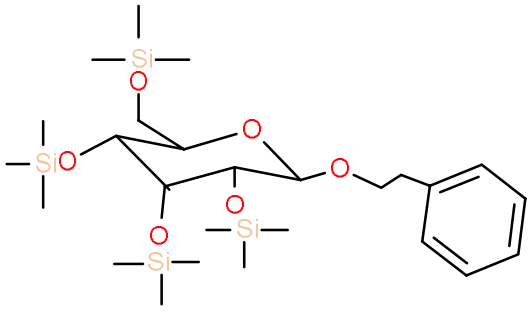

Figure 3. Schematic presentation of a structure that was looked for with GC-MS.

IV. CONCLUSIONS

Mechanochemical treatment of cotton in the presence of styrene seems to have different outcome to a system of bacterial cellulose and methyl methacrylate [4]; no copolymer is formed. In our system the milling time was shorter than in the study of Sakaguchi *et al.* [4] but the values are not comparable because the milling devices as well as other details in the experimental setup were different. In our study, special attention was given to samples milled for 40 min since that was the time that gave the highest radical content. However, copolymer formation did not occur, meaning that it is more likely that the cellulosic mechanoradicals initiate homopolymerization in styrene.

V. ACKNOWLEDGEMENT

The authors gratefully acknowledge Multidisciplinary Institute of Digitalisation and Energy (MIDE), Aalto University, for the financial support that enabled this collaboration.

VI. REFERENCES

[1] Boldyreva, E. Mechanochemistry of inorganic and organic systems: what is similar, what is different? *Chem. Soc. Rev*. **2013**, *42*, 7719-7738.

[2] Kleine, T.; Buendia, J.; Bolm, C. Mechanochemical degradation of lignin and wood by solvent-free grinding in a reactive medium. *Green Chem.* **2013**, *15*, 160-166.

[3] Hon, D. Formation and behavior of mechanoradicals in pulp cellulose. *J. Appl. Polym. Sci.* **1979,** *23* (5), 1487-1499.

[4] Sakaguchi, M. Ohura, T.; Iwata, T.; Takahashi, S.; Akai, S.; Kan, T.; Murai, H.; Fujiwara, M.; Watanabe, O.; Narita, M. Diblock copolymer of bacterial cellulose and poly(methyl methacrylate) initiated by chain-end-type radicals produced by mechanical scissionof glycosidic linkages of bacterial cellulose. *Biomacromolecules* **2010,** *11*, 3059-3066.

[5] Borrega, M.; Tolonen, L.; Bardot, F.; Testova, L.; Sixta, H. Potential of hot water extraction of birch wood to produce high-purity dissolving pulp after alkaline pulping. *Bioresource Technol.* **2013,** *135*, 665-671.

[6] Willför, S.; Pranovich; A.; Tamminen, T.; Puls, J.; Laine, C.; Suurnäkki, A.; Saake, B.; Uotila, K.; Simolin, H.; Hemming, J.; Holmbom, B. Carbohydrate analysis of plant materials with uronic acid-containing polysaccharides - a comparison between different hydrolysis and subsequent chromatographic analytical techniques. *Ind. Crop. Prod.* **2009,** *29*, 571-580.

[7] Laine, C.; Tamminen, T.; Vikkula, A.; Vuorinen, T. Methylation analysis as a tool for structural analysis of wood polysaccharides. *Holzforschung* **2002,** *56* (6), 607-614.

[8] Hasegawa, M.; Kimata, M.; Kobayashi, S.-I. Mechanochemical polymerization of styrene initiated by the grinding of quartz. *J. Appl. Polym. Sci.* **2001**, *82*,2849-2855.

IDENTIFICATION AND PRODUCTION OF XYLANASES DERIVED FROM *PIRIFORMOSPORA INDICA*

Aleksandra Sominka[1], Bernd Mueller-Roeber[1,2,*] and Hakan Dortay[1,#]

[1]University of Potsdam, Institute of Biochemistry and Biology, Karl-Liebknecht-Straße 24-25, 14476 Potsdam-Golm, Germany; [2]Max-Planck Institute of Molecular Plant Physiology, 14476 Potsdam-Golm, Germany; [#]Present address: Berlin University of Technology, Institute of Photoacoustic Imaging and Spectroscopy, Straße des 17. Juni 135, 10623 Berlin, Germany (*bmr@uni-potsdam.de)

ABSTRACT

Lignocellulosic biomass from different sources such as agricultural products (e.g. wheat), industrial waste (e.g. woodchips) or household waste (e.g. used paper) can be used as substrate for the production of biofuels, chemicals or animal feed. There are two basic approaches to convert biomass into low-molecular-weight sugar polymers: i) physical treatment allowing an improved access of enzymes to cellulosic fibers of lignocellulosic biomass and ii) enzymatic hydrolysis. The typical chemical composition of lignocellulosic material is cellulose, hemicellulose and lignin. Xylan is the major component of hemicellulose and the most abundant non-cellulosic polysaccharide in hardwood and annual plants. Complete degradation of hemicellulose requires a complex mixture of hemicellulose degrading (e.g. endoxylanases, β-xylosidases) or modifiying (e.g. acetyl xylan esterase, α-glucuronidase, feruloyl esterase, α-L-arabinofuranosidase) enzymes. Endo-1,4-β-xylanase (EC.3.2.1.8) catalyzes the hydrolysis of β-1,4-D-xylosidic linkages in xylan. Xylanases isolated from fungi or bacteria have been widely used in industry (e.g. pulp and paper). In this work we expressed putative xylanases from the root-colonizing fungus *Piriformospora indica* using the *Pichia pastoris* expression system. Enzymes were characterized with respect to pH and temperature dependencies as well as hydrolysis products in the presence of xylan as substrate.

I. INTRODUCTION

In nature, plant cell wall decomposition is performed by bacteria and fungi that secrete a wide range of lignocellulolytic enzymes. Xylanases (endo-β-1,4-xylanases) are increasingly recognized to be important for the deconstruction of lignocellulosic biomass [1]. Most characterized xylanases belong to the GH families 10 and 11. Enzymes of both families are produced by fungi and bacteria, whereas xylanases indentified so far in plants exclusively belong to the GH10 family [2,4]. Typically, xylanases of GH family 10 have a comparatively high molecular masses (of ~35 kDa) and a low pI, while GH family 11 xylanases have a low molecular mass (~20 kDa) with a high pI [6]. GH11 xylanases use exclusively xylan as substrate and hydrolyse only unsubstituted regions of the sugar polymer, whereas GH10 enzymes exhibit activity on cellulosic substrates and substituted xylans [8]. *Piriformospora indica* is a root-colonizing fungus of the order Sebacinales. Recent studies focus on studying the mutualistic relationship between plants and *P. indica*. Notably, *P .indica* promotes plant growth and increases the resistance against abiotic (salt) and biotic (fungal pathogen) stresses [9]. In this study we demonstrate that *P. indica* can also serve as a new source for lignocellulolytic enzymes.

II. EXPERIMENTAL

Pichia pastoris transformation and screening of transformants. The recombinant plasmids were transformed into *P. pastoris* X-33 cells using the "Pichia EasyComp Kit" (Life Technologies) following the manufacturer´s instructions. The transformation reactions were spread on YPDS agar plates containing 100 µg/ml zeocin. Small-scale expression analysis was performed in 24-deep-well plates to detect formation of recombinant protein. Randomly selected transformants were used for screening of well expressing clones. To this end clones were inoculated in wells of 24-deep-well plates supplemented with 2 ml of BMMY medium (induction medium containing 0.6% methanol) and incubated for four days at 28ºC on a rotary shaker (190 rpm). The cell free supernatants were collected after centrifugation and stored at -80°C until further analysis such as immunological detection of expressed xylanases, and enzymatic activity assays were performed. Clones showing xylanase activity were used for large-scale protein production and purification.

Purification of recombinant xylanases. Proteins were purified using Protino Ni-IDA 150 packed columns (Macherey and Nagel, Germany) according to the instructions of the manufacturer. Purified protein concentrations were determined by the Bradford assay [3] using bovine serum albumin (BSA) as standard. Molecular sizes of purified proteins were tested by SDS-PAGE separation followed by western blot analysis.

Xylanase activity assay. Xylanase activity was analysed by i) DNS assay and ii) Congo Red staining/destaining of xylan containing agar plates. i) The DNS (3,5-dinitrosalicylic acid) method determines the concentration of released reducing ends [10]. Activity was determined at 50˚C using 1% (w/v) beech wood xylan (Sigma, Germany) in 50 mM sodium acetate buffer (pH 6.0). After 15 min the reaction was stopped by adding DNS reagent, and the reducing sugars released were quantified, using xylose as a standard. ii) Congo Red staining/ destaining of substrate containing agar plates was performed by dropping enzyme solution on LB-agar plates containing 0.2% beech wood xylan and incubation at 37˚C. After incubation, plates were flooded with Congo Red staining solution (0.5% Congo Red solution, 10% ethanol) and stained by shaking and destaining with 1M NaCl solution. A clear zone (yellow halo) around the drops indicated xylanase activity. All enzymatic assays were performed in triplicate, and results are presented as mean values.

pH optimum, temperature optimum and thermal stability. The effect of pH on xylanase activity was measured at 50°C in a pH range of 3.5 to 10.0 using appropriate buffers, i.e., 50 mM sodium acetate (pH 3.5 - 6.5) and Tris - HCl (pH 7.0 - 10.0). The temperature optimum was determined by performing the reaction at different temperatures ranging from 20°C to 60°C at optimum pH. To evaluate the thermal stability, xylanases were incubated at the optimum temperature in the absence of substrate for different periods. The residual xylanase activity was then determined by DNS assay.

Hydrolysis products. Purified enzymes were incubated with 2% beech wood xylan in 50 mM sodium acetate buffer at determined optimal conditions for 0 h, 0.5 h, 8 h and 24 h. The oligosaccharide composition in the reaction mixture was analyzed by HPAEC-PAD (ICS-5000 Dionex) equipped with 250 x 3 mm CarboPAC PA200 column. The column was equilibrated with 100 mM NaOH and elution was performed using a multi-gradient method with 5 mM - 500 mM sodium acetate and 100 mM sodium hydroxide for 60 min. All analyses were carried out at a temperature of 30˚C and a flow rate of 0.4 ml/min. Standards were used as follows: 1,4β-D-xylo-oligosaccharides (xylobiose, xylotriose, xylotetraose, xylopentaose, xylohexaose from Megazyme), D-(+)-glucose BioUltra and D-(+)- Xylose BioUltra (Sigma).

III. RESULTS AND DISCUSSION

Eighteen putative GH10 and 15 GH11 family xylanases are listed in the CAZY database (www.cazy.org/). Using computational tools (Uniprot at www.uniprot.org, and Expasy at www.expasy.org/) we selected putative xylanases of the smallest molecular sizes. According to Pu et al. (2013) [6] small enzymes can easily penetrate into the structure of the plant cell wall. Amino acid sequence alignments of all potential xylanases using ClustalW (www.genome.jp/tools/clustalw) demonstrated highly conserved and characteristic motifs of GH11 family members: the amino acid stretch IEYYI and two catalytic Glu residues (Glu131 and Glu 217). The active site of GH10 family members contains many aromatic residues important for substrate binding [11].

Heterologous expression of xylanases in Pichia pastoris and screening for active enzymes. To achieve maximal protein expression, we used codon-optimized synthetic open reading frames (without their cognate N-terminal signal peptides) in frame with a secretion signal peptide (α-MF factor) from *Saccharomyces cerevisiae*. The cell free supernatants of selected transformants were assayed for xylanase activity. In **Figure 1A** yellow halo zones indicate active xylanases after Congo Red staining/destaining of substrate (xylan or CMC) containing agar plates. All analysed enzymes were active on xylan agar plates**.** Additionally xylan from different sources were tested by the DNS method. The highest activity was observed when beech wood xylan was used as a substrate (not shown). The concentrations of the purified proteins were around 100 - 200 µg/ml. SDS-PAGE separation followed by western blot analysis showed the expected molecular weights of all xylanases (**Figure 1B**).

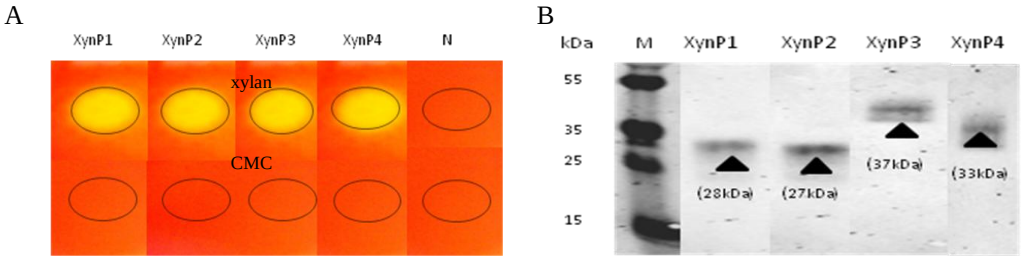

Figure 1. Analysis of xylanase activities and molecular masses**. A.** Activity assay. Congo Red staining/ destaining on xylan/CMC-containing agar plates. Formation of yellow halo indicates xylanase acitivity. Circles indicate areas of a drop of xylanase-containing cell-free supernatant. N, negative control. **B.** Immunological detection of xylanase proteins after SDS-PAGE separation. Black arrows indicate protein bands; molecular weights are given. Lane M, protein marker.

Effect of temperature on the activity and thermal stability of xylanases. Effects of pH and temperature changes on the activity of purified xylanases were analyzed using beech wood xylan as substrates. Xylanase XynP2 showed the highest activity at pH 5.5, while XynP1, XynP3 and XynP4 were most active at pH 4.5. Substantial activity was detected for all enyzmes in the pH range of 4.0 to 8.0 **(Figure 2A)**. Similar results were published for xylanases isolated from *Fusarium proliferatum* with highest activities within the acidic region [7]. The optimum temperature for XynP2 was 45˚C. XynP1 and XynP3 showed the highest activities at 35˚C, and XynP4 showed an optimum at around 30˚C (**Figure 2B**). Thermal stability analysis showed that XynP2 was the most stable xylanase (**Figure 2C).**

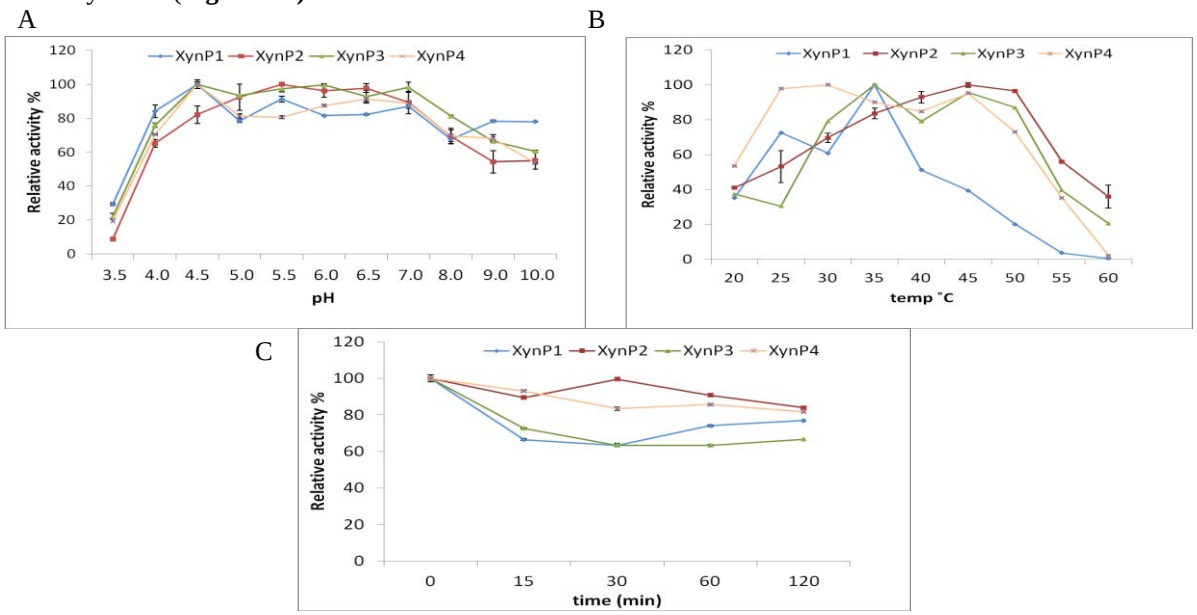

Figure 2. Characterization of purified xylanases**. A.** Effect of pH on xylanase activity. The assay was performed at 50˚C in buffers with different pH values ranging from 3.5 to 10.0 for 15 min in the presence of 1% (w/v) beech wood xylan. **B.** Effect of temperature on xylanase activity. Assays were carried out using 1% (w/v) beech wood xylan as a substrate at pH optimum and at temperatures ranging from 20˚C to 60˚C. **C.** Thermostability of purified proteins. The enzymes were pre-incubated at optimal temperature in the absence of substrate for varying periods of time. In (A) and (B), the highest activity determined for each enzyme was set as 100%. In (C), enzyme activity before heat incubation (time point 0 min) was set to 100%. Data are means ± SD (n = 3).

Identification of hydrolysis products. Hydrolysis products generated by the purified enzymes from beech wood xylan were analyzed by HPAEC-PAD. An extended incubation of enzymes with the substrate led to the formation of sugar oligomers while polymers decreased. Candidate XynP1 required a longer incubation time with substrate, after 0.5 h only slightly hydrolysed fractions were detected. After 24 h the following main hydrolysis products were detected: xylotriose (1.54 µg/ml), xylotetraose (1.39 µg/ml), xylopentaose (1.47 µg/ml) and xylohexaose (1.08 µg/ml) **(Figure 3A)**. For candidate XynP2 hydrolysis products were detected already within 0.5 h of incubation with the substrate. Extended incubation increased the amount of hydrolysed fractions. The main hydrolysis products were xylobiose (9.01 µg/ml) and xylotriose (11.15 µg/ml) **(Figure 3B**). Intermediate incubation times for substrate hydrolysis were observed for enzymes XynP3 and XynP4. For XynP3, the main fractions released after 24 h were xylobiose (4.22 µg/ml), xylotriose (8.13 µg/ml) and xylotetraose (3.77 µg/ml). The end hydrolysis products of XynP4 were xylobiose (4.98 µg/ml) and xylotriose (5.99 µg/ml) **(Figure 3C, D).**

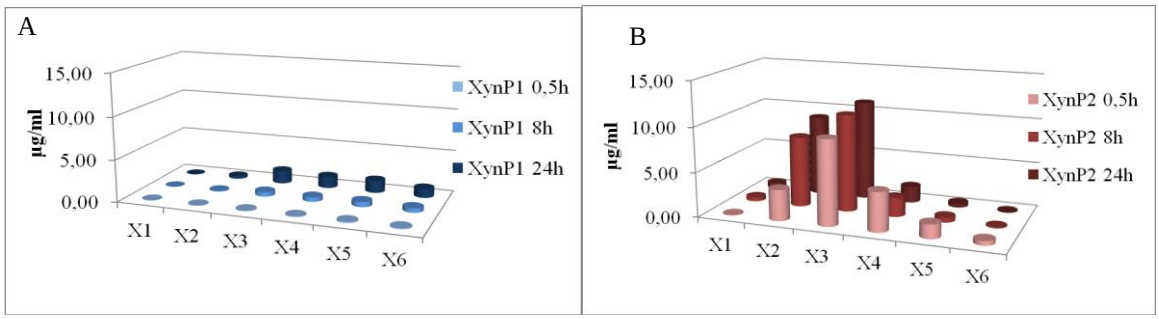

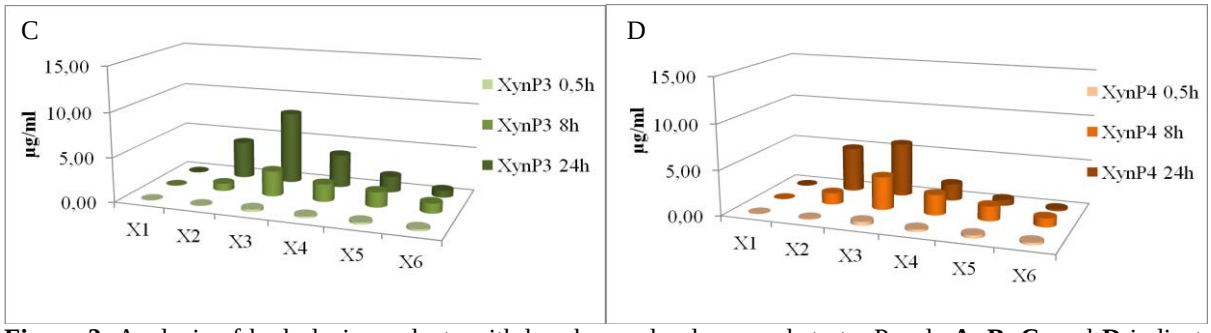

Figure 3. Analysis of hydrolysis products with beech wood xylan as substrate. Panels **A**, **B**, **C**, and **D** indicate hydrolysis product for the enzymes XynP1, XynP2, XynP3 and XynP4, respectively, at the incubation times indicated; x1, xylose; x2, xylobiose; x3, xylotriose; x4, xylotetraose; x5, xylopentaose; x6, xylohexaose.

IV. CONCLUSIONS

In conclusion, *P. indica* is a further source of lignocellulolytic enzymes. In the present study we succeeded in expressing selected *P. indica* xylanases free of cellulase activity. Further studies aiming at the production of more thermostable enzymes by genetic engineering are in progress.

V. ACKNOWLEDGEMENTS

The project was supported by the Ministry for Economic and European Affairs of the State Brandenburg, Germany.

VI. REFERENCES

[1] Beaugrand J, Chambat G, Wong VWK, Goubet F, Rémond C, Paës G. Impact and efficiency of GH10 and GH11 thermostable endoxylanases on wheat bran and alkali-extractable arabinoxylans. *Carbohyd. Res.* **2004**, 339:2529-2540.
[2] Biely P, Vrsanská M, Tenkanen M, Kluepfel D. Endo-beta-1,4-xylanase families: differences in catalytic properties**.** *J. Biotechnol.* **1997**, 571:51-66.
[3] Bradford, MM. Rapid and sensitive method for the quantitation of microgram quantities of protein utilizing the principle of protein-dye binding. *Anal. Biochem*. **1976**, 72:248-54.
[4] Cantarel BL, Coutinho PM, Rancurel C, Bernard T, Lombard V, Henrissat B. The Carbohydrate-Active EnZymes database (CAZy): an expert resource for Glycogenomics. *Nucl. Acids Res.* **2009,** 37:D233-8.
[5] Henrissat B. A classification of glycosyl hydrolases based on amino acid sequence similarities. *Biochem. J*. **1991**, 280:309-16.
[6] Pu Y, Hu F, Huang F, Davison B, Ragauskas A. Assessing the molecular structure basis for biomass recalcitrance during dilute acid and hydrothermal pretreatments *Biotech. Biofuels* **2013**, 6:15.
[7] Saha BC. Production, purification and properties of xylanase from a newly isolated *Fusarium proliferatum* capable of utilizing corn fiber xylan. *Process Biochem.* **2002**, 36:1279-84.
[8] Sridevi B, Charaya Singara, MA. Isolation, identification and screening of potential cellulose-free xylanase producing fungi. *Afr. J. Biotechnol*. **2011,** 10:4624-30.
[9] Verma S, Varma A, Rexer K-H, Hassel A, Kost G, Sarbhoy A, Bisen P, Bütehorn B, Franken P. *Piriformospora indica*, gen. nov. sp. nov., a new root-colonizing fungus. *Mycologia*. **1998**, 90:896-903.
[10] Warwicki L, Gray P, Grego J, Quilan M. Evaluation of the DNS method for analyzing lignocellulosic hydrolysates. *Chem. Tech. Biotechnol.* **1982**, 32:1016-22.
[11] Zhang J, Tuomainen P, Siika-Aho M, Viikari L. Comparison of the synergistic action of two thermostable xylanases from GH families 10 and 11 with thermostable cellulases in lignocellulose hydrolysis *Biores. Technol.* **2011**, 526:9090-95.

EFFECT OF XYLANASE ORIGIN ON REMOVAL OF XYLAN-ASSOCIATED CHROMOPHORE STRUCTURES IN BLEACHED *E. GLOBULUS* KRAFT PULP

Joana I. T. Sousa [1,2*], Dmitry V. Evtuguin[1], M. Graça V. S. Carvalho[2]

[1]*CICECO, Department of Chemistry, University of Aveiro, 3810-193 Aveiro, Portugal*

[2]*CIEPQPF, Dep. of Chemical Eng., University of Coimbra, Portugal*

**joanaisousa@ua.pt*

ABSTRACT

An enzymatic stage (X) applied to DEDD/DEDP bleached *E. globulus* kraft pulp before or after the final D/P stages allowed a significant improvement in brightness and brightness stability of bleached pulp while decreasing the consumption of chlorine dioxide or hydrogen peroxide. The industrial DED pre-bleached *E. globulus* pulp (87.8% ISO) was subjected to enzymatic treatment with three commercial *endo* - xylanases of different origin, designated as X1, X2 and X3. The treated pulps were chemically characterised and analysed on brightness gain and reversion. The analysis of chromophores was accomplished employing UV-Resonance Raman and UV–visible Diffuse Reflectance spectroscopy. Isolated xylan from DED and DEDX pulps were characterised by wet chemistry analyses and 1D and 2D NMR spectroscopy. The molecular weight was assessed by SEC. The topochemistry of xylanase´s action in X stage was assessed using enzymatic peeling with pure commercial xylanase of GH10 family. Xylanases X1-X3 hydrolysed primarily non-branched regions of xylan molecules, whereas xylan hydrolysis profiles in fibre depth varied depending on the xylanase applied. These findings were discussed in the relation to the xylanase performance in X stage.

I. INTRODUCTION

The pulp bleaching process is a multi-stage technology aiming to increase the reflectance of visible light from the brownstock wood pulp. This is achieved by removal or modification of chromophore groups which are assigned to residual lignin and its degradation products, besides to some carbohydrates, extractives and metal ions complexed with pulp components. The chemistry of the final bleaching process in the production of bleached chemical pulp has remained a less investigated area mainly because of the difficult assessment of the nature of the remaining chromophores [1]. In the final bleaching process cellulose and hemicelluloses are especially vulnerable to oxidation with bleaching reagents. The brightness gain and reversion are also expected to be sensitive to the oxidation patterns of carbohydrates with these chemicals. Xylan is the most abundant hemicellulose and it was proved that play an important role in a brightness development and stability [2]. A xylanase treatment in final bleaching release resistant chromophores attached to the xylan backbone and contributes in this way to the brightness gain and reduces chemicals consumption [3-5].

An enzymatic stage (X) applied to DEDD/DEDP bleached *E. globulus* kraft pulp before or after the final D/P stages provide a positive effect on the brightness and brightness stability of bleached pulp and allow significant savings in chlorine dioxide or hydrogen peroxide [3]. It was notified, however, that the origin of commercial xylanase applied in X stage plays an extremely important role. In this work the effect of xylanase origin on removal of xylan-associated chromophore structures in bleached E. globulus kraft pulp was studied. Accordingly, an industrial DED pre-bleached *E. globulus* pulp (87.8% ISO) was subjected to enzymatic treatment with three commercial xylanases, designated as X1 and X2 (Pulpzyme HC$^{@}$1000 and HC$^{@}$2500, respectively, of Novozyme S/A, both from *Baccilus sp.*) and X3 (BioBrite$^{@}$100 of Iogen Corp., from *Trichoderma spp.*), under optimised conditions and similar xylanase load in term of AXU/(g of pulp). The treated pulps were chemically characterised and analysed on brightness gain and reversion (PC number). The analysis of chromophores was accomplished employing UV-Resonance Raman (UV-RR) and UV–visible Diffuse Reflectance (UV–vis DR) spectroscopy. Isolated xylans from partially (DED) and fully (DEDX) bleached eucalypt kraft pulps were characterized employing wet-chemistry methods (1D/2D NMR spectroscopy and size exclusion chromatography). In addition xylanase action in X stage was assessed using enzymatic peeling with pure commercial xylanase of GH10 family.

II. EXPERIMENTAL

The starting industrial semi-bleached DED *E. globulus* kraft pulp (87.8% ISO and 0.46 PC number) was subjected to enzymatic treatment with xylanases under laboratory conditions.

Xylanase bleaching

Three commercial xylanases, designated as X1 and X2 (Pulpzyme HC1000 and HC2500, respectively, of Novozyme S/A, both from *Baccilus sp*.) and X3 (BioBrite@100 of Iogen Corp., from *Trichoderma spp*.) were used under optimised conditions and similar xylanase load in term of AXU/ (g of pulp) in the final bleaching. The conditions were as follows: xylanase X1(pH = 8; T = 60°C; t = 120min; xylanase dosage = 0.15% odp; ~1,5 U/g odp); xylanase X2 (pH = 7; T = 70°C; t = 60min; xylanase dosage = 0.05% odp; ~5 U/g odp); xylanase X3 (pH = 6; T = 60°C; t = 60min; xylanase dosage = 0.011% odp; ~5 U/g odp). Enzyme solutions were diluted in water and pH was adjusted with NaOH or HCl solutions. The bleaching trials were run in sealed polyethylene bags in a reciprocal shaking water bath with temperature control and using 20 g odp at 10% consistency. After bleaching, the pulps were thoroughly washed with distillate water and finally conditioned in a dark room at 4ºC.

Xylan isolation

The xylan was isolated from DED and DEDX pulps by DMSO extraction. The xylan dissolution was allowed to proceed at 60ºC for 12h with stirring and temperature control. The suspension was then vacuum filtered and the filtrate was kept at room temperature in the dark. The filtered pulp cake was inserted into the same flask and the procedure was repeated with fresh solvent (DMSO). Thereafter, the pulp was carefully washed with water (40 mL) in three consecutive steps. All the filtrates were collected in the same flask. The xylan dissolved in DMSO was precipitated by addition into a mixture of ethanol (400 mL) and methanol (200 mL) under vigorous stirring. This solution was later acidified with formic acid (10 mL) to reach a pH~3. The xylan suspension was then centrifuged and washed with anhydrous methanol (five times) and finally dried in vacuum at room temperature.

Enzymatic accessibility

Five hundred mg of pulp were added with 50 mL of tampon solution in a flask for 12h with stirring. The suspension was then filtered and the filtrate was put in a reactor with 10 mL of tampon solution. When temperature stabilized (~45ºC) was added 0.5 mL enzymatic solution. At 0 min collected 200 µL of sample to an eppendorf, then sample was centrifuged for 1min. In a tube were added 100 µL of sample and 300 µL of DNS to put in a bath (100ºC) for 5 min. Then was putted a cold bath and added 3 ml distillate water and was analysis for UV (λ: 540 nm). Measurements were made at 5, 10, 15, 25, 35, 60 and 80 min.

Solid-state characterization

To determine brightness and brightness after reversion, pulp sheets were made according to ISO 3688 Standard. Brightness was measured according to ISO 2470 Standard using a Lorentzen and Wettre Spectrophotometer Elrepho SE 070. To study brightness reversion, pulp sheets were submitted to an ageing process at 100ºC and 100% humidity, during 1 h, in a closed vessel (the water is heated until its boiling point producing a vapour phase with 100% humidity), according to Tappi T280. The sheets were then dried in a ventilated chamber during 1 h, pressed and the ISO brightness after reversion was measured. The lost in brightness can be expressed as the post colour number (PC number). The bleached pulp samples were pressed into pellets using 100 mg of pulp. The analysis of chromophores was accomplished employing UV-Ressonance Raman (UV-RR) and UV-visible Diffuse Reflectance (UV-vis DR) spectroscopy. UV-vis DR spectra were recorder at room temperature on JASCO V-560 spectrophotometer equipped with JASCO ISV-469 integrating sphere and using $BaSO_4$ standard as background reference. UV-RR spectra were recorder using a Jobin Yvon (Horiba) LabRam HR 800 micro-Raman spectrometer@325nm and @442 (He-Cd UV laser, Kimmon IK Series) under backscattering configuration using a 40xNUV objective.

Wet-chemistry characterization

The xylans were analysis by 1D/2D H NMR spectroscopy and molecular weight distribution by size exclusion chromatography (SEC). NMR: the xylans were dissolved in D_2O and using sodium 3-(trimethylsilyl)-propionate-d_4 as internal standard. The ^1H NMR spectra were recorded at ambient temperature on a Bruker AMX 300 spectrometer operating at 300.1 MHz. A relaxation delay of 12 s and r.f. angle of 90º was used and 1000 scans were collected. Two dimensional ^1H–^1H TOCSY (Total Correlation Spectroscopy) spectra (τ_{mix}= 0.050 s) were acquired at a spectral width of 2185 Hz in both dimensions at 50◦C. The relaxation delay was 2.0 s. For each FID, 128 transients were acquired; the data size was 1024 in t_1×512 in t_2. The delay between scans was 2 s.

SEC: four mg of xylan were dissolved in 50 µL of 8% LiCl/N, N-dimethylacetamide (DMAc) solution at 105 ºC during 15 min and then further diluted with 600 µL DMAc. The SEC was carried out on two PLgel 10 µm MIXED B 300×7.5 mm columns protected by a PLgel 10 µm pre-column (Polymer Laboratories, UK) using a PLGPC 110 system (Polymer Laboratories). The columns, injector system and the detector (RI) were maintained at 70 °C during the analysis. The eluent (0.1 M LiCl in DMAC) was pumped at a flow rate of 0.9 mL/min. The analytical columns were calibrated with pullulan standards (Polymer Laboratories).

Xylan was characterized by acid methanolysis for analysis of sugars. The samples were dissolved by addition of 70µL pyridine. For silylation, 150µL hexamethyldisiloxane and 80µLtrimethylchlorosilane were added and the samples were shakenwell. GC–MS analysis was performed using a Hewlet-Packard Gas Chromatograph 5890 equipped with a mass selective detector MSD series II, using helium as carrier gas (35 cm/s), equipped with a DB-1 J&W capillary column (30 m×0.32 mm i.d. 0.25µm filmthickness).

III. RESULTS AND DISCUSSION

Final bleaching stage

DED pulp was bleached in a final stage with xylanase X1 (DEDX1), xylanase X2 (DEDX2) and xylanase X3 (DEDX3). The aim of these bleaching assays was to evaluate the brightness development and stability after an enzymatic treatment with different xylanases. In previous studies an enzymatic stage applied to DEDD/DEDP bleached *E. globulus* kraft pulp before or after the final D/P stages allowed a reduction the requirement for oxidizing chemicals while increasing brightness and brightness stability of bleached pulp [3]. These observations suggest that effect of xylanase action and growth of microorganism rendered the pulp fibers more accessible to chemical bleaching agents. With a final xylanase treatment the achieved brightness is similar, but the brightness stability is different, as observed in **Table 1**. Pulp treated by fungi xylanase X3 exhibit slightly higher brightness and PC number, but to achieve the same brightness a lower xylanase dosage is needed.

In previous studies using UV-RR spectroscopy coupled to UV-vis DR spectroscopy, xylan was highlighted as an important source of chromophores in bleached eucalypt pulps [6, 7]. Particular selectivity in the detection and identification of chromophores in pulps is achieved using 325 nm laser beam excitation. This band (325 nm) at the diffuse reflectance (DR) spectra corresponds to the absorption of polyunsaturated chromophore structures [7]. The DR spectra of DEDX bleached pulps are presented in **Figure 1(a)** and showed that DEDX3 pulp has the highest absorption at 220-350 nm assigned to chromogens, which explains it highest brightness reversion (**Table 1**). The UV-RR spectra @325 nm (**Figure 1 (b)**) show a characteristic signal at ca.1600 cm $^{-1}$ assigned to polyunsaturated conjugated chromophore structures [6,7]. It was observed that DED pulp treatment by bacterial xylanase (X2) has reduced the amount of polyconjugated chromophore/chromogen structures detected at ca. 1600 cm^{-1} in the UV-RR spectra much more than by fungi xylanase (X3). In addition, based on intensity and shifts of signals in UV-Vis DR and UV-RR spectra, it may be proposed that not only the amount of chromophores but also their nature in pulps treated with this variety of xylanases is different.

Xylanase treatment (DEDX), independently of xylanase used, led to 1.5-2.0 ISO brightness gain. This finding confirms once more the role of xylan as a source of chromophores [2, 3]. The hydrolytic action of xylanase is supposed to remove chromophores attached to xylan backbone. However, the contribution of xylanases from different donors is not yet clear. Thus, it is important to understand the difference in xylan accessibility towards xylanases of different origin. Such a study was done using enzymatic peeling of DED and DEDX pulps with pure commercial xylanase of GH10 family.

Table 1. Effect of the final X bleaching stage applied to the industrial DED pulp.

Sequence	DEDX1	DEDX2	DEDX3
X charge, % odp	0.15	0.05	0.01
Brightness ISO, %	89.2	89.0	89.4
PC number	0.28	0.22	0.31

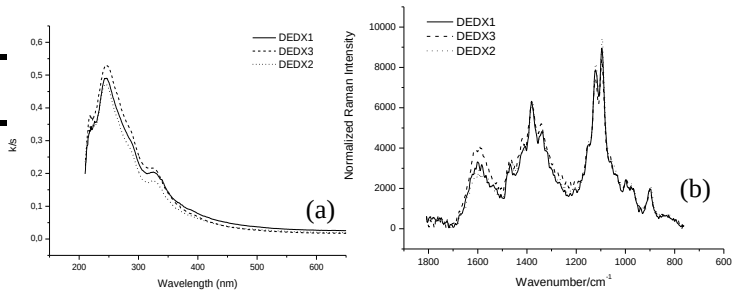

Figure 1.UV-vis DR (a) and UV-RR (b) spectra of the DEDX1, DEDX2 and DEDX3 bleached pulps.

The content of released xylose during enzymatic peeling by xylanase was assessed as reducing sugars. The integral curves were differentiated giving rise the velocity profiles upon the hydrolysis of residual xylan in pulps (**Figure 2**). It was assumed that bulk accessibility is proportional to the hydrolysis time. The comparison of xylan removal profiles from DED and DEDX pulps allowed a conclusion that xylan was removed preferentially from the fiber surface independently of xylanase used. However, it seems fungal xylanase (X3) showed more efficient hydrolysis of xylan on the outer fibre layers and less efficient in bulk than bacterial xylanase X2. This finding may explain the higher brightness of DEDX3 than DEDX2 pulp but not the reversion (**Table 1**).

Wet chemistry and NMR analysis of residual xylans

The quantitative structural features of residual xylans in DED and DEDX pulps were studied by ^{1}H NMR based on assignments of anomeric signals confirmed by ^{1}H-^{1}H correlation spectra (TOCSY) (**Figure 3**). Xylans from pulps subjected to enzymatic hydrolysis possessed not only lower molecular weight (**Table 2**) but also almost double degree of substitution with uronic moieties when compared to xylan from initial DED pulp (**Table 3**). The last fact may be explained by preferential hydrolysis of non-branched regions of xylan backbone by industrial xylans X1-X3, which are essentially of GH11 family according to provider's information. The similar proportion between xylopyranose and 4-O-methyl-α-D-glucuronic acid residues in residual xylans after enzymatic stage, suggested based on ^{1}H NMR data, was confirmed by sugars analysis employing acid methanolysis (**Table 4**). At the same time, the molecular weights of xylans isolated from all DEDX pulps were very similar (**Table 2**), which can indicate comparable efficiency of X1-X3 in the hydrolysis of xylan in pulp.

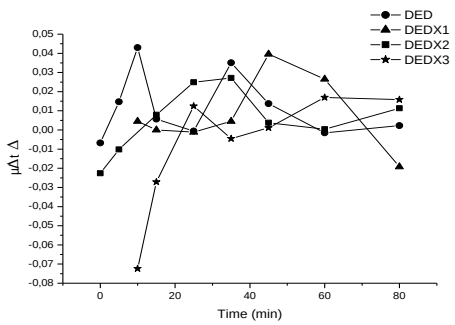

Figure 2. Profiles of xylans (differential curves) removed during enzymatic peeling by xylanase in DED, DEDX1, DEDX2 and DEDX3 bleached pulps.

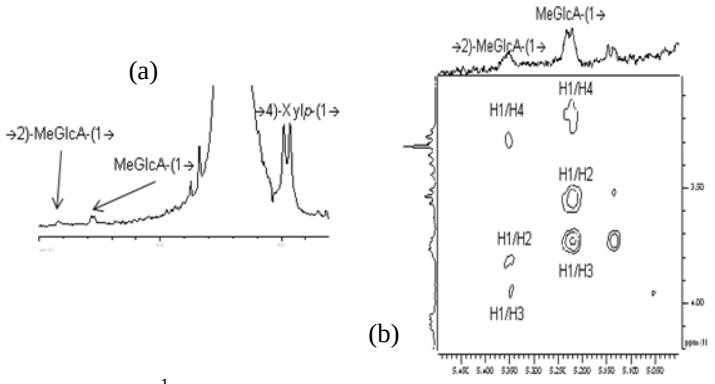

Figure 3. ^{1}H NMR (a) and 2D NMR (b) spectra of the xylan isolated from DEDX3 bleached pulp (D_2O, 30 ºC).

Table 3. Results of linkage analysis of xylan (per 100 Xyl*p* residues).

	→4)-Xyl*p*-(1→	MeGlc*p*A-(1→	→2)-MeGlc*p*A-(1→
DED	100	5	2
X1	100	9	4
X3	100	8	4

Table 4. Carbohydrate composition of isolated xylan as revealed by acid methanolysis (mol%).

	X1	X2	X3
Xyl	94	95	95
4OMeGlc*p*A	5	4	4
Gal*p*	1	1	1

Table 2. Weight average molecular weight (Mw), number molecular weight (Mn), and polydispersity (PD) values of the isolated xylan from SEC analysis.

Xylan	M_w (KDa)	M_n (KDa)	PD
DED	15.5	9.2	1.67
X1	9.5	6.9	1.39
X2	9.8	7.1	1.39
X3	9.7	7.8	1.24

The observed differences in accessibility of xylans in pre-bleached kraft pulp, while applying xylanases of different origin (**Figure 2**), may be due to the presence of concomitant hydrolytic enzymes (both cellulases and hemicellulases) promoting the xylanase penetration inside pulp fibers, rather than due to the differences in xylanase hydrolytic efficiencies.

IV. CONCLUSIONS

A xylanase treatment is a promising tool to improve brightness and brightness reversion of ECF bleached eucalypt kraft pulp. The different performance of commercial xylanases from different donor cultures in X stage not necessarily relates to the xylanase hydrolytic efficiency but rather to the presence of concomitant enzymatic complexes promoting the xylanase penetration inside pulp fibers.

V. ACKNOWLEDGEMENT

Authors are grateful to FCT (Portuguese Foundation for Science and Technology) and UE - FEDER (European Fund for Regional Development) through the Competitiveness Factors Operational Programme (COMPETE) for the financial support of this work within the scope of Project PTDC/EQU-EQU/113547/2009 (COMPETE, ref. FCOMP-01-0124-FEDER-015254). Novozymes A/S is acknowledged for supplying the xylanases.

VI. REFERENCES

[1] Rosenau, T., Potthast, A., Kosma, P., Suess, H.U., Nimmerfroh, N. Isolation and identification of residual chromophores from aged bleached pulp samples. *Holzforschung*. **2007**, 61, 656 – 661.

[2] Loureiro, P.E.G., Domingues, M.R.M., Fernandes, A.J.S., Carvalho, M.G.V.S., Evtuguin, D.V. Discriminating the brightness stability of cellulosic pulp in relation to the final bleaching stage. *Carbohydr. Polym*. **2012**, 88, 726 – 733.

[3] Loureiro, P.E.G., Sousa, J.I.T., Carvalho, M.G.V.S., Evtuguin, D.V. Contribution of xylan to the brightness development and stability in the final ECF bleaching of eucalypt (*Eucalyptus globulus* Labill.) kraft pulp. *Holzforschung*. **2013**, 67(5), 497–503.

[4] Buchert, J., Bergnor, E., Lindblad, G., Viikari, L., Ek, M. Significance of xylan and glucomannan in the brightness reversion of kraft pulps. *Tappi Journal.* **1997**, 80 (6), 165-171

[5] Simeonova, G., Sjodahl, R., Ragnar, M., Lindstrom, M.E., Henriksson, G. On the effect of a xylanase post-treatment as a means of reducing the yellowing of bleached hardwood kraft pulp. *Nord. Pulp Pap. Res. J.* **2007**, 22 (2), 172 -176.

[6] Loureiro, P., Fernandes, A., Carvalho, M. G., Evtuguin, D. The assessment of chromophores in bleached cellulosic pulps employing UV-Raman spectroscopy. *Carbohyd. Res*. **2010**, 345 (10), 1442-1451.

[7] Loureiro, P., Fernandes, A., Carvalho, M.G., Evtuguin, D. UV-resonance Raman micro spectroscopy to assess residual chromophores in cellulosic pulps. *J. Raman Spectr*. **2011**, 42, 1039-1045.

ALGINATE ANALYSIS AND CHARACTERISATION BY TWO DIFFERENT FRACTIONATION TECHNIQUES

Irina Sulaeva,[1] Ute Henniges,[1] Wolfgang Harreither,[2]
Christian Rohrer,[2] Thomas Rosenau,[1] Antje Potthast[1*]

[1] University of Natural Resources and Life Sciences, Department of Chemistry, Christian Doppler Laboratory "Advanced Cellulose Chemistry and Analytics", Konrad-Lorentz-Str. 24, A-3430 Tulln
[2] Lohmann & Rauscher GmbH, Kirchengasse 17, A-2525 Schönau an der Triesting
*(*antje.potthast@boku.ac.at)*

ABSTRACT
Solutions of seven different alginate samples were analyzed with two different fractionation techniques – gel-permeation chromatography (GPC) and asymmetric flow field-flow fractionation (AsFlFFF), both coupled to multi-angle laser light scattering (MALLS). GPC analysis was performed in 0.153M NaCl, 0.1M $NaNO_3$ and 0.01M Na-EDTA. The study disproved a significant influence of the mobile phase on the elution pattern of the alginate. Various AsFlFFF system parameters were tested and optimized, among them cross flow, detector flow and focus flow rates, and injected sample mass. The data obtained from both studies were compared and showed good overall agreement. However, AsFlFFF performed better with respect to separation over a wide range of molar mass due to increased accuracy, particularly in regions which are unfavorable for GPS analysis.

I. INTRODUCTION

Alginate is a naturally occurring polymer isolated from cell walls of algae. It can be applied to solve a number of problems that occur in biomedical science and engineering due to its favorable properties, such as biocompatibility, non-toxicity and ease of gelation. Alginate hydrogels are widely used in wound healing, drug delivery and tissue engineering. The properties of alginates are governed mainly by its primary structure, i.e. the ratio between its β-D-mannuronic and α-L-guluronic acid units (M/G ratio), their along-chain pattern, the molecular weight distribution and polydispersity [1]. Hence, there is a substantial need in fast and simple, yet effective, methods for routine alginate characterization.
Various fractionation techniques, such as gel permeation chromatography (GPC) or flow field-flow fractionation (FlFFF) followed by detailed sample analysis with different detectors (differential refractive index, dynamic or static laser light scattering) provide comprehensive information about molecular weight distribution, polydispersity index, and hydrodynamic radius of the molecules.
For alginate characterization, GPC methods in combination with multi-angle laser light scattering, UV or viscosity detection are widely used. The effect of critical parameters, such as ionic strength of mobile phases, sample concentration, temperature as well as chemical composition of the alginates are discussed in detail in pertinent literature [2, 3, 4, 5].
As an alternative to gel permeation chromatography, the FlFFF technique was initially introduced already in 1966. Being a powerful tool for sample separation over a wide size range (10^{-3}-10^{2} µm), the method however requires comprehensive optimisation of experimental conditions for each individual analyte. Thus far, reports concerning alginate characterization by FlFFF are rather scarce. Investigations have been performed on system parameters optimizations, such as cross flow rate, carrier liquid concentration and injected sample mass of sodium alginate solutions [6, 7]. Besides, calcium alginate nanogel particles [8] and metal-alginate complexes [9] were characterized by asymmetrical FlFFF coupled with MALLS detection. There are no studies so far that compare different separation techniques for alginate analysis.
The present study provides optimized system parameters for alginate analysis by AsFlFFF, along with a comparison of the results to those from GPC measurements and a discussion of the pros and cons of the used analytical methods.

II. EXPERIMENTAL

Materials
Mobile phase solutions were prepared by dissolving of respective amount of salt in 2L volumetric flask with deionized water. Stock solution was filtered through a 0.2 µm vacuum filter (VacuCup Supor membrane). Following solutions were used for alginate analysis: 0.153M NaCl, 0.01M Na-EDTA, and 0.1M $NaNO_3$.
All alginates were present in the form of sodium salts. Typically, a 2 mg/mL solution of alginate was prepared by direct dissolution in the freshly prepared mobile phase. The samples were stirred for 2 hours to achieve complete dissolution and filtered through 0.45 µm syringe filter (PTFE Membrane).

Gel Permeation Chromatography (GPC)

GPC was performed using a Agilent Technologies 1260 Infinity pump equipped with online Dionex DG-1210 degasser and Agilent G1367C autosampler. The samples were chromatographed on two GPC columns (Agilent PL Aquagel-OH Mixed-H, pore size, 8µm) and monitored by a MALLS detector (Wyatt Technology DAWN HELEOS with 120mW solid-state laser operating at 658 nm) equipped with online QELS detector (Wyatt Technology WyattQELS at 100^{o} measuring angle) and a RI detector (Shodex RI-101). Measurements were performed at room temperature. The following system parameters were used: 0.8 mL/min flow rate; 100 μL injection volume; 30 min run time. Data collection and molecular weight calculations were performed by ASTRA software Version 6.0.1 (Wyatt Technology). The refractive index increment (d*n*/d*c*) used for calculations was 0.145.

Asymmetric Flow Field-Flow Fractionation (AsFlFFF)

Sample fractionation was performed by an Eclipse AF4 (Wyatt Technology) separation system consisting of a flow control system and separation channel. The system was complemented by an Agilent 1260 pump with Dionex DG-1210 degasser, Agilent Technologies G1367C autosampler, Wyatt Technology DAWN HELEOS as given above and an RI detector (Wyatt Technologies Optilab T-rEX).

The long channel with 275 mm length was assembled with a 350µm spacer (350W spacer type) and a regenerated cellulose membrane with a cut-off of 10 kDa (Millipore). Sample injection into the channel was performed at the flow rate of 0.2 mL/min for 3 min, injection volume 200 μL.

The optimized program for alginate analysis required 45 min to complete. **Figure 1** represents the flow diagram. Detector flow V_d = 1 mL/min and focus flow V_f = 2 mL/min were constant for all the measurements. Within the first 2 min the system was stabilized under the constant cross flow V_x = 1 mL/min, and then focus flow was set. The sample injection started after 1 min of focusing and was followed by the sample relaxation phase. Thereon the sample was eluted from the channel within 15 min, the cross flow was decreased linearly during this time from 1 to 0.1 mL/min. Then the system was flashed with low cross flow V_x = 0.1 mL/min to make sure that all sample was eluted from the channel. This step was followed by channel elution under zero cross flow with the aim to remove traces of the sample. As the last step the cross flow was adjusted to the initial value to stabilize the system for a new run. Data were collected and analyzed by ASTRA 6.1.0 (Wyatt Technology) software.

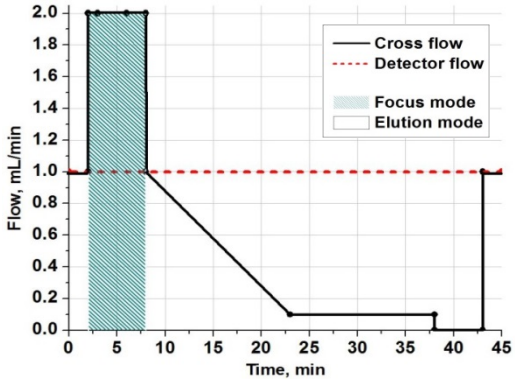

Figure 1. Flow rates changes during the AsFlFFF separation process.

III. RESULTS AND DISCUSSION

GPC results

Mobile phase selection is a major topic for the method development in GPC, especially when charged polysaccharides are analyzed due to the interaction processes occurring during chromatography between solvent or sample and column packing material, even though these are not desired. This interaction is often reduced by increasing the ionic strength of the stock solution. In order to achieve better separation and peak resolution three different eluents were tested: 0.153M NaCl, 0.1 M $NaNO_3$ and 0.01M Na-EDTA with ionic strengths of 0.153, 0.1 and 0.085 respectively. The M_n and M_w values obtained for all solutions are in a good agreement; no significant differences in the elution profiles and sample characteristics were observed. $NaNO_3$ was selected as mobile phase for further experiments.

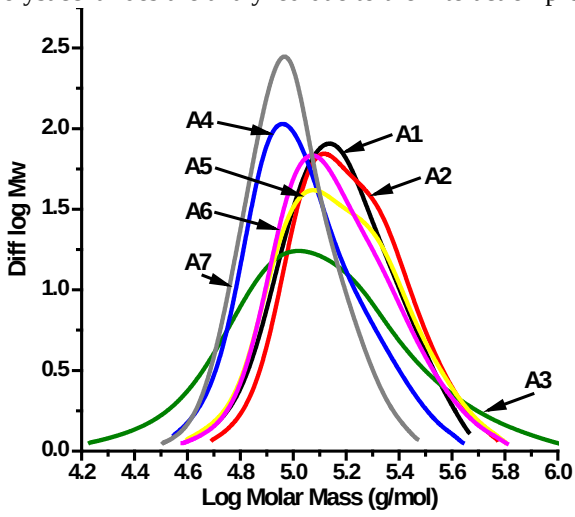

Figure 2. Differential molar mass distribution of the samples, alginate samples A1 – A7, eluent: 0.1M $NaNO_3$.

Calculated molecular weight distributions for all the samples are shown at **Figure 2**. All the samples are polydisperse with average molecular weights in the range of 100-185 kDa. Detailed information is given in **Table 1**.

AsFlFFF results

In the normal operation mode based on *Brownian* motion of the analyte, the elution speed of the particles from the channel is determined by their diffusion coefficient, which is in direct correlation with particle size. Sample fractions with higher diffusion coefficient diffuse back into the bulk to a larger extent and experience a higher velocity vector in the parabolic flow profile of the narrow channel which consequently leads to faster elution from the channel compared to a fraction with a lower diffusion coefficient. Analyte nature may also cause interaction with the membrane leading to peak broadening. Sample motion along the channel can be controlled by method settings. Thus, higher cross flow moves the samples closer to the membrane, where the flow has a lower speed.

Thereby, the first step toward system optimization was to study the influence of cross flow on alginate retention time. Experiments were performed with 2, 1.5, 1, 0.5 and 0.1 mL/min constant cross flows. Elution mode with established constant cross flow lasted 40 min and was followed by elution under zero cross flow to wash out sample residues. Surprisingly no sample was eluted under V_x = 2, V_x = 1.5 and V_x = 1 mL/min, however, the peak was observed during the channel washing step. In the case of 0.5 mL/min cross flow, the sample was eluting constantly in a small portion leading to noisy baselines, yet no reasonable peak was obtained. A broad peak was observed when the cross flow was 0.1 mL/min, however, data interpretation was not possible due to the peak overlapping with the channel void peak, its asymmetrical shape and poor resolution.

To improve peak shape and resolution, gradient cross flow was adjusted. The high cross flow (V_x) at the beginning prevents the peak from being eluted together with the void peak, meanwhile decreased cross flow provides reasonable elution time and optimized peak shape. Different speeds of cross flow were tested, decreasing from 1.5 mL/min to 0 within 8 min (1.875mL/min flow decreasing rate), 15 min (1.5 mL/min flow decreasing rate) and 20 min (0.75 mL/min flow decreasing rate). The elugrams are shown in **Figure 3**.

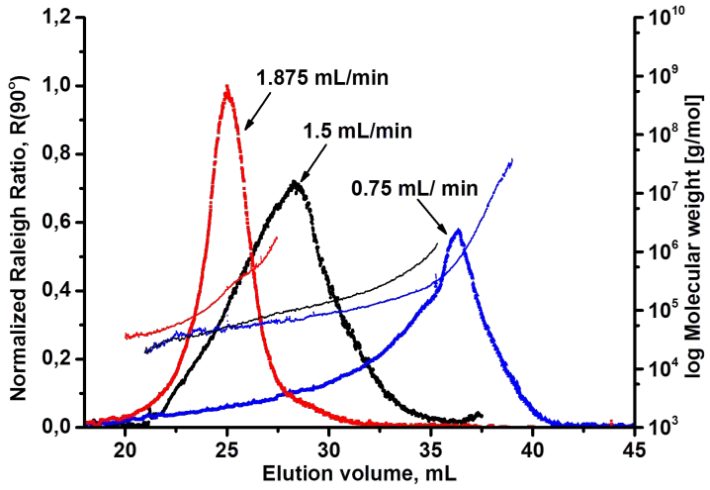

As an optimal parameter, a cross flow decrease rate of 1.5 mL/min was implemented for further analysis. Other parameters tested are sample injection volume, detector and focus flows (data are not presented here).

Figure 3. Light scattering at 90° and calculated molar mass for the FlFFF runs with different cross flow decreasing speed (sample A7).

Comparison of FlFFF and GPC data for characterization of alginates

The data obtained for all alginate samples after FlFFF analysis together with GPC data are presented in **Table 1**.

Table 1. GPC and FlFFF results.

Sample Name	GPC Data			FlFFF Data		
	M_w, kDa	M_w/M_n	rms radius, nm	M_w, kDa	M_w/M_n	rms radius, nm
A1	164.8 (±0.2%)	1.266 (±0.3%)	57.3 (±3.4%)	189.8 (±0.7%)	2.619 (±1.4%)	46.1 (±26.1%)
A2	182.4 (±0.2%)	1.226 (±0.2%)	62.2 (±2.7%)	284.4 (±9.3%)	3.108 (±12.6%)	54.7 (±16.6%)
A3	161.5 (±0.4%)	1.374 (±0.7%)	70.5 (±3.3%)	227.7 (±8.5%)	4.087 (±11.9%)	43.1 (±22.6%)
A4	123.9 (±0.2%)	1.252 (±0.2%)	55.2 (±3.8%)	355.0 (±8.6%)	6.301 (±12.3%)	52.0 (±19.9%)
A5	176.8 (±0.1%)	1.303 (±0.2%)	103.2 (±2.4%)	249.0 (±6.5%)	2.957 (±11.9%)	43.1 (±26.6%)
A6	167.3 (±0.2%)	1.269 (±0.2%)	57.5 (±4.2%)	284.0 (±6.2%)	3.564 (±9.9%)	40.5 (±21.3%)
A7	103.9 (±0.3%)	1.164 (±0.2%)	40.6 (±9.3%)	165.9 (±7.8%)	2.272 (±11.1%)	37.1 (±32.5%)

As evident from Table 1, the molecular weight data obtained by FlFFF, as well as the polydispersity indices are higher than those for GPC analysis. A closer look at the molar mass distribution of the same sample (A5) obtained after different fractionation procedures shows that FlFFF provides more precise information about molecular distribution, specifically in the range of very low and very high molar masses (**Figure 4**). In both cases 80% of the mass of the polymer was in the range between 20 to 220 kDa. However, GPC separation did

not show any fractions in the range below 70 kDa. Meanwhile FlFFF shows two groups of molecular weights between 20 – 40 kDa (Figure 4, region I) and 40 – 70 kDa (Figure 4, region II). A similar effect was observed in the region of high molar masses. GPC did not reportthe presence of molecules larger than 900 kDa, but FlFFF was able to distinguishes regions up to 1000 kDa (Figure 4, region V) and separates them from the small fractions in one run. Apparently, the contribution of these rather large molecules within the total size distribution was the reason of overall increased Mw values. A more precise detection of the particles outside average values subsequently leads to higher PDI numbers.

However, the FlFFF method requires tedious system testing to find a combination of optimal parameters for every new sample to be analyzed. In this respect, GPC is a good alternative for routine sample analysis providing fast, reproducible and accurate results. When more detailed information about molar mass variations in the sample is required, or when some limitations of using a GPC system have to be overcome, the column-free AsFlFFF technique is a powerful tool for both polymer separation and molar mass characterization, especially concerning samples of high molar mass.

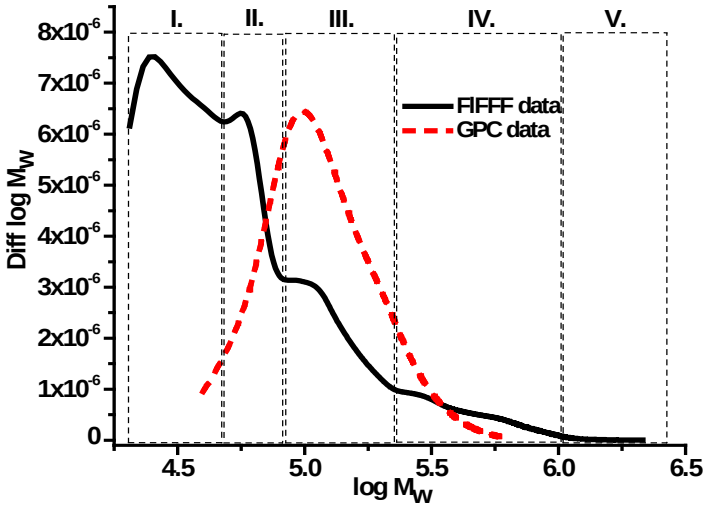

Figure 4. Differential molecular weight distribution of the sample A5 according to GPC and FlFFF separation.

IV. CONCLUSIONS

In this study seven alginate samples have been analyzed by GPC and FlFFF separation techniques. The data obtained from both methods are in good correlation. FlFFF separation power allows more precise information for a wider range of molar masses. However, to achieve the desired fractionation, constant and gradient cross flows with different rates have to be examined and optimized. GPC is a useful standard technique to obtain basic information on molar mass characteristics of alginates.

V. ACKNOWLEDGEMENT

Financial support of the Austrian Christian Doppler Research Society through the Christian Doppler Laboratory "Advanced cellulose chemistry and analytics" and Lohmann & Rauscher GmbH are gratefully acknowledged.

VI. REFERENCES

[1] Gacesa, P. Alginates. *Carbohyd. Polym.* **1988**, *8*, 161−182.
[2] Fujuhara, M.; Nagumo T. Determination of the molecular weights of alginates by agarose gel filtration. *J. Chromatogr.* **1989**, *465*, 386 −389.
[3] Díaz Baños, F.G; Díaz Peña, A.I.; Hernánez Cifre, J.G.; López Martínez, M.C.; Ortega, A.; de la Torre, J.G. Influence of ionic strength on the flexibility of alginate studied by size exclusion chromatography. *Carbohyd. Polym.* **2014**, *102*, 223–230.
[4] Gómez-Ordóñez, E.; Jiménez-Escrig, A.; Rupérez, P. Molecular weight distribution of polysaccharides from edible seaweeds by high-performance size-exclusion chromatography (HPSEC). *Talanta.* **2012**, *93*, 153– 159.
[5] Mackie, W.; Noy, R.; Sellen, D.B. Solution properties of sodium alginate. *Biopolymers.* **1980**, *19 (10)*, 1839–1860.
[6] Alasonati, E.; Benincasa, M.-A.; Slaveykova, V.I. Asymmetrical flow field-flow fractionation coupled to multiangle laser light scattering detector: Optimization of crossflow rate, carrier characteristics, and injected mass in alginate separation. *J. Sep. Sci.* **2007**, *30*, 2332 – 2340.
[7] Van de Ven, W.; Pünt, I.; Kemperman A.; Wessling, M. Unraveling ultrafiltration of polysaccharides with flow field flow fractionation. *J. Memb. Sci.* **2009**, *338*, 67–74.
[8] Hong, J.S.; Vreeland, N.W.; DePaoli Lacerda, S.H.; Locascio L.E.; Gaitan, M.; Raghavan S.R. Liposome-Templated Supramolecular Assembly of Responsive Alginate Nanogels. *Langmuir.* **2008**, *24*, 4092-4096.
[9] Alasonati, E.; Stolpe, B.; Benincasa,M.-A.; Hassellöv, M.; Slaveykova, V.I. Asymmetrical Flow Field Flow Fractionation–Multidetection System as a Tool for Studying Metal–Alginate Interactions. *Environ. Chem.* **2006**, *3*, 192–198.

ISOLATION AND CHARACTERISATION OF LIGNOSULFONATES FROM SPENT SULFITE LIQUORS

Ivan Sumerskii*, Philipp Korntner, Thomas Rosenau, Antje Potthast*

Division of Chemistry of Renewable Resources, Department of Chemistry, University of Natural Resources and Life Sciences, Konrad-Lorenz-Str. 24, A-3430 Tulln, Austria.
*(*ivan.sumerskii@boku.ac.at, *antje.potthast@boku.ac.at)*

ABSTRACT

New methods for lignin isolation and purification from spent liquors, which could rapidly provide lignin with high purity and yield, are currently of great interest for both analytical purposes and industrial recovery to obtain lignins for added value products.
A novel approach for isolation of lignosulfonate from spent sulfite liquor was established, the sorption on macroreticular non-ionic poly(methyl methacrylate) particles (XAD-7 resin) and subsequent desorption with organic solvents to obtain lignosulfonates with high purity. The method proved to be reasonably fast, robust and efficient for lignosulfonate isolation and subsequent purification.
The isolated lignosulfonate was characterised by spectroscopic, chromatographic and thermogravimetric methods. Its basic characteristics were compared with that of lignosulfonate purified by an alternative ultrafiltration method.

I. INTRODUCTION

Lignosulfonates (LS) are the major - but by far not the only - component of spent sulfite liquor which is generated in the sulfite pulping processes. The presence of other components and the difficulties with their neat separation cause certain limitations in the application of the entire sulfite liquor as well as problems in chemical analysis of LS in general. Thus, rapid isolation and purification approaches for LS are highly needed.
Currently, several methods for the isolation of LS are available. Among them, the isolation by formation of lignosulfonate-amine complexes [1, 2], dialysis [3] and ultrafiltration [2] are the most common approaches. These techniques have certain drawbacks as they require additional purification steps to reach the necessary purity, which is important for further analytical characterization.
Recently it was proposed to apply polymeric resins of different matrices, for example polyacrylic [4] or polyaromatic [5-7], for adsorption of phenolic compounds in wastewater treatment, removal of inhibitors from fermentation media, isolation of high added value products, like ferulic acid etc. [4-8]. Such resins possess high capacity, they are able to resist elevated temperatures (max. 150^{o}C), and they are stable at the whole pH range. The resins can adsorb polymers with molar masses (MM) up to 60000 g mol^{-1}and can easily be regenerated and applied repeatedly.
The aim of the present study was to evaluate LS adsorption and desorption on XAD-7 polymer resin at different pH and adsorbent/adsorbate ratio and, thus, elaborate optimal conditions at which the highest LS adsorption capacity could be reached.

II. EXPERIMENTAL

Materials and Chemicals
Industrial spent liquor from magnesium-based acidic sulfite pulping was supplied by Sappi Papier Holding GmbH (Gratkorn, Austria). Macroporous polyacrylate resin Amberlite XAD-7 (20–60 mesh), strongly acidic cation-exchange resin Dowex 50WX8 (50-100 mesh), ethanol, diethyl ether, chloroform, sodium hydroxide, sodium tetraborate anhydrous were obtained from Sigma-Aldrich Co. Other chemicals were of p.a. grade.

Preparation of XAD7 and Dowex50WX8 resins
The XAD-7 resin was washed and Soxhlet-extracted to remove micro particles and low molar mass contaminants according to [9]. XAD-7 resin was stored in ethanol. Prior to adsorption experiments ethanol was removed from XAD-7 resin by exhaustive washing with deionized water. The resin was filtrated on a glass filter #3 at constant reduced pressure (900 mbar). For further adsorption experiments the resin was used in the wet state, because the complete removal of moisture negatively influences its adsorption capacity [5]. The moisture content was estimated by oven drying at 100 °C until constant weight was reached. Two parallel experiments yielded 70% moisture content, which was used for further calculations of the lignosulfonate adsorption.

The Dowex 50WX8 resin was exhaustively washed with distilled water. The resin was regenerated by stirring with diluted HCl solution according to following protocol: 0.5 M HCl (10 min, 3 times), then 1 M HCl (10 min, 3 times), and finally 2 M HCl (10 min, 3 times). The regenerated resin was filtered on a glass filter and stored in a closed flask. Directly before use the resin was washed with distilled water to neutral pH.

Equipment

The ultrafiltration of LS was carried out on Millipore stirred ultrafiltration cell model 8200 equipped with a membrane NMWL: 1000 [2], diameter 63.5 mm, at 100 rpm stirring and 3 bar pressure. Approximately 1.5 g of LS was used in each ultrafiltration process. The volume of LS solution in the cell was kept over 50 ml. The total volume of the permeate collected was 600 ml. The retentate, which contained purified LS, was quantitatively transferred to a plastic bottle and freeze-dried. Three parallel experiments were performed.

UV absorption spectra of dissolved LS were determined with a PerkinElmer Lambda 35 UV/VIS spectrometer using quartz cells.

GC-MS analysis was performed on an Agilent 6890N GC and a Agilent 5975B inert XL MSD quadrupole mass selective detector (EI, 70 eV) using a Agilent HP-5MS capillary column (30 m x 0.25 mm i.d.; 0.25 µm film thickness) and helium as carrier gas with a pressure 13.68 psi, flow rate of 1.1 ml min^{-1} and a split flow rate of 7.5 ml min^{-1}, split ration 7:1. The column oven temperature profile was as follows: initial temperature 140°C (1 min), raise up to 210°C with a heating rate 4°C, raise up to final temperature 300°C with a heating rate 30°C min^{-1}. The injector temperature was 260°C; the temperature of the GC-MS transfer line 290°C, and that of the ion source 230°C.

Thermogravimetric (TG) analysis in air atmosphere was carried out on NETZSCH TG 209 F1 Iris instrument. TG analysis was performed at temperature range of 25-1000°C; the heating rate was 10 °C min^{-1}, the purge gas velocity was 30 ml min^{-1} and the sample weight was 8-10 mg.

Extinction coefficient determination

A buffer solution with pH 12, containing 4.02 g of anhydrous borax $Na_2B_4O_7$ and 2.4 g of NaOH in 1 L of distilled water was used for LS dissolution. A LS stock solution with concentration 0.25 mg ml^{-1} was prepared. Probes of stock solution in the range from 0.5 to 5 ml were quantitatively transferred to 25 ml volumetric flasks. The volume in the flasks was adjusted with the prepared buffer solution. The absorbance of solutions was measured at 280 nm against buffer solution. The extinction coefficient was calculated from the linear equation of dependence of LS concentration and UV absorbance [10].

Lignosulfonate adsorption

The industrial LS sample (4 g) with concentration of solids 47.5% was weighed to a beaker. The sample was diluted approximately five times with deionized water and acidified with 10% sulfuric acid to pH 2. As an alternative, acidification by treatment with cation-exchange Dowex 50WX8 resin (10 g) which gave pH 1.3, was used.

The sample was quantitatively transferred to a 50 ml volumetric flask and the volume was adjusted with deionized water. For the experiments on XAD-7 resin capacity, a LS stock solution was prepared in the same way. The LS solution (50 ml) was quantitatively transferred to a 100 ml glass bottle with a screw cap containing certain amount of wet XAD-7 resin. The closed bottle was gently shaken in a water bath. The pH of LS solution remained unchanged after resin addition and upon the adsorption process. Aliquots (85 µl) of the liquid phase were taken every 15 min during the first two hours, every 30 min during the next 9 hours and then after 12 hours. Each aliquot was transferred to a 25 ml volumetric flask and dissolved in borax buffer solution with pH 12. The content of LS remaining in the solution was investigated by measuring the UV absorbance at 280 nm. The extinction coefficient determined for LS isolated by the XAD-7 adsorption method was applied in calculations.

The amount of LS adsorbed on XAD-7 resin was analysed gravimetrically. XAD-7 resin with adsorbed LS was filtrated off on a glass filter #3 under reduced pressure (800 mbar). Then the resin was washed first 4 times (10 ml per 10 g of wet XAD-7 resin) with acidified water (pH level of corresponding experiment) and then 4 times with deionised water (10 ml per 10 g of wet XAD-7 resin). Each time the resin was transferred to a bottle, gently shaken during 15 min and then filtered off.

The LS was desorbed from the resin with ethanol. The resin was transferred to a bottle, gently shaken in ethanol (15 ml per 10 g of wet XAD-7 resin) for 30-40 min at 50 °C and filtered on the same glass filter under reduced pressure (250 mbar). Overall, the resin was washed 4-5 times with ethanol and 1-2 times with deionised water. The ethanol in the filtrate was partially removed at 40 °C. The remaining water solution of LS was quantitatively transferred to a plastic bottle and freeze-dried.

III. RESULTS AND DISCUSSION

Extinction coefficient

The specific extinction coefficient of LS, purified by the XAD-7 adsorption method at optimal conditions, which will be discussed later, was determined to be 8.79 $g^{-1} \cdot cm^{-1}$. This coefficient was used for indirect semi-quantitative determination of LS remaining in the solution upon the adsorption process.

Lignosulfonate adsorption

Experiments of LS adsorption on the XAD-7 resin revealed that the temperature of the process and the speed of mixing of LS with resin did not have a strong effect. Moreover, vigorous mixing caused mechanical destruction of resin beads. pH level, resin capacity and time of contact were found to be the most critical factors.

It is well investigated that the pH level influences the surface charge of the adsorbent and the degree of ionization of the adsorbate [4-8]. The highest adsorption of aromatic hydrophobic compounds was achieved at pH below 4. **Figure 1** clearly demonstrates that adsorption at the genuine pH 10.7 of LS is very weak. The adsorption pattern at pH 4 and 2 was rather similar and led to maximum LS adsorption after approximately 8-10 hours. pH 2 was found to be optimal and was applied for further experiments. The XAD-7 resin capacity at the selected pH 2 and constant LS concentration and temperature, showed a non-linear dependence of absorbable LS and resin amount (**Figure 2**). The optimal adsorbate/adsorbent ratio in a one-stage adsorption process was approximately 1 g of LS per 6 g of XAD-7 resin based on dry weight. The equilibrium was reached after 8-10 hours. Further contact of LS and resin did not significantly increase the amount of adsorbed LS. The data obtained correlate with those given in the literature [5-8]. However, it is necessary to mention that the data in **Figures 1 and 2** give only semi-quantitative values due to the presence of extractives and polysaccharide degradation products typical for industrial lignosulfonates, which cause overestimation of UV absorption and, as a consequence, the LS content [4].

Adsorbed LS was quantitatively desorbed with ethanol and analyzed gravimetrically [4]. The highest yield of lignosulfonate, which is present in acidic form, at optimal conditions was approximately 35.3% based on dry matter of the original material.

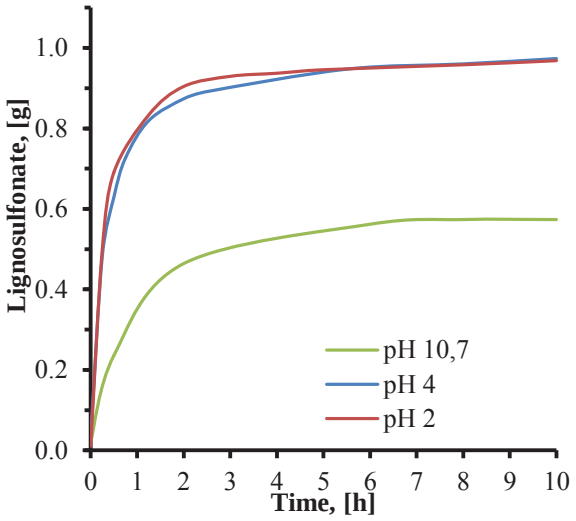

Figure 1. Effect of pH on the adsorption of lignosulfonate on XAD-7 resin (6 g base on dry weight) at 25°C.

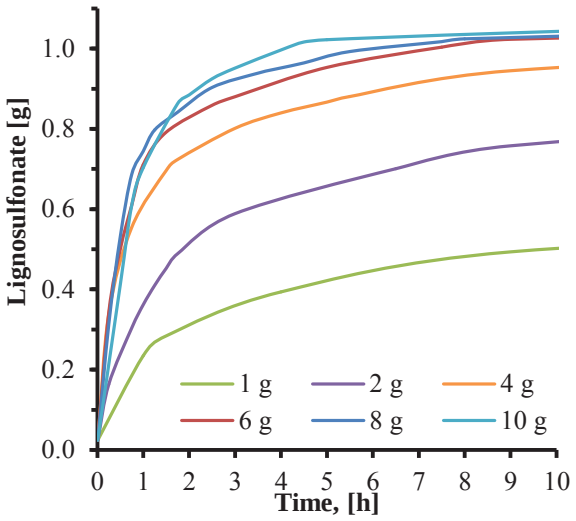

Figure 2. Adsorption of lignosulfonate by different amounts of XAD-7 resin at pH 2 and 25°C.

Ultrafiltration of LS, as an alternative to XAD-7 adsorption, required more experimental time (12-14 h) and yielded approximately 45.8% of purified LS based on dry matter. [2]. However, the treatment of the obtained purified LS with a cation-exchange resin led to substitution of the present magnesium ions for hydrogen ions and hence decreased the yield to approximately 36.9%, which is again comparable to the results obtained via XAD-7 adsorption.

Characterization of purified lignosulfonate

Purified LS contained less than 0.5% of residual, mainly non-cellulosic polysaccharides, composed predominantly of galactose, glucose and mannose, as determined according to [11]. Approximately 1.5% of low molar mass compounds, which comprise various fatty and resin acids (predominantly stearic and dehydroabietic acids).

Thermogravimetric analysis (**Figure 3**) gave similar degradation pattern for LS purified by both methods. Typical for lignin preparations, thermo-oxidative degradation rate maxima were found at approximately 190, 340 and 420 °C [12]. No charcoal residue, which is inevitable for unpurified LS, was found.

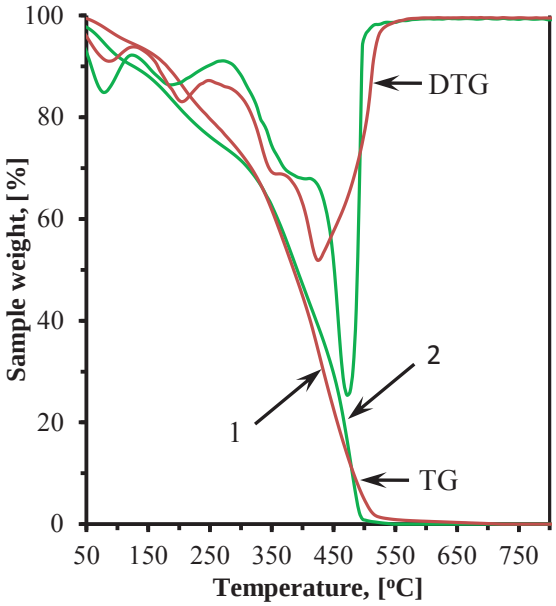

Figure 3. Thermogravimetry (TG) and differential thermogravimetry (DTG) curves of lignosulfonate purified by XAD-7 adsorption (1) and ultrafiltration (2) techniques.

IV. CONCLUSIONS

It was demonstrated that industrial lignosulfonate can be nicely purified by adsorption to XAD-7 resin with subsequent desorption by ethanol.

The highest adsorption of lignosulfonate was achieved at pH levels below 4 and after 8-10 hours of contact time and an adsorbate/adsorbent ratio of 1:6.

At optimal conditions the yield of purified lignosulfonate was approximately 35% based on dry matter of the original material. Lignosulfonate isolated by the XAD-7 adsorption method had a very low content of residual mainly non-cellulosic polysaccharides (<0.5%) and extractives (<1.5%), and contained no inorganic thermostable components. The thermo-oxidative degradation pattern of the purified lignosulfonate was comparable to that of authentic lignin preparations.

V. ACKNOWLEDGEMENT

We appreciate the possibility to use the TGA equipment at the Institute of Wood Science at BOKU, Vienna. The authors acknowledge the company partners of the FLIPPR° project for their generous financial support.

VI. REFERENCES

[1] Lin, S.Y.; Dence, C.W. Commercial Spent Pulping Liquors. Methods in Lignin Chemistry. *New York: Springer Verlag, Berlin Heidelberg*. **1992**, 75-80.

[2] Ringena, O.; Saake, B.; Lehnen, R. Isolation and fractionation of lignosulfonates by amine extraction and ultrafiltration: A comparative study. *Holzforschung*. **2005**, 59, 405-412.

[3] Marques, A.P.; Evtuguin, D.V.; Magina, S.; Amado, F.M.L.; Prates, A. Structure of lignosulfonates from acidic magnesium-based sulfite pulping of Eucalyptus globulus. *J. Wood Chem. Tech*. **2009**, 29(4), 337-357.

[4] Pranovich, A.; Reunanen, M.; Sjöholm R.; Holmbom, B. Dissolved lignin and other aromatic substances in termomechanical pulp waters. *J. Wood Chem. Technol*. **2005**, 25, 109-132.

[5] Davila-Guzman, N.E.; Cerina-Cordova, F.J.; Diaz-Flores, P.E.; Rangel-Mendez, J.R.; Sanchez-Gonzalez, M.N.; Soto-Realado, E. Equilibrium and kinetic studies of ferulic acid adsorption by Amberlite XAD-16. *Chem. Engineering J*. **2012**, 183, 112-116.

[6] Schwartz, T.J.; Lawoko, M. Removal of acid-soluble lignin from biomass extracts using amberlite XAD-4 resin. *BioResources*. 2010, 5(4), 2337-2347.

[7] Li, C.; Xu, M.; Sun, X.; Han, S.; Wu, X.; Liu, Y.N.; Huang, J.; Deng, S. Chemical modification of Amberlite XAD-4 by carbonyl groups for phenol adsorption from wastewater. *Chem. Engineering J*. **2013**, 229, 20-26.

[8] Soto, M.L.; Moure, A.; Dominguez, H.; Parajo, J.C. Recovery, concentration and purification of phenolic compounds by adsorption: A review. *J. Food Engineering*. **2011**, 150, 1-27.

[9] Sjöström, J. Detrimental Substances in Pulp and Paper Productin. Åbo Akademi University, Finland, **1990**.

[10] Lin, S.Y.; Dence, C.W., Ultraviolet Spectroscopy. Methods in Lignin Chemistry. *New York: Springer Verlag, Berlin Heidelberg*. **1992**, 42-48.

[11] Sundberg, A.; Sundberg, K.; Lillandt, C.; Holmbom, B. Determination of hemicelluloses and pectins in wood and pulp fibres by acid methanolysis and gas chromatography. *Nord. Pulp Pap. Res. J*. **1996**, 11, 216–219.

[12] Faix, O.; Jakab, E.; Till, F.; Szekely, T. Study on low mass thermal degradation products of milled wood lignins by thermogravimetry-mass-spectrometry. *Wood Sci. Technol*. **1988**, 22, 323-334.

ELECTROSPINNING AND CHARACTERIZATION OF CELLULOSE/POLYMER NANOCOMPOSITE FIBER MATS

Anna Sutka[1,2]*, Silvija Kukle[1], Janis Gravitis[2],

[1] *Institute of Textile Technology and Design, Riga Technical University, Riga, LV-1048, Latvia*
[2] *Laboratory of Biomass Eco-Efficient Conversion, Latvian State Institute of Wood Chemistry, Dzerbenes Street 27, Riga LV-1006, Latvia*
**anna.sutka@rtu.lv*

ABSTRACT

In this study, cellulose nanowishkers (CNW) and poly (vinyl alcohol) (PVA) composite fibers were prepared via needle-free high voltage, free liquid surface electrospinning with cylindrical electrode. CNW were obtained from hemp shives as a result of various treatments including steam explosion pretreatment, ball milling and ultrasonication technologies. The electrospinning of PVA /CNW composite solution has been successfully used to produce nano- and micro fibers. The goals of this paper are to determine the morphology of electrospun mats and study the mechanical and optical properties of nanofibre composites.

I. INTRODUCTION

Electrospinning is one of the fast growing nanofibre producing technologies and at the present only a single method for industrial scale nanofibres production. Although a wide range of application possibilities have already been proven, nevertheless scientists are trying to find more and more opportunities to produce nanofibres from biodegradable and non-toxic materials with eco-friendly technologies. Cellulose is the most widely used biomass material in nature. Major studies have shown that cellulose nanosized particles could be used as fillers to improve mechanical properties of biocomposites [1-4]. Recently, the production of submicron-scale cellulose fibers via direct dissolution has been proposed, but this issue remains demanding due to the difficulty of cellulose dissolution into common solvents [5].

II. EXPERIMENTAL

Hemp shives used in experiments represent the woody parts of stems of plant - Cannabis sativa that is free from plant fibers. Hemp variety Bialobrzeskie grown on the experimental fields of the Latgalian Agriculture Research Center LLZC (Latvia, district Vilani). Cellulose nanowhiskers were prepared from hemp shives using steam explosion (SE) pretreatment, ball milling and ultrasonication as described in our previous research [6].

The PVA powder of molecular weight 145 000 g/mol and hydrolysis grade ~99.0 – 99.8 mol% purchased from Sigma Aldrich Europe GmbH, Germany.

X-ray XRD patterns were determined on a Bruker D8 Discover diffractometer using copper radiation (CuKα) at a wavelength of 1.54180 Å. The tube voltage and amperage were set to 40 kV and 40 mA. The divergence slit was set at 0.6 mm, and the anti-scattering slit was set at 8.0 mm. The diffraction pattern was recorded using a scanspeed 0.5s/0.02° from 5–45° in 2θ scale and LynxEye position sensitive detector.

The crystallinity index (CI), which is a measurement of the amount of crystalline cellulose with respect to the global amount of amorphous materials, was evaluated using Segal empirical method. The Segal method is used for empirical measurements to allow rapid comparison of cellulose samples. The CI has frequently been determined by means of the empirical Segal equation [7];

$$C,\% = \frac{I_{crystalline} - I_{amorphous}}{I_{crystalline}} x100$$

The PVA solutions in the concentration 9 and 10 wt% were prepared by dissolving the PVA powder in distilled water at 90°C for 2 hours with a magnetic stir bar. Distilled water was used as a solvent in all compositions. After that the CNW were added to the PVA solution in amounts to obtain final nanocomposite concentration 10 wt% relative to mass ratio to PVA, the stirring continued for 2 more hours.

Viscosity of the PVA/CNWs solutions was measured by a HAAKE Viscotester 6 plus (Germany) at the temperature of 22 ± 0.5°C. The conductivity of the solutions was measured using a conductivity meter (Win-Lab® DataLine Conductivity Meter) at 22± 0.5°C.

Electrospinning of the solutions was carried out using Nanospider^{TM} NS Lab 200 (Elmarco, Czech Republic) electro-spinning equipment on the spun-bonded polypropylene substrate (surface density Q = 21.5 ± 3 g/m^2). Electrospinning parameters were fallowing: distance between spinning and collector electrodes - 12 cm, applied voltage to ensure spinning 65 kV, speed of substrate 0,2 m/min, speed of the spinning solution feeding roll 4 rpm. The temperature of the environment 22 ± 1 °C and the humidity γ = 35 ± 2%.

Morphology of the PVA and the electro-spun PVA/CNWs blend fibres were studied by Scanning Electron Microscopy (SEM), Field Emission Gun (Tescan Mira/Lmu, Czech Republic) equipment. A CorelDRAW Graphics Suite X6 software was used to measure the diameter of electro-spun fibres from micrographs.

To measure light absorbance of PVA and CNW reinforced PVA nanofiber mats, the instrument UV-Visible spectrophotometer Shimadzu, UV-3700 (Shimadzu Scientific Instruments Kyoto, Japan) with barium sulfate-coated integrating sphere ISR-240A (wavelength range from 400 to 700 nm) was used.

Mechanical properties of the electrospun composite nanomats were measured by Instron Universal Tester (Model 2519-107) with Bluehill software applying deformation speed 1 mm/min and load 1N. Samples 20 mm in length and 10 mm

III. RESULTS AND DISCUSSION

X-ray method was used for identification of changes in the amount of crystalline cellulose in SE treated hemp shives in comparison to untreated shives. From X-ray diffraction patterns in Figure 1(A) can be concluded that SE hemp shives with following water and alkaline after-treatment crystallinity index increased to 72%, comparing to 48% of untreated shives associated with removing of amorphous regions, where lignin and polyose layer such as hemicellulose surrounding the hemp fibres. Figure 1 (B) shows nanowhisker size after following pretreatments. It is visible from Figure 1 (B) that after several treatments of shives the nanosized particles and nanowhiskers can be obtained

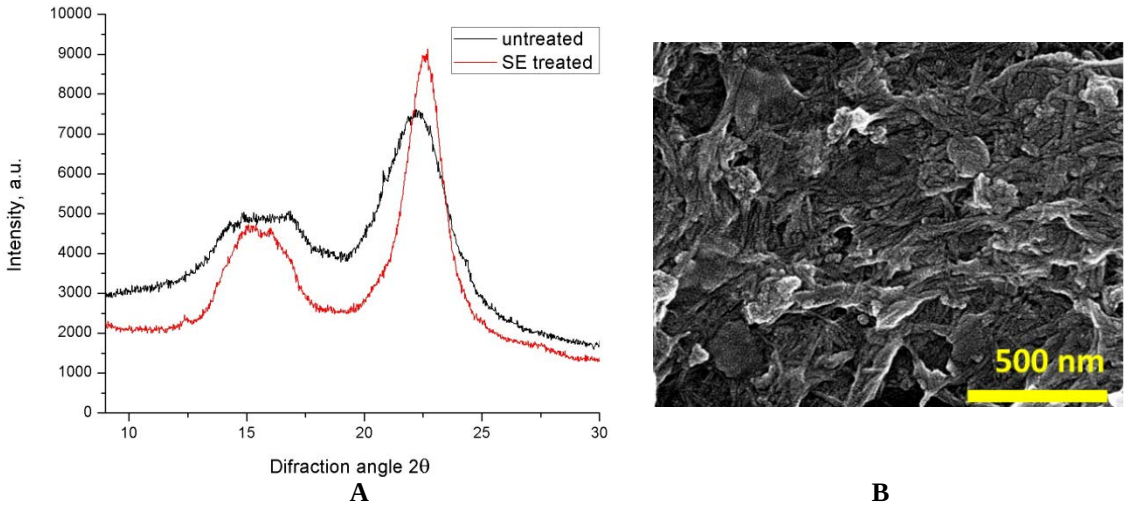

Figure 1. X-ray diffraction patterns for untreated and SE treated hemp shives (A); SEM micrograph of CNW from hemp shives after various treatments (B)

Solution properties have been found to affect the morphology of the fibers. One of the major parameter influencing the fiber diameter is the solution viscosity. The viscosity of the solution is related to the extent of polymer molecule chains entanglement within the solution. A higher viscosity results in a large fiber diameter. The solution viscosity decrease from 856 to 952 mPa.s in result of PVA replacement into spinning mixture with CNW.

The morphology of pure PVA (A) and PVA/CNWs (B) composite mats produced by electrospinning shown in Figure 2. No cellulose nanowhiskers appears to be protruding from the outer surface of the PVA fibres, indicating that they are embedded in PVA matrix and also they may be aligned along the fibre axis during electrospinning process under the electrical field. Addition of CNW to the PVA solution led decrease nanofiber diameter from 500 to 300 nm, because CNWs increase electrical conductivity of pure PVA solution from 383µS to 420 µS. The conductivity of the fiber solution is important to initiate the electrospinning process.

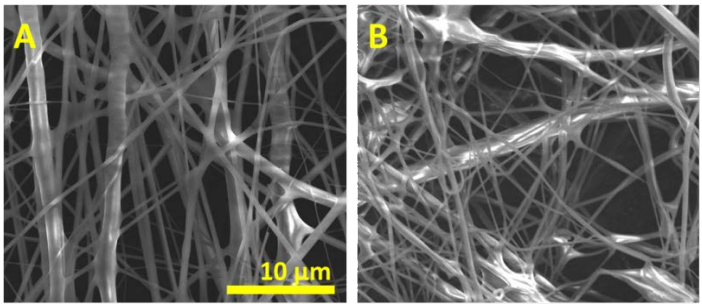

Figure 2. SEM micrographs of electrospun nanofibre mats (a) PVA and (b)10 wt% CNWs

Figure 3 shows the visible light absorption spectra (Kubelka-Munk) of PVA and PVA/CNW nanomats in the wavelength range from 400 to 700 nm. The absorption in wavelength range from 400 to 700 nm increases for PVA/CNW nanomat vindicating the presence of CNW in the electrospun nanomat. It may be attributed to the presence of small amount of lignin in CNW because of it dark brown color therefore absorbing more light.

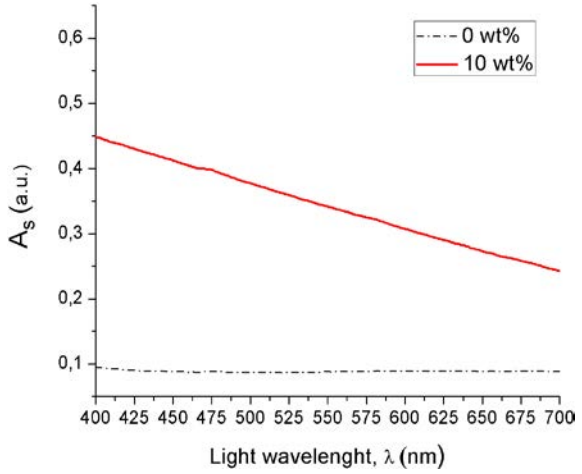

Figure 3. Visible light absorbance (Kubelka-Munk) of PVA nanofibre mat and of PVA/CNW nanofibre composite mat

The tensile strength of PVA and PVA/CNWs nanocomposite mats are shown in Figure 4. Each datum is obtained by averaging the test results of ten samples. The addition of CNW (10%) results in an increase in tensile strength from to 1.4 to 8.5 MPa and the Young's modulus from 0.07 to 0.5 GPa.

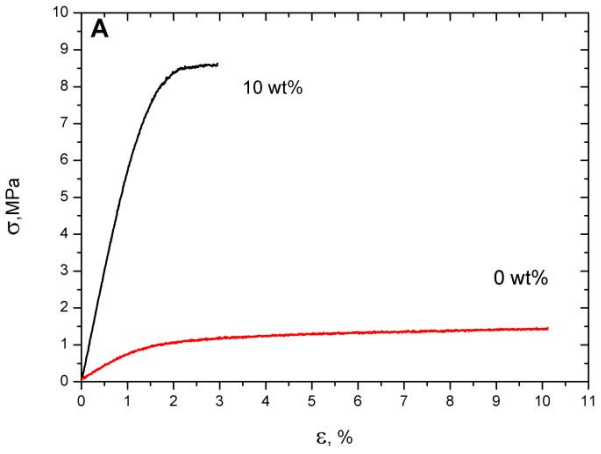

Figure 4. Tensile strength (δ, MPa) of pure PVA and PVA/CNWs electrospun fibers (10 wt %)

IV. CONCLUSIONS

Nanofibre mats were produced from electrospinning dispersions of compositions containing poly (vinyl alcohol) (PVA) and cellulose nanowhiskers (CNW) obtained from hemp shives. The morphology of bicomponent fibers

depending on composition was examined by SEM. The presence of the cellulose component in the obtained composite samples is confirmed by visible light absorbance spectra. The intermolecular interactions between the polymer matrix and the dispersed CNW (10 wt %) played an important role proving mechanical properties of electrospun composite mats. Electrospun PVA nanofibre composites reinforced with CNW can be used effectively as reinforcing material in electrospinning. Nanocomposite mats are expected to have potential use in many particular fields as new functional materials.

V. ACKNOWLEDGEMENT

The study has been supported by the European Social Fund within the project "Support for the implementation of doctoral studies at Riga Technical University" and by the National Research Programme No. 2010.10-4/VPP-5 "Sustainable Use of Local Resources (Entrails of the Earth, Forest, Food and Transport) – New Products and Technologies (NatRes)" (2010-2014).

VI. REFERENCES

[1] Siqueira, G.; Bras, J.; Dufresne, A. Cellulosic Bionanocomposites: A Review of Preparation, Properties and Applications. *Polymers* **2010**, *2*, 728-765.

[2] Z. X. Cao, Y. Chen, P. R. Chang, M. Stumborg, M. A. Huneault, Green Composites Reinforced with Hemp Nanocrystals in Plasticized Starch, *J of Appl Polym Sci* ,**2008,**109 (63), 804–3810.

[3] M. S. Peresin, Y. Habibi, J. O. Zoppe, J. J. Pawlak, O. J. Rojas, Nanofiber composites of polyvinyl alcohol and cellulose nanocrystals: Manufacture and characterization, *Biomacromolecules* ,**2010**,11, 674–681.

[4] M. Samir, F. Alloin, A. Dufresne, Review of recent research into cellulosic whiskers, their properties and their applications in Nanocomposite field, *Biomacromolecules*, **2005,** 6, 612-626.

[5] Kim C.W. et al. *Polymer*, **2006**, 47, 5097.

[6] Sutka A, Kukle S, Gravitis J., Milašius R,Malašauskiene J. *Advances in Materials Science and Engineering*, **2013**, 2013, article number 932636.

[7] Segal L, Creely JJ, Martin Jr, Conrad CM. An empirical method for estimating the degree of crystallinity of native cellulose using the Xray diffractometer. *Text Res J* **1959**, 29,786–94.

IMMOBILIZATION OF LACCASE ON BACTERIAL CELLULOSE: OPTIMIZATION OF ENZYME STABILITY, ACTIVITY AND CHARACTERIZATION

Ana P. M. Tavares[1]*, Cláudio J. R. Frazão[2], Nuno H. C. Silva[2], Carmen S. R. Freire[2], Armando J. D. Silvestre[2], Ana M. R. B. Xavier[2]

*[1]Laboratory of Separation and Reaction Engineering (LSRE), Associate Laboratory LSRE/LCM, Departamento de Engenharia Química, Faculdade de Engenharia, Universidade do Porto, Rua Dr. Roberto Frias, 4200-465 Porto, Portugal; [2]Centre for Research in Ceramics and Composite Materials (CICECO), Departamento de Química, Universidade de Aveiro, 3810-193 Aveiro, Portugal. (*atavares@fe.up.pt)*

ABSTRACT

Commercial laccase was immobilized on bacterial cellulose membranes. The immobilization conditions such as enzyme concentration, contact time and pH were optimized in terms of activity recovery of the immobilized laccase. For this purpose a 3^3 experimental design and response surface methodology was applied. Enzyme concentration played a critical role on laccase immobilization. Under optimized conditions the predicted and experimental response of recovery enzyme activity was equal to 48 and 49 %, respectively. The thermal stability studies showed a notably increase at 60 and 70 ºC which corresponds to a stabilization factor of 1.79 and 2.11, respectively. The immobilized laccase presented high operational stability, since it retained 86 % of its initial activity after 7 consecutive biocatalytic cycles of reaction with ABTS. The kinetic reaction followed the Michaelis-Menten model and upon immobilization the K_M increase 9.9 fold and V_M decreased 1.6 fold.

I. INTRODUCTION

Immobilized enzymes have several advantages over free enzymes, such as enzyme stability improvement, biocatalyst reuse and easier product separation [1]. In order to increase the industrial use of laccases, there is a high interest in discovering the ideal support

to immobilize such enzymes. Laccases (benzenediol: oxygen oxidoreductases, EC 1.10.3.2) are multicopper oxidases, belonging to the so called blue oxidases group of enzymes [2]. Numerous potential industrial applications have been reported for laccases, such as dye decolourization [3-5], pulp delignification [6], soil bioremediation [7] and detection of specific analytes [8].

Bacterial cellulose (BC) is a singular form of cellulose produced by some bacteria. Namely those belonging to *Gluconacetobacter genus*, are able to produce an unique form of cellulose, called bacterial cellulose [9]. Owing to its unique properties (e.g. high mechanical strength and excellent water absorption capacity), BC is attracting a lot of interest as a new functional material. Additionally, BC contains a lot of functional groups, which makes it a potential suport for enzyme immobilization. Because of its singular characteristics which differ from those of plant cellulose, BC has attracted attention as a new functional material [10].

The aim of the present work was to immobilize laccase onto bacterial cellulose and to optimize the experimental conditions (enzyme concentration, pH and contact time) by 3^3 factorial design and response surface methodologies (RSM). Thermal, operational and storage stability, kinetic properties, as well as structural characterization were investigated.

II. EXPERIMENTAL

Enzyme and support of immobilization

Commercial laccase was supplied by Novozymes (Denmark). Bacterial cellulose membranes (99 % water content) were produced by bacteria *Gluconacetobacter sacchari*, purified and lyophilized as described by Trovatti *et al.* [11].

Immobilization of laccase

Lyophilized BC pieces (6 mg) were incubated at room temperature in 0.50 mL of appropriated buffered laccase solution under stirring at different conditions as explained below (Experimental design). After immobilization, the supports were washed three times with the same buffer solution used for enzyme immobilization.

Assay of enzyme activity

Free and immobilized laccase activity was determined using 2,2'-azinobis-(3-ethylbenzothiazoline-6-sulfonic acid) (ABTS) as previously reported [12]. Recovery activity of immobilized laccase was calculated from **Eq. (1)**:

$$R(\%) = \left(\frac{A_i}{A_f}\right) \times 100 \qquad (1)$$

where R is the activity recovery of immobilized enzyme (%), A_i the activity of immobilized enzyme ($U.g^{-1}$), and A_f the theoretical activity of immobilized enzyme (Ug^{-1}).

Experimental design and statistical analysis

RSM and a 3^3 factorial design [13] were employed in this optimization study. The variable levels were: i) enzyme concentration ($\mu L L^{-1}$): 0.15; 1.05 and 1.95; ii: contact time (h): 1.0; 3.0 and 5.0; iii) pH 5.0; 7.0 and 9.0. From the experimental data, analysis of variance (ANOVA) was performed using MATLAB® software (v8.0, The MathWorks, Inc., USA).

Characterization of free and immobilized laccase

Thermal stability studies were carried out at 60 and 70 ºC in 0.10 M sodium carbonate/0.10 M sodium bicarbonate buffer (pH 9.0) and 0.05 M citrate/0.10 M phosphate buffer (pH 5.4), respectively. Immobilized laccase was incubated in 3.0 mL of the buffer solution. The thermal parameters were calculated according to the simplified deactivation model proposed by Henley and Sadana (**Eq. (2)**) [14]:

$$A = [100 - \alpha] \times e^{-kt} + \alpha \qquad (2)$$

where A is the residual enzyme activity, α the ratio of specific activity (residual activity), k the thermal inactivation parameter and t the time. Enzyme's half-life ($t_{1/2}$) was calculated assuming A equal to 50 %.

To evaluate the storage stability, free and immobilized laccase was stored in buffer solution pH 9 at 4 ºC for 42 days. The operational stability was investigated in 7 consecutive operating cycles.

Michaelis-Menten kinetic parameters (K_M and V_{max}) were determined by measuring the reaction rates with ABTS 0.005–0.300 mM for free enzyme and 0.010–1.000 mM for immobilized enzyme.

Immobilized laccase morphology was evaluated by SEM. The presence of functional groups on the support and on the immobilized enzyme was determined by ATR-FTIR.

III. RESULTS AND DISCUSSION

The first aim of this study was to optimize the laccase immobilization in order to maximize the activity recovery of immobilized laccase. The values of the independent variables corresponding to the optimal response (Y=47.88 %) were the following: enzyme concentration 0.15 $\mu L.L^{-1}$, contact time 4.8 h and pH 5.4. A maximum activity recovery of 49.30 % was reached under these conditions and was used for further studies.

Thermal stability tests suggest that the heat-deactivation of free and immobilized laccase followed the thermal deactivation model presented in **Eq. (2)**. The results show that the immobilized enzyme exhibited improved thermal stability at 60 ºC as compared with the free enzyme. Both free and immobilized laccase were practically inactivated at 70 ºC. The analysis of kinetic parameters of thermal deactivation can support these results. For both temperatures, the free laccase showed higher values of the thermal deactivation rate constant (k) than the immobilized laccase. Consequently, in contrast to the values of k, the values of α, residual activity, improved after laccase immobilization. At 60 and 70 ºC, the half-life time was higher for the immobilized enzyme (3.6 and 0.3 h, respectively) than for the free one (2.0 and 0.14 h, respectively).

Results from storage stability show that free enzyme retained 99 and 94 % of its initial activity after 7 and 42 days of storage, respectively. On the other hand, the immobilized enzyme maintained 78 and 54 % of its original activity after 7 and 42 days of storage, respectively. Such results show that free laccase presented better storage stability than its immobilized form. The operational stability of the immobilized laccase was investigated for 7 consecutive cycles of ABTS oxidation. The relative activity of the immobilized enzyme decreased slightly along the cycles. The immobilized enzyme maintained 97 and 86 % of its original activity after 5 and 7 cycles, respectively. This indicates a notable operational stability and reusability of the immobilized biocatalyst. Enzyme reuse can lead to significant cost reduction, which is of utmost relevance for the industry.

Kinetic parameters of the free and immobilized enzyme were determined by fitting the experimental data to Michaelis-Menten kinetics model. The K_M value increases 9.9 times upon laccase immobilization. Such fact shows that immobilization caused a decrease in the enzyme's affinity for ABTS. V_M of the free laccase (2.68 µM

min^{-1}) was found to be higher than that of the immobilized laccase (1.70 µM min^{-1}), probably due to diffusional limitations between the substrate and the enzyme.

SEM images of BC support particles before (**Figure 1a**) and after laccase immobilization (**Figure 1b**) shows that BC displays its typical tridimensional nanofibrillar structure with numerous open free spaces. After immobilization, the presence of immobilized laccase on the free spaces in BC structure was demonstrated and it was clear that the immobilized enzyme was distributed homogeneously by a smooth layer with most of the pore entrances being blocked. FTIR spectra of BC **(Figure c1)** and BC after enzyme immobilization (**Figure c3**) shows strong bands at 3300, 2800 and 1100 cm^{-1}, typical attributed to the vibrations of OH, CH and C–O–C groups of cellulose, respectively. On the other hand, the spectrum of laccase presents strong bands at 3300 (OH and NH), 2800 (CH), 1630 (CONH) and 1100 cm^{-1} (COC) that reflects the characteristic chemical group composition of proteins (**Figure c2**). As, expected, after enzyme immobilization, the spectrum of BC was found to be a sum of those of BC and laccase (Figs. 6A–C). However, the band associated with the vibrations of the CONH group is slightly deviated when compared to that of laccase. Such fact may be due to the establishment of hydrogen bounds and/or interactions enzyme–BC–enzyme during laccase immobilization. Thereby, no new bands appeared, thus indicating that laccase was not covalently immobilized on BC. Considering such data, probably laccase was immobilized on the BC support by adsorption.

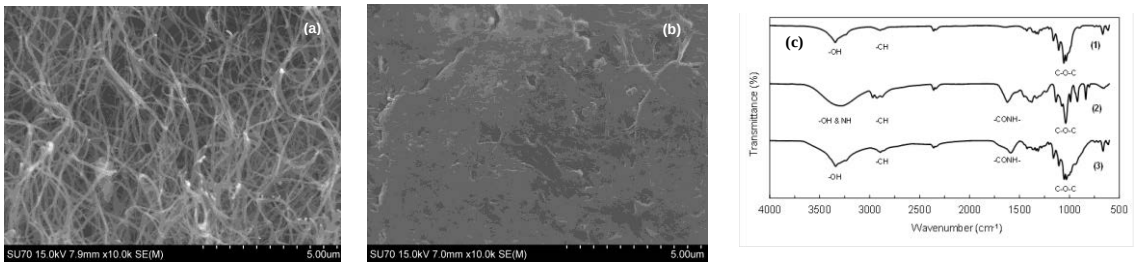

Figure 1. Transverse SEM micrograph of BC: (a) before immobilization; (b) after enzyme immobilization on bacterial cellulose. (c) FTIR spectra of: (1) bacterial cellulose particles; (2) laccase; (3) bacterial cellulose particles after enzyme immobilization on bacterial cellulose.

IV. CONCLUSIONS

Laccase was successfully immobilized on BC particles. Enzyme concentration was found to have the highest impact on the activity recovery of immobilized laccase. The predicted activity recovery of immobilized laccase, the response value, was 47.9% and the experimental one was 49.3% showing a good agreement of the results. After immobilization, laccase exhibited an improved stability against heat denaturation. The immobilized enzyme also presented a very successful reusability with no significant loss of activity (14 %) after 7 consecutive cycles. This study shows that BC is an efficient support for laccase immobilization. The developed immobilization system provides not only an effective, but also a simple and inexpensive process for different industrial applications of laccase. From these findings, the use of immobilized laccase on bacterial cellulose offers an interesting tool for industrial biocatalytic applications.

V. ACKNOWLEDGEMENT

This work was funded by FEDER funds through COMPETE (Programa Operacional Factores de Competitividade) and national funds through FCT (Fundação para a Ciência e Tecnologia) under project PEst–C/CTM/LA/0011/2013 and PEst-C/EQB/LA0020/2013. Ana P.M. Tavares and C.S.R. Freire ackowledge the financial support from FCT (Programs “Ciência 2008” and “Investigador FCT 2012”, respectively).

VI. REFERENCES

[1] Sheldon, R.A. Enzyme immobilization: the quest for optimum performance. *Adv. Synth. Catal.* **2007**, *349*, 1289-1307.

[2] Fernández-Fernández, M.; Sanromán, M.Á..Moldes, D. Recent developments and applications of immobilized laccase. *Biotechnol. Adv.* **2013**, *31*, 1808-1825.

[3] Tavares, A.P.; Cristóvão, R.O.; Gamelas, J.A.; Loureiro, J.M.; Boaventura, R.A..Macedo, E.A. Sequential decolourization of reactive textile dyes by laccase mediator system. *J. Chem. Technol. Biotechnol.* **2009**, *84*, 442-446.

[4] Cristovão, R.; Tavares, A.; Ferreira, L.; Boaventura, R..Macedo, E. Optimisation of reactive dye degradation by laccase using Box–Behnken design. *Environ. Technol.* **2008**, *29*, 1357-64.
[5] Cristóvão, R.O.; Tavares, A.P.; Ferreira, L.A.; Loureiro, J.M.; Boaventura, R.A..Macedo, E.A. Modeling the discoloration of a mixture of reactive textile dyes by commercial laccase. *Biores. Technol.* **2009**, *100*, 1094-1099.
[6] Xavier, A.M.; Tavares, A.P.M.; Agapito, M.S..Evtuguin, D.V. Sequential batch reactor for eucalypt kraft pulp effluent treatment with Trametes versicolor. *J. Chem. Technol. Biotechnol.* **2008**, *83*, 1602-1608.
[7] Strong, P.; Claus, H. Laccase: a review of its past and its future in bioremediation. *Crit. Rev. Environ. Sci. Technol.* **2011**, *41*, 373-434.
[8] Gomes, S.; Rebelo, M. A new laccase biosensor for polyphenols determination. *Sensors* **2003**, *3*, 166-175.
[9] Gomes, F.P.; Silva, N.H.; Trovatti, E.; Serafim, L.S.; Duarte, M.F.; Silvestre, A.J.; Neto, C.P..Freire, C.S. Production of bacterial cellulose by Gluconacetobacter sacchari using dry olive mill residue. *Biomass Bioenerg.* **2013**, *55*, 205-211.
[10] Fu, L.; Zhang, J..Yang, G. Present status and applications of bacterial cellulose-based materials for skin tissue repair. *Carbohydr. Polym.* **2013**, *92*, 1432-1442.
[11] Trovatti, E.; Serafim, L.S.; Freire, C.S.; Silvestre, A.J..Neto, C.P. *Gluconacetobacter sacchari*: An efficient bacterial cellulose cell-factory. *Carbohydr. Polym.* **2011**, *86*, 1417-1420.
[12] Cristóvão, R.O.; Tavares, A.P.; Brígida, A.I.; Loureiro, J.M.; Boaventura, R.A.; Macedo, E.A..Coelho, M.A.Z. Immobilization of commercial laccase onto green coconut fiber by adsorption and its application for reactive textile dyes degradation. *J. Mol. Catal. B-Enzym.* **2011**, *72*, 6-12.
[13] Box, G.E.; Behnken, D. Some new three level designs for the study of quantitative variables. *Technometrics* **1960**, *2*, 455-475.
[14] Henley, J.P.; Sadana, A. Categorization of enzyme deactivations using a series-type mechanism. *Enzyme Microb. Technol.* **1985**, *7*, 50-60.

ELECTROKINETIC PROPERTIES (CATIONIC DEMAND) OF CELLULOSE SUSPENSIONS

Antonio Tijero[1]*, MªDolores Hernández[2], Ana Moral [2], Roberto Aguado[1], Mª Jesús de la Torre[2]

[1]*Grupo de Celulosa y Papel, Chemical Engineering Dpt, Faculty of Chemistry, Complutense University of Madrid, 28040 Madrid, Spain; (*e-mail: atijero@quim.ucm.es)*
[2] *Chemical Engineering Dpt. Experimental Sciences Faculty, Pablo de Olavide University.41013 Seville, Spain*

ABSTRACT

Currently, cellulose is a raw material used in a lot of industrial processes such as papermaking. Cellulose can be treated in order to increase its economic value, to favor chemical processes or to decrease the environmental and economic effect of the use of reagents that can be substituted by treated cellulose.
One of the most interesting treatments of the cellulose is its cationization. Cationized cellulose can be used to substitute the cationic flocculants used in papermaking. These cationic additives are used mainly to decrease the overall negative charge of process waters, and therefore increase the attractive force between particles in the process water.
The cellulose was obtained from cotton linter from Aldrich Sigma. The linter underwent a mercerization in strong alkali at different temperature and concentration values. Mercerized cellulose was analyzed by X-ray diffraction in order to determine the relationship between the different cellulose allomorphs and the proportion of elemental nitrogen incorporated as quaternary ammonium. Later, the mercerized cellulose was cationized by reaction of OH groups of the carbon 6 of the cellulose with the epoxy formed by alkaline reaction of 3-Chloro-2-hydroxypropyltrimethylammoniumchloride *(CHPTAC).* Cationic demand of the cellulose samples was measured by colloidal titration with a Mutec sensor.
This work evaluates the relationship between the cationization degree and the cationic demand of various samples, aiming to obtain the highest possible cationization performance.

I. INTRODUCTION

Cellulose is one of the most abundant raw materials on earth, as the main constituent of plants, particularly the stalks, stems and woody parts of plants. It is also present in bacteria, fungi, algae and even in animals. Literature suggests that the cellulose is formed into or out of the plasma membrane [1, 2].

Through the obtaining of cationic derivatives of cellulose pulp, free methoxyl groups of cellulose become alcoxy groups containing a quaternary ammonium. Due to the substituted nitrogen group, this cellulose derivative has positive charges, which confers physicochemical properties that enable a number of innovative applications.

The mercerization process causes swelling of the cell walls of native cellulose fibres (cellulose I) with alkali, leading to cellulose II [3]. Thereby, altering the chemical structure fibre converts native cellulose into a polymorphic structure, thermodynamically more favourable. This change is irreversible and usually accompanied by a decrease in crystallinity and a reduction in polymerization degree due to hydrolysis of the glycosidic bonds [4]. Adding alkali leads to improved properties such as fibre strength, gloss and dye affinity [5, 6]. The improvement of these properties is considerably influenced by the duration of the treatment and the concentration of alkali solution [7].

Cationization is the reaction of a substrate with an electrophilic reagent containing quaternary ammonium salt. Cationization of cellulose fibres can improve the absorption of dye [8]. In the case of cotton, this mechanism can alter the surface electrical properties, which has caused great impact on textile industry [9, 10]. A wide variety of cellulosic materials has been modified functionally by addition of sodium hydroxide as well as covalent binding of quaternary ammonium in order to obtain a derivative with an overall positive charge [8].

Cationic starches are widely used in the field of papermaking, due to its capability to improve the mechanical properties, strength and drainage of the sheets, and retention of fines, fillers and dyes. Also, cationic starches can be used to decrease of BOD (biological oxygen demand) of the paper mill effluents [11].

Another application of the cationic starches is as flocculants in wastewater treatment, or as additives in the manufacture of textiles, cosmetics, detergents and adhesives [12, 13]. In addition, studies on the use of cationic starches in drug delivery and recovery of oils are booming. The wide use of cationic starch in the industry is also due to their low cost, excellent properties, and high biodegradability [9]

The objective of this work is to study the relationship between the cationization degree, determined by nitrogen elemental analysis, and the cationic demand of the different samples studied, to obtain the highest cationization performance that could lead to develop products to be applied as flocculants, retention agents and adsorbents. Also, the use of biopolymers is an interesting alternative to the use of chemical because they are a renewable resource and biodegradable [14].

II. EXPERIMENTAL

Raw material

The raw material used during the experiments was medium cellulose fibre from cotton linter supplied by Sigma Aldrich. The reagents used in the mercerization process and cationization were sodium hydroxide, isopropyl alcohol and 3-chloro-2-hydroxypropyltrimethylammonium chloride (CHPTAC), from Aldrich. Copper (II) Ethylenediamine, purchased from Panreac, was used to determine pulp viscosity.

Mercerization

The mercerization process was carried out using a strong alkali (NaOH) at different concentrations and different operation times in order to obtain different mercerization grades. Table 1 shows the mercerization times used thorough the experimentation.

Table 1. Mercerization conditions.

Alkali concentration (% P/V)	Time (min)		
	60	120	180
10	A_1T_1	A_1T_2	A_1T_3
20	A_2T_1	A_2T_2	A_2T_3
30	A_3T_1	A_3T_2	A_3T_3

The mercetization process was carried out at different sodium hydroxide concentrations (10, 20 and 30%) and operation times (60, 120 and 180 minutes), with periodic stirring. Next, the treated sample was filtered on a glass fiber filter with a porosity of 2.7 micrometers, washed with water and ethanol and dried in a vacuum oven at 45 ° C.

Cationization

The cationization-mercerization process was carried out in a three necked round bottom flask mounted with a variable speed magnetic stirrer and heating mantle. The cationization agent used during the experimentation was CHPTAC. The alkalized cellulose was dissolved in a mix of sodium hydroxide and isopropyl alcohol in the flask. When the mixture reached the set temperature (70 °C), cationization agent CHPTAC was added. Next, mix samples were taken every 30 minutes up to 300 minutes. The samples were filtered on a glass fiber filter of 7 micrometers, washed with water. Table 2 shows the cationization times form each of the samples analyzed.

Table 2. Cationization time for each sample.

Sample	1	2	3	4	5	6	7	8	9	10
Time (min)	30	60	90	120	150	180	210	240	270	300

Sample characterization

The samples obtained were characterized by elemental analysis and cationic demand (zeta potential). Nitrogen elemental analyses were carried out with carbon, nitrogen and sulfur analyzer LECO CNS-2001. The degree of nitrogen substitution (DNS) of cellulose was calculated from the nitrogen content (% N) and the molecular weight of the anhydroglucose unit, 162.15, using equation I:

$$DNS = \frac{162.15 \cdot \%N}{1401 - 151.64 \cdot \%N} \qquad \text{(I)}$$

The zeta potential is the electric potential in the interfacial double layer (DL) at the location of the slipping plane versus a point in the bulk fluid away from the interface. Z potential was measured by an analyzer Zetasizer Nano from Malvern

III. RESULTS AND DISCUSSION

Elemental analysis

Figure 1 shows the results of the degree of nitrogen substitution calculated from Equation 1, measured for various concentrations of NaOH versus cationization time.

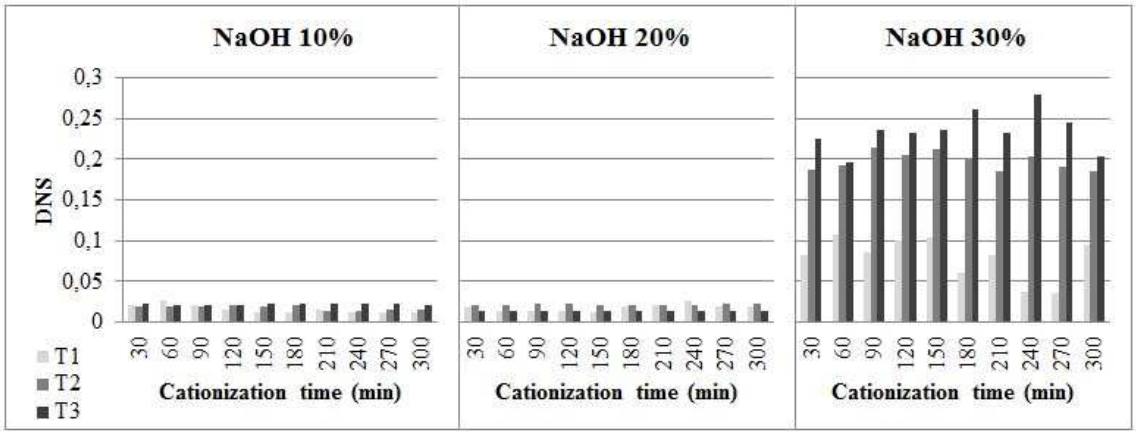

Figure 1. Degree of nitrogen substitution.

The results shown than the highest degree of nitrogen substitution were found at the highest alkali concentration. The optimal cationization time was at 240 minutes, after this time the DNS decreased with time. This decrement could be due to a degradation of cellulose by the alkali solution that affects the DNS of the cellulose treated.

Zeta potential

The Z potential results are shown in the Figure 2. In all cases, the cationization led to an appreciable increase of the zeta potential value. The highest Z potential obtained was found at the two trials with the highest cationization times. The Z potential values obtained at the highest cationization time were very similar to those obtained with the previous trial conditions. That could be due to the maximum DNS% being obtained at 240 minutes and, therefore, without an increment of the %DNS an increase of the Z potential is not possible.

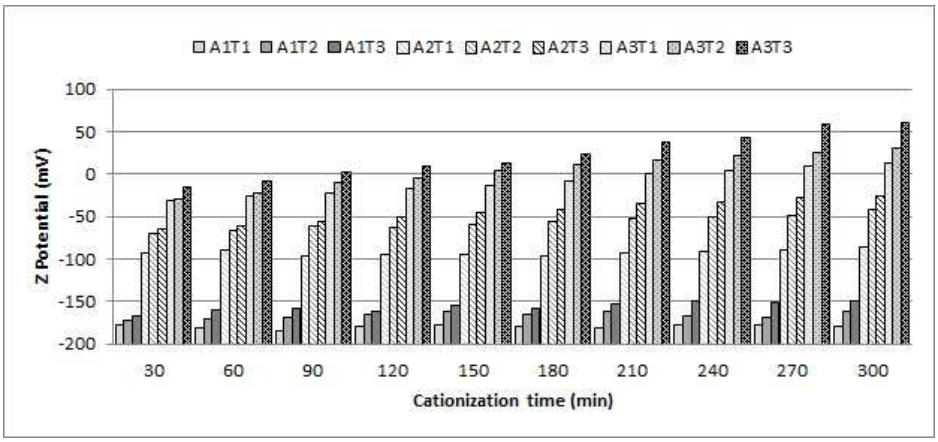

Figure 2. Z potential.

IV. CONCLUSIONS

The maximum degree of substitution, inside of the experimental interval studied, was obtained with the cellulose with the lowest crystallinity. This DNS was obtained at high alkali concentrations.

All the trials carried out showed an increase of the cationic characteristics of the cellulose studied. The highest Z potential was found in the cellulose samples mercerized at the highest mercerization time and alkali concentration.

V. ACKNOWLEDGEMENT

The authors wish to acknowledge the Ministry of Science and Innovation of Spain for the financial support of the Project CTQ2010-21660-C03-01 in which the present study is framed.

VI. REFERENCES

[1] Lamport, D. T. A. Cell wall metabolism. *Ann. Rev. Plant Physiol*. **1970**, *21*, 235–270.

[2] Breett, C. T.; Waldron, K. Physilogy and Bychemistry of Plant Cell walls. (Black, M.; Charlwood, B. ed.). London, UK: *Echapman& Hall*. **1990**.

[3] Bel-Berger, P.; Von Hoven, T.; Ramaswamy, G.N.; Kimmel, L.; Boylston, E. Textile Technology: Cotton/Kenaf Fabrics: a Viable Natural Fabric. *J. Cotton Sci*. **1999**, *3*, 60–70.

[4] Buschle-Diller, G.; Zeronian, S.H. 1992. Enhancing the reactivity and strength of cotton fibres. *J. Appl. Polym. Sci*. **1992**, *45(6)*, 967–979.

[5]Zuber, M.; Mahmood, K.; Ahmad, I.; Ali, Z.; Umair, M.;Jawwad, M. Modification of cellulosic fibers by UV-irradiation . Part II: After treatments effects. *Int. J. Biol. Macromol*. **2012**, *51(5),* 743–748.

[6] Sarko, A. Cellulose How much do we know about its structure. In: Wood and Cellulosics: Industrial utilization, biotechnology, structure and properties (J. F. Kennedy, ed.). Chichester, UK: *Ellis Horwood*. **1987**. 55–70.

[7] Bhatti, I., A., Zia, K., M., Ali, Z., & Zuber, M. Modification of cellulosic fibers to enhance their dyeability using UV-irradiation. *Carbohydr. Polym*. **2012**, *89(3)*, 783–787.

[8] Biswas, S.; Huang, X.; Badger, W.R.; Nantz, M.H. Nucleophiliccationization reagents. *Tetrahedron Lett*. **2010**, *51*, 1727–1729.

[9] Fang, K.; Wang, C.; Zhang, X.; Xu, Y. Dyeing of cationised cotton using nanoscale pigment dispersions. *Color. Technol.* **2005**, *121*, 325–328.

[10] Hao, L.; Wang, R.; Liu, J.; Liu, R. The adsorptive and hydrolytic performance of cellulase on cationised cotton. *Carbohydr. Polym*. **2012**. *89(1)*, 171–176.

[11] Wurzburg, O. B. (1986). Modified Starches: Properties and Uses. . In: O. B. Wurzburg (Ed.), Modified starches: Properties and uses. Boca Raton: *CRC Press Inc*. **1986**, 113-129.

[12] Solarek, D. B. Cationic starches. In: O. B. Wurzburg (Ed.), Modified starches: Properties and uses. Boca Raton: *CRC Press Inc*. **1986**, 114–129.

[13] Qin, C.; Soykeabkaew, N.; Xiuyuan, N.; Peijs, T. The effect of fibre volume fraction and mercerization on the properties of all-cellulose composites. *Carbohydr. Polym*. **2008**,*71(3)*, 458–467.

[14] Zhao, H.; Kwak, J.H.; Zhang, Z.C.; Brown, H.M.; Arey, B.W.; Holladay, J.E. Studying cellulose fiber structure by SEM, XRD, NMR and acid hydrolysis. *Carbohydr. Polym*. **2007**, *68*, 235–241.

RELATIONSHIP AMONG CATIONIZATION DEGREE, CRYSTALLINE STRUCTURE AND VISCOSITY OF THE CATIONIZED CELLULOSE

Antonio Tijero[1]*, Mª Dolores Hernández[2], Ana Moral [2], Roberto Aguado[1], Mª Jesús de la Torre[2]

[1]*Grupo de Celulosa y Papel, Chemical Engineering Dpt, Faculty of Chemistry, Complutense University of Madrid, 28040 Madrid, Spain; (*e-mail: atijero@quim.ucm.es)*
[2] *Chemical Engineering Dpt. Experimental Sciences Faculty, Pablo de Olavide University.41013 Seville, Spain*

ABSTRACT

Polysaccharides are the most abundant biopolymers in nature and chemical modifications of these can be used in the development of new materials. These polymers are the principal raw material in papermaking industry and, due to their anionic character, lead to a decrease in the retention of fines and fillers. The traditional method to control these issues is by means of the addition of cationic polymers. These cationic additives are used mainly to decrease the overall negative charge of process waters, and therefore increase the attractive force between particles in the process water. However, the cationic flocculant added can be the origin of several additional problems in papermaking. The addition in excess of cationic polyelectrolyte can lead to formation adherent flocs that decrease the process performance and increase the amount of contaminant in the process waters. The cellulose studied come from cotton linter supplied by Aldrich Sigma. An alkali mercerization of the cellulose was carried out followed by a cationization. The mercerization was carried out at different times and sodium hydroxide concentrations. The linter underwent a mercerization in strong alkali at different temperature and concentrations, and was analyzed by X ray diffraction in order to determine the relation between the crystalline structure of the cellulose and the cationization degree reached. The mercerized cellulose was cationized by reacting with a cationization agent, 3-Chloro-2-hydroxypropyltrimethylammoniumchloride (CHPTAC).
The objective of this study was the evaluation of the properties, cationization degree, crystalline structure and viscosity related to the sequential process of mercerization-cationization of cellulosic fibers, to develop products to be applied as flocculants, retention agents and adsorbents.

I. INTRODUCTION

Traditionally, one of the main applications of the cellulose has been papermaking. Cellulose has been widely studied, but nevertheless, the structural characteristics of cellulose have not been fully identified and knowledge of them is being improved by the use of new technologies [1]. The use of modified biopolymers is an interesting alternative to the use of chemical agents due to being a renewable resource [2], thus minimizing costs and environmental impact. Cationic cellulose derivatives can interact in a similar way to the cationic polyacrylamides used traditionally in wastewater treatment and therefore could be use as flocculating agents [3]. Through the obtaining of cationic derivatives of cellulose pulp, a nucleophilic addition of alkali-activated cellulose hydroxyl groups to the epoxy moiety of 2,3-epoxipropyl trimethyl ammpnium chloride takes place. Due to the substituted group, this cellulose derivative has positive charges, which confers physicochemical properties that enable a number of innovative applications. The mercerization process causes swelling of the native cellulose fibre cell walls (cellulose I) with alkali, leading to cellulose II [4] and, therefore, altering the chemical structure of the fibre, converting native cellulose into a polymorphic structure, thermodynamically more favourable. This change is irreversible and usually accompanied by a decrease in crystallinity [5] and a reduction in polymerization degree due to hydrolysis of the glycosidic bonds [5, 6]. Adding alkali leads to improved properties such as fibre strength, resistance, gloss and dye affinity. [7, 8]. The improvement of these properties is considerably influenced by the treatment time and the concentration of alkali [9].

Cationization is the reaction of a substrate with an electrophile reagent containing a quaternary ammonium salt. Cationization of cellulose fibres can improve dye absorption [10]. With cotton, this mechanism can alter surface electrical properties, which has caused great impact on textile industry [10, 11]. A wide variety of cellulosic materials has been modified functionally by addition of sodium hydroxide as well as by covalent binding in order to obtain an overall cationic charge [2].Cationic starches are widely used in the field of papermaking due to its capacity to improve the mechanical properties, strength and drainage of sheets, retention of fines, fillers and

dyes. Also, the use of cationic starches can decrease the biological oxygen demand of the paper mill effluents [13] Another application of the cationic starches is as flocculants in wastewater treatment, or as additives in the manufacture of textiles , cosmetics, detergents and adhesives [14]

II. EXPERIMENTAL

Raw material

The raw material used in the experiments was medium cellulose fibre from cotton linter supplied by Sigma Aldrich. The reagents used in the mercerization process and cationization were sodium hydroxide, isopropyl alcohol and 3-chloro-2-hydroxypropyltrimethylammonium chloride (CHPTAC), purchased from Aldrich. Copper (II) Ethylenediamine, provided by Panreac, was used to measure pulp viscosity.

Mercerization

Mercerization process was carried out at various strong alkali conditions in order to obtain different degrees of mercerization. The cellulose used was treated with sodium hydroxide at various concentrations values, 10, 20 and 30%, that corresponding to the acronyms C1, C2 and C3, respectively, and, various times, 60, 120 and 180, minutes, that corresponding to the acronyms T1, T2 and T3, respectively, with periodic stirring. Next, the treated sample was filtered on a glass fibre filter with a porosity of 2.7 micrometers, washed with water and ethanol and vacuum-dried at 45 °C.

Cationization

The cationization agent used was CHPTAC. The cationization-mercerization process was carried out in a three necked round bottom flask with a variable speed magnetic stirrer and heating mantle. The alkalized cellulose was dissolved in a mixture of sodium hydroxide and isopropyl alcohol in the flask. When the mixture reached the set temperature (70 °C), cationization agent CHEPTAC was added. Samples were taken every 30 minutes up to 300 minutes. The samples were filtered on a glass fibre filter of 7 micrometers, washed with water and air-dried.

Sample characterization

The samples were subjected to the following analysis: nitrogen elemental analysis, X-ray diffraction and determination of viscosity. Nitrogen elemental analyses were carried out with a carbon, nitrogen and sulphur analyzer LECO CNS-2001.Measurements of X-ray diffraction were carried out with PANanalytica equipment using X'Pert MPD software. The computer software used for the acquisition, processing and evaluation of data was DIFFRACplus Diffractometric. The crystallinity index of cellulose is expressed as the unity minus the ratio of the amount of the amorphous part and the crystalline cellulose area, as show in equation 1. The value of the diffraction intensity of the amorphous cellulose is taken as 118, and the diffraction intensity of the crystalline cellulose, 225. Cellulose II is expressed by the intensity of bands, according to the expression of Equation 2.

$$\mathrm{CI(XD)} = 1 - \frac{\mathrm{ham}}{\mathrm{hcr}} = 1 - \frac{\mathrm{ham}}{\mathrm{htot} - \mathrm{ham}} \quad \text{(I)} \qquad \mathrm{CII} = \frac{\mathrm{Ir12.1}}{\mathrm{Ir12.1} + 0.5 \cdot (\mathrm{Ir14.6} + \mathrm{Ir16.11})} \quad \text{(II)}$$

The intrinsic viscosity of the pulps was obtained with an Oswald viscometer following the standard UNE 57-039 [15].

III. RESULTS AND DISCUSSION

Elemental Analysis

Figure 1 shows percentage of crystallinity versus mercerization time with different parameters studied in the mercerization stage. The crystallinity indexes shown in Figure 1 were obtained from X-ray diffractograms. The results showed a decrease of Cellulose I with an increase of the alkali concentration and time. The results at 10 and 20 % of alkali concentration show a low variability. The results of the trials carried out at 30% of alkali concentration showed an increase of the amount of amorphous cellulose with time.

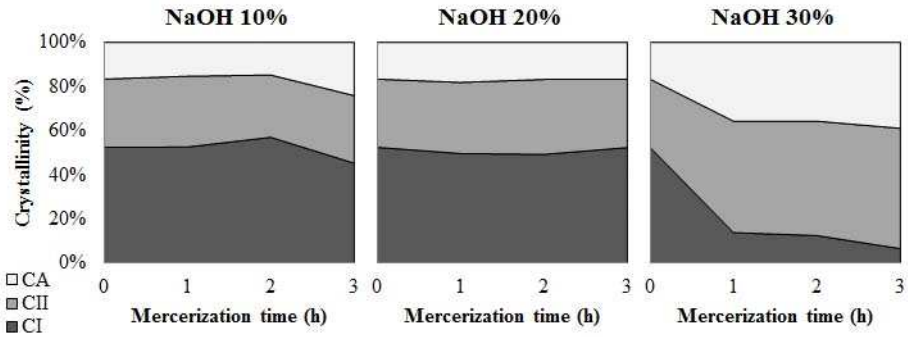

Figure 1. Crystallinity of the alkalised cellulose

The increase of amorphous cellulose should lead to increase of the cationization capacity of the cellulose. All the samples were submitted to an elemental analysis in order to obtain the percentage of nitrogen in its compositions. The best results were obtained in the trials at the highest alkali concentration. Figure 2 shows the percentage of nitrogen for the cellulose samples at the highest alkali concentration.

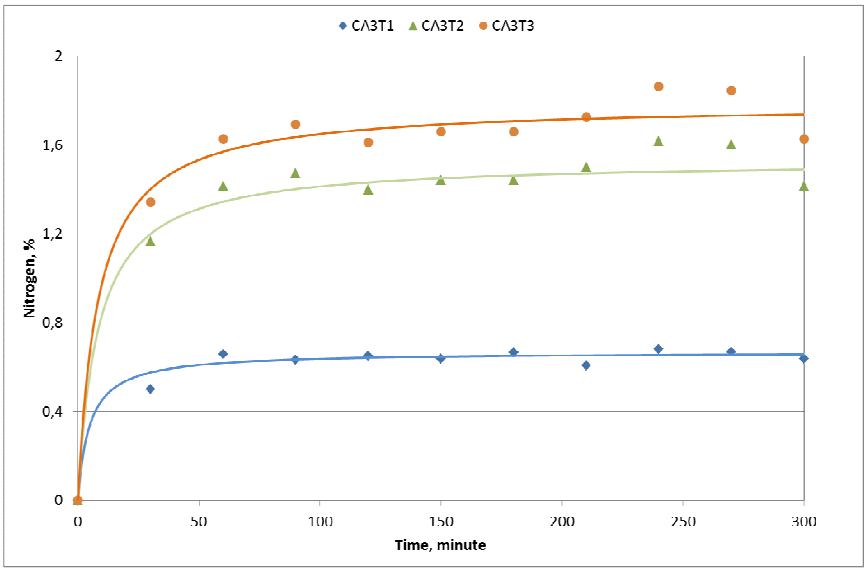

Figure 2. Percentage of nitrogen versus cationization time.

The higher the percentage of nitrogen in the cellulose sample analyzed is, the higher the cationization degree is, since this percentage is due to nitrogenised groups introduced in the cellulose. The best performance was obtained with cellulose mercerized for three hours. The content of nitrogen reaches its highest value at 100 minutes of cationization and remains relatively constant at higher cationization times.

Viscosity

The results obtained in the measurement of viscosity of cationized and alkalized cellulose are shown in Figure 3. The viscosity of the solution depends on the molecular weight of the compounds in it. An increase of the crystallinity does not lead to an increase of viscosity.

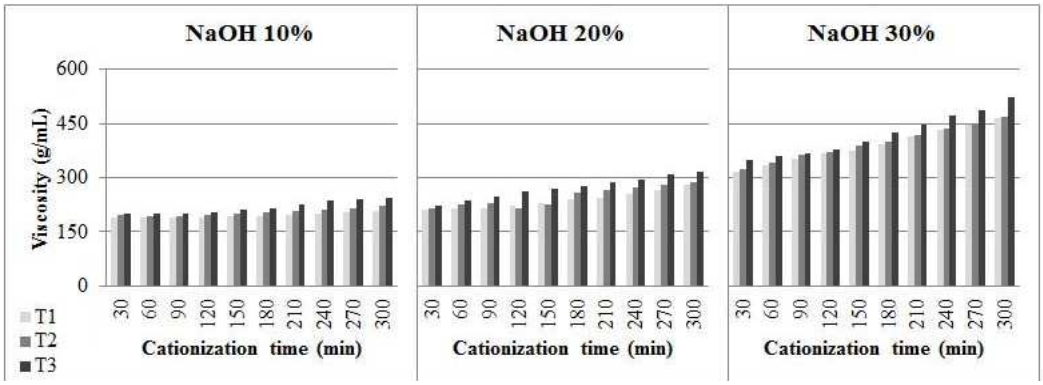

Figure 3. Viscosity of alkalised and cationized cellulose.

IV. CONCLUSIONS

The best results of cationization were obtained with cellulose that had been submitted to a mercerization of 3 h at high alkali concentration (30%). The best substitution degree and nitrogen percentage were obtained in trials with high amorphous cellulose content. [1, 2].The amorphous cellulose, being more reactive than the crystalline cellulose, leads to higher substitution degree. The reaction of substituting is relatively quick, reaching the substitution degree equilibrium at relatively short cationization times.

The results of viscosity showed an increase of it with the cationization times at all the samples analyzed. This increment can be due to, with increasing of the alkali concentration and residence time in the cationization reactor, the cationization degree increasing the rate of formation of (2,3-epoxypropyl)trimethylamonium chloride with the hydroxide group of the carbon six of the anhydroglucose unit.

V. ACKNOWLEDGEMENT

The authors wish to acknowledge the Ministry of Science and Innovation of Spain for the financial support of the Project CTQ2010-21660-C03-01 in which the present study is framed.

VI. REFERENCES

[1] Le Moigne, N.; Montes, E.; Pannetier, C.; Höfte, H.; Navard, P. *Macromol. Symp*., **2008**, 262, 65–71.

[2] Biswas, S.; Huang, X.; Badger, W.R.; Nantz, M.H. Nucleophiliccationization reagents. *Tetrahedron Lett*. **2010**, *51*, 1727–1729.

[3] Prado, H.J.; Matulewicz, M.C.; Bonelli, P.R.; Cukierman, A.L. Potential use of a novel modified seaweed polysaccharide as flocculating agent. *Desalination*, **2011**, *281*, 100–104.

[4] Bel-Berger, P.; Von Hoven, T.; Ramaswamy, G.N.; Kimmel, L.; Boylston, E. Textile Technology: Cotton/Kenaf Fabrics: a Viable Natural Fabric. *J. Cotton Sci*. **1999**, *3*, 60–70.

[5] Buschle-Diller, G.; Zeronian, S.H. 1992. Enhancing the reactivity and strength of cotton fibres. *J. Appl. Polym. Sci*. **1992**, *45(6)*, 967 –979.

[6] Sarko, A. Cellulose: How much do we know about its structure. In Wood and Cellulosics: Industrial utilization, biotechnology, structure and properties (J. F. Kennedy, ed.). Chichester, UK: *Ellis Horwood*, **1987**, 55–70.

[7]Zuber, M.; Mahmood, K.; Ahmad, I.; Ali, Z.; Umair, M.;Jawwad, M. Modification of cellulosic fibers by UV-irradiation . Part II: After treatments effects. *Int. J. Biol. Macromol*. **2012**, *51(5),* 743–748.

[8] Qin, C.; Soykeabkaew, N.; Xiuyuan, N.; & Peijs, T. The effect of fibre volume fraction and mercerization on the properties of all-cellulose composites. *Carbohyd. Polym*. **2008**. *71(3)*, 458–467.

[9] Bhatti, I., A., Zia, K., M., Ali, Z., & Zuber, M. Modification of cellulosic fibers to enhance their dyeability using UV-irradiation. *Carbohydr. Polym*. **2012**, *89(3)*, 783–787.

[10] Biswas, S.; Huang, X.; Badger, W.R.; Nantz, M.H. Nucleophiliccationization reagents. *Tetrahedron Lett*. **2010**, *51*, 1727–1729.

[11] Fang, K.; Wang, C.; Zhang, X.; Xu, Y. Dyeing of cationised cotton using nanoscale pigment dispersions. *Color. Technol.* **2005**, *121*, 325–328.

[12] Hao, L.; Wang, R.; Liu, J.; Liu, R. The adsorptive and hydrolytic performance of cellulase on cationised cotton. *Carbohydr. Polym*. **2012**. *89(1)*, 171–176.

[13] Wurzburg, O. B. (1986). Modified Starches: Properties and Uses. . In: O. B. Wurzburg (Ed.), Modified starches: Properties and uses. Boca Raton: *CRC Press Inc*. **1986**, 113-129.

[14] Solarek, D. B. Cationic starches. In: O. B. Wurzburg (Ed.), Modified starches: Properties and uses. Boca Raton: *CRC Press Inc*. **1986**, 114–129.

[15] Pulps. Cellulose in dilute solutions. Determination of limiting viscosity number. Part 1: method in cupri-ethylene-diamide (ced) solution. UNE 57039-1:1992. Spain, AENOR 2001.

WATER PREHYDROLYSIS OF PINE WOOD IN A CONSECUTIVE RECIRCULATION/PERCOLATION MODE FOLLOWED BY KRAFT PULPING FOR THE PRODUCTION OF AN ACETATE-GRADE PULP

Terhi Toivari[1]*, Lidia Testova[1], Vahid Jafari[1], Agnes Stepan[1], Herbert Sixta[1]

[1]*Department of Forest Products Technology, School of Chemical Technology, Aalto University*
P.O. Box 16300, 00014 Helsinki, Finland
**terhi.toivari@aalto.fi*

ABSTRACT

The limited availability of cotton linters encourage utilizing wood as a raw material for dissolving pulps with the highest purity demand, even though the production of wood dissolving pulp is more challenging. The aim of this study is to develop a simple process that would remove most of the pine wood hemicelluloses during a modified prehydrolysis only, while avoiding an additional cold caustic extraction step. At the same time the removed hemicelluloses should be available in the form of intact oligo- and monosugars in the prehydrolysate. Here, a prehydrolysis with consecutive recirculation and percolation of water is used. The entire process consist only of four steps; prehydrolysis, Kraft cooking, oxygen stage, and bleaching. The results show that by applying this method it is possible to produce pulp with a minimum amount of non-cellulosic impurities. However, the viscosity of the pulp is still unacceptably low due to a very high viscosity loss during the ECF bleaching sequence applied.

I. INTRODUCTION

Cotton linters is the preferred raw material for the manufacture of cellulose products which do not tolerate presence of even very small amounts of hemicelluloses or demand very high viscosity. However, the availability of this raw material is limited and thus it is quite expensive. Alternatively, wood is the most important raw material for high purity pulps, but the production of dissolving wood pulp meeting all quality requirements at a reasonable yield is challenging. Today approximately half of the dissolving wood pulp is manufactured by the prehydrolysis-Kraft (PHK) process, in which the non-cellulosic polysaccharides are removed from wood by the prehydrolysis before the Kraft pulping. However, conventional application of aqueous-phase prehydrolysis, as opposed to its steam equivalent, has been limited due to the formation of sticky lignin precipitates. On the other hand, steam prehydrolysis does not allow the recovery of the hemicellulose-rich dissolved organic fraction. Here, a prehydrolysis by consecutive recirculation and percolation modes is seen as a process combining the advantages of both the aqueous-phase in batch and flow-through prehydrolysis. In this process a prehydrolysis in recirculation mode is performed at elevated temperatures until the removed hemicelluloses start to react to unwanted degradation products. Subsequent percolation mode with a continuous fresh water feed is then applied in order to increase the removal of hemicelluloses while avoiding carbohydrate degradation and lignin recondensation. The aim is to simultaneously achieve increased removal of hemicelluloses and maximize the utilization potential of the organic fraction in the hydrolysate.

II. EXPERIMENTAL

The prehydrolysis experiments were performed in a 10-liter reactor that allows recirculation and percolation of liquid. In the prehydrolysis, 750g of OD pine wood chips were treated at temperatures 170 and 200°C. The liquid to wood –ratio was adjusted so that the chips were covered by liquid during the experiments. The reference prehydrolysis treatments consist of a hydrothermolysis with water recirculation only (batch mode). The studied prehydrolysis concept applies combined recirculation/percolation of water. During the percolation mode fresh water was fed continuously from the top of the reactor. In order to investigate the effects of the prehydrolysis on wood composition, these experiments were repeated with various treatment times. Samples of hydrolyzed wood chips were air dried, refined and their carbohydrate and lignin compositions were analyzed according to method NREL/TP-510-42618 and Janson's method [1]. These results were then used to determine suitable conditions for the pulping experiments.

The aim was to adjust the pulping process conditions so that pulp with Kappa number around 25 and a high purity in cellulose would be produced. The chosen prehydrolysis conditions for reference experiments (batch mode) were 90 minutes at 170°C and 15 minutes at 200°C, resulting in P-factors of 1000 and 1300, respectively. Experiments with consecutive recirculation and percolation of the water were also performed at 170°C and 200°C and the total treatment times were equal to the reference experiments. Kraft cooking was performed in an air bath digester at 160°C with effective alkali of 22%, sulfidity of 40%, and liquor to wood -ratio of 4:1. When bleaching the PHK pulp samples, following sequence was applied: First, a two-stage oxygen delignification was performed in an air bath digester at 120°C. Samples were then bleached by sequence D_0-EO_p-D_1-P. The conditions of each stage are described in **Table 1**. The bleached pulp samples are represented by numbers 1, 4, and 5 in **Table 2**.

Table 1. Applied bleaching sequence.

Bleaching stage	D_0	EO_P	D_1	P
Consistency, %	10	10	10	10
Temperature, °C	50	80	70	75
Time, min	60	60	120	180
Bleaching chemicals	Kappa factor 0.25 as active chlorine Final pH adjusted to 2.3 by using H_2SO_4	NaOH 20 kg/t H_2O_2 3 kg/t O_2 pressure 3bar EPSOM 3kg/t	Kappa factor 6.0 as active chlorine Final pH adjusted to 3 by using NaOH	H_2O_2 8 kg/t NaOH 10 kg/t EPSOM 0.5kg/t (Mg)

III. RESULTS AND DISCUSSION

The applied prehydrolysis and Kraft cooking conditions and the main pulp properties of the non-bleached samples are shown in **Table 2**. With the exception of the H-factor, cooking conditions were similar for all of the samples, as described above in experimental part. Carbohydrate and lignin compositions of samples 1, 4, and 5 after prehydrolysis and Kraft cook are shown in **Figure 1**.

Table 2. Prehydrolysis and Kraft cook circumstances and main pulp properties of the non-bleached samples. C stands for circulation mode and P stands for percolation. Sample number 6 is bleached softwood acetate-grade pulp.

	Prehydrolysis	Kraft cook	Pulp properties						
Sample	Temperature, time, L:W	Temperature, H-factor	Yield, %	Kappa number	Viscosity, mL/g	Cellulose, % on pulp	Glucomannan, % on pulp	Xylan, % on pulp	Lignin, % on pulp
1	170°C 90 min, 7:1	160°C, 1200	37.3	18	860	93.4	1.3	2.4	2.9
2	170°C 90 min, 7:1	160°C, 1600	34.6	16	795	93.8	1.0	2.5	2.7
3	170°C 60 min(C) + 30 min(P), 53:1	160°C, 1600	34.7	15	725	93.9	1.2	2.3	2.6
4	200°C 15 min, 7:1	160°C, 1600	30.6	25	590	95.0	0.3	1.2	3.5
5	200°C 10 min(C) + 5 min(P), 16:1	160°C, 1600	31.2	25	615	94.9	0.3	1.4	3.3
6	Commercial SW acetate-grade pulp				826	97.5	0.9	1.6	0.0

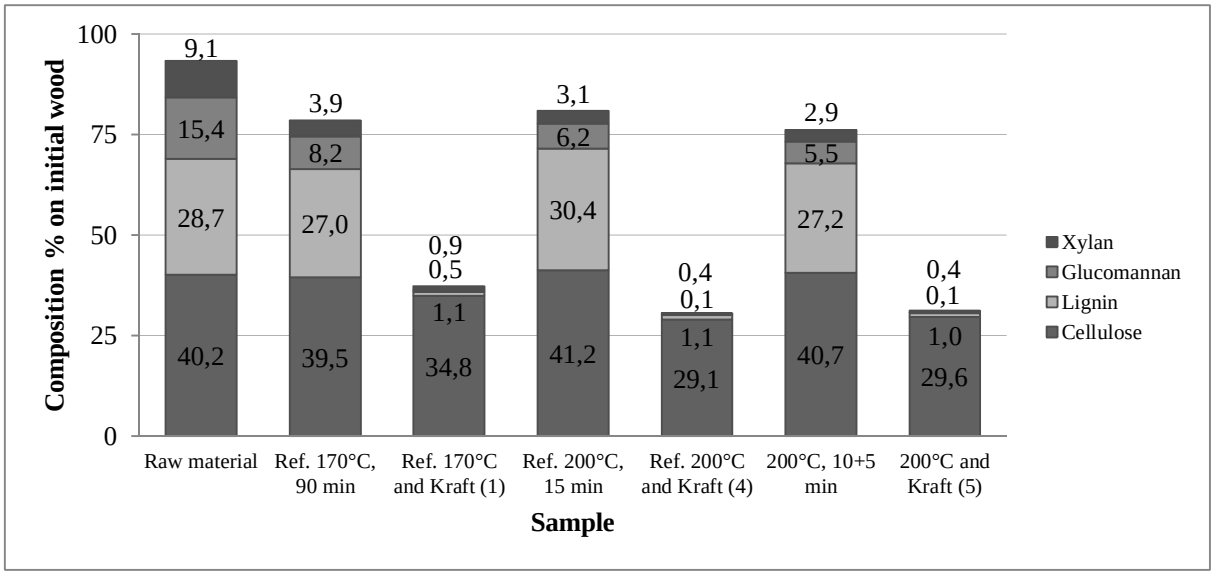

Figure 1. Carbohydrate and lignin compositions of raw material (*pinus sylvestris*) and samples 1, 4, and 5 after prehydrolysis and Kraft pulping as % on initial wood.

Figure 1 illustrates that at 200°C a remarkable share of the hemicelluloses can be removed after relatively short prehydrolysis without any significant losses of cellulose or lignin. After 15 minutes of prehydrolysis with recirculation of water, 62.0% of the hemicelluloses is removed, while after 10 minutes of circulation followed by a 5 minutes percolation treatment, 65.7% of the hemicelluloses is removed. In order to remove an equal amount of hemicelluloses at 170°C, a substantially longer treatment time would be needed; after 90 minutes of batch mode prehydrolysis 50.6% of hemicelluloses is removed. As shown in **Figure 1**, cellulose and lignin do not degrade to a large extent during the prehydrolysis and, therefore, most of the organic compounds found in hydrolysate are originated from the hemicelluloses. When it comes to collection and utilization of the removed hemicelluloses in hydrolysate phase, higher prehydrolysis temperature might be more favorable due to increased hemicellulose removal.

Based on the chemical composition of the pulp samples shown in **Table 2** and **Figure 1**, most of the lignin and remaining hemicelluloses are removed during the Kraft cooking. The results show differences in total yield of the first two stages caused by the prehydrolysis temperatures. After a prehydrolysis at 200°C and Kraft cooking, the total yield is almost 4% lower compared to pulps with prehydrolysis at 170°C, even though the H-factors were similar. However, as regards acetate-grade pulp production, the pulp compositions of the samples with prehydrolysis at 200°C are more favorable. According to carbohydrate and lignin analyses, higher temperature during the prehydrolysis results in higher amount of cellulose (95% compared to approximately 94% on pulp) and lower amount of hemicelluloses (approximately 1.5% compared to 3.5% on pulp) which is a prerequisite for acetate-grade pulp. The main disadvantage of the used method is the effect of the prehydrolysis on viscosity: viscosities decrease below the level of commercial dissolving pulp already before the bleaching. The effect of increased prehydrolysis temperature on higher loss in viscosity is obvious. When comparing the pulps cooked with H-factor of 1600, after prehydrolysis at 170°C and a Kraft cook viscosity varies between 725 – 795mL/g, while prehydrolysis at 200°C and Kraft cook results in viscosities around 600mL/g. After the Kraft cooking pulp samples 1, 4, and 5 were bleached. **Table 3** provides the properties of these pulp samples after the bleaching.

Table 3. Properties of the pulp samples after each bleaching stage.

	Oxygen 1		Oxygen 2		D_0-EO_P		D_1-P	
Sample	Kappa number	Viscosity, mL/g	Kappa number	Viscosity, mL/g	Kappa number	ISO-brightness, %	ISO-brightness, %	Viscosity, mL/g
1	10	650	4	485	0.8	83.8	92.2	345
4	12	445	4	365	0.8	82.6	91.8	270
5	14	500	4	400	0.6	84.4	92.0	285

The initial Kappa number of sample 1 was notably lower than the Kappa number of the samples 4 and 5, 18 v. 25, respectively, but already after the oxygen stages the Kappa numbers decrease to same level. When bleaching is continued, Kappa numbers and ISO-brightness values of all three samples become consistent. Bleachability of the samples is good and the final ISO-brightness values of about 92% are at the target level. However, viscosity losses are significant also during the oxygen stages and bleaching. Especially during the oxygen delignification viscosities of all three samples decrease greatly. The viscosities were relatively low already before bleaching and the final viscosities around 300mL/g are not on acceptable level for an acetate-grade pulp.

IV. CONCLUSIONS

The main outcome of this study is that by using the developed method it is possible to produce dissolving softwood pulp with a minimum amount of impurities. However, the level of the viscosity does not yet conform to the requirements for acetate-grade pulp. Next steps of this study will focus on modifying the bleaching sequence so that the decrease of viscosity would be avoided. The chemical composition analyses of prehydrolyzed chips show that most of the softwood hemicelluloses can be removed when using studied consecutive recirculation/percolation prehydrolysis concept at elevated temperatures. Further investigation to characterize the constituents of the hydrolysates is needed in order to evaluate the possibilities to utilize this removed fraction.

VI. REFERENCES

[1] Janson, J. Calculation of the polysaccharide composition of wood and pulp. *Paperi ja puu*. **1970**, 52, 323 – 329.

[2] Testova, L.; Borrega, M.; Tolonen, L.; Penttilä, P.; Serimaa, R.; Larsson, P.; Sixta, H. Dissolving-grade birch pulps produced under various prehydrolysis intensities: quality, structure and applications. *Cellulose.* **2014**, Published online, DOI 10.1007/s10570-014-0182-x

AGEING OF CELLULOSIC PULP UNDER SIMULATED MARINE ATMOSPHERE

Tereza Tribulová[1,2]*, Dmitry V. Evtuguin[1], František Kačík[2], António J. S. Fernandes[3]

*[1]CICECO, Department of Chemistry, University of Aveiro, 3810-193 Aveiro, Portugal; [2]Department of Chemistry and Chemical Technologies, Faculty of Wood Sciences and Technology, Technical University in Zvolen, T.G. Masaryka 24, 960 53 Zvolen, Slovakia; [3]I3N, Department of Physics, University of Aveiro, 3810-193 Aveiro, Portugal. (*Tereza.Tribulova@gmail.com)*

ABSTRACT

The brightness reversion of dissolving eucalypt sulphite pulp under conditions simulating the marine atmosphere during pulp shipping has been studied. Accelerated aging of seawater sprayed pulp has been monitored by wet chemical methods (viscosimetry, determination of carbonyl and carboxyl groups) and by UV–VIS Diffuse Reflectance (UV–VIS DR) spectroscopy and VIS–Resonance Raman (VIS–RR) spectroscopy. The results of this study clearly showed that the marine atmosphere has a detrimental effect on the brightness stability of bleached pulps. Pulp cellulose suffered from oxidative depolymerization in the presence of seawater salts under conditions of wet-thermal aging. This process was accompanied by the formation of new oxidised structures containing carbonyl and carboxyl groups, which were extensively converted into chromophore structures. The oxidative depolymerization of cellulose in the presence of seawater upon aging was associated with certain seawater salts, i.e. mineral components, such as alkaline carbonate salts and transition metal cations provoking base-induced autoxidation reactions. This work is the first evidence for the increasing of pulp brightness reversion under conditions of marine atmosphere.

I. INTRODUCTION

Bleached cellulosic pulps are vulnerable to environment conditions during its storage and transportation. Under increased humidity/temperatures and UV irradiation pulp components suffer a series of autocatalytic reactions leading to polysaccharide degradation and formation of chromophores (aging), which is highly undesirable for customers. According to industrial experience the pulp aging during transportation of unprotected pulp bales by marine transport is particularly noticeable. However, practically nothing is known how marine atmosphere can enhance the ageing of bleached pulps. The main objective of this work was to evaluate the effect of marine atmosphere on brightness reversion of bleached pulp using the model pulp samples treated by seawater under laboratory condition and subsequently subjected to wet-thermal aging.

II. EXPERIMENTAL

Materials

The dissolving TCF bleached sulphite pulp sheets of 91.8% ISO brightness (denominated as P0) supplied by CAIMA pulp mill (Portugal) were involved in experiences on combined accelerated ageing, i.e. dry assay (T=70°C for 24 hrs) followed by a wet-thermal step according to TAPPI T260 om-91 (T=100°C and RH=100% for 1 hour). Dissolving pulp contained less than 0.1% of lignin and less than 3% of pentosans. In order to model the condition of marine atmosphere, pulp sheets were treated by spray of seawater sampled at the Atlantic Ocean coast in Portugal. Analysis of the seawater (pH≈8) with salinity of 3.7 wt.% showed the presence of the most abundant anions (Cl^- 58.2 wt.% and SO_4^{2-} 7.7 wt.%,) and cations (Na^+ 24.0 wt.% and Mg^{2+} 3.1wt.%). Other anions (e.g. CO_3^{2-}, NO_3^-, Br^-, I^-, etc.) and cations (Ca^{2+}, K^+, Sr^{2+}, etc.) were presented in much lower amounts. Two levels of seawater spray were applied, one with lower content (ca 4.5 g/m^2, P2) and one with higher content (ca 20.0 g/m^2, P3) of salts. For the comparative reason also a spray of distilled water was applied as well (P1).

Methods

The measurement of ISO brightness according to TAPPI T452 om-92 was carried out using an L&W Elrepho SE 070 spectrophotometer. ISO brightness/ISO yellowness was determined for all samples three times: before aging/after first dry step of aging/after combined aging. Post Color (PC) Number was determined in the relation to the first dry step of aging process (PC Number I) and to the combined double step aging (PC Number II) [1].

The determination of the intrinsic viscosity of the pulps was performed using a cupriethylenediamine (CED) solution according to ISO 5351/1. Degree of polymerization (DP) of cellulose chains in pulps were calculated based on measured intrinsic viscosity values according to equation developed by Evans and Wallis [2]. The quantification of carbonyl group content was determined according to the Sabolks method [3]. The carboxyl groups in pulps were determined according to TAPPI T237 om-1993.

UV–VIS DR spectra of samples were recorded on a JASCO V-560 spectrophotometer equipped with a JASCO ISV-469 integrating sphere and using $BaSO_4$ standard as a background reference. The measured range was 200–800 nm with scanning speed of 200 nm/min and bandwidth of 5 nm. The reflectance spectra were also converted into k/s spectra using known Kubelka-Munk equation.

Micro-Raman spectra of samples were recorded on a Jobin Yvon (Horiba) LabRam HR 800 micro-Raman spectrometer under backscattering configuration and using 40 × NUV objective. Measurement was performed in a visible region of the spectrum at @442 nm (He-Cd UV laser, Kimmon IK Series). The recorded spectral range was 800–1800 cm^{-1}. The spectra were collected during 30 s of acquisition time to avoid photodegradation. For each pulp sample at least 3 points were analysed in order to obtain an average spectra. The spectral data were subjected to background correction (linear fluorescence) and normalised to the ca. 1380 cm^{-1} band [4].

III. RESULTS AND DISCUSSION

Optical Properties

The brightness of initial pulp (P0) before aging was 91.79 ± 0.21% ISO (**Table 1**) and decreased by 2.13% after two combined (dry and wet) aging steps (P0-CA). The blank pulp P1, which were sprayed by distilled water, showed almost the same brightness and yellowness as P0. It was also evidenced that with increasing amounts of sprayed salts on cellulose its brightness decreases progressively and the yellowness has a contrary growing trend (**Table 2)**. For a series of samples subjected to wet-thermal aging the brightness decreases in the range from 2.1 to 2.9% and the yellowness increases in the range 25.2 to 29.5%. Between the PC Number I (dry aging step) and the PC Number II (wet aging step) there is a very good linear relationship: pulp samples after combined aging have universally double tendency to the brightness reversibility comparing to the same samples after only the first dry phase of the combined aging. In conclusion, the presence of seawater salts during accelerated aging has promoted brightness reversion, i.e. the content of chromophores in pulp cellulose was increased. Note worthy the brightness reversion of pulp was not linearly proportional to amount of sprayed seawater salts, because PC numbers of P2 and P3 were similar while the amount of sprayed seawater was almost 5 times higher in the case of P3 than with P2.

Table 1. Effect of seawater on the optical properties of pulps under conditions of wet aging.

Sample	NON-AGIED		AFTER COMBINED AGING (CA)		PC number I	PC number II
	ISO Brightness (%)	ISO Yellowness (%)	ISO Brightness (%)	ISO Yellowness (%)		
P0	91.79 ± 0.21	4.97 ± 0.07	89.84 ± 0.24	6.22 ± 0.12	0.111	0.213
P1	91.78 ± 0.06	5.01 ± 0.03	89.83 ± 0.12	6.48 ± 0.14	0.133	0.275
P2	91.27 ± 0.14	5.22 ± 0.03	88.69 ± 0.24	6.60 ± 0.08	0.152	0.305
P3	90.79 ± 0.14	5.50 ± 0.07	88.21 ± 0.12	7.12 ± 0.16	0.138	0.323

Changes of the Degree of Polymerization, Carbonyl and Carboxyl Content

Accelerated aging of both non-sprayed and sprayed initial pulp P0 with distilled water (P0-CA and P1-CA, respectively) revealed small increase in carbonyl groups and insignificant cellulose depolymerization (**Table 2).** However, pulp samples sprayed by seawater (P2-CA and P3-CA) exhibited after aging rather significant growth in carbonyl and carboxyl groups and about 15-23% decrease in DP compared to P0. These data evidenced significant oxidative depolymerization of cellulose upon aging and formation of new oxidised structures in pulp. Note worthy that the formation of new carbonyl groups in cellulose was less accentuated than carboxyl groups (e.g. for sample P3-CA the increase of CO groups was of 59% and COOH groups of 208%). Again, as in the case of brightness reversion of pulp discussed above, the increase in oxidised structures was not proportional to amount of sprayed seawater salts, because P2-CA and P3-CA showed comparable rise in CO and COOH groups while the amount of sprayed seawater was almost 5 times higher in the case of P3 than with P2. Randomly oxidised polysaccharide chains appeared in the presence of seawater salts could suffer extensive hydrolytic cleavage of weakened glycosidic bonds. The newly formed carboxyl groups have a known catalytic effect in aging reactions [5]. Oxidised structures containing CO and COOH groups are particularly vulnerable to formation of chromophores during aging. The positive correlation between oxidised structures in pulp and it yellowing was previously reported [6]. In fact, a clear correlation between the amount of oxidised structures in aged pulps (**Table 2**) and their susceptibility towards brightness reversion have been observed (**Table 1**).
The oxidation of cellulose could be induced by basic salts presented in seawater, mostly sodium and potassium carbonates. After drying of seawater, a local concentration of basic salts on the surface of pulp fibres could be high enough to provoke base-induced autoxidation reactions. However, taken into consideration the diversity of seawater salts composition, other mechanisms of cellulose degradation under aerobic conditions may be also

proposed (e.g. oxidative catalysis with ferric, copper or strontium salts, with iodine or bromine presented in seawater or produced by disproportionation reactions, etc.).

Table 2. Results on pulps analysis for intrinsic viscosity, degree of polymerization and oxidised groups (CA–samples after combined aging).

Sample	Intrinsic viscosity (cm^3/g)	Degree of polymerization	Carbonyl (CO) content (mmol/kg)	Carboxyl (COOH) content (mmol/kg)
P0	498 ± 1	1732	5.7 ± 0.15	41.1 ± 0.30
P0-CA	474 ± 1	1640	6.4 ± 0.20	62.3 ± 0.15
P1-CA	470 ± 1	1624	6.4 ± 0.25	65.1 ± 0.35
P2-CA	429 ± 1	1468	7.8 ± 0.05	119.0 ± 0.20
P3-CA	395 ± 1	1339	9.1 ± 0.15	126.5 ± 0.25

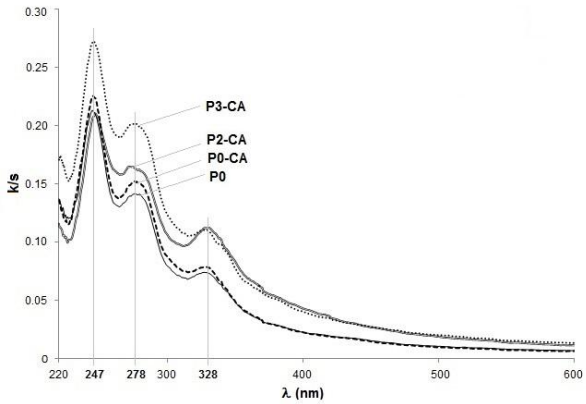

Figure 1. UV–VIS DR spectra of the selected model pulp samples.

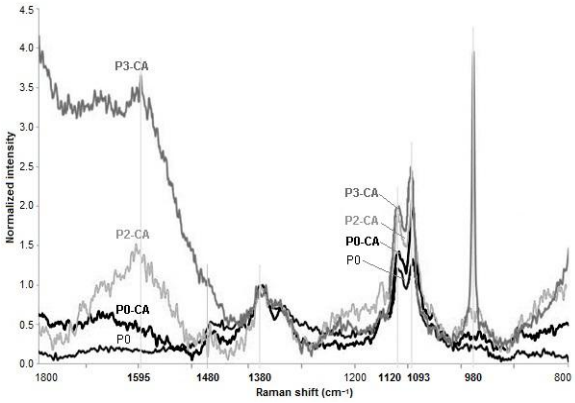

Figure 2. VIS–RR spectra of the selected model pulp samples.

Analysis of Pulps by UV–VIS DR and VIS–RR Spectroscopy

Aged P0–P3 pulps were analysed by UV–VIS DR and VIS–RR spectroscopy to evaluate the origin of chromogens/chromophore structures. Thus, absorbance curve of P0 (**Figure 1)** exhibited three intensive bands at ca 247, 278 and 328 nm, which were increased after aging of non-sprayed (P0-CA) and, especially, of sprayed pulps with seawater (P2-CA and P3-CA). The absorption maxima at 247 nm in pulp is frequently assigned to structures with single double bonds conjugated with carboxyl group ($\pi \rightarrow \pi^*$ transition), whereas band at ca 280 and 325 nm could be assigned to aromatic structures and to carbonyl/carboxyl-containing structures with conjugated multiple double bonds, respectively [4]. The strong increasing in absorbance at 247, 278 and 328 nm upon aging of pulp sprayed with seawater evidences the formation of aforementioned polyunsaturated structures. At the lowest content of seawater salts applied in pulp P2-CA the band at 278 and 328 nm are increased significantly, whereas at highest content of seawater salts applied in pulp P3-CA the bands at 247 and 278 nm were risen pronouncedly, unlike to the band at 328 nm. Hence, structures absorbed at 328 nm were almost independent on amount of seawater sprayed on pulp before the accelerated aging.

The chromophore structures formed upon aging were also assessed by VIS–RR spectra using laser excitation beam at 442 nm (@442 nm) just nearby the wavelength normally used for the determination of pulp brightness at 457 nm (**Figure 2**). Since cellulose content of samples was presumed to remain nearly constant, all spectra were normalized to cellulose CH bending band at 1380 cm^{-1}. Chromophores contribute essentially to the VIS–RR spectra at 1550–1750 cm^{-1}. Two major bands were observed in this region at ca 1595 and at ca 1660 cm^{-1}. The band about 1600 cm^{-1} is usually assigned to aromatic/quinonic structures or structures containing multiple conjugated double bonds with carbonyl groups and the band at about 1660 cm^{-1} to the structures with double bond conjugated to carboxyl group (e.g. HexA) or with aromatic structures [4]. Interestingly, the intensity of the band of 278 nm in the UV–VIS DR spectra (assigned to series of conjugated double bonds or aromatic structures) correlated well with the band of 1595 cm^{-1} in the VIS–RR spectra, whereas the band of 247 nm, correlated with the less pronounced signal of 1660 cm^{-1} (**Figure 2**). Hence, the formed chromophore structures in aged pulps may be assigned to carbonyl groups containing structures with conjugated multiple double bonds and moieties with double bonds linked to carboxyl groups. Moreover, the amount of these structures increase drastically after pulp spraying with seawater before the aging tests.

After cellulose oxidation a variety of oxidized groups may appear at various positions of glucopyranose rings (most likely at C2, C3 and C6), apart from the terminal positions. At least part of these oxidized structures may provide a contribution to the band centred at around 1600 cm^{-1} in Raman spectra due to the formation of conjugated double bonds formed as a result of tautomerization of carbonyl groups to the corresponding enols [8]. The growing intensity of signal at 1595 cm^{-1} is coherent with increase of unsaturated and carbonyl structures in the samples and inversely with pulp brightness, which decreases in order: P0, P0-CA, P2-CA, and P3-CA. The structures of quinone type derived from hydrothermal degradation products of carbohydrates upon wet-thermal aging may be suspected [5]. The band at ca. 1480 cm^{-1} correlate directly with the furan derivates, an eventual chromogen structure in pulps treated with seawater salts. The bands at ca. 1093 cm^{-1} and at 1120 cm^{-1} includes the contributions of C-O-C and O-C-O stretching of glucopyranosyl unit and β-(1→4) glycosidic linkages in cellulose (glycosidic O-C-O symetric and asymetric stretching modes of vibrations from carbonyl moieties in its hemiacetal and hydrate configurations) [4, 7]. A major part of carbonyl groups (both ketone and aldehyde) are present in oxidized polysaccharides in hydrated or hemiacetal forms [5] thus contributing to the intensity of bands at ca. 1093 cm^{-1} and at 1120 cm^{-} [4]. These changes in Raman band intensity (**Figure 2**) are therefore proportional to the increase in carbohydrate oxidation after aging of seawater sprayed pulps **(Table 2**). A very sharp signal Raman signal at ca 980 cm^{-1} in P3-CA and less intensive in P2-CA were assigned to ν_1 vibrations in SO_4^{2-} belonging to seawater salts.

IV. CONCLUSIONS

The results of this study clearly showed that the marine atmosphere have a detrimental effect on brightness stability of bleached pulps. Pulp polysaccharides suffered oxidative depolymerisation in the presence of seawater salts under conditions of wet-thermal aging with formation of new oxidised structures containing carbonyl and carboxyl groups. At least part of these oxidised structures has been transformed into chromophore structures upon aging. The combined spectroscopic analysis of aged pulps by UV–VIS DR and VIS-RR (@442 nm) showed the appearance of structures containing carbonyl/carboxyl groups coupled with polyconjugated double bonds including quinone structures. The increase of pulps absorbance at 247 and 278 nm in UV–VIS DR spectra upon aging corroborated with intensities of bands at ca 1660 and 1600 cm^{-1}, respectively, in VIS-RR (@442 nm) spectra. The oxidative depolymerization of cellulose in the presence of seawater upon aging was associated with it certain mineral components, such as alkaline carbonate salts and transition metal cations provoking base-induced autoxidation reactions.

V. ACKNOWLEDGEMENT

Authors wish to acknowledge the FCT (Fundação para a Ciência e Tecnologia) and CICECO for financial support within the scope of the project Pest-C/CTM/LA0011/2013. This research work was also supported by the Slovak Scientific Grant Agency VEGA under contract No. 1/0454/12.

VI. REFERENCES

[1] J.-E. Levlin, J.-E.; Söderhjelm, L. (Eds.) Pulp and Paper Testing. Fapet Oy, Helsinki, **1999**, 128–129.

[2] Evans, R.; Wallis, A.F.A. Cellulose molecular weights determined by viscometry. *J Appl Polym Sci*. **1989**, *37(8)*, 2331–2340.

[3] Obolenskaya, A.V.; Elnitskaya, Z.P.; Leonovitch, A.A. Determination of aldehyde groups in oxidized pulp. In *Laboratory Manipulations in Wood and Cellulose Chemistry*. Ecologia, Moscow, **1991**, 211–212.

[4] Loureiro, P.E.G.; Fernandes, A.J.S.; Carvalho, M.G.V.S.; Evtuguin, D.V. The assessment of chromophores in bleached cellulosic pulps employing UV-Raman spectroscopy. *Carbohyd Res*. **2010**, *345(10)*, 1442–1451.

[5] Rosenau, T.; Potthast, A.; Krainz, K.; Yoneda, Y.; Dietz, T.; Shields, Z.P.I.; French, A.D. Chromophores in cellulosics: VI. First isolation and identification of residual chromophores from aged cotton linters. *Cellulose*. 2008, *18(6)*, 1623–1633.

[6] Barbosa, L.C.A.; Maltha, C.R.A.; Demuner, A.J.; Cazal, C.M.; Reis, E.L.; Colodette, J.L.A. Rapid method for quantification of carboxyl groups in cellulose pulp. *BioResources*. **2013**, *8(1)*, 1043–1054.

[7] Edwards, H.G.M.; Farwell, D.W.; Williams, A.C. FT–Raman spectrum of cotton: a polymeric bimolecular analysis. *Spectrochem Acta*, Part A. **1994**, *50*, 807–811.

REMOVAL OF LIGNIN AND HEXENURONIC ACIDS FROM SISAL FIBERS WITH NOVEL XYLANASES BELONGING TO DIFFERENT GH FAMILIES

Susana V. Valenzuela[1]*, Cristina Valls[2], Mª Blanca Roncero[2], Teresa Vidal[2], Pilar Diaz[1] y F. I. Javier Pastor[1]

*[1]Department of Microbiology, Faculty of Biology. Av. Diagonal 643, E-08028 Barcelona. [2]Department of Textile and Paper Engineering, Polytechnic University of Catalonia. Colom 11, E-08222 Terrassa (*susanavalenzuela@ub.edu)*

ABSTRACT

The aim of this study was to evaluate five different preparations of xylanases from *Paenibacillus barcinonensis*, a highly xylanolytic species, who is able to grow on xylan as a sole carbon source.
As raw material to assess, fibers from sisal (*Agave sisalana*) were chosen. Sisal pulps were bleached by an XP sequence, where X denotes the enzyme treatment and P a hydrogen peroxide extraction stage. Kappa number, brightness, viscosity and hexenuronic acid content of samples were determined. Sugars released from sisal pulps, other non-wood fibres and also eucalyptus fibres, by the treatment with the xylanases were also analysed. The best results were obtained with the GH10 xylanase and with crude supernatants of *P. barcinonensis*, which produced a lignin removal of 23% and a reduction of 25% in the hexenuronic acid content of sisal pulps without a significant loss of viscosity. The xylanases of family GH30 showed good performance, being more efficient when applied as a single catalytic domain. On the contrary, Xyn11E did not show any significant effect on pulp properties.
The release of sugars in the effluents from the X stage applied to sisal correlated with the effectiveness of the xylanases tested. The xylan content of wood and non-wood fibres, the type of xylan and its accessibility also had an influence on the xylanase activity on pulps.

I. INTRODUCTION

The use of xylanases as bleaching agents of fibers is a sustainable alternative to the traditional chemical bleaching used in the paper industry. However, the bleaching capacity is not distributed among all of these enzymes, and generally the xylanases belonging to the GH11 family are considered more efficient than the members of the GH10 family. Recent reports show that xylanase application in pulps can also reduce the content of hexenuronic acids (HexA), formed during the alkaline cooking of wood [1]. HexAs can increase kappa number and brightness reversion, and besides produce a consumption of bleaching reagents and can retain metal ions [2]. Xylanase-assisted bleaching of wood and non-wood pulps is the focus of several studies designed to identify the most appropriate enzymes and the optimum conditions of application.
In this study, the effects of five different xylanase preparations from *Paenibacillus barcinonensis*, were assayed to remove HexAs and lignin from unbleached sisal pulps. The first xylanase evaluated was Xyn10A [3], which belongs to the GH10 family of glycosyl hydrolases. This xylanase was cloned by amplification with degenerate primers designed from the amino terminal sequence of the protein. The second xylanase tested, Xyn30D belongs to family GH30 and has a modular structure GH30-CBM35 [4]. This xylanase was recently identified by proteomic analysis of secretome of *P. barcinonensis*. Xyn30D was assayed as a complete modular protein and, alternatively, devoid of its carbohydrate binding module CBM35. A fourth xylanase tested was Xyn11E, a new family GH11 xylanase cloned with primers deduced from the genome of *Paenibacillus polymyxa* [5]. Finally, the supernatants of *P. barcinonensis* grown on rice straw were evaluated as a crude xylanase [6].
Commercial non-wood pulp production has been estimated to account for about 10% of global pulp production and is expected to increase in the next few years. Sisal (*Agave sisalana*) is a good candidate for such use because of its commercial price, ease of availability and renewability [7]. Sisal fibres, moreover, offer attractive properties, such as their high tear strength, cellulose content, porosity, and folding endurance, for the production of a variety of specialty and high value papers, such as those used in surgical gauze, filters, condensers or even for tea bags [8]. Sisal fibers have not been evaluated in detail for its enzymatically assisted bleaching, a fact that gives more interest to the analysis performed. Our study reports for the first time the application of non-commercial xylanases to sisal fibres.

II. EXPERIMENTAL

Raw material

Sisal (*Agave sisalana*) pulps were supplied by CELESA (Tortosa, Spain). Initial pulp properties were 47.8% ISO brightness, kappa number 8.1, viscosity 778 mL/g and hexenuronic acid content (HexA) 42.0 µmol/g oven-dried pulp (odp). Flax (*Linum usitatissimum*), showing 40.1% ISO brightness, kappa number 10.5 and 12.5 µmol HexA /g odp; and kenaf (*Hibiscus cannabinus*), showing 35.1% ISO brightness, kappa number 12.9 and 50.1 µmol HexA /g odp were also supplied by CELESA. Eucalyptus (*Eucalyptus globulus*) kraft pulp, 38.3% ISO brightness, kappa number 14.3 and 36.5 µmol HexA /g odp was supplied by ENCE (Pontevedra, Spain).

Xylanase treatments

The xylanases (EC 3.2.1.8) assayed were Xyn10A [3], Xyn30D and Xyn30Dcat [4], and Xyn11E [5]. Pba crude xylanase consisted in the supernatant of cultures of *P. barcinonensis* grown for 3 days at 37ºC on LB broth supplemented with 0.5% rice straw. Xylanase treatments (X stage) were performed on 12 g of dried pulp using 10 xylanase Units per gram of odp in 50 mM phosphate buffer, pH 6.0 at 10% consistency. The treatments were carried out in polyethylene bags at 50 °C for 2 h. The control reaction contained all the components with the exception of the enzyme. Xylanase activity was determined as described [3].

Bleaching treatment

The X stage was followed by a hydrogen peroxide bleaching stage (P stage). The P stage was carried out using 2% H_2O_2, 1.5% NaOH, 0.5% DTPA (diethylenetriaminepentaacetic acid) and 0.2% $MgSO_4$ (percentages referring to odp), at 5% pulp consistency, at 90 °C for 2 h, in an Ahiba Spectradye dyeing apparatus (Datacolor).

Analysis of pulp properties

Kappa number, pulp brightness and viscosity were determined according to ISO 302, ISO 2470-1 and ISO 5351/1, respectively. The HexA content was determined following the Gellerstedt and Li method [9].

III. RESULTS AND DISCUSSION

Xylanase activity on sisal fibres

In a first approach to evaluate the activity of the xylanases belonging to different GH families on sisal fibres, the effluents obtained from the enzyme treatments (X stage) were analyzed to quantify their reducing sugar content. Xyn10A and Pba crude xylanase released high amounts of reducing sugars from sisal fibres, Xyn30Dcat and Xyn11E released lower amounts, while treatment with Xyn30D released only a very small amount of these sugars (Table 1). The amounts of sugars obtained with Pba crude xylanase was very similar to that obtained with Xyn10A, which is in line with the fact that it is the predominant xylanase in the supernatants of *P. barcinonensis* cultures as it has been shown by SDS-PAGE and zymographic analysis [6].

Table 1. Reducing sugars released by xylanase treatment of pulps

	µg of xylose equivalent per mL of effluent			
	Sisal	Eucalyptus	Flax	Kenaf
Control	23.1 ± 17.6	21.6 ± 17.0	27.0 ± 17.7	39.2 ± 17.9
Xyn10A	589.4 ± 28.5	1045.8 ± 40.2	88.1 ± 30.8	697.2 ± 16.7
Xyn30D	54.9 ± 16.7	62.4 ± 17.9	62.4 ± 27.3	142.1 ± 34.4
Xyn30Dcat	138.7 ± 32.0	162.8 ± 19.1	122.1 ± 25.0	182.7 ± 16.7
Xyn11E	132.1 ± 43.7	117.2 ± 20.3	45.8 ± 20.3	111.4 ± 23.8
Pba crude xylanase	323.8 ± 28.5	830.0 ± 40.2	154.5 ± 30.8	464.9 ± 40.2

Analysis of sisal pulp properties

Pulp samples taken after the X and P stages respectively were analyzed in order to evaluate and compare the ability of the xylanases to increase lignin and chromophore removal. Table 2 shows kappa numbers and brightness values of the pulp samples after these two stages. Xylanase treatment led to a decrease in kappa number of most of the samples. These decreases were in accordance with the amount of sugars released by each enzyme. The maximum effects were obtained with Xyn10A and with Pba crude xylanase, which produced kappa number decreases of 22 and 21% respectively after the X stage and 23 and 18% respectively after the P stage, compared to control values. Xyn30Dcat also presented a marked decrease in kappa number (11%) after the P stage (Table 2).

Brightness analyses of the pulp samples after the X stage showed that treatment with Xyn10A, Pba crude xylanase and Xyn30Dcat increased brightness by 8.3, 2.8 and 1.5% ISO respectively, compared to control values

(Table 2). After the P stage, all samples, including controls, showed a notable increase in brightness of around 25% ISO, indicative of the bleaching effect of alkaline peroxide. Xylanase treatment led, in most instances, to an additional increase in brightness between 0.9 and 2.4% ISO. Surprisingly, yet in accordance with the absence of any significant contribution to lignin removal, treatment with Xyn11E did not increase pulp brightness, showing that, contrary to what has been suggested, not all family GH11 xylanases are suitable candidates for bleaching.

Our results show that xylanase effects were less evident after the P stage than they were after the X stage, probably because of an excess of bleaching agent during the second stage. Nevertheless, the bleaching capacity of the xylanases could be detected immediately after the X stage by evaluating changes in pulp properties [10]. Xyn10A was found to be the best candidate among those assayed for improving the bleachability of sisal fibres. However, Pba crude xylanase performed similarly to Xyn10A, the predominant enzyme in the multicomponent xylanase. Thus, it would be considerably cheaper to use Pba crude xylanase, the supernatant of *P. barcinonensis* cultures, than to employ recombinant Xyn10A, due to the costs that its production can imply. A comparison of Xyn30D and Xyn30Dcat shows that better results were obtained by the latter, which is a truncated derivative of Xyn30D. As Xyn30D is a modular xylanase containing the carbohydrate-binding module 35 (CBM-35), it is of greater size (62 kDa) than Xyn30Dcat, which comprises no more than the catalytic module of the enzyme (47 kDa). Even when the catalytic domain is responsible for xylan hydrolysis (and hence its bleaching capability), the extra size provided by CBM-35 could interfere with xylan accessibility. Previous results from the performance evaluation of a modular 120 kDa xylanase from *P. barcinonensis* on eucalyptus fibres showed that the enzyme did not produce any effects on bleaching [11]. These results suggest that the accessory modules may decrease the bleaching efficiency of an enzyme, because of the difficulties a larger molecule encounters to access the lignin trapped in pulp fibres. The lower bleaching capacity of xylanase Xyn30D could also be caused by its glucuronoxylan binding ability [4] as this might decrease the free diffusion of the enzyme between fibres.

Even when all treatments with recombinant xylanases were cellulase free, the Pba crude xylanase contained a small amount of cellulase (11.6 U/ml of xylanase activity vs. 0.13 U/ml of CMCase activity). Moreover, enzyme treatments can cause damage to the structural integrity of the cellulose. For this reason in order to assess the effect of each treatment on cellulose, the viscosity of the pulps was determined after the P stage (Table 2). In all cases a small decrease in viscosity was observed.

Table 2. Sisal pulp properties after each bleaching stage

	X		P		
	KN	Br (%ISO)	KN	Br (%ISO)	Viscosity (mL g^{-1})
Control	7.7 ± 0.02	47.6 ± 1.9	5.6 ± 0.09	72.6 ± 0.3	772 ± 25
Xyn10A	6.0 ± 0.02	55.9 ± 0.4	4.3 ± 0.08	73.8 ± 0.1	724 ± 18
Xyn30D	8.1 ± 0.11	47.4 ± 0.3	5.5 ± 0.18	73.8 ± 0.1	662 ± 12
Xyn30Dcat	7.2 ± 0.12	49.1 ± 0.5	5.0 ± 0.02	75.0 ± 0.1	620 ± 52
Xyn11E	7.1 ± 0.01	48.2 ± 1.3	5.5 ± 0.18	72.0 ± 0.3	658 ± 18
Pba crude xylanase	6.1 ± 0.02	50.4 ± 0.2	4.6 ± 0.21	73.5 ± 0.1	753 ± 10

Hexenuronic acid content of sisal fibres

The HexA content of pulps was measured after the P stage. All xylanase treatments reduced HexA content (Fig. 1). Once more the best results were obtained with Xyn10A and Pba crude xylanase, which reduced the total HexA of the pulp samples by around 25%. Xyn30D and Xyn30Dcat treatments led to a HexA reduction of between 11 and 14%, which contrasted with previous findings that report a smaller effect of the xylanases belonging to family GH30 in HexA removal from eucalyptus fibres [11]. A more detailed analysis with more xylanases and a wider range of raw materials is needed to clarify the effect of xylanase application on HexA content of pulps.

Xylanase application on other non-wood and wood fibres

As the amount of reducing-sugar release in the X stage correlated with xylanase bleaching efficiency and their HexA removal capacity, a further three raw materials were assayed to determine the potential effectiveness of the xylanases on these fibres. Eucalyptus, flax and kenaf fibres were treated, as above, with the enzymes under study and the effluents from all treatments were analyzed to measure the amount of reducing-sugar release (Table 1). Maximum activity on eucalyptus fibres was observed with Xyn10A and Pba crude xylanase, which released a considerably greater amount of reducing sugars than they did from sisal. Xyn30, Xyn30cat and Xyn11E presented similar results on eucalyptus as they did on sisal fibres, suggesting a similar behaviour in bleaching. Xylanase treatment of flax fibres released only small amounts of sugar in each case, which can probably be attributed to the low xylan content of these fibres. Kenaf fibres, in contrast, recorded slightly better results than those obtained with sisal, indicating that an enzyme-aided bleaching with Xyn10A or Pba crude

xylanase could produce promising results. We believe this result is remarkable since to the best of our knowledge no xylanases have previously been tested in the bleaching of kenaf fibres.

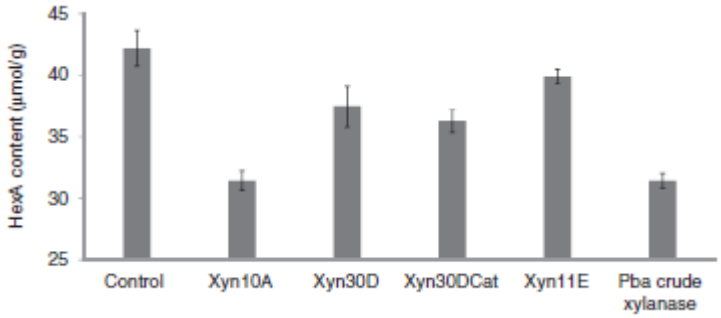

Figure 1. Hexenuronic acids content of pulps.

IV. CONCLUSIONS

Xyn10A from family GH10 was the most efficient xylanase for the lignin removal of sisal fibres and the reduction of their HexA content. Similar results were obtained with Pba crude xylanase, an enzyme cocktail which contains Xyn10A as its predominant component. Xylanases belonging to family GH30 were more efficient when applied as single catalytic domain. By contrast, Xyn11E did not have any significant effects on pulp properties. The release of sugars in the X stage effluents correlates with the effectiveness of the enzymes tested. Moreover, the effectiveness of a xylanase depends on the xylan content of fibres and on the type and accessibility of these xylans.

V. ACKNOWLEDGEMENT

The study was supported in part by the Spanish Ministry of Education and Science, grant CTQ2010-20238-C03-01, CTQ2010-20238-C03-02, CTQ2009-12904 and AGAUR from Generalitat de Catalunya, grant 2009 SGR 819.

VI. REFERENCES

[1] Shatalov A., Pereira H. Impact of hexenuronic acids on xylanase-aided bio-bleaching of chemical pulps. *Bioresour Technol*. **2009**, 100, 3069–75.

[2] Cadena E., Du X., Gellerstedt G., Li J., et al. On hexenuronic acid (HexA) removal and mediator coupling to pulp fiber in the laccase/mediator treatment. *Bioresour Technol*. **2011**, 102, 3911–7.

[3] Valenzuela S., Díaz P., Pastor F. Recombinant expression of an alkali stable GH10 xylanase from *Paenibacillus barcinonensis*. *J Agric Food Chem*. **2010**, 58, 4814–8.

[4] Valenzuela S., Diaz P., Pastor F.I.J. Modular Glucuronoxylan-Specific Xylanase with a Family CBM35 Carbohydrate-Binding Module. *Appl Environ Microbiol*. **2012**, 78, 3923–31.

[5] Valenzuela S., Diaz P., Pastor F.I.J. Xyn11E from *Paenibacillus barcinonensis* BP-23: a LppX-chaperone-dependent xylanase with potential for upgrading paper pulps. *Appl Microbiol Biotechnol*. **2014.** DOI 10.1007/s00253-014-5565-2

[6] Blanco A., Vidal T., Colom J.F. and Pastor F.I.J. Purification and properties ofxylanase A from alkali-tolerant *Bacillus* sp. strain BP-23. *Appl Environ Microbiol.* **1995**, 61, 4468–4470.

[7] Li Y., Mai Y., Ye L. Sisal fibre and its composites: a review of recent developments. *Compos Sci Technol*. **2000**, 60, 2037–55.

[8] Aracri E., Vidal T. Enhancing the effectiveness of a laccase–TEMPO treatment has a biorefining effect on sisal cellulose fibres. *Cellulose*. **2012**, 19, 867–77.

[9] Gellerstedt G., Li J. An HPLC method for the quantitative determination of hexeneuronic acid groups in chemical pulps. *Carbohyd Res*. **1996**, 294, 41–51.

[10] Wong K., Nelson S., Saddler J. Xylanase treatment for the peroxide bleaching of oxygen delignified kraft pulps derived from three softwood species. *J Biotechnol*. **1996**, 48, 137–45.

[11] Valls C., Vidal T., Gallardo O., Diaz P., et al. Obtaining low-HexA-content cellulose from eucalypt fibres: Which glycosil hydrolase family is more efficient? *Carbohydr Polym.* **2010**, 80, 154–60.

EVALUATING THE IMPACT OF COMBINING MEDIATORS IN THE LMS FOR BIOBLEACHING OR FUNCTIONALIZATION

Cristina Valls, Teresa Vidal and M. Blanca Roncero*

CELBIOTECH_Paper Engineering Research Group. Universitat Politècnica de Catalunya-BarcelonaTech. Colom 11, E-08222 Terrassa, Spain.
**E-mail: roncero@etp.upc.edu, Phone n: (+34) 937398210*

ABSTRACT

In this work, a laccase from *Cerrena Unicolor* (CuL) supplied by Fungal Bioproducts® was firstly applied in combination with VA in *Eucalyptus globulus* in order to compare its biobleaching effect with the well-known laccase from *Trametes villosa* supplied by Novozymes®. However, the main purpose of this work was to apply the CuL in presence of two different mediators like VA (as synthetic compound) or *p*-coumaric acid (PCA), acetosyringone (AS) or syringaldehide (SA) (as natural compounds). Each compound was applied alone or in combination with another one in order to find a possible biobleaching or functionalising boosting effect between them. Concerning the biobleaching effects, the highest delignification and brightness increase was produced with the VA applied alone. The natural mediators failed to increase delignification and contrary, they hindered the effect of VA due to possible interactions with the natural phenols and fibres. Concerning the grafting effects, the highest increase in kappa number and in colour properties was produced with the combination of PCA and AS. Finally, the best way of applying these mediators, together in one step (L_{AS+PCA}), or in two steps with (L_{AS}-washing-L_{PCA}) or without (L_{AS}-L_{PCA}) washing was evaluated.

I. INTRODUCTION

The use of biotechnology to bleach pulp has attracted enormous attention and provided very interesting results. It has been proven that laccases, in combination with natural or synthetic mediators can make several effects on wood and non-wood fibres: they can produce an oxidative degradation of lignin (biobleaching effect) [1] or they can induce the grafting of phenols into fibre surface (biografting or functionalization effect) [2]. Several laccases have been tested for this purpose being the laccase from *Trametes villosa* one of the most efficient enzymes [3]. However, new laccases need to be discovered. The synthetic mediator violuric acid (VA) has been evidenced to be one of the most interesting mediators for producing a biobleaching effect [1, 4]. Due to environmental concerns, there has been an increased interest in using natural mediators for biobleaching. However, their effectiveness in producing delignification cannot be compared with the synthetic ones. By contrast, they are grafted into fibres providing pulps with new functionalities [5].

The main purpose of this work was to apply several combinations of mediators in order to find a boosting effect between them in producing a biobleaching or a biografting effect. All these treatments were performed with a laccase from *Cerrena unicolor*.

II. EXPERIMENTAL

Raw material

A hardwood kraft pulp (*Eucalyptus globulus* oxygen-delignified) produced by the Torraspapel S.A mill (Spain) was used. The initial kappa number and brightness after washing were 8.4 and 51.2 % ISO, respectively.

Enzymatic and chemical treatments

Oxygen-delignified eucalyptus pulps were subjected to an enzymatic stage (L) followed by a chemical bleaching stage (P) resulting in a biobleaching sequence named LP.
In the enzymatic stage (L), laccases from *Trametes villosa* (TvL) supplied by Novozymes® and from *Cerrena unicolor* (CuL) supplied by Fungal Bioproducts® were used. Both laccases were applied with the synthetic mediator violuric acid (VA) and the CuL was also applied with the natural mediators syringaldehyde (SA), acetosyringone (AS) and *p*-coumaric acid (PCA). Enzymatic treatments on pulp were performed in a Datacolor Easydye individual reactor with a laccase dose of 20 U g^{-1} odp, 0.5% odp of mediator, 50ºC for 4 h in the presence of 50 mM tartrate buffer at pH 4 at 5% consistency. A few drops of 0.05% w/v of the surfactant Tween 20 were also added. Combinations between all the mediators were also performed: VA+AS, VA+SA, VA+PCA, AS+SA, AS+PCA, SA+PCA, being 0.5% odp the dose of applied for each one. The results of each process were compared with a control treatment with laccase and without mediator (K_{TvL} or K_{CuL}). During the P stage, fibre samples, at 5% consistency, were treated with 2% odp H_2O_2, 1.5% odp NaOH, 1% odp DTPA and 0.2% odp

$MgSO_4$ in a Datacolor Easydye AHIBA oscillating individual reactor at 90ºC for 2h. After each stage, pulp samples were filtered and extensively washed for further processing.

Pulp properties

Kappa number and brightness were determined according to ISO 302 and ISO 5351/1, respectively. Colour coordinates (CIE *L*a*b**) were also measured.

III. RESULTS AND DISCUSSION

The biobleaching effects produced by the *Cerrena unicolor* lacase (CuL) were firstly compared with the well-known and efficient laccase from *Trametes villosa* (TvL). Both laccases were applied with VA for being this synthetic mediator one of the best efficient ones [1, 4]. As can be appreciated on **Table 1**, the addition of VA to the laccase treatments produced a reduction on kappa number and an increase on brightness after both, the enzymatic and P stages. This effect was similarly produced by both laccases during the enzymatic stage; interestingly, after the LP sequence this effect was slightly higher with the CuL. Therefore, it can be assumed that the CuL was a very efficient enzyme for producing a biobleaching effect.

Table 1. Kappa number and ISO brightness after enzymatic (L) and P stages for both laccases applied with or without violuric acid (VA) as mediator

	L		LP	
	Kappa number	Brightness (%ISO)	Kappa number	Brightness (%ISO)
K_{CuL}	7.2	51.3	6.3	72.2
VA_{CuL}	6.0	55.5	4.6	79.6
K_{TvL}	7.8	50.5	6.4	69.1
VA_{TvL}	6.7	54.2	5.1	76.3

Secondly, the CuL was applied in combination with VA and three natural mediators in order to observe an increased biobleaching effect (**Table 2**). However, the opposite effect was produced and all the natural mediators applied in combination with VA reduced brightness after L and P stages in comparison with the VA applied alone. After P stage, kappa number was increased in all the mediator combinations suggesting coupling of natural mediators on the fibre surface. The highest increase in kappa number as well as the highest decrease on brightness was attained with the VA+PCA combination.

Table 2. Kappa number and ISO brightness after enzymatic (L) and P stages when the CuL was applied with VA combined with natural mediators

	Kappa number		Brightness (%ISO)	
	L	P	L	P
K_{CuL}	7.94	5.22	52.25	66.91
VA_{CuL}	7.77	4.14	53.48	78.4
$VA+AS_{CuL}$	6.58	5.96	47.1	68.84
$VA+SA_{CuL}$	7.52	6.03	47.17	67.62
$VA+PCA_{CuL}$	8.7	6.94	45.09	62.81

When natural mediators were applied alone with the CuL (**Table 3**) brightness only increased slightly after LP sequence with SA and AS, but the values obtained failed to attain the brightness levels acquired with VA (78% *vs.* 70%). Therefore, the natural mediators cannot be comparable with the VA in terms of biobleaching. On the other hand, the increase on kappa number produced during the L stage suggested that these mediators were grafted on the fibre surface. The highest result was obtained with the PCA. In order to find a boosting effect in functionalising the fibre, combinations of natural mediators were performed. The maximum increase in kappa number was obtained with PCA combined with AS or SA.

Table 3. Kappa number and ISO brightness after enzymatic (L) and P stages when the CuL was applied with several natural mediator combinations

	Kappa number		Brightness (%ISO)	
	L	P	L	P
K_{CuL}	7.94	5.22	52.25	66.91
AS_{CuL}	7.98	6.05	49.3	70.11
SA_{CuL}	9.07	6.72	47.4	70.36
PCA_{CuL}	10.43	6.6	50.24	67.83
$AS+SA_{CuL}$	7.81	5.91	45.57	66.38
$AS+PCA_{CuL}$	10.64	7.01	47.33	61.6
$SA+PCA_{CuL}$	10.97	6.87	48.51	63.03

Another simple way to observe if the mediator is coupled on the fibre surface are the colour coordinates that can be expressed as the chroma value (C*). In **Figure 1** can be appreciated that all the natural mediator combinations increased C*, but the highest value was provided by the AS+PCA combination.

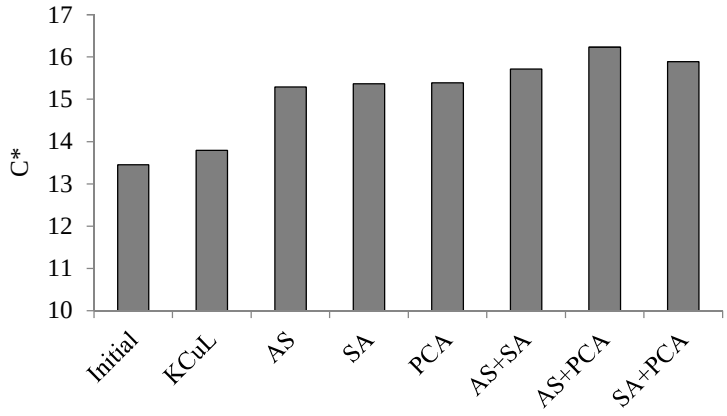

Figure 1. Crhoma value (C*) of pulps treated with the CuL and several natural mediator combinations, after the enzymatic stage.

Finally, the best way of applying the AS+PCA combination on pulp was evaluated in order to attain the maximum grafting effects. They were applied together in one step (L_{AS+PCA}), or in two steps with (L_{AS}-washing-L_{PCA}) or without (L_{AS}-L_{PCA}) washing. The highest increase in the kappa number property and also in the colour coordinates was produced when the pulp was washed between the laccase-natural mediator treatments: L_{AS}-washing-L_{PCA}.

IV. CONCLUSIONS

In this work the laccase from *Cerrena unicolor* produced by Fungal Bioproducts® has been shown to be a very efficient enzyme to be applied with synthetic or natural mediators for biobleaching or functionalizing. The best biobleaching effect was obtained with the synthetic mediator violuric acid applied alone. However, the best biografting effect was obtained with the combination of the natural mediators *p*-coumaric acid and acetosyringone. Moreover, results can be enhanced if an interstep washing between them is performed.

V. ACKNOWLEDGEMENT

This work was supported by the Spanish MICINN BIOSURFACEL-CTQ2012-34109 and BIOFIBRECELL-CTQ2010-20238-C03-01 projects. The authors are grateful to the consolidated group with the Universitat de Barcelona (UB) AGAUR 2009SGR 00327.

VI. REFERENCES

[1] Valls,C.; Cadena, E.M.; Roncero, M.B. Obtaining biobleached eucalyptus cellulose fibres by using various enzyme combinations. *Carbohydr. Polym*. **2013**, *92*, 276–282.

[2] Cusola, O.; Valls, C.; Vidal, T.; Roncero, M.B. Rapid functionalisation of cellulose-based materials using a mixture containing laccase activated lauryl gallate and sulfonated lignin. *Holzforschung*. **2014**, 1–9.

[3] Valls, C.; Vidal, T.; Roncero, M.B. Enzymatic strategies to improve removal of hexenuronic acids and lignin from cellulosic fibers. *Holzforschung*. **2014**, *68*, 229-237.

[4] Quintana, E.; Valls, C.; Vidal, T.; Roncero, M. B. An enzyme-catalysed bleaching treatment to meet dissolving pulp characteristics for cellulose derivatives applications. *Bioresour. Technol.* **2013**, *148*, 1–8.

[5] Andreu, G.; Barneto, A.G.; Vidal, T. A new biobleaching sequence for kenaf pulp: Influence of the chemical nature of the mediator and thermogravimetric analysis of the pulp. *Bioresour. Technol*. **2013**, *130*, 431–438

SHORTEN FUNGAL TREATMENT OF LIGNOCELLULOSIC WASTE WITH ADDITIVES TO IMPROVE RUMEN DEGRADABILITY

S.J.A. van Kuijk[1]*, A.S.M. Sonnenberg[2], J.J.P. Baars[2], W.H. Hendriks[1], J.W. Cone[1]

[1]*Animal Nutrition Group, Wageningen University, De Elst 1, 6708 WD Wageningen, The Netherlands;*
[2]*Plant Breeding, Wageningen University, Droevendaalsesteeg 1, 6708 PB Wageningen, The Netherlands (*Sandra.vankuijk@wur.nl)*

ABSTRACT

Selective lignin degrading fungi can be used as pre-treatment to make cellulose in plant cell walls accessible for rumen microbes. According to previous studies, *Ceriporiopsis subvermispora* and *Lentinula edodes* can increase the *in vitro* rumen degradability of lignocellulosic biomass in 7 to 8 weeks. To shorten this treatment three additives, urea (1 µg/g or 10 µg/g), manganese (15 µg/g or 150 µg/g) and linoleic acid (0.5 mM or 1 mM), were tested during *C. subvermispora* or *L. edodes* treatment of wheat straw and wood chips. After 2 and 4 weeks samples were taken to analyse the *in vitro* rumen degradability and fibre content. Two weeks of fungal treatment did not increase the *in vitro* rumen degradability of wheat straw or wood chips and additives did not have an effect on this. Addition of manganese (both concentrations) to *C. subvermispora* on wood chips did result in more lignin degradation. Linoleic acid (1 mM) and manganese (15 µg/g) enhanced lignin degradation of wood chips by *L. edodes* after 2 weeks of treatment. Fungal treatment for four weeks increased the *in vitro* rumen degradability. However additives did not enhance this. Urea and manganese did result in higher lignin degradation after 4 weeks of treatment of wheat straw with *C. subvermispora*. The cellulose content was not changed during the fungal treatment, without or with either additive.

I. INTRODUCTION

In plant cell walls lignin is bound to hemicellulose and cellulose, preventing rumen microbes to break down the carbohydrates. De-lignification is needed to improve the nutritional value of lignocellulosic biomass. Physical and chemical treatments have proven to be a fast and effective way to improve the cellulose accessibility in lignocellulosic biomass. However these treatments are expensive, have high energy demands, require special equipment and toxic waste is produced [1].

Biological pre-treatment using lignin degrading white rot fungi is a cheap and environmentally friendly method. After colonization, selective fungi produce lignin degrading enzymes and when fruit bodies are formed they start on the cellulose. The process should be stopped after the lignin degradation and before the cellulose is degraded and thus becomes available for rumen microbes. Cellulose availability for rumen microbes can be measured in the *in vitro* gas production technique, in which rumen fluid is added to the material and due to anaerobic fermentation by rumen microbes, gas is produced [2]. The amount of gas produced is directly related to organic matter fermentation in rumen fluid, and is therefore related to a better availability of cellulose and hemicellulose.

Previous experiments have shown that certain white rot fungi are very effective and selective lignin degraders. *Ceriporiopsis subvermispora* and *Lentinula edodes* significantly increased the *in vitro* degradation by rumen microbes of wheat straw, rice straw (only *C. subvermispora* showed significant increases), sugarcane bagasse, miscanthus (only *L. edodes* tested) and wood chips (only *L. edodes* tested) [3][4]. After 7 to 8 weeks of aerobic fungal treatment the *in vitro* degradability by rumen microbes reached a plateau. Fungal pre-treatment was shown to be a successful method for delignification, however it is a time consuming process. Optimization of the process is needed before fungal pre-treatments can be used in practice. Adding additives can have an effect on the growth rate and on the enzyme production. Three different additives have been tested. Urea as a nitrogen source for a faster colonization [5], manganese to stimulate the manganese peroxidase activity, which is involved in lignin degradation [6], and linoleic acid to stimulate manganese peroxidase to degrade more of the non-phenolic part of the lignin [7]. These additives have been added to *C. subvermispora* and *L. edodes* grown on wheat straw or wood chips. The *in vitro* rumen degradability and fibre content were measured to see whether additives enhance the fungal treatment.

II. EXPERIMENTAL

Fungal treatment

The fungal strains used in this experiment (*Ceriporiopsis subvermispora* (strain MES 13094) and *Lentinula edodes* (strain MES 11910)) were preserved in liquid nitrogen at Wageningen UR Plant Breeding. Initial culturing of the fungi was done on malt extract agar plates at 24°C until mycelium was covering most of the plate surface. Pieces of colonized agar culture were added to sterilized sorghum grains and this was incubated at 24°C until all grains were colonized by mycelium. The spawn was kept at 4°C until further use. Wheat straw and wood chips (oak, *Quercus rubra* L.) were used as substrates. All substrates were chopped into pieces of about 3 cm. Samples were taken as untreated non-autoclaved control. To the substrates an excess of water was added and left for 3 days to let the water fully penetrate the material. After the excess of water was removed, substrates were sprayed with additives dissolved in ethanol (maximum 0.1% ethanol was added). Single additives were added to all three substrates. Urea was added in concentrations of 1 µg or 10 µg per gram dry substrate, manganese was added in concentrations of 15 µg or 150 µg per gram dry substrate and linoleic acid in concentrations of 0.5 mmol or 1 mmol per liter moisture in the substrate. Substrates were weighed into 1.2 L polypropylene containers with filter cover. To sterilize, the material was autoclaved for 1 hour at 121°C. After cooling down the containers with sterilized substrate were kept at room temperature until further use. For each substrate about 5 gram of spawn was added to each 50 gram dry matter and mixed to distribute the spawn equally over the substrate. The samples were incubated for 0, 2 or 4 weeks at 24°C. All conditions were tested in duplicate. After incubation the substrate was air-dried at 70°C until a constant weight. The dried materials were ground through a 1 mm sieve.

Chemical analysis

Fibre analysis was done on air-dried, ground material, according to the Van Soest et al. (1991) method, using Ankom fiber analyser 2000 [8]. Hemicellulose content was calculated as the difference between neutral detergent fibre (NDF) and acid detergent fibre (ADF). Cellulose content was calculated as the difference between ADF and acid detergent lignin (ADL). For dry matter determination air-dried material was dried at 103°C. Ash content was determined by combustion for 3 hours at 550°C in a muffle furnace.

In vitro gas production technique

The *in vitro* gas production (IVGP) technique was performed according to the procedure described by Cone et al. (1996) [2]. In summary, rumen fluid from fistulated non-lactating cows was collected. To each 500 mg air dried sample 60 ml buffered rumen fluid was added. During 72 hours of incubation at 39°C, the amount of gas produced by anaerobic fermentation was measured. Total gas production was related to organic matter (OM) content of the samples.

Statistical analysis

Chemical composition and *in vitro* gas production by the fungal treatment compared to the control of each substrate were subject to generalized linear model (GLM) analysis in SAS 9.2. Post-hoc multiple comparison with Tukey's significant test at level of $\alpha = 0.05$ was performed to determine the significance between the treatments. The following model was used:

$$Y_{ij} = \mu + \alpha_i + \omega_{ij}$$

In which Y_{ij} is the observation j in treatment i; μ is the overall mean; α_i is the fixed effect of treatment i; ω_{ij} is the random error.

III. RESULTS AND DISCUSSION

Untreated wheat straw had an IVGP of 200 ml/g OM, untreated wood chips 85 ml/g OM. Additives did not have an effect on IVGP of untreated material. Fungal treatment for 2 weeks did not have an effect on IVGP of wheat straw. Additives did not enhance IVGP or ADL degradation after two weeks of treatment of wheat straw by *C. subvermispora* or *L. edodes*. Wheat straw treated for 4 weeks with *L. edodes* did increase IVGP with 56 ml/g OM to 270 ml/g OM ($P<0.05$). *C. subvermispora* could not significantly increase the IVGP of wheat straw in a 4 week's treatment (**Figure 1**). In literature an increased IVGP of wheat straw was found after 3 weeks treatment

with *L. edodes* or *C. subvermispora* [3]. A different batch of wheat straw used might explain the difference. Additives could not stimulate the fungi to increase the IVGP. Addition of manganese (15 µg/g) resulted in 30% and urea (1 µg/g) resulted in 16% more lignin degradation in wheat straw by *C. subvermispora* after 4 weeks than without any additive (P<0.05) (**Figure 1**).
Both *C. subvermispora* and *L. edodes* did not decrease the cellulose content of wheat straw throughout the treatment period.

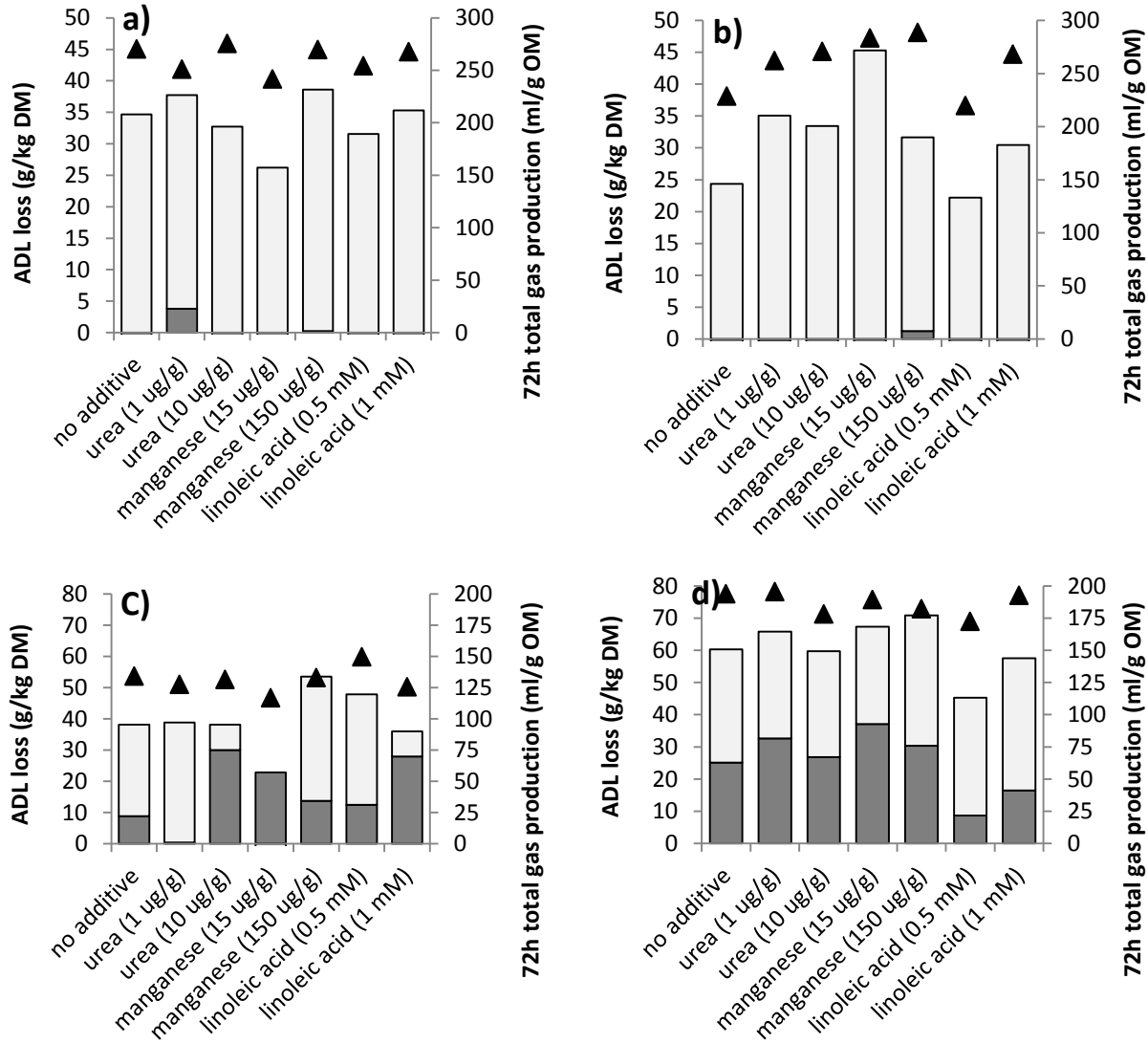

Figure 1. ADL loss after 2 and 4 weeks of fungal treatment compared to *in vitro* gas production. Dark grey bars: ADL loss after 2 weeks of incubation, light grey bars: ADL loss after 4 weeks of incubation, ▲ *in vitro* gas production after 4 weeks of treatment. a) wheat straw treated with *L. edodes*, b) wheat straw treated with *C. subvermispora*, c) wood chips treated with *L. edodes*, d) wood chips treated with *C. subvermispora*.

IVGP of wood chips did not increase significantly after 2 weeks of treatment as compared to the untreated control. Additives did not have an effect on the IVGP after 2 weeks. Without additives, the ADL content of wood chips was not significantly lowered by *C. subvermispora* or *L. edodes* as compared to the control. However when manganese (15 µg/g or 150 µg/g) was added to *C. subvermispora* on wood chips a lower ADL content than the control was found after 2 weeks (P<0.05) (**Figure 1**). Upon adding linoleic acid (1 mM) or manganese (15 µg/g) to *L. edodes* on wood chips, a lower ADL content was found than in the control after 2 weeks (P<0.05) (**Figure 1**). Four weeks of treatment of wood chips with *C. subvermispora* resulted in a 200% higher IVGP as compared to the untreated control (P<0.05). Additives did not have an additional effect on the IVGP or lignin degradation by *C. subvermispora* grown on wood chips for 4 weeks (**Figure 1**). *L. edodes* could not significantly increase the IVGP of wood chips after 4 weeks of treatment. However addition of manganese

(150 µg/g) to the culture resulted in more lignin degradation (P<0.05) (**Figure 1**). The cellulose content did not change during the treatment of wood chips with *C. subvermispora* or *L. edodes*.
Literature describing an additional effect of urea, manganese and linoleic acid on fungal treatments uses a different fungal strain and/or substrate [5][6][7][9]. Both linoleic acid and manganese target the enzyme manganese peroxidase. The effect of linoleic acid might be enhanced when manganese is added to the culture [9]. In future research a combination of both additives will be tested.

IV. CONCLUSIONS

Four weeks of incubation with *C. subvermispora* and *L. edodes* improves the *in vitro* rumen degradability of wheat straw or wood chips. Additives do not result in a higher *in vitro* rumen degradability after 2 or 4 weeks of fungal treatment. *C. subvermispora* degraded more lignin in wood chips after 2 weeks when manganese (15 µg/g or 150 µg/g) was added. *L. edodes* degraded more lignin in wood chips after 2 weeks when manganese (15 µg/g) or linoleic acid (1 mM) were added. Urea (1 µg/g) and manganese (15 µg/g) did result in a higher lignin degradation after four weeks of treatment of wheat straw with *C. subvermispora*. Cellulose content of the substrate did not change during the fungal treatment. Although in this experiment manganese had the highest effect, a combination of linoleic acid and manganese might result in an additional effect.

V. ACKNOWLEDGEMENT

This research was supported by the Dutch Technology Foundation (STW), which is part of the Netherlands Organization for Scientific Research (NWO), which is partly funded by the Dutch Ministry of Economic Affairs. This research was co-sponsored by Agrifirm, Purac, DSM, Den Ouden, Hofmans and Wageningen University.

VI. REFERENCES

[1] Agbor, V.B.; Cicek, N.; Sparling, R.; Berlin, A.; Levin, D.B. Biomass pretreatment: Fundamentals toward application. *Biotechnology Advances* **2011**, *29*, 675-685.

[2] Cone, J.W.; Van Gelder, A.H.; Visscher, G.J.W.; Oudshoorn, L. Influence of rumen fluid and substrate concentration on fermentation kinetics measured with a fully automated time related gas production apparatus. *Animal Feed Science and Technology* **1996**, *61*, 113-128.

[3] Tuyen, V.D.; Cone, J.W.; Baars, J.J.P.; Sonnenberg, A.S.M.; Hendriks, W.H. Fungal strain and incubation period affect chemical composition and nutrient availability of wheat straw for rumen fermentation. *Bioresource Technology* **2012**, *111*, 336-342.

[4] Tuyen, D.V.; Phuong, H.N.; Cone, J.W.; Baars, J.J.P.; Sonnenberg, A.S.M.; Hendriks, W.H. Effect of fungal treatments of fibrous agricultural by-products on chemical composition and *in vitro* rumen fermentation and methane production. *Bioresource Technology* **2013**, *129*, 256-263.

[5] Tripathi, J.P.; Yadav, J.S. Optimization of solid substrate fermentation of wheat straw into animal feed by *Pleurotus ostreatus* - a pilot effort. *Animal Feed Science and Technology* **1992**, *37*, 59-72.

[6] Kerem, Z.; Hadar, Y. Effect of manganese on preferential degradation of lignin by *Pleurotus ostreatus* during solid-state fermentation. Applied and Environmental Microbiology 1995, 61, 3057-3062.

[7] Kapich, A.; Hofrichter, M.; Vares, T.; Hatakka, A. Coupling of manganese peroxidase-mediated lipid peroxidation with destruction of nonphenolic lignin model compounds and 14C-labeled lignins. Biochemical and Biophysical Research communications 1999, 259, 212-219.

[8] Van Soest, P.J.; Robertson, J.B.; Lewis, B.A. Methods for dietary fiber, neutral detergent fiber, and nonstarch polysaccharides in relation to animal nutrition. Journal of Dairy Science 1991, 74, 3583-3597.

[9] Cunha, G.G.S.; Masarin, F.; Norambuena, M.; Freer, J.; Ferraz, A. Linoleic acid peroxidation and lignin degradation by enzymes produced by *Ceriporiopsis subvermispora* grown on wood or in submerged liquid cultures. Enzyme and Microbial Technology 2010, 46, 262-267.

CELLULASE-ASSISTED REFINING OF BLEACHED CHEMICAL PULP AND ITS EFFECT ON THERMAL DURABILITY OF PAPER

Emilia Vänskä[1]*, Tapani Vuorinen[1]

[1]*Aalto University, School of Chemical Technology, Department of Forest Products Technology, P.O. Box 16300, 00076 Espoo, Finland (*emilia.vanska@aalto.fi)*

ABSTRACT

Increasing environmental awareness is advocating the use of cellulosic fiber-based packaging materials. However, the thermal stability of natural fibers is insufficient for several food packaging solutions. Meanwhile, an emerging need for reducing energy consumption has drawn the paper industry's interest toward enzymatic pretreatments prior to refining of pulp. Despite the industrial utilization of enzymes, the effect of enzymatic hydrolysis on the thermal stability of paper is still not properly understood.

An evaluation of the properties of a cellulase-treated kraft pulp at high refining degrees revealed various important aspects relevant for the study of the thermal stability of paper. We were able to show by means of Schopper-Riegler drainability number, water retention value, fiber width, molar mass distribution, and intrinsic viscosity that the cellulase treatment affects the depolymerization of cellulose during refining.

The cellulase pretreatment of the bleached softwood pulp changed the thermal durability (at 225 °C) of paper remarkably. After the thermal treatment the sheets made of the enzymatically treated pulp were weaker and more brittle than the sheets made of untreated pulp. Overall, our findings contribute to the current understanding of how enzymatic treatment of chemical pulp affects the thermal durability of paper aiming at food packaging applications.

I. INTRODUCTION

Natural fiber based webs are becoming an increasingly important raw material for food packaging applications due to the growing demand of replacing plastics with more sustainable materials. Unfortunately, the insufficient temperature resistance of cellulosic fibers limits their more extensive utilization in the food industry.
The thermal degradation of cellulose has been widely studied and it is known to proceed via oxidation of the glucopyranose ring and hydrolysis of glycosidic bonds [1].

Cellulases have been applied to reduce the energy consumption in pulp refining and to improve the strength properties of paper [2]. However, little is known about the influence of the enzyme treatment of pulp on the thermal stability of paper. Cellulases catalyze the hydrolysis of cellulose [3] and the mechanical refining process fractures the cell wall, which has already been weakened by the enzymes, resulting in the strength loss of the pulp [4].

Herein, we report the effect of cellulase treatment on the thermal durability of a paper, made of bleached softwood kraft pulp, at high temperature (225 °C). The depolymerization of cellulose during the pulp refining was followed by measurements of the intrinsic viscosity and molar mass distribution (MMD). Changes in fiber morphology after the cellulase-assisted refining was monitored with the Schopper-Riegler drainability (°SR) number, water retention value (WRV) and fiber width. Finally, the thermal degradation of the cellulase-treated paper was investigated with the tensile strength and stretch.

II. EXPERIMENTAL

Refining of pulp

Metsä Fibre Oy, Rauma mill (Finland) supplied fully bleached (bleaching sequence DE_PDP) softwood kraft pulp. Oy Banmark AB (Finland) provided a commercial mixture of endo-1,4-β-D-glucanase and cellobiohydrolase with an reported enzyme activity of 90,000 ECU/g.

Before refining with a conical refiner, the pH of the pulp was adjusted to 5. Prerefining was performed at a specific energy consumption (SEC) level of 102 kWh/t and a specific edge load of 3.0 J/m, with a rotation speed of 750 rpm, and pulp consistency of 3.5%. After prerefining the pulp was divided into two batches of which one was treated with the cellulase solution (250 g/ADt). To activate the cellulase, the EFB pulp was incubated at ~60 °C for 90 minutes before further refining. The primary refining of the pulps was accomplished at the specific edge load of 1.5 J/m, rotation speed of 1500 rpm and consistency of 3.5%. The target of the refining was to obtain comparable °SR numbers for the reference and cellulase-treated pulps (determined according to the standard ISO 5267-1). WRV was measured according to the standard SCAN-C62. The effect of the enzyme treatment and refining on the fiber width was studied with the Kajaani FS-300 instrument, according to the standard ISO 16065.

Preparation of paper sheets, their thermal treatments, and properties

Paper sheets were prepared following the standard EN ISO 5269-1:1998. The basis weight of the sheets was measured according to the standards ISO 5270:1998 and ISO 534:2005. The thermal treatment procedure, based on a method described earlier [4], was adapted to evaluate the effect of the cellulase treatment on the thermal durability (20 min at 225 °C) of the paper.

Tensile strength and stretch of the sheets were measured before and after thermal treatments in accordance with the standards ISO 5270:1998, and ISO 5270:1998 and EN ISO 1924-2:1994, respectively. Deviating from the standards, the thermally treated paper sheets were not conditioned before the strength measurements.

The intrinsic viscosity of the paper sheets was measured as defined by the standard ISO 5351:2004. The viscosity-based average DP of cellulose was calculated via the Mark-Houwink-Sakurada equation: $[\eta] = K_p DP_v^a$, where constants K_p = 1.7 ml/g and a = 0.80 were chosen as suggested for the 0.5 M copper(II) ethylene diamine (CED) solvent. [5] The technical details for molar mass distribution (MMD) determination with gel-permeation chromatography (GPC) can be found in Borrega et al. [6].

III. RESULTS AND DISCUSSION

Table 1 demonstrates that after the cellulase treatment comparable pulp properties were obtained at lower SEC level during refining. The cellulase-treated pulp showed more extended swelling (fiber width) and retained more water in the fiber matrix (WRV) than the reference pulp, which can be explained by the loosened structure and higher amount of accessible hydroxyl groups [7].

Table 1. Characteristics of pulp before and after cellulase treatment and refining.

	Refining energy	Pulp properties		
Pulp type	SEC (kWh/t)	°SR	WRV (ml/g)	Fiber width (μm)
Reference	0	14	1.2	23.0
	605	94	2.3	18.9
Cellulase-treated	102	22	1.6	23.5
	404	89	2.7	21.1

The degradation of cellulose was monitored by means of intrinsic viscosity and MMD measurements. **Figure 1** shows pronounced mechanical degradation in terms of DP decrease of the cellulase-treated pulp during the refining. This is in line with the MMD results, which showed expanded polydispersity of the pulp after the refining. Interestingly, the results indirectly indicate that the refining led to the formation of new reducing end groups which corroborates with an earlier finding [8] on homolytic chain cleavage of cellulose under intensive mechanical treatment.

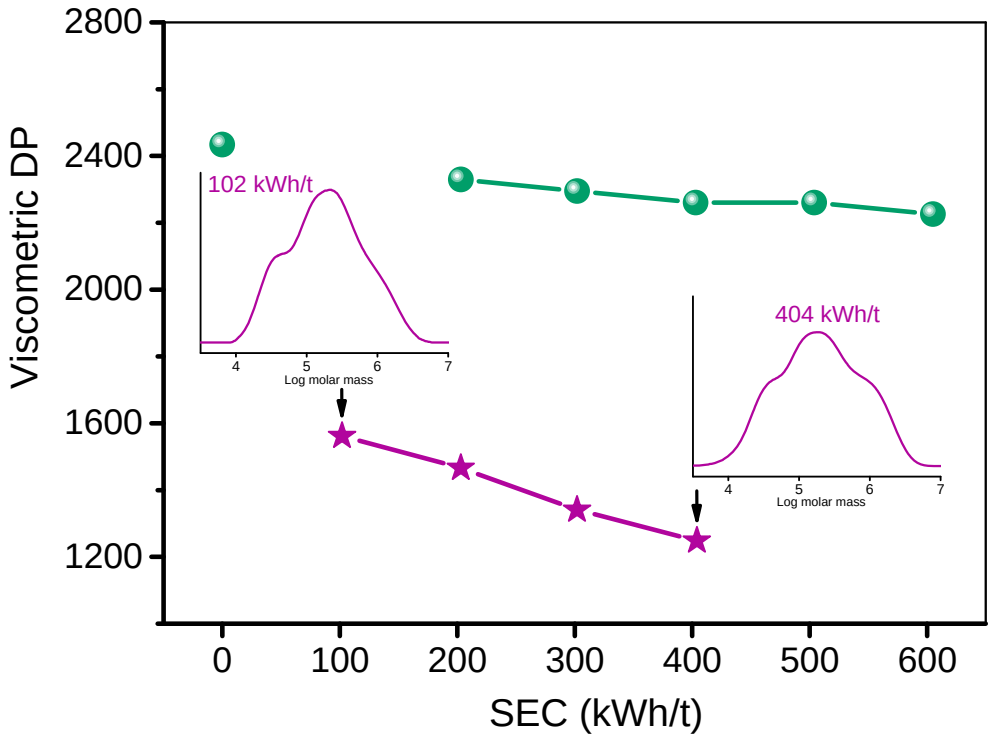

Figure 1. Decrease in the DP of cellulose and shift in MMD of untreated (circles) and cellulase-treated (stars) pulps as a function of SEC during refining.

High strength is typically desired for paper-based packages. The stretch of paper is an indicator of fiber web toughness, while the tensile strength is affected by both inter-fiber bonding and individual fiber strength. **Table 2** shows that the tensile strength of paper made of both untreated and cellulose-treated pulps developed as a result of the extended refining. Contrastively, stretch of the sheet made of the cellulase-treated pulp decreased by the action of refining.

Table 2. Mechanical properties of paper sheets before and after 20 min thermal treatment at 225 °C.

Paper	Tensile index (Nm/g)	Stretch (%)
Reference, 0 kWh/t	27	3.4
After heat: reference, 0 kWh/t	34	3.0
Reference, 605 kWh/t	99	3.9
After heat: reference, 605 kWh/t	109	1.4
Cellulase-treated, 102 kWh/t	56	3.3
After heat: cellulase-treated, 102 kWh/t	56	1.9
Cellulase-treated, 404 kWh/t	85	2.8
After heat: cellulase-treated, 404 kWh/t	94	1.1

Surprisingly, an increase in the tensile strength of the paper sheets after their thermal treatment was observed, while the stretch was reduced significantly. These findings may possibly be explained with covalent cross-linking between fibers [9]. Furthermore, the formed cross-links in the sheets of refined pulps seemed to be sensitive to thermal degradation. The sheet properties summarized in **Table 2** along with the DP results in **Figure 1** may indicate that the homolytic cleavage of glucosidic linkages at high refining degrees possibly affects the thermal durability of the intensively-refined paper particularly.

IV. CONCLUSIONS

The cellulase-treated fibers were more swollen (increased fiber width and WRV) already prior to intensive refining. In addition, it was found that the cellulase treatment of pulp enhanced the refining efficiency, indicated by similar °SR number at lower SEC level. However, the tensile strength of sheets made of cellulase-treated pulp remained lower than the strength without the enzyme treatment, explained also by lower DP of cellulose after the cellulase treatment.

The main contribution from this study was to demonstrate how an enzyme pretreatment affects the performance of paper in food packaging applications where the product is subjected to high temperature. Overall, our results imply that the thermal durability of paper made of intensively-refined reference pulp was superior to paper of cellulase-treated pulp.

V. ACKNOWLEDGEMENTS

This work was part of EffFibre program of Finnish Bioeconomy Cluster Ltd and was funded by Metsä Fibre Ltd.

VI. REFERENCES

[1] Castro, K.; Princi, E.; Proietti, N.; Manso, M.; Capitani, D.; Vicini, S.; Madariaga, J. M.; De Carvalho, M. L. Assessment of the weathering effects on cellulose based materials through a multianalytical approach. *Nucl. Instrum. Methods. Phys. Res. Sect. B.* **2011**, *269*, 1401-1410.

[2] Lecourt, M.; Sigoillot, J.-C.; Petit-Conil, M. Cellulase-assisted refining of chemical pulps: Impact of enzymatic charge and refining intensity on energy consumption and pulp quality. *Process Biochem.* **2010**, *45*, 1274-1278.

[3] Henrissat, B. Cellulases and their interaction with cellulose. *Cellulose.* **1994**, *1*, 169-196.

[4] Vänskä, E.; Luukka, M.; Solala, I.; Vuorinen, T. Effect of water vapor in air on thermal degradation of paperat high temperature. *Polym. Degradation Stab.* **2014**, *99*, 283-289.

[5] Kasaai, M. R. Comparison of various solvents for determination of intrinsic viscosity and viscometric constants for cellulose. *J. Appl. Polym. Sci.* **2002**, *86*, 2189-2193.

[6] Borrega, M.; Tolonen, L. K.; Bardot, F.; Testova, L.; Sixta, H. Potential of hot water extraction of birch wood to produce high-purity dissolving pulp after alkaline pulping. *Bioresour. Technol.* **2013**, *135*, 665-671.

[7] Pala, H.; Mota, M.; Gama, F. M. Enzymatic modification of paper fibres. *Biocatal. Biotransform.* **2002**, *20*, 353-361.

[8] Sakaguchi, M.; Ohura, T.; Iwata, T.; Takahashi, S.; Akai, S.; Kan, T.; Murai, H.; Fujiwara, M.; Watanabe, O.; Narita, M. Diblock copolymer of bacterial cellulose and poly(methylmethacrylate) initiated by chain-end-type radicals produced by mechanical scission of glycosidic linkages of bacterial cellulose. *Biomacromolecules.* **2010**, *11*, 3059-3066.

[9] Kato, K. L.; Cameron, R. E. A review of the relationship between thermally-accelerated ageing of paper and hornification. *Cellulose.* **1999**, *6*, 23-40.

EXTRACTIVES IN THE WOOD TISSUE OF WOUNDED AND RED HEARTED BEECH

Viljem Vek[1], Primož Oven[1]*, Ida Poljanšek[1], Miha Humar[1], Thomas Ters[2]

[1] *Department of Wood Science and Technology, Biotechnical Faculty, University of Ljubljana, Rožna dolina, cesta VIII/34, 1000 Ljubljana, Slovenia;* [2] *Vienna University of Technology, Institute of Chemical Engineering, Karlsplatz 13, 1040 Vienna, Austria (*primoz.oven@bf.uni-lj.si)*

ABSTRACT

The composition of extractives in the wound-associated wood and knots of common beech (*Fagus sylvatica* L.) was investigated. Low-molecular compounds were extracted from wood by means of cyclohexane and methanol. Obtained lipophilic and hydrophilic extractives were examined with gas chromatography and high performance liquid chromatography. Further on, an antifungal potential against *Trametes versicolor* and *Gloeophyllum trabeum* was estimated by the paper disc screening test. The chromatographic analysis of lipophilic extractives revealed the presence of saturated and unsaturated fatty acids, fatty alcohols and triterpenoids, mainly free sterols. The largest contents of identified lipophilic extractives were measured in discoloured tissues and knots. The hydrophilic extractives consisted of mono- and oligosaccharides, sugar alcohols and acids, di- and tricarboxylic acids, various simple phenols and flavonoids. Catechin was referred to as the dominant and characteristic compound of beech wood extracts. The largest concentrations of phenolic extractives were measured in wound-wood, knots, and sapwood whereas the tissues of red heart contained the lowest amounts. A screening test indicated the fungistatic potential of particular wood tissues in a living tree. A schematic diagram of distribution of phenolic extractives in the wood of wounded and red hearted beech tree is proposed and the role of wound-associated tissues is discussed.

I. INTRODUCTION

Common beech represents one of the economically most important deciduous tree species in Europe due to its prevalence and high application potential. It accounts approximately 32 % of the wood stock in Slovenian forests. It is also known as the tree species, which is characterized by the formation of facultative discoloration at the location of ripewood [1]. Discoloration in a beech stem, also called the red heart, is frequently formed as a negative consequence of mechanical wounding caused by selective harvesting and logging activates in forests. After all, the negative effects of mechanical injuries can drastically affect the quality of wood biomass and consequently lower the economic income. Such like traumatic events represents the first phase in a sequence of complex processes that can lead to spatially defined changes (discolouration, biological decay, tree hollow). Restriction of these changes can be explained by the concept of compartmentalization, which suggests that living trees can limit the affected regions by existing and newly formed tissues and by chemical substances on a minimal volume. For a general description of the complex compartmentalization processes, three basic models are used, i.e. the conceptual model CODIT [2], model of reaction zones [3] and model of microenvironmental changes [4]. Furthermore, a compartmentalization in wood of living trees can be understood in the frames of the passive and active functions of the defense and protective systems as the constitutive protection and induce defense [5, 6]. These protective and defensive mechanisms in wood are being accompanied by the anatomical and chemical changes. Besides anatomical specialties, e.g. aspiration of pits, formation of tyloses or suberisation of cell walls, the chemical aspect is crucial for tree survival after traumatic event. Chemical changes are associated with the cell necrosis and the consequent formation and accumulation of both low molecular compounds and phenolic polymers, i.e. extractives. Extractives are the non-structural components of wood and are from physiological aspect of view interpreted as the primary or secondary metabolites. Regarding the solvent which are soluble in, extractives can be further divided as the lipophilic and hydrophilic extractives. It is generally believed that in a living tree lipophilic extractives represent physical protection, e.g. as the hydrophobic barrier, while the hydrophilic extractives occur as the chemical inhibitors. Lignans, stilbenes and flavonoids are well known as the compounds with antioxidant, antimicrobial and antifungal properties. Therefore, extractives have been treated as the substances with very important physiological function in a survival strategy of living tree.

The aim of this study was (*a*) to investigate the composition of lipophilic and hydrophilic extractives in wounded wood of stem and knots of common beech and (*b*) to estimate the antifungal potential of hydrophilic extracts of beech wood against representative white and brown rot fungi.

II. EXPERIMENTAL

Material

Investigation was performed on more mechanically wounded beech trees (*Fagus sylvatica L.*) fallen in Slovenia. Discs with a direct injury and discs containing living and dead branches were taken from each harvested tree. Samples of wound-wood (W), intact sapwood (S), reaction zone (RZ), discolored wood (DW) and knots of living (LK) and dead branches (DK) were sawn out from the discs and grinded. Before the extraction, samples were being freeze dried for 24 hours.

Extraction

For the purposes of GC-MS analyses different types of wound-associated stem tissues and knots of beech were extracted for lipophilic and hydrophilic extractives in a Büchi speed extractor E-916. Sequential extraction was performed by means of cyclohexane (90°C, 110 bar under N_2, two 15 min static cycles) and methanol/water (95:5 (v/v), 100°C, 110 bar under N_2, two 15 min static cycles). Beech wood samples were extracted in a Soxhlet apparatus as well. Therefore, lipophilic extractives were removed from 2.5 g of wood sample by extraction with 250 mL of cyclohexane for 4 hours, while hydrophilic extractives were subsequently extracted for 6 hours with 250 mL of methanol/water mixture (95:5, v/v). Extracts obtained with the Soxhlet extraction were examined by HPLC and exposed to wood decaying fungi. The amounts of total lipophilic and hydrophilic extractives were determined gravimetrically.

Chromatographic analyses

The extractives in wounded wood and knots of beech were chemically characterized by means of gas chromatography (GC-MS) and liquid chromatography (HPLC). Before GC analysis, all the extracts were silylated according to Willför et al. [7]. Heneicosanoic acid and betulinol were used as internal standards. Quantitative evaluation of the separated extractives was performed on an Agilent 7890A GC-FID system quipped with an Agilent 7693 auto sampler and a HP-5 column (30 m × 0.32 mm i.d.; 0.25 μm film thickness). The injection volume was 1 μL. Temperature program: 150°C (1 min)→ 4°C/min to 220°C→ 20°C/min to 320°C (6.5 min); flow of helium was 1.4 mL/min, split ratio of 10:1; the injector and FID temperatures were 260°C and 330°C, respectively. The results were expressed in milligrams per gram of dry wood (mg/g). The identification of lipophilic and hydrophilic extractives was done by an Agilent 5975 GC-MS system, using similar column and the same temperature program as described above. MS parameters: source temperature 250°C, quadropole temperature 150°C, EI at 70 eV, and mass range 35 - 750 m/z.
The results obtained by gas chromatography were upgraded with the high performance liquid chromatography (HPLC). Separation was done on a Thermo Accela 600 HPLC-PDA system. Methanol extracts were filtered and 3 μL of each sample was directly injected on an Accucore PFP column (150 × 2.1 mm, 2.6 μm particle size). The column was heated at 30°C. The mobile phase consisted of water with 0.1 % of formic acid (v/v) and methanol containing 0.1 % of formic acid. The 10 minutes gradient from 5 - 65 % of methanol was applied. Flow rate was defined at 400 μL/min. The detection wavelength was adjusted to 275 nm and UV spectra from 200 to 400 nm were recorded for peak identification. Quantitative analysis was based on a calibration curves consisting of standard solutions. Peak identification was achieved by comparison of retention times and UV spectra of separated compounds with analytical standards. The content of extractives was expressed in milligrams per gram of dry sample (mg/g).

Antifungal properties of extractives

The antifungal potential of lipophilic and hydrophilic extractives towards the growth of white rot (*T. versicolor*) and brown rot (*G. trabeum*) fungi was investigated by means of a paper disc screening test. Extracts of sapwood, wound-wood, reaction zone and knot (K) were applied in the test. Cellulosic antibiotic assay discs were used as the carriers, where each disc was impregnated ten times with a volume of 100 mL of extract. Cyclohexane and methanol served as the controls (C). White and brown rot fungal inoculums were placed in the center of the Petri dish and stored in a growth chamber at 25°C and 75 % relative humidity. Growth of mycelium was monitored after 3, 4, 7 and 10 days. Fungal growth toward the paper discs with different extracts was visually estimated and compared to the growth in control direction. Since some of the extractives promotes fungal growth while other retarded it, the scale chosen covered all possible responses (+, promotes the growth of mycelia; /, normal growth, no retardation; -, inhibits the growth of mycelia; - -, markedly inhibits the growth of mycelia).

III. RESULTS AND DISCUSSION

The differences in the content of lipophilic extractives among different types of beech wood were not significant, whereas the highest amounts of hydrophilic extractives were determined, gravimetrically, in knots and wound-wood. Relative high amounts of hydrophilic extractives were characteristic for the intact sapwood as well. Significantly lower contents of hydrophilic extractives were measured in the samples from the discoloured part of a beech stem.

The chromatographic analysis of the lipophilic extractives in cyclohexane extracts of beech wood revealed the presence of saturated and unsaturated fatty acids (palmitic, stearic, behenic, linoleic and oleic acid), fatty alcohols (behenyl and lingoceryl alcohol) and triterpenoids (squalene, stigmstadiene, β-sitosterol and β-sitostanol), among which β-sitosterol was found as the most abundant one. The largest contents of identified lipophilic extractives were determined for the discoloured tissues and knots, as presented by a **Figure 1**.

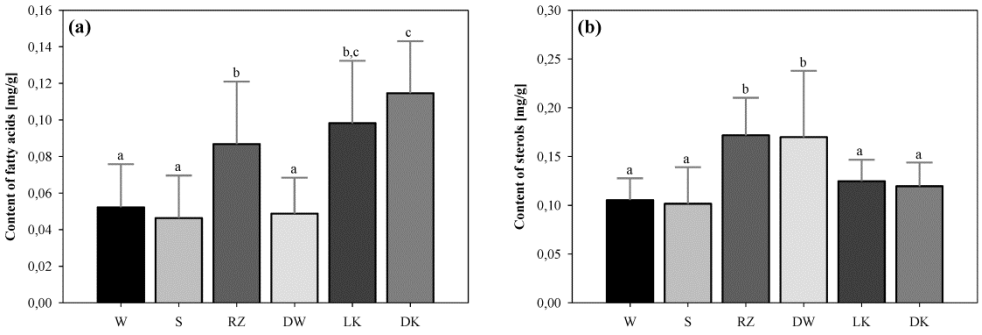

Figure 1. The contents of identified lipophilic extractives as determined by chromatographic analysis. [a - c] The different letters at the top of the error bars indicate the statistically significant differences (LSD test at a 95 % confidence level). (a) Fatty acids; (b) Free sterols.

In comparison to the lipophilic extractives the yield of hydrophilic extractives was significantly larger. The hydrophilic extractives consisted of mono- and oligosaccharides (trehalose, saccharose and raffinose), sugar alcohols (erytritol, syringol and arabitol) and inositols, sugar acids (ribonic, threonic, gluconic and glucuronic acid), di- and tricarboxylic acids (malic, malonic and citric acid), various simple phenols (vanilyl alcohol, syringol, vanillic acid, syringic acid, gallic acid, sinapyl alcohol and coniferyl alcohol) and flavonoids (catechin, epicatechin and taxifolin). Chemical analysis of methanol extracts revealed also the presence of unidentified lignan-type compounds. Catechin was referred to as the dominant and characteristic compound of beech wood extracts. The largest concentrations of identified phenolic extractives were measured in wound-wood and knots, as well as in the sapwood, whereas the tissues of discolouration contained the lowest amounts of identified hydrophilic extractives (**Figure 2**).

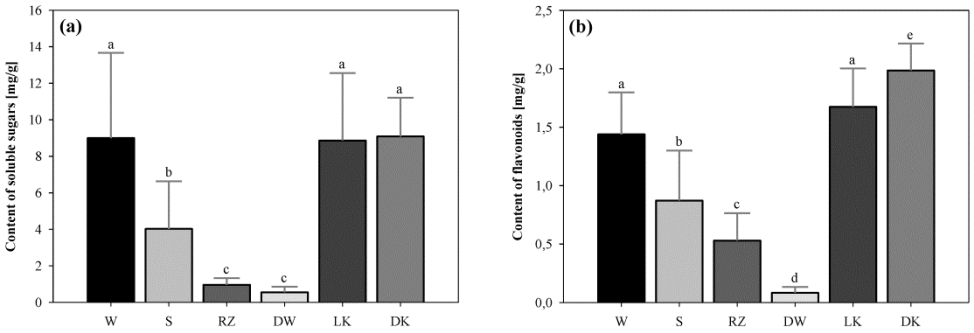

Figure 2. The contents of identified hydrophilic extractives as determined by chromatographic analysis. [a - e] The different letters at the top of the error bars indicate the statistically significant differences (LSD test at a 95 % confidence level). (a) Fatty acids; (b) Sterols.

Table 1. Inhibition of *Trametes versicolor* and *Gloeophyllum trabeum* by cyclohexane and methanol extracts of different categories of wound-associated wood and knot of beech (*Fagus sylvatica* L.). Sample abbreviations: C, control; S, intact sapwood; RZ, reaction zone; W, wound-wood; K, knot.

Extractives	*Trametes versicolor*					*Gloeophyllum trabeum*				
	C	S	RZ	W	K	C	S	RZ	W	K
Hydrophilic	/	- -	+	- -	-	/	- -	/	- -	- -
Lipophilic	/	-	/	-	/	/	-	-	-	/

Chromatographic results were confirmed by the performed paper disc screening test, which indicated the fungistatic potential of particular wood tissues in a living tree (**Table 1**). The relevant antifungal potential was demonstrated by both the lipophilic and hydrophilic extractives of beech wood, the inhibiting effect of the latter being more pronounced. A clear inhibition was demonstrated in the case of the methanol extracts of wound-wood, intact sapwood and knot, especially with regard to the initial stages of development of brown rot fungi *G. trabeum*. In spite of the important compartmentalization function of reaction zones in wood of living trees, extracts of these morphological barriers did not reveal a relevant antifungal effect. Therefore, a function of physical barriers rather than chemical protection can be ascribed to the reaction zone in a beech tree [8].

IV. CONCLUSIONS

Results of present investigation complement the concept of compartmentalization in the sense that a more important protective role is attributed to the tissues located at the exposed sites in a living tree, i.e. wound-wood, older parts of sapwood and bases of living and dead breaches. The extractive compounds which accumulate in the oldest parts of sapwood are mobilized at the time of formation of reaction zones, which, in the case of beech, perform the function of a protective physical barrier. A key role for tree survival after mechanical wounding and an important repairing function can be ascribed to wound-wood. Therefore, the constitutive protection of wood, which is intensified in tissues that are exposed to the penetration of atmospheric oxygen and invasive organisms, represents an important part of protective and defensive systems of living trees. The role of phenolic extractives in these tissues can be understood as the protection for functional and vital parts of trees. Our results also indicate that different types of wound-associated tissues describes an important source of variability in content of extractives in the wood of a tree, in addition to regular structures described in literature (heartwood, knots).

V. ACKNOWLEDGEMENT

The authors would like to thank to the COST Action FP0901 and to the Slovenian Research Agency for financial support.

VI. REFERENCES

[1] Torelli, N. The ecology of discolored wood as illustrated by beech (*Fagus sylvatica* L.). IAWA Bull. **1984**, 5, 121-127.

[2] Shigo, A.L., Marx, H.G. Compartmentalization of decay in trees. USDA For. Serv. Agric. Bull. **1977**, 405, 1-73.

[3] Shain, L. Dynamic responses of differentiated sapwood to injury and infection. USA, American Phytopathological Society: Symposium on wood decay in living trees. **1979**, 69, 1143-1147.

[4] Boddy, L., Rayner, A.D.M. Origins of decay in living deciduous trees: the role of moisture content and a re-apprasial of the expanded concept of tree decay. New Phytol. **1983**, 94, 623-641.

[5] Duchesne, L.C., Hubbes, M., Jeng, R.S. Biochemistry and molecular biology of defense reactions in the xylem of angiosperm trees. In Defence mechanisms of woody plants against fungi, R.A. Blanchete and A.R. Biggs, eds (Berlin: Springer-Verlag). **1992**, 133-146.

[6] Franceschi, V.R., Krokene, P., Christiansen, E., Krekling, T. (2005) Anatomical and chemical defenses of conifer bark against bark beetles and other pests. New Phytologist. **2005**, 167, 353-375.

[7] Willför, S.M., Ahotupa, M.O., Hemming, J.E., Reunanen, M.H.T., Eklund, P.C., Sjoholm, R.E., Eckerman, C.S.E., Pohjamo, S.P., Holmbom, M.R. Antioxidant activity of knotwood extractives and phenolic compounds of selected tree species. J. Agric. Food Chem. **2003**, 51, 7600-7606.

[8] Schwarze, F.W.M.R., Baum, S. Mechanisms of reaction zone penetration by decay fungi in wood of beech (*Fagus sylvatica*). New Phytol. **2000**, 146, 129-140.

CHIMERIC SIGNAL PEPTIDES FOR THE FUNCTIONAL EXPRESSION OF ARYL-ALCOHOL OXIDASE IN *Saccharomcyes cerevisiae*.

Javier Viña-González[1], David González-Pérez[1], Angel T. Martínez[2] and Miguel Alcalde[1]*.

*[1]Institute of Catalysis, CSIC, Cantoblanco, 28049 Madrid, Spain; [2]Centro de Investigaciones Biológicas, CSIC, Ramiro de Maeztu 9, 28040 Madrid, Spain (*malcalde@icp.csic.es)*

ABSTRACT

Among the ligninolytic oxidoreductases secreted by white-rot fungi, aryl-alcohol oxidase (AAO) plays an outstanding role as H_2O_2 supplying enzyme during lignin decay. With high enantioselectivity and broad substrate specificity, this flavo-enzyme is also a promising departure point for directed evolution studies towards different biotechnological fates, but the lack of heterologous functional expression levels precludes further advances in the field. In this study, the native signal peptide of AAO from *Pleurotus eryngii* was replaced by those of the mating α-factor, the toxin K_1 Killer, as well as combinations of pre- and pro-regions from both leaders to achieve secretion in *Saccharomyces cerevisiae*. AAO expression in yeast was measured with the help of an *ad-hoc* dual high-throughput screening protocol based on the detection of H_2O_2 with a chemical and an enzymatic assay (the latter using horseradish peroxidase). All constructs were successfully processed and secreted by yeast showing extracellular AAO activities with several aryl alcohols, which opens new paths for future developments.

I. INTRODUCTION

Aryl-alcohol oxidase (AAO, EC 1.1.3.7) is a FAD-containing enzyme sorted in the GMC (glucose-methanol-choline) oxidoreductase superfamily whose members share a canonical ADP-binding domain near the N-terminus [1]. This monomeric flavoprotein is produced by white-rot fungi and plays an essential role during lignin "enzymatic combustion" in nature. Accordingly, AAO generates H_2O_2, which is demanded by different high-redox potential ligninolytic peroxidases to start the plant cell-wall attack. Besides, H_2O_2 produced by AAO is an efficient vehicle to generate highly reactive hydroxyl radicals through the Fenton reaction ($Fe^{2+} + H_2O_2 \rightarrow OH^{\bullet} + OH^- + Fe^{3+}$): $OH^{\bullet}$ acts as diffusible oxidizer being able to depolymerize lignin and cellulose [2]. It is worth noting that the hydride abstraction process mediated by AAO shows a high enantio-selectivity, which could be very valuable in organic synthesis.

Directed molecular evolution has become the favorite strategy to engineer novel enzymes in tune with industrial standards. Unfortunately, there are no reported data about the engineering of AAO by directed evolution due to the lack of suitable functional expression systems with which to tackle this approach. Indeed, AAO has only been heterologous expressed in *Aspergillus nidulans*, an unsuited microorganism for directed evolution, [3] and in *Escherichia coli* as inclusion bodies, which can be *in vitro* refolded for rational studies although this strategy is not suitable in the high-throughput frame of a directed evolution experiment [4].

In the current work, the native signal peptide of the AAO was replaced by several signal sequences used for functional expression in *Saccharomyces cerevisiae* [5]. We first tested the signal prepro-leader of the mating α-factor of *S. cerevisiae*, which was successfully used in our laboratory to evolve different ligninolytic oxidoreductases. Besides, we fused to the AAO both the signal prepro(δ)-leader and the γ-spacer-segment of the K_1 killer preprotoxin, which were previously used for directing β-lactamases secretion in yeast [6]. Engineered fusion genes contained chimeric versions of the leaders that combined different pre- and pro-regions were also studied for a successful exocytosis by yeast. Hybrid constructs were evaluated with a dual high-throughput screening (HTS) assay to detect AAO activity from yeast supernatants permitting directed AAO evolution.

II. EXPERIMENTAL

All chemical were reagent-grade purity. Ferrous ammonium sulfate, xylenol orange, sorbitol, veratryl (3,4-dimethoxibenzyl) alcohol, 4-methoxybenzyl alcohol, ABTS (2,2'-azino-bis(3-ethylbenzothiazoline-6-sulphonic acid)), Horseradish peroxidase (HRP) and the Yeast Transformation Kit were purchased from Sigma (Madrid, Spain). Zymoprep Yeast Plasmid Miniprep, Yeast Plasmid Miniprep Kit I and Zymoclean Gel DNA Recovery Kit were from Zymo Research (Orange, CA). Restriction enzymes *Bam*HI and *Xho*I were from New England Biolabs (Hertfordshire, UK). pJRoC30-αVP (containing α-factor prepro-leader) comes from former work [5]; pflag1-AAO (containing cDNA of AAO from *P. eryngii*) was donated by Dr. Aitor Hernández-Ortega (CIB, CSIC, Madrid); and pRE1219 (containing prepro(δ)-leader of K_1 killer toxin) and pJRoC30-δN1C2 (containing the γ-spacer-segment of the K_1 killer toxin) were donated by Dr. Susana Camarero (CIB, CSIC, Madrid).

Fusion genes and signal chimeric leaders

Four fusions were designed to address functional expression in *S. cerevisiae* using *in vivo* overlap extension [7]. First, AAO mature protein was fused to the α-factor prepro-leader and also to the prepro(δ)-γ regions of the preprotoxin K_1 killer from *S. cerevisiae*. In addition, two chimeric signal peptides were constructed and attached to the AAO: i) the α-factor pre-leader fused to the γ segment of the K_1 Killer toxin, (preαproK); and ii) the prepro(δ) signal sequence of the K_1 Killer toxin fused to the α-factor pro-leader (preKproα).

AAO functional expression and HTS-screening assays

For each fusion gene, two 96-well plates were prepared. Individual clones containing the autonomous replicating vector were picked and cultured in sterile 96-well plates containing 50 µL of minimal medium (SC). In each plate, well H1 was inoculated with URA3$^-$ *S. cerevisiae* as a negative control. Plates were sealed to prevent evaporation and incubated at 30°C, 225 rpm and 80% relative humidity in a humidity shaker (Minitron-INFORS, Biogen Spain). After 48 hours, 160 µL of expression medium were added to each well and cultured for additional 48 hours. Finally, 20 µL of microcultures were screened for activity with the FOX and HRP assays describe below, using two different alcohol substrates.

Chemical (direct) assay: FOX (Ferrous Oxidation in Xylenol orange presence)

Aliquots of 20 µL of yeast supernatants were incubated with 20 µL substrate (2 mM 4-methoxybenzyl alcohol or 10 mM veratryl alcohol in 100 mM phosphate buffer, pH 6.0) during 30 min at room temperature. Then 160 µL of FOX reagent were added to assess H_2O_2 production with a final concentration of FOX mixture in the well of 100 µM xylenol orange, 250 µM $Fe(NH_4)_2(SO_4)_2$ and 25 mM H_2SO_4. Plates were recorded in end-point mode at 560 nm using a spectrophotometer SPECTRAmax 384 PLUS (Molecular Devices); it took around 20 min of incubation to develop an intense colorimetric response. Responses were amplified by adding 100 mM sorbitol as signal enhancer. All measures were performed by triplicate. In each microtiter plate, columns A, B and C were employed to prepare a H_2O_2 calibration curve (from 0 to 8 µM). Detection limits were assessed applying the *Blank determination* method on a 96-well plate with triplicate standards (0, 0.5, 1, 1.5, 2, 2.5, 3 y 4 µM H_2O_2) in yeast supernatants of URA3$^-$. FOX signal stability was tested with different H_2O_2 concentrations (0, 2, 4, 6, 8, 10, 15 and 18 µM) throughout 300 min.

Enzymatic (indirect) assay: HRP-ABTS

Aliquots of 20 µL of yeast supernatants were added to 180 µL of HRP-ABTS reagent (final concentrations of HRP-ABTS reagent in the well: 1 mM 4-methoxybenzyl alcohol or 5 mM veratryl alcohol, 2.5 mM ABTS, 1µg/mL HRP in 100 mM phosphate buffer pH 6.0). The plates were incubated at room temperature and measured in end-point mode at 418 nm (ε_{ABTS}•+ = 36,000 M^{-1} cm^{-1}).

DNA sequencing

All the fusion genes were verified by DNA sequencing (BigDye Terminator v3.1 Cycle Sequencing Kit). The primers used were common to the four constructions: primers sense, RMLN and AAOsec1F 5'-GTGGATCAACAGAAGATTTCGATCG-3'and primers antisense RMLC 5'-GCTTACATTCACGCCCTCCC-3', AAOsec2R 5'-GTGGTTAGCAATGAGCGCGG-3' and AAOsec3R 5'-GGAGTCGAGCCTCTGCCCCT-3'.

III. RESULTS AND DISCUSSION

Fusion genes and signal chimeric leaders

To direct the secretion of AAO in *S. cerevisiae*, two different prepro-leaders from the mating α-factor and from the K_1 killer toxin, along with their chimeric combinations, were tailored and attached to the mature AAO. The mating α-factor signal sequence is formed by 19 and 64 amino acids for the pre- and pro-leader, respectively, **Fig. 1A**. The pre-leader initiates endoplasmic reticulum translocation being finally removed by the action of a signal peptidase. The pro-leader is supposed to be involved in proper folding and maturation before protein is packed into vesicles for exocytosis. In particular, the pro-leader is processed by the action of KEX2, STE13 and KEX1 proteases at the Golgi compartment, although the latter is not necessary for heterologous protein secretion. Likewise, K_1 prepro-toxin is leaded by a prepro-sequence of 44 residues (prepro-δ), which follows a similar processing pathway as described above for the α-factor prepro-leader but without the requirement of STE13 and KEX1, **Fig. 1B**. Besides, the prepro-toxin contains an internal γ segment of 85 residues with three extra KEX2 recognition sites for processing at the Golgi. Bearing in mind the common features of these prepro-leaders in terms of processing and secretion routes, we decided to create several fusions genes containing single and combined versions of the genetic elements to study the AAO functional expression in yeast. Accordingly, four fusions were designed: i) α-AAO formed by AAO fused to the α-factor prepro-leader; ii) K-AAO formed by AAO linked to the prepro(δ) of K_1 toxin and directly attached to a truncated version of the γ segment. The

truncated segment comprised from position 149 to 170, thereby preserving the three N-glycosylation sites (N108, N203 and N216), which may be important for a proper processing since it has been reported that longer K_1 prepro-fusions show 10% or even less secretion efficiency compared with shorter γ segment versions [6]; iii) preαproK-AAO was a chimeric leader formed by the α-factor pre-leader fused to the aforementioned truncated γ segment; and iv) preKproα-AAO, a chimeric leader formed by the prepro(δ) of K_1 toxin linked to the α-factor pro-leader. In an attempt to promote secretion, all the prepro(δ) containing constructs were modified by site directed mutagenesis to change the KEX2 recognition site Pro43-Arg44 to Lys43-Arg44, since it has been reported 50-fold enhancements in the KEX2 catalytic efficiency with such substitutions [8].

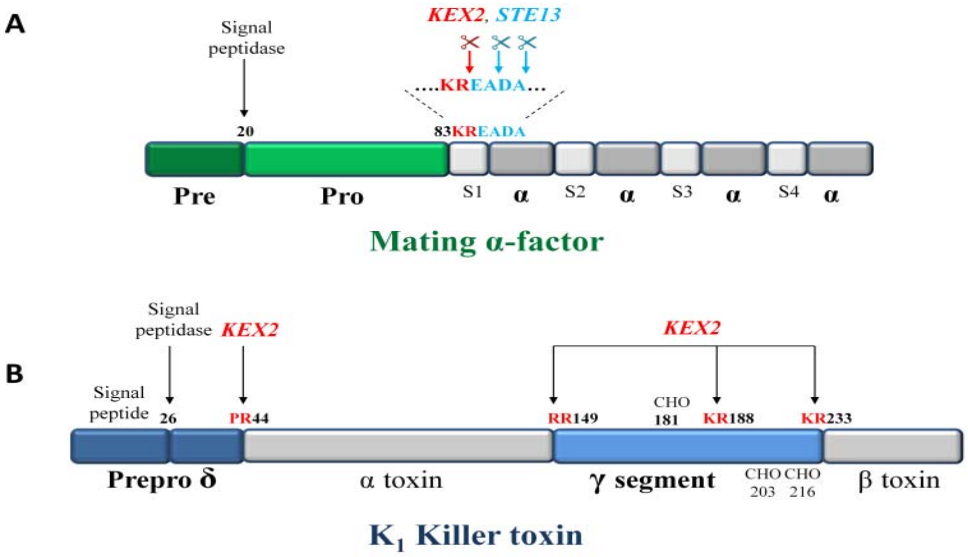

Figure 1. Mating α-factor (A) and K_1 Killer preprotoxin (B). Yeast mating pheromone α prepro-polyprotein precursor contains hydrophobic N-terminal pre-sequence (dark green) followed by potentially N-glycosylated pro-sequence (light green). Killer K_1 toxin is derived from a 316 reside preprotoxin. The unprocessed precursor consist of prepro(δ)-sequence (dark blue), which contains 26 residue signal peptide, and γ segment (light blue) separating α- and β- toxin subunits.

All hybrid fusions were spliced and repaired in *S. cerevisiae*. Taking advantage of the high frequency of homologous DNA recombination of this yeast, overlapping areas of ~40 bp were enough to guarantee a correct DNA assembly of the different genetic products and the linearized plasmid without altering the ORF. Each construction was assayed for AAO activity (with the dual chemical/enzymatic HTS-assay described in Methods Section) in the presence of veratryl alcohol as substrate. The four fusion genes reported detectable levels of AAO activity in the culture broth and they were consistent between the two colorimetric assays. The secretion levels relationship between the corresponding constructs was as follows: α-AAO> preαproK-AAO> preKproα-AAO> K-AAO. To check the constructs, individual plasmids were isolated and sequenced. It was verified that none of the constructions incorporated mutations neither in the mature protein nor in the prepro-sequences and all the elements were properly assembled as planned. Fermentations were translated from HT-format to larger volumes (10 mL) for each construct under study, **Fig. 2**. Regardless of the substrate (4-methoxybenzyl or veratryl alcohol), the order of activity between fusion genes was maintained: α-AAO, (1.5 U/L); preαproK-AAO (0.5 U/L); preKproα-AAO (0.35 U/L) and K-AAO (0.06 U/L) (all Units measured with 4-methoxybenzyl alcohol).

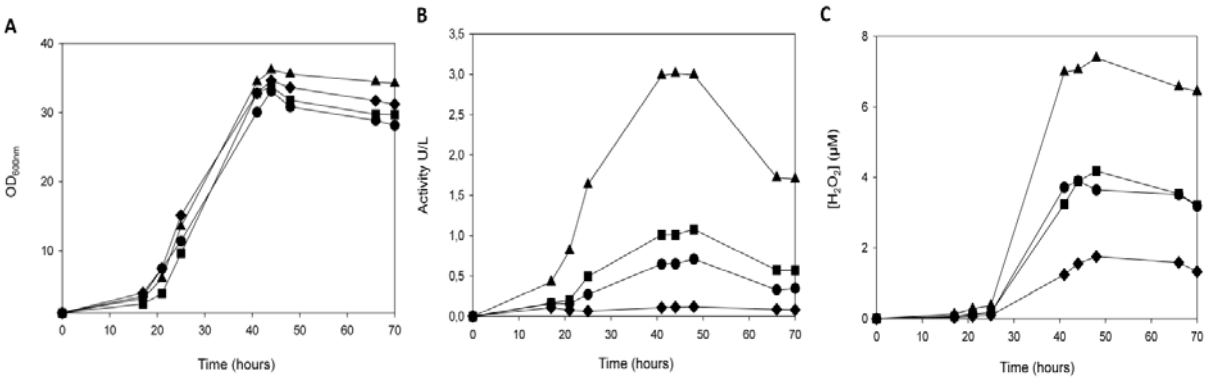

Figure 2. Shake flask fermentation monitorized throughout 70 hours. Growth curve (A), enzymatic activity through HRP-ABTS method (B) and hydrogen peroxide production measured by FOX assay (C). Construction α-AAO (triangles) (achieved the highest yields in cell growth and enzymatic activity (OD_{600} = 36 and 1.5 U/L after 44 hours), followed by preαproK-AAO (squares), preKproα-AAO (circles) and K-AAO (diamonds). Clone activity and H_2O_2 production were evaluated by triplicated.

IV. CONCLUSIONS

We have presented a platform for de directed evolution of AAO from *P. eryngii* based on: i) the AAO functional expression in *S. cerevisiae* and ii) the design of a dual HTS-assay for the detection of AAO activities. Our study have showed that all the constructions based on α-factor and K_1 toxin prepro-peptides as well as their chimeric versions yielded detectable levels of secreted AAO being valuable departure points for further engineering. This result indicates that all the fusions were successfully processed and exported by yeast. From a more general point of view, the engineering of these chimeric leaders opens a novel strategy to secrete foreign proteins so that they could be tested with other eukaryotic genes not easily handled by *S. cerevisiae*. Finally, the dual HTS-assay described in this work (based on the detection of H_2O_2 produced by AAO regardless of the substrate oxidized) opens many paths for evolving AAO towards challenging purposes, including the oxidation of secondary aromatic alcohols.

V. ACKNOWLEDGEMENTS

This work was supported by European Commission Projects PEROXICATS (FP7-KBBE-2010-4-26537), INDOX (FP7-KBBE-2013-7-613549), COST-Action CM1303-Systems Biocatalysis; and the National Project EVOFACEL (BIO2010-19697).

VI. REFERENCES

[1] Cavener, D.R. GMC oxidoreductases: a newly defined family of homologous proteins with diverse catalytic activities. *J. Mol. Biol.* **1992**, *223*, 811-814.

[2] Hernández-Ortega, A.; Ferreira, P.; Martínez, A.T. Fungal aryl-alcohol oxidase: a peroxide-producing flavoenzyme involved in lignin degradation. *Appl. Microbiol. Biotechnol*. **2012**, *93*, 1395-1410.

[3] Varela, E.; Guillén, F.; Martínez, A.T.; Martínez, M.J. Expression of *Pleurotus eryngii* aryl-alcohol oxidase in *Aspergillus nidulans*: purification and characterization of the recombinant enzyme. *Biochimica et Biophysica Acta*. **2001**, *1546*, 107-113.

[4] Ruiz Dueñas, F.J.; Ferreira, P.; Martínez, M.J.; Martínez, A.T. In vitro activation, purification, and characterization of *Escherichia coli* expressed aryl-alcohol oxidase, a unique H_2O_2-producing enzyme. *Protein Expression and Purification*. **2006**, *45*, 191-199.

[5] Garcia-Ruiz, E.; Mate, D.M.; Gonzalez-Perez, D.; Molina-Espeja, P.; Camarero, S.; Martínez, A.T.; Ballesteros, A.O.; Alcalde, M. Directed evolution of ligninolytic oxidoreductases: from functional expression to stabilization and beyond. *In*: Cascade Biocataysis, Riva, Fessner Eds. Wiley-VCH. In press.

[6] Cartwright C.; Zhu Y.; Tipper D.J. Efficient Secretion in Yeast Based on Fragments from K1 Killer Preprotoxin. *YEAST*. **1992**, *8***,** 261-272.

[7] González-Perez, D.; García-Ruiz, E.; Alcalde M. *Saccharomyces cerevisiae* in directed evolution. An efficient tool to improve enzymes. *Bioengineered Bugs* **2012**, *3*, 172-177.

[8] Brenner, C.; Fuller, S.R. Structural and enzymatic characterization of a purified prohormone-processing enzyme: Secreted, soluble Kex2 protease. *Proc. Natl. Acad. Sci. USA.* **1992**, *89***,** 922-926.

ACTIVATED H_2O_2 DISCOLORATION OF A MODEL AZOIC DYE-COLORED PULP

WALGER Elsa[1]*, RIVOLLIER Camille, MARLIN Nathalie, MORTHA Gérard
[1]*LGP2, UMR 5518, Institut National Polytechnique de Grenoble, 461 rue de la papeterie, CS 10065, F-38402 Saint-Martin-d'Hères, France (*elsa.walger@pagora.grenoble-inp.fr)*

ABSTRACT

Recovered fibers can be reused for the manufacture of bright paper, provided efficient fiber discoloration can be operated in recycling mills. Generally, hydrogen peroxide is applied in alkaline medium as a final bleaching stage (P) of the deinking line, after paper disintegration and ink removal by flotation. But the efficiency of P bleaching is often limited because of the low reactivity of H_2O_2 on the azo (N=N) groups of azoic dyes. The purpose of the research was to improve the efficiency of the P stage for the removal of these azoic dyes.

The Direct Yellow 11 dye was used as a model azoic dye. ECF-bleached kraft pulp was colored with the dye and submitted to activated H_2O_2 discoloration treatments. Pure phenanthroline (Phen) and Copper(II)-Phenanthroline complex (Cu-Phen) were used as activating compounds, since they had already proven their efficiency during P stage or O stage (oxygen) delignification of chemical pulps. The herein presented color-stripping tests using hydrogen peroxide involved the reaction of H_2O_2 alone, H_2O_2+Phen and H_2O_2+Cu-Phen. All the tests were carried out at near-neutral or alkaline pH for comparison. The results were evaluated in terms of Dye Removal Index (DRI), cellulose degree of polymerization (DPv) and H_2O_2 consumption.

Results show the improvement achieved with the use of Copper-Phenanthroline, which is a first step towards more efficient peroxide bleaching of recycled fibers. However, the use of this activator is responsible for cellulose degradation, imparted to the formation of hydroxyl radicals. This degradation has to be controlled by modifying some conditions found to be of key importance, such as the reaction pH.

I. INTRODUCTION

Hydrogen peroxide is commonly used in alkaline conditions in mechanical pulp bleaching. Its anion form, the perhydroxyl anion HOO^- (pKa=11.6), oxidizes the conjugated carbonyls of lignin into carboxylic acids, which are partially dissolved, leading to a higher brightness of the pulp. Hydrogen peroxide is also used for bleaching of wood-containing deinked pulps. In this case, it is often combined with a reducing agent - such as sodium dithionite or formamidine sulfinic acid - in order to achieve better results [1], although these chemicals are more expensive. Indeed, unlike hydrogen peroxide, they are quite efficient for dye color-stripping.

Dyes absorb the visible light because of their highly conjugated structures, containing several groups with π-electron clouds, such as azoic groups. These structures constitute the chromophore part of the molecule. Most dyes used in the industry are azoic dyes, such as Direct Yellow 11 (**Figure 1**). The conjugated structure constitutes the chromophore part of the molecule and the sulfonic and hydroxyl groups are the auxochrome part.

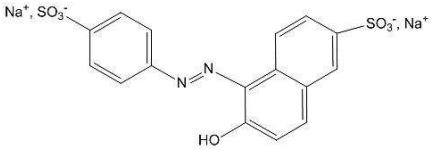

Figure 1. Molecular structure of the Direct Yellow 11 dye

Direct dyes have a good affinity with bleached and unbleached chemical pulps. They represent more than half of the dyes present in the pulp and textile industries [2] and they usually contain at least one azo group and some sulfonic acid groups. Since N=N links are not oxidizable by HOO^-, direct azo dyes are not degraded by H_2O_2.

Several works were conducted on the activation of H_2O_2 for chemical pulp delignification in alkaline conditions [3,4], leading to patents [5,6]. They have shown that the action of H_2O_2 could be enhanced by the action of copper-phenanthroline complexes. Some studies focused on the catalytic action of Cu-Phen complexes for the oxidation of lignin by either O_2 [7–11] or H_2O_2 [4,11], especially with lignin model compounds such as veratryl alcohol. Trials with deinked pulps and dyed pulps were also carried out and showed that the dye removal index – indicating the loss of color in the CIE L*a*b* color space, as defined by Sharpe and Lowe [12] – was improved in a P stage activated with a copper-phenanthroline complex [4,13].

The aim of our work was to study the effect of the copper-phenanthroline complex during hydrogen peroxide bleaching of a bleached chemical pulp colored with the Direct Yellow 11 dye.

II. EXPERIMENTAL

Pulp dyeing - The Direct Yellow 11 dye used was a commercial liquid dye solution (23%) provided by Clariant. Two doses were applied on an ECF-bleached eucalyptus kraft pulp (FIBRIA, Brasil, DPv: 1156, ISO brightness: 85.7±0.2): 0.1% concentration on o.d. pulp, corresponding to a standard color depth of 1/25, and 1% on o.d. pulp. Dyeing was carried out without any fixative agent, at 1% pulp consistency with 30 min contact time.

Color-stripping trials - Commercial chemical products of analytical grade were used: NaOH (99%, reagent grade, Carl Roth), H_2O_2 (35%, Carl Roth), $CuSO_4$, 5 H_2O (98.0%, ACS reagent, Sigma Aldrich), 1,10-phenanthroline (99.0%, Acros Organics). The color-stripping stages were carried out in polyethylene bags at 10% consistency during 1 hour at 80°C. P stages used 2% H_2O_2 and 0.12% or 1% NaOH (weak and strong alkaline conditions). Activated P stages (Pact) were carried out using Phen or Cu-Phen complex (previously dissolved in water), in the same operating conditions as for the P stage (activators were added after NaOH and before H_2O_2). 140.9 µmol of Phen were added for the H_2O_2+Phen trial and 140.9 µmol of Phen and 44.9 µmol of Cu were added for the H_2O_2+Cu-Phen trial (one trial used 30 g o.d. pulp). Controls without H_2O_2 were also performed: 0.12% and 1% NaOH alone and with the activators.

Characterization - Color-stripping efficiency was quantified by optical measurements on pulp handsheets, prepared according to TAPPI Standard T 272 sp-12. L*a*b* values were measured on a spectrophotometer (Elrepho Datacolor) according to ISO 5631-2:2008. The Dye Removal Index (DRI), developed by Sharpe and Lowe [12], was then calculated. It indicates the percentage of discoloration in the CIE L*a*b* color system.
The degrading effect of the P and Pact stages on cellulose was evaluated by measuring the cellulose polymerization degree DPv (TAPPI Standard T 230 om-13). The DPv accuracy was estimated to be ±20.

III. RESULTS AND DISCUSSION

Results of all the color-stripping trials are presented in **Table 1**.

Table 1. Color-stripping efficiency of P, activated P stages and controls

% Dye	% NaOH	Assay	L*	a*	b*	DRI	DPv	% H_2O_2 consumed	Final pH
0	/	fully bleached ECF pulp	97.1 ±0.0	-0.3 ±0.0	5.5 ±0.0	/	1156	/	/
0.1	/	unbleached colored pulp	93.4 ±0.1	1.3 ±0.0	24.3 ±0.2	0.0	1191	/	/
	1	NaOH	92.0 ±0.1	4.6 ±0.0	20.2 ±0.2	22.6 ±0.8	1145	/	11.4
		NaOH+Cu-Phen	90.5 ±0.0	6.2 ±0.0	18.0 ±0.1	28.9 ±0.8	1040	/	11.9
		NaOH+H_2O_2	94.8 ±0.1	0.0 ±0.1	18.8 ±0.3	40.4 ±1.4	779	100	11.2
		NaOH+H_2O_2+Cu-Phen	95.1 ±0.1	-0.4 ±0.0	13.9 ±0.1	65.8 ±0.2	676	100	10.5
		NaOH+H_2O_2+Phen	95.8 ±0.1	-0.6 ±0.0	12.9 ±0.1	71.0 ±0.3	728	82	11.0
	0.12	NaOH	94.0 ±0.1	0.8 ±0.0	20.7 ±0.2	26.9 ±1.2	1208	/	9.5
		NaOH+Cu-Phen	93.4 ±0.0	6.2 ±0.0	18.0 ±0.1	36.3 ±0.8	1122	/	9.0
		NaOH+H_2O_2	93.2 ±0.1	0.0 ±0.1	18.8 ±0.3	37.5 ±1.3	320	89	6.2
		NaOH+H_2O_2+Cu-Phen	94.0 ±0.1	0.6 ±0.0	16.0 ±0.1	53.9 ±0.0	289	93	4.7
		NaOH+H_2O_2+Phen	95.3 ±0.1	-0.2 ±0.0	15.9 ±0.1	57.0 ±0.1	815	92	6.8
1	/	unbleached colored pulp	87.8 ±0.1	9.8 ±0.1	51.5 ±0.6	0.0	1193	/	/
	1	NaOH	86.2 ±0.1	11.2 ±0.1	47.9 ±0.1	10.1 ±0.2	1191	/	/
		NaOH+Cu-Phen	86.6 ±0.1	9.6 ±0.1	41.6 ±0.1	31.0 ±0.4	1069	/	12.2
		NaOH+H_2O_2	89.4 ±0.1	6.3 ±0.1	46.3 ±0.1	20.8 ±0.3	958	69	11.2
		NaOH+H_2O_2+Cu-Phen	91.1 ±0.1	2.6 ±0.1	35.3 ±0.1	54.1 ±0.2	586	99	11.5
		NaOH+H_2O_2+Phen	89.6 ±0.1	4.7 ±0.1	36.2 ±0.2	50.3 ±0.4	704	93	11.0
	0.12	NaOH	88.6 ±0.1	8.0 ±0.1	45.3 ±0.1	22.7 ±0.3	1203	/	/
		NaOH+Cu-Phen	88.2 ±0.1	6.9 ±0.2	44.5 ±0.2	25.3 ±0.6	1200	/	/
		NaOH+H_2O_2	87.1 ±0.1	7.5 ±0.1	43.7 ±0.1	26.7 ±0.2	603	60	/
		NaOH+H_2O_2+Cu-Phen	88.8 ±0.1	4.4 ±0.1	34.6 ±0.1	53.8 ±0.2	294	80	/
		NaOH+H_2O_2+Phen	88.9 ±0.1	6.0 ±0.1	41.1 ±0.1	36.4 ±0.2	754	55	/

Color-stripping of the 0.1% dyed pulp

The pulp was first treated in classical conditions: 2% H_2O_2 and 1% NaOH (NaOH+H_2O_2 in the table). Two controls without H_2O_2 were carried out: NaOH alone and NaOH+Cu-Phen, to examine the possible color-stripping effect of the complex itself. Activated P stages were performed with the addition of Cu-Phen (NaOH+Cu-Phen+H_2O_2) or Phen (NaOH+Phen+H_2O_2).
With NaOH alone (1% or 0.12%), a slight color-stripping effect was observed (DRI=23% or 27%, respectively), probably due to the partial solubilization of the dye in alkaline medium. With the complex, the dye removal was slightly better. In addition to the alkaline effect, the complex itself influenced the color of the pulp. Two explanations could be given: the color of the complex is responsible for the DRI variation (decrease of the b* and L* values due to the blue color of the complex) or the complex has a chemical effect on the dye.

With 2% H_2O_2 and 1% NaOH, the dye removal surprisingly reached 40%: H_2O_2 alone had thus a positive effect although the dye molecular structure does not contain any H_2O_2 sensitive groups. The dye may have been degraded by the action of highly oxidative hydroxyl radicals generated in presence of metal ions traces coming from the pulp and certainly also from the commercial dye solution.
The effect of Cu-Phen or Phen activators was much more important since the DRI reached 66 and 71% for NaOH+H_2O_2+Cu-Phen and NaOH+H_2O_2+Phen respectively. Phen alone activated the P stage as much as Cu-Phen. The presence of free copper ions in the dyed pulp probably led to the formation of active Cu-Phen complexes.
In terms of cellulose DPv, as expected, NaOH had almost no effect (DPv=1145 *vs* 1191 for the unbleached pulp), whereas NaOH+Cu-Phen induced a slight pulp degradation (DPv=1040). The addition of complex thus favored cellulose oxidation. H_2O_2 alone, without activator, had a detrimental effect, which might be explained by the action of hydroxyl radicals generated by the H_2O_2 decomposition with metal ions traces, in the absence of any chelating agent in the pulp. As far as the activated P stages are concerned, the DPv values were lower than with H_2O_2 alone. The NaOH+H_2O_2+Phen treatment was the most interesting one since the DRI was high and cellulose DPv was not so much affected. The final pH was actually similar to the pH obtained after H_2O_2 bleaching, leading to similar degradation (DPv=728 *vs* 779). Regarding the Cu-Phen activated stage, the final pH was lower, meaning that more acidic molecules were formed. This lower pH is certainly correlated to a higher generation of hydroxyl radicals due to the higher metal ions content in the pulp with Cu-Phen.
The treatments with 1% NaOH leading to a high H_2O_2 consumption (82 to 100%), the amount of NaOH was reduced in order to limit the environmental impact of the bleaching. The assays were thus conducted with 0.12% NaOH instead of 1%. As observed before, sodium hydroxide alone was still able to dissolve part of the color (DRI=27 *vs* 23% with 1% NaOH), although the NaOH concentration was much lower. In the same manner, NaOH+Cu-Phen had a slight color-stripping effect. The DRI was higher than with 1% NaOH (DRI=36 *vs* 27%) and the pH lower. This better result obtained in weaker alkaline conditions may be due to different and more or less active copper-phenanthroline species, that are known to depend on the pH conditions.
Conventional P stage conducted at low alkalinity (0.12% NaOH) removed 38% of the dye, which was similar to the 40% obtained with 1% NaOH, although the consumption of H_2O_2 was reduced. However, much more cellulose degradation was observed (DPv=320), which could be related to the lower pH (6.2). The color-stripping mechanisms involved with H_2O_2 in alkaline or acidic/near neutral conditions are probably very different. With activators (NaOH+H_2O_2+Cu-Phen and NaOH+H_2O_2+Phen), the DRI were higher but cellulose was also more degraded, probably by the action of highly reactive hydroxyl radicals, as already discussed.
To conclude, Cu-Phen added in a P stage improved color-stripping efficiency but it should be used in conventional alkaline conditions (around 1% NaOH) to avoid any additional cellulose degradation.

Color-stripping of the 1% dyed pulp

Overall, the DRI followed the same trend as for the 0.1% dyed pulp. However, the H_2O_2 consumption was lower, probably because of the higher quantity of dye.
The dyed pulp was first treated in standard conditions using 1% NaOH. As discussed before, the dye was partly dissolved with NaOH alone (DRI=10%) and NaOH+Cu-Phen had a beneficial effect (DRI=31%). With NaOH+ H_2O_2, the DRI was similar (DRI=21%). Likewise, the activated P stages led to efficient color-stripping (DRI=54% after Cu-Phen Pact and DRI=50% after Phen Pact).
In terms of DPv, same tendencies were observed: no effect of NaOH (DPv=1191), slight degradation with Cu-Phen and higher degradation with H_2O_2 due to the hydroxyl radicals generation in presence of metals coming from the dyed pulp. However, the 1% dyed pulp was less degraded than the 0.1% dyed pulp (DPv=958 *vs* 779) probably because the higher quantity of dye plays a protecting role on the cellulose chains. With the Cu-Phen activator, the consumption of H_2O_2 increased up to 99% and the DPv dropped (DPv 586): radicals were certainly produced in huge quantity. With Phen, the H_2O_2 consumption was slightly lower (93%) and the DPv higher (DPv=704), probably due to a lower quantity of copper, inducing lower radical generation.
In weak alkaline conditions (0.12% NaOH), the P stage was not able to efficiently color-strip the pulp (DRI=27%). However, with the activators, especially with Cu-Phen, H_2O_2 was more active on both dye (DRI=54%) and cellulose (DPv=294). As described before, the cellulose DPv was strongly affected as soon as H_2O_2 combined with the activator was applied in a near neutral environment. This confirms that Cu-Phen or Phen should not be used in weak alkaline conditions.

IV. CONCLUSIONS

The activated P stages were efficient: the DRI was improved with the use of Cu-Phen as a hydrogen peroxide activator. Phenanthroline alone may also be used as an activator since it probably forms Cu-Phen complexes with copper ions present in the pulp. However, the cellulose degree of polymerization dropped, especially in weak alkaline conditions. Whatever the conditions used, color-stripping came along with cellulose degradation, which is illustrated by **Figure 2** with the example of the 1% dyed pulp.

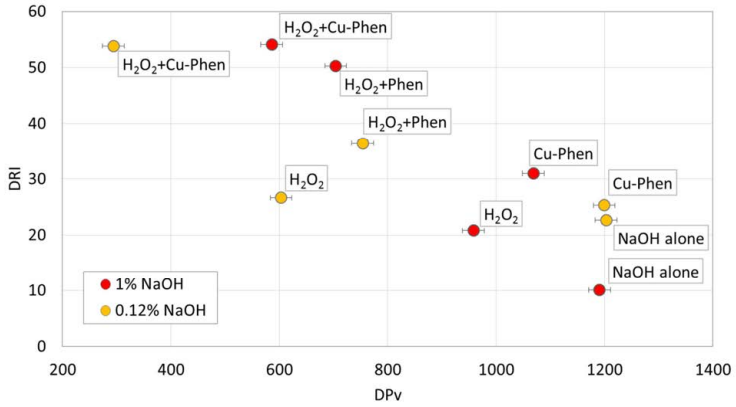

Figure 2. DRI *vs* DPv after bleaching of 1% dyed pulp

The effect of activated peroxide bleaching of colored pulp is probably mainly due to the generation of hydroxyl radicals. This very oxidative species also degrades cellulose, which induces a drop in pulp quality. However, it was shown that a compromise could be found between efficient color-stripping and cellulose preservation. The activated P stage may be improved by optimizing the dose of NaOH and by protecting cellulose with sodium silicate or magnesium sulfate.

V. ACKNOWLEDGEMENT

To Dr. POUYET Frédéric and the following students of Grenoble INP – Pagora (international school of paper, print media and biomaterials): DECHAMBENOY Laure, GUIGON Valentin, LELEU François, QUINET Lucas, QUINOT Déborah, SYTY Luc, who carried out a preliminary work for this study.

VI. REFERENCES

[1] Göttsching, L.; Pakarinen, H.; Seifert, P. Bleaching of Deinked Pulp. In *Recycled fiber and deinking*; Papermaking Science and Technology; Fapet Oy: Helsinki, **2000**.

[2] Alén, R. Papermaking Additives. In *Papermaking Chemistry*; Papermaking science and technology; Fapet Oy: Helsinki (Finlande), **2007**.

[3] Coucharriere, C. Mise au point et étude d'un système d'activation du peroxyde d'hydrogène en délignification et blanchiment des pâtes chimiques. PhD thesis, France, **2000**.

[4] Marlin, N.; Coucharriere, C.; Mortha, G.; Lachenal, D.; Larnicol, P.; Hostachy, J.C. Use of o-phenanthroline as a catalyst in hydrogen peroxide stages. In *Proceedings of the International Symposium on Wood Fibre and Pulping Chemistry*; Auckland, New Zealand, **2005**, 29–34.

[5] Cabanne, L.; Larnicol, P.; Coucharriere, C. Hydrogen Peroxide Activation in Delignification and Bleaching of Wood Pulp Using a Phenantroline-Copper Complex. WO03080925 (A2), October 2, **2003**.

[6] Blanc, J.; Calais, C.; Dubois, J.L. Process for Delignification and Bleaching of Paper Pulp Using Activated Hydrogen Peroxide, June 29, **2012**.

[7] Korpi, H.; Lahtinen, P.; Sippola, V.; Krause, O.; Leskelä, M.; Repo, T. An Efficient Method to Investigate Metal-Ligand Combinations for Oxygen Bleaching. *Appl. Catal. Gen.*, **2004**, *268*, 199–206.

[8] Korpi, H.; Figiel, P.J.; Lankinen, E.; Ryan, P.; Leskelä, M.; Repo, T. On In Situ Prepared Cu–Phenanthroline Complexes in Aqueous Alkaline Solutions and Their Use in the Catalytic Oxidation of Veratryl Alcohol. *Eur. J. Inorg. Chem.*, **2007**, *2007*, 2465–2471.

[9] Lahtinen, P.; Korpi, H.; Haavisto, E.; Leskelä, M.; Repo, T. Parallel Screening of Homogeneous Copper Catalysts for the Oxidation of Benzylic Alcohols with Molecular Oxygen in Aqueous Solutions. *J. Comb. Chem.*, **2004**, *6*, 967–973.

[10] Korpi, H. Copper Di-Imine Complexes: Structures and Catalytic Activity in the Oxidation of Alcohols by Dioxygen. PhD thesis, Laboratory of Inorganic Chemistry Department of Chemistry University of Helsinki: Finland, **2005**.

[11] Sippola, V.O.; Krause, A.O.I. Bis(o-Phenanthroline)copper-Catalysed Oxidation of Lignin Model Compounds for Oxygen Bleaching of Pulp. *Catal. Today*, **2005**, *100*, 237–242.

[12] Sharpe, P.E.; Lowe, R.W. The Bleaching of Colored Recycled Fibers. In *1993 pulping conference : Marriott Copley Place Hotel, Boston, MA november 1-5*; TAPPI Press: Atlanta (Ga.), **1993**, Vol. 3, 1205–1217.

[13] Marlin, N.; Fernandes, J.; Benattar, N. New Ways to Improve Color-Stripping of Deinked Pulps and Dyed Effluents. In *International Symposium on Wood Fiber and Pulping Chemistry (ISWFPC) Proceedings*, **2007**.

Covalent immobilization of $(ZnS)_x(CuInS_2)_{1-x}$/ZnS (core/shell) quantum dots in (bacterial) cellulose aerogels

Huiqing Wang, Thomas Rosenau, Falk Liebner*

*Division of Chemistry of Renewables, University of Natural Resources and Life Sciences Vienna, Konrad-Lorenz-Straße 24, A -3430 Tulln, Austria (*falk.liebner@boku.ac.at)*

ABSTRACT

Photoluminiscent (PL) cellulose aerogels of variable shape containing homogeneously dispersed and surface-immobilized alloyed $(ZnS)_x(CuInS_2)_{1-x}$/ZnS (core/shell) quantum dots (QD) have been obtained by 1) dissolution of hardwood prehydrolysis kraft pulp in the ionic liquid 1-hexyl-3-methyl-1*H*-imidazolium chloride, 2) addition of a homogenous dispersion of quantum dots in the same solvent, 3) molding, 4) coagulation of cellulose with ethanol as antisolvent, and 5) $scCO_2$ drying of the resulting composite aerogels. Both compatibilisation with the cellulose solvent and covalent attachment of the quantum dots onto the surface of the regenerated cellulose was achieved through replacement of the 1-mercaptododecyl ligands, typically used in alloyed $(ZnS)_x(CuInS_2)_{1-x}$/ZnS QD synthesis, by 1-mercapto-3-(trimethoxysilyl)-propyl ligands.
The obtained materials have densities of 37.9 to 57.2 mg cm^{-3}, and have BET surface areas of 296 to 686 m^2 g^{-1} comparable with non-luminiscent cellulose aerogels obtained according to the NMMO, TBAF/DMSO or $Ca(SCN)_2$ routes. Depending mainly on the ratio of QD core constituents and to a minor extent on the cellulose/QD ratio, the emission wavelength of the novel aerogels can be controlled within a wide range of the visible light spectrum. Increasing the QD/cellulose ratio shifts the photoluminescence peak position towards longer wavelengths and increases the photoluminescence. Reinforcement of the cellulose aerogels and hence significantly reduced shrinkage during $scCO_2$ drying is a beneficial side effect when using α-mercapto-ω-(trialkoxysilyl) alkyl ligands for QD capping and covalent QD immobilization onto the cellulose surface.

I. INTRODUCTION

Quantum dots (QD) are colloidal, mostly semiconductor-based nanoparticles of a size typically being equal to or smaller than the exciton Bohr radius (ca. 2 to 15 nm). At such small dimensions continuous band structures, such as those in bulk semiconductors, are no longer possible as quantum confinement of excited electron-hole pairs ("excitons") causes quantization of energy levels [1].
The multifaceted response of QDs towards photons of different energy (low energy such as UV, visible light, NIR radiation: photoabsorption or photosensitation; high energy such as X-rays or γ-rays: photoelectric ionization or photon annihilation on an atom nucleus and generation of an electron-positron pair) render QDs very interesting materials for a wide range of applications [2].
Covalent immobilization of QDs on the surface of suitable matrices is considered to be a prerequisite to many applications, and a means of reducing the health risk related to respirable particulate matter. By grafting QDs onto the large inner surface of lightweight aerogels, novel functional materials advantageously employing the large interconnected porosity and void surface area can be created. Next to opto-electronic or photovoltaic applications, QD containing aerogels could be used for true volumetric 3D displays as it has been recently successfully demonstrated for CdSe/ZnS-silica hybrid aerogels or as highly specific sensors reporting the occurrence of specific biomolecules or gene sequences as it would be required for tracking cancer cells [3].
Covalent immobilisation of QDs equipped with ligands that contain terminal anchor groups on the surface of aerogels, can be accomplished in two ways by synthesizing QD aerogels from sols of quantum dots, or by embedding prefabricated QDs in the supporting aerogel matrix of another material [3]. Following these two ways aerogels from both bacterial cellulose and regenerated cellulose containing homogeneously dispersed and covalently immobilized alloyed $(ZnS)_x(CuInS_2)_{1-x}$/ZnS (core/shell) quantum dots (QDs) have been prepared. Experimental details and the properties of the obtained materials will be presented.

II. EXPERIMENTAL

Materials: Eucalyptus pre-hydrolysis kraft pulp (hwPHK; TCF bleached; MW 80.3 kg mol^{-1}, CCOA: 4.7 µmol g^{-1} C=O, FDAM: 8.8 µmol g^{-1} COOH; [4].Octadecene, 1-mercaptododecane, toluene, CuI, $In(OAc)_3$, $Zn(OAc)_2$, 1-hexyl-3-methyl-1*H*-imidazolium chloride (HMImCl) and 3-(mercaptopropyl)-trimethoxysilane (MPtMS) were purchased from Sigma-Aldrich (Sigma-Aldrich HandelsGmbH, Vienna, Austria). Pressurized CO_2 was purchased from Linde Gas, Austria.

Preparation and purification of alloyed $(ZnS)_x(CuInS_2)_{1-x}$ core / ZnS shell QDs of variable shell thickness and 1-mercaptododecane ligands grafted onto the particle surface was accomplished as described elsewhere (Wang et al. 2013). For compatibilization of the QDs with ionic liquids and covalent binding onto the cellulose surface, 1-mercapto-*n*-dodecyl ligands were replaced by MPtMS via phase transfer. In brief, a solution of 0.05 mL of MPtMS in 5.0 mL of HMImCl was added to 5.0 mL of a solution that contained the $(ZnS)_x(CuInS_2)_{1-x}$/ZnS (alloyed core/shell) nanoparticles solubilized in toluene by the presence of lipophilic 1-mercapto-*n*-dodecyl ligands. The resulting two-phase system was vigorously stirred at ambient temperature for 30 min whereupon the QDs moved from the supernatant toluene into the lower ionic liquid phase which was then separated from the supernatant.

Preparation of cellulose-$(ZnS)_x(CuInS_2)_{1-x}$/ZnS (core/shell) QD composite aerogels
Eucalyptus prehydrolysis kraft pulp (hwPHK) was dissolved in HMImCl at 100 °C to afford solutions that contained 1 - 3 wt% of cellulose. Based on microscopic evaluation (Novex B series binocular microscope BBS Led for bright field contrast) dissolution was assumed to be complete within 2 hours for all variants. The solutions were cooled down to 60 °C before different aliquots of the suspension of the 3-(trimethoxysilyl)-propyl-functionalized $(ZnS)_x(CuInS_2)_{1-x}$/ZnS (core/shell) QDs in HMImCl were added dropwise under argon and vigorous stirring. Then, the solutions containing 0.01-0.3 wt% of QDs were transferred into PTFE molds. Disk-like alcogels (Ø 30 mm, height 3 mm) were obtained by coagulation of cellulose with either absolute or aqueous (50 v%) ethanol and replacing the coagulation media by fresh solvent every four hours for three times at least. If aqueous ethanol was used for coagulation, the samples were thoroughly equilibrated in absolute ethanol prior to $scCO_2$ drying (three times, four hours each).
Supercritical CO_2 drying: The composite alcogels were placed onto stainless steel filter panels inside the autoclave (SFP-200, Separex, Champigneulles, France). The system was then pressurized through the bottom valve with liquid, pre-heated CO_2 using a HPLC pump until the operation pressure of 10 MPa was reached. The top valve was opened and the bottom valve was subsequently switched to the separator, where ethanol and CO_2 were separated by an isothermal flash. Drying was accomplished at 40°C using a drying time of 5 hours. Finally the top valve was closed and the autoclave was depressurized over the separator.

Analytical methods. *ATR-FTIR* spectra (500–4000 cm^{-1}) of the pure and composite aerogel discs were recorded on a L128-0099 PerkinElmer Spectrometer (Waltham, MA, USA), *fluorescence* experiments on a PerkinElmer LS55.
Transition electron microscopic (TEM) pictures of cellulose-$(ZnS)_x(CuInS_2)_{1-x}$/ZnS (core/shell) QD composite aerogels were obtained on a JEM-2010 FEF (UHR; JEOL, Tokyo, Japan). *Scanning electron microscopy(SEM)*: Hitachi X-650. Gold sputtering (5 nm) was performed at a voltage of 2.5 kV under argon. *Energy-dispersive X-ray (EDX):* Horiba EX-250 coupled with SEM. *X-ray diffractometry* of cellulose and cellulose-$(ZnS)_x(CuInS_2)_{1-x}$/ZnS composite aerogels was performed in reflection mode (Rigaku RINT 2000, Japan) using monochromatic Cu K_α radiation (λ = 0.15406 nm).
Nitrogen sorption experiments at 77 K were conducted on a Micrometrics ASAP 2020 analyzer. Specific surface areas were calculated from the BET equation, the average pore diameter being evaluated by the BJH equation on the desorption branch of the isotherm. All samples were kept under vacuum overnight prior to the measurements. *Thermogravimetric analysis (TGA)*: NETZSCH TG209 F1. A constant heating rate of 20 °C min^{-1} was used throughout the entire temperature range studied (25-800°C). *Mechanical response to compression stress* was investigated with a Zwick/Roell Materials Testing Machine Z020. A 50 N load cell was used to measure the force required to achieve a deformation rate of 2.4 mm min^{-1}.
^1H, ^{13}C, and ^{29}Si NMR spectroscopy was performed on a BrukerAvance II 400 spectrometer with a 5 mm broadband probe head equipped with z-gradient in DMSO-d_6 (^1H frequency 400.13 MHz, ^{13}C: 100.61 MHz, and ^{29}Si: 79.49 MHz) at room temperature with standard Bruker pulse programs.

III. RESULTS AND DISCUSSION

The synthesis of alloyed core / shell QDs according to the applied thermolytic approach involves embedding of lipophilic ligands such as 1-mercaptododecane and 1-aminooctadecane into both core and shell which promotes surface deactivation, increased PL lifetimes, quantum yields, and imparts good dispersibility in non-polar liquids, such as toluene. Grafting of this type of QDs onto the surface of cellulose, however, requires ligands that carry suitable, reactive groups and – if cellulose-QD composite aerogels are produced by grafting of cellulose in solution state and subsequent coagulation of the modified cellulose – a solvent that is able to dissolve cellulose and to disperse QDs at the same time.
These obstacles have been overcome by replacing part of the 1-mercaptododecyl ligands by 1-mercapto-3-(trimethoxysilyl)-propyl ligands. It has been accomplished by phase transfer into 1-hexyl-3-methyl-1*H*-imidazolium chloride (HMImCl) which has the capability of both dispersing the QDs after ligand exchange and dissolving cellulose. The ligand exchange has been accomplished by adding a suspension of the 1-

mercaptododecyl-capped QDs in toluene to a solution of 1-mercapto-3-(trimethoxysilyl)-propane inHMImCl. Exchange of 1-mercaptododecane ligands by 1-mercapto-3-(trimethoxysilyl)-propyl ligands was shown to facilitate the transfer of QDs from the supernatant toluene into the lower ionic liquid phase. The occurrence of a ligand exchange followed by QD phase transfer is evident from the color transfer between the two phases and was confirmed by GC/MS analysis of the toluene phase that revealed a strong correlation between the amounts of QDs added and the 1-mercaptododecane concentration in the upper toluene layer.
Replacement of 1-mercaptododecyl- by 1-mercapto-3-(trimethoxysilyl)-propyl ligands allows not only for a homogenous dispersion of the QDs in the cellulose/HMImCl solution, but also for the QDs to get covalently immobilized on the large inner surface of the cellulosic aerogels. This is considered to be advantageous for two reasons: It reduces the potential health risk immanent to nanoparticles and renders the quantum dots more resistant towards extraction during $scCO_2$ drying.
Figure 1 summarizes the steps required to obtain cellulose aerogels that contain covalently immobilized, capped $(ZnS)_x(CuInS_2)_{1-x}/ZnS$ (core/shell) quantum dots: a) joint dissolution of 1, 2, or 3 w% of cellulose (ca. 60 min) and dispersing 0 or 0.3 w% of QDs in HMImCl at 60°C, b) casting, c) coagulation of cellulose by adding ethanol, and d) converting the alcogels into aerogels by supercritical carbon dioxide (40°C, 10 MPa).

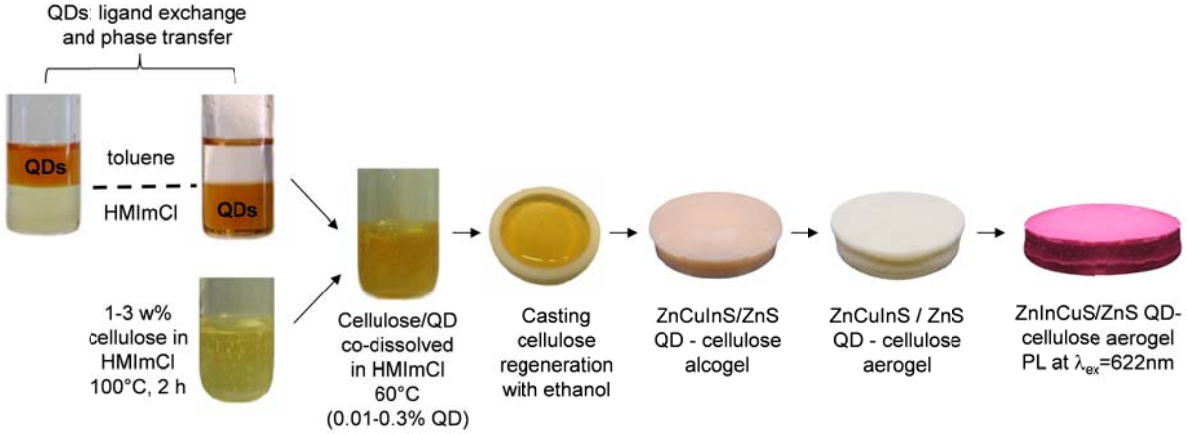

Figure 1: Schematic presentation of the approach to photoluminiscent cellulosic aerogels containing covalently grafted $(ZnS)_x(CuInS_2)_{1-x}/ZnS$ (core/shell) quantum dots [5].

Grafting of 1-mercapto-3-(trimethoxysilyl)-propyl (MPTmS)-capped QDs onto cellulose occurs mainly within the first one hour of the joint dissolution/dispersion of cellulose and QDs at 60°C and has been confirmed by XRD, EDX, FT-IR, and indirectly by liquid-state, gradient-selected ^{1}H-^{13}C HSQC NMR and long-range ^{1}H-^{29}Si HMBC NMR spectroscopy using methyl D-glucopyranoside as a cellulose model compound and 3-mercaptopropyl-trimethoxysilane instead of the MPTmS-capped QDs.
Coagulation of cellulose and the progress and endpoint of the solvent exchange (HMImCl was replaced by ethanol) can be monitored by fluorescence spectroscopy as the photoluminescence (PL) intensity largely increases with ethanol concentration. Similarly, the PL peak position depends also on the type of dispersant used, next to the stoichiometric ratio of core constituents, core size and shape, core/shell ratio, ligand type and concentration. The presence of water present in both the cellulose solvent and anti-solvent should be avoided as it promotes both shrinking of the samples and self-condensation of QDs via residual methoxysilyl groups not consumed by grafting. Aggregation of QDs, in turn, leads to PL quenching, reduced photoluminiscence and a slight red-shift for the final aerogels.
Scanning electron microscopy confirms that grafting of 1-mercapto-3-(trialkoxysilyl)-propyl-capped QDs onto cellulose has no negative impact on the morphology of the obtained aerogels and a largely homogeneous dispersion of the grafted QDs across the cellulosic network. This is supported by TEM which also confirms that the initial size of the core/shell QDs (10-13 nm *vs.* ≈15 nm) was not significantly affected by the different process steps from joint co-dissolution with cellulose in HMImCl to $scCO_2$ drying.
Fluorescence experiments reveal that the photoluminescence of both cellulose hybrid alcogels and aerogels containing covalently immobilized $(ZnS)_x(CuInS_2)_{1-x}/ZnS$ (core/shell) quantum dots can be controlled over a wide range (460-710 nm) of the visible light by varying the stoichiometric composition of the QD core's constituents, the core size (duration of particle growth) and the thickness of their ZnS shell.

Disk-like cellulose-QDs composite alcogels are largely transparent and feature a uniformly high fluorescence across the samples. This confirms homogeneous distribution of the $(ZnS)_x(CuInS_2)_{1-x}/ZnS$ (core/shell) nanoparticles within the cellulosic network as also evident from SEM and TEM spectroscopy. After $scCO_2$-drying the obtained aerogels are off-white at daylight (figure 2c) tending to a hue that corresponds to the color observed under UV light.

Apart from the parameters discusses above, the photoluminescence intensity of both cellulose-$(ZnS)_x(CuInS_2)_{1-x}$/ZnS (core/shell) QD hybrid alcogels and aerogels can be also controlled by the amount of QDs covalently grafted onto cellulose. The slight red shift of the PL peak position which increases with the amount of QDs added has been observed for both alcogels and aerogels and is likely due to QD aggregation by van der Waals forces.
Grafting of the core/shellQDs onto cellulose aerogels has been demonstrated to reduce shrinkage during both cellulose coagulation and $scCO_2$ drying leading to higher internal surface areas. Furthermore, increased stiffness (Youngs modulus, increased capability of absorbing energy by elastic deformation) and strength (measured at 0.2% off-set strain) has been calculated from the results of respective compression tests.
Nitrogen sorption experiments at 77K reveal that the obtained cellulose-QD composite aerogels are dominated by (narrow-sized) mesopores (IUPAC type IV-a/b). A small fraction of macropores have been shown to be also present (low BET intercepts, small N_2 volumes adsorbed at $P/P_0 = 0.02$; approx. 2-100 $cm^3\ g^{-1}$).

IV. CONCLUSIONS

$(ZnS)_x(CuInS_2)_{1-x}$/ZnS (core/shell) quantum dots obtained according to the thermolytic approach have been successfully subjected to ligand exchange. Replacement of 1-mercaptododecyl ligands by 1-mercapto-3-(trimethoxysilyl)-propyl ligands allow covalent binding of the respective QDs to cellulose. Co-dispersion of the 1-mercapto-3-(trimethoxysilyl)-propyl-capped $(ZnS)_x(CuInS_2)_{1-x}$/ZnS (core/shell) quantum dots in solutions of cellulose in ionic liquids, such as HMImCl, at slightly elevated temperature (45-60°C) and subsequent addition of a cellulose-anti-solvent affords largely transparent, fluorescent organogels. Their photoluminescence can be tuned within a wide range of the visible light by varying the composition of the core constituents, thickness of shell and the cellulose/QD ratio. Conversion of the organogels to aerogels by $scCO_2$ drying preserves the PL properties to a large extent. The weak blue shift caused by $scCO_2$ drying is superimposed by a somewhat less pronounced bathochromic shift that occurs when increasing the amount of QDs at constant density of the cellulosic network. Grafting of $(ZnS)_x(CuInS_2)_{1-x}$/ZnS (core/shell) quantum dots onto cellulose increases the mechanical stability of the hybrid aerogels compared to their QD-free counterparts which benefits high pore surface area, overall porosity, and dimensional stability of the samples during $scCO_2$ drying. Cellulose organogels and aerogels containing covalently immobilized QDs of group Ia, III and VI elements are expected to have a large application potential and will be studied further.

V. ACKNOWLEDGEMENT

The financial support by the *Chinese Academy of Sciences and the Beijing Institute of Technology ("Advanced materials based on cellulosic aerogels")* and by the Austrian Science Fund (FWF, Austrian-French Project CAP-Bone) is thankfully acknowledged.

VI. REFERENCES

1. Zhang, Y.; Clapp, A. Overview of stabilizing ligands for biocompatible quantum dot nanocrystals. Sensors 2011, 11 (12), 11036-11055.
2. Juzenas, P.; Chen, W.; Sun, Y.-P.; Coelho, M.A.N.; Generalov, R.; Generalova, N.; Christensen, I.L. Quantum dots and nanoparticles for photodynamic and radiation therapies of cancer. Advanced Drug Delivery Reviews 2008, 60 (15), 1600-1614.
3. Marinov, V.R.; Lima, I.T.; Miller, R. Quantum dot dispersions in aerogels: A new material for true volumetric color displays. Proc. SPIE 2010, 7690, 76900X.
4. Liebner, F.; Haimer, E.; Potthast, A.; Loidl, D.; Tschegg, S.; Neouze, M.-A.; Wendland, M.; Rosenau, T. Cellulosic aerogels as ultra-lightweight materials. Part II: Synthesis and properties. Holzforschung 2009, 63 (1), 3-11.
5. Wang, H.; Shao, Z.; Bacher, M.; Liebner, F.; Rosenau, T. Fluorescent cellulose aerogels containing covalently immobilized (ZnS)x$(CuInS_2)_{1-x}$/ZnS (core/shell) quantum dots Cellulose 2013, 20, 3007-3024.
6. Primeau, N.; Vautey, C.; Langlet, M. The effect of thermal annealing on aerosol-gel deposited SiO_2 films: A FTIR deconvolution study. Thin Solid Films 1997, 310 (1), 47-56.

STABILISATION OF POLYSACCHARIDES DURING ALKALINE PRETREATMENT OF WOOD FOLLOWED BY ENZYME-SUPPORTED EXTRACTIONS

Yan Wang[1], Shoaib Azhar[1], Mikael Lindström[1, 2] and Gunnar Henriksson[1, 2] *

[1] *Wallenberg Wood Science Center, KTH Royal Institute of Technology, SE-100 44 Stockholm, Sweden;* [2] *Division of Wood Chemistry and Pulp Technology, KTH Royal Institute of Technology, SE-100 44 Stockholm, Sweden*

* *Corresponding author: ghenrik@kth.se*

ABSTRACT

The possibilities to increase the extraction of wood polymers were tested with a prior use of specific enzymes. An open wood structure is needed for the enzymatic treated which was achieved by extended impregnation of the wood. However, some of the hemicelluloses, primarily glucomannan, and lignin were lost during the impregnation. In order to improve the carbohydrate yield in the impregnated wood different glucomannan modification agents were used. Through the use of additives, most of the glucomannan could be retained in the wood while still allowing the enzymes to penetrate the wood and attack the polymers. The additives were able to retain the carbohydrates and increased the extraction yield afterwards from 9 to 12% w/w wood. Gamanase treatment prior to the extraction increased the extraction yield to 14%. Of the three stabilising agents, sodium borohydride was the most efficient, providing the highest extraction yields.

I. INTRODUCTION

Nowadays biomass materials are very promising renewable raw material selection to replace the petroleum for its abundant resources in the nature [1]. Biomass materials are complex in composition, plant materials, for example, contain three major components: cellulose, hemicellulose, and lignin. All of these three components have broad use in varying areas. So, if a chemical process uses only one component and the others become wastes that must be disposed, the process often becomes uneconomic. In traditional wood pulping, for example, cellulose for cellulose fiber and chemical production is separated from lignin and hemicellulose fractions, which are usually wasted. New wood production processes should also have to include higher-value uses for the lignin and hemicellulose. Due to the compact lignin carbohydrate complex (LCC) wood structure, the separation of the components of lignocellulose materials without intensive use of chemicals and energy, as is done in traditional wood pulping, is no easy matter. But intensive use of chemicals and energy will result in large damage and lost of the wood components. A new idea was introduced here, which introduced enzymes to treat the wood before the components separation [2]. The enzymes are specified and in relatively mild working condition. The extraction process was done on the hemicellulases attacked materials and the result showed that all enzymatic treatments increased the yield of extraction and the polymers extracted from the xylanase treated material had higher degree of polymerization than non-enzymatically treated controls [3]. The chemo-enzymatic extraction concept was set here to separate the wood components. One problem is however, that the valuable glucomannan to large extent was degraded during these treatments. The sensitivity of this polysaccharide is probably mainly due to the "peeling" reaction that degrade the glucomannan from the reducing end [4]. To improve chemo-enzymatic extraction process concept, modification of extended impregnation should be done to inhibit the peeling reaction from the alkaline attack.

Preservation of the glucomannan against alkali degradation can be done with conversion of carbonyl groups with a reducing or an oxidizing agent to prevent the further peeling reaction [5]. In this paper, we provide insight into three common chemicals, sodium borohydride ($NaBH_4$), polysulfide (PS), anthraquinone (AQ), which are used in kraft pulping to see whether they can do the modification on the extended impregnation process. And then we should demonstrate that after the modified work, if the enzyme also can penetrate into the materials and work on them.

II. EXPERIMENTAL

Extended impregnation (EI) of 1 kg (o.d. weight) of Norway spruce (*Picea abies*) chips was carried out in a pilot scale circulation digester with white liquor, at conditions adapted from traditional kraft cooking process. Modified extended impregnation of wood chips was performed with the addition of $NaBH_4$, elemental sulphur or

anthraquinone see **Table 1**. After impregnation, wood chips were washed with deionised water for more than 12 hours to remove the alkaline residue. Pretreated wood chips were disintegrated through 50,000 revolutions in a disintegrator designed according to ISO 5263-1:2004.

Table 1. Extended impregnation conditions and additives

Extended Impregnation (EI)	L:W	7
	$[OH^-]$	25 g/L
	Sulfidity	60 % w/w wood
	Maximum temperature	110°C
	Impregnation time	120min
Modified Extended Impregnation Additive charge, %w/w wood	$NaBH_4$	3
	PS	4
	AQ	0.15

The incubation process was performed by suspending 5 mg (dry weight) wet samples of each type of impregnated wood in 20 mM sodium phosphate buffer (pH 7) with 5 µL Novozym 342 (90 EGU/g) at 40 °C for 5 h in a final volume of 1 mL. Gammanase was used for the treatment of impregnated wood prior to extraction. A 10 g (o.d. weight) of each tyoe of impregnated wood was incubated with 300 mL of 50 mM (pH 5) sodium acetate buffer at 60°C for 24 h. Gammanase dosage was 1000 VHCU units /g (1 mL/g). The enzymatic treatment was terminated by increasing the temperature above 90 °C.

For extraction experiments, a 10 o.d. g of impregnated wood was subjected to a mixture of 50% w/w methanol containing 5% w/w alkali charge on wood at 130°C for two hours with a liquor-to-wood ratio of 10:1 [9]. Liquid-containing dissolved solids were separated from the wood material by vacuum filtration using a wire cloth (mesh size: 71 microns) followed by washing with deionised water. Aliquots of the residual wood were heated at 105 °C to determine the amount of extracted material. The liquids containing dissolved solids were lyophilized.

Reducing sugar analysis was performed by the method described by Miller [6]. Klason lignin content in the wood material was measured in accordance with Tappi standard T 222 om-02. Carbohydrate composition of the filtrates after acid hydrolysis (SCAN-CM 71:09) was analysed using high-performance anion-exchange chromatography. Molar mass distribution of the lyophilised extracts was determined using a size exclusion chromatography calibrated with pollulan standards with specific molecular weights ranging from 320 to 400 000 Da.

III. RESULTS AND DISCUSSION

The addition of additives during extended impregnation considerably increased the yield, with sodium borohydride to be the most efficient as compared to polysulphide and anthraquinone, **Table 2**. Because the oxidized structure does possess a double bound oxygen, a peeling type reaction might occur, although more slowly than in the original structure, whereas the reduced structure contains no double bond that can initiate the peeling reaction. Thus, reduction is most likely an efficient way to prevent the peeling reaction, as previously suggested [8].

Even though more glucomannan was retained in the material the enzymes can still penetrate into the wood and attack the polymers from the released reducing sugar results shown in **Figure 2**. One possible explanation is that approximately 20% of the extractable lignin was lost during the impregnation process, as shown in **Table 2**. The non-phenolic β-O-4 ethers in lignin are cleaved under alkaline conditions [7], and such a reaction may partly degrade the lignin-carbohydrate networks in wood, making the structure of the wood "looser" and more flexible, thereby allowing enzymes to penetrate into the structure and access the polysaccharides. In addition to the lignin aspect, some hemicelluloses were also lost even in the modified EI. This loss may also lead to the cleavage of the lignin carbohydrate complex. Due to still more glucomannan was preserved in the modified extended impregnated samples, the reducing sugar contents from the respective samples were slightly lower than that from the non-modified extended impregnated sample, except for the AQ-modified material. That may due to the reduced form of AQ i.e. AHQ, prevented an undesirable side reaction (e.g., condensation) of the lignin, and thus, the solubilising reactions of delignification were enhanced.

Table 2. Composition of wood material after extended impregnation with and without additives in %w/w wood

Sample	Yield	Lignin	Ara	Gal	Glu	Xyl	Man
Spruce	(100)	28.3	1.57	2.23	46.89	6.88	13.56
EI	76.6	22.4	0.88	0.77	44.16	4.85	4.01
EI-$NaBH_4$	89.5	23.2	1.03	1.37	48.52	5.91	10.17
EI-PS	80.0	22.8	0.94	1.12	45.97	5.53	5.76
EI-AQ	81.3	22.7	0.84	0.70	45.21	5.68	5.52

EI: extended impregnation, EI-$NaBH_4$: extended impregnation with $NaBH_4$, EI-PS: extended impregnation with elemental sulphur, EI-AQ: extended impregnation with anthraquinone.

The carbohydrates were stabilized by the additives during extended impregnation, which were then isolated during the extraction stage. In cases where no additive was used, the yield of extracted material was 9% w/w wood whereas the gamanase treatment did not noticeably affect the extraction yield. However, 11% w/w wood was extracted from sodium borohydride treated wood, which increasing to 14% with gamanase treatment. With polysulphide and anthraquinone, the amount of extracted material was 11-12% w/w wood (**Figure 1**) but the yield was not considerably increased after gamanase treatment. This result may be because the polysulphide and anthraquinone did not preserve as many polysaccharides as in the case of sodium borohydride.

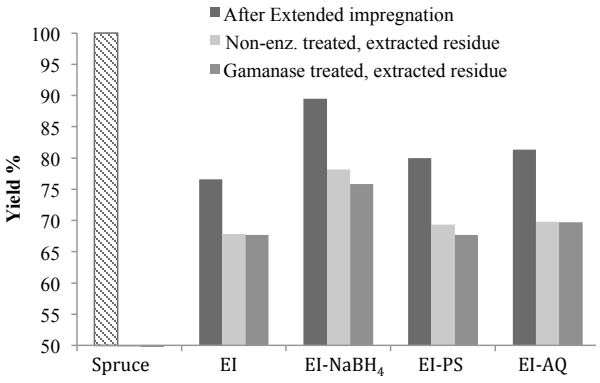

Figure 1. The extraction yields of enzyme-treated and non-enzyme-treated wood after impregnation. Modified extended impregnation preserved more material in the wood, and hence more material was extracted than from the wood undergoing extended impregnation. Sodium borohydride showed larger effects

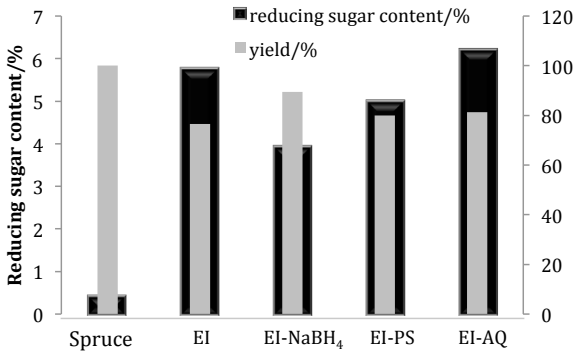

Figure 2. Released reducing sugar analysis and yield comparison. The yield increased from 76.6% to 80.0% (PS), 81.3% (AQ) and 89.6% ($NaBH_4$), respectively, under the same conditions, and the reducing sugar analysis data indicated that the enzymes could penetrate and attack the wood.

Because the mannose content in the impregnated wood was low, i.e., 4%, hence only 13% of mannose was extracted, which increased to 20% after the gamanase treatment (**Table 3)**. Sodium borohydride preserved a significant amount of mannose in the wood, and hence, it was possible to extract a comparatively larger 25% of mannose, whereas gamanase treatment increased it to 30%. The material extracted from non-enzyme treated wood has a molecular weight ranging up to 20000 Da, which means that the opened wood structure enables the extraction of high molecular weight material regardless of the addition of additives. However, the molecular weight of the material extracted from gamanase treated wood was not very high, and most of the extracted hemicelluloses appear in the oligomeric region, with some larger LCCs. This result is most likely because gamanase has degraded the polysaccharides.

Xylose was less extracted from the gamanase-treated samples for all three pretreatment methods. This result is unexpected and difficult to explain. However, gamanase contains some xylanase activity, and as xylan has a rather high solubility in alkali, the xylan in the pretreated material might have been partly dissolved and precipitated and thereby very accessible for enzymatic degradation. Thus, xylanase-free enzyme products might be interesting for this type of application.

The lignin content in the extracted material from gamanase-treated wood is also slightly high, which may be because gamanase can cut glucomannan, producing more free LCCs to be extracted.

Table 3 Amount of lignin and anhydro-monosugars extracted from impregnated wood samples

% based on wood		Lignin	Ara	Gal	Glu	Xyl	Man
EI	Non-enzyme treated	5.77	0.07	0.09	2.62	0.20	0.53
	Gamanase treated	6.77	0.08	0.15	2.10	0.20	0.88
EI-$NaBH_4$	Non-enzyme treated	4.64	0.26	0.48	2.98	1.20	2.51
	Gamanase treated	5.86	0.11	0.52	4.36	0.50	3.02
EI-PS	Non-enzyme treated	5.76	0.02	0.53	3.64	1.41	1.54
	Gamanase treated	7.27	0.10	0.57	4.08	0.62	1.81
EI-AQ	Non-enzyme treated	5.01	0.11	0.09	2.18	1.32	2.18
	Gamanase treated	6.40	0.10	0.18	1.16	0.58	2.25

IV. CONCLUSIONS

The three additives successfully achieved the preservation of glucomannan during modified extended impregnation. The yield increased from 76.6% to 80.0% (PS), 81.3% (AQ) and 89.6% ($NaBH_4$). After the modification, the impregnated wood was also opened up to enzymes. The additives during extended impregnation enhance the yields of extracted materials with molecular weight up to 20 000 Da. Gamanase treatment improved the extraction yield even more, but the polymers are degraded to oligomers or less. Thus, a monocomponent such as endo-mannanase would be a better option than gamanase.

VI. REFERENCES

[1] Lucia, L. A. Lignocellulosic biomass: Replace petroleum, *BioResources* **2008,** 3(4), 981- 982.

[2] Wang, Y., Lindström, M. E., & Henriksson, G. Alkaline pretreatment to open the wood structure for enzymatic modification, *BioResources* **2011** 6(3), 2425-2434.

[3] Azhar, S., Wang, Y., Lawoko, M., Henriksson, G., and Lindström, M.E. Extraction of polymers from enzyme-treated softwood, *BioResources* **2011** 6(4), 4606-4614.

[4] Gellerstedt G. Chemistry of chemical pulping In Pulp and Paper Chemistry and Technology 2 Pulping Chemistry and Technology Eds: Ek M, Gellerstedt G and Henriksson G *de Guyter*, Berlin, Germany. **2009** ISBN 978-3-11-021341-6 pp 35 – 120.

[5] Courchene, C.E. The tried, the true and the new - getting more pulp from chips – modifications to the kraft process for increased yield, *Proceedings of the breaking the pulp yield barrier symposium*. *Tappi Press, Atlanta* **1998** , 11-20.

[6] Miller, G. L. Use of dinotrosalicylic acid reagents for determination of reducing sugars, *Anal. Chem*. **1959** 31, 426-428.

[7] Gierer, J. Chemical aspects of kraft pulping, Wood Sci. Technol. **1989**, 14, 241-266.

[8] Istek, A., Özkan, I. Effect of sodium borohydride on Populus tremula L. kraft pulping. *Turk. J. Agric.* **2009** 32, 131–136.

[9] Muurinen, E. Organosolv pulping: A review and distillation study related to peroxyacid pulping. *University of Oulu, Finland.* **2000**.

CELLULOSE NANOCRYSTALS USED FOR IMMOBILIZATION OF POLYMER ADDITIVES

Sabrina Weigl[1]*, Klaus Bretterbauer[1] and Christian Paulik[1]

[1]*Institute for Chemical Technology of Organic Materials, Johannes Kepler University Linz, Altenbergerstraße 69, 4040 Linz, Austria (*Sabrina.Weigl@jku.at)*

ABSTRACT

Antioxidants were grafted to cellulose nanocrystals (CNC), characterized and compounded to polypropylene (PP). Antioxidizing di-*tert*-butylphenol groups were covalently bound to previously synthesized carboxymethyl cellulose nanocrystals via amide formation. Characterization was carried out using fourier transform infrared spectroscopy, NMR measurements and elemental analyses. Stabilization tests and dispersion of CNC samples within the PP matrix were verified using oxidative induction time and scanning electron microscopy measurements. We display that carboxymethyl cellulose nanocrystals do show a weak stabilizing effect while antioxidant grafted cellulose nanocrystals do not possess this ability with the herein described method of compound preparation.

I. INTRODUCTION

Cellulose Nanomaterials are of increasing interest for nanocomposites due to their natural abundance and biodegradability. They are known as fillers and reinforcements for polymers to increase mechanical, thermal and barrier properties [1]. Furthermore, additivation of cellulose follows the trend to biobased materials and the raw product is cheap [2]. Physical loss and migration of commercially available additives in polymers is discussed in literature as it affects the service life of a product [3,4]. Additionally, additives can contaminate its surrounding area, for example in water pipeline systems or food through packaging [5–7]. In this work additive molecules are covalently bound to CNC and their migration is hindered. Hence, reinforcing properties are combined with the immobilization of polymer additives.

II. EXPERIMENTAL

Materials and methods

Solvents and reagents were purchased from standard chemical suppliers. Reagents were of p.a. quality and used without further purification. Solvents were dried by conventional means if necessary. Cellulose nanocrystals (CNC) were purchased from the University of Maine process development center in dry form with a purity of 90 to 100 %. Unstabilized PP powder with a melt flow index of 0.02 g min^{-1} at 240 °C and 2.16 kg was purchased from Borealis Polyolefine GmbH (Linz, Austria). Fourier transform infrared (FT-IR) spectroscopy was recorded using a Perkin Elmer Paragon 1000 PC FT-IR spectrometer. Static oxidative induction time (OIT) measurements were carried out on a Perkin Elmer DSC 8000. Samples were prepared by cutting a cylindrical sample out of extruded compounds with 5 mm diameter, ~0.5 mm thickness, and 14-16 mg weight. Measurement consisted of heating from 30 °C to 220 °C at 20 °C min^{-1}, holding for 5 min, cooling to 190 °C at 20°C min^{-1}, and holding 5 min before applying oxygen. The oxidative induction time is indicated by an exothermal reaction. ^{1}H nuclear magnetic resonance (NMR) spectra were performed on a Bruker Avanve III 300 MHz spectrometer using standard pulse sequences as provided by the manufacturer. Deuterated solvents were used as internal calibration standards for NMR spectroscopy. A Zeiss 1540XB CrossBeam equipped with an Oxford Instruments EDX system was used for scanning electron microscopy (SEM) and energy-dispersive x-ray spectroscopy (EDX). For SEM/EDX measurements, samples were cut with a knife and the surface spattered with gold. Elemental analyses were done on a Thermo electron corporation Flash EA 1112 CHNS-O analyzer.

*Synthesis of carboxymethyl cellulose nanocrystals (CM-CNC) **2***

Cellulose nanocrystals (CNC) **1** (1 g) are dispersed in a mixture of 50 mL isopropyl alcohol and 5 mL H_2O on an ultrasonic bath for 30 min. Sodium hydroxide solution (6 mL, 30 %) is added resulting in a translucent reaction mixture followed by the addition of 1.8 g chloroacetic acid. The reaction mixture is then stirred for 2.5 h at

70 °C, neutralized with acetic acid (80 %), filtered and washed with a mixture of methanol and H_2O. The resulting sodium salt is suspended in 0.1 N hydrochloric acid on an ultrasonic bath for 1 h, filtered and washed with methanol to yield **2** in 90 %.

*Synthesis of AO-grafted cellulose nanocrystals (CNC-AO) **4***

CM-CNC **2** (145 mg) are dispersed in 5 mL absolute *N,N*-dimethylformamide (DMF) under Argon on an ultrasonic bath for 1 h. Dicyclohexyl carbodiimide (610 mg) dissolved in 3 mL DMF is added and the mixture stirred at room temperature for 5 min followed by the addition of 4-dimethylamino pyridine (95 mg) dissolved in 3 mL DMF and amine **3** dissolved in 5 mL DMF. The reaction mixture is then stirred at room temperature under Argon for 120 h, filtered and washed eight times with acetone to yield **4** [8].

Preparation of polypropylene compounds

Compounds were prepared with a Thermo Scientific Minilab II Haake Rheomex CTW5 twin-screw compounder at 175 °C and a speed of 60 min^{-1} for 5 min mixing time. The ratio of compounded CNC-AO to polypropylene (PP) was fixed at 0.5 wt.% based on di-*tert*-butylphenol groups grafted to the CNC [9].

III. RESULTS AND DISCUSSION

Synthesis

Antioxidant (AO) grafted cellulose nanocrystals **4** were synthesized by coupling of an amine functionalized AO **3** to carboxymethyl cellulose. Raw cellulose nanocrystals **1** were converted to carboxymethyl cellulose nanocrystals **2** with chloroacetic acid (Figure 1).

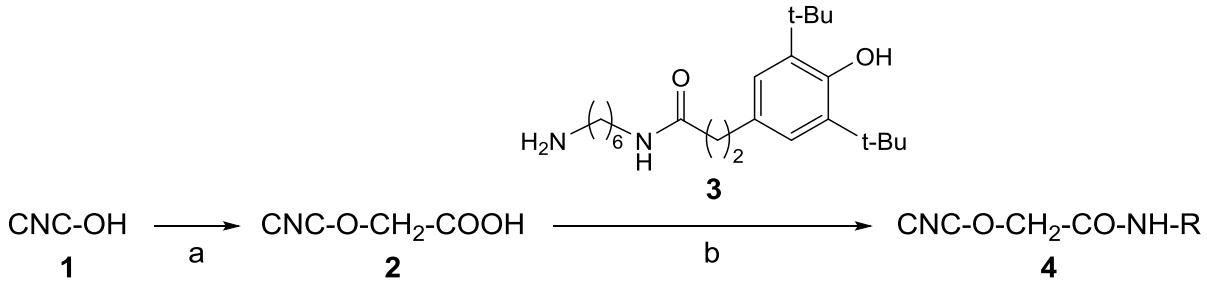

Figure 1: Synthesis of AO-functionalized CNC via CM-CNC. Reaction conditions: (a) CM-CNC: i-Prop/H_2O, ultrasonic bath (30 min), addition of NaOH (30%), addition of $ClCH_2COOH$, 70 °C, 2.5 h, then HCl (0.1 N) and ultrasonic bath (60 min) to the corresponding acid; (b) CNC-AO: DMF, DCC, DMAP, r.t., 120 h

Analytics

Fourier transform infrared spectroscopy *(*FT-IR) is a method to qualitatively characterize functionalized cellulose. Figure 2 compares pristine CNC with CM-CNC and AO-grafted CNC. AO precursor **3** shows a characteristic peak for the phenolic hydroxyl group at 3635 cm^{-1}, which is additionally found in **4**. Two peaks at 2930 and 2850 cm^{-1} are associated to the aliphatic groups of **3** and **4**. Compared to pristine CNC, CM-CNC **2** show a signal at 1730 cm^{-1} arising from the C=O stretching vibration of the carboxylic acid group. For CNC-AO **4** the C=O stretching vibration is shifted to 1610 cm^{-1} according to the conversion from carboxylic acid to amide group. Additionally, signals at 1540 and 1430 cm^{-1} corroborate the presence of amide groups. The intactness of the phenolic AO groups was additionally verified by ^1H NMR measurements since **4** is slightly soluble in DMSO-*d6*. The degree of functionalization was verified using elemental analysis by evaluation of the nitrogen content since it is only introduced through AO precursor **3**. The degree of substitution is 1 which means one phenolic AO group per glucose unit.

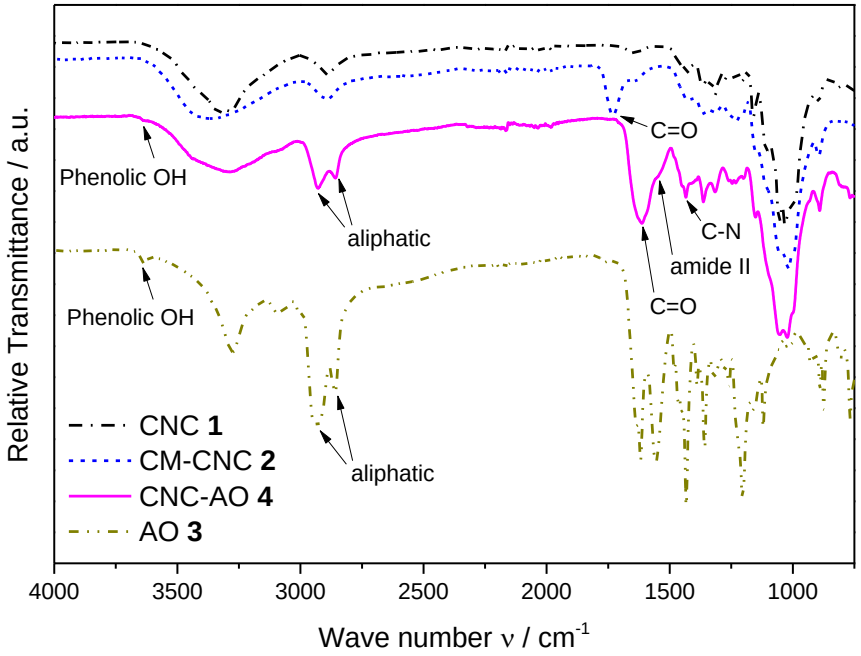

Figure 2: FT-IR spectra of pristine CNC **1**, CM-CNC **2**, CNC-AO **4,** and raw AO **3**.

Analytics of compounded samples

To determine the stabilizing ability of CNC-AO **4** it was compounded to commercially available isotactic PP and the oxidative induction time (t_{OIT}) was measured. Pristine CNC, and CM-CNC were also compounded to PP and compared to non-stabilized PP. Table 1 and Figure 3 illustrate the results of OIT measurements. Surprisingly, CM-CNC **2** show a weak stabilizing ability whereas AO-grafted CNC **4** do not possess this effect. One possible explanation is the missing dispersion of CNC in the polymer matrix as SEM images show (Figure 4).

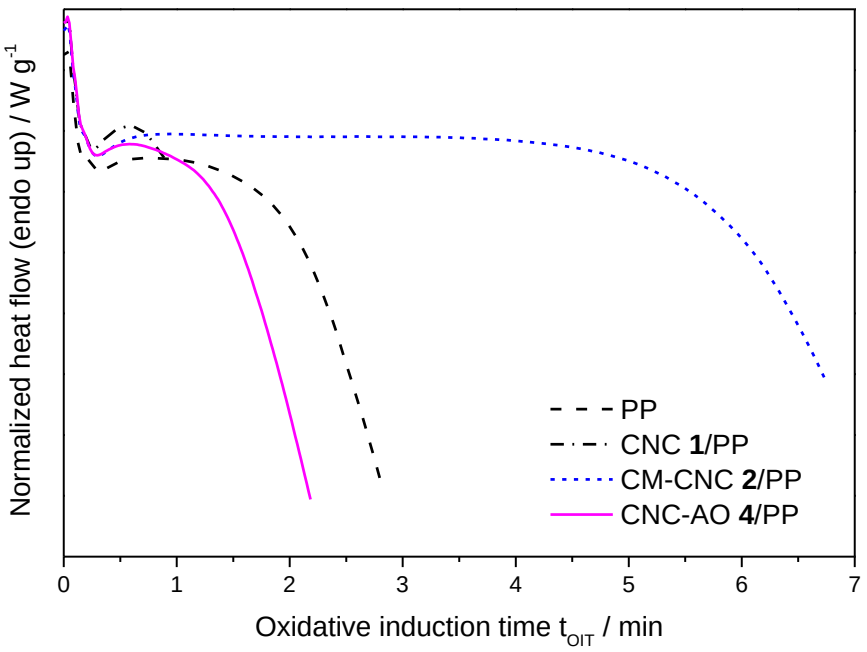

Figure 3: OIT measurements of compounded samples **1**/PP, **2**/PP, and **4**/PP compared to non-stabilized PP

Table 1: OIT values for compounded samples **1**/PP, **2**/PP, and **4**/PP compared to non-stabilized PP

Sample	t_{OIT} / min
PP	2.26
CNC **1**/PP	1.34
CM-CNC **2**/PP	6.41
CNC-AO **4**/PP	1.83

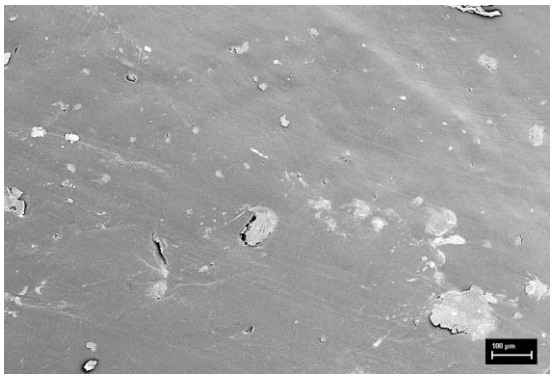

Figure 4: SEM image of CNC-AO **4**/PP compound, darker matrix is PP, lighter areas are CNC-AO **4**.

IV. CONCLUSIONS

CNC were grafted with an amino-functionalized phenolic AO via carboxymethylation of raw CNC and subsequent amide formation with DCC/DMAP. Characterization was performed by FT-IR and NMR measurements which proof the intactness of the phenolic AO group and elemental analyses to determine the degree of functionalization. Nevertheless, compounded CNC-AO/PP samples do not show stabilizing properties as OIT measurements illustrate. CNC-AO dispersion in PP compounds is inhomogeneous as SEM images show. Further research will concentrate on the homogenization of CNC-AO/PP compounds for example through chemical modification of CNC and thus a better compatibility with the PP matrix.

V. ACKNOWLEDGEMENT

The NMR spectrometer was acquired in collaboration with the University of South Bohemia (CZ) with financial support from the European Union through the EFRE INTERREG IV ETC-AT-CZ program (project M00146, "RERI-uasb").

VI. REFERENCES

[1] Siro I., Plackett D., Microfibrillated cellulose and new nanocomposite materials: a review, *Cellulose (Dordrecht, Neth.)* **2010**, *17*(3), 459–494.

[2] Siqueira G., Bras J., Dufresne A., Cellulose Whiskers versus Microfibrils: Influence of the Nature of the Nanoparticle and its Surface Functionalization on the Thermal and Mechanical Properties of Nanocomposites, *Biomacromolecules* **2009**, *10*(2), 425–432.

[3] Billingham N. C., Chapter 4 - THE PHYSICAL CHEMISTRY OF POLYMER OXIDATION AND STABILIZATION, In: *Atmospheric Oxidation and Antioxidants : Atmospheric Oxidation and Antioxidants* **1993**, Vol. 2, Elsevier, Amsterdam, 219–277.

[4] Gächter R., Müller H., Plastics Additives Handbook, *Stabilizers, Processing Aids, Plasticizers, Fillers, Reinforcements, Colorants for Thermoplastics* **1990**, 3rd Edition, Hanser Publishers, Munich-Vienna-New York.

[5] Thörnblom K., Palmlöf M., Hjertberg T., The extractability of phenolic antioxidants into water and organic solvents from polyethylene pipe materials – Part I, *Polymer Degradation and Stability* **2011**, *96*(10), 1751–1760.

[6] Brocca D., Arvin E., Mosbaek H., Identification of organic compounds migrating from polyethylene pipelines into drinking water, *Water Res.* **2002**, *36*(15), 3675–3680.

[7] Lundbaeck M., Strandberg C., Albertsson A.-C., Hedenqvist M. S., Gedde U. W., Loss of stability by migration and chemical reaction of Santonox R in branched polyethylene under anaerobic and aerobic conditions, *Polym. Degrad. Stab.* **2006**, *91*(5), 1071–1078.

[8] Lucente-Schultz R. M., Moore V. C., Leonard A. D., Price B. K., Kosynkin D. V., Lu M., Partha R., Conyers J. L., Tour J. M., Antioxidant Single-Walled Carbon Nanotubes, *J. Am. Chem. Soc.* **2009**, *131*(11), 3934–3941.

[9] Shi X., Wang J., Jiang B., Yang Y., Hindered phenol grafted carbon nanotubes for enhanced thermal oxidative stability of polyethylene, *Polymer* **2013**, *54*(3), 1167–1176.

STRUCTURAL ELUCIDATION OF WHOLE LIGNIN FROM EUCALYPTUS BASED ON PRESWOLLEN AND ENZYMATIC HYDROLYSIS

Jia-Long Wen[1], Tong-Qi Yuan[1], Shao-Long Sun[1], Run-Cang Sun[1,2]*

[1]*Beijing Key Laboratory of Lignocellulosic Chemistry, Beijing Forestry University*
[2]*State Key Laboratory of Pulp and Paper Engineering, South China University of Technology, Guangzhou, China, rcsun3@bjfu.edu.cn*

ABSTRACT

A comprehensive understanding of the structures of whole lignin in the plant cell wall is extremely significant for developing effective biomass processing and utilization. In the present study, a robust method based on mild alkaline preswollen and *in-situ* enzymatic hydrolysis for the isolation of "swollen residual enzyme lignin, SREL" from *Eucalyptus* wood was presented. The SREL obtained was investigated as compared to the corresponding cellulolytic enzyme lignin (CEL) and alkali lignin (AL). Remarkablely, the yield of SCEL (95%) was significantly higher than that of CEL (20%) and AL (12%). The isolated lignin polymers have been comparatively investigated by a combination of elemental analysis, 2D HSQC NMR, ^{31}P-NMR, and GPC techniques. The major lignin linkages (β-O-4′, β-β′, and β-5′, etc.) were thoroughly assigned and the frequencies of the major lignin linkages were quantitatively obtained. In particular, *p*-hydroxyphenyl (H) units were observed in SREL and AL rather than CEL, suggesting that H-type lignin units, which are difficult to be extracted with 96% dioxane, could be obtained by this method. Inspiringly, the effective method gives us an integrated vision to understand the intrinsic structural features of whole lignin from plant cell wall and helps to develop more effective plant deconstruction or pretreatment strategies in the current biorefinery process.

I. INTRODUCTION

Isolation and structural characterization of lignin has been also extensively investigated and developed in wood and lignin chemistry. However, the complex and irregular structure of lignin as well as fundamental chemistry of the lignin during current biorefinery has not been completely elucidated although the primary structure has been well depicted [1]. Traditionally, isolation methods for structural analysis of lignin have been proposed during the past decades, such as MWL[2], CEL[3], and EMAL[4]. All the above-mentioned lignin preparations have played a very significant role in structural elucidation of lignin in wood chemistry. However, these methods could not provide panoramic structural features of the whole lignin components via an un-extracted approach, i.e., *in situ* approach.

Ideally, it is important to find a pretreatment that two premises should be satisfied simultaneously: 1) enhancing the enzymatic hydrolysis of the pretreated plant cell wall to remove most of carbohydrates; 2) keeping the structure of the lignin in the raw material unchanged as far as possible. If the pretreatment exist, the whole lignin can be isolated as a residue after sufficient enzymatic hydrolysis. Most publications demonstrated that enzymatic hydrolysis efficiency is related to the crystallinity and accessibility of the pretreated substrates. In addition, due to the swelling action of alkaline treatments, the aqueous alkaline treatment causes a reduction in both cellulose crystallinity and crystallite size of the plant cell wall [5]. Under these enlightenments, mild alkaline treatments and subsequent in-situ enzymatic hydrolysis were applied to the ball-milled plant cell wall to remove more carbohydrates as far as possible, obtaining swollen residual enzyme lignin (SREL) as residual lignin, instead of extracting lignin with neutral solvent (i.e. dioxane). Based on the above-mentioned enlightenments, a new paradigm of lignin isolation method from *Eucalyptus* wood was proposed for the first time. In addition, to evaluate the effect of mild alkaline treatments and enzymatic hydrolysis on the structural features of the SREL, the corresponding alkaline lignin (AL) and cellulolytic enzyme lignin (CEL) isolated under the same condition was used as a control.

In this study, the lignin preparation obtained from the novel method was scientifically evaluated by comparing the yield, composition, and structural features of the SREL with those of corresponding CEL and AL. More importantly, quantitative information, including functional groups, syringyl/guiaiacyl (S/G) ratio as well as major substructures (β-O-4′, β-β′, β-5′, and β-1′), were obtained according to the advanced ^{13}C, 2D-HSQC, and ^{31}P-NMR spectra. It is believed that the application of this method in biomass chemistry will enlarge our understanding of structural features of whole lignin in the plant cell wall.

II. EXPERIMENTAL

Materials

Eucalyptus sawdust (2×0.5×0.5 cm) was prepared from *Eucalyptus* grandis × *Eucalyptus* urophylla wood. The extractive-free *Eucalyptus* wood (30 g, 40-60 mesh) was milled (5 h, 450 rpm) in a Fritsch planetary ball mill. The composition of Eucalyptus was 37.5% glucan, 16.2% xylan, 0.26% arabinan, 0.99% galactan, 32.3% Klason lignin, 2.0% acid-soluble lignin, which was analyzed by the standard of NREL.

Preparation of Swollen Residual Enzyme Lignin (SREL)

The ball-milled *Eucalyptus* powder was firstly slowly dissolved into 4% sodium hydroxide (1/25, g/mL) for 24 hour under stirring at room temperature. After the preswollen, the pH value of the mixture solution was directly adjusted to 4.8 with acetic acid. The resulted mixtures were subjected to enzymatic hydrolysis, with the loading large amounts of cellulase (50 FPU/g) and β-glucosidase (50 IU/g). The reaction mixture was incubated at 50 °C in a rotary shaker (200 rpm) for 48 h, afterward, the solution was centrifuged to remove hydrolyzed carbohydrates, and the residue named "swollen residual enzyme lignin, (SREL)". The SREL was thoroughly washed with boiling water (pH=2.0) to eliminate the residual enzyme and free sugars. Eventually, the purified SREL was freeze-drying.

Isolation of Cellulolytic Enzyme Lignin (CEL) and Alkali Lignin (AL)

The isolation of CEL was according to a previous publication[3], while the alkali lignin (AL) was isolated from the ball-milled Eucalyptus powder (5 g) at room temperature for 24 h (solid to liquid ratio, 1:25) according to a previous publication with some modifications[6].

Characterization of Lignin Samples

Carbohydrate analysis, molecular weight, 2D-HSQC NMR spectra were analysed according to a previous publication[7].

III. RESULTS AND DISCUSSION

Table 1. Yield, carbohydrate contents and the elemental analysis of the lignin preparations

Sample	SREL	CEL	AL
Yield	95%	20%	12%
Carbohydrate	8.7%	13.4%	0.4%
C_{900} formula	$C_{900}H_{935}O_{332}(OCH_3)_{150}$	$C_{900}H_{895}O_{316}(OCH_3)_{139}$	$C_{900}H_{823}O_{316}(OCH_3)_{146}$

One of the most used methods to isolate wood lignin for structural studies is CEL method. The method uses cellulolytic enzyme mixtures (containing cellulases and hemicellulases) to remove most of the carbohydrate fraction prior to lignin extraction with aqueous dioxane. However, the yield of CEL is only 20% based on the Klason lignin of the *Eucalyptus* wood. Considering the highest yield of SREL (95%), SREL was an ideal lignin sample for structural analysis. Surprisingly, after evaluating the associated carbohydrate contents in these lignin samples, it was found that SREL contained a small quantity of associated sugars (8.7%, w/w), while CEL and AL contained 13.4% and 0.4% sugars based on dry lignin (w/w), respectively (**Table 1**). In light of the results obtained (super-high yield and low associated sugars), it was concluded that SREL can better represent for the whole lignin in the plant cell wall. After carefully examined the composition of associated carbohydrates, it was observed that glucose was the major sugar in SREL, while xylose was major sugar in CEL. The differences of associated sugars could be attributed to the different isolating methods, e.g. the higher content of glucose is related to the small amount of obstinate cellulose in SREL, while the abundant xylose is ascribed to the potential lignin-carbohydrate complex (LCC). The elemental composition and methoxy group (OMe) contents of the lignin samples, together with the calculated approximate C_{900} formulas, are also listed in **Table 1**. As shown in the C_{900} formulas, the OMe contents in the SREL and AL are higher than that of CEL. The numbers of oxygen are 332, 316, and 316/C_{900} and those of OMe groups are 150, 139, and 146/C_{900} in SREL, CEL, and AL, respectively. It is known that higher oxygen contents in lignins approximating the theoretical limit of 300/C_{900} (or above) are indicative for carbohydrate residues originating from lignin-carbohydrate linkages, implying that the associated carbohydrates in these lignin are potentially originated from LCC linkages. However, the oxygen content of lignins could be elevated by large amounts of carboxylic group, which are resulted from alkaline treatments.

To investigate the composition and detailed chemical structures of the lignin obtained, the lignin samples (SREL, CEL, and AL) were analyzed with 2D HSQC NMR technique according to the publications[8,9]. The main structural characteristics of the lignins, including basic composition (S, G, and H units) and various substructures linked by ether and carbon-carbon bonds (β-*O*-4′, β-β′, β-5′, and β-1′, etc.), can be observed in the 2D HSQC spectra. The side-chain and aromatic regions of 2D HSQC spectra and the main substructures are depicted in **Figure** 1.With respect to the relative content of different linkage types (not shown), all the lignin samples display a predominance of β-*O*-4′ aryl ether units (A, 75.7%–81.1% of total side chains) followed by β-β′ resinol-type units (B; 15.1%–18.8%) and lower amounts of β-5′ phenylcoumaran-type (C; 2.8%–6.7%). It was observed that the relative content of β-*O*-4′ linkages is higher in SREL and AL, probably resulting from the abundant S-type lignin units in these lignin samples. Basically, monolignol addition to a syringyl unit has essentially only a single pathway available, β-*O*-4′ linkage [8]. In contrast, the abundance of phenylcoumaran structures decreased in the order of CEL>SREL>AL, which is most probably related to the decrease in G lignin observed in these lignin samples.

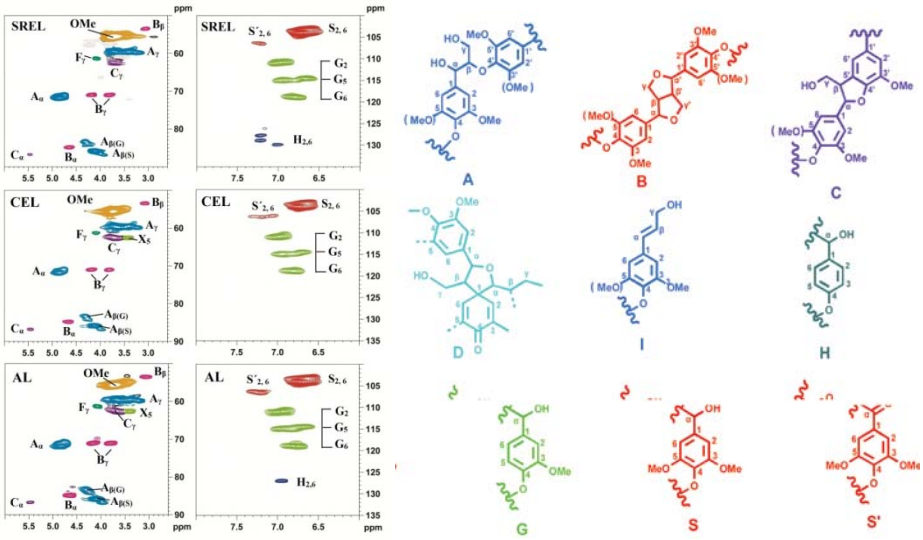

Figure 2. 2D HSQC NMR spectra and the identified structures of the lignins

The ^{31}P spectra results were listed in **Table 3**. For SREL, CEL, and AL, the content of S-type OH was less than that of corresponding G-type OH. This suggested that most of S-type lignin unit involves in the formation of β-*O*-4′ linkage in these lignins and only a small amount of free S-OH could be detected by ^{31}P- spectra. Generally, cleaved β-aryl ether linkages give raise to phenolic hydroxyl groups, while oxidation reactions may result in oxidative fragmentation of the lignin macromolecule with concomitant creation of carboxylic acid group. Less amount of phenolic OH in SREL than CEL suggesting that SREL probably contains more etherified units, that is, phenolic OH is linked as β-*O*-4′ linkages and phenyl glycoside linkages. By contrast, the contents of COOH in SREL and AL were abundant, resulting from the oxidative of aliphatic OH during alkaline treatment, as revealed by the decreased aliphatic OH in REL and AL. Moreover, non-condensed H-type phenolic OH was found in SREL and AL rather than CEL, reconfirming the existence of H-type lignin units in these lignins.

Table 3. Quantification of the functional groups by quantitative ^{31}P-NMR method.

Samples	SREL	CEL	AL
Aliphatic-OH	3.74	5.23	2.90
Condensed S-OH	0.07	0.02	0.02
Non-condensed S-OH	0.12	0.24	0.17
Condensed G-OH	0.03	0.05	0.04
Non-condensed G-OH	0.18	0.43	0.27
Non-condensed H-OH	0.01	N.D	0.03
COOH	0.13	0.03	0.19

Figure 3 shows the curves of weight-average (M_w) and number-average (M_n) molecular weights and polydispersity index (PDI, M_w/M_n) of the lignin samples obtained from *Eucalyptus* wood. It was found that CEL has a higher M_w than that of AL and SREL; however, the highest M_w of CEL is probably related to the associated carbohydrates[10]. By contrast, considering the molecular weight, higher β-*O*-4′ linkages, and less phenolic OH of SREL, it was concluded that the isolation of lignin as "SREL" could be serves as an effective method to prepare lignin samples for structural analysis.

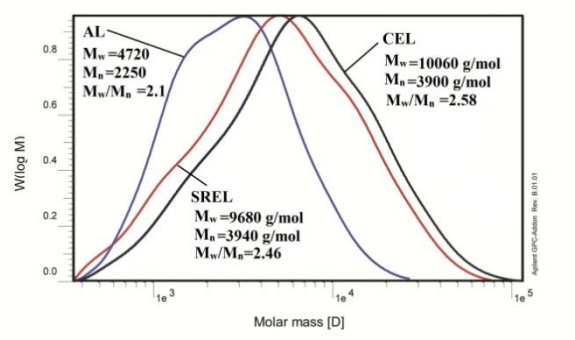

Figure 3. Molecular weight distributions of the lignins

IV. CONCLUSIONS

It has been demonstrated that preswelling/dissolution pretreatment with sodium hydroxide significantly improves enzymatic hydrolysis of polysaccharides in ball-milled wood, and thus increasing the yield and purity of SREL. SREL was demonstrated to be an ideal sample to characterize the structural features of lignin in the plant cell wall. The data presented indicated that the lignin extracted by this method is a syringyl-rich lignin, having more abundant β-O-4′ linkages and less phenolic hydroxyl groups. More importantly, H-type lignin units, which are difficult to be extracted with traditional methods (MWL and CEL) were obtained by this method. Comparing with the CEL, AL, and SREL preparations, by using various analysis approaches revealed that all these samples have similar structural features and compositions. Surprisingly, this method also gives some inspirations for better deconstruction of plant cell wall in an easily approach, which is crucial to pretreated process in the current biorefinery process.

V. ACKNOWLEDGEMENT

This work was supported by the grants from the National Natural Science Foundation of China (31110103902).

VI. REFERENCES

[1] Ralph, J.; Lundquist, K.; Brunow, G.; Lu, F.; Kim, H.; Schatz, P. F.; Marita, J. M.; Hatfield, R. D.; Ralph, S. A.; Christensen, J. H. Lignins: Natural polymers from oxidative coupling of 4-hydroxyphenyl-propanoids. *Phytochem Rev.* **2004**, *3*, 29–60.

[2]Björkman, A. Studies on finely divided wood. Part I. Extraction of lignin with neutral solvents.*Sven.Papperstidn.***1956**, *59*, 477–485.

[3] Chang, H. M.; Cowling, E. B.; Brown, W. .Comparative studies on cellulolytic enzyme lignin and milled wood lignin of sweetgum and spruce. *Holzforschung* **1975**, *29*, 153–159.

[4] Wu, S.; Argyropoulos, D. An improved method for isolating lignin in a high yield and purity. *J. Pulp Pap. Sci.* **2003**, *29*, 235–240.

[5] Mittal, A.; Katahira, R.; Himmel, M. E.; Johnson, D. K. Effects of alkaline or liquid-ammonia treatment on crystalline cellulose: changes in crystalline structure and effects on enzymatic digestibility. *Biotechnol Biofuels.* **2011**, *4*, 1–16.

[6] Sun, R.C.; Lawther, J.M.; Banks, W.B. Effects of extraction time and different alkalis on the composition of alkali-soluble wheat straw lignins. *J. Agric. Food Chem.***1996**, *44*, 3965–3970.

[7] Wen, J. L.; Xue, B.L.; Xu, F.; Sun, R.C.; Pinkert, A. *Ind. Crops Prod.* **2013**, *42*,332–343.

[8] Kim, H.; Ralph, J. Solution-state 2D NMR of ball-milled plant cell wall gels in DMSO-d_6/pyridine-d_5. *Org. Biomol. Chem.* **2010**, *8*, 576–591.

[9] Rencoret, J.; Marques, G.; Gutierrez, A.; Ibarra, D.; Li, J.; Gellerstedt, G.; Santos, J. I.; Jiménez-Barbero, J.; Martinez, A. T.; del Río, J. C. Structural characterization of milled wood lignins from different eucalypt species. *Holzforschung* **2008**, *62*, 514−526.

[10] Jääskeläinen, A.; Sun, Y.; Argyropoulos, D.; Tamminen, T.; Hortling, B. The effect of isolation method on the chemical structure of residual lignin. *Wood Sci. Technol.* **2003**, *37*, 91−102.

OXALIC ACID FORMATION AND ANALYSIS IN PULPING AND PAPERMAKING

Stefan Willför*, Matti Häärä, Anna Sundberg

*Process Chemistry Centre, c/o Laboratory Wood and Paper Chemistry, Åbo Akademi University, Porthansgatan 3, 20500, Åbo/Turku, Finland (*swillfor@abo.fi)*

ABSTRACT

Calcium oxalate scaling is a major problem in pulping and papermaking. Oxalic acid is coming into the processes with the wood raw material, especially with the bark, and it is furthermore formed from other wood components especially in oxidative bleaching stages, e.g. in the alkaline peroxide bleaching of mechanical pulps. The low solubility of calcium oxalate is a challenge also for oxalate analysis, especially concerning the pretreatment and storage methods used.
Isolated wood components and representative sugars for spruce wood were treated in a laboratory peroxide-stage and the oxalic acid formation was analysed with ion chromatography. Sample pretreatment and storage methods were studied and evaluated both for soluble and total oxalate analysis of pulp samples by ion chromatography.
The major source of oxalic acid formed in the peroxide stage was the lignin, but also uronic acids and xylans contributed to the formation to a large extent. Considering the bark, in addition to oxalates already present especially in the outer bark, it also formed more oxalic acid during the peroxide treatment. Effective debarking is therefore important for preventing oxalate related scaling.
Suitable and simple pretreatment methods were established for analysis of soluble oxalate, as well as for the acidification of pulp samples prior to total oxalate analysis. Filtration must be done at process temperature immediately after sampling for getting the soluble oxalate content correct, but afterwards the sample can be stored in a freezer without problem. Considering the total oxalate analysis, acidification with 2 M HCl to pH 1 under heating and mixing at 70°C for 30 min is sufficient to render all oxalate in soluble form for the analysis. Frozen pulp samples can be treated the same way, but it is recommended that the pulp sample should be acidified directly after sampling to make the solubilisation easier. Additionally, if metal ions like calcium are not of interest, strongly acidic cation exchange resins can be used for oxalate solubilisation with good recovery.

I. INTRODUCTION

Calcium oxalate scaling is a common problem in many pulp and paper mills, as well as in sugar plants, breweries, other biorefineries, and in the form of urinary and kidney stones also in medicine [1]. In pulping and papermaking, oxalic acid (OA) is coming into the processes with the wood raw material, especially if it is poorly debarked, and then it is formed from other wood components especially in oxidative bleaching stages, like in the alkaline peroxide bleaching of mechanical pulps [2]. Calcium oxalate is actually one of the most problematic scale salts occurring in pulp and paper production processes. Calcium oxalate scaling in a paper machine system often leads to disturbances in the process, production losses due to downtime needed for cleaning, as well as impaired paper quality. Calcium oxalate scale in paper mills is also a source for so-called hickeys, a particular type of print defect. In many mills, the calcium oxalate phenomenon is well known and a lot of resources are used to monitor and solve the problem. However, there is still a lack of a thorough understanding of the formation of the scale salt in pulping and papermaking, and therefore the actions taken are often ineffective. For monitoring the oxalate balance in the processes or for evaluating the efficacy of chemical anti-scale treatment, reliable methods for oxalate analysis are a must [3]. Analysing or monitoring oxalate balances between soluble and precipitated form are important to evaluate the efficiency of anti-scale agents.

In this work, isolated wood components and representative sugars for spruce wood were treated in a laboratory peroxide-stage and the OA formation was analysed with ion chromatography [2]. The effect of pulp sample pretreatment and storage methods was evaluated both for soluble and total oxalate analysis by ion chromatography [3].

II. EXPERIMENTAL

Materials

In total 20 different substances (cellobiose, mannose, glucose, galactose, xylose, arabinose, glucuronic acid, galacturonic acid, acetic acid, birch xylans (both commercial and laboratory-prepared) and then spruce-related galactoglucomannans, milled wood lignin, TMP lignin, EMAL lignin, wood resin, hydroxymatairesinol lignans, inner bark, outer bark, and groundwood pulp) were studied for oxalate formation after alkaline peroxide treatment [2].

Alkaline peroxide treatment (P)

The various substances were treated with P-stage chemicals at 2% consistency in test tubes, and the amount of OA released was determined by ion exchange chromatography (IEC) [2].

Sample pretreatment procedures

Three parallel samples of peroxide-bleached groundwood pulp were kept in process temperature, room temperature, and in a freezer before filtration and analysis of soluble oxalate [3]. The filtrates were also stored in a freezer and analyzed after melting. Precipitation of calcium oxalate was induced in a suspension of unbleached groundwood pulp by adding oxalate and calcium solutions. Different methods were evaluated for recovery of oxalate for analysis, including acidification with 2 M HCl to different pH values and utilization of acidic cation exchange resin.

Analyses

All oxalate analyses were carried out by IEC by means of a Dionex DX-500 IEC equipped with an autosampler and suppressed conductivity detector (details in [2,3]) after filtration of the samples with Whatman ME25 membranes (0.45 µm pore size). The residual peroxide level was determined by Merckoquant® 1.10081.0001 peroxide test strips (Merck KGaA, Darmstadt, Germany) in 100 times diluted samples, which is better suited for small sample amounts than iodimetric titration.

III. RESULTS AND DISCUSSION

From the monosaccharides, most oxalic acid was formed from the uronic acids, i.e. from galacturonic and glucuronic acid, during the alkaline peroxide treatment. More oxalic acid was formed from pentoses, i.e. xylose and arabinose, compared to hexoses, i.e. mannose, glucose, and galactose. These results are due to the fact that uronic acids and pentoses are more easily degraded than hexoses, and give an indication that xylans and pectins are a more significant source of oxalate than galactoglucomannans in alkaline peroxide bleaching.

Among the isolated wood components, xylans were the largest single source for oxalic acid formation in the alkaline peroxide treatment. However, when considering the relatively low xylan content in spruce wood, its contribution is less significant compared for example to lignin. Both lignin and xylans have been pointed out as major sources of oxalate in alkaline peroxide bleaching [4, 5]. Spruce bark samples were found to contain large amounts of native oxalates, and more oxalic acid was further formed in alkaline peroxide treatment. Hence, good debarking is essential for preventing calcium oxalate scaling. In **Figure 1** the relative contributions of different wood components on oxalic acid formation have been estimated from the results by calculation based on their average contents in spruce wood. Based on these results it can be concluded that lignin is the principal source of oxalate in alkaline peroxide bleaching, but the contribution of hemicelluloses and pectins can also be regarded as significant.

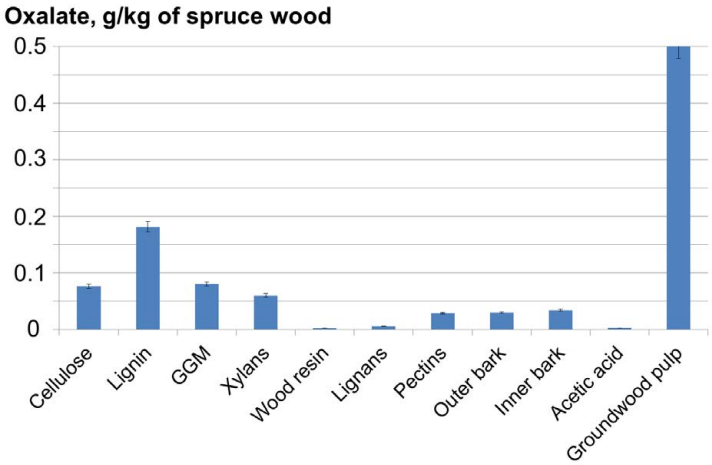

Figure 1. Relative contribution of different wood components on oxalate formation in alkaline peroxide treatment based on their average content in Norway spruce (The values used in the calculations for the individual components were the following: cellulose: 40%; lignin: 27.5%; GGM: 17.5%; xylans: 7.5%; wood resin: 1%; lignans: 1%; pectins: 1.5%; outer bark: 0.2%; inner bark: 0.5%; acetic acid: 2%; groundwood pulp: 100%)

The amounts of soluble oxalate in peroxide-bleached groundwood pulp sample analysed by IC after different sample pretreatments are listed in **Table 1**. It can clearly be seen that the amount of soluble oxalate in the sample

is decreased by the delay and the temperature drop between sampling and filtration. Not even re-heating of the pulp sample to the process temperature (63°C in this case) can bring the original soluble oxalate back to the soluble form once it has been precipitated, which is shown here for a frozen pulp sample. It can thereby be concluded that for reliable determination of soluble oxalate in a specific process stage, the sample filtration has to be done directly after sampling at the ambient process temperature. Thereafter, the filtrate can be stored in a freezer without any major impact on analysis result, if the analysis cannot be carried out right away (Table 1).

Table 1. Effect of sample pretreatment procedure on soluble oxalate analysis by IC (peroxide-bleached groundwood pulp)

Sample	**Oxalate, mg/L**
Filtrated at 63°C	18.0
Filtrated at 63°C → Frozen → Melted	17.8
Filtrated at 25°C	6.2
Frozen → Heated to 63°C → Filtrated	8.1

Some variation in the results for total oxalate amount in the peroxide-bleached groundwood pulp was observed, when the end-pH varied in sample acidification with 1 M HCl. Therefore, oxalate recovery experiments with different acidification procedures were carried out using unbleached groundwood pulp suspension, where calcium oxalate precipitation was induced by addition of oxalate (50 mg/L) and calcium (200 mg/L) ions. **Table 2** summarises the results from the recovery experiments. In the Blank sample that was filtrated in room temperature without any acidification, only a minor amount of the total oxalate could be analysed, indicating a strong precipitation of calcium oxalate in the pulp suspension. The analysed oxalate amount gradually increased with decreased acidification pH (2 M HCl) when the sample was heated and mixed for 30 min at 70°C, the highest recovery rate obtained at end-pH 1. The effect of acidification pH and temperature on oxalate solubilisation has been shown in earlier studies for pulp samples [6], urine samples [7], and plant material [8]. A good recovery of oxalate was also obtained by mixing with acidic cation exchange resin, although the end-pH was only ~ 2. Drawbacks of using this type of resins are the fairly high consumption and the need to wash the resin properly before use. Also the analysis of metal ions like calcium in the same sample is not possible as these are bound to the resin.

Table 2. Effect of sample acidification method on oxalate recovery after induced precipitation from unbleached groundwood pulp suspension for IC analysis (IE resin=cation exchange resin Amberlite IR-120). (Added oxalate amount: 50 mg/L; added calcium amount: 200 mg/L. Contribution of pulp to the total oxalate amount ~ 2 mg/L).

Sample	**Total oxalate, mg/L**
Blank (25°C)	5.7
pH 1.7 (2 M HCl, 70°C)	42.1
pH 1.4 (2 M HCl, 70°C)	49.8
pH 1 (2 M HCl, 70°C)	54.2
IE resin (70°C)	49.5

IV. CONCLUSIONS

From spruce wood components, lignin was found to be the major source of oxalic acid formed in alkaline peroxide treatment, considering its high content in wood. Large amount of oxalate was also formed from pectic acids and xylans, but as their content in spruce is much lower, their contribution is at the same level as that for galactoglucomannans. However, the total amount of oxalic acid formed from hemicelluloses, pectins, and even lignans can be regarded as significant, especially when they can occur in high concentrations as dissolved substances in the process waters. This makes them well exposed for bleaching chemicals. A probable reason for the high oxalic acid formation from xylans is its composition from pentose units, i.e., xylose and arabionose, as

well as from methyl glucuronic acid side groups. Spruce bark, especially the outer bark, was found to contain large amount of native oxalates, and a substantial amount of OA was further formed under P-conditions. Accordingly, a good debarking is an essential part of calcium oxalate scale control in pulp and paper mills.

Proper sample pretreatment procedures are essential for reliable oxalate analysis, especially if the target is to monitor oxalate solubility and balances in a process. For analysis of soluble oxalate in a pulp or filtrate sample, the filtration has to be carried out at process temperature directly after sampling. Otherwise the soluble part of the oxalate will start to precipitate. The membrane filtrate can be acidified with hydrochloric acid to pH<2 to ensure oxalate solubility and stored in freezer without affecting the results. For total oxalate analysis, acidification with 2 M hydrochloric acid to pH 1 with heating and mixing at 70°C for 30 min is enough to ensure that all the oxalate is in soluble form for analysis. This can be carried out also for pulp samples that have been stored frozen, but it is recommended that also acidification and filtration for total oxalate analysis is done just after sampling as this will make the solubilization easier. Also strongly acidic cation exchange resins can be used for oxalate solubilization with good recovery, if analysis of metal ions like calcium is not desired.

V. ACKNOWLEDGEMENT

We acknowledge Kemira Oyj, Sappi Fine Paper Europe, and the International Doctoral Programme in Bioproducts Technology (PaPSaT) for financing of the work. This work was also part of the activities at Åbo Akademi Process Chemistry Centre.

VI. REFERENCES

[1] Häärä, M.; Sundberg, A.; Willför, S. Calcium oxalate - a source of "hickey" problems - A literature review on oxalate formation, analysis and scale control. *Nord. Pulp Pap. Res. J.* **2011**, *26*, 263–282.

[2] Häärä, M.; Sundberg, A.; Pranovich, A.; Willför, S. Formation of oxalic acid in alkaline peroxide treatment of different wood components. *Holzforschung*, online first, DOI: 10.1515/hf-2013-0123.

[3] Häärä, M.; Konn, J.; Sundberg, A.; Willför, S. Sample pretreatment for oxalate analysis and the effect of peroxide bleaching parameters on oxalate formation. *Nord. Pulp Pap. Res. J.* **2013**, *28*, 42–50.

[4] Yu, L., Ni, Y. Oxalate formation during peroxide bleaching of mechanical pulps. *Appita J.* **2005**, *58(2),* 138-142, 148.

[5] Sjöde, A., Jönsson, L.J., Nilvebrant N.-O. Oxalic acid in bleaching processes - formation and control, *Proc. 13th International Symposium on Wood, Fibre and Pulping Chemistry*, 16-19 May, **2005**, Auckland, New Zealand, 2: 303-309.

[6] Reimann, A., De Sousa, F., Jansson, M.B. A method for the analysis of oxalic acid and calcium oxalate in kraft mill bleaching samples. Poster presentation, *6th European Workshop on Lignocellulosics and Pulp (EWLP 2000)*, 3-6 Sep, **2000**, Bordeaux, France, 543-546.

[7] Hodginson, A. Sampling errors in the determination of urine calcium and oxalate: solubility of calcium oxalate in HCl-urine mixtures. *Clin. Chim. Acta* **1981**, *109*, 239-244.

[8] Holmes, R.P., Kennedy, M. Estimation of the oxalate content of foods and daily oxalate intake. *Kidney Int.* **2000**, *57*, 1662-1667.

NANOFIBRILLATED CELLULOSE PREPARED FROM TEMPO OXIDATION ACTING AS TEMPLATES FOR SYNTHESIS OF CONDUCTING POLYMERS AND IN SITU FORMATION OF BIOCOMPOSITES

Chunlin Xu[1]*, Ann-Sofie Leppänen[1], Jun Liu[1], Patrycja Bober[1,2], Xiaoju Wang[1],Tom Lindfors[1], Rose-Marie Latonen[1], Stefan Willför[1]

[1]Process Chemistry Centre, Åbo Akademi University, Porthansgatan 3, 20500, Turku, Finland;
*[2]Institute of Macromolecular Chemistry, Academy of Sciences of the Czech Republic, 162 06 Prague 6, Czech Republic; (*cxu@abo.fi)*

ABSTRACT

Nanofibrillated cellulose (NFC), also termed as cellulose nanofiber, can be prepared by 2,2,6,6-tetramethylpiperidine-1-oxyl radical (TEMPO)-mediated oxidation, which introduces anionic carboxylate groups on the fibril surfaces. Here, we present a novel approach for fabricating NFC/conducting polymer composites using anionic NFC as a synthesis template and constructing matrix. Firstly, we developed chemo-enzymatic processes to utilize anionic water-soluble polysaccharides or their derivatives, i.e. κ-carrageenan or TEMPO-oxidized spruce *O*-acetyl galactoglucomannan (GGM) as a template instead of conventional synthetic polymers for polymerization of aniline. Afterwards, the optimized process was applied to anionic NFC. Moreover, these templates could be directly processed with polyaniline (PANI) and utilized as construction components of the final PANI-biocomposites. Another conducting polymer, i.e. polypyrrole (PPy) was synthesized using anionic NFC as a template. Notably, the resulted NFC/conducting polymer hydrogel can be directly processed to various forms of biocomposites with good mechanical strength, which may find potential applications in biosensors and biomedical engineering.

I. INTRODUCTION

Cellulose, the most abundant biorenewable material on this planet with its promising properties such as excellent mechanical strength and flexibility, biocompatibility, and environmentally-friendly nature, has found its potential applications in a broad spectrum of areas, e.g. organic electronics, biosensors, and biomedical engineering [1, 2]. NFC has recently been extensively studied and can be prepared by mechanical, chemical, and enzymatic treatments. Isogai et al. has developed an oxidation approach using TEMPO to selectively convert primary hydroxyls exposed on the surface of crystalline cellulose fibrils to anionic carboxylate groups (–COOH) [3]. High available surface area and high mechanical performance make NFC a good material as loading matrix and carriers to build up nanostructured composites in the forms of hydrogels [4], aerogels [5], sheets, and fibers for applications such as cosmetics, water or oil absorbents, electronic actuators, and other functional materials. Hemicelluloses, the second most abundant biorenewable materials, are water-extractable with controlled pH values depending on their structures and origins [6]. GGMs, which are the main softwood hemicelluloses and water soluble, can be isolated from Norway spruce (*Picea abies*) [7]. The good water solubility of those polysaccharides has made them easy to be modified in water targeting different applications. One approach to utilize cellulose and other polysaccharides is to tailor structured composites by incorporating functionalities, e.g. conductivity, from other composite component while keeping the intrinsic properties of polysaccharides.

Conducting polymers, particularly PANI and PPy, have attracted a lot of attention ascribed to numerous potential applications in electrical, chemical, biomedical, and sensing materials due to their advantages such as chemical stability, tunable conductivity, and the ease to synthesize [8]. However, the limited water solubility and poor mechanical properties are restricting their application potential ability. For instance, the anionic template polystyrene sulfonate has been used as a template for synthesis of PANI to increase the water solubility of PANI and to avoid branching caused by the unselectivity of the reaction, which could lower the conductivity of the resulting PANI [9]. To increase the mechanical properties, formation of composites of polymeric material with desired mechanical strength may broaden their potential in various applications.

We report new approaches for fabricating conducting biocomposites using anionic NFC from TEMPO oxidation as a template. A chemo-enzymatic approach was applied to utilize natural polysaccharides as templates instead of conventional synthetic polymers for laccase-catalyzed polymerization of aniline [10]. Firstly, anionic κ-carrageenan (κ-CGN, a naturally occurring anionic polysaccharide from algae) and TEMPO-oxidized GGM (GGM_{PolyU}) were assessed as anionic templates. Moreover, the study was extended to use anionic NFC as a template. For the polymerization of pyrrole, anionic NFC was used as a template, while silver nitrate or iron(III) nitrate or their mixtures were used as oxidants. The resulted conducting composite hydrogel was injectable and could be directly processed to a flexible free-standing film or other forms of biocomposites with good mechanical strength, which may find potential applications in biosensors and biomedical engineering [3, 7].

II. EXPERIMENTAL

Materials

Aniline (99%, Riedel de Haën) and pyrrole (≥98%, Sigma Aldrich) were purified either by extraction or by distillation prior to use. Laccase from *Trametes versicolor* (EC 1.10.3.2, 13.6 U/mg), κ-CGN, silver nitrate and iron(III) nitrate were purchased from Sigma-Aldrich (Steinheim, Germany) without further purification prior to use. GGM was isolated from a process water of thermomechanical pulping as was previously reported by Willför et al. [7] Bleached birch kraft pulp was obtained from UPM-Kymmene as a gift.

Preparation of NFC.

Procedures were optimized from [3] and briefly described as follows: Cellulose fibers (2 g) were dispersed in 100 mL distilled water and stirred for 4 h at room temperature and oxidized by adding 32 mg TEMPO (0.1 mmol/g fiber), 200 mg sodium bromide (1.0 mmol/g fiber), and 10% NaClO dropwise (10 mmol/g fiber). The pH value was kept at 10.5 by the addition of 0.5 M NaOH. The resulted oxidized fibers were purified by precipitation in ethanol with a ratio of 1:3 (v/v) and thoroughly washed with distilled water by filtration and further fibrillated by a domestic blender (OBH Nordica 6658, Denmark) for 2 min at an output of 300 W. The carboxylate content was determined by conductometric titration.

TEMPO oxidation of GGM

Fully oxidized polyuronic acid derivative of GGM (GGM_{PolyU}) was prepared by TEMPO oxidation according to the method modified by Parikka et al. [11] Shortly, GGM (500 mg) in aqueous solution (50 mL) was oxidized by adding NaBr (750 mg), TEMPO (5 mg), and NaClO (10-15% solution, pH adjusted to 10, 10 mL) at 2-4 °C. The pH value of the solution was kept at 10 by adding 0.5 M NaOH. The product was then purified by dialysis against distilled water (membrane cut-off 12000-14000 g/mol) and freeze-dried.

Synthesis of polyaniline

Polymerization of aniline was performed in aqueous phase containing anionic polysaccharides: κ-CGN, GGM_{PolyU}, or NFC, respectively [10]. Laccase was used as a catalyst. The pH value was adjusted and kept to 3-4 using phosphoric acid. The reaction mixture was stirred at room temperature for overnight. The resulted dark-green PANI-based hydrogel was purified by dialysis against 1 mM HCl (pH 3) for three days (membrane cut-off 12000-14000 g/mol).

Synthesis of polypyrrole

Polymerization of pyrrole was performed in aqueous phase containing NFC by oxidation of pyrrole with silver nitrate or iron(III) nitrate or their mixtures of various composition. The oxidant-to-pyrrole molar ratio was 2.3. The reaction mixture was left to stand at room temperature for 24 h or for one week in case of oxidation just with silver nitrate. The product was isolated by filtering through a membrane with 0.2 µm pores (Durapore PVDF, hydrophilic).

Processing of the conducting composites

For spray coating, an office copy paper was covered by a patterned mask using ELISA microarray as a template. The PANI composite hydrogel was sprayed using an air-brush. Both PANI-based hydrogels and PPy-based suspensions were filtrated through a membrane with pore size of either 0.05 µm (Whatman Nuclepore Track-Etch polycarbonate) or 0.22 µm (Durapore PVDF, hydrophilic) and dried in vacuum desiccator at 40 °C. Conducting films were obtained.

Characterization

UV-VIS spectra were recorded on a Perkin-Elmer Lambda 40 UV/VIS spectrometer for the aqueous solutions at room temperature. Fourier transform infrared spectroscopy (FTIR) spectra were recorded on an FTIR spectrophotometer with the ALPHA platinum Attenuated Total Reflectance (ATR) - single reflection diamond ATR module. The spectra were obtained in the frequency range of 4000–400 cm^{-1} at a resolution of 2 cm^{-1} in the transmittance mode. The electrical conductivity of the samples was characterized by 4-point probe measurements, in a linear configuration, having a tip spacing of 1.79 mm. A constant bias current was applied over the sample and the corresponding voltage was measured (Keithley 2400 SourceMeter®). The conductivity of the samples was calculated using finite-size corrections. The electrochemical characterization on the biocomposites was performed in cyclic voltammetry mode with an IviumStat potentiostat (Ivium Technologies BV, the Netherlands) connected to a conventional three-electrode cell, which was equipped with an Ag/AgCl/KCl (saturated) reference electrode and platinum wire auxiliary electrode. ITO glass with a defined project area coated by casting the hydrogels of polysaccharide/PANI composites was used as the working electrode. All measurements were carried out at room temperature in 0.1 M HCl solution containing 0.1 M NaCl as a supporting electrolyte.

III. RESULTS AND DISCUSSION

To polymerize PANI, the amount of aniline used in the reactions was adjusted in correspondence to the amount of anionic groups in the polysaccharide templates (Table 1), which are sulfate in κ-CGN (2.6 mmol/g) and carboxylate in GGM_{PolyU} (4.5 mmol/g) and NFC (0.8 mmol/g), respectively. The pH value of the reaction was critical for aniline polymerization using the laccase *Trametes hirsuta*. It was adjusted to ~2 in κ-CGN reaction and 3.7 in GGM and NFC reactions. Green color was observed when conducting PANI was formed. The formation of the conducting form of PANI was verified in the UV-VIS spectra (Figure 1), in which a broad absorption band between 700-800 nm and a shoulder at 400-420 nm appeared and can be assigned to the polaron of conducting PANI [12].

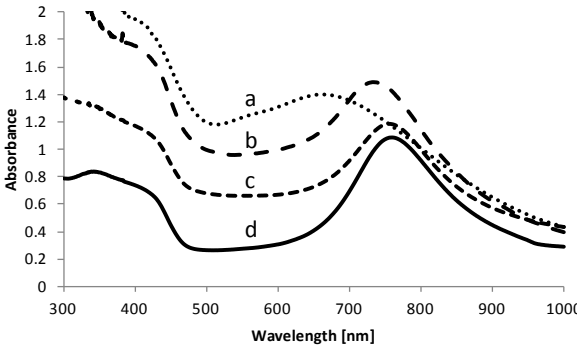

Figure 1. UV-VIS of PANI polymerized using different polysaccharide templates: a) GGM; b) GGM_{PolyU}; c) NFC; and d) κ-CGN[10].

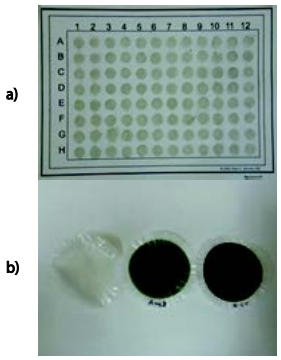

Figure 2. a) A dot array of κ-CGN/PANI mask-spray coated on office copy paper with dots (d=7 mm); b). Films of NFC; NFC/PANI (-COOH-aniline 1:2); NFC/PANI (-COOH-aniline 1:10) (from left to right) [10].

In situ polymerization of PPy in the presence of anionic NFC was assessed by FTIR (not shown). The amount of pyrrole was adjusted in correspondence to the amount of anionic groups of NFC (1.55 mmol/g). After polymerization, appearance of the bands at 1305 cm^{-1} assigned to the C–N in-plane bending and 1571 cm^{-1} assigned to C=N stretching vibration proves the formation of PPy [13].

The good water solubility of the PANI-based composites and good dispersibility of the PPy-based composites prepared using our approaches offers a variety of facile processing means for further application. The hydrogel of κ-CGN/PANI composite was micropatterned on an office copy paper by mask-spray coating using normal ELISA microarray plates as template (Figure 2a).

Owed to the high mechanical properties of NFC, both PANI-based hydrogel and PPy-based suspension were directly processed to films (Figure 2b). In the composite films, the NFC formed a matrix of nanofibers, which was coated by conducting polymers during synthesis. The conductivity was measured on those resulted films by a four-point probing method. The highest conductivity of the PANI films investigated was $5x10^{-3}$ S/cm for the κ-CGN/PANI composite at a sulfate-aniline ratio of 1:2. The highest value obtained for GGM_{PolyU}/PANI film was$1.4x10^{-7}$ S/cm at a carboxylate-aniline ratio of 1:1. The highest conductivity of NFC/PANI composites was $9x10^{-7}$ S/cm at a carboxylate-aniline ratio of 1:10. The conductivity of NFC/PPy composite film reached as high as 2 x 10^{-3} S/cm which is in the same range of conductivity values obtained as previously reported for tunicate cellulose/PPy film (10^{-3} to 10^{-4} S/cm) [13].

Moreover, the PANI hydrogel was also deposited on an ITO glass. The cyclic voltammetry profile confirmed the electrochemical nature of the PANI composite. Two sets of redox peaks at $E_{1/2}$ = 0.22 V and $E_{1/2}$ = 0.42 V over full potential window from -0.2 V to 1.2 V were observed and it is consistent with previous studies on the conducting PANI in template-growing complexes [14].

Table 1. The conductivity of PANI- and PPy-based composite films.

Samples	Anionic group/Anilne or Pyrrole ratio	Conductivity, S/cm
κ-CGN/PANI	1:1	$6x10^{-7}$
κ-CGN/PANI	1:2	$5x10^{-3}$
GGM_{PolyU}/PANI	1:1	$1.4x10^{-7}$

NFC	-	$3x10^{-8}$
NFC/PANI	1:10	$9x10^{-7}$
NFC/PPy	1:10	2×10^{-3}

IV. CONCLUSIONS

We have developed new approaches for fabricating conducting biocomposites using anionic polysaccharides as templates. NFC obtained from TEMPO oxidation and other anionic polysaccharides can be used as templates for laccase-catalyzed polymerization of aniline. NFC can also be used as a template in the polymerization of pyrrole. The resulted conducting composite hydrogels or suspensions are injectable and can be directly processed to flexible and conducting films or other forms of biocomposites with good mechanical strength, which may find potential applications in biosensors and biomedical engineering.

V. ACKNOWLEDGEMENT

The Graduate School for Biomass Refining (A.-S.L.), Johan Gadolin Scholarship Programme (P.B.) at the Process Chemistry Centre at Åbo Akademi University (Finland), the Chinese Scholarship Council, and the Graduate School of Chemical Engineering (J.L.) are acknowledged for funding the research. Dr. Markus Pesonen is thanked for the conductivity measurements.

VI. REFERENCES

[1] Cheng, C.; Martinez, A.; Gong, J.; Mace, C.; Philips, S.; Carrilho, E.; Mirica, K.; Whitesides, G. Paper-based ELISA. *Angew. Chem. Int. Ed.* **2010**, *49*, 4771-4774.

[2] Xu, C.; Spadiut, O.; Araújo, A.; Nakhai, A.; Brumer, H. Chemo-enzymatic assembly of clickable cellulose surfaces via multivalent polysaccharides. *ChemSusChem* **2012**, *5*, 661-665.

[3] Saito, T.; Isogai, A. TEMPO-Mediated Oxidation of Native Cellulose. The effect of oxidation conditions on chemical and crystal structures of the water-insoluble fractions. *Biomacromolecules* **2004**, *5*, 1983-1989.

[4] Pääkkö, M.; Ankerfors, M.; Kosonen, H.; Nykänen, A.; Ahola, S.; Österberg, M.; Ruokolainen, J.; Laine, J.; Larsson, P.; Ikkala, O.; Lindström, T. Enzymatic hydrolysis combined with mechanical shearing and high-pressure homogenization for nanoscale cellulose fibrils and strong gels. *Biomacromolecules* **2007**, *8*,1934-1941.

[5] Olsson, R.T.; Azizi Samir, M.A.S.; Salazar-Alvarez, G.; Belova, L.; Ström, V.; Berglund, L.A.; Ikkala, O.; Nogués, J.; Gedde, U.W. Making flexible magnetic aerogels and stiff magnetic nanopaper using cellulose nanofibrils as templates. *Nature Nanotech.* **2010**, *5*, 584-588.

[6] Willför, S.; Sundberg, A.; Hemming, J.; Holmbom, B. Polysaccharides in some industrially important softwood species. *Wood Sci. Technol.* **2005**, *39*, 245-257.

[7] Willför, S.; Rehn, P.; Sundberg, A.; Sundberg, K.; Holmbom, B. Recovery of water-soluble acetylgalactoglucomannans from mechanical pulp of spruce. *Tappi J.* **2003**, 2, 27-32.

[8] MacDiarmid, A.G. "Synthetic Metals": A novel role for organic polymers (Nobel Lecture). Angew. Chem. Int. Ed. **2001**, *40*, 2581-2590.

[9] Samuelson, L.; Anagnostopoulus, A.; Alva, K.; Kumar, J.; Tripathy, S. Biologically derived conducting and water soluble polyaniline. Macromolecul. **1998**, *31*, 4376-4378.

[10] Leppänen, A.-S.; Xu, C.; Liu, J.; Wang, X.; Pesonen, M.; Willför, S. Anionic polysaccharides as templates for the synthesis of conducting polyaniline and as structural matrix for conducting biocomposites. Macromol. Rapid Commun. **2013**, *34*, 1056-1061.

[11] Parikka, K.; Leppänen, A.-S.; Xu, C.; Pitkänen, L.; Eronen, P.; Österberg, M.; Brumer, H.; Willför, S.; Tenkanen, M. Functional and anionic cellulose-interacting polymers by selective chemo-enzymatic carboxylation of galactose-containing polysaccharides. Biomacromolecules **2012**, *13*, 2418-2428.

[12] Shumakovich, G.; Vasil'eva, I.; Morozova, O.; Khomenkov, V.; Staroverova, I.; Budashov, I.; Kurochkin, I.; Boyeva, J.; Sergeyev, V.; Yaropolov, A. A comparative study of water dispersible polyaniline nanocomposites prepared by laccase-catalyzed and chemical methods. J. Appl. Polym. Sci. **2010**, *117*, 1544-1550.

[13] Zhang, D.; Zhang, Q.; Gao, K.; Piao, G. A nanocellulose Polypyrrole Composite Based on Tunicate Cellulose. Int. J. Polym. Sci. **2013**, Article ID *175609*, 1-6.

[14] Chan, H.; Ho, P.; Ng, S.; Tan, B.T.G.; Tan, K. A New Water-Soluble, Self-Doping Conducting Polyaniline from Poly(o-aminobenzylphosphonic acid) and Its Sodium Salts: Synthesis and Characterization. J. Am. Chem. SoC. **1995**, *117*, 8517-8523.

AVAP® PROCESS: CONVERSION OF LIGNOCELLULOSICS INTO VALUE-ADDED CHEMICALS

Xiang You[1,*], Adriaan van Heiningen[1,2], Herbert Sixta[1] and Mikhail Iakovlev[1]

[1] *Department of Forest Products Technology, School of Chemical Technology, Aalto University, P.O. Box 16300, FI-0076, Aalto, Finland*

[2] *Department of Chemical and Biological Engineering, University of Maine, 5737 Jenness Hall, Orono, ME, USA*

[*] *Corresponding author: xiang.you@aalto.fi*

ABSTRACT

The AVAP® process utilizes SO_2-ethanol-water cooking liquor to fractionate lignocellulosics into its three principal components. In addition to complete conversion of biomass polysaccharides to biofuels, this process is capable of producing traditional pulp and paper products, dissolving pulp as well as nanocellulose. The advantages of the AVAP® process are absence of base, higher dissolved sugar yields due to absence of oxidation, higher flexibility in raw materials (pine and larch are readily digestible), and considerably lower overall duration due to absence of impregnation stage.

INTRODUCTION

The depletion of conventional petroleum reserves is one of the pressing global issues. Due to the environmental concerns as well as energy security issues, it is necessary to promote alternative solutions to reduce the consumption of fossil fuels. Therefore, the routes for conversion of renewable materials are being developed which cover an extensive range of combined technologies aiming to produce bio-fuels (for example, ethanol or butanol), bio-materials (for example, fibres, pulp for paper manufacture) and bio-chemicals (for example, lactic, succinic acids, etc.). The importance of the biorefinery concept is now widely accepted throughout the world. This implies utilization of various renewable feedstocks (softwoods, hardwoods and annual plants) by applying various technologies. Numerous pathways are developed to satisfy low energy requirement, low waste generation, high resource efficiency, low operation time and equipment size, and efficient chemicals recovery [1]. The aim of this emerging bio-industry is to utilize biomass for the production of bio-based materials as progressive replacement for conventional fuels [2]. Unfortunately, the conventional acid sulfite and Kraft processes have significant limitations to meet the requirements of the biorefinery concept [3-4].

In acid sulfite pulping, the cooking liquor contains hydrosulfites (referred to as combined SO_2) and sulfur dioxide (called free SO_2). The employed cations are calcium, magnesium, sodium, or ammonium [5]. The recovery of the base represents a major problem (not possible for calcium, limited recovery rate of about 75-80% for magnesium, [6]). The sulfite process is suitable for some softwoods (such as spruce, fir, and hemlock), and hardwoods (such as poplar and eucalyptus). However, resinous softwoods and tannin-containing hardwoods are more difficult to handle. An important disadvantage of acid sulfite pulping is a wasteful oxidation of monosaccharides by hydrosulfite anions [6]. The Kraft process suffers from extensive carbohydrate losses, whereby most of the dissolved hemicelluloses are degraded to hydroxycarboxylic acids. Prehydrolysis-kraft (PHK) process was developed to produce dissolving pulp and also offers the possibility to recover the hemicelluloses. It consists of two steps: first wood chips are pre-treated in a high temperature prehydrolysis step to remove hemicelluloses, and, secondly, the hemicellulose-lean wood chips are subjected to kraft pulping to remove lignin [7]. There are a few serious disadvantages associated with this concept, 1) the precipitation of sticky lignin while handling the prehydrolysate, 2) highly reactive intermediate products formed during water prehydrolysis and undergoing condensation reactions, 3) high capital cost due to increased recovery requirements (the released sugars cannot be recovered since they are displaced to the neutralization liquor and burnt). This paper describes the advantages of a new Biorefinery technology in comparison to acid sulfite and PHK processes.

American Value Added Pulping (AVAP®) is a process utilizing SO_2-ethanol-water (SEW) solutions to fractionate lignocellulosic feedstocks into the principal components – cellulose, hemicellulose sugars and lignin, at full yields. AVAP® pulping was studied as a promising fractionation process to be used as a core component of the forest biorefinery. The chemistry of the process is close to that of acid sulfite pulping with the difference being that the base is replaced by ethanol. The presence of SO_2 leads to dissolution of hemicelluloses in high yield mostly as monomeric sugars, while lignin becomes soluble through sulfonation. This process can be considered a hybrid between acid sulfite and organosolv pulping. The absence of base (such as Na, Mg or Ca) leads to very low hydrosulfite anion concentrations, which greatly simplifies the recovery cycle. Sulfonation is therefore achieved by sulfur dioxide itself [8]. Furthermore, ethanol increases the impregnation rate of dissolved SO_2 into wood, thereby avoiding the impregnation stage. In this way the fractionation time of a continuous SEW cook will be very much shorter than the cover-to-cover cooking time of a batch acid sulfite cooking. The acidity of the SEW cooking liquor at pulping temperature is similar to that of acid sulfite cooking, due to an increased pK_a of $SO_2 \cdot H_2O$ in an ethanol-water solution. In addition to complete conversion of biomass polysaccharides into bio-fuels and chemicals, this process is capable of producing high quality traditional pulp and paper products.

A wide range of lignocellulosics including low-quality forest (such as branches and tree tops; softwoods/hardwoods) and agricultural (such as wheat straw and palm empty fruit bunches) residues is used as feedstock for AVAP® fractionation, producing relatively pure cellulosic fibers and monomeric hemicellulose sugar solution [9]. Exceptional ability to delignify softwoods is due to the high nucleophilicity of SO_2, while the advantages for annual plants include efficient chemicals recovery as well as avoiding scaling problems related to alkaline solubilization of silica. The fibers can then be enzymatically hydrolyzed to produce glucose. Low residual lignin content and increased lignin hydrophilicity result in high sugar yields at low enzyme charges. The sugars serve as platform for further biochemical/chemical transformation to value-added products.

REFERENCES

[1] Morais, A. and Bogel-Lukasil, R., 2013. Green chemistry and the biorefinery concept. Sustainable Chemical Processes. 1:18, 1-3.

[2] Cherubini, F., 2010. The biorefinery concept: Using biomass instead of oil for Producing Energy and chemicals. Energy Conversion and Management. 51,1412-1421.

[3] Yamamoto, M., Iakovlev, M. and van Heiningen, A., 2014. Kinetics of SO_2-ethanol-water (SEW) fractionation of hardwood and softwood biomass. Bioresource Technology. 155, 307-313.

[4] Sixta, H., Iakovlev, M., Testova, L., Roselli, A., Hummel, M., Borrega, M., van Heiningen, A., Froschauer, C. and Schottenberger, H., 2013. Novel concepts of dissolving pulp production. Cellulose. 20, 1547-1561.

[5] Deslauriers, M., Trozzi, C. and Woodfield, M., 2006. Processes in wood, paper pulp, food, drink and other industries-Paper pulp (acid sulphite process). In EMEP/CORINAIR Emission Inventory Guidebook. SNAP code 040603. Chapter B463, European Environment Agency.1-12.

[6] Sixta, H., Potthast, A. and Krotchek, A.W., 2006. Chemical Pulping Processes. Handbook of Pulp, Vol 1. Ed. H. Sixta. Publ. WILEY-VCH Verlag GmbH & Co. KgaA, Weinheim. 109-510.

[7] Saeed, A., Jahan, M.S., Li, H., Liu, Z., Ni, Y. and van Heiningen, A., 2012. Mass balance of components dissolved in the pre-hydrolysis liquor of kraft-based dissolving pulp production process from Canadian hardwoods. Biomass and Bioenergy. 39, 14-19.

[8] Iakovlev, M., You, X., van Heiningen, A. and Sixta, H., 2014. SO_2-ethanol-water (SEW) fractionation process: production of dissolving pulp from spruce. Cellulose. DOI 10.1007/s10570-014-0202-x. Published online: 19 February 2014.

[9] Iakovlev, M., You, X., van Heiningen, A. and Sixta, H., 2014. SO_2-ethanol-water (SEW) fractionation of spruce: kinetics and conditions for paper and viscose-grade dissolving pulps. RSC Advances. 4, 1938-1950.

CONVERSION OF LIGNIN INTO HIGH-VALUED LIGNIN-PHENOL–FORMALDEHYDE (LPF) RESIN ADHESIVE AND IMPROVING THE ECONOMICS OF THE BIOREFINERY

Tong-Qi Yuan[1]*, Sheng Yang[1], Feng Xu[1], Run-Cang Sun[1,2]

*[1]Beijing Key Laboratory of Lignocellulosic Chemistry, Beijing Forestry University, Beijing, 100083, China; [2]State Key Laboratory of Pulp and Paper Engineering, South China University of Technology, Guangzhou, 510640, China. (*ytq581234@bjfu.edu.cn)*

ABSTRACT

The objective of this study was to produce high performance lignin-phenol-formaldehyde (LPF) resin adhesives and offset the cost of the biorefinery. A new method was applied to calculate the active sites of technical lignin for substitution of phenol based on quantitative ^{31}P NMR analysis. The results showed that phenol could be partially replaced by lignin in the range of 10%-60%, and high performance LPF adhesives could be prepared as compared with control phenol formaldehyde (CPF) resin adhesive. According to the corresponding Chinese National Standard, the bonding strength and formaldehyde emission of poplar plywoods bonded by the LPF adhesives can meet the requirement of the first grade and E_0 grade of plywood, respectively. NMR analyses indicated that the LPF and CPF adhesives have similar chemical structure and curing behavior.

I. INTRODUCTION

Phenol-formaldehyde (PF) resin adhesive is widely used in plywood industry. It provides high strength and is extremely resistant to moisture, which prevents delamination and gives excellent temperature stability. With the increasing demand for plywood, the requirement for PF adhesive is increasing. However, the phenol is an expensive and high-toxic substance, which is produced from the non-renewable petroleum resource. In fact, both the high price and the emission of harmful substances have restricted the utilization of PF adhesive. Lignin is structurally similar to phenol, which makes it possible for technical lignin to be used as substitute for phenol in the synthesis of PF resin [1]. Besides, the technical lignin is an abundant, cheap, nontoxic, and renewable resource. It is obviously that the substitution of technical lignin for phenol in the synthesis of PF resin will not only alleviate the dependence on petroleum resource but also provide an avenue for high value-added application of technical lignin.

Various technical lignins have been used for the production of lignin-phenol-formaldehyde (LPF) resin adhesives and some of the LPF have been produced in pilot scale. However, the low activity and heterogeneity of technical lignins restrict their large scale application in adhesive industry. Technical lignins have been used in LPF adhesive with two methods, copolymerization with phenol and formaldehyde or blending with PF resin. Generally, the properties of the adhesive products, which were produced by lignin as substitution of phenol directly, were inferior to pure phenolic resin adhesive. In addition, a high substitution rate was also hard to be achieved. There are two major reasons for these disadvantages; one is the complexity of different technical lignins and the other is the unreasonable determination of the active sites in lignin. In order to increase the reaction active of lignin for the PF adhesive synthesis, some modification processes have been applied [2-4]. However, these processes inevitably increased the cost and offset the price advantage of the technical lignins. Thus, a reasonable method, in which technical lignin is directly used for PF adhesive production with a high substitution rate, is needed to produce low toxic and high performance LPF adhesives.

In this study, a novel method was applied to calculate the active sites of technical lignin for substitution of phenol based on quantitative ^{31}P NMR analysis and a reasonable formulation was obtained. The technical lignin was analyzed by ^{31}P NMR to get the exact amount of different –OH groups of lignin units. Then, the active sites, which could react with formaldehyde, could be calculated according to the ^{31}P NMR results. A reasonable proportion between lignin and formaldehyde could be achieved through this method. The LPF adhesives, which were produced based on the reasonable formulation, were characterized by chemical, structural, and thermal analyses. The effects of substitution rate on the properties of the LPF adhesives were also investigated.

II. EXPERIMENTAL

Materials

Technical lignin extracted from corncob was kindly supplied by Longlive Biotechnology Company, Shandong province, China. The lignin obtained was placed in a vacuum dryer at 50 ºC for 16 h to constant weight before used. Phenol, formaldehyde solution (37%), sodium hydroxide, and urea were of reagent grade and used as obtained without purification. The control PF adhesive was purchased from Beijing Taier Chemical Co., Ltd.

Characterization of the Technical lignin

The chemical and structural features of the lignin were determined according to a previous literature [5].

Preparation of LPF adhesives

The total formaldehyde was calculated according to the molar ratio of total phenol to formaldehyde 1:1.8. The NaOH weight was 20% of the total weight of phenol and technical lignin. The substitution rates were in the range from 10% to 60%. In the first step, phenol, technical lignin, 1/2 of the formaldehyde, and 1/2 of the NaOH solution (30% concentration) were mixed in a three flask. The mixture was heated for 1 h at 80 ºC. Then, another 1/2 of the formaldehyde and 1/4 of the NaOH solution were added in the flask for 1.5 h at 80 ºC. Finally, the temperature of the mixture was decreased to 65 ºC, and then the remaining 1/4 NaOH solution and urea (5% of total weight of phenol and technical lignin) were added in the flask for 0.5 h. When the reaction was completed, the LPF adhesive was rapidly cooled to 40 ºC. A LPF adhesive, which regarded lignin as pure phenol completely with a 40% substitution rate, was also produced as a comparison.

Preparation and characterization of plywoods

The three-layer poplar plywoods (400 mm×400 mm×4.5 mm) were prepared. Wheat flour was added into the adhesive as filler, and the proportion is 20wt% to the CPF/LPF adhesives. The core veneer was coated with 140-160 g/m^2 adhesive each sides. The coated veneers were hot-pressed at 145 ºC under 1.0 MPa for 7.0 min. The bond strength and formaldehyde emission of the plywoods were measured according to the Chinese National Standard (GB/T 17657-1999).

Characterization of CPF and LPF adhesives

The properties of the adhesives were determined in accordance with the Chinese National Standard (GB/T 14704-2006). The liquid state ^{13}C-NMR spectra and CP/MAS ^{13}C-NMR spectra of the CPF and LPF adhesives were characterized according to previous papers [5,6].

III. RESULTS AND DISCUSSION

Technical lignin characterization

The technical lignin contained 88.5% acid-insoluble lignin, 4.7% acid-soluble lignin, and 0.3% polysaccharides. Moisture and ash contents were determined gravimetrically to be 6.45 and 2.12%, respectively. Both M_w and M_n of the acetylated lignin were relative low (3258 g/mol and 2260 g/mol), which suggested that the technical lignin used was more suitable for the condensation with phenol and formaldehyde due to the less steric hindrance [7].

Table 1. Characterization of the technical lignin by quantitative ^{31}P NMR spectroscopy.

Parameter	Technical lignin
^{31}P-NMR analysis (mmol/g)	
Aliphatic ―OH	1.77
Condensed phenolic―OH in S units	0.10
Noncondensed phenolic―OH in S units	0.55
Condensed phenolic―OH in G units	0.22
Noncondensed phenolic―OH in G units	0.42
Noncondensed phenolic―OH in H units	0.65
―COOH	1.09
Active sites	1.72

The contents of different hydroxyl groups of the technical lignin were calculated based on previous literatures and the results are summarized in Table 1 [5]. In this research, the amount of unsubstitude ortho and para sites of

phenolic hydroxyl groups in lignin units was calculated as active sites. The proportion of 1g lignin equal to pure phenol could be got based on the value of active sites, which was given in Table 1. The weight of the technical lignin equal to the weight of pure phenol in each experiment was calculated based on this proportion. The equaled phenol weight of lignin and the weight of pure phenol used in each experiment were regarded as total phenol weight. Then a reasonable formulation could be got based on this result for the production of low cost, low toxic, and high quality LPF adhesive.

Performance of CPF and LPF resins as plywood adhesives

Table 2 shows the properties of the CPF and LPF adhesives. The content of free formaldehyde in the different LPF adhesives produced according to our reasonable formulation, were lower than that of the CPF adhesive except for the 60% LPF. However, the contents of free formaldehyde in the LPF adhesives were significantly lower than the value of 40% LPF^{-1} adhesive. This indicated that the formaldehyde can fully participated in hydroxymethylated reaction with an appropriate amount in the synthesis process. The contents of free phenol in the LPF adhesives were higher than that of the CPF adhesive. This may due to the reduction of formaldehyde content in our formulation. However, the contents of free phenol in the LPF adhesives were still far below the limit requirement of Chinese National Standard (GB/T 14732-2006).

With increase of the substitution rate of lignin to phenol from 10% to 60%, the bonding strength of plywoods decreased from 1.35 MPa to 0.84 MPa. However, the bonding strength can meet the requirement of the first grade of plywood (⩾0.7 MPa). The formaldehyde emissions of plywood samples bonded by the LPF adhesives were all lower than the value of the CPF adhesive except for 40% LPF-1. These results confirmed that all the plywoods bonded by the LPF adhesives can meet E_0 grade (⩽0.5 mg/L). It could be found that the substitution rate can reach 50% at most, without influencing the properties and applicability of adhesives significantly. Thus, the 50% LPF adhesive could be regarded as an adhesives product with good comprehensive properties. The LPF adhesive with 60% substitution rate was difficult in coating on the wood, owing to its high viscosity (17696 mPa•s). These results indicated that the formulation based on accurate analysis of the active sites in lignin with ^{31}P NMR could produce low formaldehyde emission, high substitution rate, and superior quality LPF adhesives.

Table 2. Various adhesives and their performances.

Adhesive	Adhesive performances					Plywood performances	
	pH	Viscosity	Solid	Free	Free	Bonding	Formaldehyde
CPF	12.6	132.9	43.96	0.241	0.11	1.53	0.25
10% LPF[a]	11.3	54.0	51.35	0.082	1.68	1.35	0.24
20% LPF	11.4	115.8	54.12	0.086	1.46	1.30	0.20
30% LPF	11.5	283.1	56.23	0.099	1.15	1.28	0.19
40% LPF	11.5	415.7	56.29	0.136	1.41	1.15	0.17
40% LPF-1[b]	11.2	722.0	53.87	0.710	0.34	1.26	1.29
50% LPF	11.6	1239	58.22	0.181	1.15	1.00	0.13
60% LPF	12.1	17696	59.54	0.289	0.96	0.84	0.11
GB/T 14732	≥7	≥60	≥35	≤0.3	≤6	≥0.7	≤0.5

[a] 10% LPF is the adhesive of technical lignin substituted phenol by 10 wt%. The following 20~60% LPF et al. are the same meaning. [b] The technical lignin was regarded as pure phenol completely in this experiment.

NMR analysis

Liquid state ^{13}C NMR spectra of the uncured CPF adhesive, the uncured LPF (20% LPF and 50% LPF) adhesives, and the technical lignin are shown in Figure 1a. The spectra of the uncured LPF adhesives were similar with that of the uncured CPF adhesive. However, some differences between the two types of adhesives could also be observed as the co-condensation of lignin. Such as the signals from G units (117 ppm, unsubstituted position in benzene ring) and $-OCH_3$ groups (56 ppm). The broad signals around 129-131 ppm are assigned to the ortho and para carbon sites, which have been substituted on the aromatic ring. The peaks around 61-64 ppm and 35-40 ppm are assigned to the methylol groups and the methylene bridges, respectively. These results indicated that the technical lignin had been embedded into the adhesive system during the synthesis process of the LPF adhesives.

^{13}C CP/MAS NMR spectra for the cured CPF adhesive and the cured LPF adhesives are shown in Figure 1b. As compared with the spectra of the uncured adhesives, the increase of the signals at 35-40 ppm was accompanied by the decrease of the signals at 61-64 ppm. The peaks of unsubstitued positions at around 117 ppm also decreased significantly. These results indicated that the polymerization of both adhesives occurred via the

condensation of methylol groups with active sites to form methylene bridges. The similarity of curing behavior and cured structure between the CPF adhesive and the LPF adhesives indicated that the formulation which was used to produce the LPF adhesives in this research was reasonable.

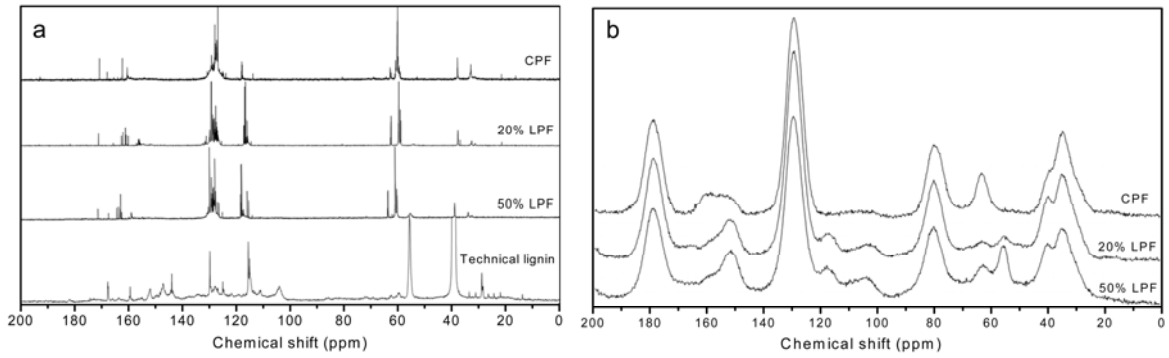

Figure 1. (a) Liquid state ^{13}C NMR spectra of the uncured LPF and CPF adhesives, and the technical lignin; (b) solid state CP-MAS ^{13}C NMR spectra of the cured LPF and CPF adhesives.

IV. CONCLUSIONS

LPF adhesive with good comprehensive performance can be synthesized according to the formulation based on quantitative ^{31}P NMR analysis of the technical lignin. The properties of the LPF adhesives and plywoods prepared could meet the corresponding Chinese National Standard successfully. Both the LPF and CPF adhesives have similar structure and curing behavior. The LPF adhesive with 50% substitution rate could be regarded as an ideal product. It is believed that the development of value-added LPF adhesive from lignin will greatly improve the economics of the biorefinery.

V. ACKNOWLEDGEMENT

We are grateful for financial support of this research from National Science Foundation of China (31110103902) and Major State Basic Research Projects of China (973-2010CB732204).

VI. REFERENCES

[1] Pizzi, A.; Mittal, K.L. Handbook of adhesive and technology, in Pizzi, A.; (Eds.), Natural Phenolic Adhesives II: Lignin. Introduction to the Electronic Age. Marcel Dekker Inc., New York, **2003**, pp. 589-599.

[2] Sudan, V. Process for preparing a black liquor-phenol formaldehyde thermoset resin. US Patent, **2003**, 6632912.

[3] Vázquez, G.; González, J.; Freire, S.; Antorrena, G. Effect of chemical modification of lignin on the gluebond performance of lignin-phenolic resins. *Bioresour. Technol.* **1997**, *60*, 191–198.

[4] Xiao, Z.G.; Li, Y.H.; Wu, X.R.; Qi, G.Y.; Li, N.B.; Zhang, K.; Wang, D.H.; Sun. X.Z.S.S. Utilization of sorghum lignin to improve adhesion strength of soy protein adhesives on wood veneer. *Ind. Crop. Prod.* **2013**, *50*, 501–509.

[5] Yuan, T.Q.; Sun, S.N.; Xu, F.; Sun, R.C. Structural characterization of lignin from triploid of Populus tomentosa Carr.. *J. Agric. Food Chem.* **2011**, *59*, 6605–6615.

[6] Yuan, T.Q.; Sun, S.N.; Xu, F.; Sun, R.C. Homogeneous esterification of poplar wood in an ionic liquid under mild conditions: Characterization and properties. *J. Agric. Food Chem*. **2010**, *58*, 11302–11310.

[7] El Mansouri, N.E.; Salvadó, J. Structural characterization of technical lignins for the production of adhesives: Application to lignosulfonate, kraft, soda-anthraquinone, organosolv and ethanol process lignins. *Ind. Crop. Prod*. **2006**, *24*, 8–16.

REACTIONABILITY OF ACID AND ORGANOSOLV PRETREATED ASPEN WOOD IN THE PROCESS OF ENZYMATIC HYDROLYSIS

Zorov I.N. [1,2], Rozhkova A.M.[1,*], Osipov D.O.[1], Sinitsyn A.P.[1,2]

*[1]A.N. Bach Institute of Biochemistry RAS, 119071, Russia, Moscow, Leninskii pr-t 33/2, Tel.:+7(495) 954-52-83; [2] M.V. Lomonosov Moscow State University, Dept. of Enzyme Chemistry, 119991, Moscow, Russia, Vorobievi gori 1-11, Tel.:+7(495) 939-16-71 (*amrojkova@mail.ru)*

ABSTRACT

The comparative study of the efficacy of aspen wood biomass pretreatment process followed by enzymatic hydrolysis was performed. Pretreatment includes semi-coarse milling (200-300um particles) followed by prehydrolysis by aqueous solutions of sulfuric and nitric acids, and by organosolve. The influence of acid concentration, temperature, organic phase ratio, and pressure on the efficacy of pretreatment was studied. The increase of organosolve pretreated aspen wood biomass reactionability was 3,5-4 fold to compare to untreated substrate. Nitric acid pretreatment leads to over 5 fold increase of the substrate reactionability.

I. INTRODUCTION

Aspen is a fast-growing but relatively low value wood culture to compare to pine and fur-tree, that are most abandon in Russia. Aspen wood has a limited implementation in pulp-and-paper, and is used mainly in production of plywood, wood particleboards, and matches [1]. Despite of aspen is considered as a low value product and even as a by-product in industrial forestry, it has a huge potential as a feedstock for biorefinery processes. Variable value-added organic acids, biofuels, and other building blocks for chemical industry could by obtained through microbiological or chemical conversion of C5 and C6 sugars derived from plant polysaccharides [2-4]. Efficient biochemical conversion of natural polysaccharides into fermentable sugars requires pretreatment procedures that lead to cellulose crystallinity index reduction and partial reduction of lignin content [5]. Typical aspen wood contains 42-50% of cellulose, 19-22% of hemicelluloses, and relatively low (around 21-22%) percentage of lignin. Such polysaccharides/lignin ratio in addition to fast-growing makes aspen a promising nonfood feedstock for biotechnological transformation and applications.

The efficiency of different types of woody biomass pretreatment varies in terms of costs and simple sugars yield after the following enzymatic hydrolysis [6-8]. High efficacy of pretreatment with diluted aqueous solutions of inorganic acids or with acidic solutions of different organic solvents (mainly alcohols) was shown for woody materials [9,10].

The main goal of the study was to search for optimal aspen wood pretreatment conditions that yield in high simple sugars content after enzymatic saccharification.

II. EXPERIMENTAL

Pretreatment

Chips of aspen (*Populus tremula,* collected at Tver' region, Russia) were milled to form the particles of 200-300 um at the industrial impeller mill Microxylema IM-450 ("Monolit-stroj", Russia). 4,5 grams of milled aspen wood (dry weight) were placed into the high pressure SS container (length 174 mm, diameter 29 mm, net volume 30 cm^3, total volume 55 cm^3) and aqueous or water-organic solutions containing different concentration of sulfuric or nitric acid were added. The containers were tightly stoppered and placed into the bath (approx. 2L) containing preheated paraffin. After certain time the containers were cooled down in room temperature water. The reaction mixture was centrifuged (10 minutes, 4000g), the precipitate was washed twice with 50% ethanol solution and neutralized by 1M NaOH to the pH 4,8-5,0. The suspension was recentrifuged and precipitate was used for enzymatic hydrolysis.

Enzyme preparations

Lyophilized cultural fluids of *Penicillium verruculosum* cellulase and β-glucosidase strains (B1 #3.147.2 and F10 #3.201.2) were used for enzymatic hydrolysis of pretreated aspen wood. *Penicillium* cellulase preparations exhibits higher saccharification ability to compare to commercial *Trichoderma* cellulases [11,12].

Activities of enzyme preparations

Medium viscosity carboxymethylcellulose sodium salt (*CMC*, Sigma C4888), birchwood xylan (*Xyl*, Sigma X0502), 4-nitrophenyl β-D-glucopyranoside (*pNPG*, Sigma N7006), chromatography filter paper #1 (*FP*, Whatman, England),

microcrystalline cellulose (avicel PH-101, *MCC*) (Serva, Germany), cellobiose (*G2*, Merck 2352, Germany) were used for determination of enzymatic activity [13]. One Unit corresponds to the amount of enzyme which will release 1 μmoL of reducing sugar equivalents (expressed as glucose) per minute at pH 5.0 and 40 °C or 50 °C. Initial concentration of polymeric substrates was 5g/L, and 1mM for cellobiose and 4-nitrophenyl β-D-glucopyranoside. Protein concentration in enzyme preparations was measured using Lowry assay.

Enzymatic hydrolysis of pretreated aspen wood

Enzymatic hydrolysis was performed in 50 mL plastic containers using the shaking flask thermostat (50 ^{o}C, 250 RPM, pH 5.0). Reaction mixture (20 mL total volume) consists of 100 g/L of pretreated substrate in 0.1M sodium acetate buffer. Enzymes content was 10mg of B1 and 3 mg of F10 per 1 gram of substrate (dry weight). Glucose and reducing sugars concentration were measured in aliquots after 3, 6, 24, and 48 hours using glucoseoxidase/peroxidase and Nelson-Somogui assays [13]. The reactionability of pretreated substrates mean the reducing sugars and glucose release after 48 hours of enzymatic hydrolysis.

III. RESULTS AND DISCUSSION

Relatively low reactionability of natural, untreated wood biomass during enzymatic hydrolysis by cellulolytic enzymes is due to unproductive absorption of enzymes on lignin, screening of cellulose by non-cellulosic polysaccharides, and resistance of cellulose crystalline regions towards enzymatic attack. Pretreatment methods can resolve the problem of low reactionability but there is no universal pretreatment method yet suitable due to high variety of the components for different biomass stocks. Pretreatment method selection or the combination of different methods for particular regional biomass feedstock and cost-efficient process optimization is usually needed. Energy consumption during pretreatment as well as the price of enzyme preparation impacts primarily on fermentable sugars net costs. The formation of various inhibitors during pretreatment process is another considerable issue.
Based on *Penicillium verruculosum* recombinant strains the highly efficient and relatively low cost cellulase and β-glucosidase enzyme preparations have been developed. Total and specific enzyme activities of the preparations used are presented at **Table 1**. These preparations were used in the process of enzymatic hydrolysis of pretreated aspen wood.

Table 1. Total and specific enzyme activities of *P. verruculosum* B1 и *P. verruculosum* F10 preparations.

Substrate / Enzyme preparation	*FP*	*MCC*	*CMC*	*pNPG*	*G2*	*Xyl*
	50ºC, pH5,0	40ºC, pH5,0	50ºC, pH5,0	40ºC, pH5,0	40ºC, pH5,0	50ºC, pH5,0
Total enzymatic activity, U/g of preparation						
B1	760	580	15120	1400	605	25030
F10	147	853	4575	35260	46660	620
Specific activities, U/mg of protein						
B1	0,92	0,9	18,3	1,70	0,73	30,3
F10	0,19	1,1	5,9	45,5	60,2	0,8

Fine (2-5um) milling and activation is an efficient but expensive and not scalable method for biomass pretreatment. The combination of low cost coarse milling of biomass followed by diluted acid or organosolve pretreatment was studied.
Sulfuric acid is widely used for pretreatment of various cellulosic substrates – corn cobs, bagasse, straw, and wood. Diluted acid pretreatment at 100-180 ^{o}C leads to partial degradation and dissolution of hemicelluloses as well as partial decrystallization of cellulosic fibrils that make cellulose molecules more available for hydrolytic enzymes. The pretreatment of aspen wood with 0.9-12.5% sulfuric acid in the temperature range 120-180^{o}C were performed in our work. The acid concentration 7% at 140 ^{o}C did not lead to any further increase in reactionability and yield in 58 mg/ml of reducing sugars or 74% of polysaccharide conversion after 48 hours of enzymatic hydrolysis. The conversion rate decreases to 58%, 55% and 50% at sulfuric acid concentration of 4.4, 2.0 and 0.9% respectively.
In despite of relatively high yield of reducing sugars the yield of former transformation of above sugars to ethanol or butanol by yeast and bacterial strains was very low probably due to various inhibitors (acetate, furfural) generation at high concentration of sulfuric acid.
The initial concentration of sulfuric acid could be significantly reduced in case of organosolve pretreatment with ethanol or butanol as an organic component. The concentration of sulfuric acid at 0.3-0.6% during organosolve pretreatment provided the conversion of aspen polysaccharides at the range of 56-77% after 48 h of enzymatic hydrolysis.

The impact of ethanol and butanol concentrations and their ratio in organic phase on the efficacy of organosolve pretreatment of aspen was studied. In general, butanol acts as a more efficient extracting agent to compare to ethanol, however different ratio of ethanol/butanol mixtures in organosolve leads to promising results (**Figure 1**).

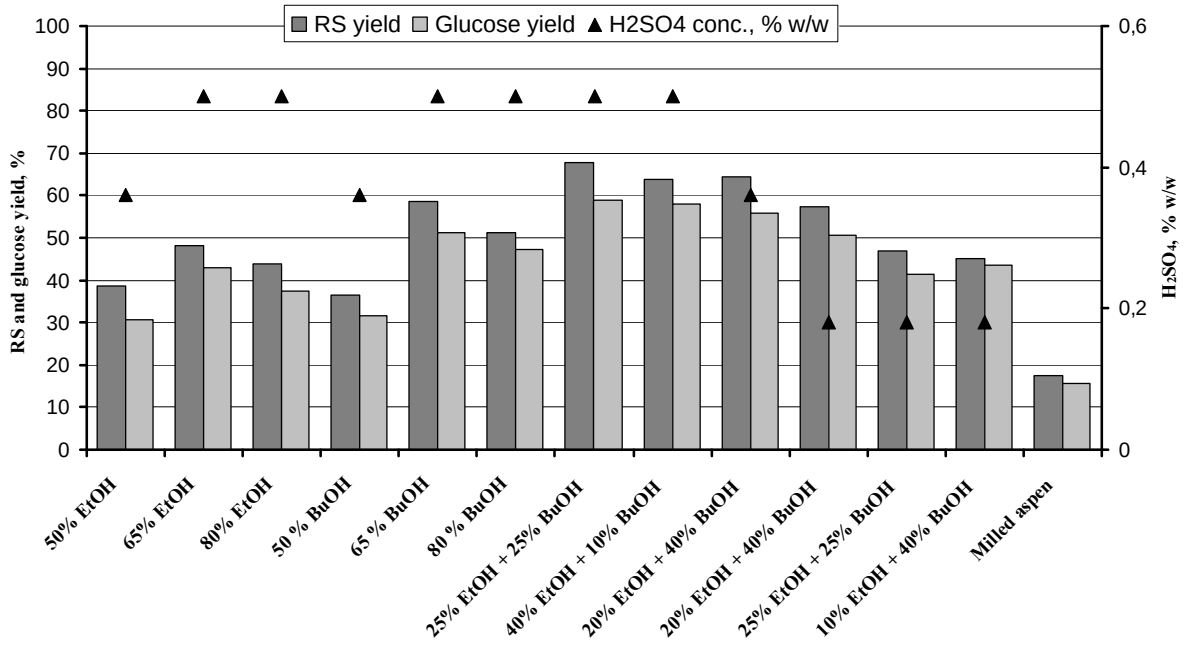

Figure 1. Reducing sugars (RS) and glucose yield, % from total polysaccharides of organosolve pretreated aspen wood after 48 hours of enzymatic hydrolysis.

Nitric acid could be an alternative to sulfuric acid used widely in biomass pretreatment processes. Sulfuric salts and sulfonated derivatives of plant polymers could be environmentally unfriendly while nitric derivatives, that is formed in pretreatment process appears to be the significant nitrogen source for microbial transformation step, following the enzymatic hydrolysis.

The effect of aspen wood pretreatment with diluted nitrogen acid under various conditions was studied. RS and glucose yield is shown at **Figure 2** for some selected cases. The yield of reducing sugars and glucose after 48 hours of enzymatic hydrolysis of wood pretreated for 10 minutes by 4.8% nitric acid at 100^{o}C and by 1.0% at 130^{o}C were comparable to the best results obtained for organosolve pretreated samples (see **Figure 1**). The increase of pressure inside the reaction vessel impacts highly in the increase of substrate reactionability. Close to 100% conversion rate of cellulose and hemicellolose was obtained after 10 minutes pretreatment of aspen with 4% nitric acid at 18-20 bars overpressure. In general much shorter time is needed for pretreatment with nitric acid to reach plant polymers conversion comparable to organosolve pretreatment. Temperature and acid concentration windows are much wider for nitric acid pretreatment in comparison with sulfuric acid or organosolve.

IV. CONCLUSIONS

- Pretreatment of aspen wood with sulfuric acid appears efficient only at relatively high acid concentration at temperatures not exceeding 140 ^{o}C.
- Organosolve pretreatment requires much less sulfuric acid to reach the same 3.5-4 fold increase of aspen wood reactionability in enzymatic hydrolysis processes.
- Nitric acid pretreatment of aspen is an alternative to sulfuric acid or organosolve pretreatment. 5 fold and over increase of reactionability of initially milled aspen substrate can be reached.

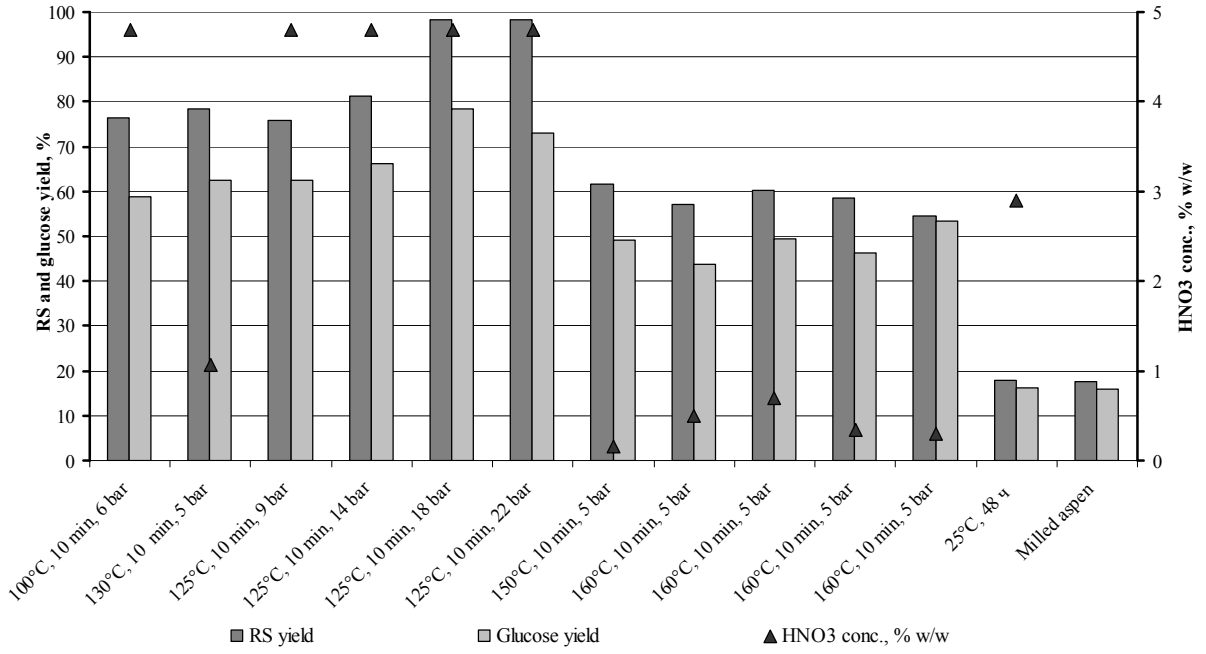

Figure 2. Reducing sugars (RS) and glucose yield, % from total polysaccharides of aspen wood, pretreated by nitric acid after 48 hours of enzymatic hydrolysis.

V. ACKNOWLEDGEMENT

The project was supported by Russian Federal Target Program "Research and development on priority Areas of Science and Technology complex of Russia for 2014-2020"

VI. REFERENCES

[1] Bukshtinov, A.D., *Groshev, B.I., Krylov , G.V.* Forests. *Moscow-Misl,* **1981**. 316.
[2] Johansson T. Increment and biomass in 26- to 91-year-old European aspen and some practical implications. *Biomass and Bioenergy*. **2002**, *23*, 245–255.
[3] Zhu J.Y., Gleisner R., Scott C.T., Luo X.L., Tian S. High titer ethanol production from simultaneous enzymatic saccharification and fermentation of aspen at high solids: A comparison between SPORL and dilute acid pretreatments. *Bioresource Technol.* **2011**, *102*, 8921–8929.
[4] Goshadrou A., Karimi K., Lefsrud M. Characterization of ionic liquid pretreated aspen wood using semi-quantitative methods for ethanol production. *Carbohydrate Polymers.* **2013**, *96,* 440– 449.
[5] Dotsenko, G.S., Chekushina, A.V., Kondrat'eva, E.G. et.al. Reactionability of various lignocellulosic substrates during enzymatic hydrolysis *Lesnoj vestnik*. **2012**, *8*, 129-135.
[6] Conde-Mejíaa C., Jiménez-Gutiérreza A., El-Halwagi M. A comparison of pretreatment methods for bioethanol production from lignocellulosic materials. *Process Safety and Environmental Protection*. **2012**, *90*, 189–202.
[7] Alvira P., Tomás-Pejó E., Ballesteros M., Negro M.J. Pretreatment technologies for an efficient bioethanol production process based on enzymatic hydrolysis: A review *Bioresource Technol*. **2010**, *101*, 4851–4861.
[8] Eggeman T., Elander R.T. Process and economic analysis of pretreatment technologies. *Bioresource Technol.* **2005**, *96*. 2019–2025.
[9] Papatheofanous M.G., Billa E., Koullas D.P., Monties B., Koukios E.G. Two stage acid-catalyzed fractionation of lignocellulosic biomass in aqueous ethanol systems at low temperatures *Bioresource Technol*. **1995**, *54*. 305–310.
[10] Park N., Kim H., Koo B., Yeo H., Choi I. Organosolv pretreatment with various catalysts for enhancing enzymatic hydrolysis of pitch pine (*Pinus rigida*) *Bioresource Technol.* **2010**, *101*, 7046-7053.
[11] Chekushina, A.V., Dotsenko G.S., Kondrat'eva, E.G., Sinitsyn, A.P. Enzyme preparations from *Penicillium verruculosum* for biomass conversion – an alternative to *Trichoderma*-based enzymes. *Biotechnologia*. **2013**, *3,* 69-80.
[12] Zorov, I.N., Gusakov, A.V., Baraznenok, V.A., Bekkarevich, A.O., Okunev, O.N., Sinitsyn, A.P, Kondrat'eva, E.G. Isolation and properties of cellobiase from *Penicillium verruculosum*. *Prikl. Biokhim. Mikrobiol*. **2001**, *37,* 687-693.
[13] Ghose T.K. Measurement of cellulase activities *Pure Appl. Chem.* **1987**, *59*, 257-268.

Author Index

D

E

F

G

H

I

J

K

L

M

N

O

P

Q

R

S

T

U

V

W

X

Y

Z

http://www.irnas.csic.es/users/delrio/Proceedings-13thEWLP.pdf